PROCEEDINGS OF THE EUROPEAN POLYMER CONGRESS 2011

June 26 - July 1, 2011 - Granada, Spain

European Polymer Congress 2011

European Polymer Federation

Specialized Group of Polymers (GEP)

Institute of Polymer Science and Technology

ISBN: 978-84-694-3124-5

EPF 2011

EUROPEAN POLYMER CONGRESS

GEP

European Polymer Congress 2011

XII Congress of the Specialized Group of Polymers

Congress Program

European Polymer Federation

Specialized Group of Polymers (GEP)

Institute of Polymer Science and Technology (ICTP-CSIC)

ISBN: 978-84-694-3124-5

TABLE OF CONTENTS

Dear friends and colleagues:

On behalf of the Organizing Committee I would like to welcome you to the European Polymer Congress EPF 2011 and XII GEP, in this special year of Chemistry and in the worldwide recognized city of Granada, meeting point of legendary cultures and world heritage site with a long history in the contributions to Science and Culture of different civilizations.

The European Polymer Congress is the main activity of the European Polymer Federation and has become a world reference in the field of Polymer Science and Technology with increasing interest of the Scientific Community. This edition has been carefully organized to present the most relevant and advanced vision of the Chemistry, Physics, Technology and Applications of the broad field of Polymers and composites. Thanks to the enormous interest of the most relevant researchers in the field, we have prepared an exciting program with 12 plenary leader speakers, six parallel sessions, 58 selected invited speakers, 432 podium presentations and more than 600 posters presentations that will be exhibited permanently during the five days of the congress.

The great attendance of excellent professionals in all of the Polymer Science and Technology fields will offer the best scenario to find colleagues and common interest with specialists all over the world. In addition, the legendary city of Granada will provide the complementary and excellent scenario for the success of an unforgettable meeting.

This congress could not have been organized without the work and contribution of individuals, groups and referential schools. Therefore, I would like to acknowledge to all the speakers, exhibitors, committee members, chairpersons, reviewers and all the people that have been involved in the organization and presentation of relevant results and perspectives.

Enjoy the EPF 2011 congress and breathe the special atmosphere of Granada and the “Alhambra Palace”.

Julio San Roman

Chair of the EPF2011 Congress

Dutch Polymer Institute will grant DPI Invention Award

The Dutch Polymer Institute (DPI) will grant the DPI Invention Award for the third time at the European Polymer Congress 2011 in Granada, Spain. The award will be granted to a researcher who has significantly contributed to the development of polymer research and technology in Europe and who has enabled scientific knowledge to be quickly converted into industrial applications.

The winner of the 2011 edition of the DPI Invention Award is Prof. Cor E. Koning of the Eindhoven University of Technology in The Netherlands. The organization of the European Polymer Congress and DPI have created a special session dedicated to this award on Wednesday 29 June from 14.30 – 16.15 hrs. The session features three lectures from academics working in the same field as the award winner. There will also be a lecture by Prof. Koning.

The research performed by Prof. Koning's group at Eindhoven University of Technology within the DPI programme has resulted in several inventions that were filed for patent because the inventions attracted the interest from industrial partners of DPI. In many cases this resulted in follow-up projects and/or transfers to parties who are now further developing the technologies.

Prof. Koning's work in the fields of bio-based as well as biocompatible/biodegradable polymers and conductive polymer nanocomposites (such as carbon nanotubes and graphene) fits perfectly with the societal and environmental responsibilities that are taking shape in DPI's research programme.

Dutch Polymer Institute

DPI was established in 1997 as a public-private partnership to perform pre-competitive research into polymers and their application, linking scientific knowledge to the industrial need for innovation. This results in added value for universities in the form of scientific publications and for companies in intellectual property rights and the possibilities to execute new activities. Some 200 researchers (PhDs and Post-Docs) are involved in DPI projects at known institutes throughout the world. DPI connects more than 30 national and international companies and almost 50 highly ranked knowledge institutes.

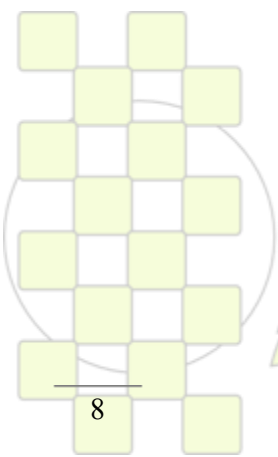

SPONSORS


CSIC
CONSEJO SUPERIOR DE INVESTIGACIONES CIENTÍFICAS


bio
CSIC
BIOMATERIALS GROUP


epf


GEP


ESB


GOBIERNO
DE ESPAÑA
MINISTERIO
DE CIENCIA
E INNOVACIÓN


ciber-bbn
Centro Investigación Biomédica en Red
Bioingeniería, Biomateriales y Nanomedicina


JUNTA DE ANDALUCIA


DPI
Dutch Polymer Institute

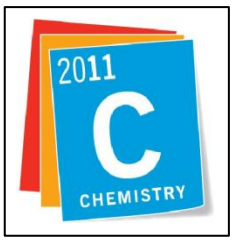
2011
C
CHEMISTRY


iesmat

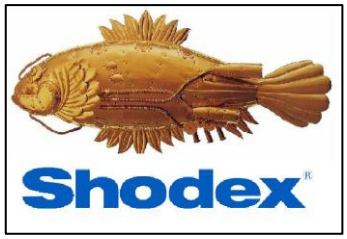
Shodex


WILEY


iFi

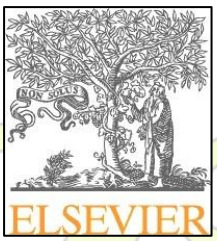
ELSEVIER


Iberlaser, s.a.
Electro-Óptica Científica e Industrial
Instrumentación y Láseres


TA
Instruments
Análisis Térmico, Reología y Microcalorímetría


Wyatt
Technology
www.wyatt.com


Malvern


ACS Publications
MOST TRUSTED. MOST CITED. MOST READ.


REPSOL


TOSOH BIOSCIENCE
TOSOH


Telstar
Instruments for solutions

INTERNATIONAL ADVISORY BOARD

Julio San Roman (President), *Spain*
Andrej Krzan (Gen. Secretary), *Slovenia*
Franz Stelzer (past President), *Austria*
Stanislaw Slomkowski (past Gen. Sec.), *Poland*
Majda Zigon, *Slovenia*
Christian Paulik, *Austria*
Hugo Berghmans, *Belgium*
Ivan Schopov, *Bulgaria*
Marica Ivankovic, *Croatia*
Søren Hvilsted, *Denmark*
Jukka Seppala, *Finland*
Daniel Grande, *France*
Hans-Wilhelm Engels, *Germany*
Klaus Mecke, *Germany*
Joachim Steinke *Great Britain*
Richard Jones, *Great Britain*
Nikos Hadjichristidis, *Greece*
Giancarlo Galli, *Italy*
Gundars Teteris, *Latvia*
Ludo Kleintjens, *Netherlands*
Andrzej Duda, *Poland*
Antonio Correia-Diogo, *Portugal*
Alexei R. Khokhlov, *Russia*
Piet J. Lemstra
Maria Omastova, *Slovakia*
Ann-Christine Albertsson, *Sweden*
Harm-Anton Klok, *Switzerland*
Teoman Tincer, *Turkey*
Jean Pierre Vairon, *France*
Akira Harada, *Japan*
Jean Francois Gerard, *France*
Allan Hoffman, *USA*
Christopher K. Ober, *USA*
Samuel Stupp, *USA*
Teruo Okano, *Japan*
Jean M. J. Frechet, *USA*
Hiroyuki Nishide, *Japan*
Krzysztof Matyjaszewski, *USA*
Jung-Il Jin, *Korea*
Eric Baer, *USA*
Cor Koning, *Netherlands*
M. Eugenia Muñoz, *Spain*
Virginia Cadiz, *Spain*
Luis Oriol, *Spain*
Begoña Peña, *Spain*
Jose M. Pereña, *Spain*
Concepcion Valencia Barragan, *Spain*
Sebastian Muñoz Guerra, *Spain*
Carmen Ramirez, *Spain*
Francisco Cimadevila, *Spain*
Jose C. Rodriguez Cabello, *Spain*
Jose M. Lagaron, *Spain*

LOCAL ORGANIZING COMMITTEE

Julio San Román (Chair)
Blanca Vazquez (Co-Chair)
Luis García-Fernández (Scientific Secretary)
Manuel Toledano
Raquel Osorio
Maria Rosa Aguilar
Luis Rodriguez-Lorenzo
Eva Maya Hernández
Antonio López Bravo
Mar Fernández Gutiérrez
María Luisa López Donaire
Belén Fernández-Montes Moraleda
Cristina Abradelo
Pablo Caracciolo
Álvaro González Gómez
Gema Rodríguez Crespo
Juan Parra
Francisco Parra
Patricia Suárez
Felisa Reyes
Jordi Girones
Jose Alberto Méndez
Concepción Domingo
Isabel Goñi
Marilo Gurruchaga
Raquel Palao Suay
Hazel Peniche

OFFICIAL LANGUAGE

The official language at the congress is English. No simultaneous translations will be provided.

REGISTRATION AND INFORMATION DESK

The registration desk for the European Polymer Congress 2011 will be located in the *Palace of Congress and Exhibitions of Granada Main Hall* and will be open from Sunday to Friday:

Sunday, June 26, 2011	14:00 – 19:00
Monday, June 27, 2011	8:00 – 19:00
Tuesday, June 28, 2011	8:00 – 19:00
Wednesday, June 29, 2011	8:00 – 19:00
Thursday, June 30, 2011	8:00 – 19:00
Friday, July 1, 2011	8:00 – 11:00

CONFERENCE IDENTIFICATION BADGE

A conference identification badge will be included in the conference material provided upon registration. Conference participants are required to wear their named badges in order to gain entry to the scientific sessions and social activities.

INTERNET CONNECTION

Free Wi-Fi will be available in the *Palace of Congress* during the five days of the meeting.

COFFEE BREAKS

During the session breaks, coffee, tea and refreshments will be served free of charge to participants wearing conference identification badges in the *Poster and Sponsor Area*.

LUNCHES

Informal lunches are included in the registration fee and will be served in the *Poster and Sponsor Area.*

INSTRUCTIONS FOR ORAL PRESENTATIONS

- Each lecture hall will be equipped with a computer and an overhead projector.
- The duration of the presentations is limited to:
  - 45 min for plenary lectures.
  - 30 min for invited lectures including discussion.
  - 15 min for oral presentations including discussion.
- File type: Microsoft Power Point. Please do not use fonts smaller than 16 pt.
- Please upload your file to the appropriate computer and check the presentation one day before your presentation. Please contact the support staff for assistance.
- It is strictly necessary that all podium speakers keep to their presentation times given. Chairpersons will have to control the timeframe in order to assure timely running parallel sessions.

INSTRUCTIONS FOR POSTER PRESENTATIONS

Poster session will take place during the coffee breaks over the five days of the congress.

The poster board will be marked with the poster number. Please refer to the Final Program for the poster number assigned to you.

Posters boards are 95 cm wide and 110 cm high. The preferred poster form is 90 cm wide and 100 cm high. Alternatively presenters may present their material on several smaller sheets, however please observe the maximum poster board size.

The title and author's names as stated in the submitted abstract should appear at the top of the poster. The text, illustrations, etc. should be of an appropriate size to be read from a distance of 1.5 meter (4.5 feet).

Tacks and technical equipment for hanging the poster will be available in the *Poster and Sponsor Area*.

The presenting authors are kindly requested to stay at their posters for discussion during the poster session.

Posters will be displayed during the entire congress in the *Poster and Sponsor Area*. The poster session and all breaks will provide excellent opportunities for in-depth discussions. All delegates are encouraged to visit and discuss the posters.

SOCIAL EVENTS

Sunday, June 26, 2011

20:00

Welcome reception at the TERRACE of the Palace of Congress with beautiful views of the Granada city and surrounding mountains at sunset.

Tuesday, June 28, 2011

21:00

Special dinner for chairpersons and invited speakers in an exclusive restaurant "La Chumbera" in the area of "Sacromonte" with beautiful views of the Alhambra Palace at night.

Transport by bus will be organized with departure from the Palace of Congress at 20:30.

Thursday, June 30, 2011

21:00

Gala dinner in the Restaurant "La Mamunia" near to Granada, with a nice decoration inspired in Nazari Period.

Transport by bus will be organized with departure from the Palace of Congress at 20:30.

CONFERENCE AREA FLOOR PLAN

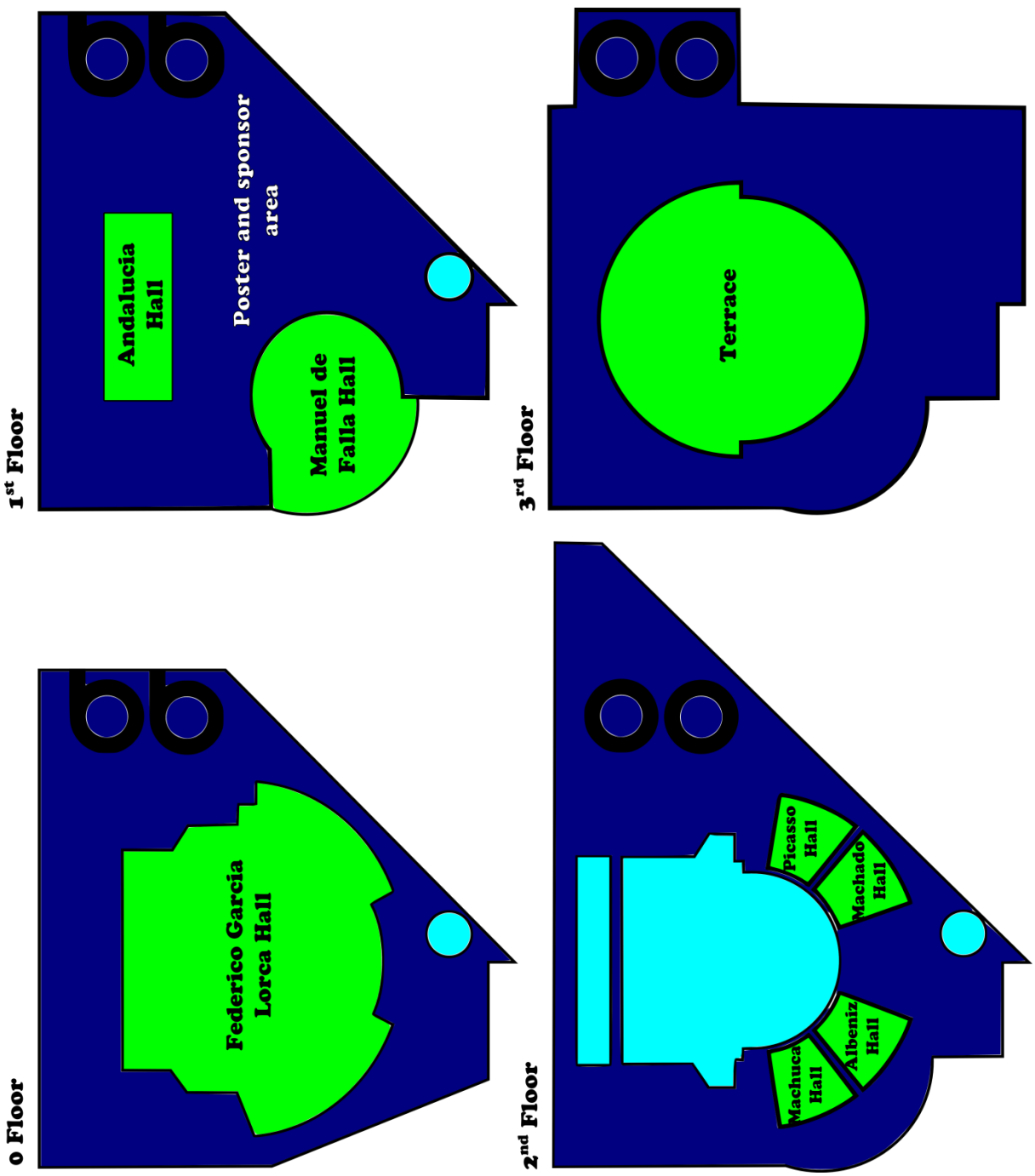

CONGRESS PROGRAM

SUNDAY, JUNE 26, 2011

14:00-17:30	**REGISTRATION**	
	FEDERICO GARCIA LORCA	
17:30-18:00	Official Opening	
18:00-18:45	OC - 1	**Cristopher K. Ober:** Life without polymers.
18:45-19:30	OC - 2	**Allan Hoffman:** Smart polymer applications in drug delivery and diagnostics.
	TERRACE	
20:00	Welcome Reception	

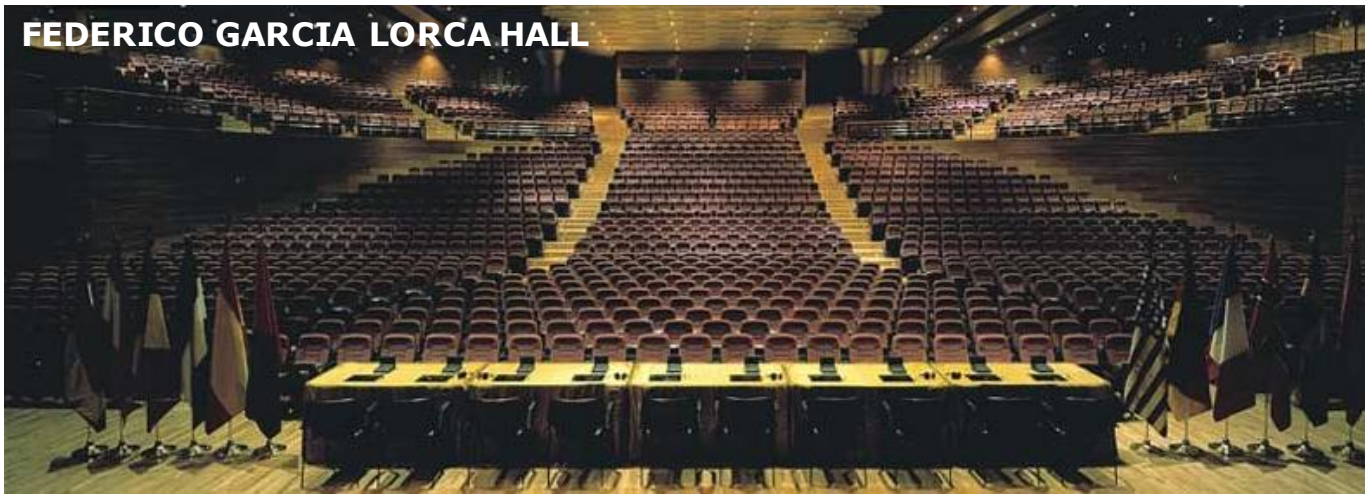

MONDAY, JUNE 27, 2011

8:00-9:00	**REGISTRATION**	
	FEDERICO GARCIA LORCA	
9:00-9:45	PL - 1	**Krzysztof Matyjaszewski:** Macromolecular engineering for nanostructured materials via ATRP.

	MACHUCA Chair J. Ronda	ALBENIZ Chair R. Alamo	MACHADO Chair J. Kenny	M. FALLA Chair J. de Abajo	ANDALUCIA Chair G. Galli	PICASSO Chair B. Vázquez
9:45-10:00	**BREAK**					
10:00-10:30	T1 - IL1	T2 - IL1	T3 - IL1	T4 - IL1	T5 - IL1	T6 - IL1
10:30-10:45	T1 - OP1	T2 - OP1	T3 - OP1	T4 - OP1	T5 - OP1	T6 - OP1
10:45-11:00	T1 - OP2	T2 - OP2	T3 - OP2	T4 - OP2	T5 - OP2	T6 - OP2
11:00-11:30	**COFFEE BREAK AND POSTER SESSION**					
	MACHUCA Chair J. Forcada	**ALBENIZ** Chair C. Lacabanne	**MACHADO** Chair G. Maron	**M. FALLA** Chair A. del Campo	**ANDALUCIA** Chair C. Mijangos	**PICASSO** Chair A. García
11:30-11:45	T1 - OP3	T2 - OP3	T3 - OP3	T4 - OP3	T5 - OP3	T6 - OP3
11:45-12:00	T1 - OP4	T2 - OP4	T3 - OP4	T4 - OP4	T5 - OP4	T6 - OP4
12:00-12:15	T1 - OP5	T2 - OP6	T3 - OP5	T4 - OP5	T5 - OP5	T6 - OP6
12:15-12:30	T1 - OP6	T2 - OP7	T3 - OP6	T4 - OP6	T5 - OP6	T6 - OP7
12:30-12:45	T1 - OP7	T2 - OP8	T3 - OP8	T4 - OP7	T5 - OP7	T6 - OP8
12:45-13:00	T1 - OP8			T4 - OP8	T5 - OP8	
13:00-14:30	**LUNCH**					
	FEDERICO GARCIA LORCA					
14:30-15:15	PL - 2	**Ann-Christine Albertsson:** A holistic view on the biodegradable macromolecular design.				

	MACHUCA Chair N. Hadjichristidis	ALBENIZ Chair H.W. Spiess	MACHADO Chair J.P. Pascault	M. FALLA Chair A. Diogo	ANDALUCIA Chair L. Oriol	PICASSO Chair A. Prieto
15:15-15:30	**BREAK**					
15:30-16:00	T1 - IL2	T2 - IL2	T3 - IL2	T4 - IL2	T5 - IL2	T6 - IL2
16:00-16:15	T1 - OP9	T2 - OP9	T3 - OP9	T4 - OP9	T5 - OP9	T6 - OP9
16:15-16:30	T1 - OP10	T2 - OP10	T3 - OP10	T4 - OP10	T5 - OP10	T6 - OP10
16:30-16:45	T1 - OP11	T2 - OP11	T3 - OP11	T4 - OP11	T5 - OP11	T6 - OP11
16:45-17:00	T1 - OP12	T2 - OP12	T3 - OP12	T4 - OP12	T5 - OP12	T6 - OP12
17:00-17:30	**COFFEE BREAK AND POSTER SESSION**					
	MACHUCA Chair R. Herrero	**ALBENIZ** Chair E. Piskin	**MACHADO** Chair M. Zigon	**M. FALLA** Chair J. Vancso	**ANDALUCIA** Chair A. Pandit	**PICASSO** Chair S. Hvilsted
17:30-17:45	T4- OP13	T4 - OP19	T5 - OP13	T2 - OP13	T6 - OP13	T5 - OP19
17:45-18:00	T4- OP14	T4 - OP20	T5 - OP14	T2 - OP15	T6 - OP14	T5 - OP20
18:00-18:15	T4- OP15	T4 - OP21	T5 - OP15	T2 - OP16	T6 - OP15	T5 - OP21
18:15-18:30	T4- OP16	T4 - OP22	T5 - OP16	T2 - OP17	T6 - OP16	T5 - OP22
18:30-18:45	T4- OP17	T4 - OP23	T5 - OP18	T2 - OP18	T6 - OP17	T5 - OP23
18:45-19:00	T4- OP18	T4 - OP24			T6 - OP18	T5 - OP24

TUESDAY, JUNE 28, 2011

8:00-9:00	**REGISTRATION**	
	FEDERICO GARCIA LORCA	
9:00-9:45	PL - 3	**Eric Baer:** Layered polymeric systems – lessons from biology.
9:45-10:00	**BREAK**	

	MACHUCA Chair A. M. van Herk	**ALBENIZ** Chair D. Mecerreyes	**MACHADO** Chair B. Rivas	**M. FALLA** Chair J. Vidal	**ANDALUCIA** Chair M.J. Vincent	**PICASSO** Chair D. Cohn
10:00-10:30	T1 - IL3	T2 - IL3	T3 - IL3	T4 - IL3	T5 - IL3	T6 - IL3
10:30-10:45	T1 - OP13	T2 - OP19	T3 - OP13	T4 - OP25	T5 - OP25	T6 - OP19
10:45-11:00	T1 - OP14	T2 - OP20	T3 - OP14	T4 - OP26	T5 - OP26	T6 - OP20
11:00-11:30	**COFFEE BREAK AND POSTER SESSION**					

	MACHUCA Chair L.H. Tagle	**ALBENIZ** Chair S. Kazarian	**MACHADO** Chair J.M. Lagaron	**M. FALLA** Chair J.M. Garcia	**ANDALUCIA** Chair D. Lopez	**PICASSO** Chair R. Reis
11:30-11:45	T1 - OP15	T2 - OP21	T3 - OP15	T4 - OP27	T5 - OP27	T6 - OP21
11:45-12:00	T1 - OP16	T2 - OP22	T3 - OP16	T4 - OP28	T5 - OP28	T6 - OP22
12:00-12:15	T1 - OP17	T2 - OP23	T3 - OP17	T4 - OP29	T5 - OP29	T6 - OP23
12:15-12:30	T1 - OP18	T2 - OP24	T3 - OP18	T4 - OP30	T5 - OP30	T6 - OP24
12:30-12:45	T1 - OP19	T2 - OP25	T3 - OP19	T4 - OP31	T5 - OP31	T6 - OP25
12:45-13:00	T1 - OP20	T2 - OP26	T3 - OP20	T4 - OP32	T5 - OP32	T6 - OP26
13:00-14:30	**LUNCH**					
	FEDERICO GARCIA LORCA					
14:30-15:15	PL - 4	**Samuel Stupp:** Ordered supramolecular polymers and their hybrids with covalent chains.				
15:15-15:30	**BREAK**					

	MACHUCA Chair J. Rodriguez	**ALBENIZ** Chair S. Paz	**MACHADO** Chair J. Suay	**M. FALLA** Chair D. Grande	**ANDALUCIA** Chair A. Martinez Richa	**PICASSO** Chair M. Monleon
15:30-16:00	T1 - IL4	T2 - IL4	T3 - IL4	T4 - IL4	T5 - IL4	T6 - IL4
16:00-16:15	T1 - OP21	T2 - OP27	T3 - OP21	T4 - OP33	T5 - OP33	T6 - OP27
16:15-16:30	T1 - OP22	T2 - OP28	T3 - OP22	T4 - OP35	T5 - OP34	T6 - OP28
16:30-16:45	T1 - OP23	T2 - OP29	T3 - OP23	T4 - OP36	T5 - OP35	T6 - OP29
16:45-17:00	T1 - OP24	T2 - OP30		T4 - OP37	T5 - OP36	T6 - OP30
17:00-17:30	**COFFEE BREAK AND POSTER SESSION**					

	MACHUCA Chair J.M. Pereña	**ALBENIZ** Chair R. Williams	**MACHADO** Chair S. Slomkowski	**M. FALLA** Chair M.E. Muñoz	**ANDALUCIA** Chair E.M. Hart	**PICASSO** Chair F. Rasoul
17:30-17:45	T4- OP43	T4 - OP38	T6 - OP37	T5 - OP43	T5 - OP38	T6 - OP31
17:45-18:00	T4 - OP44	T4 - OP39	T6 - OP38	T5 - OP44	T5 - OP39	T6 - OP32
18:00-18:15	T4 - OP45	T4 - OP40	T6 - OP39	T5 - OP45	T5 - OP40	T6 - OP33
18:15-18:30	T4 - OP46	T4 - OP41	T6 - OP40	T5 - OP46	T5 - OP41	T6 - OP34
18:30-18:45	T4 - OP47	T4 - OP42	T6 - OP41	T5 - OP47	T5 - OP42	T6 - OP35
18:45-19:00	T4 - OP48		T6 - OP42	T5 - OP48		T6 - OP36
	"LA CHUMBERA" RESTAURANT					
21:00	CHAIRMAN'S DINNER					

WEDNESDAY, JUNE 29, 2011

8:00-9:00	**REGISTRATION**	
	FEDERICO GARCIA LORCA	
9:00-9:45	PL - 5	**Hiroyuki Nishide**: Radical polymers for an organic-based rechargeable battery and photovoltaic cell.
9:45-10:00	**BREAK**	

	MACHUCA Chair Y. Gnanou	ALBENIZ Chair R. Benavente	MACHADO Chair J.C. Rgez. Cabello	M. FALLA Chair M. Salmerón	ANDALUCIA Chair M. Moeller	PICASSO Chair S. Deb
10:00-10:30	T1 - IL5	T2 - IL5	T3 - IL5	T4 - IL5	T5 - IL5	T6 - IL5
10:30-10:45	T1 - OP25	T2 - OP32	T3 - OP25	T4 - OP49	T5 - OP49	T6 - OP43
10:45-11:00	T1 - OP26	T2 - OP33	T3 - OP26	T4 - OP50	T5 - OP50	T6 - OP44
11:00-11:30	**COFFEE BREAK AND POSTER SESSION**					

	MACHUCA Chair S. Muñoz Guerra	ALBENIZ Chair J.I. Moreno V.	MACHADO Chair C. Domingo	M. FALLA Chair A. Lozano	ANDALUCIA Chair A. Khokhlov	PICASSO Chair B. Voit
11:30-12:00	T1 - IL6	T2 - IL6	T3 - IL6	T4 - IL6	T5 - IL6	T6 - IL6
12:00-12:15	T1 - OP27	T2 - OP34	T3 - OP27	T4 - OP51	T5 - OP51	T6 - OP45
12:15-12:30	T1 - OP28	T2 - OP35	T3 - OP28	T4 - OP52	T5 - OP52	T6 - OP46
12:30-12:45	T1 - OP29	T2 - OP36	T3 - OP29	T4 - OP53	T5 - OP53	T6 - OP47
12:45-13:00	T1 - OP30		T3 - OP30	T4 - OP54	T5 - OP54	T6 - OP48
13:00-14:30	**LUNCH**					

	FEDERICO GARCIA LORCA **Special Session in honor of the DPI Invention Award** Chairman: Jacques Joosten	
14:30-14:50	SL - 1	**Michael Meier:** Plant oils: the perfect renewable resource for polymer science.
14:50-15:10	SL - 2	**Sebastian Muñoz-Guerra:** Carbohydrate-based polycondensation polymers.
15:10-15:30	SL - 3	**Joachim Loos:** On the importance of carbon allotrope network organisation in nanocomposites.
15:30-16:15	PL - 6	**Cor Koning:** Sustainable coatings, plastics and fibers from novel biomass-based polymers.
16:15-16:45	**SPECIAL BREAK HOSTED BY THE DUTCH POLYMER INSTITUTE (DPI)**	

	MACHUCA Chair E. Valles	ALBENIZ Chair J. Girones	MACHADO Chair A. Krzan	M. FALLA Chair A. Muller	ANDALUCIA Chair M. Strumia	PICASSO Chair R. Osorio
16:45-17:00	T4 - OP55	T4 - OP63	T4 - OP71	T5 - OP55	T5 - OP63	T6 - OP49
17:00-17:15	T4 - OP56	T4 - OP64	T4 - OP72	T5 - OP56	T5 - OP64	T6 - OP50
17:15-17-30	T4 - OP57	T4 - OP65	T4 - OP73	T5 - OP57	T5 - OP65	T6 - OP51
17:30-17:45	T4 - OP58	T4 - OP66	T4 - OP74	T5 - OP58	T5 - OP66	T6 - OP52
17:45-18:00	T4 - OP59	T4 - OP67	T4 - OP75	T5 - OP59	T5 - OP67	T6 - OP53
18:00-18:15	T4 - OP60	T4 - OP68	T4 - OP76	T5 - OP60	T5 - OP68	T6 - OP54
18:15-18:30	T4 - OP61	T4 - OP69	T4 - OP77	T5 - OP61	T5 - OP69	T6 - OP55
18:30-18:45	T4 - OP62	T4 - OP70	T4 - OP78	T5 - OP62	T5 - OP70	T6 - OP56

THURSDAY, JUNE 30, 2011

8:00-9:00	**REGISTRATION**	
	FEDERICO GARCIA LORCA	
9:00-9:45	PL - 7	**Teruo Okano:** Design of intelligent surfaces for cell sheet tissue engineering.
9:45-10:00	**BREAK**	

	MACHUCA Chair G. Bataglia	**ALBENIZ** Chair M. Meier	**MACHADO** Chair A. Serra	**M. FALLA** Chair I. Morfin	**ANDALUCIA** Chair C. Abradelo	**PICASSO** Chair M. Refojo
10:00-10:30	T1 - IL7	T2 - IL7	T3 - IL7	T4 - IL7	T5 - IL7	T6 - IL7
10:30-10:45	T1 - OP31	T2 - OP37	T3 - OP31	T4 - OP79	T5 - OP71	T6 - OP57
10:45-11:00	T1 - OP33	T2 - OP38	T3 - OP32	T4 - OP80	T5 - OP72	T6 - OP58
11:00-11:30	**COFFEE BREAK AND POSTER SESSION**					
	MACHUCA Chair V. Cadiz	**ALBENIZ** Chair A. Marcos	**MACHADO** Chair M. Galia	**M. FALLA** Chair A. Santamaria	**ANDALUCIA** Chair M. Stenzel	**PICASSO** Chair S. Madrigal
11:30-11:45	T1 - OP34	T2 - OP39	T3 - OP33	T4 - OP81	T5 - OP73	T6 - OP59
11:45-12:00	T1 - OP35	T2 - OP40	T3 - OP34	T4 - OP82	T5 - OP74	T6 - OP60
12:00-12:15	T1 - OP36	T2 - OP41	T3 - OP35	T4 - OP83	T5 - OP75	T6 - OP61
12:15-12:30	T1 - OP37	T2 - OP42	T3 - OP36	T4 - OP84	T5 - OP76	T6 - OP62
12:30-12:45	T1 - OP38	T2 - OP43	T3 - OP37	T4 - OP85	T5 - OP77	T6 - OP63
12:45-13:00		T2 - OP44	T3 - OP38	T4 - OP86	T5 - OP78	T6 - OP64

13:00-14:30	**LUNCH**	
	FEDERICO GARCIA LORCA	
14:30-15:15	PL - 8	**Pilar Martí:** Trainer project: research on self- and inteligent healing materials.
15:15-15:30	**BREAK**	

	MACHUCA Chair J.Galbis	**ALBENIZ** Chair P. Boch	**MACHADO** Chair J.L. Gardette	**M. FALLA** Chair M.R. Aguilar	**ANDALUCIA** Chair M. Gurruchaga	**PICASSO** Chair D.W. Grijpma
15:30-16:00	T1 - IL8	T2 - IL8	T3 - IL8	T4 - IL8	T5 - IL8	T6 - IL8
16:00-16:15	T1 - OP39	T2 - OP46	T3 - OP39	T4 - OP87	T5 - OP79	T6 - OP65
16:15-16:30	T1 - OP40	T2 - OP47	T3 - OP40	T4 - OP88	T5 - OP80	T6 - OP66
16:30-16:45	T1 - OP41	T2 - OP48	T3 - OP41	T4 - OP89	T5 - OP81	T6 - OP67
16:45-17:00	T1 - OP42		T3 - OP42	T4 - OP90	T5 - OP82	T6 - OP68
17:00-17:30	**COFFEE BREAK AND POSTER SESSION**					
	MACHUCA Chair F. Stelzer	**ALBENIZ** Chair L. Rojo	**MACHADO** Chair Y. Lee	**M. FALLA** Chair G. Lligadas	**ANDALUCIA** Chair D. Puppi	**PICASSO** Chair J.A. Mendez
17:30-17:45	T4 - OP91	T4 - OP103	T4 - OP97	T5 - OP83	T5 - OP89	T5 - OP95
17:45-18:00	T4 - OP92	T4 - OP104	T4 - OP98	T5 - OP84	T5 - OP90	T5 - OP96
18:00-18:15	T4 - OP93	T4 - OP105	T4 - OP99	T5 - OP85	T5 - OP91	T5 - OP97
18:15-18:30	T4 - OP94	T4 - OP106	T4 - OP100	T5 - OP86	T5 - OP92	T5 - OP98
18:30-18:45	T4 - OP95	T4 - OP107	T4 - OP101	T5 - OP87	T5 - OP93	T5 - OP99
18:45-19:00	T4 - OP96	T4 - OP108	T4 - OP102	T5 - OP88	T5 - OP94	T5 - OP100
	"LA MAMUNIA" RESTAURANT					
21:00	CONGRESS DINNER					

FRIDAY, JULY 1, 2011

	FEDERICO GARCIA LORCA	
9:00-9:45	PL - 9	**Jean Francois Gerard:** Self-assembling processes of organic-inorganic nanobuilding blocks and supramolecular units as new routes for nanostructured polymer networks.

	BREAK
9:45-10:00	

	MACHUCA Chair E. Maya	**ALBENIZ** Chair L. Rodriguez	**MACHADO** Chair J.L. Vilas	**M. FALLA** Chair S. Mikhalovsky	**ANDALUCIA** Chair R.G.Rubio	**PICASSO** Chair M. Toledano
10:00-10:30	T1 - IL9	T2 - IL9	T3 - IL9	T4 - IL9	T5 - IL9	T6 - IL9
10:30-10:45	T1 - OP43	T2 - OP49	T3 - OP43	T4 - OP109	T5 - OP101	T6 - OP69
10:45-11:00	T1 - OP44	T2 - OP50	T3 - OP44	T4 - OP110	T5 - OP102	T6 - OP70
11:00-11:30	T1 - IL10	T2 - IL10		T4 - IL10	T5 - IL10	
11:30-11:45	T1 - OP45	T2 - OP51	T3 - OP45	T4 - OP111	T5 - OP104	T6 - OP71
11:45-12:00	T1 - OP46	T2 - OP52	T3 - OP46	T4 - OP112		T6 - OP72

	BREAK
12:00-12:15	

	FEDERICO GARCIA LORCA
12:15	CLOSING SESSION

ORAL CONTRIBUTIONS

OPENING CONFERENCES

OC – 1	**Life without polymers.** *Cristopher K. Ober*
OC – 2	**Smart polymer applications in drug delivery and diagnostics.** *A. S. Hoffman; P. S. Stayton; P. Yager; A. Convertine; J. Lai; M. Nash; C. Duvall; D. Benoit*

SPECIAL LECTURES

SL – 1	**Plant oils: the perfect renewable resource for polymer science?!** *M. Meier*
SL – 2	**Carbohydrate-based polycondensation polymers.** *S. Muñóz-Guerra*
SL – 3	**On the importance of carbon allotrope network organisation in nanocomposites.** *J. Loos*

PLENARY LECTURES

PL – 1	**Macromolecular engineering for nanostructured materials via ATRP.** *K. Matyjaszewski*
PL – 2	**A holistic view on the biodegradable macromolecular design.** *A. Albertsson*
PL – 3	**Layered polymeric systems - lessons from biology.** *E. Baer*
PL – 4	**Ordered supramolecular polymers and their hybrids with covalent chains.** *S. Stupp*
PL – 5	**Radical polymers for an organic-based rechargeable battery and photovoltaic cell.** *H. Nishide*
PL – 6	**Sustainable coatings, plastics and fibers from novel biomass-based polymers.** *C. E. Koning; B. Noordover; L. Jasinska; J. Wu; D. Tang; I. van der Meulen; M. de Geus; A. Heise; D. van Es; J.van Haveren; M. Villani; S. Rastogi*
PL – 7	**Design of intelligent surfaces for cell sheet tissue engineering.** *T. Okano*
PL – 8	**Trainer project: Research on self- and inteligent healing materials.** *P. Martí*
PL – 9	**Self-assembling processes of organic-inorganic nanobuilding blocks and supromolecular units as new routes for nanostructured polymer network.** *J.F. Gerard; J. Duchet; J. Galy; J. Bernard; L. Dai; F. Lortie*

INVITED LECTURES

TOPIC 1: Synthetic Routes: Monomers and Polymers from Bioresources and Advanced Methodologies

T1 - IL1	**Cyclic and multiblock polystyrene-b-polyisoprene copolymers by combining anionic polymerization and azid/alkyne "click" chemistry.** *A. Touris; N. Hadjichristidis*
T1 - IL2	**Vegetable oils as platform chemicals for polymer synthesis.** *J.C. Ronda; G. Lligadas; M. Galià; V. Cádiz*
T1 - IL3	**Hybrid nanoparticles for biotechnological applications.** *J. Ramos; J. Forcada*
T1 - IL4	**Synthesis of multicompartment nanoparticles.** *A. Van Herk; S. Imran Ali; H. Heuts*
T1 - IL5	**Synthesis and characterization of multivalent dendritic glycopolymers.** *B. Voit; D. Appelhans*
T1 - IL6	**Polyester synthesis using enzymatic catalysis by Yarrowia lipolytica Lipase.** *A. Martinez-Richa; K. Barrera-Rivera; A. Marcos-Fernandez*
T1 - IL7	**RAFT polymerization and various click reactions to develop a micellar drug delivery system for albendazole.** *M. Stenzel; Y. Kim; Y. Zhao; F.M. Yhaya*
T1 - IL8	**Hybrid brushes nanoparticles: synthesis and properties.** *J. Paez; A. Cappelletti; M. Strumia*
T1 - IL9	**Organocatalysis of polymerizations: the contribution of N-heterocyclic carbenes.** *J. Raynaud; J. Pinaud; M. Fèvre; J. Vignolle; D. Taton; Y. Gnanou*
T1 - IL10	**Self-assembly of nanocomposite polymer latex and structural color films.** *L. Wu; Z. Shen; L. Duan; B. You*

TOPIC 2: New Analytical and Characterization Tools

T2 - IL1	**New opportunities with spectroscopic imaging.** *S. Kazarian*
T2 - IL2	**Elucidation of macromolecular structure using the MHS plot.** *B. Sabagh; S. Olivier; P.G.Clarke*
T2 - IL3	**The use of analytical techniques in the study and development of structural adhesives: ambient cure.** *S. Paz; A. Moreno-Cid; P. Prendes; R. Meizoso*
T2 - IL4	**Solid state NMR methods for studying functional macromolecular and supramolecular systems.** *H. W. Spiess*
T2 - IL5	**Effect of (3,1) chain-walking defects compared with other regio and constitutional defects in the crystallization and melting of isotactic poly(propylene).** *R. Alamo; C. Ruiz-Orta1; J. Fernandez-Blazquez; A. Anderson; G. Coates*
T2 - IL6	**Towards complex and integrated platforms in nanotechnology employing responsive polymer-metal-semiconductor hybrid materials.** *G. J. Vancso*
T2 - IL7	**Broad band dielectric relaxation for identification of gene mutation in plant model.** *A. Léonard ; J.F. Capsal; F. Roig; J. Dandurand; E. Dantras; P. Demont; C. Lacabanne*
T2 - IL8	**Two photon fluorescence microscopy and small angle X ray and neutron scattering: tools for the structural characterization of complex polymer architectures.** *I. Morfin*
T2 - IL9	**Combined mechanical and electrical characterization of polymers by atomic force microscopy.** *A. Mednick; C. Li; S. Lesko*
T2 - IL10	**Transient rheology: improving measurements at very short time.** *A. Diogo*

TOPIC 3: Advanced Processing and Recycling Technologies

T3 - IL1	**Inducing supramolecular structures in polymers by the combined effects of nanoparticles and flow.** *G. Marom*
T3 - IL2	**Processing of thermosetting matrix nanocomposites: modelling and characterization of the electrical behaviour.** *J. Kenny; L.Torre; M. Monti; M. Natali*
T3 - IL3	**Polymers processing using supercritical fluid technology.** *C. Domingo; C.A. García-González; A. López-Periago*
T3 - IL4	**How to use block copolymers for processing of thermosets and composites?!** *J. Pascault; F. Lortie; D. Portinha; J. Gérard*
T3 - IL5	**Functional polymers with capability to remove pollutant ions.** *B. Rivas*
T3 - IL6	**Preparation of advanced soft tissue engineering scaffolds by stereolithography.** *S. Schüller-Ravoo; S.M. da Silva Texeira; J. Feijen; D. Grijpma*
T3 - IL7	**Electrospinning of biopolymers: biomedical, pharmaceutical and food related application.** *J. M. Lagaron*
T3 - IL8	**Recombinamer-based, coomplex and highly functional systems attained by mild, clean and biocompatible processing technology.** *J.C. Rodríguez Cabello*
T3 - IL9	**Influence of polymer microstructure and post-treatment on the performance of latex-based pressure sensitive adhesives.** *M. Dubé; L. Qie*

TOPIC 4: Polymers for Advanced Applications Including Energy, Transport, Packaging and Environmentally Friendly Activities

T4 - IL1	**Polymer membranes for water purification.** *B. Freeman; D. R. Paul; J. E. McGrath; H. B. Park; A. J. Hill; B. McCloskey; W. Xie; J. Cook; D. Miller; G. Geise; S. Kasemset; A. Lee*
T4 - IL2	**Bioinspired reversible adhesives.** *A. Del Campo*
T4 - IL3	**Macroporous cryopolymer and hybrid hydrogels: biomedical and environmental applications.** *S. Mikhalovsky; S. James; L. James; R. Shevchenko; I. Allan; I. Savina; R. Whitby; A. Cundy*
T4 - IL4	**Polymer electrolyte membranes based on poly(phenylene ether)s with pendant perfluoroalkyl sulfonic acids.** *M. Ueda; K. Nakabayashi; T. Hiagshihara*
T4 - IL5	**Biobased/biodegradable/compostable polymers/blends/nanocomposites for packaging and agro-based uses.** *E. Piskin; F.Y. Ekinci*
T4 - IL6	**Thermally rearranged polymer membranes with tuned microcavities for CO_2 capture.** *Y. M. Lee*
T4 - IL7	**RAFT polymerization and various click reactions to develop.** *F. Stelzer; R. Saf; C. Slugovc; G. Trimmel; F. Wiesbrock*
T4 - IL8	**Porous polycyanurates: new film materials derived from old polymers.** *D. Grande; O. Grigoryeva; A. Fainleib*
T4 - IL9	**Epoxy polymers and composites for advanced applications.** *R. Williams*
T4 - IL10	**Ageing and long-term durability of polymer-based solar cells.** *J. Gardette; A. Rivaton; S. Thérias*

TOPIC 5: Chemistry and Physics of Nanomaterials and Nanotechnologies

T5 - IL1	**A direct way to fabricate polymer and polymer-based composite nanostructures.** *C. Mijangos; J. Martin; I. Blaszczyk-Lezak; Y. Maíz; J. Sacristán*
T5 - IL2	**Polymer films with nano-to micro-structured surfaces for marine biofouling-release coatings.** *G. Galli*
T5 - IL3	**Mimicking nature using copolymers.** *G. J. Bataglia*
T5 - IL4	**Synthesis and functionalization of "nanosponges" to enhance the efficacy of a broad range of therapeutics.** *D. M. Stevens; G. Hariri; J. N. Dobish; E. Harth*
T5 - IL5	**Microphase separation for diblock-copolymers: Novel aspects of an old problem.** *A. Khokhlov*
T5 - IL6	**Morphology, nucleation and crystallization kinetics of biodegradable double crystalline PLLA-b-PCL diblock copolymers.** *A. J. Müller; R. V. Castillo; J. M. Raquez;P. Dubois*
T5 - IL7	**Polymer conjugates as single agents or in combination therapy: Versatile platform technology for tissue repair and cancer therapy.** *M. Vincent*
T5 - IL8	**Nanomaterials based on poly(ε-caprolactone) - a versatile and intriguing biomedical building block.** *S. Hvilsted; I. Javakhishvili*
T5 - IL9	**Homo- and block copolymers of poly(β-benzyl-l-aspartate)s and poly(γ-benzyl-l-glutamate)s of different architectures.** *B. Brulc; E. Zagar; M. Gadzinowski; S. Somkowski; M. Zigon*
T5 - IL10	**Light-responsive block copolymers based on azobenzene.** *J. Barrio; E. Blasco; P. Forcén; C. Berges; R.M. Tejedor; J.L. Serrano; M. Piñol; C. Sánchez; R. Alcalá; L. Oriol*

TOPIC 6: Bioinspired Polymers, Bioengineering and Biotechnology

T6 - IL1	**Material considerations for annulus fibrosus and nucleus pulposus composite structures.** *S. Deb*
T6 - IL2	**Scaffold functionalisation strategies for modulation of inflammation.** *A. Pandit*
T6 - IL3	**Recent progress on the use of natural origin polymers and stem cells in tissue engineering strategies.** *R. L. Reis*
T6 - IL4	**Polyethylene glycol hydrogels for therapeutic vascularization.** *E. A. Phelps; A. J. Garcia*
T6 - IL5	**Polymer-silica nanocomposites: Structure, properties, bioactivity and biological performance of their scaffolds.** *M. Monleón Pradas*
T6 - IL6	**Rational design and synthesis of amphilphilic biodegradable polymers for alveolar bone regeneration.** *F. Rasoul; D. Wang; D. Hill; A. Symons; S. Varanasi; A. Whittaker*
T6 - IL7	**Polymeric endograft for the treatment of abdominal aortic aneyrysms.** *D. Cohn; R. Abbas; I. Pelled; R. Malal*
T6 - IL8	**Additive manufacturing of wet-spun scaffolds for bone tissue engineering.** *E. Chiellini; D. Puppi*
T6 - IL9	**Nano- and microparticles with controlled surface properties; synthesis, properties, selected medical applications.** *S. Slomkowski; M. Gosecki; M. Gadzinowski; M. Gosecka; T. Basinska; P. Wozniak*

ORAL PRESENTATIONS

TOPIC 1: Synthetic Routes: Monomers and Polymers from Bioresources and Advanced Methodologies

T1 - OP1	**Ferrocenyl-containing compounds as modifying additives for radical polymerization of vinyl monomers.** *R.M. Islamova, O.I. Golovochesova, S.V. Nazarova, Y.B. Monakov*
T1 - OP2	**New biobased epoxy resins.** *S. Caillol; B. Boutevin; H. Fulcrand; H. Nouailhas*
T1 - OP3	**Effective catalytic systems for atom transfer radical polymerization based on the carborane complexes of ruthenium.** *I. Grishin; E. Turmina; I. Chizhevsky; D. Grishin*
T1 - OP4	**Polylactic acid and Polyamide11 with controlled macromolecular architecture** *G. Di Silvestro, M. Ortenzi, H. Farina, C.M. Yuan, L. Basilissi, E. Zini, L. Martino; M. Scandola*
T1 - OP5	**Ring-opening co- and terpolymerization of an alicyclic oxirane with carboxylic acid anhydrides and CO_2 in the presence of chromium porphyrin and salen or zinc aryloxide catalysts.** *E. Hosseini Nejad; R. Duchateau; C. Koning*
T1 - OP6	**Polyurethane elastomers from castor oil and chemically modified yucca starch: synthesis and physical-chemical, physical-mechanical and thermical properties.** *M. F. Valero Valdivieso*
T1 - OP7	**New degradable aminovalerolactone-based copolyesters for biomedical applications: synthesis, characterization and biocompatibility.** *S. Blanquer; M. Patterer; V. Darcos; D. Domurado; X. Garric; B. Nottelet; J. Coudane*
T1 - OP8	**Renewable hybrid materials through living radical polymerization.** *U. Edlund; J. Voepel; A.C. Albertsson*
T1 - OP9	**Synthetic route effect on macromolecular architecture: from block to gradient copolymers based on acryloyl galactose monomer using RAFT polymerization.** *P. Escalé; S. R. Ting; A. Khoukh; L. Rubatat; M. Save; M. H. Stenzel; L. Billon*
T1 - OP10	**Bio-inspired cationic polymerization of isoprene initiated by allylic alcohols/b$(C_6F_5)_3$.** *S. Ouardad; F. Peruch; A. Deffieux*
T1 - OP11	**Synthesis and characterization of antibacterial polyurethanes coatings from novel quaternary ammonium functionalized soybean oil based polyol.** *H. Bakhshi; H. Yeganeh; M.A. Shokrgozar; A. Yari*
T1 - OP12	**Dextran-poly(deoxycholate) block copolymers as new biodegradable materials.** *M. Nichifor; M.C. Stanciu*
T1 - OP13	**Π-conjugated polymers with functional endgroups through modified nickel initiators.** *A. Smeets; K. Van Den Bergh; P. Willot; J. De Winter; P. Gerbaux; T. Verbiest; G. Koeckelberghs*
T1 - OP14	**Step growth polymerization of starch-derived dianhydrohexitol stereoisomers: versatile platform for the design of linear polymers and polymer networks with original properties.** *C. Besset; E. Fleury; J.P. Pascault; J. Bernard; E. Drockenmuller*
T1 - OP15	**New functional materials from polysaccharides modified by copper catalyzed azide-alkyne cycloaddition.** *M. Bertoldo; G. Zampano; S. Nazzi; F. La Terra; F. Ciardelli*
T1 - OP16	**Production of polyether polyols with phosphorous initiators.** *M. M. Velencoso; M. J. Ramos; J.C. García-Martínez; A. de Lucas; J. F. Rodriguez*
T1 - OP17	**Towards ring opening metathesis polymerisation: special initiators for special applications.** *A. Leitgeb; E. Pump; A. Szadkowska; K. Grela; C. Slugovc*
T1 - OP18	**New polyurethanes from natural and synthetic rubbers.** *N. Kébir; I. Campistron; A. Laguerre; J.F. Pilard; C. Bunel*
T1 - OP19	**Chitosan-graft-polyaniline-based hydrogels: eloboration and properties.** *P. Marcasuzaa; S. Reynaud; J. Desbrières*

T1 - OP20	**BODIPY-conjugated thermo-sensitive fluorescent polymers based on 2-(2-methoxyethoxy)ethyl methacrylate.** *M. Liras; I. Quijada; O. García; R. Paris*
T1 - OP21	**Malic acid as key building block for the synthesis of OH-functional polyesters.** *C. Hahn; H. Keul; M. Möller*
T1 - OP22	**Synthesis of biobased polyols by thiol-ene 'click chemistry' from vegetable oils.** *M. Desroches; S. Caillol; R. Auvergne; B. Boutevin*
T1 - OP23	**Crosslinking of epoxidized natural rubber by dicarboxylic acids: monitoring crosslinking density, polar interactions and kinetics rate.** *M. Pire; S. Norvez; I. Iliopoulos; B. Le Rossignol; L. Leibler*
T1 - OP24	**Synthesis of terpolymers based acrylamides by RAFT polymerization and their application in the synthesis of goldnanoparticles.** *V. J. Gonzalez Coronel; J. A. Corcino Campos; E. R. Rodriguez; N. Tepale Ochoa*
T1 - OP25	**Preparation of furfuryl functionalised polystyrenes by atom transfer radical polymerization and their use in the surface chemical modifications of multi-wall carbon nanotubes by "grafting to".** *R. Paris, M. M. Bernal, M. Liras, R. Verdejo, I. Quijada-Garrido, M. A. López-Manchado.*
T1 - OP26	**Cationic polymerization of isobutylene using $AlCl_3OBu_2$ as a co-initiator: synthesis of highly reactive polyisobutylene.** *S. Kostjuk; I. Vasilenko; A. Frolov*
T1 - OP27	**Functionalisation of unsaturated polyesters from enzymatic ring-opening polymerisation of macrolactones by thiol–ene click chemistry.** *Z. Ates; I. van der Maulen; P. D. Thornton; A. Heise*
T1 - OP28	**Structure of polyamides made from aldaric acids.** *S. Leon; C. E. Fernández; A. Díaz; M. Bermúdez; M. G. García-Martín; M. Mancera; J. A. Galbis; S. Muñoz-Guerra*
T1 - OP29	**One-pot multistep reactions based on thiolactones: extending the realm of thiol-ene chemistry in polymer synthesis.** *P. Espeel; F. Goethals, F. Du Prez*
T1 - OP30	**Polymeric platforms based on thiolactone monomers for post-polymerization functionalization.** *P. Espeel; L. Petton; M. Stamenovi; F. Goethals; F. Du Prez*
T1 - OP31	**"Click" synthesis of fatty acid derivatives as polyanhydride precursors.** *C. Lluch; G. Lligadas; J. C. Ronda; M. Galià; V. Cádiz*
T1 - OP33	**Controlled synthesis of reactive polyethers: application to free-isocyanate polyurethane.** *A. Brocas; G. Cendejas; A. Deffieux; S. Carlotti*
T1 - OP34	**Sol-gel transition and gelatinization kinetics of wheat starch.** *F. Teyssandier; P. Cassagnau; J. Gérard; N. Mignard*
T1 - OP35	**Aliphatic polyesters from the carbohydrate-based bicyclic monomer methyl di-o-methylene-galactarat.** *C. Lavilla; A. Alla; A. Martínez de Ilarduya; E. Benito; M. G. García-Martín; J. A. Galbis; S. Muñoz-Guerra*
T1 - OP36	**Controlled release of polyphenols from cellulose-based hydrogels.** *D. Ciolacu; A. Oprea; G. Cazacu; M. Cazacu*
T1 - OP37	**Microwave-assisted nitroxide-mediated radical polymerization of acrylamide in aqueous solution.** *J. Rigolini; B. Grassl; L. Billon; S. Reynaud; O.Donard*
T1 - OP38	**Unique fully aliphatic or aliphatic/aromatic copolyesters containing biobased w-hydroxy fatty acids: Molecular structures and properties.** *A. Celli; P. Marchese; S. Sullalti; C. Berti; R. A. Gross*
T1 - OP39	**Pyridinium and picolinium ionic liquids as a media for biphasic ethylene polymerizaton.** *K. Dziubek, W. Ochędzan-Siodłak, K. Czaja*

T1 - OP40	**Novel poly(carboxybetaine methacrylamides) synthesized via Living/controlled aqueous RAFT polymerization.** *C. Rodriguez-Emmenegger; B. Schmidt; Z. Sedláková; V. Šubr; E. Brynda; A. Bologna Alles; C. Barner-Kowollik*
T1 - OP41	**Zinc powder-alkyl halide: a novel initiation system for living radical polymerization of vinyl monomers.** *G. Cankaya; N. Bicak*
T1 - OP42	**Microwave-assisted synthesis of PAMAM type dendrimers & their analytical applications.** *C. Dizman; T. Parali; A. S. Ertürk; M. Tulu*
T1 - OP43	**Ring-opening polymerization of D,L-lactide using Zinc(II) octoate as catalyst.** *R. Mazarro; G. Storti; M. Morbidelli*
T1 - OP44	**Emulsion polymerization of oleic acid-based monomers.** *M. Moreno; M. Goikoetxea; M. J. Barandiaran*
T1 - OP45	**Synthesis of functionalised hyperbranched polymers via catalytic chain transfer polymerisation and thiol-ene click chemistry.** *J. Menzel; D. Haddleton; E. Khoshdel*
T1 - OP46	**Reaction and mass-transfer in polycondensation process of PA-MXD6.** *Z. Xi; Y. Zhao; L. Zhao*

TOPIC 2: New Analytical and Characterization Tools

T2 - OP1	**IR and raman two dimensional correlation vibrational spectroscopy and QM modeling applied to the study of fluorinated polymers.** *S. Radice*
T2 - OP2	**High temperature asymmetrical flow field-flow fractionation (HT-AF4) - New possibilities for characterizing polyolefins.** *T. Otte; T. Klein; E. Moldenhauer*
T2 - OP3	**Characterization and applications of aromatic-aromatic interactions between water-soluble polymers and low molecular-weight molecules.** *I. Moreno-Villoslada; J. P. Fuenzalida-Werner; R. Araya-Hermosilla; E. Araya-Hermosilla; C. Torres-Gallegos; J. Gómez-Manosalba; D. Muñoz; V. Barrueto; M. Flores; N. Sano; W. Tomita; F. Oyarzun-Ampuero; H. Nishide*
T2 - OP4	**Raman structural analysis of olefin – based materials.** *Y.V. Zavgorodnev; K. Prokhorov; G. Nikolaeva; E. Sagitova; P. Pashinin*
T2 - OP6	**Semiflexible macromolecules in nanoslit confinement.** *P. Cifra*
T2 - OP7	**Behaviour of water during temperature-induced phase transition in poly(vinyl methyl ether) aqueous solutions. NMR and optical microscopy study.** *J. Spevacek; L. Hanykova; J. Labuta*
T2 - OP8	**Co-crystallization process of syndiotactic polystyrene/naphthalene revealed by the measurements of angular distributions of polarized fluorescence intensities.** *T. Sago; H. Itagaki*
T2 - OP9	**Tandem mass spectrometry of poly(2-oxazoline)s by electrospray ionization (ESI), matrix assisted laser desorption/ionization (MALDI), and atmospheric pressure chemical ionization (APCI).** *E. Altuntas; K. Kempe; A. Crecelius; U. S. Schubert*
T2 - OP10	**Characterisation of viscoelasticity and dynamics in polymers and proteins using DLS microrheology.** *C. Rega; S. Amin; H. Jankevics*
T2 - OP11	**Relating performance and structure of nanocomposites by new methods in time-resolved X-ray scattering.** *N. Stribeck; A. Zeinolebadi; M. Ganjaee Sari*
T2 - OP12	***In situ* SAXS investigation of transient nanostructure of thermoplastic polyurethane elastomers during thermal treatments.** *N. Stribeck, A. Zeinolebadi, M. Ganjaee Sari*
T2 - OP13	**Determination of the macromolecular dimensions of hydrophobically modified polymers by micellar size exclusion chromatography coupled with multiangle light scattering.** *G. Dupuis; J. Rigolini; G. Clisson; D. Rousseau; R. Tabary; B. Grassl*
T2 - OP15	**Characterization of nanogels by a combination of light and small-angle x-ray scattering.** *G. Roshan Deen; T. Alsted; W. Richtering; J. S. Pedersen*
T2 - OP16	**Mechanism of degradation of acrylic-melamine thermoset. Relating material properties to structure evolutions.** *J.F. Larché; P.O. Bussiere; P. Wong-Wah-Chung; J.L. Gardette*
T2 - OP17	**Keeping track of water in complex multilayered films with NMR imaging.** *H.P. Huinink; V. Baukh; S.J.F. Erich; O.C.G. Adan; L.G.J. van der Ven*
T2 - OP18	**NMR for determining the structure of new polysulphones.** *M. Gorbunova; A. Vorob'eva; R. Muslukhov*
T2 - OP19	**The glass transition of thin polystyrene films - heterogeneity studies by single molecule fluorescence spectroscopy.** *D. Wöll; B. Flier; M. Baier; S. Mecking; K. Müllen; A. Zumbusch*
T2 - OP20	**TD-NMR investigation of nanoconfined soft phase in SEBS.** *M. Mauri; L. Mauri; R. Simonutti*

T2 - OP21	**Kinetics and modeling of aqueous-phase N-vinylformamide free radical polymerization studied by reaction calorimetry.** *J. Zataray; J. C. De la Cal; J. R. Leiza*
T2 - OP22	**Characterization of polyfurfuryl alcohol resin - a new biomass-based resin for advanced composite materials.** *J. C. Domínguez; B. Madsen*
T2 - OP23	**Effect of architecture and molecular weight of PEO based electrolytes on the ionic conductivity and viscosity.** *D. Devaux; D. Glé; T. Phan; R. Denoyel; D. Bertin; D. Gigmes; R. Bouchet*
T2 - OP24	**Investigation of the morphology of elastomeric blends.** *M. Merlin; J. Majesté; C. Carrot; V. Pelissier; M. Eloy; I. Anselme-Bertrand*
T2 - OP25	**Non-linear rheological parameters for characterization of molecular structural properties in polyolefins.** *K. Klimke; S. Filipe; A.T. Tran*
T2 - OP26	**Rheology behavior and study of payne effect in natural rubber/regenerated cellulose/ montmorillonite clay nanocomposites.** *R.M. Mariano; R.C.R. Nunes; L.L.Y. Visconte*
T2 - OP27	**Two-dimensional liquid chromatography of complex polymers: PDMS-PS block copolymers.** *M.I. Malik; P. Sinha; G.W. Harding; H. Pasch*
T2 - OP28	**Imaging polymer nanostructures with scanning transmission X-ray spectro-microscopy.** *B. Watts; C.R. McNeill; J. Raabe*
T2 - OP29	**Comprehensive molecular characterization of complex polymer systems with liquid chromatography.** *D. Berek*
T2 - OP30	**Uptake of water and ions in nylon 6 as studied by MRI imaging.** *N.J.W. Reuvers; H.P. Huinink; H.R. Fischer; O.C.G. Adan*
T2 - OP32	**Recent progress of polymer investigation using SAXS and WAXS laboratory setups.** *P. Panine; S. Rodrigues*
T2 - OP33	**Phosphorus dendrimers functionalized with TEMPO radicals. Synthesis and study by electron paramagnetic resonance spectroscopy.** E. Badetti; V. Lloveras; R.M. Sebastián; A.M. Caminade; J.P. Majoral; J. Veciana; J. Vidal-Gancedo
T2 - OP34	**A new generation dual controlled-stress/rate extensional rheometer for polymer melts.** *R.J. Andrade; P. Harris; J.M. Maia*
T2 - OP35	**Evaluation of polyethylene films photodegradation by analitycal fractionation techniques.** *M.T. Exposito; C. Dominguez; J. Codina; R.A. García;*
T2 - OP36	**Microstructure characterization of polyolefins by high temperature HPLC.** *B. Monrabal*
T2 - OP37	**Photochromic reaction of fluorescent rhodamine 6G-polyelectrolyte complexes and the sensitivity of the complexes to Mercury in solution.** *R. Araya-Hermosilla; C. Alarcón; E. Araya-Hermosilla; M. Flores; I. Moreno-Villoslada*
T2 - OP38	**Local thermomechanical analysis of polymers on the sub-µm scale using heated SFM-probes.** *T. Fischinger; S. Hild*
T2 - OP39	**Dielectric properties of poly(vinyl alcohol) hydrogels prepared by freezing/thawing technique.** *M.E. Londoño López; J.M. Jaramillo Ocampo; R. Sabater i Serra; J.M. Vélez Restrepo*
T2 - OP40	**The creep behavior of linear low density polyethylene.** *Y. Unigovski; A. Bobovitch; E. Gutman*
T2 - OP41	**The advantages of TOPEM in studying the cure of a trifunctional epoxy resin (TGAP).** *J. Hutchinson; F. Shiravand; Y. Calventus; I. Fraga*
T2 - OP42	**Real-time raman spectroscopy measurements to study the uniaxial tension of isotactic polypropylene.** *P. Bourson; J. Martin; S. Chaudemanche; M. ponçot; J. Hiver; A. Dahoun*
T2 - OP43	**Investigation of the dispersion process of different PP/nanoclay composites at different processing conditions during extrusion by on-line near infrared and ultrasonic spectroscopy.** *D. Fischer; S. Kummer; J. Müeller; B. Kretzschmar*

T2 - OP44	**Monitoring atom transfer radical polymerisation (ATRP) and the resulting polymers using ^{14}C radio-labeled initiators.** *M. Long; S. Rogers; D. Thornthwaite; F. Livens; S. Rannard*
T2 - OP46	**Molecular structure and local dynamic in impact polypropylene studied by preparative TREF and subsequent 2D solid-state NMR spectroscopy.** *R.A. García; A. Fernández; M.T. Expósito; B. Peña; B. Coto; I. Suarez; J. Shu; R. Graf; H.W. Spiess*
T2 - OP47	**Mass spectrometry reveals the degradation product patterns of biodegradable polyesters.** *A. Höglund; M. Hakkarainen; A.C. Albertsson*
T2 - OP48	**Carbon dioxide plasticized polymer melts – An interpretation of the plasticizing effect by means of the free volume concept.** *B. Duscher; A. Schausberger; W. Stadlbauer*
T2 - OP49	**Development of a thermoplastic starch to be used in the co-injection process.** *E. Benavent; B. Galindo; O. Menes; A. Pascual; F. Marti*
T2 - OP50	**Monitoring of the epoxy curing with different methods.** *G. Teteris; W. Stark*
T2 - OP51	**Modeling of phase separation of polymer blends using spectrum method.** *M. A. Parsa; M. Ghiass*
T2 - OP52	**Evolution of elastomers network structures during the vulcanization process as investigated by ^{1}H low-field multiple-quantum NMR.** *J. L. Valentín; I. Mora-Barrantes; M. A. Malmierca; P. Posadas Bernal; A. Fernandez-Torres; Á. Marcos-Fernández; A. Rodríguez; L. Ibarra*

TOPIC 3: Advanced Processing and Recycling Technologies

T3 - OP1	**Photoelectrochemical properties of doped polyaniline: application to hydrogen production upon visible light upon visible light.** *Z. Benabdelghani; G. Rekhila; M. Trari; A. Etxeberria*
T3 - OP2	**T.T.T & C.C.T diagrams for PP/SGFR PA 66 reinforced blends: Effect of PP-g-MAH as a compatibilizer.** *Z. Safidine; A. Belhadj; S. Fellahi; D. Benachour; H. J. Radusch*
T3 - OP3	**Ternary blends: morphology and properties.** *L. Gonzalez-Gomez; M. Alvarez-Lainez*
T3 - OP4	**Formation of self-assembled buffer layer from fullerene end-capped poly(ethylene glycol) for high performnace of P3HT/PCBM heterojuction solar cells.** *J. W. Jung; W. H. Jo*
T3 - OP5	**Cryostructured polymer/clay aerogel materials.** *D.A. Schiraldi; M.D. Gawryla; Y. Wang; J.R. Johnson*
T3 - OP6	**Preparation of polyether-block-amide copolymer/organoclay composite via freeze-drying.** *Y. Wang; S.M. Alhassan; D.A. Schiraldi*
T3 - OP8	**Controlled chain-cleavages of polydienes by oxidation and by metathesis: Application to the waste tire recycling.** *F. Sadaka; I. Campistron; A. Laguerre; J.F. Pilard*
T3 - OP9	**Anomalous mechanical anisotropy of extruded polypropylene sheet with beta-form crystallites.** *P. Phulkerd; Y. Uchiyama; M. Yamaguchi*
T3 - OP10	**New methodology to produce a polyetherimide (PEI) via chloro-displacement by SABIC innovative plastic.** *P. Forcén*
T3 - OP11	**Polypropylene functionalization using acid, anhydride and alcohol monomers by reactive extrusion.** *T. Sadik; F. Becquart; M. Taha; V. Massardier*
T3 - OP12	**Polymeric surface modification of capillaries for the separation of DNA by capillary electrophoresis.** *K. Allan; C. Lenehan; H. Kobus; A. Ellis*
T3 - OP13	**Radiation induced vulcanization of SBR blends containing pristine silica and silica modified by polybutadiene grafting: reaction mechanisms and physicochemical properties of the vulcanizates.** *D. Dondi; A. Lostritto; L. Conzatti; M. Castellano; A. Turturro;, S. Bracco; M. Galimberti; A. Buttafava; A. Faucitano*
T3 - OP14	**Preparation of polystyrene nanocomposite nanofibers by electrospinning.** *N. Reshad; M. Najafi; H. Roughani-Mamaqani; M. Salami-Kalajahi; V. Haddadi-Asl*
T3 - OP15	**The effect of partially crosslinking of high density polyethylene on its structure and rheology.** *K. Montaser Asadi; J. Morshedian; Y. Jahani; A. Pakdaman*
T3 - OP16	**Precision design of novel copolymers and nanohybrids by cobalt-mediated radical polymerization (CMRP).** *C. Detrembleur; M. Hurtgen; Y. Piette; J.M. Thomassin; C. Jérôme; A. Debuigne*
T3 - OP17	**Synthesis and characterization of poly(fatty alkyloylethylacrylate-*co*-methylmethacrylate) as solid solid phase change materials for thermal energy storage.** *T.G. Ertuğral; O.F. Ensari; C. Alkan*
T3 - OP18	**New recycling polymer-immobilizing catalysts for the controlled/living radical polymerization.** *E. Geraskina; M. Lazarev; D. Grishin*
T3 - OP19	**Effet of coupling agent on the mechanical properties of cellulose fiber/polystyrene composites II. Dependent on the fiber content** *C.D. Zanrosso; M. Poletto; A. Zettera; M. Zeni*
T3 - OP20	**Mechanical recycling of polymers from real WEEE deposits: morphology, blend composition, impact strength.** *S. Ausset; M. Barthès; O. Mantaux; M. Pedros; M. Dumon*

T3 - OP21	**Polymers with hydrogen bonding moieties via ROMP.** *S. Kurzhals; W.H. Binder*
T3 - OP22	**Large-scale nacre-mimetic hybrid films and paper via rapid self-assembly.** *A. Walther; L. Berglund; O. Ikkala*
T3 - OP23	**Recycling of polyurethane-based shape memory polymers.** *M. Ahmad; J.K. Luo; H. Purnawali; W.M. Huang; M. Miraftab*
T3 - OP25	**Advances in small scale processing equipment for polymers and additives.** *B. Jakob*
T3 - OP26	**Role of rheology on quality of polymeric articles.** *F. Aghazadeh; H. Hosseini*
T3 - OP27	**Re-use and recycling of PLA and its mechanical properties.** *R. Forstner; J. Pleiner*
T3 - OP28	**Characterization of iron oxide nanoparticles created in a polymer brush matrix.** *S. Neuhaus; C. Padeste; N. D. Spencer*
T3 - OP29	**Chain architecture modifications of poly(lactic acid) by reactive extrusion.** *O.O. Santana; J. Callioux; E. Franco-Urquiza; J. Bou; F. Carrasco; J. Gámez-Pérez; M. Ll. Maspoch*
T3 - OP30	**Electromechanical characterization of styrene-butadiene-styrene / carbon nanotube composites for deformation sensors.** *P. Costa; J.C. Viana; S. Lanceros Mendez*
T3 - OP31	**High velocity compaction: a fast process insensitive to viscosity.** *N. Doucet; O. Lame; G. Vigier; F. Doré*
T3 - OP32	**Microphase separation in asymmetric coil-coil and coil-amphiphilic comb block copolymers in strong segregation limit.** *M. Asad Ayoubi; K. Zhu; B. Nyström; U. Olsson; K. Almdal; A. Khokhlov; L. Piculell*
T3 - OP33	**Influence of polymer and process characteristics on microstructure and physical properties of SLS parts.** *S. Dupin; O. Lame; C. Barres; J.Y. Charmeau*
T3 - OP34	**Key issues in re-processing aged polyamide-12 powders by selective laser sintering: influence of polymer features evolution upon part properties.** *C. Barrès; S. Dupin; A. Msakni; O. Lame; J.Y. Charmeau*
T3 - OP35	**Poly(D,L-lactide)-b-poly(2-hydroxyethyl acrylate) block copolymers as potential biomaterials for peripheral nerve repair.** *T. Trimaille; B. Clément; F. Féron; P. Decherchi; D. Bertin; K. Mabrouk; D. Gigmes; T. Marqueste*
T3 - OP36	**A new building block concept for polymers based on multifunctional coupling agents.** *F. Böhme; L. Jakisch*
T3 - OP37	**Amorphous silica obtained from rice husk: Study of the enhanced surface area for use as reinforcement of rubber.** *D. Mosca; C. Mantero; P. Raimonda*
T3 - OP38	**Recycling of Poly(ethylene terephthalate) bottle waste with modified styrene butadiene rubber through reactive mixing.** *O. Moini Jazani; A. Ghaemi; A. Ebrahimi Jahromi*
T3 - OP39	**Grafting of a biodegradable pH-sensitive copolymer based on poly(ethylene glycol) methyl ether and poly(ethyl glyoxylate) onto maghemite nanoparticles.** *C.H. Brachais; L. Hu; F. Xu; A. Percheron; D. Chaumont; G. Boni; J.P. Couvercelle*
T3 - OP40	**Epoxy/amine: simulation of reactive rotational molding.** *E. Mounif; S. Khelladi; F. Bakir; A. Tcharkhtchi*
T3 - OP41	**Biodegradation in compost of recycled low density polyethylene/polycaprolactone blends.** *J. J. Bou; L.M. Marroyo; A. Alla; L. Ollé, A. Bacardit; O.O. Santana; M. L. Maspoch*
T3 - OP42	**Thermoplastic elastomer/organoclay nanocomposites: morphology, thermal and mechanical properties.** *A. Szymczyk; S. Paszkiewicz; Z. Roslaniec*

T3 - OP43	**A comparison in dispersion of carbon nanotubes in aqueous media.** *V. Ghamgosar khorshidi; G.R. Bakhshandeh; A. Salimi; G. Naderi*
T3 - OP44	**X-ray investigation of iPP and propene/ethylene random copolymers solidification during ultra fast cooling.** *G. Portale; D. Cavallo; L. Balzano; G. Alfonso*
T3 - OP45	**The behaviour of the inorganic nano-filler in polypropylene composite fibres.** *E. Borsig; A. Augustinova; A. Ujhelyiova; A. Marcincin*
T3 - OP46	**Synthesis and characterization of natural oil based alkyd–acrylic copolymers.** *P. Rämänen; S.L. Maunu*

TOPIC 4: Polymers for Advanced Applications Including Energy, Transport, Packaging and Environmentally Friendly Activities

T4 - OP1	**Multiarm star poly(glycidol)-block-poly(ε-caprolactone) of different arms lengths and their use as modifiers of diglycidylether of bisphenol A thermosets.** *M. Morell; A. Lederer; X. Ramis; B. Voit; A. Serra*
T4 - OP2	**Dynamics of uniaxially oriented natural rubber using dielectric spectroscopy.** *M. Hernández; T. Ezquerra; M. López-Manchado*
T4 - OP3	**Adhesion properties of polycaprolactones and polycaprolactone based polyurethane prepolymers.** *M. García Ruiz; J. L. Valentin; A. Marcos-Fernandez*
T4 - OP4	**Polyvinyl butyral furfural: molecular structure and thermomechanical properties.** *A.G. Rodionov; N.K. Kobyakova; Y.A. Kursky; I.V. Blagodatskikh; E.A. Litmanovich; V.M. Aleksashin*
T4 - OP5	**Transmissive to black electrochromic aramids based on electroactive tetraphenylbenzidine units.** *H.J. Yen; K.Y. Lin; G.S. Liou*
T4 - OP6	**Charge-transporting polymers and molecular glasses for optoelectronic applications.** *J.V. Grazulevicius*
T4 - OP7	**Model poly(dimethylsiloxane-*b*-ε-caprolactone) obtained by anionic ring opening polymerization.** *A.J. Satti; F.G. Nador; E.M. Vallés; M.A. Villar; A.E. Ciolino*
T4 - OP8	**Synergistic effect of H-bond and chain mobility in enhancing proton transfer: a study case in urocanic acid system.** *C. Jarumaneeroj; S. Chriachanchai*
T4 - OP9	**New crystalline-crystalline diblock copolymers of poly(3-hexylthiophene-*b*-steryl acrylate) for field effect transistors.** *J.C. Lin; C.C. Kuo; W.Y. Lee; J.C. Hsu; W.C. Chen*
T4 - OP10	**Nanocomposite functional membranes for biomedical applications.** *A.M. Popa; F. Teixeira; S. Zuber; R. Rossi*
T4 - OP11	**Foamed nanocomposites: a system in which nanofillers play a multifunctional role.** *M.A. Rodríguez-Pérez; C. Saiz-Arroyo; J.A. de Saja*
T4 - OP12	**Poly(meth)acrylates obtained by cascade reaction.** *H. Keul; D. Popescu; E. Hrsic; M. Möller*
T4 - OP13	**High speed polymer semiconductors for applications on printed integrated circuits.** *K.J. Baeg; Y.Y. Noh; D.Y. Kim; A. Facchetti; S.W. Jung; J.B. Koo; I.K. You*
T4 - OP14	**Electrically bistable memory devices based on poly(3-hexylthiophene)-*block*-poly(3-phenoxylthiophene) and Its PCBM composite films** *Y.C. Lai; K. Ohshimizu; W.Y. Lee; T. Higashihara; M. Ueda; W.C. Chen*
T4 - OP15	**Effect of composition on the properties of sulfonated poly(indene)/poly(vinyl alcohol) membranes.** *N. Löser; B. Santos; R. Cavalheiro, M. M. Camargo Forte*
T4 - OP16	**Unimolecular polymeric nanoparticles: from conventional to highly efficient 'click'chemistry routes.** *J. A. Pomposo; L. Buruaga; J. Colmenero*
T4 - OP17	**Thermally rearranged (TR) poly(ether-benzoxazole) membranes for gas separation.** *M. Calle; Y. M. Lee*
T4 - OP18	**One single composite for chemical sensor or heating purposes.** *M. Bouhadid; J. Desbrières; C. Pillon; N. Redon; S. Reynaud*
T4 - OP19	**Synthesis and applications of copoly(*p*-phenylene)s containing bipolar triphenylamine and 1,2,4-triazole groups.** *C. Wu; Y. Chen*
T4 - OP20	**Synthesis of new two-dimensional thiophene-based conjugated copolymers and their applications to thin film transistors and photovoltaic cells.** *H.W. Lin; J.H. Tsai; C.J. Lin; H.C. Wu; C. Lu; Y.W. Lin; Y.C. Lai; W.C. Chen*

T4 - OP21	**Physicochemical study of the gelation kinetics and mechanism of polyacrylamide-based copolymers and polyethyleneimine hydrogels.** *R.V. Castillo; B. Grassl; S. Dagreou; N. Blin; G. Dupuis; A. Karam*
T4 - OP22	**Viscoelastic and generalized newtonian fluid flows simulation in single screw extruder using computational flow dynamics.** *A. Ahmadian; Y. Tamsilian; A. Ramazani S. A.*
T4 - OP23	**Ion exchange and electron exchange properties of polycalixresorcinarene.** *H.N. Altshuler; E.V. Ostapova*
T4 - OP24	**Working with water insoluble organic molecules in aqueous media: piperazinedione derivative-containing polymers as sensory materials for the fluorogenic sensing of biomolecules.** *S. Vallejos; P. Estévez; H. El Kaoutit; M. Trigo; F. Serna; F. García; J. L. Peña; J. M. García*
T4 - OP25	**Electrospun aligned nanofibers of two-dimensional conjugated P4TDPP for high performance field effect transistors.** *C.J. Lin; J.C. Hsu; J.H. Tsai; C.C. Kuo; W.C. Chen*
T4 - OP26	**Preparation of open submicron cell structure by $scCO_2$ foaming of highly oriented isotactic polypropylene.** *J.B. Bao; T. Liu; L. Zhao; G.H. Hu*
T4 - OP27	**Design rules for fuel cell membranes.** *G. Maier; M. Groß; T. Fuller; S. MacKinnon; C. Gittleman; C. Mittelsteadt*
T4 - OP28	**Dextran based micro-/nano-gels as injectable device for controlled release system.** *S.V. Ghugare; E. Chiessi; M. Telling; G. Paradossi*
T4 - OP29	**Structure and supramolecular formations of star-shaped fullerene-containing polymers in solution.** *V.T. Lebedev; G. Torok; L.V. Vinogradova*
T4 - OP30	**Phase segregation and thermal degradation of polycarbonatediol-based polyurethanes. Effect of hard segment content and soft segment length.** *A. Nohales; V. Costa; J. Latorre; C. Guillem; P. Félix; C. M. Gómez*
T4 - OP31	**Characterization of a microbial fucose-containing polysaccharide produced from glycerol byproduct.** *C. A. Torres; F. Freitas; M. A. Reis; I. de Sousa; V. D. Alves*
T4 - OP32	**Block copolymers containing photocleavable side groups : Formation and disruption of micelles by light.** *O. Bertrand; J.M. Schumers; C.A. Fustin; J.F. Gohy*
T4 – OP33	**Carbon atom volume as indicator for biodegradation susceptibility in highly oxidized species.** *A. Kržan; J. Mavri*
T4 - OP35	**Design of complex polymersomes structures and "one pot" loading of hydrophilic model drug using simple co-flow microfluidic chip.** *A. Perro; C. Nicolet; J. Angly; A. Colin; S. Lecommandoux; J.F. Le Meins*
T4 - OP36	**Click chemistry to fluorescent hyperbranched polymeric sensors: synthesis and characterization.** *S. Medel; V. Abenza; P. Ramírez-López; M. C. De La Torre; C. Peinado; P. Bosch*
T4 - OP37	**Solid state properties of fluorinated polyimides containing perylene and oxadiazole moieties.** *M.D. Damaceanu; R.D. Rusu; M. Bruma*
T4 - OP38	**Characterization, melting and crystalline properties of isotactic (4,2)-enchained poly(1-butene).** *C. Ruiz-Orta; R.G. Alamo*
T4 - OP39	**SU8 - carbon nanotubes composites: preparation, characterisation and patterning.** *M. Mionic; R. Gaal; L. Forro; S. Jiguet; M. Judelewicz; A. Magrez*
T4 - OP40	**Synthesis of highly soluble polymer-coated magnetic nanoparticles using a combination of diazonium salt chemistry and the iniferter method.** *N. Griffete; A. Lamouri; F. Herbst; S. Ammar; C. Mangeney*
T4 - OP41	**Monitoring the swelling/deswelling of stimuli-responsive hydrogels with magneto-resistive methods.** *K. Arndt; I. Moench; C. Kaiser; R. Koseva*
T4 - OP42	**Synthesis of microcapsules via reactive surfactants.** *F. Gayet; A. Limer; N. Jagielski; A. Heming; I. Shirley; D. M. Haddleton*

T4 - OP43	**Nanocomposites based on polyamidoimides with hydrosilicate nanotubes for membrane technology.** *G. Gubanova; S. Kononova; M. Vilegzhanina; T. Sukhanova; E. Korytkova; D. Timpu; M. Cristea; V. Harabagiu*
T4 - OP44	**Study of diffusion of jeffamines into reactive "surface-attached" polymer networks.** *R. Navarro; M. Pérez Perrino; O. Prucker; J. Rühe*
T4 - OP45	**Fabrication of low density foam shells using TMPTMA aerogel by UV polymerization.** *C. Lattaud; L. Guillot; C.H. Brachais; B. Reneaume; E. Fleury; O. Legaie; J.P. Couvercelle*
T4 - OP46	**Self-assembling of polyelectrolyte multilayers.** *E. Guzmán; R. Chulia; J. Cavallo; F. Ortega; R. Rubio; M. Strumia; C. Gómez*
T4 - OP47	**Aggregation and chain dynamics in supramolecular polymers by dynamic rheology: cluster formation and self-aggregation.** *F. Herbst; K. Schröter; I. Gunkel; S. Gröger; T. Thurn-Albrecht; J. Balbach; W.H. Binder*
T4 - OP48	**Functionalized nanoporous materials from photocleavable block copolymers.** *J.M. Schumers; A. Vald; C.A. Fustin; J.F. Gohy*
T4 - OP49	**Photostable polymer/clay nanocomposite encapsulant for organic solar cells.** *J. Gaume; S. Therias; A. Rivaton; S. Cros; S. Guillerez; J.L. Gardette*
T4 - OP50	**Advanced organic-soluble polymers for optical and electronic application: new colorless, transparent and thermally stable polynorbornenes via ROMP.** *W.R. Lian; K.L. Wang; J.C. Jiang; D.J. Liaw, K.R. Lee; J.Y. Lai*
T4 - OP51	**Solvent induced morphology in polymer-based systems for organic photovoltaics.** *M. A. Ruderer; S. Guo; R. Meier; H.Y. Chiang; V. Körstgens; J. Perlich; S. V. Roth; P. Muller-Buschbaum*
T4 - OP52	**Convenient method for functional biocompatible hyperbranched polymers.** *T. Loontjens; F. Xiang; L. Asri; J. Yin; S. Roest*
T4 - OP53	**Fabrication of clickable thin-film composite membranes for reduced biofouling.** *M. Haeussler; S. Harrisson; G. Li; J. Habsuda; E. Rizzardo; M. Jasieniak; H. Grieser; C. Barner-Kowollik; M. Le Hellaye; V. Chen; J. Mansouri, I. Dagley*
T4 - OP54	**Applying post polymerisation hypercrosslinking on polyHIPE material.** *I. Pulko; P. Krajnc*
T4 - OP55	**Composites of semiconductive polyelectrolytes for optoelectronic applications.** *J. Pfleger; S. Kazim; V. Sluneckova; D. Bondarev; J. Vohlidal*
T4 - OP56	**Supramolecular poly(3-hexylthiophene)s for solar cells: synthesis and electronic properties.** *C. Enders; A. Shaigan Nia; W.H. Binder*
T4 - OP57	**Fluorene based core-polymers for efficient white oled: correlation between molecular structure and photophysical properties.** *S. Destri; U. Giovanella; F. Samperi; S. Battiato*
T4 - OP58	**Obtention of modified polypropylene using the trifunctional cyclic initiator DEKTP as the radical initiator in the presence of different crosslinking co-agentes.** *G. Morales; L. García-Salazar; F. Avalos*
T4 - OP59	**Aggregates of constant size in dilute solutions of associating polyelectrolyte.** *E. Korchagina; O. Philippova*
T4 - OP60	**Magnetic, molecular imprinted polymeric nanoparticles for developing optical sensors.** *A. Medina-Castillo; G. Mistlberger; J. Fernández-Sánchez; I. Klimant; A. Fernández-Gutiérrez*
T4 - OP61	**Effect of masterbatch dilution on the structure and mechanical properties of carbon-based nanocomposites.** *E.V. Kuvardina; S.S. Abramchuk; V.G. Krasheninnikov; S.M. Lomakin*
T4 - OP62	**3D optical waveguides produced by two photon photopolymerisation of a flexible silanol terminated polysiloxane containing acrylate functional groups.** *R. Woods; S. Feldbacher; G. Langer; D. Zidar Satzinger; W. Kern*
T4 - OP63	**Bioinspired polymeric foam-lattice composite combining stochastic and periodic systems at two different length scales: Lightweight materials for absorption applications.** *R. Rinaldi; C. Hammetter; J. Bernal-Ostos; A.J. Jacobsen; F.Z. Zok*

T4 - OP64	**Polymeric sensors based on polymer phase transition and thiazole dyes.** *C. Pietsch; R. Menzel; R. Hoogenboom; R. Beckert; U.S. Schubert*
T4 - OP65	**Cancer drug targeting by a magnetic polymer – *in vivo* proof of concept.** *J. L. Arias; L. H. Reddy; P. Couvreur*
T4 - OP66	**Synthesis, characterization and application of amphiphilic elastomeric polyurethane networks in drug delivery.** *C. S. Pita; P. C. Caracciolo; G. A. Abraham; J. Gironès; J. A. Méndez; M. A. Pèlach*
T4 - OP67	**Double hydrophilic copolymer poly(ethylene oxide)-*block*-poly(2-ethyl oxazoline) as a carrier of cobalt bis(dicarbollide) conjugates designed as HIV protease inhibitors.** *P. Matejicek; V. Dordovic; M. Uchman; K. Prochazka; B. Gruner; A. Nykanen; J. Ruokolainen; M. Gradzielski*
T4 - OP68	**Polyesters and polyesterimides containing phosphaphenanthrene bulky groups for high performance applications.** *D. Serbezeanu; T. Vlad-Bubulac; C. Hamciuc; M. Aflori*
T4 - OP69	**From polymers to well-patterned membranes by mimicking the nature.** *A. Gugliuzza*
T4 - OP70	**Preserving cytokines' stability and activity: a novel controlled release polymeric drug delivery approach.** *H. Younes; M. Shaker*
T4 - OP71	**Phase-morphology and structure of model fullerene - polymer materials.** *D. Bucknall; G. Bernardo; M. Shofner; N. Deb; D. Raghavan; B. Sumpter; S. Sides; A. Karim*
T4 - OP72	**Liquid crystal homo and alternating (co)polymers based on π-conjugated backbone for organic Electronics.** *F. Mathevet; I. Tahar-Djebbar; D. Zeng; B. Heinrich; B. Donnio; D. Guillon; D. Kreher; A. Attias*
T4 - OP73	**Light microstructuring of thiol-yne photopolymers: cell adhesion on surface relief patterns.** *M. Lomba; L. Oriol; C. Sánchez; R. Alcalá; J. L. Serrano; M. Moros; J. Martínes de la Fuente; V. Grazú*
T4 - OP74	**PHEMA based polymer dielectrics for gravure-printed OTFTs** *J. Farmer; B. Muir; N. Vaklev; A. Campbell; J. Steinke*
T4 - OP75	**Modified epoxy resin as electrolytes for structural supercapacitors.** *A. Bismarck; S. Carreyette; Q. P. Fontana; E. S. Greenhalgh; G. Kalinka; A.Kucernack; M. Shaffer; N. Shirshova; J. H. Steinke; M. Wienrich*
T4 - OP76	**Kinetics of thermo-stimulated volume phase transition in poly(2-(2-methoxyethoxy)ethyl methacrylate) hydrogels; Raman and dielectric spectroscopy studies.** *M. Pastorczak; Y. A. Yoon; M. Kozanecki; L. Okrasa; S. Kadlubowski; R. Kisiel; T. Kowalewski; K. Matyjaszewski; J. Ulanski*
T4 - OP77	**Electro - responsive MWNT-PMAA hydrogel composites for controlled drug delivery.** *A. Servant; K.T. Al-Jamal; C. Bussy; K. Kostarelos*
T4 - OP78	**Exploiting adsorption to taylor the behavior of polymers at the nanoscale.** *S. Napolitano; C. Rotella; M. Wübbenhorst*
T4 - OP79	**New insights in the synthesis of rod-like polyamides. Dependence of molecular weight on the synthetic method.** *G. Hernández; C. Álvarez; J. G. de la Campa; J. de Abajo; A. E. Lozano*
T4 - OP80	**Heterocomplementary H-Bonding RAFT agents: new tools for the preparation of tailor-made supramolecular block copolymers.** *S. Chen; A. Bertrand; P. Alcouffe; C. Ladaviere; J.F. Gérard; F. Lortie; J. Bernard*
T4 - OP81	**Copolymers of trimethylene carbonate and glycolide: synthesis and relationship between microstructure and properties.** *E. Díaz-Celorio; L. Franco; A. Rodríguez-Galán; J. Puiggalí*
T4 - OP82	**Innovative polyelectrolytes for advanced applications.** *D. Mecerreyes; A. Pascual; A. Abouzadheh*
T4 - OP83	**Improving thermal energy storage in rpu foams by incorporating microcapsules containing PCMs.** *A. M. Borreguero; J. L. Valverde; J. F. Rodríguez; M. Carmona*

T4 - OP84	**Design of high inorganic content organic-inorganic hybrids based on a fluorinated polymer via combination of sol-gel chemistry and reactive extrusion.** *F. Niepceron; V. Bounor-Legaré; J. Gérard; P. Buvat; H. Galiano*
T4 - OP85	**Synthesis of phenylphosphine oxide containing urethane acrylates and their applications.** *B. Türel Erbay; I. E. Serhatli*
T4 - OP86	**Hybrid macroporous hydrogels with iron oxide nanoparticles.** *I.N. Savina; C. J. English; R. L.D. Whitby; S. V. Mikhalovsky; A. B. Cundy*
T4 - OP87	**Design of functional S/DVB microspheres: from hydrophilic particles to superhydrophobic surfaces.** *J. Rodríguez-Hernández; A. Muñoz-Bonilla; C. Labrugere; E. Ibarboure; E. Papon*
T4 - OP88	**Novel functional chromatographic supports: from preparation to application.** *A. Lamprou; A. F.M. Gavriilidou ; G. Storti; M. Morbidelli*
T4 - OP89	**New developments on hybrid coloidal materials for applications in magnetic hyperthermia.** *R. Hernández; C. Echeverria ; V. Zamora; C. Mijangos*
T4 - OP90	**Multi-shape memory effect of thermo-responsive semi-crystalline polymeric blends.** *J.M. Cuevas; L. German; R. Rubio; J.M. Laza; F. Mijangos; J.L. Vilas; L.M. León*
T4 - OP91	**Multi-armed, biodegradable polyphosphazenes and their use as macromolecular anti-cancer drug carriers.** *S. Wilfert; I. Teasdale; I. Nischang; O. Brüeggemann*
T4 - OP92	**Effects of parameters on emittance of thermal control coatings based on polyurethane and titanium dioxide.** *M. Taheran; A. H. Navarchian; R. Shoja Razavi*
T4 - OP93	**Functional particles obtained by emulsion polymerization using glycopolymer surfactants.** *A. Muñoz-Bonilla; V. Bordegé; O. León; R. Cuervo-Rodríguez; M. Sánchez-Chaves; M. Fernández-García*
T4 - OP94	**Fundamentals aspects of crosslinking control of PDMS rubber at high temperatures for development of new thermoplastic silicone vulcanizate (super-TPV).** *S. Mani; P. Cassagnau; M. Bousmina; P. Chaumont*
T4 - OP95	**Thermodegradable polyaldehydes: from amiphiphilic block-copolymers to advanced materials patterning.** *S. Köstler; D. Wachter; B. Zechner; H. Pichler; A. Rudorfer; S. Spirk; H. Fasl; B. Trathnigg; V. Ribitsch*
T4 - OP96	**Poly(2-oxazoline)-based non-cytotoxic hydrogels with tailor-made swelling degrees for drug delivery.** *F. Wiesbrock; A. M. Kelly; A. Hecke; B. Wirnsberger*
T4 - OP97	**Magnetic properties of neutral substituted poly(thiophenes)s.** *S. Vandeleene; A. Stesmans; M. Van Bael; T. Verbiest; G. Koeckelberghs*
T4 - OP98	**Optimization of multilayer heat sealing.** *E. Planes; L. Flandin*
T4 - OP99	**Characterization of soluble and precipitated chitosan adsorption onto cellulose viscose fibres.** *T. Ristic; L. Fras Zemljic*
T4 - OP100	**Modification of surface properties of organically modified clay particles for preparation of nanocomposite hydrogels.** *M. Kurecic; S. Hribernik; M. Tomsic; A. Jamnik; K. Stana Kleinschek; M. Sfiligoj-Smole*
T4 - OP101	**An elegant and facile single-step UV-curing approach to self-assembled metallopolymer capacitors.** *J. R. Nair; C. Gerbaldi; V. s. Ijeri; R. Bongiovanni; N. Penazzi*
T4 - OP102	**Synthesis and characterization of photoactive and extrudable polymers in view of developing a new solvent-free process for production of organic solar cells.** *L. Perrin; A. Nourdine; E. Planes; L. Flandin; N. D. Alberola*
T4 - OP103	**Multiscale gold and silver plasmonic plastics by melt compounding.** *N. García; P. Tiemblo; E. Benito; A. Esteban; R. Pina; C. Pecharromán;*
T4 - OP104	**Block copolymer coated magnetic nanoparticles as hybrid systems for imaging and therapeutic Applications.** *C. Schatz; S. Louguet; S. Lecommandoux; R. Epherre; E. Duguet; S. Mornet; C. Boiziau; A. Vekris; K. Petry;*

T4 - OP105	**Effect of polymer structure of acrylic pressure-sensitive adhesives on light leakage phenomenon in TFT-LCD panel.** *I. Nam; K. Ha; K. Lee; L. J. Kim; C. Lee; M. Kim; T. Chang*
T4 - OP106	**Nanofiber networks of aromatic polybenzimidazole.** *J. Gong; T. Uchida; S. Yamazaki; K. Kimura*
T4 - OP107	**Self-assembling of tapered dendrons of various nature and functionality.** *M. Shcherbina; A. Bakirov; V. Percec; U. Beginn; M. Moller; S. Chvalun*
T4 - OP108	**Towards chromogenic and fluorogenic sensing materials via molecular imprinting.** *R. Wagner; I. Lazraq; J. Fernández Sánchez; J. L. Urraca-Ruiz; M. Biyikal; K. Rurack; E. Benito-Peña; M. Moreno-Bondi; G. Orellana; B. Sellergren*
T4 - OP109	**Conformational behavior of conjugated polymers with oligo(phenylenevinylene) side chains.** *H. Peeters; W. Vanormelingen; T. Verbiest; G. Koeckelberghs*
T4 - OP110	**Nanocomposites: dispersion quality and percolation threshold.** *N. Watzeels; H. E. Miltner; C. Block; G. Van Assche; B. Van Mele; H. Rahier*
T4 - OP111	**Poly(ethylene oxide) based block copolymers : synthesis, characterization and applications.** *T. N.T. Phan; D. Bertin; D. Gigmes; E. Bloch; V. Hornebecq; P. Llewellyn; G. Bonniol; D. Quémener; A. Deratani*
T4 - OP112	**Synthesis and characterization of biodegradable polyurethane sealants containing rosin resin.** *P. Carbonell-Blasco; J.M. Martín-Martínez*

TOPIC 5: Chemistry and Physics of Nanomaterials and Nanotechnologies

T5 - OP1	**Development of light responsive membranes for controlled drug release.** *L. Baumann; E. Aslan-Gürel; D. de Courten; M. Wolf; R. M. Rossi; L. J. Scherer*
T5 - OP2	**Polyesterification catalyzed by hydrotalcite modiefied nanoparticles.** *Z. Boncza-Tomaszewski; M. Kedzierski*
T5 - OP3	**Epitaxial growth from the crystalline cores of cylindrical polyferrocenylsilane (PFS) block copolymer micelles.** *S. F. Mohd Yusoff; J. B. Gilroy; I. Manners*
T5 - OP4	**From heterogeneous to homogeneous nucleation of isotactic poly(propylene) confined in nanoporous alumina.** *H. Duran; M. Steinhart; H. Butt; G. Floudas*
T5 - OP5	**Polyethylene/graphene nanocomposites obtained by *in situ* polymerization.** *F.C. Fim; N.R.S. Basso; D.S. Azambuja; G. Barrera Galland;*
T5 - OP6	**Impact of synergy between carbon nanotubes and carbon black on the rheological and electrical properties of an EPDM rubber.** *M. Charman; F. Leonardi; C. Bissuel; C. Derail*
T5 - OP7	**Ordered lithium-ion-conducting polymer electrolytes.** *D. Golodnitsky; K. Shvartsman; E. Peled; L. Adler-Abramovich; E. Gazit; A. Greenbaum; S. Greenbaum*
T5 - OP8	**Atmospheric pressure plasma jet deposition of gas and vapour barrier coatings onto polymer films for packaging applications.** *R. Sulcis; P. Scopece; M. Muzio; I. Kulyk; A. Patelli*
T5 - OP9	**Preparation, surface properties and applications of nanometric cellulose model films.** *R. Kargl; T. Mohan; S. Köstler; M. Reischl; A. Doliška; K. Stana-Kleinschek; V. Ribitsch*
T5 - OP10	**Formulation and optical study of ordered phases of copolymers and nanoparticles.** *V. Ponsinet; B. Maxit; C. Tallet; D. Bendejacq*
T5 - OP11	**Nanostructures from tunable self-assembly of a simple diblock copolymer.** *A. Bianchi; M. Mauri; R. Simonutti*
T5 - OP12	**The melting and non-isothermal crystallization behaviors of polypropylene/montmorillonite (MMT)nanocomposites under high pressure CO_2.** *C. Jie; L. Tao; Z. Ling; Y. Wei-Kang*
T5 - OP13	**Mechanical properties of PA66/PA6/multi-walled carbon nanotube ternary nanocomposite prepared by melt mixing method** *M. Hadizade ; A. Shojaei; R. Bagheri*
T5 - OP14	**Nanocomposites based on carbonaceous nanoestructures oxidized by solar energy.** *M. López; M. Blanco; E. Aranzabe; A. Marcaide*
T5 - OP15	**Tailored designed cellulosic nanoparticles for possible pharmaceutical and biotechnological applications.** *M.R. Kulterer; V.E. Reichel; M. Reischl; R. Kargl; J. Schaller; K. Stana-Kleinschek; V. Ribitsch*
T5 - OP16	**Preparation and characterization of nitrile butadiene rubber-nanoclay composites with maleic acid anhydride as compatibilizer- Part I: Rheometric and swelling characteristics.** *E. Sadek; D. El-Nashar*
T5 - OP18	**Transition behavior of block copolymer films on controlled interaction.** *D. Y. Ryu; E. Kim; H. Ahn; J. Gong*
T5 - OP19	**Morphology evolution driven by transreactions in a polyurethane / α, ω-aminopropyl polydimethylsiloxane blend.** *F. Fenouillot; F. Méchin; F. Boisson; P. Alcouffe; T. Pokropski; T. Kallel; M. Mnif*
T5 - OP20	**Effect of clay/polymeric modifier combination on structure and properties of epoxy nanocomposite.** *I. Kelnar; J. Rotrekl; L. Kaprálková*

T5 - OP21	**Structural changes in liquid crystal polymer vesicles induced by temperature variation and magnetic field.** *A. Brulet; S. Hocine; L. Jia; J. Yang; A. Di Cicco; L. Bouteiller; M.H. Li*
T5 - OP22	**Preparation of fluoroalkyl end-capped oligomers possessing nonflammable and flammable characteristics in silica gel matrices.** *H. Sawada*
T5 - OP23	**Synthesis, micelle formation, and gelation of (PEG – P(MA-POSS)) amphiphilic hybrid block copolymers.** *H. Hussain; B. Tan; C. He*
T5 - OP24	**Thermoset nanosphere formation: a model case from SEBS and benzoxazine molecular assembly system.** *S. Chirachanchai; W. Rungswang*
T5 - OP25	**Effect of carbon nanotubes on thermo-mechanical properties of polyimide-carbon nanotube nanocomposites.** *R. Misiego; B. Pipes*
T5 - OP26	**Antimicrobial activity of nanocomposites based on polycaprolactone/MMT-(PCL-*b*-DEAEMA).** *I. Larraza; C. Abrusci; J. Pablos; M. Luzón; F. Catalina; C. Peinado; T. Corrales*
T5 - OP27	**Phase diagrams of the mobility of charge carriers in conducting polymers.** *L. F. Roncaratti; P. H. Neto; W. F. Cunha; R. Gargano; J. F. Teixeira; G. M. E Silva*
T5 - OP28	**Non conventional methods to prepare conducting polymer nanocomposite.** *W.M. de Azevedo; R.A. de Barros; J.F. Felix; E.F. da Silva Jr*
T5 - OP29	**Concentration and temperature influenceon the rheological behavior of a filled polymer.** *A.I. Gómez-Merino; M.H. Spillman; F.J. Rubio-Hernández*
T5 - OP30	**Properties of thin films of amphiphilic block copolymers based on *N*-vinylpyrrolidone and 2,2,3,3-tetrafluorpropylmethacrylate.** *I.V. Deniskina; O.G. Zamyshlyayeva; M.A. Batenkin; G.A. Shandryuk*
T5 - OP31	**Hierarchically structured polymeric films used as a model substrate for the investigation of adhesion and wettability.** *P. Escalé; M. Save; C. Derail; L. Billon; L. Rubatat*
T5 - OP32	**Complex architectures of hybrid nanoparticles controlled by amphiphilic copolymers.** *C. Geidel; K. Schmidtke; M. Klapper; K. Muellen*
T5 - OP33	**Theory and self-consistent field modeling of dendritic polymer brushes.** *T. Birshtein; A. Polotsky; O. Borisov*
T5 - OP34	**Solutions of amphiphilic polyelectrolytes: effect of electrostatic interactions on self-organization.** *S. Venev; I. Potemkin*
T5 - OP35	**Mesoscale simulation of network formation and structure,combining molecular dynamics and kinetic monte carlo approaches.** *A. V. Berezkin; P. U. Biedermann; A. A. Auer*
T5 - OP36	**Surface modifications of polymeric materials with functional Ag nano-particles; a comparative study of different immobilization techniques.** *D. Breitwieser; S. Lenz; R. Kargl; M. Wu; H. Fasl; K. Stana-Kleinschek; V. Ribitsch*
T5 - OP38	**Network formation by thiol-ene 'click' chemistry / by controlled radical polymerization: a 'single-molecule' view.** *K. Goossens; W. Van Camp; H. Uji-i; D. Wöll; K. Müllen; F. Du Prez; J. Hofkens*
T5 - OP39	**The sharp thermal transition of the diblock copolymers methoxy-poly(ethylene glycol)-*block*-poly(*N*-isopropylacrylamide) (PNIPAAM-*b*-MPEG).A combined analytical-ultracentrifugation and dynamic-light-scattering study.** *A. Ortega; R. Pamies; J. García de la Torre*
T5 - OP40	**Ionic liquids: structuration agents in a fluorinated matrix.** *S. Livi; J.F. Gérard; J. Duchet-Rumeau*

T5 - OP41	**Dynamic dielectric spectroscopy and thermo stimulated current for identification of gene mutation in a model plant.** *F. Roig; E. Dantras; J. Grima-Pettenati; C. Lacabanne*
T5 - OP42	**"Amphiphilic" ionic liquid in a mixte of nonionic liquids: theoretical study.** *A.A. Aerov; A.R. Khokhlov; I.I. Potemkin*
T5 - OP43	**Thermal and electronic conduction in conjugated polymers.** *L. Roncaratti; P. H. de Oliveira Neto; W. F. da Cunha; R. Gargano; G. Magela e Silva*
T5 - OP44	**Quantum dots functionalised with polymers via RAFT polymerisation for the fluorescent detection of latent fingerprints.** *J. Dilag; H. Kobus; A. Ellis*
T5 - OP45	**Polyacrylate core-shell stars – synthesis and application.** *A. Kowalczuk; N. Koseva; S. Rangelov; B. Trzebicka; A. Dworak*
T5 - OP46	**Water-soluble polymer-*grafted* platinum nanoparticles for the subsequent binding of enzyme: synthesis and SANS study.** *G. Carrot; F. Gal; H. Perez*
T5 - OP47	**Full exfoliation of clay and nanocomposite preparation.** *Y. Seo; K. Oh; Y. Seo; S. M. Hong*
T5 - OP48	**Synthesis and study of random amphiphilic polymers for molecular encapsulation of pyrene and clofazimine.** *M. Schott; C. Barbaud; J. Coudane; D. Domurado*
T5 - OP49	**Modification of the electrical properties of TPU by modified expanded graphites.** *J. Pionteck; F. Piana*
T5 - OP50	**Processing and properties of carbon nanotube-polymer composite fibers.** *C. Mercader, A. Lucas, P. Miaudet, A. Derré, M. Maugey, P. Poulin, C. Zakri*
T5 - OP51	**Phase behavior and structure formation under fast cooling of syndiotactic poly(propylene) nucleated with 1,3:2,4-bis(3,4-dimethylbenzylidene)sorbitol.** *A.M.J.T. Meijer-Vissers; J.G.P. Goossens*
T5 - OP52	**Study of the effect of carbon nanofillers on the foaming evolution of polyurethane foams.** *M. M. Bernal; A. Mortamet; M. A. López-Manchado; A. J. Ryan; R. Verdejo*
T5 - OP53	**Crystallinity and chain conformations in polymer / layered silicate nanohybrids.** *K. Chrissopoulou; K. Andrikopoulos; S. Bollas; S. Fotiadou; G. Voyiatzis; S. H. Anastasiadis*
T5 - OP54	**New hybrid core-shell star-like architectures made of poly(*n*-butylacrylate): synthesis and properties.** *S. Pensec; F. Périneau; G. Hu; L. Rozes; F. Ribot; C. Sanchez; C. Creton; L. Bouteiller*
T5 - OP55	**Crystallization in co-continuous nanostructured blends and composites.** *S. Tencé-Girault; L. Gani; T. Périé; L. Leibler*
T5 - OP56	**Electrical conductivity of carbon nanotube/polymer composite fibers in extensional shear.** *F. Grillard; C. Zakri; P. Poulin; A. Korzhenko; P. Gaillard*
T5 - OP57	**Maleinized polybutadienes as clay modifiers for sbr-based rubber nanocomposites.** *G. Colucci; R. Bongiovanni; A. Priola; M. Alessi; L. Conzatti; P. Stagnaro*
T5 - OP58	**Directing self assembly of RAFT polymers using end group functionalization.** *H. Willcock; R. O'Reilly*
T5 - OP59	**Effect of acrylic acid hairy layer length on film formation and properties.** *E. González; A. Chuvilin; M. Paulis; M. J. Barandiaran*
T5 - OP60	**Evolution of the electrical conductivity of MWCNT/PUR nanocomposites from non-quiescent molten state to solid state.** *M. Fernández; M. Landa; M. E. Muñoz; A. Santamaría*
T5 - OP61	**Semi-interpenetrating networks based on poly(*N*-isopropylacrylamide) reinforced with nano-clays and linear hydrophilic polymers.** *J. Djonlagic; D. Zugic; A. Lancuski; M. Nikolic; Z. Petrovic*

T5 - OP62	**Generation of metal polymer nanohybrids in the irradiated polyelectrolyte metal complexes of different architecture.** *A. Zezin; V. Feldman; S. Abramchuk; E. Zezina; A. Danchenko*
T5 - OP63	**Step-and repeat assembly of molecularly controlled ultrathin polyaramide layers.** *M. Perez; N. Lomadze; H. Reinecke; O. Prucker; J. Rühe*
T5 - OP64	**Synthesis of core-branched ABC block copolymer nanoparticles having incompatible functional moieties.** *E. Hasan; J. V. Weaver; D. J. Adams*
T5 - OP65	**Polyesteramide nanofibers – preparation and properties.** *J. Brožek; L. Malinová; V. Benešová; D. Lubasová; L. Martinová; J. Roda*
T5 - OP66	**Polyurethane functionalized with hydroxyapatite nanostructures by a non-conventional route. Thermal behavior as a function of pressure.** *L. Popescu; R. M. Piticescu; T. Buruiana; E. Vasile; R. Trusca*
T5 - OP67	**Nanostructured polymer composites based on carbon nanotubes.** *M. Galimberti; M. Coombs; I. Tritto; A. Ravasio; T. Riccò; S. Passera; L. Conzatti; C. D'Arrigo; S. Senatore*
T5 - OP68	**Preparation and characterization of sol-gel functionalized polysaccharides.** *H. M. Ehmann; S. Spirk; K. Stana-Kleinschek; V. Ribitsch*
T5 - OP69	**Nano-hybrid PDMA/silica hydrogels: from structure to mechanical properties.** *S. Rose; A. Marcellan; T. Narita; D. Hourdet*
T5 - OP70	**Structure/highly electrical conductivity relationships of gold nanowires/P(VDF-TrFE) nanocomposites.** *A. Lonjon; L. Lafffont; P. Demont; E. Dantras; C. Lacabanne*
T5 - OP71	**Design of "all-supramolecular" nanocapsules made of low-molecular weight bis-ureas through interfacial reaction in miniemulsion.** *E. Groison; S. Adjili; A. F. Ferrand; F. Lortie; N. Sintes-Zydowicz; D. Portinha*
T5 - OP72	**Synthesis and characterization of PCL-*b*-PLA di-block copolymers.** *L. Peponi; L. Casaban; A. Marcos-Fernández; J. M. Kenny*
T5 - OP73	**Foaming in CO_2 *sc* medium as an efficient way to produce electromagnetic interference shielding materials.** *L. Monnereau; J. Thomassin; N. Quiévy; P. Bollen; S. Eggermont; T. Pardoen; C. Bailly; I. Huynen; C. Jérôme; C. Detrembleur*
T5 - OP74	**Ag(PbS)/Poly-*p*-xylylene nanocomposites by VDP-method.** *S. Ozerin; A. Gusev; K. Mailyan; A. Pebalk; I. Ryzhikov; S. Zavyalov; S. Chvalun*
T5 - OP75	**Relaxation dynamics in ultrathin polymer films investigated at the nanoscale.** *K. H. Nguyen; D. Prevosto; M. Labardi; S. Capaccioli; M. Lucchesi; P. Rolla*
T5 - OP76	**Tuning thermomechanical properties of polystyrene/polybutadiene-based thermoplastic elastomers by grafting.** *J. Prévost; M. N. Nguyen; I. Iliopoulos; L. Leibler*
T5 - OP77	**Dielectric properties of poly(ethylene-*co*-butylene) modified MWCNT/polypropylene composites.** *A.E. Daugaard; K. Jankova; J. Bøgelund; J.M.R. Marín; S. Hvilsted*
T5 - OP78	**Electrosynthesis study of poly(*N*-methyl aniline)/Ag nanocomposite.** *S. M. Seyed Mohaghegh; F. Ansari; B. Najafzadeh*
T5 - OP79	**New approaches to development of equipment for nanoscale investigations in aqueous solutions of polymers.** *D. Shaltykova; V. Bublik; D. Bobrovnokov; N. Semenyakin; E.E. Kopishev; I.K. Nam; A. Timofeyev*
T5 - OP80	**Interpolyelectrolyte complexes based on star-like polyionic species.** *D.V. Pergushov; I.A. Babin; A. Wolf; H. Schmalz; A.B. Zezin; A.H. Mueller*
T5 - OP81	**Hybrid carbonaceous and plasmonic nanostructures as efficient elements in energy conversion devices.** *D.H. Kim; Y.H. Jang; Y.J. Jang*
T5 - OP82	**Voltage-induced swelling and de-swelling of weak polybase brushes.** *M.P. Weir; S.Y. Heriot; S.J. Martin; A.J. Parnell; S.A. Holt; J.R.P. Webster; R.A.L. Jones*
T5 - OP83	**Fabrication and ordering of noble metal nanoparticles through functional polymers.** *A. Ledo-Suárez; M.A. López-Quintela; M. Lazzari*

T5 - OP84	**PVC modified with well dispersed nano silica spheres.** *M. Conradi; M. Zorko; I. Jerman; B. Orel*
T5 - OP85	**Viscoelastic behavior of magnetic elastomers depending on composition and magnetic field.** *E.Y. Kramarenko; G.V. Stepanov; N.S. Perov; A.V. Chertovich; A.R. Khokhlov*
T5 - OP86	**Polyelectrolyte-clay multilayers for surface modification of biopolymers: preparation and possible applications.** *G. Findenig; S. Nowitsch; R. Kargl; M. Reischl; A. Doliska; T. Heinze; K. Stana-Kleinschek; V. Ribitsch*
T5 - OP87	**Block-gradient copolymers of styrene and acrylic acid synthesized by nitroxide-mediated radical polymerization.** *O. Borisova; L. Billon; M. Zaremski; B. Grassl; Z. Bakaeva; A. Lapp; P. Stepanek; O. Borisov*
T5 - OP88	**Self-organization of amphiphilic macromolecules in semidiluted and concentrated solutions.** *V.V. Vasilevskaya; A.A. Glagoleva; M.K. Glagolev*
T5 - OP89	**Local structure around nano-clay agglomerates in PP composites – a scanning X-ray diffraction study with sub micron resolution.** *M. Feuchter; G. Maier; M. Burghammer; M. Kracalik; S. Laske; J. Keckes; G. Pinter*
T5 - OP90	**Poly(ethylene oxide)/sepiolite and poly(ethylene oxide)/sepiolite/Li salt nanocomposites: Confinement effects and preliminary results on their performance as solid electrolytes.** *A. Mejía; J. Guzmán; N. García; P. Tiemblo*
T5 - OP91	**Nanocomposites prepared with montmorillonite modified by quaternary polyesters.** *M. Huskic; M. Žigon*
T5 - OP92	**Polymeric micelles using pseudo-amphiphilic block copolymers and their cellular uptake.** *M. Benaglia; E. Spisni; A. Alberti; A. Papi; E. Treossi; V. Palermo*
T5 - OP93	**Patterning polymer brush microstructures by colloidal lithography.** *T. Chen; R. Jordan; S. Zauscher*
T5 - OP94	**Penetrants interacting with matrix of polymeric membrane. Problems and perspective.** *I.V. Vorotyntsev; N.A. Petukhova*
T5 - OP95	**From bulk to attograms of matter: dynamics and phase transitions of polymeric materials.** *A. Serghei; T.P. Russell*
T5 - OP96	**Effect of organoclay surface treatment on the property profile of recycled PET nanocomposites.** *M. Kracalik; A. Witschnigg; S. Laske; C. Holzer*
T5 - OP97	**Effect of two different surfactants on the properties of PET nanocomposites.** *I.F. Leite; A.P.S. Soares; O.L. Malta; S.M. de Lima Silva*
T5 - OP98	**Optical writing in self-assembled azobenzene block copolymers and their blends with PMMA.** *S. Menghetti; M. Alderighi; F. Tantussi; F. Fuso; M. Allegrini; R. Solaro; G. Galli*
T5 - OP99	**Generating hierarchical nanostructures in polymer surfaces.** *J.P. Fernández-Blázquez; A. del Campo*
T5 - OP100	**Electric conductivity of aqueous solutions of partially neutralized poly(thiophene-3-ylacetic acid) as predicted by different polyelectrolyte theories – comparison with experiment.** *J. Cerar; D. Bondarev; J. Vohlidal; V. Vlachy*
T5 - OP101	**Characterization of the morphology of co-extruded, thermoplastic/rubber multi-layer tapes.** *J.G.P. Goossens; R.M.A. l'Abee; A.M.J.T. Meijer-Vissers; A.B. Spoelstra; M. van Duin*
T5 - OP102	**Cationized nanofibrillated cellulose by aqueous free radical polymerization: synthesis, structure, and antibacterial properties.** *K. Littunen; U. Hippi; J. Seppälä*
T5 - OP104	**A new approach to peptides encapsulation.** *B. Trzebicka; A. Dworak; B. Robak; P. Weda; J. Silberring*

TOPIC 6: Bioinspired Polymers, Bioengineering and Biotechnology

T6 - OP1	**Some novel applications of biodegradable elastomers.** *S. Venkatraman; V. Lipik; K.J. Fong; H. Yingying; N. V; F. Boey*
T6 - OP2	**Amyloid peptides and peptide copolymers: from self-assembly, towards therapeutics.** *I.W. Hamley; V. Castelletto*
T6 - OP3	**New smart heparin-based bioconjugates synthesized by ATRP and click chemistry.** *F. Reyes; G. Rodriguez; M.R. Aguilar; J. San Román; W. Li; S. Averick; K. Matyjaszewski*
T6 - OP4	**Synthesis of PLA-*b*-PHEA block copolymers as precursors of tubular guides for peripheral nerve repair.** *B. Clement; T. Trimaille; K. Mabrouk; D. Bertin; D. Gigmes*
T6 - OP6	**Polymer hydrogels with a 'memory' effect to drugs.** *S.S. Ivanchev; V.F. Danilichev; V.N. Pavlyuchenko; O.N. Primachenko; S.Y. Khaikin*
T6 - OP7	**Synthesis and characterization by lipase-catalyzed ring-opening polymerization of poly(ε-caprolactone) with different reaction mediums.** *E. Özsağıroğlu; B. İyisan, Y. Avcıbaşı Güvenilir*
T6 - OP8	**Polyesters from natural macrolactones for biomedical applications.** *I. Van der Meulen; C.E. Koning; A. Heise; R. Deumens*
T6 - OP9	**Developing and evaluating mucoadhesive polymers and mucosa-mimetic materials.** *V. Khutoryanskiy*
T6 - OP10	**Macromolecular nanoparticles with cholesterol for solid tumour targeting: how do they look like from inside. The origin of functionality.** *S.K. Filippov; P. Chytil; P.V. Konarev; D.I. Svergun; J. Plestil; A. Jugunov; T. Etrych; K. Ulbrich; P. Stepanek*
T6 - OP11	**Photo cross-linked and pH sensitive polymersomes as bionanoreactors.** *J. Gaitzsch; D. Appelhans; D. Gräfe; P. Schwille; B. Voit*
T6 - OP12	**Enzyme sensitive dendrimers with defined chirality via 'click' coupling of enantio-pure building blocks.** *B. Yeniad; H. Naik; R. Amir; C. Koning; C. Hawker; A. Heise*
T6 - OP13	**Design of bioinspired asymmetric diblock copolypeptides for DNA-template self assembled coating.** *A. Hernández-García; M. Werten; F. de Wolf; R. de Vries*
T6 - OP14	**Modification of polymers materials to achieve antibacterial properties.** *J. Casimiro; P. Roger; B. Lepoittevin; C. Boisse Laporte*
T6 - OP15	**Core-shell type nanofibrous scaffolds using coaxial electrospinning for bioapplication.** *H. Park; H. Yoo; T. Hwang; T. Park; I. W. Cheong; J. H. Kim*
T6 - OP16	**Vinyl sulfonate terminated polyglycidol for biomedical applications.** *D. Haamann; H. Yoshida; H. Keul; M. Akashi; D. Klee; M. Möller*
T6 - OP17	**Biosynthesis – structure – property relations for branched polysaccharides as revealed by two-dimensional macromolecular size/branch chain-length distributions** *F. Vilaplana; M.A. Sullivan; J. Hasjim; R.G. Gilbert*
T6 - OP18	**Compositionally-tunable surface nanostructuration of microspheres obtained from a self-stabilizing copolymerization of methylmethacrylate and vinylpyrrolidone.** *I. Aranaz; H. Reinecke; C. Elvira; A. Gallardo*
T6 - OP19	**Matrix protein dynamics on polymer surfaces** *C. González-García, P. Rico, M. Cantini, J. Ballester-Beltrán, V. Llopis-Hernández, M. Salmerón-Sánchez*
T6 - OP20	**Thermo-responsive self assembled nanoparticles from elastin-like recombinamers.** *L. Martín; C. García-Arévalo; F.J. Arias; M. Alonso; J.C. Rodríguez-Cabello*
T6 - OP21	**Lysine dendrimers and their conjugates and complexes with amyloid-like peptides.** *I. Neelov*
T6 - OP22	**Poly(ester amide)s based on α-amino acids and α-hydroxy acids oligomers: Synthesis, characterization and biodegradation studies** *A.C. Fonseca; P.N. Simões; M.H. Gil;*

T6 - OP23	**Nanoengineered polymeric capsules for drug delivery.** *G. Such; C.J. Ochs; Y.Y. Yan; F. Caruso*
T6 - OP24	**A water-based antibacterial nanohybrid solution for coating stainless steel.** *C. Falentin-Daudré; E. Faure; C. Jérôme; C. Van de Weerdt; J. Martial; C. Archambeau; A.S. Duwez; C. Detrembleur*
T6 - OP25	**Bioinspired protein imprinted poly(dopamine)-silica composite as separation materials in high-pressure liquid chromatography.** *A. Nematollahzadeh; B. Selleregren; A. Shojaei; M.J. Abdekhoadie*
T6 - OP26	**Development and characterization of antimicrobial PCL fibres for surgical suture applications.** *L. Botta; R. Scaffaro; M. Sanfilippo; G. Gallo; A.M. Puglia*
T6 - OP27	**Enzymatically cross-linked proteins: hierarchical biopolymers.** *Y. Saricay; P. Wierenga; R. de Vries*
T6 - OP28	**Polymer-cooperative blocking the viruses - strategy, synthesis, and effectiveness.** *A.V. Serbin; E.N. Karaseva; O.L. Alikhanova; V.B. Tsvetkov*
T6 - OP29	**Non-linear viscoelastic models for random coil polysaccharide solution rheology over a broad range of concentrations.** *W.M.H. Verbeeten*
T6 - OP30	**Porous protein based scaffolds produced using a freeze-thawing technique.** *H. Kirsebom; L. Elowsson; M. Durbeej; B. Mattiasson*
T6 - OP31	**Galactomannan in imidazolium-based ionic liquids.** *E. Sultan; A. Bussard; E. Fleury; A. Charlot*
T6 - OP32	**Hierarchically self-organized PS-*b*-P4VP Honeycomb films with reversible pH-responsive wettability.** *P. Escale, M. Save, C. Derail, L. Rubatat; L. Billon*
T6 - OP33	**Lipase catalyzed synthesis of biopolyester and related clay-based nanohybrids.** *H. Öztürk Düşkünkorur; E. Pollet; P. Debeire; V. Phalip; L. Avérous*
T6 - OP34	**Intelligence polymers behavior and its application idea in treatment of some diseases of centeral nervous system.** *M. Abolhassani; A. Yavari; P. Abolhassani; S. Shouli*
T6 - OP35	**Hydrogels based on poly(vinyl alcohol)/phosphoester and poly(ethylene glycol)/phosphoester for biomedical applications.** *T. Vlad-Bubulac; A. Oprea; D. Serbezeanu; C. Hamciuc*
T6 - OP36	**The missing lactam – thermoresponsive poly(*N*-vinylpiperidone).** *C. Ieong; R.K. O'Reilly*
T6 - OP37	**Polysaccharide capsules with engineered hydrophobic drug-loaded multilayers.** *J. Jing; D. Cui, I. Pignot-Paintrand; B. De Geest; C. Picart; R. Auzély-Velty*
T6 - OP38	**Non-monotonic variation of polymer size with increasing confinement.** *D. Chaudhuri; B. Mulder*
T6 - OP39	**Poloxamines for injectable scaffolds with osteogenic activity.** *C. Alvárez-Lorenzo; A. Rey-Rico; M. Silva; J. Couceiro; A. Concheiro*
T6 - OP40	**The key factors driving *in vivo* immobilization of proteins to PHA.** *N. Dinjaski; J.L. García; M.A. Prieto*
T6 - OP41	**Polymeric bio-functionalisation to generate enzyme-responsive biomaterials.** *P.D. Thornton; A. Heise*
T6 - OP42	**Nanohybrides and composites as perspective biomedical materials.** *V.P. Zubov; D.V. Kapustin; A.N. Generalova; I.V. Bakeeva*
T6 - OP43	**Sol-Gel coatings for metal implants.** *M. Hernández-Escolano; M.J. Juan-Díaz; M. Martínez; M.D. Gurruchaga; M.I. Goñi; J.J. Suay*
T6 - OP44	**Spray dried hydroxyapatite-chitosan biocomposites.** *T. Başargan; G. Nasün-Saygılı*
T6 - OP45	**Antiheparin activity of cationic dextran derivatives in rats *in vivo*.** *K. Kaminski; K. Szczubialka; M. Nowakowska; B. Kalaska; W. Buczko*

T6 - OP46	**Trimethyl chitosan-based complexes as nanocarriers for pH-triggered lysosomal delivery of therapeutic proteins.** *M. I. Giannotti; O. Esteban; M. F. García-Parajo; F. Sanz*
T6 - OP47	**Modeling of nanotubes penetration through a phospholipid bilayer.** *S. Pogodin; N.K.H. Slater; V.A. Baulin*
T6 - OP48	**Zinc oxide protects etch&rinse adhesive resin-dentin hybrid layers from MMPs degradation.** *M. Toledano; M. Yamauti; P. Suarez; M. Quintana; E. Osorio; R. Osorio*
T6 - OP49	**Preparation and characterisation of glycopolymers by CCTP and click chemistry.** *Y. Gou; D.M. Haddleton*
T6 - OP50	**Recognition and release of biological catechols in NIPAM-based copolymers bearing phenylboronic acid receptors.** *N. Martin; S. Norvez; I. Iliopoulos*
T6 - OP51	**Chitin-immobilized lipase catalyst for ring opening polymerization of ε-caprolactone.** *B. Iyisan; E. Özsağıroğlu; N. Deveci Aksoy; Y. Avcıbaşı Güvenilir*
T6 - OP52	**Novel bioimaging probes combining well-defined multifunctional polymers and two-photon absorption chromophores.** *C. Cepraga; S. Adjili; S. Marotte; T. Gallavardin; J. Massin; J.C. Mulatier; C. Monnereau; O. Maury; Y. Bretonnière; A. Favier; Y. Leverrier; J. Marvel; P.L. Baldeck; C. Andraud; M.T. Charreyre*
T6 - OP53	**Blends and composites of biodegradable polyesters with cellulosic fibers. Effect of chemical modification on the morphological, thermal and mechanical properties.** *M. Pracella; M.U. Haque; M. Errico; G. Gentile; V. Alvarez*
T6 - OP54	**Synthesis and (bio)conjugation of polypeptides from *N*-carboxyanhydride (NCA) polymerization.** *J. Huang; G. Habraken; A. Heise*
T6 - OP55	**Study on biodgradability of xenobiotic polymers based on numerical simulation and experimental outcomes.** *M. Watanabe; F. Kawai*
T6 - OP56	**Presence of nano precursors in lignin of hevea brasiliensis (rubber wood): a sem, ftir study.** *S. Tabassum; O. Sulaiman; R. Hashim*
T6 - OP57	**Cellulose nanostructure in natural fibers from position resolved SAXS and WAXS measurements.** *C.J. Garvey; M.P. Weir; K.J. Jarrett; C.E. Buckley*
T6 - OP58	**Polymeric lipidic membrane permeabilizers displaying densely packed arrays of crown ether lateral substituents.** *M Liu; N.Illy; B.Brissault; K.Ondrias; J.Penelle; V.Barbier*
T6 - OP59	**Synthesis of monodisperse linear poly(oxazolines) with minimised structural defects as model compounds for elucidating cell membrane properties.** *B. Monnery; S. Shaunak; M. Thanou; J. Steinke*
T6 - OP60	**Proteins as mechanophores in damage self-reporting polymeric materials.** *N. Bruns; S. Lörcher; T. Winkler*
T6 - OP61	**Synthesis and characterization of redox and pH-sensitive poly(aspartic acid) hydrogels.** *B.S. Gyarmati, Á. Némethy, T. Gyenes, A. Szilágyi*
T6 - OP62	**Copoly(2-oxazoline)s exhibiting side chains for thiol-ene reactions – synthesis of glycopolymers and their potential for biological applications.** *K. Kempe; C. Biskup; M. Gottschaldt; U. S. Schubert*
T6 - OP63	**Engineering Alg-PEG hybrid microspheres for biomedical applications.** *R. Mahou; C. Gonelle; G. Parnnaud; F. Schmitt; G. Kollárikova; L. Jullierat; I. Laçik; C. Wandrey*
T6 - OP64	**Degradation of polyglycidol in aqueous solution by UV light.** *A. Utrata-Wesolek; R. Trzcinska; B. Trzebicka; A. Dworak*
T6 - OP65	**DNA complexes with charged compounds, that are useful for nanotechnology.** *N. Kasyanenko; B. Dribinsky; A. Puchkova; P. Sokolov*

T6 - OP66	**Viscoelastic and thermal behavior of polyurethane films prepared as shape memory polymer.** *C. Citak; I. Yavuz; M. Bonfil; F. S. Guner*
T6 - OP67	**Wavelength-responsive polymer materials.** *V. San Miguel; A. Del Campo*
T6 - OP68	**Photoresponsive polymer brushes.** *J. Cui; A. Del Campo*
T6 - OP69	**Properties of cyanoacrylate adhesives with different alkyl chain length.** *R. Torregrosa-Coque; A.M. Villarreal-Gómez; J. M. Martín-Martínez*
T6 - OP70	**Multi-block copolymers of polyamide 6 and diepoxy propylene adipate obtained by solid state polymerization.** *S. Cakir; C. Koning; M. Eriksson; M. Martinelle*
T6 - OP71	**Dynamics of hydrogen bonds and protein in hydrated elestin.** *V. Samouillan; D. Tintar; F. Delaunay; J. Dandurand; C. Lacabanne*
T6 - OP72	**The effect of degradation on PLLA/PCL scaffolds prepared by freeze extraction.** *L. A. Gaona Corral; J. L. Gómez; J.E. Perilla; M. Lebourg*

POSTER CONTRIBUTIONS

TOPIC 1: Synthetic Routes: Monomers and Polymers from Bioresources and Advanced Methodologies

T1-001	**Low temperature photoinitated RAFT of vinyl acetate.** *M. K. Ham; S. H. Shim; Y. Jeong; Y. K. Kwon; Y. J. Kwark*
T1-002	**Towards sustainable polymerization of stimuli-responsive polyglycerol hydrogels.** *S. Salehpour; M. A. Dube*
T1-003	**Biocomposites based on elastomeric polyurethane and cellulose nanocrystals.** *L. Rueda; B. Fernández d'Arla[1]; M.L. González; A. Valea; I. Mondragon; M.A. Corcuera; A. Eceiza*
T1-004	**Polyurethanes derived from renewable resources: effect of polyol structure.** *A. Saralegui; L. Rueda; B. Fernández d'Arlas; M. D. Martín; I. Mondragon; A. Eceiza; M. A. Corcuera*
T1-005	**Synthesis of polyesters from castor oil and their use as polymer matrix for magnetic nanocomposites.** *P. A. Ziani Suarez; F. Machado Silva; E. U. Xavier Péres; F. Gomes de Souza Jr*
T1-006	**Thermosensitive copolymers based on alginate and poly(N-isopropylacrylamide) obtained by gamma-radiation.** *M. S. Lencina; N. A. Andreucetti; M. A. Villar*
T1-007	**Study of incorporation of vegetable waste as filler in flexible polyurethane foam.** *F. J. Melero Muñoz; M. V. Navarro Bañon; J. R. Vega Baudrit; M. R. Sibaja*
T1-008	**Lyocell fibers reinforced with anisotropic nanofiller.** *A. J. Uddin; A. Yamamoto; Y. Gotoh*
T1-009	**Castor oil based poly(urethane-co-pyrrole)s as novel electroactive anticorrosive coatings for steel.** *R. Gharibi; M. Yousefi; H. Yeganeh*
T1-010	**Synthesis of isotactic poly(hydroxy acrylic acid) by radical polymerization of methylene dioxolanone prepared from lactic acid.** *H. Tanaka; Y. Matsubara; K. Okuda; M. Niwa*
T1-011	**Investigation of the type of the bridge on the activity of supported metallocene catalyst in ethylene polymerization.** *A. Talaei*
T1-012	**Biopolymers from natural oils.** *A. Remeikyte; J. Ostrauskaite; J. Vidas Grazulevicius*
T1-014	**Synthesis of polystyrene waterborne nanoparticles by miniemulsion polymerization.** *L. Ronco; R. J. Minari; J. R. Vega; L. M. Gugliotta*
T1-015	**Lithium naphthalenide initiators for controlled anionic polymerization.** *V. A. González; A. J. Satti; M. D. Ninago; E.M. Vallés; M. A. Villar; A. E. Ciolino*
T1-016	**A new method for synthesis of photocurable low molecular weight chitosan.** *L. Solhi; M. Atai; A. Nodehi; M. Imani*
T1-017	**Study of rare earth metal triflates as new catalyst for the formation of oxazolidone-isocyanurate-ether networks from DGEBA and 4-toluene-2,4-diisocyanate.** *M. Flores; X. Fernández-Francos; J. M. Salla; A. Mantecón; A. Serra; E. Jimenez-Piqué; X. Ramis*
T1-018	**Binuclear carbonyl complexes of transition metals of VI Group in homo- and copolymerization of methyl methacrylate and styrene.** *M. V. Pavlovskaya; A. A. Zolotukhin; D. F. Grishin*
T1-019	**Amphiphilic copolymers based on sucrose methacrylate and acrylic monomers.** *H. F. N. de Oliveira; M. I. Felisberti*
T1-020	**Non isocyanate polyurethane obtained from different vegetable oils.** *P. Mazo; L. Rios*

T1-021	**Kinetic study of 2-acrylamido-2-methylpropanesulfonic acid in free-radical polymerization method by differential scanning calorimetry.** *E. Nadim; H. Bouhendi; F. Ziaee, R. Bazhrang*
T1-022	**Synthesis and characterization of novel bio-based polyesters based on curcumin as a natural diol monomer and commercially available aromatic dicarboxylic acids.** *A. Shockravi; A. Javadi; S. Hajavi*
T1-023	**The oxypropylation of olive stone and the use of the ensuing polyols for the synthesis of novel polyesters and polyurethanes based on renewable resources.** *M. Matos; F. Barreiro; A. Gandini*
T1-024	**Microwave synthesis: an alternative approach to synthesize conducting end-capped polymers.** *P. Marcasuzaa; S. Reynaud; B. Grassl; J. Desbrières; O. F. Donard*
T1-025	**Synthesis and characterization of new sensitive copolymer of poly-2,7-fluorene-1,4-(2,3-diamine)naphthalene for aqueous media.** *R. Vázquez-Guilló; A. Calero; A. Salinas-Castillo; C.R. Mateo; R. Mallavia*
T1-026	**Copolymers from poly(lactic acid) (PLA) and chain extenders or branching agents.** *A. Hitos-Rodríguez; A. Bacardit; L. Olle; O. O. Santana; M. L. Maspoch; J. J. Bou*
T1-028	**Synthesis of photocleavable block copolymers based on p-methoxyphenacyl groups.** *O. Bertrand; C .A. Fustin; J. F. Gohy*
T1-029	**Semi-IPNs based on poly(n-vinylpyrrolidone) and poly(L-lactide): synthesis and characterization.** *A. P. R. Camilo; M. I. Felisberti; V. Mano*
T1-030	**Evaluation of yam agriculture wastes to obtain fructans.** *M. Esquivel; A. Aguilar; R. Sibaja; J. Vega-Baudrit; S. Madrigal-Carballo*
T1-031	**Synthesis of low formaldehyde emission urea-formaldehyde resins and their application to the manufacturing of particleboards.** *P. Estévez; S. Vallejos; H. El Kaoutit; M. Trigo-López; F. Serna; F. García; J. L. de la Peña: J. M. Pérez*
T1-032	**Controlled free-radical copolymerization of 4-vinyl pyridine and tert-butyl acrylate via reversible addition-fragmentation chain transfer (RAFT) technique: kinetics and mechanism.** *E. Sivtsov; A. Gostev; E. Chernikova*
T1-033	**Conventional and RAFT copolymerization of N-vinyl succinimide and 4-vinyl pyridine.** *A. Gostev; E. Sivtsov*
T1-034	**Aromatic copolyesters containing cyclic diacetalized D-glucitol.** *C. Japu; A. Martínez de Ilarduya; A. Alla; E. Benito; M. G. García-Martín; J. A. Galbis; S. Muñoz-Guerra*
T1-035	**Eco-friendly aliphatic polyesters containing 1,4-cyclohexane dicarboxylate units: effect of diol chain length on thermo-mechanical properties.** *A. Celli; P. Marchese; S. Sullalti; J. Boyenval; S. Commereuc*
T1-036	**Synthesis and modification of biopolymers with unsatured terminal groups.** *C. Berti; A. Celli; L. Cruciani; P. Marchese; L. Sisti; M. Vannini*
T1-037	**Synthesis and characterization of lactide-graft-poly(vinyl alcohol) and miscibility study with poly(ethylene oxide).** *A. Lejardi; A. Etxeberria; E. Meaurio; J. Fernandez; J. R.Sarasu*[1]
T1-038	**Oleic and undecylenic acids-based diols and derived polyurethanes via thiol-ene coupling.** *R. J. González-Paz; G. Lligadas; J. C. Ronda; M. Galià; V. Cádiz*
T1-039	**Synthesis and microbiologic assays of new polymers based on antibacterial biomolecules.** *B. Lepoittevin; J. Casimiro; C. Rinfray; J. M. Herry; M. N. Bellon-Fontaine; P. Roger*

T1-040	**Carbohydrate-based polyurethanes: a comparative study of polymers made from isosorbide and 1,4-butanediol.** *R. Marín; A. Alla; A. Martínez de Ilarduya; S. Muñoz-Guerra*
T1-041	**Thermal and hydrolytic degradability of polyesters containing cyclic acetalized carbohydrate units.** *C. Lavilla; C. Japu; M. G. García-Martín; J. A. Galbis; S. Muñoz-Guerra*
T1-042	**Polyhydroxybutyrate nanocomposite microcapsules with brazilian smectitic clays.** *M. G. da Silva Valenzuela; W. H. Shu; H. Wiebeck; F. R. Valenzuela Diaz*
T1-043	**Structural features of copolymers of styrene and macromers of a vegetable oil.** *S. Gómez Robles; M. I. Felisberti*
T1-044	**Synthesis and characterization of poly(L-lactide-co-ε-caprolactone) random copolymers.** *J. Fernández; A. Etxeberria; E. Zuza; E. Meaurio; S. Petisco; J. R. Sarasua*
T1-045	**Thermosets from methyldiphenolic acid-based benzoxazine and diphenolic acid mixtures.** *C. Zuñiga; G. Lligadas; J. C. Ronda; M. Galià; V. Cádiz*
T1-046	**Polybenzoxazine foams from renewable diphenolic acid.** *C. Zúñiga; G. Lligadas; J. C Ronda; M. Galià; V. Cádiz*
T1-047	**Aminoalkylphosphonic acids and glycylaminoalkylphosphonic acids as antibacterial additives in textile chemistry.** *M. H. Kudzin; Z. H. Kudzin; J. Drabowicz*
T1-048	**Amphiphilic poly(4-vinylpyrine) (P4VP) block copolymer micelles for metal binding.** *N. Abdul Rahim; F. Audoin; J. G. Vos; A. Heise*
T1-049	**Sunflower oil-modified polyester synthesis by ring opening polymerization and its use in organic coatings.** *C. Tasdelen-Yucedag; A. Tuncer Erciyes*
T1-050	**Synthesis and optical, electrochemical and electroluminescence properties on new series of copoly-2,7-fluorene-1,4-(2/3-amino)benzene.** *A. Calero; R. Vazquez-Guilló; A. Salinas-Castillo; F. Montilla; C. Coya; A. L. Alvarez; C. R. Mateo; R. Mallavia*
T1-051	**Metathesis degradation of natural rubber in the presence of avocado and mandarin oils using ruthenium alkylidene catalysts.** *A. Martínez; M. A. Tlenkopatchev*
T1-052	**Thiol-yne coupling to undecylenic acid derivatives. Synthesis of polyurethanes.** *Z. Beyazkilic; R.J. González-Paz; G. Lligadas; J. C. Ronda; M. Galià; V. Cádiz*
T1-053	**Phosphorus-containing high oleic sunflower oil flame retardant thermosets.** *M. Moreno; G. Lligadas; J. C. Ronda; M. Galià; V. Cádiz*
T1-054	**Amphiphilic triblock copolymers of poly(ethylene glycol) and L-lactide: a possible mechanism of polymerization for coordination/insertion catalysts.** *R. Bergamo Trinca; H. F. Nunes de Oliveira; M. I. Felisberti*
T1-055	**Styrenated oil synthesis by "click" chemistry approach.** *P. Yazgan; A. Tuncer Erciyes; N. Alemdar; Y. Yagci*
T1-056	**Effect of organoclay preparation and the processing conditions on the extent of exfoliation in nylon 6/ modified clay nanocomposites.** *E. Erdmann; M. A. Toro; H. A. Destéfanis; M. Modesti*
T1-057	**Thermoplastic polyurethanes with undecylenic acid-based soft segments: synthesis and properties.** *C. Lluch; G. Lligadas; J. C. Ronda; M. Galià; V. Cádiz*
T1-058	**Polybenzoxazine prepolymers from renewable fatty acid derivatives.** *A. Tüzün; G. Lligadas; J. C. Ronda; M. Galià; V. Cádiz*
T1-059	**Molecularly imprinted nanoparticles prepared by non-aqueous emulsion polymerization.** *G. Dvorakova; R. Hashick; K. Chiad; M. Klapper; K. Müllen; J. Vohlidal; A. Biffis*

T1-060	**Synthesis of functionalized polyesters via ring-opening polymerization of ε-caprolactone initiated by Al-based catalysts.** *Y. A. Piskun; I. V. Vasilenko; S. V. Kostjuk; K. V. Zaitsev; S. S. Karlov*
T1-061	**Styrenated oil production by RAFT method.** *N. Caglar; A. Tuncer Erciyes; N. Alemdar; N. Bicak*
T1-062	**Starch containing polyurethanes: structure and biodegradability.** *T. Travinskaya; E. Mishchuk; Y. Savelyev*
T1-063	**Preparation of ordered Au/PEO-b-PFOMA hybrid films through phase transition of micellar thin films.** *E. J. Yoon; N. T. Hoai An; D. H. Kim; K. T. Lim*
T1-064	**In situ micelle formation and inter-block crosslinking of PAA-b-PS via RAFT polymerization.** *E. S. Lim; L. T. Bao Tran; K. T. Lim*
T1-065	**Ethylene/1-octene copolymerization with supported salen-type complexes. Effect of metal type.** *A. Pietruszka; M. Białek; K. Czaja*

TOPIC 2: New Analytical and Characterization Tools

T2-001	**Fractionation analysis techniques for the characterization of copolymers with bimodal chemical composition distribution.** *B. Paredes; A. Carrero; R. van Grieken; I. Suarez*
T2-002	**Novel method for the in-situ estimation of curing shrinkage using FTIR/ATR spectroscopy and refractive index measurements.** *X. Fernández-Francos; X. Ramis; À. Serra; M. Sangermano*
T2-003	**Raman evaluation of the structure of organic materials by analyzing the region of stretching vibrations of CH_2 and CH_3 groups – benefits and limitations.** *P. Donfack; K. Prokhorov; E. Sagitova; Y.V. Zavgorodnev; G. Nikolaeva; M. Guseva; V. Gerasin; A. Materny; E. Antipov; P. Pashinin*[2]
T2-004	**Polymer film analysis.** *R. M. Zacur; D. R. Ercoli; G. S. Goizueta*
T2-005	**Interplay between raman scattering and atomic force microscopy in characterization of polymer blends.** *P.Dorozhkin; A. Shelaev; S. Magonov*
T2-006	**Characterization of different polymer systems via asymmetric flow field-flow fractionation (AF4).** *E. Altuntas; N. Fritz; M. Hage; U. S. Schubert*[1]
T2-007	**Thermogravimetric analysis of an acrylic copolymer.** *T. G. Oberti; M. S. Cortizo; J. L. Alessandrini*
T2-008	**Structural analysis of synthetic polymer by high-energy CID using MALDI SpiralTOF-TOF.** *T. Satoh; A. Kubo; Y. Ito; M. Hashimoto; M. Ubukata; T. Sato; J. Tamura; A. Kusai*
T2-009	**Mechanical characterization of a linear polyethylene by means of depth sensing indentation (DSI) measurements.** *V. Lorenzo; M. Ulagares de la Orden; R. Claramunt; J. Martínez-Urreaga*
T2-010	**Characterization of different varieties of cassava flour by solid state NMR spectroscopy.** *G. C. V. Iulianelli; M. I. B. Tavares*
T2-011	**Kinetic investigation of thermal degradation for low molecular weight 1,2-polybutadiene.** *M. Ronagh Baghbani; F. Ziaee; H. Bouhendi; F. Ziaie*
T2-012	**Three-dimensional modeling of mold filling process in injection process using OpenFOAM.** *N. Jafari Esfad; B. Azinfar; A. Ramazani*
T2-013	**Derivatives of coumarin as fluorescent probes for monitoring photopolymerization processes by fluorescence probe technology.** *J. Ortyl; R. Popielarz*
T2-014	**Study of thermo-mechanical and thermo-oxidative degradation of polylactide by MALDI-TOF-MS. A statistical design of experiments to optimize the sample preparation procedures.** *J. D. Badía; E. Strömberg; A. Ribes-Greus; S. Karlsson*
T2-015	**Diffusion during radical bulk polymerization of styrene and methyl methacrylate.** *B. K. Stempfle; M. Dorfschmid; D. Wöll*
T2-016	**PVT analysis of chemical reactions: polymerization, transesterification, crosslinking.** *J. Pionteck*
T2-017	**In situ studies of phase structure and crystalline development of poly(L-lactide/ε-caprolactone)/poly(ethylene glycol) blends by atomic force microscopy.** *N. Hernández Montero; J. M. Ugartemendia; T. Suárez; J. R. Sarasua*
T2-018	**SEC-DAD as a powerful tool for characterization of conjugated polymers.** *O. Trhlíková; D. Bondarev; J. Sedlácèk; J. Vohlídal*
T2-019	**Heterogeneity during controlled radical polymerization – a single molecule fluorescence microscopy investigation.** *J. Martin Nölle; K. Goossens; W. van Camp; D. Wöll*
T2-020	**Continuous-flow off-line pyrolysis-GC/MS for detection of poly(vinylpyrrolidone).** *M. Antic; V. Antic; A. Kronimus; K. Oing; J. Schwarzbauer*

T2-021	**Investigation of the miscibility (solubility) of molten polypropylene-polyethylene blends by means of rheometry.** *M. Mihalic; A. Schausberger*
T2-022	**Comparative study of various grades of polyethylene by raman spectroscopy: microstructural attribution of bands.** *R. Jumeau; P. Bourson; M. Ferriol; F. Lahure*
T2-023	**Characterisation of morphology of uniaxial oriented PET – films and pressure-induced i-PP via confocal and polarised μ-RAMAN spectroscopy.** *K. Vincze-Minya; S. Hild; T. Keplinger; S. Jilg; W. Stadlbauer; M. Aigner; J. Miethlinger*
T2-024	**A thermoset-thermoplastic blend: spectroscopy characterization.** *F. A. Mesa Rueda; A. Cuellar Burgos; C. Vargas Hernandez; J. E. Perilla*
T2-025	**Characterization of the mechanical properties of EVA foams by TMA.** *M. I. Beltrán; A. Marcilla; I. Pelaez; A. Otero*
T2-026	**Molecular weight distribution changes in irradiated films of vinyl ketone copolymers.** *S. Sánchez-Ballester; J. D. Badia; A. Martinez-Felipe; A. Ribes-Greus; V. Soria*
T2-027	**Study of the thermal behavior of syndiotactic and atactic polystyrene by raman spectroscopy.** *N. Brun; P. Bourson; S. Margueron; M. Duc*
T2-028	**Study, by raman spectroscopy, of the microstructure evolution of isotactic polypropylene during tensile test and relaxation: measuring the chains orientation.** *S. Chaudemanche; M. Ponçot; J. Martin; J. M. Hiver; P. Bourson; A. Dahoun*
T2-029	**Chromatographic characterization of PS-block-PEO.** *M. Grabowsky; M. I. Malik; P. Sinha; H. Pasch*
T2-030	**Nanoparticle characterisation by field-flow fractionation.** *W. van Aswegen; I. Malik; T. Otte; H. Pasch*
T2-032	**Predicting the slow crack growth resistance of polyethylene resins using alternative short-time performance tests** *C. Dominguez; A. Adib; J. Rodríguez; C. Martín; R. A. García*

TOPIC 3: Advanced Processing and Recycling Technologies

T3-002	**Phase behaviour of blends of poly(4-vinylphenol-co-methyl methacrylate) / poly(styrene-co-4-vinylpyridine).** *Z. Benabdelghan; A. Etxeberria*
T3-003	**Chemical characterization of organic-inorganic coating for dental applications.** *M. J. Juan-Díaz; M. Martinez; M. Hernández-Escolano; J. Suay; M. Gurruchaga; I. Goñi*
T3-005	**Low-temperature polymerization of vinyl monomers controlled by metallocomplexes based on C2B8-carborane ligand.** *I. Grishin; A. Ohapkin; I. Chizhevsky; D. Grishin*
T3-006	**Morphological characterization of PP for different foam injection molding processes with chemical blowing agents.** *V. Contreras; N. Villarreal-Bastardo; J. C. Merino ; J. M. Pastor*
T3-007	**Development of glass reinforced PVC composite.** *D. Gomes de Araujo; E. Hage Jr.; L. H. Grizzo*
T3-008	**New copolymer of tautomerizable monomer.** *J. M. Giussi; P. E. Allegretti; M. S. Cortizo*
T3-009	**"Smart pellet" additives for reinforcement in polypropylene composite.** *Y. Wang; D. A. Schiraldi*
T3-010	**Carbon nanotube imprinting technique using brownian motion in polymer melt.** *M. Yamaguchi; H. W. Yoon*
T3-011	**Polymerisation of pyrrole with phenyliodine bis(trifluoroacetate).** *E. Ateş; N. Kızılcan*
T3-012	**Performance improvement of silicone rubber/carbon fiber composites.** *E. S. Kim; Y. H. Jeon; M. Y. Jo; J. S. Yoon*
T3-013	**Novel mechanochemistry reactor and its use for rubber degradation studies in presence of stabilizers under controlled reactive gas atmosphere.** *D. Dondi; A. Buttafava; M. Bianchi; A. Zeffiro; A. Faucitano*
T3-014	**Ion-imprinted silsesquioxane polymers: synthesis and structure.** *M. Barczak; K. Michalak; Y. L. Zub*
T3-015	**Free radical melt grafting of polyolefins by using nitroxide radicals.** *D. Bélékian; P. Chaumont; E. Beyou; P. Cassagnau; S. Quinebèche; J. J. Flat*
T3-016	**Polyvinylchloride: synthesis and modification of properties by copolymerization.** *E. Kotlova; M. Pavlovskaya; M. Filippova; D. Grishin*
T3-017	**Photodegradation and bacterial biodegradation of polyethylene-vinyl acetate (EVA) mulching films. Effect of calcium and iron stearates as pro-oxidant additives.** *J. L. Pablos; C. Abrusci; I. Marín; E. Espi; T. Corrales; F. Catalina*
T3-018	**Evaluation of photodegradation of polyethylene films with pro-degradant agents II. Morphological analysis.** *J. M. Klein; A. M. C. Grisa; R. N. Brandalise; M. Zeni*
T3-019	**Chemical modification of ethylene butyl acrylate copolymer with hindered amine light stabilizer HALS. Photostabilization study.** *L. López-Vilanova; E. Espí; A. I. Real; M. Calvo; A. Fontecha; J. L. G. Fierro; C. Peinado; F. Catalina*[1]
T3-020	**Synthesis of low formaldehyde emission urea-formaldehyde resins and their application to the manufacturing of particleboards.** *P. Estévez; S. Vallejos; H. El Kaoutit; M. Trigo-López; F. Serna; F. García; J. L. de la Peña; J. M. Pérez*
T3-021	**Modeling of butadiene polymerization using neodymium catalyst complex.** *A. M. Gumerov; I. M. Davletbaeva*
T3-022	**Effects of incorporating waste rigid polyurethane foam in polymer compounds based on polypropylene.** *S. Fontana Pereira; E. Hage Jr*
T3-023	**Parallel versus perpendicular lamellar-within-lamellar self-assembly of A-b-(B-b-A)$_n$-b-C and (B-b-A)$_n$-b-C ternary multiblock copolymer melts: SSL theory, DPD, SCFT investigation.** *V. A. Markov; Y. A. Kriksin; A. V. Subbotin; G. ten Brinke*

T3-024	**Aminoiminophosphoranate complexes of platinum and palladium in radical polymerization of vinyl monomers.** *E. V. Kolyakina; M. V. Pavlovskaya; N. A. Ustynyuk; D. F. Grishin*
T3-025	**Atom transfer radical polymerization of methyl methacrylate in the presence of four-coordinated cobalt complex with sterically hindered o-iminobenzoquinone ligand.** *E. V. Kolyakina; A. A. Poddel'sky; D. F. Grishin*
T3-026	**Nitroxide-mediated (Co) polymerization of vinyl monomers with high-molecular-weight alkoxyamines, derived from C-phenyl-N-tert-butylnitrone.** *A. Shchepalov; D. Grishin*
T3-027	**Synthesis and singlet-singlet energy transfer studies of copolymers involving fluorene-carbazole units as energy donor and porphyrin as pendant acceptor group.** *S. M. A. Pinto; M. J. F. Calvete; H. D. Burrows; M. M. Pereira; A. Salinas-Castillo; R. Mallavia*
T3-028	**Degradation kinetics of electron beam irradiated poly (propylene-co-ethylene) heterophasic copolymer.** *M. Koosha; N. Ebrahimi; Y. Jahani; S. A. Seyed Sajadi*
T3-029	**Effect of process conditions on the compatibilization of in-reactor alloys.** *H. Bagheri; M. Nekoomanesh; S. Hakim; Y. Jahani; Z. Q. Fan*
T3-030	**Investigation of expanded graphite nanoplatelet its properties and composites applied in EMI shielding.** *C. P. Chang; C. S. Tsai; J. W. Lu; C. Y. Huang*
T3-032	**Electrosedimentation thromboresistant polymeric coverings on purely iron electrode.** *S. H. Sargsyan; A. S. Sargsyan; K. S. Margaryan*
T3-033	**Temperature effects in the dynamics of bipolaron in polymer chains.** *J. F. Teixeira; W.F da Cunha; P.H.O. Neto; L. F. Roncaratti; R. Gargano; G. M. e Silva*
T3-034	**Excitons dissociation in semiconducting polymers PN junctions.** *W. F. da Cunha; P. H. O. Neto; L. F. Roncaratti; F. V. Moura; R. Gargano; G. M. e Silva*
T3-035	**Modification of linear low-density polyethylene in single-screw extruder.** *K. Ono; M. Yamaguchi*
T3-036	**PET modification using PLA and chitosan.** *D. Palma Ramírez, A. M. Torres Huerta, M. A. Domínguez Crespo, E. O. Bustamante*
T3-037	**Mechanical properties of postconsumer agave/polyethylene biocomposites.** *R. Jimenez Amezcua; I. Reyes Gonzalez; S. Garcia Enriquez; R. Gonzalez Nunez*
T3-038	**Study of conductivity of PANI compounds processed by extrusion and compression.** *J. Ruiz; B.Gonzalo; J. L.Vilas; J. M. Laza; L. M. León*
T3-039	**Rheological modeling of single-screw extruders.** *H. Hosseini; F. Aghazadeh*
T3-040	**Preparation of core-shell, organic-inorganic, hybrid latexes via a new single-step pickering emulsion polymerization method.** *A. Pakdel; H. Eslami; S. Pourmahdian*
T3-041	**Influence of crosslinker and stabilizer additives on the mechanical and the rheological properties of recycled plastic mixtures.** *J. Acosta García; C. Fonseca Valero; T. Aguinaco Castro; M. U. de la Orden; J. Martínez Urreaga; C. González Sánchez*
T3-042	**The effect of oil content on the grinding EPDM elastomers and on the structure of rubber powders** *D. V. Solomatin; O. P. Kuznetsova; E. V. Prut*
T3-043	**Characterization of induced thermo-mechanical degradation on poly (ethylene terephthalate).** *J. D. Badía; E. Strömberg; S. Karlsson; A. Ribes-Greus*
T3-044	**Influence of the multi-walled carbon nanotubes on morphology and material properties of PC/ABS nanocomposites obtained by extrusion.** *M. Wegrzyn; I. Buezas; E. Gimenez*

T3-045	**Effect of nano particles on mechanical properties of biodegradable LDPE/ starch/nanoclay composite.** *A. Oromiehie; P. Gusheh*
T3-046	**Antimicrobial gluten-gelatin films containing fatty-acids.** *F. Fakhouri; S .M. Martelli; A. Teixeira; F. Yamashita; L. H. Innocentini-Mei; F. P. Collares-Queiroz*
T3-047	**The development of a new co-polymer for immobilizing an optical Hg^{2+}-sensitive probe.** *F. J. Orriach-Fernández; A.L. Medina-Castillo; J.F. Fernández-Sánchez; A. Muñoz de la Peña; A. Fernández-Gutiérrez*
T3-048	**Study of structural features of fluorinated paraffins.** *V.M. Bouznik; Y. E. Vopilov; M. V. Doroshkevich; L. N. Ignatieva;M. D. Nivikova; M. A. Smirnov; V. P.Tarasov; A. N. Toropov; E .P. Kharitonova; A. V. Chernyak; G. Y. Yurko[1]*
T3-049	**Bioactive textile materials covered with polymers as continuous layers, microparticles or microcapsules.** *G. Mocanu; M. Nichifor; D. Mihai; L. C. Oproiu*
T3-050	**Rheology applied to the study of processing behaviour of PVC-PBA block copolymers.** *M. I. Calafel; B. Pascual; J. I. Conde; M. Boix; A. Santamaría; M. E. Muñoz*
T3-051	**Effects of reprocessing cycles on the structure and properties of polypropylene/cloisite 15A nanocomposites.** *S. Bruzaud; N. Touati; M. Kaci; Y. Grohens*
T3-052	**Obtaining porous polyimides with controlled pore size.** *E. Rangel-Rangel; E. M. Maya; J. de Abajo; A. E. Lozano; J. G. de la Campa*
T3-053	**Advanced polymeric composites for self-healing structural materials.** *M. Raimondo; R. Corvino; L. Guadagno; P. Longo; C. Naddeo; A. Mariconda*
T3-054	**Relationships between structures and physical properties of PVDF/MWNT composite.** *S. M. Hong; J. M. Koo*
T3-055	**Thermoplastic composites reinforced with keratin fibers.** *F. Giunco; L. Conzatti; P. Stagnaro; A. Aluigi; E. Marsano; M. Castellano; C. Marano*
T3-056	**Interfacial interactions in flax fibre/PLA biocomposite: from model surfaces to real fibres.** *E. Balnois; G. Raj; C. Baley; Y. Grohens*
T3-057	**Valorisation of maghnite-H^+ as a catalyst for the synthesis of various biodegradable polyesters and polyacetals.** *S. Bennabi; N. Sahli; M. Belbachir; C. H. Brachais; J. P. Couvercelle*
T3-059	**Thermal decomposition of PVC plastisol foams. Influence of the concentration of plasticizer.** *A. Marcilla; A. Zoller; M. I. Beltrán*
T3-060	**Waste recycling and public awareness "the case of plastic waste".** *A. R. Abay; M. Öksüz*
T3-061	**Thermal decomposition of PVC plastisol foams. Influence of the type of plasticizer.** *A. Marcilla; A. Zoller; M.I. Beltrán*
T3-062	**Monitoring of Recycled AAO Templates. An Exhaustive Characterization after Polymer Extraction.** *Iwona Blaszczyk-Lezak, Jon Maiz, Javier Sacristan, Carmen Mijangos*

TOPIC 4: Polymers for Advanced Applications Including Energy, Transport, Packaging and Environmentally Friendly Activities

T4-001	**Fluoropolymer dispersions: new environment-friendly products and technology.** *S. Musio; V. Kapeliouchko; T. Poggio*
T4-002	**Properties enhanced PU coating using (Desmodure Z 4470) as isocyanate and the different Desmophens as polyalcohols.** *A. Shokuhi Rad*
T4-003	**New epoxy thermosets obtained from DGEBA and hyperbranched polyesters having reactive/ unreactive chain ends using adipic dihydrazide as latent curing agent.** *Adrian Tomuta; Xavier Ramis; Francesc Ferrando; Àngels Serra*
T4-004	**Inhibition of the migration of low molecular weight moieties to rubber-polyurethane coating interface by incorporating filler.** *R. Torregrosa-Coque; J. M. Martin-Martinez;*
T4-005	**Epoxy polymers and composites for advanced applications.** *R. J. J. Williams*
T4-006	**Development of flexible temperature sensors - realization and characterization of multifilaments based on immiscible polymers loaded with carbon nanotubes.** *A. Cayla; C. Campagne; M. Rochery; E. Devaux*
T4-007	**New polytricyclnonenes and polytricyclononadienes: from monomer synthesis to polymer gas permeability.** *B. Bulgakov; M. V. Bermeshev; L. E. Starannikova; E. S. Finkelshtein*
T4-008	**Enhancement of epoxy thermosets by modification with commercially available hyperbrached poly(ethyleneimine)s (LUPASOLTM) as polymeric modifiers.** *X. Ramis; D. Santiago; X. Fernández-Francos; J. M. Salla; A. Cadenato; J. M. Morancho; À. Serra*
T4-009	**Preparation of L-arabinitol-based functional polyurethanes.** *C. Ferris; M. V. de Paz; F. Zamora; B. Begines; J. A. Galbis*
T4-010	**Thiol-ene coupling reactions: a new approach to functionalized polyurethanes.** *M. V. De Paz; C. Ferris; J. A. Galbis*
T4-011	**Biodegradable linear sulfur-containing polyurethanes derived from carbohydrates.** *B. Begines; F. Zamora; V. de Paz; C. Ferris; J. A. Galbis*
T4-012	**Sugar-based polyurethanes and polyureas.** *F. Zamora; B. Begines; I. Roffé; M. Mancera; J. A. Galbis*
T4-013	**Synthesis and properties of aromatic polyamides derived from isomeric biphenyldicarboxylic acids. theoretical study of the polycondensation reaction.** *G. Hernández; J. M. Pérez; F. García; Á. E. Lozano; J. G. de la Campa; J. de Abajo*
T4-014	**Silarylene –containing poly(amide)s based on 4-(4-((4-(4-aminophenoxy)phenyl)dimethylsilyl)phenoxy) benzenamine. Effect of dicarboxylic acid structure used.** *C. A. Terraza; L. H. Tagle; A. Tundidor; D. Coll*
T4-015	**Thermal rearrangement in poly(o-hydroxyimide)s. Isomeric effects on physical and gas separation properties.** *B. Comesaña; P. Cuadrado; C. Álvarez; A. Hernández; M. Calle; Y. M. Lee; J. G. de la Campa; J. de Abajo; A. E. Lozano*
T4-016	**Peculiarities of water emulsion copolymerization of tetrafluoroethylene with perfluoro(3,6-dioxa-4-methyl-7-octene)sulfonyl fluoride to obtain proton conducting copolymers.** *S. S. Ivanchev; V. S. Likhomanov; A. Y. Menshikova; O. N. Primachenko; S. Y. Khaikin*
T4-017	**Application of pulverized concrete cement powder as filler in PVC pipe.** *M. Natamai Subramanian; T. Arunachalam*
T4-018	**New copolymers of norbornene and vinyl monomers.** *D. S. Popov; V. I. Bykov; K. L. Makovetskii; M. V. Bermeshev; T. A. Butenko; E. S. Finkelshtein*

T4-019	**Macromolecular design of energetic tetrazole-containing olygomers and polymers.** *V. N. Kizhnyav; F. A. Pokatilov; L. I. Vereschagin; A. I. Smirnov*
T4-020	**The effect of fiber orientation on the thermal behavior of polypropylene fibers.** A. Parviz; F. Dadashian
T4-021	**Generation of conductivity through transfer charge properties in flourene and diphenylsilane-containing poly(ester)s and poly(amide)s.** *C. González-Herríquez; L. H. Tagle; C. A. Terraza; A. Barriga; A. Cabrera; U. Volkmann*
T4-023	**Barrier performance of gelatin coated pla films.** *M. Leobono; C. Frova; R. Zacur; D. Ercoli; G. Goizueta*
T4-024	**Polypropylene films of high oxygen and water vapor permeability for MAP applications.** *M. Acosta; D. Ercoli; G. Goizueta; J. Lozano; N. Capiati*
T4-025	**Studies on preparation and properties of novel photoluminescence hydrogels.** *W. F. Lee; H.H. Tsai*
T4-026	**Photovoltaic cell based on lead sulfide\conjugated polymer bilayer heterojunction.** *F. Mighri; J. Patel; A. Ajji*
T4-027	**Photoinduced electron transfer in an oligo-meta-phenylene ethynylene donor-bridge-acceptor complex.** *B. Bingöl; A. C. Durrell; A. J. Di Bilio; R. H. Grubbs; H. Gray*
T4-028	**Synthesis and photopolymerizations of new hydrolysis-stable dental monomers containing phosphonic acids.** *B. Akgün; D. Avci*
T4-029	**Nanocomposite membranes based on nafion and $TiSiO_4$ nanoparticle.** *Y. Devrim; N. Bac; I. Eroglu*
T4-030	**Effect of processing conditions on the performance of polymer-based materials for biomedical applications.** *J. S. Gonzalez; L. N. Ludueña; V. A. Alvarez*
T4-031	**Changing essential characteristics of poly(vinylalcohol) cryogels by thermal treatments.** *J. S. Gonzalez; V. A. Alvarez*
T4-032	**Highly-ordered nanoporous TiO_2 films with hierarchical order directed by self-assembly.** *W. Kim; S. Y. Choi; Y. C. Kim; S. H. Kim*
T4-033	**Synthesis of regioregular poly(3-hexylthiophene) with low polydispersity using zincate complex: toward a purification-free system.** *T. Higashihara; M. Ueda*
T4-034	**Improvement of mechanical properties of soy protein-based films.** *P. Guerrero; T. Garrido; S. Cabezudo; K. de la Caba*
T4-035	**Polyaniline–silver composites: oxidation of aniline with silver nitrate accelerated by p-phenylenediamine.** *P. Bober; M. Trchova; J. Stejskal*
T4-036	**Light triggered solutes release from covalent DNA gels.** *D. Costa; A. J. M. Valente; M. Miguel; B. Lindman*
T4-037	**Surface properties of cationic polyelectrolytes hydrophobically modified.** *H. E. Ríos; J. González; M. D. Urzúa*
T4-038	**Release of amoxicillin embedded in cellulose acetate-poly(vinyl pyrrolidone) fibers by coaxial electrospinning.** *M. M. Castillo-Ortega; A. L. Nájera-Luna; D. E. Rodriguez-Felix; F. Rodriguez-Felix; J. Romero-García; P. J.Herrera-Franco*
T4-039	**Effect of fatty acids on the functional properties of biofilms for packaging applications.** *P. Guerrero; I. Leceta; N. Gabilondo; K. de la Caba*
T4-040	**Block copolymers of polypyrrole with 4-vinylaniline modified cyclohexanone formaldehyde resin.** *E. Ates; N. Kızılcan*
T4-041	**Sustainable anaerobic adhesive technology development.** *D. Birkett*

T4-042	**Nanoporous membranes with controlled pore dimensions.** *Y. Gonzalez-Lemus; D. J. Broer*
T4-043	**Incorporation of bioactive molecules in polymer matrix for food packaging.** *C. Nguimjeu; M. Kurek; F Sadaka; L Tighzert; I Vroman; C-H Brachai;, J. P. Couvercelle*
T4-044	**Modeling migration of colored food compounds into thermoplastic polymers: application to food cooking in reusable polymer bags**. *S. Narses; N. Lautard; T. Fichu; F. Sadaka; C. H. Brachais; J. P. Couvercelle*
T4-045	**Poly lactic acid active packaging: migration of natural and synthetic antioxidants.** *M. Jamshidian; E. Arab-Tehrany; S. Desobry*
T4-047	**New polyester obtained from ethylketene.** *N. Hayki; N. Desilles; F. Burel*
T4-048	**Synthesis of cyclo-aliphatic polyamide precursors by polycondensation of diamines with ketene symetric dimers.** *N. Kébir; M. Ben Haddi; N. Hayki; F. Burel*
T4-049	**Self-assembling waves in nanocomposites on hydrophilic polymer base and their advanced applications.** *I. E. Suleimenov*
T4-050	**Effect of poly(amic acid)-treated $BaTiO_3$ on the dielectric and mechanical properties of $BaTiO_3$/polyimide composites.** *J. Kim*
T4-051	**New phenolic resins for advanced materials.** *G. Konishi*
T4-052	**Covalent attachment of cholesterol oxidase on transparent polyaniline film for cholesterol sensing.** *T. Del Castillo Castro; M. M. Castillo Ortega; A. Ortiz Rascón; E. F. Placencia Fontes*
T4-053	**Synthesis of new two-dimensional thiophene-based conjugated copolymers and their applications to thin film transistors and photovoltaic cells.** *H. W. Lin; J. H. Tsai; C. J. Lin; H. C. Wu; C. Lu; Y. W. Lin; Y. C. Lai; W. C. Chen*
T4-054	**Obtaining and stability of iodine-cationic starch complexes.** *R. Klimaviciute; J. Bendoraitiene; R. Rutkaite; A. Zemaitaitis*
T4-055	**Stabilization of liposomes by multilayer films of modified polysaccharides.** *A. Karewicz; D. Bielska; A. Socha; M. Nowakowska*
T4-056	**Polysaccharide coating of liposomes via layer-by-layer self-assembly as novel delivery system for proteins.** *S. Madrigal-Carballo; M. Esquivel; J. Vega-Baudrit; M. Sibaja; A. O. Vila*
T4-057	**Microparticles of the natural polymer chitosan in aqueous suspension: stability of particle size distribution.** *A. C. R. N. Barboza; F. B. T. Pessine*
T4-058	**Preparation and evaluation of novel absorptive and antibacterial polyurethane membranes for wound dressing application.** *A. Yari; H. Yeganeh; H. Bakhshi*
T4-059	**Swelling behavior of macroporous polymer networks.** *C. G. Gómez; G. Pastrana; D. Serrano; E. Zuzek; M. A. Villar; M. C. Strumia*
T4-060	**On the morphology of drawn UHMWPE gel films and PTFE extrudates.** *H. M. Shabana*
T4-062	**Nonvolatile memory transistors using ferroelectric p(VDF-TrFE) and printed semiconducting channel.** *S. W. Jung; K. J. Baek; S. M. Yoon; J. B. Koo; Y. S. Yang; K. D. Kim; I. K. You*
T4-063	**Drawing and tensile properties of polyamide 6 / calcium chloride composite fibers.** *J. T. Yeh; Y. C. Lai; H. P. Chen; L. Qiu; F. C. Tsai; C. Y. Yeh*
T4-064	**Drawing properties of modified polyamide 6 fibers.** *J. T. Yeh; F. C. Tsai; Z. W. Liu; D. R. Wu; Y. C. Lai; C. R. Yeh; K. H. Hsieh*

T4-065	**Ultradrawing properties of ultra-high molecular weight polyethylene/functionalized carbon nanotube fibers.** *J. T. Yeh; C. H. Tsou; Y. C. Lai; W. H. Wang; H. P. Zhou; C. Y. Yeh*
T4-066	**Investigation of argon plasma modification on peel strength of woven type ultra high molecular weight polyethylene.** *C. Y. Huang; J. T. Yeh; K. N. Chen; C. S. Tsai; S.K. Lin; K. Y. Tsao; J. Y. Wu; C. P. Chang*
T4-067	**Design and synthesis of low refractive index, organosoluble, and thermally stable fluorinated polyamides having *ortho*-linked aromatic units in the main chain.** *A. Javadi; A. Shockravi*
T4-068	**Multiple bicolor fluorescent micropattern formation on a single polymer film based on the polymeric photobase generator containing oxime-urethane and anthracene groups** *K. H. Chae; H. S. Kim*
T4-069	**Starburst triarylamine-containing electroactive aramids with ultra-stable near-infrared and multicolor electrochromism.** *G. S. Liou; H. J. Yen; H. Y. Lin*
T4-070	**Synthesis of copolymer based on polydimethylsiloxane and alkylamine.** *L. Leymarie; P. Chaumont; E. Fleury; N. Sintes*
T4-071	**Ion conducting solid electrolytes based on differents macromolecular architecture containing PEO.** *D. Glé; D. Devaux; T. Phan; R. Bouchet; M. Robinet; D. Bertin; D. Gigmes*
T4-072	**Block copolymers via macromercaptan initiated ring opening polymerization.** *D. Glé; C. Lefay; M. Rollet; D. Gigmes; D. Bertin; C. Schmid; C. Barner-Kowollik*
T4-073	**Batch anionic polymerization of octamethylcyclotetrasiloxane in emulsion using cationic and nonionic emulsifiers.** *I. Mohoriè; U. Šebenik;*
T4-074	**Kinetic study of aqueous free- radical polymerization of 2-acrylamido-2-methyl-1-propanesulfonic acid via on-line ^{1}H NMR technique.** *E. Nadim; H. Bouhendi; F. Ziaee; A. Nouri*
T4-075	**Continuous synthesis of polyesteramides via a reactive extrusion process.** *M. Gupta; F. Siegmund; X. Zhu; M. Möller; E. Haberstroh; M. Fijten*
T4-077	**Electromagnetic properties of polyaniline hybrid nanocomposite application to gas sensing and EMI shielding.** *N. El Kamchi; J. L. Wojkiewicz; N. Redon; T. Lasri*
T4-078	**Graft copolymers via ROMP and Diels–Alder click reaction strategy.** *N. Cerit; H. Durmaz; A. Dað; O. Sirkecioglu; G. Hizal; U. Tunca*
T4-079	**Branching polyethylenimine functionalized with methylbenzimidazole: an approach to enhance proton conductivity via multi-direction of heterocycles.** *A. Pangon; K. Tashiro; S. Chirachanchai*
T4-080	**Preparation and characterization of impregnated PVA/PSSA_MA/THS-PSA membranes into porous polyethylene membranes for fuel cell applications.** *C. J. Park; I. H. Kim; S. P. Kim; H. M. Lee; J. W. Rhim*
T4-081	**Dual 'stimuli' responsive hydrogel: effect of ionizable monomer on the swelling behavior.** *G. Roshan Deen; V. Chua; X. Jun Loh*
T4-082	**Copolymerization of 2,2-diallyl-1,1,3,3-tetraethylquanidiniumchloride with maleic and fumaric acides .** *M. Gorbunova*
T4-083	**Influence of microcrystalline cellulose on thermal properties of polypropylene composite nonwovens.** *K. Bujnicka; J. Kałużka*
T4-084	**Contact polymerization of the composition on the basis of acrylamide and formaldehyde on metal surfaces.** *L. Kolzunova; M. Karpenko*

T4-085	**Synthesis and characterization of poly(L-lactic acid) nanocomposites with vermiculite of different modification.** *I. Aranburu; M. D. Fernandez; M. J. Fernandez*
T4-086	**Upon the synthesis possibilities of 2 - hydroxyethyl methacrylate copolymer with a comonomer with spiroacetal moiety.** *A. P. Chiriac; L. E. Nita; M. T. Nistor*
T4-087	**The temperature influence upon the complexation process between poly(aspartic acid) and poly (ethylene glycol).** *L. E. Nita; A. P. Chiriac; M. Bercea; I. Neamtu*
T4-088	**Light-driven wettability changes on a photoresponsive electrospun mat.** *M. Chen; F. Besenbachor*
T4-089	**Polymeric nanocomposites produced from polypropylene and nanocellulose whiskers.** *H. A. Önen; N. Ucar; E. Bahar; M. Öksüz; Y. Wang; M. Ucar; O. Ayaz; A. Demir*
T4-090	**High molecular weight polymers for gas separation applications.** *L. Escorial; A. Tena; A. E. Lozano; J. de Abajo; A. Hernández; P. Prádanos; L. Palacio*
T4-091	**Synthesis of poly(o-acyloxyamide)s for gas separation applications.** *B. Díez; A. Marcos-Fernández; P. Cuadrado; A. Hernández; J. G. de la Campa; J. de Abajo; A. E. Lozano*
T4-092	**Design of experiment - versatile tool for structure-property relationship investigations.** *A. Buryak*
T4-093	**Synthesis and characterization of star-shaped conjugated systems with triphenylamine core for photovoltaic applications.** *N. Metri; X. Sallenave; C. Plesse; L. Beouch ; P.H. Aubert ; G. Sini ; F. Goubard ; C. Chevrot*
T4-094	**Functionalization of polystyrene surfaces.** *A. Del Prado Abellán; N. Briz; A. Gallardo; C. Elvira; H. Reinecke*
T4-096	**Enhancing the formation of the new trigonal polymorph in iPP-1-pentene copolymers.** *E. Perez; M. L. Cerrada; R. Benavente; J. M. Gomez-Elvira*
T4-097	**Persistence of order in liquid crystalline copolymers.** *V. Rodriguez-Amor; J. P. Fernandez-Blazquez; M. L. Cerrada; A. Bello; E. Perez*
T4-099	**Mineralization ability of HEMA-AMPSA copolymers incubated in simulated body fluid.** *P. Stanescu; C. Zaharia; C. Cincu; F. Miculescu*
T4-100	**Experimental investigation of crosslinkedpolymer formulation for drilling fluid approach to modified rheological properties in carbonate wells.** *T. Yousef; S. A Ahmad Ramazani*
T4-101	**Hybrid composites based on polypropylene (PP): mechanical properties of PP/talc composites reinforced with different calcium based inorganic fillers.** *M. Yazdani-Pedram; H. Aguilar; P. Toro; R. Quijada*
T4-102	**Hot melt poly-ε-caprolactone/poloxamine implantable blends that sustain the release of ciprofloxacin.** *A. M. Puga; C. Alvarez-Lorenzo; B. Magariños; A. Concheiro*
T4-103	**Monomers vs polymers of Cu(III) corroles on reduction of O_2.** *J. Velez; F. Isaac; M. J. Aguirre*
T4-105	**Electrical resistance behavior under strain of in situ polymerized polyaniline in swollen NBR.** *J. C. Encinas; M. M. Castillo Ortega; T. Del Castillo Castro; P. J. Herrera Franco*
T4-106	**Ultra-thin electronic nanocomposites of carbon nanotubes and self assembled block copolymers.** *C. Park; J. Sung; Y. S. Choi; S. H. Cho*
T4-107	**Polymer electrolyte membranes based on poly(phenylene ether)s with pendant perfluoroalkyl sulfonic acids.** *K. Nakabayashi; T. Hiagshihara; M. Ueda*
T4-108	**Study of the new functionalized dimethacrylate copolymers for biochemical applications.** *B. Podkoscielna; B. Gawdzik; A. Bartnicki*
T4-109	**Rheologhical properties of poly (acryl amide with 2-acrylamido-2-methy-1-propane sulphonic acid) microgel via precipitation polymerization..** *M. Fathollahi; H. Bouhendi; M. J. Zohurian-Mehr; K. Kabiri; S. Roostamizadeh*

T4-110	**A feasible route to disperse bacterial cellulose nanowhiskers in polymers by melt compounding of interest in packaging applications and physical characterization of the optimized nanocomposites.** *M. Martinez-Sanz; A. Lopez-Rubio; J. M. Lagaron*
T4-111	**Synthesis of novel oligoimides and their applications to non-volatile memory.** *T. Kurosawa; W. Y. Lee; T. Higashihara; M. Ueda; W. C. Cheng*
T4-112	**Click chemical modifications of PVC surfaces for antibacterial applications.** *J. Lafarge; N. Kebir; F. Burel*
T4-114	**Sensory coumarin-containing polymers.** *S. Vallejos; P. Estévez; H. El Kaoutit; M. Trigo; F. Serna; F. García; J.L. Peña; J.M. García*
T4-115	**High performance gas separation membranes with aging and plasticization resistance.** *A. Tena; A. E. Lozano; A. A. Marcos-Fernández; J. G. de la Campa; J. de Abajo; L. Palacio; P. Prádanos; A.Hernández*
T4-116	**Gas separation membranes derived from rigid, high-free-volume, fluorinated polyimides.** *M. Juan y Seva; C. Álvarez; Á. E. Lozano; J. de Abajo; J. G. de la Campa*
T4-117	**Direct patterning of regioregular poly(3-hexylthiophene).** *Y. Saito; T. Higashihara; M. Ueda*
T4-118	**Asymmetric porous membranes from PEG modified aromatic polyamides.** *S. Molina; A. Martínez-Gómez; Á. E. Lozano; J. G. de la Campa; J. de Abajo*
T4-120	**Photophysical properties of some copoly(1,3,4-oxadiazole-ether)s.** *A. Airinei; R. I. Tigoianu; M. Homocianu; C. Hamciuc; E. Hamciuc*
T4-121	**Spectral-luminescent properties of polyurethanesiloxane polymers doped by Rhodamine 6G.** *A. I. Akhmetshina; I. M. Davletbaeva; A. M. Gumerov; T. N. Kopylova; L. G. Samsonova*
T4-122	**Acrylates block copolymers with N-trityl-L-serine methyl ester and pyrene prepared by ATRP.** *E. C. Buruiana; V. Podasca; T. Buruiana*
T4-123	**Hybrid composites based on photopolymerizable urethane dimethacrylates and silver nanoparticles.** *T. Buruiana; V. Melinte; F. Jitaru;; L. Balan; E. C. Buruiana*
T4-124	**Organic-inorganic gels for heterochain polymers modification.** *O. R. Gumerova; R. S. Davletbaev*
T4-125	**Novel polymetacrylamides containing a triazole moiety. Application to the extraction/elimination of metal cations from aqueous media.** *M. Trigo; A. Gómez; P. Estévez; S. Vallejos; H. El Kaoutit; F. Serna; F. García; J. L. de la Peña; J. M. García*
T4-126	**Polyurethanes based on sterically hindered esters of boric acid.** *O. Y. Emelina; R. S. Davletbaeva*
T4-127	**Epoxy polymers for medical applications. In vitro biological properties.** *F. Gonzalez Garcia; M. E. Leyva; A. A. Alencar de Queiroz; O. Z. Higa*
T4-128	**Polymer chemosensoring materials with crown-ether derivatives for advanced application in environmental monitoring.** *D. O. Soloveva; I. S. Zaitsev; M. S. Tsarkova; A. N. Timonin; S. Y. Zaitsev; S. K. Sazonov; A .I. Vedernikov; S. P. Gromov*
T4-129	**Gradient in viscoelastic properties of polymers to control adhesion.** *F. Tanguy; R. Even; I. Uhl; A. Lindner; C. Creton*
T4-130	**Comparative study for tin and zinc catalysts for lactide polymerization.** *J. Wojtaszak; J. Ejfler; I. Czeluœniak*
T4-131	**Magnesium catalysts design for ring-opening polymerization of lactides.** *J. Ejfler; S. Szafert; K. Mierzwicki; P. Sobota*
T4-132	**Fluorene-derivative containing polymers as sensory materials for the colorimetric and fluorogenic sensing of analytes.** *H. EL Kaoutit; P. Estévez; S. Vallejos; M. Trigo-López; F. C. García; F. Serna; J. L. de la Peña; J. M. García*
T4-133	**Study of surface energy of polypropylene films treated by corona at ambient temperature and above.** *H. C. de Sena; J. S. C. Campos*

T4-134	**Background and new opportunities with the aromatic thermosetting copolyesters.** *Z. Parkar; J. Economy*
T4-136	**Effect of acrylic copolymer dispersants bearing epoxy groups on dielectric properties of carbon black-filled epoxy system.** *B. T. Son; J. Y. Bae*
T4-137	**Synthesis and characterization of novel graphited polythiophene.** *A. Takahashi; K. Ohshimizu; T. Higashihara; M. Ueda*
T4-139	**Synthesis and characterization of thianthrene-based poly(phenylene sulfide)s with very high refractive index over 1.8.** *Y. Suzuki; K. Murakami; S. Ando; T. Higashihara; M. Ueda*
T4-140	**Surface and foam characteristics of PPG-b-PDMS-b-PPG tri-block copolymer as an anti-foaming agent.** *B. Kekevý; H. Berber; H. Yıldırım*
T4-141	**Synthesis of water-soluble polyamide dendrimers for DNA sensors.** *Y. Ito; C. Y. Chen; T. Higashihara; W. C. Chen; M. Ueda*
T4-142	**Synthesis and characterization of polyurethane-based shape memory polymers with low transitional temperature for medical applications.** *M. Ahmad; J. K. Luo; B. Xu; H. Purnawali; P. J. King; P. Chalker; Y. Q. F;, W. M. Huang; M. Miraftab*
T4-143	**Amphiphilic multiarm star block copolymer via Diels-Alder click reaction.** *N. Cakir; A. Dag; H. Durmaz; G. Hizal; U. Tunca*
T4-144	**Synthesis and characterization of biodegradable polyester resins.** *S. Theiler; H. Keul; M. Möller*
T4-145	**MWCNT- epoxy composite- electrodes for environmentally friendly detection of pharmaceutical compounds.** *A. Remes; F. Manea; A. Pop; N. K. K. Kowlgi; S. J. Picken; J. Schoonman*
T4-146	**Electrospun nanofibers of a biodegradable poly(ester amide). Scaffolds loaded with antimicrobial agents.** *A. Rodriguez-Galán; M. Roa; A. Díaz; J. Puiggalí; L. J. del Valle*
T4-147	**Surface modification of titanium dioxide by a modified emulsion/dispersion polymerization with an aid of ultrasonication.** *A. J. Ho; M. J. Kim*
T4-148	**The sulfobetaine-type surfactants applied for Nafion 212 on PEMFC.** *T. H. Chiang; Y. M. Hsieh; L.M. Chen*
T4-149	**Semiconducting properties of irradiated polyethylene sheets.** *F. Latif; M. H. Yaakob; R. Mohamed; K. Z. Mohd Dahlan*
T4-151	**Thermal conductivity of plastic materials in embedded electronics applications.** *J. Sarlin; M. Koponen; A. Sitomaniemi*
T4-152	**Modification of polysulfones by click chemistry: amphiphilic graft copolymers and their protein adsorption and cell adhesion propertie.** *L. Torun; G. Yilmaz; H. Toiserkani; D. Odaci Demirkol; S. Sakarya; S. Timur; Y. Yagci*
T4-154	**Chalcone Modified Urethane Acrylates.** *H. A. Önen; B. Güler; I. E. Serhatlý*
T4-155	**Usage of grafted chitosan beads as adsorbents for copper(II) ions removal from aqueous solutions.** *A. Bal; B. Ozkahraman; I. Acar; G. Guclu; M. Özyürek*
T4-156	**Effect of glass fiber and glass beads content on mechanical and tribological properties of polyamide-6.** *A. Mimaroglu; H. Unal*
T4-157	**The Influence of Nature of Nickel Complexes and Halide-Containing Initiators on the Polymerization of Vinyl Monomers** *Natalya Valetova, Galina Malysheva, Ilya Ilitchev, and Dmitry Grishin*
T4-158	**First linear-soluble poly (p-phenylenemethylene) via boron ester of benzyl alcohol.** *D. Gunes; Y. Yagci; N. Bicak*
T4-159	**Block-brush copolymers via romp and sequential double click reaction strategy.** *A. Dag; H. Sahin; H. Durmaz; G. Hizal; U. Tunca*

T4-160	**New mixed matrix composite membranes made from polymers able to undergo thermal rearrangement processes. Gas separation study.** *B. Bayón Alonso; L. Escorial López; Á. E. Lozano; Y. M. Lee; P. Prádanos; A. Hernández; L. Palacio*
T4-161	**Effects of types and amounts of plasticizer on the curing kinetics of unsaturated polyester.** *Z. Dogruyol; M. A. Kaya; S. Keskin Dogruyol; H. Yildirim; N. Arsu*
T4-162	**Use of waste polymer as thickener agent in lubricating greases.** *J. E. Martín Alfonso; C. Valencia; M. Sánchez; J. Franco; C. Gallegos*
T4-163	**Thermal properties of polymer composites containing ultrasonicated cellulose.** *D. M. Panaitescu; A. N. Frone; C. I. Spataru; D. Donescu; P. Stanescu; M. D. Iorga*
T4-164	**Application of microencapsulated phase change materials to improve thermo-regulating properties of textiles.** *L. Sanchez-Silva; J. F. Rodriguez; P. Sanchez; A. M. Borreguero*
T4-165	**Removal of crystal violet from aqueous solution by thermosensitive hydrogels: Investigation the effect of hydrophilic comonomer amount.** *B. Ozkahraman; I. Acar; S. Emik*
T4-166	**The synthesis and physico-chemical properties of dextran phosphates.** *M. Zhyhala; N. Yurkshtovich; N. Golub; V. Alinovskaya; T. Yurkshtovich; R. Kosterova*
T4-167	**New branched oligophenylenefluorenes for luminescent applications.** *I. Khotina; A. Kovalev; A. Shapovalov; N. Kushakova*
T4-168	**Synthesis, morphological characterization and antimicrobial application of nanostructured membranes of cellulose acetate.** *S. Nista; K. Segala; L. Cordi; O. Bagnato; N. Duran; L. Lona; L. Mei*
T4-169	**Synthesis and characterization of silicon containing membranes for PEM fuel cells.** *M. A. Kaya; H. Yildirim*
T4-170	**Optical and transport properties of poly(thiophene-3-ylacetic acid) and its sodium salt.** *J. Cerar; D. Bondarev; P. Nachtigall; J. Vohlidal; V. Vlachy*
T4-171	**Influence of type of methacrylic esters on properties of acrylic core/shell dispersions.** *K. Burja; E. Žagar; S. Skale*
T4-172	**Synthesis and self-assembly of block copolymers bearing o-nitrobenzyl side groups.** *O. Bertrand; J. Schumers; C. Fustin; J. Gohy*
T4-173	**Zinc metal as catalyst for direct grafting of vinyl acetate from PVC.** *G. Cankaya; N. Bicak*
T4-174	**Development of stimuli-responsive polymers for liposome based drug delivery systems.** *P. Alves; J. Coelho; H. Gil; P. Simões*
T4-175	**Rapid removal of copper from ATRP mixtures by chemical reduction with wetted zinc powder.** *F. Canturk; N. Býçak; B. Karagoz*
T4-176	**Solid supported benzoquinone as a click component for facile immobilization of amino acids and proteins.** *K. Yuksel; G. Cankaya; O. Sirkecioglu; N. Bicak*
T4-177	**Preparation and characterization of a polyetherimide/polyaniline composite.** *E. M. Alexandrino; M. I. Felisberti*
T4-178	**Cationic homo and copolymerization of indene and other olefins.** *F. J. Bento Brum; M. M. C. Forte; F. N. Laux*
T4-179	**Poly(ethylene imine) tedhered microspheres for selective extraction of aldehydes from organic mixtures.** *B. Gure; D. Gunes; B. Karagoz; N. Bicak*
T4-180	**Sulfonated polystyrene brushes tethered to PS-DVB microspheres as new generation of ion exchange polymers.** *O. Ozer; A. Ince; N. Bicak*
T4-181	**Butyl sulfonium sulfate as cationic initiator for synthesis of poly(cyclohexeneoxide)-b- poly(2-methyl-2-oxazoline) copolymers.** *C. Elci; O. Sirkecioglu; N. Bicak*
T4-182	**Modeling of precipitation co-polymerization of water-soluble polymers in organic solvent.** *R. Mazarro; P. Arosio; G. Storti; M. Morbidelli*

T4-183	**Ultrafast relaxation dynamics of exciton in poly-p-phenylenevinylene oligomers.** *F. Moura; P. Neto; W. Cunha; L. Roncaratti; R. Gargano; G. Silva*
T4-184	**Corrosion and adhesion study of hybrid coatings on 3l6l stainless steel.** *D. del Angel; M. Dominguez; A. Torrres; A. Flores*
T4-185	**Enhancement on redox-stability and electrochromic performance of aromatic polyamides incorporating 3,6-dimethoxycarbazolyl-substituted triphenylamine units.** *S. Hsiao; H. Wang*
T4-186	**Synthesis and properties of novel triptycene-based polyimides.** *S. Hsiao; H. Wang*
T4-187	**Preparation of conducting polypyrrole/polytetramethylene ether (ptme) composites.** *W. M. De Azevedo; J. Batista; E. H. L. Falcão*
T4-189	**Synthesis of new membrane of fuel cells based on sulfonated block copolyimide.** *M. Oroujzadeh; S. Mehdipour-Ataei*
T4-190	**Functional polyHIPE materials for metal adsorption.** *E. H. Mert; M. A. Kaya; H. Yýldýrým*
T4-191	**Development of gel-like dispersions for bio-lubricant applications using castor oil and different cellulose pulp samples.** *N. Nuñez; J. E. Martín-Alfonso; J. M. Franco; C. Valencia; M. J. Díaz; C. Gallegos*
T4-192	**Modification of high ortho novolac: a novel si/acrylate modified resin and its surface coating properties.** *S. Emik; T. B. Ýyim; S. Özgümüþ*
T4-193	**Polyynic benzoxazines. Synthesis and polymerization.** *S. Szafert; N. Gulia*
T4-194	**Investigation long-chain and short chain crosslinkers on microgel networkd with precipitation polymerization method.** *H. Es-Haghi; H. Bouhendi; g. Bagheri marandi; M. J. Zohurian-Mehr; K. Kabiri*
T4-195	**Synthesis and characterization of hybrid acrylic copolymers with and without (isobutyl)propylmethacrylate polysilsesquioxane (POSS).** *A. Carvalho; E. Veludo; J. Machado; M. H. Gil*
T4-196	**Synthesis, characterization and applications of *N*-vinyl pyrrolidone and itaconic acid based hydrogels.** *I. Acar; M. Evren; G. Güçlü; K. Güçlü*
T4-197	**Removal of cationic dyes from aqueous solution by *N*-vinyl pyrrolidone and crotonic acid based hydrogels.** *I. Acar; M. Akar; G. Güçlü*
T4-198	**Biodegradable thermo-sensitive polyurethane-based foams for tissue engineering.** *J. Girones; J. A. Mendez; J. San Roman*
T4-199	**Development of green coatings made from biopolymers for environmental friendly packaging.** *B. Rullier; J. Bonino; M. Menu; M. Gressier; F. Ansart*
T4-200	**Post-curing of photo-polymeric dental composites - effects on mechanical and dielectrical performance.** *J. Steinhaus; B. Moeginger; D. Lyssek; B. Hausnerova*
T4-201	**Hybrid chitosan-hydrolised collagen films for burn injuries. A preliminary study.** *E. Franco-Marquès; J. A. Méndez; J. Gironès; M. A. Pèlach*
T4-202	**Preparation of poly (norbornene) and poly-(dicyclopentadiene-co-norbornene) polyHIPEs.** *S. Kovacic; P. Krajnc; C. Slugovc*
T4-203	**Influence of different cross-linking mechanisms on the material properties of a silicone-based TPA-functional polymer for optical waveguides.** *S. Feldbacher; R. Woods; S. Bichler; V. Satzinger; V. Schmidt; G. Jakopic; G. Langer; W. Kern*
T4-204	**Supramolecular block copolymers: synthesis and investigation of the crystallization behavior.** *E. Ostas; K. Schröter; T. Thomas Thurn-Albrecht; G. K. Gupta; I. Gunkel; M. Beiner; W. Binder*
T4-205	**New thio-click hyperbranched polymers as macroinititators for the dual curing of cycloaliphatic epoxy resins.** *D. Foix; X. Ramis; À. Serra; M. Sangermano*

T4-206	**Synthesis of new methacrylates bearing phosphonic acid groups for an application in dental materials.** *Y. Catel; U. Fischer; N. Moszner*
T4-207	**Resonance effect on conductivity of poly(esters)s containing silarylene and thiophene moieties after polarized by application of an external field.** *C. González-Henríquez; L. H. Tagle; C. A. Terraza; A. Cañete; A. Leiva; A. Barriga; U. Volkmann; A. Cabrera; E. Ramos; M. Pavez*
T4-208	**Poly(amide-imide)s containing silarylene and L-aminoacid moieties. Relation with electrical conductivity and raman active vibrations.** *C. González-Henríquez; L. H. Tagle; C. A. Terraza; A. Barriga; U. Volkmann; A. Cabrera; E. Ramos; M. Pavez*
T4-209	**Synthesis, characterization and thermal studies of halogenated poly(imide-diamides) containing silicon in the main chain.** *L. H. Tagle; C. A. Terraza; D. Coll; A. Tundidor-Camba; A. Leiva*
T4-210	**Inclusion of cytidine in nanoparticles as a model for HIV drugs.** *J. P. Fuenzalida Werner; I. Moreno Villoslada; F. Goycoolea; H. Nishide*
T4-211	**Thioxanthone containing novel dendritic photoinitiators.** *T. Parali; Z. Dogruyol; G. Temel; N. Arsu; M. Tulu*
T4-212	**Characterization, melting and crystalline properties of isotactic (4,2)-enchained poly(1-butene) .** *C. Ruiz-Orta; R. G. Alamo*
T4-213	**Synthesis and properties of a self-doped polyacetylenes via the activated polymerization of ethynylpyridines by the ring cleavage reaction of cyclic compounds.** *Y. Gal; S. Jin; J. Park; W. S. Lyoo; K. T. Lim*
T4-214	**Porous polymer surfaces with superhydrophobic/superhydrophilic micropatterns: towards genome-on-a-chip cell microarrays.** *F. Geyer; U. Liebel; E. Ueda; P. Levkin*
T4-215	**Photoelectrochemical properties of doped polyaniline: application to hydrogen production upon visible light.** *Z. Benabdelghani; G. Rekhila; M. Trari; A. Etxeberria*
T4-216	**Poly(2-isopropenyl-2-oxazoline): hydrogel formation and potential applications.** *V. Schenk; L. Ellmaier; F. Wiesbrock*
T4-217	**Ionic liquid based membranes: water sorption properties.** *K. Fatyeyeva; S. Rogalskyy; O. Tarasyuk; S. Marais*
T4-218	**Thermophysical, electrical and mechanical properties of ethylene-vinylacetate copolymer (EVA) filled with wollastonite fibers coated by silver.** *I. Krupa; V. Cecen; R. Tlili; A. Boudenne; L. Ibos; J. Prokes*
T4-219	**Synthesis of functionalised polymer microspheres with ultra-high specific surface areas and their applications in selective chemical extractions.** *P. A. Cormack; A. Davies; N. Fontanals*
T4-220	**Synthesis and in vitro biocompatibility of copolymers, telomers, and hydrogels of polyvinylpyrrolidone with sulphonic and carboxylate groups.** *M. Gomez; C. Elvira; Y. Rochev; H. Reinecke; A. Gallardo*
T4-221	**Addition of polymer to viscoelastic solutions of living micellar chains.** *V. Pletneva; V. Molchanov; O. Philippova*
T4-222	**Copolymerization of monomer systems based on *N*-vinylpyrrolidonefor advanced applications.** *D. Soloveva; V. Zaitseva; A. Shtonda; T. Tyurina; I. Opeia; S. Z. Yu*
T4-223	**A Study of cationic polymerization of 1-(2-hydroxyethyl)aziridine.** *A. Sakalyte; M. Giamberini; J. A. Reina*
T4-224	**Homeotropic alignments of nematic liquid crystals on polar substrates.** *K. Song; Y. J. Kim; M. Lee*
T4-225	**Surface properties of silica modified by silane with polybutadiene oligomer tail.** *M. Castellano; A. Turturro; A. Bertora; E. Marsano; L. Conzatti; G. Colucci*

T4-226	**Reinforcement of SBR with silica modified by silane with polybutadiene oligomer tail.** *M. Castellano; A. Turturro; E. Marsano; A. Bertora; P. Stagnaro*
T4-227	**Modulation of the charge carrier transport in conjugated polymers by means of polar additives.** *P. Toman; W. Bartkowiak; J. Pfleger*
T4-228	**Thermal and mechanical properties of flexible bioplastics based on modified starch and gelatin.** *F. Fakhouri; R. Cardoso; D. Costa; F. Yamashita; L. H. Innocentini-Mei; F. P. Collares-Queiroz*
T4-229	**Desarrollo de una espuma polimérica atóxica con propiedades de resilencia.** *J. Heba; C. García; L. Warcok; M. F. Gómez; M. Calatayud; O. Ferré*
T4-230	**Thermoplastic elastomers based on graft copolymers.** *G. Tuzcu; M. van Duin; B. Klumperman*
T4-232	**Fluorescent labeling of calcium alginate beads with rhodamine 6G assisted by polyaromatic-anion.** *E. Araya-Hermosilla; I. Moreno-Villoslada; F. Oyarzun-Ampuero; S. Orellana; A. Yañez; H. Silva*
T4-233	**Structure, morphology and transport properties of nanocomposites films prepared from starch, montmorillonite and silver nitrate.** *F. Gouanve; M. Meyer; E. Espuche*
T4-234	**Design of novel, fluorescent-tuneable, pH-sensing, water-insoluble, lineal copolymers synthesized by ATRP and its application in the development of pH-sensing nanofibres made by electrospinning.** *A. L. Medina Castillo; J. F. Fernández Sánchez; A. Fernández Gutierrez*
T4-235	**Block copolymer surfactants in emulsion polymerization: the influence of the miscibility of the hydropho block on kinetics, particle morphology and film formation.** *A. Muñoz-Bonilla; S. I. Ali; A. del Campo; M. Fernández-García; A. M. van Herk; J. P. Heuts*
T4-236	**Side-chain liquid-crystalline copolyethers with tapered mesogenics groups.** *S. Bhosale; J. A. Reina; M. Giamberini; M. Rasool*
T4-237	**Hybrid electrospun fibres showing spin-crossover properties.** *D. Lopez; G. Mitchell; M. Rubio; A. Roig*
T4-238	**Dissolution modeling of smart nano-scale coated polymer particles in polymer flooding process.** *A. Ramazani; M. Ashrafizade; S. Sadeghnejad*
T4-239	**Nanoclay composite barrier coating for plastic substrate of flexible display .** *S. S. Kim; H. Ra*
T4-241	**New phenol functionalized polyamides: a new polymer family for multiple applications.** *S. Jeol; F. Touraud; C. Corriol; J. Marchand*
T4-242	**Optical CO_2-sensing film for clinical applications based on a fluorescent pH-sensitive and water-insoluble lineal copolymer.** *P. Contreras-Gutierrez; A. Medina-Castillo; J. Fernandez-Sanchez; A. Fernandez-Gutierrez*
T4-243	**Properties of conductive layers printed by ink-jet printing.** *M. Rom; J. Janicki; S. Przybylo; E. Sarna; R. Fryczkowski*
T4-244	**Polymethacrylamides´s synthesis. Dendronized polymers.** *N. Alvarado; D. Radic*
T4-245	**Zinc dithiocarbimates as accelerators for natural rubber vulcanization.** *L. M. Cunha; M. M. Rubinger; M. R. Oliveira; L. L. Visconte*
T4-246	**Characterization of gas-barrier coated polyethersulfone substrate for flexible display application.** *Y. Ahn; M. Kim; S. Paek; Y. C. Kim*
T4-247	**Aromatic polyimides containing methyl substituents and study of their physical properties.** *S. Chisca; I. Sava; V. Musteata; M. Bruma*
T4-248	**Synthesis and photophysical properties of donor-acceptor block copolymers.** *E. Bicciocchi; M. Chen; E. Rizzardo; K. Ghiggino*
T4-249	**New highly thermostable phthalonitrile-containing aromatic polyamides and poly(amide imide)s for high performance applications.** *I. Carja; C. Hamciuc; E. Hamciuc; T. Vlad-Bubulac*
T4-250	**Polyaniline synthesis using fenton reagent: effect of substitution of aniline.** *M. Blaha; J. Zednik; J. Svoboda; J. Vohlidal*

T4-251	**UV cured acrylic membranes reinforced by cellulose microfibrils for lithium batteries.** *A. Chiappone; R. Bongiovanni; J. Nair; C. Gerbaldi; E. Zeno*
T4-252	**Photoinduced surface relief gratings of azopolymers with rigid and flexible chains.** *I. Sava; N. Hurduc; L. Sacarescu; V. Damian*
T4-253	**Heterocyclic polynaphthaleneimides containing siloxane groups in the main chain.** *R. Rusu; M. Damaceanu; M. Bruma*
T4-254	**Study on the crystallization of poly(nonamethylene azelate) and its copolymers incorporating pimelate moeities .** *A. Díaz; L. Franco; R. Díaz; M. T. Casas; J. Puiggalí*
T4-255	**Combination of ionic and covalent cross-links on elastomeric ionomers: Effect on the structure-properties relationship.** *M. Alonso Malmierca; L. Ibarra; A. Rodríguez; I. Mora-Barrantes; J. López Valentín*
T4-256	**Preparation of HDPE/MMTHDTMA/PVA nanocomposites: morphology, structure and mechanical properties.** *M. Carrera; E. Erdmann; H. Destéfanis; J. Pastor Barajas*
T4-257	**Nitrate remove from drinking water using polymer/MWCNTs nanocomposites.** *N. Mousavi Rad; R. Sedghi; R. Sharifi; M. Reza Nabid*
T4-258	**Influence of the swelling behavior on the electrochemistry of redox hydrogel gels.** *G. Osterwinter; C. Bunte; O. Prucker; J. Rühe*
T4-259	**Non aqueous polyHIPEs as novel polymer separators for lithium ion batteries.** *N. Shirshova; E. Kot; A. Bismarck; J. H. Steinke*
T4-260	**Natural antioxidants for polymer.** *A. Masek; A. Kosmalska; M. Zaborski*
T4-261	**Polymers silver electrodes plating.** *J. S. Campos; E. H. Geraldo*
T4-262	**Synthesis and characterization of a ionic polymers derived from disubstituted acetylenes.** *R. Sivkova; D. Bondarev; J. Zedník; J. Sedlaček; J. Vohlídal*
T4-263	**Polyacetylenes with cyclopropyl pendant groups: precursors for polyacetylene-based polymer networks.** *V. Hanková; E. Slováková; J. Zedník; J. Vohlídal; J. Sedláèek*
T4-264	**The studies of polymer nanocomposites based on thermoplastics and binary conductive nanofillers.** *E. Beyou; V. Levchenko; Y. Mamunya; G. Boiteux; P. Alcouffe; E. Lebedev*
T4-265	**Synthesis and complexation properties of terpyridine derivatives: building of supramolecular polymers .** *T. Vitvarova; J. Zednik; P. Stenclova; J. Vohlidal; J. Svoboda*
T4-266	**Study on the copolymerization of potassium chloroacetate and potassium n-chloroacetyl-6-aminohexanoate.** *S. Murase; A. Rodríguez-Galán; L. Franco; J. Puiggalí*
T4-267	**Solvent-free aqueous polyurethane dispersions.** *I. Fernandes; M. Barreiro; M. R. Costa*
T4-268	**Thermoresponsive polyether-grafted hyaluronan: synthesis and reversible gelation behavior.** *J. Areguian; R. Auzely-Velty*
T4-269	**Electrochemical response of host-guest assemblies of polysaccharides immobilized on surfaces.** *J. Mergy; G. Dubacheva; P. Labbé; L. Guérente; R. Auzély-Velty*
T4-270	**Semiconducting materials based on block and graft copolymers having donor and acceptor functionalities for molecular electronics.** *J. Kallitsis; S. Kourkouli; A. Stefopoulos; A. Andreopoulou; A. Siokou*
T4-271	**Study on adsorbing chromium (VI) into hyperbranched copolymers from aqueous solution.** *M. Luzón; T. Corrales; C. Peinado; V. San Miguel; F. Catalina*
T4-272	**Synthesis and characterization of a molecularly imprinted polymer optosensor for TEXs-screening in drinking.** *F. J. Sainz-Gonzalo; A. L. Medina-Castillo; J. F. Fernández-Sánchez; A. Fernández-Gutiérrez*
T4-273	**Synthesis and properties of aromatic poly(disubstituted acetylene)s.** *J. Zednik; Z. Duchoslavova; J. Svoboda; J. Sedlacek; V. Hankova; D. Vrbata; J. Vohlidal; R. Sivkova*

T4-274	**Composite polymer materials for stabilization of washing liquid of oil and gas wells.** *S. Negmatov; K. Negmatova; B. Sobirov; S. Isakov; H. Qobilov; M. Negmatova; J. Haydarov*
T4-275	**Developing of antifriction wear-resistant polymer composite materials and products from them for working bodies of facilities of mechanization of the cotton industry.** *N. Abed-Negmatova; D. Musabekov; G. Gulyamov; S. Negmatov; M. Negmatova; S. Kodirov; B. Sobirov*
T4-276	**Developing of wood polymer composite materials and sliding bearing for cotton machines and mechanisms.** *D. Musabekov; N. Abed-Negmatov; G. Gulyamov; S. Negmatov; A. Shernaev; S. Kodirov; B. Sobirov*
T4-277	**Polymer reagents for stabilization of drilling mud, used in the process of drilling of oil wells.** *K. Negmatova; G. Sharifov; S. Isakov; S. Negmatov; B. Sobirov; K. Rahimov*
T4-278	**Atom transfer radical polymerization of polymerization of MMA and styrene initiated by 3,5-bis(perfluorobenzyloxy)benzyl 2-bromopropanoate.** *T. Cakir Canak; M. Selcukoglu; E. Hamuryudan; I. E. Serhatli;*
T4-279	**Release behavior of biodegradable polyesters reinforced with triclosan loaded polylactide micro/nanofibers.** *L. J. Del Valle; A. Díaz; M. Royo; A. Rodríguez-Galán; J. Puiggalí*
T4-280	**Adhesive properties of low tg polymers bearing hydrogen bonding moieties.** *S. Pensec; J. Courtois; H. Wang; C. Fonteneau; G. Ducouret; L. Bouteiller; C. Creton*
T4-281	**Preparation of cationic polymer brushes on silicon wafer surface via RAFT polymerization.** *S. Demirci; T. Çaykara*
T4-282	**Engineering of magnetic poly(ε-caprolactone) nanomedicines against arthritis.** *E. Saez-Fernandez; V. Gallardo; M. A. Ruiz; A. V. Delgado; J. L. Arias*
T4-283	**Development of a poly(ε-caprolactone)-based magnetic biodegradable nanoplatform against cancer.** *E. Saez-Fernandez; V. Gallardo; M. A. Ruiz; A. V. Delgado; J. L. Arias*
T4-284	**Fabrication of pH responsive copolymer brushes on silicon wafer surface via reversible addition-fragmentation chain transfer polymerization.** *S. Kýnalý Demirci; S. Demirci; T. Çaykara*
T4-285	**Microencapsulation of butyl stearate with melamine-formaldehyde resin: Effect of decreasing pH value on composition and thermal stability of microcapsules.** *B. Ališ; U. Šebenik; M. Krajnc*
T4-286	**Polymerization of octamethylcyclotetrasiloxane in a microtube reactor with liquid-liquid slug flow pattern.** *E. Šinkovec; M. Krajnc*
T4-287	**Conductive polymer composites obtained from urea–formaldehyde resin and copper powder.** *G. Pinto; A. Maaroufi; R. Benavente; J. M. Pereña*
T4-288	**Ruthenium olefin metathesis initiators bearing one or two N_2O chelating coligands in the triggered polymerization of DCPD.** *J. Wappel; C. Slugovc*
T4-289	**Biocide finishing of poly(isoprene) by thiol-ene click chemistry.** *J. Kienberger; N. Noormofidi; C. Slugovc*
T4-290	**From emulsion templating of poly(cyclooctene) towards elastic, porous monolithic materials.** *F. Preishuber-Pfluegl; C. Slugovc; P. Krajnc*
T4-291	**Water-soluble polymers prepared by Ring opening metathesis polymerization.** *K. Gallas; T. Wrodnigg; C. Slugovc*
T4-292	**Thermal studies of interpenetrating methacrylate/epoxy resins.** *N. M. Florea; A. Lungu; H. Iovu; R. Stan*
T4-293	**Electromechcanical performance of epoxy/vapour grown carbon nanofiber composites||for pressure sensor applications.** *A. Ferreira; P. Cardoso; A. Paleo; D. Klosterman; J. Covas; F. Van Hattum; S. Lanceros-Mendez*
T4-294	**Study of the basalt fibers' damage assessment due to different sizing removal processes.** *J. Kano; R. Hernandez; A. M. Zaldua; T. Guraya; I. Mondragon*
T4-295	**Synthesis and study of new poly(amide imide)s as advanced materials.** *I. Bacosca; E. Hamciuc; V. E. Musteata; M. Bruma*
T4-296	**Synthesis of bimodal polypropylene through binary metallocene catalysts.** *R. van Grieken; A. C. Carrero; B. P. Paredes; M. E. Lopez*

T4-297	**Ethylene-propylene copolymers synthesized with homogeneous and supported metallocene catalyst in the whole range of compositions.** *J. Arranz-Andrés; I. Suárez; R. Benavente; E. Pérez*
T4-298	**Microstructure characterization and influence on gamma form content of polypropylene copolymers and terpolymers.** *S. Caveda; R. Benavente; E. Pérez; E. Blazquez; B. Peña; R. van Grieken; I. Suárez*
T4-299	**Synthesis and analysis of properties of Poly(vinyl alcohol)composites.** *G. Nasar; M. Saleem Khan; U. Khalil*
T4-300	**Synthesis and characterization of conjugated ionic polymers with potential applications in optolectronic devices.** *D. Bondarev; J. Zedník; J. Vohlídal; J. Pfleger; S. Kazim; V. Sluneèková*
T4-301	**Synthesis and FTIR analysis of nanocomposite UV crosslinkable acrylic pressure sensitive adhesives|.** *J. Kajtna; M. Krajnc*
T4-302	**Synthesis and photo-responsive behavior or spiropyran end-functionalized polymers by ATRP.** *C. Ventura; R. Byrne; F. Audouin; D. Diamond; A. Heise*
T4-303	**Synthesis of hybrid materials via photopolymerization of benzoin functionalized silica nanoparticles.** *M. D. Karahasanoðlu; A. Önen; Ý. E. Serhatlý*
T4-304	**Hybrid photosensitizers for the removal of trace pollutants from water.** *A. Karewicz; D. Bielska; M. Kumorek; K. Szczubia³ka; M. Nowakowska*
T4-305	**Structure and conductivity of the copolymers of 2-methoxyaniline with aminobenzoic and aminobenzenesulfonic acids.** *D. Pahovnik; I. Mav-Golez; M. Zigon; J. Vohlídal*
T4-306	**Morphological characterization and mechanical properties of poly(lactic acid) blends.** *M. Taipina; M. Ferrarezi; L. Silva; M. D. Gonçalves*
T4-307	**Photocatalytic activity of TiO_2 nanocomposites on degradation of water pollutions.** *M. R. Nabid; R. Sedghi; S. Gholami*
T4-308	**Spectroscopic and thermodynamic study of phase transition in solutions of acrylamide/ nisopropylmethacrylamide-copolymers.** *J. Stastna; L. Hanykova; J. Spevacek*
T4-309	**Innovative perfluoropolyether-based copolymers: another breakthrough in fluorine chemistry.** *M. Avataneo; P. A. Guarda; G. Marchionni*
T4-310	**Novel liquid crystal ionomers for polymeric electrolyte membranes in direct methanol fuel cells.** *A. Martinez-Felipe; L. Santonja-Blasco; R. Teruel-Juanes; P. Henderson; M. Giacinti-Baschetti; G. Sarti; C.T. Imrie; A. Ribes-Greus*
T4-311	**Crosslinked PVA membranes for direct methanol fuel cells.** *A. Martinez-Felipe; L. Santonja-Blasco; M. Rosado-Gil; A. Ribes-Greus*
T4-312	**Developing of effective multipurpose polymer-bitumen compositions.** *S. Negmatov; B. Rahmonov; B. Sobirov; A. Abdullaev; Y. Salimsakov; M. Negmatova; A. Sobirov*
T4-313	**Nanostructures, morphology and properties of Poly[N-(2-cyanoethyl)pyrrole].** *G. Fabregat; E. Armelin; C. Alemán*
T4-314	**Development of effective technologies of heat and frost resistant composite materials for sealing the joints and cracks of asphalt roads, bridges and airfields.** *B. Rahmonov; S. Negmatov; B. Sobirov; A. Abdullaev; Y. Salimsakov; R. Soliev; D. Mahkamov; A. Bozorov; A. Sobirov*
T4-315	**Study of composition and technology of highly filled composite polymeric materials for asphalt roads, which can be used in hot climates and increasing their operation life.** *B. Sobirov; B. Rahmonov; S. Negmatov; A. Abdullaev; K. Inoyatov; Y. Salimsakov; D. Mahkamov; R. Soliev*
T4-316	**Compatibility studies of poly(ether imide) with liquid crystal mixtures.** *F. Çakar; H. Ocak; B. Bilgin-Eran; Ö. Cankurtaran; F. Karaman*
T4-317	**Development of polyester coating using branched polymers and silanes.** *J. Gamez-Perez; M. Puig; J. Gracenea; A. Jiménez; J. Suay*

T4-318	**Synthesis, structure and properties of poly(urethane-urea-siloxane)s.** *V. Antic; M. Balaban; M. Pergal; I. Francolini; A. Martinelli*
T4-319	**Physical aging of melt-blown PLA fibres.** *J. Janicki; M. Rom; J. Fabia*
T4-320	**Recovery of copper with sulfonated microcapsules containing DEHPA.** *Á. Alcázar; A.M. Borreguero; M. Carmona; A. de Lucas; J. F. Rodríguez*
T4-321	**A comparison of the morphology and thermoresponsive switching behavior in thin films of cyclic and linear poly(N-isopropylacrylamide).** *D. Magerl; X. Qiu; F. Winnik; M. Rawolle; G. Herzog; S. V. Roth; P. Müller-Buschbaum*
T4-322	**Incorporating nanostructured polypyrrole counter electrodes into dye-sensitized solar cells.** *S. S. Jeon; C. Kim; j. Ko; S. S. Im*
T4-323	**The preparation of nanofiber composites of Poly(butylene succinate)/TS-1 zeolite for drug delivery system.** *S. Hwang; E. Yoo; S. Im*
T4-324	**Morphology control of poly(p-oxybenzoyl) crystals using direct polymerization of p-hydroxybenzoic acid in the presence of boronic anhydrides.** *M. Kihara; S. Kohama; S. Umezono; K. Wakabayashi; S. Yamazaki; K. Kimura*
T4-325	**Selective synthesis of aromatic copolyester using reaction-induced crystallization under shear flow - Influence of shearing on composition of copolyester.** *T. Ichimori; S. Yamazaki; K. Kimura*
T4-327	**Facile, single-step preparation of versatile, high surface area nanoporous hybrid materials.** *I. Teasdale; I. NIschang; O. Brueggemann*
T4-328	**Emulsion polymerization of styrene: Simulation the effects of mixed ionic and non-ionic surfactant system in presence of coagulation .** *S. Feiz; A. H. Navarchian*
T4-329	**Wear resistance optimization of PU/TiO_2 coatings on aluminium surfaces.** *M. Taheran; A. H. Navarchian; R. Shoja Razavi*
T4-330	**Changes of supermolecular structure and selected properties of polymer matrix of polyamide fibres caused by addition of LCO modifier.** *M. Baczek; J. Janicki*
T4-331	**Kinetic study on photopolymerization of acrylates by Photo-DSC and RT-FTIR: the effect of thioxanthone based dendritic photoinitiators and light intensity.** *Z. Doğruyol; T. Parali; M. A. Kaya; Mm. Tülü; N. Arsu*
T4-332	**Effect of nanofillers on curing kinetics and thermal properties of epoxy amine thermosets.** *A. K. Ghosh; G. Van Asche; B. Van Mele*
T4-333	**Preparation of organometallic polymers with conjugated building blocks.** *P. Stenclova; J. Zednik; T. Vitvarova; J. Vohlidal; J. Svoboda*
T4-334	**Synthesis of porous polymeric organic frameworks (POFs) with C_{3v} symmetry and controlled pore size.** *E. Verde; E. M. Maya; J. G. de la Campa; J. de Abajo; Á. E. Lozano*
T4-335	**Enhancing properties of piezoelectric polyimides by copolymerization.** *M. San Sebastián; A. Maceiras; J. L. Vilas; T. Breczeswki; M. A. Perez-Jubindo; M. R. de la Fuente*
T4-336	**Plastics with reduced flammability, containing graphite halogen-free additives.** *P. Jankowski; M. Kêdzierski*
T4-337	**Water transport properties in biodegradable copolyesters.** *N. Follain; E. Dargent; F. Chivrac; F. Girard; S. Marais*
T4-338	**Isothermal crystallisation study of P3HT:PCBM blends as used in bulk heterojunction solar cells based on fast scanning calorimetry techniques .** *N. Van den Brande; F. Demir; S. Bertho; B. Van Mele; D. Vanderzande; J. Manca; G. Van Assche*
T4-339	**Solvent and substrate contributions to the formation of breath figure patterns in polystyrene films.** *E. Ferrari; P. Fabbri; F. Pilati*
T4-340	**Collapse of polyelectrolyte star. Theory and modeling.** *O.V. Rud; A.A. Mercurieva; T.M. Birshtein*

T4-341	**Polylactide and β-tricalcium phosphate composite fibers by electrospinning technique for tissue engineering applications.** *L. Tammaro; R. Wyrwa; J. Weisser; U. Müller; M. Schnabelrauch*
T4-343	**Azobenzene block copolymers and blends: microstructure, photoinduced anisotropy and holographic storage.** *C. Berges; E. Blasco; N. Gimeno; P. Forcén; L. Oriol; M. Piñol; C. Sánchez; R. Alcalá*
T4-344	**Diastereoselective synthesis of azanorbornenes from enantiomerically pure precursors and subsequent polymerizations.** *E. Rossegger; F. Stelzer; F. Wiesbrock*
T4-345	**Screening of new developed copolymers as potential antidotes against radionuclides.** *Z. Farmazyan; G. Harutyunyan; L. Hayriyan; V. Sargsyan; K. Stepanyan; A. Pogosyan*
T4-346	**Poly(ferrocenylsilane) hydrogels.** *M. Hempenius; X. Sui; C. Cirmi; J. Song; G. J. Vancso*
T4-347	**Synthesis and characterization of stimuli-responsive amphiphilic block copolymers.** *E. Blasco; C. Berges; R. Alcala; C. Sánchez; L. Oriol; M. Piñol*
T4-348	**Development of active flexible packages by the incorporation in bulk of antimicrobial natural additives.** *R. Gonzalez-Leyba; B. Galindo-Galiana; C. Gadea-Tomás; F. Martí-Ferrer*
T4-349	**Synthesis of superparamagnetic magnetite/poly(butylcyanoacrylate) (core/shell) nanoparticles for drug delivery purposes.** *D. Alioto; M. Lopez-Viota; E. Saez-Fernandez; M. A. Ruiz; J. L. Arias*
T4-350	**Batch foaming and cellular structure of biodegradable PLA/Graphene Nanocomposites.** *E. Gimenez; A. C. Cárcel; L. Cabedo; W. Zhai; C. B. Park*
T4-351	**Synthesis and photopolymerization of hydrolytically stable crosslinkers for dental composites.** *A. Altin; D. Avci*
T4-352	**Plasma modification of MWCNTs and their use in the preparation of PA6/MWCNT nanocomposites.** *R. Scaffaro; A. Maio*
T4-353	**Flexible nanoskin-core poly(ethylene-co-acrilic acid)/polyaniline hybrids.** *R. Scaffaro; G. Lo Re; C. Dispenza; M. A. Sabatino; L. Armelao*
T4-355	**Associative and segregative phase behaviour of poly(N-diethylacrylamide)/poly(4-vinylphenol) mixtures. Effect of solvent.** *L. Ruiz Rubio; N. Rioja; M. T. Garay; M. Rodríguez; E. Bilbao; J. E. Figueruelo*
T4-356	**Formation study of biocomposite films synthesized from chitosan.** *J. A. Cavallo; M. López-González; M. C. Strumia; E. Riande; C. G. Gómez*
T4-357	**Self-curable PDMS-containing PU oligomers for water repellent textile treatment.** *R. Wu; J. Hwang; K. Chen*
T4-358	**Novel reactive polymeric supports for synthesis of polymer drug conjugates.** *G. Tanriver; R. Sanyal*
T4-359	**Thiol reactive hydrogels for biomolecular immobilization via photopolymerization.** *T. N. Gevrek; E. Park; A. Sanyal*
T4-360	**Dynamic covalent reorganization of polymer/polymer systems: alcoholysis catalyst effect on kinetic and secondary reactions.** *F. Becquart; M. Taha; S. Touhtouh*
T4-361	**Mechanical properties of crosslinked hybrid PVA membranes for DEFCs applications.** *A. Gomes; J. C. Dutra Filho*
T4-362	**Study of natural aging of PVC flat-plate absorber used for low cost solar collectors.** *J. R. Bartoli; B. R. Prado; R. C. Pereira*
T4-364	**Synthesis of organic/inorganic composite hydrogels with embedded clay particles.** *M. Kurecic; S. Hribernik; M. Sfiligoj Smole*
T4-365	**SEC-MALS and molecular dynamics characterization of an amphiphilic poly(acrylic acid-b-styrene-b-styrene-b-acrylic acid) symmetric block-copolymer synthesized by RAFT.** *M. P. Tarazona; G. Marcelo; J. G. Martinho; J. P. Farinha;*

T4-366	**Development of conducting nanofillers based on polypyrrole and nanoclays.** *L. Cabedo; I. Mróz; J. M. Lagarón Cabello; E. Giménez Torres*
T4-367	**Strippable deactivating coatings: case of modified polyvinylalcohol.** *Z. Farmazyan; G. Harutyunyan; L. Hayriyan; V. Sargsyan; N. Dalalyan; K. Stepanyan; K. Pyuskyulyan; J. Abramyan; I. Shahazizyan*
T4-368	**Production and characterization of starch and starch based composite biodegradable films crosslinked by glutaraldehyde.** *I. Gonenc; F. Us*
T4-369	**Validation of an elasto -viscoplastic model for polyvinilidene fluoride (PVDF).** *V. Gonçalez; I. Pasqualino; M. Costa*
T4-370	**Characterization of poly(lactide-co-glycolide) (PLGA) obtained via ring-opening polymerization: effect of the LA/GA molar ratio.** *J. C. Ramirez-Contreras; E. Vargas-Reyes; P. Hernández-Belmares; J. C. Ortiz-Rodriguez*
T4-371	**Internal and external gelling method for alginate hydrogels preparation with planar geometry.** *E. Papajová; Z. Kroneková; M. Stach; D. Chorvát; C. Hoesli; D. Horne; J. Piret; I. Lacík*
T4-372	**Porous methacrylate copolymers as stationary phases for HPLC.** *M. Grochowicz; M. Maciejewska*
T4-373	**Crosslinked membranes of PVA/MMT for direct ethanol fuel cells.** *A. Gomes; J. C. Dutra Filho; G. Gomes*
T4-374	**Synthesis and characterization of polymeric microspheres based on styrene / divinylbenzene containing silver nanoparticles.** *K. Segala; D. Cruz; L. Cordi; O. Bagnato; N. Duran; L. Lona; L. Mei*
T4-375	**Photorresponsive bifunctional side chain polymers.** *J. Royes; L. Oriol; M. Piñol; R. M. Tejedor*
T4-376	**Characterization of the functional properties of commercial polyhydroxyalkanoates (PHA).** *Y. Corre; S. Bruzaud Grohens*
T4-377	**Preparation and characterization of polystyrene-graft-polyethylene glycol copolymers as solid–solid phase change heat storage material.** *A. Biçer; C. Alkam; A. Sari Karaipekli*
T4-378	**Synthesis and characterization of poly (fatty alkyloylethylmethacrylate-co-methylacrylate) as solid-solid phase change materials for thermal energy storage.** *T. Güngör; Ö. F. Ensari; C. Alkan*
T4-379	**Polyethers as phase change materials for passive thermal energy storage.** *D. Kahraman; C. Alkan; Ö. Ülkü*
T4-380	**Synthesis of paramagnetic polymers using ionic liquid chemistry.** *M. Döbbelin; V. Jovanovski; L. J. Claros Marfil; G. Cabañero; J. Rodríguez; D. Mecerreyes*
T4-381	**Environmentally friendly polyurethane foams.** *Y. Savelyev; L. Markovskaya; I. Yanovych; E. Akhranovych*
T4-382	**Effect of salt concentration on strength and morphology of natural degradable additive PP film upon immersion in water.** *M. Rahmad; S. M. Zarith; A. F. Abdullah*
T4-383	**Synthesis of flexible polymer-ceramic composites for RFID tagging of people.** *C. Ortiz; M. Suárez; S. Ver Hoeye; E. De Cos; M. Fernández; C. Vázquez; R. Camblor; G. Hotopan; R. Hadarig; F. Las Heras; J.L. Menéndez*
T4-384	**Multifunctional properties of PLA composites based on silver nanoparticles and crystalline cellulose: role of crystal micro and nano-dimension.** *E. Fortunati; I. Armentano; Q. Zhou; A. Iannoni; E. Saino; L. Visai; L. Berglund; J. Kenny*
T4-385	**Solid-state polymerized conducting polymers for highly efficient, iodine-free dye-sensitized solar cells.** *J. Kim; J. Kwan Koh; B. Kim; J. Hak Kim; E. Kim*
T4-386	**Towards innovating polymer materials for a new generation of organic laser sources.** *F. Lincker; V. Barret-Vivin; D. Kreher; F. Mathevet; A. Barsella; A. Boeglin; A. Fort; A. Attias*

T4-387	**Preparation and characterization of waste leather reinforced polymeric composite .** *S. Nahar; M.A. Khan; F. Karim; R. Islam; S. Hussain; A. K. Deb; H. Lal Paul; F. Pervin; S. Rahman*
T4-388	**Studying PMMA/PVC polymer blend for its use as lithium polymer electrolyte.** *L. Zubizarreta; A. García Bernabé; M. Gil Agustí; P. Llovera*
T4-389	**Ionic conductivity vs. thickness on the cast Nafion® polymer.** *M. Gil-Agustí; L. Zubizarreta; J. Calleja-Langa; R. Iserte*
T4-390	**Chitosan-collagen sponge-like 3d scaffolds as potential biomaterials for tissue engineering.** *M. Ramos; V. Zamora-Moral; S. Madrigal-Carballo; M. Lopretti; M. Sibaja*
T4-391	**Studies on toughening of polylactic acid by melt-blending with thermoplastic polyurethanes.** *K. Hsieh; C. Huang; Y. Lai; J. Han*
T4-392	**Multifunctional PDMS-PEG coatings for the finishing of cotton.** *R. Ronge; A. Körner; M. Möller*
T4-393	**Osteoconductive and bioresorbable composites based on poly(L,L-lactide) and pseudowollastonite.** *D.T-J Barone; Z.Luklinska; O. Persenaire; J-M. Raquez; Ph. Dubois*
T4-394	**Onion-like superabsorbent microspheres with PS-DVB core and PAA-b-crosslinked(PMMA) capsules via SI-ATRP.** *A. Ince, B. Karagoz, N. Bicak*

TOPIC 5: Chemistry and Physics of Nanomaterials and Nanotechnologies

T5-001	**Morphology and fracture behaviour of phenoxy/layered silicate nanocomposites.** *M. A. Corres; A. Mugica; M. Zubitur; M. Cortázar*
T5-003	**Quantum-chemical study of the low molecular polyethylene fluorination.** *L. Ignat'eva; V. Bouznik*
T5-004	**Characterization and thermal properties of poly(L-lactid acid)/clay bionanocomposites.** *A. Oyarzabal; A. Mugica; M. Zubitur; M. Cortázar*
T5-005	**Textile strain sensors based on conductive polymer nano-composite.** *C. Cochrane; M. Lewandowski; V. Koncar*
T5-006	**Influence of the aminopropylisobutyl POSS nanoparticles on the thermal behavior of isotactic.** *R. Bouza; C. Ramírez; L. Barral; B. Montero; R. Bellas*
T5-007	**Microstructural and morphological analysis of SBR/nanoclay composites.** *R. Bellas; R. Bouza; J. Díez; J. López; C. Ramírez; M. Rico*
T5-008	**Preparation and characterization of polyethylene nanocomposites including titanium oxide nanoparticles.** *P.A. Zapata; F.M. Rabagliati*
T5-009	**A new way to improve PC/ABS blends: use of nano-sepiolite.** *F.C. Basurto; D. García-López; N. Villarreal-Bastardo; J.C. Merino; J.M. Pastor;*
T5-010	***In situ* formation of polystyrene magnetic particles via batch suspension polymerization.** *J.S. Neves; F.G. Souza Jr.; P.A.Z. Suarez; A.P. Umpierre; F. Machado*
T5-011	**Cracking in thin polymer films promoted through physical ageing.** *M. Chowdhury; C. Calers; A.C.M. Yang; U. Steiner; G. Reiter*
T5-012	**Strategy to improve the mechanical properties of electroactive materials: preparation of PEDOT-montmorillonite and multilayer PEDOT/poly(*N*-methylpyrrole)/montmorillonite exfoliated nanocomposites.** *F. Estrany; D. Aradilla; D. S. Azambuja; M. T. Casas; C. A. Ferreira; C. Alemán*
T5-013	**Effect of binary organoclay mixture on the properties of ABS-clay nanocomposites prepared by melt intercalation.** *D. Galvan; J. R. Bartoli; M. A. D'Avila; M. Mazzuco; F. Massucato*
T5-014	**Synthesis, characterization and nonlinear optical properties of micellar nanohybrids based on Pd nanoparticlesand carbazole-containing block copolymers.** *M. Demetriou; T. Krasia; I. Papagiannouli; S. Couris; G. Chatzikyriakos*
T5-015	**Inducing microdomain orientation of thermoplastic elastomer in As-spun electrospinning fibers through study cases of SEBS triblock copolymer.** *W. Rungswang; M. Kotaki; S. Sakurai; S. Chirachanchai*
T5-016	**Computational modeling of nanocomposites' mechanical behavior at different environments parameters (moisture and thermal loadiing).** *K.M. Simeonova*
T5-017	**Fluoroalkyl end-capped oligomers/polyaniline and /phenyl-capped aniline dimer nanocomposites: controllingphotochromism between these nanocomposites induced by UV-light-responsive titanium oxide nanoparticles.** *H. Sawada; T. Tsuzuki-ishi; M. Iizuka; M. Yoshida*
T5-018	**Hybrid materials based on unsaturated polyester resins and polyhedral oligomericsilsesquioxanes (POSS).** *F. Constantin; S.A. Garea; H. Iovu*
T5-019	**Micellization and gelation of PEO/PPO block copolymers and their carboxyl-terminal derivatives.** *J. Dybal; A. Sturcova; A. Braunova; M. Pechar; A. Jigounov; J. Kriz*
T5-020	**A plasma reactor for the surface modification of silica based fillers: description and the apparatus and EPR investigation of reactive intermediates.** *A. Buttafava; D. Dondi; D. Grassi; F. Pepori; A. Faucitano*
T5-021	**Effect of sodium dodecylbenzene sulfonate on carbon nanotubes dispersion.** *V. Ghamgosar khorshidi; G.R. Bakhshandeh; A. Salimi; Gh. Naderi*

T5-022	**Optical and electrochemical properties of temperature fractions of nanodispersed polytetrafluoroethylene Forum®.** *A. Tsvetnikov; L. Matveenko; S. Suchoverchov; V. Kuryaviy; D. Opra; K. Galkin; S. Gnedenkov*
T5-023	**Influence of dopants on properties of polypyrrole nanocoated poly(styrene-*co*-methacrylic acid particles).** *I. Carrillo; M. González-Tejera; J. Fierro; E. Sánchez de la Blanca; I. Redondo; M. García; E. Enciso*
T5-024	**Effect of silane grafting and post cross-linking of HDPE on compatibilization and oxygen barrierity of HDPE/clay nanocomposite.** *A. Sharif Pakdaman; J. Morshedian; Y. Jahani*
T5-025	**PLA/PCL/montmorillonite nanocomposite systems: morphology and properties.** *V. Vascotto; A. Brunetin; R. Sulcis; P. Schiavuta*
T5-026	**Synthesis and characterization of superparamagnetic and thermoresponsive hydrogels based on functionalmethacrylates and oleic acid-coated magnetite nanoparticles.** *T. Krasia-Christoforou; P.C. Papaphilippou; A. Pourgouris; O. Marinica; A. Taculescu; G.I. Athanasopoulos; L. Vekas*
T5-027	**Biosensory function of self-assembled fluorescent nanotubes.** *C. Kim; J. Lee; S. K. Park; H. S. Kim*
T5-029	**Luminescent gold–poly(thiophene) nanoaggregates prepared by one-step oxidative polymerization.** *J.H. Kim; Y. J. Jung; S. J. Lee; S. M. Lee; H. Park; I. W. Cheong*
T5-030	**The influence of thermodynamic quality of solvent on properties of molecular nanoobjects.** *A. Amirova; E. Belyaeva; A. Kovina; E. Tarabukina; N. Sheremet'eva; A. Muzafarov; A. Filippov*
T5-031	**Colloidal crystallization of poly(*N*-isopropylacrylamide) microgels.** *H. Takeshita; S. Nakano; M. Miya; K. Takenaka; T. Shiomi*
T5-032	**Effect of orientation on structure and thermal properties of constrained polypropylene nanocomposite fibres.** *A. Marcincin; K. Marcincin; M. Hricova; A. Ujhelyiova; E. Borsig.*
T5-033	**Polyurethanes from agroindustrial wastes: pineapple case.** *J. Vega-Baudrit; S. Madrigal; L. Benavides; M. Sibaja-Ballesteros*
T5-034	**Hybrid block copolymer precursors carrying reactive triethoxy silyl side groups: synthesis, micellar behaviour and hydrolysis-condensation.** *C. G. Gamys; E. Beyou; E. Bourgeat-Lami*
T5-035	**Mechanical and thermal properties of nanocomposites based on heterophasic polypropylene/multiwalled carbon nanotubes functionalized with itaconic acid or monomethylitaconate.** *M. Yazdani-Pedram; J. Miranda; R. Quijada; P. Toro; R. Benavente*
T5-036	**Microspherical aniline oligomers and their nitrogen-containing carbon analogues.** *Z. Rozlívková; M. Trchová; E. N. Konyushenko; J. Steskal*
T5-037	**Porous titanium dioxide nanocomposite materials.** *O. Gaer; J. U. Wieneke; M. Ulbricht*
T5-040	**Nitrate remove from drinking water using polymer/MWCNTs nanocomposites.** *M. R. Nabid; S. J. Tabatabaei Rezaei; Y. Bide*
T5-041	**Spherulite growth rate in polypropylene/silica nanoparticle composites: effect of particle morphology and compatibilizer.** *H. Palza; J. Vera; M. Wilhelm; P. Zapata*
T5-042	**Supramolecular assembly of end-functionalized polymer mixture confined in nanospheres.** *J. Huh; C. Park; W.H. Jo*
T5-043	**Graphene-wrapped conductive nanospheres.** *S. Lee; K. Kim; S.A. Ju*
T5-044	**Behavior of ZrO_2/SiO_2 nanoparticles on the properties of the PVC/ABS blend.** *M.A. Reyes Acosta; A. Flores Vela; J.L. Rivera Armenta; A.M. Torres-Huerta; M.A. Domínguez Crespo*
T5-046	**Coarse-grained molecular dynamics simulations of Nylon-6 nanofibers.** *A. Milani; M. Casalegno; C. Castiglioni; G. Raos*

T5-047	**Testing 'double percolation' of carbon nanotubes in copolymer latexes by means of reverse addition fragmentation transfer polymerisation.** *G.T.H. Hill; G. Van Assche; B. Van Mele; C.E. Coning; M.C. Hermant*
T5-048	**Aqueous microgels modified by wedge-shaped amphiphilic molecules: hydrophilic microcontainers with hydrophobic nanodomains.** *L. Li; C. Cheng; X. Zhu; A. Pich; M. Möller*
T5-049	**Simulation of end-coupling reactions at a polymer-polymer interface: the kinetics and mechanism of interfacial roughness development.** *A. Berezkin; D. Guseva; Y. Kudryavtsev*
T5-050	**Low temperature process of Inkjet-printed ZnO Oxide transistor.** *S.C. Lim; S.Y. Kang; J.Y. Oh; S.D. Ahn; H. Kim; K.I. Cho*
T5-051	**Electrospinning of poly(γ-benzyl-L-glutamate) nanofibres: the effect of polymer molecular weight and spinningconditions in various solvents.** *J. Svobodova; F. Rypacek*
T5-052	**Investigation of structure and resistance of electroless copper sulfide nanoparticles in different deposition time. NSC 99-2221-E-036-002-MY3** *C.Y. Huang; Y.M. Fan; C.S. Tsai; K.Y. Tsao; C.P. Chang*
T5-053	**Study of the film formation and mechanical properties of the latexes obtained by miniemulsion co-polymerizationof the butyl acrylate, methyl acrylate and 3-methacryloxypropyltrimethoxysilane.** *J.M. Ramos-Fernández; C. Guillem; A. Lopez-Buendía*
T5-054	**Investigation of porous structure and thermal properties of sulphur containing copolymers.** *B. Podkoscielna*
T5-055	**Unexpected enhancement of polymerization rate in solution polymerization with nano CeO_2 particles.** *M. Aguirre; M. Paulis; J. R. Leiza*
T5-056	**Stimuli-responsive and electically conducting hydrogel nanocomposites from *N*-isopropylacrylamide and polyaniline.** *K. Depa; A. Strachota; P. Bober; J. Stejskal*
T5-057	**Instantaneous electric dipole moment in conjugated polymers.** *L. Roncaratti; R. Gargano; P. H. Oliveira Neto; W. Ferreira da Cunha; G. M. e Silva*
T5-059	**Effect of reaction parameters on the conductivity of nano polyaniline particles using Taguchi experimental design.** *R. Arefinia; A. Shojaei; H. Shariatpanahi .*
T5-060	**Influence of different nanofillers on the phase behavior of epoxy/polystyrene blends.** *M. Culebras; I. S. Monzó; C. M. Gómez*
T5-061	**Successive AGET ATRP of cationic methacrylate and PEO macromonomer yielding water soluble stiff cylindrical molecular brushes with cationic tail.** *C. Visnevskij; A. Baceviciute; R. Makuska*
T5-062	**Preparation and optical properties of novel bioactive photonic crystals obtained from core-shell hydrophilic microspheres.** *T. Basinska; M. Goseka; M. Griffete; M. Mangeney; M. Chehimi; M. Slomkowski*
T5-063	**Microspheres of poly(3-hydroxybutyric acid-*co*-3-hydroxyvaleric acid) loaded with holmium-166 for braquitherapy.** *J. R. De Souza; J. R. Martinelli; J. A. Osso Júnior; N. Nascimento; M. De Burgos Martins De Azevedo*
T5-064	**Microspheres of poly(lactic acid) loaded with holmium-166 for braquitherapy.** *G. Pires; J. R. de Souza; J. R. Martinelli; J. A. Osso Jr; N. Nascimento; M. De Burgos Martins De Azevedo;*
T5-066	**Exciton diffusion length in conjugated polymers.** *P.H.O. Neto; W.F. da Cunha; L. F. Roncaratti; F.V. Moura; R. Gargano; G.M. e Silva*
T5-067	**Bamboo charcoal supported silver particle by polyol process.** *C. Tzu Hsuan; L. Guan-Ting*
T5-068	**Theory of polyelectrolyte solutions.** *A. Karatrantos*

T5-069	**A new method for size controlled synthesis of zinc oxide nanocrystallites and their nanocomposite films.** *B. Karagoz; N. Bicak*
T5-070	**Influence of SiO_2 nanoparticles on ionic conductivity of PEI-LiTFSI electrolytes.** *I. Bayrak Pehlivan; C.G. Granqvist; P. Georen; R. Marsal; G. A. Niklasson*
T5-071	**Disiloxyl and dihydroxyl functionalized polymers by controlled/living polymerization methods.** *N.A. Mputumana; G. J. Summers*
T5-072	**Structures of the thermo-responsive poly(*N*-isopropylacrylamide) grafted from cotton fabric substrate.** *H. Yang; H. Zhu; D. Wang; J. H. Xin*
T5-073	**Raspberry–like silica particles to design superhydrophobic surfaces.** *R. de Francisco; N. García; T. Pilar*
T5-074	**Preparation and characterization of polyester resin-layered silicate containing reactive groups.** *S. Calvo; C. Arribas; R. M. Masegosa; M. G. Prolongo; C. Salom*
T5-075	**Analysis of polyhedral oligomeric silsesquioxanes, POSS, influence in properties of epoxy thermoset materials.** *B. Montero; A. Serra; C. Ramírez; X. Ramis*
T5-076	**Obtaining of biodegradable polymer films containing silver nanoparticles.** *Kh. E.Yunusov, A. A. Atakhanov, A. A.Sarymsakov, S. Sh.Rashidova*
T5-077	**First-principles simulations of IR spectra of polymers: nylon-6 polymorphs.** *A. Milani; C. Castiglioni; C. Quarti*
T5-078	**Covalent modification of MWCNT for styrene-isoprene-styrene block copolymer-based nanocomposites.** *M. Ilcikova; M. Mrlik; A. Juhari; K. Koynov; K. Csomorova; J. Mosnacek;*
T5-079	**Influence of montmorillonite (Cloisite 30B) content on water and oxygen barrier properties of polylactic acid films.** *N. Tenn; N. Follain; K. Fatyeyeva; S. Alix; J. Soulestin; S. Marais .*
T5-080	**Organo modified clay - biodegradable PHB/PCL nanocomposites: morphology, mechanical and barrier properties evaluation as function of blend composition.** *A. Botana; M. Mollo; P. Eisenberg*
T5-081	**Behavior of polyelectrolyte solutions in a wide temperature range.** *S.K. Filippov; T.A.P. Seery; P. Cernoch; J. Panek; P. Stepanek*
T5-082	**The influence of nanoparticles on the crystallization behaviour and the local deformation mechanism of poly(ε-caprolactone).** *M. Eriksson; P. Pichon; T. Peijs; H. Goossens*
T5-083	**Preparation and characterization of PLA-hydrotalcite nanocomposites.** *R. Scaffaro; L. Botta;*
T5-084	**Investigation of relationship between morphology and thermal stability of polystyrene & polymethylmethacrylate/Na-MMT nanocomposites prepared by emulsion polymerization.** *M. Rezaei; H. bouhendi; V. Haddadi-Asl; M. Nekomanesh-Haghighi*
T5-085	**Viscoelasticity of graphite oxide based suspensions in PDMS.** *A. Guimont; E. Beyou; G. Martin; P. Sonntag; P. Cassagnau*
T5-086	**Synthesis and characterization of new polyamides bearing 2,2'-thio, sulfinyl and sulfoxobis(1- naphthoxy) units in the main chain under microwave irradiation.** *E. Rostami*
T5-087	**Optical properties of 83 Titanium mono layers on glass substrateby Kramers Kronig method.** *H. Kangarlou; M. Motallebi Aghdam*
T5-088	**Production and investigation of optical and structural properties of MgF_2/TiO_2/glass and MgF_2/Ag/glass multi layers.** *H. Kangarlou; E. sattarpoor Isa Kan*
T5-089	**Synthesis of thermoresponsive nanocomposite hydrogels by alternative methods.** *B. Ferse; A. Große; K. Arndt*
T5-091	**PVDF/copper nanocomposites: preparation and properties.** *J. Arranz-Andrés; E. Pérez; M. L. Cerrada*

T5-092	**The effect of organoclay nature on the nanostructure andmechanical properties of polyamide-12 nanocomposites.** *N. Aramburu; J. I. Eguiazabal; J. Nazabal*
T5-093	**Crystallization studies on clay nanocomposites of Nylon 47.** *L. Franco; L. Morales; M. T. Casas; J. Puiggalí*
T5-094	**Characterisation and cure kinetics of epoxy-clay nanocomposites cured using an anionic initiator.** *F. Roman; Y. Calventus; P. Colomer; J. M. Hutchinson*
T5-095	**Biocompatible nanofibrous constructs targeted for controlled delivery of selected drugs.** *J. Michalek; J. Sirc; R. Hobzova; M. Pradny; N. Kostina; V. Holan; M. Munzarova*
T5-096	**Effect of dispersed phase modulus on brittle/tough transition of toughened polypropilene based nanocomposites.** *A. Zabaleta; I. González; J. I. Eguiazábal; J. Nazabal*
T5-097	**A low-temperature preparation of polymer-ZnO hybrid materials and/or ZnO nanoparticles from poly(zinc-methacrylate).** *G. Ambrozic; S. D. Skapin; M. Zigon; Z. Crnjak Orel*
T5-098	**Thermal stability of PMMA/ZnO nanocomposites.** *A. Anzlovar; Z. Crnjak Orel; M. Zigon*
T5-099	**Influence of the epoxy /amine stoichiometry on the thermomechanical properties of nanocomposites based on high T_g epoxy and organophilic clays.** *M. A. García del Cid; M. G. Prolongo; R. M. Masegosa; C. Arribas; C. Salom*
T5-100	**Biodegradable polyesters reinforced with mesoporous silica particles.** *J. Campos; M. R. Ribeiro; A. Deffieux; F. Peruch; J. . Lourenzo; M. L. Cerrada*
T5-101	**Fluorinated epoxy resin nanocomposites reinforced with amine functionalized MWNTs.** *C. M. Damian; S. A. Garea; C. Andronescu; A.M. Pandele; E. Vasile; H. Iovu*
T5-102	**Fluorescent polynorbornene/oxazine-1 loaded fluoromica nanocomposites by *in situ* polymerization for solution processable electronics.** *G. Leone; U. Giovanela; W. Porzio; C. Botta; G. Ricci*
T5-103	**Novel rheological and electrical results of polyamide/graphene nanocomposites.** *J. Canales; M. Fernandez; M. E. Muñoz; A. Santamaria*
T5-104	**Evaluation of polymeric micelles as potential carriers of antifungal agents.** *A.F. Olea; I. Fuentes; H. Carrasco; R. Martínez; I. Montenegro*
T5-105	**Isothermal titration calorimetry as a tool for elucidating the cobalt bis(dicarbollide) interaction with hydrophilic polymers.** *M. Uchman; K. Prochazka; M. Gradzielski; P. Matejicek*
T5-106	**Synthesis of polymeric nanoparticles by miniemulsion evaporation for the development of optical sensing phases.** *M. Marín Suárez Del Toro; J. F. Fernández Sánchez; T. Galeano Díaz; A. Fernández Gutiérrez*
T5-107	**NAOB® – Nanocomposites of natural rubber filled with organophillic clay and other reinforcers carbonous materials.** *G. R. Martín Cortés; F. José Esper; A. de Almeida Cutrim; A. de Almeida Dantas; W. Theodoro Hennies; F. R. Valenzuela Díaz*
T5-108	**Hierarchical structure and its formation process in liquid crystalline block copolymers.** *T. Shiomi; H. Takeshita; S. Adachi; S. Taniguchi; K. Takenaka*
T5-109	**Polyimide/silica nanocomposite thin films for advanced applications.** *E. Hamciuc; C. Hamciuc; I. Bacosca; L. Okrasa*
T5-110	**Dynamic mechanical relaxations and free-volume holes in polypropylene/carbon nanotubes composites.** *G. Zamfirova; N. Djourelov; J. M. Pereña; R. Benavente; E. Pérez; M. L. Cerrada; S. Peneva; V. Gaydarov*
T5-111	**New nanocomposites based on unsaturated polyester resin and modified halloysite.** *A. Ghebaur; S. A. Garea; H. Iovu*
T5-112	**Influence of silane treatment on the filler-coupling agent interactions.** *A. Lungu; N. Florea; C. Parvu; E. Vasile; H. Iovu*

T5-113	**Sphere-to-cylinder transition in mixed PS-*b*-PEO/TiO_2 micellar systems.** *D. Scalarone; M. Lazzari; F. Caldera; O. Chiantore*
T5-114	**Microstructure analysis of the layers containing nanoparticles hybrids ZnO-SiO_2, TiO_2-SiO_2 on textile fabrics.** *J. Sojka-Ledakowicz; J. Olczyk; A. Walawska; T. Jesionowski*
T5-115	**Synthesis of multi-walled carbon nanotubes using hydrocarbon as carbon sources in an arc discharge.** *M. Teymourzade; H. Kangarlou; K. Kazemikia;*
T5-116	**Synthesis of novel macroporous copolymer resins via aggregation/ breakage and post-polymerization.** *A. Lamprou; I. Koese; M. Soos; G. Storti; M. Morbidelli*
T5-117	**Crystallization kinetics of polypropylene nanocomposites.** *H. P. Nogueira; E. M. Alexandrino; M. I. Felisberti*
T5-118	**Magnetite-montmorillonite hybrid materials for wastewater treatment.** *G. Marcelo; I. Larraza; M. Lopez; T. Corrales; C. Peinado*
T5-119	**Analysis of the dispersion of nanofillers in PVC plastisols via rheological and morphological characterizations.** *C. Barres; A. Gueye; J. Duchet-Rumeau*
T5-120	**Intermolecular Interactions in polyacrylic acid solutions and gels.** *D. Shaltykova; E. Kalacheva; E. Shadrova; D. Kaldybekov; Z. Konyrbayeva*
T5-121	**Polymeric ionic liquids: homo- and copolymers in water.** *E. Karjalainen; H. Tenhu*
T5-122	**Functional poly(vinylpyrrolidone)s for the controlled synthesis of Ag nanoparticles.** *A. Ledo-Suárez; I. Rielo-Rodríguez; M. A. López-Quintela; M. Lazzari; M. G. Tardajos; H. Reinecke; A. Gallardo*
T5-123	**Study of nanocomposites processing containing polyaniline and carbon nanotube as use with radar absorbing structures.** *L. Folgueras; M. Rezende*
T5-124	**Single macromolecule as neural network.** *S. Panchenko; I. Suleimenov*
T5-125	**Novel fluorescence properties of syndiotactic polystyrene and its derivative.** *T. Sago; H. Itagaki*
T5-126	**Polymers as nanocarbon presursors in template method characterization and sorption properties of the obtained products.** *M. Sobiesiak, B. Podkościelna, M. Podgórski, A.M. Puziy, O.I. Poddubnaya, C.A. Reinish, M.M. Tsyba*
T5-128	**How affect the shape and modifier of clay on polymer blends?.** *R. Gallego; D. García-López; J. C. Merino Senovilla; J. M. Pastor*
T5-129	**Role of polymer-to-filler grafting in dispersion of CNTs in rubbers..** *P. Verge; S. Peeterbroeck; L. Bonnaud; P. Dubois*
T5-130	**Synthesis of colloidal stable silica containing blockcopolymer-nanoparticles.** *N. Köken Öz; K. Tauer; N. Weber*
T5-131	**Characterization of conducting polymer nanocomposites with poly(vinylidene fluoride) used in devices electroluminescents.** *A. Linardi Gomes; J. Sinézio de C. Campos; E. Armelin; C. Aleman; R. A. Ricci Jr; M. Beny P. Zakia; M. A. Canesqui; A. R. Vaz; J. G. Filho; J. A. Diniz*
T5-132	**Formation and size tuning of colloidal microcapsules via host-guest molecular recognition at the liquid-liquid interface.** *K. M. Turksoy; A. Sanyal*
T5-133	**Characterization, bioactivity and *in vitro* cellular response of sol-gel silica-polymer hybrid nanocomposites.** *S. Iváshchenko; D. M. García Cruz; A. Campillo Fernández; M. Monleón Pradas; J. L. Escobar Ivirico; G. Gallego Ferrer*

T5-134	**Unusual blue-shifted photoluminescence of MDMO-PPV films.** *H. Méndez; C. Hernández; B. Páez-Sierra; J. C. Salcedo-Reyes*
T5-135	**The thermodynamics of formation and structure peculiarities of nanostructured polyurethane/poly(2-hydroxyethyl methacrylate) interpenetrating polymer networks.** *L. Karabanova; Y. Gomza; S. Nesin*
T5-136	**Polyurethane urea nanocomposites: synthesis and characterization.** *A. Cuellar-Burgos; F. A. Mesa-Rueda; J. E. Perilla-Perilla*
T5-137	**Applications of broadband dielectric spectroscopy in polymer nanoscience.** *A. Serghei; F. Kremer; T. P. Russell*
T5-138	**Charge transport mechanism and thermal properties of novel polycyanurates/MWCNTs nanocomposites.** *L. Bardash; G. Boiteux; J. Ulanski; R. Grykien; I. Glowacki; A. Fainleib; P. Cassagnau*
T5-140	**Templating functional nanoporous materials with macromolecular architectures of controlled degradability.** *R. Majdoub; D. Grande*
T5-141	**Preparation and characterization of EVA nanocomposites obtained from montmorillonite and methylene-blue.** *M. Beltrán; A. Marcilla; V. Marchante; V. Benavente; I. Pelaez*
T5-142	**Nanostructures in polymer surfaces controlled by mechanical orientation.** *C. Fuentes; J. Feznández-Blasquez; A. Del Campo*
T5-143	**Estimation of cross-link density into networks in the polymerization of acryl-furanic compounds by mathematical modelling.** *J. Lanje*
T5-144	**Polymer shell nanocapsules for footwear applications.** *M. Sánchez; F. Arán; C. Orgilés; A. Marcilla*
T5-145	**Stable dispersions of chemically functionalized carbon nanofibers in waterborne polyurethanes.** *E. Orgilés-Calpena; F. Arán-Alís; A. M. Torró-Palau; C. Orgilés-Barceló*
T5-146	**Conformation and aggregation behavior of polymer-coated gold nanoparticles studied by dynamic light scattering experiments and Monte Carlo computer simulation.** *R. Pamies; J. G. Hernández Cifre; J. García de la Torre*
T5-147	**Chain dimensions, entanglement features and linear rheology of short chain branched polyethylene models: simulations and experiments.** *J.F. Vega; J. Ramos; J. Martínez-Salazar*
T5-148	**Particles composed of oppositely charged polyelectrolytes: effect of polymer molecular weight.** *F. Lima; A. Morán; F.E. Antunes; H. Chaimovich; M.G. Miguel; B. Lindman*
T5-149	**Transparent flexible electrodes using carbon nanotubes.** *J. Figueras; J. Pérez-Puigdemont; O. López; A. Fabregas; A. Abiad-Monge; N. Ferrer-Anglada*
T5-150	**Mesoporous Cuo as new catalyst for advanced energetic composites of polyurethane matrix.** *J. L. de la Fuente*
T5-151	**Evaluation of the phase inversion in HIPS/silver nanoparticles nanocomposites through UV-Vis spectrophotometry.** *G. Morales; F. Soriano*
T5-152	**Biopolymers / clays nano-biocomposites: impact of clay organo-modification on the morphology and properties of these hybrid materials.** *E. Pollet; L. Averous*

TOPIC 6: Bioinspired Polymers, Bioengineering and Biotechnology

T6-001	**Production of poly(lactic acid) microsphere loaded with holmium-166 for braquitherapy.** *G. Pires; J. Martinelli; J. Osso; N. Nascimento; M. de Burgos; M. Azevedo*
T6-002	**Morphology and properties of porous thermosensitive cryogels based on poly(*N*-isopropilacrylamide) systems.** *H. Peniche; F. Reyes; G. Rodriguez; M. R. Aguilar; C. Peniche; J. San Román*
T6-003	**Biologically inspired polymer scaffold development for artificial skin.** *M. Marimuthu; J. An; S. Kim*
T6-004	**Phenol biosensor based on electrochemically controlled integration of tyrosinase in a redox polymer.** *H. B. Yildiz; J. Castillo; D. A. Guschin; L. Toppare; W. Schuhmann*
T6-005	**Characterization and properties of PCL / PDIPF matrices for biomedical applications.** *J.M. Fernandez; S.M. Cortizo; A.M. Cortizo; G.A. Abraham;*
T6-006	**Reducing fibrillation tendency of polyvinyl alcohol fiber by incorporating cellulose nanowhiskers.** *A.J. Uddin; J. Araki; Y. Gotoh*
T6-007	**Synthesis and characterisation of well-defined optically active methacrylate-based block copolymers.** *M. Achilleos; D. Kafouris; S. Holder; T. Krasia-Christoforou*
T6-008	**Immobilization of soy bean peroxidase into nanotubes of natural halloysite and its application in the polyaniline synthesis.** *J. Romero-Garcia; E. Tierrablanca-Maldonado; R. Cruz-Silva*
T6-009	**Bioactive alginate-nanosiver-anthocyanin hybrid composite.** *J.H. Choi; S.Y. Seo; G.H. Lee; S.G. Lee; E.J. Oh; H.Y. Chung; J.H. Yeum; S.I. Han*
T6-010	**Degradation of polyethylene by a thermophilc bacterium.** *Y. S. Jeong; M. N. Kim*
T6-012	**Stimuli-responsive hydrogels for recognition of ions and biomolecules.** *T. Hennecke; N. Adrus; D.M. Balster; M. Ulbricht*
T6-013	**Novel pH-sensitive hydrogel for nano-pearl powder delivery.** *H.R. Lin; Y.C. Chen; Y.J. Lin; M.H. Ling*
T6-014	**Reinforced composites based on biodegradable polymer matrix and microcrystalline cellulose.** *F.A. dos Santos; M.I.B. Tavares; R.P.C. Neto*
T6-015	**Combined effect of temperature and humidity on the biodegradation behaviour of polylactic acid (PLA) and its nanocomposites.** *E. Kontou; P. Georgiopoulos; M. Niaounakis*
T6-016	**New copolymers derived from pyrrolidine and cyclodextrin with applications in gene therapy.** *J. A. Redondo; D. Velasco; A. Gallardo; H. Reinecke; A. Fernandez-Mayoralas; G. Corrales; E. García-Doyagüez; A. Pandit; C. Elvira*
T6-017	**Biomimetic block copolymer membranes for functionalized surfaces.** *S. Toughraï; E. Rakhmatullina; V. Malinova; N. Bruns; W. Meier*
T6-018	**Biodegradable micellar polymer drug carriers based on *N*-(2-hydroxypropyl)methacrylamide copolymers.** *P. Chytil; T. Etrych; K. Ulbrich*
T6-019	**PEG and tartaric acid: crosslinking agents and spacers for targeting delivery of chitosan nanogels.** *L. Perez; M. Artetxe; L. C. Cesteros*
T6-020	**Immobilization of glucose oxidase in conducting graft copolymers and determination of glucose amount in orange juices with enzyme electrodes.** *H.B. Yildiz; S. Kiralp; L. Toppare; Y. Yagci*
T6-021	**Elaboration of functionalized polylactide nanoparticles from *N*-acryloxysuccinimide-based block copolymers for drug delivery applications.** *N. Handké; T. Trimaille; E. Luciani; M. Rollet; T. Delair; B. Verrier; D. Bertin; D. Gigmes*
T6-022	**Preparation of pluronic micelles for ophthalmic delivery using ethyl acetate as a dispersion agent.** *H.R. Lin; P.C. Chang; H.J. Kao*

T6-023	**Effect of the crosslinker in molecularly imprinted polymers.** *I. Iturralde; M. Paulis; J. R. Leiza*
T6-024	**Chitosan based microspheres with good swelling characteristics.** *M. Maciejewska; J. Osypiu-Tomasik*
T6-025	**Purification and characterization of adhesive proteins for footwear.** *N. Cuesta; M.J. Escoto; C. Orgilés*
T6-026	**Flocculation by cationic amphiphilic polyelectrolytes: relating efficiency with polymer characteristics and concentration.** *L. Ghimici; M. Nichifor*
T6-027	**Composting of some biodegradable synthetic polyesters can be influenced by sample shape and surface quality.** *M. Koutny; P. Stloukal; S. Commereuc; V. Verney*
T6-028	**Synthesis and characterization of organic-inorganic hybrid biomaterials based on 2-hydroxyethylmethacrylate/triethoxyvinylsilane composites.** *L. John; M. Baltrukiewicz; P. Sobota*
T6-029	**Controlled delivery of gentamicin antibiotic from bioactive electrospun polylactide-based ultrathin fibers.** *S. Torres-Giner; A. Martinez-Abad; M.J. Ocio; J.M. Lagaron*
T6-030	**Stress-strain analysis of poly(lactic-*co*-glycolic) acid / poly(isoprene) blend for use as implants.** *D.R. Marques; L.A. dos Santos*
T6-031	**Comparative study of the polymer – lipase complexes.** *D.O. Solovieva; S.Y. Zaitsev; E.V. Tulskaya*
T6-032	**Magnetic nanoparticles coated with a molecularly imprinted polymer synthesized by RAFT polymerization.** *C. Gonzato; P. Pasetto; K. Haupt*
T6-033	**Novel biodegradable copolyesters of poly(butylene succinate) containing ether-oxygen atoms: correlation between chemical and architectural modification and enzymatic hydrolysis.** *M. Gigli; A. Negroni; M. Soccio; G. Zanaroli; N. Lotti; F. Fava; A. Munari*
T6-034	**Synthesis and characterization of hydrogels based on copolymers 2-hydroxyethyl methacrylate –*co*-zwitterionic carboxybetaine (meth)acrylamide for tissue engineering.** *N.Y. Kostina; C. Rodriguez-Emmenegger; J. Michalek; E. Brynda*
T6-035	**Norfloxacin-impregnated intraocular lenses: supercritical fluids technology vs. aqueous immersion.** *C. Gonzalez Chomon; M.E.M. Braga; H.C. de Sousa; A. Concheiro; C. Alvarez-Lorenzo*
T6-036	**Synthesis of biodegradable polymer and evaluation of its elastic properties available for stent coating layer.** *M.J. Kim; J. An; D.J. Chung*
T6-037	**Bio-FET using biotinylated F8T2.** *S.H. Kim; S.C. Lim; Y.S. Yang; H.T. Kim*
T6-038	**Correlation of physical and surface properties of polyurethane films with their chemical structure.** *C. Citak; A. Sirkecioglu; F.S. Guner*
T6-039	**Aging of a medical device surface after a cold plasma treatment.** *O. Mrad; J. Saunier; C. Aymes-Chodur; V. Mazel; V. Rosilio; F. Agnely; J. Vigneron; A. Etcheberry; N. Yagoubi*
T6-040	**A comparative kinetic study of the controlled drug release ability of the hydrogels synthesized from diepoxy-terminated poly(ethylene glycol)s and aliphatic polyamines.** *B. Cursaru; M. Teodorescu; C. Boscornea; P. O. Stanescu; S. Stoleriu*
T6-041	**Computer simulation of lysine based peptide dendrimers.** *I. Neelov; S. Falkovich; A. Darinsky; H. Tenhu*
T6-042	**Improved properties of cross-linked sodium hyaluronate films.** *J. A. Calles; J.A. Ressia; J. M. Llabot; P. Chetoni; S. D. Palma; E. M. Vallés*
T6-043	**Thermoset biodegradable elastomers with tunable mechanical properties and degradations.** *A. Harrane; H. Nouailhas; A. Leroy; B. Nottelet; J. Coudane*

T6-045	**Synthesis, characterization and application in controlled drug release of chitosan hydrogels obtained from *aspergillus niger*.** *N. E. Valderruten; E. Ruiz; H. F. Zuluaga; Z. Lentini; G. A. Muñoz; E. L. Romero; G. Álvarez; C. Suárez; L. Trujillo; J. de la cruz*
T6-046	**The use of a novel polymer to measure and classify plantar surface skin stresses.** *S. Stucke; D. McFarland; B. Davis; L. Goss; S. Fonov; R. Forlines; N. Berme; H. C. Guler; C. Bigelow*
T6-047	**Removal of heavy metals from waste water by naturally occurring bio-waste.** *F. Alsewailem; S. Aljlil*
T6-049	**Amphiphilic segmented elastomeric polyurethane bio-based on PLLA: Synthesis and characterization.** *J.M. Bergamaschi; M.I. Felisberti*
T6-050	**Polyhydroxyalkanoates (PHAs) produced by *cupriavidus necator* employing by-products from industrial biodiesel production as carbon source.** *J.A. López; I. López; A. Koutinas; M.A. Villar*
T6-051	**Synthesis of caffeic acid molecularly imprinted polymer microspheres and HPLC evaluation of their sorption properties.** *A. Valero Navarro; M. Gómez Romero; J.F. Fernández Sánchez; A. Segura Carretero; P. A.G. Cormack; A. Fernández Gutiérrez*
T6-052	**Nano and micro phospholipid/block copolymer hybrid vesicles: a new approach for the design of carriers for cancer therapy.** *M. Chemin; P. M. Brun; O. Sandre; S. Lecommandoux; J. F. Le Meins*
T6-053	**Removal of textile dyes with chitosan-polyacrylic acid (PAA) polymer conjugates.** *M. Celebi; Z.O. Ozdemir; H. Yildirim*
T6-054	**Effect of redox mediator (HOBT) on biodecolorization of textile dyes.** *M. Celebi; M. Altikatoglu; Z. Akdeste*
T6-055	**Novel synthetic route for covalent coupling of biomolecules on super-paramagnetic hybrid nanoparticles.** *A.L. Medina-Castillo; J. Morales- Sanfrutos; A. Megia-Fernandez; J. F. Fernández Sánchez; F. Santoyo-Gonzalez; A. Fernández Gutierrez;*
T6-056	**Thermal degradation of poly(hexamethylene terephthalate-*co*-dioxanone) copolyesters.** *G. Giammanco; A. Martinez de Ilarduya; A. Alla; S. Muñoz-Guerra*
T6-057	**Microwave assisted conjugation of BSA & chitosan.** *Z.O. Ozdemir*
T6-058	**Investigation of cellulase-dextran conjugates.** *L. Karagoz; Z.O. Ozdemir*
T6-059	**Thermal degradation of polyuronic acids and their ionic complexes.** *A. Tolentino; A. Alla; A. Martínez de Ilarduya; S. Muñoz-Guerra*
T6-060	**Electrospun fibrous scaffolds from novel poly(ester urethane urea) and poly(dioxanone) for vascular tissue regeneration.** *I. Stanishevskaya; V. Thomas; P. Caracciolo; G. Abraham; Y. Vohra*
T6-061	**Hydrophilic nanoparticles based on a three star poloxamer for ophthalmic applications.** *J. Marinich; I.T. Molina-Martínez; F.J. Parra; V. Andrés-Guerrero; R. Herrero-Vanrell; M.B. Vázquez-Lasa; J. San Román*
T6-063	**Erythrocyte aggregation induced by cationically-modified biopolymers.** *K. Kaminski; M. Plonka; J. Ciejka; K. Szczubialka; M. Nowakowska; B. Lorkowska; R. Korbut*
T6-064	**Polymer-cooperative blocking the viruses: *in silico* modeling the *in vitro* HIV-1 entry inhibitors.** *V.B. Tsvetkov; A.V. Veselovski; A.V. Serbin*
T6-065	**Novel bioactive resin adhesives inhibit dentin MMPs mediated collagen degradation.** *R. Osorio; M. Yamauti; S. Sauro; T.F. Watson; M. Quintana; M. Toledano*
T6-066	**Actin networks at interfaces: microrheology of reconstituted cell cortex.** *D. Ershov; J. Vander Gucht*
T6-067	**Surface nanostructuring and biofunctionalization through PAMAM chemical immobilization.** *A. Lungu; D. Dragusin; E. Rusen; A. Mocanu; E. Vasile; I. Stancu; H. Iovu*

T6-068	**Transport properties in plasticized biodegradable polymers.** *A. Chaos; E. Agirrezabal; A. Gonzalez; A. Etxeberria*
T6-069	**Development of PVA-based polyurethane microparticles for enzyme immobilization.** *S. Budriene; A. Straksys; T. Romaskevic*
T6-070	**Preparation of polyurethane-gold and polyurethane-silver nanoparticles conjugates for immobilization of enzyme.** *T. Romaskevic; S. Budriene; A. Ramanaviciene; N. Ryskevic*
T6-071	**Nanoparticles of glycopolymers as tumor-specific polymeric drugs.** *M.L. Lopez-Donaire; M. Fernández-Gutierrez; B. Vázquez-Lasa; E. Sussman; B. D. Ratner; J. San Román*
T6-072	**Self-assembling enzyme-polyelectrolyte nanofilms for sensor applications.** *L.V. Sigolaeva; H.A. Tarhonskaya; N.A. Krainova; M.S. Gromova; A.V. Kondrashina; A.V. Eremenko; A.H.E. Mueller; I.N. Kurochkin*
T6-073	**Bioactive alginate-nanosilver-anthocyanin hybrid composite.** *J.H. Choi; S.Y. Seo; G.H. Lee; S.G. Lee; E.J. Oh; H.Y. Chung; J.H. Yeum; S.I. Han*
T6-074	**Characterization and biocompatibility evaluation of novel segmented polyurethanes based on poly(ε-caprolactone)-poly(dimethylsiloxane)-poly(ε-caprolactone).** *M.V. Pergal; V.V. Antiæ; G. Tovilovic; J. Nestorov; J. Djonlagic*
T6-075	**Amphiphilic bioactive polymers and preparation of self assembled nanostructures.** *P. Suárez; A. González-Gómez; L. Rojo; J. San Román*
T6-077	**Viability and proliferation analysis of culture from human mesenchymal stem cells onto bioinspired collagen membranes for guided tissue regeneration..** *A.F. Fraga; H.S. Tavares; R.F.C. Marques; H. Tómas; J.L. Santos ,*
T6-078	**Modular and tunable polymeric systems containing dual biologically active ions.** *F.J. Parra; M. Fernández-Gutiérrez; B. Vázquez-Lasa; N. Dinjaski; A. Prieto; J. San Román*
T6-079	**Surfactant influence in obtaining hyaluronic acid micro and nanoparticles for *Arrabidaea chica* encapsulation and its effects on cicatrization.** *V. Ferre-Souza; D. Giacobbe; J. Lima; M.P. Jorge; A.L.T.G. Ruiz; I.M.O. Sousa; R.A.F.R. Rodrigues; J. E. Carvalho; M.A. Foglio; M.H.A. Santana*
T6-080	**Synthesis and characterization of porous hydroxyapatite/polymer biocomposite scaffolds.** *D. Kranzelic; M. Ivankovic; H. Ivankovic*
T6-081	**Polymer brushes grafted on polymer foils as platforms for enzyme immobilization.** *S. Neuhaus; C. Padeste; N. D. Spencer*
T6-082	**Photochemicaly promoted degradation of poly(ε-caprolactone).** *K. Borska; M. Danko; I. Janigova; J. Mosnacek*
T6-083	**Gene vectors with anticancer drugs based on DNA-polycationic complexes.** *N. Kasyanenko; L. Lysyakova; O. Nazarova; E. Panarin*
T6-084	**Synthesis and the characterization of poly(L,L-lactide)-*b*-poly(ethylene glycol) diblock copolymers as plasticizers and their effect on the hydrophilicity of the polymer matrix to promote cellular affinity.** *G. Lo Re; F. Meyer; J.M. Raquez; P. Dubois; R. Scaffaro*
T6-085	**The role of poly(ethylenglycol) molecular weight on viability and cell adhesion in polylactide-based scaffolds.** *G. Lo Re; R. Scaffaro; S. Rigogliuso; G. Ghersi*
T6-086	**PLA nanocomposites reinforced by cellulose nanowhiskers: influence of the preparation on the final properties.** *B. Ruelle; L. Bonnaud; P. Dubois*
T6-087	**Novelty linear (*N*-ethyl pyrrolidine methacrylamide-*co*-1-vinylimidazole) copolymers for gene therapy applications.** *D. Velasco; G. Réthore; B. Newland; J. Parra; C. Elvira; A. Pandit; L. Rojo; J. San Román*
T6-088	**Polymer-cooperative blocking the viruses: cholesten modified polyanions for raft-tropic antivirals.** *A.V. Serbin; Y.A. Egorov; E.N. Karaseva; O.L. Alikhanova; V.B. Tsvetkov*

T6-089	**Protein nanoreactors for atom transfer radical polymerization.** *K. Renggli; G. Kali; N. Bruns*
T6-090	**Amino functionalization of poly(lactic-*co*-glycolic acid) (PLGA) films with low-temperature plasma treatments.** *C. Riccardi; S. Zanini; E. Grimoldi; E. Ranucci; A. Manfredi; S. M. Doglia; A. Natalello*
T6-091	**Effect of photo, thermal and biodegradation on molar mass and crystallization of polylactide.** *L. Santonja-Blasco; A. Ribes-Greus; R.G. Alamo*
T6-092	**Chitosan and layered silicates bionanocomposites of preparation to be used as drug carrier vehicle.** *I. F. Leite; S.F. Oliveira; T.M. Marinho; O.L. Malta; S.de L. Silva*
T6-094	**Plasma polymerization of methyl methacrylate on zirconium oxide particles for use in the preparation of bone cements.** *M. Escamilla-Coral; A. Avila-Ortega; J.M. Cervantes-Uc*
T6-095	**Three-dimensional porous biocompatible and biodegradable scaffolds based on PHAs.** *J. Ramier; E. Renard; V. Langlois; D. Grande*
T6-096	**Preparation of polyvinylpyrrolidone (PVP) /polyethyleneglycol dimethacrylate (PEGMA) scaffolds for tissue engineering.** *B. Fernandez-Montes Moraleda; L. Rodríguez-Lorenzo; M. Fernández-Gutierrez; J. San Román*
T6-097	**Chitosan and layered silicates bionanocomposites of preparation to be used as drug carrier vehicle.** *I. F. Leite; S.F. Oliveira; T.M.A. Marinho; O. L. Malta; S.M. de L. Silva*
T6-098	**Synthesis and biocompatibility studies of poly(HEMA-*co*-DMAEMA) based scaffolds obtained by cryopolymerization.** *T. Volkmer; J. Magalhães; F. Blanco; E. Burguera; V. Sousa; L. A. Santos; L. Rodriguez-Lorenzo; J. San Román*
T6-099	**DOPA crosslinked biopolymers.** *L. Pastor-Pérez; Z. Shafiq; V. San Miguel; A. Del Campo*
T6-100	**Novel caged RGDs for photocontrol of cell attachment to artificial surfaces.** *M. Wirkner; A. García; A. Del Campo*
T6-101	**Two novel poly-ether-ether-ketone (PEEK) applications for bone repair: assessment of dental implants and craniotomy closure devices.** *B. Pérez-Köhler; A. Cifuentes-Negrete; A. Rodríguez; S. Llas; J. M. Aragoneses; J. Buján; N. García-Honduvilla*
T6-102	**Sol-gel synthesis of silica-chitosan hybrids for bone regeneration.** *M. Suarez; E. Valliant; J. R. Jones*
T6-103	**Hemoglobin binding from human blood hemolysate with poly(glycidyl methacrylate) beads .** *E. Banu Altıntas; D. Türkmen; V. Karakoç; H. Yavuz; A. Denizli*
T6-104	**Biodegradable fibrous polymer materials and composites prepared on the basis of plant biomass.** *A. Okruszek*
T6-105	**Bioactive alginate based drug delivery microgels for skeletal tissue engineering.** *L. Rojo; H. Autefage; S. McCullen; E. Gentleman; M. M. Stevens*
T6-106	**Preparation of protein-like amphiphatic polymers with antimicrobial activity.** *A. Plum; E. Heine; H. Keul; M. Möller*

ABSTRACTS

OPENING CONFERENCES

Life without Polymers

Christopher K. Ober

Cornell University, MSE, 310 Bard Hall, Ithaca, NY 14853

cko3@cornell.edu

Polymers play a vital role in all aspects of today's society. It is therefore difficult to imagine life without polymer materials. Nevertheless, it is a valuable exercise to consider the impact that polymers have on life today, particularly in the role of advanced technology.

The field of polymer science and engineering is a vibrant contributor to the world economy, not only in its own right, but also because of the wide array of industries and technologies made possible by the use of polymer materials. Polymers have unique, molecularly definable properties and process advantages unattainable in any other kind of material. Their attractiveness comes, in part, from the wide varieties of structure, molecular weight, and functionality available via rational synthesis of polymers and their characteristically broad range of processing modes. Polymers thus offer the potential for high performance at lower cost, sustainable use, and in many cases possible replacement of other materials in many fields. Polymers have become indispensable items in everyday life in uses ranging from clothing, paints, secure food packaging to major parts of automobiles but also as essential components in virtually every emerging advanced technology. A recent workshop report from the US National Science Foundation neatly summarizes the many contributions made by polymer science and future possibilities[1].

Polymers are needed to address many of the most critical challenges we face today in areas such as:

- Energy;
- Sustainability;
- Clean water;
- Healthcare;
- Informatics;
- And security.

A major opportunity for the field of polymer science lies in the direct integration of functional polymers into an energy-generating device. Polymers will play an important role in the shift to alternate fuels and energy sources. Polymers serve as the basis of advanced batteries, the membranes used in efficient, low temperature fuel cells and as the polymer photovoltaic diodes (solar cells) for energy production that are now being developed.

Polymers are ideally positioned to impact most of the key aspects of economic, social, institutional and environmental sustainability. Polymers play a central part in the membranes used in water purification and desalination. Polymers are critical components in food production and in the storage of delicate, time sensitive materials such as food and medicine. Polymers are being developed that come from biological sources, do not compete with food for their feedstock as many biofuels do, and can be much more readily recycled than in the past. Polymers are used because they are light, robust, low cost, extremely effective materials.

Polymers possess another critically important attribute, namely their similarity to biomacromolecules, the molecular basis of living organisms. In healthcare recent advances in biomedicine in areas such as artificial skin for wound healing and new methods of drug delivery such as that used in drug eluting stents are vitally dependent on discoveries in the creation, processing and understanding of polymers. As a result of the features they share with biomolecular materials, the impact of polymers will continue to grow, as their use expands further into human tissue repair, disease detection, food supply monitoring and other aspects of homeland defense, and future medical technologies. In the near future, advances in polymers will enable superior healthcare to reach greater numbers of people in a more economical manner.

Without polymers our lives, our health, our well being would be severely diminished. Most of the things we depend on would no longer be available. Simply put, without polymers much of life as we know it would no longer be possible.

---

[1] C.K. Ober, S. Cheng, P. Hammond, M. Muthukumar, E. Reichmanis, K. Wooley, "Interdisciplinary, Globally Leading Polymer Science and Engineering: 2007 NSF Workshop Report", Cornell University, Ithaca (2008).

Smart Polymer Applications in Drug Delivery and Diagnostics

Allan S. Hoffman[a], Patrick S. Stayton, Paul Yager, Anthony Convertine, James Lai, Michael Nash, Craig Duvall and Danielle Benoit

Department of Bioengineering, University of Washington, Seattle, WA 98195 USA
also WCU Distinguished Professor, Kyungpook National University Medical School, Daegu, South Korea

hoffman@uw.edu

In the first part of my talk I will describe our work with smart polymer carriers for intracellular delivery of biomolecular drugs. Such drugs include peptides, proteins and nucleic acid drugs (eg, pDNA and siRNA). Many of these drugs act at intracellular sites; however, the effective intracellular delivery of these "fragile" drugs remains a significant challenge. Endocytosis of drug formulations usually results in localization within the endosome, where the predominant fate is fusion with lysosomes and enzymatic degradation of the biomolecular drug. Inspired by the principle behind the ability of many viruses to deliver their genomic cargo from the endosome to the cytosol, we have designed and synthesized a family of biomimetic, "smart" acid-responsive polymeric carriers that can enhance the escape of fragile biomolecular drugs from the endosome to the cytosol.

In the second part of my talk I will describe our application of smart T- and pH-responsive polymers for point-of-care (POC) immunoassays. In this work, we have synthesized smart polymers using RAFT polymerization techniques, and conjugated them to: a) capture antibodies, b) porous membrane surfaces, c) magnetic nanoparticles, and d) gold nanoparticles. We have also coated the smart polymer-antibody conjugates onto magnetic and gold nanoparticles. These smart nanoparticles are used to capture and concentrate the target, biomarker molecules and then to release them as a concentrated pulse for downstream assay. We have used microfluidic devices and lateral flow strip assay formats for these POC assays.

ABSTRACTS

SPECIAL LECTURES

Sesion in honor of

Prof. C. Koning

Plant Oils: The Perfect Renewable Resource for Polymer Science?!

Michael A. R. Meier

Karlsruhe Institute of Technology (KIT), Institute of Organic Chemistry, Karlsruhe, Germany

m.a.r.meier@kit.edu

In ages of depleting fossil reserves and an increasing emission of greenhouse gases it is obvious that the utilization of renewable feedstocks is one necessary step towards a sustainable development of our future. Especially plant oils bear a large potential for the substitution of currently used petrochemicals, since a variety of value added chemical intermediates can be derived from these resources in a straightforward fashion taking full advantage of nature's synthetic potential. Here, new approaches for the synthesis of monomers as well as polymers from plant oils as renewable resources will be discussed.[1]

For instance, we could show that different chain length α,ω-diester monomers can be obtained from fatty acid esters via olefin cross-metathesis (CM) with methyl acrylate taking advantage of natures "synthetic pool" of fatty acids with different chain lengths and positions of the double bonds.[2] Similarly, we could show that the cross-metathesis with allyl chloride and other functional olefins allows for the synthesis of α,ω-difunctional compounds. Moreover, thiol-ene click chemistry offers a complementary approach for the introduction of different functional groups to fatty acids in a straightforward and efficient manner, as demonstrated for the functionalization of the castor oil derived methyl 10-undecenoate with a variety of thiols.[3] The thus obtained renewable platform chemicals are valuable starting materials for a variety of polyesters and polyamides.

Moreover, olefin metathesis as well as thiol-ene click chemistry were used to prepare renewable polymers. For instance, we could demonstrate the synthesis of telechelics as well as ABA triblock copolymers via ADMET in a one-step procedure.[4] During these ADMET polymerizations we observed more or less pronounced olefin isomerization side reactions. Therefore, we developed a strategy to monitor and quantify these side reactions during ADMET polymerizations and were able to correlate their amount to the applied catalyst as well as reaction conditions.[5] In a subsequent study, we could also demonstrate how to efficiently supress these unwanted side reactions.[6] Very recently, we could show that ADMET, a typical step-growth polymerization, can be used to prepare block- and star-shaped polymers by taking advantage of the CM selectivity between terminal olefins and acrylates.[7] Moreover, thiol-ene chemistry is also perfectly suited for the polymerization of fatty acid derived monomers, as will be shown with the synthesis of biopolymers with tuneable degradation behaviour.[8] Last but not least, we recently reported a strategy to highly functionalized renewable monomers and polymers based on multi-component reactions that offers manifold synthetic opportunities for polymer chemistry.[9]

In summary, we will thus demonstrate the versatility of plant-oil derived platform chemicals for the synthesis of a large variety of monomers and polymers. Plant oils are therefore a perfectly suited renewable resource for the polymer industry.

References:

[1] L. Montero de Espinosa, M. A. R. Meier, Eur. Polym. J. 2011, 47, 837.

[2] A. Rybak, M. A .R. Meier, Green Chem. 2007, 9, 1356.

[3] O. Türünç, M. A. R. Meier, Macromol. Rapid Commun. 2010, 31, 1822.

[4] A. Rybak, M. A. R. Meier, ChemSusChem 2008, 1, 542.

[5] P. A. Fokou, M. A. R. Meier, J. Am. Chem. Soc. 2009, 131, 1664.

[6] P. A. Fokou, M. A. R. Meier, Macromol. Rapid Commun. 2010, 31, 368.

[7] L. Montero de Espinosa, M. A. R. Meier, Chem. Commun. 2011, 47, 1908.

[8] O. Türünç, M. A. R. Meier, Green Chem. 2011, 13, 314.

[9] O. Kreye, T. Tóth, M. A. R. Meier, J. Am. Chem. Soc. 2011, 133, 1790.

Carbohydrate-based polycondensation polymers

Sebastián Muñóz-Guerra

Departament d'Enginyería Química, Universitat Politècnica de Catalunya, ETSEIB, Diagonal 647, 08028 Barcelona

sebastian.munoz@upc.edu

Polyamides and polyesters are thermoplastics of primary importance for both domestic and technological applications, in which they are consumed in huge amounts. In terms of sustainability, the total or partial replacement of the petrochemical monomers currently used for the industrial production of these polymers by others of natural origin is highly desirable. However to do it without detriment of the genuine properties and at acceptable costs is very challenging.

Carbohydrates constitute an excellent platform for the synthesis of step-growth polymers because their easy accessibility and wide variety.[1] If properly modified and protected, sugar derivatives may be used in polycondensation to produce thermoplastic polymers with inedited properties. First incursions in this area were made in the sixteen of the past century,[2] and more recently a good number of works exploring the potential of both acyclic and cyclic carbohydrate-based monomers in the synthesis of step-growth polymers have been reported.[3]

In these last years we have prepared an assortment of bifunctional monomers from easily accessible monosaccharides and used them as building-blocks for the synthesis of linear polyamides and aromatic copolyesters.[1] Both asymmetrical configurations and configurations containing a two-fold axis leading to non-stereoregular and stereoregular chains respectively, were explored (Figure 1).

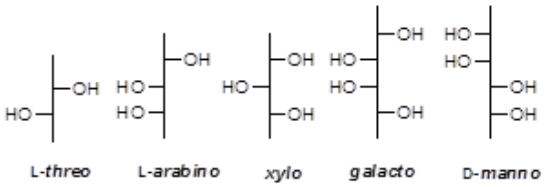

Figure 1. Sugar configurations explored in the preparation of polyamides and polyesters.

Polyaldaramides (**PAld-*n,m***) were prepared by polycondensation in solution from 1,*n*-alkanediamines (*n* = 4 to 12) and aldaric acids activated as pentachlorophenyl esters with their secondary hydroxyl groups protected either as methyl ether or as cyclic methylene acetal (Figure 2).

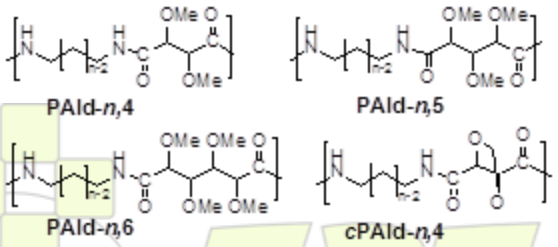

Figure 2. Polyaldaramides prepared from aldaric acid derivatives.

Most of polyaldaramides were crystalline polymers regardless the configuration of the aldaric acid. They adopt a common crystal structure made of kinked chains with the sugar unit located at the kinks and the polymethylene segment arranged in *all-trans* extended conformation.[4] These polyamides display higher hidrophilicity and hydrodegradability than their unsubstituted nylon homologues, and in some cases they show appreciable biodegradability.

Alditols with the secondary hydroxyl groups protected in the same way as done in aldaric acids were reacted in bulk with terephthalic acid or its dimethyl ester to obtain aromatic copolyesters derived from poly(ethylene terephthalate and poly(butylene therephthalate) (Figure 3).[5]

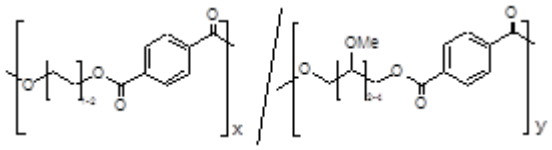

Figure 3. Sugar containing PET and PBT copolyesters.

PET and PBT copolyesters containing alditols units had a random microstructure for all compositions and showed increased solubility and hydrodegradability. Their *T*g were largely sensitive to composition, and both crystallinity and crystallization rate of the copolyesters decreased with the content in sugar residues. Crystalline copolyester have the same crystal structure than their parent homopolyesters with the alditols units being excluded from the ordered phase.

Dedicated to Prof. Cor E. Koning on the occasion of his Dutch Polymer Institute Invention Award.

References

[1]Galbis, J.A.; García-Martín, M.G. *Chem. Curr. Top.* **2010**, *295*, 147-176.

[2]Bird, T.P.; Black, W.A.P.; Dewar, E.T.; Hare J.B. *Chem. & Ind.* **1961**, *28*, 1077-1077.

[3]a) Thiem, J.; Bachmann, F.; *Trends Polym. Sci.* **1994,** *2*, 425–432. b) Kricheldorf , R.; Chatti, S., Schwarz, G., Krueger, R.P. *J. Polym. Sci. A Polym. Chem.* **2003,** *41*, 3414–3424. c) Noordover, B.A.J.; van Staalduinen, V.G.; Duchateau, R.; Koning, C.E.; van Benthem, R.A.T.M.; Mak, M.; Heise, A.; Frisen, A.E.; van Haveren, J. *Biomacromolecules* **2006**, *7*, 3406.

[4]Muñoz-Guerra, S; Fernández, C.E. Benito, E.; Marín, R.;García-Martín, MG, Bermúdez, M.; Galbis, J. *Polymer* **2009**, *50*, 2048–2057.

[5]Alla, A., Hakkou, K.; Zamora, F.; Martínez de Ilarduya, A.; Galbis, J.A.; Muñoz-Guerra, S. *Macromolecules* **2006,** *39*, 1410-1416.

On the Importance of Carbon Allotrope Network Organisation in Nanocomposites

Joachim Loos

Kelvin Nanocharacterisation Centre, Scottish Universities Physics Alliance (SUPA) and School of Physics and Astronomy, University of Glasgow, Glasgow, G12 8QQ, Scotland, UK

joachim.loos@glasgow.ac.uk

Polymer composites filled with carbon allotropic nanoparticles like carbon black (CB), carbon nanotubes (CNT) and graphene are applied as lightweight and easy processable materials with specific functionality. For very low nanofiller loading substantial improvement of the mechanical, thermal and electrical behaviour can be achieved. For instance, polyolefin composites could be prepared reaching electrical conductivity in the semiconductive range already for nanofiller concentrations far below 1 wt.%. However, until today critical processing parameters influencing nanofiller distribution and network formation in the polymer matrix are not clearly identified. One reason for our limited knowledge in this field is the difficult access to local morphological data that allows for identification of the individual nanofiller particles, their interface organisation in contact with the polymer matrix, their local functional properties and the overall macroscopic network organisation. In this study I will introduce some examples on how smart tuning of the involved processing conditions/routes helps tailoring the electrical properties of CNT and graphene filled composites, and I will introduce several advanced microscopy methods that allow for in-detail observation of the formed nanofiller networks with nanometer resolution in all three dimensions.

ABSTRACTS

PLENARY LECTURES

Macromolecular Engineering for Nanostructured Materials via ATRP

Krzysztof Matyjaszewski

Carnegie Mellon University, Pittsburgh, PA, 15213, USA

matyjaszewski@cmu.edu

Copper-based ATRP (atom transfer radical polymerization) catalytic systems with polydentate nitrogen-based ligands are among most efficient controlled/living radical polymerization systems.[1] Recently, by applying new initiating/catalytic systems, Cu level in ATRP was reduced to a few ppm. Various reducing agents, including metals, organometallic species, sugars, amines, phenols or even some monomers and ligands, as well as radical initiators have been successfully applied.[1-2] Similar control can be achieved with ppm of Fe-based catalysts.[3]

ATRP of acrylates, methacrylates, styrenes, acrylamides, acrylonitrile and many other vinyl monomers provides polymers with molecular weights in a large range $200<M_n$ 20,000,000 and with low dispersities.[4] Polymers can be formed quantitatively in bulk, in solution and in dispersed media. Water can serve both as solvent for many water soluble polymers and also as medium for microemulsion, miniemulsion, dispersion and suspension polymerization.[5] Block, graft, star, hyperbranched, gradient and periodic copolymers, molecular brushes and various hybrid materials as well as bioconjugates have been prepared.[5-6] The (co)polymers made by ATRP have many potential applications as components of advanced materials such as coatings, elastomers, adhesives, surfactants, dispersants, lubricants, additives, but also as specialty materials in biomedical and electronic areas and will affect the market of ~$20 billion/year.[7] Macromolecular engineering comprising design, synthesis, characterization and applications of nanostructured multicomponent polymeric materials prepared via ATRP will be presented.

References:

1. (a) Matyjaszewski, K.; Xia, J. *Chem. Rev.***2001**, *101*, 2921-2990;(b) Tsarevsky, N. V.; Matyjaszewski, K. *Chemical Reviews (Washington, DC, United States)***2007**, *107*, 2270-2299.

2. (a) Jakubowski, W.; Matyjaszewski, K. *Angew. Chem.***2006**, *45*, 4482-4486;(b) Min, K.; Gao, H.; Matyjaszewski, K. *J. Am. Chem. Soc.***2005**, *127*, 3825-3830;(c) Matyjaszewski, K.; Jakubowski, W.; Min, K.; Tang, W.; Huang, J.; Braunecker, W. A.; Tsarevsky, N. V. *Proceedings of the National Academy of Sciences of the United States of America***2006**, *103*, 15309-15314;(d) di Lena, F.; Matyjaszewski, K. *Prog. Polym. Sci.***2010**, *35*, 959-1021;(e) Matyjaszewski, K.; Coca, S.; Gaynor, S. G.; Wei, M.; Woodworth, B. E. *Macromolecules***1997**, *30*, 7348-7350;(f) Matyjaszewski, K.; Tsarevsky, N. V.; Braunecker, W. A.; Dong, H.; Huang, J.; Jakubowski, W.; Kwak, Y.; Nicolay, R.; Tang, W.; Yoon, J. A. *Macromolecules (Washington, DC, United States)***2007**, *40*, 7795-7806.

3. (a) Wang, Y.; Matyjaszewski, K. *Macromolecules (Washington, DC, U. S.)***2010**, *43*, 4003-4005;(b) Matyjaszewski, K.; Wei, M.; Xia, J.; McDermott, N. E. *Macromolecules***1997**, *30*, 8161-8164;(c) Teodorescu, M.; Gaynor, S. G.; Matyjaszewski, K. *Macromolecules***2000**, *33*, 2335-2339.

4. (a) Patten, T. E.; Xia, J.; Abernathy, T.; Matyjaszewski, K. *Science***1996**, *272*, 866-868;(b) Listak, J.; Jakubowski, W.; Mueller, L.; Plichta, A.; Matyjaszewski, K.; Bockstaller, M. R. *Macromolecules (Washington, DC, U. S.)***2008**, *41*, 5919-5927.

5. (a) Min, K.; Matyjaszewski, K. *Macromolecules***2005**, *38*, 8131-8134;(b) Min, K.; Jakubowski, W.; Matyjaszewski, K. *Macromolecular Rapid Communications***2006**, *27*, 594-598;(c) Min, K.; Gao, H.; Yoon, J. A.; Wu, W.; Kowalewski, T.; Matyjaszewski, K. *Macromolecules (Washington, DC, U. S.)***2009**, *42*, 1597-1603;(d) Min, K.; Matyjaszewski, K. *Central European Journal of Chemistry***2009**, *7*, 657-674.

6. (a) Gao, H.; Matyjaszewski, K. *Prog. Polym. Sci.***2009**, *34*, 317-350;(b) Lee, H.-i.; Pietrasik, J.; Sheiko, S. S.; Matyjaszewski, K. *Prog. Polym. Sci.***2010**, *35*, 24-44;(c) Sheiko, S. S.; Sumerlin, B. S.; Matyjaszewski, K. *Prog. Polym. Sci.***2008**, *33*, 759-785;(d) Coessens, V.; Pintauer, T.; Matyjaszewski, K. *Progress in Polymer Science***2001**, *26*, 337-377;(e) Matyjaszewski, K. *Progress in Polymer Science***2005**, *30*, 858-875;(f) Oh, J. K.; Drumright, R.; Siegwart, D. J.; Matyjaszewski, K. *Progress in Polymer Science***2008**, *33*, 448-477.

7. (a) Matyjaszewski, K.; Spanswick, J. *Materials Today (Oxford, United Kingdom)***2005**, *8*, 26-33;(b) Matyjaszewski, K.; Tsarevsky, N. V. *Nature Chemistry***2009**, *1*, 276-288.

A holistic view on the biodegradable macromolecular design

A.-C. Albertsson

Fibre and Polymer Technology Royal Institute of Technology, KTH

aila@kth.se

Biodegradable polymeric materials have formidable potential in a broad spectrum of applications, from high volume disposable items to specialized biomedical purposes. Presented here is a holistic perspective on how to engineer and optimize the polymer structure, from a nano-molecular to a macro-functional level. Our research approaches comprise all steps from macromolecular design, adopting new monomers, better initiator systems, creating polymers with advanced structures to surface modification, device formulation, production of scaffolds and assessments of in vivo behavior and degradation pattern. A range of pathways have been used to synthesize polymers with various architectures with the aim to control and vary the properties and function. Varying the chemistry and architecture changes the polymer behavior with respect to their physical, thermal, and mechanical properties. Ring-opening polymerization, anionic polymerization, enzymatic polymerization and living and controlled radical polymerization using a range of initiators and catalysts have allowed us to attain materials with narrow molecular weight distributions, varying architectures, easily controlled compositions, hydrophilicity, conductivity, and mechanical properties. Synthesis strategies are further developed to offer benign conditions. Strategies for covalent surface modification and are also developed and utilized for the subsequent biofunctionalization and/or nanopatterning.

The prepared biomaterials show great potential for usage in porous scaffolds in tissue engineering applications with respect to cell attachment, proliferation and stem cell differentiation. In any biological environment, the human body included, the fate of a degradable polymer is of imperative concern. The amount, diversity and structures of generated degradation products directly influence the environmental adaptability of a material. Chromatographic tools are developed to probe how the polymer structure, formulation, additives and processing affect the degradation in terms of rates, mechanisms, product patterns, and reproducibility.

Layered Polymeric Systems – Lessons From Biology

Eric Baer

Department of Macromolecular Science and Engineering.
Center for Layered Polymeric Systems
Case Western Reserve University

Lessons from biology have revealed that natural materials systems have architectures that are specifically designed to accommodate a unique spectrum of required properties. These architectures always have many scale levels that are bound together by interfacial coupling or adhesion. In recent years, new synthetic approaches have been used to develop macromolecular architectures that "self-assemble" into nano-scale morphologies. This lecture addresses another approach – the "forced-assembly" of synthetic polymers by continuous nanolayer coextrusion. Films can readily be created with thousands of layers containing two or more alternating polymers using a multilayer coextrusion system illustrated in Figure 1. Layer thicknesses have been made in the range of several microns down to less than ten nanometers by varying the number of layers and the layer composition.

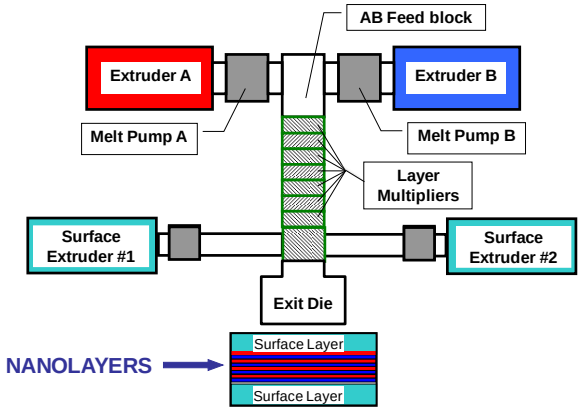

Figure 1: Two component multilayer coextrusion system comprised of extruders, pumps, feedblock, multiplying dies, surface layer extruders, and exit die.

Nanolayered films are of interest because of a potential for developing materials systems with novel mechanical, transport, electrical and optical properties. Since the radius of gyration of macromolecules can readily exceed the nanolayer thickness, the surrounding layers can be used to impart dimensional constraint at the molecular level. The novel effects that accompany a decrease in layer thickness from the microscale to the nanoscale will be illustrated with three examples related to the polymer interphase, confined crystallization, and finally, the development of graded index lens (GRIN) systems inspired from biomimetics.

When two immiscible polymers are brought into intimate contact, highly localized mixing creates an "interphase" region that is of considerable importance to polymer blends. We characterized the size and properties of the interphase by reducing the layer thickness in nanolayer assemblies to the size scale of the interphase. Films that were completely interphase were obtained with the thinnest nanolayers.

Confined two-dimensional crystallization of polymers presents unique challenges and opportunities due to the long chain, covalently bonded nature of the macromolecules. We discovered a unique morphology that emerges as confined polymer layers are made progressively thinner. When the thickness is confined to 20 nm, the PEO crystallizes as single, high aspect ratio lamellae that resemble single crystals. This may be the first time that large polymer single crystals are obtained by melt processing. Unexpectedly, the unique crystallization habit imparts two orders of magnitude reduction in the gas permeability.

The unique capabilities of biological optics arise from sophisticated features such as gradient index (GRIN) lenses and dynamic shape change. These GRIN lenses comprise thousands of layers that vary in protein concentration. It is reported that the human eye comprises greater than 20,000 layers and can change shape to accommodate near and far focus. The refractive index range (Δn) within a spherical lens in a human eye is about 0.03. In other cases like fish eye and octopus eye lenses, larger Δn compensates for an inability to change shape. The refractive index range within octopus eye is about 0.15 and fish eye is about 0.22. We have developed new nanolayered polymeric lenses with bio-inspired designs that have the structure and the properties of biological lenses. Specifically, polymeric nanolayered systems will be described that are used to mimic the lens in an octopus eye.

References

1. Liu, R.Y.F.; Bernal-Lara, T.E.; Hiltner, A.; Baer, E.; *Macromolecules*, 2004, 37 (18), 6972–6979.
2. Wang, H.; Keum, J.K.; Hiltner, A.; Baer, E.; Freemann, B.; Rozanski, A.; Galeski, A.; Science, 2009, 323, 757-760.
3. Beadie,G.; Shirk, J.; Rosenberg, A.; Lane, P.; Fleet, E.; Kamdar, A.; Jin, Y.; Ponting, M.; Kazmierczak, T.; Yang, Y.; Hiltner, A.; Baer, E.; Optics Express, 2008, 16, 11540-11547.

Ordered Supramolecular Polymers and their Hybrids with Covalent Chains

Samuel I. Stupp

Departments of Chemistry, Materials Science and Engineering, and Medicine
Northwestern University

s-stupp@northwestern.edu

Supramolecular polymers formed through self-assembly of monomers offers the potential to create ordered aggregates that can collectively emulate the shape persistence of proteins and many other filamentous structures in biological systems. One of the targets by several groups has been been the design of monomers that can self-assemble into conducting nanowires of interest in electronic applications. Efforts in our laboratory have also focused on fibrils that present groups with known biological functionality in highly favorable orientation and density, resulting in unprecedented efficiency of cell signaling for regenerative medicine. The future of the field needs to include programming of molecules for self-assembly that create more complex structures with order on scales that exceed the dimensions of the supramolecular polymers they form.

Another important goal is the design of hybrid structures that integrate supramolecular and covalent polymers as well as supramolecular and inorganic structures. This lecture discusses self-assembly pathways that produce cell-like objects or virus-like structures containing both supramolecular and covalent polymers and potential for biomedical functions. The lecture will also describe crystals of supramolecular polymers, and hybrid structures of supramolecular polymers with inorganic semiconductors with great potential in solar energy applications

Radical Polymers for an Organic-based Rechargeable Battery and Photovoltaic Cell

Hiroyuki Nishide

Department of Applied Chemistry, Waseda University, Tokyo169-8555, Japan

nishide@waseda.jp

We have focused on aliphatic polymers bearing organic robust radicals as pendant groups per repeating unit. For the radical groups, tetramethylpiperidinoxyl (TEMPO), nitronyl nitoxide, galvinoxyl, and viologen are typically employed. The so-called radical polymers are characterized by an ultimate population of unpaired electrons or singly occupied molecular orbitals, which allow efficient redox-driven electron transport throughout the polymer layer through self-exchange reactions. The high electron-transport reactivity of radical polymers provides very fast charge-propagation and reversible charge-storage in a rechargeable battery. A pair of two radical polymers with different redox potentials are used as a cathode- and an anode-active material in this organic radical battery. Organic and Li-ion free batteries offer several advantages over conventional batteries, including higher safety, adaptability to wet fabrication processes, easy disposability, and capability of fabrication from less-limited resources. Challenges toward a slim, paper-like battery and bust-power battery by molecular designing of the radical polymers will be demonstrated. We are also fabricating dye-sensitized photovoltaic cells to replace the iodine-containing electrolyte and/or the titanium oxide semiconductor in Graetzel-type one with the radical polymer layers for charge-separation and -transport in the cell. The cells displayed significantly high open-circuit voltage of almost 1 V. Radical polymers are emerging as a new class of electroactive materials useful for various kinds of wet-type energy storage and conversion devices.

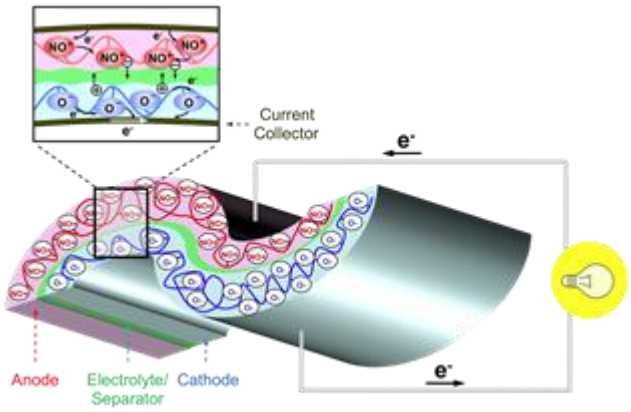

1. H. Nishide, K. Oyaizu, Science, 319, 737 (2008)
2. K. Oyaizu, H. Nishide, Adv. Mater., 21, 2339 (2009)
3. T. Suga, S. Ohshiro, K. Oyaizu, H. Nishide, Adv. Mater., 21, 1627 (2009)
4. F. Kato, N. Hayashi, T. Murakami, C. Okumura, K. Oyaizu, H. Nishide, Chem. Lett., 39, 464 (2010)
5. T. Ibe, A. Lachowicz, S. Kyo, H. Nishide, Chem. Commun., 46, 3475 (2010)
6. K. Oyaizu, A. Hatemata, W. Choi, H. Nishide, J. Mater. Chem,. 20, 5404 (2010)
7. K. Koshika, N. Sano, K. Oyaizu, H. Nishide, Green Chem., 12, 1573 (2010)
8. T. Suga, S. Sugita, K. Oyaizu, H. Nishide, Adv. Mater., 23, 751 (2011)

Sustainable Coatings, Plastics and Fibers from Novel Biomass-based Polymers

Cor E. Koning,[1,5] Bart Noordover,[1,5] Lidia Jasinska,[1,2,5] Jing Wu,[1,3,5] Donglin Tang,[1,5] Inge van der Meulen,[1,5] Matthijs de Geus,[1,5] Andreas Heise,[1,4,5] Daan van Es,[3,5] Jacco van Haveren,[3,5] Maurizio Villani,[1,5] Sanjay Rastogi,[1,5]

[1]Laboratory of Polymer Chemistry and Technology, Eindhoven University of Technology
[2]Department of Polymer Technology, Chemical Faculty, Gdansk University of Technology
[3]Food and Biobased Research (FBR)
[4]Dublin City University, School of Chemical Sciences
[5]Dutch Polymer Institute (DPI)

c.e.koning@tue.nl

Introduction

Striving for a more sustainable society and in their search for sustainable materials, many academic and industrial research groups focus their activities on biomass-based or renewable polymers. The most obvious approach is to synthesize renewable monomers, e.g. by using fermentation technology or by submitting biomass to mature industrial chemical engineering processes, and subsequently replace petrochemistry-based monomers by these renewable monomers in existing industrial processes and polymerization plants. Until quite recently any biomass like e.g. starch, suitable to be transferred into polymerizable chemicals, was considered as being attractive, but more recently it is realized that the generation of new monomers from biomass should not compete with the food chain, and sources like castor oil, cellulose and other biomass that cannot be digested by most living creatures is strongly preferred.

This work describes the synthesis and characterization of renewable polyesters, polyamides, polycarbonates and poly(urea urethane)s and also presents a selection of the physical and mechanical properties of powder coatings, injection moldable plastics and melt-spun fibers manufactured from these biobased polymers.

Experimental

Materials 1,4;3,6-Dianhydro-D-glucitol (isosorbide, IS, 98+%) was a gift from Roquette Frères. All other renewable monomers used in this study were either synthesized by FBR (Wageningen) or purchased from Aldrich and used as received.

Results and Discussion

Hyperbranched, fully biobased polyesters (Fig.1) were successfully synthesized from succinic acid, isosorbide and glycerol via bulk polycondensation. These renewable polymers were evaluated as solvent-casted films and as powder coatings and showed very promising properties. With respect to the yellowing behavior in sunlight, important for outdoor applications, these materials outperform the commercial petro-based powder coatings. Also by bulk polycondensation isosorbide-based polycarbonates were made. Coatings based on these renewable polymers showed superior toughness, solvent resistance, UV-resistance and gloss. Promising melt-processable, semi-crystalline (*Tm*=160-230°C), renewable polyamides were made from the isoidide diamine, putrescine and sebacic acid (Fig. 2)

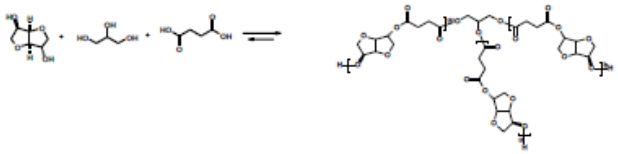

Fig 1. Renewable amorphous, branched polyester from isosorbide, glycerol and succinic acid for powder coatings.

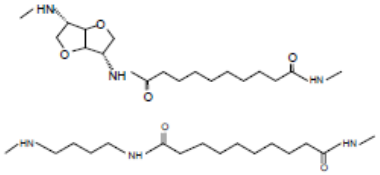

Fig 2. Repeat units of renewable, semi-crystalline polyamides from isoidide diamine, putrescine and sebacic acid.

Fully biobased poly(urea urethane)-polyester multiblock copolymers, consisting of renewable elastomeric polyester blocks and renewable urea-urethane blocks as physical cross-links, were prepared via an isocyanate-free route. These materials exhibit promising properties as renewable and biodegradable thermoplastic elastomers.

By enzymatic polymerization of the biobased macrocyclic musk lactone cyclopentadecanolide, high molecular weight aliphatic polyesters were synthesized and melt-spun into strong fibers which after drawing exhibited a tensile strength of 0.6-0.7 GPa.

Conclusions

Fully or nearly fully biobased cycloaliphatic polyesters, polycarbonates, polyamides, poly(urea urethane)s and linear aliphatic polyesters have been successfully synthesized and showed very promising behavior when evaluated as coatings, plastics or fibers, sometimes even outperforming their petro-based counterparts.

This work forms part of the research program of the Dutch Polymer Institute.

Design of Intelligent Surfaces for Cell Sheet Tissue Engineering

Teruo Okano, Ph.D.

Institute of Advanced Biomedical Engineering and Science. Tokyo Women's Medical University
8-1 Kawada-cho, Shinjuku-ku, Tokyo 162-8666 Japan

tokano@abmes.twmu.ac.jp

Our research has been focused on constructing a novel form of co-culture consisting layered tissue structure. For our goal, we first developed unique tissue culture dishes which equipped their inner-bottom surface coated with the temperature-responsive polymer poly(*N*-isopropyl acrylamide) (PIPAAm). The "intelligent surface" of these dishes possessed the hydrophobicity similar to regular tissue culture polystyrene dishes at 37℃. However, the surface reversibly became hydrophilic at a lower temperature and spontaneously released the cultured cells as a single layer without the need for trypsin or EDTA, thus leaving the cell layer with extracellular matrix (ECM) intact. All the cultured confluent cells were harvested as a single contiguous cell sheet from the temperature-responsive culture dishes and readily applied to other biological and non-biological surfaces, thanks to the intact ECM. We here propose this novel system of cells and cell-layers arrangement called "cell sheet engineering."

We initiated human clinical studies of cell sheet engineering therapy using oral mucosal cell sheet for treatment of cornea epithelium deficient disease and recovery from endoscopic submucosal dissension surgery for esophageal epithelial cancer, and we also succeeded in treating cardio-myopathy using myoblast cell sheet. However, these applications only required primarily two dimensional manipulations of the cultured cells without prevascularized networks, which would be essential for the development of biological structures to treat or replace dysfunctional organs and tissues in human patients, the next stage of cell sheet tissue engineering. While they were vital, there were no known feasible methods to introduce effective vascular networks to sustain the fundamental functions of the regenerated organs and tissues, e.g., the liver and capillary blood vessels. Therefore, a new strategy was required, and the construction of cell sheets which had more than one type of cells became necessary in attempt to create the desired prevascular networks in three dimensional biological constructs.

In order to overcome the challenges of developing crucial and functional prevascular networks, first the copolymers with different phase transition temperatures were coated on the surface of culture dishes to produce a patterned dual phase thermo-responsive cell culture surface using electron beam polymerization method and porous metal masks. On the patterned surface of the dishes, site-selective adhesion and growth of hepatocytes and endothelial cells yielded a patterned co-culture layer based on the hydrophobic-hydrophilic surface chemistry regulated by simple temperature change. In addition, the recovered co-cultured cell sheets could be modified and multilayered, and other types of cells could even be inserted between the cell sheets. The experimental results demonstrated that this method could provide a new approach for the development of organ-like structures with the essential vascular networks found in normal human organs. Therefore, cell sheet engineering with the intelligent surface is a highly promising tool for tissue engineering and regenerative medicine.

References

1. N. Yamada, T. Okano, K. Sakai, F. Karikusa, Y. Sawasaki, Y. Sakurai, *Makromol. Rapid Commun.***1990**, *11*, 571.

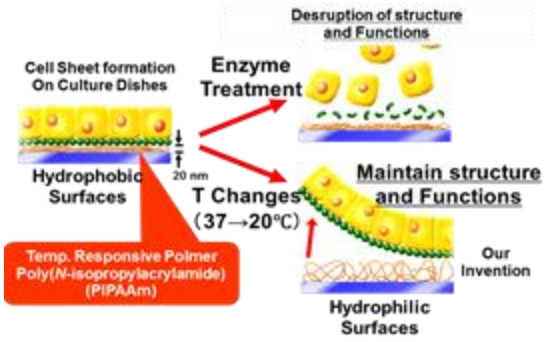

Figure. Cell Sheet Manipulation by Temperature Change.PIPAAm-grafted surfaces enable non-invasive cell harvest without need for proteolytic enzymes simply by lowering the temperature

2. T. Okano, N. Yamada, H. Sakai, Y. Sakurai, *J. Biomed. Mater.Res.***1993**, *27*, 1243.

3. T. Okano, N. Yamada, M. Okuhara, H. Sakai, Y. Sakurai, *Biomaterials***1995**, *16*, 297.

4. A. Kikuchi, T. Okano, *J. Controlled Release***2005**, *101*, 69.

5. M. Yamato, T. Okano, *Mater. Today***2004**, *7*, 42.

6. J. Yang, M. Yamato, H. Sekine, S. Sekiya, Y. Tsuda, K. Ohashi, T. Shimizu, T. Okano, *Adv. Mater.***2009**, *21*, 3404.

Trainer project: research on self- and inteligent healing materials

Pilar Martí; Directora de Tecnología Química.Repsol YPF.

Pmartip@repsol.com

Repair or healing is a well-known property in Nature, which provides inspiration for both academic and industrial researchers to invest in the development of artificial materials with self-healing capability. These self-healing materials attempt to mimic the ability of living organisms to heal an injury by themselves.

And this is the purpose of the TRAINER* project. Thirteen Spanish companies from different sectors (construction, renewable energies, transport,...), are part of this consortium, among which Repsol along with 21 research centres and universities collaborate under the leadership of ACCIONA. The project was launched in 2010 and will be completed by the end of 2013. The consortium is working on the development of self-repairing systems and their implementation in different materials, not only polymers but also others such as concrete and asphalt. Besides, specific tests and protocols for evaluating the healing capability of the new materials developed are an important outcome and contribution of this project.

Materials are often internally or superficially damaged by mechanical causes (impacts, scratches, sudden temperature changes, etc.) and/or environmental factors (corrosion, UV radiation, humidity, temperature, etc.). Maintenance can be costly and time-consuming, especially in cases that require the replacement of the damaged part. Traditional measures establish high safety factors, periodic inspections and preventive maintenance. The implementation of the technologies developed in the TRAINER project would reduce CO_2 emissions, waste generation, costs and risks associated with maintenance and repairing operations. Additionally, service stops would be avoided, thus reducing costs and increasing end user satisfaction.

Following the chronological order of appearance in the state of the art of self-regeneration technologies for materials, there are three generations:

- 1st generation: The first developments of this technology published in 2001 are based on micro-capsules embedded in the matrix containing the healing agent. The healing agent spreads after rupture of the capsule due to the propagation of a crack and repairs the failure.
- 2nd generation: In 2007 a new generation emerged mimicking the human body's vascular network through the incorporation of hollow fibers containing the healing agent.
- 3rd generation: In 2009, a new concept was introduced based on the recombination of the broken bonds to regenerate the deteriorated material.

The TRAINER project aims to overcome barriers in the implementation of the present self-healing technologies and also to develop novel healing agents such as microorganisms, expansive agents, conductive fibers, etc. that will suppose a major technological breakthrough in the state of the art.

*(*CENIT project funded by the Centre for the Development of Industrial Technology (CDTI) and the Ministry of Science and Innovation of Spain*).

Self-Assembling Processes of Organic-Inorganic Nanobuilding Blocks and Supramolecular Units as New Routes for Nanostructured Polymer Networks

J.F. Gerard[1], J. Duchet[1], J. Galy[1], J. Bernard[1], L. Dai[2], F. Lortie[1]

[1]Ingénierie des Matériaux Polymères – UMR CNRS #5223
Université de Lyon – INSA Lyon
F-69621 Villeurbanne Cedex – France
[2]College of Materials, Xiamen University, Xiamen Fujian 361005 China

jean-francois.gerard@insa-lyon.fr

Self-assembling processes could be used to generate nanostructures within polymer networks in order to design innovative materials. In fact, non-conventional physical behaviours and combination of functionalities could be expected from the definition of morphologies of polymer networks at nanoscale. This lecture will review the different routes for nanostructuration of polymer networks and offer new approaches for designing inorganic-rich or organic supramolecular nanostructures from self-assembling processes.

Pre-formed nano-objects such as organic or inorganic nanoparticles or nanotubes are usely considered. Nevertheless, poorly ordered nanocomposites are obtained and the final dispersion depends strongly to the mixing procedure. Another route deals with the *in situ* generation of inorganic-rich nanodomains from a reaction-induced phase separation occurring during sol-gel reactions of (functional) metal alkoxides. The morphology could be tailored from the reaction conditions such as temperature, pH, concentration, etc. A third promising route to hybrid materials involves well-defined inorganic clusters such as polyhedral oligomeric silsesquioxanes (POSS), 1-3 nm $(SiO_{1.5})_n$ structures that can be considered as the tiniest silica nano-objects. Non-reactive organic substituents (such as isobutyl, iBu, or cyclohexyl, Cy) on the POSS cages will be used to trigger supramolecular assembling process whereas a reactive group will be used to covalently connected the metal-oxo cluster to polymer backbones via (co)polymerization with organic monomers, such as methacrylate ones. The ability to the POSS-cages to self-assemble in poly(MACyPOSS-co-MMA) copolymers and in well-defined hybrid block copolymers poly(MACyPOSS-b-MMA) and poly(MAiBuPOSS-b-MMA) synthesized by RAFT polymerization exhibiting high POSS weight content will be demonstrated. In a second part, the self-assembling of functional (amine or epoxy) POSS or the previous O/I block copolymers in epoxy networks will be evidenced. The hybrid block copolymers self-assembled within the epoxy precursors into micelles possessing an inorganic core and a PMMA corona. Thanks to the presence of the PMMA blocks that remain miscible until the end of the reaction, curing of the resulting blends afforded nanostructured hybrid organic/inorganic networks with well-dispersed inorganic-rich nanodomains with diameters on the order of 20 nm. Such an approach offers a new route for designing nanocomposites based on polymer networks as matrices from the in-situ generation via self-assembling of inorganic nanoparticles..

The second approach for nanostructuration of polymer networks consists in self-organization and freezing of a multi-scale hydrogen-bonded and π-stacked assemblies in an epoxy-amine network matrix. The self-assembly units are ureidopyrimidinones (UPy) introduced from a ureido-pyrimidinone-terminated polyoxypropylene ami-ne which can introduce both covalent crosslinks in the final network and supramolecular crosslinks from the self-assembling of the UPy units. The UPy-functionalized amine can self-assemble in the epoxy monomer (diglycidyl ether of Bisphenol-A) as a gel-like behaviour is observed for a critical content of associating units and below 90°C, i.e. the temperature above which the dimer's hydrogen-bonds are destroyed. This UPy-functionalized amine has been considered at different contents to nanostructure epoxy (DGEBA) non-functionalized amine reactive systems. After polycondensation, transparent materials have been obtained and characterized. The 3D-polymerization induces a (reaction-induced) phase separation between the associative UPy units and the polyoxypropylene chains. RIPS occurs from a decrease of solubility the supramolecular macromolecules into the growing network species. As the α-NH_2-ω-UPy-polyoxy propylene are mixed with the corresponding neat polyoxypropylene diamine, no phase separation is observed as the later ones improve the miscibility of UPy units all along construction of the networks, i.e. during curing. Nevertheless, SAXS evidences the existence of nanoscale domains with correlation distance between scattering objects depending upon concentration. Such an homogeneous (nano)phase separation leads to the construction of networks based on multifunctional nano-objects as supramolecular crosslinks in addition to the covalent ones. As a consequence, the mechanical properties in the rubbery state could be fully tailored from the coexistence of these physical and chemical crosslinks by changing the UPy content and temperature. In fact, the crosslink density could be tuned below and above 90°C, the temperature at which the dissociation of UPy occurs. Temperature-tuned crosslink density networks (as the association and dissociation processes of supramolecular assembling are fully reversible) could be designed from such a route for intelligent materials and integrated in devices.

ABSTRACTS

INVITED LECTURES

Topic 1: Synthetic Routes: Monomers and Polymers from Bioresources and Advanced Methodologies

Cyclic and Multiblock Polystyrene-*b*-Polyisoprene Copolymers by Combining Anionic Polymerization and Azide/Alkyne "Click" Chemistry

Athanasios Touris and Nikos Hadjichristidis

Department of Chemistry, University of Athens, Athens, Greece
hadjichristidis@chem.uoa.gr

Introduction

The unique characteristics of alkyne/azide "click" reaction[1] have contributed considerably to the popularity of "click" chemistry within the polymer and materials science communities. However, in the case of anionic polymerization, apart from the use of post- polymerization reactions to introduce active "clickable" groups, with subsequent loss of the lithium site, "clickable" groups have never been simultaneously present with the lithium-propagating sites. Such species would have the potential to take advantage of both the lithium and active "clickable" sites, thereby combining two ideal methods, for the synthesis of well-defined complex macromolecular architectures.

Along these lines, we report here a new strategy for the synthesis of well-defined cyclic block and multiblock copolymers of polystyrene (PS) and polyisoprene (PI).

Experimental Part

The purification of monomers, solvents and other compounds used here, to the standards required for anionic polymerization, has been described elsewhere.[2] All manipulations were done in vacuo in all-glass vessels, washed with *n*-BuLi, and rinsed with solvent. Additions were made through break-seals and removals through heat sealing of constrictions. Size exclusion chromatography (SEC) experiments were conducted at 40 °C in THF at a flow rate of 1 mL/min. All nuclear magnetic resonance (NMR) spectra were recorded in chloroform-*d* at 25 °C with a Varian Unity Plus 300/54 NMR spectrometer. A Perkin-Elmer Spectrun One model was used for the FTIR characterization.

Results and Discussion

Synthesis of the initiator 5-triethylsilyl-4-pentynyllithium (TESPLi). The synthesis of TESPLi, from (5-chloro-1-pentynyl)trimethylsilane and lithium, was conducted in benzene, as it is very well documented[3] that pentynylalkyllithiums undergo intramolecular cyclization reaction, at room temperature in hexane.

The general reactions for the synthesis of the linear diblock precursor, the cyclic diblock, and the multiblock copolymer are given in the **Scheme.**

Intramolecular "click" cyclization of α-acetylene-ω-azido-PS-*b*-PI. The reaction was conducted in cyclohexane ($c < 6 \times 10^{-5}$ g/mL), which is a rather poor solvent for the PS, a condition which favors the intramolecular reaction {M_n(PS)=8.1K, M_n(PS-b-PI)=14.9, PDI=1.05}.

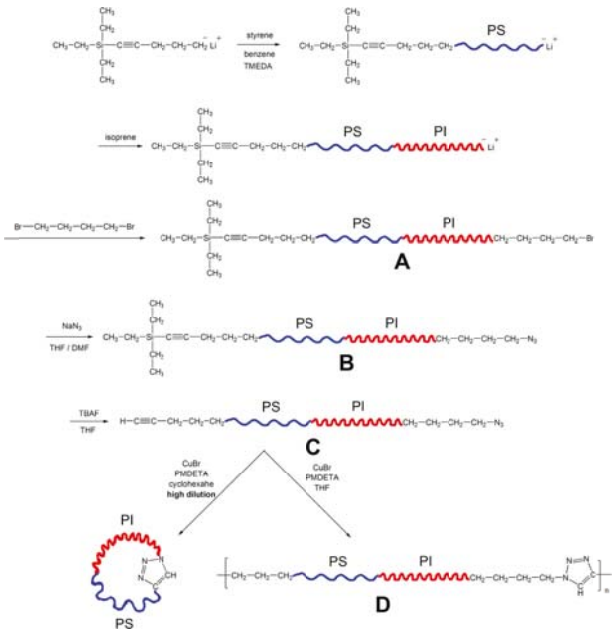

The successful cyclization reaction was evidenced by: a) the shift of the SEC trace of the cyclic copolymer to a slightly higher elution volume and b) the disappearance of the azido and acetylene characteristic peaks in FTIR spectrum. The unreacted linear precursor α-acetylene-ω-azido-PS-*b*-PI was eliminated with an azido-functionalized Merrifield resin.

Intermolecular "click" coupling of α-acetylene-ω-azido-PS-*b*-PI. The intermolecular "click" reaction was conducted in THF, a good solvent for both blocks, which favors the intermolecular coupling reaction and thus leading to multiblock copolymers. The evolution of the reaction was monitored by SEC {highest peak, M_p=849K, DP=57}.

Conclusions

By using TESPLi and appropriate post-polymerization reactions, anα-acetylene-ω-azido-PS-*b*-PI was prepared, which led to cyclic block (intra-click, dilute cyclohexane solution) and multiblock (inter-click, concentrate THF solution) copolymers. These are only two architectures out of myriads this strategy (combination of two ideal methods) can produce.

References

(1) Kolb, H. C.; Finn, M. G.; Sharpless, K. B. *Angew. Chem. Int. Ed.* **2001**, *40*, 2004-2021.

(2) Hadjichristidis, N.; Iatrou, H.; Pispas, S.; Pitsikalis, M. *J. Polym. Sci. Polym. Chem. Ed.* **2000**, *38*, 3211-3234.

(3) Bailey, W. F.; Ovaska, T. V. *J. Am. Chem. Soc.* **1993**, *115*, 3080-3090.

Vegetable Oils as Platform Chemicals for Polymer Synthesis

Ronda, J.C.; Lligadas, G.; Galià, M.; Cádiz, V.

Departament de Química Analítica i Química Orgánica
Universitat Rovira i Virgili
Marcel.li domingo s/n, Tarragona, Spain

juancarlos.ronda@urv.cat

The replacement of petroleum-based raw materials by renewable resources constitutes a major contemporary challenge in terms of both economical and environmental aspects[1].Natural vegetable oils are considered to be one of the most important classes of renewable sources because of the wide variety of possibilities for chemical transformations, universal availability, and low price and they are preferred by the chemical industry as alternative[2]. The main components of the triglyceride vegetable oils are saturated and unsaturated fatty acids which in its pure form are also available as platform chemicals for polymer synthesis

To convert vegetable oils and their derivatives to useful polymeric materials, three main different approaches can be used: the direct polymerization of the double bonds, the chemical modification and posterior polymerization and the polymerization of monomers synthesized using vegetable oil-derived platform chemicals. The purpose of our research is to develop new biobased thermoplastic and thermosetting polymers from vegetable oils by using these three approaches.

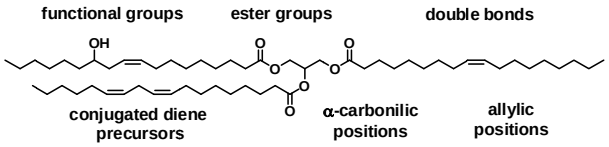

The direct polymerization of vegetable oils themselves is generally considered difficult due to their lack of active functional groups. Moreover the aliphatic nature and the light crosslinking that characterize the triglyceride-based materials make them incapable of displaying the necessary rigidity and strength required for structural applications. These drawbacks can be overcome for instance by cationic copolymerization of natural oils with styrene and divinylbenzene[3]. Even the resulting materials have the appropriate properties for a specific application, they must be inherently safe to be commercialized which involves to posses flame resistance and non toxic characteristics. One approach that we have explored is the preparation of styrene-soybean oil based copolymers containing phosphorus, silicon or boron as effective environmentally friendly flame-retardant systems.

The functionalization of the triglyceride double bonds is another common strategy for obtaining high performance polymeric materials and various chemical pathways for functionalising triglycerides have been described. We developed an environmentally friendly chemical procedure to obtain an enone-containing triglyceride from high oleic sunflower oil that could be an interesting alternative to epoxidized vegetable oils to produce thermosets. We studied their chemical crosslinking through aza-Michael and phospha-Michael reactions using aromatic diamines and aromatic secondary phosphine oxides in order to infer flame retardancy to the final material in the second case.

The use of fatty acids or its chemical derivatives to obtain useful polymers has also been considered by us. Starting from 10-undecenoic acid or 10-undecenyl alcohol, we synthesized a set of glycerol derived α,ω-dienes and trienes containing free hydroxylic groups. Acyclic diene metathesis (ADMET) polymerization of these monomers has been shown as an efficient tool for the synthesis of polymer architectures that are not available using other polymerization methods[4]. It has been demonstrated that ADMET polymerization can proceed in the presence of heteroatoms and a variety of functional groups, as long as the terminal olefins are far enough apart from them. So we used this synthetic procedure to prepare a set of lineal and branched polyether and polyester polyols with different molecular weight and hydroxyl content that were used to prepare conventional and segmented polyurethanes with shape memory properties in some cases. The transformation of fatty acids in the corresponding oxazolines and its living cationic polymerization has also been explored as a convenient route to produce polyols with control of molecular weight, hydroxyl content and hydroxyl group distribution which allows tuning the properties of the resulting polyurethanes.

Finally, 10-undecenoic, 10-undecynoic and oleic acid derivatives have been exploited as platform chemicals to obtain renewable diols, polyols, diacids and polyacids that have been used to produce linear and crosslinked polyurethanes and polyanhydrides. The coupling between a thiol and a carbon double or triple bond has received recently a growing interest. Thiol-ene and thiol-yne couplings comply with most of the requirements of the concept of a click reaction[5] and so it has been used with hydroxyl and carboxyl-functionalized thiols such as 2-mercaptoethanol, 1-thioglycerol and 3-mercaptopropanoic acid to obtain well defined functionalized structures.

---

[1] Bozell J.J., Patel M., eds. ACS Symposium Series 921.WashingtonDC: American Chemical Society, 2006.
[2] Biermann U., Friedt W., Lang S., Lühs W., Machmüller G., Metzger J.O., Klaas M.R., Schäfer H.J., SchneiderM.P. Angew Chem Int Ed2000; 39: 2206-2224.
[3] Lu Y., Larock R.C. ChemSusChem 2009, 2:136-147.
[4] Schwendeman J. E., Church A. C., Wagener K. B. Adv Synth Catal 2002, 344, 597-613
[5] Dondoni A. Angew. Chem. Int. Ed. 2008, 47, 8995-8997

Hybrid Nanoparticles for Biotechnological Applications

Jose Ramos[1] and Jacqueline Forcada[2]

[1] Grupo de Física de Fluidos y Biocoloides, Departamento de Física Aplicada, Facultad de Ciencias, Universidad de Granada, 18071 Granada, Spain

[2] Institute for Polymer Materials POLYMAT and Grupo de Ingeniería Química, Facultad de Ciencias Químicas, Universidad del País Vasco/EHU, Apdo. 1072, 20080 Donostia-San Sebastián, Spain

jacqueline.forcada@ehu.es

Superparamagnetic iron oxide nanoparticles with appropriate surface chemistry can be used for numerous in vivo applications, such as magnetic resonance imaging (MRI) contrast enhancement, immunoassays, detoxification of biological fluids, hyperthermia, drug delivery, and cell separation. All of these biomedical applications require nanoparticles with high magnetization values, a size smaller than 100 nm, and a narrow particle size distribution. These applications also need peculiar surface coating of the magnetic nanoparticles, which has to be nontoxic and biocompatible, and must also allow for a targetable delivery with particle localization in a specific area. Such magnetic nanoparticles can bind to drugs, proteins, enzymes, antibodies, or nucleotides and can be directed to an organ tissue or tumor using an external magnetic field. In this way, due to the existing interest in new hybrid particles in the colloidal range based on both magnetic and polymeric materials for applications in biotechnological fields, an overview on the preparation and characterization of hybrid (polymeric/inorganic) nanoparticles will be presented focusing on the preparation of magnetic polymer nanoparticles and silica/polymer nanoparticles by different polymerization processes developed to achieve a better control in the morphology of the nanocomposite particles. The different morphologies (from a typical core-shell to a homogeneously distributed morphology) obtained depending on reaction conditions will be revised, emphasizing on the reaction conditions and polymerization processes in dispersed media used [1-6].

In brief, this contribution is focused on the synthesis, characterization, and biotechnological applications of hybrid nanoparticles. The challenge in all the synthesis strategies is their optimized production depending on necessity or biotechnological application in which they could be used. The target is the optimization of the encapsulation of the inorganic nanoparticle into the polymeric matrix (shell) avoiding the production of pure polymeric nanoparticles.

References

[1] Lu, S.; Forcada, J. J. Polym. Sci. Part A: Polym. Chem., 44, (2006) 4187.

[2] Lu, S.; Ramos, J.; Forcada, J., Langmuir, 23, (2007) 12893.

[3] Lu, S.; Qu, R.; Forcada J., Materials Letters, 63, (2009) 770.

[4] Lu, S.; Qu, R.; Forcada J., Materials Letters, 63, (2009) 2539.

[5] Costoyas, A; Ramos, J; Forcada, J., J. Polym. Sci. Part A: Polym. Chem., 47, (2009) 935.

[6] Ramos, J.; Forcada, J., Langmuir, (submitted, March 2011).

Acknowledgments

The Spanish Ministerio de Ciencia e Innovación (MICINN)/Programa Nacional de Materiales (MAT2009-13.155-C04-01) finances this work.

Synthesis of Multicompartment Nanoparticles

Alex M. van Herk, Syed Imran Ali, Hans Heuts

Eindhoven University of Technology
P.O. Box 513, 5600 MB Eindhoven, The Netherlands

a.m.v.herk@tue.nl

In the field of encapsulation of many types of particles like pigments, fillers and clay particles [1,2] tremendous progress has been made and applications of encapsulated inorganic particles are known, for example in car coatings. Core-shell latex particles are applied for many decades.

A new challenge is in the encapsulation of clay platelets striving towards a high aspect ratio of the resulting nanostructured particles. One is struggling with surface tensions there and the thermodynamic driving force to small surface area. Similar problems exist in the field of vesicle polymerization [3]. After careful studies it turned out to be very difficult to produce a thin wall of polymer inside the hydrophobic domain of the vesicle double layer. The most common structure produced is that of the parachute, a latex particle connected to the vesicle structure. Apparently only with strong interactions or covalent bonds between the surfactant and the polymer one is able to produce hollow particles through vesicle polymerization. The field of vesicle polymerization opens many possibilities to produce many different and interesting new nanostructured particles. The phenomenon of phase separation in latex particles not only is controlled by thermodynamic factors (mainly interfacial tensions) but alsoby kinetic factors. Specialty applications like intraocular eye lenses bases on transparent latices are showing the enormous potential of nanocomposites in the area of specialties [4].

So the field of emulsion polymerization is maturing to a science where control on a nanolevel becomes common practice and moreover the synthesis and application of these nanostructured particles can be on bulk scale.

Added to this is the introduction of controlled radical polymerization techniques as an additional means to control molecular microstructure and morphology in latex systems. It will be shown that many different multicompartment structures can be produced while applying the general principles of thermodynamics and kinetics in emulsion polymerizations. One example are the so-called nanobottles where a hollow structure is combined with a latex particle, making a lid for the ‘nanobottle’.

The use of RAFT agents has made it possible to produce flat latex particles during clay encapsulation [5] and responsive nanocapsules [6].

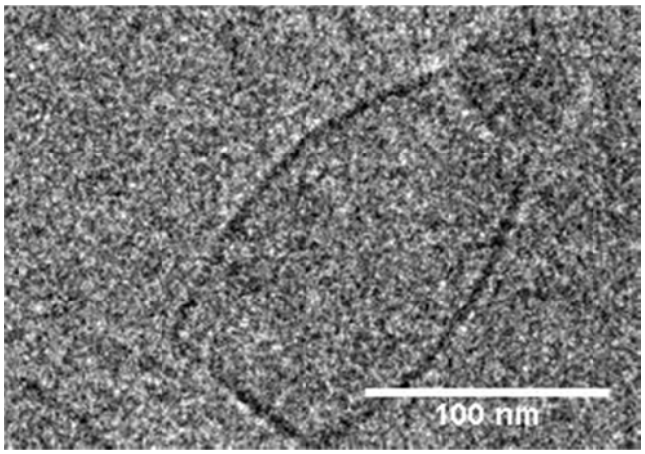

One of a kind nanobottle produced in vesicle polymerization (normal particles look more spherical)

References

1. D.J. Voorn, W. Ming, A.M. van Herk, Clay Platelets Encapsulated Inside latex Particles, *Macromolecules* **2006**, 39, 4654-4656

2. A.M. van Herk and A.L. German, "Microencapsulated pigments and fillers", contribution to the book 'Microspheres, Microcapsules & Liposomes', vol 1 : Preparation & Chemical Applications, Citus Books, London , ed Prof. R Arshady (**1999**)

3. M. Jung, D.H.W. Hubert, P. Bomans, P.M. Frederik, A.M. van Herk, A.L. German

Advanced Materials 12 **2000** 210-213

4. J. Pusch, A.M. van Herk *Macromolecules* 38 **2005**, 6939-6945

5 S.I. Ali, J.P.A. Heuts, B.S. Hawkett, A.M. van Herk, *Langmuir,* 25(18), 10523-10533.

6 S.I. Ali, J.P.A. Heuts, A.M. van Herk

Langmuir, 26, 7848-7858 2010

Synthesis and Characterization of Multivalent Dendritic Glycopolymers and their Use in Life Science Applications

Brigitte Voit and Dietmar Appelhans

Leibniz-Institut für Polymerforschung Dresden e.V., Hohe Strasse 6, 01069 Dresden, Germany

e-mail: voit@ipfdd.de

Introduction Dendritic polymers – both, perfectly branched dendrimers and hyperbranched polymers - can be prepared in a broad variety of structures and exhibit interesting properties like high solubility and functionality, dense globular structure and low solution viscosity.[1] The high control over structure, molar mass and size in dendrimers renders them specifically interesting as functional nanomaterials in biomedical applications.

Results and Discussion Very high biocompatibility as well as specific interactions can be achieved by modifying e.g. poly(propylene imine) dendrimers with dense sugar shells through reductive amination.[2,3]The materials have been synthesized successfully varying the dendritic scaffold and the degree of modification[2,4,5] and we were able to demonstrate their usefulness as nanoscopic delivery system for drugs, biomacromolecules, metal clusters and nanoparticles as well as RNA and DNA into cells in in-vitro and in-vivo experiments.[6]Also, nanodiamands[7] as well as various nanoparticles, prepared in the presences of dendritic glycopolymers, can be decorated with a highly biocompatible oligosaccharide shell.

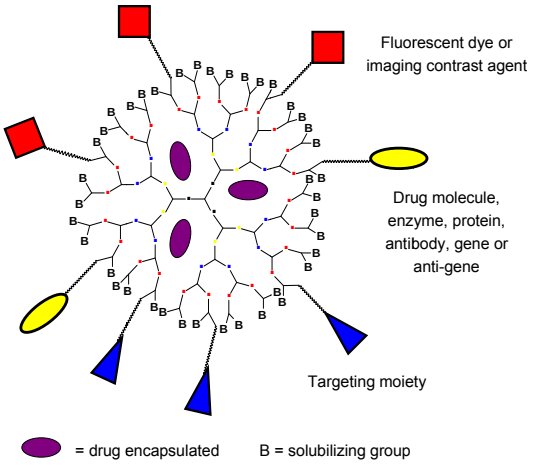

In addition, densely maltose shelled glycodendrimers showed very promising effects to prevent prion aggregation, a first step in the potential treatment of prion and Alzheimer disease.[2,8]Ongoing work is directed to the understanding of the interactions of dendritic glycopolymers towards drugs and biomolecules in solution, including their aggregation behavior under physiological and serum conditions, but also the uptake behavior of the dendritic glycopolymers and their nanocarrier properties towards cells and organs. Further studies are engaged in the bio-distribution and blood circulation of those dendritic glycopolymers and their drug complexes with regard to selective targeting of the drug-nanocarrier complexes towards organs and brain under in-vivo conditions.

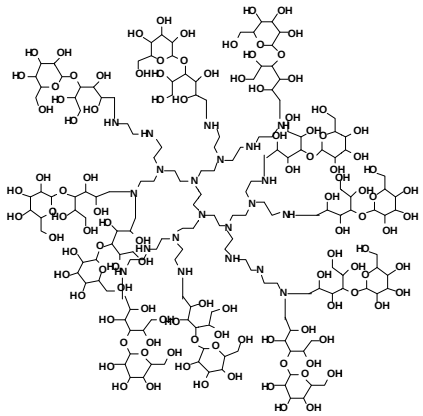

Maltose modified polyethylene imine

Hyperbranched (hb) polymers like polyethylene imine (PEI), which are less well-defined but more easily available than the perfectly branched dendrimers, can as well be modified with various sugar moieties and are highly promising in the field of biosensors and diagnostics.[5] We were able to prove that stable films can be prepared on surfaces which show extremely low unspecific protein adsorption, and allow e.g. the selective adsorption of ATP and other biological relevant molecules.[9] These materials can be further decorated with specific binding units.

References

1. B. Voit, A. Lederer, *Chem. Rev.* **109**, 5924, 2009.

2. B. Klajnert, D. Appelhans, H. Komber, N. Morgner, S. Schwarz, S. Richter, B. Brutschy, M. Ionov, A. K. Tonkikh, M. Bryszewska, B. Voit, *Chem. Eur. J.***14**, 7030, 2008.

3. B. Voit, D. Appelhans, *Macromol. Chem. Phys.* **211**, 727, 2010.

4. D. Appelhans, U. Oertel, R. Mazzeo, H. Komber, J. Hoffmann, S. Weidner, B. Brutschy,B. Voit, M. Ottaviani, *Proc. R. Soc. A,***466**,1489, 2010.

5. D. Appelhans,H. Komber, M.A. Quadir, S. Richter, S. Schwarz,J. van der Vlist, A. Aigner,M. Müller,K. Loos, J. Seidel, K.-F. Arndt, R. Haag, B. Voit, *Biomacromolecules,* **10**, 1114, 2009.

6. S. Höbel, A. Loos, D. Appelhans, S. Schwarz, J Seidel, B. Voit, A. Aigner, *J. Control. Release***149**, 146, 2011.

7. M. Mkandawire, A. Pohl, T. Gubarevich, V. Lapina, D. Appelhans, G.Rödel, W. Pompe, J. Schreiber, J. Opitz, *J. Biophoton.***2**, 596, 2009.

8. M. Fischer, D. Appelhans, B.Klajnert,M.Bryszewska, B. Voit, M. Rogers, *Biomacromolecules*, ***11***, 1314, 2010

9. A. Richter, A. Janke, S. Zschoche, R. Zimmermann, F. Simon, K.-J. Eichhorn, B. Voit, D. Appelhans, *New J. Chem.***34**, 2105, 2010.

Polyester synthesis using enzymatic catalysis by *Yarrowia Lipolytica* lipase

Antonio Martinez-Richa[1,*], *Karla A. Barrera-Rivera*[1] *and Angel Marcos-Fernández*[2]

1. Departamento de Química, Universidad de Guanajuato, Noria alta s/n, Guanajuato, Gto., 36050, México.

2. Departamento de Química y Tecnología de Elastómeros, Instituto de Ciencia y Tecnología de Polímeros (CSIC), Juan de la Cierva No. 3, 28006 Madrid, Spain

*richa@quijote.ugto.mx

Application of biocatalysis to the synthesis of biodegradable polyesters from lactones has been studied in the Polymer group of the University of Guanajuato for the last five years. An efficient process to quantitatively isolate *Yarrowia lipolytica* (YLL) strains was developed in our laboratory, and the extracted lipase was proved to induce ring-opening polymerization (ROP) of lactones (Barrera *et al*, (2008))[1]. Recently, research has been focused to (a) studies on the immobilization of YLL onto different matrices (b) kinetics studies of ROP of lactones under different reaction conditions using immobilized YLL (reaction times, solvent effect, temperature)[2], (3) studies on acylation of isosorbide by immobilized YLL[3]. and (4) chemo-enzymatic synthesis of polyester urethanes

Keyword: Yarrowia lipolytica lipase (YLL); biocatalysis; biodegradable polymers; isosorbide; ROP (ring-opening polymerization)

Introduction

Polymerization reactions catalyzed by enzymes proceed through quimioselective, regiospecific and stereoselective pathways. Lipases are one of the most versatile biocatalysts that bring about a wide range of bioconversion reactions, including ring-opening polymerization (ROP) of cyclic esters. *Yarrowia lipolytica* is a yeast species widely used in industrial applications. Strains of this yeast secrete a set of proteins (alkaline or acid proteases, lipases) that can be quantitatively isolated from the production culture medium[1].

In this presentation, results on the synthesis of biodegradable polyesters using YLL as biocatalyst will be discussed.

Materials and Methods

Polymerizations were carried out in 10 mL vials previously dried and purged with dry nitrogen. In a typical run, monomer (ε-CL), catalyst (immobilized enzyme) and in some cases solvent or ionic liquid were added under dry nitrogen atmosphere. Vials were stoppered with a rubber septum and placed in a thermostated bath at predetermined temperatures and time periods.

Immobilization of lipases: Before immobilization, Lewatit 1026 beads were activated with ethanol (1:10 beads: ethanol), washed with distilled water and dried under vacuum for 24 h at room temperature. The beads (1g) were shaken in a rotatory shaker in 15 mL of lipase solution with 0.1568 mg/mL of YLL at 4ºC for 24 h. After incubation, the carrier was filtered off, washed with distilled water and then dried under vacuum for 24 h at room temperature.

Final polymers were crystallized from chloroform/methanol, separated from the insoluble enzyme by filtration through 10-15 µm glass-fritted filters and dried under vacuum. Molecular weights and conversions during reaction were monitored by ^{1}HNMR. The crystallized polymers were in general analyzed by FT-IR, MALDI-TOF, DSC, WAXS, solution (proton and carbon-13) and solid-state-NMR.

Results and Discussion

Lipase performance is improved in the presence of ionic liquids[2]. Immobilization of enzymes in general improves biocatalytic performance. Immobilized Yarrowia lipolytica lipase (YLL) catalyzes bulk ring opening polymerization of ε-caprolactone in the presence of isosorbide. Biodegradable amphiphilic oligomers can be obtained using this methodology[3]. PCL diols can be synthesized using immobilized YLL. These diols can be quantitatively converted to biodegradables polyurethanes[4].

Conclusions

Various methods to obtain biodegradable polyesters using YLL as catalyst were developed. Information on chemical structure and morphology were derived using different characterization techniques.

References

1. Barrera-Rivera K. A., Flores-Carreón A., Martínez-Richa A., (2008) *Journal of Applied Polymer Science* 109(2), 708-719.

2. Barrera-Rivera K. A., Marcos-Fernández A., Vera-Graziano R., Martínez-Richa A., (2009) *Journal of Polymer Science Part A: Polymer Chemistry*, 47, 5792– 5805.

3. Barrera-Rivera K. A., Martínez-Richa A., (2009) *Macromolecular symposia* 283-284, 144-151.

4. K.A. Barrera-Rivera, A. Marcos-Fernández and A. Martínez-Richa, Chemo-Enzymatic Syntheses of Polyester-Urethanes, in H.N. Cheng and R. A. Gross eds., *Green Polymer Chemistry: Biocatalysis and Biomaterials*, ACS Symposium series 1043, Washington DC, **2010**, Chapter 16, p. 227-235

RAFT polymerization and Various Click Reactions to Develop a Micellar Drug Delivery System for Albendazole

Martina Stenzel, Yoseop Kim, Yue Zhao, Firdaus Mohd Yhaya

Centre for Advanced Macromolecular Design (CAMD), University of New South Wales, Sydney, Australia

Introduction

Albendazole (ABZ), methyl[5-(propylthio)-1-H-benzimidazol-2yl]carbamate, is a benzimidazole derivative containing a broad activity spectrum against intestinal helminth infections. Recently, it has been discovered that ABZ is also highly effective as anti-cancer agent.

Treatment is however hampered due to the poor aqueous solubility of ABZ. The encapsulation of a drug into a polymer matrix such as nanospheres and microspheres is expected to increase the efficacy of a drug as well as to decrease potential side effects. The slow release of drug from the carrier ensures its long-term supply. Block copolymer micelles have been widely studied as a drug carrier system. micelle to protect the drug from immediate renal elimination. Here, the development of a drug delivery system for albendazole is discussed. The block copolymers are synthesized via RAFT polymerization [1], but in order to achieve a more stable drug carrier, micelles were crosslinked using amine- or thiol-isocyanate click reactions. In addition, to increase drug loading and delay drug release, the polymers are conjugated with β-cyclodextrin, which can host ABZ as guest.

Results and discussion

Group Contribution Method was used to estimate the partial solubility parameters for the drug (ABZ) and various polymers. Poly(methyl methacrylate) (PMMA) was identified as an optimum candidate using this predictive tool while poly(lauryl methacrylate) (PLMA) was calculated to have only a low compatibility with ABZ. Block copolymers were prepared via reversible addition fragmentation chain transfer (RAFT) polymerization resulting using poly(polyethylene glycol methyl ether methacrylate) as the water-soluble block and various ratios of MMA and LMA to determine the optimum polymer composition of the core of the micelle to achieve highest drug loading. Drug loading of the micelles with ABZ confirm that the different compatibilities affect the loading and retention time of the drug with most drug being loading in micelles with PMMA in the core while increasing amount of LMA decrease the amount of loaded drug and also lead to faster drug release. The micelles are readily taken up by tumour cell, OVCAR-3, although the uptake abruptly stops when the concentration reaches a certain critical low value. The uptake could be enhanced by decorating the micelles with RGD, which could be conjugated to the polymer endgroup when a aldehyde containing RAFT agent was employed.

However, the low stability of the drug carrier and the associated low uptake of micelles at low concentration led to the further evolution of the current drug carrier. The stable micelles, which can be created by crosslinking, should in addition have features that encapsulate the drug safely in the blood stream, but release the drug rapidly once the micelle has been taken up by the cell. A block copolymer, with reactive isocyanate units was prepared via the RAFT process and self-assembled into micelles. Addition of 1,8 diamino octane leads to crosslinking of the micelles, but also to excess amine groups that can respond to changes of pH value. The drug, albendazole (ABZ), was encapsulated tightly at pH7, but released suddenly at pH5. Cell experiments using OVCAR-3 cell lines show the efficient uptake of these nanoparticles and the fast release of the drug.

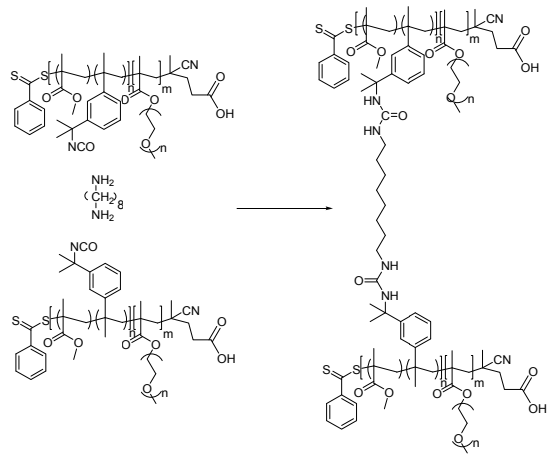

Figure 1: Synthesis of pH-responsive core-crosslinked block copolymers micelles; excess diamines will lead to amine pendant group

Instead of using amine-isocyanate click reaction, this approach has also been tested using thiol-isocyanate click reaction, which will not result in pH-responsive, but in a system with disulfide groups.

An alternative route to generate drug delivery carriers is by attaching monofunctional β-cyclodextrin to a reactive polymer. Two techniques were employed, azide-alkyne click reaction and thiol-ene reaction, both leading to high conjugation yields. The β-cyclodextrin polymers were found to enhance the toxicity of ABZ/

Conclusion

The combination of RAFT polymerization with various click reaction can be used to build up molecular architectures for a specific drug delivery problem shown here using the drug albendazole. Both approaches, cross-linked micelles and micelles with β-cyclodextrin, were found to be equally promising carriers

References

1. Stenzel, M. H. *Chemical Communications* **2008**, (30), 3486-3503.

Hybrid Brushes Nanoparticles: synthesis and properties

Julieta Paez, Ariel Cappelletti and Miriam Strumia

IMBIV (Conicet). Facultad de Ciencias Químicas. Universidad Nacional de Córdoba. Ciudad Universitaria. (5000) Córdoba. Argentina.

mcs@fcq.unc.edu.ar

Introduction

Recently, the preparation of organic-inorganic hybrid materials that utilizes various supramolecular driving forces has been progressing rapidly. In particular, organic molecular or nanoscale materials that are tethered on solid supports such as spherical particles, thin solid films, or metal surfaces form self-assembling monolayers with specific functions. This possibility of the creation of well-defined nanohybrid materials with specific properties is of great significance for fundamental research and for their use in numerous potential applications, such as engineering, communications, robotic and medicine for therapeutic drug delivery and the development of treatments for a variety of diseases and disorders. The rise of nanomaterials correlates with further advances in these disciplines[1].

One of the fundamental aspects of research in nanochemistry is the synthesis and morphological control of metallic nanoparticles (NPs). The funtionalization the surface of NPs and to improve the particles compatibility with different environments by the proper attachment of organic monomer or polymer groups has therefore attracted much interest.

In nanochemistry, the term "dendronization" describes the covalent or supramolecular interaction between dendrons and non-dendritic substrates, allowing the preparation of new hybrid materials with outstanding properties.[2] In this context, making use of dendritic structures as building blocks is based on the possibility of systematically and rigorously controlling properties of the system such as size, shape, number and type of functional groups. Following this approach, it has been reported the preparation of protein-resistant surfaces,[3] and the design of electroactive surfaces as well. Moreover, the combination of dendritic molecules with metallic or oxide nanoparticles has led to the construction of hybrid materials with a huge variety of applications, for example in the preparation of nanoelectronic materials, sensor devices, or nanocatalysis, among others.[4]

Our research group is working on the chemical modification of polymers and different substrates using dendritic molecules as building blocks. In aprevious work[5], we presented the study of the hydrophobic/hydrophilic balance of a family of dendrons synthesized in our labs bearing a different number and nature of functional groups on their surface. The selection of the structure in the construction of these molecules was based on a synthetic strategy to generate a branched effect on the properties of the resulting building block and the subsequently constructed product. Similarly, we reported[6-8] the use of some of those grafting molecules to modify the chemical/physical properties of linear and crosslinked polymers, films and electrodes. Important changes on the properties of these dendronized products were observed and they are strongly dependent on the chemical nature of the dendrons used.

In this occasion, we will describe different synthetic routes used to obtain functionalized gold and magnetic NPs. The methodologies of "*grafting from*" and "*grafting to*" were choosed for the chemical surface modification of the NPs. They were modified by polymerization of thermosensible monomers and by the covalent bond of different dendrons previously synthesized in our labs. The characterization and the physical/chemical properties were determined. The results found and the comparative analysis on the surface chemical modification of the gold and magnetic nanoparticles, will be presented.

Acknowledgement*:* The authors wish to thank FONCYT, CONICET and SECYT of UNC for their financial assistance, and CONICET for the fellowships awarded to Julieta Paez and Ariel Cappelletti.

REFERENCES:

1.A. Faraji, P. Wipf. Bioorganic & Medicinal Chemistry, 17, 2950-62, 2009.

2. D. Tomalia. *Aldrichimica Acta*, *37*, 39, 2004.

3. M. Wyszogrodzka, R. Haag. *Langmuir, 25 (10)*, 5703,2009.

4. X. Zhang, Q. Guo, D. Cui. *Sensors*, *9*, 1033,2009.

5. Calderón M, Monzón L, Martinelli M, Yudi L, Strumia M. *Langmuir*; *24*:6343-6350, 2008.

6. Marisa Martinelli, Marcelo Calderón, Esteban Rodríguez, Juan J. Freire, Miriam C. Strumia. *Eur. Polym. Journal*. 43, 1978-85, 2007**.**

7. Martinelli M, Calderón M, Rodríguez E, Freire JJ, Strumia MC. *Eur. Polym. J.*; *43*: 1978-1985, 2007.

8. J. Paez, P. Froimowicz, A. Baruzzi, M. Strumia, V. Brunetti. *Electrochem. Commun., 10*, 541, 2008.

Organocatalysis of Polymerizations: The Contribution of *N*-Heterocyclic Carbenes

Jean Raynaud, Julien Pinaud, Maréva Fèvre, Joan Vignolle, Daniel Taton and Yves Gnanou,

Université de Bordeaux & Centre National de la Recherche Scientifique
Laboratoire de Chimie des Polymères Organiques, 16 avenue Pey-Berland
Pessac cedex, F-33607 France

gnanou@enscpb.fr

Introduction:

Carbene chemistry has received a considerable attention in molecular synthesis, and more recently, in macromolecular chemistry as well. Among organocatalysts, *N*-heterocyclic carbenes (NHCs) have emerged as the most efficient and versatile for a variety of organic transformations.

Results and discussion:

After Hedrick, Waymouth *et al.* established that NHCs could catalyze the ring-opening polymerization (ROP) of cyclic esters, we have expanded the use of these organic activators to various polymerization reactions, including ROP of epoxides,[1-3] group transfer polymerization (GTP) of (meth)acrylics,[4] and step-growth polymerization of terephtaldehyde.[5]

For instance, NHCs can trigger the GTP of both methacrylic and acrylic monomers initiated by a silyl ketene acetal (SKA) both in polar and apolar media,[4] by an associative (concerted) mechanism allowing the synthesis of all acrylic block copolymers by sequential GTP.[4]

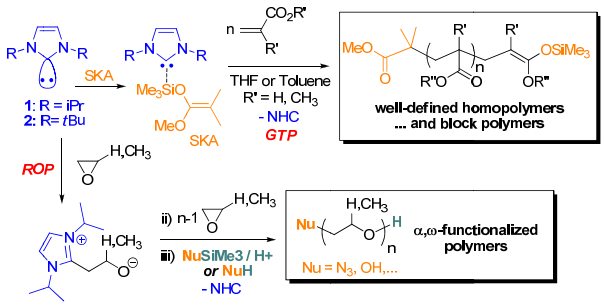

NHC-induced GTP of (meth)acrylics and ROP of epoxides

The same NHCs can serve either as organic initiators or as true organocatalysts for ROP of both ethylene and propylene oxides, *via* the formation of a zwitterionic imidazolium alkoxide intermediate.[1-3] Use of a functionalizing agent of NuE-type (e.g. Nu= -OH; $-N_3$; $-OCH_2C{\equiv}CH$ and E= -H or $-SiMe_3$) as a quencher [1-3] or as a chain moderator at the beginning of the reaction,[2] gives a direct access to well-defined heterodifunctionalized poly(ethylene oxide)s and poly(propylene oxide)s.

The lecture will also describe the design of recyclable poly(NHC)s generated from polymeric ionic liquids (PILs) that are anionic-responsive polyelectrolytes. These poly(NHC)s have been evaluated for homogeneous and heterogeneous catalysis of model reactions, namely benzoin condensation and transesterification.

Conclusions:

This presentation summarizes the recent advances in organocatalyzed polymerizations. It highlights the advantages associated with the use of organic catalysts and namely of NHCs which now appear as viable substitutes for classical metallic catalysts, in a context where the demand for sustainable and environmentally-friendly reactants and processes steadily increases. The lecture will unveil and review those among NHCs that can trigger polymerization and also monomers amenable to organocatalysis by these NHCs. Will also be thoroughly discussed the mechanisms involved in each pair of NHC and monomer and the controlled/ living character for chain polymerizations.

References:

1)Raynaud, J.; Absalon, C.; Gnanou, Y.; Taton, D. *J. Am. Chem. Soc.*,**2009**, *131*, 3201;

2) Raynaud, J.; Absalon, C.; Gnanou, Y.; Taton, D. *Macromolecules,* **2010**, *43*, 2814 ;

3) Raynaud, J.; Nzahou Ottou, W.; Gnanou, Y.; Taton, D. *Chem. Commun.***2010**, 3203 ;

4) (a) Raynaud, J.; Ciolino, A.; Baceiredo, A.; Destarac, M.; Bonnette, F.; Kato, T.; Gnanou, Y.; Taton, D. *Ang. Chem. Int. Ed.*, **2008**, *47*, 5390. (b) Raynaud, J.; Gnanou, Y.; Taton, D. *Macromolecules,***2009**, *42*, 5996 ; 5) Pinaud, J.; Vijayakrishna, K.; Taton, D.; Gnanou, Y. *Macromolecules,***2009**, *42*, 4932.

Self-Assembly of Nanocomposite Polymer Latex and Structural Color Films

*Bo You, Lingli Duan, Zhehong Shen, Limin Wu**

Department of Materials Science and the Key Laboratory of Molecular Engineering of Polymers of MOE , Fudan University, Shanghai 200433, China

lmw@fudan.edu.cn

In recent years, the assembly of colloidal spheres into two-dimensional and three-dimensional ordered structures has attract great attention since it is a simple, cost-efficient strategy to fabricate crystal films for some important potential applications, such as photonic crystals, biosensors, templates, and even paints, photonic papers and cosmetics due to the structural colors of the crystal films.

Recently, we have report for the first time that the "soft" polymer spheres can also form three-dimensional ordered structure with the aid of nanosilica particles. In this method, monodisperse "soft" polymer spheres colloids are synthesized by surfactant-free emulsion polymerization and then blended with colloidal silica to obtain nanocomposite polymer latex. When this nanocomposite polymer latex is cast on a glass substrate and dried at room temperature, these "soft" polymer spheres could periodically arrange, forming three-dimensional ordered films in large-scale area.

Figure 1 shows the cross-sectional SEM images and the typical TEM image of the polymer films with various nanosilica contents. It can be seen that the pure latex polymer film appears no visible ordered structure (Figure 1a), just as typical polymer latex. When 2 wt%, 5 wt% or even 10 wt% of nanosilica was blended with this polymer latex, the films present an ordered array of polymer spheres in the cross-sections (Figure 1b−1d). But more nanosilica would cause irregular array (Figure 1e). The typical TEM image (Figure 1f) clearly indicates a hexagonal face centered cubic (fcc) array of the polymer spheres. The corresponding live Fast Fourier Transform Algorithm image, as displayed in the inset of Fig. 1f, also strongly suggests that the three-dimensional ordered structure exists in the nanocomposite film. The reason why the "soft" polymer spheres can self-assemble into three-dimensional structure with the aid of nanosilica particles, is probably attributed to the interaction between the −SiOH groups of nanosilica particles and −COOH groups of polymer spheres. It is this interaction that nanosilica particles can be adsorbed on the surfaces of the polymer spheres, which can interdict the deformation and coalescence of "soft"

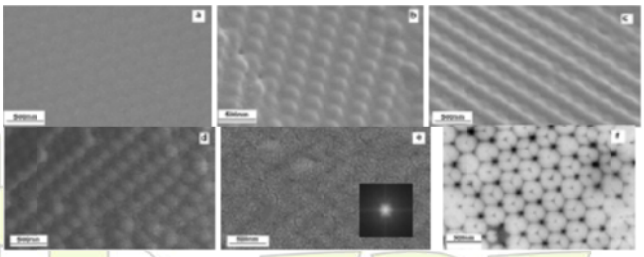

Figure 1. The cross-sectional SEM images and TEM image of films with various nanosilica contents. a) pure polymer, b) 2 wt%, c) 5 wt%, d) 10 wt%, e) 20 wt%, f) typical TEM image of the film.

These ordered films display brilliant green color, while the pure polymer film appears colorless and transparent just as the typical latex polymer film and too much nanosilica causes a white film. And the peak position of the stop band and the color of the film depend on the refractive index contrast between polymer and nanosilica, relatively filling ratio and the diameter of polymer spheres. For example, when the sphere size increases from 180, 210, 240, 260, 270, 310 to 340 nm, the film exhibits different brilliant colors transiting from blue to red (Figure 2). And their corresponding photonic band red-shifts from a wavelength of 435, 450, 505, 530, 545, 605 to 640 nm. This means that the structural color is tunable.

Figure 2. The photographs of films with various sizes of polymer spheres.a) 180, b) 210, c) 240, d) 260, e) 270, f) 310, g) 340 nm

Furthermore, we can fabricate a reversible solvatochromic--responsive coatings and films, as demonstrated in Figure 3.

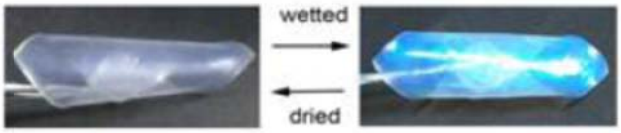

Figure 3. Reversible color change of the crystal film

And the chroma of the structural colors can be obviously improved by doping carbon black into the self−assembly of colloidal polymer spheres and nanosilica particles, as shown in Figure 4.

Figure 4. Intuitionistic comparison between the structural colors of CC films and peacock feathers. The CC films with carbon black (up) and without carbon black (down)

References

[1] B. You, N. Wen, L. Shi, L. Wu, J. Zi, *J. Mater. Chem.*, **2009**, 19, 3594.

[2] Z. Shen, Y. Zhu, L. Wu, B. You, J. Zi, *Langmuir*, **2010**, 26, 6604

[3] L. Duan, S. Zhou, B. You, L. Wu, *J. Mater. Chem.*, **2010**, DOI:10.1039/C0JM02484H

[4] L. Duan, B. You, L. Wu, M. Chen, *JCIS,* **2010,** 353, 163

[5] S. Zhang, S. Zhou, B. You, L. Wu, *Macromolecules*, **2009**, 42, 3591

[6] B. You, L. Shi, N. Wen, X. Liu, L. Wu, J. Zi, *Macromolecules,* **2008**, 41, 6624

[7] Z. Shen, L.Shi, B. You, L. Wu, *J. Mater. Chem.,* submitted.

ABSTRACTS

INVITED LECTURES

Topic 2: New Analytical and Characterization Tools

New Opportunities with Spectroscopic Imaging

Sergei G. Kazarian

Department of Chemical Engineering, Imperial College London, UK

s.kazarian@imperial.ac.uk

FTIR spectroscopic imaging has emerged as a powerful tool for characterisation of polymeric materials. This talk will outline the research we are developing in this area with focus on micro- and macro ATR (Attenuated Total Reflection)-FTIR spectroscopic imaging applied to heterogeneous materials. Main advantage of micro ATR-FTIR imaging using a germanium microscope objective is its enhanced spatial resolution. The advantages of macro ATR-FTIR imaging include its versatility and the relative ease of sample preparation. Recent new developments in macro ATR-FTIR imaging with the use of inverted prism crystals show good potential with applications to polymer interdiffusion, mixing and phase separation, studies of polymer blends and layered polymeric structures. New opportunities exist to obtain ATR-FTIR images of the same sample from different depths using a diamond ATR imaging accessory. This approach involved the introduction of a movable aperture to restrict the angles of incidence to certain values. [1, 2]

Results and Discussions

A most recent application of this new approach has been demonstrated for layered polymeric structures. As the evanescent wave in ATR spectroscopy is not limited by diffraction, it was possible to resolve thin sandwiched polymer-layers non-destructively within a layered polymer system. Chemical images were obtained from the layers of different thickness of the sample by moving a lab-made aperture to specific positions on the condenser lens of the ATR accessory. Sequences of spectroscopic images illustrate the successive appearance of thin, sandwiched layers of polybutylmethacrylate (400 nm thick) and polycarbonate (300 nm thick) in different depths of the stack of polymer layers. The depth resolution of variable angle ATR-FTIR imaging in the z-direction is sufficiently high to detect surface roughness at the interface between different polymer layers. Two different stacks of polymers with reordered sandwichlayers were imaged simultaneously, demonstrating the potential of variable angle ATR-FT-IR for 3D-imaging of a sample with 3D-heterogeneity which can be a powerful analytical technique for characterisation of polymeric materials.

Another exciting recent application of this imaging approach has been demonstrated by the first FTIR images of flows in the channels of microfluidic devices. This opens many new possibilities of using macro ATRFTIR imaging as a novel detection method in the studies of microfluidics. [3, 4]

Conclusions

Significant potential exists in the applications of FTIR spectroscopic imaging to polymeric materials using attenuated total reflection in micro and macro imaging modes.

Macro ATR imaging with variable angle of incidence provided opportunity of destructive, three-dimensional chemical imaging of polymeric materials with high z-resolution. This approach may have considerable impact in the investigation of thin or buried layers in coating and lamination industry, in studies of polymer interdiffusion. Many opportunities are also present for applications of ATR-FTIR imaging in macro mode for studying dynamic systems.

Acknowledgements

SGK acknowledges the research funding from the European Research Council under the *European Community's* Seventh Framework Programme (*FP7/2007-2013)* / ERC *advanced grant agreement* n° [*227950*] and thanks Drs. T. Frosch, K.L. A. Chan, JT Cabral, F.H. Tay and Mr. H. C. Wong.

References

[1] S. G. Kazarian, K. L.A. Chan *Applied Spectroscopy* **64**, 135A-152A (2010).

[2]T. Frosch, K. L. A. Chan, H. C. Wong, J.T. Cabral, G. Kazarian *Langmuir* **26**, 19027–19032 (2010).

[3] S. G. Kazarian *Anal. Bioanal. Chem* **388**, 529-532 (2010)

[4] K. L. A. Chan, X. Niu, A. J. de Mello, S. G. Kazarian S. G. *Lab on a Chip* **10**, 2170-2174 (2010).

Elucidation of Macromolecular Structure using the MHS Plot

Bassem Sabagh, Sandrine Olivier, Paul G Clarke.

Malvern Instruments

Bassem.sabagh@malvern.com

Abstract: The Mark-Houwink-Sakurada (MHS) plot is a powerful tool for analysing the structure of macromolecules because it describes the relationship between the intrinsic viscosity and the molecular weight of polymer molecules in solution.

$$IV = KM^{\alpha}$$

The traditional construction of the plot from discrete intrinsic viscosity and molecular weight measurements is a laborious and difficult task, but over the last 20 years, the introduction and then improvement and simplification of Triple Detection GPC has given rapid access to accurate MHS plots. This paper will describe how these plots are so easily accessed and illustrate how they are used to analyse the structure of a variety of polymers. It will look into the information that can be obtained and use this to compare samples qualitatively describing conformation, or quantitatively with calculation of branching number and frequency via the Zimm-Stockmayer approach.

The Use of Analytical Techniques in the Study and Development of Structural Adhesives

Senén Paz Abuín

GAIRESA

senen@gairesa.com

In a pure sense the adhesion is a measurement of the attractive/s force/s which maintains two surfaces intimately bonded[1]. According to this definition it is clear that if the attractive forces increase, the value of adhesion should increase in the same direction. In the case of solid surfaces, even a fractured material, it is highly difficult to reach a reasonable contact area between two surfaces. A liquid, capable to wet both surfaces, can fill all irregularities and make a new imperfections-free surface. This liquid can be very suitable for many purposes if it keeps the two surfaces bonded together through an adhesive/cohesive joint. Such a liquid, either in the initial state or when converted into a solid, is called an adhesive. Keeping in mind this idea of an adhesive, it is clear that mainly epoxy, acrylic and polyurethane prepolymers can be suitable as raw material for adhesives. They can wet most surfaces and develop different types of chemical groups capable of originating very high attractive and interactive forces with many solids.

The knowledge of the evolution of reaction is extremely important due to the great influence on final properties and behaviour of the adhesive. A partially cured or incompletely cured adhesive contains unreacted compounds that can result in reduced bond strength and poor environmental resistance and durability. Cure monitoring requires the measurement of a selected material property in order to assess the level of cure. Many different test methods are used to measure the cure rate and cure evolution of polymeric adhesives. The cure implies a study under different temperatures and conditions and several analytical techniques as Fourier Transform Infrared Spectroscopy (FTIR), Differential Scanning Calorimetry (DSC), Rheology and Dynamomechanical Analysis (DMA) can be used to follow the reaction.

1. FT-IR. Due to the fact that in the fingerprint region there are many bands, the near region[2] is the preferred option for quantification purposes.

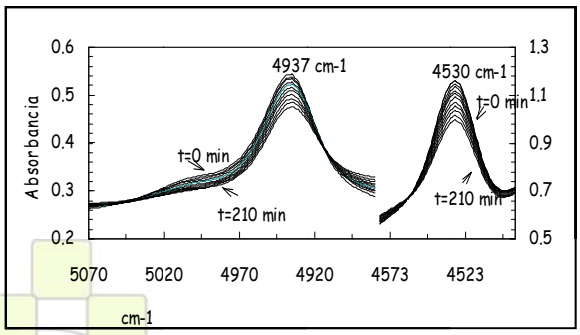

Figure 1. Quantitative FT-NIR experiment to follow the epoxy-amine cure

2. DSC. In spite of that this technique does not give information on the evolution of monomers separately, it is a very powerful method to follow the cure and thermal transitions[3].

3. RHEOLOGY. Rheological properties such as the viscosity and the dynamic modulus can be directly correlated to the evolving physical and mechanical properties of the polymer during cure[4]. Oscillation tests in a controlled stress rheometer can provide a total curing profile for polymeric adhesives.

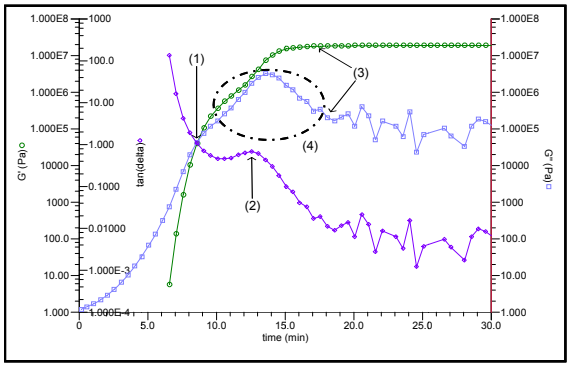

Figure 2. Stages in an epoxy-amine cure reaction by rheology

4. DMA. The cohesive body of an adhesive can be properly evaluated with the help of this technique. DMA is a sensitive probe of molecular mobility. Thus, measurement of loss modulus provides a convenient method for the identification of mechanical relaxation temperatures.

REFERENCES

1. S. Paz Abuín in "Epoxy Polymers.New Materials and Innovations", J.P. Pascault and R.J.J. Williams, Ed., Wiley-VCH, Weinheim (2010).

2. A. López-Quintela, P. Prendes, M. Pazos-Pellín, M. Paz and S. Paz-Abuín, *Macromolecules,* 31(15), pp 4770-4776 (1998).

3. J. P. Pascault, H. Sauterau, J Verdu and R. J. J. Williams in "*Thermosetting Polymers"*. Ed. Marcel Dekker, New York (2002).

4. P. J. Halley, M. E. Mackay and G. A. George.*High Performance Polymers*, 6 pp 405-414 (1994).

Solid State NMR Methods for Studying Functional Macromolecular and Supramolecular Systems

Hans Wolfgang Spiess

Max Planck Institute for Polymer Research, Ackermannweg 10, 55128 Mainz, Germany

spiess@mpip-mainz.mpg.de

Nanostructures are in the focus of current materials science. They occur in advanced synthetic as well as in biological systems through self-assembly of carefully chosen building blocks. Secondary interactions such as hydrogen bonding, aromatic π-π interactions, electrostatic forces and attachment to surfaces are of central importance. Despite being highly ordered on a local scale, such systems often do not crystallize. Therefore, their structures cannot be determined by conventional X-ray crystallography or neutron scattering. Alternatives are needed which should provide structural and dynamic information, preferably requiring only small amounts of as-synthesized samples, without the need of isotopic labeling.

High resolution solid state NMR can meet these requirements [1], provided that sufficiently selective information can be extracted from the corresponding spectra. For that purpose solid state ^{1}H, ^{13}C, and ^{15}N NMR techniques have been developed combining fast MAS and DQ NMR spectroscopy, which make use of the homonuclear and heteronuclear dipole-dipole couplings. These techniques have provided new insight in hydrogen bonded structures in the solid state [2], columnar stacking and molecular dynamics of discotics [3, 4], as well as self-assembly and dynamics of polypeptides [5]. For full structural elucidation, the spectroscopic data have to be combined with other techniques such as scattering and computer simulation [1]. The techniques will be introduced and the findings from NMR will be related to the function of such materials, such as proton conductivity [2] and photoconductivity [5].

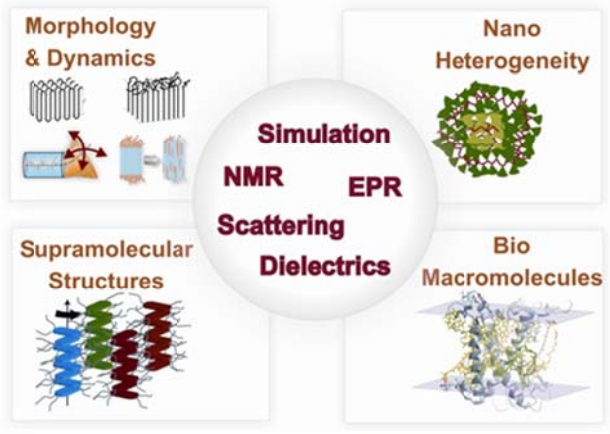

Figure 1: Overview of systems, phenomena and techniques for studying structure and dynamics in functional macromoleular and supramolecular systems.

References

[1] H. W. Spiess, Macromolecules, **43**, 5479–5491 (2010)

[2] Ü. Akbey, S. Granados-Focil, B. Coughlin, R. Graf, H. W. Spiess, J. Phys. Chem. **B 113**, 9151–9160 (2009).

[3] M. M. Elmahdy, X. Dou, G. Floudas, M. Mondeshki, H.W. Spiess, H.-J.Butt, and **K**. Müllen, J. Am. Chem. Soc. **130**, 5311-5319 (2008).

[4] M. R. Hansen, T. Schnitzler; W. Pisula, R. Graf; K. Müllen, H.W. Spiess, Angew. Chem. Int. Ed. **48**, 4621 – 4624 (2009).

[4] G. Floudas, H. W. Spiess, Macromol. Rapid Commun.**30**, 278–298 (2009).

[5] H. N. Tsao, D. M. Cho, I. Park, M. R. Hansen, A. Mavrinskiy, Do Y. Yoon, R. Graf, W. Pisula, H. W. Spiess, K. Müllen, Am. Chem. Soc. **133**, in press (2011)

.

Effect of (3,1) Chain-Walking Defects Compared with Other Regio and Constitutional Defects on the Crystallization and Melting of Isotactic Poly(propylene)

R. G. Alamo[*], *C. Ruiz-Orta, J.P. Fernandez-Blazquez, A. M. Anderson, G.W. Coates*

[1]FAMU/FSU College of Engineering, Department of Chemical and Biomedical Engineering, Tallahassee, FL, USA
[2]Department of Chemistry and Chemical Biology, Baker Laboratory, Cornell University, Ithaca, NY

alamo@eng.fsu.edu

Introduction. The commercial success of novel polyolefins and the extended range of applications compared to classical commodity polyethylenes and poly(propylenes) used in the past are due by in large to a variety of possible modifications of the basic material. These modifications are feasible in situ, i.e. in the polymerization reactor, due to the development of new catalysts able to copolymerize olefin monomers with non-polar and polar comonomers and at a much higher levels of incorporation while controlling molecular weight and comonomer distribution. Recently, a new family of polypropylene has been synthesized via living polymerization with late metal, nickel α-diimine catalysts. These polymers differ from polypropylene produced by early metal catalysts due to chain-walking events which often result in unique defect microstructures. The comparison of (3,1) *i*PP crystalline properties with those of random propylene ethylene (PE) copolymers is of interest due to the generation in the novel *i*PP of backbone ethylene runs via (3,1) enchainments that are, in principle, of a similar nature to the ethylene runs resulting from copolymerization with ethylene. Alternatively, if chain walking defects are generated as random events and are excluded from the crystalline regions, their melting and crystalline properties should parallel the behavior of propylene 1-hexene (PH) (< 13 mol% comonomer) and propylene 1-octene (PO) since both co-units are known to be excluded from the crystals. With complexes for the isotactic polymerization of propylene in hand, a detailed ^{13}C NMR study on polypropylene microstructure and crystalline properties was pursued.

Materials and Methods. Two series of (3,1) iPP were synthesized using two living nickel α-diimine complexes (*rac-1*and *rac-4*) activated with methylaluminoxane (MAO) as described in prior works (1,2). Detailed defect characterization was obtained from high resolution ^{13}C NMR spectra in tetrachloroethane-d_2 using a Varian spectrometer with a frequency of 700 MHz on ^{1}H. The total point defect content encompasses a range between 3 and ~ 18 mol% for both series. The melting peaks, T_m, heat of fusion, ΔH, and overall crystallization kinetics were followed by DSC. Levels of crystallinity, polymorphic behaviour and crystal thicknesses were obtained from wide and small angle x-ray diffractograms (SAXS, WAXD) using a Bruker Nanostar diffractometer operating at ambient temperature on samples that were previously isothermally crystallized either in the DSC or in thermostated baths. Molecular weights (M_n and M_w) and polydispersities were determined by high temperature gel permeation chromatography (GPC) in a Waters Alliance GPCV 2000 GPC equipped with a Waters DRI detector and viscometer.

Results and Discussion. The thermodynamic, structural and mechanical properties of isotactic polypropylene depend strongly on the type, content and distribution of defects (other than isotactic (1,2) additions) generated during synthesis. Novel iPP synthesized with late metal catalysts (*rac-1*and *rac-4*) contained unique defects characterized by isolated and successive groups of (2,1) and (3,1) enchainments, all identified by solution state ^{13}C NMR spectroscopy. Although the nature of the defects is similar to addition of ethylene units, the impact in sequence packing and development of the crystalline state is rather different. The ethylene unit enters the *i*PP crystal, while the (3,1) defect is rejected. Compared with earlier metallocene *i*PP, PH and PO copolymers used as control, *i*PP with chain-walking defects melt at lower temperatures and display a dramatic depression of crystallinity on a customary point defect molar composition per 100 monomers. These features, coupled with reduced crystallization rates, lower crystallite thicknesses and enhanced contents of crystallites in the gamma phase, are associated with a shortening of isotactic sequence lengths which are caused by the bulky nature of most (3,1) associated defects when compared with random copolymers. Chain-walking defects, such as (3,1) enchainments, decrease the level of *i*PP crystallinity at a much faster rate than the more common defects found in Ziegler-Natta or early metallocene made *i*PP as well as propylene random 1-alkene copolymers.

The experimental increasing gap in crystallinity between (3,1) *i*PP and propylene copolymers with increasing defect concentration is also explained by equilibrium basis. Plotted on the basis of Flory's equilibrium theory, the melting temperature-composition behavior of late metal catalyzed iPP closely follows the behavior of PH and PO random copolymers indicating that the defects are *random-blocky* or generated on a random fashion but of a defined blocky monomer nature.

Conclusion. In reference to defects generated in iPP by earlier metal catalysts, iPP synthesized with α-diimine Ni(II) late metal catalysts have (3,1) enchainments with well defined structures. These defects cause a shortening of crystallizable sequence length with a dramatic effect on decreasing crystallinity level.

References

1. Rose, J. M.; Cherian, A. E.; Coates, G. W. *J. Am. Chem. Soc.* **2006**, *128*, 4186–4187

2. Rose, J. M.; et al. *Macromolecules***2008**, *41*, 9548-9555.

Acknowledgements: We acknowledge funding of this work by the USA National Science Foundation.

Towards Complex and Integrated Platforms in Nanotechnology Employing Responsive Polymer-Metal-Semiconductor Hybrid Materials

G. Julius Vancso

University of Twente, MESA+ Institute for Nanotechnology, P.O. Box 7500 AE, Enschede, The Netherlands

g.j.vancso@utwente.nl

Nanotechnology deals with the design, fabrication, study, and applications of materials structures, platforms, and devices that have enhanced or novel properties and functions due to nanoscale control of the elementary materials objects that constitute them. These objects can include atoms, molecules, nanoparticles and their simple assemblies. Although these building blocks often can be further divided using physical or chemical methods, they constitute from the nanotechnological point of view the smallest i.e. elementary constituents. As breaking up matter to smaller units in materials nanotechnology is not sensible beyond these building blocks, nanotechnology has often been recognized as "the ultimate production technology".

At the early stages of nanotechnology focus was laid on surface structures and their assemblies. These could be studied and manipulated by scanning probe techniques "bottom up" from the length scale of the individual objects in a directly controlled fashion, either between two nanoobjects, or between a micro (or macro) object and a nanoobject. Top down miniaturization approaches, most notably in semiconductor industries, have reached control of structures at the length scales of single polymer chains,

e.g. in Intel's 3-gate transistors featuring 32-22 nm technologies. Due to the swift development of materials chemistry used in preparing the elementary nanotechnology building "bricks", as well as due to the tremendous progress in the development of experimental technologies such as scanning probe techniques, single molecule optics, optical tweezers, single molecule 3-dimensional (3D) NMR, etc..., a paradigm shift is emerging in materials nanotechnology. This paradigm shift expands the horizons of materials technology to include full 3D "bottom up" control of complex, integrated materials nanostructures for advanced functions. Essential for this paradigm shift is the use of complementary materials including hybrid systems of synthetic and biological polymers, metal-as well as semiconductor nanostructures, and other nanoobjects such as dendrimers, fullarenes, tailored nanotubes, etc. For advanced functions, on the other hand, addressability and responsiveness of the active elements of these integrated nanostructures become indispensable.

In this presentation we shall provide examples for complex, functional metal nanoparticle-polymer nanostructures first, from the perspective of macromolecular nanotechnology. Corresponding case studies obtained in our laboratories will include description of the design, synthesis, characterization and applications of a stimulus-responsive polymer brush-gel platform [1] grafted from the walls of a microreactor which is first used to obtain designer metal nanoparticles with catalytic activity, embedded in the brush gels. Such microreactors exhibit substantially enhanced catalytic activity in various reactions. Polymer-semiconductor nanocrystal integrated systems allow one to fabricate complex water soluble platforms featuring fluorescent semiconductor nanocrystals (Quantum Dots, QDs) as robust optical labels, versatile optical transducers and active constituents in medical applications and for possible initiation of controlled cancer cell apoptosis. As a representative example, huisgen 1,3-dipolar cycloaddition "click" reaction with functional quantum dots and magnetic nanoparticles in water is presented [2]. The introduction of "click" enabling groups on the surface of the nanoparticles is combined into one step with a transfer into water process. The reaction between acetylene and azide groups is used for the fabrication of covalent spherical assemblies encompassing QDs or iron oxide magnetic particles in solution. Finally, detection of an analyte via supramolecular host-guest binding and quantum dot (QD)-based fluorescence resonance energy transfer (FRET) signal transduction mechanism is demonstrated [3]. Surface patterns consisting of CdSe/ZnS QDs functionalized at their periphery with β-cyclodextrin (β-CD) were obtained by immobilization of the QDs from solution onto glass substrates patterned with adamantylterminated poly(propylene imine) dendrimeric "glue." Subsequent formation of host-guest complexes between vacant β-CD on the QD surface and an adamantyl-functionalized lissamine rhodamine resulting in FRET was confirmed by fluorescence microscopy, spectroscopy, and fluorescence lifetime imaging microscopy.

On the basis of the above examples we shall sketch possible avenues, and speculate about constituents of the technology toolbox needed to achieve the next leap in integrated materials nanotechnologies for complex functional systems.

[1] Benetti, E.M., Sui, X., Zapotoczny, S., Vancso, G.J. (2010) *Adv. Func. Mater.*, **20** (6), pp. 939-944.

[2]Janczewski, D., Tomczak, N., Liu, S., Han, M.-Y., Vancso, G.J. (2010) *Chem. Comm.,* **46** (19), pp. 3253-3255.

[3] Dorokhin, D., Hsu, S.-H., Tomczak, N., Blum, C., Subramaniam, V., Huskens, J., Reinhoudt, D.N., Velders, A.H., Vancso, G.J. (2010) *Small,* **6** (24), pp. 2870-2876.

Dielectric and anelastic relaxations for the characterization of polymeric materials

Aurelie Léonardi, Jean-Fabien Capsal, Frédéric Roig, Jany Dandurand, Eric Dantras, Philippe Demont, Colette Lacabanne

Physique des Polymères, Institut Carnot CIRIMAT, UMR CNRS 5085
Université Paul Sabatier, 31062 Toulouse Cedex 09, France

lacabane@cict

Introduction

Low frequency molecular mobility reflects the various levels of organization of polymeric materials from micronic till nanometric scales. The mechanical parameters are very sensitive to molecular mobility so that the analyses of viscoelasticity by Dynamic Mechanical Spectroscopy (DMS) and Thermo Stimulated Creep (TSCr) give original data in apolar polymers. For polar polymeric materials, dielectric measurements take advantage of dipolar relaxation with kinetics that are characteristic of local environment. By combining Dynamic Dielectric Spectroscopy (DDS) and Thermo Stimulated Current (TSCu), a broad frequency range (10^{-3} to 10^{6}Hz) becomes accessible so that the whole range of molecular mobility can be explored.

Transition and molecular dynamics

In semicrystalline polyolefins, it is difficult to locate transitions in the amorphous phase. Those events are associated with anelastic relaxations with kinetics that are governed by the density of physical bonds: The discontinuity gives an order of magnitude of the glass transition. Data obtained by DMS and TSCr on a series of polyethylenes will be shown as example.

Heterogeneity of the amorphous phase of semi crystalline polymer with rigid chain

As example of semi crystalline polymer with a rigid chain, Poly(ether ether ketone) (PEEK) has been investigated by DDS and TSCu. For isolating the dipolar contribution from DDS data, the Kramers- Kronig transform has been used. The main α relaxation is observed close to the glass transition temperature Tg. The parameters of the relaxation times correspond to a delocalized cooperative mobility of the mobile amorphous phase.

At Tg+20°, a higher temperature component has been resolved: The kinetics are characteristic of the rigid amorphous phase confined by crystallites. This description of the PEEK heterogeneous amorphous phase significantly improves the understanding of mechanical behavior at a molecular level.

Influence of inorganic fillers on the structure of polymeric matrix in synthetic composites

Hybrid 0-3 composites Polyamide 11/ Barym titanate (PA11 / $BaTiO_3$) [1] might associate the ductility of PA11 and the piezoelectric properties due to $BaTiO_3$. Interesting piezoelectric coefficients have been obtained forparticles of 700 nm in diameter.The challenge is to maintain the volume fraction Φ of the ceramic low enough for preserving the mechanical properties of PA 11. Consequently, the physical structure of the amorphous phase of PA 11 has been analysed by TSCu.

The molecular mobility in the liquid state is not perturbed by $BaTiO_3$. In the glassy state, an evolution of the mobile amorphous phase is exhibited by the distribution of activation enthalpy. When Φ is increasing, the maximum value of the activation enthalpy is decreasing. This restriction of the delocalized molecular mobility shows that $BaTiO_3$ favours physical interactions. An optimum value for Φ is 24%.

Molecular interactions in natural composites

Dielectric relaxations in vegetal cell wall have been compared with the response of its major macromolecular components (cellulose and lignin) [2]. The objective is to extract information on macromolecular interactions in wood: Considering the polar character of the vegetal components, DDS and TSCu have been used.

Both cellulose and lignin dynamics are described by an Arrhenius law across the glass transition due to a significant density of hydrogen bonds. The comparison with the dynamics in the cell wall shows two different behaviours according to the frequency. At frequencies lower than the characteristic frequency (Fc) of the glass transition, two segregated components respectively due to lignin and cellulose are observed in the order of increasing temperature. Contrarily, at frequencies higher than Fc, a global response is recorded; it reflects molecular interactions between the various components.

Conclusion

The analysis of low frequency molecular mobility complements the characterization of polymeric materials despite their complexity and allows us to establish correlations between structure and mechanical or dielectric properties

Références

[1]Molecular mobility in piezoelectric hybrid nanocomposites with 0-3 connectivity: Particles size influence; Capsal JF, Dantras E, Dandurand J, Lacabanne. C; J. Non Crystalline Solids, 357, 2, 2011.

Capsal JF, PhD Thesis, 2009.

[2] Influence of hydrogen bonds on glass transition and dielectric relaxations of cellulose ; Roig F , Dantras E , Dandurand J , Lacabanne C ;J. Phys. D, 44, 2011.
Roig F, PhD Thesis, 2010.

Two-Photon Fluorescence Microscopy and Small Angle X ray and Neutron Scattering : tools for the structural characterisation of complex polymer architectures.

Isabelle Morfin,

Laboratoire Interdisciplinaire de Physique, UMR 5588 CNRS/UJF, Grenoble 1, France.

Nowadays, scientists are able to build more and more complex polymer architectures often used for biotechnological or biomedical applications. The complexity of such materials comes not only from the number of chemical or biological components involved in the preparation but also from the multi-scale structures found in materials. For the characterization, it is essential to use tools able to give information on the multi-scale structure, from the atomic to the macroscopic length scale but also on the internal structure, i.e. how the different components are organized ones compared to the others). The aim of the communication is to report the structural information extracted from several techniques, using examples coming from recent studies: Two-Photon Fluorescence Microscopy and Small Angle X-ray Scattering for cryogel and small Angle Neutrons Scattering for polyelectrolyteprotein complexes. We will focus on the particularities of each technique and will compare the respective advantages and disadvantages.

pNIPA cryogels observed by TPFM and SAXS :

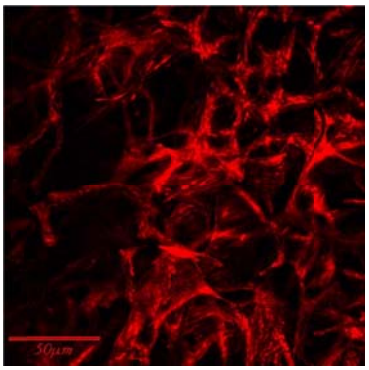

Figure 1. TPFM Image of the pNIPA cryogel in water

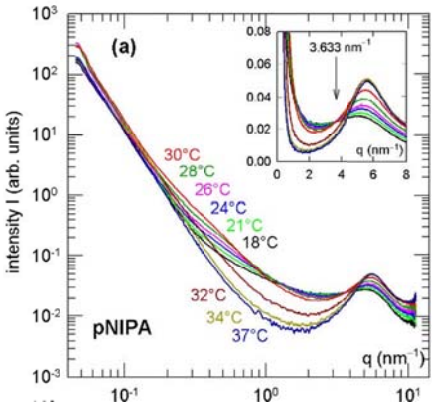

Figure 2. Temperature dependence of the SAXS intensity profile of the thermosensitive pNIPA cryogel.

Combined Mechanical and Electrical Characterization of Polymers by Atomic Force Microscopy

Chunzeng Li, Adam Mednick, Samuel Lesko

Nano Surfaces Business, Bruker Corporation,112 Robin Hill Road, Santa Barbara, CA93117, USA

Combining co-localized information at the nanoscale is a major trend in polymer science, resulting in a better and more complete understanding of complex, multi compound materials such as organic electronic devices, lithium batteries or composite materials. So far, Atomic Force Microscopy has successfully achieved correlation of topography with phase repartition (Phase Imaging) or with electrical properties (Electric Force Microscopy / Kelvin probe / Conductive AFM). However, Phase Imaging does not lead to unambiguous mapping of mechanical properties and characterization of electrical conductivity remains challenging because of the use of Contact Mode which is known to disturb soft polymer surfaces.

To address those limitations, we present new AFM methods that combine real time and simultaneous mapping of topographic, electrical and mechanical properties together with unprecedented tip-to-sample interaction control. The AFM operation relies on Peak Force Tapping Mode: force curves are collected at 1kHz rate while scanning the surface. In this mode, the AFM feedback loop maintains a constant maximum interaction force (Peak Force) down to tens of pN allowing one to routinely image fragile samples at high resolution. Mechanical parameters such as Young's Modulus, adhesion, dissipation and deformation are extracted simultaneously from these force curves, resulting in complete mechanical maps. For conductivity mapping, the tip is connected to a high performance current allowing one to record current during the vertical modulation cycle at (and near) the Peak Force. The amplifier bandwidth reaches 15kHz at sensitivities as high as 20pA/V while retaining the capability to also measure larger currents (1μA).

To illustrate the synergistic power of these new methods, we will show a correlation between electrical conductivity and crystallinity of PEDOT:P3HT [poly(3,4-ethylenedioxythiophene:poly-3(hexylthiophene)] samples. Other examples presented include Lithium cathode composites for which the simultaneously acquired elastic modulus and conductivity maps unambiguously identify the 3 different functional components of the electrode (metal oxide, polymer binder and conductive additives).

Transient rheology: improving measurements at very short time.

A.C. Diogo,

Instituto Superior Técnico (Dep. Chemical and Biological Engineering), Technical University of Lisbon
Av. Rovisco Pais, 1049-001 Lisbon, Portugal

acdiogo@ist.utl.pt

Introduction

Stress relaxation experiments, creep-recovery experiments and start-up of shear flows are transient experiments which can be very useful in assessing constitutive models of linear and branched polymers, as well as for multiphase systems such as polymer blends, foams, emulsions, asphalts, and so on. A number of examples can be found in literature [1]; for instance, the double step strain experiment has been the touchstone for different constitutive models of polymer melts in the last decades [2]. On the other hand, transient experiments may provide fast and accurate means of getting some of the most important viscoelastic constants such as the zero-shear viscosity, the recoverable creep compliance, among others.

However, the analysis of the experimental data can be perturbed by interference of the apparatus response functions, in most of the cases. Moreover, the sensitivity to this interference is predominant at short times where the intensity of the signal is higher.

It is shown that the quality of the data can be significantly improved by a number of procedures based on deconvolution. Some examples are considered.

Stress relaxation

Stress relaxation measures the response to a step strain, either in shear or in extension. For shear, the relevant material function is the shear relaxation modulus G(t), given by the ratio between the time-dependent shear stress $\sigma(t)$ and the amplitude γ_0 of the step strain. No actuator can provide a perfect step strain: instead, a step-like transient function $\gamma(t)$ is generated, which can be measured, in general. Moreover, it is generally believed that after some characteristic actuator growth time t_1 ($\gamma(t)$ becomes constant after t_1) the shear relaxation modulus is given by $\sigma(t)/\gamma(t)$; the software of most rheometers indeed assumes it. The main issues are that $\sigma(t)/\gamma(t)$ is not equal to G(t) for $t < t_1$ as well as for $t > t_1$, and that $\sigma(t)/\gamma(t)$ may not approach G(t) even at very long times. Numerical simulation can easily provide several realistic examples where $\sigma(t)/\gamma(t)$ does not converge to G(t) even at very large t.

Since the strain $\gamma(t)$ provided by the actuator can be measured, the relaxation modulus G(t) can be extracted from the measured time-dependent shear stress $\sigma(t)$ and the strain growth function $\gamma(t)$ by deconvolution. A procedure to perform such deconvolution was developed, and used on different sets of data from a RMS-800 mechanical spectrometer. Here, a constant strain is attained after 80 ms from startup, but the convergence of $\sigma(t)/\gamma(t)$ to G(t) is much slower: it takes about 0.3 s after startup.

It is shown that our deconvolution procedure extends the available G(t) data for about two orders of magnitude (down to about 10 ms). In particular, it becomes possible to get rather accurate values of the zero shear viscosity η_0, by using the following equation

$$\eta_0 = \int_0^\infty dt'.G(t') \qquad (1)$$

As a matter of fact, equation (1) is quite sensitive to short time values of G(t). It must be stressed that eq.(1) provides a much faster way of getting the zero-shear viscosity as compared to the standard method.

Creep-recovery experiments

The rheological behaviour of foams, emulsions and other multiphase systems (e.g. bitumen) is mainly controlled by interface properties. Stress controlled rheometers are more appropriate for these systems since stresses are low and strain must be kept small enough. The number n of relaxation processes is small and so must be the number (n-1) of retardation times.

A creep experiment followed by elastic recovery does provide the needed information to get the time dependent creep compliance J(t). It is possible to get G(t) from J(t) once the retardation spectrum is discrete. The inverse problem difficulties are also avoided if the breadth of the retardation times is kept small. Preliminary data on bitumen shows that creep-recovery data as well as stress relaxation data can be analysed in terms of a few relaxation (retardation) processes. These processes can be correlated to bitumen microstructure as sensed by atomic force microscopy (AFM).

Conclusions

Transient experiments can provide fast and valuable information about a number of rheological material functions and rheological constants which are difficult to obtain by standard means. In particular, for multiphase systems or other systems where a reduced number of relaxation mechanisms can be identified, most of the difficulties which come from the inverse problem can be overcome. For these cases, transient data can give an insight on the dynamics of these relaxation processes.

References

[1] Macosko, CW, "Rheology: Principles, Measurement and Applications", Wiley-VCH, (1994)

[2] Venerus, DC, CM Vrentas, JS Vrentas, "Step strain deformations for viscoelastic fluids: experiment", J. Rheol. 34, 657-683 (1990).

ABSTRACTS

INVITED LECTURES

Topic 3: Advanced Processing and Recycling Technologies

Inducing Supramolecular Structures in Polymers by the Combined Effects of Nanoparticles and Flow

Gad Marom

The Institute of Chemistry, The Hebrew University of Jerusalem

gadm@vms.huji.ac.il

Introduction: The application of flow to polymers results in stretching and aligning some polymer chains, allowing them to form orientated structures that can eventually develop into orientated crystalline domains. This behavior is a function of several factors, including processing conditions (e.g., temperature, deformation rate, and deformation strain) and polymer properties (e.g., molecular weight and distribution). In polymers that are reinforced by acicular inclusions, such as short aramid fibers and carbon nanotubes, flow generates orientation of the acicular inclusions parallel to the flow lines – in addition to the shear flow that promotes chain stretching, disentanglement, and alignment. The combined effects of the aligned polymer chains on the one hand and the inclusion on the other can produce various types of supramolecular structures.

Experimental: A typical experimental procedure is based on melt mixing of polymer pellets filled with about 1.5 wt-% of nanoparticles, it was carried out in a twin-screw microcompounder (DSM, Netherlands). Mixing was performed at temperature above the melting point of the corresponding polymer for a period of about 10 min at about 100 rpm, according to the procedure published elsewhere [1]. This was followed by extrusion through a 900 □m die and drawing of fiber-like filaments with diameters decreasing from 900 μm to 30 μm (with corresponding draw ratios DR = 1 to 900). A range of experimental techniques based on electron microscopy and X-ray diffraction methods was used to analyze the structure morphology of the various polymers.s

Results & Discussion: This lecture will attempt to underline the main common factors that relate the mechanical performance to the structural morphology and, in turn, to the combined effects of flow and nanoparticles. An example of carbon nanotube (CNT) based polyacrylonitrile (PAN) composites shows how specific interfacial interactions in multi-component systems such as composites improve the chemical compatibility between the filler and the matrix. Scanning electron micrographs (SEM) attest to a fairly uniform dispersion of apparently single CNT within the PAN matrix. The study explains the nature of CNT/PAN interaction by a model of charge-transfer of CNT □-electrons from the highest occupied molecular orbital to the empty nitrile π** orbital of PAN [1-2]. Another example describes a nanocomposite monofilament composed of a nematic thermotropic liquid crystalline polymer (TLCP) mixed with carbon nanoparticles (CNP) prepared by melt extrusion [3-4]. It shows that the tensile strength and modulus of the fibers increase with the draw down ratio of the filament; specifically, a positive effect on the tensile modulus is displayed by fibrous CNP, achieving extremely values. At high draw down ratio, addition of CNP also increased the relative amount of orientated polymer chains and contributed to sharpening of the mesomorphic transition. Additionally, the solid state crystallization in drawn thermoplastic polyimide (PI) films is studied as a function of draw ratio (DR) under the effect of vapor grown carbon fiber (VGCF) nanoinclusions [5]. The nucleating effect of the nanoinclusions coupled with the orientation effect of drawing, as can be seen in the figure, generates a unique orientated layered lamellar structure, characteristic of smectic-like mesophase. The degree of draw induced orientated crystallization increases with the content of nanoinclusions and with the DR, and is reflected in the mechanical behavior of the film. Generally, the young's modulus and the yield point of the drawn crystalline films in the drawing direction are significantly higher compared with the noncrystalline counterparts. Finally, nanocomposite filaments composed of isotactic polypropylene (iPP) and VGCF were prepared by melt mixing extrusion, followed by melt drawing [6]. The effect of composition and flow on the morphology was investigated by X-ray diffraction and high resolution scanning electron microscopy. It is found that melt mixing followed by extrusion of monofilaments is a highly effective procedure for the preparation of uniform mixtures of individually dispersed nanofibers in a polymeric matrix. The extrusion process produces axial alignment of nanofibers and of stretched polymer molecules along the flow direction. The level of the alignment of both the nanofibers and the polymer chains can be raised further by extensional drawing up to almost perfect orientations at draw ratios of around 20. The orientated nanofibers together with the stretched polymer chains nucleate other polymer molecules to form a highly orientated crystalline bulk. The high anisotropic mechanical properties in the flow direction of the resulting nanocomposites are attributed to the combined contributions of the orientated crystalline structure and the nanofiber reinforcement.

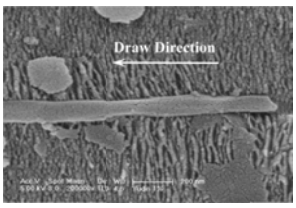

Reference

[1] Vaisman L, Larin B, Davidi I, Wachtel E, Marom G, Wagner HD. Compos. Pt. A-Appl. Sci. Manuf. 2007;38(5):1354-1362.

[2] Vaisman L, Wachtel E, Wagner HD, Marom G. Polymer. 2007;48(23):6843-6854.

[3] Kalfon-Cohen E, Marom G, Wachtel E, Pegoretti A. Polymer. 2009;50(7):1797-1804.

[4] Kalfon-Cohen E, Pegoretti A, Marom G. Polymer. 2010;51(5):1033–1041.

[5] Smirnova VE, Gofman IV, Yudin VE, Dobrovolskaya IP, Shumakov AN, Didenko AL, Svetlichnyi VM, Wachtel E, Shechter R, Harel H, Marom G. Polym. Eng. Sci. 2009;49(2):217-222.

[6] Larin B, Lyashenko T, Harel H, and Marom G. Compos. Sci. Technol. 2011;71(2):177-182.

Processing of thermosetting matrix nanocomposites: modelling and characterization of the electrical behavior

José M. Kenny, L.Torre, M. Monti*, M. Natali**

Institute for Polymer Science and Technology (ICTP-CSIC). Juan de la Cierva, 3 – 28006 Madrid, Spain

kenny@ictp.csic.es

*Materials Science and Technology Centre, University of Perugia. Pentima 4, 05100 Terni, Italy

Carbon nanotubes (CNTs), carbon nanofibres (CNF) and graphenes are carbon structures with extraordinary mechanical, chemical and electrical properties. These unique properties make these carbon nanoobjects (CNOs) extremely valuable in a wide range of end-use applications. However, the achievement of these properties requires a careful definition of processing routes and conditions able to produce nanocomposites with designed and controlled nanofiller dispersion, orientation and alignment.

In past years, we have contributed to demonstrate that although carbon nanotubes are difficult to disperse in liquid suspensions, they can be oriented by application of electric, magnetic and shear fields. These approaches have been applied for the production of thermosetting matrix films and bulk nanocomposites containing aligned nanotubes, which exhibit strong anisotropic properties. In particular, the measurement of the electric current during the electric field application to polymer nanocomposites mwith CNTs, before and during matrix curing, has been used an indicator of the formation of a CNT network oriented in the direction of the electric field itself. In fact, the electric field induces the formation of a dipole moment which results in a rotational force which tends to orient them in the field direction. Driven by the opposite charges of their ends, CNTs also gradually move closer toward each other, forming a network of tubes connected each other, head-by-head, aggregating in chain-like structures. This network represents a path for electric current.

We propose a physical modelling based, on classic electrodynamics and fluid dynamics, which describes all the phenomena appearing when a suspension of single-wall nanotubes in a viscous polymer is subjected to the action of a DC electric field, based on classical electrodynamics: rotation, orientation, migration, network formation and relaxation when the field is released. The main result of this modelling approach is the optimization of the processing conditions for the production of a bulk polymer nanocomposite with aligned carbon nanotubes via DC electric fields.

Polymers Processing Using Supercritical Fluid Technology

C. Domingo, C.A. García-González, A. López-Periago

Instituto de Ciencia de Materiales de Barcelona (CSIC), Campus UAB, Barcelona, Spain,

conchi@icmab.es

Introduction

Te architecture of a polymeric scaffold plays an important role in modulating tissue growth and response behavior of cultured cells. Required characteristics include high porosity and an interconnected 3D macroporous network necessary for cell proliferation, and high surface area to promote cell adhesion [1]. The main drawbacks of conventional scaffolds production methods involve a reduced capability to control pore size and pore interconnectivity. Technology based on supercritical carbon dioxide ($scCO_2$) has been already proposed for the processing of a great range of biopolymers with excellent control on morphology, surface properties and purity [2-4]. It is used to produce polymer foams by pressure-induced phase separation. Furthermore, spray processes involving $scCO_2$ have achieved considerable success in addressing polymer particles and fibers production. Finally, the potential role of CO_2 in assisting the blending of polymers has been studied. The main objective of this work is to follow a line of research that explores the possibilities of using the $scCO_2$ for the processing of different biopolymers: semi-crystalline, amorphous and blends, either pure or as a part of hybrid composites.

Materials and Methods

Poly(lactic acid) (L-PLA), poly(e-caprolactone) (PCL) and poly(methylmethacrylate) (PMMA) were the used polymers. Both the production of monolithic foams and the precipitation of fibers were attempted.

(i) Polymer foaming in $scCO_2$ was performed in a high pressure equipment running in the batch mode. In a typical experiment, the autoclave (70 mL, TharDesign) was initially loaded with ~ 1g of polymer. The system was heated with resistances to the selected temperature and pressurized at 20 MPa using a syringe pump (Thar SP240). The system was stirred at 300 rpm.

(ii) Fibers precipitation was carried out in a semicontinuous antisolvent equipment, where the spray chamber consisted on a high pressure vessel (Autoclave Engineers) of 5 cm i.d. x 25 cm long. The CO_2 was pumped using a reciprocating pump (Lewa EK3). Dichloromethane solutions of polymer were sprayed into the precipitation chamber using a reciprocating dual-piston minipump (Milton Roy LDC). Two types of nozzles were used for liquid solution injection: a plain orifice (disk) and a conical spray (swirl). The precipitated polymer was dried with a CO_2 flow.

Results and Discussion

Macroporous sponges of the amorphous PMMA were fabricated using $scCO_2$ as a porogen agent [5]. This type of processing led to a partially closed pore structure which is disadvantageous for cell-migration in 3-D scaffolds. However, for systems formulated with molecularly dispersed drugs, swellable polymers are mainly used as matrixes. Hence, the molecular impregnation of PMMA matrixes with active agents was studied using a similar $scCO_2$ process. Homogeneously distributed loadings of *ca.* 20 wt% of active agent in PMMA were obtained [6].

$scCO_2$ was also used for the solvent induced crystallization of L-PLA and for their thermal annealing and crystallization from the melt. The use of $scCO_2$ dropped the glass, crystallization and melting temperature of the raw material during processing. Treatment with $scCO_2$ at different temperatures allowed obtaining L-PLA samples having different structures with respect to the crystallinity, crystallite size, and crystal morphology [7]. For the semicrystalline L-PLA, the induced nucleation and/or crystallization effect in the amorphous fraction prevented the molecular dispersion of organic active compounds in the matrix.

The development of a $scCO_2$ antisolvent technique for the production of template-free fibrous polymeric scaffolds, as an alternative to macroporous sponges, has been carried out for PMMA and L-PLA homopolymers and PMMA/PCL blend [8]. A modification of the antisolvent technique was used to precipitate a composite of L-PLA loaded with hydroxyapatite nanoparticles used as reinforcing filler [9]. The introduction of small quantities of nanosized inorganic particles can significantly improve the mechanical and physical properties of the polymeric matrix. These composites have gained much recognition as bioactive bone grafts, owing to their compositional and structural similarity to natural bone.

References

1. Czerwonatis N, Eggers R, Chem. Eng. Technol., 24, 619, 2001.

2. Cooper AI, Adv. Mater, 15, 1049, 2003.

3. Tomasko DL, Li H, Liu D, Han X, Wingert MJ, Lee, LJ, Koelling KW, Ind. Eng. Chem. Res., 42, 6431, 2003.

4. Quirk RA, France RM, Shakesheff KM, Howdle SM, Curr. Opin.Solid.State Mater.Sci., 8, 313, 2004.

5. López A, Argemí A, Andanson JM, Fernández V, García CA, Kazarian SG, Saurina J, Domingo C, J. Supercrit. Fluids, 48, 56, 2009.

6. Andanson JM, López A, García, CA, Domingo C, Kazarian SG, Vib. Spectr., 49, 183, 2009.

7. López AM, García CA, Domingo C, J. App. Pol. Sci., 111, 291, 2009.

8. Vega A, Subra P, López A, Domingo C, Eur. Pol. J., 44, 1081, 2008.

9. García CA, Vega A, López A, Subra P, Domingo C, Acta Biomater., 5, 1094, 2009.

How to use Block Copolymers for Processing of Thermosets and Composites?

J.P. Pascault, F. Lortie, D. Portinha, J.F. Gérard

Université de Lyon, F-69003, Lyon, France - INSA Lyon, F-69621, Villeurbanne, France - CNRS, UMR5223, Ingénierie des Matériaux Polymères.

(Jean-Pierre.Pascault@insa-lyon.fr)

Thermoset precursors are frequently formulated with modifiers like small molecules, oils, low- or high-molar mass rubbers or thermoplastics. One application which has been an interesting and challenging topic for over four decades is the toughening of thermosetting polymers for adhesives, coatings and composites [1-2]. In recent years, a new thermoset toughening approach using self-assembling amphiphilic block copolymers, BCPs has drawn significant attention. The incorporation of a small amount of dispersed microphase-separated BCP can produce significant improvements in fracture toughness without compromising other propertiesof the neat epoxy network [3-16].

Thermosetting polymers are widely used as matrices of fiber-reinforced composites constituting structural parts in the transportation industry. For instance, epoxies are largely involved in carbon-reinforced parts for aeronautical applications while polyesters are constitutive of SMC (Sheet Moulding Compound) for automotive applications. These composites have also to be improved in terms of impact resistance, damage tolerance and surface aspect, and the use of BCP may be a way of enhancing both mechanical and aspect properties of the parts.

But BCPs as modifiers of thermosetting polymers and fiber-reinforced composites have also many other interests [17,18]. By controlling the chemistry (choice of the thermoset precursors, right hardener and accelerator) and the processing (the Order Disorder Transition, ODT temperature of the BCP in the thermoset precursors), the initial viscosity of the formulation and the viscosity increase during the curing process, it is possible to develop innovative technologies like thermoplastic films or fibers, thermoset powders, prepregs for infusion or resin transfer molding (RTM). Depending on the involved reactive process (RTM or SMC), different strategies have been optimized to integrate the BCP and to obtain the desired BCP morphologies and localizations inside the final parts.

Some examples of the use of BCPs for preparing advanced (and also functional) materials will be given during this presentation.

REFERENCES

1. a) Yee A.F., Pearson R.A., J. Mat. Sci., 1986, 21, 2462-2474;
b)Pearson R.A., Yee A.F., J. Mat. Sci., 1986, 21, 2475-2488;
c)Pearson R.A., Yee A.F., J. Mat. Sci., 1989, 24, 2571-2580;
d)Pearson R.A., Yee A.F., J. Mat. Sci., 1991, 26, 3828-3844.

2. Pascault JP, Williams RJJ. In Polymer Blends, Ed. by Paul D.R. and Bucknall C.B., a Wiley Interscience publication, 2000; Vol.1:379

3. Dean JM, Lipic PM, Grubbs RB, Cook RF, Bates FS. J Polym Sci, Part B: Polym Phys 2001; 39:2996.

4. Dean JM, Grubbs RB, Saad W, Cook RF, Bates FS. J Polym Sci, Part B: Polym Phys 2003; 41:2444.

5. Dean JM, Verghese NE, Pham HQ, Bates FS. Macromolecules 2003; 36:9267.

6. Ritzenthaler S, Court F, Girard-Reydet E, Leibler L, Pascault JP. Macromolecules 2003; 36:118.

7. J. Liu, H.-J. Sue, Z.J. Thompson, F.S. Bates, et al, *Macromolecules*, 2008, *41*, 7616.

8. J. Liu, H-J. Sue, Z.J. Thompson, F.S. Bates, et al, *Acta Materialia* 2009, *57*, 2691.

9. Hillmyer MA, Lipic PM, Hajduk DA, Almdal K, Bates FS. J Am Chem Soc 1997; 119:2749

10. Lipic PM, Bates FS, Hillmyer MA. J Am Chem Soc 1998; 120:8963.

11. Meng F, Zheng S, Zhang W, Li H, Liang Q. Macromolecules 2006; 39:7111.

12. Ritzenthaler S, Court F, David L, et al, Macromolecules 2002; 35:6245.

13. Mijovic J, Shen M, Sy JW, Mondragon I. Macromolecules 2000; 33:5235.

14. Guo Q, Thomann R, Gronski W, Thurn-Albrecht T. Macromolecules 2002; 35: 3133.

15. Guo Q, Thomann R, Gronski W, Staneva R, Ivanova R, Stühn B. Macromolecules 2003; 36:3635.

16. Maiez-Tribut S, Pascault J.P, Soulé E.R, Borrajo J, Williams R.J.J. Macromolecules, 2007; 40:1268

17. Pascault J.P, Williams R.J.J, « Epoxy Polymers: New Materials and Innovations", Wiley-VCH, 2010.

18. Lamy Y., Gille F., Lortie F., Portinha D., Gérard J.F., Pascault J.P., umpublished results.

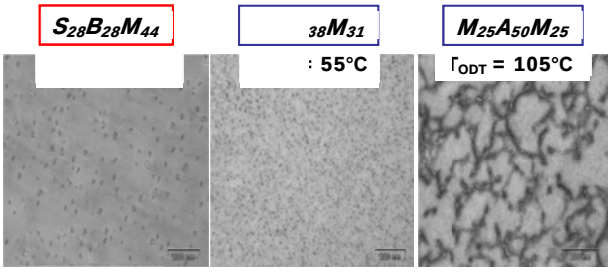

Figure: One example of the role of the Order-disorder Transition T°C (measured by oscillatory shear rheology before curing) on cured epoxy /BCP blend morphologies; TGMDA/MDEA+MMIPA) and 20 wt.%BCP.TS curing conditions = 1h @ 130°C; 2°C.min-1 up to 180°C, 2h @ 180°C. TEM: no staining agent used

"Functional polymers with capability to remove pollutant ions"

Bernabé L. Rivas

Polymer Department, Faculty of Chemistry, University of Concepción, Casilla 160-C, Concepción, Chile

brivas@udec.

The need to mitigate the environmental impact of industrial development has resulted in an important development of processes and technologies to remove pollulant ions from a variety of sources. Presently, there are various techniques available to separate metallic ions, including; differential precipitation, solvent extraction, distillation, ion exchange, flotation, and filtration membranes.

Ion exchange resins are the most widely used materials to remove ions from aqueous sources. They have several applications, such as in water softening, wastewater treatment, hydrometallurgy, and chromatography.

To face the problem of separation of ions bound to the polymer and non-bound, one of the most promising techniques used is the application of separation methods based on membrane processes (1-3). Membrane filtration easily allows this separation by means of the method known as the *liquid-phase polymer-based retention(LPR)* technique. Applications of water-soluble polymers, WSP, to the homogeneous enrichment or selective separation of various metal ions from dilute solutions have been reported. Ultrafiltration is found as the most suitable technique for LPR studies. To be used in homogeneous ions recovery, the appropriate water-soluble polymers may present high solubility in water, and easy and cheap route of synthesis, an adequate molecular weight and molecular weight distribution, chemical stability, high affinity for one or more metal ions, and selectivity for the metal ion of interest.

All the polymers are synthesized by radical polymerization, purified by membrane filtration, and characterized by FT-IR and ^{1}H-NMR spectroscopy. The molecular weight is determined by GPC.

The ion retention properties are investigated by LPR technique (washing and enrichment methods) under different experimental conditions.

Interactions of metal cations:Co(II), Ni(II), Ca(II), Mg(II), Pb(II), Cd(II), Zn(II), and Cu(II), and anion As(V) species with water-soluble polymers were studied at different pH and filtration factor, Z.

It is useful to quantify the separation process by plotting the retention of the metal species versus the filtration factor. The filtration factor (Z) is defined as the volume ratio of the filtrate (V_f) versus volume in the cell (V_o). Retention (R) is defined for any species as the fraction per unit of the species under study remaining in the cell during filtration. The ion (M) remaining in the cell during filtration consists of the sum of the ion bound to the polymer chain and the ion free in the solution.

To obtain the retention profiles a polychelatogen : ion 40:1.0 relationship is used. It corresponds to 0.2 mmol : 0.005 mmol. This ratio obeys to ensure an excess of the ligand groups respect to the ion. The ion retention ability of the water-soluble polymer depends strongly on the pH. As the pH increases the metal ion retention increases. This is due to at higher pH, the majority of carboxylic acid groups are non-protonated. Therefore, the carboxylate is more available to bind metal ions. Particularly, at pH >5, which is above to the pKa value for an acrylic acid.

The interactions between the polymer and the metal ions are mainly due to electrostatic forces and to formation of coordinating bonds. Other weak interactions may appear such as trapping metal ions in the bulk of the polymer phase.

Respect to the removal of metal ions at higher pH, as pH 5 and pH 7, increased the ability to bind metal ions and there is not an important decrease on the retention as increases Z. That means that the sulfonic/sulfonate-metal ion interaction is strong. The polymer-metal ion interaction may be intramolecular, intermolecular or both.

As(V) species are removed by polymers containing ammonium groups. The highest retention ability was observed at higher pH (6 and 8). The retention of arsenic occurs basically by ion-exchange between the counter ion of the ammonium group with the anion species of the arsenic.

The retention of arsenic(V) occurs basically for ion-exchange of the anioonic specie with the counter ion of the polycation.

In addition, water-soluble polymers containing carboxylic acid and sulfonic acid groups showed a high affinity for metal ions. It depends on the structure of the polymers and on the pH, and filtration factor, Z. The functional polymer group-metal ion interaction would occur through different mechanisms. For carboxylate groups should be by complexing process and for sulfonic acid it should be by electrostatic process.

Acknowledgements. The authors thank to FONDECYT (Grant No 1110079), PIA (Anillo ACT-130), and CIPA the financial support

References

[1] Spivakov BYa, Geckeler K, Bayer E. *Nature* 1985; 315: 313

[2] Rivas BL, Pereira ED, Moreno-Villoslada I. *Progr. Polym. Sci.* 2003; 28: 173.

[3]Rivas BL, Pereira ED, Palencia M, Sánchez J. *Progr. Polym. Sci*. 2011; 36: 294.

Preparation of Advanced Soft Tissue Engineering Scaffolds by Stereolithography

S. Schüller-Ravoo,[1] S.M. da Silva Texeira[1], J. Feijen[1], D.W. Grijpma[1,2]

[1]University of Twente, Enschede,
[2]University Medical Center Groningen, Groningen, The Netherlands

d.w.grijpma@tnw.utwente.nl

Introduction: Stereolithography (SLA) is a rapid prototyping technique that allows the building of complex 3D structures. Designed porous structures that varying in shape, porosity, pore size, pore geometry and pore interconnectivity can be prepared at high resolutions. It is envisaged that flexible and elastic scaffolds that resorb in the body will be highly applicable in the engineering of soft tissues such as cartilage or cardiovascular tissues. Currently, no resins are available that can be processed by SLA to yield suitable porous structures.

This work describes the development of photo-crosslinkable resins based on biodegradable poly(trimethylene carbonate) (PTMC) and the processing of these resins by stereolithography to yield flexible porous and non-porous network structures.

Materials and Methods: Three-armed oligomers were synthesized by ring opening polymerization of TMC using glycerol as initiator. By varying the monomer to glycerol ratio, the molecular weight of the oligomers can be adjusted. The oligomers were functionalized using methacryic anhydride to yield photo-crosslinkable macromers.

Resins of the different macromers, varying in molecular weight between 3000 g/mol to 21000 g/mol, were formulated using a photo-initiator (Lucirin TPO-L, 5 wt %), a dye (Orasol Orange G, 0.15 wt %) and a non-reactive diluent. The resins were processed by SLA (EnvisionTec, Germany) at temperatures between room temperature and 65 ºC.

Results: Porous structures with different mathematically defined architectures were prepared from the different macromers. While the macromers with the lowest molecular weights could be readily processed at room temperature, the higher molecular weight ones required the addition of diluent or increased temperatures.

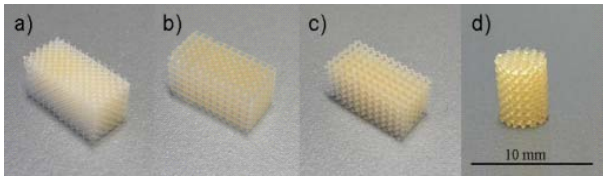

Fig.1. Scaffolds with different pore architectures prepared by SLA using PTMC3000.

a) diamond-, b) cubical-, c,d) gyroid geometry.

Disk-shaped specimens were used to assess the adhesion and proliferation behaviour of human umbilical vein endothelial cells (HUVECS) on extracted networks. After 3h of culture, the cells show good cell adhesion and proliferate well on the surfaces (Fig. 2). The SEM images show the stretched morphology the cells adopt. No substantial differences were found between networks prepared from the different macromers.

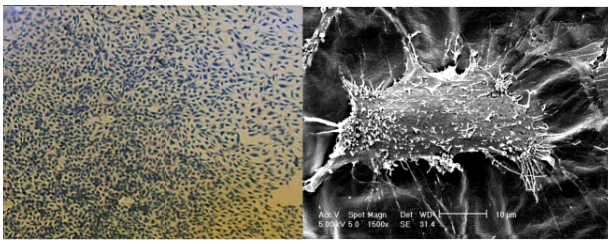

Fig. 2. Methylene Blue staining of HUVECS on PTMC21000 networks (left). SEM image of HUVEC on PTMC8000 networks (right).

Conclusions: PTMC macromers of different molecular weights were formulated into photo-crosslinkable resins, and successfully used to prepare 3D-structures with pre-designed pore characteristics. HUVECs show good adhesion and proliferation on these networks.

Electrospinning of Biopolymers: Biomedical, Pharmaceutical and Food Related Applications

Jose M. Lagaron

Novel Materials and Nanotechnology Group, IATA, CSIC, Avda. Agustín Escardino 7, 46980, Burjassot, Spain;

e-mail: lagaron@iata.csic.es

Abstract Body:

Looking genuinely at nature, nanofibers often serve as a basic platform where either organic or inorganic components are built upon. For instance, cellulose nanofibers would represent the building block in plants while collagen nanofibers in the animal body. The fiber structure exhibits, from a structural point of view, the certain ability to transmit forces along its length and, thus, reducing the amount of materials required. While strong enough for their designed purpose, nanofibers have the added advantage of giving high porosity to the natural supports which allows faster diffusion of chemicals to the inner structure. To follow this extraordinary nature's design, a process that is able to fabricate fiber nanostructures from a variety of materials and mixtures is an indispensable pre-requisite. Control of the nanofibers arrangement is also necessary to optimize such structural requirements.

Electrospinning is a physical process used for the formation of ultrathin fibers by subjecting a polymer solution to high electric fields. At a critical high voltage (5-25 kV), the polymer solution droplet at the tip of the needle distorts and forms a Taylor cone to be ejected as a charged polymer jet. This stretches and is accelerated by the electrical field towards a grounded and oppositely-charged collector. As the electrospun jet travels through the electrical field, the solvent completely evaporates while the entanglements of the polymer chains prevent it from breaking up. This results in the ultrathin polymer fibers deposition on a metallic collector to habitually assemble the fibers as non-woven mats.

Since the electrospinning is a continuous process, fibers when winded can be as long as several metres or even kilometres. The formed fibers are not only ultrathin and relatively large in length but also fully inter-connected to form a three-dimensional network.

The current paper will highlight some recent advances carried out within our research group in which various applications of the high voltage spinning processing technique making use of biopolymers and biopolymeric blends will be reviewed (1-10). These include examples in which new antimicrobial nanostructured fiber mats with strong biocide efficiency were successfully developed, as well as nanostructured systems for bone implant interfaces with significant bioactivity, antiinflamatory and antibiotic properties and also novel nanoencapsulation of active and bioactive food ingredients.

References:

(1) Martínez-Sanz, M., Olsson, R.T., Lopez-Rubio, A., Lagaron, J.M., 2010, *Cellulose*, pp. 1

(2) Torres-Giner, S., Lagaron, J.M., 2010 *Journal of Applied Polymer Science* 118 (2), pp. 778

(3) Torres-Giner, S., Martinez-Abad, A., Ocio, M.J., Lagaron, J.M. 2010 *Journal of Food Science* 75 (6), pp. N69

(4) Olsson, R.T., Kraemer, R., López-Rubio, A., Torres-Giner, S., Ocio, M.J., Lagarón, J.M., 2010 *Macromolecules* 43 (9), pp. 4201

(5) López-Rubio, A., Sanchez, E., Sanz, Y., Lagaron, J.M. 2009, *Biomacromolecules* 10 (10), pp. 2823

(6) Fernandez, A., Torres-Giner, S., Lagaron, J.M. 2009 *Food Hydrocolloids* 23 (5), pp. 1427

(7) Torres-Giner, S., Ocio, M.J., Lagaron, J.M. 2009 *Carbohydrate Polymers* 77 (2), pp. 261

(8) Torres-Giner, S., Ocio, M.J., Lagaron, J.M. 2008 *Engineering in Life Sciences* 8 (3), pp. 303

(9) Torres-Giner, S., Gimenez, E., Lagaron, J.M., 2008 *Food Hydrocolloids* 22 (4), pp. 601

(10) Torres-Giner, S.; Gimeno-Alcañiz, J.V.; Ocio, M.J.; Lagaron, J.M. *ACS Appl. Mater. Interfaces* 2009, 1, 218

Acknowledgements:

Contract grant sponsor: MICINN, MAT2009-14533-C02-01 and EUI2008-00182 and the EU FP7 IP ECOBIOCAP, FREESBE and NEWBONE

Recombinamer-based, complex and highly functional systems attained by mild, clean and biocompatible processing technology

J.C. Rodríguez Cabello

GIR Bioforge, Universidad de Valladolid, Edificio I+D, Paseo de Belén 1, 47011 Valladolid

E-mail: roca@bioforge.uva.es

Recombinamers are recombinant protein-based polymers. They are produced as recombinant proteins by genetically engineered microorganisms by the use of a synthetic DNA. This DNA has generally been designed and synthesised from the scratch and can contain both naturally and non naturally occurring DNA sequences. Generally speaking, the macromolecules obtained by this new technology are much more complex and much more controlled in composition and, therefore, show higher degree of functionality, than their synthetic polymer counterparts[1].

The peculiar properties of the recombinamers place them in the diffused interface among material science, nano(bio)technology, biomedicine, biomedical engineering and others. Additionally, the protein nature of those functional macromolecules and the biotech route by which they are produced enables the use of mild processing technologies[2]. For example, water uses to be the exclusive solvent, and the processing conditions are characterised by being moderate in parameters such as temperature or pH. Additionally, the molecular complexity of some of the recombinamers now-a-days produced can be used to drastically simplify the processing stages since, concepts of biological inspiration such as self-assembly are common in this new class of materials[3].

Examples of recombinamers designed and produced for different uses will be presented. Those include recombinamers with smart nature, self-assembling properties, acute bioactivity for advanced drug delivery and regenerative medicine, and biomimetic functionality such as that for biomimicked mineralization. Those can be processed to obtain from nanoparticles or nanofibres to macro-hydrogels under the easiness and cleanliness characteristic of this new class of materials.

References.

1. Developing Functionality in Elastin-Like Polymers by Increasing their Molecular Complexity: The Power of the Genetic Engineering Approach. J. C. Rodríguez-Cabello, J. Reguera, A. Girotti, M. Alonso, A. M. Testera. Prog. Polym. Sci. **2005**, 30 (11), 1119-1145.
2. "Recombinamers" as Advanced Materials for the Post-oil Age. J. Carlos Rodríguez-Cabello, Laura Martín, Matilde Alonso, F. Javier Arias, Ana Mª Testera. Polymer **(2009).** Vol 50, Issue 22, 5159-5169
3. Emerging Applications of Multifunctional Elastin-Like Recombinamers. Rodríguez-Cabello J.C., Martin L., Girotti A., García-Arévalo C., Arias F.J., Alonso M. Nanomedicine (**2011**),Vol. 6, 111-122.

Influence of Polymer Microstructure and Post-Treatment on the Performance of Latex-based Pressure Sensitive Adhesives

Marc A. Dubé and Lili Qie

Department of Chemical and Biological Engineering, Centre for Catalysis Research and Innovation University of Ottawa, Ottawa, ON Canada

Marc.Dube@uOttawa.ca

Introduction: Pressure sensitive adhesives (PSAs) produced via solution polymerization tend to have much better performance (i.e., much larger shear strength at similar tack and peel strength levels) than those produced via emulsion polymerization. This is because the gel network is continuous in solvent-based PSAs but discontinuous in emulsion- or latex-based PSAs[1]. Since the production and use of latex-based PSAs is more environmentally friendly than that of solventbased PSAs, significant effort has been made to improve the performance of latex-based PSAs so that they can replace their solvent-based counterparts. One approach involves the addition of functionalized monomers followed by post-treatment of the PSA films to encourage the reaction of the functional groups and transform the discrete gel into a continuous structure[1,2].

Tobing et al. [1,2]showed the influence of Mw (molecular weight of sol polymers), Mc (molecular weight between two adjacent cross-linking points) and Me (molecular weight between entanglements) on the production of a continuous gel network using latexbased PSAs. Post-treatment by heating the PSA films resulted in significantly larger shear strengths. However, up to now, the performance of post-treated PSAs has still not attained that of solvent-based PSAs.

This study focused on improving the performance of heat-treated latex-based PSA films by optimizing the polymer properties of the original PSAs. The influence of very small and/or very large sol polymers was studied. In addition, PSAs with similar gel contents but different Mc and Mw were used to study if simultaneously increasing Mc and Mw could lead to the formation of a continuous gel network and larger shear strengths in the treated PSAs.

Materials and Methods: Butyl acrylate/acrylic acid/2-hydroxyl methacrylate (BA/AA/HEMA, weight ratio: 96/2/2) latexes were produced via starved seeded semi-batch emulsion polymerization. The microstructure of the latex polymers was controlled by varying the amount of chain transfer agent (1-dodecanethiol) and cross-linker (allyl methacrylate) used.

PSA films were cast using standard procedures[3] and were then dried and conditioned (24 h at 23ºC and relative humidity of 50%). For post-treatment, the PSA films were first heated at 90 ^{o}C for 10 min to remove water and then heated at a higher temperature (e.g., 120 or 126 ºC) to react the carboxyl and hydroxyl groups from the AA and HEMA units. The post-treated PSA films were also conditioned as above prior to testing.

The latexes were characterized for gel content, Mc, Mw and Me[3]. Tack, peel strength and shear strength of the PSA films were measured according to the Pressure Sensitive Tape Council standards[4].

Results and Discussion: In the figure below is a representation of the PSA film formation process. In “a”, the original latex is shown as separate particles with cross-linked networks (in red), very large sol polymers (Mw>20Me, in blue), and medium-sized sol polymers (2Me ≤Mw<20Me, in pink). In “b”, the PSA film shows how the medium-sized sol polymers have migrated and entangled with neighbouring networks. In the post-treated PSA film, “c”, new cross-linking points (in green) have formed. Improved connections between microgels in the untreated PSAs could be achieved by: (1) simultaneously and properly increasing Mc and Mw for similar gel content PSAs; (2) decreasing the amount of very small sol polymers (i.e., Mw < 2Me). The negative effect of very small sol polymers is due to its incapability to effectively entangle with microgels as well as other sol polymers; and (3) decreasing the amount of very large sol polymers (i.e., Mw > 20 Me), due to their lower mobility.

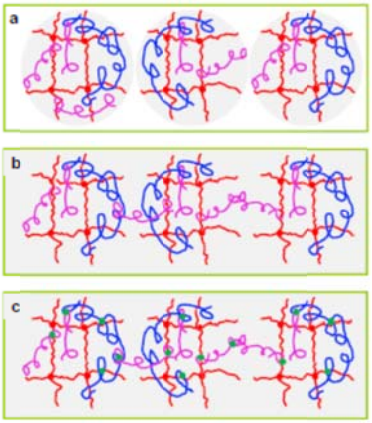

Conclusions: Post-treatment by heating was shown to be an effective way to improve latex-based PSA performance. The effectiveness of the post-treatment was observed to depend on the polymer microstructure (Mc relative to Me relative to Mw) of the untreated latexbased PSAs and on the gel content. Finally, it was possible, by optimizing polymer microstructure of the latex-based PSAs, to generate a treated latex-based PSA with even better performance than that of a solventbased PSA with similar polymer properties.

References:

1 S. D. Tobing, A. Klein, Journal of Applied Polymer Science 2001, 79: 2558-2564.

2 S. D. Tobing, A. Klein, L. H. Sperling, Journal of Applied Polymer Science 2001, 81: 2109-2117.

3 L. Qie, M. A. Dubé, European Polymer Journal 2010, 46(6): 1225-1236.

4 Pressure Sensitive Tape Council Test methods for pressure sensitive adhesive tapes. Pressure Sensitive Tape Council, Northbrook, Illinois, 2004, 14th Edition.

ABSTRACTS

INVITED LECTURES

Topic 4: Polymers for Advanced Applications Including Energy, Transport, Packaging and Environmentally Friendly Activities

Polymer Membranes for Water Purification

Benny D. Freeman[1], Donald R. Paul[1], James E. McGrath[2], Ho Bum Park[3], Anita J. Hill[4], Bryan McCloskey[5], Wei Xie[1], Joe Cook[1], Dan Miller[1], Geoff Geise, Sirirat Kasemset[1], and Albert Lee[1]

[1]Department of Chemical Engineering.The University of Texas at Austin.Austin, TX

[2]Department of Chemistry.Virginia Tech. Blacksburg, VA

[3]Department of Chemical Engineering.Hanyang University.Seoul, Korea

[4]CSIRO Materials Science and Engineering, Victoria, Australia

[5]IBM Almaden Research Laboratory.San Jose, CA

freeman@che.utexas.edu

An urgent need in the 21st century is access to secure, sustainable sources of fresh water. Membrane-based desalination has been recognized as an energy efficient, low environmental impact route to produce clean water for a variety of applications. Additionally, ultrafiltration and microfiltration of aqueous streams have become important unit operations in many industries, including the water purification and wastewater purification industries. This presentation focuses on 2 new classes of polymers to attack critical problems in membrane-based water purification: (1) chlorine-tolerant desalination membranes and (2) fouling-resistant membrane nanolayers based on polydopamine.

Commercially available RO membranes are prepared mainly from aromatic polyamides (PA). However, PA membranes suffer from poor resistance to continual exposure to oxidizing agents such as chlorine. Chlorine is the most widely used oxidizing biocide in water treatment because it is inexpensive and highly effective when present in water at levels of a few ppm. Disinfection of feed water to membrane desalination units is required to prevent biofilm growth on the membranes, which significantly degrades their performance. However, PA membranes cannot tolerate continuous exposure to water containing more than a few ppb of chlorine. This presentation discusses results from a systematic study of the desalination properties of a new family of highly chlorine tolerant, sulfonated polysulfones. These polymers are prepared via a novel synthesis involving direct copolymerization of non-sulfonated monomers with a disulfonated monomer. By controlling the content of disulfonated monomer in the final polymer, desalination properties, such as water permeability and salt rejection, can be varied over a wide range. A family of materials, based on random copolymers, phase-separated block copolymers, blends, and crosslinked materials may be prepared from these starting blocks to provide a new platform for desalination membranes.

Across many platforms of membranes, fouling mitigation is a major challenge to be addressed to achieve the most energy-efficient, cost-effective membrane filtration processes. Previously, many surface modifications and functionalized polymers were reported to prevent fouling. However, most of these techniques and materials are practically difficult to implement in water purification membranes. We have discovered surface treatment methodologies that can be used to prepare high permeability polymeric membranes from all common water purification membrane classes. These surface-modified membranes have persistent tolerance to fouling by proteins and emulsified oil, two ubiquitous contaminants in a variety of wastewaters. These membranes were prepared by depositing bio-inspired, self-polymerized hydrophilic polydopamine nanolayers on their surfaces.To demonstrate scalability of this modification, the nanolayers were also applied to entire membrane modules. Upon nanolayer deposition, the membranes could be further functionalized using fouling-resistant macromolecules, such as poly(ethylene glycol), to promote improved fouling resistance and, therefore, high membrane flux. The simplicity, versatility, and broad applicability of the nanolayer deposition technique on membranes provide distinct advantages over other modification strategies to reduce fouling.

Bioinspired Reversible Adhesives

Aránzazu del Campo

Max-Planck-Institut für Polymerforschung. Ackermannweg 10, 55128 Mainz, Germany

delcampo@mpip-mainz.mpg.de

Amongst a number of animals, geckos, some insects and frogs have developed adhesive pads in the course of biological evolution. These consist of non-compact material in the form of either foam-like (wet adhesion) or fibre-like (dry adhesion) structures with a hierarchical arrangement of thin walls or fibres with decreasing dimensions when approaching the outer pad surface. They allow the animal to effectively attach to and easily release from surfaces during locomotion, even on vertical walls or across ceilings. In some cases, adhesion is also guaranteed under extreme environmental conditions such as hurricanes (gecko) or waterfalls (torrent frogs).

We will present micro and nanostructured surfaces as biomimetic models to study and understand the mechanisms behind these biological systems that may lead to practical exploitation of a new concept of adhesion. Bioinspired surface structures are combined with responsive materials to obtain reversible adhesive systems in both dry and wet conditions.

Macroporous Cryopolymer and Hybrid Hydrogels: Biomedical and Environmental Applications

S. Mikhalovsky, S. James, L. James, R. Shevchenko, I. Allan, I. Savina, R. Whitby, A. Cundy

University of Brighton, Brighton, UK

s.mikhalovsky@brighton.ac.uk

Introduction. Cryopolymer hydrogels are produced in a frozen solvent, usually water. Ice crystals formed are used as a porogen, which is removed by thawing rather than freeze drying. Cryopolymers thus obtained have large interconnected pores in the range of 10-200 μm size. The most interesting applications of cryopolymers are related to their porosity combined with mechanical strength unusual for hydrogels. Here a few examples of biomedical and environmental applications of cryopolymers and cryopolymer-nano-iron oxide hybrid materials are presented and discussed.

Regenerative medicine. Various artificial skin products are currently available, however they are costly and not very efficient. We have produced a novel supermacroporous gelatin cryopolymer scaffold with an ordered anisotropic pore structure. The material was characterised and assessed *in vitro* and *in vivo* in porcine full-thickness wound model as a skin substitute.

It was found to be biocompatible and non-toxic to human skin cells, supporting active cellular migration and proliferation. The keratinocytes formed a continuous differentiated layer on the surface of the gelatin scaffold, mimicking the native skin bilayered structure. Gelatin-based cryopolymers successfully integrated into the *in vivo* wounds exhibiting an early host cellular influx into the matrix, neocollagen deposition within the scaffold. A scaffold biointegration was followed by the scaffold remodelling, which occurred earlier when compared with Integra®, a commonly used commercial skin substitute.

The large size of interconnected gradient pores, biocompatibility and small production costs of gelatin cryopolymers make them a promising material for tissue engineering and regenerative medicine, to treat burns and chronic wounds.

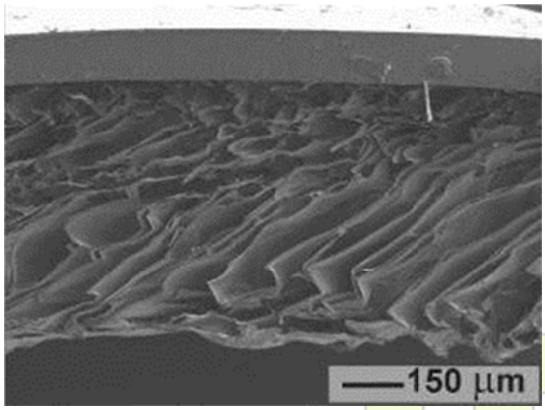

Figure 1SEM image of gelatin cryopolymer cross-section

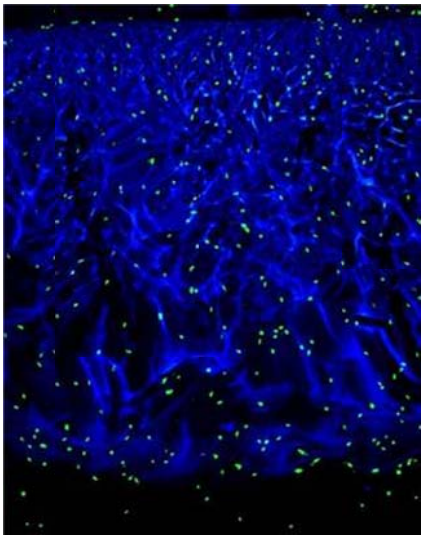

Figure 2 Confocal microscope image of gelatin cryopolymer populated with human skin fibroblasts

Environmental cleanup. Flexibility of cryopolymer synthesis allows manufacturing of various 3-D constructs, in which particles of other materials can be incorporated thus producing mechanically robust hybrid materials with low flow resistance. A filtration device made of a monolithic poly(hydroxyethylmetacrylate) macroporous cryopolymer with embedded iron oxide nanoparticles efficiently removed heavy element ions (arsenic, lead and copper) from water.

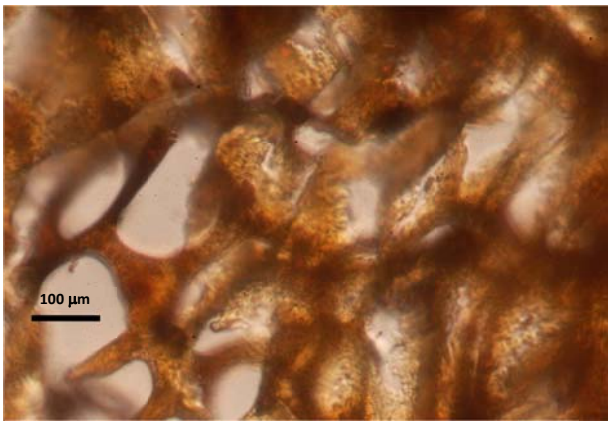

Figure 3 Light microscopy image of a thin slice of Poly-HEMA-Fe_2O_3 hybrid material.

Acknowledgments: FP6-IAP 'MATISS', Protista AB (Bjov, Sweden) and StratiCell (Namur, Belgium).

Polymer Electrolyte Membranes Based on Poly(phenylene ether)s with Pendant Perfluoroalkyl Sulfonic Acids

Kazuhiro Nakabayashi, Tomoya Higashihara, and Mitsuru Ueda

Department of Organic and Polymeric Materials, Tokyo Institute of Technology, 2-12-1-H120, O-okayama, Meguro-ku, Tokyo 152-8552, Japan

ueda.m.ad@m.titech.ac.jp

Development of polymer electrolyte membranes (PEMs) based on aromatic polymers have been investigated over the past decades to realize alternatives of sulfonated perfluoropolymers (e.g., Nafion® and Flemion®). For example, PEMs based on sulfonated multiblock copolymers have been widely studied as the promising polymer architecture for high-performance PEMs.[1]Recently, the introduction of perfluroalkyl sulfonic acids into aromatic polymers also demonstrated drastic improvement of proton conductivity due to its high acidity (pK_a~ –6).[2] Thus, as well as sulfonated multiblock copolymers, this approach can be a promising way to improve performances of aromatic PEMs.

Hence, in this work, novel poly(phenylene ether)s containing pendant perfluoroalkyl sulfonic acids with ion exchange capacity (IEC) of1.17–1.83 mequiv/g(**4a–5a**) were synthesized by the aromatic nucleophilic substitution reaction of a perfluoro monomer (decafluorobiphenyl or hexafluorobenzene) with 2,5-bis(4'-iodophenyl)hydroquinone, followed by the Ullman coupling reaction with potassium 1,1,2,2,-tetrafluoro-2-(1,1,2,2-tetrafluoro-2-iodoethoxy)ethanesulfonate (**PTES**). These poly(phenylene ether)s consist of the rigid polymer backbones with the high fluorine content and the flexible perfluoroalkyl sulfonic acid side chains, that is, the structure mimics that of the sulfonated perfluoropolymers (Figure 1). Their IEC values could be readily controlled by changing the equivalent of **PTES** in the Ullman coupling reaction. The structure of polymers was confirmed by ^{1}H and ^{19}F NMR spectra.

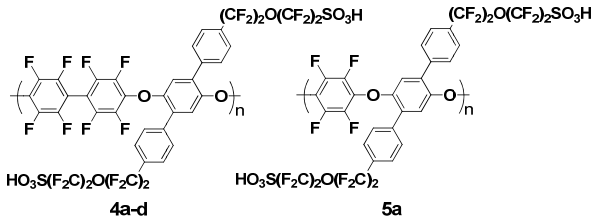

Figure 1. Structure of **4a–5a**.

The **4a–5a** membranes prepared by solution casting showed significantly low water uptake (19.3–28.0 wt %) and excellent dimensional stability even in the hydrated state, which were due to the strong hydrophobicity of the polymers (i.e., the high fluorine content). Besides, the high oxidative stability against hot Fenton's reagent (3% H_2O_2 aqueous solution containing 2 ppm $FeSO_4$ at 80 °C) was achieved. Humidity dependence of water uptake was evaluated in the **4a–5a** membranes at 80 °C. The **4a** and **4b** membranes with IEC = 1.17 and 1.38 mequiv/g showed low water uptake comparable to the Nafion 117 membrane in a whole range of relative humidity. The **5a** membrane with IEC = 1.83 mequiv/g showed the highest water uptake (24.0, 20.1, 12.6, and 8.8 wt % at 95, 80, 50, and 30% RH, respectively), which corresponded to λ (the number of water molecules per a sulfonic acid) = 7.3, 6.1, 3.8, and 2.7, respectively. These λvalues are as high as those of the Nafion 117 membranes. Figure 2 shows humidity dependence of proton conductivity of the **4a–5a** membranes at 80 °C. All membranes show high proton conductivity comparable to the Nafion 117 membrane at 95% RH. The proton conductivity of the **4a–d** membranes, however, decreases rapidly with decreasing relative humidity from 95 to 30% RH. On the other hand, the **5a** membrane with IEC = 1.83 mequiv/g maintains high proton conductivity comparable to the Nafion 117 membrane to 30% RH. The high λ values of the **5a** membrane should contribute to high proton conductivity. As for sulfonated aromatic polymers with the same IEC values, high proton conductivity like the **5a** membrane has never been achieved, which obviously indicates that the high acidity of perfluoroalkyl sulfonic acids contributes to drastic improvement of proton conductivity.

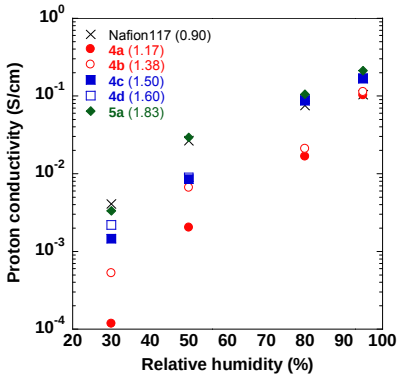

Figure 2. Humidity dependence of proton conductivity of **4a–5a** and Nafion 117 membranes at 80 °C.

In summary, novel poly(phenylene ether)s containing pendant perfluoroalkyl sulfonic acid with IEC = 1.17–1.83 mequiv/g (**4a–5a**) were successfullysynthesized. All membranes showed high dimensional and oxidative stability. Among them, the **5a** membrane with IEC = 1.83 mequiv/g accomplished high proton conductivity comparable to the Nafion 117 membrane in the range of 30–95% RH, which resulted from the strong acidity of perfluoroalkyl sulfonic acids.

References: (1)(a) Yu, X. et al. *Macromol.Symp.***2006,***245,* 439-449. (b) Nakabayashi, K. et al. *J. Polym. Sci. Part A: Polym. Chem.***2010,***48,*2757-2764. (2)(a)Miyatake, K. et al. *Chem. Commun.* **2009,** 6403-6405. (b) Yoshimura, K. et al. *Macromolecules***2009,***42*, 9302-9306.

Biobased/biodegradable/compostable polymers/blends/nanocomposites for packaging and agro-based uses

Erhan Pişkin[1], F.Yeşim Ekinci[2]

[1]Hacettepe Univ., Chem.Eng.Dept.and Bioeng.Div., and Bioeng. R&D Center - Biyomedtek, Beytepe, Ankara, Turkey

[2]Yeditepe Univ., Food Eng.Dept., Kayışdağı, İstanbul, Turkey

piskin@hacettepe.edu.tr

Industrial product made of fossil fuel based synthetic raw materials have been produced in very large quanties and consumed since 1970s which is also the reality today. Fuels (petroleum, natural gas and coal) are considered as non-renewable resources. The annual consumption of fossil fuel feedstock is about about 7.3 Gton, and we are consuming about 93% of it for energy production. Only 7% is used for polymer and raw chemicals production. **Fossil fuel feedstock will finish** as a result of this very high consumption rates. More than 30% of the polymers produced are consumed for packaging (including agro-chemical uses such as mulching films) which has a relatively short life (< 1 year). This means that packaging waste accumulating in the environment quite rapidly which may cause very undesirable adverse effects that we have already facing today. **We have to be more environmentally conscious.** Even only because of these two main concerns one can easily prospect that naturally derived resources (also called biobased resources) will be again a major contributor to the production of industrial and commodity products. There is a great potential market of biobased polymers. They are mainly made of renewable resources of agricultural origin desirably agroindustrial waste not interfering with food chain. After use they are disposed of as organic waste, and return to the earth through processes of biodegradation and composting - completing a virtuous circle- **A very environmentally friendly approach.** Here, in this short presentation, one important biopolymer, i.e. starch, and important biodegradable polyester, polylactic acid and its clay nanocomposites are briefly overviewed.

Starch: Polysaccharides, such as starch, cellulose and chitin are in one of the most important categories of biobased polymers, as biopolymers. Corn is the primary source of starch, although considerable amounts of starch are produced from potato, wheat and rice starch in Europe. In order to produce thermally processable starch (thermoplastic starch, TS) several modifications have been proposed in which the starch -after milling of the raw material- is destructured and chemically modified (converting hydroxyl groups to aldehyde groups) to obtain amorphous (noncrystalline-more stable in aqueous media, since more hydrophobic). In order to further improve its processabilities and also final product properties (mechanical strength, gas permeability, etc.) TS is compounded with plasticizers (e.g., glycerol) and/or complexion agents (e.g., vegetable oils). Alternatively, several more hydrophobic biodegradable and nondegradable polymers are used to prepare blends that are more suitable for injection molding and blowing films. Compatibility is an important issue when these types of blends and laminates are considered, and therefore compatibilizers and other additives should be used as processing aids. The price of starch especially in US is competitive with petroleum therefore it has been processed into several compostable products.

Polylactic acid (PLA): Lactic acid is the most widely occurring carboxylic acid, having a prime position due to its versatile applications in food, pharmaceutical, textile, leather, and other chemical industries. Lactic acid is widely used in the food related applications but recently it has gained many other industrial applications like biodegradable plastic production. Lactic acid, is the monomer for PLA, may easily be produced by fermentation of carbohydrate feedstock. There is a huge list of studies for the production of lactic acid from different resources nicely reviewed recently.

Lactic acid is an α-hydroxy acids, and as being bifunctional molecules, it can be homopolymerized into linear polymers by heating with or without using a catalyst by direct polycondensation reactions (or in other terms by intermolecular esterification).This technique produces only low-molecular-weight polymers (oligomers). In order to produce polyesters with higher molecular weights that lactic acid is first converted to the respective cyclic dimer, i.e. "lactides". These processes are usually based on the transformation of lactic acids into a low molecular weight polymer by heating or also using a catalyst (e.g., antimony trioxide, zinc chloride), and then heating the polymer under reduced pressure to generate the desired cyclic ester. Then, ring-opening polymerization of cyclic dimers using various catalysts (e.g., stannous octoate) are being conducted, usually in bulk or in reactive extruders which is the main approach for the synthesis of polyesters with high molecular weights.

Polymer nanocomposites are prepared by dispersion of nano-sized materials (nanofillers) into the polymer matrix usually less than 10%. Layered clays and silicates (e.g., montmorillonite, hectorite, saponite) are the most widely used nanofillers. Incorporation of nanofillers, due to huge interfacial surface area improves polymer properties (such as mechanical properties; thermal stability; flame retardance; barrier properties, etc.) drastically. Dispersion of the layered silicates into discrete monolayers is hindered by the intrinsic incompatibility of hydrophilic layered silicatesand hydrophobic (usually) polymer matrices. Therefore they have to be **"intercalated"** or even converted into a better form, **"exfoliated**" using several organo-modifier, usually organic onium ions which are then dispersed in the polymer matrix (both in solution or in melt) to prepare the nanocomposites.

PLA is a very promising material, as also mentioned above, since it is commercially available with reasonable prices, exhibit good thermal plasticity and mechanical properties suitable for many applications including packaging films. However, some of its properties, like flexural properties, gas permeability and heat distortion temperature, are too low for widespread applications. Therefore, PLA have been one of the most widely studies bio-based polymers to prepare nanocomposites in order to improve its properties. Several parameters affect nanocomposite properties, includingboth organoclay type, size/shape and clay content, and also organomodifier type and content which will be discussed in this presentation.

References

Bordes P, Pollet E, Avérous L, Nano-biocomposites: Biodegradable polyester/nanoclay systems.

Prog in Polym Sci 34: 125-155, 2009.

Garlotta D. A literature review of poly(lactic acid). *J Polym Environ*, 9:63-84, 2001.

John RP, Anisha GS, Nampoothiri KM, Pandey A, Direct lactic acid fermentation: Focus on simultaneous

saccharification and lactic acid production, *Biotechnol Adv* 27:145-152,2009.

Lima LT, Aurasb R, Rubino M, Processing technologies for poly(lactic acid), *Prog Polym Sci* 33:820-852, 2008.

Yu J, Peter R, Chang PR, Ma X, The preparation and properties of dialdehyde starch and thermoplastic

dialdehyde starch, *Carbohydrate Polym* 79:296-300, 2010

Zobel H F (1998). Molecules to granules: A comprehensive starch review. *Starch-Starke,* 40:44-50, 1998.

Thermally Rearranged Polymer Membranes with Tuned Microcavities for CO2 Capture

Young Moo Lee

WCU Department of Energy Engineering, College of Engineering, Hanyang University, Seoul 133-791, Republic of Korea

ymlee@hanyang.ac.kr

Microporous materials have various beneficial properties (e.g. large surface area, high pore volume and appropriate pore width in the materials) for enhanced sorption, diffusion, and the improved permeation properties beyond conventional nonporous materials. Compared to inorganic microporous materials such as silica, alumina, zeolite and metal-organic frameworks (MOFs), organic microporous materials are advantageous in their synthesis, mass production, and processability for numerous applications. Since T. Matsura reported a novel poly[1-(trimethylsilyl)-1-propyne] with high fractional free volume in 1983, in the last few decades, polymeric materials retaining microporous characteristics have been developed: poly(substituted acetylene)s, amorphous fluoropolymers, polymers with intrinsic microporosity (PIMs) and thermally rearranged (TR) polymers.

Thermal rearrangement of ortho-functional polyimides is a robust and irreversible process to render thermally and chemically stable rigid-rod polymers. The thermal conversion in stiff, rigid heteroaromatic rings cause increase of free volume elements as well as change of polymer structure confirmed by various analytic method such as FT-IR, NMR, TGA, DSC, WAXD, density, PALS, SAXS and gas permeation measurements. TR-polymers have bimodal cavity sizes of 0.3-0.4 nm and 0.7-0.9 nm, and narrow cavity size distributions as a shape reminiscent of aquaporins which has bottlenecks connecting adjacent chambers so that those can yield both high permeability and high selectivity based on high diffusivity of small gas penetrants.

Most of all, the greatest benefit of these TR-polymers is the ability to control their separation performances for specific gas applications including CO_2 capture from flue gas by using various polymer structures and templating molecules with heating time and temperature. Copolymerizations with pristine polyimide or polypyrrolone in the main chain as well as the control of conversion ratio of precursors provide simple and convenient method to govern diffusivities and diffusion selectivities. Changes of ortho-functional groups also contribute to the physical properties because the side groups can affect the intermolecular distances and topologies of precursor and the resulting TR polymer membranes as well as act as templating molecules during thermal rearrangement. Moreover, other precursor polymers such as poly(hydroxyl amide) and schiff-base polymers can be thermally treated in solid states and bring in microcavities and high separation performances for specific gas pairs such as H_2/CO_2 and H_2/N_2.

Understanding of these diverse routes correlated with the cavity size and distribution of the materials can provide the evidence to the high gas separation performances and also the method of controlling the microcavities in TR-polymers for targeted applications. Here, gas transport properties of various precursors and TR-polymer membranes will be summarized overall and analyzed with microcavities.

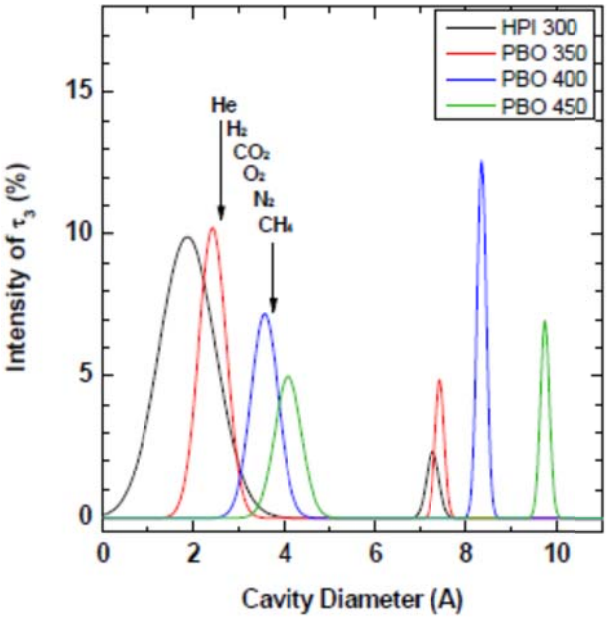

Figure 1. Cavity size and distribution of TR-PBOs

Acknowledgement

This research was supported by a grant (2009K000673) from the Carbon Dioxide Reduction & Sequestration Research Center, one of 21st Century Frontier R&D Programs funded by the Ministry of Education, Science and Technology (MEST) of the Korean Government.

References

[1] Park, H. B.; Jung, C. H.; Lee, Y. M.; Hill, A. J.; Pas, S. J.; Mudie, S. T.; Wagner, E. V.; Freeman, B. D.; Cookson, D. J. *Science* **2007**, 318, 254-258.

[2] Park, H. B.; Han, S.H.; Jung, C.H.; Lee, Y. M.; Hill, A. J.;*J. Membr. Sci*. **2010**, 359, 11-24.

[3] Jung, C.H.; Lee, J.E.; Han, S.H.; Park, H. B.; Lee, Y. M.; *J. Membr. Sci*. **2010**, 350, 301-309.

[4] Han, S.H.; Lee, J.E.; Lee, K.J.; Park, H. B.; Lee, Y. M.; *J. Membr. Sci*. **2010**, 357, 143-151.

[5] Han, S.H.; Misdan, N.; Kim, S.; Doherty, C.M; Hill, A. J.; Lee, Y. M.; *Macromolecules* **2010**, 43, 7657-7667.

[6] Calle, M.; Lee, Y. M.; *Macromolecules* **2011**, in press.

Functional Polymers for Electronics and Packaging - Synthesis, Chracterisation and Application

Franz Stelzer, Robert Saf , Christian Slugovc, Gregor Trimmel, Frank Wiesbrock

Institute for Chemistry & Technology of Materials, Graz University of Technology, Stremayrgasse 9/Z5east

A-8010 Graz, Austria

franz.stelzer@tugraz.at

Functional polymers are gaining more and more importance concerning various fields of application. In this contribution we will present some examples of polymers developed for application as biocidic food packaging material, as matrix in hybrid photovoltaic cells or in sensor applications, as smoothening layer in printed boards and many more.

Our synthetic working horse is the ring opening metathesis polymerization (ROMP). Because of its living character it allows a far going control of polymer structures, sequences in copolymers and finally even morphology of the resulting block-copolymers.

Furthermore, in addition to these synthetic polymers some biopolymers will be presented that are produced via fermentation processes (PHAs), where the properties can be defined by applying a multi-step process. These polymers are modified chemically in order to meet the demands of the applications, in this case in medical applications.

In addition to traditional characterization methods some special methods especially connected to the applications will be presented and discussed.

Porous Polycyanurates: New Film Materials Derived from Old Polymers

Daniel Grande,[1] *Olga Grigoryeva,*[2] *Alexander Fainleib*[2]

[1] "Complex Polymer Systems" Laboratory, Institut de Chimie et des Matériaux Paris-Est, 2 rue Henri Dunant, 94320 Thiais, France (E-mail: grande@icmpe.cnrs.fr)

[2] Institute of Macromolecular Chemistry, National Academy of Sciences of Ukraine, Kharkivske shose 48, 02160 Kiev, Ukraine

Introduction

Porous polymer films are widely used in many branches of industry as membranes, adsorbents and filters for separation, purification or filtration, as well as low-permittivity films for microelectronics.[1] Numerous advanced technologies require a combination of properties for polymer films, including high thermal stability, inertness, excellent resistance towards solvents and aggressive media, etc. Polycyanurates (PCNs) represent a family of thermosetting polymers that meet such requirements, in addition to their attractive intrinsic features, *i.e.* excellent dimensional stability, low dielectric constants (2.6-3.2), inherent flame-retardancy, and high adhesion to conductor metals and composites.[2] To the best of our knowledge, few reports on the design and synthesis of porous PCNs have hitherto been published.[3] Accordingly, engineering porous PCN thermosets still remains challenging.

Results and Discussion

We have undertaken a thorough investigation of the scope and limitations associated with the use of miscellaneous PCN systems as precursors to (nano)porous thermosetting film materials.[4,5] Three original approaches have been developed to prepare new mesoporous films. First, the PCN synthesis was performed in the presence of a reactive oligomeric modifier, *i.e.* poly(ε-caprolactone) (PCL). During the synthesis of PCL-modified PCN networks, PCL was partially incorporated chemically into the PCN structure. Porous frameworks were then derived from such PCN/PCL hybrid networks by hydrolysis of PCL segments under mild conditions (pH 7). Alternatively, the PCN-based films were bombed by α-particles, and subsequently the tracks formed were chemically etched to generate nanopores. The last route entails the preparation of pure PCN networks in the presence of high-boiling solvents, such as dimethyl or dibutyl phthalate, and their subsequent removal upon extraction.

The cyanurate-based precursors and the resulting porous films were characterized using FTIR, DSC, TGA, and pycnometry. In this communication, the potentialities afforded by these versatile and effective approaches will be addressed, and we will particularly focus our attention on the investigation of correlations between the structure and properties of the precursors and those of the corresponding porous thermosets. SEM and DSC-based thermoporometry analyses demonstrated the presence of well-defined mesopores (average diameters around 50 nm) within these novel film materials, and pore sizes generally ranged from 10 to 150 nm –at most– (*Figure 1* as examples).

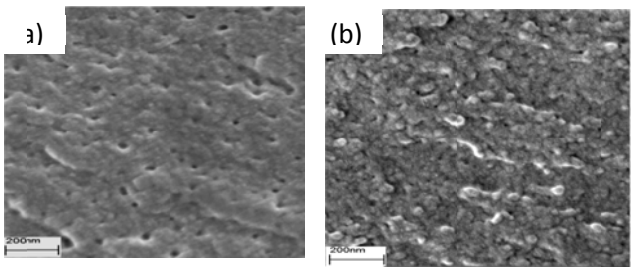

Figure 1. SEM images of nanoporous PCN-based films: (a) "track-etch" membrane, (b) membrane derived from the phthalate extraction in a PCN precursor.

Conclusions

While the most straightforward approach to these novel nanoporous PCN films relies on the use of high-boiling liquids as porogens, the narrower pore size distributions can be obtained by resorting to the track-etching technique. Such crosslinked film materials may find miscellaneous applications, and especially in membrane technologies requiring polymeric materials with thermal and dimensional stability.

Acknowledgements

The CNRS (France) and the NASU (Ukraine) are gratefully acknowledged for financial support through a French-Ukrainian international project for scientific cooperation.

References

1. *Membrane Technology in the Chemical Industry, 2nd edition*; Pereira-Nunes, S., Peinemann, K.-V., Eds.; Wiley-VCH: Weinheim, 2006.
2. *Chemistry and Technology of Cyanate Ester Resins*; Hamerton, I., Ed.; Chapman & Hall: Glasgow, 1994.
3. (a) Kiefer, J; Hilborn, J.G.; Hedrick, J.L.; Cha, H.J.; Yoon, D.Y.; Hedrick, J.C. *Macromolecules* **1996**, *29,* 8546. (b) Hedrick, J.L.; Russell, T.P.; Hedrick, J.C.; Hilborn, J.G. *J. Polym. Sci., Part A: Polym. Chem.* **1996**, *34*, 2879.
4. (a) Fainleib, A.; Grigoryeva, O.; Garda, M.R.; Saiter, J.M.; Lauprêtre, F.; Lorthioir, C.; Grande, D. *J. Appl. Polym. Sci.* **2007**, *106*, 3929. (b) Grande, D.; Grigoryeva, O.; Gusakova, K.; Fainleib, A.; Lorthioir, C. *Eur. Polym. J.* **2008**, *44*, 3588.
5. Grande, D.; Grigoryeva, O.; Fainleib, A. In *Thermostable Polycyanurates: Synthesis, Modification, Structure, and Properties*;Fainleib, A., Ed.; Nova Science Publishers: New York, 2010; chap. 9, pp. 297-320.

Epoxy Polymers and Composites for Advanced Applications

Roberto J. J. Williams

Institute of Materials Science and Technology (INTEMA), University of Mar del Plata and National Research Council (CONICET), Av. J. B. Justo 4302, 7600 Mar del Plata, Argentina

e-mail: williams@fi.mdp.edu.ar

Introduction: Due to their excellent properties epoxy polymers are extensively used in traditional applications such as adhesives, coatings and composites. In recent years there has been an increasing use of epoxies in the development of advanced functional materials.[1] Some examples will be given in this presentation.

Reversible Epoxy Networks: The reaction of diglycidylether of bisphenol A (DGEBA) with an *n*-alkylamine leads to a linear epoxy polymer. However, linear chains can be assembled by tail-to-tail associations between *n*-alkyl groups leading to a network with physical crosslinks. The strength of the physical bonds decreases with temperature and with the length of the *n*-alkyl group.[2] By increasing temperature the material reversibly transforms from a gel to a liquid, a fact that may used to develop self-healing epoxies.

Shape Memory Epoxies: When epoxies are heated above their glass transition temperature (T_g) they can be deformed to a temporary shape by applying a relatively small stress. By fixing the deformation and cooling below T_g, a glass is obtained that stores elastic energy in chain conformations removed from their equilibrium values. When the material is released from any constraint and is heated again above T_g, a rapid recovery of the initial shape is obtained as chains recuperate their equilibrium conformations. But if the heating step is performed keeping the initial deformation, the material develops a recovery stress. Actuators based on epoxies can make use of the shape recovery or the stress recovery. They can be designed for large tensile elongations (e.g., 75 % or higher) or large recovery stresses (e.g. 3 MPa or higher). However, meeting both requirements simultaneously is a difficult task because changes in the crosslink density affect both variables in opposite ways. An epoxy formulation based on the reaction of DGEBA with *n*-dodecylamine (DA) and *m*-xylylenediamine (MXDA) gives a network with both chemical and physical crosslinks that can be used for a shape memory material verifying both requirements.

Epoxy Networks Containing Silver Nanoparticles (NPs): Ag NPs can be introduced into epoxy coatings to obtain specific electrical or antimicrobial properties. Different methods can be employed to obtain a uniform dispersion of NPs. A DGEBA/DA gel was swollen with a 6mM solution of $AgNO_3$ in THF/H_2O (90:10). After rinsing with THF and drying in vacuum, the epoxy network was heated at 100 ºC for 1 h, generating a uniform dispersion of Ag NPs with an average size close to 10 nm.[3] The reduction was performed by the secondary alcohols present in the epoxy backbone. The T_g increased from 20 ºC (neat epoxy) to 28 ºC (nanocomposite). A different strategy to obtain a uniform dispersion of Ag NPs in an epoxy matrix was to introduce reactive groups in the organic chains stabilizing the NPs. Silver NPs with an average size of 4nm and stabilized with an organic group containing secondary hydroxyls, were synthesized and dissolved in DGEBA. The epoxy was polymerized using a tertiary amine as initiator. Ag NPs were covalently bonded to the epoxy network through chain transfer reactions to the secondary hydroxyls of the organic ligands. The nanocomposites were strongly colored and showed a dependence of T_g on the concentration of NPs.[4]

Epoxy Networks Containing Single-Wall Carbon Nanotubes (SWCNT): Epoxy nanocomposites containing SWCNT exhibit significant improvements in mechanical, thermal or electrical properties. Surface functionalization of SWCNT enables to obtain an adequate dispersion of the nanotubes in the epoxy formulation. A problem that is present in some formulations is the different partition of the epoxy monomer and the hardener in the interphase, a process favored by the large specific area per unit volume. This leads to a heterogeneous network characterized by two relaxation peaks and a significant decrease of the glass transition temperature. This problem was avoided by a convenient functionalization of the SWCNT, producing a localized formation of bundles of nanotubes in the course of polymerization. The T_g of the nanocomposite was the same as the one of the neat epoxy.[5]

Epoxy Networks Containing POSS Crystalline Platelets: The dispersion of intercalated/exfoliated clays in polymers decreases their permeability due to geometrical effects. However, processing is difficult due to the initial high viscosity. An alternative is to produce the crystallization of an initially soluble precursor during polymerization. The feasibility of this idea was proved using a polyhedral oligomeric silsesquioxane (POSS) dissolved in the epoxy precursors.[6]

References

1. Pascault, J.P.; Williams, R.J.J.; Eds., Epoxy Polymers: New Materials and Innovations, Wiley-VCH, Weinheim, 2010.

2. Puig, J.; Zucchi, I.A.; Hoppe, C.E.; Pérez, C.J.; Galante, M.J.; Williams, R.J.J.; Rodríguez-Abreu, C. Macromolecules 2009, 42, 9344-9350.

3. Ledo-Suárez, A.; Puig, J.; Zucchi, I.A.; Hoppe, C.E.; Gómez, M.L.; Zysler, R.; Ramos, C.; Marchi M.C.; Bilmes S. A.; Lazzari, M.; López-Quintela, M.A.; Williams, R.J.J. J. Mater. Chem. 2010,20, 10135-10145.

4. dell'Erba, I.E.; Hoppe, C.E.; Williams, R.J.J. Langmuir 2010, 26, 2042-2049.

5. Auad, M.L.; Mosiewicki, M.A.; Uzunpinar, C.; Williams, R.J.J. Polym. Eng. Sci. 2010, 50, 183-190.

6. Di Luca, C.; Soulé, E.R.; Zucchi, I.A.; Hoppe, C.E.; Fasce, L.A.; Williams, R.J.J. Macromolecules 2010, 43, 9014-9021.

Ageing and long-term durability of polymer-based solar cells

Jean-Luc Gardette[1,2] ,*A. Rivaton*[1,2] , *S. Thérias*[1,2]

[1]Clermont Université, Université Blaise Pascal, Laboratoire de Photochimie Moléculaire et Macromoléculaire.

[2]CNRS, UMR 6505, LPMM, F-63173 Aubière

luc.gardette@univ-bpclermont.fr

Introduction. As the world energy demand continues growing and the cost of natural resources is rising, new solutions for cheaper and cleaner energy production are required. Among the various options, solar cells are expected to be a major contributor to fulfil the future needs. However, alternatives to silicon-based devices must be developed to reduce the power production costs. Devices that mediate energy conversion by way of light-sensitive organic polymers may be attractive because of the low cost of the materials and manufacturing methods required to produce the cells. Organic solar cells, although less efficient than silicon ones, exhibit a unique combination of properties including low cost, flexibility and large surface processability. Organic photovoltaic could then prevail for some applications alongside silicon, such as nomad or indoor. To achieve this objective, the control and the improvement of the initial properties are required, but the sustainability of these properties in conditions of use of the cell could be a lock to the emergence of these devices in the market. Organic solar cells (OSC) are indeed known to exhibit low resistance to environmental constraints, in particular to the combined action of sunlight, oxygen and water. Among all of the known conducting polymers used in organic solar cells, polyphenylenevinylene derivatives and poly(3-alkylthiophenes) have been the focus of particular attention due to their good electrical and mechanical properties [1,2]. It is however surprising that the photochemical behaviour of these polymers in the solid state remains so scarcely documented, since most of their applications are optical in nature. Similar to numerous other conjugated macromolecules, MDMO-PPV and P3HT have low photochemical stability, which leads to reduced operating lifetimes of OSCs.

Results and discussion. Understanding the degradation processes that result from the interaction of conducting polymers with solar light seems relevant to improve the stability of devices that integrate such polymers. We present results on the photochemical ageing of two polymers, poly(2-methoxy-5-(30,70-dimethyloctyloxy)-1,4-phenylenevinylene(MDMO-PPV) and poly(3-hexyylthiophene) (P3HT), and their blends with [60]PCBM (methano-fullerene[6,6]-phenyl C61-butyric acid methyl ester), a fullerene derivative [3-6].

We present in details the mechanism of photooxidation and photolysis of MDMO-PPV and P3HT monitored by various analytical tools, including IR spectroscopy, fluorescence emission, X-ray photoelectron spectroscopy, SEC, isotopic labelling experiments. The obtained results evidenced that P3HT is much more resistant to light irradiation than MDMO-PPV. This improved stability was explained on the basis of the different chemical structures of the two materials and, more precisely, considering their respective side chains. It was also observed that the degradation rate was strongly attenuated, and even nearly suppressed, when the polymers were blended with PCBM. This behaviour was attributed both to the radical scavenging properties of the fullerene and to its ability to quench excited singlet states. Complementary information was obtained by transient absorption spectroscopy [7]. It was demonstrated that the oxidation of both MDMO-PPV and P3HT proceeds via a free-radical chain reaction route, thus forming various oxidation products that were identified, and also includes cross-linking. It was shown that singlet oxygen played no decisive role in the phootoxidation [8]. The photodegradation mechanisms of these polymers were elucidated[9].

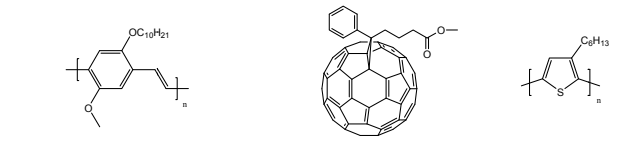

Figure 1. Chemical structures of MDMO-PPV, $PC_{60}BM$ and P3HT

Conclusion. The results showed that, if deposited on an inert substrate and well protected from oxygen, P3HT:PCBM based active layer should be intrinsically stable for long exposure periods. The extrapolation of the data obtained in conditions of artificial accelerated ageing to natural ageing suggested that the P3HT:PCBM blend would be stable for at least three years under use conditions if well protected from oxygen with a convenient

References

Roncali J. *Chem Rev* 1992; 92(4):711–38.

[2]McCullough R D. *Adv Mater* 1998; 10(2):93–116.

[3]Chambon S, Rivaton A, Gardette J-L, Firon M, Lutsen L. *J Polym Sci Part A Polym Chem* 2007; 45:317–331.

[4]Chambon S, Manceau M, Firon M, Cros S, Rivaton A, Gardette J-L. *Polymer* 2008; 49(15):3288–94.

[5]Chambon S, Rivaton A, Gardette J-L, Firon M. *Sol Energy Mater Sol Cells* 2008; 92(7):785–92.

[6]Chambon S, Rivaton A, Gardette J-L. Firon M. *Sol Energy Mater Sol Cells* 2007; 91(5):394–8.

[7] Chambon S, Rivaton A, Gardette J-L. Firon M. *J Polym Sci Part A Polym Chem* 2009; 47:6044-6052

[8] Manceau M, Rivaton A, Gardette J-L. *Macromol Rapid Commun* 2008 ; 29:1823-1827

[9] Manceau M, Rivaton A, Gardette J-L, Guillerez S, Lemaitre N. *Polym Deg Stab* 2009; 94:898-907

ABSTRACTS

INVITED LECTURES

Topic 5: Chemistry and Physics of Nanomaterials and Nanotechnologies

A direct Way to Fabricate Polymer and Polymer-based Composite Nanostructures

Carmen Mijangos,Jaime Martin, Iwona Blaszczyk-Lezak, Yon Maíz, Javier Sacristán

Instituto de Ciencia y tecnologia de Polimeros, CSIC
Juan de la Cierva 3, 28006, Madrid

cmijangos@ictp.csic.es

One of the most promising aspects in the fabrication of polymer nanostructures is the ability to generate a variety of different morphologies with structural definition on the nanometric scale. The properties of the nanostructured materials will depend on both the nature of its molecular constituents and the precise spatial positioning of them and, as the structure becomes smaller than a characteristic length, may be different from those of the bulk. With recent progress in synthetic routes and continuous emerging technologies, it is possible to reproducibly fabricate polymer nanostructures such as spherical functional gels, polymer and polymer based composite nanotubes and nanowires, etc. These materials are initiating development of new miniature devices and functional materials that exhibit unique capabilities.

Nowadays, the self-ordered porous alumina template (AAO) is recognized as one of the most versatile external shape-defined process to fabricate 1D polymer nanostructures. During the last few years our group has been working on the fabrication of AAO templates of adjustable size and the subsequent polymer infiltration methods (1); the morphological and chemical characterization of polymer nanostructures (2); the determination of polymer properties under confinement (3,4); the potential applications of tailored polymer-based nanofibers and nanotubes (5,6) and, more recently, on recycling methods of AAO templates. This last aspect is motivated by the fact that in order to expand the use of nanostructured polymers and composites it is necessary to develop an easier and scale-up the fabrication process from laboratory to an industrial level. But because of the time needed for preparation and the price of aluminum, it is first necessary to try to recover used AAO templates.

The aim of this work is to give a brief presentation of the current progress and the most important aspects related tothe fabrication of 1D polymer nanostructures on the basis of our research group developments. It includes, i) examples of fabrication of polymer nanotubes and nanofibres of very different chemical nature and their nanostructured arrays, as well as, of polymer-based nanocomposites functionalised with magnetic, electrical, gold, etc, nanoparticles obtained by the same procedure; ii) the compositional distribution characterisation of polymer nanofibre&nanotubes, determined by confocal Raman microscopy; iii) related to confined polymer properties, we will show how the behaviour of polymer composites under nanoscale confinement seems to holdout a new perspective to deal with some classical problems in polymer composites physics, i.e. the early stages of the crystallization, the glass transition, and so on. iv) few examples on the perspectives to produce miniaturise polymer materials, directly related to applications and new strategies to prepare large are of 1D nanostructured polymers. v) the possibility of reusing the AAO template (recycling) by high temperature treatment of infiltrated AAO membranes.

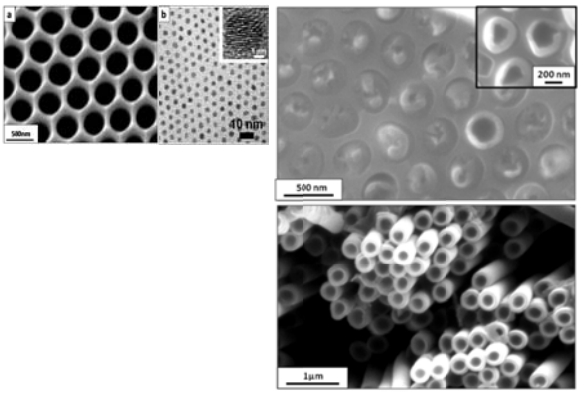

[1]J. Martín, C. Mijangos. Langmuir 2009, 25, 1181

[2]J. Maiz, J. Sacristán, C. Mijangos. Chemical Physics Letters 484 (2010) 290

[3]J. Martín, C. Mijangos, A. Sanz, T. A. Ezquerra, A. Nogales. Macromolecules 2009, 42, 5395

[4]J. Martin, M. Krutyeva, Mijangos, J. Colmenero, D.

Richter, et al Phys. Rev. Letters 104 (2010) 197801.

[5]S Grimm, J Martín, G Rodriguez, U Gosele, J San Roman, C Mijangos, M Steinhart et al J. Mater. Chem., 20, 3171–3177, 2010

[6]J Martin, M Vazquez, C. Mijangos et al, sent to Nanotechnology

Polymer films with nano- to micro-structured surfaces for marine biofouling-release coatings

Giancarlo Galli

Dipartimento di Chimica e Chimica Industriale, UdR Pisa INSTM,
Università di Pisa, via Risorgimento 35, 56126 Pisa, Italy

Email: gallig@dcci.unipi.it

Introduction

With an increasing drive towards environmentally benign, non-toxic marine coatings, there is an increasing interest in developing novel polymer coatings in which a functional, nanostructured surface can result in improved resistance to and release of marine biofoulig organisms.[1]

Most recent and innovative advances include use of hybrid polymer nanocomposites, biomimetic polymer-analogue platforms, lithographically patterned monolayers and plasma assisted chemical modifications of polymeric surfaces. Although highly diversified in their individual architecture and function, all such technologies share the underpinning concept to exploit the interactions intervening between the fouling organisms and the specific surface features at the nanoscale[2].

Materials and Methods

In keeping with this rationale, we devised novel low elastic modulus and low surface energy coatings by the homogeneous dispersion of variously engineered fluorinated polymer additives in an elastomeric polymer matrix. Surface segregation of low surface tension polymers in fact can be an additional tool to nanostructure a coating in such a way to comply with the nanosized cues of the foulants, thereby effecting an antifouling activity or favouring removal of those foulants that do adhere.

Results

We studied the surface morphological, topological and compositional nano- to micro-scale complexities of the polymer film surface[3,4] and show how they add to enhance release of marine biofouling organisms in laboratory bioassays[5,6].

Moreover, amphiphilic polymers were also used, as we perceive that the 'ambiguous' character of the coating surfaces, due to the simultaneous presence of hydrophilic and hydrophobic domains, would result in distinct biological performances against micro- and macro-organisms with contrasting tendencies to interact with the substratum.

Conclusion

The amphiphilic polymers can be formulated in fouling release coatings for application in the marine environment with a proven potential in field trials, notably for shipping.

Acknowledgments

This work would have not been possible without the dedicated efforts of my coworkers (E. Martinelli) or the collaboration with the research groups at the Universities of Birmingham (J. A. Callow and M. E. Callow) and Newcastle (A. S. Clare), Cornell (C. K. Ober) and Akzo-International Paint (D. Williams). I am indebted to E. Chiellini for his invaluable support.

Funding of the work from the EU-FP6 IP 'AMBIO' and, more recently, from the EU-FP7 Marie Curie ITN 'SEACOAT' and the Italian MiUR (fondi PRIN 2008) is gratefully acknowledged.

References

1. S. Krishnan, C. J. Weinman, C. K. Ober, J. Mater. Chem., 18, 3406 (2008).

2. A. Rosenhahnan, T. Ederth, M. E. Pettitt, Biointerphases, 3, IR1 (2008).

3. E. Martinelli, A. Glisenti, B. Gallot, G. Galli, Macromol. Chem. Phys., 210, 1746 (2009).

4. W. Zhang,Y. Zheng, L. Orsini, A. Morelli, G. Galli, E. Chiellini, E. Carpenter, K. J. Wynne, Langmuir, 26, 5848 (2010).

5. E. Martinelli, S. Agostini, G. Galli, E. Chiellini, A. Glisenti, M. E. Pettitt, M. E. Callow, J. A. Callow, K. Graf, F. W. Bartels, Langmuir, 24, 13138 (2008).

6. I. Marabotti, A. Morelli, L. M. Orsini, E. Martinelli, G. Galli, E. Chiellini, E. M Lien,M. E. Pettitt, M. E. Callow, J. A. Callow, S. L. Conlan, R. J. Mutton, A. S. Clare, A. Kocijan, C. Donik, M. Jenko, Biofouling, 25, 481 (2009).

Mimicking nature using copolymers

Giuseppe Battaglia

Department of Biomedical Science.University of Sheffield

http://battaglia.group.shef.ac.uk/

We are interested in studying and developing self-assembled structures formed in water exploiting weak supramolecular interactions such as hydrophobic effect, hydrogen bonds, and columbic forces. We often take inspiration from biological structures such as extracellular matrix, cells and virus and try to reverse engineer their functionalities. This is achieved by working closely with synthetic chemists combining effective molecular and macromolecular design with our supramolecular engineering approach. We are interested in a variety of structures often polymeric such as hydrogels, polymer emulsions and polymer vesicles and micelles. Polymer vesicles and polymersomes have attracted most of our interest making us one of leading groups in the field. These are vesicles formed by the self-assembly in water of amphiphilic copolymers. We have characterized the different molecular parameters that control polymersome structural features as well as the kinetics and thermodynamics that regulate their formation. We have used this fundamental understanding to optimize methods of fabrication as well as to formulate new systems that comprise more functionality. In parallel to this, we are also working on series of projects aimed towards the engineering of soft materials with controlled topology, exploiting controlled polymer/polymer phase separation with the aim to generate cell-instructive and bioactive materials.

References:

- LoPresti et al. ACS Nano 2011, 22, 1775-84

- Howse et al. Nature Mater. 2009, 8, 507-511

- Gill et al. Nature Chem. 2009 1, 662-667

- Massignani et al. Small, 2009, 5 (21), 2424-2432

- Battaglia et al., Angew. Chem. Int. Ed. 2006, 45, 2052-2056

- Battaglia et al. Nature Mater. 2005, 4, 869-876

Synthesis and Functionalization of "Nanosponges" to Enhance the Efficacy of a Broad Range of Therapeutics

*David M. Stevens, Ghazal Hariri, Julia N. Dobish and Eva Harth**

Department of Chemistry, Vanderbilt University, Stevenson Center 7619, Nashville, TN, 37235-1822

eva.harth@vanderbilt.edu

Controlled degradable nanoscopic structures have been investigated to design delivery systems that target, solubilize and increase the efficacy of therapeutics. Most of the current degradable polyester based nanoparticles are self-assembled structures that are difficult to further modify and tailor due to the dissolution of the 3-D architecture in organic solvents.

The developed strategy to design optimized drug delivery systems is to create tailorable nanoscopic networks that degrade and release the drug in linear fashion. The cross-linked, in organic solvents completely solvatized nanosponge, can be loaded after nanoparticle formation and is with this a valuable tool in drug discovery, drug efficacy and drug combination studies.

Based on an intramolecular crosslinking technique, the linear polyester precursor made from ring-opening polymerization procedures and functionalized monomers from the valerolactone family are cross-linked with diamines, diazides or dithiols to achieve a controlled nanoparticle formation depending on the amount of cross-linker reacted with the linear precursor.

In view of the tailorable degradation profile the cross-linking density of the prepared particle can be adjusted by the percentage of the cross-linking partner in the linear polymer precursor such as epoxides, alkynes and allyl groups. The versatility to react the two cross-linking partners makes the developed method a powerful tool to design a personalized drug delivery system.

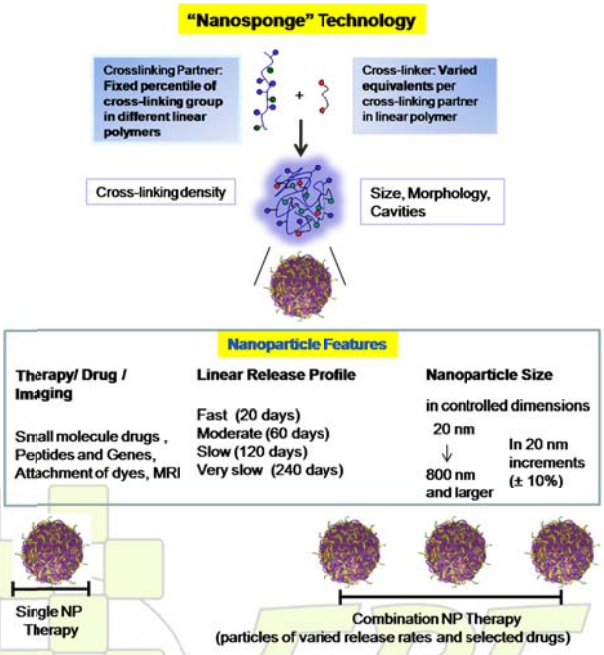

We will present functionalization chemistries to target tissues and cells and will demonstrate the superior targeting ability of the nanosponge. The mentioned versatility in the ability to load a number of different drugs into the particles lead to the further optimization of drug therapies not only based on their increased targeting and solubilization but also newly discovered powerful drug combinations. The increased efficacy of therapeutics is presented in three tumor models and the efficacy of drug combinations are tested with a variety of newly discovered and traditional drugs.

The designed system with its versatility in the cross-linking chemistry provides a multitude of possibilities to attach ligands and load the particles with a broad range of therapeutics.

Microphase Separation for Diblock-Copolymers: Novel Aspects of an Old Problem

Alexei R. Khokhlov

Moscow State University, Moscow, Russia

khokhlov@polly.phys.msu.ru

In the first part of the talk, the review of the recent results concerning the microphase separation of the diblock copolymers in the bulk will be given. In particular, it will be shown (both theoretically and by computer simulation) that for the case of amphiphilic blocks the local chemical structure can dictate the global morphology of block copolymer melts. Furthermore, "inverse" morphologies are possible when minority component forms a matrix and majority complexes form micelles in the matrix.

In the second part of the talk I will discuss a simple and robust approach to control the orientation of cylindrical microdomains in diblock copolymer films. This approach is based on the so-called double phase separation occurring in the binary blend of incompatible compositionally asymmetric block copolymers and their selective adsorption on a homogenous surface. As a proof-of-concept, we performed mesoscale simulations, using dynamic density functional theory and dissipative particle dynamics, and show that the target morphology with perpendicularly oriented cylinders can be thermodynamically stable for rather thick films when the intrinsic hexagonal period of the majority bulk phase is commensurate with the surface-induced pattern formed by the strongly adsorbed minority component.

In the third part of the talk I will describe recent study of self-assembly of cylinder-forming diblock-copolymers near homogenous surfaces having periodically distributed regions of different wettability. The methods used were self-consistent field theory and dissipative particle dynamics. The patterned surfaces were demonstrated to provide an effective means to enhance the stability of vertically aligned cylindrical domains in thin films. The template-guided control over ordering and orientation is strongly dependent of affinity between the minority domains and the pattern. For some cases doubling the pattern frequency in the resulting array of microdomains is possible.

Morphology, nucleation and crystallization kinetics of biodegradable double crystalline PLLA-b-PCL diblock copolymers

Alejandro J. Müller[1], Reina Verónica Castillo[2], Jean-Marie Raquez[3] and Philippe Dubois[3]

[1]Grupo de Polímeros USB, Departamento de Ciencia de los Materiales, Universidad Simón Bolívar, Caracas, Venezuela.
[2]Laboratorio de Polímeros, Centro de Química, Instituto Venezolano de Investigaciones Científicas IVIC, Miranda, Venezuela.
[3]Center of Innovation and Research in Materials & Polymers CIRMAP, Service des Matériaux Polymères et Composites SMPC, Université de Mons-UMONS, Mons, Belgium.

amuller@usb.ve

Introduction

The crystallization process in double crystalline diblock copolymers can lead to structures within structures. Crystallization can be either confined within the copolymer microdomain structure for strongly segregated systems, or it can drive structure formation for weakly segregated melts (overwriting any previous microdomain structure) or homogeneous systems. In the case of double crystalline diblock copolymers, the situation can be even more complicated, since the crystallization of one block may affect the crystallization and morphology of the second block. In fact, the second block could be nucleated or its crystallization could be confined within the microdomain structure or within the previously formed lamellar stacks of the first block. Confined crystallization can lead to fractionated crystallization. The fractionated crystallization phenomenon has been explained as the crystallization of a series of micro domains at specific and independent supercoolings, i.e., the crystallization of the isolated domains of a semicrystalline polymer dispersed in an immiscible matrix, where the number of domains is higher than the number of active heterogeneous nuclei.

Experimental

The morphology, nucleation and crystallization kinetics of biodegradable and double crystalline poly(L-lactide)b-poly(ε-caprolactone) diblock copolymers (PLLA-b-PCL) was studied in a wide composition range by differential scanning calorimetry (DSC) and polarized light optical microscopy (PLOM).[1-4] We have also gathered previously information on their weak segregation strength by SAXS experiments in the molten state.[1-2]

Results, discussion and conclusions

The two blocks were found to be partially miscible according to the variations of their thermal transitions with composition. PLOM results showed that PLLA crystallizes in a wide composition range with a spherulitic superstructural morphology. Only when the PLLA content is as low as 10 wt % axialites are formed. These results were in good agreement with the overall crystallization kinetics obtained by DSC isothermal experiments and analyzed by the Avrami equation. Both overall crystallization rates and spherulitic growth rates of the PLLA block decrease with PCL content, since PCL acts as a diluent for the PLLA block in view of their miscibility.

Reorganization processes revealed as double melting peaks for the PLLA block (not observed for the PLLA homopolymer) were observed during heating scans performed after isothermal crystallization. The reorganization ability of the PLLA block was found to increase with PCL content, a fact that quantified the perturbation caused by molten PCL block chains during the isothermal crystallization of the PLLA block. The PCL block crystallizes within previously formed PLLA spherulites or axialites. In spite of the partial miscibility, unexpected and novel fractionated crystallization of the PCL occurs at contents of PCL in between 40-19 wt %. For the lowest PCL content (i.e., 19%), a homogeneous nucleation process was detected as indicated by the large supercooling needed for crystallization and by the first order crystallization kinetics obtained (i.e., Avrami index close to 1). Due to the partial miscibility, the glass transition temperature of the PLLA block ($T_{g,PLLA}$) decreases with PCL addition, so at PCL contents lower than 40 wt % the $T_{g,PLLA}$ values are close or higher than the crystallization temperature of the PCL block. Thus, PCL fractionated crystallization is induced by hard confinement of the PLLA amorphous and crystalline regions. This is the first time that a homogeneous nucleation process has been documented for a crystallizable component in a miscible or weakly segregated diblock copolymer. The PCL block can also be nucleated by previously formed PLLA crystals depending on the crystallization degree of the PLLA, which was varied by self-nucleation experiments. The crystallization rate of PCL strongly decreased with increasing PLLA content. The crystallization and morphology of the biodegradable polymers PLLA and PCL can be strongly influenced by coupling them in double crystalline diblock copolymers, a fact that will also influence their performance in possible biomedical applications.

References

1. Hamley, W.; Castelletto, V.; Castillo, R.V.; Müller, A.J.; Martin, C.M.; Pollet, E.; Dubois, Ph. Macromolecules, 2005, 38, 463
2. Hamley, I.W.; Parras, P.; Castelletto, V.; Castillo, R.V.; Müller, A.J.; Pollet, E.; Dubois, Ph.; Martin, C.M. Macromolecular Chemistry and Physics, 2006, 207, 941
3. Castillo, R. V.; Müller, A. J. Progress in Polymer Science, 2009, 34, 516
4. Castillo, R. V.; Müller, A. J.; Raquez, J. M.; Dubois, Ph. Macromolecules, 2010, 43, 4149

Polymer Conjugates as Single agents or in Combination Therapy: Versatile Platform Technology for Tissue Repair and Cancer Therapy

María J. Vicent

Polymer Therapeutics Lab. Centro de Investigación Príncipe Felipe.
Av. Autopista del Saler 16 E-46012, Valencia (Spain)

mjvicent@cipf.es

Polymer conjugates are nanosized hybrids that covalently combine a bioactive agent with a polymer to ensure not only its efficient release to the required intracellular compartment, but also its availability within a specific period of time. Clinical proof of concept for these multicomponent constructs has been already achieved as anticancer agents, both as single agents or as elements of combinations[1]. Orthodox anticancer drugs were preferentially chosen in the development of the first conjugates[2]. The fast evolution of polymer chemistry and bioconjugation techniques and deeper understanding of cell biology opened up exciting new opportunities. However, many challenges still lay ahead providing scope to develop this platform technology further.

Delivery of new anticancer agents focusing on novel molecular targets and their combination, development of both new and exciting polymeric materials with defined architectures and treatment of diseases other than cancer, in particular looking at promoting tissue repair, are the most exciting and promising areas[3], and therefore, are the driven research lines in the Polymer Therapeutics laboratory at CIPF.

Our research lines include the design of novel nanoconjugates for the treatment of hormone-dependent

cancers by using novel concepts, such as, bioresponsive systems with controlled architecture and the active drug incorporated within a pH-triggered biodegradable polymeric mainchain[4] or the use of polymer-based combination therapy (endocrine + chemotherapy or antiangiogenics + chemotherapy in the same polymer)[5]. Novel polymeric carriers with controlled architecture and high versatility are also being developed.[6] On the other hand, the design of conjugates for other diseases[7] and in particular promoting tissue repair is a key area in the group, in this sense, novel hybrid systems are being developed for cardiorregeneration, ischaemia and neurodegenerative diseases.

Acknowledgements.

This work is supported by grants from EU-FP7 (Livimode, proposal n. 241919); MICINN (CTQ2007-60601, CTQ2010-18195/BQU, EUI2008-03904, EUI2008-00116), Generalitat Valenciana (AP036/10) Fundación GentxGent and CIPF.

References

(1) Vicent, M.J. and Ducan R. Eds. *Ad. Drug.Deliv.Rev.* **2009**, *61(13)*, whole issue.

(2) Duncan, R. *Nature Rev Cancer* **2006**, *6,* 688.

(3) a) Greco, F. and Vicent, M.J. *Frontiers Biosci.* **2008**, *13*, 2744. b) Sanchis J., Canal F., Lucas R., Vicent MJ. *Nanomedicine (Lond)***2010**, *5*, 915–935

(4) a) Vicent, M.J.; Tomlinson, R.; Brocchini, S.; Duncan, R. *J Drug Target* **2004**, *12*, 491. b) Giménez V., James C., Paul A., Vicent, M.J. *Macromol Rapid Comm.* **2011**

(5) a) Vicent, M.J.; Greco, F.; Nicholson, R.I.; Paul, A.; Griffiths, P.C.; Duncan, R. *Angew Chem Int Ed* **2005**, *44*, 4061. b) Eldar-Boock A., Miller K., Sanchis J., Lupu R., Vicent MJ., Satchi-Fainaro R. *Biomaterials***2011**doi:10.1016/j.biomaterials.2011.01.073.

(6) Barz M., Luxenhofer R., Zentel R. Vicent M.J. *Polym. Chem.***2011**DOI: 10.1039/c0py00406e

(7) a) Vicent, M.J., Cascales, L., Carbajo, R.J., Cortés, N., Messeguer, A., Pérez Payá, E. *J. Control. Rel.* **2010***, 142*, 277 b) Vicent, M.J.; Pérez-Payá, E. *J Med Chem* **2006**, *49*, 3763. b) Pérez-Payá, E.; Orzáez, M.; Mondragón, L.; Wolan, D.; Wells, J.A.; Messeguer, A.; Vicent, M.J. *Med. Res. Rev.* Jan 22 **2010**. DOI: 10.1002/med.20198

Nanomaterials Based on Poly(ε-caprolactone) - A Versatile and Intriguing Biomedical Building Block

Søren Hvilsted and Ikrakli Javakhishvili

Danish Polymer Centre. Department of Chemical and Biochemical Engineering. Technical University of Denmark

sh@kt.dtu.dk

The classical medical material workhorse, poly(ε-caprolactone) (PCL), has been employed as a viable scaffold for design of several novel nanomaterials with intri-guing, potentially therapeutic and biological properties. Living ROP strategies have afforded telechelic PCLs that can be utilized in either ATRP to make amphiphilic block copolymers or various "click" reactions resulting in multicomponent nanomaterials as outlined in Scheme 1. Three different examples will be elaborated.

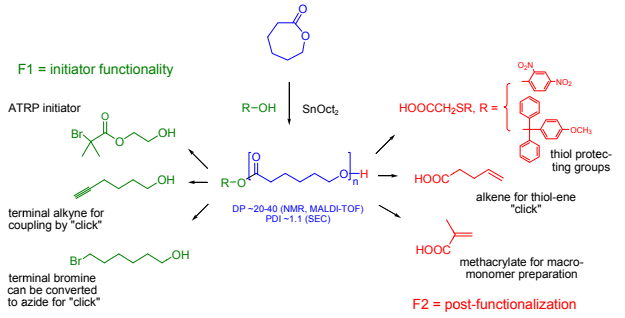

Scheme 1. Various options for creating hetero bifunctional PCL building blocks by use of functional initiators (F1) and post-functionalization (F2).

In the first case gold nanoparticles protected with a polymeric shell may combine ablative therapy and site-specific drug delivery in bladder cancer therapy [1]. This may be accomplished by tailoring the surface properties and the size of the gold clusters. The former may be addressed by devising polymeric ligands with desirable features and functional groups. Thus the preparation of the PCL-*b*-PAA corona will be outlined as shown in Scheme 2.

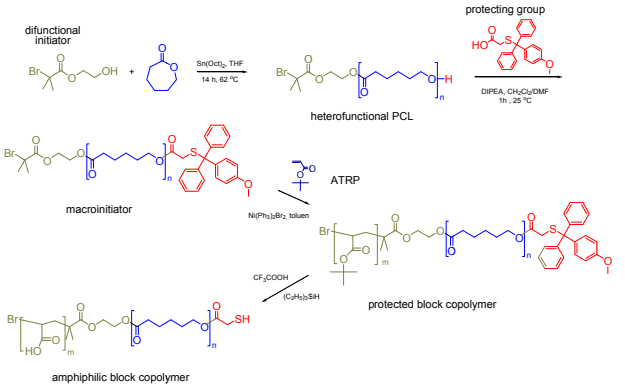

Scheme 2. Synthetic sequence for preparation of amphiphilic block copolymer precursor.

The synthesis of the effective macro-ligand that allows preparation of the stable gold cluster and provides nanoenvironment for hydrophobic anticancer drugs and mucoadhesive anchoring on mucous membranes is one of the objectives of this study.

The second approach is the ligation of biologically active moieties to the termini of a hydrophobic polymeric chain (PCL) to afford the amphiphilic linear-dendritic macromolecule that comprises rod-like, coil-like, and dendritic fragments [2]. Furthermore this may self-assemble in solid state as well as in aqueous solution. The facile route to linear-dendritic cholesteryl-*b*-PCL-*b*-(L-lysine)$_{G2}$ by thiol-ene and azide-alkyne "click" reactions is illustrated in Scheme 3. Here the driving motivation was to contrive a robust, facile, and effective synthetic strategy.

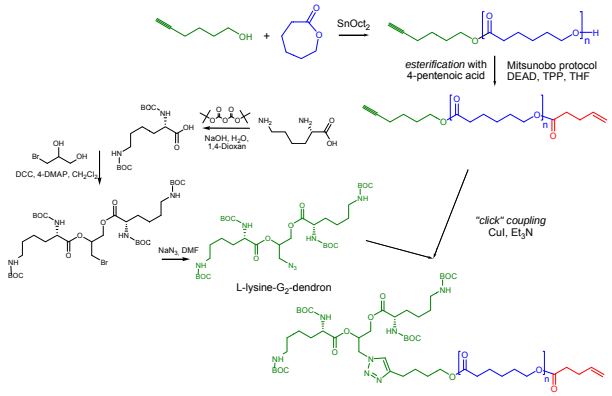

Scheme 3. Preparation of α-hexynyl-ω-pentenoate PCL, L-lysine-G_2-dendron, and the CuAAC coupling to the L-lysine-G_2-dendron-PCL.

Finally, the preparation of PCL-based miktoarm core-crosslinked amphiphilic star copolymers (CCS) with hydrophobic interior, charged hydrophilic surface, and targeting motifs are elaborated as shown in Scheme 4.

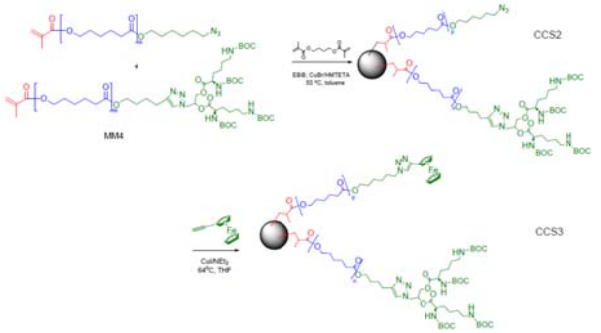

Scheme 4. Preparation of miktoarm CCS copolymers by copolymerization of functional macroinitiators.

Such nanoscopic core-shell type architectures are envisioned to be excellent candidates as drug delivery devices owing to the enhanced stability in biological fluids [3]. Moreover, they may permit site-specific delivery of their potential cargo due to the presence of biologically active moieties on the peripheries.

References:

1) I. Javakhishvili, S. Hvilsted, *Biomacromolecules* **10** (2009) 74-81.

2) I. Javakhishvili, W. H. Binder, S. Tanner, and S. Hvilsted, *Polymer Chemistry* **1** (2010) 506-513.

3) I. Javakhishvili and S. Hvilsted, *Polymer Chemistry* **1** (2010) 1650-1661.

Homo- and Block Copolymers of Poly(β-benzyl-L-aspartate)s and Poly(γ-benzyl-L-glutamate)s of Different Architectures

Blaž Brulc[1], Ema Žagar[1,2], Mariusz Gadzinowski[3], Stanisław Słomkowski[3], and Majda Žigon[1,4,5]

[1]Laboratory for Polymer Chemistry and Technology, National Institute of Chemistry, 1000 Ljubljana, Slovenia
[2]EN→FIST Centre of Excellence, 1000 Ljubljana, Slovenia
[3]Department of Engineering of Polymer Materials, Center of Molecular and Macromolecular Studies, Polish Academy of Sciences, 90-363, Łódź, Poland
[4]Center of Excellence for Polymer Materials and Technologies, 1000 Ljubljana, Slovenia
[5]Polymer Technology College, 2380 Slovenj Gradec, Slovenia

majda.zigon@ki.si

We present a systematic study of the synthesis of poly(β-benzyl-L-aspartic acid)s (PBAs) and poly(γ-benzyl-L-glutamic acid)s (PBGs) using monoamino functional nucleophilic initiators, such as a primary amine (n-hexylamine – HEX) and its hydrochloride salt (HEX–C), as well as simple multifunctional amines (1,6-diaminohexane,DAH, and tris(2-aminoethyl)amine, TAA, the lysine-based tetraamino dendritic initiator, LD4) [1]. Benzylic-protected aspartic acid and glutamic acid *N*-carboxyanhydrides (Glu NCA, Asp NCA) were used as the monomers. We studied both NCA ring-opening polymerizations (ROP) by varying the key reaction parameters, i.e., the monomer-to-initiator ratio, the initial monomer concentration, and the reaction temperature. The molar-mass characteristics of the reaction products were determined by size-exclusion chromatography coupled to a multi-angle light-scattering photometer (SEC-MALS). NMR and DSC were used for a determination of the monomer's purity. NMR spectroscopy was also used to determine the products' structure and as a complementary method to the SEC-MALS technique for a determination of the polypeptide number-average molar masses ($\overline{M_n}$).

Polypeptides (PBAs and PBGs) from Monofunctional Initiators

The polymerizations were run for 3 hours, with the exceptions for the slower reactions involving initiator HEX–C. The PBA–Hs obtained from the HEX -initiated Asp NCA polymerizations at room temperature had lower molar-mass averages than predicted from the [M]:[I] ratios (50, 100, 200), but the results are in agreement with the trend of $\overline{M_n}$ increase with the increasing [M]:[I] ratios. The molar-mass dispersities ($Đ_M$s) of PBA–Hs remain fairly low (below 1.30) but have a general tendency to increase somewhat with an increasing [M]:[I] ratio (from 1.04 for [M]:[I]=50 to 1.24 for [M]:[I]=200). PBG–H polymers with [M]:[I] ratios 50, 100, and 200 exhibited narrow molar-mass distributions (MMDs) and their $\overline{M_n}$ were in excellent agreement with the theoretical values. From the NMR and SEC-MALS data it can be seen that Glu NCA polymerizes much faster under the given experimental conditions than its Asp NCA analog.

When using HEX–C instead of HEX the polymerization rates are much slower than those of PBA-H and PBG-H polymerizations and almost free of side-reactions [2].The obtained PBA–Cs and PBG–Cs are all monomodal with narrow MMDs even for longer reaction times.

Differences in polymerization rates of both monomers were studied by the kinetics measurements using ^{1}H NMR spectroscopy. Both reactions can be described by the first-order kinetics. The HEX-initiated Glu NCA polymerization proceeded faster ($k_p = 1.4 \times 10^{-4}$ s^{-1}) than its analogous Asp NCA polymerization ($k_p = 5.5 \times 10^{-5}$ s^{-1}). A possible reason for this difference in the reaction rates could be the intramolecular H-bonding interactions, which are more pronounced in PBAs than in PBGs. The quasi-6-membered ring which can be completed with an N-H---O hydrogen bond is thermodynamically more stable than the 7-membered ring in the case of PBGs. The NH_2 terminus of the growing PBA macromolecule is thus somewhat deactivated in comparison to the PBG polymer.

Polypeptides from Di, Tri-, and Tetrafunctional Initiators

Using DAH we synthesized PBA2s and PBG2s with narrow MMDs ($Đ_M$=1.02–1.25), whose molar-mass averages were in fairly good agreement with the values calculated from the [M]:[I] feed ratios. The PBA3 polymers also have very narrow MMDs but slightly lower molar-mass averages than their calculated values.

Using the lysine-based dendrimer LD4 as an NCA polymerization initiator [M]:[I]=52, $\overline{DP}$ =13 per polypeptide arm, we prepared four-arm, star-like PBA–LD4 and PBG–LD4 with fairly narrow monomodal MMDs, ĐMs<1.3 (Fig.1).

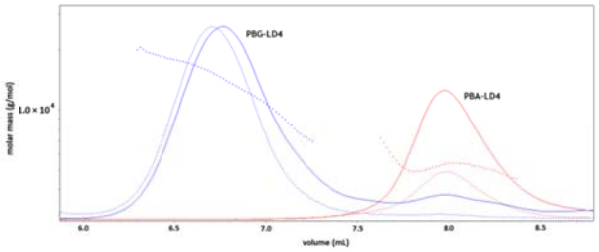

Figure 1. SEC-MALS chromatograms (– DRI response, - - LS response at 90° angle) and molar mass vs. elution volume curves for PBA–LD4 and PBG–LD4 polymers (points).

References

[1] B. Brulc, E. Žagar, M. Gadzinowski, S. Słomkowski, M. Žigon, *Macromol. Chem. Phys.* DOI:10.1002/macp.201000710.

[2] (a) T. J. Deming, *Prog. Polym.Sci.* 2007, 32, 858. (b) T. J. Deming, *Adv. Polym. Sci.* 2006, 202, 1. (c) G.J.M. Habraken, M. Peeters, C.H.J.T. Dietz, C.E. Koning, A. Heise, *Polym. Chem.* 2010, 1, 514. (d) C. Simó, W. Vayaboury, O. Giani, M. Pelzing, A. Cifuentes, *Anal. Chem.*2004, 76, 335.

Light-responsive Block Copolymers based on Azobenzene

J. Barrio[1],E. Blasco[1],P. Forcén[1],C. Berges[2],R.M. Tejedor[1],J.L. Serrano[1],M. Piñol[1],C. Sánchez[2],R. Alcalá[2],

L. Oriol[1,]*

[1]Dpto. Química Orgánica. Instituto de Ciencia de Materiales de Aragón, Universidad de Zaragoza-CSIC,Zaragoza, Spain.

[2]Dpto. Física de la Materia Condensada. Instituto de Ciencia de Materiales de Aragón, Universidadde Zaragoza-CSICZaragoza, Spain.

e-mail: loriol@unizar.es

Block copolymers (BCs) are of particular interest in the design of novel functional materials based on self-assembling properties. It is well-known that block copolymers can segregated into nanostructures either in bulk or solution. Besides, the incorporation of adequate functional moities in polymeric materials may allow the response of these materials to external stimuli. Furthermore, the response and the self-assemblies properties of BCs can be mutually affected.

On the other hand, light-responsive polymers have received great attention, being azopolymers (containing azobenzene as photochromic units) one of the most investigated, e.g. as optical data storage materials or photomechanical actuators[1]. Azobenzene molecules undergo isomerization between the *trans*and the *cis* states when they are irradiated in their absorption bands. Molecular motions and photoinduced anisotropy may be generated by irradiation using linearly polarized light.

We have previously described the synthesis and characterization of polymethacrylates having cyanoazobenzene as pendant groups, as well as the photoinduced anisotropy and holographic storage in thin films. Nevertheless, thick films are required for volume holography (higher storage capacity). For this last application, BCs can be a good alternative. The block copolymer architecture allows: (1) the confinement of azobenzene into nanodomains, which favors the cooperative motions induced by light, and (2) the dilution of the photochromic units, which allows the processing of thicker films.

We first accomplished the synthesis of linear-linear BCs (Figure 1) containing azobenzene units by ATRP using PMMA-macroninitiators[2]. BCs of high molecular weight have better been approached by a separate ATRP-synthesis of both blocks and coupling by a click reaction.

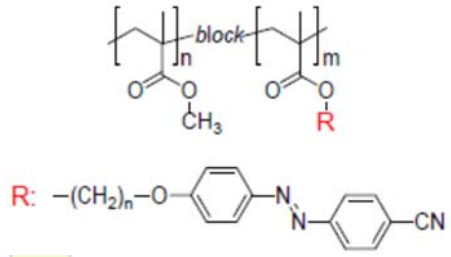

Figure 1. Chemical structure of linear-linear BCs

Synthesis, characterization, morphology and optical properties of films processed from these block copolymers will be discussed and compared with homopolymers.

In order to introduce a precise number of photochromic units, a new kind of azo-BCs were attempted having a linear-dendritic structure (Figure 2).

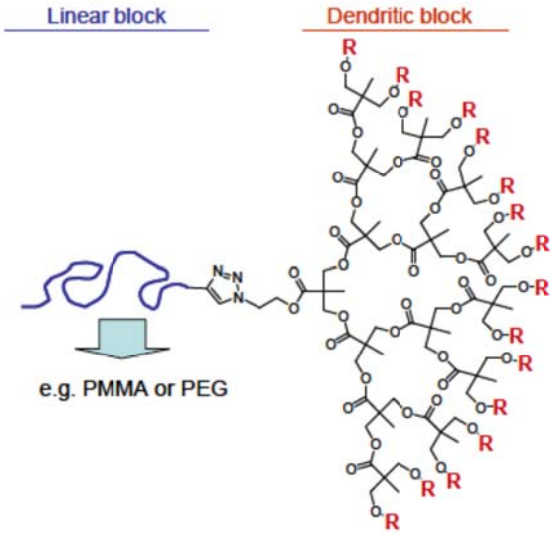

Figure 2.Chemical structure of linear-dendritic BCs.

The click coupling of linear and dendritic blocks (having photochromic units at the periphery) gives rise to different series of BCs[3]. In the case of amphiphilic BCS, self-assembly in aqueous solutions gives rise to different nanoobjects, ranging from nanofibers to vesicles, depending on the generation of the dendritic blocks (Figure 3)[4].

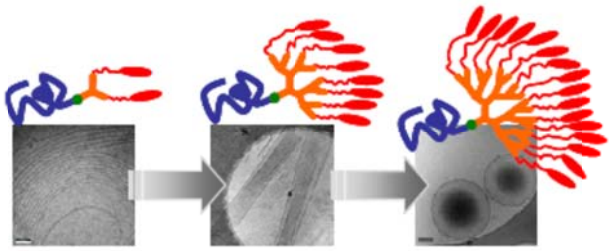

Figure 3.Self-assemblies of linear-dendritic BCs.

Acknowledgment. Work supported by the MICINN, Spain, under the project MAT2008-06522-C02, FEDER and DGA.

References

1 A. Natashon, P. Rochon *Chem. Rev.* **2002**, *102,* 4139

2 P. Forcén, L. Oriol, C. Sánchez, R. Alcalá, S. Hvilsted, K. Jankova, J. Loos, *J. Polym. Sci. Pol. Chem.* **2007**, *45*, 1899

3. J. del Barrio, L. Oriol, R. Alcalá, C. Sánchez, *Macromolecules* **2009**, *42*, 5752; J. Del Barrio, L. Oriol, R. Alcala, C. Sanchez, *J. Polym. Sci. Pol. Chem.* **2010**, *48*, 1538

4 J. del Barrio, L. Oriol, C. Sánchez, J. L. Serrano, A. Di Cicco, P. Keller, M. H. Li *J. Am. Chem. Soc.* **2010**, *132*, 3762

ABSTRACTS

INVITED LECTURES

Topic 6: Bioinspired Polymers, Bioengineering and Biotechnology

Material considerations for annulus fibrosus and nucleus pulposus composite structures

Sanjukta Deb

Department of Biomaterials, Biomimetics & Biophotonics.King's College London, Dental Institute, Tower Wing, Guy's Hospital, London Bridge, London SE1 9RT, UK

Intervertebral disc (IVD) degeneration is a common problem that is the leading cause of low back pain worldwide, which seriously affects the health of the working population. The main approaches for treating the condition with discectomy and fusion provides good short term results however the altered biomechanics of the spine causes complications such as further degeneration. Artificial IVD discs have been developed to act as a functional prosthetic replacement unit for intervertebral units, however, current treatment modalities provide less than satisfactory outcomes.

The intervertebral disc (IVD) is composed of 3 distinct tissues, namely, the nucleus pulposus (NP), outer annulus fibrosus, and inner annulus fibrosus (AF), with cartilaginous end plates on the superior and anterior surfaces. Each of the components of the disc is composed of morphologically distinct cellular populations with a specific role. The different components of the healthy disc are an important determinant in the absorption and distribution of the forces arising in the spinal column. With disc degeneration a loss in fluidity occurs that compromises the elasticity resulting in the inability to absorb the normal compressive loads.

In this paper we report the synthesis of a set of novel hydrogels that have been synthesized using different methods of polymerization. Novel hydrogel scaffolds were synthesised using free radical solution and photo-polymerisation techniques under physiological conditions with the aim of creating a seamless construct that would comprise of a stiffer composite matrix forming the annulus fibrosus and a hydrogel forming the nucleus pulposus. In the first approach the monomer 2-hydroxyl ethyl methacrylate (HEMA) in conjunction with a phosphate containing comonomer, namely ethylene glycol methacrylate phosphate (EGMP) with ethylene glycol dimethylacrylate (EGDMA) as a cross-linker was used with the second approach involving the use of HEMA interacting with the adhesive, comonomer pyromellitic glycerol dimethacrylate (PMGDM) in 50% triethyleneglycol dimethacrylate (TEMA) as a crosslinker, introducing carboxyl groups into the copolymer. The different reaction conditions were explored to optimize a method that would allow the incorporation of biological entities during the polymerization reaction. Furthermore Bioglass particles were introduced to develop a composite with the phosphate containing hydrogels to enable the study of their interaction and produce a stiffer matrix suitable for annulus fibrosus.

Scaffold Functionalisation Strategies for Modulation of Inflammation

Abhay Pandit

Network of Excellence for Functional Biomaterials, National University of Ireland, Galway

Abhay.pandit@nuigalway.ie

Most degenerative diseases are characterised by an inflammatory response. Regenerative strategies employed to date do not attempt to address this response. Inflammatory response is often characterised by lack of oxygenation, apoptosis and presences of inflammatory cells. This microenvironment is often not-conducive for a regenerative response. An example of such a microenvironment is that of myocardial infarction (MI). Myocardial infarction (MI), which is literally the death of cardiac tissue due to lack of oxygenation, accounts for the majority of deaths associated with cardiovascular disease. This death of cardiac tissue leads to a loss of cardiac function as the damaged area becomes a non-contractile scar. Reversal of this process is the main aim of regenerative cardiac strategies such as stem cell transplantation. While initial studies were promising, subsequent clinical trials yielded disappointing results. Stem cell therapy may be limited by the poor survival rate of the cells after implantation into the infarcted heart, which is likely due to the inflammatory response. We have functionalised a collagen scaffold seeded with mesenchymal stem cells with an anti-inflammatory gene (interleukin-10 (IL-10)) to modulate the inflammatory response after implantation of a MSCs. IL-10 is considered the most potent anti-inflammatory cytokine produced naturally and has been used in a number of studies to decrease or control inflammation. It was hypothesized that IL-10 gene therapy could be used to increase the retention rate of stem cells in a collagen scaffold when delivered to the ischemic myocardium. The primary objectives were to develop a controlled release scaffold-based gene therapy system suitable for stem cell delivery to the infarcted myocardium. The efficacy of this system was evaluated by assessing stem cell retention, overall cardiac function and the inflammatory response. A crosslinked collagen scaffold was developed and optimised for rMSC culture in vitro. Non-viral plasmid-dendrimer polyplexes were optimized for transfection in both two and three-dimensional culture. When cells were seeded into polyplex loaded scaffolds, relatively high levels of transgene expression were observed for up to three weeks of culture. When the polyplex-loaded scaffolds were implanted in rat skeletal muscle, increased retention of rMSCs was observed. This was associated with decreased inflammation and a change in macrophage phenotype from cytotoxic to regulatory. Similarly, when the polyplex-loaded scaffolds were implanted over the surface of infarcted rat hearts, rMSC retention was increased, the inflammatory and remodelling responses were modulated and, most importantly left ventricular ejection fraction – a measure of cardiac function – was significantly improved. A similar strategy has been employed in peripheral nerve repair. A peripheral nerve conduit was fabricated with a neuro-regenerative factor and an anti-inflammatory factor. Down regulation of the inflammatory response permitted enhanced recovery of neural function. Thus, combining biomaterial, gene and cell therapy can improve functional outcomes if a key response such as inflammation is addressed. This combinatorial strategy can be utilised to provide functional efficacy in disease targets.

Recent Progress on the use of Natural Origin Polymers and Stem Cells in Tissue Engineering Strategies

Rui L. Reis [1,2 *]

[1] *Director of the 3B´s Research Group - Biomaterials, Biodegradables and Biomimetics,* University of Minho, Headquarters of the European Institute of Excellence on Tissue Engineering and Regenerative Medicine, Taipas – Guimarães, Portugal; *www.3bs.uminho.pt;*

[2] Director of the ICVS/3B´s - PT Government Associated Laboratory, Braga/Guimarães, Portugal

rgreis@dep.uminho.pt

Abstract

The selection of a scaffold material is both a critical and difficult choice that will determine the success of failure of any tissue engineering (TE) strategy. In our research we believe that natural origin polymers are the best choice for many approaches. In addition, we have been developing an all range of processing methodologies to produce adequate scaffolds for different TE applications. Furthermore an adequate cell source should be selected. In many cases efficient cell isolation, expansion and differentiation methodologies should be developed and optimized. In our research we have been using different human cell sources namely: mesenchymal stem cells from bone marrow, mesenchymal stem cells from human adipose tissue, human cells from amniotic fluids and membranes and cells obtained from human umbilical cords. The potential of each type of cells, to be used to develop novel regeneration therapies will be discussed.

Their uses and their interactions with different natural origin degradable scaffolds and distinct nano and micro-carriers, and smart release systems, will be described. A great focus will be given to the different sources of stem cells, the isolation of distinct sub-populations, ways of differentiating them, as well as their interactions with different 3D architectures and materials for culturing them. During the all lecture we will try to distinguish what is a fact, a trend and a real clinical open possibility. The use of bioreactors to control cell differentiation, as well as the surface modification of the materials in order to control cell adhesion and proliferation will also be illustrated. The results will be mainly based on our research in the areas of bone, cartilage and osteochondral tissue engineering. Several biomimetic and nanotechnology based strategies to engineer mineralized tissues will be described. We will also pay attention to the role of interfaces and controlled surface characteristics on the performance of different constructs.

* Editor-in-Chief of the Journal of Tissue Engineering and Regenerative Medicine (TERM), John Wiley & Sons - Blackwell, CEO of the European Institute of Excellence on Tissue Engineering and Regenerative Medicine.

Polyethylene Glycol Hydrogels for Therapeutic Vascularization

Edward A. Phelps and Andrés J. García

Petit Institute for Bioengineering and Bioscience, Georgia Institute of Technology

andres.garcia@me.gatech.edu

Clinically viable vascularization therapies will lead to better treatment for patients with peripheral artery disease and coronary heart disease as well as enhanced survival of cell and tissue transplants. Many clinical trials to induce new vascular growth have focused on delivery of a single angiogenic gene or growth factor, or activation and delivery of progenitor cells. We have engineered functionalized polyethylene glycol (PEG)-based hydrogel matrices with bioactive motifs to serve as engineered platforms for cell-demanded delivery of angiogenic growth factors and supportive environments for tissue ingrowth.

In one application, we have engineered PEG-maleimide hydrogels to incorporate VEGF as supportive matrices to improve pancreatic islet engraftment and vascularization. This hydrogel chemistry is advantagous for cell delivery due to mild crosslinking that occurs rapidly enough for in situ delivery, while easily lending itself to "plug-and-play" design variations. Precursor solutions of 4-arm PEG-maleimide were functionalized with RGDS adhesion peptide and VEGF.

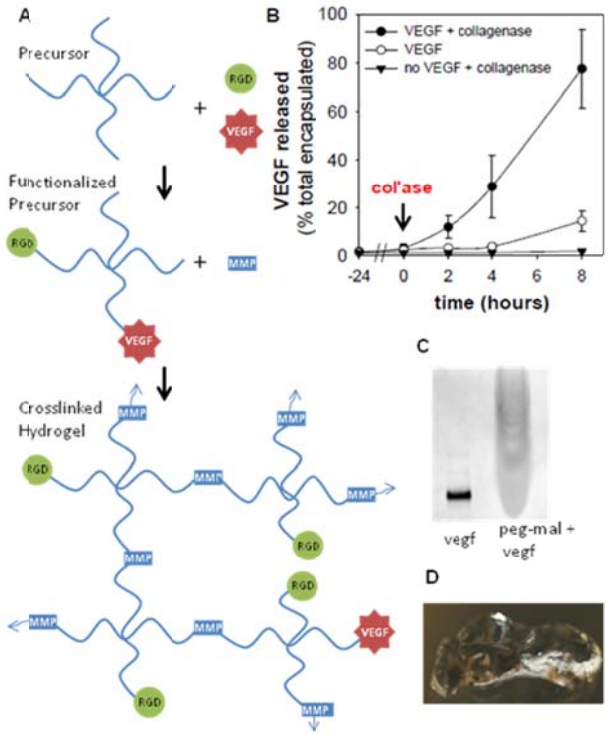

Fig. 1. PEG-maleimide hydrogel: (A) Reaction scheme. (B) VEGF release from hydrogels is MMP-dependent. Hydrogels were incubated in collagenase for different time points and VEGF in supernatant was quantified by ELISA. No VEGF was released prior to treatment with collagenase, indicating minimal passive (diffusion) release. (C) Western blot confirming pegylation of growth factor. (D) Sample of PEG-maleimide hydrogel.

The precursor molecules were crosslinked into a hydrogel by addition of cysteine-flanked MMP-degradable peptide sequences (Fig 1A). A collagenase gel degradation study measured release of growth factor from the matrix (Fig 1B). In a pilot *in vivo* study, approximately 500 islets isolated from inbred Lewis rats were transplanted into 3 sites in the small bowel mesentery of recipient Lewis rats by delivery in 5% (wt/vol) PEG-maleimide matrix with 2 μM RGDS adhesive peptide and 80 ng/mL VEGF or FGF. The matrix was crosslinked with MMP-degradable peptide *in situ* to adhere the graft to the mesentery tissue. After 7 days, the rats were perfused with fluorescein-lectin to label vasculature and the grafts were examined histologically for neovascularization, insulin expression, and immune / inflammatory response.

Release studies indicate that PEG-maleimide bound growth factors incorporated into the matrix were released primarily in a proteolytic manner (Fig. 1B). Islets/matrix delivered to the small bowel mesentery exhibited vascular reperfusion (as shown by lectin staining) by 7 days *in vivo*. Furthermore the hydrogel itself exhibited a high degree of vascular invasion (Fig 2A) with markedly stronger vascular response in grafts with FGF or VEGF. Immunostaining revealed a concentration of grafted islets expressing insulin at the transplant site (Fig 2B). Histological staining indicated vessel penetration into the bulk of the hydrogel with no fibrous encapsulation and low presence of primary inflammatory cells (negative for CD11b).

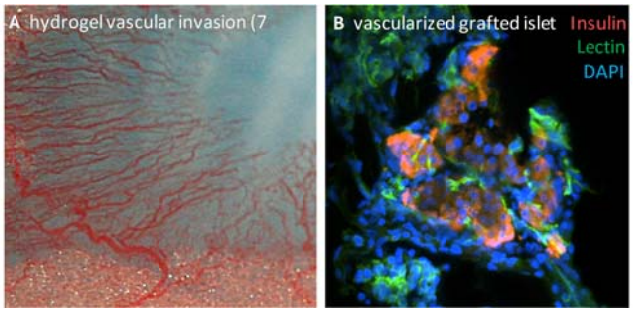

Fig. 2. (A) Hydrogel vascular ingrowth (7 days)

(B) Engrafted islet showing vascularization and insulin.

We present the use of an engineered matrix that supports islet activities and promotes vascularization *in vivo*. This project establishes novel biomaterial strategies for islet delivery that support islet viability and function via the induction of local vascularization. To our knowledge these PEG-maleimide hydrogels have never been used for cell culture or delivery.

Funding provided by CHoA/GT Center for Pediatric Healthcare Technology Innovation and GTEC/ACTSI.

Polymer-Silica Nanocomposites: Structure, Properties, Bioactivity and Biological Performance of Their Scaffolds

Manuel Monleón Pradas

Centro de Biomateriales, Universidad Politécnica de Valencia, Spain
Centro de Investigación Príncipe Felipe, Valencia, Spain

mmonleon@upvnet.upv.es

Introduction

Sol-gel silica polymer nanocomposites are an interesting class of materials in that their properties may be varied within a wide range of values, thus satisfying requirements which cannot be met with homo- or copolymers. If biomedical applications are considered, the important properties may be the mechanical strength, the dimensional stability upon water sorption, and the bioactivity, or ability to nucleate the growth of hydroxyapatite, the mineral component of bone tissues. A silica phase in an organic matrix can improve these aspects in one stroke. Depending upon the chemical functionalities of the matrix, materials more or less hydrophilic, and more or less rigid, can be modified to different degrees as a function of the silica content in the nanocomposite formulation. The silica phase obtained by a sol-gel reaction has terminal silanol groups in a number which depends on the connectivity of the network, and thus the silica to polymer ratio influences not only the mechanical properties of the composite, but also its hydrophilicity. Here we review work of our laboratory on a series of hybrid matrices and scaffolds made thereof aimed at regenerating mineralized tissue.

Materials and Methods

TEOS was used as precursor for silica. Different acrylate comomers (EA, HEA, CLMA and EMA) were employed to produce the nanohybrid matrices in a sol-gel reaction were both the silica network and the organic matrix polymerize simultaneously. Scaffolds with aligned channels of these matrices were obtained by a porogen-template method. The properties of the hybrid matrices and the silica structure therein were investigated by FTIR, DSC, dynamic-mechanical and dielectric relaxation measurements, contact angle, water sorption, EDS, SEM, AFM, thermogravimetry and densimetry. *In vitro* bioactivity was studied with SBF immersion tests. *In vivo* performance of nanohybrid scaffolds was studied in subcutaneous implants in nude mice with histological techniques.

Results and Discussion

Issues of interest in these systems include: the efficiency of the condensation reaction; the degree of interpenetration of both (organic and inorganic) networks; the topology and percolation threshold of the silica phase throughout the matrix; the confinement effects of the silica structure upon the mobility of the organic chains and the ensuing relaxation behaviour; the mechanical reinforcement effects as a function of silica contents; the effect of silica upon the specific hydrophilicity and surface energy of the material; the different silica structure build-up due to different hydrophilicity of the organic phase monomers; the specific mechanism leading to the *in vitro* bioactivity (hydroxyapatite nucleating ability) of the materials; the role of the connectivity of the silica phase in explaining the bioactivity of these systems; and finally, the interaction of the organic and the inorganic phase with cells *in vitro* and *in vivo*.

Conclusions

Sol-gel nanocomposites based on these organic matrices are finely interpenetrated networks with marked property changes at the percolating threshold; formulations around this composition exhibit better biological performance. Scaffolds with well defined pore order mimicking specialized bony tissues such as dentin can be made from these hybrid matrices, which get invaded by odontoblast-like cell processes *in vivo*.

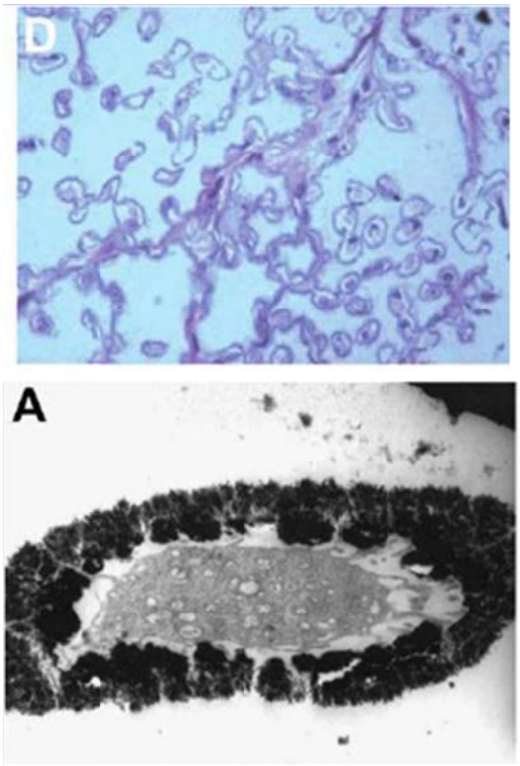

Figure Caption. Upper figure: histological cut of a tubular-channelled nanocomposite hybrid scaffold after in vivo implantation, showing a structural pattern similar to dentinal tissue. Lower figure: a detail thereof, showing a cell process within a microtubule of the scaffold (white area: nanocomposite matrix; dark area: hydroxyapatite; grey region: cell process) (*taken from* [4])

References

[1] Gómez Tejedor J A, et al, *J Macromol Sci, Part B: Phys* 46 (2007) 43

[2] Vallés Lluch A, et al, *Polymer* 50 (2009) 2874

[3] Stathopoulos A, et al, *Eur Polym J* 46 (2010) 101

[4] Vallés Lluch A, et al, *Tissue Eng Part A* 16 (2010) 2783

Rational Design and Synthesis of Amphilphilic Biodegradable Polymers for Alveolar Bone Regeneration

Firas Rasoul[1,2], David Wang[1], David Hill[1,2], Anne Symons[3], Srinivas Varanasi[3] and Andrew Whittaker[1,2]

[1]Australian Institute for Bioengineering and Nanotechnology, [2]Centre for Advanced Imaging and [3]School of Dentistry. The University of Queensland, Brisbane, Queensland, 4072 Australia

f.rasoul@uq.edu.au

Alveolar bone is the supporting bone structure of the maxilla (top jaw) and the mandible (bottom jaw) which are the tooth-bearing bones in humans. The primary cause of alveolar bone loss is periodontal disease (Periodontitis) which is an inflammatory gum infection caused by the convergence of bacteria that adheres to and grows on the tooth surface below the gum line. It involves progressive and irreversible loss of the alveolar bone around the teeth and eventually leads to the loosening and subsequent loss of teeth. Periodontitis is very common and has a prevalence of 40-50% of the population above 30 years old. The principal goal for this research program is to develop an effective method for the treatment of periodontitis through controlled delivery of bone-healing bioactives from biodegradable hydrogels.

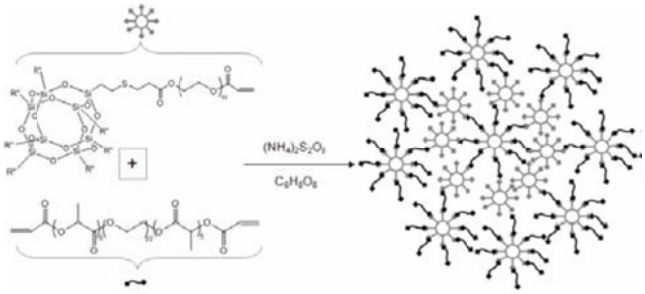

Figure 1: Copolymerization Reaction of Acrylated POSS-macromer with acrylated PLA-PEG-PLA tri-block copolymer

Hydrogels based on acrylated poly(lactic acid)-b-poly¬(ethylene glycol)-b-poly(lactic acid) (PLA-b-PEG-b-PLA) macromers were designed to maintain all of the advantages of a PEG-based material while also permitting tuneable degradability1. As the utilization of PLA-b-PEG-b-PLA based gels has increased, this characteristic of tuneable degradability has become extremely useful in the biomedical field to modulate the delivery rates of drugs or growth rates of cells encapsulated within cross-linked gel matrices.

However, PLA-b-PEG-b-PLA based hydrogels are falling short in some of their requirements for this particular application; such as high swelling ratios which can compromise the integrity of the dental implant, also high swelling ratios will results in high rates of degradation and therefore faster drug release.

In the current study we report the synthesis of new hydrogel copolymer systems based on multi-functional arms macromers as crosslinkers and acrylated PLA-b-PEG-b-PLA tri-block copolymer. Two examples of multi-functional arms macromers will be discussed: the first is based on polyhedral oligomeric silsesquioxane (POSS), which was pegylated through thiol-ene"click chemistry" followed by acrylation reaction to produce multi-functional arms "acrylated POSS-macromer" (see Fig 1) and the second is based on a hyperbranched polyester polymer (BoltornTM) which was also decorated with PEG using Cu(I) catalyzed azide-alkyne "click-chemistry" and then acrylated to produce "acrylated-Boltorn macromer". The effect of the multi¬arms macromers contents on the PLA-PEG-PLA hydrogels morphology, swelling ratios and degradation rates will be also presented. According to the developed degradation models of hydrogels based on polylactide and lactide copolymers, the hydrolytic degradation in aqueous media is known to be affected by two main parameters2, namely the kinetics of hydrolysis of the ester bonds within the hydrogel network, and the physical structure of the gel. Both parameters control the process of network degradation which makes the entire gel degradation process very complex. In the current study, it is important to understand the factors controlling the degradation behavior of the newly developed hydrogels including the effect of the molecular weight of the PEG segment (structural effect), the number of the lactide unites (kinetic effect) and the level of the multi-arms macromers in the hydrogel (morphological effect).

Furthermore, for the first time since the discovery of the Cu(I)-catalyzed click reaction, we have been able to show the presence of complexed Cu(II) residues in polymerized gels and that Cu(II) can play an important role in the hydrolytic degradation of polyester-based gels as elucidated by the cryoSEM and EPR spectroscopic studies (Fig 2). Moreover, the ability to tailor hydrogel cross-linking density can also be used to control network mesh size and diffusivities of encapsulated drugs. We have shown that multi¬functional arms macromers have tremendous effect on the hydrogel morphology and therefore on the rate of degradation. The results showed that hydrogels with high molar ratios of multi-arms macromers produce highly porous microstructures (Fig 2). This behaviour can be attributed to the formation of clusters of multi¬arms aggregates due to hydrophobic interaction, which give rise to phase separation during copolymerization process[3].

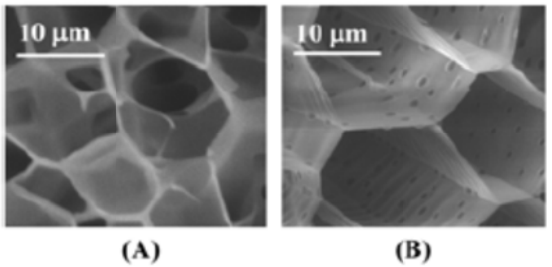

Figure 2: CryoSEM micrographs of the hydrogels at (A) 1 & (B) 8 weeks of immersion in water.

[1]Shah, Pool and Metters, *Biomacromolecules* **2006**, 7, 3171
[2]Lu and Anseth, *Macromolecules* **2000**, 33 (7), 2509;
[3]Wang et al, *Polym. Degradation & Stability* **2011**, 96, 123

Acknowledgements: The authors would like to thank The Queensland State Government-NIRAP for financial support.

Polymeric Endograft for the Treatment of Abdominal Aortic Aneurysms

Daniel Cohn, Randa Abbas, Itai Pelled and Ram Malal

Institute of Chemistry, The Hebrew University of Jerusalem, Jerusalem, Israel

dcohn18@gmail.com

Introduction

The formation of aneurysms is an extremely dangerous degenerative pathology of arterial tissues, especially common in adult and elderly populations, whereby the wall of the artery weakens locally and largely expands. In more than 80% of the cases, the rupture of the aneurysmal sac is fatal.

Until 1991, the only treatment available entailed a fully open surgical procedure, whereby the dilated segment of the artery was replaced by an artificial vascular graft. An endograft consisting of a vascular prosthesis mounted on a stent and deployed intra-luminally at the aneurysmal site using a balloon, was implanted in 1991 for the first time.

This minimally invasive technique, called EndoVascular Aneurysm Repair (EVAR), represented a breakthrough in the field both conceptually as well as technologically. Unfortunately, though, there are various factors that restrict considerably the use of this technique, mainly. The key problems of these devices are the occurrence of renewed leakage into the aneurysmal sac (endoleaks), despite the presence of the stent/graft device and its migration downstream. Additionally, strict anatomical considerations pertaining to the dimensions of the artery both proximal and distal to the aneurysmal site, may prevent the use of the endograft.

This lecture will introduce a polymeric device for AAA treatment that will be deployed intra-luminally at the aneurismal site and then expanded so it tightly attaches to the aorta, proximally and distally to the aneurysm.

The implantation of these devices is divided into two parts: {a} the insertion through the iliac artery, navigation to the site and expansion stages, during which the flexibility of the device is critical, and {b} its performance at the aneurismal site, where the device is required to display appropriate mechanical properties.

Two strategies were pursued: (1) the device is thermally softened using a balloon filled with warm saline, so it can be easily brought to the site and then expanded, followed by its firm and conformable attachment to the arterial wall, proximally and distally to the aneurysm. While in its expanded configuration, the endograft is then cooled down to 37^{o}C and attains the mechanical properties and strong attachment required. (2) The endograft consists of an Expandable Component (EC) and a "Smart" Component (SC), with the latter being present within the former. The EC is responsible for the large change in dimensions the endograft undergoes during its deployment at the aneurysm. The SC is a low molecular weight, polymerizable or crosslinkable precursor that fulfills two different roles: {a} It acts as a plasticizer during the early stages of the procedure (navigation and expansion), rendering it with the required flexibility, and, {b} It stiffens the device after its expansion and snug attachment to the vessel wall, once it polymerizes or crosslinks, imparting to the endograft the necessary mechanical properties.

Materials and Methods

PEU thermoplastic elastomers softening between 50 and 60 degrees were used when following the first strategy, while polymethacrylates and polyacrylates performed as the EC, and methacrylates such as HEMA and EGDMA were used as the SC. The various polymers were characterized by NMR, DSC, GPC and their mechanical properties were determined using an Instron Universal Testing Machine. Their ex-vivo performance was assessed in pig aorta segments and the acute in vivo feasibility of the device was evaluated by implanting it in a pig for eight hours.

Results and Discussion

Following the basic working concept of this study, various expandable conduits were generated, differing in their composition, the technique used to produce them, their mechanical properties and expandability ratio. The straightforward expandability of the devices created was demonstrated in cadaveric pig aorta sections using a balloon filled with warm saline. The diameter of the conduits increased more than three times and they became tightly attached to the luminal surface of the vessel. Moreover, it was extremely difficult to pull them out, once deployed at the site.

Figure 1 present the mechanical behavior of a PMMA/HEMA system, where HEMA softens the PMMA expandable component during the early stages of the implantation procedure, and remarkably stiffens when it polymerizes, after the device is expanded and tightly attached to the aortic wall, proximally and distally to the aneurismal sac.

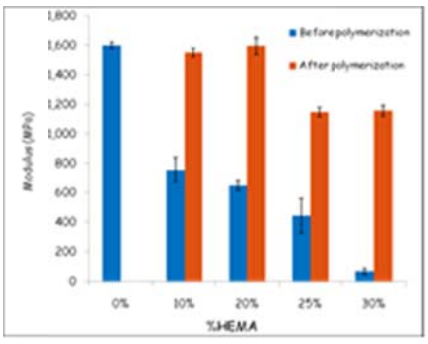

Figure 1.The mechanical behavior of an EC/SC PMMA/HEMA device.

The *in vivo* Proof of Principle of these devices, namely their ability to be deployed and inflated at the site following minimally invasive procedures that are routinely used in the clinic, and generate a stable and safe conduit, was demonstrated acutely (eight hours) in the abdominal aorta of pigs.

Additive manufacturing of wet-spun scaffolds for bone tissue engineering

Prof. Emo Chiellini

Laboratory of Bioactive Polymeric Materials for Biomedical and Environmental Applications (BIOlab), Department of Chemistry and Industrial Chemistry, University of Pisa, Italy.

emochie@dcci.unipi.it

Concept

The main result attained during the present research activity was the development of a layer-by-layer Additive Manufacturing (AM) technique allowing for a better control over shape, size and microarchitecture of tissue engineered polymeric scaffolds produced by wet-spinning. Layers composed of parallel fibers were fabricated by extruding a polymeric solution through a computer-controlled translating spinneret into a coagulation bath, and 3D structures were built up by collecting layers with different fiber orientation one on top of the other.

Motivations and Objectives

In recent years, some published studies have proposed non-woven polymeric meshes of wet spun microfibers, fabricated by physical bonding of prefabricated fibers or by a single-step method, as scaffolds for tissue engineering [1, 2]. However, these fabrication methods suffer from lack of structure reproducibility as well as control over external shape and internal morphology. The aim of the present activity was to develop an AM technique for the design and fabrication of wet-spun polymeric constructs, with customized architecture and shape, suitable for tissue engineering purposes.

Results and Discussion

Poly(ε-caprolactone) (PCL) and PCL/hydroxyapatite (HA) nanoparticles composite scaffolds, composed by layers of parallel microfibers with a diameter in the range 200 – 300 μm, were produced layer-by-layer with a 0-90° lay-down pattern (Figures 1a and 1b). Different architectures were obtained by changing the interfiber distance and fiber staggering between layers. The phase inversion process governing polymer solidification led to highly porous fibers both in the outer surface and in the cross section, with a pore size of few micrometers (Figure 1b). Uniaxial compression testing showed higher compressive modulus and strength of HA-loaded constructs in comparison with bare PCL constructs. Scaffolds with two different architectures were tested for their *in vitro* compatibility to MC3T3 preosteoblastic cells showing encouraging results in terms of cell adhesion, viability, ALP activity andmineralization. After 31 days most of the fibres throughout the scaffolds were completely covered by cells that were also able to colonize the inter-fibre gap, forming cellular bridging between adjacent fibres (Figure 1c).

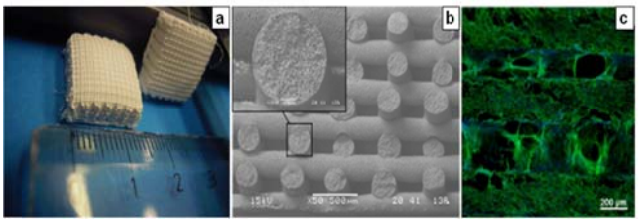

Fig. 1. a) Photograph of 3D PCL scaffolds fabricated by AM; b) Scanning Electron Microscopy micrograph of scaffold cross section; c) Confocal Laser Scanning Microscopy micrograph of top view of PCL tissue engineered construct.

References

[1] D. Puppi, F. Chiellini, A.M. Piras, E. Chiellini. *Progress in Polymer Science*, 35 (2010) 403–440.

[2]D. Puppi, D. Dinucci, C. Bartoli, C. Mota, C. Migone, F. Dini, G. Barsotti, F. Carlucci, F. Chiellini. *Journal of Bioactive and Compatible Polymers*. In press.

Nano- and Microparticles with Controlled Surface Properties; Synthesis, Properties, Selected Medical Applications

Stanislaw Slomkowski, Mateusz Gosecki, Mariusz Gadzinowski, Monika Gosecka, Teresa Basinska, Pawel Wozniak

Center of Molecular and Macromolecular Studies, Polish Academy of Sciences
Sienkiewicza 112, 90-363 Lodz, Poland

staslomk@cbmm.lodz.pl

Introduction

Polymer nano- and microparticles found many applications in medicine. Dimensions of these objects are close to the dimensions of large proteins, intracellular organelles and whole cells. Therefore, such particles can be used as convenient tools probing properties of living systems on the cellular, subcellular and molecular level. Initially polymer microparticles were used for preparation of simple diagnostic tests (see Ref. 1,2 and references therein). Later it was found that particles composed of (bio)degradable polymers could be used also as drug carriers [3,4]. For all the mentioned above applications there are needed particles with tailored surface properties, allowing for their controlled interactions with tissue, cells and macromolecules of the immune system. The lecture will present results of our recent studies on preparation of nano- and microparticles with interfacial properties tuned for diagnostic purposes, drug delivery and tissue engineering. The attention will be focused on particles with shells containing hydrophilic polyglycidol suitable for controlled binding of proteins and other biomolecules.

Particles for diagnostic applications

Particles for diagnostic applications should allow for selective covalent immobilization of antibodies or antigens with elimination, or at least efficient reduction, of the adventitious protein adsorption during the diagnostic tests. In the last years we developed methods for synthesis of microspheres by copolymerization of styrene with polyglycidol macromonomers. In the lecture we will present our recent findings on the mechanism of particle nucleation, growth and formation of their interfacial layer. The TEM, SEM and AFM observations revealed that microspheres are decorated with nanoparticles, presumably formed at the early stage of polymerization. XPS studies did prove that the interfacial layer of microspheres is strongly enriched (up to 45 %) in polyglycidol. The high polyglycidol content and special morphology of particles' interfacial layer resulted in their superhydrophilicity and strong reduction of the uncontrolled protein adsorption. Moreover, activation of polyglycidol with trichloro-triazine allowed for the covalent immobilization of proteins yielding systems suitable for the immunotests.

Polyglycidol containing nnoparticles for drug delivery

Polyglycidol can be used also for protection of the outer layer of biodegradable nanoparticles. Particularly interesting are nanoparticles formed by dialysis of poly(L,L-lactide)-*b*-polyglycidol copolymer solutions against water. This approach allowed preparation of nanoparicles loaded with insulin and ovalbumin. Their diameters ranged from 25 to 70 nm, depending on the copolymer composition. It is worth noting that suspensions of the poly(L,L-lactide)-*b*-polyglycidol nanoparticles were colloidally stable for pH from 2 to 9. Kinetics of protein release revealed absence of the initial burst. Thus, the particles can be considered as interesting candidates for oral protein delivery.

Polyglycidol and poly(ethylene oxide) containing nanoparticles for scaffolds for tissue engineering

The proper adjustment of hydrophilic/hydrophobic balance of interfacial layer is important in the case of materials used for preparation of scaffolds for tissue engineering. Especially interesting are materials which could adapt hydrophilicity/hydrophobicity of their surface to the environment. Recently we developed the method suitable for preparation of nano- and microsilica with tethered pairs of polyglycidol (or poly(ethylene oxide)) and poly(L,L-lactide) chains. First, silica particles are modified with 3-glycidoxypropyl trimethoxysilane. This step yields particles with epoxy groups at their surface. An exposure of silica particles with epoxide groups to solution containing living poly(1-ethoxyethylglycidol) with alkoxide propagating species yielded silica with tethered polyether chains and alkoxide groups generated by opening the epoxide rings. The subsequent grafting of poly(L,L-lactide) from silica yielded particles with almost equal number of hydrophilic polyglycidol chains (formed by deprotection of hydroxyl groups in poly(1-ethoxyethylglycidol)) and hydrophobic poly(L,L-lactide) chains. In a similar way the silica particles with poly(ethylene oxide) and poly(L,L-lactide) chains were obtained. The coil-to-globule and globule-to-coil transition of polyether and polyester chains, induced by changing media surrounding silica particles resulted in adaptation of their surface properties to environment. The modified silica particles with adaptable interfacial properties were used for preparation of silica fortified scaffolds for the hard tissue engineering.

References

1. S. Slomkowski, Macromol. Symp. **2010**, *288*, 121
2. T. Basinska, Macromol.Biosc. **2005**, *5*, 1145
3. Microspheres, microcapsules and liposomes, vol. 2 Medical and biotechnological applications, R. Arshady, Ed.; Citus Books, London, 1999, pp 1-695
4. S. Slomkowski, Acta Polon. Pharm.; Drug Res. **2006**, *62*, 351

ABSTRACTS

ORAL PRESENTATIONS

Topic 1: Synthetic Routes: Monomers and Polymers from Bioresources and Advanced Methodologies

Ferrocenyl-containing Compounds as Modifying Additives for Radical Polymerization of Vinyl Monomers

Regina M. Islamova, Olesya I. Golovochesova, Svetlana V. Nazarova, Yurii B. Monakov

Institute of Organic Chemistry of Ufa Scientific Centre of the Russian Academy of Sciences 71, pr. October, Ufa, 450054, Russian Federation

rmislamova@mail.ru

Introduction

Ferrocene and its derivatives are successfully used in various polymerization processes [1]. Ferrocenyl containing monomers have been synthesized and related polymers with improved electrophysical characteristics were synthesized [2]. In [3], effective initiation systems based on ferrocene and diacyl peroxides have been studied. To extend the range of using ferrocenyl containing substances and to study the influence of new azinylferrocenes (AFC) and ferrocenyl containing semiclathrochelates and clathrochelates of Fe(II) (FCC) on the process of radical polymerization of vinyl monomers (by the example of methyl methacrylate – MMA and styrene) are tasks of great interest and importance.

Materials and Methods

Azinylferrocenes and clathrochelates of Fe(II) were synthesized and purified as described in [4, 5]. The kinetic of bulk polymerization was studied by dilatometric and gravimetric methods. Molecular weight characteristics were determined by gel penetrating chromatography using a "Waters GPC 2000 System" chromatograph. Polymer microstructure was determined using ^{1}H NMR-spectra. Interactions of organic molecules were studied by IR, UV and NMR spectroscopy.

Results and Discussion

When catalytic amounts of AFC as modifying additives were used in the polymerization of vinyl monomers the synergic effect of metal containing and nitrogen containing groups on kinetic parameters of process and on molecular characteristics of obtained polymers was observed. It was shown that AFC in combination with diacyl peroxides form effective initiation systems, especially in polar MMA, which are more active in comparison with initiation systems based on unsaturated ferrocene, all other conditions being the same [3]. The increase of MMA and styrene polymerization rate in the presence of azo initiator (azo-bis-isobutironitrile - AIBN) is distinguishing feature of AFC. The influence of AFC on propagating and termination stages was confirmed by the results of study of interaction of AFC with monomers, by the increase of syndiotactic triads content in polymer chains (in the case of polymethyl methacrylate - PMMA) and by the increase of polymers thermo stability (in the case of PMMA and polystyrene).

The choice of ferrocenyl containing semiclathrochelates and clathrochelates of Fe(II) as modifying additives for radical polymerization of vinyl monomers caused by presence of both ferrocenyl group and ligand of special kind – macrocyclic clathrochelate with transition metal central atom – in their structure. It was found that ferrocenyl containing semiclathrochelates and clathrochelates of Fe(II) in combination with diacyl peroxides form initiation systems which are more active than ferrocene and its derivatives. The using of clathrochelates makes it possible to reduce the concentration of initiator. Concentration of added FCC was less by 1-2 order than in the case of using of ferrocene and its derivatives. By variation of initiation system components ratio high weight polymers and low weight polymers can be synthesized. Obtained polymers were characterized by high content of syndiotactic triads and high thermo stability. When AIBN was used as initiator, metal complexes additives at studied concentrations had almost no effect on kinetic parameters of MMA and styrene polymerization processes.

Conclusions

Thus, AFC and FCC are promising modifying additives for carrying out the radical polymerization of vinyl monomers. It is most probable, that polymerization follows the complex-radical mechanism.

References

1. Perevalova E.G., Reshetova M.D., Grandberg K.I. Methods of organoelement chemistry. Organoiron compounds. Ferrocene. M.: Nauka. 1983. [in Russian]

2. Pomogailo A.D., Savost`yanov V.S. Metall-containing monomers and related polymers. M.: Khimiya. 1988. [in Russian]

3. Puzin Yu.I., Yumagulova R.Kh., Kraikin V.A. // Europ. Polym. J. 2001. V. 37. No. 9. P. 1801-1812.

4. Chupakhin O.N., Utepova I.A., Kovalev I.S., Rusinov V.L., Starikova Z.A. // Eur. J. Org. Chem. 2007. No. 5. P. 857-862.

5. Voloshin Y.Z., Makarov I.S., Vologzhanina A.V., Monakov Yu.B., Islamova R.M., Polshin E.V., Bubnov Yu.N. // Russian Chemical Bulletin, International Edition. 2008. Vol. 57. No. 6. P. 1223-1230.

This work was supported by the Russian Foundation of Basic Research (grants No. 10-03-00027-a).

New Biobased Epoxy Resins

Dr Sylvain CAILLOL[a], *Pr Bernard Boutevin*[b], *Dr Hélène Fulcrand*[c], *Dr Hélène Nouailhas*[d]

[a] Institut Charles Gerhardt ChemSuD Montpellier, France; sylvain.caillol@enscm.fr

[b] Institut Charles Gerhardt Montpellier, France; bernard.boutevin@enscm.fr

[c] Inra, Montpellier, France; fulcrand@supagro.inra.fr

[d] Innobat, Clapiers, France; nouailhas@innobat.fr

Introduction

In the field of green chemistry development, scientists and especially chemists are facing new stakes and have to deal with new constraints. Among these constraints, we find new regulations concerning chemicals, and especially concerning reduction and substitution of Carcinogen, Mutagen Reprotoxic (CMR) classified substances. Among many of these substances we can note several molecules constituting of widely used plastics, and particularly bisphenol A (BPA) (CMR R3), one of the main components of epoxy resins.

BPA has been commercially used for over 50 years and is currently produced in huge quantities: over 3.3 Mt/y in the world. Since the year 2000, lots of publications studied the effects of bisphenol A on human health. Hundreds of publications deal with the toxicity of BPA in animal, human and environment. This recent awareness on BPA toxicity implies necessary changes in the world of epoxy resins. Major issues are to find alternative to the typical synthesis route for epoxy resins and to find substitutes to BPA. To find a substitute to BPA and amines are the two goals of this study. Polyphenols and especially condensed tannins extracted from waste produced by the wood and wine industries are proposed as substitutes to BPA to produce "green resins". Amines synthesized from renewable resources could be proposed as "green" hardener for these "green resins".

The aim of this study is to qualify natural tannins as potential substitutes to BPA. However, before working on tannins, we intended to focus on smaller molecules, such as catechin, tannins reactivity model molecule, to study the reactivity of polyphenols and their ability to produce epoxy resins (**¡Error! No se encuentra el origen de la referencia.**, **¡Error! No se encuentra el origen de la referencia.**). Indeed, catechin molecule corresponds to repetition unit of tannins.

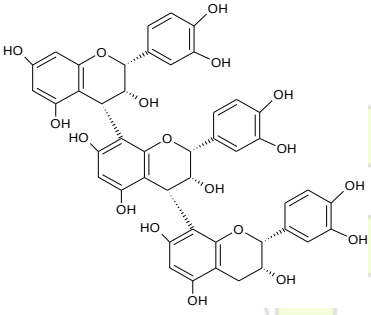

Figure 4 : tannins structure

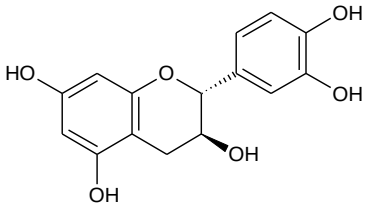

Figure 5 : catechine molecule

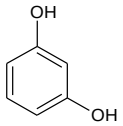

Figure 6 : resorcinol

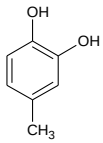

Figure 7 : methylcatechol

Results

We first studied the epoxydation of monoaromatic phenolic molecules such as resorcinol and methylcatechol that constitute the two aromatic rings of tannins (Figure 6, Figure 7). We obtained different yield of epoxydation owing to different positions and then different reactivity when reaction with amine hardener.

Then we studied the epoxydation of catechin, tannin monomer model. We synthesized glycidyl catechin. We isolated and characterized this new reactive molecule. We identified epoxydation loci and reactivity. Finally, we elaborated green resins from glycidyl tannins[i] with amine hardeners. We characterized these resins with mechanical and thermal properties and compared to classic resins made from diglycidyl ether of BPA (BADGE).

Conclusion

We obtained succeeded in replacement of BPA by natural tannins and elaborated epoxy resins from glycidyl tannins. We obtained similar thermal properties with epoxy resins elaborated from glycidyl tannins compares to resins from commercial BADGE.

[i] Nouailhas H, Burguiere C, Caillol S, Boutevin B, Fulcrand H, Rapior S, patent WO 2010136725

Effective catalytic systems for Atom Transfer Radical Polymerization based on the carborane complexes of Ruthenium

Ivan Grishin[a], *Elena Turmina*[a], *Igor Chizhevsky*[b], *Dmitry Grishin*[b]

[a]Research Institute of Chemistry of Nizhny Novgorod State University,

[b]A.N.Nesmeyanov Institute of Organoelement Compounds Russian Academy of Sciences

grishin_i@ichem.unn.ru

Introduction

Atom Transfer Radical Polymerization **(ATRP)** is a very effective and convenient tool for obtaining polymer samples with predicted molecular-weight parameters, and controlled topology. It opens wide opportunities for the synthesis of polymer materials with unique properties. So, the development of novel catalytic systems for ATRP is an actual and challenging task. Here we report about the use of novel ruthenium carborane complexes in ATRP of methyl methacrylate and the obtaining block copolymers based on them.

Materials and Methods

Ruthenium complexes were synthesized using standard Schlenk-line techniques under an atmosphere of dry argon. Monomers were dried over CaH_2 and distilled under reduced pressure prior to use. The polymerization was conducted at 80˚C in sealed glass tubes under reduced pressure in monomer bulk. The obtained polymer samples were purificated from monomer and catalyst by dissolving ion chloroform and precipitating in petroleum ether. The molecular-weight distributions of the polymers were analyzed by Size-exclusion chromatography on a Knauer instrument equipped with two polystyrene gel columns (Phenomenex, pore size 10^3-10^5Å).

Results and discussion

In this work paramagnetic ruthenium complexes **1-4** containing C_2B_9-dicarbollide ligand were used as catalysts for ATRP:

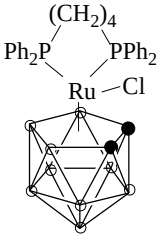

1

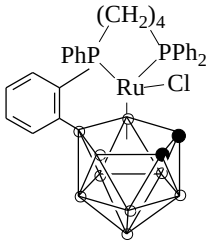

2

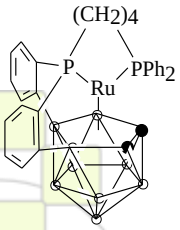

3

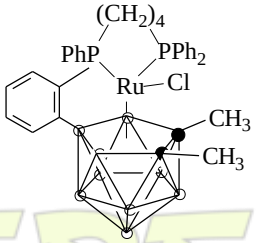

4

The obtained results have shown that these paramagnetic derivatives of ruthenium (III) are perfect catalysts for ATRP of MMA and allow to obtain polymer samples with polydisperstity of 1.1-1.2. The molecular weight of the obtained samples linearly increases with conversion indicating the "living" nature of the process. It should be mentioned that all the complexes show similar degree of control over process, but compound **2** is the most preferable one due to its higher stability.

The obtained poly MMA samples may be used as macronintiators for post polymerization and block-copolymerization with styrene and methacrylic monomers indicating "living" nature if the process. The obtained block-copolymers have unimodal molecular weight distribution indicating the absence of "dead" chains in the polymer.

It was established that amine additives can significantly increase the rate of polymerization in the presence of complexes **1-3** leaving process controlled. The use of amines as co-catalysts for ruthenacarboranes allows to decrease catalyst concentration ten times. We suppose that amine interacts with carborane complex of ruthenium giving novel organometallic species which are responsible for the reversible deactivation of growing chains.

It was shown that complex **4**, based on dimethylcarborane ligand is less effective catalyst than its nonsubstituted counterparts. The use of systems based on **4** results in the formation of polymers with M_w/M_n=1.4. We suppose that methyl groups are enough bulky to disturb the interaction between catalyst and growing polymer chain. This results in the loss control over polymerization. Moreover systems based on **4** and amines are incapable to control polymerization of MMA leading to polymers with broad polydispersity and high molecular weights.

Conclusions

A novel carborane complexes of ruthenium (III) were synthesized. These compounds have shown themselves as perfect catalysts for ATRP. Introduction of amine additives allow to increase polymerization rate and decrease catalyst concentration which is necessary for synthesis of polymers.

Acknowledgements: This work was supported by Russian foundation for basic researches (project №11-03-00074) and Russian Ministry of Education and Science ("Federal target program of scientific and scientific-pedagogical personnel of innovation of Russia on 2009-2013").

Polylactic acid and Polyamide11 with controlled macromolecular architecture

G. Di Silvestro[a], M. Ortenzi[a], H. Farina[a], C.M. Yuan[a], L. Basilissi[a], E. Zini[b], L. Martino[b] and M. Scandola[b]

a) University of Milan and INSTM UdR Milan , Italy; b) University of Bologna and INSTM UdR Bologna, Italy

Giuseppe.disilvestro@unimi.it

Introduction

The synthesis of polymers with controlled macromolecular architecture according to well tested models of chain growth [1] is important from both academic and industrial points of view. Upon correlation of structure with properties in such polymers and by application of the developed models, new polymeric materials with optimized physical properties can be obtained. An example of the application of such a strategy is PA6 with low [2] or high viscosity [3] recently produced by Rhodia. The present work reports the synthesis, according to chain growth models recently developed by some of the Authors [1], of star, tree and star-tree PA11 and PLA, together with their melt and solid-state characterization.

Materials and Methods

For the synthesis of PLA and PA11 with complex architectures, monomer and proper concentrations of multifunctional comonomers (pentaeritrol, cyclodextrin, trimethylolpropane) were polymerised at 190°C (2 hours) and at 270°C (4 hours), respectively, in inert atmosphere. Lactide present at equilibrium in PLA was eliminated at 150°C under vacuum. SEC analyses were performed at room temperature with a 6 column set using CH_2Cl_2 as eluent. PA11 was analysed after trifluoroacetylation. Specimens for stress-strain measurements were cut from compression molded films (0.2-0.4 mm thick).

Results and Discussion

The model predicts [1] that, when an AB monomer is polymerised in the presence of a comonomer having 6 reactive groups, all possible species (linear and thee-to-six branched chains) are present even at very high conversion. In this work, such model predictions were confirmed by SEC and NMR analyses, by oligomerisation and MALDI-TOF [4], not only for PLA and PA11, but also for PA6 and PA12 [5].

The model also suggests [1] a means to obtain star PLA having higher melt viscosity than commercially available PLA. As an example, the figure compares the rheological behaviors of a linear PLA (DPn = 950) with the one of two different star PLA (three arm and DPn = 400; 21 arms and DPn = 10000) and a star-tree PLA. It is worth pointing out that star-polycondensates are commonly synthesized for their low melt viscosity, due to their smaller hydrodynamic volume than their linear counterparts (with the same DPn) and to the absence of intermolecular entanglements. The example in the figure instead concerns a PLA with a high number of branches with very high arm length suitable for intermolecular interaction that results in a remarkable increase of melt viscosity.

Interestingly, tree- or star-tree-branched PLAs display even higher melt viscosities than equivalent star-shaped macromolecules. An analogous behaviour is shown by PA11 polymers with different architectures. The mechanical properties of PLA and PA11 are quite different (i.e. tensile modulus 2400 MPa and 1050 MPa, elongation at break 3-5% and > 100%, respectively), but the measurements carried out in this work on the synthesized polymers indicate that solid-state properties are not significantly affected by macromolecular architecture.

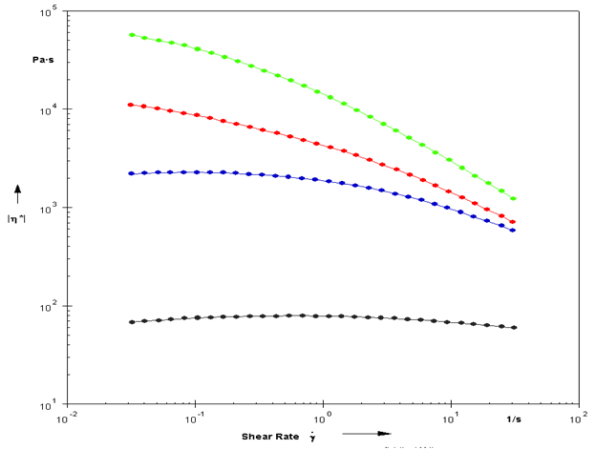

Melt viscosity of a three arm star (black curve), of a linear (blue curve), of a star-tree (red curve) and of a 21-arms branched (green curve) PLA's

Conclusions

PLA and PA11 with complex macromolecular architectures can be obtained according to the models originally proposed for PA6. The macromolecular architecture strongly affects the melt behaviour. The solid-state characterization results show that the rheological properties can be tuned to processing requirements without altering the material's mechanical performance.

Acknowlegments: Authors thank Regione Lombardia, INSTM and Fondazione Cariplo for financial support.

References:

[1] C.M. Yuan, G. Di Silvestro, F. Speroni, C. Guaita, H. Zhang, Macromolecular Chemistry and Physics (2001), 202(10), 2086-2092.

[2]. A. Cucinella,G. Di Silvestro,C. Guaita, F. Speroni, H. Zhang, PCT Int. Appl. (1997) WO 9724388 A1 19970710.

[3]. G. Di Silvestro, C. Guaita, F. Speroni, C.M. Yuan, H. Zhang. PCT Int. Appl. (1999) 19 pp. WO 9903909 A1 19990128.

[4] C.M. Yuan, G. Di Silvestro, C. Guaita, H. Zhang. Macromolecular Symposia (2003), 199, 109-124.

[5]. H. Farina, C.M. Yuan, M. Ortenzi, G. Di Silvestro. Macromolecular Symposia (2004), 218, 51-60.

Ring-opening co- and terpolymerization of an alicyclic oxirane with carboxylic acid anhydrides and CO2 in the presence of chromium porphyrin and salen or zinc aryloxide catalysts

Elham Hosseini Nejad, Rob Duchateau, Cor Koning

Department of Chemical Engineering and Chemistry, Laboratory of Polymer Chemistry, Eindhoven University of Technology, P.O.Box 513, 5600MB Eindhoven, The Netherlands

e.hosseininejad@tue.nl

In recent years polyesters have gained increasing attention due to their suitability for an ever-broadening range of applications ranging from packaging materials to biomedical devices. Polyesters can be synthesized via several routes. One path is the copolymerization of diols with anhydrides or dicarboxylic acids through step-growth polymerization, whereas another and very attractive path is to synthesize them through a catalytic ring-opening polymerization of the corresponding anhydrides and oxirane monomers, using different selective catalysts for this type of polymerization.

In this study, our primary main goal is to synthesize fully hydroxide end-capped aliphatic polyesters with relatively high Tg by the catalytic copolymerization of cyclohexene oxide (CHO) and different anhydrides such as phthalic anhydride (PA) or succinic anhydride (SA). While CHO residues will exhibit a rigid structure and result in relatively high Tg polyesters, the succinic anhydride residues will provide some flexibility to the polymer chain structure.

On the other hand, carbonate segments in polyester chains have also been very appealing during the recent few years due to the advantages they pertain to the polymer chain. The introduction of a carbonate linkage into the polyester chain has the beneficial effect of improving hydrolytic stability and impact strength. Like polyesters, polycarbonates are useful as biodegradable products and have shown to have adjustable degradation rates. So another pathway in this research is the catalytic terpolymerization of CHO and PA (or SA) with carbon dioxide (CO2) to obtain poly (ester-co-carbonate)s and investigate the properties of this class of copolymers.

Porphyrin and salen type catalysts have been used extensively in this research to investigate their selective role in both aforementioned attractive catalytic ring-opening polymerization pathways. On the other hand, a more environmentally friendly catalyst; viz zinc bis aryloxide (Zn(OAr)2) has also been investigated for the same co- and terpolymerizations.

Extensive characterization of the obtained polyesters and poly (ester-co-carbonate)s has been performed by conventional SEC, NMR and MALDI-ToF-MS methods. The results obtained show that the copolymerization of epoxides and anhydrides yields completely alternating polyesters whereas introducing the third monomer, CO2, into the polymerization reaction results in a terpolymer with a random/blocky structure.

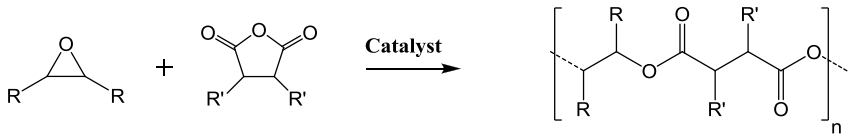

Polyester

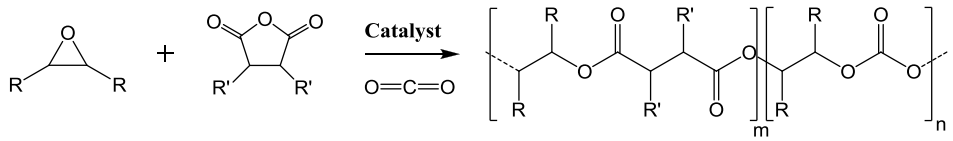

Poly(ester-*co*-carbonate)

Polyurethane elastomers from castor oil and chemically modified yucca starch: synthesis and physical-chemical, physical-mechanical and thermical properties

Manuel F. Valero

Programa de Ingeniería Química, Universidad de La Sabana, Chía, Colombia.

manuel.valero@unisabana.edu.co

Abstract: Chemical modification of cassava starch was conducted through an acylation reaction by using pyridine and propionic anhydride to replace the functional groups of starch. The design variables were the temperature of preactivation, the pre-activation time and temperature of acylation. The process was carried out using a 23 factorial experimental design. The most favorable conditions for cassava starch modified by acylation with propionic anhydride are pre-activation temperature of 95 °C, pre-activation time of 2 h and acylation temperature of 65 °C. Under these conditions reached a rate of 38% replacement of hydroxyl groups by propionyl groups. The purpose of the modification was to replace the hydrogen in the hydroxyl groups of the molecule of amylose by a propionyl group of propionic anhydride in the acylation reaction. The original starch (S) and modified starch (AMP) were mixed with castor oil (CO) to obtain a suspension. The suspensions were characterized by means of tests based on The Fourier Transform Infrared Spectroscopy and the Hydroxyl Index. Polyurethane elastomers were prepared using suspensions of the mixture obtained from castor oil and yucca starch that was modified by a propionic anhydride reaction. By modifying the hydroxyl groups of starch ester groups of the PU properties varied.

The PUs were characterized by their physical-mechanical properties like tension- deformation and Shore A. hardness, thermal gravimetric analysis and swelling test. The density cross-linking of from swelling tests was determined by applying the Flory-Rehner equation. The goal of this work was to understand what the effect of changing the chemical structure of starch by acylation on the physical chemical properties, thermal and physicochemical properties of PU elastomers and compared with the counterparts obtained from oil-native starch suspensions, depending on the interfacial adhesion between the starch granule and the original and modified polyurethane matrix.

It was found that the increase in the tensile strength and shore A hardness is higher for PU from oil-AMP than for counterparts obtained from oil-pure starch, while elongation at break decreases for materials obtained from AMP-oil suspensions.

In PU systems suspensions obtained from castor oil-AMP was found that the decrease in crosslink density due to an increase in the interfacial adhesion between the PU and the AMP. Intermolecular forces present between groups were calculated by Coulomb's law based on links-length and the ratio of Van der Waals forces between two polar molecules.

These properties were due to increased interfacial adhesion present between AMP granules (dispersed phase) and the PU matrix (continuous phase) due to attractive forces (related to the polarity of the molecules) are higher for PU AMP that PU and native starch, under the synthesis conditions have the same NCO / OH and an equal percentage of modifying agent. The results of crosslink density from swelling tests of the materials obtained from oil-AMP suspensions support the increase in interfacial adhesion due to the crosslinking density increased with the concentration of AMP in response to increased affinity and not related to the change in the crosslinking of the polymer network.

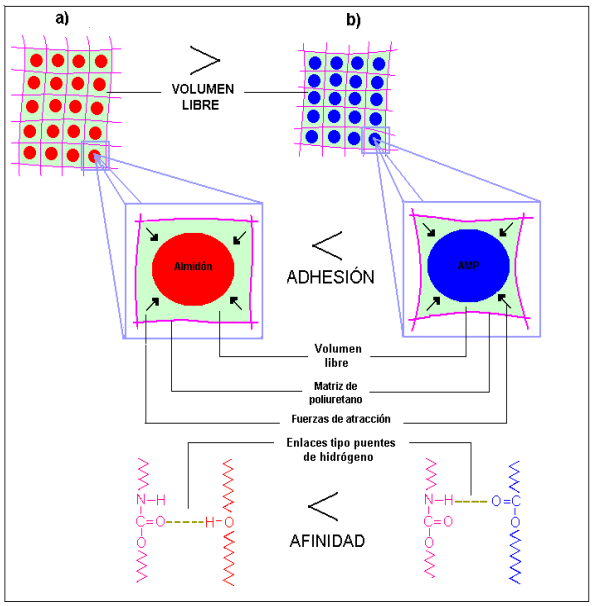

New Aminovalerolactone-based Degradable Copolyesters for Biomedical Applications: Synthesis, Characterization and Biocompatibility.

S. Blanquer, M. Patterer, V. Darcos, D. Domurado, X. Garric, B. Nottelet and J. Coudane

IBMM, Artificial Biopolymers Group, UMR-CNRS 5247, UM1-UM2, 15 Av. C. Flahault, 34093 Montpellier, France

Benjamin.Nottelet@univ-montp1.fr

Introduction: As a consequence of their tremendous development in environmental and biomedical applications, most efforts have been focused in the recent years on the functionalization of biodegradable aliphatic polyesters. Among others, one possible strategy is to synthesize and polymerize lactones substituted by a group of interest. Various functional lactones have thus been described ranging from 4- to 7-membered functionalized monolactones or even dilactones of the substituted glycolide-type.[1,2] However, although amino-polyesters possess great potential for many biomedical applications due to their cationic nature (vectorization, transfection,…), only two examples of amino-functionalized lactones have been reported so far: one butyrolactone derived from serine,[3] and one glycolide-like derived from lysine.[4] But the number of steps required for their syntheses and their tricky required purification ultimately lead to poor yields.
We describe here a facile two steps synthesis of the novel 5-NHZ-valerolactone and its subsequent (co)polymerization to generate aliphatic amino-functionalized copolyesters. Biocompatibility, hemocompatibility as well as proof of concept for biomedical use are reported.

Materials and Methods: Synthesis of 5-NHZ-valerolactone was recently described by our group starting from ZGlu(OtBu)OH (**1**) (**Scheme 1**).[5] (Co)-polymerization was carried out by ROP using $Sn(Oct)_2$ as a catalyst and BzOH as an initiator under nitrogen. Amino-deprotection was achieved under acidic conditions with AcOH/HBr (33%). Biocompatibility and hemocompatibility were assessed according to previous protocols.[6,7]

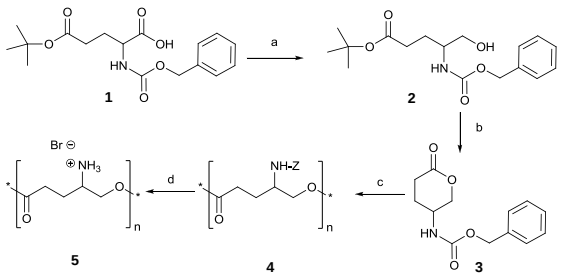

Scheme 1. Synthesis of 5-NHZ-VL and of poly(NH3+-VL)

Results and Discussion: Consecutive activation of the ester and reduction of the free carboxylic group were obtained using *N,N'*-diisopropylethylamine/BOP and $NaBH_4$ to yield **2** after purification on column chromatography (yield 90%). The second step consisted in the simultaneous *in situ* carboxylic acid deprotection and intramolecular cyclization of **2** in a CH_2Cl_2/TFA (1:1) mixture at room temperature. The final 5-NHZ-valerolactone **3** (5-NHZ-δ-VL) was purified by column chromatography and recovered as white crystals (yield 55%).
3 was copolymerized with ε-caprolactone (ε-CL) to yield a family of poly(5-NHZ-VL_x-co-ε-$CL_{(1-x)}$) with x varying from 10 to 100 (**Figure 1**). Copolymers were obtained in good yields by ROP in bulk at 110°C under nitrogen for 24h. Molecular weights were slightly lower than expected with $\overline{Mn}$ ranging from 3500 to 8600 g/mol for x = 100 and x = 10, respectively. Amino-group deprotection led to the quantitative conversion of NH-Z group to free ammonium groups.

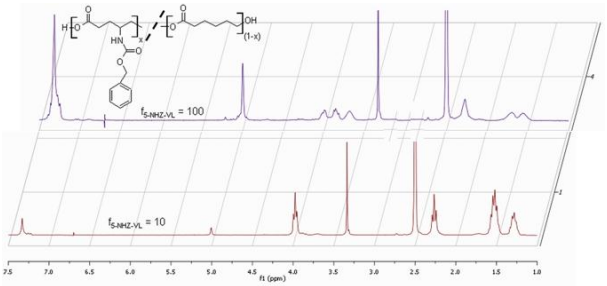

Figure 1. ^{1}H NMR (300 MHz; DMSO-d_6) spectra of poly(5-NHZ-VL_{10}-co-ε-CL_{90}) and poly(5-NHZ-VL)

Copolymers were tested for biocompatibility and hemocompatibility. No acute toxicity was found compared to poly(L-Lysine) with decreased toxicity with ε-CL content. Cell viability was unchanged for concentrations <100 µg/mL. Neither aggregation nor hemolysis was observed at 2mM (**Figure 2**). Small erythrocytes shape modification occurred only at concentrations > 10 mM. Finally, a model molecule was conjugated to poly(5-NHZ-VL-co-ε-CL) as a proof of the potential of this new class of aminated degradable polyesters to be used as macromolecular prodrugs.

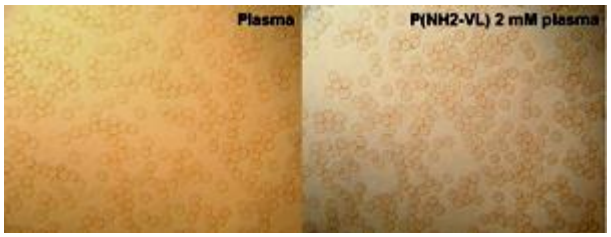

Figure 2. Hemocompatibility of poly(5-NHZ-δ-valerolactone)

Conclusion: Novel 5-NHZ-VL allows the easy synthesis of bio- and hemocompatible aminated degradable (co)polyesters which constitute a new class of cationic degradable polyelectrolytes for biomedical applications.

References: **1.** *El-Habnouni S. et al. Macromol. Rapid Commun., 2009, 30, 165* **2.** *Saulnier B. et al., Macromol. Biosci., 2004, 4, 232* **3.** *Zhou Q. et al. Macromolecules, 1990, 23, 3399* **4.** *Gerhardt W. et al. Biomacromolecules, 2006, 7, 1735.* **5.** *Blanquer S. et al. J.Pol.Sci.PA, 2010, 48, 5891.* **6.** *Hansen, MB. et al. J. Immun. Meth., 1989, 119, 203.* **7.** *Moreau, E. et al. J. Drug Target. 2002, 10, 161.*

Renewable Hybrid Materials through Living Radical Polymerization

U. Edlund, J. Voepel, A.-C. Albertsson

Fibre and Polymer Technology Royal Institute of Technology, KTH

edlund@kth.se

The conversion of forestry biomass to added value materials and products is a conceivable and powerful route to realize the forest as a biorefinery and to provide renewable, inexpensive and ethically non-controversial alternatives in a future sustainable lifestyle. Non-cellulosic poly- and oligosaccharides from wood are typically released to the liquid fractions in a range of wood processing operations. Optional and customized strategies for extraction, upgrading and refining yield hemicelluloses of varying purities and types. This family of branched and highly hydrophilic heteropolysaccharides offers a great potential for chemical modification through numerous hydroxyl functionalities. Presented here is a new approach to covalent functionalization of hemicelluloses, offering a fast pathway to the design of thermoplastic glycopolymers with a high level of control.

Single-electron-transfer mediated living radical polymerization (SET-LRP) is a powerful and versatile synthetic technique for living and controlled polymerization, viable in a range of solvents and for a range of vinyl monomers. The mechanism involves a reversible activation of a halide-terminated macroradical into an active propagation chain caused by a single electron donated from the metal catalyst, typically a Cu species.

O-acetyl-galactoglucomannan (AcGGM) from spruce was synthetically converted to a macro initiator mediating the SET-LRP of vinyl monomers, achieving brush-like hybrid polymers. In a first step, some anomeric hydroxyl groups on the heteropolysaccharide backbone were functionalized with bromo- or chlorine moieties through immidazole assisted esterification. The resulting macro initiators were explored with respect to their potency in the SET-LRP of four different monomers in three different solvents using Cu^0 as a catalyst. The kinetics in terms of $\ln([M]_0/[M])$ over time is linear and conversions of up to 99,98% are achieved.

Synthetic Route Effect on Macromolecular Architecture: From Block to Gradient Copolymers Based on Acryloyl Galactose Monomer using RAFT Polymerization

Pierre Escalé [†,‡], *S.R. Simon Ting*[‡], *Abdel Khoukh*[†], *Laurent Rubatat*[†], *Maud Save*[†], *Martina H. Stenzel* [‡] *and Laurent Billon*[†]

[†] IPREM Equipe de Physique et Chimie des Polymères, UMR 5254 CNRS, Université de Pau et des Pays de l'Adour, Hélioparc, 2 Avenue du Président Angot, 64053 Pau Cedex, France

[‡] Centre for Advanced Macromolecular Design, School of Chemical Sciences and Engineering, University of New South Wales, Sydney NSW 2052, Australia

pierre.escale@etud.univ-pau.fr

In recent few years glycopolymers (i.e. polymers carrying pendant carbohydrate moieties) have received increasing attention due to the numerous biological mechanisms in which carbohydrates are implicated such as cell to cell recognition, inflammation, signal transmission and infection[1]. These polymers could be also used for drug delivery nanoreactors, radio-labeled sugar-nucleotide donors and cell surface receptor[2].
Glycopolymers can be obtained by post polymerization glycosylation reaction or polymerization of galactose containing monomers.[3]
The purpose of the present study is to synthesize amphiphilic gradient and block copolymers by RAFT polymerization using a carbohydrate based monomer (AcGalEA) and styrene (Sty). The final aim is to compare the properties of the copolymers depending on their microstructure to self-assemble into Honeycomb films (Figure 1). The carbohydrate moiety will provide a bioactivity of the polymer film and the hydrophobic polystyrene part is required for the honeycomb film formation by the Breath Figure approach.[3-4]

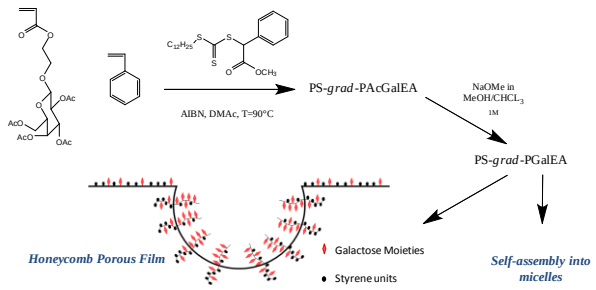

Figure 8- Schematic Approach to honeycomb structured porous film and micelles with glycopolymer based gradient copolymer.

Indeed, glycopolymers are not only of interest in solution because they could serve as screening devices when there are immobilized onto surface. Also, gradient copolymers, made in one pot synthesis, are of great interest because there are time and cost saving in comparison with block copolymers.
Here, we report for the first time the determination of the reactivity ratio of both monomers by comparing the results obtained with Skeist, Kelen-Tudos and Finemann-Ross methods. These three methods tend to a same conclusion: styrene is much more reactive than glycomonomer with r(Sty) = 0.7 ± 0.1 and r(AcGalEA) = 0.07 ± 0.01. Figure 2A displays the evolution of the AcGalEA composition in the monomer mixture ($f_{AcGalEA}$) as a function of the global conversion (X_n) and Figure 2B shows the evolution of the copolymer composition in styrene (F_{Sty}) as a function of the monomer mixture composition in styrene (f_{Sty}).

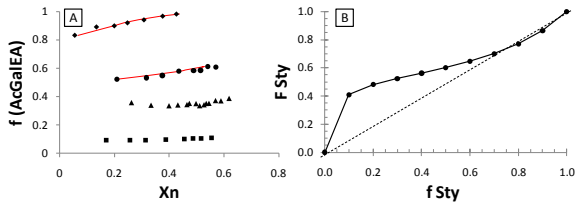

Figure 9- (A) Plots of $f_{AcGalEA}$ versus X_n for different initial S/AcGalEA compositions: (square) 90/10, (triangle) 70/30, (circle) 50/50, (rhomb) 20/80; (B) composition diagram: F_{Sty} versus f_{Sty}.

Considering the reactivity of both monomers, spontaneous gradient copolymer with high content in glycomonomer and forced gradient copolymer with high content in styrene can be obtained. The more hydrophilic gradient copolymer will be able to self-assemble into galactosylated micelles for drug delivery purpose or lectins complexation whereas the more hydrophobic one was appropriate to elaborate honeycomb porous films (Figure 3).

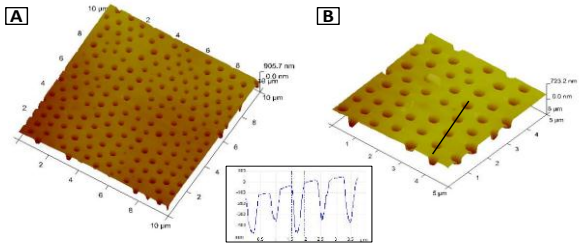

Figure 3- AFM images of honeycomb porous films made with PS-b-(PS-*grad*-PGalEA) copolymer.

1. Spain, S. G.; Gibson, M. I.; Cameron, N. R., *Journal of Polymer Science Part A: Polymer Chemistry* **2007,** 45, (11), 2059-2072.
2. Cairo, C. W.; Gestwicki, J. E.; Kanai, M.; Kiessling, L. L., *Journal of the American Chemical Society* **2002,** 124, (8), 1615-1619.
3. Ting, S. R. S.; Min, E. H.; Escale, P.; Save, M.; Billon, L.; Stenzel, M. H., *Macromolecules* **2009,** 42, (24), 9422-9434.
4. Stenzel, M. H.; Barner-Kowollik, C.; Davis, T. P., *Journal of Polymer Science Part a-Polymer Chemistry* **2006,** 44, (8), 2363-2375.

BIO-INSPIRED CATIONIC POLYMERIZATION OF ISOPRENE IP INITIATED BY ALLYLIC ALCOHOLS / $B(C_6F_5)_3$

Samira OUARDAD, Frédéric PERUCH, Alain DEFFIEUX.

Laboratoire de Chimie des Polymères Organiques (LCPO), 16 Avenue Pey Berland, 33607 Pessac Cedex, France

ouardad@enscbp.fr

Introduction

More than 2500 plants are able to produce polyisoprenes (PI) but *Hevea Brasiliensis* is the only one to produce PI with high molar mass with a 100% 1,4-*cis* structure in sufficient yield. Whereas isoprene (IP) is the monomer employed for the chemical synthesis of PIs, isopentenyl pyrophosphate (IPP) is the monomer used for the biosynthesis of NR (Figure 1). From the polymer chemist point of view, these enzymatic processes can be seen as electrophilic additions, comparable to cationic polymerizations. Both during initiation and propagation reactions, the pyrophosphate moiety is released to give an allylic carbocation able to add IPP to yield a tertiary carbocation. One α proton is then eliminated to give back an allylic pyrophosphate. Moreover, it has been shown that divalent cations are necessary. In a "pseudo-cationic" pathway, they could act as Lewis acids, assisting the cationation[1,2].

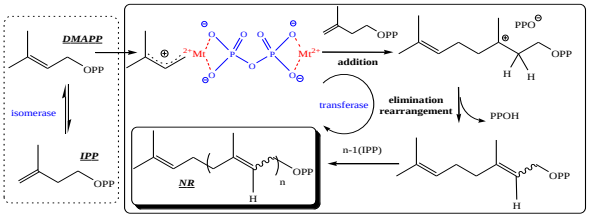

Figure 10. Biosynthesis of NR.

The goal of this study is to investigate the cationic polymerization of IP in the presence of different allylic alcohol initiators and in the presence of $B(C_6F_5)_3$ as Lewis Acid.

Experimental

Materials. 2-methyl-3-buten-1-ol, DMAOH (Aldrich) was dried over a sodium cube and cry-odistilled. Isoprene was dried over CaH_2 and cryo-distilled prior to use. $B(C_6F_5)_3$ (TCI Europe) was used as received. Dichloromethane (Atlantic Labo) was dried over CaH_2 and cryo-distilled prior to use.

Instrumentation. Size Exclusion Chromatography (SEC) was used to determine molar masses and molar masses distributions of polymer samples with respect to polystyrene standards. ^1H and ^{13}C NMR spectra were recorded on a Bruker Avance 400. Matrix-assisted laser desorption ionization time-of-flight (Maldi-Tof) mass spectrometry was performed using a Voyager-DE STR (Applied Biosystems) spectrometer.

Polymerization reactions. Polymerizations were carried out under a dry nitrogen atmosphere using standard Schlenk techniques.

Results and Discussion

Initiation step. The ability of $B(C_6F_5)_3$ to generate an allylic carbocation from DMAOH was studied by ^1H NMR, varying the DMAOH/LA ratio. At the initial stage, the chemical shift of the hydroxyl group is highly affected, in relation with the amount of the LA (Figure 2). Besides, the formation of isoprene is detected. This latter which is produced by rearrangement of an allylic carbocation, followed by proton elimination (Figure 2) and is a proof that allylic carbocations are formed by interaction of DMAOH and $B(C_6F_5)_3$

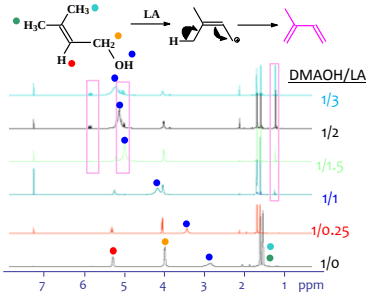

Figure 2. ^1H NMR spectra of DMAOH and $B(C_6F_5)_3$ at different ratios.

Polymerization

By combining NMR, Maldi-Tof and SEC a full characterization of the microstructures have been determined . Many side reactions have been characterized: Cyclization (by NMR), branching (by SEC), protic intiation andd transfer (by Maldi-Tof).

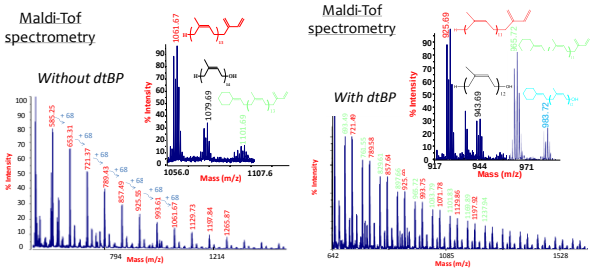

Figure 3. Maldi-Tof spectrum of polyisoprenes obtained with or without DtBp

Conclusions

It was shown that allylic alcohols associated to $B(C_6F_5)_3$ were able to initiate the cationic polymerization of isoprene. In all cases, only oligomers are formed, probably due to the presence of transfer reactions. They were characterized by NMR and Maldi-Tof spectrometry. The addition of isoprene proceeds via 1,4-*trans* addition, which is the opposite of the NR structure. Nevertheless, oligomers structure is fairly complicated with the presence of cyclized sequences and is not completely elucidated yet.

It was also shown that the polymerization yield is strongly reduced when a proton trap is added, due to the reduction of side protic initiation coming from protons generated during transfer reactions.

Acknowledgements

Financial support from ANR is gratefully acknowledged. Cesamo for Maldi-Tof spectrometry.

References

([1]) Puskas, J. E.; Gautriaud, E.; Deffieux, A.; Kennedy, J. P. *Prog. Polym. Sci.*, **2006**, 31, 533.

([2]) Puskas, J. E.; Li, H.; Dabney, D. E.; Wesdemiotis, C.; Lindsay, A.; Peruch, F.; Deffieux, A. *J. Polym. Sci. A: Polym. Chem.*, **2009**, *47*, 2172.

Synthesis and Characterization of Antibacterial Polyurethanes Coatings from Novel Quaternary Ammonium Functionalized Soybean Oil Based Polyol

Hadi Bakhshi[1], *Hamid Yeganeh*[1]*, *Mohammad Ali Shokrgozar*[2], *Abbas Yari*[1]

1)Polyurethane Department, Iran Polymer and Petrochemical Institute, P.O. Box: 14965/115, Tehran, Iran

2) National Cell Bank of Iran, Pasteur Institute of Iran, Tehran, Iran

h.yeganeh@ippi.ac.ir

Introduction

Coatings with antibacterial properties are useful in many areas such as hospitals, food manufacturing, building trades and antifouling applications. There are several methods for the introduction of biocidal functions in polymers. Chemical grafting of a biocide to polymer matrix can provide many advantages for polymers, especially for biomedical applications such as non-volatility, good environmental and chemical stability, low toxicity, extended lifetime, lack of skin irritation and/or skin-permeability as well as better bactericidal activity due to higher density of biologically active groups [1, 2].

In the present work for the first time both quaternary ammonium groups with well-known biocidal function and reactive hydroxyl groups were introduced on the back bone of soybean oil. These new renewable resource based functional polyols were used for the preparation of polyurethane coatings via reaction with proper diisocyanate monomers. The biocompatibility and antibacterial properties as well as some mechanical and physical properties were evaluated for these new materials.

Materials and Methods

Quaternary ammonium containing polyols were prepared by reacting epoxydized soybean oil (ESBO) with diethylamine at 80 ºC using anhydrous zinc chloride as catalysis. This intermediate compound bearing tertiary amine groups was further quaternized with either benzyl chloride or methyl iodide. Polyurethane films were prepared via one-shot reaction of polyols and various diisocyanates including MDI, TDI, HDI and IPDI (Scheme 1).

Results and Discussion

The structure of prepared polyols was confirmed using ^{1}H-NMR and FTIR spectroscopies and elemental analysis. The physical, mechanical and viscoelastic properties of polyurethane films including gel content, phase transitions, tensile strength, elongation at break, surface hydrophilicity, and solvent resistance were evaluated. All of the cured films showed complete curing with gel content more than 95%. DMTA thermograms showed two phase structure with soft and hard segment glass transitions in the range of 0-15 °C and 140-170 °C respectively. According to stress-strain curves, the prepared films showed tensile strength and elongation at break of 5-9 MPa and of 16-87% correspondingly. The contact angle data of water droplet on the surface of films were in the range of 68-80 degree. Depends on the quaternizing group and diisocyanate structure the surface hydrophilicity of films were altered. Samples made from aliphatic diisocyanates and methyl iodide as quaternizing group showed higher surface hydrophilicity. The solvent resistant of coatings based on MEK rub test was excellent.

Cell culture test and MTT assay based on mouse L929 fibroblast cells were used to evaluate both cytotoxicity and cytocompatibility of the specimens. The evaluation of cell morphology showed cells survived and grew with spindle shape morphology, during full three days of the test, and none of the polymers appeared to give off any toxic or inhibitory leachates, since cells grew to confluence on the all samples. The MTT assay showed excellent level of biocompatibility with cells viability in the range of 95-120%. These are indications of noncytotoxcicity and cytocompatibility of prepared polyurethanes.

Examination of antibacterial property of specimens by shaking flask and agar plate methods using *Escherichia coli* and *Staphylococcus aureus* microorganisms showed strong dependency to the chemical structure of polyurethanes. Films prepared from benzyl chloride based quaternized polyol had no biocidal function, however, the samples made from polyol quaternized with methyl iodide showed significant bacterial reduction in the range of 79-88%. To find the reason behind this observation, the concentration of active quaternary ammonium groups was examined by measuring the halogen counter ion content using energy-dispersive X-ray analysis (EDXA). Although the EDXA maps showed uniform distribution of halogen atoms, the concentration of quaternary ammonium groups were much higher for methyl iodide based samples (0.53-0.60 mole %) than benzyl chloride based specimens (0.20-0.23 mole %). Therefore, sufficient concentration of quaternary ammonium groups was the determining factor.

Conclusions

It was concluded that via proper functionalization of Soybean oil, it is possible to use it for making polyurethane coatings with excellent biocompatibility and antibacterial properties. Simple chemical modification route, low cost of starting material and possibility to use an environmentally friendly and renewable resource based raw material are some fascinating features of these newly developed polyurethanes.

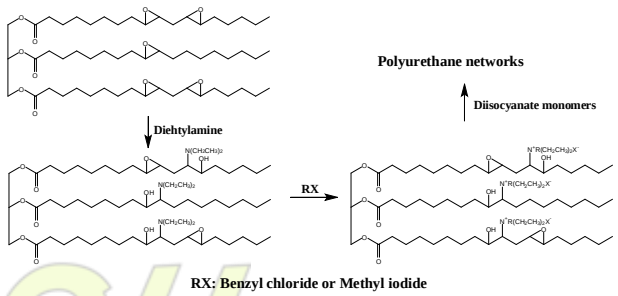

Scheme 1

References

1. K.Y. Chen, et al. J. Biomater. Sci. 21, 429, 2010.
2. E. Kenawy, et al. Biomacromolecules 8, 1359, 2007

Dextran-Poly(deoxycholate) Block Copolymers as New Biodegradable Materials

Marieta Nichifor and Magdalena Cristina Stanciu

"Petru Poni" Institute of Macromolecular Chemistry, Iasi, Romania

nichifor@icmpp.ro

Introduction

Amphiphilic block copolymers able to form self-assembled core-shell nanoparticles have a great potential in application for drug and gene delivery. Presence of bioerodible blocks gives the possibility for a more efficient control of rate and site of the bioactive compound delivery.

In the attempt to obtain new biocompatible and biodegradable materials containing naturally occurring compounds, we have prepared amphiphilic block copolymers, with a polysaccharide (dextran) as the hydrophilic block and an oligoester of a bile acid - deoxycholic acid (**DCA**) - as a lipophilic block. These polymers based on natural compounds have the advantage of forming only biocompatible degradation products (mainly **DCA**, a product found in small intestin).

Materials and Methods

Cholic and deoxycholic acid, dextran of MW 6000 and the other reagents were from Aldrich and were used as received.

FT-IR (KBr pellets), ^{1}H and ^{13}C-NMR (in $CDCl_3$ or DMSO-d6) spectroscopical analyses were used for determination of polymer structure and composition. Size exclusion chromatography (with polystyrene standards and THF solvent) provided the polyester molar mass. Thermal decomposition (TG and DTG), thermal properties (DSC), X-rays diffraction spectroscopy, and electronic microscopy (SEM images) provided information about the physico-chemical properties of the block copolymers and their intermediate products. Degradation rate of polymers in the physiologically similar media (phosphate buffered saline of pH 7.4, 37°C), as well as the release rate of a model drug (diclofenac) from block copolymer nanoparticles, were studied by reverse phase HPLC.

Results and discussion

Preparation of the desired block copolymer required the synthesis of several intermediates:(i) 3α-(succinoyloxy) - 12α-hydroxy-5β-cholan-24-carboxylyc acid (**ScDCA**), (ii) the poliester of **ScDCA** and diethylene glycol (called here poly(deoxycholate or **PDCA**)), and (iii) dextran (MW 6000) aminated at the reductive end. The block copolymer (**Dex-PDCA**) was obtained by attachment of **PDCA** to aminated dextran. Chemical structures of the **PDCA** and **Dex-PDCA** were confirmed by IR and NMR spectroscopy and are depicted in Scheme 1.

PDCA had a molar mass of 3500, T_g = 48.24°C, started to decompose at 332 °C and was partially crystalline (about 30 % crystallinity). **Dex-DCA** had a T_g = 78°C, displayed two decomposition steps (T_i = 183 and 340°C), and was less crystalline than **PDCA** (Fig. 1).

Nanoparticles (100-400 nm), loaded or not with diclofenac, were prepared from **Dex-PDCA** by solvent diffusion method. The degradation of the polyester block, with formation of **DCA** and **ScDCA**, was slow (about 20% in 24 h), and followed zero order kinetics. The release rate of diclofenac loaded in nanoparticles was only slightly higher than polyester degradation rate, indicating a predominance of erosion as a release mechanism, with a small contribution of drug diffusion.

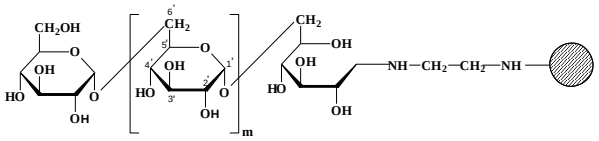

Dex-PDCA

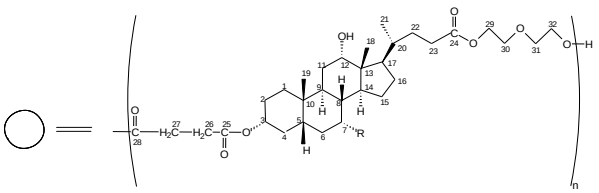

PDCA

Scheme 1. Chemical structure of the dextran-poly(deoxycholate) block copolymer

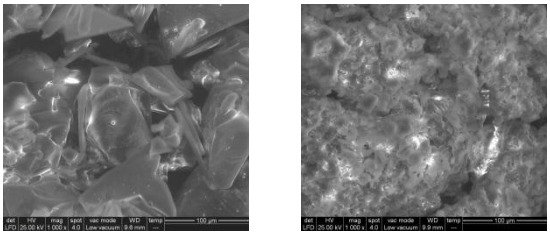

Fig. 1. Electronic micrographs of PDCA (left) and dex-PDCA(right)

Conclusion

Newly synthesized biodegradable amphiphilic block copolymers containing two natural compounds, dextran and deoxycholic acid, can form nanoparticles with potential application as carriers for drug delivery systems. The release of the drug is controlled mainly by erosion, and can be easily tailored by changing the length of the two blocks.

References

M. Nichifor, M. C. Stanciu, X. X. Zhu. *React. Funct. Polym.* 59, 141-148, 2004.

M.C. Stanciu, M. Nichifor, B.C. Simionescu, *Rev. Roum. Chim*, 54, 951 -956, 2009.

Π-Conjugated Polymers with Functional Endgroups through Modified Nickel Initiators

Alfons Smeets, Karlien Van den Bergh*, Pieter Willot*, Julien De Winter°, Pascal Gerbaux°, Thierry Verbiest* and Guy Koeckelberghs**

° Mass Spectrometry Center, Organic Chemistry Laboratory, University of Mons, 20 Place du Parc, B-7000 Mons, Belgium

*Laboratory of Molecular Electronics and Photonics, Katholieke Universiteit Leuven, Celestijnenlaan 200F, B-3001, Heverlee, Belgium

Alfons.smeets@chem.kuleuven.be

Introduction

Π-Conjugated polymers (CPs) are becoming increasingly viable candidates for replacing silicon based materials in electro-optical applications, such as field effect transistors (FETs), light emitting diodes (LEDs) and photovoltaic cells (PVs). In order to achieve satisfactory performance and stability of these devices, the supramolecular organization of the active material is of great importance. Therefore, conjugated block copolymers and supramolecular structures based on CPs, for example core shell particles, should provide the desirable supramolecular properties for these applications.

Materials and Methods

Contemporary methods to prepare block copolymers and supramolecular structures rely on living polymerizations and either consist of subsequent addition of different monomers or by performing endcapping with functional groups, which are then employed in coupling reactions. However, these methods cannot be generally applied to CPs, as only a few of them can be prepared through living polymerizations. We want to circumvent this limitation by introducing the desired functional group at the start of the polymerization, using a functional initiator. Subsequent post-polymerization reactions should then allow the preparation of block copolymers or supramolecular structures of choice. Because a living polymerization is no longer a necessity, the scope of this protocol would be expanded to many different CPs.

Results and Discussion

From a synthetic point of view, the protocol is based on a nickel complex carrying the desired functional group, which initiates the polymerization while inserting the functional group at the beginning of each chain. More specifically, we first synthesized nickel initiators with (protected) alcohol, amine, carboxylic acid and ethynylene functionalities. These initiators were then used to initiate the polymerization of poly(3-alkylthiophene)s, poly(3-alkoxythiophene)s, poly(3-thioalkylthiophene)s and poly(*para*-phenylene)s. Through post-polymerization reactions we were able to quantitatively convert the alcohol moiety to tosylates and azides. Finally, we coupled azide functionalized poly(3-alkylthiophene)s with ethynylene functionalized poly(3-alkoxythiophene)s, forming block-copolymers composed of electronically different blocks (Figure 1).

Conclusions

We successfully established a protocol for the synthesis of nickel initiators with different functional groups and subsequently employed those initiators for the synthesis of different CPs with different functional groups[1]. We also demonstrated that the functional groups could be used in post-polymerization reactions to form block-copolymers.

References

1) Alfons Smeets, Karlien Van den Bergh, Julien De Winter, Pascal Gerbaux, Thierry Verbiest and Guy Koeckelberghs, Macromolecules, 2009, 42 (20), pp 7638–7641

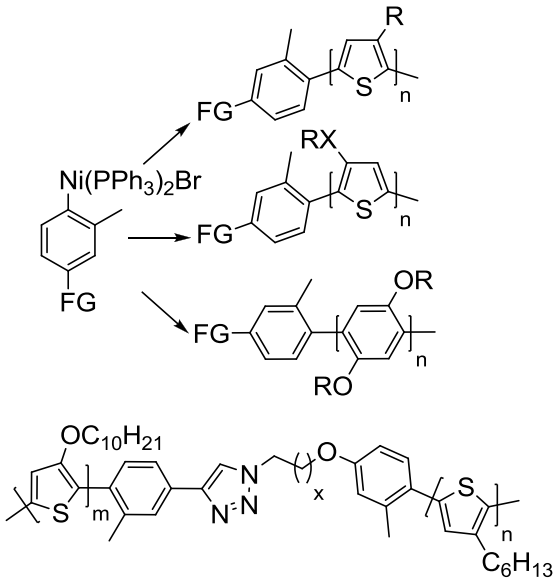

Figure 1: Synthesis of end-functionalized CPs and Π-conjugated block-copolymers

Step growth polymerization of starch-derived dianhydrohexitol stereoisomers: versatile platform for the design of linear polymers and polymer networks with original properties.

Céline Besset,[1,2,3] Etienne Fleury,[2,3] Jean-Pierre Pascault,[2,3] Julien Bernard,[2,3] Eric Drockenmuller[1,3]

[1]: Université de Lyon 1, [2]: INSA de Lyon, [3]:Ingénierie des Matériaux Polymères (IMP)

eric.drockenmuller@univ-lyon1.fr

Introduction

Starch-derived 1,4:3,6-dianhydrohexitol stereoisomers (i.e. isosorbide, isomannide, and isoidide) are particularly interesting difunctional building blocks (Figure 1).[1]

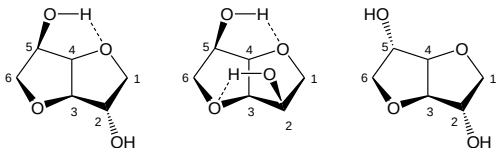

Figure 1: 3D structure of (from left to right) isosorbide (SR), isomannide (RR) and isoidide (SS) dianhydrohexitols.

Results and Discussion

Taking advantage of organic chemistry procedures several homo- or hetero-difunctional monomers suitable for click chemistry polyaddition were prepared. In a first approach diazide, dialkyne and α-azide,ω-alkyne monomers of every dianhydrohexitol stereosiomers were obtained in high yields (Figure 2).

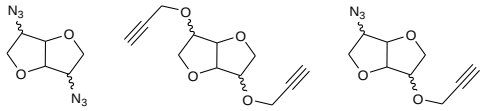

Figure 2: Diazide, dialkyne and α-azide,ω-alkyne dianhydrohexitol monomers suitable for click chemistry polyaddition.

Linear polytriazoles and corresponding networks were then obtained by copper catalyzed azide-alkyne cycloaddition (CuAAC) as well as thermally initiated 1,3-dipolar Huisgen cycloaddition (Figure 3). The influences of monomer stereochemistry, processing conditions and polyaddition regiospecificity on the physico-chemical properties of the resulting polymers have been thoroughly examined using ^{1}H NMR, DSC, TGA, SEC and rheological measurements.[2]

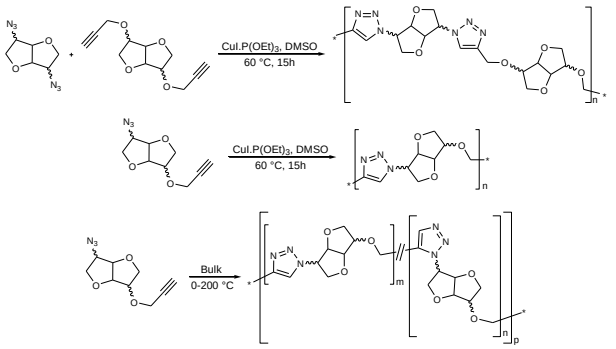

Figure 3: Polyaddition of diazide, dialkyne and α-azide,ω-alkyne dianhydrohexitol monomers.

Following the discussion of these preliminary results, our latest results regarding their polyaddition of functionalized bio-sourced monomers using other types of click chemistry processes will be presented.

References

[1] Fenouillot, F.; Rousseau, A.; Colomines, G.; Saint-Loup, R.; Pascault, J-P. *Prog. Polym. Sci.* **2010**, *35*, 578-622.

[2] (a) Besset, C.; Binauld, S.; Ibert, M.; Fuertes, P.; Pascault, J-P.; Fleury, E.; Bernard, J.; Drockenmuller, E. *Macromolecules* **2010**, *43*, 17-19. (b) Besset, C.; Bernard, J.; Fleury, E.; Pascault, J-P.; Cassagnau, P.; Drockenmuller, E.; Williams, R. J. J. *Macromolecules* **2010**, *43*, 5672-5678. (c) Besset, C.; Pascault, J-P.; Fleury, E.; Drockenmuller, E.; Bernard, J. *Biomacromolecules* **2010**, *11*, 2797-2803.

New Functional Materials from Polysaccharides Modified by Copper Catalyzed Azide-Alkyne Cycloaddition

Monica Bertoldo[1], *Giovanni Zampano*[2], *Samuele Nazzi*[1], *Federico La Terra*[1], *Francesco Ciardelli*[3]

[1]Istituto per i Processi Chimico Fisici, Consiglio Nazionale delle Ricerche, via G. Moruzzi, 1 56124, Pisa Italy

[2] c/o,MENARINI SpA,Firenze,

[3] SPIN_PET;srl.Pontedera Italy

monica.bertoldo@ipcf.cnr.it

Natural macromolecular materials such as polysaccharides are very attractive not only for environmental reasons but also for their physical and chemical properties. Indeed peculiar reactive groups such as amines, amides, carboxylic and sulfonic acids are present , in addition to typical hydroxyl groups. These last provide polysaccharides with specific properties such as gelling capability, positive or negative charge, chelating ability, mucoadhesive property, etc.... The reactivity of these groups offers also many opportunities to modify polysaccharide by introducing new functionalities. However, the mentioned modification can affect some original properties which can be partially or totally lost. In this contribution some examples are presented concerning polysaccharide modification with preservation of the original polysaccharide structure. The very selective copper catalyzed azide-alkyne cycloaddition (click) [1] was used as key step.

Materials and Methods

Chotosan (~300 kDa, DAC 0.75) amylose from potato and glycogen from mollusc were purchased from Aldrich. Modified polysaccharides were characterized by FT-IR and NMR spectroscopies, elemental analysis and TGA. TEM, dynamic and static light scattering, UV-Vis and swelling analyses were carried out to characterize the new polysaccharide properties.

Results and Discussion

Two different modification strategies were adopted, respectively of chitosan (scheme 1), a polysaccharide bearing amine and amide groups into its backbone, and of linear amylose and hyperbranched glucan glycogen (scheme 2), bearing just hydroxyl groups in their backbone. The first step in chitosan modification was a reaction with phtalic anhydride to protect the amine groups and to make chitosan soluble in organic solvents such as DMF and DMSO. The derivative was then brominated and successively azidated in two consecutive "one pot" reactions [2]. This azido-functionalized chitosan (PH-N_3) was then converted to new functional materials under click condition (scheme 1). In particular, a biopolymer exhibiting distinct photocromic response and a very low thermal decay of the photogenerate state [3] was obtained by covalent bonding of a chromophoric spiropiran derivative bearing an alkyne group (SPCC). Gels with pH dependent swellability (higher at acid pH) were prepared by crosslinking with dialkines and amine deprotection at 80°C with hydrazine [2].

Periodate oxidation and subsequent reductive amination with propargylamine was adopted for the controlled functionalization of glucans with alkyne groups, while ATRP polymerization was exploited to obtain end-azide functionalized poly(meth)acrylates to be used as "click" reagents. Finally, polysaccharide-g-polymethacrylate copolymers were prepared by "click" grafting "onto" method with complete grafting yield (scheme 2) [4].

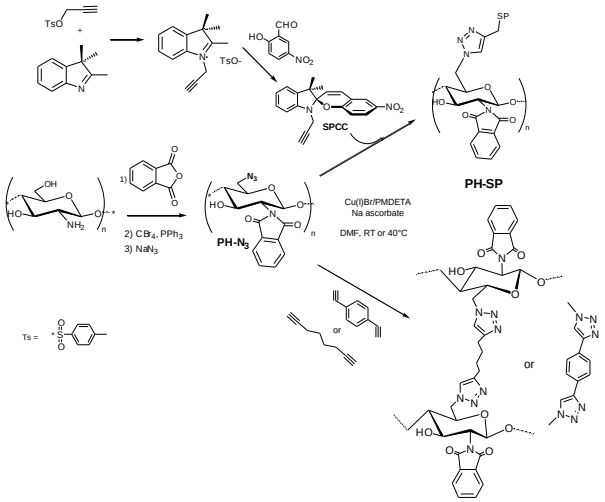

Scheme 1: Chitosan modification strategies

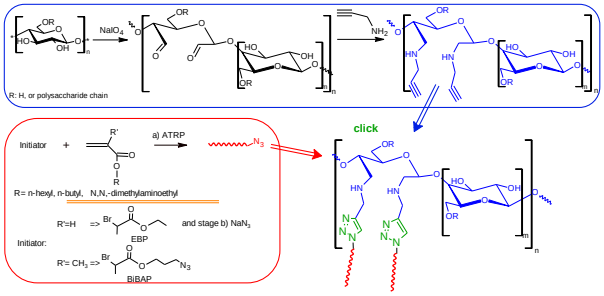

Scheme 2: Preparation of graft copolymers by "click" promoted grafting "onto" method

The most amphiphilic among amylose graft copolymers self-assembled in water yielding nanoparticles with ca. 30 nm diameter, while glycogen natural nanoparticles became the core of core-corona nanoparticles stable in toluene dispersion.

References

[1] H.C. Kolb; M.G. Finn; K.B. Sharpless *Angew. Chem. Int. Ed.* 40 (2001) 2004-2021

[2] G. Zampano; M. Bertoldo; F. Ciardelli; *React. Funct. Polym.* 70 (2010) 272–281

[3] M. Bertoldo; S. Nazzi; G. Zampano; F. Ciardelli, *Carbohydr. Polym.*, accepted

[4] M. Bertoldo; G. Zampano; F. La Terra; V. Villari; V. Castelvetro, *Biomacromolecules*, DOI: 10.1021/bm101143q.

Production of Polyether Polyols with Phosphorous Initiators

M.M. Velencoso[1], M.J. Ramos[1], J.C. García-Martínez[2], A. de Lucas[1] and J.F. Rodriguez[1]

[1]Institute of Chemical and Environmental Technology (ITQUIMA), Department of Chemical Engineering, University of Castilla-La Mancha, Avda. Camilo José Cela s/n 13004 Ciudad Real, Spain

[2]Department of Organic Chemistry, Faculty of Pharmacy, University of Castilla-La Mancha, 02071 Albacete, Spain

Maria.MVelencoso@uclm.es

Polyurethanes (PUs) are an important class of polymers that have wide application in a great number of different industrial sectors. One of the main concerns of PUs producers are the complement of flammability regulations. Phosphorous compounds have been widely used as flame retardant materials because of their high flame-retardancy efficiency, lower production of corrosive and toxic gases in flames, and lower destruction to the earth's environment (1). Therefore there is an increasing interest on the incorporation of phosphorous compounds as additives or even as moieties on the PUs formulations to improve their flammability resistance.

The aim of this work was the synthesis of polyols including a phosphorous moiety in order to obtain a polyol with high flame retardancy. For this purpose, an appropriate phosphate as initiator was selected. A study of the ring-opening polymerization process and the structural characterization of products obtained were made. This kind of phosphorylated polyether has not been previously described in literature.

In the reaction has been used glycerol phosphate calcium salt and glycerol phosphate disodium salt as initiators and caesium hydroxide and potassium tert-butoxide as catalysts of the process (Sch. 1).

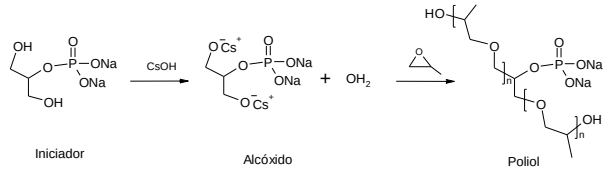

Sch. 1. Synthesis of polyether polyol

The kinetic studies revealed that there was a linear relationship between the propylene oxide consumption and time. Fig 1 presents the dependence of reaction time on propylene oxide consumption for catalyst/initiator molar ratio of 1:2 CsOH.

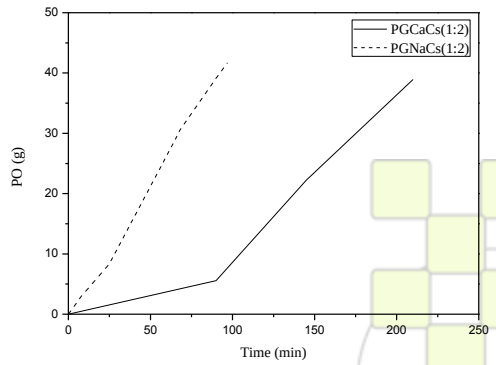

Fig 1. Relation of reaction time with propylene oxide consumption using CsOH with molar ratio 1:2.

It can be seen (Fig. 1) that the rate of addition of propylene oxide for sodium salt was higher than calcium salt. In both cases the reaction rate during the induction period is much slower than in the case of the commercial process using glycerol as initiator. This apparent lower reactivity during the first step could be attributed to low homogeneity of the glycerol phosphate salt hydrate. The solubility of propylene oxide (PO) in the reaction mass is an important parameter, because the reaction takes places in the liquid phase and the gaseous monomer is transferred from the gas phase to the liquid phase (2). From this point, the optimum amount of polyol to dissolve the initiator solution is formed in the reactor thereby increasing the consumption of PO, avoiding the problems of miscibility and diffusion of PO. The number and weight average molecular weight of the different polyols obtained ranged between 1500-5000 g/mol and 3500-9500 g/mol, respectively. The polydispersity indexes were between 1.2 and 1.6 (3, 4).

The IR spectra of the products obtained showed the characteristics bands of polyols, similar to conventional ones obtained using glycerine as initiator (5). ^{1}H NMR of polyols showed a new signal at 4 ppm, corresponding to the link P-O-C**H** and also the ^{31}P NMR presented a single signal at -3.60 ppm for glycerol phosphate calcium salt and at -0.02 ppm for glycerol phosphate disodium salt (6). So that, NMR data revealed that the phosphate was incorporated into the polymer chain.

References:

1. Chen, H., Luo, Y., Chai, C., Wang, J., Li, J. and Xia, M. (2008) Journal of Applied Polymer Science, 110, 3107.
2. Ionescu, M. Chemistry and Technology of polyols for Polyurethanes, Ed. Rapra Technology Limited: Shropshire, UK, 65-69, 2005.
3. De Lucas, A., Rodríguez, L., Pérez-Collado, M. and Sánchez, P. (2002) Polym Int., 51, 1041-1046.
4. De Lucas, A., Rodríguez, L., Pérez-Collado, M., Sánchez, P. and Rodríguez J.F. (2002) Polym Int., 51, 1066-1071.
5. Wang, D., Zhang, G., Zhang, Y., Gao, Y., Zhao, Y., Zhou, C., Zhang, Q. and Wang, X. (2007) Journal of Applied Polymer Science, 103, 417-424.
6. Huang, Y., Qi, G. and Wang, Y. (2002) Journal of Polymer Science: Part A: Polymer Chemistry, 40 1142-1150.

Acknowledgments: The authors gratefully acknowledge the support of the Ministerio de Ciencia e Innovación through the project Ref. CTQ2008-06350.

Towards Ring Opening Metathesis Polymerisation: Special Initiators for Special Applications

Anita Leitgeb[1], *Eva Pump*[1], *Anna Szadkowska*[2], *Karol Grela*[2] *and Christian Slugovc*[1]*

[1] Graz University of Technology, Institute for Chemistry and Technology of Materials, Stremayrgasse 9/5, A-8010 Graz, Austria

[2] Institute of Organic Chemistry, Polish Academy of Science, Kasprzaka 44/52, 01-224 Warsaw, Poland

anita.leitgeb@tugraz.at

Ring opening olefin metathesis polymerisation has gained much attention due to a great potential for the synthesis of specialty polymers. Since the introduction of ruthenium based initiators the robustness of this versatile polymerisation method has largely increased. An outstanding functional group tolerance and stability at ambient conditions allow for the use of demanding, highly functionalized monomers as well as bulk polymerisation of the commodity material DCPD (dicyclopentadien).[1] Regarding industrial processes like ink jet printing or RIM (reaction injection moulding) the introduction of a thermal trigger that will allow polymerisation only above a certain temperature has been a major subject in initiator design.[2]

Within this contribution various olefin metathesis catalysts based on commercially available complexes like M2, M31 or the Hoveyda-Grubbs catalyst will be presented. The effect of ligand modifications such as the introduction of electron shifting groups or change of the sterical impact are discussed in the context of ring opening metathesis polymerisation. An emphasis will be given on latent complexes featuring a chelating carbene ligand.

Monomers used comprise various norbornene derivatives and DCPD. Obtained poly(norbornenes) have been investigated by means of gel permeation chromatography, thermal switchability of the initiators was investigated by dynamic thermal analysis techniques. Moreover, the impact of the catalyst loading on mechanical properties of poly(DCPD) has been investigated.

Monomers

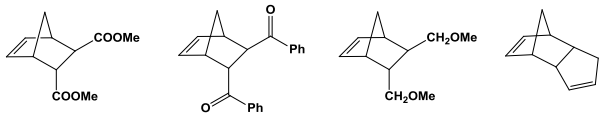

Highly active initiators

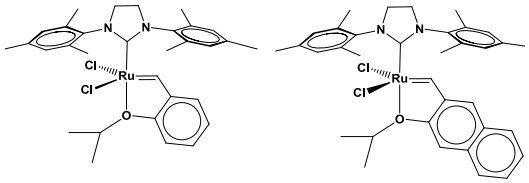

Latent initiators

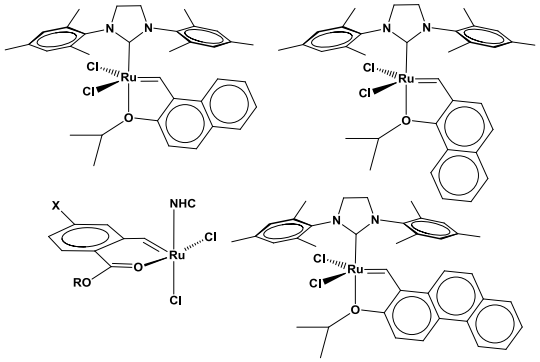

Figure 11: Exemplary structures of employed monomers and initiators

[1] A. Leitgeb, J. Wappel, C. Slugovc; *Polymer*, **2010**, *51*, 2927 - 2946

[2] (a) C. Slugovc, D. Burtscher, K. Mereiter, F. Stelzer; *Organometallics*, **2005**, *24*, 2255. (b) X. Gstrein, D. Burtscher, A. Szadkowska, M. Barbasiewicz, F. Stelzer, K. Grela and C. Slugovc, *J. Polym. Sci., Part A: Polym. Chem.*, **2007**, *45*, 3494.

New polyurethanes from natural and synthetic Rubber

Nasreddine Kébir [1], Irène Campistron [2], Albert Laguerre [2], Jean-François Pilard [2], Claude Bunel [1]

[1] INSA Rouen, UMR CNRS 6270 FER 3038 (PBS), F-76801 Saint-Etienne du Rouvray, France

[2] Université du Maine, Laboratoire de Chimie Organique Macromoléculaire, UMR CNRS 6011 (UCO2M), Avenue Olivier Messiaen, F-72085 Le Mans cedex 9, France

nasreddine.kebir@insa-rouen.fr

The synthesis of functional polymers from renewable resources has attracted considerable attention from polymer scientists throughout the world, because of their potential attributes as substitute petrochemical derivatives. With petroleum production facing exhaustion day over day, scientists and technologists focus their attention on renewable resources because these materials may act as potential raw materials for the manufacture of polymers in the 21st century.

In the polyurethane industry, conventional polyether polyols, which account for 80% of the total worldwide consumption of oligopolyols, are mostly produced from petroleum-based alkylene oxides. Due to uncertainty about the future cost of petroleum as well as the desire to move toward more environmentally friendly feedstocks, many recent efforts have focused on replacing all or part of the conventional petroleum based polyols with those made from renewable resources such as vegetable oils and Natural Rubber.

Materials and Methods

The general procedures of synthesis of Telechelic Liquid Natural Rubbers (TLNR) and their polyurethanes as well as the characterization methods were described elsewhere.[1-6]

Results and discussions

Telechelic Liquid Natural Rubbers (TLNR) can be considered as precursors of a very wide range of polymers. The selective cleavage of high molecular weight polymers for the obtaining of TLNR and the chemical modification of such oligomers has been the center of a lot of activities.[1]

During the last decade, our group focused its work on selective degradation of natural and synthetic Rubber (cis-1,4-polyisoprene) using well controlled oxidative chain-cleavage leading to new carbonyltelechelic cis-1,4-polyisoprene (CTPI). Chemical modifications of carbonyl end-groups and carbon-carbon double bonds led to new hydroxyl and amino telechelic cis-1,4-polyisoprenes with various functionalities in terms of number and distribution as well as with various degree of hydrogenated and epoxidiezed moieties.[2,3] Polyurethanes with different soft and hard segment backbones based on these new oligomers and different isocyanates were synthesized and their thermo-mechanical properties were investigated.[4-6] A large property spectrum was obtained including elastomers, thermoplastic and thermosets properties. Moreover, polyurethane materials bearing ammonium groups and exhibiting antibacterial properties against Staphylococcus epidermidis and Pseudomonas aeruginosa were also prepared.[6]

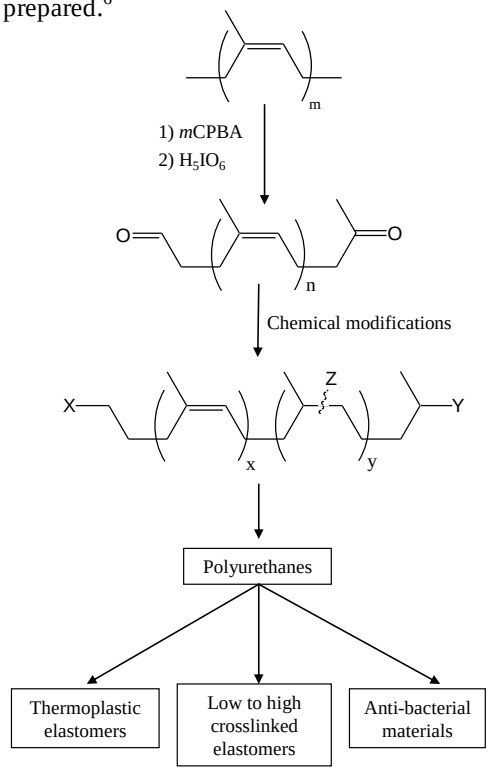

Scheme 1. Synthesis of new polyurethanes from Natural Rubber.

Conclusion

This work showed the potentialities of making new polymer materials from natural Rubber, a renewable resource.

(1) Nor, H.M.; Ebdon, J.R. Progress in Polym. Sci. **1998**, 23, 143-177.
(2) Kébir, N.; Morandi, G.; Campistron, I.; Laguerre, A.; Pilard, J. F. Polymer **2005**, 46, 6844-6854.
(3) Morandi, G.; Kébir, N.; Campistron, I.; Gohier, F.; Laguerre, A.; Pilard, J. -F. Tetrahedron Lett. **2007**, 48(43), 7726-7730.
(4) Kébir, N.; Campistron, I.; Laguerre, A.; Pilard, J. F ; Bunel, C.; Couvercelle, J. P. Polymer **2005**, 46, 6869-6877.
(5) Kébir, N.; Campistron, I.; Laguerre, A.; Pilard, J. F ; Bunel, C.; Couvercelle, J. P. e-Polymers **2006**, 48, 1-14.
(6) Kébir, N.; Campistron, I.; Laguerre, A.; Pilard, J. F ; Bunel, C.; Jouenne, T. Biomaterials **2007**, 28(29), 4200-4208.
(7) Kébir, N.; Campistron, I.; Laguerre, A.; Pilard, J. F ; Bunel, C. Journal of applied polymer science, **2011**, under production.

Chitosan-*graft*-Polyaniline-Based Hydrogels: Elaboration and Properties

Pierre Marcasuzaa, *Stephanie Reynaud*, *Jacques Desbrières*

IPREM / Equipe de Physique et Chimie des polymères, Hélioparc, 2 avenue du Président Angot, 64053 Pau Cedex

pierre.marcasuzaa@univ-pau.fr

Intrinsically conducting polymers are of great interest for a large number of applications. But among the major drawbacks are their low solubility in common solvents and their poor mechanical properties. Elaboration of composites associating a matrix, bringing its mechanical properties, and polyaniline, as the conducting polymer, is a way of overcoming these disadvantages. For that, differents works related the synthesis of PANI in hydrogel (PAA, PVA…)[1-4]. But, in lot of cases, aniline is introduced in the network, which is before synthesized, and polymerized in order to obtain conducting composite. The main problem of these composites is the heterogeneousness of PANI inside of gel, and the mobility of conducting chains which leads to observe migration phenomena. In order to avoid these negatives points, the aim of this work is to obtain an homogeneous conducting hydrogels where PANI is linked covalently with the network.

To reach our objective[5], the idea was to incorporate PANI onto a polymer which is able to be cross-linked. Chitosan is a good candidate to obtain required properties. Indeed, chitosan holds amine groups which are able to initiate aniline polymerization, morever this natural polymer is well-known to react with a cross-linking agent (di-aldehyde) to lead to a tri dimensional network (**Figure 12**).

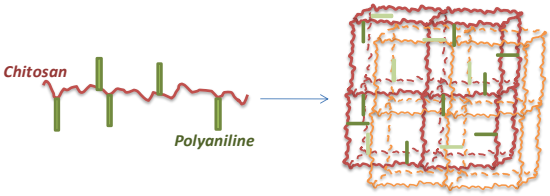

Figure 12: Schematic representation of copolymer and hydrogel structures.

At first, this talk will treat about the optimization of grafting reaction between chitosan and PANI, the characterization of obtained copolymer and a method to determinate the rate of PANI grafted onto chitosan. This study demonstrates that, with appropriate conditions, more than 99% PANI is grafted onto polymer and chitosan keeps his coating properties after grafting. The copolymer exhibits a conductivity of 10^{-1} S.cm. But, it becomes insulating below 33 % of PANI. This phenomena can be explained by a break of conducting way which is demonstrated by microscopy.

At second, it will be shown the cross-linking conditions between copolymer and glutaraldehyde. The kinetic of gelation is followed by rheological measurement. It was shown that cross-linking reaction is most efficient when precursor polymer is a blend of chitosan and chitosan-*graft*-PANI. Conductivities values as high as the precursor graft copolymer were obtained after dehydration and drying of hydrogel. Different properties of this hydrogel were studied. Results obtained for swelling tests make the composite hydrogel eligible for the development of applications as the inclusion and release of active matter as already demonstrated for semi-interpenetrating polyacrylamide-PANI gels[2,6]. More specifically, the presence of intrinsic conducting polymers within these hydrogels allows electrochemical control release of active matter[2]. The hydrogel was actually used like actuators. In this work, we studied the ability of the composite hydrogel to convert mechanical work into electrical energy, as referred to previous articles, and the so called "reverse actuators". Experiments demonstrated the feasibility of a mechano-electric actuator using our new composite hydrogel as sensing material (Figure 13).

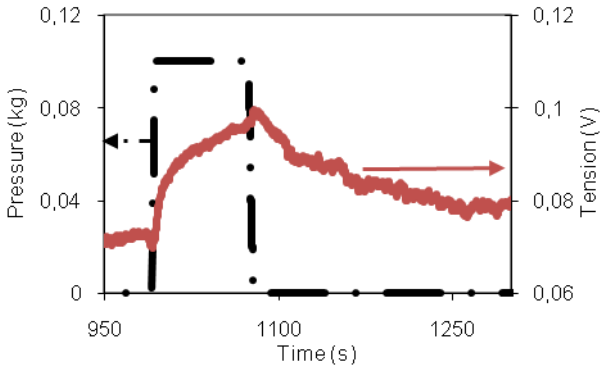

Figure 13: Pressure testing as an actuator.

This work allowed to obtain different forms of conducting materials from film to tri dimensional network (**Figure 14**). The particularity of these material is the covalent link between matrix and conducting polymer. Thus, problems of diffusion and heterogeneity are avoided. Hydrogels of Chitosan-*graft*-PANI exhibit rheological, swelling and mechano-electric properties.

Figure 14: Images of PANI based film and hydrogel.

[1] Tang, Q. L., J.; Wu, J.; Zhang, C.; Hao, S. . Carbohydrate Polymers 2007, 67, 332.
[2] Lira, L. M. C. d. T., S. I. . Electrochemistry Communications 2005, 7, 717.
[3] Liu, Z. L., Y.; Zhang, K. . Journal of Biomaterials Science, Polymer Edition 2008, 19, 1503.
[4] Tang, Q. W., J.; Sun, H.; Fan, S.; Hu, D.; Lin, J. . Carbohydrate Polymers 2008, 73, 473.
[5] Marcasuzaa, P.; Reynaud, S.; Ehrenfeld, F.; Khoukh, A.; Desbrieres, J. Biomacromolecules, 11, 1684.
[6] Xu, X.; Ren, G.; Cheng, J.; Liu, Q.; Li, D.; Chen, Q. Journal of Materials Science 2006, 41, 3147.

BODIPY-Conjugated Thermo-Sensitive Fluorescent Polymers Based On 2-(2-methoxyethoxy)ethyl methacrylate

Marta Liras, Isabel Quijada, Olga García, Rodrigo París,

Instituto de Ciencia y Tecnología de Polímeros (CSIC) Juan de la Cierva, 3 28006 Madrid SPAIN

martaliras@ictp.csic.es

A methacrylic monomer containing the dye 4,4-difluoro-4-bora-3a,4a-diaza-s-indacene (BODIPYMA)[1] was synthesized to provide fluorescence properties to three different thermo-sensitive families of polymers based on 2-(2-methoxyethoxy)ethyl methacrylate (MEO2MA).

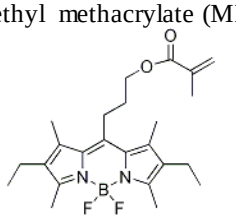

BODIPYMA

Initially, linear random terpolymers of MEO2MA, oligo(ethylene glycol) methyl ether methacrylate (OEG8-9MA) with Mn= 475 g mol^{-1}, and a very low proportion of BODIPYMA were synthesized by atom transfer radical polymerization (ATRP).

Polymers based on MEO2MA and (OEG8-9MA) are thermo-sensitive.[2] They undergo a thermal transition in water solution, becoming reversibly nonsoluble when the solution temperature is higher than the LCST. The LCST values (cloud points) of the synthesized polymers were determined by turbidimetry. As expected, these values linearly increase when the MEO2MA ratio in the polymer decreases.[3] But the most important issue here is that the system shows a remarkable increase in the fluorescent intensity when the polymer collapses, which means at temperatures above the LCST. Thus, Figure 1 shows the dependence of the absorbance at 600 nm (cloud point determinations) and the quantum yield of fluorescence on the temperature for each polymer water solution.

Apart from the relevant change in the optical and luminescent properties of the polymers in water solution at the LCST, it is also important to point out that this change is reversible. Second, a family of diblock copolymers was formed by the ATRP of MEO2MA and a very short block of BODIPYMA. They also behave as a fluorescent thermometer in water but, in this case, the fluorescence quantum yield decreased due to the intermolecular π-π stacking of BODIPY dyes that produces H- aggregates.

In addition, a MEO2MA-BODIPYMA based hydrogel was prepared to show that the optical and fluorescence properties also exhibit a sudden and reversible change at the volume transition temperature (VTT) of the hydrogel. In this case, this transition takes place independently on the BODIPYMA units. However, the novelty of the present system is again that the hydrogel is fluorescent due to the presence of BODIPY side groups. Analogous to their homologues linear polymers, the intensity of the fluorescence depends on the temperature. Thus, for temperatures higher than the VTT the equilibrium swelling decreases, the system becomes opaque and the fluorescence emission intensity increases. Therefore, it is experimentally demonstrated that the cross-linked structures show the same interesting results of fluorescence observed for the linear polymers. It is important to mention that the VTT of this kind of hydrogels can also be easily modulated by the incorporation of low proportion of other oligo(ethylene glycol) side chain macromonomers, as it was found previously by our research group.[4]

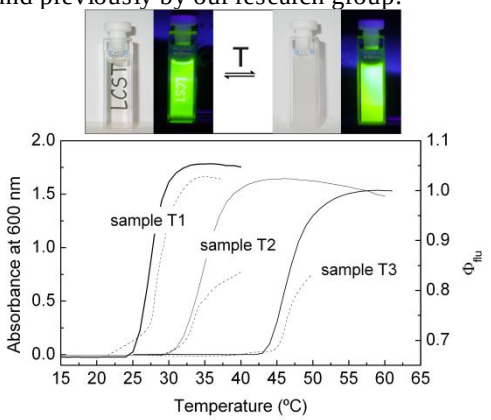

Figure 1. Absorbance at 600 nm(solid lines) and fluorescence quantum yield (dashed lines) vs temperature of the P(MEO2MA-co-OEG8-9MAco-BODIPYMA) terpolymers dissolved (0.36 mg mL-1) in PBS (pH 7, μ = 0.1 M). Photographs under visible and UV irradiation taken at temperatures below LCST (left part) and above LCST (right part) of sample T1 are included.

In conclusion, three different families of thermo-sensitive polymers based on MEO2MA with a very low proportion of a fluorescent monomer based on BODIPY have been synthesized to study their thermosensitive/fluorescent behavior in aqueous solution: (i) Well-controlled random P(MEO2MA-*co*-OEG8-9MA-*co*-BODIPYMA) terpolymers, in which the monomeric feed ratio establishes the values of the LCST. In this system, the intensity of the fluorescence strongly increases in a reversible way at the LCST. (ii) Well controlled diblock P(MEO2MA-*b*-BODIPYMA) copolymers, in which the H-aggregation between the BODIPY units reduces the emission properties. (iii) A random P(MEO2MA-*co*-BODIPYMA) hydrogel that becomes opaque and exhibits an increase of the fluorescence intensity rising the VTT, in the same way that its linear homologues.

Acknowledgment: The authors express thanks for the financial support of the Consejo Superior de Investigaciones Científicas (CSIC), Ministerio de Ciencia e Innovación, through Project CTQ 2008-03229. R.P. thanks the Ministerio de Ciencia e Innovación for a Juan de la Cierva contract and M.L. thanks the CSIC for a JAE-Doc contract.

[1] Amat-Guerri, F.; Liras, M.; Carrascoso, M. L.; Sastre, R. *Photochem. Photobiol*. **2003**, *77*, 577–584.

[2] a) Lutz, J. F.; Weichenhan, K.; Akdemir, O.; Hoth, A. *Macromolecules* **2007**, *40*, 2503–2508. b) Badi, N.; Lutz, J. F. *J. Controlled Release* **2009**, *140*, 224–229.

[3] Lutz, J. F. J. *Polym. Sci., Polym. Chem*. **2008**, *46*, 3459–3470.

[4] París, R.; Quijada-Garrido, I. *Eur. Polym. J*. **2009**, *45*, 3418–3425.

Malic Acid as Key Building Block for the Synthesis of OH-Functional Polyesters

Christian Hahn, *Helmut Keul*[*], *Martin Möller*[*]

Institute for Technical and Macromolecular Chemistry, RWTH Aachen University and

DWI an der RWTH Aachen e.V., Pauwelsstr. 8, 52056 Aachen, Germany

E-mail: keul@dwi.rwth-aachen.de

Introduction

Much interest in current research is focused on bio-based, biocompatible and biodegradable materials. It is often an important requirement to have functional groups in the polymer chain as they allow further functionalization and/or modification and therefore lead to tailor-made materials which are particularly useful in the biomedical field. To prepare such materials multifunctional building blocks are needed. Malic acid, a natural hydroxy-dicarboxylic acid, is a building block suitable for the preparation of hydroxy-functional polyesters. A wide range of copolymers, which are accessible by using dicarboxylic acids with hydroxy or similar functions as building blocks, will be presented.

Materials and Methods

Hydroxy-functional polyesters were synthesised in a polycondensation reaction using mono- and polydisperse diols, based on oligocaprolactone (OCL) or alkane diols, and malic acid as hydroxy-functional dicarboxylic acid (Scheme 1). The reactions were performed at 60 °C either in bulk or in solution with scandium triflate [$Sc(OTf)_3$] as catalyst, which discriminates between primary and secondary OH-groups.[1] OCL used as diol was afore oligomerised by means of ring-opening polymerisation using an alkane diol as initiator and $Sc(OTf)_3$ as catalyst.

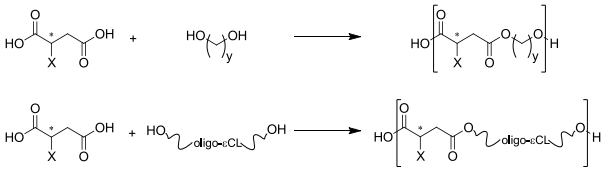

X = H, OH, Hal, SH; y = 6,8,10,12

Scheme 1: Polycondensation reaction of a mono- or polydisperse diol and malic acid without participation of the secondary OH-groups by using $Sc(OTf)_3$ as catalyst.

Results and Discussion

The thermal properties of the malic acid based polyesters were analysed by means of DSC and compared with their non-functional analogues based on succinic acid. Thus the influence of the OH-groups onto the thermal properties was studied. Malic acid based polyesters show a wide range of thermal properties – highly crystalline to completely amorphous – depending on the monomer ratio, adjusted in the feed (Table 1).

The thermal properties, which are important for many material properties, are easily adjustable in a certain range by varying the monomer type and ratio. This precisely leads to the desired hydroxy-functional polyester.

Table 1: SEC and DSC data of several polyesters.

Entry	Diol:CL	M_n [g·mol^{-1}][a)]	M_w/M_n[a)]	T_m [°C]	T_g [°C]
PHMM[b)]	–	6 800	2.57	–	11.3
POMM[d,e)]	–	10 300	2.00	–	-20.4
PDeMM[d,f)]	–	17 300	2.37	–	-35.8
PDoMM[d,g)]	–	17 800	2.03	1.1	–
POCLM a[b)]	1 : 2	4 000	2.17	–	-53.0
POCLM b[b)]	1 : 4	11 400	1.31	6.7	-57.5
POCLM c[b)]	1 : 8	10 200	1.62	29.1	-58.7
POCLM d[b)]	1 : 12	9 300	1.54	36.8	-60.2
POCLM e[e)]	1 : 2	18 200[d)]	1.59[d)]	–	-49.9
POCLM f[f)]	1 : 2	1 900	2.12	-3.9	-52.9
POCLM g[g)]	1 : 2	2 600	1.96	6.4	–

[a)] SEC in THF using PMMA standards, [b)] hexane diol, [c)] without precipitation, [d)] precondensation in $CHCl_3$ with a dean-stark-apparatus, [e)] octane diol, [f)] decane diol, [g)] dodecane diol, [h)] 5 mol-% $Sc(OTf)_3$ instead of 1 mol-%.

To show the prospects these new hydroxy-functional polyesters offer, additionally a wide range of post polymerisation modifications starting from the OH-groups was performed. For example L-lactide (LLA) was grafted directly from the free OH-groups. Here trans-esterification was suppressed by the use of $Zn(oct)_2$ as catalyst.[2] The direct reaction of the OH-group with an acid chloride showed elimination as a competitive reaction depending on the base used.[3]

Conclusion

Malic acid as monomer in a polycondensation with scandium triflate as catalyst makes it possible to directly synthesise hydroxy-functional polyesters.

First, investigations of the thermal properties were systematically performed to get a deeper understanding of the behaviour of these new polymers.

Further modifications of these polyesters show the possibility of preparing tailor-made materials especially for medical applications.

References

[1] A. Takasu, Y. Oishi, Y. Iio, Y. Inai, T. Hirabayashi, *Macromolecules* **2003**, *36*, 1772.

[2] C. Hahn, H. Keul, M. Möller, *Macromolecular Chemistry and Physics* **2010**, *211*, 752.

[3] C. Hahn, H. Keul, M. Möller, *Macromolecular Symposia* **2010**, *296*, 366.

Synthesis of Biobased Polyols by Thiol-ene "Click Chemistry" from Vegetable Oils

Desroches Myriam, Caillol Sylvain, Auvergne Rémi, Boutevin Bernard

Institut Charles Gerhardt Montpellier UMR 5253 - Equipe Ingénierie et Architectures Macromoléculaires, Ecole Nationale Supérieure de Chimie de Montpellier, 8 rue de l'Ecole Normale 34296 Montpellier Cedex 5, France

myriam.desroches@enscm.fr

Introduction

Polyurethanes are versatile plastics which are traditionally prepared by reacting an oligomeric polyol and a diisocyanate. Whereas the isocyanate component is always derived from petrochemical feedstocks, the polyol component can be provided from bio-based resources[1]. Vegetable oil-based polyols are synthesized from varied oils which, except castor oil, have to be chemically modified to meet the polyurethane production requirements. Transesterification[2] and epoxydation[3] are already industrially used for the production of polyols from oleochemicals.

The thiol-ene reaction represents another attractive toolbox for the functionalization of unsaturated vegetable oils[4, 5]. Indeed, this reaction of click chemistry[6] requires mild conditions and leads to high yields with basic purification procedures.

Our team used 2-mercaptoethanol to functionalize vegetable oils[7], ester[8] and amide oleo derivatives.

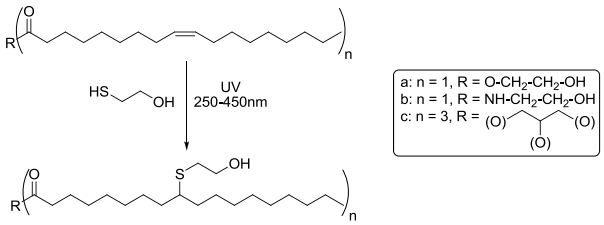

2-Mercaptoethanol photo-addition onto fatty compounds bearing one double bond per chain

The synthesized oleo polyols were used as precursors for polyurethanes.

Materials and Methods

Photochemical thiol-ene reactions were performed in quartz reactors of 20 mL equipped with an Ultracure 100SS plus/ Novacure lamp (unfiltered radiation between 250 and 450 nm) and a magnetic stirrer under air for 6 hours. The total reaction mixture weight was 5 g. During the reaction, the conversion of double bonds was monitored by ^{1}H NMR spectroscopy (vinyl proton signals at 5.40 ppm). After reaction, the viscous liquid was dissolved in ethyl acetate (20 mL) and extracted with water (3×20 mL) to eliminate the excess of 2-mercaptoethanol. The organic layer was dried over anhydrous magnesium sulfate and filtered. A pale yellow viscous liquid was recovered after evaporation of the solvent under reduced pressure (3.10^{-2} mbar).

Polyols were characterized by NMR ^{1}H, ^{13}C, FT-IR, LC-MS, SEC THF, and titrations. Polyurethanes were analyzed by ATG and DSC.

Results and discussion

To evaluate the efficiency and the robustness of thiol-ene reaction, experimental parameters were varied, such as the irradiation intensity (ranging from 0.5 to 15.0 W/cm^2), the thiol/double bond ratio (ranging from 1.2/1 to 5.0/1), the solvent/double bond ratio (ranging from 0/1 to 500/1) and the number of double bonds per fatty chain. It was especially shown that the higher the content of polyunsaturated fatty chains, the lower the rate of 2-mercaptoethanol grafting. Side reactions, identified by NMR, FT-IR, LC-MS, and iodine titration, were upon disulfide formation, double bond isomerization, and inter and intramolecular bond formation. Despite these side-reactions, by-products were found to exhibit alcohol functions. Optimized conditions were then applied to functionalize vegetable oil, fatty ester and fatty amide. Thus, the formed polyol mixtures were used to synthesize polyurethane with methylene diphenyl-4,4'-diisocyanate.

Polyurethanes based on modified vegetable oil, fatty amide diol and fatty ester diol were analyzed by ATG and DSC. The thermal properties of elastomeric products were found to be similar to those from a commercial polyol (Desmophen 1150).

Conclusions

2-Mercaptoethanol was efficiently grafted onto vinyl groups of vegetable oils and derivatives to yield various biobased polyols. The thiol-ene reaction was performed under mild conditions. The oleo polyols were then used to synthesize polyurethanes. The synthetic method can readily undergo incorporation of different reactive functions onto vegetable oils and their derivatives, thus leading to functional precursors suitable for polymer synthesis.

References

1. Ionescu, M. In *Chemistry and technology of polyols for polyurethanes*, Rapra Technology Limited Eds.; 2005; p 586.
2. Lubguban, A. A.; Tu, Y.-C.; Lozada, Z. R.; Hsieh, F.-H.; Suppes, G. J., *J. Appl. Polym. Sci.* **2009,** *112*, (1), 19-27.
3. Guo, A.; Javni, I.; Petrovic, Z., *J. Appl. Polym. Sci.* **2000,** *77*, (2), 467-473.
4. Bantchev, G. B.; Kenar, J. A.; Biresaw, G.; Han, M. G., *J. Agric. Food Chem.* **2009,** *57*, (4), 1282-1290.
5. Türünç, O.; Meier, M. A. R., *Macromol. Rapid Commun.* **2010,** *31*, (20), 1822-1826.
6. Kade, M. J.; Burke, D. J.; Hawker, C. J., *J. Polym. Sci., Part A: Polym. Chem.* **2010,** *48*, (4), 743-750.
7. Desroches, M.; Caillol, S.; Auvergne, R.; Lapinte, V.; Boutevin, B., *Macromolecules* **2011,** *submitted*.
8. Desroches, M.; Boutevin, B.; Caillol, S.; Auvergne, R., *Polym. Bull.* **2011,** *submitted*.

Crosslinking of Epoxidized Natural Rubber by Dicarboxylic Acids: Monitoring Crosslinking Density, Polar Interactions and Kinetics Rate

Myriam Pire[1], *Sophie Norvez*[1], *Ilias Iliopoulos*[1], *Benoît Le Rossignol*[2] *and Ludwik Leibler*[1]

[1] Matière Molle et Chimie, ESPCI ParisTech – CNRS, UMR-7167, 10, rue Vauquelin, 75005 Paris, France

[2] Hutchinson SA Centre de Recherche, Rue Gustave Nourry, BP31, 45120 Chalette sur Loing Cedex, France

myriam.pire@espci.fr

Epoxidized natural rubber (ENR) is a material of great interest obtained from renewable resources. It exhibits a dual functionality for cross-linking (double bonds and epoxy sites) while retaining most of the properties of natural rubber. In this work, the crosslinking reaction of ENR with dodecanedioic acid was followed by rheology and the properties of the cured materials were tested by dynamic mechanical analysis, stress-strain experiments, and DSC measurements.

We first studied the crosslinking of simple binary blends of dodecanedioic acid and ENR of different grades (10 and 25% mol epoxide groups), as well as the mechanical properties of the resulted materials after curing at 180 °C [1]. Properties of cured rubbers are governed by crosslinking density and glass transition temperature. It was found that mechanical properties were optimal for a certain amount of diacid (Figure 1). For high concentrations of crosslinking agent, DSC measurements on ENR25 revealed a nonlinear behaviour in the increase of glass transition temperature. By comparing crosslinking with dodecanedioic acid and reaction with monofunctional lauric acid, this behaviour was attributed to polar interactions due to free carboxylic groups of pending diacid grafts.

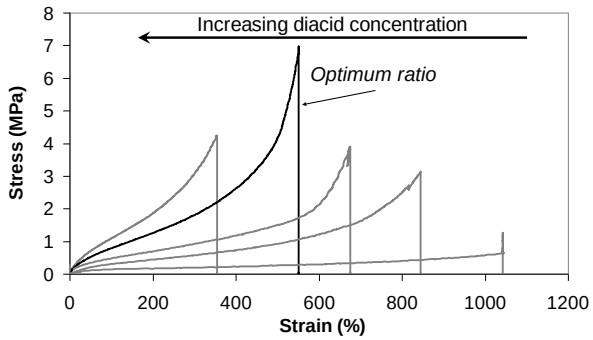

Figure 1: Strain-stress measurements for vulcanized ENR10-dodecanedioic acid blends, containing increasing amount of diacid.

The long heat treatment (3 hours at 180 °C) has however detrimental effects on the mechanical properties of cured rubbers. Curing behaviour of blends of ENR and dodecanedioic acid was thus investigated in presence of usual catalysts of the acid-epoxy reaction. Among all the accelerators tested, 1,2-dimethylimidazole (DMI) was found the only one able to activate in bulk the crosslinking of these high molecular weight elastomers. As seen on Figure 2, the rate of the reaction was efficiently accelerated in presence of DMI. An equimolar amount of accelerator and carboxylic functions was required to give rise to optimum tensile properties. This was associated to a non-catalytic crosslinking mechanism involving the quantitative formation of an imidazolium carboxylate. The formation of this intermediate was further highlighted by DSC experiments.

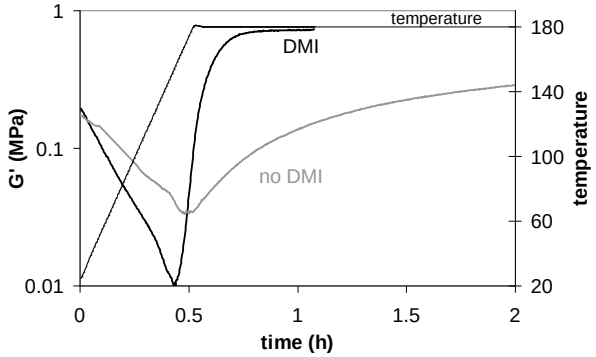

Figure 2: Effect of 1,2-dimethylimidazole (DMI) on the crosslinking of ENR25 with dodecanedioic acid.

Our system thus enables the efficient crosslinking of functionalized natural rubbers without the use of sulphur or any non-environmentally-friendly vulcanization additives.

[1] M. Pire, S. Norvez, I. Iliopoulos, B. Le Rossignol and L. Leibler, "Epoxidized natural rubber/dicarboxylic acid self-vulcanized blends", *Polymer*, 51, 5903-5909 (2010).

Synthesis of terpolymers based acrylamides by RAFT polymerization and their application in the synthesis of goldnanoparticles

V.J. González-Coronel, J.A. Corcino-Campos, E.R. Rodríguez, N. Tepale-Ochoa,

Facultad de Ingeniería Química, Benemérita Universidad Autónoma de Puebla

valeriajordana@yahoo.com.mx

Introduction

Recent developments in controlled radical polymerizations enable the synthesis of functional polymers with controlled molar mass, narrow molecular weight distribution, and well-defined architectures and functionalities. The systems include atom transfer radical polymerization, nitroxide-mediated radical polymerization, and reversible addition-fragmentation chain transfer (RAFT) polymerization. Among these controlled radical polymerizations, RAFT has been successfully applied for controlled polymerization of acrylamide derivatives, such as N,N-dimethylacrylamide, N-isopropylacrylamide, and N-acryloylmorpholine.

In this study, we investigated radical polymerization of a acrylmide with a monosubstituted acrylamide, in the presence of a chain transfer agent (CTA).

Experimental Section

The terpolymers were prepared by reversible addition-fragmentation transfer radical polymerization using acetonitrile as solvent. The PAm-b-PDAm-b-Pam was synthesized starting from the preparation of RAFT agent benzyl dithiobenzoate (BDB) (Figure 1)which was synthesized according to the method in the literature. [ref]

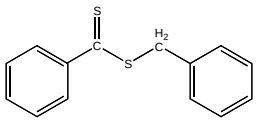

Figure 1. Benzyl dithiobenzoato

Preparation of PAm-b-PDAm-b-Pam

The PAm-b-PDAm-b-Pam was obtained in three steps. First Am, BDB and acetonitrile were added into a 1000mL reactor equipped with condenser and mechanical stirrer. The mixture was vigorously agitated, purged with nitrogen during 1 h, and heated to 82°C under agitation. Then, the initiator ACVA was added to the mixture to start the reaction, and bubbling was maintained during all the polymerization reaction, this step was run for 5 h. The polymer obtained was insoluble in acetonitrile. The polymer was recovered by filtration and washed with methanol to remove traces of residual monomer and initiator, and finally filtered and dried under reduced pressure at 40°C for 48 h. In the second step were added the PAm, dodecilacrylamide (DAm) and acetonitrile. The procedure was similar than the first step. The block copolymer was recovered, washed and dried. In the next step were added PAm-b-PDAm, Am. The reaction was run like in the past steps.

Preparation of gold nanoparticles

The synthesis of gold nanoparticles has been achieved at 25°C and different polymer concentration (0.5,1,1.5 and 2 wt. %) were studied. The formation of gold nanoparticles were monitored by observing changes (in time function) in the absorption spectra using a UV-visible spectrometer (Perkin Elmer, Lambda 35); the absorption band centered at ≈220nm that originates from the gold (III) chloride solutions and the band centered at ≈540nm that originates from the surface plasmon of the gold nanoparticles.

Results

The transfer agent was characterized by ^{1}H NMR. The Mn of each block of the terpolymer was obtained by ^{1}H NMR. The composition of the terpolymer was $AM_{5500}DAM_{1000}AM_{5000}$. Also we determined the Tg by DSC.

Table 1. Terpolymer properties

Block	Time (h)	%conversion	Mn ^{1}HNMR	Tg °C DSC
PAm	2	72	5500	60.68
PDam	1	80	6500	67.41
PAm	2	78	11500	62.94

The gold nanoparticles was characterized by SEM and TEM, and the average diameter was 99 nm.

Acknowledgment

This work is suppoted by the proyect PROMEP/103.5/09/4194.

References

[1]R.T. Mayadunne,. *Macromolecules*, **2006**, 39, 2729.

[2]A.B. Lowe, E. Rizzardo. *J. Am. Chem. Soc.*, **2002**,*124*, 11562.

[3] T. Sakai, P. Alexandridis, *Chem. Mater*, 18(10), 2577-2583, 2006.

[4] T. Sakai, P. Alexandridis, *Langmuir*, 20, 8426-8430, 2004.

[5] V. J. González-Coronel, E.J. Jímenez-Regalado, *Polym. Bull*., 62 (6), 727-736, 2009.

Preparation of Furfuryl Functionalised Polystyrenes by Atom Transfer Radical Polymerization and Their Use in the Surface Chemical Modifications of Multi-wall Carbon Nanotubes by "grafting to"

Rodrigo Paris, M. Mar Bernal, Marta Liras, Raquel Verdejo, Isabel Quijada-Garrido, Miguel A. López-Manchado.

Instituto de Ciencia y Tecnología de Polímeros, Consejo Superior de Investigaciones Científicas (ICTP-CSIC)

rparis@ictp.csic.es

Atom transfer radical polymerisation (ATRP) is one of the most powerful and versatile controlled radical polymerisation methods employed for the preparation of very diverse and well-controlled polymeric materials[1]. One the main advantages of ATRP is that it can be used to obtain functionalised polymers. Thus, four different synthetic strategies can be employed: i) use of functional monomers, since ATRP is generally tolerant of various functional groups, ii) post-polymerisation modification of monomeric units, using monomers with "protected" groups, iii) use of functional initiators and iv) end-group transformation by post-polymerisation nucleophilic substitution reactions, obtaining well-defined α and/or ω end-functionalized polymers.

In addition, ATRP has been extensively used for the incorporation of polymers onto several surfaces. Thus, three main routes have been employed for this aim, called "*grafting from", "grafting to" and "grafting through"* [2,3]. The former methodology establishes the incorporation of an ATRP-initiator on the surface and then, the polymerisation process obtaining a very high surface grafting density. The second requires a functionalised polymer that, in a second step, is incorporated to the surfaces by chemical reactions. Its advantage is the previous control over the properties of the grafted polymers. The third and the least used route is based on the incorporation of actives species for polymerisation on the surface.

Several approaches for the preparation of functionalised polymers by ATRP have been used by our research group. In fact, they have been attached to different surfaces in order to improve some of their properties. Thus, silica nanoparticles, polyhydroxyalkanoates and so on, were coated with polymers prepared by ATRP.

In this contribution a simple and single-step "*grafting to*" approach based on a Diels-Alder (DA) reaction is described to functionalise multi-wall carbon nanotubes (MWCNTs) with polystyrene (PSt). Thus, several fluorescent and furfuryl functionalised PSts were synthesised by the ATRP of styrene, furfuryl methacrylate (FMA) and low proportion of a fluorescent monomer (BODIPYMA) in a first step.

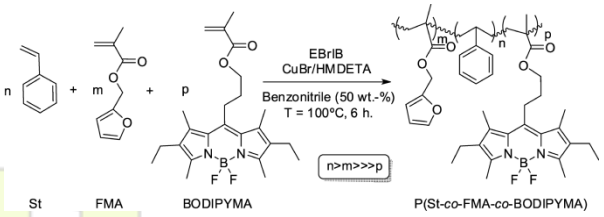

Scheme 1: Preparation of furfuryl functionalised and fluorescent styrene-based polymers, P(St-*co*-FMA-*co*-BODIPYMA), by ATRP.

Thus, several P(St-*co*-FMA-*co*-BODIPYMA) polymers were prepared in a controlled way using different monomer feed compositions. All of them were characterized by FT-IR, NMR, GPC, TGA, DSC, absorbance and fluorescence measurements, observing that their properties were those expected.

In a second step, these furfuryl functionalised PSts were covalently attached onto pristine MWCNTs. Furfuryl (diene) groups of FMA monomeric units allowed the chemical attachment of the PSt polymer onto the as-synthesised nanotubes by a DA reaction. On the other hand, the incorporation of fluorescent groups in the polymer offers two main advantages. It permits to determine the attachment of the polymer onto the nanotubes and, in further applications, it will allow to follow the dispersion of these modified MWCNTs in a matrix.

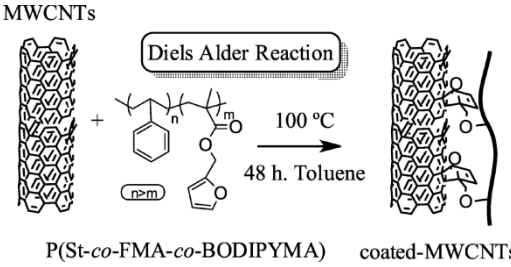

Scheme 2: Modification of MWCNTs with P(St-*co*-FMA-*co*-BODIPYMA) polymers by Diels-Alders reaction.

The efficiency of the proposed MWCNT functionalisation with the described methodology based was verified by FT-IR, Raman spectroscopy, TEM, AFM and fluorescence techniques. As an example, some results of TEM and fluorescence measurements are included in Figure 1, where it can be observed the polymeric coating (left) and the fluorescence of the modified carbon nanotubes (right).

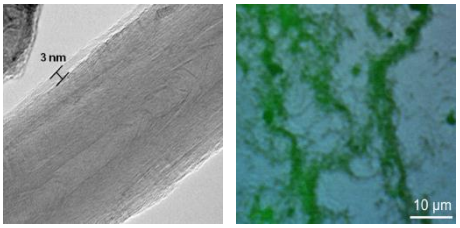

Figure 1: (left part) TEM image and (right part) combined light and fluorescent microscopy of modified MWCNTs.

Acknowledgment: Financial support provided by the Ministerio de Ciencia e Innovación (MCINN) through the Project CTQ 2008-03229 and MAT 2010-18749. R. P. and M.M.B. thank the MICINN for a "Juan de la Cierva" contract and a FPI grant, respectively. M. L. thanks the CSIC for a JAE-DOC contract.

[1] Coessens, V.; Pintauer, T.; Matyjaszewski, K. *Prog. Polm. Sci.* **2001**, 26, 337-377.

[2] Polymer Grafting and Crosslinking. Eds : Bhattacharya, A.; Rawlings, J.W.; Ray, P..*Willey & Sons*, **2009**.

[3] Xu, F.J.; Neoh, K.G.; Kang, E.T. *Prog. Polm. Sci.* **2009**, 34 719-761.

Cationic Polymerization of Isobutylene Using $AlCl_3OBu_2$ as a Coinitiator: Synthesis of Highly Reactive Polyisobutylene

Sergei V. Kostjuk, Irina V. Vasilenko, Alexander N. Frolov

Research Institute for Physical Chemical Problems of the Belarusian State University

kostjuks@bsu.by or kostjuks@rambler.ru

Introduction. The low-molecular weight polyisobutylenes (M_n<5,000 g mol^{-1}) with high content of the vinylidene end groups, i.e. so-called highly reactive polyisobutylenes (HR PIB*s*), represent the most important industrial class of isobutylene (IB) polymers due to their use as a raw material for manufacturing of lubricants and fuel additives. Recently, BASF, the worldwide leader in the production of HR PIB*s*, increased the capacity for their production mainly due to the new fuel requirements. These polymers under trade mark Glissopal® with M_n ranging between 550 and 2300 g mol^{-1}, molecular weight distribution (MWD) less than 2.0 and containing 75–85% of *exo*-olefin end groups are produced via cationic polymerization of IB using alcohols/BF_3 initiating system. In this work we report new $AlCl_3$-based initiating systems, 2-phenyl-2-propanol (CumOH)/$AlCl_3OBu_2$ and H_2O/$AlCl_3OBu_2$, for the synthesis of HR PIB containing 88-95 % of *exo*-olefin terminal groups under mild experimental conditions. These initiating systems are originated from our systematic investigations of the controlled cationic polymerization of styrene using of complex of $AlCl_3$ with Bu_2O as an coinitiator.[1,2] The use of such kind of complexes of $AlCl_3$ allows to solubilize the Lewis acid in polymerization media and decrease its instantaneous concentration that leads to totally different behavior of these complexes in the polymerization processes in comparison with a neat $AlCl_3$.[1,2]

Results and discussion. Table 1 summarizes the main results obtained during the cationic polymerization of isobutylene using $AlCl_3$-based initiating systems.

Table 1. $AlCl_3OBu_2$-coinitiated cationic polymerization of IB in CH_2Cl_2/*n*-hexane 80/20 v/v during 3 min [a]

run	T (ºC)	conv (%)	M_n (g/mol)	M_w/M_n	*exo* (%)
1	–60	85	2330	1.81	86
2	–40	62	1560	1.46	91
3[b]	–40	73	1200	1.20	90
4	–20	49	1150	1.16	91
5[c]	–20	46	1750	2.25	92

[a] Conditions: [CumOH]=18 mM; [$AlCl_3OBu_2$]=22 mM; [IB]=0.91 M; [b] [CumOH]=36 mM; [$AlCl_3OBu_2$]=44 mM. [c] no initiator; time: 7 min.

The increase in the reaction temperature from –60 ºC to –20 ºC led to the gradual decrease of monomer conversion, molecular weight (from M_n=2300 g mol^{-1} to M_n=1150 g mol^{-1}) and to the narrowing of MWD down to M_w/M_n<1.2 at –20 ºC. Importantly, increasing the temperature did not influence significantly the content of *exo*-olefin end groups (see Table). Higher initiator concentration resulted in higher monomer conversion and narrower molecular weight distribution (MWD) (compare runs 2 and 6). In the absence of initiator, the cationic polymerization of isobutylene proceeded at lower reaction rate than with initiator affording polymers with high content of vinylidene end groups (92 %) and acceptable MWD (M_w/M_n=2.25) (runs 4, 5).

A mechanism of IB polymerization with CumOH/$AlCl_3OBu_2$ initiating system was proposed.[3] According this mechanism, free Lewis acid, which is generated by dissociation of $AlCl_3OBu_2$ complex, participates in the initiating and propagating steps of reaction.[3] Basically, the polymerization proceeds in two stages. During the first stage, a fast polymerization occurs due to the initiation by cumyl alcohol followed by β-H abstraction by Bu_2O to generate double bond-terminated PIB and $H^+AlCl_3OH^-$. The latter species either participate in a competitive initiation of the polymerization, which is considerably slower than CumOH-initiated polymerization, or decompose with the formation the week Lewis acid $AlCl_2OH$, which is inactive in the polymerization.[3] We also propose that the predominant formation of *exo*-olefin terminal groups occurs through reaction of growing carbocation with free base (Bu_2O), which is formed due to the $AlCl_3OBu_2$ complex dissociation. Indeed, the decrease of the basicity of corresponding ED in $AlCl_3$×ED leads to a dramatic lowering of *exo*-olefin end group content: Bu_2O (pK_a=–3.59, *exo* =91 %); EtOAc (pK_a=–6.5, *exo* =53 %); Ph_2O (pK_a=–6.54, no *exo*-olefin end groups).

Conclusions. CumOH in combination with $AlCl_3OBu_2$ provides a very efficient initiating system for the synthesis of HR PIB*s* (M_n=1000–5000 g mol^{-1}) with rather narrow MWD (M_w/M_n=1.2–1.9) containing 86–95 % of *exo*-olefin end groups at elevated reaction temperatures (–40…–20 ºC). The predominant formation of *exo*-olefin-terminated polyisobutylenes during the cationic isobutylene polymerization with CumOH/$AlCl_3OBu_2$ initiating system is consistent with a selective β-H abstraction by free Bu_2O formed due to the dissociation of $AlCl_3OBu_2$ complex.

References

(1) Kostjuk, S. V.; Dubovik, A. Yu.; Vasilenko, I. V.; Frolov, A. N.; Kaputsky, F. N. *Eur. Polym. J.* **2007**, *43*, 968–979.

(2) Frolov, A. N.; Kostjuk, S. V.; Vasilenko, I.V.; Kaputsky, F. N. *J. Polym. Sci.: Part A.: Polym. Chem.* **2010**, *48*, 3736–3743.

(3) Vasilenko, I.V.; Frolov, A. N.; Kostjuk, S. V. *Macromolecules* **2010**, 43, 5503–5507.

Acknowledgment. BASF SE is acknowledged for financial support of this research.

Functionalisation of Unsaturated Polyesters from Enzymatic Ring-Opening Polymerisation of Macrolactones by Thiol–ene Click Chemistry

Zeliha Ates[1], *Inge van der Maulen*[2], *Paul D. Thornton*[1] *and Andreas Heise*[1,2]

[1]School of Chemical Sciences, Dublin City University, Dublin 9, Ireland.

[2]Technische Universiteit Eindhoven, Den Dolech 2, P.O. Box 513, 5600 MB, Eindhoven, The Netherlands

zeliha.ates2@mail.dcu.ie

Introduction: Aliphatic polyesters have received significant recent attention owing to their use in a number of biomedical applications, with key research focussed particularly on their use as degradable drug delivery vehicles and in tissue engineering.[1] Despite the suitability of incorporating polyesters into biomaterials, their use in highly sophisticated biomedical applications is hindered by the difficulty of polyester side-chain functionalisation. Material modification to allow specific interactions within biological systems significantly enhances biomaterial performance, potentially offering the material a dynamic role in its application.

In this work we propose the chemically straightforward modification of aliphatic polyesters by utilising highly efficient and robust thiol–ene 'click' reactions directly on unsaturated polyesters obtained from ring-opening polymerization (ROP) of the unsaturated macrolactone globalide (Gl).[2]

Results and Discussion: The ROP of globalide was carried out in toluene with Novozym 435 (*Candida antarctica* Lipase B (CALB) immobilised on macro-porous resin) to a molecular weight of 16000 g mol^{-1} and a polydispersity of 2.5.[3] The thiol–ene functionalisation of polyglobalide (PGl) was undertaken by a thermally initiated reaction catalysed by AIBN in the bulk above the melting point of PGl or with a minimum amount of solvent when required to enable complete reactant miscibility. Obtained thiol–ene functionalised polymers were characterized by ^{1}H NMR, DSC and GPC analysis.

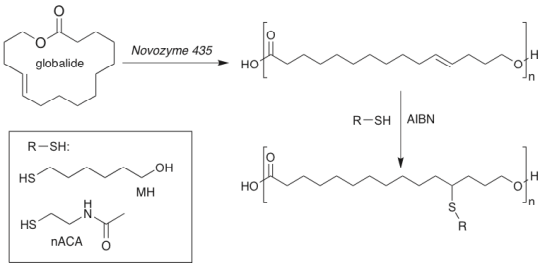

Scheme 1. Polymerisation of globalide and thiol–ene reaction of polyglobalide with 6-mercapto-1-hexanol (MH) and *N*-acetylcysteamine (nACA).

6-Mercapto-1-hexanol (MH) and *N*-acetylcysteamine (nACA) were selected as suitable candidates for the introduction of a primary alcohol and amine functionality to the polymer *via* the methodology proposed (Scheme 1). The ^{1}H NMR obtained for MH and nACA functionalised PGl reveals characteristic peaks corresponding to the repeat units of PGl and signals from the thiol fuctional groups, which suggests a successful reaction. By comparing the integration of the peaks that correspond to the double bond in PGl at around 5.4 ppm with the peaks representative of the methylene group adjacent to hydroxyl terminal group, it was determined that the fraction of thiol–ene coupling was in excess of 95%.

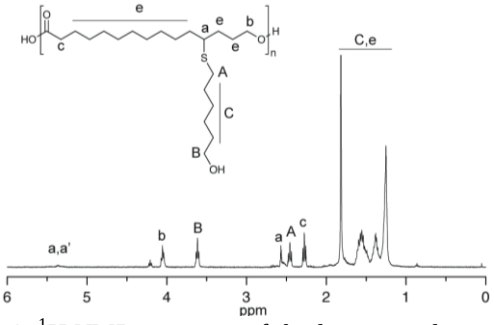

Figure 1. ^{1}H NMR spectrum of thiol-ene coupling product of PGl and 6-mercapto-1-hexanol.

Moreover, using multifunctional thiols transparent cross-linked films were obtained under UV radiation from PGl homo and copolymers.

Figure 2. P(Gl-co-CL) (30/70) obtained via thiol-ene cross-linking using UV radiation for 15 min

Conclusions: Thiol–ene click chemistry may be utilised to functionalise and cross-link unsaturated polyester obtained by enzymatic ROP of macrolactones. This approach therefore readily enables the highly efficient and chemically simplistic biofunctionalisation of a polyester compound to yield significant products of potential biomedical importance.

References:

1. A. C. Albertsson, I. K. Varma, *Biomacromolecules* **2003**, *4*, 1466–1486.
2. Z. Ates, P. D. Thornton. A. Heise, *Polym. Chem.* **2011**, *2*, 309-312.
3. I. van der Meulen, M. de Geus, H. Antheunis, R. Deumens, B.E.A.J. Joosten, C.E. Koning, A. Heise Biomacromolecules **2008**, *9*, 3404-3410.

Acknowledgement

Most of this work was conducted under a Science Foundation Ireland (SFI) funded Principle Investigator Award 07/IN1/B1792. AH is a SFI Stokes Senior Lecturer (07/SK/B1241). IvdM acknowledges the financial support from the Dutch Polymer Institute (DPI, project number 608).

Structure of Polyamides Made from Aldaric Acids

S. León,[a] C.E. Fernández,[b] A. Díaz,[b] M. Bermúdez,[b] M.G. García-Martín,[c] M. Mancera,[c] J.A. Galbis,[c] S. Muñoz-Guerra[b]

[a] Dept. de Ingeniería Química Industrial, Universidad Politécnica de Madrid, ETSII, Gutiérrez Abascal 2, 28006 Madrid
[b] Dept. d'Enginyeria Química, Universitat Politècnica de Catalunya, ETSEIB, Diagonal 647, 08028 Barcelona
[c] Dept. de Química Orgánica y Farmacéutica, Universidad de Sevilla, Profesor García González 2, 41012 Sevilla
salvador.leon@upm.es

Introduction

The incorporation of carbohydrate units into polycondensates is attracting a great interest as a tool for the development of sustainable polymers with improved properties. Here, we present a systematic study on the conformation and crystal structure of polyaldaramides, which are polyamides prepared from alkanediamines and aldaric acids (sugar-based monomers). The influence on the structure of both the size of the polymethylene segments and the nature of the monosaccharide-based unit is considered.

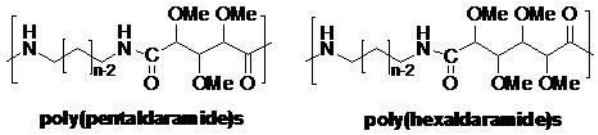

Scheme 1. Chemical structure of polyaldaramides.

Materials and Methods

The polyaldaramides studied in this work include derivatives of pentoses (LAr and DXy) and hexoses (D-Gal and DMan). Their synthesis and chemical characterization have been reported in detail elsewhere.[1,2] The crystal structure has been analyzed by combination of transmission electron microscopy, X-ray (WAXS) and electron diffraction (ED) techniques, and force-field based atomistic simulations.

Results and Discussion

These polyaldaramides were stretched in more or less oriented fibers that were analyzed by WAXS and crystallized from solution to render lamellar single crystals susceptible to be analyzed by electron diffraction.

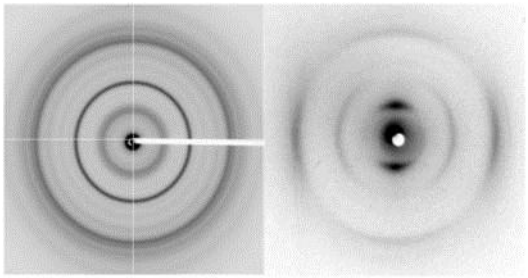

Figure 1. Powder (left) and fiber (right) WAXS obtained for PA-10LAr.

The analysis of the X-ray and electron diffraction patterns produced by crystallized samples of these polymers is consistent with a crystal structure characterized by the occurrence of a highly contracted conformation of the chains. Thus, the axial repeat of the structure appears to be shorter than the length that should be expected if the chains were in a fully extended conformation[3].

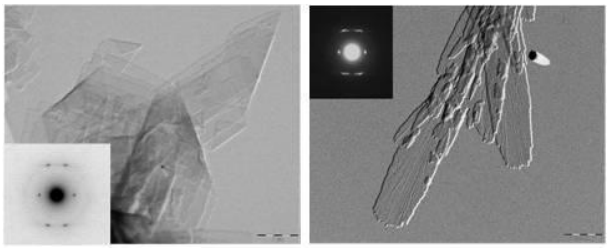

Figure 2. TEM of lamellar crystals of PA-10LAr (left) and PA-12-Mn (Inset: DE from lamella).

Molecular modeling simulations show that in this type of polymers, the monosaccharide-derived moieties tend to adopt a skewed arrangement that leads to a folded conformation in which the polymethylene segments of the same chain are bending with respect to each other. The resulting crystal structure consists on chains arranged in sheets with intermolecular hydrogen bonds between the amide groups.

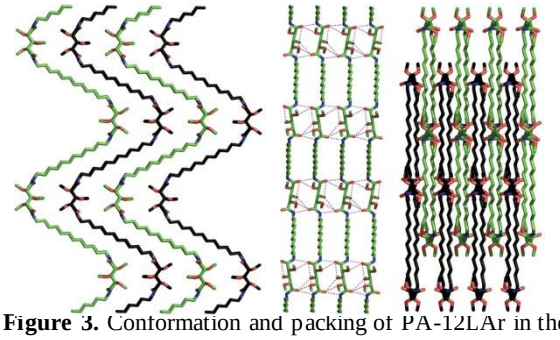

Figure 3. Conformation and packing of PA-12LAr in the crystal lattice obtained from molecular modeling simulations.

Conclusions

The presence of aldaric units within the backbone of polyaldaramides favors the adoption of folded conformations with the sugar moieties located at the skew of the bended chain. Such conformation allows an optimal occupancy of the space in a stratified structure.

References

[1] García-Martín, MG.; Benito E.; Ruiz R.; Alla, A.; Muñoz-Guerra, S.; Galbis, JA. *Macromolecules* **2004**, 37, 5550.
[2] Mancera, M.; Zamora, F.; Roffé, I.; Bermúdez, M.; Alla, A.; Galbis, JA.; Muñoz-Guerra, S. *Macromolecules* **2004**, *37*, 2779-2783.
[3] Muñoz-Guerra, S., Fernández, C., García-Martín, MG., Marín-Bernabé, R., Benito, E., Bermúdez, M., Galbis, JA. *Polymer* **2009**, *50*, 2048.

Acknowledgements

Authors acknowledge the Spanish MICINN for project grant MAT-2009-14053-CO2

One-pot Multistep Reactions Based on Thiolactones: Extending the Realm of Thiol-Ene Chemistry in Polymer Synthesis

Pieter Espeel, Fabienne Goethals, and Filip E. Du Prez

Department of Organic Chemistry, Polymer Chemistry Research Group, Ghent University, Krijgslaan 281 S4-bis, B-9000 Ghent, Belgium

Filip.Duprez@Ugent.be

Introduction

Recently, many organic reactions, generally labeled as 'click' chemistry and originally developed and applied in the synthesis of low-molecular-weight compounds, infiltrated the toolbox of synthetic macro- and supramolecular research groups.[1-3] As Malkoch et al.[4] expressed the need to increase the range of available 'click' reactions that can be achieved without the need of metal catalysts and to develop libraries of compatible reactions, our ongoing interest is to develop an efficient one-pot process based on metal-free radical thiol-ene chemistry. In addition to the fact that the availability of thiols as starting materials is rather limited, thiols usually have an unpleasant smell and a poor shelf life due to oxidation reactions. Therefore it can be advantageous to generate thiols *in situ* and convert them in a one-pot process. The readily available *N*-acetylhomocysteine thiolactone **1** was already used for the introduction of sulfhydryl groups in natural proteins, through the nucleophilic ring-opening by the ε-NH_2 groups of lysine residues.[5] We anticipated the ability to adapt this methodology and combine it with the radical thiol-ene process in a one-pot fashion as a mild approach for the synthesis of polymeric architectures starting from stable amine containing compounds, as very recently published in *JACS*.[6] This *amine-thiol-ene conjugation* (Scheme 1) as a simple, efficient, and modular linking process is considered to be a relevant extension of the currently quite popular thiol-ene chemistry, especially in polymer science.

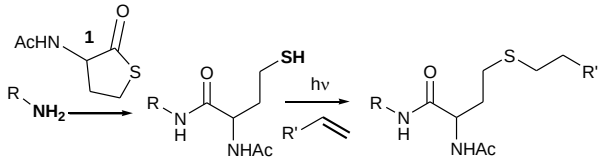

Scheme 15 – General concept of the Investigated Metal-Free One-Pot Reaction: Nucleophilic Opening of a Thiolactone (Aminolysis), Followed by a Radical *Thiol-Ene* Conjugation

Results and Discussion

In the first stage of this study, the one-pot two-step sequence was performed on low-molecular-weight model compounds in order to investigate the reaction kinetics and to analyze the composition of the obtained reaction mixture. Encouraged by the positive results of this model study, we investigated the synthesis of a monomer containing both a double bond and a thiolactone unit. Since a thiolactone moiety can be considered as a precursor of a thiol functionality, the combination with a double bond results in an AB' type monomer. The valorization of the reactivity of this monomer, *N*-(allyloxy)carbonylhomocysteine thiolac-tone (Alloc-TL) **2**, upon aminolysis and subsequent UV-curing, would enable us to develop convenient and accelerated protocols for the synthesis of novel polymeric architectures. Radical (photo)polymerization reactions between a thiol and an alkene occur in a stepwise fashion. In order to obtain high-molecular weight polyaddition compounds, the ratio between the involved functional groups should equal 1. The aminolysis of the thiolactone in the Alloc-TL monomer **2** to generate a thiol should therefore efficiently reach full conversion. In the presence of a 2-fold excess of the nucleophile ethanolamine and DMPA as photoinitiator, the polyaddition occurred and, after 1h of UV-curing, a white precipitate was obtained (Scheme 2).

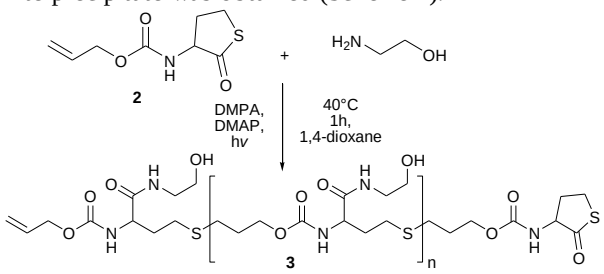

Scheme 2 – Stepwise Photopolymerization of the Alloc-TL Monomer **2** in a One-Pot Process Yielding a Hydroxyl-Functionalized Polymer **3** with a Polyurethane Backbone

A mild and efficient one-pot polyaddition process yielded a polymer **3** with a polythioether/polyurethane backbone and pendant hydroxyl groups with a molecular weight of 7.8 kDa (^{1}H NMR). It should be noted that standard synthetic methods for the synthesis of functionalized polyurethanes would certainly require a protection/deprotection strategy. To further extend the scope of this thiolactone methodology in material science, polymer networks based on the AB' type monomer **2** were targeted. The use of 4,9-dioxadodecanediamine as a cross-linker yielded a clear, non-tacky and mechanically stable network film.

Conclusion

We have demonstrated that a thiolactone entity can serve as a precursor for thiols in a one-pot amine-thiol-ene reaction. Functional, linear polymers and networks were obtained using this methodology.[6] Further investigations will focus on the development and valorization of the analogous *amine-thiol-yne reaction*. Moreover, we are strongly convinced that this methodology will be useful for the modification of double/triple bond containing materials.

References

(1) Golas, P.; Matyjaszewski, K. *Chem. Soc. Rev.* **2010**, *39*, 1338-1354. (2) Sumerlin, B. S.; Vogt, A. P. *Macromolecules* **2009**, *43*, 1-13. (3) Hawker, C. J.; Wooley, K. L. *Science* **2005**, *309*, 1200-1205. (4) Lundberg, P.; Hawker, C. J.; Hult, A.; Malkoch, M. *Macromol. Rapid Commun.* **2008**, *29*, 998-1015. (5) Benesch, R.; Benesch, R. E. *Proc. Natl. Acad. Sci. U.S.A.* **1958**, *44*, 848-853. (6) Espeel, P.; Goethals, F.; Du Prez, F. E. *JACS* ASAP DOI: 10.1021/ja1098098.

Polymeric Platforms Based on Thiolactone Monomers for Post-Polymerization Functionalization

Pieter Espeel, Lionel Petton, Milan Stamenović, Fabienne Goethals and Filip E. Du Prez

Department of Organic Chemistry, Polymer Chemistry Research Group, Ghent University, Krijgslaan 281 S4-bis, B-9000 Ghent, Belgium

pieter.espeel@ugent.be

Introduction

At the beginning of the 21st century, polymer science is entering a new era. Never before has the need for polymeric structures that are both functional and modular been so important. In order to meet the challenges required for new applications, polymer chemists have to come up with original routes that are straightforward and wide in scope. It is with this aim in mind that we developed a strategy to produce controlled polymers that are amenable to very efficient post-polymerization functionalization. In order to make the strategy as universal as possible, different monomers and polymerization techniques were used. The polymeric platforms created could then be used to form networks or introduce desired functional groups through thiol-click chemistry.

Results & discussion

The new copolymers are based on thiolactone containing monomers, inspired by a new one-pot efficient conjugation methodology developed in our laboratory[1] (**Scheme 16**). The two monomers (styrene-thiolactone and acrylamide-thiolactone) were synthesised from a bioresource material. The advantage of the thiolactone group is that it allows for the introduction of thiol groups along the backbone while preventing side reaction from occurring. As long as the thiolactone ring remains closed, the polymer is stable under air and at room temperature for prolonged times. However, in the presence of an amine, the ring opens and a thiol is generated. The key point is that the opening of the thiolactone followed by reaction of the thiol can be performed in one-pot.

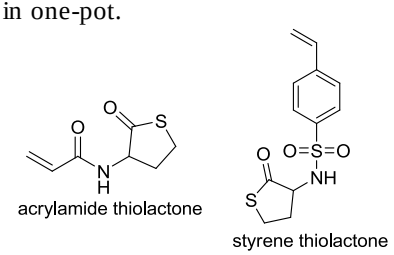

Scheme 16 Thiolactone monomers

Controlled-radical polymerization methods were chosen for their ease of use and flexibility to synthesize the copolymers. The versatility of the methods employed, namely nitroxide-mediated polymerization (NMP) and reversible addition-fragmentation chain transfer (RAFT) polymerization, allow for the production of a wide range of polymer structures for post-polymerization functionalization. Furthermore, random copolymerization gave control over the density of the thiolactone side groups within the polymer chains.

The following copolymers were synthesised: poly(styrene-*co*-styrene thiolactone), poly(*N*-isopropylacrylamide-*co*-acrylamide thiolactone) and poly(methyl methacrylate-*co*-styrene thiolactone).

RAFT copolymerization of styrene with styrene thiolactone was performed in dioxane at 70°C using S-1-dodecyl-S'-(α,α'-dimethyl-α"-acetic acid) trithiocarbonate (DDMAT) as RAFT agent and AIBN as radical initiator. Copolymers of $M_n \approx 12{,}000$ g/mol and polydispersities (PDI) as low as 1.1 were obtained. The polymerization proceeded faster for higher amounts of styrene thiolactone (up to 20 mol%). Different compositions were studied to determine the reactivity ratios of the two comonomers under those conditions. A similar procedure was applied to synthesize poly(*N*-isopropylacrylamide-*co*-acrylamide thiolactone).

Methyl methacrylate (MMA) cannot by homopolymerized in a controlled manner by NMP[2]. However, small addition of styrene thiolactone was found to control the polymerization of MMA by NMP. The copolymers were synthesized with MAMA-SG1 in DMF at 80°C and high conversions were obtained in about 3h. The amount of styrene thiolactone in the polymer feed was varied from 5 mol% to 15 mol%.

The different polymers were then used to generate networks or to introduce other functional groups by opening thiolactone units along the backbone to generate thiols (**Scheme 2**).

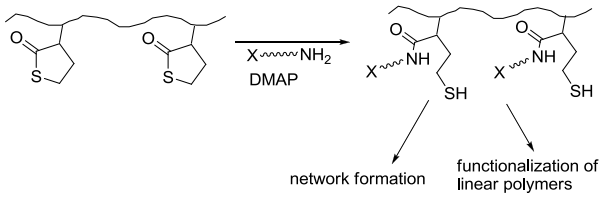

Scheme 2 Post-modification of the thiolactone containing copolymers

Conclusion

New and versatile thiolactone containing copolymers were synthesized by NMP and RAFT polymerization. As these thiolactone units represent latent thiol functionalities, these copolymers were used as efficient platforms for post-polymerization modifications.

References

(1) Espeel, P.; Goethals, F.; Du Prez, F. E. *JACS* ASAP DOI: 10.1021/ja1098098. (2) Nicolas, J.; Dire, C.; Mueller, L.; Belleney, J.; Charleux, B.; Marque, S. R. A.; Bertin, D.; Magnet, S.; Couvreur, L. *Macromolecules* **2006,** *39*, 8274-8282

"Click" Synthesis of Fatty Acid Derivatives as Polyanhydride Precursors

Lluch, C.; Lligadas, G.; Ronda, J.C.; Galià, M.; Cádiz, V.

Department of Analytical Chemistry and Organic Chemistry, Rovira i Virgili University,

Marcel.li Domingo s/n, 43007 Tarragona (Spain)

gerard.lligadas@urv.cat

Introduction

The field of polymers derived from non-petrochemical feedstocks has recently attracted a great deal of interest from both economic and environmental sense. Vegetable oils, made up of triglycerides molecules, are considered to be one of the cheapest and most abundant biological sources available, and their use as annually renewable platform chemicals has numerous advantages, including low toxicity and inherent biodegradability.

Polyanhydrides (PAs) are useful biodegradable vehicles for localized drug delivery.[1] In aqueous media the breaking of the anhydride bonds resulting in gradually polymer fragments collapse and release drugs in a controlled manner. Fatty acids are good candidates for the preparation of biodegradable and biocompatible PAs, as they are natural body components.[2] Unfortunately, fatty acids are monofunctional and cannot serve as monomers for polymerization. One methodology to convert fatty acids into PA precursors is by dimerization of unsaturated fatty acids such as oleic and erucic acid. Alternatively, dicarboxylic fatty acid derivatives can also be obtained by modification of hydroxyl-containing fatty acids with cyclic anhydrides.

Due to its ability to add a broad range of functionalities in lieu of double bound, thiol-ene coupling is a promising route that can be used for the synthesis of novel PA intermediates from renewable resources.

Materials and Methods

Three novel oleic and undecylenic acids-based polyacids (Figure 1a) were synthesized using photoinitiated thiol-ene click chemistry. OLS, UDS and UDTGS were used to prepare linear and crosslinked PAs via melt-condensation under vacuum. The characterization of these polymers was performed using a combination of NMR spectroscopy, FTIR and thermal analysis. The hydrolytic degradation of some of these polymers in phosphate buffer of pH 7.4 at 37ºC was investigated by GPC, gravimetry, FTIR and ESEM. The release characteristics of drugs from some of these PAs were determined using rhodamine B as model hydrophobic compound.

Results and Discussion

OLS, UDS, and UDTGS polyacids were synthesized in high yields applying thiol-ene coupling with 3-mercaptopropionic acid, and were used to prepare homo and copolyanhydrides. OLS and UDTGS homopolymers were isolated as a viscous liquid and rubbery solid, respectively.

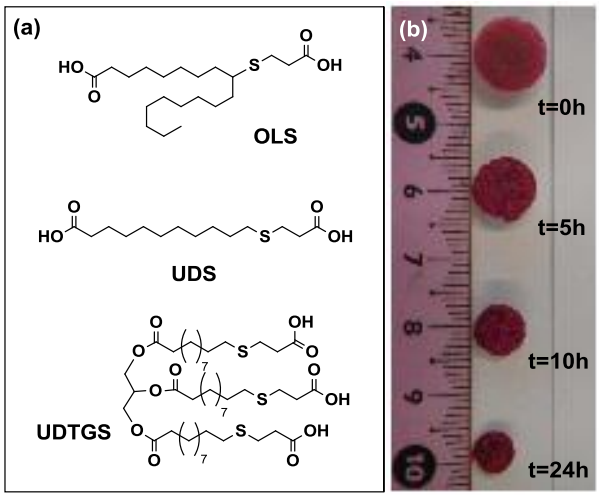

Figure 1. (a) Chemical structures of fatty acids-based polyacids. (b) Reduction in the size of rhodamine B loaded PA (UDS:UDTGS, 80:20) device with time.

Linear UDS and crosslinked UDS:UDTGS, 80:20 PA formulations showed melting points at around 75ºC and therefore were considered to be suitable for drug incorporation via melting process and delivery through degradation process. Hydrolytic degradation study revealed that both PAs show a fast decrease in the weight and anhydride content during the first hours of degradation, loosing 70% and 50% of its initial weight after 24h. When rhodamine B was incorporated into PA devices, UDS:UDTGS 80:20 PA showed a more sustained release of drug during the first stages of degradation in agreement with its crosslinked structure but in both cases up to 90% of loaded drug was released after 3 days. The progressive size reduction of the PAs devices over time (Figure 1b) and the porous eroded surface observed by SEM suggest a degradation mechanism governed by surface erosion.

Conclusions

Thiol-ene click chemistry has been applied to oleic and undecylenic acids to prepare biobased polyacids as PAs precursors. The studied PA systems showed fast-degrading properties and therefore could be useful in specific fast-acting applications such as wound care.

References

1. Jain, J.P.; Chitkara, D.; Kumar, N. *Expert Opin. Drug Deliv.* **2008**, *5*, 889-907

2. Jain, J.P.; Sokolsky, M.; Kumar, N.; Domb, A.J. *Polym. Rev.* **2008**, *48*, 156-191.

Experimental and Theoretical Investigation on the Synthesis of High-molecular Weight Linear and Branched Polylactides

T. Mantourlias [a,b], *A. Seretis* [a,b], *K. Karidi* [a], *P. Pladis* [a], *S. Parouti* [a] and *C. Kiparissides* [a,b]

[a] Chemical Engineering Department, Aristotle University of Thessaloniki, P.O.Box 472, 54124 Thessaloniki,
[b] Chemical Process Engineering Research Institute, P.O.Box 60361, 57001 Thessaloniki; Greece

cypress@cperi.certh.gr

Polylactide is a well-known biodegradable polymer with a broad range of applications, including packaging, surgical sutures, drug delivery systems, internal bone fi xation, etc. It is produced either from lactic acid by direct polycondensation or via ring-opening polymerization of lactide with the latter being the most widespread method. In order to extent the applications range of biodegradable polymers very high molecular weight PLA should be produced. The preferred route of preparation is the bulk polymerization of L-lactide in the presence of a suitable catalyst such as stannous octoate (Sn(Oct)2). In addition, branched or star-shaped polylactides that exhibit different physical and degradation properties compared with the linear polylactide may be produced via the utilization of various co-initiators (e.g., pentaerythritol, 1,4 butanediol, polyglycidol, etc.).

The present work deals with the experimental and theoretical investigation of the ring-opening polymerization of lactide with Sn(Oct)2 as a catalyst for the production of high molecular weight polymers with improved physical and mechanical properties. It should be pointed out that the production of high molecular weight polylactides strongly depends on the high purity of all reagents employed since the presence of reactive impurities or traces of moisture can significantly lower both the polymerization rate and the polymer molecular weight. For this reason, high vacuum technique and very careful purification procedures were used for all reagents. Initially, the homopolymerization of lactide was experimentally studied at various temperatures (i.e., 140, 160 and 180 0C) and different monomer to initiator concentration ratio values (i.e., [M/I] = 5000, 10000 and 20000). The monomer conversion was determined by using 1H NMR spectroscopy and the corresponding molecular weight distributions by GPC. Subsequently, co-intitiators with different number of hydroxyl groups were utilized to obtain branched or star shaped polymers. The produced polylactides were fully characterized concerning their thermal and mechanical properties (i.e., DSC, TGA, DMA). It is demonstrated that the polymerization temperature, the monomer to initiator ratio as well as the co-initiator type greatly affect the monomer conversion and the molecular properties of the produced polymer, during the ringopening polymerization of L-lactide, which in turn affect its end-use properties. It should be pointed out that in the absence of co-initiator the obtained molecular weights were higher than those presented in the open literature (e.g., Mw = 700000 with PD < 2.5, at 160 0C and [M/I] = 10000) indicating the efficiency of the purification procedure.

Moreover, a comprehensive mathematical model was developed based on a detailed kinetic mechanism to simulate the dynamic evolution of the monomer conversion and molecular weight developments (i.e., Mn, Mw, PD). The proposed kinetic mechanism of the ring-opening L-lactide polymerization comprises a series of elementary reaction steps, including catalyst activation, chain initiation, propagation, chain transfer to wat er and octanoic acid, transesterification, etc.

Dynamic material balance equations were derived to describe the conservation of the various molecular species (i.e., monomer, catalyst and moments of the live and dead polymer number chain length distributions) during the polymerization. The predictive capabilities of the proposed kinetic model for the ringopening polymerization of L-lactide are demonstrated by a direct comparison of the theoretical predictions with experimental results on monomer conversion and molecular properties (Figures 1, 2).

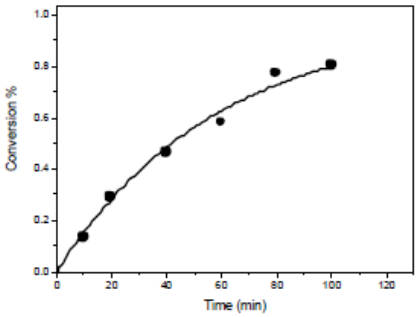

Figure 1: Comparison between model prediction and experimental data on monomer conversion (Monomer/Catalyst = 20000, 160 ^{0}C).

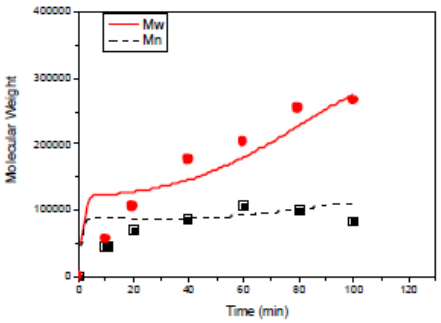

Figure 2: Comparison between model prediction and experimental data on number and weight average molecular weight (Monomer/Catalyst = 20000, 160 ^{0}C).

Controlled synthesis of reactive polyethers: application to free-isocyanate polyurethanes

Brocas Anne-Laure, Cendejas Gabriel, Deffieux Alain and Carlotti Stéphane

Université Bordeaux, Laboratoire de Chimie des Polymères Organiques, CNRS, ENSCBP, 16 avenue Pey Berland, 33607 Pessac Cedex, France

brocas@enscbp.fr

Polyurethane materials, thanks to their versatile properties, found many applications in various areas like building, coating, automobile or aeronautic industries. Because of the increasing energy demand, the decrease of petroleum products and recent regulations, newroutes for the synthesis of bio-based polymers and materials derived thereof have to be developed. The approach presented here is based on the use of epoxides like epichlorohydrin (ECH) and glycidol issued from glycerol directly coming from vegetal oils. These epoxides allow the synthesis of glycidyl methyl ether (GME) and also reactive allylglycidyl ether (AGE).

In this presentation, the controlled copolymerizations between AGE and ECH or GME or protected glycidol will be discussed. The synthetic approach was based on monomer-activated anionic polymerization[1,2,3](scheme 1). The method required an organic initiator (tetraoctylammonium bromide) and an activator (triisobuylaluminum) in slight excess (~2 eq) compared to the initiator to get fast (a few hours) and controlled polymerization in hydrocarbons.

Scheme 1

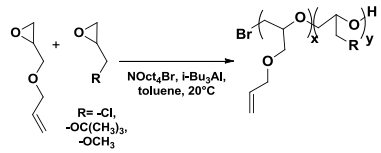

Functional copolymers, with various compositions and molar masses from 2000 to 30000 g/mol were prepared. In addition, complete conversions and low dispersities were obtained. The pendant allylic unsaturation enables various functions to be introduced, in particular, epoxide and cyclic carbonate groups by reaction with metachloroperbenzoic acid and carbon dioxide (scheme2).

Scheme 2

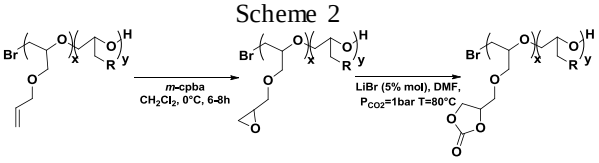

The occurrence of the different functionalizations was checked by ^{1}H (figure1) and ^{13}C NMR analysis. It showed the total disappearance of double bounds after the epoxydation reaction, then the disappearance of epoxides after reaction with $CO_2$and the formation of new signals attributed to the ethylene carbonate group.

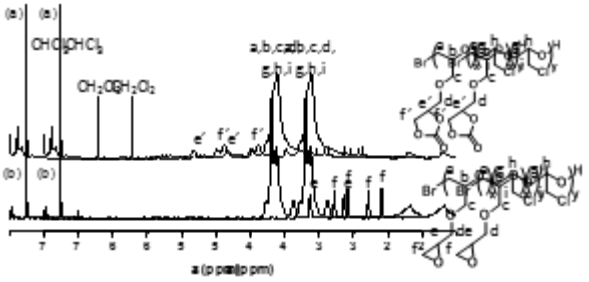

Figure 1: ^{1}H NMR (400MHz, $CDCl_3$) spectrums

Five members cyclic carbonate groups were then reacted with primary amines to form hydroxyurethane functions. As shown in Figure 2, the reaction was followed by FT-IR spectroscopy with the disappearance of the peak corresponding to carbonyl group at 1795 cm^{-1} and the appearance of peaks characteristic of the urethane functions at 1710 and 1610 cm^{-1}.

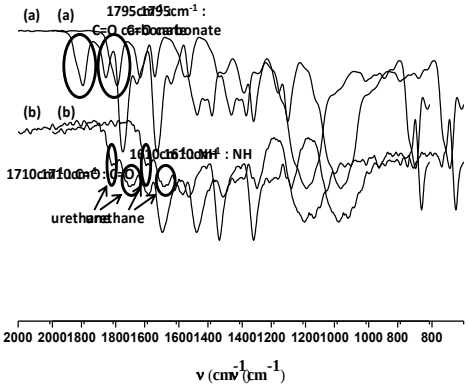

Figure 2: FT-IR spectrums

The mechanical properties of various reactive polyethers and crosslinked polyurethanes were then investigated.

[1] Labbé A.; Carlotti S.; Billaud C.; Deffieux A., Macromolecules, 2007, 40, 7842-7847

[2] Carlotti S.; Labbé A.; Rejsek V.; Dourges S.; Gervais M.; Deffieux A., Macromolecules, 2008, 41, 7058-7062.

[3] Gervais M.; Brocas A. L.; Cendejas G.; Deffieux A.; Carlotti S., Macromolecules, 2010, 43, (4), 1778-1784

Sol-Gel Transition and Gelatinization Kinetics of Wheat Starch

F. Teyssandier [a], P. Cassagnau [a], J. F. Gérard [b], N. Mignard [c]

[a] Université de Lyon, CNRS UMR 5223, Ingénierie des Matériaux Polymères/ Laboratoire des Matériaux Polymères et Biomatériaux, Université Lyon1, Villeurbanne, F-69622 Lyon, France.

[b] INSA de Lyon, CNRS UMR 5223, Ingénierie des Matériaux Polymères/ Laboratoire des matériaux macromoléculaire, 17 rue Jean Capelle, Villeurbanne, F-69622 Lyon, France.

[c] Université Jean Monnet, CNRS UMR 5223, Ingénierie des Matériaux Polymères/ Laboratoire de Rhéologie des Matières Plastiques, 23 rue docteur Paul Michelon, St Etienne, F-42023, France.

Philippe.cassagnau@univ-lyon1.fr

Introduction: During the last decades, biopolymers and particularly starch-based materials showed growing interest in replacing oil-based materials. Their large availability and very low cost make thermoplastic starch one of the main renewable resource materials to be used as a raw material or to be blended with synthetic polymers. Compared to other natural polymers, their processing properties are very complex since they involve numerous physical processes and chemical reactions [1-2]. Gelatinization, which is closely connected to the other phase transitions, is the main phenomenon involved in the conversion process from starch to thermoplastic starch since it refers to the destruction of the crystalline structure that includes granular swelling, native crystalline melting and molecular solubilization [2].

Materials and Methods: Wheat starch from Sigma-Aldrich at 10% moisture content was employed during all this study. Several plasticizers such as glycerol, propylene glycol and polyethylene glycol 200 (PEG 200 - Mw = 200 g/Mol) were evaluated and compared. Rheology experiments were carried out on a controlled stress AR2000 (TA instruments) rheometer equipped with a Peltier module, in oscillatory mode with parallel-plate geometry. The swelling of the granules was monitored thanks to an optical microscope equipped with a video camera and a heating plate.

Results and Discussion: Time sweep measurements at different volume fractions at constant temperature and frequency using glycerol as the plasticizer have been done to characterize the influence of the volume fraction on the sol-gel transition. The gelation process is directly influenced by the volume fraction. To determine the maximal packing fraction (Φ_m) in the suspension, rheological experiments and precisely frequency sweep tests were carried out. By fitting the Krieger-Dougherty equation [3] on the experimental data of the evolution of the zero-shear viscosity as a function of volume fraction for suspensions of particles we were able to calculate Φ_m and the intrinsic viscosity [η] which we found equal to 0.341 and 2.5 respectively.

As a consequence of the formation of an elastic, three dimensional polymer network, the increase of G' is wider than the G'' and thus the tangent delta is decreasing progressively with time. Viscoelasticity experiments have been performed at several frequencies at constant temperature and volume fraction to characterize the independency of tan (δ) with frequency at the gel point. The gel point can be determined from the crossover of the different curves. In this case tan (δ) ≈ 2.2 leading to a relaxation exponent equal approximately to 0.73. This value is very close to that obtained by De Gennes, meaning that this gelation process is described by percolation and supports De Gennes analogy between the viscosity of the gelation bath and percolating superconductivity.

The gelation time is greatly influenced by the temperature. When the gelation is kinetically controlled, apparent activation energy of gelation (Ea) can be obtained from the integration of the kinetic Arrhenius equation. The gelation times were determined from the crossover of the elastic and viscous moduli of the isothermal experiments by assuming that the relaxation exponent was constant as a function of temperature. As expected the variation logarithmic of t_{gel} versus the inverse of the absolute temperature was linear for each volume fractions. To predict the t_{gel} evolution with temperature for any composition of the system, we have re-scaled the Y-axis with a shift factor, acquired from the Dickinson model [4], to obtain a master curve. From the linear regression we have been able to calculate the apparent activation energy that we found equal to Ea = 112 KJ.mol^{-1}.

In addition to the rheological experiments, the kinetic of gelatinization has been monitored using an optical microscope. During isothermal heating (from 60 to 100°C), the growth of an isolated grain in glycerol has been observed. In the same way that we did with the rheological results, we were able to calculate an activation energy that we found equal to 100 KJ.mol^{-1}.

Conclusions and References: To characterize the sol-gel transition occurring during the gelatinization of starch using glycerol as a plasticizer, dynamic rheology and optical microscopy were used. The maximal packing fraction was calculated and was found to be equal to 0.341. Thanks to isothermal frequency sweep tests, the relaxation exponent has been determined and the value (n = 0.73) provided us the information that the gelation process was described by the percolation theory. The apparent activation energy was worked out by both instruments and the variation of t_{gel} for any composition of glycerol/starch suspension was described using the Dickinson model.

Septo RFT, *Macromol. Symp.* 2003;201:203–212.

Liu H, Xie F, Yu L, Chen L, Li L. *Prog. Polym. Sci.* 2009;34:1348–1368.

Krieger IM, Dougherty TJ, *J. Rheol.* 1959;3(1):137–152.

Dickinson E. *J. Chem. Soc., Faraday Trans.* 1997;93(1):111–114.

Aliphatic Polyesters from the Carbohydrate-based Bicyclic Monomer Methyl Di-*O*-methylene-galactarate

C. Lavilla,[a] *A. Alla*,[a] *A. Martínez de Ilarduya*,[a] *E. Benito*,[b] *M.G. García-Martín*,[b] *J.A. Galbis*,[b] *S. Muñoz-Guerra*[a]

[a]Dept. d'Enginyeria Química, Universitat Politècnica de Catalunya, ETSEIB, Diagonal 647, 08028 Barcelona
[b]Dept. de Química Orgánica y Farmacéutica, Universidad de Sevilla, Profesor García González 2, 41012 Sevilla

cristina.lavilla@upc.edu

Introduction

The use of cyclic monomers derived from carbohydrates has been scarcely explored, with most of work made up to now devoted to isosorbide,[1] which is obtained by dehydration of D-glucitol. Other types of cyclic carbohydrate-derived monomers are those generated by intramolecular acetalization of either alditols or aldaric acids.[2] Dimethyl 2,3:4,5-di-*O*-methylene-galactarate (Galx) is a bicyclic acetalized aldarate which has not yet been explored to prepare polyesters.

Scheme 1. Chemical structure of isosorbide (left) and dimethyl 2,3:4,5-di-*O*-methylene-galactarate (right).

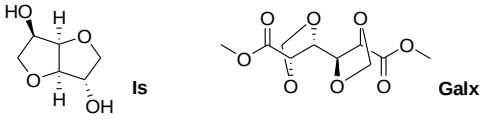

Materials and Methods

The monomer Galx was obtained by reacting commercial galactaric acid with paraformaldehyde, methanol and sulphuric acid. Poly(alkylene 2,3:4,5-di-*O*-methylene-galactarate) polyesters (PE-*n*Galx) were obtained by melt polycondensation of Galx with an aliphatic α,ω-alkanediol (1,6-hexanediol, 1,8-octanediol, 1,10-decanediol or 1,12-dodecanediol).

Results and Discussion

PE-*n*Galx polyesters were obtained with intrinsic viscosities between 0.51 and 0.62 $dL \cdot g^{-1}$ and weight-average molecular weights ranging from 34,700 to 43,100.

The thermal behavior, mechanical properties and biodegradability of these polyesters were evaluated and compared with those displayed by their homologous n-alkylene adipate polyesters (PE-*n*Ad).

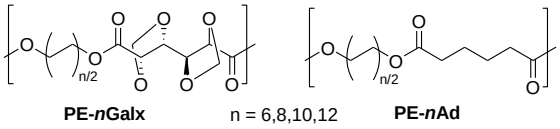

Scheme 2. Chemical structure of PE-*n*Galx (left) and PE-*n*Ad (right).

Glass transition temperatures (T_g) of PE-*n*Galx varied from -17 to 6 ºC, decreasing with an increase of the length of the polymethylene chain, which acted as soft segment. T_g of PE-*n*Galx were invariably higher than those observed for PE-*n*Ad.

All PE-*n*Galx from synthesis were semicrystalline, and melting temperatures were in the range of 70-86 ºC. The introduction of cyclic acetal groups improved the thermal stability of polyesters, thus increasing onset temperature ($^oT_{5\%}$), temperature for maximum decomposition rate (T_d) and remaining weight at 600 ºC.

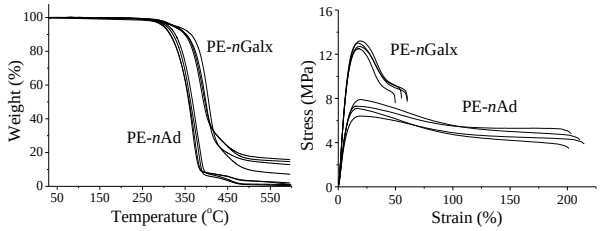

Figure 1. Compared TGA traces (left) and stress-strain curves (right) of PE-*n*Galx and PE-*n*Ad.

Regarding mechanical properties, the presence of the cyclic acetal units in the polyester chain caused an increase in the elastic modulus and the tensile strength of the polyesters, and produced a reduction in the elongation at break at the same time.

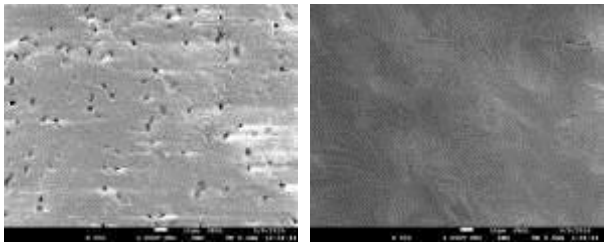

Figure 2. SEM micrographs of PE-8Galx (left) and PE-8Ad (right) after hydrolytic degradation at pH 2.0 for 56 days.

The hydrolytic degradation in aqueous buffer (pH 2.0, 7.4 and 10.5) and the enzymatic degradation in the presence of either lipase from porcine pancreas or lipase from *Pseudomonas fluorescens* were evaluated. The degradation study revealed that PE-*n*Galx were biodegradable polyesters, and that they degraded faster than PE-*n*Ad.

Conclusions

Aliphatic polyesters derived from a novel carbohydrate-based cyclic monomer, which might be an alternative to isosorbide, displayed thermal and mechanical properties highly influenced by the presence of the cyclic groups, and were hydrodegradable and biodegradable.

Acknowledgements

Authors acknowledge the Spanish MICINN for project grant MAT-2009-14053-CO2 and Spanish MEC for the FPU grant awarded to C. Lavilla.

References

[1]F. Fenouillot, A. Rousseau, G. Colomines, R. Saint-Loup, J.-P. Pascault, *Prog Polym Sci* **2010**, *35*, 578-622.

[2]J.A. Galbis, M.G. García-Martín, In *Monomers, Polymers and Composites from Renewable Resources*; Belgacem, M.N.; Gandini, A. Eds.; Elsevier: Oxford, UK, **2008**; pp 89-114.

Controlled Release of Polyphenols from Cellulose-Based Hydrogels

D. Ciolacu, A. Oprea, G. Cazacu, M. Cazacu

"Petru Poni" Institute of Macromolecular Chemistry, Alea Gr. Ghica Voda 41A, 700487, Iasi, Romania

dciolacu@icmpp.ro

Introduction: Cellulose is considered an almost inexhaustible source of raw material for environment friendly and biocompatible products [1]. Cellulose based superabsorbent hydrogels are finding increasing interest in the scientific and industrial field due to their biodegradable character and the high swelling capacity [2,3]. Lignin, a natural phenolic polymer, is the second most abundant polymer after cellulose. There is an increasing interest in the potential health application of lignin, such as antitumoral, antiviral, anticarcinogenic activities, as well as, antibacterial and antiparasite action [4,5]. The aim of this paper is to present the preparation of novel cellulose-lignin hydrogels with special properties and to demonstrate their possible application as delivery device by incorporating the polyphenols from grapes seeds.

Materials and Methods: Microcrystalline cellulose (Fluka), C, was dissolved in 8.5% NaOH solution, at –30°C. Steam explosion lignin from aspen wood (L) was supplied by ENEA, Italy. Epichlorohydrin (Fluka) was used without further purification. Polyphenols (PF) were obtained by extraction from grape seeds from the *Chambourcin* type and analysed according to ISTA methods. For the preparation of cellulose/lignin hydrogels (CL), the cellulose was firstly dissolved in alkaline solution at low temperature (-30ºC). Different percents of lignin (Table 1) and epichlorohydrin were added in the obtained cellulose solution, under continuously stirring. The obtained composition was kept for 8h, at 80°C when cross-linking occurred. The hydrogel was washed successively with warm and cold water and then the sample was dried in vacuum, at room temperature.

Results and Discussion: By chemical crosslinking of CL mixtures, in presence of epichlorohydrin, hydrogels with high swelling capacities were obtained, maximum swelling degree in a mixture water:ethanol = 19:1 ranging between 2300-3060 % wt. (Figure 1).

Table 1. The main characteristics of the obtained hydrogels

Sample	Reaction mixture composition		Hydrogel features	
	C, g	L, g	Yield, %	Qmax, %
C	0.500	0.000	99.90	1145
CL1	0.375	0.125	99.91	2358
CL2	0.335	0.165	99.52	2446
CL3	0.250	0.250	92.34	2642
CL4	0.165	0.335	78.28	2737
CL5	0.125	0.375	71.70	3061

Direct evidence for the cross-linking reaction is the formation of ether bonds between cellulose and lignin, as FT-IR spectrum of hydrogels revealed by the increasing intensity of the aryl ether band (C-O-C stretching) at 1265 cm^{-1}, and alkyl ether bands at 1120 cm^{-1} (C-O-C stretching) and 1062 cm^{-1} (C-O stretch from alkyl substituted ether) (spetra not shown). The DSC curve of hydrogels determines a shifting of the endothermic peak between the corresponding temperatures of the initial samples, fact which certifies the formation of the cross-linked network. These hydrogels proved to be suitable to incorporate grapes seed polyphenols from water/ethanol solutions. The amount of the incorporated polyphenols was estimated by UV-VIS spectral measurements and the obtained values increased as a function of swelling capacity of the hydrogels.

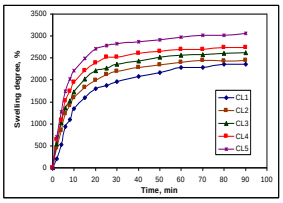

Fig. 1. Variations of the hydrogel's swelling degrees as a function of time and composition

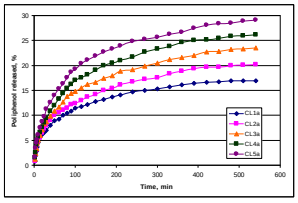

Fig. 2. Release profiles of polyphenols from CL hydrogels in water:ethanol medium, at 37 °C

Spectral studies regarding the release of polyphenols from CL hydrogels showed its dependence on the lignin content from matrices (Figure 2). Thus, higher lignin content leads to increasing the percentage of released polyphenol. A simple, semi-empirical equation using Korsmeyer and Peppas model was used to kinetically analyze the data regarding the polyphenols release from systems. Both the swelling and polyphenols release can be controlled by the composition of the hydrogels.

Conclusions: The cellulose-lignin based hydrogels were investigated by FT-IR and UV-VIS spectroscopy, differential scanning calorimetry (DSC) and optical microscopy. The obtained hydrogels may be potential candidates for biomedical applications.

Acknowledgements: This research was financially supported by European Social Fund – „Cristofor I. Simionescu" Postdoctoral Fellowship Programme (ID POSDRU/89/1.5/S/55216), Sectoral Operational Programme Human Resources Development 2007/2013 and by the European Union's Seventh Framework Programme (FP7/2007-2013), under grant agreement n°264115 - STREAM.

References

1. D. Klemm, B. Heubletin, H.-P. Fink, A. Bohn, *Angew. Chem., Int. Ed.*, 44(22), 3358-3393 (2005).
2. R.-N. Chena, H.-O Hob, C.-Y. Yub, M.-T. Sheub, *European Journal of Pharmaceutical Sciences*, 39, 82–89 (2010).
3. S. Trombino, R. Cassano, E. Bloise, R. Muzzalupo, L. Tavano, N. Picci, *Carbohydrate Polymers*, 75, 84–188 (2009).
4. V. Ugartondo, M. Mitjans, M.P. Vinardell, *Industrial Crops and Products*, 30, 184–187 (2009).
5. K. Toh, H. Yokoyama, H. Noda, Y. Yuguchi, *Journal of Food Biochemistry*, 34(1), 192 – 20 (2010).

Microwave-Assisted Nitroxide-Mediated Radical Polymerization of Acrylamide in Aqueous Solution

Julien Rigolini, Bruno Grassl, Laurent Billon, Stephanie Reynaud and Olivier F. X. Donard

Institut Pluridisciplinaire de Recherche sur l'Environnement et les Matériaux (IPREM) UMR 5254 CNRS / Université de Pau et des Pays de l'Adour (UPPA), Hélioparc Pau Pyrénées, 2 Avenue du Président Angot, 64053 Pau Cedex 09, France

julien.rigolini@univ-pau.fr

In a recent work[1], we demonstrated that the combined use of microwave irradiation as a heating source and water as a solvent provides a reasonable living/controlled polymerization of acrylamide by nitroxide mediated polymerization (NMP). To conduct the reaction, a combination of a conventional hydrosoluble radical initiator (Vazo56) and a β-phosphonylated nitroxide (SG1) were employed.

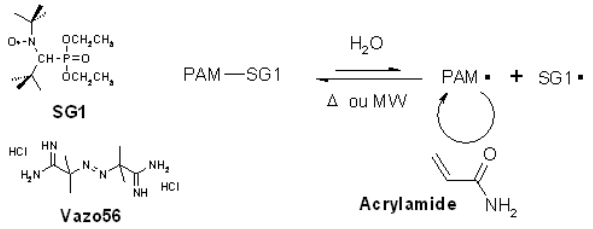

When using the DYN mode which corresponds to a dynamic control of the temperature with a high initial microwave power, no specific microwave effect was observed even for temperatures ranging between 90° and 105°C. While the Arrhenius plots obtained by both the DYN mode and conventional heating (CH) were in good agreement at 90°C, a deviation was noticed at 105°C and was attributed to the experimental errors. The absence of microwave effect was explained by the DYN parameters themselves, *i.e.*, a high microwave power at the beginning of the polymerization increasing the bulk temperature to the set point as quickly as possible. Upon reaching the target temperature, the microwave power decreases or completely shuts off to maintain the target bulk temperature, T_p, without exceeding it.

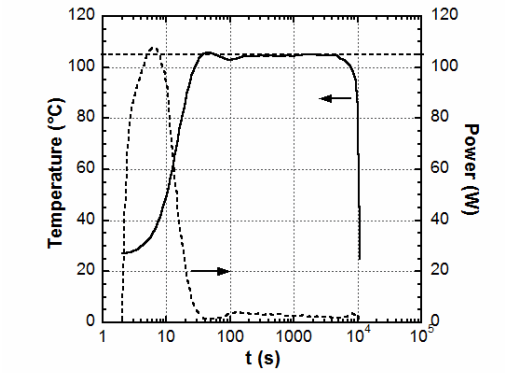

Figure 1: Temperature and power profiles during microwave irradiation in DYN mode.

In the absence or near absence of microwave irradiation, we concluded that classical thermal chemistry was taking over and that the full advantage of microwave synthesis was lost. It is however worth noticing that the temperature was only measured by an external IR sensor. The use of IR sensors may be inappropriate for temperature measurements in microwave-heated reactions[2]. The reason for this is that they may easily lead to a misinterpretation of the results since the real reaction temperature is unknown in particular when operating with simultaneous air cooling. The existence of a microwave effect was ascertained with a complementary series of reactions carried out between 130 and 160°C using the DYN mode and a microwave apparatus equipped not only with an external IR sensor but also with an internal temperature sensor, an optic fiber, which allowed the monitoring of the bulk temperature of the reactive media[3].

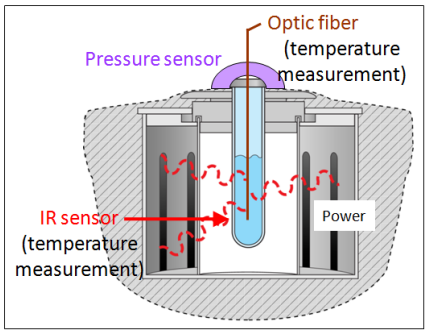

Figure 2: Schematic of the Monowave 300 from Anton-Paar GmbH used in this study.

Using the microwave-assisted nitroxyde-mediated polymerization, we also extended the field of AB hydrophilic diblock copolymer. Using a tertiary SG1-based macroalkoxyamine, we were able to synthesize in homogeneous aqueous media poly(acrylamide-*b*-sodium 2-acrylamido-2-methylpropanesulfonate), *i.e.* a neutral-*b*-anionic diblock copolymer, and poly(acrylamide-*b*-3-dimethyl(methacrylamidopropyl)ammonium propanesulfonate), *i.e.* a neutral-*b*-zwitterionic diblock copolymer[3].

References

1. Rigolini, J.; Grassl, B.; Billon, L.; Reynaud, S.; Donard, O. F. X., *Journal of Polymer Science: Part A: Polymer Chemistry* **2009,** *47* (24), 6919-6931.
2. Herrero, M. A.; Kremsner, J. M.; Kappe, C. O., *Journal of Organic Chemistry* **2008,** 73, (1), 36-47.
3. Rigolini, J.; Grassl, B.; Reynaud, S.; Billon, L., *Journal of Polymer Science: Part A: Polymer Chemistry* **2010,** 48, (24), 5775-5782.

Unique Fully Aliphatic or Aliphatic/Aromatic Copolyesters Containing Biobased ω-Hydroxy Fatty Acids: Molecular Structures and Properties

Annamaria Celli[a], *Paola Marchese*[a], *Simone Sullalti*[a], *Corrado Berti*[a], *Richard A. Gross*[b],

[a] Department of Civil, Environmental, Materials Engineering, Via Terracini 28, 40131 Bologna, Italy
[b] Polytechnic Institute of NYU, Six Metrotech Center, Brooklyn, NY, 11201 http://www.poly.edu/grossbiocat/

annamaria.celli@unibo.it

Introduction

The development of biobased polymers that bring unique properties desired by consumers at acceptable prices is a major challenge and opportunity. Recently, Gross and collaborators reported the development of an engineered *Candida tropicalis* strain capable of producing commercially viable yields of ω-hydroxyfatty acids. This required the identification and elimination of 16 genes from the diploid yeast *Candida tropicalis* genome. After reintegration of a P450 and process optimization, volumetric yields higher than 150 g/L of 14-hydroxytetradecanoic acid (14HA) was produced using methyl myristate as substrate.[1] In this work, 14HA was used in two-step polycondensations to obtain novel copolyesters with 1,4-cyclohexylene units or terephthalate moieties along chains. The introduction of aliphatic or aromatic rings into the main chain aims at improving thermal and mechanical performances.

Materials

14-hydroxytetradecanoic acid (14HA) was prepared by a literature method.[1]
1,4-dimethyl cyclohexanedicarboxylate (DMCD) (containing 100 and 22 mol% of trans isomer), dimethyl terephthalate (DMT), 1,4-butanediol (BD), titanium tetrabutoxide (TBT) were purchased from Aldrich.

Results and Discussion

Scheme 1 describes the synthetic route to prepare two series of novel fully aliphatic and aliphatic/aromatic terpolymers built from 14HA/BD/DMCD and 14HA/BD/DMT, respectively. The biocontent of terpolyesters is from 14HA, however, it is anticipated that commercial sources of bio-BD will soon be available.[2] The presence of cyclohexane and phenyl rings along chains results in corresponding copolyesters with attractive thermo-mechanical properties: for example, P14HA-*co*-PBT and P14HA-*co*-PBCHD, containing 20 mol% of 14HA, have melting temperatures of about 190 and 135°C, respectively. In contrast, homopolyesters of 14HA melt at about 91°C. Elastic modulus of the copolyesters, measured by DMTA, is similar to that of PBT or Ecoflex (poly(butylene terephthalate-*co*-butylene adipate)). Moreover, the 1,4-cyclohexylene units show some further advantages: they provide copolyesters with resistance to weather, light, and support material biodegradability.[3] Finally, according to the cis/trans isomeric ratio of the aliphatic rings, the phase behaviour of copolyesters can change from a semicrystalline, at high trans content, to amorphous copolyesters when the cis isomer predominates. Therefore, by modifying the stereochemistry of the aliphatic ring, the molecular structure or the copolymer composition can be specifically manipulated in order to fine-tune copolyester physical-mechanical properties.

Conclusions

Novel biobased copolyesters were successfully synthesized. They contain long aliphatic chains, which impart flexibility and rapid crystallizability. In conjuction with biobased 14HA aliphatic repeat units, copolyesters contain aliphatic or aromatic rings, which enables to molecular design of materials with adjustable physico-mechanical properties. Thus, by judicious selection of monomers, there is ample ability to fine-tune material properties so a desired balance of material rigidity, ductility, sufficiently high melting point and good mechanical performance can be realized.

References

[1] W. Lu, J. Ness, W. Xie, X. Zhang, J. Minshull, R.A. Gross, *Journal of the American Chemical Society* **2010**, *132*, 15451.
[2] J.M. Burk , *Int. Sugar J.* **2010**, *112*, 30.
[3] C. Berti, A. Celli, P. Marchese, G. Barbiroli, F. Di Credico, V. Verney, S. Commereuc, *Europ. Polym. J.* **2009**, *45*, 2402.

Scheme 1: Scheme of the synthesis of copolymers

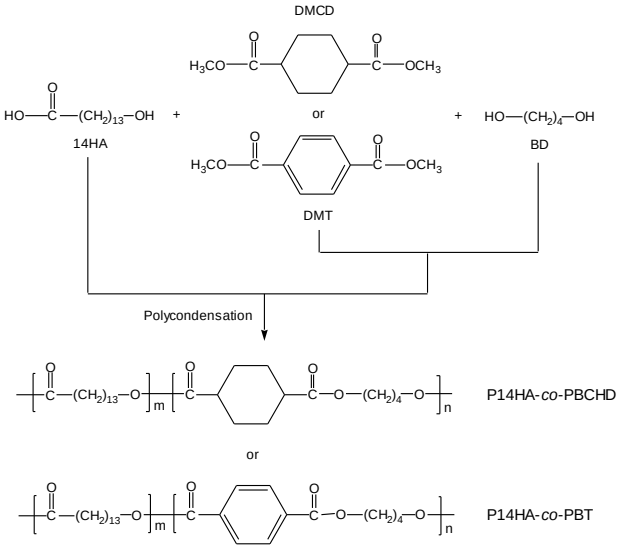

Pyridinium and Picolinium Ionic Liquids as a Media for Biphasic Ethylene Polymerizaton

Katarzyna Dziubek, Wioletta Ochędzan-Siodłak, Krystyna Czaja

Opole University, Faculty of Chemistry, Opole, Poland

katarzyna.dziubek@pwr.wroc.pl

Introduction

Two-phase solvent systems are attractive alternative to homogenous and heterogeneous catalysis. In these systems the catalyst is retained in one phase and the product remains in another, which allows the catalyst recovery and easy product separation [1].

In the last decade, particular attraction has been devoted to biphasic systems, in which one phase constitutes a ionic liquid. Ionic liquids have been shown to have a significant benefit over conventional solvents due to a variety of interesting and useful physical and chemical properties depending on the choice of either cation and anion of ionic liquid [1, 2].

In our recent search, we have focused our attention to the biphasic polymerization of ethylene with using ionic liquids as a medium of titanocene catalyst activated by alkylaluminium compounds. The studied ionic liquids constituted by the chloroaluminate anion and pyridinium cations with different number, length, and the position of the alkyl substituent at the pyridinium cation.

It was found that not only the performance of polyreaction but also the properties of the obtained PE depend on physical properties, especially viscosity, of the ionic liquids, which again, depends on the structure of the pyridinium cation. Furthermore, the pyridinium ionic liquids has recently been shown to be generally more environmentally friendly, regarding their biodegradation pathway, than the most popular imidazolium analogues [3].

Materials and Methods

As presented previously [4, 5]

Results and Discussion

In our investigations, the alkylpyridinium (C_n-py) and alkylpicolinium (C_n-3-mpy, C_n-4mpy) chloroaluminate ionic liquids (where alkyl was butyl or octyl) were applied in the biphasic ionic liquid/hexane ethylene polymerization as a medium for titanocene (Cp_2TiCl_2) catalyst activated by $AlEtCl_2$ and $AlEt_2Cl$ alkylaluminium compounds. It was found that the catalyst was immobilized in the ionic liquid phase and no catalyst leakage was observed. Polyethylene (PE), formed in the ionic liquid phase, has been progressively transferred to the hexane phase. Thus, the polymer was characterized by a high purity and can be easily separated from the reaction mixture by simple decantation. The structure of the ionic liquid cation, the kind of alkylaluminium compound, and the activator/catalyst (Al/Ti) molar ratio have a considerable effect on the polymerization performance.

In the biphasic systems, where [C_4-3-mpy][$AlCl_4$], [C_4-4-mpy][$AlCl_4$], and [C_8-4-mpy][$AlCl_4$] picolinium ionic liquids were applied, the PE yields were higher that those with use of imidazolium analogues, previously investigated [4]. An increase of the total polymerization yield with an increase of Al/Ti molar ratio was observed, regardless of the ionic liquid used. It was found that the ionic liquid with the alkyl substituent at the para (*gamma*) position is favoured. Maintenance of the PE product in the ionic liquid phase at higher activator/catalyst molar ratio is a disadvantageous feature of these biphasic systems, despite of a satisfactory total yield of PE.

The total PE yield decreases when the pyridinium ionic liquid ([C_4-py][$AlCl_4$] or [C_8-py][$AlCl_4$]) were used as a medium for catalyst. It should be noted, however, that the greater amount of PE was obtained in hexane phase, regardless of activator/catalyst molar ratio, which is the great advantageous feature of systems.

These results are related to physical properties, especially viscosity, of the ionic liquids used. The viscosity of the studied ionic liquids increases with the length and number of alkyl substituents. Low viscosity improves the dispersion of the ionic liquid in the hexane phase and increases the access of the monomer to the active site. For that reason the best results was obtained for ionic liquids with butyl alkyl chain in pyridinium cation.

Additionally, regardless of the ionic liquid used, for the same activator/catalyst molar ratio the polymerization yield was much higher when $AlEtCl_2$ was applied than $AlEt_2Cl$.

The structure of the ionic liquid cation has an influence also on the PE yield and properties. A distinguishing feature of the PE produced were the high bulk density (up to 520 g/dm^3) and the high crystallinity degree (≈95%), non-typical for polyethylene obtained over metallocene catalyst.

Conclusions

The studied ionic liquids as a medium metallocene catalyst enable to develop an unique system for the metallocene-catalyzed biphasic ethylene polymerisation with wide-range control of the polyreaction and the product properties.

References

[1] Wasserscheid P., *J. Ind. Eng. Chem.* 2007, 13, 325.

[2] Olivier-Bourbigou H., Magna L., *J. Mol. Catal. A* 2002, 182, 419.

[3] Docherty K. M., Dixon J.K., Kulpa Ch. F., *Biodegradation* 2007, 18, 481.

[4] Ochędzan-Siodłak, W., Dziubek K., Siodłak D., *Eur. Polym. J.* 2008, 44, 3608

This work is supported by The Ministry of Science and Higher Education for Grant No N N209 335337. Katarzyna Dziubek is a recipient of a Ph.D. fellowship from a project funded by the European Social Fund.

Novel poly(carboxybetaine methacrylamides) Synthesized via Living/Controlled Aqueous RAFT Polymerization

C. Rodriguez-Emmenegger[1], B.V.K.J. Schmidt[2], Z. Sedlákova[1], V. Šubr[1], A. Bologna Alles[1], E. Brynda[1], and C. Barner-Kowollik[2]

[1]Institute of Macromolecular Chemistry AS CR, Heyrovskeho Sq. 2, Prague 6, 162 06, Czech Republic [2]Preparative Macromolecular Chemistry, Karlsruhe Institute of Technology (KIT), Institut für Technische Chemie und Polymerchemie, Germany.

e-mail: rodriguez@imc.cas.cz, brynda@imc.cas.cz, christopher.barner-kowollik@kit.edu

Introduction

Water-soluble zwitterionic polycarboxybetaine polymers (poly(CB)) are a highly interesting class of materials being applied to a broad range of biomedical and engineering applications. Among other zwitterionic polymers, poly(CB) is unique, emerging as the only ultra-low fouling material known allowing the preparation of biosensors, fouling resistant nano-particles, and non-adhesive surfaces for bacteria.[1, 2] Poly(carboxybetaine methacrylate) and poly(carboxy-betaine acrylamide) have been prepared via ATRP however a controlled polymerization has not been yet achieved. Herein the first successful living/controlled RAFT polymerization of the novel (3-acryloylamino-propyl)-(2-carboxy-ethyl)-dimethyl-ammonium (carboxybetaine methacrylamide) (CBMAA-3) monomer in acetate buffer is presented.

Materials and Methods

CBMAA-3 polymerizations were performed in acetate buffer, pH 5.2, at 70 or 25ºC using variable ratios of 4-cyanopentanoic acid dithiobenzoate as chain transfer agent (CTA) and 4,4'-azobis(4-cyanovaleric acid) or 2,2'-azobis[2-(2-imidazolin-2-yl)propane] dihydrochlo-ride as initiators (I) with target molecular weigths in the range between 55000 and 222000 g mol^{-1}. The conversion was determined by on-line ^{1}H-NMR. After 48 hour dialysis, samples were lyophylized and the absolute M_n, *PDI* and hydrodynamic radius were determined by aqueous size exclusion chromatography (ASEC-MALLS) and dynamic light scattering.

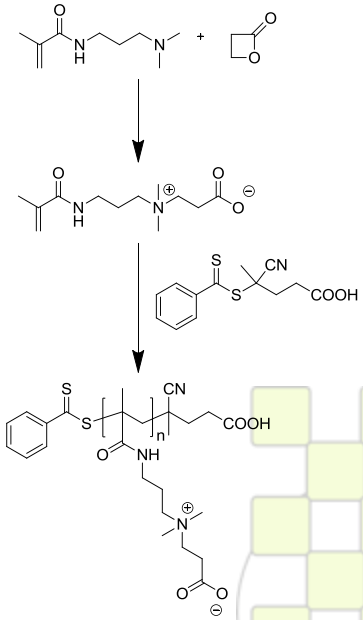

Scheme 1. Preparation and polymerization of CBMAA-3.

Results and Discussion

Poly(CBMAA-3) was obtained with M_n ranging from 14000 to 250000 g mol^{-1} in acetate buffer with conversions exceeding 90% in 24 hours. The controlled/living character of the polymerization was evidenced by a linear increase of the molecular weight with conversion with concomitantly decreasing *PDI*s. No induction period was observed when the CTA/I ratio was 2 and the propagating species concentrations was constant as evidenced by a linear first order relation.

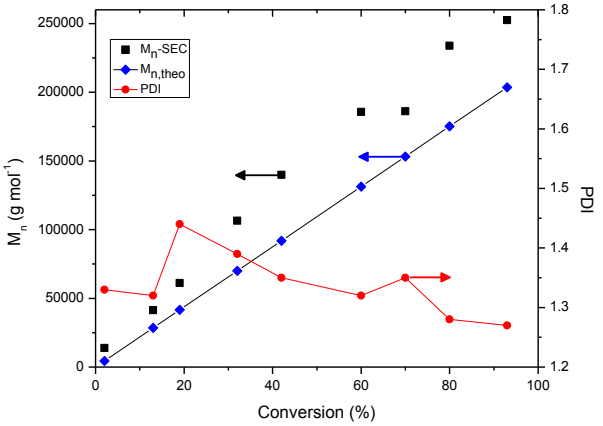

Figure 2. M_n (black squares) and *PDI* (red circles) determined by ASEC-MALLS and theoretical M_n (blue diamonds) as function of conversion (CTA:I 2:1)

Conclusions

The novel carboxybetaine monomer CBMAA-3 was synthesized for the first time and was utilized for the first living/controlled polymerization of carboxybetaine monomers. Aqueous RAFT polymerization afforded polymers with high molecular weight and low *PDI*.

References

(1) Rodriguez Emmenegger, C.; Brynda, E.; Riedel, T.; Sedlakova, Z.; Houska, M.; Alles, A. B., *Langmuir* **2009,** 25, (11), 6328-6333.

(2) Jiang, S.; Cao, Z., *Adv. Mater.* **2010,** 22, (9), 920-932.

Acknowledgements:

This research was supported by the Academy of Sciences of the Czech Republic under Contract No KAN200670701 and by Grant Agency of the Academy of Science of the Czech Republic (IAAX00500803). C.B.-K. Acknowledges support from the Karlsruhe Institute of Technology (KIT) within the context of the Excellence Initiative.

Zinc Powder-Alkyl Halide: A Novel Initiation System for Living Radical Polymerization of Vinyl Monomers

Gokhan Cankaya, Niyazi Bicak

Istanbul Technical University, Department of Chemistry, Maslak 34469 Istanbul, Turkey

bicak@itu.edu.tr

Introduction: Synthesis block copolymers based mainly on controlled radical polymerization (CRP) techniques, such as ATRP, RAFT and NMP methods. Among those ATRP is most favorable due to its good control over the chain growth[1]. However ATRP is almost confined to styrenic and acrylic monomers and it can not be employed in polymerization of vinyl ester or vinyl amide monomers. Therefore preparation of block copolymers constituting with monomers polymerizing by different mechanisms is difficult task and can be achieved by end-group transformation of the first block to be used as macro-initiator.

In this presentation we'll introduce activated zinc powder-alkyl halide as novel initiation system applicable for controlled/living polymerization of vinyl monomers, including vinyl acetate.

Result and Discussion: The initiation of VAc, MMA and styrene in the presence of ethyl bromoacetate or benzyl bromide was demonstrated to be effective in dry conditions around 70 °C. The zinc-alkyl halide system is sluggish to start the polymerization at room temperature (Table-1). The system does not give polymers in the presence of trace water, due to reductive dehalogenating effect of the activated zinc. This was evidenced by a model reaction of zinc with ethyl bromoacetate in the absence of the monomer.

Table-1: The polymerization yields (in bulk) of Zn-ethylbromoacetate initiation system in various conditions.

Monomer	*Water*	*Condition*	*Yield*
VAc	-	RT/ 48 h	No polymer
VAc	+	70 °C /24 h	No polymer
VAc	-	70 °C /24 h	81 %
MMA	-	RT/ 24 h	No polymer
MMA	-	70 °C /6 h	59 %
Styrene	-	55 °C /24 h	No polymer
Styrene	-	90 °C /8 h	48 %

Kinetic investigations revealed about 2 h of induction periods and nearly first order kinetics ($k=1.82\times10^{-5}$ 1.79×10^{-5} and 4.26×10^{-5} s^{1} for VAc, styrene and MMA respectively) in bulk conditions.

GPC traces of the resulting polymers showed relatively narrow polydispersities ((PDI: 1.12-2.6) up to 60-80 % conversions. Logically cationic, radicalic or insertion mechanisms can be considered for this polymerization system. However, polymerizability of MMA eliminates the cationic mechanism. In order to determine the mechanim operating, polymerization of MMA was studied in the presence of 0.5 mL methyl isobutyl ketone, which is well-known radical inhibitor. Surprisingly no polymer was obtained after 24 h of reaction. This result clearly eliminates the insertion mechanism and the system works in radicalic fashion as depicted in Scheme-1. Recently Arriola *et al.* demonstrated radical generation of dialkyl zincs by ESR and used atactic olefin polymerization the presence of a hafnium complex[2].

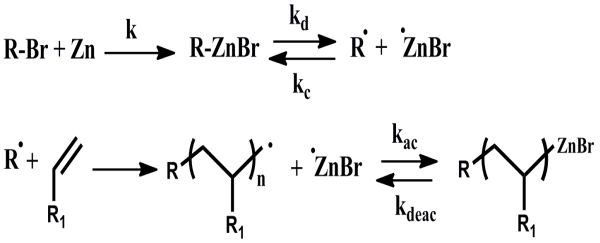

Scheme-1: Possible mechanism of the polymerization system with zinc-alkyl halide.

Regarding with reaction of alkyl halides with zinc metal, the polymers obtained by this method must bear ZnBr end-group which is highly reactive towards hydrogen donating compounds such as water or acids.

Indeed, the polymers isolated in ordinary conditions were not living due to easy destruction of the reactive end groups by hydrogen transfer. However, chain extension of PVAc (obtained by EBA and zinc powder) with MMA yielding PVAc-*b*-PMMA revealed livingness of the system in dry conditions, as evidenced by molecular weight increment in GPC traces and ^{1}HNMR spectrum of the resulting polymers (Fig-1).

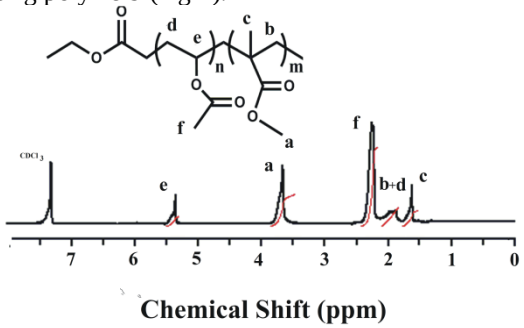

Figure-1: ^{1}HNMR spectrum of the polymer obtained by chain extension of PVAc with MMA.

Conclusion: The initiation system described is a living radical system which is especially useful for synthesis of block copolymers of VAc with ATRP grown acrylic and styrenic pre-polymers by direct initiation from their terminal haloalkyl groups.

References

1-W. A. Braunecker, K. Matyjaszewski. *Prog. Polym. Sci.* 32 (2007) 93–146

2- D.J. Arriola, E.M. Carnahan, P.D. Hustad, R. L. Kuhlman, T.T. Wenzel. *Science* (312 714-719, 2006

Microwave-Assisted Synthesis of PAMAM Type Dendrimers & Their Analytical Applications

*Cemil Dizman[1], Tezcan Paralı[2], Ali Serol Ertürk[3], Metin Tülü[3] **

[1]Istanbul Technical University Dept. of Chem., Istanbul 34469, İstanbul
[2] Fatih University Dept. of Chem., Istanbul 34500, Turkey
[3] Yildiz Technical University, Dept. of Chem. Istanbul 34220, Turkey

Dendrimers are highly branched three dimensional supra(macro)molecules with well-defined structures constructed around a multifunctional central core. These structural characteristics exhibit good physical and chemical properties. Their synthesis are arising from a core, symmetrically additions of new groups help the dendrimer to grow exponentially. The functionalities of the dendrimers depend on cores, terminal groups and internal void spaces. PAMAM-type dendrimers with different functional groups on their peripheries by using Newkome[1] and Tomalia[2] repeating units were synthesized. Depending on the necessity, conventional and microwave-assisted reaction methods have been alternatively used. Poly (ethylene glycol) diacid 600, Jeffamine® (polyoxypropylene triamine), Trimesic acid, and Tren (tris (2-aminoethyl) amine) have been chosen as the cores. In order to prevent any undesired lactam formation, all amidation reactions related to Behera's amine[1] have been carried out under normal pressure and at room temperature. Acryl groups have been added to the corresponding amines by Michael addition reaction under microwave conditions. First and second generation dendrimers of corresponding cores have been successfully obtained[3]. After the characterization of the dendrimers, the metal complexing properties were studied for Cr(III), Co(II), Ni(II), Cu(II),Zn(II), Cd(II), Pb(II) and Ag(I) ions in aqueous solution using the Liquid-Phase Polymer-Based Retention (LPR) method.

General Outlook

In general, most divergently generated 1-2 branched dendrimers were assembled by addition of simple nonbranched monomers by means of a Michael reaction, whereas most of the 1-3 branched dendrimers have been prepared using preformed 1-3 branching (mini)dendrons or monomers, which were constructed via a predendron. Utilizing these precursors or monomers in the convergent synthesis with a central core gives the synthetic advantage of having fewer reactions occurring within a single molecule. This greatly reduces the number of branching and focal defects within the macromolecule, compared with those constructed using the purely divergent method of synthesis, yielding near uniformity and monodispersity in many cases. Upon construction of the layers or generations as they are commonly called, the number of surface groups on a tetravalent core for a 1-3 branched dendrimer increases faster than that of a 1-2 branched dendrimer. Using branched monomers offers unique opportunities to instill controlled polyfunctionalization and localized steric hindrance or protection.

The novel features of these fractal-like molecular architectures are their rich chemistry associated with the untappedinternal regime(s) as well as limitless uniform and combinatorial surface possibilities. There is unlimited potential for a wide range of utilitarian applications. Since these 1-3 branched dendritic assemblies generally utilize branching centers associated with the starting monomer, the creation of new novel functionalized monomers and their subsequent combination to generate different synthetic patterns will open doors to vast new families of synthetically generated structural organic architectures. The creation of new monomers will afford new avenues to specific nanostructures that will spark the imagination of future inventors[4].

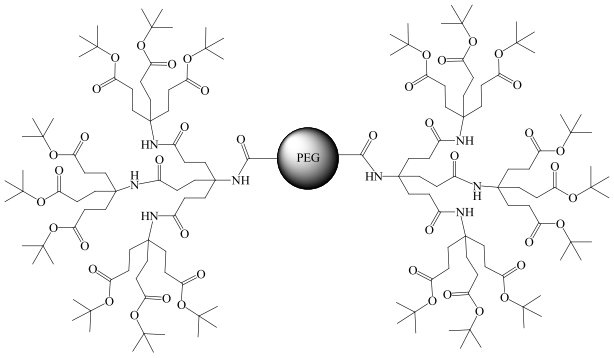

Scheme 1. Second Generation PEG based dendrimer.

References:

1. Newkome, G. R.; Weis, C. D. *Org. Prep. Proc. Int*. 28 (1996) 485.
2.Tomalia, D. A.; Naylor, A. M.; Goddard, W. A., *Angew. Chem., Int. Ed*. 29 (1990) 113.
3. Tulu M. ; Senel M., *Journal of Applied Polymer Science*, 109 (2008) 2808.
4. Newkome, G. R and Shreiner, C. *Chem. Rev*. 110 (2010) 6338

Ring-opening Polymerization of D,L-lactide using Zinc (II) Octoate as Catalyst

Rosario Mazarro[1], *Giuseppe Storti*[1], *Massimo Morbidelli*[1], *Ignacio Gracia*[2], *Juan F. Rodríguez*[2]

[1]Institute for Chemical and Bioengineering, ETH Zurich, Wolfgang-Pauli-Str. 10, 8093 Zurich, Switzerland

[2]Department of Chemical Engineering, Faculty of Chemistry, University of Castilla – La Mancha, Avda. Camilo José Cela 12, 13071 Ciudad Real, Spain

rosario.mazarro@chem.ethz.ch

Introduction: Poly(lactic acid) (PLA) is typically produced either by direct polycondensation or by Ring-Opening Polymerization (ROP). For high molecular weight polymers and large-scale applications, ROP is the reaction of choice and it is in fact used in various commercial processes.[1-3] PLA can effectively replace conventional plastics in several different applications. In addition, it has the key advantage of degradability, which makes it environmentally compatible[4] and suitable for medical applications.[5]

The most popular industrial catalyst is Stannous Octoate ($Sn(Oct)_2$). However, although some debate in the scientific community, cytotoxicity and difficulties in removal from the resulting polymer have limited its use in several cases, especially in the case of biomedical applications.[6,7] Several groups are currently studying alternative and more biocompatible catalysts, as recently reviewed by Williams et al.[8] Among them, Zinc Octoate ($Zn(Oct)_2$) seems to be an attractive substitute of Stannous Octoate.[9,10] However, most of these studies are purely experimental, with almost no discussion about the corresponding mechanisms and kinetic scheme and very uncertain parameter values.

Aimed to study the kinetics of ROP of PLA using $Zn(Oct)_2$ as catalyst, a set of experimental data of bulk melt ROP of D,L–lactide using methanol as co-catalyst has been collected at different temperatures (140-180°C). The values of the Arrhenius parameters for propagation and intermolecular transesterification reactions are reported and a previous model[11] based on the "alkoxide initiation mechanism"[12] has been successfully applied to simulate the experimental results of conversion and molecular weights.

Results and Discussion: The livingness of the reacting system in the examined temperature range has been checked up to conversion values around 90%.

The activation energy and the pre-exponential constant of the propagation reaction were determined as: E_p = 68.33 ± 8 kJ mol^{-1} and k^0_p = 1.90 10^{11} L mol^{-1} h^{-1}. The measured value of activation energy is quite similar to the literature ones for L-lactide polymerization with $Sn(Oct)_2$.[13,14] Nevertheless, the reaction rate using $Zn(Oct)_2$ is slower than the one with $Sn(Oct)_2$, as previously observed by Penczek et al.[10] A model which includes catalyst activation, reversible propagation, reversible deactivation, inter-molecular transesterification and non-radical random chain scission has been developed to describe the evolutions of conversion and molecular weight distribution. Comparing experimental results and model predictions, the reliability of the model and of the corresponding parameter values is proved.

Conclusions: As expected, the "alkoxide initiation mechanism" has been successfully applied to the model description of D,L–lactide ROP using $Zn(Oct)_2$ as catalyst and an alcohol as co-catalyst.[12] In addition, the relevance of some side reactions, mainly transesterification and thermal non-radical random chain scission, has been verified all over the studied temperature range. On the one hand, the transesterification rate constants have been estimated. On the other hand, the role of non-radical random chain scission has been experimentally observed mainly at higher temperatures: a decrease of average molecular weight along with a broadening of the molecular weight distribution (Figure 1). According to the estimated values of the activation energies of the main reactions, an increase in temperature favors always the broadening of the molecular weight distribution by a major contribution of the abovementioned side reactions.

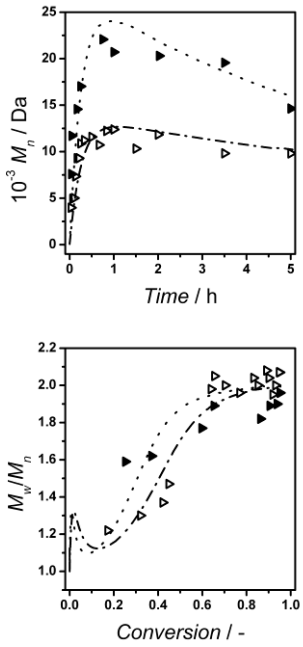

Figure 1. Number-average molecular weight versus time (above) and dispersity versus conversion (below) for D,L-lactide polymerization at 180°C, M/C = 10,000 and different ROH/C ratios. Symbols: experimental data. Lines: model results.

ROH/C: ▷ and dash-dotted line = 100; ▶ and dotted line = 50.

References:

1. Jacobsen et al. *Poly. Eng. Sci.* **1999**, *39*,1311.
2. Drumright et al. *Adv. Mater.* **2000**, *12*, 1841.
3. Datta and Henry, *J. Chem. Technol. Biotechnol.* **2006**, *81*, 1119.
4. Lim et al. *Prog. Polymer Sci.* **2008**, *33*, 820.
5. Gilding and Reed, *Polymer* **1979**, *20*, 1459.
6. Schwach et al. *J. Poly. Sci. Part A: Poly. Chem.* **1997**, *35*, 3431.
7. Dobrzynski et al. *J. Biomed. Mater. Res. Part A* **2006**, *79A*, 865.
8. Platel et al. *Polym. Rev.*, **2008**, *48*, 11.
9. Libiszowski et al. *Macrom. Chem. Physic.* **2002**, *203*, 1694.
10. Kowalski et al. *Polymer* **2007**, *48*, 3952.
11. Yu et al. *Macromolecules* **2009**, *42*, 8187.
12. Kowalski et al. *Macromolecules* **2000**, *33*, 7359.
13. Witzke et al. *Macromolecules* **1997**, *30*, 7075.
14. Ryner et al. *Macromolecules*, **2001**, *34*, 3877.

Emulsion Polymerization of Oleic Acid-based Monomers

Mónica Moreno, M. Goikoetxea, M. J. Barandiaran

POLYMAT, University of the Basque Country, Avda. Tolosa 72, 20018, Donostia-San Sebastián,Spain

monica.moreno@ehu.es

Introduction. The macromolecular materials that surround us today are mostly derived from petrochemical feedstock. However, the dwindling of fossil resources in the early future, together with the likely increase in price and the sense of urgency related to sustainability has pushed the scientific community to develop new synthetic routes to produce polymeric materials using renewable resources[a].
Vegetable oils, which are triglycerides composed by fatty acids, are one of the most promising renewable resources. Among the several known vegetable oils, olive and sunflower oil are the most abundant commodity oils in the Mediterranean basin. The oleic is the main component of these oils and therefore, it appears as a strong candidate as bio-based starting material.
The aim of this work is the synthesis of emulsion polymers by using oleic acid based-monomer. This strategy combines the advantages of bio-based monomers with a solvent-free polymerization technique. Nevertheless, the oleic acid double bond is not reactive enough for free radical polymerization and the incorporation of a more reactive group is required. For this purpose glycidyl methacrylate (GMA) was used since it allows the incorporation of a vinyl group at the end of the polymeric chain through a simple addition reaction between the carboxylic acid and the epoxide group of GMA[b]. On the other hand, because diffusion through the water phase of highly hydrophobic monomers is limited, conventional emulsion polymerization is precluded, and miniemulsion polymerization was found to be a suitable technique to overcome this drawback.

Materials and Methods. Stoichiometric amounts of oleic acid and glycidyl methacrylate, both purchased from Aldrich, were used to synthesize the monomer, methacrylated oleic acid. The synthesis was carried out with two different metal complex catalysts (Figure 1). Acid number titration was used to measure the amount of unreacted acid in the system. Miniemulsification of the monomer mixture and the aqueous surfactant solution was performed by sonication followed by high pressure homogenization. The miniemulsion homopolymerization reactions as well as the copolymerization reactions with the renewable monomer α-methylene γ-butyrolactone (TCI Europe), were performed in a stirred jacketed tank glass reactor equipped with a condenser and a nitrogen inlet. In all the reactions Dowfax 2A1 (Dow Chemicals) was used as emulsifier.

Results and discussion. The monomer synthesis was successfully carried out with two different transition metal catalysts, as ^{1}H-NMR spectroscopy reveals. It was also found that the aliphatic chain unsaturation was not affected during the functionalization process.

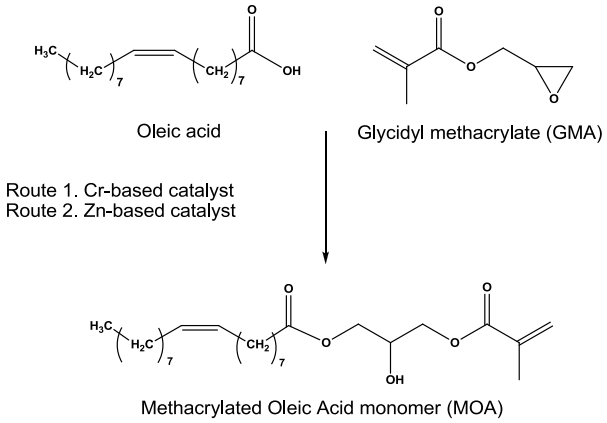

Figure 1. Synthesis of the oleic acid-based monomer

In order to analyze the role of the two catalysts in the polymerization process and the end-polymer properties, a comparative study of the polymerization kinetics as well as polymer microstructure of the two different monomers was developed by varying the initiator type. All the polymerization reactions led to high conversion. To further improve the thermal and mechanical properties of the homopolymers, the copolymerization reaction with a high Tg and bio-based monomer such as α-methylene-γ-butyrolactone is reported. The copolymers were synthesized with 5, 10 and 15% weight based monomer of comonomer and their mechanical properties were evaluated by means of tensile strength experiments as well as stickiness and hardness measurements. The thermogravimetric analysis results suggest that either the homopolymers or the copolymers presented high thermal stabilities.

References

a. Gandini A. Macromolecules **2001**, 41, 24
b. Goikoetxea, M., Minari, R.J., Beristain, I., Paulis, M., Barandiaran, M.J., Asua, J.M. Polymer **2010**, 51, 5313

Acknowledgments

We acknowledge the financial support provided by the Spanish Ministerio de Ciencia e Innovación (CTQ2006-03412)

Synthesis of functionalised hyperbranched polymers via Catalytic Chain Transfer Polymerisation and Thiol-ene Click Chemistry

Jasmin P. Menzel[1], *David Haddleton*[1], *Ezat Khoshdel*[2]

[1] University of Warwick, UK
[2] Unilever R&D Port Sunlight, UK

j.p.menzel@warwick.ac.uk

Introduction: Catalytic Chain Transfer Polymerisation (CCTP) is an excellent tool to synthesise vinyl terminated polymers with low molecular weights and various architectures. Using dimethacrylates hyperbranched polymers can be formed via cascade trimerisation.[1-3] In combination with thiol-ene click chemistry[4,5] a wide range of highly functionalized polymers can be synthesised with possible applications in hair and personal care or medical sciences.

Materials and Methods: All polymerisations and thermal thiol-ene click reactions were carried out under inert atmosphere. Schlenk flasks were degassed by three freeze-pump-thaw cycles.

Polymerisations: The monomer(s) (1 eq) and initiator dimethyl 2,2'-azobis(2-methylpropionate (V-601) (0.01 eq) were dissolved in an equivalent volume of 1,2-dichloroethane (DCE). A stock solution of cobalt oxime boron fluoride (COBF) in DCE was then added. Polymerisations were carried out for up to 24 h at 70 °C and samples for GPC and ^{1}H NMR were taken at regular intervals.

Phosphine catalysed thiol-ene click reactions: Thiol (1.1 eq) was added to a crude polymer mixture, followed by addition of the catalyst dimethylphenyl-phosphine (DMPP) (0.2 eq). Samples for ^{1}H NMR were taken every 30 min until completion of the reaction. Thiols used were benzyl mercaptan, 1-dodecanethiol and triisopropylsilanethiol.

Thermal thiol-ene click reaction: The initiator (0.5 eq,), macromer and thiol (5 eq) were dissolved in methylethylketone and heated to 70 °C after degassing. Samples for ^{1}H NMR were taken every 30 min until completion of the reaction. Thiols used were 11-mercapto-1-undecanol, thioglycerol, thioglycolic acid, 11-mercaptoundecanoic acid, and PEG monomethyl ether thiol (MW 1000 g/mol).

All samples were analysed by GPC (eluent THF or $CHCl_3$, both on 2 Mixed-D columns) and ^{1}H NMR (Bruker, 400 MHz).

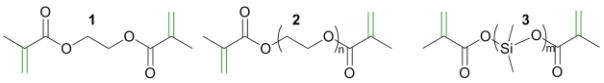

Fig. 1: Ethylenglycol dimethacrylate (EGDMA) (**1**), polyethylenglycol dimethacrylate (PEGDMA)(**2**), polydimethylsiloxane dimethacrylate (PDMSDMA) (**3**).

Results and Discussion: In this work highly functionalised hyperbranched polymers with low molecular weights were synthesised via CCTP of EGDMA and PEGDMA and subsequent DMPP catalysed Thiol-ene click reactions with different thiols (Fig. 2). GPC and ^{1}H NMR analysis showed that polymerisation up to a conversion of nearly 82 % (64 %) is possible without gelation, providing molecular weights up to 7700 g/mol (14000 g/mol) for EGDMA and PEGDMA respectively. Thiol-ene click reactions showed complete conversion in ^{1} H NMR, except for triisopropylsilanethiol where steric hindrance might have prevented inner double bonds to react.

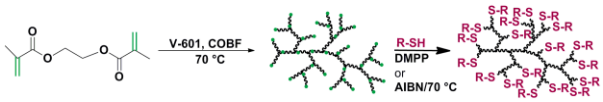

Fig. 2: Polymerisation of EGDMA and subsequent thiol-ene click reaction

Furthermore the macromonomer PDMSDMA was synthesised and functionalised via thermal thiol-ene click reactions because the catalyst DMPP caused hydrolysation of the macromonomer. Hydrolysation in different solvents over time was monitored by ^{1}H NMR (Fig. 3). It started within a few hours in DMSO whereas the compound was stable for weeks in $CHCl_3$. This shows that after functionalisation via thiol-ene click reactions small molecules can be released over time, leaving behind the plain PDMS polymer. Possible applications for this concept can be found in personal care industry or medical sciences.

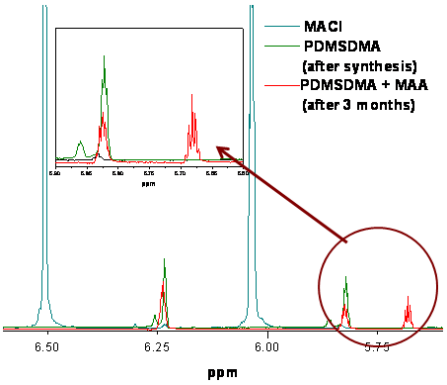

Fig. 3: Vinyl peaks of methacryloylchloride (MACl) (blue), PDMSDMA after the synthesis (green) and after partial hydrolysation into PDMS and methacrylic acid (MAA) (red).

Polymerisation of the PDMSDMA macromonomer and subsequent functionalisation are currently being investigated and will lead to even more interesting materials.

References:

1 Guan, Z., *J. Amer. Chem. Soc.*, 2002, **124**, 5616.
2 Gridnev, A., *J. Polym. Sci. Part A: Polym. Chem.*, 2000, **38**, 1753.
3 P. Davis, T., D. Zammit, M., P.A. Heuts, J., Moody, K., *Chem. Commun.*, 1998,
4 Hoyle, Charles E., Bowman, Christopher N., *Angew. Chemie Int. Ed.*, 2010, **49**, 1540.
5 Campos, L.M. *et al.*, *Macromolecules*, 2008, **41**, 7063.

Reaction and Mass-transfer in Polycondensation Process of PA-MXD6

Zhenhao Xi[1,*], *Yong Zhao*[1] *and Ling Zhao*[1]

[1] State Key Laboratory of Chemical Engineering, East China University of Science and Technology

zhhxi@ecust.edu.cn

Poly(m-xylene adipamide) or PA-MXD6 is finding increasing use in multilayer food packaging applications due to its inherent high oxygen barrier properties, excellent heat resistance and its comparable rheology and processing conditions to polyethylene terephthalate, e.g. for use in carbonated beverage bottles. The main polycondensation reaction of PA-MXD6 is a reversible reaction which can be written as $C_E + C_E \Leftrightarrow Z + g$, and the volatile by-products especially the water have to be continuously removed to obtain desired high molecular weight. As reaction and mass-transfer are coupled in polycondensation process, the rate depends not only upon the chemical kinetics of polycondensation reaction but also upon the mass-transfer of volatile by-product through the melts. With the sharp increase of melts viscoelasticity and the decrease of the amount of by-product, the removal of the small molecules become more and more difficult, and the polycondensation process change to be mass-transfer controlled gradually. The complex interconnection between the chemical reaction and mass-transfer problem in PA-MXD6 melt polycondensation process poses a serous challenge to make process control and optimization.

In the paper, a realistic model has been proposed for the melt polycondensation process of PA-MXD6. Since chain growth reaction is equilibrium controlled, if the small molecule is removed in time, the concentration of end groups would decrease and DP would increase, chain growth reaction would go forward and reach new reaction equilibrium. By the assumption that the process could reach pseudo-steady state between the reaction and mass-transfer, the overall apparent rate of PA-MXD6 melt polycondensation process can be inferred as,

$$\frac{d[g]}{dt} = k_T([Ce]^2 - \frac{4[Z][g]^*}{K})$$, and

$$\frac{1}{k_T} = \frac{1}{k} + \frac{[Z]/K}{K_L s_w}$$

where K_L is the mass transfer coefficient, denoting the interfacial area per unit weight of polymer, k is the rate constant of forward reaction and K reaction equilibrium constant, and $[Ce]$, $[Z]$, $[g]^*$ represent the concentration of end groups, amido groups and concentration of the small molecules at the gas-liquid interface respectively.

The characteristics of reaction and the effects of mass-transfer of the PA-MXD6 melt polycondensation process were studied by using stagnant film experiments in this paper, see Fig.1. The experiments were carried out using pre-polymers with different molecular in the range of the temperature 240-280℃, pressure 50-1500Pa and film thickness 1-10mm, and the change of end groups in melts with time of the process were investigated, see Fig.2. It was shown experimentally that the devolatilization in this process is form-devolatilization. The results indicated that with thinner film which means the greater mass-transfer specific interfacial area, the intrinsic viscosity increases faster; the apparent rate of the polycondensation process was also increased under high temperature and low degree of vacuum. Based on the experiments, the parameters of above model were fitted and the apparent kinetics of polycondensation process could be showed as follows,

$$\frac{d[g]}{dt} = (\frac{1}{\frac{1}{0.2418e^{-40703/RT}} + \frac{1}{1.0611Ks_w}})([Ce]^2 - \frac{4[Z][g]^*}{K})$$

And the interfacial concentration of small-molecules $[g]^*$ can be calculated by the limit of reversible reaction as follows,

$$[g]^* = A\exp(E_g/T) \times P = 9.5513 \times 10^{-8} \exp(1396.1/T) \times P$$

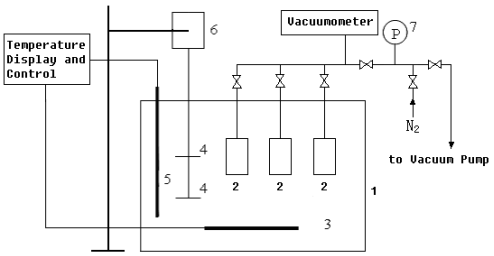

Fig.1 Schematic of experimental apparatus
1 silicone oil bath; 2 thin-film reactor; 3 electric heating elements; 4 agitator; 5 thermocouple; 6 motor; 7 pressure-and-vacuum gauge

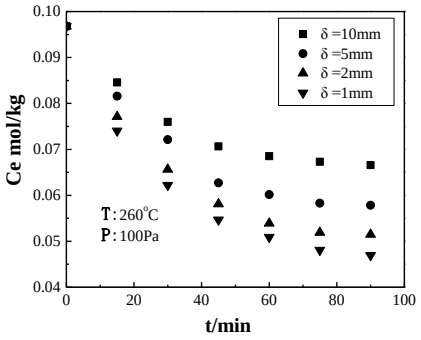

Fig.2 Effect of film thickness on polycondensation of PA-MXD6

References:

[1] Mitsubishi Gas Chemical Catalog, MX-Nylon, 2000: 5
[2] F. G. Lum, E. F. Carlston, *Ind. Eng. Chem.[J]*. 1957, (47): 1239
[3] U.S. Pat. 2,997,463 (1961); 3,968,071 (1975); 4,433,136 (1984); 4,398,642 (1983); 6,596,803 (2003); Int. Pat. WO 98/58790 (1998)
[4] Y. S. Hu, V. Prattipati, S. Mehta, et.al., *Polymer*, 2005 (46) : 2685
[5] O. George, *Principles of Polymerization*. New York. John Wiley&Sons.1981
[6] S. K. Gupta, A. Kumar, *Reaction Engineering of Step Growth Polymerization*, Plenum Press, New York, 1987
[7] J. A. Biestenberger, D. H. Sebastian, *Principle of Polymerization Engineering*. New York. John Wiley & Sons. 1983
[8] L. Zhao, Z. Zhu, G. Dai, *Proc. 17th Int. Symp. Chem. React. Eng.* Hong Kong, 2002, MS# 0663
[9] Z. Xi, L. Zhao, W. Sun, et.al., *J. Chem. Eng. Japan*,2009(42): s96
[10] B. Deroover., *J. Polym. Sci. Part A: Polym. Chem.*, 1996(34):1039

ABSTRACTS

ORAL PRESENTATIONS

Topic 2: New Analytical and Characterization Tools

Two Dimensional Correlation Vibrational Spectroscopy and QM modeling applied to the study of Fluorinated Polymers

Stefano Radice[1], Alberto Milani[2], Chiara Castiglioni[2]

[1] Solvay Solexis R&D Center, Viale Lombardia 20 20021 Bollate (MI) Italy,

[2] Politecnico di Milano, Piazza Leonardo da Vinci , Milano, 20100, Italy

stefano.radice@solvay.com

Introduction

Fluorinated polymers play an important and innovative role in various technological and scientific industrial sectors. They may show outstanding and peculiar properties when high demanding requirements, such as thermal and chemical stability, are needed.

The development of new materials needs the support of analytical tools suitable to give precise and useful structural information.

In this respect vibrational spectroscopy (IR, Raman) contributed in the past and is still contributing in the determination of chemical composition, microstructure (sequence of monomers/chemical groups) and functional end groups [1-3]. More recently, the approach of Two Dimensional Correlation spectroscopy [4,5] has been successfully applied to the study of different phenomena:

i) kinetics of chemical reactions (deblocking and crosslinking) [6]
ii) spectral trends as a function of composition [7]
iii) hydrogen bonded systems and aggregation phenomena [8]

The description of the above topics is here presented and summarised.

Materials and Methods

The examples reported are related to Perfluoropolyether products available on the market with the trademark names of FOMBLIN® and GALDEN®. Their chain backbone has the general chemical formula: $(CF_2CF_2O)_n(CF_2O)_m$ (statistical copolymers with n>m).

Most of their applications are in the field of high vacuum and lubrication technology.

Results and Discussion

The kinetic experiment (carried out on a sample inside the spectrometer) was aimed to follow the formation of the three dimensional urethane network. Fluorinated macromeric diols and hydrogenated isocianate structures reacted to build up the material.

The kinetic model has been developed using intensity data and 2D correlation maps, mainly the asynchronous maps. The experiments and data analysis allowed to achieve information on reaction order and helped to select the best blocking agent and time/temperature conditions for effective crosslinking.

The normal modes analysis as a function of composition allowed to identify characteristic normal modes (Raman active) arising due to the presence of peroxide groups. The overall effect of such moieties have been studied and analysed in details also by means of DFT modeling [7]. Indeed, QM modeling has been necessary to provide detailed eigenvectors description: as a matter of fact, most of the vibrations in fluorinated polymers may be considered as cooperative (not topologically localised) normal modes of vibration. The information obtained allowed to identify a localised normal mode due to the -O-O- bond stretching of peroxide moieties which is useful for analytical purposes.

The third example is focused on the study of fluorinated macromers with amidic functional groups; we observed clear spectroscopic evidences of aggregation throught hydrogen bonding. The nature and the amount of aggregates strongly depend on chemical environment, concentration and temperature. By means of accurate experimental data and QM modeling the experimental findings have been explained; three possible types of dimers and two types of trimers have been proposed for the description of the relevant aggregates. The 2D correlation approach has been applied using as perturbation both concentration and temperature [8]. The study allowed us to describe the fluorinated system also from a quantitative point of view, providing the aggregates distribution.

Conclusions

The approach combining IR and Raman experimental data with QM molecular modeling (DFT calculations) allowed to identify and assign normal modes suitable for analytical purposes in the characterisation of Fluorinated Polymers. The use of Two Dimensional Correlation spectroscopy provided us complementary piece of information with respect to usual 1D spectroscopic data and suggested further investigation on the observed spectral features.

References

[1]S.Radice et al: Macromolecules, 27, 2194 (1994).
[2]S.Radice et al.: Polymer, 38(11), 2753 (1997).
[3]S.Turri et al.: "Fluoropolymers: synthesis and properties" G.Hougham et al., eds. Vol.II pag.145. Plenum Press , New York, 1999.
[4] I. Noda, *Bull. Am. Phys. Soc.*, 31, 520 (1986)
[5] I. Noda, *Appl. Spectrosc.*, 47, 1329 (1993)
[6]S.Radice et al.: Applied Spectroscopy, 58[5] 535-542 (2004).
[7]S.Radice et al.: Journal of Molecular Structure, Vol.974 , pag.73-79 (2010)
8]S.Radice et al.: Macromolecular Symposia (accepted, to be published)

High Temperature Asymmetrical Flow Field-Flow Fractionation (HT-AF4) - New possibilities for characterizing polyolefins

Tino Otte, Thorsten Klein, Evelin Moldenhauer

Postnova Analytics, Max-Planck-Str. 14, D-86899 Landsberg/Lech (Germany)

Tino.Otte@postnova.com

In many applications which require particular mechanically stability polyolefins with ultra-high molar mass (UHMWPE) are used. These materials often contain molecules with masses above 10^6 g/mol. Depending on the polymerization technique the material can additionally be highly branched. These two facts make a correct analysis by the common HT-SEC-procedures impossible. Shear degradation and late co-elution of large material occurs in HT-SEC caused by the porous column packing and the implemented frits.

Asymmetrical Flow Field-Flow Fractionation (AF4) is a powerful technique which widely overcomes the above mentioned limitations of SEC. The recently developed High Temperature-AF4 system from Postnova Analytics now offers the possibility to analyze ultra-high molar mass or excessively branched polyolefins correctly over the whole size range without disturbing effects like shear scission or abnormal elution.

The size-separation is determined by the different abilities of the molecules to diffuse in a cross-flow field. An empty channel is used for size separation instead of a packed column which makes the separation very gentle.

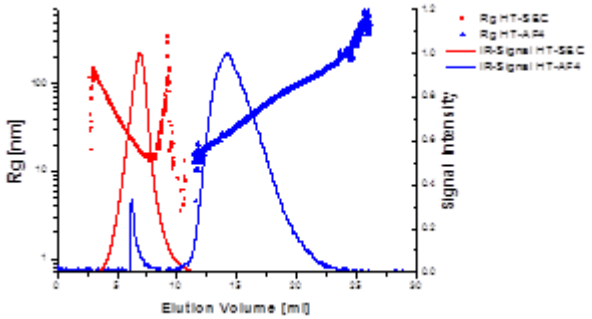

Fig. 1: Comparison of HT-SEC- and HT-AF4 separation of an UHMWPE sample

For detection infrared (IR) and static light scattering (SLS) detectors are used.

In Fig. 1 a fractogram from HT-AF4 is compared with the corresponding SEC elugram of the same UHMWPE sample. It is visible that larger radii can be detected by HT-AF4 while the SEC results are prone by shear degradation and abnormal late elution of branched species visible as a re-increase of the radius at high retention times.

While comparing results from both techniques the advantages of HT-AF4 over HT-SEC will be demonstrated in this presentation.

The efficiency of the adjustable cross-flow gradient will be shown especially with regard to the enhanced separation of the high molecular weight species. Finally the quality of the new HT-AF4 membrane is validated with narrow distributed standards and reference material.

Characterization and Applications of Aromatic-Aromatic Interactions between Water-Soluble Polymers and Low Molecular-Weight Molecules

Ignacio Moreno-Villoslada[1], Juan Pablo Fuenzalida-Werner[1], Rodrigo Araya-Hermosilla[1], Esteban Araya-Hermosilla[1], César Torres-Gallegos[1], Jorge Gómez-Manosalba[1], Daniel Muñoz[1], Víctor Barrueto[1], Mario Flores[2], Naoki Sano[3], Wataru Tomita[3], Felipe Oyarzun-Ampuero[1], and Hiroyuki Nishide[3]

[1] Instituto de Química, Facultad de Ciencias, Universidad Austral de Chile, Valdivia, Chile
[2] Departamento de Ciencias de los Materiales, Facultad de Ciencias Físicas y Matemáticas, Universidad de Chile, Santiago de Chile, Chile
[3] Department of Applied Chemistry, School of Science and Engineering, Waseda University, Tokyo, Japan

imorenovilloslada@uach.cl

Polyelectrolytes are suitable building blocks that can lead to nanoscale structures by means of their association with complementary charged polyelectrolytes, multivalent counterions, surfactants, or low molecular-weight molecules susceptible to undergo self-association such as liquid crystals and dyes. Long-range electrostatic interactions may be considered primary interactions between polyelectrolytes and their counterions. However, when additional secondary interactions such as hydrogen bonding, coordination binding, or aromatic-aromatic interactions are held, the general picture for the polyelectrolyte-counterion interaction may change dramatically, and is by means of these secondary interactions that supramolecular assemblies based on charged molecules can be achieved with controlled structure and geometry. Nanoscale architectures with different functionalities may thus be designed under the so-called ionic self-assembly (ISA).[1]

Aromatic-aromatic interactions are one of the principal noncovalent forces governing molecular recognition and biomolecular structure. They are important in the stabilization of DNA and its association with intercalators. They also play an important role in protein stabilization and protein functionality, as in enzymes, trans-membrane channels, etc. The major contribution to aromatic-aromatic interactions arises from van der Waals interactions, including solvofobic effects, while short-range electrostatic interactions determine the geometry of the interaction. As a result of the planar geometries of aromatic molecules, the molecular surface/volume ratio is high compared to that of spherical particles. Then, the aggregation of aromatic groups in water may produce the release of higher amounts of surface-solvating water molecules and, consequently, an increase on the favorable entropic and enthalpic contributions to the free energy by means of classical and nonclassical hydrophobic effects. In addition to these solvent contributions, site-specific interactions such as short-range electrostatic interactions, hydrogen bond formation, π-π interactions, or cation-π interactions may also contribute to the free energy and define the geometry of the complexes.

By means of these short-range interactions, site-specific binding between the counterion and the polymeric aromatic functional groups is held, and hydrophobic ion pairs are formed; these ion pairs tend to aggregate depending on the polyelectrolyte / counterion ratio, a fact that may be crucial for the behavior, structure, and properties of the systems.[2,3]

Under appropriate conditions the self-stacking tendency of aromatic counterions such as charged dyes may be overcome by the polymers, thus inhibiting the cooperative binding tendency of the counterions and showing a high dispersant ability. The dispersant ability of polyaromatic-ions may be of potential use in controlling counterion properties such as redox, luminescent, and acid-base properties. On the other hand, trapping low molecular-weight molecules as drugs, dyes, or other functional molecules in polymeric matrices of nano-, micro-, and macrometric size may need strong interactions between the species. Thus, new materials containing functional molecules, whose properties may be tuned to afford a desirable functionality, may be synthesized.

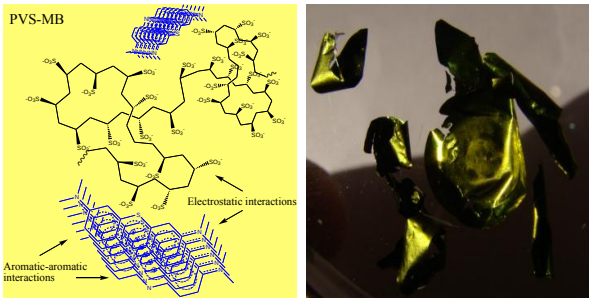

Figure 1: Metallic-like films made of organic molecules

Bibliography:

1. Faul, C.F.J.; Antonietti, M. *Adv. Mater.* **2003**, *15*, 673.
2. Moreno-Villoslada, I.; González, F.; Arias, L.; Villatoro, J.M.; Ugarte, R.; Hess, S.; Nishide, H. *Dyes and Pigments* **2009**, *82*, 401.
3. Moreno-Villoslada, I.; González, F.; Rivas, B.L.; Shibuhe, T.; Nishide, H. *Polymer* **2007**, *48*, 799.

Acknowledgements: The authors thank Fondecyt grant 1090341 for financial support.

Raman Structural Analysis of Olefin – Based Materials

Yu.V. Zavgorodnev, K.A. Prokhorov, G.Yu. Nikolaeva, E.A. Sagitova, and P.P. Pashinin

A.M. Prokhorov General Physics Institute, Russian Academy of Sciences, 38 Vavilov St., 119991 Moscow, Russia

nikolaeva@kapella.gpi.ru

Introduction

We present Raman study of polymeric materials such as polyethylene (PE), isotactic polypropylene (PP), random ethylene/olefin and propylene/olefin copolymers, PE/clay and PP/clay nanocomposites, and PE/PP blends. These materials are successfully used in industry, and its applications could be expanded, if the materials properties would be additionally improved or adjusted to pre-specified consumer requirements. This task can be efficiently solved by minor modification of the current material production technologies.

Raman spectroscopy is very informative and convenient technique for evaluation of a polymer structure in terms of the chemical composition, the degree of crystallinity, the phase and conformational states, and the orientational order of macromolecules. One of important advantages of this method is the possibility to analyze the state of macromolecules in both crystalline and amorphous phases.

Results

For PE and isotactic PP we carried out theoretical and experimental study of the intensity dependence of some Raman lines on the degree of molecular orientation. It was found that the second and the fourth coefficients in the expansion of the orientation distribution function could be determined by measurement of two depolarization ratios of the Raman lines. These depolarization ratios should be measured at parallel and perpendicular orientations of the axis of molecular orientation with respect to the direction of the laser polarization.

We studied Raman spectra of the samples, oriented uniformly to certain draw ratios, and spectra, recorded in the sample necking region during the spatial scanning from isotropic part to oriented one. Degree of molecular orientation in the crystalline and amorphous phases of PE and isotactic PP is shown to grow rapidly in the initial stages of plastic deformation and change insignificantly afterwards.

For intercalated PE/clay and PP/clay nanocomposites, the presence of the filler, that is modified clay, results in reduction of the orientational ability of the macromolecules, localized in the amorphous phase of the polymer matrix. The filler does not affect the orientational ability of the PE and PP crystallites.

For the first time we proposed the novel Raman method to determine the crystallinity of uniaxially drawn PE and PE/clay nanocomposites [1]. It is based on the analysis of two spectra, recorded at parallel and crossed polarizations of the exciting and scattered radiation. This allows discriminating the influence of the molecular orientation and the degree of crystallinity on the Raman intensities.

For neat PE and PE/clay nanocomposites, the degree of crystallinity is found to enhance with the increasing draw ratio. The results of the Raman method are shown to be in a good agreement with the data, obtained by the differential scanning calorimetry (DSC).

It was found out that the Raman method of analysis of neat isotactic PP structure [2] can be also applied for propylene/olefin copolymers, namely, for evaluation of the content of crystalline phase of isotactic PP and conformational composition of macromolecules. In this case, the Raman method data are in a good agreement with the investigation results of our samples by X-ray analysis and DSC.

The degree of crystallinity of the olefins copolymers was shown to depend on the relative content and chemical structure of the comonomers, and the type of the catalyst, used for the synthesis. For the propylene copolymers we have observed reduction in the content of crystallites of isotactic PP as well as in the content of the isotactic chains in the amorphous phase with decrease in the propylene content. The content of the isotactic chains in the crystallites is found to decrease faster than that in the amorphous phase. At the same propylene content, value of the total amount of the macromolecules in the helical conformation decreases with increase in length of the side chain of the incorporated monomer.

For the first time, we have measured and analyzed Raman spectra for the neat γ modification of the isotactic PP with the degree of crystallinity around 70%, and compared it with the spectra for the neat α and smectic modifications of the isotactic PP. Although the Raman spectra for the α and γ modifications were found to be very similar, the identification of the polymorph modifications was possible and could be based on measurement of the peak positions and relative intensities of the doublet, assigned to the asymmetric stretching vibrations of the CH_3 groups.

Raman spectra of the reactor and melt-mixed PE/PP blends were also studied. For both series it was shown that the ratio of the integral intensities of two Raman lines, assigned to the fundamental vibrations of the PE and PP, can be used for quantitative analysis of the PE and isotactic PP contents in the blends.

This work is supported by the Russian Foundation for Basic Research (project code 09-02-00587-a) and the Grant of the President of the Russian Federation for the Support of Leading Scientific Schools (3675.2010.2).

References

1. E.A. Sagitova, “Raman structural study of polyethylene – based nanocomposites” (PhD thesis, A.M. Prokhorov General Physics Institute, Moscow, 2008).

2. A.S. Nielsen, D.N. Batchelder, and R. Pyrz, Polymer 43, 2671 (2002).

Semiflexible Macromolecules in Nanoslit Confinement

P. Cifra

Polymer Institute, Slovak Academy of Sciences, Dúbravská cesta 9, 845 41 Bratislava 45, Slovakia

cifra@savba.sk

Recent experiments in nanofluidic channel devices are used to manipulate and analyze single DNA macromolecules. The experiments in nanofludic devices are oriented towards the channel or the slit-like confinements. The understanding of macromolecular confinement of real excluded volume chains started, however, by a prediction of behavior for pure slits by Daoud and de Gennes (1). Only recently we go back to the situation of pure slit and we verify experimentally by single molecule experiments the basic principles, which are modified, however, for semi-flexible chains relatively to the original predictions for flexible macromolecules.

Important question remains still opened for the semiflexible chains under the slit confinement. Is there a clear chain stretching transition of the coil size in slit in the range between a weak and a strong confinement, similar to that in channel as predicted by Odijk for the semiflexible chains? Some recent experiments show this behavior also in the slit (2), but other experiments and simulations (3), show only a broad and gradual crossover from the de Gennes blob regime to a strong confinement regime with no distinct transition as that predicted and observed for the channel. The radius of gyration of excluded volume chain of N segments in blob regime in direction parallel to the slit of width h is predicted to behave as $R_{g\parallel} \sim N^{x} h^{-y}$, with exponents $x = 0.75$ and $y = 0.25$. We refine here molecular simulation results on slit confinement for stiff macromolecules and find only a weak transition between the blob regime and the regime of strong confinement approximately at the ratio $h/P \approx 1$, where P is the persistence length of the chain. This weak transition is visible as a change in the slope of coil size *vs* h and occurs at the same ratio as corresponding pronounced coil size transition in the channel. The scaling of coil size in the blob regime deviates also from the theoretical prediction.

For a flexible chain the exponent y is close to 0.25 as predicted for the blob regime but the scaling with N shows a mixed 2D/3D regime. The 2D exponent $x = 0.75$ is found only at a strong confinement of h close to the monomer size, while at confinement in the blob regime the exponent is 0.72. For stiffer chains we observe for the blob regime considerably smaller exponent than predicted $y = 0.25$. The strong confinement regime starts approximately at $h/P \approx 1$, similar as in the channel but the crossover is not like the saturation-like/chain stretching transition in channel according to Odijk. Instead, at stronger confinement there is only a smaller change of coil size with increasing confinement than in blob regime. The scaling with N at confinement approximately of the transition shows exponent 0.61 instead of 0.75. This change is attributed to a crossover of dimensionality and also to deviations of stiffer chains from the excluded volume regime towards the ideal chain statistics.

Both flexible and semiflexible chains indicate thus that in the slit we have only a pseudo-2D behavior in accordance with recent experiments (4) on DNA in slits of h=110 nm, approximately one Kuhn length of chain. Accepted predictions for the blob regime in slit, however, assume a 2D-behavior. More details on the chain behavior are revealed by a structure factor of the chain and orientation correlations along chain. At the smallest scale the chain behaves as a rigid rod, within the scale of the blob size (of the slit width h) structure factor corresponds to a chain in 3D and on a larger scale the coil has the expected 2D-character.

In this report we answer the question what is the main effect responsible for the observed differences from theoretical predictions. Our results indicate a combination of two effects. The first is the crossover of dimensionality, a quasi-2D-behavior of the chain in slit. The second is the tendency of stiff chain towards the ideal chain statistics as observed for the free chain and also the chain confined in channel(5), which also contributes to the lowering of the exponent x for the coil size in slit together with the crossover of dimensionality. While these results apply for realistic chain lengths also much longer chain simulations are still needed to investigate the long chain limit behavior of semiflexible macromolecules. Our results provide deeper understanding for single macromolecule manipulations in nanofluidic devices with respect to different shapes of nanoconfinement and different stiffness of macromolecules.

(1) M. Daoud, P.G. de Gennes, *J. Phys. (Paris)* **38**, 85, (1977) (2) D.J. Bonthuis, Ch. Meyer, D. Stein, C. Dekker, *Phys. Rev. Lett.* **101**, 108303, (2008) (3) J. Tang, S.L. Levy, D.W. Trahan, J.J. Jones, H. Craighead, P.S. Doyle, *Macromolecules*, 43, 7368 (2010) (4) Po-Keng Lin, Chi-Cheng Fu, Yan-Ru Chen, Pei-Kuen Wei, C.H. Kuan, W.S. Fann, *Phys. Rev.* **E76**, 011806 (2007) (5) P. Cifra, *J. Chem. Phys.* **131**, 224903, (2009)

This work was supported by the Science and Technology Assistance Agency under the contract No. APVV-0079-07, VEGA grant 2/0144/09 and in part by the Centre of Excellence Program of the Slovak Academy of Sciences (COMCHEM).

Behaviour of Water during Temperature-Induced Phase Transition in Poly(vinyl methyl ether) Aqueous Solutions. NMR and Optical Microscopy Study

Jiří Spěváček[a], *Lenka Hanyková*[b], *Jan Labuta*[c]

[a]Institute of Macromolecular Chemistry, Academy of Sciences of the Czech Republic, Heyrovsky Sq. 2, 162 06 Prague 6, Czech Republic;
[b]Faculty of Mathematics and Physics, Charles University, V Holešovičkách 2, 180 00 Prague 8, Czech Republic;
[c]Supermolecules Group, WPI Center for Materials Nanoarchitectonics, National Institute for Materials Science, 1-1 Namiki, Tsukuba, Ibaraki 305-0044, Japan
spevacek@imc.cas.cz

Introduction: It is well known that some polymers with amphiphilic character, including poly(vinyl methyl ether) (PVME), exhibit in aqueous solutions a lower critical solution temperature (LCST). These polymers are soluble at lower temperatures but heating above the LCST results in phase separation which, especially for polymer concentrations $c \geq 1$ wt%, manifests itself by milk-white turbidity of solutions. On the molecular level, phase separation is a macroscopic manifestation of a coil-globule transition followed by aggregation and formation of so called mesoglobules [1]. Their thermosensitivity makes these polymers interesting for biomedical and technological applications, e.g., as drug release polymers. Of various methods used in investigations of phase separation behaviour, NMR spectroscopy can play an important role providing information on phase-separated globular structures and interactions in these systems [2]. Several years ago we used ^{1}H NMR spectroscopy to investigate changes in the structure and dynamics during temperature-induced phase separation in PVME/D_2O solutions. [3,4] Here we present some new results especially on behaviour of water during the transition using NMR methods combined with optical microscopy.

Materials and Methods: PVME (Aldrich, molecular weight M_w = 60 500, $M_w/M_n \cong 3$, 59% of isotactic diads) was used to prepare PVME/D_2O solutions in the range c = 6-50 wt %. ^{1}H NMR spectra were recorded with a Bruker Avance 500 spectrometer operating at 500.1 MHz. A modified double pulsed-field-gradient spin-echo (DPFGSE) NOE pulse sequence [5] was used in one-dimensional exchange ^{1}H NMR experiment. Photomicrographs were obtained under nitrogen atmosphere using an Olympus BX51 microscope equipped with Olympus MP5Mc/OL digital camera.

Results and Discussion: For semidilute D_2O solutions of PVME (c = 2-10 wt %) we have found that ^{1}H NMR spin-spin relaxation times T_2 of HDO molecules at temperature above the LCST phase transition (309.5 K) are 1 order of magnitude shorter than those at temperature below the phase transition (305 K). This shows that at temperatures above the transition there is a portion of HDO bound in globular-like structures. In all cases there was a single line of HDO in ^{1}H NMR spectrum and the T_2 relaxation curves were exponential, indicating a fast exchange between bound and free sites. The exchange time τ_{ex} = 1.2 ms was found for PVME/D_2O solution (c = 6 wt%) from dependence of spin-spin relaxation rate on the time interval between pulses in CPMG pulse sequence. For highly concentrated PVME/D_2O solutions (c = 20-60 wt%) the existence of the separate signal of the bound HDO with ~0.74 ppm smaller chemical shift in comparison with the main HDO signal suggests a slow exchange process. To detect a slow exchange in highly concentrated PVME/D_2O solutions (c = 20-50 wt%) we applied an one-dimensional exchange ^{1}H NMR experiment with selective excitation of the main HDO signal and detection of the changes in the intensity of the signal of the bound HDO as a function of the mixing time in the modified DPFGSE NOE pulse sequence. These measurements have shown that the residence time of bound water τ_B is independent of polymer concentration in the range c = 20-50 wt% with $\tau_B \cong 2$ s, i.e., a three orders of magnitude larger value than the residence time of bound HDO in semidilute PVME/D_2O solution with c = 6 wt%. To explain this substantial difference we assumed that exchange between free and bound water is associated with diffusion process and that the observed difference in the exchange rate might be mainly in connection with different size of globular-like structures in both cases. The evidence supporting this hypothesis was obtained by optical microscopy which revealed that very large agglomerates are formed in highly concentrated PVME/D_2O solutions with dimensions ~20 times larger than the diameter ~2.5 μm of the mesoglobules formed in PVME solution with c = 6 wt%.

Conclusion: We have found that at temperature above the LCST transition the exchange between water bound in mesoglobules and free water is in highly concentrated PVME/D_2O solutions ($c \geq 20$ wt%) three orders of magnitude slower in comparison with semidilute solution. This substantial difference is in accord with our optical microscopy findings that globular-like structures are in highly concentrated solutions ~20 times larger than in PVME solution with c = 6 wt%.

Acknowledgment: Support by the Czech Science Foundation (Project 202/09/1281) is gratefully acknowledged.

References:

1. V. O. Aseyev, H. Tenhu, F. M. Winnik, *Adv. Polym. Sci*. 2006, *196*, 1-85.
2. J. Spěváček, *Curr. Opin. Colloid Interface Sci*. 2009, *14*, 184-191.
3. J. Spěváček, L. Hanyková, L. Starovoytova, *Macromolecules* 2004, *37*, 7710-7718.
4. J. Spěváček, L. Hanyková, *Macromolecules* 2005, *38*, 9187-9191.
5. H. Hu, K. Krishnamurthy, *J. Magn. Reson*. 2006, *182*, 173-177.

Co-crystallization process of syndiotactic polystyrene/naphthalene revealed by the measurements of angular distributions of polarized fluorescence intensities

Tomohiro Sago[1*] *and Hideyuki Itagaki*[1,2]

Department of Chemistry, [1]Graduate School of Science and Technology, and [2]School of Education, Shizuoka University, 836 Ohya, Suruga-ku, Shizuoka 422-8529, Japan

f5944001@ipc.shizuoka.ac.jp

Introduction

Syndiotactic polystyrene (sPS) is known to have five crystalline forms (α, β, γ, δ and ε). In particular, the δ and ε crystalline forms are nanoporous and can cocrystallize with guest molecules in clathrate or intercalate form.

The measurements of polarized fluorescence of a chromophore in a film by rotating it around the excitation light beam, abbreviated as PFR method, are quite efficient for the determination of the arrangement of the chromophores oriented in the film. We have already successfully applied this PFR method to some systems where fluorescent molecules are highly oriented: guest molecules in a clathrate crystalline form of polymer [1] and molecules doped into polymer films [2]. In the present study, we monitored the change of positions of guest naphthalene (NP) molecules in sPS accompanied with co-crystallization process due to the exposure of NP vapors to stretched sPS films by using PFR together with WAXD mesurements.

Experimental Section

sPS films were prepared by hot-pressed method and stretched uniaxially at drawing ratio, $\lambda \approx 3$ by manual stretching machine. Drawn samples were exposed to NP vapors by changing temperatures and exposure time.

Fluorescence depolarization was measured on a Hitachi F-4500 spectrofluorometer. All the films containing NP were stuck on a holder with a circle hole whose diameter was 2.0 mm. Films were rotated by every 10° in the same plane whose center was at 60° to the exciting beam.

Results and Discussion

No crystallization occurred when sPS films were exposed to NP vapor at room temperature. Nevertheless, PFR method clarified well that the NP molecules staying in the films were distributed not uniformly but rather with a sort of orientation in the stretched amorphous sPS. On the other hand, some regular structures were found to be produced when the films were exposed at 60°C or 80°C (Figure 1). The WAXD patterns of the films exposed by NP vapor at 60°C and 80°C for 120 hrs show trans planar mesomorphic form and sPS/NP δ co-crystalline form, respectively. We examined the exposure time dependence on crystallization due to NP vapor exposure by means of PFR and WAXD.

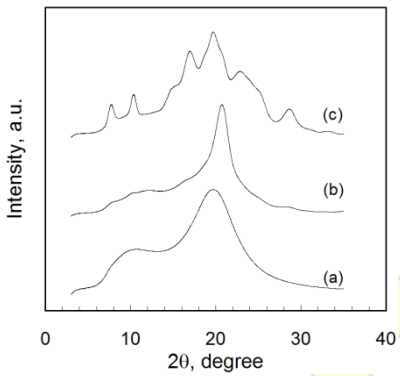

Figure 1. WAXD patterns of stretched sPS films that were exposed of NP vapor at 60ºC for 3 hrs (a), 120 hrs (b) and at 80ºC for 120 hrs (c).

Although WAXD measurements could not monitor the initial process of developing structure at all, the crystallization of sPS/NP δ cocrystals or the reaction of forming a mesomorphic structure of sPS with NP were found to proceed even after the exposure of NP at 60°C for 3 hrs by PFR method. Furthermore, we could follow the structural change with the progress of exposing time by measuring NP orientations. The NP molecules staying in the amorphous region were shown to be oriented due to the formation of a trans planar mesomorphic phase. Finally, we have succeeded to show the detail of the amorphous region of the film exposed at 60°C for 120 hrs where most NP molecules being absorbed in sPS are staying with an oriented arrangement (Figure.2). It suggested most NP molecules were oriented with an inclination: the short and long axes of NP molecule were 79º and 169 º against the stretching direction, namely the direction of the sPS polymer chains.

Moreover, we will show the PFR change that was observed along with the formation of sPS/NP cocrystals when drawn sPS films were exposed by NP vapor at 80ºC.

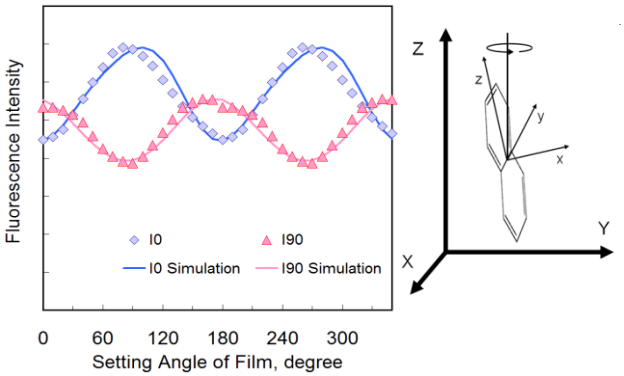

Figure 2. Angular distributions of I0 (◆) and I90 (▲) of NP in the film exposed to NP at 60ºC for 120 hrs. The solid lines show the best fitting curves of I0 and I90 for the simulated position of the NP molecule in an sPS film (Z is the stretching direction and X is the depth direction of the film).

References

[1] Itagaki, H.; Sago, T.; Uematsu, M.; Yoshioka, G.; Correa, A.; Venditto, V.; Guerra, G.; *Macromolecules* 2008, 41, 9156-9164.

[2] Sago, T.; Itagaki, H.; *J. Photopolymer Sci. Tech.* 2010, 23, 357-362.

Tandem Mass Spectrometry of Poly(2-oxazoline)s by Electrospray Ionization (ESI), Matrix Assisted Laser Desorption/Ionization (MALDI), and Atmospheric Pressure Chemical Ionization (APCI)

Esra Altuntaş,[1] *Kristian Kempe,*[1] *Anna Crecelius*[1,2] *and Ulrich S. Schubert*[1,2]*

[1]Laboratory of Organic and Macromolecular Chemistry (IOMC), Jena Center for Soft Matter (JCSM), Friedrich-Schiller-Universität Jena, Humboldtstrasse 10, 07743 Jena, Germany, Fax. +49 3641 948 202
[2]Dutch Polymer Institute (DPI), P.O. Box 902, 5600 AX Eindhoven, The Netherlands.

E-mail: ulrich.schubert@uni-jena.de; www.schubert-group.com

Introduction

Mass spectrometry has become an important tool for the characterization of different macromolecules in recent years based on the development of electrospray ionization mass spectrometry (ESI-MS)[1], matrix-assisted laser desorption ionization mass spectrometry (MALDI-MS)[2-3] and atmospheric pressure chemical ionization (APCI). Although involving different processes in ion formation, all of these techniques generally allow the ionization of various macromolecules with little or no fragmentation, enabling accurate molar mass determination by making the unfragmented structure amenable to mass separation. A combination of these techniques to high-resolution mass analyzers such as quadrupole-time-of-flight (Q-TOF) instruments provides exact molar masses for the polymers analyzed with mass accuracies in the ppm region. As a result, valuable information on the chemical constitution of the macromolecule can be derived. Data from ESI, MALDI and APCI can be utilized to determine the size of repeating units as well as end group masses, average molar masses and polydispersity index values. Further structural characterization of the polymer requires oligomer ions to be fragmented in collision-induced dissociation (CID) experiments[4-5].

Materials & Methods

The polymerizations of different 2-ethyl-2-oxazolines have been performed using the microwave-assisted living cationic ring-opening polymerization. ESI-Q-TOF-MS and APCI-Q-TOF MS measurements were performed with a micrOTOF Q-II (Bruker Daltonics) mass spectrometer equipped with an automatic syringe pump from KD Scientific for sample injection. MALDI-TOF MS experiments were performed with an Ultraflex III TOF/TOF (Bruker Daltonics, Bremen, Germany) equipped with a Nd:YAG laser and a collision cell.

Results & Discussion

In this study, ESI-Q-TOF-MS, MALDI-TOF-MS, and APCI-Q-TOF-MS have been used for the detailed characterization of various poly(2-oxazoline)s with different end groups, which were synthesized via a microwave-assisted living cationic ring-opening polymerization. The detailed tandem mass measurements were performed to evaluate these methods as structural characterization tool for the detailed analysis of poly(2-oxazoline)s. The results obtained provided an understanding about the fragmentation mechanism of the poly(2-oxazoline)s. Tandem mass analysis of the poly(2-oxazoline)s revealed the elimination of small molecules such as ethene and hydrogen in their fragmentation patterns. Moreover, a McLafferty rearrangement can be a possible fragmentation route for these polymers. The information gained from this study will also help to build a tandem MS product ion library of poly(2-oxazoline)s with different end groups including fragmentation pathways which will provide necessary knowledge for the future to make a fast and automated identification of these polymers possible.

References

[1] Fenn, J. B., *Angew. Chem. Int. Ed.* **2003**, *42*, 3871-3894.
[2] Karas, M., Hillenkamp, F., *Anal. Chem.* **1988**, *60*, 2299-2301.
[3] Tanaka K., Waki, H., Ido, Y., Yoshida, Y., Yoshida, T., *Rapid Commun. Mass Spectrom.* **1988**, *2*, 151-153.
[4] Altuntaş, E., Kempe, K., Crecelius, A., Hoogenboom, R., Schubert, U. S. *Macromol. Chem. Phys.* **2010**, 211, 2312–2322.
[5] Baumgaertel, A.; Altuntaş, E.; Kempe, K.; Crecelius, A.; Schubert, U. S. *J. Polym. Sci., Part A: Polym. Chem.* **2010**, 48, 5533–5540.

Characterisation of viscoelasticity and dynamics in polymers and proteins using DLS microrheology

Carlos A Rega, Samiul Amin and Hanna Jankevics

Malvern Instruments Ltd, Malvern WR14 1XZ, Worcestershire, UK

samiul.amin@malvern.com

The ability to precisely detect the onset of protein aggregation and draw insights into microstructural characteristics of the evolving microstructure plays a critical role in a variety of biotechnological applications, with therapeutic protein stability being a key one[1].

Rheological techniques are very sensitive to evolution of an aggregating network and although such techniques are being utilized in other fields such as foods, their use has been limited in the biotechnology area. This is primarily due to large sample volume and moderately high viscosity requirements in traditional mechanical rheometry techniques.

We propose the application of a method based on optical microrheology for the detection of the onset of protein aggregation and for developing an understanding of the nature of the evolving network structure. Optical tracer microrheology relies an determining the behaviour of tracer particles embedded in the sample of interest, and originates, with the seminal work of Phillies [2], and has evolved significantly over the last decade [3,4]. The tracer microrheology approach overcomes the limitations of mechanical rheometry, as measurements can be effectively carried out on comparatively dilute samples and require only small sample volumes.

The technique relies on the determination of the mean square displacement of the tracer particles, from which several properties of the sample can be determined, such as viscosity, the exponent of the tracer mean squared displacement power law fit and the viscoelastic modulus.

Sample viscosity can be directly obtained from the slope of the mean squared displacement using the Stokes-Einstein relation in the Newtonian regime. For non-Newtonian samples the frequency dependent viscoelastic modulus and complex viscosity can be calculated using the Generalised Stokes-Einstein relation. The elastic modulus G' emerges as a key parameter in the detection of the on-set of protein aggregation and in understanding the nature of the evolving microstructure.

Choosing the correct probe chemistry and size is highlighted as an important part of the experimental design.

In this work we present applications of the technique to the determination of the viscoelastic modulus of PEG model solutions. We also use the tracer microrheology technique to determine the transition from purely viscous (Newtonian) behaviour to viscoelastic behaviour in a range of concentrations of BSA, as well as to track the gelation process during thermal denaturation of BSA.

[1] A Saluja et al, "Ultrasonic rheology of a monoclonal antibody (IgG2) solution: implication for physical stability of proteins in high concentration formulations" Journal of Pharmaceutical Sciences (2007) **96**, 3181-3195

[2] K Ullmann, G S Ullmann and G D J Phillies "Optical probe study of a nonentangling macromolecule solution -- bovine serum albumin:water" Journal of Colloid and Interface Science (1985) 105, 315-324

[3] T A Waigh "Microrheology of complex fluids" Reports of Progress in Physics (2005) **68**, 685-742

[4] D Weihs et al, "Bio-microrheology: a frontier in microrheology" Biophysical Journal (2006) **91**, 4296-4305

Relating Performance and Structure of Nanocomposites by new Methods in Time-Resolved X-ray Scattering

N. Stribeck, A. Zeinolebadi, M. Ganjaee Sari

Dept. of Chemistry, University of Hamburg, 20146 Hamburg, Germany

norbert@stribeck.de

Introduction

Structure evolution in nanocomposites during exposure to load can be monitored with increasing time- and spatial resolution at synchrotron light sources by X-ray scattering. In such experiments voluminous data series are collected. Each scattering pattern must be evaluated. For this purpose automated analysis methods are required. We apply newly developed methods [1-3] to mechanical tests of pure polymer materials and nanocomposites containing multi-wall carbon nanotubes. We are aiming at the elucidation of structure evolution mechanisms. The experiments have successfully been carried out recently. Results from a quantitative automated analysis will be presented in the contribution in movies and graphs.

Methods

Small-angle X-ray scattering (SAXS) of materials with uniaxial orientation is monitoring mechanical tests. The recorded 2D patterns are normalized and corrected for the machine background. Blind areas are filled either considering symmetry or by 2D extrapolation [4]. Applying spatial frequency filtering, the Laplacian, and Fourier transform the multidimensional chord distribution is computed [4]. The peaks in the CDFs can be associated to information related to size and arrangement of domains in the material. Movies of the peak evolution help with the choice of relevant peaks. Chosen peaks are tracked automatically. Their shape and position is automatically evaluated [1] and yield information on the nanostructure evolution. Macroscopic mechanical parameters are related to the nanostructure parameters.

Materials

Commercial thermoplastic polyurethanes (TPU) (Trelleborg Sealing Solutions) and polypropylene (PP) Moplen HP400R (LyondellBasell Industries) are the basic materials. Nanocomposites have been manufactured from these materials by blending with multi-wall carbon nanotubes (MWCNT) in different amounts and with varying compatibilization.

Results

It is observed that the mechanical properties of the TPU can considerably be improved by addition of small amounts of MWCNT, whereas the preparation of nanocomposites from the PP does not show a considerable change of the properties.

Already the raw SAXS patterns exhibit clear differences between the different preparations. Moreover, the pattern evolution is different for both basic material if nanocomposites and pure polymers are compared.

Conclusions

From a full analysis of the scattering pattern series as a function of mechanical load we expect novel insight in the mechanisms of structure evolution in two classes of polymers as a function of nanofiller content and blend composition similar to those documented in a previous study [5].

References

[1] N. Stribeck, "X-ray Scattering for the Monitoring of Processes in Polymer Materials with Fiber Symmetry". *Polymer Reviews*, Vol. 50, No. 1, pp 40-58, 2010.

[2] A. ZEINOLEBADI, N. STRIBECK "EXPLORING A PATHWAY FOR TIME-RESOLVED STUDIES OF POLYMER FATIGUE RELATED TO NANOSTRUCTURE EVOLUTION". IOP CONF. SER.: MATER. SCI. ENG., VOL. 14, , 0120010, 2010.

[3] N. Stribeck, "Advanced X-Ray scattering methods for the study of structure and its evolution in soft materials with fiber symmetry". MIOP Conf. Ser.: Mater. Sci. Eng., Vol. 14, 012003, 2010.

[4] N. STRIBECK, "X-RAY SCATTERING OF SOFT MATTER". 1ST EDITION, SPRINGER 2007.

[5] N. Stribeck, U. Nöchel, S. S. Funari, T. Schubert, A. Timmann "Nanostructure Evolution in Polypropylene During Mechanical Testing". *Macromol. Chem. Phys.*, Vol. 209, No. 19, 1992-2002, 2008.

In-situ SAXS Investigation of Transient Nanostructure of Thermoplastic Polyurethane Elastomers During Thermal Treatments

N. Stribeck, A. Zeinolebadi, M. Ganjaee Sari

Dept. of Chemistry, University of Hamburg, 20146 Hamburg, Germany

zeinoleb@chemie.uni-hamburg.de

Introduction: Thermoplastic polyurethane elastomers (TPEs) are a class of polymers with versatile applications as medical devices, piezoresistive sensor elements, shape memory materials, and many others. Segmented polyurethanes are able to form several morphologies due to their special molecular architecture. Usually the soft domains form a rubbery matrix while the hard segments phase separate (crystallize) into hard domains and act as physical cross-links. Physical and mechanical properties of TPEs depend on their morphology; namely shape, size and orientation of the domains. Hence, understanding the mechanisms of morphology development has a crucial role in obtaining the desired microstructure and properties. Thermal annealing is a simple route by which the microstructure can be easily varied. During heating (cooling) TPEs go through several transitions. Accordingly, it is important to follow the transient structures in order to devise the optimum pathway toward the desired morphology. Therefore, it is essential to apply characterization methods by which the variations of microstructure can be monitored without disturbing the heating process and affecting the microstructure. X-rays do not interact with polymers and x-rays can be applied to investigate microstructure development of polymeric materials under thermal/mechanical loads from molecular level up to several hundreds of nanometers [1-4]. Thus, it is possible to follow transient microstructures of polymers and study mechanisms of microstructural developments.

Materials: Commercial grade polyurethane (soft segments: linear polycaprolactone diol, chain extender: HQEE and Hard segments: MDI) is used. The soft segment/hard segment ratio is 7/1. The material has a hardness equal to 95 based on Shore A scale. The granules are injected molded into dog-bone form at 205 °C.

Experimental Methods: SAXS is performed at the synchrotron beamline A2 at HASYLAB, Hamburg, Germany. Scattering patterns are collected by a two-dimensional position sensitive marccd 165 detector. The TPE sample is first scanned during heating up to 250 °C in order to find transition temperatures. The samples are then heated in different thermal cycles. In cycle A the sample is heated up to maximum temperature of 215 °C and then kept at this temperature for 2 minutes and then rapidly cooled down to 150 °C and kept at this temperature for 10 minutes and finally quenched to room temperature. In cycle B and C the maximum temperature is raised to 235 °C and 250 °C, respectively and the rest of the the program is the same as in cycle A.

Results: The peak intensity of SAXS patterns increased with increasing temperature until ca. 215 °C. This was attributed to the enhancement of contrast between the soft segment matrix and hard segment domains. At about 215°C the two meridional peaks disappeared and a broad strong meridional streak appeared. This pattern was attributed to dispersed laminar structures. This structure existed until 245 °C and above this temperature a typical pattern of an amorphous melt was observed. Based on these initial observations, three different thermal treatment cycles were designed in order to follow transient structures during heating and cooling. By quenching the sample from 215 °C to 150 °C a highly oriented structure developed and it was stable during quenching to 30 °C. Cooling the sample from 235 °C resulted in the same observation as the first cycle. However, cooling the sample from 250 °C resulted in a completely isotropic structure.

Conclusions: By applying synchrotron x-ray radiation it is possible to follow nanostructure transition of TPEs during heat treatment. It has been shown in this study how to obtain a highly ordered material from a partially oriented material by a simple heat treatment. The investigation of the influence of heat treatments on the mechanical and physical properties are in progress

References

[1] N. Stribeck, "X-ray Scattering for the Monitoring of Processes in Polymer Materials with Fiber Symmetry". *Polymer Reviews*, Vol. 50, No. 1, pp 40-58, 2010.

[2] A. Zeinolebadi, N. Stribeck "Exploring a pathway for time-resolved studies of polymer fatigue related to nanostructure evolution". *IOP Conf. Ser.: Mater. Sci. Eng.*, Vol. 14, , 0120010, 2010.

[3] N. Stribeck, "Advanced X-Ray scattering methods for the study of structure and its evolution in soft materials with fiber symmetry". *MIOP Conf. Ser.: Mater. Sci. Eng.*, Vol. 14, 012003, 2010.

[4] N. Stribeck, *"X-Ray Scattering of Soft Matter"*. 1st edition, Springer 2007.

Determination of the Macromolecular Dimensions of Hydrophobically Modified Polymers by Micellar Size Exclusion Chromatography Coupled With Multiangle Light Scattering

Guillaume Dupuis[1-2], Julien Rigolini[1], Gérald Clisson[1], David Rousseau[2], René Tabary[2], and Bruno Grassl[1]

1: Institut Pluridisciplinaire de Recherche sur l'Environnement et les Matériaux (IPREM) UMR CNRS, Université de Pau et des Pays de l'Adour (UPPA) 5254, Hélioparc Pau Pyrénées, 2 Avenue du Président Angot, 64053 Pau Cedex 09, France
2: IFP Energies Nouvelles, 1 & 4 Avenue de Bois Préau, 92852 Rueil-Malmaison, France

bruno.grassl@univ-pau.fr

The present work demonstrates that the use of a nonionic surfactant in the mobile phase together with light scattering coupled to size exclusion chromatography (SEC) provides an accurate determination of macromolecular dimensions of hydrophobically modified water-soluble polymer and polyelectrolyte, *i.e.*, weight-average molar mass M_w and polydispersity I_p. This method, called micellar SEC, is based on the dissociation of the aggregates in aqueous solution and the formation of mixed micelles between the surfactant and the polymer hydrophobic groups.

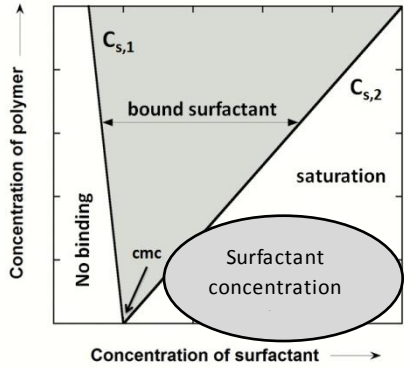

The methodology and its application are presented for synthetic sulfonated polyacrylamides (5 and 20 mol % of AMPSNa) modified with three hydrophobic alkyl side groups (C8, C12, and C18) and with Triton X-100 as a nonionic surfactant and are discussed according to the associativity of the polymers.

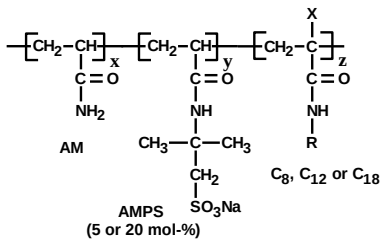

R	X	z (mol%)
C_8 : $C(CH_3)_2CH_2C(CH_3)_3$	H	0 or 0.5
C_{12} : $(CH_2)_{11}CH_3$,	CH_3	0, 0.1, 0.2, 0.5 or 1.0
C_{18} : $(CH_2)_{17}CH_3$,	H	0, 0.1, 0.2, 0.5 or 1.0

The method consists in the measurement of the apparent refractive index increment of the polymer-surfactant complex ($(dn/dc)_{app}$) in the mobile phase with surfactant by injecting different volumes of polymer-surfactant solution. The measurements are made using classical light scattering and concentration detectors such as multi-angle light scattering (MALS) and refractometer instruments.

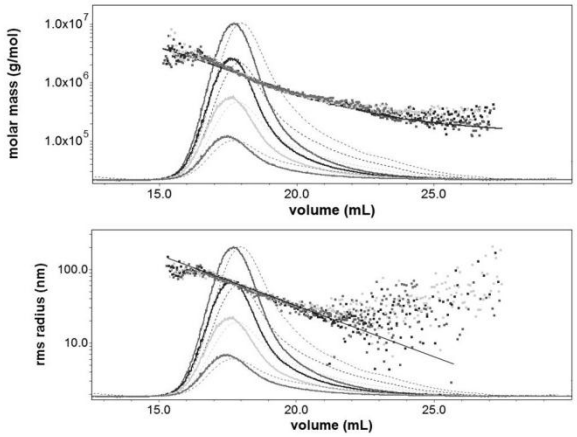

The figure above shows representative chromatograms obtained for a highly associative polymer (insoluble in aqueous media) along with molar mass and *rms* radius for four amounts of injected mass. The apparent *dn*/*dc* is determined by linearization of the refractometer surface signal and the injected mass. This value is used in the ASTRA software to extract the molar mass and the *rms* radius according to the following modified Zimm-Debye equation:

$$\left(\frac{K\left(\frac{dn}{dc}\right)_{app}^2 c_p}{I(q,c_{ps})}\right) = \frac{1}{M_{w,p}}\left(1+\frac{q^2R_{g,ps}^2}{3}\right)$$

The results are compared to those obtained by classical SEC in 0.1 M $NaNO_3$ and by static light scattering (SLS) in formamide solution. First of all, MSEC-MALS allows the characterization of all the samples even those insoluble in salt solution. Secondly, the values of the weight-average molar mass determined by each of the mentioned techniques are very close. Also comparing the results obtained from MSEC-MALS and SLS shows the non-retention of the surfactant-polymer complex on the columns.

Associated publication:

Dupuis et *al. Analytical Chemistry* **2009,** 81, (21), 8993-9001.

Characterization of Nanogels by a combination of Light and Small-Angle X-ray Scattering

G. Roshan Deen[1], Thomas Alsted[2], Walter Richtering[3], and Jan Skov Pedersen[2]

[1]Natural Sciences and Science Education, NIE, Nanyang Technological University, Singapore 637616.
[2]Department of Chemistry and Interdisciplinary Nanoscience Center (*iNANO*), Aarhus University, Aarhus Denmark.
[3]Institute of Physical Chemistry, RWTH Aachen University, Aachen, Germany.

Introduction

Polymer nanogels are cross-linked particles with a three-dimensional network structure that are swollen in a suitable solvent. Over the last decades these materials have been studied in relation to theoretical studies of soft matter and in applied fields such as in materials science for drug delivery, separation media, coatings, cosmetics, and sensors[1]. Depending on the type of monomers used in the synthesis of nanogels they can be made to respond to a variety of external stimuli such as pH, temperature, ionic strength, illumination, magnetic field etc [2,3]. Among the monomers reviewed in the sysnthesis of nanogels, *N*-isopropyl acrylamide (NIPAM) is the most widely studied owing to its excellent temperature-responsive behaviour.

In this work, thermo-responsive nanogels of PNIPAM were prepared by an emulsion polymerization method. The purpose of this work is to investigate the systematic influence of the added surfactant on the final size and structure of the nanogel particles. A further aim of the study is to demonstrate that the nanogels can be structurally characterized by a combination of static light scattering (SLS) and small-angle X-ray scattering (SAXS) techniques. This combination can be of a great advantage as SLS and SAXS are laboratory based techniques as opposed to small angle neutron scattering (SANS) that is carried out at large scale facilities.

Materials and Method

The nanogels particles were prepared by emulsion polymerization at 70 °C for 5 h. Different sizes of nanogels were obtained by systematically varying the amount of emulsifier in the reaction mixture. The reactants feed used in the synthesis of the nanogels are summarized in Table 1.

Table 1. Monomer feed ratios in the synthesis of nanogels at 70 °C.

Nanogel	NIPAM (g)	MBA (g)	SDS (g)	KPS (g)	Water (mL)
A	7.86	0.15	0.15	0.32	500
C	7.87	0.15	0.23	0.31	500
D	7.87	0.15	0.41	0.31	500

Static and dynamic light scattering measurements were performed on a commercially available instrument (ALV, Langen, Germany) consisting of an ALV/CGS-8F goniometer equipped with an ALV-6010/EPP multi-tau digital correlator. SAXS measurements were performed on the NanoSTAR instrument (Bruker AXS) at Aarhus University[4], which is optimized for solution scattering. The instrument in the high-resolution (low-*q*) configuration provides a range of scattering vector moduli *q* from 0.004 to 0.22 $Å^{-1}$ with a flux of 106 photons per second.

Results and Discussion

The light scattering results of the nanogels as function of emulsifier content are summarized in Table 2. With increase in the emulsifier content, nanogels of smaller size are obtained.

Table 2. Light scattering results of the nanogels in water (0.01 wt %) at 20 °C.

Nanogel	Emulsifier (g)	R_g (nm)	R_h (nm)[a]
A	0.15	117.7	153.0
C	0.30	97.2	119.0
D[b]	0.40	58.0	82.1

[a]measured at θ = 90°, [b]molar mass = 2.8×10^7 g mol^{-1}.

The combined SLS and SAXS data for the nanogel is shown in Figure 1 for the lowest (25 °C) and highest temperature (40 °C).

A very large change in the scattering with temperature is observed. One also sees a large difference in size between the two temperatures as the Guinier region is at much lower *q* values at 25 °C compared to 40 °C. The described model[6] fits the data very well at all temperatures. The radical volume fraction of the particles was also determined. At 25 °C, the particles are swollen with a broad graded outer surface. The values of *z*-average radius of gyration calculated agreed well with that obtained from Zimm analysis.

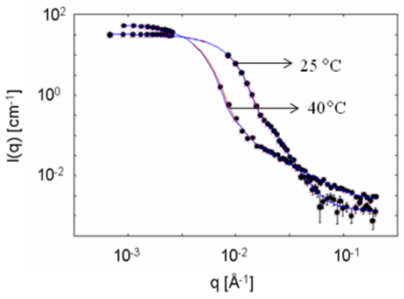

Figure 17 Combined SLS and DLS data for nanogel dispersion.

Conclusion

The combination of SLS and SAXS as applied to the microgels in the present study is an attractive method for particle characterization on a very broad length scale of almost three orders of magnitude as it spans a very large range of scattering vector from $q = 0.0004$ to 0.22 $Å^{-1}$.

References

1. M. Karg and T. Hellweg, *Curr. Opin. Colloid Interface Sci.*, 2009, 14, 438.
2. R. Pelton, *Adv. Colloid Interface Sci.*, 20008, 85, 1.
3. J. E. Wong and W. Richtering, *Curr. Opin. Colloid Interface Sci.*, 2008, 13, 403.
4. J.S. Pedersen, *J. Appl. Crystall.*, 2004, 37, 369.
5. M. Stieger, W. Richtering, J.S. Pedersen and P. Lindner, *J. Chem. Phys.*, 2004, 120, 6197.

Mechanism of degradation of acrylic-melamine thermoset. Relating material properties to structure evolutions.

J.-F. Larché[1,2], P.-O. Bussière[1,2], P. Wong-Wah-Chung[1,2], J.-L. Gardette[1,2]

1Clermont Université, Université Blaise Pascal, LPMM, BP 10448, F-63000 Clermont-Ferrand / 2CNRS, UMR 6505, LPMM, F-63173 Aubière

e-mail : p-olivier.bussiere@univ-bpclermont.fr

ABSTRACT

Several techniques were used to study the photo-oxidation of acrylic-melamine used for automotive applications: spectroscopy, micro-hardness, DMA, HS-SPME-GC-MS, and AFM. This set of attractive complementary techniques allows us to propose a new mechanism of degradation.. In order to quantify degradation, mechanical analysis were performed, which confirmed that crosslinking reactions are prevalent during ageing. Quantitative correlations were made between the main relevant criteria of degradation, from the chemical structure to the mechanical properties.

EXPERIMENTAL

A high solid thermoset acrylate polymer was used in this study. It was a solvent-based acrylic-melamine which is commonly employed as automotive clearcoat. It consists of a mixture of an acrylate-polyol copolymer and a butyl-oxylated melamine crosslinker.. Irradiations were carried out in artificial ageing conditions. The ageing device used was a SEPAP 12/24 [1] unit from Atlas.

RESULTS & DISCUSSION

1. Proposed mechanism of degradation of acrylic-melamine clearcoat

UV, IR and micro-hardness measurements of the irradiated samples were performed. The obtained results indicated that the degradation of the melamine ethers at 1085 cm^{-1}, the apparition of a CN bond at 1250 cm^{-1} and the increase of the micro-hardness are linked and can be directly correlated. On the basis of these results and on results obtained in previous works [2], we propose a new mechanism of degradation. As reported in scheme 1, this mechanism can explain the close relationship between the modifications of the chemical structure and the mechanical properties.

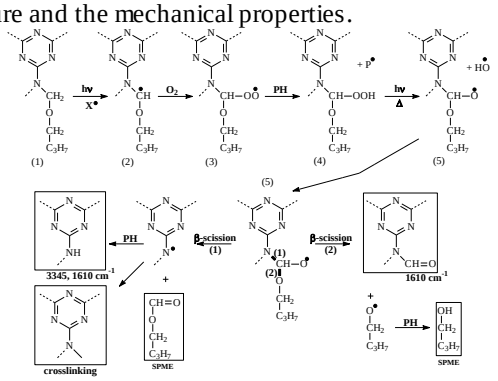

Sch. 1. Mechanism of photo-oxidation of acrylic-melamine.

2. Evolutions of the physical properties by DMA, DSC and AFM

DMA, DSC and AFM measurements were performed. By DMA, an increase of Tanδ, a decrease of Mc (average molecular weight between two crosslinking points) and so an increase of the crosslink density ρ was demonstrated. As shown in figure 1, these results were confirmed by the increase of Tg and surface hardness measured by DSC and AFM.

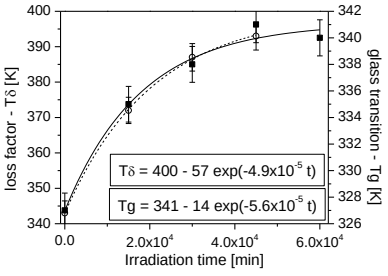

Fig. 1. Tg (black square) and Tδ (circles) versus irradiation time.

These sets of data, whatever the studied scale, confirm the network densification as well at the extreme surface of the clearcoat as in the bulk.

3. Calculation of correlation factors

Relationships between the molecular changes and the mechanical properties were attempted by using previous degradation criteria. Tg, Tan δ and micro-hardness were quantitatively correlated using *Fakirov et al.* [3] linear law. Different criteria (which were based on chemical, mechanical or physical properties) were studied using a first order kinetic law. The obtained degradation rates k were compared. As shown in table 1, very good agreement was found between all the data, which is consistent with the photo-oxidation mechanism proposed above. These kinetic constants were finally compared with k values from previous works [4-6] to validate our results.

Tab. 1. Degradation rates k for the various parameters.

Parameters	k ($min^{-1}.10^{-5}$)	standard error ($min^{-1}.10^{-5}$)	C.coeff - X^2
COC (1085cm^{-1})	4.5	± 0.1	1
CN (1250cm^{-1})	3.0	± 0.2	0.99
Hv	3.0	+/- 0.7/0.5	0.99
Tg	5.6	-	0.99
Tδ	4.9	-	1

CONCLUSIONS

This paper deals with the photo-oxidation of acrylic-melamine clearcoat. On the basis of both spectroscopic analysis/identification of the photoproducts and characterisation of the mechanical properties, we have shown that chain scissions process is not the predominant route of degradation. It has been shown that the increase of the mechanical properties can be attributed to the degradation of the residual unreacted melamine ethers, which induce the formation of new crosslinks. These new crosslinks lead to a global increase of the polymer network density, which explains the formation of cracks, as observed during the service life of coatings. We have also proved that all these evolutions are well correlated, from the microscopic scale to the macroscopic scale.

REFERENCES

[1] Lemaire J, Arnaud R, Gardette J-L. *Rev. Gen. Caout. Plast.* 1981 ;613 :87-92 / [2] Lemaire J, Siampiringue N. *Ser Life Pred Orgc Coat : ACS.* 1999:246-256 / [3] Fakirov S, Baltá Calleja FJ, Krumova M. *J. Polym. Sci. Pol. Phys.* 1999;37:1413-1419 / [4] Gerlock JL, Dean MJ, Korniski TJ, Bauer DR. *Ind. Eng. Chem. Prod. Res. Dev.* 1986;25:449-453 / [5] Luckey CA. *Prog. Org. Coat.* 2001;41:129-134

Keeping track of water in complex multilayered films with NMR imaging

H.P.Huinink[1], V. Baukh[1], S.J.F. Erich[1,2], O.C.G. Adan[1,2], L.G.J. van der Ven[3]

[1]Department of Applied Physics, Eindhoven University of Technology, Eindhoven, The Netherlands
[2]TNO, Delft, The Netherlands
[3]AkzoNobel Automotive & Aerospace Coatings, Sassenheim, The Netherlands

h.p.huinink@tue.nl

Introduction: Polymeric coatings are applied for esthetical and protective reasons on cars, planes, walls, etc. Good barrier properties for water are needed for protection. Several developments have renewed the interest in water migration. Coatings have become highly complex multilayered structures and the market has shifted to waterborne products, which are more susceptible to water. Standard techniques (gravimetry, EIS) only access average or surface properties (FTIR). They are useful for homogeneous single films, but data interpretation is difficult for multilayer and multiphasic films. Knowledge of the water distribution is crucial for better understanding. NMR imaging with a resolution of 3-5 µm is now possible with the GARField method [1]. Recently we have proven that this technique is very useful for studying cross-linking reactions in polymer layers [2] and water migration [3,4]. The presented study illustrates how water migration in multilayer coatings can be traced with NMR imaging.

Materials and methods: Water uptake and drying experiments were performed on two-layer polymeric films typical for automotive applications. In all cases the top coat (TC) was a cross-linked acrylic/PUR film and the base coat (BC) consisted of acrylic, polyurethane and pigment particles. Profiles with a resolution 5 µm were obtained with GARField NMR. Polymer-water interactions were studied on the basis of T_2 relaxation of the NMR signal.

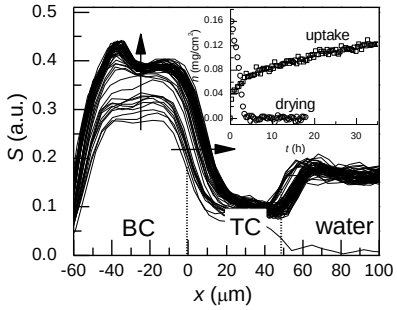

Figure 1 – *NMR profiles of a two-layer coating during water uptake. BC and TC refer to the base and top coat respectively. The vertical and horizontal arrows mark the water uptake and swelling of the BC layer. Total amounts of water in the BC layer during uptake and drying are plotted in the insert.*

Water migration: The measured signal profiles for water uptake in a typical sample are presented in the Fig.1. The base coat takes up water and swells. Water is already observed near the base coat/substrate interface in the first profiles, indicating a quick redistribution of water in this BC layer. Therefore, the kinetics of water uptake is determined by penetration through the top coat. The total amount of water in the base layer during uptake and drying is calculated from the profiles, see the insert of Fig. 1. Whereas uptake takes 100 hours before saturation, drying occurs in less then 5 hours. This asymmetry can be understood on the basis of the non-linear shape of the sorption isotherm.

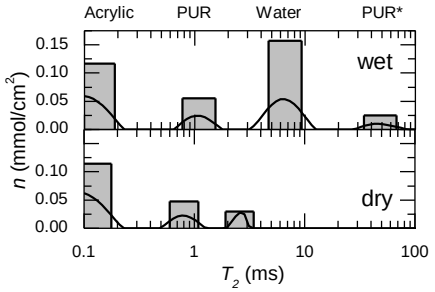

Figure 2 – *T_2 spectra of a wet (upper) and dry (lower) base coat. The lines represent spectra and the height of a bar is a measure for the intensity of a peak.*

State of water and plasticization: A typical T_2 relaxation spectrum of the wet base coat is shown in Fig. 2. Peaks of water, acrylic and the polyurethane phases are visible. The state of the water depends on the water content: the mobility of water strongly increases with the water content. Whereas at low water contents water is bounded to the polymer matrix, water is organised in big clusters at high water contents. In a completely saturated sample water has a diffusion constant a ten times smaller then the diffusion constant in liquid water. The spectra also make clear that the PUR particles in the base layer are plasticized by water.

Conclusion:
GARField NMR is very useful for probing water uptake in multilayer coatings. A huge difference in uptake and drying rates has been observed, which can be understood on the basis of the non-linear shape of the sorption isotherm.
The T_2 spectra show that water goes from a bound to a mobile state with increasing water content. Further, plasticization of the polyurethane particles is observed.
GARField NMR proves to be a versatile tool for studying water in coating films with a high spatial resolution.

References: [1] P.M. Glover et al., *A novel high-gradient permanent magnet for the profiling of planar films and coatings*, J. Mag. Res. 139, 90 (1999). [2] S.J.F. Erich et al.; *Comparison of NMR and confocal Raman microscopy as coatings research tools*, Prog. Org. Coat., 52, (2005). [3] V. Baukh et al., NMR *Imaging of Water Uptake in Multilayer Polymeric Films: Stressing the Role of Mechanical Stress*, Macromolecules, 43, 3882 (2010). [4] V. Baukh et al., *Water-polymer interaction during water uptake*, submitted (2011).

NMR for Determination the Structure of New Polysulfones

Gorbunova M., Vorob'eva A., Muslukhov R.

Institute of Technical Chemistry, Ural Branch of Russian Academy of Sciences
Institute of Organic Chemistry Ufa Scientific Centre of Russian Academy of Sciences

mngorb@newmail.ru

The primary motivation for determining the structure of a polymer chain is to relate the structure to the performance properties of the polymer in end use. If a polymer chain is completely characterized and the structural basis of its properties is known, the polymerization can be optimized and controlled to produce the best possible properties from the chemical system. NMR spectroscopy has proven to be the most effective technique in chemical structure characterization, which not only permits the determination of the copolymer composition but also provides information on detailed structure of the copolymer chains.

The interest in the purposive synthesis of polyfunctional polymers is growing steadily. It is conditioned by a wide set of useful properties of mentioned polymers [1–3]. Among allyl monomers only quaternary salts of diallylammonium found an application as monomers for the synthesis of polyfunctional polymers [4]. *N*-allyl derivatives of hydrazine, diethylaminoguanidine, aminophosphonium salts are promising as monomers from this point of view. Results of investigations concerning synthesis of new polysulphones and determination of their structure by NMR are shown in presented paper.

Allyl compounds, destinguished by a tendency to degradative chain transfer to the monomer, are known to exhibit low activity in reactions of radical polymerization [5]. It was determined that new monomers – *N,N*-diallyl-*N'*-acylhydrazines, 2,2-diallyl-1,1,3,3-tetraethylguanidiniumchloride, tris(diethylamino) diallylaminophosphonium tetrafluoroborate and chloride are active in copolymerization with sulphur dioxide exhibiting high electron-acceptor activity. The study of copolymerization of new monomers with SO_2 showed the content of copolymers obtained to be of no dependence on the monomers ratio, reaction conditions - temperature, nature of initiator, medium, polymerization degree and to correspond to DAAH:SO_2 ratio 1 to 1.

Composition constancy regardless of the monomer ratio in the reaction mixture allowed to suppose that copolymerization of new allyl monomers with SO_2 proceed via formation of the complexes.

The shifts of the signals of the double bond carbon atoms denote distribution of π-electron density in molecule and formation of donor-acceptor complex [monomer···SO_2]. Magnetic equivalence of the carbon atoms of allyl groups indicates the complex structure to be symmetric.

The carried out investigations have shown that these new allyl monomers copolymerize with SO_2 both double bonds participating with formation of cis-, trans-stereoisomeric pyrrolidine structures in a cyclolinear polymer chain. The cyclolinear copolymers obtained are soluble due to the intramolecular cyclization of allyl monomers during the formation of the polymer chain and to the absence of intermolecular crosslinks.

Our results indicate that the proposed approach based on ^{13}C NMR - spectroscopy is suitable for the characterization of new polysulphones.

Financial support by the Russian Foundation for Basic Reseach (grant № 09-03-00220) is gratefully acknowledged.

References

1. Kirsh, Yu.E.. 1988. Poly-N-vinylpyrrolidone and other poly-N-vinylamides: Synthesis and physico-chemical properties. p. 252. Moscow: Nauka.
2. Al-Issa, M.A., Davis, T.P., Huglin, M.B., Yip, D.C.F. 1985. Polymer. 26: 1869 – 1874.
3. Soundararajan, S., Reddy, B.S.R. 1993. Polymer. 34: 2224 – 2226.
4. Vorob'eva, A.I., Prochuhan, Yu.A., Monakov, Yu.B. 2003. Polymer sci. 45: 2118-2136.
5. Kabanov, V.A., Zubov, V.P., Semchikov, Yu.D. 1987. Complex-radical polymerization. p. 256. Moscow: Khimiya.

The glass transition of thin polymer films – heterogeneity studies using single molecule fluorescence spectroscopy

Dominik Wöll,[1,2] *Bente Flier*,[2] *Moritz Baier*,[2] *Stefan Mecking*,[2] *Klaus Müllen*,[3] *Andreas Zumbusch*[2]

[1] Zukunftskolleg, University of Konstanz
[2] Faculty of Chemistry, University of Konstanz
[3] Max-Planck-Institute for Polymer Research, Mainz

dominik.woell@uni-konstanz.de

Introduction

The glass transition is a ubiquitous phenomenon in many materials.[1] Despite its high importance and considerable research efforts, a full understanding of this property is still lacking. In thin polymer films, interfaces complicate things as they alter the glass transition in their vicinity. Experimental approaches to study the influence of interfaces on relaxation of polymer chains are thus very challenging.[2] As a result, the glass transition at interfaces has mainly been investigated using simulations.[3]
In our contribution, we present single molecules fluorescence spectroscopy as a new methods to investigate such interfacial effects on the glass transition of polymers.

Materials and Methods

Polystyrene (M_W = 3000 g/mol, polydispersity = 1.07, bulk T_g 69 °C) was dissolved in toluene, and a sub-nM amount of perylene diimide derivatives was added as fluorescent probes. This solution was spin-coated onto ITO-glass slides, and the film tension was allowed to relaxed at 80 °C for 24 h. The fluorescence of single molecules was observed using a fluorescence microscope set to widefield-illumination and recorded with a CCD camera. Observation of the motion of single molecules at different temperatures and tracking of their motion allowed us to determine the distribution of their diffusion coefficients. To investigate the influence of the interfaces, different film thicknesses were prepared and measured. Their thickness was determined using AFM.

Results and discussion

The dynamics of single perylene diimide dye molecules embedded in a thin polystyrene film was detected using widefield fluorescence microscopy. We measured the translational diffusion coefficients of single dye molecules in thin polystyrene films up to temperatures of 150 °C and analyzed their distributions. It was shown that translational motion of different molecules was homogeneous at high temperatures and became heterogeneous at T < 105 °C.[4] We attribute the observation of heterogeneities to differences in the glass transition temperature T_g which is known to vary in the vicinity of interfaces (in our case the polymer-air and the silicon glass-polymer interface).

At high temperatures the T_g profile is obscured since the function of viscosity versus temperature is rather flat in this range. Thus, we found a homogeneous distribution of single molecule diffusion coefficients. However, when the temperature approaches bulk T_g, the molecules gradually become immobile starting from high T_g regions in the center of the film to low T_g regions at its polymer-air interface. This distance dependent relaxation time profile of the film results in significant spatial heterogeneity of single molecule motion (see Figure).

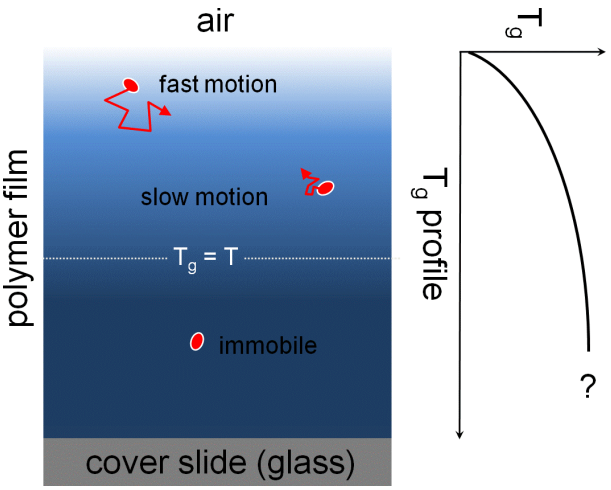

We found that interface effects in our systems reach quite far, up to ca. 100 nm, into the polymer films. Assuming a homogeneous distribution of dye molecules in the polymer film, we could construct a T_g profile and compare these profiles for films of different thicknesses.

Conclusion

We demonstrated the power of single molecule fluorescence microscopy to investigate interface-dependent glass transition profiles in thin polymer films. Our results show that surface effects have to be accounted for when motion in thin polymer films is measured and conclusions on heterogeneities are drawn.

References

[1] E. Donth, *The Glass Transition - Relaxation Dynamics in Liquid and Disordered Materials*, Spinger **2001**.
[2] C. J. Ellison, J. M. Torkelson, *Nat. Mater.* **2003**, 2, 695.
[3] J. L. Barrat, J. Baschnagel, A. Lyulin, *Soft Matter* **2010**, 6, 3430.
[4] B. M. I. Flier, M. Baier, J. Huber, K. Müllen, S. Mecking, A. Zumbusch, D. Wöll, Phys. Chem. Chem. Phys. **2011**, DOI:10.1039/C0CP01801E

TD-NMR investigation of nanoconfined soft phase in SEBS.

Michele Mauri, *Lucio Mauri and Roberto Simonutti*

Dipartimento di Scienza dei Materiali, Università di Milano-Bicocca, Via R. Cozzi 53 20125 Milano (Italy)

michele.mauri@mater.unimib.it

Introduction: Polymer chain dynamics can be investigated effectively by Time-Domain NMR (TD-NMR). The application of advanced pulse sequences based on exciting multiple-quantum coherences provides rich information, like crosslink density in rubbers, even with moderate technical requirements (e.g. low magnetic field). In this work we address directly the mobility of soft ethylene-butilene phases confined by glassy polystyrene (PS) blocks.

Materials and Methods: We studied two samples of polystyrene-block-poly(ethylene-co-bu-1-ene)-block-polystyrene triblock copolymers (SEBS) with 20 and 65% (mol) butene content in the midblock. Samples were cast from toluene, letting polymer organize in the lamellar morphology. [1] TEM and SAXS confirmed a lamellar structure, with alternating PS and EB blocks with few nanometers thickness. All TD-NMR experiments were performed on a Bruker Minispec mq20. DSC was performed with a Mettler-Toledo calorimeter, at 10 K/min.

Results and Discussion:
DSC analysis (Fig. 1) showed a broad endothermic transition in the sample with 20% butene (SEBS_L) upon heating from 221K to 300K. The transition was absent in the high butene copolymer (SEBS_H) that displays only a T_g at around 230K.

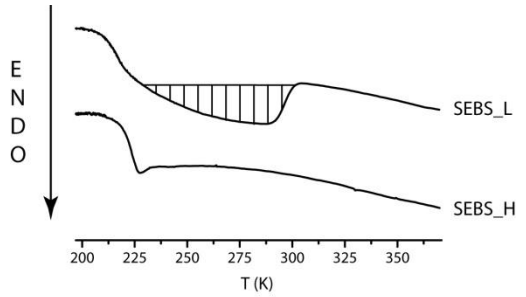

Figure 1: Comparison of thermal analysis of the copolymer samples. SEBS_H and SEBS_L contain High and Low percentage of butyl respectively.

This peculiar transition was observed in literature [2] and attributed, on the basis of indirect evidence, to a complex pseudo crystalline rearrangement of the mobile phase starting immediately above the glass transition.
Between 230 and 370K, the PS layers are below T_g and have a distinctively short T_2 while EB phase is comparatively softer, and can be investigated in depth by MQ experiments. Double quantum coherence intensity (DQ) of the mobile phase alone is normalized against a reference curve [3] and plotted versus excitation time in Fig. 2. The resulting dataset was fitted as a sum of contributions from protons with different residual dipolar coupling (D_{res}). Tichonov regularization procedure provides a distribution of D_{res} without any preliminary assumption on its functional form.

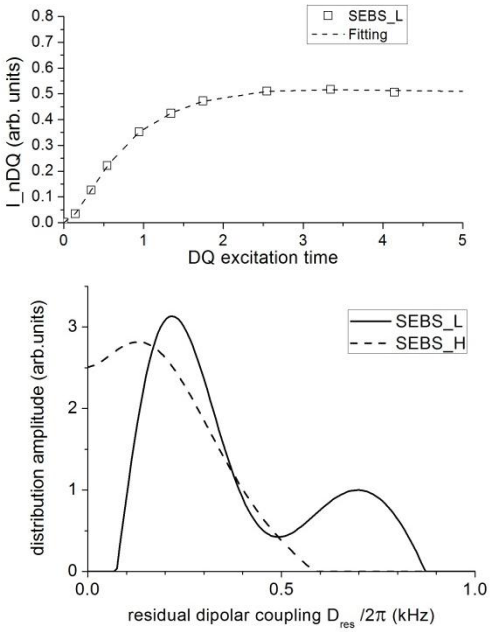

Figure 2: (above) best fitting of the normalized DQ intensity. (below) RDC distribution at 353K for the two samples.

In SEBS_H the D_{res} are rather disperse but centered around a single value. SEBS_L instead has a bimodal distribution. Because of the extremely high number of butyl side chains in the SEBS_H, the mobile phase is fully amorphous. SEBS_L, while having a number of bulky side groups that is too large for proper crystallization, exhibits areas of increased order that are compatible with a rotator phase.

Conclusions:
TD-NMR relaxometry of the EB phase of SEBS_L detects the presence of two populations of protons that are distinguished by their motional regime. This behaviour, reminiscent of EP copolymer rotator phase, is recorded directly for the first time and is probably made possible by tethering of the EB chains on both sides to PS blocks and by the resulting confinement.

Acknowledgements: We thank Prof. Kay Saalwaechter and Walter Chassé for kindly providing the nDQ fitting program and for inspiring discussion.

References:
[1] Jeong, U.; Lee, H. H.; Yang, H.; Kim, J. K. *Macromolecules* **2003**, 36, 1685-1693
[2] Fredrikson, G.H. And Bates, F.S. *Annu. Rev. Mat. Sci.* **1996**, *26*, 501-526.
[3] Saalwaechter, K. *Prog. Nucl. Mag. Reson.* **2007**, *51*, 1-35.

"Kinetics of the Aqueous phase polymerization of N-Vinylformamide "

Julieta Zataray, José Carlos De la Cal, Jose Ramon Leiza

POLYMAT-The University of the Basque Country

julietapaulina.zataray@ehu.es

INTRODUCTION

Functional polymers such as polyacrylamides, poly(N-vinylamides), poly(acrylic acid), and their copolymers find widespread applications in pharmaceuticals, waste water treatment, consumer products, paper manufacturing, and cosmetics.[1] These polymers are mostly produced by free-radical polymerization. Despite their importance, the reaction systems have been the focus of only a relative small number of academic studies.

N-Vinylformamide (NVF) is an isomer of acrylamide, is of interest because it has low toxicity, and high reactivity for homo- and copolymerization.[2] The monomer was developed as a precursor for the synthesis polyvinylamine.[3]

The goal of the present work was to study the kinetics and the mechanisms involved in the polymerization of NVF in aqueous media. For this purpose, the effect of temperature, concentration of initiator and concentration of NVF in the kinetics and molecular weight distribution (MWD) of the polyNVF produced was experimentally assessed.

A mathematical model to predict the kinetics and MWD for the aqueous phase polymerization of NVF has been developed.

MATERIALS AND METHODS

NVF monomer (Aldrich inc.) was distilled under vacuum and stored at ≤10˚C before polymerization. The free radical initiator, 2,2'-azobis(2-methylpropio-namidine)dihydrochloride (AIBA) (Aldrich Inc.) was used as received. Distilled water was used for the preparation of the polymerization solutions.

Monomer in distilled water was heated to the reaction temperature under constant stirring and nitrogen atmosphere. Once the reaction temperature was reached to the set value, polymerization was initiated by the addition of a know amount of AIBA initiator in distilled water.

All the experiments were carried out in a commercial calorimetric reactor (RC1, Mettler-Toledo). The thermal polymerization conversion was determined by the integration of the heat generation rate.

SEC-MALS for the MWD analysis was performed in the mixed eluent water/acetonitrile.

RESULTS AND DISCUSSION

The kinetics and MWD obtained in the experiments carried out at different temperatures ([I]=1.47 x 10^{-3} mol•l^{-1} and [M]=1.27 mol•l^{-1} or 9 wt%) and at different initiator concentrations ([M]=1.27 mol•l^{-1} or 9 wt% and 70˚C) presented the expected trend, which is increasing temperature and initiator concentration the polymerization rate increased and the molecular weights decreased. However, by increasing the monomer concentration the results were not expected. The conversions and Mw of the experiments were the concentration of the monomer was varied, is presented in figure 1.

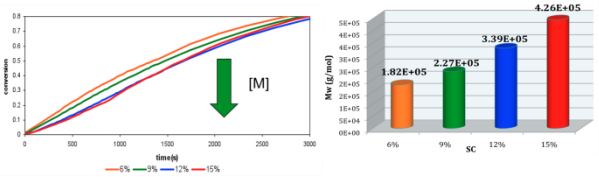

Fig.1.Time evolution of the thermal conversion (left) and Mw (right) of NVF aqueous solution polymerization, [I]=1.47x10-3 mol•L-1,T=70˚C.

As it can be seen in the conversion plot, the conventional solution polymerization was not as expected.

The mathematical model was used to analyze the whole set of experiment results. It was found that the model predicts all the trends observed when the propagation rate coefficient (Kp) was considered to depend on the temperature and monomer concentration (recently reported by PLP-SEC studies [4]) and chain transfer to polymers was taking into account.

CONCLUSIONS

Free radical polymerization kinetics of NVF was investigated in aqueous phase.

It was found that behavior of this polymerization differs from the conventional solution polymerization in organic solvents. This feature is consistent with the results previously obtained for other water-soluble monomers like non-ionized methacrylic acid, and N-Vinyl pyrrolidone [5]

REFERENCES

[1] Z.Amjad,Water Soluble Polymers: Solution properties and Applications, Plenum Press, New York.

[2] K.B MacAuley, J. Physics, 2004, 3,29-33.

[3] K.Marcus, H. Corneliu, D. Rainer, B.Klaus, M. Angew, Chem Int Ed. 2003,42,4687-4690.

[4] M.Stach,I. Lacik,P. Kasak,D.Chorvat,A.J.Sauders,S. Santanakrishnan,R.A.Hutchinson,Macromol.Chem.Phys20 10,211,580-593

[5] S.Santanakrishnan,L.Tang,R.A.Hutchinson,M.Stach, I.Lacik,J.Schrooten,P.Hesse,M.Buback,Macromol. React.Eng, 2010,4,499-509.

Characterization of Polyfurfuryl Alcohol Resin - A New Biomass-Based Resin for Advanced Composite Materials

Domínguez, J.C.; Madsen, B.

Materials Research Division, Risø National Laboratory for Sustainable Energy, Technical University of Denmark, Frederiksborgvej 399, DK-4000 Roskilde, Denmark

jucar@risoe.dtu.dk

Furfuryl alcohol is the most widely used furanic compound for production of resins due to the simple reduction process used for its synthesis from furfural.[1] Furfural can be obtained from pentosan-rich biomass, such as sugar cane bagasse. Therefore, polyfurfuryl alcohol resins, produced from furfuryl alcohol monomer through condensation reactions, become a relatively cheap and easily produced eco-friendly type of thermosetting polymer that can be used to manufacture advanced composite materials for structural applications, such as rotor blades for wind turbines. The furan resin composites can be reinforced with traditional fibres such as carbon and glass fibres, or with natural fibres such as flax and jute fibres to make fully biomass-based composite materials.

The process development of composite materials is traditionally performed by a trial-and-error methodology based on practical experience. This methodology can be expensive and time-consuming and, ultimately, the developed composite materials might not be fully optimised. Therefore, a more rational and scientific methodology is needed to establish the optimal processing conditions with a reduced amount of experimental work. A general model for the process development of composite materials which includes several sub-models was proposed by Kenny (see Figure 1).[2]

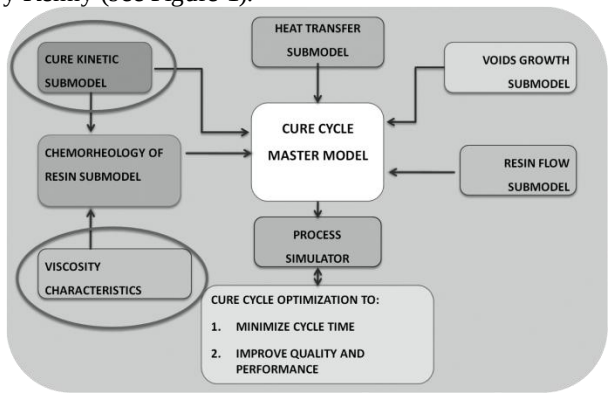

Fig. 1. General model for process development of composite materials.[2]

In order to develop such a process model, knowledge of the chemical and physical phenomena that govern the behaviour of the resin when used as matrix in the composite should be achieved. Thus, initial characterization of the resin is essential to enable a correct choice of operating conditions used in the manufacturing process of the composite materials.

The work presented here is part of a larger study of polyfurfuryl alcohol resin. It involves the determination of the curing kinetics of the resin, as well as its rheological and chemorheological parameters (the boxes indicated by ellipses in Figure 1).

Polyfurfuryl alcohol (FA) resin was supplied by TransFurans Chemicals BVBA (Belgium). The kinetics of the curing process of the FA resin was studied using a STA449 F1 Jupiter TGA-DSC equipment with low pressure pans. Non-isothermal DSC runs were carried out from 30 to 250°C using seven different heating ramps under Ar atmosphere: 4, 6, 8, 10, 12, 16 and 20°C/min. Sample weight was fixed between 30 and 35mg. Three different amounts of catalyst were tested: 2, 4 and 6% w/w.

Rheological runs were performed using an AR Rheometer with either a 25 or a 60 mm ϕ upper plate and a peltier lower plate. Normal force was zeroed and fixed during the tests to prevent contact loss between sample and plates. Gap was changed automatically to maintain constant normal force.

An nth order model was applied to analyse the values of the degree-of-cure of the resin obtained from the DSC curves. The values of the activation energies calculated for the curing of the FA resin were in the range between 187 and 193 kJ/mol for the amounts of catalyst tested.

The viscosity of the FA resin as a function of temperature was found to be linear in the range from 0 to ca. 30°C, as predicted by the Andrade model. As the temperature is increased above 30°C, the relation begins to deviate from being linear. This deviation may be due to that the tested temperature range is within the range T_g+100°C. Therefore, a WLF model was applied to the measured viscosities as well as a VTF model to describe the viscosity dependence on temperature of the FA resin.

Future work is planned to complete the characterization of the FA resin by isoconversional methods. In addition, the chemorheological behaviour of the resin will be analyzed. Finally, the general process model will be used to select the best possible operating conditions for the manufacturing of FA resin composite materials.

Acknowledgement:

The authors are grateful for the support from "Ministerio de Educación" (Spanish Government) for financial support (Programa Nacional de Movilidad de Recursos Humanos del Plan Nacional de I-D+i 2008-2011). The research has been funded by the European Community's Seventh Framework Programme (FP7/2007-2013) under grant agreement nº 210037 (WOODY).

References:

1. Gandini, A.; Belgacem, M. N. Prog Polym Sci 1997, 22, 1203-1379.
2. Kenny, J. M. Compos Struct 1994, 27, 129-139.

Effect of architecture and molecular weight of PEO based electrolytes on the ionic conductivity and viscosity.

Didier Devaux, David Glé, Trang Phan, Renaud Denoyel, Denis Bertin, Didier Gigmes, Renaud Bouchet

Laboratoire Chimie Provence - UMR 6264
Université Aix-Marseille, centre St Jérôme
13397 Marseille Cedex 20 - France

Didier.devaux@etu.univ-provence.fr

Safety is the ever-growing concern in electrochemical energy storage systems with, for example in liquid electrolyte battery technologies, the possibility of leaks, flammable reaction products and internal short-circuits. A solution to this problem is the development of solid polymer electrolytes (SPE). In fact, the major drawback of SPE is that mechanical strength and conductivity generally vary in opposite manner. Ionic conduction in solid polymer electrolytes depends on the movement of polymer chains [1]. High chain mobility results in high ionic conductivity but poor mechanical properties. Therefore, both properties are usually in conflict. Among the dry SPE materials available, poly(ethylene oxide) PEO and its derivatives are the most widely studied because PEO contains ether coordination sites and has a flexible macromolecular structure, which assists in dissociation of salts and improves ionic transport. A strong research effort has been devoted to the improvement of not only the ionic conductivity but also of the mechanical strength of PEO based polymer electrolytes at room temperature. Notably to improve the mechanical properties of low molecular weight (M_w) PEO, many attempts have been made to graft it to a synthetic polymer backbone to produce block copolymers [2] or comb-like polymers [3, 4]. The idea is that the polymer backbone gives the mechanical stability while preserving locally the high molecular dynamics of the small grafted PEO chains. Despite many efforts were devoted in this direction, up to now, none of the systems proposed in the literature fulfils the targeted criteria. The objective of the study is thus to model at a given temperature the ionic conductivity of such polymeric systems depending on their overall architecture and molecular weight.

For this purpose, we studied the ionic conductivity of model electrolytes based on linear PEO complexes with LiTFSI in comparison with the results of branched poly[(meth)acrylate of ethylene oxide] doped with the Li salt, using different lengths of grafted EO as well as different molecular weights. Isotherms conductivity at different temperatures enable to monitor the influence of the EO chain length and the impact of the macromolecular architecture (linear vs. branched). Based on the seminal work of Shi and Vincent[1], the data are modelled using a molecular dynamic concept in polymers which is:

- Above a critical weight, M_w^*, (called De Gennes region [5]) the conductivity is considered as constant due to chain entanglement. The backbone flexibility pilots the chain dynamic leading to the introduction of a specific excluded volume concept which depends on the architecture of the host polymer.

- Below M_w^* (called Rouse region [6]), the conductivity decreases linearly with $1/M_w$. In this domain, the macromolecular friction coefficient and the impact of the end-groups, determined by rheological experiments, significantly affect the ionic dynamic.

References:

[1] J. Shi and C. A. Vincent, Solid State Ionics 60 (1993) 11.
[2] A. Ghosh and P. Kofinas, ECS Transactions 11 (2008) 131.
[3] W-H.Hou, C-Y. Chen, C-C. Wang, Y-H. Huang, Electrochimica Acta 48 (2003) 679.
[4] Y.-H. Liang et al., European Polymer Journal 44 (2008) 2376.
[5] P.G. de Gennes, J. Chem. Phys. 55 (1971) 572.
[6] P.E. Rouse, J. Chem. Phys. 21 (1953) 1272.

Investigation of the morphology of elastomeric blends

M. Merlin[1,2], J.C. Majesté[1], C. Carrot[1], V. Pelissier[2], M. Eloy[2], I. Anselme-Bertrand[3]

[1] Université de Lyon, F-42023, Saint Etienne, France ; CNRS UMR 5223, IMP@UJM, France ; Université de Saint Etienne, Jean Monnet, F-42023, Saint Etienne, France.
[2] MFP Michelin, Centre de Technologie de Ladoux, 63040 Clermont-Ferrand Cedex 9, France.
[3]Centre de Microscopie Electronique Stéphanois, Université Jean Monnet, 42023 Saint Etienne Cedex 2, France.

Contact : marie.merlin@univ-st-etienne.fr

Introduction : Elastomeric blends are frequently used in the rubber industry, especially in tire manufacturing, in order to balance the properties that can not be obtained with any single elastomer. Such compounds can be used notably for tire tread band. The aim of this work is to investigate the morphology of two types of blends and to find a relation, as general as possible, between morphology and properties.

Materials and Methods : Three elastomers were used for this study : polybutadiene CB 22 (high 1,4-cis isomer) from Bayer (PB), styrene butadiene rubber (SBR) and natural rubber (NR), both supplied by Michelin. Two types of blends were realised in an internal mixer (Rheomix R600) at 80°C with a filling factor of 70 % : PB/SBR and NR/SBR from 100wt % PB and NR to 100wt % SBR by steps of 10 % (weight fraction). In this study, the blends are uncured and unfilled. All these blends were analysed by differential scanning calorimetry (DSC Q10 from TA Instruments) between -170°C and 100°C under helium with a 25mL/min flow. Solid state rheology was carried out between -130°C and 0°C with a strain control (ARES from Rheometrics). Pictures of morphology (for NR/SBR blends) were obtained by transmission electron microscopy (Hitachi H800-3) with a 200kV acceleration voltage. For the TEM analysis, samples were prepared with an ultra-cryomicrotome, at -120°C with a diamond knife.

Results and Discussion :

In the PB/SBR blends case, the microscopy [1] and the melt state rheology [2] were not relevant. There was no contrast between the two phases and no extra-elasticity of the storage modulus G' at low frequencies. However, some important variations of glass transition temperature, Tg PB and crystallization temperature, Tc PB, were observed in solid state rheology and DSC, respectively. These changes in Tg are linked with a change of morphology and/or a composition effect. These variations originate from the difference between the volume expansion coefficients of the two elastomers [3]. Three domains which correspond to different morphologies are observed : a droplet/matrix system under 30wt % and over 65wt % of SBR. These limits are confirmed by the selective extraction of the SBR phase. The DSC analysis shows a strong decrease of Tc PB when the quantity of SBR increases in the blend, which is explained by a partial miscibility of the two components. (This drop in Tc can not be explained by confined cristallization for low fractions of SBR) [4]. This partial miscibility leads to an interphase between the two components. The superposition of these results highlights a complex morphology with droplet/matrix systems which border a complex transition with interphases percolation (between 30wt % and 65wt % of SBR).

In the NR/SBR blends case, the close chemical structure prevents the selective solvent extraction, and none of the components crystallize. Nevertheless, the variation of Tg NR is similar to the one of Tg PB previously observed in solid state rheology. These variations of Tg NR show a change of morphology around 25wt % and 60wt % of SBR. The two elastomers NR and SBR are totally immiscible so the TEM analysis give good micrographs of the morphology over the entire composition range of NR/SBR compounds. The TEM micrographs are in good agreement with the solid state rheology results. The morphology changes from a droplet/matrix system to a co-continuity-like morphology and then a matrix/droplet system.

Conclusions : The superposition of different analytical methods was necessary for having an overview of the morphology of PB/SBR and NR/SBR blends on the entire composition range. The Tg from solid state rheology is a new way for investigating the morphology of elastomer blends. The knowledge of the morphology will now be used for studying the influence of fillers on the morphology. Carbon black will be added to these compounds. Its location and the blends morphology will be studied.

References

[1] S.C. George, K.N. Ninan, G. Groeninckx, S. Thomas, *J. Appl. Polym. Sci.*, 78, 1280-1303, **2000**.

[2] S. Chaput, C. Carrot, M. Castro et F. Prochazka, *Rheol. Acta*, 43, 417-426, **2004**.

[3] F.S. Bates, R.E. Cohen et A.S. Argon, *Macromolecules*, 16, 1108-1114, **1983**

[4] J. Portal, C. Carrot, J.C. Majeste, S. Cocard, V. Pelissier, I. Anselme-Bertrand, *Polym. Eng. Sci.*, 49, 1544-1552, **2009**.

Non-linear rheological parameters for characterization of molecular structural properties in polyolefins

K. Klimke, S. Filipe, A.T. Tran

Borealis Polyolefine GmbH,
Innovation & Technology,
St.-Peter- Strasse 25, 4021 Linz, Austria

katja.klimke@borealisgroup.com

Introduction: The appropriate tailoring of molecular structure and topology requires suitable and sensitive analytical techniques with the ability to provide insight into the amount and type of long-chain branching (LCB) incorporated during either in-reactor polymerization or post-reactor modification.

Materials and Methods: A series of different industrial polyethylene and polypropylene based systems were analyzed with respect to their rheological behavior under both uniaxial extensional flows and Large Amplitude Oscillatory Shear (LAOS). The uniaxial extensional flow experiments were used to calculate the Strain Hardening Factors (SHF) while the LAOS experiments measured the LAOS Non-Linearity Factors (LAOS-NLF).

Results and Discussion:

SHF: The SHF parameter provides a measure of the non-linearity in a material by calculating the deviation of the uniaxial extensional viscosity with respect to the linear viscoelastic envelope (LVE) [1, 2].

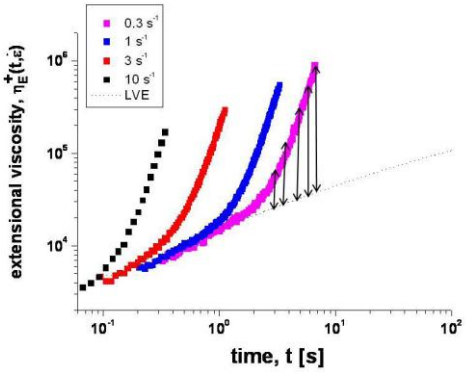

It was found that the SHF parameter can provide not only a quantitative but also a qualitative description of LCB.

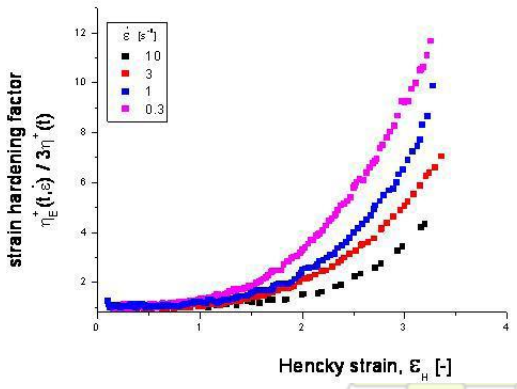

The absolute SHF values were found to increase with increasing LCB content (as measured via the standard Rheotens method). However, additional analysis of the complete set of SHF curves, measured at different Hencky strain rates, also allowed insight into the quality or "homogeneity" of the branching.

LAOS-NLF: The LAOS-NLF parameter detects the non-linearity in a material under shear and is an indirect measure of the amount of LCB in the system [3, 4].

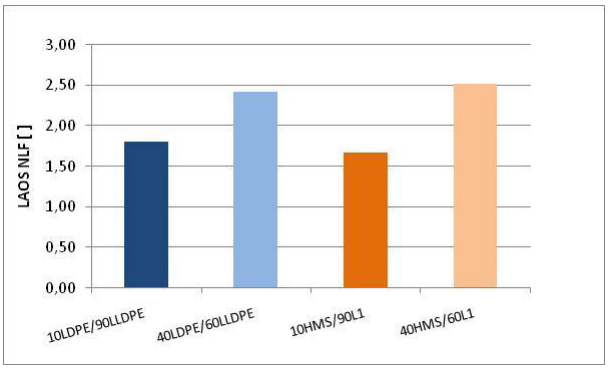

The LAOS-NLF parameter was found to provide a good quantitative description of LCB. The measured LAOS-NLF values correlated well with the LCB content. Due to its high speed and accuracy the LAOS-NLF method also has the potential to be used for quality control purposes.

Conclusions: A qualitative and quantitative description of the molecular topology for both polyethylene and polypropylene was shown to be possible by the use of specific non-linear rheological parameters determined from uniaxial extensional flow and LAOS experiments.

References:

1. E. Kabamba et al, Polym. Eng. Sci. 48, 11 (2008)
2. S. Filipe et al., Appl. Rheo. 19, 23345 (2009)
3. I. Vittorias et al., Macrom. Mat. Eng. 292, 935 (2007)
4. S. Filipe et al., Macrom. Mat. Eng. 293, 57 (2008)

Rheology Behavior and study of Payne Effect in natural Rubber/Regenerated Cellulose/ Montmorillonite clay nanocomposites

Roberta M. Mariano (MSc.)[1], *Regina C. R. Nunes*[1]*(DSc.), *Leila L. Y. Visconte*[1] (DSc.)

[1] Universidade Federal do Rio de Janeiro/ Instituto de Macromoléculas Professora Eloísa Mano, Caixa Postal 68.525, 21.970-170 Rio de Janeiro, RJ;

e-mail: *rcnunes@ima.ufrj.br

Introduction

Sodium montmorillonite (Na-MMT) clay minerals have been used as reinforcement in rubber compositions *in nature* and in the organofilled form [1]. By exfoliating these layered silicates in water, which is accomplished by mechanical stirring at high speeds, it is possible to have the separated layers of Na-MMT and the formation of an aqueous suspension. This exfoliation process of Na-MMT can be observed by wide angle x-ray diffraction [2]. The gain in strength given by the clay-rubber nanocomposites is attributed to the structure resulting from the rubber and clay, built during processing [1,2].

Natural rubber (NR) elastomeric nanocomposites with regenerated cellulose (CEL) have been developing by this research group allowing that two polymers, one amorphous (NR) and other extremely crystalline, are incorporated in nanomaterial forms showing good physical and mechanical properties [3]

In this work, Na-MMT clay was added as filler, to nanocomposites of NR and CEL II (regenerated cellulose) in amounts varying from 0 to 5 phr (per hundred resin). NR/CELII/MMT nanocomposites were prepared by co-coagulating NR latex, montmorillonite aqueous suspension and cellulose xanthate.

Materials and Methods

Natural rubber latex (solid content 61.9%) was kindly supplied by Comércio e Beneficiamento de Látex Talismã Ltda – São Paulo, Brazil; Na-montmorillonite (Na-MMT) (Volclay SPV 200) from Wyoming, EUA was provided by Bentonit União Nordeste S. A.; and cellulose xanthate (cellulose content 9.8%) by Vicunha Têxtil S/A, São Paulo, Brazil. The vulcanizing ingredients and others additives were used as received.

Na-MMT was purified according to the literature [4]. The clay was previously exfoliated in water and the resulting suspension was then added to the mixture of NR latex with cellulose xanthate.

Results and discussion

Morphological and mechanical properties of the NR nanocomposites with and without cellulose were evaluated and an increase in tensile strength, elastic modulus as well as tear strength were observed. The rheological properties were also studied. It was observed that the addition of cellulose to NR / MMT compositions promoted increase in storage modulus as well as in the other parameters studied. By studying the Payne effect it was observed good filler-filler and filler-matrix interactions, thus allowing the identification of the best clay content to be present in the elastomeric composition [5]. Figure 1 shows the variation of storage modulus with the amplitude of deformation. It can be observed an increase in storage modulus on increasing MMT addition, attributed to the occurrence of the Payne Effect. The graph shows that the concentration limit of MMT addition is 3 phr.

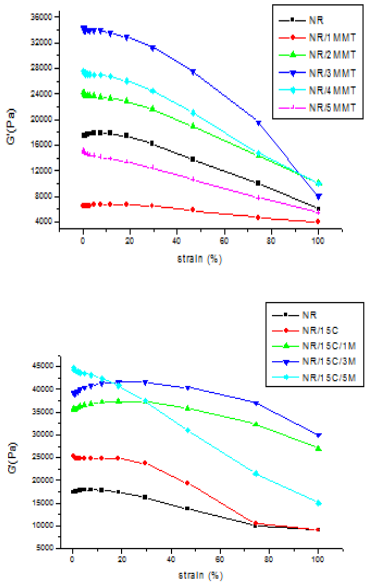

Figure 1. Payne effect study by strain sweep analysis of NR/CELII/clay nanocomposites.

Conclusions

The results show the advantage in using cellulose as a nanopolymer as well as MMT as nanofiller. The results showed that the concentration limit of MMT addition is 3 phr, which corroborates the XRD analysis. This effect can also be found in other compositions with addition of cellulose.

References

[1] Wang, Y.; Zhang, H.; Wu, Y.; Yang, J.; Zhang, L. J Appl Polym Sci 2005, 96, 318.

[2] Y. Kojima; A. Usuhi; M. Kawasumi; A. Okada; T. Kurauchi; O. Kamigaito *J. Appl. Polym. Sci.* 1993, 49, 1259.

[3] Reis-Nunes, R. C.; Compañ, V.; Riande, E.; "*Gas Transport in Vulcanized Natural Rubber-Cellulose. II. Composites*", **Journal of Polymer Science: Part B: Polymer Physics 38**, p. 393 – 402, 2000.

[4] Ferreira, H. S.; Menezes, R. R.; Ferreira, H. S.; Martins, A. B.; Neves, G. A.; Ferreira, H. C. Cerâmica 2008, 54, 77.

[5] Fröhlich, J.; Niedermeier, W.; Luginsland, H.-D.; *Composites Parte A: Applied Science and Manufacturing* 2005, 36, 449.

Two-dimensional liquid chromatography of complex polymers: PDMS-PS block copolymers

Muhammad Imran Malik, Pritish Sinha, Gareth W. Harding, Harald Pasch*

Department of Chemistry and Polymer Science, University of Stellenbosch, South Africa

Fax: +27218084967, e-mail: imran@sun.ac.za

Polymers are complex materials with distributions in many properties. These distributions include molar mass distribution, chemical composition distribution, functionality type distribution etc. amongst others. Naturally, these distributions can have enormous effects on the final properties of the materials. The development of reliable and fast characterization methods for such complex polymeric systems is one of the challenges for polymer scientists and technologists. Better and faster characterization methods lead to better and faster screening of products and helps enormously in developing improved synthesis procedures. A single technique is not sufficient for the comprehensive analysis of such complex polymers since SEC provides only relative MMD irrespective of chemical composition and the spectroscopic techniques like NMR, FTIR etc. provide only average chemical composition without any information of molar masses. Furthermore, it is more time consuming to do an analysis of two different properties by two independent runs. In addition, it has been shown previously that important information can be missed during the analysis of block copolymers if each single technique is used independently. In principle one needs N number of techniques or dimensions for the analysis of N number of properties. There must be a hyphenation of these techniques or there must be modes of characterization which are capable of analyzing the products according to a single property, ideally without or at least with only minimal effects of the other distributions.

In this study, PDMS-PS block copolymers are characterized by two-dimensional liquid chromatography. Comprehensive two dimensional liquid chromatography using LCCC as first dimension and size exclusion chromatography as second dimension reveals very important information about composition and molar masses of different fractions which were not possible by using both techniques independently.

Furthermore, by an offline approach; fractions are collected from first dimension and subjected to analysis in the second dimension. Block copolymer fractions are subjected to LCCC of the other block in the second dimension to see if there is any homopolymer of second block present in the sample. Fractions from LCCC are also analyzed qualitatively as well as quantitatively by FTIR. Different collection modes of FTIR namely ATR, transmission, reflectance and transmission in solution are compared for qualitative as well as quantitative analysis of fractions and raw samples.

Imaging Polymer Nanostructures with Scanning Transmission X-ray Spectro-Microscopy

Benjamin Watts[1], *Christopher R. McNeill*[2] *and Jörg Raabe*[1]

[1] Swiss Light Source, Paul Scherrer Institut, 5232 Villigen, Switzerland.
[2] Cavendish Laboratory, University of Cambridge, J J Thomson Ave, Cambridge CB3 0HE, United Kingdom.

benjamin.watts@psi.ch

Introduction

Polymer composite materials are of great, and increasing, technological importance in many industries. In particular, there is currently much interest in the development of polymer-based optoelectronic devices such as LEDs, lasers, FETs and solar cells. [1] However, the morphology of such materials is complex, often displaying three dimensional composition structure or molecular alignment effects. The structure of the polymer film incorporated into a device can strongly affect its performance characteristics, e.g. via the connectedness between of polymer domains and to the device electrodes, or due to anisotropic material properties due to molecular alignment. [2]

Scanning transmission x-ray spectro-microscopy (STXM) has proven to be a powerful tool for the investigation of polymer nanostructures due to its high resolution and variety of strong contrast mechanisms. Of particular interest to polymer imaging, is the molecular-structure based contrast that is achieved by tuning the incident photon energy to near-edge resonances that correspond to electronic transistions from the C 1s orbital to unoccupied π* and σ* anti-bonding orbitals. This mechanism allows strong contrast to be achieved (without labelling) between materials which differ only in molecular structure.[3,4]

Materials and Methods

STXM spectro-microscopy was performed at the PolLux beamline at the Swiss Light Source, Paul Scherrer Institut, Villigen, Switzerland.[5] The Swiss Light Source are open-access facilities, available to all researchers and free of charge for non-proprietary work.[52] TEM grid-supported films of poly(9,9'-dioctylfluorene-co-bis(N,N'-(4,butylphenyl))bis(N,N'-phenyl-1,4-phenylene)diamine) (PFB) and poly(9,9'-dioctylfluorene-co-benzothiadiazole) (F8BT) were mounted in the sample chamber. The transmitted X-ray intensity through the film was recorded using a scintillator and photo-multiplier tube and measured as a function of energy (280.0 to 320.0 eV with a resolution of 0.1 eV) and sample position (with X-ray focus better than 25 nm diameter and X-Y sample position resolution better than 1 nm).

Computation of quantitative composition maps for blend samples was achieved by fitting each pixel of the sequence of images to known spectra of the component materials. For computation of domain orientation and molecular order a rotation stage was used to rotate the sample with respect to the fixed linear polarization of the synchrotron.

Results and Discussion

Recent work at the PolLux STXM has demonstrated two new developments in the imaging of thin polymer films. Figure 1 demonstrates simultaneous imaging of the sample bulk and surface regions has been enabled by the installation of a channeltron detector (operated in TEY mode) next to the standard phosphor-coated PMT detector.[6] Secondly, Figure 2 displays a mapping of the molecular orientation within an annealed F8BT polymer film.[7] This molecular orientation mapping has been achieved via imaging at the energy of an anisotropic resonance combined with rotation of the sample and can be extended to include the out-of-plane direction through knowledge of the physical constraints of the sample material.

References

[1] C. R. McNeill, N. C. Greenham, *Adv. Mater.* **21**, 3840 (2009).
[2] M. Redecker, D. D. C. Bradley, M. Inbasekaran, E. P. Woo, *Appl. Phys. Lett.* **74**, 1400–2 (1999).
[3] O. Dhez, H. Ade, and S. Urquhart, *J. Electron Spectrosc. Relat. Phenom.* **128**, 85 (2003).
[4] B. Watts, S. Swaraj, D. Nordlund, J. Lüning, and H. Ade, *J. Chem. Phys.* **134**, 024702 (2011).
[5] J. Raabe et. al, *Rev. Sci. Instrum.* **79**, 113704 (2008).
[6] B.Watts and C. R. McNeill, *Macromol. Rapid Commun.* **31**, 1706 (2010).
[7] B. Watts, T. Schuettfort and C. R. McNeill, *Adv. Func. Mater.* accepted (DOI: 10.1002/adfm.201001918

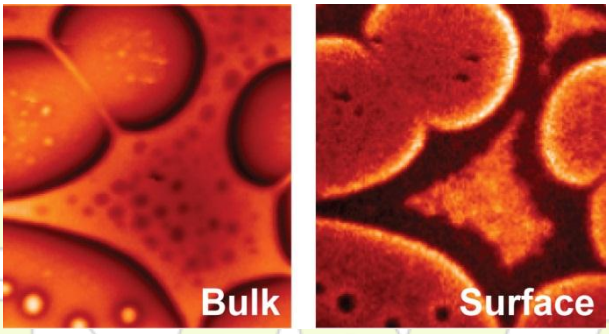

Figure 1: 7x7 µm bulk and topside surface images of a 1:1 PFB:F8BT polymer blend film spincast from xylene, measured at the 285 eV PFB π* resonance.[6]

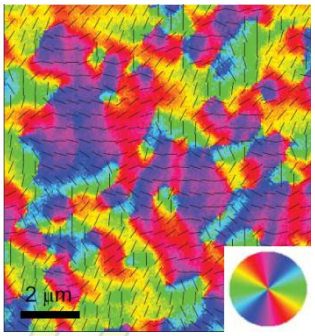

Figure 2: False color plot showing molecular orientation in an annealed F8BT film via the 284.7 eV F8BT π* resonance.[7]

Comprehensive Molecular Characterization of Complex Polymer Systems with Liquid Chromatography

Dušan Berek

Polymer Institute, Slovak Academy of Sciences, 84541 Bratislava, Slovakia
Dusan.Berek@savba.sk

Molecular characteristics of macromolecules that co-determine the end-use properties of resulting polymeric materials are molar mass, chemical structure (composition) and physical architecture. All molecular characteristics of synthetic polymers exhibit a distribution. *Complex polymers* possess more than one distribution in their molecular characteristics. Typical examples are various copolymers, functional, and stereoregular polymers, as well as blends of linear homopolymers. A mixture of a complex polymer with other macromolecular substances of distinct nature is called *complex polymer system*. The quantitative data on molecular characteristics of distributed polymers are assessed by the separation methods; the field is at present dominated by high performance liquid chromatography (polymer HPLC). Molar mass distribution of synthetic polymers is most often determined by size exclusion chromatography, SEC called also gel permeation chromatography. SEC separates macromolecules according to their size in solution, which depends not only on molar mass but also on other molecular characteristics of polymers to be characterized. Therefore, SEC cannot directly produce exact, quantitative data on the molar mass averages and distributions of complex polymers and complex polymer systems. Still, SEC provides valuable information on the *tendencies* of molar mass evolution during polyreactions. As a rule, SEC cannot discriminate polymer species of different nature that possess similar size in solution. Quantitative assessment of minor (<1%) constituents of multicomponent polymers systems with help of SEC is not possible even if their molecular sizes differ substantially. This results from the low sensitivity of the SEC detectors and from the limited both sample capacity and selectivity of the SEC columns. To quantitatively characterize complex polymers and complex polymer systems, the exclusion, entropy controlled separation mechanism of SEC is to be combined with one or several interaction, enthalpy driven separation mechanisms. This approach is called coupling of retention mechanisms, and the resulting procedures are designated *coupled methods of polymer liquid chromatography*. The representatives of coupled methods of polymer HPLC are *eluent gradient liquid chromatography*, EG LC, *liquid chromatography under critical conditions of enthalpic interactions*, LC CC and *liquid chromatography under limiting conditions of enthalpic interactions*, LC LC. The principle, advantages and limitations of LC CC and LC LC methods will be elucidated and compared in the contribution. The coupling of separation mechanisms within one single HPLC column is often insufficient for separation of complex polymers, and especially for separation and molecular characterization of complex polymer systems. It is necessary to combine two different HPLC procedures executed in two independent chromatographic systems. Such combination is denoted *two-dimensional polymer high performance liquid chromatography*, for short 2D-LC or also LCxLC. Principles and limitations of the existing 2D-LC procedures will be briefly reviewed. A novel approach will be presented, namely a combination of LC LC and SEC, LC LC x SEC called *sequenced two-dimensional polymer liquid chromatography*, S2D-LC. The procedure includes fast separation of multicomponent complex polymer systems with help of appropriate LC LC procedure into defined fractions while the latter are in their entirety online transported into SEC column(s). In this way, constituents of complex polymer systems can be comprehensively characterized as to their amount and molar mass average and distribution. Minor macromolecular admixtures well below one percent can be analyzed with help of S2D-LC: this was not possible by the existing analytical methods. Typical examples of sequenced two-dimensional separations will be presented; the separation and molecular characterization of parent homopolymers in block copolymers being the important application. The aim is to facilitate the start-up experiments by selection of appropriate chromatographic system for S2D-LC and to prevent misleading, erroneous results.

Acknowledgement: This work was supported with Slovak Grant Agency VEGA (Project 2/0171/09).

Uptake of Water and Ions in Nylon 6 as studied by MRI Imaging.

N.J.W. Reuvers[1], H.P. Huinink[1], H.R. Fischer[2] and O.C.G. Adan[2].

[1] Department of Applied Physics, Eindhoven University of Technology, Eindhoven, The Netherlands
[2] TNO, Delft, The Netherlands

n.j.w.reuvers@tue.nl

Introduction

Polyamides or nylons are important engineering plastics because of their mechanical properties. Water acts as a solvent on nylon and therefore it is important to understand the water uptake process. Our study is also concerned with the uptake of electrolyte solutions because of the well known effect of ions on the mechanical properties[5] of nylon.

Materials and Methods

The water uptake process is measured using ^{1}H-MRI imaging on thin films (200 μm) of nylon 6. The used GARField[1] set-up is especially developed for measuring on thin films. This set-up enables us to follow water distributions non-destructively in time. The spatial resolution (1D) is in the order of 10 μm and the time resolution is 17 minutes.

Water Uptake

The diffusion coefficient and the moisture content profiles (inset) as obtained from the NMR measurements are shown in the figure below. Profiles show the penetration of water from the top (left side of inset figure). The moisture content (Θ) is defined as the percentage of mass increase with respect to the dry mass.

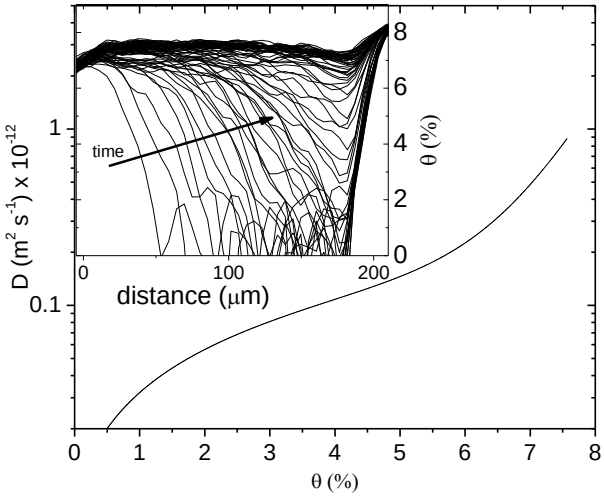

Figure 1: The relation between diffusion coefficient and moisture content. Moisture content profiles (inset).

The relation between the moisture content and the diffusion coefficient is obtained by application of the Boltzmann transformation[2]. The relation for the diffusion coefficient appeared to be highly non-linear, in contrast to other studies[2,3]. To investigate plasticization the nylon is exposed to heavy water (D_2O). In this way only hydrogen nuclei on the polymer backbone appear in the MRI signal. This reveals that the polymer contributes half of the signal during a water uptake measurement. Only a small part of the amorphous phase is plasticized enough to be detected which leads to the conclusion that the amorphous phase is heterogeneous[4] and water is absorbed into preferential zones.

Ion Ingress

Ion uptake has been studied with different salt solutions.

In the figure below profiles are shown of a nylon film is exposed to a 5M $CuCl_2$ solution. Two stages can be observed in the process. In figure 2 the first and second stage are indicated as solid and dotted lines. The first step (1) is the ingress of water in the film indicated by a signal increase at the top of the film. A second stage (2a,b), slower than the first one, is the ingress of Cu^{2+} into the nylon. The presence of copper is given away by the signal lowering (2b). The magnetic field of the copper ion causes a fast relaxation and blanks the hydrogen signal.

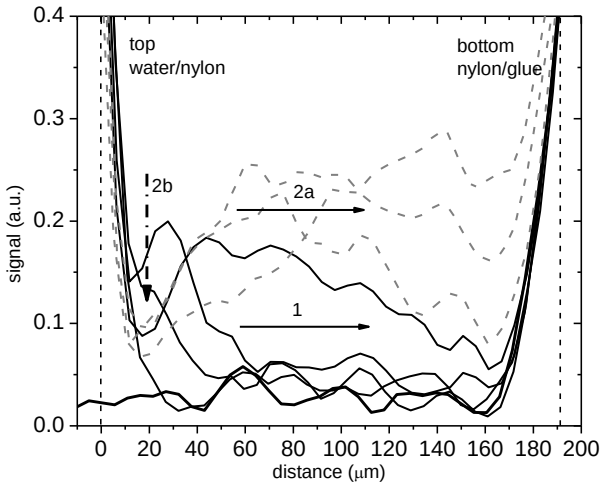

Figure 2: A nylon film exposed to a 4M $CuCl_2$ solution. Water precedes (1) the copper ions into the film (2).

For mono-valent salts such as NaCl, LiCl and KCl no ion ingress or interaction is detected. The absence is caused by the preferential hydration shell of the ions in water. Divalent ions however, can form complexes and interact with the amine group on the polyamide.

Conclusion

Water and electrolyte uptake in nylon 6 has been measured using MRI. The NMR signal is quantified and the relation between the moisture content and the diffusion coefficient is extracted. Based on the ingress of ions a distinction can be made between mono-valent or divalent ions. The paramagnetic effects of the copper ions gives away its presents while moving through the nylon.

References

1.P.M. Glover et. al., J. Mag. Res., 1999
2.P. Mansfield et. al., J. Mag. Res., 1992
3 J.E.M. Snaar et. al., J. Mag. Res. Img., 1998
4 V.M. Litvinov et. al., Macromol. Chem. Phys., 2004
5. A. Siegmann et. al., Pol. Eng. Sci., 1981

Recent progress of polymer investigation using SAXS and WAXS laboratory setups

Pierre Panine and Sergio Rodrigues*

XENOCS SA, 19 rue François Blumet, F-38360 Sassenage, France

Keywords : small angle x-ray scattering, collimation, microfocus source, multilayer optic

pierre.panine@xenocs.com

The quality of a small angle scattering setup, the experimental time and its ultimate performances expected at low values of q-wave vector are strongly related to the flux density on the sample and the propagation towards the detector of the beam used for the experiment. In the laboratory, two strategies are coexisting, the first one is to use a convergent beam focused on the detector and the second is based on a parallel beam and long sample-to-detector distances. In the convergent case, the flux level is privileged while in the parallel beam configuration lowest values of wave vector are sought. The aim of this paper is to present the recent progress of single reflexion multilayer optics [1] and collimation devices [2]. The decisive contribution of scatterless slits in the optimization of SAXS setup will be also described. Advantages in term of brightness preservation and range of wave vector reachable, both for compact-focused and for long-collimated setups will be reviewed. Advantages of improved collimation and of new optics for the study of macromolecular solutions and for solid polymer films will be described. Performances and data of experimental SAXS and WAXS measurements on various platforms will be presented.

References:

[1] Wohlschlögel, M.; Schülli, T.U.; Lantz, B.; Welzel, U. *J. Appl. Cryst.* **2008**, 41, 124–133

[2] Li, Y.; Beck, R.; Huang, T.; Choi M.C. and Divinagracia, M; *J. Appl. Cryst.* **2008**, 41, 1134–1139

Phosphorus Dendrimers functionalized with TEMPO Radicals. Synthesis and Study by Electron Paramagnetic Resonance spectroscopy.

Badetti, E.[a]; Lloveras, V.[a]; Sebastián, R.-M.[b]; Caminade, A.-M.[c]; Majoral, J.-P.[c], Veciana, J.[a]; Vidal-Gancedo, J.[a]

[a]Instituto de Ciencia de Materiales de Barcelona – CSIC; Campus UAB, 08193 Bellaterra, Barcelona (Spain). [b]Universitat Autònoma de Barcelona; Campus UAB, 08193 Bellaterra, Barcelona. (Spain) [c]Laboratoire de Chimie de Coordination – CNRS, Route de Narbonne 205, 31077 Toulouse (France).

e-mail: j.vidal@icmab.es

Dendrimers are a very special class of hyper branched macromolecules for which, in many cases, we can control the number of substituents and their distribution on the dendrimer surface. Our interest is focussed in the study of molecular materials based on organic radicals and their magnetic or electric properties.

There are only a few examples of self- assembled monolayers based on organic radicals[1] and fully functionalized dendrimers with organic radicals to study the magnetic behaviour.[2]

We present a series of dendrimers built with phosphorus as branching points and with ending groups that can be easily functionalized. Moreover fully branch substitution can be controlled.[3]

Molecules with many unpaired electrons, which possess high-spin ground state and stability at room temperature, are particularly challenging and promising targets. The interaction between pendant stable radicals
at the exterior of the dendritic surface and their dynamic behaviour can be studied using Electron Paramagnetic Resonance (EPR) spectroscopy. This is very important to understand the magnetic properties of these functionalized dendrimers. Here we describe four generations of phosphorus dendrimers with stable radicals ending groups as well as the crystal structure of the zeroth generation obtained by X-ray diffraction. The nitroxyl radicals at the exterior of the phosphorus containing dendrimers are found to exhibit an exchange interaction, which depends from the core and the generation of the dendrimer.

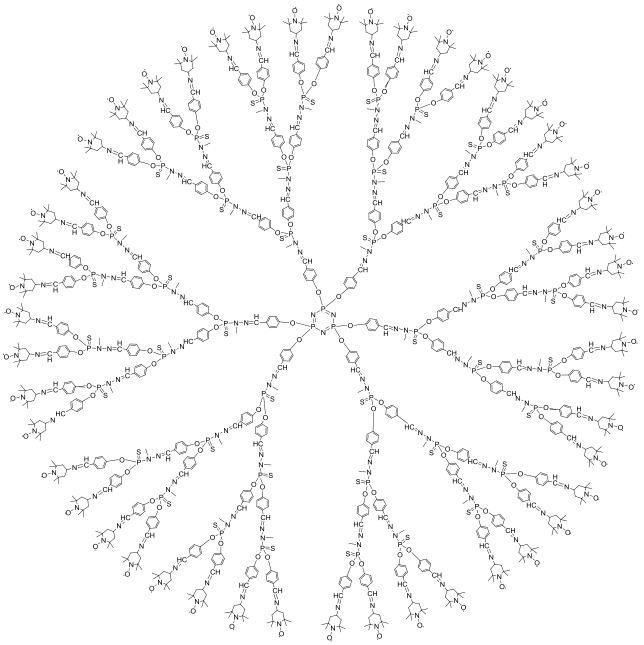

Extended structure of dendrimer **3-Gc$_3$T**

1 N. Crivillers, M. Mas-Torrent, S. Perruchas, N. Roques, J. Vidal-Gancedo, J. Veciana, C. Rovira, L. Basabe-Desmonts, B. Jan Ravoo, M. Crego-Calama y D. N. Rinhoudt. Angew. Chem.Int. Ed., 2007, 46, 2215-2219. N. Crivillers, M. Mas-Torrent, J. Vidal-Gancedo, J. Veciana and C. Rovira. J. Am. Chem. Soc, 2008, 120 (16), 5499-5506.

2 See for example: A. W. Bosman, R. A. J. Janssen and W. Meijer. Macromolecules, 1997, 30, 3606-3611.

3 A-M. Caminade, V. Maraval, R. Laurent, C-O Turrin, P. Sutra, J. Leclaire, L. Griffe, P. Marchand, C. Baudeoin-Dehoux, C. Rebout and J.-P. Majoral, C. R. Chimie, 2003, 6, 791-801 and references therein.

A New Generation Dual Controlled-Stress/Rate Extensional Rheometer for Polymer Melts

R. J. Andrade, P. Harris and J. M. Maia

Department of Macromolecular Science & Engineering, Case Western Reserve University, 2100 Adelbert Rd., Cleveland, OH 44106, USA

e-mail: ricardo.andrade@case.edu, patrick.harris@case.edu, joao.maia@case.edu

INTRODUCTION

Over the last 30 years Extensional Rheometry has been continually at the forefront of research in Rheometry because of its relevance to real-world flow situations and the difficulty in performing well-controlled, physically relevant experiments. In fact, the rheological properties of polymer melts in extensional flows are recognized to have a great relevance for polymer processing even when the elongational component of the flow is present to very low extents. Our group has been working in this area since the late 1990's, having developed its own experimental capability in the form of a controlled-rate extensional rheometer that is based on the Meissner principle of extension between pairs of counter-rotating rollers [1] while keeping sample length constant, albeit in our case the extension is only performed at one end, and adapts onto a rotational TA Instruments Weissenberg rheogoniometer [2]. Recently we introduced a second generation instrument working under the same basic principle but able to perform experiments in controlled stress mode in addition to the usual controlled strain [3-4].

In this work we introduce our third generation rheometer, which is a dual controlled-stress/rate extensional rheometer for high viscosity systems, again adapted to a rotational rheometer and based on the Meissner principle, but that this time uses two pairs of counter-rotating rollers to ensure deformation homogeneity. Due to its unique combination of geometrical set-up and feed-back control loop it now is possible for the first time to perform experiments on polymer melts both in controlled rate and controlled stress modes up until the point of physical rupture, whilst guaranteeing optimal deformation homogeneity, which is not the case with other instruments such as the SER, the Munstedt type of rheometers and even our previous ones. The new instrument is designated the CSER – Controlled Stress Extensional Rheometer.

MATERIALS AND METHODS

The polymer used in this work was a low-density polyethylene, reference material, Lupolen 1840H, which is a benchmark melt, and is the only material characterized in the literature in both controlled rate and controlled stress deformation modes [5-7]. The test temperature was 150 ^{o}C.

RESULTS AND DISCUSSION

The focus of the presentation will be on the validation of the CSER concept, which will be accomplished *via* the comparison of the results for LDPE with those obtained both by other authors [5,7] and with our previous instrument [3]. We will show that samples can be indeed deformed homogeneously until physical rupture occurs and that this allows us to study not only the flow behavior in both tensile creep and controlled-rate situations, but also the failure and rupture mechanisms, especially the transition from ductile to cohesive rupture at high strain rates and/or tensile stresses.

REFERENCES

[1] Meissner, J., "Elongation behavior of polyethylene melts," Rheol. Acta 10, 230-242 (1971).

[2] Maia, J. M., J. A. Covas, J. M. Nobrega, T. F. Dias, and F. E. Alves, "Measuring uniaxial extensional viscosity using a modified rotational rheometer," J. Non-Newtonian Fluid Mech. 80, 183-197 (1999).

[3] Maia, J. M., R. J. Andrade, J. A. Covas, and J. Laeuger, "A New Dual Controlled Stress/Rate Extensional Rheometer for High Viscosity Systems", The XV International Congress on Rheology: The Society of Rheology 80th Annual Meeting Volume 1027, 1111-1113 (2008).

[4] Andrade, R.J. and J. M. Maia, "A study on the flow, failure and rupture mechanisms of branched polyethylene in controlled-stress uniaxial extensional flow", J. Rheol. 2011, *in press*.

[5] Münstedt, H., S. Kurzbeck, and L. Egersdorfer, "Influence of molecular structure on rheological properties of polyethylenes—Part II: Elongational behavior," Rheol. Acta 37, 21-29 (1998).

[6] Gabriel, C., J. Kaschta, and H. Münstedt, "Influence of molecular structure on rheological properties of polyethylenes. I. Creep recovery measurements in shear," Rheol. Acta 37, 7-20 (1998).

[7] Sentmanat, M. L., B. N. Wang, and G. H. McKinley, "Measuring the transient extensional rheology of polyethylene melts using the SER universal testing platform," J. Rheol. 49, 585-606 (2005).

Evaluation of Polyethylene Films Photodegradation by Analitycal Fractionation Techniques

M.T. Expósito[a,*], *C. Domínguez*[b], *J. Codina*[c], *R.A. García*[a]

[a] Department of Chemical and Environmental Technology, Rey Juan Carlos University, Móstoles (Madrid), Spain
[b] Polymer Technology Laboratory (LATEP) , Rey Juan Carlos University. Móstoles (Madrid), Spain
[c] Applus-LGAI Technological Center S.A, Bellaterra (Barcelona), Spain

*e-mail: teresa.exposito@urjc.es

Introduction

The wide use of polymers in many industrial and domestic fields causes ecological problems connected with their utilization. Some synthetic plastics including polyolefins, as low density polyethylene (LDPE), are characterized by relatively high stabilities under both photochemical and environmental conditions for tens of years. Thus, in the presence of sunlight LDPE undergoes a series of reactions such as photolytic, photo-oxidative and thermo-oxidative, leading to chemical degradation. And as consequence its brittleness, loss of brightness, colour change, opacity and crack formation [1]. In the laboratory, this degradation might be accelerated by ultraviolet (UV) irradiation of LDPE. During irradiation activated molecules are formed, and then processes such as chain scission, cross-linking and oxidation take place [2]. The main process is the reduction in molecular weight, however the formation of carbonyl, hydroxyl and vinyl groups take also place in the LDPE molecules [3]. The presence of chains with very low molecular weight and functional groups promote and accelerate the LDPE biodegradation.

Material and Methods

In this study, LDPE film placed in both coloured and white part of store bags has been analysed. These LDPE bags have been cut into small pieces. Then, sample is irradiated with a UV source in order to cause an accelerated aging, which simulates ca. 10 year-equivalent weathering. For evaluation of the samples before and after treatment different conventional techniques have been employed such as: Fourier transformed infrared spectroscopy (FTIR) to analyse the absorption peak of functional groups, and gel permeation chromatography (GPC) to determine the molecular weigh and its distribution. As new, the analytical technique temperature rising elution fractionation (TREF) applied to diluted solution have been also used to study in and quantify the number of chains with different molecular weight. Finally, standard biodegradation experiments have been carried.

Discussion and Conclusion

Simultaneous exposure to UV light and oxygen gave as result the photo-oxidative degradation of LDPE films. As a consequence an increase of functional groups and a shift in molecular weight distribution to lower values were observed, as expected. TREF results show three crystallization peaks corresponding to three chains set with molecular weights which differ in one or more order of magnitude. Beside this, the ratio among areas under crystallization peaks indicates the photo-oxidative degradation is a homogeneous and independent process of characteristic chain (Figure 1).

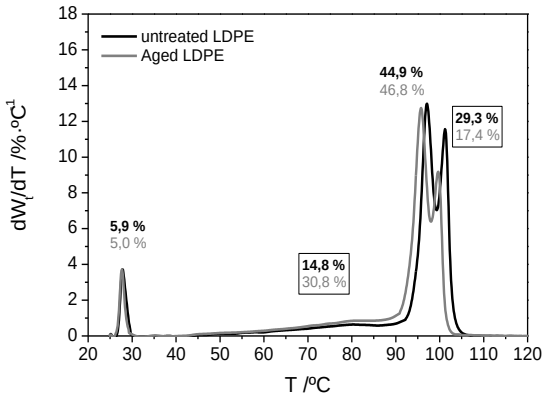

Figure 1. TREF profiles of LDPE film untreated (black color) and after accelerated aging (gray color). Areas under each crystallization peak are also indicated.

References

1. Andrady AL, Hamid SH, Hu X., Torikai A., J. Photochem. Photobiol. B, 46, 96, 1998.
2. Tse KCC, Ng FM F, Yu KN, Polym. Degrad. Stab., 91, 2380, 2006.
3. Sousa AR, Amorin KLE, Medeiros ES, Melo TJA, Rabello MS, Polym. Degrad. Stab., 91, 1504, 2006.

Microstructure characterization of polyolefins by high temperature HPLC

Benjamin Monrabal

Polymer Char, Valencia SPAIN

benjamin.monrabal@polymerchar.com

The introduction of single site catalysts in the polyolefins industry has opened new possibilities in polymer design through multiple reactor-catalyst systems. Very often this approach results in bimodal or trimodal composition distributions and unique composition-molar mass dependence; the performance of these resins is very sensitive to small microstructure variations. The analysis of the Chemical Composition Distribution has been, in those cases, the most important analytical task.

Typically the Chemical Composition Distribution is analyzed by crystallization techniques such as temperature rising elution fractionation. TREF (1), crystallization analysis fractionation, CRYSTAF (2) and crystallization elution fractionation, CEF (3).

The application of high temperature HPLC has been extended in the past years to the analysis of the composition distribution in polyolefins by Solvent Gradient Interaction Chromatography (4-9) and a new mode of separation by Thermal Gradient Interaction Chromatography combined with carbon based column has been introduced recently with significant success for the analysis of less crystalline polyolefins (10-11).

Recent advances in high temperature HPLC applications to Polyolefins will be presented and compared to existing crystallization techniques.

References

1. L. Wild, Adv. Polym. Sci. 1990, 98, 1.

2. B. Monrabal, J. Appl. Polym. Sci. 1994, 52, 491.

3. B. Monrabal, J. Sancho-Tello, N. Mayo, L. Romero, Macromol. Symp. 2007, 257, 71.

4. T. Macko, H. Pasch, Y.V. Kazakevich, A.Y. Fadeev, J. Chromatogr. A, 988 (2003) 69.

5. L.Ch. Heinz, H. Pasch, Polymer 46 (2005) 12040.

6. T. Macko, H. Pasch, Macromolecules 42 (2009) 6063.

7. H. Pasch, A. Albrecht, R. Bruell, T. Macko, W. Hiller, Macromol. Symp. 2009, 282, 71.

8. T. Macko, R. Brull, R. Alamo, Y. Thomann, V. Grumel, Polymer 2009, 50, 5443.

9. R. Abhishek, M. Miller, D. Meunier, W. deGroot, W. Winniford, F.Van Damme, R. Pell and J. Lyons, Macromolecules 2010, 43, 3710.

10. R. Cong, W. deGroot, A. Parrott, W .Yau, L. Hazlitt, R .Brown, M. Miller and Z. Zhou. 3rd ICPC conference Shanghai 2010, to be published in Macromol. Symp. 2010.

11. B. Monrabal, N. Mayo and R. Cong 3rd ICPC conference Shanghai 2010, to be published in Macromol. Symp. 2010.

Photochromic reaction of fluorescent rhodamine 6G-polyelectrolyte complexes and the sensitivity of the complexes to Mercury in solution

Rodrigo Araya-Hermosilla[1], *Carlos Alarcón Alarcón*[1], *Esteban Araya-Hermosilla*[1], *Mario Flores*[2], *Ignacio Moreno-Villoslada*[1].

[1] Instituto de Quımica, Facultad de Ciencias, Universidad Austral de Chile, Valdivia, Chile
[2] Departamento de Ciencias de los Materiales, Facultad de Ciencias Físicas y Matemáticas, Universidad de Chile, Santiago de Chile, Chile

raarayah@gmail.com

Complex formation between rhodamine 6G and the polyelectrolytes poly(sodium 4-styrenesulfonate) (PSS) and poly(acrylic acid-*co*-maleic acid) (P(AA_1-*co*-MA_1)) is investigated by UV-Vis spe ctroscopy of absorbance and emission, and diafiltration. The responses in the presence of divalent metal ions were assessed with the aim of developing sensors to metal ions in aqueous environments.

It was found that the self-aggregation properties of R6G on the environment of theses polyelectrolytes change as a function of their relative concentrations and the presence of charged aromatic groups in the polymers.[1-2] In the case of the R6G-PSS complex, short-range aromatic-aromatic interactions with the benzene sulfonate groups are dominant, and the dye tends to distribute randomly on the polymeric binding sites. Association of these ion pairs can be controlled, with a consequent modulation of the system fluorescence. When long-range electrostatic interactions dominate the overall interaction between the dye and polyelectrolyte as in the case of P(AA_1-*co*-MA_1), a higher local concentration of the dye around the polymer can be found, resulting in dye self-aggregation and fluorescence quenching. When non fluorescent complexes are irradiated with UV light, a photochromic change is observed. The fluorescence of the system P(AA_1-*co*-MA_1) / R6G is enhanced, but not that of the system PSS / R6G.

The irradiated P(AA_1-*co*-MA_1) / R6G complex showed fluorescence quenching in the presence of Hg^{2+} at micromolar concentrations (Figure 1), but not in the presence of Cu^{2+} or Cd^{2+}. This behavior is attributed to a new conformational ordering of the dye on the surface of the polymer due to the influence of the metal. Contrarily, the R6G-PSS complex did not show any spectroscopic change in the presence of the metals. This behavior can be due to the high capacity of the functional aromatic groups of the polymer to held short-range interactions with the dye.

The standardization of this photochromic reaction can be tuned to develop new applications in analytical chemistry and to create devices sensitive to hazardous heavy metals in aqueous environment with high selectivity.

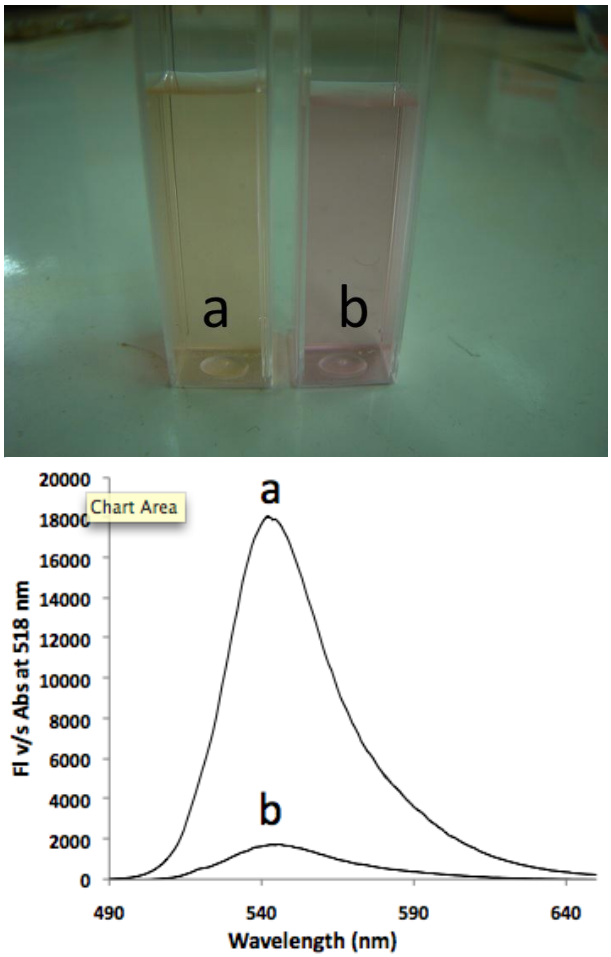

Figure 1: Emission at 600 nm versus absorbance at 520 nm (excitation wavelength) of irradiated R6G $1x10^{-5}$ M in presence of $1x10^{-4}$ M of P(AA_1-co-MA_1): (a) in absence of Hg^{2+} and (b) in prescence of $1x10^{-6}$ M of Hg^{2+}.

Bibliography:

4. Ignacio Moreno-Villoslada; Juan Pablo Fuenzalida; Gustavo Tripailaf; Rodrigo Araya-Hermosilla; Guadalupe del C. Pizarro; Oscar Guillermo Marambio; Hiroyuki Nishide. *J. Phys. Chem. B.* **2010**, 114, 11983-11992.
5. Ignacio Moreno-Villoslada, Mario E. Flores, Oscar G. Marambio, Guadalupe del C. Pizarro and Hiroyuki Nishide. *J. Phys. Chem. B.* **2010**, 114, 7753–7759.

Acknowledgements: The authors thank Fondecyt grant 1090341 for financial support.

Local thermomechanical analysis of polymers on the sub-µm scale using heated SFM-probes

Thomas Fischinger and Sabine Hild

Department of Polymer Science, Johannes Kepler University Linz, Altenbergerstrasse 69, 4040 Linz, Austria

Thomas.Fischinger@jku.at

Instruction: Detailed information of physical and chemical properties of advanced polymers are needed to satisfy the demands of our lifestyle. Therefore, thermal analysis methods are mainly used, to provide important and reliable data. However, up to now mainly bulk properties have been detected. In order to close this gap a combination between common thermal analysis and Scanning Force Microscopy (SFM) referred to as Micro Thermal Analysis (µTA)[1)] has been designed to close this gap. In particular, due to the development of a new generation of heatable cantilever probes, in our work analysis in the sub-µm range has been realized and a variety of promising applications are offered.

Materials and Methods: Our method is based on an appropriate temperature calibration, which provides a reliable correlation between measured deflection signal and tip-temperature. For this purpose different calibration methods, such as tracking of the raman peak shift as a function of temperature as well as measurements on standard materials, has been investigated. Thermoplastic polymer standard, covering a range from 60 °C to 250 °C, serve for calibration.
With our basic experimental set-up, see Figure 1a, conventional Local Thermal Analysis (LTA) in an unpresented range of scale is available. Thus a precise detection of transition points such as melting point and softening point is possible. However, the determination of the glass transition point has reached its limits here.

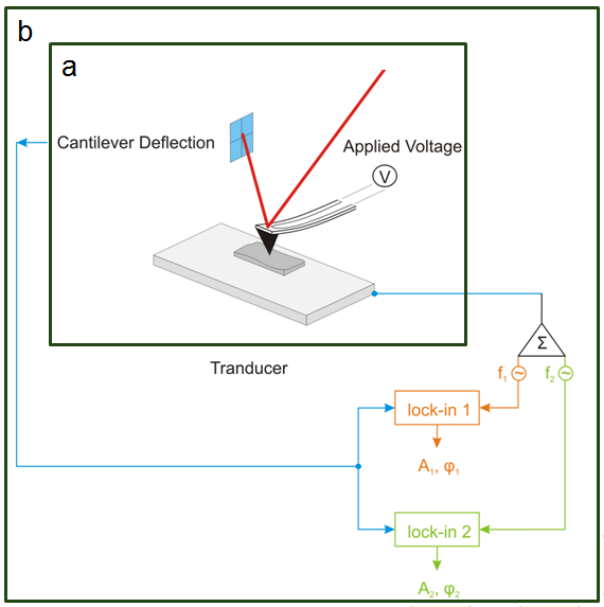

Figure 18: a) Typical LTA measurement results of a thermoplastic polymers, b) Simplified scheme of the Dual AC Resonance Tracking System.

Therefore, the LTA method is being replaced by a new technique. Dual AC Resonance Tracking (DART)[2)] is a combination of atomic force acoustic microscopy[3)] and band excitation[4)], which enables the unambiguous detection of temperature-induced changes in the contact stiffness of the tip–surface junction. As illustrated in Figure 1b, the sample is attached to a transducer element, which is modulated by two frequencies around resonance frequency. Changes in phase transition through the thermal probe, however, influence the contact stiffness of the tip-sample system and the resonance frequency. Consequently, phase transition phenomena can be detected by tracking of the resonance frequency.

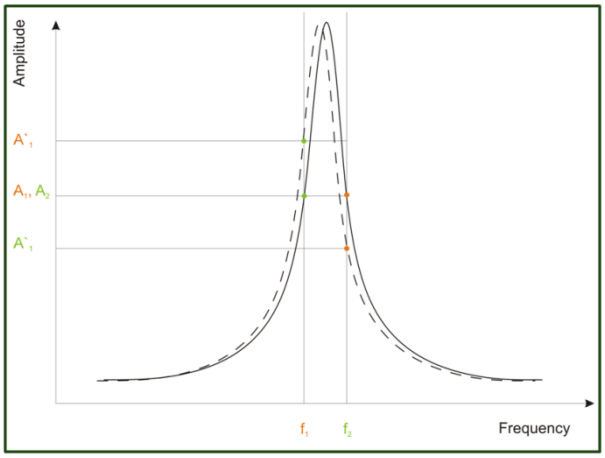

Figure 19: Resonance frequency tracking of the tip-sample system.

Results and Discussion: LTA curves measured on thermoplastic polymers, have been verified as an appropriate method to measure phase transition points. Therefore, the maximum of the derivative with respect to z-sensor signal has been proven to describe the melting point accurate. Furthermore this method is used for tip-temperature calibration. However, there is an insensitivity of glass transition detection, that results from changing contact area between tip and sample, while feedback loop keeps the force of the cantilever constant. In cotrast, the DART system is controlled by the frequency shift and independent of influences such as thermal extension and varying contact area.

References:

[1] R. Häßler and E.z. Mühlen, Thermochimica Acta, 361 (2000)
[2] B. J Rodriguez et al, Nanotechnology, 18 (2007)
[3] U. Raabe and W. Arnold, Appl. Phys. Lett., 64 (1994)
[4] St. Jesse et al, Nanotechnology, 18 (2007)

Dielectric properties of poly(vinyl alcohol) hydrogels prepared by freezing/thawing technique

Martha Elena Londoño López[*], *Juan Manuel Jaramillo Ocampo*[**], *Roser Sabater i Serra*[***], *Juan Manuel Vélez Restrepo*[****].

[*]Associated Professor, Biomedical Engineering Research Group EIA-CES, Engineering School of Antioquia
Address: km 2 variante al aeropuerto José María Córdova, Envigado - Colombia – South America PBX: (574) 354 9090 FAX: (574) 3861160
e-mail: pfmalon@eia.edu.co
[**]Titular Professor EAFIT University, Electromagnetism Applied Group,
Address: Carrera 49 N° 7 Sur - 50 - Medellín - Colombia – South America. Jjaram44@eafit.edu.co
[***]Centre de Biomaterials i Enginyeria Tissular -Universitat Politècnica de València
Camí de Vera 14 - 46022 València – Spain. rsabter@die.upv.es
[****]Titular Professor Nacional of Colombia University, Science and Technology of Material Group,
Address: carrera 80 65 – 223 Facultad de Minas - Medellín – Colombia - South America
PBX: (574) 425 5008
jmvr@epm.net.co

Introduction

Heterogeneous systems composed of two or more phases show interfacial polarization, termed the Maxwell-Wagner-Sillars effect (MWS) (1). In heterogeneous polymeric materials interfacial polarization is almost always present. Phenomenological behavior of electrical relaxation processes in PVA hydrogels obtained by freezing/thawing technique was examined, using electric modulus (2).

Experimental

PVA with molecular weight of approximately 89,000 to 98,000 and a degree of hydrolysis 99+% (SIGMA-ALDRICH) was used to prepare 15% wt PVA hydrogel by freezing/thawing technique at 4,6 and 12 cycles. The crosslinked polymer is produced by the clustering of chains caused by the association of polar group of the dissolved polymer followed by polymer crystallization (3).

Results and discussion

The dielectric spectra obtained from -50 °C to 25 °C shows a broad secondary relaxation process, figure 1, associated to local mobility, β relaxation, which is related to the terminal polar groups (OH) this process is strong affected by the freezing/thawing cycles applied. The interfacial relaxation processes in PVA hydrogels are best described by the Havriliak-Negami model.

References

1. Tsangaris, G. M., Psarras, G. C., and Kouloubi, N. J. of Mat. Sci, 1998, 33, 2027-2037.
2. Macdonald, J. R. J. Phys. Chem. Sol. 2009,70, 546-554.
3. Hassan, C. M.; Peppas, N. A. Adv. Poly. Sci. 2000, 153, 37-65.

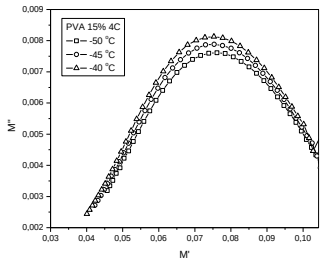

Figure 1. Cole-Cole plot of the PVA xerogel at 4 cycles of freezing/thawing

The Creep Behavior of Linear Low Density Polyethylene

Yakov Unigovski[1)], *Arthur Bobovitch*[2)] & *Emmanuel Gutman*[1)]

[1)] Ben-Gurion University of the Negev, 84105, Beer-Sheva, Israel
[2)] Syfan Saad (99) Ltd

e-mail: yakovun@bgu.ac.il

Introduction

The effect of density *d* and processing parameters on the creep behavior of linear low-density polyethylene (LLDPE) films with a broad range of densities has not been studied in-depth yet.

Materials and Methods

Creep behavior of 40- and 80-micron-thick films of linear low-density polyethylene with density of 0.902, 0.912, 0920 and 0.930 g/cm^3 produced by blowing and casting processes was investigated at room temperature and 70^{o}C. As a criterion for ductile creep failure, strain-to-failure was chosen, which amounts to the maximum elongation characterized by necking of the whole sample.

Results and discussion

At room temperature under the stress of 8 MPa, strain-to-failure increases by one order of magnitude (from 0.08 to 0.80) with a decrease in density from 0.930 g/cm^3 to 0.902 g/cm^3. The most marked decrease in the total strain and creep compliance as a function of *d* was found with the density increase more than 0.912 g/cm^3 both at room temperature (RT) and 70^{o}C (Fig. 1).

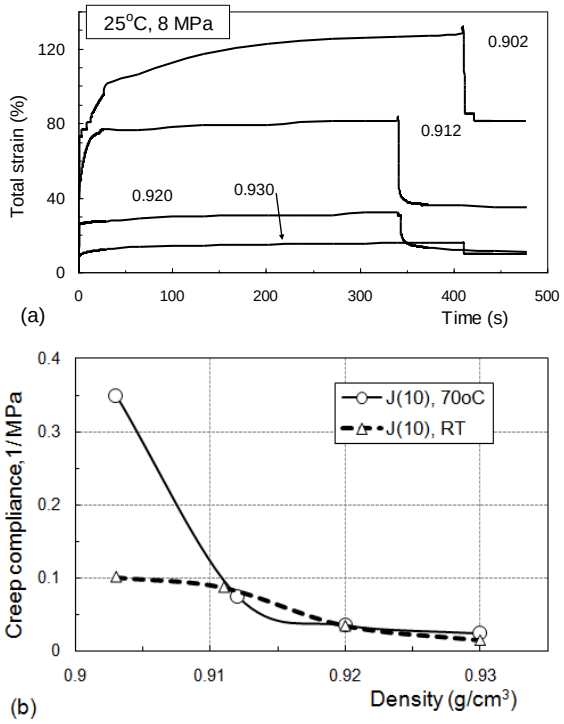

Fig. 1. Total strain (a) and creep compliance for 10 s (b) depending on the film density and the temperature.

Processing affects creep deformation much less significantly in comparison with density. The crystalline structure of cast films is much more deformed as compared to that of blown ones due to a higher cooling rate in the casting process and a higher orientation in cast film. That is confirmed by a much broader peak of orthorhombic reflection (110) in cast films in comparison to that of blown films.

It is found that under loading at room temperature, some amount of orthorhombic phase in films with the densities of 0.902 g/cm^3 and 0.912 g/cm^3 transforms into the monocline phase. For the last film a short-term loading for 0.3 h at room temperature leads to the appearance of a marked reflection (010) of monocline phase near the angle 2θ of 19.5^o (Fig. 2). With a longer test duration, the intensity of the (010) peak decreases slightly and then remains unchanged up to 165 hours (Fig. 2). Two other reflections of the monoclinic phase are heavily overlapped with the second orthorhombic reflection. Monoclinic reflection does not appear at 70^{o}C due to the instability of this phase at elevated temperatures. However, for the film with the highest density (0.930 g/cm^3) both creep load and the test temperature do not affect the morphology of orthorhombic phase.

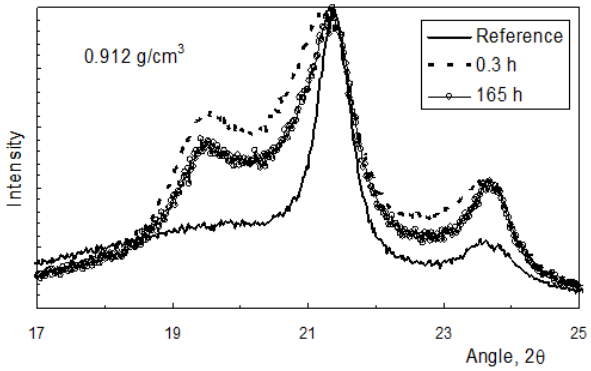

Fig. 2. X-ray patterns for the blown film with density of 0.912 g/cm^3 before and after the creep tests.

Calorimetric spectra for the polyethylene show that the crystallinity percentage and melting peak temperature of blown films increase from 29.7% to 39.7% and from 87.0^{o}C to 122^{o}C, respectively, with density increasing from 0.902 g/cm^3 to 0.930 g/cm^3. The crystallinity of blown films was slightly higher than that of cast films with the same density that can be attributed to a lower cooling rate at the production of blown films in comparison with the cast film processing.

Conclusions

-The creep strain of films is higher at lower densities, in the interval from 0.930 g/cm^3 to 0.902 g/cm^3.

-The secondary crystallization of the monoclinic phase (strain-induced crystallization) was found in films with density less than 0.920 g/cm^3 under the action of the applied stress at room temperature.

-The cast films have a less perfect crystalline structure than blown ones. However, processing affects creep much less significantly in comparison with density.

The Advantages of TOPEM in Studying the Cure of a Trifunctional Epoxy Resin (TGAP)

J M Hutchinson, F Shiravand, Y Calventus, I Fraga

Departament de Màquines i Motors Tèrmics, ETSEIAT, Universitat Politècnica de Catalunya

hutchinson@mmt.upc.edu

Introduction Epoxy resins are versatile thermosetting polymers which are widely used in various applications, including the matrix material of polymer layered silicate (PLS) nanocomposites. For high performance applications, such as the aerospace industry, there has been interest recently in the use of a trifunctional epoxy resin, triglycidyl *p*-amino phenol (TGAP), which not only has excellent mechanical properties as a result of a very highly cross-linked network structure, but also exhibits a very high glass transition temperature, T_g [1,2]. An important consequence of this last aspect is that conventional differential scanning calorimetry (DSC) cannot detect either the vitrification which occurs during isothermal cure or the $T_{g\infty}$ of the fully cured and highly cross-linked material. These are important drawbacks, since the cure kinetics is a crucial aspect of PLS nanocomposite fabrication. In this paper, we show how TOPEM, an advanced temperature modulated DSC technique, overcomes these problems, and allows a clear description of the cure kinetics of this epoxy resin.

Materials and Methods The TGAP epoxy resin (Araldite MY0510) is cured with 4,4-diamino diphenyl sulphone, DDS (Aradur 976-1), both from Huntsman Advanced Materials, in a mixture with excess epoxy (1:0.9 molar, 1:0.52 mass, epoxy:DDS). Isothermal cure temperatures of 120ºC and 150ºC were used, for times from 1 to 6 hours, followed by a second scan (non-isothermal) to obtain complete cure, and a third scan to determine $T_{g\infty}$. In the DSC experiments (DSC821e, Mettler-Toledo), the second and third scans were made at 10 K/min from 50 to 300ºC. In the TOPEM technique (DSC823e, Mettler-Toledo), stochastic temperature pulses are superimposed on the isotherm, or on the underlying heating rate of 2 K/min from 50 to 300ºC, with an amplitude of alternately ±0.5 K and random intervals between 15 and 30 s. The frequency-dependent heat capacity, C_{p0}, is obtained from the analysis, which allows vitrification to be identified during isothermal cure, and vitrification and devitrification during the non-isothermal second scan [3].

Results and Discussion A typical isothermal cure at 150ºC in the DSC is shown in Figure 1(a). Though not evident here, the sample vitrifies, as can be seen by the appearance of a glass transition and a residual cure reaction in the second scan, shown in Figure 1(b). In the third DSC scan, it is not possible to identify $T_{g\infty}$.

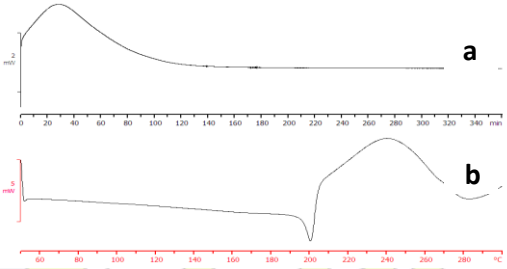

Figure1. DSC cure, 150ºC (a), DSC 2nd scan (b)

With TOPEM, on the other hand, vitrification during the first scan is clearly evident from the change in C_{p0}, as seen in Figure 2. The vitrification time of ~100 min is in excellent agreement with the value that can be found from a series of DSC experiments with increasing cure times to determine the time for which T_g in the second scan is equal to the cure temperature.

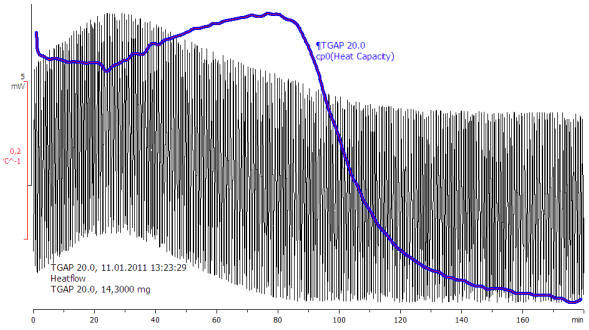

Figure 2. TOPEM isothermal cure at 150ºC

The second scan in TOPEM, shown in Figure 3, is also much more informative than is DSC. The C_{p0} curve shows three separate transitions: the glass transition of the sample after isothermal cure, vitrification almost immediately after that as the T_g increases during the residual cure, and then another devitrification at 256ºC. This temperature corresponds very closely to $T_{g\infty}$.

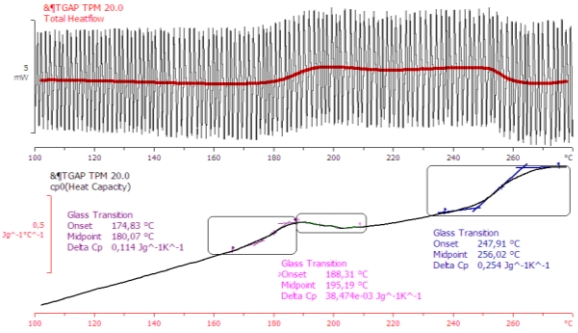

Figure 3. TOPEM second scan

Conclusions TOPEM has significant advantages over conventional DSC in characterising the isothermal cure of TGAP/DDS systems. Not only can the vitrification time be identified directly, but also the T_g of the fully cured resin can be determined with precision.

References

1. R.J. Varley, J.H. Hodgkin, D.G. Hawthorne, G.P. Simon, J. Appl. Polymer Sci., **60**, 1996, 2251
2. M. Frigione, E. Calò, J. Appl. Polymer Sci., **107**, 2008, 1744
3. I. Fraga, S. Montserrat, J.M. Hutchinson, Macromol. Chem. Phys., **211**, 2010, 57

Acknowledgements We thank CICYT for grant MAT 2008-06284-C03-03 and Huntsman Advanced Materials for providing Araldite MY0510 and Aradur 976-1.

Real-time Raman spectroscopy measurements to study the uniaxial tension of isotactic polypropylene

P. Bourson1, J. Martin[1,2], S. Chaudemanche1[2], M. Ponçot[2], J.M. Hiver[2], A. Dahoun[2]

1 - Laboratoire Matériaux Pptiques Photonique et Systèmes, Université Paul Verlaine de Metz, 2 rue Edouard Belin, 5 7070 Metz, France

2 - Institut Jean Lamour,départ. Science et Ingénierie des Matériaux et de la Métallurgie, UMR CNRS 7198, Nancy Université, Parc de Saurupt, 54042

A better comprehension of the mechanisms of deformation of polymers is a requirement with the optimization of their mechanical properties [1]. We propose the Raman micro-spectroscopy to characterize the microstructure of isotactic polypropylene (thermoplastic semi crystalline) during its deformation by uniaxial traction.

A testing bench, coupling a tensile testing machine controlled by the VidéoTractionTM system and a Raman spectrometer (Figure 1) was especially developed to satisfy two experimental requirements, often neglected in former work:

I) First of all, the use of the VidéoTractionTM system gives access the true mechanical behavior of material by the instantaneous measurements of the deformation in the necking of the test-sample [2].

II) Moreover, the measurement by Raman diffusion practiced in real-time with the deformation of the test-sample makes it possible to make correspond a microstructural state in a state of deformation true all while being freed from the relieving of material observed during characterizations post-mortem [3,4].(figure 2)

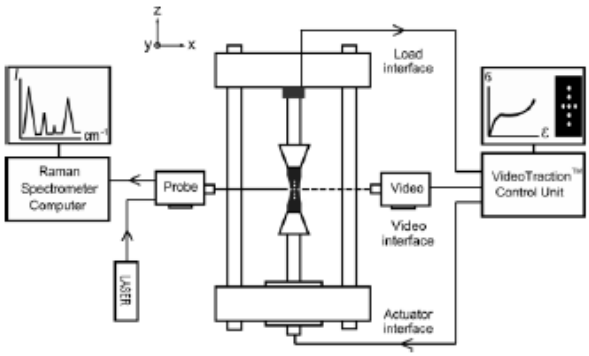

Figure 1: Schematic view of the experimental set-up coupling the VidéoTraction™-controlled tensile machine and a Raman spectrometer

On the basis of preliminary result validating the use of Raman spectral signatures suitable for the quantification of the rate of crystallinity, of the orientation of the macromolecules (amorphous and crystalline phase) and of the voluminal damage, we could follow the microstructural evolution of isotactic polypropylene during its deformation [3,4]. The results of this work make it possible to consolidate and specify certain descriptive models of the microphone-mechanisms concerned in the deformation of isotactic polypropylene and more generally of semicrystalline polymers [5,6]. (Figure 3)

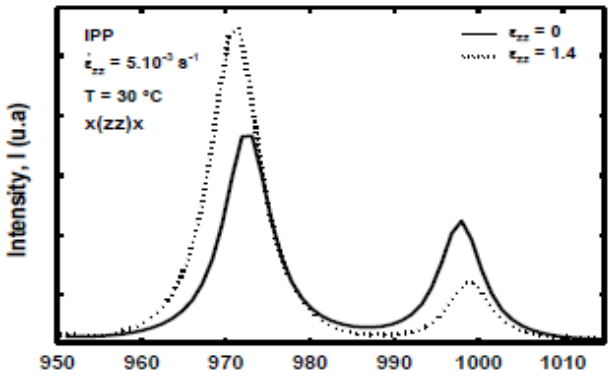

Figure 2: Polarized x(zz)x Raman spectra of iPP stretched at different strain levels.

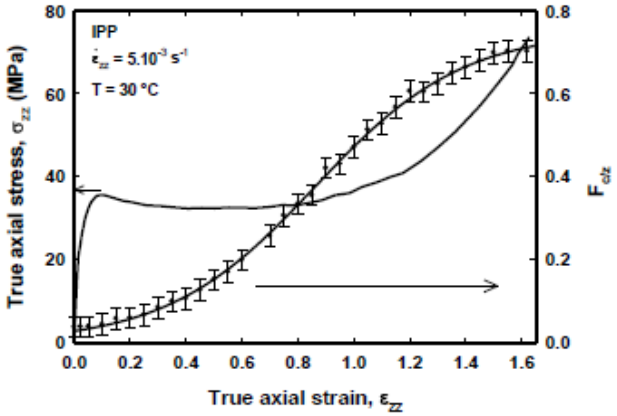

Figure 3 : Evolution of the true axial stress, σzz, and the orientation function of the crystalline phase, $F_{c/z}$, in function of the true axial strain, ε_{zz}, of iPP uniaxially stretched at T = 30 °C under a constant true strain rate ε_{zz} = 5.10-3 s^{-1}.

Lastly, this study brings an answer to the present needs (industrial and academic) for a fast, reliable method analytical, nondestructive and easily integrated in processes of workings such as the injection or extrusion.

References

[1] Ward I.M., Mechanical Properties of Solid Polymers, Eds Wiley-Interscience, London, 1971

[2] G'Sell C., Hiver J.M., Dahoun A., Int. J. Solids Struc., 2002, 39, p. 3857-3872

[3] Martin J., Thèse de Doctorat, Université Paul Verlaine de Metz, Metz, 2009

[4] J. Martin, S. Margueron, M. Fontana, M. Cochez and P. Bourson, *Polym. Eng. Sci.*, **50**, 138-143 (2009).

[5] Peterlin A., J. Mater. Sci., 1971, 6, p. 490-508

[6] Schultz J., Polymer Materials Science, Eds Printice- Hall, Englewood Cliffs, 1974

Investigation of the dispersion process of different PP/nanoclay composites at different processing conditions during extrusion by on-line near infrared and ultrasonic spectroscopy

Dieter Fischer[1], *Sven Kummer*[2], *Jan Müller*[3], *Bernd Kretzschmar*[1]

[1]Leibniz Institute of Polymer Research Dresden, Germany
[2]Topas GmbH Dresden, Germany, [3]Plastic Logic GmbH Dresden, Germany

fisch@ipfdd.de

Introduction

Extrusion is one of the most applied technologies for polymer processing of nanocomposites (NC). Application markets for NC are in automotive, electrical and electronic and packaging sectors. NC can offer improvements in several of the properties of thermoplastics including flame retardancy, tensile strength, modulus, barrier and heat distortion temperature, surface properties and electrical properties.

During the processing there is a need to control the dispersion of the nanofillers in the polymer matrix and to control the influence of the processing conditions on the dispersion in real time. The crucial point is the determination of the degree of exfoliation of the nanofillers as an indicator for the dispersion. Spectroscopic on-line measurements at different positions along and at the end of the extruder can determine the state of dispersion during processing. Our concept was to calculate the shear thinning exponent (STE) from shear viscosity measurements as a quantitative degree for the state of exfoliation. The STE was than correlated with on-line near infrared (NIR) and Ultrasonic measurements using multivariate data analysis. These methods are described in [1-4].

Materials and Methods

The polymers used are different polypropylenes (PP HP500 and HP522) modified with maleic anhydride (mPP). For the determination of dispersion we measured the degree of exfoliation of different nanoclays in mPP. These nanoclays were layered silicates (montmorillonite, MMT) without and with different organic modifications (Cloisite 15A and 20A, Dellite 67G).

All experiments were done at two twin screw extruders (Leistritz Micro 27 and a Maris TM45) with measuring adapters at the die and at two different positions along the extruder. These adapters were assembled with sensors for NIR and ultrasonic measurements. For the variation of the process conditions we used different screw profiles, different screw speeds, different processing temperatures and different output rates during extrusion.

For the off-line determination of the NC dispersion we used Raman Imaging, Electron microscopy and rheologic measurements by an oscillatory rheometer to measure the shear viscosity. The initial slope at low frequencies was used to calculate the shear thinning exponents (STE) [5] between 0 and 1. A value better 0.8 of the STE indicates a good exfoliation state and a low value below 0.2 indicates a bad exfoliation state.

Results and Discussion

Shear viscosity measurements at low frequencies show a pseudo-solid behavior for NC with layered silicates [5]. With decreasing frequency, an increasing viscosity is induced by interaction of the single layers of the layered silicates. The initial slope (0.05 – 0.20 Hz) of this increasing viscosity was used to calculate the STE as a quantitative degree of exfoliation. The STE were correlated with the on-line NIR and Ultrasonic spectra and show a good correlation between on-line data and off-line STE measurements. It was possible to determine the degree of exfoliation for different modified nanoclays in mPP. The investigation of the NC at the different process conditions could show the strong influence of these conditions on the exfoliation behavior of the NC. This is shown in the Figure for the real time determination of the STE for the NC mPP/Cloisite 20A at different screw speeds (100 to 300 rpm) calculated using NIR spectra.

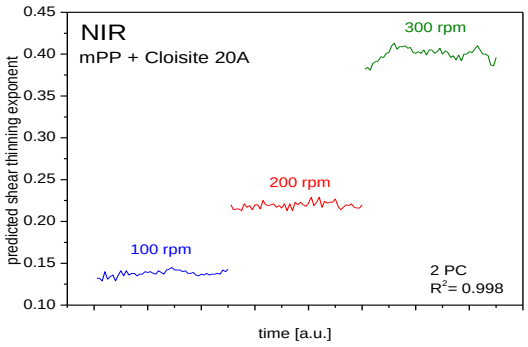

Furthermore we investigated the dispersion process in real time along the extruder at different measurement points. The NIR and the Ultrasonic data at these different positions illustrate the improvement of the exfoliation of modified nanoclays in the mPP matrix along the extruder.

Conclusions

NIR and Ultrasonic spectroscopy can determine on-line in real-time in the melt during extrusion the degree of exfoliation of polymeric NC. It is possible to measure different dispersion states caused by different processing conditions and different modified nanofillers and to describe the dispersion process along the extruder.

References

[1] I. Alig, D. Fischer, D. Lellinger, B. Steinhoff
Macromol Symp 2005, 230, 51-58.
[2] D. Fischer et. al.
Compt Rendus Chem 2006, 9, 1419-1424.
[3] J. Müller, S. Kummer, D. Fischer
Meas. Sci. Technol. 2009, 20, 097002.
[4] D. Fischer, S. Kummer, J. Müller, B. Kretzschmar
Macromol Symp 2011, in press.
[5] R. Wagener, R., T.J.G. Reisinger
Polymer 44 (2003) 7513-7518

Monitoring Atom Transfer Radical Polymerisation (ATRP) and the resulting polymers using ^{14}C radio-labeled initiators

Mark Long[a], *Suzanne H. Rogers*[a], *David W Thornthwaite*[a], *Francis R Livens*[b] *and* *Steve P Rannard*[c]

[a]Unilever Research and Development Port Sunlight Laboratories, Quarry Road East, Bebington, Wirral, UK CH63 3JW; [b]University of Manchester, Oxford Road, Manchester, UK, M13 9PL; [c]Department of Chemistry, University of Liverpool, Crown Street, Liverpool, L69 7ZD, UK.

e-mail:srannard@liv.ac.uk

Introduction: Controlled polymerisation has been utilised for many years to generate polymers of increasing complexity for potential applications requiring increasingly stringent operating conditions or technical performance. Areas such as energy generation, data storage, light harvesting, tissue engineering, drug delivery and stimuli-responsive encapsulation/release have been the focus of much research.

Applications involving the interaction of polymer-based technologies with biological systems are often studied for their therapeutic benefit, eg drug delivery, enhanced bioavailability or efficacy. It is extremely rare that the polymers themselves are studied for residence time within the body, accumulation in tissues or cellular interactions. This is due to the difficulty in monitoring the fate of polymers used as drug carriers or tissue scaffolds etc.

To visualise and quantify the behaviour of a polymer in a highly dilute environment, it is not uncommon to label with a fluorescent dye, however it is clear that such a hydrophobic modification may affect water-soluble polymer behaviour. Radio-labeling of polymers has also been utilised, providing high levels of detection, however it is common for radio-labels to be introduced to polymers by reaction with the preformed polymer. Such chemical modification results in the evaluation of the modified polymer and extrapolation to unmodified polymer behaviour. Reactive labelling approaches also generate a distribution of labelled products which can lead to inaccuracies.

Recently we have employed ^{14}C radio-labeled Atom Transfer Radical Polymerisation (ATRP) initiators to generate polymers of controlled chain length with a single radio-labelled site (the chain end) and have studied the behaviour of the materials in simple surface adsorption experiments. Mechanistic understanding of the utilisation of ATRP initiators throughout the polymerisation has been developed and considerable variation of adsorption behaviour has been observed, driven by the nature of the initiator-derived end group.

Results and Discussion: Initially we sought to create a generic strategy for ^{14}C-labeled ATRP initiator synthesis and establish the validity of our approach through labelling at different sites within the same initiator. ^{14}C-labeled benzyl-2-bromoisobutyrate was therefore synthesised using two strategies (one utilising ^{14}C-labeled benzyl alcohol and the second involving the synthesis of ^{14}C-labeled 2-bromoisobutyric acid (Scheme 1)), and used in the polymerisation of 2-hydroxypropyl methacrylate. Through this approach it was possible to establish that all data generated through monitoring of radioactivity was consistent, indicating no cleavage of the ester end-group during polymerisation. The utilisation of the initiator

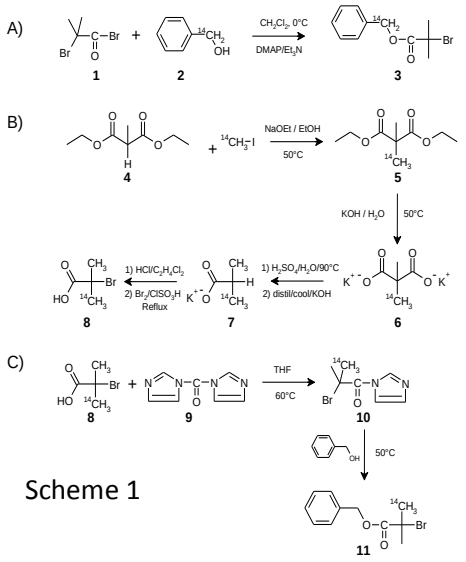

Scheme 1

throughout the polymerisation was also studied and the surprising result that new chains were being formed at high monomer conversion and long polymerisation times was observed using a combination of radio-TLC and liquid-scintillation during GPC analysis.

Two further ^{14}C-labeled ATRP initiators were synthesised

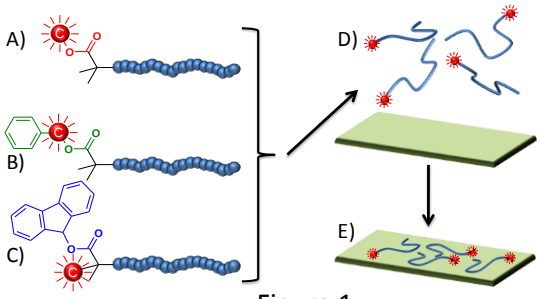

Figure 1

and, together with the benzyl-2-bromoisobutyrate, used to polymerise N,N-diethylamino ethyl methacrylate to near-identical chain lengths (Figure 1). The adsorption of the materials was then studied in a simple experiment using hair, filter paper and photographic paper. It was clearly shown that the nature of the end-group considerably directed the adsorption of the polymer. If adsorption had been measured by fluorescence and the observed behavior attributed to the unmodified polymer, the adsorption would have been considerably overestimated.

Data monitoring the ATRP polymerisation, characterisation of the initiators and polymers and the adsorption of the materials onto various substrates will be shown.

Molecular structure and local dynamic in impact polypropylene studied by preparative TREF and subsequent 2D solid-state NMR spectroscopy

R.A. García[a], A. Fernández[b], M.T. Expósito[a], B. Peña[c], B. Coto[b], I. Suárez[b], J. Shu[d], R. Graf[d], H.W. Spiess[d]

[a] Department of Chemical and Environmental Technology, Rey Juan Carlos University, Móstoles (Madrid), Spain
[b] Department of Chemical and Energy Technology, Rey Juan Carlos University, Móstoles (Madrid), Spain
[c] Centro de Tecnología REPSOL, Ctra. de Extremadura, Km. 18, Móstoles (Madrid), Spain
[d] Max-Planck-Institute for Polymer Research, Mainz, Germany

*e-mail: rafael.garcia@urjc.es

Introduction

Isotactic polypropylene (iPP) shows poor impact strength and is brittleness at low-temperatures, which limits its applications. Increase in the low-temperature impact strength of polypropylene (PP), is a key to further broadening its and end-use properties in areas like infrastructure, automotive and packaging. Therefore, in the last years, the development of new systems such as random or heterophasic polypropylene copolymers (called also impact polypropylene), which show an improved balance between properties, represent therefore one of the major challenges to PP industry [1].

Extensive investigations have been focused to study the compositional heterogeneity, chain and phase structure as well as phase morphology by using different analytical techniques for this kind of impact polypropylene [2-4]. Several papers based on ^{13}C nuclear magnetic resonance (^{13}C NMR) in the liquid state, transmission electron microscopy (TEM), scanning electron microscopy (SEM), X-ray diffraction (XRD), have been published on the characterization, but only little information about local morphologies and local molecular mobility in the solid state is known. In particular, the broad variety of methods available in solid state NMR ranging from simple ^{13}C CP-MAS measurements to multidimensional experiments have not been applied so far.

Material and Methods

In this work, we try to deep in the microstructure, structure-properties relationship and local dynamic of four impact polypropylenes (P-EP-1, P-EP-2, P-EP-3 and P-EP-4), with different ethylene content, by using preparative Temperature rising elution fractionation (TREF). Once the raw material has been fractionated in several components according to its chemical composition distribution, subsequent characterization by multidimensional solid state NMR spectroscopy has been carried out, in order to provide additional information non-accessible by other techniques. Thus, and by combination of ^{1}H wideline NMR, cross polarization (CP) and ^{13}C MAS spectroscopy in a 2D experiment is possible to obtain information about the mobility of the different structural units, being potentially valuable for many industrial applications.

Discussion and Conclusion

The complete characterization of the impact polypropylene by using different analytical techniques has been undertaken. First of all the raw materials were analyzed but little information were extracted. The study of the fractions using conventional techniques like analytical TREF, differential scanning calorimetry (DSC) and gel permeation chromatography (GPC) showed different families in each fraction. Despite these interesting differences in comparison with the raw materials, to get a more comprehensive sense of the molecular structure and species mobility subsequent analysis of the fractions by NMR solid-state using 2D WISE experiments were developed. Accordingly, fraction 1 resulted to be composed by sequences of elastomeric ethylene/propylene rubber (EPR) with high ethylene content and atactic PP, which however could as well be a sequence in the EPR. Fraction 2 contains long ethylene sequences with capability to crystallize and propylene segments with also capacity to crystallize but not highly isotactic (Figure 1). Fraction 3 consists of reasonably highly iPP, incorporating some small amount of ethylene sequences into the PP matrix, and finally fraction 4 is constituted by the matrix of iPP.

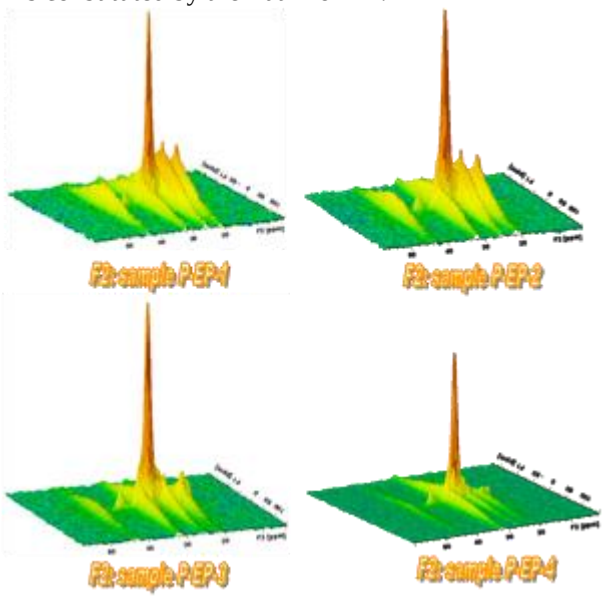

Figure 1. 2D WISE-NMR spectra corresponding to the fraction 2 of all studied impact polypropylenes

References

1. E. Tomasettia, R. Legras, B. Henri-Mazeaud, B. Nysten, Polymer (2000) 41, 6597-6602.
2. C. Hongjun, L. Xiaolie, C. Xiangxu, M. Dezhu, W. Jianmin, T. Hongsheng, J. Appl. Polym. Sci. (1999) 71, 103-113.
3. H. Tan, L. Lib, Z. Chen, Y. Song, Q. Zheng, Polymer (2005) 46, 3522-3527.
4. Y. Chen, Y. Chen, W. Chen, D. Yang, Polymer (2006) 47, 6808-68.

Mass Spectrometry Reveals the Degradation Product Patterns of Biodegradable Polyesters

Anders Höglund, Minna Hakkarainen and Ann-Christine Albertsson

Department of Fibre and Polymer Technology, School of Chemical Science and Engineering, Royal Institute of Technology, Stockholm, SE-100 44 Sweden.

anhog@kth.se

Controlling the degradation rate and the release of degradation products are crucial steps in the design of biodegradable polymers. Today, much is known of the factors affecting the degradation and degradation rate, and the continuous development of mass spectrometry techniques (e.g. MALDI-TOF-MS, ESI-MS) has paved the way for characterizing individual polymer chains on a molecular level. However, despite the large research efforts within the field of polymer degradation, less attention has been paid to the low molar mass products formed during the degradation. This is a key aspect to take into consideration in the design of new materials.

In this work, different polymer modification techniques were used to control the release rate of monomeric and oligomeric degradation products of various homo- and copolymers of lactic acid (LA), ε-caprolactone (CL) and 1,5-dioxepan-2-one (DXO). The influence of architecture, hydrophilicity, surface modification and plasticization on the degradation product patterns were revealed by different mass spectrometry techniques. Gas Chromatography-Mass Spectrometry (GC-MS), Electrospray Ionization-Mass Spectrometry (ESI-MS), and Matrix Assisted Laser Desorption Ionization-Time of Flight-Mass Spectrometry (MADI-TOF-MS) were used to monitor the released monomeric and oligomeric degradation products.

The results showed that the release pattern of monomeric degradation products was tailored by varying the distribution of the more hydrolysis susceptible DXO units.[1] Cross-linking entailed a shift in the degradation product patterns from water-soluble oligomers toward monomeric hydroxyacids, and the hydrophilicity of the networks could be altered to control the degradation product patterns.[2] The PDXO-PCL-PDXO triblock ESI-MS spectra were similar to the corresponding PDXO spectra, indicating preferential hydrolysis of the DXO blocks which was also confirmed by NMR.[3]

Oligomers up to heptadecamer were observed after hydrolysis of hydrophilic PDXO,[4] whereas only oligomers up to hexamer were observed after hydrolysis of hydrophobic PCL.[3] Large amounts of oligomers with attached cross-linking agent were detected after prolonged hydrolysis of DXO-rich networks showing an extensive disruption of the network structure.[5]

It was also shown that surface modification leads to rapid formation of water-soluble degradation products, and the degradation product pattern of acrylic acid surface grafted PLA varied with hydrolysis time.[6] Plasticizing PLA with a hydrophobic plasticizer protects the material against hydrolytic degradation but the plasticizer still migrates to aging medium and there undergoes further hydrolysis contributing to the spectrum of degradation products.[7]

References

1. Hakkarainen, M., Höglund, A., Odelius, K., Albertsson, A.-C. *J. Am. Chem. Soc.* **2007**, *129*, 6308-6312.
2. Höglund, A., Odelius, K., Hakkarainen, M., Albertsson, A.-C., *Biomacromolecules* **2007**, *8*, 2025-2032.
3. Hakkarainen, M., Adamus, G., Höglund, A. Kowalczuk, M., and Albertsson, A.-C. *Macromolecules* **2008**, *41*, 3547-3554.
4. Hakkarainen, M., Höglund, A. Kowalczuk, M., Adamus, G., and Albertsson, A.-C., *J. Polym. Sci., Part A: Polym. Chem.* **2008**, *46*, 4617-4629.
5. Höglund, A. and Albertsson, A.-C. *J. Polym. Sci., Part A: Polym. Chem.* **2008**, *46*, 7258-7267.
6. Höglund, A., Hakkarainen, M., Edlund, U., and Albertsson, A.-C. *Langmuir* **2010**, *26*, 378-383.
7. Höglund, A., Hakkarainen, M., Edlund, U., and Albertsson, A.-C. *Biomacromolecules* **2010**, *11*, 277-283.

Carbon dioxide plasticized polymer melts. An interpretation of the plasticizing effect by means of the free volume concept

Duscher Bernadette[a,b], *Schausberger Alois*[b], *Stadlbauer Wolfgang*[a]

[a] Transfercenter für Kunststofftechnik GmbH, Franz-Fritsch-Str. 11, A-4600 Wels,
[b] Institute of Polymer Science, Johannes Kepler University Linz, Altenberger Str. 69, A-4040 Linz

Bernadette.Duscher@jku.at

Introduction Carbon dioxide is well known for its particular properties as a processing solvent. According to its noticeable solubility in polymer melts it is used for polymer modification, blending as well as plasticizing during the process. Furthermore it is well established as a physical foaming agent especially for long chain branched polymers. Dissolving carbon dioxide strongly affects the rheological properties of the melt and causes viscosity reduction. Hence processing properties of polymer/CO_2 – solutions exhibit a remarkable change.

Materials Commercially available polymers (polypropylene - PP, polystyrene - PS) with varying molar mass distribution and different glass transition temperatures are used. Isotactic PPs with different molecular structures are investigated.

Pressure is brought to bear upon the cell via a carbon dioxide pressure cylinder. By this working pressure is up to 40 bar.

Methods A newly developed pressure cell is used for rheometry in shear. The setup used is developed to perform rheological experiments with a common MCR rheometer by Anton Paar. With a plate-plate-system in the pressure cell material functions in rotation and oscillation are measured. By this means widespread rheological information is gained. Gas diffusion processes and pressure effects are observed as well as the effect of gas dissolution on the material functions of poymer melts. Relations based on the free volume concept are used to interpret the experimental results.

Results Depending on the concentration of dissolved carbon dioxide dynamic functions can be shifted to the dynamic moduli of the neat polymer. By this a mastercurve is constructed and the shift factors a_c for the shift on the frequency axis and b_c for the shift on the modulus axis are determined.

In case of linear polymers (polystyrene, polypropylene) this time-concentration-superposition is simple, i.e. the shifted curves correspond in the investigated frequency range. By use of a generalized Doolittle relation of Fujita and Kishimoto[1] the concentration dependent horizontal shift factors are calculated

$$\ln a_c = B(1/f_c - 1/f_2) \qquad (1)$$

For this purpose the relation

$$f_c = f_2 + A/M_{n,c} \qquad (2)$$

is used. A is the product of the free-chain-end volume per mole and the density of the polymer.[2] The rheological properties of carbon dioxide plasticized polymer melts as well as the molar plasticizing activity A of an additive can be predicted.

By the use of a van-Gurp-Palmen-plot modified by Mavrides and Shroff[3] the shift factors a_c and b_c can be determined independently of each other. Hence, an additional shift along the modulus axis is found. By this, the relation of Schausberger[4] is applied

$$G_{0,d} = \rho RTw^2 / M_{e,0} = G_{0,u} w^2 \qquad (3)$$

and the vertical shifts $b_c = w^2$ are calculated. (w is the weight fraction of the entangled polymer).

The solubility parameters are in accordance to literature.[5,6]

Discussion The setup used is an appropriate possibility to determine time-concentration dependent horizontal and vertical shifts independently of each other. The shift factors are interpreted similarly to the shift created by solvents and additives. The moduli are reduced by the square of the polymer weight fraction and the frequency (time) shift is interpreted with the aid of the free volume concept. In this context long chain branched polymers show particular properties.

References

1. Fujita, H.; Kishimoto, A. J Chem Phys 1961, 34, 393-398
2. Knoglinger, H.; Schausberger, A.; Janeschitz-Kriegl, H. Rheol Acta 1987, 26, 460-467
3. Mavridis, H.; Schroff, R. N. Polym Eng Sci 1992, 32, 1778-1791
4. Schausberger, A.; Ahrer, I. V. Macromol Chem Phys 1995, 196, 2161-2171
5. Sato Y.; Yurugi, M.; Fujiwara, K.; Takishima, S.; Masuoka, H. Fluid Phase Equilibr 1996, 125, 129-138
6. Royer, J. R; DeSimone, J. M.; Kahn, S. A. J Polym Sci Part B: Polym Phys 2001, 39, 3055-3066

Development of a thermoplastic starch to be used in the co-injection process.

E. Benavent, B. Galindo, O. Menes, A. Pascual, F. Marti

Instituto Técnologico del Plástico C/ Gustave Eiffel, 4; 46980 Paterna (València).

fmarti@aimplas.es

Introduction. Packaging plays a vital role in modern integrated product supply systems. It does not only protect a product from the production line to the consumer (impact on health and safety), but also facilitates production, distribution and storage. Packaging technology is currently making huge strides in the development and application of new products and processes. About 15% of the total enterprises of the EU plastic sector are devoted to packing goods. In fact, *long life rigid/semi-rigid plastic* in food and drink packaging market represents a very important share of the current global packaging market.

COBAPACK project[1] aims to develop a new high barrier long life, low cost, recyclable packaging through a special injection molding process (co-injection) specially addressed to applications in the food sector. The core of the new packaging will be made of a renewable material (native thermoplastic starch) whereas the skin layer is polypropylene providing the required physic-mechanical and chemical properties for its optimum production and use.

Starch is an inexpensive abundant product available annually from different crops. Due to its high molecular weight, starch must be destructurized (to destroy its cristallinity) applying shear stress, heat and plasticizers in order to be processed as a thermoplastic.

The processability and properties of the unmodified starch have been studied[2]. However, there are very few products for packaging applications manufactured with non-chemically modified starch due to its low melt strength, moisture sensitivity, high tendency to stick to metal surfaces and limited mechanical and thermal properties[3].

Materials and Methods. For this work four different types of native starch (potato, maize, pea and wheat) was studied using glycerin as a plasticizer. The percentage of glycerin was between 25-50% w/w. To avoid sticking problems during injection molding a low amount of inorganic filler was used.

The selection of the most suitable native starch for the project was carried out in a twin screw extruder with a diameter of 16 mm. A pre-mix of starch and plasticizers is needed to ensure that all the plasticizer is completely absorbed by the starch. The destructurization process of the starch must be optimized for pilot plant scale twin screw extruder. The screw design and machine parameters were optimized employing a compounding simulation software.

The viscosity of the different compounds was characterized by capillary rheology at a temperature of 180 ºC and shear ratebetween 10 and 5000 1/s.

The main thermal, mechanical and oxygen barrier properties of selected thermoplastic starches were determinated.

Results, Discussion and Conclusions Figure 1 shows the rheological curves of the prepared compounds.

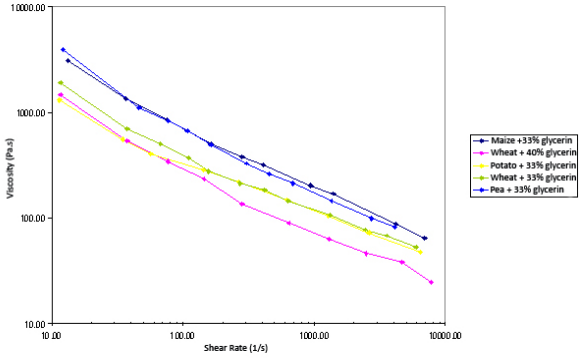

Figure 1. Capilary rheology curves of five different starch-glycerin compounds

Taking into account the ranges of viscosity and shear rate for the injection process it can be concluded that wheat starch with 40% wt of glycerine is the best compound.

However, compounds with 33% wt glycerin have good processing properties. Starch with 40% wt glycerin is very sticky, which makes the dosage of the material in the injection machine more difficult[4]. Starchwith 33% w/w glycerin has good oxygen barrier properties and limited thermal and mechanical properties. Protection of starch to be used in the packaging industry is needed.

Figure 2 shows a co-injected package obtained using wheat starch compound as core layer and polypropylene as skin layer.

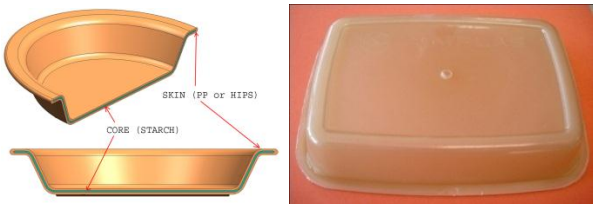

Figure 2 Co-injected package obtained in the COBAPACK project.

Acknowledgements. The authors thank the European Commission and the Research Executive Agency for financial support.

References

[1] "Development of a new recyclable long life co-injected high barrier packaging for food applications, with broad design possibilities and reduced manufacturing costs " FP7-SME-2008-1 Contract No: 231106.

[2] R. Stepto, Macromolecular Symposia, 245-246, 2006.

[3] O. Martin , E. Schwach, L. Avérous, Y. Couturier, Starch – Stärke, 53, 372-380, 2001.

[4] L. Avérous, J. Macromolecular Science, part C, 44, 231-274 2004.

Monitoring of the Epoxy Curing with Different Methods

G. Teteris[1,2], *W. Stark*[2]

[1] Institute of Polymer Mechanics, Latvian University, Aizkraukles 23, LV 1006 Riga, Latvia
[2] Federal Institute for Materials Research and Testing, Unter der Eichen 87, 12205 Berlin, Germany

e-mail: gundars.teteris@tu-berlin.de

Thermosetting resins play an important role in lot of industry branches such as aerospace, automotive light weight constructions, wind energy plants and other. Each of these branches has different requirements on process parameters and curing degree. Nevertheless, all they have some common: reducing of the production costs. One of the possibilities is the optimization of the cure process with the aim to decrease the cyclus time and energetical input decrease. Therefore an effective, at the best online, process control method is necessary.

The methods used for monitoring the progress of the cure can be divided into the two main categories: methods based on measurement the changes in chemical level such as monitoring concentration of reactive groups consumed or produced during the reaction, and methods based on monitoring the effects of network formation on to the parameters of physico-mechanical properties of the substrates. Only a few of them can be used to follow the whole curing process from the beginning of the reaction till the end of network structure building. From the data of mechanical properties is then possible to win the knowledge about chemical structures and their changes. Technically there is a problem with the wide scale of material properties: they change often in logarithmic scale, the sensors have linear sensitivity. Therefore combination of different measurements or methods with building of mastercurve from single experiments is necessary.

IR spectroscopy deals with atomic and molecular bond twisting and vibration, DSC registers the reaction heat flow, rheometry, DMA and other mechanical methods obtained their information from macromolecular chain and block “stiffness” as reaction on oscillatory deformation within their frequency band. So the question on compatibility of the results of different methods is still entitled.

DSC is the most used method for curing monitoring, but this method is not always useful in the final stages of curing. It looks likely that the chemical bond building heat that excreats during the final stage of the reaction are too small to be detected by DSC, but the result of these structural changes is strong enough to affect properties that can be measured. There are also some proposals, that the change of properties at the final stage of curing is related to relaxation that proceeds without thermal effects.

Observing curing process with rheological methods, changes in modulus and/or complex viscosity are measured. These changes draw up by many orders of magnitude. However, interpretation of the data in compliance with changes in chemical structure is not quietly simple. The results from different studies of epoxy resin cure analyzed with rheological methods can be summarized into the development of a methodology to predict the relative reactivity of curing systems from the complex dynamic viscosity value development during the process.

DMA became widespread for curing control with the works of Gillham. This method deals with rubber elasticity and glass transition, what results on dependence of rubbery modulus and T_g of network formation. With DMA method is not always possible to receive absolute values of modulus because due to the low viscosity of monomers/oligomers at the early process stages it is necessary to use special soft carriers and only relative characterisation can be provided.

With IR spectroscopy the dynamic of the curing process can be observed by changes of different specific chemical bonds such as decrease of the absorption bands of the oxirane ring.

Ultrasonic technique is used successful since a long time in non destructive testing and medicine. In the last years there are new developments on hardware, what allows investigation of curing processes. Generally ultrasonic waves act as a high frequency dynamic-mechanical deformation of material (compression deformation). If during the chemical reactions, such as curing, physical changes of material occurs, the evolution of the changes of an elastic compression modulus L^* can be monitored. This modulus is related to the complex bulk K^* and shear G^* moduli and can be displaced with one of its parameters: ultrasonic longitudinal velocity.

Therefore it is necessary to compare the results of various methods used by cure monitoring and after that to receive the relationships between the results obtained with different methods and optimize the measurement parameters for each of the methods. Nevertheless, it must be noted, that also within one and the same method using different parameters from the same experiment differences in the curing parameter values are not rarely.

The curing process was studied on different commercial, room and high temperature curing epoxy resin compounds using five measuring methods:

DSC, IR, rheology with a plate–plate geometry by oscillation, DMA and ultrasonic measurements. The objective of the study was to compare the effectiveness and sensitivity of these methods and the correlation of the results of the methods with each other.

The results obtained with all 5 methods will be compared and the advantages and disadvantages explored. Their practical usability for prepreg characterisation will be discussed. Our experimental data demonstrate that the obtained results give comparable results of curing kinetics and curing grades.

Modeling of Phase Separation of Polymer Blends Using Spectrum Method

*M. Ali Parsa, Majid Ghiass**

School of Chemical Engineering, Iran University of Science and Technology (IUST), Iran

majidghiass@iust.ac.ir

Introduction: Polymer blends are a very important class of engineering materials with specialized applications. [1-4] The morphology of the final polymer blend is either a droplet-like or bicontinuous pattern is a key characteristic of the properties and application of the polymeric material. It is very demanding to develop a quantitative realistic model to predict the polymer blend system, capture and control the desired morphology in a phase separation process. The Cahn-Hilliard nonlinear theory has been effectively employed for quantitative modeling of the dynamics of temperature-induced phase separation of polymer (TIPS) blends.[5] For incompressible polymer blend the Flory-Huggins lattice model have been extensively successfully applied to determine the free energy of the polymer system. The solution of nonlinear Cahn-Hilliard equation provides the information for dynamic morphology evolution of a polymer blend during the temperature-induced phase separation process, TIPS. For the unsymmetric blends with different molecular weights (chain length), which is very common in blend processes, the phase equilibrium information leads to an unsymmetric phase diagram which introduces mathematical complexities in computational procedures for determination of the spatial dynamic concentration field. This research provides a new mathematical framework to model the dynamic behavior of temperature-induced phase separation for unsymmetric polymer blends.

Method of Solution: Substitution of the Flory-Huggins free energy model in the Cahn-Hilliard equation leads to a nonlinear fourth order dynamic pde whose solution provides information of the concentration in a phase separation domain. Several attempts have been employed to solve this equation by conventional finite difference, finite elements, and even stochastic methods.
Here we used the discrete cosine method (DCT) which is a general procedure for solution of the partial differential equation.[5,6] The DCT method, among the spectral methods, provides a very robust, and computationally feasible algorithm for solution of the Cahn-Hilliard equation.

Results: To solve the Cahn-Hilliard equation, a 2D square 256×256 grid field has been selected. To validate the applicability of the model, the properties of an industrial relevant polymer blend system, polystyrene (PS) and polyvinylmethylether (PVME) which have been widely experimentally studied, have been used [1-4]. Figure 1 shows a LCST behavior for this system in which polymer blend phase separates into two equilibrium phases upon temperature increases (Fig. 1)

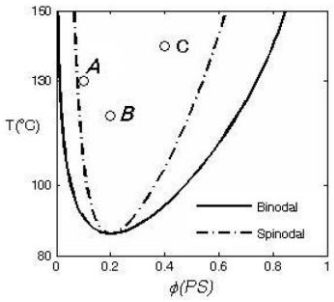

Figure 20. Phase diagram of PS/PVME blend

The phase separation dynamic has been studied for different initial concentrations which lead to different final morphologies of the polymer blend. Figure 2 shows a 2D image represents the dynamic phase separation as microstructure evolution of a PS/PVME blend at the initial concentration of 0.2 and at temperature 120°C namely an on-critical quench. The Figure shows the initial sudden appearance of microdomains followed by growth and coalescence leads the formation of larger droplets.

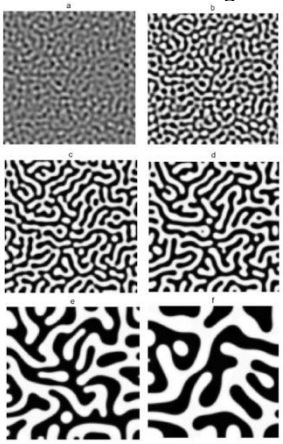

Figure 21. Morphology evolution during temperature-induced phase separation of a PS/PVME blend

Conclusion: A dynamic mathematical model for study of the kinetics of phase separation upon temperature changes in phase separation of a polymer blend of PS/PVME has been developed and solved with use of the discrete cosine transform method to predict the microstructure evolution of phase separated blend.

References:

1. Utracki, L.A., Polymer Alloys and Blends: Thermodynamics and Rheology. Hanser Pub. 1989, New York.
2. Higgins, D.A., Advanced Materials 2000, 12, 251–264.
3. Mucha, M., Progress in Polymer Science 2003, 28, 837–873.
4. Tran, T. L., Chan, P. K., Rousseau, D. Computational Materials Science 2006,37,328–335.
5. Cahn, J. W., 1965. J Chem Phys 965, 42, 93–99.
6. Eyre, D. J., SIAM J. Appl. Math. 1993, 53, 1686-1712.

Evolution of elastomers network structures during the vulcanization process as investigated by ^{1}H low-field multiple-quantum NMR

*J. L. Valentín**, I. Mora-Barrantes, M. A. Malmierca, P. Posadas, A. Fernández-Torres, A. Marcos-Fernández, A. Rodríguez, L. Ibarra*

Instituto de Ciencia y Tecnología de Polímeros (CSIC)
c/ Juan de la Cierva, 3. 28006 Madrid, Spain

* *email:* jlvalentin@ictp.csic.es

Introduction:

Elastomers are important polymeric materials because of their unique long-range elasticity. This property is obtained after the vulcanization process, where a plastic polymer is transformed into an elastic material by formation of a three-dimensional network of cross-links that connect the different polymeric chains. For this reason, it is not surprising that the most important properties of rubbers depend on the network structure, and its study allows us to reach a better understanding of the correlation between the micro-structure and the macroscopic properties of rubber compounds.

As long as the detailed reaction pathways of the most-used processes in rubber technology are unclear and remain too complex to be unveiled, the most useful approach to control and to be able to obtain tailor-made properties of elastomeric materials is clearly the direct study of the meso-scale network structure formed during the vulcanization reactions. A complete description of the network structure should contain information about non-elastic network defects, number of cross-links, their chemical nature and functionality, the spatial distribution of cross-links, and information about entanglements. The main problem is the difficulty to obtain this local information from a complex matrix in solid state. In this sense, it has been demonstrated that solid-state NMR could be considered as a powerful tool to study the structure and chain dynamics in elastomers[1]. This information is encoded in the dipolar coupling constant. Nowadays, the double quantum (DQ) NMR experiments are the most versatile and powerful tool to study, not only the residual dipolar couplings, related with both chemical (cross-links) and physical (entanglements) constrictions, but also their distribution and associated dynamics[1].

Results and Discussion:

By the use of DQ experiments (performed in inexpensive low field NMR spectrometers) it was quantitatively demonstrated that sulfur-based and peroxide vulcanization systems for dienic elastomers, e.g. NR and BR, are characterized by different reaction pathways, leading to substantial variations in the fraction of elastically non-active network defects, the vulcanization efficiency, the spatial distribution of cross-links, and the segmental dynamics. While sulfur vulcanization generates rather homogeneous networks, peroxide-cured systems exhibit a heterogeneous and even bimodal structure (Figure 1) with unexpectedly high amounts of network defects[2].
These results can be explained via the radical mechanism that dominates peroxide vulcanization process[3], as it partially leads to polymerization-type cross-linking involving addition to the double bonds, leading to highly cross-linked clusters which we could observe directly by NMR. The final structure of the network strongly depends on the polymer backbone structure, temperature, and proportion of cure system.

Figure 1 Effect of vulcanization systems (C: conventional, E: efficient, P: peroxide) on the distribution

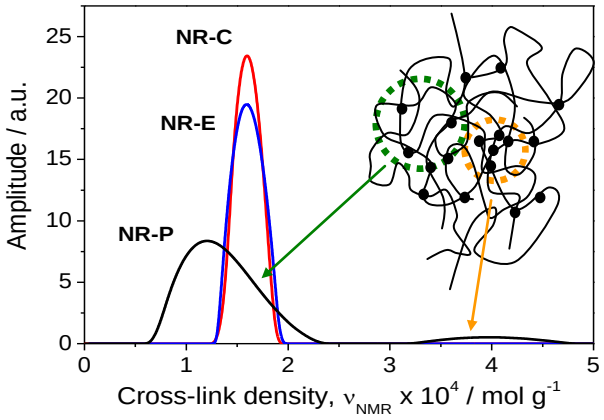

of cross-link density in NR samples. Note that the samples have the same average cross-link density.

Deeper studies about the evolution of the network structure during the vulcanization process reveal that sulphur vulcanization is heterogeneous process based on located nucleus of cross-linking. However these cure systems generate, at the end of the process, networks with extremely narrow cross-links distribution and excellent elastic properties. On the opposite side, peroxide vulcanization is a homogeneous (random) process. However in the last steps, higher cross-linked areas (clusters) are formed because the existence of polymerization-type reactions. This fact generates network inhomogeneities that deeply affect the elastic properties of these materials.

References:

1. Saalwächter, K. *Prog. Nucl. Magn. Reson. Spectrosc.* **2007**, *51*, 1.
2. Valentín, J. L.; Posadas, P.; Fernández-Torres, A.; Malmierca, M. A.; González, L.; Saalwächter, K. *Macromolecules*. **2010,** *43*, 4210.
3. Valentin, J. L.; Fernandez-Torres, A; Posadas, P.; Marcos-Fernandez, A.; Rodriguez, A. Gonzalez, L. *J Polym Sci Part B: Polym Phys.* **2007**, *45*, 544.

ABSTRACTS

ORAL PRESENTATIONS

Topic 3: Advanced Processing and Recycling Technologies

Photoelectrochemical Properties of Doped Polyaniline: Application to Hydrogen Production Upon Visible Light

Z. Benabdelghani[1], G. Rekhila[1], M. Trari[1], A. Etxeberria[2]*

[1]Laboratory of Storage and Valorization of Renewable Energies, Faculty of Chemistry, USTHB, P.O.Box 32,El Alia, Algiers 16111, Algeria.
[2]Departamento de Ciencia y Tecnologia de Polimeros and Instituto de Materiales Polimericos (POLYMAT). Universidad del Pais Vasco UPV/EHU. P.O. Box 1072. 20080 San Sebastian (Spain).

* To whom all correspondence should be addressed to e-mail address: Ben_Zit@yahoo.fr

Introduction:

Over the last years, the conducting polymers found a new interest from both academic and industrial points of view due to their interesting properties and possible applications, in the conversion of solar energy into electrical and/or chemical forms. In order to diminish the dependence of the fossil fuels and in this way the greenhouse gases, the solar power is considered as eco-friendly energy, an attractive alternative due its large abundance and consistency [1,2].
For this purpose, the use of polymer semiconductors as photoactive electrodes and photovoltaic devices attracts much attention of a large scientific community [3]. Such materials are not only able to function in a similar way to inorganic semiconductors but have additional advantages including environmental friendliness, low cost, light weight, easy fabrication, and potentially manufacturable as large-area coatings. They have been considered as promising materials for organic light conversion devices, in particular, for solar cells and photodetectors.

Our aim in this contribution was focused on a study of photoctalytic process in order to product the hydrogen using polymer semiconductor materials such as doped polyaniline (emeraldine salt).

2. Experimental

The powder was cold pressed into pellets under 1 kbar. In order to minimize the contact resistance, silver paint was deposited on the back pellet by spot welding a copper wire. The pellets were mounted in Teflon holders to give a projected surface area of 1.32 cm^2.
PEC measurements were done in NaOH (1 M) electrolyte under potentiostatic conditions using a three electrode cell with a large Pt counter electrode and a saturated calomel reference electrode (SCE). The electrode potential was monitored by a computer controlled potentiostat (Voltalab PGZ 301, Radiometer).
The electrode was illuminated through a flat optical window by a 200 W tungsten lamp.
Prior each run, A nitrogen stream was passed over the solution to remove dissolved oxygen, the purging rate was maintained constant at 10 mL mL^{-1} during 35 min.
50 mg of powder (PANI) was suspended by magnetic stirring in a double walled Pyrex reactor in 250 mL of aqueous Na_2SO_3 (0.1 M) solution.
The light source was an assembly of three tungsten lamps which are predominantly in the 400-900 nm (max. 650 nm), disposed around the reactor.
Hydrogen in the outgoing gas was identified by gas chromatography. The amount was collected volumetrically with a water manometer in an inverted burette via water displacement. Blank runs were carried out and no hydrogen was evolved in the dark.
The experiments were repeated three times with very reproducible results

Results and discussion:

The photoelectrochemical properties of polyaniline (emeraldine-salt) (PANI) doped was investigated by the photocurrent technique and capacitance measurements in various electrolytes. The volume evolved of H_2 as showed in Figure 1 reveals the applicability of this material for the photocatalytic conversion. The photocatalytic properties have been evaluated for the first time according to the H_2 evolution under visible light.

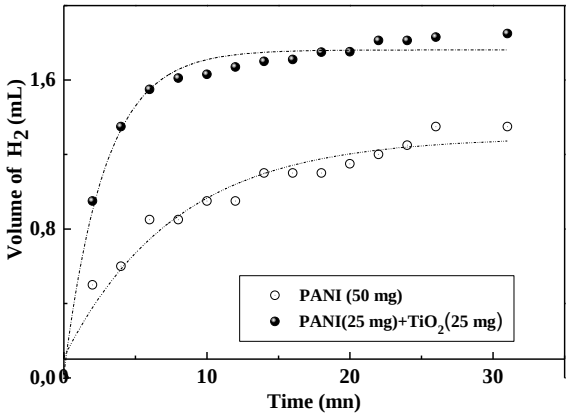

Figure 1: Volume evolved H_2 versus irradiation time on Na_2SO_4 solution (0,1 M)

Therefore, favorable valence band position for water reduction makes the PANI as an ideal photocathode. Our results indicate that the doped PANI is able to generate incident photon to chemical chemical efficiency of 4% under an intensity of 20 mW cm^{-2}.

References

1. Djellal L, Omeiri S, Bouguelia A, Trari M, J of Alloys and Compounds 2009, 476: 584-589.
2. Benabdelghani Z, Etxeberria A, J of Appl Polym, in Press.
3. Hsu C.W., Wang L.W, Su. F, J of Colloid and interface science 2009, 329: 182-187.

TTT & CCT diagrams for PP/SGFR PA 66 reinforced blends: Effect of PP-g-MAH as a compatibilizer

Zitouni Safidine[1], *Amina Belhadj*[1], *Said Fellahi*[1], *Djafer Benachour*[2], *Hans Joachim Radusch*[3]

[1] Macromolecular Chemistry Laboratory, EMP BP 17; Bordj El Bahri City; 16111 Algiers, Algeria
[2] Laboratoire de préparation, modification et application des matériaux polymériques multiphasiques, 19000, UFA-Sétif, Algeria
[3] Martin Luther University Halle-Wittenberg, Centre of Engineering Sciences, D06099 Halle, Germany.
Safi192003@yahoo.fr

Abstract: The Differential Scanning Calorimetry (DSC) was used as a useful method for the study of the global crystallization of the reinforced blends based on the dispersion of polypropylene (PPh) in a short glass fibber reinforced polyamide 66 (SGFR PA 66) as a matrix and with the presence of polypropylene grafted maleic anhydride (PP-g-MAH) as a compatibilizer. These reinforced blends were previously prepared by the twin screw extruder (TSE) and injected in the moulding machine to get specimens from which the all samples were taken. The new approaches emanating from the modern metallurgy were performed and applied for the study of the global crystallisation; these later are named Temperature-Time-Transformation (T.T.T) diagrams of the relative (absolute) crystallinity under isothermal conditions and Continuous Cooling Transformation (CCT) diagrams under non-isothermal conditions. Using these diagrams, the overall crystallization was described and it is found that the compatibilizer affects greatly the crystallization behaviour of the minor phase (PPh), in which, 2.5 wt. % of PP-g-MAH should be enough to enhance the crystallization temperature. The increasing of the crystallisation aptitude gives evidence of improvement of mechanical properties. Meanwhile the major phase (PA 66 component) still no affected by the presence of the PP-g-MAH having the lower melting point.

Key words: Polypropylene, polyamide 66, reinforced blends, glass fibber, compatibilizer, crystallization, DSC, TTT and CCT.

Literature cited:

1- Z. Safidine, S. Fellahi, and N. D. Alberola, International *conference: Polymeric materials 2002, Halle (Saale) Germany, properties, processing, modification, application*. Vol. 2: Posters, 180, (2002).
2- Z. Safidine, S. Fellahi and A. Frick, *Proceedings of the **PPS 21st** Annual Meeting*, Leipzig, Germany, [CD-ROM]; Lecture **SL 9.24**; Polymer Processing Society (2005).
3- Z. Safidine, S. Fellahi and A. Frick, *J. Appl. Polym. Sci*., **104**, 1620 (2007).
4- Z. Safidine, S. Fellahi, H. J-Radusch and D. Benachour, *Proceedings of the **PPS 24th** Annual Meeting*, Salerno, ITALY, [CD-ROM]; Lecture **S10-175;** Polymer Processing Society (2008).

Ternary Blends: Morphology and Properties

L. González Gómez[1], *M. Álvarez-Laínez*[2]

Grupo de investigación en materiales de ingeniería, Universidad Eafit, COLOMBIA

1. lgonza48@eafit.edu.co
2. Malvar26@eafit.edu.co

Abstract

The high annual consumption requirements of polypropylene and polyethylene explain the significant percentage of these materials in the total solid waste stream and become their blends an important deal of study from the viewpoint of recycling [1-5]. It has been shown that is possible the improvement of mechanical properties of polyolefin blends without the use of compatibilizers, just by controlling composition and processing conditions [3, 6-8].

The aim of this work is study ternary blends like as PP/LDPE/HDPE by changes in composition without a chemical compatibilization.

Experimental design chosen was a mixture design called simplex-centroid using statsgraphics software, besides was decided it to add additional runs (the extreme vertices) in order to improve the surface response methodology. There were five replicates of each blend. The idea of this design is to find the optimum setting of the experimental components according to the response variables (compressive strength, flexural strength, modulus, etc). Figure 1, shows the ternary blends used in this study.

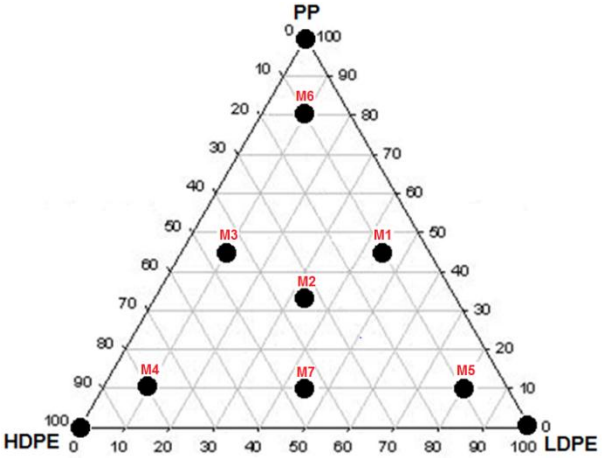

Fig 1. Experimental design region used in this study.

All the blends were performed in a Haake Rheomix 600 at 60 rpm at temperature of 200°C. Morphology blends was studied by SEM (Scanning electron microscopy) and mechanical properties were tested in an Instron 3366.

In figure 2 is present it M4 Blends (10PP/80HDPE/10LDPE) morphology, show it a heterogeneous morphology suggesting immiscible polymer blends. However, the identification of phases could not be possible due to chemistry similarity of polyolefins.

Figure 3 shows the flexural modulus of the blends. The blend 4 (M4) had a flexural modulus value higher than the target PP. This ternary blend displayed the highest and synergistic level of flexural modulus (1432 MPa) among all blends (pure and ternary) studied.

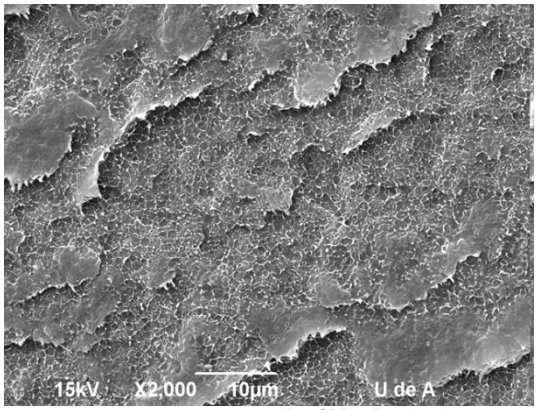

Fig 2. SEM micrograph of blend 4 (M4)

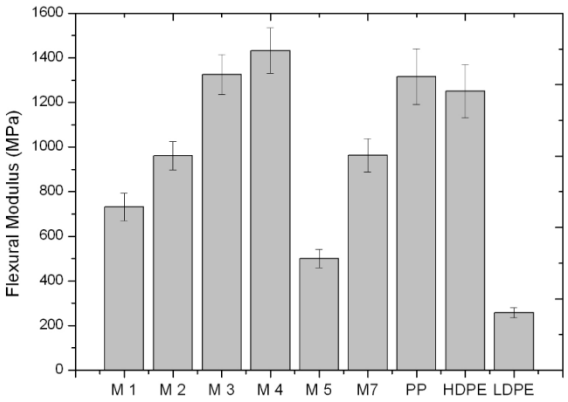

Fig. 3. Flexural modulus of ternary blends and their constituents.

References

[1]. Goforth et al. Patent No. 5088910. 1992

[2]. S. Bertin; J. Robin. European Polymer Journal: 2255-2264, 2002.

[3]. M. Polaskova; R. Cermak. Polymer composites: 1-6, 2009

[4].P. Noriega. Plásticos, 2009

[5]S. Tall; A.C. Albertsson. Polymer Science: 2381-2390, 1998

[6] A. Hamid; I.Mourad. Materials and design: 918-929, 2010.

[7]N.Kukaleva; G.P. Simon. Polymer Engineering and science:431-443, 2003.

[8] R.W Renfree; T.J. Nosker; D.R. Marrow. Paper 292, 1992

Formation of Self-Assembled Buffer Layer from Fullerene End-Capped Poly(ethylene glycol) for High Performance of P3HT/PCBM Heterojunction Solar Cells

Jae Woong Jung and Won Ho Jo

Department of Materials Science and Engineering, Seoul National University, Seoul 151-742, Korea

whjpoly@snu.ac.kr

One of the most important issues of polymer solar cells (PSCs) is lower efficiency than conventional Si-based solar cells or dye-sensitized solar cells. Various approaches for morphology control such as thermal annealing, solvent annealing, and use of additive, have been proposed to increase the efficiency. These methods have been very effective to afford nano-scaled phase-separated morphology in horizontal direction (parallel to film surface). However, the methods have a limitation to control the vertical distribution of the components in active layer, although the vertical distribution is very critical for effective transport of charge carriers.

It has been agreed that an ideal bulk heterojunction (BHJ) PSC must have the vertical distribution of components where the p-type conjugated polymers are rich near the anode and n-type fullerenes are rich near the low work-function metal cathode. This ideal vertical morphology renders holes and electrons to move more efficiently to anode and cathode, respectively. However, such ideal vertical distribution in the active layer cannot be developed during film casting due to the lower surface energy of P3HT (26.9 mJ/m^2) than PCBM (37.8 mJ/m^2).

We report here enhanced performance of PSC by controlling the vertical morphology with the addition of a self-assembled additive. We synthesized fullerene end-capped poly(ethylene glycol) (PEG-C_{60}) (Figure 1) and added it to P3HT/PCBM blend.

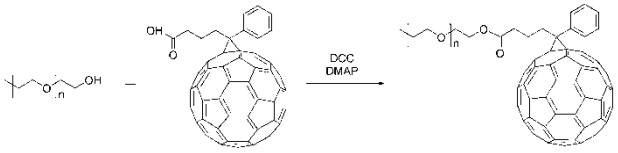

Figure 1. Synthesis Scheme of PEG-C_{60}.

Since it has been reported that the addition of small amount of PEG in P3HT/PCBM blend induces spontaneous vertical phase separation with formation of PEG thin layer on top of the P3HT/PCBM, it is expected that PEG-C_{60} molecules also migrate to the surface of the P3HT/PCBM active layer to form nano-scaled buffer layer between active layer and metal cathode (see Figure 2a). As this buffer layer with high dielectric constant induces an interfacial dipole between active layer and metal cathode, the vacuum level of the cathode is increased and the energy barrier for electron collection is decreased (see Figure 2b). Consequently, the exciton dissociation at the interface and the charge collection at the cathode become more efficient, affording increased open circuit voltage (V_{OC}) and short circuit current density (J_{SC}). Another important feature with addition of PEG-C_{60} is to induce segregation of PCBM near PEG-C_{60} layer, which makes an ideal vertical distribution of PCBM in the active layer: P3HT becomes rich near the anode and PCBM becomes rich near the cathode. Furthermore, since the PEG-C_{60} layer may protect the active layer from oxygen as well as the invasion of Al to the active layer during metal deposition, the stability of PSC will be improved.

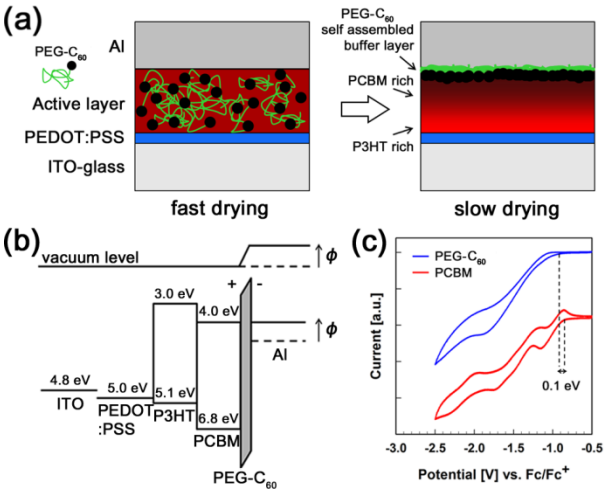

Figure 2. Schematic illustration of (a) bulk hetero- junction solar cell with PEG-C_{60} as buffer layer and (b) the energy level diagram of the polymer solar cell with PEG-C_{60} buffer layer. (c) Cyclic voltammetry reduction curves of PEG-C_{60} (blue) and PCBM (red).

To investigate the effect of PEG-C_{60} buffer layer on the performance, the power conversion efficiencies (PCEs) of PSCs with different amount of PEG-C_{60} were compared. While the reference device (0 wt% PEG-C_{60}) exhibits 3.60% PCE, the device with 5 wt% PEG-C_{60} shows 4.41% PCE (see Table 1). The enhancement of V_{OC} by addition of PEG-C_{60} is originated from the effect of dielectric buffer layer between active layer and metal cathode, and the increase of *FF* is due to development of an ideal vertical-morphology. Therefore, it is concluded that both the formation of buffer layer and the development of ideal vertical-morphology in the active layer enhance the device performance.

Table 1. Performance of PSCs with different amount of PEG-C_{60}.

PEG-C_{60} [wt%] [a]	V_{OC} [V]	J_{SC} [mA/cm]	*FF*	PCE [%]
0	0.61	10.17	0.58	3.60
5	0.66	10.27	0.65	4.41

[a] Weight ratio to the total amount of P3HT and PCBM.

Cryostructured Polymer/clay Aerogel Materials

David A. Schiraldi, Matthew D. Gawryla, Yuxin Wang, Jack R. Johnson III
Department of Macromolecular Science and Engineering, Case Western Reserve University,
Cleveland, OH-44106, United States.
Das44@case.edu

Introduction

Traditional polymer foams are largely based on petrochemical feedstocks, require environmentally-unfriendly foaming agents, are generally flammable and difficult to recycle or biodegrade. Over the last several years we have been developing polymer/clay aerogel composites, materials which match foam mechanical properties, but offer significant environmental and performance improvements over existing products.

Materials and Methods

Sodium montmorillonite clay (Nanocor PGW grade, Na-MMT), and a wide range of commercial polymers were used as received. Deionized water (DI water) was prepared using a Barnstead RoPure reverse osmosis system.

In a typical aerogel preparation, 5 g Na-MMT was mixed with 100 mL DI water in a Waring laboratory blender to prepare 5 % wt/v clay suspension. An equal volume of an aqueous polymer solution was combined with the clay suspension with mechanical stirring, then this mixture to 18 mL polystyrene cylindrical vials and frozen using low temperature cooling baths. The samples were then freeze dried using a Virtis Advantage EL-85 lyophilizer with an initial shelf temperature of 25^{o}C, condenser temperature of -80^{o}C and an ultimate 5 µ bar vacuum.

The microstructure of clay aerogels were imaged using an FEI Quanta 3D scanning electron microscope. Prior to imaging, all samples were sputter coated with gold and were studied with the microscope operating at 5 kV.

Compressive tests were carried out using an Instron 5566 Universal testing machine with a crosshead speed of 1mm/min. Skeletal density measurements of these clay and PVOH/clay aerogels were carried out using an Ultra pycnometer 1000.

Results and Discussion

Polymer/clay aerogels exhibiting bulk densities in the range of 0.05 – 0.15 g/cm3 were readily prepared by freeze drying of aqueous polymer/clay suspensions. These materials made use of biopolymers, such as casein, pectin, natural rubber latex and poly(hydroxybutyrate) as well as synthetic polymers including poly(vinyl alcohol), poly(ethylene oxide), poly(ethylene imine), expoxies, poly(ether-amides) and poly(amide-imides). Thermal conductivies in the range of 0.025 – 0.05 W/m-K were typical of these composites, depending in large part upon the bulk density of the material. Compressive moduli from 50 kPa to over 100 MPa are also possible, depending on the composite density and polymer composition. The spacing of polymer/clay composite layers were determined to be highly sensitive to both the freezing temperature and the ionic strength of the starting solutions employed. When the milk protein, casein was used, it was found that the polymer/clay aerogel is biodegradable with or without chemical crosslinking of the polymer; with crosslinking, mechanical properties of the casein aerogel can match those of commercial expanded polystyrene foam products. Incorporation of nanocrystalline cellulose whiskers can improve aerogel mechanical properties, as can addition of cut fibers. Single walled carbon nanotubes increase both mechanical and electrical properties of the aerogels. Functionalization of the clays with metal nanoparticles can result in composite materials that are magnetic and/or catalytically active. Post-treatment of the aerogels with inorganic precursors can generate layered, bio-mimetic mineralized structures.

Conclusions

Freeze-drying can be used to prepare low density, cryostructured polymer/clay aerogels, which can serve as replacements for traditional polymer foams. These materials exhibit very low thermal conductivities, low flammability, and can range from elastomeric to rigid mechanical properties. By utilizing bio-based and biodegradable polymers in such composite materials, and using water as the processing solvent, environmentally benign materials for consumer, packaging, and industrial applications can be produced. The effects of processing parameters, along with post freeze-drying processing steps will be discussed, opening up the possibility for producing highly functional (conductive, magnetic, catalytic) materials.

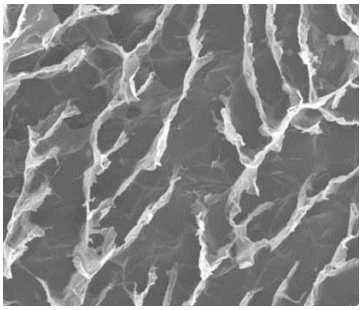

Figure 1. The structure of a poly(vinyl alcohol)/clay aerogel (SEM image)used for absorbing animal waste

References

T. Pojanavaraphan, R. Magaraphan, B.-S. Chiou. D. A. Schiraldi, *Biomacromolecules*, **2010**, *11*, 2640-6.
S. M. Alhassan, S. Qutubuddin, D. A. Schiraldi, *Langmuir*, **2010**, *26*, 12198-202.
M. D. Gawryla, D. A. Schiraldi, *Macromolec. Mater. Eng.*, **2009**, *294*, 570-4.
E. Arndt, M. D. Gawryla, D. A. Schiraldi, *J. Mater. Chem.*, **2007**, *17*, 3525-29.

Preparation of Polyether-block-amide Copolymer/organoclay Composite via Freeze-drying

Yuxin Wang , Saeed M. Alhassan, David A. Schiraldi
Department of Macromolecular Science and Engineering, Case Western Reserve University, Cleveland, OH-44106, United States.
Das44@case.edu

Introduction

Polymer/clay nanocomposites have long been studied since nylon-6/clay composites originally burst onto the scientific scene. As an alternative to directly melt mixing polymer with clay, or to a solvent-casting method, would be an 'aerogel method' in which clay is added to a polymer solution, the mixture freeze-dried to produce a porous, lamellar aerogel, with a typical density in the 0.08 to 0.15 g/cc range, then this structure would be pressed into a film. This method allows for producing composite containing very high levels of aligned fillers.

Materials and Methods

Polytetramethyleneoxide-block-nylon12 copolymer (Pebax® 2533) was used as received from Alkema. Sodium montmorillonite (MMT) clay (Nanocor, PGW) was modified with dodecyltrimethylammonium bromide (DTAB) from Sigma Aldrich. Deionized (DI) water used was prepared using a Barnstead ROpure low-pressure reverse osmosis which was connected to NANOpure ultrafiltration system. 2 g organoclay was mixed with 50 mL t-butanol using the blender. 4 g Pebax® was dissolved in 50 mL t-butanol at 80°C with reflux and vigorous stirring. Then this organoclay suspension was mixed with Pebax® solution using a low shear rate hand mixer. This final suspension was poured into 18 mL polystyrene cylindrical vials and frozen in ethanol/dry ice cooling bath. All aerogels were prepared via freeze-drying process using a Virtis Advantage Model EL-85 lyophilizer, with an initial shelf temperature of -70°C and an ultimate temperature at 25°C with 5 μ bar pressure.

The microstructures were imaged using an FEI Quanta 3D scanning electron microscope. The finished Pebax®/organoclay aerogel samples were compression molded into films along vertical direction at 180°C using a Carver Laboratory Press (Model C). Films were characterized in terms of clay dispersion and gas barrier properties and mechanical properties. X-ray diffraction (XRD) patterns were obtained using Rigaku diffractometer (RINT 2000 series) with CuKα source (1.5418 Å). Oxygen flux was measured with a MOCON OX-TRAN 2/20 at 25°C, 0% relative humidity and 1 atm. Tensile tests were conducted using an Instron 5566 Universal testing machine at a crosshead speed of 10 mm/min.

Results and Discussion

PEBAX®/organoclay aerogels with organoclay contents varing from 0.5 vol% to 16.7 vol% (1wt % to 33.3 wt%) were prepared and compression-molded into films. XRD showed no clay intergallery peak around 5-6° (2 theta) for 0.5 vol% organoclay composite, indicating complete exfoliation. When clay loading was increased to 1 and 2 vol%, two domains appeared. One with unexfoliated clay (2 theta ~ 5.2° and d-spacing is 1.6 nm) and one with intercalated clay (2 theta ~ 2.5° and d-spacing is 3.5 nm). The existence of domains has been observed in polymer-clay aerogel. However, for film prepared from traditional blending, no exfoliation has been achieved even at the lowest clay loading.

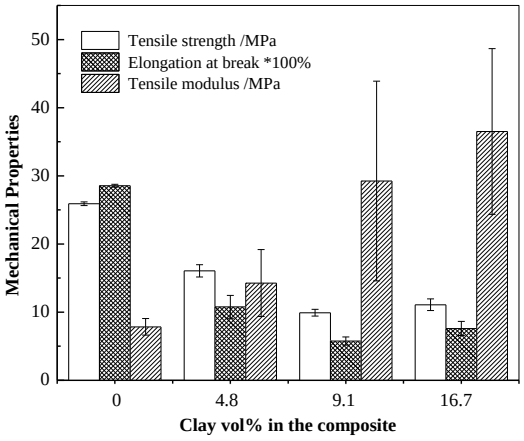

Figure 1.The tensile properties of Pebax® composite films via freeze-drying

Up to 16.7 vol% organoclay was added via freeze-drying method, creating homogenous films. As organoclay amount increased, increases in tensile modulus were observed (Figure 1), which is consistent with clay reinforcement. The tensile strength and elongation at break decreased due to the rigidity or less deformability of filler under external force.

Gas permeability of both oxygen and carbon dioxide were also studied. Addition of 16.7 vol% organoclay decreased O_2 permeability by approximately 60% and CO_2 permeability by 70%.

Conclusions

Freeze-drying method showed its superiority by environmentally processing and higher levels of aligned fillers, compared with traditional polymer/clay blending method. Both mechanical and gas barrier properties for O_2 and CO_2 were improved.

References

S. M. Alhassan, S. Qutubuddin, D. A. Schiraldi, *Langmuir*, **2010**, *26*, 12198-202.

L. S. Somlai, S. A. Bandi, L. J. Mathias, D. A. Schiraldi. *AIChE J.*, **2006**, *52*, 1162-1168.

I. Yang, P. Tsai. *Polym. Eng. Sci.*, **2007**, *47*, 235-243

Controlled chain-cleavages of polydienes by oxidation and by metathesis: Application on the waste tires rubber recycling

Faten Sadaka[1], *Irène Campistron*[2], *Albert Laguerre*[2], *Jean-François Pilard*[2]

[1]ICMUB-UMR CNRS 5260, University of Bourgogne- 9 avenue Alain Savary, 21078 Dijon, France
[2]UCO2M-UMR CNRS 6011, University of Maine-Avenue Olivier Messiaen, 72085 Le Mans, France

faten.sadaka@u-bourgogne.fr

Only in the EU, USA and Japan around 6 millions tons per year of scrap tires are produced[1]. The huge quantity of waste tires presently produced in the world will certainly increase in the future as the associated automotive industries grow. Since polymeric materials do not decompose easily, disposal of waste polymers is a serious environmental problem. Two major approaches to solve this problem are the recycle and the reuse of used and waste rubber, and the reclaim of rubber raw materials[2]. All of these recycling methods are effective and have been successful; however, they lead to environmental pollution.

The overall aim of our work was to find a method to recycle waste tires rubber by chemical controlled degradation focusing on efficient methods easier to implement, with an appropriate cost for industrial development. Two methods are choosen: the degradations using periodic acid[3] (H_5IO_6) and by metathesis[4].

The studies have firstly been carried out on polyolefins as standard raw materials because of the complexity of the formulations of waste tires.

The first degradation pathway consisted on the use of periodic acid in THF medium for the degradation of *cis*-1,4-polyisoprene (PI), Natural Rubber (NR) and carbonyltelechelic natural rubber (CTNR). In fact, periodic acid is an interesting reagent used for the selective cleavage of weak epoxidized units[5]. However, in our work we realized this degradation on one-step reaction.

As expected, we obtained telechelic polymers with aldehydic and ketonic chain ends showed by ^{1}H NMR spectroscopy (scheme 1).

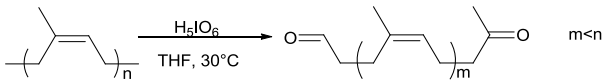

Scheme 1: Oxidative cleavage of Natural Rubber using periodic acid

The molecular weight and molecular weight distribution of polymers have been determined using size-exclusion chromatography. The telechelic polymer weights decrease with the increase of time reaction or the increase of periodic acid quantity.

This method allows us to obtain end-functionalized polyisoprenic oligomers in a high yield in a specific range of molecular weight (500–7 000 g.mol^{-1}).

The second approach involved degradation by metathesis reaction on PI and styrene-butadiene rubber (SBR) using second generation Grubbs catalysts in presence of 1,4-diacetoxy-but-2-ene as chain transfer agent, to achieve acetoxytelechelic oligomers (scheme 2).

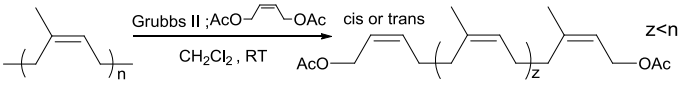

Grubbs II:

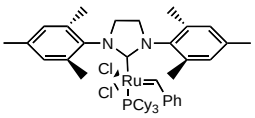

Scheme 2: Metathetic cleavage of cis-1,4-polyiso-prene using Grubbs II catalyst.

The degradation by metathesis is a complementary approach; it allows high molecular weight liquid polyisoprene (molecular weight > 100 000 g.mol^{-1}) to be obtained in a well controlled manner.

These modeling allows us to show the feasibility of degradation, the efficiency of the oxidizing agent or initiator and to determine the optimal conditions for the degradation reaction. We then extended the reaction to crumbs and granulates waste tires rubber. The results of this work have been the subject of a patent[6].

1. M. Juma, Z. K., J. Markoš, L. Jelemensky, M. Bafrnec, Polym. Adv. Technol. 2007, 18, 144-148.
2. Adhikari, B.; De, D.; Maiti, S., Prog. Poly. Sci. 2000, 25, 909-948.
3. Gillier-Ritoit, S.; Reyx, D.; Campistron, I.; Laguerre, A.; R.P.Singh, J. Appl. Polym. Sci. 2003, 87, 42.
4. Solanky, S. S.; Campistron, I.; Laguerre, A.; Pilard, J. F., Macromol. Chem. Phys. 2005, 206, 1057.
5-Reyx, D Campistron, I.,Angew. Makromol. Chem., 1997, 247(1): 197-211.
6- Sadaka, F.; Campistron, I.; Laguerre, A.; Pilard, J.-F.; French Patent, PCT/FR2010/050292, February 19, 2010.

Anomalous mechanical anisotropy of extruded polypropylene sheet with β-form crystallites

Panitha Phulkerd[1], *Yohei Uchiyama*[2], *Masayuki Yamaguchi*[1]

[1] Japan Advanced Institute of Science and Technology
[2] New Japan Chemical Co., Ltd.

Email: m_yama@jaist.ac.jp

Abstract

An extruded polypropylene (PP) sheet in which PP molecules and crystalline lamellae orient perpendicular to the flow direction is obtained by addition of a specific nucleating agent, *N,N'*-dicyclohexyl-2,6-naphthalenedicarboxamide. According to the measurements of dichroic ratio of infrared absorption, Hermans orientation function of crystalline phase is a large negative value whereas that of amorphous phase is close to zero. The sample shows anomalous anisotropy in dynamic tensile modulus, in which the storage modulus in the machine direction (MD) is lower than that in the transversal direction (TD) in the low temperature range and vice versa at high temperatures. Moreover, the tensile test reveals that Young's modulus and yield stress in MD direction are larger than those in TD direction at room temperature. These results indicate that PP crystallites are mechanically connected in MD direction. It can be explained by the existence of tie chains in the flow direction.

Introduction

β-form crystal of isotactic polypropylene (PP) is widely accepted in terms of mechanical properties to achieve pronounced toughness,[1,2] which is one of the most important properties for PP. In general, addition of β nucleating agents and control of mixing and processing conditions are inevitable to obtain PP with high level of β form crystals. Recently, our research group succeeded to prepare PP sheets in which c-axis of PP orients perpendicular to the flow direction employing a new type of a β nucleating agent. The nucleating agent exists as needle crystals in a molten PP, which orients to the flow direction at extrusion processing by hydrodynamic force. Then, PP molecules crystallize on the surface of the nucleating agent in which the growth direction of lamellae is perpendicular to the long axis of the needle nucleating agent. Furthermore, c-axis of PP molecules in crystalline phase also orients perpendicular to the long axis of the needle crystals as shown in *Fig.1*.[1,2]

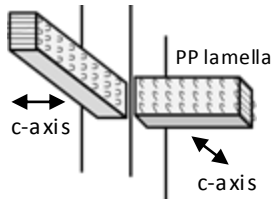

Fig.1: PP lamellae on a

Materials and Methods

Commercially available PP was used in this study. Further, *N,N'*-dicyclohexyl-2,6-naphthalene dicarboxamide (New Japan Chemical, NJ Star[TR] NU-100) was employed as a β nucleating agent. Mixing of PP with 0.1% of the nucleating agent was performed at 260°C by a twin-screw extruder. The mixed pellets were fed into a single screw extruder equipped with a T-die controlled at 200°C to obtain a sheet sample with a thickness of 200 μm. The molecular orientation of extruded sheets was characterized by the infrared (IR) dichroism, dynamic mechanical analysis (DMA), and tensile testing.

Results and Discussion

The molecular orientation of the extruded sheet is characterized by dichroic ratio of infrared absorption peaks at 841 and 973 cm^{-1}, which are ascribed to crystalline and amorphous regions, respectively. Hermans orientation function, *F* is evaluated to be -0.053 (crystal) and 0.007 (amorphous), demonstrating that PP molecules in crystalline phase orient perpendicular to the flow direction. On the contrary, orientation function of amorphous chains is closed to zero, i.e., random orientation on average. The temperature dependence of tensile storage modulus *E'* shows that the magnitude of *E'* in MD is significantly lower than that in TD in the low temperature region whereas vice versa at high temperatures. A similar phenomenon was reported for injection-molded PP, although the order of modulus was completely opposite to our result. This seems to be reasonable because the present sample shows perpendicular orientation to the flow direction. Moreover, the obvious crossing behavior in E' can be explained by the oriented crystalline phase. Because the crystalline lamellae and PP chains in the lamellae orient perpendicular to the flow direction, suggesting that the fragmentation of the lamellae can not be avoided in TD stretching. It is expected that the yield stress in TD is higher than that in MD. However, it is found from the experimental results that the yield stress in MD is higher. The result indicates that many amorphous chains connect neighbor lamellae along to the flow direction. The MD orientation of PP chains during processing is responsible for a large amount of tie chains.

Conclusions

Anisotropy of dynamic mechanical properties is studied employing an extruded sheet of PP containing *N,N'*-dicyclohexyl-2,6-naphthalenedicarboxamide. It is found that PP molecules orient perpendicular to the flow direction and thus the mechanical anisotropy is opposite to those of conventional processing products. Further, crystallites are connected each other along to the flow direction, although both crystalline lamellae and PP chains in crystals orient perpendicular to the flow direction. The amorphous chains which orient to the flow direction by the applied flow are responsible for the mechanical connection.

References

1. Y. Uchiyama, S. Iwasaki, C. Ueoka, T. Fukui, M. Yamaguchi, J Polym Sci B, 47, 424-433 (2009).
2. M. Yamaguchi, T. Fukui, K. Okamoto, S. Sasaki, Y. Uchiyama, C. Ueoka, Polymer, 50, 1497-1504 (2009).

New methodology to produce a Polyetherimide (PEI) *via* Chloro-Displacement by SABIC Innovative Plastics

Patricia Forcén

SABIC Innovative Plastics

patricia.forcen@sabic-ip.com

SABIC Innovative Plastics has recently launched the production of a polyethermide (PEI) by a novel synthetic pathway demonstrating SABIC's commitment to innovation.

Traditionally, the synthesis of polymers has primarily been approached by ionic, free radical, or condensation step-growth polymerizations in the industry. These synthetic routes mainly produce commodity polymers. The need for high tech devices and designs requires polymers with higher mechanical and thermal performance. This has driven industry to the innovation of new and more sophisticated monomers and the subsequent development of new polymerization methodologies.

One example is the commercial production of a high performance polyetherimide ***(Fig. 1)*** via a chloro-displacement process by SABIC Innovative Plastics.

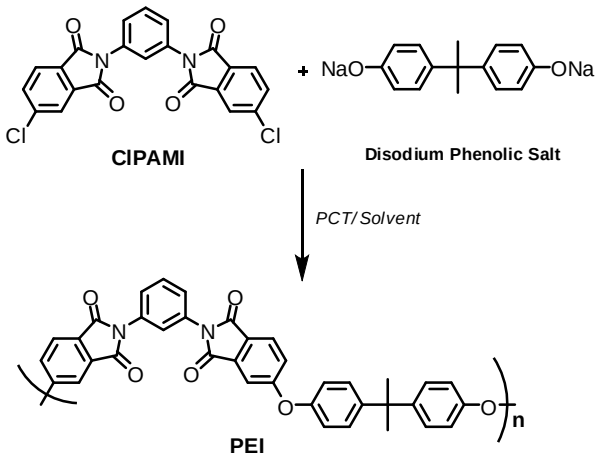

Fig.1

A previous methodology [1] was by the condensation of a proprietary dianhydride (Bis-DA), synthesized by nitro-displacement from 4-nitro-N-methylphthalimide (4-NPI) and the disodium salt of 4,4'-dihydroxy-2,2-diphenylpropane (disodium phenolic salt) with m-phenylene diamine (mPD) to produce PEI.

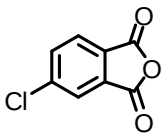

4ClPA

The new route [2] to obtain this polymer is by the reaction of the disodium salt of 4,4'-dihydroxy-2,2-diphenylpropane, with a di-halo-aromatic molecule, 1,3-bis[N-4-chlorophthalimido)]benzene (ClPAMI), using a phase transfer catalyst (PTC) in the nucleophilic displacement reaction ***(Fig. 1)***. The ClPAMI compound is made by reacting a di-amino compound, mPD, with a halophthalic anhydride, 4-chlorophthalic anhydride (4-ClPA), which has recently been produced on a commercial scale with a high purity ***(Fig. 2)***.

Fig.2

This new chloro-displacement process not only permits the synthesis of this particular polyetherimide, it also allows the opportunities to synthesize other novel polymers that were previously difficult to obtain with the traditional polymerization approaches.

Moreover, this route has also led to the availability of an array of intermediates that are now finding there way into other markets. (i.e. ClPA is a key intermediate for production of other molecules such as: specialty monomers, chain extenders, hardeners or cross linkers) allowing this SABIC technology to expand beyond thermoplastic applications.

REFERENCES

[1] D. M White, Schenectady, N.Y. US Patent 3852242
[2] D. J. Brunelle *et al*. US Patent 2006/0173158 A1

Polypropylene Functionalization using acid, anhydride and alcohol by reactive extrusion

T. SADIK[1], F. BECQUART[1], M. TAHA[1] and V. MASSARDIER[2]

[1]Université de Lyon, F-42023, CNRS, UMR 5223, IMP@UJM, Université de Saint Etienne, Jean Monnet, F-42023, Saint Etienne, France

[2]INSA-Lyon, IMP, UMR5223, Université de Lyon, F-69621 Villeurbanne, France

tarik.sadik@univ-st-etienne.fr

Abstract: Polypropylene (PP) was functionalized in the melt by grafting polar monomers. 2,5-bis (tertbutylperoxy)-2,5-dimethylhexane (Luperox 101) and dicumyl peroxide (DP) were used as radical initiators. A Haake Rheomix mixer and corotative twin screw extruder were used for the experiments. The polar monomers used in this work were itaconic acid (IA), 2-hydroxyethyl methacrylate (HM), 3-allyloxy-1,2-propanediol (AP) and 2-octen-1-ylsuccinic anhydride (OY). The existence of grafting PP was confirmed by FTIR and Elemental Analysis. The degree of grafting obtained was 4% by weight of PP for IA, 4% for AP, 9% for HM and 2,1% for OY. Thermal analysis indicates the polarity of PP increase by grafting reaction and GPC showed that the grafting was not accompanied by a M_w decrease.

Introduction: The radical functionalization of polypropylene by reactive extrusion is a very challenging industrial process. The occurrence of side reactions such as chain scission makes the grafting process quite critical for the production of grafted polymers with high graft contents while preserving the mechanical properties or processability. Besides, it is also very challenging to control the chemical structure of the grafts during processing and the co-existence of several types of grafts is usually observed in commercial products [1-3].

The well studied modification of PP is with maleic anhydride, but grafting reaction is accompanied by chain scission, and the grafting degree and efficiency are relatively low.

The purpose of this work was to study the melt functionalization of PP by reactive extrusion with (IA), (HM), (AP) and (OY). Some properties of modified PP were also reported.

Experimental: Polypropylene homopolymer Moplen HF500R was kindly supplied by LyondellBasel Industries. IA, HM, AP and OY were purchased from Sigma Aldrich. Free radical initiator Luperox 101 was generously supplied by Arkema, dicumyl peroxide initiator was obtained from Aldrich.

PP was functionalized with polar monomers with Luperox 101 and DP as initiators in a reactive melt polymer processing. The grafting reactions were carried out in a Haake Rheomix mixer and corotative twin screw extruder. Prior to any analysis, the modified PP was purified. The evidence of grafting as well as an estimation of its extent, expressed as weight percent of grafting, was determined by FTIR spectroscopy. Molecular weights were determined by high temperature gel permeation chromatography (GPC). The thermal properties of modified PP were determined by DSC under a nitrogen atmosphere. The rheological measurements were performed using a Rheometric Scientific ARES N2 with parallel plate geometry.

Results and Discussion: The evidence of grafted polar function in PP was confirmed by FTIR. For the grafting reactions carried out in Haake Rheomix, the FTIR spectrum of the grafted PP with acid shows two absorption bands in carbonyl region. The absorption band at 1712cm^{-1} is due to stretching vibrations of the carbonyl groups of carboxylic acid. The second absorption band centered at 1770cm^{-1} is due to carbonyl absorption band coming from monomer grafted as anhydride during the grafting reaction. In the case of PP grafted alcohol, the FTIR spectrum showed an absorption band at 3640cm^{-1} due to stretching vibrations of hydroxyl groups of the alcohol. For PP grafted anhydride, the appearance of a low absorption band near 1792cm^{-1} is assigned to symmetric C=O stretching of anhydride functions grafted on PP. FTIR has been combined with elemental analysis to get an estimate of the grafting rate expressed as weight percent wich reaches 4wt% for PP grafted acid, 4wt% for PP grafted alcohol and 2wt% for PP grafted anhydride. In the same way, an estimate of the grafting rate was determined for the grafted PP prepared by twin-screw extruder. When IA was used as functional polar monomer, a maximum of 3% of grafting was reached. A maximum of 6,7% by weight of HM was incorporated in PP and grafting of AP is estimated to be 1,2%

The control of chain scission was verified by GPC, the molecular weight remains about constant. In order to characterize grafted PP, a sample of each modified PP was analysed by DSC and rheology. Thermal properties indicate slightly higher crystallinity of the functionalized polymer due to the polarity of modified PP.

Conclusion: It is concluded from this study that IA, AP, HM and OY can be successfully grafted onto PP in the melt without M_w decrease. The combination of FTIR with elemental analysis determines the extent of grafting obtained where higher percentage of grafting was obtained for HM.

Reference:

[1] G. Moad, Prog. Polym. Sci., 24, 81–142, 1999

[2] Drooghaag, D.D.J. Rousseaux, G.R.P. Henry, M. Sclavons, V. Carlier, J. Marchand-Brynaert , Poly Deg and Stab, 95, 342-345, 2010

[3] M. Yazdani-Pedram, H. Vega, R. Quijada, Polymer, 42, 4751-4758, 2001

This study is a part of the FUI-MATORIA Program

Polymeric Surface Modification of Capillaries for the Separation of DNA by Capillary Electrophoresis

Kerrilee Allan[1], *Claire Lenehan*[1], *Hilton Kobus*[1], *Amanda Ellis*[1,2]

[1]School of Chemical and Physical Sciences, Flinders University, GPO Box 2100, Adelaide SA, 5001
[2]Flinders Centre for Nanoscale Science and Technology, School of Chemical and Physical Sciences, Flinders University

kerrilee.allan@flinders.edu.au

Introduction:
Capillary electrophoresis (CE) separates components in a solution based on charge and size, however, DNA has a constant mass to charge ratio regardless of base pair length. At present DNA is separated using polymer gel filled capillaries, however, these have a limited life time due to the deterioration from run to run, the inability to regenerate the gel, and the formation of air bubbles[1]. Consequently in order to overcome these issues, recent research is focusing on direct surface modification of the capillary to selectively retard DNA based on size[1]. In particular, extensive research is being conducted into the use of surfaces modified with polymers in order to manipulate DNA transport through the capillary[2-3]. These dynamic-type coatings are becoming the method of preference for capillary surface modification due to the wide range of polymers available and the capacity for capillary regeneration[4-6]. Here we describe a capillary electrophoretic method of separating double-stranded oligonucleotides (oligo-dsDNA) with 1 - 4 base pair resolution using a fused-silica capillary dynamically coated with *Poly*(ethylpyrrolidine methacrylate-*co*-methyl methacrylate) PEPYM-*co*-PMMA copolymer. Separation is compared to analysis using a capillary coated with a novel PEPYM-*block*-PMMA copolymer.

Materials and Methods:
PEPYM-*co*-PMMA copolymer was synthesised by free-radical co-polymerisation of EPYM (25%) and MMA (75%) in THF using benzoyl peroxide as the radical initiator. PEPYM-*block*-PMMA was prepared by RAFT polymerisation by first synthesising a PMMA macro-RAFT agent in DMF using 2-cyanoprop-2-yl dithiobenzoate as the RAFT agent and 4,4′-azobis(4-cyanovaleric acid) as the initiator. The block copolymer was prepared in the same way from the PMMA macro-RAFT agent and EPYM. The copolymers were characterised by NMR, FTIR and GPC. The dynamic coating was prepared by dissolving the copolymer in ethanol with aqueous ammonia and formic acid (1 mg/ml) and flushing the polymer solution through the capillary using the CE system.
All DNA separations were carried out on an Agilent 3D Capillary Electrophoresis Instrument with diode array UV detection at 260 nm and negative polarity (cathodic flow) at -131.6 V/cm.

Results and Discussion:
Isolation of the copolymers resulted in a fine yellow powder, with free radical polymerisation exhibiting greater yields than RAFT polymerisation. FTIR analysis of copolymers of EPYM and MMA indicated the presence of the ester bonds, pyrrolidine ring, and C-H stretching. These results were confirmed by ^{1}H NMR.

In order to determine the effectiveness of the coating, the electroosmotic flow (EOF) was determined for the buffer in both a non-coated and coated capillary. Results show a reduction in EOF for the coated capillary due to the replacement of the surface silanol groups with polymer reducing the negative surface charge distribution. In addition, the shorter strands of DNA are screened more by the positively charged dynamic coating than longer strands, and hence are retained by the capillary surface to a greater extent (Figure 1).

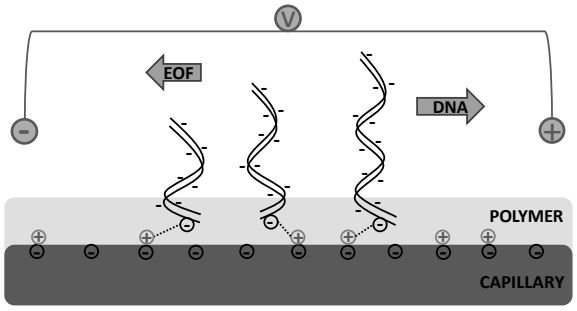

Figure 1: Proposed charge dependent separation of DNA strands due to polymer interactions.

The DNA interaction with the surface differs for the random and block copolymers. This is most likely due to the copolymer arrangement on the surface.

Conclusions:
Capillaries dynamically coated with random and block copolymers of EPYM and MMA are capable of separating short strands of dsDNA with well resolved peaks. The migration times of the ds-oligonucleotides decreased with increasing size and all oligonucleotides investigated exhibited very good reproducibility, less than 1 % RSD (n = 3). This coating can be simply accomplished within one hour affording a greatly reduced capillary preparation time and was shown to effectively reduce the EOF. A capillary lifetime of over 70 injections was observed.

References:
[1] K. Klepárník, P. Bocek, *Chem. Rev.*, **107**, 5279-5317 (2007).
[2] S. Hjertén, *J. Chromatogr.*, **347**, 191-198 (1985).
[3] N. González, C. Elvira, J.S. Román, *J. Polym. Sci.*, **41**, 395-407 (2002).
[4] J. Bernal, I. Rodríguez-Meizoso, C. Elvira, E. Ibáñez, A.J. Cifuentes, *J. Chromatogr. A*, **1204**, 104-109 (2008).
[5] M. Chiari, M. Cretich, F. Damin, L. Ceriotti, R. Consonni, *Electrophoresis*, **21**, 909-916 (2000).
[6] P. Zhang, J. Ren, *Anal. Chim. Acta*, **507**, 179-184 (2004).

Radiation induced vulcanization of SBR blends containing pristine silica and silica modified by polybutadiene grafting: reaction mechanisms and physicochemical properties of the vulcanizates

Daniele Dondi[1], *Angela Lostritto*[2], *Lucia Conzatti*[3], *Maila Castellano*[4], *Antonio Turturro*[4], *Silvia Bracco*[5], *Maurizio Galimberti*[2], *Armando Buttafava*[1], *Antonio Faucitano*[1]

[1] Dipartimento di Chimica Generale, Università di Pavia, V. le Taramelli 12, 27100 Pavia (Italy)
[2] Pirelli Tyres, Milano-Bicocca, Milano (Italy)
[3] Istituto per lo Studio delle Macromolecole – UOS CNR ,Genova (Italy)
[4] Dipartimento di Chimica e Chimica Industriale, Università di Genova (Italy)
[5] Dipartimento di Scienza dei Materiali, Università di Milano-Bicocca (Italy)

daniele.dondi@unipv.it

Introduction

In normal thermal sulphur vulcanization, silica-rubber chemical links are not formed unless coupling agents like bis (3-trietoxy silyl propyl) tetrasulfide (TESPT) are used. A different situation applies when high energy ionizing radiations are used as initiator since reactive species are formed in both silica and the rubber matrix thus allowing silica-rubber chemical reactions to take place.

The aim of this work is to exploit the γ ray induced vulcanization of SBR-silica blends to develop silica-rubber chemical links, with a focus on the mechanism leading to said links and on the cured blends mechanical properties. Related to the mentioned aim is also the attempt to enhance the formation of silica-rubber chemical links through the grafting onto silica of vinyl rich polybutadiene olygomers with the role of free radical scavengers.

Materials and Methods

Silica Zeosil 1165 with a surface area 160 m^2/g was used as received from Rhodia. Blends were prepared by mixing 30-40 % of pristine and modified silica with 40 % SBR (30% styrene, 45 % vinyl and 25 % aromatic oil). Modified silica was prepared (1-3) by impregnation and subsequent radiation grafting of polybutadiene olygomers with average molecular weight $\overline{M}_n$ = 5000 and 1000 and vinyl double bond content 20% and 45% respectively.

γ irradiations were performed under nitrogen atmosphere in a 60-Co source with total doses ranging from 100 to 400 kGy.

Information concerning the mechanism of crosslinking and silica-rubber chemical links were obtained by EPR spectroscopy and 13-C, 29-Si CP/MAS NMR spectroscopy.

Mechanical behaviour of compounds was investigated by tensile and dynamic-mechanical measurements.

Results and Conclusions

During the irradiation, radicals and radical-ions are formed both in silica and the rubber matrix. In silica a powerful free valence migration mechanism exists leading to radicals decay and diffusion toward the surface. The species attaining the surface react with SBR vinyl double bonds thus generating grafted radicals and silica-rubber chemical links. When modified silica is used, the formation of silica-rubber chemical link is enhanced since a greater fraction of silica radicals escapes mutual coupling being scavenged at the surface by polybutadiene vinyl bonds. With SBR blends containing pristine silica, the crosslinks yields, as determined by the Flory-Rhener method, grows almost linearly with the radiation dose attaining a value > $2.5x10^{-4}$ moles/kg at about 400 kGy (both physical and chemical links, fig 1). When using modified silica, lower initial yields are observed followed by an acceleration period which ultimately leads to a full recovery of the overall crosslinks yields with respect to pristine silica. The initial lower yields are thought to arise from the weakening of the silica-rubber physical links due to the attenuation of the silica surface energy by the olygomer grafting. The subsequent acceleration is related to the taking over of the mechanism leading to silica-rubber chemical links. Mechanical measurements are consistent with this interpretation showing that blends containing modified silica show lower initial mechanical strength followed by a faster response to the radiation dose.

In order to evaluate the effect of the radiation dose on the dispersion of pristine and modified silica, a thorough investigation by TEM has been carried out.

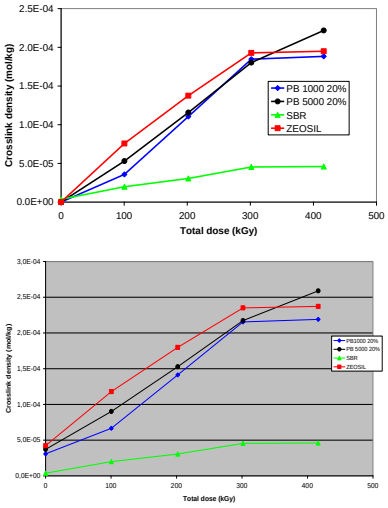

Fig 1 Crosslinks density vs. radiation dose for SBR blends containing pristine and modified silica. The curve pertaining pure SBR is shown for comparison

Bibliography.

1) D.Dondi, C.Palamini, F.Pepori, A.Buttafava, P.Galinetto, A.Faucitano Nukleonica, 54, 71-75, (2009)

2) D.Dondi, A.Buttafava, P.Stagnaro, A.Turturro, A.Priola, S.Bracco, P.Galinetto, A.Faucitano
Radiat. Phys. Chem. 78, 525-530, (2009)

3) D. Dondi , C. Palamini, A.Buttafava, A.Faucitano, P.Galinetto, M.Nahmias, L.Giannini, A.Lostritto
Macromol. Symp.2010, 296, 38-43

Preparation of Polystyrene Nanocomposite Nanofibers by Electrospinning

Niloofar Reshad[1], *Mohammad Najafi*[1], *Hossein Roughani-Mamaqani*[2], *Mehdi Salami-Kalajahi*[1,2], *Vahid Haddadi-Asl*[2]

[1] Polymer Engineering Division, Research Institute of Petroleum Industry (RIPI), 1485733111, Tehran, Iran.
[2] Department of Polymer Engineering, Amirkabir University of Technology, Tehran, Iran.

niloofar.reshad@yahoo.com

Abstract: The electrospun nanofibers have attracted great attention since they were employed in a wide variety of applications, such as scaffolds for tissue engineering, sensors, molecular electronics, and protective clothing.[5] Electrospinning, a versatile route which can be applied to various polymers, polymer blends, sol-gels, and composites, is well known to be a useful tool to prepare nanowebs of the ultrathin fibers having a diameter of about few hundred nanometers.[6] Incidentally, considering the variety of polymerization techniques, one cannot ignore the prominent role of controlled/"living" radical polymerization (CRP) in the synthesis of polymers with narrow molecular weight distribution and well-defined topology. CRP has attracted much attention in recent years for providing simple and robust routes to the synthesis of tailor-made polymers. In this context, nitroxide-mediated polymerization (NMP), reversible addition-fragmentation chain transfer polymerization (RAFT), and atom transfer radical polymerization (ATRP) have extensively been studied. Some advantages of the latter over the former systems are the applicability to a wide variety of monomers and systems of polymerization and its being less sensitive to impurities. [7]

The SEM and TEM images of polystyrene nanocomposite nanofibers prepared via electrospinning technique are depicted in **Fig. 1** and **Fig. 2** respectively. The morphology and average diameter of the prepared nanofibers can easily be observed in **Fig. 1**. Fibers with the average diameter ranging from 450-700 nm are obtained by this process. The smallest variations in the accelerating voltage, solution flow rate, and the distance between needle and collector result in the instability of the nanofiber morphology and thereby production of nanofibers with uneven diameters. The TEM results confirm the intercalation of clay layers in the polymer matrix of polystyrene nanocomposite nanofibers (**Fig. 2**); the clay layers are specified by the tactoids in the TEM image. The light and dark areas represent polystyrene matrix and silicate layers respectively. The lack of space between the clay platelets and the polymer matrix affirms that there is an interaction between the clay layers and the host polymer matrix; this facilitates delamination of the clay stacks by the polymerization process.[8]

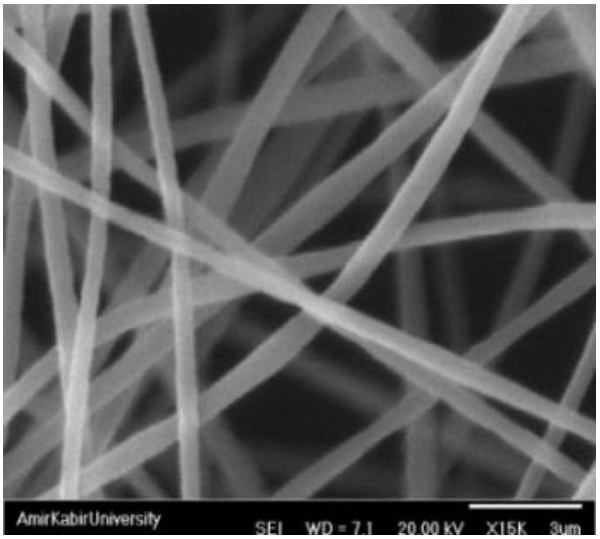

Figure 1. SEM image of the polystyrene nanocomposite nanofibers containing 4 wt% of nanoclay

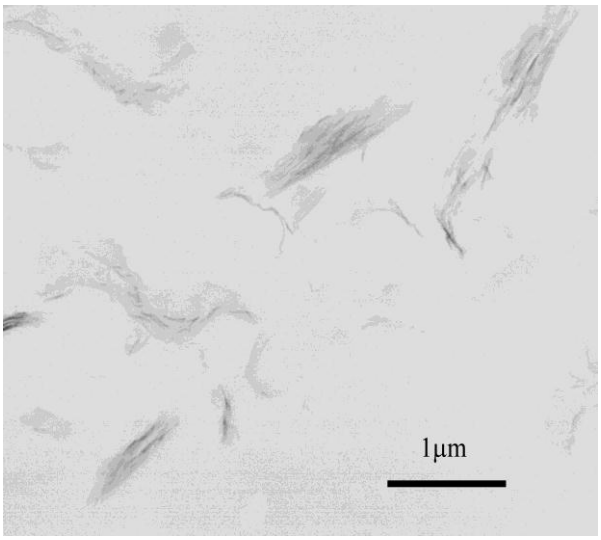

Figure 2. TEM image of the polystyrene nanocomposite nanofibers containing 4 wt% of nanoclay

To summarize, ATRP and electrospinning were jointly employed to produce "fit for function" polymeric nanofibers. The delamination of nanoclay stacks was achieved during the ATRP process and nanofibers with the average diameter ranging from 450-700 nm were obtained by electrospinning of the synthesized nanocomposite.

[5] P. W. Gibson, H. L. Schreuder-Gibson, D. Rivin, *AIChE J.*, **1999**, *45*, 190.
[6] P. D. Dalton, D. Grafahrend, K. Klinkhammer, D. Klee, M. Moller, *Polymer*, **2007**, *48*, 6823.
[7] W. Jakubowski, K. Matyjaszewski, *Angew. Chem*, **2006**, *118*, 4594.
[8] H. Roughani-Mamaghani, V. Haddadi-Asl, M. Najafi, M. Salami-Kalajahi, *Polymer Composites*, **2010**, Early View.

The Effect of Partially Crosslinking of High Density Polyethylene on Its Structure and Rheology

K. Montaser Asadi, J. Morshedian, Y. Jahani, A. Pakdaman

Plastic Processing & Engineering Department, Iran Polymer and Petrochemical Institute, Tehran, Iran

E-mail: kourosh.m.a@gmail.com

Introduction: It has been recognized for quite some time that crosslinked polyethylene has superior properties such as higher operating temperature and better chemical and environmental resistance in comparison with uncrosslinked PE [1]. However the main drawback of crosslinked PE of common degree of crosslinking (above 60% of gel content) is that its crosslinking must occur in the final product, i.e. crosslinked PE cannot be processed and its products cannot be recycled. Better flowability of partially crosslinked PE leads to processable raw materials and recycleable products with desired properties [2]. So, it is of crucial importance to find the optimum limit of crosslinking in such materials.

Partially crosslinked PE can be used in low shear processes such as rotational molding (to produce tanks), film blowing (to produce packaging films) and processing of crosslinked PE foams (to achieve high quality closed-cell structure) [3, 4]. In this work limit of crosslinking degree of HDPE for flowing through an extruder was determined. Crosslinking was achieved by both chemical and physical methods. Some properties of prepared lightly crosslinked PEs were determined and compared.

Materials and Methods: High density polyethylene with density of 0.956 gr/cm^3 and melt flow index (MFI) of 1.2 gr/min was partially crosslinked through a chemical method using dicumyl peroxide in HAAKE SYS 90 HIB internal mixer and an irradiation method with electron beam by Rhodotron TT200 Ion Beam Application.

At first, the processability of crosslinked products was assessed using a single extruder, HAAKE SYS 90 HIB, equipped with a rod die.

In chemical method various amounts of DCP were mixed with the polymer and fed into the reactive extruder in order to form strands after crosslinking occurrence, while in physical method the irradiated granules were directly used for flowability.

Gel content of flowable lightly crosslinked samples were determined. Some typical amounts of peroxide and irradiation doses were selected to give close values of gel contents.

Rheological behavior of samples was studied using Rheometer, MCR300, from Paar Physica Co. Molecular weight of uncrosslinked polymer and partially crosslinked samples (the sol fraction) were determined by Ubbelohde viscometer. MCR was used as an alternative method to calculate an approximate value for Mw from readings of zero-shear rate viscosity. MFI at different loads was also measured for an estimation of

Results and Discussion: Chemical and irradiated samples of up to 40% gel content were found to still flow through the employed rod die of 0.5 cm in diameter. Hence for properties investigation, only samples with less than 40% gel were chosen, some of which are shown in Figure 1. The results obtained from MFI, viscometry and rheology indicated that with increasing of crosslinking degree in both methods higher and broader molecular weight polymers were obtained [5]. Molecular weights were estimated from zero-shear rate viscosity using the relationship $\eta_0=k.Mw^{\alpha}$ with k and α parameters obtained for rubbery behavior are indicated in Table 1.

It was also observed that with increasing the amount of peroxide or radiation dose, molecular weight of the sol fraction was decreased compared to the neat polymer, i.e. crosslinking mostly occurred between longer chain molecules and chain scission in shorter ones. Moreover, the sol fractions of irradiated samples had lower molecular weight than those of peroxide crosslinked samples of the same gel content. Rheological results showed that while zero-shear rate viscosity was increased with crosslinking, its shear sensitivity was also increased. This indicated the higher flowability of partially crosslinked samples in the processing shear range. G' and G" curves versus frequency implied a solid-like behavior in low shear rates with a yield stress. Higher value of G' in comparison with G" (tan δ<1) over whole frequency range confirmed a rubber-like behaviour of samples in the molten flow.

Figure1

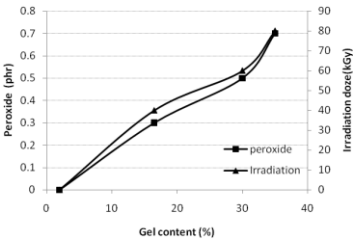

Table 1

Samples	η_0 (Pa.s)	M_w(gr/mol)
0.3 DCP	2255100	1110530
0.5 DCP	4181100	1329540
0.7 DCP	4656700	1371960
40 KGy	738650	802100
60 KGy	1917800	1059300
80 KGy	1613400	1007240

Conclusions: Crosslinked HDPE samples of less than 40% gel content are still processable in conventional single screw extruders. Although the average molecular weight increases with crosslinking, the sol fractions have lower molecular weight in comparison with the uncrosslinked samples.

The effect of crosslinking on Mw of sol fraction and polydispersity index is more pronounced in the irradiation method.

In the processing shear range, shear sensitivity and hence flowability increases while elasticity also increases for lightly crosslinked HDPE.

References

[1] S. Ultsch et al., Plast. Rubber. Process. Appl. 3, 81-91, 1990.
[2] M. Narkis et al., Polym. Eng. Sci. 9, 153-158, 1969.
[3] A. Marcilla, et al., Polym. Eng. Sci. 47, 1804-1812, 2007.
[4] S.M. Tamboli, et al., Indian J. Chem. Technol. 11, 853-864, 2004.

Precision design of novel copolymers and nanohybrids by Cobalt Mediated Radical Polymerization (CMRP)

Christophe Detrembleur, Marie Hurtgen, Yasmine Piette, Jean-Michel Thomassin, Christine Jérôme, Antoine Debuigne

Center for Education and Research on Macromolecules (CERM), University of Liège, Sart-Tilman B6a, 4000 Liège, Belgium

christophe.detrembleur@ulg.ac.be

Introduction. Cobalt Mediated Radical Polymerization (CMRP) using bis(acetylacetonato)cobalt(II) ($Co(acac)_2$) is the most efficient technique for controlling the radical polymerization of vinyl acetate until high molar masses and low polydispersity.[1-4] In this process the cobalt complex ($Co(acac)_2$) reversibly forms a Co-C bond at the chain-end of the polymer. At any time, a large number of polymer chains capped by a cobalt complex are in equilibrium with a tiny amount of propagating species such that irreversible termination reactions that occur between radicals by coupling or dismutation are avoided. The reversibility of the deactivation is ensured by homolytic cleavage of the Co-C bond by thermal treatment or radical exchange. By carefully adjusting the polymerization conditions, this CMRP process allows to control efficiently both conjugated (n-butyl acrylate (nBuA)[5], acrylonitrile (AN)[6]) and non-conjugated monomers (vinyl acetate (VAc)[1-4], N-vinyl pyrrolidone (NVP)[7]) using the same cobalt complex. Block copolymerization between these two monomers families is also possible by the fine-tuning of the Co-C bond at the polymer chain-end by metal coordination, giving access to novel copolymers.[1]

The importance of this system in the field of the macromolecular engineering is best illustrated by the recent development of a fast, efficient and quantitative radical polymer chain coupling reaction called Cobalt Mediated Radical Coupling (CMRC)[8-10]. Treatment of well-defined polymers prepared by CMRP by a conjugated diene such as isoprene exclusively leads to the coupling product with high coupling efficiencies (~ 95%) even when the molecular weight of the precursor is high (about 25000g/mol)[8-10]. This Cobalt-Mediated Radical Coupling (CMRC) method also proved efficiency for preparing symmetrical triblock copolymers when applied to a diblock precursor and for the efficient mid-chain functionalization of polymers.

Results and discussion. This communication aims at presenting recent advances in the field of CMRP, more particularly in the precision design of novel copolymers for advanced applications. Recent developments in our laboratory have demonstrated the possibility to promote the n-butyl acrylate homopolymerization with control until high molar masses (~ 6 10^5 g/mol) in mild conditions using $Co(acac)_2$ as controlling agent.[5] In the frame of synthesizing novel materials useful for bio-applications, we were interested in controlling the polymerization of poly(ethylene oxide) methyl ether acrylate (APEO) and in copolymerizing this monomer with vinyl acetate. We will show that controlling the APEO polymerization is not trivial and the reactivity of the CMRP system for APEO is different than that of nBuA. After discussing the optimal conditions for control, we will describe the synthesis of poly(vinyl acetate)-b-poly(poly(ethylene oxide) methyl ether acrylate) (PVAc-b-PAPEO), a novel block copolymer of interest in the field of drug delivery systems and surfactants.

Conditions for controlling the vinyl chloride (VC) homopolymerization and for synthesizing poly(vinyl chloride)-b-poly(vinyl acetate) (PVC-b-PVAc) block copolymers in mild conditions by CMRP will also be described. These new results open new avenues in the design of novel PVC based block copolymers.

In the last part of the talk, we will report on the preparation of novel well-defined nanohybrids of fullerene and carbon nanotubes grafted by poly(vinyl alcohol) based copolymers for photodynamic cancer therapy and electromagnetic protection purposes, respectively. A universal radical grafting onto approach of poly(vinyl acetate) based copolymers prepared by CMRP in mild conditions is used for the formation of the nanohybrids.

Conclusions. This talk will therefore emphasize the versatility of the CMRP process for the precise design of unprecedented copolymers and nanohybrids of interest using a cheap and commercially available cobalt complex ($Co(acac)_2$). Ways for adjusting the reactivity of the system in regards to the polymerized monomers will be highlighted.

References. [1]Debuigne, A.; Poli, R.; Jerome, C.; Jerome, R.; Detrembleur, C. *Prog. Polym. Sci* **2009**, *34*, 211-239 ; and references therein. [2]Debuigne A., Caille J.-R., Detrembleur C., Jerome R. *Angew. Chem., Int. Ed.* **2005**, *44*, 3439-3442. [3]Debuigne, A.; Caille, J.-R.; Jerome, R. *Angew. Chem.* **2005**, *44*, 1101-1104. [4] Debuigne, A.; Champouret, Y.; Jerome, R.; Poli, R.; Detrembleur, C. *Chem. Eur. J.* **2008**, *14*, 4046-4059. [5]Hurtgen M., Debuigne A., Jerome C., Detrembleur C. *Macromolecules* **2010**, *43*, 886-894. [6]Debuigne, A.; Michaux, C.; Jerome, C.; Jerome, R.; Poli, R.; Detrembleur, C. *Chem. Eur. J.* **2008**, *14*, 7623- 7637. [7]Debuigne A., Willet N., Jerome R., Detrembleur C. *Macromolecules* **2007**, *40*, 7111-7118. [8]Debuigne, A.; Jerome, C.; Detrembleur, C. *Angew. Chem., Int. Ed.* **2009**, *48*, 1422-1424. [9]Debuigne A., Poli, R., De Winter J., Laurent P., Gerbaux, P., Dubois P., Wathelet J.-P., Jérôme C., Detrembleur C. *Chem. Eur. J.* **2010**, *16*, 1799-1811.[10]Debuigne A., Poli R., De Winter J., Laurent P., Gerbaux P., Wathelet J-P., Jerome C., Detrembleur C. *Macromolecules* **2010**, *43*, 2801–2813.

Synthesis and Characterization of Poly (alkyloyloxyethylmethacrylate-co-methylacrylate) as Solid-Solid Phase Change Materials for Thermal Energy Storage

Tuğba Güngör Ertuğral[1], *Ömer Faruk ENSARİ*[2], *Cemil ALKAN*[2]

[1]Giresun University, Şebinkarahisar Vocational School, Department of Food Technology, Giresun, Turkey
[2]Gaziosmanpaşa University Department of Chemistry 60240 Tokat, Turkey

tuba.gungr@hotmail.com

Phase change material is a substance with a high heat of fusion which, melting and solidifying at a certain temperature, is capable of storing and releasing large amounts of energy. Heat is absorbed or released when the material changes from solid to liquid and vice versa; thus, PCMs are classified as latent heat storage (LHS) units. Total amount of energy absorbed or released by a phase change material can be calculated by equation 1.

$$Q = m\Delta H_M + \int_i^M mC_p dT + \int_M^f mC_p dT \quad (1)$$

PCMs should be encapsulated for usage and they are mostly encapsulated in polymers for the ease of application. Polymeric solid solid phase change materials are promising for their easy applicability and expected long lasting property. In this work, 2-hydroxyethyl methacrylate esterified with acyl chlorides of three different fatty acids to obtain monomers with phase changing property at convenient temperatures with high storage density so that copolymerization of these monomers with methylacrylate will result in polymers with solid solid phase changing property at variable phase change temperatures. 9 different polymers have been synthesized as a result of the reaction between produced monomers and methylacrylate at 3 different weight ratios. Produced copolymers were characterized by structural and thermal aspects. For the synthesis of the novel PCMs, myristic acid, palmitic acid, and stearic acid were chosen and they were transformed to acyl chlorides by thionyl chloride in the presence of dimethylformamide catalyst. Fatty acid acyl chlorides were bound to 2-hydroxyethylacrylate monomer from hydroxyl group as shown in the following Figure.

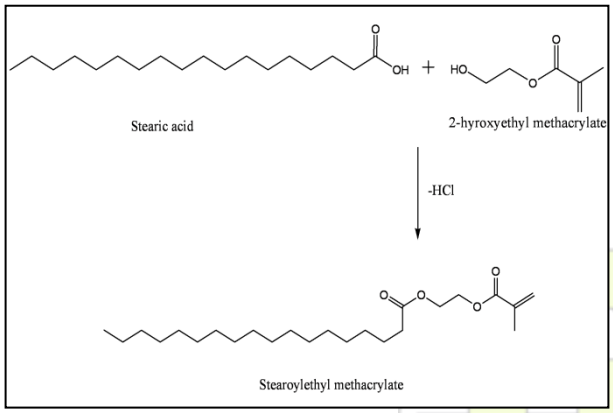

FT-IR and NMR spectroscopy techniques were used to characterize the produced PCMs structurally as molecular weight measurements were done using Gel Permeation Chromatography (GPC) technique. Molecular weight of the polymers produced decreased by the fatty alkyloylethylmethacrylate monomer content and with increasing paraffinic side length. Phase change temperatures and enthalpies and degradation temperatures of the synthesized PCMs were investigated using Differential Scanning Calorimetry (DSC) and Thermal Gravimetric Analysis instruments respectively and it was found that produced polymers have potential to be used as thermal energy storage materials and stable up to considerably high temperatures. On the other hand structural and thermal consistency of the polymers was confirmed by FT-IR and DSC measurements after accelerated thermal cyclings.

Thermal conductivity of the polymers was found to be in the range of the thermal conductivities of fatty acids.

Besides polarize optical microscopy was used for morphology investigation of polymers below and above phase transition temperatures.

Key words: 2-hydroxyethyl methacrylate, methylacrylate, phase change material, fatty acid

References

Baran, G., Sarı, A., 2003. Phase change and heat transfer characteristics of a eutectic mixture of palmitic and stearic acids as PCM in a latent heat storage system. Energy Conversion and Management 44: 3227–3246.

Feldman, D., Khan, M. A. Banu, D., 1989. Energy storage composite with an organic PCM, Solar Energy Materials, 18(6), 333-341

Feldman D., M.M. Shapiro, D. Banu and C.D. Fuks, Fatty acids and their mixtures as phase change materials for thermal energy storage, *Solar Energy Materials* 18 (1989), pp. 201–216.

Hong K., Park S., Preparation of polyurethane microcapsules with different soft segments and their characteristics. Reactive and Functional Polymers 42, (1999) 193.

Jiang Y., Ding E. Y., Li G. Study on transition characteristics of PEG/CDA solid-solid phase change materials Polymer 43 (2002) 117–122.

Su J. C., Liu P. S. A novel solid-solid phase change heat storage meaterial with polyurethene blok copolymer structure Energy Conversion and Management 47, (2006) 3185.

Yuan X. P., Ding E. Y. Synthesis and Characterization of Storage Energy Materials Prepared from Nano Crystalline Cellulose/Polyethylene Glycole Chinese Chemical Letters 17(8), (2006) 1129.

New Recycling Polymer-Immobilizing Catalysts for the Controlled/living Radical Polymerization

Evgenia Geraskina, Mikhail Lazarev (Dr), Dmitry Grishin (Prof)

Research Institute of Chemistry of Nizhny Novgorod State University,
23/5 Prospekt Gagarina, 603950 Nizhny Novgorod, Russia. Fax: (+7) 831 465 8162
E-mail: garaskinaev@mail.ru

Introduction. Cu-mediated ATRP has become one of the most powerful tools for the synthesis of well-defined polymer materials. However, one remaining drawback of ATRP is the difficulty to effectively separate the homogeneous ATRP catalysts from products. Therefore it can limit one of the processes of choice for large-scale production of special polymers such as thermoplastic elastomers and materials with medical and pharmaceutical applications, among others. Although many post-polymerization purification workup methods have been devised to remove the soluble catalyst from the polymer,[1-3] a solid, recoverable, and recyclable catalyst is the most attractive solution. However, these techniques offer limited control over the polymerization of vinyl monomers, originating from the heterogeneous nature of the process.

We believe that immobilized catalysts (using functional polymers that interact with the transition metal as stabilizers) can overcome this diffusion limitation. In our case the catalyst is copper complexes coordinated with nitrogen atoms of the pyridine units of poly-2- and poly-4-vinylpyridine. Moreover, the catalysts based on copolymers with styrene or C12-C14 esters of methacrylic acid, and the non-soluble in organic solvents copolymers cross-linked with divinylbenzene (2%) were obtained. Such supported catalysts would act similarly to homogeneous catalysts and can be considered as an "quasi-soluble".

Materials and Methods. The poly-2- and poly-4-vinylpyridine, 2-vinylpyridine were got from Sigma-Aldrich. The poly-2-vinylpyridine-co-styrene was synthesized in bulk at 70^0C initiated with AIBN (1 mol%). The poly-2-vinylpyridine-co-divinylbenzene, poly-2-vinylpyridine-co-styrene-co-divinylbenzene and poly-2-vinylpyridine-co-methacrylate C12-C14-co-divinylbenzene were prepared via emulsion polymerization in the presence of sodium dodecylsulphate (0.5 mass%, Sigma-Aldrich) and AIBN (1 mol% to monomer mixture) as initiator at 70ºC for 5 hours. The catalytic complexes were prepared by ligand change reaction. The polymerization of methyl methacrylate (MMA) was performed in a glass tube equipped with magnetic stirrer under vacuum. The catalytic complex, monomer, ethyl-2-bromoisobutyrate (EBiB, initiator) and solvent were put to the tube, then degassed and heated during adjusted time. Poly(MMA) was separated via fractional precipitation to methanol in the case of soluble homopolymers and was extracted from the mixture with catalyst via acetonitrile after precipitation to hexane in the case of insoluble homopolymers. The cross-linked catalysts were separated via filtration through PTFE membrane filter. Purified polymers were dried under vacuum.

Synthesized poly(MMA) was characterized by SEC with two Phenomenex phenogel column 7.8×250 mm, 10 μm (10^3 and 10^5 Å) on Knauer WellChrom equipment with RI and UV-detectors.

Results and Discussion. The influences of temperature, the ratio of the components in the initial mixture, the nature of solvents and polymer matrix on the polymerization have been investigated.

The polymerization in polar solvent (DMSO) is characterized in high polymer yield and PDI values, and in non polar solvents (benzene and dioxane) in low rate. In Single Electron Transfer – Living Radical Polymerization (SET-LRP) the balance between dormant and active chains is provided by an outer-sphere heterolytic SET-mediated by the appropriate choice of solvent. THF is the optimal solvent that allows the controlled radical polymerization of MMA to provide.

We suppose that the lack of controllability of the immobilized catalysts in ATRP may be caused by the change of coordination angle. The best results were achieved in the presence of soluble and insoluble poly-2-vinylpyridine-co-styrene copolymers. The backbones, connecting with different donor functions bonded to the same Cu ion, are enough long and enough flexible to provide the desired stability for the metal species.

Kinetic studies of the polymerization were performed with both of copolymer catalyst systems. These homogeneous catalysts produce polymers with low PDI. In the presence of the cross-linked catalysts the level of control over the polymerization decreased insignificantly. The molecular weights of the resulting polymer increased linearly with conversion, indicating a living character of polymerization.

Conclusions. It has been established that temperature in the range 90-110^0C, the molar ratio MMA : initiator : Cu = 100 : 1 :1, THF as the solvent and the catalysts based on the copolymer of 2-vinylpyridine with styrene (soluble or non-soluble) are the optimal conditions for providing the controlled polymerization. The immobilized catalysts were removed by simple filtration or sedimentation, and can be recycled, affording a colourless transparent polymer solution.

Acknowledgements. This work has been supported by the Russian Federal Agency for Education "Federal target program of scientific and scientific-pedagogical personnel of innovational of Russia" on 2009-2013 and by Russian foundation for basic researches (project №11-03-00074).

References.

(1) Matyjaszewski, K.; Pintauer, T.; Gaynor, S. *Macromolecules* **2000**, *33*, 1476-1478.

(2) Angot, S.; Ayres, N.; Bon, S. A. F.; Haddleton, D. M. *Macromolecules* **2001**, *34*, 768-774.

(3) Honigfort, M. E.; Brittain, W. J.; Bosanac, T.; Wilcos, C. S.*Macromolecules* **2002**, *35*, 4849.

Effet of coupling agent on the mechanical properties of cellulose fiber/polystyrene composites II. Dependent on the fiber content

*C.D. Zanrosso, M. Poletto,A. J. Zattera, M. Zeni**

Center of Exact Sciences and Technology (CCET) Caxias do Sul University (UCS), Caxias do Sul, RS, Brazil

(mzandrad@ucs.br)

Abstract

The usage of natural fibers as reinforcement in thermoplastic composites has gained a rapid growth in the last few years, due to a several advantages that the natural fibers offer over conventional inorganic fibers, such as, abundance, renewability, low density, high specific strength and stiffness, almost no health hazards, and relatively low cost [1, 2]. However, one difficulty that have prevented a more extended utilization of natural fibers, and it is a challenge for cellulose fiber reinforced thermoplastic composites, is a lack of good interfacial bonding between the hydrophilic nature of fibers to a hydrophobic matrix [1]. This study is focused on evaluating the effect of coupling agent by mechanical properties of cellulose fiber and polystyrene composites.

In this study, cellulose fiber/polystyrene composite were processed on a twin-screw extruder, with 10wt%, 20wt% and 30wt% of cellulose fiber, with 2wt% of SMA, poly(styrene-co-maleic anhydride) with 30wt% of maleic anhydride groups, as a coupling agent and without SMA. Flexural and unotched IZOD impact test were performed according to ASTM D790-03 and ASTM D256, respectively(Fig.1).

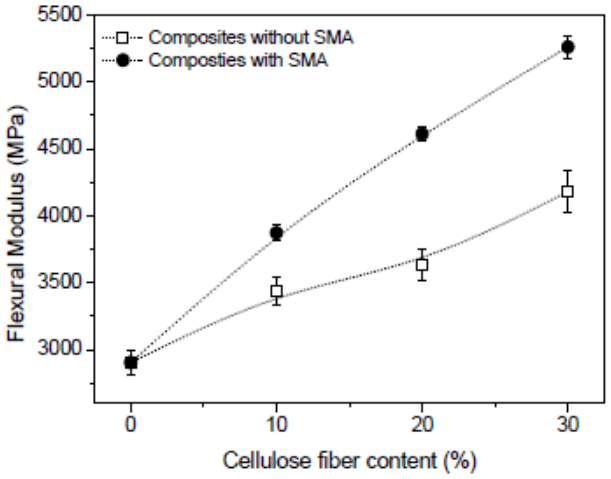

Figure 1: Flexural modulus of PS/Cellulose composites

The flexural modulus as a function of fiber content is shown in Figure 1. The modulus increases almost linearly when increasing the fiber content; this behavior may be related to the fact that the cellulose fibers have a greater modulus than the matrix [2]. The modulus also increases, significantly, with the addition of SMA, as related by Bengtsson et al, the increase in modulus upon the addition of SMA is most likely caused by an improvement in Dispersion of cellulose fibers on the polystyrene matrix [1].

However, another explanation is an improvement on the interface between the fibers and the matrix caused by the coupling agent, which leads to a better efforts transference from the matrix to the fiber, increasing the flexural modulus [3].

From to analyse the be less dependent on the fiber content, as also reported by several researches. The improvement on the interfacial adhesion improves the impact strength, since weak interface is the weakest part of the composites; however, a strong interfacial adhesion will reduce polymer mobility and prevent fiber pull-outs from the matrix leading to a decrease in impact strength (Fig.2)[1].

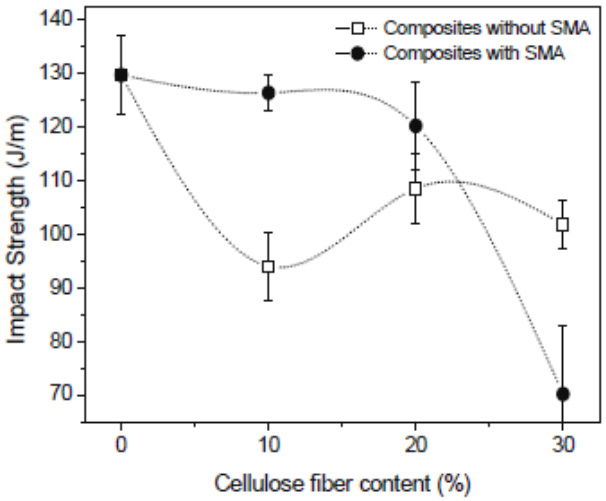

Figure 2: Impact strength of PS/Cellulose composites

The results confirm that SMA promoted a better fibermatrix interfacial interaction, due to a number of polar groups introduced into de matrix resulting in the interfacial adhesion improvement between cellulose fiber and PS matrix, reflecting on mechanical properties improvements.

Keywords: thermoplastic composites; cellulose fiber / polystyrene; coupling agent.

Acknowledgement

The authors would like to thank Cambará S/A, Sartomer Company and Innova S/A for supplying the materials.

References

[1] Bengtsson, M.; Bailif, M. L.; Oksman, K. Composites: Part A. Vol. 38, p. 1922-1931, 2007.

[2] Bledzki, A. K.; Gassan, J. Prog. Plym. Sci. Vol. 24, p. 221-174, 1999.

[3]Correa, C. A.; Razzino, C.A.; Hage Jr, E. Journal of Thermoplastic Composite Materials, Vol 20, p. 323 – 338, 2007.

Mechanical recycling of polymers from real WEEE deposits: morphology, blend composition, impact strength.

Sandrine Ausset [(1)], *Marie-Lise Barthès* [(1)], *Olivier Mantaux* [(1)], *Matthieu Pedros* [(1)], *Michel Dumon* [(1)(2)]

[(1)] I2M MPI, IUT Bordeaux 1, 15 rue Naudet CS 10207 33175 GRADIGNAN Cedex, France
[(2)] LCPO, ENSCBP, IPB, 16, Avenue Pey-Berland 33607 Pessac Cedex, France

sandrine.ausset@etu.u-bordeaux1.fr

The production of electric and electronic equipment is one of the fastest growing areas of manufacturing industry. These advanced technologies generate a huge volume of waste of electric and electronic equipment (WEEE). In order to contribute to a sustainable development, the European Commission adopted the 2002/96/EC and 2002/95/CE directive. Among other principles, these regulations require an increasing rate of materials recycling. WEEE contain about 15-30% plastics [Achilias2009; Vilaplana2008], that is why it is necessary to develop efficient processes to recycle these plastics. The recycling of WEEE plastics is a complex technological challenge for many reasons. Firstly, WEEE plastics are composed of approximately 15 different types of engineering polymers. It is difficult to obtain an all-pure material from real deposits and sorting is never completely achieved. Indeed, with efficient sorting technique, a significant amount of impurities remains in the recycled material, reducing its mechanical properties. Secondly, in recycled plastics issued from WEEE, many grades of polymers exist. If a recycled plastic without impurities could be elaborated, its mechanical properties would be automatically lower than the virgin plastic.

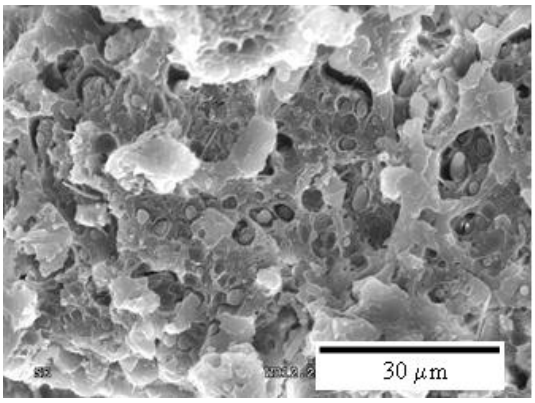

Figure 22: SEM micrograph of impact fractured surfaces of ABS-PC containing 5wt% of HIPS.

A way to solve this problem and upgrade recycled plastics is firstly to compensate for the impurities inclusion by adding compatibilizer or specific additives. Secondly, recycled plastic blends can be developed in order to associate their properties into the recycled matter.
In this work, mechanical recycling of polymers from real waste deposits is studied i.e. neat ABS, PC-ABS alloys, blends between ABS and PC. The aim of our work is to discuss, illustrate and compare the mechanical behaviour, mainly impact strength, of either new or aged recycled material. The presentation deals with blend properties (morphologies vs impact strength) and optimization of blending process to produce competitive recycled materials. Examples of PC-ABS blends over the whole concentration range will be discussed and analysed in terms of process, morphology and mechanical properties.

[Achilias2009] Achilias D., Antonakou E., Koutsokosta E. & Lappas A.; *J Appl Polym Sci*; **114**; pp. 212-221 (2009).
[Vilaplana2008] Vilaplana F. & Karlsson S.; *Macromol Mater Eng*; 293; pp. 274-297 (2008).

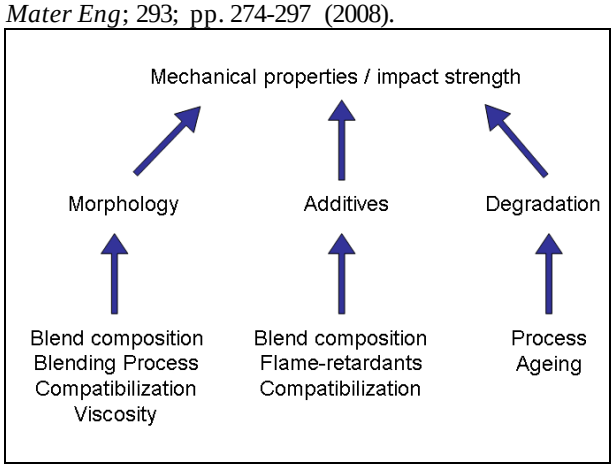

Figure 23: synopsis of main interacting parameters on performance of recycled polymers.

Polymers with hydrogen bonding moieties via ROMP

Steffen Kurzhals, Wolfgang H. Binder

Martin-Luther-University Halle-Wittenberg, Faculty of Natural Sciences II, Institute of Chemistry / Chair of Macromolecular Chemistry / Von-Danckelmann-Platz 4 / 06120 Halle / Saale, Germany

Steffen.Kurzhals@chemie.uni-halle.de

Supramolecular polymers[1] represent an interesting group of materials due to their reversible assembly and disassembly which allows them to respond on external stimuli. These materials are held together by weak interaction e.g. hydrogen bondings, metal-ligand bonding which are directive forces. This allows to transform a random chain assembly into an ordered structure. By combining the supramolecular interaction with a functional polymer it might be possible to improve its properties e.g. conjugated polymers. These polymers, which find application in display technology or solar cells, are attractive alternatives to inorganic analogues due to their lower manufacturing costs and lower weight.

The aim of this work is the synthesis of functionalized polymers (polynorbornenes, poly-*p*-(phenylene vinylenes) via ring opening metathesis polymerization (ROMP) (Figure 1) to prepare sheet like structures. The polymers should be modified with hydrogen bonding donors and acceptors (e.g. thymine, barbiturate) which are introduced via quenching reaction with symmetric olefins.[2] The quenchers are synthesized from the corresponding α-olefins via homometathesis under microwave irradiation. This method for the introduction of functional groups offers a facile approach to functional polymers with no need for post functionalization reactions.

As model system for the introduction of hydrogen bonding moieties we have chosen a norbornene-derivate which could be polymerized in a living fashion with commercial available Grubbs catalysts (1st- and 3rd-generation) as judged by the control over the molecular weight and the small polydispersities (1.1-1.3). These living polymers were then reacted with an excess of the symmetric quenching agents. Quantification via MALDI-TOF MS[3] revealed an increasing fraction of functionalized polymer with time and amount of added quencher.[4] Additionally, the desorption ratios showed a strong influence of the end group on the desorption of the different polymer species. After proving the successful incorporation of the functional moieties in the polymer backbone we transferred this quenching approach to conjugated poly-p-phenylene vinylenes. Since the synthetic access to the corresponding cyclic olefins is limited, we have chosen a 7 step process for the preparation of the barrelene derivates starting from commercial available myo-inositol.[5,6] Various metathesis catalysts (Grubbs, Umicore and Schrock) are investigated for the preparation of soluble PPV-precursor polymers aiming at a living polymerization, which is a requirement for the crossover reaction with the symmetric olefins.

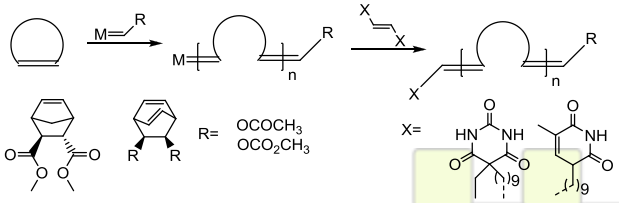

Figure 1. Synthesis of hydrogen bonded polymers

References:

1. Binder, W.; Zirbs, R., Hydrogen Bonded Polymers. In *Adv. Polym. Sci.*, **2007**; Vol. 207, pp 1-78.
2. Matson, J. B.; Grubbs, R. H. *Macromolecules* **2010,** 43, 213-221.
3. Binder, W. H.; Pulamagatta, B.; Kir, O.; Kurzhals, S.; Barqawi, H.; Tanner, S. *Macromolecules* **2009,** 42, (24), 9457-9466.
4. Kurzhals, S.; Binder, W. H. *J. Poly. Sci., Part A: Polym. Chem.* **2010,** 48, (23), 5522-5532.
5. Fabris, F.; Rosso, E.; Paulon, A.; De Lucchi, O. *Tetrahedron Lett.* **2006,** 47, (28), 4835-4837.
6. Conticello, V. P.; Gin, D. L.; Grubbs, R. H. *J. Am. Chem. Soc.* **1992,** 114, 9708-9710.

Large-Scale Nacre-Mimetic Hybrid Films and Paper via Rapid Self-Assembly

Andreas Walther[a], *Lars Berglund*[b], *Olli Ikkala*[c]

[a]DWI at the RWTH Aachen, Pauwelst. 8, D-52056 Aachen, Germany and
[b] Fiber and Polymer Technology, Royal Institute of Technology, SE-10044 Stockholm, Sweden
[c]Molecular Materials, Aalto University, FIN-00076 Aalto, Finland

Walther-andreas@web.de

Nature provides us with the prime examples of lightweight, strong, stiff and yet tough materials. The unique and exceptional properties are realized via a hierarchical ordering of hard (inorganic) and soft (organic, polymeric) building blocks. Nacre serves as an excellent example with its highly ordered brick and mortar structure. In terms of materials science, nacre is considered to be a perfect marriage of hard and soft materials and thus biomimetic materials of this structure are in the focus of research. Significant efforts have been devoted to the generation of nacre-mimics by various sequential multilayer techniques. Although the materials exhibit superior properties, their preparation suffers from being laborious, step-wise and extremely time-consuming. Days to weeks are necessary to prepare films with thicknesses of only a few micrometers. Thus, all these strategies face tremendous obstacles to allow a transfer of concepts beyond the laboratory scale. To promote these structures into true 21st century biomimetic materials with advanced properties, we have to think of more innovative strategies.

Herein, we will show how to overcome many obstacles and how to create large-area brick-and-mortar nacre-mimics (Figure 1a) with sub-millimeter thicknesses and potentially unlimited lateral dimensions via continuous roll-to-roll processes. We combine concepts of colloid chemistry with hierarchical self-assembly and well-developed up-scaled preparation strategies. Our concept makes use of solution-based self-assembly of polymers onto nanoclay platelets to create ideal building blocks with intrinsic hard/soft character. Subsequently, these core-shell bricks are forced to self-order on a second length scale. The resulting materials show a highly ordered layered arrangement of the platelet-shaped inorganics, surrounded by an organic polymer matrix (Figure 1). Due to the utilization of well-defined building blocks, the structures are composed of an optimized hard/soft ratio and a majority fraction of hard reinforcing material. Hence, the resulting material properties demonstrate outstanding stiffness and strength, being in the range or even surpassing the values of natural nacre. We will also show how the mechanical characteristics can be tuned and improved via chemical and physical crosslinking.

The strategy allows for the rapid, economic and environmentally friendly production of nacre-mimetic sub-millimeter thick films with superior material properties.

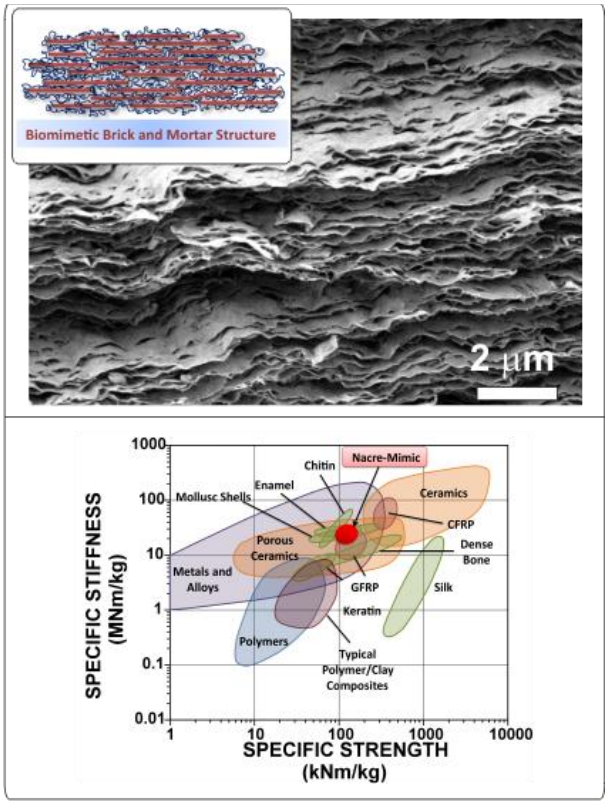

Figure 24. Top: SEM image demonstrating the strongly aligned layered orientation of the platelet-shaped inorganics. The inset schematically shows the biomimetic brick and mortar structure. Bottom: Specific mechanical property selector chart adapted from Ashby et al. The mechanical properties of our materials are in range with strong biological materials and can compete with metals, ceramics and glass fiber reinforced composites (GFRP).

References:

Walther, A.; Bjurhager, I.; Malho, J.-M.; Ruokolainen, J.; Berglund, L.A.; Ikkala, O.: *Angew. Chem. Int. Ed.*, 49, 6448 **(2010)**

Walther, A.; Bjurhager, I.; Malho, J.-M.; Pere, J.; Ruokolainen, J.; Berglund, L.A.; Ikkala, O.: *Nano Letters*, 10, 2742 **(2010)**

Recycling of Polyurethane-based Shape Memory Polymers

M. Ahmad[a], J.K. Luo[a], H. Purnawali[b], W.M. Huang[b] and M. Miraftab[a]*

[a]Institute of Materials Research & Innovation, University of Bolton, Bolton, BL3 5AB, U.K

[b]School of Mechanical and Aerospace Engineering, Nanyang Technological University, 50 Nanyang Avenue, Singapore,

*Corresponding author's email: J.Luo@bolton.ac.uk

Polyurethane shape memory polymers (SMPUs) are one of the most studied and developed shape memory polymers (SMPs), and have found tremendous applications in engineering, space exploration and medical devices owing to their superior properties of large deformation, light weight, low density, low cost and easy processing etc. Chemical resins are available commercially for synthesis of SMPUs, and ready-made SMPU products can be also obtained and used for various applications. However, the waste and disposal of SMPUs have been treated no exception as to other polymers, and little effort has been made to study the recycle and re-usage of SMPUs, and to investigate the relevant physical and chemical properties of the SMPUs. With the increasing concerns over the impact on environment and global warming caused by chemical synthesis, disposal and waste, recycling of polymers becomes increasingly important and urgent. Meanwhile, successful recycle of SMPUs would increase the value of SMPs and further widen their applications. This paper is to report recycling of SMPUs and the relevant study on the material properties of the recycled SMPUs.

Recently we have developed various polyurethane-based shape memory polymers (SMPUs) with low transitional temperatures, Tg, suitable medical application in human body using polyols as soft segment and combination of diisocyanates: isophorone diisocyanate (IPDI) and 4,4′-diphenylmethane diisocyanate (MDI) as hard segments. This is continuous work of the development.

The SMPUs used for the recycling experiments were SMPUs made from poly(caprolactone) (PCL) and MDI/IPDI hard segment[5]. The PCL-samples were used for various thermal mechanical, tensile and shape memory (SME) tests and are longer suitable for further use. The used PCL-SMPUs with different MDI/IPDI rates were dissolved in various solvents, and it was found that N,N-dimethylformamide (DMF) is the best solvent which dissolves the SMPUs and form resin-type polymers without losing originality significantly. The details of the process will be reported at conference. The processed polymer resins were recast into thin films for various characterizations: thermo-gravimetric analyzer (TGA), differential scanning calorimetry (DSC), X-ray, SEM, tensile tests and SME tests.

It was found that the recycled SMPUs with original largely retained their properties of the freshly made samples regardless the concentration of polyols, and concentration ratios of MDI to IPDI used. TGA measurements showed slight changes in material loss rate at high temperature, while DSC showed Tg and heat of fusion increased slightly at recycle as summarized in Table (samples with -R are the recycled ones), indicating increased crystallinity once recycled.

Thermal mechanical and tensile tests showed the recycled SMPUs retained most of the SME effects with deterioration rates less than 10% with results shown in Fig.1-3. Since the recycled SMPUs with proper MDI to IPDI ratios still possess high performance such as 830% elongation at break, high than 80% shape recovery rate and fixity, they can be used for various applications as the original shape memory polymers do.

SAMPLE	Peak Temp. (Tpm) (°C)	ΔH (J/G)	Stress at break (MPa)	Strain at break (%)
PCL (P)	**53.03**	**65.27**		
PCL-PU-1	43.06	7.68	6.99	930
PCL-PU-3	40.03	13.79	5.64	790
PCL-PU-7	41.06	28.47	2.21	37
PCL-PU-1R	43.08	14.45	5.85	834
PCL-PU-3R	45.42	23.84	4.36	558
PCL-PU-7R	42.74	25.26	3.79	17

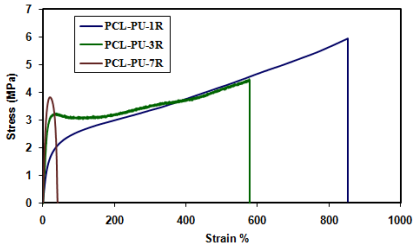

Fig.1 Elongation at break for recycled SMPs.

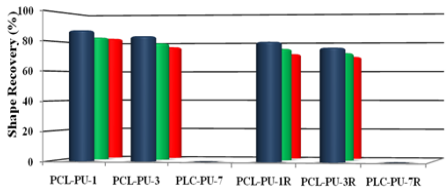

Fig.2 Shape recovery for SMPs before and after recycling.

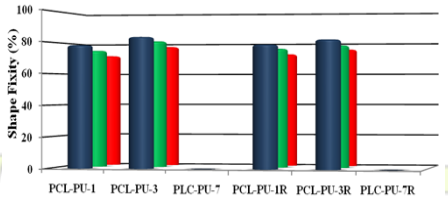

Fig.3. Shape fixity for SMPs before and after recycling.

Advances in Small Scale Processing Equipment for Polymers and Additives

Bernd Jakob - Thermo Fisher Scientific, Karlsruhe, (Germany)

bernd.jakob@thermofisher.com

Abstract: The use of a conical twin screw extruder with backflow channel combines the aspects of mixing and extrusion in a batch process. With a small force feeder and a conveyor belt the micro compounder operates continuously producing a strand or a small sheet. With a total filling volume of 7 ml and a built in slit capillary die the applications focus is on compounding and reactions of small amounts of polymers in the molten stage. Two great areas of application: mixing and rheological recording of the melt characteristics are combined in the micro compounder. For further tests the polymer melt can be transferred into a micro injection moulding machine to shape different kind of test specimens for further analyses.

Compounding: To analyze small batches different test setups are possible. Either continuous or batch processes with defined mixing times can be selected. Co- or counter rotating screws are used to melt and mix the polymer pellets or powders. The influence of additives is show in graph 1.

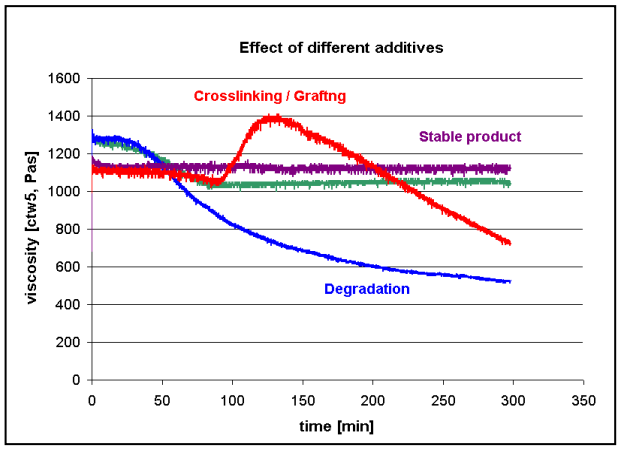

Graph 1 The Effect of different additives

The effect of different additives is obvious. *One compound is stable for 5 hours and no change in the viscosity is observed*. Where as the other compound degrades after about 30 minutes visible by a decreasing the viscosity. A third compound shows a viscosity increase after about 120 minutes due to a reaction of the product followed by degradation

Viscosity: The backflow channel of the micro compounder is designed as a slit capillary. Two pressure transducers in the backflow channel measure the pressure drop. From this pressure drop a shear stress is calculated. To determine the shear rate, the mass flow in the flow is correlated with the screw speed of the Thermo Scientific Haake MiniLab. To record a flow and viscosity curve, different screw speeds are set and the pressure drop (shear stress) at those different screw speeds is measured.

The correlation between the screw speed and the mass flow is for each polymer slightly different. So the calculated shear rate and therefore also the calculated viscosity can only be a relative value which is accurate enough to compare different batches.

Test Specimens: With the compound produced in the Haake MiniLab various test specimens can be produced very efficiently with the Thermo Scientific Haake MiniJet, a micro injection moulding machine. The instrument is build as a piston injection machine with a removable heated cylinder with injection piston to collect the melt from the Haake MiniLab. Also pellets or powders can be molten direct in the heated cylinder. The amount of required sample material is minimized to less than 5 g Almost the whole amount of polymer melt is completely trans-formed into test specimens. This is a major advantage as the waste material of conventional screw driven injection moulding machines can be avoided by this principle. With the exchangeable moulds disks, plates, DMA and tensile bars can be prepared for hardness tests, breaking strength,

Dynamical Mechanical Analyses (DMA): For testing of the solid polymer according to DIN/ISO 6721-1 a DMA bar is mounted with solid clamps in the Thermo Scientific Haake MARS monitoring the effect of additives over a wide temperature range. The effect of the additives is seen in the shift of the glass transition temperature. In graph 2 the result of a DMA test is shown.

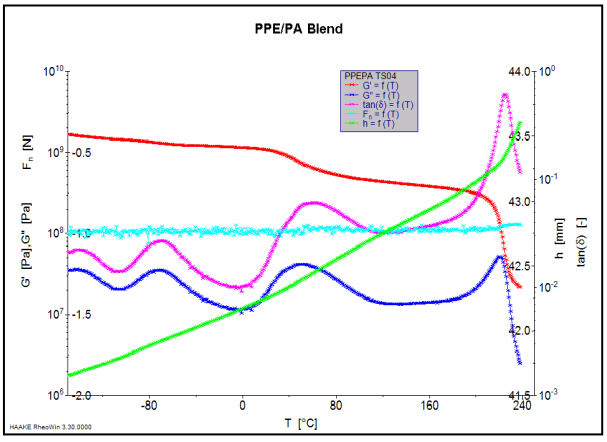

Graph 2 DMA test of a PPE/PA Blend

Conclusion: The micro compounder Haake MiniLab is a useful tool to process small amounts of polymers and additives. Especially in the stage of development of new products and the screening process for promising candidates of new compounds reproducible results are obtained in a shorter time. For further tests the compound can be shaped to a variety of different test specimens with the micro injection moulding machine Haake MiniJet.

Role of Rheology on Quality of Polymeric Articles

Faezeh Aghazadeh[1] *and Hossein Hosseini*[2]

[1] R&D Center, Tabriz petrochemical Company, Tabriz, Iran
[2] Department of Chemical Engineering, University of Tabriz, Iran

f.aghazadeh@hotmail.com

Polymer processing for production of all forms of polymeric articles has found a great place in chemical industries. Thermoforming process is one of the most popular techniques in this field. The fundamental defects inherent to the thermoforming technology are wall-thickness variation and warpage of the products. A nonlinear viscoelastic rheological model is implemented for developing the process model. This model describes deformation process of a sheet in thermoforming process. Because of relaxation pause after plug-assist stage and also implementation of two stage thermoforming process have minor wall-thickness variation and consequently minor warpage and better mechanical properties of thermoformed articles. For model validation, a quantitative relation between stress and technical parameters of plug-assist thermoforming is determined by comparison of theoretical and experimental results. This model could be suggested for prevention from some technical defects such as wall thickness variations, physical instability during inflation-shrinkage, and warpage exhibited in the final part of a polymeric article.

It is well known that the stage of vacuum-forming with a pre-stretched sheet occurs too quickly for experiencing of relaxation processes in the polymeric sheet. This will result in this fact that almost all accumulated deformations in polymeric sheet within this stage are elastic. Consequently, the minimization of the accumulation may be realized only by minimizing of the general deformations accumulated in polymeric sheet during this stage. For practical purposes, this means that the profile of the pre-stretched sheet should be maximally approximated by the profile of the final product which could be assured based on the application of a plug with the respective radius.

In contrast to the second stage, the stage of plug-assisted can be regulated in the sense that it is technically possible to control the motion of the plug. This creates a practical opportunity that at this stage to organize the relaxation process of elastic deformations accumulated in a polymeric sheet during the process of plug-assist forming. The essence of the simplest of many variants used in the realization of this process lies in the creation of a relaxation pause period between the first and the second stage. During this period the accumulated elastic deformations are completely or partially relaxed and consequently minor wall-thickness variation. So, because of relaxation pause after plug-assist stage and also implementation of two stage thermoforming process have minor wall-thickness variation and consequently better mechanical properties of thermoformed articles.

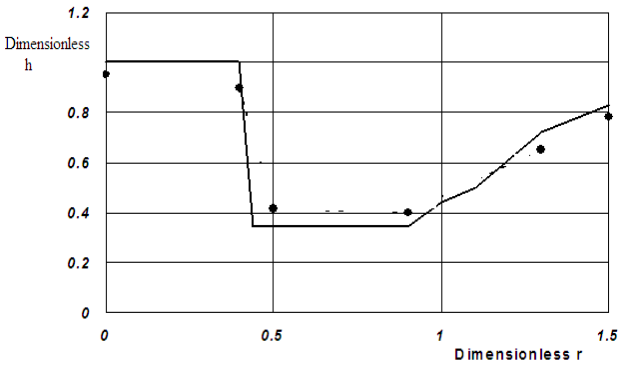

Fig.1. Comparison of model simulation (___) and experimental (●) wall-thickness distribution for PP (h_0 = 1mm).

References

1. J.L. Throne, Thermoforming. Hanser publishers, Munich, 1987.

2. N. Rosenzweig, M. Narkis and Z. Tadmor, Polym Eng Sci 1979; 19: 946.

3. G. J. Nam, K. H. Ahn and J. W. Lee, Polym Eng Sci 2000; 40: 2232.

4. Z. Ayhan and Q.H. Zhang, Polym Eng Sci 2000; 40: 1

5. H. Hosseini, H., B.V. Berdyshev and A. Mehrabani, Euro. Poly. J., 2006; 42: 1836.

Re-Use and recycling of PLA and its mechanical properties

Reinhard Forstner, *Julia Pleiner*

Transfercenter für Kunststofftechnik, Franz-Fritsch-Straße 11, A-4600 Austria

Reinhard.forstner@tckt.at

Introduction: In recent years Poly-(lactic acid) as a green polymer has attracted scientific and industrial attention since PLA can be processed similar to polyolefins and is known to be compostable. Polylactide, an aliphatic polymer, which can be obtained from renewable resources by fermentation [1,2] and was mainly used in medical applications [3] Meanwhile PLA has entered the packaging market and pushes also into technical applications such as housings of cell phones. In production in house waste material is produced in amounts of several tons/a, which is a costly problem for the industry.
The goal of this study was to investigate the mechanical and thermal degradation of PLA in a re-use situation in a lab compounder to mimic recycled material or the re-fill of in-house waste.

Materials: In this study two different PLA grades with different molecular weight and melt flow rate of MFI~8 (PLA 1) and MFI~30 (PLA2) were used.

Methods: The PLA grades were compounded and re-compounded in a parallel twin screw lab compounder up to fifteen times and samples were taken at five, ten and fifteen repetitions. For each fraction tensile, impact and flexural properties were determined according to ISO standards and dynamic mechanical viscosity as well as gloss measurements were performed.

Results: The results showed that the moduli and the impact properties hardly changed for all repetitions. Only the tensile strength and the flexural strength decreased as well as rheology data showed a decrease of zero shear viscosity with increasing numbers of repetitions, which indicated a change in molecular structure.

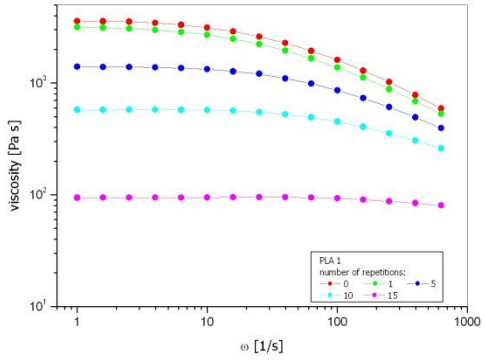

Figure 1: Viscosity data of PLA 1

Molecular weigth of the re-used fractions were calculated from viscosity data, which confirmed the decrease of the molecular weigth with increasing numbers of repetitions.

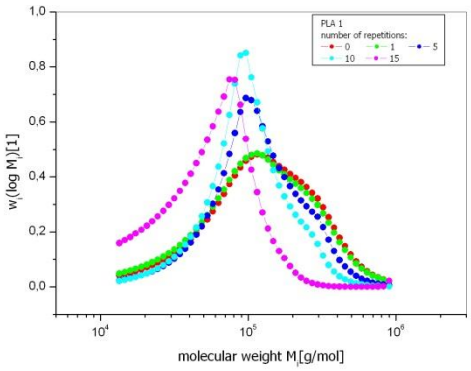

Figure 2: calculated molecular weight distribution

Conclusions: As this study showed, PLA can be reprocessed several times with hardly any change to mechanical properties, but serious change in viscosity and molecular weight respectively.

References:

[1] A. Södergard, M. Stolt, Properties of lactic acid based polymers and their correlation with composition, Prog. Polym.Sci., **27**, 1123-1163, (2002)

[2] E.T.H. Vink, K.R. Rabago, D.A. Glassner, P.R. Gruber, Applications of life cycle assessment to Nature WorksTM polylactide (PLA) production, Polym. Degrad. Stab., **80**, 403-419, (2003)

[3] K.E. Uhrich, M.S. Cannizzaro, R.S. Langer, K.M Shakesheff, Polymeric Systems for Controlled Drug Release, Chem. Rev., 99, 3181-3198, (1999)

Characterization of Iron Oxide Nanoparticles Created in a Polymer Brush Matrix

Sonja Neuhaus[1,2], *Celestino Padeste*[1], *Nicholas D. Spencer*[2]

[1]Laboratory for Micro- and Nanotechnology, Paul Scherrer Institut, 5232 Villigen PSI, Switzerland
[2]Laboratory for Surface Science and Technology, ETH Zurich, 8093 Zurich, Switzerland

sonja.neuhaus@psi.ch

Introduction

A strategy for creating a polymer brush / nanoparticle composite layer on a flexible polymer foil substrate is presented. Polymer brushes with carefully selected functionality are ideal templates for the formation of nanoparticles, as the size of the particles should be limited by the metal content of the brush matrix and the confined space therein.

Materials and Methods

Poly(4-vinylpyridine) (P4VP) brushes were grown from poly(ethylene-*alt*-tetrafluoroethylene) (ETFE) foils. (Hydro)peroxide radicals for the initiation of a free radical polymerization were created by exposure of the foils to EUV light at the Swiss Light Source (SLS) or by activation with cold, atmospheric-pressure helium plasma [1]. The pyridine moieties abundant in the polymer brush were used to complex iron. In a subsequent annealing step under alkaline conditions, iron oxide nanoparticles were created.

Results and Discussion

The different steps of the production sequence as well as the resulting polymer brush / iron oxide nanocomposites were characterized with a number of methods. Upon iron complexation, a strong shift of the ring skeleton vibration bands was observed with attenuated total reflectance-infrared micro-spectroscopy (ATR-IR) (Figure 1). The initial spectrum was retrieved after the oxidative treatment, suggesting that the pyridine ligands were regenerated and again available for complexation. UV spectra recorded in transmittance proved that the amount of iron oxide could indeed be increased by multiple loading and oxidation steps.

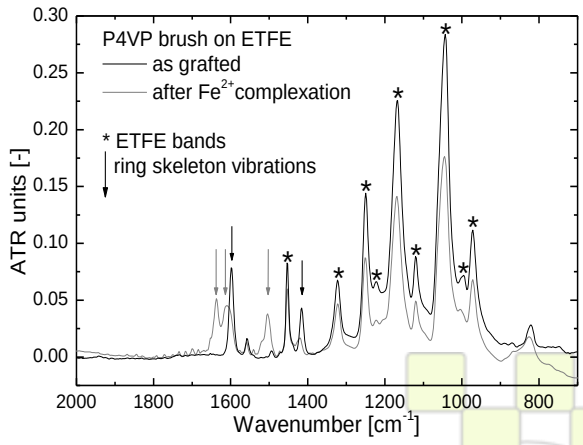

Figure 1: ATR-IR spectra of P4VP brushes as grafted, after the complexation of iron and after the oxidative treatment.

Microtome cuts of the samples were prepared in order to image the P4VP / iron oxide composite layer with transmission electron microscopy (TEM) (Figure 2). Particle sizes were found to be in the range of 1 nm, but larger clusters were observed as well. The presence of iron in the brush was confirmed by energy dispersive x-ray spectroscopy.

In a further step, the composite material will be investigated using the unique capabilities of the scanning transmission x-ray microscope (STXM) at the PolLux beamline of the SLS. Apart from element specific imaging of the nanoparticles and the interface to the substrate with high resolution, x-ray absorption spectra will help to identify the type of iron oxide produced. Moreover, the nanoparticles will be tested for their magnetic properties with x-ray magnetic circular dichroism measurements.

Conclusion

Ultimately, the aim is to implement several types of functionalities on one surface. In the presented approach, the *chemical* functionality of the brush is used for capturing iron for subsequent particle formation. It will be interesting to see whether the particles endow the brush with *magnetic* responsiveness as shown for an anionic polymer brush on a silicon/gold substrate [2].

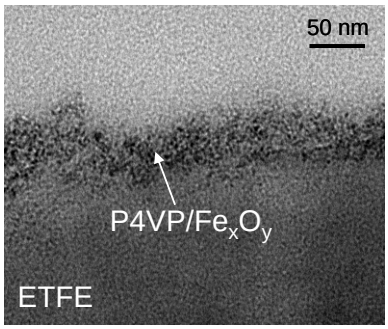

Figure 2: TEM image of a microtome cut showing a P4VP brush with iron oxide nanoparticles on ETFE.

References

[1] S. Neuhaus, C. Padeste, H. H. Solak, N. D. Spencer, *Polymer* **2010**, *51*, 4037.
[2] W. S. Choi, H. Y. Koo, J. Y. Kim, W. T. S. Huck, *Adv. Mater.* **2008**, *20*, 4504.

Chain architecture modifications of Poly(Lactic Acid) by reactive extrusion.

O. O. Santana[1], J. Callioux[1], E. Franco-Urquiza[1], J.J. Bou[2], F. Carrásco[3], J. Gámez-Pérez[4], M. Ll. Maspoch[1]

1. Centre Català del Plàstic – Universitat Politècnica de Catalunya
2. Universitat Politècnica de Catalunya - Dept. Eng. Quimica
3. Univesitat de Girona - Dept. Eng. Química
4. Universitat Jaume I - Polymers and Advanced Materials Research Group (PIMA)

orlando.santana@upc.edu

Introduction: Poly(lactic acid) (PLA) is a semi-crystalline biodegradable polymer that has been used for several years in medical and biocompatible applications, packaging, food and agriculture. Due to the chiral nature of lactic acid, two types of monomer (L or D) could be used in PLA synthesis. Control of the ratio of L to D monomer has a large effect on material properties primarily through affecting the percent of crystallization.

One of the main drawbacks of PLA is its high sensitivity to hydrolytic degradation during processing (similar to PET). Moreover, due to its linear molecular architecture has a low melting strength which limits its application on single-use disposable items produced by low density foaming, vacuum thermoforming, highly oriented film and blow molding. It is well known that the branching and low degree cross-linking of molecules can offer the enhancement of rheological properties, and give new opportunities for PLA markets. Following the PET approaches, there have been studied some reactive modifications during processing with chain extenders or branching agents. Among these, the glycidyl acrylates-based copolymers have shown excellent versatility in these issues.

The aim of this communication is to show some results of the rheological, thermal and mechanical properties of two grades of PLA modified by a glycidyl methacrylate-based branching agent. In order to study the scaling-up of processing conditions (main key problem for industrial processing), the modifications have been made by: a) internal mixer at laboratory scale and b) pilot plant scale (twin screw extrusion - continuous calendar).

Materials and methods: Two extrusion grades of PLA from NatureWorks (PLA 2002D and PLA4032D) with similar MFI (7 g/10min at 210ºC/2,16 kg) differing only in the L:D ratio (96:4 and 98:2 respectively) have been used in this study. As branching agent it has been used a low molecular weight copolymer Styrene-acrylic-glycidyl methacrylate kindly supplied by BASF (Joncryl 4003-C) with a EEW of 443. It was added in a proportion of 0.5 and 1 % wt of PLA.

Previous to any processing PLA and branching agent were dried for 5 h at 80ºC in a PIOVAN hopper with dew point of -40ºC. Two processing systems were used:

a) Internal mixer compounding (laboratory scale, 50 g/batch): T = 180ºC, 50 rpm, N_2 atmosphere, t = 15 min. Sheet (1 mm in thickness) were compression molding at 180ºC during 10 min.

b) Twin screw extrusion-continuous calendar (pilot plant scale): L/D =36, plane temperature profile at 180ºC, variable screw rotation speed (80, 60 and 40 rpm (residence time of 2, 3 and 4 min). Sheets of 0.9 mm in thickness were obtained.

Rheological measurements were performed on a AR-G2 RDA (TA Instruments) in parallel plate geometry at 180ºC and 1 % of strain (Linear viscoelastic range, LVR). N_2 atmosphere was used during the tests.

For the thermal characterization it was used a DSC Pyris 1 (Perkin-Elmer) at 10ºC/min per scan. Additionally, thermal fractionation (SSA) were performed in the same equipment. Dynamic Thermo-mechanical tests were conducted in a Q-800 DTA (TA Instrument) at 2ºC/min of heating scan (from 30 to 170ºC) at 0.5 % of strain and 1 Hz (LVR). MWD has been determined by GPC (25ºC, HFIP) and from the relaxation spectrum obtained from the master rheological curves

Results: One of the interesting aspects focused on the rheological properties obtained. As shown in Fig. 1, the rheological changes achieved are consistent with a branching system. At high shear rate region (>100s^{-1}) (range of extrusion) it seems that as higher the D enantiomer content, the greater the increase in viscosity. This trend seems reversed at low shear rate. However, differences on MWD between grades must be considered. These and other aspects of change and the comparison of results with extruded systems will be discussed during the presentation.

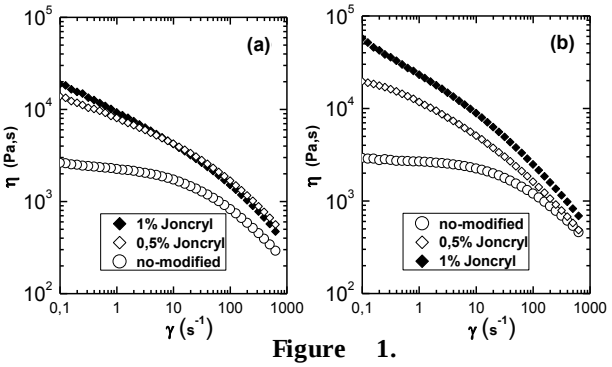

Figure 1. Rheological curves,after Cox-Merz correspondence of **a)** 2002D and **b)** 4032D preparations at 180ºC.

Acknowledgements: This work has been financially supported by MICINN, grants nº MAT2010-19721-C02-01 and MAT2010-19721-C02-02.

Electromechanical characterization of styrene-butadiene-styrene / carbon nanotube composites for deformation sensors

P. Costa[1], *J. C. Viana*[2], *S. Lanceros Mendéz*[1]

[1]Centro de Física da Universidade do Minho, Campus de Gualtar, 4710-057 Braga, Portugal.
[2]IPC-Institute for Polymers and Composites, University of Minho, 4800-058 Guimarães, Portugal

pcosta@fisica.uminho.pt

Rubbers and thermoplastic elastomers play an important part in industrial applications and biomaterial development. The thermoplastic elastomer styrene-butadiene-styrene (SBS) is widely studied and used due to its interesting characteristics, in particular, its high elongation at break and insulation properties. In order to increase the application range of this material to sensors and actuators, for example, it is necessary to tailor its electrical response. One possibility to tailor conductivity in SBS is to add carbon nanotubes (CNT) to the polymeric matrix. Several theoretical and experimental studies showed that the composites reinforced with carbon nanofillers have the percolation threshold lower than with other conductive materials. In this work, SBS/CNT composites were prepared by solution casting at various concentrations raging to 8 wt% of incorporation of CNT. The dielectric properties (dielectric constant and losses), electrical conductivity and piezo-resistance were measured for all composites. The dielectric constant increases with the inclusion of CNT, being $\varepsilon' \sim 50$ for the higher concentrations of CNT while de pure SBS is around the $\varepsilon' \sim 2$. The addition of CNT increases considerably the initial modulus of the composite compared to neat SBS, being ~160 MPa for the composite with 5% CNT and around 50 MPa for nonfilled SBS. The elongation to break, on the other hand is above 1000%, even for the nanocomposites with higher concentrations of CNT. The performance of the composites as piezo-resistive sensors was also evaluated through the measurement of the longitudinal gage factor.

Acknowledgements: Science and Technology Portugal, for financial support through projects PTDC/CTM/69316/2006, PTDC/CTM-NAN/112574/2009, PTDC/CTM/73465/2006 and NANO/NMed-SD/0156/2007, and grant SFRH / BD/ 64267/ 2009.

Keywords: Thermoplastic elastomers, carbon nanotubes, nanocomposites

High Velocity Compaction: A Fast Process Insensitive To Viscosity

*Nolwenn DOUCET[1], *, Olivier LAME[1], Gérard VIGIER[1] and Florence DORÉ[2]*

[1] Materiaux : Ingénierie et Sciences (MATEIS) – INSA de Lyon, Bât. B. PASCAL, 7 av. Jean CAPELLE, 69621 Villeurbanne Cedex

[2] Centre Technique des Industries Mécaniques (CETIM) – 7 rue de la presse, BP 802,42952 Saint Étienne Cedex 9

e-mail: nolwenn.doucet@insa-lyon.fr

Introduction

One of the main issue of high molecular weight or strongly filled polymers is their very high viscosity. For these polymers, sintering is often required instead of injection or extrusion. This process needs a long time (few hours) at high temperature (170 °C for UHMWPE) to sinter the polymer.

The High Velocity Compaction (HVC) is an original and in development processing. The melting of nascent polymer powder occurs by impacting the powder in a heated die. Parameters are the energy, the number and the frequency of impacts. HVC allows obtaining a part close to the final shape in a few minutes. Quick processing and low starting temperature (~115 °C) prevent the thermal degradation of the polymer. The main advantage of HVC is the possibility to adjust the quantity of nascent phase remaining in the material after processing. DSC measurements allow to evaluate the recrystallized phase fraction (Fr) [1].

In this study we are going to show that HVC can process a UHMWPE 6 x 10^5 g/mol to 10.5 x 10^6 g/mol with only small changes in process parameters. Moreover it is possible to choose the mechanical behavior (fragile or ductile) and the mechanical properties of the material by adjusting the ratio of nascent powder which remains in polymer. SAXS and WAXS allow to understand relationship between micr structure and properties of HVC materials.

Materials and methods

Ticona provided the different powder of UHMWPE (GHR 8810 and GUR's 4113, 4120, 4130, 1050, 4170). Tivar 1000 obtained by hot-compaction is our reference material. Before compaction, we heat the powder

DSC analysis has been performed on a Perkin Elmer DSC 7 at an heating rate about 10 °C/min.

Tensile tests have been realised with an Instron device at 0.2 s^{-1}.

Results

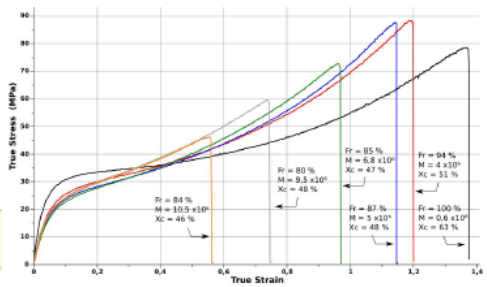

Figure 1: Tensile test for all grades with the same process parameters (M: molecular weight, Fr: recrystallized fraction, Xc: crystallinity)

Fig. 1 shows that we can be sinter all of our powder with the same parameters. Nevertheless the recrystallised fraction depend on the grade: Fr vary from 80% to 100% and the break occurs for a true strain between 0.58 and 1.39.

Fig. 2 shows, for one UHMWPE, the variations of the mechanical behavior according to the recrystallized phase ratio. For Fr = 46 %, the mechanical properties are lower because of a lack of interparticular cohesion.

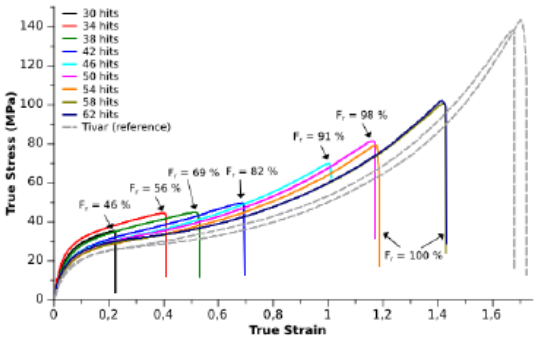

Figure 2: Mechanical behavior according to the recrystallized phase ratio and the number of hits

Discussion

The ratio of residual nascent phase drives the mechanical behavior (fig. 2). HVC material can be described as an "autocomposite", the residual nascent phase acts as filler [2]. With a large amount of residual nascent phase Young modulus can be 70 % higher than material processed by hot-compaction.

Surprisingly, when the material is completely melt during the process (Fr = 100 %), it is stiffer than the reference material. Is also highlighted by microindentation test, depth penetration is 30 % higher on Tivar than nascent phase free HVC material. According to the x-ray scattering studies, this stiffening is not due to some residual stress but more due to the thickening of the crystals.

Conclusion

HVC can process, with the same parameters, a wide range of UHMWPE grades. Surprisingly the quality of sintering seems to be nearly independent of the molecular mass. The materials obtained are autocomposites where the nascent phase acts as filler.

However, it has been shown that even when the nascent phase is completely melted, the stiffness of the HVC material remains higher than the reference. The result is probably due to the higher crystallite thickness observed on the HVC material. The thermo-mechanical treatment applied to the powder during HVC is probably the cause of this thickening.

References

[1] D. Jauffrès et al., Polymer, 2007, 48-21, 6374-6383

[2] D. Jauffrès et al, Macromolecules, 2008, 41 (24), pp 9793–9801

Microphase Separation in Asymmetric Coil-Coil and Coil-Amphiphilic Comb Block Copolymers in Strong Segregation Limit

Mehran Asad Ayoubi[1], *Kaizheng Zhu*[2], *Bo Nyström*[2], *Ulf Olsson*[1], *Kristoffer Almdal*[3], *Alexei Khokhlov*[4], *and Lennart Piculell*[1]

[1]Division of Physical Chemistry, Lund University, Sweden
[2]Department of Chemistry, University of Oslo, Norway
[3]Department of Physics, Moscow State University, Russia
[4]Departmnet of Micro and Nanotechnology, Technical University of Denmark, Denmark

email: Mehran.Asad_Ayoubi@fkem1.lu.se

Coil-Coil Block Copolymer: For a series of asymmetric coil-coil block copolymers of poly(styrene)-*b*-poly(methacrylic acid) (PS-*b*-PMAA) type, effects of polydispresity of the minority block (PMAA) on the melt self-assembly in the strong segregation limit SSL have been addressed. It was observed that in a PMAA volume fraction window of $0.03 \leq \Phi_{PMAA} \leq 0.30$ spherical microdomains exist in disordered liquid-like state and ordered liquid-crystalline state with body-centered-cubic BCC symmetry. Polydispersity of the minority block has two main effects. First, the existence of a BCC phase at a high value of Φ_{PMAA} (=0.30), where conventionally cylindrical hexagonally ordered microdomains are expected (Figure 1, left). This can be explained by the fact that polydispersity in PMAA blocks reduces entropic elasticity of these microdomains and facilitates formation of an interface curved toward them. Second, an increase in polydispersity index of minority PMAA block (PDI_{PMAA}) results in a linear increase of relative microdomain size (defined as the ratio of the observed microdomain size to the one calculated from SSL model of Helfand and Wasserman for monodisperse blocks, R/R_{HW}) and a linear decrease of relative interfacial area per molecule ($A_{mol}/A_{mol.HW}$) (Figure 1, right). When one of the blocks is polydisperse (in our case PMAA block) the entropic penalty paid for packing the chains at the interface becomes lower, compared to the case of monodisperse blocks. This is because shorter blocks do not extend so far from the interface, which gives a chance for longer blocks to fill the space further away from the interface without sacrifice in configurational entropy. The net result is that polydisperse chains will pack more densely, which leads to a lower interfacial area per molecule and, consequently, an increase in the microdomain size.

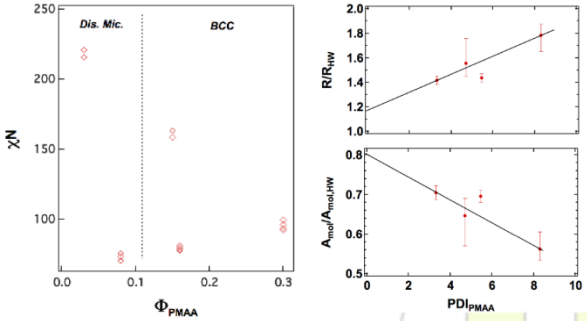

Figure 25: (left) phase diagram of PS-*b*-PMAA block copolymer with polydisperse PMAA block, (right) relative size (top) and interfacial area per molecule (bottom) of PMAA domains vs. PDI_{PMAA}

Coil-Amphiphilic Comb Block Copolymer: Recently Khokhlov *et al.* [1] reported computer simulation results of diblock copolymers in which one of the blocks is non-polar and the other is made of composite amphiphilic (non-polar/polar) repeat units. They found that the existence of amphiphilic monomer units induces two main effects: 1) microphase separation on a short length scale (inside the block with composite amphiphilic monomer units), and 2) microphase separation on a large length scale (between non-polar and amphiphilic blocks) with a considerable asymmetry in phase diagram with respect to Φ_{Amph}. Our aim is to test experimentally these theoretical predictions. For this purpose we have attached non-polar alkyl chains to the PMAA block of the previously presented PS-*b*-PMAA block copolymers via electrostatic interactions. This is achieved by an ion-exchange reaction between the acidic groups of the PMAA and the hydroxide form of alkyltrimethylammonium salts with 8, 12 and 16 carbons in alkyl tails (C8, C12 and C16) for various degrees of side chain grafting densities. Strong incompatibility between the polyelectrolyte backbone (PMA-trimethyl ammonium, PMA-TMA) and alkyl chain results in a comb-like block with strongly amphiphilic monomer units.

As an example we have presented a phase map of these coil-amphiphilic comb block copolymers (Figure 2) based on a PS-*b*-PMAA block copolymer with $\Phi_{PMAA} = 0.15$

A number of effects are observed: 1) microphase separation at two length scales are realized in most of the data points presented in phase map on Figure 2, 2) phase boundaries have shifted considerably to low values of $\Phi_{AmphComb}$, 3) a new regime has emerged (l), in which small length scale microphase separation dominates the self-assembly behavior.

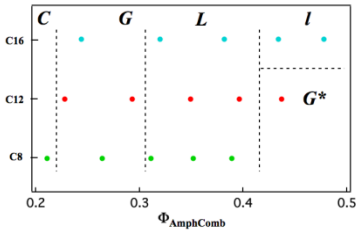

Figure 26: C: normal hexagonally packed cylinders, G: normal gyroid phase, G*: reverse gyroid phase L: large scale lamella, l: small length scale lamella with no large scale microphase separation

References:

[1] Y. A. Kriksin, P. G. Khalatur, I. Y. Erukhimovich, G. Ten Brinke and A. R. Khokhlov Soft Matter 5 (2009) 2896.

Influence of polymer and process characteristics on microstructure and physical properties of SLS parts

S. Dupin[1], *O. Lame*[2], *C. Barres*[1], *J.Y. Charmeau*[1]

Université de Lyon, CNRS

1- INSA-Lyon, IMP, UMR5223, F-69621Villeurbanne, France

2- INSA-Lyon, MATEIS, UMR5510, F-69621Villeurbanne, France

stephane.dupin@insa-lyon.fr

Introduction

The selective laser sintering (SLS) process is an additive manufacturing technology. It consists in 4 stages:

- a roller or blade system spreads a layer of polymer powder in the build chamber (1)
- a laser beam scans the area that corresponds to a "slice" of the object to be built (2)
- the platform in the building chamber moves downwards by a layer thickness (about 100µm) (3)
- another powder layer is spread and steps 1-4 are repeated (4).

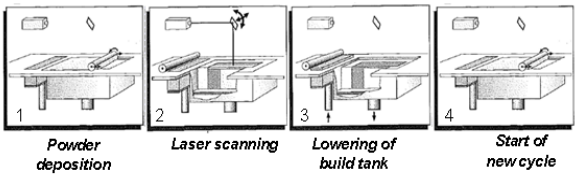

Principles of selective laser sintering (SLS)

This results in building the object layer by layer in the vertical direction.

It is well known that such objects have low mechanical properties compared to injection moulded parts. Therefore, the improvement of mechanical properties (notably elongation at break) is a major technological issue for this process.

To reach this objective, fundamental scientific issues have to be overcome. Indeed, very complex physical phenomena occur during sintering (heat transfers, partial melting, coalescence and densification, ageing), which have to be understood more deeply than in the current state of the art. During sintering, many process parameters play crucial roles, like the temperature of the build chamber, the laser power or the scan spacing. Furthermore, powder particle size, size distribution and polymer rheological features, have also a key influence on the densification of the sintered material, especially during the coalescence process.

Consequently, the aims of this study are:

- to emphasize and explain the role of polymer features and process parameters on the microstructure and properties of sintered parts
- to correlate these properties to a unique energy criterion call "supplied energy density" (SED) enclosing the main process parameters [1].

Material and methods

Polyamide12 is widely used in selective laser sintering because of its thermal properties [2]. During this study we used two types of polyamide 12 materials: DuraformPA obtained from 3D systems and InnovPA obtained from Exceltec.

Samples have been sintered with different SED by varying laser power and scan spacing.

Powder morphology was studied by scanning electron microscopy. The characterisation of the thermal properties and the degree of cristallinity was carried out by DSC. Porosity was measured by weighing. Microstructural investigations of the final parts were made by optical and electron microscopies on microtomed sections and by 3D X-ray tomography. Finally, tensile, flexural and impact properties were measured on the sintered parts.

Results and discussion

In our investigation we have shown that the SED and polymer characteristics (molecular weight, thermal properties) have a great effect on the microstructure by influencing the degree of porosity and the remaining fraction of nascent polymer in the sintered parts. Because of this microstructure, the elongation at break reduces strongly compared to injection moulded parts. However, the rigidity increases due to higher degree of crystallinity in sintered parts.

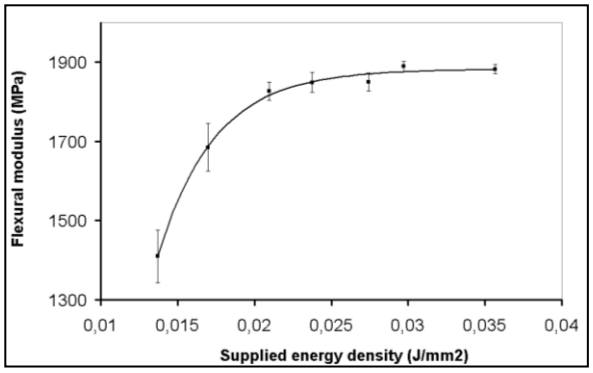

Evolution of flexural modulus versus supplied energy density for polyamide 12 sintered parts

Conclusion

As a conclusion, this study enables a better understanding of the complex relations between process parameters, polymer characteristics and final part properties.

References

[1] R. Morgan, C. J. Sutcliffe, W. O'Neill. Journal of materials science 39 (2004), 1195–1205.

[2] B. Wendel, D. Rietzel, F. Kühnlein, R. Feulner, G. Hülder, E. Schmachtenberg. Macromol. Mater. Eng. 293 (2008), 799–809.

Key Issues in Re-Processing Aged Polyamide-12 Powders by Selective Laser Sintering : Influence of Polymer Features Evolution on Part Properties

Claire Barrès, Stéphane Dupin, Amir Msakni, Olivier Lame, Jean-Yves Charmeau*

Université de Lyon, F-69361 Lyon, France; CNRS, UMR 5223, Ingénierie des Matériaux Polymères, Villeurbanne, France; *CNRS, UMR 5510, MATEIS, F-69621, Villeurbanne, France ;INSA-Lyon, Villeurbanne, France
claire.barres@insa-lyon.fr

Introduction

The selective laser sintering (SLS) process is an additive (layer by layer) manufacturing technology. Using a CAD file in which the object to be built is numerically "sliced" into successive sections in the vertical direction, the polymer processing consists in spreading layers of powder and scanning areas that correspond to "slices" of the object with a laser beam. This causes local melting and fuses the particles with their neighbours and with the previous layer. This cycle is repeated until the part is completed in the vertical direction. SLS has been used up to now to make prototype parts from PA12 mostly. Its potential for "rapid manufacturing" of custom-designed or small to mid-size series of parts is very attractive since no tool nor mold are needed [1].

However, since only ca. 20% of the powder is actually melted and sintered, the re-use of the remaining powder is a real issue, in order to improve the economic and environmental balances of such technologies. Moreover, the whole building tank is maintained for hours 30 to 10°C below the melting temperature of the polymer, which degrades powder features and limit its re-processability. Our purpose is therefore to contribute to process optimization by understanding in which manner the evolution of the powder physico-chemical properties upon ageing affects its processability and, ultimately, the sintered part properties.

Materials and Methods

Commercial PA12 powders were used and re-used in 5 successive manufacturing batches in an SLS machine (3D Systems, USA). Both sintered parts and remaining powder samples from each batch were collected for further analysis. In parallel, the powders were also aged in controlled conditions in a laboratory oven, at 170°C for 3 to 120 hours, for comparison purposes.

Powder morphology was studied by scanning electronic microscopy (SEM). The evolution of molecular mass was followed by intrinsic viscosity measurements in a phenol-1,2-dichlorobenzene mixture and by rheological measurements in the melt. The characterisation of the thermal properties was made by differential scanning calorimetry (DSC). Nanostructure modification was evidenced by X ray diffraction (SAXS). 3D Xray tomography, porosity measurements, and mechanical testing completed the characterizations of sintered parts.

Results and Discussion

Morphological analysis reveals a strong aggregation of fine particles upon ageing. This phenomenon is partly responsible for the degradation of powder flowability. Flowability is crucial to achieve the spreading of even, about 100 µm-thick powder layers.

Then, intrinsic viscosity measurements have shown a strong increase of the molecular weight during ageing, due to post-condensation of PA12. This phenomenon has been confirmed by rheological measurements in the melt. This increase of molecular weight has a great impact on the properties of final parts. Indeed, molecular weight governs the melt viscosity which is a key parameter of the coalescence, as show models such as Frenkel's [2]. An increase of the melt viscosity induces an increase of the coalescence time. The exposition time of the powder grains to the laser radiation is very short (some milliseconds). Therefore an increase of coalescence time greatly impacts the properties of final parts by promoting porosity due to incomplete coalescence of the particles.

The characterisation of thermal properties by DSC has shown an increase of the PA12 melting point upon ageing, which is a consequence of crystallites growth. Moreover a decrease of the crystallisation temperature with ageing is also observed. This modification can be explained by the increase of the molecular weight.

Finally, tensile, flexural and impact properties of parts made with new and used powder were measured. Some of these properties improved with used powder (e.g. elongation at break). More generally, they display a complex dependence on the number of re-using cycles, which results from simultaneous degradation processes: postcondensation and degradation of the polymer chains, alteration of particle shape, increase of viscosity and then of porosity, evolution of the ratio between re-crystallized and nascent crystalline fractions.

Conclusions

Although promising, selective sintering technologies presently still have their industrial development hindered by different factors, among which the difficulties met in reusing the un-sintered powder. Thus, we have undertaken a scientific approach aimed at showing how PA12 ageing affects both the powder processability and the final microstructure of sintered parts. The large range of characterization methods implemented here is original in the field of SLS studies. By improving the scientific knowledge in the field, this work will contribute to a better control of the process.

References

[1] Hopkinson N, Hague RJH, Dickens PM, in *Rapid Manufacturing: An Industrial Revolution for the Digital Age*. John Wiley & Sons, 2006, pp. 1–4.

[2] Frenkel J. *J Phys*. 1945;9:385-391.

Poly(D,L-lactide)-*b*-poly(2-hydroxyethyl acrylate) block copolymers as potential biomaterials for peripheral nerve repair

Thomas Trimaille[1], *Benoît Clément*[1], *François Féron*[2], *Patrick Decherchi*[3], *Denis Bertin*[1], *Kamel Mabrouk*[1], *Didier Gigmes*[1], *and Tanguy Marqueste*[3]

[1]Laboratoire Chimie Provence (UMR CNRS 6264), Université de Provence, Av. Escadrille Normandie-Niemen, 13397 Marseille Cedex 20, France

[2]Neurobiologie des Interactions Cellulaires et Neurophysiopathologie (UMR CNRS 6184), Faculté de Médecine Nord, Université de la Méditerranée, Boulevard Pierre Dramard, 13916 Marseille Cedex 20, France

[3]Institut des Sciences du Mouvement : Etienne-Jules Marey (UMR CNRS 6233), Université de la Méditerranée, 163, Av. de Luminy, 13288 Marseille Cedex 09, France

thomas.trimaille@univ-provence.fr

Introduction

The use of synthetic polymer materials as guide scaffolds for nerve repair is a promising approach as alternative to natural ones, such as collagen, that present several drawbacks (reproducibility between samples, cost, possible contamination with pathogen agents,…). Among synthetic polymers, poly(2-hydroxyethyl (meth)acrylate) (PHE(M)A) polymers are attractive for nerve repair,[1] due to their hydrophilic and hydrogel-like properties. Aliphatic polyesters such as polylactide (PLA) are also choice candidates due to their biodegradability.[2] We aimed at combining the properties of these both kinds of polymers in a single homogeneous material. This can be achieved through the use of block copolymers of PLA and PHEA. Their synthesis through the combination of ring-opening polymerization (ROP) and nitroxide mediated polymerization (NMP) and their properties by means of degradation and Schwann cell adhesion are here described.

Materials and Methods

The ROP of D,L-lactide (Purac) was performed in toluene at 100°C using tin (II) 2-ethylhexanoate ($Sn(Oct)_2$) as catalyst and 2-hydroxyethyl acrylate (HEA) as initiator. The intermolecular radical 1,2-addition (IRA) of the BlocBuilder® (10 eq.) on the obtained acrylate end-capped PLA was performed in THF at 100°C. The NMP of HEA from the PLA macro-alkoxyamine was carried out in bulk at 120°C in presence of free SG1. The block copolymers were characterized by ^{1}H NMR and size exclusion chromatography (SEC). *In vitro* and *in vivo* degradation studies were performed on samples obtained by solvent casting from THF, in phosphate buffer pH 7.4 at 37°C and in rats by subcutaneous implantation, respectively. Schwann cell adhesion was studied on spin-coated polymer films from THF.

Results and Discussion

Our approach to obtain the targeted block copolymers relies on the preparation of SG1-terminated PLA macro-alkoxyamine for further initiation of the NMP of HEA (Scheme 1). For this, an acrylate end-capped PLA (**1**) of M_n~15000 g.mol^{-1} was first prepared by ROP of the D,L-lactide using HEA as initiator and $Sn(Oct)_2$ as catalyst. This PLA was further involved in the IRA with the BlocBuilder®, leading to the PLA-SG1 macro-alkoxyamine (**2**) with a high functionalization yield (~95%). The NMP of HEA from this macro-alkoxyamine led to the block copolymers (**3**) in a controlled manner.

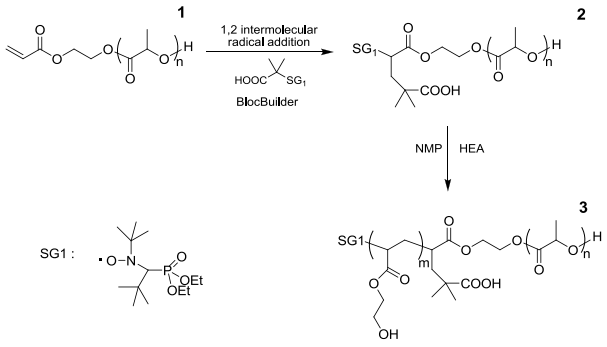

Scheme 1. Synthesis pathway for PLA-b-PHEA.

In vitro / *in vivo* (rat) degradation properties of the PLA-*b*-PHEA block copolymers were then investigated and compared to those of parent PLA homopolymer. Over 12 weeks, we observed mass loss and molecular weight decrease. *In vitro* and *in vivo* findings were very similar for each polymer tested. When a short PHEA block was used (PLA-*b*-PHEA 15000-3000 g.mol^{-1}, 85/15 wt%), the degradation process was found to be very similar to that of homo-PLA, and was typical of a bulk erosion mechanism, with no mass loss observed until week 7 and continuous decrease of molar mass within this time frame. For a longer PHEA block length within the block copolymer (PLA-*b*-PHEA 15000-7000 g.mol^{-1}, 65/35 wt%), the degradation mechanism was modified, with a significant mass loss observed at early times and only a slight decrease in molar mass. The latter finding is related to the pronounced hydrophilicity and softness of the material induced by the PHEA block, which allow easy diffusion and rapid escape of the degradation residues from the material towards the aqueous medium. Schwann cells were found to better adhere on spin coated films of PLA-b-PHEA (85/15 wt%) than on PLA ones.

Conclusion

These results show the potential of such hydrophilized PLA-based copolymers for use in peripheral nerve repair.

References

[1] Flynn, L.; Dalton, P. D.; Shoichet, M. S. *Biomaterials*, 2003, *24*, 4265–4272.

[2] Hurtado, A.; Moon, L. D. F.; Maquet, V.; Blits, B.; Jérôme, R.; Oudega, M. *Biomaterials* 2006, *27*, 430–442.

A New Building Block Concept for Polymers Based on Multifunctional Coupling Agents

Frank Böhme, Lothar Jakisch

Leibnitz Institute of Polymer Research Dresden, Germany

Boehme@ipfdd.de

Introduction:

Reactive compatibilization is a frequently used principle in polymer blending. Reactions between the blend components result in the formation of block or graft copolymers during processing which stabilize blend structures and improve mechanical performance. Usually, such reactions occur mainly in the interface and comprise only a small part of the whole mixture whereas most of the polymer chains remain unreacted. Because of these incomplete conversions, it is difficult to obtain pure block or graft copolymers with defined structures by reactive blending.

To overcome this problem, we developed new coupling agents containing at least two different reactive groups such as oxazinone, oxazoline, or lactamate groups [1-3]. It could be shown that these groups react under certain conditions very selectively in high yields with amino, carboxylic, and hydroxy groups, respectively. The reactivity of these groups is high enough so that the conversions could be performed under the conditions of reactive extrusion. Provided stoichiometry of the reacting groups is warranted, mixing of two oligomers containing different reactive terminal groups with respective multifunctional coupling agents allows obtaining block and graft copolymers with defined block lengths.

In this paper we introduce a new building block concept based on bi-, tri-, and tetrafunctional coupling agents containing oxazinone and lactamate groups. Consecutive conversion of the coupling agents with amino and hydroxy functionalized oligomers allows tailoring the polymer structure in a wide range. Besides alternating polymers, graft and starlike polymers are available.

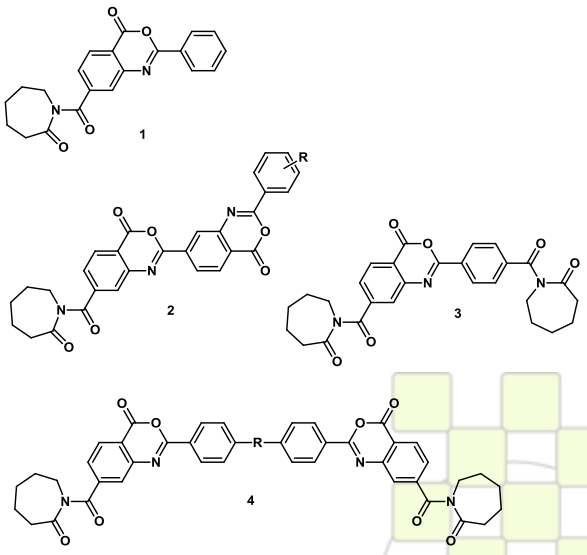

Materials

Coupling agents **1-4** were synthesized according to the procedures described in reference [3].

As oligomers, amino terminated PA12 and hydroxy terminated polycaprolactones (PCL) were used.

The conversion of the oligomers with the coupling agents was preferably done in melt using glass flasks equipped with stirrers or in a mini-melt-mixer.

Results

Coupling agents **1-4** possess different numbers of oxazinone and lactamate groups. It could be shown that the hydroxy groups of PCL oligomers reacted preferably with the lactamate groups. After complete conversion of the lactamate groups, the reaction of the amino terminated PA12 with oxazinone group was performed. Using mono and bifunctionalized oligomers, different structures were available.

As an example, a series of PA12/PCL block copolymers with different block length was synthesized with coupling agent **1**. The mechanical properties are presented in Figure 1.

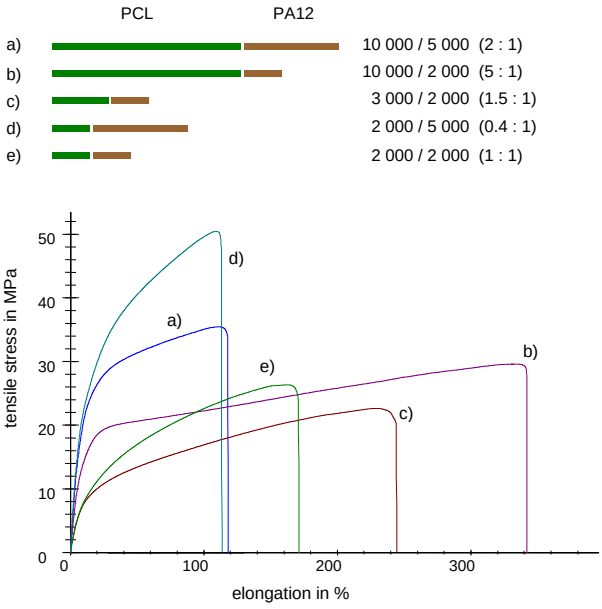

Figure 1 Tensile test curves of PA12/PCL block copolymers with different block length

References

1) L. Jakisch, H. Komber, F. Böhme *J. Polym. Sci., Polym. Chem.* 2003, *41*, 655

2) L. Jakisch, H. Komber, R. Wursche, F. Böhme *J. Appl. Polym. Sci.*, 2004, *94*, 217

3) L. Jakisch, H. Komber, F. Böhme *Macromol. Mater. Eng.*, 2007, *292*, 557

Amorphous silica obtained from rice husk: Study of the enhanced surface area use as reinforcement of rubber

D. Mosca[1] *C. Mantero*[2] *P. Raimonda*[3]

[1, 2, 3] Instituto de Ensayo de Materiales, Facultad de Ingeniería, UDELAR

praimonda@fing.edu.uy

With a production of approximately a million tons of rice,[1] its husk, obteined during the process of production of grain, with a high silica content, is a real problem for Uruguay; a South American country with a surface area of 176,215 Km^2. Silica, is a filler often used in the rubber industry and notes that worldwide demand for this product is increasing, with a production that fails to satisfy the same and therefore with a tendency for prices to rise. In order to find a solution of the problem of environmental pollution, in a previous study, we evaluated the use of the ash with a composition of around of 90% in silica obtained from the controlled calcination of the husk as a filler in rubber compound.

The aims of this paper is to study how the husk acid treatment does increase the surface area of the ash, obtained by controlled burning, in order to maximize it´s effects and compare the results with commercial products.

RESULTS AND DISCUSSION

It was observed that the boil rice husk treatment with hydrochloric acid solutions at 10% was the best option for increasing the surface area of the structure of the silica from the ash and that this increase was achieved through the removal of sodium, potassium and calcium ions in it. In fact, we verified that we can extract 6 more times calcium, and 1.5 more times potassium in acid solutions at 10% than the same treatment with distilled water without affecting the silicon content of ash. Table I summarizes the results of the increased surface area of the structure of silica ash as a function of the concentration of hydrochloric acid.

Tabla I: Resumen de los datos obtenidos del área superficial de la ceniza de cáscara de arroz en función del % de HCl

HCl %	Sup. area in m^2/g
2	188
5	198
10	208
20	208

We studied, using a base formulation, how varied the mechanical properties of a compound based on SBR rubber wich was aded ash as a fill, whose specific surface area was increased by chemical pretreatment of extraction of alkali earth ion of the rice hulls. Controlled burning shell was performed at 600 °C, in order to obtain a residue of silica with amorphous structure, otherwise the product obtained with a crystalline structure is ineffective for the intended application. The results were compared with the values of the compound without charge, with ash obtained without treatment to increase surface area, and amorphous precipitated silica for industrial use. Characterization tests are summarized in Table II and were conducted under ASTM standards, with the exception of abrasion, which was conducted by the DIN ones.

Tabla II. Resumen de los ensayos de caracterización realizados sobre probetas.

Tensile		*Tear Resistance*	*hardness*	*Abrasion*	*Density*	*Compression set*	*Water absorption*
Mpa	*% Elon*	*KN/m*	*Sh A*	*mm^3*	*g/cc*	*%*	*%*
2.6	450	7.7	57	200	1.287	11.6	5.8
1.6	160	8.5	83	161	1.253	15.8	4.3
3.5	550	12.0	64	159	1.261	14.3	2.9
16	595	47.8	77	105	1.334	10.2	2.5
10	560	27.2	70	132	1.346	11.1	2.7

. Notes: Firt line, test specimen witout fill.
Second line, test specimen with rice husk.
Third line, test specimens with ash without tratment.
Fouth line, test specimens with comercial Silica. Refrence
Fifth line, test specimens with ash husk treated with HCl

CONCLUSIONS

In summary we concluded that with the acid treatment of the rice husk was possible to increase the silica content in the ash, and in turn, improve significantly the specific surface area of the structure of the silica particles obtained by extracting the metal ions present in the husk. However we not achieved the expected results in the values of the mechanical properties of the formulated compound.

REFFRENCES

[1]Ministerio de Ganadería Agricultura y Pesca. www.aca.com.uy/publicaciones/revista_38_situacio

Recycling of Poly(ethylene terephthalate) Bottle Waste with Modified Styrene Butadiene Rubber Through Reactive Mixing

O.Moini Jazani[1], A.Ghaemi[2], A.Ebrahimi Jahromi[3]*

1. Polymer Engineering Department, Islamic Azad University omidieh Branch, Omidieh, Iran
2. Polymer Engineering Department, Amir Kabir University of Technology, Tehran, Iran
3. Polymer Engineering Department, Islamic Azad University South Tehran Branch, Tehran, Iran

*Corresponding author : o_moini@yahoo.com

Abstract

Styrene butadiene rubber (SBR) was modified by the grafting reaction of maleic anhydride (MAH) in the presence of the initiator benzoyl peroxide (BPO). This modified elastomer was then blended with poly(ethylene terephthalate) (PET) bottle waste, and the mechanical and morphological properties of the resulting blends were studied. The amount of grafted MAH was determined by chemical titration. The results revealed that the concentrations of MAH and BPO strongly affected the grafting process. The morphology of the dispersed phase for blends of PET waste and SBR-*g*-MAH was quite different from that of a simple blend of PET waste and SBR. The enhanced compatibility resulted in better impact properties. The better compatibility was concluded to result from bond formation between the carbonyl group of SBR-*g*-MAH and the hydroxyl or carboxyl end groups of PET

.Keywords: reactive processing-blending-morphology-recycling

Grafting of a biodegradable pH-sensitive copolymer based on poly(ethylene glycol) methyl ether and poly(ethyl glyoxylate) onto maghemite nanoparticles

Claire-Hélène Brachais[1], *Ling Hu*[2], *Fan Xu*[1], *Aurélien Percheron*[2],

Denis Chaumont[2], Gilles Boni[1], Jean-Pierre Couvercelle[1]

[1]ICMUB - UMR CNRS 5260, 9 avenue Alain Savary, BP 47870, 21078 Dijon Cedex, France

[2]ICB - UMR CNRS 5209, 9 Avenue Alain Savary, BP 47870, 21078 Dijon Cedex, France

e-mail: brachais@u-bourgogne.fr

Introduction :

Magnetic nanohybrids based on inorganic cores encapsulated by a biocompatible polymeric corona have been widely studied due to their broad range of potential applications in ferrofluids[1], drug delivery[2] and biological cell labeling and bioseparation[3]. For these last applications, poly(ethyleneglycol methyl ether) (mPEG) is an ideal material with biocompatible properties (nonimmunogenic, nonantigenic and protein-resistant)[4]. Poly(ethylglyoxylate) (PEtG) or polymethylglyoxylate (PMG) are a family of new biodegradable and biocompatible polymers[5,6]. Recently, the synthesis of poly (mPEG-co-PEtG) as a new pH-sensitive material was described[7]. The purpose of this work is to synthesize by a "grafting to process", new core-shell structured nanohybrid materials composed of a maghemite γ-Fe_2O_3 core and a biodegradable block copolymer mPEG-co-PEtG shell.

Synthesis of the nanohybrides:

The maghemite nanoparticles were first synthesized by precipitation of magnetite from iron (II) and (III) chlorides (according to the procedure developed by Mornet) followed by oxidization of magnetite into maghemite using nitric acid[8]. Then, copolymers synthesis were carried out by anionic polymerization of ethyl glyoxylate (EtG) starting from methoxy-PEG with $\overline{Mn}$ = 2000 g.mol^{-1} . Ethyl glyoxylate was previously purified by distillation under vacuum over phosphorus pentaoxide (100 °C, 70mbar). Polymerizations proceed at room temperature in THF solutions, using triethylamine (NEt_3) as initiator, followed by functionnalization with IPTS. Grafting of silanated mPEG-co-PEtG onto nanoparticles was conducted in THF at 80 °C under N_2 flow with a polymer/nanoparticle ratio equal to 10.

Results and discussion :

The presence of maghemite was evidenced by FTIR spectrum showing three peaks around 631, 573 and 438 cm^{-1}. The particles exhibit a diameter of 14 ± 2 nm which was established by XRD patterns from measurement of the half-height width of the strongest reflection planes. The synthesis of copolymer mPEG-co-PEtG was performed according to the mechanism presented in Figure 1.

SEC characterization was used to investigate the average molar mass of obtained copolymers. Average molar masses are comprised between 2250g/mol and 5600g/mol instead of 2000 g.mol^{-1} for the starting mPEG. FTIR spectra of pure maghemite nanoparticles and nanohybrids obtained after different grafting time revealed the presence of the copolymer at the surface of the nanoparticles. The grafted amount of biodegradable copolymer was estimated by TGA (figure 2).

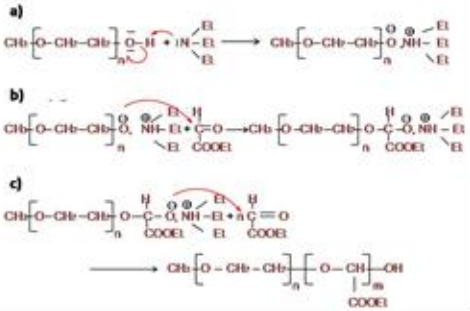

Figure 1 : Synthesis of mPEG-co-PEtG: (a) acido-basic reaction, (b) initiation and (c) propagation.

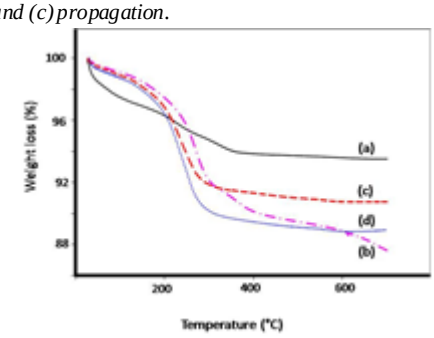

Figure 2 : TGA curves of pure maghemite nanoparticles (a) and nanohybrids obtained after different grafting time: 1h (b), 2h (c) and 5h (d).

The weight loss of grafted copolymer on the nanoparticles, is about 5 % (*w*/*w*) after 1h, 3 % (*w*/*w*) after 2h and 5 % (*w*/*w*) after 5h. Even if the weight loss are rather low these results revealed the aibility of mPEG-co-PEtG be grafted onto maghemite nanoparticles.

Conclusion :

This study is a first exploration of the grafting of a copolymer based on mPEG and PEtG onto maghemite nanoparticles. These preliminary results are quite encouraging and further work is still needed in order to improve the grafting rate of the nanoparticles.

References :

[1] Soler MAG, Alcantara GB, Soares FQ, Viali WR, Sartoratto PPC, Fernandez JRL, Silva SWD, Garg VK, Oliveira AC, Morais PC (2007) Surf Sci 601:3921

[2] Gupta AK, Curtis ASG (2004) J Mater Sci:Mater in Med 15:493

[3] Gupta AK, Gupta M (2005) Biomaterials 26:3995

[4] Zhang Y, Kohler N, Zhang M (2002) Biomaterials 23:1553

[5] Brachais CH, Duclos R, Vaugelade C, Huguet J, Capelle-Hue ML, Bunel C (1998) Int J Pharm 169-1:23

[6] Belloncle B, Burel F, Oulyadi H, Bunel C (2008) Pol Deg Stab 93:1151

[7] Kim JK, Garripelli VK, Jeong UH, Park JS, Repka M, Jo S (2010) Int J Pharm 401: 79

[8] Mornet S, Grasset E, Portier J, Duguet E, (2002) Eur Cells Mat 3:110.

Epoxy/amine: simulation of reactive rotational molding

E. Mounif[a] S. Khelladi[c] F. Bakir[c] A. Tcharkhtchi[b]

[a]Department of physics, Higher Institute for Applied Sciences and Technology, Damascus, Syria
[b]Procédés et Ingénierie en Mécanique et Matériaux, Arts et Métiers ParisTech, Paris, France
[c]Laboratoire de Dynamique des Fluide, Arts et Métiers ParisTech, Paris, France

eskandar.mounif@hiast.edu.sy

Introduction

Rotational Molding (RM)[1] is a suitable process which allows fabricating hollow plastic parts. In the Reactive Rotational Molding (RRM)[2] process, synthesis is taking place during the molding. The initial viscosity of the epoxy/amine reactive mixture (DGEBA/DETDA) at the processing temperature (120-160°C) is very low (<0.001Pa.s) and it increases until gel point. A complete rehokinetic study was realized in a previous work [3]. In order to predict the flow of the reactive mixture at the starting steps of the process, we tried to simulate it using a meshless method. In this paper we study the simulation of reactive rotational moulding (RRM) of complex geometry mould using Smoothed Particle Hydrodynamics (SPH) method[4] .

After testing our code in the case of breaking dam problem, the free flow surface inside horizontally rotating mold is considered as a modelling of the process. More complex geometry of a turbine blade mold was also used.

Method

The Smoothed Particle Hydrodynamics is a meshless lagrangian numeric method. In this method the reactive fluid is represented by discrete particles. In the SPH method, the dynamic pressure p as a function of the density ρ is computed by the equation of state (1):

$$p = \frac{c_s^2 \rho_0}{\gamma}\left[\left(\frac{\rho}{\rho_0}\right)^{\gamma} - 1\right] \qquad (1)$$

To compute the momentum we used the following expression[5]:

$$\frac{dv_j}{dt} = -\sum_i m_i \left[\left(\frac{p_i}{\rho_i^2} + \frac{p_j}{\rho_j^2}\right) - \frac{\xi}{\rho_i \rho_j}\frac{4\eta_i\eta_j}{(\eta_i+\eta_j)}\frac{v_{ji}.r_{ji}}{r_{ji}^2+\varepsilon^2}\right]\nabla_j W_{ji} + g \qquad (2)$$

The density was calculated via the commonly used SPH expression for continuity equation:

$$\frac{d\rho_j}{dt} = \sum_i m_i (v_j - v_i)\nabla_j W_{ji} \qquad (3)$$

To assure the adherence of liquid resin to the internal walls of the mold we applied the non-penetration boundary condition. Time integration was done using Euler scheme

Results and Discussion

We compared between experimental and SPH code results for water dam breaking case (Fig.1).

The method was applied for horizontal rotating cylinder and to more complex geometry like the 2D turbine blade mold (Fig.2).

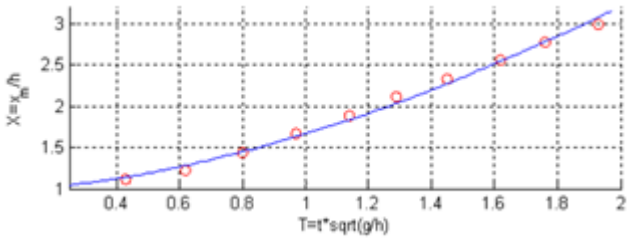

Fig.1 .Front location in broken dam problem, experimental results (o) and SPH (-)

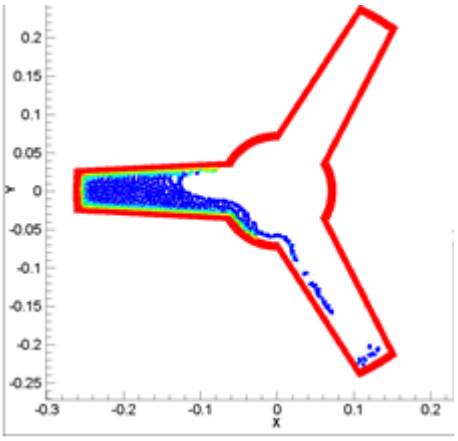

Fig.2. Flow of reactive fluid after 1s inside a turbine mold during the RRM process.

Conclusions

We simulated the free surface flow of a reactive liquid polymer during the first steps of the rotational molding. The Smoothed Particle Hydrodynamics numeric method was applied to simulate the flow. Free surface variation was tracked and easily obtained.

The first results were promising and we are working to optimize the different interactions aspects of the flow such as chemical crosslinking kinetics[3] and thermal transfer.

References

1. Crawford RJ. Prog. Rubber Plast. Technol. 1990;6(1):1-29.
2. Throne JL and Gianchandani J. Polymer Engineering and Science 1980;20(13):899-919.
3. Mounif E, Bellenger V, and Tcharkhtchi A. Journal of Applied Polymer Science 2008;108(5):2908-2916.
4. Monaghan JJ. Reports on Progress in Physics 2005;68(8):1703-1759.
5. Cleary PW. Applied Mathematical Modeling 1998;22(12):981-993.

Biodegradation in Compost of Recycled Low Density Polyethylene/Polycaprolactone Blends

Jordi J. Bou[2], L.M. Marroyo[2], Abdel Alla[2], Lluis Ollé[2], Anna Bacardit[2], Orlando O. Santana[1] and M. Lluisa Maspoch[1]

1. Centre Català del Plàstic – Universitat Politècnica de Catalunya
2. Departament Enginyeria Química – Universitat Politècnica de Catalunya

maria.lluisa.maspoch@upc.edu

Introduction

Plastic bags are very controversial goods due to their apparent environmental impact. To minimize impact, solutions like biodegradable bags from polycaprolactone (PCL), Mater-bi or starch-polyethylene blends have been proposed. In general, economic reasons have been responsible of low market success. Recycled low density polyethylene is commonly used in a large variety of items with low requirements, one of them rubbish plastic bags which have a very low lifetime. Recycled LDPE is very cheap; it is easy molded and also can be obtained sustainably from bioethanol. However it is not compostable or biodegradable like PCL, starch or Poly(Lactic Acid) (PLA).

It is known that recycled polyolefins are slightly degraded due to a little amount of oxidative reactions that reduce their properties compared with virgin materials. In addition, more chemical or biological reactions can be produced due to the presence of new functional groups like hydroxyls, carbonyls or double bonds.

In this study we have prepared different blends from used LDPE and PCL, as biodegradable polymer that could induce degradation of LDPE. In spite of PCL and LDPE are not compatible, blends with both plastics can be made with reasonable properties [1]. These blends (as thin film) have been treated in a compost plant up to 15 weeks and characterized by weight loss, IR spectroscopy, DSC and mechanical properties. The objective of this study is to determine if blends of recycled LDPE and PCL have been biologically degraded, as blown-extruded film. Potential application as biodegradable plastic bags is the motivation of this project.

Materials and methods

LDPE from own plastic bag plant (blue colored with copper phtalocyanine) was our raw material (MFI = 0.5 g/10 min). PCL was obtained from Union Carbide, TONE 787 grade (MFI = 0.5 g/10 min) which is specially designed for film blow molding applications. Blends containing from 0 % to 50 % of PCL were prepared in a pilot plant extruder and blow molded. For every composition was necessary to adjust processing conditions (BUR), in order to obtain to 20 micron thickness films. These films could be easy characterized by FT-IR (Perkin Elmer 1000) and mechanically with a Polymer Laboratories Minimat testing machine for very little samples (50 mm long). Films were 500x500 mm cut and introduced in a homemade rigid iron rack, as container to be inserted in compost piles. Aerating static piles composting were developed in an urban plant in Torrelles (Barcelona – Spain), that works with organic urban waste. Every 4 weeks, a sample iron rack was retired and characterized. The composting process was completed in 15 weeks.

Results

Up to five blends were produced (0, 10, 20, 30, 40, 50 % PCL by weight). Sample with no PCL showed a very little absorption at 1720 cm^{-1}, in infrared spectrum, that indicates some extent in oxidative degradation of polyethylene. After 4 weeks of composting only 40 and 50 % PCL showed visually changes; little weight loss is detected. After 8 weeks 30 % PCL blend began to degrade, according to mechanical properties (break strain). After 15 weeks only 30, 40 and 50 % PCL clearly showed symptoms of degradation. Other samples did not display changes. IR spectra did not show significant changes at any of degraded films, due to PCL degradation mechanism does not modify its chemical structure [2]. After complete composting process, between 15 and 3 % weight loss in 50, 40 and 30 % PCL films were observed. Only strongly degraded samples (50 and 40 % PCL) lost completely their integrity after 12 weeks. These samples after 8 weeks reached elongations at break not more than 9 %. The 30 % PCL sample showed a constant decrease in mechanical properties; at 15 weeks of composting break strain were 11 %. Young modulus was around 1500 MPa and it did not vary notably during biodegradation process for undegraded blends.

The morphological study of these blends is currently being carried out.

Conclusion

Film samples obtained from blow molding of blends of PCL and recycled LDPE were produced and biodegraded by composting. Blends with high content of PCL degrade easily. A blend formulated with 30 % of PCL can be considered as potential material to be used as environmental friendly plastic bag, in spite of LDPE does not biodegrade.

References

[1] G.C Eastmond Adv Polym Sci 1999, 149, 187

[2] N. Lucas Chemosphere 2008, 73, 429.

Acknowledgements

This work has been financially supported by MICINN, grants nº MAT2010-19721-C02-02 and MAT2010-19721-C02-01

Thermoplastic elastomer/organoclay nanocomposites: morphology, thermal and mechanical properties

Anna Szymczyk[1], Sandra Paszkiewicz[2], Zbigniew Rosłaniec[2]

[1]Institute of Physics, [2]Institute of Materials Science and Engineering, Faculty of Mechanical Engineering and Mechatronics, West Pomeranian University of Technology, Piastów Av. 17,70-310 Szczecin, Poland

Abstract

Resent interest on polymer matrix based nanocomposites has attracted much attention due to the interesting observations involving polymer composites with exfoliated clay and more recent studies nanocomposites with carbon nanofibers, carbon nanotubes, exfoliated graphite and metal nanoparticles [1-2]. These nanocomposites have shown that at low loading nanofillers can be used as reinforcing agents to improve the physico-mechanical properties of many polymers.

In this study our objectives is to established the possibility of the improvement of the tensile properties of semicrystalline thermoplastic elastomers. Nanofil 32 was used as nanofiller and poly(trimethylene terephthalate)-*block*-poly(tetramethylene oxide) (PTT-PTMO) segmented block copolymer was used as elastomeric matrix. The morphology of this copolymer consisted of semicrystalline PTT domains dispersed in the soft matrix of amorphous non-crystalizable PTMO.

The nanocomposites containing from 0.5 to 3 wt% of nanoclay (Nanofil 32, Rockwood Additives) were prepared *in situ* by introducing the filler into a reaction mixture for synthesis of PTT-PTMO segmented copolymer by polycondensation in the molten state [3-4]. In order to obtain nanocomposites with well exfolited nanoclay, Nanofil 32 was sonicated and mechanicallly stired in liqiud monomer (1,3- propanediol) and then introdced to the reaxtion mixture.

The properties of polymer-clay nanocomposites depend strongly on the dispersion of the clay layers and the interaction between the polymer chains and their surface. Therefore, the effect of the presence of the nanoclay on the phase separated structure and mechanical properties of the net PTT-PTMO copolymer and nanocomposites were studied by DSC, DMTA and tensile testing.

Structure and morphology evolution during tensile deformation of the net copolymer and nanocomposites were investigated by using synchrotron wide and small-angle X-ray scattering (WAXS, SAXS). The obtained nanocomposites form an exfoliated structure which can be observed by TEM. The DSC results have shown that glass transition and melting behaviour of PTT-PTMO copolymer was not significantly affected by the presence of nanoclay, but increase of crystallization rate and the decrease of supercooling degree required for crystallizing nucleation. Modulus and strength of the PTT-TMO elastomer was improved significantly in the presence of nanoclay attributed to the stiffness, rigidity, reinforcing effects and exfoliation of nanocaly. Besides, the elastic modulus increases without any worsening of the elongation at break. It was established that optimal concentration of Nanofil 32 in PTT-PTMO matrix is 0.5 wt%.

Acknowledgements

The authors thank the financial support from the Polish Ministry of Science and High Education and HASYLAB at DESY in Hamburg (Proposal II-20080143EC).

References

[1] Y.-W. Mai, Z.-Z. Yu; Polymer Nanocomposites, Woodhead Publishing, 2006.

[2] W. Kim, A. A. Abdala, C. W. Macosko, Macromolecules, 2010, *43* (16), 6515–6530

[3] A. Szymczyk, J. Nastalczyk, R.J. Sablong, Z. Roslaniec; Polym. Adv. Technol. 2011, 22(1), 72-83.

[4] A. Szymczyk, E. Senderek, J. Nastalczyk, Z. Roslaniec; Eur. Polym. J. 2008, 44(2), 436-443.

A comparison in dispersion of Carbon Nanotubes in aqueous media

Ghamgosar khorshidi V., Bakhshandeh G.R., Salimi A., Naderi Gh*

Iran Polymer and Petrochemical Institute, P. O. Box: 14965/115, Tehran, Iran

a.salimi@ippi.ac.ir

Introduction

Due to their unique properties, Carbon Nanotubes (CNTs) have been attracted much attentions in modern polymer nanocomposites [1]. In polymeric aqueous media, the effective surfactant must be loaded to achieve a good degree of CNT dispersion [1, 2]. The purpose of this work is to study and evaluate the ability of surfactants in CNT dispersion in aqueous media. The work was performed using two individual surfactants in non-functionalized and functionalized multi walled carbon nanotubes (MWNTs) dispersion.

Materials and Methods

The OH functionalized and non-functionalized MWNTs (diameter 10-30 nm, length 10 µm, purity 95%) were supplied by Institute of Petroleum Industry (Tehran, Iran). The surfactant sodium dodecylbenzene sulfonate (SDBS) from Fluka and sodium lauryl sulfate (SLS) from Merck was used as received. All dispersions were prepared in deionized water at surfactant concentration of 0.075 g/L and constant 1wt% of functionalized and non-functionalized MWNT. The samples were ultrasonicated for 5 minutes using (Bandelin HD 3200, Germany) and then filtered after centrifuging at 3000 rpm for 20 min. The dispersion of CNTs was characterized using UV-vis spectrophotometer model UV-1650 PC (SHIMADZU, Japan) [3].

Results and Discussions

Fig 1 shows the UV spectra of dispersions of non-functionalized and functionalized MWNTs using SDBS and SLS, individually. The functionalized CNTs showed higher absorption comparing with non-functionalized CNTs. The higher absorption in wavelength of 250-400 nm indicates for higher dispersion in functionalized CNTs in both SDBS and SLS containing dispersions [2, 3]. The functionalized CNT provides hydrogen bonding between the –OH group and the hydrophilic group of each surfactant and hence greater attractions to CNTs surface [3].

In comparison between two surfactants, the increase in absorption is more pronounced using SDBS for the same level of surfactant loading, i.e. 0.075 g/L. This behavior was observed in both functionalized and also non-functionalized MWNTs. Due to the existing benzene ring in SDBS structure, higher attraction to CNTs surface and hence better dispersion can be obtained [3]. The existing OH group in CNTs and also the benzenering of surfactants provide the highest degree of disperion for the SDBS-functinalizes MWNTs.

Conclusions

The existing functional group in CNTs and also the structure of surfactants are two main factors playing influence on dispersion of MWNTs. The disersion was better in functionalized CNTs due to hydrogen bonding and in SDBS containg disperion due to the benzene ring. These two parameters provides the highest degree of disperion for the SDBS-functinalizes MWNTs.

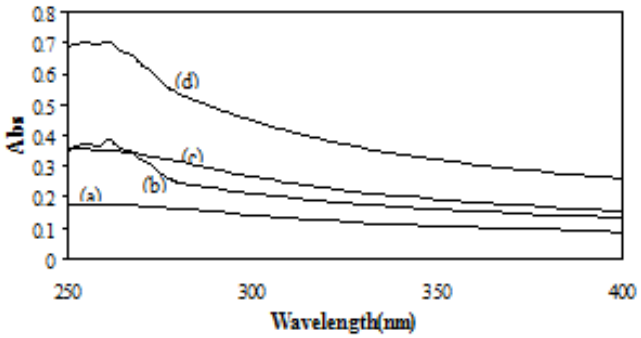

Fig 1. UV–vis spectra of (a) SLS-non functionalized CNTs (b) SDBS- non functionalized CNTs (c) SLS-functionalized CNTs (d) SDBS- functionalized CNTs

References

1- Uddin, N. M., thesis, Drexel University, March (2010).
2- Rastogi R., Kaushal R., Tripathi S. K., Sharma A. L., Kaur I., Bharadwaj L. M., Journal of Colloid and Interface Science, 328 (2008) 421- 428.
3- Bystrzejewski M., Huczko A., Lange H., Gemming T., Buchner B., Rummeli M. H., Journal of Colloid and Interface Science, 345 (2010) 138- 142.

X-ray Investigation of iPP and Propene/Ethylene Random Copolymers Solidification During Ultra Fast Cooling

G. Portale[1], D. Cavallo[2], L. Balzano[3], G. C. Alfonso[2]

[1]BM26-Dubble, ESRF, Grenoble, France. Netherlands Organization for Scietific Research (NWO)
[2]Dip. di Chimica e Chimica Industriale, University of Genova, Genova, Italy
[3]Dept. Mechanical Engineering, Eindhoven University of Technology, Eindhoven, The Netherlands

portale@esrf.fr

Introduction

It is well known that the crystallization behaviour of semi-crystalline polymeric materials is strongly affected by the thermo-mechanical history during processing. For instance, the wide range of cooling rates (from few to hundreds of degrees per second) employed in industry for polymer processing results in strong differences on the morphology development. For many polymers, fast cooling implies structuring at extreme undercoolings, with the possibility to develop kinetically driven metastable structures. In particular, on quenching, polypropylene develops a mesomorphic structure with a degree of order intermediate between that of the monoclinic -phase and of the amorphous supercooled liquid.[1] Its formation and transformation have been extensively investigated.[2] However, the role of molecular features in the development of this polymorph is not fully assessed yet. For example, the effect of stero-defects on mesophase formation is controversial,[3] while the role of constitutional defects (i.e. random copolymers) has been reported only in a few papers and the results are still not exhaustive.[4] Recently a Continuous-Cooling-Curves (CCC) approach has been applied to investigate the development of the mesomorphic structure in propene/ethylene random copolymers.[5]

Results and Discussion

The present work reports recent results on structure development of iPP and its copolymers with ethylene during fast cooling as obtained by coupling on-line thermal analysis with ultra-fast in-situ synchrotron radiation wide-angle X-ray scattering (WAXS).[6] Fast cooling was performed using an home-built quenching device, which enables controlled heating and rapid cooling of thin polymer samples by blowing compressed air on its surface. Simultaneous collection of WAXS patterns and sample temperature (i.e. CCC curves) was carried out with perfect synchronization. Thanks to novel photon counting Pilatus 300K detector, high quality WAXS patterns were collected, allowing to quantitatively describe the kinetics of mesophase and -phase development during ultrafast cooling, which last only a fraction of a second.As an example, Figure 1a shows the mesophase formation during fast cooling of a propene/ethylene copolymer thin film with 7.3 mol% of comonomer at 160 ºC/s. The evolution of the calculated mesophase fraction formed during cooling for two propene/ethylene copolymers (3.4 and 7.3 mol%) is shown in Figure 1 b.

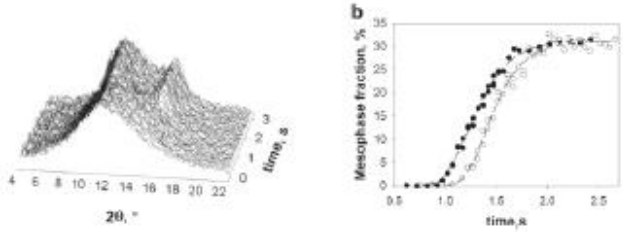

Figure 1 a (left) WAXS time evolution during cooling 160 °C/s for random propene/ethylene copolymers 7.3 mol % of ethylene; Figure b (right) Time evolution of mesophase fraction during cooling at 160 °C/s for random propene/ethylene copolymers with 3.4 (•) and 7.3 (○) mol % of ethylene.

Thus, the evolution of the mesophase fraction can be calculated in real-time for different cooling rates and different copolymer composition. In this manner, the coupling of X-ray with CCC data allows us to obtain quantitative diagrams indicating at what temperature the phase transition takes place as well as the content of the different phases.

A general concept can be stated on basis of our results: anything that negatively affects the crystallization kinetic of the α-phase (including regio-, stereo- and constitutional defects) decreases the minimum cooling rate required to obtain a prevailing mesomorphic sample. On the other hand, when the crystallization kinetics of the monoclinic structure is promoted (e.g. by nucleating additives) the formation of the mesophase can only take place at cooling rates which are practically inaccessible.

References

[1] P. Corradini; V. Petraccone; C. De Rosa; G. Guerra Macromolecules 1986, 19, 2699
[2] Q. Zia; R. Androsch; H.J. Radusch; S. Piccarolo, Polymer 2006, 47, 8163
[3] T. Konishi; K. Nishida; T. Kanaya; K. Kaji Macromolecules 2005,38, 8749
[4] D. Mileva; Q. Zia; R. Androsch; H.J. Radusch; S. Piccarolo Polymer 2009,50, 5482
[5] Cavallo, D.; Azzurri, F.; Floris, R.; Alfonso, G.C.; Balzano, L., Peters, G.W. Macromolecules 2010, 43, 2890-2896.
[6] Cavallo D., Portale G., Balzano L., Azzurri F., Bras W., Peters G.W., Alfonso G.C. Macromolecules 2010, 43, 10208–10212

The Behavior of the Inorganic Nano-Filler in Polypropylene Fibres

*E. Borsig, A. Augustinova, A. Ujhelyiova, A. Marcincin

Institute of Polymer Materials, Faculty of Chemical and Food Technology, Slovak University of Technology in Bratislava, Radlinskeho 9, 812 37 Bratislava, Slovakia
Institute of Polymers, Slovak Academy of Sciences, Dubravska cesta 9, 845 41 Bratislava 45, Slovakia

eberhard.borsig@stuba.sk

Introduction

From our last, partly already published, works we would like to show the results we obtained in studies of the influence of inorganic nano-filler on the morphology and mechanical properties of polypropylene (PP) fibres and what behavior is different in comparison with testing of bulky plastics material. Since, the fibers is a material containing oriented crystallites and macromolecules, the aim was to follow the influence of degree of orientation of PP fibres (what is attained with different drawing ratios at the spinning of PP composite) on the efficiency of nano-filler reinforcement, and also influence of the spinning process of the PP/filler nano-composite on the morphology of the fibres was investigated.

Materials and Methods

For preparation of PP/nano-composite, various kind and types of nano-filler based on clay or boehmite at our experiments were used. Silicate nanofiller: SOMASIF, Co.Chemical Yapan, modified with talcum and Na_2SiF_6. Boehmite: Disperal 40 and 60 (Sasol, Hamburg). Polypropylene: PP-HPF Slovnaft, a.s. Bratislava.

Laboratory spinning apparatus – VUCHV, a.s. Svit. TEM – Frieburg Material Forschung. Mechanical properties - Instron 1122.

Results and Discussion

An example, where the influence of the Nanofil type on some mechanical properties of PP nano-composite fibres is indicated, shows the Table 1. At these experiments also a compatibilizer AR 504 (based on grafted PP with maleic anhydride) was used. It seems to be interesting, that the maximal tenacity of fibres was obtained already at about 1 wt. % of Nanofil, and at higher content of filler the tenacity decreases up to the tenacity of neat PP fibres (till 3 wt. % of filler) and then also to more lower values [1]. The maximal tenacity of the PP nano-composite fibres at used conditions in Table 1, increases with drawing ratio of nano-composite fibres, but the quotient of the effect of the filler on their tenacity with respect to tenacity of the neat PP fibres decreases.

The influence of filler Nanofil on the elongation of the PP nano-composite fibres is very different. At low content of filler about 1 wt. %, the elongation of fibres decreased relatively considerably in comparison with neat PP fibres, but with further increase of filler, a slightly decreases of elongation was observed. For example: elongation ε of neat PP fibres achieved 109.8 % and but at 1 wt. % of filler ε decreased to 93.3 and then at 2 and 3 wt. % increases to 110 and 114 % resp. [2].

Table 1 The influence of filler Nanofil and compatibilizer AR 504 on tenacity (σ), of PP fibres at different drawing ratios (λ)

Nanofil wt. %	AR 504 wt. %	cN/dtex		
		λ = 2	λ = 3	λ = 4
0	0	1.49	2.19	3.86
1	2.8	1.85	2.81	4.22
2	5.6	1.61	2.65	4.15
3	8.4	1.47	2.46	3.97
4	11.2	1.48	2.20	3.48

The knowledge about the influence of filler on the viscosity of PP melt we have used at spinning the syndio-tactic (sPP) [3]. The laboratory spinning apparatus did not allowed to spine the neat sPP. Using sPP compounded with a silicate filler M-ODA the obtained sPP polymer composite was spinned. TEM micrographs of the sPP M-ODA fibres prepared at presence and without a compatibilizer showed the difference in exfoliation of filler particles. Without the compatibilizer the M-ODA particles were only partly exfoliated and some of them were seen on "fibre-skin" surface. Also a boehmite nano-filler Disperal compounded with iPP was spinned without use of compatibilizer and obtained fibres were tested. The original filler Disperal contained aggregated crystalline particles of size several hundred microns were dispersed without compatibilizer to nano-particles less than 200.

Conclusion

At these conditions prepared PP fibres containing Disperal 40 and Disperal 60 or silicate nanofiller showed some positive mechanical properties applicable for practical use. The observed properties of PP nano-composite fibres will be discussed.

Acknowledgement

The support of the National Grant Agency of Slovakia VEGA 1/0444/09 is appreciated.

References

1. Andrea Augustinova, Thesis, Slovak University of Technology in Bratislava, "Study of geometric and structural non-uniformity polypropylene nano-composite fibres", 2005, p. 34
2. Jana Čarná, Thesis, Slovak University of Technology in Bratislava, Influence of the compatibilizer on properties of nano-composite fibres", 2003, p. 32
3. Z. Mlynarcikova, D. Kaempfer, R. Thomann, R. Mulhaupt, E. Borsig, Polymer for Advance technologies, 2005, 16:1-8

Synthesis and Characterization of Natural Oil Based Alkyd–Acrylic Copolymers

Pirita Rämänen and Sirkka Liisa Maunu

University of Helsinki, Laboratory of Polymer Chemistry
P.O. Box 55, FIN-00014 Helsinki, Finland

pirita.ramanen@helsinki.fi

Introduction

Alkyd-acrylic copolymers have been widely studied as coating materials due to their attractive properties. By copolymerization it is possible to combine the positive properties of both: auto-oxidative drying and high gloss of alkyd resin and fast drying of acrylates. The aim of this study is to develop new environmentally friendly copolymers with special properties to be focused, for example, on various coating applications. The challenge and the novelty of this research is to utilize abundant renewable raw materials, such as tall oil fatty acids and rapeseed oil.

Materials and Methods

In this study acrylate monomers were polymerized in the presence of natural oil based alkyd resin, when acrylic macroradicals were grafted to the double bonds of the unsaturated fatty acid chains in the alkyd resin [1]. The polymerization was done via miniemulsion method due to the smaller particle size achieved and more stable emulsion created when compared to conventional emulsion polymerization. Films of these copolymers were prepared by drying the copolymer dispersions at ambient conditions and the effect of the product composition on the film properties was studied, e.g. the mechanical properties of films were studied with dynamic mechanical analysis (DMA). In addition solid state NMR spectra and IR spectra of copolymers and copolymer films were measured.

Results and Discussion

Solid state NMR studies showed that the drying of copolymer films occurred, in addition to physical drying via water evaporation, also chemically via double bond oxidation, which can be seen in NMR spectra as a diminution of the double bond peaks at 125 – 135 ppm (Fig. 1). From liquid state NMR studies it was observed that copolymerization between alkyd resin and acrylic monomers was occurred based on the decreased amount of double bonds.

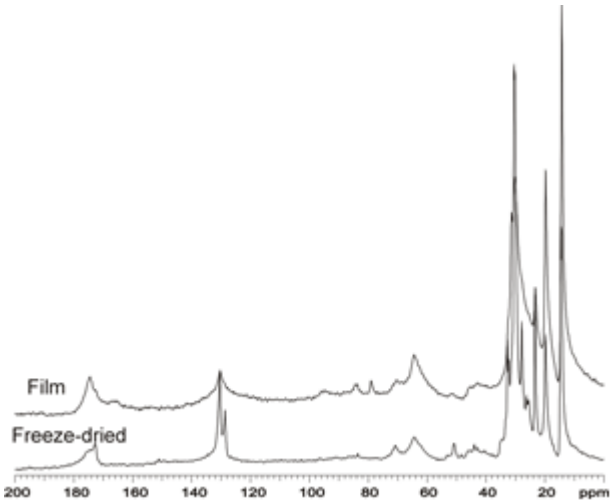

Figure 1. Solid state NMR spectra of freeze-dried copolymer and copolymer film.

The mechanical properties of films were studied with DMA. The stress-strain measurements prove that increased the alkyd content makes the films harder and more brittle.

Conclusions

The results show that copolymerization occurs and alkyd resin and acrylate monomers form copolymers and the prepared dispersions are stable for several months. Besides physical drying, drying of copolymer films was noticed to take place autoxidatively as with pure alkyd resins. It was observed that varying alkyd-acrylate ratio, alkyd resin type and acrylate monomer combination affect the copolymer and copolymer film properties.

References

1. Uschanov, P., Heiskanen, N., Mononen, P., Maunu, S. L., Koskimies, S. Prog. Org. Coat. 63 (2008) 92.

ABSTRACTS

ORAL PRESENTATIONS

Topic 4: Polymers for Advanced Applications Including Energy, Transport, Packaging and Environmentally Friendly Activities

Multiarm star poly(glycidol)-*block*-poly(ε-caprolactone) of different arms lengths and their use as modifiers of diglycidylether of bisphenol A thermosets

Mireia Morell[1], *Albena Lederer*[2], *Xavier Ramis*[3], *Brigitte Voit*[2], *Àngels Serra*[1]

[1] Department of Analytical and Organic Chemistry, Universitat Rovira i Virgili, Tarragona, Spain.
[2] Leibniz-Institut für Polymerforschung Dresden e.V., Dresden, Germany.
[3] Thermodynamics Laboratory, ETSEIB Universitat Politècnica de Catalunya, Barcelona, Spain.

e-mail: mireia.morell@urv.cat

Introduction

The main objectives of our research on epoxy based materials are the control of shrinkage and the enhancement of toughness especially required in many applications. Employing reactive modifiers such as hyperbranched polymers (HBPs) a significant improvement of these properties was observed without affecting the thermomechanical characteristics due to the high free volume of the HBP and its chemical incorporation into the epoxy network [1,2].

In the present work, we propose the use of star polymers capable to improve not only the mechanical properties of the resulting thermosets but even the processability of the reactive mixtures. Until now the use of multiarm star copolymers based on poly(glycidol)-*b*-poly(ε-caprolactone) (PGOH-*b*-PCL_x) of different arm lengths as chemical modifiers of DGEBA (diglycidylether of bisphenol A) has not been reported. Our aim is to investigate the influence of this new polymer topology and of the arm length variation on the rheological behaviour, curing and gelation processes and on the final properties of the resulting PGOH-*b*-PCL_x/DGEBA thermosets.

Materials and Methods

Poly(glycidol) (PGOH, $\overline{M}_n$=12.200 g/mol, PDI:1.31) was synthetized according to [3]. ε-caprolactone (ε-CL) was dried over CaH_2 and distilled. Tin (II) 2-ethylhexanoate ($Sn(oct)_2$) and 1-methylimidazole (1MI) were used without further purification. Diglycidylether of bisphenol A (DGEBA) Epikote Resin 827 was provided by Shell Chemicals (EEW=182.08 g/eq).

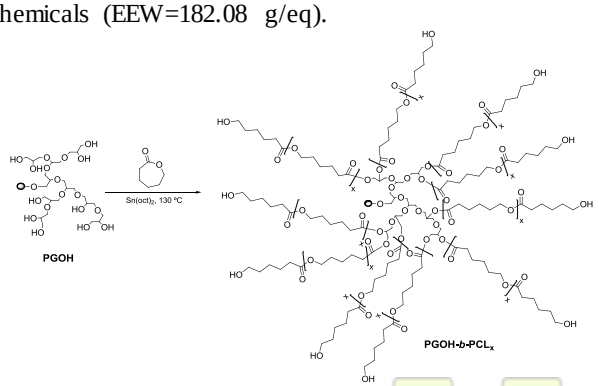

Scheme 1. Synthetic route to PGOH-*b*-PCL_x, where x is the average degree of polymerization of ε-CL (x = 10 or 30).

Varying the monomer/initiator ratio (ε-CL:OH), two star copolymers with 165 arms/molecule and 1.000 g/mol or 3.000 g/mol of arm length were obtained by cationic ring-opening polymerization of ε-CL from poly(glycidol) employing $Sn(oct)_2$ as catalyst (**Scheme 1**). Both stars were used in a proportion of 5 wt% and 10 wt% to modify DGEBA. The curing kinetics was studied by DSC. The complex viscosity (η*) and the gelation process were evaluated by rheometry and DSC. Thermal characteristics were studied by DSC, DMTA and TGA. Curing shrinkage was evaluated by density measurements. Cryofractured samples were observed by ESEM.

Results and Discussion

The addition of PGOH-*b*-PCL_x to DGEBA retards the curing process, when 5 phr of 1MI was used as initiator. In comparison with pure DGEBA, the modified formulations reach the gelation at longer times and higher epoxy conversion which permits a better processabilitiy of the thermoset and the reduction of internal stresses.

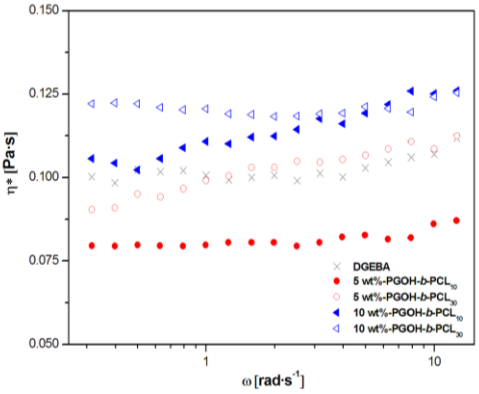

Figure 1. Complex viscosity (η*) versus angular frequency (ω) of reactive mixtures at 30 ºC.

In **Figure 1** it is observed that the incorporation of 5 wt% of PGOH-*b*-PCL_{10} diminishes the η* of the mixture, but increasing the arm length of the star, the viscosity rises significantly. The shrinkage during curing is reduced for all the formulations but using 10 wt% of PGOH-*b*-PCL_{30} the highest reduction is obtained. From all the studies done, we can conclude that the better coating improvements are obtained when a short arm length star copolymer is used.

References

[1] Voit, B.; Lederer, A. Chem. Rev. 2009, 109:5924-5973.
[2] Morell, M.; Ramis, X.; Ferrando, F.; Yu, Y.; Serra, A. Polymer 2009, 50:5374-5383.
[3] Sunder, A; Hanselmann, R.; Frey, H.; Mülhaupt, R. Macromolecules 1999, 32:4240-4246.

Acknowledgements

To MICINN, FEDER and Generalitat de Catalunya (MAT2008-06284-C03-01/02, 2009-SGR-1512). M.M. to the grant FI-DGR 2009 from the Catalonian Government and the mobility fellowship from MEC.

Dynamics of uniaxially oriented natural rubber using dielectric spectroscopy

Marianella Hernández[a], *Tiberio A. Ezquerra*[b], *Miguel A. López Manchado*[a]

[a]Instituto de Ciencia y Tecnología de Polímeros, CSIC, Madrid 28006, Spain
[b]Instituto de Estructura de la Materia, CSIC, Madrid 28006, Spain

marherna@ictp.csic.es

Introduction

Natural rubber (NR) is a well studied elastomer. Of particular interest is the ability of NR to crystallize, specifically the strain-induced crystallization that takes place whilst the material is stretched. Moreover, in many elastomer applications, network chain dynamics under external stress/strain are critical for determining ultimate performance[1]. Thus, a study on how the strain-induced crystallization affects the dynamics of a rubbery material is of outmost importance. This research studies the effect of orientation on the segmental dynamics as a function of the draw ratio, focusing on the relationship between the network structure and the strain-induced crystallization behavior of NR using Broad-band dielectric spectroscopy.

Materials and Methods

NR was kindly supplied by Malaysian Rubber (Berhad, Malaysia) under the trade name CV 60 (Mooney viscosity: ML(1 + 4) 100 ºC = 60). The curing system employed expressed as parts per hundred parts of rubber (phr) was: sulphur (2.5), zinc oxide (5), stearic acid (1) and MBTS (benzothyazyl disulfide) (1).

The uniaxial deformation measurements were carried out in a dynamometer (INSTRON, model 3366) at 25 ºC, and at a cross-head speed of 500 mmmin^{-1}. Stretching ratios from 250 to 750% were performed.

Broad-band dielectric relaxation spectroscopy (BDS) measurements were performed on an ALPHA□□ high resolution dielectric analyzer (Novocontrol Technologies GmbH, Hundsangen, Germany). The complex permittivity ($\varepsilon^* = \varepsilon' - i\varepsilon''$) of the stretched NR compounds was measured over a frequency window of $10^{-1} < F/Hz < 10^{7}$ in the temperature range from -60 to 25 ºC in 5 ºC steps. The dielectric relaxations were empirically described in terms of the Havriliak-Negami (HN)function[2]:

$$\varepsilon^*(\omega) = \varepsilon_\infty + \frac{\varepsilon_S - \varepsilon_\infty}{\left[1 + \left(i\omega\tau_{HN}\right)^b\right]^c}$$

Results and Discussion

After 300% strain, a noticeable upturn in stress is observed while stretching proceeds, as expected (see Figure 1a). This outstanding property of NR is believed to be due to the increased crystallization by stretching of the rubber causing molecular alignment in the stretching direction. This peculiarity gives NR a self-reinforcement character, since the strain-induced crystallites form an additional physical cross-linking network, carrying most of the applied load.

Concerning dielectric behavior, the α-relaxation, attributed to the segmental mode, manifests itself as a maximum in ε''(F); this maximum shifts to lower frequencies while stretching proceeds, slowing down the segmental motion of NR chains. Figure 1b shows an important rise in ε'' for the strained samples compared to unstretched NR, which can be associated with the increase in density as a consequence of the orientation suffered by chains. Also, from 300% strain on, a decrease in the intensity of ε''_{max} is observed. This behavior can be associated to a decrease with the drawing process in the total number of dipole groups in the crystalline regions, which can move easily in the external field[3].

From these results we can infer that the emergence of rubber crystals starts after 300% extension. In consequence, as the tie molecules in the crystalline-amorphous interphase become part of the crystalline regions, the degree of crystallinity increases since the orderly arrangement of molecules in the crystalline structure limits the chain mobility (see Figure 1c).

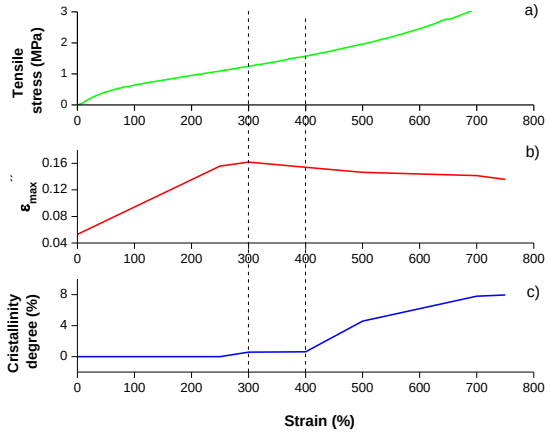

Figure 1. a) Tensile stress, b) dielectric loss maxima ε'', and c) crystallinity degree for stretched NR samples at different extension ratios.

Conclusions

Segmental dynamics of NR seem to be affected by uniaxial stretching since a slowing down of the α-relaxation is achieved. Also, the results presented herein are evidence of an amorphous/semi-crystalline transition between 300% and 400% strain: below this transition, molecular chains show orientation, but no crystallization takes place and dielectric strength increases dramatically; while above this transition, the crystalline structure formed limits the segmental dynamics of NR.

References

1.Toki, S.; Hsiao, B. S. *Macromolecules* **2003,** 36, (16), 5915-5917.

2.Schönhals, F. K. A., *Broadband Dielectric Spectroscopy*. Springer: 2003.

3.Ozkazanc, E.; Guney, H. Y.; Oskay, T.; Tarcan, E. *Journal of Applied Polymer Science* **2008,** 109, (6), 3878-3886.

Adhesion Properties of Polycaprolactones and Polycaprolactone Based Polyurethane Prepolymers

Monica Garcia Ruiz, Juan L. Valentin, A. Marcos-Fernandez

Instituto de Ciencia y Tecnología de Polímeros (C.S.I.C.)

mgarciarui@repsol.com

Introduction

Polycaprolactones are a type of aliphatic crystalline polyesters with very good mechanical properties.

Although polycaprolactones (PCLs) are widely used in several applications, including polyurethane adhesives, there are not many bibliographic references about their adhesive properties.

On the other hand, poyurethanes are a very versatile family of polymers with properties spanning from soft to very rigid materials used in many applications including adhesives.

For adhesives, one of the major applications is in the footwear field, more specifically, in the adhesion of shoe soles to instep materials. Current trends lead towards the use of 100% solids adhesives, avoiding the use of solvents and water. For a 100% solids adhesive, the main properties it must fulfil are: good wettability of the substrate, good adhesion properties and good processability. The aim of this work is to evaluate the adhesion properties of PCLs and of PCL based polyurethane prepolymers (isocyanate capped) and correlate the results with their molecular weight and their chemical structure respectively.

Materials and Methods

Materials

Polycaprolactones were kindly provided by Perstop. In the following table, nominal Mn for high molecular weight polycaprolactones is indicated.

PCL	Mn
CAPA® 6250	25000
CAPA® 6400	40000
CAPA® 6430	43000
CAPA® 6500	65000
CAPA® 6800	80000

Isocyanate-terminated prepolymers were synthesized in bulk at 120ºC using MDI as diisocyanate and PCL diols kindly provided by Perstop. A series of prepolymers with different molecular weight of the PCL diol and different molecular weight of the resulting prepolymer were prepared, as listed in the following table:

Mn PCL diol	Mn prepolymer	%NCO
2000	25000	0.34
	50000	0.17
	100000	0.08
4000	25000	0.34
	50000	0.17
	100000	0.08
8000	25000	0.34
	50000	0.17
	100000	0.08

Methods

Thin films of PCLs and prepolymers were applied from the MEK solutions onto PVC strips, used as substrate for the adhesion tests, and solvent removed at ambient temperature. The covered PVC strips were heated at 80ºC in an oven until adhesive was melted, pressed for 15 seconds and stored at room temperature for 72 hours before performing the T-peel test.

Results and Discussion

For PCLs, a critical value of molecular weight was found to reach high adhesion values. Crystallinity was measured, and rheology and low-field RMN experiments for the melted PCLs was performed in order to correlate with the adhesion values.

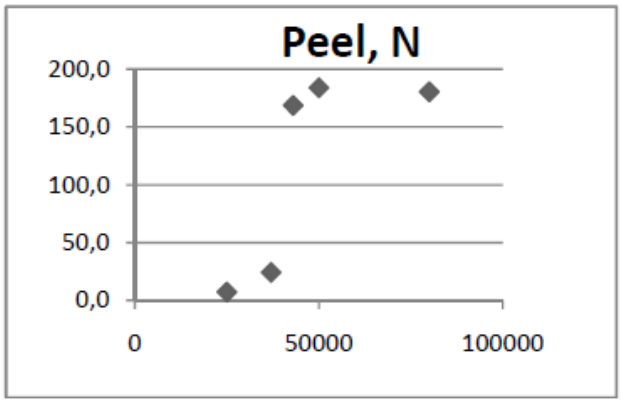

Figure 1. Adhesion results for PCLs

High adhesion values for isocyanate terminated prepolymers were obtained for PCL 4000 and 8000, with high PCL crystallinity. For short PCL diol, with lower crystallinity, only at high isocyanate contents adhesion values approached the values for the others. Isocyanate content also influenced the adhesion values, increasing adhesion when isocyanate content increased.

Conclusions

PCL has very good adhesion properties to PVC when molecular weight exceeds 40000 Da. This limiting value is not related to crystallinity, and do not correlate with mechanical properties. Adhesion properties of prepolymers were dependent on the crystallinity of PCL and isocyanate content, higher at longer PCL and higher isocyanate content.

References

- M.P. Grosvenor, J.N. Staniforth. Int.J.Pharm., 135, 103-109 (1996)
- A.L. Daniel da Silva, J.M. Matín-Martínez, J.C. Moura Bordado. Int.J.Adh.Adh., 26, 355-362 (2006)
- M.S. Sánchez-Adsuar, E. Papon, J.-J. Villenave. J.Appl.Polym.Sci., 76, 1602-1607 (2000)

Polyvinyl Butyral Furfural: Molecular Structure and Thermomechanical Properties.

A.G. Rodionov[1], *N.K. Kobyakova*[2], *Y.A. Kursky*[3], *I.V. Blagodatskikh*[4], *E.A. Litmanovich*[5], *V.M. Aleksashin*[6].

[1] – Open Joint-Stock Corporation "Plastpolymer", St. Petersburg;
[2] - V.A. Kargin Polymer Chemistry And Technology Research Institute, Dzerzhinsk;
[3] - G.A. Razuvaev Institute of Organometallic Chemistry of RAS, Nizhny Novgorod;
[4] - A.N.Nesmeyanov Institute of Organoelement Compounds of RAS, Moscow;
[5] – Lomonosov Moscow State University, Moscow;
[6] – All-Russian Scientific Research Institute of Aviation Materials, Moscow.

e-mail: agr2049@yandex.ru

Polyvinyl butyral furfural (PVBF) is a mixed acetal of polyvinyl alcohol of general formula

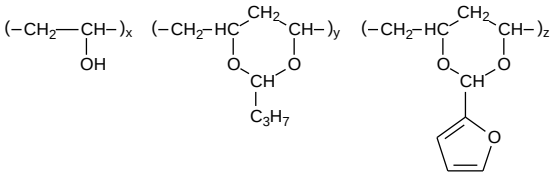

having high adhesion, cohesion and heat resistance, which allows to use it as a component of construction, heat-resistant adhesives and thermosetting laminated plastics.

The present work is concerned with developing of methods and analysis of PVBF molecular structure, as well as determining their thermomechanical properties.

We have developed NMR technique for determining of PVBF chemical and stereoisomeric composition.

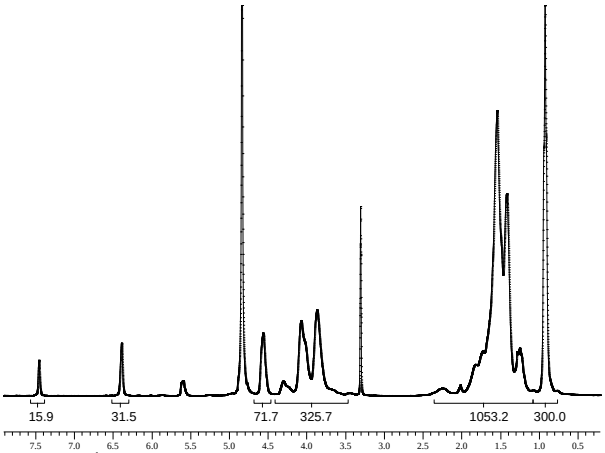

PVBF ^{1}H NMR spectrum at 400 MHz in CD_3OD. Under the spectrum regions of integration and the integral intensities of different group signals are shown.

PVBF Composition from ^{1}H NMR Spectroscopy Data.

PVBF Sample Nos.	Substituted Alcoholic Groups, %	Content of Polymeric Moieties mole %			Mesomeric Butyral Rings, %
		X	Y	Z	
28	65.8	50.9	43.0	6.1	78
34	66.4	50.3	41.4	8.3	77
35	69.9	46.3	46.9	6.9	74
36	71.3	44.5	47.9	7.6	72

For determining of PVBF molecular mass characteristics gel permeation chromatography and static and dynamic light scattering were used.

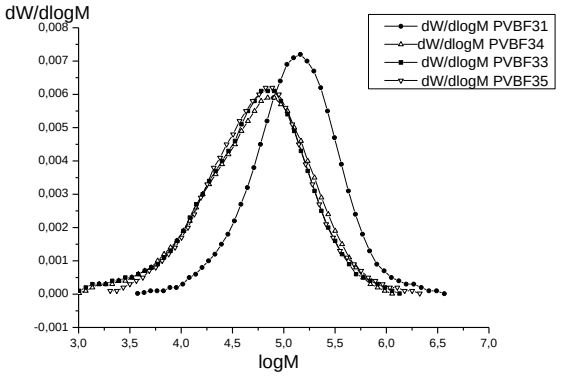

Molecular Mass Distribution (MMD) of PVBF samples.

Test Nos.	Mn	Mw	Mz	Mw/Mn
31	76700	203000	537000	2,65
33	22200	89800	227000	4,05
34	25500	94500	218000	3,71
35	29800	106000	366000	3,55

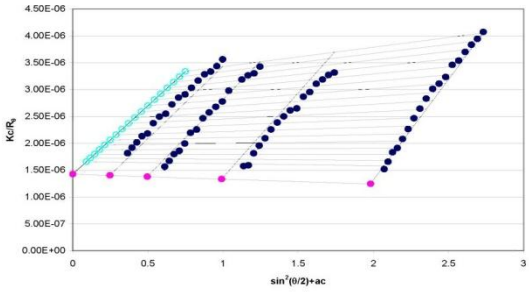

Static light scattering for PVBF.

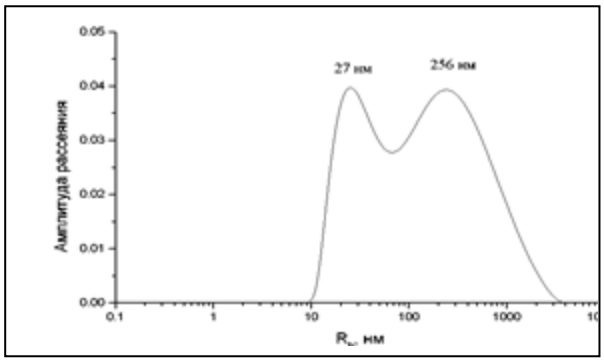

Dynamic light scattering for PVBF.

Sample	Insoluble fraction %	Soluble fraction %	Coarse fraction %	R_1, nm	R_2, nm
PVBF -31	0	96.4	3.6	27	256
PVBF -34	5	90.1	4.9	11	120
PVBF -33	2.7	85.6	11.7	20	189
PVBF -35	6	≈80	≈20	16	175

Transmissive to Black Electrochromic Aramids Based on Electroactive Tetraphenylbenzidine Units

*Hung-Ju Yen, Kun-Ying Lin, and Guey-Sheng Liou**

Functional Polymeric Materials Laboratory, Institute of Polymer Science and Engineering, National Taiwan University, 1 Roosevelt Road, 4th Sec., Taipei 10617, Taiwan

E-mail: d96549005@ntu.edu.tw (Yen, H.-J.) and gsliou@ntu.edu.tw (Liou, G.-S.)

Electrochromic materials exhibit a reversible optical change in absorption or transmittance upon electrochemically oxidized or reduced, such as transition-metal oxides, inorganic coordination complexes, organic molecules, and conjugated polymers.[1]

According to Robin and Day,[2] the *N*, *N*,*N*',*N*'-tetraphenyl-*p*-phenylenediamine (TPPA) cation radical have been reported as a symmetrical delocalized class III structure with a strong electronic coupling while *N*,*N*,*N*',*N*'-tetraphenylbenzidine (TPB) cation radical was demonstrated as a class II structure with a weakly electronic coupling, both leading intervalence charge transfer (IV-CT) absorption bands in the NIR region.[3] These result made aryldiamine-containing molecule a interesting anodic electrochromic system for NIR applications.

our strategy is to design and synthesize TPB-based ECPs with a longer distance between two electroactive nitrogen centers and higher absorption wavelength than the TPPA-based ones.[3b] Furthermore, by the copolymerization of these two series ECPs, the absorbing bands and reflected coloration could be merged and offer the potential for the preparation of ECPs possessing either highly saturated or darker colors.

In this contribution, we synthesized the TPB-based diamine monomer, *N*,*N*'-bis(4-aminophenyl)-*N*,*N*'-di(4-methoxyphenyl)-4,4'-biphenyldiamine, and its derived aromatic polyamides containing *para*-substituted methoxy groups which could not only enhance the solubility by a high steric hindrance for close packing but also greatly prevent the electrochemical coupling reactions by affording stable cationic radicals. The result TPB-based polyamides are expected to reveal a slightly bathochromic shift when compared with the reported TPPA-based ones in the oxidized stages due to the longer conjugating length between two electroactive nitrogen atoms. In addition, by random copolymerization of TPB and TPPA-based diamine monomers, the resulting copolymer **IIb** could exhibit extensive absorption ranging of 400-750 nm required for a black electrochromism. To the best of our knowledge, copolymer **IIb** is the first transmissive to black ECP absorbing virtually the whole visible spectrum in the oxidized state.

Transmissive to Black Electrochromic Aramids Based on Electroactive Tetraphenylbenzidine Units

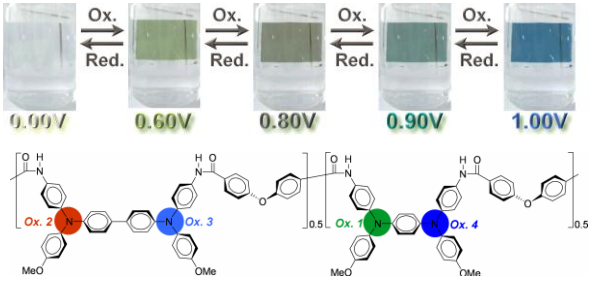

References and Notes

1. (*a*) P. M. S. Monk, R. J. Mortimer and D. R. Rosseinsky, *Electrochromism and Electrochromic Devices*; Cambridge University Press, Cambridge, UK, 2007; (*b*) P. M. Beaujuge and J. R. Reynolds, *Chem. Rev.*, 2010, **110**, 268.
2. M. Robin and P. Day, *Adv. Inorg. Radiochem.*, 1967, **10**, 247.
3. (*a*) C. Creutz and H. Taube, *J. Am. Chem. Soc.*, 1973, **95**, 1086; (*b*) C. Lambert and G. Noll, *J. Am. Chem. Soc.*, 1999, **121**, 8434; (*c*) A. V. Szeghalmi, M. Erdmann, V. Engel, M. Schmitt, S. Amthor, V. Kriegisch, G. Noll, R. Stahl, C. Lambert, D. Leusser, D. Stalke, M. Zabel and J. Popp, *J. Am. Chem. Soc.*, 2004, **126**, 7834.

Charge-transporting polymers and glasses forming molecular materials for optoelectronic applications

J.V. Grazulevicius

Kaunas University of Technology

juozas.grazulevicius@ktu.lt

Introduction. Charge-transporting polymers and molecular glasses are widely used in (opto)electronic devices, such as electrophotographic photoreceptors of copying machines and laser printers, light-emitting diodes, solar cells, organic thin film transistors [1]. In this presentation the resent results of the work on the synthesis and properties of charge-transporting polymers and molecular glasses performed in the author's laboratories are reviewed.

Materials and Methods. Carbazole was used as the main building block in the design and synthesis of charge-transporting polymers and molecular glasses [2]. We used electron photoemission technique for estimation of ionization potentials and xerographic time of flight technique for the investigation of charge-transporting properties of the materials. Thermal transitions of the materials were estimated by thermogravimetric anlyis and differential scanning calorimetry

Results and Discussion. We prepared soluble charge-transporting polymers and oligomers by chain growth (photo)polymerization of oxiranes, oxetanes, thiiranes, vinyl ethers bearing different electroactive groups [3] also by polycondensation and polyaddition of bifunctional electroactive monomers [4]. We use cationic and radical photocross-linking of bifunctional monomers bearing electroactive moieties for the preparation of insoluble charge-transporting layers [5]. Such layers are useful in the fabrication of multi-layer optoelectronic devices if they are prepared by the solution casting techniques.

We also synthesized hole-transporting glass-forming molecular materials belonging to the families of condensed aromatic amines [6], hydrazones [7], enamines [8], ethynylenes, stilbenes and electron-transporting materials belonging to the families of thioxanthenes and aromatic imides [9]. The ionization potentials of hole-transporting materials range from 4.80 to 5.80 eV. Time-of-flight hole drift mobilities in the amorphous films of 2,7-substituted derivatives of carbazole [10] and carbazole-based enamines [8] exceed 10^{-2} cm^2/V. Electron mobilities in the layers of the newly synthesized perylene diimide derivatives exceed 10^{-3} cm^2 V^{-1} s^{-1} at high electric fields. for disordered organic solids these are state-of-the-art charge mobilities. Glass-forming stable free radicals have appeared to be very effective ambipolar organic semiconductors [11]. Well defined carbazole oligomers have appeared to be effective host materials for blue organic electrophosphorescent devices [12]. The triplet energies of these materials approach 3.0 eV. Using these host materials, blue phosphorescent OLEDs having efficiencies of up to 15 %, 31 cdA^{-1}, and 28 lmW^{-1} were demonstrated [13]. Some of the recently synthesized high-triplet-energy glass-forming hosts have appeared to be effective ambipolar semiconductors. They were successfully used for the development of single layer organic light emitting diodes.

Conclusions. We have prepared and studied charge-transporting monomers, polymers and glass-forming molecular materials, with the wide range of ionization potentials and high charge mobilities. The selected materials were successfully used in organic light emitting diodes.

References

[1] P. Strohriegl, J.V. Grazulevicius. *Adv. Mater*., 14, 1439, 2002.

[2] V. Grazulevicius, P. Strohriegl, J. Pielichowski, K. Pielichowski, *Prog. Polym. Sci*., 28, 1297, 2003.

[3] R. Lazauskaite, J.V. Grazulevicius, *Polym. Adv. Technol*., 16, 571, 2005.

[4] V. Getautis, J.V. Grazulevicius, M. Daskeviciene, T. Malinauskas, V. Gaidelis, V. Jankauskas, J. Sidaravicius, Z. Tokarski, *Polymer***,** 46, 7918, 2005.

[5] S. Lengvinaite, J.V Grazulevicius, S. Grigalevicius, R. Gu, W. Dehaen, V. Jankauskas, B. Zhang, Z. Xie, *Dyes. Pigm.* 85, 183, 2010

[6] A. Tomkeviciene, J. Simokaitiene, J.V. Grazulevicius, V. Jankauskas, *J. Polym. Sci. A: Polym. Chem*., 46, 4674, 2008.

[7] R. Lygaitis, V. Getautis, J.V. Grazulevicius, *Chem. Soc. Rev*., 37, 770, 2008.

[8] E. Puodziukynaite, E. Burbulis, J.V. Grazulevicius, V. Getautis, J. Jankauskas, *Synth. Met*., 158, 993, 2008.

[9] S. Vajiravelu, R. Lygaitis, J.V. Grazulevicius, V. Gaidelis, V. Jankauskas, S. Valiyaveettil, *J. Mater. Chem*., 19, 4268, 2009.

[10] A. Tomkeviciene, J.V. Grazulevicius, V. Jankauskas, *Chem. Lett*, 37, 344, 2008.

[11] S. Castellanos, V. Gaidelis, V. Jankauskas, J.V. Grazulevicius, E. Brillas, F. Lopez-Calahorra, L. Julia, D. Velasco, *Chem. Commun*., 46, 5130, 2010.

[12] N. Seidler, S. Reineke, K. Walzer, B. Lussem, A. Tomkeviciene, J.V. Grazulevicius, K. Leo, *Appl. Phys. Lett*., 96 (9)**,** article No 093304, 2010.

[13] M. H. Tsai, Y. H. Hong, C. H. Chang, H. C. Su, C.-C. Wu, A. Matoliukstyte, J. Simokaitiene, S. Grigalevicius, J. V. Grazulevicius, C. P. Hsu, *Adv. Mater*., 19, 862, 2007.

Model Poly(dimethylsiloxane-*b*-ε-caprolactone) Obtained by Anionic Ring Opening Polymerization

Angel J. Satti[1,2], Fabiana G. Nador[2], Enrique M. Vallés[1], Marcelo A. Villar[1], and Andrés E. Ciolino[1]

[1]Planta Piloto de Ingeniería Química, PLAPIQUI (UNS-CONICET), Departamento de Ingeniería Química, Universidad Nacional del Sur, Camino "La Carrindanga" Km. 7, (8000) Bahía Blanca, Argentina.
[2]Instituto de Química del Sur, INQUISUR (UNS-CONICET), Departamento de Química, Universidad Nacional del Sur, Av. Alem 1253, (8000) Bahía Blanca, Argentina.

e-mail: valles@plapiqui.edu.ar, mvillar@plapiqui.edu.ar, aciolino@plapiqui.edu.ar

Introduction: Poly(ε-caprolactone) (PCL) is a biodegradable polyester which can be used as drug carrier because of its excellent drug permeability. Poly(dimethylsiloxane) (PDMS) is a biocompatible hydrophobic polymer with good properties as surface modifier. This combination makes PDMS-based copolymers excellent candidates for several biomedical applications. Thus, many synthetic strategies have been developed in order to synthesize block copolymers of siloxane/ε–caprolactone for specific applications [1-4]. In this work, we report the synthesis of these block copolymers under different reaction conditions by using anionic polymerization. We explored the use of PDMS macroinitiators to promote the anionic ring opening polymerization (AROP) of ε-caprolactone (ε-CL).

Experimental: The controlled synthesis of poy(dimethylsiloxane–*b*–ε-caprolactone) copolymers (PDMS-*b*-PCL) was studied by employing hexamethyl-cyclo(trisiloxane) (D_3) and ε-caprolactone monomers, a mixture of benzene/tetra-hydrofuran, and sec-Bu^-Li^+ as initiator. The reactions were carried out in whole-sealed glass reactors according to standards procedures for anionic polymerization (high-vacuum techniques). The molar mass, molar mass distribution, and composition of the resulting copolymers were obtained by Size Exclusion Chromatography (SEC), ^{1}H-Nuclear Magnetic Resonance (^{1}H-RMN), and Fourier Transform Infrared Spectroscopy (FTIR).

Results and Discussion: The synthesis of (PDMS-*b*-PCL) copolymers was carried out in two steps by using sequential addition of monomers. In the first step, D_3 polymerization was promoted by adding THF [5]. Under these circumstances, the living macrosilanolate initiators were obtained. Then, the ε-CL monomer was added to the reaction media in order to promote its co-polymerization. To achieve this, we hypothesized a nucleophilic attack of the PDMS macroinitiator already formed to the carbonylic carbon of the ε-CL monomer:

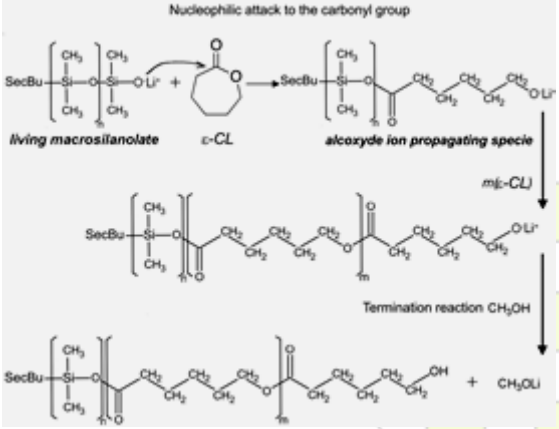

The results obtained are shown in Table 1. ε-CL incorporation seems to be temperature-dependant. At 50 ºC, the incorporation of ε-CL is close to the theoretical amounts expected by stoichiometry. At 40 ºC, there is lower incorporation, whereas at room temperature (RT) no incorporation is detected. These results suggest that temperature reaction is a fundamental parameter to promote higher ε-CL incorporation in the resulting PDMS-*b*-PCL copolymer.

Table 1: Synthesis of PDMS-*b*-PCL copolymers

Copolymer	T (ºC)	$x_{\varepsilon\text{-CL}\ t}$ a)	$x_{\varepsilon\text{-CL}\ e}$ b)	Mn (g/mol) c)	PD d)
PDMS-*b*-PCL 82	50	0.82	0.86	140,800	1.25
PDMS-*b*-PCL 67	50	0.67	0.61	94,500	1.25
	RT		0.00	-	-
PDMS-*b*-PCL 47	50	0.47	0.55	22,400	1.12
	40	0.47	0.10	17,900	1.15

a) Theoretical ε-CL molar fraction according to the initial monomer content, **b)** Experimental ε-CL molar fraction obtained by ^{1}H-NMR, **c)** Experimental Mn of copolymers from SEC and ^{1}H-NMR, and **d)** Polydispersity Index of copolymers according to SEC.

Conclusion: PDMS-*b*-PCl copolymers with different monomer compositions were obtained by AROP of the ε-caprolactone ring using PDMS macroinitiators, sequential addition of monomers, and anionic polymerization (high-vacuum techniques). The reaction is temperature-dependant: at 50 ºC, the ε-CL incorporation in the resulting copolymer is close to the theoretical amounts expected by stoichiometry; at 40 ºC, there is lower ε-caprolactone incorporation; and at room temperature no incorporation is detected.

The reaction will also be tested using (trimethylsilyl-methyl)lithium initiator with other siloxane monomer tetravinyl, tetramethyl, cyclo(tetrasiloxane) (V_4).

ACKNOWLEDGMENTS

We express our gratitude to CONICET, the Agencia Nacional de Promoción Científica y Tecnológica (ANPCyT), and the UNS for their financial support to this study, and Drs. Gabriel Radivoy and Cristian Vitale (INQUISUR) for their helpful advise.

REFERENCES

[1] M.A. Childs, D.D. Matlock, J.R. Dorgan, T.R. Ohno, *Biomacromolecules*, 2 (2001) 526-537.
[2] L. Tang, M.S. Sheu, T. Chu, Y.H. Huang, *Biomaterials*, 20 (1999) 1365-1370.
[3] G. Zhu, S. Xu, J. Wang, L. Zhang, *Rad. Phys. Chem.*, 75 (2006) 443-448.
[4] Z. Xu, S. Zheng, *Polymer*, 48 (2007) 6134-6144.
[5] M.D. Ninago, A.J. Satti, J.A. Ressia, A.E. Ciolino, M.A. Villar, E.M. Vallés, *J. Polym. Sci. Part A: Polym. Chem.*, 47 (2009) 4774–4783.

Synergistic Effect of H-bond and Chain Mobility in Enhancing Proton Transfer: A Study Case in Urocanic Acid System

Chatchai Jarumaneeroj[1], *Suwabun Chirachanchai*[1,2]

[1] The Petroleum and Petrochemical College, Chulalongkorn University, Soi Chula 12, Phyathai Rd., Pathumwan, Bangkok 10330, Thailand.

[2] Center for Petroleum, Petrochemicals, and Advanced Materials, Chulalongkorn University, Thailand

e-mail: csuwabun@chula.ac.th

Nafion® membrane is a commercial membrane for PEMFC; however, the operation of Nafion® membrane at high temperature is limited due to an evaporation of water cluster resulting in decreasing of proton conductivity.[1, 2] Heterocyclic compounds such as imidazole, pyrazole, benzimidazoles are accepted as the compounds for proton transfer. The mechanism is suspected to relate to the hydrogen bond and structural reorientation through the resonance N-HN without the need of water molecules.[3,4] The proton conductivities of those heterocycles are about 10^{-4} S/cm[5] at intermediate temperature which still needs an improvement to compete with that of Nafion® membrane (10^{-2} S/cm at below 80 °C).[1,2] In order to develop the conductivity efficiency, here, we propose a synergistic effect between H-bond and chain mobility to enhance the proton transfer from a heterocycle to another. The present work focuses on a model case by using urocanic acid backbone with different alkyl chain length (**Scheme**) to satisfy the conditions related to the hydrogen bond and chain mobility.

Scheme

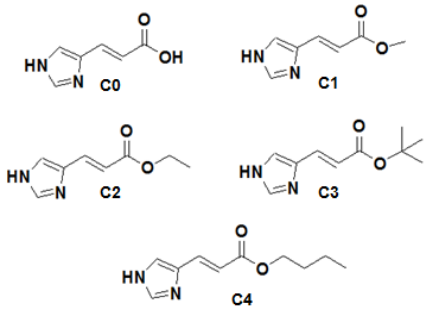

The number of methylene groups was varied from **C1** to **C4**. FTIR spectra of all derivatives showed an ester peak at 1710 cm^{-1}. The structural characterization identified by ^{1}H NMR confirmed imidazole ring at 9.18 ppm (1H, s) and 8.04 ppm (1H, s) with CH=CH at 7.59 ppm (1H, d) and 6.84 ppm (1H, d).

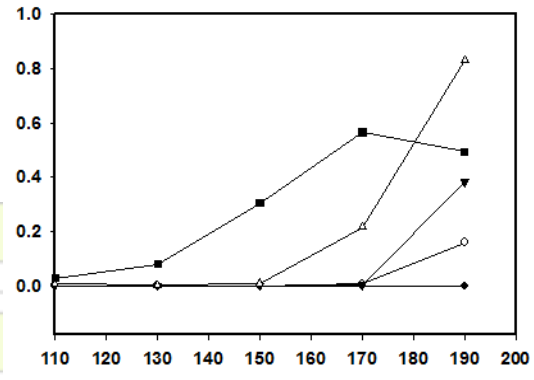

The proton conductivities of **C0**-**C4** in neat solid form were measured by using electrochemical impedance spectrometer (**Figure**). The fact that **C3** shows the significant proton conductivity for 0.8 mS/cm at 190 °C whereas urocanic acid did not perform the conductivity, this clearly informs us how the chain mobility plays an important role in proton transfer. The presentation will cover the temperature dependence FTIR, T_1 relaxation time, and thermal properties to clarify the plausible mechanism related to the proton transfer on the chain mobility under hydrogen bond network.

Figure Proton conductivities of **C0** to **C4** in neat compounds.

The authors would like to acknowledge the Thailand Research Fund (the Royal Golden Jubilee (RGJ) program) for the Ph.D. scholarship.

References

1. V. Neburchilo, J. Martin, H. Wang, J. Zhang, *Journal of Power Sources*, 2007, **169**, 221-238.
2. U. Sen, S. U. Celik, A. Ata, A. Bozkurt, *International Journal of Hydrogen Energy* 2008, **33**, 2808- 2815.
3. S. D. Mikhailenko, K. Wang, S. Kaliaguine, P. Xing, G. P. Robertson, M. D. Guiver, *Journal of Membrane Science*, 2004, **223**, 93-94.
4. W. Munch, K.-D. Kreuer, W. Silvestri, J. Maier, G. Seifert, Solid State Ionics, 2001, **145**, 437–443.
5. B. Smitha, S. Sridhar, A. A. Khan, *Journal of Membrane Science*, 2005, **259**, 10–26.

New Crystalline-Crystalline Diblock Copolymers of Poly(3-hexylthiophene-b-steryl acrylate) for Field Effect Transistors

Jung-Chuan Lin,[a] *Chi-Ching Kuo,*[b] *Wen-Ya Lee,*[a] *Jung-Ching Hsu,*[a] *Wen-Chang Chen,*[a,b,*]

[a] Department of Chemical Engineering, National Taiwan University, Taipei 106 Taiwan
[b] Institute of Polymer Science and Engineering, National Taiwan University, Taipei 106 Taiwan;

email: chenwc@ntu.edu.tw

SABIC Innovative Plastics has recently launched the Synthesis, morphology and charge transport of new crystalline-crystalline diblock copolymers, poly(3-hexylthiophene-b-steryl acrylate) (P3HT-b-PSA), with various PSA segment lengths are reported in this study. The hole mobilities of P3HT-b-PSA diblock copolymers were investigated by field-effect transistors on both bare SiO_2- and phenyltrichlorosilane (PTS)-treated dielectric surfaces. On the bare SiO_2-surface, the mobility of the copolymers was decreased with the increased PSA contents. On the contrast, the mobility of the diblock copolymers on the PTS-treated substrates was enhanced to be $3.92*10^{-3}$ $cm^2V^{-1}S^{-1}$ as the PSA content was increased to be 85.7 mol%. The hydrophobic PTS-surface facilitated the orientation and the fiber-like self-assemblied structure of P3HT segments. Nevertheless, the mobility was reduced after the thermal treatment at a high temperature. It might be due to the thermally enhanced aggregation of P3HT nanofibers, which increased the amount of boundaries and led to the reduced mobility. This study indicated the significance of the P3HT/PSA ratio, surface modification, and thermal treatment on the morphology and charge-transporting characteristics of conjugated crystalline-crystalline block copolymers for high-performance organic electronics.

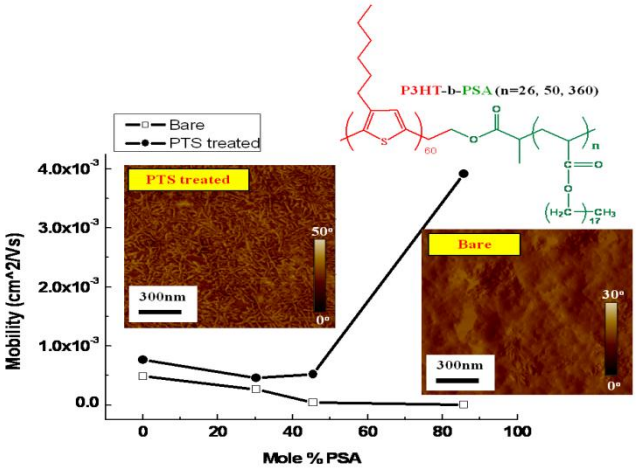

Nanocomposite Functional Membranes for Biomedical Applications

Ana Maria Popa, Francisco Teixeira, Stefanie Zuber, René M. Rossi

EMPA, Swiss Federal Laboratories for Materials Science and Technology, Laboratory for Protection and Physiology

ana-maria.popa@empa.ch

Introduction

Thermo-responsive polymers have been extensively studied in the last years, due to their potential applications in the biomedical field (e.g. controlled drug delivery). Their low mechanical stability however limits their application range. In this work we have investigated a novel class of thermo-responsive copolymers based on oligoethylene methacrylate (OEGMA) and vinyl caprolactam. These copolymers display tunable LCSTs in the physiological range which makes them extremely interesting for biomedical applications. We have explored different techniques for immobilizing these materials onto novel supports, as to extend their range of applications in the field of medical textiles, namely as active gating systems for moisture management in wounds or immobilized drug-delivery reservoirs.

Results and discussion

The random copolymers based solely on OEGMA monomers were grafted on functionalised track-etched polymeric membranes by controlled radical polymerization techniques (ATRP) as to obtain polymer-polymer nanocomposite membranes. The temperature-dependent permeation of caffeine molecules through the functionalized membranes has been demonstrated.

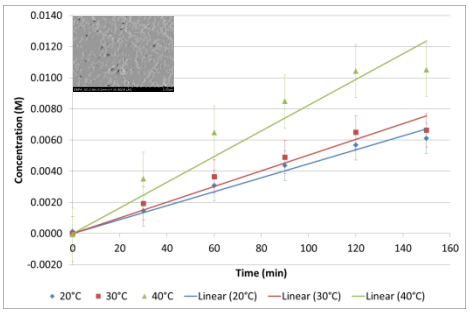

Figure 1. Temperature responsive permeation of caffeine through an OEGMA-functionalised track-etched membrane. Insert shows an SEM image of the modified membrane.

Additionally we have demonstrated a temperature-responsive permeation of water vapors through the functional pores, an effect which could be exploited for medical textiles where moisture management is necessary.
A second direction explored the synthesis of novel VCL-OEGMA copolymers. We demonstrated that minute amount of OEGMA can be incorporated into PVCL chains by simple free radical polymerization techniques and the LCST of these systems can be tuned in the physiological range.

Since their mechanical resistance is low, these polymers have been processed into microporous membranes by electrospinning together with poly(lactic acid), a biopolymer with superior tensile properties. The temperature responsiveness of these membranes has also been demonstrated.

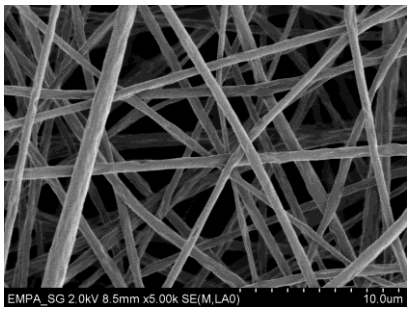

Figure 2. PLA-PVCL Composite microporous membrane obtained by electrospinning

Conclusions

We have presented two straight-forward processes for taking advantage of the very interesting properties of OEGMA and VCL based copolymers – biocompatibility and temperature-dependent behavior – by incorporating them in easy-to-handle materials with increased stability, such as microporous membranes and non-wovens. These new polymer/polymer nanocomposites open the perspective for numerous applications in the biomedical field, ranging from sensing to drug delivery.

Foamed Nanocomposites: A System in which Nanofillers Play a Multifunctional Role

M.A. Rodriguez-Perez, C. Saiz-Arroyo, J.A. de Saja

Cellular Materials Laboratory (CellMat), Condesed Matter Physics Department, University of Valladolid, 47011 Valladolid, Spain

e-mail: marrod@fmc.uva.es

Foamed nanocomposites constitute a novel class of materials combining the advantages of nanocomposites and cellular materials. Although the potential of these materials is very high the research and technology of these new materials is still at an embryonic stage[1,2].

Merging two types of materials and processing technologies poses new challenges compared to generic materials. It has been concluded that nanofillers enhance nucleation efficiency in the foaming process[2], but it is not clarified what is the mechanical reinforcement efficiency of nanofillers embedded within a cellular structure and how these two property attributes interact for giving required property values at macro-scale. When considering the main challenges to developers of foamed nanocompoites questions regarding the foaming behaviour and underlying physics; interaction at gas/polymer/nanofiller interfaces; homogeneity of cell sizes and fillers dispersions; and physical mechanisms responsible for local deformation pattern at nano / microscale resulting in a macroscopic mechanical response, cannot simply be answered by looking at the properties of the nanocomposites on the one hand and cellular materials on the other. *Strong interactions between these two groups of materials are to be expected in a final cellular nanocomposite material.*

During the last years our group has been studying different foamed nanocomposite systems proving that with a proper selection of the matrix and the nanoparticles, the nanoaditive can play a multifunctional role acting in very different ways:

1. Acting as nucleating agent for the cells, which allows reducing cell size and narrowing the cell size distribution which in turns also affect the physical properties.
2. Acting as nucleating agent for the polymer crystals, modifying the morphology of the base polymer.
3. Improving the polymer rheology, increasing the melt strength and as a consequence improving the stability of the molten foam.
4. Improving the foamability due to gas barrier effects
5. Improving the thermal and mechanical properties of the base polymer and as a consequence enhancing the physical properties of the foams.

To show the previous concepts this paper presents some examples regarding the fabrication of foamed low density polyethylene silica nanocomposites. Foams with cell sizes well below 100 microns and very homogeneous structure have been produced [3] (figure 1). It was found that the nanoparticles modified both the cellular structure and polymer morphology, acting as nucleating agent of the cells and polymer crystals. It was also found a strong improvement of the physical properties, much bigger in the cellular materials than in solid nanocomposites with similar compositions (figure 2), indicating the strong interaction (synergetic effect) between the nanoparticles and the cellular structure.

.

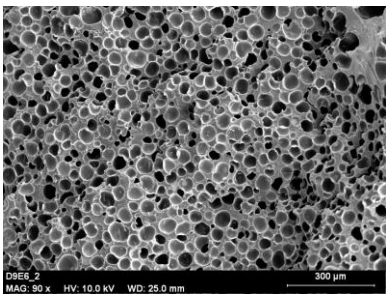

Figure 1. Morphology of a foamed LDPE/silica nanocomposite with 6% wt of silica.

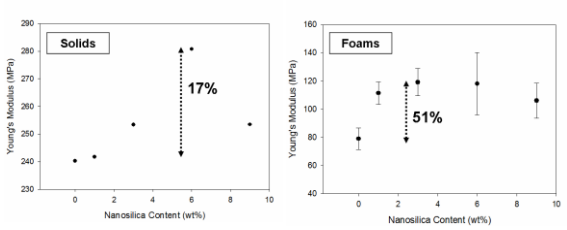

Figure 2. Improvement in the Young's modulus of solids and foams as a function of the silica content

References.

1.K.T. Okamoto, Microcellular Processing, Hanser Publishers, Munich 2004.

2.C.B. Park in Foam extrusion: Principles and Practice, Ed. S. T. Lee, Technology Publishing Company, USA, 2000.

3. M.A. Rodriguez-Perez, J.Lobos, C. A. Perez-Muñoz, J.A. de Saja, Cell. Polym., 27, 327, 2008.

Poly(meth)acrylates obtained by Cascade Reaction

Helmut Keul, Dragos Popescu, Emin Hrsic, Martin Möller

Institute of Technical and Macromolecular Chemistry, RWTH Aachen and DWI an der RWTH *Aachen e.V.*

keul@dwi.rwth-aachen.de

Introduction

Preparation, purification and stabilization of functional (meth)acrylates with a high dipole moment are complex, laborious and expensive processes. In order to avoid purification and stabilization of the highly reactive functional monomers, a concept of cascade reactions was developed comprising enzymatic monomer synthesis and radical polymerization. Transacylation of methyl acrylate (MA) and methyl methacrylate (MMA) with different functional alcohols, diols and triols (1,2,6-hexanetriol and glycerol) in the presence of Novozyme 435 led to functional (meth)acrylates. After the removal of the enzyme by means of filtration, removal of excess (meth)acrylate and/or addition of a new monomer, e.g. 2-hydroxyethyl (meth)acrylate the (co)polymerization via free radical (FRP) or nitroxide mediated radical polymerization (NMP) resulted in poly[(meth)acrylate]s with predefined functionalities. Hydrophilic, hydrophobic as well as ionic repeating units were assembled within the copolymer. The transacylation of MA and MMA with diols and triols carried out under mild conditions is an easy and rapid in process and is suitable for the preparation of sensitive monomers.

Materials and Methods

Methyl methacrylate (MMA), methyl acrylate (MA), functional alcohols, diols and triols were used without further purification. All solvents were used as received. A commercial lipase, Novozyme 435 (Lipase B from Candida antarctica immobilized onto a macroporous acrylic resin, 10 000 U/g) was dried in vacuum at room temperature for 24 h and stored under nitrogen before it was used as a biocatalyst for the transacylation reactions. All reactions were carried out in nitrogen atmosphere. All reaction products were analized via ^{1}H NMR spectroscopy and size exclusion chromatography.

Lipase-catalyzed transacylation reactions: Methyl methacrylate or methyl acrylate, a functional alcohol, and Novozyme 435 were stirred for 24 h at 70°C. The reaction was quenched by cooling the mixture to ambient temperature and the enzyme was filtered off. The molar ratio of (meth)acrylates was determined via ^{1}H NMR spectroscopy. Excess MMA or MA was removed by distillation and new monomers were eventually added before polymerization.

Copolymerization of monomers obtained by trans-acylation reaction: (i) Free radical polymerization. To a mixture of monomers obtained by transacylation reaction was added AIBN and reacted at 90°C for 24 h. The reaction was quenched by cooling the mixture to room temperature. The polymer was isolated by precipitation in a suitable solvent and dried in vacuo. *(ii) Nitroxide mediated polymerization:* To a mixture of monomers obtained by transacylation was added Blocbuilder™ initiator and SG-1 free nitroxide and immersed into an oil bath, preheated to 110°C. After 8 hours polymerization time, the reaction mixture was cooled to room temperature. The polymer was isolated by precipitation or dialysis and analysed by NMR and SEC.

Results and Discussion

Different functional polyacrylates were prepared by free radical polymerization as well as by nitroxide mediated polymerization of functional monomers prepared by in situ lipase-catalyzed transacylation. After the enzymatic transacylation of MA with different diols and triols a mixture of mono- and bisacrylates is obtained. We have shown that by free radical polymerization of the monomer solution directly obtained from the enzymatic catalyzed transacylation, a concentration up to 6 mol% bisacrylate is tolerated in order to get non cross linked polymers. Starting with 7 mol% bisacrylate significant polymer coupling was observed, while a concentration of 10 to 12 mol% bisacrylate leads to gel formation. Functional poly(meth)acrylates showing bacteriostatic or thermoresponsive properties were prepared.

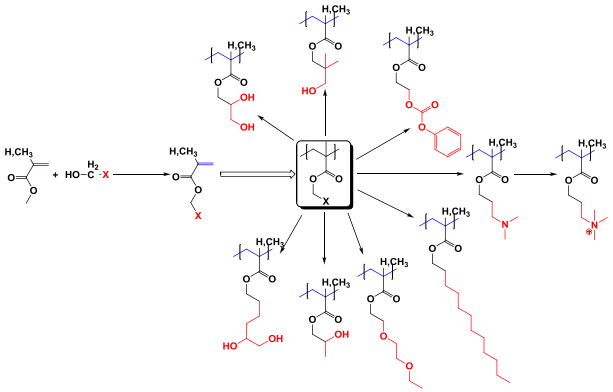

Scheme 1. Cascade reaction for the preparation of functional Poly(acrylates) and poly(methacrylates)

Conclusions

The cascade reaction comprising an enzymatic transacylation and a nitroxide mediated polymerization or free radical polymerization represents a mild, easy and rapid process for functional polyacrylates and polymethacrylates. Well defined functional poly(meth)acrylates were prepared suitable for various application.

References

[1] D. Popescu, R. Hoogenboom, H. Keul, M. Möller *J. Mol. Catal. B-Enzym.* **2010**, *62*, 81-90

[2] D. Popescu, R. Hoogenboom, H. Keul, M. Möller *Journal of Polymer Science, Part A: Polymer Chemistry,* **2010**, *48*, 2610-2621.

High Speed Polymer Semiconductors for Applications on Printed Integrated Circuits

Kang-Jun Baeg[1,*], *Yong-Young Noh*[2], *Dong-Yu Kim*[3], *Antonio Facchetti*[4], *Soon-Won Jung*[1], *Jae Bon Koo*[1], *In-Kyu You*[1]

[1]Convergence Components and Materials Research Laboratory, Electronics and Telecommunications Research Institute, [2] Department of Chemical Engineering, Hanbat National University, [3]Heeger Center for Advanced Materials, Gwangju Institute of Science and Telecommunications, [4]Polyera Corporation

e-mail: kangjun100@etri.re.kr

Solution processed conjugated molecules enable to manufacture low-cost a variety of opto/electronic devices by unconventional patterning methods, such as inkjet, screen, or gravure printing, with high throughput. The charge carrier mobility of state-of-the-art conjugated polymer semiconductors are comparable with a-Si so that it is expected that many applications will be replaced by cost-effective solution-processed organic field-effect transistors (OFETs) in near future. To realize advanced printed integrated complementary circuits, those p- or n-channel conjugated molecules must be patterned. Novel patterning methods have researched so far, but among those novel patterning methods, inkjet have a variety of advantages, such as removal of need for masks, which lead to cost-savings, efficient use of materials and waste elimination, non-contact deposition method [1].

Here we demonstrate high performance inkjet-printed p- and n-channel top-gate/bottom-contact polymer FETs, and applications to complementary inverter and ring oscillator circuits [2]. The various semiconducting polymers, such as p-channel [poly(3-hexylthiophene) (P3HT) and Polyera ActivInk P2100] and n-channel [poly{[N,N'-bis(2-octyldodecyl)- naphthalene-1,4,5,8-bis(dicarboximide)-2,6-diyl]-alt-5,5'-(2,2'-dithiophene)} (P(NDI2OD-T2))] were inkjet-printed using 50 μm diameter Microfab single nozzle in air. After formation of the stable inkjet droplets, p- and n-type organic semiconductors were directly patterned on glass or plastic substrate. Uniform printed lines on substrate can be obtained, which verified using optical microscope image.

Inkjet-printed P3HT FET devices showed good p-type characteristics, whose hole mobility was as high as 0.1 cm^2/Vs. Moreover, P3HT FET devices showed high on/off ratio more than 10^6, very low gate leakage current, little contact resistance, and no significant bias hysteresis. Moreover, newly developed ActivInk P2100 showed excellent p-channel OFET characteristics with very high hole mobility as high as 1.0 cm^2/Vs. For development of the polymeric complementary inverter circuits, where the combination of p- and n-channel transistors results in far greater circuit speeds, lower power dissipation and more stable operation, high performance and easily printable both p- and n-channel polymer semiconductors must be developed. We can obtain high electron mobility as high as 0.3 - 0.4 cm^2/Vs using P(NDI2OD-T2) and conventional PMMA gate dielectrics with proper selection of orthogonal solvents. Similar with those of P3HT FETs, P(NDI2OD-T2) transistors also showed high on/off ration, low threshold voltage, very low gate leakage current, little contact resistance and no significant bias hysteresis.

It is noted that n-type polymer, P(NDI2OD-T2), OFET characteristics are critically affected by selection of the gate dielectric and orthogonal solvent. Because of the very large solubility of P(NDI2OD-T2) (~60 g/L) and the location of the lowest unoccupied molecular orbital (LUMO) level at ~4.0 eV [3], an hydroxyl-free polymer dielectric and a perfectly orthogonal solvent are needed to prevent electron trapping and semiconductor surface roughness via swelling/dissolution of the underlying conjugated polymer. A poly(methyl methacrylate) (PMMA) dielectric solution in 2-ethoxyethanol (2E) was found to optimize the performance of both transistor type, which is essential for CMOS circuit fabrication.

By appropriate combination of p-channel and n-channel polymer FETs, we can demonstrate top-gated and inkjet-printed polymeric complementary inverter and ring oscillators. The inverter circuits were well operated at low operation voltage range as low as 5 V with a high voltage gain more than 30. Maximum and typical operation frequency of our printed ring oscillators is as high as 50 KHz and 1 – 50 KHz.

In conclusion, the first inkjet-printed high-performance polymeric complementary devices have been demonstrated. We believe that the operating frequency can be further improved by fine-tuning of the device architecture and optimization of the p-channel semiconductor processing. Based on a rough estimation, f_{OSC} >10 MHz are possible for a ActivInk P2100 and P(NDI2OD-T2)-based ring oscillator by reducing the FET channel lengths to ~1 μm and by minimizing the overlap capacitance (0.2–0.6 pF/mm) via self-aligned gate printing method.

References

[1] Y.-Y. Noh, N. Zhao, M. Caironi, H. Sirringhaus, *Nat. Nanotechnol.* **2007**, *2*, 784.
[2] K.-J. Baeg, D. Khim, D.-Y. Kim, S.-W. Jung, J. B. Koo, I.-K. You, H. Yan, A. Facchetti, Y.-Y. Noh, J. Poly. Sci. Part B: Poly. Phys. **2011**, *49*, 62.
[3] H. Yan, Z. Chen, Y. Zheng, C. Newman, J. R. Quinn, F. Dotz, M. Kastler, A. Facchetti, *Nature* **2009**, *457*, 679.

Electrically Bistable Memory Devices Based on Poly(3-hexylthiophene)-*block*-poly(3-phenoxylthiophene) and Its PCBM composite films

Yi-Cang Lai,[a] *Kaoru Ohshimizu*,[c] *Wen-Ya Lee*,[b] *Tomoya Higashihara*,[c] *Mitsuru Ueda*,[c] *Wen-Chang Chen*[a,b]

[a] Institute of Polymer Science and Engineering, National Taiwan University, Taipei 106 Taiwan;
[b] Department of Chemical Engineering, National Taiwan University, Taipei 106 Taiwan;
[c] Department of Organic and Polymeric Materials, Graduate School of Science and Engineering, Tokyo Institute of Technology, 2-12-1 O-okayama, Meguro-ku, Tokyo 152-8552, Japan

email: chenwc@ntu.edu.tw

The memory characteristics of rod-rod diblock all-conjugated copolymers, poly(3-hexylthiophene) -*block*-poly(3-phenoxymethylthiophene) (**P3HT**-*b*-**P3PT**), and Its blends with PCBM were investigated. The field-effect transistors prepared from **P3HT**-*b*-**P3HT** showed a significant hysteresis between forward and backward gate-bias scans in the transfer curve, indicating the occurrence of the charge trapping. The charge trapping may be due to the amorphous P3PT moieties, reducing charge transport and trapping charge. **$P3HT_{102}$**-*b*-**$P3PT_{37}$** exhibited the dynamic random access memory (DRAM) behaviors in the sandwich configuration of ITO/**P3HT**-*b*-**P3PT**/Al. On the other hand, **P3HT** only showed the semiconductor characteristics, suggesting that the electrical switching behavior could be tuned through the **P3HT**/**P3PT** ratio. By blending a small amount (5-10%) of PCBM into **$P3HT_{102}$**-*b*-**$P3PT_{37}$** and **$P3HT_{89}$**-*b*-**$P3PT_{23}$**, based memory devices showed a write-once-read-many times (WORM) behavior with the switching voltages of -2.5∼-3.1 V and high ON/OFF ratios (10^5 -10^6). The mechanism associated with the memory characteristics was the charge transfer from the donor the polymers to acceptor PCBM, which stabilized the charge separated state and retained the high conductance state for a long time. The ON state of the **$P3HT_{102}$**-*b*-**$P3PT_{37}$**/PCBM device could remain more than 30 min after the power was turned off, whereas the pure **$P3HT_{102}$**-*b*-**$P3PT_{37}$** device relaxed from the on state to the off state quickly after removing the applied voltages. These experimental results provide the new strategies of designing block copolymers for tuning the memory characteristics for advanced flexible electronic devices.

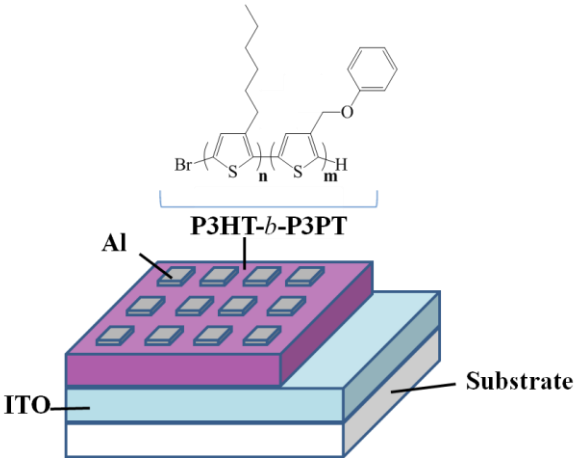

Figure 1. A schematic diagram of the memory device consisting of **P3HT**-*b*-**P3PT** thin film sandwiched between an ITO bottom electrode and an Al top electrode.

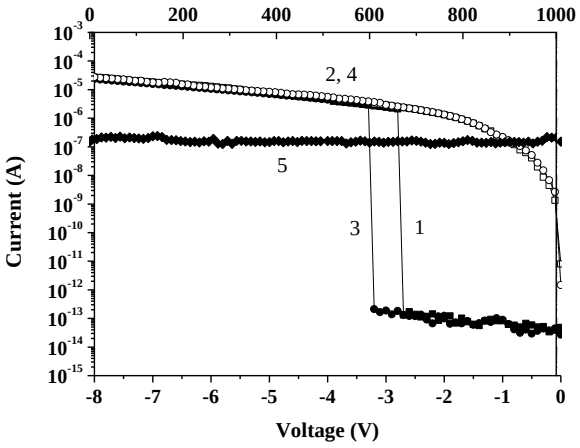

Figure 2. Current-voltage (I-V) characteristics of **$P3HT_{102}$**-*b*-**$P3PT_{37}$** memory device.

Effect of Composition on the Properties of Sulfonated Poly(indene)/Poly(vinyl alcohol) Membranes

Neiva Löser, Bruna dos Santos, Ricardo Cavalheiro, Maria Madalena Camargo Forte

Federal University of Rio Grande do Sul/Engineering School/Department of Materials – Porto Alegre/Brazil

mmcforte@ufrgs.br

Studies[1-5] has been carried out on exploring the possibilities of hydrocarbon-based membranes as potential candidate for polymer electrolyte fuel cells (PEMFC). The transport of charges across the membrane occurs by the migration of hydrogen's sulfonic groups, as well established for the DuPont trademark Nafion®[3], a perfluorinated membrane. On the other hand, sulfonation of molecular chains[4,5] can establish this feature to some appropriate hydrocarbon polymers, in which the sulfonic groups $-SO_3H$ is attacked in the macromolecule. Sulfonated aromatic polymers, inorganic composites, and polymer blends[2,7] electrolyte membranes have been explored and heterocyclic-based polymers have attracted special interest. In this work, membranes of sulfonated poly(indene) (SPInd) and poly(vinyl alcohol) (PVA) were investigated according to their composition.

The membranes SPInd/PVA were prepared as semi-interpenetrating polymer network (semi-IPN) by crosslinking PVA with a crosslinking agent (CA) glutaraldehyde (GA) or sulfosuccinic acid (SA). The membranes were evaluated by termogravimetry (TGA), dynamic-mechanic analyses (DMA), Water uptake (WU), Ion exchange capacity (IEC), and electrochemical impedance spectroscopy (EIS) under anhydrous conditions. The SPInd was obtained according to Makowsky[8] using acetyl sulfate. The SPInd/PVA membranes (**Table 1**) (0.8 ± 0.4mm) were obtained by mixing water solutions of SPInd (M_W=1,15x10^{6}g/mol and SD=56±2% (mol/molInd), produced in the lab, and of PVA (VETEC HD=99%; M_W=10^{5}g/mol), followed by the CA addition (5% w/w) at 60ºC. To avoid bubble formation, the solutions were prepared in an ultrasonic bath, and cast into plastic dishes (r = 8 cm) maintained at 60ºC for 48 h in an oven. The water uptake was calculated by correlating weight differences of the wet and dry membrane, after this be soaked 24h at R.T. and oven dried at 45°C until constant weight. The membrane IEC (meq/g) was determined by acid–base titration method.

Table 1. Designation and composition of the membranes

Designation	Ratio (wt%)	SPInd x10^{3}mol	PVA x10^{3}mol	CA mol
SPInd/PVA2-GA	80/20	5.17	3.41	7.5x10^{-5a}
SPInd/PVA3-GA	70/30	4.52	5.11	1.1x10^{-5a}
SPInd/PVA4-GA	60/40	3.88	6.81	1.5x10^{-4a}
SPInd/PVA2-SA	80/20	5.17	3.41	3.7x10^{5b}
SPInd/PVA3-SA	70/30	4.52	5.11	5.6x10^{5b}
SPInd/PVA4-SA	60/40	3.88	6.81	7.5x10^{5b}

[a]glutaraldehyde (GA); [b]sulfosuccinic acid (SA)

The SPInd has higher thermal stability than the non-sulfonate PInd, since at 1000ºC both presented residue of 0.3 and 16.7%, respectively. In the former ring condensation must occur due to a high interaction between the polymer chains caused by the $-SO_3H$ groups. The loss of $-SO_3H$ groups have occurred in a broad temperature range from 160 to 400 ºC. On the other hand, higher amount of PVA in the membrane did not depress the thermal stability of the SPInd since the mass loss occurs at the same temperatures as can be seen in **Figure 1**.

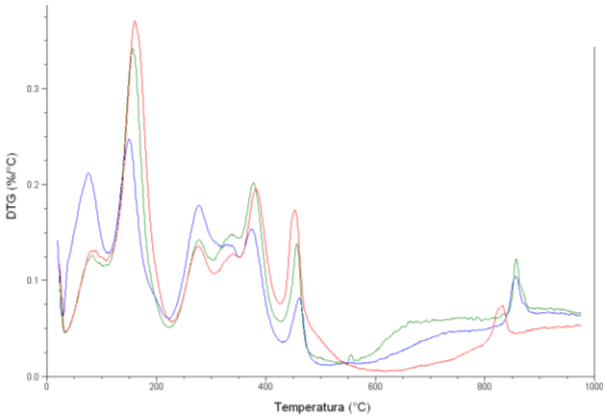

Figure 1. DTG curve of the SPInd/PVA-GA (5%) membranes with 20 (blue), 30 (green) and 40% (red) of PVA.

Table 2 shows the water up take, ion exchange capacity, resistance and conductivity of the SPInd/PVA-CA membranes. The type of CA affected the chain crosslinking and membrane characteristics. The membrane IEC depends on the $-SO_3H$ access to the ion sodium during the titration. The GA attaches to four –OH groups the PVA chains while the SA attaches only to two groups. Thus the number of –OH solvated by water in the former is lower than in the last. On the other hand, as higher the PVA content in the membrane higher the occurrence of intermolecular crosslink, that hindered the membrane swelling and water up take. Decreasing in the WU was observed for the membranes with SA. Although the membranes with SA have more $-SO_3H$ groups, the resistance in these membranes was higher and consequently lowers the conductivity.

Table 2. Ion exchange capacity (IEC) and water uptake (WU) of the SPInd/PVA-CA membranes

Membranes	IEC (meq/mol)	WU (%)	R (Ω)	δ(S.cm^{-1})
SPInd/PVA2-GA	3.36	444	5.88x10^6	1.97x10^{-7}
SPInd/PVA3-GA	3.31	811	7.32x10^5	1.59x10^{-6}
SPInd/PVA4-GA	2.78	570	1.76x10^7	6.17x10^{-8}
SPInd/PVA2-SA	2.75	1449	3.01x10^8	2.73x10^{-9}
SPInd/PVA3-SA	2.30	1201	1.07x10^8	1.51x10^{-8}
SPInd/PVA4-SA	2.35	981	1.77x10^6	6.61x10^{-7}

The composition affected the SPInd/PVA-CA membrane performance and the these with sulfosuccinic acid presented higher water uptake since it has more –OH sulfonic groups. The crosslinking agents were not so effective in hindering the membrane swelling.

Acknowledgements

The authors thank the Agencies CNPq and CAPES.

References

[1] J. Rozière; D.J. Jones, Annual Rev. Mat. Research 33 (2003) 503. [2] C.W. Lin et al., J. Power Sources 171 (2007) 340. [3] A. Mahreni et al., J. Membrane Sci. 327 (2009) 32. [4] B. Smitha at al., J. Membrane Sci 259 (2005) 10. [5] F. Kucera; J. Jancar, J. Polym. Eng. Sci. 38 (1996) 783. [6] J. Won et al., J. Membrane Sci. 214 (2003) 245. [7] Y.F. Huang, L.C. Chuang, A.M. Kannan, C.W. Lin, J. Power Sources, 186 (2009) 22. [8] H. S. Makowski; R. D. Lundberg. U.S. Pat 3870841 (1975).

Unimolecular Polymeric Nanoparticles: From Conventional to Highly-Efficient "Click" Chemistry Routes

José A. Pomposo[1,2], *Lorea Buruaga*[1], *Juan Colmenero*[1,3,4]

[1]Centro de Física de Materiales (CSIC, UPV/EHU), Paseo Manuel de Lardizabal 5, 20018 San Sebastián, Spain.
[2]IKERBASQUE - Basque Foundation for Science, Alameda Urquijo 36, 48011 Bilbao, Spain.
[3] DIPC - Donostia International Physics Center, Paseo Manuel de Lardizabal 4, 20018 San Sebastián, Spain
[4]Departamento de Física de Materiales, Universidad del País Vasco (UPV/EHU), Apartado 1072, 20800 San Sebastián, Spain.

e-mail: Josetxo_pomposo@ehu.es

Introduction

The design of functional soft nanoparticles is of current interest for several traditional (*e.g.* polymer processing industry) and emerging (*e.g.* nanomedicine) fields due to the interesting and sometimes unique properties displayed by such nano-objects. For instance, potential applications for unimolecular nanoparticles cover from processing additives to artificial enzymes, photostable bio-imaging agents and *in vivo* drug / siRNA-delivery systems.

In recent years, the irreversible intramolecular collapse of individual polymer chains to unimolecular nanoparticles in the sub-20 nm size range has become an efficient avenue to functional soft nano-objects free from emulsifiers/steric stabilizers.

In this communication we review the main chemical routes to unimolecular polymeric nanoparticles, with special emphasis on emerging, highly-efficient "Click" chemistry methodologies. Additionally, some examples of new nanoscale effects induced by unimolecular polymeric nanoparticles are illustrated.

Conventional Routes to Unimolecular Nanoparticles

Classical routes to well-defined, unimolecular nanoparticles in the sub-20 nm size range include, among others, the use of functional polymers containing pendant vinyl functional groups across the linear polymer chain.[1]

Under appropriate dilute conditions, selective intramolecular cross-linking of the vinyl functionality allows the synthesis of unimolecular nanoparticles with size < 20 nm.

Photo-cross-linking of cinnamoyl units[2] and the use of low-molecular homobifunctional cross-linking compounds are other related, well established techniques.[3]

"Click" Chemistry Routes to Unimolecular Nanoparticles

Significant progress in the field of unimolecular nanoparticle synthesis was made by the introduction of latent Diels-Alder functionalities and a continuous addition technique, even when harsh reaction conditions were required (250 ºC).[4]

A great breakthrough was the application of the intramolecular "Click" chemistry concept[5] to the efficient, room-temperature synthesis of functional unimolecular nanoparticles through intramolecular coupling of azide and alkyne functionalities resulting in permanent triazole cross-linking joints (see **Figure 1**).

This concept has been recently extended to the preparation of nanoparticles by intramolecular cross-linking of isocyanate functionalized copolymers.[6] Also, the formation of metastable polymeric nanoparticles has been demonstrated through a supramolecular approach.[7]

Current work by our Group involves the development of alternative, alkyne-homocoupling "click" chemistry procedures, as well as the introduction of innovative metal-free routes for the synthesis of multi-functional unimolecular nanoparticles.

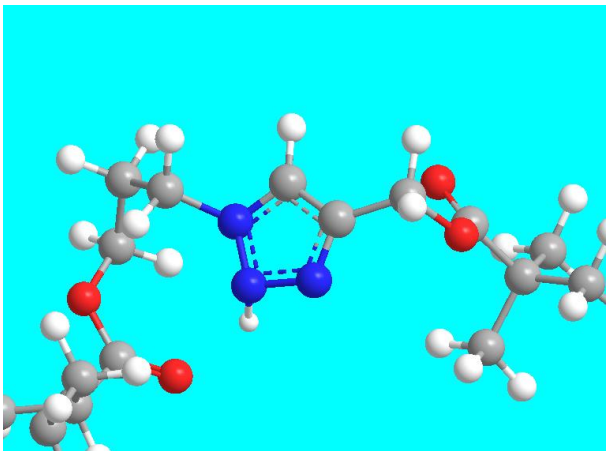

Figure 1. *Azide-alkyne "click" chemistry concept for the highly-efficient synthesis of biofunctional unimolecular nanoparticles at room temperature.*[5] *Intramolecular cross-linking joints result from the formation of conjugated triazole rings in the presence of copper(I) catalyst.*

Nanoscale effects

Illustrative examples of unimolecular-nanoparticle-induced nanoscale effects are: i) reduction of viscosity in thermoplastic and rubber melts,[8,9] ii) increase of quantum efficiency in organic, fluorescence-based nanoparticles,[10] and iii) arresting of phase-separation in polymer blends.[11]

References

[1] R. D. Miller et al. *Adv. Mater.* **2001**, *13*, 204
[2] G. J. Liu et al. *Macromolecules* **1997**, *30*, 2408
[3] J. A. Pomposo et al. *Macromol. Symp.* **2011**, 296, 303
[4] C. J. Hawker et al. *J. Am. Chem. Soc.* **2002**, *124*, 8653
[5] J. A. Pomposo et al. *Macromol. Rapid Commun.* **2008**, *29*, 1156
[6] C. J. Hawker et al. *Macromolecules* **2009**, *42*, 5629
[7] E. W. Meijer et al. *J. Am. Chem. Soc.* **2009**, *131*, 6964
[8] M. E. Mackay et al. *Natur. Mat.* **2003**, *2*, 762
[9] J. A. Pomposo et al. *Adv. Mater.* **2010**, *22*, 3038
[10] E. Harth et al. *Macromolecules* **2009**, *42*, 5786
[11] J. A. Pomposo et al. *Macromol. Rapid Commun.* **2011**(in press)

Acknowledgment

L. B. acknowledges financial support by Basque Excellence Research Center – Materials Physics Center (BERC–MPC).

Thermally Rearranged (TR) Poly(ether-benzoxazole) Membranes for Gas Separation

Mariola Calle and Young Moo Lee

WCU Department of Energy Engineering, College of Engineering, Hanyang University, Seoul 133-791, Republic of Korea

ymlee@hanyang.ac.kr

Thermally rearranged polybenzoxazole (TR-PBO) membranes have emerged as a new class of microporous organic materials showing extraordinarily fast molecular transport, as well as molecular sieving effect for small gas molecules.[1,2] Their microporous structure and size distribution results from thermally driven structural rearrangements in the solid state of precursor aromatic polyimides, containing *ortho*-hydroxy groups, into the highly rigid, ladder-like polybenzoxazole structure. Free volume elements and their size distribution can be tuned easily by varying the monomer structures of the precursor polyimides and by using different thermal treatment protocols. Thus, in our previous studies, the thermal conversion of a series of *o*-hydroxy polyimides prepared from diverse commercially available dianhydrides and bis(*o*-amino phenol)s was carried out and their gas transport behaviour was examined by varying the heat treatment protocol.[2-5] Most of these TR polymers showed outstanding gas separation performance, overcoming polymeric upper bounds for gas separation, but strongly dependent on the chemical structure of the precursor polyimides and also on the thermal rearrangement treatment. Thus, TR-PBO membranes containing six bulky fluorine groups, derived from 4,4'-(hexafluoroisopropilidene) diphthalic anhydride (6FDA) and 2,2'-bis (3-amino-4-hydroxy-phenyl) hexafluoropropane (bisAPAF) displayed the highest fractional free volumes and permeabilities among all the TR-PBO reported.[1,2] Moreover, as a rule, the gas permeability increased dramatically and the gas selectivity decreased slightly by increasing the heat treatment temperature.

As a continuation on the study and development of new high free volume polymer membrane materials using the thermal rearrangement concept, we have considered the possibility of tuning the formation of free volume elements in TR-PBO polymers, in terms of temperature and rate of conversion, by increasing the flexibility of the polybenzoxazole backbone. Hence, here we describe for the first time the synthesis and characterization of poly(ether-benzoxazole) membranes by thermal rearrangement of a novel fluorinated ether-containing poly(*o*-hydroxy imide) (**HPEI**).[6] The effect of increased chain flexibility on the physical and transport properties of the resultant TR polymer membranes for different thermal treatment protocols (e.g. final temperature and thermal dwell time), have been examined and will be presented in detail.

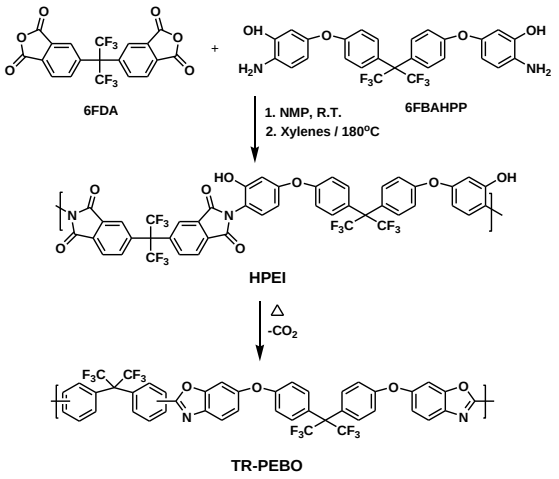

Figure 1. Synthesis of Thermally Rearranged Poly(ether-benzoxazole) (**TR-PEBO**)

Acknowledgment

This research was supported by the WCU (World Class University) program, National Research Foundation (NRF) of the Korean Ministry of Science and Technology (R31-10092), which we gratefully acknowledge.

References

[1] Park, H. B.; Jung, C. H.; Lee, Y. M.; Hill, A. J.; Pas, S. J.; Mudie, S. T.; Wagner, E. V.; Freeman, B. D.; Cookson, D. J. *Science* **2007,** 318, 254-258.

[2] Park, H. B.; Han, S.H.; Jung, C.H.; Lee, Y. M.; Hill, A. J.; . *J. Membr. Sci.* **2010,** 359, 11-24.

[3] Jung, C.H.; Lee, J.E.; Han, S.H.; Park, H. B.; Lee, Y. M.; *J. Membr. Sci.* **2010,** 350, 301-309.

[4] Han, S.H.; Lee, J.E.; Lee, K.J.; Park, H. B.; Lee, Y. M.; *J. Membr. Sci.* **2010,** 357, 143-151.

[5] Han, S.H.; Misdan, N.; Kim, S.; Doherty, C.M; Hill, A. J.; Lee, Y. M.; *Macromolecules* **2010,** 43, 7657-7667.

[6] Calle, M.; Lee, Y. M.; *Macromolecules* **2011**, in press.

One Single Composite For Chemical Sensor Or Heating Purposes.

Myriam Bouhadid[1], Jacques Desbrières[1], Caroline Pillon[1], Nathalie Redon[2] and Stéphanie Reynaud[1]

[1]IPREM-EPCP, UMR 5254 (CNRS/UPPA), Hélioparc, 2 avenue du président Angot, 64053 Pau cedex 9, France ; [2]Ecole des Mines de Douai, 941 rue Charles Bourseul, BP 10838, 59508 Douai cedex, France

stephanie.reynaud@univ-pau.fr

The major target of intrinsic conducting polymer (ICP) development is to combine the electrical properties of these materials with the mechanical and processability properties of commodity bulk polymers. Among ICPs, polyaniline (PAni) received a great deal of attention because of its easy preparation with low costs and its stability under environmental atmosphere. Moreover, the electrical conductivity of PAni can be closely controlled over a wide range coming from 10^{-4} to 10 $S.cm^{-1}$ which makes PAni a good candidate for many applications[1-4] as antistatic films, electromagnetic shielding layers, sensors, technical packaging and anticorrosion.

The IPREM-EPCP group focused on the optimization of a simple way of synthesis to yield to a conducting composite in one-step[5-6]. The final aqueous dispersion contains composite particles mad of polymer matrix and polyaniline and is used without post formulation. Conducting films are obtained by spaying or automatic film applicator methods. The conductivity and the chemical composition of the final composite may be in line with the target application.

The same conducting composite was then successfully used as chemical sensor and heating surface. The whole process, *i.e.* from the synthesis to the film forming, remain as simple as possible and are carried out in soft experimental conditions, that is, without external acid or organic solvent.

After a brief presentation of the synthesis and the characterization of the conducting films, the performances of chemical sensors and heating surface will be discussed. The study of chemical sensor demonstrated the feasibility of whole polymer sensors to detect ammonia[7-9]. Moreover, all performances of this new chemical sensor are in line with the market needs in terms of response time, sensitivity, reproducibility. At last, these sensors introduce a breakthrough technology since their response is reversible with no need of servicing or calibration between two exposures (Figure 27). This feature is very interesting in terms of time-life and cost.

The same composite films have been successfully tested as heating surface. The temperature of the films is measured via an Infra-Red camcorder and the results are reported Figure 28. Its heating performances and its processability (soft final material, easy to cut and pattern) allow considering its development as heating devices suitable for low energy building (tunable size, thin film, easy to handle).

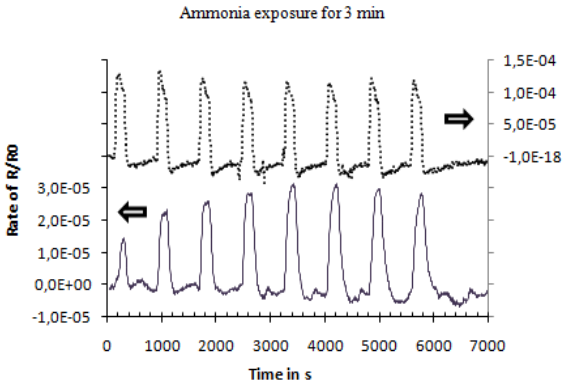

Figure 27. Sensor performances under several exposures to ammonia. Resistance evolution vs. time for composite film containing HCl doped PAni (plain line) and H_3PO_4 doped PAni (dashed line)

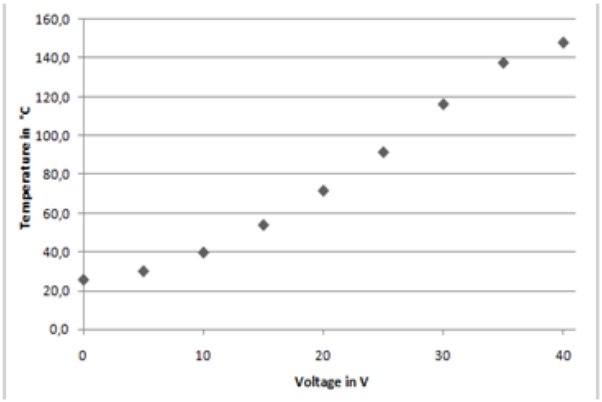

Figure 28. Heating performances of a composite film (50µm) containing HCl doped PAni.

(1) Stejskal, J.; Trchova, M.; Blinova, N. V.; Konyushenko, E. N.; Reynaud, S.; Prokes, J. *Polymer* **2008,** *49*, 180. (2) Koul, S.; Chandra, R.; Dhawan, S. K. *Polymer Guildford* **2000,** *41*, 9305. (3) Wessling, B. *Synthetic Metals* **1998,** *93*, 143. (4) Kang, E. T.; Neoh, K. G.; Tan, K. L. *Progress in Polymer Science* **1998,** *23*, 277. (5) Kohut-Svelko, N.; Dinant, F.; Magana, S.; Clisson, G.; François, J.; Dagron-Lartigau, C.; Reynaud, S. *Polymer International* **2006,** *55*, 1184. (6) Kohut-Svelko, N.; Joubert, M.; Reynaud, S. *Synthèse one-step de films conducteurs*. 0508172, 2005. (7) Joubert, M.; Bouhadid, M.; Bégué, D.; Iratçabal, P.; Redon, N.; Desbrières, J.; Reynaud, S. *Polymer* **2010,** *51*, 1716. (8) Bouhadid, M.; Thévenot, C.; Ehrenfeld, F.; Redon, N.; Desbrières, J.; Grassl, B.; Reynaud, S. *Sensor Letters* **2008,** *6*, 548. (9)Bouhadid, M.; Redon, N.; Plaisance, H.; Desbrières, J.; Reynaud, S. *Macromolecular Symposia* **2008,** *268*, 9.

Synthesis and Applications of Copoly(*p*-phenylene)s Containing Bipolar Triphenylamine and 1,2,4-Triazole Groups

Chia-Shing Wu and Yun Chen

Department of Chemical Engineering, National Cheng Kung University, Tainan, Taiwan

n3895120@mail.ncku.edu.tw

Abstract: Two novel copoly(*p*-phenylene)s (**P1**-**P2**) containing bipolar groups (12.8 mol% and 6.8 mol%, respectively), directly linked hole-transporting triphenylamine and electron-transporting aromatic 1,2,4-triazole, was synthesized to enhance electroluminescence of poly(*p*-phenylene vinylene) (PPV) derivatives. The bipolar groups not only enhance thermal stability but also promote electron- and hole-affinity of the resulting copoly(*p*-phenylene). Blending the bipolar copoly(*p*-phenylene)s (**P1**-**P2**) with PPV derivatives (**d6-PPV**) as an emitting layer effectively improve the emission efficiency of its electroluminescent devices [ITO/PEDOT:PSS/polymer blend/Ca(50 nm)/Al(100 nm)]. The maximum luminance and maximum luminance efficiency were significantly enhanced from 310 cd/m^2 and 0.03 cd/A (**d6-PPV**-based device) to 1450 cd/m^2 and 0.20 cd/A (blend device with **d6-PPV**/**P1**=96/4 containing *ca.* 0.5 wt% of bipolar groups), respectively. Our results demonstrate the efficacy of the copoly(*p*-phenylene)s with bipolar groups in enhancing electroluminescence of PPV derivatives.

Keywords: bipolar; conjugated polymers; light-emitting diodes (LED); poly(*p*-phenylene) (PPP); triazole (TAZ); triphenylamine (TPA)

Introduction: Since the polymeric light-emitting diodes (PLEDs) using poly(*p*-phenylenevinylene) (PPV) as an emitting layer was first reported by Holmes *et al.* in 1990, PLEDs have attracted much research interest over the past two decades because of their potential applications in large-area display and solid-state lighting. An efficient PLED requires a balanced injection and transport between electrons and holes. Unfortunately, electron injection is usually more difficult than hole injection in conjugated polymers, such as PPV derivatives, leading to the imbalance between electron and hole injection and transport, which greatly reduces the luminescence efficiency of their PLEDs. In this study, to enhance both hole and electron transport/injection we synthesized two novel copoly(*p*-phenylene)s (**P1**-**P2**) containing 12.8 mol% and 6.8 mol% bipolar group, respectively. The copoly(*p*-phenylene)s exhibit not only good thermal stability but also enhanced hole and electron injection relative to homo-poly(*p*-phenylene) (**P0**) due to the presence of the bipolar units. Finally, the influence of bipolar contents on device performance is investigated, using blends of the bipolar copoly(*p*-phenylene) and **d6-PPV** as emitting layer. Both maximum luminance and maximum luminance efficiency of the blend devices are greatly enhanced.

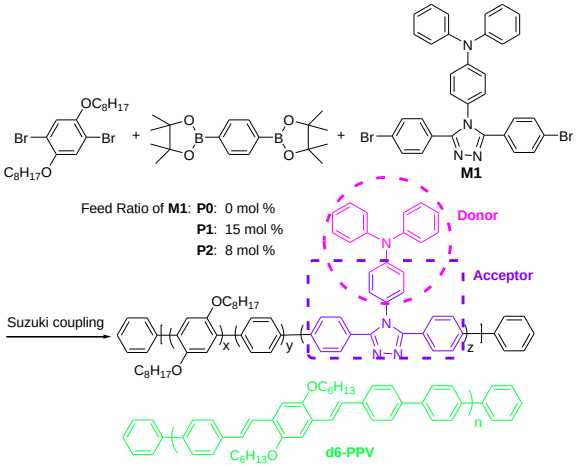

Scheme. Synthesis of Copoly(*p*-phenylene)s (**P1**-**P2**), Poly(*p*-phenylene) (**P0**) and Chemical Structure of **d6-PPV**.

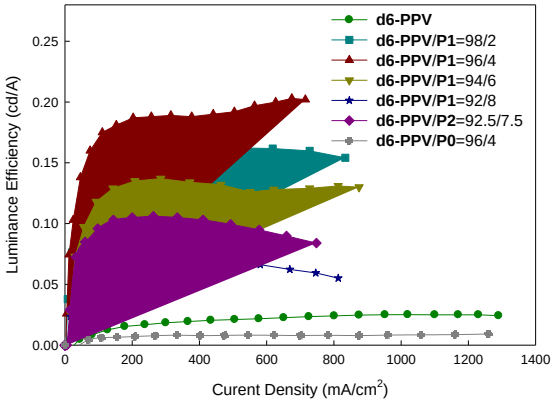

Figure. Luminance efficiency versus current density characteristics of PLEDs using blends of **d6-PPV** and **P1** (2~8 wt%), **P2** (7.5 wt%) or **P0** (4 wt%) as emitting layer. Device configuration: ITO/PEDOT:PSS/ **d6-PPV** + **P1**, **P2** or **P0** (80~100 nm)/Ca(50 nm)/Al(100 nm).

Conclusion: The function of the bipolar structure is to balance charges recombination in **d6-PPV**-based devices. Blending the copoly(*p*-phenylene)s containing bipolar moieties are promising additives to enhance device performance of **d6-PPV** due to improved carriers injection and transport.

Reference:

1. Wu, C.-S.; Chen, Y. Macromolecules 2009, 42, 3729-3737.
2. Wu, C.-S.; Chen, Y. J Mater Chem 2010, 20, 7700-7709.
3. Wu, C.-S.; Chen, Y. J Polym Sci Part A Polym Chem 2010, 48, 5727-5736.

Synthesis of New Two-Dimensional Thiophene-Based Conjugated Copolymers and Their Applications to Thin Film Transistors and Photovoltaic Cells

Hsiang-Wei Lin,[a] *Jung-Hsun Tsai,*[b] *Chih-Jung Lin,*[b] *Hung-Chin Wu,*[b] *Chien Lu,*[b] *Yu-Wei Lin*[a] *Yi-Cang Lai,*[a] *and Wen-Chang Chen,*[a,b,*]

[a] Institute of Polymer Science and Engineering, National Taiwan University, Taipei 106 Taiwan;
[b] Department of Chemical Engineering, National Taiwan University, Taipei 106 Taiwan

e-mail: chenwc@ntu.edu.tw

Two-dimensional 4T-acceptor conjugated polymers have been shown to have excellent charge-transport characteristics and solar cell performances.[1] In this study, new two-dimensional conjugated homopolymer poly(5,5'''-di- (2-ethylhexyl)[2,3';5',2'';4'',2''']quarterthiophene) (P4T) and their copolymers, P4TT, P4TSe, P4TFT, P4TBDT, and P4TDTS, were synthesized by Stille coupling reactions under microwave heating. The effects of chemical structures on the electronic energy level, charge transport, and photovoltaic properties were explored systematically. Among these copolymers, P4TFT showed the highest
organic field effect transistor (OTFT) hole mobility of 0.12 $cm^2 V^{-1} s^{-1}$ due to its highly crystalline packing structure. The performances of bulk heterojunction polymer solar cells based on the blends of these 4T-based copolymers and 1-(3-methoxycarbonyl) propyl-1 - phenyl-[6,6]-C-71 ($PC_{71}BM$) were also characterized. P4TSe/ $PC_{71}BM$ based photovoltaic device showed the highest power conversion efficiency (PCE) of 2.6% under AM 1.5 illumination ($100mW/cm^2$). The above results exhibited that two-dimensional conjugated copolymers emerged as a promising candidate for organic electronics.

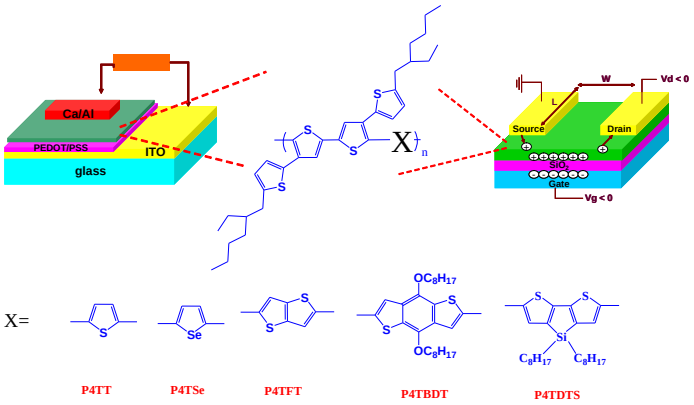

1. C. Y. Yu, B. T. Ko, C. Ting, and C. P. Chen, *Sol. Energy Mater. Sol. Cells*, **93**, 613 (2009).

Physicochemical Study of the Gelation Kinetics and Mechanism of Polyacrylamide-based Copolymers and Polyethyleneimine Hydrogels.

Castillo, R.V.[1,3]; Grassl, B.[1]; Dagreou, S.[1]; Blin, N.[2]; Dupuis, G.[2]; Karam, A.[3]

[1]Institute Pluridisciplinaire de Recherche sur l'Environnement et les Matériaux (IPREM) UMR CNRS, Université de Pau et des Pays de l'Adour (UPPA) 5254, Hélioparc Pau Pyrénées, 2 Avenue du Président Angot, 64053 Pau Cedex 09, France. [2]Poweltec, 3 Rue Paul Héroult, 92500 Rueil-Malmaison, France. [3]Laboratorio de Polímeros, Centro de Química, Instituto Venezolano de Investigaciones Científicas (IVIC), Apartado 20632, Miranda 1020-A, Venezuela.

rcastill@ivic.gob.ve

Introduction. Gels based of polyacrylamides (PAM) and modified-polyacrylamides (PAMs) and cross-linker(s) have been used in treatment of injection and productions wells to improve production of oils and gas [1]. Polyethyleneimine (PEI) is an organic cross-linker with a low toxicity that has been also used with PAM's and PAM derivatives for hydrogel systems. However, the mechanism of gelation of these systems is not yet well understood. This work evaluates the physicochemical properties of the polymer-crosslinker solution before, during and after the gel transition. Synthesized and well characterized: anionic poly(acrylamide-*co*-2-acrylamido-2-methyl-1-propane sulphonic acid) copolymer (PAM-*co*-AMPS) with 5, 10 and 20 mol-% of AMPS; hydrophobic poly(acrylamide-*co*-*tert*-butyl acrylate) (PAM-*co*-tBuA) with 1 and 5 mol-% of tBuA; and neutral PAM homopolymer were used. The presence of the co-monomers changes the charge density and chemical functionality of the PAM which can be conveniently used to modulate the gelation time [2]. The physicochemical mechanism of gelation was study by nuclear magnetic resonance (NMR), dynamic light scattering (DLS) and rheology. Also the viscoelastic properties of the gels were evaluated and the influence of crosslink density and polymer characteristics on the behavior of the gel was established.

Materials and Methods. Acrylamide (AM), 2-acrylamido-2-methyl-1-propanesulfonic acid sodium salt (AMPS) and hydrophobic *ter*-butyl acrylate (tBuA) were used as monomers. Sodium dodecyl sulfate (SDS), 2,2-azobis(2-methylpropionamidine) dihydrochloride, denoted VAZO56, were employ as surfactant and initiator, respectively. All these products were used without any further purification. Salt-free Milli-Q water (resistivity: 18.3 MΩ· cm) was used to prepare all brines for polymer dissolution. PAM and PAM-*co*-AMPS copolymers were synthesized via radical polymerization. PAM-*co*-PtBuA were synthesized via micellar copolymerization method [3]. The surfactant (SDS) was used at an excess value to ensure a number of hydrophobic units per block (assumed to be equal to the number of hydrophobic monomers) equal to 20 (N_H=20).

Results and Discussions. The mechanism of gelation and also the kinetics was found to be sensitive to the chemical structure of PAMs, besides the concentration of both polymer and crosslinker, and also temperature and pH. The mechanism of gelation was deeply studied using ^{13}C and ^{16}N RMN allowing to established the chemical groups responsible of the covalent links. Dynamic LS measurements performed at scattering angle of 90º allows to calculate the intensity time correlation function (TCF) $g_2(t)$ and the electric field TCF $g_1(t)$. The power-law behavior or not of $g_1(t)$ at the gel point was evaluated, as the behavior of the relaxation modes. Finally, the gelation process was monitoring recording by rheology the elastic (G') and viscous (G'') moduli during the in situ gelation of PAMs with the cross-linker PEI. Figure 1 illustrates the evolution of G' during gelation at constant temperature of 80 ºC, and a concentration of 0.5 wt% for both PAMs and PEI. From the G'(t) plot (Figure 1), three different periods in gelation process can be defined: (1) an initiation period where G` remains almost constant, (2) a sol-gel transition period where G` increases dramatically, and (3) an almost plateau regimen where G` slightly increases but did not reach a final equilibrium value before 24 h (results not shown). It is notorious from the Figure 1 that the gelation kinetic for the PAM-*co*-AMPS copolymers it is not the same from those of PAM and PAM-*co*-tBuA. The insert in Figure 1 shows the evolution of gel strength from ¨flowing¨ to ¨non-flowing gel¨ which revealed a behavior apparently not in accord with the formally gel definition. Different models and relationships between the different parameters were finally established.

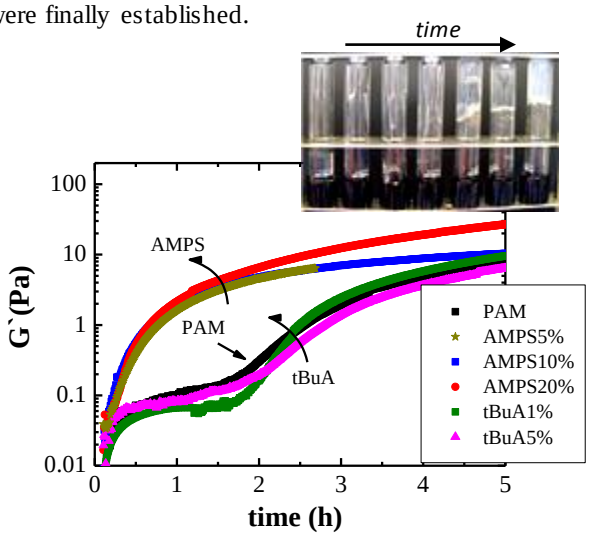

Figure 1. Variation of G' during gelation of PAM and PAM copolymers (0.5 wt%) with PEI (0.5 wt%) at 80 ºC under dynamis oscillations using ω = 1Hz and γº < 0.02. *Insert*: Gel evolution in time.

References.

1. Moradi-Araghi, AJ. Pet. Sci. Eng. 2007 ;55 :56-66.
2. Travas-Sejdic, A, Easteal, AJ. Polymer 2000;41:2535-2542.
3. Dupuis, G.; Rigolini, J.; Clisson, G.; Rousseau, D.; Tabary, R. ; Grassl, B. *Anal. Chem* **2009**, *81*, 8993-9001.

Viscoelastic and Generalized Newtonian Fluid Flows Simulation in Single Screw Extruder Using Computational Flow Dynamics

*Amirhosein Ahmadian, Yousef Tamsilian, Ahmad Ramazani S.A**

Sharif University of Technology Chemical, and Petroleum Engineering Department, Tehran, Iran.

*Email: ramazani@sharif.edu, Tel: +982166165431

This manuscript is presented to simulation of viscoelastic and generalized Newtonian fluid flows in an extruder considering that screw is turning instead of barrel turns which normally was considered in most simulation as assumption. A three dimensional finite-volume scheme is used to solve momentum and fluid equations. The real geometrical configuration of the channel is investigated to obtain best result and show effective profiles same as pressure, shear stress, velocity, and normal stress. The simulations concern incompressible fluids obeying different constitutive equations such as generalized Newtonian with shear-thinning properties (Carreau–Yasuda model), and viscoelastic differential model, the Phan–Thien/Tanner (PTT). The obtained results are shown in contour and vector form based on special position onto axial flow. Numerical results can demonstrate influence of boundary condition (fixed barrel and mobile barrel assumption) and rheological properties upon flow characteristics in considered geometry. The results show that screw moving as realistic conditions instead of mobile barrel assumption in single extruder has significant effects on pressure, stress, and velocity profiles comparing to results obtained from simulation with assumption of fixed barrel boundary that currently are used to model extruder flows. In other hand, in this study, we easily can observe two different behaviors of two different fluid models (viscoelastic and generalized Newtonian fluids) to compare the profiles

Ion exchange and Electron Exchange Properties of Polycalixresorcinarene

Altshuler H.N. and Ostapova E.V.

Institute of Coal Chemistry and Material Science, Siberian Branch of Russian Academy of Sciences

e-mail: ostapovaev@bk.ru

Introduction

Polycalixresorcinarenes as electrode materials for fuel elements of new generation was offered by us [1]. The oxidation-reduction processes with participation of hydrogen, oxygen and metals proceeding in polycalixresorcinarene matrix are investigated [1]. High electric conductivity of polycalixresorcinarenes equilibrated with aqueous solutions of electrolytes was established [2]. The goal of the present research was to study the ion exchange and electron exchange abilities of sulfonated polytetraphenylcalixresorcinarene

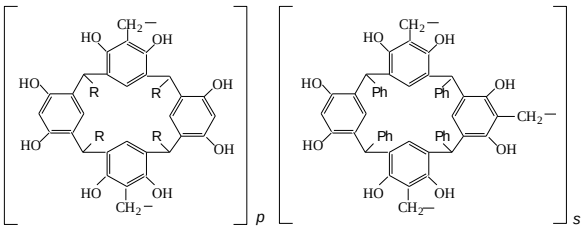

R= Ph-SO_3H .

Materials and Methods

The sulfonated polycalixresorcinarene was prepared by twice sulfonating of the network polymer synthesized by the resol polycondensation of tetraphenylcalixresorcinarene with formaldehyde following the procedure described in [3].

The dynamic ion exchange capacities of the polycalixresorcinarene were determined by passing the 0.1 M NaOH or 0.1 M NaCl through the polymers bed until the concentrations of H^+ in solutions at the inlet and outlet of the column became identical.

The dynamic electron exchange capacity of the polycalixresorcinarene was determined by passing the 0.01 M $Ce(SO_4)_2$ through the polymer bed until the concentrations of Ce^{4+} in solutions at the inlet and outlet of the column became identical. The value of the exchange capacity per kg of the H^+ form of the polymer dried at 105°C was calculated.

Electron exchange ability of polycalixresorcinarene were determined in the electrometric titration of polymer in 0.25 M H_2SO_4 with 0.01 M $Ce(SO_4)_2$ in 0.25 M H_2SO_4 using a bright platinum electrode referred to a saturated chlorine-silver electrode.

Results and Discussion

An analysis of the material balance indicates that the ion exchange from aqueous solutions involves protons of all sulfo groups and four protons of eight resorcinol OH groups (one per each resorcinol fragment) of repeating units of polycalixresorcinarene. The total ion exchange capacity of polymer (with respect to 0.1 M NaOH) is 5.65 moles per kg. The ion exchange capacity for polymer respect to the sorption of 0.1 M NaCl from neutral solutions corresponds to the concentration of sulfo groups in the polymer. It equals to 2.45 moles per kg.

It is revealed that the polymeric matrix of nanocomposite based on polycalixresorcinarene containing palladium participates in oxidation-reduction transformations according to the scheme

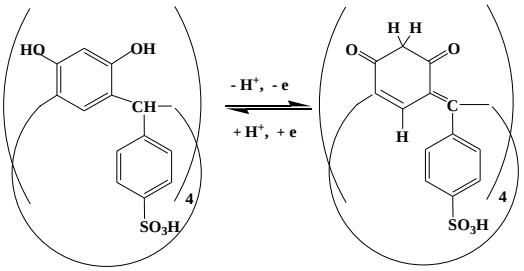

Thus after oxidation the resorcinol fragments of calixarene were transformed in quinoid structures. The analysis of FTIR-spectra of nanocomposite has shown that the basic fragments of macrocyclic structures of initial polymer are kept after treatment of nanocomposite by oxygen. The wide intensive strip in the rang of 3400 sm^{-1} corresponding to intramolecular hydrogen bonds in diols is observed in initial nanocomposite spectrum but the strip at 3400 sm^{-1} disappears in the spectrum of oxidized composite. In a spectrum of oxidized composite the intensity of strips at 2850 sm^{-1}, 2940 sm^{-1}, and 2920 sm^{-1} corresponding to asymmetric and symmetric valence vibrations of C-H bonds of methyl-methylene groups increases considerably.

The electron-exchange capacity of sulfonated polycalixresorcinarene equals to 3 electron moles per kg of polymer.

Conclusions

Polycalixresorcinarene is capable to exchange the protons by the cations from electrolyte solutions. The operating sorption pH interval of polymer ranges from 1 to 14.

Polycalixresorcinarene possess the electron-exchange ability caused by reversible oxidation of the resorcinol fragments.

References

1. Sapozhnikova L., Altshuler O., Malyshenko N., Shkurenko G., Ostapova E., Altshuler H. International Journal of Hydrogen Energy. L. 2010. doi:10.1016/j.ijhydene.2010.06.124.

2. Ostapova E.V., Altshuler H.N. International Conference Hydrogen Materials Science & Chemistry of Carbon Nanomaterials (ICHMS'2009). Yalta. Ukraine. 2009. P. 892-895

3. Altshuler H., Ostapova E., O. Fedyaeva, L. Sapozhnikova, O. Altshuler, Macromol. Symp., 181 (2002). P.1.Authors

Working with Water Insoluble Organic Molecules in Aqueous Media: Piperazinedione Derivative-Containing Polymers as Sensory Materials for the Fluorogenic Sensing of Biomolecules.

S. Vallejos, P. Estévez, H. El Kaoutit, M. Trigo, F. Serna, F. García, J.L. Peña, J.M. García

Departamento de Química, Facultad de Ciencias, Universidad de Burgos, 09001 Burgos, Spain

jmiguel@ubu.es

Introduction. Naturally, recognition in biological systems takes place in aqueous environments. The active sites, for example in an enzyme, have the shape needed to fit the guest molecule, or a part or the guest molecule, and the interaction relay on feeble bonds then takes place due to the hydrophobic microdomain in a hydrophilic general domain provided by the chemical and by the quaternary structure of a protein. In a very simplified manner, the competitiveness of the water molecules to establish these weak integrations is locally diminished or altered by the active site microsurroundings.

Mimicking nature, water insoluble receptors may be chemically anchored to a linear or crosslinked hydrophilic polymer, giving rise to water-soluble sensing polymers or to water-swelled sensing networks. The later approach permits easy control of swelling by means of increasing the crosslinking ratio. That is, the hydrophilic character of a polymer, derived from the chemical composition of the monomers, may be controlled not only by the monomer nature, but also by increasing the crosslinking monomer content of the network; thus, mechanically impairing the water uptake. Thus, an induced partially hydrophobic character may be addressed with an overall hydrophilic polymer associated with the mechanical stretching of the network upon swelling with water, as we have previously described.[1,2] Moreover, the polymers usually have good thermal and mechanical properties, can be easily transformed into end materials, such and films or coatings, to produce cheap sensing devices (e.g., user-friendly "naked-eye" film sensors). These polymers may also be incorporated as coating at the end of an optic fibre connected to a portable UV/Vis diode-array or fluorescence detector.[3]

Results and discussion. Thus, we prepared a methacrylamide monomer containing a piperazinedione derivative as the fluorogenic mercury sensing motif (**II**) and copolymerized them with a hydrophilic monomer (N-vinyl-2-pyrrolidone, **I**). The cross-linking agent, 1,2-ethanedioldimethacrylate, was used to obtain the dense, 100 μm thick polymer film or membrane (Scheme 1), with a water swelling percentage of 200 %. This membrane is optically transparent and demonstrates good mechanical properties, even after water or DMSO swelling. Upon soaking the film in aqueous solutions at physiological pH (pH= 7.4), the film exhibited selective fluorescence quenching behavior with increasing Hg(II) concentration, achieving a very low detection limit of 10 ppt (Fig. 1).

To test the fluorogenic anion and cation sensing selectivity of **II**, different anions and cations were tested. The addition of mercury cations resulted in a change in the gradual diminishing of the fluorescence intensity (F) of the 591 nm band. The fluorescent quenching was 8-fold when the relationship of **II** to Hg^{2+} was equimolar. In contrast, upon adding an equimolar amount of Cr^{6+} and Fe^{3+}, only a 1 and 0.5-fold fluorescence quenching was observed, respectively. The addition of a broad set of anions (sulfonate, chloroacetate, *p*-toluenesulfonate, oxalate, acetate, benzoate, cyanide, hydroxyl, nitrite, nitrate, carbonate, phosphate, fluoride, bromide, chloride), on the other hand, caused no effect.

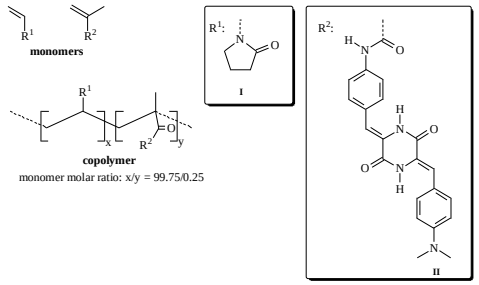

Scheme 1. Chemical structure of monomers and copolymer

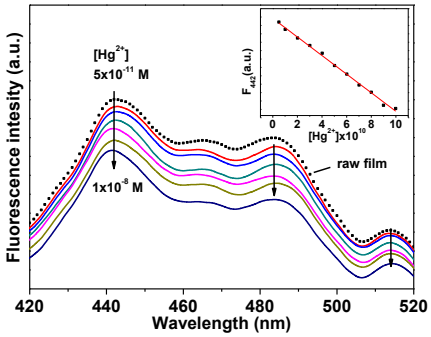

Figure 1. Selected titration curves of copolymer film with mercury cations in water at physiological pH (7.4) (inset: Hg^{2+} concentration vs. fluorescence intensity at 442 nm, F_{442})

Regarding biological molecules, the membrane showed a fluorogenic quenching upon adding increasing concentration of CoA, cysteine, and the tripeptide glutathione, with a lower detection limit of $1x10^{-6}$ M. Interestingly, and following the displacement-approach, the monomer in DMSO/water (90/10) solution, with the fluorescence quenched by an equimolar amount of Hg(II), recovered the fluorescence upon addition of the bimolecular mentioned above, improving the detection limit in one order of magnitude. The sensing performance of the hybrid organic/inorganic membrane is currently being carried out.

Refereces

1 F. García, J.M. García, B. García-Acosta, R. Martínez-Mañez, F. Sancenón, N. San-José, and J. Soto, J. *Chem. Commun.*, 2005, 2790.

2 B. García-Acosta, F. García, J.M. García, R. Martínez-Mañez, F. Sancenón, N. San-José, and J. Soto, *Org. Lett.*, 2007, **9**, 2429.

3 J.M. García, F.C. García, F. Sena, and J.L. de la Peña, *Prog. Polym. Sci.*, 2010, **35**, 623.

Electrospun Aligned Nanofibers of Two-Dimensional Conjugated P4TDPP for High Performance Field Effect Transistors

Chih-Jung Lin,[1] *Jung-Ching Hsu*,[1] *Jung-Hsun Tsai*,[1] *Chi-Ching Kuo*,[2] *Wen-Chang Chen*[1,2,*]

1: Department of Chemical Engineering, National Taiwan University, Taipei 106 Taiwan
2: Institute of Polymer Science and Engineering, National Taiwan University, Taipei 106 Taiwan

E-mail: chenwc@ntu.edu.tw

High performance field effect transistors (FET) were fabricated by electrospun (ES) aligned nanofibers using two-dimensional regioregular polythiophene derivatives: poly[2',5''-5,5'''-di-(2-ethylhexyl),3';5',2'';4'',2''']-quaterthiophene-*alt*-3,6-dithien-2-yl-2,5-di(2-ethylhexyl)-pyrrolo[3,4-c]pyrrole-1,4-dione-5',5''-diyl] (**P4TDPP**), the molecular structure is shown in chart 1. The **P4TDPP** precursor solution was treated with gel-induced procedure to enhance crystallinity and further promoted FET mobility.

Figure 1 shows the normalized absorption spectra of polymer solution, thin film and nanofibers with different processing conditions. The intensity of **Solution-G** (polymer solution treated gel induced procedure) is increased evidently at 752 nm shoulder. It indicates the **P4TDPP** can self-organize to form crystallites through the gel-induced procedure. The maximum absorption wavelength of thin film (pristine procedure: **Spin-P**; gel induced procedure: **Spin-G**) and nanofibers (**ES-G**) is observed at 780 nm. It implies the three samples exhibit the identical π−π interaction of **P4TDPP**. The inset of Figure 1 shows that the absorption coefficient of **Spin-G** is 1.5 times larger than **Spin-P**, suggesting the crystallinity of **Spin-G** is higher than that of **Spin-P**.

The average FET mobility, on/off ratio and threshold voltage of nanofiber transistors are 0.305 $cm^2\ V^{-1}\ s^{-1}$, 1.30 × 10^5 and -1.25 V, respectively. It exhibited a higher mobility than those of thin film transistors (**Spin-P**: 0.029 $cm^2\ V^{-1}\ s^{-1}$; **Spin-G**: 0.152 $cm^2\ V^{-1}\ s^{-1}$). The high mobility is ascribed to order molecular stacking and regular orientation within aligned nanofibers discovered through synchrotron grazing incidence small angle X-ray scattering (GISAXS), as shown in Figure 2. Each layer consists of the parallel conjugated main chains stacked by π−π interaction. The (100) peak of all sample is displayed at q_z = 0.322 $Å^{-1}$ (plane spacing is 18.87 Å). Figure 2(c) and 2(d) show the 2D-GISAXS patterns of the incident beam vertical (**ES-G_V**) and horizontal (**ES-G_H**) to the long axis direction of aligned ES nanofibers collected onto ODTS modified SiO_2/Si wafer, respectively. The schematic representation of the polymer packaging is shown in Figure 2(e). Compared to the 2D-GISAXS patterns of **Spin-P** (Figure 2(a)), **Spin-G** (Figure 2(b)) and **ES-G_H** (Figure 2(d)), the **ES-G_H** exhibited stronger intensity of (100) peak (**ES-G_H** > **Spin-G** > **Spin-P**) and weaker intensity of (100) rings (**ES-G_H** < **Spin-G** < **Spin-P**). It suggests that **ES-G_H** has a higher crystallinity and more order packing structures with (100)-axis normal to the substrate. In contrast, the intensity of (100) peak of **ES-G_V** is lower 0.5 times than **ES-G_H**. It suggests that the (010)-axis (normal vector of π−π stacking plane) is parallel to long axis of nanofibers, as shown in Figure 2(e). The above result indicates that the ES **P4TDPP** nanofibers could form order stacking and high orientation lamella with high carrier mobility. The present study demonstrates that the combination of ES nanofibers and the gel-induced structure is a simple process to fabricate conjugated polymers for high performance FET.

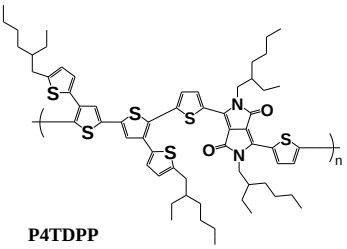

P4TDPP

Chart 1. Molecular structure of the **P4TDPP** polymer.

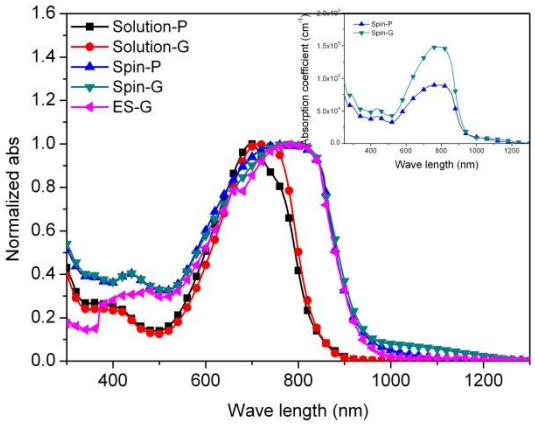

Figure 1. Normalized absorption spectra of **P4TDPP** prepared from different processes. The inset figure is absorption coefficient diagram of **Spin-P** (▲) and **Spin-G** (▼).

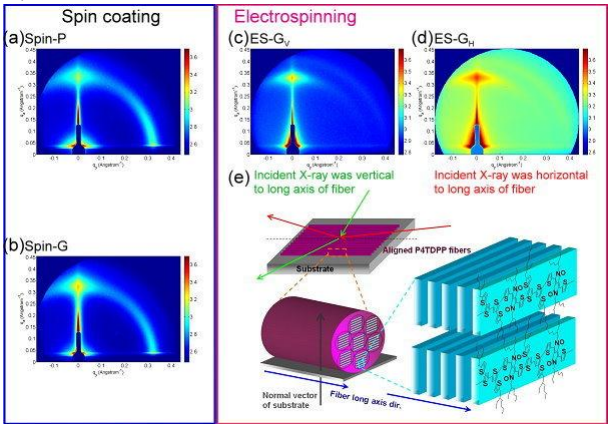

Figure 2. GISAXS pattern of **P4TDPP** thin film were fabricated on ODTS-treated wafer by the following procedures: (a) **Spin-P**, (b) **Spin-G**, (c) **ES-G_V**, and (d) **ES-G_H**. (e) Schematic representation of GISAXS measurement for aligned ES nanofibers. Suffix H (V) represents incident beam vector is horizontal (vertical) to the long axis direction of the fiber.

Preparation of Open Submicron Cell Structure by $scCO_2$ Foaming of Highly Oriented Isotactic Polypropylene

Jin-Biao BAO[a,b], *Tao Liu*[a], *Ling Zhao*[a*], *Guo-Hua Hu*[b,c]

a) State Key Laboratory of Chemical Engineering, East China University of Science and Technology, Shanghai, 200237, China.
b) Laboratory Reactions and Process Engineering, CNRS-Nancy Université-INPL-ENSIC, 1 rue Grandville, BP 20451, 54001 Nancy, France.
c) Institut Universitaire de France, Maison des Universités, 103 Boulevard Saint-Michel, 75005 Paris, France.

Email: baojinbiao@gmail.com, zhaoling@ecust.edu.cn

Introduction

Conventional $scCO_2$ foaming, in which CO_2 is introduced into polymeric matrix and depressurized quickly to foam, normally produce microcellular foams with average cell sizes of about 10 μm and cell densities greater than 10^9 cells/cm^3 [1]. Polymer foams in nano or submicron cells with a well-defined open pore structure and tunable mass transport characteristics by CO_2 foaming have been brought into focus as their unique application (drug delivery devices and porous membrane materials) and the process non-polluting [2-3].In this work, we report a method to prepare open submicron cell structure by $scCO_2$ foaming of highly oriented iPP. Optical light microscopy (OM), differential scanning calorimetry (DSC), small-angle X-ray scattering (SAXS) and scanning electron microscopy (SEM) were employed to investigate the effect of the crystalline structure and the foaming conditions on the final cell morphologies.

Materials and Methods

A commodity iPP (RS 1684) with broad molecular weight and high melt strength, was purchased from Basell Co., America to obtain highly oriented iPP samples by injection molding. CO_2 (purity: 99.9% w/w) was purchased from Air Products Co., Shanghai, China. CO_2 foaming of the highly oriented iPP samples was performed in a high-pressure vessel placed in a homemade oil bath with a temperature controller and its accuracy was ±0.2 °C [4].

Results and Discussion

Figure 1a shows a typical skin-core structure of the injection molded iPP sample, and figure 1b indicates the presence of shish-kebab crystalline structure in the shear zone ("A" zone in figure 1a). The equatorial streak in SAXS pattern was attributed to the formation of oriented structure or shish, oriented parallel to the flow direction; meridional maxima were attributed to the layer-like oriented structure or kebab, oriented perpendicular to the flow direction [5].

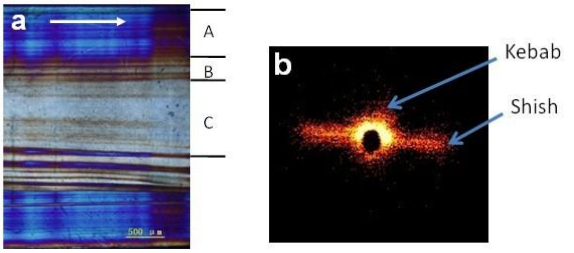

Fig. 1. (a) Optical micrographs of cross-sections of the injection molded iPP sample with a typical multiple layers distribution: (A) the 'shear layer'; (B) the 'intermediate layer' and (C) the 'isotropic core'. The white arrow indicates flow direction. (b) 2D SAXS image of the "A" zone in part (a).

It is generally accepted that crystallites are impenetrable for most non-reactive molecules including CO_2. In our previous work, we studied the effect of crystalline structure on the cell formation in an iPP during a solid-state foaming process, and found that the crystalline structure exerted a significant impact on the cell morphology of foamed iPP as cell nucleation and growth only occur in the amorphous regions where CO_2 dissolved [4].Therefore, with the restriction of the shish-kebab crystalline structure, the uniform nano or submicron size cell morphology must be obtained by CO_2 foaming under the certain foaming condition like figure 2 illustrated.

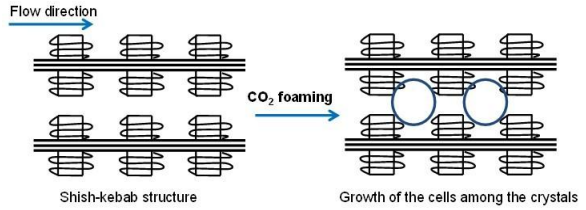

Fig. 2. Schematic of the restriction of cells growth in the amorphous and molten crystal regions of iPP.

To get the desirable cell morphology, we took the "A" zone in figure 1a to foam under CO_2 saturation pressure of 25 MPa and various temperatures. As shown in figure 3a, the un-foamed region still revealed the shish-kebab like structure when the foaming temperature was 140 °C. With the temperature increased, the open submicron cell structure was achieved (figure 3b) as more crystals, which restricted the growth of cells under the lower temperature, were molten.

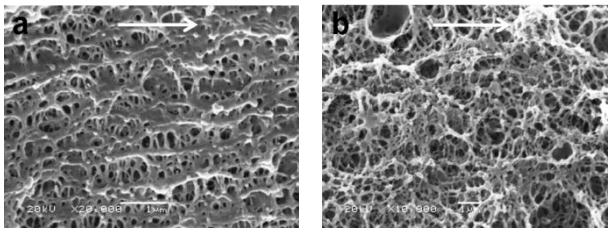

Fig. 3. SEM photographs of highly oriented iPP samples foamed at CO_2 saturation pressure of 25 MPa and (a) 140 °C, (b) 143 °C, respectively. The arrows indicate the flow direction, and the white bars in (a) and (b) are both 1 μm.

Conclusions

Open submicron cell structure was successfully achieved by $scCO_2$ foaming of highly oriented iPP. The crystalline structure and the foaming temperature have a significant impact on the final cell morphologies.

References

[1] S. K. Goel, E. J. Beckman. Polym. Eng. Sci. 1994, 34, 1137.
[2] B. Krause, et al. Macromolecules 2002, 35, 1738-1745.
[3] Seyed H. Tabatabaei, et al. J. Membrane Science, 2008 325, 772-782.
[4] Xiu-Lei Jiang, et al. J. of Supercritical Fluids, 2009, 48, 167-175.
[5] Rajesh H. Somani, et al. Polymer 47 2006 5657-5668.

Design Rules for Fuel Cell Membranes

Gerhard Maier[1], *Markus Groß*[1], *Tim Fuller*[2], *Sean MacKinnon*[2], *Craig Gittleman*[2], *Cortney Mittelsteadt*[3]

[1]Polymaterials AG, Kaufbeuren, Germany, [2]GM Fuel Cell Activities, Honeoye Falls, NY, USA, [3]Giner Electrochemical Systems, Newton, MA, USA

g.maier@polymaterials.de

Introduction: Fuel cells are considered a potential alternative to batteries for portable electronics, internal combustion engines for cars, and even boilers and generators for stationary applications. Most technical problems solved now on the pathway to commercial success. However, depending on the specific application, there are still improvements desired concerning the proton conducting membranes in PMFCs. For automotive use, conductivity at low humidity and durability are most important.
Many different polyelectrolytes have been synthesized over the past decades for application as proton conducting membrane in fuel cells. While many of them (polymers as well as membranes) are well studied, it is often hard to identify the specific benefits and drawbacks of one chemical structure over another. Based on observations of the effects of certain chemical structures as well as the architecture of the polymer chains on membrane properties such as proton conductivity, water uptake, and durability, we have found some principles during the development of several series of ion conducting polymers that may serve as general guidelines for optimization.

Approach: Our approach to improve the proton conductivity of sulfonated hydrocarbon polymers at low humidity is to increase the "efficiency" of the proton transport, i.e. to reduce the amount of water required for proton transport.

Results and Discussion: Microphase separated polymers allow a very high local acid content (IEC) without excessive swelling of the membrane. The water that is present is located in hydrophilic domains, e.g. in segmented block copolymers. (Figures 1 and 2)
In addition, attaching sulfonic acid groups in side chains rather than the polymer main chain can enhance interaction of the ionic groups and improve phase separation.
Increasing the hydrophobicity of the non-sulfonated segments, especially avoiding groups that interact strongly with water by hydrogen bonding, further improves the water management by pushing most water from the hydrophobic domains into the hydrophilic domains, where it supports acid dissociation and proton transport. (Figure 3)
Another very important factor is the morphology of microphase separated block copolymers. Regular, ordered morphologies lead to better conductivity than when there is no phase separation. However, the highest conductivity can be achieved with microphase separated polymers with disordered morphologies, because in a disordered morphology the proton conducting domains are more interconnected than in a well ordered morphology with long range order [1].

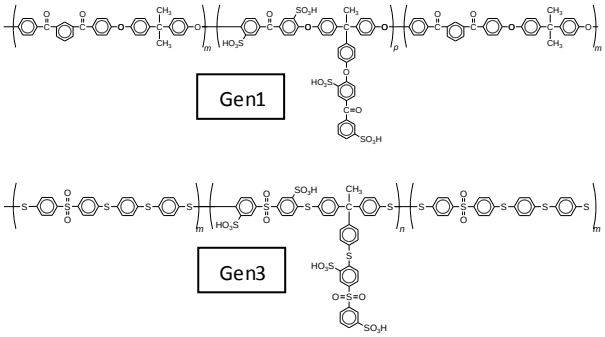

Figure 1: Side-chain sulfonated block copolymers

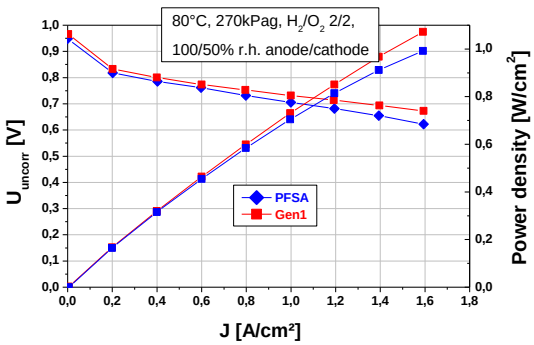

Figure 2: Fuel cell performance of Gen1 membrane (red) in comparison with Nafion 112 (blue)

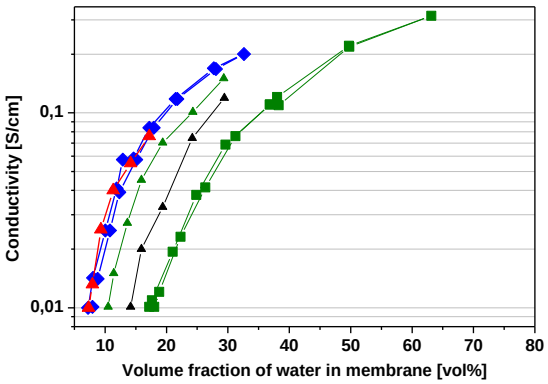

Figure 3: Proton conductivity in dependence of water content of the membrane. Gen3 membrane (red), Nafion 112 (blue), Gen1 (black), poly(thioether sulfone) (green)

References:

[1] M. Gross, G. Maier, T. Fuller, S MacKinnon, C. Gittleman, in Handbook of Fuel Cell, Vol. 5, W. Vielstich, H. A. Gasteiger, and H. Yokokawa (Editors), Wiley-VCH, (2009).

Dextran based Micro-/Nano-gels as Injectable Device for Controlled Release System

S. V. Ghugare,[1] *E. Chiessi*,[1] *M. Telling*[2] *and G. Paradossi*[1*]

[1]Dipartimento di Scienze e Tecnologie Chimiche, Università di Roma Tor Vergata and SOFT, CNR-INFM, Roma, Italy.
[2]ISIS Facility, Rutherford Appleton Laboratory, Chilton Didcot, Oxfordshire OX11 0QX, UK

e-mail: gaio.paradossi@stc.uniroma2.it

The design of materials (especially micro-/nano-gels) that biodegrade and switch their physio-chemical properties in response to external stimuli constitutes a main research activity in controlled drug release. Biodegradation of the microgel matrix not only circumvents removal of the empty device but also can be used to modulate the release of loaded drugs for a long period of time. Dextran based polymers have been extensively studied for sustained release of protein drugs in recent years, because dextran is enzymatically degradable, hydrophilic and biocompatible. In particular, thermoresponsive polymers are a class of the environmentally switchable materials and poly(*N*-isopropyl acrylamide) (PNiPAAm) has been most intensively studied.

The structure and dynamics of such devices are characterized in terms of diffusive processes with time scales covering several decades. Scattering methods including small-angle neutron scattering (SANS), quasi elastic neutron scattering (QENS), small-angle x-ray scattering (SAXS), and dynamic light scattering (DLS) are well suited to investigate thoroughly the overall structure and the detailed architecture of the microgels.

Here we report a new simple method to obtain the dextran based microgels, DexM, with four different degrees of substitution using water-in-water microemulsion technique combined with ultrasonication. Size and size distribution of the microgels and degree of swelling were investigated as well. In order to evaluate the average pore size of the microgel network, we used confocal laser scanning microscopy (CLSM) combined with size exclusion experiments. The dynamics of confined water molecule in the microgel system was studied by using quasi elastic neutron scattering technique (QENS). Furthermore we have investigated the enzymatic degradation of DexM microgels.

In addition we have prepared novel dextran based "smart" microgels with nano/micro size using water-in-water microemulsion technique. In order to check the possiblity to use injectable device in controlled release, we have investigated the size, size distribution and thermoresponsivity of microgels. Furthermore we have investigated structural information using small angle neutron scattering (SANS).

Dextran microgels described in this contribution have an average diameter < 2 μm with relatively narrow size distribution (**Figure 1 (left)**). An increase of the degree of substitution (DS) of methacryloyl dextran polymers decreases the overall microgel size up to DS 25 % as well as the degree of swelling. Size exclusion/confocal microscopy experiments evidenced that the average pore size is < 3 nm.

A complex pattern characterizes the diffusion of water in DexM networks. The diffusion of bound water in the microgels showed a supercooling behaviour due to the hydrophilic character of dextran chains (**Figure 1 (right)**). Moreover, the dynamics of the associated water depends strongly on the pore size.

Finally, the biodegradation of microgels was investigated during the action of different hydrolytic enzymes, leading to the conclusion that the degradation is directly linked to the structural and interfacial features of the dextran based microgels.

In addition we have designed dextran based microgels modified with the incorporation of NiPAAm residues in network. Combining features such as dimensions in the micro/nano size domains and thermal responsivity in physiological conditions is the main characteristic of the microgels studied.

The structural details of "smart" microgels have been studied by SANS. At low Q values and above the volume phase transition temperature, VPTT, the scattered intensity vs. the scattering vector, Q, , approaches a Q^{-4} trend (Porod's behaviour) (**Figure 2**).

This leads to the conclusion that the microgels are characterized by a smooth surface at temperatures higher than VPTT. Below VPTT, the I(Q) shows a $\propto Q^{-2}$ trend indicating a higher roughness of the surface due to the presence of polymers chains projected toward the solvent. The analysis of the data at higher Q values allows the evaluation of a correlation length characterizing the average pore size across the volume phase transition.

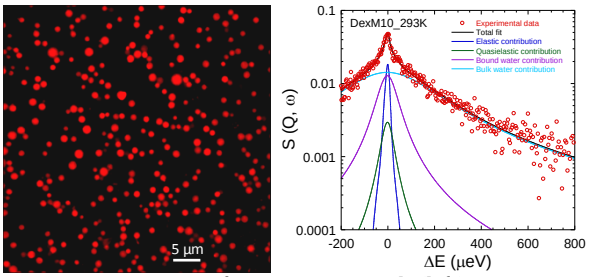

Figure 1: CLSM image of DexM25 Microgels (left), QENS spectra (IRIS) of DexM10 microgels at 293 K (right).

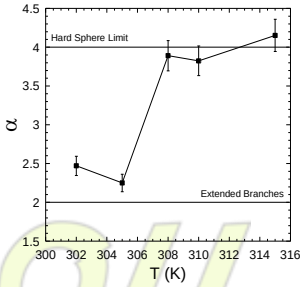

Figure 2: Exponent α as a function of temperature during the swelling process of DexMN50 microgel (SANS

Structure and supramolecular formations of star-shaped fullerene-containing polymers in solution

V.T.Lebedev, Gy. Torok**, L.V.Vinogradova****

* Petersburg Nuclear Physics Institute, 188300 Gatchina, St-Petersburg distr., Russia
** Research Institute for Solid State Physics and Optics POB-49, 1525 Budapest, Hungary
*** Institute of Macromolecular Compounds of RAS, 199004 St-Petersburg, Bolshoy pr.31 , Russia

vlebedev@pnpi.spb.ru

Self-organization of protonated star-shaped polymers composed of six polystyrene (PS) arms and six arms of polar polymer attached to common fullerene(C_{60})-centre have been studied by small-angle neutron scattering (SANS) in deuterated toluene at ambient temperature below the threshold of macromolecules' overlapping (concentration ~ 1 g/dl).

The samples of Li-polystyril (linear precursors) were synthesized by anionic polymerization of styrene in benzene. There was used oligopolystyrillithium (PSLi, polymerization degree 6-8). Star-shaped 6-arm PS with centre C_{60}, $(PS)_6C_{60}$, have been obtained by grafting fullerene C_{60} using living PS chains with lithium counterion in the mixture benzene-toluene at ambient temperature (the PSLi:C_{60} ratio was 6:1, Fig.1) [1].

The comparison of these data with properties of 6-arm PS-star has shown that the addition of six polar arms leads partially to the collapse of star when its polar arms become coiled in non-polar solvent (toluene). In solvent hetero-arm stars demonstrated the formation of supramolecular structures being clusters those size and density depend on chemical nature of polar arms.

Stars with PS and poly(2-vinylpyridine) are found weakly associated (average number of macromolecules in associate ~ 1.3) while hybrid polymers containing the arms of PS and poly(tert-butylmethacrylate) revealed a trend to be interpenetrated and associated into large-scale entities (diameter ~ 50 nm, ~ 12 macromolecules, Fig.2).

On the other hand, the hybrid stars with PS and diblock arms, poly(2-vinylpyridine)-poly(tert-butylmethacrylate), have exhibited a moderate self-assembly resulted in the formation of chain-like clusters (~ 4 particles, Fig.3). These SANS-results are discussed regarding to modern theories of polymers association.

1. E.Yu. Melenevskaya, L.V.Vinogradova, L.S. Litvinova et al. // Polymer Science, A. 1998. V.40. P.115.

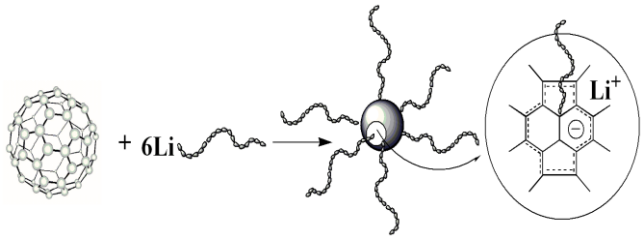

Fig.1. Synthesis of star-shaped fullerene-containing polymers.

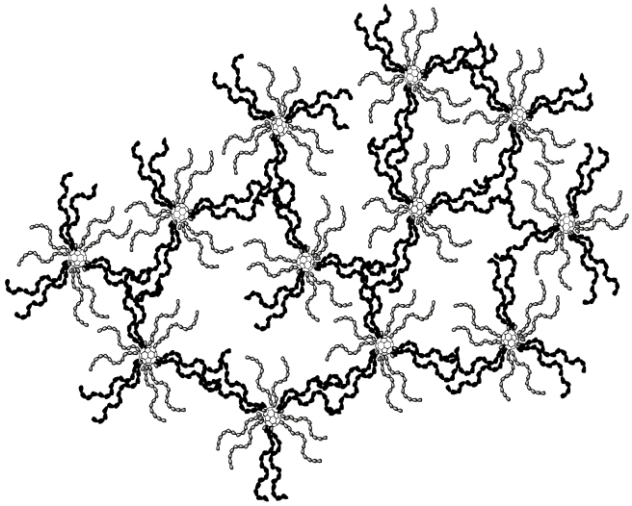

Fig.2. Formation of superstructures of star-shaped hetero-arm macromolecules in toluene.

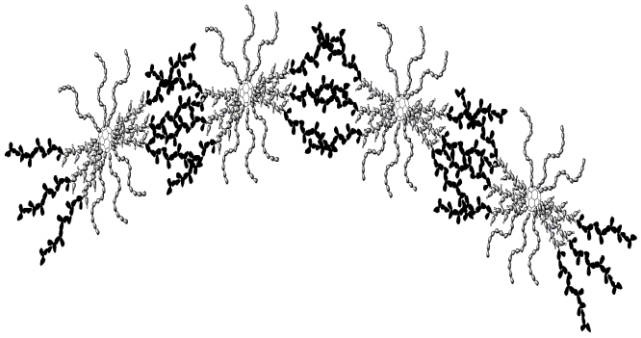

Fig.3. Chain-like clusters of star-shaped polymers with diblock-arms.

Phase Segregation and Themal Degradation of Polycarbonatediol-based Polyurethanes. Effect of Hard Segment Content and Soft Segment Length

Andrés Nohales[1], Victor Costa[1], Julio Latorre[2], Carmen Guillem[2], Paula Félix[2] and Clara M. Gómez[2]

[1]R&D Department UBE Corporation Europe, S.A., Castellón (Spain)
[2]Institut de Ciència dels Materials, Universitat de València, 46980 Paterna, Valencia (Spain)

a.nohales@ube.es; clara.gomez@uv.es

Introduction

Thermoplastic polyurethanes, due to the wide range of compositions available, have found extensive use in numerous commercial applications such as coatings, foams adhesives, sealants, synthetic leathers , membranes, elastomers as well as in many biomedical applications. Polyurethane elastomers are lineal segmented copolymers formed by thermodynamically incompatible segments named as the hard and the soft ones. The hard segments consist of a diisocyanate and a low molecular weight diol. The soft segments are high molecular weight polyols. In general, microphase separation between hard and soft domains is not complete and this conferee unique elastomeric properties at room temperature. Many factors such as type of polyol and diisocyanate, mass fraction, molecular mass, polydispersity of hard and soft segments, manufacturing conditions etc affect on morphological factors and define final properties, such as hardness, stiffness, tensile strength, and clarity of materials. A proper selection of the raw materials and molar composition becomes crucial as it provides the required properties that meet customers' needs. Commonly employed soft segments are derived from polyether or polyester polyol. However, nowadays, considerable attention have been devoted at the industrial level to new polycarbonate-based polyurethane elastomers due to their improved mechanical performance and their better anti-hydrolyzation and anti-oxidation properties compared to the traditional polyurethanes. The aliphatic polycarbonate based polyurethane can be used for industrial parts, building materials, sports goods, medical equipment, and even artificial tissues. New types of polycarbonate diols which are liquid at room temperature, such as the PH series used in the present work, are easy for handling, and show improved polyurethane flexibility and chemical resistance compared with the conventional commercially available (solid at laboratory conditions) polycarbonate diols, highly used since now. The aim of the present work was to synthesize thermoplastic polyurethanes based on aliphatic and liquid at room temperature polycarbonate diols (PCD). Two PCD molar masses (1000 and 2000) and three hard segment compositions (37, 48 and 62 wt%) have been selected to build up the polyurethane chains. Influence of the composition on the phase segregation and thermal stability has been investigated.

Experimental

The hard segment consists of 4,4'-diphenylmethane diisocyanate (MDI) and 1,4-butanediol (BD) as chain extender, both supplied by Aldrich. The soft segments are polyhexamethylene-pentamethylene carbonate diol of molar mass 1000 and 2000, and with trade name PH100 and PH200, both supplied by UBE Chem Eur.

Fourier Transform Infrared-Attenuated Total Reflection Spectroscopy (FTIR-ATR) were performed with a Thermo Nicolet Nexus FTIR spectrometer equipped with a multiple internal reflection accessory ATR single bounce.

Thermogravimetric analysis (TGA) experiments were performed using a Setaram Setsys 16/18 under oxygen atmosphere at 5ºC/min.

Differential scanning calorimetry (DSC) thermograms were carried out in a Mettler Toledo DSC821 Differential Scanning calorimeter at 10 ºC/min under dry nitrogen purge. The midpoint of the heat capacity change has been chosen to represent the glass transition temperature and melting point refers to the endotherm peak temperature.

Results and Discussion

FTIR spectroscopy was used to investigate the isocyanate conversion and hydrogen bond formation in polyurethanes. No isocyanate peak at ca. 2270 cm^{-1} was observed indicating full NCO conversion and absence of residual isocyanate groups. Also, it is observed the absence of the stretching vibration peak at 3640 cm^{-1} of free amidic NH groups not engaged in H-bonds. The only NH signal is a vibration peak of hydrogen-bridged amidic NH groups at 3326 cm^{-1}, which indicates that practically all NH groups participate in the formation of hydrogen bonds. To study the influence of the hard segment content on the formation of hydrogen bonds the "-C=O amide I" stretching region has been analyzed. The result of the deconvolution of the C=O stretching band in four Gaussian curves corresponding to free and bonded carbonate and urethane groups gives an idea of the degree of H-bonding. An increase in the hard segment content causes a decrease in the fraction of free to associated urethanes and a decrease in the fraction of free carbonate-carbonyl groups.

DSC analysis displays several transitions associated with the soft phase in the low temperature range and with the hard segment in the high temperature range. The glass transition temperature of the soft segments suffers a considerable increase when forms part of the polyurethane copolymer. This increase results from partial mixing between hard and soft segments, and restriction of the mobility of the polyurethane soft segment at the hard/soft segment junction.

Thermal decomposition of polyurethanes occurs as a result of a multitude of physical changes and is not dominated by a single process. TG/DTG curves show that up about 300 ºC the polymeric material is chemically stable. The first weight drop increases as the hard segment content decreases for both polycarbonate molar masses used.

Characterization of a Microbial Fucose-containing Polysaccharide Produced from Glycerol byproduct

Cristiana A. V. Torres [1], *Filomena Freitas* [1], *Maria A. M. Reis* [1], *Isabel de Sousa* [2], *Vítor D. Alves* [2]

[1]REQUIMTE/CQFB, Chemistry Department, FCT/Universidade Nova de Lisboa, 2829-516 Caparica, Portugal. [2]CEER-Biosystems Engineering, Institute of Agronomy, Technical University of Lisbon, Tapada da Ajuda, 1349-017 Lisbon, Portugal.

cristiana.torres@dq.fct.unl.pt

Microbial polysaccharides are environmental friendly and versatile polymeric materials with a wide range of distinct properties (e.g. thickening, emulsifying, flocculating and film-forming capacity) and industrial applications (e.g. food, pharmaceutical, cosmetics). When compared to plant and algae-derived polysaccharides, microbial production presents the advantage of being more productive and less resource intensive. Furthermore, microbial production processes are more amenable to control product composition, yield and productivity. Despite that, industrial microbial production is limited by the high cost of the carbon sources (e.g. sucrose, glucose, fructose) usually used. To overcome this limitation, those traditional substrates can be replaced by low cost carbon sources (agro or industrial residues/byproducts), such as glycerol byproduct from the biodiesel industry.

In this work, a fucose-containing EPS was produced by *Enterobacter* A47 DSM 23139 using glycerol byproduct from the biodiesel industry as substrate. The fucose-containing EPS is composed by neutral sugars, such as fucose, galactose and glucose and acyl groups substituents (acetate, pyruvate and succinate). Pyruvate and succinate confers to the polymer polyelectrolyte behaviour. It is a homogeneous polymer (PD = 1.3) with a high molecular weight (5.8×10^{6}).

The intrinsic viscosity of the fucose-containing EPS in 0.1 M NaCl was 8.03 ± 0.68 dL/g, with a Huggins coefficient (k_H) of 0.62 ± 0.21, suggesting some molecular aggregation. The EPS is a viscosity enhancer, forming viscous aqueous solutions which present a non-Newtonian shear thinning behaviour and a mechanical spectrum suggesting a viscous solution with entangled polymer chains. The EPS exhibits surface-active properties, showing potential to substitute current synthetic commercial products as emulsion forming and stabilizing agent. It might also be used in colloid and cell aggregation due to its high flocculating activity (comparable to $Al_2(SO_4)_3$). In addition, it is able to produce cohesive and flexible films. Beyond that, the presence of fucose (a bioactive component) envisages its application provides a great potential to be applied on pharmaceutical and cosmetic industries.

Considering all the characteristics presented the novel fucose-containing EPS has enormous potential to be used as viscosity enhancer on several industries, and in biomaterials, such as, scaffolds bioadhesives or drug delivery systems.

Block copolymers containing photocleavable side groups : Formation and disruption of micelles by light

Olivier Bertrand, Jean-Marc Schumers, Charles-André Fustin and Jean-François Gohy

Université chatholique de Louvain, Institut de la matière condensée et des nanoscience/Bio et Soft Matter

olivier.bertrand@uclouvain.be

Block copolymers are the focus of a sustained interest since they can be used for preparing micellar structures with various morphologies and functionalities when they are dissolved in a selective solvent for one of the blocks [1-2]. Moreover, the family of stimuli responsive block copolymers shows great potential for application in diverse fields due to their ability to change their properties when submitted to a stimulus (pH, temperature, light irradiation) [2]. Among all the existing stimuli light is particularly interesting [3] since it can be localized in time and space, it can be triggered from outside of the system, and it does not require particular reagents which limit byproducts. In this contribution, we combine the concepts of block copolymer micelles and light-sensitive polymers.

We report on block copolymers containing photocleavable side groups. The copolymer synthesis and the light induced formation or the disruption of micelles is discussed. The light induced micellization is studied with *o*-nitrobenzyl derivative. The block copolymers are composed of a polystyrene (PS) block and a poly(nitrobenzyl acrylate) or poly(dimethoxynitrobenzyl acrylate) block bearing photocleavable side-groups (PNBA-*b*-PS and PDMNBA-*b*-PS). The light induced disruption of micelles is studied with block copolymers containing p-methoxyphenacyl side groups. The block copolymer are composed of a poly(*p*-methoxypenacyl methacrylate) (PMPMA) block bearing photocleavable side-groups and a poly(oligoetheyleneglycol methacrylate) block (PMPMA-*b*-POEGMA).

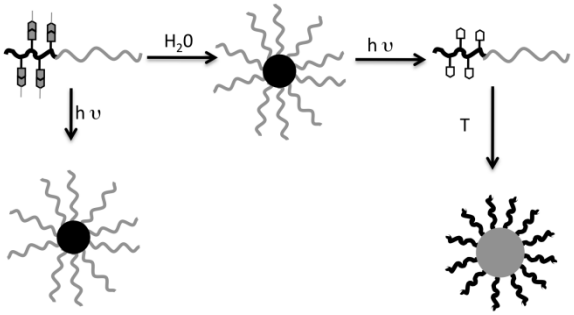

Figure 1 : Light induced formation and disription of micelles

[1] J-F. Gohy, *Adv. Polym. Sci.,* **2005**, 190, 65-136
[2] N. Rapoport, *Prog. Polym. Sci.,* **2007**, 32, 962-990
[3] J-M. Schumers, C-A. Fustin, J-F. Gohy, *Macromol. Rapid Commun.*, **2010**, 31, 1588-1607

Carbon Atom Volume as Indicator for Biodegradation Susceptibility in Highly Oxidized Species

Andrej Kržan, Janez Mavri

National Institute of Chemistry, Ljubljana Slovenia

andrej.krzan@ki.sI

Introduction

In general, biodegradation of organic substances occurs through oxidation or hydrolysis, however the oxidation level of the substrate is of great importance for the process since it defines the amount of energy a living organism can extract by aerobic digestion.

The oxidation level of the substrate can also be linked to the susceptibility of the substrate toward biodegradation: in inverse correlation to the energy content, un-oxidized hydrocarbons are less likely to biodegrade while more oxidized substrates are often good substrates for biodegradation. This empirical "rule" can be illustrated by polyethylene – a fully reduced hydrocarbon, which is not biodegradable (but can be made at least partially biodegradable by catalytic oxidation as in oxo-degradable technology), and the numerous natural polymers with medium oxidation levels: polysaccharides, proteins, polyesters, etc., which readily biodegrade. On the far end of this spectrum is the fully oxidized form of carbon - carbon dioxide, and it's unstable polymeric forms, which do not biodegrade due to their obvious lack of extractable energy content. These examples also points to a relation between stability and biodegradation: stable but reactive compounds of medium oxidative levels biodegrade best, while very stable or indeed very reactive species are not that likely to biodegrade.

In our earlier work we showed a stability/ biodegradability correlation.[1] We now quantified these observations through the analysis of carbon atom electronic structure[2] in a series of esters and related structures (Table 1) that were examined by the use of the Atoms in Molecules (AIM) quantum theory. This allows to divide the molecular physical space and electron density and assign them to individual atoms.[3] Through this method atomic charge and atomic volume can be derived directly from electron density.

Table 1. Structures studied. Formula: X-C(=Z)-Y

Compound /abrev.	X	Y	Z
Formic acid /fa	H	OH	O
Acetic acid /aa	CH_3	OH	O
Glycolic acid /ga	CH_2OH	OH	O
Oxalic acid /oa	COOH	OH	O
Urea /u	NH_2	NH_2	O
Thiourea /tu	NH_2	NH_2	S
Isobutene /ib	CH_3	CH_3	CH_2
Carbonic acid /ca	OH	OH	O
ca trimer /ca3	OCOOH	OCOOH	O
ca decamer /ca10	$O(COO)_4H$	$O(COO)_5H$	O
caNN	OH	OH	NH
caSS	OH	OH	S
caN	NH_2	OH	O
caS	SH	OH	O

Computational

All structures were geometry optimized in the Gaussian 2003 suite of programs. *Ab-initio* quantum chemical calculations were performed using the Hartree-Fock method in conjunction with the 6-31G(d) basis set. For some species, the calculations were also performed at the MP2/6-31++G(d,p) level. Wavefunction coefficients obtained from these calculations were then used as the input for AIM analysis performed using the AIMPAC software.

Results and Discussion:

AIM analysis of the examined structures surprisingly showed very little variation in the bond critical point (BCP, position on the bond path where neighboring atomic basins meet) position as well as the charges of atoms bound to the central carbon atom.

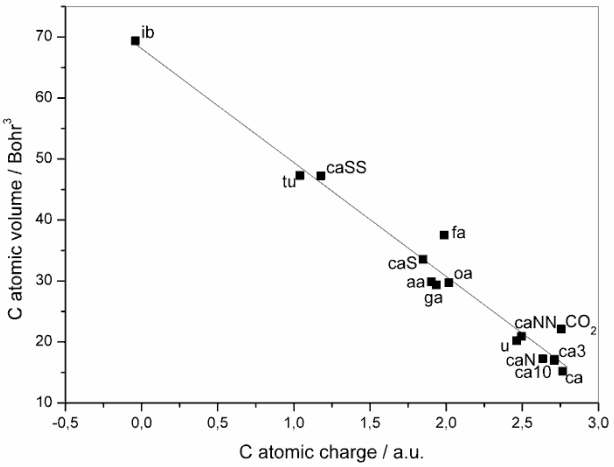

Figure 1. Carbon atom charge and volume obtained by Atoms in Molecules (AIM) quantum theory.

On the other hand the atomic charge and volume of the central carbon atom underwent a significant change and followed the electronegativity of its neighboring atoms and groups. High electron depletion due to electronegative neighbors is associated with small atomic volumes and unstable (unreal) structures, whereas medium depletion results in charge separation associated with reactive real molecules. The correlation is valid throughout the range from carbonic acid (ca) to isobutene (ib). Compounds in which carbon volume is below 18 bohr^3 appear to be unstable under normal conditions. Our approach is practical from the computational point of view since expensive calculation of the transition states associated with several mechanisms is avoided. The proposed application of the AIM approach is useful for design of novel biodegradable polymers.

Conclusions:

AIM calculated atomic volume of the central carbon atom is a sensitive descriptor for the electronic strain of oxidized carbons, which can be correlated to susceptibility towards biodegradation.

References:

[1] Kržan, A.; J. Mol. Struct.(THEOCHEM)2009, 902, 49.
[2] Kržan, A., Mavri J.; J. Org. Chem 2011,
[3] Bader, R. F. W.; Chem. Rev. 1991, 91, 893.

Design of complex polymersomes structures and "one pot" loading of hydrophilic model drug using simple co-flow microfluidic chip

Perro A.[2], Nicolet C.[2], Angly J.[2], Colin A.[2], Lecommandoux S[1], Le Meins JF[1]

[1] Université de Bordeaux, ENSCBP, 16 avenue Pey Berland, 33607 Pessac Cedex, France
CNRS Laboratoire de Chimie des Polymères Organiques, (UMR CNRS 5629), Pessac Cedex,
[2] Rhodia Laboratoire du Futur, Unité mixte Rhodia-CNRS, Université Bordeaux I, Bordeaux, France

e-mail: lemeins@enscbp.fr

Introduction In the field of drug delivery, block copolymers are widely investigated because of their ability to form complex morphologies able to encapsulate drugs and release them in controlled way: micelles, nanoparticles,[1] and more recently polymersomes.[2] Considering the loading of hydrophilic compounds different approaches have been developed: direct dissolution, film rehydration or electroformation are mainly used but the encapsulation efficiency is low and purification procedures are systematically required. Recently, microfluidic ships have been used to create giant polymersomes and to encapsulate compounds using co-flow and flow focusing geometries.[3,4,5] We propose here a simple approach based on a co-flow geometry,in which polymersomes containing model hydrophilic molecules in a "one pot" process are elaborated *via* a double emulsion, controlled in the chip.[6]

Results.The chip proposed, (illustrated in Figure 1), thanks to the relative simplicity of the flow inside the capillaries allows a good control of the double emulsion (size of internal and external drop, number of water drop inside one organic drop...) Globally the morphology of the double emulsion can be predicted, knowing interfacial tensions (water/solvent –solvent/water) and the flow rates Q_1,Q_2,Q_3.

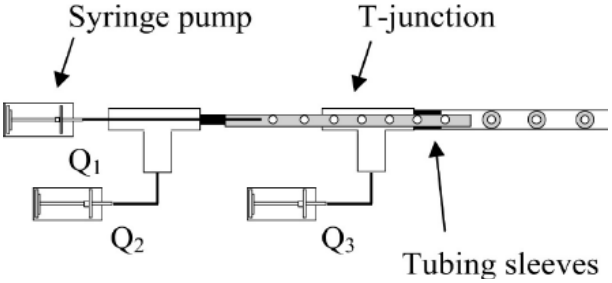

Figure 1:Picture of the device for the generation of double emulsion. Q_1 andQ_3: aqueous phases. Q_2: organic phase

The amphiphilic block copolymers stabilize the water/solvent interface (Figure 2), allowing the formation of polymersomes whose membrane consists of one or more bilayers of block copolymers after solvent evaporation.

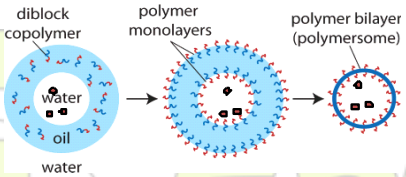

Figure 2: Solvent evaporation leading to the formation of polymersomes

Material and methods We have essentially worked on polybutadiene-block-poly(ethylene-oxide) solubilized in chloroform/cyclohexane mixtures and used an hydrophilic fluorescent probe (Fluorescein) as a model drug to evaluate the encapsulation efficiency of the process. In some cases Nile red has been solubilized in organic phase for better visualization.

Results and discussion We have obtained a good relationship between the morphologies of the resulting polymersomes and those of the double emulsion inside the microfluidic chip as illustrated in Figure 3.

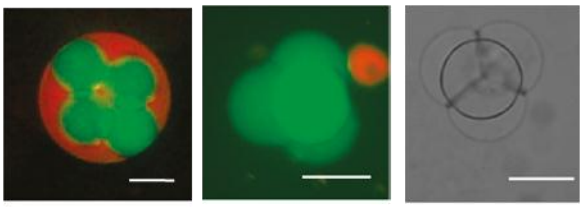

Figure 3: Multiple emulsion (four internal aqueous droplets) leading to tetrahedral polymersomes. (White bar=100µm)

Interestingly, the final size of the polymersomes corresponds to the size of the internal aqueous droplets, showing that the double emulsion created by the microfluidic device can be considered as atemplate for the microstructures obtained.In addition, Fluorescein used as a model drug in this study remains in majority in the aqueous internal compartment. Depending on the solvent mixture used, a "one pot" encapsulation can be reached with absolutely no leakage of the hydrophilic drug thus eliminating eventual purification steps.

Conclusion Using very simple microfluidic capillary device, we are able to prepare in a "one pot" process giant complex polymersomes structures in which model hydrophilic compound are encapsulated. This method is not only very interesting for application areas such as controlled release of drugs, but can be also considered for the construction of synthetic biomimetic structures, such as a cell or virus.

References

1. Bromberg, L. *J. Cont. Rel.* 128 (2), 99-112 (2008)
2. Discher et al. Prog. Pol. Sci.,32, 8-9, 838-857 (2007)
3. Ho Cheung Shum, et al. JACS 130 (29), 9543-9549 (2008)
4. Hayward, R.C., et al. Langmuir 22 (10), 4457-4461 (2006)
5. Thiele J. et al. Langmuir, 26 (9) 6860-6863 (2010)
6. Perro A. et al. Langmuir (2011) DOI: 10.1021/la1037102

Click Chemistry to Fluorescent Hyperbranched Polymeric Sensors: Synthesis and Characterization

S. Medel, V. Abenza, P. Ramírez-López, M.C. de la Torre, C. Peinado, P. Bosch

Instituto de Ciencia y Tecnología de Polímeros (ICTP), CSIC

s.medel@ictp.csic.es

Introduction

Multifunctional sensors have exceptional sensitivity and specificity for analytes detection. A way to obtain them is functionalizing dendrimers[1], but this method has disadvantages, because precursors are expensive and only few different structures are available.

Hyperbranched polymers (HBP) are a special type of dendritic polymers that have attracted major attention because of their interesting properties resulting from the branched architecture as well as the high number of functional groups.[2] Many different structures are currently commercialized, being them much more available than dendrimers.

Cu-catalysed Huisgen 1,3-dipolar cycloaddition ("click reaction") between terminal alkynes and organic azides has recently been extensively used and found wide applications in polymer and materials science because of its high efficiency, versatility and excellent functional-group compatibility.[3]

In this work we present the functionalization of HBP through click chemistry for the fluorescent labeling of azide-functionalized hyperbranched polymers.

Materials and Methods

Hyperbranched polymers, Hybrane®, were kindly provided by DSM. All the other materials were from Aldrich and used as received. The polymers were characterized through conventional methods (^{1}H NMR and ^{13}C NMR, FTIR-ATR, SEC, UV-Vis spectroscopy and Fluorescence spectroscopy).

Results and Discussion

In our approach, we locate azide group onto the HBP skeleton and the alkyne function on the selected fluorophore. Azide-terminated polymers were preferred to those incorporating terminal alkynes.[4] Fluorophores like dansyl chloride, 9-chloroacridine and naphthalimide were chosen to prepare the fluorescent polymers. Scheme I describes the reactions of HBP and fluorophore functionalization. Final structure of the multifunctional HBP-sensors is illustrated in Scheme II.

The behaviour of the multifunctional HBP-sensors was studied by fluorescence response measurements towards both changes in polarity and addition of a strong organic acid. The fluorescence emissions of the different polymers were strongly affected by solvent polarity and they also showed fluorescent changes upon addition of protons.

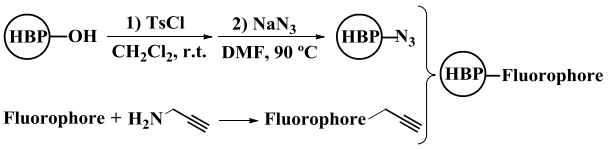

Scheme I. Reactions of HBP and fluorophore functionalization.

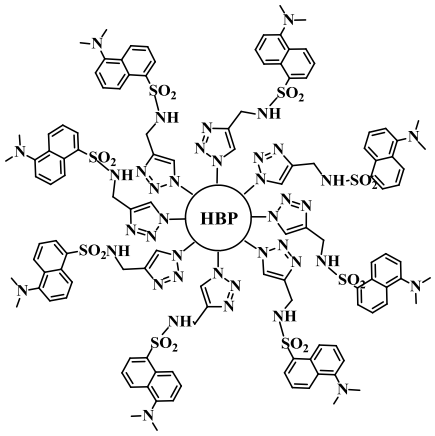

Scheme II. Ideal structure of dansylated HBP-fluorescent multifunctional sensors.

Conclusions

A new series of fluorescent hyperbranched polymers have successfully been prepared by "click chemistry", introducing different fluorophores into the side-chain of HBP.

In addition, the fluorescence properties of these compounds appeared to be highly sensitive to the polarity and the pH.

Acknowledgements

This work was financially supported by the Spanish Science and Innovation Ministry (MAT2009_09671).

References

[1] Villavieja M.M., **2007**. Thesis, (PhD). University UCM of Madrid, carried out at the Applied Photochemistry Group, ICTP, CSIC.

[2] *Chem. Rev.* **2009,** *109*, 5924–5973.

[3] *Eur. J. Org. Chem.* **2010,** 2395-2405.

[4] *Macromolecules* **2006**, 39, 2113-2120.

Solid State Properties of Fluorinated Polyimides Containing Perylene and Oxadiazole Moieties

Mariana-Dana Damaceanu, Radu-Dan Rusu, Maria Bruma

"Petru Poni" Institute of Macromolecular Chemistry, Aleea Grigore Ghica Voda 41A, Iasi-700487, Romania

e-mail: damaceanu@icmpp.ro

Introduction

The increasing demand of advanced technologies for new materials offering high thermal, chemical and mechanical resistance and other special properties as electron-transporting ability, electroluminescence, optical and electrical conductivity stimulates the growing interest in aromatic polymers containing heterocyclic units [1,2]. The inclusion of imide rings together with other electron-rich rings, such as perylene, and with electron-withdrawing units, such as 1,3,4-oxadiazole, could be a good way to obtain polymers having a desired balance of properties [3]. However, the practical application of polyperyleneimides is very difficult due to their insolubility and lack of processability. In order to improve the solubility of perylene-containing polyimides, novel copolymers have been designed and synthesized by introducing flexible hexafluoroisopropylidene groups in the main chain. These polyimides based on aromatic diamines containing oxadiazole rings and a mixture of perylenetetracarboxylic dianhydride and hexafluoroisopropylidene-diphthalic dianhydride, dissolved in polar amidic solvents and gave flexible films, by casting their solutions onto glass plates. Here we present a study of these films by dynamo mechanical analysis (DMA), dielectric and X-ray photoelectron spectroscopy (XPS).

Materials and methods

Copolyimides **I**, **II** and **III** were prepared by one-step polycondensation reaction of three different aromatic diamines containing oxadiazole ring with a mixture of perylenetetracarboxylic dianhydride and 4,4'-hexafluoroisopropylidene-diphthalic dianhydride taken in various molar ratios (scheme below).

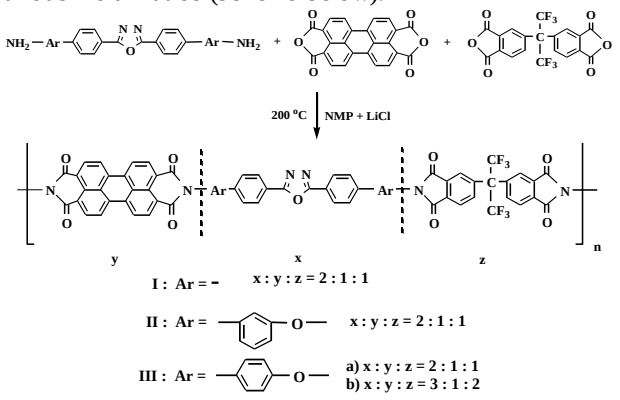

The reactions were carried out in NMP with 3.5% LiCl, at a concentration of 7% total solids, under nitrogen stream, at high temperatures (200-210°C). For comparison, a related copolyimide, **IV**, based on 4,4'-oxydianiline and a mixture 1:1 of the same dianhydrides was synthesized. All these polymers possess film forming ability. The free-standing films having a thickness in the range of tens of micrometers were flexible, tough, and maintained their integrity after repeated bending, except for films prepared from polymer **IIIa**, which were brittle. The properties of these copolyimides such as solubility, thermal stability, glass transition, composition of the films, dielectric behaviour and subglass relaxations were investigated.

Results and discussion

The synthesized copoly(peryleneimide)s are soluble in a convenient aprotic amidic solvent which is NMP, at a concentration of 0.5-1%. The polymers are highly thermostable, with initial decomposition temperature being in the range of 465-475°C. The glass transition temperatures as evaluated by DMA using thin films, are above 300°C. The chemistry of the films was analyzed by XPS. The survey spectra for fluoropolymers **I-III** are dominated by C, O, N and F, with some minor components (Si, Cl, Li). Complex chemistry was observed in each film, and variations between the film samples were clear. It is likely that solvent, silicone and hydrocarbon contaminants are present, and perhaps water. Electrical insulating properties of the polymer films were evaluated on the basis of the dielectric constant, ε' and dielectric loss, ε'' and their variation with frequency and temperature. Figures below present the dependence of the real (a) and imaginary (b) part of the complex permittivity, on frequency, at low, moderate and high temperatures. The sub-glass relaxations taking place in the polymer films were studied, as well.

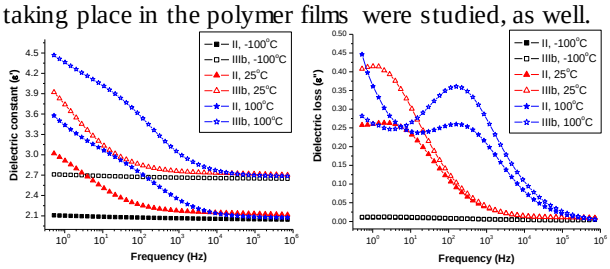

Conclusions

Thermostable polyimides containing oxadiazole and perylene units were prepared and thin films having a complex chemistry were made therefrom. The dielectric constant varies with frequency and temperature, taking low values even at high temperatures. The films displayed γ and δ relaxation processes connected with local movements of polymer chains.

Acknowledgements

The financial support provided by CNCSIS-UEFISCDI through the Project PN II-RU, code TE_221, no. 31/2010 is acknowledged with great pleasure.

References

1. Schmidt-Mende, L.; Fechtenkotter, A.; Müllen, K.; Moons, E.; Friend, R. H.; MacKenzie, J. D., *Science* **2000**, *293*, 1119–1122.

2. Liu, Y. J.; Zhuang, P.; Liu, H.; Li, Y.; Lu, F.; Gan, H.; Jiu, T.; Wang, N.; He, X.; Zhu, D., *ChemPhysChem.* **2004**, *5*, 1210–1215.

3. Rusu, R. D.; Damaceanu, M. D.; Marin, L.; Bruma, M., *J. Polym. Sci., Part A: Polym. Chem.* **2010**, 48, 4230–4242.

Characterization, Melting and Crystalline Properties of Isotactic (4,2)-Enchained Poly(1-Butene)

Carolina Ruiz-Orta, Rufina G. Alamo

FAMU-FSU College of Engineering, Chemical and Biomedical Engineering Department, 2525 Pottsdamer St., Tallahassee, FL 32310

Alamo@eng.fsu.edu, Carolina@eng.fsu.edu

Introduction. The availability of new crystalline polyolefins by control of catalyst "chain-walking" offers the opportunity to study crystalline properties of new polymer structures similar to the most common polyolefin commodities. Living polymerization of 1-butene with an α-diimine Ni(II) catalyst generates new crystalline polybutenes with unique chain microstructures.[1] A normal (1,2) insertion followed by a subsequent chain-walking to the fourth carbon results in a (4,2) addition. Conversely, a regio (2,1) inversion followed by chain-walking produces (4,1) linkages leading to a sequence of four consecutive methylenes in the backbone chain. In addition, when high selectivity for (4,2)-enchainment is exhibited a (4,2)-enchained poly(1-butene) is obtained. This polybutene is isostructural with poly(*trans*-2-butene). In this work we study crystalline properties of the novel polybutenes with a similar content of (4,2) and (4,1) additions and different content of stereo defects.

Materials and Methods. The molecular characteristics of the two polybutene samples studied are as follows. From ^{13}C NMR, (4,2) additions (~96 mol%), stereo errors (9 or 16 mol%); (4,1) additions (~ 4 mol%), and zero (1,2) additions in both samples. The combined (4,2) and stereo defects are 12, (4,2PB12) and 21 mol% (4,2PB21) for the most and the least crystalline samples studied. From GPC, Mw = 54,000 Dalton, Mw/Mn = 1.5.

The melting peaks, T_m, heat of fusion, ΔH, and overall crystallization kinetics were followed by DSC (Perkin Elmer DSC7). Wide and small angle x-ray diffractograms (SAXS, WAXD) were obtained at ambient temperature on samples that were previously isothermally crystallized either in the DSC or in thermostated baths. The degree of crystallinity derived by WAXD, X_c, was determined from the x-ray powder diffraction profiles of samples isothermally crystallized at different temperatures, T_c. The WAXS pattern of molten 4,2PB was used as amorphous halo. Crystal and interlamellar thicknesses were obtained from SAXS profiles via one-dimensional correlation function analysis. Spherulitic morphology and linear growth rates were analyzed by polarized optical microscopy and a Linkam hot stage, and lamellar morphology by AFM in non-contact AC mode. The densities were measured at room temperature in a water/isopropanol density gradient column calibrated with standards glass floats.

Results and Discussion. *Crystalline Structure*. In spite of a relatively low tacticity (mm <0.8), and a significant content of (4,1) defects, WAXD patterns exhibit two relatively sharp crystallographic reflections at 2θ = 16.9 and 19.7 degrees, consistent with high order chain-packing symmetry. Unlike *i*PP and poly(1-butene) that display polymorphism with increasing stereo defects or increasing crystallization temperature, the crystallographic phase of 4,2PB is maintained with increasing T_c or defects. The WAXD-derived degree of crystallinity (X_c) is low (<30 %) in 4,2PB21, and exhibits a modest 37 to 52 % increase in a large T_c range in the sample with 12 mol% defects.

Under isothermal crystallization, 4,2PB12 develops relatively thick lamellar crystallites (~ 95 Å thick by AFM) that aggregate in highly ordered spherulites. This feature and the relatively high crystallinity content for a copolymer with a high content of structural defects suggests co-crystallization of the stereo defects, similarly to the inclusion of stereo defects in *i*PP crystallites. With increasing chain defects the structural irregularities break down the spherulitic and lamellar habits.

Thermodynamic Parameters. Degrees of crystallinity of isothermally crystallized specimens were combined with density measurements, heat of fusion, and lamellar thicknesses to estimate the densities of the crystalline and amorphous phases, ρ_c = 0.9494 g/cm^3 and ρ_a = 0.8698 g/cm^3, respectively, and the heat of fusion per mole of crystalline unit (ΔH° = 132.6 J/g). Accounting for a re-structuring of crystallites during melting, the crystallites thicknesses and melting temperatures were analyzed with the simplified Gibbs-Thompson equation to extract values of the equilibrium melting temperature and the basal surface free energy of the crystallites. The value of T_m° = 135 ± 4°C. The defects reduce the T_m° value of 4,2PB in reference to expectations for the defect free chain and values. At a 12 mol% defect level, the T_m° is similar to the value for form I of *i*poly(1- butene), and significantly lower than for *i*PP and *s*PP. However, the heat of fusion per mole of crystalline units (8670 J/mol) is similar to the values of *i*PP and *s*PP in spite of a larger repeat unit. From the Gibbs-Thompson relation, the interfacial free energy is σ_e = 77 erg/cm^2. This value is supported by a basically identical σ_e value obtained from an analysis of lamellar growth rates according to secondary nucleation theory. The σ_e value of 4,2PB is similar to values obtained for polyethylene and *i*PP homopolymers (~ 70 erg/cm^2), and lower than for *i*PP copolymers with about the same content of defects. This feature suggests a relatively flexible conformation that favours chain folding in the novel poly(butenes).

Conclusion. The thermodynamic and structural properties of 4,2PB synthesized with a α-diimine Ni(II) catalyst have been analyzed. Stereo and (4,1) regio are defects that hinder the crystallization, as given by the decreasing rates, decreased levels of crystallinity and lowered melting temperatures with increasing defect content.

Acknowledgment. We gratefully acknowledge G.W. Coates from Cornell University for synthesis, and the USA National Science Foundation for funding.

[1] J.M. Rose, A.E. Cherian, G.W. Coates. J. Am. Chem. Soc. 2006, 128, 4186-7.

SU8 – Carbon Nanotubes: Preparation, Characterization and Patterning

Marijana Mionić,[1] Richard Gaál,[1] László Forró,[1] Sébastien Jiguet,[2] Moshe Judelewicz[2] and Arnaud Magrez[1]

1) Ecole Polytechnique Fédérale de Lausanne (EPFL), Switzerland
2) Gersteltec SARL

arnaud.magrez@epfl.ch

Introduction: SU8 polymer consists of rigid epoxy oligomers allowing the micro-fabrication of structures with vertical walls and with high aspect ratio (>50). [1] Thanks to its photo-patterning abilities, SU8 is widely used in nano-engineering for MEMS, sensors, batteries, flat panel displays, fluidic and packaging applications.

However, SU8 is an insulating polymer and is brittle with high internal stress although it has high Young's modulus (Ey) as compared to other polymers.

Consequently, the synthesis of conducting SU8 composites with improved mechanical properties is highly demanded but remains very challenging.

Materials and Methods: Multiwalled carbon nanotubes (MWCNTs) were synthesized by CCVD of acetylene over Fe–Co catalyst supported by CaCO3.

Details of the supported catalyst preparation and MWCNTs synthesis procedure have been reported elsewhere [2, 3]. In brief, stoichiometric amount of metal salts corresponding to Fe2Co composition are dissolved in distilled water. CaCO3 and base are subsequently added inducing the precipitation of Fe and Co salts onto the CaCO3 support. The supported catalyst is subsequently dried by sublimation of water, and placed afterwards into a 80mm diameter CVD reactor for MWCNTs synthesis.

Composites precursors were prepared by first dispersing MWCNTs in gamma-butyrolactone (GBL). Long term stability is obtained by the addition of dispersing agent. SU8 powder is subsequently added to this mixture under vigorous stirring. The resulting solution with adjustable viscosity can be easily processed and patterned while polymerisation is can be achieved thermally or by photolithography.

Results and Discussion: Although we prepared successfully composites exhibiting exciting electrical and mechanical properties without surfactant [4,5], the appropriate use of surfactant results systematically in better CNTs distribution in the polymer matrix (figure 1). A percolating network of CNTs is formed above 0.2w% of CNTs at the end of the first step when GBL is fully evaporated. During crosslinking and polymerisation, composites shrink and the percolation threshold is reduced below 0.2w%. It has to be noted that the resistivity is reduced by 8 orders of magnitude as compared to pure SU8 with only 1w% of CNTs. This corroborates, together with SEM analysis (figure 1), the high quality of the CNTs produced in this project as well as the excellent dispersion of the CNTs within the polymer matrix by using surfactants.

Dip coating of glass substrates in the solution of composite precursor results in transparent coatings. Coatings can also be patterned by photolithography, screen or inkjet printing. Objects with complex structures can be easily produced. The mechanical and thermal properties of the composites are being characterized.

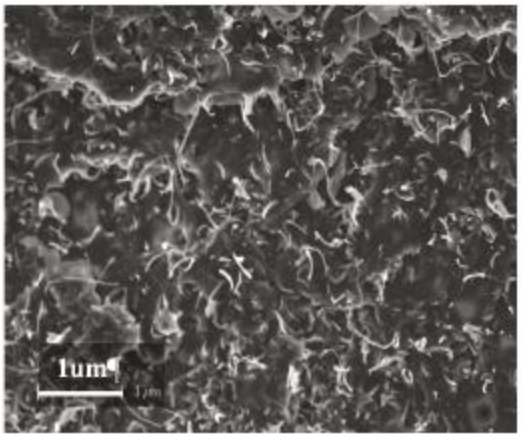

Figure 1: SEM analysis of analysis of the composites (3w%of CNTs after complete polymerisation) reveals a perfect dispersion of the carbon nanotubes in the SU8 matrix. Possible holes left by GBL evaporation are absent from the samples.

Conclusions: Here, we will present the synthesis,application and characterisation of conductive SU8-CNTs composites.

References:

[1] H. Lorenz, M. Despont, N. Fahrni, N. LaBianca, P. Renaud and P. Vettiger, Journal of Micromechanics and Microengineering 7, 121-124, **1997**

[2] A. Magrez, J.W. Seo, V.L. Kuznetsov and L. Forró, Angewandte Chemie International Edition 46, 441-444, **2007**

[3] A. Magrez, J.W. Seo, R. Smajda, B. Korbely, J.C. Andresen, M. Mionic, S. Casimirius and L. Forró, ACS Nano 4, 3702-3708, **2010**

[4] M. Mionić, S. jiguet, M. Judelewicz, L. Forró and A. Magrez, Physica Status Solidi B, 246, 2461-2464, **2009**

[5] M. Mionić, S. jiguet, M. Judelewicz, A. karimi, L. Forró and A. Magrez, Physica Status Solidi B, 247, 3072-3075, **2010**

Synthesis of highly soluble polymer-coated magnetic nanoparticles using a combination of diazonium salt chemistry and the iniferter method

Nébéwia Griffete, Aazdine Lamouri, Frédéric Herbst, Souad Ammar and Claire Mangeney

ITODYS, Université Paris Diderot (UMR 7086), 15 rue Jean de Baïf, 75013 Paris, France

griffetenebewia@hotmail.fr

Introduction

The grafting of polymer brushes from metal oxide nanoparticles via surface-initiated controlled radical polymerization has been the subject of intense research these last years[1].

One of the key steps for obtaining stable hybrid metal oxide cores/polymer shells nanostructures relies on the grafting of an appropriate coupling agent between the nanoparticle surface and the polymer coating. Although many coupling agents have been explored to this end, the anchoring groups of the chelate type often fail on metal oxide surfaces in aqueous or protic media due to the hydrolytic instability of the surface attachment and/or the dynamic nature of the interaction. Therefore, the development of versatile and efficient surface modification strategies for obtaining strong and stable linkages in aqueous media, between the metal oxide NP surface and the polymer coating still remains challenging.

Results and discussion

In this talk, we address this issue by proposing a novel and facile methodology for the *in-situ* surface functionalization of Fe_3O_4 nanoparticles, based on the use of diazonium salts chemistry as coupling agents. Such unique chemistry has never been extended to the spontaneous functionalization of metal oxyde nanoparticles, probably due to the poor reducing character of this type of material inhibiting the generation of aryl radicals able to bind to the NP surface. We circumvented this difficulty by taking advantage of the transformation of diazonium species to diazoates in basic media which dediazonize spontaneously to give aryl radicals able to bind to the iron oxide surface through highly stable covalent linkages.

These aryl grafted groups were then used as macro-initiators for the growing of pH-sensitive poly(methacrylic acid) polymer chains (PMAA) from the NPs surface, by the iniferter method. This strategy provided individually dispersed, highly soluble and pH-sensitive PMAA-coated magnetic nanoparticles.

IR spectra after each treatment steps were made : a very intense band is seen at *ca.* 1715 cm^{-1} due to the C=O stretching mode. This feature, characteristic of poly(methacrylic acid), indicates that the polymerization step has been effective.

XPS confirmed the efficiency of the grafting procedure as well as the living caracter of the polymerization process. The magnetic properties of the functionalized Fe_3O_4 nanoparticles were then examined. The saturation magnetization of surface functionalized Fe_3O_4 nanoparticles appeared significantly reduced compared to pure Fe_3O_4 nanoparticles.

The stability of the NP-PMAA colloids in water was checked qualitatively. Fig. b reveals that the pH strongly influences the dispersion with flocculated NPs in deionized water (pH 5.5) while they appear highly stable in basic medium (pH 8).

Conclusion

Our approach offers several advantages over conventional methods: (i) ease and rapidity of the diazonium-based coupling agent grafting at the NP surface; (ii) presence of a covalent bonding between the polymer and the NP surface; (iii) opportunities offered by the living character of the polymerization process. We believe this synthetic approach will not only pave an additional way for the preparation of water-soluble and pH-sensitive PMAA-coated Fe_3O_4 nanocrystals but also provide a new general functionalization strategy for magnetic nanoparticles.

a)

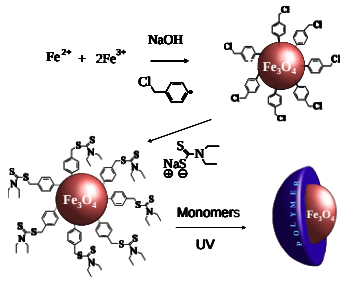

b)

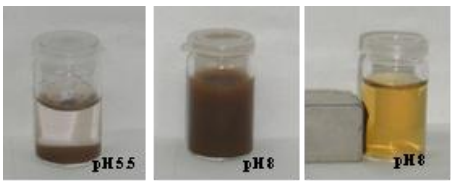

Figure: a) Surface functionalization strategy of Fe_3O_4 NPs; b) Numerical photographs of aqueous dispersions of NP-PMAA particles.

References

[1] R. Barbey, L. Lavanant, D. Paripovic, N. Schuwer, C. Sugnaux, S. Tugulu, and Harm-Anton Klok, ***Chem. Rev.***, 2009, 109, 5437; F. Hu, K. G. Neoh, L. Cen and E. Kang, *Biomacromolecules*, 2006, **7**, 809.

[2] N. Griffete, K. Chen, F. Herbst, J. Pinson, S. Ammar and Claire Mangeney, ***J. Am. Chem. Soc.***, 2011, ASAP

Monitoring the Swelling/Deswelling of Stimuli-Responsive Hydrogels with Magneto-Resistive Methods

Karl-Friedrich Arndt[a], *Ingolf Moench*[b], *Claudia Kaiser*[a], *Radinka Koseva*[b]

[a] Department of Chemistry and Food Chemistry, Physical Chemistry of Polymers, Technische Universität Dresden, Mommsenstr. 13, D-01062 Dresden, Germany

[b] Institute for Integrative Nanosciences, IFW Dresden, Helmholtzstrasse 20, D-01069 Dresden, Germany

karl-friedrich.arndt@chemie.tu-dresden.de

Introduction

Stimuli-responsive gels react on external stimuli with a drastic change of their degree of swelling. Such stimuli can be, e.g., temperature, pH, ionic strength, pH, salt concentration, composition of swelling agent. A unique feature of such hydrogels is that they serve as sensors and actuators at the same time. Therefore, responsive hydrogels are chemo-mechanical transducers converting chemical energy into mechanical energy and vice versa. A recent review on application of hydrogels as sensors and actuators is given in [1].

Magneto-resistive sensors have been proposed as detection components in biological devices such as biosensors and biochips. They directly provide an electrical signal that can evaluated with standard electronics. The change of a magnetic field can be followed by giant magneto-resistive (GMR) elements or sensors based on the Hall-effect.

Planar Hall sensors were applied in detection of magnetic micro-beads and nano-beads. Superpara-magnetic beads (diameter in µm-range) were coated with streptavidin and attached via bonding with biotin on a sensor-surface. The immobilization of the micro-beads on the sensor by biochemical interactions results in a change of the Hall voltage [2]. A biosensor plat-form combining on-chip integration of magnetic field generation with GMR sensors for magnetic label detection is described in [3]. Again, the signal is based on the immobilization of magnetic beads due to the high affinity between streptavidin and biotin. The magneto-resistive detection of magnetic particles by GMR sensor array is discussed on example of binding forces between magnetic micro-beads to a solid substrate [4].

A theoretical description of magnetic-hydrogel trans-duction principle based on GMR is given in [5].

Materials and Methods

The application of a stimuli-responsive hydrogel as a sensor layer in combination with a Hall-effect sensor was firstly demonstrated in our groups on example of monitoring the swelling/deswelling of a hydroxypropyl cellulose (HPC) foil decorated with magnetic particles [6]. The distance between magnetic particles and the Hall sensor depends on the degree of swelling. The Hall voltage measures the degree of swelling and therefore the properties of the liquid environment.

Now, we demonstrate the application of the GMR-effect as a transduction principle in hydrogel-based sensors.

Magnetic particles are fixed in a sensitive hydrogel. The measuring signals represent the response of the sensor signals to a relative change of the thickness of the filled hydrogel. The thickness is proportional to the degree of swelling, which depends, e.g., on an analyte concen-tration (composition sensitive hydrogel), or pH (polyelectrolyte gel).

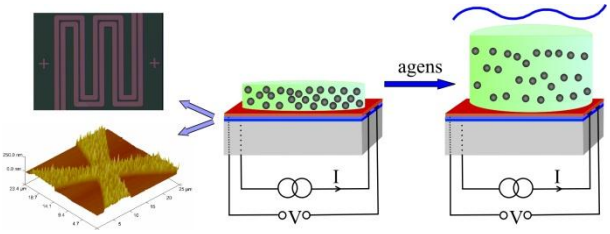

Fig. 1: Scheme of hydrogel-based magneto-resistive senor (left: GMR-meander and planar Hall sensor)

Results and Discussions

The presented paper describes our design of a magneto-resistive device based on a GMR platform (Figure1). GMR and a responsive polymer are coupled in different geometries (planar, tube, reaction vessel). The used stimuli-sensitive polymers (cross-linked HPC and PNIPAAm) are filled with different magnetic particles. The functionality of the designs is demonstrated on different tasks: Following the swelling/deswelling curve (Figure 2), monitoring the change of an analyte concentration, and counting of gel containers in a flow stream. On example of the used test arrangements the main properties of a GMR-based sensor are discussed, even in comparison with the Hall-based principle.

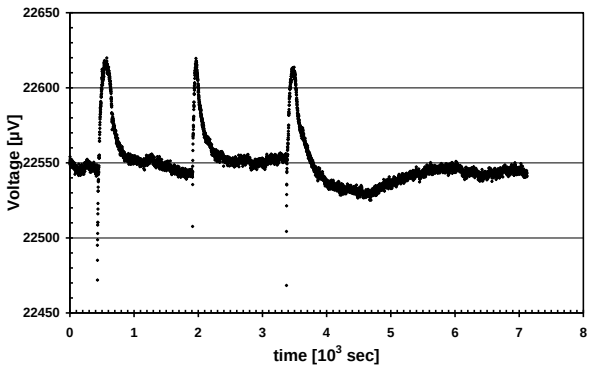

Fig 2: Swelling of HPC in water (298K); deswelling in air

The work was financed by DFG (Ar 193/11-2; Mo 887/1-2).

References

[1] Hydrogel sensors and actuators, ed. G. Gerlach, K.-F. Arndt, Springer series on chemical sensors and actuators, Springer-Verlag Heidelberg 2009.

[2] A. Lapicki, H. Sanbonsugi, T. Yamamura, N. Matsushita, M. Abe, H. Narimatsu, H. Handa, A. Sandhu, IEEE Trans. on Magnetics 41 (2005) 4134-4136.

[3] B.M. Boer, J.A.H.M. Kahlmann, T.P.G.H. Jansen, H. Duric, J. Venn, Biosens.& Bioelec. 22 (2007), 2366-2370

[4] D.R. Baselt, G.U. Lee, M. Natesan, S.W. Metzger, P.E.Sheehan, R.J. Colton, Biosens. & Bioelec. 13 (1998),731-739.

[5] M.P.B. van Bruggen, J.B.A. van Zoon, Sensors Act. A. 2010 (158), 240-248.

[6] R. Koseva, I. Mönch, J. Schumann, K.-F. Arndt, O. G. Schmidt, Thin Solid Films (2010), 518(17), 4847-4851.

Synthesis of Microcapsules via Reactive Surfactants

*Florence Gayet,[1] Adam Limer,[1] Nicole Jagielski,[1] Alex Heming,[2] Ian Shirley[2] and David M. Haddleton[1]**

[1]Department of Chemistry, University of Warwick, Coventry CV4 7AL, United Kingdom; [2]Syngenta, Jealotts Hill Research Station, Bracknell, RG42 6EY, United Kingdom

d.m.haddleton@warwick.ac.uk

Introduction:

Controlled/''living''radical polymerisation techniques (C/LRP) enables the synthesis of many polymers using ATRP or similar methods.[1] By combining hydrophobic and hydrophilic moieties[2] amphiphilic block copolymers can be obtained. Those bearing polymerisable functionalities can be used as reactive surfactants in emulsion, dispersion and suspension techniques to obtain particles.[3] In this study, we present the synthesis of well-defined ionic and non-ionic amphiphilic block copolymers of P(MMA/HEMA)-*b*-PDMAEMA and PEG-*b*-P(MMA/HEMA) synthesised via ATRP, further modified to active surfactants in order to prepare core-shell microcapsules using soap-free emulsion polymerisation.

Materials and methods

Methyl methacrylate and butyl methacrylate were purified by passing through activated basic alumina prior to use. 2-(Dimethylamino)ethyl methacrylate, 2-hydroxyethyl methacrylate and toluene were degassed for 30 minutes prior to use. The ethyl-2-bromo isobutyrate (EBIB) was used as supplied. *N*-Propyl and *N*-octyl-2-pyridylmethanimine (PrMI, OcMI)[4] and the poly(ethylene glycol methyl ether) macroinitiators[5] were prepared as described previously. All reactions were carried out with standard Schlenk techniques under a dry nitrogen atmosphere using Cu(I)Br and all Schlenk solutions were degassed by three freeze-pump-thaw cycles. Molar mass distributions were measured using size exclusion chromatography (SEC) with differential refractive index detection on two PL-gel 5 µm mixed C columns and a PL-gel 5 µm guard column used with THF/TEA (95:5, vol/vol) at 1.0 mL/min as the eluent. NMR data were obtained on a Bruker DPX400 and cryogenic scanning electron microscopy was performed on ZEISS SUPRA 55-VP equipped with cold stage and sample preparation chamber.

Results and discussion

Copolymers with various amount of MMA and HEMA were synthesised at 75°C in toluene using EBIB and methoxy poly(ethylene) glycol (PEG, D_p113) as initiators. All polymers were targeted to have a low DP (~20). For all polymerisations M_n increased linearly with conversion and PDi remained low, 1.17 to 1.26 and from 1.20 to 1.23 (for the EBIB and the PEG initiated block copolymers) as expected for a LRP process. The statistical copolymers synthesised from EBIB were further used as macroinitiators in the synthesis of amphiphilic block copolymers P(MMA/HEMA)-*b*-PDMAEMA. All reactions were conducted at 100°C in toluene with a target DP ~ 50. All SEC chromatograms showed a monomodal peak and narrow PDi indicating the amphiphilic copolymers were obtained in controlled manner (Fig 1). Target degrees of quaternization (10, 25 and 50%) were readily achieved by adjusting the molar ratio of methyl iodide to PDMAEMA and integration from ^{1}H NMR analysis confirm degrees of 13.8%, 28.4% and 47.7% leading to ionic amphiphilic polymers. These ionic diblock copolymers (P(MMA/HEMA)-*b*-PDMAEMA) where then transformed into ionic surfmers reacting the hydroxyl group of HEMA part with methacrylic anhydride.

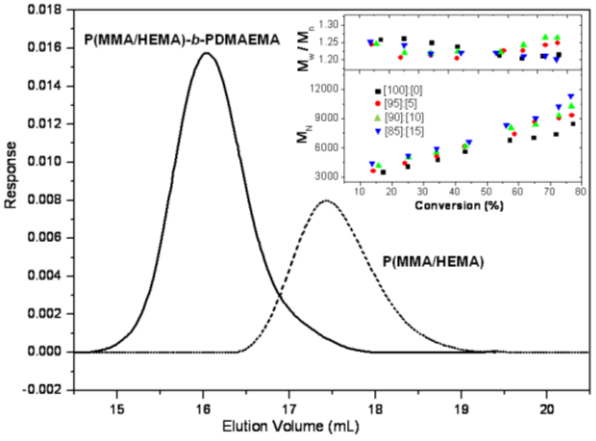

Figure 1: SEC traces of P(MMA/HEMA) macroinitiator and P(MMA/HEMA)-*b*-PDMAEMA diblock and evolution of M_n and M_w/M_n with time for the polymerisation of DMAEMA with various P(MMA/HEMA) macroinitiators.

Polymeric BMA microparticles were synthesised using ionic surfmers (25% quaternized) via emulsion polymerisation in which hexadecane was encapsulated. Up to 33% of hexadecane could be incorporate to the oil phase to obtain colloidal stable systems. Cryo-scanning electron microscope confirmed the core-shell morphology of the particles and differentiated between shell and core material.

Conclusions and References

A range of well defined ionic and non-ionic block copolymers were used as active surfactants to prepare particles with soap-free emulsion polymerisation technique.

1- J. S. Wang and K. Matyjaszewski, J. Am. Chem. Soc., 1995, 117, 5614-5615.

2- H. Kukula, H. Schlaad, M. Antonietti and S. Forster, J. Am. Chem. Soc., 2002, 124, 1658-1663.

3- F. Stoffelbach, K. Matyjaszewski and B. Charleux, Macromolecules, 2007, 40, 8813-8816.

4- D. M. Haddleton and A. J. Shooter, Macromolecules, 1999, 32, 2110-2119.

5- D. M. Haddleton, S. Perrier and S. A. F. Bon, Macromolecules, 2000, 33, 8246-8251.

Acknowledgements. The authors thank EPSRC and Syngenta for funding and Birmingham Science City (AWM/ERDF AM2 Project) for the GPC equipment.

Galina Gubanova[1], *Svetlana Kononova*[1], *Milana Vilegzhanina*[1], *Tatiana Sukhanova*[1], *Eleonora Korytkova*[2], *Daniel Timpu*[3], *Mariana Cristea*[3], *Valeria Harabagiu*[3]

[1] Institute of Macromolecular Compounds, St.-Petersburg, Russia
[2] Institute of Silicate Chemistry, St.-Petersburg, Russia
[3] "Petru Poni" Institute of Macromolecular Chemistry, Iasi, Romania

e-mail: gubanovagn@yandex.ru

Introduction: The development of nanocomposites based on polyamidoimides and nanotubes (NT) of different morphology and size is the perspective direction for obtaining new materials for the membrane application. In previous investigation it was shown that the introduction of inorganic tubular nanoparticles in to the matrix of poly(diphenyloxideamino-N-phenylphthalimide) leads to the formation of nanocomposite with improved mechanical properties permeable to a greater extent than the pure polymer in the process of pervaporation of polar liquids, in particular of water and alcohol [1]. In this paper the nonporous composite films based on aromatic polyamidoimides differing by the structure of diamine component, containing equal amount of silicate nanotubes $Mg_3Si_2O_5(OH)_4$ were obtained and their structure, morphology, thermal, transport properties were investigated.

Materials and Methods: The polyamidoimides as the matrices for nanocomposite were synthesized by the low-temperature polycondensation of dicarboxyphenyl-phtalimide dichloride with 4,4'-diaminodiphenyl ether (PAI-1,M 68000), or, 3,5-diaminobenzoic acid (PAI-2, M 57000) in solution [1]. As inorganic filler were used nanotubes $Mg_3Si_2O_5(OH)_4$ with chrysotile structure, synthesized under hydrothermal condition [1].

Results and Discussion: The transport properties both PAI-1, PAI-2 and their nanocomposites were tested at the pervaporation (Fig.1,2) in relation to a wide range of penetrating substances (water, methanol, cyclohexane, methyl-tert-butyl ether).

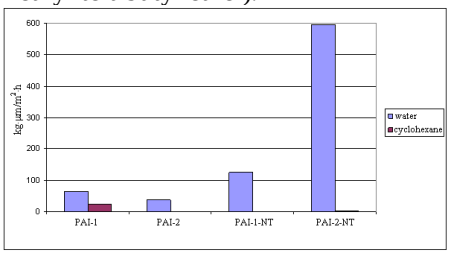

Fig.1 Separation of (a)methanol-methyl *tert*-butyl ether mixtureat 40°C;(b)methanol-water at 20°C on PAI1-NT

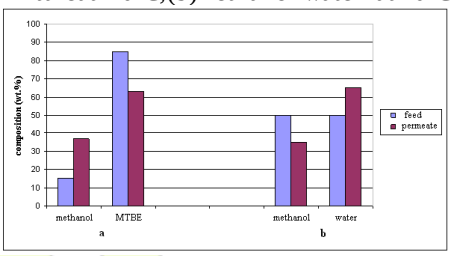

Fig.2 Permeability by water and cyclohexane of non-porous membranes PAI-1,PAI-2, PAI-1-NT, PAI-2-NT.

Polymer PAI-2 (more hydrophilic polymer than PAI-1) is twice more permeable by water than PAI-1, like in the case of PAI-1-NT compared to PAI-1. The introduction of nanotubes in the PAI-2 enhances the ability of the composite membrane to pass the water more than 4-fold, which makes the material 5-fold more permeable for water than PAI-1-NT.

Nanotubes were not found on both surfaces of nanocomposite films when content of NT in polymer matrix does not exceed 2wt%. The NT's fragment on the film surface can be recognized by AFM when the content of nanofillers attains 5wt% (Fig.3). In this case adhesion between Nts and PAI is broken (Fig.3b)

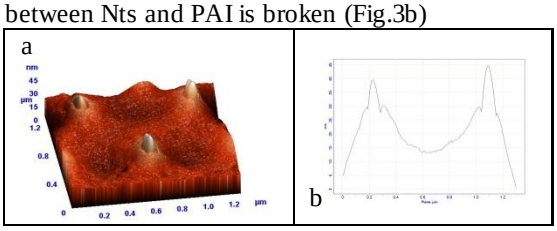

Fig.3. 3D image (a) and line profile (b) for composite PAI–NT-1 (5wt% of NT).

It was found by SEM and AFM that NTs combine into aggregates which regularly distributed in the inner layers of polymer. In the PAI-2-NT the aggregates are observed of 2-3 nanotubes whereas the number of NT's in agglomerate in PAI-1-NT increase up to 10-15.

Thermal properties of PAI-1, PAI-2 and their nanocompositis were also investigated. For the PAI-1-NTs composite, two steps of the mass loss have been registered. First step extends to 260°C, thus indicating a slower solvent evaporation as compared with the PAI-1. The second step related to the PAI-NT degradation is shifted to higher temperature, compared to pure PAI-1 (420°C and 360°C correspondingly).Thus, thermal stability of the PAI-1-NT composite increases in comparison with that for the PAI matrix.

Nt's introduction into polymer matrix leads to increasing of glass transition temperature for PAI-1-NT and PAI-2-NT in comparison with pure polymers.

Conclusions: New polymer-inorganic composites with improved thermalphisic properties (thermal stability and glass transition) are developed. Nanotubes in the composite form the aggregates in spite of the NT's content in polymer matrix. Dimension of aggregates is dependent from chemical structure of PAI.

Introduction into polymer matrix of $Mg_3Si_2O_5(OH)_4$ nanotubes leads to increase flow of water and lower aliphatic alcohols through the corresponding membrane film, which may be interest of practical application.

References:

[1] Kononova,S.V.,Korytkova, E.N., Romashkova,K.A. at al. Zh.Prikl.Khim., 2007,V.80, 12, p.2064

Study of Diffusion of Jeffamines into Reactive "Surface-attached" Polymer Networks

R. Navarro, M. Pérez Perrino, O. Prucker, J. Rühe

University of Freiburg – IMTEK. Department of Microsystems Engineering
Laboratory for Chemistry & Physics of Interfaces. Georges-Köhler-Allee 103 D-79110 Freiburg Germany
rodrigo.navarro-crespo@imtek.de

Introduction

The diffusion of linear polymer molecules into confined space scaffolds is an important topic of practical importance about which there is little fundamental understanding[1]. From a practical point of view, the study of the diffusion of macromolecules into the networks plays an important role if "surface-attached" networks or coatings are to be modified or functionalized. The diffusion of free polymer chains depends on the shape of the concentration profile at an interface between the incoming macromolecules and polymer network. In the present study the influence of copolymer composition regarding to PEGylation of these scaffolds has been studied. The penetration depth of free H_2N-PEGs into the reactive networks and the molecular weight dependence on the modification degree have also been determined.

Materials and Methods

A series of copolymers with "active ester" (AE) units and benzophenone (BP) moieties has been prepared. Their chemical structures were confirmed by conventional techniques, such as ^{1}H-NMR, ^{13}C-NMR, FTIR and GPC. The preparation of surface-attached networks was carried out by UV-light illumination of a thin polymer layer deposited on modified silicon wafer. The photocrosslinking reaction takes places by non-specific insertion of benzophenone units into C-H bonds. The modification reaction was carried out introducing PEG-NH_2 to these scaffolds using Et_3N as a catalytic agent. In this way the PEG chains were selectively grafted to reactive points (active esters moieties). The diffusion of H_2N-PEGs and the reactivity of these monomers are schematically shown in figure 1.

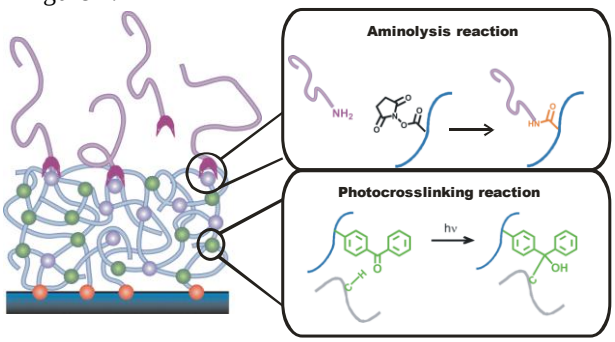

Figure 1: Schematic representations of diffusion of PEG-NH_2, aminolysis and photocrosslinking reaction.

In order to determine the degree of modification, the layer thickness has been measured by ellipsometry before and after PEGylation reaction. The modified polymeric networks were characterized by contact angle, XPS and SPR.

Results and Discussion

The functionalization of the surface-attached networks has been studied as a function of important reaction parameters, such as crosslinking density, reactive group content (AE content) and PEG-NH_2 molecular weight. Results are shown in figure 2.

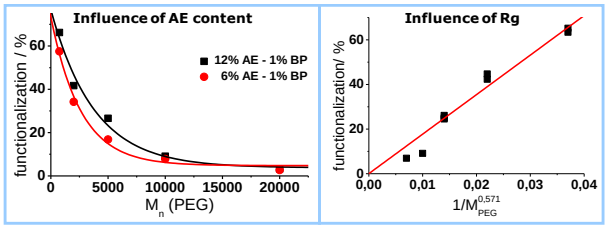

Figure 2: Variation of functionalization degree respect to Active ester (2a) and Radius of Gyration (2b).

The functionalization exponentially decreases from 65% for PEG750 to 5% for PEG20000, which indicates a strong influence of the molecular weight of free PEG chains. The penetration into the surface-attached networks depends on the radius of gyration (Rg) of the incoming macromolecules, which is according to the literature $Rg \sim M^{0.571}$ within the investigated molecular weight region[2]. This relation is clearly evident from the result plotted in figure 2b.

Under selective hydrolysis of most external AE units, the corresponding variation of funtionalization degree indicates that the PEG chains are able to diffuse into deeper layers and react with inner AE moieties. However under this reactive zone, there are still more reactive points, which are not accessible for free PEG-NH_2 (even for the lowest Mw) due to the shape of the concentration profile of surface-attached network and the *entropic shielding*. This entropic reason is related with the adopted conformation of these polymer networks during the modification reaction. Therefore, it was also possible to measure the depth of this interpenetration zone and our measurements estimate it to about 20 nm approximately.

Conclusions

The experiments described in this contribution show surface-attached polymer networks are systems that are barely penetrable for other large molecules. Typically functionalization degrees stay well below 10% if the Mw increases to as far thousand g/mol. These systems are therefore rather interesting candidates as layers to repel large molecules

References

[1] Murata H.; Prucker O.; Rühe J. Macromolecules, **2007**, *40* (15), 5497-5503.
[2] Lee, H.; de Vries, A.H.; Marrink, S.J.; Pastor, R., J. Phys. Chem. B **2009**, *113*, 13186-13194.

Fabrication of low density foam shells using TMPTMA aerogel by UV polymerization

Cecile Lattaud[1,2], *Lyonel Guillot*[1], *Claire-Hélène Brachais*[2], *Benoit Reneaume*[1], *Emmanuel Fleury*[1], *Olivier Legaie*[1], *Jean-Pierre Couvercelle*[2]

[1]Commissariat à l'Energie Atomique, Direction des Applications Militaires, Valduc, F-21120 Is-Sur-Tille, France
[2]Equipe SYMS (Systèmes Hybrides Multifonctionnels), Institut de Chimie Moléculaire de l'Université de Bourgogne (ICMUB) - UMR CNRS 5260, 9 avenue Alain Savary, BP 47870, 21078 Dijon cedex

cecilelattaud@gmail.com

Abstract :
Targets for fusion preparation on the French high power laser LMJ (Laser Mega Joule) require low density organic foam shells. These foam shells are composed of C, H and O, with a 2 mm diameter, 100 µm thickness and 250 mg.cm^{-3} density. The TMPTMA foam shells are synthesized by a microencapsulation technique giving a double emulsion water-in-oil-in-water. The foam shells have to fulfill severe specifications: diameter ranging from 1.7 to 2.3 mm, 100 µm thickness, 250 mg.cm^{-3} density, sphericity > 99.9% and non-concentricity < 1%. The diameter, density and thickness criteria are reached by using a droplet generator, whereas the shell shape (sphericity and non-concentricity) depends on several parameters of the process such as density, kinetics of polymerization, deformations of the shells, interfacial tensions and viscosity. The influence of the kinetics of polymerization upon the non-concentricity (NC) of the foam shells obtained is being studied here.

Introduction :
Water-in-oil-in-water (W/O/W) double emulsions are complex systems where a water droplet is entrapped within an oil droplet that in turn is dispersed in a continuous water phase [1]. Double emulsions can be produced using either a two steps drop break-up method with a mere succession of two T junctions [2], [3], or a single step process with parallel co-flowing streams [4], [5]. The monomer oil phase can later be polymerized either by a thermal or a UV process in order to fix the shell's shape (non concentricity and sphericity). In this work, a double emulsion W/O/W is obtained by using a droplet generator with parallel co-flowing streams. Once the shell's shape is set the organic phase is polymerized at 60°C with a thermal initiator. This process leads to a gelation time of 23 minutes. In the microfluidic area, the UV-polymerization is used to polymerized beads within a few minutes [4]-[7]. We thought that a faster polymerization kinetics may lead to better results of shells NC. Thus, a photo-polymerization process was investigated focusing on the effects of the incident light intensity and the amount of photo-initiator used on the shells NC.

Materials and Methods :
The external water phase of the double emulsion is a solution of 5% polyvinyl alcohol in water. The organic solution is composed of a monomer (trimethylolpropane trimethacrylate, TMPTMA), a mixture of two solvents (dibutyl phthalate and ethylbenzene), a surfactant (Span® 80) and a photo-initiator (2,2-dimethoxy-2-phenylacetophenone). The internal water phase solution is a mixture of water and deuterated water. The shells are produced by a microencapsulation technique using a triple orifice generator. The shells generated are then collected into an agitated horizontal flask. This flask is placed into a heated water bath at 60°C and under a nitrogen flow of 60 mL.min^{-1}. The shells are then photo-polymerized by illumination with a UV light (λ = 365 nm).

Results and discussion :
The UV-polymerization was performed with different amount of photo-initiator (5, 10 and 15%) and two incident light intensities. The results obtained are summarized in the table below.

incident light intensity (mW.cm^{-2})	% of photo-initiator	average NC (%)	% of shells with NC < 8 %
2	5	23	8
	10	21	9
	15	23	6
2,3	5	23	9
	10	17	29
	15	22	9

The best results of NC are obtained with 10% of photo-initiator for both incident light intensities. The highest light intensity seems to give better results of NC than the lowest light intensity.

Conclusion :
From the results of the experiments, we can conclude that the better results of NC are obtained with 10% of photo-initiator and a light intensity of 2.3 mW.cm^{-2}. However, these results of NC are really low compared to the results obtained with a thermal polymerization process (average NC: 98%). Thus, the UV- polymerization process still has to be improved to get results as good as with the thermal polymerization process.

References :
[1] F. Leal-Calderon, V. Schmitt, J. Bibette, "Emulsion Science: Basic Principles", Springer (2007).
[2] S. Okushima, T. Nisisako, T. Torii, T. Higushi, Langmuir. 20, 9905 (2004).
[3] P. PAnizza, W. Engl, C. Hany, R. Backov, Colloids Surfaces A. 312, 24 (2008).
[4] A. S. Utada, E. Lorenceau, D. R. Link, P. D. Kaplan, H. A. Stone, D. A. Weitz, Science. 308, 537 (2005).
[5] Z. Nie, S. Xu, M. Seo, P. C. Lewis, E. Kumacheva, J. Am. Chem. Soc. 127, 8058 (2005).
[6] S. Xu, Z. Nie, M. Seo, P. Lewis, E. Kumacheva, H. A. Stone, P. Garstecki, D. B. Weibel, I. Gitlin, G. M. Whitesides, Angew. Chem. Int. Ed. 44, 724 (2005).
[7] T. Nisisako, T. Torii, T. Higuchi, Chemical Engineering Journal. 101, 23 (2004).

Self-assembling of polyelectrolyte multilayers

Eduardo Guzmán[1], Raquel Chulia[1], Jesica Cavallo[2], Francisco Ortega[1], Ramón G. Rubio[1], Miriam Strumia[2], Cesar Gómez[2].
[1]Universidad Complutense de Madrid, Departamento de Química Física I, 28040-Madrid, Spain
[2] Universidad Nacional de Córdoba, Departamento de Química Orgánica, CP-5000 Córdoba, Argentina

After the seminal works of Decher and co-workers using polyelectrolytes with charges of opposite sign, [1, 2], the sequential electrostatic self-assembling of oppositely charged materials has attracted considerable attention as a simple and versatile method for constructing nanostructured materials. The reason of this interest is the existence of a large amount of promising applications in different fields as sensors, functional coatings, selective membranes and drug delivery [3]. Even though much has been advanced in the understanding or self-assembled multilayers of polyelectrolytes [4], less effort has been dedicated to the study of the adsorption kinetics, and to the desorption of drugs adsorbed within the multilayer.

In this work we have carried out a multi-technique experimental study of the adsorption kinetics of multilayers formed by Chitosan and Poly(acrylic acid) -PAA- as a function of the number of layers at different pH's, and of the same system including Propanolol. The main techniques used were a dissipative quartz microbalance (D-QCM) and ellipsometry. The combination of the results obtained using D-QCM and ellipsometry have allowed calculating the water content of the films as a function of number of layers [5].

The results show that the polymer adsorption is an almost irreversible process. In our studies, we have observed a very important effect of pH on the thickness and the water content of the films. The strongly non-linear dependence of the film thickness on the number of layers is due to the polymer diffusion within the film, which leads to high roughness and to a homogeneous chemical structure within the multilayer. The pH modifies the charge densities of the polymers, thus modifying their interactions and their mutual diffusion. Fig. 1 shows a set of representative results obtained by D-QCM. It can be observed that, in general, the addition of a chitosan layer leads to a lower increase on the thickness than the addition of a PAA layer. Additionally, the increase on the thickness of chitosan layers is almost the same for all the pH conditions studied, whereas the PAA layers changes very significantly. The thickness obtained by D-QCM for a given number of layers and for a pH is higher than that obtained by ellipsometry. This is a consequence of the fact that D-QCM is sensitive not only to the amount of polyelectrolyte adsorbed, but also to the water content of the multilayer.

In a second series of experiments, Propanolol, as a third component, has been adsorbed after each PAA layer. As expected the increase of thickness after each propanolol layer is much smaller than for each polymer layers. We have studied desorption kinetics studies in water using 22-layers films using the QCM technique, which point out that the desorption of Propanolol (remember that the adsorption of polymers is irreversible) lasts for at least six days, although some of the Propanolol remains adsorbed in the multilayer.

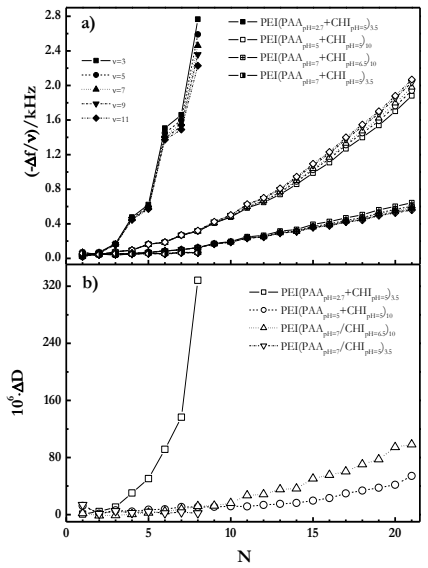

Fig.1 Multilayers PEI(PAA+CHI)$_n$ built using different pH combinations for the assembling of layers of PAA and CHI. (a) Number of layers dependence of the reduced frequency of the quartz crystal for the different overtones measured (b) Dissipation factor for the third overtone of the quartz crystal.

Acknowledgments:
This work was supported in part by MEC under grants FIS2009-14008-C02-01, and by EC Marie Curie ITN-MULTIFLOW.

References

[1] G. Decher, J.D. Hong, J. Schmitt. *Thin Solid Films*. **1992**, *210*, 831-835.
[2] G. Decher. *Science.* **1997**, *277*, 1232-1237
[3] X. Qiu, E. Donath, H. Möhwald. *Macromolecular Materials and Engineering* **2001**, *51*, 591-597
[4] *Multilayer Thin Films*, G. Decher, J.B. Schlenoff Eds. 2003
[5] E. Guzmán et al. Soft Matter **2009**, *5*, 2130-2142

Aggregation and Chain Dynamics in Supramolecular Polymers by Dynamic Rheology: Cluster Formation and Self-Aggregation

Florian Herbst, Klaus Schröter, Ilja Gunkel, Stefan Gröger, Thomas Thurn-Albrecht, Jochen Balbach and Wolfgang H. Binder

Martin-Luther-University Halle-Wittenberg – Institute of Chemistry and Institute of Physics

Wolfgang.Binder@chemie.uni-halle.de

Supramolecular polymers are of great interest in material science, since they exhibit remarkable properties including self-assembly and self-healing. The introduction of supramolecular motifs into the main-chain or at the chain-end of different polymers has been reviewed extensively, highlighting the wide scope of structural and dynamic features.[1]

Aim of this investigation was the synthesis of mono- and bivalent telechelic polyisobutylenes (PIBs) (**3-7**) bearing polar functional groups at their chain ends, which are capable to undergo self-assembly via hydrogen bonds. Melt rheology and SAXS measurements of the supramolecular polymers/mixtures were performed in order to become a deeper insight in the dynamics of the hydrogen bonds. Thereby the formation of clusters was observed.[2]

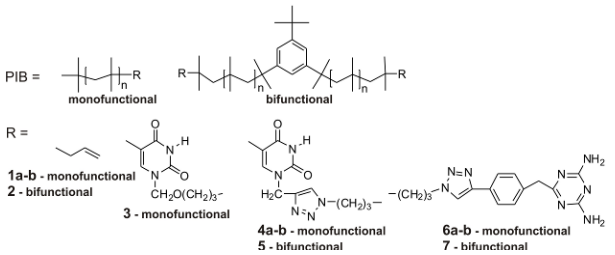

As used hydrogen bonding motif, the thymine/2,6-diaminotriazine interaction was applied. Since the mechanism of the living carbocationic polymerization of isobutylene does not permit the direct introduction of hydrogen bonding units, they were affixed onto the polyisobutylene chain via azide/alkyne "click"-reactions starting from azido-telechelic polyisobutylenes.[3] The resulting polymers were obtained in high purity and characterized by means of ^{1}H- and ^{13}C-NMR spectroscopy, as well as MALDI-TOF measurements, indicating completely telechelic PIB-polymers. Mixtures of the functionalized PIBs were made in order to achieve supramolecular A-B or $(\text{-A-B-})_n$ pseudo BCP's.[3] The dynamic-mechanical behavior of the resulting supramolecular blockcopolymers was investigated via bulk-rheology measurements (frequency sweep). It was shown that a equimolar mixture of monovalent thymine-telechelic PIB (**3**) and monovalent 2,6-diaminotriazine-telechelic PIB (**6a**) (both M_n ~ 3500 g/mol) exhibits a 40-times higher viscosity when compared to a non-functionalized PIB (**1a**) (allyl-telechlic species) with a similar molecular weight at room temperature. Furthermore, the supramolecular mixture shows strong temperature dependence in the range of 20 to 80 °C, explainable by the dynamics of the hydrogen bonds, due to a decrease of the virtual molecular weight.

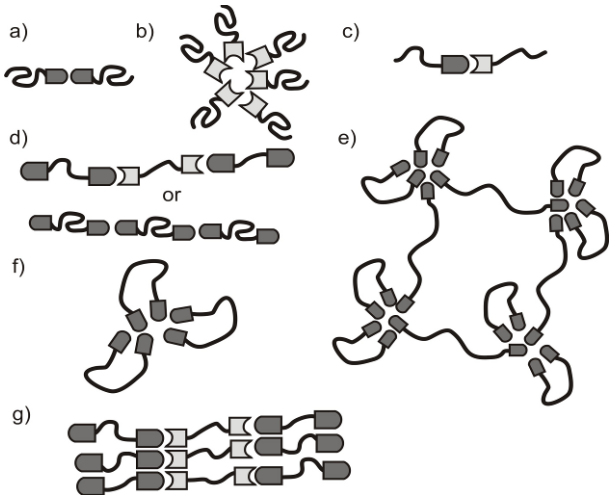

It is noteworthy that the pure functionalized PIBs (**3-7**) show a strong increase of the viscosity, indicating an undefined clustering of the functional groups, as confirmed by additional SAXS-measurements. Possible modes of clusters/aggregates are displayed above (**a-g**). Monofunctional PIBs with a higher molecular weight (10000 g/mol) were investigated revealing a similar behavior. While all monofunctional PIBs flow at small angular frequencies, their bifunctional analogues (**5, 7, 5+7**) were rubber-like materials. The observed plateau modulus (~10^7 Pa) was higher than reported for a linear high molecular weight PIB (~10^5), indicating a serious amount of supramolecular cross-links between the polymer chains (**e**). By increasing the temperature to 60 °C the materials (**5, 7, 5+7**) start to flow, indicating a cleavage of the supramolecular cross-links. All the materials completely recover their properties at 20 °C after being heated at 80 °C within 20 minutes even after repeated heating-cooling cycles. Therefore the bifunctional (rubber-like) samples can be treated as a low molecular weight polymer melt at high temperatures and used as a strong rubber at room temperature which also exhibits self-healing properties.

1. Binder, W.; Zirbs, R., *Adv. Polym. Sci.*, 2007; pp 1- 78.
2. Herbst, F.; Schröter, K.; Gunkel, I.; Gröger, S.; Thurn-Albrecht, T.; Balbach, J.; Binder, W. H., *Macromolecules* **2010,** *43* (23), 10006-10016.
3. (a) Binder, W. H.; Bernstorff, S.; Kluger, C.; Petraru, L.; Kunz, M., *Adv. Mater.* **2005,** *17* (23), 2824-2828; (b) Binder, W. H.; Kunz, M. J.; Ingolic, E., *J. Polym. Sci. A: Polym. Chem.* **2004,** *42* (1), 162-172; (c) Binder, W. H.; Kunz, M. J.; Kluger, C.; Hayn, G.; Saf, R., *Macromolecules* **2004,** *37* (5), 1749-1759; (d) Binder, W. H.; Machl, D., *J. Polym. Sci. A: Polym. Chem.* **2005,** *43* (1), 188-202.

Functionalized Nanoporous Materials from Photocleavable Block Copolymers

Jean-Marc Schumers, Alexandru Vlad, Charles-André Fustin, Jean-François Gohy.

Institute of Condensed Matter and Nanosciences (IMCN),
Université catholique de Louvain, Place L. Pasteur, 1, Louvain-la-Neuve, Belgium.

jean-marc.schumers@uclouvain.be

Block copolymers have become nowadays powerful tools for the preparation of nanostructured materials.[1-3] They are indeed able to self-assemble at the nanoscale into well-ordered structures that can be used, among other things, for the preparation of nanoporous materials by selectively removing the minor phase. These materials exhibit the pore topology and the pore size of their parent structures and can be further used as separation membranes or templates for other nanomaterials.[1-7]

Most methods reported up to now for the creation of nanopores rely on the degradation of the sacrificial minor block. This degradation is often performed under harsh conditions and offers thus a rather poor control over the chemical functionality inside the pores.

This presentation will present an alternative and milder strategy based on the introduction of a photocleavable junction ($h\nu$) between the blocks of a polystyrene-*block*-poly(ethylene oxide) diblock copolymer (PS-$h\nu$-PEO).[8]

This diblock was synthesized by a one-pot simoultaneous ATRP–CuAAC ‘‘click’’ reaction process.[9] After its synthesis, the diblock was self-assembled into thin films displaying perpendicular PEO cylinders in a PS matrix. The films were then irradiated with UV light in order to cleave the junctions between the blocks. The nanoporosity was then generated by a simple soaking of the film in a water/methalol mixture, enabling the selective removal of the PEO minor phase.

[1] I. W. Hamley, *Angew. Chem. Int. Ed.* **2003**, *42*, 1692.
[2] C. Park, J. Yoon, E. L. Thomas, *Polymer* **2003**, *44*, 6725.
[3] H. C. Kim, S. M. Park, W. D. Hinsberg, *Chem. Rev.* **2010**, *110*, 146.
[5] M. A. Hillmeyer, *Adv. Polym.* Sci. **2005**, *190*, 137.
[6] I. W. Hamley, *Prog. Polym. Sc.* **2009**, 34, 1161.
[7] J.Bang, U. Jeong, D. Y. Ryu, T. P. Russell, C. J. Hawker, *Adv. Mater.* **2009**, *21*, 4769.
[8] J.-M. Schumers, C.-A. Fustin, J.-F. Gohy, *Macromol. Rapid Commun.* **2010**, 31, 1588.
[9] J.-M. Schumers, J.-F. Gohy, C.-A. Fustin, *Polym.Chem.* **2010**, *1*, 161

Photostable polymer/clay nanocomposite encapsulant for organic solar cells

J. Gaume[1,2], S. Thérias[1,2], A. Rivaton[1,2], S. Cros[3], S. Guillerez[3], J.L. Gardette[1,2]

(1) Clermont Université, Université Blaise Pascal, BP 10448, F-63000 Clermont-Ferrand
(2) CNRS, UMR 6505, Laboratoire de Photochimie Moléculaire et Macromoléculaire, F-63177 Aubière
(3) CEA-Grenoble DRT/LITEN/DTS/LCP, INES-RDI, Laboratoire des Composants Photovoltaïques, 50 avenue du Lac Léman BP 332, F-73377 Le Bourget du Lac

e-mail : sandrine.therias@univ-bpclermont.fr

INTRODUCTION

New photovoltaic technologies as organic and copper-indium-selenium (CIS and CIGS) allows thinner and more flexible modules. To growth the market shares of these flexible technologies, it needs to reach sufficient lifetimes by limiting considerably the insertion of water and oxygen in the device. High barrier materials, which are optically transparent in the visible domain, flexible, and low cost have to be developed. Furthermore these materials must have a good stability under exposure to solar light [1].

To obtain high barrier encapsulating foils, stacks alternating dense inorganic layers (such as SiOx, ≈ 300 nm) and organic layers (≈ 1µm) are deposited on a thick polymeric substrate [2]. The organic layers have to be as barrier as possible. Insertion of nanoclays in the organic layer brings improvement on the barrier properties [3], but nanoclays could decrease the photostability of the polymer [4]. The goal is to prepare barrier, transparent and flexible nanocomposite films which are photostable when inserted in the multilayer encapsulation. The nanocomposites are based on polyvinylalcohol (PVA) as the polymeric matrix and two different clays, natural and synthetic.

MATERIALS AND METHODS

PVA $(-CH_2-CH(OH)-)_n$ was 98% hydrolyzed with molecular weight ≈16,000 $g.mol^{-1}$. Clays were either natural clay such as sodium montmorillonite (Cloisite® Na+) or synthetic clay (Laponite). The nanocomposite films at different clay concentrations (up to 10 wt %) were characterized by several analytical techniques: UV-visible and infrared spectroscopies, XRD, TEM, DSC and permeability measurements. UV-light irradiations ($\lambda > 300$ nm, 60°C) were carried out in a SEPAP 12/24 unit [5], under accelerated artificial conditions in order to simulate natural ageing..

RESULTS & DISCUSSION

Characterizations of PVA/clay nanocomposites

Figure 1 shows the IR spectra of PVA/clay nanocomposites with various contents of Cloisite®Na^+. One observes a linear increase of absorbance at 1050 cm^{-1} (ν_{Si-O}) as a function of clay content, which clearly indicates the good distribution of the clay in PVA..

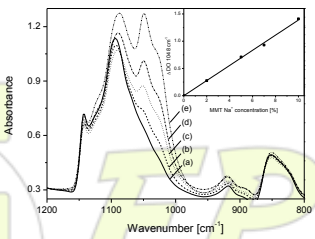

Figure 1 : FTIR spectra of PVA (a) and PVA/Cloisite®**Na^+** nanocomposites (b-e) with different clay content: (b) 2 wt%, (c) 5 wt%, (d) 7 wt%, (e) 10 wt%. Insert: ΔOD at 1050 cm^{-1} as a function of clay content.

DRX and TEM characterizations (Figure 2) reveal coexistence of silicate layers in intercalated and exfoliated states.

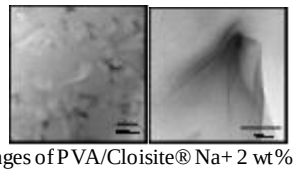

Figure 2: TEM images of PVA/Cloisite® Na+ 2 wt% at (a) low magnification and (b) high magnification.

Gas permeability of the nanocomposites decreases with increasing clay content up to 5%. This effect can be attributed to tortuosity effect of the clay platelets. However, the barrier properties are better in the case of Cloisite® Na+ than in the case of Laponite, which comes from the higher aspect ratio of Cloisite® Na^+ platelets.

Photostability of PVA/clay nanocomposites

In presence of both clays, the same photoproducts of PVA are formed, but a discrepancy on the photooxidation rate of PVA is observed depending on the clay: Cloisite® Na^+ displays a prodegradant effect whereas Laponite has no influence on the oxidation rate of PVA (figure 3). However, in the absence of oxygen, PVA nanocomposites are photostable and no modification of their chemical structure and morphologies are observed. This can be achieved when the nanocomposite layer is protected by an inorganic one, which is the case in the multilayer material.

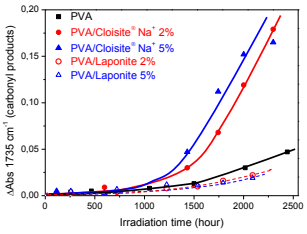

Figure 3: Photooxidation rate of PVA, PVA/Cloisite® Na+ and PVA/Laponite nanocomposite films as a function of irradiation time.

CONCLUSIONS

Cloisite® Na^+ and Laponite/PVA nanocomposites with intercaled/exfoliated silicate layers of clay homogeneously dispersed in the polymeric matrix have been developed. The best gas barrier properties were obtained in the case of Cloisite® Na^+. In multilayer encapsulant coating alternating inorganic and nanocomposite layers, these nanocomposites are photostable.

REFERENCES

[1]Rivaton A, Chambon S, Manceau M, Gardette J.L, Lemaître N, Guillerez S, Polym. Degrad. Stab 2010;95(3): 278-284
[2]Charton C et al., Thin Solid Films 2006;502(1-2):99-103
[3]Yeun J.H. et al., Journal of Applied Polymer Science 2006;101(1):591-596
[4]Morlat-Therias S et al., Polymer Degradation and Stability 2006;91(12):3033-3039

Advanced Organic-soluble Polymers for Optical and Electronic Application :New Colorless, Transparent and Thermally Stable Polynorbornenes via ROMP

Wei-Ren Lian[a], Kun-Li Wang[b], Jyh-Chiang Jiang[a], Der-Jang Liaw[a], Kueir-Rarn Lee[c] and Juin-Yih Lai[c]

a. Department of Chemical Engineering, National Taiwan University of Science and Technology, Taipei 10607, Taiwan
b. Department of Chemical Engineering and Biotechnology, National Taipei University of Technology, Taipei 10608, Taiwan
c. R&D Center for Membrane Technology, Department of Chemical Engineering, Chung Yuan University, Chung-Li 32023, Taiwan

liawdj@mail.ntust.edu.tw; liawdj@gmail.com; liawdj@ntu.edu.tw; liawdj@yahoo.com.tw

Abstract : The novel near-infrared (NIR) electrochromic polynorbornenes, poly(NBDTPA) and poly(HNBDTPA), containing electroactive chromophores were prepared, respectively, via ring opening metathesis polymerization from a new norbornene derivative (NBDTPA) using different Grubbs' catalysts, and followed hydrogen reduction. The glass transition temperatures (Tg) of poly(NBDTPA) and hydrogenated poly(HNBDTPA) were 141 ^{o}C and 91 ^{o}C, respectively. The 10% weight-loss temperatures of hydrogenated poly(HNBDTPA) and poly(NBDTPA) were up to 440 ^{o}C and 397 ^{o}C, respectively. Poly(NBDTPA) and poly(HNBDTPA) were highly soluble in common organic solvents such as toluene, xylene, chlorobenzene, 1,2-dichlorobenzene, tetrahydrofuran and benzene at room temperature. Hydrogenated poly(HNBDTPA) film showed excellent transparency (up to 91%). Poly(HNBDTPA) film exhibited three reversible oxidation redox couples at 0.63, 0.82 and 1.23 V v.s. Ag/Ag+ in acetonitrile solution. Poly(HNBDTPA) showed excellent stability and reversibility, with multi-staged color changes from its colorless neutral form to green, light-blue and dark-blue as applying potentials from 0 to 1.75 V. The color switching time and bleaching time of the poly(HNBDTPA) were 7.1 s and 4.2 s in near-infrared region (1230 nm) and 7.4 s and 4.5 s in UV-Vis region (420 nm), respectively.

Introduction: Electrochromism has been reported in redox-active inorganics, organic small molecules as well as in polymer materials such as conjugated polymers.[1-8] polyamides[5] and polyimides.[6] The colored polymers are disliked as electrochromic materials, and the native color is one of disadvantages for practical uses in optical devices.[9] It is well-known that hydrogenated polynorbornene derivatives are colorless, amorphous and readily solution-processed polymers with high thermal stability, optical transparency. Ring-opening metathesis polymerization (ROMP) offers an effective way in polymerization of norbornene monomers with different side chain substitutes. Grubbs' ruthenium (Ru) carbene complexes efficiently catalyzed ROMP under ambient conditions, with high tolerance toward polar functional groups. Thus, ROMP using Ru-based catalyst is a promising route to prepare polynorbornenes and hydrogenated polynorbornenes which has colorless, transparent and easily solution-processed properties.

Conclusion: The novel near-infrared (NIR) electrochromic polynorbornenes, poly(NBDTPA) and poly(HNBDTPA), were successfully prepared via ring opening metathesis polymerization from electroactive chromophore-containing monomer, NBDTPA, and followed hydrogenation, respectively. Poly(NBDTPA) and hydrogenated poly(HNBDTPA) exhibited similar electrochemical and electrochromic behaviors with high contrast and electrochromic reversibility. Thus, these characteristics suggest that the prepared colorless polynorborenes are good candidates for the electrochromic materials.

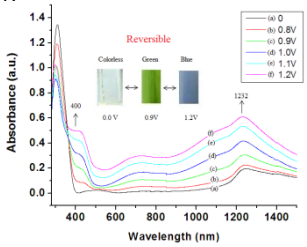

Absorption spectra of poly(NBDTPA) E_{appl}: (a) 0.00, (b) 0.80, (c) 0.90, (d) 1.00, (e) 1.10 and (f) 1.20 V.

1. H. Y. Wu, L. K. Wang, D. J. Liaw, K. R. Lee and J. Y. Lai, *J. Polym. Sci., Part A: Polym. Chem.*, 2010, **48**, 1469
2. H. Y. Wu, K. L. Wang, J. C. Jiang, D. J. Liaw, K. R. Lee, J. Y. Lai and C. L.Chen, *J. Polym. Sci., Part A: Polym. Chem.*, 2010, **48**, 3913
3. W. H. Chen, K. L. Wang, D. J. Liaw, K. R. Lee and J. Y. Lai, *Macromolecules* 2010, **43**, 2236
4. W. H. Chen, K. L. Wang, W. Y. Hung, J. C. Jiang, D. J. Liaw, K. R. Lee, J. Y. Lai and C. L. Chen, *J. Polym. Sci., Part A: Polym. Chem.*, 2010, **48**, 4654
5. C. H. Chang, K. L. Wang, J. C. Jiang, D. J. Liaw, K. R. Lee, J. Y. Lai, K. Y. Chiu and Y. O. Su, *J. Polym. Sci., Part A: Polym. Chem.*, 2010, **48**, 5659
6. C. H. Chang, K. L. Wang, J. C. Jiang, D. J. Liaw, K. R. Lee, J. Y. Lai and K. H. Lai, *Polymer*, 2010, **51**, 4493
7 D. J. Liaw, J. S. Tsai, P. L. Wu, *Macromolecules*,, 2000, **33**, 6925
8. D. J. Liaw, T. P. Chen, C. C. Huang, *Macromolecules*,, 2005, **38**, 3533.
9. K. Tajima, Y. Yamada, S. Bao, M. Okada and K. Yoshimura, *Appl. Phys. Exp.*, 2008, **1**, 0670071

Solvent induced morphology in polymer-based systems for organic photovoltaics

Matthias A. Ruderer[1], Shuai Guo[1], Robert Meier[1], Hsin-Ying Chiang[1], Volker Körstgens[1], Jan Perlich[2], Stephan V. Roth[2], Peter Müller-Buschbaum[1]

[1] Physik-Department, Lehrstuhl für Funktionelle Materialien, Technische Universität München, D-85747 Garching, Germany
[2] HASYLAB at DESY, D-22603 Hamburg, Germany

muellerb@ph.tum.de

Introduction

Photoactive semi-conducting polymers have shown to be interesting candidates for organic photovoltaics due to their high absorption coefficient, easy processibility, mechanical flexibility and low costs [1-3]. At present, polymer-based systems reached already 6% to 8% in photovoltaic efficiency. However, despite promising efficiencies a detailed understanding is still limited.

In a typical organic solar cell the active layer contains two components, namely an electron-donor and an electron acceptor, to enhance exciton separation. It was found that besides fitting in electronic properties the inner film morphology of the two components is crucial for the photovoltaic performance [4]. In contrary to conventional layered systems, with a relative small interface, in the bulk heterojunction concept a donor and an acceptor material are blended which results in a much higher interfacial area [5-7]. Consequently, more excitons reach the interface between both and are separated. Besides, the high interfacial area also the structural length scales, which have to fit the small exciton diffusion length in organic materials (in the order of 10 nm), and percolation paths to the electrodes are of utmost importance. As the bulk heterojunction concept is commonly based on simple blending of two components, the structure develops in a self assembly process. Therefore the morphology of the active layer can only be controlled indirectly by several parameters such as the chemical composition, the solvent used and post production treatments.

Materials and Methods

In this investigation we probe the influence of the used solvent on the morphology formation of polymer-based bulk heterojunction systems for photovoltaic applications. Films are spin coated from different solvents. We chose the bulk heterojunction system consisting of the conjugated polymer P3HT (poly(3-hexylthiophene-2,5-diyl)) and the methano fullerene PCBM ([6,6]-phenyl-C61 butyric acid methyl ester). Both components fit very well concerning their electronic behaviors and this combination is probably the best investigated system in organic photovoltaics so far. Besides imaging methods such as atomic force microscopy (AFM), the advanced scattering techniques X-ray reflectivity and grazing incidence small and wide angle X-ray scattering (GISAXS and GIWAXS) reveal a full understanding of the inner film structure on molecular to mesoscopic length scales. Spectral characterization, such as absorption and photoluminescence, and optical microscope investigations complete this study.

Results and Discussion

In combination with topography imaging we are able to reconstruct schematic morphologies from the scattering experiments for the films made from the different solvents. Depending on the solvent, enrichment layers at the interfaces as well as varying structural length scales inside the active layer are found. As an example, **figure 1** summarizes the structures detected in this investigation in case of annealed P3HT:PCBM films made from the solvent chlorobenzene in a schematic morphology. Black areas illustrate pure PCBM and white areas pure P3HT phases. Possible phases containing portions of both components, P3HT and PCBM, are neglected in this presentation for clarity.

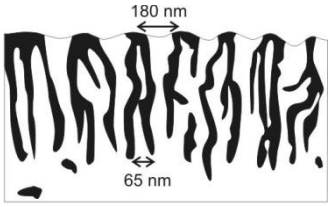

Figure 1. Black-and-white schematic morphology of annealed P3HT:PCBM film

Conclusion

It is found that the choice of solvent has direct influence on the lateral and vertical material arrangement and therefore on the device performance [8].

References

[1] J. Y. Kim, K. Lee, N. E. Coates, D. Moses, T. Q. Nguyen, M. Dante, A. J. Heeger, *Science* **2007**, *317*, 222.
[2] C. J. Brabec, F. Padinger, J. C. Hummelen, R. A. J. Janssen, and N. S. Sariciftci, *Synthetic Metals*, **1999**, *102*, 861.
[3] C. R. McNeill, A. Abrusci, J. Zaumseil, R. Wilson, M. J. McKiernan, J. J. M. Halls, N. C. Greenham, R. H. Friend, *Appl. Phys. Lett.* **2007**, *90*, 193506.
[4] C. R. McNeill, A. Abrusci, I. Hwang, M. A. Ruderer, P. Müller-Buschbaum, N. C. Greenham, *Adv. Funct. Mater.*, **2009**, *19*, 3103.
[5] M. A. Ruderer, S. M. Prams, M. Rawolle, Q. Zhong, J. Perlich, S. V. Roth, P. Müller-Buschbaum, *J. Phys. Chem. B*, **2010**, *114*, 15451.
[6] W. Wiedemann, L. Sims, A. Abdellah, A. Exner, R. Meier, K. P. Musselman, J. L. MacManus-Driscoll, P. Müller-Buschbaum, G. Scarpa, P. Lugli, L. Schmidt-Mende, *Appl. Phys. Lett.*, **2010**, 96, 263109.
[7] M. A. Ruderer, E. Metwalli, W. Wang, G. Kaune, S. V. Roth, P. Müller-Buschbaum, *ChemPhysChem*, **2009**, *10*, 664.
[8] M. A. Ruderer et al., to be published

Convenient Method for Functional Biocompatible Hyperbranched Polymers

J.A.Loontjens, F. Xiang, L. Asri, J. Yin, S. Roest

University of Groningen, Nijenborgh 4 9747AG, Groningen, The Netehrlands

J.A.Loontjens@RUG.nl

Introduction

Due to aging of the world populations the need for polymeric auxiliaries for biomedical devices is rapidly growing. Tissue engineering, antibacterial coatings, micelles for drug delivery and the like attract therefore in the last two decades much attention. However, the body is extremely complex and therefore the requirements for biomedical polymers are highly demanding. Most of the studies tackle only one biomedical property, but we are deemed to cope with a number of requirements. The aim of our research is to make hyperbranched polyurethanes with multiple functional groups as depicted in Figure 1.

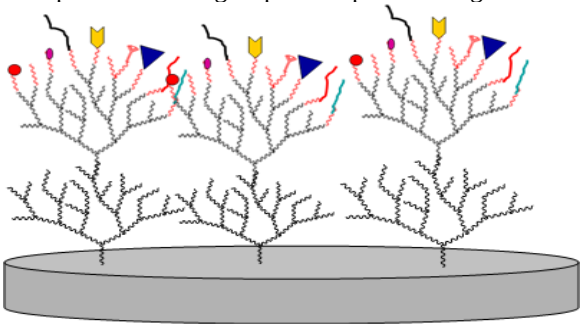

Figure 1: Schematic presentation of multifunctional hyperbranched coating.

Materials and Methods

The key element of this research is our discovery of the extremely high selective reaction between primary amines and carbonyl biscaprolactam (CBC). In toluene at 80 °C compounds comprising primary and secondary amines form in 6 hours quantitatively caprolactam blocked isocyanates. By this approach AB_2 monomers were prepared in a one step reactions starting for example from bishexamethylene triamine. The consecutive polymerization of the AB_2 monomers, as well as the successive functionalization, is done at 145 °C in bulk or in DMF.

Results and discussion

Primary amines react with carbonyl biscaprolactam (CBC) quantitatively yielding blocked isocyanates [1, 2, 3]. More remarkably, when a polyamine comprises primary and secondary amines (or esters) exclusively primary amines react. Hence this methodology offers the possibility to make in one step blocked isocyanates comprising secondary amino groups (or esters), as depicted in scheme 1. Triamines, such as bishexamethylene triamine, comprise two primary and one secondary amino groups. Through the reaction with CBC the primary amino groups are converted into blocked isocyanates (B-groups), whereas the secondary amino group remains unaffected (A-group) below 100 °C. On heating at 145 °C the polymerization starts by the substitution of caprolactam of the B-group by the secondary amine (A-group).

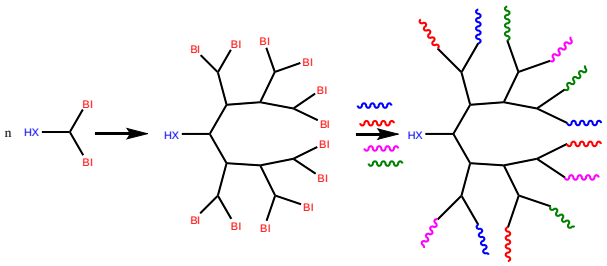

Scheme 1: The synthesis of AB_2 monomers, the corresponding hyperbranched polymers and the corresponding modified hyperbranched polymers (BI = blocked isocyanate, X = O or NH).

We purposely designed the AB_2 monomer in such a way that the B-groups are the blocked isocyanates. To this end, the HB polymers comprise numerous blocked isocyanates (up to more than 30), which can be functionalized. Indeed every compound comprising hydroxyl or amino groups can be coupled onto the end of each polymer chain. Obviously, various compounds can be used, as each polymer chain comprises an abundant amount of BI's.

The conversion of lysine into the corresponding blocked isocyanate proceeds as well quantitatively, although it takes more time for complete conversion. The ester side group is used to introducing functional groups. The modified lysine blocked isocyanates yielded functional polyurethanes when heated with polyols.

Conclusions

We have developed a feasible novel method to make in one step in quantitative yield AB_2 monomers or functionalized amino acids (lysine). The polymerization of the AB_2 monomers starts simply on heating, yielding hyperbranched polymers furnished with blocked isocyanate end groups. The blocked isocyanate groups enabled us to tether hydroxyl of amino functional compounds provide with special properties. The polymerization of lysine blocked isocyanates yield linear polymers with functional side groups.

References

1. Carbonylbiscaprolactam (CBC) a versatile reagent for organic synthesis and isocyanate-free urethane chemistry. S. Maier, J.A. Loontjens, B. Scholtens, R. Mülhaupt, Angew. Chem., **42**, 5094, (2003).

2. Modular Approach for Novel Nanostructered Polycondensates Enabled by the Unique Selectivity of Carbonyl BisCaprolactam. J.A. Loontjens, Polym Sci Part: Polym Chem 41 (21), 3198, 2003.

3. Process for preparation of functionalized polymers and intermediate products, compositions and shaped parts, J.A.Loontjens, B. Plum, A. van Geenen, W. Ming, WO 03/070785.

Fabrication of Clickable Thin-Film Composite Membranes for Reduced Biofouling

Matthias Haeussler, Simon Harrisson, Guoxin Li, Jana Habsuda, Ezio Rizzardo, Marek Jasieniak, Hans Grieser, Christopher Barner-Kowollik, Maude Le Hellaye, Vicki Chen, Jaleh Mansouri, Ian Dagley

CRC for Polymers, 8 Redwood Drive, Notting Hill, Vic 3168, Australia

Matthias.Haeussler@csiro.au

Introduction

Huisgen 1,3-dipolar cycloaddition of azides and alkynes is the reaction most commonly associated with 'click'-chemistry, a term coined by K. Barry Sharpless 0 in 2001. The Cu^{I}-catalyzed cycloaddition affords 1,2,3-triazoles 0 and can be performed in an aqueous system across a wide range of temperatures and pH, and thus is compatible with chemically and hydrolytically sensitive thin film composite membranes. Click functionalization is insensitive to acid and amine functional groups on the membrane surface, and can be complementary to other functionalization strategies that target these groups (e.g. with epoxy-functional polymers). Click chemistry is a versatile technique for the functionalization of thin film composite reverse osmosis membranes to reduce biofouling.

Experimental

TFC polyamide membranes were prepared from *m*-phenylene diamine (MPD) and trimesoyl chloride (TMC) via interfacial polymerization. Azide-functionalized membranes were fabricated of azide-functionalized acidchloride monomer analog, 5-(azidomethyl)isophthaloyl dichloride (AMID), which was prepared from commercially available starting material diethyl 5-(hydroxylmethyl) isophthalate in three steps [3,4]. Alkyne-functionalized polymers were prepared by esterification of polyethylenglycol (PEG) with 5-hexynoic acid or by aminolysis of trithiocarbonate-functionaled pNIPAM, obtained from reversible addition fragmentation chain transfer (RAFT) polymerization, and *in situ* Michael addition to propargyl acrylate. The procedure for click-grafting was adapted from a previously published procedure 0.

Results and Discussion

The new azide-functionalized TFC polyamide membranes were prepared by interfacial polymerization on ultrafiltration polysulfon and polyethersulfon membranes supports, using an aqueous solution of MPD and a mixture of TMC and AMID in decane.

Different amounts of AMID were used for the membrane preparation ranging from 0-50%. The TFC polyamide membranes were characterized via FTIR-ATR spectroscopy and the presence of azide functions on the surface of the membranes confirmed by the presence of the azide band located at 2105 cm^{-1}.

Different cycloaddition conditions for the PEG-alkyne grafting were tested. Best results were obtained at 60°C in 11% K_2SO_4 (cloud point conditions). Under these conditions, nearly complete disappearance of the azide absorption in the IR spectrum was obtained after 1 h.

The performance of the surface-modified membranes was evaluated in a dead-end cell and flux and salt rejections typically in the range of 20-50 LMH and 95-100% were determined, respectively, for AMID contents up to 25%.

Model PEG and pNIPAM brush surfaces were prepared by click reaction of alkyne-functionalized polymer with azide-functional surfaces. The azide-functional model surfaces were prepared by plasma polymerization of allyl glycidyl ether on polyethersulfone substrate, followed by reaction with sodium azide to introduce surface epoxide groups. Surfaces were characterized by XPS to follow the introduction of azide groups and their reaction under click conditions.

The model surfaces showed no measurable fouling on exposure to solutions of human serum albumen. By contrast, unmodified polyethersulfone showed significant adsorption of HSA under the same conditions.

When PEG and PNIPAM-modified surfaces were exposed to *S. epidermidis* bacteria, very limited attachment of isolated bacteria was observed after 6h. This may be associated with defects in the polymer brush. By contrast, untreated polyethersulfone samples showed significant colonization and biofilm formation after exposure to *S. epidermidis* for 6h under the same conditions.

Conclusion

The technology comprises a method of synthesising azide-functional reverse osmosis membranes, which can be functionalized with alkyne-functional polymers to impart antifouling properties to the membrane. Membranes prepared with up to 25% AMID content exhibit >95% salt rejection in dead end cell testing. The membranes have been successfully grafted with alkyne-functionalized polymers, which are readily prepared from commercially-available end-functionalized polymers or polymers which contain RAFT endgroups. Model polyethersulfone surfaces which have been grafted with the alkyne-functionalized polymers exhibit significantly improved antifouling behaviour compared to unmodified polyethersulfone surfaces.

References

Kolb, H. C.; Finn, M. G.; Sharpless, K. B. *Angew. Chem. Int. Ed.* **2001**, *40*, 2004-2021.

Bock, V. D.; Hiemstra, H.; van Maarseveen, J. H. *Eur. J. Org. Chem.* **2006**, 51-68.

Zhang, X.; Nirschl, A. A.; Zou Y.; Priestley, E. S. *US Patent* WO2007/002313.

Dimick, S. M.; Powell, S. C.; McMahon, S. A.; Moothoo, D. N.; Naismith, J. H.; Toone, E. J. *J. Am. Chem. Soc.* **1999**, *121*, 10286-10296.

Bergbreiter, D. E.; Chance, B. S. *Macromolecules* **2007**, *40*, 5337-5343.

Applying post polymerisation hypercrosslinking on polyHIPE material

Irena Pulko[a,b], *Peter Krajnc*[c,b]

[a]Polymer Technology College, Pod gradom 4, Slovenj Gradec, Slovenia
[b]Centre of Excellence PoliMaT, Tehnološki park 24, Ljubljana, Slovenia
[c]University of Maribor, Faculty of Chemistry and Chemical Engineering, Smetanova 17, Maribor, Slovenia

peter.krajnc@uni-mb.si

Poly(high internal phase emulsion) material utilizes high volume fraction of an internal phase of an emulsion to template highly porous polymeric material. Pores are created due to the droplets of internal phase and additionally due to the shrinkage of the polymeric material produced from the polymerisation of the continuous phase of the emulsion. Result is a highly porous polymer with large pores in place of the droplets of the internal phase and smaller interconnecting pores between them. Such material, termed polyHIPE[1] (see Figure 1 for morphology) is permeable due to the interconnected porous structure and can be used in monolithic form as columns for synthesis facilitation[2], chromatography[3], reactive filtration[4], etc. However, because of the large diameters of pores (usually in the micrometer range), the surface area of such materials is rather low. In order to address this issue, we have introduced a second generation of pores to the polyHIPE material, utilizing a post polymerisation hypercrosslinking method. In this manner, much smaller pores can be generated by creating additional crosslinks in the material by a chemical method. Poly (4-vynilbenzyl chloride) polyHIPE material was prepared and a Friedel-Crafts method was applied in order to connect neighbouring chloromethyl groups with benzene rings. This resulted in a material with a much higher surface area, in the range of 1000 m^2/g (ranging 20 m^2/g prior to procedure) and controlled kinetics enabled tailored properties of the material. We have applied the material for the immobilisation of an organocatalyst[5] and for the immobilisation of piperazine for the removal of atrazine from water.

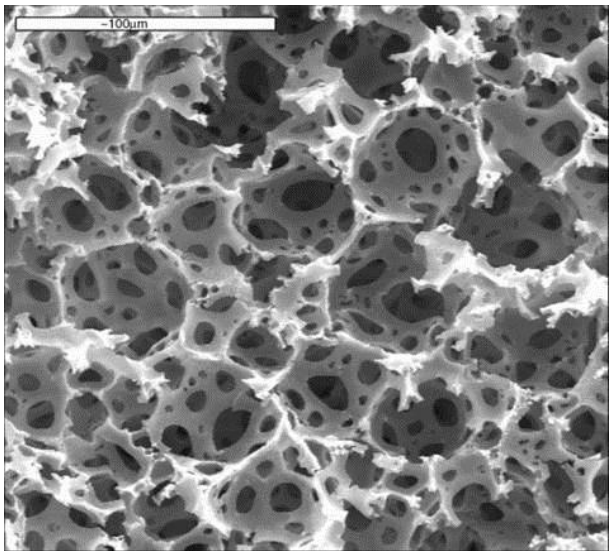

Figure 1: SEM image of a polystyrene polyHIPE

References
1 D. Barby, Z. Haq, Eur. Pat. 60138, 1982
2 S. Kovačič, P. Krajnc, J. Polym. Sci. Part A, Polym. Chem. 2009, 47, 6726.
3 P. Krajnc, N. Leber, D. Štefanec, S. Kontrec, A. Podgornik, J. Chromatogr. A 2005, 1065 (1), 69-73; I. Junkar, T. Koloini, P. Krajnc, D. Nemec, A. Podgornik, A. Strancar, J. Chromatogr. A 2007, 1144 (1), 48-54.
4 I. Pulko, M. Kolar, P. Krajnc, Sci. Total Environ. 2007, 386 (1/3), 114-123.
5 I. Pulko,J. Wall, P. Krajnc,N. R. Cameron, Chem. Eur. J. 2010, 16, 2350.

Composites of Semiconductive Polyelectrolytes for Optoelectronic Applications

Jiří Pfleger[1], *Samrana Kazim*[1], *Veronika Slunečková*[1], *Dmitrij Bondarev*[2], *Jiří Vohlídal*[2]

[1]Institute of Macromolecular Chemistry, AS CR, v.v.i., Heyrovsky Sq. 2, 162 06 Prague 6
[2]Faculty of Sciences, Charles University in Prague, Czech Republic

pfleger@imc.cas.cz

Introduction

Nanocomposites based on semiconducting polymers and metal or inorganic semiconductor nanofillers have gained recently an increasing interest due to their promising application in nonvolatile rewritable memories, optical sensors, SERS probes and phototovoltaic devices; the applications based on a resonance excitation of surface plasmons or charge transfer at the polymer/inorganic semiconductor interface. A well controlled nanostructuring of the inorganic phase as well as its immediate contact with the semiconducting polymer is desirable for achieving high efficiency of photonic or electronic processes. It was shown recently, that conjugated polymers comprising ionic or ionizable groups, i.e. semiconducting polyelectrolytes, are easily adsorbed to oppositely charged inorganic surfaces and by careful mixing the polymer with inorganic nanoparticles a desirable nanostructures can be obtained. For example, by mixing Ag nanoparticles (NPs) hydrosols with polyelectrolytes solutions nanocomposites can be easily prepared, which show very strong surface enhanced Raman (SERS) signals.

Materials

Regioregular *poly{3-[6-(1-methylimidazolium-3-yl)-hexyl]thiophene-2,5-diyl bromide}*, PMHT-Br, and *poly [(thiophene-3-yl)acetic acid]*, PTAA, shown in Fig. 1 were used as soluble π–conjugated polymers bearing cationic and anionic groups, respectively.

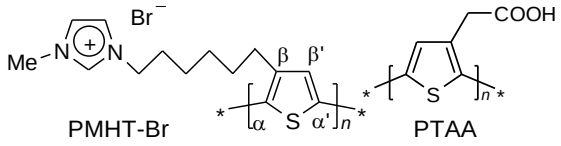

Figure 29: Ionic polythiophenes used in the study

PMHT-Br was synthesized using recently developed two step procedure.[1] The resulting cationic polythiophene is soluble in water, common polar solvents like dimethyl sulfoxide, dimethylformamide and some alcohols. Silver and gold NPs were prepared by the reduction of a proper metal salt with sodium borohydride or citrate. Mesoporous TiO_2 layers prepared according recently published procedure[2] were used as received.

Results and Discussion

The measured electrical conductivity of the pure cationic PMHT-Br in vacuum was found to be $3x10^{-10}$ S/cm while the nanocomposites with Au NPs showed higher conductivity depending on the concentration of the Au NPs. The conductivity of composites and of the pure polymer showed a linear dependence on reciprocal temperature up to 80 °C with the average activation energy 0.32 eV (see Fig. 2 also compared with P3HT).

Mixed ionic and electron conductivity was detected with a steep increase of the ionic mobility at higher temperatures due to the increased segmental motion of the polymer confirmed by impedance spectroscopy. The I-V characteristics showed a nonlinear behavior and electrical bistability in forward and reversed directions.

Figure 30: Dependence of the electrical conductivity on reciprocal temperature. ● - PMHT-Br, ♦ - P3HT

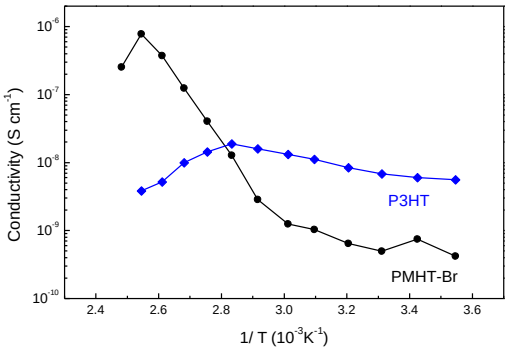

When Ag or Au NPs and PMHT-Br are mixed in components ratios providing the charge balance between Ag-NPs and cationic polythiophene, NPs aggregated with interparticle distances enabling marked interparticle plasmon interactions, demonstrated by a red shift of optical absorption and strong SERS signals. The SERS activity of such NPs assemblies was preserved when the sol was cast on a substrate forming a thin solid film. The electrostatic interactions were successfully utilized also for the preparation of multilayered structures of alternating PMHT-Br, Au NPs and PTAA using layer–by–layer deposition technique on charged surfaces, even inside the mesoporous TiO_2. The surface plasmon resonance of metal nanoparticles contributed markedly to the overall extinction of the composite showing a red shift of optical absorption with increasing number of layers due to an increased electronic coupling of plasmons in the multilayer structure.

Conclusions

The electrostatic interactions between ionic polythiophenes, metal NPs and TiO_2 nanostructured surface were exploited for building aggregated or multilayered systems as a new materials with strong plasmonic effects and mixed ionic and hole conductivity.

Acknowledgements: Financial support of the Czech Science Foundation projects P208/10/0941 and 203/08/H032, COST OC1007 (Czech MEYS) and EU NoE project FlexNet are greatly acknowledged.

References

[1]Bondarev, D.; Zedník, J.; Šloufová, I.; Sharf, A.; Procházka, M.; Pfleger, J.; Vohlídal, J.; J. Pol. Sci: A - Polym. Chem. 2010, 48, 3073-3081.

[2]Zukalova M., Prochazka J., Zukal A., Yum J. H., Kavan L, Grätzel M.; J. Electrochem. Soc. 2010, 157, H99-H103.

Supramolecular Poly(3-hexylthiophene)s for Solar Cells: Synthesis and Electronic Properties

CLAUDIA ENDERS , ALI SHAYGAN NIA, WOLFGANG H. BINDER

Martin-Luther-University Halle-Wittenberg, Faculty of Natural Sciences II (Chemistry and Physics), Institute of Chemistry/Division Technical and Macromolecular Chemistry, Von- Danckelmann-Platz 4, 06120 Halle (Saale) (Germany)

claudia.enders@chemie.uni-halle.de

The sun is the largest supplier of carbon-neutral energy. Although there are a variety of inorganic solar cells for harvesting efficiently solar energy, the costs of processing are too high to be economically viable. Therefore a major motivation is the development of organic photovoltaic (OPV) materials and devices which are envisioned to exhibit advantages such as low cost, flexibility and unlimited availability. The state-of-the-art organic solar cell is built from a bulk heterojunction (BHJ) composed of electron-donating semiconducting polymers and electron-withdrawing fullerides or perylenes. Significant progress has been made on the structural enlightenment of these materials to increase the power conversion efficiencies over 7% up to now. However, many factors limit the performance of BHJ solar cells. Especially the morphology of the active composite layer plays an important role. Hence, we have combined the knowledge about microphase separated oligomers and polymers (well-known as supramolecular pseudo-block copolymers), which we have already gained[1], with the composition of BHJ solar cell materials.

Thus we have synthesized active layer materials based on postfunctionalized poly(3-hexyltiophene)s (P3HT) bearing hydrogen bonding moieties on the end groups and perylene derivates with the corresponding equivalent for attractive supramolecular interactions (see figure 1). Via these postfunctionalization reactions we synthesized telechelic P3HTs bearing trimethyl-silylacetylene moieties by microwave supported Sonogashira reactions.

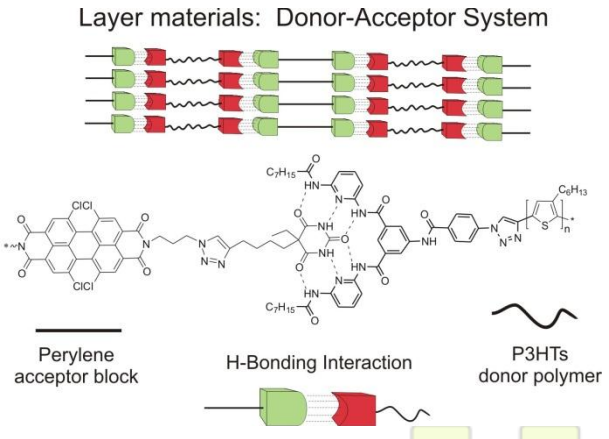

Fig.1 Selfassembly of postfunctionalized P3HT and perylene units to active layer material (D-A system)

After deprotection of the acetylene group we introduced hydrogen bonding units onto the polymer chain ends via the azide/alkyne "click" reaction (see figure 2). The defined end group structure analysis is therefore essential and was realized via LC-ESI-TOF mass spectrometry[2]. Beside this we investigated the electrochemical properties of all telechelic P3HTs, perylenes and their blends via cyclic voltammetry (CV), UV-vis and fluorescence spectroscopy to determine the electronic and optical band gap.

In a single active-layer organic solar cell the power conversion efficiency (PCE) will be measured. These results give us knowledge about the interface interaction between electron acceptor and conjugated polymer which are crucial for the photophysical performance in organic photovoltaic devices.

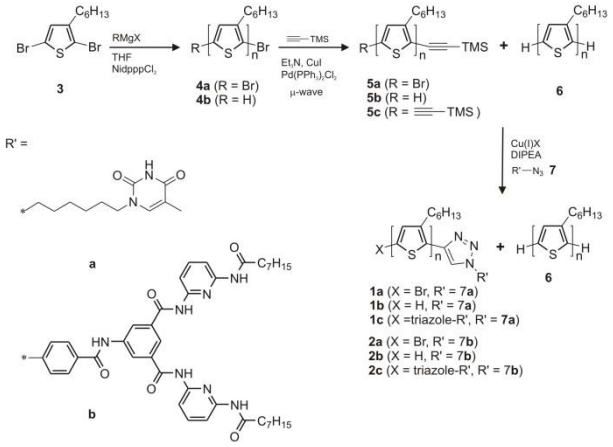

Fig.2 Postfunctionalization of poly(3-hexylthiophene)s via Sonogashira and azide/alkyne "click" reaction

References:

1. Binder, W. H.; Bernstorff,S.; Kluger, C.; Petraru, L.; Kunz, M.J., *Advanced Materials* **2005**, 17,(23), 2824-2828.
2. Enders, C.; Tanner, S.; Binder, W. H., *Macromolecules* **2010,** 43, (20), 8436-8446.

Fluorene Based Core-Polymers for Efficient White Oled: Correlation between Molecular Structure and Photophysical Properties.

Silvia Destri[1], *Umberto Giovanella*[1], *Filippo Samperi*,[2] *Salvatore Battiato*[2]

[1]Istituto per lo Studio delle Macromolecole (ISMAC) via E. Bassini 15, 20133- Milano, Italy
[2]Institute of Polymer Chemistry and Technology (ICTP) Sez. Catania – CNR, Via Gaifami 18, 95126 Catania , Italy

s.destri@ismac.cnr.it

Efficient white electroluminescence can be obtained from a fully miscible blend of core-type polyfluorene-based copolymers prepared by using Suzuki coupling reaction between a properly functionalized fluorene prepolymer coming on its turn from a Suzuki polycondensation and the di-bromide derivative of either a green or a red dye.[**1]**

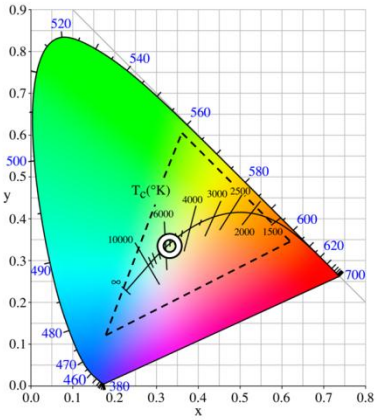

Fig.1 CIE 1931 chromaticity space, also showing Planckian locus

The chemical composition of the materials is a key factor to tune the emission colour, particularly the white shade (correlated colour temperature see Figure 1) which dramatically depends on the percentage of the three polymers constituting the blend. A deep molecular characterization of three polyfluorenes (PF) has been carried out combining different techniques such as (^{1}H- and ^{13}C)-NMR, and MALDI-TOF MS. Their exact molar mass distributions were calculated applying the absolute calibration curves builds by SEC-MALDI TOF MS analysis of selected SEC fractions of opportune choice PF samples. More than ten clusters of homologous peaks separated by about 1039.2÷1039.6 Da which correspond the mass of the PF repeating units (1039.4 Da), were envisaged in the prepolymer samples, each cluster has been assigned to linear PF chains bearing different end groups corroborating NMR observations. Reactive boronate linear chains are present together with unprofitable bromide terminated ones and un-reactive chains ending with phenyl or hydroxylic or hydrogen groups. Even more families are present in the final core PF. The identification of macromolecules terminated with hydrogen, hydroxyl and phenyl groups suggests that, in accordance to the literature[2], side reaction occur during the Suzuki polycondensation reaction between dibromide and diboronate monomers. The formations of PF chains terminated with bis(boronic pinacol) diester in the prepolymer samples suggests that this group, in the Suzuki polycondensation, is more stable with respect to the bis(boronic 1,3-propanediol) diester end groups.

Moreover, by applying a gel permeation cromatography to separate the samples as a function of the chains molecular weight we were able to discriminate among the different situations obtaining in the high molecular weight range only the polymeric chains which contain in a core or end position the dye (red or green emitting depending on the chosen sample).

Photophysical characterization (absorption and photoluminescence) has been carried out on diluted solution of the different fractions to investigate intramolecular energy transfer mechanism as a function of both the molecular weight and the acceptor dye position within the polymer chain (core or end-type copolymers), and its effect on the overall photoluminescence quantum efficiency.

[1] U. Giovanella, P. Betti, A. Bolognesi, S. Destri, M. Melucci, M. Pasini, W. Porzio, C. Botta, *Org. Electron*.**2010**.***11*** 2012-2018.

[2] Kappaun, S.; Zelzer, M.; Bartl, K.; Saf, R.; Stelzer, F.; Slugovc, C. *J. Polym. Sci. part A: Polym. Chem.* **2006**, *44*, 2130-2138.

Obtention of modified Polypropylene using the trifuntional cyclic initiator DEKTP as the radical initiator in the presence of different crosslinking co-agents

Graciela Morales[*], *Lizet García-Salazar*[*], *and F. Avalos*[**]

[*]Centro de Investigación en Química Aplicada, E. Reyna 140, 25253, Saltillo, Coah. México.
[**]Fac. CC. Químicas, UADEC, Blvd. V. Carranza s/n 25000, Saltillo, Coah. México.

e-mail:gmorales@ciqa.mx

Introduction. Long chain branched (LCB) polymers have value in processing techniques which demand high melt strength, including thermoforming, film blowing, extrusion coating, and blow molding processes. Due to the difficulties in the synthesis of branched polypropylenes, there hasbeen an increased interest in the chemical modification of polypropylene (PP).Among the most successful processes, reactive extrusion[1,2]is the most used, which degrades the polypropylene in a controlled fashion to create branches.

The rheological importance of these types of materials is the effect of long chainbranches on the extensional flow of the polymers. Linear and branched polypropylenes have been examined in a similar manner[3,4]. Polypropylene containing long chain branches strain-hardened while a linear polypropylene did not. Thesedifferences in rheology make branched polymers beneficial forsome polymer processing operations, such as blow molding andfilm blowing.

Experimental. Homopolypropylene HG009 fromValtec (MFI = 7.0, 230°C, 2.16 Kg and Mw: 232,400 g/mol) from Indelpro SA de CV. (México), was modified by a reactive-extrusion process with the addition of a small amounts of cyclic peroxide and a multifunctional co-agent. The peroxide was Diethyl ketone Triperoxide (DEKTP) synthetized in our laboratories and multifunctional co-agents were Trimethylolpropanetriacrylate (TM), Trimethylolpropanepropoxylate (TMPPTA), Pentaerythritoltetraacrylate (PETA) and N'N'-1,3-Phenylene dimaleimida (FDM) were supplied by Aldrich Chemical Co. (Fig.1)

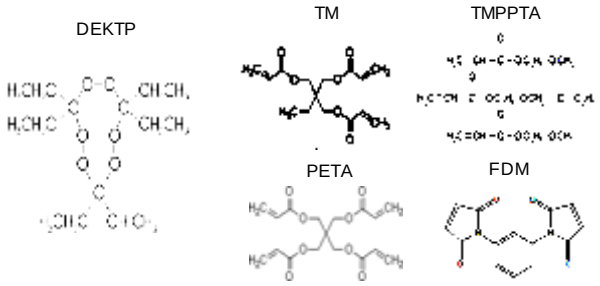

Figure 2.Initiator and co-agents used in PP modification

The PP melt modification was performed in an internal mixer Brabenderat 60 rpm, 180°Cfor 30min. Before 6 min of mixing,the co-agent was added and at 8 min the peroxide was added. The total reaction time was 30 min.The molar rate concentrations of the multifunctional co-agents/ peroxide were 10/1 (0.25/025 and 0.50/0.05).

In order to characterize the modified PP's, MFI, Mw, and gel content were measured. The chemical groups present in modified PP's were analysed by FTIR.

Results and discussion. Fig.2presents the evolution of the torque as a function of time for the system co-agent/peroxide = 0.5/.05 where all thesystems show a decrease of the torque with time except for TM and PETA, where the final torque is slightly increased.

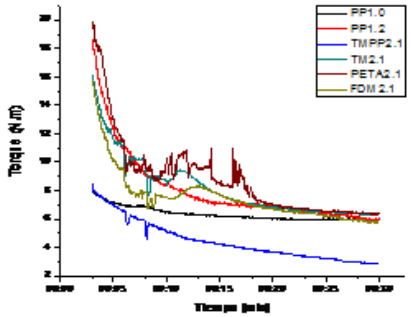

Figure 2. Evolution of the torque as a function of reaction time for the different evaluated systems

The results of MF, Mw, Mn and polydispersityindex (IP = Mw/Mn) are shown in the Table below.

System	[TPDEC] % mol	[Coagent] % mol	MFI (g/10 min)	MW (g/mol)	Mn (g/mol)	IP
PP1.0			7.31	223 331	53 843	4.14
PP1.1	0.025		7.42	210 143	56 043	3.74
PP1.2	0.050		15.285	206 294	49 542	4.16
TMPP1.1	0.025	0.25	15.266	217 285	51 715	4.20
TMPP2.1	0.050	0.50	31.33	181 489	63 236	3.69
TM1.1	0.025	0.25	12.537	214 538	54 050	3.96
TM2.1	0.050	0.50	9.89	289 399	71 430	5.25
PETA1.1	0.025	0.25	8.716	234 870	88 336	2.65
PETA 2.1	0.050	0.50	9.748	259 115	79 959	2.73
FDM2.1	0.025	0.25	14.66	188 846	52 014	3.63
FDM1.1	0.050	0.50	14.057	188 048	65 711	3.24

In all cases the MFI is higher than the pristine PP due to themacromolecular break up in the presence ofthe formed from the peroxide, attack the β hydrogen of PP. In the presence of the co-agents TM and PETA,the Mw increases with respect virgin PP. In these casesthe increase in MFI is related to the IP, since the low molecular chains gives a lubricant effect to the melt flow ofthe modified materials.A more extended discussion will be presented through the analysis of theglobal results in the extended paper.

Conclusions. It could be demonstrate that with theuse of the studied co-agents and in the presenceof the polyfunctionalperoxide DEKTP, the polypropylene radical functionalization can be achieved to obtain LCB PP.

References.

1)Langston J.A., Colby R.H., Mike Chung T. C.,F., T. Suzuki, Aoki M., *Macromolecules***2007**, 40, 2712-720
2) Graebling, D. *Macromolecules* **2002**, *35*, 4602.
3) Yoshii, F.; Makuuchi, K.; Kikukawa, S.; Tanaka, T.; Saitoh, J.;Koyama, K. *J. Appl. Polym. Sci*. **1996**, 60, 17.
4) Gabriel, C.; Münstedt, H. *J. Rheol*.**2003**, 47, 619.

Aggregates of Constant Size in Dilute Solutions of Associating Polyelectrolyte

Korchagina Evgeniya, Philippova Olga

Physics Department, Moscow State University, Moscow 119991, Russia

e-mail: phil@polly.phys.msu.ru

Introduction. Study of the self-assembly of associating polyelectrolytes in dilute solutions is quite important for the preparation of new functional polymeric systems. For instance, multichain aggregates of nontoxic, biocompatible and biodegradable polymers are very promising for various applications in pharmacy, biotechnology, cosmetics etc. In particular, it concerns aggregates formed by chitosan and its hydrophobic derivatives. In most of the papers the effect of the content of hydrophobes on the size of multichain aggregates of hydrophobically modified (HM) chitosan was studied. At the same time, the impact of such an important parameter as the main chain length of polymer on the dimensions of aggregates is not yet understood. Also, little is known about the aggregation numbers of multichain aggregates.

The aim of the present paper is to study the effect of the chain length of chitosan and HM chitosan macromolecules on the size and on the aggregation numbers of multichain aggregates formed in dilute aqueous solutions of these polymers.

Materials. Solutions of **c**hitosan and HM chitosan (containing 4 mol% of n-dodecyl side groups) with molecular weights of 55 000, 70 000 and 125 000 g/mol in 0.3M acetic acid and 0.05M sodium acetate.

Methods. Light scattering was used to determine the size of the aggregates, transmission electron microscopy (TEM) was used to visualize the aggregates.

Results and Discussion. In the dilute regime the solutions of chitosan were investigated by light scattering. For all the samples under study the correlation functions $g^{(1)}(q,t)$ of polymer concentration fluctuations show a bimodal relaxation behavior with fast and slow relaxation modes, which are due to the translational diffusion of unimers and aggregates, respectively.

It was observed that the hydrodynamic radius $R_{h\ agg}$ of aggregates does not depend on the length of individual chitosan chains. The same behavior is observed for the gyration radius $R_{g\ agg}$ of aggregates obtained from static light scattering data. To the best of our knowledge, this is the first observation of aggregates keeping a constant size independently of the length of individual chains in any associating polyelectrolyte solution. Such behavior is due to the presence of unscreened charges on the polymer chains. For dilute solutions of associating polyelectrolytes the equilibrium mean-field theory developed by Potemkin et al. predicts[1] that the size of aggregates is determined only by the content of associating groups and charged units as well as by the fraction of counterions escaped from the aggregate. At the same time, the size of aggregates should be independent of the chain length of individual macromolecules.[1] This result follows from the electrostatic nature of stabilization of the aggregates and is related to the classical Rayleigh problem of the charged droplet: a spherical droplet whose charge exceeds some critical value disintegrates into a set of smaller droplets of a certain size carrying charge lower than the critical one.

At the same time, the aggregation numbers of the multichain aggregates drop with increasing length of individual polymer chains,[2] which is also in perfect agreement with the theoretical predictions.[1] This result can be explained as follows. The energy of association is determined by the number of attracting groups. As shorter polymer chains have smaller amount of associating groups, their aggregates should include more chains in order to get a necessary gain in the energy of association.

The aggregation behavior for chitosan and HM chitosan is rather similar, but the size and the aggregation numbers of aggregates in HM chitosan are much larger than in its unmodified precursor, i.e. the incorporation of alkyl moieties into chitosan promotes the aggregation.[2]

The R_g/R_h ratio observed in aggregates of HM chitosan (0.58-0.59) lies within the range 0.3-0.6 characteristic for microgels that have a surface layer with much lower density than the core. Such structure of aggregates is confirmed by TEM data.[2]

Conclusions. Intermolecular association in dilute aqueous solutions of chitosan and HM chitosan of different molecular weights was studied by light scattering. It was observed that with increasing length of individual chains the aggregates keep constant size and almost constant number of hydrophobic and charged units; simultaneously, the content of polymeric chains in one aggregate decreases. When comparing the association phenomena in chitosan and HM chitosan, one can conclude that the introduction of hydrophobic substituents leads to larger and denser aggregates with higher content of polymeric chains. Analysis of light scattering and TEM data suggests that both in chitosan and HM chitosan the aggregates can be regarded as highly swollen nanogels with more dense core and loose shell with some dangling chains on the surface. Unique combination of properties of chitosan (biocompatibility, biodegradability, positive charge, nontoxicity, and bioadhesiveness) makes such aggregates very promising for the use as nanosize drug carriers.

References.

1. Potemkin, I. I.; Andreenko, S. A.; Khokhlov, A. R. *J. Chem. Phys*. **2001**, *115*, 4862-4872.

2. Korchagina, E. V.; Philippova, O. E. *Biomacromolecules* **2010**, *11*, 3457-3466.

Acknowledgment. The financial support of the program "Scientific and educational staff of innovative Russia" in 2009-2013 is gratefully acknowledged.

Magnetic, Molecular Imprinted Polymeric Nanoparticles for Developing Optical Sensors

A.L. Medina-Castillo[1], G. Mistlberger[2], J.F. Fernandez-Sanchez[1], I. Klimant[2], A. Fernandez-Gutierrez[1]

[1]Department of Analytical Chemistry, UGR, Granada, Spain.
[2]Institute of Analytical Chemistry and Food Chemistry, Graz Uni, Graz, Austria.

jfferan@ugr.es

Introduction

Molecular imprinting is a method of inducing molecular recognition properties in synthetic polymers in response to the presence of a template species during formation of its three-dimensional structure. The show a lot of advantages, however the application of MIPs for optical sensors was only successful in a few cases due to the difficulty of its implementation in optical devices.

The incorporation of magnetic properties allows the *in situ* formation of sensor spots by magnetic separation and, consequently, optical readout from the outside.[1] Several magnetic MIPs have been synthesized and characterized, highlighting that both the amount and distribution of magnetite are essential for producing a good material;[2] evidencing that well-organized structures are needed to design magnetic-MIP which can be used as optical sensors. Thus, in this work we propose a novel strategy to design well-organized, highly magnetic MIP particles to be used as optical sensors.

Materials and Methods

For the synthesis of Magnetic hybrid nanoparticles encapsulated by EDMA/MMA (EDMA/MMA-Fe_3O_4-OA), 2 g of magnetite coated with oleic acid (Fe_3O_4-OA) were dispersed in 5 mL of n-heptane and added to 400 mL of milli-Q water containing 250 mg of SDS. The ice-cooled mixture was sonicated for 20 min in a high energy sonifier. The resulting miniemulsion was transferred slowly to a double-necked flask containing 1.5 mL of 40 wt% MMA and 60 wt% EDMA. The mixture was stirred during 2 hours at room temperature. Then, 180 mg of KPS was added to start the polymerization and the reaction system was heated to 65 ºC under a gentle stream of nitrogen.

Magnetic-MIPs were synthesized by solution polymerization (sMIP), emulsion polymerization (eMIP) and precipitation polymerization (pMIP) using 4-VP as functional monomer, DVB as crosslinker, pyrene as template, AIBN as radical initiator and EDMA/MMA-Fe_3O_4-OA as magnetic seeds.

Results and Discussion

The first experiment consisted in the study of the effect of amount and distribution of magnetite over the optical recognition of pyrene. Thus, mag-MIPs with different amounts of Fe_3O_4-OA (1, 2 and 5 wt%) were prepared by solution polymerization (sMIP) and emulsion polymerization (eMIP). We determined that 1) at least 5 wt% Fe_3O_4-OA are necessary; 2) Magnetite had to be homogeneously distributed among the single particles and phase separation had to be avoided; and 3) Fe_3O_4-OA had to be isolated from the MIP in order to avoid filter effects and self-absorption of luminescence emission.

Therefore, we proposed the synthesis of new magnetic microparticles of MIPs in which the magnetite is located inside the particle and the MIP is covering these magnetic cores. It allows the use of a higher amount of magnetite and the isolation between magnetite and sensing material. They were prepared in two steps: 1) magnetic nanoparticles of Fe_3O_4-OA were encapsulated in a crosslinked polymer (EDMA/MMA) by a miniemulsion polymerization; 2) Then, these magnetic particles were embedded into the structure of a MIP which was prepared by precipitation polymerization (see Fig. 1). The preparation of these particles is simple and provides a sensing material which is highly magnetic (approximately 5 wt%) and sensitive (detection limit of 7 ng mL^{-1} of pyrene in water). In addition, this material shows a very high affinity characteristic (MIP/NIP ratio of 2.41) and very high selectivity; none of the tested luminescent PAHs (ACE, FLU, ANT, BaP and BaA) interfered with the determination of pyrene.

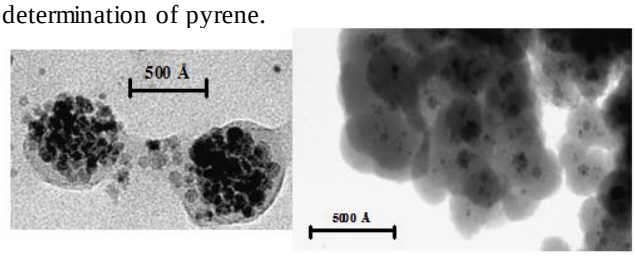

Fig. 1. HREM images of EDMA/MMA-Fe_3O_4-OA and mag-MIP produced by their encapsulation.

Conclusions

In this work we introduce a new synthetic route to a well-controlled magnetic imprinted material based on a two-step process: Firstly, the incorporation of the magnetite into a matrix which does not negatively influence the molecular imprinting phenomenon, and secondly, the embedding of these magnetic nano precursors in the MIP structure which can be used for optical sensing. To the best of our knowledge, this is the first time that a magnetic MIP can be used as optical sensor.

Acknowledgment

The authors thank the Spanish Ministry of Education (FPU grant reference AP2006-01144 and Project CTQ2008-01394), the Regional Government of Andalusia (Excellence projects P07-FQM-02738 and P07-FQM-02625) for their financial support.

References

1. Wang, X. B.; Ding, X. B.; Zheng, Z. H.; Hu, X. H.; Cheng, X.; Peng, Y. X., Macromolecular Rapid Communications 27, 14 (2006) page 1180 – page 1184.
2. Zhang, Y.; Liu, R.; Hu, Y.; Li, G., Analytical Chemistry 81, 3 (2009) page 967 – page 976

Effect of masterbatch dilution on the structure and mechanical properties of carbon-based nanocomposites.

Kuvardina E.V.[1], *Abramchuk S.S.*[2], *Krasheninnikov V.G.*[1], *Lomakin S.M.*[3]

[1] Semenov Institute of Chemical Physics, Russian Academy of Science
[2] Moscow State University, Electron Microscopy Center
[3] Emanuel Institute of Biochemical Physics, Russian Academy of Science

e-mail: janekuvardina@yandex.ru

Introduction: Carbon nanoparticles are thought to be very interesting objects as fillers for polymer composites. It is caused by their high mechanical characteristics, electrical and thermal conductivity. In this term it is important to consider these particles as fillers for large-scale polymers such as polypropylene. As the most of polymer goods manufacturers prefer using masterbatch as the input material it is interesting to analyze the effect of masterbatch dilution on the properties of carbon nanocomposite that plays a key role in further commercial application. The goal of this work is to investigate the effect of dilution on the structure, mechanical and thermal properties of the result composites depending on particle shape, size and volume loading.

Materials: Two types of carbon nanofillers (multiwall carbon nanotubes – MWNT and exfoliated graphite nanoplatelets of different lengths – xGnP™ with fiber-like and plate-like particle shape respectively) have been explored. Polypropylene was used as matrix.

Methods: Nanocomposites were fabricated by melt mixing on two-roller mixing chamber. Materials with maximum filler volume loading about 10% were obtained as a masterbatch and then were diluted to 0,5, 2,5 and 5 vol.%.

Results and Discussion: It was found that dilution of composites based on carbon nanotubes leads to shortening of the nanotube length that crucially effects on the mechanical properties of these composites. Reinforcing effect of MWNT in diluted composite with filler loading 5 vol.% is ~8% lower than in straight-mixed one. Relative tensile moduli of masterbatch-derived materials based on xGnP(5) with less length well correlate with those of straight-mixed composites. However Young's modulus of composites with xGnP(10) slightly increases after dilution that can indicate the increasing of particle quantity. In dynamic conditions, the relative storage modulus of masterbatch-derived composites based on both graphite nanoplatelets and carbon nanotubes rise up with temperature to 50-60°C and then slightly decrease. In case of xGnP(5), the masterbatch dilution is accompanied by the glass temperature shift in the higher temperature area caused by decreasing of polymer chains mobility.

Acknowledgement: This work was supported by the Russian Foundation for Basic Research, project no. 09-03-12232, and by the Federal Agency for Science and Innovations, project no. 02.740.11.0406.

3D Optical Waveguides produced by Two Photon Photopolymerisation of a Flexible Silanol Terminated Polysiloxane containing Acrylate Functional Groups

Rachel Woods [b,d]*, *Sonja Feldbacher* [b], *David Zidar* [b,d] *Gregor Langer* [a], *Valentin Satzinger* [c], *Wolfgang Kern* [d]

[a] AT&S AG, Fabriksgasse 13, A-8700 Leoben, Austria.
[b] Polymer Competence Center Leoben GmbH, Roseggerstraße 12, A-8700 Leoben, Austria
[c] Institute of Nanostructured Materials and Photonics, Joanneum Research, A-8160 Weiz, Austria
[d] Institute of Chemistry of polymeric Materials, Montanuniversität Leoben, A-8700 Leoben, Austria

Rachel.Woods@pccl.at

This work concerns the recent development and characterisation of a new polysiloxane material, which is used in the application of the integration of optical interconnections on printed circuit boards. To produce optical interconnects, two-photon photopolymerisation, induced by a femto-second laser is utilised in the fabrication of three-dimensional optical waveguides, embedded in a silanol terminated polysiloxane matrix material. The high photon density obtained in the focus of the laser results in the polymerisation of acrylate functional groups, which are attached to a polysiloxane backbone, causing an increase in the refractive index. A silanol terminated polysiloxane, cured by condensation reaction at room temperature in the presence of a Sn catalyst, has been investigated for this application. The material needs to fulfill a number of requirements to be a suitable candidate in this field. This includes having a low curing temperature, a high refractive index contrast between the matrix cladding material and the written waveguide core and the material must have sufficient flexibility and high thermal stability to withstand harsh processing conditions. High chemical and long-term stability is also required. The material currently being investigated has been characterised by FTIR spectroscopy, simultaneous thermal analysis and the refractive index of the cladding and core material was determined by ellipsometry measurements. Two Photon Absorption (TPA) material testing has been carried out on thin films to produce 3D waveguide structures with cross sections of up to 40 µm. The waveguides are characterised by phase contrast microscopy and cut back investigations to determine the optical losses. Optical interconnects have also been fabricated on specially designed printed circuit boards, with waveguide structures aligned correctly between optoelectronic components resulting in high photocurrents at the photo diodes. Recently produced demonstrators, consisting of optical interconnects mounted on fully flexible substrates, show low optical losses, which remain stable even at elevated temperatures and during long term storage. Room temperature curing enables fast and straightforward material processing, with the matrix material also being compatible with a specific two photon photoinitiator. This recently developed flexible polymeric material is highly suitable for applications in two photon processing of three dimensional optical waveguides

Bioinspired Polymeric Foam-Lattice Composite Combining Stochastic and Periodic Systems at two Different Length Scales: Lightweight Materials for Absorption Applications

R.G. Rinaldi[1], *C. Hammetter*[2], *J. Bernal-Ostos*[1], *A.J. Jacobsen*[3], *F.W. Zok*[1]

[1]University of California, Materials department, Santa Barbara, CA, 93106,
[2]University of California, Mechanical Engineering department, Santa Barbara, CA, 93106,
[3]HRL Laboratories, LLC, Malibu, CA 90265.

rrinaldi@engineering.ucsb.edu

Abstract: Many systems found in nature are hierarchical multi-scale materials in which periodicity and porosity are prominent features [(1)]. Such hierarchy suggests that different mechanisms are operative at distinct length-scales, potentially enhancing mechanical performance beyond that which could be obtained in simpler systems. Inspired by examples provided by nature, we aim to develop, characterize and understand hierarchical composites combining periodic lattices with stochastic foams.

The system of present interest combines a periodic polymer lattice at the mm scale with a stochastic foam at the μm scale, yielding a hierarchical co-continuous composite. Stochastic systems (*i.e.* foams) are well-known for exhibiting enhanced absorption performance whereas periodic lattices are mostly designed to improve strength resistance [(2)]. The system developed here aims to combine those advantageous effects in designing lightweight materials with enhanced mechanical properties.

The lattice is produced via a self-propagating polymerization process [(3)] and is then filled with polyurethane foam. The final composite and its constituents are illustrated in the figure1 below:

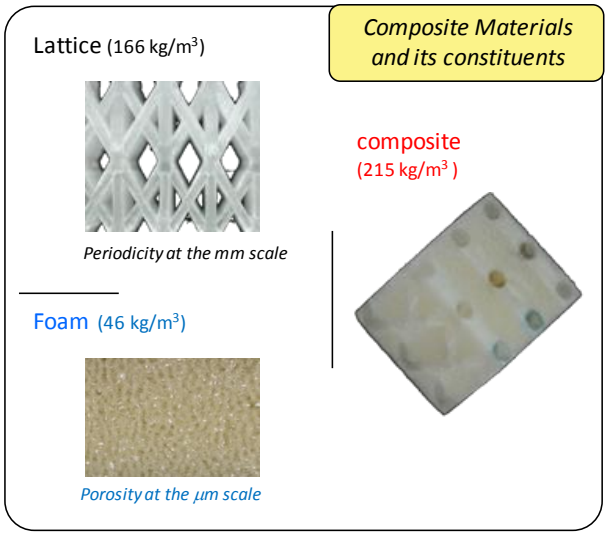

Figure 31: the composite designed consists of a lattice which interstices are filled with low density polyurethane foam.

The study focuses specifically on the efficacy of this composite structure on energy absorption capability. To this end, experimental measurements have been made of the compressive stress-strain response and parametric numerical studies using finite element analysis have been instrumental in clarifying the key design parameters of the lattice and in guiding the optimization process. Special cautions are devoted to the intrinsic mechanical response of the polymeric constituents: mainly, the strain rate sensitivity of both constituents [(4)] and its effect on the composite performance are under investigation.

References:

(1) Chen P-Y. et al., Structure and Mechanical Properties of Selected biological materials, J. Mech. Behav. Biomed. Mat. I (2008) 208-226.
(2) Fleck N.A. et al., Micro-Architectured materials: past, present and future, Proc. R. Soc. A (2010) 2495-2516.
(3) Jacobsen A.J. et al., Compression behavior of micro-scale truss structures formed from self propagating polymer waveguides, Act. Mat. (2007) 6724-6733.
(4) Mulliken, A.D., Boyce, M.C., Mechanics of the rate-dependent elastic-plastic deformation of glassy polymers from low to high strain rates, Int. J. of Sol. & Struct. (2006) 1331-1356.

Polymeric sensors based on polymer phase transition and thiazole dyes

C. Pietsch,[a] *R. Menzel,*[a] *R. Hoogenboom,*[b] *R. Beckert,*[a] *U. S. Schubert,*[a]*

[a] Institute of Organic Chemistry and Macromolecular Chemistry (IOMC), Friedrich-Schiller-University Jena, Jena Center for Soft Matter (JCSM), Humboldtstr. 10, 07743, Jena, Germany,
[b] Supramolecular Chemistry group, Department of Organic Chemistry, Ghent University, Krijgslaan 281 S4, 9000 Ghent, Belgium.

email: ulrich.schubert@uni-jena.de, www.schubert-group.de

In recent years, the interest in dye-functionalized responsive polymers, which respond to changes in the environmental conditions, strongly increased. Such 'smart' polymers are used for the development of new sensory materials for a wide range of applications in various fields, such as biomedical or optical sensing.[1] The approach allows simple and fast detection of, e.g. the temperature by measuring the absorbance or fluorescence of the solution. The high sensitivities arise from the incorporated solvatochromic dye molecules, which respond to minor local environmental changes that occur upon the temperature induced polymer phase transition. This phase transition is called lower critical solution temperature (LCST) behavior when the polymer precipitates upon heating. Recently, it was reported by our group that combining a solvatochromic dye with a temperature-responsive polymer leads to a color change upon changing the temperature, which can be used for optical sensing.[2]
Here, we present the synthesis of well-defined di(ethylene glycol) methyl ether methacrylate (DEGMA) based responsive copolymers by the reversible addition fragmentation chain transfer (RAFT) polymerization method. In this copolymerization we introduced a dye-functionalized monomer into the polymer backbone. The dye-functionalized monomer is based on 4-hydroxythiazoles, with a non classical chromophore structure similar to the luciferin dye of glowworms.[3] The obtained polymers revealed PDI values below 1.3 and were fully characterized and will be discussed in detail in the present contribution. Furthermore, the polymeric sensor was studied with temperature controlled UV/Vis and fluorescence spectroscopy and the effect of the polymer chain collapse upon passing the LCST transition on the attached dye emission and absorption behavior will be discussed in detail.
These non-classical chromophores show interesting photophysical properties and may open avenues for the construction of new multifunctional polymers.

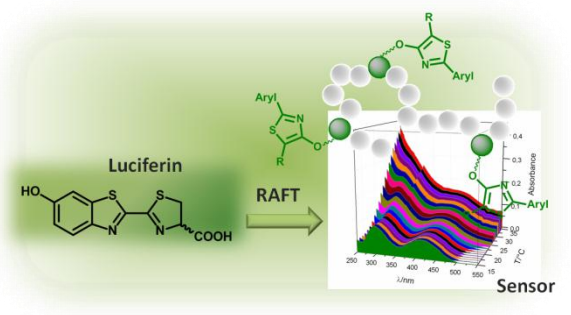

References:

[1] Schmaljohann, D. *Adv. Drug. Deliv. Rev.* **2006**, *58*, 1655.
[2] Pietsch, C.; Hoogenboom, R.; Schubert, U. S. *Angew. Chem. Int. Ed.* **2009**, *48*, 5653.
[3] Menzel, R.; Breul, A.; Pietsch, C.; Schäfer, J.; Friebe, C.; Täuscher, E.; Weiß, D.; Dietzek, B.; Popp, J.; Beckert, R.; Schubert, U.S. *Macromol. Chem. Phys.* **2011**, in press

Cancer Drug Targeting by a Magnetic Polymer – *In Vivo* Proof of Concept

José L. Arias[1], *L. Harivardhan Reddy*[2], *Patrick Couvreur*[2]

[1]Department of Pharmacy and Pharmaceutical Technology, University of Granada, Spain.
[2]Université Paris-Sud XI, Faculté de Pharmacie, UMR CNRS 8612, Châtenay-Malabry Cedex, France.

jlarias@ugr.es

Introduction. The efficacy and safety of anticancer therapy is conditioned by the very high drug doses needed to obtain an efficient therapeutic activity, the poor pharmacokinetics of chemotherapy molecules, and the frequent multi-drug resistance of tumor cells. The application of nanotechnology strategies in oncology (nano-oncology) has revolutionized the transport of drugs to cancer, allowing the appearance of new treatments with improved specificity [1]. For instance, magnetic nanoparticles (NPs) have shown their capability to assure a controlled and efficient accumulation of anticancer drugs into the tumor mass. As well, these nanoplatforms can also result in a triggered drug release into the targeted site [2].
In this work, we describe the formulation of magnetic core/shell NPs made of magnetic nuclei (magnetite, Fe_3O_4) and a polymeric shell (chitosan). An extensive physicochemical characterization of this magnetic nanoplatform has been done. More interestingly, we have further carried out an *in vivo* proof of concept on the possibilities in controlling the biological fate of the magnetic NPs by the use of an external magnetic field (accumulation at the tumor periphery investigated by Prussian blue staining).

Materials and Methods. Superparamagnetic Fe_3O_4 NPs (size ≈ 10 nm) were prepared by chemical co-precipitation [3]. The formulation of magnetically responsive Fe_3O_4/chitosan nanocomposites was based on the coacervation method for the synthesis of chitosan NPs [4]. Briefly, chitosan (1 %, w/v) was dissolved in an aqueous solution of acetic acid (2 %, v/v) containing 1 % (w/v) pluronic® F-68, and 0.75 % (w/v) Fe_3O_4. 12.5 mL of a solution of Na_2SO_4 (20 %, w/v) were added dropwise to the chitosan solution under mechanical stirring. Stirring was continued for 1 hr to obtain the aqueous suspension of core/shell NPs. The suspension was then subjected to a cleaning procedure by magnetic separation. Mean particle size was determined in triplicate by PCS. To confirm the size measurements, the nanocomposites were checked by HRTEM. The magnetic properties of the Fe_3O_4/chitosan NPs were determined by using a vibrating magnetometer.
Animal experiments were done according to the French and European Community guidelines for the care and use of experimental animals. DBA/2 mice (4 weeks old) weighing ≈ 15 g were used for this study. L1210 *wt* murine subcutaneous tumor model was developed by subcutaneous injection of the exponentially growing L1210 *wt* leukemia cells in suspension containing 30 % growth factor reduced Matrigel™. When mice developed palpable tumors, they were randomly divided into 3 groups of 6 each, i.e. untreated, treated with magnetic NPs, and treated with magnetic NPs under the influence of a 400 mT extracorporeal magnetic field. The accumulation of the NPs was qualitatively evaluated in terms of iron content using Prussian blue staining technique [5].

Results and Discussion. The coacervation method allowed the formation of well-stabilized Fe_3O_4/chitosan nanocomposites with an average diameter of 190 ± 30 nm and a narrow size distribution (polydispersity index: 0.071). HRTEM microphotographs of the magnetic composites proved that the iron oxide nuclei were covered by a polymeric shell. No presence of aggregates or bulky sediments was observed. In addition, no appreciable change in the size of the magnetic colloid was detected after 2 weeks of storage at 4.0 ± 0.5 ºC in water.
The very good magnetic responsiveness of Fe_3O_4/chitosan nanocomposites was quantitatively investigated by the hysteresis cycle, and qualitatively confirmed by direct observation and microscope visualization of the performance of nanocomposite suspensions under exposure to a 400 mT permanent magnet.
Tumor sections of the mice treated with Fe_3O_4/chitosan NPs without exposure to magnetic field revealed a negligible presence of the iron content as indicated by faible staining. On the contrary, tumor sections of mice treated with the magnetically-guided Fe_3O_4/chitosan NPs showed significant accumulation of iron, mainly deposited at the tumor periphery, where the external magnet was placed.

Conclusions. We have demonstrated that it is possible to reproducibly coat Fe_3O_4 NPs with a shell of chitosan. Prussian blue staining investigation of the tumor biopsies clearly evidenced their accumulation at the tumor site. The very important magnetic responsiveness of Fe_3O_4/chitosan (core/shell) NPs opens promising possibilities to improve drug delivery to cancer.

Acknowledgements. The research leading to these results has received funding from the European research Council under the European Community's Seventh Framework Programme FP7/2007-2013 (grant agreement nº 249835).

References. [1] Arias, J.L., et al., Mini-Rev. Med. Chem. 11 (2011) 1. [2] Laurent, S. Chem. Rev. 108 (2008) 2064. [3] Massart, R., IEEE Trans. Magn. 17 (1981), 1247. [4] Arias, J.L., et al. Drug Develop. Industrial Pharm. 36 (2010) 744. [5] Gang, J., J. Drug Target. 15 (2007), 445.

Synthesis, characterization and application of amphiphilic elastomeric polyurethane networks in drug delivery

S. Pita C.[1,3], Caracciolo P.C.[1], Abraham G.A.[1], Gironès J.[2], Méndez J.A.[3], Pèlach M.A.[3]

1. Institute of Materials Science and Technology (INTEMA), National University of Mar del Plata–National Research Council (CONICET). Mar del Plata, Argentina
2. Dept. of Biomaterials, Instituto de Ciencia y Tecnologia de Polimeros (ICTP–CSIC), Spain
3. Lepamap group. University of Girona, Spain

e-mail: jalberto.mendez@udg.edu

Introduction

Since the 60's, polyurethanes have been playing a key role in the development of biomedical devices due to their versatility, mechanical properties and excellent tissue compatibility. Polyurethanes have been extensively studied as biodegradable and/or injectable materials and have found several applications. Polyurethane networks (PUN) are synthesized by incorporating at least one reactant with functionality higher than 2, and depending on their composition PUN can be hydrophilic/hydrophobic, elastomeric/rigid and degradable/non-degradable.

Although linear segmented polyurethanes and multiblock copolymers with controlled hydrophilicity have been extensively studied, investigation on hydrophilic crosslinked polyurethanes is limited.

PUN composed of hydrophilic and hydrophobic segments can provide controlled swelling and allow homogeneous dispersion of drugs. For this reason, the characteristics of PUN are ideal for the design of controlled drug release systems. However, the use of polyurethanes in this field remains largely unexplored.

In this work, a series of crosslinked poly(ester-ether urethane)s with a range of hydrophilic character were synthesized. The effect of composition-morphology on the PUN swelling behavior and their application as drug-delivery vehicles has been investigated.

Materials and methods

Initiated by glycerol, poly(ε-caprolactone)s (PCL triol) were synthesized by ring-opening polymerization of ε-caprolactone. Molecular weight (M_n=1060 and 3130Da) were determined by titration of hydroxyl groups. Commercial PCL triol (M_n≈900Da), polyethylene glycol (M_n≈400Da), 1,6-hexamethylene diisocyanate (HDI) and DMAc were purchased from Aldrich. Prior to reaction, all polyols were exhaustively dried under vacuum. DMAc was dried over molecular sieves and distilled under reduced pressure. Dibutyltin dilaurate was used as catalyst in PUN synthesis.

Preparation of PUN: Predetermined amounts of PCL triol, PEG and catalyst were dissolved in DMAc. After adding HDI the reactive mixture was vigorously mixed and degassed under reduced pressure. Films were prepared by casting from the degassed colorless mixtures and allowed to cure at 60ºC for 24 h. Although the composition of PUN was changed, they all comply with the following molar ratio: $([OH]_{PCL\ triol} + [OH]_{PEG}) \times 1.05 = [NCO]_{HDI}$. The polyol component contained 10, 30, 50, 70, 90 and 100 % by weight of PCL triol. Samples were coded as P*X*-*Y*, where *X* and *Y* correspond to PCL triol and PEG mass percentages, respectively.

Results and discussion

Three series of PUN (PUN_{900}, PUN_{1060} and PUN_{3130}) with different PCL and PEG content were successfully synthesized. Infrared analysis confirmed the complete reaction of isocyanate groups. In all cases, sol content in PUN increased with the increase of PEG. Networks having PEG content higher than 70% underwent partial dissolution during extraction.

The DSC analysis revealed the presence of a single T_g, indicating that PUN consisted in a non-segmented polymeric network. The absence of a long chain macrodiol avoided the formation of hard/soft microphases. In all series, PUN exhibited T_g values higher than the starting PCL triol with T_g increasing with PEG content.

PUN_{1060} P100-0 displayed a small melting endotherm, whereas the other samples of this series were amorphous. PUN_{3130} series presented lower T_g values due to its semicrystalline character. Both series displayed the same T_g value for P10-90 samples, indicating that networks with low PCL content had a thermal behavior not dependent of PCL chain length. In PUN_{900} series all the samples were amorphous, showing T_g values almost constant with composition.

All the PUN series exhibited close equilibrium swelling values for the same PEG content. Equilibrium was achieved in approximately 1 h. The water uptake, as expected, was controlled by the content of hydrophilic monomer and it was not dependent on the chain length or crystallinity of the hydrophobic monomer. For PUN_{1060} P30-70 hydrolytic degradation was observed after 3 h.

Finally drug release capacity was studied by loading some PUNs with paracetamol. Drug release profiles showed paracetamol was released progressively within 8-12 days depending on PUN formulation.

Conclusions

Polyurethane networks having non-segmented structure and different hydrophilic-to-hydrophobic ratio were synthesized. Water uptake was controlled by the PEG content, with star-shaped PCL chain length not affecting the swelling degree. Based on experimental results, PUN with varying degrees of hydrophilicities have considerable interest as non-toxic controlled drug delivery devices in the form of implants (i.e. depot systems for localized drug delivery), and antimicrobial coatings. Profiles of paracetamol release have shown promising results.

Double Hydrophilic Copolymer Poly(ethylene oxide)-*block*-poly(2-ethyl oxazoline) as a Carrier of Cobalt bis(dicarbollide) Conjugates Designed as HIV Protease Inhibitors

Pavel Matejicek,[1] *Vladimir Dordovic*,[1] *Mariusz Uchman*,[1] *Karel Prochazka*,[1] *Bohumir Gruner*,[2] *Antti Nykanen*,[3] *Janne Ruokolainen*,[3] *Michael Gradzielski*[4]

[1]Department of Physical and Macromolecular Chemistry, Faculty of Science, Charles University in Prague, Hlavova 2030, 128 40 Prague 2, Czech Republic
[2]Institute of Inorganic Chemistry, ASCR, v.v.i., Area of Research Institutes 1001, 25068 Husinec-Řež, Czech Republic
[3]Aalto University, Department of Applied Physics, Nanotalo, Puumiehenkuja 2, FI-02150 Espoo, Finland
[4]Stranski-Laboratorium für Physikalische Chemie und Theoretische Chemie, Institut für Chemie, TU Berlin, Sekr. TC 7, Strasse des 17. Juni 124, D-10623 Berlin, Germany

matej@lynette.natur.cuni.cz

Introduction: It has been recently discovered that cobalt bis(dicarbolide) and its derivatives act as potent inhibitors of HIV protease.[1] Since the metallacarborane conjugates are sparingly soluble in water, suitable drug delivery carriers are needed. We can take advantage from the fact that cobalt bis(dicarbollides) interact with water soluble polymer poly(ethylene oxide), PEO, via unusual dihydrogen bonds and insoluble nanocomposite forms as a result.[2] In order to prepare stable polymeric nanoparticles with embedded metallacarboranes, we chose biocompatible double-hydrophilic diblock copolymer poly(ethylene oxide)-*block*-poly(2-ethyl oxazoline), PEO-PEOX.

Materials: Sodium salt of metallacarborane anion [3-cobalt(III) bis(1,2-dicarbollide)](-1) was a kind gift of Dr. Bohumír Grüner and Dr. Jaromír Plešek (Institute of Inorganic Chemistry, ASCR, Řež near Prague). Poly(ethylene oxide) was purchased from Fluka (M_w is 41.5×10^3 and PDI 1.10). Poly(2-ethyl-2-oxazoline) was purchased from Aldrich (M_w is 50.0×10^3). Poly(ethylene oxide)-*block*-poly(2-ethyl oxazoline) was purchased from Polymer source, Inc. (Dorval, Quebec, Canada), (M_w of PEO and PEOX: 5.0×10^3 and 6.5×10^3, respectively, PDI 1.10).

Results and Discussion: First we studied nanoparticles based on interaction of PEO-PEOX with parent sodium cobalt bis(dicarbollide) to elucidate their mutual interaction. In NaCl solutions with sufficiently high metallacarborane content, we observed stable spherical nanoparticles with radius 69 nm. Their structure was studied by means of light scattering, AFM, cryo-TEM and 1H NMR (the cryo-TEM micrograph is shown in Figure 1). Thermodynamics during their formation was studied by ITC.

As the second step, we mixed PEO-PEOX solutions differing in NaCl concentrations with several metallacarborane-based HIV protease inhibitors, which are almost insoluble in water. The increase in their solubility was estimated spectrophotometricaly. The nanoparticles were characterized by means of light scattering and AFM.

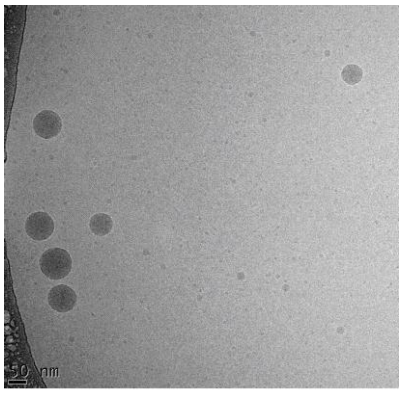

Figure 1: PEO-PEOX/metallacarborane nanoparticles imaged by cryo-TEM technique.

References: (1) Cigler, P.; Kozisek, M.; Rezacova, P.; Brynda, J.; Otwinowski, Z.; Pokorna, J.; Plesek, J.; Gruner, B.; Doleckova-Maresova, L.; Masa, M.; Sedlacek, J.; Bodem, J.; Krausslich, H. G.; Kral, V.; Konvalinka, J. *Proc. Natl. Acad. Sci. USA*. **2005**, *102*, 15394.
(2) Matejicek, P.; Zednik, J.; Uselova, K.; Plestil, J.; Fanfrlik, J.; Nykanen, A.; Ruokolainen, J.; Hobza, P.; Prochazka, K. *Macromolecules* **2009**, *42*, 4829.

Polyesters and Polyesterimides Containing Phosphaphenanthrene Bulky Groups for High Performance Applications

Diana Serbezeanu, Tăchiţă Vlad-Bubulac, Corneliu Hamciuc, Magda Aflori

"Petru Poni" Institute of Macromolecular Chemistry, Aleea Gr. Ghica Voda 41A, Iasi-700487, Romania

e-mail: diana.serbezeanu@icmpp.ro

Introduction: Thermotropic liquid-crystalline polymers (LCPs) have generated much interest in material science in recent years because of their various industrial and commercial applications, such us optical devices and engineering plastics [1]. The main chain wholly aromatic thermotropic polyesters and polyesterimides have received considerable interest for technological applications because of their good thermal stability, excellent chemical resistance, high glass transition temperatures, in addition to good processing and mechanical properties. In order to design aromatic polymers with lowered melting transitions, which allows appearance of the liquid crystalline phases below the temperatures corresponding to the thermal degradation or isotropization, several approaches have been taken into consideration: copolymerization, insertion of flexible spacer, use of laterally attached bulky groups, introduction of bent or crankshaft sequences etc. [2]. Introduction of lateral bulky groups to *p*-oriented monomers has also been applied to lower the melting points of LCPs. The incorporation of phosphaphenanthrene bulky structure (9,10-dihydro-9-oxa-10-phosphaphenanthrene-10-oxide (DOPO)) into polymers resulted in polymers with good solubility, resonable thermal stability, good adhesion, low birefringence etc. [3,4]. In addition, phosphorus-containing polymers meet the requirements of low toxicity and low smoke during burning for environmental and health considerations. In the present work we describe the results of the polycondensation of different aromatic bisphenols containing phosphaphenanthrene groups with a diacid chloride containing two preformed ester groups and various aliphatic diols.

Materials and Methods:

Terephthaloyl-bis-(4-oxybenzoyl-chloride), 2-(6-oxido-6H-dibenz<c,e><1,2>oxaphosphorin-6-yl)-1,4-naphthalene diol, 2-(6-oxido-6H-dibenz<c,e><1,2>oxaphosphorin-6-yl)-1,4-benzene diol and 1,4-bis[N-4-hydroxyphenyl)phthalimidyl-5-carboxylate]-2-(6-oxido-6H-dibenz<c,e><1,2>oxaphosphorin-6-yl)-naphtalene were synthesized in our lab. The aliphatic diols, 1,3-propanediol, 1,4-butanediol, 1,5-pentanediol, 1,6-hexanediol and 1,12-dodecanediol, were purchased from commercial sources. The molar ratio of aromatic bisphenol to aliphatic diol was varied to generate copolyesters and copolyesterimides with tailored physicochemical properties, structure-properties relationships being established.

Results and Discussion:

The polymers were synthesized by polycondensation reaction at high temperature. Their structure was confirmed by FT-IR, ^{1}H NMR, ^{31}P NMR spectroscopy and elemental analyses. The general structure of the polymers is depicted in following image.

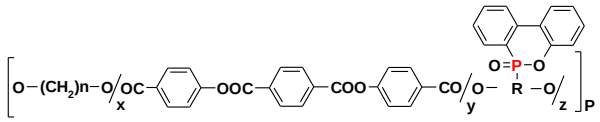

The thermo-oxidative stability of the polymers was evaluated by TGA in air at a heating rate of 10 °C min^{-1}. TGA revealed that the polymers were stable up to 350°C. The effect of the phosphorus content on the thermal properties and the flame retardancy was evaluated by means of thermogravimetric analysis (TGA), TGA-FTIR, and scanning electron microscopy. The char yield at high temperature increased by increased the content of phosphorus-containing bisphenol. The effect of the aliphatic content on the liquid crystalline behavior was investigated by polarized light microscopy, differential scanning calorimetry, and X-ray diffraction. The influence of the content of the aliphatic unit on the phase behavior of the polymers has been examined. It has been found that the transition temperatures become smaller by increasing the aliphatic content. Smectic phases were observed from polymers with a higher content of aliphatic moieties when polymers were heated upon their mesomorphic transition. Broad mesophase temperature ranges were observed for these polymers, making them interesting from practical point of view. The degree of crystallinity increased upon increasing the content of aliphatic moieties.

Conclusions:

A comprehensive study on the synthesis and on the relationship between the aliphatic/aromatic ratio, polymer liquid crystalline phase structure and thermo-oxidative stability of thermotropic liquid crystalline aromatic-aliphatic polymers derived from various ratios of phosphaphenanthrene-containing bisphenols, various aliphatic diols, and terephthaloyl bis-(4-oxybenzoyl-chloride) is presented.

Acknowledgements:

This research was supported by the FP7 Grant Agreement No 264115 – STREAM (CSA – SA_FP7-REGPOT-2010-1).

References:

[1] A.M. Donald, A.H. Windle and S. Hanna, in *Liquid crystalline polymers*, Cambridge University Press; 2nd edition, Cambridge, 2006, pp. 504–543.

[2] Y. Xu, Q. Yang, Z. Shen, X. Chen, X. Fan and Q. Zhou, Macromolecules 42(7) (2009), pp. 2542–2550.

[3] D. Serbezeanu, T. Vlad-Bubulac, C. Hamciuc and Magdalena Aflori, J Polym Sci Part A Polym Chem 48(23) (2010), pp. 5391–5403.

[4] C. Hamciuc, T. Vlad-Bubulac, O. Petreus and G. Lisa, Eur Polym J 43(3) (2007), pp. 980–988.

From Polymers to Well-Patterned Membranes by Mimicking the Nature

Annarosa Gugliuzza

Institute on Membrane Technology-National Research Council (ITM-CNR),
Via P. Bucci, Cubo 17/C, I-87030 Rende (CS), Italy

a.gugliuzza@itm.cnr.it

Introduction: The membranes are well-structured films with associated separation, catalysis, controlled storage, (bio)conversion, sensing, and (bio)mimetic properties.

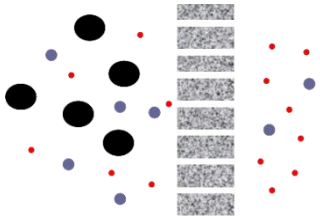

Representative scheme of a permselective porous membrane

Despite many efforts have been done over the years, the building up of complex and sophisticated polymeric structures at the nanometer scale remains a current challenge for many membranologists.
The ambitious target is to decide on nanoscale any desired macroscopic interplayed membrane properties such as transport and surface functions.
To select ideas and principles directly from nature and apply them to the membrane design takes advantage over conventional manufacturing procedures, because controlled chemical composition and tight placement of various components are attractively allowed at the nanometer and micrometer length scales, yielding programmable properties.
Materials: Poly(ethersulphone) (*PSU, Solvay-Solexis, USA*) and modified poly(etherketone)s (*PEEK-WCs, Department of Chemistry, IFM, University of Turin, Italy and Chang Chung Institute, Cina*)
Results and Discussion: Here, we propose an advanced bio-inspired procedure to build-up high-definition polymeric membranes according to a bottom-up approach. Water droplets are used as natural building blocks to template polymeric patterns through self-assembly events. Droplets are caused to arrange in semi-crystalline lattices by thermocapillary and Marangoni forces, yielding interfaces that challenge lithographic precision.
Depending on the operating conditions, the dynamics of the water droplets can be controlled and directed towards the formation of polymeric patterned architectures that exhibit well-defined packed pore geometry, uniform pore size and spatial distribution.

Representative scheme of membrane pore formation

The singular topology of the polymeric films causes very high interfacial area and surface roughness, which efficiently affect the final transport and surface properties of the membranes.
These new polymeric interfaces well meet the requirements of an advanced branch of the membrane science: the membrane contactor technology. When equipping a contactor device, these 3D well-ordered membranes exhibit ability to establish long-term stable interfaces between two aqueous phases at the entrance of each single pore, causing transfer of large amount of water vapour from one phase to the other.

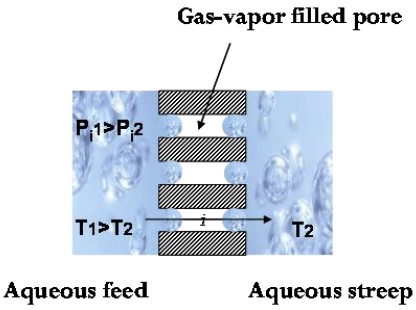

Scheme of a membrane contactor

Higher performance has been observed for these polymeric interfaces than commercial membranes. The reason is the highest surface porosity enabling simultaneous events to occur in all region of the membrane surface.
The surface porosity causes also high surface roughness responsible for enhanced hydrophobicity, yielding controlled mutual liquid-membrane interactions at the entrance of the pores. The intrusion of liquid inside the channels is prevented, resulting in long term stability of the interface and long operational time.
Conclusions: Regular polymeric membranes with structural features and surface properties have been realised by a bio-inspired approach. High-definition architectures have been constructed by exploiting the ability of water droplets to template liquid films through spontaneous rearrangement in ordered arrays. Macroscopic properties including transport and water repellence have been programmed through the control of structural features on nanoscale. Ideal interfaces for advanced membrane unit contactors have been realised.

References

Speranza V., Trotta F., Drioli E., Gugliuzza A., ACS Appl. Mater. Interfaces 2 (2) (2010) 459.
Gugliuzza A., Speranza V., Trotta F., Drioli E., Chemical Engineering Transactions, 17 (2009) 1537-1542
Gugliuzza A., Aceto M.C., Macedonio F., Drioli E., J. Phys. Chem B 112 (34) (2008) 10483-10496.

Preserving Cytokines' Stability and Activity: A Novel Controlled Release Polymeric Drug Delivery Approach

Husam M Younes[1,2] *& Mohamed Shaker*[2]

[1]Pharmaceutics & Polymeric Drug Delivery Research Laboratory, Department of Pharmaceutical Sciences, College of Pharmacy, Qatar University, Doha, Qatar. Email: husamy@qu.edu.qa

[2]School of Pharmacy, Memorial University of Newfoundland, Health Sciences Center, St. John's, NL, Canada

Introduction: The application of therapeutic proteins and cytokines like Interleukin-2 (IL-2) for long-term, localized delivery has been hindered by a lack of a delivery device that releases active protein at a concentration within their therapeutic window [1]. The purpose of this oral presentation is to report on the osmotic-driven controlled-release from novel visible-light photocrosslinked biodegradable elastomeric devices recently designed in an attempt to overcome this limitation.

Materials and Methods: All chemicals were purchased from Sigma-Aldrich and used as received. Novel biodegradable and biocompatible poly (decane-co-tricarballylate) [PDET] elastomers were synthesized by polycondensation reaction between tricarballylic acid and alkylene diols, followed by acrylation and photo-curing (Figure 1A) [2-3]. IL-2 loaded micro-cylinder and disk-shaped elastomeric devices were prepared by intimately mixing IL-2 lyophilized powder with the acrylated prepolymer prior to photocrosslinking (Figure 1 B) [4]. IL-2 release was analysed through using IL-2 ELISA system and the *in vitro* bioactivity of released IL-2 was assessed using C57BL/6 mouse cytotoxic T lymphocyte. The influence of various parameters such as the elastomer crosslinking density, the volumetric drug loading percentage and the incorporation of osmotic excipients like trehalose on the release kinetics of the drug was also examined.

Results and discussion: The disk-shaped specimens showed faster IL-2 release profiles than microcylinders, with drug release proceeding via typical zero-order release kinetics. The increase in the device's surface area and the incorporation of trehalose in the loaded lyophilized mix increased the IL-2 release rate. As well, it was shown that the decrease in the degree of prepolymer acrylation of the prepared devices increased the IL-2 release rate. Cell based bioactivity assays showed that IL-2 released over a period of 28 days, retained more than 94% of its initial activity. These bioactivity results represent a highly significant improvement over the other previously published data provided with a quantitative analysis of the actual percentage of bioactive IL-2 released during the period of the release study.

Conclusion: The novel PDET elastomeric drug delivery systems demonstrated to be promising as protein drug delivery vehicles for localized and sustained IL-2 immunotherapy.

References:

1- Shaker M and Younes HM. Interleukin-2: Evaluation of Routes of Administration and Current Delivery Systems in Cancer Therapy. *J Pharm Sci* **2009**; 98: 2268-2298.

2- Younes HM, inventor, Genesis Group/MUN, assignee. Biodegradable elastomers prepared by the condensation of an organic di-, tri- or tetra-carboxylic acid and an organic diol. *International Patent* (PCT) Number PCT/CA/2008/000870. **2008** December 4th.

3- Shaker M, Doré J and Younes HM. Synthesis, Characterization and Cytocompatibility of Poly (diol-tricarballylate) Visible Light Photocrosslinked Biodegradable Elastomer. *J Biomat Sci: Polym Ed* **2010**; 21: 507-528.

4- Shaker M and Younes HM. Osmotic-Driven Release of Papaverine Hydrochloride from Novel Biodegradable Poly (Decane-co-Tricarballylate) Elastomeric Matrices. *Therap Deliv* **2010**; 1: 37-50.

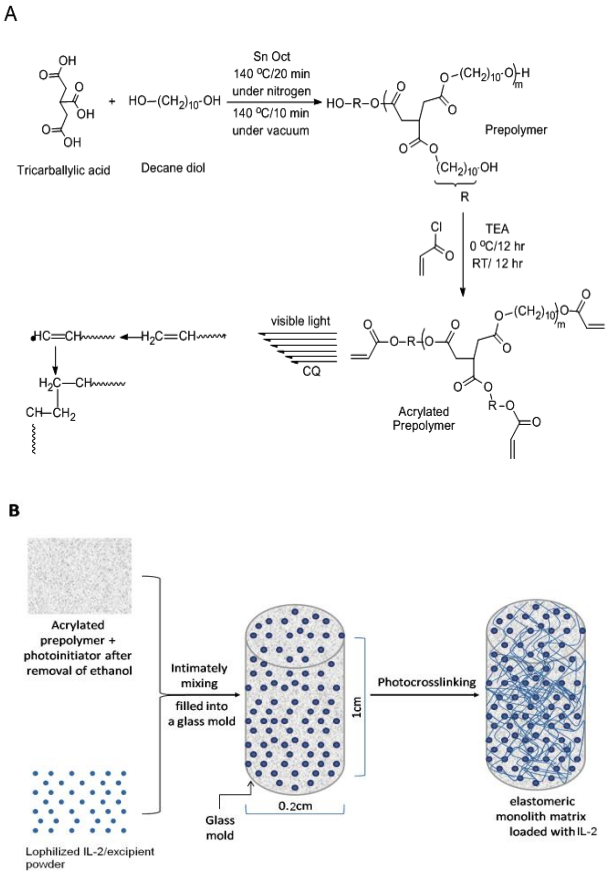

Figure 1. A schematic representation of the synthesis, acrylation and photo-crosslinking of the PDET elastomers. The step-reaction polymerization of tricarballylic acid and decane diol was catalyzed by stannous 2-ethylhexanoate. The acrylation process was done by reacting with acryloyl chloride in the presence of triethylamine. To photo-crosslink, acrylated prepolymer was mixed with the photoinitiator, poured into a sealed glass mold and crosslinked under visible light (40mW/cm2).

Phase-Morphology and Structure of Model Fullerene - Polymer Materials

D. G. Bucknall (Georgia Tech), G Bernardo (Univ. Minho), M Shofner (Georgia Tech), N Deb (Georgia Tech), D. Raghavan (Howard U.), B. Sumpter (ORNL), S. Sides (TechX), and A. Karim (U. Akron)

Bucknall@gatech.edu

Introduction Organic or polymer based photovoltaic devices promise solar technologies that are inexpensive enough to be widely exploited and therefore provide a significant fraction of the Nation's future energy needs. Nanoscale heterojunction systems consisting of fullerenes dispersed in conjugated block copolymers are promising materials candidates for achieving high performance devices. The fullerenes can be functionalized to change their electronic properties or to alter their interactions with the different components of the block copolymer. The block copolymer ratio or composition may be varied to produce different microphase morphologies and these morphologies may be further altered or oriented by the choice of processing conditions or substrates. This versatility is also a challenge to the rational exploration of these materials because the number and types of possible variations are far too large to investigate without predictive models or well-established data and guidelines to expected behavior.

Approach In order to guide the use of electron acceptor fullerenes in these systems we are using multi-scale molecular modeling coupled with neutron and X-ray scattering to determine the structure behavior of model polymer-fullerene mixtures. Neutron scattering is particularly useful for these types of studies since the fullerene generally have a high scattering contrast with respect to most polymers. This natural contrast, enhanced in some cases by careful selective deuteration allows us to carefully probe the atomic and molecular interactions in these complex systems.

Results and Discussion An initial model system we investigated was vinyl polymer and C_{60} blends. This system allowed us to probe the molecular interactions between fullerenes and polymers. We used scattering methods to determine miscibility as well as computational density functional theory (DFT) methods to evaluate binding energies. These studies have shown the role of π-π interactions in controlling interactions between the polymer and the fullerene. We recently we have been studying the phase behavior in model conjugated polymer-fullerene blends. This paper will describe the latest results in predicting miscibility and ultimately the phase behavior in such blends. The influence of processing conditions on the phase behavior and molecular structure in blends of, for instance P3HT and PCBM, is known to directly affect electronic performance, such as photovoltaic efficiency. In our studies we are exploring a number of approaches to control phase domain structure and orientation, using for instance block copolymers, and control of surface interactions.

Our neutron reflectivity measurements have shown that processing time scales of thin film spinning from dilute solutions can affect the through thickness thin film composition of polymer-fullerene blends (see Figure 1). These data show that segregation and selective absorption to the substrate from the polymer-fullerene solution is time dependent and can dominate the composition profile.

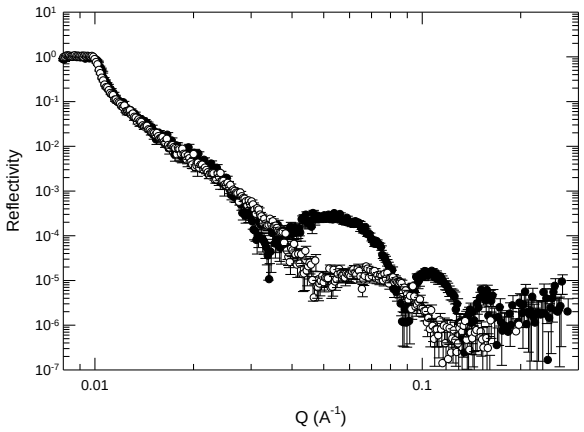

Figure 1: *NR plots of films of PS-C_{60} blends spun immediately after (open circles) and 5 minutes after solution deposition (filled circles).*

We are also examining processing conditions such as casting solvent, thermal gradient zone annealing and substrate surface energy on film structure. As example, we are developing a top down soft contact method using UVO treated PDMS for orientation control of block copolymers thin films. The flexibility of PDMS ensures conformal contact with the top surface of the BCP film, whereas its surface energy was tuned by controlled UVO exposure. The PDMS film was delaminated from the BCP surface after annealing and the BCP film structure characterized (see Figure 2).

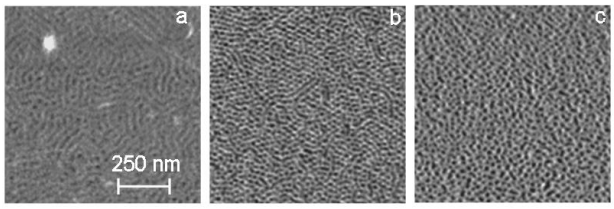

Figure 2: *Tapping mode AFM Phase images of the micro-phase separated cylindrical PS-PMMA BCP films (a) annealed without PDMS film cover and top surface covered by (b) partially hydrophilic PDMS films exposed to UVO and (c) hydrophobic PDMS films (unexposed to UVO).*

Conclusions A comprehensive effort involving theoretical methods as well as experimental studies of polymeric-nanoparticle donor-acceptor (D-A) thin films has been launched. Key objectives are to examine the correlation between polymer –nanoparticle system processing parameters vs. film morphology vs. OPV properties. We examine a wide range of nanostructures offered by block copolymer systems for this purpose.

Liquid Crystal Homo and Alternating (Co)polymers Based on π-Conjugated Backbone for Organic Electronics

F. Mathevet[a], *I. Tahar-Djebbar*[a], *D. Zeng*[a], *B. Heinrich*[b], *B. Donnio*[b], *D. Guillon*[b], *D. Kreher*[a], *A.-J. Attias*[a]

[a] Laboratoire de Chimie des Polymères, Université P. et M. Curie, 4 Place Jussieu 75005, Paris, France
[b] Departement des Matériaux Organiques, IPCMS, Strasbourg, France

fabrice.mathevet@upmc.fr

The self-organization of π-conjugated organic materials forming highly ordered supramolecular architectures has been extensively investigated in the last two decades in view of optoelectronic applications.[1] Indeed, the control of both the mesoscopic and nanoscale organization within thin semiconducting films is the key issue for the improvement of charge transport properties and achievement of high charge carrier mobilities. These well-ordered materials are currently either self-organized semiconducting polymers[2] or liquid crystals.[3] Indeed, on the one hand previous studies have shown that well-defined polymer architectures such as a regioregular poly(3-alkylthiophenes)[4] promote self-organizations in a two-dimensional sheet-like lamellar structures due to the high planarity of the polymer chains. More recently it has been reported that a semiconducting main-chain liquid-crystalline thieno[3,2-b]thiophene polymer exhibited enhanced charge-carrier mobility, when crystallized from the mesophase, due to the formation of large, well organized lamellar domains.[5] On the other hand, it has been demonstrated that discotic mesogens self-assembling into columns can exhibit high charge carrier mobilities due to the efficient one-dimensional anisotropic charge transport along the columnar axis.[6] However the supramolecular architecture resulting from the phase separation at the nanoscale of two covalently linked π-conjugated systems able to self-assemble individually in a lamellar and a columnar nanostructure respectively, has never been investigated to the best of our knowledge.
In this context, we endeavored to investigate the self-organization of a side-chain liquid crystal (SCLC) semiconducting polymer where (i) the backbone is a π-conjugated polymer and (ii) the side groups are π-conjugated discotic mesogens.

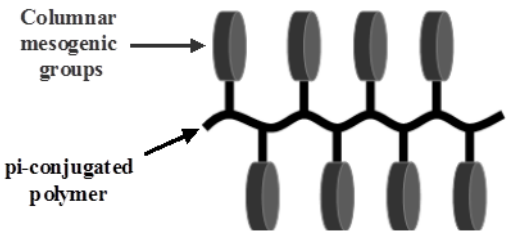

Here we describe the design and synthesis of columnar side-chain liquid crystal homo and alternating (co)polymers with triphenylene mesogens as side groups, and well-defined regioregular polythiophene as backbone.

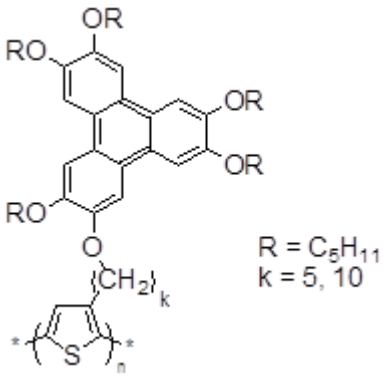

These different kinds of architectures prepared following the Grignard methathesis (GRIM),[7] allow the control of the triphenylene side group ratio along of the polymer chains, and lead to tunable electronic properties and nanostructures.
In this work, we will give the details on the synthesis and structural characterization studied by Polarized-light Optical Microscopy (POM), Differential Scanning Calorimetry (DSC) and Temperature-dependent, small-angle X-ray diffraction. Moreover, their photophysical properties and the preliminary charge transport results will also be depicted in view of applications for organic optoelectronics.

([1]) Special issue on ''Supramolecular Approaches to Organic Electronics and Nanotechnology'' *Adv. Mater.* **2006**, *18*, 1227.
([2]) Sirringhaus, H.; Brown, P. J.; Friend, R. H.; Nielsen, M. M., Bechgaard, K.; Langeveld-Voss B. M. W.; Spiering, A. J. H.; Janssen, R. A. J., Meijer, E. W.; Herwig, P.; de Leeuw, D. M. *Nature* **1999**, *40*, 685.
([3]) Sergeyev S.; Pisula W.; Geerts Y. H. *Chem. Soc. Rev.* **2007**, *36,* 1902.
([4]) Osaka I.; McCullough R.D. *Acc. Chem. Res.* **2008**, *41*, 1202.
([5]) McCulloch, I.; Heeney, M.; Bailey, C.; Genevicius, K.; MacDonald, I.; Shkunov, M.; Sparrowe, D.; Tierney, S.; Wagner, R.; Zhang, W. *Nature Materials* **2006**, *5*, 328.
([6]) Van de Craats, A. M.; Warman; J. M.; Fechtenkötter, A.; Brand, J. D.; Harbison, M. A.; Müllen, K. *Adv. Mater.* **1999**, *11*, 1469.
([7]) a) Loewe, R. S.; Khersonsky, S. M.; McCullough, R. D. *Adv. Mater.* **1999**, *11*, 250. b) Zhai, L.; Pilston, R. L.; Zaiger, K. L.; Stokes, K. K.; McCullough, R. D. *Macromolecules* **2003**, *36*, 61.

Light Microstructuring of Thiol-yne photopolymers: Cell adhesion on surface relief patterns.

M. Lomba [a], L. Oriol [a], C. Sánchez [b,], R. Alcalá [b], J.L. Serrano [c], M. Moros, J. M. de la Fuente [c], V. Grazú [c]*

[a]Departamento de Química Orgánica y Química Física. Facultad de Ciencias-Instituto de Ciencia de Materiales de Aragón, Universidad de Zaragoza-CSIC, 50009 Zaragoza, Spain.
[b]Departamento de Física de la Materia Condensada. Facultad de Ciencias-Instituto de Ciencia de Materiales de Aragón, Universidad de Zaragoza-CSIC, 50009 Zaragoza, Spain.
[c]Instituto Universitario de Nanociencia de Aragón, Universidad de Zaragoza-CSIC, 50009 Zaragoza, España

* carloss@unizar.es

Fibres forming the extracellular matrix (ECM) of a live tissue have a specific orientation and structure that heavily influences its response and therefore its function. Apart from this anisotropy, biomimetic scaffolds try to emulate the natural ECM with structure architectures having geometries, pore sizes and surface textures that favors the cell adhesion, proliferation, transport of nutrients and residues and the formation of a vascularate. Photopolymerization is a suitable technique for the preparation of complex artificial structures since allow a good spatial control of the polymerization reaction so it is a very convenient technique for the production of polymeric microstructures with well defined features of interest in tissue engineering applications.

Acrylate based systems have been widely studied for the preparation of scaffolds. Usually they comprise biodegradable segments functionalized with acrylate reactive end groups. The chain growth polymerization mechanism of acrylates results in nondegradable hydrocarbon polymeric chains that may be difficult to eliminate by the body after in vivo degradation leading sometimes to side effects in the patient.[1] Anseth and coworkers have investigated thiol-ene biodegradable photopolymers that result in a controlled homogeneous network architecture generated via a step-growth mechanism obtaining as a result an improved control of the degradation-elimination process.[2] Only very recently the thiol-yne reaction has been proposed to be used in photopolymerizable systems that result also in homogeneous network architectures[3] however the thiol-yne reaction has not been tested as a biomaterial.

In the present communication we demonstrate the use of the thyol-yne reaction to produce microstructured biomaterials which can be used as a versatile platform for cell culture. Our material is based in a hyperbranched polyester functionalized with alkyne groups, a multifunctionalized thiol and a UV photoinitiator Citotoxity and cell viability essays have shown that the material is biocompatible. We have also created two dimensional structures with controlled geometries using direct laser writing followed by a solvent etching step. We have studied the cell growth and proliferation in bidimensional relief structures with different geometric parameters. The influence of the polymeric structure geometry on cell morphology will be discussed.

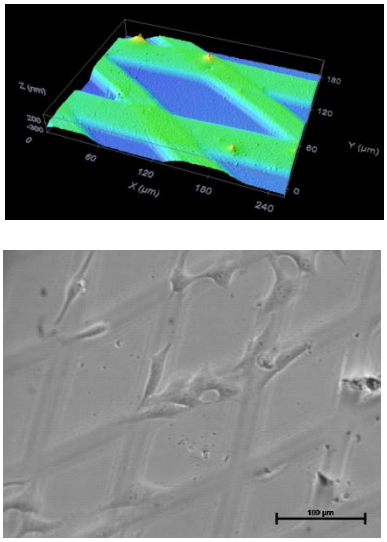

Figure 1. (a) Topography image, obtained using a confocal microscope, of a two dimensional structure generated by direct laser writing onto a casted film followed by subsequent solvent etching step (two sets of parallel stripes arranged at an oblique angle). (b) Phase contrast microscope images of HeLa cells cultured onto patterned polymeric structures.

Acknowledgments: This work was supported by the Gobierno de Aragon under the project ARAID jovenes investigadores, MICINN under the project MAT2008-06522-C02, FEDER fundings and CSIC (Project PIE200960I168). M.L. acknowledges to the DGA for his grant.

References:

1. B.Baroli. "Photopolymerization of biomaterials: issues and potentialities in drug delivery, tissue engineering, and cell encapsulation applications", Journal of Chemical Technology and Biotechnology, 81, 491 (2006).
2. A.E. Rydholm, C.N. Bowman, K.S. Anseth. "Degradable thiol-acrylate photopolymers: Polymerization and degradation behaviour of an in situ forming biomaterial", Biomaterials 26, 4495 (2005).
3. B.D Fairbanks, T.F. Scott, C.J. Kloxin, K.S. Anseth, C.N. Bowman, Thiol-yne photopolymeriations: novel mechanism, kinetics, and step-growth formation of highly cross-linked networks. Macromolecules 42, 211 (2009).

PHEMA based Polymer Dielectrics for gravure-printed OTFTs

Julian Farmer[1], *Beinn Muir*[1,2], *Nikolay Vaklev*[2], *Alasdair J. Campbell*[2], *Joachim H.G. Steinke*[1]

1. Chemical Biology Section, Department of Chemistry, Imperial College London, South Kensington Campus, London, SW7 2AZ, UK. 2. Department of Physics, Imperial College London, South Kensington Campus, London, SW7 2AZ, UK.

j.steinke@imperial.ac.uk

There is a wide variety of dielectric materials, which include polymers, SAMs, inorganic compounds and hybrids. With the increasing interest in the study and fabrication of OTFTs there is a need for new dielectrics that can be easily printed. These polymer dielectric films need to be thin and robust. It is also favourable, when gravure printing the films, to be able to adjust the molecular weight and thus the viscosity of the polymer blends. PHEMA and crosslinked PHEMA (XL-PHEMA) has already been gravure printed and used as a dielectric in organic electronic devices. XL-PHEMA has been shown to be robust, easy to process and high performing in gravure printed OTFTs (Figure 1).[1]

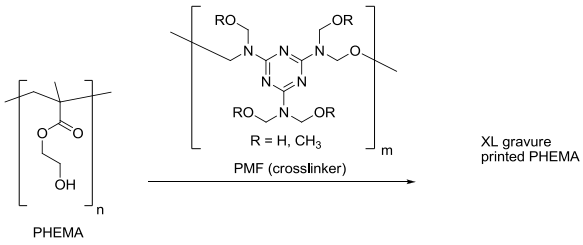

Fig 1. PHEMA as a low temperature crosslinkable dielectric for gravure printing.

In order to retain the advantageous properties of PHEMA while being able to produce much thinner gravure printed films, we have begun to develop PHEMA-based copolymers to improve the deposition characteristics of PHEMA.[1,2]

ATRP is the preferred controlled polymerisation method (over RAFT and NMP) as it has been shown to polymerise a wide variety of methacrylates with good control over molecular weight and gives narrow polydispersity (typically $M_w/M_n < 1.3$).[3,4] ATRP can also give access to obtain well-defined copolymers such as block-polymers and gradient polymers (Fig 2) to further tune the physical and chemical properties.[2,5]

Specific functionality has to be introduced to the PHEMA "base" dielectric to improve the performance. Therefore, co-monomers providing specific interactions to enhance adherence of the dielectric to the substrate, and in our case to gold electrodes, have been synthetically introduced to achieve thinner films and a more controlled ink transfer during gravure printing.

One such functional inclusion is the introduction of thiol groups into the dielectric to enhance the affinity to the gold electrodes. (Fig 2)

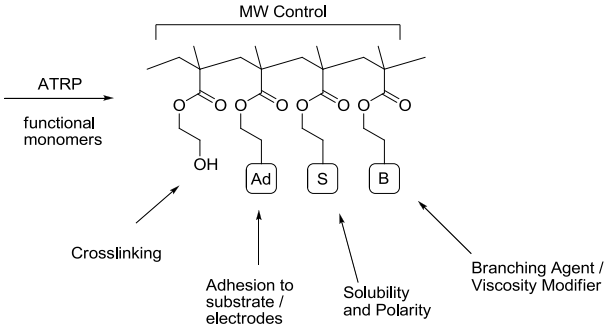

Fig 2. Synthesis of PHEMA copolymers for the introduction of specific functionalities.

Films of PHEMA copolymers containing thiol group as adhesion promoters have been both thermally- and UV-cured using a variety of crosslinkers. We will show data comparing spin coated and gravure printed PHEMA films both thermally- and UV-cured and their performance as dielectrics for OTFTs.

References:

1. M.M. Voigt, A. Guite, D.-Y. Chung, *et al.*, *Adv. Funct. Mater.* **2010**, 20, 239.
2. W. Xiao-song, L. Ning, Y. Sheng-kang, *Polymer*, **1999**, 40, 4157
3. K. Matyjaszewski, J. Xia, *Chem. Rev.* **2001**, 101, 2921
4. J.-S. Wang, K. Matyjaszewski, *J. Am. Chem. Soc.* **1995**, 117, 5614
5. K. Matyjaszewski, M.J. Ziegler, S.V. Arehart, D. Greszta, T. Pakula, *J. Phys. Org. Chem.* **2000**, 13, 775

Modified Epoxy Resin as Electrolytes for Structural Supercapacitors

Alexander Bismarck[1], Shuaijin Carreyette[2], Quentin P.V. Fontana[2], Emile S. Greenhalgh[3], Gerhard Kalinka[4], Anthony Kucernack[5], Milo Shaffer[5], Natasha Shirshova[1], Joachim H.G. Steinke[5], Malte Wienrich[4]

[1]Department of Chemical Engineering, Polymer and Composite Engineering (PaCE) Group, Imperial College London, London, U.K.
[2]UMECO Composites Technology Centre, Heanor, Derbyshire, U.K.
[3]Composite Centre, Imperial College London, London, U.K.
[4]Bundesanstalt fuer Materialforschung und –pruefung (BAM), Berlin, Germany
[5]Department of Chemistry, Imperial College London, London, U.K.

n.shirshova@imperial.ac.uk, j.steinke@imperial.ac.uk

Introduction

Multifunctional materials have received widespread attention their ability to perform simultaneously two or more functions make them attractive materials for applications from biomedical to aerospace encompassing many disciplines [1]. Energy storage is one of the areas where the introduction of multifunctional materials is expected to save weight and volume by combining the features of structural materials with those responsible for the electrochemical performance.

Our focus in this area is on supercapacitors where the main components are the electrodes, separator and electrolyte. We have opted to combine epoxy resin with liquid electrolyte to provide a resin which retains its desirable mechanical performance while exhibiting sufficient levels of ionic conductivity. Despite these contradicting requirements, it was shown earlier [2] that it is possible to cure epoxy resins in the presence of ionic liquid. However authors found that ionic liquid content significantly affects both mechanical performance and ionic conductivity and samples which were ionically conducting had low Young's Modulus.

Results and discussion

A commercially-available epoxy resins was studied. It was found that at only 30 wt.% of resin monolithic tough plaques with a thickness of 2-3 mm could be made which showed ionic conductivities of 1 mS/cm (measured at 25 °C) and Young's Modulus 0f 200 MPa. A clear correlation was found between resin content and performance of the cured product. An overall trend similar to that found by Endo [2] was observed. Figure 1 gives an indication of the morphology encountered in one of these multifunctional resins. At the meeting we will provide details on the effect of additives on the curing kinetics, phase separation, ionic conductivity and morphology of the resultant resin. We consider these initial results as an important step towards the materials developments required for structural supercapacitors.

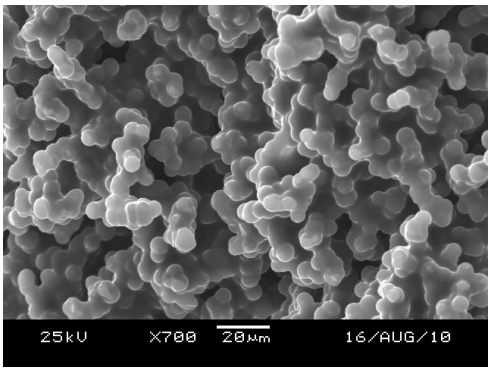

Figure 1. SEM micrograph of multifunctional resin

Acknowledgements

Funding from the EU as part of the FP7 project "Storage" (Grant Agreement No. 234236) is gratefully acknowledged.

References

Gibson, R.F. Composite Structures, 2010(92): p. 2793-2810.

K. Matsumoto and T. Endo. Macromolecules, 2008. **41**: p. 6981-6986.

Kinetics of Thermo-Stimulated Volume Phase Transition in Poly(2-(2-methoxyethoxy)ethylmethacrylate) Hydrogels – Raman and Dielectric Spectroscopy Studies

M. Pastorczak[1], Y.A. Yoon[2], M. Kozanecki[1], L. Okrasa[1], S. Kadlubowski[3], R. Kisiel[1], T. Kowalewski[2], K.Matyjaszewski[2], J. Ulanski[1]

1 Department of Molecular Physics, Technical University of Lodz, Zeromskiego 116, 90-924, Lodz, Poland
2 Department of Chemistry, Carnegie Mellon University, 4400 Fifth Avenue, Pittsburgh, Pennsylvania 15213
3 Institute of Applied Radiation Chemistry, Technical University of Lodz, Wroblewskiego 15, 93-590 Lodz, Poland

marcin.pastorczak@p.lodz.pl

Introduction

Stimuli-responsive hydrogels are a group of materials which reveal relatively large and abrupt change in the properties in response to even small modification in environmental conditions [1, 2]. Because of such properties going together with their good biocompatibility and biodegradability, they are expected to be perfect materials in various biomedical and pharmaceutical applications. The biggest disadvantage of these amazing materials preventing them from commercialisation is their insufficiently quick response to an applied stimulus. Hence, many studies have been performed lately to improve response kinetics of hydrogels. The most important factor that slows down the squeezing rate of a hydrogel is the formation of a dense skin layer which is impenetrable by water molecules and slows down further diffusion processes. One of the most promising strategies of solving this issue is introducing hydrophilic dangling chains into a polymer network. Their role is to prevent to some extent aggregation of hydrophobic chains and maintain channels for water diffusion. The additional advantage should be caring out such modification with use of atom transfer radical polymerisation (ATRP) which allows to control well the architecture of synthesised polymer [3].
The analytical problem to solve is finding a proper methodology to analyze kinetics of thermo-stimulated volume phase transition, and control of potential skin formation.

Experimental

Thermo-responsive hydrogels both “mother gel” and “daughter gel” based on 2-(2-methoxyethoxy)ethyl methacrylate (MEO2MA) were prepared by ATRP method with crosslinking agent (EGDMA; ethylene glycol dimethacrylate) concentration 1:100. Mother gel does not contain any dangling chains and daughter gel contains dangling chains (MEO2MA) with degree of polymerization of 65 [4].Relaxations of polymer chains during volume phase transition (VPT) were analyzed with use of Novocontrol Alpha Analyser Concept 80 apparatus. In order to keep good contact between hydrogel sample and electrodes and to avoid flowing of water out of a cell the measurements were performed using the Novocontrol Liquid Sample Cells BDS 1308.

Water-molecular interactions during volume phase transition were studied with Bruker FT-Raman spectrometer combined with confocal microscope Ramanscope.

Results

Broadband dielectric spectroscopy results revealed that α-process (related to segmental relaxation of the polymer) accelerates ca. 1.5 decade (from 5x104 Hz to 1.3x106 Hz) after heating of the hydrogels above VPT (temperature of ca. 20C). After cooling down below this temperature it slows down again. Such behaviour is probably related to the facts that polymer chains in their hydrated state (hydrogel in equilibrium swelling degree) are stretched and after desorption of water they relax and change their conformation. Analysis of shifts of bands related to particular hydrophilic centres at polymer chain during VPT shows that various centres release water at different stages of the transition. For example, desorption of water from the $–OCH_3$ groups ends just in the initial stage of the hole process.

Acknowledgments

his project was supported by Polish Ministry of Science and Higher Education (grant no. NN209200738)

References

1. Gil, E.S., Hudson, S. M., Stimuli-responsive polymers and their bioconjugates. Prog. Polym. Sci., 2004. 29: p. 1173–1222.
2. Qiu, Y., Park, K., Environment-sensitive hydrogels for drug delivery. Advanced Drug Delivery Reviews, 2001. 53: p. 321-339.
3. Matyjaszewski, K., Xia, J., Atom transfer radical polymerization. Chem. Rev., 2001. 101: p. 2921-2990.
4. Yoon, J.A., et al., Comparison of the Thermoresponsive Deswelling Kinetics of Poly(2-(2-methoxyethoxy)ethyl methacrylate) Hydrogels Prepared by ATRP and FRP. Macromolecules, 2010. 43(10): p. 4791-4797

Electro - Responsive MWNT-PMAA Hydrogel composites for Controlled Drug Delivery

Ania Servant[1], *Khuloud T. Al-Jamal*[1,2]*, *Cyrill Bussy*[1], *Kostas Kostarelos*[1]*

[1]Nanomedicine Lab, Centre for Drug Delivery Research, The School of Pharmacy, University of London WC1N 1AX, UK.
[2]Drug Delivery Group, Institute of Pharmaceutical Science, King's College London, Franklin-Wilkins Building, London SE1 9NH, UK.

ania.servant@pharmacy.ac.uk; kostas.kostarelos@pharmacy.ac.uk

Introduction

The development of controlled drug delivery systems offers the possibility to deliver drugs at predefined periods of time and at predetermined rates. This provides an alternative to the shortcomings of conventional drug delivery formulations[1].Hydrogels have been extensively used in the development of 'smart' controlled delivery systems[2] for their ability to swell and de-swell in response to external stimuli. Electro-responsive drug delivery systems have been developed using polyelectrolyte hydrogels based on poly(methacrylic acid) PMAA matrices[3]. The mechanism of such controlled drug delivery system is based on the chemo-mechanical changes of the gel matrix, such as shrinkage and contraction upon application of an electrical field[4]. Although previously reported systems offer interesting responses regarding pulsatile drug release with ON/OFF electrical field application, the maximum percentage of drug released of 35% after one hour.
Multi-walled carbon nanotubes (MWNTs) have attracted a lot of interest in biomedical applications due to their unique mechanical, thermal, and electrical properties. In this work, we present the development of an electro-responsive PMAA-MWNT hydrogel composite for the generation of 'smart' controlled drug delivery systems.

Materials and Methods

MWNT-PMAA hybrid gels were prepared by *in-situ*radical polymerization (at 70°C for 20 hours) in the presence of pristine MWNTs. Methacrylic acid (MAA),N,N'-methylene bisacrylamide (BIS) and potassium persulfate were used as backbone monomer, cross-linker and initiator, respectively. The incorporation of individualised MWNTs into the polymeric network was characterized by SEM and Raman spectroscopy.

Results and discussion

Homogeneous PMAA-MWNT hydrogel composites with different MWNT concentrations were successfully fabricated.The response of the gels to electrical stimulation was studied by measuring matrix de-swelling as a result of water release upon application of an electrical field. Introduction of MWNTs into the gel matrix decreased the bulk resistivity of the gels and led to an enhanced gel response to electrical stimulation. ^{14}C-sucrose was selected as model hydrophilic drug and drug release was monitored over time while applying ON/OFF electrical field at 15 min exposure interval every one hour. Drug release up to 50% was reached after an hour, in a pulsatile manner for the hybrid gel synthesized with the highest MWNT concentration. The presence of MWNTs seemed to enhance gel damage after exposure to the electrical field as confirmed by SEM.

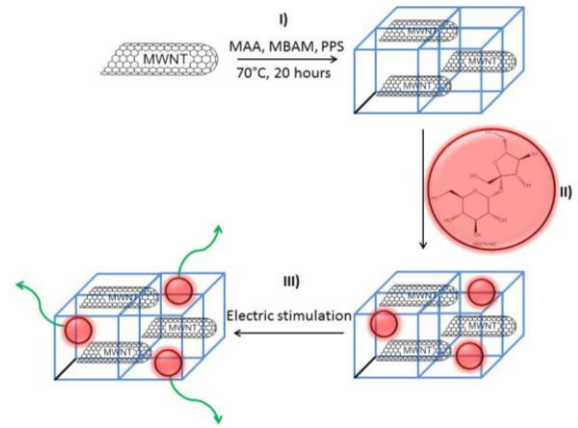

Scheme 1: Synthesis protocol of the MWNT-PMAA hydrogel hybrids

Conclusion

The incorporation of MWNTs into the gel polymeric network has enhanced the electrical responsiveness of the gel and led to significant improvement in drug release, using the model drug ^{14}C-sucrose, up to 50% after an hour of ON/OFF electrical field application, in a pulsatile manner. This offers a great alternative for the development of more efficient controlled drug delivery systems.

Acknowledgments:
Financial support is acknowledged by the EPSRC Grant Challenge of Nanotechnology in Healthcare in Collaboration with Swansea University.

References:

1. Y. Qyu, K. Park, Adv. Drug Deliv. Rev., 2001, 53, 321-339
2. K. Kamasth, K. Park, Adv. Drug Deliv. Rev., 1993, 11 59-84
3. K. Sawahata, M. Hara, H. Yasunaga and Y. Osada, J Contr. release, 1990, 14, 253-262
4. T. Tanaka, I. Nishio, S-T. Sun, S. Ueno-Nishio, Science, 1982, 218, 467-469

Exploiting Adsorption to Taylor the Behavior of Polymers at the Nanoscale

Simone Napolitano, Cinzia Rotella, Michael Wübbenhorst

Department of Physics and Astronomy, KULeuven

simone.napolitano@fys.kuleuven.be

Presence of free surfaces and attractive interfaces might dramatically alter the behavior of polymer chains: deviations from bulk behavior are observed already at hundreds of nanometers, a length scale which cannot be explained in terms of finite size effects.

A large number of experimental works highlighted how properties of ultrathin polymer films (<200 nm) depend on the annealing conditions used during their preparation [for a review see Reiter and Napolitano, Journal of Polymer Science, part B: Physics, **48** (2010), 2544-2547]. We show clear evidence that the changes ultrathin films undergo during annealing are strongly correlated to the amount of chains irreversibly adsorbed at the interface.

A careful analysis of the time evolution of the dielectric function during annealing steps above T_g revealed three different regimes: at short times (in comparison to the adsorption time) the thickness of the adsorbed layer is constant and the interface mimics the effect of a free surface (packing frustration, see Napolitano et al. ACSNano, **4** (2010). 841-848); upon increase of surface coverage, the films undergo a series of metastable states characterized by the largest changes in the deviations from bulk behavior; finally the system approach a new equilibrium whose properties are fixed by the new interfacial configurations.

Our picture is confirmed by further investigation of the impact of annealing on tracer diffusivity and on the crystallization kinetics, as well as on the determination of the distribution of glass transition temperature and dielectric relaxation strength at different distances from the adsorbing interface. Measurements of the local dielectric properties were achieved by selectively placing layers of dye-labeled polystyrene at different depth inside films of neat polystyrene (Rotella, Napolitano et al., Macromolecules, **43** (2010), 8686-8691).

Finally, we show that during annealing ultrathin films evolve towards a steady state whose properties might still differ from bulk. In particular, for polystyrene, the lack of specific interactions with the substrate results in slow adsorption kinetics, keeping the deviations from bulk behavior in steady states with an extremely long lifetime.

New insights in the synthesis of rod-like polyamides. Dependence of molecular weight on the synthetic method

Guiomar Hernández, Cristina Álvarez, José G. de la Campa, Javier de Abajo. Ángel E. Lozano

Instituto de Ciencia y Tecnología de Polímeros, CSIC., Madrid, Spain.

lozano@ictp.csic.es

Introduction

In order to attain materials with improved properties for advanced applications, polymers with the highest possible molecular weight should be synthesized. During the development of the macromolecular chemistry, many synthetic methods have been refined to obtain total conversion of reactive groups, use of mild conditions to limit the hazard of side secondary reactions, easiness of operation and a long so forth.

With regard to aromatic polyamidation, the most common method both in the industry and academia consists of the reaction between diacid chlorides and aromatic diamines in aprotic polar solvents. However, it is necessary to add Ia and/or IIa salts when seeking to obtain wholly rod-like aromatic polyamides (aramids) [1-4].

A milestone in the synthesis of aromatic polyamides was the use of silylated diamines from the 1980s. These monomers are more reactive and produce higher molecular weight (MW) polyamides. It is noteworthy that Imai [5] realized that gelation point for aramids, such as poly(*p*-phenylene terephthalamide), **PPD-T,** was achieved at longer times than when the reaction was made using the classical conditions. This result seems to point out to a different mechanism.

Afterwards, our group developed a new synthetic method by using *in situ* formed silylated diamines, obtaining aramids with higher Mw values than ever reported [6].

This communication deals with the synthesis and characterization of polyamide **PPD-T** synthesized using three methods, as shown in the following scheme:

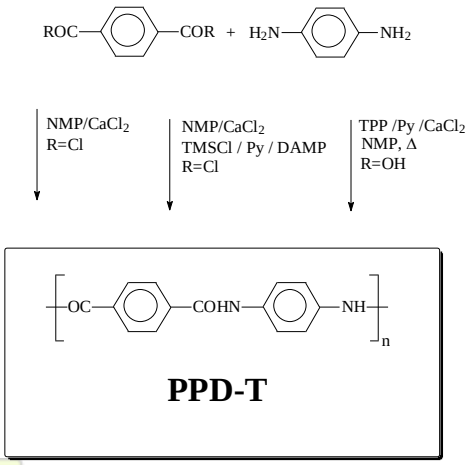

Both classical and in situ silylation polyamidation were performed. The activated reaction using phosphorous compounds was also made for comparison purposes [7]. The target was finding a method which rendered very high Mw PPD-T.

Materials and Methods

Terephthaloyl chloride (TCl, Aldrich) was recrystallized from hexane and subsequently sublimed at high vacuum just prior to use. 1,4-Phenylene diamine (PPD, high- purity Aldrich) was sublimed before being used. Terephthalic acid (TA, Amoco) was used after drying under vacuum at 100°C. Calcium and lithium chloride (Scharlau) were dried at 250°C overnight and kept in a desiccator with phosphorous pentoxide under vacuum. Other materials and solvents were commercially available and used as received

A typical polymerization reaction is as follows: a double-walled glass flask was charged with diamine and polar aprotic solvent under a blanket of nitrogen. After diamine dissolved, the stirred solution was cooled to 0ºC and diacid chloride was added. The mixture was allowed to react under nitrogen for 1h at 5ºC, and then for 12h at 20ºC. Polymers were thoroughly washed with hot water and ethanol and finally dried at 100°C under vacuum. Yields were quantitative for all samples of PPD-T. The *in situ* silylation reaction conditions reported in [6] were used.

Results and Discussion

Samples of PPD-T obtained in 5 batches under different reaction conditions of in situ silylation, were compared with those prepared by the classical polyamidation and the phosphorous assisted reaction. The inherent viscosity data permitted to assert that much higher molecular weight were obtained by the silylated promoted method.

The time to reach the gel point was also determined. The critical point of PPD-T via *in situ* polyamidation was attained at longer times than those obtained with other methods. This fact was explained by pressuming that the amide groups formed during the reaction were being silylated. A tertiary base (pyridine and a mix of pyridine and N,N-dimethylamino pyridine) was used in order to favor the -silyl amide moieties and then it was possible to confirm this assumption. A model NMR study and molecular modeling has justified this assumption. Finally, optimization of the method has produced a polymer with very high viscosity.

References

1. H. Blades, US. Pat. 3,767,756 (1973) and 3,869,429 (1975).
2. S. L. Kwolek, P. W. Morgan, and W. R. Gorenson, US. Pat. No. 3,063,966 (1962).
3. T. I. Bair, P. W. Morgan, and F. L. Killian, *Macromolecules*, 1977, **10**, 1396
4. S. L. Kwolek, Br. Pat. No. 1,283,064 (1970).
5. Y. Oishi, M. Kakimoto, Y. Imai, *Macromolecules*, 1987, **20**, 703
6. A. E. Lozano, J. de Abajo, J. G. de la Campa; *Macromolecules* 1997, **30**, 2507
7. S. Russo, Alberto Mariani, V. N. Ignatov, I. I. Ponomarev; *Macromolecules* 1993, 26, 4984

Acknowledgements

Authors gratefully acknowledge the financial support provided by MICINN project MAT2010-20668. Also, authors are indebted to Mediodia project for economical support. G. Hernández kindly acknowledges CSIC for a grant JAE-Intro

Heterocomplementary H-Bonding RAFT Agents: New Tools for the Preparation of Tailor-made Supramolecular Block Copolymers

Senbin Chen, Arthur Bertrand, Pierre Alcouffe, Catherine Ladavière, Jean-François Gérard, Frédéric Lortie and Julien Bernard

Université de Lyon, INSA-Lyon, Université Claude Bernard Lyon 1, IMP, F-69621, Villeurbanne Cedex (France)

e-mail: julien.bernard@insa-lyon.fr

Introduction-Despite the increasing attention paid to the construction of supramolecular edifices, the development of block copolymers from self-assembly of tailor-made H-bonding macromolecules remains in its infancy in comparison with covalent analogues. Strategies affording the incorporation of H-bonding units at a specific region of a polymer backbone (chain ends, centre of the chain) are indeed rather limited. Introduction of such motifs can be achieved through postpolymerization functionalization.[1] However, this approach suffers from incomplete transformation of the macromolecules. Surprisingly, the alternative approach consisting in incorporating H-bonding units during the polymerization by using functionalized initiators, chain transfer agents (CTA) or chain terminators in order to optimize the chain functionalization has been scarcely explored so far.[2] Herein, we report a new straightforward approach to the preparation of well-defined sticker-functionalized polymers by RAFT polymerization from original CTAs bearing heterocomplementary H-bonding motifs and the generation of supramolecular block copolymers thereof.[3]

Materials and methods-All reagents were purchased from Aldrich. Monomers were filtered prior to use by passing through a column of basic aluminium oxide. H-bonding CTAs were synthesized as previously described.[3] NMR spectra were recorded on a Bruker AVANCE400 spectrometer using $CDCl_3$. Polymers were analyzed with a SEC apparatus running in THF at 25°C (1mL.min^{-1}) and equipped with a Viscotek VE1121 automatic injector, three columns (Waters HR2, HR1 and HR0.5), and a differential RI detector (Viscotek VE3580). Molar masses were derived from a calibration curve based on a series of PS standards. TEM was performed on a Philips CM120 microscope.

Results and discussion-Aiming at generating a library of well-defined H-bonding polymers, a series of monofunctional and difunctional CTAs bearing either thymine (T) or 2,6-diamidopyridine (D) heterocomplementary recognition units have been prepared (Scheme 1). The capability of the heterocomplementary CTAs to associate through H-bonding interactions was first evidenced by ^{1}H NMR (K_{ass}= 110-140 M^{-1} in $CDCl_3$ at 20°C). Radical polymerizations of vinyl acetate (CTA1), methyl methacrylate (CTA2), isoprene (CTA3), *n*-butyl acrylate (CTAs 3-5) or styrene (CTAs 3-5) were subsequently investigated.

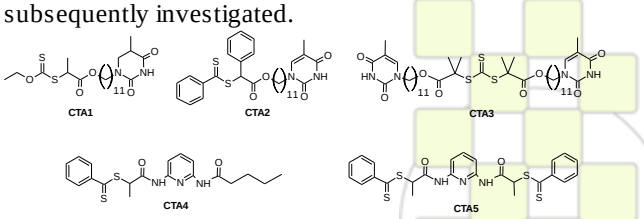

Scheme 1: T and D-functionalized CTAs.

All CTAs were proven to effect a good control of the polymerizations. Sticker-functionalized polymers grew linearly with conversion and polydispersity indices remained narrow (PDI<1.5 excepting for PI samples). Experimental molar masses (1.5-22K) were in good agreement with those expected and polymerizations proceeded with pseudo-first order kinetics indicative of a constant number of propagating centers. ^{1}H NMR/MALDI-TOF analyses demonstrated the incorporation of T/D units on the polymer chains and molar masses evaluated from relative integration of polymer backbone protons and T/D motifs protons were in excellent agreement with theoretical values.

The formation of supramolecular block copolymers and miktoarm stars was demonstrated by ^{1}H NMR with a significant downfield shift of the NH thymine proton ($\Delta\delta$=0.7-0.8 ppm; [T]=[D]=3 × 10^{-3} mol.L^{-1} in $CDCl_3$ at 20°C) observed after adding an equivalent of D-functionalized chains to T-functionalized chains. K_{ass} for the T-D association between H-bonding PS, PBuA, PVAc, PI or PMMA were comparable (80-90M^{-1}) suggesting that the chemical nature of the polymer does not interfere with the recognition process. Supramolecular block copolymer formation in the bulk was further confirmed by TEM (Scheme 2). Indeed whereas blends of unfunctionalized PVAc and PS-D-PS exhibited poorly dispersed domains, macrophase separation was prevented for H-bonding polymer blends owing to supramolecular assembly of the blocks.

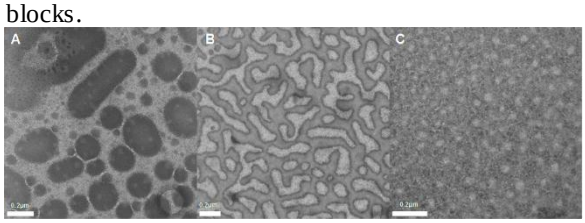

Scheme 2: TEM pictures of PVAc/PS-D-PS 1/1 blend (A), 0.5/0.5/1 PVAc/T-PVAc/PS-D-PS blend (B) and T-PVAc/PS-D-PS 1/1 blend (C).

Conclusions- we have designed a series of original heterocomplementary H-bonding CTAs allowing the generation of well-defined H-bonding macromolecules. The self-assembly of these polymer chains afforded the straightforward generation of synthetically challenging supramolecular miktoarm stars and block copolymers.

References

(1)Folmer, B.J.B; Sijbesma, R.P; Versteegen, R.M.; van der Rijt, J.A.J.; Meijer, E.W. *Adv.Mater.* **2000**, *12*, 874.

(2) (b) Yang, S.K.; Ambade, A.V.; Weck, M. *J. Am. Chem. Soc.* **2010**, *132*, 1637.

(3) (a) Chen, S.; Bertrand, A.; Chang, X, Alcouffe, P.; Ladavière, C.; Gérard, J-F.; Lortie, F.; Bernard, J. *Macromolecules* **2010**, *43*, 5981. (c) Bertrand, A.; Chen, S.; Ladavière, C.; Fleury, E.; Bernard, J. Submitted to *Macromolecules*.

Copolymers of Trimethylene Carbonate and Glycolide: Synthesis and Relationship between Microstructure and Properties

E. Díaz-Celorio, L. Franco, A. Rodríguez-Galán, J. Puiggalí

Departament d'Enginyeria Química, Universitat Politècnica de Catalunya, ETSEIB, 08028-Barcelona

Jordi.Puiggali@upc.edu

Great efforts are nowadays focused on developing polymers for specialized uses (e.g. surgical sutures, scaffolds for tissue engineering or controlled drug delivery systems). In general, polymers that should be employed in the biomedical field must accomplish strict requirements and consequently an improvement of properties appears necessary to extend their application range.

Glycolide and its copolymers with different lactones and/or cyclic carbonates are widely employed due to their biodegradability, biocompatibility and physical properties. In particular, the copolymerization of glycolide and trimethylene carbonate is interesting since may provide materials with controlled properties. Thus, the stiffness of polyglycolide can be compensated by the elastomeric characteristics of poly(trimethylene carbonate). Despite the commercial uses of some glycolide/trimethylene carbonate copolymers, it is clear that they have been designed to accomplish specific requirements. Thus, a complete understanding of the influence of composition and microstructure on properties is still necessary.

Copolymers with different architectures (i.e. random, blocky and segmented) were synthesized under a nitrogen atmosphere in a stainless steel jacketed batch reactor with a capacity of 250 mL at 0.2 MPa and temperatures that ranged between 180 and 220 ºC. Synthesis followed a two step strategy where firstly a soft segment with a theoretically random distribution was prepared by reaction of the two monomers, and then two hard segments were incorporated at each end of the middle soft segment by a subsequent polymerization of glycolide. Block copolymers were obtained from a soft segment constituted only by trimethylene carbonate units whereas random copolymers corresponded to those attained after the first polymerization step.

Analysis of polymer microstructure (Figure 1) and occurrence of transesterification reactions (Figure 2) were evaluated by means of NMR spectroscopy. Mechanical properties were measured from fibers and rectangular shaped samples prepared by using a small-scale melt spinning apparatus and by melt pressing, respectively. Thermal properties were determined by DSC and related to the hard segment content (Figure 3). All the studied copolymers showed similar thermal degradation behaviour although the stability of the corresponding homopolymers was significantly different. Hydrolytic degradation rate in pH 7.4 phosphate buffer was dependent on the microstructure and specifically of the crystallinity of the samples. Influence of the soft segment content and composition on the crystallization process was evaluated by optical microscopy and synchrotron radiation experiments.

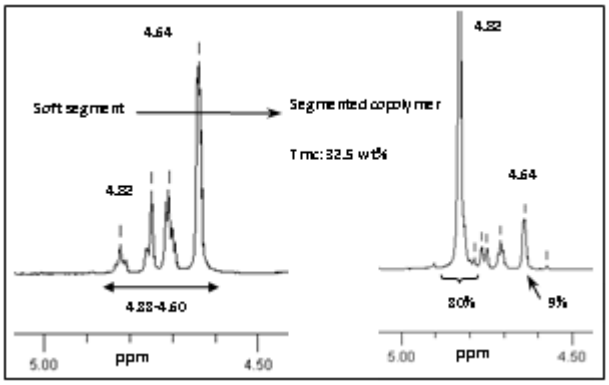

Figure 1. ^{1}H-NMR spectra of representative samples showing glycolide signals of different sequences.

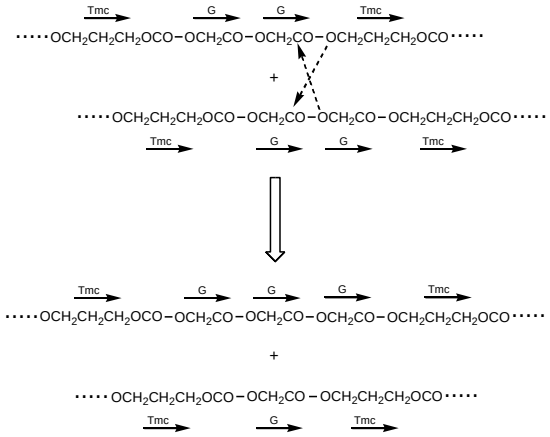

Figure 2. Transesterification reactions that lead to new TmcGTmc sequences.

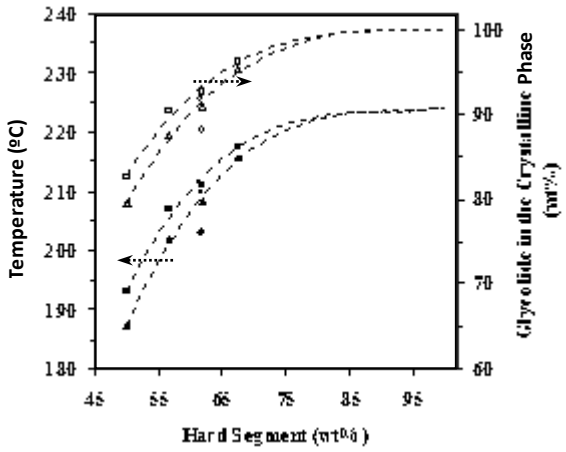

Figure 3. Dependence of the melting temperature with the hard segment content.

Acknowledgements: This research has been supported by a grant from MCYT/FEDER (MAT2009-11503). We want also to express our gratitude to B.BRAUN Surgical S. A. for the collaboration and support.

Innovative Polyelectrolytes For Advanced Applications

David Mecerreyes, Ana Pascual, Ali Aboudzadeh

Institute for Polymer Materials, POLYMAT, University of the Basque Country, Joxe Mari Korta Center, Avda. Tolosa 72; 20018 Donostia-San Sebastian, Spain

e-mail: david.mecerreyes@ehu.es

The properties and classical applications of polyelectrolytes are being outspreading in the last years by the introduction of new ionic moieties (cations and anions) into the polymeric backbone [1]. These new ionic moieties are being developed due to the scientific and technological interest in the field of ionic liquids and for this reason, some of the new polyelectrolytes are being named polymeric ionic liquids (PILs). Examples are found in the figure including polycations and polyanions having i.e. new cations; imidazolium, pyridinium, guanidinium, pyrrolidonium and anions including tetrafluoroborates, hexafluorophosphates, triflates, amidotriflates, and carboxylates. In the last few years, those innovative polyelectrolytes have been finding a wide range of applications in different technological fields such as polymer electrolytes for batteries, electrochromic devices, biosensors, solar cells, gas membranes, anion sensitive block copolymer micelles, smart surfaces and nanocomposites [3-4].

In this presentation, we will review the recent developments in the synthesis and application of innovative polyelectrolytes by introducing the author's work and his perspectives for the field.

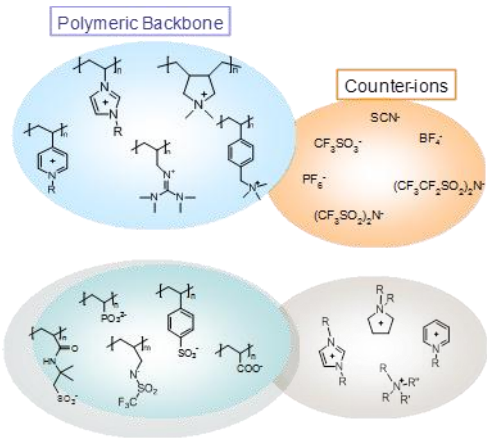

Fig 1. Chemical structure of Innovative Polyelectrolytes

References

[1] Mecerreyes D, Polymeric ionic liquids: Broadening the properties and applications of polyelectrolytes; Progress in Polymer Science 2011.

[2] Vijayakrishna K, Jewrajka SK, Ruiz A, Marcilla R, Pomposo JA, Mecerreyes D, Taton D, Gnanou Y. Synthesis by RAFT and ionic responsiveness of double hydrophilic block copolymers based on ionic liquid monomer units. Macromolecules 2008; 41:6299-6308;

[3] Dobbelin M, Tena-Zaera R, Marcilla R, Iturri J, Moya S, Pomposo JA, Mecerreyes D. Multiresponsive PEDOT-Ionic Liquid Materials for the Design of Surfaces with Switchable Wettability. Adv. Func. Mater. 2009:19;20;3326-333

[4] Pont AL, Marcilla R, De Meatza I, Grande H, Mecerreyes D. Pyrrolidinium-based polymeric ionic liquids as mechanically and electrochemically stable polymer electrolytes. J Power Sources 2009;188:558–63

Improving Thermal Energy Storage in RPU Foams by incorporating Microcapsules containing PCMs

Ana M., Borreguero; Jose L, Valverde; Juan F, Rodríguez ; Manuel, Carmona

Department of Chemical Engineering, University of Castilla – La Mancha, Av. Camilo José Cela s/n, 13071 Ciudad Real, Spain; Phone:+34 926 295300 ext. 6362; Fax:+34 926 295242

e-mail: Anamaria.Borreguero@uclm.es

Introduction

Nowadays, the environmental impact of fossil fuels is undergoing an important attention due to the CO_2 emissions associated with their combustion, which are strongly believed to be contributing to global warming [1]. According to the EU directive 2002/91/EC, close to 40 % of the final energy consumption and also the 36% of CO_2 emissions in the Europe Community in 2002 were due to the residential and tertiary sectors [2] and the new EU directive 2010/31/UE [3] establishes in a 20% the reduction in the green house gases emissions. In the USA, where the energy consumption in buildings is the 30% of the total consumption, the situation is quite similar [4]. The energy demand in the residential sector can be reduced by using the solar energy that reaches the buildings surface. Phase Change Materials (PCMs) can be used to storage the solar energy and release it when external temperature goes down. On the other hand, rigid polyurethane foams (RPU foams) are widely used as insulating materials in buildings due to their low thermal conductivity and high mechanical and chemical stability [5]. However, the thermoregulating properties of the RPU foams can be improved by incorporating PCMs in them [6,7]. Therefore, in this work polyurethane foams have been incorporated with different contents of microencapsulated PCMs and their thermal and mechanical properties have been studied. A special experimental set up has been designed for measuring their thermal behavior and thermal energy storage (TES) capacity.

Materials and Methods

Polyol used was Alcupol R-458 from Repsol YPF S.A. As isocyanate, diphenylmethane-4,4'-diisocyanate (MDI) supplied by Merck Group was used. Catalyst Tegoamin 33 and surfactant Tegostab B8404 were supplied by Evonik Degussa International AG. Deionized water was used as blowing agent. Spherical microcapsules containing Rubitherm® RT27 with a particle size between 1 to 5 μm were obtained following the method described in the Patent EP2119498 [8]

RPU foams were synthesized by weighting and mixing the polyol, silicone, water, amine and the microcapsules and stirring the mixture during 1 min. Then, the isocyanate was added and the solution was stirred for 5 seconds, curing the foams at room temperature.

The foams rising process was measured by an ultrasonic system sqs-01. The microcapsules distribution in the foam was studied by DSC analysis. Cellular structure was depicted by SEM and the cellular size distribution was determined by the program Image Plus. Foam densities were calculated by weighting and measuring the volume of the samples. Uniaxial compression tests were performed according to ASTM D1621 by using using the Model 5584 of an INSTRON universal testing instrument. The thermal behavior and the thermal energy storage (TES) capacity of the foams were studied by measuring the inlet and outlet heat flux to a foam slab subjected to an external heat source.

Results and Discussion

The RPU foams rises properly even when they are incorporated with a 21wt% of microcapsules. However, the higher the microcapsules content, the lower the rising rate and the final height of the foam. The rising process was successfully fitted by a model of reaction curve of 4 tank-in-series. The decrease in the height promoted an increase in the foam density. It can be pointed out that all the synthesized foams satisfied the Spanish regulations for the use of foams in buildings (UNE 92120) that demands a minimum density of 30 kg/m^3. SEM analyses showed that the higher the microcapsules content, the lower the cell size. However, for the higher studied concentrations 18 and 21wt%, microcapsules agglomerate and promote the rupture of struts, giving place to some big cells. On the other hand, the TES capacity increases with the microcapsules content, observing an enhancement of 16.5 kJ/kg in this property when a 21 wt% of microcapsules have been incorporated. Finally, the mechanical tests indicated that, synthesized foams exhibited mechanical properties similar to those reported in literature.

Conclusions

RPU foams with thermo-regulating properties can be developed by incorporating microcapsules containing PCMs. The characterization analyses of these foams allowed to select 18 wt% as the microcapsule content to synthesize foams with a high TES capacity and a good structure and mechanical resistance. According to the experimental results, this foam is able to storage an amount of energy of 12.1 kJ/kg or 23.6kJ/m^2.

Acknowledgments

A fellowship from the Spanish Ministry of Science and Innovation is acknowledged.

References

[1] Gerpen JV. Fuel Process Technology 86 (2005) 1097-1107.
[2] EU Directive 2002/91/EC European Parliament, Brussels; 2003.
[3] EU Directive 2010/31/UE, European Parliament, Strasburg, 2010.
[4] Wang X and Niu J. Energy Conversion and Management 50 (2009) 583-591.
[5] Sarier N. and Onder E. Termochimica Acta 2007; 454:90-98.
[6] Borreguero AM, Valverde JL, Peijs T, Rodríguez JF, Carmona M, *Journal of Material Science*. 2010; 45:4462. doi: 10.1007/s10853-010-4529-x
[7] Borreguero AM, Rodriguez JF, Valverde JL, Arévalo R, Peijs, T, Carmona M. *Journal of Material Science 46:* 347-356.
J. Gravalos, I. Calvo, J. Mieres, J. Cubillo, A.M Borreguero, M. Carmona, J.F Rodriguez, J.L. Valverde, Patent EP2119498 (A1), 2009

Design of high inorganic content organic-inorganic hybrids based on a fluorinated polymer via combination of sol-gel chemistry and reactive extrusion

F. NIEPCERON[1], V. BOUNOR-LEGARE[1], J.F. GERARD[1], P. BUVAT[2], H. GALIANO[2]

(1) UMR CNRS#5223 Université de Lyon – F-69621 Villeurbanne France
(2) CEA-DAM – LSTP - Centre Le Ripault – F-37260 Monts France

bounor@univ-lyon1.fr

Hybrid organic-inorganic materials based on a fluorinated polymer matrix have a large interest as several functionalities could be combined such as enhancement of mechanical properties, electrical and thermal conductivities, use for photovoltaics, antibacterial properties, etc. In addition, numerous papers describe the design of materials based on a polymer matrix and a phase which allows a ionic migration for purification, electrochromic devices, batteries, or fuel cells. The conventional approaches consist in the introduction of already pre-formed nanoparticles such as layered silicates, carbon nanotubes, or nanoclusters whereas the sol-gel chemistry allows to synthesize *in-situ* a nanoscale and hierarchical inorganic phase within the organic polymer medium from the hydrolysis and condensation of metal alkoxides.

This paper proposes a description of the design of hybrid O/I materials based on a fluorinated polymer (polyvinylidene fluoride PVDF) and silicon alkoxides precursors including organofunctional ones (fluorinated, thiol) via an extrusion process.

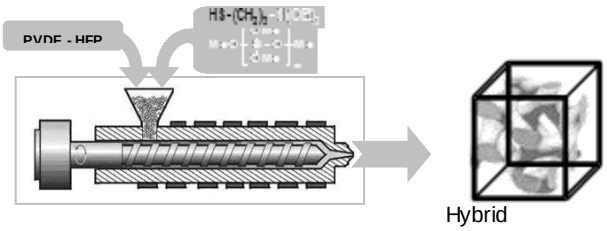

In fact, this approach allows to generate *in situ* in molten PVDF a silicon-rich phase at high contents of eq. SiO_2 (up to 25 wt. %) and tailored interfaces without the introduction of organic solvents which are conventionally used, i.e. enabling the direct processing of O/I films. The influence of the nature of the silicon alkoxide precursors and their degree of pre-condensation, as well as the extrusion process conditions, on the resulting morphologies of the O/I hybrids are detailed.

Synthesis of Phenylphosphine Oxide Containing Urethane Acrylates and Their Applications

Betül Türel Erbay[1], *I. Ersin Serhatli*[2]

[1]Istanbul Technical University, Institute of Science and Technology, Polymer Science and Technology, Istanbul, Turkey
[2]Istanbul Technical University, Faculty of Science and Letters, Department of Chemistry, Istanbul, Turkey

betul_turel@yahoo.com, serhatli@itu.edu.tr

Introduction

Polyurethanes gives excellent performance properties such as toughness, flexibility, elongation, low Tg, low modulus, etc. Because of these inherently good qualities, it made sense to use urethane backbone by adapting as ultraviolet (UV)-curing format. The isocyanates are reacted with diols and polyols to form NCO terminated prepolymers. Then these prepolymers reacted with small acrylated monomers (hydroxyethyl acrylate and methacrylate, etc.), it was shown that the active NCO group of the polymer was replaced by a terminal acrylate functionality.[1,2]

Polyurethane acrylates constitute a class of materials widely used in UV-curable formulations to produce flexible and abrasion resistant coatings.[2] The advantages offered by the UV-curing process; including high speeds of curing that lead to high productivity, lower energy consumption, generation of polymer materials without emission of volatile organic compounds, pollution reduction, cost-effectiveness. and industrial applications such as adhesives, printing inks, photoresist, biomaterials, protective coatings.[2-5]

Curing based on UV radiation allows fast, almost istant, transformation of wet coating composition into a solid material by polymerization at ambient temperature without emission of volatile compound.[6]

The electron pair of the phosphine structure has been donated to an oxygen atom, the phosphine oxide group is unreactive, although it is very polar and subject to strong hydrogen bonding.[7] Phosphine oxide moiety is known to be very good in enhancing thermal and mechanical properties.[8-10]

Materials and Methods

In this study bis[(4-β-hydroxyethoxy)phenyl] phenylphosphine oxide (BHEPPO) was synthesized as mentioned in the literature.[6,11] Different polyols (polyester polyol, polyetherpolyol, and polycarbonate diol) and a diol (BHEPPO) as the soft segment, isophorone diisocyanate (IPDI) and toluene diisocyanate (TDI) as hard segment, hydroxyethyl methacrylate (HEMA) as the blocking agent were used to synthesize reactive urethane acrylate. Coating performance of the polyurethane acrylates on plexiglass substrates was determined by the analysis technique, such as contact angle, pendulum hardness, pencil hardness, gloss. Water absorption, gel content, solvent and chemical resistance values are observed. Also stress-strain test were enhanced.

Results and Discussion

The gloss values of the synthesized polyurethane acrylates (PUA) increased with the increasing BHEPPO content. The pendulum hardness, pencil hardness, tensile strength and e-modulus values increased with increasing BHEPPO content. The value of elongation at break decreased with increasing BHEPPO content. This is totally related with the rigid phenylphosphine oxide groups in the main backbone of PUA's. The contact angle values which were tested with water, decreased by increasing the BHEPPO content. This is related with the hydrophilicity of the phenylphosphine oxide groups.

The chemical and solvent resistance was tested by using hydrochloric acid 10%, Acetic acid 10%, sodium hydroxide 10%, chloroform, xylene, and methanol. The appearance of the samples was good except chloroform treated samples.

Conclusions

Different types of PUA's have been synthesized. The effects of soft segment types (different polyols and BHEPPO) on their physical and thermal properties have been investigated.

The excellent mechanical properties such as pendulum hardness, pencil hardness, tensile strength, e-modulus of the PUA's could be observed by the incorporation of BHEPPO into the PUA's backbone with increasing the content of BHEPPO. The gloss values of all the PUA films were good.

References

S. Oprea, *J. Appl. Polym. Sci.*, **2007**, *105*, 2509.
PH. Barbeau, J. F. Gerard, B. Magny, J. P. Pascault, *J. Polym. Sci*., **2000**, *38*, 2750.
H. Miao, Z. Huang, L. Cheng, W. Shi, *Prog. Org. Coat*., **2009**, *64*, 365.
J. Zhang, P. Xiao, S. Shi, J. Nie, *Polym. Adv. Tech*., **2009**, *20*, 16.
J. Zhang, P. Xiao, S. Shi, J. Nie, *J. Appl. Polym. Sci.*, **2009**, *113*, 896.
S. Karatas, Z. Hosgor, Y. Menceloglu, N. Kayaman-Apohan, A. Gungor, *J. Appl. Polym. Sci*., **2009**,*102*, 1906.
H. F. Mark, J. I. Kroschwitz, *Encyc. of Pol. Sci. and Tech*., **2003**, *11*, 96.
C. W. Lee, S. M. Kwak, T. H. Yoon, *Polym.*, **2006**, *47*, 4140.
M. F. Martinez-Nunez, V. N. Sekharipuram, J. E. McGrath, *Polym. Prepr*., **1994**, *35*, 709.
Y. J. Lee, A. Güngör, T. H. Yoon, J. E. McGrath, *J. Adhesi*., **1995**, *55*, 165.
D. J. Liaw, W. C. Shen, *D. Angew. Makrom. Che.*, **1992**, *199*, 171.

Hybrid Macroporous Hydrogels with Iron Oxide Nanoparticles.

Irina N. Savina[1], Christopher J. English[1], Raymond L. D. Whitby[2], Sergey V. Mikhalovsky [2], Andrew B. Cundy[1]*

[1] School of Environment and Technology, University of Brighton, UK
[2] School of Pharmacy and Biomolecular Sciences, University of Brighton, UK

i.n.savina@brighton.ac.uk

Introduction

Nanoscale particles are used or been evaluated for use in many fields. Because of large surface area and high surface reactivity nanoscale particles provide cost effective solutions to many challenging environmental remediation problems. However there are more concerns rising about toxicity of manufactured nanoparticles for microbes, plants and mammals and the impact of free nanoparticles release to the environment. Embedding the nanoparticles into polymer or other substrates however significantly reduces the environmental risk, while retaining the bulk of the particle reactivity.

In this work novel hybrid material with iron oxide nanoparticles imbedded into a macroporous polymer structure were produced, and their efficiency for removal of heavy metals from aqueous media was tested.

Results and conclusions

Hybrid macroporous hydrogels containing iron oxide nanoparticles were prepared in the form of monoliths by polymerization of 2-hydroxyethyl methacrylate and acrylamide in semi-frozen conditions. Nanoparticle distribution was improved by adding nanoclays to polymer solution. The effect of nanoclays on the structure and physical properties of multicomponent hybrid hydrogels were studied. The material has unique structure of large interconnected pores which provide high permeability (*ca*. 3 * 10^{-3} m s^{-1}). Fe_2O_3 and Fe_3O_4 nanoparticles were physically embedded within the macroporous polymer preventing their release into the environment.

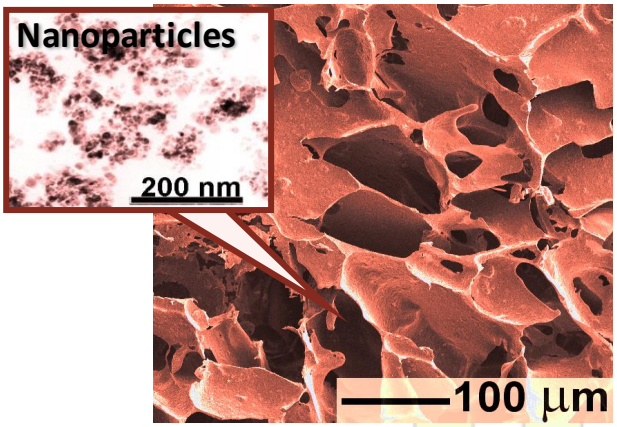

Figure 1. TEM image of a transverse section through the hydrogel with the iron oxide nanoparticles randomly distributed inside the polymer wall (top) and SEM image of the hydrogel cross-section (bottom).

Adding of nanoclays improve the mechanical properties of hydrogel and distribution of iron oxide in the matrix. The hybrid macroporous hydrogel showed promising results for the removal of trace concentrations of As(III), Pb, Cu and Ni from solution. The leaching of iron was minimal and the device could operate at a pH range 3.0 – 9.0.

Hybrid hydrogel can be produced in different configurations that can be adapted to specific applications: monolithic blocks, polymer sheets, discs or columns for through-flow (or flow-over) applications (Figure 2).

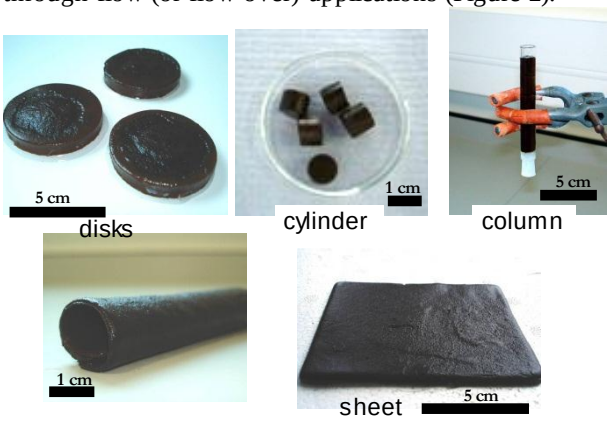

Figure 2. Hybrid macroporous hydrogel in different configurations

The interconnected large pores, mechanical stability and low flow resistance of hybrid macroporous hydrogels make them promising materials to be used as a support for nanoparticles in developing absorption/filtration devices for the clean-up ground water, surface waters and drinking water.

References

1. Plieva F.M., Galaev I.Y., Mattiasson B. Monolithic gels prepared at subzero temperatures as novel materials for chromatography of particulate-containing fluids and cell culture applications. J. Sep. Sci. 30 (2007) 1657.
2. Savina IN, Cnudde V, D'Hollander S, Van Hoorebeke L, Mattiasson B, Galaev IYu, Du Prez F. Cryogels from poly(2-hydroxyethyl methacrylate): macroporous, interconnected materials with potential as cell scaffolds. Soft Matter 3 (2007) 1176.

Acknowledgement

This work was financially supported by FP7 project PIEF-GA-2008-220212-MACRO-CLEAN.

Design of Functional S/DVB microspheres: from hydrophilic particles to superhydrophobic surfaces

J. Rodriguez-Hernandez[1], *A. Muñoz-Bonilla*[1], *C. Lagrugère*[2], *E. Ibarboure*[3], *E. Papon*[3]

[1]Instituto de Ciencia y Tecnología de Polímeros (ICTP), CSIC. C/ Juan de la Cierva n°3 28006 Madrid, SPAIN
[2]Institut de Chimie de la Matière Condensée de Bordeaux, ICMCB-CNRS, 87, Avenue du Docteur Schweitzer 33608 Pessac-Cedex, FRANCE
[3]Laboratoire de Chimie des Polymères Organiques, LCPO-CNRS-Université Bordeaux 1. ENSCPB-16, Avenue Pey Berland, 33607-Pessac-Cedex FRANCE.

jrodriguez@ictp.csic.es

Introduction

Microspheres largely used in coatings, adhesives or inks have been recently employed for other purposes such as medical and biological applications. However, the final use of particles for a targeted purpose is conditioned by different parameters such as suitable and uniform sizes, colloidal stability, but requires also control over the nature and density of the surface functional groups. The preparation of systems able to respond and adequate their properties depending on the environmental conditions is a current center of interest. Systems that exhibit such behavior needs necessarily to incorporate in its structure either responsive polymers or different functional groups (multifunctional interfaces). In particular, the development of multifunctional materials that may adapt their surface properties by orientation of one or other functionality depending on the environmental conditions appears to be an interesting approach. To the best of our knowledge there are only few examples of multifunctional particles. In these cases the authors generally prepared microspheres enveloped with a second polymer shell or modified them chemically to introduce the multifunctional groups: single functional groups or polymer chains.

We describe an approach to prepare environmentally responsive multifunctional particles with hydrophobic (fluorinated moieties) and hydrophilic functional groups (carboxylic acid) able to modify their surface functionality depending on the environment of exposure.

Materials and methods

The particles employed throughout this study were prepared by precipitation copolymerization of divinylbenzene and 2,3,4,5,6-pentafluorostyrene (DVB/5FS 55/45 v/v) with AIBN as initiator (Fig. 1) and using a Acetonitrile/Toluene (95/5 v/v) mixture as solvent. To this mixture and prior to the initiation step, an amphiphilic block copolymer, i.e. polystyrene-block-polyacrylic acid (PS_{31}-b-PAA_{21}) was added. The reaction was carried out during 4 h at 85°C.

Results and Discussion

The presence of the appropriated surface functionality was verified by XPS analysis of the microspheres. XPS analysis revealed that whereas the O1S signal was missing upon annealing to air at 90°C during 3 days, a further annealing to water (80°C, 2 days) increases the oxygen content at the surface as evidenced by the presence of a signal at ~532 eV. Since the oxygen comes exclusively from the PAA segment of the diblock copolymer, annealing to water enhances the migration of the diblock copolymer towards the interface. On the opposite, the F1S signal (~ 687 eV) is larger when the particles are annealed in air. In contact to air the hydrophilic diblock copolymer tends to migrate beneath the surface, so that the surface is now enriched in the fluorinated groups provided by the monomer 2,3,4,5,6-pentafluorostyrene employed for the polymerization.

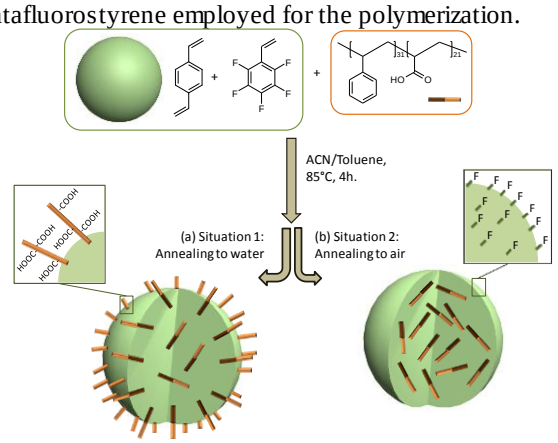

Fig 1. Approach for the preparation of the environmentally responsive particles by combining hydrophobic moieties (fluorinated monomer) and hydrophilic functional groups (carboxylic acid groups present in the poly(acrylic acid) block).

We employed the particles annealed to air to obtain superhydrophobic surfaces and the particles annealed to water to both disperse the fluorinated microspheres in aqueous solution and analyze their response to pH. The elaboration of films from particles annealed to air by solvent casting lead to the formation of superhydrophobic surfaces with contact angles of 165±1.6°. A completely different wettability is observed when the particles are annealed to water under stirring at 80°C during 2 days. Under these conditions, the contact angle of the particle films decreases below 30±1.9°.

Conclusions

We present a new and versatile methodology for the fabrication of switchable (super)hydrophobic /hydrophilic smart surfaces prepared from multifunctional particles containing both hydrophobic (fluorinated) and hydrophilic moieties.

References

a) A. Muñoz-Bonilla et al. Langmuir, 2010, 26(22), 16775.
b) J. Rodríguez-Hernández et al. Langmuir, 2010, 26(24), 18617.

Aknowledgement

The authors gratefully acknowledge financial support from the CNRS, the ANR (Jeunes Chercheurs program ANR-07-JCJC-0148). Equally, this work was supported by the Spanish National Research Council (CSIC) through the PI 200860I037, CCG08-CSIC/MAT-3643 and MAT2009-12251.

Novel Functional Chromatographic Supports: from Preparation to Application

Alexandros Lamprou[1], *Agni Faviola Mika Gavriilidou*[2,1], *Giuseppe Storti*[1], *Massimo Morbidelli*[1]

[1] Inst. for Chemical & Bioengineering, Department of Chemistry & Applied Biosciences, ETH Zurich, Switzerland
[2] Department of Chemical Engineering, Aristotle University of Thessaloniki, Greece
alexandros.lamprou@chem.ethz.ch

Intoduction: The most widespread method for downstream purification of therapeutic proteins, like monoclonal antibodies, is chromatography. Our work's objective is the introduction of novel functional polymeric stationary phases, with advantageous mass transport properties, in order to address different chromatographic modes and solutes after proper surface modification.

Materials and Methods: Initially, primary latex hard core-dual soft shell nanoparticles, surface-modified with an ATRP initiator, are produced by a 3-step semi-batch miniemulsion polymerization. Subsequently they are aggregated in a controlled fashion by gradient salt addition under shear, in combination with the "reactive gelation"[1] technique.

The resulting microparticles are used to pack a conventional HPLC column and consequently their pores are functionalized in situ with polyelectrolytic or environmentally responsive chains, grafted from the pore surface by continuous ATRP. The growth of polymer brushes bearing ionic units and their respective application performance is currently under optimization. Nevertheless, apart from the possibility to carry out conventional ion-exchange protein separations, temperature-controlled purification emerges as an attractive alternative.

Results and Discussion: The microclusters produced are irregularly shaped, yet monodisperse, macroporous (N_2 & Hg porosimetry) and mechanically rigid (SEM), with compact internal structure (DLS). The packed column exhibits exceptionally high total porosity (Inverse Size Exclusion Chromatography) and pressure drop comparable to commercial chromatographic supports. Moreover, due to the large pore size there are no diffusion limitations (Van Deemter analysis), which is ideal for purification of large biomolecules.

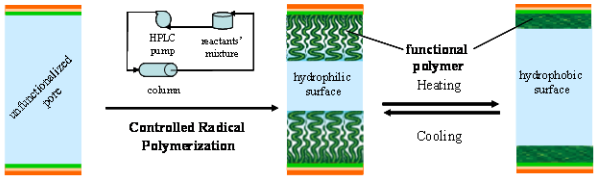

Figure 1: Pore functionalization scheme.

ATRP allows for sufficient functionalization tuning; the degree of polymerization is quantified and correlated with the column's hydraulics and on-line separation performance. For the environmentally responsive functionality, the effect of grafting density, as well as eluent salinity and polarity on the retention of a range of small hydrophobic pharmaceuticals was investigated.

Conclusions: Our results confirm the ability of this novel functional environmentally responsive support to perform analytical separations based on hydrophobic interactions, by responding to temperature cycles. Commonly employed salt of solvent control gradients could thus be substituted by mere temperature changes.

References: 1 N. Marti, F. Quattrini, A. Butté and M. Morbidelli, Macromol. Mater. Eng., 2005, **290**, 221-229

New Developments on Hybrid Colloidal Materials for Applications in Magnetic Hyperthermia

Rebeca Hernández, Coro Echeverría, Vanessa Zamora, Carmen Mijangos

Instituto de Ciencia y Tecnología de Polímeros

rhernandez@ictp.csic.es

Introduction

Magnetically mediated hyperthermia (MMH) consists of the localization of magnetic nanoparticles (NPs) within tumour tissue followed by exposure to an externally applied alternating magnetic field to cause them to heat to temperatures around 40-43 0C. For MMH, superparamagnetic and ferrimagnetic iron oxides have been explored extensively. The encapsulation of these particles on polymer nanogels, crosslinked particles whose dimensions are in the nanoscopic range, allows the intracellular delivery of entrapped drugs combined with magnetic hyperthermia and protects the biological tissue from the contact with the inorganic particles [1].

In this communication, we will present new methods implemented in our group for the synthesis of polymer gels containing magnetic NPs and their response to remote heating by applying a magnetic field [2,3]. In addition, recent results on the encapsulation of magnetic nanoparticles on polymer nanogels [4], will also be presented with emphasis on the relation between viscoelastic and structural organization of these systems. This systematic study is essential for the development of applications.

Materials and Methods

Polymer nanogels with dimensions around 400-500 nm with encapsulated 10 nm magnetic iron oxide nanoparticles prepared from synthetic polymers such as poly (acrylamide-co-acrylic acid) (PAAm-AA) and biopolymers such as chitosan will be considered. Specific power absorption measurements were performed using a homemade ac applicator working at 260 kHz and field amplitudes up to 16 mT and equipped with an adiabatic sample space (0.5 mL) for measurements in liquid phase. Rheological studies were carried out using the AR-G2 TA Instruments stress-controlled oscillatory rheometer. To visualize the morphology and distribution of magnetic nanoparticles, transmission electron microscopy (TEM) at 300 kV was used.

Results and discussion

Figure 1a shows a TEM image where it can be observed that 10 nm iron oxide nanoparticles are encapsulated within a polymer nanogel and that they are not aggregated. Likewise, in situ formation of iron oxide nanoparticles inside polymer gels (figure 1b) allows the homogeneous dispersion of iron oxide nanoparticles and, in addition, the polymer matrix controls the NPs polydispersity

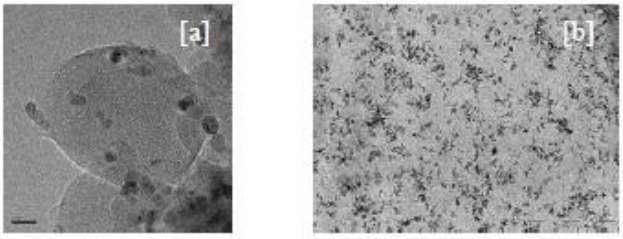

Figure 1. TEM microscopy corresponding to (a) PAAm-AAc nanogel with a 5 wt% Fe3O4 nanoparticles. (b) Fe3O4 nanoparticles synthesized inside a polymer hydrogel derived from alginate.

Interestingly, rheological measurements have shown that for both systems, the elastic modulus is independent of the frequency and that the elastic component (G′) is higher than the viscous one (G″) which is characteristic of gel behavior. In both cases, the introduction of iron oxide nanoparticles causes a reinforcement of the system as demonstrated through the increase of the elastic modulus with the iron oxide NPs concentration. The heating response is also dependent on the iron oxide NPs concentration as shown in remote heating experiments.

Conclusions

Hybrid polymer nanogels and gels have been obtained through two different methods: encapsulation and in situ synthesis of iron oxide nanoparticles. Both methods have proven useful to obtain systems with response to magnetic fields and hence for the development of applications in magnetic hyperthermia.

References

[1] Omid C. Farokhzad; Robert Langer; ACS Nano, 2009, 3, 16-20

[2] R. Hernández, J. Sacristán, C.Mijangos, L. Asín, T.E.Torres, M.R.Ibarra, G.F.Goya Journal of Physical Chemistry B, 2010, 114, 12002-12007

[3] R.Hernandez, V. Zamora, M. Sibaja, J. Vega, D. López, C.Mijangos Journal of Colloid and Interface Science, 2009, 339, 53-59

[4] C. Echeverría, D. López, C.Mijangos Macromolecules, 2009, 42 (22), pp 9118–9123

Multi-shape memory effect of thermo-responsive semi-crystalline polymeric blends

J. M. Cuevas, L. German, R. Rubio, J. M. Laza, F. Mijangos, J. L. Vilas and L. M. León

Gaiker Technology Centre, Parque Tecnológico de Bizkaia, Ed. 202, Zamudio 48170, Spain.
Departamento de Química Física, FCT/ZTF, Universidad del País Vasco/EHU, Apdo.644, Bilbao E-48080, Spain.

cuevas@gaiker.es

Introduction: Smart materials start playing a fundamental role in materials engineering due to their capability to respond actively to external stimulus. In particular, shape memory polymers (SMPs) are stimuli-responsive materials able to adaptively store a temporary shape and recover a 'memorized' permanent shape under specific changes in heat, light, moisture or magnetic fields, among others.
In contrast to most common dual-SMPs able to move from one shape to another, increasing attention is focused on recent thermo-responsive SMPs with multi-shape memory effect upon heating. These exciting discoveries enable further applications in, e.g. deployable structures, biomedicine, adaptive optical devices, smart fasteners and intelligent textiles.
In this work, covalently crosslinked semi-crystalline polymeric blends with thermally-induced triple-shape actuation capabilities, characterized by programmable recovery process from one temporary shape to an intermediate shape before returning to the permanent shape, were developed. The concept was based on forming two segregated crystalline domains, each having its own transition temperature, by combining semi-crystalline polymers, with adjusted respective melting temperatures and elasticity through controlled density of covalent knots. Consequently, applying two-step programming process it was able to create multiple subsequent intermediate shapes, which were not necessarily unidirectional.

Materials and methods: Thermo-responsive crosslinked semi-crystalline polymeric blends were manufactured by melt-compounding and free-radical crosslinking process of double bond containing low broad molecular weight *trans*-polyoctenamer (PCO) and linear medium-density polyethylene (PE).
Thermogravimetric analysis (TGA), differential scanning calorimetry (DSC) and dynamical-mechanical-thermal analysis (DMTA) were used to characterize the formulations, as well as shape memory features like multiple shape fixities (R_{f1} and R_{f2}), shape recoveries (R_{r2} and R_{r1}) and actuation temperatures were evaluated by thermo-mechanical bending experiments.

Results and discussion: Apart from high thermal stability (main thermal decomposition above 430ºC for all developed formulations), evaluation of thermal and thermo-mechanical properties allowed demonstrating two different crystalline domains from both segregated components. Furthermore, corresponding melting temperatures, considered the respective transition temperatures ($T_{trans-1}$ and $T_{trans-2}$) of shape memory features for multiple shape effect, were adjusted by controlling the crosslinking density.

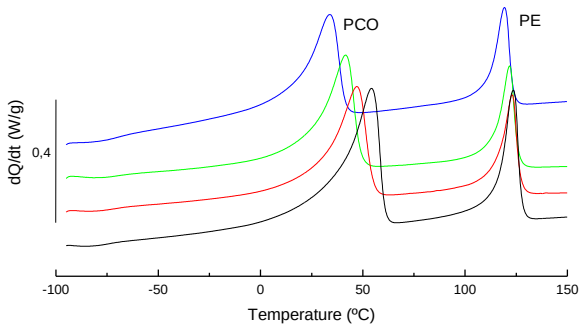

DSC thermograms demonstrating two crystalline domains.

Original permanent shape, thus, was defined by covalent knots along polymeric network, whereas multiple intermediate temporary shapes could be determined by the semi-crystalline domains from PE and PCO, respectively, by two-step thermo-mechanical programming process.

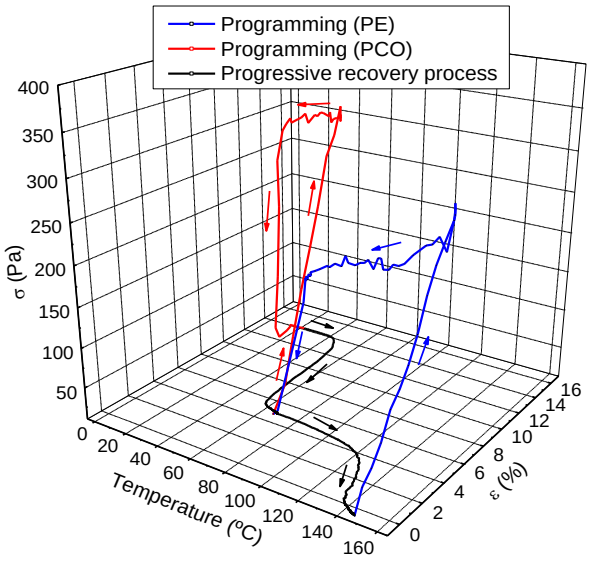

Triple-shape memory capabilities (thermo-mechanical cycling test).

Conclusions: Polymers with multi-shape functionality demonstrate promising applications in temperature sensing/actuating elements. The described approach, thus, allowed developing a series of thermo-responsive triple shape memory polymers with adjustable individual activation temperatures and progressive recovery ratios close to 95-100% for programmable temporary and original shapes.

References:

1- Xie T 2010 *Nature* **464** 267-270.
2- Sun L, Huang W M 2010 *Soft Matter* **6** 4403-4406.
3- Behl M *et col.* 2009 *Adv. Funct. Mater.* **19** 102-108.
4- Bellin I, *et col.* 2006 *PNAS* **103** 18043-18047.
5- Li J, Xie T 2011 *Macromolecules* **44** 175-180.

Multi-armed, biodegradable polyphosphazenes and their use as macromolecular anti-cancer drug carriers

S. Wilfert, I. Teasdale, I. Nischang, O. Brüggemann.*

Institute of Polymer Chemistry (ICP), Johannes Kepler University Linz

Sandra.wilfert@googlemail.com

Biocompatible, biodegradable polymers have gained increasing interest for their role in the development of drug delivery systems. Due to their structural variability, hydrolytic degradability and non-toxic degradation products, polyphosphazenes offer tremendous potential for drug delivery applications. Since the hydrodynamic volume plays a crucial role in the pharmacokinetics and biodistribution of polymeric drug carriers, the synthesis of polymers with well-defined architectures and controlled molecular weights is essential.

In this work we present the synthesis of novel multi-armed polyphosphazenes with controlled architectures and narrow molecular weight distributions. For this purpose, various end-capped phosphoranimines were polymerized with chlorophosphoranimine in a living cationic polymerization. The functionality, solubility and biodegradability of the polymers were adjusted via the side substituents of the polyphosphazene chains.

The ability to carefully control and tailor molecular weight and architecture via the polyphosphazene backbone is important for the design of macromolecular carriers.

To illustrate the versatility of the synthetic procedure to prepare polyphosphazene-drug conjugates, we also synthesized branched, hydrophilic polyphosphazenes carrying tumor-targeting ligands and anthracycline antibiotics attached to the polyphosphazene backbone via a cleavable hydrazone linkage. The conjugates showed a controlled release of the anti-cancer drug in a pH-triggered response. Furthermore, the rate of degradation of the polyphosphazenes could be controlled through careful selection of substituents. These biodegradable, multi-functional polyphosphazenes represent extremely promising candidates for the use as polymeric carriers for the tumor-targeted delivery of anti-cancer drugs.

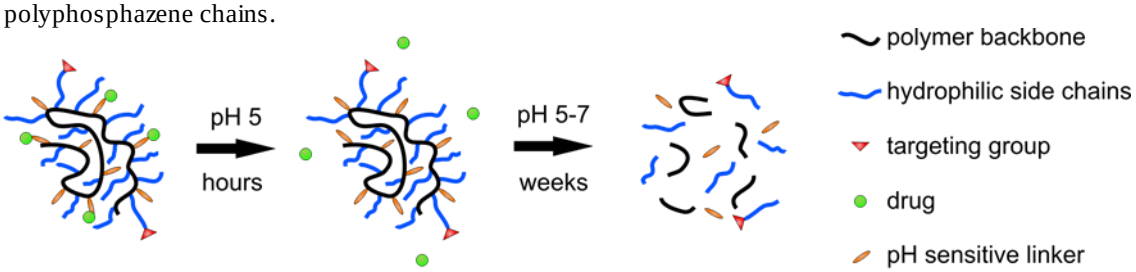

Anti-cancer drug-loaded polyphosphazenes prepared by living cationic polymerization. Drug release via a pH response is followed by degradation of the macromolecular carrier.

Effects of Parameters on Emittance of Thermal Control Coatings Based on Polyurethane and Titanium Dioxide

Mehrdad Taheran[1], *Amir H. Navarchian*[1], *Reza Shoja Razavi*[2]

[1] Department of Chemical Engineering, Faculty of Engineering, University of Isfahan, Isfahan, Iran
[2] Department of Material Engineering, Malek Ashtar University of Technology, Shahin Shahr, Isfahan, Iran

Navarchian@eng.ui.ac.ir

1. Introduction:

Polyurethanes (PUs) are widely used in different industries such as aerospace [1]. The coatings that are used for coating of satellites surfaces should have specific optical properties including maximum total emittance (ε) to maintain the thermal balance of spacecraft and so to protect it against the extreme temperature variations. Because of this characteristic these kinds of coatings are called "Thermal Control Coatings: TCCs". The aim of this work is to develop a coating on aluminum surface based on PU binder and TiO_2 pigment having maximum total emittance. The influences of polyol molecular weight, diisocyanate type, surface pretreatment, NCO/OH ratio and pigment volume concentration (PVC), on total emittance of PU coatings have been statistically investigated.

2. Experimental:

To synthesize the prepolymer, 40 g of PTMG (MW = 1000 or 2000) was reacted with diisocyanate (Hexamethylene diisocyanate (HDI), isophorone diisocyanate (IPDI)) according to specified NCO/OH ratio (1.4, 1.6 or 1.8). The reactions were carried out at 80°C for 6 hrs in a three-necked flask. The prepared resin was dissolved in solvent (xylene /n-butyl acetate: 50/50, v/v) and the specified amount of TiO_2 was added to the mixture. TiO_2 pigments (particle size 10μm) were dispersed in resin with a pearl mill apparatus at 800 rpm [2]. Chemical (using alcoholic phosphoric acid cleaner) and anodic (sulfuric acid anodic) methods were used for surface pretreatment. A L_{16} Taguchi array was employed for experimental design, using S/N response.

3. Result and discussion

3.1. Analysis of variance

Table 1 shows the ANOVA statistical terms for total emittance of PU/TiO_2 coatings. The critical F-ratios for two and three-level factors at confidence level of 95% are 5.33 and 4.46, respectively [3]. It is clear from Tables 1 that the important contributors to variability of the results are pigment volume concentration (E), NCO/OH ratio (D), polyol molecular weight (A), and diisocyanate type (B), respectively. In the present study, factor C (surface pretreatment) represents the lowest F-ratio in the ANOVA tables which implies that both surface pretreatment methods have a same effect on the response.

Table 1. ANOVA table for total emittance (ε)

Factor	DOF	Sum of squares	Variance	F-ratio	Contribution%
A	1	0.0291	0.0297	262.13	12.11
B	1	0.0122	0.0122	109.78	5.04
C	1	0.0026	0.0026	23.62	1.05
D	2	0.0436	0.0218	196.15	18.09
E	2	0. 1513	0.0756	680.21	62.99
Other/error	8	0.0009	0.0001		.071
Total	**15**	**0.239**			**100**

3.2. Influence of operating variables on ε

The effects of factors on ε are shown in Fig. 1. TiO_2 particles strongly reflect the rays within infrared wavelength range, so that TiO_2 can be assumed as a non-absorbing pigment [4]. On the other hand PU resin containing C=O and N-H functional groups absorb and then emit rays in infrared wavelength range [5]. Therefore increasing PVC% or decreasing polymeric phase results in decreasing ε [4]. The use of polyol with higher MW for synthesis of PU resin results in less C=O and N-H absorptive bonds in unit mass, and thus reduction in ε. A same reason justifies also the effect of NCO/OH ratio on the response. IPDI indicates a greater emissivity due to its cyclic structure [4,5].

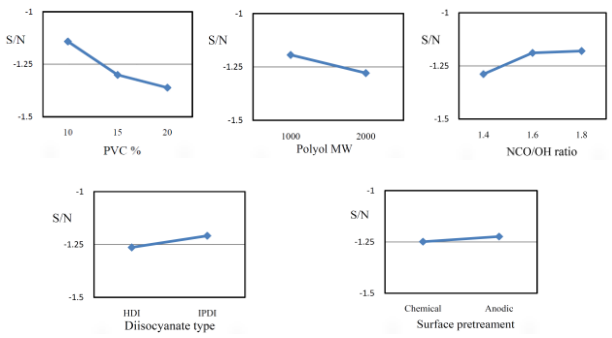

Fig. 1. The effect of factors on total emittance of PU/TiO_2 coating

3.3. Optimum conditions

The optimum conditions to attain a PU/TiO_2 coating with maximum emittance can be determined from maximum points in main effect plots (Fig.1). The predicted value for ε at optimum conditions was therefore obtained as 0.891. In order to verify the validity of the recommended optimum conditions, a new sample was prepared according to proposed optimum factor levels. The predicted value for ε in optimum conditions (0.891) was found reasonably in agreement with the experimental data (0.887).

4. Conclusion

The ε of PU/TiO_2 coating strongly depends on the PVC% and the best performance is obtained at high pigment content. The NCO/OH ratio, polyol MW and diisocyanate type, have also intermediate effects, so that the higher ε is obtained with NCO/OH ratio = 1.8, and with IPDI reacted with high MW polyol. The surface treatment method does not affect ε, and thus the chemical method can be chosen for pretreatment in order to decrease the costs and energy consumption.

References

[1]. Chen et al., 2007. Eur. Polym. J., 43, 4151– 4159.
[2]. Taheran & Navarchian, 2008. 13th National Iranian Chemical Engineering Congress, Kermanshah, Iran.
[3]. Roy, K. R., 2001, John Wiley & Sons,New York.
[4]. Baneshi, M., 2009, Ther Sci. Tech., 32, 131- 145.
[5]. Wang, Z., 2009, Macromolecules, 42, 4972–4976.

Functional Particles Obtained By Emulsion Polymerization Using Glycopolymer Surfactants

Alexandra Muñoz-Bonilla,[1] Vanesa Bordegé,[1] Orietta León,[1] Rocío Cuervo-Rodríguez,[2] Manuel Sánchez-Chaves,[1] Marta Fernández-García[1]

1 Chemistry and Properties of Polymeric Materials Department, Institute of Polymer Science and Technology (CSIC), C/ Juan de la Cierva 3, 28006 Madrid, Spain.
2 Organic Chemistry I Department, Faculty of Chemistry (UCM), Avenida Complutense s/n, Ciudad Universitaria, 28040 Madrid, Spain.

e-mail: martafg@ictp.csic.es

Introduction

Glycopolymers, typically, containing cyclic saccharides are used in biomolecular recognition processes. In contrast, polymers with an open-chain sugar structure seem to be more efficient on enhancing the hydrophilicity of the polymer surface than those containing cyclic saccharides. To this respect, glycopolymers containing the sugar groups in the open-chain form, such as lactone, can be used to modify polymeric materials surface to prevent the undesirable adhesion of protein, cell, or other molecules.

In this work, we report the synthesis of statistical glycopolymers by conventional radical polymerization and their posterior employment as stabilizers in the emulsion polymerizations of methyl acrylate. This is an easy method to prepare particles bearing saccharides by using only classical radical polymerization.[1]

Experimental part

Materials

2-Hydroxyethyl methacrylate, HEMA, and methyl acrylate, MA, were purified by conventional methods. 2,2'-Azobisisobutyronitrile, AIBN, was purified by successive crystallizations from methanol. *p*-Nitrophenyl chloroformate, glucono-1,5 lactone and 1,4-diaminobutane were used without further purification. Sodium persulfate and thiosulfate were used as received. Dimethyl sulfoxide, DMSO, and triethylamine were previously distilled; methanol, ether dioxide and ethanol were used as received.

Synthesis of Glycomonomer, HEMAG

The aminosaccharide, N-(4-aminobutyl)-D-gluconamide, NABG, and activated HEMA with p-nitrophenyl chloroformate, HEMAN were prepared by following the literature. The glycomonomer, 2-[({[4-(D-gluconamid-N-yl) butyl]amino}carbonyl)oxy] ethyl methacrylate, HEMAG, was prepared according to the following Scheme.

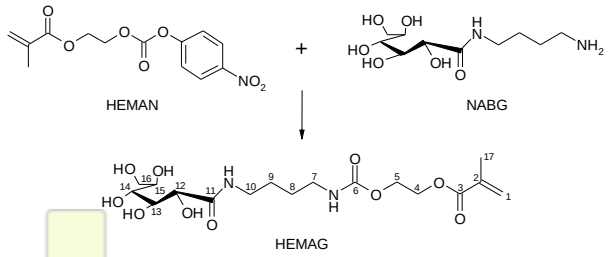

Copolymerization Reaction

The HEMAG and MA monomers were polymerized with AIBN as an initiator ($3 \cdot 10^{-2}$ mol/L) and with DMSO as a solvent (1 mol/L) at 70 ºC. The copolymerization was monitored in-situ by proton NMR using tube sealed under argon atmosphere.

Emulsion Polymerization

Water-soluble glycopolymers obtained at very high conversion ($f_{HEMAG} \cong F_{HEMAG} \geq 0.5$) were used as surfactants in the emulsion polymerization of MA. All the reactions were carried out in batch, in a three-neck reactor with a reflux condenser, an argon inlet, and a mechanical stirrer. At different reaction times, samples were withdrawn by syringe under an argon flow. Hydroquinone was added to quench the polymerization, and the monomer conversion was determined by gravimetry.

Results and discussion

A series of amphiphilic statistical glycopolymers were synthesized by conventional radical polymerization of methyl acrylate and a synthesized glycomonomer with the glucose groups in the open-chain form, HEMAG. The monomer reactivity ratios were calculated from the cumulative feed and copolymer molar fraction data obtained during the reaction. The HEMAGl-MA system is fairly described by the Mayo-Lewis terminal model. The thermal properties of the obtained glycopolymers such as their glass transition and thermal stability temperatures, which resulting to be dependent on the carbohydrate composition, were studied to evaluate their operability for the application of these materials as antifouling coating. The incorporation of NABG into HEMA could leads to a considerable decrease in Tg due to the diaminobutyl flexible spacer. However, the inter- and intramolecular hydrogen bonds between carbohydrate hydroxyl groups compensate this diminishment.

The water soluble statistical glycopolymers, i.e. those with compositions higher than 0.5 in glycomonomer, were used as polymeric surfactants in the MA emulsion polymerization. In this sense, increasing the molar fraction of MA in the copolymer improves the performance of the glycopolymers as surfactants, and smaller and more monodisperse particles are obtained, varying their size in the range of 200 nm and 1 μm.

Acknowledgment

The financial support of Ministerio de Ciencia e Innovación (Project MAT2010-17016) is gratefully acknowledged. V. Bordegé and O. León thank Comunidad de Madrid and Universidad de Zulia for their fellowships, respectively. A. Muñoz-Bonilla thanks CSIC for her JAE-DOC postdoctoral contract.

References

1. V. Bordegé, A. Muñoz-Bonilla, O. León, R. Cuervo-Rodríguez, M. Sánchez-Chaves, M. Fernández-García, *J. Polym. Sci. Part A: Polym. Chem*. 49: 526–536, 201

Fundamentals aspects of crosslinking control of PDMS rubber at high temperatures for development of new Thermoplastic Silicone Vulcanizate (Super-TPV)

Skander Mani[1,2*], *Philippe Cassagnau*[2], *Mosto Bousmina*[3], *Philippe Chaumont*[2]

1) Department of Chemical Engineering, Laval University, Quebec G1V 0A6, Canada
2) Université de Lyon, France, F-69003, Université de Lyon 1, France, F-69622, CNRS UMR5223, Ingénierie des Matériaux Polymères: Laboratoire des Matériaux Polymères et Biomatériaux, 15 Boulevard Latarjet, F-69622 Villeurbanne (France)
3) Institute for Nanomaterials and Nanotechnology (INANOTECH), Hassan II Academy of Science and Technology, Rabat, Morocco

*skander.mani.1@ulaval.ca

Abstract:

The control of macromolecular structure has recently become an important facet of polymer science from both an academic and an industrial point of view.

Indeed, free-radical crosslinking of Polydimethyl-vinylmethyl-siloxane (vinyl-PDMS) rubber by organic peroxide suffers from premature crosslinking at high temperatures, which is called scorching. Consequently, the basic aim of the investigations described in this work is to widen and explore the network topology-crosslinking kinetics relationships and find a novel way to control free-radical crosslinking chemistry and topological parameters of final PDMS networks. The work is primarily focused on the extensive study of the crosslinking control of PDMS rubber at high temperatures. A novel composition using 2,2,6,6-tetramethylpiperidinyloxyl (TEMPO) and dicumyl peroxide (DCP) for scorch delay and control of the final network topology of the PDMS has been proposed. The work specified in this investigation is therefore directed to find a proper [TEMPO]/[DCP] ratio provided the development of a new biphasic material such as PA12/PDMS blend type Super-TPV (Super Thermoplastic Vulcanizated). For this purpose a new method based on the relationship between the kinetics of the macro-radicals coupling [Rcc(t)] was derived from a fundamental kinetic model and the viscoelastic changes of the complex shear modulus (G'(t)ω and G''(t)ω). The kinetic model takes into account the initiator (DCP) decomposition and the trapped PDMS macro-radicals in the presence of a radical scavenger such as TEMPO. As a main result, the rheological modelling shows that this new method accurately predicts the time variation of complex shear modulus at any temperature and [TEMPO]/[DCP] ratio (Figure 1). Interestingly, addition of TEMPO to the TPV novel composition provided the PA12/PDMS blend compatibilization in the dynamic process and gives a new material having a controlled structure and morphology. A better insight in understanding the blend composition and the morphology development relationships is aimed at.

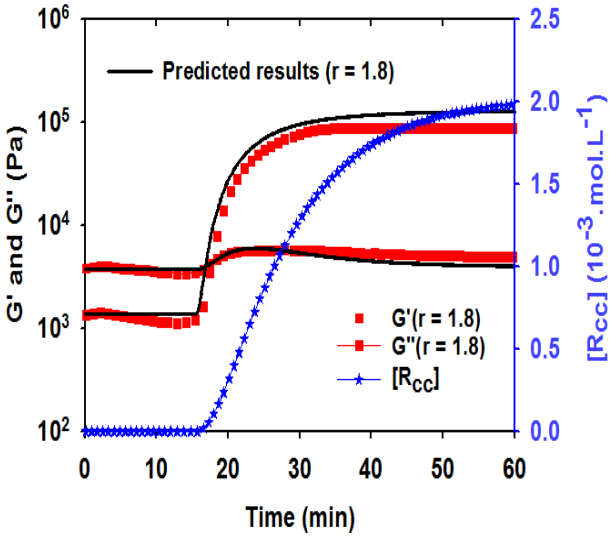

Figure 1: Rheological modelling of the free-radical crosslinking of PDMS rubber in presence of TEMPO nitroxide.

Keywords: TPV, rheological modelling, crosslinking, compatibilization, silica nanoparticles, morphology

Thermodegradable Polyaldehydes: From Amiphiphilic Block-Copolymers to Advanced Materials Patterning

Stefan Köstler[1], *Daniela Wachter*[2], *Barbara Zechner*[2], *Heinz Pichler*[1], *Andreas Rudorfer*[1], *Stefan Spirk*[2], *Hubert Fasl*[2], *Bernd Trathnigg*[2], *Volker Ribitsch*[1,2]

[1] JOANNEUM RESEARCH, Materials – Institute for Surface Technologies and Photonics, Graz, Austria
[2] University Graz, Institute of Chemistry, Graz, Austria

stefan.koestler@joanneum.at

Introduction:

Polyaldehydes are a very special class of polymeric materials. Their most distinguishing property is that many of them have ceiling temperatures close to or below room temperature. Therefore they can be depolymerized following a well defined unzipping reaction and are converted back into the monomers at moderate temperatures. Although this type of unzipping reaction has been recognized long ago [1] and such polymers were used as self-developing photoresists [2], the responsive properties of polyaldehydes were so far not explored for other applications. This interesting class of materials remains to be rediscovered for the preparation of smart functional materials. Recently it could be shown that polyaldehydes allow for the preparation of amphiphilic block copolymers [3] and the construction of chemoresponsive materials [4]. In this contribution we report on the preparation and characterization of poly(phthalaldehyde) and poly (glyoxylate) and amphiphilic block-copolymers. We also show applications of these thermoresponsive materials as dispersants, in the preparation of organic nanoparticles [5], or for inkjet formulations. Moreover the potential for further applications such as the synthesis of organic/inorganic hybrid materials will be discussed.

Materials and Methods:

Polyaldehydes from phthalalehyde and ethylglyoxylate were prepared by ionic polymerization. Block copolymers were obtained by coupling of preformed telechelic blocks. Molar mass and polymer composition were characterized by dual-detection size exclusion chromatography among other techniques. The thermal behaviour and depolymerisation reactions were investigated using scanning thermal analysis coupled with mass spectroscopy. Colloidal and self-assembly properties of amphiphilic polymers were investigated using dynamic light scattering, fluorescence probe techniques and by use for nanoparticle stabilization. Polyaldehyde homopolymers were investigated for the formulation of conductive inkjet printing inks. Inks were evaluated using rheology and printing tests using a piezoelectric drop-on-demand materials printer.

Results and Discussion:

Homopolymers of phthalaldehyde were polymerized with cationic and anionic initiators and their properties were compared. In order to prevent immediate depolymerisation the polymer endgroups were blocked using isocyanate capping reagents. For the preparation of block copolymers, poly(phthalaldehyde) blocks were endcapped with bifunctional reagents in order to obtain telechels. Telechelic polyaldehyde blocks having isothiocyanate endgroups can be isolated and subsequently coupled to amino-terminated poly (alkyleneoxide) to form amphiphilic block-copolymers. The poly(phthalaldehyde) blocks can selectively be depolymerized at moderate temperature (Fig. 1). These blockcopolymers were shown to be able to form micellar aggregates in solution. Consequently they were found to be effective dispersants. They were for example successfully applied for in-situ stabilization of organic nanoparticles during direct condensation synthesis.

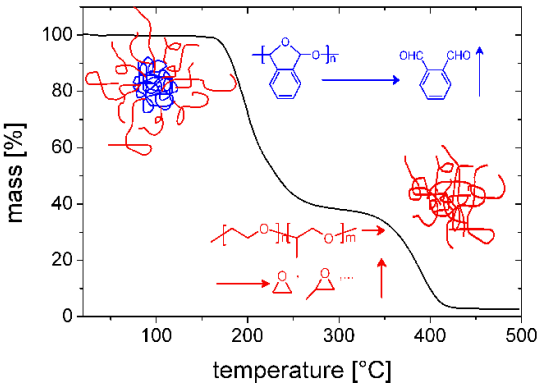

Figure 1: Thermogravimetry of poly(phthalaldehyde) – poly(alkyleneoxide) block-copolymer showing well defined depolymerisation/decomposition steps.

Different aldehyde polymers were also investigated as key components in the formulation of inkjet inks for printing of electrically conductive metal structures. Depending on their molecular structure and chemical composition, polyaldehydes can contribute various functionalities to the ink formulation. After printing, they can be easily and almost completely removed from the printed pattern by a simple heating step at moderate temperature. Such functional ink formulations are expected to have a major impact in fields like plastic and printed electronics, sensors and photonics.

Conclusions:

Due to their special thermodynamic properties, poly-aldehydes show a huge potential for the design of smart, stimuli-responsive materials. A few first examples could be demonstrated so far but many others can be expected for the future.

References:

[1] O. Vogl, J.Polym.Sci. Part A, 1964, 2, 4621.
[2] H. Ito, et al., J. Electrochem. Soc., 1989, 136, 241.
[3] S. Köstler, et al., J. Polym. Sci. Part A: Polym. Chem., 2009, 47, 1499.
[4] W. Seo, S.T. Philips, J. Am. Chem. Soc., 2010, 132, 9234.
[5] S. Köstler et al., Adv. Mater. 2009, 21, 2505.

Poly(2-oxazoline)-Based Non-Cytotoxic Hydrogels with Tailor-Made Swelling Degrees for Drug Delivery

Frank Wiesbrock,[1;*] *Andrew M. Kelly*,[1;2] *Angela Hecke*,[1;2] *and Bianca Wirnsberger*[2]

[1] Graz University of Technology, Institute for Chemistry and Technology of Materials, Stremayrgasse 9/V, AT-8010 Graz, Austria.
[2] Polymer Competence Center Leoben GmbH PCCL, Roseggerstrasse 12, AT-8700 Leoben, Austria.

e-mail: f.wiesbrock@tugraz.at

Introduction: As the population of the world ages, new and more effective means of medical care will invariably have to be developed, integrating many fields of science. The diverse nature of polymer materials and the degree of specification which can be engineered via various functionalities allows for use in applications such as drug delivery, where stealth characteristics and biocompatibility of polymers allow for effective and safe use within the body,[1] surgical procedures such as suturing, bone grafting and tissue adhesion,[2] and in the growing field of tissue engineering and its reliance upon materials more biocompatible and functional than existing artificial implants.[3]

Materials and Methods: 2-Ethyl- and 2-phenyl-2-oxazoline were chosen as monofunctional oxazolines because of the food&drug administration FDA approval of the corresponding homopolymers.[4] Crosslinking of the propagating chains during copolymerization was provided by phenylene-1,3-bis-oxazoline. Hydrogel syntheses were performed in solvent-free one-pot routines under microwave irradiation benefiting from the acceleration of reaction speed under autoclave conditions.[5-6] The cationic ring-opening polymerization of 2-oxazolines was initiated by methyl tosylate (Scheme 1) and completed within reaction times of 1 h or shorter. Yields were 95% or higher (determined after repeated swelling/drying cycles). Organic compounds present in the polymerization mixtures were trapped in the polymer networks and not released during swelling.

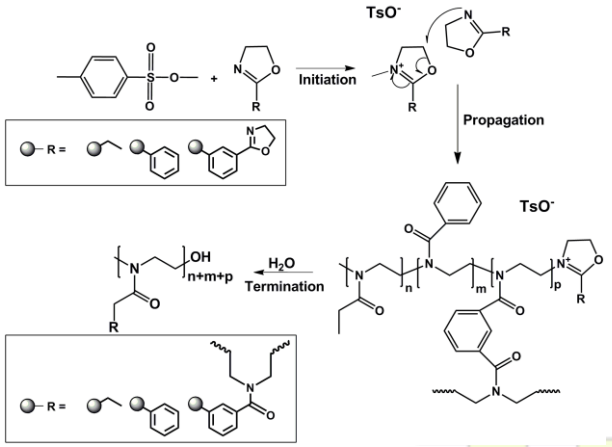

Scheme 1: Hydrogel syntheses from the cationic ring-opening copolymerization of 2-ethyl-, 2-phenyl-2-oxazoline, and phenylene-1,3-bis-oxazoline.

Results and Discussion: Benefiting from the different hydrophilic/lipohilic characters of poly(2-ethyl-2-oxazoline) and poly(2-phenyl-2-oxazoline),[5] a 32-membered library of hydro-, lipo- and amphigels was prepared. Swelling degrees could be fine-tuned by careful balance of the three 2-oxazoline monomers (Figure 1). Representative hydrogels composed of all three monomers did not show any cytotoxicity effects according to ISO 10993-5, -12. Hydrogels with cross-linking degrees of 1:25 or lower quantitatively trapped organic compounds eventually present during polymerization in the polymer network. Degradation of the polymer networks by amide bond cleavage and concomitant release of the trapped compounds like pharmaceuticals was found to be triggered by acidic environments as they are characteristic in cancer cells.

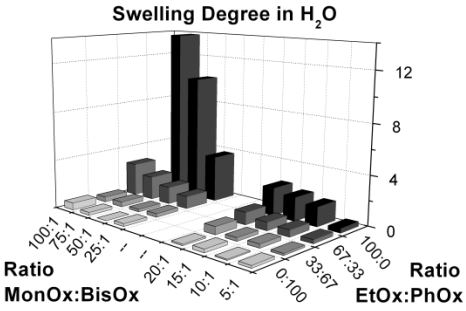

Figure 1: Maximum swelling degrees of the hydrogels in aqueous environments.

Conclusions: The rapid and facile synthesis of tailor-made oxazoline-based hydrogels with applicability in medicinal fields, in particular for pH-mediated drug delivery is reported.

Notes and References

[1] Langer, R. *Science* **1999**, *249*, 1527.
[2] Nguyen, K.T.; West, J.L. *Biomaterials* **2002**, *23*, 4307.
[3] Ikada, Y.; Tsuji, H. *Macromol. Rapid Commun.* **2000**, *21*, 117.
[4] 21 CFR 175.105
[5] Wiesbrock, F.; Hoogenboom, R.; Leenen, M.A.M.; Meier, M.A.R.; Schubert, U.S. *Macromolecules* **2005**, *38*, 5025.
[6] Ebner, C.; Bodner, T.; Stelzer, F.; Wiesbrock, F. *Macromol. Rapid Commun.* **2011**, *32*, 254.

Magnetic Properties of Neutral Substituted Poly(thiophenes)s

Steven Vandeleene, André Stesmans, Margriet Van Bael, Thierry Verbiest, Guy Koeckelberghs

Laboratory of Molecular Electronics and Photonics, Katholieke Universiteit Leuven, Celestijnenlaan 200F, B-3001 Heverlee, Belgium

guy.koeckelberghs@chem.kuleuven.be

Introduction:

Research on conjugated polymers has shown a great evolution since it became a topic of interest a few decades ago. While conjugated polymers were initially recognized as potential plastic electrical conductors, they are nowadays mainly investigated for applications based on their optical and electronic properties, such as field-effect transistors, light-emitting diodes and solar cells. The magnetic properties of materials based on conjugated polymers have also been investigated, but in these materials spins were deliberately introduced by oxidation (formation of polarons) or by the incorporation of spin-carrying moieties, such as radicals or carbenes. Here, we investigated the magnetic properties of neutral, substituted poly(thiophene)s.

Materials and methods:

The poly(thiophene)s studied (Figure 1) differ in the nature of the substituent (alkyl, alkoxy, thioalkyl) and regioregularity, the substitution pattern (head-to-tail (HT) versus HH-TT) and the molar mass. The poly(thiophenes)s were prepared using methodologies which result in defect-free structures and were thoroughly purified. Prior to the measurements, the polymers were treated with hydrazine. The measurements were carried out under inert atmosphere to avoid any oxidation.

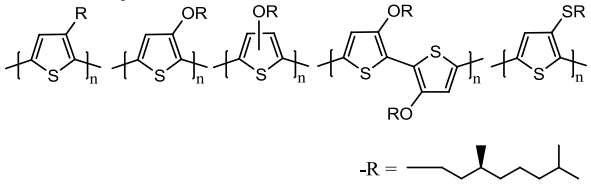

Figure 1. *Structure of the poly(thiophene)s studied.*

Results and discussion[1]:

The powders were subjected to ESR spectroscopy and SQUID magnetometry. ESR spectroscopy reveals the presence of unpaired electrons in all samples. The spin density is independent on the substitution pattern or regioregularity, but depends on the nature of the substituent. Slight oxidation of the samples (by exposure to ambient air) increases the spin density. The spins give rise to a paramagnetic behavior, demonstrating that no interactions occur, which is in line with S = ½. SQUID magnetometry reveals the presence of a second spin system. The amount of Bohr magnetons measured by SQUID is typical much higher than the amount of electron spins, measured by ESR. Moreover, they give rise to a superparamagnetic behaviour and the magnetization curves are not affected by oxidation. These results demonstrate that (at least) two systems are present: electron spin, sensed by ESR and a second spin systems, which is different from electron spins and ESR-inactive.

At low temperature (5K), most poly(thiophene)s show a ferromagnetic behavior. The coercivity does not depend on the amount of Bohr magnetons, but a clear correlation is present with the presence and strength of a absorption band, arising from stacked polymer chains which interact via π-interactions. This hypothesis was further investigated by measuring samples of HT-poly(3-alkylthiophene)s of different molar mass and by applying different annealing conditions. In both series, the degree of crystallinity is varied. In addition, annealing can also result in a different stacking. While the amount of Bohr magnetons is clearly affected by an increase of the crystalline fraction, the coercivity is not. Therefore, it must be concluded that the coercivity depends on the strength of the π-interactions.

Conclusions:

The magnetic properties of neutral, substituted poly(thiophene)s were studied. Two spin systems were identified. One is the electron spins, which gives rise to paramagnetism. A second spin system results in superparamagnetism at room temperature and ferromagnetism at low temperature. The number of Bohr magnetons depends on the fraction of lamellar stacked polymer chains, while the coercivity is governed by the strength of the π-interactions between the stacked chains.

References:

(1) Steven Vandeleene, Mihaela Jivanescu, André Stesmans, Jo Cuppens, Margriet J. Van Bael, Hitoshi Yamada, Norio Sato, Thierry Verbiest, Guy Koeckelberghs, *Macromolecules* **2010**, *43*, 2910-2915.

Optimization of multilayer heat sealing

E. Planes[1*], *L. Flandin*[1]

[1]LMOPS UMR CNRS 5041 – Université de Savoie, Campus Scientifique, Bat. IUT F-73376 Le Bourget-du-Lac Cedex, France

*Emilie.planes@univ-savoie.fr

Introduction.

Polymer-metal multilayer have been widely used for decades in packaging industry and more recently in building, as the envelope of vacuum insulation panels (VIP). The use of multilayer structures enables to have good level of barrier to gas combine with sufficient mechanical properties. In both cases the seal corresponds to the weakest zone. Even if the optimization of the heat sealing parameters of single layer films have been the subject of many investigations [1, 2], the heat sealing of multilayer has been less studied [3, 4]. Thus the aim of this study is to investigate the heat sealing properties of multilayer film, and to compare them to that of a single layer.

Materials and Methods

Materials The multilayer films are composed of one polyethylene (PE) layer and one (PETM) or three (F1Bis) polyethylene terephtalate coated or not with aluminum [5]. The low density polyethylene (LDPE) was employed as the sealing material: a control film was sealed and characterized for comparison.

Methods

Sealing Heat-seals were performed in the laboratory using Medsealer 460 MSID (K) heat sealer (Francopack). The pressure was fixed at 240 kPa and different experimental conditions were tested, varying dwell times: from 1 to 90s and sealing temperatures from 110 to 180°C.

T-peel test Strips of 25 mm wide were used for T-peel test at 90°. The samples were peeled at room temperature in an Instron mechanical testing machine, using a 2kN load cell. The constant rate of loading 100 $mm.min^{-1}$ was chosen and the force F (N) and displacement (mm) were recorded during the test. In this report, the raw data shows the force divided by the width (F/W) as a function of the displacement. The maximum force (F_{max}) divided by the nominal width (W) and the thickness (e) of the film is commonly employed to quantify the quality of the seals and defined as apparent seal strength SS. In addition, the failure modes of each test were carefully examined and will be described later.

Results and Discussion

As shown previously in the literature for monolith film, the most influencing heat-sealing parameter is the temperature and this is also valid for multilayer films. In addition the sole observation of failure modes enables to estimate the set of parameters to optimize the mechanical strength of the seal. In fact, the "peeling and tearing mode" (named (C)) corresponds to the maximal seal strength of the seal. This is confirmed by the evolution of the seal strength versus sealing temperature or dwell time.

Even if the study of multilayer sealing presents some similarities with one of simple film: the range of optimal heat sealing parameters, which was included within that of LDPE film, some differences were evidenced. A reduction of the optimal time-temperature range was observed: this latter becomes much smaller with an increasing number of PET layers. A very interesting advantage of multilayer was highlighted in this study: it concerns the influence of stiffer layers (*i.e.* PET), compared to flexible sealant layer (*i.e.* LDPE), on the mechanical behavior of the seal, since its maximal strength increases with the number of PET layers.

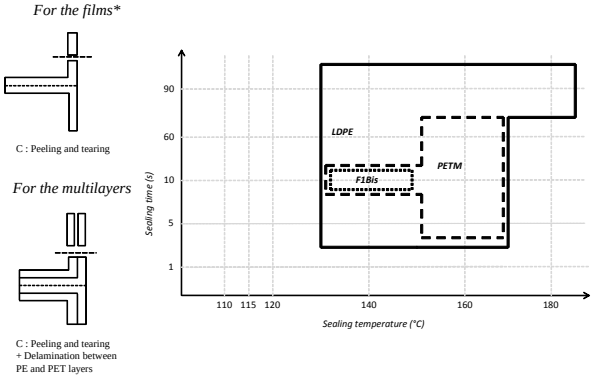

Figure 32: (left) Schematic illustration of failure mode (C) observed for monolith and multilayer films, (right) Range of optimal heat sealing parameters for three studied films

Conclusions and References

In this study, a method of optimization of heat sealing parameters was developed based on the observation of failure modes after peeling tests.

This work has allowed highlighting the interest of multilayer for sealing: an overlap of the range the optimal heat sealing parameters with the one of the sole sealant material and a more elevated mechanical strength of seal in the case of multilayer.

It would now be interesting to study other sealant materials in multilayer and more particularly the influence of the number, the nature (in chemical and mechanical terms) of the different layers of the multilayer.

1. Meka P. and Stehling F.C., J. Appl. Pol. Sci., 51:89-103, 1994
2. Stehling F.C. and Meka P., J. Appl. Pol. Sci., 51:105-119, 1994
3. Van Malsen J., Tenpierick R.H.J, Cauberg J.M.M., J. Plast. Film Sheeting, 24:35-52, 2008
4. Yuan C.S., Hassan A., Ghazali M.I.H., Ismail A. F., J. Appl. Pol. Sci., 99:974-985, 2006
5. Garnier G., Yrieix B., Brechet Y., Flandin L., J. Appl. Pol. Sci., 115 :3110-3119, 2010

Characterization of soluble and precipitated chitosan adsorption onto cellulose viscose fibres

Tijana Ristić [a], *Lidija Fras Zemljič* [b]

[a] Tosama d.d., Vir, Šaranovičeva 035, 1230 Domžale, Slovenia

[b] University of Maribor, Faculty of Mechanical Engineering, Institute for Engineering Materials and Design, Smetanova 17, SI-2000 Maribor, Slovenia

tijana.ristic@tosama.si

Trends in developing new high-quality medical and healthcare textiles are in surface functionalization of textiles with intention to introduce bioactive properties with emphasis on antimicrobial activity. Due to the fact that consumers are becoming more and more concerned and watchful of their health and well-being, there is a significant interest in cellulose materials' functionalization using natural biodegradable and non-toxic reagents – as, for example, less employed polysaccharides and their derivates possessing antimicrobial properties From among the various polysaccharide products, amino-functional polysaccharides has recently gained considerable attention for use in pharmaceutical and medical applications.

One of the most promising amino polysaccharide is chitosan, a chitin derivative, obtained by alkaline deacetylation. Chitosan is a natural, renewable resource; a polycationic biopolymer that possesses a well-documented and wide-spectrum of biological activity, including antibacterial and antifungal activities. Therefore, chitosan's incorporation into the cellulose matrix offers many advantages over traditional treatments of cellulose fibres because of its non -toxicity, biodegradability, and biocompatibility. Several techniques are available for introducing chitosan onto cellulose fibres. These methods have been mainly limited to the treatment of cellulose fibres with cross-linking agents, the soaking of cotton fibres into chitosan solutions or impregnation by chitosan solutions, etc. The adsorption of chitosan and its interactions with cellulose material are not only affected by the surface physicochemical characteristics of the cellulosic substrates but may also be strongly influenced by the chitosan aggregate's nature. The introduced amounts of amino groups onto cellulose fibres and, consequently the fibre antimicrobial activity, may increase with the attachment of polysaccharides in colloidal form, in comparison with attaching a totally-soluble form of chitosan, such as chitosan acidic solution.

Thus, the aim of this work was to compare the adsorption of fully soluble chitosan (acidic solution) with the adsorption of precipitated chitosan particles, onto cellulose viscose fibres. The content of amino groups in the functionalized cellulose fibres was studied using potentiometric titration, and a conventional spectrophotometric method C.I. Acid Orange 7. Surface modification and adsorption of chitosan were, in addition, monitored by using XPS analysis. The antimicrobial activity of the functionalized cellulose fibres was examined against common pathogenic bacteria and fungus.

Modification of Surface Properties of Organically Modified Clay Particles for Preparation of Nanocomposite Hydrogels

Manja Kurecic, Silvo Hribernik*,+, Matija Tomsic**, Andrej Jamnik**, Karin Stana Kleinschek*, Majda Sfiligoj-Smole*,+*

*Faculty of Mechanical Engineering, University of Maribor, Smetanova 17, Maribor, Slovenia
**Faculty of Chemistry and Chemical Technology, University of Ljubljana, Askerceva cesta 5, Ljubljana, Slovenia
+Centre of Excellence PoliMat, Tehnoloski park 24, Ljubljana, Slovenia

manja.kurecic@uni-mb.si

Various types of montmorillonite (MMT) and closely related minerals are the most important and widely used phillosilicate fillers in polymer composites, due to their large active surface area (MMT: 700-800 m^2/g) and ability to swell remarkably in water. On the other hand, organically modified clay particles are known for their adsorption capacity for heavy metals, organic dyes and pollutants. This property makes them a very attractive component to be introduced into polymer matrices, but their intrinsic hydrophobic nature presents a challenge when inclusion into hydrogels is required.

Aim of our study was to modify surface of organically-modified clay particles in order to ensure a sufficiently stable aqueous dispersions, which would be later on used in the preparation of polymer hydrogels. We have used a non-ionic polysaccharide-based surfactant system – Inutec SP1 (based on chicory inulin) for the improvement of wettability of clay particles and consequently, enhancement of their dispersion ability in water-based systems. Different concentrations of surfactants were tested. Properties of the particulate surfactant-stabilized aqueous colloidal system were determined by zeta potential, electrophoretic mobility and dynamic light scattering measurements. Determination of contact angles gave us insight into the particles' surface interaction ability with water and non-polar solvents. Structure of dried particles in powdered form was investigated by small-angle X-ray scattering. Combination of electrokinetic and scattering data and established hydrophobic/hydrophilic character with analysis of particles sedimentation behaviour, allows us to use these findings to plan and predict the influence of such modified MMT particles on the formation of hydrogels and their subsequent properties. By modifying surface properties of clay particles with non-ionic surfactant, we have managed to reduce the size of particles and consequently achieved better incorporation of clay particles in hydrogel matrix. Increased surface area due to the reduction of particle size results in more active functional sites.

An elegant and facile single-step UV-curing approach to self-assembled Metallopolymer Capacitors

Jijeesh R. Nair[1,*], *C. Gerbaldi*[2], *V.S. Ijeri*[1], *R. Bongiovanni*[1], *N. Penazzi*[1]

[1]Department of Materials Science and Chemical Engineering, Politecnico di Torino, Turin, Italy
[2]IIT@POLITO Center for Space Human Robotics, Italian Institute of Technology, Turin, Italy

*jijeesh.nair@polito.it

Introduction

The current widespread interest in silver-metalized polymeric materials is driven largely by their potential applications in printed circuit boards, contact devices in microelectronics, flexible polymer electronics, catalysis, space applications etc. Silver-polymer nanocomposites have also been studied with the purpose of enhancing the dielectric constant for applications in embedded capacitors[1].

Free-radical photopolymerization (UV-curing) is a well established polymerization technique that takes place under UV light to obtain a highly cross-linked polymeric thermoset matrix. The process is well-known for being fast and environmentally friendly[2].

Here we report the first example of dual surface nanosilvering of a methacrylate polymer film by a simple UV-curing process. During the process the metalized film is directly developed from a single homogeneous solution that contains both the native metal precursor (i.e., Ag^+) and the desired reactive precursors of the final polymeric network. That is, the sample is obtained in a single stage and no subsequent distinct metallization stage is involved. To the best of our knowledge, such an approach has not been reported so far. This kind of polymeric film metalized on both sides is conceptually a capacitor, well-suited for flexible and/or nonplanar electronics.

Materials and Methods

The reactive formulations were prepared as follows: $AgNO_3$ was dissolved in 50% (v/v) CH_3OH + H_2O mixture. To this solution, BEMA, pyrrole and initiator were added subsequently and mixed thoroughly. A molar ratio of 2:1 or higher for pyrrole to silver nitrate was maintained to ensure complete reduction of Ag(I). The mixtures were then poured into Petri dishes and exposed to UV-radiation for 3 min on each side. The photochemical curing was performed by using a medium vapor pressure Hg UV lamp (Helios Italquartz, Italy), with a radiation intensity on the surface of the sample of 30 mW cm^{-2}. For this process, the samples were held under a pure N_2 atmosphere in small sealed boxes equipped with a quartz window. These conditions ensure maximum curing. Free films were easily detached from the dishes (see the figure below).

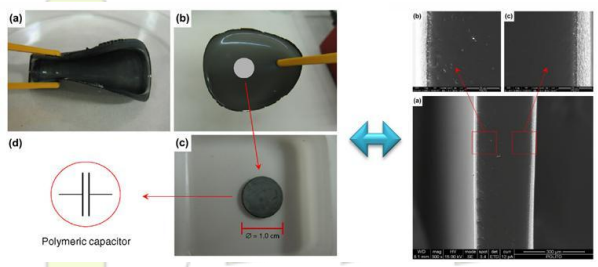

Results and Discussion

Current-voltage (*I-V*) curves were recorded for the surfaces of the samples to know how conductive they are. The I-V curves obtained for the top surface of sample were perfectly linear, suggested an ohmic behavior. Moreover, the overlapping of the multiple curves recorded over different points on the surface indicates a highly homogeneous distribution of Ag nanoparticles and polypyrrole on the surface.

Circular discs of 1.0 cm in diameter were cut out from the master film and tested for capacitive properties. The figure below shows the capacitance vs. potential curve for a sample at a frequency of 100 Hz.

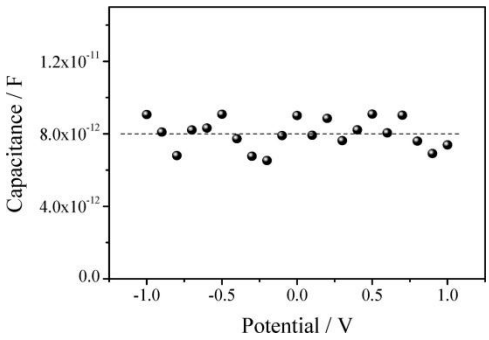

It is similar to the curve obtained by Liu et al.[3] for a polymeric capacitor prepared by inkjet printing with polyimide in the center and poly(3,4-ethylenedioxythiophene) on the surfaces, and the capacitance value is also similar, i.e., in the picofarad range.

Conclusion

In summary, we have successfully introduced a novel, simple but efficient method that allows excellent dual surface metallization of a methacrylic-based polymer network, in a single step. The formation of two conducting layers on either sides of an insulating polymer in a single step opens up possibilities of rapid production of highly flexible polymeric capacitors, which until now are made by time-consuming multiple steps procedures. The whole process is remarkably convenient, with short reaction time, "environmentally friendly", and no need for any complex equipment or manipulation.

References

1. V.S. Ijeri et al (2010) ACS Appl. Mater. Interfaces, 2:3192
2. J. Nair et al (2008) J. Power Sources 178: 751
3. Y. Liu et al (2003) Solid-State Electron. 47: 1543.

Synthesis and characterization of photoactive and extrudable polymers in view of developing a new solvent-free process for production of organic solar cells.

L. PERRIN, A. NOURDINE, E. PLANES, L. FLANDIN, N.D. ALBEROLA*

LEPMI-UMR CNRS 5279/LMOPS-Université de Savoie
Bâtiment IUT-Savoie Technolac, F-73376 Le Bourget-du-Lac Cedex

**e-mail: lara.perrin@univ-savoie.fr*

Introduction:

The performance of organic photovoltaic solar cells depends on the active layer morphology, especially the arrangement of the donor and acceptor materials. A common way to improve the performance of organic solar cells would be to increase the amount of donor / acceptor interfaces. Different ways have already been explored[1]. A new approach could consist in developing nano-multilayers of donor and acceptor polymers by forced assembly.

Materials and Methods:

Poly(3-octylthiophene) P3OT was chosen as the donor polymer and Poly(styrene-co-NC_{60}-methylstyrene) $PSNC_{60}MS$ as the acceptor polymer. The first part of the work focused on synthesis and characterization of various acceptor polymers with different amounts of C_{60}. To determine the optimal composition of the fullerene C_{60} in polystyrene matrix the electrical (charges mobility and conductivity), optical (absorption, optical gap energy) and photovoltaic properties (tests in bi-layer and bulk-heterojonction photovoltaic solar cells using P3OT as donor polymer and $PSNC_{60}MS$ as acceptor polymer) have been measured. Finally, the rheological behaviour and characteristic temperatures of both polymers were studied to confirm their plausible processability by extrusion.

Results and Discussion:

The work presented here is part of a broader project, which will consist in using a new solvent-free process[2] to produce nano-multilayers organic solar cells, with alternating donor and acceptor. Two polymers were designed and synthesized taking into account several criteria, like special processing conditions and photovoltaic properties.

The polythiophene family is well known in the field of solar cells. A good compromise between photovoltaic and processing properties[3] is easy to find using the commercial P3OT with an octyl side chain.

The $PSNC_{60}MS$ combines photovoltaic properties (good acceptor characteristic) of the fullerene C_{60} and processing properties of polystyrene. A large range of polystyrene grafted by a various percentage of C_{60} was synthesized in the laboratory, by a three steps method[1b].

Both physicochemical and photovoltaic properties were characterized as a function of C_{60} percentage. This enables us to determine the lowest amount of C_{60} required for an application in solar cell.

A percolation threshold of 4.4%vol (7.1%wt) was identified for both conductivity and mobility measurements (Figure 1).

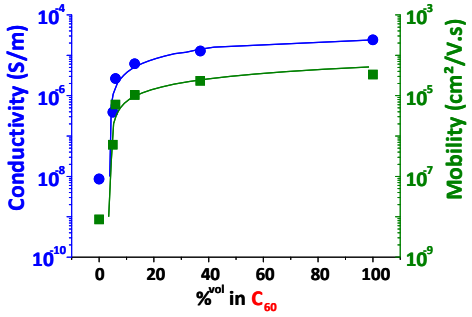

Figure 1: *Conductivity and Mobility values obtained for $PSNC_{60}MS$*

Then, the 'extrudability' of both selected polymers (donor and acceptor) was estimated using TGA and DSC in order to detect the possible range of processing temperature (180-300°C). In addition, the rheological behaviour (Figure 2) was qualified with a plan-plan rheometer to estimate possible processing conditions[2].

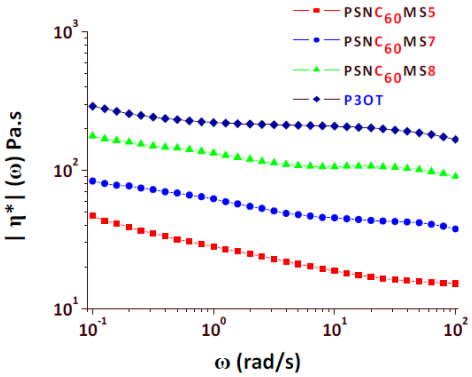

Figure 2: *Comparison of rheological behaviour of P3OT and $PSNC_{60}MS$ with different C_{60} percentages.*

Conclusions and References:

As a conclusion, the study summarized here confirms both chosen polymers are compatible with the aimed application, and suitable for coextrusion process.

Next steps of the study will be a large scale production of these polymers, in order to do the first processing of solar cells active layer by nano-multilayers forced assembly.

1 a) Yang X. and Loos J. Macromolecules, 40(5):1353–1362, 2007.
b) Van der Veen M. H., De Boer B., Stalmach U., Van de Wetering V. I., Hadziioannou G. Macromolecules, 37(10):3673–3684, 2004.
c) Botiz I. and Darling S. B. Macromolecules, 42(21):8211–8217, 2009.
2 Liu R. Y. F., Bernal-Lara T. E., Hiltner A. and Baer E. Macromolecules, 37(18):6972–6979, 2004.
3 a) Al-Ibrahim M., Roth H. K., Schroedner M., Konkin A., Zhokhavets U., Gobsch G., Scharff P. and Sensfuss S. Organic Electronics, 6(2):65 – 77, 2005.
b) Hu X. and Xu L. Polymer, 41(26):9147 – 9154, 2000.

Multiscale Gold and Silver Plasmonic Plastics by Melt Compounding

Nuria García,[a] *Pilar Tiemblo*,[a] *Esperanza Benito*,[a] *Antonio Esteban*,[c] *Raúl Pina*[b] *and Carlos Pecharromán*[b]

[a]Instituto de Ciencia y Tecnología de Polímeros (CSIC)
[b]Instituto de Ciencia de Materiales de Madrid (CSIC)
[c]Tolsa S. A. R&D Department

ngarcia@ictp.csic.es

Among the most interesting new phenomena arising from the nanosizing of materials are those derived from specific interactions between electromagnetic radiation and nanoparticles, as for instance optical properties. Selected metals (typically Au, Ag and Cu) present the so called, **Surface Plasmon Resonance** (SPR),[1] a property which can be recognized by naked eye, as such metal nanoparticles present vivid colorations. Although this phenomenon requires a full quantum dynamic formulation for its complete description, it classically manifests itself as an absorption band in the visible spectrum, originated by large electronic movements due to a notable increase of the local electric field at the metal/matrix interface.

The main interest of this effect is that the local field enhancement allows observing several non-linear processes with conventional illumination sources. However, to take full advantage from SPR-derived physical processes it is in many cases mandatory to embed the nanoparticles into a homogeneous and transparent matrix which enables the handling of the material. The embedding process poses two main problems, first how to integrate the particles in the matrix without aggregating them and second, how far do the properties stay the same when the particles change their environment. Matrixes for embedding can be inorganic, like glasses or porous silica, though integrating the nanoparticles in polymeric matrixes has many practical advantages, mainly related to the light weight and mechanical properties of these materials.

Two main strategies have been used to prepare **metal-polymer nanocomposites**: (i) *ex situ* methods based on the dispersion of metal nanoparticles in polymer solutions or in monomer mixtures to be afterwards polymerized[2] or (ii) *in situ* methods in which metal nanoparticles are generated in the midst of the polymer matrix by the spontaneous or induced reduction of the metallic precursor.[3] Both methods fail to offer a simple way to prepare well dispersed nanocomposites in a varied range of polymer matrixes.

The alternative presented in this work is based on a **multiscale** approach in which metallic nanoparticles are supported on an inorganic carrier, **sepiolite**. Sepiolite is a magnesium silicate which presents a needle-like structure that can be relatively easy to disperse in polymers by conventional processing techniques.[4] To embed Ag and Au nanoparticles in the fibers, sepiolite was subjected to acid and thermal treatments previously reported.[5] The as-obtained *metallic sepiolites* were afterwards dispersed in the polymer matrixes: low density polyethylene (LDPE) and polystyrene (PS) by melt compounding in a lab extruder. The inorganic content ranged from 2 to 40%.

The resulting materials were macroscopically homogeneous as a consequence of an optimal dispersion of the metallic sepiolite as checked by microscopy techniques (SEM and TEM). Sepiolite has a similar refractive index as those of the polymer matrix avoiding light scattering and, thus, the materials show an excellent optical transparency. The multiscale composites exhibit plasmon bands at all loading coatings regardless of the film thickness. Plasmon maxima for Ag and Au-sepiolite composites are located at 445-426 nm and 530-537 nm, respectively, depending on the polymer matrix. In addition, the composites not only behave as plastic materials, but also they are mechanically reinforced and thermally stabilized by the addition of the sepiolite fibers.

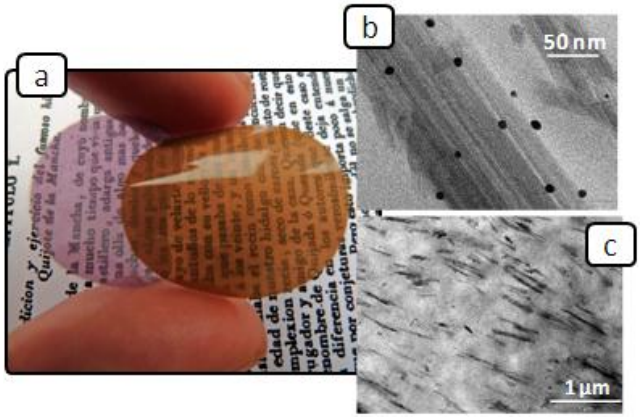

Figure. a) Visual appearance of films (50-µm width) prepared from the multiscale gold and silver nanocomposites. b) and c) TEM micrographs showing the metallic nanoparticles (Au) supported on the sepiolite carrier and the sepiolite dispersed in the polymer matrix (LDPE), respectively.

References

[1] P. Mulvaney. *Langmuir* **1996**, *12*, 788.
[2] D.I. Uhlenhaut, P. Smith, W. Caseri, *Adv. Mater.* **2006**, *18*, 1653.
[3] R. Abargues, K. Abderrafi, E. Pedrueza, R. Gradess, J. Marqués-Hueso, J.L. Valdés, J. Martínez-Pastor. *New J. Chem.* **2009**, *33*, 1720.
[4] P. Tiemblo, N. García, j. Guzmán, E. Benito, A. Esteban-Cubillo, J. Santarén, E. Aguilar. *Langmuir* **2011** (in press).
[5] C. Pecharromán, A. Estebán-Cubillo, I. Montero, J. S. Moya, E. Aguilar, J. Santarén, A. Alvarez. *J. Am. Ceram. Soc.* **2006**, *89*, 3043.

Acknowledgments. The authors thank financial support from the Spanish Ministry (MAT2008-06725-C03-01).

Block Copolymer-Coated Magnetic Nanoparticles for Imaging and Therapeutic Applications

C. Schatz, S. Louguet, S. Lecommandoux, R. Epherre, E. Duguet, S. Mornet, C. Boiziau, A. Vekris, K. Petry

University of Bordeaux, France

schatz@enscbp.fr

Introduction

Magnetic nanoparticles (NPs) are used in life sciences as contrast agents for imaging applications as well as heating sources for hyperthermia.[1] However, their lack of stability in *in vivo* conditions, their potential toxicity and their poor targetability must be improved through chemical modifications of their surface. Herein, we report on a new method to modify the surface of magnetic NPs by adsorption of a double hydrophilic poly(ethylene oxide)-*block*-poly(L-lysine) (PEO-*b*-PLL) copolymer end-functionalized by a targeting peptide and/or fluorescent probe. The physical entrapment of anticancer drug (doxorubicin) within the adsorbed polymer layer was achieved to combine both imaging and therapeutic capabilities in a single system. In addition, the co-adsorption of PEO-*b*-PLL copolymer with thermoresponsive copolymers was explored from a fundamental point of view at first and then as a mean to trigger the drug release by applying an alternative magnetic field.

Materials and Methods

Silica coated perovskite nanoparticles, PEO-*b*-PLL and Jeffamine-*b*-PLL (thermosensitive) copolymers were synthesized and characterized according to previous reported protocols.[2,3] The functionalization of the copolymers with fluorescent probes and targeting peptide was achieved through thiol/maleimide coupling reaction. Block copolymer adsorption onto nanoparticle surface was performed in 10 mM phosphate buffer pH 7.4. Doxorubicin was physically entrapped in the polymer layer during this adsorption step as well.

Results and discussion

Magnetic nanoparticles used in this study are based on manganite perovskite nanoparticles (Tcurie = 43°C) of 60 nm in diameter surrounded by a 5 nm thick silica shell. The silica layer confers to the particles a strong negative charge at physiological pH. A series of PEO-*b*-PLL copolymers with different block lengths were physically adsorbed onto modified magnetic NPs. The gradual addition of silica particles to an excess of PEO-*b*-PLL copolymer solution was the preferred method for particle coating as it favoured equilibrium conditions where the copolymer layer has good stabilizing properties against flocculation. A combination of analytical techniques such as dynamic light scattering (DLS) and isothermal titration calorimetry (ITC) evidenced the higher affinity of PLL blocks with silica surface over PEG blocks. Indeed, we showed that PLL interacts with silica surface through both electrostatic interactions with SiO^- groups and hydrogen bonding with silanols. PEO_{113}-*b*-PLL_{10} was found to be the most interesting copolymer composition since it affords high colloidal stability in time and in protein rich media. Actually, such physico-chemical properties are related to the conformation of the PEO block at the particle surface. Interestingly, we showed that this conformation is set by the length of the anchoring block (PLL), short or large PLL blocks favouring a brush-like or mushroom conformation of the PEO blocks, respectively. Jeffamine-*b*-PLL copolymers where jeffamine is a random copolymer of ethylene oxide and propylene oxide with a LCST of 70°C was co-adsorbed with PEO-*b*-PLL copolymers to confer thermosensitivity to the polymer layer. High doxorubicin loading contents of 30 and 70% were achieved by incubating NPs with doxorubicin at room temperature and 50°C, respectively. This underlines the higher hydrophobicity of the mixed copolymer layer when temperature increased. In a similar manner we showed that the doxorubicin release was fastened when the temperature increased.

As expected, we demonstrated that the hyperthermia induced heat could enhance the bioavailability of doxorubicin entrapped within the thermosensitive polymeric shell. (see opposite figure)

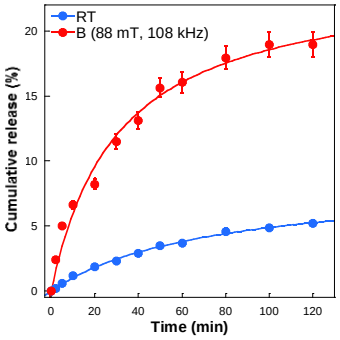

Lastly, the NPs were functionalized by AlexaFluor 488 and a cyclic targeting peptide. A brain inflammation was induced in rat by inoculation of a proinflammatory cytokine (IL-1β/LPS). NPs were intravenously injected in the caudal vein.

Fluorescence imaging of brain slices showed a preferential accumulation of NPs along endothelial cells close to the inflammation site. (see opposite image)

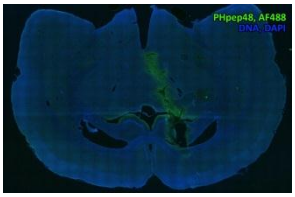

This result was also confirmed by magnetic resonance imaging (MRI) where a negative contrast was observed at the inflamed site.

Conclusion

We reported the synthesis of multifunctional magnetic NPs affording targeting, hyperthermia and therapeutic properties. Preliminary biological evaluations have confirmed their potential use for brain diseases.

References

1. Dave SR, Gao X Interdisciplinary Reviews: Nanomedicine and Nanobiotechnology 2009, 1, 6 1.
2. Mornet S, Vasseur S, Grasset, Duguet E Journal of Materials Chemistry 2004, 14, 2161
3. Agut W, Brûlet A, Taton D, Lecommandoux S Langmuir 2007, 23, 11526

Effect of Polymer Structure of Acrylic Pressure-Sensitive Adhesives on Light Leakage Phenomenon in TFT-LCD Panel

Irina Nam, Kyoungjin Ha, Kilsung Lee, Lee June Kim, Changmin Lee, Misun Kim, Tuwon Chang

Polymer Synthesis and Dispersion Group, Manufacturing Materials R&D Center, Electronic Chemical Materials Business Unit, Cheil Industries Inc., Samsung

nam.irina@samsung.com

Introduction.

Thin film transistor liquid crystal display (TFT-LCD) are widely used in desktop computer monitors, laptop computers, mobile phones, digital cameras, navigation systems, video game systems, etc. With continuously increasing consumer demands, manufactures pay lots of efforts in perfection of their products. Nowadays, one of the main problems in TFT-LCD panels is a phenomenon called "light leakage", seriously affecting black-white contrast and color brightness (Figure 1).

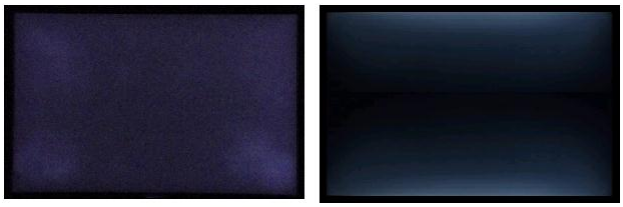

a) corner light leakage at AV mode b) edge light leakage at TN mode

Figure 1. Examples of light leakage in LCD in a) vertical alignment and b) twist nematic modes.

It occurs due to thermal stress in the polarizing film, one of the main parts of TFT-LCD panel, caused by a heat from the back light unit [1]. A pressure-sensitive adhesive (PSA) used for assembling of the polarizing film is believed to provide stress relaxation to the polarizing film and prevent its thermo-induced shrinkage, and thus minimize the light leakage [2,3].

Results and discussion.

In this paper, we supposed that introduction of acrylic/methacrylic monomers having an aliphatic or aromatic cycle in ester radical position will result in improved heat-resistant and visco-elastic properties of the PSA. As such, eight commercially available monomers were selected, as given in Figure 2.

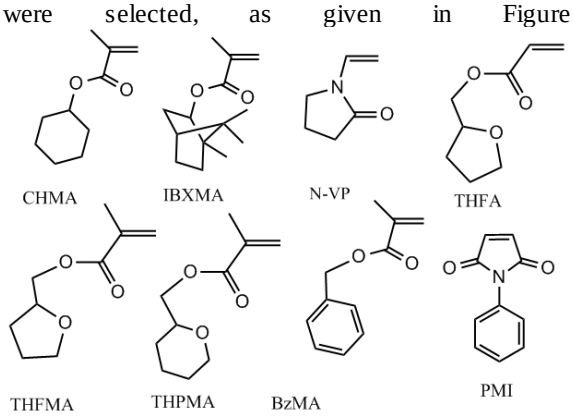

Figiure 2. Structure of the monomers.

Effect of the polymer structure and glass transition temperature on light leakage performance was investigated in complex with other two important characteristics of PSA system, as creep and peel strength. It was found that the polymers with the lowest and the highest glass transition temperatures (Tg) were excellent in prevention of light leakage. Zero light leakage was achieved through synergy of two mechanisms: resistance to thermo-induced shrinkage and stress relaxation. We also succeeded in making our PSA suitable for universal application in TFT-LCDs from 2.5 to 19 inch with obvious technological and economical benefit.

Reference

1. M.S.Yang, S.W.Ko, and H.J.Choi, J. Industrial and Engineering Chemistry 16, p.162-165 (2010).
2. T.Arai, M.Kashio, and E. Kosoukue, US 2009/0118434 A1: May 7 (2009).
3. M.S.Yang, S.W.Ko, and H.J.Choi, J. Macromolecular Sci., Part A, 46, p. 1142-1150 (2009).

Nanofiber Networks of Aromatic Polybenzimidazole

Jin Gong [1], Tetsuya Uchida [2], Shinichi Yamazaki [1], Kunio Kimura [1]

[1] Graduate School of Environmental Science, [2] Graduate School of Natural Science and Technology, Okayama University

E-mail: polykim@cc.okayama-u.ac.jp

Introduction

Aromatic polybenzimidazoles possess the outstanding performances, and they have been paid much attention from both the academic and industrial aspects.[1,2] Materials down-sized to the nanometer scale can show very different properties, enabling unique applications, and hence polybenzimidazole nanofibers will become more indispensable in high-technology field. Reaction-induced phase separation during isothermal solution polymerization is a very useful method for the morphology control of poor processable polymers, and we studied the morphology control of poly[2,6-(1,4-phenylene)-benzobisimidazole] (PPBI) during the polymerization of 1,2,4,5-tetraaminobenezene and diphenyl terephthalate. [3] PPBI crystals obtained by this method exhibited very unique brush-like morphology, whereas the nanofibers could not be prepared so far. This study aims to prepare the PPBI nanofibers by the self-polymerization of 2-(1,4-carbophenoxyphenyl)-5,6-diaminobenzimidazole (CPAB).

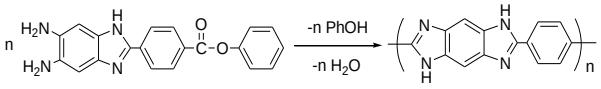

CPAB PPBI

Experimental

CPAB was synthesized according to previously reported procedures. [14] Liquid paraffin (LPF) from Nacalai Tesque and a mixture of structural isomers of dibenzyltoluene (DBT) from Matsumura Oil (Barrel Therm 400) were purified by vacuum distillation.

Polymerization in DBT was described as an example. DBT was placed into a cylindrical flask and heated up to 350°C under slow stream of nitrogen. When the temperature reached to 350°C, CPAB was added under stirring. The mixture was stirred to dissolve CPAB entirely, and then polymerization was carried out for 6 h at 350°C without stirring. Polymerization concentration was 1 wt%. Precipitated polymers were isolated by filtration at 350°C, and then washed with acetone. PPBI crystals were obtained with the yield of 85%.

Results and Discussion

Table presents polymerization results. Spheres with smooth surface and those with short needles on the surface were formed in LPF with the yield of 75 %. The diameter of the spheres with smooth surface ranged from 0.4 to 0.8 μm. The polymerization in DBT/LPF (DBT content: 50 wt%) afforded brush-like crystals with the yield of 65 %. The brush-like crystals were comprised of plate-like crystals and needles. Small needles, of which the length and width were averagely 80 and 20 nm, grew on the surface of the plate-like crystals. The polymerization in DBT gave the nanofibers successfully with the yield of 85 % as shown in Fig. The width of the fibers ranged from 30 to 110 nm and the fibers fused each other, resulting in the formation of three-dimensional network structure like nonwoven fabrics. The length is longer than 1 μm between the fused points. IR spectrum of the nanofiber network is identical with that of PPBI. The inherent viscosity (η_{inh}) of the nanofiber network was 0.65 $dL \cdot g^{-1}$ and it is the highest value among the PPBIs prepared in other solvents. The nanofiber network possesses the highest crystallinity. In order to evaluate the molecular orientation, the nanofiber network and the brush-like crystal were observed in details on a TEM. Fig. shows morphologies and SAED patterns. Sharp reflection spots were clearly observed in SAED of the nanofiber and the fiber identity period 1.06 nm was correspond to the length of one repeating unit 1.26 nm, suggesting that the molecules might align along the long axis of nanofibers. Oligomers left in DBT at 350°C were analyzed by MALDI-TOF mass spectrometry. Oligoimidazoles up to tetramers were detected and those larger than pentamers must crystallize to form the nanofibers. The molecular weight increased by the polymerization in the precipitated crystals.

Table Polymerization of CPAB in three kinds of solvent

Solvent	Yield (%)	η_{inh} [a] ($dL \cdot g^{-1}$)	Morphology	$T_{5\%}$ [b] (°C)
LPF	75	0.59	sphere, SN [c]	413
DBT/LPF-50	65	0.60	brush	422
DBT	85	0.65	fiber	457

[a] η_{inh} was measured in 97% sulfuric acid at a concentration of 0.2 $g \cdot dL^{-1}$ at 30°C. [b] Temperature of 5% weight loss measured on a TGA at a heating rate of 20°C·min^{-1} in N_2. [c] SN stands for spheres with needles on surface.

Thermal stability of these products was measured by TGA in N_2 and temperatures of 5 % weight loss are in the range of 413 - 457°C. The nanofiber network possesses the highest thermal stability due to high molecular weight and high crystallinity.

Conclusions

The nanofiber networks were formed by the polymerization of CPAB in DBT. The width of the nanofiber ranged from 30 to 110 nm. Molecules were aligned along the long axis of nanofibers. The nanofiber networks exhibit the highest thermal stability.

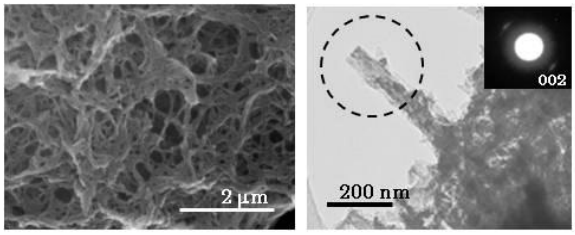

Fig. SEM and TEM of PPBI nanofiber networks

References

[1] P. E. Cassidy, *Thermally Stable Polymers, Syntheses and Properties*, Marcel Dekker, New York, 1980. [2] H. Vogel, C. S. Marvel, *J. Polym. Sci.* **1961**, 50, 511. [3] J. Gong, S. Kohama, K. Kimura, S. Yamazaki, K. Kimura, *Polymer* **2008**, 49, 3928.

Self-Assembling of Tapered Dendrons of Various Nature and Functionality

Maxim A. Shcherbina[1], *Artem V. Bakirov*[1], *Virgil Percec*[2], *Uwe Beginn*[3], *Martin Moller*[4], *Sergey N. Chvalun*[1]

[1] Enikolopov Institute of Synthetic Polymer Materials, 70 Profsoyuznaya str., 117393 Moscow, Russia;
[2]University of Pennsylvania, Philadelphia, PA 19104-6323 USA;
[3]Organic Materials Chemistry, Institute for Chemistry, University Osnabrueck, Barbarastr. 7, D-49069 Osnabrueck, Germany;
[4]Institute of Technical and Macromolecular Chemistry, RWTH Aachen and DWI e.V., Pauwelsstr. 8, D-52056 Aachen, Germany;

e-mail: shcherbina@ispm.ru

Supramolecular chemistry and molecular technology are among the most claimed fields of modern materials science. Attention of researchers is concentrated on fundamental principles of self-assembling, embracing molecular recognition of exo- and endoreceptors, as well as on the possibilities for manipulating the nanosystem structure by moderate changes of environment conditions and of outer fields of different nature (including geometrical confinement). Self-assembling is a co-operative process, giving substantial benefits for manufacture rates. Moreover, it is a “bottom-up” process, in which molecules of particular compound form supramolecular aggregates to be used as building blocks of the macroscopic system. Thus, the use of self-assembly process allows for much more accurate manipulation by the material structure and for the design of neat, precise structures.

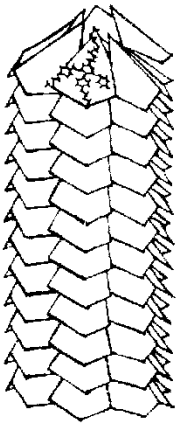

We have carried out comparative analysis of the structure of supramolecular aggregates formed by tapered and conical dendrons, ordered by different driving forces: van-der-Vaals (compounds on the basis of gallic acid), ionic (symmetric and asymmetric benzene-sulfonates of alkaline metals), fluorophobic effect etc. It was shown that at room temperature tapered dendrons form usually ordered 2-d hexagonal phase. Internal structure of cylinders is determined by a complex of different factors, such as the type of focal group, length and chemical structure of aliphatic chains. With increasing temperature compounds studied undergo a transition to the disordered columnar phase, followed by isotropization. It was shown that ϕ_{bh} - ϕ_h transition is a co-operative process of consecutive "melting" of alkyl tails and mesogen groups. In benzene-sulfonates this effect has a very important consequence. In ordered state, cylinders formed by such compounds, have an axial channel, its diameter being a function of the metal counter-ion. During transition to disordered columnar phase, increasing mobility of mesogens causes channels to close, thus giving the way to design of membranes with temperature controlled ion transmission.

Further heating of disordered columnar phase results in significant decrease of column diameter, with negative thermal coefficient $\beta=-(1\div2)\times10^{-3}$ K^{-1}. Such behavior can be explained by polymer chain unwinding in the column upon heating. In several cases we also observed high-temperature cubic micellar or bicontinuous phases. Although isotropization strongly depends of the chemical structure of tails, it takes place at the same critical column diameter due to the Rayleigh instability of the cylinder because of the increased fluctuations of its diameter with increasing temperature. Intensity of these fluctuations is a function of interactions between mesogenic groups and aliphatic matrix. For the cylinders with rigid cores, ordering of high-temperature fluctuations may lead to the development of 3D ordered structures. This effect was found upon heating of monomers with partially fluorinated alkyl tales: bicontinuous gyroid phase develops near the temperature of isotropization. Its structure was thoroughly studied by the reconstruction of electron density maps (see Figure on the right).

We studied self-assembling structures, formed by tapered dendrons (including chiral molecules on the basis of gallic acid and dipeptides) in bulk and in solutions. It was found that in the solution dendrons form elongated aggregates similar to those in bulk.

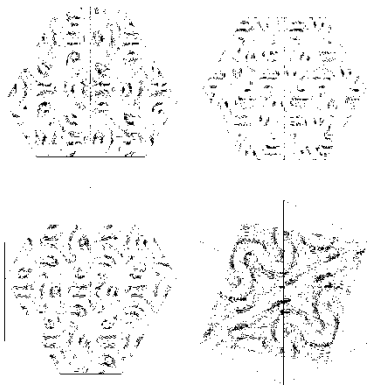

This work was supported by the Russian Foundation for Basic Research, project no. 08-03-01095a and by Russian President grant for young scientists MK-4006.2010.3

Towards Chromogenic and Fluorogenic Sensing Materials via Molecular Imprinting

Wagner, R., Dortmund/DE[1], Lazraq, I., Dortmund/DE[1], Fernández Sanchez, J., Granada/ES[2], Urraca-Ruiz, J.L., Dortmund/DE[1], Biyikal, M., Berlin/DE[3], Rurack, K., Berlin/DE[3], Benito-Peña, E., Madrid/ES[4], Moreno-Bondi, M., Madrid/ES[4], Orellana, G., Madrid/ES[5], Sellergren, B., Dortmund/DE[1]

[1]Institute of Environmental Research (INFU),TU Dortmund, Germany
[2]Analytical Chemistry Department, Faculty of Sciences, University of Granada, Spain
[3]Federal Institute for Materials Research and Testing, Berlin, Germany
[4]Analytical Chemistry Department, Faculty of Chemistry, Complutense University of Madrid, Spain
[5]Organic Chemistry Department, Faculty of Chemistry, Complutense University of Madrid, Spain

ricarda.wagner@infu.tu-dortmund.de

Introduction

The need for materials allowing rapid testing is constantly growing. Being cheap and robust, molecularly imprinted polymers (MIPs) based on responsive host monomers may be employed as sensing materials, e.g. in handheld devices or fibre-optic sensors operating with miniaturised optical equipment and a chromo- and/or fluorogenic-sensing matrix.[1-3]

Materials

We previously reported on the use of urea-based monomers for imprinting oxyanion templates.[4]

We present here a compilation of novel urea-based monomers designed for imprinting various molecules of biological and environmental importance such as amino-acids, peptides and proteins. The monomers are designed to have the dual ability to specifically bind a target molecule and to report the binding in the form of quenching or enhancement of their fluorescence emission or shifts in their UV-visible spectra.

Fig 1.: Induced colour changes of solutions of a urea-based monomer in the presence of increasing concentration of guest TBA-Benzoate (0 – 10 eq) in DMSO.

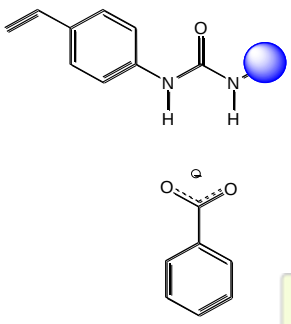

Fig. 2: Proposed complexation mode of Urea-based monomers with Benzoate

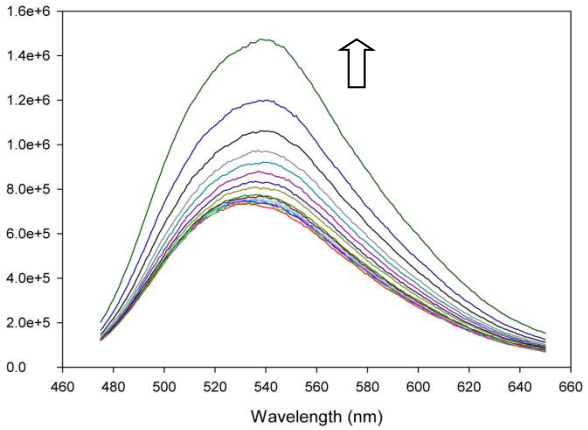

Fig. 3: Induced change in fluorescence emission intensity of urea-based monomer upon addition of increasing concentration of guest molecule TBA-Benzoate (0 – 40 eq) in DMSO.

The most promising of the novel urea-based monomers were successfully employed as building blocks in the synthesis of molecularly imprinted polymers.

Monolithic as well as nano- and hierarchically structured bead formats were applied for a variety of targets, including small- molecule anions such as amino acids up to antibiotics and proteins.

The monolithic polymers were evaluated chromato-graphically to test their molecular recognition behaviour, whereas their chromogenic and fluorogenic properties were investigated in response to various targets in different solvents for comparison with the behaviour of the soluble host monomer alone.

Literature:

[1] Wolfbeis, O.S., *Anal.Chem.*, **2006**, *78*, 3859-3874
[2] Lee,T. M.-H, *Sensors*, **2008**, *8*, 5535-5559
[3] Orellana, G., Haigh, D., *Curr. Anal., Chem.*, **2008**, *4*, 273-295
[4] Hall, A.J. et al., *J. Org. Chem.*, **2005**, *70*, 1732-1736

Conformational Behavior of Conjugated Polymers with Oligo(PhenyleneVinylene) Side Chains

Helmuth Peeters, Wouter Vanormelingen, Thierry Verbiest, Guy Koeckelberghs

Laboratory of Molecular Electronics and Photonics, Katholieke Universiteit Leuven, Celesijnenlaan 200F, B-3001 Heverlee, Belgium

helmuth.peeters@chem.kuleuven.be

Introduction:

During the last decades there has been a great interest in conjugated polymers, as they are implemented in polymeric photovoltaic cells, field-effect transistors and light-emitting diodes. In most cases the electric and optical properties solely arise from the polymer main chain. The function of the side chain, very often an aliphatic chain, is limited to ensure good solubility and to stabilize the supramolecular organisation. Preceding research[(1)], that focused on a system with oligo(phenylenevinylene) (OPV) side chains implemented on a dithienopyrrole polymer main chain, demonstrated that the side chain is also of critical importance for the conformation of the polymer. More specifically, substitution of the β position of the OPV side chain has a crucial influence. The bulkiness of the latter determines the conformation of the polymer, i.e. – short chains will favour a helical conformation, while bulky chains force the polymer in a lamellar supramolecular structure.

Materials and methods:

The polymers are synthesized using a Stille polycondensation of a dibromo OPV derivative and a distannate, for instance a distannylated thienothiophene. These polymers all have the same molecular structure - the same polymer main chain and the same OPV side chain, except the bulkyness of the R' alkyl group differs. the polymers were investigated with UV-Vis, CD and emission spectroscopy

Results and discussion:

Given the fact that the nature of the polymer backbone and OPV side chain is the same, possible differences in the optical and electronic properties must originate from a different conformation or supramolecular structure. The polymers will adopt a coil like structure with identical UV-Vis spectra for the polymers, regardless the length of the R' substituent. It is also important to note that no CD signal will be expected in a good solvent. In a poor solvent on the contrary, a polymer with a short R' chain, will preferably adopt a (one handed) helical conformation due the space filling substituted gallic moiety (Figure 1).

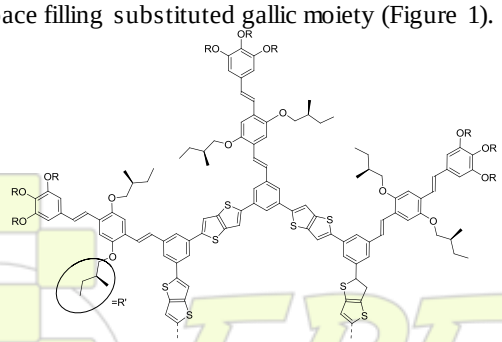

Figure 1: Preferred helical conformation for a polymer with a short R' chain (-R = -C_8H_{17}).

When substituting the polymer with a long R' chain, the polymer will be sterically unable to adopt a helical conformation in a poor solvent (Figure 2A). A planar, zig-zag conformation on the other hand is allowed and this will result a lamellar, supramolecular structure (Figure 2 B).

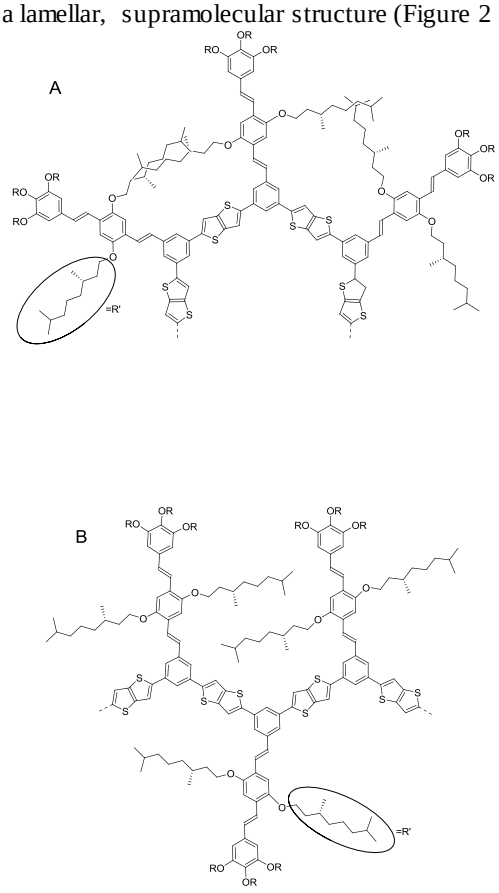

Figure 2A: The long R' chains prevent a helix conformation and B: the lamellar zig zag conformation of the polymer with long R' chains(-R = -C_8H_{17}).

Conclusions:

Small alterations in structure of the polymer, i.e. a change in length of the R' chain, has a tremendous influence on the conformation of the polymer. Applying this on polymers with another main chain, the conformation can easily be altered from a helical conformation to a supramolecular structure, by just tuning the length of the R' group.

References:

1 Wouter Vanormelingen, Lesley Pandey, Mark Van der Auweraer, Thierry Verbiest and Guy Koeckelberghs, Macromolecules, 2010, 43, 2157–2168.

Nanocomposites: dispersion quality and percolation threshold

Nick Watzeels, Hans E Miltner, Christophe Block, Guy Van Assche, Bruno Van Mele, Hubert Rahier

Vrije Universiteit Brussel (VUB), Physical Chemistry and Polymer Science (FYSC), Pleinlaan 2, B-1050 Brussels, Belgium

Email: nick.watzeels@vub.ac.be

Introduction

The last two decades a lot of research was spent on nanocomposite. The key factor in attaining the superior properties of these novel hybrid materials is the achievement of high levels of nanofiller dispersion of the incorporated low amounts of nanosized filler particles, resulting in a vast amount of polymer/filler interphase. [1]

Materials and Methods

The nanocomposites used in this work were prepared by melt mixing techniques, using Poly(ε-caprolactone) (PCL) or Poly(propylene) (PP) as polymer matrix. As nanofiller particles we used silicates based on natural montmorillonite (exchanged with quaternary alkyl ammonium ions), multi walled carbon nanotubes (MWNTs) and cellulose nanocrystals.

The nanocomposites of this work were prepared by melt mixing

Morphological information was obtained from atomic force microscopy (AFM), Transmission electron microscopy (TEM) and Wide-angle X-ray scattering (WAXS). Small angle oscillatory shear rheometry ('dynamic rheometry') experiments were carried out using a cone-and-plate geometry. Thermal characterization was performed using Modulated Temperature Differential Scanning Calorimetry (MTDSC). The mechanical properties of the various materials were assessed by determining their secant modulus (3-point bending mode).

A simulation program called Macropac (Version 6.1) (Intelligensys Ltd) was used to model the packing of objects into a simulation container.

Results and discussion

A comprehensive overview of available methods for assessing nanofiller dispersion is presented for a wide range of layered silicate-based nanocomposites, carbon nanotube-based nanocomposites and nanocomposites containing cellulose nanocrystals. [2]

Focusing on their respective strengths and weaknesses, rheological, mechanical and thermal characterization approaches are evaluated in direct relation to morphological information. [3] An advanced thermal analysis methodology (using MTDSC) is employed for the characterization of the PCL and PP nanocomposites. During quasi-isothermal crystallization, the presence of high aspect ratio nanofillers strongly affects the amount of crystalline-amorphous interface, thus increasing the recorded excess heat capacity (Cpexcess). This increase is in direct relation to the nanofiller dispersion quality. [4]

In a second part of the work, the minimum loading of nanofiller particles needed to obtain a physical network (percolation network) was studied using a simulation program called Macropac (Intelligensys Ltd). [5] Macropac uses a Monte Carlo approach to place particles at random in a simulation box (see Figure 1).

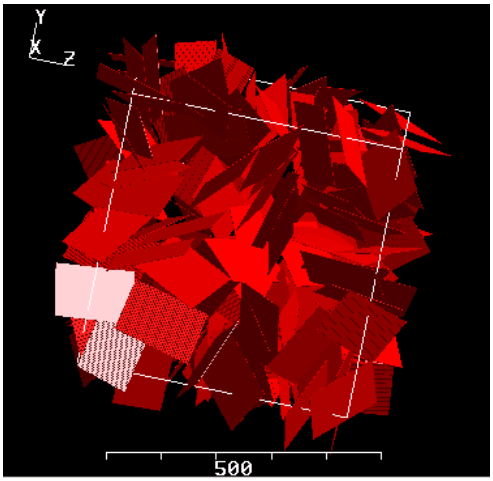

Figure 1: 3-D visualization of a packing of plate-like structures, mimicking silicate platelets, obtained using Macropac simulation software.

Conclusions

It is observed that the degree of filler dispersion is strongly influenced by the specific matrix/filler interactions and the processing conditions.

It is concluded that each techniques used to study the nanofiller dispersion in nanocomposites provides information on a different level of the quality of the dispersion. In other words, a combination of different techniques is needed to make a qualitative assessment of the nanofiller dispersion.

References

[1] M. Alexandre, P. Dubois, Materials Science and Engineering. (2000), 28, 1-63.

[2] Y. Habibi, A.-L. Goffin, et al. Journal of Materials Chemistry (2008), 18, 5002-5010.

[3]H.E. Miltner, N. Watzeels, et al., European Polymer Journal (2010), 46, 984-996.

[4] H.E. Miltner, N. Watzeels, et al., Journal of Materials Chemistry (2010), 20, 9531–9542.

[5] Shiho Akagawa, Takashi Odagaki, Physical Review E (2007), 76, 051402(5).

Poly(ethylene oxide) based block copolymers : synthesis, characterization and applications

Trang N. T. Phan,[1] *Denis Bertin*,[1] *Didier Gigmes*,[1] *Emily Bloch*,[1] *Virginie Hornebecq*,[1] *Philippe Llewellyn*,[1] *Guilhem Bonniol*,[2] *Damien Quémener*,[2] *André Deratani*[2]

[1]Laboratoire Chimie Provence-UMR 6264, Universités d'Aix Marseille 1, 2 et 3, Centre Saint Jérôme, 13397 Marseille Cedex 20, France

[2] Institut Européen des Membranes, Université Montpellier 2, C.C. 047, Place E. Bataillon, 34 095 Montpellier Cedex 05, France

E-mail: trang.phan@univ-provence.fr

Amphiphilic block copolymers, comprised at least two incompatible homopolymers covalently connecting at their ends lead to a fascinating class of self-assembling materials and present unique properties in selective solvents. Copolymers containing poly(ethylene oxide) (PEO) as hydrophilic segment and polystyrene (PS) as hydrophobic segments in PS-*b*-PEO diblock or PS-*b*-PEO-*b*-PS triblock copolymers were widely studied in the literature. The only way, which allows synthesizing block copolymers with well-defined structure, is the living/controlled polymerization techniques, namely ionic polymerization and radical controlled polymerization (CRP). Contrary to the PS-*b*-PEO diblock copolymers, the PS-*b*-PEO-*b*-PS triblock copolymer cannot be prepared directly by anionic polymerization. There were relatively few studies, which have exploited CRP for the synthesis of PS-*b*-PEO-*b*-PS copolymers. In this work, we describe the synthesis of PS-*b*-PEO-*b*-PS and PSAN-*b*-PEO-*b*-PSAN (PSAN for poly(styrene-*co*-acrylonitrile)) triblock copolymers using a new method: nitroxide mediated polymerization of styrene with a difunctional PEO macroalkoxyamine.

Difunctional PEO macroalkoxyamines were characterized by ^{1}H, ^{31}P NMR and mass spectroscopy (EIS-MS and MALDI-Tof),[1] whereas a series of block copolymers with different molar masses and compositions were characterized by ^{1}H NMR, size exclusion chromatography and 2D chromatography.[2] The character self-assembling in ordered structure of obtained PS-*b*-PEO-*b*-PS triblock copolymers was studied by AFM and different morphologies (spherical, hexagonally packed cylindrical and lamellar) were observed according to the copolymer compositions.

A rational synthesis of mesoporous silicas with ultralarge accessible pores by using PS-*b*-PEO-*b*-PS copolymer as templates was studied. Mesoporous silicas have a uniform large pores size of up to 38 nm and high BET surface area of ~ 500 m^2/g. This study demonstrated that the pore diameter of obtained silica increases linearly with the M_n values of the PS block.[3]

3D construction of nanomaterials from the assembly of PSAN-*b*-PEO-*b*-PSAN triblock copolymer micelles was studied. We demonstrated that by playing with the solvent system, spherical or worm-like micelles are formed in situ during the spin coating of copolymer solution and assembled into two different nanomaterials, the nanoparticle (Fig. 1) and the "spider web" films (Fig. 2).[4] These materials are nanoporous materials with pore size controlled by the interspaces between particles or by the superposition of "spider web" layers. Their use in membrane technology is also undertaken.

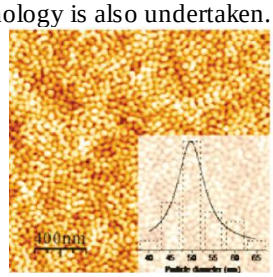

Figure 1: AFM image of the self-standing nanoparticle superlattice film prepared from a DMF/toluene (50/50, v/v) copolymer solution.

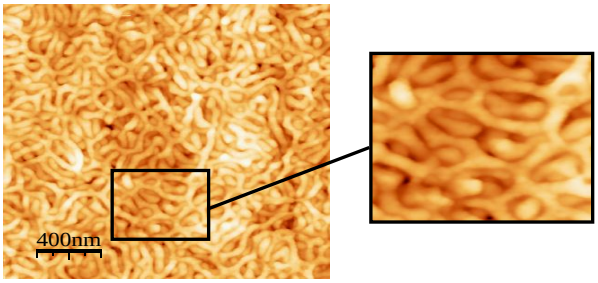

Figure 2: AFM image of the Self-standing "spider web" superlattice film obtained from a DMF/toluene (25/75, v/v) copolymer solution.

References

(1) M. Mazarin, T.N.T. Phan, L. Charles *Rapid Commun. Mass Sp* **2008**, *22*, 3776

(2) L. Perrin, T.N.T. Phan, S. Querelle, A. Deratani, D. Bertin *Macromolecules* **2008**, *41*, 6942

(3) E. Bloch, T. Phan, D. Bertin, V. Hornebecq, P. Llewellyn *Micropor. Mesopor. Mat.* **2008**, *112*, 612

(4) D. Quémener, G. Bonniol, T. N. T. Phan, D. Gigmes, D. Bertin, A. Deratani. *Macromolecules* **2010**, 43 (11), 5060

Synthesis and characterization of biodegradable polyurethane sealants containing rosin resin

Pilar Carbonell-Blasco, José Miguel Martín-Martínez

Adhesion & Adhesives Laboratory. University of Alicante. 03080 Alicante (Spain)

pilar.carbonell@ua.es, jm.martin@ua.es

Introduction

Polyurethanes are proposed as potential sealants for disc defects in spine in the FP7 European project DISC REGENERATION. One of the properties absent in these sealants is their biodegradability. One strategy to impart biodegradability to polyurethane sealants is the modification of their structure by incorporating natural biodegradable moieties. In this study, different amounts of rosin resin were incorporated as part of the chain extender during polyurethane synthesis. Because of the existence of one carboxylic moiety in the rosin resin structure, the reaction with the isocyanate end groups in the prepolymer is feasible, anchoring the rosin resin molecules at the extreme of the polyurethane chains. Furthermore, an additional drawback of the polyurethane sealants is their lack of sufficiently strong initial adhesion, i.e. the polyurethane needs some time to allow the immobilization in their application site. Rosin resin is a natural tackifier obtained from pine exudates and it is added in adhesive formulations to impart high initial strength. Therefore, the objective of this study was to increase the initial adhesion of polyurethane sealants in disc defects imparting potential biodegradability at the same time.

Materials and Methods

The polyurethane sealants were obtained by using the prepolymer method and different mixtures of rosin resin and 1,4 butane diol were used as chain extenders. The polyurethanes were characterized by ATR-IR spectroscopy, plate-plate rheometry, Differential Scanning Calorimetry (DSC), Dynamic Mechanical Thermal Analysis (DMTA), Thermal Gravimetric Analysis (TGA), ºShore A hardness, contact angle measurements, and Laser Confocal Microscopy. The adhesion properties of the polyurethane sealants were tested by T-peel test of plasticized PVC/polyurethane sealant/plasticized PVC and leather/polyurethane sealant/leather joints, and single lap-shear tests of aluminum/polyurethane sealant joints.

Results and Discussion

Polyurethanes with different mixtures of rosin resin and polyadipate of 1,4 butane diol in the chain extender were prepared (Table 1).

Table 1. Nomenclature of the polyurethanes with different content of rosin resin in the chain extender.

Polyurethane	*Amount of rosin resin (wt%)*
100BD	0
75BD+25RR	25
50BD+50RR	50
25BD+75RR	75
100RR	100

Figure 1 shows that the addition of the rosin resin in the chain extender changes the rheological properties of the polyurethanes, imparting higher storage modulus (i.e. higher cohesion), particularly at higher temperature. The higher the amount of rosin resin in the chain extender, the higher the increase in storage modulus (the mixture 25 eq% butane diol+75 eq% rosin resin is an exception).

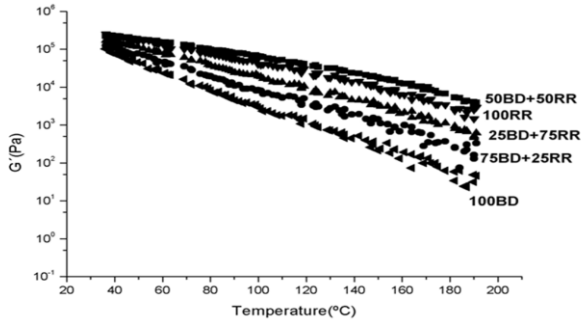

Figure1: Variation of the storage (G´) modulus as a function of the temperature of the polyurethanes.

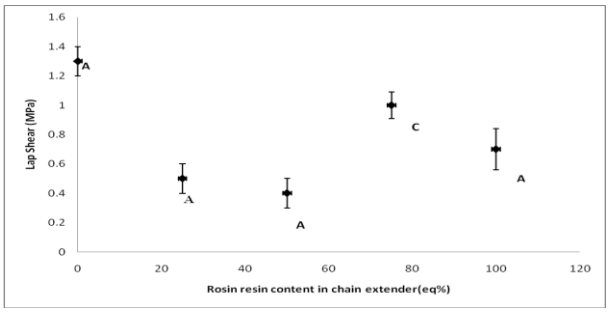

Figure 2: Lap shear values of aluminum/polyurethane adhesive/ aluminum joints as a function of the rosin resin content. Values tested 72h after joint formation. Locus of failure: A= Adhesion failure; C= Cohesive failure in the adhesive.

The single lap shear values of aluminum/polyurethane adhesive joints were relatively high and shows an adhesion failure (Figure 2), except for the mixture of 25eq% of 1,4 butane diol and 75eq% of rosin resin (cohesive failure in the polyurethane is produced).

Conclusions

The addition of rosin resin in the chain extender modifies the viscoelastic properties of the polyurethane sealants. The use of the mixture of 50 eq% of 1,4 butane diol and 50 eq% of rosin resin as chain extender imparted improved the properties to the polyurethane. Furthermore, the adhesion properties are reasonable.

Acknowledgements. Financial support by FP7 European Project DISC REGENERATION and MAT 2009-10234 project is acknowledged. Authors also thank Synthesia Española S.A. for providing the polyester polyol, and La Unión Resinera Española S.A. for providing the rosin resin used in this study.

ABSTRACTS

ORAL PRESENTATIONS

Topic 5: Chemistry and Physics of Nanomaterials and Nanotechnologies

Development of Light Responsive Membranes for Controlled Drug Release

*L. Baumann[1], E. Aslan-Gürel[1], D. de Courten[2], M. Wolf[2], R. M. Rossi[1], L. J. Scherer[1]**

[1] EMPA St. Gallen, Lerchenfledstrasse 5, 9014 St. Gallen, Switzerland
[2] University Hospital Zurich, Frauenklinikstrasse 10, 8091 Zürich, Switzerland

lukas.scherer@empa.ch

In recent years, there has been a rapidly increasing interest in membranes with switchable properties. As a result, the diffusion process of gases, liquids and dissolved molecules can be controlled. The working principle of switchable gate membranes mostly relies on membrane pores, which are coated with stimuli-responsive molecules or polymers. Stimuli responsive polymers are the most important building blocks for such smart membranes in the design of novel functional macromolecular systems with applications for instance in drug release systems. Stimuli can include changes in pH, temperature, light and others.
Alumina or silica based membranes are mostly used. However, nanoporous alumina or silica membranes are very brittle, so it is difficult to manufacture an actual device. In contrast, many polymeric materials have superior flexibility and are therefore investigated as an alternative.
The basic condition for the accomplishment of photoregulative release of drugs is to design a polymer membrane with chromophores capable of transforming light energy into a change in conformation and/or a change in surface polarity. This condition can be achieved by incorporating the photoisomerizable chromophores into the side or main chains of the polymer by covalent bonds. For porous membranes, tailored grafted functional polymer layers on the pore walls can be used to reversibly change the permeability and/or selectivity of the membrane. Switching of material properties with light is of particular interest because this stimulus can be addressed locally, very fast and with high selectivity. Especially for biological applications, the use of light offers unique opportunities, as light fluxes are easier to control temporally than most other stimuli and can be adjusted not to perturb delicate biological structures.
Spirobenzopyrans are well-characterized molecules and exhibit both thermo- and photochromic responses that reversibly transform a colourless, non-polar closed form into a strongly coloured, polar merocyanine opened form through rupture of the spiro carbonoxygen (C–O) bond (Figure 1).

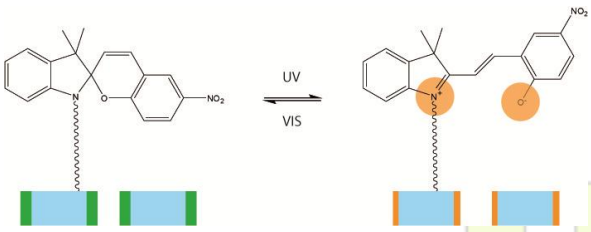

Figure 1: Photochromic spirobenzo-pyran molecule (left, uncharged), immobilized on a porous membrane surface (blue) converts into its merocyanine form (charged, orange) when irradiated with UV light (365 nm). The back reaction is induced by visible light (450-550 nm).

The increased conjugation of the merocyanine form shifts the absorption to longer wavelengths, thus giving rise to visible colour. The merocyanines can return either thermally or with visible light to the colourless spirobenzopyran.
Photochromism is accompanied by a large change in the structure and in the dipole moment. These changes suggest that such molecules are useful in light controlled, "smart surface" applications.

Different surface modification methods of several porous organic membranes were studied like dip-coating, plasma-coating and grafting from the surface. The most promising results were obtained with membranes with plasma inducedpolymerization (Figure 2). Starting from those radicals, co-polymerization of either hydroxyethyl acrylate (HEA) or hydroxyethyl methacrylate (HEMA) with an acrylate decorated spirobenzopyran provided a membrane systemwhich had switchable transport velocities of studied molecules in aqueous medium.

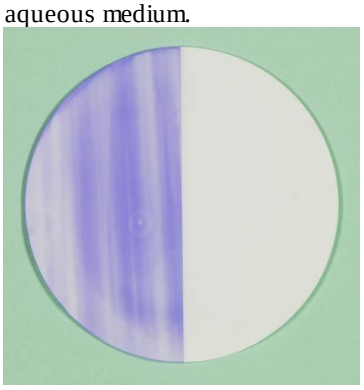

Figure 2: Surface modified PVDF membrane. The right half of the membrane was covered during irradiation of the membrane with 360nm.

Due to this switchability of the membrane resistance, it was possible to change and control the diffusion rate of several molecules across the membrane.
By choosing an appropriate matrix material, specific pore size, the right surface modification conditions and the optimal photochromic molecule, the system was fine-tuned for the diffusion of different specific molecules.

Polyesterification Catalyzed by Hydrotalcite Modiefied Nanoparticles

Zbigniew Boncza-Tomaszewski, *Michal Kedzierski*

Industrial Chemistry Research Institute
Department of Polyesters, Epoxides and Polyurethanes
01-793 Warszawa, ul. Rydygiera 8, POLAND

e-mail: zbigniew.boncza-tomaszewski@ichp.pl

INTRODUCTION

Polyesterification of dimethyl terephthalate (DMT) with neopentyl diol (NPG) has been studied in melt reaction system using a variety modified hydrotalcite (MHT) nano particles as catalyst and nano-filler.

Hydrotalcite (HT), a magnesium-aluminum hydroxy-carbonate, is a naturally occurring mineral of chemical composition $Mg_6Al_2(OH)_{16}[CO_3]4H_2O$ exhibiting a layered crystal structure. The carbonate ion in the interlayer can be exchanged with other anions, and the thickness of the layer is determined by the ionic radius of the anion. The introduction of various guest substances into the gallery and leads to the material with permanent microporosity across the range of molecular size. This process being known as PILSs (pillared interlayers clays) since the calcinated anions acts as pillars. The convenient method, commonly applied for this purpose, is the replacement of alkaline metal cations in clay gallery with organic ions by ion exchange. The modified Mg/Al, Zn/Al and Sn/Al hydrotalcite-type clay compositions containing large, pillaring organic anions were synthesised by ion exchange and used as catalysts and nano-filler in polycondensation reaction.

EXPERIMENTAL

1.*The preparation of modified anionic clays (MHT)*

The pillared Mg/Al hydrotalcites (PILSMHTs) were obtained by co-precipitation at pH=10 with respective salts of the following organicer then acids: p-dodecyl-benzenesulphonic acid (DDS), terephthalic acid (TPA) and aminolauric acids (ALA):

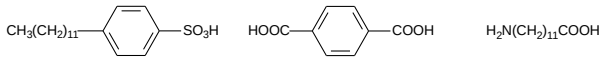

DDS TPA ALA

In the similar way wwere obtained zinc/aluminum hydrotalcite (HT-ZnAl) and tin/aluminum hydrotalcite pillared with terephtalic acid (HT-SnAlTPA)

2. *Polyesterification*

Polyesters were obtained by melt condensation from dimethyl terephthalate (DMT) and neopentyl glycol (NPG) in the presence (0.5% w/w) of modified HT (HT DDS, HT-TPA and ALA-HT, respectively) as catalyst at temperature range 185-195ºC. The progress of reactions was monitored by measuring of amount of condensed methanol and the acids number of polyesters.

RESULTS and DISCUSSION

The MHTs structures were characterized by elemental analysis, FTIR, DTG and XRD. XRD spectra shown that pillaring of HT with organic anion contained long aliphatic chain caused the exfoliation of HT layers from 0.8 nm to 3 nm. The DTG analysis shown that the most thermal stable is hydrotalcite modified with DDS which has decomposition temperature range 659-687ºC (Table 1).

Table 1: Differential Thermal Gravimetry (DTG) analysis of MHT

MHT	$T_{10\%}$ (°C)	Max.temp. range of decomposition (°C)	DTG_{max}(°C)	Weight loss at 700°C(%)
DDS-HT	209	659-687	308,460, 687	74.9
TPA-HT	189	562-582	361,369	66.5
ALA-HT	189	444-525	375,457,490	71.0

The catalytic activity of Mg/Al hydrotalcite pillared with DDS, TPA or ALA are higher then non modified Mg/Al hydrotalcite and increased as the acid strength of pillaring agent increased. The highest catalytical activity shown Zn/Al hydrotalcite (HT-ZnAl) and Sn/Al hydrotalcite pillared with terephthalic acid (HT SnAL TPA). All modiefied hydrotalcite have higher catalytic activity than Fascat 4100 $[C_4H_9SnO(OH)]$.(Fig. 1)

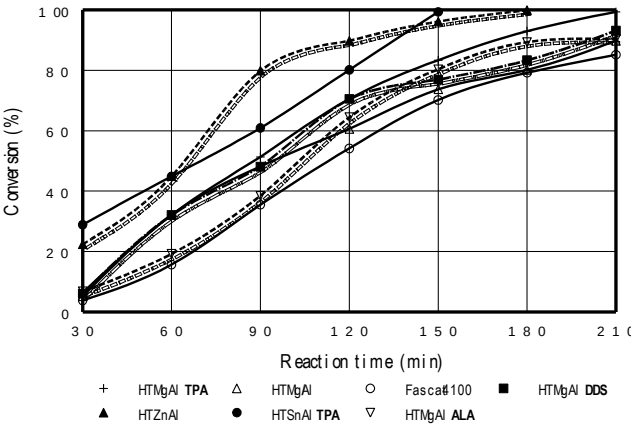

Fig.*1 The catalytical activity of modiefied hydrotalcite obtained by calcination of Mg/Al hydrotalcite precursor*

CONCLUSION

- The modified Mg/Al, Zn/AL and Sn/Al hydrotalcite-type clay compositions containing pillaring organic anions DDS, TPA and ALA are attractive catalyst in polycondnesation reaction.
- All modified hydrotalcite have higher catalytic activity than Fascat 4100 $[C_4H_9SnO(OH)]$.
- The modified hydrotalcites act as nano filler to increase softening point and Tg and thermal degradation of polyester resins.

REFFERENCES

1. S. Cheng, *Catalysis Today*, 49, **1999**, 303.
2. Kumar A.P., Depan D., Tomar N.S. and Singh R.P., *Prog. Pol. Sci.*, **2009**, 34, 479-515.
3. Costa F.R., Saphiannikova, M., Wangenknecht U., Heinrich, G., *Adv. Polym. Sci.*, **2007,** 270, 101.
4. Chan Y-N, Yuang T-Y, Liao I-L, Day S.A., Lin J-J., *Polymer*, **2008**, 49, 4796.
5. Costa F.R., et all, *Appl Clay Sci*, **2008**, 38, 153.

Epitaxial Growth from the Crystalline Cores of Cylindrical Polyferrocenylsilane (PFS) Block Copolymer Micelles

Siti F. Mohd Yusoff, Joe B. Gilroy, Ian Manners

School of Chemistry, University of Bristol, United Kingdom

chzsf@bris.ac.uk

The introduction of metal centers can introduce a wide range of additional functionality to polymeric and supramolecular materials. Block copolymers consist of two or more chemically distinct polymer segments, or blocks, connected by a covalent link. PFS block copolymers with a short crystalline PFS block form core-corona cylindrical micelles in selective solvent for the longer block. The terminii of these micelles are found to be active towards further addition of new PFS block copolymer, a process reminiscent of a living covalent polymerization and can therefore be regarded as living supramolecular polymerization.[1-3] We demonstrate that living polymerizations driven by the epitaxial crystallization of a core-forming metalloblock represent a synthetic tool that can be used to generate complex and hierarchical micelle architectures from diblock copolymers. Using this novel concept, homoepitaxial growth using the addition PFS homopolymers and PFS diblock copolymer to the cylincrical micelles seeds can be studied. This talk presents living supramolecular for the formation of complex micelle architectures including block co-micelles and network-like structure.

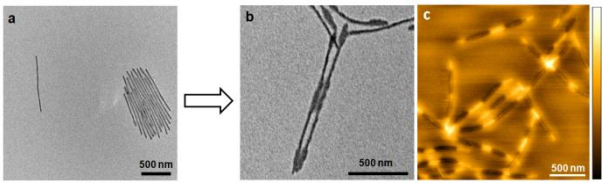

TEM images of (a) long seed micelles of PI_{324}-b-PFS_{54} (b) micelle networks after addition 40 μg of PI_{76}-b-$PFDMS_{76}$ block copolymer added as a 10 mg/mL solution in THF into seed micelles of PI_{324}-b-PFS_{54} (c) tapping mode AFM height of micelles network.

References

[1] Wang, X. S.; Guerin, G.; Wang, H.; Wang, Y. S., Science, **317** (2007) 644.
[2] Gädt, T.; Ieong, N. S.; Cambridge, G.; Winnik, M. A., Nature Materials, **8** (2009) 144.
[3] Gilroy, J. B.; Gädt, T.; Whittell, G. R.; Chabanne, L.; Mitchels, J. M.; Richardson, R. M.; Winnik, M. A.; Manners, I., Nature Chemistry, **2** (2010) 566.

From heterogeneous to homogeneous nucleation of isotactic poly(propylene) confined in nanoporous alumina

Hatice Duran,[†,‖] *Martin Steinhart*,[ǀ] *Hans-Jurgen Butt*[†] *and George Floudas*[‡,§,*]

[†] Max Planck Institute for Polymer Research, Ackermannweg 10, 55128 Mainz, Germany
‖ TOBB University of Economics and Technology, 06560 Ankara, Turkey
[ǀ] Institut fuer Chemie, Universitaet Osnabrueck, D-49069 Osnabrueck, Germany
[‡] University of Ioannina, Department of Physics, 451 10 Ioannina, Greece
[§]Foundation for Research and Technology (FORTH), Biomedical Res. Inst., Ioannina, Greece

hduran@etu.edu.tr, * gfloudas@cc.uoi.gr

Abstract: The crystallization of highly isotactic polypropylene (iPP) confined to self-ordered nanoporous alumina has been studied by differential scanning calorimetry. The pore size ranges from 25nm to 400nm with a pore depth of 80-100μm. A transformation from predominantly heterogeneous to predominantly homogeneous nucleation takes place if the pore diameter becomes smaller than 65 nm. The dependence of the heat of fusion on the pore diameter was determined. The pore diameter below which crystallization is completely suppressed was derived. The predicted suppression of crystallization in nanopores having diameters below 20 nm indicates the critical nucleus size.

Introduction: Polypropylene is a thermoplastic of outstanding commercial importance. Thus, it has attracted many researchers around the globe. Understanding the development of the crystalline phase during solidification of semicrystalline polymers is important in setting-up optimum processing conditions as well as predicting properties of final products[1]. The mechanical performance and optical properties of polymeric materials are significantly influenced by crystallinity and crystal morphology, which varies with the thermal history during processing[2]. Generally, the crystallization of bulk iPP is initiated by heterogeneous, athermal nucleation followed by a 3D spherulitic crystal growth.[3] Controlling crystallization of semicrystalline polymers by geometric confinement has attracted considerable interest as it has been shown that confinement can affect crystal nucleation, crystal growth and crystal orientation.[4, 5].

Nanoporous anodic aluminum oxide (AAO) has been widely used a an inorganic model matrix as it contains arrays of straight, cylindrical nanopores uniform in length and diameter that can easily be infiltrated with polymeric melts[6]. It is already known that segmental dynamics of polymers is altered in the presence of the hard pore walls of AAO.[7] With respect to polymer crystallization, some authors have reported heterogeneous surface nucleation of polyethylene confined to AAO nanopores small enough to neglect the presence of other types of heterogeneous nuclei.[8] This finding leads to several open questions about the type of nucleation under hard confinement typical for AAO: Is the crystallization process always heterogeneous within the small AAO nanopores? Can hard confinement completely suppress polymer crystallization and if so, what is the required size? In this research study, we explore these issues using iPP confined within the nanopores of self-ordered AAO.

Materials and Methods: AAO was prepared according to literature:[9] The iPP (PSS, Mainz) had a number-average molecular weight M_n=32500 g/mol and a polydispersity index M_w/M_n=3.32. Infiltration of the iPP was performed by placing neat iPP on the surface of the self-ordered AAO at 473 K for 20h. Thermal analysis was carried out using a Mettler Toledo Star differential scanning calorimeter.

Results and Discussion: The Figure shows the total enthalpy of crystallization and relative crystallization change as a function of pore diameter. The heat of fusion strongly decreases as the pore diameter decreases. Linear extrapolation reveals that iPP infiltrated into AAO with pore diameters below about 20 nm would be unable to crystallize. The predicted complete suppression of crystallization within the 1D hard confinement of AAO contrasts with results reported for 2D crystallization of poly(ethylene oxide) and iPP in multi-layer nano-assemblies. These experiments revealed that these polymers could still crystallize as single lamellae with large aspect ratios.

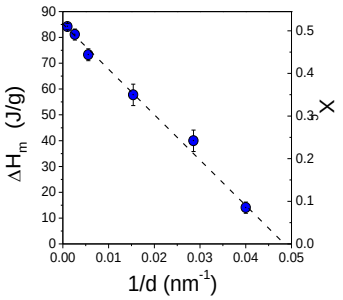

Figure. Heat of fusion and degree of crystallinity of iPP plotted as a function of inverse self-ordered AAO pore diameter.

References:

([1]) Suh, J.; White, J. L.; *J. Appl. Polym. Sci.* 2007, 106, 276-282.
([2]) Chiu, W. Y.; Fan-Chiang, K. H.; Chen, L. W. *Mater. Chem. Phys.* 1993, 34, 46-51.
([3]) Chiu, J *Anal. Chem*. 1964, 36, 2058-2061.
([4]) Steinhart, M.; Göring, P.; Dernaika, H.; Prabkukaran, M.; Gösele, U.; Hempel, E.; Thurn-Albrecht, T. *Phys. Rev. Lett.* **2006**, *97*, 027801-1.
([5]) Wu, H.; Wang, W.; Huang, Y.; Su, Z. *Macromol. Rapid. Commun.* **2009**, *30*, 194-198
[6] Steinhart, M. *Adv. Polym. Sci.* **2008**, *220*, 123
[7] Duran, H.; Gitsas, A.; Floudas, G.; Mondeshki, M.; Steinhart, M.; Knoll, W. *Macromolecules* **2009**, *42*, 2881-2885.
[8] Woo, E.; Huh, J.; Jeong, Y.G.; Shin, K. *Phys. Rev. Lett.* **2007**, *98*, 136103-1.
[9].Masuda, H. and Fukuda, K. *Science* **1995**, 268, 1466–1468

Polyethylene/Graphene Nanocomposites Obtained By *In Situ* Polymerization

Fabiana de C. Fim[1], Nara R. de S. Basso[2], Denise S. Azambuja[1], Griselda Barrera Galland[1]

[1]Instituto de Química – UFRGS, Av. Bento Gonçalves 9500, Porto Alegre/RS, 91570-970 –
[2]Faculdade de Química PUC/RS, Av. Ipiranga 6681, Porto Alegre/RS, 90619-900, Brazil.

griselda.barrera@ufrgs.br

Introduction

Polymeric nanocomposites are hybrid materials formed by an organic polymeric matrix in which the inorganic fillers are dispersed in nanometric dimensions[1]. The nanometric fillers normally used are: clay, alumina, carbon nanotubes, gold, silver and graphite[2]. The polymer/graphite nanocomposites are interesting due to the potential conductive properties. Graphite is chemically similar to carbon nanotubes and structurally analogous to layered silicate and hence is a potential nanofiller to improve the properties of neat polymer. Graphite can be introduced into the polymeric matrix to form nanocomposites through fusion of the polymeric matrix, intercalation in solution and *in situ* polymerization. There are some works in the literature related with the synthesis of polymer/graphite nanocomposites using *in situ* polymerization but the monomers used have been methylmethacrylate[3], aniline[4] and styrene.[5-7] The use of graphite and polyolefins as starting materials is convenient because both are inexpensives and with very different properties, one is conductive and the other is insulating, the formation of a nanocomposite of them will extend the applicability of both materials.

This work describes the synthesis of polyethylene/graphene nanocomposites through *in situ* polymerization of ethylene in the presence of graphene nanosheets, using the catalytic system Cp_2ZrCl_2/MAO ((bis(cyclopentadienyl)zirconium(IV)dichloride/methylalu minoxane). The main objective of this work is to prepare graphite nanoparticles with a well defined structure, and to grow polyethylene within the pores and galleries of this laminated material to obtain a well dispersed nanocomposite to evaluate the thermal, mechanical and electrical properties this new material.

Materials and Methods

Graphene nanosheets (GNS) previously treated with methylaluminoxane (15wt%), were added into the reactor as filler at percentages from 1 to 14 % (wt.%). The polymerization reactions were carried in a 100 mL PARR reactor. Toluene was used as solvent, MAO as cocatalyst (Al/Zr=1000) and Cp_2ZrCl_2 as catalyst (2.10^{-6} mol). The reactions were done at 70ºC, using an ethylene pressure of 2.8 bar during 30 min. The characterization of the GNS and the PE/GNS nanocomposites were done by SEM, TEM, AFM and XRD. The nanocomposites properties were studied by TGA, DSC and DMA. The mechanical and conductivity properties were also investigated.

Results and Discussion

XRD and TEM analysis of GNS showed that the chemical and thermal treatments of graphite produced graphene sheets of about 10 graphenes. Polyethylene/graphene nanocomposites, with graphene amounts of 1.2, 2.8, 5.6 and 14.3 wt%, were obtained by *in situ* polymerization, with good catalytic activity. XRD and TEM analysis showed that the GNS were further exfoliated by the ethylene polymerization, giving graphite crystals with smaller number of graphene layers than the exfoliated graphite initially added. TEM micrographs of the nanocomposites showed the presence of regions where the graphite maintained an organized structure (intercalated graphite) and others where it was more disorganized (exfoliated graphite).

The onset degradation temperature increased by 30°C in the nanocomposites with 2.8 and 5.6 wt.% of GNS. All the nanocomposites presented higher storage modulus than neat polyethylene. This indicates that the GNS have a reinforcing effect on the polyethylene matrix. The impedance measurements showed an increase of electrical conductivity of the nanocomposites. This enhancement is related to an increase in mobility in the network and in the density of the potential charge carriers.

Conclusions

Polyethylene/Graphene nanosheets nanocomposites were successfully obtained by *in situ* polymerization of ethylene using a metallocene catalyst. Nanocomposites showed higher thermal stability, rigidity and conductivity than the polymeric matrix.

References

1. Schaefer, D.W.; Justice, R.S. *Macromolecules*, **40**, 8501-8517, 2007.
2. Gopakumar, T. G.; Pagé, D. J. Y. S. *Polym. Eng. Sci.*, **44** (6), 1162-1169, 2004.
3. Chen, G.; Weng, W.; Wu, D.; Wu, C. *Eur. Polym. J*, **39** (12), 2329-2335, 2003.
4. Du, X. S.; Xiao, M.; Meng, Y.Z., *J Euro. Polym.* **40**, 1489-1493, 2004.
5. Chen, G.; Wu, C.; Weng, W.; Wu, D.; Yan, W., *Polymer*, ***44***, 1781-1784, 2003.
6. Uhl, F.M., Wolkie, C.A. *Polym. Degradation and Stability*, **76**, 111-122, 2002.

Xiao, M.; Sun, L.; Liu, J.; Li, Y.; Gong, K., *Polymer*, **43**, 2245-2548, 2002.

Impact of synergy between carbon nanotubes and carbon black on the rheological and electrical properties of an EPDM rubber

M. Charman[1,2], *F. Léonardi*[1], *C. Bissuel*[2], *C. Derail*[1]

1 - Institut Pluridisciplinaire de Recherche sur l'Environnement et les Matériaux
Equipe de Physique et Chimie des Polymères, Université de Pau et de Pays de l'Adour
2 - EMAC Elastomères, BP 52, 64130 Mauléon

e-mail : m.charman@emac.fr

Introduction

The outstanding properties of carbon nanotubes (high tensile modulus [1], high electric conductivity [2], and high aspect ratio) make them ideal candidates for use in nanocomposites, and particularly in those based on rubber matrix [3]. However, to obtain an improvement of the properties, a good degree of dispersion of the CNT in the matrix is crucial. It was shown that the grafting of blocks copolymer onto nanotubes surface [4, 5] or their encapsulation by a copolymer [6] improved this individualization. Nevertheless, an approach of the CNT surface modification or a polymerization in the presence of the NTC (polymerization in situ) [7] seems two ways which are very difficult to be transposed in the industry.

The CNT dispersion in an EPM rubber is investigated here by using a statistical copolymer as dispersing agent. An association between the EPM and the ethylene-*co*-vinyl acetate (EVA) being very current in the rubber industry, and we chose to investigate this way because EVA exhibits a good affinity with the CNT and improve their dispersion [8].

Materials and methods

We studied more exactly the influence of various parameters (EPM/EVA ratio, matrix viscosity) on the CNT dispersion and prepared an EPM-EVA master batch loaded with 20% of CNT. We dilute this master batch on an EPDM matrix and we compared the influence of carbon nanotubes, carbon black or the blend of both on the rubber properties.

We work with the classic methods used for rubber mixing, like an internal mixer and an open two roll mill, which are soft mixing techniques.

Results and discussion

Firstly, we demonstrate that matrix viscosity and EPM-EVA ration influence the CNT dispersion. We observe a better CNT dispersion with a low matrix viscosity. We obtain EPM-EVA composites with very good conductive properties (fig 1). The master batch loaded at 20wt% has a surface conductivity equal to 2,6S/cm.

We will present the influence of fillers and their possible synergy on the rheological and electrical properties of an EPDM rubber. In particular, we will compare the rheological and electrical percolation thresholds in the presence of fillers and will quantify their impact on the vulcanization kinetics of elastomers. We will demonstrate that the dilution of the master batch allows to obtain a rubber filled with a constant Mooney viscosity.

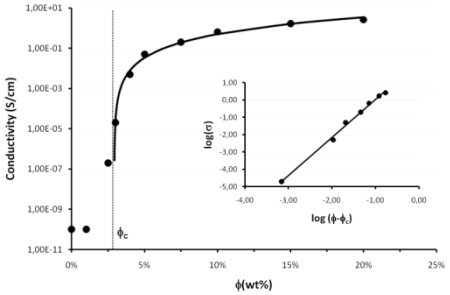

Fig. 1: Effect of CNT content on surface conductivity. The inset shows the variation of logs versus log (ϕ–ϕ_c) with ϕ_c =2,93wt% and t = 2,20

The synergistic effect between carbon black and carbon nanotubes will be shown on the mechanicals properties but not on the electrical properties [9].

Conclusion

We demonstrated that it is possible to prepare a rubber, with industrial techniques, which exhibits very good electrical properties. The synergy between carbon black and CNT was only demonstrated on mechanical properties.

References

[1] M.M.J. Treacy, T.W. Ebbesen, J.M. Gibson, *Nature*, 381, 678, 1996
[2] N. Hamada, S. Sawada, A. Oshiyama, *Phys. Rev. Lett.*, 68,1579-1581, 1992
[3] L. Bokobza, *Polymer*, 48, 4907-4920, 2007
[4] V. Datsyuk, L. Billon, C. Guerret-Piécourt, S. Dagréou, N. Passade-Boupatt, S. Bourrigaud, O. Guerret, L. Couvreur, *J. Nanomaterials*, 2007
[5] I. Do, *Nanocomposites Nanotubes de Carbone/Elastomère: Propriétés Rhéologiques et Electriques*, PhD, Université de Pau et des Pays de l'Adour, Pau, 2007
[6] A.R. Bhattacharyya, P. Pötschke, M. Abdel-Goad, D. Fischer, *Chemical Physics Letters*, 392, 28–33, 2004
[7] A.C. Courbaron Gilbert, N.E. El Bounia, E. Péré, L. Billon, C. Derail, *Adv. Mat. Res.*, 112, 29-36, 2010
[8] S. Peeterbroeck, L. Breugelmans, M. Alexandre, J.B. Nagy, P. Viville, R. Lazzaroni, P. Dubois, *Composites Science and Technology*, 67, 1659–1665, **2007**
[9] L. Bokobza, M. Rahmani, C. Belin, J-L Bruneel, N-E EL Bounia, *J. Polymer Science: Part B : Polymer Physics*, 46, 1939-1951, **2008**

Ordered Lithium-Ion-Conducting Polymer Electrolytes

D. Golodnitsky[1], K. Shvartsman [1], E. Peled[1], L. Adler-Abramovich[2], E. Gazit[2], A. Greenbaum[3], S. Greenbaum[4]

1-School of Chemistry, 2- Faculty of Life Sciences, Tel Aviv University, Tel Aviv, 69978, Israel; 3- Department of Applied Physics, - The Hebrew University of Jerusalem, 91904 Jerusalem, Israel, 4-Hunter College of CUNY, Park Avenue 695, 10065 NY, USA

golod@post.tau.ac.il

Introduction

More than 30 years ago it was proposed by Armand that the helical structure of polyether chains, like polyethylene oxide (PEO), might provide a framework for ion transport in crystals of these polymers. This suggestion was considered not feasible in view of the mounting evidence that long-range transport of lithium ions is inhibited in crystalline phases of the host materials and that ionic mobility in such systems is intimately connected with the segmental motions of the host. By contrast, our experimental data on thin-film stretched polymer electrolytes (PE) obtained more than 10 years ago and aimed at longitudinal alignment of PEO helices unambiguously showed that ordering of polymer electrolytes enhances both intrachain cation motion and its interchain hopping. This finding was supported by other researchers and mathematical models. It was shown that the less tangled the channel, the lower the activation energy required to overcome the potential barriers of the hopping from site to site, created in the PEO by structural loops.

In addition, we recently presented a procedure for the perpendicular orientation of the helical PEO segments by casting the PEs under a magnetic field. This enhances the ionic conductivity (σ) in the Z direction (perpendicular to the film plane) by about one order of magnitude. The magnetic-field effect is even more pronounced in polymer electrolytes with incorporated diamagnetic and ferromagnetic nano-fillers.

Results and Discussion

In this work we have found that casting, under a gradient magnetic field, of PEs comprising only 1% of aromatic dipeptide nanotubes coated with ferrofluid (FF-PNT) increased the total PE conductivity at room temperature by a factor of about eight, as compared to the PE with 14% content of hematite and by 2 orders of magnitude, as compared to pristine PEs. The FF-PNT-modified PE cast under MF is thermally stable. Even after 1 month of storage at 70°C it retains conductivity values that are very close to that of the freshly-cast film. As opposed to other fillers tested so far, the incorporation of FF-PNT to the pristine typically-cast PE, eliminates formation of large spherulites. A highly–homogeneous, fine-grained morphology with well-defined round-shaped crystallites develops in this composite PE under an applied MF (Fig.1). The XRD patterns make it clear that the applied magnetic field influences the crystallinity of the PE containing FF-PNTs more strongly than it does that of pristine films.

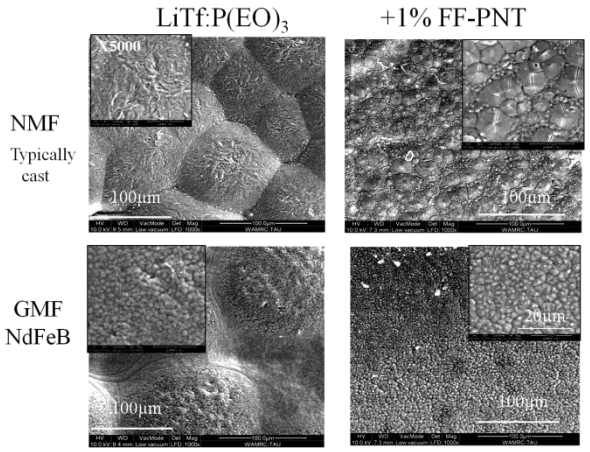

Fig.1 ESEM images of typically-cast pristine and composite polymer electrolytes

Finally we present the original approach to promote orthogonal orientation of PEO helices by the attachment of gold-coated maghemite nanoparticles to the thiol- or amine-end groups of the polymer chain. The "bridging" properties of mercaptoundecanoic acid (MUA) enabled preparation of -γFe_2O_3 particles covered by the nano-seeds of Au. The core-shell structure of the nanoparticles was verified by XRD, XPS and TEM-EDS analysis. The Au-maghemite nanoparticles have been incorporated into the PE by two-step procedure and cast under a gradient magnetic field. The conductivity values of these electrolytes are close to those of PE with FF-PNTs.

Acknowledgements

We thank the United States-Israel Binational Science Foundation (research grant 2006149) for financial support of the project

Atmospheric Pressure Plasma Jet Deposition of Gas and Vapour Barrier Coatings onto Polymer Films for Packaging Applications

R. Sulcis, P. Scopece*, M. Muzio*, I. Kulyk*, A. Patelli**

* CIVEN, Via delle Industrie 5 Marghera (VE) Italy

sulcis@civen.org

Introduction

The increase of gas and vapour barrier coatings is one of the most important issues in packaging applications. The packaging of carbonated drinks, food requiring modified atmosphere, preservation of aromas or biscuits friability usually need complex multilayer structures. Many efforts are done for the obtainment of packaging characterized by high barrier properties to water vapour or gases and simple production.

In the last years very interesting results were obtained by using organically modified silicate layers. In this case the modification of the polymer is usually obtained by melt blending the polymer with these nanoclays; however actually no clear indications on the risk of the contact of the nanocomposite materials obtained by using organically modified nanoclays are available and EU regulation still does not regulate nanocomposites for food contact use.

One of the most interesting alternative ways to increase gas barrier properties of polymers is the development of silica barrier coatings. Transparency, microwave compatibility and chemical inertness are the most important characteristics of SiOx-based film. The use of plasma enhanced chemical vapour deposition technique (PECVD) for the obtainment of barrier coatings onto different substrates is nowadays well established[1,2]. Layers like SiNx and SiOx, usually obtained by PECVD, can decrease the gas permeation through polymer substrates by several orders of magnitude.

Nevertheless, the known costs of vacuum systems in terms of technological reason and on-line processing limits have generated increasing interest to develop atmospheric condition alternatives. For these reasons atmospheric pressure plasma deposition represents an interesting solution in order to reduce equipment costs and to increase the on-line processing capability, which is a fundamental parameter for continuous productions, as in the case of traditional packaging production.

Next to traditional, low pressure techniques, normal pressure plasmas have been employed successfully for surface treatment. The use of an atmospheric pressure plasma jet (APPJ), compared to other non-equilibrium, normal pressure plasmas, is advantageous in particular for local film deposition or for the coating of 3D forms e.g. inner walls of wells, trenches or cavities. The jet geometry offers the advantage that the surfaces to be treated are not placed between electrodes thus allowing better flexibility in terms of substrate distance and electrical field[3].

In this work we present the application of this technology for the obtainment of silica barrier coatings onto different polymer substrates, ranging from poly(propylene), which is one of the most used polymers in flexible packaging applications, to poly(lactic acid), which is receiving more and more attentions for packaging applications, but which most important drawback is the very low thermal stability.

Different silica precursor were evaluated and results on adhesion, mechanical properties, carbon content, and gas transmission rate are presented together with thickness information and coating morphology.

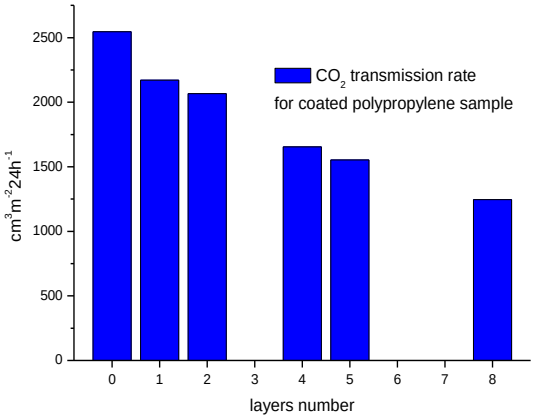

Fig. 1. Decrease of CO_2 transmission rate by increasing barrier nanostructured coatings onto PP substrate

[1] A.G. Erlat' R.J. Spontak, R.P. Clarke, T.C. Robinson, P.D. Haaland, Y. Tropsha, N.G. Harvey, and E.A. Vogler. *J. Phys. Chem. B*, (1999) **103** (29), pp 6047–6055

[2] A. Bieder, A. Gruniger and Ph.Rudolf von Rohr, *Surf. Coat. Technol.*, (2005) **20**, pp. 928–931

[3] M. Laroussi and T. Akan, *Plasma Process. Polym.*, (2007) **4**, 777-788

Preparation, Surface Properties and Applications of Nanometric Cellulose Model Films

Rupert Kargl[1], Tamilselvan Mohan[2], Stefan Köstler[3], Martin Reischl[1], Aleš Doliška[2], Karin Stana-Kleinschek[2], Volker Ribitsch[1,3]

[1] Karl-Franzens University Graz, Institute of Chemistry, AT-8010 Graz, Heinrichstraße 28, Austria
[2] University Maribor, Faculty of Mechanical Engineering, SI-2000 Maribor, Smetanova Ulica 17, Slovenia
[3] Joanneum Research, Materials, Institute for Surface Technologies and Photonics, Steyrergasse 17-19, AT-8010 Graz

rupert.kargl@uni-graz.at

Introduction: Well defined model surfaces of polymeric materials are important tools to study adsorption, wettability, adhesion or other interfacial phenomena. Model substrates of cellulose, the most abundant biopolymer, are of interest because this polymer can contribute significantly to a sustainable and renewable way in the utilization of natural resources. Several methods and film preparation techniques for cellulose model films are know from literature [1]. Besides their characterization cellulose model films were utilized for principle investigations like polymer adsorption studies or enzymatic degradation of cellulose [2]. Usually, cellulose model films are prepared from trimethylsilyl cellulose (TMSC), a derivative that is soluble in organic solvents and can be regenerated to pure cellulose under hydrochloric acid vapors [3]. A scheme of this desilylation reaction is depicted in figure 1.

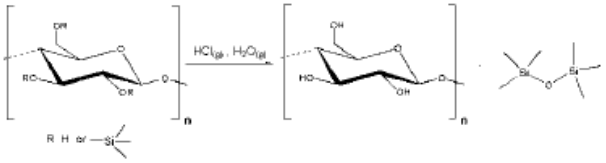

Figure 1: Reaction scheme for the desilylation of trimethylsilylcellulose (TMSC) to pure cellulose

Even though this kind of model film is used widely, little is known about the time dependent desilylation of TMSC to cellulose. In this work we therefore investigated the preparation and surface properties ofcellulose model films that were regenerated from TMSC for different regeneration times. Furthermore we showed a practical example how these model films can be structured by soft-lithography and how model films in general can be used to study interfacial phenomena at cellulose surfaces.

Materials and Methods: TMSC dissolved in toluene was spin coated on silicon wafers. The time dependent regeneration to cellulose was studied by contact angle measurements, X-ray photoelectron spectroscopy (XPS), infrared spectroscopy and optical thickness measurements (Sarfus). Atomic force microscopy was applied for morphological investigations. Selected cellulose surfaces derived in this way were structured by a new soft-lithographic method applying enzymes and polydimethylsiloxane (PDMS) moulds.

Results and Discussion: The time dependent regeneration of TMSC to cellulose allowed the targeted manufacturing of cellulose model films with different degrees of desilylation. The degree of desilylation can be followed easily by contact angle measurements and

XPS analysis. It is assumed that during the course of desilylation volatile silicon species tend to adsorb on the cellulose model films. These species can be removed under reduced pressure. Atomic force microscopy showed that the surface morphology of the films is not immediately influenced during the desilylation even though morphology changes are observable after drying or vacuum treatment.
In addition pure cellulose model surfaces regenerated from TMSC with a thickness in the nanometer range can be structured using an enzymatic treatment in combination with a soft-lithographic mould. A typical structured cellulose film is shown in figure 2, where separated cellulose lines with 50µm spaces and a thickness of 40 nm are depicted.

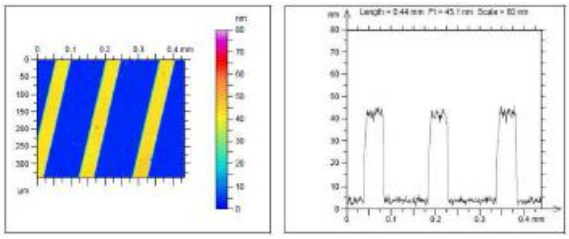

Figure 1: Soft-lithographically structured cellulose films on a silicon substrate. The left image shows a top view of a Sarfus-image whereas the right image depicts the cross-section of the structured film.

Conclusion: In this work we could show how the time dependent regeneration of cellulose model films from TMSC is reflected in the wettability and elemental composition of the surfaces. Furthermore a new oftlithographic technique was introduced to structure a biopolymeric thin film with the aid of enzymatic degradation. The research leading to these results has received funding from the European Union Seventh Framework Programme (FP7/2007-2013) under grant agreement n° 214653.

References

1 E. Kontturi, M. Österberg, Chem. Soc. Rev. 35 (2006) 1287.
2 S. Ahola, X. Turon, M. Österberg, J. Laine, O.J. Rojas, Langmuir. 24 (2008) 11592.
3 S. Köhler, T. Liebert, T. Heinze, J. Polym. Sci. 12 (2008) 4070.

Formulation and optical study of ordered phases of copolymers and nanoparticles

Virginie Ponsinet[1], *Benoit Maxit*[2], *Clémence Tallet*[1], *Denis Bendejacq*[3]

1 University of Bordeaux, CNRS-CRPP, Pessac, France
2 Cordouan Technology - Pessac, France
3 Rhodia - Aubervilliers, France

ponsinet@crpp-bordeaux.cnrs.fr

New "bottom-up" fabrication techniques are now effectively explored for the production of nanostructured functional materials. Specifically, controlling the spatial organization of nanoparticles in a material would allow taking full advantage of the nanoparticles specific properties. For example, interesting optical properties in the visible range are foreseen when assembling plasmonic nanoparticles. Such spatial control can be obtained by template-assisted self-assembly, using matrices presenting a spontaneous molecular organization. Among the promising self-assembled systems are the diblock copolymers made of two molecular chains of distinct chemical nature linked together, which present solid state spontaneous structures with long-range order and tunable characteristic sizes between 10 and 100 nm. In particular, alternating lamellar and hexagonally-ordered cylindrical structures are described in many diblock copolymers systems. Such copolymers have proven useful templates for ordering nanoparticles with long-range order.

In this presentation, we will describe an original methodology for the preparation of ordered nanocomposites of block copolymers and nanoparticles, using the specific swelling properties of amphiphilic diblock copolymers, as well as the study of the prepared materials.
Poly(styrene)-block-poly(acrylic acid) amphiphilic copolymers form hexagonal and lamellar phases in the melt state, depending on their molecular structure.

These ordered phases can be swollen in water while preserving their morphology and long range order,

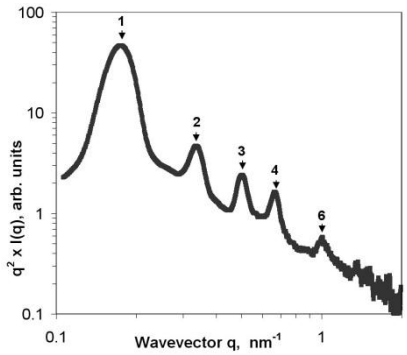

Figure 1: Small-angle X-ray scattering curve of the solid lamellar phase of a symmetric PS-b-PAA copolymer, plotted as $q^2I(q)$. The structure factor peaks, indicated by arrows and numbers corresponding to the peak order, are characteristic of the lamellar symmetry of the lattice. The position of the first order peak gives access to the lattice parameter, here d=36.4 nm.

thanks to the glassy nature of the poly(styrene) core. The stability of the swollen phases, and their behavior in dispersion, are linked to the properties of the poly(acrylic acid) polyelectrolyte brushes and can be monitored via the pH or ionic strength of the dispersion.

We use these properties to propose a original methodology for introducing solid nanoparticles, which present two advantageous specificities. First, it is possible to reach high densities of introduced particles. Second, aqueous sols of nanoparticles can be used. The copolymer ordered phases are indeed swollen with the aqueous sol instead of water, and the nanoparticles can penetrate within the copolymer dispersions. Provided an attractive interaction is tuned between the nanoparticles and the hydrophilic block of the copolymers, which can be done in this case by playing on the pH of the dispersions,and depending on the particle sizes, the nanoparticles can be trapped within the structure upon drying. We will present our study of the incorporation of 15-nm diameter silica nanoparticles, 7-nm diameter cerium oxyde nanoparticles and 10-nm diameter gold nanoparticles in the 18-nm thick poly(acrylic acid) layers of the ordered lamellar phase of a poly(styrene)-*block*-poly(acrylic acid) copolymer. Volume fraction of nanoparticles was varied in both thin films on silicon wafer and bulk samples. We will show how small-angle scattering and reflectivity of X-rays, ellipsometry, atomic force and electron microscopies were used to get a detailled structural description of the nanostructured composites and validate the control of the density and organization of the nanoparticles. We will finally discuss first results of optical measurements with the gold nanocomposites.

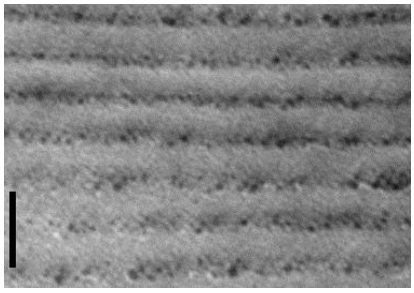

Figure 2: Transmission electron micrograph (side view) of an ordered lamellar composite film of gold nanoparticles and poly(styrene)-b-poly(acrylic acid) copolymer. Bar = 50 nm.

Acknowledgments – The support of the Région Aquitaine, the French Agence Nationale de la Recherche (NANODIELLIPSO, ANR-09-NANO-003) and the European Union's Seventh Framework Programme (FP7/2008) under grant agreement n° 228762 (METACHEM) is acknowledged.

Nanostructures from tunable self-assembly of a simple diblock copolymer

Alberto Bianchi, Michele Mauri and Roberto Simonutti

Department of Materials Science, Università di Milano-Bicocca, Via R. Cozzi 53 20125 Milano (Italy)

roberto.simonutti@mater.unimib.it

Introduction:
Amphiphilic block copolymers with low polidispersity (D) are thermodynamically driven to auto-assemble forming regular nanosized morphologies when dissolved in selective solvents [1]. We focused on producing controllable structures from commonplace monomers like styrene or dimethylacrylamide (DMA). The assembly was tuned by chemical nature of the solvent, providing several different structures that can be the basis for the preparation of materials.

Materials and Methods: RAFT synthesis was performed based on literature [2] using an optimized transfer agent. The PS block was synthesized first in bulk with 3-(benzylsulfanylthiocarbonylsulfanyl) propionic acid as RAFT agent, with M_{nNMR} = 11000, M_{nGPC} = 11920, and D = 1.06 measured by GPC. After copolymerization of the PDMA block, quantitative NMR was used to establish the polymer as $PS_{105}PDMA_{817}$. T_g was measured by DSC at about 84°C for the PS block and 120 °C for the final copolymer.
^{1}H NMR was performed on a Bruker Avance III 500 MHz instrument.

Results and Discussion: the polymer was diluted in different solvents at room temperature using several tens of mg per mL. $CDCl_3$ provides a clear solution indicating solvatation of both blocks. D_2O and toluene formed colloids with a cloudy appearance, indicating presence of structures in the tens to hundreds of nm size range.

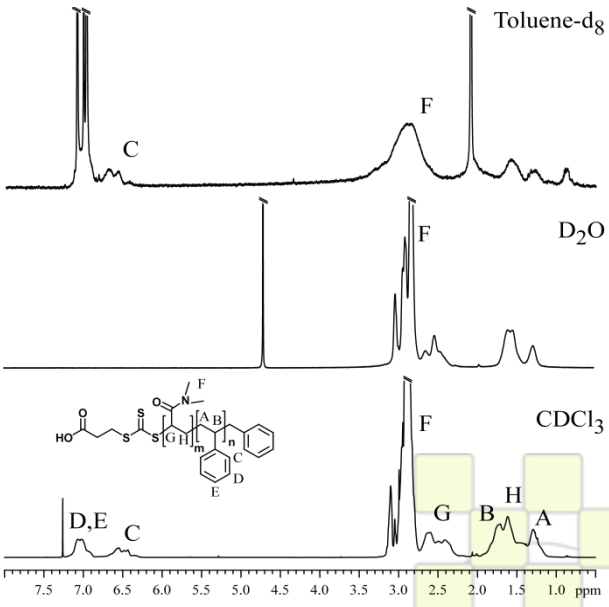

Figure 1: ^{1}H NMR spectra of PS-b-PDMA in different solvents. C and F peaks are fingerprints of PS and PDMA respectively.

Dynamic Light Scattering of the aqueous colloid confirmed the presence of particles with average diameter of 120 nm and sharp distribution.
^{1}H NMR spectra are shown in Figure 1. Each block has specific signals, namely from 6.5 to 7 ppm for PS while PDMA is around 2.8 ppm.
Solution NMR is optimized for fast moving molecules and does not detect solid-like fractions because of extremely low T_2 relaxation time [3]. The presence or absence of peaks in the spectra can be interpreted as a function of mobility. The spectrum in $CDCl_3$ contains peaks relative to all protons in the sample. The peaks of the styrenic block disappear in water, meaning the hydrophobic block is behaving as a rigid solid. In toluene, the styrenic block is solvated and provides full signal intensity, while the PDMA is also visible but with a significant line broadening corresponding to reduced but not solid like mobility.
A direct investigation of the nanostructures was performed by TEM. As seen in figure 2, the sample deposed from aqueous solution contains small circular objects arranged in a pseudohexagonal layer. In toluene, the polymer chains arrange in worm-like shapes, that aggregate in interconnected structures.

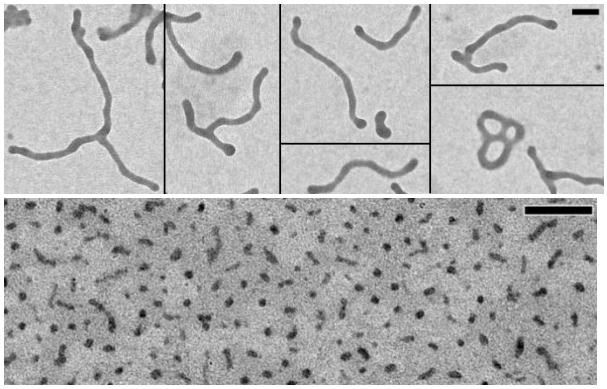

Figure 2: TEM images of PS-b-PDMA deposed from toluene (above, selection of worm-like shapes) and water (below). All scale bars are 200 nm.

Conclusions: Despite the simple starting monomers, PS-b-PDMA copolymer has not been studied extensively but has a rich capability to form different sharp nanostructures that we show here for the first time. Self-assembly provided hard, stable, core shell particles in water and less defined worm-like micelles in toluene. Work is under way to verify if such structures can then be assembled in the solid state.

References:
[1] Battaglia G. et al. *Nanotoday* **2008**, *3*, 38-46.
[2] Wong, K.H., Davis, T.P., Barner-Kowollik, C. and Stenzel, M.H. *Polymer* **2007**, *48*, 4950-4965.
[3] Viajayakrsishna K., Mecerreyes D., Gnanou Y. And Taton D. *Macromolecules*, **2009**, *42*, 5167-5174.

The melting and non-isothermal crystallization behaviors of polypropylene/montmorillonite (MMT) nanocomposites under high pressure CO_2

Jie Chen, Tao Liu, Ling Zhao and Wei-kang Yuan*

State Key Laboratory of Chemical Engineering, East China University of Science and Technology, Shanghai 200237, P. R. China.

email: chenjie851127@gmail.com, zhaoling@ecust.edu.cn

Introduction:

Due to their enhanced mechanical properties, polypropylene(PP)/montmorillonite(MMT) nanocomposites foams have attracted increasing interest as an alternative for pure PP foamed counterparts[1]. The crystallization behavior of semicrystalline polymer composites under high pressure CO_2 plays a critical role in the CO_2 foaming process. In the industrial foaming process, such as extrusion and injection foaming, semicrystalline materials experience a nonisothermal process due to the cooling. Numerous research work have been done on both isothermal and nonisothermal crystallization kinetics of PP composites[2,3]. Several authors have studied the effect of CO_2 on isothermal crystallization behavior of PP[4-6], while limited research data is available on nonisothermal crystallization under CO_2[7]. To the authors' best knowledge, no detailed research work has been reported on nonisothermal crystallization kinetics of PP/MMT nanocomposites under CO_2. In this work, non-isothermal crystallization behaviors PP/MMT nanocomposites under CO_2 were carefully studied and the nonisothermal crystallization kinetics was also analyzed from the DSC data.

Materials and Methods

PP/MMT nanocomposites containing 1%, 2% and 4% MMT were prepared by melting blending of commercial PP and nano MMT in a Haake Minilab system (Thermo Electron). Neat PP was also prepared by the same process.

Nonisothermal crystallization measurements of both PP and PP composites were conducted in a high-pressure DSC at constant rates of 5, 2, 1, and 0.2 K/min under ambient N_2 and 5, 20, 40 and 60 bar CO_2.

Results and Discussion

In this work, both the melting and non-isothermal crystallization behaviors of polypropylene (PP) and PP/montmorillonite (MMT) nanocomposites under atmospheric N_2 and high pressure CO_2 were studied using high-pressure differential scanning calorimeter (DSC). High pressure CO_2 had strong plasticization effect on both PP and PP composites, and depressed their T_m and T_c. Due to the heterogeneous nucleation effect of MMT, PP composites showed a lower melting peak temperature (T_m) and a higher crystallization peak temperature (T_c) in comparison with PP at the same atmospheric condition, as shown in Fig. 1.

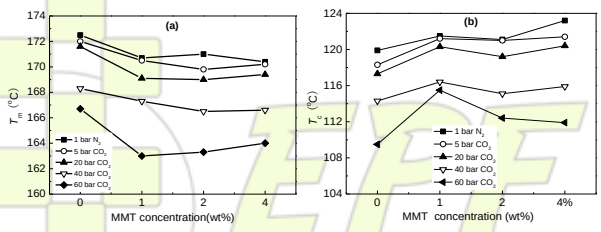

Fig.1. Effect of MMT on T_m and T_c of PP/MMT composites under CO_2

Jeziorny modified Avrima method and Mo's method were applied to analyze the non-isothermal crystallization kinetics of PP and PP/MMT composites under high pressure CO_2. Mo's approach demonstrated a success for all the system investigated. *F(t)* obtained from mo's method showed that the crystallization rates of both PP and PP composites first decreased with increasing CO_2 pressure, reached a minimum, and then increased. This trend was flattened after introducing nano-MMT into PP.

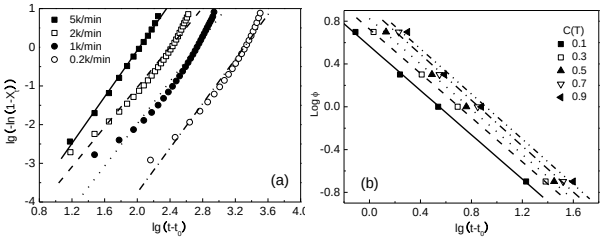

Fig.2 Fitting results for the non-isothermalcrystallization of PP/1%MMTin the presence of CO_2 at 20 bar (a) Jeziorny modified Avrima method, (b) Mo's method

The activation energy, ΔEa, for the non-isothermal crystallization kinetics of PP and PP/MMT composites was also evaluated by Kissinger method. ΔEa increased in the presence of nona-MMT. However, the overall crystallization rate characterized by half crystallization time, $t_{1/2}$, showed an increase in PP/MMT nanocomposites, indicating that the heterogeneous nucleation effect of fillers still played a critical role to enhance the overall crystallization rate although nano-MMT inhabited the transport of the polymer chains to the growing surface.

Table 1 The activation energy based on Kissinger method

	ΔEa(KJ/mol)				
	N_2	CO_2			
	0.1MPa	0.5MPa	2MPa	4MPa	6MPa
PP	291.4	287.5	278.3	283.5	231.2
PP-1%	301.3	301.3	295.7	295.5	348.9
PP-2%	316.2	321.5	298.9	305.6	309.0
PP-4%	351.0	320.6	311.9	352.2	285.0

Reference

[1] Han, X.; Shen, J.; Huang, H.; Tomasko, D. L.; Lee, L. J. Polym. Eng. Sci 2007, 47, 103.

[2] Park,C.B.; Cheung,L.K.; Song S.-W. Cell Polym. 1998,17,221.

[3] Beck, H.N. J.Appl. Polym. Sci.1967,11,673.

[4] Takada, M.; Tanigaki, M.; Ohshima, M. Polym. Eng. Sci. 2001, 41, 1938.

[5] Takada, M.; Ohshima, M. Polym. Eng. Sci.2003, 43, 479.

[6] Takada, M.; Hasegawa, S.; Ohshima, M. Polym. Eng. Sci. 2004,44, 186.

[7]Naguib, H.E. Park,C.B Ind Eng Chem Res 2005, 44, 6685.

Mechanical properties of PA66/PA6/multi-walled carbon nanotube ternary nanocomposite prepared by melt mixing method

Maryam Hadizadeh[a], *Akbar Shojaei*[a], *and Reza Bagheri*[b]

a. Department of Chemical and Petroleum Engineering, Sharif University of Technology, P. O. Box 11155-9465, Tehran, Iran, akbar.shojaei@sharif.edu.

b. Department of Materials Science and Engineering, Sharif University of Technology, Tehran, Iran.

Abstract

In this investigation, the blends of polyamide 66 (PA66)/polyamide 6 (PA6) were prepared by internal melt mixing method in a full range of PA6 concentrations, from 0 up 100 wt%, with an interval of 25 wt%. Additionally, the corresponding nanocomposites for the blends were prepared by the same mixing method via the incorporation of 1 wt% of multi-walled carbon nanotube (MWCNT). All the blends and the corresponding nanocomposites were characterized by tensile testing, dynamic mechanical thermal analyzer (DMTA), impact strength and differential scanning calorimeters (DSC). The result indicated that the PA66/PA6 blend is a miscible system in all concentrations of PA6, as was expected. Additionally, it was found that incorporation of MWCNT into PA66, improves the mechanical properties, however, the addition of PA6 into PA66/MWCNT, improves the effectiveness of MWCNT much higher.

Introduction

Carbon nanotubes (CNTs) have found great attraction in recent literature for producing polymer nanocomposites due to its superior multifunctional properties such as excellent mechanical, electrical and thermal properties as well as unique geometry, i.e. tubular shape with very high aspect ratio. However, incorporation of CNTs into the polymeric matrix is a challenging task, particularly through the melt mixing method. This is originated from the significant interaction between the CNTs bundles and the entanglement of CNT bundles, restricting their efficient dispersion in the polymeric matrix. Literature shows diversity in the enhancement of mechanical properties of PA6 with incorporation of CNTs. Some authors reported a significant enhancement in the mechanical properties of PA with CNTs[1], while others reported a low or moderate improvement[2] . Recently, the dispersion state of MWCNT in both PA6 and PA66 in the melt mixing method was compared[3]. It was found that the dispersion state of MWCNT in PA6 is better than that of PA66.

In this work, the effect of incorporation of PA6 on the mechanical performance of PA66/MWCNT was well investigated. To do this, the mechanical performance of PA66/PA6 blends was compared to that of PA66/PA6/MWCNT at the same PA66/PA6 loadings.

Materials and procedures

PA66, PA6 were purchased from Radici Group and Hyosung, respectively, and MWCNT (TNMC3, COOH content of 2 wt%) was procured from Timesnano, china. PA66/PA6 blend and PA66/PA6/MWCNT were prepared by a Brabender 350E internal melt mixer with a cavity size of 370 cm^3. The ternary nanocomposites always included 1 wt% MWCNT. The compounds were injection molded into dumbbell shaped and notched impact bars. Tensile properties, DMTA, DSC and impact strength of the samples were determined according to the related standards.

Results

Fig. 1 exhibits the elastic moduli of PA66/PA6 and PA66/PA6/MWCNT, obtained by static tensile testing and DMTA, versus the content of PA6. As can be seen the elastic modulus of PA66/PA6 decreases by increasing the PA6 content linearly justifying the miscibility of this blend. The miscibility was also corroborated by DSC and DMTA analysis. By incorporation of MWCNT, the elastic modulus shows an increase, however, the extent of enhancement with respect to unfilled blend, increases by increasing the PA6 content.

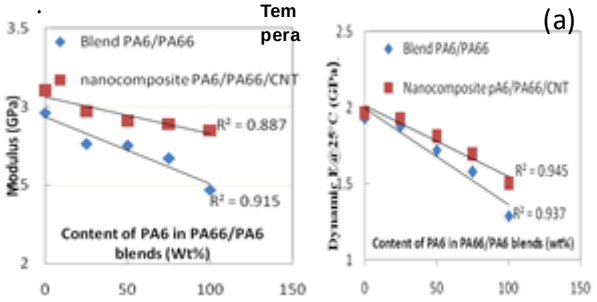

Fig. 1. Elastic modulus of PA66/PA6 blends and their nanocomposites with 1 wt% MWCNT (a) tensile modulus and (b) Dynamic elastic modulus.

Conclusion

It was found that the effectiveness of MWCNT on the mechanical performance of PA66 was improved by incorporation of PA6 in the nanocomposite. This could be explained by the improvement of dispersion of MWCNT in the matrix and enhancement of crystallinity of the matrix by incorporation of PA6.

References

1. Liu T., et al., Macromolecules 2004:37;7214-7222.

2. Logakis E., et al., Journal of Polymer Science B 2009: 47;764-774.

3. Krause B., Potschke P., Haubler L., Composites Science and Technology 2009:69;1505-1515.

Nanocomposites based on carbonaceous nanoestructures oxidized by solar energy

M López, M Blanco, E Aranzabe, A Marcaide

Fundación Tekniker, Av Otaola 20, 20600 Eibar Gipuzkoa (Spain)

mblanco@tekniker.es

Introduction: Carbon nanotubes (CNTs) have attracted much interest during the recent years due to their inherent extraordinary electrical, thermal, structural and mechanical properties [1]. Nowadays, the incorporation of nanotubes into ceramic and polymeric matrices is a vast area of study and research However, the pure CNTs are generally insoluble in common solvents and polymers, and they usually form stabilized bundles due to van der Waals force. So, it is extremely difficult to align and disperse the CNTs in a polymer matrix.[2]. One of the routes to increase the interaction between matrix and reinforcement is submitting CNTs to functionalization by aggressive chemical processes that insert functional groups on the sidewall of CNTs. The main disadvantage of these treatments is that CNT structure can be damaged during the process thus affecting CNT properties. Moreover, the high consume of solvents and energy required for these treatments point out the necessity of more environmentally friendly processes.
In the present work, an alternative method based on photoFenton treatment assisted by solar radiation to oxidize CNT is proved that overcomes main problems associated to conventional processes. The Fenton process consists on the generation of hydroxyl radicals, which have a high oxidation potential, using H_2O_2 as source of OH• radicals and Fe^{2+} salt as catalyser in an aqueous medium (pH=2.7) [3]. When the process rate is enhanced by UV radiation, it is call photoFenton process. The process conditions such as reactive concentration, reactant ratio and time of reaction have been optimized using a parabolic collector to concentrate solar radiation. In the figure 1 an scheme of the overall process of photoFenton modified nanotubes is observed.

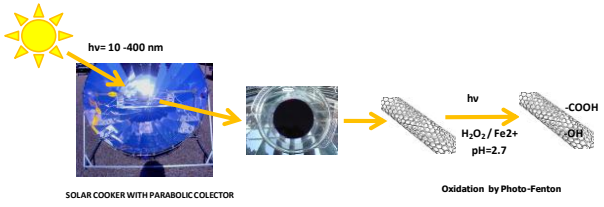

Figure 1. Scheme of the overall process of photoFenton modified nanotubes.

Results and Discussion: The PhotoPhenton process promotes the generation of carboxylic (-COOH), carbonylic (C=O) and/or hydroxylic (-OH) groups onto CNT surfaces without affecting their structural integrity as was shown by Fourier transform infrared (FTIR) spectroscopy and thermogravimetric analysis (TGA) in Figure 2 and by scanning electron microscopy (SEM). The photoFenton process achieves an increase in the oxidation degree in comparison with a usual oxidation method using HNO_3 concentrated acid.

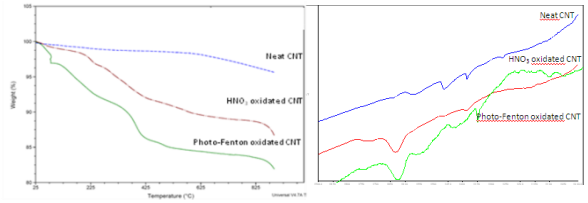

Figure 2. TGA thermograms and FTIR spectra of MWCNT pristine and oxidized with HNO3 and photoFenton treatment

PhotoFenton modified and oxidized by HNO_3 carbon nanotubes were incorporated into a thermoplastic matrix, polyamide 6 (PA 6) using a twin screw corrotating microextruder. SEM micrographs show that a homogeneous CNT dispersion into the matrix was obtained with the applied processing conditions for the three types of CNT, as it is shown in Figure 3.

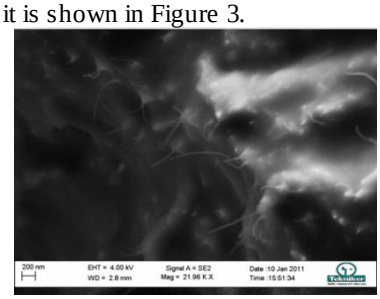

Figure 3. SEM micrograph of photoFenton oxidized CNT in PA 6 matrix

The effect of CNT content and CNT oxidation treatment in thermal and mechanical behavior of nanocomposites were analyzed by dynamic mechanical analyzer (DMA), differential scanning calorimetry (DSC) and TGA. The obtained results show a similar performance of nanocomposites based on CNT oxidized by both methods.

Conclusions: In summary, CNT oxidation by the photoFenton process assisted by solar energy is proved a suitable alternative environmentally friendlier and less costly to conventional chemical oxidation processes. Composites obtained by the incorporation of CNT oxidized with the photoFenton process into polyamide 6 show a similar behaviour than the obtained by the incorporation of CNT oxidized with common chemical methods.

References

[1] V. Datsyuk, M. Kalyva, K. Papagelis, J. Parthenios, D. Tasis, A. Siokou, I. Kallitsis, C. Galiotis, Carbon 46 (2008) 833–840
[2] S. Pegel, P. Potschke, G. Petzold, I. Alig, S.M. Dudkin, D. Lellinger, Polymer 49, (2008) 974–984
[3] L. Zhang, J. Li, Z. Chen, Y. Tang, Y. Yu, Applied Catalysis A: General 299 (2006) 292–297

Tailored designed cellulosic nanoparticles for possible pharmaceutical and biotechnological applications

Martin R. Kulterer[1], Victoria E. Reichel[1], Martin Reischl[1], Rupert Kargl[1], Jens Schaller[3], Karin Stana-Kleinschek[3], Volker Ribitsch[1]

1) Karl-Franzens University Graz, Institute of Chemistry, Heinrichstraße 28, AT-8010 Graz, Austria
2) Thüringisches Institut für Textil- und Kunststoff-Forschung e.V., Breitscheidstraße 97, D-07407 Rudolstadt, Germany
3) University of Maribor, Laboratory for Characterization and Processing of Polymers, Smetanova Ulica 17, SI-2000 Maribor, Slovenia

martin.kulterer@uni-graz.at

Introduction

Polysaccharides (PS) are cheap, stable, renewable, biodegradable, natural polymers comprising a huge chemical and structural variability. PS are used for the preparation and modification of many different nanoparticle systems [1,2]. The applicability of such PS NPs is often limited by their hydrophilicity, which does not allow the entrapment of active hydrophobic substances (i.e. drugs or fluorescent dyes) into the NP core. Hydrophobic PS NPs can be generated from cellulose acetate [3]. Their applicability for i.e. pharmaceutical purposes or surface modifications is limited by the hydrophobic nature of the NP surface which lacks reactive functional groups. A suitable way to generate hydrophobic core / hydrophilic shell PS NPs is the self assembly of amphiphilic PS based copolymers [1,4]. The main drawback of this method is the time consuming chemical synthesis of PS based copolymers. We present here a new way to generate CA NPs with tailored designed functional hydrophilic PS surfaces (CA/hPS NPs).

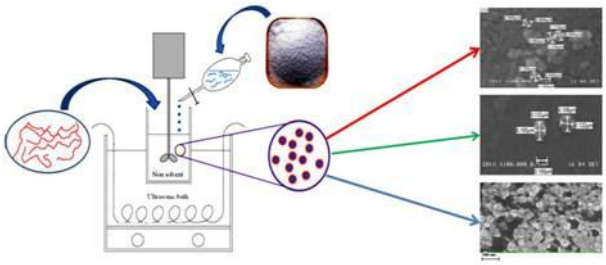

Figure 1: Preparation of in situ functionalized CA NPs

Experimental

CA/hPS NPs were prepared in one step analogous to a recently published nanoprecipitation method [5]. Briefly, CA was dispersed in an aqueous hPS solution under continuous stirring and sonication (Figure 1). CA/hPS NPs were characterized by dynamic and electrophoretic light scattering, charge titration and scanning electron microscopy and fluorescence spectroscopy.

Results/Discussion

Using amino cellulose (AC), low molecular weight chitosan (CHI) carboxymethyl cellulose (CMC) and hydroxyethyl cellulose (HEC), we generated CA NPs with shells carrying different functional groups and surface charges (Figure 2a). Hence, varying the hydrophilic PS allows the tailored design of the CA NP surface for designated applications. The pH dependent zeta potential (Figure 2a) and charge titration experiments showed clearly the successful functionalization of the NP surface.

In addition we demonstrated that CA/hPS NPs can be utilized for the entrapment of hydrophobic substances like drugs or dyes (Figure 2b) and the design of nanostructured, functional surfaces (Figure 3).

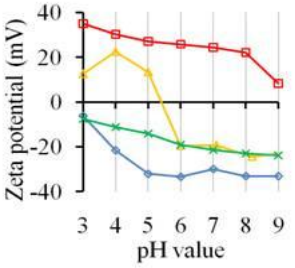

Figure 2a: pH dependent Zeta potential. □CA/AC, △CA/CHI, ×CA/HEC, and ◇CA/CMC NPs

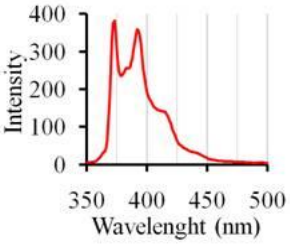

Figure 2b: Fluorescence spectra of pyrene encapsulated into CA/CMC NPs

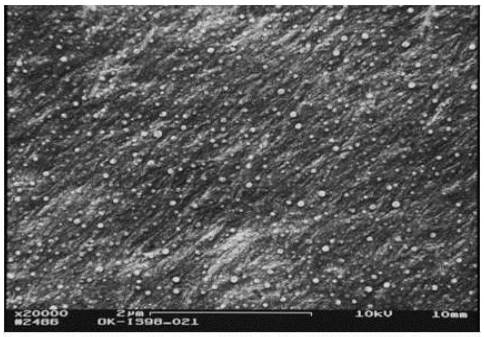

Figure 3: Chitosan surface modified with CA/CMC NPs

Conclusion

We successfully generated functional CA NPs with tailored designed PS surfaces. Future possible applications for CA/hPS NPs are the development of targeted drug delivery systems, and the design of nanostructured surfaces i.e. for the immobilization of active biomolecules.

Acknowledgement

The research leading to these results has received funding from the European Union Seventh Framework Programme (FP7/2007-2013) under grant agreement n° 214653.

References

(1) Z. Liu et al., *Adv. Drug Delivery Rev.* **2008**, 60, 1650
(2) C. Lemarchand et al., *Eur. J. Pharm. Biopharm.* **2004,** 58, 327
(3) S. Hornig et al., *Biomacromolecules* **2008**, 9, 1487
(4) J.H. Park et al., *Adv. Drug Delivery Rev.* **2010,** 62, 28
(5) M.R. Kulterer et al., *Colloids Surf. A* **2011**, 375, 23

Preparation and characterization of nitrile butadiene rubber-nanoclay composites with maleic acid anhydride as compatibilizer- Part I: Rheometric and swelling characteristics

E.M. Sadek *[1], *D.E. El-Nashar* [2]

[1] Petrochemical Department, Egyptian Petroleum Research Institute (EPRI), Nasr City, Cairo, Egypt
[2] Polymer & Pigment Department, National Research Center (NRC), Dokki, Cairo, Egypt.

E-mail address: elham_sadek@hotmail.com

Nitrile butadiene rubber (NBR)-nanoclay composites have been prepared in an open two-roll mixing mill and vulcanized using a conventional sulphuric system. Some sort of compatibilizer like maleic acid anhydride (MAH) can be utilized safely to improve the distribution of the nanoclay in the rubber matrix . Maleic acid anhydride-treated organoclay (MOC) was successfully synthesized. The synthesis method involves two possible reaction routes: (1) intercalation of ammonium cations of cetyl trimethyl ammonium bromide (CTAB) inside the untreated sodium bentonite clay galleries in order to obtain organoclay with average particle size = ~ 4nm as observed by transmission electron microscope (TEM). A higher basal spacing was obtained as indicated by X-ray diffraction (XRD). (2) Maleic acid anhydride dissolved in water was mixed with the prepared organically modified clay to give (MOC). The prepared clay structures were analyzed by Fourier transform infrared (FTIR) spectroscopy. Also, FTIR investigation confirmed the incorporation of (MOC) in NBR matrix, XRD analysis indicated that an exfoliated structure was obtained, and scanning electron microscope (SEM) images displayed the good interaction between the MOC and the rubber matrix. The influence of the MOC content (i.e. 1,3,5,10,20 phr) relative to the micrometer clay (i.e. 10, 20phr) on the NBR compounds was analyzed through rheometric and swelling characteristics. Rheometric study demonstrated an increase in minimum and maximum torques, delayed scorch time and optimum cure time for the MOC (3phr) incorporated NBR compound compared to pure NBR. The cure rate index followed the same trend. In addition, these particular compounds showed decreased equilibrium swelling in toluene solvent, increased cross linking density, more volume fraction and bound rubber content compared to the corresponding rubber filled with micrometer clay

References.

- Rajasekar,R., Pal, K., Heinrich, G., Das,A., Das,C.K., "Development of nitrile butadiene rubber–nanoclay composites with epoxidized natural rubber as compatibilizer" Materials&Design 2009,30, 3839-3845.
- Rajasekar,R., Heinrich,G., Das,A., Das,C.K., " Development of SBR-nanoclay composites with epoxidized natural rubber as compatibilizer" Research Letters in Nanotechnology 2009,2009,1-5.
- Yehia,A.A., Akelah,A.M., Rehab,A., El Sabbagh,S.H.,El-Nashar,D.E., Koriem,A.A., "Preparation and characterization of polymer-clay nano composites for Specific Applications"KGK Kautschuk Gummi Kunststoff, 2009, 2009, 580-588.
- Chakraborty,S.,Kar,S.,Dasgupta,S.,Mukhopadhyay,R.,Bandyopadhyay,S.,Joshi,M., Ameta,S.C., Material Properties " Study of the properties of in-situ sodium activated and organomodified bentonite clay – SBR rubber nanocomposites – Part I: Characterization and rheometric properties" Polymer Testing 2010,29,181-187.
- Chakraborty,S., Kar,S., Dasgupta,S., Mukhopadhyay,R., Bandyopadhyay,s.,Joshi,M., Ameta,S.C., Material Properties " Study of the properties of in-situ sodium activated and organomodified bentonite clay – SBR rubber nanocomposites – part II: Physical property " Polymer Testing 2010,29,679-684.
- Chiu,F. C., Yen,H.Z., Chen,C.C., " Phase morphology and physical properties of PP/HDPE/organoclay (nano) composites with and without a maleated EPDM as a compatibilizer " Polymer Testing 2010,29(6),706-716.
- Liao,M., Zhang,W., Shan,W., Zhang,Y., " Structure and properties of polybutadiene/montmorillonite nanocomposites prepared by in situ polymerization" JAppl.Polym Sci 2006,99,3615-3621.
- Chung,J.W., Han,S.J., Kwak,S.Y., "Dynamic viscoelastic behavior and molecular mobility of acrylonitrile–butadiene copolymer nanocomposites with various organoclay loadings" Composites Science and Technology 2008,68,1555-1561.
- Ahmadi,S.J., G'Sell,C., Huang,Y., Ren,N., Mohaddespour,A., Hive,J.M.," Mechanical properties of NBR/clay nanocomposites by using a novel testing system" Composites Science and Technology 2009,69,2566-2572.
- Sadhu,S., Bhowmick,A.K., "Morphology study of rubber based nanocomposites by transmission electron microscopy and atomic force microscopy" J Mater Sci 2005,40,1633-1642.

Transition Behavior of Block Copolymer Films on Controlled Interaction

Du Yeol Ryu, Eunhye Kim, Hyungju Ahn, and Jinsam Gong*

Department of Chemical and Biological Engineering, Yonsei University, Seoul, Korea

dyryu@yonsei.ac.kr

Block copolymer (BCP) self-assembly in thin films has recently been the focus of increased research interest due to their potential use as templates and scaffolds for the fabrication of nanostructured materials [1-2]. These potential applications have stimulated numerous studies on the influence of controlled interfacial interactions, confinement structure, and morphology of BCPs in thin films. The Flory-Huggins interaction parameter (χ) between the two block components is inversely proportional to temperature (χ decreases with increasing temperature) and the order-to-disorder transition (ODT) is governed by the product of $\chi \cdot N$, where N is the overall number of segments. Hence, a phase-mixed or disordered state can be observed when $\chi \cdot N < 10.495$ in the weak segregation regime. In addition, the phase behavior in a thin film geometry that confines polymer chains to the interfaces will be influenced by the interfacial interactions at substrate/polymer and polymer/air and the commensurability between the equilibrium period (L_0) of the BCP and the total film thickness.

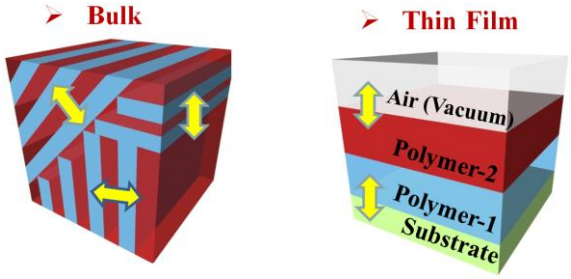

Generally, the microdomains in BCP films orient normal to the film surface when the interfacial interactions are balanced (or neutral towards the two block components) and film thickness is commensurate with L_0[3-5]. In contrast, the preferential interactions of one block component with an interface and/or the difference of surface tension between two block components will lead to an orientation of the BCP microdomains parallel to the film surface. In developing neutral surfaces, random copolymer (A-*r*-B) approaches to balancing interfacial interactions have been successfully developed for surface modification using either a chemical grafting or cross-linking strategy, enabling the microdomains of block copolymer (A-*b*-B) to orient normal to the film surface [3-5].

In this presentation, we investigated the phase transitions for the films of block copolymers (BCPs) on the modified surface, like the order-to-disorder transition (ODT) by in-situ grazing incidence small angle x-ray scattering (GISAXS) and transmission electron microscopy (TEM). The selective interactions on the surface by a PS-grafted substrate provide the preferential interactions with the PS component of the block, while a random copolymer (PS-*r*-PMMA) grafted substrate do the balanced interfacial interactions on the surface. The thickness dependence of transition temperatures for PS-*b*-PMMA films on preferential surfaces in terms of the temperature dependence of χ between two block components will be discussed in comparison to that for PS-*b*-PI films on the PS-grafted substrate.

Interestingly, with decreasing film thickness, typical behavior of the BCP films on the preferential interactions indicates an increase of transition temperature. This behavior is in quite contrast to a decrease of transition temperature for the films on the balanced interfacial interactions because the random copolymer grafted substrate provide a surface-induced compatibilization toward two block components.[6-8]

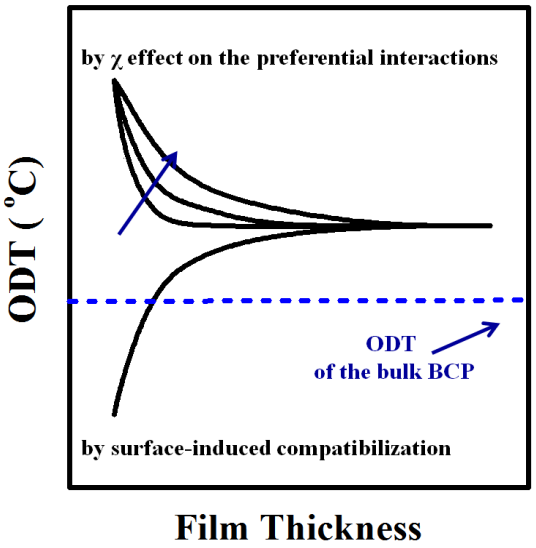

References

1. Hamley IW. Progress in Polymer Science 2009;34(11):1161-1210.
2. Bang J, Jeong U, Ryu DY, Russell TP, and Hawker CJ. Advanced Materials 2009;21(47):4769-4792.
3. Mansky P, Liu Y, Huang E, Russell TP, and Hawker C. Science 1997;275(5305):1458-1460.
4. Ryu DY, Shin K, Drockenmuller E, Hawker CJ, and Russell TP. Science 2005;308(5719):236-239.
5. Ham S, Shin C, Kim E, Ryu DY, Jeong U, Russell TP, and Hawker CJ. Macromolecules 2008;41(17):6431-6437.
6. Shin C, Ahn H, Kim E, Ryu DY, Huh J, Kim K-W, and Russell TP. Macromolecules 2008;41(23):9140-9145.
7. Shin C, Ryu DY, Huh J, Kim JH, and Kim K-W. Macromolecules 2009;42(6):2157-2160.
8. Kim E, Choi S, Guo R, Ryu DY, Hawker CJ, Russell TP. Polymer 2010; 51:6313-6318.

Morphology evolution driven by transreactions in a polyurethane / α, ω-aminopropyl polydimethylsiloxane blend

Françoise Fenouillot[1], *Françoise Méchin*[1], *Fernande Boisson*[1], *Pierre Alcouffe*[1], *Tomasz Pokropski*[1], *Tasnim Kallel*[2], *Mahdi Mnif*[2]

1) Université de Lyon, CNRS; INSA-Lyon, IMP, UMR5223, F-69621, Villeurbanne, France.
2) Ecole Nationale d'Ingénieurs de Sfax (ENIS), Département Génie des Matériaux, Route Soukra km3 3038 Sfax – Tunisia

Françoise.Fenouillot@insa-lyon.fr

An originality of the present work is that α,ω-aminopropyl polydimethylsiloxane (PDMS) and thermoplastic polyurethane (TPU) have been reacted in bulk at high temperature. Generally, PDMS/TPU copolymers are obtained via a reaction involving TPU precursors and functional PDMS oligomers and most often the reaction is done in solution at moderate temperature. Here, the elevated temperature allowed observing specific behaviour detailed below.

Experimental. Different α,ω-aminopropyl and α,ω-hydroxyethyl PDMS oligomers have been mixed with a thermoplastic polyurethane in the molten state at 200°C. Samples have been collected at different mixing/reaction times and analysed by HNMR spectroscopy and size exclusion chromatography (SEC). The morphology of the material has been characterised by scanning (SEM) and transmission electron microscopy (TEM).

Results. At 200°C the splitting of the urethane group of the TPU is releasing hydroxyl and isocyanate terminated TPU chains. It has been demonstrated that the splitting was followed by the fast reaction of the amino-siloxane with the released isocyanate. This reaction formed aryl-alkyl ureas and promoted the insertion of PDMS units inside the TPU chains, forming TPU-co-PDMS copolymer with a very fine morphology. An example of such morphology is depicted in figure 1 A). The visual aspect of the sample which was highly transparent is shown in figure 1 B). The transparency is linked to the very small size of the PDMS phase (~20nm). However, the morphology was not stable and coarsening was observed for longer reaction times. In figure 1 C) and D), the morphology and visual aspect of a sample reacted during 27 minutes is depicted. The PDMS phase size is between 50 and 150nm diameter and the material is totally opaque. This morphology evolution was unexpected and had to be explained. The following interpretation was proposed.

After the formation of the aryl-alkyl ureas several reactions can proceed. One possibility is the cleavage of unsymmetrical aryl-alkyl urea groups into alkyl isocyanate and primary aromatic amine. The reaction of the former with primary alkyl amine borne by the siloxane leads to alkyl-alkyl urea as was shown by Lu et al. on small model molecules [1].

In terms of macromolecular structure, the formation of alkyl-alkyl ureas has one important consequence: it implies that two siloxane units are now consecutive in the copolymer chain (figure 2).

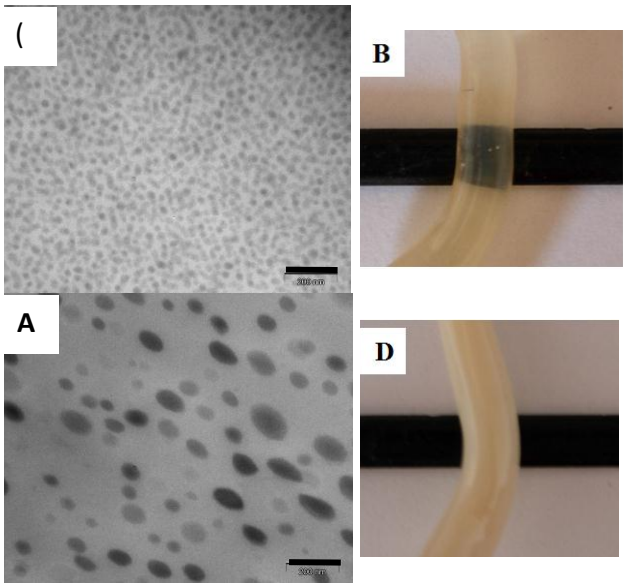

Figure 1. Transmission electron micrographs and corresponding macroscopic views of the reactive blend TPU/amino-PDMS 90/10 wt%
A) and B) after 3 minutes mixing. The blend is transparent. C) and D) after 27 minutes mixing time the morphology coarsens, the blend is opaque.
The silicone appears in dark grey. The scale bar is equal to 200 nm.

Thus, the formation of alkyl-alkyl urea leads to an increase in the average length of the siloxane segments that can then segregate in the shape of larger domains (about 100 nm or more) depending on the composition of the material.

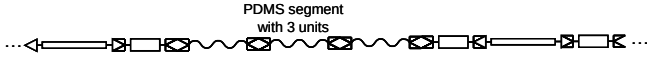

Figure 2. Scheme of the proposed structure of the TPU/PDMS when more and more aryl-alkyl ureas are replaced by alkyl-alkyl ureas formed later in the reactive process.

[1] Lu Q.W., Hoye T.R., Macosko C.W., J. Polym. Sci.: Part A: Polym. Chem., 2002, 40, 2310.

Effect of clay/polymeric modifier combination on structure and properties of epoxy nanocomposite

Ivan Kelnar, Jakub Rotrekl, Ludmila Kaprálková

Institute of Macromolecular Chemistry AS CR, v.v.i. Heyrovského sq. 2, 162 06 Prague, Czech Republic
kelnar@imc.cas.cz

Introduction

Inorganic nanofiller exhibit not only enhancement of most material parameters, but also significantly affect phase structure of multiphase polymer systems. In the case of epoxy containing polymeric modifiers dissolved in uncured epoxy affecting of reaction induced phase separation (RIPS) come into account. At the same time, formation of various complex structures (both in thermoplastics and epoxy) may lead to the synergy between these components and thus enhanced and/or better balanced mechanical behaviour. This study deals with the effect of nanofiller content, type and modification and/or functionality on structure and properties of polymer-modified epoxy. The effect of simple combination is compared with modifier/clay adduct obtained by ionic exchange.

Materials and Methods

Epoxy was DGEBA (Epilox A 19-02) with cycloaliphatic amine hardener (Laromin C 260)

Clay/polymer adducts were prepared by ionic exchange of Na+ ions of montmorillonite (MMT) by protonated aminated polymers.

In the case of aminated polyoxypropylene (APOP), water was applied as reaction medium whereas for aminated butadiene-acrylonitrile rubber (ATBN) and aminated polybutadiene (LBA) THF/water mixture was used.

Results and Discussion

In the case of simultaneous clay and liquid rubber addition, the increasing clay content influences size of RIPS generated particles. Both enlargement and diminishing occurred. E. g., with epoxy/APOP no remarkable affecting at ambient curing temperature is accompanied by significant decrease at 70°C whereas with epoxy/POP enlargement over 2.5% Cloisite 30B content was found.

The interplay between clay-affecing of viscosity, curing kinetics and nucleating effect of clay (together with possible influencing of miscibility) was evaluated by simultaneous (chemo)rheological and cloud point measurements. Results obtained with several liquid elastomers with different structure, molecular weight and functionalities combined with layered silicates, layered double hydroxides and TiO_2-based nanotubes are discussed. With most of systems studied, addition of clay to rubber modified epoxy leads to improved balance of mechanical behaviour. The synergy between dispersed components occurred at different clay content ranges and was most significant in the case of blended inclusions formation (Fig. 1a)

Very interesting results were obtained with modifier/clay adduct prepared mostly by ionic exchange, especially in comparison with single combination of these components. This modification promotes self assembly leading in some cases to nanolayered structure of polymer embedded platelets, which was most significant for LBA/MMT adduct (Fig. 1b), i.e., for polymeric component with low affinity to epoxy. In this way, very fair balance of mechanical properties (exceeding simple combination of components) can be achieved. At the same time, unusually significant dependence on concentration, adduct composition and polymer chain length indicate some new kind of influencing mechanical behaviour of epoxy. This fact is confirmed also by the significant deteriorative effect of a low adduct content on properties, not found for simultaneous addition of separated components. Effect of adduct on structure of polymer-modified epoxy is also evaluated. Though its effect on phase structure is comparable with commercial clay, significant difference in mechanical properties between epoxy/APOP and epoxy/POP systems further confirm different effect of adduct on epoxy systems behaviour.

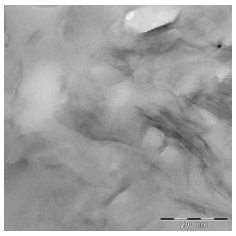

a)

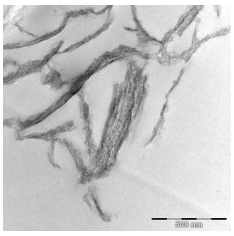

b)

Fig 1a) TEM of blended inclusions of epoxy/APOP/Cloisite 30B 90/5/5 system b) TEM picture of epoxy containing 6% of LBA-MMT adduct

Conclusions

Combination of clay and low-molecular-weight rubbers is a tool for improving balance in mechanical behaviour of epoxy nanocomposite.

Best mechanical behaviour was found when adduct of aminated rubbers with MMT was used. This is caused by the formation of elastically embedded nanosized planar arrays of elastomer-modified clay and an increase in T_g of epoxy network, leading to a new effective way of affecting the mechanical behaviour of epoxy.

This work was supported by the Grant Agency of the Academy of Sciences of the Czech Republic (grant No IAA200500904)

Structural Changes in Liquid Crystal Polymer Vesicles induced by Temperature variation and Magnetic field

Annie Brûlet,[1*] *Sabrina Hocine*,[2] *Lin Jia*,[2] *Jing Yang*,[2] *Aurélie Di Cicco*,[2] *Laurent Bouteiller*,[3] *and Min-Hui Li*[2]

[1]Laboratoire Léon Brillouin, UMR12 CEA CNRS, CE Saclay, F-91191 Gif sur Yvette, France
[2]Institut Curie, Physico-Chimie Curie, UMR168, F-75248 Paris, France
[3] UMPC, Université Paris VI, Chimie des Polymères, UMR 7610, F-75005 Paris, France

*annie.brulet@cea.fr

The supramolecular organization of amphiphilic block copolymers in water is an interesting strategy to design smart nanoparticles for applications such as drug delivery or nanoreactors. A challenging requirement for these applications is the ability in response to external stimuli to destabilize these supramolecular organization so as to release the encapsulated substances.

To address this goal, polymer vesicles, commonly called polymersomes, have been developed in which a specific stimulus destabilizes the vesicle structure.[1] We thus study a new class of polymersomes, in which the hydrophobic part is a liquid crystal polymer (LCP).[2] Recently, we have shown that light inducing by using the isomerization from *trans* to *cis* configuration of the azobenzene group in the LCP, could destabilize asymmetric azobenzene-containing liquid crystal polymersomes.[3] It is also well-known that certain LCP can undergo conformational changes, from a rod to a coil shape at the nematic-isotropic transition upon temperature variation.[4] On the other hand, aromatic LCP can change orientation under magnetic field. Therefore, the temperature changes and the magnetic field may be used as physical stimuli to induce modification of the structures of vesicles membrane.

We have studied two series of amphiphilic block copolymers in which the hydrophobic block was a side-on nematic LCP, poly((4''-acryloxybutyl) 2,5-di(4'-butyloxybenzoyloxy) benzoate) (PA444) or poly(4-butyloxy-2'-(4''-methacryloyloxybutyloxy)-4-(4-butyloxybenzoyloxy) azobenzene) (PMAazo444), and the hydrophilic block was polyethyleneglycol (PEG).[2] By combining both Small Angle Neutron Scattering (SANS) measurements under *in situ* temperature change and magnetic field application and cryo- transmission electron microscopy (cryo-TEM), we have studied the thermo- and magneto-responses of LCP vesicles.[6]

Large changes in membrane thickness, vesicle size and interior compartment volume are observed for both LCP–*b*-PEG vesicles. At room temperature, block copolymers self-assemble and form vesicles with a radius of 450-500 nm and a bilayer membrane thickness of 10-15 nm. Upon heating, the membrane thickness, d, started to increase dramatically from a temperature (~55°C) above T_g but below T_{NI} of the LC polymer block, and reached up to 120 nm at $T > T_{NI}$. The thickness of the membrane was inconsistent with a bilayer structure. The vesicles were transformed into thick-walled capsules, which surprisingly remained stable even for temperatures above T_{NI}.
The PEG chains should partially dehydrate when increasing temperature, but this cannot explain a so huge increasing of membrane thickness. We propose that the membrane reorganized into a structure consisting of microphase separated LC and PEG domains.

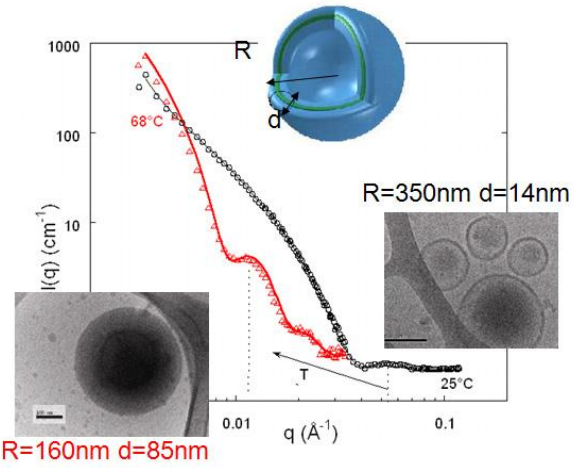

Changes upon temperature of SANS curves (25°C, 68°C) and of Cryo TEM images (20°C (right) and 90°C (left); scale bar is 100nm) of PEG-b-PMAazo444 vesicles. The vesicle radius is reducing while the membrane thickness increases.

This structure would account for the large membrane thickness and the domains would be very similar to those of LC block copolymers in pure state, except that the PEG domains would be partially hydrated in the capsule membrane. Such structural transition is not reversible and the polydomain membrane remains even when the sample is cooled back down to room temperature. The system is thus very different from other thermo-responsive systems with LCST polymer block, which formed larger hydrophobic spherical particles when increasing the temperature. Analysis of changes in structural parameters such as the internal aqueous volume and the polymer membrane volume suggest that capsule scission and fusion also occurred during the transition.

Finally, these polymersomes were also sensitive to applied magnetic field, but in a limited temperature range: application of a magnetic field of 1.4Tesla substantially increased the membrane thickness due to the induced mesogen alignment.

[1] (a) D. E. Discher and A. Eisenberg, Science, 2002, **297**, 967. (b) M. Antonietti and S. Forster, Adv. Mater., 2003, **15**, 1323. (c) M.H. Li, P. Keller. Soft Matter, 2009, **5**, 927.
[2] (a) J. Yang, D. Levy, W. Deng, P. Keller and M.-H. Li, Chem. Commun, 2005, 4345; (b) J. Yang, R. Pinol, F. Gubellini, P.-A. Albouy, D. Levy, P. Keller and M.-H. Li, Langmuir, 2006, 22, 7907.
[3] E. Mabrouk, D. Cuvelier, F. Brochard-Wyart, P. Nassoy and M.H. Li, PNAS, 2009, **106**,18, 7294.
[4] J.P. Cotton, F. Hardouin, Prog. Polym. Sci., 1997, **22**, 795.
[5] M.-H. Li, P. Keller, J.-Y. Yang, P.-A. Albouy, *Adv. Mater.* 2004, **16**, 1922.
[6] S. Hocine, A. Brûlet, L. Jia, J. Yang, A. Di Cicco, L. Bouteiller and M.-H. Li, accepted in Soft Matter 2011. DOI:10.1039/C0SM00751J

Preparation of Fluoroalkyl End-Capped Oligomers Possessing Nonflammable and Flammable Characteristics in Silica Gel Matrices

Hideo Sawada

Department of Frontier Materials Chemistry,
Graduate School of Science and Technology, Hirosaki University
Hirosaki 036-8561, Japan

e-mail: hideosaw@cc.hirosaki-u.ac.jp

From the developmental viewpoints of a higher thermally stable fluorinated polymeric materials, it is in particular interest to study the hybridization of fluorinated polymers with inorganic materials such as silica gels. For example, Lee et al. reported that PTFE [poly(tetrafluoroethylene)]/SiO_2 organic-inorgnic hybrids can be prepared through a sol-gel process with tetraethoxysilane.[1] Kim et al. have very recently reported the preparation of perfluoroalkyl methacrylate polymer/silica organic/inorganic hybrids in supercritical carbon dioxide.[2] However, these fluorinated polymers/silica hybrids exhibit a clear weight loss behavior corresponding to the contents of parent fluorinated polymers in the hybrids around 600 ~ 700 °C or 400 ~ 600 °C, respectively.[1, 2] In a variety of fluorinated polymers, especially, fluoroalkyl end-capped oligomers are attractive materials, because they exhibit various unique properties such as high solubility, surface active properties, and nanometer size-controlled molecular aggregates which cannot be achieved by the corresponding non-fluorinated and randomly fluoroalkylated ones.[3]

Here, we have succeeded in applying these fluoroalkyl end-capped oligomers to nonflammable fluorinated polymeric materials through the sol-gel reactions with silica nanoparticles under alkaline conditions. Especially, in these fluorinated oligomers, fluoroalkyl end-capped N-(1,1-dimethyl-3-oxobutyl)acrylamide oligomer [R_F-$(DOBAA)_n$-R_F]/silica nanocomposites have been verified to exhibit a nonflammable characteristic even after calcination at 800 °C through the formation of hexafluorosilicate anion during the nanocomposite reactions; although the parent fluoroalkyl end-capped oligomer can decompose completely around 500 °C. In contrast, no formation of hexafluorosilicate anion during the composite reaction affords a usually flammable behavior for fluoroalkyl end-capped acrylic acid oligomer [R_F-

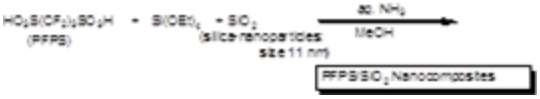

$(ACA)_n$-R_F]/silica nanocomposites.

In addition, we have found that not only R_F-$(DOBAA)_n$-R_F oligomer but also perfluoro-1,3-propanedisulfonic acid (PFPS) are applicable to nonflammable fluorinated materials through the sol-gel reactions with silica nanoparticles under alkaline conditions as shown in the following Scheme.

References:

1. Y.-C. Chen, C.-C. Tsai, Y.-D. Lee, J. Polym. Sci.: Part A: Polym. Chem. 42 (2004) 1789 - 1807.

2. J. Shin, D. W. Cho, W. Bae, H. Kim, Colloid Polym. Sci. 288 (2010) 63 - 72.

3. (a) H. Sawada, Chem. Rev. 96 (1996) 1779 – 1808;
(b) H. Sawada, Prog. Polym. Sci. 32 (2007) 509 - 533;
(c) H. Sawada, J. Fluorine Chem. 121 (2003) 111 - 130;
(d) H. Sawada, Polym. J. 39 (2007) 637 - 650.

Synthesis, Micelle Formation, and Gelation of (PEG – P(MA-POSS)) Amphiphilic Hybrid Block Copolymers

H. Hussain, B.H. Tan, C.B. He*

Institute of Materials Research and Engineering (IMRE), A*STAR (Agency for Science, Technology and Research), 3 Research Link, Singapore 117602

*h-hussain@imre.a-star.edu.sg

Abstract

Amphiphilic block copolymers combine characteristic features of the constituent blocks in a unique way creating hybrid materials that have the ability to self-assemble forming well-defined nanostructures of various morphologies in solution and thin film. The current work focuses on the synthesis, self-assembly and gelation in aqueous medium, of well-defined amphiphilic hybrid block copolymers with poly(ethylene glycol) (PEG) and poly(methacrylisobutyl polyhedral oligomeric silsesquioxane) P(MA-POSS) as the hydrophilic and hydrophobic blocks respectively.

The synthesis was carried out via a living radical polymerization technique; namely atom transfer radical polymerization (ATRP), employing PEG as the macroinitiator. Two types of block copolymers; diblock copolymers (PEG_{5k}-*b*-P(MA-POSS)) and triblock copolymers (P(MA-POSS)-*b*-PEG_{10k}-*b*-P(MA-POSS)) were prepared.

Synthesis Scheme

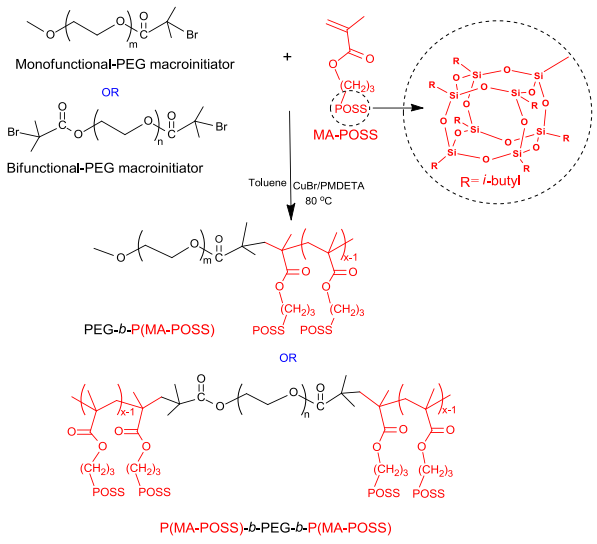

The hybrid amphiphilic block copolymers could self-assemble into nanoparticles-micelles in aqueous solution. Using the dynamic light scattering (DLS) technique, the hydrodynamic particle radii, R_h was calculated and found to be varying with the degree of polymerization (DP) of P(MA-POSS), for example, for diblock copolymer; PEG_{5k}-*b*-P(MA-POSS), it increased from R_h ~ 13.3 ± 1.1 nm to ~ 17.5 ± 1.4 nm with change in the DP of P(MA-POSS) from 4 to 6. The micellar structures formed by the P(MA-POSS)-*b*-PEG_{10k}-*b*-P(MA-POSS) triblocks were 'flower-like', where the PEG middle block assumed a loop conformation in the corona. Larger aggregates formed by P(MA-POSS)-*b*-PEG_{10k}-*b*-P(MA-POSS) were also detected in solution, whuich were interpreted as a contribution from some PEG chains adopting an extended conformation with one end dangling in solution, causing gelation at higher concentrations via intermicellar interactions. The gel formation at relatively lower copolymer concentrations (< 9 wt. %) and their rheological behavior was investigated.

The influence of hydrophobic POSS nanoparticles (Octavinyl-POSS), added to block copolymer solutions, was also investigated on their micelle formation, gelation, and rheological performance. Thus, the hydrodynamic size of the particles, formed by PEG_{5k}-*b*-$P(MA\text{-}POSS)_{3.6}$, increased more than four times to 56.9 ± 3.7 from 13.6 ± 1.0, with the addition of 0.1 wt% POSS nanoparticles. In case of P(MA-POSS)-*b*-PEG_{10k}-*b*-P(MA-POSS) triblock copolymers, which is associative in character, addition of POSS nanoparticles resulted hydrogel, with a significantly higher storage modulus, G', yield strengths, σ_y, and lower critical gelation concentration, c_g as compared with the pure triblock copolymer. Furthermore, gelation was induced in aqueous solutions of diblock copolymer by introducing P(MA-POSS)-*b*-PEG_{10k}-*b*-P(MA-POSS) triblock copolymer chains and the rheological performance was investigated.

Thermoset Nanosphere Formation: A Model Case from SEBS and Benzoxazine Molecular Assembly System

Suwabun Chirachanchai[1,2] *and Wonchalerm Rungswang*[1]

[1]The Petroleum and Petrochemical College, Chulalongkorn University, Soi Chula 12, Phyathai Road, Pathumwan, Bangkok, Thailand 10330.

[2]Center for Petroleum, Petrochemicals, and Advanced Materials, Chulalongkorn University, Bangkok, 10330, Thailand

Polymeric nanospheresaremainly referred to thermoplastic material due to the ease of controlling morphology and variety of materials. However, the preparations are complicated involving multi-step synthesis whereas. The most of nanospheres areloosely bound via secondary forces which maintain their structures only in specific conditions. In the case of thermoset nanospheres, the ease of handling is the advantage but the difficulty in controlling morphology during curing is the short-coming.

The present work, developsa novel approach to formthermoset nanospherevia molecularassembly mechanism through a study case of polystyrene-b-poly(ethylene-co-1-butene)-b-polystyrene triblock copolymer (SEBS)and benzoxazine monomer (BZ).

By simply blending BZin SEBS followed by thermal curing, well-defined nanometer sized thermoset particles were easily obtained. For example, the ratio of SEBS:BZ / 75:25 (S75BZ25) gave polybenzoxazine (polyBZ)nanospheres after thermally curing about 170 ± 43 nm (Figure, A). The less content of BZ brought the small nanospherical size. The proposed mechanism is related to the molecular interaction between BZ and PS segments in SEBS under π-π stacking. The molecular interactionmight lead to a pocket-like structure where the BZ starts crosslinking in a confined space.

To clarify the proposed mechanism, a series of thermoplastics, such as PS, polycarbonate (PC) and chlorinated polyethylene (CPE) which may form molecular interaction with BZ in different manner were selected. The resultsshowed that only PS gives the spherical polyBZ for all blending ratios but in micrometer sizes of 10 ± 3 μm for PS25BZ75 (Figure, B).The molecular interaction between two benzene rings belonging to BZ and SEBS, or BZ and PS via π-π stacking was also confirmed by using nuclear magnetic resonance (NMR) technique based onspin-lattice relaxation (T_1) and Nuclear Overhauser effect spectroscopy (NOESY).

When the confined space becomes as small as micrometer sized fibers, the thermoset nanospheres also reduces their sizes significantly. The electrospun fibers obtained from the blends of BZ and SEBS with the size about 6±0.8 μm gives the polyBZnanospheres with the size of 87± 14 nm.

In conclusion, the present work, for the first time, shows that we can simply develop thermoset nanospheres when the molecular interaction between polymer matrices and thermoset monomer is effective and at that time the factors to control the size is the content of thermoset monomer as well as the confined space of the matrices.

The authors would like to acknowledge the Royal Golden Jubilee Program (the Thailand Research Fund (PHD/0058/2550)) for the financial support.

Figure. TEM micrographs of Thermoset BZ nanosphere (A) and microsphere (B) extracted from cured S75BZ25 and PS25BZ75, respectively

Selected References

1. Rungswang, W. and Chirachanchai, S. Macromol. Mater. Eng., In Press, (10.1002/mame.201000315).

Effect of Carbon Nanotubes on Thermo-Mechanical Properties of Polyimide-Carbon Nanotube Nanocomposites

C. R. Misiego and *R. B. Pipes*

School of Chemical Engineering, Purdue University. 480 Stadium Mall Dr., West Lafayette, IN 47907-2100 USA

cmisiego@purdue.edu

Introduction

Addition of carbon nanotubes (CNT) to polyimide (PI) is an attractive alternative to tailor PI properties, since CNTs can improve, for instance, elastic modulus or electrical conductivity [1, 2]. In order to modify PI properties, good CNT dispersion is necessary. CNT agglomeration makes CNT dispersion especially difficult. Several techniques can be used for CNT dispersion in PI, such as high and low energy sonication [3], chemical modification of CNTs [4] and use of surfactants [5].

PI-CNT nanocomposites have been synthesized and characterized in order to determine the effect of CNT concentration on PI thermo-mechanical properties. As shown in Figure 1, composites with CNT concentrations ranging from 0.1 to 1%wt were synthesized via modified diester-diamine route [6]. The dispersion of carboxyl functionalized multi-walled carbon nanotubes (MWCNT-COOH) was achieved by combination of surfactants and *in-situ* polymerization under sonication.

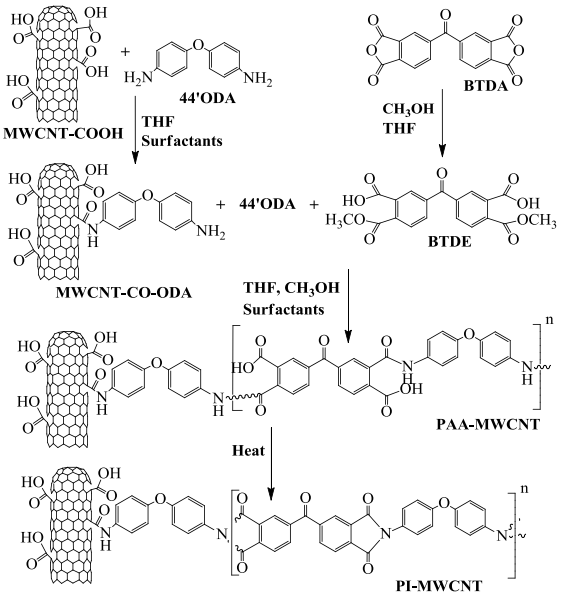

Fig. 1. Modified diester-diamine route for synthesis of PI-CNT composites

Materials and Methods

MWCNT-COOH were bath and horn sonicated in tetrahydrofuran (THF) with Sodiumdodecylbenzene sulfonate and 4,4'-oxydianiline (4,4'ODA). Methanol was reacted at 70°C with 3,3',4,4'-benzophenone tetracarboxylic dianhydride (BTDA) to produce diester. The diester solution was added to CNT-44'ODA solution and reacted under bath sonication at 65°C. After solvent volatilization, PI-CNT composites were obtained by thermal imidization at 300°C.

Results and Discussion

PI glass transition temperature (Tg) increased with CNT concentration from 287 to 335°C for the nanocomposite containing 0.3%wt CNTs and decreased for nanotube concentrations greater than 0.3%wt (Figure 2). Maximum increase in elastic modulus was also achieved for the 0.3%wt CNT nanocomposite.

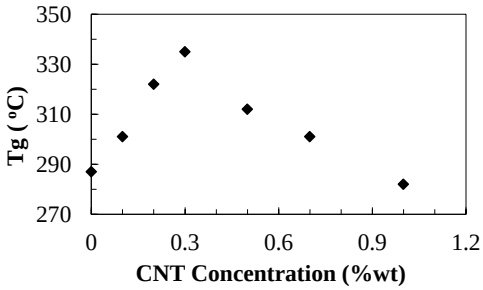

Fig. 2. Tg of PI-CNT composites (Measured by DSC)

Reduction of CNT dispersion quality as nanotube concentration increases is proposed as an explanation for the maximization of property improvement in the 0.3%w nanocomposite. Different CNT dispersion methods are studied in order to verify this hypothesis. The effect of monomer ratio (molecular weight) and crosslink agents in thermo-mechanical properties of polyimides is also investigated as a potential root cause for maximization of property modification at a particular CNT concentration.

Conclusions

Addition of CNTs to PI matrices can improve their thermo-mechanical properties, such as glass transition temperature. For this improvement to take effect, appropriate CNT dispersion is necessary: if CNT dispersion is not adequate, no significant property improvement is observed.

References

1. Zhu *et al*. *Comp. Sci. Tech*. 2006. 66. 548–554
2. Smith *et al*. *Polymer*. 2004. 45. 825–836
3. Park *et al*. *Chem. Phys. Lett*. 2002. 364. 303–308
4. Yuen *et al*. *Comp Sci. Tech*. 2007. 67. 2564–2573
5. Hamon *et al*. *Adv. Mater*. 1999. 11(10). 834-840
6. Weiser *et al*. *High Perform. Polym*. 2000. 12(1). 1-12

Antimicrobial activity of Nanocomposites based on Polycaprolactone/MMT-(PCL-b-DEAEMA)

I. Larraza[1], C. Abrusci[2] J. L. Pablos[1], M. Luzón[1], F. Catalina[1], C. Peinado[1], T. Corrales[1]

[1]Departamento de Fotoquímica, Instituto de Ciencia y Tecnología de Polímeros, CSIC, C/ Juan de la Cierva 3, 28010-Madrid
[2]Departamento de Biología Molecular, Facultad de Ciencias, Universidad Autónoma de Madrid, Cantoblanco, 28049-Madrid.

larraza@ictp.csic.es

Introduction.

Polycaprolactone (PCL) is a semicrystalline, biodegradable and biocompatible polymer. Due to its slow degradation rate, its application in the tissue engineering field has importantly increased [1, 2]. In this work, PCL nanocomposites containing organomodified montmorillonite (MMT), that simultaneously act as a substrate for cellular growth and prevent infections by microorganisms were prepared. The clay was modified with a block copolymer (PCL-b-DEAEMA) synthesized by ATRP. The different blocks contain PCL and quaternary ammonium species that attach to the clay surface and also act as cationic antiseptics [3]. The effect of the clay on the mechanical and superficial properties along with the thermal stability and its biodegradation rate was studied. The thermooxidative degradation process was monitored by the analysis of chemiluminescence emission [4]. Bacterial biodegradation was studied by determination of CO_2 using indirect impedance measurement.

Materials and Methods.

PCL with different proportions of clay were prepared. In order to compare the effect of the clay in the matrix, nanocomposites with neat clay were prepared too. All the samples were prepared by melt processing in a Haake MiniLab mixer. Nanocomposites morphology was characterized by XRD and TEM. The mechanical analysis was carried out by tensile testing and the superficial properties were analyzed by contact angle measurements. Thermooxidative stability was studied by TGA and chemiluminescence emission analysis. The biodegradation of the samples by *B.subtilis* and *P.Putida* was carried out at 30ºC and evaluated by measurement of the carbon dioxide produced using a Bac-Trac 4300 (SY-LAB Geräte GmbH, Neupurkerdorf, Austria).

Discussion

The modification of the clay produced an increase in the interlayer space and in the compatibility with the polymer leading to an intercalated/exfoliated morphology. The nanocomposites prepared with organomodified clay MMT-(PCL-b-DEAEMA) present an improvement on the mechanical properties with the clay content. The presence of the block copolymer in the clay/polymer interphase modifies the hydrophobic nature of the nanocomposites and an increase on the contact angle with water was observed. TGA analysis showed a higher thermal stability of the nanocomposites regarding to the neat PCL, this effect is due to the good barrier properties of the clay and was improved in the case of those samples with organomodified clay. The better stability of nanocomposites was confirmed by chemiluminescence (QL) emission analysis, which is related to the amount of oxidation species (hydroperoxides) generated during the thermooxidative degradation process, Figure 1A. PCL showed a higher QL intensity than the samples with clay. And for a given clay amount, those with modified clay showed a lower intensity. By CO_2 determination, it was observed that the presence of the quaternary ammonium species in the clay, decreases the biodegradation with respect to the materials with natural MMT mirroring the bactericide effect of the organomodified clay. Figure 1B shows the biodegradation by *B.Subtilis* in a period of 70 days.

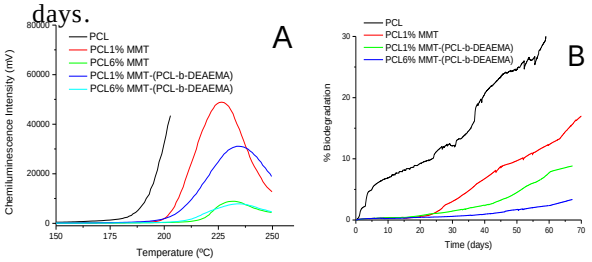

Figure 1. Chemiluminescence emission of PCL and nanocomposites *vs* temperature under O_2 (A). Biodegradation rate during a period of 70 days in the presence of *B. subtilis* (B).

Conclusions

The modification of the clay led to an improvement of the compatibility and dispersion of the filler in the matrix, showing better mechanical properties and higher thermal stability with respect to the neat PCL and the materials prepared with natural MMT. Contact angle measurements showed the effect of the organic surfactant by increasing the contact angle values in the materials prepared with MMT-(**PCL-b-DEAEMA)**. The presence of the ammonium cations of the block copolymer in the interphase matrix/filler, delays the biodegradation of the nanocomposites with respect to the materials with natural MMT and neat PCL, in presence of *B. subtilis y P. putida*, evidencing the biocide effect of the presented nanoclay.

References

[1] Okada, A., Usuki, A, Macromolecular Materials and Engineering 2006, 291 (12), 1449-1476.
[2] Darder, M., Aranda, P., Ruiz-Hitzky, E. 2007, Advanced Materials 19 (10), 1309-1319.
[3] Gilbert, P., Moore, L. E. Journal of Applied Microbiology 2005, 99, 703–715.
[4] Abrusci C., Marquina D., Santos A., Del Amo A., Corrales T., Catalina F. Journal of Photochemistry and Photobiology A: Chemistry 185 (2007) 188-197.

Phase Diagrams of the Mobility of Charge Carriers in Conducting Polymers

L. F. Roncaratti, P. H. O. Neto, W. F. da Cunha, R. Gargano, J. F. Teixeira, and G. M. e Silva

Institute of Physics, University of Brasilia, Brasília, Brazil

magela@fis.unb.br

Introduction

A model of the temperature and electric field dependence of the mobility of polarons and bipolarons in conjugated polymers in terms of an Hückel and stochastic approach is presented. Polarons and Bipolarons are self-localized, charged quasi-particles associated with characteristic distortions of the polymer backbone and with quantum states in the energy gap due to strong electron-lattice coupling[1]. The mobility is shown to have a strong dependence on the electric field, with two distinct regimes of temperature dependence. Lattice thermal oscillations enhance polaron mean velocity for electric fields of 1 mV/Angs or higher. In contrast, its mobility is damped by thermal oscillations under weaker electric fields.

The electroluminescence in conjugated polymers has a great impact in optoelectronic devices such as organic light emitting diodes (OLED's). The microscopic description of the temperature dependence of the charge carriers mobility in these materials is of fundamental importance. Our results are in good agreement with experimental data.

Methods

The essential physics of the mobility is contained in an Hückel model Hamiltonian with the hopping integral between neighboring carbon atoms explicitly dependent on the carbon-carbon distance,[2] and the Langevin approach to treat the sites motion where a random force term acts on each site simulating a thermally excited lattice. The electric field E is included in terms of a time dependent vector potential, A, by a Peierls substitution.[3] We obtain the wave functions, site positions and velocities at time t by numerical integration of the Schrödinger equation and the Langevin lattice equation of motion.

The effects of the external electric field and the thermal bath on the mobility are obtained by varying systematically E and T. The electric field takes the values from zero to 3.25 mV/Angs. The temperature values vary from zero to 300 K. The dynamics of the system is followed during 400 fs (time step t=0.004 fs). We have considered polymeric chains with N=200 sites with periodic bound conditions and containing initially one single positively charged polaron or bipolaron.

Results and Discussion

We considered the charge carrier trajectories and their velocities. When T=0 K, and after 100 fs, these trajectories are smooth and linear so, the velocity is constant. When E=0 mv/Angs, the bipolarons and polarons execute a brownian motion around the initial position and their averaged velocity are zero. We can see that the polaron kinetic energy is a linear function of temperature as it should be expected.

Two specific cases where the polaron mobility changes considerably with E and T are shown in the figure. In (a) we show polaron trajectories for E=0.5 meV/Angs. For this value of the electric field the polaron velocity is damped by thermal oscillations

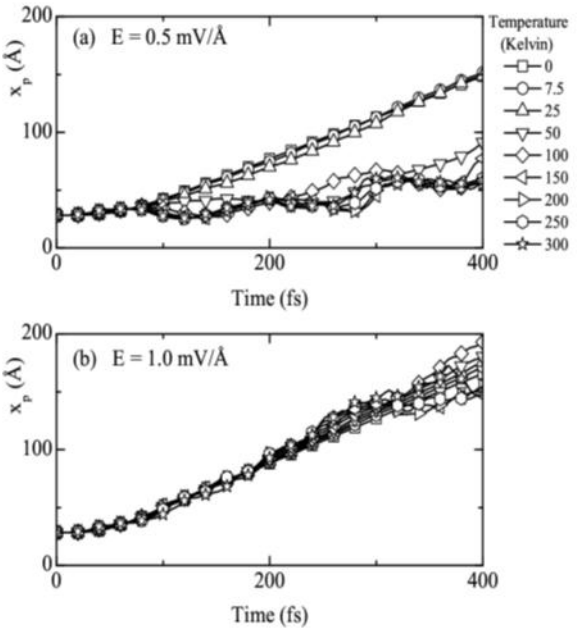

when T > 25 K. In (b) E=1.0 meV/Angs, in this case the thermal bath enhances the polaron velocity[4].

Conclusions

We solved the time-dependent Schrödinger equation for the pi-electrons and the equations of motion for the lattice displacements with temperature and electric field effects. This electric field-temperature-dependent model clearly presents two regimes for charge carrier mobility for field values used in physical devices like OLED's and OFET's. The presence of two different regimes for the temperature dependence of the mobility is shown to be consistent with the large mobility differences reported for conjugated polymers. It is shown that the temperature could enhance or damp the carrier mobility depending on the external electric field strength. For electric fields of about 1 mV/Ang or higher, the temperature works to increase the mobility of the charge carriers with a presented mechanism, that is distinct from the conventional semiconductor mechanism.

References

[1] G. M. e Silva, Phys. Rev. B **61**, 10777 (2000).

[2] G. M. e Silva, P. H. Acioli, and Y. Ono, J. Phys. Soc. Jpn **67**, 3881 (1998).

[3] M. P. Lima and G. M. e Silva, Phys. Rev. B **74**, 224304 (2006).

[4] L. F. Roncaratti, R. Gargano, and G. M. e Silva, J. Phys. Chem. A **113**, 14591 (2009).

Non conventional methods to prepare Conducting polymer nanocomposite

W.M. de Azevedo[1], R.A. de Barros[1], J. F. Felix[2] E. F. da Silva Jr[3].

[1]Departamento de Química Fundamental, CCEN
[2]Programa de Pós-Graduação em Ciência de Materiais, CCEN
[3]Departamento de Física CCEN, Universidade Federal de Pernambuco, 50670-901, Recife-PE, Brazil
e-mail wma@ufpe.br

Abstract

Conducting polymers have been investigated intensively over the last thirty years or so and the reason for this seems to be the fact that although they are organic material, their conductivity can achieve values that are comparable to semiconductors and metals. Moreover, their conductivity, electrochemical and optical proprieties make these materials excellent candidates to the development of high technological devices such as batteries, gas separating membranes, sensors, microelectronic devices, corrosion protection, electrochromic display devices and all-optical devices.
Amongst the most studied CP, polyaniline (PAni) is the preferred conducting polymer since it offers several advantages over the inherently conducting polymer family. Although its conductivity is not as high as other conducting polymers, its conductivity does not degrade upon exposure to environmental conditions.

Usually, PAni can be synthesized by a chemical, electrochemical, or photopolymerization process. Each one of these methods of synthesis provides an as made conducting polymer material with slightly different morphologies, and consequently, slightly different physical and chemical properties. Amongst these methods, the photopolymerization process has come to be more in evidence nowadays after our pioneering work, which used Ag^{+}, assisted by UV light to promote the polymerization of aniline monomer, which results in a composite material consisting of PAni and Ag^{0}. As a consequence of this research work, we also developed a new method for storing optical information and drawing patterns of conducting polymers that can be used for the development of all electronic device applications that use polymers.

In this work we extend the energy range of the light using x-ray and gamma ray and also use another non conventional source, the ultrasound waves to induce the conducting monomer polymerization.
Polyaniline (PANI) and polyaniline/silver nanocomposites composite were obtained through sonication of an aqueous solution of aniline and silver nitrate at room temperature and by the interaction of the x-ray and γ ray with the aqueous monomer solution. Also we propose a mechanisms to explain the formation of these products which is based on the fact that both methods produce hydroxyl radical •OH and hydrogen radical •H, which acts as an oxidizing agent for the polymerization of aniline monomer and as reducing agent for silver ions, respectively. Spectroscopic, X-ray and scanning electron microscope (SEM) measures showed that polyaniline and silver nanoparticles of 40nm of average diameter are obtained when ultrasonic technique is used whereas silver nanoparticles of 60nm average, and highly fibrillar polyaniline network with diameter of 60 nm is obtained when γ radiation is used.
Comparing the morphology of the chemical synthesized polyaniline with polyanianile obtained by x-ray and γ radiation, we observe that the morphology somehow seems to be correlated with the energy of the ionization radiation. The morphology for the chemical synthesis is globular whereas it is Fibril like for the gamma radiation, one the other hand for the x-ray synthesis it's appear to be a medium term, the fiber seems to be formed by the fusion of several globules.

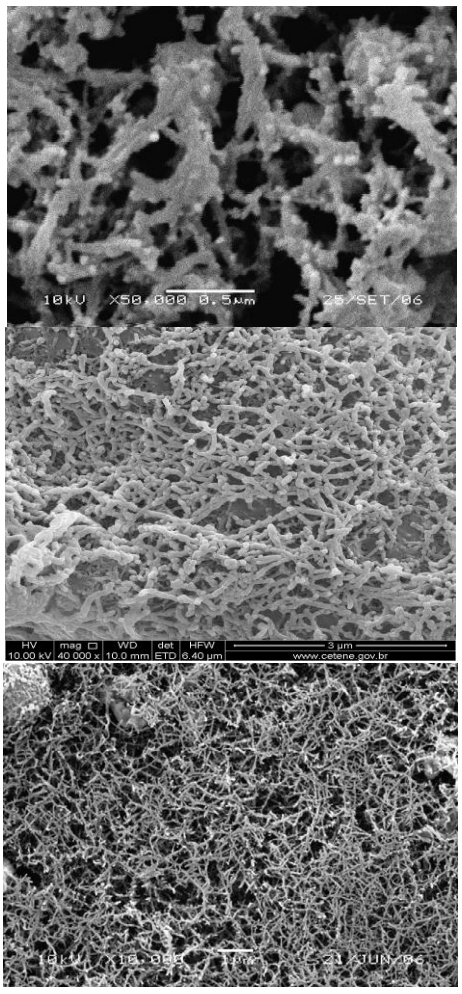

Fig. 1. Scanning electron microscopy images of polyaniline/silver nanocomposite grown from a solution of aniline nitrate and silver nitrate (a) under ultrasonic irradiation for 2 h, (b) under x-ray dose of 5 kGy and (c) under γ ray dose of 10 kGy

Concentration and temperature influence on the rheological behavior of a filled polymer

A.I. Gómez-Merino, M.H. Spillman, F.J. Rubio-Hernández

Department of Applied Physics II, University of Málaga (Spain)

aimerino@uma.es

Introduction

Over the years many products have been invented and tried in order to improve body armour. Shear thickening fluids are very much appreciated for protective applications in ballistics and stab. The shear thickening fluid (STF) is a combination of hard metal oxide particles suspended in a liquid polymer. This mixture of flow and hard components at a particular composition, results in a material with remarkable properties [1]. The shear thickening trend can take place in concentrated colloidal suspensions that have been shown to exhibit reversible shear thickening resulting in large, sometimes discontinuous, increases in viscosity above a critical shear rate, after a shear thinning behaviour at low shear rate and followed by a shear thinning region at high shear rate. In order to fit this phenomenon with a mathematic model, several attempts have been made [2]. But they use different equations to fit each region. In this work, we propose a function which fit all the experimental results.

Materials and Methods

The fumed silica used was Aerosil R-816 (Degussa Corporation). This is a hydrophobic silica, with a specific surface area of 190 m_2/g and a primary spherical particle size of 12 nm. Fumed silica primary particles are irreversibly fused into larger structures called aggregates whose particle size is under 100 nm. The continuous phase in our studies is a polyetylene glycol having an average molecular weight of 400 (PPG400) (Aldricch Chemicals). Each suspension was prepared by adding the liquid to the silica in a blender and mixing for approximately 60 minutes at 15 s^{-1}. Steady-shear viscosity has been measured using a parallel plate geometry on a stress-controlled rheometer (Haake Rheo-Stress RS600). The diameter of plates was 20 mm.

Discussion and results

Viscosity curves have been used to study the dependence of the rheological behavior of a polar polymer filled with hydrophobic silica fumed nanoparticles with particle concentration and temperature variation. At room temperature, shear-thickening behavior has been observed in between two shear-thinning regions when solid concentration is higher than 5% v/v. When temperature increases to 35-40ºC, this behavior is observed when solid concentration is higher than 11% v/v [3]. A new apparent viscosity function has been used to fit the experimental results [4]. Fig 1 shows the experimental results. As can be seen, this model fit the experimental results fairly well, specially at temperatures close to the room temperature (in between 15-25ºC).

As a very low shear rate Newtonian behavior was observed, Krieger-Dougherty equation was used to fit shear zero viscosity/solid concentration curves.

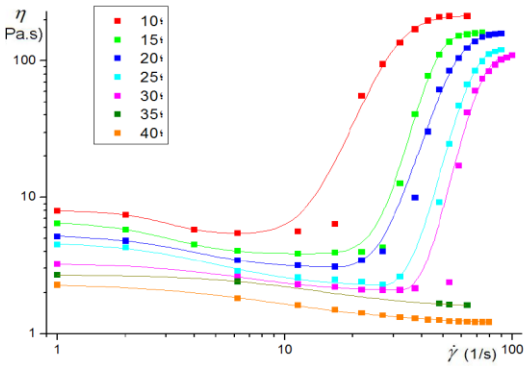

Figure 1. Apparent viscosity curves of silica in PPG 400 suspensions at 0.110137 v/v, at different temperatures.

The intrinsic viscosity calculated from the fitting process is much higher than 2.5 (hard spheres model) and the maximum packing fraction is much lower than 0.7, which is interpreted as the manifestation of the formation of aggregates of aggregates. This result leads us to justify the shear-thickening behavior here observed on the basis of "hydroclusters" formation, which are being generated by the action of hydrodynamic forces on silica aggregates.

Conclusions

Fumed silica suspensions in polypropylene glycol (PPG400) exhibit shear-thickening under steady flow. The shear-thickening behavior can be explained through a clustering mechanism, which attributes the thickening phenomena to the presence of temporary, flow-induced clusters. The calculated intrinsic viscosity value, which is a measure of the solute contribution to the suspension viscosity, is 23, and the maximum packing fraction is 0.22. These values are far away from those obtained for the hard sphere model, supporting the cluster theory.
The mathematic model here developed is able to fit the experimental results in the two regions observed in this STF fluid.

References

[1] H.A. Barnes, J. Rheol. 33 (1989) 329.
[2] J. Non-Newtonian Fluid Mech., 34 (1990) 181.
[3] M. Kamibayashi, H. Ogura, Y. Otsubo, J. Colloid Interface Sci. 321 (2008) 294.
[4] F.J. Galindo-Rosales, F.J. Rubio-Hernández, A. Sevilla, An apparent viscosity function for shear-thickening fluids, J. Non-Newtonian Fluid Mechanics, doi 10.1016/j.jnnfm.2011.01.001.

Properties of thin films of amphiphilic block copolymers based on Nvinylpyrrolidone and 2,2,3,3-tetrafluorpropylmethacrylate

Deniskina I.V, Zamyshlyayeva O.G., Batenkin M.A., Shandruk G.A.

Amphiphilic block copolymers have attracted much research interest because of the unusual properties associated with the processes of surface segregation and selforganization in solution and in films.

The study of surface morphology, physical and mechanical properties and thermo-mechanical characteristics of thin films of amphiphilic block copolymers can provide useful information for their application as gas separation membranes, photoresist in nanolithography processes, emulsifiers and stabilizers for emulsions and dispersions, compabilizators, nanocontainers [1-3].

Objects of study in this work are films of amphiphilic diblock copolymers based on the linear structure of the hydrophilic poly-N-vinylpyrrolidone (PVP) and hydrophobic poly-2,2,3,3-tetrafluorprorylmethacrylate (PFMA) previously obtained by radical polymerization of the first in the presence of the transmitter chain bis-(pentafluorophenyl)-germane to follow postpolimerization in the monomer FMA [4]. The method investigated AFM surface morphology of hybrid diblock copolymers, the individual PVP and PFMA, as well as a mechanical mixture of homopolymers in a weight ratio of 10% PVP and 90% of the PFMA. Patterns of regular granular relief spherical particles 0.78 microns and mesh size of about 2 microns.

Determined contact angles for films of block copolymers, the individual PFMA and the mechanical mixture of PVP and PFMA. The values of surface tension and its components.

Defined glass transition temperature for a given number of polymers using the method of DSC. Shows the shift of glass transition temperatures of block copolymers to a temperature of individual PFMA.

Films of copolymers, PVP, and the mechanical mixture were tested for tensile strength. The tests were conducted on tensile testing machine Zwick / Roel Z005 in the mode of uniaxial tension. Shown improvement in strength of the hybrid copolymers as compared to the fragile film PFMA.

This work was supported by the Russian Foundation for Basic Research project number 09-03-00662

References

[1]. Hamley I.W. / / Progress in polymer Sciense. 2009. V. 34. P.1161-1210.

[2]. Reining B., Helmut K., Hocker H. / / Polymer. 2002. V. 43. P. 7145-7154.

[3]. OG Zamyshlyaeva, TE Ganicheva, GA Shandryuk, JD Semchikov, Journal of Applied Chemistry, 2010. V.83. Vol. 7. P. 1193-1198.

[4]. O.G. Zamyshlyaeva, I.V. Deniskina, A.P. Filippov, J.D. Semchikov / / Polymer Science 2011. V 53. Vol. 9. P.1-12. In press.

Hierarchically structured polymeric films used as a model substrate for the investigation of adhesion and wettability

P. Escale, M. Save, C. Derail, L. Billon and L. Rubatat

IPREM / EPCP, UMR 5254, Université de Pau et des Pays de l'Adour, FRANCE

laurent.rubatat@univ-pau.fr

This work concerns the elaboration and the study of hierarchically structured films made of block copolymers in the aim of investigating the wettability and adhesion properties. The first level of structuring is a micrometer honeycomb morphology (left and center figures) obtained by a controlled solvent evaporation method under humid atmosphere. The second level of structuring is achieved via the self-assembly of diblock copolymers at the nanometer length scale (center & right figures). The challenge of the present study relies on the design of appropriate block copolymers that will spontaneously arrange into honeycomb films and concomitantly form the nanostructures during the fast solvent evaporation, i.e. less than a minute.

The selected block copolymers are poly(*n*-butylacrylate-*b*-styrene) and poly(*ter*-butylacrylate-*b*-styrene) synthesized via nitroxide-mediated polymerization, NMP. Two series of copolymers with different block ratio were synthesized in order to reach the regular copolymer morphologies (lamellar, cylindrical, etc.). The choice of the copolymers allowed us to investigate the effect of the polymer glass transition and of the Flory interaction parameter on the structures. The film morphology characterization, done by optical microscopy (left figure), atomic force microscopy (AFM, center figure) and small angle neutron scattering (SANS, right figure), revealed the nanostructuration of the acrylate-based coil-coil diblock copolymer within the walls of the highly ordered microporous polymer films. Preliminary contact angle measurements as well as tack and peeling experiments using the honeycomb films as a model substrate will be discussed.

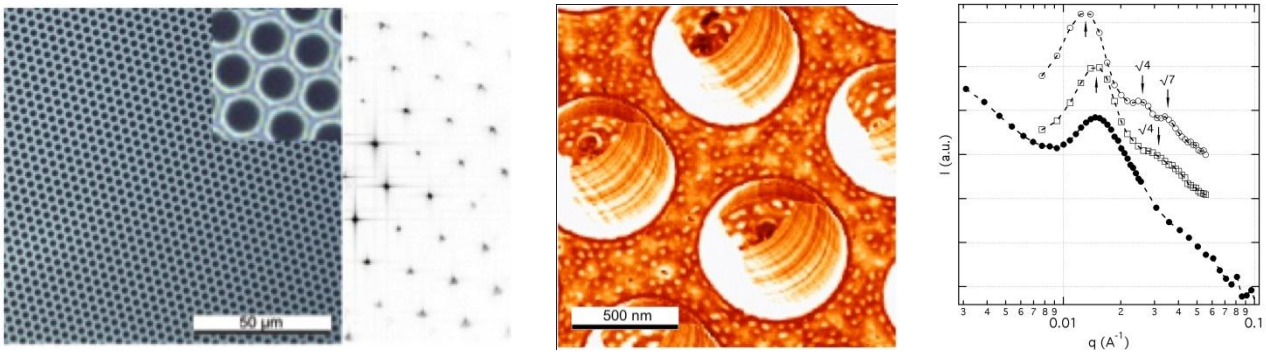

(left) Optical micrograph and the corresponding 2D-FFT of a honeycomb structure obtained with a PtBA-*b*-PS copolymer. **(center)** AFM phase image scanned on a PBA-*b*-PS copolymer films. **(right)** SANS scattering curves measured in the PBA-*b*-PS copolymer films (log-log plot) : solvent cast film (open square) thermally annealed solvent cast film (open circle) and honeycomb film (solid circle).

Complex Architectures of Hybrid Nanoparticles Controlled by Amphiphilic Copolymers

C. Geidel, K. Schmidtke, M. Klapper, K. Muellen

Max Planck Institute for Polymer Research, Ackermannweg 10, 55128 Mainz, Germany

geidel@mpip-mainz.mpg.de, klapper@mpip-mainz.mpg.de

Introduction

The controlled synthesis of inorganic nanocrystals or hybrid inorganic-organic materials with specific size is a rapidly developing field in science since physical and chemical properties, such as composite transparency and catalytic activity, are strongly influenced by the shape and morphology of the nanoparticles. For example, zinc oxide has been used in solar cells, sensors, as activator for organic accelerators and as co-accelerator in the vulcanization process. For these applications the fabrication of morphologically distinct nanostructures is required. Most of the nanoparticles are used in nanocomposites. In this case, compatibility between the inorganic and the organic components is normally achieved by hydrophobization with an organic shell in an additional step.

Results and Discussion

A universal approach for the preparation of functionalized inorganic nanoparticles through the inverse emulsion technique (**Figure 1**) has been developed.[1,2] In this method, the formation and hydrophobization was achieved in one step. The emulsions were stabilized by a statistical amphiphilic copolymer. In the micelles of the inverse emulsion, the inorganic nanoparticles were formed from a precursor salt by adding a precipitation agent. Various types of hydrophobized inorganic nanoparticles like metal oxides, sulfides and metals were accessible, which could be generated by sol-gel reaction or precipitation process. More complex structures were also available, like perovskites and zinc oxide particles coated with a silica shell, dedicated for UV protection.[3,4]

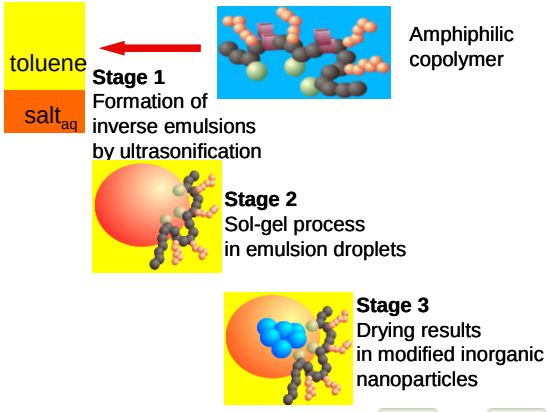

This inverse emulsion process has been extended to produce *in-situ* hydrophobized, shape-anisotropic, inorganic nanoparticles in a single step.[5] In a first approach, the stabilizing as well as the hydrophobizing property of the copolymers was combined with the ability to control the crystallization in one polymer (structure directing emulsifier - SDE). In a second approach, a mixture of two polymers was applied: an amphiphilic copolymer for hydrophobizing/stabilizing the inorganic nanoparticles and a polar or double hydrophilic polymer that induced the anisotropic growth of the inorganic nanocrystals (structure directing agents - SDA). Homopolymers and block copolymers, consisting of phosphonic acid, polyethylene oxide and propylene oxide groups, were used as SDAs. The suitability of this process has been demonstrated by the fabrication of zinc oxide nanorods, shape-anisotropic cadmium sulfide nanoparticles and porous anatase nanoparticles (**Figure 2**). The homogeneous incorporation of such particles into a composite could be easily achieved as the emulsifiers could be adopted to any polymeric matrix by varying the hydrophobic monomer in the amphiphilic copolymer. Consequently, new types of hybrid materials based on shape-anisotropic inorganic nanoparticles are now accessible.

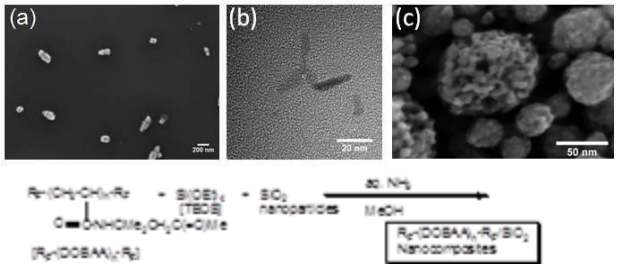

Figure 2. SEM and TEM images of hydrophobized, shape-anisotropic ZnO (a), CdS

Conclusion

The presented approach offers a fast and efficient method for obtaining a broad variety of *in-situ* hydrophobized inorganic nanoparticles of different shapes and morphologies. This technique is based on the precipitation of the particles in inverse emulsions in the presence of specially designed (co)polymers. By the choice of structure-directing polymers not only the shape and morphology of the inorganic nanoparticles obtained but also the size can be controlled. The avoidance of a complex polymer synthesis makes the process attractive for industrial applications, especially when focusing on other systems such as nanocomposites.

References

[1] V. Khrenov, F. Schwager, M. Klapper, M. Koch, K. Muellen, *Colloid Polym. Sci.* **2006**, *284*, 927.

[2] M. Klapper, C. G. Clark Jr., K. Muellen, *Polym. Int.* **2008**, 57, 181.

[3] K. Schmidtke, G. Lieser, M. Klapper, K. Muellen, *Colloid Polym. Sci.* **2010**, *288*, 333.

[4] K. Schmidtke, S. H. Stelzig, C. Geidel, M. Klapper, K. Muellen, *Macromol. Symp.* **2010**, 296, 28.

[5] C. Geidel, K. Schmidtke, M. Klapper, K. Muellen, *Polym. Bull.* **2011**, submitted.

Theory and Self-Consistent Field Modeling of Dendritic Polymer Brushes

T.M. Birshtein [1,*], *A.A. Polotsky* [1], *O.V. Borisov* [1,2]

Institute of Macromolecular Compounds of the Russian Academy of Sciences, St. Petersburg, Russia
IPREMUMR5254 CNRS/UPPA, Pau, France

[*] e-mail: birshtein@imc.macro.ru

The polymer brush is among the best studied systems in polymer science. Brushes, formed by long polymer chains densely grafted to a solid-liquid or to a liquid-liquid interfaces, received ample attention from both theoretical and experimental perspectives. In the meantime, advanced synthetic approaches now allow the making of macromolecules with a virtually arbitrary complex and well-controlled branched architecture (stars, combs, dendrons). Moreover, the technology to attach these to surfaces becomes available. It is believed that brushes from branched architectures may introduce novel desired features, such as enhanced stimuli responsiveness, outstanding nanomechanical properties, and tuned biointeractivity. From a physical point of view, brushes of branched macromolecules are challenging because the distribution of the elastic tension and the fluctuations of the individual molecules is far from trivial as these properties will differ from the behavior of the same molecules in solution.

In the present work, equilibrium structural properties of polymer brushes formed by dendritic polymer chains (dendrons), Figure 1, are studied by means of Scheutjens-Fleer self-consistent field (SF-SCF) modeling and scaling analysis.

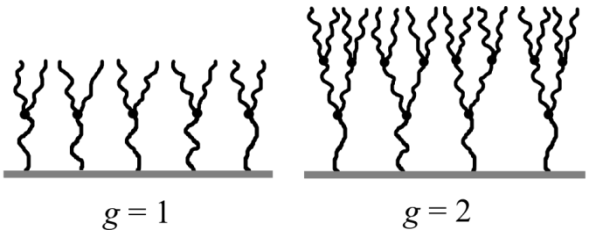

Figure 1. Schematic illustration for polymer dendritic brush. In this example, the branching functionality q =2, and g=1 and 2 is the number of generations on the left and right, respectively

Limiting cases of minimal and maximal possible losses of conformational entropy corresponding to different assumptions concerning distribution of elastic tension in the end-grafted dendrons are analyzed on the basis of the Flory-type scaling approach. The numerical SCF modeling indicates that the effective exponent of the power-law dependence for the height of dendritic brush on the grafting density differs from that derived within the Flory-type approximation. This is explained by changing of the intramolecular elastic tension distribution upon an increase in grafting density.

The distributions of end and branching points are wide and exhibit multiple maxima, pointing to a broad distribution in the chain stretching, Figure 2. This distribution leads to monotonically decreasing overall density profiles.

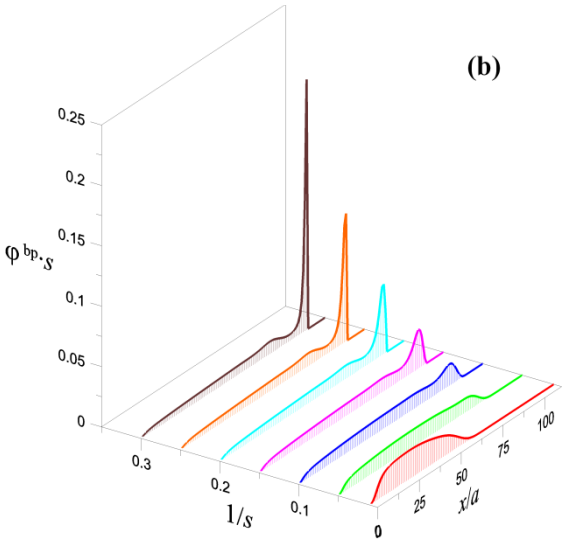

Figure 2. Number distribution of the branching points, scbp(z), for a firstgeneration dendritic brush with g=1 and branching point functionality q=3 for different grafting densities 1/s as indicated.

This implies an intrabrush segregation of dendrons having contributions that belong to different subpopulations. For the brushes formed by the first generation dendrons we made a detailed analysis of this phenomenon. Near the surface the brush is enriched by dendrons that have only weakly extended spacers. The second population of the dendrons are characterized by a strongly, at high grafting density almost completely, stretched root spacer and are predominantly found in the periphery of the brush. In brushes formed by dendrons of higher generations, multimodal distributions were found both for the terminal segments and for the branching points. These correspond to multiple populations which are stratified throughout the brush.

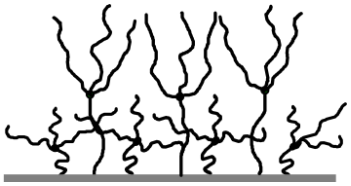

Figure 3. Schematic illustration of the occurrence of two populations of conformations of dendrons in a g=1 dendritic brush.

Reference

A.A. Polotsky,T. Gillich, O.V. Borisov, F.A.M. Leermakers, M. Textor, T.M. Birshtein. *Macromolecules* **2010**, *43*, 9555.

Solutions of Amphiphilic Polyelectrolytes: Effect of Electrostatic Interactions on Self-Organization

Sergey V. Venev and Igor I. Potemkin

Physics Department, Moscow State University, Leninskie Gory 1-2, Moscow 119991, Russian Federation
Institute of Polymer Science, University of Ulm, Albert-Einstein-Allee 47, Ulm 89069, Germany

e-mail: igor@polly.phys.msu.ru

Amphiphilic block copolymers are known to form micelles in selective solvents: insoluble blocks form the core of the micelle and the soluble (polyelectrolyte) blocks form the corona. Local violation of electric neutrality in polymer systems due to entropy-driven escape of counterions can induce long-range electrostatic forces which together with mobility of counterions play very important role in micellization. Therefore, one can expect that (i) the local violation of electric neutrality in micellar solutions and (ii) the composition of the block copolymer are responsible for the size of the micelles and their morphology. To the best of our knowledge, the simultaneous effect of these two factors on the morphology of the micelles in solutions of diblock copolymer with neutral (insoluble)
and charged block has not been studied yet.

In the present paper, we develop a mean-field theory of micelle formation in salt-free solution of diblock copolymers with a soluble polyelectrolyte block and an insoluble neutral block [1]. The so-called three-zone model is used which is a simplified alternative of the Poisson-Boltzmann approximation. This model allows analyzing an inhomogeneous distribution of counterions outside the corona (an analogue of Gouy-Chapman layer and Manning condensation). We study both dilute and concentrated solutions. Conventional spherical, cylindrical and planar morphologies of "direct" (soluble) micelles are considered in the crew-cut regime (short soluble blocks). We also analyze the stability of inverse (insoluble) spherical and cylindrical micelles, which form a dense phase. In this phase, the soluble blocks with the solvent form spherical (cylindrical) cores which are embedded in a matrix of the insoluble blocks. Phase diagrams of the solution are constructed on the basis of conditions of the true equilibrium, i.e., they include one- and two-phase stability regions as well as triple points, Fig. 1.

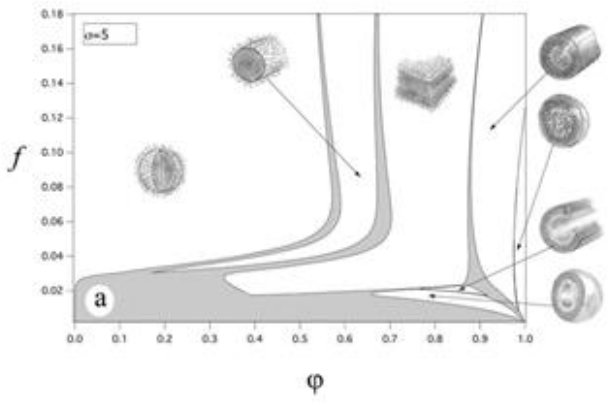

Fig. 1. Phase diagram of diblock polyelectrolyte in a selective solvent in variables: polymer volume fraction *f* and the fraction of the soluble block in the copolymer *f*. The fraction of charged groups 1/s=0.2. Grey areas correspond to the phase coexistence regions.

We demonstrate that the presence of charged groups practically does not change the phase behavior of the solution at high polymer concentrations. In this regime, the main factor governing the swelling of the coronae is the polymer concentration. On the other hand, the role of the charged groups at low polymer concentrations is very important. The Rayleigh instability prevents formation of nonspherical micelles at low polymer concentrations. The charged groups promote stability of the spherical micelles: they remain stable at conditions when the neutral spherical micelles change morphology or precipitate.

References.

[1] Venev, S. V.; Reineker, P.; Potemkin, I. I. *Macromolecules* **2010**, *43*, 10735.

Mesoscale Simulation of Network Formation and Structure, Combining Molecular Dynamics and Kinetic Monte Carlo Approaches

Anatoly V. Berezkin, P. Ulrich Biedermann, Alexander A. Auer

Max-Planck Institut für Eisenforschung GmbH,
Max-Planck-Straße 1, 40237 Düsseldorf, Germany

a.berezkin@mpie.de

Introduction

Structure and physical properties strongly depend on the network topology. As opposed to linear polymers, prediction of this topology is not so straightforward, and usually requires sophisticated theoretical approaches: random graph theory, diagram techniques, field theory etc. In case of multiple competing chemical reactions, substitution effects, topological confinements, and polymerization-induced phase transitions theoretical treatment becomes too complicated or impossible, especially at high monomer conversions. Due to this a direct molecular simulation of curing is a simple, but powerful alternative to analytical theory. Since the time scale accessible in such simulations is limited, mesoscale models, parameterized on the basis of phenomenological kinetics or quantum-mechanical calculations, seem to be more preferable here than the atomistic molecular dynamics exploiting reax force fields.

Methods and Results

In this work application of a hybrid scheme, combining mesoscale or coarse-grained molecular dynamics, and stochastic kinetics (Monte Carlo) is illustrated by two simulations: 1) mesoscale simulation of organic-inorganic nanocomposite formation by twin-polymerization of a spirocyclyc monomer, and 2) coarse-grained simulation of polyurethane network formation. While segregation forces in these polymers are relatively weak, nanostructure formation is a chemically-controlled process strongly dependent on the reaction mechanisms.

Cationic ring-opening twin polymerization[1] starts from a spirocyclic compound and yields phenolic resin/silicon resin nanocomposite:

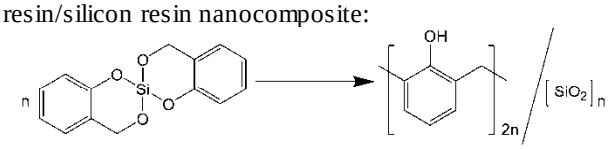

Cleavage of four unequal bridging units (-O-, and –CH_2-O-) and formation of new bonds leads to two chemically connected and topologically entangled networks. This process was simulated using dissipative particle dynamics modified to allow for multiple competing chemical reactions. These reactions "proceed" with probabilities derived from DFT *ab initio* calculations.[2] Diverse competing reactions of different mechanisms were described with a specially developed script language.[3]

The influence of catalysis, relative rates of reactions in phenol resin, and siloxane network, as well as incompatibility of components on the nanocomposite structure was studied systematically. It was shown, that polycondensation typically begins with phenolic resin formation, simultaneously yielding silanol groups. These groups initiate subsequent formation and growth of SiO_2 domains in the cross-linked organic matrix. Limited mobility and small size of inorganic fragments suppress physical segregation of chemically-different molecular fragments, resulting in a fine inorganic network with domain diameter about 2 nm. Even weak segregation disperses this network into small siloxane nanoparticles. Morphology and dimensions of the domain structure are in a good agreement with experiment.

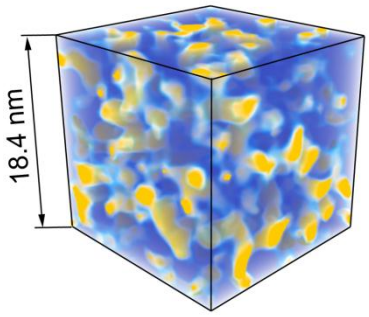

Figure. Simulated nanocomposite structure. Phenol resin is shown with blue, and siloxane net with yellow colors.

Coarse-gained molecular dynamics followed by reinsertion of atomistic details is highly promising, when influence of crystallization, glass transition, or growing viscosity has to be addressed, or time evolution of mechanical and relaxation properties is of interest. Different aspects of such chemically-oriented coarse-graining are considered for the case of polyurethane network formation from standard industrial formulations. The coarse-grained character of "reacting" beads requires correction of reaction probabilities to accurately reproduce phenomenological kinetics, observed in experiment. First steps in this direction will also be presented.

Acknowledges: Financial support of DFG (FOR 1497) is highly appreciates. Authors acknowledge Prof. Pavel G. Khalatur, and Prof. Nico van der Vegt for fruitful discussions.

References

[1] S. Spange, P. Kempe, A. Seifert, A. A. Auer, P. Ecorchard, H. Lang, M. Falke, M. Hietschold, A. Pohlers, W. Hoyer, G. Cox, E. Kockrick, S. Kaskel, Angew. Chem. Int. Ed. 2009, **48**, 8254-8258.

[2] A. Richter, A. V. Berezkin, A. A. Auer and S. Spange, to be submitted.

[3] A. V. Berezkin, P. G. Khalatur et al., DPDChem version 1.0, http://polymer.physik.uni-ulm.de/~khalatur/exchange/DPD_Chem/index.htm.

Surface modifications of polymeric materials with functional Ag nano-particles; a comparative study of different immobilization techniques

Doris Breitwieser[1], *Simon Lenz*[1], *Rupert Kargl*[1], *Ming Wu*[3], *Hubert Fasl*[1], *Karin Stana-Kleinschek*[2], *Volker Ribitsch*[2]

[1]Karl-Franzens-University Graz, Institute of Chemistry, Heinrichstraße 28, A-8010 Graz
[2] University of Maribor, Laboratory for Characterizing and Processing Polymers, Smetanova Ulica 17 SI-2000 Maribor
[3] Dept. of Chemical Technology of Materials, Graz University of Technology, Stremayrgasse 9, A-8010 Graz

doris.breitwieser@edu.uni-graz.at

Introduction

The synthesis and immobilization of stable and well defined silver nanoparticles (AgNPs) is a rapidly expanding field in nano-sciences. Especially their size-dependent electronic, optical, and chemical properties make them attractive targets for the synthesis of new materials.[1-2] Like colloidal silver[3], AgNPs are known for antibacterial and antimicrobial properties.[4] AgNPs are currently used in various applications such as catheters, scaffolds and wound dressings[5]. Beside their medical applications they are also applied in textile finishing [6]. Generally, the immobilization of AgNP on (renewable) polymer surfaces offers a promising new way to extend the application and use of these polymers. Furthermore a combination of the well known properties of AgNPs with the biocompatibility and antithrombogenicity of a polysaccharide, namely sulfated chitosan, allows the manufacturing of particles that are functionalized on their surface fAgNPs.[7] Particles modified in this way can be used for surface modifications of polymeric materials. For the immobilization of fAgNPs on polymer surfaces several strategies can be followed. In this work we compare two of these strategies namely the electrostatic adsorption and the covalent binding of fAgNPs that are functionalized with sulfated chitosan. The immobilization was followed via contact angle measurements and atomic force microscopy (AFM). Additionally, the antimicrobial properties of different immobilization methods were compared.

Materials and Methods

fAgNPs were synthesized using the functional, water soluble, polysaccharide sulfonated chitosan (S-Chi) as stabilizing and reducing agent. The synthesized fAgNP were immobilized on different polymeric surfaces namely poly(methylmethacrylate-acrylicacid-copolymer (PMMA-Co-AA), poly(methylmethacrylate) (PMMA), and regenerated cellulose. Electrostatic immobilization which was achieved using a polyethyleneimine (PEI) pre-coating was compared with covalent binding via 1-ethyl-3-(3-dimethylaminopropyl)-carbodiimide (EDC) over the activation of carboxylic groups. The PMMA surface was hydrolyzed under alkaline conditions to create carboxylic groups on the surface which are needed for the covalent immobilization using EDC. The immobilizations steps and their stability were followed by contact angle measurements and AFM. Furthermore the antibacterial properties of the surfaces were examined and compared with respect to the immobilization method.

Results and Discussion

All mentioned polymeric surfaces were successfully modified with fAgNPs. As can be seen in Figure 1 a denser surface packing is obtained with electrostatic adsorption as shown on Fig 1 with PMMA-Co-AA surfaces. Even if a less dense coverage is obtained using covalently immobilized fAgNP, it shows a much better stability then the electrostatic bound ones. Long term experiments showed that covalently immobilized particles retain their stability and wettability on modified polymer surfaces.

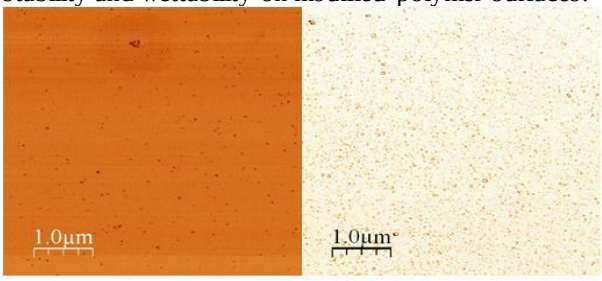

Figure 1: AFM images of S-Chi stabilized fAgNPs electrostatic immobilized (right) and covalently bound (left)

Conclusions

In summary, two methods for the immobilization of functionalized silver nanoparticles on different polymeric materials could be demonstrated. On the one hand the electrostatic adsorption is shown which leads to a dense surface coverage. On the other hand we successfully could show covalent immobilization with EDC. This technique leads to better immobilization stability of the particles.

References

[1] R. W. Murray, *Chem. Rev.* **2008**, *108*, 2688.
[2] D. D. Evanoff, G. Chumanov, *ChemPhysChem* **2005**, *6*, 1221
[3] A. Lottermoser, *J. Prakt. Chem.* **1903**, *68*, 357.
[4] V. K. Sharma , R. A. Yngard, Y. Lin, *Advances in Colloid and Interface Science* **2009**, *145* 83.
[5] X. Chen, H. J. Schluesener, *Toxicol. Lett.* **2008**, *176*, 1.
[6] M. H. El-Rafie, A. A. Mohamed, T. I. Shaheen, A. Hebeish, *Carbohydr. Polym.* **2010**, *80*, 779.
[7] H. Fasl, J. Stana, D. Stropnik, S. Strnad, K. Stana-Kleinschek, V. Ribitsch, *Biomacromolecules* **2010**, *11*, 377.

Network Formation by Thiol-Ene 'Click' Chemistry / by Controlled Radical Polymerization: a 'Single-Molecule' View

Karel Goossens,[a] *Wim Van Camp,*[b] *Hiroshi Uji-i,*[a] *Dominik Wöll,*[c] *Klaus Müllen,*[d] *Filip Du Prez,*[b] *and Johan Hofkens*[a]

[a] Katholieke Universiteit Leuven, Department of Chemistry, Celestijnenlaan 200F (PO box 2404), 3001 Heverlee, Belgium.
[b] Universiteit Gent, Polymer Chemistry Research Group, Krijgslaan 281 S4-bis, 9000 Gent, Belgium.
[c] Universität Konstanz, Zukunftskolleg/Department of Chemistry, Universitätsstraße 10, 78464 Konstanz, Germany.
[d] Max-Planck-Institut für Polymerforschung, Ackermannweg 10, 55128 Mainz, Germany.

karel.goossens@chem.kuleuven.be

Diffusional limitations during polymerization determine the reaction kinetics, as well as the properties of the final polymer (molecular mass, polydispersity index, etc.). An understanding of the fundamental processes influencing diffusion and dynamics in polymers and polymer solutions is therefore of great interest. **Single-molecule spectroscopy and microscopy (SMS/SMM)** have already proved to be suitable techniques for this purpose.[1,2] Unlike 'ensemble' measurements on polymerizing samples, which only yield data averaged over a large number of molecules, measurements on individual molecules provide information about distributions and the time dependence of the parameters studied. In particular, SM techniques allow to examine **heterogeneity** in systems on a molecular level.

SMS/SMM techniques have recently been used for the first time to follow the free radical polymerization (FRP) of styrene.[3,4] Investigation of the polymerization reaction over the entire conversion range is possible by combining *fluorescence correlation spectroscopy (FCS)* and *wide-field microscopy (WFM)* to follow diffusion of **individual, fluorescent probe molecules** (present in a concentration of ~ 10^{-9} M). In FCS, confocal excitation of the dye molecules is applied, and the fluorescence signal is recorded with an avalanche photodiode (APD) point detector. In WFM, on the other hand, a 24 × 24 μm^2 sample area is illuminated at once (wide-field excitation), and movies are recorded by means of a CCD camera, which has a limited time resolution. Both SM techniques complement each other, since FCS is a powerful method to follow diffusion processes that are characterized by a diffusion constant $D >$ ~ 10^{-13} m^2 s^{-1}, whereas WFM is a suitable technique to track slowly moving molecules with $D <$ ~ 10^{-12} m^2 s^{-1}. Because the viscosity of a polymerizing reaction mixture gradually increases, the average velocity of diffusing reporter dye molecules decreases; the first stage of the polymerization reaction ('low' viscosity) can be followed by FCS, but from a certain conversion onwards ('high' viscosity) one needs to switch to WFM. The experimentally obtained, time-dependent diffusion constant(s) of the reporter dye molecules can give direct, fundamental information about the polymerization process.

We are applying this methodology to the study of **thiol-ene 'click' chemistry reactions** and ***controlled* radical polymerization (CRP) processes**. Both reaction types allow, in principle, to obtain highly homogeneous networks. This is in contrast to free radical polymerizations, for which a high degree of heterogeneity is observed during network formation: at moderate conversion, local nanogel clusters act as dye traps that slow down/immobilize some dye molecules, while others can still move *quasi* freely in the regions where no network has been formed yet.[3] One of the main questions is how the 'bulk' homogeneity observed for CRP and 'click' chemistry is reflected on a molecular level, and whether genuinely no heterogeneity at all can be found on this length scale. The results are compared with the FRP of the same monomers. Furthermore, differences between linear (or possibly star-shaped) and cross-linked polymers are investigated (to elucidate differences between temporary and permanent cross-links), as well as the influence of the probe size. Both ATRP (more specifically, ARGET and ICAR ATRP) and NMP have been selected as CRP processes.

We will also present a new experimental setup that is dedicated to the study of polymerizing samples. The **single-molecule fluorescence microscopy setup** consists of (i) an FCS part; (ii) a WFM part; and (iii) a Raman part. It allows to investigate a polymerizing reaction mixture over the entire monomer conversion range while monitoring conversion by Raman spectroscopy measurements, all of this completely *in situ* on the microscope. Home-made sample holders allow to keep the mixture under an inert atmosphere, and to heat the sample – if required. Raman spectroscopy was validated as a suitable technique to determine the conversion of different monomers in a multi-component mixture. For the Raman measurements, either a high-boiling solvent is used as an internal standard, or a calibration is performed by reference measurements on polymer standards.

[1] D. Wöll, E. Braeken, A. Deres, F. C. De Schryver, H. Uji-i, Johan Hofkens, *Chem. Soc. Rev.* **2009**, *38*, 313-328.
[2] F. Kulzer, T. Xia, M. Orrit, *Angew. Chem., Int. Ed.* **2010**, *49*, 854-866.
[3] D. Wöll, H. Uji-i, T. Schnitzler, J. Hotta, P. Dedecker, A. Herrmann, F. C. De Schryver, K. Müllen, J. Hofkens, *Angew. Chem., Int. Ed.* **2008**, *47*, 783-787.
[4] M. Dorfschmid, K. Müllen, A. Zumbusch, D. Wöll, *Macromolecules* **2010**, *43*, 6174-6179.

The sharp thermal transition of the diblock copolymers methoxy-poly(ethylene glycol)-block-poly(N-isopropylacrylamide) (PNIPAAM-b-MPEG). A combined analytical-ultracentrifugation and dynamic-light-scattering study.

Álvaro Ortega, Ramón Pamies, and José García de la Torre

Departamento de Química Física, Facultad de Química, Universidad de Murcia, Spain

jgt@um.es

Introduction:

Poly(N-isopropylacrylamide) (PNIPAAM) is one of the most extensively investigated thermoresponsive polymers due to its interesting and novel properties and applications. One of the most interesting aspects of PNIPAAM is its thermoresponsive sensitivity, which gives the possibility of a local and temporal release by changing the temperature of the environment slightly above the low critical solution temperature (LCST), which can be tuned with the molecular weight of both blocks. Below this critical temperature, the polymer stays soluble in water but above LCST the hydrophobicity of the molecules is increased and the system exhibits a macroscopic phase separation. The characterization of PNIPAAM and PNIPAAM-based copolymers and their self-assembled structures is usually done by means of scattering and microscopy techniques but Analytical Ultracentrifugation (AUC) has been scarcely used for these purposes [1].

In the present work, diblock copolymers containing a constant length of a PNIPAAM block but with different lengths of the hydrophilic block monomethoxy-capped poly(ethylene glycol) (MPEG), were synthesized by utilizing atom transfer radical polymerization (ATRP). The prepared product is methoxy-poly(ethylene glycol)-block-poly(N-isopropylacrylamide) with the composition: $MPEG_n$-*b*-$NIPAAM_{71}$, where *n* adpots values of 0, 12, 23 and 114. We have performed experiments with AUC at different temperatures to evaluate the thermoresponsive behavior of the single chains and the self-assembled aggregates of these diblock copolymers. An evaluation of the influence of the length of the MPEG block at different concentrations and temperatures has been carried out.

Materials and Methods:

All the chemicals used for the synthesis of the block copolymers were purchased from Aldrich and Fluka. The polymers were synthesized by means of atom transfer radical polymerization (ATRP) as reported in a previous work [2]. AUC experiments were performed on a Beckman Optima XL-I ultracentrifuge (Beckman coulter, Palo Alto, CA), using for detection the Rayleigh interference optics. Sedimentation velocity experiments were performed in a range of temperatures from 5 to 35ºC at 40000 rpm.

Results and Discussion:

Firstly, we carried out the determination of the specific volume ($\bar{V}$) by means of the sedimentation coefficients in H_2O and D_2O. Although the composition changes significantly, the $\bar{V}$ value was 0.84 cm^3/g for all the polymers.

After the determination of $\bar{V}$ values, we have obtained the sedimentation (s) and the diffusion coefficients (D_t) of the copolymers at several temperatures by means of a velocity study at 40000 rpm at 0.1, 0.5 and 1wt% concentrations. Therefore, we were able to extrapolate these values to ideal conditions (c=0). By means of Stoke-Einstein equation, from D_t^o we determined the values of hydrodynamic radii (R_h), depicted in the figure, with good agreement with Dynamic Light Scattering (DLS) data [2].

In order to study the self-assembly of these copolymers, we attempted experiments at 3wt% concentration. All the experiments for the evaluation of the aggregated species at temperatures over 30ºC were conducted at 5000 rpm, to be able to appreciate larger species which would sediment too fast to be detected at 40000 rpm. Interestingly, even at this slow rotor speed an enormous aggregate can be observed that sediments in less than 2 minutes, forming a band at the bottom of the sedimentation cell that exceeds the linearity in the interference detection system, making it impossible to determine the concentration at this area. We conclude that at this temperature, and after the sedimentation process the high local concentration existing at the bottom of the cell can reach a condition where a phase separation is clearly visible, even by direct eye observation of the centrifuge cell, indicating the formation of a gel phase or even a precipitate.

Conclusions.

The determination of the unimeric chains is possible by AUC with good agreement with DLS data. Presence of oligomers was detected at high. Specific volume of the polymers can be calculated by AUC.

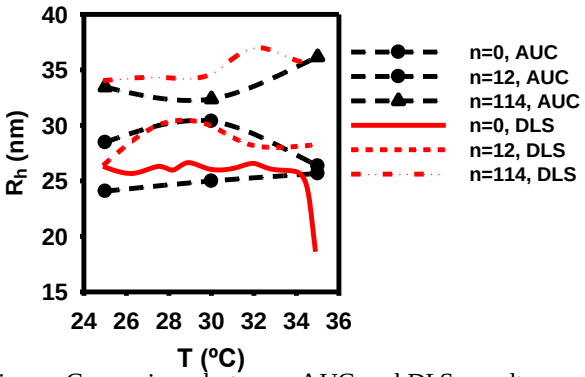

Figure. Comparison between AUC and DLS results.

References.

[1] D. Kucking and C. C. V., H.-J. P. Adler , A. Völkel and H. Cölfen. *Macromolecules*, **39**, 1585-1591, 2006.

[2] K. Zhu, R. Pamies, A.-L. Kjøniksen and B. Nyström. *Langmuir*, **24**, 14227-14233, 2008.

Ionic Liquids : Structuration agents in a fluorinated matrix

Sebastien LIVI, Jean-François GERARD, Jannick DUCHET-RUMEAU

Université de Lyon, F-69003, Lyon, France; INSA Lyon, F-69621, Villeurbanne, France; CNRS, UMR 5223.

jannick.duchet@insa-lyon.fr

Introduction

The ability to create regularly shaped nanoscale objects which serve as the building block is an extremely important goal in materials science. One of the key issues is to design and create new polymer materials with unprecedented improvements in their physical properties. Different self-assembly pathways are described to lead to hierarchical structures formed from heterogeneous chemical species, like organic molecules, polymers, organic-inorganic nanobuilding blocks [1]. Ionic liquids (ILs), which are organic salts with a melting point below 100 °C, with unique properties such as their chemical stability, excellent thermal stability, inflammability, low vapor pressure and high ionic conductivity have become more attractive in material science. This work reports for the first time the achievement of a nanoscale structuration from ILs into a polymer matrix. This structuration can be tuned by a wide choice of cation-anion combinations including pyridinium, imidazolium, and phosphonium as cation associated to iodide, bromide, or fluorinated anions. The preparation of IL nanostructured films from a fluorinated polymer solution could open many applications in energy and materials fields.

Materials and Methods

A general and simple method for the synthesis of a serie of organic halide and fluorinated salts is reported based on i) Iodide (I^-), bromide (Br^-) and hexafluorophosphate (PF_6^-) combined phosphonium cations with one long alkyl chain denoted $C_{18}P\ I^-$, $C_{18}P\ Br^-$, $C_{18}P\ PF_6^-$, respectively. ii) Iodide associated imidazolium cation with two long alkyl chains denoted $C_{18}C_{18}Im\ I^-$. iii) Iodide combined pyridinium salt denoted $C_{18}Py\ I^-$ [2]. The chemical structure of ILs combined to iodide anion is described in Figure 1.

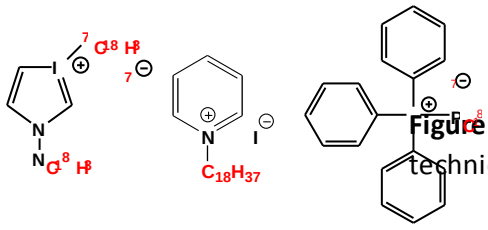

Figure 1. Chemical structure of synthesized ionic liquids

To prepare supramolecular ionic networks, the three functional ionic liquids have been introduced in very low quantities (1 wt%) in a aqueous suspension of polytetrafluoroethylene (PTFE) under stirring. Then the suspension was spread on stainless steel plates to get 50 µm-thick wet layer. A thermal treatment at 400 °C for 10 minutes was applied to obtain the final polymer film.

Results and Discussion

The hydrophobic nature of polytetrafluoroethylene and the strong interactions between the ionic domains and the PTFE matrix generate a phase-separated morphology. It is the balance of interactions between polymer medium and anion-cation pairs that leads to different morphologies [3]. TEM micrographs reveal different types of structuration which are tuned by the chemical nature of cation and of anion as well. For example, by using the same phosphonium cation combined with different anions, Figure 2 shows final morphologies varying between an agregated one with the fluorinated or bromide anion and a fine structuration at nanoscale with the iodide conteranion. The morphologies characterized by SAXS and XPS analysis are comparable to those observed in ionomers [4].

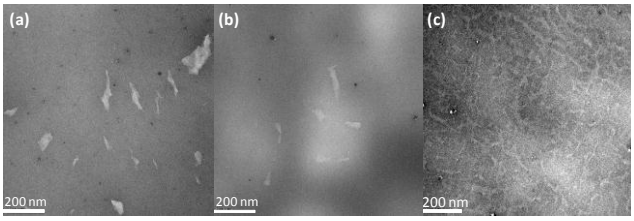

Figure 2. TEM micrographs of the nanocomposites (a) PTFE/$C_{18}P\ PF_6^-$, (b) PTFE/$C_{18}P\ Br^-$, (c) PTFE/$C_{18}P\ I^-$

The distribution of ionic liquids in the polymer matrix plays a key role on the elongation at break of films. We have highlighted that the 'spider web' structuration leads to a dramatic increase of 190% of the elongation at break as shown in Figure 3. Thus, the formation of this network can play a retardant role against the beginning of catastrophic cracking.

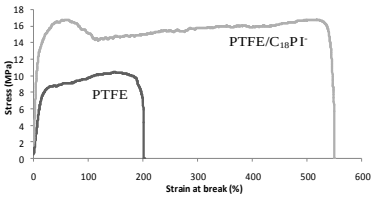

Figure.3 Effect of the phosphonium ionic liquid (1wt%) on the mechanical properties determined by uniaxial tensile tests at room temperature and 0.004 s^{-1}

Figure 1. Scheme of the applied inverse emulsion technique.

Conclusions

The use of ionic liquids as functional building blocks based on pyridinium, imidazolium and phosphonium cations to achieve materials combining a structuration at nanoscale with the dramatic mechanical properties of the resulting ionomers has been successfully demonstrated for the first time in a fluorinated matrix.

References

1. A. Vermogen, S. Boucard, J. Duchet-Rumeau, K. Masenelli-Varlot, P. Prele and R. Seguela, *Macromolecules*, 2005, **38**, 9661.
2. S. Livi, J. Duchet-Rumeau, T. N. Pham and J. F. Gerard, *J. Coll. Interface Sci.*, 2010, **349**, 424.
3. A. Eisenberg, B. Hird, R.B. Moore, *Macromolecules* 1990, **23**, 4098.
4. I. Capek, *Adv. Coll. Interface Sci.*, 2005, **118**, 73.

Dynamic Dielectric Spectroscopy and Thermo Stimulated Current for identification of gene mutation in plant model

Frédéric Roig[1], Eric Dantras[1], Jacqueline Grima-Pettenati[2], Colette Lacabanne[1]

[1]Physique des Polymères, Institut Carnot CIRIMAT, UMR CNRS 5085

[2]Surfaces cellulaires et signalisation chez les végétaux, Pôle de Biotechnologies Végétales, UMR 5546 CNRS Université Paul Sabatier, 31062 Toulouse Cedex 09, France

Abstract: The Arabidopsis Thaliana is considered by geneticists as a model plant because of its rapid growth, ease of laboratory culture and complete sequencing of its genome. The strategy of geneticists is to focus research on a plant genome with the smallest possible in order to analyze it, and then use information acquired to begin the exploration of more complex genomes. However, the biochemical analysis did not differentiate at the molecular level mutants and natural plant.

Dynamic Dielectric Spectroscopy (DDS) and Thermo Stimulated Current (TSC) have been applied to the investigation of such complex systems. The combination of dielectric techniques by accessing a wide frequency and temperature range can probe the molecular mobility of delocalized to localized molecular mobility of the composite plant. The majority of structural components of plant cell walls are cellulose and lignin. First, the molecular mobility of the two major components has been characterized. Then the composite plant is studied in its natural state and finally in its mutant state. DDS shows that the same relaxation modes are observed in both states. Contrarily, TSC exhibits differences in their fine structure.

Analysis of TSC data allows us to define the macromolecular dynamic by the activation enthalpy and entropy that are plotted on compensation diagrams, respectively for natural Arabidopsis Thaliana (Figure 1) and its mutant CAD C / D (Figure 2). We observe three segments showing discrete compensation phenomena corresponding to three relaxation modes.

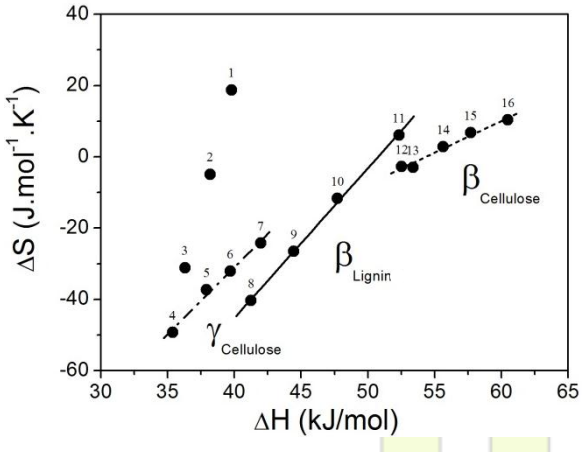

Figure 1: Compensation diagram of Arabidopsis Thaliana

The relaxation mode in the lowest enthalpy ($\gamma_{cellulose}$) is characteristic of the polar groups of cellulose, (-CH_2OH and -OH) [1,2]. The β_{Lignin} mode is associated with the molecular mobility of polar groups (-OH) of lignin and $\beta_{cellulose}$ mode corresponds to the molecular mobility of the cycles of glucose via glycosidic linkages. In Figure 2, we observe only two modes $\gamma_{cellulose}$ and β_{Lignin} with comparable slopes in contrast to Figure 1.

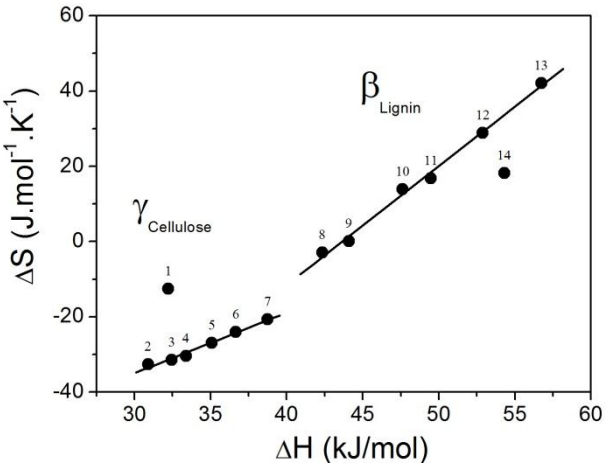

Figure 2: Compensation diagram of Mutant CAD C/D

Similar behaviour is observed between the two modes due to a common origin of these two modes. Indeed in this mutant plant, the genetic modification changes the chemical structure of lignin by increasing the proportion of alcohol function [3,4].

Thermo Stimulated Current coupled with Dynamic Dielectric Spectroscopy proves to be a suitable set of methods to identify the influence of gene mutation on the dynamic structure of the natural plant. The evolution of nanometric mobility is clearly exhibited by the compensation diagrams.

References:

[1] Einfeldt J, Meißner D and Kwasniewski A **(**2004) *Cellulose* **11** 137-505

[2] Roig F, Dantras E, Dandurand J and Lacabanne C J. Phys. D: Appl. Phys. **44** (2011) 045403 (8pp)

[3] Ralph J, Lapierre C, Marita J.M, Kim H, Lu F, Hatfield R.D, Ralph S, Chapple C, Franke R, Hemm M.R, Doorsselaere J.V, Sederoff R.R, O'Malley D.M, Scott J.T, MacKay J.J, Yahiaoui N, Boudet A-M, Pean M, Pilate G, Jouanin L, Boerjan W Phytochem. **57** (2001) 993-1003

[4] Grima-Pettenati J, Goffner D, Review in Plant Science **145** (1999) 51-65

"Amphiphilic" Ionic Liquid in a Mixture of Nonionic Liquids: Theoretical Study[1]

*Artem A. Aerov**, *Alexei R. Khokhlov*+*, *Igor I. Potemkin*+*

*Moscow State University, Department of Physics
+University of Ulm, Institute of Polymer Science

aerov@polly.phys.msu.ru

Introduction. In the last time ionic liquids (ILs) strongly attract interest of researchers because it was found out that these substances possess some unique and very useful properties. ILs are solely composed of anions and cations. Nevertheless they are liquid at around room temperature. Main advantageous peculiarity of ILs is the fact that they are very good as solvents and reaction media. This is because ILs are almost nonvolatile and at the same time they can dissolve a wide range of both organic and inorganic substances. For example, an important achievement related to the high solvent power of ILs is the invention of the novel effective and environment friendly cellulose processing technique.

Properties of an individual IL are explained by its chemical structure. At the same time, it is evident that the useful properties of ILs are somehow generally inherent to ILs nature, i.e. there are some laws which are valid for all ILs as a *whole class* of substances. The goal of our research is to reveal the laws. It is evident that general properties of ILs are somehow related to the main basic feature of ILs: they are composed of ions only. We show that because of it ILs can have a unique dual nature that can explain some of their interesting unusual for common liquids properties. The reason is that the properties of an IL's cations can strongly differ from the properties of the IL's anions. The contradictious properties of the two types of particles would immediately make them segregate if (just hypothetically!) the electrostatic interactions vanished. But the coulomb attraction makes these "incompatible" particles stay together in an intermixed state and compose thus a substance (the IL) having the unusual dual nature.

Method. We use the dual nature concept together with a Flory-Huggins like lattice model in which it is supposed that each elementary cell is occupied by one particle, and each ion of an IL is treated as an individual independently moving particle, noncoulombic interactions of two particles are described by the Flory-Huggins parameters. With the help of this method we have explained the high solvent power of ILs[2], the micpophase separation in a IL/nonionic liquid (nIL) mixture[3,4] and predicted that a polymer microgel swelling ratio can depend on the amount of polymer the gel consists of if the solvent is an IL[5]. In the present part of the work[1] we analyze the properties of the system consisting of an IL and of two types of nonionic molecules, **A** and **B**. We suppose that the duality of the IL shows up in different affinities of the IL's cations and the IL's anions to **A** and to **B**: the cations are attracted stronger to **A** than to **B** and anions vise versa are stronger attracted to **B** than to **A**.

We consider a two phase system in which the two phases are formed because the nonionic components **A** and **B** are incompatible with each other (they can't form a homogeneous mixture). We investigate how the ions of the IL are distributed near the phase boundary and how the IL contributes to the value of the phase boundary surface tension. We consider for that the two-phase system as a sequence of flat elementary layers parallel to the phase boundary. Each of them is composed of elementary cubic cells and it is one cell thick. We find the concentrations of the components and the electrostatic potential in each if the layers by means of the free energy minimization. Our method allows to calculate concentrations profiles near the phase boundary and the surface tension of the phase boundary at any concentration of ions in the bulk of the phases (i.e. in the case of an IL when ions volume fraction is of order unity and in the case of low concentrations of ions as well). The method is applicable both for systems that are far from the crtitical point or close to it.

Results. We have shown that a double electrostatic layer is formed at the phase boundary. The width of the double layer increases as the concentration of ions approaches either zero or the value corresponding to the critical point. The ratio of the maximal cations (anions) concentration in the layer to their concentration in the bulk far from the boundary is the larger the lower is the concentration of IL and the higher is the difference in the affinities of the cations and the anions to **A** and to **B**.

We have also shown that the surface tension of the phase boundary is the smaller the higher is the difference of the affinities and the higher is the concentration of the IL. The surface tension can even reach zero at a concentration of IL lower than the one corresponding to the critical point, what means that at the corresponding values of the parameters characterizing the system the mixture is to be microheterogeneous. One can say that an amphiphilic IL behaves as a surfactant, but instead of a monomolecular layer it forms at the phase boundary a double electrostatic layer which can be up to several hundred molecules thick.

Acknowledgements. This work was supported by the Federal Education Agency of the Russian Federation (state contract No. П1365, signed 02.09.2009) in the framework of the realization of the federal task program "Scientific and scientific-educational personnel of innovational Russia" in the years 2009-2013.

References.

Aerov, A.A.; Khokhlov, A.R.; Potemkin, I.I *Journal of Physical Chemistry B.*
[1] **2010,** *114 (46),* 15066.
[2] **2006**, *110 (33),* 16205
[3] **2007**, *111 (34), 10189.*
[4] **2007**, *111 (13), 3462-3468.*
[5] Aerov, A.A.; Potemkin, I.I *Journal of Physical Chemistry B,* **2009**, *111 (13), 113 (7), 1883.*

Thermal and Electronic Conduction in Conjugated Polymers

Luiz F. Roncaratti, Pedro H. de Oliveira Neto, Wiliam F. da Cunha, Ricardo Gargano, Geraldo Magela e Silva

Instituto de Física, Universidade de Brasília, Brasil

lz@fis.unb.br

Introduction

The synthesis and applications of semiconducting organic polymers has created a demand for scientific understanding of thermal and electronic transport in nanomaterials [1,2].
The macroscopic description of the thermal and electronic conduction in conjugated polymers is obtained from a microscopic model of an one-dimensional lattice of coupled atoms, the first and the last of which interact also with a quantum thermal bath.

Methods

Our system is defined by a model Hamiltonian containing an interaction potential that depend on relative atomic coordinates [3], plus a Tight-Binding term as approximation for the π electrons-phonons interaction [4]. The last term includes also a modified hopping term to take into account an external electric field [5]. Each boundary atom is also coupled to a set of reservoir oscillators representing two independent thermal baths.
To time evolve the system, we prepare a stationary state fully self-consistent with the degrees of freedom of electrons and phonons. To perform the dynamics we solve the Schrödinger one-particle equations coupled with the Euler-Lagrange equations to treat the lattice. Since our main objective is to characterize the dynamics under a temperature regime we eliminate the reservoir degrees of freedom in the usual way and obtain a quantum Langevin equation [6] for the boundary atoms. These equations are defined by an exponential correlated noise and its respective memory kernel [7]. The set of equation of motion was integrated numerically [8] using a fourth-order Runge–Kutta method.

Results and Conclusion

In our model thermal conductivity can be directly calculated through the temperature gradient along the chain. This value can be tuned to fit experimental data adjusting few parameters of the model. Topological defects over the conjugated pattern (solitons, polarons, exitons…) allowed by our model Hamiltonian are responsible for the electronic conduction. We also found that the behavior and intrinsical properties of theses quasi-particles are defined by the temperature effects. These results and their analysis shed new light on several experimental controversies [9,10,11,12].

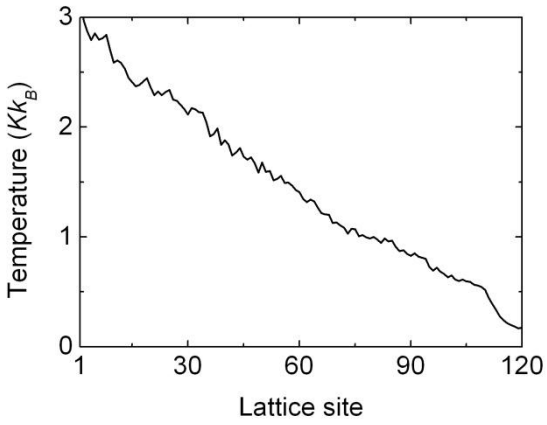

References

[1]D. G. Cahill, W. K. Ford, K. E. Goodson, G. D. Mahan, A. Majumdar, H. J. Maris, R. Merlin, S. R. Phillpot, J. Appl. Phys. **93**, 793 (2003).
[2]S. Lepri, R. Livi, A. Politi, Phys. Rep. **377**, 1 (2003).
[3]D. Ceperley, M. H. Kalos, J. L. Lebowitz, Macromolecules **14**, 1472 (1981).
[4]W. P. Su, J. R. Schrieffer, A. J. Heeger, Phys. Rev. B **22**, 2099 (1979).
[5]G. M. e Silva, Phys. Rev. B **61**, 10777 (2000).
[6]G. W. Ford, J. T. Lewis, R. F. O'Connell, Phys. Rev. A **37,** 4419 (1988).
[7]D. Banerjee, B. C. Bag, S. K. Banik, D. S. Ray, J. Chem. Phys. **120**, 8960 (2004).
[8]R. F. Fox, I. R. Gatland, R. Roy, G. Vemuri, Phys. Rev. A **38**, 5938 (1988).
[9]L. F. Roncaratti, R. Gargano, G. M. e Silva, J. Phys. Chem. A **113**, 14591 (2009).
[10]P. H. de Oliveira Neto, W. F. da Cunha, R. Gargano, G. M. e Silva, J. Phys. Chem. A **113**, 14975 (2009).
[11]P. H. de Oliveira Neto, W. F. da Cunha, L. F. Roncaratti, R. Gargano, G. M. e Silva, Chem. Phys. Lett. **493**, 283 (2010).
[12]P. K. Schelling, S. R. Phillpot, P. Keblinski, Phys. Rev. B **65**, 114306 (2002).

Quantum Dots Functionalised with Polymers via RAFT Polymerisation for the Fluorescent Detection of Latent Fingerprints

Jessirie Dilag[1,2], *Prof. Hilton Kobus*[1], *and Assoc. Prof. Amanda Ellis*[1,2]

[1] School of Chemical and Physical Sciences, Flinders University, Sturt Rd. Bedford Park, S.A 5042 Australia
[2] Center for Nanoscale Science and Technology, Flinders University, Sturt Rd. Bedford Park, S.A 5042 Australia

jessirie.dilag@flinders.edu.au

Introduction

In recent years Reverse Addition Fragmentation Chain Transfer (RAFT) polymerisation has emerged as an attractive method for polymer synthesis, providing control of molecular weight and molecular weight distributions with narrow polydispersity indexes [1]. There has also been a unique twist in fingerprint research which has involved the implementation of nanotechnology into the function of novel fluorescent fingerprint reagents, based on Quantum Dots (QDs) [2]. QDs are semi-conducting nanostructures that possess unique intrinsic luminescent properties that are size dependent at the nanoscale [3]. Here we combine advantages of RAFT polymerisation with nanotechnology using QDS in the synthesis of fluorescent nanocomposites for fingerprint detection. The polymeric surface modifications provide stability and solubility of the QDs. QDs investigated in this study were Cadmium Sulphide (CdS) and Oxidised Carbon QDs in various polymers, in particular, polydimethylacrylamide (PDMA). The polymers also play a role in the adherence to latent fingerprints (produced by sweat excretions on the palmer of the hand).

Materials and Methods

Size tuneable CdS QDs capped with 2-mercaptoethanol were first synthesised, with the appropriate amounts of sodium sulphide and cadmium chloride in DMF. The 2-mercaptoethanol on the surface of CdS was coupled, with an ester link, to a C12-carboxyl-terminated RAFT agent. From then RAFT polymerisation of a chosen monomer was performed via a grafting-from mechanism. Similar chemistry was applied to Oxidised Carbon QDs; synthesised via acid treatment of activated carbon and dialysis membrane filtration.

Fingerprint subjects were prepared by depositing fingerprints onto non-porous surfaces such as glass, and aluminum foil. Aqueous solutions of each nanocomposite (CdS/Polymer and Oxidised Carbon QDs/Polymer) were spotted onto the fingerprint substrate, followed by washing with water. Fluorescently developed fingerprints by these nanocomposites were visualised and photographed under UV light.

Results and Discussion

QD size was determined by computational methods with UV-Vis spectrophotometry. The band gap energy ($E_{g(QD)}$) was determined from the QDs absorbance, and the hyperbolic band model (equation 1) was used to estimate the nanostructure diameter (r) ($E_{g(bulk)}$= Band gap energy of the bulk, m*= effective electron mass, $\hbar$ =The Dirac Constant) [4].

Equation 1: $$E_{g(QD)} = \sqrt{\frac{E_{g(Bulk)}^2 + 2\hbar^2 E_{g(Bulk)}(\pi/r)^2}{m^*}}$$

Fluorescence spectrophotometry showed how the QDs fluorescence was retained after each step of synthesis of the nanocomposite. Broad fluorescence allowed the developed fingerprints to be visualised as two different colours. Filters were used with photography to capture this property (Figure 1).

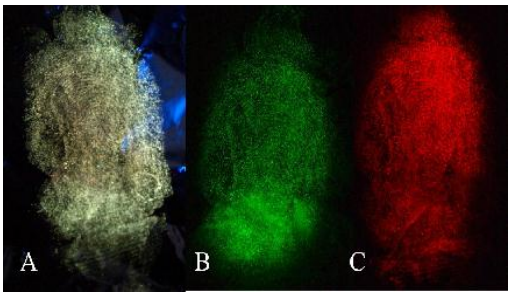

Figure 1. Fingerprints detected on aluminum foil (A) no filter (B) 525 ± 40 nm filter (C) > 555 nm filter.

Research with the Oxidized Carbon QDs showed similar results with respect to fingerprint detection on non-porous surfaces.

^{1}H NMR, FTIR and GPC was utilised to monitor the RAFT polymerisation of the chosen polymers, and to verify their successful synthesis.

Conclusions

CdS and Oxidised Carbon QDs were synthesised and functionalized with a RAFT agent. RAFT polymerisation of desired monomers from the surface of these QDs was performed. The resulting fluorescent nanocomposites were used to detect latent fingerprints deposited on non-porous surfaces. The photographs taken of fingerprints developed with the QD/polymer nanocomposites under UV light prove these fluorescent properties.

References

[1] Moad, G., Y.K. Chong, A. Postma, E. Rizzardo, and S.H. Thang, Advances in RAFT Polymerization: the synthesis of polymers with defined end-groups. Polymer 2005. 46(19), p. 8458-8468..

[2] Dilag, J.; Kobus, H.; Ellis, A. V., Nanotechnology as a New Tool for Fingermark Detection: A review, Current Nanoscience, 2011, 7, p. xxxx-xxxx (In Press)

[3] Jorge, P.; Martins, M. A.; Trindade, T.; Santos, J. L.; Farahi, F., Optical Fiber Sensing Using Quantum Dots, Sensors 2007, 7, p. 3489-3534.

[4] Y. Wang, A. Suna, W. Mahler and R. Kasowski, PbS in polymers. From molecules to bulk solids, J. Chemistry and. Physics 1987, 87 p. 7315–7322

Polyacrylate Core-Shell Stars – Synthesis and Application

Agnieszka Kowalczuk[1], *Neli Koseva*[2], *Stanislav Rangelov*[2], *Barbara Trzebicka*[1], *Andrzej Dworak*[1]

[1]Centre of Polymer and Carbon Materials, Polish Academy of Sciences, M. Curie Sklodowskiej 34, 41-819 Zabrze Poland
[2]Institute of Polymers, Bulgarian Academy of Sciences, Acad. G. Bonchev bl. 103A, 1113 Sofia, Bulgaria

akowalczuk@cmpw-pan.edu.pl

Introduction: Macromolecules of star geometry are of substantial interest because of their unique properties and possible applications. The branched topology defines the shape and physicochemical properties of a single macromolecule in the solution and together with the presence of large number of functional groups and the cavities created in star interiors offers interesting perspectives to applications as nanoscale materials for encapsulation and release of active compounds and as polymer-drug conjugated delivery vehicles [1-3].
Here, we report the synthesis of core-shell star polymers with the hyperbranched cores and polyacrylic or polymethacrylic acid arms. Stars obtained via atom transfer polymerization of *tert*-butyl acrylate and methacrylate were subjected to acidic hydrolysis to obtain structures with poly(acid) arms. The applicability of the star polymers as anticancer drug *cis*-diammine-dichloroplatinum (II) carrier was explored addressing two challenging aspects: achieving high drug payload, and evaluating the therapeuticactivity of the *cis*-platin-star polymer conjugates in vitro towards different cancer cell lines.

Materials and Methods: *tert*-Butyl acrylate and *tert*-butyl methacrylate were distilled over CaH_2 prior to use. CuBr, PMDETA, $CuBr_2$ and trifluoroacetic acid (TFA) were used as received. Anisole, dichloromethane, 1,4-dioxane were purified by distillation prior to use. The syntheses of hyperbranched macroinitiators were carried out as described in our previous reports [4, 5] yielding poly(arylene oxindole) of M_n=20 000 g/mol and poly[p-(iodomethyl)styrene] of M_n=2400 g/mol.
The polymers were characterized by NMR (Bruker Ultrashield 600) and FTIR (Nicolet FTIR 6700) spectroscopy. The molar mass and the dispersity of star poly(meth)acrylates was determined by GPC with multiangle light scattering detector (DAWN EOS,Wyatt Technologies). Light scattering (Brookhaven) experiments were performed to provide information about the size and shape of macromolecules in solution.

Results and Discussion: Synthesis of new star polymers of controlled structure, shape and charge was performed using controlled radical polymerization (ATRP) of *tert*-butyl acrylic and methacrylic monomers onto hyperbranched polymeric cores. The synthetic route involved the "core first" method and consisted of two main steps: the synthesis of the star macromolecules with active ester functionalities followed by their conversion to carboxylic groups.
Such polymerization processes were reasonably well controlled and leaded to well-defined star polymers with the number of arms 10 and 28 and M_n up to 280 000 g/mol. The resultant star structures were characterized by GPC with triple detection. The evidenced much more compact structure of these polymers, as compared with their linear counterparts, supported the star formation. The hydrolysis of polyacrylate and polymethacrylate arms in the presence of TFA proceeded smoothly at the ambient temperature, yielding polymers with branched hydrophobic interior and poly(acrylic acid) external shell. The representative stars which differed considerably in the degrees of polymerization of the arms and, consequently, in total molar mass were selected for LS measurements to obtain the information about the size of particles formed in water by star copolymers with a change of pH. In the case of stars with 10 poly(acrylic acid) arms no aggregation upon the change of pH was observed, the size of nanoparticles was around 10 nm.
Key features for drug conjugation, such as hydrophilic shell of stars and high density of functional carboxylate groups were used for reversible exchange of ligands with *cis*-platin and therefore to regeneration the nanocarrier at physiological salt concentrations. A high drug payload (up to 85%) was achieved – higher than the one obtained with the linear alternating copolymers, or dendrimer macromolecules. The platinum (II) complexes were released in sustained manner without initial burst effect. In vitro studies revealed lower cytotoxicity of the conjugates consistent with the sustained release of the agent and slower cellular uptake of the conjugated drug compared to that of free *cis*-platin.

Conclusions: Core–shell type star poly(meth)acrylates were synthesized using controlled radical polymerization via "core-first" approach, followed by acidic hydrolysis to obtain structures with polyacid arms. Light scattering investigations were performed to provide information about the size of stars in solution. In some cases, preliminary studies on immobilization of anticancer drug, *cis*-platine, were performed.

Acknowledgments: This work was done in the frame of Polish Ministry of Science and Higher Education grant no. N N209 100237.

References:

[1] Wang F. et al. Bioconjugate Chem 2005, 16, 397
[2] Zou J. et al. J. Phys. Chem. B 2006, 110, 2638
[3] Gillies E. et al. Pure App. Chem. 2004, 76, 1295.
[4] Kowalczuk A. et al. Polymer 2005, 46, 8555.
[5] Kowalczuk A. et al. J. Polym. Sci: Part A 2009, 47, 1120.

Water-Soluble Polymer-*grafted* Platinum Nanoparticles for the Subsequent Binding of Enzyme: Synthesis and SANS study.

Géraldine Carrot, François Gal, Henri Perez

LLB-LFP CEA/CNRS
IRAMIS- CEA/Saclay

geraldine.carrot@cea.fr

The convergence of nanoscience and biotechnology has showed an extensive development in the recent few years, particularly due to the attractive use of nanoparticles as a platform for various biological applications.[1] The unique properties of metal nanoparticles (NPs) together with well-reproductible synthetic and functionnalization procedures (surface-capping ligands), lead to a wide range of elementary building units for the construction of such hybrid structures. On the other side, biomolecules are interesting with their unique recognition, transport and catalytic properties. Therefore, conjugation of NPs with biomolecules could provide electronic transduction of biological phenomena, particularly beneficial for the development of biosensors.[2] Functionalized platinum nanoparticles (PtNPs) possess catalytic properties which represent a great interest in the elaboration of electrochemical biosensors. To improve the understanding of phenomena involved in such systems, we designed platinum-polymer-enzyme model structures, according to a bottom-up approach. These structures have been elaborated from 2-nm platinum nanoparticles grafted with polymer.[3]
In previous work, we have particularly showed that Surface-Initiated ATRP (*SI*-ATRP) of *n*-butyl methacrylate from PtNPs leads to polymer-*grafted*-PtNPs with controlled chain lengths. We also showed that free initiator was not necessary to maintain a good control of the surface polymerization. The platinum core is small enough with a sufficiently high grafting density of the initiator at the surface to be considered as a usual macroinitiator.
We therefore used the same method to polymerize *ter*-butyl methacrylate (*t*BuMA) because the polymer could further be hydrolyzed to generate poly(methacrylic acid) chains. Poly(methacrylic acid) (PMAA) cannot be polymerized directly from ATRP due to the complexation of copper with carboxylic acid groups. Routine characterization of the objects has been performed via thermogravimetric analysis and ^{1}H-NMR. The structure of these objects, the molecular weight and the grafting density of polymer chains were principally elucidated by small-angle neutron scattering (SANS). This technique is particularly well-adapted for the characterization of such multi-components materials (Figure 1). By using index matching, it is possible to study either preferentially the inorganic core, or the polymer chains. We particularly showed, the strong complementarities of SANS and chemistry, and particularly, how SANS could detect deviation or lead to characteristic data that other routine techniques could not. The polymer corona signal has been particularly studied in deuterated dimethylacetamide (*d*-DMAC).

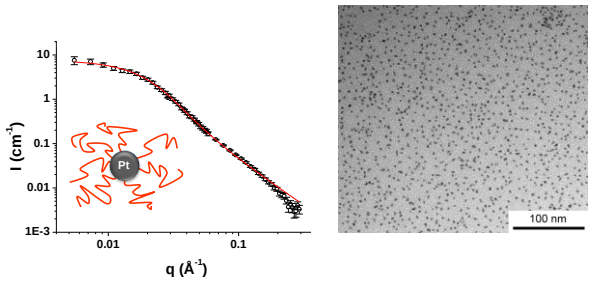

Figure 1. SANS spectrum of P(*t*BuMA)-*g*-PtNPs in *d*-DMAc and Transmission Electron micrograph of PtBuMA-*g*-PtNPs.

We therefore designed hybrid structures in solution through the modification of the poly (methacrylic acid)-*grafted* Pt nanoparticles (PMAA-*g*-PtNPs) to graft an enzyme via an activated ester reaction (Scheme 1).

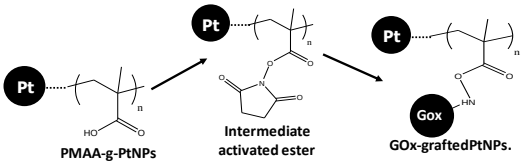

Scheme 1. Activation of the PMAA-*g*-PtNPs with *N*-hydroxy-succinimide (NHS) and subsequent grafting onto the glucose oxydase.

Both UV spectroscopy, SANS and SEM (scanning electron microscopy) will be used to characterise the structure of the hybrid nanostructure, after checking the remaining activity of the grafted enzyme.
To study the electrochemical properties of protein/polymer-*grafted*-PtNPs, it is necessary to transfer these nano-objects onto electrodes. Using Langmuir-Blodgett (LB) technique, we also elaborated two different thin-film architectures (LB films and polymer brushes) where enzymes were subsequently grafted. The control of the homogeneity, thickness and roughness was attested by neutron reflectivity measurements and TEM. After the physical characterization of these systems, the study of their electrochemical behavior towards H_2O_2 and glucose revealed significant differences due to their structure and their composition.

1. De, M.; Ghosh, P. S.; Rotello, V. M., *Adv. Mater.* **2008,** 20, 4225-4241.
2. Bahshi, L.; Frasconi, M.; Tel-Vered, R.; Yehezkeli, O.; Willner, I., *Anal. Chem.* **2008,** 80, 8253-8259.
3. Carrot, G.; Gal, F.; Cremona, C.; Vinas, J.; Perez, H., *Langmuir* **2009,** 25, 471-478.

Full Exfoliation of Clay and Nanocomposite Preparation

Youngwook P. Seo[1], Kyounghwan Oh[1], Yongsok Seo[1], Soon Man Hong[2]*

[1]ITRC & Department of Materials Science and Engineering, Seoul National University, Seoul, Korea
[2] Hybrid Materials Research Center, Korea Institute of Science and Technology, Seoul, Korea

ysseo@snu.ac.kr

Introduction

In this study, we explore further the role of nanoclay particles in the foaming of PP/clay nanocomposites.[1,2] The nanoclay particles were doing dual role as a nucleating agent for CO_2 gas or fluid and polypropylene molecules. We tried to figure out the relation between the cell generation and the processing variables.

Experimentals

Polypropylene terpolymer (poly(propylene-co- ethylene -co-1-butene), with a composition of 94.5wt% of polypropylene unit, 3wt% of ethylene unit, and 2.5wt% 1-butene unit, was obtained from Honam Petrochemicals Co. (Korea). Foamed terpolymer was prepared by injecting out the blowing-agent submerged terpolymer particle in an autoclave through a nozzle. In order to aid the compatibilization between PP terpolymer and the annoclay particles, small amount of maleic anhydride grafted polypropylene (MAPP) was added. Surface modified monmorillinite (Cloisite 20A, Southern Clay) was used. Terpolymer and premade master batch were mixed in a twin screw extruder (Prism) and extruded. Weight ratio between the matrix polymer and the master batch compound was controlled to set the clay amount s 0.2 wt% and 1wt%.

Results and Discussion

Small angle X-ray diffraction (SAXD) patterns for pristine organoclay 20A, two sc CO_2 foamed nanocomposites are illustrated in Figure 1 (0.2 wt% of clay)). Unfoamed samples show a diffraction peak of Cloisite 20A. The peak of unfoamed sample is shifted to lower angle compared to that of clay, which indicates that unfoamed samples have intercalated morphology. This expansion could be attributed to the diffusion of CO_2 and compatibilizer polymer chains into the clay galleries. SAXD patterns of all foamed samples show no peaks, which indicate full exfoliation of the nanoclay particles. The samples foamed under the subcritical condition show no peak at all. This means the foaming by CO_2 caused the exfoliation. The polymer chains are not in the fully melt state in this condition. This means that further smearing of polymer molecules into the gallery was not the cause of exfoliation or most of the exfoliation was done by the CO_2 molecules adsorption and growth by later pressure release.

Figure 2 shows the cell morphology of the foamed structure of PP and three composite samples. The pure PP foam has but smaller than composite foamed one. All the foaming temperatures were lower than the melting temperature of PP at the applied pressure, hence the crystal lamellae later split by the cell growth to form the walls of the cell. Nanocomposites show uniform cell size.

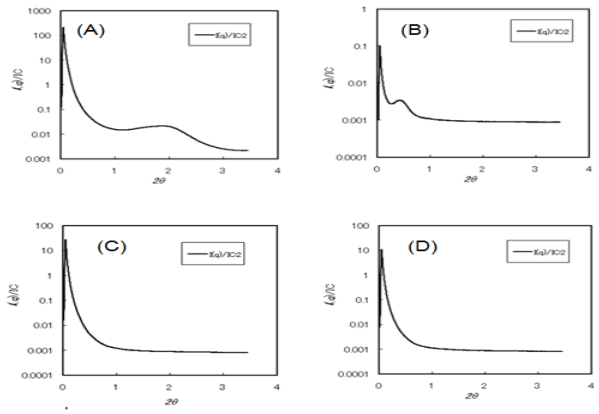

Figure 1. SAXS pattern for (A) Cloisite20A (B) Unfoamed (C) Subcritical CO_2 (D) Supercritical CO_2

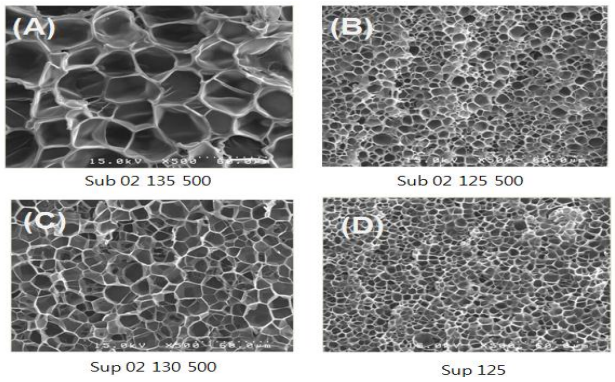

Figure 2. SEM photos of the fractured surfaces (A) Sub CO_2 (135°C foaming), (B)Sub CO_2 (125°C foaming), (C) Sup CO_2 (130°C foaming), (D) PP Sup CO_2 (125°C foaming).

Conclusions

The SAXD analyses showed that the foaming process facilitates dispersion of clay particles. Fully exfoliated structures were obtained for all foamed samples. Clay layers provide more heterogeneous nucleating sites for foaming. Nanocomposites of better dispersion of clay platelet produces more cells and more uniform structure. More details will be presented at the conference.

Acknowledgements

Support from SNU CTL Undergraduate Research Program as well as ITRC through ERC program (RIAM R11 - 2005-065) is greatly appreciated.

References

[1] Q. T. Nguyen, D. G. Baird *Polymer* 48, 6923 (2007)
[2] Y. Seo, T. Kang, S. Hong, H. Choi *Polymer* 48, 3844 (20007)

Synthesis and Study of Random Amphiphilic Polymers for Molecular Encapsulation of Pyrene and Clofazimine

Marc-Alexandre SCHOTT [a], *Christel BARBAUD* [b], *Jean COUDANE* [a], *Dominique DOMURADO* [a]

[a] Institut des Biomolécules Max Mousseron (IBMM), Artificial Biopolymer Team, UMR CNRS 5247, Université Montpellier 1, Université Montpellier 2 Faculté de Pharmacie, 15 avenue Charles Flahault 34093 Montpellier cedex 5

[b] Laboratoire de Bio-ingénierie des Polymères Cardio-vasculaires (LBPC), Institut Galilée, INSERM U698, Université Paris 13, 99 avenue Jean-Baptiste Clément 93430 Villetaneuse

e-mail : marc-alexandre.schott@univ-montp1.fr

Introduction

For more than twenty-five years, random amphiphilic polyelectrolytes have been known to enhance the apparent water solubility of highly hydrophobic compounds[1,2]. Poly(dimethylmalic acid) (PDMMLA), a degradable polymer, polyanionic at neutral pH, can be easily obtained in a partially hydrophobized form through copolymerization of malolactones with different pendant aliphatic or aromatic groups[3,4].

In this work, we synthesized various malolactones to obtain a range of amphiphilic copolymers with varying hydrophobic substituent rate and chain length. The influence of these parameters, of pH and of the presence of sodium chloride upon the apparent solubility of pyrene and clofazimine in aqueous solutions of these polymers was studied.

Materials and methods

The monomers and polymers were synthesized following the method described by Barbaud *et al.*[3,4] adapted to the ratios and side chains used in this work.

Molecular weight determinations were done by SEC analysis in THF, with PS as a standard.

Results and discussion

The monomers (fig.1a) were obtained from commercial diethyloxalpropionate in five steps with yields of 15-20%, in accordance with litterature.

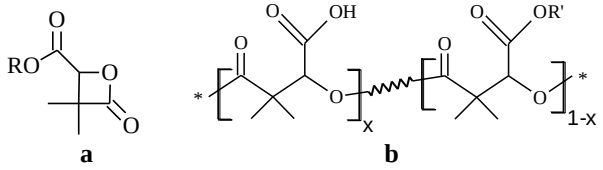

a **b**

Figure 1 : PDMMLA monomers (a) and polymers (b)
R = benzyle, hexyle or decyle
R' = hexyle or decyle

Ring opening copolymerization of the benzylated and either hexylic or decylic lactones with defined ratios followed by hydrogenolysis yielded the desired random copolymers (fig.1b), with molecular weights ranging from 50,000 to 150,000 and polydispersity between 1.1 and 1.3. ^{1}H-NMR spectra confirmed that the hydrophilic-hydrophobic ratios corresponded to the initial ratios of the lactones.

As expected, solubility studies monitored by UV-visible spectroscopy showed that water solubility for both pyrene and clofazimine was improved by increasing the hydrophobicity of the polymer. However, the solubility in moles of hydrophobic compound per mole of monomeric unit was up to ten times higher for clofazimine than for pyrene. For the latter, solubilization is achieved solely by hydrophobic interactions with the polymer side groups, whereas for clofazimine, which is polar and protonable, there is a combination of both hydrophobic and electrostatic interactions with the negatively charged polymer.

The presence of sodium chloride increased the solubility of pyrene, but decreased the solubility of clofazimine (fig.2). In the case of pyrene, shielding the charge of the polymer allows the latter to coil more, and to form bigger hydrophobic domains where pyrene can solubilize. The charge on clofazimine is also shielded by the salt, thus resulting in a weaker interaction with the polymer and a poorer apparent solubility. This confirms the major role of charge interaction in the solubilization of clofazimine.

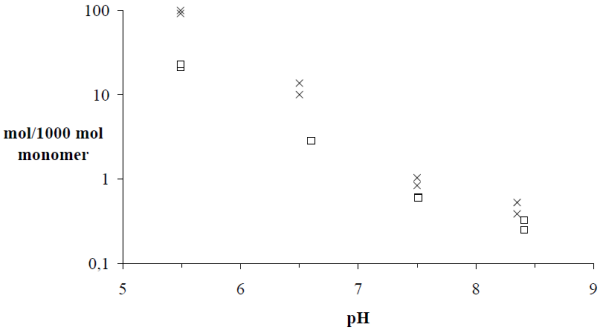

Figure 2 : Apparent solubility of clofazimine in a 1% solution of 30%-hexylated PDMMLA with (▫) or without (×) sodium chloride

Conclusion

Degradable PDMMLA derivatives improved the apparent water solubility of pyrene and clofazimine, with or without sodium chloride. However, it is still lower than with non-degradable poly(methyl vinyl ether-*alt*-maleic acid) derivatives[2].

Future work will aim at synthesizing more hydrophobic degradable copolymers with other side groups, in order to further increase the solubility of these compounds. Analyses are also under way to characterize the objects formed in solution, notably to determine if monomolecular or polymolecular micelles are involved.

[1] J. Huguet *et al.*, *J. Controlled Release*, **1985**, *1*, 217.
[2] I. Hernandez-Valdepeña, *et al.*, *Eur. J. Pharm. Sci.*, **2009**, *36*, 345.
[3] C. Barbaud *et al.*, *Des. Monomers Polym.*, **2003**, *6*, 353.
[4] C. Barbaud *et al.*, *Macromol. Chem. Phys.*, **2004**, *205*, 199.

Modification of the Electrical Properties of TPU by Modified Expanded Graphites

Jürgen Pionteck, Francesco Piana

Leibniz Institute of Polymer Research Dresden, Dept. Polymer Reactions and blends
Hohe Str. 6, 01069 Dresden Germany

pionteck@ipfdd.de

Introduction: For some applications it is necessary that polymers exhibit a certain degree of conductivity, which can be reached by mixing conventional isolating polymers with electrically conductive fillers. We analyzed the influence of the processing conditions of nano-composites based on thermoplastic polyurethanes (TPU) and expanded graphite (EG) or graphene oxide (GO) on their properties with focus on the electrical conductivity.

Materials and Methods: The TPUs used were commercial products from Elastolan varying in hart segment content, polarity and crystallinity, and self-made TPU based on diisocyanates (MDI, H12-MDI, or IPDI) and 1,4-butanediol (forming the hart segments) and PTHF as soft segment.
Melt mixing was done by means of a DSM 5 mL Microextruder in a one step process or in a two step process, preparing first a masterbatch from solution followed by diluting the masterbatch to the desired EG concentration by melt mixing with pure TPU. The composites were compression molded to 1.5 or 1 mm thick plates for testing electrical and mechanical properties, respectively. TPU composite powder mixtures were obtained by dissolution of TPU in an EG/DMAc dispersion followed by precipitation in ethanol. In-situ TPU/EG composites were obtained by dispersion of the graphites in the PTHF/BD mixture, which was then polymerized after addition of the diisocyanate. In all cases sonic treatment was used to improve the graphite dispersion.

Results and Discussion: When melt mixing, the TPU with the highest Shore hardness (C74D50) gave a conductivity of 1.3 10^{-5} S/cm already at 2 wt.% EG content, while the percolation concentration of the other TPU (1185A, S60A15) was between 6 and 4 wt% EG. Interestingly, at higher EG concentrations of up to 10 wt% the conductivity increased just slightly. Precipitated powder mixtures containing 10 wt.% EG exhibit higher conductivities than the extruded composites, in case of C74D50 as high as 0.07 S/cm. Using these composites as masterbatch for the preparation of composites containing 2 to 8 wt.% EG by melt mixing resulted in somewhat lower conductivities when compared to the directly melt mixed composites of the same composition (Fig. 1).
There is a strong influence of the melt-mixing conditions on the conductivity, as shown exemplary for composites in Fig. 2.

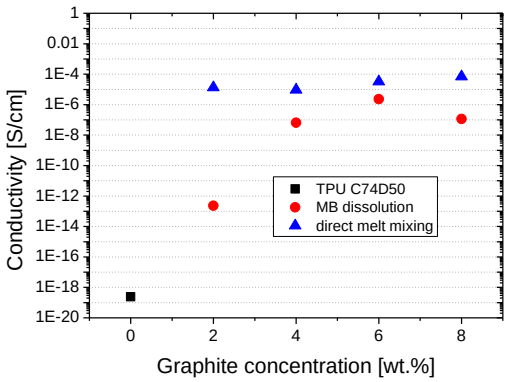

Figure 1: Conductivity versus filler content of TPU C74D50/EG composites prepared by direct melt mixing or by dissolution of the precipitated master batch

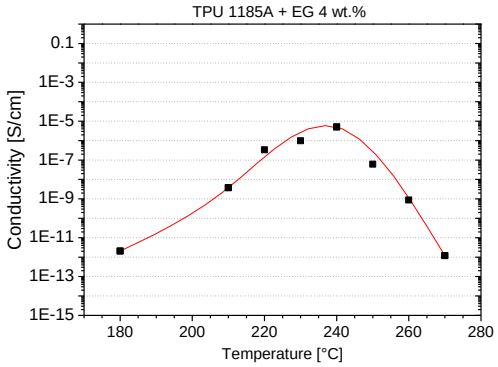

Figure 2: Dependence of conductivity of TPU 1185A containing 4 wt.% CNT on melt-temperature

The in-situ syntheses of TPU/EG composites resulted in materials with rather poor conductivities, widely independent of the used diisocyanates and composition. There seems to be no big influence of the aromaticity, polarity and crystallinity on the electrical behaviour of the composites. These effects and the use of oxidized graphites are still under investigation.

Acknowledgements: We are grateful for the support of the project by the Deutsche Forschungsgemeinschaft (DFG) and to SGL Carbon for providing the graphites.

Processing and Properties of Carbon Nanotube-Polymer Composite Fibers

C. Mercader, A. Lucas, P. Miaudet, A. Derré, M. Maugey, P. Poulin, C. Zakri

University of Bordeaux / Centre de Recherche Paul Pascal – CNRS– 115, avenue Schweitzer – 33600 Pessac – France

zakri@crpp-bordeaux.cnrs.fr

In nanocomposite materials, the final properties are strongly related to the distribution of the carbon nanotubes (CNTs) inside the polymer matrix, adding new performances to the material. To a certain extent, the composite structure can be tuned during processing, through the control of the dispersion or interactions between the nanotubes and the polymer, and the spatial re-arrangement of the structure. Trying to aim these objectives, our team has been working for several years on dispersion and processing of CNTs into various composites, like films, coatings and fibers [1].

The presentation will be dedicated to the synthesis and properties of carbon nanotube fibers. We spin CNT fibers by a coagulation process which consists in injecting a CNT dispersion in a poly(vinyl) alcohol solution (PVA) [2]. The method has been scaled-up and a new pilot for continuous production has recently been set-up. Moreover, an original method has been developed in order to characterize the strength of the fiber during the process [3]. This in-situ characterization method can be extended to various fiber processes, as many synthetic or natural polymer fibers are produced via the transformation of a liquid solution into a solid filament.

The fibers we obtain via this wet-spinning process have a nanocomposite structure with a large fraction of oriented CNTs and polymer. They exhibit electrical conductivity and exceptional mechanical properties. With strain to failure up to 450%, the energy needed to break the fibers exceeds that of any other known materials. We will discuss the different routes we follow to increase the electrical, structural and mechanical properties of these fibers, leading to markedly improved energy absorption and new thermo-mechanical properties [4,5].

[1] S. Badaire *et al.*, Langmuir 2004, 20, 10367 ; B. Vigolo *et al*, Science 2005, 309, 920 ; K. Saint-Aubin *et al.*, Langmuir 2009, 25-22,13206.
[2] B. Vigolo *et al*, Science, 2000, 290, 1331.
[3] C. Mercader *et al.*, PNAS 2010, 107-43, 18331.
[4] P. Miaudet *et al*, Nanoletters, 2005, 5, 2212.
[5] P. Miaudet *et al*, Science, 2007, 318, 1294.

Phase Behavior and Structure Formation under Fast Cooling of Syndiotactic Poly(propylene) Nucleated with 1,3:2,4-bis(3,4-dimethylbenzylidene)sorbitol

A.M.J.T. Meijer-Vissers, J.G.P. Goossens

Eindhoven University of Technology, Department of Chemical Engineering and Chemistry, Laboratory of Polymer Technology, P.O. Box 513, 5600 MB Eindhoven, The Netherlands

A.M.J.T. Meijer-Vissers@tue.nl

Syndiotactic poly(propylene) (s-PP) has some interesting properties such as high ductility and high optical transparency. However, it is less commercially successful than isotactic poly(propylene) (i-PP). This is mainly a result of the fact that it is a slow-crystallizing polymer.[1]

One way to improve this is by adding nucleating agents. Nucleating agents are a family of additives which are used to speed up processing rates of polymers by providing more nucleation sites and therefore reducing the cycle time. In the case of i-PP, 1,3:2,4-bis(3,4-dimethylbenzylidene)sorbitol (DMDBS) is a very efficient nucleating agent and so-called clarifying agent. Since DMDBS is a polar molecule, and i-PP is fully apolar, this leads to a rich phase behavior when i-PP and DMDBS are mixed together. From the application point of view, the most interesting concentration regime extends from ~ 0.1 wt% to 1 wt% of DMDBS, where i-PP exhibits a high clarity and low haze. In this regime, the temperature at which gelation occurs depends on the concentration of the additive,[2] which also governs the mechanical properties.[3] Further, the main crystal modification found for i-PP/DMDBS systems is the α-modification.

Previous research showed that DMDBS can also nucleate s-PP.[4] In this study, we investigate the phase behavior of s-PP with DMDBS. The cooling rates that are generally employed are 5-20 °C/min. However, polymers solidify under actual processing conditions at cooling rates which can range from only a few to hundreds of degrees Celcius per second, which is far beyond those accessible by common laboratory instrumentation.

Fast cooling results in the development of structural order at extreme undercooling and, for some polymers, this leads to formation of metastable states. The development of the mesophase in i-PP based materials was recently studied by Cavallo et al. through continuous cooling curves (CCC) diagrams.[5] In a similar fashion, we constructed continuous cooling curves for several blends of s-PP and DMDBS during fast cooling with in-situ WAXD.

Acknowledgement

This study is part of the Research Program of the Dutch Polymer Institute (DPI) project #708. We acknowledge L. Gardella and prof. G. Alfonso (University of Genova) for the use of the cooling unit and dr. G. Portale and dr. D. Hermida Merino (DUBBLE@ESRF) for assistance during the WAXD experiments.

References

[1]Supaphol, P.; Spruiell, J.E. J. Appl. Polym. Sci. 2000, 75, 44-59.

[2]Kristiansen, M.; Werner, M.; Tervoort, T.; Smith, P.; Blomenhofer, M.; Schmidt, H.-W. Macromolecules 2003, 36, 5150-5156.

[3]Kristiansen, M.; Tervoort, T.; Smith, P.; Goossens, H. Macromolecules 2005, 38, 10461-10465.

[4]Supaphol, P.; Charoenphol, P.; Junkasem, J. Macromol. Mater. Eng. 2004, 289, 818–827.

[5]Cavallo, D.; Azzurri, F.; Floris, R.; Alfonso, G.C.; Balzano, L., Peters, G.W. Macromolecules 2010, 43, 2890-2896.

Study of the Effect of Carbon Nanofillers on the Foaming Evolution of Polyurethane Foams

M. Mar Bernal[1,2], *Anne-Cecile Mortamet*[2], *Miguel Angel López Manchado*[1], *Anthony J. Ryan*[2], *Raquel Verdejo*[1]

[1]Institute of Polymer Science and Technology, (CSIC), Madrid, Spain
[2]Department of Chemistry, University of Sheffield, Sheffield, UK

mbernal@ictp.csic.es

Introduction

The use of nano-sized fillers in polymer foams provides unique thermal, electrical and mechanical properties compared to conventional micro-sized fillers, which cannot be accommodated in the cellular structure of the foams.[1] Polymeric foams are important and versatile materials which account for 10% of the total volume of polymer market share. Foams have outstanding strength to weight ratio, resilience, electrical, thermal, and acoustic insulating properties, among other characteristics.[2]

Materials and Methods

Flexible polyurethane foams are produced by the exothermic reaction of a diisocyanate with polyether polyol (gelling reaction) and water (blowing reaction). These reactions form a segmented block copoly(urethane-urea) and carbon dioxide gas which is responsible for the foam formation.[3] Two series of PU foams were synthesised with 25% and 32.5% of hard segment (HS) by adjusting the water and isocyanate content.

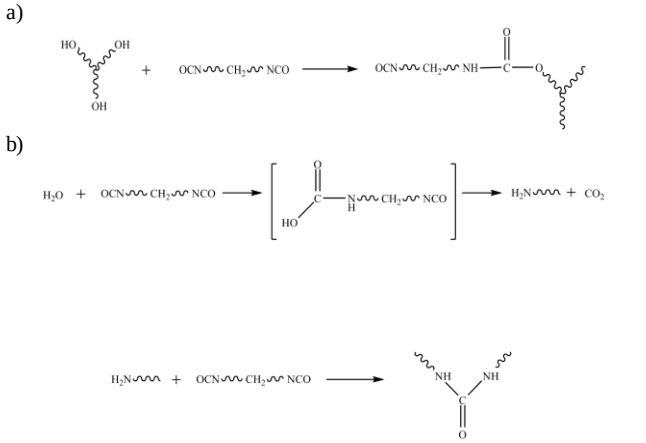

Scheme 1. Chemistry of PU foams: a) Gelling reaction and b) Blowing reaction.

Carbon nanotubes (CNTs) were synthesised in-house by a chemical vapour deposition (CVD) process[4] from the decomposition of ferrocene-toluene vapour injected at 5ml/h under an inert atmosphere at 760ºC. Functionalisation of CNTs was carried out in a mixture of acids at 120ºC for 30 minutes and then filtered with distilled water until neutral pH. Functionalised graphene sheets (FGS) were produced from the adiabatic expansion at 1000ºC of graphite oxide under argon atmosphere[5]. Nanofillers were mixed in the polyol to achieve a good dispersion before adding the isocyanate.

A fixed concentration, 0.5 pphp in polyol, of carbon nanofillers was selected for comparison purposes.

Results and Discussion

Polymerisation kinetics as well as hydrogen bonding development were analysed by FT-IR in order to gain an understanding of the effect of carbon nanofillers on the rate of reaction and the structure development of the resultant PU foams. The reaction kinetics was strongly influenced by the HS content and the decrease in the rate and isocyanate conversion was ascribed to an increase in the viscosity of the systemand, hence, a restriction of the chain mobility due to the larger HS content. At equivalent HS content, the onset of microphase separation (MST) occurred at an earlier isocyanate conversion for foams filled with carbon nanofillers compared to the unfilled foams. From SAXS data we observed that the average distance in samples with 32.5% HS content was affected by the presence of carbon nanofillers while no differences were observed for samples at 25% HS content.

Conclusions

Carbon nanofillers with different morphology and functionality delayed the onset of microphase separation of flexible polyurethane foams without significantly changing the interdomain spacing. Hence, carbon nanofillers affected the reaction kinetics of the polymerisation reaction but not the final morphology of the nanocomposite foams. Thus, any changes on the mechanical properties of this type of system would be related to reinforcing effect of the fillers rather than a change of the microstructure.

References

1. Xu, J. H.; Chatterjee, S.; Koelling, K. W.; Wang, Y. R.; Bechtel, S. E. *Rheol. Acta* **2005,** 44, (6), 537-562.
2. Klempner, D.; Sendijarevic, V., *Handbook of polymeric foams and foam technology*. Hanser Publishers: 2004.
3. Elwell, M. J.; Ryan, A. J.; Grunbauer, H. J. M.; VanLieshout, H. C. *Polymer* **1996,** 37, (8), 1353-1361.
4. Singh, C.; Shaffer, M. S. P.; Windle, A. H. *Carbon* **2003,** 41, (2), 359-368.
5. Verdejo, R.; Barroso-Bujans, F.; Rodriguez-Perez, M. A.; de Saja, J. A.; Lopez-Manchado, M. A. *Journal of Materials Chemistry* **2008,** 18, (19), 2221-2226.

Crystallinity and Chain Conformations in Polymer / Layered Silicate Nanohybrids

K. Chrissopoulou,[1] *K. Andrikopoulos*,[2] *S. Bollas*,[1] *S. Fotiadou*,[1,3] *G. Voyiatzis*,[4] *and S. H. Anastasiadis*[1,5]

[1]Institute of Electronic Structure and Laser, Foundation for Research and Technology-Hellas, Heraklion Crete, Greece
[2]Physics Division, School of Technology, Aristotle University of Thessaloniki, Thessaloniki, Greece
[3] Department of Chemical Engineering, Aristotle University of Thessaloniki, Thessaloniki, Greece
[4] Institute of Chemical Engineering and High Temperature Chemical Processes, Foundation for Research and Technology-Hellas, Patras, Greece
[5]Department of Chemistry, University of Crete, Heraklion Crete, Greece

kiki@iesl.forth.gr

Introduction: Polymer / layered silicate nano-composites constitute an interesting class of materials which allow the investigation of basic scientific problems and, at the same time, are utilized in many applications.[1] Mixing polymers with layered inorganic materials can lead to three types of structure, depending on the interactions between the two components: the phase separated, where the two components are immiscible, the intercalated, in which the polymer chains reside within the inorganic galleries forming thin polymer films, and the exfoliated one, where the interactions between the chains and the surfaces are very favorable so that the inorganic layered structure is destroyed resulting in dispersed platelets within the polymer matrix.[2] Despite the large number of studies in this area,[3,4] the influence of the addition and the state of dispersion of the nanofillers on chain conformation and/or crystallization has been largely overlooked. In this work, we aim to systematically study the effect of incorporation of inorganic material and/or elucidate the influence of the severe confinement on the structure and conformations of polymer chains in PEO / Na^+-MMT nanohybrids.[5]

Materials and Methods: Poly(ethylene oxide), PEO, with molecular weight M_w=100,000 gr/mol, glass transition temperature, T_g, -67°C and melting temperature, T_m, of 65°C, was utilized and mixed with a hydrophilic montmorillonite, Na^+-MMT (Southern Clay). The nanocomposites were prepared by direct melt intercalation; the two components were mixed in the appropriate amounts, grinded in a mortar to get a fine powder and annealed in a vacuum oven at 100°C for 2 days. A series of composites with PEO content that covers the whole regime from pure polymer to pure clay were prepared and were characterized by X-ray diffraction, XRD, and differential scanning calorimetry, DSC. Moreover, the conformations of the polymer chains in the crystal and in the amorphous state were investigated utilizing Raman and infrared spectroscopi.

Results and Discussion: XRD measurements reveal that for all hybrids, intercalated nanocomposites with mono- and bi-layers of PEO chains are obtained. Moreover, for nanohybrids with low polymer concentration, where all polymer chains are intercalated or in close proximity to the inorganic surfaces, the peaks that correspond to the crystalline structure of PEO can not be observed indicating that PEO is purely amorphous. It is only when there is plenty of excess polymer outside the completely filled galleries that polymer crystallization is observed. In agreement with XRD, DSC measurements show the melting and crystallization transitions only for hybrids with high polymer content. To investigate the conformations of the chains in the hybrid material in relation to that of pure PEO more quantitatively, Raman and IR spectroscopy have been applied.

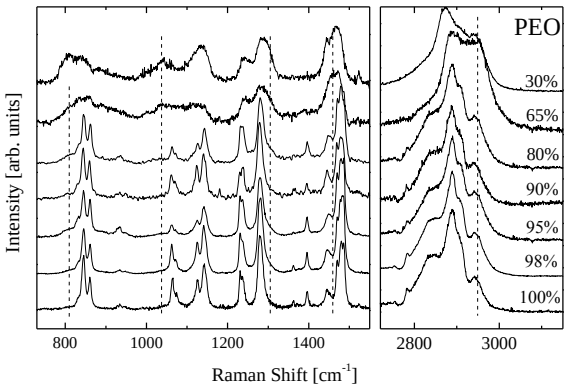

Figure 1: Raman spectra of PEO and of PEO / Na^+-MMT nanohybrids with different polymer content at 25°C.

Figure 1 shows Raman spectra of nanohybrids with different compositions, which show that, indeed, it is only at high polymer concentrations that the sharp peaks attributed to crystalline PEO are observed. Moreover, quantitative analysis reveals that the intercalated chains are more disordered and liquid-like than even the PEO melt measured at higher temperatures.

References

[1] Giannelis, E. P. et al., *Adv. Polym. Sci.* **138**, 107 (1999); Usuki, A. et al., *Adv. Polym. Sci.* **179**, 135 (2005).
[2] Giannelis, E. P. *Adv. Mater.* **8**, 29 (1996).
[3] Chrissopoulou, K. et al., *Polymer* **46**, 12440 (2005); Chrissopoulou, K. et al., *J. Polym. Sci. Part B : Polym. Phys.* **46**, 2683 (2008).
[4] Anastasiadis, S. H. et al., *Phys. Rev. Lett.* **84**, 915 (2000); Elmahdy, M. M. et al., *Macromolecules* **39**, 5170 (2006) ; Chrissopoulou, K. et al., *J. Chem. Phys.* **127**, 144910 (2007); Fotiadou, S. et al., *J. Polym. Sci. Part B : Polym. Phys.* **48**, 1658 (2010).
[5] Chrissopoulou, K. et al., *submitted*.

Acknowledgements: Part of this research was sponsored by the Greek GSRT (ΠΕΝΕΔ 03ΕΔ581 and ΣΥΝΕΡΓΑΣΙΑ 09ΣΥΝ-42-580), by the European Union (grant agreement CP-IP 246095-2) and by NATO Scientific Affairs Division (Science for Peace Programme).

New Hybrid Core-Shell Star-Like Architectures Made of Poly(n-butylacrylate): Synthesis and Properties.

Sandrine Pensec[1], *Fabien Périneau*[1,2], *Guangjun Hu*[3], *Laurence Rozes*[2], *François Ribot*[2], *Clément Sanchez*[2], *Costantino Creton*[3], *Laurent Bouteiller*[1]

[1] *UPMC* Univ Paris 06, *UMR 7610 CNRS, Chimie des Polymères*, 3, rue Galilee, *F*-94200 Ivry, *France*
[2] UPMC Univ Paris 06, UMR 7574, Chimie de la Matière Condensée de Paris, Collège de France, 11 place Marcelin Berthelot, F-75005 Paris, France
[3] Physico-Chimie Des Polymères Et Des Milieux Dispersés, UMR 7615, UPMC-CNRS-ESPCI, 10 Rue Vauquelin 75231 Paris Cedex 05

sandrine.pensec@upmc.fr

The preparation of organic/inorganic hybrid materials composed of organic polymers and inorganic components are described as a route to combine and even increase the advantageous properties of both classes of molecules in one material. A particularly attractive strategy to build nanostructured hybrid materials is based on the use of well-defined clusters that keep their molecular integrity and therefore their intrinsic properties during the assembly of superstructures. For example, a recent approach is based on the use of molecular titanium oxo-clusters, which constitute structurally well defined nanosized building blocks. These titanium oxo-clusters have well defined size and shape, and their surface can be chemically modified in order to bear functional ligands for further hybrid materials elaboration. In the case of $Ti_{16}O_{16}(OEt)_{32}$ cluster for example, the ethoxyde group present at the surface of the metallic oxo-core could be exchanged by transalcoholys reactions.[1] The present work will report the design of a hybrid star-like architecture by post-modification of a titanium oxo-cluster with polymer chains following the grafting onto and grafting from strategies.[2] In the second strategy, starting from a well-defined multifunctional titanium oxo-cluster initiator, a "grafting from" approach based on atom transfer radical polymerization (ATRP) has been develop. Conditions to prevent possible side reactions between monomer, polymer and titanium oxo-cluster ligands will be discussed. The kinetics of polymerization and the final structure will be carefully investigated. Rheological properties of the materials will be also described.[3]

1. Fornasieri, G.; Rozes, L.; Le Calve, S.; Alonso, B.; Massiot, D.; Rager, M. N.; Evain, M.; Boubekeur, K.; Sanchez, C. *J. Am. Chem. Soc.* **2005**, 127, 4869-4878.
2. Périneau, F.; Pensec, S.; Sassoye, C.; Ribot, F.; Van Lokeren, L.; Willem, R.; Bouteiller, L.; Sanchez, C.; Rozes, L. *J. Mater. Chem.*, **2011**, DOI 10.1039/c0jm04047a.
3. Périneau, F. ; Hu, G. ; Rozes, L. ; Ribot, F. ; Sanchez, C. ; Creton, C. ; Bouteiller, L. ; Pensec, S., submitted.

Crystallization in Co-continuous Nanostructured Blends and Composites

Sylvie Tencé-Girault, Léa Gani, Thomas Périé, Ludwik Leibler

Matière Molle et Chimie (ESPCI-CNRS, UMR 7167), ESPCI ParisTech
10 rue Vauquelin 75005 Paris - France

sylvie.girault@espci.fr

Co-continuous thermodynamically stable nanostructured blends of functionalized polyolefin (FPE) and polyamide-6 (PA6) have been designed and synthesized by reactive blending[1,2]. The grafting reaction occurs between the PA6 amino end-group and maleic anhydride units randomly distributed along the backbone of FPE. Depending on the chemical structures of FPE and PA6, blends with various nanostructures are obtained. These blends exhibit both solvent resistance and outstanding mechanical properties at low and high temperatures.
First, the relationship between these attractive properties and the structure and crystallization at the nano and micro-scales is studied. Then, we show that these blends are particularly nice matrices for carbon nanotubes (CNT) composites.

Due to the high reactivity of the maleic anhydride / amino couple, a large amount of graft copolymers is created *in-situ* during the reactive extrusion. As the two components of this graft copolymer are incompatible, a nanostructure is formed. The polydispersity of the backbone and the grafts helps to stabilize a co-continuous disordered structure and facilitates the incorporation of the unreacted homopolymers in the nanostructure. While keeping the PA6 as minority phase, the co-continuous nanostructure is observed in a wide composition range (Figure 1).

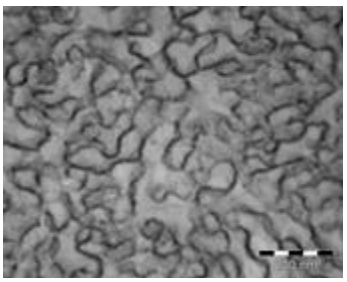

Figure 1: Morphology of a FPE/PA6 80/20 wt % blend observed by TEM (PA6 in black).

The blend is transparent and crystalline. Two melting temperatures are observed at 87°C and 216°C, attributed to the FPE and the PA6, respectively. The blend exhibits outstanding solvent resistance and thermo-mechanical properties. Indeed, with a low amount of PA6 (20 wt %) the blend does not flow at the melting temperature of the majority phase, FPE, but at 200°C. Morever, a storage modulus of 7MPa is measured between the two melting temperatures. These properties are due to the crystallization of the PA6. A crystallization study enables us to propose a model for the organization of graft copolymer and homopolymer chains in the co-continuous structure (Figure 2). PA6 crystallizes in a lamellar morphology inside the co-continuous nanostructure, it is confined in thin domains of 12 nm thickness. FPE crystallizes in this morphology as well.

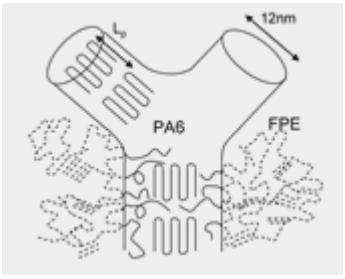

Figure 2: Schematic representation of the FPE and PA6 chains in the blend.

CNT are dispersed in these blends by melt blending in a micro compounder. On the TEM picture of the composite, we still observe the continuous PA6 phase (Figure 3). CNT are not confined in one phase, but they cross over the two phases FPE and PA6.

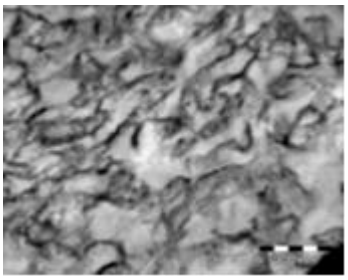

Figure 3: TEM image of the composite morphology (PA6 in black).

The mechanical and electrical properties of the composite are significantly enhanced by the CNT incorporation. This is due to a double interconnected network: a network of crystalline PA6 with high melting temperature and a conducting CNT network. The crystallinity of the blend is preserved and the formation of trans-crystalline lamellae of PA6 surrounding the nanotubes in confined domains is observed.

[1] H. Pernot, M. Baumert, F. Court, L. Leibler; Nature Materials, 2002, 1, 54-58
[2] L. Gani, S. Tencé-Girault, M. Milléquant, S. Bizet, L. Leibler; Macromol. Chem. Phys. 2010, 211, 736–743

The authors thank EU in the frame of the 7th Framework Program research project ''HARCANA'' (GrantAgreement No: NMP3-LA-2008-213277), the ESPCI-ParisTech and Arkema for financial support.

Electrical conductivity of carbon nanotube/polymer composite fibers in extensional shear

F. Grillard [1], *C. Zakri* [1], *P. Poulin* [1], *A. Korzhenko* [2], *P. Gaillard* [2]

[1] Centre de Recherche Paul Pascal, CNRS UPR 8641, Avenue du Dr Schweitzer, 33600 Pessac, France
[2] Groupement de Recherches de Lacq – ARKEMA, BP 34, RN 117, 64170 Lacq, France

grillard@crpp-bordeaux.cnrs.fr

Because of their high aspect ratio and small size, carbon nanotubes (CNTs) are well-suited for the inclusion in textile polymer fibers. CNTs intrinsically exhibit remarkable mechanical properties [1,2] and are electrically conductive [3]. They are therefore promising candidates to develop new composite fibers with improved properties and novel functionalities potentially useful in several industrial textile applications. We investigated in this work the properties of melt spun CNTs/polymer composite fibers.

First, CNTs and polymer are mixed via an extrusion process at high temperature. Homogeneous mixing is critical in order to achievable spinnable materials. The melt spinning device is composed of a single-screw extruder, two winders separated by an oven and a wind-up roll to collect the fiber at the end of the process. Several parameters can be varied such as screw extruder speed, the extruder temperature, the winding apparatus speed or the post-drawing ratio (ratio between the second and the first winding apparatus speed). The fiber production and processing are associated to fiber elongation in strong extensional flow fields. Those physical mechanisms strongly affect the structure and properties of the fibers. In particular, electrical characterizations show a great increase of the resistivity with the fiber elongation rate. According to X-ray scattering measurements, this decrease is not dominated by the orientation of CNTs as observed in other nanocomposites [4,5,6]. We discuss other effects of structural changes and consider variations of inter-tube contact probabilities. We propose an analytical model that quantitatively accounts for the observed variations of resistivity. The progresses achieved in this work should allow a much better control of the properties of fibers and other CNT composites produced by extrusion processes.

[1] F. Yu, B.S. Files, S.Arepalli, R.S. Ruoff, Phys. Rev. Lett., 84, 5552 (2000)
[2] M. Yu, O. Lourie, M.J. Dyer, T.F. Kelly, R.S. Ruoff, Science, 287, 637 (2000)
[3] T.W. Ebbesen, H.J. Lezec, H. Hiura, J.W. Bennett, H.F. Ghaemi, T. Thio, Nature, 382, 54 (1996)
[4] F. Du, J.E. Fischer, K.I. Winey, J.Polym Sci, Part B : Polym Phys 41 (2003) 3333-3338
[5] F. Du, J.E. Fischer, K.I. Winey, Phys. Rev. B 72 (2005) 121404
[6] S.I. White, B.A. DiDonna, M. Mu, T.C. Lubensky, K.I.Winey, Phys. Rev. B 79 (2009) 024301

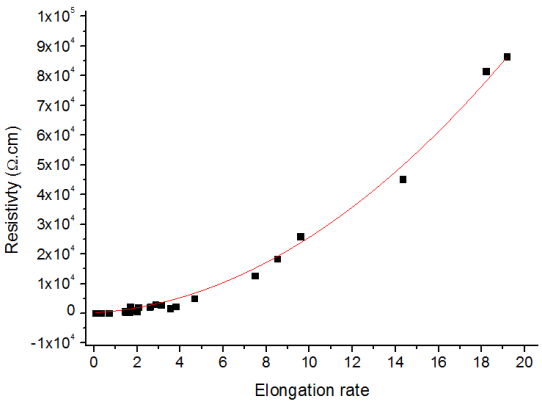

Figure: Electrical resistivity as a function of elongation rate (experimental results: black points, theoretical model: red curve)

Maleinized Polybutadienes as Clay Modifiers for SBR-based Rubber Nanocomposites

G. Colucci[1], R. Bongiovanni[1], A. Priola[1], M. Alessi[2], L. Conzatti[2], P. Stagnaro[2]

[1]Dipartimento di Scienza dei Materiali e Ingegneria Chimica, Politecnico di Torino, C.so Duca degli Abruzzi, 24, 10129, Torino, Italy

[2] Istituto per lo Studio delle Macromolecole – UOS Genova CNR, Via de Marini 6, 16149, Genova, Italy

giovanna.colucci@polito.it

Introduction: The development of rubber-clay nanocomposites attracts great interest because layered silicates can be used as new ''white'' reinforcing agents to replace carbon black in rubber compounds [1-3]. These materials are currently prepared by solution blending, latex compounding, melt intercalation and in situ polymerization[1-3]. From an industrial point of view, melt intercalation is the most direct, cost effective and environmentally friendly technique to make nanocomposites. One of the most critical issue for their preparation is the dispersion of the clays inside a rubber matrix, due to their high hydrophilic nature.

Therefore, organophilic montmorillonites, made by cation exchange of onium salts, have been preferred; however, although the compatibility is good, they do not guarantee fully exfoliation of the clay in the rubber matrix[2-3].

In this paper we report the modification of Cloisite 30B by intercalation of low MW polybutadienes (LPBs) and their maleinized homologues (LPB-MAs) with the same maleic anhydride content. We describe the reaction between the pendant succinic rings of maleinized LPBs and the hydroxyl groups of the clay modifier; moreover, we study the effect of the modifications on the properties of the clays. Morphological and structural investigations of the SBR-based composites obtained by melt blending are described and structure-properties relationships deeply discussed.

Materials and Methods: The commercial organo-clay Cloisite 30B (C30B, Southern Clay Products, USA), was used as starting material (see below the formula of the onium cation).

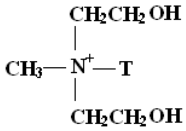

T= (65% C_{18}, 30% C_{16}, 5% C_{14})

The clay modifiers were two LPBs, MW 5000 and 1500, and two homologues LPB-MAs, with the same maleic anhydride content of 7.5 wt.%. LPBs used as modifiers were kindly supplied by Synthomer Ltd. UK. The modification procedure was reported in an our previous published work [4].

A styrene-butadiene emulsion copolymer (SBR) trade name Europrene 1739 (24 wt.-% styrene content, extended with 35 phr of oil) was used as matrix for the preparation in internal batch mixer of the rubber-based nanocomposites.

Results and Discussion: In Table 1, data describing clays modified either with LPBs or with LPB-MAs are reported. A first evidence of the modification is given by the amount of organic matter estimated by TGA.

Upon modification, in all samples a clear increase of the organophilicity of the clay is achieved, testified by contact angle values around 100°. XRD analysis reveals a remarkable increase of the interlayer distance when C30B is modified with LPB-MAs, while using simple LPBs the interlayer distances remain the same or show a slight increase depending on LPB MW.

Table 1. Characterization of modified clays.

Sample	Contact Angle with H_2O (°)	d_{001} (nm)	Organic Content @800°C (%)
C30B	60	1.8	32
C30B +LPB-1500	97	1.9	64
C30B + LPB-MA-1500	107	7.0	71
C30B + LPB-5000	98	3.6	62
C30B + LPB-MA-5000	96	7.6	76

FT-IR analysis clearly shows that the succinic rings pendant from the LPB-MA chains effectively react with the OH groups of C30B.

TEM images of the SBR-based composites containing the modified clays show the influence of the nature of the polybutadiene modifier. Using the clay modified by LPB-MA (Fig.1a) a large number of particles are well dispersed and in the form of isolated lamellae; the modification of the clay with a not maleinized LPB results in a lower number of isolated lamellae and larger tactoids (Fig.1b).

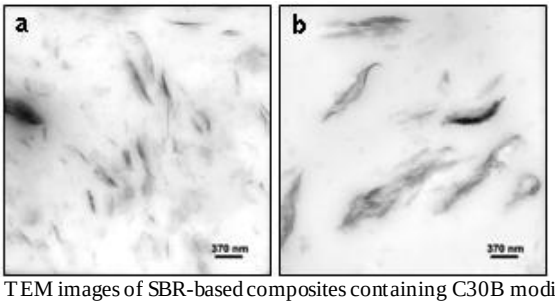

Fig.1 TEM images of SBR-based composites containing C30B modified with maleinized (a) and not maleinized (b) LPBs.

Conclusions: The succinic functional groups grafted onto the LPBs chains play a crucial role in modifying and increasing the interlayer distance to achieve a good dispersion of the new organo-clays within the rubber matrix. Rubber-based composites containing maleinized clays exhibit intercalated structures independently from the MW of maleinized LPBs.

This work was supported by the MIUR-FIRB Project ELASTORAD RBIP062Z4M_002.

References

[1] R.Sengupta et al.,*Polym. Eng. Sci.*, 47, 1956 (2007).
[2] M.Galimberti, A.Lostritto, A.Spatola, G.Guerra, *Chem. Mater.*, 19, 2495 (2007).
[3] M.Galimberti, S.Senatore, A.Lostritto, L.Giannini, L.Conzatti, G.Costa, G.Guerra, *e-Polymers*, 057 (2009).
[4] A. Priola, A. Di Gianni, G. Colucci, L. Conzatti, M. Alessi, P. Stagnaro, *Macromol. Mater. Eng*, 294, 705 (2009).

Directing self assembly of RAFT polymers using end group functionalisation

Dr Helen Willcock[1], *Dr Rachel K. O'Reilly*[1]

[1]University of Warwick

h.willcock@warwick.ac.uk

It is well documented that amphiphilic block copolymers can be assembled into a range of nanostructures such as spherical micelles, vesicles, toroids and cylinders when placed in a selective solvent for one of the blocks, in order to reduce energetically unfavourable interactions between the none-soluble block and the solvent.[1-2] Although the morphology formed is dependent upon a number of factors, it is proposed that the volume ratio between the hydrophobic and hydrophilic blocks is the most important. Specific structures can be targeted by considering the inherent molecular curvature and how this affects the packing of the polymer chains. This is described by the dimensionless packing parameter, *p*, and is shown in Figure 1.[3]

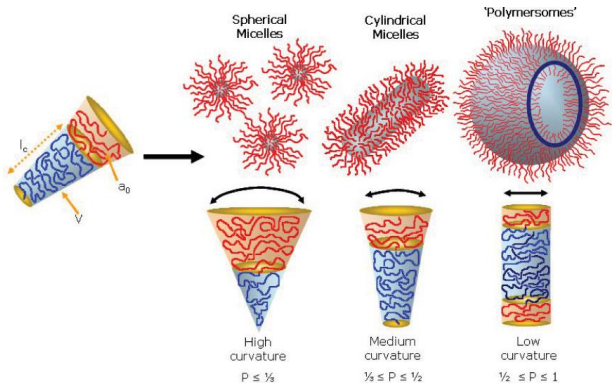

Figure 1 *Self-assembled structures formed by amphiphilic block copolymers in a block selective solvent.*

It has also been shown that secondary forces such as H-bonding or π-π interactions can aid the self-assembly process, and more recently the self-directed assembly of hydrophilic polymers with hydrophobic contents as low as 6 wt % have been described, and the work demonstrates that the presence of two spacially close rigid rings (such as in the pyrene end group) is a crucial structural requirement for vesicle formation. [4]

Reversible addition–fragmentation chain transfer (RAFT) polymerisation is one of the most versatile CRP techniques as it exhibits good tolerance to a diverse range of functional groups in monomers, solvents and initiators and offers control over a wide range of monomers through the use of different classes of chain transfer agents (CTAs).[5] As polymerisation occurs by insertion of monomer units into the C-S bond (at the α end), end-functionalised polymers can be easily achieved by incorporating the functional groups into the RAFT agent (groups R and Z) and by post-polymerisation reaction of the thiocarbonyl-thio group at the ω end (Figure 2).[6]

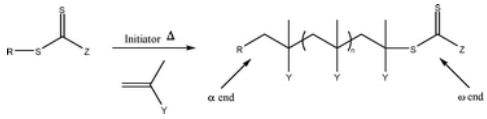

Figure 2 *Schematic representation of RAFT polymerisation showing α- and ω- ends of the resulting polymer.*

RAFT polymerisation has been used to synthesise polymers with both α and ω chain-end functionality by incorporating a hydrophilic, chargeable pyridine group into the R group of the RAFT chain transfer agent, followed by post-polymerisation introduction of a bulky, planar fluorescent group at the ω end. This was achieved by aminolysis of the trithiocarbonate end group, followed by Michael Addition of the resulting thiol to the activated alkene of hostasol acrylate. The successful incorporation of the fluorescent group has been confirmed by GPC using UV detection, and the effect of this bulky planar group on the self assembly properties of the homopolymers will be discussed.

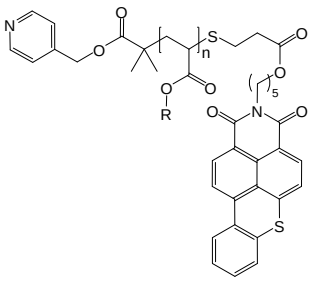

Figure 3 *Structure of dual end-functionalised homopolymer.*

1 Alexandridis, P., Lindman, B. "*Amphiphilic Block Copolymers: Self-Assembly and Applications*", 1st ed., Elsevier, Amsterdam 2000.

2 O'Reilly, R. K., Hawker, C. J., Wooley, K. L. *Chem. Soc. Rev.*, **2006**, *35*, 1068-1083.

3 Blanazs, A., Armes, S. P., Ryan, A. J. *Macromol. Rapid. Commun.* **2009**, *30*, 267-277.

4 Xu, J., Tao, L., Boyer, C., Lowe, A. B., Davis, T. P. *Macromolecules*, **2011**, *44*, 299-312.

5 J. Skey and R. K. O'Reilly, *Chem. Commun.*, **2008**, 4183–4185.

6 Willcock, H., O'Reilly, R. K., *Polym. Chem.*, **2010**, *1*, 149-157.

"Effect of acrylic acid hairy layer length on film formation and properties"

Edurne González[1], *Andrey Chuvilin*[2,3], *María Paulis*[1], *María J. Barandiaran*[1]

[1]POLYMAT, University of the Basque Country, Avda. Tolosa 72, 20018, Donostia-San Sebastián, Spain
[2]CIC nanoGUNE Consolider, Avda. Tolosa 76, 20018, Donostia-San Sebastián, Spain
[3]IKERBASQUE, Basque Foundation for Science, 48011, Bilbao, Spain

edurne.gonzalezg@ehu.es

Introduction

Water-borne polymerizations (emulsion and miniemulsion) are of great importance in industrial applications as they provide environmental-friendly processes, allow the removal of the reaction heat easily and assure the feasible handling of the final product that has a low viscosity. The final application of most polymer lattices is in the form of film (i.e. as paint or adhesive). The film formation process is the transformation of a polymer dispersion into a coherent polymer film. This process is usually divided in three stages: (i) evaporation of water and particle packing, (ii) deformation of particles and (iii) interdiffusion between particles and coalescence. All these stages have a great influence in the final film properties and the used emulsifier plays an important role in them. Low molecular weight ionic emulsifiers are commonly used to stabilize polymer particles in emulsion polymerization. However, they may create drawbacks in the final film applications as they usually migrate during the drying of the latexes, leading to poor adhesion of the polymer film to the substrate and introducing high water sensitivity. An alternative for overcoming these problems is the use of polymeric surfactants, especially amphiphilic block copolymers, as they absorb strongly on the particle surface. The hydrophobic part of the block copolymer is absorbed inside the particle whereas the hydrophilic part remains outside the particle forming a hairy layer.

In this work the effect of the acrylic acid (AA) hairy layer length on the film formation and final film properties has been studied. This requires the design of hairy layers of controlled lengths, which has also been part of this work.

Materials and Methods

Initially, different amphiphilic p(AA-*b*-BA) block copolymers containing different units of each monomer were synthesized by solution polymerization via RAFT process. Then, these copolymers were adsorbed on a clean latex, as shown in Figure 1

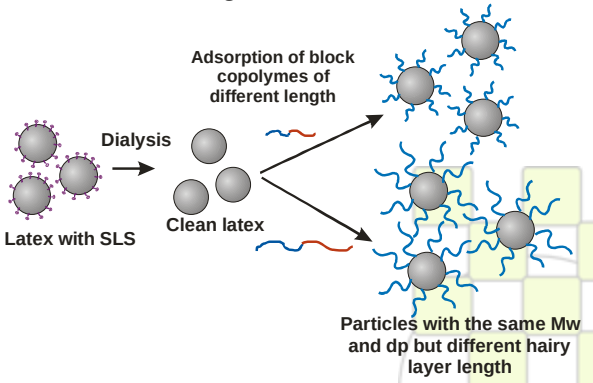

Figure 1. Steps followed to obtain polymer particles with hairy layers of different lengths.

So, a butyl acrylate (BA) /methyl methacrylate (MMA) (50/50 wt %) latex synthesized using a common anionic surfactant (sodium lauryl sulfate, SLS) was dialyzed against distilled water, in order to remove all the anionic emulsifier. Block copolymers of different lengths were added to different fractions of the clean latex. Thus, polymer particles with the same diameter and molecular weight but with different hairy layer length were obtained for comparison.

Films of the different latexes were formed and their properties such as tensile stress, static contact angle with water or water absorption were compared. Furthermore, the film formation step of each of them was studied by ESEM.

Results and Discussion

p(AA-*b*-BA) block copolymers containing different AA and BA units, with low Đ, were successfully synthesized by RAFT polymerization.

Concerning the film properties of the latexes with different hairy layer lengths, it was observed that although there were not significant differences in the contact angle values, the water absorption of the films was different. Films containing longer AA chain lengths absorbed more water. Tensile stress measurements demonstrated that the presence of AA chains on the particle surface decreased the final film properties. This effect is probably caused by the restricted interdiffusion between particles due to the high Tg of the AA (Figure 2).

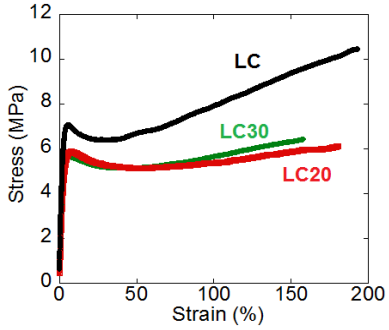

Figure 2. Stress-Strain curves for different films. LC corresponds to the clean latex and LC20 and LC30 to the clean latex stabilized by p(AA-*b*-BA) containing 20 and 30 units of each monomer respectively.

Acknowledgments

We acknowledge the financial support provided by the *Industrial Liaison Program in Polymerization in Dispersed Media* of Polymat (Arkema, Cytec Surface Specialties, Nuplex Resins, Wacker, BASF, AkzoNobel, Comex, Solvay, STAHL).

Evolution of the Electrical Conductivity of MWCNT/PUR Nanocomposites from Non-Quiescent Molten State to Solid State

Mercedes Fernández, Maite Landa, María Eugenia Muñoz and Antxon Santamaría

Departamento de Ciencia y Tecnología de Polímeros y Polymat. Universidad del País Vasco (UPV/EHU)
Centro Joxe Mari Korta, Avda Tolosa 72, 20018 San Sebastián

mercedes.fernandez@ehu.es

Introduction

The preparation of polymer/carbon nanotubes (CNT) nanocomposites with an improved electrical conductivity, implies, in general, a dispersion of the nanotubes in the polymer matrix and a subsequent solidification process. In the case of thermoplastic matrixes, dispersion is usually carried out in the molten state and then the temperature is decreased below the melting temperature or the glass transition temperature of the system. Notwithstanding this *modus operandi* is currently employed for basic studies and industrial purposes, few papers refer to a crucial aspect: The evolution of the electrical conductivity from the molten state to the solid state. Moreover, contradictory results have been found in the literature. According to Alig *et al*. [1] the effect of cooling polypropylene (PP)/ multiwalled carbon nanotubes (MWCNT) nanocomposite melts to temperatures below crystallization, is a significant decrease in the electrical conductivity. But, Lim *et al* [2] report an electrical conductivity enhancement in ethylene-co-vinylacetate (EVA)/MWCNT nanocomposites for samples cooled to the crystallization temperature.

Results and Discussion

In this contribution the electrical conductivity of dispersions of MWCNTs in a polycaprolactone based polyurethane (PUR) is investigated in the molten state, during crystallization and in the solid state. The study focuses on the effect of flow on both, electrical conductivity and dynamic viscoelastic results, establishing the percolation threshold within the framework of the "dynamic percolation" concept. The flow conditions affect the agglomeration and, eventually, the orientation of nanotubes, which gives rise to different values of the fitting parameters ϕc and t of the percolation equation $X=Xo\ (\phi-\phi c)^t$. Depending on the results obtained in the molten state, an electrical conductivity increase or a decrease is observed during crystallization process. Figure 1 shows the conductivity enhancement observed during crystallization for a PUR/2 wt % MWCNT nanocomposite.

The results are discussed considering different hypothesis, including the assumption of a distribution of the conductive particles in amorphous regions, around the crystalline regions.

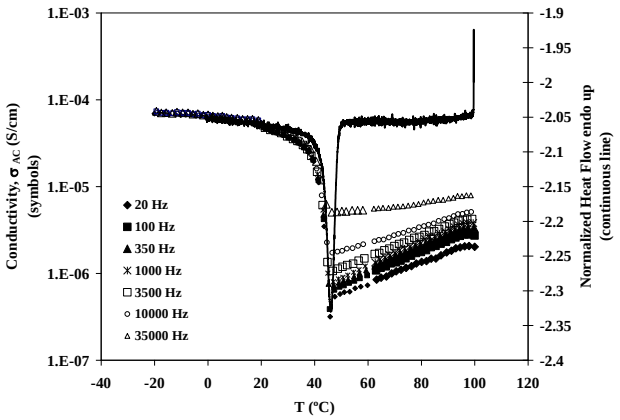

Figure 1. Temperature dependence of conductivity, σ_{AC} of the PUR/2% MWCNT nanocomposite recorded at the indicated frequencies during crystallization for 1ºC/min cooling rate (symbols). Heat Flow from DSC experiment at the same scanning rate (continuous line) is plotted for comparison purpose.

References

[1] I. ALig, D. Lellinger, S.M. Dudkin, P. Pötschke, Polymer 48 (4) 2007 pp 10020-1029

[2] G-O Lim, K-T Min, G-H Kim, Polymer Engineering and Science 50(2) 2010, pp 290-294

Acknowledgements

Financial support through MICIN MAT 2010-16-171 Project (Spanish Government) and GIC IT-441-10 (Basque Government) is acknowledged, and one of us, Maite Landa acknowledges a Thesis Grant from Basque Government.

Semi-Interpenetrating Networks Based on Poly(*N*-Isopropylacrylamide) Reinforced with Nano-clays and Linear Hydrophilic Polymers

Jasna Djonlagic [a,*] *Dragana Zugic* [a], *Anica Lancuski* [a], *Marija Nikolic* [a], *Zoran Petrovic* [b]

[a] Faculty of Technology and Metallurgy, Karnegijeva 4, 11000 Belgrade, Serbia
[b] Kansas Polymer Research Center, Pittsburg State University, Pittsburg, Kansas, USA

email: jasna@tmf.bg.ac.rs

Polymer hydrogels resemble natural living tissues more than any other class of synthetic biomaterials due to their high water content and soft consistency. However, their relatively low mechanical strength and low response rate, which mainly arise from restricted molecular motion of the chains caused by the high degree of crosslinking, affect their application. Fast responses, excellent mechanical properties, comparable to those found in living systems, are required for some specific applications, such as chemical sensors and artificial organs. The desired values of modulus and response rate of hydrogels could be achieved by molecular design. Recently, the new class of nanocomposite (NC) hydrogels based on poly(*N*-isopropylacrylamide) (PNIPA) with improved mechanical properties, high transparency and high deswelling rates has been designed.[1,2] Further improvements of properties of NC hydrogels were accomplished by addition of linear hydrophilic polymers to the networks, i.e., by forming semi-interpenetrating networks (SIPN).[3,4]

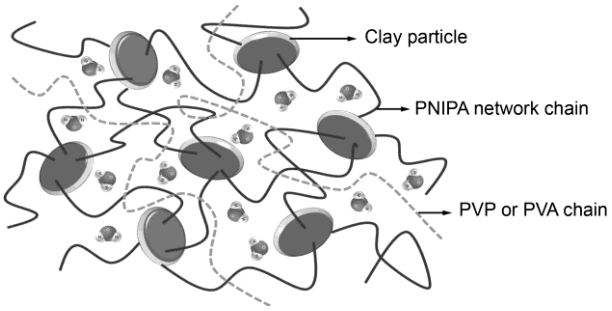

Figure 1. Schematic presentation of the structure of the PNIPA/clay network interpenetrated with linear PVP or PVA chains.

In this study, the SIPNs based on PNIPA physically crosslinked with inorganic clay and interpenetrated with linear hydrophilic poly(*N*-vinyl pyrrolidone) (PVP) or poly(vinyl alcohol) (PVA) polymers, are presented (Figure 1.). Linear PVP or PVA were used due to their high hydrophilicity and high molecular weight, which makes them capable to form entanglements and imparts some useful properties, such as good physiological inertia and biocompatibility. The hydrogels were crosslinked with 1-6 wt% of inorganic clay (hectorite, Laponite XLG). SIPN hydrogels contained linear interpenetrants in the range of 0.5 to 1.5 wt%. Hydrogels were prepared at 10 wt% of polymer in water (as-prepared state) and then swollen to equilibrium. The equilibrium degree of swelling at 25 °C, the dynamic shear modulus and the effective crosslinking density, tensile strength and elongation at the equilibrium swelling and in the "as-prepared" state are presented.

The mechanical properties and the gel structure of SIPN are compared to PNIPA hydrogels. Both hydrophilic linear polymers, PVP and PVA, modify the morphology of NC hydrogels by increasing pore size and contribute to the higher equilibrium swelling ratio and higher swelling - deswelling rates. The degree of swelling of SIPNs and PNIPA hydrogels was in the range 12 to 40 and deceased with the increasing content of clay. Kinetics of swelling and deswelling was used to estimate the responsiveness of the gels. A considerably faster deswelling and volume shrinkage of SIPN hydrogels was achieved by the addition of 1 wt% PVP and 1.5 wt% PVA. The volume phase transition temperature of hydrogels was determined by differential scanning calorimetry (DSC). The insertion of hydrophilic linear polymers slightly decreases the lower critical solution temperature, LCST, while the volume phase transition is broader as the content of clay increases. Scanning electron microscopy (SEM) was used to investigate the morphology of the PNIPA and SIPNs hydrogels. The tensile strength of the SIPNs reinforced with linear hydrophilic polymers was higher than that of the PNIPA/clay networks and was almost proportional to the clay content. The strongest hydrogels were those with 10 wt% PNIPA and 5 wt% of nano-clays, displaying tensile strengths of 85 kPa and elongation of 955 %. All properties at the equilibrium swollen state are lower than in the as-prepared state, due to the lower concentration of chains per unit volume, but the trends are maintained.

The hysteresis in the elongation-reversion curves of hydrogels observed in both as-prepared and swollen state, increased significantly with the clay content as well as with the presence of linear PVP, confirming their contribution to a slow relaxation of hydrogels. Hysteresis in the first cycle was large and it was significantly reduced in repeated cycles. It could be concluded that the elastic properties of hydrogels might be improved by pre-stretching. The SIPN and PNIPA NC hydrogels exhibited excellent elastic recovery even at high elongations.

References:

1. Haraguchi K and Takehisa T, *Adv Mater* **14:** 1120 (2002).
2. Haraguchi K, Takehisa T and Fan S, *Macromolecules* **35:** 10162 (2002).
3. Ma J, Xu Y, Fan B and Liang B, *Eur Polym J* **43:** 2221 (2007).
4. Song L, Zhu M, Chen Y and Haraguchi K, *Macromol Chem Phys* **209:** 1564 (2008).

Generation of Metal Polymer Nanohybrids in the Irradiated Polyelectrolyte Metal Complexes of Different Architecture

*Alexey Zezin**, *Vladimir Feldman***, *Sergei Abramchuk***, *Elena Zezina***, *Alexander Danchenko***

*Institute of Synthetic Polymer Materials of RAS, Profsouznaya ul.70, Moscow, 117393 Russia
**Department of Chemistry, Moscow State University, Moscow, 119991 Russia

aazezin@yandex.ru

Introduction. Design of nanocomposite polymer materials with metal particles attracts growing interest due to their specific behaviour and prospects of application. Water-insoluble interpolyelectrolyte complexes may include a wide variety of metal ions with high sorption capacity (up to 30 %wt) and may be considered as promising systems for reduction of metal ions directly in polymer matrixes [1]. On the other hand it is possible to use the solutions of stars of polyacrilic acid or micellar solutions of amphiphilic block copolymers for preparation of nanomaterials inside macromolecules. Preparation of nanomaterials with adjusted structure in polyelectrolyte metal complexes by radiation-chemical reduction of metal ions is in focus of our research.

Materials and Methods. The solutions of polyelectrolyte metal complexes (stars of polyacrilic acid (PAA) or polystyrene - polyacrilic acid block copolymers with ions Cu^{2+}) and films of interpolyelectrolyte metal complexes (polyethyleneimine (PEI) - polyacrilic acid (PAA) with ions Cu^{2+}, Ni^{2+} or Ag^{+}) were used for study of peculiarities of formation of nanocomposites materials. The samples of complexes in aqueous alcohol environment were irradiated at 293 K using e-beams, ^{60}Co and X-ray irradiation in vacuum or inert atmosphere. The degree of ion reduction was controlled by EPR or optical spectroscopy. Small angle X-ray scattering (SAXS), electron microscopy and optical spectroscopy were used for characterization of the obtained nanocomposite polymer materials. The e-beam, X-ray and γ-irradiation were used for obtaining of metal nanoparticles

Results and Discussion: The SAXS data demonstrate formation of metal particles under irradiation of polymer systems. It is shown that the type of irradiation, the type of metal ion and composition of polymer system affect on formation of metal nanoparticles and structure of resulting metal polymer hybrid materials. The formation rate and localization of reducing agents generated by irradiation, their transport in polymer matrix are main factors, which determine size distribution and spatial ordering of nanoparticles in polymer matrix. The γ-irradiation results in formation of materials with relatively narrow distribution of nanoparticles (2-5nm), while the application of X-rays leads to ensembles of nanoparticles on the surface or in the bulk of polymer matrix. The type and content of metal ions in metal films affect the structure of nanocomposites. In the case of e-beams, the structure of resulting materials is defined by energy of accelerated electrons.

It was found that irradiation of solutions of polyelectrolyte complexes of star-like PAA macromolecules with copper ions resulted in effective reduction of metal ions and subsequent formation of nanoparticles. It should be noted that obtaining of nanoparticles in aqueous complexes of copper requires higher irradiation doses. The sizes of nanoparticles are determined by the presence of star-like macromolecules. The nanoparticles with sizes 2-4 nm were obtained after radiation induced reduction of copper ions in micellar solutions of polystyrene -polyacrilic acid block copolymers. In casting films of copolymers the microphase of polyacrilic acid are filled by metal nanoparticles (fig.1).

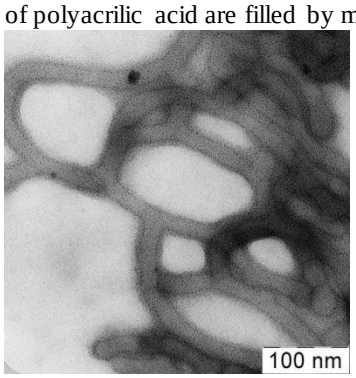

Conclusions: The high radiation-chemical yields of reduction of ions demonstrate good prospects for use of the polyelectrolyte metal complexes for the radiation-chemical synthesis of nanoparticles by this technique. The radiation-chemical approaches provide preparation of composites with uniform distribution of nanoparticles and materials with regular spatial distribution of nanoparticles including localization of metal structures in subsurface.
It was shown that complexes of macromolecules with metal ions in solutions may act as microcontainers for obtaining of nanoparticles. The approaches discussed in this paper make it possible to obtain provide wide opportunities for synthesis of nanocomposites with controlled content, size and spatial distribution of nanoparticles.

1) *Zezin A.B., Rogacheva V.B., Feldman V.I., Afanasiev P, Zezin A.A.* // Advances in Colloid and Interface Science 2010. V.158. P.84.

This work was supported by Russian Foundation for Basic Research (grant № 09-03-00877a)

Step-And Repeat Assembly of Molecularly Controlled Ultrathin Polyaramide Layers

Mónica Perez[1,2], *Nino Lomadze*[1], *Helmut Reinecke*[1,2*], *Oswald Prucker*[1], *Jürgen Rühe*[1]

[2]Instituto de Ciencia y Tecnología de Polímeros, Consejo Superior de Investigaciones Científicas, CSIC, Spain.
[1]IMTEK. University of Freiburg, Germany.

cruzdp@yahoo.es

Introduction

Surfaces of inorganic materials can be tailored through the covalent attachment of monolayers of polymer chains [1-4]. Numerous synthetic approaches were developed to allow the preparation of such surface-attached monolayers. Different types of chain polymerization have been shown to be suitable for the creation of polymer monolayers. As far as step polymerization reactions are concerned, polycondensation reactions have also been used for the preparation of monolayers consisting of terminally anchored polymer chains. However, the layer thicknesses obtained from these polymers are usually limited for thermodynamic reasons. An alternative solution for the preparation of surface-attached high molecular weight polymer chains by condensation reactions is a discontinuous process in which A-A and B-B monomers are added sequentially to form the polymer chains in a monomer-by-monomer assembly. The advantage here is that in each step the substrate with the growing reactive site may be exposed to an excess of monomer pushing the equilibrium at each step towards a complete reaction.
In the present work we follow such an approach for the formation of step-by-step polyaramide monolayers and study multi-step condensation reactions for the formation of surface-attached high molecular weight polyaramide films.

Experimental

The substrate (silica wafers) is activated in a first step by a silanation reaction which creates functional organic groups on the surface. These OH- or NH2-functionalized wafers are then sequentially dipped in a freshly prepared 10^{-3} M solution of diacid chloride in toluene (one drop of pyridine added) and a 10^{-3} solution of diamine in DMF with intermediate rinsing steps with DMF (see Fig.1). Finally the samples are washed with a mixture of NMP/ Hexamethylphosphoramide in order to asure that no monomeric or oligomeric compounds remain absorbed to the surface.

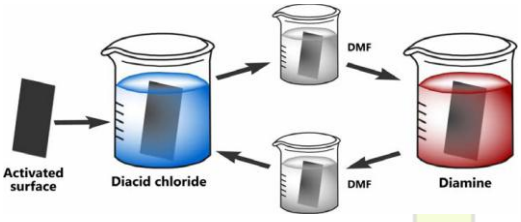

Figure1: experimental procedure for the preparation of molecularly controlled polyaramide layers

After every fifty reactions (i.e. attachment of 25 polyaramide units) an FTIR transmission spectrum of the wafer is recorded (figure 2).

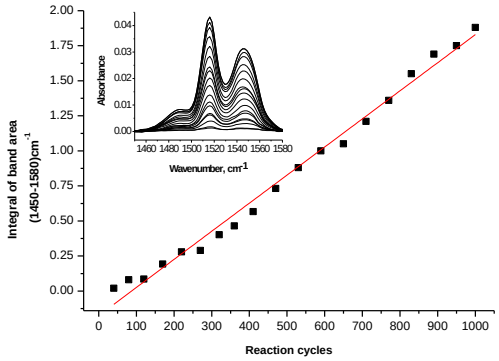

Figure 2: FTIR band area of surface-attached polyaramide monolayers in the region from 1580-1450 cm^{-1} as a function of the number of reaction cycles.

Results

It is found that polyaramide assemblies of well defined thickness and uniform topography can be synthesized by this step and repeat approach. IR, ellipsometry and AFM measurements demonstrate that the film thickness grows linearly with the number of dipping steps and that more than 1000 reaction cycles can be carried out without observing any decrease in film growth. This Merrifield-like approach of molecular assembly represents a very interesting mechanism of film growth as the layers consist of polymer chains in which the units are firmly attached to the surface and linked together either through covalent chemical links or through ionic interactions. This mechanism leads thus to a rather unusual form of formation of surface-atttached thin films. The described approach allows thus the preparation of molecularly designed assemblies of polyaramides with precisely controlled thicknesses. The synthetic effort required to generate these interesting systems is high, but might be lowered significantly through automatization of the dipping procedure.

References

Prucker, O.; Rühe, J., *Macromolecules* **1998**, *31*, 592.
Prucker, O.; Rühe, J., *Macromolecules* **1998**, *31*, 602.
Rühe J.; Knoll, W.; Ciferri, A., Ed.; M. Dekker: New York, 2000.
Whitesell, J.K., Chang, H.K. *Science*, 261-5117, (1993), 73-77.

Acknowledgements

H.R. gratefully acknowledges financial support during his stay at the University in Freiburg obtained by the Spanish Ministry of Innovation and Science (programa de movilidad).

Synthesis of Core-branched ABC Block Copolymer Nanoparticles having Incompatible Functional Moieties

Erol Hasan, [a] *Jonathan V.M. Weaver* [b] *and Dave J. Adams* [a]

[a] Department of Chemistry, University of Liverpool, Crown Street, Liverpool, L69 7ZD, UK
[b] Imperial College London, Prince Consort Road London, SW7 2AZ, UK

erhasan@liverpool.ac.uk

We demonstrate the first example of the synthesis of core-branched ABC copolymer structures having incompatible functionalities such as tertiary amino and carboxylic acid groups.

The ABC branched copolymer was prepared using a one-pot ATRP approach. The ABC copolymer structure was composed of monomethoxy polyethylene glycol (PEG) as the A-block, poly(2-dimethylaminoethyl methacrylate) (PolyDMA) as the B-block, and the C-branched block was composed of poly (t-butyl methacrylate/ ethyleneglycoldimethacrylate)(Poly(t-BMA/EGDMA)) (Figure 1). The ABC linear block copolymer analogue was prepared in same approach in absence of ethyleneglycoldimethacrylate. The ABC copolymers were characterized using NMR and GPC.

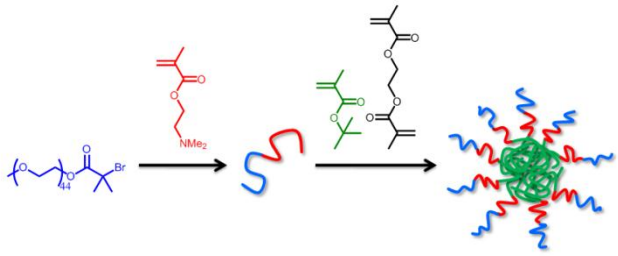

Figure 1

Both the linear and branched ABC copolymers were readily soluble in THF. DLS studies of the branched ABC structure in THF showed a well-defined single scattering mode with a radius of 12 nm, whereas the linear polymer in THF formed a poorly scattering system. Dialysis was used to form polymer nanoparticles with hydrophobic core and dual (inner/outer) shell. Both the linear and branched structures formed nanoparticles with spherical shape and hydrodynamic radius of 8 nm.

For the preparation of particles containing incompatible functional groups, hydrolysis of the poly(*tert*-butyl methacrylate) block of ABC copolymers to poly(methacrylic acid) was carried. In these ABC structures, there is the potential for interpolyelectrolytic complexation, depending on the degree of ionisation of the functional groups. The DMA group is known to have a pKa of about 7.0 while poly(methacrylic acid) is known to have a pKa of 4.9. To probe the differences in behaviour between the linear and the branched ABC polymers, the turbidity of solutions at different pH were measured.

Polyesteramide nanofibers – preparation and properties

Jiří Brožek[1], *Lenka Malinová*[1], *Václava Benešová*[1], *Daniela Lubasová*[2], *Lenka Martinová*[2], *Jan Roda*[1]

[1]Department of Polymers, Institute of Chemical Technology, 166 28 Prague, Czech Republic
[2]Technical University, 461 17 Liberec, Czech Republic

Jiri.Brozek@vscht.cz

Polyesteramides based on ε-caprolactam (CLA) and ε-caprolactone (CLO) – poly[(ε-caprolactam)-*co*-(ε-caprolactone)]s - seem to be very promising materials combining good mechanical properties of aliphatic polyamides with well-known degradability of aliphatic polyesters which makes them valuable candidates for biomaterials and environmentally friendly plastics. These polyesteramides can be prepared by an anionic[1-3] or a hydrolytic copolymerization[4] of CLA and CLO.

ε-caprolactone (CLO) ***ε-caprolactam (CLA)***

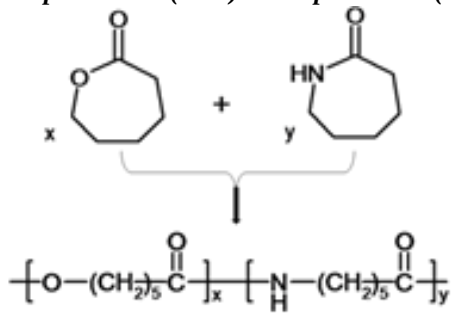

poly[(ε-caprolactam)-co-(ε-caprolactone)]

The application of ε-caprolactam magnesium bromide as an initiator of the ring-opening polymerization is rather exceptional[2,3] because it is possible to prepare copolymers containing equilibrium amount of unreacted monomers and low content of extractable portions. The copolymers thus prepared for further applications need no extraction. Glass transition temperature decreased monotonously with increasing content of lactone in the copolymer. It indicates that a random copolymer is formed. With increasing content of ester bonds in the copolymer, its impact strength and drawability increase, and modulus decreases.

Polyesteramides were subjected to biodegradation studies[5]. The hydrolyzability of PEAs increases with increasing fraction of ester bonds in macromolecules in accordance with the well-known higher sensitivity of ester bonds to hydrolysis compare to amide bonds. This was proved in both the composting tests as well as in abiotic hydrolysis test[5].

Polyesteramides prepared according to ref.[3] were used for the preparation of nanofiber sheets by electrospinning, i.e. a process for producing fibers the diameter of which is in the range below 1000 nm. In this process, fibers are formed by an action of electrostatic field from the surface of a polymer solution or melt and are put on a collector that acts as an anti-electrode. We have focused on solvent systems which allow one to prepare high aspect ratio nanofibers.

The solubility of the copolymer changes with its composition. With decreasing content of the CLO units, the polarity of the copolymer increases and the choice of the suitable solvents becomes narrower. The choice of the solvent plays an important role for electrospinning process. Polyesteramides containing from 10 to 40 mol.% of lactone structural units are soluble in polar solvents such as 1,1,1-trifluoroethanol, formic acid and formic/acetic acid mixed solvent system.

An example of very fine nanofibers prepared by electrospinning is shown in Figure for PEA with 30 mol.% CLO units.

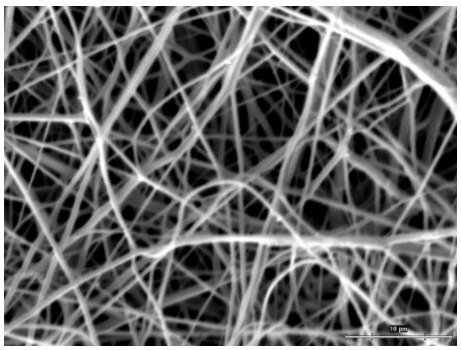

Figure: SEM image of nanofiber sheet prepared by electrospinning (polyesteramide containing 30 mol% lactone units, 10 wt.% solution, mixed solvent system formic/acetic acid 2/1)

The electrospinning process was influenced by system parameters such as solvent used, molar mass of the copolymer, its composition and solution properties.

Literature:

[1]Goodman I.; Vachon RN. *Eur Polym J* **1984**;20;529.
[2]Bernášková A.; Chromcová D.; Brožek J.; Roda J.; Polymer **2004**;45;2141.
[3]Chromcová D.; Baslerová L.; Roda J.; Brožek, J. *Eur. Polym. J.* **2008**;44;1733.
[4]Michell RM.; Müller AJ.; Castelletto V.; Hamley I.; Deshayes G.; Dubois P. *Macromolecules* **2009**;42;6671.
[5]Brožek J.; Šašek V.; Prokopová I.; Chromcová D.; Náhlík J.; Erbanová P. Folia Microbiol. **2009**;54;451.

Acknowledgement

The research was supported by Czech Science Foundation (grant no. 106/09/1378) and the research programme MSM 6046137302.

Polyurethane Functionalized with Hydroxyapatite Nanostructures by a Non-conventional Route. Thermal Behavior as a Function of Pressure

*Laura Madalina Popescu**, **, Roxana Mioara Piticescu**, Tinca Buruiana*, Eugeniu Vasile***, Roxana Trusca****

* Romanian Academy – Institute of Macromolecular Chemistry "Petru Poni", 41A Grigore Ghica Voda Alley, Iasi, 700487, Romania

** National R& D Institute for Non-Ferrous and Rare Metals, 102 Biruintei blvd., Pantelimon, 077145, Ilfov, Romania

*** METAV C-D, 31 C.A. Rosetti str., Bucharest, 020011, Romania

mpopescu@imnr.ro

Introduction

Acid polyurethane with COOH groups on its surface was functionalized with hydroxylapatite using a non-conventional synthesis route: hydrothermal method at high pressure (20-80 atm) and low temperature (60-100 ^{0}C). This technique allows formation of new phases and nanostructures and is frequently used for the preparation of inorganic nanomaterials which couldn't be obtained by solid-state fabrication route. Hydrothermal reactions take place in a sealed vessel, in aqueous medium and consist of dissolution-recrystallization of usually insoluble materials. In this study, hydrothermal reaction for hydroxylapatite (HAp) obtaining is accompanied by chemical reactions between newly formed HAp and water miscible polymer solution. In hydrothermal conditions, water and organic particles form a homogenous phase which represents an excellent reaction medium for the functionalization of inorganic nanostructures with organic polymers [1, 2].

Materials and Methods

Purity grade hydroxylapatite precursors, namely calcium nitrate tetrahydrate and ammonium dihydrogen phosphate were solubilized in water under a strict pH control, adding ammonium hydroxide as a mineralizing agent. The aqueous suspension thus obtained was further mixed with the polymer solution under vigorous stirring, followed by a hydrothermal treatment. Reactions were conducted in a closed system at low temperature (T < 100 ^{0}C) and high pressure (P > 20 atm) leading to nanostructured composite powders.

Results and discussion

The influence of pressure on the polyurethane (PU) and its bonding with hydroxylapatite has been of special interest in this study. Polymer structure is presented in figure 1.

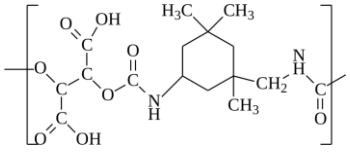

Fig. 1. Hard polyurethane-containing COOH groups.

Hybrid organic inorganic nanostructures have been prepared at various pressure values and characterized using chemical, structural and thermal methods. High-pressure synthesis could lead to structural and conformational changes of the materials, including a possible increase of H bond density in the polymer structure. The chemical structure was studied by FTIR spectroscopy and the results were corroborated with those obtained by physical characterization, *i. e.* XRD and HRTEM techniques. A representative HRTEM image is shown in figure 2.

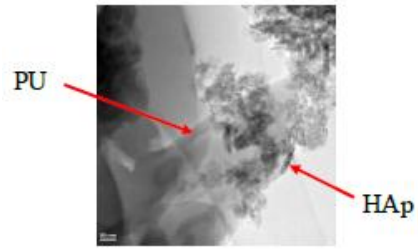

Fig. 2. HRTEM image of PU functionalized with HAp.

Thermal characterization (DSC) was used to investigate the morphostructural differences between hybrids prepared at different pressures. An example of DSC analysis at different heating rates is presented in fig. 3.

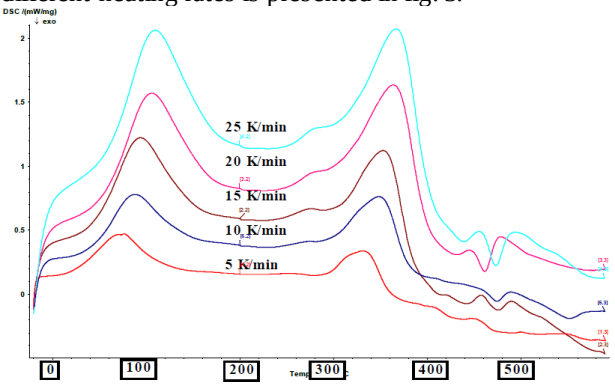

Fig. 3. DSC of PU-HAp composites at high pressures.

Conclusions

Nanostructured composites based on acid polyurethane and hydroxylapatite were prepared under hydrothermal conditions at low temperatures and high pressures. The organic/inorganic composites showed fine hydroxylapatite nano-whiskers incorporated into large polyurethane particles. Calorimetric analysis revealed the influence of pressure on chemical structure, conformation and morphology. A possible explanation could be that density of hydrogen bonds between macromolecular chains increase with pressure and in the same time the hard segmented polyurethane becomes more flexible, polar and able to interact with other molecules through carbonyl groups of the urethane structure (NH-CO-O).

References

1. L. M. Popescu, R. M. Piticescu, T. Buruiana, E. Vasile, R. Trusca, and V. Badilita, *Z. Naturforsch.* 2011, *66b*, 36 – 42;

2. R. M. Piticescu, T. Buruiana, N. Plesu, E. Vasile, C. Moldovan, B. Fartat, C. Rusti, *Optoelectr. Adv. Mater. Rapid Commun.* 2010, *4*, 401 – 406.

Acknowledgement

The financial support of the Postdoctoral Fellowship Programme ID POSDRU/89/1.5/S/55216 – 2010 is acknowledged.

Nanostructured polymer composites based on carbon nanotubes

Maurizio Galimberti[1,2], *Michele Coombs*[1], *Incoronata Tritto*[3a], *Andrea Ravasio*[3a], *Theonis Riccò*[4], *Simone Passera*[4], *Lucia Conzatti*[3b], *Cristina D'Arrigo*[3b], *Stanislao Senatore*[5]

[1] Pirelli Tyres, Viale Sarca 222, 20126 Milano (I) [2] Politecnico di Milano, Via Mancinelli 7, 20131 Milano (I); [3] CNR-ISMAC, [a]Via Bassini 15, 20133 Milano (I), [b]Via De Marini 6, 16149 Genova (I); [4] Università degli Studi di Brescia, Via Valotti 9, 25123 Brescia (I); [5]Itacanova srl, Piazza Duomo 15, 22100 Como (I)

maurizio.galimberti.ex@pirelli.com

Introduction

Fillers such as carbon black and silica are nanostructured: primary particles build up aggregates that can not be separated via thermomechanical mixing. Over the last years, new fillers have become available that can be dispersed in a matrix as individual particles having at least one dimension in the order of one or few nanometers. They are in fact known as nano-fillers and, among them, layered silicates[1] and carbon nanotubes[2] (CNT) are most investigated, both in the academic and industrial worlds, as a consequence of their outstanding properties.

This contribution is focused on CNT[3] and reports results from a research activity aimed at exploiting their huge potential in the frame of an easy large scale development.[4] A single nanotube is hundred times stronger than steel and has remarkable electrical and thermal conductivities. However, CNT are bundles, rather than single nanotubes, with a graphite inert surface. To disentangle them, developing an interaction with the matrix, for example with a polymer matrix, is still a main issue. In this work, morphology, dispersion and structure of CNT were investigated in thermoplastic and elastomeric polymer matrixes and in an aqueous dispersion medium. The synergy between CNT and a further filler was studied by using: (i) furnace carbon black in an elastomeric matrix, and (ii) an original polymeric filler polynorbornene (PN) nanoparticles in a thermoplastic matrix as well as in liquid dispersions. A poly-1.4-cis-isoprene was selected as the elastomer and an ethylene/1-octene copolymer as the thermoplastic polymer. Mixing energies and the known latex approach were primarily applied to improve the CNT dispersion, whereas hybrid filler networks, formed by CNT and the other filler, were studied as promoters of improved material properties. Dynamic-mechanical and electrical properties of the composite materials were determined, in particular assessing the percolation threshold of CNT and CNT/other filler systems. Investigations were performed with the help of transmission electron microscopy (TEM), tensile and dynamic-mechanical tests, measurements of square sheet resistance. Results are correlated with the filler structure: individual particles or aggregates or hybrid filler networks. This contribution proposes a comparative and comprehensive analysis of CNT features and behaviour in the most typical frames (thermoplastic and elastomeric matrixes and liquid dispersions) and, in particular, discusses the hybrid systems as a way to achieve an easier dispersion of CNT.

Materials and Methods

Multiwall CNT were Baytubes® C150 P from Bayer Material Science, with a chemical purity ≥ 95 wt.%, a length in the range 1-10 μm, a number of walls between 3 and 15 and outer and inner diameters of 1–16 nm and 4 nm, respectively. Synthetic cis-polyisoprene was from Nizhnekamskneftechim Export, with 70 Mooney Units (MU) as Mooney viscosity (ML(1+4)100°C). PN-based nanoparticles were obtained by freeze drying a SDS-stabilized latex prepared according to literature procedure.[5] Polymer composites were prepared via blending in an internal mixer.

Results and Discussions

CNTs were not homogeneously dispersed in a polymer matrix in the absence of a further filler; however, they were able to build up a network at a content (≅ 3 wt.%) much lower than that of a traditional filler. Mixing in a elastomeric matrix was found to favour dispersion and disentanglement of CNTs, that were also broken to shorter tubes. A further compatible filler, such as carbon black, brought to the formation of a hybrid filler network at a CNT level (≅ 1 wt.%) lower than that obtained for CNTs alone. Also the polymeric filler was observed to favour the formation of a CNT-based network. All these conclusions are based on both dynamic-mechanical and electrical measurements and are supported by TEM observations. A good correlation between formation of CNT-based networks and improvement of material properties, such as reinforcement and electrical conductivity, was found.

The latex approach was confirmed as a powerful tool to achieve nice CNTs dispersion: in particular, CNT pre-treatment with a surfactant, its dispersion/sonication and obtainment of a hybrid emulsion system with CNT and PN nanoparticles led to latexes that were either used to prepare coatings or, through liofilization, added to a thermoplastic polymer matrix. Correlation between CNT dispersion and material electrical conductivity, at a very low CNT level, are discussed.

Conclusions

Different approaches to achieve CNT dispersions, exploiting their unique properties were *vis a vis* investigated. In particular, the development of hybrid filler systems appears as a way to allow an easy development of CNT-based materials.

Bibliography.

[1] Chen B.; Evans J.R.G.; Greenwell H.C.; Boulet P.; Coveney P.V.; Bowden A.A.; Whiting A. *Chem. Soc. Rev.* **2008**, *37*, 568.

[2] Schulte, K; Gojny, Florian H.; Fiedler, Bodo; Sandler, Jan K. W.; Bauhofer, W. *Polymer Composites* (2005), 3-23.

[3] Grossiord, N.; Loos, J.; Regev, O.; Koning C.E. *Chem. Mater.*, **2006**, *18*, 1089–1099

[4] This study is supported by Cariplo Bank Fundation (Rif. 2008.2383). NANOEASY

[5] Chemtob, A.; Gilbert, R.G. *Macromolecules*, 2005, *38*, 6796–6805.

Preparation and Characterization of Sol-Gel functionalized Polysaccharides

Heike M.A. Ehmann[1,2], Stefan Spirk[2], Karin Stana-Kleinschek[1], Volker Ribitsch[2]

[1] University of Maribor, Faculty of mechanical engineering, Laboratory of characterization and processing of polymers, Smetanova ulica 17, 2000 Maribor, Slovenia

[2] University of Graz, Department of physical chemistry, Rheology and Colloidal chemistry, Heinrichstraße 28, 8010 Graz, Austria

Heike.Ehmann@uni-mb.si

Abstract

This contribution presents several hybrid materials showing different properties based on cellulose nano whiskers and chitosan functionalized with different organofunctional silane compounds. The obtained materials were characterized concerning their surface composition and their interaction abilities (Contact angle, surface free energy) and also their morphology (Atomic Force Microscopy). It is shown that properties of these materials can be tailored over a wide range choosing different organofunctional silane compounds.

Introduction

For material scientists, the combination of organic and inorganic materials offers an enormous range of possibilities to combine the functional variety of organic chemistry with advantageous properties from inorganic compounds such as thermal stability. [1] The idea of creating hybrid materials on the basis of modified polysaccharides and organofunctional-silanes has been a fascinating topic of research [2][3], during the past decades and many applications have been described e.g. as precursors for enzyme immobilization [4], for encapsulation of biomolecules in silica gels [5], anti-adhesive and antibacterial multilayers [6], bifunctional catalyst [7].

Cellulose is the most abundant natural polymer in the world and consists of ß-1-4-linked D-Glucose units. Cellulose nanowhiskers can be prepared by controlled acid hydrolysis of cellulose fibers. The incorporation of those nano whiskers into nanocomposites is very attractive due to their nanoscale dimensions, high surface area, unique morphology, low density and mechanical strength. [8]

Chitin is a ß-1-4-aminoglucan and is after cellulose the second most abundant natural polymer in the world. Chitosan is the most important chitin-derivate. It is the only pseudo natural cationic polymer in the world and is used to prepare hydrogels, films and fibers and finds applications in the biomedical sector, whereas the biocompatibility is essential. [9][10]

Materials and Methods

Cellulose nano whiskers were prepared via sulphuric acid hydrolysis [8] Chitosan was dissolved in acetic acid. All organofunctional alkoxy-silanes were prehydrolyzed via acid hydrolysis with hydrochloric acid.

The hybrid materials were prepared via solution casting and spin coating on different substrates, whereas the amount of silane to polysaccharide was varied. The surface interaction abilities were characterized using contact angle measurements with three different liquids to calculate the surface energy with different models. The surface morphology was studied using AFM.

Results and Discussion

The contact angle measurements were performed using distilled water, diiodomethane and formamide. Different model approaches have been used to calculate the total surface energy and the polar and nonpolar surface contributions. According to the nature of the functional silane side-chains, the surface energy contributions are varying. By means of AFM, the root mean square roughness and the average roughness were calculated.

Conclusions

In summary, different kinds of functional hybrid materials were prepared and characterized. Depending on the silane to polysaccharide ratio, foils and composite materials could get obtained. The incorporation of silanes into the polysaccharide matrix enhances the mechanical properties of the materials as well as their thermal stability.

References

[1] Hoffmann F. et al, Angew.Chem. Int. Ed., **2006,** 45 3216-3251.
[2] Shchipunov, Y. A et al, Langmuir, **2004**, 20, 3882-3887
[3] Silva, S. S. J.et al, Mat. Chem. **2005** 15, 3952-3961
[4] Shchipunov, Y. A. et al, J. Biochem Biophys Methods, **2004**, 58, 25-38
[5] Livage J. et al, J. Phys: Condens. Matter **2001** ,13, R613-R691
[6] Fu, J. et al, Biomaterials **2005**, 26, 6684-6692
[7] Kabib, A. E. et al, Chem. Mater. **2008**, 20, 2198-2204
[8] Habibi Y. et al, Chem. Rev. 110 **2010**, 3479-3500
[9] Rinaudo M. et al, Prog. Polym. Sci 31 **2006** 603-632
[10] Vandamme E.J. Biopolymers Vol 6: Polysacch. II, **2002**

Nano-hybrid PDMA/silica hydrogels: from structure to mechanical properties

S. Rose, A. Marcellan, T. Narita, D. Hourdet

Physico-Chemistry of Polymers and Dispersed Media, UMR 7615, ESPCI

Severine.rose@espci.fr

Introduction

Hydrogels are cross-linked polymers forming a three-dimensional network highly swollen in aqueous environment. The low fracture toughness of these systems is a limiting factor for their potential applications molecular sieves, super absorbent polymers or contact lenses. Among the different reinforcement strategies of the mechanical properties of hydrogels, we chose to focus on the impact of inorganic nanoparticles in soft polymer networks. This concept came from Haraguchi in Japan who studied polymer/inorganic clay networks[1,2]. In our laboratory, we recently started to investigate the interactions between poly(N,N-dimethylacrylamide) and silica nanoparticles and their effects on the mechanical properties of PDMA/silica hydrogels[3,4].

Materials and methods

Hybrid hydrogels have been prepared at room temperature by free-radical polymerization in water of N,N-dimethylacrylamide (DMA) in the presence of silica nanoparticles (R=17 nm), using potassium persulfate (KPS) and N,N,N',N'-tetramethylethylenediamine (TEMED) as redox initiator. A chemical cross-linking agent was also used: N,N'-methylenebisacrylamide (MBA). Several weight ratios (silica/polymer and polymer/water) and several amounts of covalent cross-linking agent were tested, keeping constant the molar ratio DMA/KPS/TEMED.

Results and discussion

Swelling experiments, performed in water and salt solutions, show that the swelling ability of the network decreases with the amount of added particles (Figure 1). These results clearly indicate that silica beads really behave as physical crosslinkers by strongly interacting with PDMA chains.

The mechanical behaviour of hydrogels was characterized using monotonic tensile tests, loading-unloading cycles and stress relaxation.

The introduction of silica highly increases the stiffness of the network, in agreement with the strong interactions taking place between PDMA chains and silica surfaces. Non-linear behaviours were also pointed out with softening at small deformation and hardening at high strain related to finite chain extensibility (Fig. 1). All these effects have been shown to strongly depend on silica content. The analysis of hysteresis and residual strains induced by cycles, clearly indicate that contrary to chemical cross-linkers, hybrid interactions increase the dissipative process. Life-time PDMA-Silica interaction seems to be key-aspect in these mechanical properties. (Fig. 2)

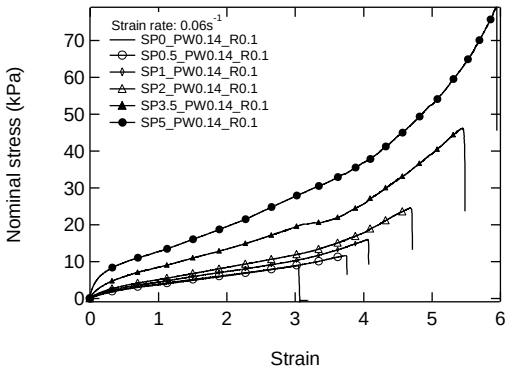

Fig. 1: Typical tensile stress-strain curves ($\dot{\varepsilon}$ ~0.06 s^{-1}) effect of filler content

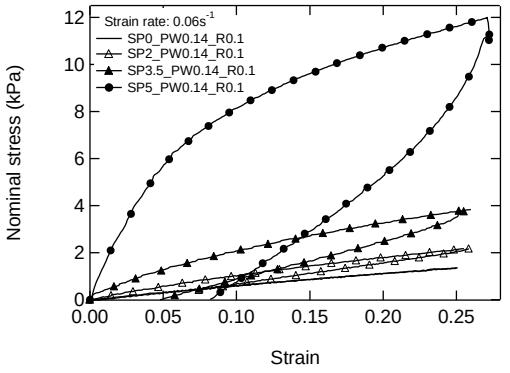

Fig. 2: First loading-unloading cycle, εmax=0.25 ($\dot{\varepsilon}$ ~0.06s^{-1})

Finally, the internal structure of hydrogels and the distribution of inorganic particles inside the organic matrix were also investigated by small angle neutron scattering. The dynamic properties at small lengths and short time scales of the networks were studied by dynamic light scattering.

Conclusion

We have successfully shown a strong and reversible interaction between PDMA and silica particles. We pointed out that silica nanoparticles greatly enhance the mechanical properties of hydrogels, keeping a high deformability.

References

4. Haraguchi, K.; Farnworth, R.; Ohbayashi, A.; Takehisa, T., *Macromolecules* **2003,** *36*, 5732 – 5741
5. Haraguchi, K.; Takehisa, T., *Adv. Mater.*, **2002,** *14*, 1120
6. Lin, W.-C., Fan, W., Marcellan, A., Hourdet, D., Creton, C., *Macromolecules*, **2010**, *43*, 2554.
7. Carlsson, L., Rose, S., Hourdet, D., Marcellan, A., *Soft Matter*, **2010**, *6*, 3619-3631.

Structure/highly electrical conductivity relationships of gold nanowires/P(VDF-TrFE) nanocomposites

Antoine Lonjon[1], Lydia Laffont[2], Philippe Demont[1], Eric Dantras[1], Colette Lacabanne[1]

[1] Physique des Polymères – Institut Carnot CIRIMAT Université Paul Sabatier, Toulouse, France
[2] Institut Carnot CIRIMAT, ENSIACET, Toulouse, France

lonjon@cict.fr

A low content of conductive fillers can significantly improve the electrical properties of an insulating polymeric matrix. These improvements are achieved through conventional processing techniques without any negative effects on mechanical behavior of the matrix. Typical mixed fillers into polymer matrix are carbon black, CNTs and metal particles. These studies showed that electrical and mechanical properties of reinforced polymer composites depend on many factors; such as particles intrinsic properties, dispersion quality, orientation, interfacial adhesion, aspect ratio and filler content. The dispersion quality was especially well-known as one of the most important factors in electrical properties with specific difficulties to control it in nanocomposites. Experimental percolation threshold was known to be strongly dependent on the apparent aspect ratio of the filler and not on their nanometric size. Very low percolation threshold were obtained with introduction of CNTs with aspect ratio ζ higher than 100 and even 1000. The literature reaches a consensus: above the percolation threshold (<5 vol %), the conductivity value of CNTs composites levels off at an upper limit[1] of about 10^{-1} S.m^{-1}. Metal nanowires (NW) have attracted much attention because of their specific properties such as intrinsic electrical conductivity.

In order to obtain higher electrical conductivity, the introduction of metallic nanowires, with a good aspect ratio sounds pertinent[2]. In this study, gold nanowires were prepared in order to elaborate high conductive nanocomposites at low Au NW volume fractions to preserve the mechanical properties of the P(VDF-TrFE) matrix. Gold nanowires were synthesized by electrochemical way giving a uniform high aspect ratio ($\zeta \sim$ 200). AuNW polymer composites were elaborated by addition of AuNW in a PVDF-TrFE matrix[3].

The conductivity of melt-pressed nanocomposite films has been studied as a function of AuNW volume fraction and it shows a very low percolation threshold (p_c) near 2.2 vol%. At the percolation threshold p_c, the volume electrical conductivity of nanocomposites exhibits a critical behaviour from 10^{-12} S.m^{-1} to 10^{2} S.m^{-1}. The influence of process on the percolation threshold value was studied. It is crucial to emphasize that electrically percolated AuNW nanocomposites reach an electrical conductivity 10^3 times higher than the one of CNTs namocomposites independently of the process. Despite moderate aspect ratio regarding CNTs, metallic nanowires represent a very promising route for improvement of the electrical conduction in polymer matrix composites

The increase of Au nanowires volume fraction on the morphology and crystallization of P(VDF-TrFE) matrix was investigated by differential scanning calorimetry[4].

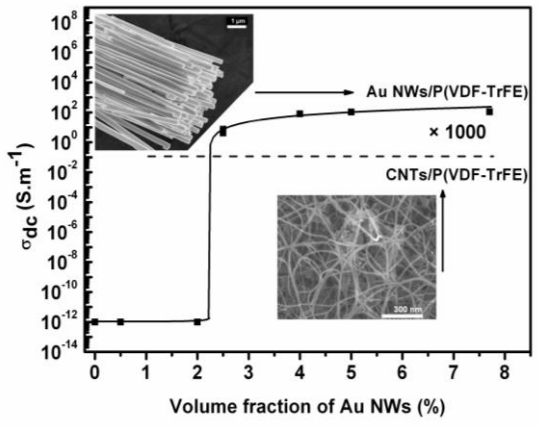

Moreover, the surface resistivity of spray coatings has been studied as a function of AuNW volume fraction and it shows the existence of a very low percolation threshold around 2 vol%. The surface resistivity above the percolation threshold reachs a low value near 4 Ω/□. This value is more than 1000 times lower than sprayed CNT coating.

1. Bauhofer W., Kovacs J.Z., A review and analysis of electrical percolation in carbon nanotube polymer composites. *Composites Science And Technology*. **69**: 1486-1498 (2009).
2. Lonjon A., Laffont L., Demont P., Dantras., Lacabanne C., New Highly Conductive Nickel Nanowire-Filled P(VDF-TrFE) Copolymer Nanocomposites: Elaboration and Structural Study. *Journal of Physical chemistry C*. **113**: 12002-12006 (2009).
3. Lonjon A., Laffont L., Demont P., Dantras., Lacabanne C., Structural and electrical properties of gold nanowires/P(VDF-TrFE) nanocomposites. *Journal of Physics D: Applied Physics*. **43**: 345401 (2010).
4. Lonjon A., Nanocomposite conducteur polymère/nanofils métalliques : élaboration et analyse des proprétés physiques. *Université de Toulouse: PhD Thesis* (2010).

Design of "All-supramolecular" nanocapsules made of low-molecular weight bis-ureas through interfacial reaction in miniemulsion

E. Groison, S. Adjili, A. Ferrand, F. Lortie, N. Sintes-Zydowicz and D. Portinha

Université de Lyon, INSA-Lyon, UCBL, CNRS, France

daniel.portinha@insa-lyon.fr@insa-lyon.fr

Introduction

The preparation of polymeric nanocapsules has attracted an intense interest in recent years due to their potential applications in fields such as controlled drug-delivery or contrast agents. In this frame, the miniemulsion process represents a well-suited strategy, due to its versatility making it possible to obtain oily or aqueous-core with different kind of polymers (vinylic, urethane, urea…) as the membrane [1-3] However, the major limitation of polymer-based nanocapsules is the lack of permeation pathway through a high molecular weight polymer membrane [4] This contribution presents a new strategy for preparing nanocapsules with a shell made of a supramolecular polymer which repeating units are held together by reversible interactions rather than covalent bonds [5]. These nanocapsules were prepared in classical miniemulsion through interfacial addition reaction of a diisocyanate (IPDI) and a monoamine (iBA), forming low-molecular weight bis-ureas moieties (M1) which are strong self-complementary interacting molecules through hydrogen-bonding. As a comparison, a diamine (DAB) was used to prepare oligo/polyurea-based nanocapsules (M2).

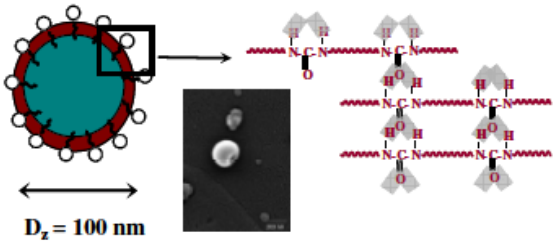

Materials and Methods

Chemicals were purchased from Aldrich and used as received. For preparing the miniemulsion, SDS (3wt% relative to the organic dispersed phase) was added to deionized water. A mixture of cyclohexane containing hexadecane (3wt%) and IPDI (10wt%) was added under magnetic stirring to the aqueous phase. The miniemulsion was then prepared by ultrasonifying the previous emulsion for 5 min. An aqueous solution of iBA was continuously added using a syringe pump operating at a flow rate of 1 ml/min, under magnetic stirring. The reaction mixture was then maintained under magnetic stirring at room temperature for 4 hours. SEM experiments were performed on a Hitachi S800. The size distribution of the nanocapsules was determined by DLS on a Malvern Nanosizer ZS. ^{1}H NMR analyses were recorded on a Bruker Avance II 250 spectrometer in d_6-DMSO at 298K. MALDI-TOF MS experiments were conducted using Voyager-DE PRO equipped with a N_2 laser (λ = 337 nm). The spectra were recorded in reflection mode.

Results and Discussion

Oily core low-molecular-weight urea-based nanocapsules were successfully obtained through interfacial reaction in direct miniemulsion between a diisocyanate and a monoamine. The control over the stability of the latex and the absence of any coagulum require a careful adjustment of the rate of addition of the amine to the miniemulsion. For the dimensions of the nanocapsules, measured by DLS, M1 nanocapsules present a D_z around 100 nm with a low PDI (0.11), while the M2 nanocapsules present a higher mean-diameter (150 nm) with a less well-defined distribution (PDI = 0.15). SEM pictures for M1 system show dented nanometric spherical objects attesting for their internal cavity, which dimensions are in the same order of magnitude than the values determined by DLS. Surprisingly, the nanocapsules from M2 could not be observed, as if the membrane was so brittle that it could not resist to the preparation of the SEM sample. Then the nanocapsules membranes were characterized by ^{1}H NMR and MALDI-TOF MS. The spectrum for M1 presents one main peak at m/z equal to 391.4 Da and some other peaks (at 587.4 and 783.6 Da) which global contribution is very small. The first peak corresponds to the cationized bis-urea molecule (MNa+), whereas the quite less intense peaks correspond to tris and tetra-urea resulting from the reaction between IPDI with isophorone diamine, the side-product of the IPDI total hydrolysis. Because of similar structures, the relative intensities of the peaks can be considered as indicative of the mixture composition. For M1, the membrane is composed of more than 95% of bis-urea molecules. In addition, the thorough examination of the ^{1}H NMR spectrum obtained for the M1 sample confirms that the membrane is mainly composed of bis-ureas, and hence asserts the MALDI-TOF MS results. For M2, MALDI-TOF spectrum of nanocapsules reveals many peaks between m/z 311.1 and 1884.4 Da, attesting that oligomers were formed: one set of peaks can be ascribed to the products of the polyaddition of the IPDI on the DAB (Δ(m/z) = 310 Da), with isocyanate and amine groups as chain ends. Another peak at m/z equal to 507.1 was also observed and assigned to a minor species.

Conclusions

This strategy opens the scope of a new type of nanomaterials exhibiting stimuli-responsiveness due to the reversible interaction linking the repeating units.

References

[1] A.J.P. Van Zyl, R.F.P Bosch, J.B. McLeary, R.D. Sanderson, B. Klumperman, *Polymer* **2005**, *46*, 3607.

[2] G. Lambert, E. Fattal, H. Pinto-Alphandary, A. Gulik, P. Couvreur, *Pharm. Res.* **2000**, *17*, 707.

[3] L.Torini, J.F. Argillier, N. Zydowicz, *Macromolecules* **2005**, *38*, 3225;

[4] A. Kishimura, A. Koide, K. Osada, Y. Yamasaki, K. Kataoka, *Angew. Chem. Int. Ed.* **2007**, *46*, 6085.

[5] E. Groison, S. Adjili, A. Ferrand, F. Lortie, D. Portinha, N. Sintes-Zydowicz, *Macromol. Rapid Comm.*, **2011**, DOI: 10.1002/marc.201000662

Synthesis and Characterization of PCL-b-PLA Di-Block Copolymers

Laura Peponi[1], *Leandro Casaban*[1,2], *Angel Marcos-Fernandez*[1], *José M. Kenny*[1]

[1]Instituto de Ciencia y Tecnología de Polímeros (C.S.I.C.)
[2] University of Perugia, Italy

lpeponi@ictp.csic.es

Introduction

Block copolymer materials have attracted a great deal of attention in the last decades due to their ability to self-assemble into different nanostructures[1-2]. While in polymer blends the constituting polymers separate at macroscopic scale ruled by enthalpic/entropic phenomena, in block copolymers the phase separation occurs in the nanometre range taking advantage of the covalent bonding between the constituting blocks. In fact, the immiscibility of the constituent blocks is responsible for this ability of block copolymers to self-assemble into well-defined ordered nanostructures with domain dimensions of 5-100 nm. The obvious interest in using these materials for patterning lays on their ability to self-assemble forming a dense array of nanostructures having dimensions and spacing which are difficult to obtain by other ways, or are prohibitively expensive to fabricate using conventional lithographic processes.

In this work di-block copolymers based on aliphatic polyesters such as polylactic acid (PLA) and poly(ε-caprolactone) (PCL) have been synthesized and characterized (PCL-b-PLA), based on the idea that both PLA and PCL are biodegradable and biocompatible polyesters[3-5] and promising materials in regenerative medicine as they degrade through hydrolytic scission of the ester group. Moreover, both of them present good processability, mechanical properties and shape memory effects.

Materials and Methods

PCL-b-PLA block copolymers have been synthesized by ring opening of the corresponding lactones using tin octoate as catalyst. After the polymerization of PCL with n-butanol as initiator to obtain different lengths, L-lactide has been added in different percentage. The copolymerization of the PCL-b-PLA block copolymers has been obtained at 180 ºC for 3 h.

Solution ^{1}H-NMR was recorded at room temperature for $CDCl_3$ on a Varian Unity Plus 300.

Matrix-assisted laser desorption ionization time-of-flight (MALDI-TOF) spectra were obtained by using a Voyager DE-PRO time-of-flight mass spectrometer (Applied Biomaterials) in the linear mode.

SAXS measurements were taken at beamline BM16 at the European Synchroton Radiation Facility (Grenoble, France).

Differential scanning Calorimetry (DSC) was performed in a Mettler Toledo 800. Samples were sealed in perforated aluminium pans. Two heating scans have been performed at 10 ºC/min.

Atomic Force Microscopy (AFM) analysis has been performed by Nanoscope IV of Digital System.

Results and Discussion

In order to make a deep analysis on the morphological changes and how the nanostructurable architectures of PCL-b-PLA block copolymers can be changed, different PCL-b-PLA block copolymers have been synthesized.

Taking into account that the self-assembled ability of block copolymer materials is influenced by their Flory-Huggins interaction parameter χ, their molecular weight, the volume fraction of the block Φ, and also by the conditions of preparation, the PCL-b-PLA block copolymers have been synthesized varying both the length of the blocks as well as the molecular weights of each block.

The chemical structure has been analysed by nuclear magnetic resonance spectroscopy, NMR and MALDI TOF experiments facilitating assignment of the block-length and the molecular weights of each synthesized PCL-b-PLA block copolymer.

The block nature of the synthesized copolymers has been demonstrated by NMR.

Morphological structure has been studied by Atomic Force Microscopy (AFM) and compared with the results obtained by Small Angle X-Ray (SAXS) experiments.

The influence of the nature of the block copolymer and the amount of each block in the amorphous and/or crystalline nature of the PCL-b-PLA block copolymers have been verified by DSC thermograms and SAXS experiments.

Finally, both the different amount such as the different length of the blocks influences the degree of crystallinity of the synthesized PCL-b-PLA block copolymers.

Conclusions

PCL-b-PLA block copolymers with different block lengths as well as different molecular weights have been synthesized. In general both Tc and Tm of PLLA blocks are affected by the presence of PCL. So, the degree of crystallinity of PLLA decreases by increasing PCL content. Moreover the amount and molecular weight of PCL influences the morphology as well as the crystallinity of PCL-b-PLA block copolymers.

References

1. L. Peponi, et al., *J. Phys. Chem. C* **2009**, *113*, 17973.
2. L. Peponi, et al. *Carbon* **2010**, *48*, 2590.
3. D. Cohn, et al., *Biomaterials* **2005**, *26*, 2297.
4. R. V. Castillo, et al., *Macromolecules* **2010**, *43*, 4149.
5. R.M. Michell, et al., *Eur. Polym. J.* **2010**, *46*, 1334.

Foaming in CO2 *sc* medium as an efficient way to produce Electromagnetic Interference Shielding Materials

*L. Monnereaua, J.-M. Thomassina, N. Quiévyb, P. Bollenb, S. Eggermontb, T. Pardoenb, C. Baillyb, I. Huynenb, C.Jérômea, C. Detrembleura**

aCenter for Education and Research on Macromolecules (CERM), University of Liège, Sart-Tilman, B6a, 4000 Liège, Belgium. bResearch Center in Micro and Nanoscopic Materials and Electronic Devices, CeRMiN, Université Catholique de Louvain, 1348, Louvain-la-Neuve, Belgium

lmonnereau@ulg.ac.be, christophe.detrembleur@ulg.ac.be

Introduction. The sharp increase in electromagnetic pollution due to the fast development of gigahertz electronic systems and telecommunications justifies a very active quest for effective electromagnetic interference (EMI) shielding materials. Most of the time, metallic boxes are used as shielding materials, acting as EMI reflectors and not as absorbers[1]. As an alternative, polymers filled with carbon fillers[2] (e.g., carbon black, carbon fibers and carbon nanotubes) have been extensively investigated for EMI shielding purposes because of unique combination of electrical conductivity and polymer flexibility. The use of carbon nanotubes (CNT) offers substantial advantages over conventional carbon fillers because they can simultaneously enhance the electrical conductivity and reinforce the mechanical performances of the filled polymers.[3] A major drawback of CNT/polymer nanocomposites[4] is a high propensity to reflect EM radiations instead of absorbing. For the particular case of electronic device protection, the emitted wave does not cross the composite material, but EMI prevails in the inner volume as a result of multiple reflections from the walls, that may alter proper operation of the device (cf. fig. 1).[5]

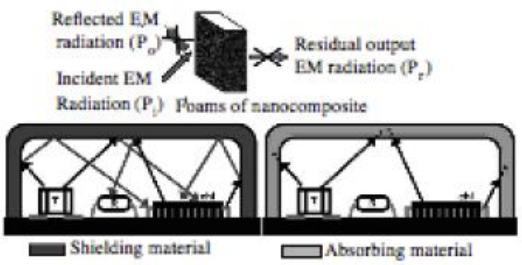

Fig. 1: a) Behavior of MWNT/polymeric foams under EMI radiation, b) schematic differences between an EMI shielding material which only reflects the wave and an EMI absorber in an electronic device.

For an EMI shielding material to absorb electromagnetic radiations, its dielectric constant must be as close to that of air as possible.[5] A straightforward approach to this highly desirable situation relies to foaming of CNT containing polymers. The relative volume of air in an open-cell foam is high, and therefore favorable for the matching of the wave impedances of the expanded material and the ambient atmosphere.

Results and Discussion. This communication reports on the preparation of novel nanocomposites foams that are efficient broadband microwave absorbers.[7] Multi-walled carbon nanotubes (MWNT) are first successfully dispersed into polymer matrix by melt-blending as confirmed by TEM microscopy and rheology. Then foaming of these nanocomposites[8] occurs under supercritical CO_2 conditions by a two-step process.[9] This physical foaming constitutes a green alternative to classical foaming agents.[10] Well-defined microcellular foams[11] were obtained with cell size around 10-50 µm and cellular density around 10^8 cells per cm3, the morphology of the foam was determined by SEM microscopy. The impact of several criteria on the morphology of the foam will be discussed. The EMI shielding efficiency of these materials are then evaluated and compared to the non-foamed nanocomposites. Finally, we will discuss about the design of the foam that is essential to optimize the performances of the EMI absorber.

Conclusions. New nanocomposite materials with high electromagnetic wave absorption effectiveness have been successfully prepared with the use of supercritical CO2 as the foaming agent. It was found that adding voids into the nanocomposite improved substantially the wave absorptive capacity, thus reducing greatly the signal reflection. The resulting material is also much lighter and more flexible than metallic counterparts currently used, making them very attractive from an industrial point of view.

References.

[1]S. Vulpe, F. Nastase, C. Nastase, I. Stamatin, Thin Solid Films, 2006, 495, 113.

[2]A. Saib, L. Bednarz, R. Daussin, C. Bailly, X. Lou, J.-M. Thomassin, C. Pagnoulle, C. Detrembleur, R. Jerome, I. Huynen, IEEE Trans. Microave. Theory Tech., 2006, 54, 2745.

[3]Y. L. Yang, M. C. Gupta, K. L. Dudley, R. W. Lawrence, J. Nanosci. Nanotechnol., 2007, 7, 549.

[4]Y. L. Yang, M. C. Gupta, Nano Letters 2005, 5, 2131.

[5]J.-M. Thomassin, C. Pagnoulle, L. Bednarz, I. Huynen, R. Jérôme, C. Detrembleur, J. Mater. Chem., 2008, 18, 792.

[7]D. M. Pozar, Microwave Engineering, Addison-Wesley, New York, 1990. H. Qian, E. S. Greenhalgh, M. S. P. Shaffer, A. Bismarck, J. Mater. Chem., 2010, 20, 4751.

[8] J. M. Thomassin, X. Lou, C. Pagnoulle, A. Saib, L. Bednarz, R. Jérôme, C. Detrembleur, J. Phys. Chem. C, 2007, 111, 11186-11192.

[9]L. Urbanczyk, C. Caldberg, C. Detrembleur, C. Jérôme, M. Alexandre, Polymer, 2010, 51, 3520.

[10]L. J. M. Jacobs, M. F. Kemmere, J. T. F. Keurentjes, Green Chemistry, 2008, 10, 731-738.

[11]S. P. Nalawade, F. Picchioni, L. P. B. M. Janssen, Progress in Polymer Science, 2006, 31, 19-43. Acknowledgements: The authors are grateful to the « Région Wallone » in the frame of the MULTIMASEC project and to the National Funds by Scientific Research (FRS-FNRS, Belgium) for financial support.

Ag(PbS)/Poly-p-xylylene Nanocomposites by VDP-Method

Sergei Ozerin[1], Alexei Gusev[2], Karen Mailyan[2], Andrei Pebalk[3], Ilya Ryzhikov[2], Sergei Zavyalov[3], Sergei Chvalun[1]

[1]Enikolopov Institute of Synthetic Polymeric Materials, 70 Profsoyuznaya str., 117393 Moscow, Russia
[2]Institute for Theoretical and Applied Electromagnetics, 13/19 Izhorskaya str., 125412, Moscow, Russia
[3]Karpov Institute of Physical Chemistry, 10 Vorontsovo pole, 105064 Moscow, Russia

e-mail: sergeoz@yandex.ru

Hybrid polymer/metal(semiconductor) nanocomposites are of great interest recently. Low cost, the simplicity of preparation, the wide spectrum of stable properties are the critical points for possible applications of hybrid nanocomposites as photovoltaic solar cells, light emitting diodes, magnetic media storage capacity, chemical sensors and others. It is important that, the properties of hybrid nanocomposites depend not only on the Coulomb blockade phenomenon and on the quantum size dependent characteristics of low-dimensional metal and semiconductor nanoparticles or nanowires, but on the interaction in the assemble of clusters, its structure and on the nature of interface between the polymeric matrix and the nanoparticles. The new VDP-based method of synthesis of hybrid nanocomposites, their structure and their electronic, magnetic, photophysical and sensoric properties will be presented.

The vapors of monomer of p-cyclophanes and of the various metals or semiconductors were simultaneously deposited in the vacuum on the substrate cooled by liquid nitrogen. The active intermediate were prepared by pyrolysis of cyclophanes at 650-700°C (Gorham's method) the metal or semiconductors were evaporated thermally or by e-beam sputtering. The following heating of the prepared cocondensate is accompanied by the several simultaneous processes, such as the polymerization and crystallization of matrix and the aggregation on inorganic into nanoparticles or into nanowires. The schematic of process is presented in the figure.

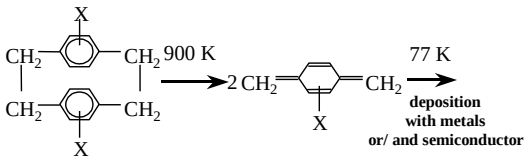

p-cyclophanes (vapor) p-xylylenes (vapor) (PX)

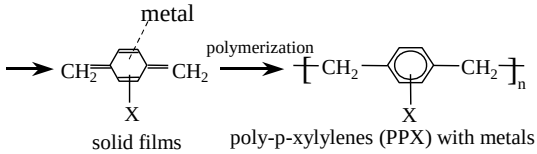

solid films poly-p-xylylenes (PPX) with metals

The thin films containing the nanoparticles of metal (Ag) and semiconductor (PbS) were prepared.

The processes of polymerization and structural organization were studied by the complex of experimental methods including UV-spectroscopy, X-ray diffraction, DSC and AFM.

On X-Ray patterns of samples, containing less, than 10 % of silver, a wide diffuse maximum, corresponding to d-spacing d ~ 0.23 nm, was observed. With increasing metal concentration, reflections 111 and 200 of silver crystal lattice, become narrower to be resolved. Correspondingly, average crystallite size increases from 2.5 to 5.0 nm.

Crystal structure of PPX is presented by a mix of β- and α-modifications, the former one being dominant. Simultaneous co-condensation of polymer and inorganic component lead to the formation of composite material, characterized by dominance of α-form in PPX matrix. This can be explained by the influence of "hot" silver atoms on PPX polymerization process.

Small-angle X-Ray studies showed, that scattering curves of composite materials with silver content less than 4% or more, than 8%, are well described by compact particle scattering model of 4nm and 6nm in size correspondingly. High-temperature vacuum annealing of the samples (30 min at 150 ºC) lead to the recrystallization of polymer matrix and to the growth of silver particles.

The structural investigations of PbS/PPX nanocomposite films showed the presence of inorganic nanoparticles embedded in the polymer matrix. Five reflections (111, 200, 220, 311, 222) corresponding to crystal lattice of PbS along with intense reflection of PPX were observed. At low concentration the PPX is polymerized in β-form and at higher concentration it formes α-structure as in the case of silver nanoparticles. The average crystallite size of PbS estimated from halfwidth of reflection 220 is equal approximately to 4.5 nm.

The presence of crystalline reflections and amorphous halo of PPX on diffraction pattern points to the semicrystalline structure of polymeric matrix. Note that the lateral crystallite size of polymer lamellae exceeds 20 nm and is significantly larger than the crystal size of inorganic compound. The volume distribution is narrow with maximum at app. 4 nm; the main population of PbS crystallites has a size much less than 10 nm. The distribution curve for the nanocomposite containing 4.7 vol.% of PbS is well described by a lognormal distribution. For higher concentrations the distribution is bimodal and each mode is described by normal distribution. We can propose mechanism of inorganic particles formation based on the shape of size distribution. The lognormal distribution corresponds to the Brownian coagulation models and in the case of normal distribution the particles formation is due to particles diffusion during the polymerization and crystallization of the polymer matrix.

The slope of the tail part of SAXS curve of PbS/PPX equals to -4.8, which is typical for the dense three-dimensional particles with the interface on the boundary.

This work was supported by the Russian Foundation for Basic Research (grant #09-03-00331, 09-03-00674)

Relaxation Dynamics in Ultrathin Polymer Films Investigated at the Nanoscale

K. H. Nguyen[1]*, *D. Prevosto*[2], *M. Labardi*[2], *S. Capaccioli* [1,2], *M. Lucchesi*[1,2], *P.A. Rolla*[1,2]

[1] Dipartimento di Fisica, Università di Pisa, Largo Pontecorvo 3, 56127 Pisa, Italy
[2] Istituto per i Processi Chimico-Fisici, CNR, Largo Pontecorvo 3, 56127 Pisa, Italy

*Email address: nguyen@df.unipi.it

Ultrathin polymer films with thicknesses of tens of nanometers have been used as an ideal sample geometry for studying the effects of one-dimensional confinement and polymer-substrate interactions on the morphology and dynamics of the polymeric materials. These effects on dynamic relaxation of ultrathin polymer films have been investigated effectively on macroscopic scale using a variety of techniques[1]. Some attempts to detect the local dielectric response have been recently performed by using electrostatic force microscopy technique. In this technique, one electrode is represented by the conductive substrate where the sample is deposited, and the second electrode is the conductive probe tip of an atomic force microscope (AFM). Most implementations until now have been exploited to measure dielectric constant of thin insulator films[2]. A possible approach to obtain highly local measurements of dynamics of ultrathin films is the local dielectric spectroscopy (LDS)[3,4].

LDS has been implemented by means of an atomic force microscope (AFM)-based method named frequency-modulated electrostatic force microscopy. In essence, an excitation voltage, $V(t) = V_{ac} \cos(\omega t)$, is applied to the conductive probe of the AFM, producing an electric field in the sample region close to the probe, which induces dielectric polarization. The force field due to interaction of the charged probe with the polarized sample induces a variation of the cantilever resonant frequency. This variation at the second harmonic, 2ω, which is related to the dielectric polarization of the sample, is measured in amplitude and phase. Information on the dielectric relaxation can be then obtained. We applied this technique to study the change in structural dynamics of poly(vinyl acetate) (PVAc) at different interfaces, such as in presence of silicate nanoparticles with high spatial resolution[4] and in ultrathin polymer films deposited on a metallic substrate.

In particular, ultrathin polymer films with a free upper surface have been studied for different values of thickness, temperature and over different substrates, in ambient pressure and controlled atmosphere (relative humidity less than 8%).

An increase in dynamics of PVAc films coated on gold has been detected when film thickness decreases down to 35 nm (Fig. 1). At smaller thicknesses the deviation respect to the bulk becomes even larger but not greater than a factor 2 for films of 18 nm thickness[5].

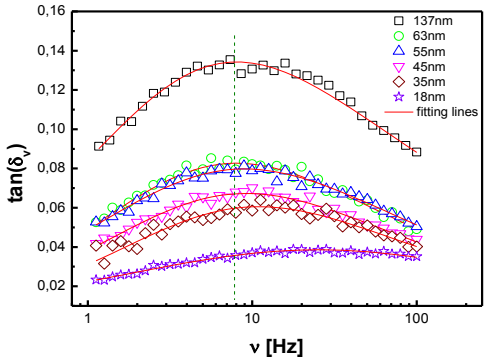

Fig. 1. Frequency dependence of the phase shift spectra ($\tan\delta_v$) on ultrathin PVAc films with different thicknesses, deposited on gold substrate, at the temperature of 324.6 K.

References

[1] C.B. Roth, J.R. Dutcher, J. Electroanal. Chem. 584, 13-22 (2005).
[2] C. Riedel, R. Arinero, Ph. Tordjeman, M. Ramonda, G. Leveque, G.A. Schwartz, D.G. de Oteyza, A. Alegria and J. Colmenero, Eur. Phys. J. Appl. Phys. 50, 10501 (2010).
[3] P.S. Crider, M.R. Majewski, J. Zhang, H. Oukris, N.E. Israeloff, Appl. Phys. Lett. 91, 013102 (2007).
[4] M. Labardi, D. Prevosto, K. H. Nguyen, S. Capaccioli, M. Lucchesi, and P. Rolla, J. Vac. Sci. Technol. B 28(3), C4D11 (2010).
[5] K. H. Nguyen, D. Prevosto, M. Labardi, S. Capaccioli, M. Lucchesi, and P. Rolla, in preparation.

Tuning Thermomechanical Properties of Polystyrene/Polybutadiene-Based Thermoplastic Elastomers by Grafting Crystallizable Side Groups

Julie Prévost[1], *Minh Ngoc Nguyen*[1], *Ilias Iliopoulos*[1], *Ludwik Leibler*[1]

[1]Matière Molle et Chimie, ESPCI ParisTech (ESPCI-CNRS, UMR 7167), 10 rue Vauquelin, 75005 Paris (France)

julie.prevost@espci.fr

Thermoplastic elastomers are of the most successful examples of nanostructured polymeric materials with numerous applications (automotive, footwear, bitumen modifiers, adhesives…)[1]. Polystyrene-*b*-Polybutadiene-*b*-Polystyrene (SBS) triblock copolymer is the archetype in this category. Because of the incompatibility between the hard (PS) and soft (PB) components, microphase separation occurs, resulting in the dispersion of polystyrene domains in a polybutadiene matrix. We propose here an efficient and easy route to tune the properties and the temperature responsiveness of these processable elastomers by grafting crystallizable side groups on the PB block.

The thiol-ene coupling is used to attach crystallizable 1-octadecanethiol (C18) on SBS. The free-radical addition of C18 on the double bonds of the PB block proceeds in solution, in the presence of an initiator, and leads to high yields. Depending on the initial amount of thiol, the degree of functionalization can be modulated in the range from 4 to 30 mol% (referring to all monomer units).

By differential scanning calorimetry (DSC), we show that the thiol-ene coupling yields to graft copolymers with modulable crystallization temperatures by varying the graft content. Dynamic mechanical analysis (DMA) shows a large increase of the glass transition of the modified block and a sharp transition of the storage modulus around the melting temperature, upon grafting C18 (figure 1). While thermal and mechanical properties of the neat SBS are largely affected by grafting alkyl side chains, the cylindrical morphology of the neat SBS is preserved even with high degrees of grafting (figure 2).

In conclusion, the thiol-ene coupling is a simple and robust strategy to graft crystallizable alkyl side chains on SBS and therefore incorpore an additional thermal transition in a classical thermoplastic elastomer. We obtain nanostructured crystallizable graft copolymers with tunable thermomechanical properties by varying the graft content.

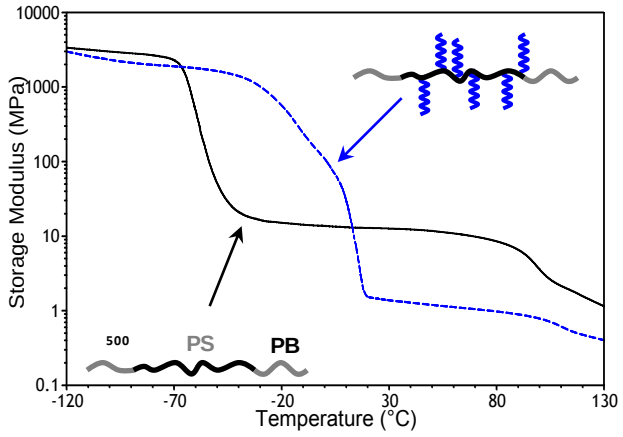

Figure 33: Storage modulus (E') as a function of temperature at 1Hz for the neat (full line) and graft SBS (50 wt % of C18) (dashed line).

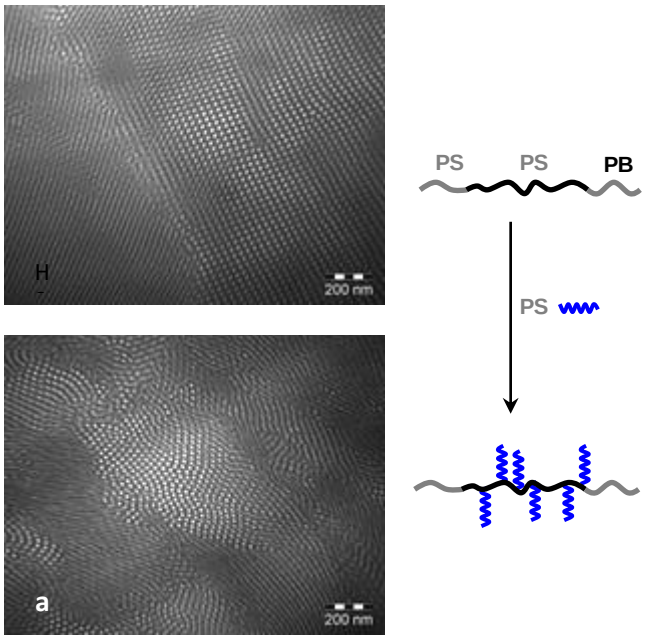

Figure 34: TEM micrographs of films prepared by solvent cast from toluene solutions followed by annealing at 180 °C for 48 h. Copolymers were stained by OsO_4. a) SBS, b) graft SBS (50 wt % of C18).

[1] G. Holden, H.R. Kricheldorf and R.P. Quirk, Editors, *Thermoplastic elastomers* (*3rd ed.*), *Hanser*, Münich (2004)

Dielectric Properties of Poly(ethylene-*co*-butylene) Modified MWCNT/Polypropylene Composites

A.E. Daugaard,[a] *K. Jankova*,[a] *J. Bøgelund*,[b] *J.M.R. Marín*,[a] *S. Hvilsted*[a]

[a]Danish Polymer Centre, Department of Chemical and Biochemical Engineering, Technical University of Denmark, Building 229, Søltofts Plads, DK-2800 Kgs. Lyngby, Denmark (adt@kt.dtu.dk).
[b]Danish Technological Institute, Taastrup, Gregersensvej 3, DK-2630 Taastrup, Denmark.

Introduction

The preparation of multi walled carbon nanotube (MWCNT) composites has received a substantial amount of attention during recent years. It is well known that functionalization of MWCNTs facilitates dispersion of the nanofiller in composite materials. However, there are few examples in the literature where the conductive properties of composites containing functionalized CNTs have been investigated. In these cases it has been shown that the functionalization has had a detrimental effect on the conductive properties of the composite.[1,2]

Here we present a method for functionalization of MWCNTs with poly(ethylene-co-butylene), which is a well known compatibilizer for polypropylene, though to our knowledge has not been used on MWCNTs.

The objective was to exploit the good properties of the compatibilizer to produce composites of functionalized MWCNTs with a relatively low degree of functionalization. The hypothesis was that good dispersion would still be obtainable due to the functionalization, while other properties such as conductive properties and potentially also mechanical improvements would not be substantially deteriorated or possibly even improved.

Methods and Materials

MWCNTs with an average diameter of 9.5 nm and average length of 1.5 µm were purchased from Nanocyl S. A. (Belgium). Poly(ethylene-*co*-butylene)-OH (M_n=7000 g/mol, Kraton Liquid Polymer L-1203) was acquired from Kuraray Co., Ltd. (Japan), all other chemicals were purchased from Sigma-Aldrich and used as received.

Results and Discussion

In the presented study a functionalization method based on nitrene chemistry, which is well known in functionalization of CNTs,[3] has been applied to obtain a low degree of functionalization of poly(ethylene-co-butylene) on an industrial grade MWCNT. For this purpose an azide functional poly(ethylene-co-butylene) was synthesized and coupled to the MWCNT as shown in Figure 1.

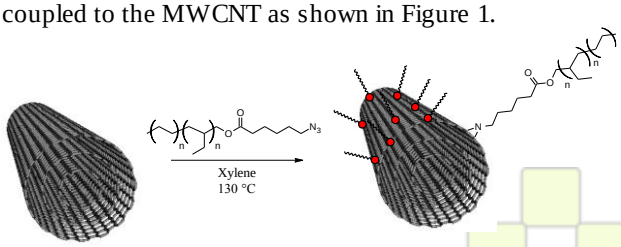

Figure 35: Preparation of Poly(ethylene-co-butylene) modified MWCNT (f-MWCNT).

The functionalization of the f-MWCNT was confirmed by both Raman spectroscopy as well as TGA. PP composites of both pristine as well as the f-MWCNT was prepared in a two step procedure, applying a new masterbatch procedure followed by extrusion on a miniextruder. The PP composites where prepared with a varied concentration of both pristine and f-MWCNT from 0.1 wt% to 1 wt%.

The composites were characterized by both rheology and dielectric resonance spectroscopy (DRS) to describe the extent of dispersion, effects of concentration as well as the conductive properties as shown in Figure 2 for DRS. The f-MWCNT/PP composite was found by DRS to have a percolation threshold below 0.3 wt%.

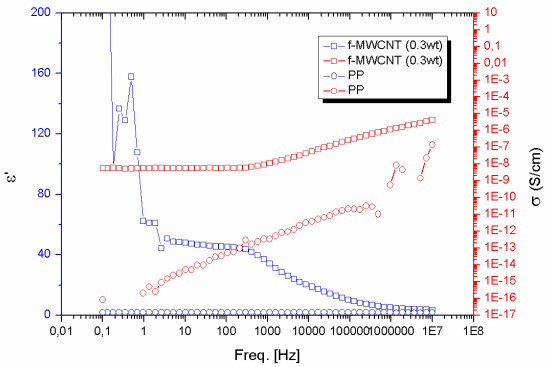

Figure 36: Dielectric resonance spectroscopy of f-MWCNT compared to PP.

Conclusions

A novel f-MWCNT/PP composite was prepared and investigated. Well dispersed materials were prepared through a masterbatch procedure. The f-MWCNT/PP composites were found to have conductivity comparable to the pristine MWCNT/PP. A low percolation threshold was identified for both the modified and unmodified materials.

Acknowledgements

The authors acknowledge the Innovation Consortium ''Extreme Materials for Extreme Environments'' funded by the Danish Ministry of Science Technology and Innovation under contract 08-034101 for financial support. In addition to this, Kuraray Co.Ltd.is thanked for supplying Kraton L-1203.

References

1. Grossiord, N.; Loos, J.; Regev, O.; Koning, C.E. *Chem. Mater.* **2006,** *18*, 1089-1099.
2. McClory, C.; McNally, T.; Baxendale, M.; Pötschke, P., Blau, W.; Ruether, M.; *Eur. Polym. J.* **2010**, *46*, 854-868.
3. Qin, S.; Qin, D.; Ford, W.T.; Resasco, D.E.; Herrera, J.E.; Macromolecules 2004, 37, 752-757.

Electrosynthesis study of poly (N-methyl aniline)/Ag nanocomposite

S.M.Seyed mohaghegh, *F.Ansari*, *B.Najafzadeh*

Iran Polymer & Petrochemical Institute (IPPI) PO Box 14965/115, Tehran, Iran

s.m.mohaghegh@ippi.ac.ir

Introduction

Au Conjugated polymers were first extensively studied for their electrical conductivity and valuable optical and electroluminescence properties [1]. Polyaniline (PANI) occupies a very significant place among these materials because of its high conductivity in the doped state. Recent developments have shown that PANI and its derivatives can also be used in the field of polymer-based light emitting diodes as an interface layer between the metal electrode and the emitting polymer layer to ease charge injection [2].

The composites of conducting polymers, such as polyaniline (PANI), with noble metals find applications in electrocatalysis [3], catalysis [4], design of fuel-cell electrodes, sensors, conducting printing inks, recovery of noble metals etc [5].

Silver has recently received considerable attention in this respect. The first method has only been used exceptionally for modifying silver nanoparticles with PANI or substituted PANI. Composites of silver and PANI have been prepared by the direct reduction of silver nitrate with PANI or PANI derivatives.

Experimental

The electropolymerisation of polyaniline (PANI) and polyaniline/Silver (PANI/Ag) and poly (N-metylaniline) (PNMA) and poly (N- metylaniline)/silver (PNMA/Ag) was carried out in a conventional three electrode electrochemical cell. Gold (Au) disc electrode was used as the working electrode (WE). An Ag/AgCl electrode and a Pt electrode as the reference electrode (RE) and counter electrodes (CE), respectively. The (PANi/Ag) and (PNMA/Ag) nanocomposite film was synthesized by the Cyclic voltammetry (CV) using cell from 0.01 M $AgNO_3$ + 0.4M aniline + 1.0M HNO_3 solution at room temperature.

Results and discussion

It is rather easy to polymerize PANI/Ag, while polymerization of PNMeANI/Ag is more difficult. It is well known that alkyl substituted anilines are oxidized at lower potentials than aniline because the alkyl substituents increase the electron density of the aromatic ring (electron-donating effect). The N-substituted PANI, PNMeANI, has a different electrochemistry from PANI and the other alkyl substituted PANIs due to N-substitution.

It is also known that N-substitution decreases the electrical conductivity of PNMeANI in comparison with PANI. In order to determine the electrochemical property of PANI/Ag and PNMAg nanocomposites film electrode, both PNMAg film and PANI/Ag nanocomposite film electrodes were investigated in 1.0MHNO3 aqueous solution by CV and the corresponding results are shown in Fig.1 and 2 (curve 1, PANI/Ag nanocomposite film; curve 2, PNM/Ag film). not only the anodic current peak but also the cathodic current peak of PANI/Ag nanocomposite film is higher than those of PNM/Ag film.

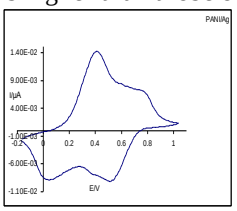

Fig.1 PANIAg in HNO_3 M

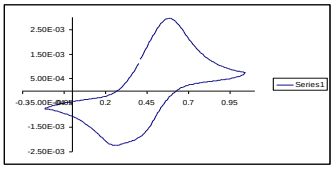

Fig.2 PNMA/Ag in HNO_3 1M

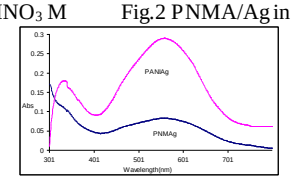

Fig.3 poly(N-alkylanilines)/Ag and PANI/Ag in NMP

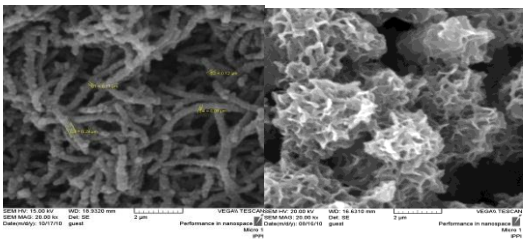

Fig.4 SEM PANIAg (a) and PNMAg(b)

The UV-VIS obtained spectra and SEM images and are given in Fig. 3, 4 respectively. The UV–vis spectra of all the synthesized poly (*N*alkylanilines)/Ag and polyaniline/Ag were in agreement with published patterns. The spectra of poly(*N*-alkylanilines) are composed of one absorption band with a maximum at λ = 325–333 nm assigned to the π–π* transition on the basis of the studies concerning polyaniline. As expected, the band in the region of λ = 560 nm was weak, due to the weak conjugation induced by the modification carried out on the nitrogen atom.

SEM images of the PANIAg (a) nanocomposite powders show non-agglomerated uniformly packed silver particles. The particles are of spherical and granular nature and seem to be nano sized, typically in the range of <50 nm (Fig. 4). SEM images of the PNMAg (b) nanocomposite powders show non-fiber uniformly packed silver particles.

References

[1] Yang Q, Wang Y, Nakano H, Kuwabata S. Polym Adv Technol 2005;16:759.

[2] Sapurina IYu, Kompan ME, Zabrodskii AG, Stejskal J, Trchova´ M. Russ J Electrochem 2007;43:528.

[3] Mourato A, Correia JP, Siegenthaler H, Abrantes LM. Electrochim Acta 2007; 53:664.

[4] Drelinkiewicz A, Waksmundzka-Go´ ra A, Sobczak JW, Stejskal J. Appl Catal A Gen 2007;333:219.

[5] Amaya T, Saio D, Hirao T. Tetrahedron Lett 2007;48:2729.

New Approaches to Development of Equipment for Nanoscale Investigations in Aqueous Solutions of Polymers

D.B.Shaltykova[1], *V.Bublik*[2], *D.Bobrovnokov*[2], *N.Semenyakin*[2], *E.E.Kopishev*[3], *I.K.Nam*[4], *A.Timofeyev*[5]

[1]National Engineering Academy of Kazakhstan
[2]Almaty University of Power Engineering and Telecommunications, Kazakhstan
[3]S.Toraigyrov Pavlodar State University, Kazakhstan
[4]Cheil Industries Inc., Samsung, Korea
[5]al-Faraby Kazakh National University, Kazakhstan

dina_65@mail.ru

Introduction

Experimental investigation of nanoscale processes in polymer aqueous solutions are of a great importance for development of nanomedicine, nanoelectronics as well as fundamental studies of physical chemistry of polymers. Nanoscale details of interpolymer reactions that yet are insufficiently studied may significantly affect structure and properties of resulting interpolymer complexes [1].

However, there are a limited number of instrumental techniques for direct observation of nanostructures only. Most of available devices such as atomic force and scanning electronic microscopes are designed primary for investigation of surfaces of solid bodies.

Therefore development of new methods for investigation of nanostructured polymer complexes in liquid phase with the same accuracy as it is for solids is of importance.

In this work we developed a construction of an instrument intended for measuring electric potential distribution within macromolecular coil per se in solution.

Concept and scheme of measurement of electric characteristics of macromolecular coil in solution

Proposed approach is based on measuring of a differential probe characteristic in solution – aqueous or organic. In case of non-charged macromolecules, a buffer electrolyte is used. The probe characteristic represents a dependence of a probe current on the probe potential; differential probe characteristic is the difference of such currents. It is determined, particularly, by contact difference of potentials probe – solution, depending on whole range of processes taking place on metal surface immersed into the electrolyte or polyelectrolyte solution.

It is shown that even short-term contact between a separate macromolecular coil and the probe results in changing the probe characteristic in correspondent time interval. Using of two closely situated probes allows register such changes by means of self-fluctuations inherent for polymer solution. Resolving power of this method is determined by distribution of electric lines between the edge points. It can be shown that main contribution is made by the macromolecules being in direct contact with the edge points.

Consequently, in the conditions when one edge point is being in contact with one macromolecule while another is not, a differential probe current appears. At chaotic movement of the macromolecules in solution, periodically occur conditions for emerging a differential signal. That signal can be measured directly with the help of differential amplifier that enables avoidance of uncontrolled factors.

The methodology worked-out in atomic-force microscopy is also applicable for fabrication probes with square as small as that of the edge point. Thus, investigation of the single macromolecule's characteristics becomes possible.

In this work we developed a new method for determination of characteristics of macromolecular coil based on measurement of radiofrequency spectrum of the probe signal. The scheme of this device is given in Figure 1.

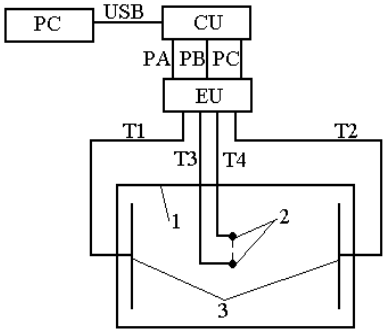

Fig.1. Scheme of the probe signal gauge; 1 – solution, 2 – wire probes coated by isolation, 3 – driving electrodes, EU, CU – controlling and measuring blocks, providing coupling with PC.

This scheme allows measurement of the differential currents up 10^{-6} A. The test measurements of the probe and differential probe characteristic of the aqueous solution of polyacrylic acid were performed. According to the results, the spectrum of the differential signal is in the range up to 5-7 MHz, which is in a good correlation with theoretical calculation. Along with the above said sensitivity, high resistance to vibrations is a considerable advantage of this scheme taking into account that the measurement is conducted in fluctuation regime.

Conclusions

A comparatively simple measurement method for investigation of characteristics of a single macromolecular coil was suggested. It allows obtaining quite accurate data without assembling expensive anti-vibration blocks.

References

1. Ergozhin E.E., Zezin A.B. Suleimenov I.E., Mun G.A. Hydrophilic polymers in nanotechnology and nanoelectronics (in Russian), Almaty-Moscow: LEM, 2008, 214 p.

Interpolyelectrolyte Complexes Based on Star-Like Polyionic Species

Dmitry V. Pergushov[1], Ivan A. Babin[1], Andrea Wolf[2], Holger Schmalz[2], Alexander B. Zezin[1], Axel H.E. Mueller[2]

[1]Department of Polymer Science, School of Chemistry, Moscow State University, 119991 Moscow, Russia
[2]Makromolekulare Chemie II, Universitaet Bayreuth, 95440 Bayreuth, Germany

pergush@genebee.msu.ru

Introduction

During the last years, polymer scientists have focused considerable attention on the easy design of multifunctional macromolecular architectures with a specific combination of properties required for their desired end-use applications. One of the possible approaches for building up such architectures is to apply macromolecular co-assembly processes, in particular, the electrostatically driven co-assembly occurring upon the simple mixing of aqueous solutions of oppositely charged polyelectrolytes (PEs), often referred to as interpolyelectrolyte complexation. This process results in the formation of interpolyelectrolyte complexes (IPECs), which represent macromolecular co-assemblies stabilized by a cooperative system of interpolymer salt bonds. IPECs are of considerable interest because of their promising applications in agriculture, water treatment, biotechnology, and medicine.

Up to now, studies on IPECs have mostly been focused on the macromolecular co-assemblies formed by the oppositely charged linear PEs. The significant progress in the controlled synthesis of well-defined polymers achieved during the last years has offered unique possibilities for designing novel macromolecular co-assemblies comprising PE species with nonlinear topologies. These co-assemblies considerably increase the complexity of the IPECs, into which new properties can be imparted.

In this contribution, we consider IPECs resulting from the interaction of the star-like polyionic species, viz., star-shaped PEs and star-like micelles of ionic amphiphilic diblock copolymers, (a) with the oppositely charged linear homopolyelectrolytes and (b) with the oppositely charged double hydrophilic diblock copolymers.

Materials

Star-shaped poly(acrylic acid) (5, 8, 21 arms, DP_n(arm) ≅ 100) or star-shaped poly([2-(methacryloyloxy)ethyl] trimethylammonium iodide) (5.6, 11, 24 arms, DP_n(arm) ≅ 170 ÷ 240) were used as star-shaped PEs. Poly(isobutylene)-block-poly(methacrylic acid) diblock copolymers (DP_n(PIB) = 20, DP_n(PMAA) = 100 ÷ 425) were used as ionic amphiphilic diblock copolymers. Exhaustively quaternized poly(vinyl pyridine)s (DP_n ≅ 35 ÷ 440) and poly(acrylic acid) (DP_n ≅ 35 ÷ 500) were used as linear homopolyelectrolytes. Exhaustively quaternized poly(vinyl pyridine)-block-poly(ethylene oxide) diblock copolymers were used as double hydrophilic diblock copolymers (DP_n(PVPq) = 40 ÷ 70, DP_n(PEO) = 210 ÷ 450).

Results and Discussion

Using a combination of various techniques, viz., turbidimetry, dynamic/static light scattering, analytical ultracentrifugation, small-angle neutron scattering, fluorescence spectroscopy (with the use of pyrene as a probe), cryogenic transmission electron microscopy, we found that, if the certain conditions are met, the interpolyelectrolyte complexation of the star-shaped polyions and star-like micelles of ionic amphiphilic diblock copolymers with the oppositely charged linear PEs or double hydrophilic diblock copolymers can result in the formation of soluble in aqueous media distinctly compartmentalized nanosized complex species. The obtained experimental results strongly suggest that the formed macromolecular co-assemblies have peculiar “core-corona” (star-shaped PEs) or “core-shell-corona” (star-like micelles of ionic amphiphilic diblock copolymers) structure. A hydrophobic core (star-shaped polyelectrolytes) or a hydrophobic shell (star-like micelles of ionic amphiphilic diblock copolymers) of each of the complex species represents an essentially water-insoluble IPEC incorporating the oppositely charged polyelectrolyte components in 1 : 1 charge ratio. In the case (a) of star-like polyionic species interacting with the oppositely charged linear homopolyelectrolyte, a hydrophilic corona is composed of free (excessive) PE branches that are not coupled with the fragments of the oppositely charged linear polyions. In the case (b) of star-like polyionic species interacting with the oppositely charged double hydrophilic diblock copolymers, a hydrophilic corona can be built up only from nonionic hydrophilic blocks of double hydrophilic diblock copolymer (at 1 : 1 charge stoichiometry) or apparently can be mixed and formed by those nonionic hydrophilic blocks and free (excessive) PE branches that do not form interpolymer salt bonds (at charge stoichiometries considerably deviating from 1 : 1).

Conclusions

The main feature of the macromolecular co-assemblies resulting from the interaction of the star-like polyionic species (star-shaped PEs or micelles of ionic amphiphilic diblock copolymers) with the oppositely charged linear homopolyelectrolytes or double hydrophilic diblock copolymers is their pronounced compartmentalized structure. We believe that such novel complex macromolecular architectures of micellar type are very promising and will be in demand for their future applications in rapidly developing nanotechnologies, for expample, as nanocontainers and nanoreactors.

Acknowledgements

This research was supported by the EU Marie Curie Research and Training Network POLYAMPHI (project MCRTN-CT-2003-505027), the Russian Foundation for Basic Research (project № 09-03-00851-a), and the Deutsche Forschungsgemeinschaft.

Hybrid Carbonaceous and Plasmonic Nanostructures as Efficient Elements in Energy Conversion Devices

Dong Ha Kim, Yoon Hee Jang, Yu Jin Jang

Department of Chemistry and Nano Science, Ewha Womans University, Seoul, Korea

dhkim@ewha.ac.kr

Introduction

It has been recognized as an urgent task to develop highly efficient and reliable energy conversion devices. Rational design and facile synthesis of nanostructured core elements necessary for the viable function with high efficiency comprise a key aspect to attain this goal. There have been tremendous efforts to suggest target-oriented nanomaterials suitable for solar cell, fuel cell, or secondary battery. Along this line, here we propose that complex nanostructures consisting of metal, semiconductor, and carbon can be programmed and fabricated by unconventional and facile self-assembly processes.

TiO_2 has been widely utilized as electrodes in dye-sensitized solar cell due to its optimum optoelectronic property and stability. A simple strategy to increase the overall cell efficiency is suggested combining surface plasmonic effects of noble metal nanoparticles (NPs). We investigate the effect of different fabrication and integration routes, as well as the morphology of hybrid nanostructures, on the ultimate function of the devices. Next, we suggest a new paradigm to fabricate hybrid carbon nanostructures decorated with highly ordered noble metal NPs (Au, Ag, Pt, Pd) or alloy metals based on a direct carbonization concept of amphiphilic copolymer nanotemplates. A unique feature of note in this method is that amphiphilic copolymer acts as a structure directing agent for controlled nanostructures and a carbon source, simultaneously. Versatile functions of the resulting hybrid nanocomposites were evaluated with a focus on their electrocatalytic activities based on which potential applications as counter electrodes in photovoltaic devices and anodes/cathodes in fuel cell can be anticipated.

Materials and Method

Polystyrene-*block*-poly(4-vinylprydine) diblock copolymers (PS-*b*-P4VP) with polydispersity index of 1.09 was purchased from Polymer Source Inc. The number of average molecular weight of PS and P4VP were M_n^{PS} = 41 Kg mol^{-1} and M_n^{P4VP} = 24 Kg mol^{-1}, respectively. Titanium tetraisopropoxide ($Ti(OCH(CH_3)_2)_4$, TTIP, 97 %) and acetylacetone (Acac) were purchased from Sigma-Aldrich. Platinum chloride ($PtCl_4$), ruthenium chloride ($RuCl_3$), sodium borohydride ($NaBH_4$), perchloric acid ($HClO_4$), and formic acid (HCOOH) were purchased from Sigma Aldrich Inc.

Solar cell was fabricated in the following way. TiO_2 nanodot arrays were fabricated on fluorine-doped tin oxide (FTO) glass substrate and then treated with $TiCl_4$ by immersing into 100 mL of 0.2 M $TiCl_4$ aqueous solution and kept in a 60 °C oil bath for 1 hr, subsequently rinsed with ethanol and annealed at 500 °C for 30 min in air. TiO_2 nanoring arrays were fabricated on previously $TiCl_4$ treated FTO glass substrate. Both of them are sensitized with ruthenium dye (*cis*-diisothiocyanato-bis(2,2´-bipyridyl-4,4´-dicarboxylato) ruthenium(Ⅱ) bis(tetrabutylammonium), N-719, Solaronix) by immersing into 0.2 mM dye/ethanol solution for 24 hrs. Platinum (Pt)-coated FTO glass was used as counter electrode, which was prepared by drop casting of 0.5 mM chloroplatinic acid (H_2PtCl_6)/isopropanol solution and directly sintering at 380 °C for 1 hr in air. Device was assembled by stacking of TiO_2 nanostructure prepared FTO (anode) and Pt-coated FTO (cathode) by insertion of spacer (25-μm-thick hot-melt sealing foil, SX1170-25, Solaronix). An ionic liquid electrolyte (0.60 M BMIM-I, 0.03 M I2, 0.50 M TBP, and 0.10 M GTC in acetonitrile/valeronitrile 85/15 (v/v) (No. ES-0004), purchased from io.li.tec (Germany) was then injected between two electrodes.

Results and Discussion

Titanium sol-gel precursors could be selectively incorporated into P4VP blocks, producing TiO_2 nanodot or nanoring arrays *via* PS-*b*-P4VP inverse micelles and micelles templates, respectively. Two kinds of TiO_2 nanostructures were applied as working electrodes of dye-sensitized solar cells.

Metal/carbon hybrid nanostructures containing both platinum (Pt) and ruthenium (Ru) NPs denoted Pt-Ru/carbon, and metal/carbon hybrid nanostructures containing exclusively Pt NPs were prepared by sequential stacking of UV-stabilized PS-*b*-P4VP inverse micelle nanotemplates followed by calcining at 500oC under an inert atmosphere.

Conclusions

In summary, we have suggested a simple approach for fabricating the TiO_2 nanostructures including nanodot or nanoring arrays from self-assembled DBCP scaffolds. The PCE of thicker TiO_2 films (5 layers) was characterized to be much higher than that of TiO_2 monolayer-thick structures. Furthermore, 5 layered TiO_2 nanoring based solar cells devices exhibited the best behavior.

A unique route for the fabrication of an exquisite configuration of hybrid metal/carbon nanostructures with a distinct electrocatalytic activity toward formic acid oxidation was introduced exploiting consecutive self-assembly and direct carbonization of BCPs.

References

(1) Jang,Y. H.; Kochuveedu, S. T.; Jang, Y. J.; Steinhart, M.; Kim, D. H. "Graphitic Thin Films with Highly Dispersed Noble Metal Nanoparticles by Direct Carbonization of Block Copolymer Inverse Micelle Templates", *Carbon*, DOI: 10.1002/chem.201002912

(2) Jang,Y. J.; Kim, D. H. "One-Step and Self-Assembly Based Fabrication of Pt/TiO_2 Nanohybrid Photocatalysts with Programmed Nanopatterns", *Chem-Eur. J.*, DOI: 10.1002/chem.201001802.

(3) Wang, Y.; Becker, M.; Wang, L.; Liu, J.; Scholz, R.; Peng, J.; Gösele, U.; Christiansen, S.; Kim, D. H.; Steinhart, M. "Nanostructured Gold Films for SERS by Block Copolymer-Templated Galvanic Displacement Reactions", *Nano Lett*. **2009**, 9(6), 2384-2389.

Voltage-induced swelling and de-swelling of weak polybase brushes

M. P. Weir[1,2], S. Y. Heriot[2], S. J. Martin[2], A. J. Parnell[2], S. A. Holt[1,3], J. R. P. Webster[3] and R. A. L. Jones[2]

[1]Bragg Institute, Australian Nuclear Science and Technology Organisation, Australia
[2]Department of Physics and Astronomy, The University of Sheffield, UK
[3]ISIS, Rutherford Appleton Laboratory, UK

Michael.Weir@ansto.gov.au

Introduction

Polymer brushes are formed when polymer molecules are grafted at one end to a surface at a sufficient density to force neighbouring chains to overlap. Repulsive interactions between chains cause them to stretch away from the surface into a brush-like structure. Careful tuning of the interactions between neighbouring chains allows control of the brush conformation. This may be achieved in neutral polymers by changing the solvent quality or temperature, while the charge present on polyelectrolyte brushes allows the manipulation of brush conformation via electrostatic interactions, e.g. by changing the pH or ionic strength.

Surface properties such as adhesion, wettability and affinity for protein adsorption are known to depend upon the presence and conformation of a polymer brush layer at a surface. Therefore, control of the brush conformation in response to external stimuli is highly desirable in the design of smart surfaces.

This work explores the use of applied voltages as a versatile, non-invasive stimulus to remotely control the conformation of charged polymer brushes. Electrical stimuli have a number of advantages over controlling the chemical environment of the brush (e.g. by changing pH or ionic strength). Electrical stimuli are easy to produce, highly repeatable and versatile, and easy to integrate into technological applications. For example, the use of patterning techniques could allow pixelation of the surface, to achieve spatial control over the brush conformation.

Materials and methods

Poly(2-(dimethylamino)ethyl methacrylate) (PDMAEMA) weak polybase brushes were grown from silicon surfaces using atom transfer radical polymerization (ATRP). Ellipsometry and neutron reflectivity were used to study the effect of electrical stimuli upon the brushes by measuring changes in their structure in response to applied voltages. DC voltages were applied in DI water or D_2O, with one electrode connected to the brush-bearing substrate and another parallel electrode a distance away in the surrounding liquid.

Spectroscopic ellipsometry data was fitted using a box model with an effective medium approximation (EMA) allowing calculation of the volume fractions of water and polymer within the layer, as well as the overall layer thickness. Neutron reflectometry data was fitted to extract the polymer brush volume fraction profile corresponding to the best fit to the reflectivity curve.

Results and Discussion

Neutron reflectometry data revealed that the polymer brushes had the Gaussian-terminated parabolic volume fraction profile predicted by self-consistent field theory. Positive voltages caused swelling of the brush while negative voltages in some cases caused de-swelling.

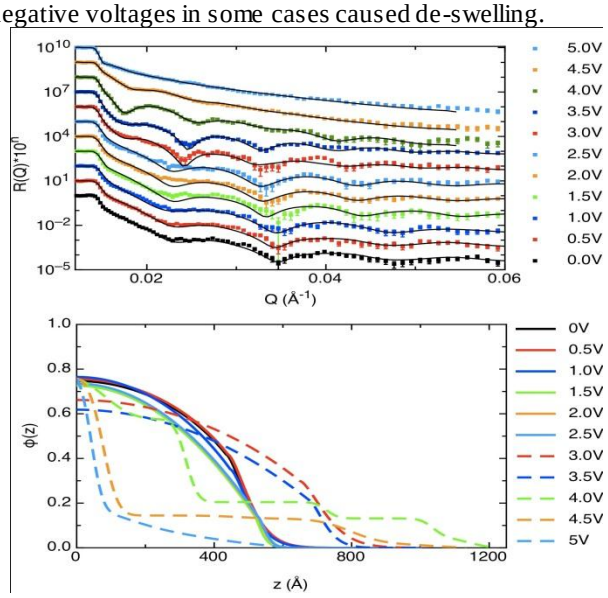

Figure 1. Top: Neutron reflectivity of a 300Å PDMAEMA brush in D_2O as a function of applied voltage, with fits shown as solid black lines. Bottom: Polymer brush volume fraction profiles corresponding to fits shown in (a), and the degree of swelling *S* of the polymer brush as a function of applied voltage (inset)

A full theoretical model is required to describe the behaviour of the brushes, and must take into account the contributions from local pH variations, charged monomers, counterions, and the physical conformation of the chains.

Conclusions

Applied voltages caused changes in the structure of PDMAEMA weak polybase brushes in water or D_2O. The brushes were swollen by positive voltages and were in some cases de-swollen by negative voltages. We have demonstrated the remote control of the conformation of a macromolecular layer. This work opens up a number of possibilities for electronically-addressed smart surfaces.

Fabrication and ordering of noble metal nanoparticles through functional polymers

A. Ledo-Suárez, M. A. López-Quintela, M. Lazzari

Department of Physical Chemistry, Faculty of Chemistry and Centre for Research in Biological Chemistry and Molecular Materials (CIQUS), University of Santiago de Compostela, 15782 Santiago de Compostela, Spain

A. Zucchi, C. E. Hoppe

INTEMA(UNMdP-CONICET) J. B. Justo 4302, Mar del Plata (Argentina)

e-mail: massimo.lazzari@usc.es

Developments in polymer synthesis and functionalization over the last decades provided a wealth of polymer and copolymer structures with well-defined morphology, controlled architecture and functionality that are converting functional polymers in a unique tool for nanotechnological applications. In particular, functional polymers and especially block copolymers [1], may be used either as nanomaterials themselves, as template or scaffold for the preparation of nanostructured materials and also for the polymer-assisted controlled fabrication of well-defined metal or metal oxide nanoparticles (NPs). As an example, different functionalized polymer matrixes were employed to prepare metallic NPs dispersed in polymer medium by *in situ* synthesis technique [2].

In this communication we present our recent results on the use of chain-end functional polymers for controlling the synthesis of noble metal NPs, with some reference to their distribution into block copolymer nanostructured morphologies. In particular, we report on the use of different ω-thiol (a functional group with high affinity for noble metal surfaces) polyacrylonitrile (PAN), poly(methyl methacrylate) (PMMA) and polystyrene (PS) ligands, opportunely prepared by controlled/living radical polymerization [3], as capping agents in the preparation of Au NPs through a one-step procedure.

The influence of molecular weight, polymer concentration and temperature was studied for different systems, also comparing the behavior of the chain-end functional polymers with those of the corresponding homopolymers without any active chain-ends. Polymer ligands and their interaction with the metal surface were mainly studied by FTIR and NMR spectroscopies, whereas TEM, UV-vis spectroscopy and thermo- gravimetric analysis allowed characterizing the metal NPs.

As an example, Figure 1 shows TEM micrographs of Au NPs prepared using $HAuCl_4$ as precursor and $NaBH_4$ as reducing agent in presence of PAN chains, either with thiol as chain-end (1A) or not (1B). In both cases stable particles were formed but only in the presence of PAN-SH size and size distribution could be efficiently controlled.

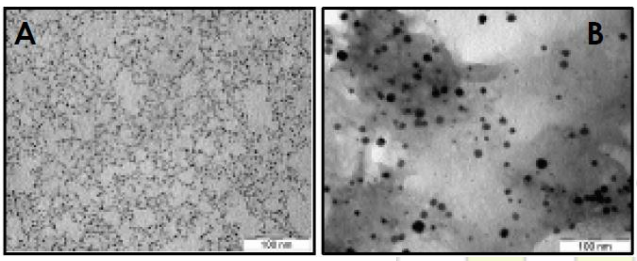

Figure 1. TEM micrographs of Au NPs prepared in presence of PAN ligands: A) PAN-SH, B) PAN-Br.

Similar results were obtained by comparing the behavior of PMMA-SH as capping agent with that of dithiobenzoate terminated PMMA.

Especially in the case of thiol chain-end PSs, a clear dependence of Au NP size and distribution was observed (see examples of Au@PS-SH systems in the insets a and b of Figure 2), and Au colloids with diameter between 1 and around 15 nm could be obtained. NP size and dispersity could be efficiently tuned by changing reaction temperature, PS molecular weight and ratio metal salt precursor to polymer

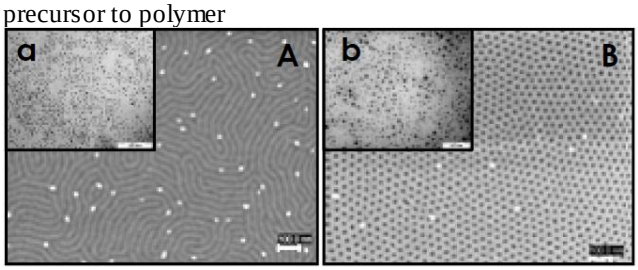

Figure 2. FESEM of thin films of PS-*b*-PMMA with Au@PS-SH NPs (A,B). Inset images show TEM micrographs of Au-capped NPs: a) $Au@PS_{27}SH$, b) $Au@PS_{167}SH$.

Finally, the preparation of block copolymer-based nanocomposites through the addition of such Au@PS-SH will also be reported. Spun-coated thin films were prepared from chloroform solutions of an asymmetric PS-*b*-PMMA block copolymer and different Au@PS-SH NP systems (Figure 2).

In particular, it was observed that depending on the NP concentration and the ligand molecular weight different orientations of the nanostructured morphology could be achieved.

Acknowledgments. The authors thank the financial support by the Spanish "Ministerio de Ciencia e Innovación" (MAT2008-06503; FPU: A.L.S.) and the Xunta de Galicia (PX2010/168-2 and PX2010/152-2)

References

[1] M. Lazzari, C. Rodríguez-Abreu, J. Rivas, M. A. Lopez-Quintela, *J. Nanosci. Nanotechnol.*, 6, 892 (2006).

[2] Z. Wang, B. Tan, I. Hussain, N. Schaeffer, M. F. Wyatt, M. Brust, A. I. Cooper *Langmuir* 23, 885 (2007).

[3] See e.g.: a) N. V. Tsarevsky, K. Matyjiaszewski, *Macromolecules*, 35, 9009 (2002); b) R. P. Quirk, M. Ocampo, M. J. Polce, C. Wesdemiotis, *Macromole-cules*, 40, 2352 (2007); c) J. Xu, J. He, D. Fan, X. Wang, Y. Yang, *Macromolecules*, 39, 8616 (2006).

PVC modified with well dispersed nano silica spheres

M. Conradi[1] , M. Zorko[2], I. Jerman[2] and B. Orel[2]

[1]Institute of Metals and Technology, Lepi pot 11, SI-1000 Ljubljana
[2]Chemistry Institute, Hajdrihova 19, SI-1000 Ljubljana

marjetka.conradi@imt.si

Poly(vinyl chloride), PVC-based composites were prepared by blending PVC with various weight ratios of submicron (i.e. 600 nm) and nano-SiO_2 spherical particles (i.e. 30 nm), which were initially treated with different surfactants: IO7 T7(OH)3 (trisilanol isooctyl polyhedral oligomeric silsesquioxane) [1], IB7 T7(OH)3 (trisilanol isobutyl polyhedral oligomeric silsesquioxane) [1] and DMOAP (N,N-dimethyl-n-octadecyl1-3-aminopropyl-trimethoxysilyl chloride). The degree of dispersion and interfacial compatibility of surface treated SiO_2 particles in PVC matrix was characterized with SEM. The best dispersion of surface modified particles and their compatibility with the PVC matrix was obtained for the silica particles (1% wt) treated with IO7 T7(OH)3, exhibiting a highly ordered 3D silica (600 nm and 30 nm)/PVC organic-inorganic composites layers. The main interest of this study was the investigation of the composites' mechanical and optical properties, which will be presented and discussed in details.

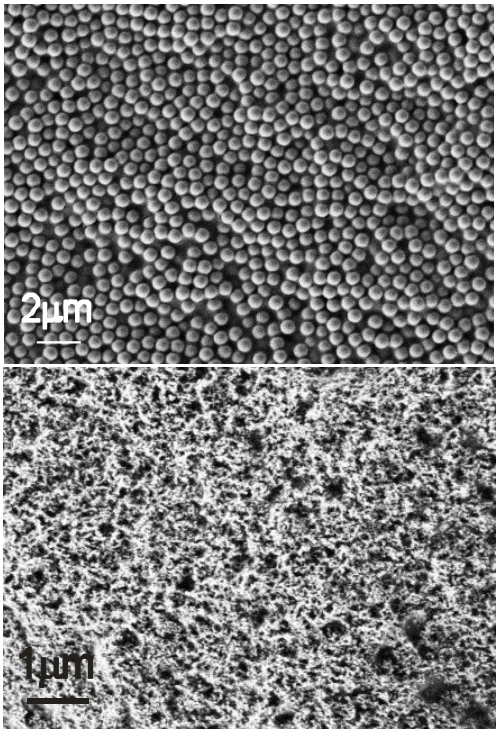

[1] P. A. Wheeler et al., Polyhedral Oligomeric Silsesquioxane Trisilanols as Dispersants for Titanium Oxide Nanopowder, J. Appl. Polymer Science, **108**, 2503–2508 (2008).

Viscoelastic Behavior of Magnetic Elastomers Depending on Composition and Magnetic Field

E.Yu. Kramarenko[1], *G.V. Stepanov*[2], *N.S. Perov*[1], *A.V. Chertovich*[1], *A.R. Khokhlov*[1]

[1] Physics Department, Moscow State University,
119991 GSP-1 Moscow, Leninskie gory, 1/2
[2] State Institute of Chemistry and Technology of Elementoorganic compounds
111123, Moscow, sh. Entuziastov, 38

kram@polly.phys.msu.ru

This work is aimed to a development of new polymer composite materials, namely, magnetic field controlled elastomers based on highly elastic polymeric matrices filled with magnetic nano- and microparticles. The novel feature of these materials is the ability to change their properties in magnetic fields and thus, perspective for design of various magnetic field controlled devices.

New elastomers have low Young's modulus (it is of the order of tens of kPa) and occupy an intermediate position between rigid magnetic composites and magnetorheological fluids. In the course of magnetic field controlled structuring of the magnetic filler within polymer matrix new materials demonstrate the following properties:

(a) a unique ability to undergo quick and controllable essential changes in elastic and viscous properties under the action of external homogeneous magnetic fields (magnetorheological effect) . More than 100-fold increase of both storage and loss moduli of the materials has been observed in an external homogeneous magnetic field of up to 0.3 T;

(b) a unique ability to undergo quick and controllable large-scale deformations in external homogeneous and gradient magnetic fields (magnetodeformational effect);

(c) new effect of shape memory or plasticity induced by magnetic field. It is found that in some cases the deformation of the material is virtually fixed by the magnetic field. One may say that the material ''remembers'' its shape in the presence of magnetic field.

In this presentation we show results of experimental and theoretical studies of these properties of new magnetic elastomers, their dependence on the material composition and strength of magnetic fields, as well as demonstrate possibilities of their practical applications.

The main attention is paid to the behavior of magnetic elastomers based on hard magnetic filler, namely, magnetic particles of FeNdB. Viscoelastic properties of these materials are studied by dynamic experiments (shear oscillations on a rheometer). In the figure we show the magnetic field dependences of the storage and loss moduli for the sample containing a mixture of iron magnetic particles (58%) and FeNdB particles (35%). The sample was magnetized in the magnetic field of 15 kOe. The shear plane was perpendicular to the direction of the internal magnetization of the samples and to the applied external magnetic field. The presence of remanent magnetization influences the effect of magnetic field on the elastic modulus. The minimum value of the modulus is reached when the direction of the external field is opposite to the sample magnetization. Thus, the elastic modulus of the magnetic elastomers can be controlled (can be both increased and decreased) by magnetic field.

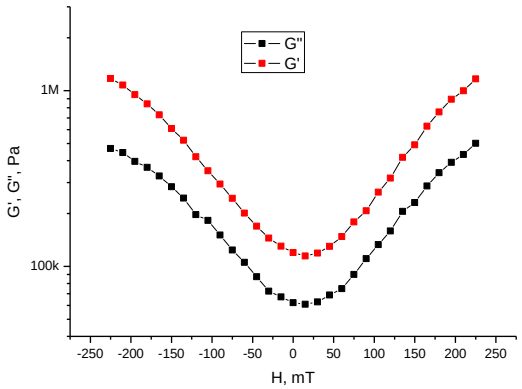

Figure. Dependences of the storage, G', and the loss modulus, G'', on magnetic field.

References

1. A.V. Chertovich, G.V. Stepanov, E.Yu. Kramarenko, A.R.Khokhlov. New composite elastomers with giant magnetic response. Macromolecular Materials and Engineering. 2010, v. 295, p. 336.

2. S. Abramchuk, E. Kramarenko, G. Stepanov, L.V. Nikitin, G. Filipcsei, A.R. Khokhlov, M. Zrinyi. Novel Highly Elastic Magnetic Materials for Dampers and Seals I.: Preparation and characterization of the elastic materials. Polym. Adv. Technol. 2007, v.18, p. 883.

3. S. Abramchuk, E. Kramarenko, D. Grishin, G. Stepanov, L.V. Nikitin, G. Filipcsei, M. Zrinyi. Novel Highly Elastic Magnetic Materials for Dampers and Seals II.: Material Behaviour in a Magnetic Field. Polym. Adv. Technol. 2007, v. 18, p. 513.

4. G.V. Stepanov, S.S. Abramchuk, D.A. Grishin, L.V. Nikitin, E.Yu. Kramarenko, A.R. Khokhlov. Effect of a Homogeneous Magnetic Field on the Viscoelastic Behavior of Magnetic Elastomers. Polymer, 2007, v.48, p. 488.

5. O.V. Stolbov, Yu.L. Raikher, G.V. Stepanov, A.V. Chertovich, E.Yu. Kramarenko, A. R. Khokhlov. Low_Frequency Rheology of Magnetically Controlled Elastomers with Isotropic Structure. Polymer Science, Ser. A, 2010, v. 52, p. 1344.

Polyelectrolyte-Clay Multilayers for Surface Modification of Biopolymers: Preparation and Possible Applications

Gerald Findenig[1], Susanne Nowitsch[1], Rupert Kargl[1], Martin Reischl[1], Aleš Doliška[2], Thomas Heinze[3], Karin Stana-Kleinschek[2], Volker Ribitsch[1]

[1] Karl-Franzens University Graz, Institute of Chemistry, AT-8010 Graz, Heinrichstraße 28, Austria
[2] University Maribor, Faculty of Mechanical Engineering, SI-2000 Maribor, Smetanova Ulica 17, Slovenia
[3] Friedrich Schiller University Jena, D-07743, Humboldtstraße 10, Germany

gerald.findenig@uni-graz.at

Introduction: Thin films prepared by the layer-by-layer technique (LbL) are meanwhile known since almost two decades [1]. The benefit of this coating method is the possibility to introduce new functionalities into the LbL-film which can be used as surface modification tool in materials science. This and the facile preparation of LbL films are making the layer-by-layer technique a powerful instrument to create customized surface coatings for different applications. Besides the choice of polyelectrolyte the incorporation of clay nanoplatelets into LbL-films provides a variety of interesting properties like flame retardance, mechanical strength, heat-seal and gas or vapor barriers [2]. The basic principle of an LbL coating with incorporated clay is shown in figure 1.

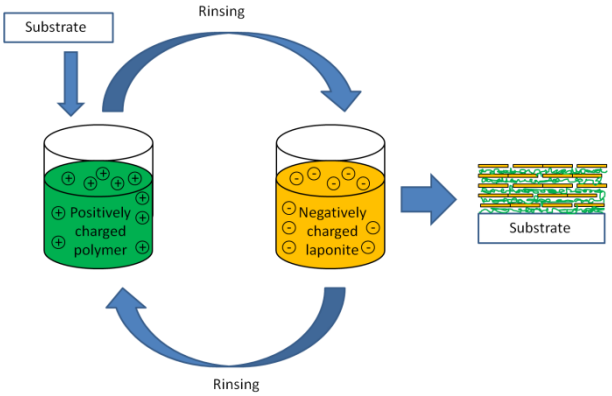

Figure 37: Preparation of a layer-by-layer coating by alternating dip-coating of a substrate, which leads to a "brick-mortar" structure of the film.

The incorporation of biopolymers into LbL-films is, with respect to sustainability, an additional big advantage of this technique. Substrates like cellulose can be modified with e.g. cationic starch and clay nanoplatelets in order to obtain a biodegradable coating. In this study we investigated different approaches to modify a cellulosic model substrate and silicon surfaces with LbL. Well defined cellulose model surfaces were prepared by spin coating and regeneration of trimethylsilyl cellulose films [3,4].

Materials and Methods: Several types of polyelectrolytes including synthetic and natural ones were investigated in order to compare the well known LbL-film forming properties of polyethyleneimine (PEI) and polydiallyldimethylammonium chloride (PolyDADMAC) with that of cationic starch. Mass changes (increase) and layer viscoelastic properties were investigated using quartz crystal microbalance with dissipation technique. The wettability of the surfaces was determined via contact angle measurements. In addition the influence of electrolyte concentration (NaCl) and the type of polyelectrolyte on the growth rate and surface properties were investigated. Finally atomic force microscopy (AFM) gave insights into the surface morphology of the thin film coatings. As an application, selected coatings were used to modify the surface of a commercial cellulose substrate in order to extent the range of applicability of this material.

Results and Discussion: The optical thickness and quartz crystal microbalance data showed a continuous increase of the layer thickness during the coating process. The contact angle measurements revealed alternating values after each coating step, which also confirmed the irreversible adsorption of the film components. Figure 2 is showing AFM images of a commercially available cellulose substrate before and after surface modification by LbL coating. A significant change in surface morphology was observed.

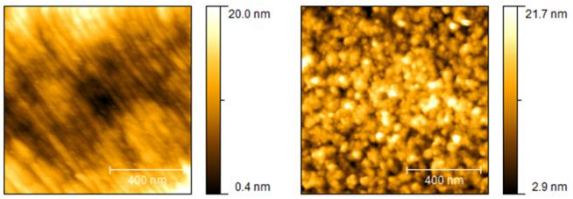

Figure 38: Surface modification of a commercially available cellulose substrate. The left image shows the untreated substrate, whereas the right image depicts the LbL coated surface.

Conclusion: Our research showed the preparation of polyelectrolyte-clay multilayers on different substrates in dependency of electrolyte concentration and polyelectrolyte type. Additionally with the introduction of starch into the film we prepared a biodegradable coating that can be used to increase the barrier properties of e.g. packaging materials.

The research leading to these results has received funding from the European Union Seventh Framework Programme (FP7/2007-2013) under grant agreement n° 214653.

References

1 E. R. Kleinfeld, G. S. Ferguson, Science 1994, 265, 5170, 370-373
2 M. A. Priolo, D. Gamboa, J. C. Grunlan, ACS Applied Materials & Interfaces 2010, 2, 1, 312-320
3 E. Kontturi, P. C.Thüne, J. W. Niemantsverdriet, Langmuir 2003, 19, 5735-5741
4 S. Köhler, T. Liebert, T. Heinze, Journal of Polymer Science 2008, 12, 4070-4080

Block-gradient copolymers of styrene and acrylic acid synthesized by nitroxide-mediated radical polymerization.

O. Borisova [a,b], L. Billon[a], M. Zaremski[b], B. Grassl[a], Z. Bakaeva[c], A. Lapp[d], P.Stepanek[c], O. Borisov[a].

[a] UPPA, CNRS UMR 5254 IPREM Equipe de Physique et Chimie des Polymères, 64053 Pau Cedex, France
[b] Department of Polymer Science, Moscow State University, Leninskie Gory, Moscow 119191, Russia
[c] Institute of Macromolecular Chemistry AS CR, v.v.i., Heyrovského nám. 2, CZ-162 06 Praha 6, Czech Republic
[d] Laboratoire Leon Brillouin/LLB CNRS/CEA Saclay, France

olga.borisova@univ-pau.fr

Amphiphilic copolymers combining in their structure hydrophilic ionic and hydrophobic moieties are very interesting in different aspects, particularly, due to their ability to self-assembly in aqueous solution giving rise to diverse nano-structures responsive to environmental changes. Here we present the results of synthesis, characterization and study of stimuli-responsive behavior of novel type of block-gradient copolymers of styrene and acrylic acid.

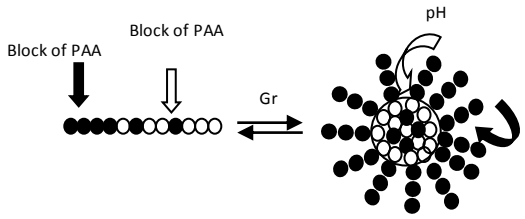

Fig.1. Dynamic micelles formed by block-gradient copolymers.

Amphiphilic copolymers each consisting of a (hydrophilic) block of polyacrylic acid and a gradient block of acrylic acid and styrene co-monomer units were synthesized by nitroxide-mediated polymerization. At the first stage we polymerized acrylic acid in the presence of nitroxide SG1 as a control agent and the alkoxyamine (MAMA) as an initiator. At the second stage we used two techniques to obtain different gradient profiles: semi-batch method with different rate of addition of styrene and addition of styrene in one step (batch method). The linear growth of molecular weight as a function of conversion during polymerization proves controlled character of the process.

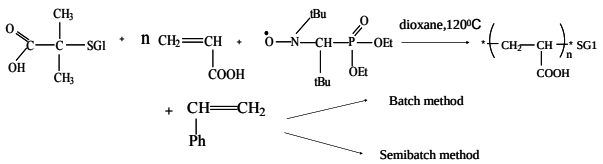

Constants of copolymerization of styrene and acrylic acid in dioxane are r_1=0,27 (AA) и r_2=0,72 (ST)[1]

The composition of copolymers and local composition along the chains were determined by means of ^{1}H NMR. Molecular weight of methylated copolymers was measured by size-exclusion chromatography.

The rate constant of decomposition of "dormant" adducts: polyacrylic acid-SG1, polystyrene-SG1, copolymer-SG1 and recombination rate constants between nitroxide SG1 and macroradicals - were determined by means of ESR. We found that with the increasing of polarity of solvent the values of constants become higher. This effect opens a new way of activating chains in nitroxide-mediated radical polymerization.

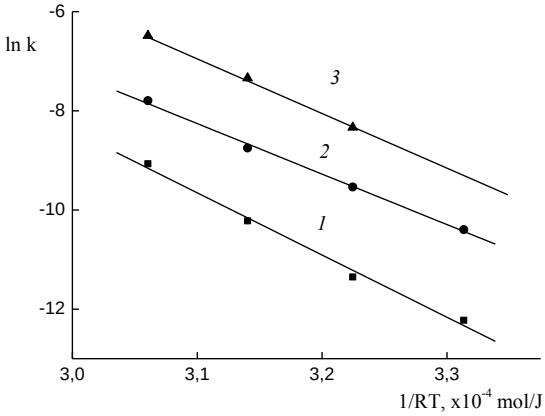

Fig.2. Energy of activation of decomposition of PAA-adducts in dioxane (1), DMF (2) and formamide (3).

The self-assembly of the obtained copolymers in water was studied by DLS and SANS. It was found that the decreasing of pH of solution leads to the increase in the hydrodynamic radius of the micelles. In the presence of salt particles demonstrate the same behavior with changing of pH, but the addition of salt causes the growth of the size of micelles. In contrast to poly(acrylic acid)-block-poly(styrene) copolymers with the same composition which form "frozen" micelles, such block-gradient copolymers can form "dynamic" micelles responding by reversible changes in the aggregation state to variation of pH and ionic strength.

This research was supported by Conseil régional d'Aquitaine and the Russian Foundation for Basic Research (project number 08-03-00269-a).

[1] L. Couvreur, B. Charleux, O.Guerret, S. Magnet. Macromol.Chem.Phys. 2003.204.2055-2063.

Self-organization of amphiphilic macromolecules in semidiluted and concentrated solutions.

Valentina V. Vasilevskaya, Anna A. Glagoleva, Mikhail K. Glagolev

Nesmeyanov Institute of Organoelement Compounds Russian Academy of Sciences

vvvas@ineos.ac.ru

It is well-known that in the large majority of real water-soluble polymers many monomer units have a dualistic (hydrophobic/hydrophilic) character, that is, repeating polymer unit, which is usually considered as pure hydrophobic or pure hydrophilic, actually incorporates both hydrophilic and hydrophobic parts concurrently. Interaction between such groups can not be be literally reduced to pure hydrophilic or pure hydrophobic interactions. To eliminate this drawback, we have introduced an extended variant of the HP model that explicitly takes into account the amphiphilic nature of hydrophilic segments [1].

In this model the hydrophilic monomer units are modeling as a "dumbbell" consisting of *H* and *P* beads linked by rigid bonds of a fixed length (Fig.1).

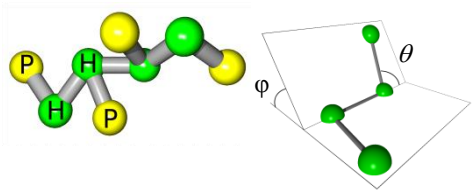

Fig. 1. Schematic representation of the semiflexible model of macromolecule with an amphiphilic monomer unit.

Using this model, we have performed an extensive molecular dynamics simulations of the hydrophobically-driven conformational transitions of macromolecules containing amphiphilic monomer units and found a variety of novel structures in a poor solvent (for review, see [2]).

In this paper we report the results on the computer modeling of self-organization of such macromolecules in semidilute and concentrated solutions.

We studied solution of semiflexible amphiphilic macromolecules with fixed bend angle θ and have found that the conformational state of macromolecules in such systems depends on the macromolecular stiffness and on the way the solution has been prepared. Thus, if the concentration of globules increased from a very diluted solution, the globules remain stable, independent of the macromolecular stiffness, and do not aggregate even in concentrated solutions. On the other hand, if the solvent quality is gradually decreased in a solution with a concentration much larger than that of a semidilute solution, then relatively flexible chains form separate globules, whereas semirigid macromolecules tend to aggregate and form braid-like conformations [3]. The aggregation number and length of complexes can vary and many of them can join with each other.

In the case of macromolecule with both bend angle θ and rotation angle φ fixed, the distribution of aggregates over aggregation number in such a systems is very narrow and moreover, we have found regimes for which the aggregates with the only aggregation number are observed (Fig. 2). The macromolecules in such complexes are interwinded in such a manner that hydrophobic core is protected by hydrophilic shell (Fig. 3) and contour length of the aggregates is equal to the contour length of single macromolecules [4].

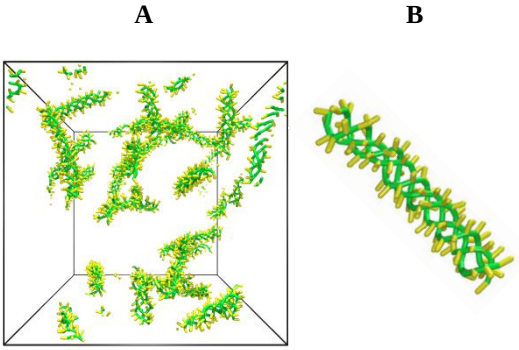

Fig. 2. Snapshot pictures illustrating the aggregate formation of semiflexible macromolecules with fixed bend and rotation angles (a) and aggregate structure (c).

We have studied the concentrated solutions of diblock copolymer containing linear ***H*** and amphiphilic ***HP*** block and found that the phase diagram for such copolymers can be significantly different from that known for the conventional linear diblocks [5].

References

[1] V.Vasilevskaya, P. Khalatur, A. Khokhlov. Macromolecules **2003**, 36, 10103

[2] V. Vasilevskaya, V. Ermilov. Polymer Science A **2011**

[3] V. Vasilevskaya, V. Markov , G. ten Brinke, A.Khokhlov. Macromolecules **2008**, 41, 7722

[4] M. Glagolev, V.Vasilevskaya, A. Khokhlov. Polymer Science A **2011**

[5] A. Glagoleva, V.Vasilevskaya, A. Khokhlov. Polymer Science A **2010**, 52, 182

This work is supported by The Ministry of Science and Education of Russian Federation, by Russian Foundation for Basic Research, by Program "Creation and study of macromolecules and macromolecular structures of new generation" of Russian Academy of Sciences.

Local structure around nano-clay agglomerates in PP composites – a scanning X-Ray diffraction study with sub micron resolution

M. Feuchter[1,2], G. A. Maier[3], M. Burghammer[4], M. Kracalik[1], S. Laske[1], J. Keckes[5,6], G. Pinter[1]

[1]University of Leoben, Department Polymer Engineering and Science, Otto Glöckel Strasse 2, 8700 Leoben, Austria
[2]Polymer Competence Center Leoben, Roseggerstrasse 12, 8700 Leoben, Austria
[3]Materials Center Leoben Forschung, Roseggerstrasse 12, 8700 Leoben, Austria
[4]European Synchrotron Radiation Facility, 38043 Grenoble, Cedex 9, France
[5]University of Leoben, Department Materialphysics, Jahnstrasse 12, 8700 Leoben, Austria
[6]Erich Schmid Institute, Austrian Academy of Science, Jahnstrasse 12, 8700 Leoben, Austria

michael.feuchter@mu-leoben.at

Introduction: Polymeric nanocomposites, especially with the filler montmorrillonite, have become of predominant interest to the scientific community and industry in the last years [1]. Especially structural details and their relationship to the mechanical, rheological, optical and permeation properties of the nano-composites are of high importance. There are different methods to produce polymer nanocomposites [1]. In this study melt compounding has been applied in order to produce intercalated polypropylene silicate nanocomposites. Isotactic polypropylene (PP) exhibits polymorphic behaviour, which can be distinguished in different modifications. Monoclinic α-form is the most common one for melt crystallized specimen, whereas the trigonal β-form can be produced only under special crystallization conditions or in the presence of nucleating agents [2]. Though much is known about bulk morphology and structure, only very few is known about local structure around agglomerates in PP composite.

Materials and method: For realisation of the melt intercalation a compounding process with an intermeshing co-rotating twin screw extruder Theysohn TSK30/40D (Korneuburg, Austria) and a string die had been used. The selected polymer was the semi crystalline isotactic polypropylene with the commercial indication HC600TF provided by Borealis Inc., Linz, Austria and as filler the smectite clay mineral montmorrillonite with the indication Nanofil 5 provided by Süd-Chemie Inc., Munich, Germany was chosen. This combination of materials was rather incompatible, so therefore additionally a compatibilizer with the indication PP–MA, Scona TPPP 2112 FA, Kometra/D, Schkopan, Germany was required. A high filled mixture with 20 wt.% nano-filler and 20 wt.% compatibilizer was produced in this way. For structural characterization the granulated material was pressed to a plate using a hydraulic vacuum press machine (Collin 200 PV, Dr. Collin Ltd., Ebersberg, Germany). This plate was cut back to a thickness of 10 µm by using a microtom (Histocom, Wiener Neudorf, Austria).
The structure of layered silicates, the arrangement of the silicate platelets, the influence of fillers on spherolithic growth and the changes in polypropylene phase content have been observed by numerous researchers [3]. All of these properties are influenced by the distribution of particles in polymeric matrix. In this paper the authors present a spatially resolved X-Ray diffraction study with sub micron position resolution. The study was performed by applying a 250 nm wide (full width half maximum) X-Ray beam at ID13 beamline at ESRF, Grenoble. From a composite containing agglomerates a thin foil was cut using microtome. In the thin sample agglomerates were visible already in the light microscope. From cutting process visually unaffected agglomerates were chosen for structural characterization. The thin sample was scanned over the area where the chosen agglomerate was located. Phase composition, local composition and interlayer distances were evaluated from the data.

Results and Discussion: In layered silicate reinforced polypropylene produced by melt intercalation more than one defined state was existing. Agglomerates as well as single platelates were coexisting; also different PP-forms could be found. This work shows structural details around an intercalated agglomerate. At the boundary of the agglomerate the interlayer distance sligthly increased and exfoliated single platelets surrounding the agglomerate could be detected. The monoclinic form of PP dominated, however β-PP was found at and near sample positions with high concentration of clay platelets. The degree of crystallinity was lower in areas of agglomerated particles.

Conclusion: Physical properties are strongly influenced by structural details and in this work we present the structural details at a sub micrometer resolution. Further research work is needed to fully understand the effects of the local structure on bulk physical properties.

References:

[1] Ray, S. S; Okamoto M. *Prog. Polym. Sci.* 2003, *28*, 1539-1641.
[2] J. Karger-Kocsis, *Polypropylene - Structure, blends and composites*, Chapman & Hall, 1995.
[3] B. Yalcin, Z. Ergungor, Y. Konishi, M. Cakmak, C. Batur, *Polymer* 2008, 49, 1635-1650.

Poly(ethylene oxide)/sepiolite and poly(ethylene oxide)/sepiolite/Li salt Nanocomposites: Confinement Effects and Preliminary Results on their Performance as Solid Electrolytes

Alberto Mejía, Julio Guzmán, Nuria García, Pilar Tiemblo

Instituto de Ciencia y Tecnología de Polímeros (CSIC), Juan de la Cierva 3, 28006 Madrid, Spain

e-mail: amejia@ictp.csic.es

For over 30 years, poly(ethylene oxide) (PEO) has been used as a matrix in the search and development of a solid polymer electrolyte[1]. In the range of operating temperatures, it is essential to suppress its crystallinity while maintaining dimensional stability. Most research has been focused on extremely confined PEO[2,3,4], however this approach leads to materials with low concentrations of PEO and high non-conducting phase. Our approach consists on using high aspect ratio nanofibers (sepiolite) optimally dispersed in the polymer matrix, with the purpose of achieving solid-like materials behaving as a pseudosolid even above the melting point.

Raw (S) and polyethylene glycol lab-modified (M) sepiolites were melt compounded by extrusion to prepare the nanocomposites with two different molecular weight PEO matrixes (Mw=5000Kg/mol; and Mw=200Kg/mol). The resulting materials were characterized by microscopy techniques, DSC and DMTA. Good compatibility with the matrix is expected for both S and M due to the hydroxylated surface of S and the polyethylene glycol coating on M. Polymer nanocomposites (PNC), with excellent transparencies up to filler levels of 40 wt% and pseudosolid behaviour from 5 wt%, were obtained.

Filler dispersion was checked by SEM and TEM, showing, in general, excellent dispersions (Figure 1).

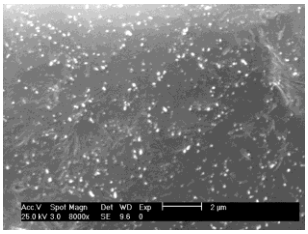

Figure 1:SEM image of 5 wt% M/PEO nanocomposite.

The crystallization behaviour of the PNCs was investigated by DSC and polarized light microscopy (PLM). DSC tests showed that crystallinity remains unaffected even at high sepiolite loadings, while the crystallization temperature (T_c) decreases clearly in M/PEO and does not increase in S/PEO. The unexpected T_c decrease suggests a confinement effect even in the composites with a 5% of M, which is confirmed by the large spherulites detected by PLM. The confinement effect is stronger in M-containing than in S-containing nanocomposites (Figure 2).

The addition of a Li salt completely alters the morphology of the composites: while salts like Li triflate (LiTF) do not strongly affect crystallinity, others like Li sulfonimide (LiTFSI) preclude crystallization and almost amorphous composites are obtained. The ability to avoid crystallization while maintaining a solid-like state above the melting point (T_m) makes these PNCs materials of great interest for the development of transport membranes. Preliminary studies on their performance as solid electrolytes have been made; being able to prepare, by extrusion, films of M/PEO-LiTFSI which are almost totally amorphous but show solid-like mechanical properties and dimensional stability. These NCPs present a Li^+ conductivity of 10^{-4} S·cm^{-1} at 40 ºC.

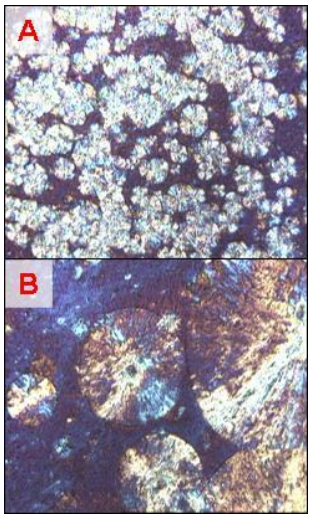

Figure 2:PLM images of A: 20 wt% S/PEO and B: 20 wt% M/PEO nanocomposites

References

[1] A. M. Stephan, K.S. Nahm. Polymer 47 (2006) 5952-5964

[2] M. Alexandre, P. Dubois. Materials Science and Engineering 28 (2000) 1-63

[3] H.-L. Chen, S.-C. Hsiao, T.-L. Lin, K. Yamauchi, H. Hasegawa, T. Hashimoto. Macromolecules 34 (2001) 671-674

[4] E. A. Stefanescu, P. J. Schexnailder, A.Dundigalla,I. I. Negulescu, G. Schmidt. Polymer 47 (2006) 7339-7348

Acknowledgements

We acknowledge financial support from the Spanish Science and Innovation Ministry (MAT2008-06725-C03-01).

Nanocomposites prepared with Montmorillonite modified by quaternary polyesters

Miroslav Huskić,[1,2] *Majda Žigon*[1,2]

1 National Institute of Chemistry, Ljubljana, Slovenia
2 Center of Excellence for Polymer Materials and Technologies, Ljubljana, Slovenia

miro.huskic@ki.si

Polymer/clay nanocomposites have attracted great interest, both in academia and industry, due to remarkable improvement in mechanical properties, heat resistance, decreased flammability etc. Various clay minerals can be used for this purpose but montmorillonite (MMT) appears to be the most studied so far.

Being hydrophilic by nature, clay minerals are not suitable for direct polymer nanocomposite preparation. Therefore, the surface has to be modified in order to make clay more hydrophobic and to reduce attractive forces between alumosilicate layers. There are several ways of clay modification, however, the most common method is a cation exchange with organic ammonium salts, which differ in a number, length and structure of long chains.[1,2]

Polycations have also been used to modify clay but have not been studied much for nanocomposite preparation[3], which is the subject of this work.

We synthesized polyesters from alkyl diethanolamine with long alkyl chains (N-octyl diethanolamine - ODEA, N-dodecyldiethanol amine – DDEA, and N-hexadecyldiethanolamine – HDEA), and succinic anhydride. Polyester synthesized from HDEA is crystalline at room temperature, polyester synthesized from DDEA is crystalline below -10°C, while P-ODEA is amorphous with glass transition temperature -58°C.

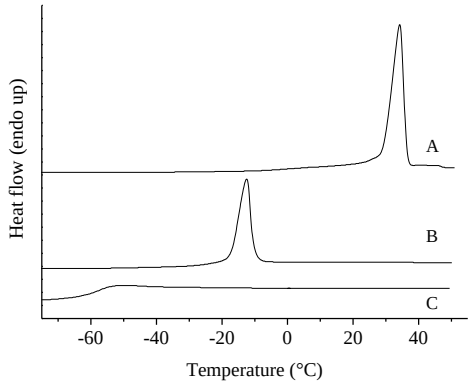

Figure1: DSC curves of polyesters: (A) P-HDEA, (B) P-DDEA, (C) P-ODEA.

The polyesters have been converted to quaternary polyesters by benzylbromide. The reaction was not quantitative and only up to 97% quaternization was achieved with P-ODEA, and up to 90% for P-DDEA and P-HDEA. Quaternization increased glass transition temperature and decreased or prevented crystallization. Polyesters with 40% and 60% quarternization were used for MMT modification. Cation ratio (MMT/polyester) 1:3 was used since our previous experiments showed that this is necessary best modification.[4] During the modification one part of quaternary polyester was bound on MMT while another part was only intercalated. The later was removed by extraction. The modified MMTs before and after extraction were characterized by X-ray diffraction (XRD) and thermogravimetric analysis (TGA). A decrease in interlayer spacing after extraction was observed as shown in Figure 2.

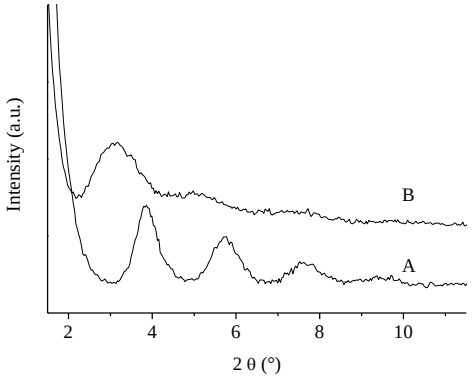

Figure 2: X-ray diffractogram of MMO modified with quaternary P-HDEA, before (A) and after extraction (B).

Unsaturated polyester and epoxy resins were used to prepare nanocomposites with the quaternary polyester modified MMT. The concentration of MMT was 1% to 5%.

Intercalation was determined by XRD and thermal stability of nanocomposites by TGA.

Mechanical properties of nanocomposites were determined by dynamic mechanical analysis (DMA). The modulus was significantly lower when non-extracted MMT was used since the excess polyester acted as a plasticizer.

Acknowledgement:
The authors acknowledge the financial support from the Ministry of Higher Education, Science and Technology of the Republic of Slovenia through the contract No. 3211-10-000057 (Center of Excellence Polymer Materials and Technologies).

[1] Alexandre M, Dubois P, Mater. Sci. Eng, R., Reports 2000; 28:1-63.
[2] Ray SS, Okamoto M. Prog. Polym. Sci. 2003;28:1539-1641.
[3] Liu P, Appl. Clay Sci. 2007;38:64–76
[4] Huskić M, Žagar E, Žigon M, Brnardić I, Macan J, Ivanković M, Appl. Clay Sci., 2009;43:420-424.

Polymeric Micelles Using Pseudo-Amphiphilic Block Copolymers and their Cellular Uptake†

Massimo Benaglia,[a] *Enzo Spisni*,[b] *Angelo Alberti*,[a] *Alessio Papi*,[b] *Emanuele Treossi*,[a] *Vincenzo Palermo*[a]

[a]ISOF - Consiglio Nazionale delle Ricerche, Area della Ricerca, 40129, Bologna, Italy. Tel: +390516398257
[b]Dipartimento di Biologia Evoluzionistica Sperimentale, Università di, Bologna, 40126 Bologna, Italy.

e-mail: massimo.benaglia@cnr.it

Introduction Nanotechnology sciences have recently benefited from controlled/living radical polymeriza-tion,[1] an extremely powerful tool that has allowed new unexploited results to be reached in polymer chemistry. Among those techniques, RAFT polymerization has been successfully used in the preparation of functional polymeric micelles[2] that can be employed for the delivery of therapeutic agents. This makes it possible to administer lipophilic drugs while protecting unstable molecules from metabolic deactivation.[3,4] Such characteristics, together with a reduced clearance, increase the efficacy of drugs that are usually toxic, thus reducing their effective dose.[5] Polymeric micelles are characterized by a low critical micelle concentration (CMC), which makes them stable under diluted conditions. Nevertheless, their high stability may not be sufficient for the in vivo physiological extreme dilution. Further stabilization can be provided to polymeric micelles by crosslinking processes.[6,7]

Results and Discussion Stable micelles are obtained starting from carboxyl terminated PS-*b*-PMA block copolymer that shows pseudo-amphiphilic properties when dispersed in methanol. Well defined mono-dispersed spherical micelles (20-30 nm) are obtained when the acidic groups carried by the unimers are deprotonated and by using dry solvents. Once assembled, the micelles can be suspended in water by osmosis because their thermodynamic stability. The micelles were also stabilized by Shell Cross Linking (SCL) using triethyleneglycol diacrylate as crosslinker and 2,2'-azobis(2-methylpropionamidine) dihydrochlo-ride as initiator. Because of electrostatic interactions this initiator settles, in its cationic form, only in proximity to the micelle surface initiating there the crosslinking polymerization process. The anionic corona that constitutes the outer shell of the micelles performs a double function: one is to direct the hyperbranching process only at the surface of the particles, the other one is to prevent micelle aggregation by electrostatic repulsion. The improved stability of SCL micelles has been proved by changing the pH of the dispersant media. The free or SCL particles were loaded with the lipophilic marker Nile Red and cell internalization of the carried fluorescent compound was followed with confocal microscopy (CLSM). Different cellular compartments were stained by free or SCL micelles. Free Nile Red loaded micelles stain the membranes while the SCL ones stain the cytosol. This evidences the intracellular stability of SCL nano-particles. Uncrosslinked micelles were also loaded with neutral doxorubicin and administered to doxorubicin resistant cells (LoVo-MDR). CLSM images showed the internalization of doxorubicin into the nucleus. This reveals that the resistance of LoVo-MDR to doxo-rubicin has been overcame. The unimers constituting the micelles were also labeled through thiol conjugation with fluorescein 5-maleimide. This has been made possible by the versatility of the RAFT group that easily affords the thiol function. Cell internalization of fluorescein labeled micelles was followed by CLSM.

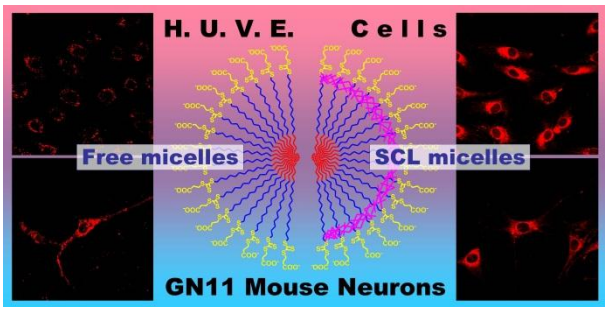

Conclusions RAFT polymerization made possible the synthesis of carboxyl terminated PS-*b*-PMA block copolymer. This material showed pseudo-amphiphilic properties when dispersed in methanol and provides stable micelles. Their thermodynamic stability allows their dispersion in water. SCL stabilization increase the intracellular stability of the micelles. These nanoparti-cles are internalized into LoVo-MDR cells delivering doxorubicin. The micelles can also be labeled in their constituent unimers which were covalently bound with fluorescein in order to trace the unimer fate *in vitro*.

References

1) W. A. Braunecker and K. Matyjaszewski, *Prog. Polym. Sci.*, 2007, **32**, 93-146.
2) H. J. Yoon and W. D. Jang, *J. Mat. Chem.*, 2010, **20**, 211-222.
3) A. S. Mikhail and C. J. Allen, *Contr. Rel.*, 2009, **138**, 214-223.
4) H. Devalapally, A. Chakilam and M. M. Amiji, *J. Pharm. Sci.*, 2007, **96**, 2547-2565.
5) Y. Matsumura and H. Maeda, *Cancer Res.*, 1986, **46**, 6387–6392.
6) B. Y. Li, I. Akiba, S. Harrisson and K. L. Wooley, *Adv. Funct. Mater.*, 2008, **18**, 551-559.
7) R. K. O'Reilly, C. J. Hawker, K. L. Wooley, *Chem. Soc. Rev.* 2006, **35**, 1068-1083.

† *J. Mater. Chem.*, 2011, DOI: 10.1039/C0JM02519D

Patterning Polymer Brush Microstructures by Colloidal Lithography

Tao Chen, [a] *Rainer Jordan*, [a] *Stefan Zauscher* [b]

[a] Department of Chemistry, Technische Universität Dresden, Dresden, 01069 (Germany)
[b] Center for Biologically Inspired Materials and Materials Systems, and Department of Mechanical Engineering and Materials Science, Duke University, Durham, NC, 27708 (USA)

tao.chen@chemie.tu-dresden.de

1. Introduction

It is well known that monodisperse colloidal microspheres easily self-assemble into hexagonal close packed (*hcp*) arrays on surfaces as a result of capillary forces arising from the evaporation of solvents.[1] Such periodic arrays were used already as shadow masks in colloid lithography (CL) for the deposition of platinum nanomaterials in early 1980 by Fischer and co-workers. [2] Since then, CL has become a simple, versatile, and cost-effective fabrication technique for a large number of researchers in the field of micro/nano fabrication.

Patterned polymer brushes are of increasing importance especially for array based platforms because of their ability to modify surface properties and their potential applications in surface-based technologies, such as protein-resistant coatings, switchable sensors, substrate for cell-growth control, and for separation of biological molecules. [3, 4] Micro- and nano-patterned polymer brushes can be grown via surface-initiated polymerization from surface confined initiator templates, fabricated by various lithographic approaches. [5-9] Among these fabricating approaches, microcontact printing (μCP) is, a simple and convenient technique, accessible to a broad range of researchers, while many of the other patterning strategies remain inaccessible due to the instrumental complexity required. This motivates our current development for new micro- and nano-patterning strategies for polymer brushes.

Here, we exploited a series of robust, but simple and convenient approach of CL using microsphere array as mask, as guiding template, and footprint as restricted geometry, and combining with surface initiated atom transfer radical polymerization (SI-ATRP) to fabricate patterned polymer brush microstructures.

2. Results and Discussion

The appropriate position of colloid microsphere structure could be as mask, as guiding template, and footprint as restricted geometry was shown in Figure 1A-C. The AFM images of subsequent patterning of polymer brush microstructures fabricated from CL and combining with SI-ATRP were given in Figure 1D-G.

3. Conclusions

We have demonstrated prototypically for the first time how colloidal lithography can provide a simple approach to fabricate various patterned polymer brush micro- and nanostructures. Our approaches rely on the spontaneous formation of well-ordered colloidal microsphere arrays that provide lithographic masks or templates for creating patterns of initiator SAMs that can be used for subsequent amplification into polymer brush patterns. The advantages of CL technique for patterned polymer brush fabricating over the aforementioned lithographic approaches that, not only providing commercially available colloid precursor at a relatively low cost, and no complex equipment required to create patterned template with features at a micro and nano scale, but also polymer brush feature are controlled simply by changing the size or chemical functionality of a microsphere.

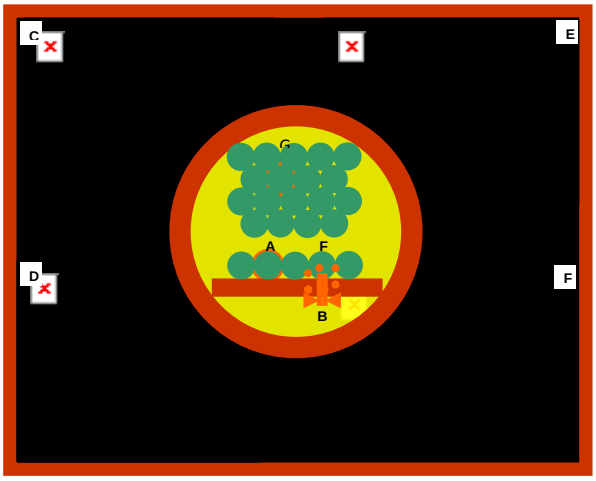

Figure 1, Schematic illustration and AFM images use of colloidal microsphere lithography for patterning polymer brush microstructures (A-C) Appropriate position for lithography. (D-G) Polymer brush microstructures fabricated from CL by using microsphere array as mask, as guiding template, and footprint as restricted geometry, and combining with SI-ATRP.

Acknowledgments: TC and RJ thank the Alexander von Humboldt Foundation for support of TC by an Alexander von Humboldt Research Fellowship. SZ thanks the National Science Foundation for support through grants NSF DMR-0502953 and NSF NIRT CBET-0609265.

References:

[1] N. D. Denkov, O. D. Velev, P. A. Kralchevsky, I. B. Ivanov, H. Yoshimura, K. Nagayama, *Nature* **1993**, *361*, 26.
[2] U. C. Fischer, H. P. Zingsheim, *J. Vac. Sci. Technol.* **1981**, *19*, 881.
[3] B. Zhao, W. J. Brittain, *Prog. Poly. Sci.* **2000**, *25*, 677.
[4] T. Chen, R. Ferris, J. M. Zhang, R. Ducker, S. Zauscher, *Prog. Poly. Sci.* **2010**, *35*, 94.
[5] S. J. Ahn, M. Kaholek, W. K. Lee, B. LaMattina, T. H. LaBean, S. Zauscher, *Adv. Mater.* **2004**, *16*, 2141.
[6] U. Schmelmer, A. Paul, A. Kuller, M. Steenackers, A. Ulman, M. Grunze, A. Golzhauser, R. Jordan, *Small* **2007**, *3*, 459.
[7] N. Ballay, S. Schilp, M. Zharnikov, *Angew. Chem., Int. Ed.* **2008**, *47*, 1421.
[8] T. Chen, J. M. Zhong, D. P. Chang, A. Carcia, S. Zauscher, *Adv. Mater.* **2009**, *21*, 1825.
[9] B. W. Maynor, S. F. Filocamo, M. W. Grinstaff, J. Liu, *J. Am. Chem. Soc.* **2002**, *124*, 522.

Penetrants interacting with matrix of polymeric membrane. Problems and perspective.

Ilya V. Vorotyntsev, *Natalia A. Petukhova*

R.Y. Alekseev Nizhny Novgorod State Technical University, N.Novgorod, Russia

postmaster@vorotyn.nnov.ru

Nowadays membrane gas separation is one of traditional physicochemical separation and purification methods such as crystallization, distillation, and sorption. Membrane gas separation is using for separation different binary system, such as N_2/O_2, CH_4/CO_2 and many others. But some systems are characterized by interaction with matrix of polymeric membrane. For example, ammonia in aromatic polyamides, polyheteroarylenes which is characterized by electron acceptors character of active groups of these polymers. Also donor-acceptor interaction in which the penetrants acting as electron acceptor is might be realized in sulphur dioxide – polyeher (ester) ureas system. Hydrogen bonds might be cause of such interaction in hydrogen containing fluorocarbons in polyurethanes. Lots of data of huge gases permeability increasing when they have higher level of humidity might be an example of ion-dipole interaction of water with polymeric matrix of membrane.

Despite the fact of wide and common use of membrane gas separation for above mentioned problems it is needed to explore the process for the case of interaction between the separated gases and membrane matrix. In this case the separation effect might increase or decrease.

In the present work we represent the results of investigation interaction between ammonia and cellulose acetate glassy polymer membrane. Ammonia and some permanent gases permeability were measured [1]. It is shown that ammonia and water interaction with cellulose acetate membrane is of reversible nature.

Features of this process determine the thermo dynamical and kinetic properties of the system penetrant (ammonia and water) – polymer caused by the types and energies of interaction realized in the system.

As we were known the donor-acceptor character of interaction of these polymer membrane matrix/penetrant can be proved by change in IR spectrums of polymer in sorption equilibrium with interacting penetrant, also by high values of partial molar enthalpy of dissolved penetrant.

The inverse gas chromatography was used for determination sorption characteristics of the investigated system. The sorption investigation for the tested systems is complicated due to non-equilibrium state of glassy polymer with micro heterogeneous which is also a swelling material. The partial thermodynamic functions were determined by thermal equation of sorption equilibrium in system of swelling polymers. This thermal equation was obtained by quasi-chemical model of sorption proposed by Laatikainen and Lindstrom. The values of partial molar enthalpy of dissolved ammonia in cellulose acetate were obtained from isotherms data.

IR-spectroscopy was used for proving specific interaction in investigated system. The tested system was obtained by ammonia purge through cellulose acetate up to sorption equilibrium at certain temperature.

The obtained IR spectrums of ammonia – cellulose acetate system is characterizing by significant increase in absorption peak which are not present in cellulose acetate without ammonia.

As a result of above-mentioned investigation the mechanism of penetration of gases interacting with membrane was proposed.

References:

[1] Vorotyntsev V.M., Drozdov P.N., Vorotyntsev I.V. High separation of substances by a gas separation method // Desalination. 2009. 240. 301-305.

This work has been financially supported by Russia Foundation of Basic Research, Grant № 11-08-00707

From Bulk to Attograms of Matter: Dynamics and Phase Transitions of Polymeric Materials

A. Serghei[1], *T.P. Russell*[2]

[1] Université Lyon 1, CNRS, UMR 5223, Ingénierie des Matériaux Polymères, F-69622 Villeurbanne, France
[2] Polymer Science and Engineering,University of Massachusetts Amherst, Amherst MA 01003, USA

russell@mail.pse.umass.edu; anatoli.serghei@univ-lyon1.fr

The present contribution is dealing with investigations on extremely small amounts of polymeric materials, i.e. attograms of matter (1 attogram=10^{-18} grams). The project is based on the novel experimental concept of using nano-containers as measurement cells (Fig. 1). Two major objectives are proposed:

(a) development of an experimental platform to address fundamental questions in soft matter physics, such as for instance: "What is the minimum amount of matter necessary to "define" the material properties?".

(b) exploring new routes to enhance the performance of macromolecular systems by means of geometrical confinement and/or external perturbations (i.e. electric fields). The concept of this approach is essentially related to a two-fold effect which is expected for sample amounts in the order of attograms: (i) the degree of disorder characteristic for bulk materials is strongly reduced in the case of small systems; (ii) small external perturbations can generate huge effects when applied on tiny amounts of material.

Different aspects of the polymer dynamics – manifested on time scales spanning more than 10 orders of magnitude (molecular fluctuations, glass transition, capillary flow) – phase transitions as well as material parameters relevant for technological applications (i.e. conductivity, permittivity, ferroelectric activity) will be discussed for polymeric systems having one, two or three dimensions on the nanometric length-scale.

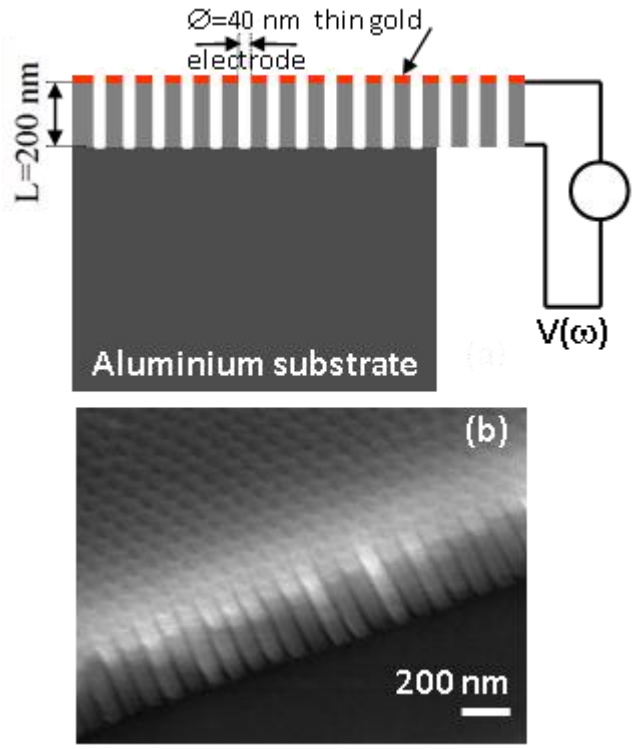

Fig. 1: Nanocontainers as experimental cells to hold and measure attograms of matter. (a) schematic representation of the sample cell; (b) SEM image of the nanocontainers in cross-section.

Effect of Organoclay Surface Treatment on the Property Profile of Recycled PET Nanocomposites

M. Kracalik, A. Witschnigg, S. Laske, C. Holzer

Montanuniversitaet Leoben, Department Polymer Engineering and Science, Otto Gloeckel Str 2, 8700 Leoben, Austria

Milan.Kracalik@unileoben.ac.at

Introduction: Nanotechnology was introduced as a new method of improvement of polymer properties in 1995. The technology involves not only incorporation of nanosized particles into the polymer but, more importantly, investigation of interactions between the polymer matrix and the enormously large nanofiller surface [1]. Especially for polymer/clay nanocomposites, the surface effects are responsible for improvement of barrier, mechanical and rheological properties, dimensional stability, heat, flame and oxidative resistance. In comparison with traditional fillers (20–40 wt. % loading), 2–5 wt. % filling of layered clays is sufficient to achieve analogous material improvement [2, 3]. Addition of nanoscaled fillers to recycled polymers represents a promising possibility of properties enhancement [4-6]. Generally, three methods of polymer/clay nanocomposites preparation are used: in situ polymerization, solution mixing and melt mixing. The melt mixing process is technologically the most interesting; nevertheless, satisfactory results with polyethylenterephthalate matrix have not been achieved. In this contribution, recycled polyethylenterephthalate (PET-R) has been compounded with differently modified commercial organoclays. Effects of organoclay surface modification on processing as well as utility properties have been investigated.

Materials and method: Colour-sorted PET-R has been compounded with 6 different organically modified layered silicates. For the compounding process, a counter-rotating twin screw extruder Brabender Plasticorder PL2000 using a string die with consequent granulation using a water bath has been employed. Processing (rotational and elongational rheometry), structural (X-ray diffraction, transmission electron microscopy) and utility properties (differential scanning calorimetry, thermogravimetric analysis, mechanical and flammability testing) of the prepared nanocomposites have been investigated.

Results and Discussion: The efficiency of the organoclay filling manifested itself as a significant increase in melt viscosity in the range of low shear rates. At higher frequencies, the complex viscosity of some PET-R nanocomposites decreased below the value of the unfilled matrix with the same processing history as the nanocomposites. It was already found that the most significant degradation during the processing of recycled PET and organoclay is attributed to chemical reactions between the functional groups of organic modifiers, free water of silicate and the polymer chains [4]. These reactions lead to a decrease in molecular weight, which explains lower viscosity values in nanocomposites at higher shear rates. The level of the mentioned degradation reactions can be assessed by viscosity decrease of the processed PET-R as compared to original PET-R before processing. Compared to the unfilled polymer matrices, all nanocomposites show significant increase in melt elasticity at lower frequencies. In the range of higher shear rates, the melt elasticity of some PET-R nanocomposites decreased below the value of the unfilled PET-R matrix due to degradation mechanism described. Considering rheological behavior in the elongational flow, all the prepared nanocomposites revealed significant increase in the melt strength as compared to unfilled polymer matrices. Results of flammability tests revealed pronounced influence of flamm rate on surface treatment applied in organoclays. Nanocomposites containing organoclays sensitive to degradation during the processing revealed even higher flamm rate than unfilled polymer matrix. On the contrary, filling with organoclays possessing higher thermal stability and lower sensitivity to degradation reactions during the processing led to reduction in the flamm rate. However, all the nanocomposites revealed significant reduction in drop-off effect in comparison with unfilled polymer matrix.

Conclusion: PET-R nanocomposites have been prepared using different organic surface modifications of layered silicate. Selected processing and utility properties have been compared. In the prepared nanocomposites both, the delamination effect (formation of 3D structure) as well as degradation phenomenon (chain scission, generation of low-molecular products) has been detected by dynamic rheological experiments. Using Rheotens equipment, effect of organoclay surface treatment on the melt strength level of different PET-R nanocomposites has been investigated. Tests of flammability revealed strong influence of the flamm rate on the surface modification used in organoclay. However, significant reduction in drop-off effect in all nanocomposite systems prepared has been obtained as compared with polymer matrix without nanofiller.

References:

[1] K. M. Lee, C. D. Han, *Macromolecules* **2003**, 36, 7165.
[2] S. S. Ray, M. Okamoto, *Prog. Polym. Sci.* **2003**, 28, 1539.
[3] H. Olphen, *Clay Colloid Chemistry*, New York, Wiley, 1977.
[4] M. Kracalik, J. Mikesova, R. Puffr, J. Baldrian, R. Thomann, C. Friedrich, *Polym. Bull.* **2007**, 58, 313.
[5] M. Kracalik, M. Studenovsky, J. Mikesova, A. Sikora, R. Thomann, C. Friedrich, I. Fortelny, J. Simonik, *J. Appl. Polym. Sci.* **2007**, 106 (2), 926.
[6] M. Kracalik, M. Studenovsky, J. Mikesova, J. Kovarova, A. Sikora, R. Thomann, C. Friedrich, *J. Appl. Polym. Sci.* **2007**, 106 (3), 2092.

Effect of two different surfactants on the properties of PET nanocomposites

Itamara F. Leite, Anna Priscilla S. Soares, Oscar M. L. Malta e Suédina Maria de L. Silva

Two types of organic modifiers as alkyl ammonium and alkyl phosphonium were employed in different amount in the organic modification of a purified bentonite clay by reaction ion exchange and utilized as filler in the preparation of poly(ethylene terephthalate)(PET) nanocomposites. PET nanocomposites containing 1 wt% of organoclays were prepared in the Rheometer Torque Haake, operating at 260 ˚C, 60 rpm for 10 min and then analyzed by X-ray diffraction and thermogravimetry analysis. This study allows evaluating the characteristics of the organic modifiers' influence on the intercalation and exfoliation processes in PET. XRD results suggested the obtaining of exfoliated PET nanocomposites when high levels of alkyl ammonium salt were used in the organic modification of purified bentonite. Improvement in the thermal stability also was observed for the sample containing high levels of alkyl ammonium as a result of exfoliated morphology.

Key-words: PET, surfactants, properties, nanocomposites.

Optical Writing in Self-Assembled Azobenzene Block Copolymers and their Blends with PMMA

S. MENGHETTI[1], M. ALDERIGHI[1], F. TANTUSSI[2], F. FUSO[2], M. ALLEGRINI[2], R. SOLARO[1], G. GALLI[1]*

[1]Dipartimento di Chimica e Chimica Industriale, INSTM UdR Pisa, Università di Pisa, 56126 Pisa (Italy)
[2]Dipartimento di Fisica, polyLab CNR, Università di Pisa, 56127 Pisa (Italy)

E-mail: gallig@dcci.unipi.it

Introduction

The attainment of ultra-high density (foreseen up to 1 Tbyte/cm^2) optical data storage, e.g., for re-writable DVDs, requires the development of materials able to sustain stable modifications of their optical properties sized on the order of tens of nm, or even less. Besides new materials, research on nanooptical writing demands non-conventional optical schemes able to access sub-diffraction spatial resolution. Block copolymers have a great potential in opto-electronics and data storage applications [1].

To these aims, we synthesized new block copolymers containing azobenzene side groups and then performed nanowriting experiments by using a scanning near-field optical microscope (SNOM) equipped with a polarization-modulation system able to catch details of the optical properties with a spatial resolution in the tens of nm range. These materials exhibit a liquid-crystalline behaviour able to improve the writing stability. The resulting morphology is not strongly influenced by liquid-crystalline order, being mostly governed by the volumetric fraction of the phase-separated blocks. We also prepared blends with PMMA and the block copolymers to dilute the azobenzene content in order to perform nanowriting in the bulk sample.

The relevance of block copolymers and their morphology in the optical writing will be discussed.

Materials and Methods

We synthesized novel block copolymers of an azobenzene-containing polymethacrylate and polymethyl methacrylate, P(MA4-b-MMA)y, with different contents y of the azobenzene block (1–20 mol% MA4) to be used as media for optical writing [Fig.1].

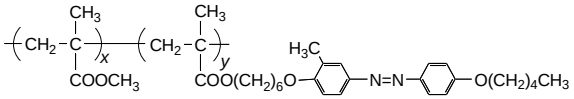

Fig.1 Chemical structure of the block copolymers P(MA4-b-MMA)y (y = 1–20 mol%).

Results and Discussion

The block copolymers are able to self-assemble in nanostructures and the segregation of the azobenzene moieties in nanodomains [Fig.2] permits high stability and high contrast in optical writing at the nanoscale to be achieved in writing/reading experiments in the near field. SNOM writing demonstrates the achievement of a stable optically nanowritten bit [Fig.3].

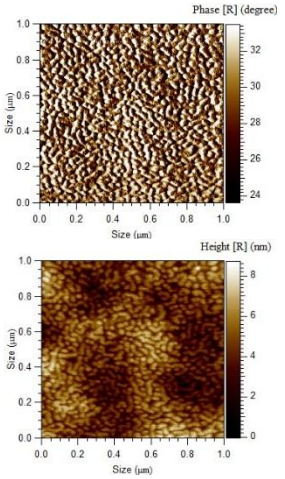

Fig.2. AFM topography (top) and phase (bottom) maps of P(MA4-b-MMA)20.

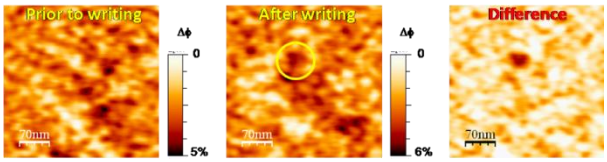

Fig.3. Maps of the optical retardation acquired by PM-SNOM on a P(MA4-b-MMA)20 film before and after optical writing (at the encircled position).

Conclusions

Self-assembled azobenzene block copolymers allow the obtainment of a pure-optical writing and the achievement of a nanoscale size of the imprinted bit.

In azobenzene block copolymer films stable optical modifications can be produced by using pulses as short as 1 ms, with the capability of pure optical writing with sub-100 nm spatial resolution. This may open avenues to ultra-high density information storage media.

References

[1] H. C. Kim, S .M. Park and W. D. Hinsberg, *Chem. Rev.* (2010) 110, 146.

Acknowledgments

The authors thank the Regione Toscana, POR OB3 Misura D4, for partial financial support of the work.

Generating Hierarchical Nanostructures in Polymer Surfaces

J.P. Fernández-Blázquez, A. del Campo

Max-Planck-Institut für Polymerforschung. Ackermannweg 10, 55128 Mainz, Germany

e-mail: fernande@mpip-mainz.mpg.de

A generic method to obtain nanostructured surfaces with different topographies upon plasma etching of polymer surfaces is presented. Special effort was paid to the generating of hierarchical structures mimicking structured surface found in nature (i.e. gecko adhesive structures or self-cleaning lotus leaves). A correlation was found between the morphology of the polymer sample (crystallinity, orientation) and the resulting nanopatterns. We propose plasma etching as a templateless method for generating polymer nanopatterns.

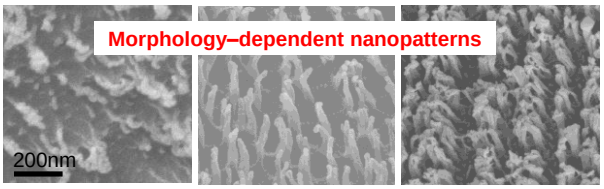

References:

E. Wohlfahrt, J. P. Fernández-Blázquez, E. Arzt, A. del Campo*, submitted

J. P. Fernández-Blázquez, D. Fell, E. Bonaccurso, A. del Campo*, *Journal of Colloid and Interface Science*, doi:10.1016/j.jcis.2011.01.082

E. Wohlfart, J.P. Fernández-Blázquez, E. Knoche, A. Bello, E. Pérez, E. Arzt, A. del Campo*, *Macromolecules* 43(23), 9908-9917 (2010)

Electric Conductivity of Aqueous Solutions of Partially Neutralized Poly(thiophene-3-ylacetic Acid) as Predicted by Different Polyelectrolyte Theories – Comparison with Experiment

J. Cerar,[a] *D. Bondarev*,[b] *J. Vohlidal*,[b] *V. Vlachy*[a]

[a]University of Ljubljana, Faculty of Chemistry and Chemical Technology, SI-1000 Ljubljana, Slovenia;
[b]Charles University, Faculty of Sciences, Dept. of Phys. and Macromol. Chem., CZ-128 40, Praha 2

janez.cerar@fkkt.uni-lj.si

Background & Methods: Conjugated polyelectrolytes (CPs) possess several interesting properties that make them an interesting material for technological use. One of these properties is their spectral characteristics in UV/Vis region which are primarily dependent on the conformation of polymer backbone. Nevertheless, the thermodynamic and transport properties of CPs in aqueous solutions are very scarce although significant portion of UV/Vis spectral studies of CPs' solutions cannot be unequivocally interpreted without known thermodynamic and transport properties. On the other hand, the information about polyelectrolyte conformation in solution can help in interpretation of conductivity studies. This is especially true when polyelectrolyte conductivity is to be interpreted also in terms of conformational changes.

As the compound that could be used in testing various polyelectrolyte conductivity theories poly(thiophene-3-ylacetic acid) (PTAA) was chosen as a typical and often studied representative of CP. For the purpose of conductivity studies the sample of PTAA was carefully dialyzed and neutralized to degree of neutralization α_n = 0.346 with aqueous NaOH solution. For the prepared stock solution of partially neutralized PTAA (PTAA/Na; α_n = 0.346) concentration dependence of electric conductivity of aqueous solutions at 25 °C was measured in dilute concentration regime.

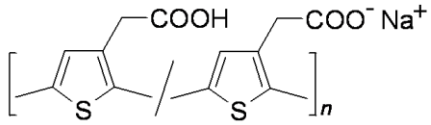

PTAA/Na (α_n = 0.346)

From the obtained specific conductivity the molar conductivity Λ, expressed to one mole of neutralized carboxylic groups, was calculated. Theoretical predictions of Λ were calculated for two Manning's models (rod-like and chain-like) and for scaling theory (for dilute and for semi-dilute regime). In order to correctly take into account fraction of free counterions, *f*, occurring in these theories, the values of *f* were evaluated from the measured transport numbers and electric conductivity. The degree of polymerization, X_n, was estimated to be $X_n \approx 39$ by size-exclusion chromatography measurements. All these data enabled application of theoretical expressions and recalculation of Λ without use of a single adjustable parameter.

Results & Discussion: Measurements of UV/Vis spectra of PTAA/Na indicated no conformational changes of polymer backbone in the concentration range where electric conductivity was measured. Both Manning's and scaling conductivity theories in principle recognizes concentration dependence of fraction of free counterions but through simplifications in their final expressions dependence of *f* on concentration is lost. Consequently, all these theories are practically always used with simplification of constant value of *f*. Results of such calculations for PTAA/Na case are presented in the figure below.

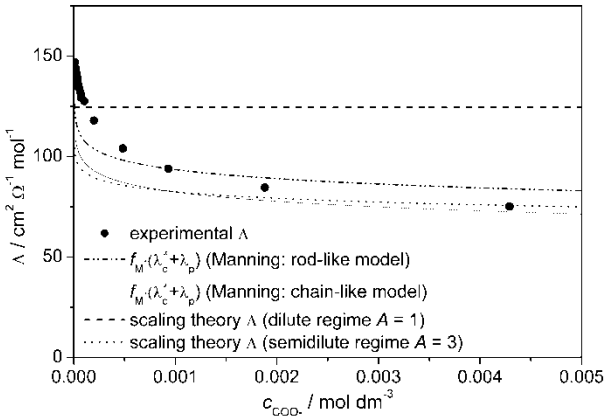

The results obtained by applying all four theoretical predictions in their standard form are rather satisfactory as judged according to their limitations. Incorporating experimentally determined and concentration dependent *f* into existing polyelectrolyte theories drastically changes some of these predictions (see figure below).

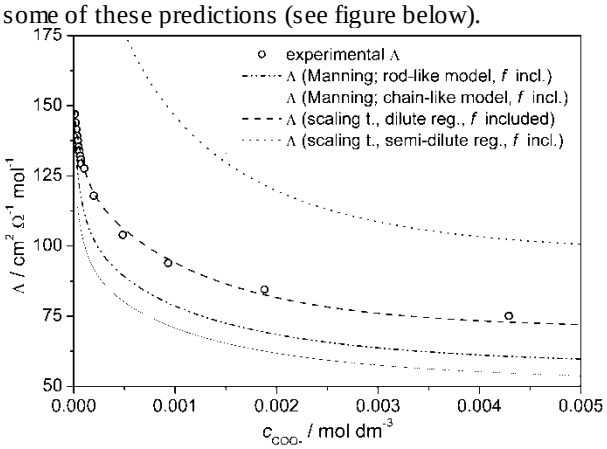

Conclusions: Introducing explicit concentration dependence of *f* on concentration can substantially change theoretically predicted Λs of polyelectrolyte. By applying this improvement for the studied case of PTAA/Na almost perfect agreement between measured Λs and those calculated from the scaling theory for dilute regime was obtained without introducing any adjustable parameter.

Acknowledgments: Financial supports of the Slovenian Research Agency (0103-0201), Czech Science Foundation (104/09/1435 and 203/08/H032), Ministry of Education of the Czech Republic (MSM0021620857) and Grant Agency of the Charles University (D. B., project 166410) are acknowledged.

Characterization of the Morphology of Co-extruded, Thermoplastic/Rubber Multi-layer Tapes

J.G.P. Goossens[a], *R.M.A. l'Abee*[a], *A.M.J.T. Meijer-Vissers*[a], *A.B. Spoelstra*[a], *M. van Duin*[a,b]

[a]Laboratory of Polymer Technology, Department of Chemical Engineering and Chemistry, Eindhoven University of Technology, P.O. Box 513, 5600 MB Eindhoven, The Netherlands
[b]DSM Elastomers R&D, P.O. Box 1130, 6160 BC Geleen, The Netherlands

e-mail: J.G.P.Goossens@tue.nl

Tapes with alternating semi-crystalline thermoplastic/rubber layers with thicknesses varying from 100 nm up to several μm's were prepared by multi-layer co-extrusion. The variation in layer thickness was obtained by varying the thermoplastic/rubber feed ratio. Various microscopy techniques were used to visualize the morphology of the layered systems. The relatively large length scales and the sample preparation make optical microscopy (OM) unsuitable to study the morphology of the multi-layer tapes. Although excellent contrast between the thermoplastic and rubber layers can be obtained, the usually applied, relatively large magnifications limit the use of transmission electron microscopy (TEM) and atomic force microscopy (AFM) to small sample areas. The large range of applicable magnifications makes scanning electron microscopy (SEM) the most suitable technique to study the morphology of the multi-layer tapes. The sample preparation for SEM with a secondary electron (SE) detector is often based on the removal of one of the components, which may induce changes in the morphology. SEM with a back-scattered electron (BSE) detector is a very convenient method to study the morphology over a wide range of length scales, where the contrast between the different layers can be enhanced by chemical staining. Finally, the crystallization behaviour of the semi-crystalline layers, as probed by differential scanning calorimetry (DSC), may provide valuable information on the layered morphology.

Cationized Nanofibrillated Cellulose by Aqueous Free Radical Polymerization: Synthesis, Structure, and Antibacterial Properties

Kuisma Littunen, *Ulla Hippi*, *Jukka Seppälä*

Aalto University School of Chemical Technology, Polymer Technology Research Group, Espoo, Finland

kuisma.littunen@tkk.fi

Chemicals with positively charged groups are known to be antibacterial, offering a nontoxic alternative to common disinfectants.[1] Combining these properties with the large specific surface area of nanofibers could yield safe and efficient antibacterial materials.

Nanofibrillated cellulose (NFC) was modified by polymers containing cationic ammonium groups. Since NFC exists as dilute water dispersions, the polymerization was conducted in an aqueous medium by redox initiated free radical grafting. Cerium ammonium nitrate was used as initiator. This method is known to be efficient for grafting polysaccharides with acrylic monomers while also preserving the nanofibrillar structure.[2]

Three different synthesis routes were investigated (Fig. 1):

- Direct grafting of cationic monomer from NFC
- Grafting NFC with a monomer containing tertiary amine groups, followed by cationization
- Grafting NFC with a monomer containing epoxide groups, amination with a secondary amine, and cationization

Chemical structure of the products was characterized by FTIR, solid-state ^{13}C NMR, and XPS. Antibacterial properties were investigated by bacterial cultivation experiments.

[1] Thome, J.; Holländer, A.; Jaeger, W.; Trick, I.; Oehr, C. *Surf. Coat. Tech.* **2003**, 174-175, 584-587.

[2] Littunen, K.; Hippi, U.; Johansson, L.; Österberg, M.; Tammelin, T.; Laine, J.; Seppälä, J. *Carbohydr. Polym.* **2011**, doi:10.1016/j.carbpol.2010.12.064.

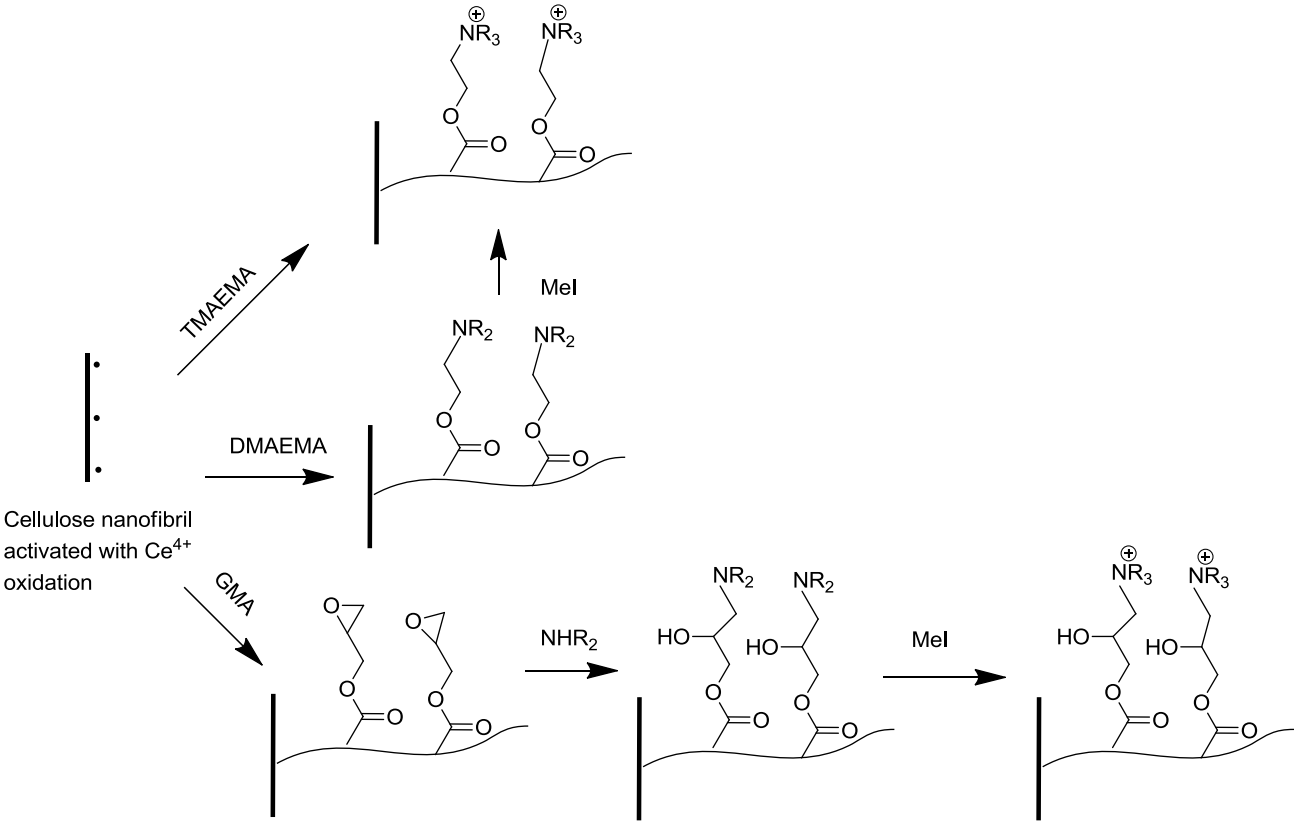

Figure 39. Synthesis routes for cationization of NFC.

Conformations, intra-molecular structures and persistence length of molecular brushes

O. Borisov [a,b], *E. Zhulina*[b], *A.Polotsky*[b], *T.M.Birshtein*[b], *L.Feuz*[c], *P.Kosovan*[d], *F.A.M.Leermakers*[e]

[a] UPPA, CNRS UMR 5254 IPREM Equipe de Physique et Chimie des Polymères, Pau, France
[b] Institute of Macromolecular Compounds, Russian Academy of Sciences, 199004, St.Petersburg, Russia
[c] Chalmers University of Technology Biological Physics, Göteborg, Sweden
[d] Institute of Computational Physics, University of Stuttgart70569 Stuttgart, Germany
[e] Laboratory of Physical Chemistry and Colloid Science, Wageningen University, 6703 HB Wageningen, the Netherlands

oleg.borisov@univ-pau.fr

Molecular brushes are composed of a long main chain onto which side chains ("grafts") are attached at regular intervals. The graft copolymers are classified as molecular brushes provided that the distance between the grafts along the contour of the main chain is small in comparison to the characteristic dimensions of the side chains.

In general case the backbone and the grafts can be chemically different, i.e., exhibit different flexibility and solubility properties. Furthermore, the grafts themselves can exhibit chemical or topological complexity. For example, "core-shell" molecular brushes are formed in the case of the block copolymer side chains. Recently, molecular brushes comprising randomly or regularly branched (dendritic) grafts have been synthesized.

The objective of our work was to establish general relationships between architecture of the grafts, types of intra-molecular interactions involved and local and large scale conformational properties of the molecular brushes. This is done on the basis of systematic combination of analytical mean-field and scaling approaches with the numerical Self-Consistent Field (SCF) modeling. Theoretical predictions are compared to experimental observations and results of numerical simulations.

The general features of molecular brushes are determined by crowding and strong steric interactions between the grafts. These interactions (repulsive under good solvent conditions) lead to radial stretching of the grafts, impose the axial tension in the backbone and affect apparent persistence length of the molecular brushes. The latter property is manifested in large-scale conformational properties, e.g. in the gyration radius of molecular brushes.

By comination of scaling and numerical SCF approaches we have proven that the apparent persistence length of molecular brushes with linear grafts comprising $10 \div 10^2$ segments is controlled by the brush thickness (i.e. by the radial extension of the grafts). This finding is in a line with results of computer simulations and with experiments on molecular brushes formed by the grafts of similar length. We have demonstrated, that the effects of induced bending rigidity (which grows proportionally to the square of the brush thickness) are manifested only in molecular brushes with the graft length $\geq 10^3$, that is beyond the up-to-date experimental and computational limits.

Conformations and induced bending rigidity of molecular brushes with dendritic grafts have been considered. These brushes are formed by dendrons attached by the end of the root spacer to the backbone of the brush. We have demonstrated that fairly uniform radial distribution of monomer unit density within the brush thickness is ensured by strong radial fluctuations in the extension of individual dendrons. The effects of induced bending rigidity on the apparent persistence length of dendritic molecular brushes become stronger upon an increase in the number of generations or/and increase in the functionality of the branching points of the dendrons.

Amphiphilic molecular brushes with block copolymer grafts have been considered. In the case of grafts with solvophobic inner block and solvophilic outer block the formation of intra-molecular core-corona cylindrical micelles was expected. We have, however, demonstrated longitudinal instability of the uniform cylindrical core and formation of multi-domain pearl-necklace structures. We predicted a similar type of necklace structure consisting of intra-molecular spherical micelles for molecular brushes with solvophilic grafts and solvophobic main chain.

Concentrational effects in semi-dilute solutions of molecular brushes have been considered on the basis of scaling approach. We demonstrated that in contrast to solutions of linear polymers the solution of molecular brushes exhibits three characteristic concentrational thresholds: the concentration c^* corresponds to the overlap of the macromolecules as a whole, the concentration c^{**} corresponds to crowding of the grafts belonging to different brushes, and only at concentration beyond c^{***} the interpenetation of the internal (proximal to the backbones) regions of different brushes occurs. Remarkably, at $c>c^{**}$ the apparent rigidity of the molecular brushes decreases as a function of polymer concentration in the solution.

A New Approach to Peptides Encapsulation

Barbara Trzebicka[1], *Andrzej Dworak*[1], *Barbara Robak*[1], *Paweł Weda*[1], *Jerzy Silberring*[1,2]

[1]Centre of Polymer and Carbon Materials, Polish Academy of Sciences, M. Curie Sklodowskiej 34, Zabrze,Poland
[2]AGH University of Science and Technology, Faculty of Materials Science and Ceramics, Al. Mickiewicza 30, Cracow, Poland
barbara.trzebicka@cmpw-pan.edu.pl

Introduction

In the last decade, an interest in formulations of peptide delivery systems that protect and stabilize biomolecules against enzymatic degradation, significantly increased [1] ."Capsules" made of polymeric materials might serve as protection carriers for biomacromolecules and provide their delivery to the desired place [2-3]. Sometimes it is also convenient to covalently attach biomolecule to the polymer, what is called bioconjugation [4]. Recently, attention has been paid to the thermosensitive materials as precursors of the stimuli-responsive drug delivery systems [5]. It was shown [6-9] that by controlling the process of heating of dilute solution of thermosensitive polymers, stable nanoparticles (mesoglobules) formed by polymer chains could be obtained.

Here we explored the idea of application of the thermosensitivity of poly(*N*-isopropylacrylamide) (PNIPAM) for encapsulation of peptides by their entrapment in PNIPAM mesoglobules or by formation of mesoglobules by peptide-PNIPAM bioconjugate.

Materials and Methods

Two peptides, the nociceptin (FGGFTGARK-SARKLANQ) and a pentapeptide (GFKRG) were synthesized. Both peptides were obtained according to the standard solid phase peptide synthesis (SPPS) and Fmoc chemistry in DMF as solvent [11] on a solid support – *Dansyl NovaTag*™ resin (Merck). Nociceptin was used in the process of physical entrapment in PNIPAM mesoglobules.

PNIPAM (Sigma-Aldrich) of M_n=84000 g/mol (according to our GPC-MALLS measurements in DMF), was used for the formation of mesoglobules with nociceptin, similarly to the protocol described in [10]. *N*-isopropylacrylamide (NIPAM) (Sigma-Aldrich) used for ATRP polymerization of polymer block in bioconjugate was purified by crystallization in hexane. Pentapeptide linked to the resin was modified with 2-bromopropionate groups capable of initiation of the ATRP polymerization of NIPAM. The resulting hybrid bioconjugate was used to obtain stable mesoglobules in water solution above bioconjugate phase transition temperature.

Peptide composition and molar masses were confirmed by ESI-MS. GPC-MALLS was used to measure molar masses and their dispersities of polymers and peptide-polymer bioconjugate. The cloud point temperature of the investigated macromolecules was taken from transmittance, observed by UV spectroscopy, vs. temperature. The size and shape of the obtained particles were determined by the light scattering techniques.

Results and Discussion

Two different peptide encapsulation methods based on the ability of thermosensitive PNIPAM to form stable mesoglobules were investigated. The physical interaction between PNIPAM and nociceptin upon heating of PNIPAM/nociceptin water solution above cloud point temperature of PNIPAM resulted in formation of mixed mesoglobules. The process of mesoglobules formation and influence of the peptide concentration on mesoglobule sizes were followed by the dynamic light scattering measurements. Physical interaction between PNIPAM and nociceptin resulted in formation of much bigger nanoparticles than those formed by the chains of PNIPAM homopolymers.

ATRP of NIPAM initiated by the solid supported peptide resulted in formation of thermosensitive peptide-PNIPAM bioconjugate. During abrupt heating of their water solutions, bioconjugate chains formed stable particles with the peptide encapsulated inside. This method provided a new approach to obtain much smaller particles than physical entrapment of the same peptide amount.

The presented encapsulation methods do not require complicated and tedious reservoir purification before peptide encapsulation and are a promising approach for peptide encapsulation and delivery.

Acknowledgments: This work was done in the frame of Polish Ministry of Science and Higher Education grant no. N N209 144136 and by the European Community from the European Social Fund within the RFSD 2 project.

References:

[1] Arhewoh I. M., Okhamaf A. O., J. Biomed. Sci. 2004, 3, 7
[2] Allemanna E., Leroux J., Gurny R., Adv. Drug Deliv. Rev. 1998, 34, 171
[3] Tan M. L., Choong P.F.M., Dass C.R., Peptides 2010, 31, 184
[4] Lutz J., Borner H. G., Prog. Polym. Sci. 2008, 33, 1
[5] Bajpa A.K., Shukla K. S., Bhanu S., Kankane S., Prog. Polym. Sci. 2008, 33, 1088
[6] Gorelov A. V., Du Chesne A, Dawson K. A., Physica A 1997, 240
[7] Dawson K. A., Gorelov A.V., Timoshenko E.G., Kuznetsov Yu. A., Du Chesne A., Physica A 1997, 244, 68
[8] Lee L-T, Cabane B. Macromolecules 1997, 30, 6559
[9] Aseyev V, Hietala S, Laukkanen A, Nuopponen M, Confortini O, Du Prez F., Polymer 2005, 46, 7118
[10] Weda P., Trzebicka B., Dworak A., Tsvetanov Ch.B., Polymer 2008, 49, 1467
[11] Chan W. C., White P. D, "Fmoc Solid Phase Peptide Synthesis (A Practical Approach)" , Oxford University Press, Oxford 2000

ABSTRACTS

ORAL PRESENTATIONS

Topic 6: Bioinspired Polymers, Bioengineering and Biotechnology

Some novel applications for biodegradable elastomers

Subbu Venkatraman, Vitali Lipik, Kong Jen Fong, Huang Yingying, Nithya V, Freddy Boey

School of Materials Science and Engineering, Nanyang Technological University, Singapore

assubbu@ntu.edu.sg

Introduction: Although several biodegradable elastomers have been reported (1), very few real applications using such elastomers have been detailed. In our laboratory, we have been targeting a few cardiovascular implant applications that require minimally invasive methods. One such example is an occluder for atrial defects (2, 3).

Cardiovascular occluders are preferably biodegradable and should be inserted via the transcutaneous method, using the femoral artery. As such the device should be compressible into a sheath, and when released should recover to its original shape. Materials for such devices must be predominantly elastomeric.

We evaluated several polymers and designs for this application, including some new polymers synthesized in our laboratory. The selection criteria for the elastomer include good recoverability and biodegradation over 6 months.

Results and Discussion: The table below gives the mechanical and compositional characteristics of various polymers evaluated:

Polymer	Modulus (MPa)	Elongation to break (%)	Recovery @50%	Recovery @150%
PCL	153 ± 23	378 ± 92	45 ± 7	-
PLC	64 ± 9	458 ± 79	86 ± 2	86 ± 1
Copoly B[1]	31 ± 4	307 ± 2	86 ± 1	83 ± 1

[1] Copoly B is a branched copolymer of PLA and PLA/CL.

PCL is a homopolymer (poly (caprolactone)) and PLC is a copolymer of PCL and Poly (l-lactide), PLA; both are commercially available polymers from Purac corporation.Star is a star-branched copolymer of PLA and PCL synthesized in our laboratory.

As can be seen from the table, PLC has good elastomeric properties, although not exhibiting 100% recoverability. In our preliminary studies we evaluated these polymers in the device design, described below.

The device design is a "double-umbrella" design, which allows for two flaps to be opened at the proximal and distal ends, so that the device is anchored at both ends of the defect.

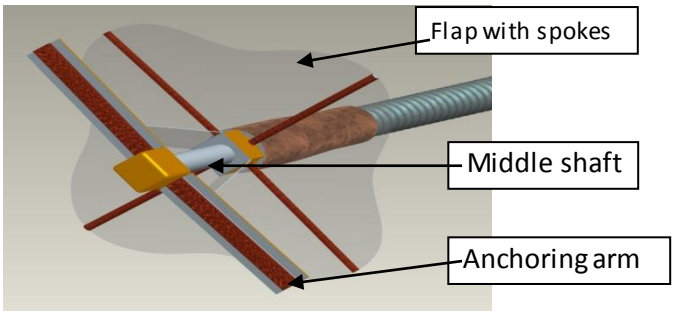

Elastomeric material is needed for the flap as well as for the shaft of the device, as explained below. This device is enclosed in a 10F or 11F sheath (diameters mm and mm) prior to insertion into a femoral artery. The sheathed device is then guided using X-ray imaging to the atrial septal defect, and the sheath withdrawn to release the device. The flaps should open fully within seconds so that the device can be positioned and anchored. Following anchoring, the sheath is withdrawn, and any wire connection to the device is severed.

We have evaluated 3 polymers (PCL, PLC and a PLA-PCL/PLA- PLA branched copolymer in this application. Although all 3 devices could be opened upon unsheathing, the time taken to unfold and the extent of opening were different, and dependent on recovery as well as on modulus. Data showing the speed and extent of opening from the sheath will be discussed.

An animal study in pigs was conducted to show the feasibility of sealing a model defect in the atrial septum1. Data clearly confirm sealing of the defect, as seen from ultrasonic testing of introduced air bubbles, as well as angiographically. Histology revealed very little tissue reaction, while at the same time confirming complete endothelial cell coverage of thedevice in one month.

References:

1. Andronova N, Albertsson AC. Resilient bioresorbable copolymers based on trimethylene carbonate, L-lactide, and 1,5-dioxepan-2-one. *Biomacromolecules* 2006;7:1489-1495.

2. D-H Duc, Y-D Tang, W.Wu, S.Venkatraman, F.Boey, J.Lim, J.Yip, Fully Biodegradable Septal Defect Occluder- A Double Umbrella Design, *Catheterization and Cardiovascular Interventions*, 76(5):711–718 (2010)

3. S.Venkatraman, F.Boey, et. al., Occlusion Device for Closing Anatomical Defects, US patent application 61/260,955; Nov 2009

Amyloid Peptides and Peptide Copolymers: From Self-assembly, Towards Therapeutics

Ian W. Hamley and Valeria Castelletto

Department of Chemistry, University of Reading, Whiteknights, Reading, RG6 6AD, UK

Email: I.W.hamley@reading.ac.uk

There has been great interest recently in the fibrillisation of peptides, especially the amyloid beta (Aβ) peptide which is involved in diseases such as Alzheimer's [1]. We have recently commenced a study of the self-assembly of peptides and peptide copolymers based on a fragment KLVFF, corresponding to the core region of Aβ(16-20). Aβ self-assembly is driven by inter-molecular β-sheet self-assembly into fibrils. A primary objective of our work is to identify fragments that bind to amyloid fibrils and disrupt fibrillisation (aggregation inhibitors based on self-recognition elements [2]). We are also interested in peptides and peptide/polymer conjugates as hydro- and organo-gelators. I will present results on the self-assembly of peptides such as AAKLVFF [3,4] and PEGylated diblock copolymers of these peptides [5,6]. Self-assembly is studied in water for hydrophilic peptides and peptide copolymers and in organic solvents for hydrophobic peptides. Gelation at higher concentration is also discussed. Peptide AAKLVFF is the subject of detailed studies (FTIR, CD, NMR, molecular dynamics simulations) of its self-assembly into nanotubes in methanol and twisted fibrils in water [4,7]. Very recently we have discovered a novel twisted ribbon fibril structure by adding β_2-amino acids to the N terminus of KLVFF to give βAβAKLVFF [8], and the fascinating structural properties of this will be discussed. We have recently examined the binding of this peptide to the amyloid β peptide Aβ(1-42), as part of a project to develop aggregation inhibitors, which may be useful in the treatment of amyloid disease [9]. In addition, we have found that a PEGylated version of this peptide forms spherical micelles in aqueous solution, pointing to the ability to modulate the self-assembled structure by introduction of amphiphilicity [10]. The enzymatic cleavage (using α-chymotrypsin) of the peptide from the PEG3000 chain (between phenylalanine residues) leads to release of unassociated peptide monomers [10]. This nanocontainer delivery and release system could be useful in therapeutic applications. As another example, we have investigated the self-assembly of a novel peptide amphiphile (PA) Matrixyl, with collagen-stimulating properties [11]. It forms self-assembled tape-like structures in aqueous solution as shown in Fig.1. These can be dispersed into amyloid-like fibrils by use of the anionic surfactant SDS.

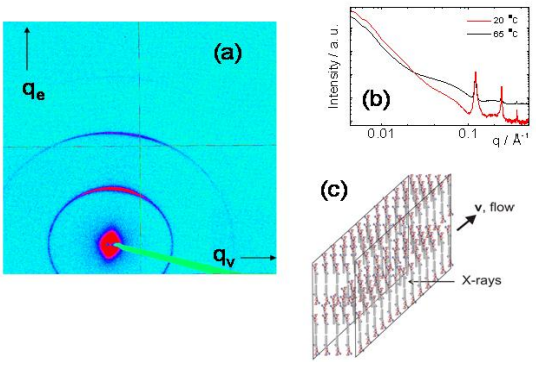

Figure 1. X-ray data and model for Matrixyl self-assembly, (a) Two-dimensional SAXS data from a sample (0.95 wt%) aligned by flow. The oriented Bragg reflections are nearly perpendicular to the horizontal flow (**v**) direction and indicate alignment of PA bilayers perpendicular to the flow direction (i.e. tapes align along the shear axis), (b) One dimensional SAXS profiles showing Bragg peak positions, and the development of diffuse scattering at high temperature, (c) Structural model for the PA bilayers.

[1] I. W. Hamley *Angew. Chem., Int. Ed. Engl.* 2007, **46**, 8128.
[2] J. Madine, A. J. Doig and D. A. Middleton *J. Am. Chem. Soc.* 2008, **130**, 7873.
[3] V. Castelletto et al *Biophys. Chem.* 2008, **139**, 29.
[4] V. Castelletto et al. *J. Phys. Chem.* B 2009, **113**, 9978.
[5] I. W. Hamley et al. *Adv. Mater.* 2008, **20**, 4394.
[6] I. W. Hamley et al. *Phys. Rev. E* 2008, **57**, 062901.
[7] I. W. Hamley et al. *J. Phys. Chem. B* 2010, **114**, 940.
[8] V. Castelletto et al. *Angew. Chem., Int. Ed. Engl.* 2009, **48**, 2317.
[9] V. Castelletto et al. *J. Pept. Sci.* 2010, **16**, 443.
[10] V. Castelletto et al. *Langmuir* 2010, **26**, 11624.
[11] V. Castelletto et al. *Chem. Comm.* 2010, **46**, 9185.

New smart heparin-based bioconjugates synthesized by ATRP and click chemistry

F. Reyes[1], G. Rodríguez[1], M.R. Aguilar[1], J. San Román[1], W. Li, S. Averick[2], K. Matyjaszewski[2]

[1] Instituto de Ciencia y Tecnología de Polímeros. CSIC. Juan de la Cierva 3. 28006 Madrid, Spain. CIBER-BBN
[2] Center for Macromolecular Engineering, Department of Chemistry, Carnegie Mellon University, 4400 Fifth Av. Pittsburgh, Pennsylvania 15213 USA.

felireyes@ictp.csic.es

Introduction

Combination of synthetic polymers with proteins and polysaccharides in order to develop bioconjugates has enjoyed a significant impact in medicine in recent years due to possess a high content of functional groups that can be utilized for bioconjugation with cell-targeting agents (1). The aim of this work was the preparation of new heparin-polymer bioconjugates via ATRP, carbodiimide chemistry and click chemistry in order to obtain new temperature-sensitive (T-sensitive) heparin-based materials with a controlled architecture that could form self-assembling systems with new properties.

Materials and Methods

Low Molecular Weight Heparin (LMWH) has been functionalized with an alkyne group via carbodiimide chemistry. MEO_2MA, $OEO_{300}MA$ and DMAEMA have been polymerized by ATRP using an initiator-N_3 to get the azide functionalization of the T-sensitive polymer (2). Heparin-alkyne and different azide functionalized polymers have been coupled by click chemistry using a copper catalyzed reaction (3). The polymers used were N_3-p(DMAEMA) and the copolymer N_3-p($OEO_{300}MA$-co-MEO_2MA) (figure 1).

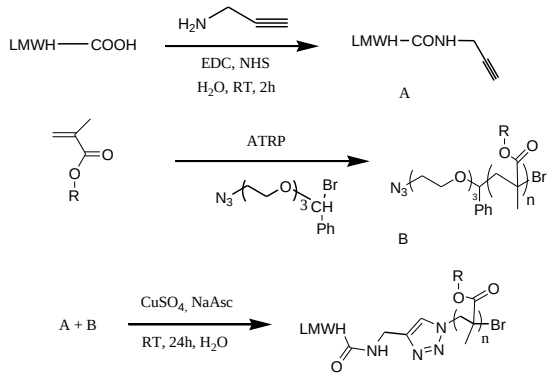

R = 2-(dimethylamino)ethyl, poly(ethyleneglycol)methylether or di(ethyleneglycol)methylether

Figure 1. Scheme of the synthesis. *Experimental conditions:* *(I):* LMWH (1.25×10^{-4} M) / EDC / propargylamine/ NHS = 1 / 10 / 20 / 5mM in distilled water, RT, 2h. *(II):* p(MEO_2MA-co-$OEO_{300}MA$) 50% (v/v) anisole, 60ºC, 2h, MEO_2MA (2.2 M) / $OEO_{300}MA$ / dNbpy / $CuBr_2$/ CuBr / N_3-In = 90 / 10 / 1 / 0.1 / 0.4 / 1. P(DMAEMA) 50% (v/v) anisole, 50ºC, 4h, DMAEMA (2.9 M)/ N_3-In/ CuCl/ $CuCl_2$/ HMTETA = 100 / 1 / 0.4 / 0.1 / 0.5. *(AB):* A (2.5×10^{-3} M) / B / sodium ascorbate / $CuSO_4$ = 1 / 1 / 0.1 / 0.05 in distilled water, RT, 24h.

Azide polymers and alkyne functionalized heparin were characterized by ^{1}H and ^{13}C-NMR, FTIR, SEC and GC techniques. Bioconjugates were characterized by NMR, FTIR and DLS.

Results and Discussion

T-sensitive polymers have been prepared by ATRP. The reactions presented a linear kinetic plot and the polymers were obtained with a low polydispersity. Alkyne functionalization of heparin has been carried out using propargyl amine and EDC/NHS to activate the carboxylic groups of heparin. A characteristic band of the alkyne group is observed at 2100 cm^{-1} in the FTIR spectra (Figure 2).

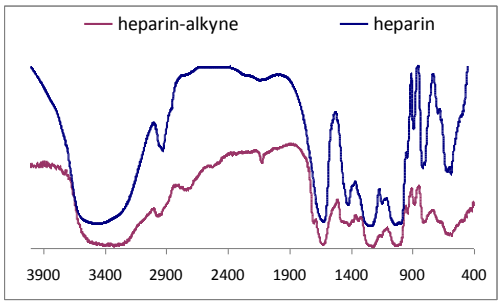

Figure 2. FTIR characterization of LMWH and LMWH-alkyne systems.

T-sensitive polymers have been grafted to heparin by click chemistry. A characteristic peak of triazole ring formed during the click reaction was observed at 7.5 ppm in ^{1}H-NMR spectra.

Low Critical Solution Temperature (LCST) was investigated in heparin polymer bioconjugates by DLS. LCST of the heparin-based bioconjugates decreased when compared with the non-modified T-sensitive homopolymer. This behavior is due to the hydrophilicity of heparin molecule.

Conclusions

T-sensitive heparin-based bioconjugates were prepared using ATRP, carbodiimide chemistry and click chemistry. These new material are very interesting for biomedical applications such as targeted drug delivery (1).

References

(1) J.K. Oh, D.I. Lee, J.M. Park. *Progress in Polymer Science 34, (2009) 1261-1282.*
(2) H. Dong, K. Matyjaszewski. *Macromolecules 43 (2010) 4623-4628.*
(3) L.A. Canalle, D.W.P.M. Löwik, J.C.M. van Hest. *Chem. Soc. Rev. 39 (2010) 329-353.*

Acknowledgements

Authors gratefully acknowledge the financial support provided by the JAE predoc program, (CSIC) and the Krzysztof Matyjaszewski Polymer Group collaboration.

Synthesis of PLA-*b*-PHEA block copolymers as precursors of tubular guides for peripheral nerve repair

B. Clement, T. Trimaille, K. Mabrouk, D. Bertin, D. Gigmes

Université de Provence, Laboratoire Chimie Provence UMR 6264, Av. Esc. Normandie Niemen, 13397 Marseille Cedex 20, France

didier.gigmes@univ-provence.fr

Introduction

The use of synthetic polymer materials[1] as guide scaffolds for nerve repair is a promising alternative to natural ones, such as collagen, that present several drawbacks (reproductibility between samples, cost, possible contamination with pathogen agents,…). Among synthetic polymers, poly(2-hydroxyehtyl acrylate (PHEA) is widely investigated in nerve repair, due to its hydrogel-like properties. Aliphatic polyesters such as polylactide (PLA) or polycaprolactone (PCL) are also choice candidates due to their biodegradability[2]. In order to fulfill the criteria of guide scaffolds for nerve repair, we aimed at combining the properties of both kinds of polymers in a single homogeneous material using block copolymers of PLA and PHEA.

Results and Discussion

More particularly, we prepared various block copolymers PLA-b-PHEA in three steps[3] (scheme 1). Typically, an acrylated end-capped PLA (PLA acrylate) was first prepared by ring opening polymerization (ROP) of the D,L-Lactide using 2-hydroxy ethyl acrylate (HEA) as initiator and $Sn(Oct)_2$ as catalyst. The PLA acrylate was further involved in a 1,2-intermolecular radical addition with MAMA-SG1 alkoxyamine, leading to the corresponding PLA-SG1 macroalkoxyamine (2). Finally, Nitroxide Mediated Polymerization (NMP) of HEA initiated from (2) led to the corresponding PLA-b-PHEA (3). The NMP of 2-hydroxyethyl acrylate (HEA) appeared to be well controlled in the presence of free SG1 nitroxide.

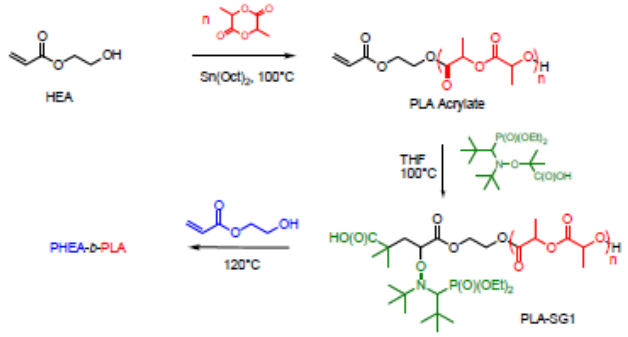

Scheme 1 : Synthesis of PLA-b-PHEA copolymers

In order to move a step closer to the clinic, we particularly focused on poly(D,L-lactide)-b-poly(2-hydroxyethyl acrylate) (PLA-b-PHEA) block copolymers and compared them to parent PLA homopolymer. For that purpose, we performed in vitro and in vivo (in rats) degradation studies and assessed Schwann cell adhesion. Over 12 weeks, we observed mass loss and molecular weight decrease. In vitro and in vivo findings were very similar for each polymer tested. The in vivo and in vitro degradation behaviour of such materials were found to be identical, and the PHEA content in the copolymer had a great impact on the degradation mechanism. The most appropriate features for further use as guides in nerve repair were found for PLA-b-PHEA presenting a sufficiently short PHEA block (PLA-b-PHEA of 85/15 wt% composition). Schwann cell adhesion on the latter copolymer substrate was improved, when compared to PLA homopolymer. No cellular death was observed after 7 days of culture.

Then, using a electrospinning process we were able to prepare a micro tube from the PLA-b-PHEA copolymer (figure 1).

Figure 1 : Scanning Electron Microscopy (SEM) pictures of the tube made from PLA-b-PHEA copolymers

Conclusion

We focused in study on the properties of novel hydrophilized PLA based materials, namely PLA-b-PHEA copolymers, in terms of degradation and Schwann cell adhesion. The obtained results show the potential of such biodegradable materials for further use in nerve guides. In vivo rat nerve regeneration experiments are currently under investigations.

References

1. Cao, H.; Liu, T.; Chew, S. Y. Adv. Drug Deliv. Rev. 2009, 61, 1055-1064. 2. Seal, B.L.; Otero, T. C.; Panitch, A. Mat. Sci. Eng. 2001, R34, 147-230 3. Clément B, Trimaille T, Alluin O, Gigmes D, Mabrouk K, Féron F, Decherchi P, Marqueste T, Bertin D. Biomacromolecules 2009, 10, 1436-1445.

Polymer hydrogels with a "memory" effect to drugs

S.S.Ivanchev[1], V.F.Danilichev[2], V.N.Pavlyuchenko[2], O.N.Primachenko[1], S.Ya.Khaikin[1]

[1] St-Petersburg Department of the Boreskov Institute of Catalysis of the Siberian Branch of the Russian Academy of Sciences, 14 prospect Dobrolubova 197198 St-Petersburg, Russia
[2] Kirov Military Medical Academy, 6 Acad. Lebedeva str. 194044 St-Petersburg, Russia

e-mail: ivanchev@SM2270.spb.edu

-The presented studies relate to the development of the synthetic approaches to obtaining polymer hydrogels featuring with a "memory" effect to antibiotics of cephalosporine and fluoroquinolone classes, characterization of sorption-desorption properties of the prepared hydrogels and obtaining therapeutic soft contact lenses (SCL) on their basis.

The hydrogels with a "memory" effect were synthesized by reacting 2-hydroxyethyl methacrylate with anionic and cationic functional comonomers using a template method in the presence of a drug extracted after the synthesis and crosslinking agents in high concentrations.
Sorption and diffusion characteristics of water and target drugs in the studied hydrogels are studied. The intrinsic parameters are determined for total, non-specific and specific sorption of the drugs by the hydrogels.
The "memory" effect is expressed as an enhanced drug sorption by the developed hydrogels in comparison with conventional hydrogels of the same composition. This phenomenon is primarily determined by a specific morphology of the hydrogels formed at the template synthesis of the copolymer in the presence of the target drug.
The considered effect is mostly prominent for cationic hydrogels but also observed for anionic and ampholitic ones. The obtained hydrogels with a "memory" effect are also featured with a prolonged drug release compared to the conventional hydrogels.
The nanostructure features of the synthesized hydrogels and effect of cephazoline immobilization at the synthesis upon their structure are studied using a small angle neutron scattering.
The developed hydrogels are shown to be efficient as polymeric carriers for drugs in therapeutic SCL saturated with three different types of drugs. The SCL based on these hydrogels are featured with an advantageous possibility to a controllable drug release into the internal structures of the eye.

Synthesis and characterization by lipase-catalyzed ring-opening polymerization of poly(ε-caprolactone) with different reaction mediums

Erhan Özsağıroğlu, Banu İyisan, Yüksel Avcıbaşı Güvenilir

ozsagiroglu@itu.edu.tr

Introduction

The development of lipase catalyzed ring opening polymerization in organic solvents has an important consideration [1]. Especially, synthesis of poly(ε-caprolactone) (PCL) is one of them because PCL has different kind of applications in biomedical area. In these reactions immobilized *Candida antarctica* lipase (Novozym 435) usually would rather than other kind of lipase enzymes. It provides higher conversions with different reaction mediums.

Previous experiments changed monomer or enzyme concentration in reactions or different solvents at one specified reaction temperature [2-4]. This work examined the effects of different reaction mediums were obtained with chancing of temperature, time and solvent types at the same time. The main purpose of the experiment is observing molecular weight distribution of polymer and understands optimum conditions of reaction mechanism with distinct mediums. Three different reaction temperatures and three different solvent types were studied in the present work. Reactions were carried out 40 ^{o}C, 60 ^{o}C and 80 ^{o}C and n-hexane, toluene and diisopropyl ether were used as solvents. Moreover, experiments were undertaken different time periods which 2h, 4h, 6h, 17h, 24h, 48h, and 72h respectively. Along the all reactions monomer, solvent and enzyme concentrations were same. For 1 ml monomer/solvent solution (0.44 M monomer and 0.56 M solvent) and 10 mg lipase were used in the experiments. All samples were analyzed by GPC and H-NMR to obtain molecular weight, conversion and chemical structures. Thermal behaviors of samples were analyzed by DSC to examine and compare polymers with one to another.

Materials and Methods

Candida antarctica lipase B, Novozym 435, (7000 PLU/g), an immobilized enzyme, was used at all reactions. ε-caprolactone was dried by activated molecular sieves before use. Organic solvents for reactions are n-hexane, toluene and diisopropyl ether.

All samples were analyzed by gel permeation chromatography (GPC). GPC was calibrated by polystyrene standards. THF was used as the eluent at a flow rate of 1 ml/min at 25 ^{o}C.

The ^{1}H and ^{13}C NMR spectra were recorded on a Bruker NMR spectrometer (250 MHz for ^{1}H NMR) and a Varian Inova 500 spectrometer (125.66 MHz for ^{13}C) using $CDCl_3$ as solvent and tetramethylsilane as an internal standard.

Differential Scanning Calorimetry (DSC) was used to analyze changing of thermal transition temperatures of polymer samples. The device model of DSC is Perkin Elmer Diamond.

ε-caprolactone were dried activated molecular sieves and a mixture (1 ml) 0.44 M monomer in n-hexane, toluene, isopropyl ether and 10 mg lipase were used in the experiments. At the end of time, reaction solution was taken and chloroform terminated by adding an excess of chloroform and removing the enzymes by filtration. The chloroform in the filtrate was in large part removed by evaporation and the polymer in the concentrated solution was precipitated in methanol. The samples were dried in an oven. Finally all samples were analyzed by GPC, NMR and DSC.

Results and Discussion

Candida antarctica lipase catalyzed ring opening polymerization of ε-caprolactone were performed in n-hexane, toluene and isopropyl ether at 40 ^{o}C, 60 ^{o}C and 80 ^{o}C with same monomer/enzyme concentrations. Analyses were made and molecular weight distributions versus time and monomer conversion versus time were figured for all solvents and temperatures. Figure 1 shows maximum M_n values for all solutions at 40 ^{o}C, 60 ^{o}C and 80 ^{o}C respectively.

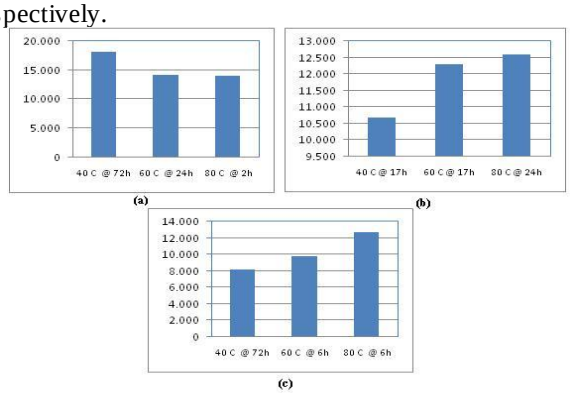

Fig. 1. Maximum M_n values at different reaction mediums (a) toluen (b) diisopropyl ether (c) n-hexane

Conclusions

Rising of molecular weight was resulted from increasing of reaction temperatures. Moreover, solvent types and reaction time has greatest effects on monomer conversions.

References

[1] **Marcilla, R., Geus, M., Mecerreyes, D., Duxbury, C.J., Koning, C.E., Heise, A.**, 2006. Enzymatic polyester synthesis in ionic liquids, *European Polymer Journal*, **42**, 1215-1221.

[2] **Kumar, A., Gross, R.A.**, 2000. *Candida antarctica* lipase B catalyzed polycaprolactone synthesis: effects of organic media and temperature, *Biomacromolecules*, **1**, 133-138.

[3] **Cordova, A., Iversen, T., Hult, K., Martinelle, M.**, 1998. Lipase-catalysed formation of macrocycles by ring-opening polymerization of ε-caprolactone, *Polymer*, **39**, 6519-6524.

[4] **Albersson, A.C., Srivastava, R.K.**, 2008. Recent developments in enzyme-catalyzed ring-opening polymerization, *Advanced Drug Delivery Reviews*, **60**, 1077-1093.

Polyesters from Natural Macrolactones for Biomedical Applications

I. van der Meulen[1], *C.E. Koning*[1], *A. Heise*[1], *R. Deumens*[2]

[1] Eindhoven University of Technology, [2] Maastricht University Medical Centre

i.v.d.meulen@tue.nl

Introduction

An interesting new class of materials is derived from macrocyclic lactones, which belong to the class of naturally occurring macrocyclic musks and are frequently used in the fragrance industry. Their eco-friendliness led to an increased demand and the development of improved synthetic routes. The goal of our research is to develop biocompatible synthetic routes to polymers from these natural monomers (Figure 1), investigate their properties and position them among other biomaterials in order to identify possible application areas. This paper will summarize our results on this interesting class of polymers.

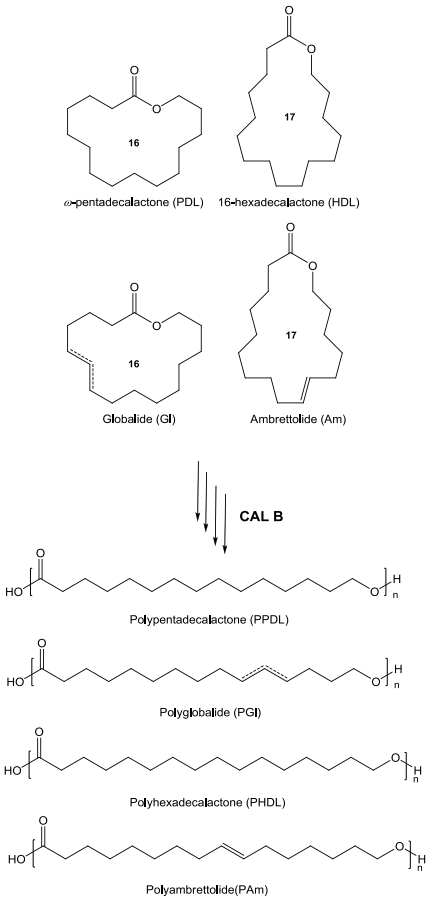

Figure 1: Structures and polymerization of various macrocyclic lactones, which form the basis of a new materials platform.

Results and Discussion

One example of such a biocompatible polyester is semi-crystalline poly(ω-pentadecalactone) (PPDL), which resembles the properties of low density polyethylene (LDPE).[1] Applying enzymatic catalysis we obtained PPDL with exceptionally high molecular weight of >300,000 g/mol (M_w). These were spun into fibers (Figure 2) revealing a tensile strength of around 0.7 GPa after elongation.[2]

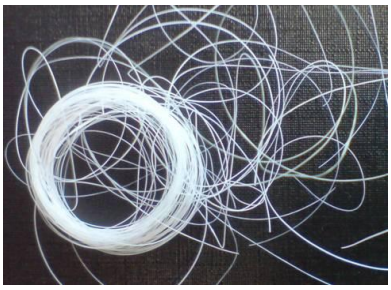

Figure 2: Fibers obtained from high molecular weight poly(ω-pentadecalactone).

The interesting structural features and properties of polymers derived from macrolactones prompted us to investigate their potential for biomedical products. Polymers were obtained via enzymatic ring opening polymerization from unsaturated macro-lactones such as globalide and ambrettolide.[3] Biocompatibility tests confirm that these polymers can be classified as non-toxic. While initially semicrystalline, thermal cross-linking of the polymers via the main chain double bonds in the solid-state produced fully amorphous materials. The degradation of the homo-polymers in buffer solution revealed the high hydrolytic stability of the materials, which can, however, be modulated by copolymerisation. By choosing the right conditions of the polymerization process and the post-polymerization methods, properties such as crystallinity, material strength, degradability (rate and percentage) and hydrophilicity can be controlled.

Conclusion

Applying this highly applicable biocompatible synthetic route to synthesize polyesters, a platform of new biomedical materials is created in which material properties can easily be tuned for the desired product.

References

[1] Focarete, M.L.; Scandola, M.; Kumar, A.; Gross, R.A. *J. Polym. Sci., Part B: Polym. Phys.* **2001**, *39*, 1721.

[2] de Geus, M.; van der Meulen, I.; Goderis, B.; Vanhecke, K.; Dorschu, M.; van der Werff, H.; Koning, C.E.; Heise, A. *Polym. Chem.* **2010**, *1*, 525

[3] van der Meulen, I.; de Geus, M.; Antheunis, H.; Deumens, R.; Joosten, E.A.J.; Koning, C.E.; Heise, A. *Biomacromolecules* **2008**, *9*, 3409.

Developing and Evaluating Mucoadhesive Polymers and Mucosa-Mimetic Materials

Vitaliy Khutoryanskiy

University of Reading, Reading School of Pharmacy, Whiteknights, PO Box 224, Reading RG6 6AD, United Kingdom

v.khutoryanskiy@reading.ac.uk

Introduction: Mucoadhesion is defined as interfacial force interactions between polymeric materials and mucosal tissues, the moist surfaces lining the walls of various body cavities such as gastrointestinal, respiratory and reproductive tracts as well as the mouth, the eyes and the nasal cavities. [1]. In this communication we will discuss our experiments on design and evaluation of various mucoadhesive dosage forms and polymeric materials able to mimic mucosal tissues.

Materials and Methods: We have studied the mucoadhesive properties for a number of polymers such as linear and weakly cross-linked poly(acrylic acid) (PAA), chitosan, various copolymers of [2-(methacryloyloxy)ethyl]trimethylammonium chloride (MADQUAT) as well as their blends with cellulose ethers. Interactions between polymers and porcine gastric mucin in solutions were studied by dynamic light scattering, zeta-potential measurements, transmission electron microscopy and turbidimetric titration. Mucoadhesive properties were studied by tensile (detachment) technique for solid dosage forms and flow-through method for liquid and semi-solid dosage forms

Results and Discussion: Investigation of the solution behaviour of chitosan and amphiphilic copolymers of MADQUAT in mixtures with porcine gastric mucin revealed a complex nature of specific interactions including electrostatic attraction, hydrogen bonding and hydrophobic effects [2, 3]. The strength of these interactions was found to be dependent on the structure of polymers and environmental conditions (solution pH, presence of inorganic ions and organic molecules). Studies of interactions between polymers and porcine gastric mucin in solutions allowed understanding and predicting mucoadhesive properties of dosage forms.

Mucoadhesive films were formulated based on blends of poly(acrylic acid) (PAA) and chitosan with cellulose ethers [4, 5]. It was demonstrated that careful selection of solution pH allows avoiding phase separation in PAA-cellulose ether blends caused by interpolymer complex formation and helps preparing homogeneous materials by casting technique. It was established that the mucoadhesive properties of the films are highly dependent on the component ratio in the blends and reduced with cross-linking of polymers.

Mucoadhesive tablets were prepared based on chitosan, half-acetylated chitosan, weakly-cross-linked poly(acrylic acid) (Carbopols®) and their blends with hydroxypropylmethylcellulose (HPMC) using direct powder compression. Mucoadhesive properties of tables were found to depend on the degree of deacetylation in chitosan, presence of model drug (ibuprofen) in the tablets and polymer ratio for Carbopol®/HPMC.

Weakly cross-linked derivatives of poly(acrylic acid) or Carbopols® in addition to excellent mucoadhesive properties exhibit unique gelation behaviour, which can be easily triggered by changes in solution pH [1]. We have shown that formation of gels in situ depends on the type of Carbopol® (71G, 940, 971PNF, 974PNF and 980NF) and presence of inorganic ions in solutions. The applicability of these polymers to provide a retention effect on the surface of ocular mucosa has been demonstrated.

Two types of hydrogels have been prepared as materials mimicking animal mucosal tissues using the following approaches: (1) Layer-by-layer (LbL) deposition of poly(acrylic acid)-methylcellulose complexes on glass surfaces with their subsequent cross-linking by thermal treatment [6, 7]. It was demonstrated that LbL approach allows preparing ultrathin hydrogel coatings with highly controlled thickness. (2) Three-dimensional copolymerisation of 2-hydroxyethylmethacrylate with 2-hydroxyethylacrylate, N-vinyl pyrrolidone, sorbitol methacrylate, and N-acryloyl glucosamine [8, 9]. Both types of hydrogels were evaluated as potential substrates to mimic mucosal tissues in experiments with mucoadhesive tablets based on Carbopol®940 and its blends with HPMC. The adhesive properties of these materials were also compared with porcine buccal mucosa, glass, polypropylene, polystyrene and polytetrafluoroethylene. It was demonstrated that synthetic hydrogels have some potential to mimic porcine buccal mucosa and the degree of their swelling, mechanical properties and chemical nature of polymers have a strong effect on the ability of these materials to mimic mucosal tissues.

Conclusions: Hydrophilic functional polymers show an excellent potential for developing mucoadhesive dosage forms for drug delivery and materials mimicking animal mucosal tissues.

References:

1. Khutoryanskiy V.V. *Macromol Biosci.* **2011**, DOI: 10.1002/mabi.201000388
2. Fefelova N.A., Nurkeeva Z.S., Mun G.A., Khutoryanskiy V.V. *Int. J. Pharm.* **2007**, 339, 25.
3. Sogias I.A., Williams A.C., Khutoryanskiy V.V. *Biomacromolecules* **2008**, *9*, 1837.
4. Dubolazov A.V., Nurkeeva Z.S., Mun G.A., Khutoryanskiy V.V., *Biomacromolecules* **2006**, 7, 1637.
5. Luo K., Yin J., Khutoryanskaya O.V., Khutoryanskiy V.V. *Macromol. Biosci.* **2008**, 8, 184.
6. Khutoryanskaya O.V., Williams A.C., Khutoryanskiy V.V. *Macromolecules* **2007**, 40, 7707.
7. Khutoryanskaya O.V., Potgieter M., Khutoryanskiy V.V. *Soft Matter* **2010**, 6, 551.
8. Khutoryanskaya O.V., Mayeva Z.A., Mun G.A., Khutoryanskiy V.V. *Biomacromolecules* **2008**, 9, 3353.

Hall D.J., Khutoryanskaya O.V., Khutoryanskiy V.V. *J. Pharm. Pharmacol.* **2010**, 62, 1452.

Macromolecular Nanoparticles with Cholesterol for Solid Tumour Targeting: How Do They Look Like from Inside. The Origin of Functionality.

S.K. Filippov[a], P. Chytil[a], P.V. Konarev[b], D.I. Svergun[b], J. Plestil[a], A. Jugunov[a], T. Etrych[a], K. Ulbrich[a], P. Stepanek[a]

[a] Institute of Macromolecular Chemistry, Academy of Sciences of the Czech Republic, , Heyrovský Sq. 2, 162 06 Prague 6, Czech Republic

[b] European Molecular Biology Laboratory, EMBL c/o DESY, Notkestrasse 85, D-22603 Hamburg, Germany

e-mail:filippov@imc.cas.cz

We report a rigorous investigation of detailed structure of nanoparticles that were already proved as a successful drug delivery nanocarrier. The basic structure of the drug conjugates consists of HPMA copolymer bearing anticancer drug doxorubicin (Dox) bound via the pH-sensitive hydrazone bond and a
defined amount of cholesterol moieties differing in their hydrophobicity (Figure 1, Table 1).

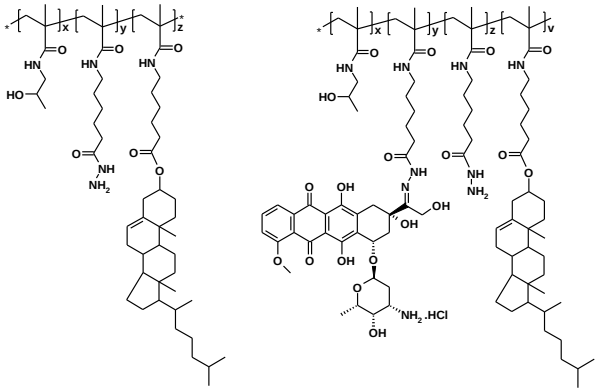

Fig. 1. The Chemical structure of conjugates.

Our study of dilute solutions of conjugates in phosphate buffer at pH5.0 and 7.2, examined by dynamic and static light scattering (DLS/SLS), small-angle X-ray and neutron scattering (SAXS and SANS), prove that the content of cholesterol has a strong influence on the system. We established that the presence of any amount of cholesterol results in formation of anisotropic nanoparticles (Figure 2).

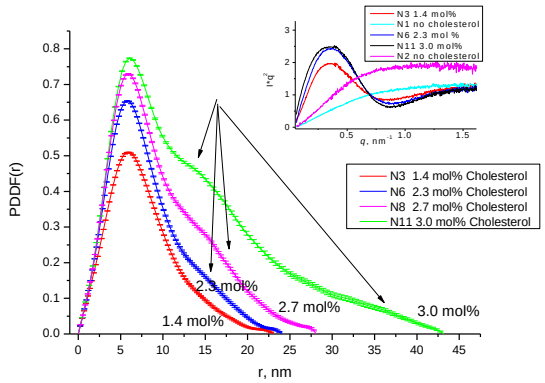

Fig. 2. Pair-distance-distribution function for the polymer N3, N6, N8, N11 at pH=5.0. Inset: Kratky plot for some polymers.

Obtained results show that the size and anisotropy of the nanoparticles grow with increase of the amount of cholesterol moieties i.e. the higher content of cholesterol groups, the higher asymmetry of a nanoparticle (Figure 3).

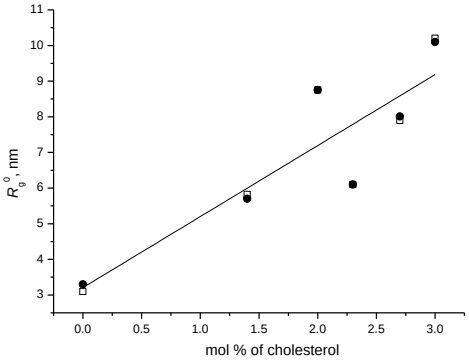

Fig. 3. The gyration radius R_g^0 extrapolated to infinite dilution as a function of cholesterol content .(●) pH=5.0; (□) pH=7.2

The similar tendency have hydrodynamic radius R_h^0 and aggregation number N_{aggr} determined by DLS and SLS methods. SAXS and SANS experiments allowed us to determine the three-dimensional low-resolution structure of the nanoparticles composed of HPMA-cholesterol conjugates (Figure 4).

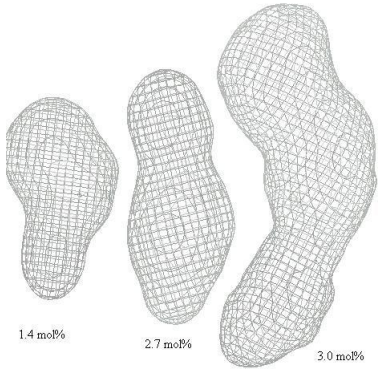

Figure 4. Ab-initio reconstructed molecular structure of nanoparticles with different content of cholesterol moieties.

Photo cross-linked and pH-sensitive polymersomes as bionanoreactors

Jens Gaitzsch[1], *Dietmar Appelhans*[1], *David Gräfe*[1], *Petra Schwille*[2] *and Brigitte Voit*[1]

[1]Leibniz-Institut für Polymerforschung Dresden e.V.
[2]Technische Universität Dresden, Biotechnological Centre

gaitzsch@ipfdd.de

Introduction:
Polymersomes consist of amphiphilic block-copolymers, which form vesicles upon a self assembly process. They show a higher mechanical and chemical stability than lipid vesicles and a great potential in synthetic biology or as drug delivery systems. The higher stability also leads to a complete loss of diffusion traffic through the polymer membrane. Usually this is overcome by incorporating transmembrane proteins into the polymersome wall. In contrast to this approach, we combine photo cross-linkable and pH sensitive monomers within the hydrophobic part of our amphiphilic block-copolymer.[1] The pH sensitivity of the polymersomes will lead to a triggered swelling and thus changes in diffusion behaviour of the membranes.

Materials and Methods:
We adapted the well-known pH-sensitive poly(ethyleneglycol)$_{45}$-block-poly(diethylaminoethyl-methacrylate)$_{81}$ (PEG_{45}-b-$PDEAEM_{81}$)[2] and integrated the photo-crosslinker 3,4-dimethyl maleic imidoethyl methacrylate[3] (DMIEM) in the hydrophobic part of the block copolymer. This resulted in a PEG_{45}-b-PDEAEM-s-PDMIEM block-copolymer with 10 mol% of DMIEM.

Results and Discussion:
The resulting polymers yielded polymersomes of approximately 100 nm in size, if produced via self-assembly in water. A production of vesicles using electroformation resulted in giant vesicles of sizes up to 100µm. (Fig. 1)

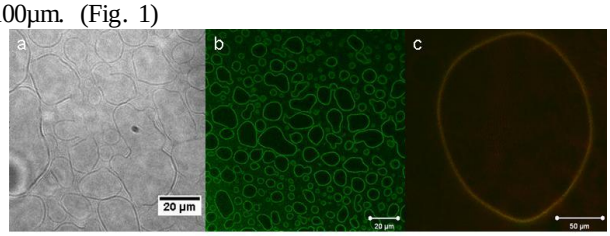

Figure 40: Bright field image of large polymersomes (a), fluorescence images of large (b) and giant (c) polymersomes

So far, only vesicles produced without electroformation showed effective cross-linking. These cross-linked vesicles show a definite pH sensitive behaviour around pH 7 by swelling in size. To check the permeability of the membrane, a solution of rhodamine B was subjected to an acidic solution of cross-linked vesicles and subsequently dialysed in basic conditions. Here, some dye still remained in the sample, while a blank sample of pure rhodamine B did not show any remaining dye after 2 days of dialysis proving effective dye enclosure (Fig. 2).
As a next step the polymersome was used as carrier for larger guest molecules. Therefore, an acidic solution of the starting polymer was mixed with dye-labeled and maltose-decorated polyethyleneimine (PEI-Mal)[4] hyperbranched polymer as a guest molecule. Upon switching to basic pH values, the PEI-Mal was partially incorporated into the vesicles. The remaining non-incorporated guest molecules were removed via dialysis. Again, a comparison with a dialysis of a pure PEI-Mal solution was carried out and revealed remaining, e.g. encapsulated, guest molecules (Fig. 3) in the polymersomes.

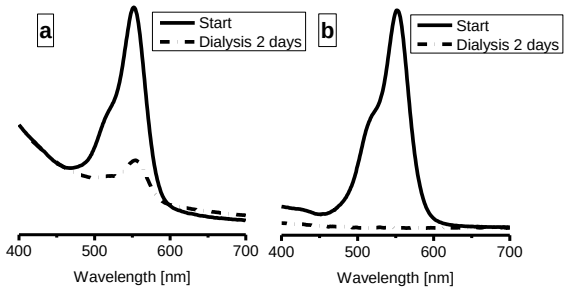

Figure 41: Dialysis with UV-Vis monitoring of rhodamin B entrapped in the vesicles (a) and pure rhodamine B (b).

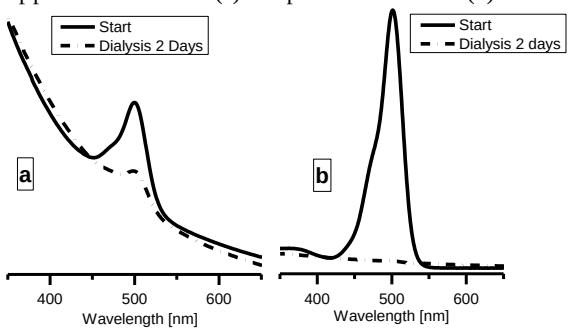

Figure 42: Dialysis with UV-Vis monitoring of dye labelled PEI-Mal entrapped in the vesicles (a) and as pure solution (b)

Conclusions:
We established a polymersome-based carrier system which enables controlled diffusion traffic through the membrane. Furthermore, large guest molecules can be incorporated into the vesicles. In further studies we want to apply our pH sensitive polymersomes as synthetic bionanoreactors for real biological questions by introducing enzymes into the polymersomes and inducing an enzymatic reaction at its substrate.

References:
[1] J. Gaitzsch, D. Appelhans, D. Gräfe, P. Schwille, B. Voit, *Chem. Commun.* **2011**, In Press.
[2] D. J. Adams, M. F. Butler, A. C. Weaver, *Langmuir* **2006**, *22*, 4534.
[3] C. D. Vo, D. Kuckling, H. J. P. Adler, M. Schonhoff, *Colloid Polym. Sci.* **2002**, *280*, 400.
[4] D. Appelhans, H. Komber, M. A. Quadir, S. Richter, S. Schwarz, J. van der Vlist, A. Aigner, M. Muller, K. Loos, J. Seidel, K. F. Arndt, R. Haag, B. Voit, *Biomacromolecules* **2009**, *10*, 1114.

Enzyme Sensitive Dendrimers with Defined Chirality via 'Click' Coupling of Enantio-pure Building Blocks

Bahar Yeniad[1], *Hemantkumar Naik*[1], *Roey Amir*[2], *Cor E. Koning*[1], *Craig Hawker*[2], *Andreas Heise*[1,3]

[1]Technische Universiteit Eindhoven,Laboratory of Polymer Chemistry, Den Dolech 2, P.O. Box 513, 5600 MB Eindhoven, The Netherlands.
[2]University of California Santa Barbara, Santa Barbara, CA93106-9510 [3]Dublin City University, School of Chemical Sciences, Glasnevin, Dublin 9, Ireland.

b.yeniad@tue.nl

The introduction of chirality within dendritic architectures has been attracted significant attention. Naturally occurring chiral building blocks such as amino acids, carbohydrates or oligonucleotides as well as synthetic monomers have been used to construct different types of chiral denrimers. Several potential applications of these chiral dendritic structures have been also envisaged such as molecular recognition processes, sensor technologies and catalysis.[1]

Here we introduce a facile and simple method to synthesize novel chiral dendrimers, which respond to enantioselective enzymatic modification as a function of their chiral composition.

In this study, first an azide functional 2,2-bis(methylol)propionic acid (bisMPA) dendrimer with 24 chain end functionality were synthesized. Then *(R)* and *(S)*-1-(4-ethynylphenyl) ethanol) were obtained via enantioselective enzymatic reductions and used as enantio-pure building blocks. These molecules bear both an alkyne functionality (for click reactions) and a chiral enzyme sensitive unit, i.e. phenyl ethanol, (for enzyme responsiveness). The periphery of the azide functional dendrimers was decorated with these building blocks via the copper(I)-catalyzed azide-alkyne cycloaddition ("click" reaction) (Figure 1). In these cycloaddition reactions, different ratios of enantio-pure building blocks were utilized changing from (R:S) 100:0 to 0:100. This resulted in chiral dendrimers with different chiral surface functionalities. When exposed to *(R)*-selective CALB enzyme (Novozyme 435) in an esterification reaction with vinyl acetate, the chiral composition encoded in the periphery of the dendrimers was successfully read-out by the enzyme, measured as the extent of the esterification reaction. The chirality of the dendrimers and the dependency of the enzymatic response to chirality are depicted in Figure 2 and Figure 3 respectively.

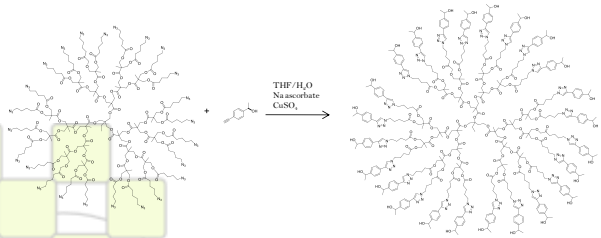

Figure 1. Synthesis of chiral bisPMA dendrimer via the copper(I)-catalyzed azide-alkyne cycloaddition

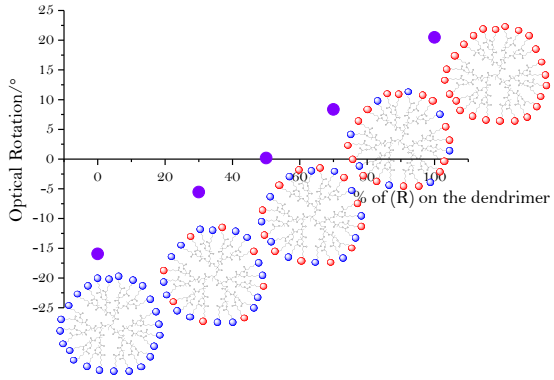

Figure 2. Optical rotation of dendrimers functionalized with different ratios of *(R)*- (red) and *(S)*-1-(4-ethynylphenyl) (blue).

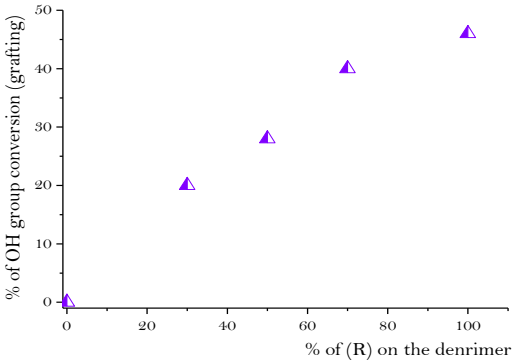

Figure 3. The extent of the esterification reaction (in terms of % of OH group conversion) on dendrimers depending on the chiral compositions of the periphery

[1] Romagnoli, B.; Hayes, W. *J. Mater. Chem.* 2002, 12, 767-799.

Design Of Bioinspired Asymmetric Diblock Copolypeptides for DNA-Template Self Assembled Coating

Hernandez-Garcia, Armando[1,2,3]; *Werten, Marc*[2]; *de Wolf, Frits*[2]; *de Vries, Renko*[1]

Wageningen university Lab of Physical Chemistry and Colloid science[1], Wageningen UR Food & Biobased Research[2], Dutch Polymer Institute[3]

e-mail: armando.hernandezgarcia@wur.nl

The development of new medical therapies involving the cellular delivery of biomolecules strongly depends on the development of efficient vehicles for encapsulation and cellular delivery. Watersoluble polypeptides are a good alternative to oil-based synthetic polymers for biomedical applications because they are biodegradable, have low toxicity, are monodisperse, and can be produced from cheap and renewable substrates at a large scale. Furthermore, functional designs can take direct inspiration from naturally evolved proteins.

For the particular case of nucleic acids delivery, viruses are the obvious benchmark. Viral capsid proteins present domains that display different functionalities necessary for an effective co-assembly with the nucleic acids (e.g. colloidal stability, self assembly and electrostatic binding). A good candidate for mimicking the functionality of viral coat proteins are unique polypeptides: these present a modular design that can be built by genetic engineering allowing insertion of independent functionalities in a linear sequence.

In this study we reported the cloning, production and characterization of one of these unique polypeptide carrying colloidal stability and DNA binding blocks (fig 1).

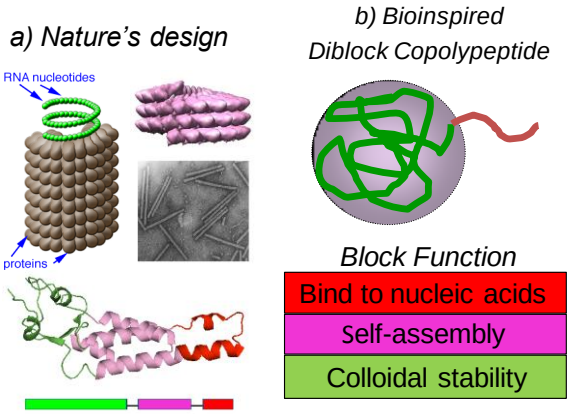

Figure 43. Biomimetics of nucleic acid-protein complexes A) Tobacco Mosaic Virus-RNA assembly B) Design of our virus-inspired diblock asymmetric copolypeptide.

The DNA binding properties were characterized by Dynamic Light Scattering and Atomic Force Microscopy (fig 2 & 3). It was found that this unique polypeptide results in controlled coating of single DNA molecules, as is the case for viral capsid proteins. The present design is intended to be a framework for adding further functional blocks to make further steps in mimicking the functionality of viral capsid proteins. Next to the above mentioned functionalities, also a high efficient production route towards this polypeptide is reported.

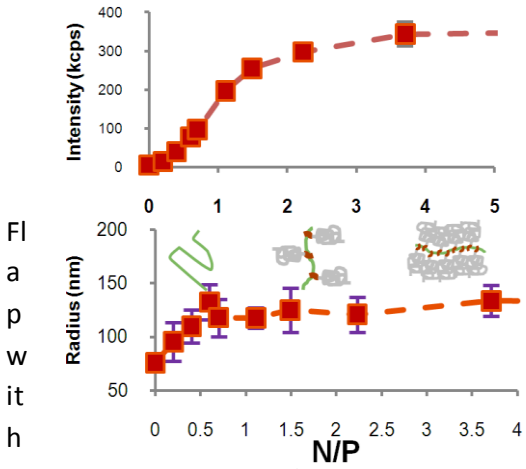

Figure 44. Dynamic Light Scattering of complexation between plasmidic DNA with diblock copolypeptide at different amino-to-phosphate ratios (N/P). A) Increment of scattering intensity B) Hydrodynamic radius calculated from diffusion coefficient and a model for pDNA coating where the DNA is drawn as a green line and diblock copolypeptide as grey-red molecule.

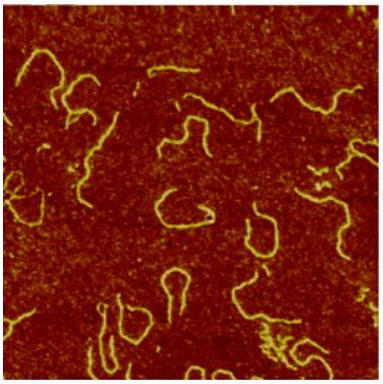

Figure 45. Atomic Force Microscopy image of diblock copolypeptide-pDNA complexes. Scale image: 2x2 µm.

Modification of polymers materials to achieve antibacterial properties

Jessie Casimiro [1], *Philippe Roger* [1], *Benedicte Lepoittevin* [1], *Caroline Boisse Laporte* [2]

[1] Laboratoire de Chimie Organique Multifonctionnelle, équipe G2M, Institut de Chimie Moléculaire et des Matériaux d'Orsay (UMR 8182), Bâtiment 420, Université Paris-sud, 91405 Orsay cedex

[2] Laboratoire des gaz et des plasmas, UMR 8578, Bat 210, Université Paris Sud 11, 91405 Orsay

Jessie.casimiro@u-psud.fr

Control surface contamination by microorganism is of great concern in a variety of areas such as food packaging, medical devices, hospitals and so on. To reduce or prevent microbial adhesion, new polymer surfaces must be developed. In this context, we investigate a new theme which deals with the modification of polymer materials containing carbohydrate molecules. [9, 10, 11] The aim of the study is to attach covalently glycopolymers or potential antimicrobial polymers on films of polyethylene terephthalate (PET) or polypropylene (PP) in order to study the biocidal or anti-fooling properties. Indeed, grafting glycopolymers on PP fibers have brought anti-fooling properties. [12]

The surfaces are prepared in several steps:

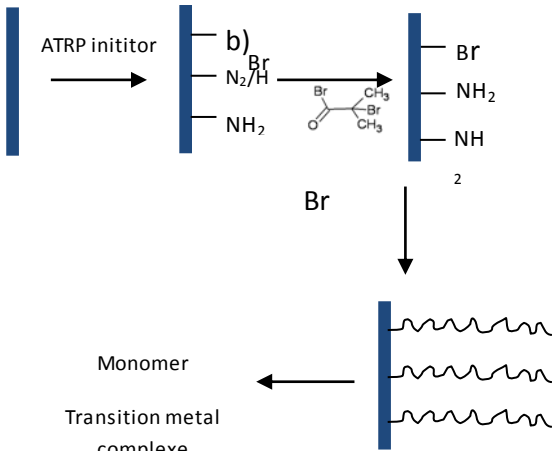

Preparation of materials

Step 1: Incorporation of primary amino groups by N_2/H_2 or NH_3 plasma treatment. The pretreatment by plasma exhibits many benefits for the surface modification, which enables to introduce functional groups at the surface without any modification of the chemical and mechanical properties of the material during the process.

Step 2: Insertion of Atom Transfer Radical Polymerization (ATRP) initiator

Step 3: Grafting from surface polymerization method of a monomer in order to control the molecular weight distribution on the surfaces. ATRP parameters of glycomonomers are studied in solution before carrying polymerization on surfaces.

Step 4: Microbial adhesion tests of modified surfaces with *Bacillus Subtilis* and *Lactoccocus Lactis* as bacterial strains.

Several analytical techniques such as X-ray photoelectron spectroscopy (XPS), Atomic Force Microscopy, size exclusion chromatography of polymers obtained in solution have been used to characterize the modified surfaces. The first step was to optimize plasma parameters in order to have a high density of primary amino group on the surfaces. Then several monomers have been studied especially a glycomonomer from galactose. Protected and deprotected glycopolymers polymerized on PET surfaces exhibit anti-fooling properties toward *Bacillus Subtilis*.

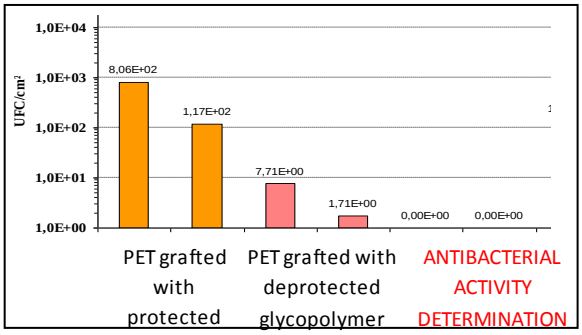

Results of counting of Bacillus Subtilis after 3 hours of adhesion at 30 °C on modified PET

Polymers containing quaternary ammonium salt or fluor have also been successfully polymerized by a grafting from method on PET films. Monomers from glucosamine are under consideration to mimic antimicrobial properties of chitosan.

[9] L. Renaudie, C. Le Narvor ,E. Lepleux , P. Roger, *Biomacromolecules*, 8, 679-685, **2007**.

[10] L. Bech, T. Meylheuc, B. Lepoittevin , P. Roger , *Journal of Polymer Science :Part A*, 45, 2175-2183, **2007**.

[11] L. Bech, B. Lepoittevin, A. El Achlab, E. Lepleux, L. Teulé-Gay, C. Boisse-Laporte, P. Roger, Langmuir, 23 10348-10352, **2007**.

[12] . Kou, Z. Xu, H. Deng, Z. Liu, P. Seta, Y. Xu, Langmuir, 19, 6869-6875, **2003**.

Core-Shell Type Nanofibrous Scaffolds using Coaxial Electrospinning for Bioapplication

Hongkwan Park[1], *Hyunhee Yoo*[1], *Taewon Hwang*[1], *Tae-Joon Park*[1], *In Woo Cheong*[2], *Jung Hyun Kim*[1,*]

[1]Department of Chemical and Biomolecular Engineering, Yonsei University, 134 Shinchon-Dong, Seodaemoon-Gu, Seoul 120-749, Republic of Korea
[2]Department of Applied Chemistry, Kyungpook National University, 1370 Sankyuk-dong, Buk-gu, Daegu 702-701, Republic of Korea

e-mail : jayhkim@yonsei.ac.kr

Core-shell type nanofibrous scaffolds were prepared using coaxial electrospinning. Poly(ε-caprolactone) (PCL) and chitosan with Levofloxacin was used as shell and core respectively, so the antibiotics Levofloxacin electrospinning would be useful for medical applications to treat acute rhinitis. PCL was used to control the release of Levofloxacin with time. SEM, TEM, and fluorescence microscope were used for the surface characterization of the core-shell fiber and the diameter measurement of the fiber core and of the total fiber. The core-shell interface was smooth and its structure was clearly visible by TEM. The total fiber diameter was about 200 nm while the core diameter was about 100 nm. 20 mg of nanofibrous scaffolds were soaked in PBS solution at 37 ℃ and the release of Levofloxacin with time was monitored by UV adsorption measurement at 331.20 nm. Since the PCL shell allowed the controlled release of Levofloxacin without an initial burst, the antibiotics-loaded core-shell type nanofibrous scaffolds show promise for treatment of wounds cause by acute rhinitis.

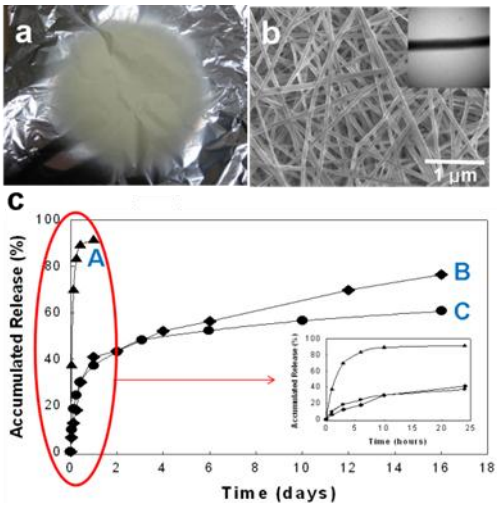

Fig.1 (a) Digital photo image of core-shell type nanofibrous scaffolds after coaxial electrospinning. (b) SEM and TEM images of core-shell type nanofibrous scaffolds. (c) Antibiotics release behavior of (A) PCL + gelatine + antibiotics nanofibrous scaffolds with single nozzle electrospinning, (B) PCL / chitosan + antibiotics nanofibrous scaffolds with dual nozzle electrospinning, (C) PCL / only solvent + antibiotics nanofibrous scaffolds with dual nozzle electrospinning.

Vinyl Sulfonate Terminated Polyglycidol for Biomedical Applications

Daniel Haamann[1], *Hiroaki Yoshida*[2], *Helmut Keul*[1], *Mitsuru Akashi*[2], *Doris Klee*[1], *Martin Möller*[1]

1) Institute of Technical and Macromolecular Chemistry, RWTH Aachen and DWI an der RWTH Aachen e.V., Pauwelsstr. 8, 52056 Aachen, Germany

2) Department of Molecular Chemistry, Graduate School of Engineering, Osaka University, 2-1 Yamada-oka, Suita 565-0871, Japan

haamann@dwi.rwth-aachen.de

During the last decade, polyglycidols and their derivates have gained much attention in biomedical applications due to their high functionality, solubility in aqueous media and biocompatibility.[1-3] Formation and application of synthetic materials in contact with biological matter remains a substantial challenge in today's biomaterial research. Therefore the combination of peptides/proteins or polypeptides with synthetic materials has gained raising interest during the last couple of years. Various reactive groups have been studied for the synthesis of polymer-peptide conjugates, e.g. maleimides or acrylates. Recently we reported the synthesis of a vinyl sulfonate terminated, linear and star-shaped polyglycidol as well as their high reactivity towards amines in organic and aqueous solution.[4-6]

In this presentation, the use of vinyl sulfonate terminated, star-shaped polyglycidol for various biomedical applications will be highlighted.

One application of the vinyl sulfonate terminated, star-shaped polyglycidol is the generation of reactive fibers in the sub-micron range for tissue engineering by electrospinning from functionalized polyglycidol/poly(ε-caprolactone) blends as shown in figure 1.[7]

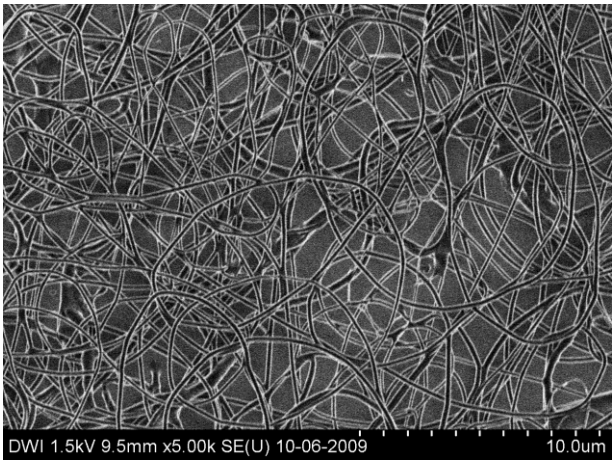

Figure 1: Electrospun fibers from polyglycidol/poly(ε-caprolactone) blends

These fibers can be further equipped with bioactive compounds using the high reactivity of the functionalized polyglycidol as shown exemplarily by reaction with an amine-group containing, fluorescent dye as shown in figure 2.

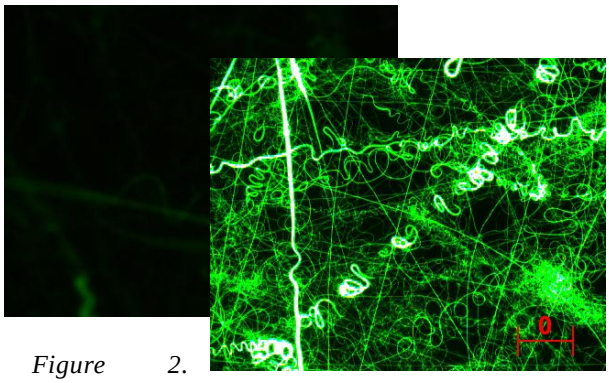

Figure 2. Fluorescence image of fibers from PCL/sPEEGE blends with no specific end groups (back) and vinyl sulfonate end groups (front) at the sPEEGE after incubation with (*R*)-(-)-4-(3-amino¬pyrrolidino)-7-nitro-benzofuran in water.[7]

Additionally, results including the use of vinyl sulfonate terminated polyglycidols for the formation of hydrogels and for hydrophilic surface coatings to minimize the unspecific protein adsorption will be presented.

Acknowledgement

The authors gratefully acknowledge funding by DFG Sonderforschungsbereich Transregio 37 "Mikro- und Nanosysteme in der Medizin – Rekonstruktion biologischer Funktionen". Furthermore, D.H. wants to thank the DFG Graduiertenkolleg 1035 "Biointerface" as well as the DFG International Research Program SeLeCa for additional funding.

References

[1] R. K. Kainthan, J. Janzen, E. Levin, D. V. Devine, D. E. Brooks *Biomacromolecules* **2006**, *7*, 703-709.
[2] H. Frey, R. Haag *Rev. Mol. Biotechnol.* **2002**, *90*, 257-267.
[3] H. Keul, M. Möller *J. Polym. Sci. Part A: Polym. Chem.* **2009**, *47*, 3209-3231.
[4] D. Haamann, H. Keul, D. Klee, M. Möller *Macromolecules* **2010**, *43*, 6295-6301.
[5] D. Haamann, H. Keul, D. Klee, M. Möller *Macromol. Symp.* **2010**, *296*, 1-4.
[6] D. Haamann, H. Keul, D. Klee, M. Möller *Manuscript in preparation.*
[7] D. Haamann, M. Bispinghoff, C. Suschek, M. Möller, D. Klee *J. Adv. Polym. Sci., submitted.*

Biosynthesis – Structure – Property Relations for Branched Polysaccharides as Revealed by Two-Dimensional Macromolecular Size/Branch Chain-Length Distributions

Francisco Vilaplana, Mitchell A. Sullivan, Jovin Hasjim, Robert G. Gilbert

Centre for Nutrition and Food Sciences, University of Queensland, 4072 Brisbane, QLD, Australia

f.vilaplana@uq.edu.au; franvila@kth.se

Introduction

Branched polysaccharides based on repeating glucose units, especially starch and glycogen, are fundamental energy storage molecules in plant and animal tissues, with significant influence on nutrition and human health. In addition, starch serves as a basic raw material for numerous industrial applications. Obtaining (bio)synthesis/(bio)degradation – structure – property relations of these molecules is fundamental to understand their functionality in biological systems and to tailor their properties through (bio)synthetic and physico-chemical modification. The structure of these polysaccharides involves a hierarchical organization at different levels: (1) the individual branches, (2) the whole branched macromolecules, and finally (3) supramolecular organizations such as crystalline and amorphous lamellae in starch, or α and β particles of glycogen [1]. Starch and glycogen are homopolymers of anhydroglucose, where the α-D-glucopyranosyl monomeric units are lineally extended by (1→4) linkages and branches are formed by (1→6) bonds at the branching points. However, this simple monomeric structure turns into a very complex branched macromolecular architecture that has defied complete characterization.

An unambiguous structural characterization of complex branched macromolecules requires multidimensional distributions based on the size and number of branches, and the position of these branches within the macromolecule [2]. Current available characterization procedures, such as size separation techniques coupled to multiple detectors (e.g. differential refractive index, viscometry or light scattering) only provide one-dimensional projections. Two-dimensional structural distributions based on macromolecular and branch size are presented here, obtained by offline multidimensional size-exclusion chromatography (SEC) and enzymatic debranching. The implications of such 2D distributions on the properties and (bio)synthetic pathways will be discussed for native rice starch, high-amylose starches, and glycogen.

Materials and methods

Commercial oyster glycogen (Sigma Aldrich, MI, USA), native starch from Malaysian rice flour (MRQ74, MARDI, Kuala Lumpur, Malaysia), and high-amylose maize starches (RMS, Gelose 50 and Gelose 80, Penford Food Ingredients Co., CO, USA) were used.

The 2D distributions were obtained by an analytical procedure combining size fractionation by preparative SEC, enzymatic debranching with isoamylase, and analysis of the branched and debranched fractions by analytical SEC with multiple detection (refractometry, viscometry and light scattering) [3].

Results and discussion

The 2D macromolecular size/branch chain-length distributions show distinct topological features for the macromolecular populations found in glycogen and native starch (see Figure). Glycogen shows a symmetrical monomodal peak, related to a single and homogeneous population of branches independent of macromolecular sizes. Starch, on the other hand, exhibits a complex surface with different peaks and foothills that differ in macromolecular size and branch length, corresponding to the main amylopectin and amylose populations, and also minor hybrid components (e.g. amylopectin with extra-long chains, intermediate components). Different starch varieties and mutants (e.g. high-amylose starches with longer branches and proven nutritional benefits) exhibit variations in the relative presence of these distinct macromolecular populations in their 2D distributions.

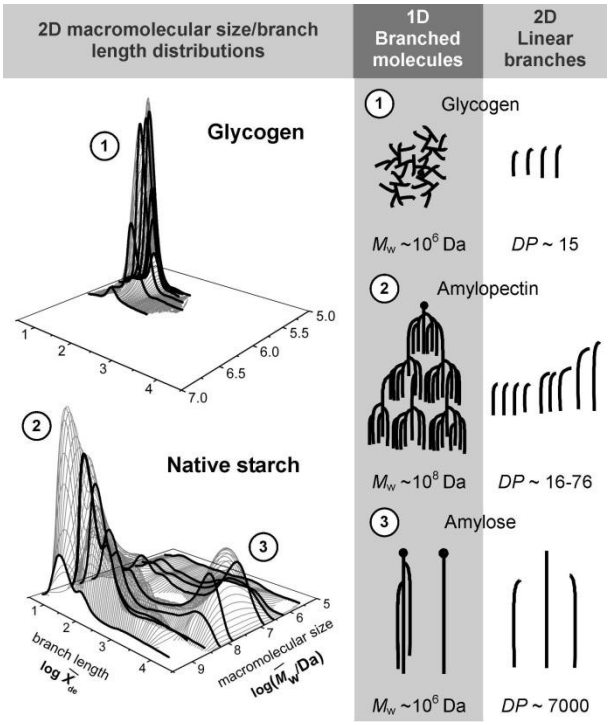

These 2D distributions reveal new knowledge on the biosynthetic pathways for glycogen and starch, with important future potential for biomedical, nutritional and industrial applications.

References:

[1] F. Vilaplana, R.G. Gilbert, Journal of Separation Science 33 (2010) 3537.

[2] A. Gray-Weale, R.G. Gilbert, J. Polym. Sci. Part A Polymer Chem. Ed. 47 (2009) 3914.

[3] F. Vilaplana, R.G. Gilbert, Macromolecules 43 (2010) 7321.

Compositionally-tunable surface nanostructuration of microspheres obtained from a self-stabilizing copolymerization of methylmethacrylate and vinylpyrrolidone

*Inmaculada Aranaz, Helmut Reinecke, Carlos Elvira, Alberto Gallardo**

Instituto de Ciencia y Tecnología de Polímeros, ICTP (CSIC). Juan de la Cierva 3, 28006 Madrid

gallardo@ictp.csic.es*

Introduction

Polymethylmethacrylate (PMMA) particles have been used in both biomedical and technological applications.12 They are commonly prepared by different heterogeneous polymerization processes being the use of surfactant molecules needed to stabilize the PMMA particles. Amphiphilic polymers as polyvinylpyrrolidone (PVP) 3 are typical surfactants used for this purpose. PVP has also many technological and biomedical applications. In this work, it is shown that MMAbased microparticles can be easily prepared in a simple and non demanding onepot procedure from copolymerization in methanol of MMA with VP, the monomeric precursors of the solid core and the polymeric surfactant mentioned above. This copolymerization leads to a high compositional heterogeneity, which actually allows the technology described in here.

Materials and Methods

Copolymerizations of MMA and VP were carried out under stirring (60º C, 24 hours,AIBN) by standard free radical reactions in different solvents (methanol, 1propanol, ethanol or dioxan). Emulsion drops formed in the reaction were hardened under vigorous magnetic stirring by slowly dropping water on the emulsion. The solutions were centrifuged and the centrifugate was resuspended in pure water. Three compositions have been studied, labeled as *MV21*, *MV11* and *MV12*, which corresponds to MMA initial feed molar fractions of 0.33, 0.5 and 0.67 respectively. Composition was determined by 1HNMR. Particles morphology and size was determined by SEM and by using a particle size analyzer.

Results and Discussion

Copolymerizations of MMA and VP on alcohols leads to a phase separated system. The high compositional heterogeneity of the reaction allows the partitioning of the copolymer chains between two phases as a function of their composition (MMArich and VPrich Chains forming the dispersed and continuous phases respectively). This emulsion can be easily hardened by adding water (Figure 1). The final result is a hydrophobic solid particle stabilized by some amphiphilic chains rich in VP. Thus, this copolymerization of MMA and VP is selfstabilizing. SEM analysis at higher magnification has shown a surprising irregular surface nanostructuration. Interestingly, changes in feed compositions leads to different sizes of the nanostructurated domains. As the amount of VP increase in the feed, these structures are bigger. Thus, the morphology is somehow compositionally driven (Fig 2).

Table 1. Samples composition and particle characterization.

Sample	f_{MMA}-copolymer phase-1[a]	f_{MMA}-copolymer phase-2[a]	Average diameter of particles[b], µm	PSD (D_w/D_N)
MV21-Me	0.79	0.41	5.570	1.91
MV11-Me	0.71	0.29	7.717	2.43
MV12-Me	0.61	0.23	3.840	1.37
MV11-Et	0.70	0.43	nd[c]	nd[c]
MV11-iPr	0.73	0.54	nd[c]	nd[c]
MV11-d	No phase separation		nd[c]	nd[c]

Me: MeoH, Et: EtOH, iPr: 1-propanol

a)Molar fraction of MMA in the copolymer as obtained from the NMR analysis.
b)Average diameter of the particles measured by using a Coulter.
c) nd: no-determined

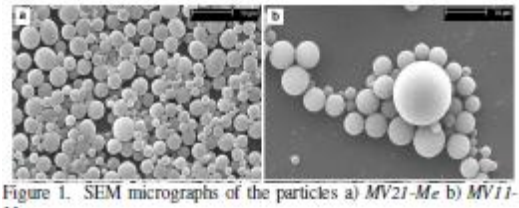

Figure 1. SEM micrographs of the particles a) *MV21-Me* b) *MV11-Me*

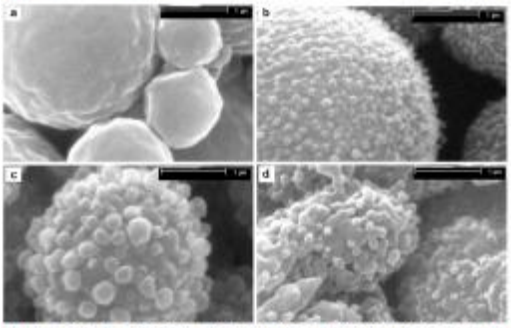

Figure 2. Details of particles surface a) *MV21* -Me b) *MV11-Me* c) *MV12-Me* d) *MV11-d.*

Conclusion

This work shows that the differential reactivity of MMA and VP may also be an opportunity in polymer chemistry. A simple onepot procedure based on the copolymerization reaction of both monomers yields solid microspheres in water. These microspheres have exhibited an irregular surface nanostructuration with a size domain that is controlled by the comonomer composition in the copolymerization.

References

1.PC Wang *et al*. Journal of Polymer Science A. 43 (2005) 13421356.

2. JH Park *et al*. Journal of Power Sources 195 (2010) 8306–8310.

3. Y Wang *et al*. Macromolecules 40 (2007) 756759.

Matrix Protein Dynamics on Polymer Surfaces

*C. González-García, P. Rico, M. Cantini, J. Ballester-Beltrán, V. Llopis-Hernández, M. Salmerón-Sánchez**

Center for Biomaterials and Tissue Engineering, Universidad Politécnica de Valencia, Spain

*masalsan@fis.upv.es

Introduction

The initial cellular events that take place at the biomaterials interface mimic to a certain extent the natural adhesive interaction of cells with the extracellular matrix (ECM). In fact, cells cannot interact directly with foreign materials, but they readily attach to the adsorbed layer of proteins such as fibronectin (FN), vitronectin (VN), fibrinogen (FG), representing the so-called soluble matrix proteins in the biological fluids. Upon longer contact with tissues many other ECM proteins, such as collagens and laminins (LN), will also associate with the surfaces, affecting the cellular interaction. The concentration, distribution, and mobility of the adsorbed protein layer on a surface play a fundamental role in the biofunctionality of a synthetic material and are clue factors to understand the biological response of a substrate. This work investigates ECM protein dynamics at the cell-material interface (FN, FG, VN, LN). Protein adsorption, cell adhesion and signaling and matrix remodeling are investigated after adsorption of model polymer substrates with controlled chemistry and surface stiffness.

Materials and Methods

The substrates employed are based on the random combination of monomers, which have either (i) a vinyl backbone chain with the side groups $–COOCH_2CH_3$ and $–COOCH_2CH_2OH$, or a vinyl backbone chain with the side groups $–COO(CH_2)_xCH_3$, with x=0, 1, 3, 5. Their copolymerization gives rise to a substrate in which the surface density of –OH groups can be varied without modifying any other chemical functionality of the system in the first case and with tailored surface stiffness in the second one. Plasma polymerization was also used for x=1 after different times. Surface properties were assessed by means of contact angle and X-ray photoelectron spectroscopy.

Protein adsorption (FN, FG, VN, LN) was performed from solutions of different concentrations (from 2μg/ml to 20 μg/ml) at different time points (from 10s to 2h). The amount of adsorbed protein on the substrates was obtained by western blot. AFM and ELISA were used to obtain protein conformation and distribution on the surfaces.

MC3T3-E1 cells were obtained from the Riken Cell Bank and cultured on the previously protein-coated substrates in serum-free conditions. Cell adhesion, actin cytoskeleton formation, intracellular signaling and matrix remodeling were correlated with the state of the protein layer on the material surface.

Results and discussion

The adsorbed amount of both FN and LN depends non-monotonically on the -OH density in the substrate, and protein surface density shows a minimum at approximately OH_{50}. Both higher and lower concentrations of hydroxyl groups in the substrate result in higher amounts of the adsorbed protein. The situation is completely different when either FG or VN is adsorbed on the same family of substrates. The amount of adsorbed protein diminishes monotonically as the OH density increases. The conformation of the adsorbed proteins can be directly observed by AFM. FN and FG tend to organize on the material surface, giving rise to protein fibrils. By contrast, cross-shaped molecules are observed for LN (which shows the change of conformation of the molecule upon adsorption) and globular aggregates are observed after VN adsorption (Figure 1).

On the other hand, the family of surfaces with different length of the side group (x=0-5), adsorbed the same FN density but in different conformations between x=0 (isolated molecules) and the other surfaces (well-interconnected network is formed). Consequently, this allows one to dispose of a set of substrates with stiffness as the main parameter able to influence the cellular behavior. Also, the conformation and amount of adsorbed FN was different on polymer surfaces obtained by plasma polymerization of x=1 after different times.

Cell behavior depends not only on the underlying chemistry, but also on the matrix protein used. Excellent adhesion is found for the more hydrophobic surfaces when using FN, FG and VN –even if they show different behavior in terms of conformation. By contrast, optimum cell interaction is found for OH_{50} if LN is used instead. Moreover, cellular reorganization of the adsorbed proteins depended on surface chemistry and was correlated to the state of the previously adsorbed protein layer and linked to the mechanical actions that cells exert on the substrate. To do that, the distribution of focal adhesion sizes was calculated. Larger focal plaques were found on those substrates on which reorganization took place more efficiently. Additionally, matrix secretion was related to reorganization abilities.

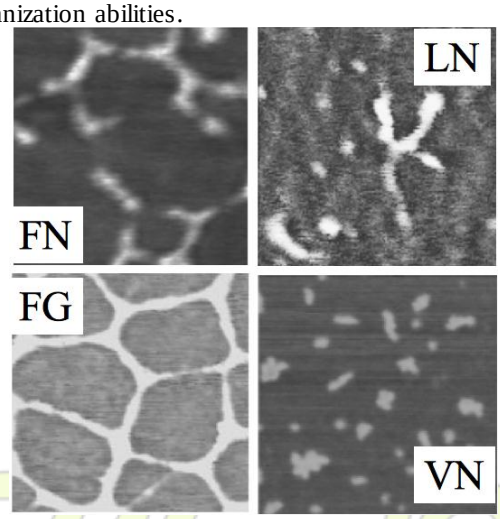

Figure 1. AFM images of ECM proteins adsorbed on substrates with controlled –OH groups from a solution of concentration 20 μg/mL.

Thermo-Responsive Self Assembled Nanoparticles from Elastin-Like Recombinamers

Laura Martín, Carmen García-Arévalo, F. Javier Arias, Matilde Alonso, J. Carlos Rodríguez-Cabello

GIR Bioforge, Universidad de Valladolid, CIBER-BBN, Paseo de Belén 11, 47010 Valladolid, Spain

e-mail: lmartin@bioforge.uva.es

In recent years, much interest has been focused on the performance of tailored stimuli-responsive self-assembled nanoparticles in aqueous solution due to their many important applications such as thickeners, coatings, drug- and gene-delivery systems, chemical or biological sensors and nanoreactors. Elastin-like recombinamers (ELRs) are made of pentameric repeat amino-acid sequences (Val-Pro-Gly-Xaa-Gly), where Xaa is any natural amino-acid except proline, or its permutations providing tunable physicochemical properties and excellent biocompatibility. This has led to extensive biological and nanotechnological applications of ELRs [1]. The absolute control over the design of ELRs allows facile manipulation of their stimuli-responsive properties and other physical and functional characteristics. Biosynthesis allows the production of strictly monodisperse polymers with no possibility of randomness in the comonomer distribution.

ELRs have shown their ability to form smart, self-assembling, protein-like micellar systems with controlled structure and function, which could be useful for drug targeting in therapeutic applications [2]. In this regard, we have biosynthesized different amphiphilic elastin-like di- and triblock corecombinamers in order to study the effect of the amino-acid composition and distribution. They are a combination of two different stimuli-responsive blocks. The first block is a pH-responsive smart polymer, and the other is a thermo-responsive polymer with no pH responsiveness [3]. We have changed the arrangement and length of the both blocks while keeping other parameters, such as the molecular weight or mean polarity, constant. The structure of the nanoparticles was investigated as a function of the temperature and concentration using turbidimetry, DLS and SLS, DSC and TEM amongst others in aqueous solution at neutral pH showing different nanostructures with several diameters The control over the molecular weight and the hydrophilic-to-hydrophobic ratio affords different nanostructures as micelles or vesicles with several sizes as well as control of the temperature at which self-assemble occurs (Figure 1).

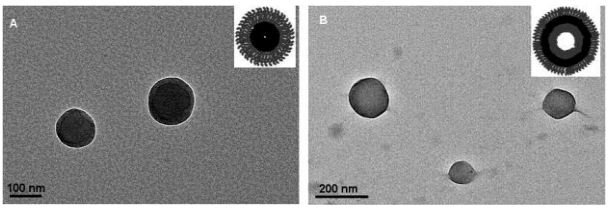

Figure 1. TEM images of micelles (A) and vesicles (B) obtained by self-assembling from elastin-like corecombinamers.

The potential of ELRs to self-assemble in response to environmental changes as pH, temperature or salt content makes them very attractive for the construction of nano-devices for use as controlled delivery and stimuli-responsive systems or advanced nanobiotechnological applications.

Acknowledgements

We acknowledge financial support from the MICINN (projects MAT 2007-66275-C02-01, MAT 2007-61604, MAT 2009-14195-C03-03 and PSE-300100-2006-1), the JCyL (projects VA034A09 and VA030A08), the CIBER-BBN (project CB06-01-0003), the JCyL and the Instituto de Salud Carlos III under the "Network Center of Regenerative Medicine and Cellular Therapy of Castilla and León".

References

[1] Rodríguez-Cabello, J. C., Martín L., Girotti A., García-Arévalo C., Arias F. J., Alonso M., Nanomedicine, **6** (2011), 111-122.

[2] MacKay, J. A., Chen, M., McDaniel, J. R., Liu, W., Simnick, A. J., Chilkoti, A. Nature Materials**, 8 (**2009), 993-999.

[3] Ribeiro, A., Arias, F. J., Reguera, J., Alonso, M., Rodríguez-Cabello, J. C., Biophysical Jounal, **97** (2009), 312-320.

Lysine Dendrimers and their Conjugates and Complexes with Amyloid-like Peptides

I.Neelov

Institute of Macromolecular Compounds, RAS, St.Petersburg, Russia

i.neelov@mail.ru

Introduction: It was shown recently[1] that charged dendrimers (PAMAM, PPI) could inhibit amyloid aggregation or even disrupt existing mature amyloid fibrils. There are also evidence that some short fragments of amyloid peptides could prevent amyloid aggregation both in full length amyloids (Aβ1-40 and Aβ1-42) and in their fragments [2]. Our goal is to understand physical mechamisms of both types of inhibition through molecular simulation of interaction of dendrimer with amyloid (or simplified amyloid-like) peptides. The lysine dendrimers are less toxic than widely used PAMAM and PEI dendrimers and thus they could be more suitable for biomedical applications and in particular for possible cure of Alzheimer's and other neurodegenerative diseases.

Materials and Methods: In present work we performed simulation of poly-L-Lysine dendrimers and their hybrids and complexes with short amyloid-like peptides. Method of molecular dynamic simulation with full atomic details (Amber99 forcefield) was used for this goal. One lysine dendrimer of 3.5 generation with 16 positively charged NH3+ terminal groups (or its hybrid with amyloid-like peptides attached to terminal groups were placed in periodic box with 7000-8000 explicit water molecules (TIP3P model). The same number of negative counterions Cl- were added to system for compensation of dendrimer charge. Complexes of lysine dendrimer or its hybrid with 8 amyloid-like peptides were studied also. We used KFFE tetrapeptides as simplest model for amyloid-like peptides. All calculations were performed at temperature T=300K. The length of each molecular dynamics trajectory was equal to 100ns. Computational package OpenMM [3] for computer simulation of molecular systems with full atomic details on graphical processor units (GPU) was used.

Results and Discussion: Structural parameters (gyration radius, asymmetry and distribution of density for all atoms and for terminal groups) around the centre mass of molecule were calculated for lysine dendrimer and hybrid of lysine dendrimer of generation 3.5 with KFFE tetrapeptides.

Time dependence of gyration radius of dendrimer was used to determine the relaxation and equilibrium parts of trajectory. Dendrimer of generation 3.5 is rather asymmetric and chemical attachment of KFFE peptides in hybrid structure doesn't influence the size and shape of dendrimer but slightly increase distance of terminal group from centre.

Adsorption of free KFFE peptides on dendrimer and on hybrid structure occurs rather quick and irreversible. Binding of adsorbed peptides to hybrid structure is stronger than to dendrimer itself. For dendrimer the adsorbed peptides are on the surface of dendrimer while for hybrid structure there are two maxima of peptide distribution around it. Adsorbed peptides are more extended than free peptides in water which help further adsorption of additional free peptides from solution. Distribution of counterions is also bimodal with maxima at the same positions as for adsorbed peptides. In the case of hybrid most number of contacts are between chemically attached and adsorbed peptides.

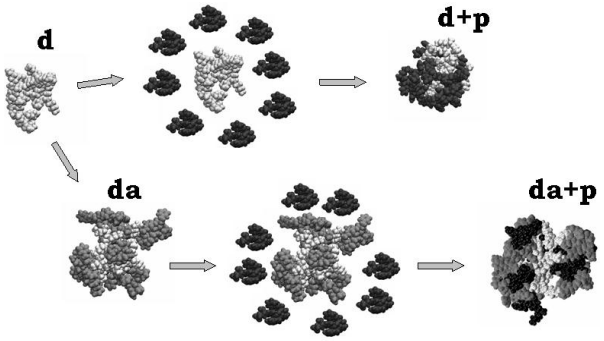

Fig.1 **d** – lysine dendrimer (light gray); **da** - hybrid of dendrimer (light gray) with chemically attached KFFE tetrapeptides (dark gray); **d+p** –complex of dendrimer (light gray) with adsorbed peptides (black); **da+p** – complex of hybrid (light gray+dark gray) with adsorbed KFFE tetrapeptides (black). Two nonamed pictures are initial conformations of dendrimer (or hybrid) and free tetrapeptides before their complexation to **d+p** or **da+p** structure correspondingly

Conclusions

Protonated lysine dendrimers and their hybrids with short peptides could adsorb significant amount of amyloid-like peptides due to strong electrostatic interactions. This spherically symmetric aggregation of amyloid-like peptides on dendrimers and hybrid structures could prevent own aggregation of free peptides in column-like linear structures (fibrils) and even lead to disruption of already existing mature amyloid fibrils.

References:

[1] Klajnert, B.; Cladera, J.; Bryszewska, M. *Biomacromolecules*, 2006, 7, 2186-2191.

[2] Gordon, D.; Sciarretta, K.; Meredith, S. *Biochemistry*., 2001, 40, 8237-8245.

[3] Friedrichs, M., et all J. Comp. Chem., 2009, 30, 864-872

Poly(ester amide)s based on α-amino acids and α-hydroxy acids oligomers: Synthesis, characterization and biodegradation studies

A.C. Fonseca[a], *P. N. Simões*[a], *M. H. Gil*[a]

[a] Department of Chemical Engineering , University of Coimbra, Rua Sílvio Lima-Pólo II, 3030-290 Coimbra, Portugal

e-mail:ana.clo.fonseca@gmail.com

Introduction: Poly(ester amide)s (PEAs) are a class of synthetic polymers whose importance in the biomedical field has increased in the last years. PEAs gather in the same entity the best properties of polyamides (good mechanical and thermal properties) and polyesters (biodegradability).[1] PEAs containing α-amino acids and α-hydroxy acids (e.g., L-lactic acid) in their structure also demonstrated their potential in biomedical applications.[2] Such PEAs release normal metabolites (α-amino acids and α-hydroxy acids) in the human body upon degradation, and for this reason the toxicity induced by these materials is very low. Because both acid and basic natures of the degradation products, a neutralization effect occurs, thus avoiding an accentuated decrease in the pH, which can cause undesirable host reactions.[3] Besides, the presence of the α-amino acid opens the possibility of these materials being degraded also enzymatically, increasing their biodegradability.

This work reports the synthesis of PEAs by an interfacial polycondensation method between diamines derived from glycine or L-phenylalanine,[3] and diacyl chlorides derived from L-lactic acid oligomers.[4] The obtained PEAs were characterized in terms of chemical structure (FTIR and ^{1}H NMR spectroscopies), thermophysical (TGA, mDSC) and thermomechanical (DMTA) properties. The biodegradation behaviour in PBS (pH=7.4) at 37ºC was also evaluated. The influence of the α-amino acid lateral group in the properties (thermal, mechanical, biodegradation) of the final PEAs was studied.

Materials and Methods: The synthesis of the diamine monomers (Monomer 1.A and Monomer 1.B) was carried out by a Fischer esterification in the presence of p-toluene sulfonic acid monohydrate as catalyst.

L-LA diacyl chlorides (Monomer 2 and Monomer 3) were obtained from the reaction between L-LA hydroxyl terminated oligomers and sebacoyl chloride.

PEAs were synthesized by interfacial polymerization between the diamines derived from the α-amino acids and the diacyl chlorides derived from L-LA oligomers, using sodium carbonate as proton acceptor. The system of solvents was water/dichloromethane. Scheme 1 presents the structure of the monomers and of the synthesized PEAs.

Results and Discussion: Both FTIR and ^{1}H NMR analysis demonstrate that PEAs were successfully obtained.

The TGA results indicate that the PEAs containing L-phenylalanine in their structure are thermally more stable than those containing glycine.

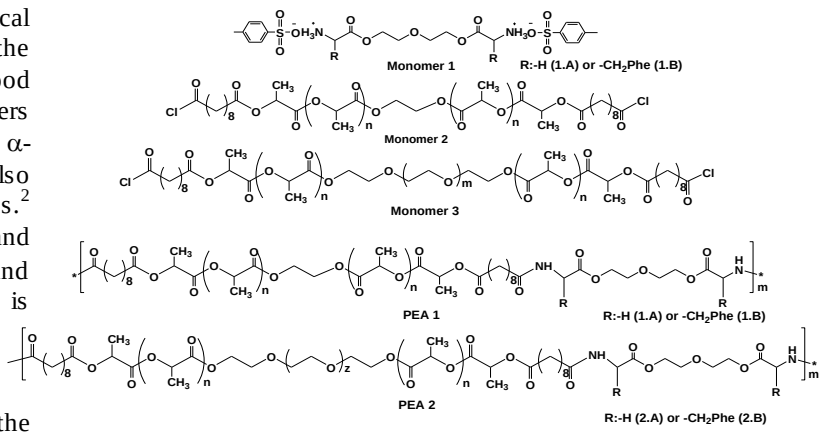

Scheme 1- Representation of the monomers and PEAs structure.

This behaviour can be attributed to the presence of the aromatic ring, which gives additional thermal stability to the PEAs.

It was observed that PEA 2 (2.A and 2.B) exhibits a lower glass transition temperature (T_g) when compared to the PEA 1 (2.A and 2.B). This is due to the higher density of ether linkages present in PEA 1.

It was observed that PEAs 2 degrade faster than PEAs 1. This is a consequence of the higher hydrophilicity of PEAs 1, due to the presence of poly(ethylene glycol). The PEAs containing L-phenylalanine (PEAs X.B) degrade slower than the PEAs containing glycine (PEAs X.A). This can be attributed to the additional hydrophobicity given by the aromatic ring in L-phenylalanine.

Conclusions: PEAs based on α-amino acids and α-hydroxy acids were successfully synthesized by interfacial polymerization. The pendant group of the α-amino acid has important influence in the thermal properties as well as in the hydrolytic degradation behaviour.

References: [1] Nair, L. S.; Laurencin, C. T. *Prog. Polym. Sci.* 2007, *32*, 762.

[2] Feng, Y.; Lu, J.; Behl, M.; Lendlein, A. *Macromol. Biosci.* 2010, *10*, 1008.

[3] Karimi, P.; Rizkalla, A.S.; Mequanint, K. Materials. 2010, *3*, 2346.

[4] D'Angelo, S.; Galletti, P.; Maglio, G.; Malinconico, M.; Morelli, P.; Palumbo, R.; Vignola, M. C. *Polym.* 2001, *42*, 3383.

Nanoengineered Polymeric Capsules for Drug Delivery

Georgina K. Such, Christopher J. Ochs, Yan Yan and Frank Caruso

Centre for Nanoscience and Nanotechnology, Department of Chemical and Biomolecular Engineering,
The University of Melbourne,
Parkville, Victoria 3010, Australia

gsuch@unimelb.edu.au

Introduction. Recently there has been significant research in the area of intelligent polymeric delivery systems for application in drug and gene therapy. Such polymeric carriers must have finely controlled and responsive properties to allow efficient and selective delivery of therapeutics within the body. One technique that has generated interest for synthesis of polymer capsules is the layer-by-Layer (LbL) technique due to the simple and versatile nature of this approach. The LbL technique is based on the serial adsorption of species with complementary interactions and can be performed on a diverse range of templates. LbL assembly on particles and subsequent template removal to form polymer capsules has generated particular interest for use as polymer carriers.

Recently, we combined click chemistry with LbL to develop new ultrathin films and capsules.[1] This approach involved assembling an alkyne-modified polymer with a corresponding hydrogen-bonding partner. After assembly, the alkyne groups were used to covalently stabilise the film by reaction with a bifunctional azide crosslinker. When these materials were incubated in phosphate buffer, the hydrogen bonding was disrupted, allowing the non-functionalised polymer to be removed. In this way single-component films and capsules could be engineered.

Herein, we report the application of the technique to design poly(*L*-glutamic acid) (PGA) capsules. We have demonstrated how these capsules can be used to load a model anticancer drug doxorubicin (DOX) in a controlled dose and position within the film (**figure 1**).[1] We have also shown that the drug-loaded capsules are active *in vitro* and can be used as an approach to partially bypass multidrug resistance.[2] The simple yet modular nature of this technique provides exciting new opportunities for the design of nanoengineered materials.

Materials and Methods. The synthetic details of the PGA capsules and PGA-DOX capsules have been described in previous work.[1,2] The main techniques used to characterise these materials included flow cytometry, ellipsometry and both confocal and fluorescence microscopy.[1]

Results and Discussion. In this work we have demonstrated alkyne-modified PGA can be assembled in alternation with poly(*N*-vinyl pyrrolidone) (PVPON) and then subsequently crosslinked with a bifunctional azide. At physiological pH, the PVPON is no longer held in the film by hydrogen bonds and thus is removed. This process can be performed on either a planar or colloidal surface, however on a colloid the sacrificial core can be removed to form a PGA capsule.

A PGA conjugate was also synthesised with both doxorubicin and alkyne functionality. It was demonstrated this conjugate could be successfully incorporated into the capsule in a specific position or dose (**figure 1**), thus allowing control over the drug loading within the capsule. The DOX loaded capsules were shown to have regular spherical morphology with uniform fluorescence due to loaded DOX. Each layer was found to load approximately 25 μg of DOX. It was also demonstrated the PGA-DOX capsule degraded in the presence of protease. This PGA-DOX capsule was found to successfully kill cells in vitro, however at a similar concentration the PGA-DOX conjugate did not effect cell viability.[1] This was thought to be due to the different uptake mechanism of the LbL carrier as compared to the polymer conjugate.

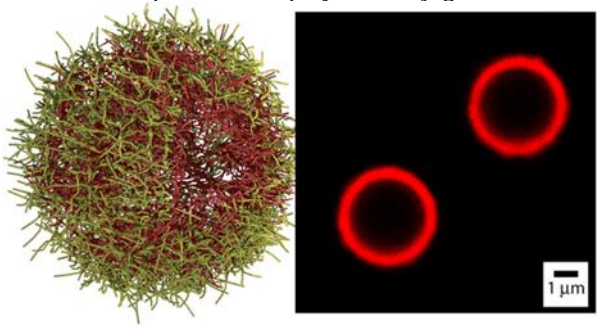

Figure 46: Schematic of a layer-by-layer (LbL) capsule and a fluorescence image of a doxorubicin loaded PGA capsule.

In later work these capsules were used to partially bypass multidrug resistance in DOX resistance cells as compared to free DOX.[2] Due to the different uptake of the capsule relative to the free drug, the DOX within the capsule could access the cell while the free DOX was excluded. In the latter case, free drug was removed by p-glycoprotein on the surface of the cell while the DOX within the capsule is protected.

Conclusion. This modular capsule design allows tunable drug loading and release of active drug once in a cell. Residual alkyne groups within the capsule also allow the possibility for post modification with antibodies or stealth materials. Thus it is expected these nanoengineered materials will have significant impact in areas such as drug or gene delivery.

References.

1. Ochs, C. J.; Such, G. K.; Koeverden, M. P.; Caruso, F. *ACS NANO* **2010**, *4*, 1653-1663.
2. Yan, Y.; Ochs, C.J.; Such, G. K.; Heath, J. K.; Nice, E. C.; Caruso, F. *Adv. Mater*. **2010**, *22*, 5398-5403.

A water-based antibacterial nanohybrid solution for coating stainless steel

Céline Falentin-Daudré[1], *Emilie Faure*[1], *Christine Jérôme*[1], *Cécile Van de Weerdt*[2], *Joseph Martial*[2], *Catherine Archambeau*[3], *Anne-Sophie Duwez*[4], *and Christophe Detrembleur**[1]

[1]Center for Education and Research on Macromolecules (CERM), University of Liège, Sart-Tilman B6a, 4000 Liège, Belgium
[2]GIGA-R, Systems Biology and Chemical Biology Unit, University of Liège, B34 Sart-Tilman, B-4000Liège, Belgium.
[3] ArcelorMittal Liège Research, Bd de Colonster B57, 4000 Liège, Belgium.
[4] Nanochemistry and Molecular Systems, University of Liège, B6 Sart-Tilman, B-4000 Liège, Belgium.

Celine.falentin@ulg.ac.be

Introduction. Due to its exceptional properties, stainless steel (SS) is widely used in the daily life (food industry, household appliances, surgery …)[1]. However, it is unable to prevent bacteria from adhering, proliferating and forming a resistant biofilm when ageing. Therefore, surface modification is needed for providing durable antibacterial properties. Various techniques are used for imparting such biocidal properties to the support such as (i) the deposition of biocidal metals (such as silver and copper) or inorganic oxides (TiO_2 anatase) by plasma[2], chemical vapor deposition (CVD)[3] or sol-gel procedures[4], (ii) the coating of the surface by paints containing antibiotics or other biocides[5], (iii) or the deposition of biocidal (bio)polymers such as antibacterial peptides or synthetic polymers containing ammonium groups[6]. Provided that the biocidal polymers are anchored to the support, they impart long tasting antibacterial properties which are highly desirable for the durability of the functionality[6].

Results and discussion. Very recently, we reported on an all-in-one approach to prepare refillable antimicrobial films[7] using the layer-by-layer (LbL) deposition of polyelectrolytes. Specifically designed biocidal multilayered polyelectrolyte films that bear 3,4-dihydroxyphenylalanine (DOPA), known as an adhesion promoter to inorganic surfaces, were deposited onto SS. DOPA was incorporated in the polycationic chains by radical copolymerisation of *N*-methacrylated DOPA with the quaternary ammonium salt of 2-(dimethylamino)ethyl methacrylate (DMAEMA+). In order to boost the antibacterial activity of the polycationic layer, $AgNO_3$ was added to the aqueous solution of P(DOPA)-*co*-P(DMAEMA$^+$), which resulted in the in-situ formation of silver based nanoparticles, Ag^0 and AgCl, sources of biocidal Ag^+. The layer-by-layer deposition of aqueous P(DOPA)-*co*-P(DMAEMA+)/AgCl/Ag^0 suspension and aqueous solution of poly(styrene sulfonate) provided high antibacterial activity against Gram-negative *E. Coli* bacteria.
Although this surface modification is highly efficient, it requires the LBL deposition of about 60 bilayers that makes the process difficult to scale-up at the industrial scale. In the present communication, we will demonstrate how the same copolymers can impart AB properties to the SS surface using only 1 or 2 layers. Novel nanohybrids are first prepared in water before being deposited on the surface.

Conclusions. The method of formation of these nanohybrids, their deposition and the characterization of the modified surface will be discussed in detail in this talk. This novel water-based approach is convenient, simple and is promising for scalable applications. It might also be used for coating other organic and inorganic surfaces in order to impart them robust AB properties.

Acknowlegments. The research was partly supported by BELSPO in the frame of IUAP VI/27 and Région Wallonne, ArcelorMittal and ULg through the PPP program BIOCOAT. C.D. is “Maître de Recherche” of the F.N.R.S. (Belgium), and thanks the F.R.S.-F.N.R.S. for financial support.

References. [1]J. A. Helsen and H. J. Breme, in *Metals as Biomaterials*, Wiley, New York, **1998**. [2](a) K. Shiraishi, H. Koseki, T. Tsurumoto, K. Baba, M. Naito, K. Nakayama and H. Shindo, *Surf. Interface Anal*., **2009**, *41*, 17-22; (b) P. K. Chu, *IEEE Trans. Plasma Sci*., **2007**, *35*, 181; (c) G. Guillemot, B. Despax, P. Raynaud, S. Zanna, P. Marcus, P. Schmitz and M. Mercier-Bonin, *Plasma Processese Polym.*, **2008**, *5*, 228. [3]P. Evans and D. W. Sheel, *Surf. Coat. Technol*., **2007**, *201*,9319. [4](a) X. Ding, J. Gao, Q. Shen, J. Liu and H. Yang, *Key Eng. Mater*., **2007**, 336-338, 1559; (b) M. Es-Souni, H. Fischer-Brandies and M. Es-souni, *Adv. Funct. Mater*., **2008**, *18*, 3179. [5]E. M. Hetrick and M. H. Schoen fisch, *Chem. Soc. Rev*., **2006**, *35*, 780. [6] G. J. Gabriel, A. Som, A. E. Madkour, T. Eren and G. N. Tew, *Mater. Sci. Eng*., **2007**, *R57*, 28. [7]A. Charlot, V. Sciannamea, S. Lenoir, E. Faure, R. Jerome, C. Jerome, C. Van De Weerdt, J. Martial, C. Archambeau, N. Willet, A.-S. Duwez, C.-A. Fustin, C. Detrembleur, *Journal of Materials Chemistry 19*, 4117-4125, **2009**.

Bioinspired Protein Imprinted Poly(Dopamine)-Silica Composite as Separation Materials in High-Pressure Liquid Chromatography

Ali Nematollahzadeh[a,b], *Börje Sellergren*[a], *Akbar Shojaei*[b] *and Mohammad J. Abdekhodaie*[b]

c. Institut fur Umweltforschung (INFU), Technical University of Dortmund, Germany
d. Department of Chemical and Petroleum Engineering, Sharif University of Technology, P. O. Box 11155-9465, Tehran, Iran,

a_nematollahzadeh@yahoo.com

Abstract

Human Serum Albumin (HSA) imprinted nano-layer of polydopamine was produced through oxidative polymerization of dopamine on HSA modified porous silica support. The coating thickness was controlled by the reaction time and, therefore, varied within 0-12 nm. The samples were characterized by elemental analysis, FT-IR, DSC, SEM, TGA, physisorption and thermoporometry. The characterization confirmed the success of the evolution and deposition of dopamine onto the silica pore surface. Batch rebinding experiment exhibited that the molecularly imprinted polymer (MIP) with 8.7 nm coating thickness in comparison with the thinner and thicker coatings, adsorbs much more the target protein. The chromatography evaluation of the materials packed in HPLC column showed that HSA imprinted polydopamine offering good mechanical stability adsorbs practically all the target protein from the HSA solution or human plasma.

Introduction

Preparation of artificial systems capable of molecular recognition and capture could uniquely be achieved by molecular imprinting technique. Generally, the technique involves the arrangement of functional monomers around template molecules in a porogenic solvent. The complex is subsequently polymerized. After removal of the template, specific cavities, which are complementary in shape, size and chemical functionality to the template, are left within the polymer matrix. These specific cavities can selectively rebind the target molecules. Surface imprinting on solid porous particle presented in this article was on the basis of mussel-inspired surface chemistry for multifunctional coatings reported by Lee et al. [1,2] Recently, we developed a general technique to obtain a hierarchically structured protein imprinted porous polymer beads by using silica porous particles as sacrificial solid support for protein recognition and capture.[3]

In this study, therefore, we present a general technique to fabricate protein imprinted composite microparticles through direct coating of DA on the pore surfaces of porous silica particles for use as stationary phases in liquid chromatography.

Materials and methods

Dopamine (DA) was purchased from Sigma-Aldrich. Tris-HCl and silica particles were received from Merck. The silica was rehydroxylated prior to use. The surface area and pore volume of the silica were measured by N_2 gas sorption (Nova-Quanatchrom4000e).

The method involves three steps including 1) immobilization of HSA on the silica pore surface, 2) polymerization of DA on the pore surface in presence of HSA and 3) removal of the template. Ten samples (5 imprinted and 5 non-imprinted) were prepared at 5 different reaction time intervals (3, 6, 12, 24 and 48 h)

Results

Different characterizations techniques (FT-IR, DSC, SEM, and TGA) confirmed the success of the evolution and deposition of dopamine onto the silica pore surface. Figure 1 shows the SEM images of bare silica and DA coated and imprinted silica. In Fig. 2A time dependency of the PDA thickness and mass evolution on the silica surface is shown. Batch rebinding experiment exhibited that 8.7 nm coating thickness which was achieved within 24 h reaction time (MIP24h) adsorbs much more target protein than the corresponding NIPs.

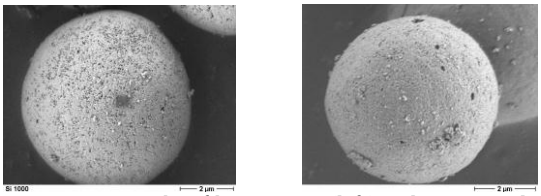

Fig. 1 SEM micrographs of bare Si1000 (left) and DA coated silica (right) particles all having an approximated mean diameter of 5 µm.

The chromatography evaluation of the materials packed in HPLC column showed (Fig. 2B) that the MIP24h adsorbs practically all the target protein from the HSA solution or human plasma, as well.

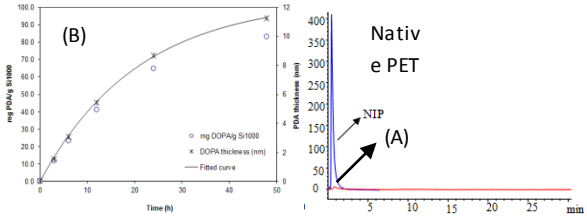

Fig. 2 Time dependency of the PDA thickness and mass evolution on the silica surface obtained by TGA (A), Chromatographs of Human Plasma 100× diluted in the HSA-MIP and NIP (B)

Conclusion

Surface imprinting on a porous solid support is an effective approach to overcome the mass transfer resistance, in particular within protein imprinted polymer, offering high mechanical robustness and a simplified procedure for producing HPLC stationary phase which can be immediately used for HPLC packing for the protein separation purposes.

References

1. Lee, H.; Dellatore, S. M.; Miller, W. M.; Messersmith, P. B., Science 318, 426 2007.
2. Lee, H.; Lee, B. P.; Messersmith, P. B., Nature 448, 338 2007.
3. Nematollahzadeh, A.; Sun, W.; Aureliano, C. S. A.; Lütkemeyer, D.; Stute, J.; Abdekhodaie, M. J.; Shojaei, A.; Sellergren, B., Angew. Chem. Int. Ed. 50, 495 2011

Development and Characterization of Antimicrobial PCL Fibres for Surgical Suture Applications

L. Botta[1], *R. Scaffaro*[1], *M. Sanfilippo*[1], *G. Gallo*[2], *A. M. Puglia*[2]

[1] Dipartimento di Ingegneria Industriale, [2] Dipartimento di Scienze e Tecnologie Molecolari e Biomolecolari
Università di Palermo, Viale delle Scienze, 90128 Palermo (Italy)

luigi.botta@unipa.it; roberto.scaffaro@unipa.it

Introduction

Actually, the preparation of antimicrobial surgical sutures is under the consideration of both academia and industry. The main problem is to find a good compromise between the effectiveness and the production costs.
Antimicrobial properties can be granted to a surgical suture by different methods that may modify or not the structure of the polymer. In all the cases it is necessary that the process does not significantly change the mechanical properties of the material.
The methods currently used for production of surgical sutures with antimicrobial properties are essentially two: coating and grafting. These methods require several steps after the spinning of the filament and, generally the use of solvents to provide the suture with antibacterial properties.
Polycaprolactone (PCL) is a synthetic biodegradable aliphatic polyester widely used for biomedical applications, such as controlled-release drug delivery systems, absorbable surgical sutures and three-dimensional scaffolds for use in tissue engineering [1].
The chlorhexidine (CHX) is a broad-spectrum antimicrobial agent belonging to the bis(biguanide) family. It is used primarily as a topical antiseptic/disinfectant in wound healing, at catheterization sites, in various dental applications and in surgical scrubs [2].
Aim of this work is to develop a method for preparing PCL monofilament with antimicrobial properties for surgical suture applications by incorporating CHX during the melt extrusion of the PCL monofilament. The effect of CHX content and of the cold drawing on antimicrobial and mechanical properties of the prepared monofilaments was investigated. Moreover, the release of CHX from the fibres was investigated too.

Materials and Methods

Both PCL and CHX (diacetate salt hydrate) used in this work were commercial samples supplied by Sigma Aldrich.
PCL has been compounded with CHX at different concentrations (1%, 2%, 4%) by using a counter rotating twin screw compounder with a thermal profile of 40-50-70-100 °C. The fibres were spun by using a capillary rheometer operating under a constant extrusion speed; the final diameter of the as spun fibres was about 250 µm.
The antimicrobial activity of filaments was determined by agar diffusion method evaluating the presence of inhibition zones against two Gram-positive (*M. luteus*, and *B. subtilis*) and a Gram-negative (*E. coli*). Moreover, bacterial growth in presence of the antimicrobial fibres was determined by plate counting test.

Results and Discussion

All the filaments containing chlorhexidine showed a clear zone of inhibition against both Gram-positive and Gram-negative bacteria. On the contrary, the pure PCL shows no antibacterial activity as reported in figure 1 for the assay against the *M. luteus*.

The effectiveness of the antibacterial properties of the filaments was also evaluated by inhibition tests in a liquid

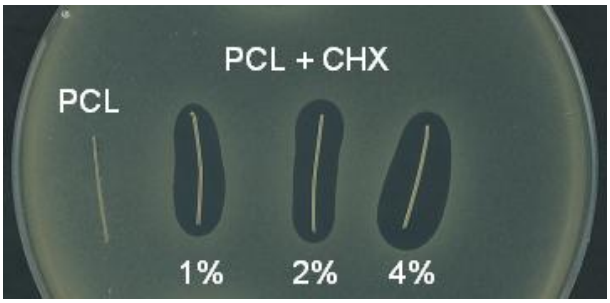

MIP

medium. The measurements of the bacterial growth revealed, in full agreement with the agar diffusion tests, that the pure PCL did not show any antibacterial activity. On the contrary all the samples added with chlorhexidine inhibited the growth of the bacterial mass.
The off-line cold drawing of the fibres induced an obvious decrease of their diameter and an increase of the mechanical properties with particular reference to the load at break. Both inhibition tests showed that also the drawn fibres clearly exhibit a strong antibacterial activity.
The evaluation of CHX release showed that, as expected, the amount of released antimicrobial agent raised on increasing the content added to the fibres. Moreover, the drawn fibres released a lower amount of chlorhexidine if compared with as spun ones.

Conclusions

This work reports a method to prepare antimicrobial PCL fibres for surgical suture applications. In particular, an antimicrobial agent, i.e. CHX, was incorporated in PCL during the melt extrusion of the monofilaments. The filaments were cold drawn in order to increase their mechanical resistance. Both as-spun fibres and drawn ones clearly exhibit a strong antibacterial activity.

References

1. E. Y. Teo, S.-Y. Ong, M. S. K. Chong, Z. Zhang, J. Lu, S. Moochhala, B. Ho, S.-H. Teoh. *Biomaterials*, 2011, 32, 279.

R. R. Arnold; Hong Hong Wei; E. Simmons; P. Tallury; D. A. Barrow; S. Kalachandra, *J Biomed Mater Res Part B: Appl Biomater*, 2008, 86B, 506

.

Enzymatically Cross-linked Proteins: Hierarchical Biopolymers

Yunus Saricay[1], *Peter Wierenga*[2], *Renko de Vries*[1]

[1]Laboratory of Colloid Science, Wageningen University and Research Center, Chemisty , Dreijenplein 6 6703 HB Wageningen, The Netherlands

[2]Laboratory of Food Chemistry, Wageningen University and Research Center, Bomenweg 2, 6703 HD Wageningen, The Netherlands

yunus.saricay@wur.nl

-Introduction. Enzymatic cross-linking has been reported to improve the food functionality (foam, emulsions, gels) of the commercially important whey proteins[1-2]. However, the relation between the mesoscale physical properties and the functionality of cross-linked "protein-polymers" has so far not been elucidated.

Materials & Methods. A Ca^{+2}-depleted-α-lactalbumin type III was supplied from sigma and used without any purification. Horseradish peroxidase type VI-a, hydrogen peroxide solution of 30% (w/w) in H_2O were purchased from Sigma-Aldrich.

Results & Discussion. In order to characterize the mesoscale properties of enzymatically cross-linked proteins, we here study the details of peroxidase-catalyzed cross-linking of the whey protein α-lactalbumin, with peroxide as a co-substrate. Crucial to our study is the integration of on-line characterization of the cross-linking chemistry (via UV-spectroscopy) and on-line characterization of the particle formation process (via dynamic light scattering) (Fig.1)

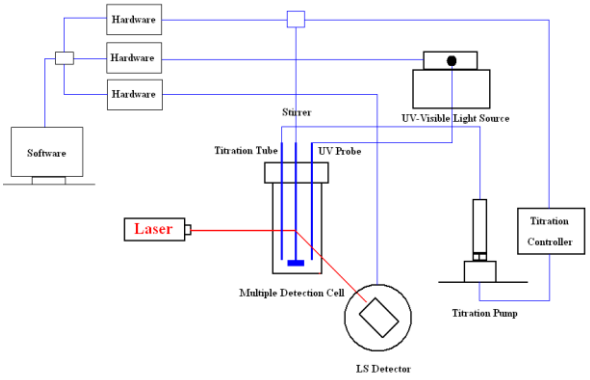

Figure.1. Scheme of multiple detection system.

We find that for our system, cross-linking is limited by the lifetime of the enzyme that is gradually inactivated by excess peroxide. For a 1 % (w/w) starting concentration of α-lactalbumin, we find final sizes for cross-linked products of about 25-30 nm (Fig.2).

Off-line analysis combining Size-Exclusion Chromatography and Light Scattering shows that the relation between the solution size and molecular weight of the reaction products is $R \sim M^{a}$, with an exponent a ≈ 0.6, indicating a very open structure of the cross-linked proteins, with molecular weights up to $M_w \approx 10^7$ Da (Fig.3).

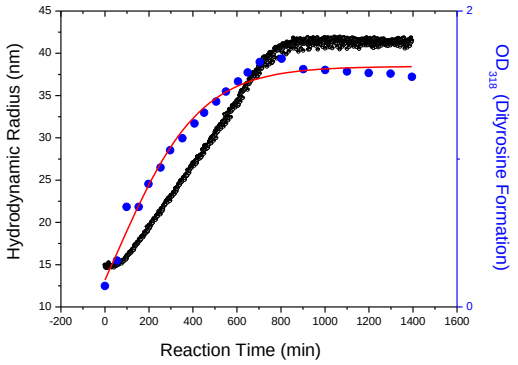

Figure.2. LS intensity and absorbance at 318 nm of reaction mixture of 1 % α-lactalbumin incubated HRP at pH 6.8 in 0.1 M NH_4Ac as a function of reaction time during online characterization of peroxidase-mediated cross-linking reaction

The open structure may be related to the rather low functionality of the monomer that contains only 4 reactive tyrosines.

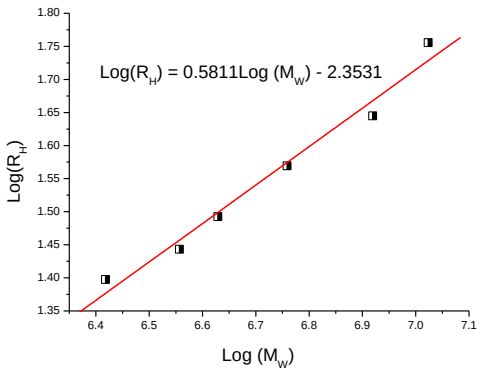

Figure.3. Double logarithmic plotting of hydrodynamic radius vs molecular weight of protein polymer fractions.

Conclusion. We achieved to characterize peroxidase-meadited cross-linking of α-lactalbumin in terms of cross-linking chemistry and particle formation process in order to relate mesoscale physical properties to functionality for the engineered protein structures with controlled size and architecture.

References.

1. Ahmed s. Eıssa, Satısha Bısram and Saad a. Khan *J. Agric. Food Chem.*, Vol. 52, No. 14, 2004

2. Eric Dickinson, Christos Ritzoulis, Yukiko Yamamoto 1, Heather Logan *Colloids and Surfaces B: Biointerfaces* 12 (1999) 139–146.

Polymer-Cooperative Blocking the Viruses – Strategy, Synthesis, and Effectiveness

Alexander V. Serbin1,2, Ekaterina N. Karaseva1,2, Olga L. Alikhanova1, Vladimir B. Tsvetkov1,2

1Biomodulators RC, Health RDF, Moscow, Russia
2Topchiev Institute of Petrochemical Synthesis, RAS, Moscow, Russia

e-mail: serbin@ips.ac.ru

The problem and objective

Polymeric macromolecules construct a fundament for all biologic systems: cell organisms, and cell parasites, including the viruses. But small molecules (**SM**) are incapable for adequate functionality, and SM drugs industry is covered by same objective law. SM cannot be effective blockers for many macromolecular targets, and blocking only sub-molecular small-scale sites fatally promote a drug resistance of mutated viruses. This fundamental course directs our efforts for systematic development of antiviral polymers (**AVP**).

Strategy

To achieve the maximal antiviral efficiency with lowest precondition for a drug resistance the polymer-cooperative approach was studied on base of controlled combining the variable polymeric backbone nature with various kinds of virus-targeting side vectors (**VTV**), designed on the principle: ***from virus bio-acceptors mimicry toward the anti-viral targeting***, for example:

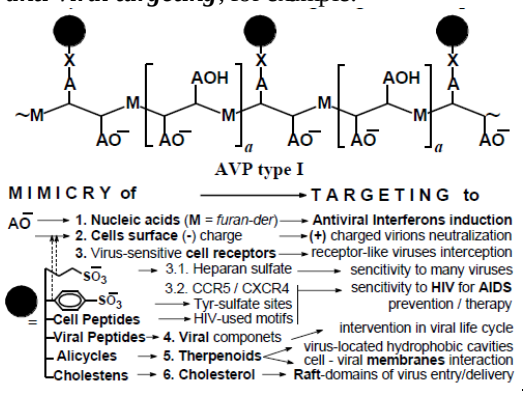

Synthesis

One of the most advanced approaches to the AVP is the tri-step scheme:

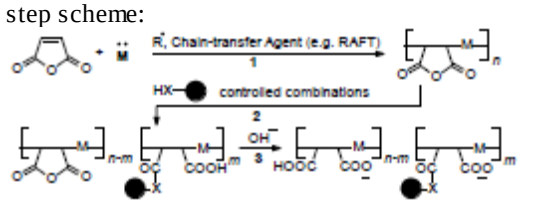

The **step 1** (free radical alternating copolymerization of maleic anhydride with suitable monomers) regulates the –M– nature, polymerization degree and polydispersity; the **step 2** allows to introduce the variable designated VTVs = in required combinations, and the **step 3** leads to the correspondent acid-anionic polyelectrolytes, biocompatible, soluble in aqua (bio) media, and maximally safe for toxicology criteria.

Antiviral Effectiveness

1. ***Imitation of nucleic acids (NA)*** by the AVP-acids leaded to NA-like induction of interferon and immune-stimulating preventive protection against lethal doses of viruses: *eastern equine encephalomyelitis-, tick-born encephalitis-, rabies-, Crimean hemorrhagic fever-, meningo-encephalomyelitis* etc. These effects were registered on immune competent experimental models (*in vivo*) [1], but not on cell cultures (*in vitro*).

2. ***Cell surface negative charge mimicry*** only via the slight anionic carboxy-acid manner resulted in slow-downing the electrostatic driven attachment to cells of viral particles, for example the HIV-1 virions, *in vitro*.

3. ***Virus sensitive cell receptors mimicry*** amplified this effect by imitation of strong anionic sulfo-acids, relative to heparan sulfate, the cellular receptor, used by many human viruses to entry into cells. Sulfated Tyr residues, take place also in chemokine receptors CCR5 / CXCR4 within the amino acid moieties used by HIV-1 (R5/R4 strains). The sulfated AVP blocked the viral entry in cells, evidently recorded as a dual protection against both human cytomegalo- and HIV-1 viruses [2]. The next generation of synthetic pseudo receptors was constructed as AVP modified by polypeptide fragments of the CCR5 or CXCR4, and the obtained substances possessed more strong protection *in vitro* against HIV- 1, including strains resistant to SM drug, AZT [3].

4. ***Viral components mimicry*** tested recently on an example of conjugates of AVP with 15-33 amino acid motifs of HIV-1 gag matrix (p17) protein, leaded to VTV interfering with the latest stage of HIV-1 reproduction, post-replication self-assembly of the viral particles [4]. And now this approach is under study.

5-6. ***Membrane tropic agents mimicry*** using variable alicyclic and cholesterol-related VTV. The AVP containing a cholesten anchor, targeted to the cholesterol-enriched "raft" domains of membranes (epicenters of virus entry - delivery risks), strongly inhibited HIV-1 and related strains replication *in vitro*.

The adamantane, norborna(e)n, and dinorbornen containing AVPs were effective against influenza (A,B) HIV-1/2, *herpesviridae*, and other viruses, including the SM drug (e.g. rimantadine) resistant strains [5]. To understand the polymer-cooperative effects a computational modeling-analysis was applied.

Conclusion

The polymer-cooperative strategy allows essentially amplify the antiviral effectiveness and to overcome / prevent the drug resistance of viruses.

References: ***1***. *Macromol Symp 2010,296:466;* ***2.*** *PMID 19227117, 19275050, 19441649 ;* ***3***.*Antivir Res 2004,62(2):18;* ***4***. *PMID 19459409;* ***5***.*10320046, 12803048, 12968467, 14598476, 15954475.*

Non-linear viscoelastic models for random coil polysaccharide solution rheology over a broad range of concentrations.

Wilco M.H. Verbeeten

Departamento de Ingeniería Civil, Área de Mecánica de los Medios Continuos y Teoría de Estructuras, Universidad de Burgos, C/ Villadiego s/n, E-09001 Burgos, Spain

wverbeeten@ubu.es

Introduction: The investigation deals with the modelling of the flow behaviour of aqueous random coil polysaccharide solutions using non-linear viscoelastic models. Up to date, most researchers and scientists use General Viscous Fluid models to describe the rheology of such biological macromolecular solutions, *e.g.* the Cross model. Although these types of models do an excellent job in modelling steady state simple shear viscosity, they are unable to describe the other three phenomena of viscoelasticity, *i.e.* time dependence, normal stresses in shear, and different behaviour in shear and elongation. Furthermore, these models are not able to describe satisfactorily the linear viscoelastic behaviour measured by dynamic oscillation experiments. Thus, when more complex flows have to be analyzed, *i.e.* flows where material elements experience various types of deformations in a transient sense rather than steady state, these General Viscous Fluid models do not suffice and more complex non-linear viscoelastic models are necessary.

Materials and Methods: A mastercurve can be constructed from experimental steady state shear data over a broad range of concentrations, from the dilute to the semi-dilute solution regime. Shift factors can be determined for the experimental data to transpose data and the linear relaxation spectrum to different concentrations, similar to the time-temperature-superposition. In the limit of small deformations, polymeric fluids show a linear viscoelastic response, which can be accurately described by a multi-mode Maxwell model. For larger strains, polymeric fluids show non-linear viscoelastic behavior, which is modeled by three non-linear viscoelastic models of the differential type: the Phan-Thien Tanner (PTT) model, the Giesekus model, and the eXtended Pom-Pom (XPP) model. The zero-shear viscosity as a function of the concentration can be described over the entire concentration range, both dilute and semi-dilute solution regimes, by a simple combination of two concentration dependent terms with different slopes. The concentration dependent term can now be divided into a part that corresponds to the relaxation time and to the plateau modulus.

Results and Discussion: The experimental linear viscoelastic and steady state shear data of various random coil polysaccharide solutions, *i.e.* polysaccharide guar galactomannan, aqueous phosphopolysaccharide "viilian" solution excreted by *Lactococcus lactis* subspecies *cremoris* SBT 0495, and aqueous *Propionibacterium acidi-propionici* polysaccharide solution, can be quantitatively predicted by the multimode Phan-Thien Tanner, Giesekus, and eXtended Pom-Pom non-linear viscoelastic models over a broad range of concentrations, from dilute to semi-dilute regimes, using a single set of parameters. Transient shear viscosity data is quantitatively and first normal stress coefficient is qualitatively predicted for a galactomannan guar solution.

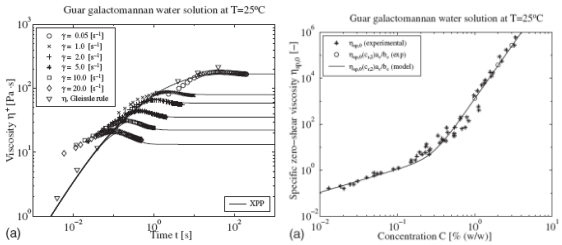

Figure 47: *Numerical and experimental data for a guar galactomannan solution in water at 25°C.*

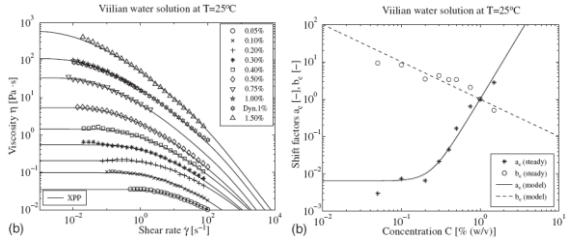

Figure 48: *Numerical and experimental data for a phosphopolysaccharide viilian solution in water at 25°C.*

Conclusions: Due to their proven performance in finite element simulations, these non-linear viscoelastic constitutive equations could help to improve predictive modelling of time-dependent complex flow problems for polysaccharide solutions. However, as a previous step, the performance of additional rheological experiments in simple flows, *i.e.* transient and steady-state extensional measurements, is recommended.

References:

1. Gorret, N., C. M. G. C. Renard, M. H. Famelart, J. L. Maubois, and J. L. Doublier, *Carbohydr. Polym.* 51, 149–158 (2003).
2. Oba, T., M. Higashimura, T. Iwasaki, A. M. Matser, P. A. M. Steeneken, G. W. Robijn, and J. Sikkema, *Carbohydr. Polym.* 39, 275–281 (1999).
3. Ren, Y., P. R. Ellis, I. W. Sutherland, and S. B. Ross-Murphy, *Carbohydr. Polym.* 52, 189–195 (2003).
4. Ren, Y., D. R. Picout, P. R. Ellis, and S. B. Ross-Murphy, Biomacromolecules 5, 2384–2391 (2004).
5. Richardson, R. K., and S. B. Ross-Murphy, *Int. J. Biol. Macromol.* 9, 250–256 (1987).
6. Robinson, G., S. B. Ross-Murphy, and E. R. Morris, *Carbohydr. Res.* 107, 17–32 (1982).
7. Tuinier, R., P. Zoon, M. A. Cohen Stuart, G. J. Fleer, and C. G. de Kruijf, *Biopolymers* 50, 641–646 (1999).
8. Verbeeten, W.M.H., *J. Rheol.* 54, 447-470 (2010).

Porous Protein based Scaffolds produced using a Freeze-Thawing Technique

Harald Kirsebom[1*], *Linda Elowsson*[1,2], *Madeleine Durbeej*[2] *Bo Mattiasson*[1]

[1] Department of Biotechnology, Lund University, Lund, Sweden
[2] Department of Experimental Medical Science, Unit of Muscle Biology, Lund University, Lund, Sweden

* Email: Harald.Kirsebom@biotek.lu.se

Introduction

Scaffolds which can sustain mammalian cell cultivation in a 3D environment are interesting for research and as potential material which can be implanted into patients. In this study cryogelation, e.g. freezing combined with chemical crosslinking, has been utilized to produce highly porous and permeable scaffolds from proteins. Cryogelation has previously been shown to be a suitable technique to produce highly porous protein-based materials either through chemical reactions or through non-covalent interactions[1, 2].

Using proteins for the preparation can raise the possibility of immunological responses if the material is implanted into a patient. In order to avoid this reaction one could use proteins from the patient to form an autologous scaffold. Blood or plasma is biological fluids which is generally present in large amounts from most patients. In this study blood or plasma of bovine origin were used as model systems in an attempt to fabricate autologous scaffolds[3].

Materials and Method

Scaffolds from blood or plasma were produced by diluting bovine blood or plasma with PBS buffer or water at a volume ratio 1:1. The mixtures were then kept on ice and subsequently glutaraldehyde was added to a final concentration of 0.25 % (w/v). Thereafter 0.5 ml aliquots of the mixture were frozen at -12 °C for 16 h. after which the samples were thawed at room temperature and washed with water before the samples were reduced using 0.05 M sodium borohydrid in carbonate buffer pH 9.2.

The mechanical properties of the produced materials were analyzed using unconfined compression and the elastic modulus was calculated in the linear range. The porous structure and the pore wall texture were analyzed using scanning electron microscopy after the samples had been critical point dried.

Prepared blood or plasma based scaffolds were then evaluated for biocompatibility through cultivation of myoblasts. Prepared scaffolds were cut into 1 mm disc and sterilized with iso-propanol and the washed with PBS. Prior to cell seeding the discs were equilibrated in cultivation media. For each disc $0.5x10^6$ myoblasts were seeded. The cells were grown in proliferation medium for three days after which the medium was changed to differentiation media. Cell viability was assayed using XTT and the myogenic phenotype of the cells was confirmed using immunofluorescence stainings.

Results and Discussion

Cryogelation of both diluted blood and plasma yielded highly porous and permeable materials. Freezing of blood or plasma mixtures causes the formation of ice crystals which expels any soluble or suspended material. Hence a two phase system is formed in which the solid ice phase acts as pore forming agent while a chemically stable crosslinked protein network is formed in the liquid water phase. Scaffolds from plasma were obtained both from dilution of water or PBS while for blood only PBS was possible to use. Diluting blood with water will change the osmolarity and thus cause lysis among the red blood cells. Undiluted blood or plasma was not possible to use since the high protein content resulted in fast gelation after glutaraldehyde were added. In order to form a interconnected and porous material, gelation must occur after freezing[4] and thus blood and plasma had to be diluted.

Both plasma and blood scaffolds exhibited pores in the range 10-80 µm which were studied using SEM. The pore walls of the plasma-based scaffolds exhibited a smooth texture while the blood-based material was highly uneven due to the red blood cells (Figure 1).

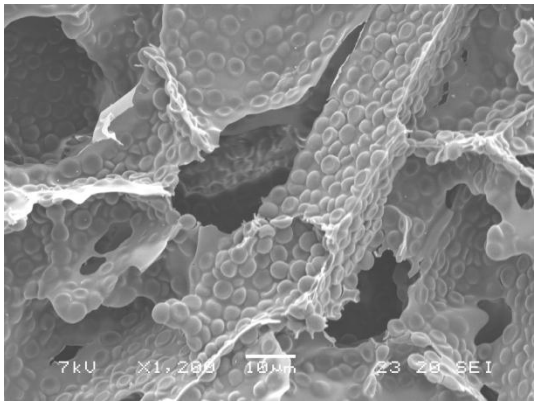

Figure 1: Scanning electron micrograph of a scaffold produced through cryostructuration of bovine blood. The intact red blood cells are clearly shown to be embedded into the pore walls.

The plasma and blood based scaffolds were shown to support cell attachment and proliferation and cell numbers increased during cultivation in proliferation medium. Furthermore, the immunofluorescense stainings confirmed that the cells maintained their myogenic phenotype during the whole cultivation time.

References:

[1] M. B. Dainiak et al., *Biomaterials* **2010**, *31*, 67-76.
[2] N. R. Konstantinova et al., *Food Hydrocolloids* **1997**, *11*, 113-123.
[3] L. Elowsson et al. *Tissue Engineering*, Submitted
[4] F. Plieva et al., *J. Mat. Chem.* **2006**, *16*, 4065-4073.

Galactomannan in Imidazolium-Based Ionic Liquids

E. Sultan, A. Bussard, E. Fleury and A. Charlot

Université de Lyon, INSA de Lyon, CNRS, France

aurelia.charlot@insa-lyon.fr

Introduction- The development of polysaccharide-based materials has attracted considerable attention due to their various properties in addition to their renewable character. In this frame, guar gum is a relevant building-block since it combines an easy availability, a low cost, biodegradability, hydrophilicity and viscoelasticity. Guar is a neutral polysaccharide extracted from the seeds of *Cyamopsis tetragonoloba*. Belonging to the galactomannan family, it is constituted of a β-1,4 mannose backbone with randomly distributed α-1,6 galactose moieties (Fig. 1).

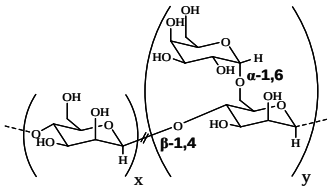

Figure 1. Chemical structure of guar

It is widely used in the food, paper, textile, petroleum, personal care and biomaterial industries. Various synthetic methods can be applied to guar chemical modifications [1] to obtain attractive materials. However, guar is difficult to be solubilised in common solvents due to the existence of strong hydrogen bonds. The use of organic solvents at high temperature leads to guar chain degradation. The solubilisation in aqueous medium generates suspensions of swollen guar particles and no homogeneous solutions (Fig. 2). Thus, there is a strong need to find eco-friendly and efficient solvents to expand the applications of guar. In this context, ionic liquids (IL), a group of salts liquid at low temperature, appear as promising "green" solvents [2] due to their high chemical and thermal stability, non flammability, negligible vapor pressure, as well as their good dissolution capability of sugar.[3] In this work, we investigated the ability of different imidazolium-based IL derivatives to solubilise guar gum with in particular a rheological analysis. Moreover, we illustrated the potential of IL as reactional medium to perform homogeneous guar chemical modifications such as esterification and copper-catalyzed azide-alkyne cycloaddition (CuAAc).

Material and Methods -Guar gums were provided by Rhodia (mannose/galactose = 1.3). EMIMAc, AMIMCl (Aldrich) and EMIMMP (Solvionic) were dried before chemical reactions. Other reagents were performed from Aldrich and used as received. The dissolution of guar in IL was performed under N_2, during 16 h at 50°C under stirring. The guar-based hydrogels by CuAAc in EMIMAc were performed as previously described in water.[1(b)] The viscosity of guar solutions in IL as well as the gelation process were analysed with a AR1000 controlled stress rheometer by using an aluminum cone/plate geometry (diameter 60 mm, angle 2°). Esterification reactions with maleic anhydride, acetic anhydride, butyric anhydride were performed under N_2, at 50°C during 4h by using 5 molar eq. between esterifying reagent and AGU unit. The products were isolated by precipitation into isopropyl alcohol and characterized by IR and by NMR spectroscopy.

Results and Discussion- We have shown the ability of various hydrophilic imidazolium derivatives with low melting points such as 1-ethyl-3-methylimidazolium methyl phosphonate (EMIMMP), 1-allyl-3-methylimidazolium chloride (AMIMCl) and 1-ethyl-3-methylimidazolium acetate (EMIMAc) to act as good solvents for guar (M_w = 50-300 kDa) without any chain degradation (Fig. 2).

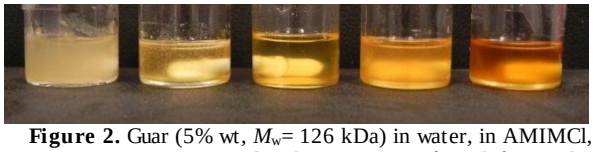

Figure 2. Guar (5% wt, M_w= 126 kDa) in water, in AMIMCl, in EMIMMP, in BMIMCl and in EMIMAc (from left to right)

The rheological properties of guar in IL and in particular the influence of temperature allowed us to determine activation energies (Arrhenius law). The high values obtained for guar/IL solutions compared to water "suspension" reflect strong physical LI/guar and guar/guar interactions. The results also demonstrated that interactions are closely dependant on the IL chemical structure (Table 1).

sample	EMIMAc	Guar in EMIMAc	EMIMMP	Guar in EMIMMP
Ea (kJ/mol)	37	43.9	31.7	42.6
sample	AMIMCl	Guar in AMIMCl	Guar in water	
Ea (kJ/mol)	61.4	64.5	10.1	

Table 1. *Activation energies for pure IL and guar dissolved (5% wt-M_w = 126 kDa) in different IL compared to dispersion in water*

Besides, we evidenced that both AMIMCl and EMIMMP constitute suitable medium to obtain homogeneously esterified guar derivatives, not described in the literature before. Also, we successfully performed CuAAc coupling in EMIMAc between diazido crosslinker and alkyne fonctionalized guar to obtain chemical networks and we have shown that the gelation process as well as the elasticity differ from those obtained in water.[1(b)]

Conclusion- Taking advantage of the efficiency of hydrophilic imidazolium-based IL to solubilise guar, we obtained attractive rheological properties and we prepared a range of homogeneously modified guar derivatives with no noticeable chain degradation.

References- 1. (a) Tizzotti, M.; Labeau, M-P. ; Hamaide, T. ; Drockenmuller, E. ; Charlot, A. ; Fleury, E, J Polym Sci Part A Polym Chem , 2010, 48, 2733. (b) Tizzotti, M.; Creuzet, C. Labeau, M-P. ; Hamaide, T. ; Boisson, F. ; Drockenmuller, E. ; Charlot, A. ; Fleury, E. Macromolecules, 2010, 43, 6843. **2**. Wilkes, J.S. Green Chemistry, 2002, 4, 73

Hierarchically self-organized PS-*b*-P4VP Honeycomb films with reversible pH-responsive wettability

P. Escale, M. Save, C. Derail, L. Rubatat and L. Billon

IPREM / EPCP, UMR 5254, Université de Pau et des Pays de l'Adour, FRANCE

laurent.billon@univ-pau.fr

Self-organized porous polymer films with pores ordered into a hexagonal pattern can be elaborated by a fast evaporation method under humid atmosphere, also called "Breath Figure" approach. [1] Honeycomb (HC) films have been fabricated from a variety of polymers using the appropriate experimental conditions for each class of polymer. [2-4] The elaboration of smart honeycomb surface with thermo or pH-responsive wettability has been proposed using poly(*N*-isopropyl acrylamide) or PS-*b*-PAA based copolymers [5-6]. In these previous studies, no reversibility of the wettability was shown.

Moreover, self-assembly of diblock copolymers are able to create a nanophase separation within the walls of the honeycomb films, which was observed by microscopy techniques and/or small angle neutron scattering.[7,8] One of the advantage of nanophase separation is that the first block confers the sufficient hydrophobicity required for the elaboration and stability of HC structure whereas the second block can provide an additional functional property.

Here, we aim to elaborate hierarchically ordered porous film from a pH-sensitive diblock copolymer able to create an inner nanostructuration while tuning the surface wettability. We report the self-assembly of well-defined high molar mass polystyrene-*b*-poly(4-vinyl pyridine) diblock copolymer (PS-*b*-P4VP), synthesized by nitroxide-mediated polymerization (NMP), into honeycomb-structured porous film prepared by simple evaporation method under humid conditions (Figure 1).

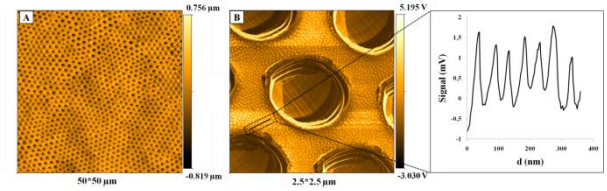

Figure 1. AFM phase images (**A** and **B**) of PS-*b*-P4VP honeycomb recorded at different scales and **(C)** variation of the signal intensity versus the distance for a cross-section of 400 nm.

Then, these films are peeled-off in order to form pincushion structures. The wettability and the impact of the pH-responsive behavior are studied by measuring the contact angle for the two honeycomb and pincushion films (Figure 2)

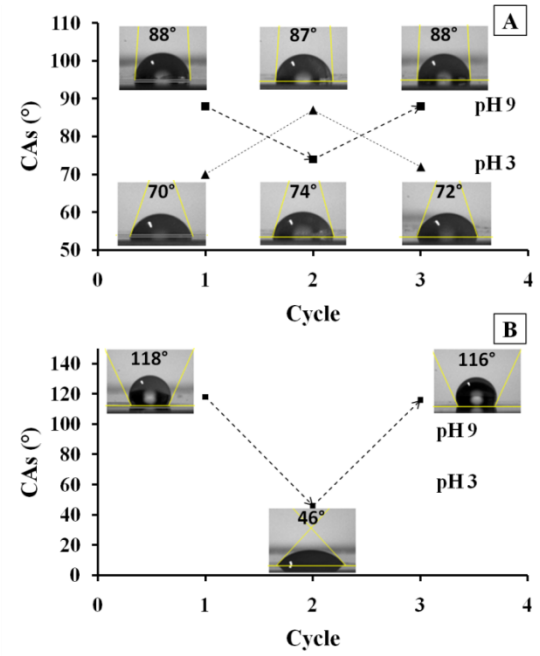

Figure 2. Reversibility of contact angles of a water droplet deposited onto **(A)** PS-*b*-P4VP honeycomb film and **(B)** peeled off PS-*b*-P4VP HC film.

First, an increase of the hydrophobicity is demonstrated when pH is tuned in a large range of values for hierarchically structured honeycomb films. The same behavior can be described with a stronger exaltation of the hydrophobicity when honeycomb films are peeled-off due to the presence of pillars which increase the roughness of the films.

1. Widawski, G.; Rawiso, M.; Francois, B. *Nature* **1994,** 369, (6479), 387-389.
2. Billon, L.; Manguian, M.; Pellerin, V.; Joubert, M.; Eterradossi, O.; Garay, H. *Macromolecules* **2009,** 42, (1), 345-356.
3. Ghannam, L.; Manguian, M.; Francois, J.; Billon, L. *Soft Matter* **2007,** 3, (12), 1492-1499.
4. Ting, S. R. S.; Min, E. H.; Escale, P.; Save, M.; Billon, L.; Stenzel, M. H. *Macromolecules* **2009,** 42, (24), 9422-9434.
5. Min, E.H.; Ting, S.R.S.; Billon, L.; Stenzel M.H. *Journal of Polymer Science Part A.* Chemistry **2010**, *48,* 3440-3446.
6. Yabu, H.; Hirai, Y.; Kojima, M.; Shimomura, M. *Chemistry of Materials* **2009,** 21, (9), 1787-1789.
7. Escale, P.; Save, M.; Lapp, A.; Rubatat, L.; Billon, L. *Soft Matter* **2010,** 6, (14), 3202-3210.
8. Hayakawa, T.; Horiuchi, S. *Angewandte Chemie-International Edition* **2003,** 42, (20), 2285-2289

Lipase Catalyzed Synthesis of Biopolyester and Related Clay-based Nanohybrids

H. Öztürk Düşkünkorur[1,2], E. Pollet[1], P. Debeire[1], V. Phalip[1], L. Avérous[1]

[1] Université de Strasbourg, France; [2] Istanbul Technical University, Turkey

eric.pollet@unistra.fr

Introduction: Enzymatic ring opening polymerization (ROP) of lactones attracts attention as a new trend of biodegradable polyesters synthesis due to its non-toxicity, mild reaction requirement and recyclability of immobilized enzyme [1]. Beside the enzyme-catalyzed synthesis of biopolyesters, key researches are conducted nowadays on the elaboration of composites materials in combination with inorganic (nano)particles. Thus far, the majority of enzymes studied for polyester synthesis have been from the lipase family. Among these lipases, lipase B from Candida Antarctica (CALB) has proven to be a dominant catalyst for these reactions [2]. In parallel, the use of clays as inorganic porous supports to immobilize enzymes has also been described. Interestingly, the use of such nanoclays as lipase carriers can bring numerous advantages such as the high specific surface availability, the high water uptake capacity, and the excellent mechanical resistance of these materials [3]. The objectives of this study is to develop original catalytic systems based on lipases which are efficient for polyester synthesis and allowing the preparation of hybrid materials based on clay nanoparticles grafted with such polyesters.

Materials & Methods: For this, ε-caprolactone (ε-CL) polymerization catalyzed by CALB was carried out in the presence of montmorillonite and sepiolite clay.
The unmodified and organo-modified forms of these two nanoclays were also used to physically adsorb CALB. The obtained catalytic systems have been tested and their efficiency has been compared. The polymerization kinetics and resulting products were characterized with NMR, SEC, DSC and TGA analyses.

Results & Discussion: Monitoring the monomer conversion and PCL molecular weight versus time shows that the presence of nanoclays does not change the reaction kinetic, the monomer conversion being higher than 90% within 2 hours. However, the addition of clay leads to lower Mn values.

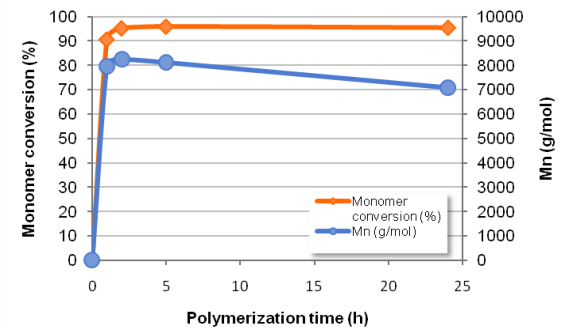

Such decrease in molecular weight depends on the added amount of montmorillonite and attests for the participation of clay hydroxyl groups in the polymerization. Analyses showed that organic/inorganic nanohybrids were obtained through polymer chains grafting and growth from the hydroxyl groups of the clay. Indeed, TGA analyses of the isolated clay fraction evidenced the presence of grafted PCL chains.

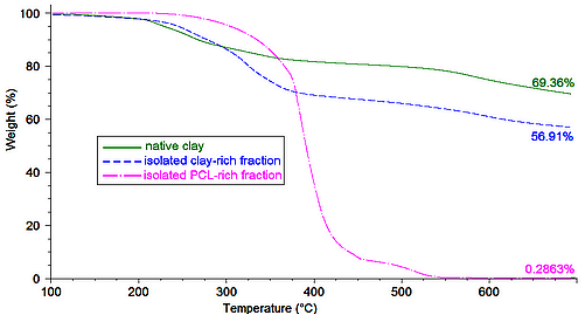

Both montmorillonite and sepiolite nanoclays were also used as carriers for CALB immobilisation. Interestingly, activity tests showed that organo-modification of the clay surface allowed to improve lipase immobilization leading to catalytic systems with higher activity.

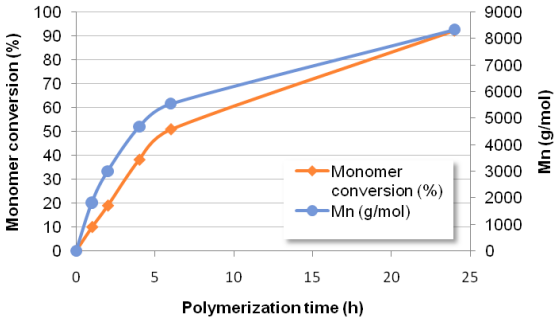

Nevertheless, polymerization kinetic was slower for nanoclay-immobilized lipases compared to commercial catalytic system.

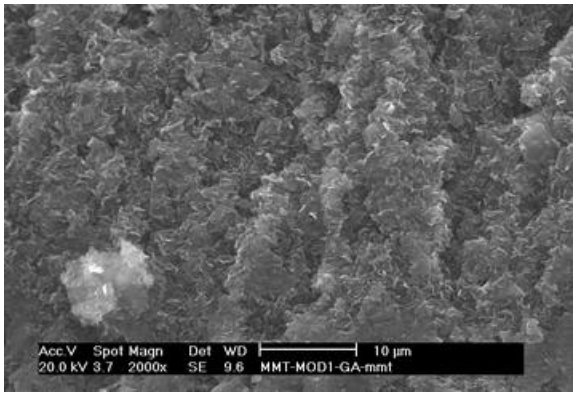

References:

1. A.C. Albertsson; R.K. Srivastava Adv. Drug. Deliv. Rev. 2008, 60, 1077.
2. Y. Mei; A. Kumar; R. Gross Macromolecules. 2003, 36, 5530.
3. I.E. Fuentes; C.A. Viseras; D. Ubiali; M.Terreni; A.R. Alcantara J. Mol. Catal. B: Enzym. 2001, 11, 657.

Intelligence polymers Behavior and Its Application Idea in Treatment of Some Diseases of Central Nervous System

Mohammad Abolhassani[1], *Amirhossein Yavari*[2], *Pegah Abolhassani*[3], *Somayeh Shouli*[4]

1. (Researcher of Polymer Department of Ariya pazhohesh Alpha Co –Ahwaz- iran.& Student MA Polymer Department of Mahshar University)
2. (Clinical Psychologist. Clinical Psychology Department of Shiraz University - Iran)
3. (Researcher of Polymer Department of Ariya pazhohesh Alpha Co & linguist)
4. (Industrial & Organizational Psychologist. Psychology Department of Shahid Chamraran University of Ahvaz - Iran)

1. Mohammad.abolhassani@gmail.com

Abstract

Intelligent polymers are pure or composed material will origin intelligence and self-comparative specialty against all instigations. Shape memory polymers are kind of intelligent materials which are reverse able to the origin shape. Instigators are controllable tools for productive work which tempretural, electronic and magnetic instigator is input and strain and mechanical work is output. According to development of intelligent polymer application, scientists newly use intelligent polymers for produce instigators. Instigators are tools which under influence of instigation get involved in strain. In fact instigators in responding to order or control signs work out. The amount of works which instigators do and the used energy are extremely depends on the way instigation. Hydro gels are kind of intelligent polymers; they have various applications in medicine. The most specialties are: hyrophilically, water absorption and softness which really similar to live weave. Natural hydro gels (collagen, alginate, and fibrin) shows good biomaterial. A crucial point is to make sure of being no non- reacted monomers in the system before apply. Hydro gel behaves both in solid and liquid. This specialty caused classification to 2 parts which is base on side gropes: neutral and ionic. According to physical and structural properties they can be divided to continuous polymer network and phantom. They also can be homo polymer or copolymer networks. In addition they can be classified non-shaped, half crystal, hydrogen bond structure, super molecule structure and association of colloid networks (hydro gel may have shown swelling behavior depend on media). The polymers are physiological responder hydro gels. In last 3 decades, scientists paid more attention to analysis and development in hydro gels responding to the physiological media. Responding to media due to the changes in pH, temperature, ionic power nature and combination of swelling elements shows different enzyme or chemical reaction. Mostly responding networks has critical point which usually transfer happens there. This hydro gel is unique because of different mechanism for drug blocking and other system. Another rare specialty for responding gels is the reversibility of polymer networks which have been changed. In this research we worked on analysis and development of this substructure mechanism of artificial nervous. According to achievements in this filed we can claim to find certain cure of demyelination and degeneration diseases of CNS, like MS and ALS and another diseases of CNS, like Alzheimer and dementia.

Hydrogels Based on Poly(vinyl alcohol)/Phosphoester and Poly(ethylene glycol)/Phosphoester for Biomedical Applications

Tăchiţă Vlad-Bubulac, Ana-Maria Oprea, Diana Serbezeanu, Corneliu Hamciuc

"Petru Poni" Institute of Macromolecular Chemistry, Aleea Gr. Ghica Voda 41A, Iasi-700487, Romania
e-mail: tvladb@yahoo.com

Introduction: Biodegradable polymers have attracted considerable attention in the very recent years. Their potential applications in biomedical and ecological fields have been generated a great deal of effort in developing new polymeric structures with a biodegradable backbone, having excellent combined properties such as biocompatibility, antifouling properties, tunable mechanical properties, no toxicity, potential functional versatility which allows introduction of bioactive molecules and extensive modification of the physical, chemical and biological properties etc. [1–3]. Actually, the development of novel, stable and economical advanced drug delivery formulations based on hydrogels, which are well known to reduce the problems of conventional dosage forms, is an important topic in the field of biomaterials science [4]. The present work focuses on the synthesis and characterization of new polymers with phosphoester functions obtained by polycondensation reaction of poly(vinyl alcohol) (PVA) or poly(ethylene glycol) with different phosphonic dichlorides. These compounds were used to prepare hydrogels for biomedical applications.

Materials and Metods:

Starting materials (poly(vinyl alcohol) of variable molecular mases, poly(ethylene glycol) 1000, phosphonic dichlorides, chondroitin sulphate (CS), epichlorohydrin, metoprolol) were purchased from commercial sources and were used as received.

Results and Discussion:

In the first step, the phosphorylated materials, poly(vinyl alcohol)/ phosphoesters and poly(ethylene glycol)/phosphoesters were synthesized by polycondensation reaction using dimethylformamide as solvent (scheme 1). The products were reacted with chondroitin sulphate and then crosslinked with epyclorohydrin. Basic structural characterization was performed and specific investigations for hydrogels were conducted.

Swelling studies were performed for all formulations and carried out by direct immersion in phosphate buffer solution (pH=7.4). The hydrogels samples were maintained for 24 hours at 37 ^{0}C, periodically removed from the solution, gently wiped with a soft tissue to remove surface solution, weighed and than placed back into the vessel as quickly as possible. The swelling degree at equilibrium was calculated according to the equation:

$$Qmax\ (\%) = (Wt - Wd)/Wd\ 100.$$

To determine the kinetics of solvent diffusion into the matrices (swelling) the following equation was used:

$$F_t = \frac{W_t}{W_{eq}} = k_{sw} t^{n_{sw}}$$

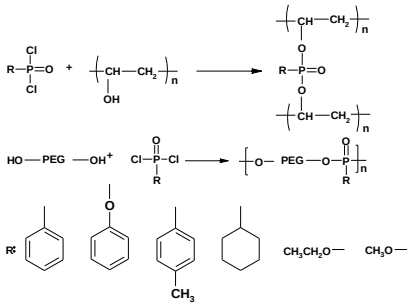

The drug loading method was performed by soaking or equilibration of superporous hydrogels samples in phosphate buffer solution (pH=7.4) with metoprolol tartrat for their complete swelling. The dissolution medium was pH 7.4 phosphate buffer solution. During dissolution testing, the media was maintained at 37 ± 0.5 ^{0}C. The concentrations of the drugs were calculated based on calibration curves determined for drug at specific maximum absorption wavelengths.

The in vitro release of metoprolol from PVA-P-CS hydrogels was carried out in intestinal pH conditions at 37 ^{0}C. The percent released is higher in case of hydrogels with an increased CS content, dependence between percent drug released and hydrogel compositions being seen. The highest cumulative metoprolol release obtained at the end of releasing period (6 hours) was 36% for 50/50 APV-P-CS composition.

Conclusion:

The PVA-P-CS hydrogels, crosslinked by epychlorohydrin provide advantages of all the components, PVA, phosphoester and CS moieties and they have potential use in controlled drug release.

Acknowledgements:

This research was financially suported by:

1. FP7 Grant Agreement N^o 264115 – STREAM (CSA – SA_FP7-REGPOT-2010-1).

2.European Social Fund – „Cristofor I. Simionescu" Postdoctoral Fellowship Programme (ID POSDRU/89/1.5/S/55216), Sectoral Operational Programme Human Resources Development 2007 – 2013.

References:

[1] Rapoport N. Progr Polym Sci 2007, 32, 962–990.

[2] Strehin I., Nahas Z., Arora K., Nguyen T., Elisseeff J. Biomaterials 2010, 31, 2788–2797.

[3] Fischbach C., Mooney D. J. Adv Polym Sci 2006, 203, 191–221.

[4] Amin S., Rajabnezhad S., Kohli K. Science Research and Essay 2009, 3, 1175–1183.

The Missing Lactam – Thermoresponsive Poly(*N*-vinylpiperidone)

Dr. Cecilia Ieong[1], *Dr. Rachel K. O'Reilly*[1]

University of Warwick[1]

n.s.ieong@warwick.ac.uk

In recent years, there has been significant interest in the development of stimuli-responsive materials as they have shown great promise in various biomedical applications.[1] In particular, temperature-responsive polymers (materials which undergo phase changes in response to a temperature trigger) have gained much current attention.

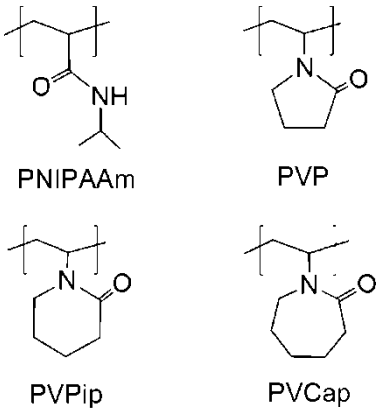

The discovery of poly(*N*-isopropylacrylamide) (PNIPAAm) as a thermoresponsive polymer in the 1950s has sparked interest in search for new classes of these 'smart' materials.[2] Amongst the numerous types of thermosensitive polymers, PEG-based polymers[3] and polyamides (such as poly(2-oxazoline)s[4], poly(*N*-vinylpyrrolidone) (PVP) and poly(*N*-vinylcaprolactam) (PVCap)[5,6] have been the most extensively studied. In particular, PVCap has received much attention due to its biocompatibility.[7] Despite the vast amount of scientific literature on the polymerization and the thermoresponsive behaviour of the 5- and the 7-membered ring poly(*N*-vinyllactam)s, there has been very little work on the 6-membered ring analogue.

In this talk, we will present a new type of thermoresponsive polymer, poly(*N*-vinylpiperidone) (PVPip) prepared by reversible-addition fragmentation chain-transfer (RAFT) polymerization using a xanthate as a chain-transfer agent.[8] All these polymers exhibited sharp and molecular-weight-dependent cloud points (CPs) with no apparent hysteresis. These water-soluble PVPip homopolymers could also be chain-extended with a hydrophobic monomer to afforded well-defined amphiphilic, thermosensitive diblock copolymers. The self-assembly and tunable thermoresponsive behaviour of these block copolymers will also be discussed.

The excellent thermoresponsive behaviour together with the promising cytotoxicity studies of the new materials demonstrated that these polymers possessed huge potential as novel biomaterials. More importantly, the possibility of incorporating PVPip into the existing family of thermosensitive materials, *e.g.* by copolymerization, suggested that the significance of this work might be much more far-reaching.

References

[1](a) Gil, E. S.; Hudson, S. M. *Prog. Polym. Sci.* 2004, *29*, 1173; (b) Schmaljohann, D. *Adv. Drug Delivery Rev.* **2006**, *58*, 1655. (c) Bajpai, A. K.; Shukla, S. K.; Bhanu, S.; Kankane, S. *Prog. Polym. Sci* **2008**, *33*, 1088. (d) Onaca, O.; Enea, R.; Hughes, D. W.; Meier, W. *Macromol. Biosci* **2009**, *9*, 129; (e) Kikuchi, A.; Okano, T. *Prog. Polym. Sci.* **2002**, *27*, 1165; (f) Chan, G.; Mooney, D. J. *Trends Biotechnol.* **2008**, *26*, 382.

[2]Schild, H.G. *Prog. Polym. Sci.* **1992**, *17*,163–249.

[3]Lutz, J.-F.; Andrieu, J.; Üzgün, S.; Rudolph, C.; Agarwal, S. *Macromolecules* **2007**, *40*, 8540-8543.

[4]Hoogenboom, R.; Thijs, H. M. L.; Jochems, M. J. H. C.; van Lankvelt, B. M.; Fijten, M. W. M.; Schubert, U. S. *Chem. Commun.* **2008**, 5758-5760.

[5]Shtanko, N. I.; Lequieu, W.; Goethals, E. J.; Du Prez, F. E. *Polym. Int.* 2003, 52, 1605-1610.

[6]Maeda, Y.; Nakamura, T.; Ikeda, I., *Macromolecules* **2002**, *35*, 217-222.

[7]Prabaharan, M.; Grailer, J. J.; Steeber, D. A.; Gong, S. *Macromol. Biosci.* **2009**, *9*, 744-753.

[8]Stenzel, M. H.; Davis, T. P.; Barner-Kowollik, C. *Chem. Commun.* **2004**, 1546-1547.

Polysaccharide capsules with engineered hydrophobic drug-loaded multilayers

Jing Jing[a], *Di Cui*[a], *Isabelle Pignot-Paintrand*[a], *Bruno De Geest*[b], *Catherine Picart*[c] *and* *Rachel Auzély-Velty*[a]

[a]Centre de Recherches sur les Macromolécules Végétales (CERMAV-CNRS), affiliated with Université Joseph Fourier, BP53, 38041 Grenoble cedex 9, France

[b]Laboratory of Pharmaceutical Technology, Department of Pharmaceutics, Ghent University, Harelbekestraat 72, 9000 Ghent, Belgium

[c]Minatec, Grenoble Institute of Technology, LMGP, CNRS, 3 parvis Louis Néel, 38016 Grenoble, France

e-mail : rachel.auzely@cermav.cnrs.fr

Introduction

Administration of drugs is often limited by problems of insolubility, inefficient distribution, enzyme hydrolysis, lack of selectivity and side-effects raising health concerns. Hollow capsules prepared by the layer-by-layer assembly of oppositely charged polyelectrolytes on a colloidal template, following by its decomposition, have recently emerged as attractive vehicles in the field of drug delivery.[1] For drug delivery applications, a prerequisite is to use biocompatible and biodegradable polyelectrolytes for the construction of the shell.[2,3] In this context, we proposed to develop tailor-made capsules from biocompatible and biodegradable polysaccharides able to entrap hydrophilic and hydrophobic drug molecules in the aqueous core and in the wall, respectively. In this presentation, we will describe an original approach to prepare in mild conditions polysaccharide capsules able to encapsulate poorly water-soluble molecules in the multilayer shell.

Materials and Methods

Materials. Chitosan Protasan with a degree of *N*-acetylation (DA) of 0.09 and a molar mass of M_w of 372000 g/mol was kindly provided by FMC BioPolymer AS, Novamatrix (Norway). Hyaluronic acid under the sodium salt form, having a molar mass of M_w of 200000 g/mol, was purchased from MEDIPOL Distribution (Switzerland). All other chemicals were purchased from Sigma-Aldrich-Fluka. The quaternized derivatives of chitosan were prepared according to literature procedures.[4,5] The alkylated derivatives of hyaluronic acid were synthesized as previously described.[6]

Polysaccharide capsules preparation. Microcapsules were prepared using calcium carbonate particles as a sacrificial template according to a procedure described previously. Incorporation of the hydrophobic molecules was performed by their pre-complexation with hydrophobically modified HA.

Results and Discussion

For the synthesis of tailor-made capsules, we selected hyaluronic acid (HA) as the anionic polyelectrolyte, due to its unique physico-chemical and biological properties that make it a particularly interesting candidate for the development of novel biomaterials for biomedical applications. In spite of its highly hydrated nature and weak polyacid character, we established the feasibility to obtain capsules consisting of HA and poly(allylamine).[2] As our goal was to obtain fully biodegradable capsules, we replaced PAH by biocompatible and biodegradable biopolymers that can form polyelectrolyte complexes with HA. We successfully prepared capsules based on HA and poly(L-lysine) (PLL) as polypeptide but shell cross-linking was required to improve capsule stability.[3] Interestingly, by replacing PLL by quaternized chitosan derivatives (QCHI), stable capsules could be obtained without cross-linking the shell,[7] which has the advantage of avoiding side reactions that may occur with the encapsulated drugs during the cross-linking reaction.

Based on these results and our previous work showing the very high affinity of hydrophobic molecules for the hydrophobic nanodomains formed by alkylated derivatives of HA in aqueous solution or in multilayer films[6], we then investigated the preparation of capsules able to entrap poorly water-soluble molecules in the polyelectrolyte shell. The LbL assembly of hydrophobically modified HA and QCHI on calcium carbonate particles followed by core decomposition afforded stable capsules. As expected shell loading with hydrophobic molecules pre-complexed with hydrophobically modified HA could be achieved making these capsules promising candidates for the solubilisation and delivery of hydrophobic drugs.

Conclusion

In summary, the present work establishes for the first time the feasibility of hydrophobic shell loading of polysaccharide capsules. The unique physico-chemical and biological properties of the polysaccharides used for the shell construction, and the close control over shell drug loading makes these capsules versatile candidates as carriers for hydrophobic drugs.

References

[1] B. G. De Geest, S. De Koker, G. B. Sukhorukov, O. Kreft, W. J. Parak, A. G. Skirtach, J. Demeester, S. C. De Smedt, W. E. Hennink, *Soft Matter* (2009), *5*, 282.

[2] A. Szarpak, I. Pignot-Paintrand, C. Nicolas, C. Picart, R. Auzély-Velty, *Langmuir* (2008), *24*, 9767.

[3] A. Szarpak, D. Cui, F. Dubreuil, B. G. De Geest, L. J. De Cock, C. Picart, R. Auzély-Velty, *Biomacromolecules* (2010), *11*, 713.

[4] J. Cho, J. Grant, M. Piquette-Miller, C. Allen, *Biomacromolecules* (2006), *7*, 2845.

[5] S.-H. Lim, S. M. Hudson, *Carbohydr. Res*. (2004), *339*, 313.

[6] S. Kadi, D. Cui, E. Bayma, T. Boudou, C. Nicolas, K. Glinel, C. Picart, R. Auzély-Velty, *Biomacromolecules* (2009), *10*, 2875.

[7] D. Cui , A. Szarpak, I. Pignot-Paintrand, A. Varrot, T. Boudou, C. Detrembleur, C. Jérôme , C. Picart, R. Auzély-Velty, *Adv. Funct. Mater* (2010), *20*, 3303.

Non-monotonic variation of polymer size with increasing confinement

Debasish Chaudhuri and Bela Mulder

Affiliations: FOM Institute AMOLF

e-mail: chaudhuri@amolf.nl

Abstract:

A number of recent experiments have provided detailed observations of the configurations of long DNA strands under nano-to-micrometer sized confinement.
We therefore will revisit the problem of an excluded volume polymer chain confined between two parallel plates with varying plate separation. We'll show that the non-monotonic behavior of the overall size of the chain as a function of plate-separation, seen in computer simulations and reproduced by earlier theories, can already be predicted on the basis of scaling arguments. However, the behavior of the size in a plane parallel to the plates, a quantity observed in recent experiments, is predicted to be monotonic, in contrast to the experimental findings.

We analyze this problem in depth with a mean-field approach that maps the confined polymer onto an anisotropic Gaussian chain, which allows the size of the polymer to be determined separately in the confined and unconfined directions. The theory allows the analytical construction of a smooth cross-over between the small plate-separation de Gennes regime and the large plate-separation Flory regime. The results show good agreement with molecular dynamics simulations in presence of Langevin heat bath, and confirm the scaling predictions.
We will also show a direct comparison between our simulations and two recent experiments on confined DNA measuring the projected radius of gyration as a function of inter-plate separation.

Poloxamines for injectable scaffolds with osteogenic activity

Carmen Alvarez-Lorenzo[1], *Ana Rey-Rico*[1], *Maite Silva*[2], *José Couceiro*[2], *Angel Concheiro*[1]

[1]Departamento de Farmacia y Tecnología Farmacéutica, Facultad de Farmacia. [2]Instituto de Ortopedia y Banco de Tejidos Musculoesqueléticos. Universidad de Santiago de Compostela, 15782-Santiago de Compostela, Spain

e-mail: carmen.alvarez.lorenzo@gmail.com

Introduction

Current research on bone regeneration tries to optimize the healing while making the treatment more economically affordable and patient-friendly (injectable scaffolds). Small polyamines, such as spermidine, spermine, ornitine and putrescine, have appeared as an alternative to the expensive recombinant growth factors for inducing the differentiation of mesenchymal stem cells into osteoblasts (1). The aim of this work was to explore the potential of poloxamine block copolymers (Tetronic®) for combining the osteoinductive capability of amine-bearing synthetic molecules with the administration by minimally invasive techniques. These X-shaped copolymers bear four PEO-PPO arms connected to a central ethylenediamine group (Figure 1) and exhibit self-aggregation and in situ gelling under physiological conditions (2). Cytocompatibility, sol-to-gel transitions and osteogenic activity tests were carried out with three poloxamines and the results compared to those obtained in the presence of rhBMP-2.

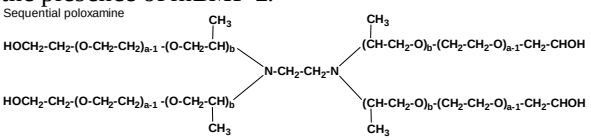

Figure 1. Poloxamines T908 (a=454.5; b=86.2), T1107 (a=238.6; b=77.6) and T1307 (a=286.4; b=93.1).

Materials and Methods

Osteoblast viability. SAOS-2 cells (HTB-85, ATCC) were cultured in D-MEM with 10% w/v FBS. 200,000 cells/well (1.5 ml) were seeded in 24-well plate and 0.5 ml polymer solution (20% w/w) was added. The plates were incubated at 37ºC for 72 hours and a calcein/propidium iodide staining was carried out.

Oscillatory rheology. The storage (G´) and the loss (G´´) moduli of 20% w/w poloxamine solutions in phosphate buffer pH 7.4 and D-MEM were evaluated before and after being autoclaved (121ºC, 20 min), using a Rheolyst AR-1000N rheometer at 5 rad/s from 15ºC to 45ºC with a heating rate of 2ºC/min (cone 6 cm diameter and 2.1 degrees; TA Instruments, UK).

ALP assay and histochemical analyses. Mesenchymal stem cells (StemPRO®, Invitrogen, Spain) were cultured in MesenPRO RSTM medium (Gibco, Invitrogen, Spain) and seeded ($3 \cdot 10^4$ cells/well, 2.5 ml) in 6-well plates. 200 µL of copolymer dispersions (20% w/w) containing or not rhBMP-2 (0.037 mg/ml) were placed into the upper compartment of 6-well plate Transwell® permeable supports. The amounts of copolymer and rhBMP-2 into each well were 40 mg and 7.4 µg, respectively. Negative and positive controls were carried out with cells in culture medium and in osteogenic differentiation medium, respectively. Plates were incubated at 37 ºC with 5% CO_2. To carry out the alkaline phosphatase (ALP) assay, cells were lysed, exposed to freezing/unfreezing cycles, and centrifuged. Each sample (50 µl) was incubated with ALP substrate (150 µl) in 96-well plates at 37ºC for 30 min and the absorbance read at 405 nm (BIORAD Model 680 Microplate Reader, USA). ALP activity measurements were normalized by the protein content. Cell proliferation was quantified with MTT assay. Alizarin red staining was used to detect the mineralization of the matrix and Oil Red O staining was performed to detect adipogenic activity and mature adipocytes. Chondrogenic differentiation was tested using Alcian blue staining.

RT-PCR analysis RNA was extracted at days 7, 10 and 14 using TRIzol (Invitrogen, Spain) and reversed transcripted into cDNA using Maloney murine leukemia virus (M-MLV) reverse transcriptase and random hexamers (Invitrogen, Spain) A semiquantitative RT-PCR method was used by assessing PCR products during the exponential phase of cDNA amplification. The generated cDNA was amplified by using primers for CBFA-1, ALP, and collagen type I, and GAPDH.

Results and Discussion

SAOS-2 cells viability was above 90% after being 24 hours in contact with 20% w/w T908, T1107, and T1307 medium. Below 20ºC, the poloxamine solutions behaved as free flowing liquids and were easily syringeable owing to their low viscosity. The gel temperature was around 25ºC for T1107 and T1307, and 33ºC for T908. At 37ºC, all systems behave as gels with storage modulus ranging between 10^3 and 10^5 Pa. Autoclaving did not modify the rheological behaviour.

The ALP activity of the cells cultured in the osteogenic medium showed a maximum at day 7. ALP activity of T1107 solely and T1307 with rhBMP-2 was no different to that of negative control. Cells cultured with T908 and T1107 gels loaded with rhBMP-2 exhibited an ALP activity pattern that resembled that obtained with the osteogenic medium. By contrast, the ALP activity of cells cultured with T1307 gel loaded with rhBMP-2 initiated at day 3, remained practically constant up to day 14, and then decreased. The highest ALP activity at day 7 was obtained for T908 gels with or without rhBMP-2. Poloxamine solely gels led to an initial proliferation of mesenchymal stem cells (1 week), followed by differentiation to osteoblasts (2-3 week). Such an intrinsic osteoinductive effect of poloxamines was confirmed by histochemical and RT-PCR analysis.

Conclusions

The osteogenic activity of poloxamines offers novel perspectives in the field of fracture healing, overcoming safety and cost/effectiveness concerns associated to the large scale clinical use of recombinant growth factors.

References

1. Tjabringa et al. J Cel Mol Med 12, 1710-1717, 2008.
2. Alvarez-Lorenzo et al. Front Biosci E2, 424-440, 2010.

The key factors driving *in vivo* immobilization of proteins to PHA

Nina Dinjaski[1], *Jose Luis Garcia*[1], *M. Auxiliadora Prieto*[1]

[1]CIB-CSIC, Ramiro de Maeztu, 9, 28040 Madrid, Spain

nina@cib.csic.es

-Introduction

Polyhydroxyalkanoates (PHAs) are biodegradable polymers, produced by different bacterial species, with important industrial and medical applications as bioplastic and potential biomaterial. PHAs are accumulated intracellularly in form of granules protected by a lipid monolayer interspersed with amphipatic phasins from highly hydrophilic cytoplasm. *Pseudomonas putida* strains contain two phasins PhaI and PhaF that is a modular bi-functional protein. PhaF behaves as a structural and also as DNA associating protein. The C-terminal region is similar to nucleoid associated proteins and plays a crucial role in granule localization within the cell and segregation during the cell division. It ensures the equal distribution of granules between daughter cells (Galán *et al*., 2011). The N-terminal region works as a functional domain (BioF domain) able to bind PHA granules and, in harmony with PhaI, acts as a major structural protein. The *BioF protocol* was established as protein immobilization/purification system based on the use of polyhydroxyalkanoate (PHA) granules and their associated phasins (Moldes *et al*., 2004). After fermentation under optimal PHA production conditions, the granules carrying the BioF-proteins fusions can be isolated from the crude cell lysate by a simple centrifugation process and directly used for some applications (Moldes *et al*., 2004). In this work, generated BioF fusions were transferred and expressed in *P. putida* KT2442 strains in the presence and absence of the natural phasins to determine the roles of these key factors for protein immobilization to PHA. The efficiency of the BioF system has been tested by using a reporter BioF-fusions. Host strains have been engineered by site-directed gene replacement, which has the environmental advantage of generating antibiotic marker-free strains. Our work provides new evidences about the minimal genetic modifications that make it suitable for producing environmental friendly active bioplastics.

Materials and Methods

In order to test the BioF system and determine localization of both N- and C-terminal region of PhaF *in vivo*, expression of their fusions with GFP was analyzed by confocal microscopy Laser Confocal espectral (CLSM) Leica TCS SP2-AOBS. Furthermore, DNA was stained with 2 µg/ml (DAPI), while the PHA granules were stained with 1 µg/ml Nile Red to analyze co-localization with C- and N-terminal region respectively. PHA-immobilized protein was extracted as described before (Moldes *et al*., 2004) and analyzed by SDS-PAGE. PHA monomer composition and cellular content were determined by GC-MS. Samples were subjected to methanolysis in the presence of 15% (w/v) sulfuric acid, and resulting methyl esters of monomers were analyzed by gas chromatography. *P. putida* strains KT42F (PhaF mutant) and KT42I (PhaF and PhaI mutant) have been engineered by site-directed gene replacement using the pK18*mobsacB* vector, which has the environmental advantage of generating antibiotic marker-free strains. The heterogeneity of the cell population concerning the PHA production was performed using Flow citometry (flow cytometer Coulter EPICS XL). Analysis was done as described before (Galan *et al*., 2011).

Results and Discussion

The role for the C-terminal and N-terminal domain of PhaF phasin of *P. putida* KT2442 was investigated by confocal microscopy and flow-cytometry studies. Our results confirm the co-localization of the fusion protein GFP::C-PhaF and nucleoid in wild type and PhaF minus cells, independently of the presence or absence of the PHA granules, demonstrating its DNA associating properties. Furthermore, PHA granules produced in the wild type cells, which contain native PhaF protein, co-localised with the nucleoid and GFP::C-PhaF reporter. However, PHA granules produced in the KT42F (PhaF minus) mutant strain were localised independently of the nucleoid and GFP reporter system. This definitively demonstrated the association of PHA granule to the chromosome driven by PhaF protein. Visualizing GFP::N-PhaF proved its co-localization with PHA granules in wild type as well as in both mutant strains when grown in PHA producing conditions. It confirms its granule binding function. However, the PHA production in the strains KT42F (PhaF mutant) and KT42I (PhaF and PhaI mutant) was reduced to 50% and 10%, respectively, when compared to the production of the wild type strain, making them non optimal hosts for expression of BioF system. When complemented with PhaF, KT42F strain recovered wild type phenotype. Furthermore, KT42I strain recovered phenotype of wild type when complemented simultaneously with both PhaF and BioF. Consequently, PhaF and, BioF or PhaI, were identified as essential requirements for BioF system host strains for optimal PHA production yields.

Conclusions

1. BioF tag or its fusion derivatives can replace PhaI role in *P. putida*.

2. The optimal host *P. putida* strain for the BioF system should express i) the whole protein PhaF and ii) PhaI or BioF tag

Acknowledgements

We are greatly indebted to Miguel Arévalo-Rodríguez from BIOMEDAL S.L, Spain, for providing genetic tools to perform this work. This work was supported by the grants BIO2010-21049 and NMP2-CT-2007-026515.

References

Galán B., Dinjaski N., Maestro B., de Eugenio L.I., Escapa I.F., Sanz J.M., García J.L. and Prieto M.A. *Mol Microbiol* 79:402-418 (2011).

Moldes, C. Garcia, J.L. and Garcia, P., *Appl Environ Microbiol* 70: 3205–3212 (2004).

Polymeric Bio-Functionalisation to Generate Enzyme-Responsive Biomaterials

Paul D. Thornton and Andreas Heise

Dublin City University, School of Chemical Sciences, Polymer Chemistry Group, Glasnevin, Dublin

Paul.d.thornton@dcu.ie

Introduction

Proteolytic enzymes have been identified to play key roles in disease states making them valuable targets for therapeutic programs. We disclose methodologies in which commercially available polymers can be adapted to possess an actuating component sensitive to the presence of targeted proteolytic enzymes. Enzyme activity stimulates a material response that may be employed in 1) drug delivery or 2) protease detection systems. In the first instance a protease-responsive release mechanism that employs a molecular gate to entrap payload molecules is described. Selective proteolysis of the specific peptide sequence results in the triggered release of payload molecules on-demand. A second protease-responsive mechanism details the peptide modification of water soluble poly(allylamine) (PAA) to generate a material capable of self-support when dissolved in water. Enzymatic disruption of the dipeptide sequence generates polarity within the structure, enabling polymer dissolution in water and offering a visible response to enzyme activity. nter your text here making certain it is in a two-column format. Please use this template only.

Materials and Methods

Material modification was achieved by synthesising peptide components directly using stepwise peptide synthesis. HBTu and DIPEA were used as coupling agents and DMF was the chosen solvent. Prior to each additional amino acid coupling piperidine and potassium carbonate were employed to remove Fmoc and acetyl protecting groups respectively. Analysis of the biomaterials produced utilised GPC, NMR, HPLC, ATR-FTIR and TGA. The release of payload molecules was analysed by confocal microscopy and UV-VIS spectrophotometry. Type the abstract title in upper and lower case letters (do not use all capitals letters) in the indicated line spanning both columns.

Results and Discussion

1) Highly Specific Dual Enzyme-Mediated Payload Release from Peptide-Coated Particles

The triggered release of macromolecular guest molecules from polymer microparticles coated with a bioactive peptide shell (Fmoc-EAAR) was demonstrated by utilising terminal Fluorenylmethyloxycarbonyl (Fmoc) groups as molecular gates.[1] Specific enzymatic hydrolysis of the peptide sequence, by elastase but not the control enzyme chymotrypsin, removes the bulky peptide-terminating Fmoc groups from the particle shell, permitting the selective release of previously entrapped guest molecules through the newly created openings. Two-stage payload release was demonstrated by coating the particles with both Fmoc-EAAR (elastase cleavable) and Fmoc-EGGR (thermolysin cleavable) (Figure 1). The system offers highly selective responsiveness and adaptability to be applied to a wide range of organic and inorganic polymeric particles of varying size ranges.

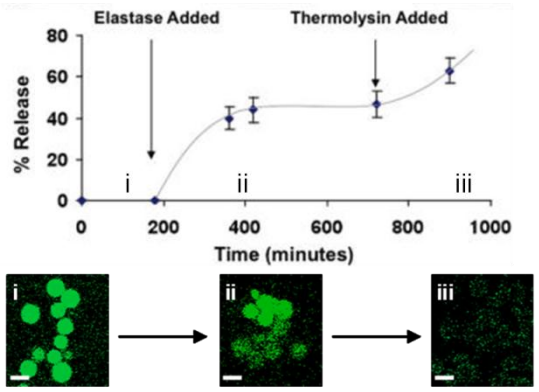

Figure 1: Payload release profile (top) and confocal images detailing enzyme-controlled release.

2) Bio-Functionalisation to Enzymatically Control the Solution Properties of a Self-Supporting Polymer

The solubility of PAA in water can be altered by the partial addition, and subsequent cleavage, of acetyl protected alanine to alanine-modified PAA.[2] Successful proteolysis by elastase generates polarity, allowing the polymer to dissolve in water, offering a visible response to the specific enzymatic activity. It is anticipated that system of controlling polymer solubility may be further employed for the label-free detection of a range of proteases or the release of guest molecules.

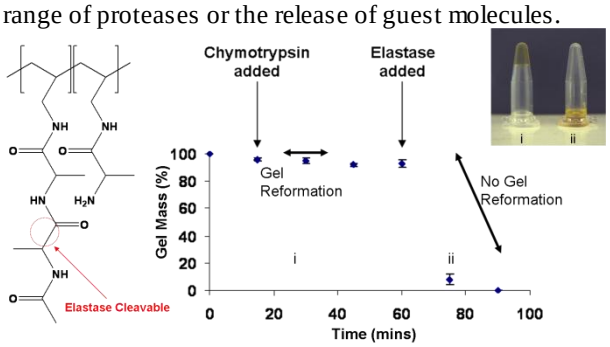

Figure 2: Left Functionalised polymer capable of self-support. Right Targeted proteolysis disrupts the structure.

Conclusions

The work presented discloses methods of polymer modification to offer materials that possess a degree of biological functionality. Possible applications involve the use of polymers in drug delivery and biodiagnostics.

References

1. P. D. Thornton and A. Heise. J. Am. Chem. Soc. 2010, 132, 2024.
2. P. D. Thornton and A. Heise. Chem. Commun. 2011, DOI: 10.1039/c0cc03647a

Nanohybrides and Composites as Perspective Biomedical Materials

Zubov V.P.[1,2], *Kapustin D.V.*[1], *Generalova A.N.*[1], *Bakeeva I.V.*[2]

[1] Shemyakin-Ovchinnikov Institute of Bioorganic Chemistry of the Russian Academy of Sciences Miklukho-Maklaya str., 16/10, Moscow 117997, Russia

[2] Lomonosov State Academy of Fine Chemical Technology, Vernadskogo av., 86, Moscow 119571, Russia

zubov@ibch.ru

A modern trend to miniaturization of bioanalytical, diagnostic and informatic functional devices down to molecular level requires development and use of nanosize elements of various chemical structure and morphology obtained mainly by direct chemical synthesis. The presentation considers three types of such hybrids and composites.

First, macroscopic solid porous and nonporous matrices have surface modified with nanothick uniform layers of various polymers (fluorinated polymers, polyanilines, etc.) and contain specific functional groups on the surface [1]. The peculiarity of preparation of such composites and their application are considered on the examples of the system for facile separation of biomacromolecules (nucleic acids [2], proteins [3], etc.) and enzyme immobilization [4].

Secondly, the presentation considers a series of bioanalytical systems where the used markers are molecular dyes, fluorophores and in particular fluorescent nanocrystals immobilized on various polymer [5] including nanoscale matrices [6] and full-size or mini-antibodies as bioligands. The efficiency of the system is demonstrated on the examples of various immunoagglutionation assays, flow cytometry, visualization of cells including tumor cells, tissues.

Thirdly, the presentation considers hybrid hydrogels based on linear water-born polymers (poly-N-vinylpirrolidone [7], poly-N-vinylcaprolactam [8], etc.) and nanosize inorganic particles (SiO_2, Si, Au, Fe_3O_4) [9]. The latter acts as cross-linker of the system and also may bring specific function (magnetic, optical, etc.) to resulting hybrid hydrogels. The hybrid hydrogels are formed under mild conditions and show high elasticity and mechanical strength. Their use as biomaterials is discussed.

References

1. Zubov VP, Kapustin DV, Generalova AN et al. *Polymer Science, Ser. A.*, **49**, 1247-1264 (2007).
2. Kapustin DV, Yagudaeva EY, Zubov VP, et al., In: "Frontiers in DNA Research", Corey R. Woods., ed. Nova Science Publishers, USA, 113 -136 (2006).
3. Yagudaeva EYu, Bukina YaA, Prostyakova AI, Zubov VP, et al. *Polymer Science, Ser. A*, **51**, 675–682 (2009).
4. Kapustin DV, Vikhrov AA, Gorokhova IV, et al. *Russian Chemical Bulletin*, 54, 452–457 (2005).
5. Generalova AN, Sizova SV, Goncova MS, et al. *Nanotechnologies* in Russia, **2**, 144-154 (2007).
6. Generalova AN, Sizova SV, Oleinikov VA, Zubov VP, et al. *Colloids and Surfaces A: Physicochemical and Engineering Aspects*, **342**, 59-64 (2009).
7. Kirilina YO, Bakeeva IV, Bulychev NA, et al. *Polymer Science Ser. B*, **51**, 135-142 (2009).
8. Loos W, Verbrugghe S, Goethals EJ, Zubov VP, et al. *Macromol. Chem. & Physics*, **204**, 98-103 (2003).

Sol-Gel coatings for metals implants.

M. Hernández-Escolano[1,3], M.J. Juan-Díaz[2]. M. Martinez[2] , M. Gurruchaga[2], I. Goñi[2], J. Suay[3]

1 Ctr. Biomaterials & Tissue Engineering, University Politecnic of Valencia, UPV (Spain)
2 Polymer Science and Technology Department, Faculty of Chemistry of San Sebastian, UPV/EHU (Spain)
3 Polymers and Advanced Materials Research Group (PIMA), Universitat Jaume I, UJI (Spain)

e-mail: miheres@doctor.upv.es

Introduction:

Metals are the most common materials used in medical implants for hard tissues due to their excellent mechanical properties. [1] However, metals have some severe limitations.[2] For example, their capacity of osseoinduction, the corrosion process that suffers in biological medium releasing metallic particles that reduce the osteoblast activity.[3] Moreover, metals can not incorporate biological or organic components as peptides or drugs. The incorporation of biological compounds and drugs to metals could be a way to obtain multifunctional prosthesis and to increase its biocompatibility.

One way to avoid these problems and to make metal implants able to delivery drugs and peptides is to create a biocompatible and bioactive coating. [4] The sol-gel process is an available technique for coating the surface of the metal. In this method, a metal alkoxide undergoes hydrolysis in the presence of water with an acid or basic catalyst. The silanols produced then condense forming a SiO_2 network. It is possible to obtain organic-inorganic coatings throw the sol-gel method by using metal alkoxides with organic chains.

The aim of this work is to prepare and evaluate sol-gel coatings. Different organic-inorganic coatings have been synthesized using as methal alkoxides vinyltrimethoxisilane (VTES), 3-glycidoxypropyl trimethoxysilane (GPTMS) and tetraethoxysilane (TEOS). The physic-chemical characterization of the materials was done and reported. This paper is focus in the biological characterization of the hybrid coating.

Materials and Methods

Synthesis of the sols
Two set of materials was prepared: VTES / GPTMS and VTES / TEOS, with different compositions. The sol was prepared by acid catalysis method, isopropanol as solvent and 0.1M nitric acid (HNO_3) in order to obtain an acid pH. The water was incorporated from the nitric acid solution in stoichiometric ratio. The molar ratio of VTES/GPTMS were 4:1; 1:1; and 1:4 and the molar ratio of VTES/TEOS were 9:1, 4:1, 7:3. The sol solutions were stirred for about 1h and set for another hour at room temperature before use.

Curing process of the sol
The curing process for VTES/GPTMS was 15 min.50ºC, 15 min. 100ºC, 45 min 140ºC. The curing process for VTES/TEOS was 15 min.50ºC, 90 min. 100ºC.
Characterization of the coatings
The chemical composition of the coating was investigated by Fourier Transformed Infrared (FTIR). The study of the cure process was done by FTIR and Differential Scanning Calorimetry (DSC). The contact angle was measured. The hydrolytic degradation of the materials was characterized. Finally, the cell response using human adipose tissue-derived mesenchymal stem cells (AMSC) in contact with the materials was studied.

Results and Discussions

The characteristic bands of the inorganic network and the presence of the organic groups was found in all spectra. The study of the VTES/GPTMS show that the increase of the quantity of GPTMS in the formulation leads to an increase of active epoxy rings in the surface of the material.

The study of the cure process was done by FTIR and DSC. Optimal cure temperatures and times were obtained for each set of materials in order to maximize Tg, adhesion and mechanical properties.

Variations of the wettability and the hydrolytic degradation ratio ware detected in different formulations of VTES/TEOS, as more TEOS is added more wet and degradation ratio is registered.

The proliferation and the induction of bone formation of AMSC has been reported for each set of materials, showing the high possibilities for using them in tissue engineering.

Acknowledgements

The research work is taking place thanks to the public support provided by the Spanish Ministry of Science and Innovation (IPT-010000-2010-004 and IPT-020000-2010-001).

References

[1] E. De Giglio, M.R. Guascito, L.Sabbatini, G.Zambonin. Biomaterials. 2001, 22, 2609
[2] Ballarre, J; López, D.A.; Schreiner, W.H.; Durán, A; Ceré, S.M. *Appl. Surf. Sci.*. **2007**, *253*, 7260.
[3] G.A. Crawford, N. Chawla, K. Das, S. Bose, A. Bandyopadhyay. Acta Biomaterialia. 2007, 3, 359.
[4] W. Khan, M. Kapoor, N. Kumar. Acta Biomaterialia. 2007, 3, 541.

Spray Dried Hydroxyapatite-Chitosan Biocomposites

Tuğba Başargan and Gülhayat Nasün-Saygılı[*]

[*] Chemical Engineering Department, Istanbul Technical University, Turkey

nasun@itu.edu.tr

Introduction

Hydroxyapatite ($Ca_{10}(PO_4)_6(OH)_2$, HAp) is a bioceramic used in the biomedical applications [1]. HAp-polymer composites are used to maintain bioactive properties and development in mechanical properties [2]. Chitosan is a natural polymer degrading to non-harmful and non-toxic compounds in the body [3]. Chitosan has gained great interest as a result of their biological activities such as antimicrobial, hypocholesterolemic, immunity enhancing, antitumor effects, drug delivery,accelerating calcium and ferrum absorption [4]. HAp-chitosan microsphere-based material may be used for bone-grafting and delivery of therapeutic agents [5]. It is claimed that HAp-polymer microspheres are perfect to the delivery of cells, proteins and drugs for the cure of defective tissues and their regeneration [6].

The aim of this study was to synthesize HAp-chitosan microspheres by spray drying technique.

Materials and Methods

Phosphoric acid (0.12 M)-chitosan (%1 wt in %2 aqueous acetic acid) mixture was added to $Ca(OH)_2$ (0.2 M) solution drop by drop at 40 ^{0}C. During the addition of acid mixture, the pH was maintained at 9 using dilute acetic acid and NaOH. After the mixture addition, the reactants were stirred for two hours more and then suspension was aged for 15 h at room temperature. The precipitate was separated from the supernatant liquid by decanting and volume was restored again by adding distilled water. The slurry was fed into a laboratory scale spray dryer at a flow rate of 500 mL/h. The inlet temperature of hot air was set to 160 $^\circ$C. For comparison, HAp sample was also prepared in the absence of chitosan using a similar way. Synthesized HAp and HAp-chitosan samples were structurally characterized using FTIR, SEM, XRF, BET and XRD. Crystallite size of the composite was calculated with TOPAS 3 software [7]. Particle size measurements were made using ZetaPals.

Results and Discussion

The XRD patterns of the samples (Fig. 1) confirmed the formation of HAp in the samples. Nano-crystalline apatite and low degree of crystallinity were observed in the samples [8-10]. Crystallite sizes of the composite were found 40.8, 10.3 and 14.3 nm when 002, 211 and 310 peaks were used, respectively [7]. According to FTIR spectra (Fig. 2) HAp-chitosan composite was successfully synthesized. After polymer addition, CH_2 (2920-2858 cm^{-1}) and amide II (1570 cm^{-1}) bands of chitosan appeared on the composite which confirmed the formation of HAp-chitosan composite.

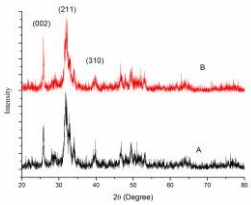

Fig. 1. XRD patterns for **A** HAp **B** HAp-chitosan.

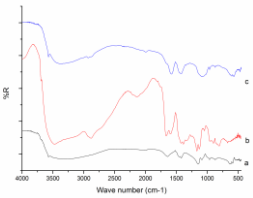

Fig. 2. FTIR spectra of **A** HAp **B** Chitosan **C** HAp-chitosan.

According to XRF analysis result, the Ca:P molar ratio of HAp and HAp-chitosan powders were 1.665 and 1.721, respectively. The particle size was found 2.7 µm. BET surface area of HAp and HAp-chitosan samples were found 78.59 and 94.82 m^2/g, respectively.

Fig. 3 indicates SEM graph of HAp-chitosan composite. Most of the granules were solid particles and the particle distribution was not uniform.

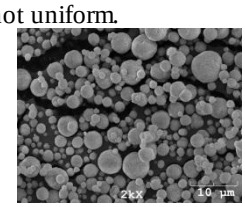

Fig.3 SEM graph of HAp-chitosan.

Conclusions

In this study, HAp-chitosan microsphere was prepared using spray dryer. This composite may be a potential material in biomedical fields.

References

1. Kalita S. J. et al, Materials Science and Engineering: C, 27:441, 2007.
2. Mollazadeh, S. *et al*, Advances in Applied Ceramics, 106:165, 2007.
3. Chen, F. *et al*, Materials Letters, 57: 858-861, 2002.
4. Xia W. et al, Food Hydrocolloids, 25(2):170-179, 2011.
5. Bumgardner, J. D., United States Patent Application 20070254007, 2007.
6. Sinha A. et al, Journal of Materials Science-Materials in Medicine, 19:2009, 2008.
7. Kern, A.A. and Gelho, A.A., TOPAS 3 (Bruker Axs), www.brukeraxs.com, 2006.
8. Sukhodub, L., Mat.-wiss. U. Werkstofftech, 40(4): 318-325, 2009.
9. Wang, A. *et al*, Powder Technology, 191:1-6, 2009.
10. Zhang, Y. and Yokogawa, Y., J., Mater. Sci: Mater. Med., 19:623-628, 2008.

Antiheparin activity of cationic dextran derivatives in rats *in vivo*

Kamil Kamiński [1], *Krzysztof Szczubialka* [1], *Maria Nowakowska* [1], *Bartłomiej Kałaska* [2], *Włodzimierz Buczko* [2]

1.Jagiellonian University, Faculty of Chemistry, Ingardena 3, 30-060 Krakow, Poland;
2. Department of Pharmacodynamics, Medical Uniwersity in Bialystok, 2C Mickiewicza Street Poland, 15-222 Bialystok,

e-mail: Kaminski@chemia.uj.edu.pl

Introduction:
Heparin is a natural polymer widely used in medicine especially during the treatment of cardiovascular diseases since it is a potent blood anticoagulant. In case of emergency, e.g. massive haemorrhage the anticoagulant activity of heparin has to be quickly stopped by the administration of a heparin reversing agent. Currently protamine sulfate, an allergenic protein is used for this purpose.

Materials and Methods
We are reporting the studies on a new polymeric substance, a cationic dextran derivative, which is able to form complexes with heparin. Dextran is a blood-compatible polymer which is also frequently applied in medicine. By substituting dextran with glicydyltrimethylamonium chloride (see reaction scheme below) a cationic polymer was obtained that binds to heparin with an efficiency similar to that with protamine[1].

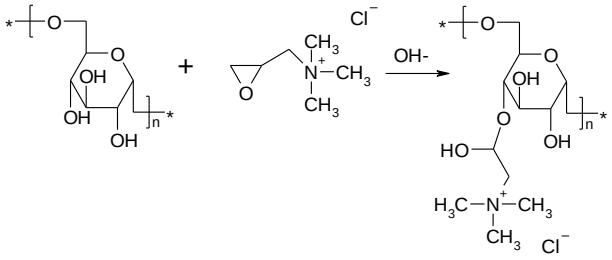

Figure 50 Schema of reaction used to obtain cationic dextran

The binding process and the complex formed were studied using UV-Vis spectroscopy, DLS and zeta potential measurements.

Results and Discussion:
Cationic dextran derivative was found to bind heparin in PBS solution. This binding is based on attractive electrostatic interaction between anionic heparin and cationic dextran. The efficiency of this processes strongly depends on the degree of cationic modification and is similar to binding of heparin by protamine, however, the size of heparin-dextran complexes is larger than that of heparin-protamine complexes (ca. 10 μg). Moreover, preliminary studies on the influence of different levels of modified dextran on the heparin activity in the rat blood using various coagulation tests were performed. They have shown a decrease in clotting time after administration of cationic dextran to heparinized rats.

Conclusions:
The preliminary data obtained show that the cationically-modified dextran may reduce anticoagulative heparin activity both under in vivo and in vitro conditions.

Acknowledgment:
The project was operated within the Foundation for Polish Science Team Programme (TEAM/208-2/6) and Ventures Programme (VENTURES/2009-4/4) cofinanced by the EU European Regional Development Fund

References:
[1] K. Kaminski, K. Szczubiałka, K. Zazakowny, R.Lach, M. Nowakowska; *J. Med. Chem.* **2010**, *53*, 4141–4147

Trimethyl chitosan-based complexes as nanocarriers for pH-triggered lysosomal delivery of therapeutic proteins

Marina I. Giannotti,[a,b,c] *Olga Esteban*,[a,d] *María F. García-Parajo*,[a,d] *Fausto Sanz*[a,b,c]

[a]CIBER de Bioingeniería, Biomateriales y Nanomedicina (CIBER-BBN);
[b]Physical Chemistry Department, University of Barcelona (UB);
[c]Nanoprobes & Nanoswitches Group and [d]BioNanoPhotonics Group, Institute for Bioengineering of Catalonia (IBEC), Spain

e-mail: migiannotti@ub.edu

Introduction. Nanopharmaceutics composed of a carrier and a protein have the potential to improve the activity of therapeutical proteins. Therapy for lysosomal diseases is limited by the lack of effective protein delivery systems that allow the controlled release of specific proteins to the lysosomes. Here, we address this problem by developing functional polyelectrolyte-based nanoparticles able to promote acidic pH-triggered release of the loaded protein. Complexes formed by self-assembly between proteins and natural or synthetic polyelectrolytes do not require harsh preparation methods and have been the focus of many recent studies.[1] Chitosan and its derivatives are cationic polymers at low pH and can interact and form complexes with proteins that bare a negative charge at pH<pI, whereas derivatives like quaternized chitosan bare positive charge and are soluble at physiological pH. α-galactosidase A (α-GAL) is a lysosomal enzyme, which deficiency leads to the Fabry disease and results in the lysosomal accumulation of globotriaocylceramide within various tissues and cells, in particular the vascular endothelium.[2] To date, the only strategy to treat this disease has consisted in ERT with exogenously administered α-GAL.[3] As an alternative, we developed functional TMC-based PEC nanocarriers with α-GAL, prepared by self-assembly via simple aqueous solution mixing and ionotropic gelation. We characterize their physicochemical properties, stability against time and temperature, behavior against the variation of the medium pH as well as intracellular trafficking and fate in human endothelial cells.[4]

Materials and Methods. Chitosan middle-viscous was used to prepare *N*,*N*,*N*-trimethyl chitosan chloride (TMC) following a two-step synthesis procedure.[5] The product was characterized by 1H NMR. Potentiometric titration was used to analyze chitosan and TMC buffering capacity (free amine moieties that can be protonated). The polyelectrolyte complexes (PECs) between TMC and the negatively charged protein α-GAL were prepared by self-assambly, adding a solution of TMC (buffer HEPES 10 mM, pH 7.4) at various concentrations (100 to 24.5 μg ml^{-1}) to the protein dissolved in the same buffer, in a volume ratio 70:30. For the cases where penta-sodium triphosphate (TPP) was used, the polianion was previously dissolved in the protein solution. Average size, polidispersity index (PDI) and Z-pontential values were determined by dynamic light scattering (DLS). TMC was conjugated to the florescent dye Atto 647N NHS ester, to visualize the nanoparticles under total internal reflection fluorescence (TIRF) microscopy (for single particle tracking) and for further *in vitro* studies. Atomic force microscopy (AFM) was used to characterize the PECs morphology and their behavior upon pH variations. Cellular uptake of the fluorescent nanoparticles by HMEC-1 cells was followed flow citometry and confocal laser scanning microscopy (CLSM).

Results and discussion. Ionically crosslinked colloidal polyelectrolyte complexes (PECs) between TMC and the lysosomal protein α-GAL were successfully obtained by self-assembly in a simple way. These α-GAL nanocarriers are homogeneous in size, as well as stable and active under physiological conditions. A relatively high protein load (around 50 wt %) per particle was achieved. The enzymatic activity of the α-GAL was not significantly affected by the encapsulation process, ensuring the integrity of the protein during and after the procedure. Finally, a rapid PEC internalization and further accumulation in lysosomal compartments of human endothelial cells was demonstrated. Following a pH drop from physiological (around 7.5) to endosomal/lysosomal (4.5-5.5) values, the PECs dissociated and released the protein (Fig. 1). Altogether, our results demonstrate that the α-GAL nanocarriers are stable and active under physiological conditions and traffick to lysosomal compartments of human endothelial cells, where the acidic conditions can trigger the release of the protein. As such, these nanocarriers represent a valuable and promising alternative for lysosomal enzyme replacement therapy with improved efficiency in Fabry disease and other lysosomal storage diseases.

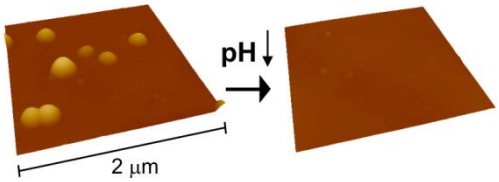

Fig. 1. 3D representations of AFM images (height, tapping mode) of TMC/α-GAL PECs on an HOPG substrate at pH 7.5 and after HCl addition (pH 3.9).

References

1. Jintapattanakit, A.; Junyaprasert, V. B.; Mao, S.; Sitterberg, J.; Bakowsky, U.; Kissel, T. *Int. J. Pharm.* **2007**, 342, 240.
2. Garman, S. C.; Garboczi, D. N. *J. Mol. Biol.* **2004**, *337*, 319.
3. Schaefer, R. M.; Tylki-Szymanska, A.; Hilz, M. J. *Drugs* **2009**, *69*, 2179.
4. Giannotti, M. I.; Esteban, O.; Oliva, M.; García-Parajo, M. F.; Sanz, F. **2011** *Submitted*
5. Sieval, A. B.; Thanou, M.; Kotzé, A. F.; Verhoef, J. C.; Junginger, H. E. *Carb. Polym.* **1998** 36, 157.

Modeling of Nanotubes Penetration through a Phospholipid Bilayer

Sergey Pogodin[1], *Nigel K. H. Slater*[2] *and Vladimir A. Baulin*[1,3]

[1]Departament d'Enginyeria Quimica, Universitat Rovira I Virgili, Av. dels Països Catalans 26, 43007 Tarragona, Spain, [2]Department of Chemical Engineering and Biotechnology, University of Cambridge, Pembroke Street, Cambridge CB2 3RA, United Kingdom, [3]ICREA, Passeig Lluis Companys 23, 08010 Barcelona, Spain

msupsg@yandex.ru

A great efficiency to penetrate into living cells is attributed to carbon nanotubes due to a number of direct and indirect observations of the nanotubes inside the cells. However the exact mechanism of such penetration still remains unknown. We performed series of computer simulations in order to study one of the possible ways of the nanotubes inside the cells, namely the spontaneous translocation through a pure phospholipid membrane induced by thermal motion.

With use of Single Chain Mean Field technique we simulated phospholipid membrane at the coarse grained level, which had been shown to represent adequately the key thermodynamic properties of the DMPC bilayer in the fluid phase [1]. A carbon nanotube was modeled by a cylinder, which diameter and surface affinity to the hydrophobic core of the membrane was varied between different sets of the simulations. Performing perpendicular insertion of the nanotube inside the membrane we were obtaining, as output of our simulation, the values of equilibrium free energy of the system at every position of the nanotube (Fig. 1), and mean field snapshots of the bilayer reorganization around its' tip (Fig. 2).

We began with consideration of the nanotubes with uniform surface properties [2]. As we found out, they hardly are able to cross the phospholipid membrane without an application of external force due to the presence on their way of energy barrier of order 40 kT and higher, depending on the nanotube size and hydrophobicity. While relatively hydrophilic nanotubes meet the positive barrier which is difficult to overcome by thermal motion, the hydrophobic ones are exposed to strong attraction to the phospholipids tails which is high enough to entrap them within the hydrophobic membrane core. The nanotubes with the intermediate hydrophobicity are exposed to the both effects. To pass through the membrane they have to overcome the steric repulsion from it due to the pore formation in the bilayer, as well as the attraction to the membrane's core.

Comparison of the energy curves (Fig. 2) of the nanotubes with uniform surface properties suggests that alternation of hydrophobic and hydrophilic regions on the nanotubes surface can reduce considerably the energy barrier of translocation. We have shown [3] that the periodical patterning of the nanotube with distinct hydrophobic and hydrophilic bands can significantly facilitate their penetration through the phospholipid bilayer. Such a patterning may occur naturally in biological systems upon the spontaneous self-assembly of biomolecules onto the surface of the nanotubes.

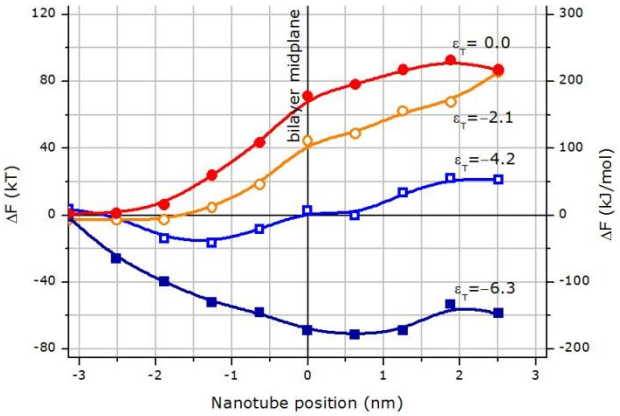

Fig. 1. Free-energy cost of the nanotube insertion into the phospholipid bilayer versus the tube position. For the nanotube with diameter 1.0 nm and hydrophobicity increasing from curve ε_T=0.0 to ε_T=-6.3.

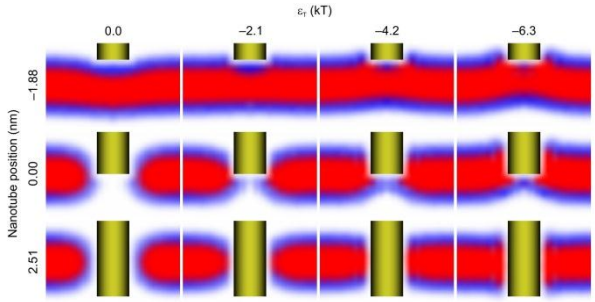

Fig. 2. Mean-field snapshots of the nanotubes insertion into the phospholipid bilayer.

References:

[1]. "Coarse-Grained Models of Phospholipid Membranes within the Single Chain Mean Field Theory", Sergey Pogodin and Vladimir A. Baulin, *Soft Matter*, **6**, 2216-2226 (2010)

[2]. "Can a Carbon Nanotube Pierce through a Phospholipid Bilayer?", Sergey Pogodin and Vladimir A. Baulin, *ACS Nano*, **4**, 5293-5300 (2010)

[3]. "Surface Patterning of Carbon Nanotubes Can Enhance Their Penetration through a Phospholipid Bilayer", Sergey Pogodin, Nigel K. H. Slater, and Vladimir A. Baulin, *ACS Nano*, Published online 10.1021/nn102763b (2011)

Zinc oxide protects etch&rinse adhesive resin-dentin hybrid layers from MMPs degradation.

Toledano M, Yamauti M, Suarez P, Quintana M, Osorio E, Osorio R.

Aim of the study: Demineralization of dentin collagen matrix by acids may represent a suitable collagen scaffold to be remineralized; in the presence of minerals.Demineralized exposed collagen can undergo degradation by endogenous matrix metalloproteinases (MMPs). Effective inhibitors of matrix metalloproteinases may be included in resin-dentin bonding interfaces to protect the seed crystallite-sparse collagen fibrils of the scaffold, from degradation before they could be re-mineralized. MMPs mediated collagen degradation in the different bonded interfaces has to be determined.

Methods: An in vitro assay with dentin beams was performed. Dentin beams were obtained and immersed in: 1) 10% phosphoric acid (PA) and impregnated with Single Bond resin or 2) Clearfil SE Bond (SE) primer and impregnated with SE bonding resin. 2% of $ZnCl_2$ or 10% of ZnO nanoparticles were added to resin mixtures. Four dentin beams were tested for each condition.

Dentin beam specimens were incubated in 500 µl of media artificial saliva at 37°C for 24 h, 1 and 3 wk. Supernatants were analyzed for the release of collagen degradation product (C-terminal telopeptide of type I collagen -ICTP-) using a radioimmunoassay. Values were analyzed by ANOVA and SNK multiple comparison ($P<0.05$).

Results and discussion: Mean and standard deviation of ICTP values and multiple comparisons results are in the table. Identical numbers in each row indicate no significant difference. In each column values with identical letters indicate no difference.

		24 h	1 wk	4 wk
Phosphoric acid		53.33 (8.3) 1A	210.11(11.20)2A	212.3(17.89) 2A
Phosphoric acid	SB	0.84 (0.03) 1B	1.49 (0.33) 2B	2.52 (0.80) 2B
	SB- 2% $ZnCl_2$	1.09 (0.10) 1B	0.97 (0.12) 1B	1.74 (0.76) 2B
	SB- 10% ZnO	0.48 (0.05) 1B	0.83 (0.05) 1B	0.60 (0.05) 1C
SEB-Primer		10.02 (1.20) 1C	41.54 (5.32) 2C	50.97 (6.54) 1D
SEB-Primer	SEB-Bond	1.37 (0.22) 1B	0.30 (0.12) 2E	0.59 (0.09) 2C
	SEB-Bond- 2% $ZnCl_2$	1.71 (0.32) 1B	2.94 (0.11) 2B	5.04 (0.87) 3E
	SEB-Bond- 10% ZnO	0.92 (0.20) 1B	1.35 (0.10) 2B	1.91 (0.54) 2B

Conclusions: Addition of 10% of zinc oxide particles serves as effective and stable inhibitor of dentin MMPs in resin/dentin hybrid layers created with the tested etch&rinse system. MMPs degradation of collagen is strongly reduced in resin infiltrated dentin.

Acknowledgments: CICYT/FEDER MAT2008-02347, JA-P07-CTS2568 and JA-P08-CTS-3944.

References:

1. Toledano M, Nieto-Aguilar R, Osorio R, Campos A, Osorio E, Tay FR, Alaminos M. Differential expression of matrix metalloproteinase-2 in human coronal and radicular sound and carious dentine. J Dent. 2010;38(8):635-40.

2. Toledano M, Osorio R, Osorio E, Aguilera FS, Yamauti M, Pashley DH, Tay F. Effect of bacterial collagenase on resin-dentin bonds degradation. J Mater Sci Mater Med. 2007a;18(12):2355-61.

3. Osorio R, Yamauti M, Osorio E, Ruiz-Requena ME, Pashley DH, Tay FR, Toledano M. Zinc reduces collagen degradation in demineralised human dentin explants. J Dent 2011;39:148-153.

4. Osorio R, Yamauti M, Osorio E, Ruiz-Requena ME, Pashley DH, Tay FR, Toledano M. Effect of dentin etching and clorhexidine application in MMPs mediated collagen degradation. Eur J Oral Sci 2011, 119(1):79-85.

Preparation and Characterisation of Glycopolymers by CCTP and Click Chemistry

*Yanzi Gou and David M. Haddleton**

Department of Chemistry, University of Warwick, Coventry CV4 7AL, United Kingdom

D.M.Haddleton@warwick.ac.uk

Introduction

Glycopolymers are important in many biological processes such as inflammation, cell-cell contacts and fertilisation.[1] For catalytic chain transfer polymerisation (CCTP), very small amount of chain transfer agent is needed to prepare low molecular weight oligomers and under well-chosen conditions, nearly all polymer chains will have an unsaturated vinyl bond at the chain end for post-functionalization.[2] Huisgen copper-catalysed azide–alkyne cycloadditions (CuAAC) click reaction has been used in the design of novel polymeric materials, bioconjugation, synthesis of lead discovery libraries, tagging of live organisms and proteins and labeling of DNA.[3, 4] In this study, CCTP and CuAAC have been combined to prepare glycopolymers with low molecular weights, which are very difficult to synthesize by other living polymerisation techniques.

Materials and Methods

3-Tri-methylsilanyl-prop-2-yn-1-ol was purchased from Alfa Aesar and used without further purification. Copper(I) bromide (Aldrich, 98%) was purified according to the method of Keller and Wycoff.[5] Triethylamine (TEA) (Fischer, 99%) was stored over sodium hydroxide pellets. All other reagents and solvents were obtained from Aldrich and used without further purification. All reactions were carried out by using standard Schlenk techniques under nitrogen. NMR spectra were obtained on Bruker DPX300 and Bruker DPX400 spectrometers. All chemical shifts are reported in ppm relative to tetramethylsilane, referenced to the chemical shifts of residual solvent resonances (^{1}H and ^{13}C). MALDI-TOF spectra were obtained on a Bruker UltraflexII TOF and analyzed using FlexAnalysis software. The MALDI contains a 337 nm wavelength N2 at a maximum repetition rate 50 Hz. The system is kept inside a vacuum at 5×10^{-6} Torr to avoid contamination of the sample reading.

Results and Discussion

Preparation of alkyne-containing double clickable polymers via CCTP. A series of TMS-protected polymers **(2)** were prepared using CoBF as catalyst and AIBN as initiator, **Figure 1**. Double clickable scaffolds **(3)** can be obtained by deprotection to remove the TMS groups with tetrabutylammonium fluoride (TBAF) and acetic acid in THF at ambient temperature. MALDI-TOF spectrum, **Figure 2,** shows the composition, structure and PDi of the double clickable polymers.

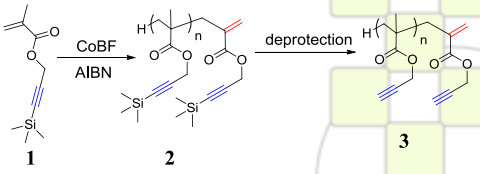

Figure 1. Preparation of polyalkyne scaffolds via CCTP.

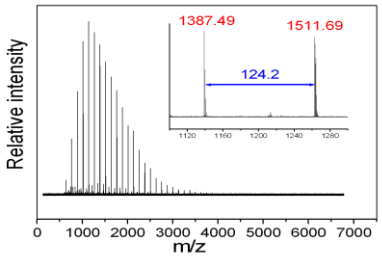

Figure 2. MALDI-TOF spectrum of polymer **(3)**.

Glycopolymers synthesized by CuAAC click reaction. Sugar azides were prepared by one-step reaction from unprotected sugars.[6] Fucose glycopolymers were synthesised by CuAAC, **Figure 3**, **Figure 4**, as were mannose and galactose glycopolymers.

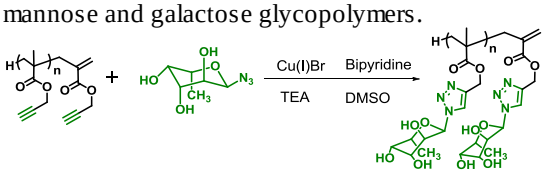

Figure 3. Synthesis of fucose glycopolymer via CuAAC.

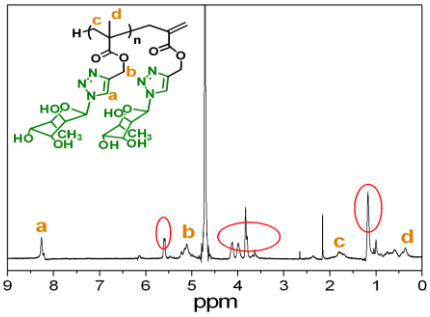

Figure 4. ^{1}H NMR of fucose glycopolymer

Conclusions and References

A series of glycopolymers have been synthesised in a modified way by combining CCTP and CuAAC. The interaction of them with specific lectins is being investigated.

(1) Spain, S. G.; Gibson, M. I.; Cameron, N. R. *J. Polym. Sci. Polym. Chem.* **2007,** 45 (11), 2059.
(2) S. C. J. *Pierik, Eindhoven Univ. of Tech*, **2002**.
(3) Lutz, J.-F. *Angew. Chem. Intl. Ed.* **2007**, 46 (7), 1018.
(4) Kolb, H. C.; Sharpless, K. B. *Drug Disc. Today* **2003**, 8 (24), 1128.
(5) Keller, R. N.; Wycoff, H. D. *Inorg. Synth.*, **1946**, 2,1.
(6) Vinson, N.; Gou, Y.; Becer, C. R.; Haddleton, D. M.; Gibson, M. I., *Polym. Chem.*, **2011**, 2 (1), 107-113.

Recognition and Release of Biological Catechols in NIPAM-Based Copolymers Bearing Phenylboronic Acid Receptors

Nicolas Martin, Sophie Norvez, and Ilias Iliopoulos

Matière Molle et Chimie, ESPCI ParisTech – CNRS, UMR-7167
10, rue Vauquelin, 75005 Paris, France

sophie.norvez@espci.fr

Responsive polymers like poly (*N*-isopropyl-acrylamide), PNIPAM, have been widely used for the preparation of stimuli sensitive systems with potential applications in drug transfer and delivery. A comonomer bearing the phenylboronic acid (PBA) functionality may be designed to recognize diol-containing biological molecules, *e.g.* catechol derivatives like dopamine or noradrenaline. Since PNIPAM is a thermosensitive polymer, PNIPAM-*co*-(acrylamido-PBA) copolymers (PNB) will exhibit both temperature and diol responsiveness. In this work, the reversible association *via* boronic ester formation between PBA-bearing NIPAM-based copolymers and biological catechols was investigated at physiological pH by experiments in the UV–visible range.

Alizarin Red S (ARS), considered here as a model for biological catechols, was chosen as an optical reporter in the visible range for the boronate ester formation (Figure 1). Dialyses experiments and numerical analysis of UV-visible titration curves resulted in the quantitative determination of the host-guest binding constants. Above the phase transition temperature of the NIPAM-based thermosensitive copolymer, the binding constant decreases significantly more than in the case of non thermosensitive copolymers. Temperature-controlled released of the dye was associated to the coil-to-globule transition of NIPAM-based copolymer [1].

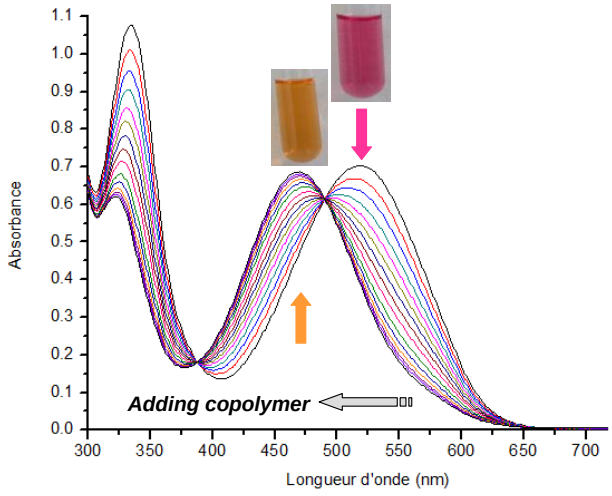

Figure 1: Quantitative study of the recognition of ARS by PNB copolymer.

Polycatechols, like tannins, are other attractive molecules because of their biofunctional properties, in particular anti-oxidative. Tannic acid (TA) is a bio-resourceful fully degradable polyphenol extracted from plants. Only a couple of studies have dealt with the TA-PNIPAM interaction, a weak association acting through hydrogen-bonding between hydroxyl groups of the phenols and amide groups of the polymer, as well as through hydrophobic interactions. In this work, turbidity studies as well as competitive experiments highlighted a very strong interaction between tannic acid and NIPAM-based copolymer bearing phenylboronic acid residues. This was in particular attested by the disappearance of the LCST of PNB (Figure 2). This huge interaction is likely rooted in the multivalent character of the polyphenol, which may bind to multiple chain sites through boronate ester formation.

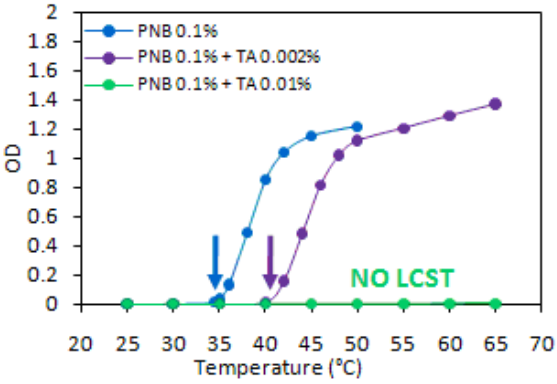

Figure 2: Disappearance of the LCST of PNB copolymer in presence of tannic acid (TA).

It is envisioned that the affinity between tannic acid and NIPAM-*co*-PBA copolymers may serve to the controlled release of catechols of significant biological importance, like dopamine or others.

[1] G. Carré de Lusançay, S. Norvez, I. Iliopoulos, "Temperature-Controlled Release of Catechol Dye in Thermosensitive Phenylboronate-Containing Copolymers: A Quantitative Study", *Eur Polym J* (2010) **46**, 1367-1373.

Chitin-Immobilized Lipase Catalyst for Ring Opening Polymerization of ε-caprolactone

Banu İyisan, Erhan Özsağıroğlu, Nuran Deveci Aksoy, Yüksel Avcıbaşı Güvenilir

Istanbul Technical University, Department of Chemical Engineering, 34469 Maslak, Istanbul, Turkey

iyisanb@itu.edu.tr

Introduction

Lipase is a kind of hydrolase that catalyze the hydrolysis of fats in living cells. They are also used in organic synthesis as a catalyst to produce organic compounds. In addition to that, their hydrolytic effect in water can be changed into ester synthesis in non-aqueous media. By utilizing this special behavior, lipases are used to catalyze ring opening polymerization (ROP) of lactones. A seven-membered lactone called ε-caprolactone (ε-CL) is used as a monomer to produce poly (ε-CL). Although novozym 435 (immobilized form of candida antartica lipase B) can catalyze ROP of ε-CL efficiently, because of the cost reasons, chitin immobilized lipase was prepared for polycaprolactone synthesis in this study [1,2].The reason why chitin was chosen as a support material for immobilization in this study is that it is a cheap, ubiquitous and nontoxic material, also it has high protein affinity and this property makes chitin a demanding support for enzyme immobilization [3,4].

In this study, chitin was immobilized to lipase by two different methods: physical adsorption and crosslinking with glutaraldehyde. To evaluate prepared catalysts for polycaprolactone synthesis, polymerizations reactions were carried out simultaneously with the same conditions by both chitin immobilized catalysts (physically immobilized and crosslinking with gluteraldehyde) and novozym 435. Among chitin immobilized lipases, crosslinking with gluteraldehyde showed higher catalytic activity. To reach optimum polymerization conditions, chitin immobilized lipase crosslinking with gluteraldehyde was used in further polymerization reactions. Effect of temperature, polymerization time and enzyme concentration on molecular weights (Mn) of polycaprolactone was investigated in this study. Also, reuse of chitin immobilized lipases was examined.

Materials and Method

Novozym 435 and free form of lipase enzyme (Novozymes CALB L) was purchased from Sigma Aldrich Company. ε-caprolactone (%99) was provided Alfa Aesar and stored under dry nitrogen over molecular sieves (3A^{o}). Toluene was supplied from Merck Company. Gluteraldehyde solution, chloroform and Chitin from crab shells were purchased from Sigma Aldrich Company.

First part of the experiments was immobilization of lipase. Gluteraldehyde pretreated chitin was prepared by adding chitin into 50 ml %0.2(v/v) gluteraldehyde/phosphate buffer solution (ph7,0.015M). Then this suspension was stirred (160 rpm) for 1 hour at 25 ^{o}C. The gluteraldehyde pretreated chitin was filtered and washed with distilled water. Secondly, determined amounts of CALB enzyme solution was diluted by phosphate buffer (ph 7, 0.015 M). 400 mg chitin and gluteraldehyde-pretreated chitin supports were suspended in prepared diluted enzyme solutions. Enzyme-support suspensions were stirred (160 rpm) for 5 hours at 25 ^{o}C. Immobilized enzymes were characterized by scanning electron microscopy.

In the second part of the study, polymerization reactions were performed at different temperatures (60 ^{o}C, 70 ^{o}C, 80 ^{o}C) in toluene (toluene to ε-caprolactone ratio, 2:1(v/v)) under dry nitrogen. At a specified time, reaction was terminated by adding chloroform and enzyme was separated by filtration. Chloroform in the filtrate was largely evaporated and resulted solution was precipitated in methanol. Polymer was filtered and dried at 35 ^{o}C.

Characterization of the resulting polymers was performed by GPC, FTIR and ^{1}H-NMR. Molecular weights and polydispersity were determined by GPC using Agilent 1100 HPLC system.

Results and Discussion

In figure 1, for 24 hours and at 70 ^{o}C, comparison of three enzymes mentioned above with respect to Mn can be seen.

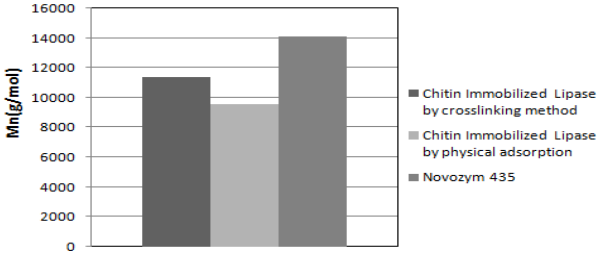

Figure 1. Comparison of enzymes with respect to Mn

Conclusions

Temperature, polymerization time and enzyme concentration had important effects on molecular weights (Mn) of polycaprolactone. Also, in comparison to novozym 435, although polymerization reaction was slower by chitin immobilized lipase, polydispersity were reduced by this type of catalyst.

References

[1] **Albertsson, A.C., Srivastava, R.K.**, 2008. Recent developments in enzyme-catalyzed ring-opening polymerization, *Advanced Drug Delivery Reviews*, **60**, 1077-1093.

[2] **Kumar, A., Gross, R.A.,** 2000. Candida antartica lipase B catalyzed polycaprolactone synthesis: effects of organic media and temperature. *Biomacromolecules*, **1**, 133-138

[3] **Gomes, M.F., Pereira, E.B., Castro, H.F.,** 2004. Immobilization of lipase on chitin and its use in nonconventional biocatalysis, *Biomacromolecules*, **5**, 17-23.

[4] **Foresti, M.L., Ferreira M.L.**, 2007. Chitosan-immobilized lipases for the catalysis of fatty acid esterifications, *Enzyme and Microbial Technology*, **40**, 769-777.

Novel Bioimaging Probes Combining Well-Defined Multifunctional Polymers and Two-Photon Absorption Chromophores

C. Cepraga[1], S. Adjili[1], S. Marotte[1,4], T. Gallavardin[2], J. Massin[2], J. C. Mulatier[2], C. Monnereau[2], O. Maury[2], Y. Bretonnière[2], A. Favier[1], Y. Leverrier[4], J. Marvel[4], P. L. Baldeck[3], C. Andraud[2], M. T. Charreyre[1]

[1]Ingénierie des Matériaux Polymères, INSA Lyon and Laboratoire Joliot Curie, ENS Lyon, France.
[2]Laboratoire de Chimie, ENS Lyon, France.
[3]Laboratoire de Spectroscopie Physique, Université Joseph Fourier Grenoble, France
[4]INSERM U851, Immunité, Infection, Vaccination, Lyon, France

Arnaud.favier@ens-lyon.fr

The development of polymer/chromophore conjugates is particularly attractive in many fields such as bioimaging. Indeed, polymers bring many advantageous features to the conjugates. First, they contribute to the solubilization of the hydrophobic organic chromophores in biorelevant media. In addition, highly fluorescent probes are obtained through the coupling of many chromophores on the same polymer backbone. Finally, multifunctional polymers can also be used to immobilize other entities like bioactive moieties (bioconjugates).

Using well-defined multifunctional polymers synthesized by RAFT polymerization [1-2], we developed biocompatible conjugates bearing a controlled number of chromophores that can be excited in the red or the near–infrared where absorption of light by the biological media and tissues is low.

Figure 51: Schematic representation of the polymer/chromophore (F) conjugates

.

In particular, high two-photon absorption (TPA) chromophores were covalently bound onto the polymers since two-photon excitation is highly localized and thus allows high 3D resolution imaging with low out-of-focus photodamages or photobleaching [3-4].

After a thorough characterization of the mono- and two-photon optical properties of the conjugates, their cytotoxicity as well as their internalization into live cells were evaluated using flow cytometry and confocal fluorescence microscopy.

[1]. Favier, A., D'Agosto, F., Charreyre, M.-T., Pichot, C., *Polymer*, **2004**, *45(23)*, 7821-7830.
[2]. Favier, A., de Lambert, B., Charreyre, M.-T., in *Handbook of RAFT Polymerization*, **2008**, Barner-Kowollik, C., Ed.; Wiley-VCH Verlag GmbH & Co. KGaA, 483-535.
[3]. Zipfel, W.R., Williams, R.M., Webb, W. W., *Nat. Biotech.*, **2003**, *21(11)*, 1369-1377.
[4]. So, P.T.C., Dong, C. Y., Masters, B. R., Berland, K. M., *Ann. Rev.of Biomed. Eng.*, **2000**, *2(1)*, 399-429.

Blends and composites of biodegradable polyesters with cellulosic fibers. Effect of chemical modification on the morphological, thermal and mechanical properties.

Mariano Pracella[1], Md. Minhaz-Ul Haque[2], Maria Errico[3], Gennaro Gentile[3], Vera Alvarez[4]

[1]Institute for Composite and Biomedical Materials, IMCB-CNR, Via Diotisalvi
[2]Pisa 56122, Italy 2Department of Chemical Engineering & Materials Science, University of Pisa, Pisa 56122, Italy
[3]Institute of Chemistry and Technology of Polymers, ICTP-CNR, Pozzuoli 80078 (NA), Italy
[4]Research Institute of Material Science & Technology, INTEMA-CONICET, Mar del Plata, Argentina

e-mail: mariano.pracella@diccism.unipi.it

Introduction

Incorporation of cellulosic fibers into polymers matrices offers the possibility to design new composite materials with reduced environmental impact, due to the biodegradability, renewability and low cost of natural fillers. The properties of these composites are strictly depending on the interactions at the interface between the components. To improve the interfacial adhesion and fiber dispersion into the polymer matrix, either addition of modified components or introduction of reactive groups can be advantageously employed [1]. The present study is focused on the preparation and characterization of new binary and ternary polyester/cellulose composites with enhanced properties and processability for packaging applications.

Materials and Methods

Poly(lactic acid) (PLA) (Hycail HM 1011, MFR[190 °C/2.16 Kg]= 2-4 g/10min), ethylene-vinyl acetate-glycidylmethacrylate (EVA-GMA) (Elvaloy AS DuPont), polycaprolactone (PCL) (CAPA 680, Solvay) were used as polymer components. Cellulose fibers (CF) of different length (Technocel 165 and 500-1, Neuchem) were used as filler. Binary and ternary composites (PCL/CF, PLA/CF, EVA/CF, and PLA/EVA-GMA/CF) were obtained by melt mixing in a Brabender Plasti-corder internal mixer at 150/180 °C (60 rpm, 10 min). The various systems were then examined by SEM, RX, FT-IR, DSC, TGA, DMTA and tensile tests.

Results and Discussion

Composites of PCL with CF were compatibilized by adding cellulose modified with butyric acid (CFB). SEM analysis of these samples pointed out an improved adhesion between PCL and fibers as compared to uncompatibilized PCL/CF composites. DSC and XRD analyses showed that the PCL crystallinity decreased from 68% to 50% by increasing the CFB content (0-10 wt%) due to miscibility effects [2] (**Figure 1**).

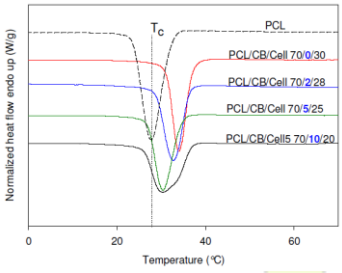

***Figure 1**. DSC cooling thermograms of PCL and PCL/CF composites*

The properties of PLA/EVA-GMA blends and PLA/EVA-GMA/CF ternary composites were investigated as a function of composition. For the blends the values of elastic modulus followed the model of Coran and Patel [3]. Tensile strength of blends decreases with increasing EVA-GMA content due to the lower strength of EVA-GMA, while elongation at break increased exponentially (**Figure 2**).

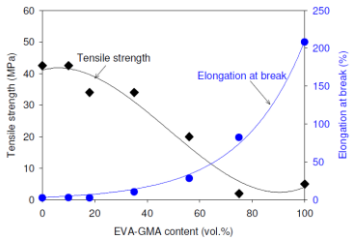

***Figure 2.** Tensile strength and elongation at break of PLA/EVA-GMA blends*

SEM microscopy pointed out a higher compatibility between cellulose and PLA/EVA-GMA matrix blends over all the composition range, as compared to PLA/CF composites (**Figure 3**). This effect was accounted for by the reaction of epoxy groups of EVA-GMA with the OH groups of cellulose and OH/COOH groups of PLA.

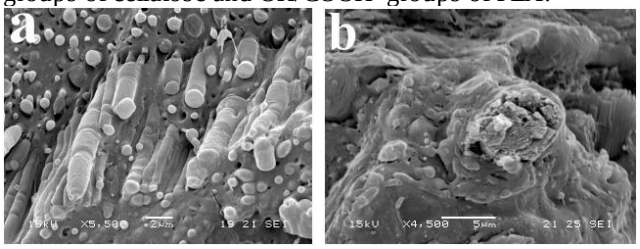

***Figure 3.** (a) PLA/EVA-GMA 50/50; (b) PLA/EVA-GMA/CF*

Moreover, a nucleating effect of cellulose fibers on the crystallization of PLA was observed with formation of transcrystalline morphology. Enhanced mechanical properties, i.e. tensile strength, elastic modulus and elongation at break, were also recorded for ternary composites.

Conclusions

For all examined systems the interfacial adhesion and properties are improved both in the presence of modified cellulose (CFB) and reactive polymer (EVA-GMA). In the case of ternary composites PLA/EVA-GMA/CF the phase morphology and mechanical properties can be advantageously modulated by varying the ratio of polymer components.

References

[1] Pracella M, Haque MM, Alvarez V. Macromol. Mater. Eng. 2010; 295: 949–957
[2] Kusumi R et al. Cellulose. 2008;15:1–16
[3] Coran AY, Patel R. J. Appl Polym Sci. 1976;20: 3005.

Synthesis and (Bio)Conjugation of Polypeptides from *N*-Carboxyanhydride (NCA) Polymerization

Jin Huang[a], *Gijs Habraken*[b], *Andreas Heise*[a,b]

andreas.heise@dcu.ie

[a]School of Chemical Sciences, Dublin City University, Dublin 9, Ireland.
[b]Technische Universiteit Eindhoven, Den Dolech 2, P.O. Box 513, 5600 MB, Eindhoven, The Netherlands

Introduction: Recent developments in the ring-opening polymerization of N-carboxyanhydrides (NCA) allow the synthesis of well-controlled polypeptides.[1] A very common and convenient method of NCA polymerization is the initiation by primary amines (amine mechanism). We investigated the effect of reaction parameters like temperature and pressure on this approach with respect to structural control and reaction kinetic. Secondly, we will present our results on the lateral as well as end-group (bio)functionalization of synthetic polypeptides for example for the synthesis of glycopeptides.

Results and Discussion:
We have systematically investigated the polymerization of various amino acid N-carboxyanhydrides (NCAs) at 0 °C.[2] Detailed MALDI-ToF analysis of homo-polymerizations clearly confirms that frequently occurring end-group termination and other side-reactions are absent at 0 °C. The polymerization is thus controlled and homo and copolypeptides with low polydispersities around 1.1 can be obtained. The controlled character of the low temperature NCA polymerization was further verified by the successful multi-block copolymer synthesis from polypeptide macroinitiators (Figure 1).

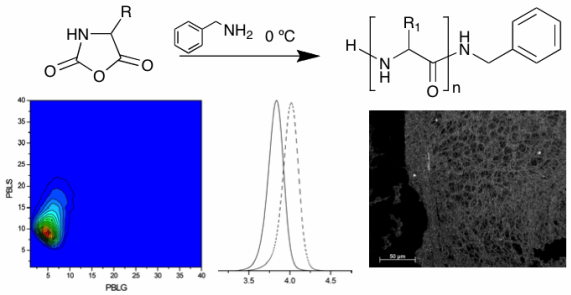

Figure 1. NCA polymerization at 0 °C: MALDI-ToF contour plot of copolymerization of benzyl-L-glutamate (BLG) and benzyl-L-serine (BLS) NCA confirming randomness of monomers (left), GPC traces of P(BLG-*b*-BLS) synthesis by macoinitiation (center) and optical microscopy picture of P(BLG-*b*-BLS).[2]

Based on these experimental procedures functional polypetides were targeted by using efficient thiol chemistry and azide-alkyne click reactions.[3,4] The latter was applied for the synthesis of glycopeptides. In the initial polymerization poly(DL-propargylglycine) and poly(BLG–*co*–DL-propargylglycine) were synthesized to yield well-defined polypeptides with polydispersity indices below 1.3. The subsequent glycosylation was achieved by Huisgen [3+2] cylcoaddition ('click' reaction) with azide-functional galactose (Figure 2). FTIR, NMR, SEC and MALDI-TOF analyses verified the successful glycosylation and suggest a high efficiency of the click reaction. Upon glycosylation a transition from β-sheet to random coil was observed for the homopolymer in the solid state. The homo-glycopeptide was found to be water-soluble and to form aggregates in water above a critical concentration of 0.079 mg/mL. Selective lectin binding experiments confirmed that the glycopeptides could be used in biorecognotion applications. The fact that no labile bond was used to link the alkyne to the amino acid allows to apply common amino acid deprotection chemistry on the glycopeptides as was shown for the γ-benzyl-L-glutamate copolymer. The isosteric linkage thus improves the chemical and potentially metabolic stability while retaining biological activity.

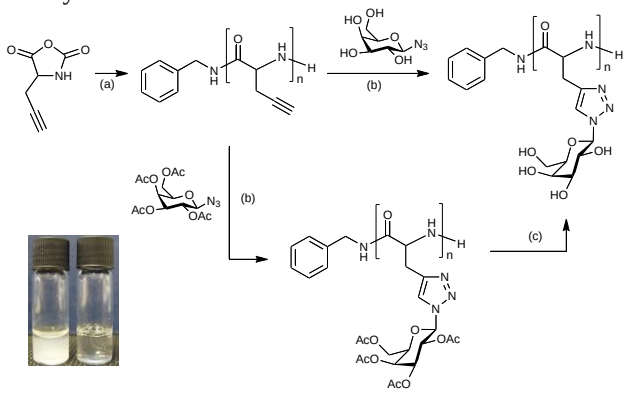

Figure 2. Synthesis of glycopeptides by NCA polymerization und subsequent glycosylation by 'click' chemistry. The inset shows positive reaction with lectin RCA_{120} (left, turbid) and negative control with lectin Con A (right).[4]

References:

1. Hadjichristidis, N.; Iatrou, H.; Pitskalis M.; Sakellariou, G. *Chem. Rev.* **2009**, *109*, 5528.
2. Habraken, G.J.M.; Peeters, M.; Dietz, C.H.J.T.; Koning, C.E.; Heise, A. *Polym. Chem.* **2010**, *1*, 514.
3. Habraken, G.J.M.; Koning, C.E.; Heuts, J.P.A.; Heise, A. *Chem. Commun*. **2009**, *24*, 3612.
4. Huang, J.; Habraken, G.; Audouin, F.; Heise, A. *Macromolecules* **2010**, *43*, 6050.

Acknowledgement

The low temperature NCA polymerization project was carried out with financial support from the Dutch Polymer Institute (DPI, project number 610). The glycopeptides project was conducted under a Science Foundation Ireland (SFI) funded Principle Investigator Award 07/IN1/B1792. AH is a SFI Stokes Senior Lecturer (07/SK/B1241).

Study on biodgradability of xenobiotic polymers based on numerical simulation and experimental outcomes

Masaji Watanabe[1] *Fusako Kawai*[2]

[1]Graduate School of Environmental Science, Okayama University
watanabe@ems.okayama-u.ac.jp

[2]Center for Nanomaterials and Devices, Kyoto Institute of Technology
fkawai@kit.ac.jp

Microbial depolymerization processes are categorized into two classes, exogenous type depolymerisation processes and endogenous type depolymerisation processes. In an exogenous depolymerization process, molecules reduce molecular weight by trancation of monomer units from their terminals. Polymers subject to exogenous depolymerization processes include polyethylene (PE). The mechanism of PE biodegradation is based on two essential factors, gradual weight loss of large molecules due to β-oxidation and the direct consumption or absorption of small molecules by cells. A mathematical model based on those factors was proposed to study PE biodegradation [1, 2, 3, 4].

Polyethylene glycol (PEG) is also subject to exogenous depolymerization processes. The mathematical techniques originally developed for the PE biodegradation was extended to study the biodegradation of PEG. Problems were formulated to determine degradation rates based on the weight distribution of PEG with respect to molecular weight

before and after cultivation of a microbial consortium E-1, and transition of the weight distribution was simulated [5, 6, 7, 8].

Unlike exogenous type depolymerization processes, molecules are cleaved at arbitrary positions in endogenous type depolymerization processes. A mathematical model for endogenous depolymerization process was proposed to study enzymatic depolymerization process of PVA [9, 10]. Mathematical model originally proposed for enzymatic degradation of PVA was extended to study enzymatic hydorolythis of polylactic acid (PLA) [11, 12].

Techiques in studies on biodgradability of xenobiotic polymers based on numerical simulation and experimental outcomes will be described, and results will be introduced.

References

[1] Fusako Kawai, Masaji Watanabe, Masaru Shibata, Shigeo Yokoyama, Yasuhiro Sudate, Experimental analysis and numerical simulation for biodegradability of polyethylene, Polymer Degradation and Stability 76 (2002) 129-135.

[2] Masaji Watanabe, Fusako Kawai, Masaru Shibata, Shigeo Yokoyama, Yasuhiro Sudate, Computational method for analysis of polyethylene biodegradation, Journal of Computational and Applied Mathematics, Volume 161, Issue 1, 1 December 2003, 133-144.

[3] Fusako Kawai, Masaji Watanabe, Masaru Shibata, Shigeo Yokoyama, Yasuhiro Sudate, Shizue Hayashi, Comparative study on biodegradability of polyethylene wax by bacteria and fungi, Polymer Degradation and Stability 86 (2004), 105-114.

[4] Masaji Watanabe, Fusako Kawai, Masaru Shibata, Shigeo Yokoyama, Yasuhiro Sudate, Shizue Hayashi, Analytical and computational techniques for exogenous depolymerization of xenobiotic polymers, Mathematical Biosciences 192 (2004) 19-37.

[5] M. Watanabe, F. Kawai, Numerical simulation of microbial depolymerization process of exogenous type, Proc. of 12th Computational Techniques and Applications Conference, CTAC-2004, Melbourne, Australia in September 2004, Editors: Rob May and A. J. Roberts, ANZIAM J. 46(E) pp.C1188--C1204, 2005.

[6] M. Watanabe, F. Kawai, Mathematical study of the biodegradation of xenobiotic polymers with xperimental data introduced into analysis, Proceedings of the 7th Biennial Engineering Mathematics and Applications Conference, EMAC-2005, Melbourne, Editors: Andrew Stacey and Bill Blyth and John Shepherd and A. J. Roberts, ANZIAM J. 47 pp.C665--C681, 2007.

[7] M. Watanabe, F. Kawai, Mathematical analysis of microbial depolymerization processes of xenobiotic polymers, Proceedings of the 14th Biennial Computational Techniques and Applications Conference, CTAC-2008, Editors: Geoffry N. Mercer and A. J. Roberts, ANZIAM J. 50 (CTAC-2008), C930--C946, 2009.

[8] M. Watanabe and F. Kawai, Effects of microbial population in degradation process of xenobiotic polymers, In P. Howlett, M. Nelson, and A. J. Roberts, editors, Proceedings of the 9th Biennial Engineering
Mathematics and Applications Conference, EMAC-2009, volume 51 of ANZIAM J., pages C682--C696, September 2010.

[9] Masaji Watanabe, Fusako Kawai, Numerical Simulation for Enzymatic Degradation of Poly(vinyl Alcohol), Polymer Degradation and Stability, Volume 81, Issue 3, 2003, 393-399.

[10] M. Watanabe and F. Kawai, Mathematical modelling and computational analysis for enzymatic degradation of xenobiotic polymers, Applied Mathematical Modelling 30 (2006) 1497--1514.

[11] M. Watanabe, F. Kawai, S. Tsuboi, S Nakatsu, and H. Ohara, Study on enzymatic hydrolysis of polylactic acid by endogenous depolymerizaion model, Macromolecular Theory and Simulations 16 (2007) 619--626.

[12] M. Watanabe, F. Kawai, Modeling and analysis of biodegradation of xenobiotic polymers based on experimental results, Proceedings of the 8th Biennial Engineering Mathematics and Applications Conference, EMAC-2007, Editors: Geoffry N. Mercer and A. J. Roberts, ANZIAM J. 49 (EMAC-2007) pp.C457--C474, 2008.

Acknowledgments

This work was supported by KAKENHI (20540118).

Presence of Nano Precursors in Lignin of Hevea Brasiliensis (Rubber wood): A SEM, FTIR study

Salma Tabassum, Othman Sulaiman, Rokiah Hashim

Division of Bio-resource, Paper and Coatings Technology, School of Industrial Technology, Universiti Sains Malaysia, 11800 Penang, Malaysia.

Email:salmazenith@gmail.com

Abstract

Lignin is biopolymer that belongs to the main components of wood. The modification in the chemical structure of lignin of rubber wood chip, Soda-Anthraquinone and total chlorine free bleached lignin content was monitored by SEM and FTIR spectroscopy. FTIR spectroscopy is an important tool for lignin characterization based on several major vibration bands associated with generally found chemical groups. In wood treated by soda pulping, there was a progressive increase in the lignin content, which is evident from increase in the relative intensities of lignin associated bands and a corresponding decrease in the intensities of carbohydrate bands. In contrast, there was a decrease in the lignin content of TCF bleached pulp. Less than half of the surface lignin was removed during bleaching process, with the oxygen stage and the final peroxide stage being the most effective. The SEM result also shows that the surface lignin remaining on TCF-bleached lignin was remnant from native rubber wood lignin having tetra functional branch points, which was never released from wood fibers, but it had undergone several structural changes during cooking.

Keywords

Lignin, Total chlorine free bleaching (TCF), Soda-Anthraquinone (soda-AQ), Rubber wood chip (RWC).

Cellulose nanostructure in natural fibers from position resolved SAXS and WAXS measurements.

Christopher J. Garvey[1], *Michael P. Weir*[1], *Kevin J. Jarrett*[2], *Craig E. Buckley*[2]

[1]Bragg Institute, Australian Nuclear Science and Technology Organisation, Australia
[2] Curtin University of Technology, Australia

Chris.Garvey@ansto.gov.au

Introduction

Cellulose is a polymer β-(1-4) linked glucose units. By contrast to synthetic polymers where crystallization is an entirely separate process from the synthesis, the nature of cellulose biosynthesis is such that cellulose crystallites are synthesized at the same time as the polymer by an array of synthetic complexes embedded with a specific orientation with respect to the cell membrane. Biosynthesis by the arrays (rosette complexes[1]) arranges cellulose chains in parallel along the length of the crystallite, rather the than the more thermodynamically favorable anti-parallel form[2]. As a result of this modern view of cellulose biosynthesis, and careful analysis of x-ray diffraction of powder (isotropic) samples, we view cellulose as a nanocrystalline (microfibrilar) solid rather than a semi-crystalline solid[3]. This stiff crystalline material is embedded in an amorphous matrix consisting of lignin and other cell wall polysaccharides. The anisotropic arrangements of the microfibrils (texture) within plant tissue is a key means by which plants may modulate their mechanical properties with little or no change in chemistry or nanostructure.

There is a renewed technological interest in natural fibres due to a dawning molecular scale understanding of biosynthesis and generation of texture[1], and the potential to economically unlock glucose locked within the crystalline microfibril. In our work we examine the response of these structures to mechanical deformations, both from the perspective of understanding mechanical performance, but also the physical changes to the packing of cellulose chains within the cellulose microfibril.

Materials and Methods

Palm nut fibres are the by-product of palm cooking oil and represent a considerable source of unexploited biomass[4]. Hemp fibres are used commercially for reinforcement of composite materials and textiles[5]. These materials have been selected because it is relatively easy to isolate single fibres for presentation to the x-ray beam and provide an interesting contrast in cellulose texture.

Small and wide angle X-ray scattering (SAXS and WAXS respectively) patterns have been collected on a two-dimensional X-ray detector from single hemp and palm nut fibres. Both measurements were made on a Bruker Nanostar instrument - operational details of the instrument may be found on its web-site[6].

Results and Discussion

The azimuthal SAXS and WAXS profiles indicate two different cellulose arrangements in the palm and hemp fibres. Azimuthal profiles of WAXS are interpreted in terms of a rectangular cellular cross-section, while the cross section of the hemp fibre would seem to be largely cylindrical. In the palm fibres the cellulose microfibrils are largely arranged in a helix around the fibre axis. The angle of this helix with respect to the fibre axis is approximately 35°. In the hemp fibres the microfibrils are arranged largely parallel to the fibre axis.

Radial averages of WAXS measurements and the Scherer equation (assuming pure size broadening of diffraction peaks) were used to calculate the lateral dimensions of the cellulose microfibril. The picture of a rectangular cross-section is consistent with the view of cellulose biosynthesis. The palm fibre microfibril is smaller than that of the hemp fibre. The relatively homogenous electron density of all cell wall polymers means that SAXS is of limited use in determining cellulose nanostructure. SAXS data is consistent with long voids in the fibre aligned largely with microfibril direction.

Conclusions

SAXS and WAXS provide, non-destructively, information about the arrangements of cell wall polymers in single fibres. Thus both measurements and the analysis outlined here are suitable and provide complementary information for the *in-situ* studies of structural re-arrangements of fibres during tensile deformation using the synchrotron radiation. These studies, which are currently underway, should provide an interesting contrast, in the case of the palm fibres it will be the cellulose helix which is deformed, and in the case of the hemp fibres the tensile stress will be applied largely along the direction of the cellulose crystallite.

References

1. Carpita, N. C. *Plant Physiol.* **155** , 171 (2011).
2. Sarko, A. Muggli, R. *Macromolecules*, **7**, 486 (1974).
3. Garvey, C.J., *et al. Macromol. Chem. Phys.*, **206**, 1568 (2005).
4. http://en.wikipedia.org/wiki/Palm_kernel_oil
5. http://en.wikipedia.org/wiki/Hemp
6. http://www.ansto.gov.au/research/bragg_institute/facilities/instruments/saxs/Bruker_SAXS

Polymeric lipidic membrane permeabilizers displaying densely packed arrays of crown ether lateral substituents

M Liu[*], *N.Illy*[*], *B.Brissault*[*], *K.Ondrias*[**], *J.Penelle*[*], *V.Barbier*[*]

*Institut de Chimie et Matériaux Paris-Est (ICMPE), 2 rue Henri Dunant, 94320 Thiais, France
** Institute of Molecular Physiology and Genetics, Slovak Academy of Sciences, Bratislava, Slovak Republic

barbier@icmpe.cnrs.fr

Introduction

Designing novel synthetic agents that are able to affect cellular membrane properties and induce a controlled permeabilization while keeping the integrity of the membrane is a major challenge for academic chemistry and biophysics, applications in pharmaceutical research, and biotechnologies.

In this context, we developed an original family of polymeric membranar permeabilizers. Their originality lies on a unique structure with single or geminated crown-ethers located on each three carbons along the main chain (Scheme 1). This particular stereochemistry induces absolutely unusual inter-substituents distances.

The communication reports the synthesis of four monomers **(1)-(4)** differing by the number and size of crown-ether substituents and the corresponding polymers. Their ion binding properties as well as their ability to permealize bilipidic membranes have been investigated.

Materials and methods

The polymers were obtained via the anionic ring-opening polymerization of the substituted cyclopropane-1,1-dicarboxylate monomers (scheme 1). A controlled polymerization was obtained by using a procedure we recently developed based on tetrameric phosphazene base $ButP_4$ in association with a protic precursor to the initiator.[1,2]

The binding efficiencies of the polymers and their monomeric analogs towards Li^+, K^+ and Na^+ were evaluated from distribution equilibria of the respective salt complex between an aqueous phase and an immiscible organic solvent.

The membrane permeabilization ability of synthesized polymers was investigated by conductance measurements on planar bilipidic membranes (*BLM experiments*).

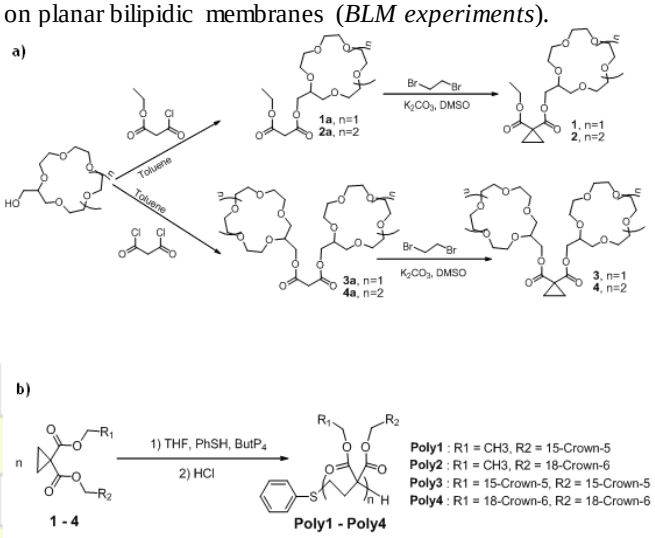

Scheme 1: monomers (a) and polymers (b) synthesis pathways

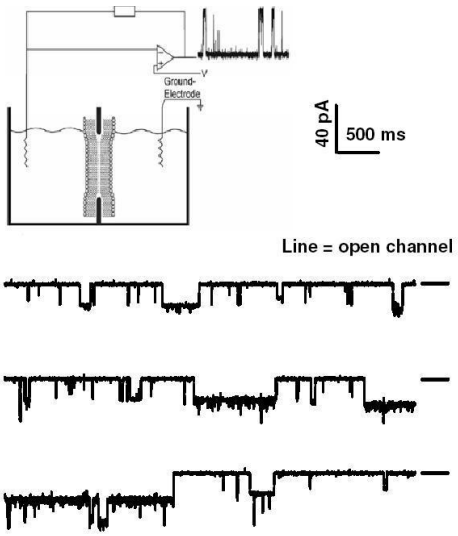

Figure 1: *BLM experiments*; (up) experimental set-up; (down) some current traces obtained with Poly(1) at 40 mV. The current jumps are characteristics of the closure and opening of well-defined pores within the bilipidic membrane.

A conventional set-up for BLM conductance measurements uses two chambers that are filled with buffer (Figure 1). The membrane is located between both chambers. The current flowing through pore in the BLM in response to an applied voltage is then recorded and used to obtain insights on the pore conductance.

Results and discussion

To span a bilipidic membrane, polymers have to be around 3-7 nm. Four oligomers corresponding to **poly(1)-poly(4)** has been successfully synthesized with a good control of molecular weights ($6.10^3<M_n<10^4$ g/mol) and narrow polydispersity index (<1.2). Results obtained on the complexation of metallic cations indicate a strong polymer effect and the possibility of obtaining sandwich structures. Finally, BLM experiments revealed no pore formation in presence of monomers, whereas well defined pores could be observed in presence of the corresponding oligomers (Figure 1).

Conclusions

Original polymeric membrane permealizers with crown-ethers located on each three carbons along a polymer backbone has been developed and studied. Their activity on biological membranes is now under investigation.

References.

[1]N. Illy, S. Boileau, J. Penelle, V. Barbier, *Macromol. Rapid Commun.* **2009**, 30, 1731-1735.

[2]Illy, N.; Boileau, S., Buchmann, W., Penelle, J.; Barbier , V. *Macromolecules* **2010**, 43(21), 8782–8789.

Synthesis of monodisperse linear poly(oxazolines) with minimised structural defects as model compounds for elucidating cell membrane properties

Bryn Monnery[1], *Sunil Shaunak*[2], *Maya Thanou*[3], *Joachim Steinke*[1]

1. Chemical Biology Section, Department of Chemistry, Imperial College London, South Kensington Campus, London, SW7
2. AZ, UK; 2: Department of Infectious Diseases and Immunity, Faculty of Medicine, Imperial College London, Hammersmith Campus, London, W12 ONN, UK;
3. Pharmacy Department, Division of Pharmaceutical Sciences, King's College London, Franklin-Wilkins Building, London, SE1 9NH, UK.

Correspondence: j.steinke@imperial.ac.uk

-Linear poly(ethylenimine) is an important polymer in the field of gene delivery as it is widely used as a cationic model gene delivery vector [1, 2]. However it is extremely cytotoxic, and this toxicity is related to the molecular weight of the polymer [3, 4, 5]. Synthesis of linear PEI (l-PEI) is typically carried out by the cationic polymerisation of a 2-alkyl-2-oxazoline followed by hydrolysis (see figure 1).

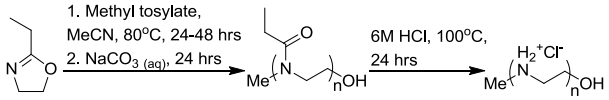

Figure 1: Commercial synthesis of l-PEI hydrochloride salt[6].

The current state of the art polymerisation of oxazolines was reported by Park and Kataoka [7] and shows low polydispersity up to a molecular weight of ~ 10 kDa. However, applying this methodology to higher molecular weights leads to a broadening of the molecular weight distribution by a chain transfer- coupling mechanism (see figure 2).

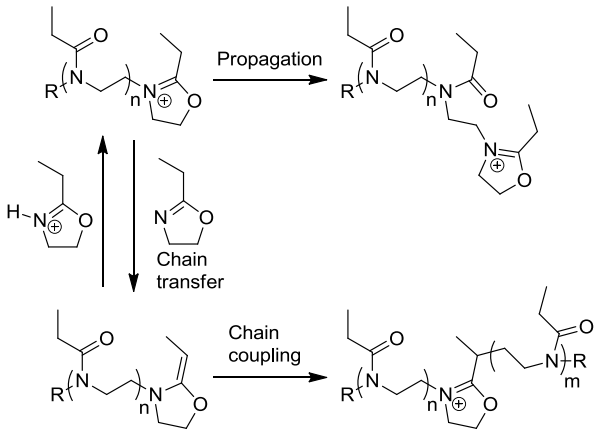

Figure 2: Competing propagation (nucleophilic substitution) and chain transfer (elimination) reactions, followed by chain coupling (alkene competing with the monomer). R = CH_3 or H (re-initiated polymers)

Optimised reaction conditions could be identified further suppressing chain-transfer lowering PDI values, for example at ~ 25 kDa polymers with PDI values of 1.03 instead of ~ 1.30 (see figure 3). This allowed us to synthesise higher molecular weight poly(oxazolines) than previously possible whilst retaining a very narrow molecular weight distribution.

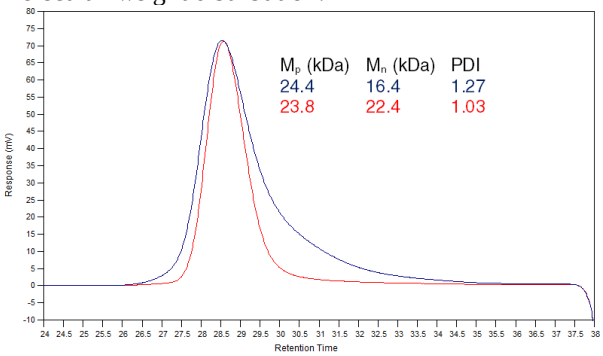

Figure 3: M_p = ~ 24 kDa poly(2-isopropyl-2-oxazoline) via (blue) the methodology of Park and Kataoka[4], and (red) the current work. Eluograms in DMF (1% TEA/ 1% acetic acid) of one drop of the crude reaction mixture in 1 ml DMF.

Polymers with a DP of around 250 have been synthesised without detectable chain transfer. Even higher molecular weight poly(oxazolines) with narrow PDI can be accessed in this way, though chain-coupling is present and crude product samples require an additional purification step via affinity chromatography. Our polymers are currently being employed to generate a rigorous data set which will allow us to determine the structure-activity relationship of l-PEI in regards to its cytotoxic properties.

References

1. Boussif, O., Lezoualch, F., Zanta, M. A., Mergny, M. D., Scherman, D., Demeneix, B., Behr, J. *et al.*, *Proc. Natl. Acad. Sci. U. S. A.* **92**, 7297-7301 (1995)
2. Boeckle, S., von Gersdorff, K., van der Piepen, S., Culmsee, C., Wagner, E. and Ogris, M., J. Gene Med. **6 (10)**, 1102-1111 (2004)
3. Fischer, D., Li, Y., Ahlemeyer, B., Krieglstein, J. & Kissel, T., *Biomaterials* **24**, 1121-1131 (2003)
4. Hunter, A. C., *Adv. Drug Delivery Rev.* 58, 1523-1531 (2006)
5. Falco, A., Encinas, P., Carbajosa, S., Cuesta, A., Chaves-Pozo, E., Tafalla, C., Estepa, A. and Coll, J. M., *Fish & Shellfish Immunology* **26**, 559-566 (2009).
6. Polyplus Transfection patent WO/2009/016507
7. Park, J.-S. & Kataoka, K., *Macromolecules* **39**, 6622-6630 (2006)

Proteins as mechanophores in damage self-reporting polymeric materials

N. Bruns, Samuel Lörcher, Thomas Winkler

Department of Chemistry, University of Basel, Klingelbergstrasse 80, CH-4056 Basel, Switzerland.

nico.bruns@unibas.ch

Living organisms have developed ways to detect and report damage of their tissue. This is usually accomplished by nerve signals, e.g., in the form of pain, or by optical signals, e.g., by the dark red color of a bleeding wound. The indication of damaged tissue is crucial for an organism in order to start to protect the respective body part. In technical applications, polymer-based materials are often used as load-bearing materials because they are lightweight, possess excellent mechanical properties and are easy to manufacture into any desired shape. Fiber-reinforced composites in particular find application in the aerospace, the automotive and the sporting goods sector. However, common polymers and composites do not visualize damage to alert the user of impeding danger. In order to avoid accidents, man-made polymeric materials that detect and report small scale structural damage before catastrophic failure occurs are highly desirable.

We have doped polymers and fiber-reinforced composites with engineered proteins. Microcracks and delamination defects due to strain or impact are reported by the proteins in the materials through a local change in the fluorescent properties of the proteins, e.g. a change in fluorescence resonance energy transfer (FRET) [1] or the vanishing of fluorescence [2]. These signals can be observed by fluorescence microscopy and other fluorescence methods.

References: [1] Bruns et al. *Angew. Chem., Int. Ed.* **2009, 48**: 5666-5669. [2] N. Bruns, S. Lörcher, GB1009280.7 **2010**.

Acknowledgements: Nico Bruns gratefully acknowledges the Marie Curie Actions of the European Commission for an Intra-European Fellowship.

Synthesis and Characterization of Redox and pH-sensitive Poly(aspartic acid) Hydrogel

B. S. Gyarmati, Á. Némethy, T. Gyenes, A. Szilágyi

Soft Matters Team, Department of Physical Chemistry and Materials Science, Budapest University of Technology and Economics, H-1521 Budapest, Hungary

e-mail: aszilagyi@mail.bme.hu

Hydrogels have been studied extensively because of their unique bulk and surface properties, as well as their responsiveness to external stimuli. Hydrogels play an important role in various biomedical applications, especially in the development of controlled drug delivery systems. Besides the stimuli responsive attribute, biocompatibility and biodegradability of the controlled drug delivery system is also important. Drug delivery systems aim to be compatible with the drug and control the rate of its release at the targeted biological disease site with little or no damage to the surrounding tissues [1]. Polymer gels based on amino acids may fulfill these requirements.

A novel preparation route was developed to synthesize chemically cross-linked poly(succinimide) (PSI) and poly(aspartic acid) (PASP) gels [2]. Several natural compounds were selected as cross-linkers. In this study we focused on PSI and PASP hydrogels containing redox sensitive cross-linkers. The resulting redox and pH sensitive gels were investigated and the interconversion between thiols and disulfides are produced in different conditions. This phenomenon is a key step in many biological processes, as well as being applicable in injectable polymeric implants.

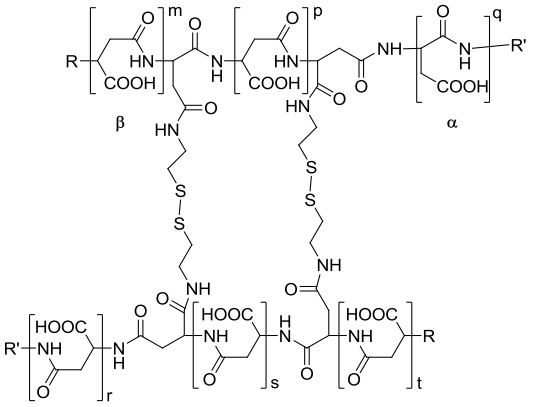

Figure 1. Chemical structure of the poly(aspartic acid) hydrogels with redox sensitive cross-linkers.

In case of cysteamine modified PASP, gelation can be carried out by oxidation. Gelation time strongly depends on the polymer concentration, but less on the modification ratio. To determine gelation time oscillation rheometry measurements were carried out. Storage modulus increased rapidly during oxidation, and gelation time determined from these measurements. Thiol and disulfide groups were characterized by Raman microscopy and it was proven that sol-gel transition occurs because of thiol-disulfide transformation in redox reaction.

With a combination of two kinds of cross-linker – redox sensitive and inert cross-linker – we could synthesize PASP hydrogel with well defined, adjustable swelling properties. The hydrogels could respond with a volume change when the environmental properties, such as the pH or redox potential, were varied.

Swelling degree of poly(aspartic acid) gels showed strong pH-dependence. They show an abrupt change at about the pKa values of poly(aspartic acid) so this property arises because of the polymer and it is independent from the cross-linkers.

Redox sensitivity was also characterized by measuring swelling degrees. Swelling - shrinking response of the hydrogels, due to the cleaving and reforming of the disulfide bonds, could be observed through several cycles. Relative change in swelling degree can be controlled by the gel composition. Elastic moduli of gels also change in the redox reaction.

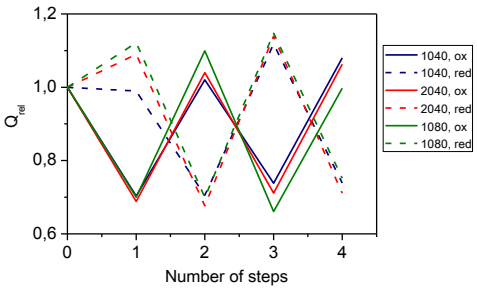

Figure 2. Repeatable swelling and shrinking of redox sensitive gels through several reduction and oxidation cycles.

Redox and pH sensitive nanogels were also synthesized. By applying these nanoparticles in drug delivery the disadvantage of macroscopic gels with slow response to environmental parameters could be overcome [3].

Acknowledgement: This research was supported by the OTKA Foundation (Grant number PD76401) and by the NKTH - A*STAR Hungarian - Singaporean Bilateral S&T International Co-operation (BIOSPONA). This research was also supported by the János Bolyai Research Scholarship of the Hungarian Academy of Sciences.

[1] S. W. Shalaby (ed.): Designed-to-Degrade Systems, Hanser Publishers, Munich, Vienna, New York (1994)
[2] T. Gyenes, V. Torma, B. Gyarmati and M. Zrinyi, *Acta Biomater* **4**, 733 (2008)
[3] J. K. Oh, R. Drumright, D. J. Siegwart and K. Matyjaszewski, *Prog. Polym. Sci.* **33**, 448 (2008)

Copoly(2-oxazoline)s exhibiting side chains for thiol-ene reactions – Synthesis of glycopolymers and their potential for biological applications

Kristian Kempe,[a] *Christoph Biskup*,[b] *Michael Gottschaldt*,[a,c] *Ulrich S. Schubert*[a,c]*

[a] Laboratory of Macromolecular and Organic Chemistry, Jena Center for Soft Matter (JCSM), Friedrich-Schiller-University Jena, Humboldtstr. 10, 07743 Jena, Germany;
[b] Biomolekulare Photonik, Universitätsklinikum Jena, Teichgraben 8, 07743 Jena, Germany;
[c] Dutch Polymer Institute (DPI), John F. Kennedylaan 2, 5612 AB Eindhoven, The Netherlands.

E-mail: ulrich.schubert@uni-jena.de; kristian.kempe@uni-jena.de.

Introduction

Poly(2-oxazoline)s are a perfectly suited class of polymers for the preparation of well-defined (co-)polymers, allowing the integration of a wide range of functionalities. Due to their known biocompatibility poly(2-oxazoline)s have the potential to find a wide range of applications in biological systems. The incorporation of manifold conjugation sites in the polymer can be achieved by both side group and end group functionalization, whereby the polymer properties can be tailored by the nature of the side chains. Besides a defined structural design by preparation of hydrophilic and hydrophobic blocks as well as the fine-tuning of the crystallinity, functionalized side chains can be utilized for subsequent efficient modification reactions, e.g. for "click chemistry", allowing the introduction of sugar-moieties, peptide sequences as well as specific dye molecules.

Results and Discussion

Here we report the synthesis of a series of copoly(2-oxazoline) consisting of 2-ethyl-2-oxazoline as hydrophilic monomer as well as 2-decenyl-2-oxazoline (DecOx), a hydrophobic double bond containing monomer (Figure 1). The incorporation of DecOx was varied from 10 to 60% yielding water-soluble and insoluble copolymers.

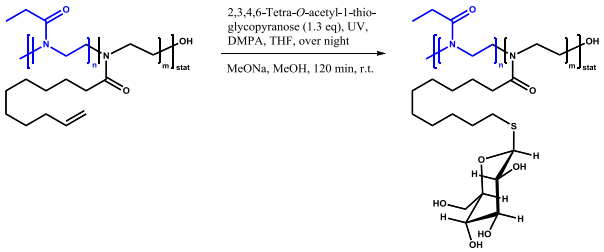

Figure 1. Schematic representation of the preparation of glycopoly(2-oxazoline)s using the thiol-ene approach.

Applying thiol-ene "click" reactions the corresponding glycopolymers were prepared and subsequently studied systematically in terms of their LCST behavior resulting in a decrease of the cloud point temperature with increasing sugar content in water. The overall hydrophobic copolymers and glycopolymers respectively, were used for the preparation of functional nanoparticles. To be able to study their cellular uptake these copolymers where labeled with fluorescein as well as fluorescein 5(6)-isothiocyanate prior to the nanoparticle formation by the nanoprecipitation technique. The particle size could be varied by the concentration used as well as the applied method encompassing the dialysis and dropping technique, respectively. Furthermore, the cellular uptake of the particles was revealed by confocal laser scanning microscopy (Figure 2).[1]

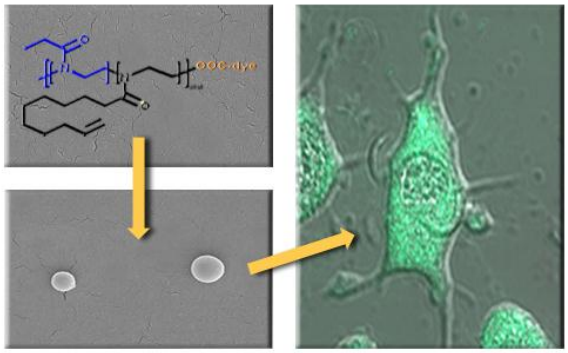

Figure 2. Confocal micrograph of fibroblasts incubated for 24 h with fluorescein labeled nanoparticles.

In addition, bulk (co-)polymerizations of the fatty acid based DecOx as well as thiol-ene reactions in environmentally friendly solvents could be performed demonstrating the green character of this copolymer system.

Reference

[1] K. Kempe, A. Vollrath, H. W. Schaefer, T. G. Poehlmann, C. Biskup, R. Hoogenboom, S. Hornig and U. S. Schubert, *Macromol. Rapid Commun.*, 2010, **31**, 1869-1873.

Engineering Alg-PEG Hybrid Microspheres for Biomedical Applications

Redouan Mahou[1], Carmen Gonelle[2], Géraldine Parnnaud[2], Frederic Schmitt[3], Gabriela Kollárikova[4], Lucienne Juillerat[3], Igor Lacík[4], Christine Wandrey[1]

[1]Ecole Polytechnique Fédérale de Lausanne (EPFL), Switzerland,
[2]University of Geneva (HUG), Switzerland,
[3]Centre Hospitalier Universitaire Vadoise (CHUV), Lausanne, Switzerland,
[4]Polymer Institute of the Slovak Academy of Sciences, Bratislava, Slovakia

redouan.mahou@epfl.ch

Introduction: For the last three decades, sodium alginate (Na-alg) based hydrogels have become one of the most studied systems for cell immobilization. Such hydrogels are obtained by ionotropic gelation of Na-alg in presence of Ca^{2+}or Ba^{2+}. However, these hydrogels suffer from mechanical stability deficiency, limited durability, and permeability drawbacks. Frequently used coating or reinforcement with polycations requires multi-step processes and can have a negative impact on the biocompatibility. Our approach aims at combining ionotropic gelation of alg and covalent cross-linking of poly(ethylene glycol) (PEG) derivatives in one step and designing a process which yields alginate-PEG hybrid microspheres (Alg-PEG-M).

Methods: Alg-PEG-M and PEG-M were prepared at 37°C under physiological conditions employing a coaxial airflow droplet generator (Fig.1)

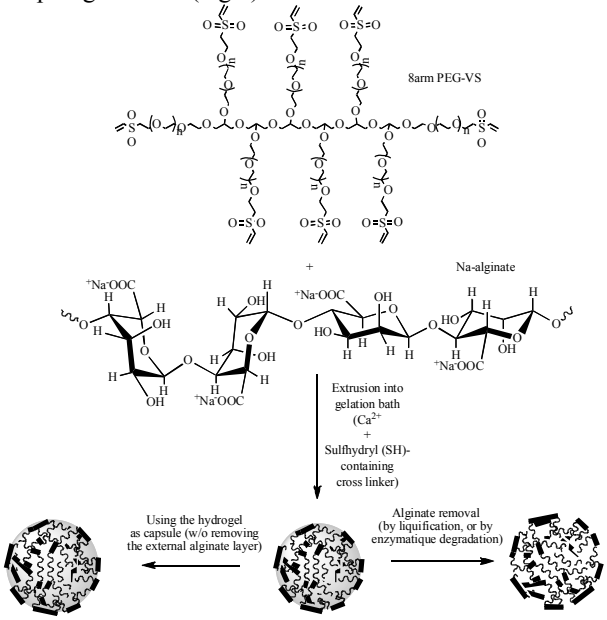

***Fig. 1**: Formation process. Both Alg-PEG-M (left) and PEG-M (right) were obtained spherical and uniform.*

Results and Discussion: Minimum swelling and maximum mechanical resistance of Alg-PEG-M were obtained for the molar ratio thiol/VS=2.75 (Fig. 2).

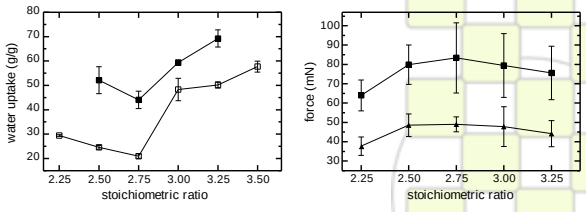

***Fig. 2**: Swelling (left) and mechanical resistance (right) of Alg-PEG-M as a function of the molar ratio thiol/VS.*

The initial precursor concentration influenced swelling and mechanical resistance. Increasing the concentration of PEG-VS creates a denser and more rigid network. Dissolution of Ca-alg slightly raised the resistance to compression (Fig.3). The permeability of the hydrogels could be tailored by adequate choice of the arm length of PEG-VS. The MWCO was tuneable in a range of 70 to 150 kg/mol.

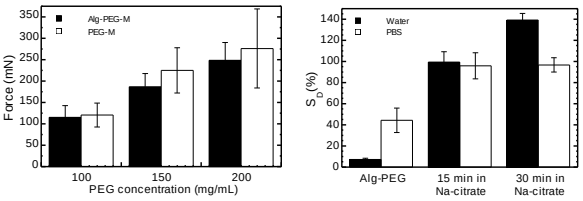

***Fig. 3:** Mechanical resistance to 80% compression for different initial PEG-VS concentrations (left), before and after Ca-alg liquefaction. Swelling degree of Alg-PEG-M after gradual dissolution of Ca-alg (right), in water and in PBS.*

In vitro cytotoxicity tests did not reveal cytotoxic effects for different cell lines after incubation with Alg-PEG-M at different concentrations (Fig.4).

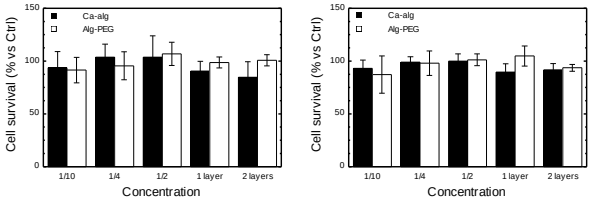

***Fig.4.** Cell survival after 24 h of incubation (percentage compared to the control). EC219 rat endothelial cells (left) and ECp23 murine endothelial cells (right).*

The immune response, cytokine production, after intraperitoneal implantation into mice was comparable to the control and pure Ca-alg microbeads. No significant increase was observed for IL-6, IL-10, IL-12p70, MCP-1, TNF and IFN. Encapsulated human islets continued insulin secretion.

Conclusions: Combining of ionotropic gelation of Na-alg and chemical cross-linking of PEG-VS in a one-step process yields hybrid Alg-PEG-M with well-controllable physical properties. Significant toxic effects were observed neither *in vivo* nor *in vitro*. Overall, microsphere properties are in a range as requested for biotechnological, biomedical, and pharmaceutical applications.

References: R. Mahou, C. Wandrey (**2010**). Macromolecules 43(3):1371-1378.

Acknowledgement: We thank the SNF, Grants 205321-116397/1205320-130572/1; COST 865 /STSM.

Degradation of Polyglycidol in Aqueous Solution by UV light

Alicja Utrata-Wesolek, Roza Trzcinska, Barbara Trzebicka, Andrzej Dworak

Centre of Polymer and Carbon Materials, Polish Academy of Sciences, M. Curie-Sklodowskiej 34, 41-819 Zabrze, Poland

alicja.utrata@cmpw-pan.edu.pl

Introduction:
In recent years, great interest in polyglycidol (PGl) based materials has increased considerably. Systems based on different molecular architectures of PGl such as block, hyperbranched, arborescent and graft copolymers have been obtained [1-3]. PGl chain modification has also been used to obtain thermoresponsive polymer materials, including hydrogels, nanogels, micelles and nanoparticles [4-6]. These thermoresponsive PGl materials can be used in biotechnology and medicine for controlled drug and genes release, bioseparation and surfaces for cell culture. Although the interest to use the PGl to obtain materials for aforementioned application is recently strongly growing, its degradation has not been previously investigated.
Here, we report the photodegradation of PGl in aqueous solution under the UV irradiation at 254 nm. The experiments were carried out in air at a constant temperature and the photodegradation of polyglycidol was compared to that of poly(ethylene oxide) (PEO), the most widely studied polyether. The mechanism of polyglycidol degradation under UV light was proposed.

Materials and Methods: The PGl was synthesized via coordination polymerization as described in [7]. PEO with a M_n = 300,000 g/mol, supplied by Aldrich was used as received.
The degradation of PGl and PEO aqueous solutions were carried out using a UVILITE LF 215S 2x15 W lamp (UVItec, Cambridge, UK) at 254 nm. The polymer solutions were irradiated vertically, 4 cm from the lamp (the intensity of the incident light was 25 mW/cm^2).
The polymers and their degradation products were characterized by SEC-MALLS (DAWN EOS, Wyatt Technologies), NMR (Bruker Ultrashield 600 MHz) and FTIR (FTS-40A, BIO-RAD).

Result and Discussion: The PGl was obtained through the anionic-coordination polymerization of ethoxyethyl glycidyl ether in the presence of partially hydrolyzed diethyl zinc as a catalyst. When the synthesis was complete, the ethoxyethyl groups were removed by hydrolysis under acidic conditions to yield a linear PGl. The molar mass of the polymer was 270,000 g/mol and the dispersity of the polymer (M_w/M_n) was equal to 2.5. PEO with molar mass of 300,000 g/mol and a dispersity of 2.0, was used to compare its photodegradation process to that of polyglycidol.
Aqueous solutions of PGl with concentrations of 2% and 8% and a 2% aqueous solution of PEO were exposed to UV irradiation at 254 nm. The change in the molar mass and molar mass dispersity of PGl and PEO was measured using SEC-MALLS. During irradiation of PGl, the shape of the chromatograms changed from monomodal to bimodal whereas the chromatograms of PEO remained monomodal throughout the entire irradiation. In all of the chromatograms, the lack of signals at higher elution volumes pointed to the absence of low molar mass oligomers as photodegradation products. This could indicate that UV irradiation of PGl solutions led to the fragmentation of the polymer chains, which occurred through scission around the midpoint of the polymer chain but not at the polymer chain end. Regardless of the polymer type or polymer concentration, the molar mass of degraded PGl and PEO gradually approached the limiting value of 17,000 g/mol and 14 000 g/mol, respectively. During the irradiation of the polymer solutions, a strong acidification was observed. The observed decrease in the pH of the PEO solution appeared to be more significant than for PGl.
To determine the structure of the degradation products of PGl and PEO created during UV irradiation at 254 nm, FTIR, ^{1}H NMR and ^{13}C NMR analyses were performed. During the irradiation of PGl formats, esters and α-hydroxyesters were formed whereas degradation of PEO led to formation of formate, ester and formic acid ions. A mechanism accounting for the main routes of polyglycidol photooxidation is proposed.

Conclusions:
The irradiation of polyglycidol in aqueous solution with the UV light at 254 nm caused damage to the macromolecular chains via chain scission around the midpoint. The molar mass of polyglycidol decreased significantly due to irradiation and reached a limiting value. The degradation of polyglycidol was accompanied by strong acidification. Based on the degradation products detected by NMR and FTIR spectroscopy, a mechanism of the photodegradation of PGl was proposed.

This work was supported by a special project of the Polish Ministry of Education and Science, Grant No. 759/N-Slowacja/2010/0. The work of R. Trzcinska was supported by the European Community from the European Social Fund within the RFSD 2 project.

[1] Backes M. et al. Macromolecules 2010, 43, 3238
[2] Walach W. et al. Polymer 2004, 45, 1755
[3] Dimitrov P. el al. Polymer 2006, 47, 4905
[4] Mendrek S. et al. Macromolecules 2009, 42, 9161
[5] Trzebicka B. et al. J Polym Sci: Part A 2010, 48, 4074
[6] Utrata-Wesołek A. et al. e-Polymers 2007, 019, 1
[7] Haouet A. et al. Eur Polym Mater 1983, 19, 1089

DNA complexes with charged compounds, that are useful for nanotechnology

Kasyanenko N., Dribinsky B., Puchkova A., Sokolov P.

Department of Molecular Biophysics, Faculty of Physics, St.-Petersburg State University

nkasyanenko@mail.ru

Introduction

DNA is a polyanion with a high charge density and unique properties (high stiffness, complementarity of base pairs, reversible denaturation). This molecule is the attractive, useful and convenient object of manipulation in the field of nanotechnology. Its interaction with cationic molecules cause the formation of different structures, including gene vectors, self-assembled ordered structures, as well as templates for nanowires.

The investigation of DNA reversible packaging in a solution (so-cold DNA condensation) induced by various agents has a long history. Nevertheless now this is of a great interest in connection with the absence of complete clarity in molecular bases of DNA condensation and due to the development of new nanobiotechnologies. For example, DNA packaging is the main step in gene transfer into target cells. Polycations and DNA form compact interpolyelectrolyte complexes (IPEC) in a solution. So synthetic polycations are known as perspective agents for the non-viral gene delivery. They exhibit many advantages over other DNA transporting means because of their ease of production, nonimmunogenicity, low risk of side effects, simplicity of DNA–polymer complex formation. DNA condensation is a collapse of swollen molecular coils into small dense particles. Since DNA is a highly-charged polyanion, the key question is how the electrostatic interaction between charged monomers changes from repulsive to attractive.

In our previous articles the key distinction in DNA organization before condensation induced by trivalent metal ions and polycations was discussed [1-3]. The model system (DNA + oligocations) can provide the more understanding of difference between influence of polycations and small multivalent ions on DNA conformation in a solution.

Materials and Methods

Calf Thymus DNA, poly- and oligolysine, spermine and spermidine (Sigma) were used. The influence of di-, tri-, penta- and oligoions as well as polycations (polylysine) with a degree of polymerization 270 and 350 on DNA conformation in a solution was studied. DNA conformational changes are examined by the methods Atomic Force Microscopy (NanoScope 4a, Veeco), Dynamic Light Scattering (PhotoCor, Russia), Low Gradient Viscometry, Flow Birefringence, Circular Dichroism (Mark IV, Jobin Ivon).

Results and Discussion

It was shown that some polycations (polylysine 270 and 350) as well as multivalent cations (La3+, hexammine cobalt (III) (CoHex), spermidine, spermine) facilitate DNA packaging in a solution into toroids. Small multivalent ions cause the change in DNA tertiary structure via intramolecular linkage with remote phosphate groups and formation of compressed coil with mutually oriented segments of macromolecule before DNA packaging. In contrast to that polycations do not induce any reorganization of DNA structure prior to condensation. In our research the influence of number of positive charges, the length of oligocation chain and the disposition of charges on polymer chain on DNA conformation. As a result of DNA interaction with multivalent ions in a solution the discrete nanoparticles (100-200 nm) were registered.

DNA complexes with charged compounds can also be used as templates for the fabrication of nanowires. It was shown that DNA complexes with silver ions provide the further silver DNA-nanowire formation on silicon surface. The method of DNA metallization is based on the reduction of silver ions on DNA bundles by means of silicon substrate.

Conclusions

High molecular DNA is a good material for the creation of nanostructures like gene vectors and nanowires. Self-organizing structures on the base of DNA complexes with charged compounds in a solution can be interesting also as model systems for the understanding of conformational properties of main biological macromolecule during functioning in vivo and in vitro.

References

1. N. Kasyanenko, D. Afanasieva, B. Dribinsky, D. Mukhin, O. Nazarova, E. Panarin DNA Interaction with Synthetic Pjlymers in Solution. Structural Chemistry (2007) 18, 4, 519-525
2. N. A. Kasyanenko, D. A. Afanasieva. DNA Self-Assembling Nanostructures Induced by Trivalent Ions and Polycations Nanomaterials for Application in Medicine and Biology (2008), pp. 29-38.
3. N.A. Kasyanenko, D.A. Mukhin, I.Y. Perevyazko Conformational Changes of a DNA Molecule Induced by Metal Complexes Formed in Solution. Polymer Science. Series C (2010), 52, 1, 122-133.

Viscoelastic and thermal behavior of polyurethane films prepared as shape memory polymer

Cansu Citak, Isık Yavuz, Mirey Bonfil, F. Seniha Güner,

Istanbul Technical University, Department of Chemical Engineering, Maslak 34469 Istanbul, Turkey

e-mail: guners@itu.edu.tr

Shape memory polyurethanes are the typical thermo-sensitive shape memory polymers, which were extensively studied in the near past decades. A shape memory polyurethane has two phases on its structures that are hard and soft segments, these segments make up phase separation. The soft segment forms reversible phase and also, it determines the shape recovery temperature.

The aim of this study is to characterize some viscoelastic and thermal properties of the polyurethane films showing shape memory property. Castor oil (CO) and polyethylene glycol (PEG) are used as polyol sources, and hexamethylene diisocyanate is used as diisocyanate component in the preparation of the films. Dibutyl-tin-dilaurate, 1,4-buthane diol and triethanol amine are used as catalyst, chain extender and crosslinking agent, respectively. The films are prepared in various CO/PEG weight ratios (50/50, 60/40, 70/30, 90/10 and 100/0); (1) with cross-linker and catalyst (WC-wc), (2) with cross-linker and without catalyst (NC-wc), and (3) without cross-linker and catalyst (NC-nc). The crystallinity of the polyurethane films is determined by using wide angle X-ray scattering. Crosslink density (υ_c) and average molecular weight between two crosslinks (M_c) are determined by the equilibrium swelling method according to the Flory-Rehner equation. The thermal and viscoelastic properties of the samples are characterized by differential scanning calorimeter (DSC), thermal gravimetric analysis (TGA) and dynamic mechanical analysis (DMA).

The crystallinity of the polymer decreases, on the other hand, the number of the crosslink center increases with increasing CO content. The glass transition temperatures (T_g) of all polyurethanes are below room temperature, consequently they are rubbery at ambient temperature. The T_g increases with increasing CO/PEG ratio. As shown in Figure 1, the polyurethanes synthesized without crosslinker show the lowest T_g for the same CO/PEG ratio except the sample prepared at 70% CO content.

An intersection point is obtained for all TGA curves at 415±10°C. Increasing the CO content in polymer structure caused a rapid decrease in the weight (increase the weight loss) of the polymer at the intersection temperature. The degradation pathway depends on the ratio of CO/PEG used in the polymer synthesis.

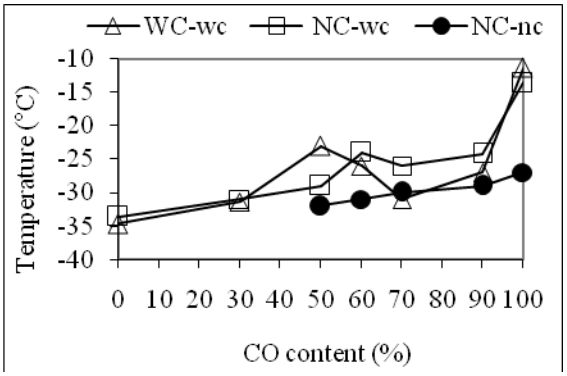

Figure 1. T_g of the polyurethanes

According to the DMA results, the polyurethanes synthesized without catalyst and chain extender have less chain mobility than the other polyurethanes containing same amount of CO, since the hight of the tan D peak is the smallest value (Figure 2). This may be due to the relatively high crystallinity of these polyurethanes compared to the samples having same CO content. This result is supported by XRD measurements.

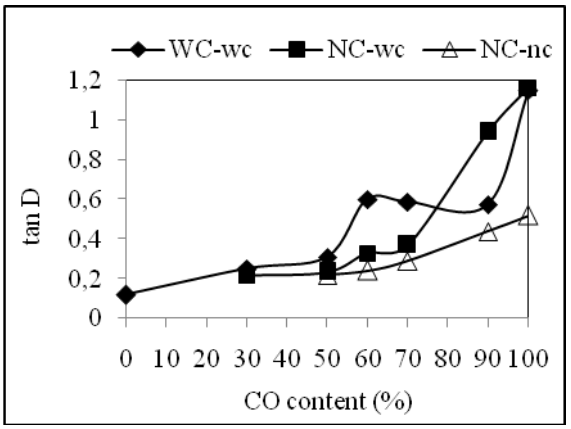

Figure 2. The value of tan D peak

.

Wavelength-Responsive Polymer Materials

V. San Miguel, A. del Campo

Max-Planck Institut für Polymerforschung. Ackermannweg 10, 55128 Mainz, Germany

e-mail: sanmigue@mpip-mainz.mpg.de

Advanced technologies require the development of materials able to respond to external triggers (temperature, pH, pressure, electrical fields, light etc) by changing their physicochemical properties. Light has important advantages as source for activating processes. Light stimulus can be readily available and focused, allowing precise temporal and spatial definition of the stimulus. Light exposure can be also precisely controlled over the irradiation time and intensity and, as a consequence, the strength of the stimulus (and the response) can easily be modulated. We present a strategy to control materials properties (reactive state, polymerisation or depolymerisation) at the surface[(1)] and in the bulk of a polymer material using chromic-tunable caging groups with sensitivity to light of different wavelengths. In addition, using two-photon excitation our strategy allows 3D control over the stimulus and response.

References:

[(1)]V. San Miguel et al. *Wavelength selective caged surfaces*, submitted; M. Alvarez et al., *Modulating surface density of proteins via caged surfaces and controlled light exposure*, Langmuir 2011; P. Stegmaier et al., *Photoresponsive surfaces with two independent wavelength-selective functional levels*, Langmuir 2009; A. del Campo et al, *Surface modification with orthogonal photosensitive silanes for sequential chemical lithography and site-selective particle deposition*, Angew. Chem. Int. Ed. 2005.

Photoresponsive Polymer Brushes

Jiaxi Cui, A. del Campo

Max-Planck Institut für Polymerforschung. Ackermannweg 10, 55128 Mainz, Germany

e-mail: cui@mpip-mainz.mpg.de

Polymer brushes (polymer chains tethered by one end to a solid substrate), can be used to modify surface properties (wettability, biocompatibility, adhesion etc.). When stimuli-responsive polymers are selected to anchor, the physicochemical properties of the brush (extended/collapsed state) can be tuned via external triggers. As a consequence, surface properties also change. Several examples of temperature and pH sensitive brushes have been reported. Here we present a novel example of a light-responsive brush. We have used the photoremovable caging group 4,5-dimethoxy-2-nitrobenzyl to cage charged side groups (i.e. COOH, NH2…) of polyacrylates and we have prepared polymer brushes via suface-initiated ATRP. Upon irradiation, the photocleavable group can be removed and this generates charged groups in the polymer chains. Consequently, the swelling state changes and the surface becomes light and pH-sensitive.

Properties of cyanoacrylate adhesives with different alkyl chain length

Rafael Torregrosa-Coque[1], Ana María Villarreal-Gómez[2], José Miguel Martín-Martínez[1]

[1]Adhesion & Adhesives Laboratory. University of Alicante. 03080 Alicante (Spain).
[2]Adhbio Corporation, 03206 Elche, Alicante (Spain).

jm.martin@ua.es

Introduction

Cyanoacrylates polymerize in the presence of bases, such as water. Skin has a high concentration of water, so cyanoacrylate adhesives can be used for surgical practice and wound closure. However, despite producing effective joining, the cyanoacrylate adhesives show exothermic cure and the polymerised product is too stiff. One simple route to reduce the exothermic reaction and stiffness of the cyanoacrylate adhesives is to increase the length of the hydrocarbon chain backbone.

To the best of our knowledge there are a few scientific studies dealing with the physico-chemical characterization of cyanoacrylate adhesives and only four of them consider the incidence of the length of the alkyl chain [1,2]. In this study, the properties of cyanoacrylate monomer and the polymer obtained after cure will be compared, paying particular attention to the modifications produced during polymerization.

Materials and Methods

Ethyl (ECN), butyl (BCN) and octyl cyanoacrylate (R=8) were used. Cyanoacrylate monomers were cured by adding water (1:1 vol%). The monomers and polymers films were characterized by ATR-IR spectroscopy, scanning electron microscopy (SEM) and thermal gravimetric analysis (TGA). Adhesion was obtained from single lap-shear tests of aluminium/cyanoacrylate adhesive joints.

Results and Discussion

The derivative curves of the TGA thermograms (Figure 1) show the thermal decompositions of the cyanoacrylate monomers. The first decomposition was found at about 120 ºC and the weight loss decreased by increasing the length of the alkyl chain. The increase in the alkyl chain length increases the decomposition temperature of the cyanoacrylate and several decompositions are obtained.

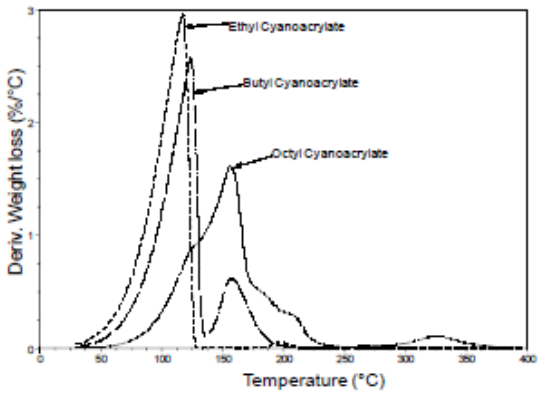

Figure 1. Derivative of the TGA thermograms of the cyanoacrylate monomers.

The thermal properties of the cyanoacrylate polymers differ from those of the corresponding monomers. The polymerization increases noticeably the temperature at which the polymer degrades (Figure 2). In general, the temperature at which decomposition is produced increases by increasing the length of the alkyl chain in the cyanoacrylate polymer. Whereas the ethyl cyanoacrylate polymer shows a unique decomposition at 199 ºC, both the n-butyl and the n-octyl cyanoacrylate polymer show two thermal decompositions corresponding to two different polymer structures.

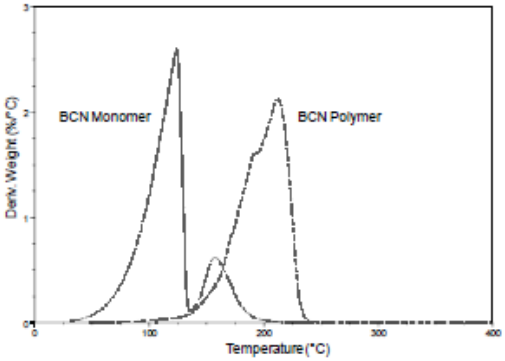

Figure 2. Derivative of the TGA thermograms of butyl cyanoacrylate monomer and polymer.

Polymerization modifies the chemical structure of the cyanoacrylate. The SEM micrograph of the ethyl cyanoacrylate polymer showed a homogeneous and smooth surface, whereas the n-butyl and, more markedly, the n-octyl cyanoacrylate polymer showed a heterogeneous topography consisting in shredded polymer chains. This is in agreement with the loss in elastic modulus and cohesion of the cyanoacrylate by increasing the length of the alkyl chain.

Conclusions

Whereas the ethyl cyanoacrylate is mainly composed of monomer, the n-butyl cyanoacrylate contains monomer and some dimmers and the n-octyl cyanoacrylate has only a minor content of monomer.

Acknowledgements. Financial support from MICYNN (MAT2009-10234 and PET2008-0264 projects) is acknowledged.

References

1. M. Dossi, G. Storti, D. Moscatelli. *Macromol. Symp.*2010, 289, pp 124–128.
2. N. G. Senchenya, T. I. Guseva, Yu. G. Gololobov. *Polymer Science*, 2007, 49(3), pp 235–239.

Multi-block Copolymers of Polyamide 6 and Diepoxy Propylene Adipate Obtained by Solid State Polymerization

Seda Cakir[1], *Cor Koning*[1*], *Magnus Eriksson*[2], *Mats Matinelle*[2]

[1]Laboratory of Polymer Chemistry, Eindhoven University of Technology, Den Dolech 2, P.O. Box 513, 5600 MB Eindhoven, The Netherlands

[2]Department of Biochemistry, School of Biotechnology, KTH, Royal Institute of Technology, SE-10691 Stockholm, Sweden

*Corresponding author e-mail: c.e.koning@tue.nl

Introduction

Polyamide 6 (PA 6) is a high-performance engineering plastic used for a wide range of applications in everyday life. However, there is an increasing demand for disposable packaging applications because of environmental considerations. The biodegradability of PA 6 could be enhanced by incorporating hydrolyzable groups into the main chain.[1] If these hydrolyzable groups are randomly introduced into the PA 6 main chain during melt polymerization, the crystallization behavior of PA 6 will be negatively affected, the melting point will be reduced and the mechanical and physical properties crucial for packaging applications (such as barrier properties) will become worse.[2] An alternative method can be incorporating these groups into the amorphous part of a relatively low molar mass PA 6 by solid state modification at reduced temperature, *viz.* below the melting point of the PA 6 crystals.[3] To achieve this, a new synthetic approach can be followed: Epoxide end-capped oligoesters and carboxylic acid end capped PA 6 can be copolymerized in the solid state.

Experimental Methods, Results and Discussion

The synthetic procedure for the preparation of multi-block polyesteramide copolymers is shown in ***Scheme 1.*** The first step included the preparation of low molar mass, fully carboxyl end-capped PA 6 by the addition of 5 mol% adipic acid during the hydrolytic ε-caprolactam polymerization. According to the number of end groups determined by titration, the number average molecular weight of the PA 6 is 2400 g/mol. Diepoxy propylene adipate (DEPA) with a molecular weight of 450 g/mol was synthesized as described before[4] and both components were mixed in HFIP with the addition of DMAP as the base catalyst. After full dissolution of all components vacuum distillation was started and continued at room temperature until full removal of the solvent. Finally, solid state polymerization was done under Argon in the temperature range of 70-100°C. An increase in molecular weight was observed by SEC analysis (M_n=10 kg/mol). The molecular weight of the copolymers can be improved by using different types of catalysts in different concentrations. Further characterization will be done by FTIR, DSC and NMR.

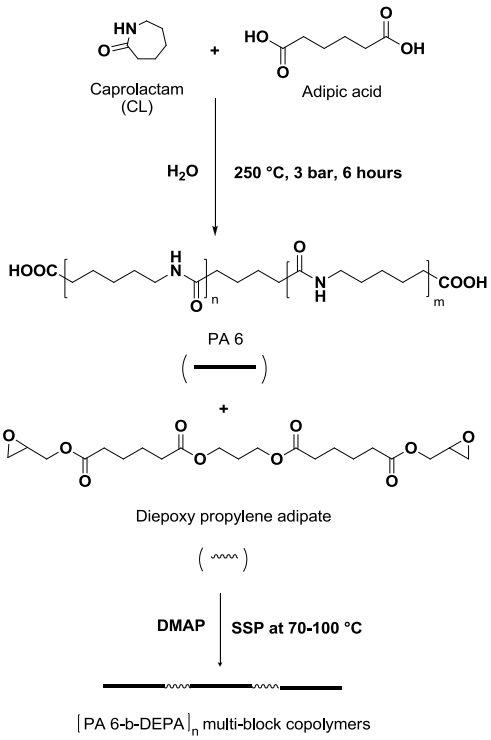

Scheme 1. Schematic drawing of stepwise synthesis of Polyamide 6-Dipeoxy propylene adipate multi-block copolymers obtained by solid state step growth polymerization.

Acknowledgements

This project is supported by DSM.

References

[1]Michell, R. M.; Muller, A. J.; Castelletto, V.; Hamley, I.; Deshayes, G.; Dubois, P. *Macromolecules* **2009,** 42, (17), 6671-6681.

[2] Jansen, M.A.G.; Wu, L.H.; Goossens, J.G.P. ; Wit, G.D.; Bailly, C.; Koning, C.E.; Portale, G. *J.Polym. Sci.: Part A: Polym. Chem.* **2008**, *46*, 1203-1217

[3] Vouyiouka, S.N.; Karakatsani, E.K.; Papaspyrides, C.D. *Prog. Polym. Sci.* **2005**, *30*, 10-37

[4] Eriksson, M.; Fogelstrom, L.; Hult, K.; Malmstrom, E.; Johansson, M. ; Trey, S.; Martinelle, M. *Biomacromolecules*, **2009**, 10, 3108-3113

Dynamics of hydrogen bonds and protein in hydrated elastin

Valérie Samouillan, Doris Tintar, Florian Delaunay, Jany Dandurand and Colette Lacabanne

Polymer Physics, Institut Carnot CIRIMAT UMR CNRS 5085, Université Paul Sabatier, 31 062 Toulouse Cédex 09 France

vsamou@cict.fr

Protein surface hydration is essential to its structural stability and flexibility and protein associated water is often an integral element in biological activities [1,2]. Protein function usually involves protein motions corresponding to transitions between conformational substates. The conformational motions imply α fluctuations that originate in the bulk solvent, and β fluctuations that originate in the hydration shell [3]. Nevertheless, a complete understanding of the underlying coupling of proteins and water motions is still lacking [4]. For a series of globular proteins, the protein dynamics were proposed to be slaved [5-7] or plasticized by water dynamics, but the mechanism remains questionable.

So it is of peculiar interest to study the temperature dependence of proteins and water dynamics. Elastin is a main protein of connective tissues such as lung, arteries and skin, and the mechanism of elasticity of this hydrophobic and insoluble protein is still subject to debate. We used Differential Scanning Calorimetry (DSC) to quantify free (freezable) water and bound (unfreezable) water [8]. Dielectric techniques - Dynamic Dielectric Spectroscopy (DDS) and Thermally Stimulated Current (TSC) -, well-suited experimental methods to characterize the system elastin-water were used to access to the dynamics of the system. The protein was studied between 123 and 313 K in the $10^{-3}/10^{6}$ Hz range, at different hydrations levels [9].

By DSC, a localized water phase is evidenced, with a maximal value of 1.2-1.3 molecules of water bound to one elastin residue. Above this value, bulk water appears in the system.
By DDS, a complex relaxation map is observed with four dipolar modes labeled β1, β2, p1 and p2. Assignments for the different modes can be proposed by the combination of DDS and TSC experiments as well as the determination of the activation parameters of the relaxation times.

The temperature dependence of the two β_1 and β_2 modes is found to be Arrhenius-like, with a direct proportionality between β_1 and β_2. The elastin dynamics are "slaved" by water dynamics.
Localized molecular mobility (at the nanometric scale), undetectable by DSC, which occur at low temperature can be observed by the combined use of DDS and TSC. In this case, the evolution of the local dipolar reorientations have been followed for different hydration contents, revealing an increasing complexity when coexist elastin, unfreezable water and freezable water. The fastest process β1 mode is attributed to reorientations of water in the hydration shell, needing the breaking of two hydrogen bonds (≈50 KJ/mol) to occur; the β1 mode drives the β2 one, associated to water/elastin local reorientations. So the dynamic nature of the localized water phase lends significant mobility to the protein, as already observed in globular proteins.

These fast processes were shown non or little cooperative when compared to the lower processes p1 and p2, which are associated with more energetic (55-80 KJ/mol) and more delocalized motions in the elastin-water system, merging at around 0°C and exhibiting a non Arrhenius-like behavior at higher temperature.

These results on hydrated elastin are a basis to help to answer the question - How the solvent influences the protein dynamics - which still remains largely unanswered. Moreover, our experimental data could be useful for the assessment of starting conditions in molecular dynamics simulations: simulation on long polypeptidic sequences of elastin could be launched with a small hydration level, typically 10°%, corresponding to detectable localized reorientations of the complex water/residues in dielectric spectroscopies.

[1] L. Zhang, Y.T. Kao, D. Zhong, J. Am. Chem. Soc. 131(2009) 10677.
[2] N. Nandi, K. Bhattacharyva, B. Bagchi, Chem. Rev. 100 (2000) 2013.
[3] H. Frauenfelder, Chem. Phys. 375 (2010) 612.
[4] S.A. Lusceac, M. Vogel, C.H. Herber, Biochim. Biophys. Acta. 1804 (2010) 41.
[5] P.W. Fenimore, H. Frauenfelder, B.H. McMahon, R.D. Young, Proc. Nat. Acad. Sci. 101 (2004) 14408.
[6] H. Jansson, R. Bergman, J. Swenson, J. Phys. Chem. B. 109 (2005) 24134.
[7] H. Frauenfelder, G. Chen, J. Berendzen, P.W. Fenimore, H. Jansson, B.H. McMahon, I. R. Stroe, J. Swenson, R.D. Young, Biophys. Comput. Biol. 106 (2008) 5129.
[8] V. Samouillan, C. Andre, J. Dandurand, C. Lacabanne, Biomacromolecules ,5, (2004) 958 .
[9] D. Tintar, PhD Toulouse/F (2010).

The effect of degradation on PLLA/PCL membranes prepared by freeze extraction

Luis Andrés Gaona[1,2], *José Luis Gómez*[1], *Jairo Ernesto Perilla*[2], *Myriam Madeleine Lebourg*[1]

[1] Centro de Biomateriales e Ingeniería Tisular, Universidad Politécnica de Valencia
[2] Grupo de Procesos Químicos y Bioquímicos, Universidad Nacional de Colombia

E-mail: luigaoco@posgrado.upv.es

Introduction

Biomaterials made with Poly l-Lactic Acid (PLLA) and Poly ε-Caprolactone (PCL) have been widely studied as suitable biodegradable materials for tissue implants. In a previous work, the freeze extraction technique was used to produce porous PLLA/PCL membranes and their properties were evaluated. So, the next step was to evaluate how PLLA/PCL scaffolds behave when degraded, and in this study the PLLA/PCL membranes made by freeze extraction were degraded hydrolytically in Phosphate Buffered Saline solution. After 11, 33 and 65 weeks of degradation the membranes were characterized using Gravimetric Analysis, Differential Scanning Calorimetry (DSC), Gel Permeation Chromatography (GPC) and Strength Compression by Indentation. Better resistance to degradation is associated with PCL composition meanwhile PLA does not let the scaffold keep its structure long time. This study demonstrates the capacity for PCL to make slower the degradation of PLLA/PCL scaffolds made by freeze extraction, giving better support to its suitability as graft biomaterial.

Materials and Methods

The scaffolds were prepared by freeze extraction of PLLA and PCL solutions in different weight ratios using Dioxane as solvent. The dissolution was poured into a Teflon mould and frozen in liquid nitrogen. The disks obtained were immersed in ethanol at -10ºC for two days. The disks were then removed, vacuum dried and stored in a dry environment. After being synthesized the membranes underwent a degradation process keeping them in PBS dissolution for 65 weeks; they were washed with distilled water and vacuum dried. After different degradation time, weight loss was measured by gravimetric analysis; crystallinity was determined by DSC heating from 0 to 200ºC at 10ºC/min; Molecular Weight Distribution was measured by Gel Permeation Chromatography (GPC) preparing the samples in Tetrahydro Furan (THF), with an elution volume of 1mL/min, obtaining a profile of signals associated to molecular weight; and Compression Strength was determined by Indentation with a Thermo Mechanical Analyzer (TMA)

Results and Discussion

Gravimetric analysis shows a significant weight loss in PLLA membranes compared to weight loss in PCL membranes. So it can be deduced that weight loss in PLLA/PCL membranes is associated the most to PLLA degradation.

DSC thermograms at different degradation ratios show how the melting temperature of PCL rises from 57 to 58ºC approximately when its fraction rises. It can be seen also that melting temperature of PLA diminishes in the same order, as its fraction is smaller, likely due to smaller crystal size or more imperfections. It is clear also, that for PLLA the peak width is bigger as its fraction rises, and the opposite case for PCL. A slightly peak of crystallization of PLLA appears as its fraction is smaller, which indicates that PLLA does not cold-crystallize in the membranes after freeze extraction due to crystallization of the whole crystallizable fraction during the process. After degradation, thermograms show practically no changes in PCL behavior, however PLA shows broader peaks, and even a second peak in blends with both higher amounts of PLLA and as the degradation time rises, because of the smaller crystals formation. The melting temperatures for PCL do not undergo significant changes in all degradation time; as opposed of PCL since the presence of smaller crystals, melting temperature of PLLA diminishes drastically in almost 20°C after the 33th degradation week.

The GPC results do not show distinct peaks as PLLA and PCL used have very similar molecular weights and only one peak is seen for both polymers. So, GPC peak was deconvoluted into smaller peaks that were associated whether to PCL or to PLLA molecular weight distribution, according with the expected composition at different degradation times. Besides the degradation of PCL is very light, it can be seen in PCL-rich blends that molecular weight drops slightly after 11 weeks of degradation, which is consistent with end chain degradation as often seen in very crystalline polymers. On the other hand, molecular weight of PLLA-rich blends decrease much more and new peaks appear, which is consistent with a random cleavage of the chains that produces more polymers with low crystallinity.

Changes in compressive elastic modulus for the PLLA/PCL membranes are somewhat puzzling, due the difficulty of defining the appropriate zone for calculation in Stress-Strain curves and the tendency to non-lineal behavior when indentated. However, a slightly drop in modulus is observed at 11th week, followed by modulus rising maybe due to re-crystallization phenomenon during degradation.

Conclusions

The degradation process affects primary to PLLA-rich phase in the membranes, not only because of terminal chain cleavage but also because random cleavage. PCL undergoes a slightly change during the degradation time in both its molecular weight and weight loss, but it seems not to affect significantly its properties, like crystallinity and melting temperature. The presence of PCL in the membrane makes it more resistant to degradation and enhances the mechanical properties in degraded state. These materials should thus be suitable for tissue engineering since the PCL/PLA ratio allows the design of a composite blend with a degradation rate that matches the regeneration rate of the tissue.

ABSTRACTS

POSTER PRESENTATIONS

Topic 1: Synthetic Routes: Monomers and Polymers from Bioresources and Advanced Methodologies

Low Temperature Photoinitated RAFT of Vinyl Acetate

Min-kyoung Ham,[1] So-Hee Shim,[1] Youngjin Jeong,[1] Young-Ku Kwon,[2] and Young-Je Kwark[1,]*

[1]Department of Organic Materials and Fiber Engineering, Soongsil University, Seoul, Korea 156-743
[2]Department of Nano-Systems Engineering, Inha University, Incheon, Korea 402-751

[*]ykwark@ssu.ac.kr

Controlling streospecificity in polymer chemistry is important because it affects properties of polymers. However it is very difficult to control stereochemistry in radical polymerization because the nature of active radical species has low energy barrier between two enantiomers. Protic solvents like fluoroalcohols or lewis acid are known to be efficient for the stereo-controlled radical polymerization of vinyl esters. Along with using protic solvents, lowering polymerization temperature is generally preferred to further improve stereoregularity of the prepared polymers, because it lowers the possibility of inter-conversion between two enantiomers.

On the other hand, controlling molecular weight (MW) and its distribution in radical polymerization can be achieved by controlled polymerization techniques, such as ATRP, NMP, and RAFT. There have been several reports of preparing polymers with controlled MW and streospecificity by controlled radical polymerizations in fluoroalcohols. However, it is not easily achievable to run the polymerization at low temperature. Since in many cases radical generation process, for example homolytic cleavage of AIBN or BPO, requires sufficient thermal energy, the polymerizations proceed at elevated temperatures, which is not favored in preparing polymers with high streospecificity. It is also the case for RAFT process. Photo-initiation can be applied to the technique to lower the reaction temperature, but thioester chain ends in RAFT process can be cleaved by UV irradiation to deteriorate the controlling characteristics of the process. This system has been known as 'photo-iniferter' system.

In this work, we used photochemically inert RAFT agent in photo-initiated polymerization of vinyl acetate (VAc) to minimize the photochemical cleavage of the chain ends. With this approach, it was possible to get polymers with better controlled MW and lower PDI. Then lower reaction temperature and fluoroalcohol solvents were applied to attain higher level of control in streospecificity.

Aside from its requisite effectiveness in controlling polymerization, the RAFT agent in a photo-initiated system must be inert under UV irradiation. Therefore, the photochemical properties of RAFT agents and photo-initiators were tested using UV-Vis spectroscopy. Among the tested compounds, bis(2,4,6-trimethyl benzoyl)phenylphosphine oxide BAPO decomposed upon the tested UV irradiation, while Methyl(ethoxy carbonothioyl)-sulfanyl acetate (MESA) was unchanged. Therefore we used BAPO as a photo-initiator and MESA as a chain transfer agent in the polymerization of VAc. Polymerization using the photo-initiation system was performed at 0 °C. The polymerization produced polymer with low PDI. It indicated that photo-initiated RAFT of VAc was well-controlled at low temperature (Figure 1).

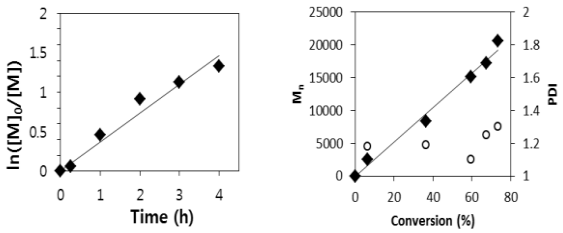

Figure 1. Kinetic plots for the photo-initiated RAFT of vinyl acetate at 0 °C.

In search of an efficient fluoroalcohol in controlling stereospecificity of the prepared polymer, $(CF_3)_2CHCOH$, $(CF_3)_3COH$, $PhC(CF_3)_2OH$, $m\text{-}C_6H_4\{C(CF_3)_2OH\}_2$ were employed as solvents in the polymerization of VAc (Figure 2). The syndiotacticity of the prepared polymer was affected by the structure of fluoroalcohol. The more acidic $(CF_3)_3COH$ yielded higher syndio- tacticity (r = 62.3) than $(CF_3)_2CHCOH$ (r = 60.1). With bulkier $m\text{-}C_6H_4\{C(CF_3)_2OH\}_2$, higher syndiotacticity (r = 61.0) could be attained, compared to the one with $PhC(CF_3)_2OH$ (r = 58.6). The fluoroalcohols also affected the control of MW. The best results was achieved with $(CF_3)_3COH$ to produce polymer with the lowest value of PDI (1.05)

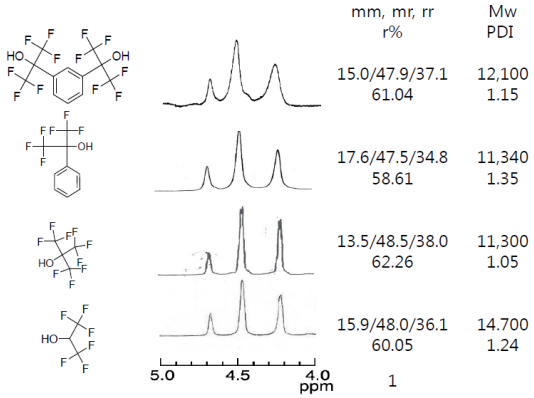

Figure 2. Effect of various fluoroalcohols on the MW and tacticity of the prepared polymers at 0 °C.

In conclusion, the simultaneous control of the molecular weight and stereospecificity of PVA has been achieved for the RAFT Polymerization in fluoroalcohol solvent. Low temperature polymerization in fluoroalcohol solvents gave polymers with higher syndiotacticity.

Acknowledgements. The authors of this paper would like to thank the National Research Foundation of Korea (KOSEF 2009-0072743) and Human Resources Development (20104010100610) of the Korea Insitute of Energy Technology Evaluation and Planning(KETEP) grant for financial support of this research.

Towards Sustainable Polymerization of Stimuli-Responsive Polyglycerol Hydrogels

Somaieh Salehpour and Marc A. Dubé

Department of Chemical and Biological Engineering,
Centre for Catalysis Research and Innovation
University of Ottawa, Ottawa, ON Canada

Ssale050@uOttawa.ca; Marc.Dube@uOttawa.ca

Introduction: There is growing interest in the use of bio-based polymers due to their lower environmental burden as an alternative to conventional polymers made from petroleum, which is a limited natural resource. Due to a significant glut in the glycerol market because of increasing biodiesel production, interest in finding economic ways to utilize the emerging surplus has grown.[1] Currently, new opportunities for the conversion of glycerol into value-added chemicals have emerged due its functionality, properties, biocompatibility and biodegradability.[2] One approach to use this glycerol surplus is polymerization. Until now, only oligomers have been synthesized directly from glycerol. On the other hand, high molecular weight polyglycerols, have been produced from toxic monomers, which are environmentally hazardous (e.g., glycidol).[3]

In this study, the step-growth polymerization of polyglycerol to relatively high molecular weight from glycerol feedstock was investigated. One focus of our investigation was the use of different catalysts to improve polymer properties. The biocompatibility and functionality of the polymer makes polyglycerol an interesting option for pharmaceutical and medical applications, such as hydrogels. Consequently, the cross-linking of polyglycerol by multifunctional electrophilic compounds was investigated to achieve a controlled increase in polyglycerol molecular weight.

Materials and Methods: Polymerizations were carried out in a 1 L glass reactor equipped with a distillation trap, a condenser, nitrogen inlet, catalyst feeding and sampling ports, temperature probe, and a mechanical stirrer. The stirring speed (250 rpm) and the temperature were controlled separately. Polyglycerol was synthesized by glycerol etherification at 414 K in the presence of various catalysts. To shift the reaction equilibrium, a vacuum pump was attached to the reactor to carry out the condensation reaction at pressures below 200 mm Hg absolute. A Dean-stark trap topped by a condenser was attached to the reactor to continuously remove water from the reaction mixture. The reaction progress was determined by monitoring the water formation in the trap. The reactants were blanketed with nitrogen throughout the polymerization.

Polymer molecular weight and distribution were measured using gel permeation chromatography. Gel content was determined by the membrane gel partitioning method.[4] Swelling ratio measurements of the hydrogels were performed using distilled water at various temperatures and pH. Sulphuric acid, calcium carbonate and calcium hydroxide were used as catalysts. Polyethylene glycol diglycidyl ether (molecular weight: 400 g/mol) was used as a cross-linker. In order to form the gels, high molecular weight polyglycerol was added to a 2M NaOH solution. The solution was heated and stirred until all the polyglycerol was dissolved. The cross-linker was added to the solution, poured into Teflon moulds and then left to cure at 120°C for 24 h.

Results and Discussion: Conversion and polymer molecular weight were greatly influenced by the type of catalyst employed. The polymerization of glycerol proceeded fastest with sulphuric acid; conversion of functional hydroxyl groups was 71 to 77 mol%, along with molecular weights between 58000 and 114000 g. mol^{-1}. The polyglycerol obtained was a mixture of polyols with linear, branched and cyclic structures of different degree of polymerization with high functionality. The predominant species was polyglycerol with a linear structure, followed by branched structures as confirmed by ^{13}C-NMR. From a practical point of view, it was important to predict the extent of reaction at the gel point in order to stop the polymerization prior to that point and avoid gelation for straightforward removal from the reaction vessel. Using theoretical models,[5] the functionality of the monomer was found to be 2.4 and the critical extent of reaction (gel point) was calculated to be 71 mol%. Hydrogels formed from this high molecular weight polyglycerol using a cross-linker showed swelling ratios as high as 600 wt%. The swelling of the hydrogel was observed to be both pH and temperature dependent.

Conclusions: Using step-growth polymerization at 140°C, polyglycerols of relatively high molecular weights were produced. The most effective catalyst for this process at the tested conditions was sulphuric acid.

Novel temperature and pH-responsive polyglycerol-based hydrogels were successfully synthesized and characterized. Hydrophilicity and biocompatibility of this hydrogel make it suitable for applications in the pharmaceutical, biomedical and biotechnological fields as hydrogel adhesives for wound dressing and drug delivery.

References:

[1] M. Pagliaro, M. Rossi, "*The Future of Glycerol*", 2nd edition, The Royal Society of Chemistry, Cambridge, 2010.
[2] A. Behr, J. Eilting, K. Irawadi, J. Leschinski, F. Lindner, *Green Chem.* **2008**, *10*, 13.
[3] D. Wilms, S. E. Stiriba, H. Frey, *Acc. Chem. Res.* **2010**, *43*, 129.
[4] USA. (1982), US 4,311,039, invs.: M. E. Koehler, T. Provder, R. A. Zander; *US patent*
[5] C. W. Macosko, D. R. Miller, *Macromolecules* **1976**, *9*, 199.

Biocomposites based on Elastomeric Polyurethane and Cellulose Nanocrystals

L. Rueda[1], B. Fernández d'Arlas[1], M.L. González[2], A. Valea[2], I. Mondragon[1], M.A. Corcuera[1], A. Eceiza[1]

[1]'Materials + Technologies' Group, Polytechnic School, University of the Basque Country, Pza. Europa 1, 20018 Donostia-San Sebastián, Spain

[2]School of Technical Industrial Engineering of Bilbao, University of the Basque Country, Pza. La Casilla 3, 48012 Bilbao, Spain

arantxa.eceiza@ehu.es

Introduction

Due to the finite nature of fossil resources and their environmental impact, alternative renewable based materials are increasingly attractive. Cellulose is one of the most abundant organic materials that can be easily obtained in nature and used as precursor for chemical modification to prepare a broad variety of commercial polymers. On the other hand, cellulose nanocrystals (CNC) have focused attention as a potential reinforcement in bionanocomposites due to the combination of their high surface area, high aspect ratio, environmental benefits and low cost as well as due to the exceptional mechanical properties. However, it is well known that to obtain an improvement in the thermo-mechanical properties of polymeric nanocomposites, is essential to carry out several challenges in using cellulose reinforcements, including the efficient separation of nanocrystals from plant resources, compatibilization of the nanoreinforcements with the matrix and development of suitable methods for processing these nanocomposites. In this work, CNC have been isolated from microcrystalline cellulose (MCC) and functionalized with hexametylene diisocyanate (HDI) through covalent attachment. On the other hand, bionanocomposites with high toughness have been prepared adding different contents of CNC to segmented thermoplastic elastomeric polyurethane (STPUE) by casting method. STPUE are versatile polymeric matrices typically constituted alternating soft (SS) and hard segments (HS). The thermodynamic incompatibility between both segments leads to nano/microphase separation of the polymeric system. Thermal, morphological and mechanical properties of bionanocomposite films have been evaluated from the viewpoint of the influence of CNC content and fucntionalization on the resulting nano/microstructure.

Materials and Methods

STPUE with 18 wt% of HS was synthesized by two step polymerization procedure using a block copolymer diol as SS and HDI and 1,4-butanediol as HS.

CNC were isolated from MCC by acid hydrolysis with concentrated sulphuric acid (64 wt%) at 44 ºC during 1h and functionalized using different CNC:HDI molar ratios at 80 ºC for 24 h.

STPUE/CNC bionanocomposite films were prepared casting suspensions of STPUE and CNC in dimethylformamide (DMF) onto Teflon dishes, which were subjected to a pressure-temperature cycle.

The isolated CNC were characterized by light scattering and transmission electron microscopy (TEM). CNC functionalization was examined by elemental analysis, nuclear magnetic resonance (^{13}C-NMR) in solid state and Fourier transform infrared spectroscopy (FT-IR).

Thermal, morphological and mechanical characterization of bionanocomposites was performed by differential scanning calorimetry (DSC), dynamic mechanical analysis (DMA), atomic force microscopy (AFM) and tensile test.

Results and Discussion

Acid hydrolysis of MCC leads to aqueous suspensions of CNC with high aspect ratio. The rod-like CNC showed an average diameter of 15 ± 5 nm and a length of about 157 ± 53 nm as estimated by TEM. The FT-IR spectra of functionalized CNC showed the $\nu_{-C=O}$ stretching vibration in the amide I region at 1710 cm^{-1} corresponding to urethane groups, the amide II band at 1560 cm^{-1} and the band assigned to amide III aliphatic urethane at 1250 cm^{-1}. Bionanocomposites showed an enhancement in storage modulus because of effective dispersion of CNC. The storage modulus plateau of nanocomposites with functionalized CNC extended to higher temperatures, showing an improvement in dimensional stability. This can be due to the preferential interactions of covalently attached HDI in functionalized CNC with polyurethane HS, in agreement with DSC results. Elastic modulus of bionanocomposites increased with CNC content.

Conclusions

CNC were extracted from MCC and functionalized with HDI. Higher functionalization efficiency was achieved with an excess of HDI. Interactions between well dispersed CNC and STPUE matrix increased the storage modulus of bionanocomposites. HDI chains attached to the stiff CNC formed a network with the surrounding STPUE matrix, leading to improved dimensional stability and mechanical properties. Functionalized CNC preferentially located in the hard domains of the STPUE matrix enhanced the HS crystallization.

Acknowledgements

The authors wish to express their gratitude to the University of the Basque Country (PIFA/01/2006/045 and SGIker) and Basque Government (S-PE09UN07 and S-PE10UN22).

References

Habibi Y., Lucia L.A., Rojas O.J. *Chem. Rev.*, 110, 3479-3500 (2010).

Eichhorn S.J., Dufresne A., Aranguren M., Marcovich N.E., Capadona J.R., Rowan S.J., Weder C., Thielemans W., Roman M., Renneckar S., Gindl W., Veigel S., Keckes J., Yano H., Abe K., Nogi M., Nakagaito A.N., Mangalam A., Simonsen J., Benight A.S., Bismarck A., Berglund L.A., Peijs T. *J. Mater. Sci.*, 45, 1-33 (2010).

Habibi Y., Goffin A.-L., Schiltz N., Duquesne E., Dubois P., Dufresne A (2008). *J. Mat. Chem.*, 18, 5002-5010 (2008).

Polyurethanes Derived From Renewable Resources: Effect of Polyol Structure

Ainara Saralegui, Lorena Rueda, Borja Fernández d'Arlas, Mª Dolores Martín, Iñaki Mondragon, Arantxa Eceiza, Mª Angeles Corcuera

"Materials + Technologies" Group, Department of Chemical and Environmental Engineering, Polytechnic School, University of the Basque Country, Pza Europa 1, 20018, Donostia-San Sebastián, Spain

marian.corcuera@ehu.es

Introduction

Polyols derived from vegetable oils are new materials from renewable sources (1,2). Combined with diisocyanates, these polyols produce polyurethanes that can compete in many aspects with polyurethanes derived from petrochemical polyols, reducing the environmental impact.

Segmented polyurethane elastomers (SPU) are block copolymers formed by soft segments (SS) and hard segments (HS). The SS, formed by the polyol, provides extensibility and the HS, formed by diisocyanate and chain extender, plays the role of physical crosslinker and acts as high modulus filler. The incompatibility between both segments causes phase separation determined by several factors (3).

In this work two polyols, of similar molecular mass and different structure, derived from castor oil were used as SS and a low molecular weight diol derived from corn sugar and an aliphatic diisocyanate as HS. The effect of the HS content and the structure and functionality of SS were analyzed on the final properties.

The aim of this work was the synthesis of SPU with a high content of carbon derived from renewable resources and their characterization by mean of physico-chemical, mechanical and morphology techniques.

Materials and Methods

SPU were synthesized by using commercial polyols, CO1 and CO2, derived from castor oil with a functionality of 2 and 2.7 respectively, 1,6-hexamethylenediisocyanate (HDI), kindly supplied by Bayer and 1,3-propanediol (1,3-PD) from Quimidroga as chain extender. The molecular weight of CO1 and CO2 (3505 and 3366 g/mol) was evaluated from the hydroxyl number determined by the standard procedure ASTM D4275-05 test method A. Prior to be used, the polyol and 1,3-PD were dried at 60ºC.

Polyurethanes with different HS content ranging from 16 wt% to 60 wt%, maintaining a NCO/OH molar ratio equal to 1 for all the compositions, were prepared using two-step bulk polymerization procedure. Firstly, the isocyanate-terminated prepolymers were prepared by the reaction between the polyol with the diisocyanate at 90 ºC for 5 h in nitrogen atmosphere. Then, 1,3-PD was added at the same temperature during 10 min with vigorous stirring. Finally, the viscous liquid was quickly poured between two Teflon coated metal plaques separated by 1.5 mm and left to cure under pressure for 10 h at 100 ºC.

Microdomain structure and properties of synthesized polyurethanes with different HS content were analyzed by attenuated total reflexion Fourier transform infrared spectroscopy (ATR-FTIR), differential scanning calorimetry (DSC), thermogravimetric analysis (TGA), and performing tensile and Shore D hardness tests.

Results and Discussion

ATR-FTIR spectroscopy was used to investigate the effect of chemical structure and HS content on the microstructure of polyurethanes, based on CO1 and CO2 castor oil derived polyols as SS, by means of hydrogen bonding formation in the amide I region. In both polyurethane systems, while the band associated with H-bonded urethane carbonyl groups in disordered (amorphous) domains at 1721cm^{-1} decreases with increasing HS content, H-bonded urethane carbonyl groups in ordered (crystalline) hard domains at 1685 cm^{-1} increases with HS content and, in this way, it provokes the formation of large HS domains that contribute to the phase separated microstructure.

The results obtained from tensile test are shown in table 1. The CO1-based SPU show higher modulus (E), strength at break (σ) and percent of elongation (EL) than those based on CO2. As observed by DSC, this may be due to the crystalline nature of CO1-based SS while not crystallinity is observed in CO2-based SS. In both SPU systems HS crystallize showing similar melting temperatures and cristallinity.

The thermal stability of SPU systems has been studied by TGA. All the analyzed systems show similar weight loss profiles in the whole temperature range. Derivative TGA curves revealed three main degradation processes and higher thermal stability of CO1-based SPU.

Polyurethane	E (MPa)	σ (MPa)	EL (%)
SPU-CO1-3	178.2±6.3	24.4±1.4	740±34
SPU-CO1-5	222.9±8.0	14.7±0.2	310±25
SPU-CO1-9	284.9±7.4	16.4±0.4	50±3
SPU-CO1-13	319.1±6.0	19.6±0.4	18±3
SPU-CO2-3	6.7±2.1	1.9±0.2	254.7±34
SPU-CO2-5	36.5±7.6	5.3±0.1	194.4±8
SPU-CO2-10	73.8±34.3	7.5±0.4	161.2±36
SPU-CO2-15	223.9±91.6	8.7±0.4	64.5±17

Table 1. Mechanical properties of the synthesized SPU

Conclusions

Two SPU systems based on renewable precursors were synthesized, analyzed and characterized. The final properties of synthesized SPU were analyzed taking into account the functionality and crystallinity of polyol and the HS content.

Acknowledgments

The authors wish to express their gratitude to the Basque Government (BFI09.167, S-PE09UN07 and S-PE10UN22)' and to the University of the Basque Country (SGIker)

References

1. Williams, C. K.; Hillmyer, M. A.; Polym. Rev. 2008, 48, 1.
2. Gandini, A.; Macromolecules 2008, 41, 9491.
3. Yilgor, I.; Yilgor, E.; Guler, I. G.; Ward, T. C.; Wilkes, G. L.; Polymer 2006, 47, 4105.

Synthesis of polyesters from Castor Oil and their use as polymer matrix for magnetic nanocomposites

Paulo Anselmo Ziani Suarez[*], *Fabricio Machado Silva, Eduardo Ulisses Xavier Péres and Fernando Gomes de Souza Junior*[1].

University of Brasília, [1]Instituto de Macromoléculas Professora Eloisa Mano

e-mail: [*]psuarez@unb.br

Introduction

The synthesis of polymeric materials derived from renewable resource has been intensely studied in the last decades.[1] Depending on the nature of the monomeric specie, the bio-based polymeric materials can present final properties similar to those usually observed in polymer materials obtained from petrochemicals. In addition, some biopolymeric material can also present biodegradability feature and can be tailored in order to be used for controlled drug delivery applications[2].

Specifically, ricinoleic acid (RA, 12-hydroxy-9-*cis*-octadecenoic acid) has been utilized as raw material to produce aliphatic polyesters and lactones. This fatty acid presents specific characteristics, intrinsically related to its chemical structure that involves two reactive functional groups (hydroxyl, carboxyl) and a double bond, which makes easy the formation of several polymeric materials through step-growth polymerization mechanism.[3]

From this point, the use of dispersions of magnetic iron oxide nanoparticles with their surface modified by organic molecules or polymers have given rise to intensive research for biomedical applications such as magnetic drug targeting, cancer treatment (hyperthermia), enzyme immobilization, or magnetic resonance imaging[4], as well as for a bottom-up approach to build nanodevices such as high density storage systems.

The aim of this work is developing new routes to prepare composites from castor oil and magnetic iron nanoparticles.

Materials and Methods

Castor oil was purchased from Celtic (São Paulo, Brazil); chloridric acid and sodium hydroxide were obtained from VETEC (Rio de Janeiro, Brazil); chloroform was acquired from Synth (São Paulo, Brazil); nitrogen was provided by White Martins Ltda (Rio de Janeiro, Brazil). All other reagents were used as received.

Synthesis of Ricinoleic Acid

Castor oil was mixed with a 3 mol L^{-1} sodium hydroxide solution and kept at 70 °C under mechanical stirring for 3 h. To the obtained soap was added a 2 M chloridric acid solution and the mixture was mechanically stirred for 30 min at 80 °C. A two phase mixture was obtained (an aqueous phase and an organic phase rich in ricinoleic acid), which were separated by decantation. The isolated organic phase was washed three times with distilled water. Then, the ricinoleic acid was dissolved in chloroform and mixed with magnesium sulphate. The mixture was filtered and chloroform was removed by distillation under reduced pressure.

Synthesis of Magnetic Nanoparticles

Magnetite (Fe_3O_4) nanoparticles were prepared by chemical coprecipitation of aqueous Fe^{2+} and Fe^{3+} salts solution and NaOH solution. Initially, 6.1 g of $FeCl_3.6H_2O$ and 3.1 g of $FeSO_4.7H_2O$ were dissolved in distilled water (125 mL) and hydrochloric acid (5 mL) and kept at 60 ºC with bubbling of nitrogen gas. Separately, NaOH (37.5 g) was dissolved in distilled water (625 mL). The base solution was added into the iron salts solution and kept under nitrogen atmosphere and vigorous stirring at 60 ºC for 30 min. The resulting black magnetic nanoparticles were isolated by magnetic decantation and washed with distilled water until neutral pH.

Surface Modification of Nanoparticles

RA (1.12 mL) was slowly dropped into a nanoparticles (1 g) suspension under mechanical stirring in water at 85 °C.

Synthesis of Polymer

Polymerizations were carried out in a 1 L five necked round-bottom flask. The flask was equipped with a mechanical stirred, nitrogen inlet tube, adjacent partial reflux condenser and a thermocouple. The reaction vessel was heated with an electrical heating mantle connected to an automatic temperature controller. The monomer RA and modified nanoparticles were introduced into the reaction vessel and purged with nitrogen. Then the mixture was kept under stirring at the desired temperature during a determined time. The composite was characterized by FT-IR (IRPrestige-21 Shimadzu) and DSC (DSC-60 Shimadzu).

Results and Discussion

The polyesterification of RA was confirmed by FT-IR. The ester formation was confirmed by two new strong stretches at 1732 cm^{-1} and 1178.51 cm^{-1}. The RA consumption was observed by the disappearance of stretches related to the carboxyl (at 1708 cm^{-1}) and hydroxyl (at 3352 cm^{-1}) groups.

The Tg observed values for polymeric materials at 190 °C was –75.2 °C. This behavior may be understood as a result of the increasing molecular weight and also related to the crosslinking of growing polymeric chains.[5]

Conclusions

The method used here was suitable to prepare composites of biopolyester from RA and surface modified magnetic nanoparticles. Measures Magnetic force realized after further showed that the material formed has superparamagnetic behavior. At this behavior there is not histerese.

References

1 Sharma, V.; Kundu, P. P. Prog Polym Sci 2006, 31, 983-1008
2 Okada, M. Prog Polym Sci 2002, 27, 87-133.
3 Slivniak, R.; Domb, A. J. Macromolecules 2005, 38, 5545-5553.
4 (a) Pankhurst, Q. A.; Connolly, J.; Jones, S. K.; Dobson, J. J. *Phys. D: Appl. Phys.* 2003, *36*, 167.
5 Slivniak, R.; Domb, A. J. Biomacromolecules 2005, 6, 1679-1688

Thermosensitive Copolymers Based on Alginate and Poly(N-isopropylacrylamide) Obtained by Gamma-radiation

M. M. Soledad Lencina[1], *Noemí A. Andreucetti*[2], *Marcelo A. Villar*[1]

[1]Planta Piloto de Ingeniería Química, PLAPIQUI (UNS-CONICET), Departamento de Ingeniería Química, Universidad Nacional del Sur, Camino "La Carrindanga" Km. 7, (8000) Bahía Blanca, Argentina.
[2]Departamento de Química, Universidad Nacional del Sur, Av. Alem 1253, (8000), Bahía Blanca, Argentina

e-mail: mlencina@plapiqui.edu.ar, mvillar@plapiqui.edu.ar

Introduction: Irradiation is a valuable technique for the modification of physical and chemical properties of polymeric materials. The use of gamma-irradiation methods has advantages, such as relatively simple manipulation and the absence of any extra agents for polymerization and/or crosslinking [1].
Alginate is a linear biopolymer of 1,4-linked β-D-mannuronate (M) and α-L-guluronate (G) residues [2]. N-isopropylacrylamide (NIPAAm) could be polymerized in order to obtain poly(NIPAAm), a thermo-responsive polymer, which shows coil-globule transformation at a lower critical solution temperature (LCST) around 32 °C [3].
The aim of this work is to obtain alginate-PNIPAAm copolymers via irradiation with gamma rays from ^{60}Co with the final goal of synthesized thermoresposive hydrogels.

Materials and Methods: The irradiation was carried out in solution. First, a water solution containing 5 % NIPAAm recrystallizated from n-hexane was prepared. Then, 1 g of alginate and the necessary amount of the NIPAAm solution to achieve alginate:NIPAAm molar ratios of 0.5:1, 1:1, and 1:0.5 were introduced in 100 mL flasks. In order to have a constant alginate concentration, the volume of final solution was 50 mL for all the cases. The flasks were connected to a vacuum line, evacuated and heat sealed having alginate-NIPAAm solutions under vacuum. Water solutions were irradiated with ^{60}Co at Centro Atómico Ezeiza (Argentina). Different doses between 0.5 and 10 kGy were applied with a low dose rate (1 kGy/h).
After irradiation, the copolymers obtained were washed in a soxhlet extractor with methanol. Percentages of grafting (% G) and grafting efficiency (% EG) were calculated from mass recovered and from elemental analysis.

Results and Discussion: Values of % G and % EG, calculated according to other authors [4], for samples irradiated with 0,5 and 1 kGy, are presented in Table 1.

Table 1. % G and % EG values of irradiated solution.

Dose	ID	Alg:NIPAAm molar ratio	% G	% EG
0.5 kGy	A1	0.5:1	67.9	30.2
	A2	1:1	45.3	39.7
	A3	1:0.5	38.1	66.9
1 kGy	B1	0.5:1	152.7	67.9
	B2	1:1	38.5	33.8
	B3	1:0.5	27.7	48.7

% EG values are function of both NIPAAm concentration and dose rate used. Then further studies must be done in order to understand the influence of each variable.
Values of percentage of carbon and nitrogen content, obtained from elemental analysis, along with % G calculated from these values are shown in table 2 for copolymers irradiated with 1 kGy.
% G increases with the increase in the content of initial solution. The values obtained from elemental analysis are in good agreement with those calculated from mass measurements.

Table 2. Elemental analysis and % G calculated.

ID	% C	% N	% G
B1	48.9	7.06	154.2
B2	41.1	4.43	65.5
B3	38.7	3.16	37.0

Fourier Transform Infrared (FTIR) spectrum of samples B1, B2, and B3 are presented in Figure 1. The presence of PNIPAAm in the copolymer is reflected in the signals at 3072, 2969, and ~1550 cm^{-1} associated to stretching ν N-H, ν^{as} CH_3, and δ N-H respectively. The mains signals for alginate are at 1413 cm^{-1} (δ O-H) and ~ 1050 cm^{-1} (ν C-O; ν^{as} C-O-C). In B1 spectra the bands for PNIPAAm are deeper than in B2 and B3, according to the degree of grafting calculated from elementary analysis.

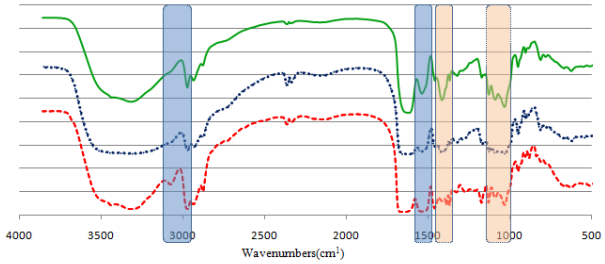

Figure 1. FTIR spectra of samples B1 (- - -), B2 (· · ·), and B3 (—).

Conclusions: Alginate-PNIPAAm copolymers were obtained by solution irradiation of alginate and NIPAAm monomer. % G is a function of NIPAAm content and % GE is a function of both NIPAAm content and irradiation dose. At higher irradiation dose a gel is produced as consequence of PNIPAAm crosslinking. For this reason, low doses with a low dose rate must be used in order to obtain soluble copolymers.

Acknowledgements: Authors thank to Consejo Nacional de Investigaciones Científicas y Técnicas (CONICET) and Universidad Nacional del Sur (UNS) for financial support.

References

1. S.B. Lee, E.K. Park, Y.M. Lim, S.K. Cho, S.Y. Kim, Y.M. Lee, Y.C. Nho, *J. Appl. Polym. Sci.*, 100 (2006), 4439-4446.
2. A. Kikuchi, M. Kawabuchi, A. Watanabe, M. Sugihara, Y. Sakurai, T. Okano, *J. Control. Release*, 58 (1999), 21-28.
3. Y. Hirokawa, T. Tanaka, *J. Chem. Phys.*, 81 (1984), 6379-6380.
4. H. Cai, Z.P. Zhang, P.C. Sun, B.L. He, X.X. Zhu, *Rad. Phys. Chem.*, 74 (2005) 26-30.

Study of Incorporation of Vegetable Waste as Filler in Flexible Polyurethane Foam

Francisco José Melero Muñoz, Mª Virtudes Navarro Bañón, José Roberto Vega Baudrit, Mª del Rosario Sibaja

Ballestero Technological Center of Furniture and Wood (CETEM), National Nanotechnology Laboratory (LANOTEC), Polymers Laboratory National University of Costa Rica (POLIUNA)

fj.melero@cetem.es

Introduction: Use of flexible polyurethane foam has been widely extended to a high range of commercial applications. Manufacturing of cushioning and sleeping devices is one of the most outstanding applications. In the foaming process, different fillers are usually added in the formulation with the aim of reduce manufacturing costs and enhance physical properties of the final product, such as increase density, strenght and mechanical resistance. Most commonly used fillers are inorganic powders, like barium sulfate, calcium carbonate, talc and inorganic fibers. The main objective of this study has consisted of characterising properties of flexible polyurethane foams in which formulation conventional fillers, that nowadays are being used, have been replaced by vegetal waste.

Materials and Methods: The raw materials employed were polyols, isocyanates and additives such as silicone, amine and tin octoate commonly used in the manufacturing of flexible polyurethane foams for its use in cushioning and sleeping devices. Calcium carbonate and rice shell previusly pulverized and sieved obtained from rice harvest were used as fillers. Optical microscopy, thermogravimetric analysis and infrared spectroscopy were used for the analysis of foams obtained. Standard test method for cellular polymeric materials were carried out to analyse their mechanical properties: hardness, static fatigue at constant deformation and tensile strenght and elongation at break.

Results and discusions: After selection and characterisation of raw materials that were used in this study, four flexible polyurethane foams were obtained and subsequently characterized, which difference between them was the kind of filler: No filler, Calcium Carbonate, Milled Rice Shell and Mix of them.

Conclusions: It has been shown that milled rice shell can be used as filler in the production of flexible polyurethane foams for it use in cushioning and sleeping devices :

- It disperses homogeneously during the foaming process.
- TGA analysis shows that flexible polyurethane foam filled with milled rice shell is thermically more stable than polyurethane foam without fillers.

Standard test methods carried out showed that flexible polyurethane foam filled with milled rice shell has a mechanical behaviour similar and even better in some aspects to polyurethane foams filled with calcium carbonate.

Lyocell Fibers Reinforced with Anisotropic Nanofiller

Ahmed Jalal Uddin, Atsushi Yamamoto, Yasuo Gotoh

Faculty of Textile Science and Technology, Shinshu University, 3-15-1 Tokida, Ueda, Nagano 386-8567, Japan

Email: jalal@shinshu-u.ac.jp

Introduction: Cellulose is one of the most abundant natural resources on earth and it is a source of biodegradable and eco-friendly regenerated fibres for both apparel and industrial applications. The cellulose fibres regenerated from NMMO solutions, known by the generic name lyocell, yield fibres with good physical properties than those produced using earlier technologies. The cellulose of lyocell is usually derived from pulp as found in hardwood tress such as eucalyptus, oak and birch. The production of pulp material from these trees is relatively costly. Conversely, bagasse, derived from the crushing of sugarcane stalks, is a much cheaper that can reduce the production cost of lyocell fibres. With our persistent efforts, we successfully prepared lyocell fiber from bagasse equivalent with the commercial lyocell. [1]

In this work, we attempted to reinforce our lyocell fiber prepared from baggase with single-walled carbon nanotubes (SWCNTs). Homogeneous suspensions of cellulose and nanotubes were extruded through the nozzle in dry-jet wet spinning method and taken up to their highest possible speed. The morphology, structure, thermal and mechanical properties of composite fibers were characterized.

Materials and Methods: The spinning solutions were prepared by taking bagasse, NMMO 0.9 hydrate (solvent), propyl gallate (antioxidant) and sodium dodecyl-sulphate (surfactant). The suspension of SWCNT with catechin, recent finding as a good dispersant of SWCNT [2], and CMC were made separately and added to the cellulose solution to become SWCNT 0.05, 0.1, 0.2 and 0.3 wt% relative to the cellulose content.

Dry jet-wet spinning was carried out with a single-hole spinneret of diameter 0.5 mm at 120°C with the injection speed of 4.0 m min^{-1}. Coagulation was taken place in water/NMMO mixture (10 wt%) at room temperature (20°C) with a 2-m coagulating bath followed by a water wash. The prepared fibers were taken up at their maximum possible speeds. The spin-draw ratio d_f/d_0 was determined by measuring the cross-sectional diameter of the solution dope at the spinneret exit (d_f) over the fiber cross-sectional diameter at the take-up point (d_0).

Results and Discussion: Table 1 shows the spin-draw ratio, and the tensile properties of neat cellulose and composite fibers. It is seen that the spin-draw ratio was drastically increased after incorporation only a small amount of SWCNTs i.e., 0.05% and the trend continued till filler loading of 0.2%. It indicates that the spinnability of cellulose is enhanced with SWCNT loadings. Tenacity and initial modulus also show the same dramatic increase with the spin-draw ratio and highest properties were obtained for 0.2% filler loading. However, the tenacity and Young's modulus of 0.2% nanotube filled fibre are 1.18 GPa and 65 GPa that are respectively 188% and 400% higher than the neat cellulose ones. Storage modulus of composite fibers increases with the loading of nanotubes in the whole temperature range. Such high-resistant fibers will hopefully be useful as tire-cord and in other industrial applications. The WAXD images, in Figure 1, support the corresponding structural development of composite fibers with the spin-draw ratio that lead to outstanding mechanical properties.

TABLE 1. Properties of neat cellulose and SWNT loaded composite fibers

Fiber	*Spin-draw ratio*	*Tenacity (GPa)*	*Young's modulus (GPa)*	*Elong. at break (%)*
Neat cellulose	*17.5*	*0.41*	*13*	*15*
SWCNTs 0.05%	*48.8*	*1.04*	*54*	*3.2*
SWCNTs 0.1%	*52.5*	*1.15*	*63*	*3.8*
SWCNTs 0.2%	*57.5*	*1.18*	*65*	*3.5*
SWCNTs 0.3%	*45*	*0.71*	*39*	*2.4*

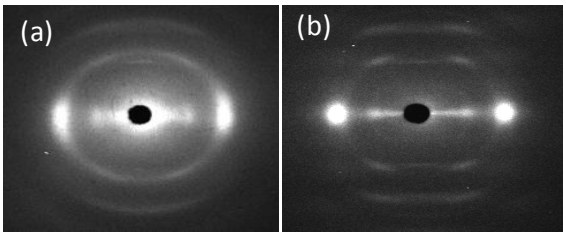

Fig 1. WAXD patterns of the neat cellulose and 0.2% loaded SWCNTs composite fibers.

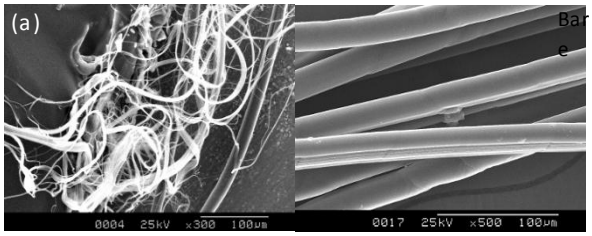

Fig 2. SEM images of the neat cellulose and 0.2% loaded SWCNTs composite fibers after pulverization in a laboratory blender.

It is well-known that lyocell fiber suffers in fibrillation against any mechanical abrasion. We checked the fibrillation property of our nanotube incorporated fibers after a harsh-beating in a laboratory blender. As shown in figure 2, it was observed that only an introduction of a small content of nanotubes resulted drastic prevention of fibrillation of our lyocell fiber.

Reference:

1. Uddin, A.J, Yamamoto, A, Gotoh, Y. and Nagura, M., Textile Res. J. 80, 1846-1858 (2010).

2. Nakamura, G, Narimatsu, K, Niidome, Y, and Nakashima, N., Chem Lett, 36, 1140-1141 (2007).

Castor Oil based Poly(urethane-co-pyrrole)s as Novel Electroactive Anticorrosive Coatings for Steel

*Reza Gharibi, Mohammad Yousefi, Hamid Yeganeh**

Iran Polymer and Petrochemical Institute, P.O. Box: 14965/115, Tehran, Iran

E-mail: h.yeganeh@ippi.ac.ir

Introduction

The discovery of the corrosion protective properties of electrochemically deposited conducting polymers such as polythiophene, polyaniline and polypyrrole (PPy) on metallic surfaces has opened a new dimension in the field of anticorrosive organic coatings [1]. Despite their considerable merits as corrosion protective coatings, poor mechanical properties, improper processability and low environmental stability are main drawbacks of these compounds [2]. To tackle these problems, preparation of copolymers or composites of conducting polymers with some tractable insulating polymers was considered [3].

In the present work, preparation of novel block copolymers of polypyrroles and polyurethanes with high flexibility and mechanical properties similar to pure polyurethane and conductivity close to pristine PPy was considered. For the synthesis of polyurethane, castor oil was used as starting material. Because, castor oil is one of the most important renewable resources raw material, due to its low cost, low toxicity and widespread availability in most region of the world.

Experimental

At the first step, hydroxyl terminated polyurethane (HCO) was prepared via the reaction of three equivalents of butane diol with one equivalent of NCO-terminated urethane prepolymer, which itself prepared from the reaction of three equivalents of isophorone diisocyanate with one equivalent of castor oil. At the second step, for the preparation of block copolymers (HCO-PPy1-4), HCO was used as initiator for oxidative polymerization of pyrrole (Py) in the presence of cerric ammonium nitrate (CAN) as catalyst. Different formulations of copolymers are tabulated in Table 1.

Results and discussion

In contrast to polypyyrole homopolymer, the prepared copolymers were readily soluble in common organic solvents; therefore, they freed from homopolymer by simple filtration of polymerization mixture. The structure of the prepared copolymers was confirmed by examination of their FTIR and ^{1}HNMR spectra. Electrical conductivity of the obtained block copolymers were measured by four-point probe technique (Table 1). Conductivity of copolymers was depended on the molar ratio of HCO/Py/CAN. The observed trend is in accordance with Kızılcan findings [4].

The PPy-HCO2 copolymer with highest conductivity was used for the coating step. The protective coating was applied on steel 316 electrode (0.6 cm^2) by electrochemical deposition of electroactive copolymer from its solution in acetonitrile solvent containing lithium perchlorate (0.1 M) as supporting electrolyte using a cyclic voltammetry technique. The electrodepositing was performed by cycling continuously the potential between -0.8 and 1.8 V versus Ag/AgCl reference electrode at a potential scan rate of 0.03 V/Sec (Figure 1). Bare and coated steel were evaluated by examination of corrosion potential (Ecorr), polarization resistance (Rp) and corrosion current (Icorr). Aqueous solutions of NaCl (3.5wt %) were used as electrolyte. The Tafel plots (Figure 2) were obtained by scanning the potential in the range of ± 250 mV around the Ecorr, at a scan rate of 5 mV/min. The coated steel electrode showed much higher Ecorr (0.254v) and Rp (7800Ω) values and lower Icorr value than uncoated steel electrode. Therefore, HCO-PPy2 can be considered as effective anticorrosive coating for steel with 0.6 V shift of corrosion potential.

Table 1: Different formulations and conductivity of copolymers

Name	CAN (mmol)	Py (mmol)	HCO (g)	Conductivity (s/cm)
HCO-PPy1	0. 25	2.3	0.62	7×10^{-3}
HCO-PPy2	0.5	2.3	0.62	1.8×10^{-1}
HCO-PPy3	0. 8	2.3	0.62	4×10^{-3}
HCO-PPy4	0.125	4.6	0.62	5.5×10^{-2}

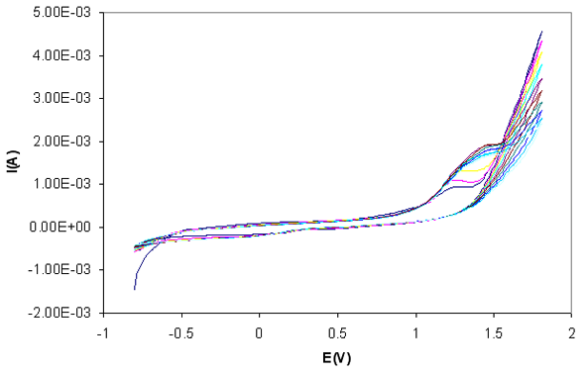

Figure 1:Cylic voltamograms of electrodeposited HCO-PPy-2

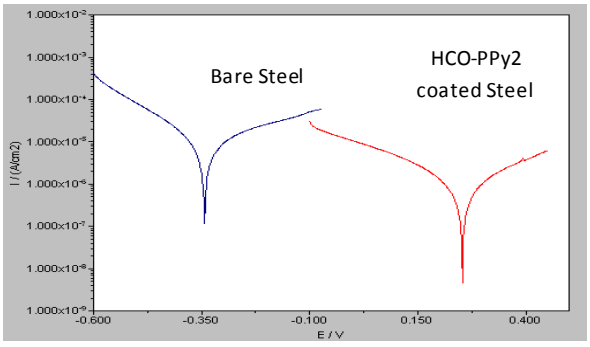

Figure 2: Tafel plots for bare and coated steel316steel

References

1. E. Armelin, et al. Corr. Sci. 50, 721, 2008.
2. J.O. Iroh, et al. Eur. Polym. J. 38, 1547, 2002.
3. J. Njguna, et al. J. Mat. Sci. 39, 4081, 2004.
4. N. Kızılcan, et al. J. Appl. Polym. Sci. 89, 2896, 2003.

Synthesis of Isotactic Poly(hydroxy acrylic acid) by Radical Polymerization of Methylene Dioxolanone Prepared from Lactic Acid

Hitoshi Tanaka, Yoshitaka Matsubara, Kazuya Okuda, and Miki Niwa

Institute of Technology and Science, University of Tokushima

tanaka@opt.tokushima-u.ac.jp

Introduction:

Control of tacticity and helicity has been known to be difficult in free radical polymerization in contrast to ionic polymerization. However, we found that the acrylates with s-cis conformation would propagate preferentially to give an isotactic helical polymer near ceiling temperature (*Tc*) in the polymerization of the acrylates including (-)-menthyl 2-acetamidoacrylate.[1] From this fact and the standpoint of sustainability, we focused on the preparation of an isotactic polymer by free radical polymerization under normal conditions, e.g. reaction temperature far from *Tc*, using a bioresource monomer. We report here the preparation of bioresource monomer and isotactic polymer as well as a conversion of the resulting polymer to a hydrophilic material according to the green chemical process for **1** and **2**.

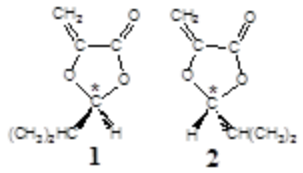

1 **2**

Materials and Methods:

1 and **2** were synthesized by mainly two steps, i.e. cyclization using lactic acid and iso-butylaldehyde and following a vinylization of resulting cyclic compound according to the literature.[2] Cyclization was carried out by refluxing a mixture of lactic acid and iso-butyl aldehyde in the presence of *p*-toluenesufonic acid. This condensation reaction gave a mixture of cis and trans dioxolanone diastereomers, with the cis isomer always predominating. Isolation of the cis dioxolanone, (*S*)-2-*iso*-propyl-(*S*)-5-methyl-1,3- dioxolan-4-one, from trans one, (*R*)-2-*iso*-propyl-(*S*)-5-methyl-1,3-dioxolan-4-one, was performed at need by silica gel column chromatography. Resulting dioxolanones were readily transformed into the required olefins by vinylization, i.e. **1** and **2** from cis and trans dioxolanones respectively by bromination with N-bromosuccinimide (NBS) and AIBN followed by a dehydrobromination with triethylamine. After dehydrobromination, crude produc was purified by distillation under reduced pressure; bp.41°C/1.5mmHg, to give a colorless liquid.

Polymerization was carried out in a sealed ampoule with shaking at given temperature. The ampoule containing required amounts of reagents was degassed several times by a freeze-thaw method and then sealed under reduced pressure and placed in a constant temperature bath. The resulting polymer was isolated by pouring the reaction mixture into methanol.

Polymer was hydrolyzed with KOH in THF at room temperature for 1 day.

Results and Discussion:

Methylene dioxolanone (mixture of **1** and **2**) which were synthesized from ferment lactic acid (LA) and chemically synthesized DL-LA as a starting LA gave a polymer with Mn=15,000~20,000 in ca.60% yield in the polymerization with AIBN for 3 hrs at 60°C. Polymerizability of both dioxolanones synthesized from ferment LA and DL-LA is similar to each other. Tacticity of the resulting polymer, however, is much different, and

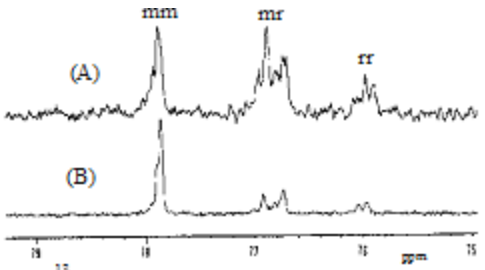

Fig.1 ^{13}C-NMR spectra of poly(hydroxy acrylate) originally obtained from the polymerization of methylene dioxolanone prepared from (A) DL- and (B)ferment lactic acid.

the polymer obtained from the monomer originated from ferment LA represents high isotacticity (mm) as seen in Fig.1, in which hydrolyzed polymer is used for the convenience of the NMR measurement. Moreover, much higher isotactic polymer was obtained by the polymerization of isolated **1**. For the study on the second structure of the polymer is now in progress.

Preparation of isotactic polymer from LA is summarized in Scheme 1. In this scheme, aldehyde is recovered by facile hydrolysis of methylene dioxolanone

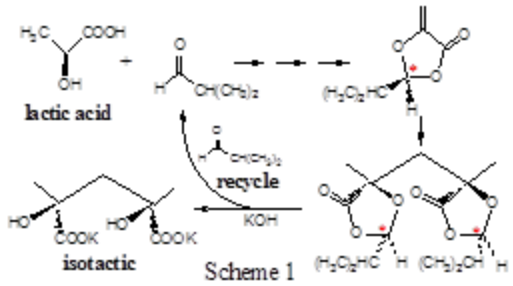

Scheme 1

polymer. Structural comparison between the present polymer and well-known poly(LA) is shown in Fig.2.

In conclusion, the monomer synthesized from a ferment LA gives an isotactic polymer, which converts to a hydrophilic material according to the green recycle process as in Scheme 1.

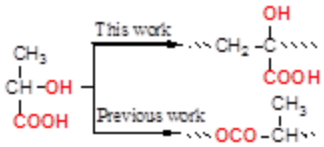

Fig.2 Two types of poly(lactic acid)

References

(1) Tanaka, H.; Niwa, M. *Polymer* **2005**, *46*, 4635-4639.

(2) Magee, D. I.; Mallais, T. C.; Mayo, P. D. M.; Strunz, G. M. *Tetrahedron* **2006**, *62*, 4153-4161.

Investigation of the type of the bridge on the activity of supported metallocene catalyst in ethylene polymerization.

A. Talaei

alirezatalaei@yahoo.com

ABSTRACT:

Ethylene polymerization was carried out with immobilization of rac-Ethylenebis(1-indenyl)zirconium dichloride ($Et(Ind)_2ZrCl_2$) and rac-Dimethylsilylbis(1-indenyl)zirconium dichloride ($Me_2Si(Ind)_2ZrCl_2$) on ES70W Silica support by indirect method. Effects of pre-activated catalyst concentration and calcination temperature of support on activity of supported catalyst were investigated. At [Zr]:[Si]= 0.04 wt% and 450 ^oC calcinating of silica temperature the maximum activity were observed. The ethylene bridge catalyst was more active than silyl bridge by the activity of 8142 kg PE. (mol Zr. h)$^{-1}$ and 4523 kg PE.(mol Zr. h)$^{-1}$ respectively. It was observed that the molecular weight of polyethylene that produced by ethylene bridge was higher than silyl bridge. The two type of bridge showed same trend in activity by changing of polymerization condition. It was observed that the reactor fouling was removed by supporting of catalyst.

Biopolymers from Natural Oils

Ausra Remeikyte, Jolita Ostrauskaite, Juozas Vidas Grazulevicius

Kaunas University of Technology

jolita.ostrauskaite@ktu.lt

Introduction

In recent years, natural oils have become the center of attraction for their potential use as starting materials for the preparation of polymers. This is an alternate route, which has the potential to augment the use of petroleum-based polymers [1].

In this study, the biopolymer films have been prepared by the cationic cross-linking in the dark or by photocross-linking of the epoxydized natural oils with or without the reactive diluents. The effect of the method of curing and of the addition of the reactive diluent on the thermal, mechanical properties, and biodegradability of the cross-linked polymers was studied.

Materials and Methods

The linseed oil, rapeseed oil, and fish oil were epoxydized with 3-chloroperbenzoic acid [2] or with methyltrioxorhenium catalyst and hydrogen peroxide as oxygen source [3]. The highest conversion of carbon double bonds reached 86% and the highest number of epoxy groups per triglyceride of 5.3 was obtained.

The epoxydized natural oils were cross-linked in the dark using ytterbium trifluoromethane sulfonate as cationic initiator at 60°C with the following reactive diluents: bisphenol A diglycidyl ether (**1**), bisphenol A propoxylate diglycidyl ether (**2**), and 3,4-epoxycyclohexylmethyl-3,4-epoxycyclohexane-carboxylate (**3**).

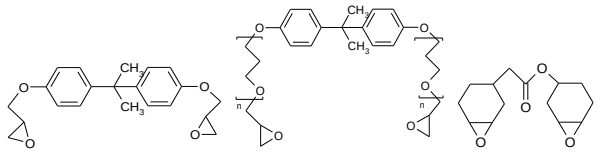

1 **2** **3**

The photocross-linking of different natural oils was carried out using diphenyliodonium hexafluorophosphate or triarylsulfonium hexafluoroantimonate as photoinitiators at the room temperature with the reactive diluents **1**-**3** as well as with the following reactive diluents: 1,4–cyclohexane dimethanol diglycidylether (**4**), resorcinol diglycidylether (**5**), bis[4-(glycidyloxy)phenyl]methane (**6**), and trimethylolpropane triglycidyl ether (**7**).

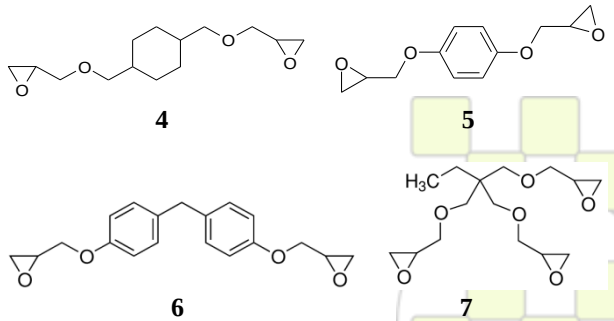

4 **5**

6 **7**

Results and Discussion

Cross-linking of epoxydized natural oils in the absence of diepoxy compounds resulted in viscous polymers. The fastest curing was observed for the layers containing reactive diluents **3** and **4**. The yield of the insoluble fraction of the polymers was found to be 59-90%. It depended on the curing method and on the ratio of the epoxydized oil and the reactive diluent in the reaction mixture.

The Young modulus of the cross-linked polymer films ranged from 2 to 861 MPa. The cross-linked polymer obtained with the reactive diluent **3** showed the highest Young modulus. The hardness of some compositions prepared from the epoxydized linseed oil was similar to that of the commodity polymer films. The thermogravimetric analysis indicated that the cross-linked polymers were thermally stable up to 200°C in nitrogen atmosphere. The 10% weight loss temperature of the polymers ranged from 250 to 420°C. The water vapour transmission rate of the cross-linked polymer films was in the range of 6-49 g/m^2/24h. The increase of the amount of the reactive diluent used leaded to the decrease of the water vapour transmission in the polymer films. The measurements of the biochemical oxygen demand indicated that the cross-linked polymers showed higher biodegradation rate than cellulose, starch and polyvinylalcohol. The composting of the polymer films showed that the cross-linked polymers of epoxydized natural oils prepared without diepoxy reactive diluents showed higher biodegrability than those prepared with the reactive diluents.

Conclusions

The biopolymer films have been prepared by the cationic cross-linking in the dark or by photocross-linking of the epoxydized natural oils with or without the reactive diluents. The thermal, mechanical properties and biodegradability of the cross-linked biopolymers depended on the curing method and on the epoxydized oil, the reactive diluent, and their ratio in the reaction mixture.

References

1. V. Sharma, P.P. Kundu, *Progress in Polymer Science*, 2006, 31, 983-1008.

2. E.A.C. Demengeot, I. Baliutaviciene, J. Ostrauskaite, L. Augulis, V. Grazuleviciene, L. Rageliene, J.V. Grazulevicius, *Journal of Applied Polymer Science*, 2010, 115, 2028–2038.

3. D.D. Andjelkovic, M. Valverde, P. Henna, F. Li, R.C. Larock, *Polymer*, 2005, 46, 9674-9685.

Synthesis of Polystyrene-Rubber Waterborne Nanoparticles by Miniemulsion Polymerization

Ludmila Ronco, Roque J. Minari, Jorge R. Vega, Luis M. Gugliotta

INTEC (Universidad Nacional del Litoral - Conicet) - Güemes 3450 - (3000) Santa Fe – Argentina

rjminari@santafe-conicet.gov.ar

Introduction: Actually research on waterborne hybrid latexes has gained a lot of interest, since it is considered as the opportunity for developing new products based on the synergy effects of the adopted compounds.[1] Polystyrene/rubber waterborne hybrid systems are expected to combine positive properties to produce nanoparticles with high impact resistance. The improvement of properties is expected to be maximum with intimate contact of both materials. Unfortunately, polystyrene (PS) and polybutadiene (PB) are not compatible. Miniemulsion (mE) polymerization allows the incorporation of hydrophobic components, like PB based rubbers, into PS particles. The molecular structure of rubber, the formulation and polymerization conditions affect the phase compatibilization.

In this work, the mE polymerization is used to synthesize waterborne PS/PB based-rubber (anionic PB and styrene-butadiene random copolymer: SBR) nanocomposites; and the effect of the process variables and rubber architecture was investigated.

Experimental Work: mE of 20-30% wt solids content, with variable rubber content, 2% wbop (weight based on organic phase) of sodium lauryl sulphate as surfactant, 4% wbm (weight based on monomer) of hexadecane as costabilizer, and $NaHCO_3$ at a 0.04 M concentration in the water phase. In order to produce the mE, organic and water phases were first strongly mixed and then treated with a Sonics VC 750 ultrasonic homogenizer (100% of amplitude with cycle of 20 sec on and 5 sec off).

Polymerizations were carried out in batch at 70ºC and under constant N_2 bubbling. Along the polymerizations the following was measured: i) monomer conversion (x) by gravimetry; ii) droplet (d_d) and particle (d_p) diameters by dynamic light scattering, using a Brookhaven BI-2030 equipment; and iii) molecular properties by size exclusion chromatographic (SEC) with a Waters 1515 chromatograph. mE stability and surface tension (ST) were measured using a turbiscan TMA2000 and a Krüss tensiometer K8, respectively.

Results and Discussions: Table 1 and Fig. 1.a,b present the results of the mE polymerization when 5 % wbop of PB (M_w=445000 g/mol) was used as preformed polymer. All mE were stable; and while in experiment ME1 the solids content was 30 %, in ME2 and ME3 it was 20%. Also, 2 kinds of initiators were employed: potassium persulfate (KPS) in ME1-2 and the redox system tert-butyl hydroperoxide/ascorbic acid (TBHP/ AA) in ME3. Independently of the initiator type and the solids content, the final x was greater than 90 %. The reduction in the solids content mainly affects d_d, thus favoring the droplet nucleation (i.e., N_p/N_d is reduced). The redox initiator produces an increment of the radical availability and increases the rates of polymerization and nucleation (Fig. 1.a,b and Table 1), with a reduction of N_p/N_d. Notice that the higher the particle fraction produced by droplet nucleation, the lower the phase separation, and the lower the collected coagulum (mainly composed by PB, according to SEC analysis.)

Table 1. Experiments with 5% wbop of PB

Experiment	*ME1*	*ME2*	**ME3**
Solid content [%]	30	20	20
Initiator (%wbm)	KPS(0.8)	KPS(1.5)	TBHP/AA(1.5)
x [%]	94.2	94.3	94
d_d [nm]	340	229	160
d_p [nm]	96	108	108
N_p/N_d [a]	44.7	9.5	3.3
Coagulum [%]	1.7	0.1	> 0.1

[a] N_p: number of particles; N_d: number of droplets

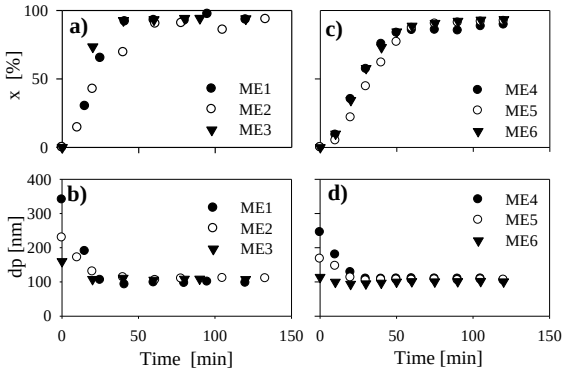

Fig. 1. mE polymerizations with PB (a, b) and SBR (c, d).

Table 2 and Fig. 1.c,d show the experimental results obtained with SBR as preformed polymer and KPS as initiator. While in ME4 and ME5 high M_w SBR (305000 g/mol) was used, low M_w SBR (65000 g/mol) was employed in ME6. Not significant effect on x of the SBR concentration and M_w was observed. As expected, the reduction of the organic phase viscosity (by decreasing the amount of SBR or its M_w) diminishes d_d, thus increasing the droplet nucleation (Table 2 and Fig. 1.d). The highest droplets nucleation efficiency ($N_p/N_d \approx 1$) was achieved in ME6 with 1 % wbop of low M_w SBR. ME6 also presents the smallest d_d and ST=49 mN/m, indicating the absence of micelles in the mE. Finally, a negligible amount of coagulum was observed in these experiments.

Table 2. Experiments with SBR and 0.75 % wbm of KPS

	ME4	*ME5*	**ME6**
SBR [% wbop]	5	1	1
x [%]	89.4	92.1	93.4
d_d [nm]	245	167	114
d_p [nm]	110	106	101
N_p/N_d	11.2	3.9	1.4

Conclusions: The effect of M_w and rubber composition was studied in order to produce compatibilized nanoparticles. The employment of low M_w SBR (a rubber more compatible with PS than PB) allows the achievement of higher droplets nucleation efficiency, with minimum phase separation.

References:

[1] Asua JM, Prog. Polym. Sci., 22:1283 (2002)

Lithium Naphthalenide Initiators for Controlled Anionic Polymerization

Verónica A. González, Angel J. Satti, Mario D. Ninago, Enrique M. Vallés, Marcelo A. Villar, Andrés E. Ciolino

Planta Piloto de Ingeniería Química, PLAPIQUI (UNS-CONICET), Departamento de Ingeniería Química, Universidad Nacional del Sur, Camino "La Carrindanga" Km. 7, (8000) Bahía Blanca, Argentina.

e-mail: valles@plapiqui.edu.ar, mvillar@plapiqui.edu.ar, aciolino@plapiqui.edu.ar

Introduction: The use of effective initiators is the key for a successful synthesis of complex macromolecular architectures by anionic polymerization techniques. In this work we report the synthesis and polymerization performance of a soluble initiator obtained by the reaction of naphthalene (Naph) and lithium metal (Li), under mild experimental conditions. Its efficiency was tested in homopolymerization reactions by using different monomers such as styrene (S), isoprene (I) and hexamethyl(cyclotrisiloxane) (D_3).

Experimental: All manipulations were performed under high vacuum in glass reactors designed according to anionic polymerization standards [1]. The apparatus employed is shown in Figure 1.

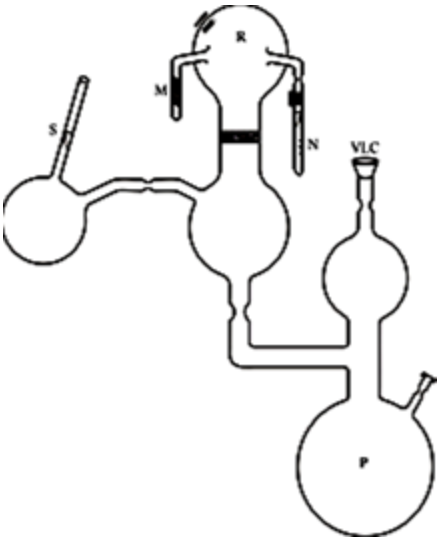

Figure 1. Apparatus used for the synthesis of lithium naphthalenide. References: **P**: Purge Section, **R**: Reactor, **VLC**: Vacuum Line Conection, **N**: Naphtalene Solution in Benzene, **M**: Lithium Metal, and **S**: Sampling Ampoule.

The synthesis was performed in a carefully cleaned apparatus by using granulated lithium and powder naphtalene as reagents and pure distilled benzene or THF/benzene mixtures as reaction solvent. Different [Li]:[Naph] molar ratios were studied. The reaction was performed during 24 h at room temperature (RT), under continuous and vigorous stirring. The crude reaction product was then filtered from the reactor to the sampling ampoule by employing a fritted glass filter between them. For each [Li]:[Naph] ratio studied, pure S monomer polymerization experiences were performed. The PS homopolymers obtained were evaluated by Size Exclusion Chromatography (SEC) in order to test the polymerization activity and the efficiency of the synthesized initiator. After testing all the experimental variables with S, similar experiences were done by using D_3 or I as monomers.

Results and Discussion: Figure 2 show the chromatograms of synthesized PS.

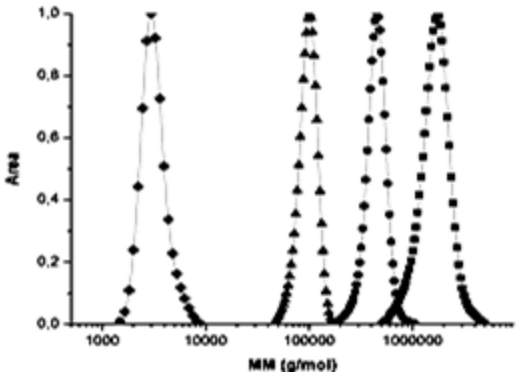

Figure 2. SEC chromatograms for model PS homopolymers synthesized in benzene (Benz.) or benzene/THF mixture. Symbols: (◆) Benz.:THF = 90:10 v/v (THF/Li = 1.5 molar), [Li: Naph] = 4:1, (■) [Li: Naph] = 4:1, (●) [Li: Naph] = 40:1, and (▲) [Li: Naph] = 400:1.

By using benzene as solvent, polymers with a monomodal distribution and high molar masses are always obtained. On the other hand, polymers with lower molar masses can be synthesized when a mixture of benzene/THF is employed,. A molar relation of THF/Li around 1 is needed to get a monomodal population. Other relations produce a bimodal signal with two polymer populations. Recent studies indicate that this result can be attributed to two different reactive species: the naphthalene radical anion and the naphthalene dianion [2], each one visually evidenced by a characteristic color: a deep purple solution (dianion) or a purple-brown solution (radical anion + dianion).

From figure 2, three facts can be clearly appreciated: **i)** all the PS synthesized show narrow molar mass distribution, without the appearance of secondary high or low molar mass peaks; **ii)** regardless the [Li:Naph] ratio, an efficient initiator is obtained; and **iii)** a broad range of molar masses (between 10^3–10^6 g/mol) can be obtained.

Conclusions: Lithium naphthalenide initiators were synthesized under mild conditions by employing different [Li:Naph] ratios, room temperature, and benzene or benzene/THF mixture as solvent. Model homopolymers such as PS, PI, or PDMS were obtained with these initiators, which clearly show the suitability of the experimental procedure employed.

ACKNOWLEDGMENTS

We express our gratitude to CONICET, the Agencia Nacional de Promoción Científica y Tecnológica (ANPCyT), and the UNS for their financial support to this study.

REFERENCES

[1] D. Uhrig, J. Mays, *J. Polym. Sci. Part A: Polym. Chem.*, 43, 6179-6222 (2005).

[2] C. Melero, A. Guijarro, M. Yus, *Dalton Trans.*, 8, 1286-1289 (2009).

A New Method for Synthesis of Photocurable Low Molecular Weight Chitosan

Laleh Solhi, Mohammad Atai, Azizollah Nodehi, Mohammad Imani

Iran Polymer and Petrochemical Institute (IPPI), P.O.Box: 14965/115, Tehran, Iran

L.solhi@ippi.ac.ir

Introduction: Light-curable polymers can undergo photopolymerization upon light exposure, which shows many advantages compared with chemical polymerization, including a high polymerization rate that overcomes the solvent effects in normal polymerization, good temporal and spatial control and resolution, ambient temperature operation and low energy consumption. Light-curable polymers may be used for in situ scaffold forming, which makes minimally invasive surgery possible. Moreover, the light-curable materials may be used for computer-aided fabrication through rapid prototyping which allows fabricating scaffolds with customized shape and reproducible microarchitecture on a large scale. Chitosan is a natural biopolymer that has been widely used in medical applications because of its biocompatibility and biodegradability [1-2]. The purpose of this study was to establish a new method for the synthesis of photocurable chitosan.

Materials and Methods: This synthetic path involves the bonding of Glycidyl Methacrylate (GM) onto the Low Molecular Weight Chitosan (LMWC) chain via glycidyl group of the monomer and the amine group of LMWC. The reaction was carried out in a way that the double bond remains intact and is then able to be polymerized. The process was carried out through a ring opening reaction of mixing the dissolved GM and Hydroquinone (HQ) in Isopropanole with an aqueous solution of LMWC with the molecular weight of about 3000. HQ was added to prevent the polymerization reaction of the double bonds of GM during the grafting reaction. After 15 hours stirring at room temperature, the product was precipitated in a large amount of Methyl Ethyl Ketone (MEK) and filtered. The precipitate was washed with MEK several times to remove the unreacted monomers and other unreacted species. MEK is a good solvent for GM, poly(GM) and HQ, but it is not able to solve the LMWC and the modified LMWC (m-LMWC). The product was then dissolved in Dimethyl Sulfoxide (DMSO) which is not able to dissolve LMWC, but is a good solvent for m-LMWC. The mixture was filtered and the clear solution of m-LMWC in DMSO was separated and freeze-dried. Figure-1 shows the scheme of the reaction. The effect of different parameters such as the temperature and the reactants concentration were investigated.

Results and Discussion: The FT-IR spectra confirmed the formation of m-LMWC. NMR spectra revealed that the reaction was performed mostly by the reaction of amine groups of LMWC and the glycidyl groups of GM. Figure-2 shows the FT-IR spectra of LMWC and m-LMWC. The appearance of the 1725 cm^{-1} peak proves the presence of carbonyl functional groups. Considering the purification process which removes the unreacted GM or Poly(GM) in the product, this peak shows the carbonyl groups of the GM-grafted-LMWC. The product was dissolved in DMSO and photo cured in the presence of 1,3-dibutanone as a photoinitiator meanwhile the solvent was evaporated. The degree of conversion, gel content, and mechanical properties of the cured polymer were also investigated.

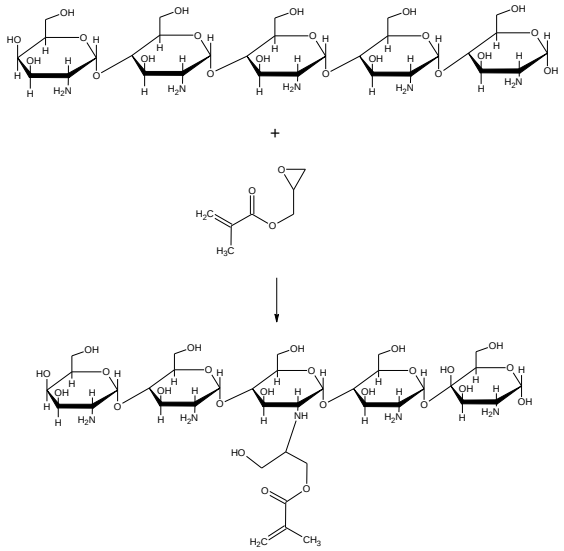

Figure-1- Scheme of the reaction of GM and LMWC

Conclusions: As a result, the synthesized photocurable chitosan seems to be a promising material for many applications. With a glance on the intrinsic wound healing properties of chitosan, this product could be applied for many biomedical and dental purposes such as in situ polymerizable scaffolds and injectable gels.

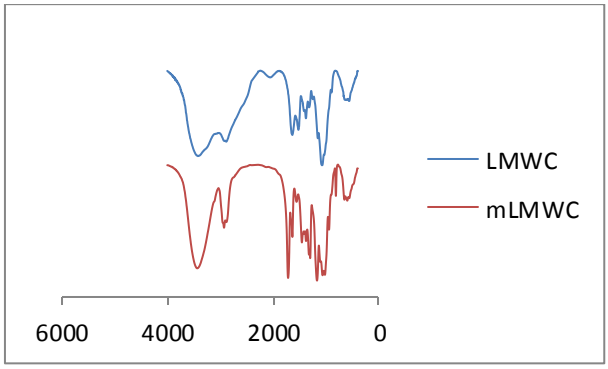

Figure-2- FT_IR spectra of LMWC and m-LMWC

References:

[1] Suh JK, Matthew HW., Biomaterials, 2000; 21, 2589–2598.

[2] Yongzhi Qiu, Ning Zhang, Qian Kang, Yuehuei An, Xuejun Wen, Journal of Biomedical Materials Research Part A, 2009, 89A, 3, 772–779.

Study of Rare Earth Metal Triflates as new Catalyst for the Formation of Oxazolidone-Isocyanurate-Ether Networks from DGEBA and 4-Toluene-2,4-diisocyanate

M. Flores[1], *X. Fernández-Francos*[1], *J.M. Salla*[2], *A. Mantecón*[1], *A. Serra*[1], *E. Jimenez-Piqué*[3], *X. Ramis*[2]

[1] Dept. Química Analítica i Química Orgànica, Universitat Rovira i Virgili, Tarragona
[2] Lab. Termodinàmica, ETSEIB, Dept. Màquines i Motors Tèrmics, Universitat Politécnica Catalunya, Barcelona
[3] Dept. Ciencia dels Materials i Eng. Metal.lúrgica, ETSEIB, Universitat Politécnica Catalunya, Barcelona

marjflores1@gmail.com

Introduction

Improving properties of epoxy resins at a lower cost is of a general great interest for certain technological applications. A good strategy is to insert heterocyclic rings in the polymer structure, increasing the distance between crosslinks while increasing the rigidity of the structure. The reaction between diepoxides and diisocyanates can lead to thermosets containing isocyanurate and oxazolidone rings in their structure. Oxazolidones act as chain extenders and isocyanurate rings play the role of crosslinking points. Although few studies report thermosets having these two kinds of heterocycles in the structure, it is accepted that these copolymers exhibit better properties, mainly higher thermal stability, than neat epoxy resins and other classical epoxy thermosets.[1-4] Usually, the curing of diepoxides/diisocyanates is catalyzed by a tertiary amine and shows short gel time and pot-life due to the formation of isocyanurate rings on the first stages of the curing. In order to offset this drawback, in the present work the amine has been substituted by a rare earth metal triflate. The aim of this work is to study the curing of mixtures of DGEBA and 4-toluene-2,4-diisocyanate (TDI) in the presence of ytterbium triflate, which is a Lewis acid, and the final properties of the materials prepared. The results obtained were compared with those obtained by using

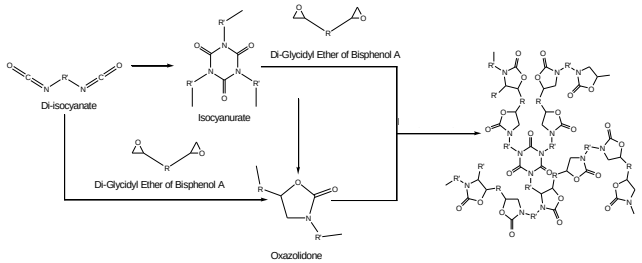

benzyldimethylamine (BDMA) as the catalyst.

Materials and Methods

Diglycidylether of Bisphenol A (DGEBA), Epikote Resin 828 from Hexion Specialty Chemicals (epoxy equivalent = 187 g/eq) was used after drying under vacuum. Ytterbium (III) trifluoromethanesulfonate (99.99%) and BDMA from Aldrich were used without further purification. TDI from Aldrich was distilled before use. TDI and DGEBA were carefully mixed with stirring and degassed under vacuum (at 80ºC) during two hours to prevent the appearance of bubbles during curing. Samples were kept at -20ºC before use to prevent polymerization. 1 phr of catalyst was added to the corresponding DGEBA:TDI mixtures at room temperature just before curing. Kinetic parameters were determined using integral isoconversional non-isothermal kinetic analysis named Kissinger-Akahira-Sunose. Conversions of the different reactive groups, epoxide, isocyanate, isocyanurate and oxazolidone, were determined by FTIR. Gelation was studied using TMA and DSC and thermal stability was determined by TGA. The morphology was investigated by SEM and DMTA. Microhardness and modulus were determined by nanoindentation tests.

Results and discussion

The initial composition of the formulation (molar ratio of isocyanate to epoxide groups), the curing conditions and the catalyst used are the parameters that control the final structure of the network formed, the evolution of the curing and the final properties of the thermosets.

By increasing the initial proportion of isocyanate the glass transition temperature, the thermal stability and the content of isocyanurate rings increase.

The curing with the tertiary amine starts with the formation of isocyanurates, and is followed by oxazolidone ring formation, epoxy homopolymerization and isocyanurate decomposition to produce oxazolidone groups on increasing the temperature. In contrast, ytterbium triflate leads to the initial formation of oxazolidone rings and then catalyzes polyetherification, formation of isocyanurates and their reaction with epoxides to form oxazolidones. Moreover, when ytterbium triflate is used urethane formation takes place at the beginning of the cure, although they disappear at higher temperature. The differences observed in the reactivity not only affect the kinetics of curing, but also the gelation and the final properties of the materials. The most relevant differences between ytterbium triflate and tertiary amine catalyzed curing processes are the longer pot-life and higher glass transition temperature of the resulting materials obtained with the former.

References

1. Caille D, Pascault JP and Tighzert L *Polym Bull* **24**:23-30 (1990).
2. Senger JS, Yilgor I and McGrath JE *J Appl Polym Sci*, **38**:373-382 (1989).
3. Kordomenos PI, Frisch KC and Kresta JE *Macromolecules* **20**:2077-2083 (1987).
4. Galante MJ and Williams RJJ *J Appl Polym Sci* **55**:89-98 (1995)

Acknowledgements

The authors would like to thank MICINN, FEDER and Generalitat de Catalunya (MAT2008-06284-C03-01, MAT2008-06284-C03-02, 2009-SGR-1512, FPI-2009).

Binuclear carbonyl complexes of transition metals of VI Group in homo- and copolymerization of methyl methacrylate and styrene

Pavlovskaya M.V., Zolotukhin A.A., Grishin D.F.

Research Institute of Chemistry, Nizhny Novgorod State University, Nizhny Novgorod, Russia

pavlovskaya@ichem.unn.ru

Introduction

Design of new effective controlling systems for polymerization of vinyl monomers is an important sphere of modern polymer chemistry. Indicated systems allow to synthesize polymer with determined molecular-weight characteristics and stereoregularity. That is why transition metal complexes in a combination with halogen-containing compounds represent doubtless interest for synthetic polymer chemistry.

Materials and Methods

Monomers were dried over $CaCl_2$ and distilled under reduced pressure. Polymerization was carrying out in sealed glass tubes in monomer bulk at 80^0C. Obtained polymer samples were purified from monomer by dissolving in chloroform or ethyl acetate and precipitating in hexane. Conversion of monomers is determined by gravimetry method. Molecular-weight properties of obtained polymer are determined by the method of Gel-Permission Chromatography.

Results and Discussion

It was established that binary systems based on $[CpM(CO)_3]_2$ (where M = Cr, Mo, W) and carbon tetrachloride initiate homopolymerization of methyl methacrylate (MMA) and styrene (St) at 80^0C. While rate of the process increases, gelation in the system is not observed, molecular weight of synthesized polymer grows with increasing of conversion in range $(20\text{-}60)\times10^3$. However, polydispersity indexes of obtained polymer samples have quiet high values. Curves of molecular-weight distribution of polyMMA and polySt samples have unimodal character in all cases. Nature of central metal atom significantly affect rate of the process. In this respect complexes can be ranked in following line: $[CpMo(CO)_3]_2$ > $[CpW(CO)_3]_2$ > $[CpCr(CO)_3]_2$ as their efficiency goes.

On the basis of obtained data scheme of initial step was proposed:

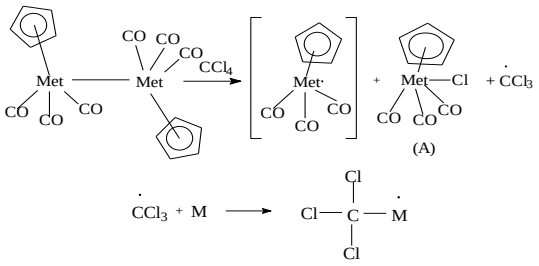

where M = monomer.

According to this scheme, metal complex interacts with carbon tetrachloride with formation of metal-centered radical, chlorine-containing complex (A) and radical $\cdot CCl_3$ which initiates polymerization.

Indicated scheme was proved by research of model systems. Formation of metal-centered radical was established by ESR method. Complex (A) was isolated and identified by IR-spectroscopy.

Research of MMA and St copolymerization patterns shows that mechanism of process is not radical purely. Type of curves of copolymer composition (Fig.1) and values of calculated copolymerization constants ($[CpCr(CO)_3]_2$: r_{MMA} = 1.53, r_{St} = 0.67; $[CpMo(CO)_3]_2$: r_{MMA} = 1.40, r_{St} = 0.47; $[CpW(CO)_3]_2$: r_{MMA} = 1.96, r_{St} = 0.14) can be considered evidence of this fact.

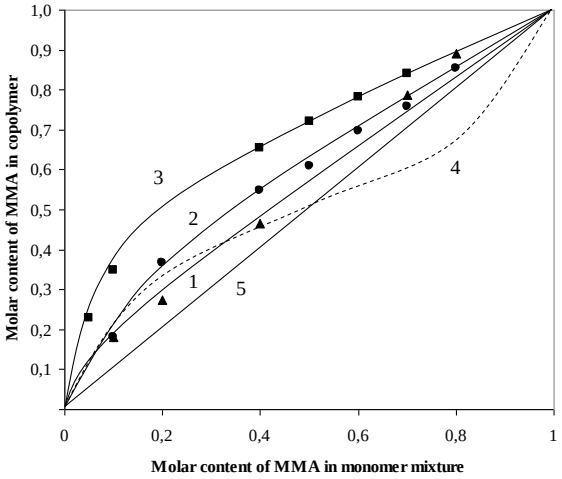

Figure 1. Curves of composition of MMA and St copolymer, synthesized in the presence of complexes $[CpM(CO)_3]_2$ (M = Cr (1), Mo (2), W (3)) and CCl_4.

Results of studying of MMA and styrene copolymerization kinetics accord to data of homopolymerization of indicated monomers. In this case proposed line of complex efficiency is also observed. In the presence of radical initiator (AIBN) studied complexes play a role of radical cages reducing molecular weight of synthesized polymer and eliminating gelation which characteristic for traditional radical polymerization of MMA and St.

According to results of researching of MMA and St copolymerization in the presence of studied complexes and AIBN, process has a radical nature (curves of copolymer composition have S-shaped character, constants of copolymerization match radical process).

Conclusion

Thus studied binuclear complexes of transition metals of VI Group $[CpM(CO)_3]_2$ (where M = Cr, Mo, W) in conjunction with either halogen-containing initiator or radical one are efficient additives in MMA and St polymerization which allow to eliminate gelation in system and reduce molecular weight of obtained polymer.

Acknowledgements: This work was supported by Russian foundation for basic researches (project №11-03-00074) and Russian Ministry of Education and Science ("Federal target program of scientific and scientific-pedagogical personnel of innovation of Russia on 2009-2013").

Amphiphilic Copolymers based on Sucrose Methacrylate and Acrylic Monomers

Heitor F. N. de Oliveira and Maria Isabel Felisberti

Chemical Institute - State University of Campinas (Unicamp)

heioliveira@iqm.unicamp.br, misabel@iqm.unicamp.br

Introduction

Sucrose is the most abundant of all sugars, presenting as advantages high world production and, low cost. The high versatility and reactivity of sucrose have been explored for many authors to obtain surfactants and monomers aiming polymers synthesis. For example, *Queneau et al.* reported a successful synthetic rote for sucrose 1'-*O*-methacrylate (SMA).[1] The high hydrophilicity of this molecule suggests high biocompatibility and biodegradability levels, and the carbon-carbon double bond is highly reactivity in radical reactions, which confers it a potential as a material for the preparation of amphiphilic polymers. These materials type are largely employed as degradable hydrogels, which are used in several biomedical applications, such as injectable matrices for drug delivery systems, temporary scaffolds for tissue engineering, and bioabsorbable surgical sutures. In this work, we will show the results and aspects of SMA-based copolymers synthesized in our research group.

Materials and Methods

Regioslective sucrose 1'-*O*-methacrylate (SMA) was synthesized, by enzymatic catalysis, purified and characterized by the methodology described in *Reference 1*. For the polymerization reactions, solutions 20 wt% of purified SMA and comonomer in dimethyl formamide (DMF) (10 to 15 mL) was prepared, and 0.1 % (mol/mol) of benzoyl peroxide (BPO) was added. This solution was added in an ampoule and cycles of freezing/degas were employed to eliminate oxygen, a radical inhibitor. The polymerization proceeded at 60 °C under nitrogen for 6 days. The product was precipitated in diethyl ether and dryed under vacuum at 40 °C. Non reactive monomers were eliminated by dialyze. The comonomers employed were methyl methacrylate (MMA) and N-isopropylacrylamide (NIPAAm), in molar ratios SMA/comonomer 1:1, 1:3, 1:5, 1:10 and 1:20. Homopolymers of SMA, MMA and NIPAAm were synthesized too. The polymers were characterized by ^{13}C NMR, GPC, DSC and TGA. Solubility, swelling ratio and phase behavior of aqueous solution (LCST behavior) were investigated.

Results and Discussion

The polymerization yields (Y), molar mass (Mw) and glass transition temperature (Tg) of the synthesized polymers are summarized in *Table 1*. These results show that the copolymers are synthesized in good yields, with high molar mass and polydispersity in the range from 1.5 to 2.0 and glass transition at temperatures dependent on the composition. The composition of the copolymers determined by ^{13}C NMR analysis shows a good agreement with the composition of the reactional medium, indicating that the copolymerization parameters of the studied monomers are close.

Table 1 – Polymerization yield (Y), molar mass (Mw) and glass transition temperature (Tg) of the polymers.

Sample	Y/ %	Mw[(a)]/ g mol^{-1}	Tg[(b)]/ °C
PMMA	100	334,000	117
P(SMA-*co*-MMA) 1:20	100	725,000	127
P(SMA-*co*-MMA) 1:10	100	385,000	131
P(SMA-*co*-MMA) 1:5	99	749,000	130
P(SMA-*co*-MMA) 1:3	90	788,000	132
P(SMA-*co*-MMA) 1:1	95	393,000	120
PSMA	100	802,000	113
P(SMA-*co*-NIPAAm) 1:1	93	822,000	124
P(SMA-*co*-NIPAAm) 1-3	71	478,000	125
P(SMA-*co*-NIPAAm) 1:5	78	1,330,000	118
P(SMA-*co*-NIPAAm) 1:10	64	673,000	143
P(SMA-*co*-NIPAAm) 1:20	41	957,000	145
PNIPAAm	78	278,000	122

(a) GPC; (b) DSC.

The copolymers with SMA present higher thermal stability in comparison with MMA and NIPAAm homopolymers, which increases with increasing SMA fraction. Residual mass increases as the SMA fraction in the copolymers increases, as consequence of condensation between SMA hydroxyl groups. No residual mass were observed for MMA and NIPAAm homopolymers.

Because SMA/MMA copolymers combine hydrophilic and hydrophobic segments, respectively, their solubility and swelling ratio are strongly dependent on the composition. As expected, copolymers richer in SMA are water soluble, while the copolymers richer in MMA swell in water and the amount of sorved water increases with increasing SMA contents.

SMA/NIPAAm copolymers are water soluble and the solutions present LCST behavior, as determined by turbidimetry of diluted solutions (0.1 wt%) at 300 nm. PNIPAAm presents LCST at 32.5 °C, in agreement with literature[2], P(SMA-*co*-NIPAAm) 1:5 at 37.0 °C and P(SMA-*co*-NIPAAm) 1:20 at 41.0 °C. How expected, the increase in the hydrophilic component (SMA) results in higher LCST for the copolymer. The other copolymers had not presented LCST.

Conclusions

These studies show that it is possible to obtain the desirable amphiphilic copolymers based on sucrose methacrylate, showing physical-chemical properties dependent on the copolymer composition.

References

1. P. Potier; A. Bouchu; J. Gagnaire; Y. Queneau; *Tetrah.: Asym.* 2001, *12*, 2409-2419.

2. H. G. Schild; *Prog. Poly. Sci.* 1992, *17* 163-249.

Non Isocyanate Polyurethane Obtained From Different Vegetable Oils

MAZO PAULA, RIOS LUIS

UNIVERSIDAD DE ANTIOQUIA

paulamazo@yahoo.com

Introduction: The NIPU can be obtained by reaction of polycyclocarbonates with polyamines to form β hydroxy urethanes [1]. The cyclocarbonates are obtained by the reaction of ethylene oxide with CO_2 by cycloaddition. Tetrabutylammonium bromide (TBAB) is the most widely used catalyst [2]. It is proposed in this paper to obtain NIPU from renewable sources (vegetable oils) and compare the properties of polymers.

Materials and Methods: Soybean Oil (SO), dehydrated Castor Oil (DCO) and Sasha Inchi Oil. Acetic acid (AA), Sulphuric acid (AS), H_2O_2 (33% v/v), Hexamethylenediamine (HEXA), CO_2, Tetrabutylammonium bromide (TBAB).
The Fig 1 shown the synthesis processes for modified oil and NIPU.

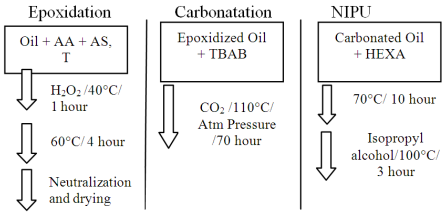

Fig. 1. Synthesis Processes for modified oil and NIPU.
Percentage of epoxy oxygen (%OO), iodo value (VI), acid value (AV), percentage of humidity (%H), viscosity, IR, Tensile Strength, Tensile module, elongation, DSC.

Results and Discussion:
The Table 1 shown the physico-chemical properties of modified oils.
TABLE I. PHYSICO-CHEMICAL PROPERTIES OF MODIFIED OILS.

		%OO (g epoxy/ 100g oil)	VI (gI/100g oil)	AV (mg KOH/g sample)	%H	Viscosity (cps)
Epox Oil	SO	5,75	1,78	0,61	0,210	450
	DCO	5,82	1,43	3,50	0,570	1530
	Sasha	7,96	2,43	1,24	0,340	425
Carb Oil	SO	2,50	0,43	0,13	0,051	13200
	DCO	3,42	0,35	2,38	0,192	19320
	Sasha	2,78	1,27	0,11	0,064	9500

Sasha Epoxidized oil has the highest content of oxirane oxygen and the lowest viscosity that is due to the increased amount of unsaturation that it has. DCO oil exhibits a similar %OO that SO Oil, but the viscosity is much higher due to ricinoleic acid remaining in it. More efficient conversion of epoxy groups to cyclocarbonates is obtained with Sasha Oil and lower conversion with DCO Oil, this is due to reduced diffusional resistance in the liquid from CO_2. Carbonated Oils have a higher viscosity than the Epoxidised Oil.
An infrared spectroscopy analysis shown that: epoxy peaks appear in 845-823 cm^{-1} for SO and DCO Oil, but Sasha Oil moving to 825-799 cm^{-1}, due to the high concentration of these. In 1803 cm^{-1} appear the signal of cyclocarbonate C=O. For the NIPU the signal are: peak 300-3400 cm^{-1} OH and NH, 1733 cm^{-1} NH-CO-O urethane group. The band 1803 cm^{-1} disappear. (See Fig 2).

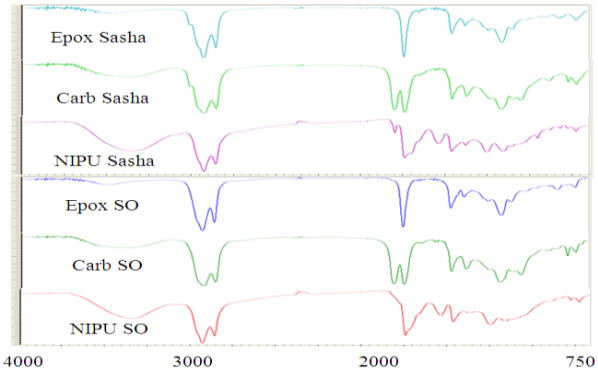

Fig. 2. Sasha and SO Oils Infrared Espectroscopy.
In the Table 2 shown NIPU properties, The Tg of NIPU Sasha is the lowest because the epoxy, amine and cyclocarbonates groups act as plasticizers decreasing the glass transition temperature and properties of polymers.
In the DCO NIPU, the ricinoleic acid can react with the cyclocarbonates, increasing the crosslinking and decreasing the elongation.
TABLE II. PROPERTIES OF NIPU

Sample	Tg (°C)	Tensil Strength MPa	% Elongation	Young Module MPa
NIPU Soja	24,5	0.35	160	0,002
NIPU DCO	12,8	0.20	50	0,003
NIPU Sasha	-10	------	------	------

The NIPU Sasha is tacky and highly viscous liquid, for this reason we could not measure their mechanical properties.

Conclusions: In this paper, polyurethane is obtained without using diisocyanates. SO oils and DCO, produce NIPU with good mechanical properties to be used as coatings and adhesives. Sasha oil is presented as a good alternative but requires a higher content of amine.

References: [1] V. Calo, A. Nacci, A. Monopoli, A. Fanizzi. Cyclic Carbonate Formation from Carbon Dioxide and Oxiranes in Tetrabutylammonium Halides as Solvents and Catalysts. Organic Letters. 4, (2002) 2561-2563.
[2] G. Wilkes, S. Sohn, B. Tamami. Nonisocyanate polyurethane materials, and their preparation form epoxidized soybean oils, US Patent 7045577 (2004)

Kinetic Study of 2-Acrylamido-2-methylpropanesulfonic Acid in Free-Radical Polymerization method by Differential Scanning Calorimetry

E. Nadim, H. Bouhendi, F. Ziaee, R. Bazhrang*

Iran Polymer and petrochemical Institute, P.O.BOX 14965/115, Tehran, Iran.

*Boouhendi@yahoo.com

Introduction

A driving force for polymerization reaction is the heat of polymerization which governs the rates and kinetics of polymerization. So, accurate measurement of thermochemical data is an appropriate method for following the kinetic of polymerization. Thus, differential scanning calorimetry is a suitable technique for recording heat production of chemical process because of its advantages such as small sample size which help better temperature control, handiness of manipulation, performance rapidity and versatility [1]. In the present work, aqueous kinetic of AMPS polymerization initiated by a thermal initiator was studied by using DSC.

Material and Methods

AMPS and potassium persulfate (KPS) were purchased from Fluka and Merck, respectively, and were recrystalized from ethanol for further purification. In this study, DSC thermograms were obtained on a NETSCH DSC 200 F3 instrument. Monomer and initiator were weighted precisely and dissolved in de-ionized water. Closed pans were loaded with 22-24 mg of the solution. In order to prevent side and retarding reactions, a hole was produced in pans and all the reactions were carried out under the nitrogen atmosphere.

Results and Discussions

If E_a is representative of overall activation energy, general rate of polymerization is given by equation 1;

$$R_p = k_0 e^{-\frac{E_a}{R}\frac{1}{T}}[M]^n[I]^p$$

or

$$\ln R_p = \ln(k_0[M]^n[I]^p) - (\frac{E_a}{R})\frac{1}{T} \qquad (1)$$

DSC thermograms at isothermal conditions were done at desired amount of monomer and initiator. In order to sure complete reaction of entire monomer for all samples a non-isothermal run, from ambient temperature to 80°C at heating rate of 1°C/min, was purposed. Absence of exothermic peak for the samples demonstrated complete conversion of monomer in isothermal run. DSC thermogram of polymerization for samples 1-3 ([I] = 0.074, 0.148, 0.185 mol/lit) are illustrated in Figure 1. Monomer conversion was calculated as a fraction of exothermic heat in a specific time to total exothermic heat of polymerization Figure 2 shows a typical calculation of monomer conversion (π) at 7 minutes in which A_p and A are peak area at 7 minutes and total peak area of polymerization, respectively. In constant initial monomer concentration, slope of $-\ln R_p$ vs.-ln [I] reveals the order of reaction with respect to the initiator concentration (p=0.52). Determined n value by slope of $-\ln R_p$ vs.-ln [M] plot was 1.56. E_a and k_0 could be deliberated from slope and intercept of $-\ln R_p$ vs.1/T plot in a constant amount of monomer and initiator. E_a was 83kj/mol.K. k_0 determined by intercept of mentioned plot was 1.2×10^{13} $mol.lit^{-1}.sec^{-1}$.

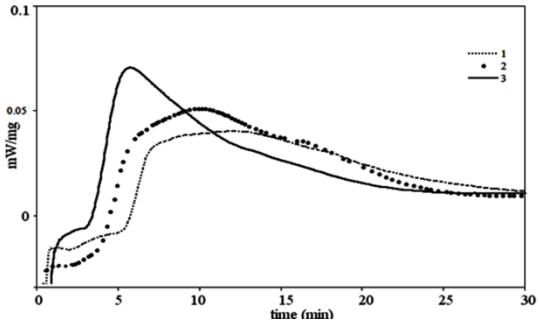

Fig1. DSC thermogram of polymerization at different initiator content.

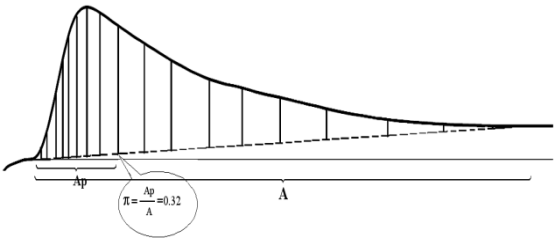

Fig2. Partial area of exothermic peak of a typical sample at 420 seconds.

Dependence of polymerization rate on monomer concentration greater than unity can be described by three theories: a) the solvent transfer theory, b) the cage effect theory, and c) the complex theory[2].

The solvent transfer theory was ignored in aqueous polymerization of AMPS because derived sulfur-containing fragment from persulfate are very reactive toward monomers. Cage effect theory is based on forming a barrier for separation of sulfur-containing fragment from the surrounding solvent molecules. In Complex theory, formation of a complex between monomer and initiator is proposed in complex theory and rate of complex decomposition is the key factor in initiation process[2]. In cage effect theory, activation energy is predicted to be smaller than that matches complex theory. Activation energy that was measured in present work was in the range of conventional activation energy of radical polymerization (80-90 kj/mol). Thus, in monomer concentration ranges from 0.966 to 2.41 mol/lit and temperature ranges 35-47 °C polymerization mechanism of AMPS in aqueous medium could be described by the cage effect theory.

Conclusion

n value and activation energy supported the assumption that polymerization kinetic was according to cage effect theory.

References

1. G Alberda, V Ekenstein, Y Tan, Eur Polym J 17, 839-843, (1981).

2. AR Mahdavian, M Abdollahi, HR Bijanzadeh, J Appl Polym Sci 93:2007–2013, (2004).

Synthesis and Characterization of Novel Bio-Based Polyesters Based on Curcumin as a Natural Diol Monomer and Commercially Available Aromatic Dicarboxylic Acids

Abbas Shockravi, Ali Javadi, Saeideh Hajavi

Faculty of Chemistry, Tarbiat Moallem University, No.49, Postal Code 1571914911, Tehran, Iran

Email: hajavi_saeideh@yahoo.com

Introduction

In recent years, interest in polymeric materials from renewable resources has increased and a great deal of efforts have been paid to utilize a wide variety of bio-resources instead of petroleum ones for the polymer industry. Also, there is a great demand to design and develop high-performance bio-based polymers because the use of such products leads to decrease carbon dioxide emission [1, 2].

Polyesters are a family of polymers of increasing significance because of their biodegradability [3]. They are one of the most versatile polymers. They contain widely different materials with large applications, which are produced by a variety of manufacturing techniques [4].

Curcumin is a natural yellow-orange dye extracted from turmeric (dry rhizomes of the plant *Curcuma Longa*) and has widely used as the spices and the cosmetics. Moreover, it possesses diverse pharmacological effects, such as anti-inflammatory, antioxidant, antimicrobial anticancer, and wound healing activities. Furthermore, it is nontoxic, even at relatively high doses. On the other hand, curcumin is a bis-*α,β*-unsaturated *β*-diketone (commonly called diferuloylmethane) that exhibits keto-enol tautomerism (Scheme 1 ***a***). It also has a predominant keto form in acidic and neutral solutions and a stable enol form in alkaline media. In addition, symmetric curcumin molecule has two phenolic hydroxyl groups which are available as polymerizable functional groups. Thus, curcumin can be regarded as a suitable monomer for synthesis of bio-based polymers [5-8]. In the field of polymer chemistry, there have been some reports using curcumin in producing various polymers [2, 6-8].

In this work, we aimed to synthesis novel series of bio-based polyesters through a polycondensation reaction between aromatic diacid chlorides and the phenolic groups of curcumin as a bio monomer. (Scheme 1 ***b***)

Materials and methods

All chemicals were purchased either from Merck or Fluka chemical Co. Cucumin used after recrystallization in 2-propanol. O-Dichlorobenzene was dried over molecular sieve. Acid chlorides were obtained from the condensation reaction of their corresponding dicarboxylic acids with excess of thionyl chloride, in the presence of few drops of pyridine as a catalyst. They were purified by crystallization with hexane. The polymerization was carried out by adding acid chloride to a suspension of an equimolar amount of curcumin in o-dichlorobenzene in the presence of TEA as HCl scavenger at 0°C under nitrogen atmosphere. Then, the resulting mixture was stirred for 30 min at room temperature and then slowly heated and reflux under magnetic stirring at 180°*C* overnight. The polymer suspension was precipitated in methanol.

Results and Discussion

The polyesters were obtained in high yields and possessed inherent viscosities in the range of 0.41-0.87 dLg^{-1}. Structure of polyesters was characterized using ^{1}HNMR, ^{13}CNMR and FTIR. In the ^{1}HNMR the methine proton was at 5.5 ppm. In the ^{13}CNMR the methine carbon of enol structure was at 101.5 ppm while peak due to methylene carbon of *β*-diketone was not observed. These results show that the β-diketone unit in the polyester backbone tends to be in the enol form. This fact is also verified by the presence of a broad OH peak at 3457 cm^{-1} in the FTIR spectrum.

In the FTIR spectrum the C=O peak of the ester bond was at 1741 cm^{-1}.

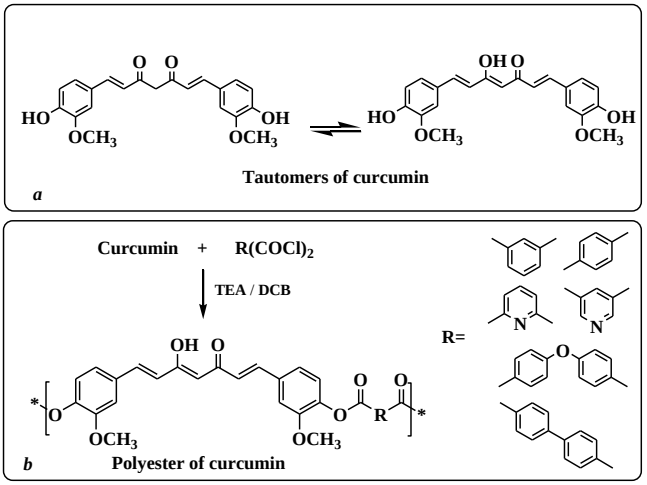

Scheme1. Tautomerism of curcumin (*a*), Preparation of polyester (*b*)

References

[1] T. Tsujimoto et al. *Polym. Deg. and Stab*, **2010**, 95, 1399.
[2] V.C. James et al. *Macromol. Symp*. **2006**, 240, 1.
[3] O. Suwantong et al. *Polymer*. **2007**, 48, 7546.
[4] D.J. Liaw et al. *polym. sci*., part A: *polym. chem*. **2001**, 39, 2951.
[5] A. Anitha et al. *Carbohydrate Polymers*. **2011**, 83, 452.
[6] W. Shi et al. *Org. Lett*. **2007**, 9, 5461.
[7] N. Matsumi et al. *Polym .J*. **2008**, 40, 400.
[8] I. Mukherjee et al. *Macromolecules*. **2010**, 43, 3277.

The Oxypropylation of Olive Stone and the Use of the Ensuing Polyols for the Synthesis of Novel Polyesters and Polyurethanes Based on Renewable Resources

Marina Matos[1,2], *Filomena Barreiro*[2], *Alessandro Gandini*[1]

1. CICECO and Chemistry Department, University of Aveiro, Campus de Santiago, 3810-193 Aveiro, Portugal
2. LSRE, Polytechnic Institute of Bragança, Campus de Santa Apolónia Ap. 1134, 5301-857 Bragança, Portugal
marina.matos@ua.pt, agandini@ua.pt, barreiro@ipb.pt

The development of polyols by the oxypropylation of abundant and renewable vegetable and animal resources constitutes an original approach to the exploitation of the biomass. Cellulose, starch, chitosan, chitin, different types of lignins, cork and more complex structures like sugar beet pulp, are among the documented examples[(1)]. All these systems displayed a similar pattern in terms of the grafting of short poly(propylene oxide) (POP) chains from the OH groups of the substrate, albeit of course each situation required a specific set of optimized experimental conditions to transform the natural solid into a viscous polyol. The transformation of these polyols into polyurethanes is the only operation which has been studied to date as a form of their exploitation into polymer materials.

In a similar vein, we have undertaken a study of the oxypropylation of olive stone, a by-product of the olive oil production, which, like many other biomass residues, is presently burnt for energy recovery. The purpose of this investigation was of course the search of a more useful and promising way to exploit this abundant and renewable Mediterranean natural material. A preliminary report on some aspects of this work has already been published[(2)], and the purpose of this communication is to provide an up-to-date account of its progress.

On the one hand, a detailed relationship was obtained between the reaction parameters applied to the oxypropylation of olive stone and the structure and physical properties of the ensuing polyols, and this for different particle sizes of the substrate. The characterization involved FTIR and NMR spectra, viscosity and OH index, as well as the proportion of POP homopolymer formed in these reactions.

On the other hand, a choice of more promising polyols was selected for chemical modifications involving first ester and urethane formations with aliphatic and aromatic monofunctional reagents. The conversion of part or all of the OH groups of the polyols into much less polar moieties brought about significant changes in the properties of the ensuing materials, which were thoroughly characterized. Thereafter, difunctional reagents were employed to transform the polyols into polyester and polyurethane networks, whose properties were again assessed as a function of the type of reaction (different modes of esterification and condensation with diisocyanates), the specific structure of the reagent (aliphatic vs. aromatic) and the extent of OH conversion (stoichiometry).

Acknowledges

Financial support from **FCT** (project PTDC/CTM/71491/2006) is acknowledged.

References

(1) Gandini, A., Belgacem, N. M., 2008. Monomers Polymers and Composites from Renewable Resources. Amsterdam: Elsevier.

(2) Matos, M., Barreiro, Maria F., Gandini, A., 2010. Olive Stone as a Renewable Source of Biopolyols. Industrial Crops and Products 32, 7-12.

Microwave synthesis: An alternative approach to synthesize conducting end-capped polymers

Pierre Marcasuzaa[1], *Stéphanie Reynaud*[1], *Bruno Grassl*[1], *Jacques Desbrières*[1], *Olivier F.X. Donard*[2]

[1]IPREM / Equipe de Physique et Chimie des polymères, Hélioparc, 2 av. du Président Angot, 64053 Pau Cedex
[2] IPREM / Laboratoire de Chimie Analytique Bio-inorganique et Environnement, Hélioparc, 2 avenue du Président Angot, 64053 Pau Cedex

pierre.marcasuzaa@univ-pau.fr

Microwave (MW) synthesis represents a major breakthrough in synthetic chemistry versus conventional heating sometimes known to be time consuming because of its low efficiency. If the microwave energy was developed for industrial application from the middle of the 20th century, first microwave-enhanced organic chemistry was not explored until the mid 1980's. In comparison to the impressive development of the microwave technique in organic synthesis during the last decades, microwave-assisted polymer synthesis[1,2] is rather new emerging field and mainly reported from the late of 1990's. The aim of our work[3] is to study the use of MW synthesis to obtain conducting HCl-doped tetraaniline (TANI) end-capped polymers while controlling the molecular weights and polydispersity. The synthesis of block copolymers containing one block of intrinsic conducting polymer[4] has already been reported. The strategies involved fastidious syntheses as multi-step routes and drastic experimental conditions. However the synthesis of these kind of polymer are still of interest because these materials are used as models to study the conduction phenomena and interface organization[4], and may be used as conducting additives in insulating matrices[5].

Our objectives were at the same time to reduce the duration of the synthesis while keeping the process as simple as possible. Special attention was also given to the comparison with the results obtained under conventional heating in order to determine the occurrence of non-thermal microwave effects which is still a controversial topic. After a brief presentation of the MW irradiation methods *i.e.* dynamic and pulsed modes, kinetic results will be presented. This poster will present the difference between polymerization performed under microwave irradiation and by conventional heating (CH = oil bath) (Figure 52).

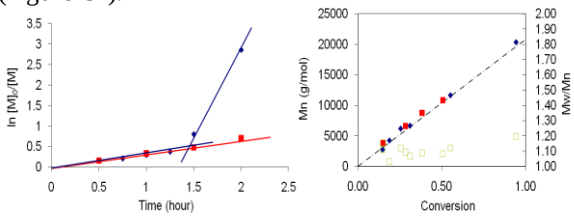

Figure 52: ATRP kinetic study of styrene/EBP/CuBr/PMDETA (200/1/1/1). (red square) CH at 98°C; (bleu rhomb) MW at 80W and 98°C; (green empty square) polydispersity of PS under MW and CH.

A sharp increase of the logarithmic conversion versus time is observed under MW while CH leads to a linear fit. This phenomenon is observed for different monomers at different powers. In spite of this acceleration of kinetic, the living/controlled nature of the polymerization is kept. Thus, the occurrence of a "microwave effect" will be discussed.

Optimized experimental conditions have been obtained from the previous kinetic study and used to perform the end-capped conducting polymer. The latter is obtain in two steps: ATRP to obtain the precursor polymer (PStyr) followed by the coupling reaction between PStyr ad TANI. A specific initiator leaded to a end-chain functionalization PSty able to react with the TANI is necessary (**Figure 53**). End-capped conducting polymers (TANI content from 2 to 7 wt%) have been obtained by both heating methods: MW and CH and fully characterized. Conductivities as high as 5 $S.cm^{-1}$ are obtained. Synthetic methods (MW and CH)are compared and MW effect has been demonstrated.

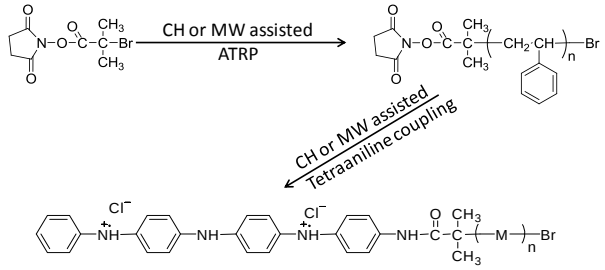

Figure 53: Synthesis routes of HCl-doped TANI end-capped polymers either by conventional heating (CH) or under microwave irradiation (MW).

Within this study, microwave assisted synthesis has been tested both in polymer synthesis and polymer functionalization. Conducting end-capped polymers with controlled architectures in terms of molecular size of both the insulating and the conducting parts as well as the chemical formulation have been obtained. The synthesis has been performed under conventional heating and microwave irradiation to highlight the effect of MW heating.

[1] Wiesbrock, F.; Hoogenboom, R.; Schubert, U. S. Macromolecular rapid communications 2004, 25, 1739.
[2] Bardts, M.; Gonsior, N.; Ritter, H. Macromolecular Chemistry and Physics 2008, 209, 25.
[3] Marcasuzaa, P.; Reynaud, S.; Grassl, B.; Preud'Homme, H.; Desbrires, J.; Trchov, M.; Donard, O. F. X. Polymer, 52, 33.
[4] Gospodinova, N.; Ivanov, D. A.; Anokhin, D. V.; Mihai, I.; Vidal, L.; Brun, S.; Romanova, J.; Tadjer, A. Macromolecular rapid communications 2009, 30, n/a.
[5] Laska, J.; Zak, K.; Pron, A. Synthetic Metals 1997, 84, 117.

Synthesis and Characterization of new sensitive copolymer of Poly-2,7-fluorene-1,4-(2,3-diamine)naphthalene for aqueous media

*R. Vázquez-Guilló, A. Calero, A. Salinas-Castillo, C.R. Mateo and R. Mallavia.**

* Instituto de Biología Molecular y Celular, Universidad Miguel Hernández, 03202 Elche, Spain.

r.mallavia@umh.es

Abstract: In this work, we report the synthesis and characterization of a new copoly-2,7-(fluorene-1,4-(2,3-diamine)naphthalene using the corresponding monomer 1,4-dibromo-2,3-diaminonaphthalene. Transformation posterior of the pendant bromide group for ammonium group, which will be provide it the properties and characteristic designed. The high reactivity of the monomer involves performing work on the amino group protection in order to obtain of copolymers composition

Introduction

Conjugated polymers have received great interest for its applications, in particular as sensing platforms [1]. In general, fluorene derivatives are interesting because they contain a rigidly planar biphenyl unit and also for the facile substitution at the remote C9 site that provides the possibility of improving the solubility and processability of polymers without significant increase of the steric interactions in the polymer backbone. For induce a change in the fluorescence response of the conjugated polymer we selected a model close to 2,3-diaminebenzene high sensitive in order to introduce it on backbone, as previously obtained analogous copolymers by Yamaguchi *et al*. [2].

Results and Discussion

We prepared the corresponding monomer 1,4-dibromo-2,3-diaminonaphthalene, as previously report [3], with a noticeable difference between the assignments realised. The ^{1}H and ^{13}C NMR spectra of the monomer were corrected assigned and contrasted with literature. FTIR spectrum confirm the structural monomer and mass their composition. Then, we proceed to the polymerization by cross-coupling Suzuki with different ratio feed 1,4-dibromo-2,3-diaminonaphthalene monomer using palladium zero (Scheme 1, first reaction). In these experimental conditions, we need a low feed ratio due to the high reactivity of the monomer. In fact, we have studied some details of the effect of carbonyl groups in the monomer using different spectroscopic techniques (UV-visible and NMR). Thus, the great reactivity of monomer with carbonyl groups, even acetone, and their copolymer will be able to as sensing of this organic compound.

The polycondensation, as indicated in Scheme 1, give only **P3**, with R_2 =-$(CH_2)_6$-Br and R_1=$(CH_2)_5CH_3$ while **P2** and **P1** were not obtained. As indicated, monomer reacts with boronic group still need a protection before to used in Suzuki polycondensation. NMR data of **P3** are well resolved indicating a well-defined structure and their spectroscopic characteristic are similar to those of the other fluorene polymer derivates. Current reactions are being carried out to achieve these stoichiometries.

The structural assignment of polymer was based on their ^{1}H and ^{13}C NMR spectra by analogy with monomer spectra. **P5** was obtained by Menschutkin reaction like before neutral precursor [4]. Now, we are measuring the distribution of molecular weight by gel permeation chromatography coupled with light scattering detector and also, other characteristic parameters are currently under progress.

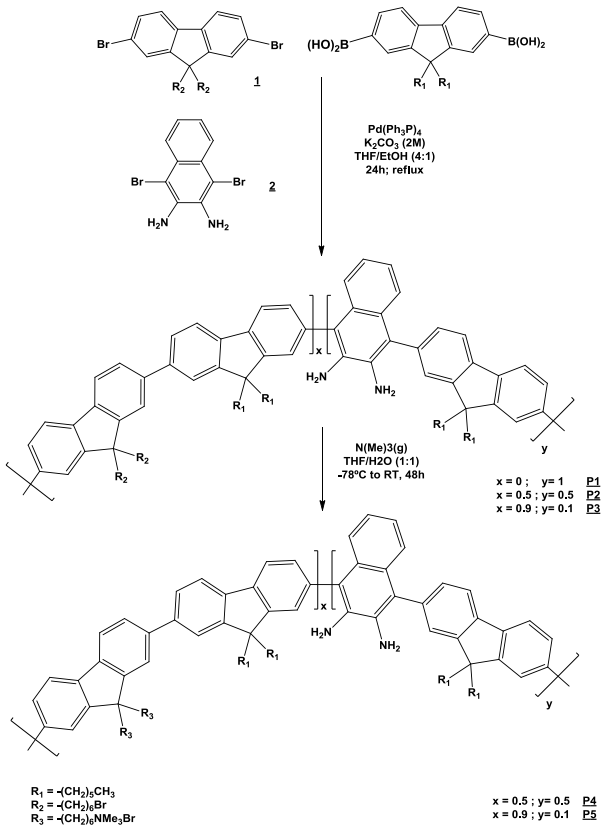

Scheme 1. Synthetic route of copoly[9,9-bis(alkyl-hexyl)fluorene-*alt*-1,4-(2,3-diamine)naphthalene].

Acknowledgments: This work was supported by research project MAT-2008-05670 and PT2009-002 of MICNN.

References:

[1] a) S.W. Thomas *et al. Chem. Rev*. **2007**;107:1339. b) B. Liu *et al, Chem. Mater*. **2004**;16: 4467. c) M.J. Tapia *et al. Adv. Coll. Inter. Sc.* **2010**, 158 (1-2): 94.

[2] I. Yamaguchi *et al, Macromolecules*, **2007**, 40: 438.

[3] a) J. Yang, et al. *Macromolecules*, **2004**, 37: 1211. b) A. Tsami *et al. J. Polym. Sci. A: Polym. Chem.*, **2007**, 45: 4773.

[4] a) R. Mallavia *et al. Bol. Soc. Esp. Ceram*. **2004** 43(2):327. b) R. Mallavia *et al. Macromolecules*, **2005**, 38: 3185.

Copolymers from Poly(lactic acid) (PLA) and Chain Extenders or Branching Agents

Angel Hitos-Rodríguez[1], Anna Bacardit[1], Lluis Olle[1], Orlando O. Santana[2], M. Lluisa Maspoch[2], Jordi J. Bou[1]*

1. Departament Enginyeria Química – Universitat Politècnica de Catalunya
2. Centre Català del Plastic - Terrassa

jordi.bou@upc.edu

Introduction

Polylactic acid (PLA) is the most used biodegradable polymer [1]. In recent years it has been applied in medicine, packaging or agriculture. Its properties are similar to polypropylene and it is therefore an excellent alternative to oil derived polymers. Three structures are known: the isotactic polymers derived from a single enantiomer (PLLA or PDLA), the syndiotactic polymer derived from the meso form of polylactide (PLDLA) and atactic form, mixture of isomers L and D.

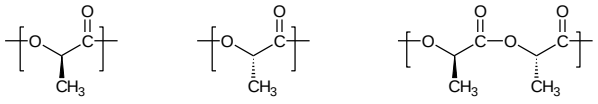

PLLA PDLA PDLLA

Since the homopolymers have insufficient mechanical properties (very fragile), copolymers based on one enantioner and small percentages from the other are put onto the market, yielding less rigid materials but more tough. However, this change causes a decrease in softening temperature and potential applications are limited to medium temperatures (less than 60 ºC). Moreover, PLA is very sensitive to hydrolytic degradation in processing, which leads to molded materials with lower molar mass polymers and, consequently, with poorer mechanical properties.
Some approaches are currently being studied for improvement, which include altering the structure of PLA with branching agents or chain extensors (bifunctional or polyfunctional compounds) and formulating materials with nanoparticles [2].

In this study we have prepared a collection of PLA copolymers with different candidates to extensors or chain branching agents and the resulting compounds have been characterized chemically. In some cases we have evaluated their biodegradability.

Materials and methods

The starting material is NatureWorks PLA 2002D, which has been copolymerized with compounds such as polycaprolactone, maleic anhydride, oligomeric polyfunctional extensors Joncryl from BASF, among others. The reactions were carried out in batch at 170 ºC with different percentages of modifier (0,5, 1, 2, 5, 10 %). In some cases, transesterification catalyst ($Ti(BuO)_4$) is used. The polymers obtained were analyzed spectroscopically (IR and NMR) and by viscometry and GPC. The degradation studies were conducted hydrolytically or biologically according to ISO 14851 and followed by GPC in HFIP.

Results

Copolymers obtained with bifunctional compounds, as polycaprolactone or maleic anhydride, have shown a loss of properties when high concentrations of modifier were added. This effect can be explained to promotion of degradation due to acid catalyst. Copolymers with low concentrations (2, 5 %) of maleic anhydride afford macromolecules with similar molar masses (around 100 kg/mol) than original PLA. However, inert atmosphere (N_2) was necessary to avoid degradation due to tertiary radicals promoted by O_2 [3]. ^{1}H-NMR spectra of these compounds show two doublets at 6.5 and 6.4 ppm indicating that maleic anhydride has reacted different ester bonds. In same region, a relatively broad singulet at 6.48 ppm is identified as maleate diester obtained by reaction of OH originated in hydrolysis of PLA; this signal is being analyzed in proof in order to not to be confused with others like fumarates or free diacids.

Reaction of PLA with oligomeric polyfunctional extensors (Joncryl from BASF) has given from slightly increased molecular size compounds (GPC) to crosslinked insoluble materials, not analyzed. Joncryl contains a number of epoxy groups (grade depending) and a very low dosage is imperative. Concentrations of 0.5, 1 and 2 % affords to polydispersed polymers (up to 4.5) in both sides of distribution curve. Analysis by NMR or IR is very difficult due to dispersed nature (structure and composition) of obtained compounds.

The polymers have been found to be readily degradable hydrolytically, similar to pure PLA. The results of biodegradation have also been positive, but less conclusive.

Conclusion

We have prepared various PLA copolymers by reactions with chain extensors agents or crosslinkers that have attractive features new materials to be processed successfully. These copolymers have been hydrolytically and biologically degraded.

Acknowledgements
This work has been financially supported by MICINN, grants nº MAT2010-19721-C02-02 and MAT2010-19721-C02-01.

References
[1] A.P. Gupta and V Kumar, Eur Polym J 2009, 43, 4053.
[2] J. Gamez-Perez et al., J Appl Polym Sci 2011, 120, 896.
[3] S. Bocchini et al., Biomacromolecules 2010, 11, 2925.

Synthesis of photocleavable block copolymers based on *p*-methoxyphenacyl groups

Olivier Bertrand, Charles-André Fustin and Jean-François Gohy

Université chatholique de Louvain, Institut de la matière condensée et des nanoscience/Bio et Soft Matter

olivier.bertrand@uclouvain.be

Block copolymers have been the focus of much interest during the last 30 years because their constituent blocks are generally immiscible, leading to phase separated structures. Since the different blocks are linked together by covalent bonds, the phase separation process is spatially limited and results in self-assembled structures in bulk, thin films or in solution (micelles) whose characteristic sizes are in the range from ca. 10 to 100 nm [1,2]. Stimuli-responsive polymers are polymers that undergo relatively large and abrupt, physical or chemical changes in response to small external changes in the environmental conditions [3]. Among all the existing stimuli light is particularly interesting [4] since it can be localized in time and space, it can be triggered from outside of the system, and it does not require particular reagents which limit byproducts.

Here, we report on the synthesis of new light-responsive block copolymers containing *p*-methoxyphenacyl photocleavable side groups. They are particularly interesting because it generally generate harmless side product after cleavage [5]. The block copolymers are composed of a poly(p-methoxypenacyl methacrylate) block and a block composed of polystyrene (PS), poly(tert-butyl acrylate) or poly(oligoethyleneglycol methacrylate) (PMPMA-b-PS and PMPMA-b-PtBA and PMPMA-*b*-POEGMA). The synthetic strategy consists in the direct polymerization of the monomers by Atom Transfer Radical Polymerization (ATRP). These polymers are then used for light induced micellization.

[1] H-C. Kim, S-M. Park, W. D. Hinsberg, *Chem. Rev.,* **2010**,110, 146-177
[2] J-F. Gohy, *Adv. Polym. Sci.,* **2005**, 190, 65-136
[3] N. Rapoport, *Prog. Polym. Sci.,* **2007**, 32, 962-990
[4] J-M. Schumers, C-A. Fustin, J-F. Gohy, *Macromol. Rapid Commun.*, **2010**, 31, 1588-1607
[5] C. G. Bochet, *J. Chem. Soc., Perkin Trans.1*, **2002**, 125-142

Semi-IPNs Based on Poly(*N*-vinylpyrrolidone) and Poly(L-lactide): Synthesis and Characterization

Ana P. R. Camilo[1], *Maria I. Felisberti*[2], *Valdir Mano*[1]

[1]Department of Natural Sciences – Federal University of São João del Rei (UFSJ); [2]University of Campinas (UNICAMP), P.O. Box 6121, Zip Code 13083-970, Campinas - SP, Brazil

mano@ufsj.edu.br; misabel@iqm.unicamp.br

Introduction

Technological applications of biodegradable polymers usually require changes in their mechanical properties or, at least, a balance between the rate of degradation and the properties of the final product, and an affordable cost [1]. In order to obtain a material with improved properties and economically acceptable, an alternative that has been widely explored is the development of new materials consisting of two or more types of polymeric materials, i.e., the formation of blends, copolymers, and polymer networks (IPNs or semi-IPNs) [2]. The specific interest in the synthesis of semi-IPNs based on poly(*N*-vinylpyrrolidone), PVP, and poly(L-lactide), PLLA, comes from the fact that these homopolymers are biodegradable and biocompatible, which allows to infer applications for the medical area such as surgical sutures, implants, matrixes for drug delivery systems, etc. [3]. The objective of this work was to prepare an amphiphilc multicomponent materials in the form of semi-interpenetrating polymer networks, based on PLLA, a hydrophobic homopolymer, and PVP, a hydrophilic component. The preparation of the semi-IPN combined the polymerization and crosslinking of *N*-vinylpyrrolidone in the presence of PLLA. The products were characterized by spectroscopic, thermal and morphological methods.

Materials and Methods

N-vinylpyrrolidone (Aldrich) was vacuum distilled prior to polymerization. Benzoyl peroxide (BPO, Sigma) was dried in vacuum at room temperature. Di(ethylene glycol)divinyl ether (DEG, Aldrich) was used as received.

The polymerization in bulk of *N*-vinylpyrrolidone occurred by radical polymerization using as initiator benzoyl peroxide; PLLA was synthesized by ring opening polymerization of L-lactide. The homopolymers were characterized by infrared spectroscopy (FT-IR), nuclear magnetic ressonance proton and carbon 13 (^{1}H NMR and ^{13}C), thermogravimetry (TG), differential scanning calorimetry (DSC) and gel permeation chromatography (GPC).

The preparation of semi-IPNs combined polymerization and crosslinking of *N*-vinylpyrrolidone in the presence of poly(L-lactide). BPO was used as initiator and DEG as crosslinker for *N*-vinylpyrrolidone (VP), mass ratios of 0.5 and 1% on the mass of VP were used, and the cure process was carried out at 70 and 90°C for different periods of time. The semi-IPNs prepared were characterized by elemental analysis (CHN), TG, DSC, dynamic mechanical analysis (DMA), scanning electron microscopy (SEM) and swelling measurements.

Results and Discussion

The applied synthesis to obtain PVP and PLLA homopolymers were effective. FT-IR, ^{1}H and ^{13}C NMR, TG and DSC analysis confirmed the formation of PLLA and PVP. PLLA presented Mn, Mw and polydispersity of 52216 Daltons, 37294 Daltons and 1.4, respectively.

The composition of the semi-IPNs was determined from the amount of nitrogen in semi-IPNs provided by elemental analysis. PVP contents in the semi-IPNs varies from 49 to 70 wt%. The thermal study of the semi-IPNs by TG showed that the semi-IPNs exhibit thermal behavior characteristics of each of the starting homopolymers, reflecting the composition in terms of PVP and PLLA components. Data obtained by DSC showed that the polymerization and the crosslinking of *N*-vinylpyrrolidone during formation of semi-IPNs hinder the crystallization of PLLA. According to the DSC results the glass transition temperature shifts to higher temperatures with increasing concentration of the stiffer component, PVP. From DMA results secondary relaxations of the polymers were detected. Scanning electron microscopy micrographs show the presence of small particles of PLLA in the form of dispersed fibers in the matrix of PVP, indicating phase separation. Swelling studies of the semi-IPNs in water showed that these materials are able to quickly absorb large amounts of solvent, proving its performance as hydrogel.

Conclusions

The synthesis of semi-interpenetrating polymers networks of PVP and PLLA was effectively carried out. The bulk polymerization and crosslinking of the VP in the presence of PLLA result in a complex mixture with phase separation. Also, it is possible to conclude that the semi-IPNs thermal properties were dependent on the homopolymer contents. Lastly, the prepared semi-IPNs presented excellent absorbing characteristics, being probably efficient hydrogel material.

References

1. Z. Jedlinski; M. Kowalczuk *Macrom.* 1989**,** *22,* 3242.
2. I. Janigová; I. Lacík; I. Chodák *Polym. Degrad. Stab.* 2002, 77, 35.
3. H. R. Kricheldorf, *Handbook of Polymer Synthesis*, Marcel Dekker, New York, 2005.

Evaluation of Yam Agriculture Wastes to Obtain Fructans

M. Esquivel, A. Aguilar, M. Sibaja, J. Vega-Baudrit, S. Madrigal-Carballo

Laboratorio de Polímeros, POLIUNA, Universidad Nacional, Heredia, Costa Rica

mesquive@una.ac.cr

In Costa Rica, the agricultural sector has been modernized over years in order to increase production and become more competitive in international markets. Because of that it had become specialized not only in the cultivation of traditional products (cocoa, coffee, bananas), but also in non-traditional products, like citrus, roots and tubers. Yam is a kind of tuber with high nutritional value, and it is within the products that Costa Rica had diversified its exports in recent years; it occurs mainly in Northern and Atlantic regions of our country. Agro-industrial activities generate large quantities of waste, those that are biodegradable, are mainly leaves and rejected products. In Costa Rica, there is no exact data about the amount of wastes produced from the yam production, however, Sandi in 2008, reported that the percentage of rejected product is about 30% of total production, which corresponds to 34.486 metric tons per year. Therefore there is an interest to obtain higher added value products, extracted from yam wastes, generated by the rejected material that do not meet the export standards (defects, appearance, quality, conservation) This investigation intends to evaluate this waste to extract fructans, due to the natural wealth of yam in this compound, it was used the *Dioscorea alata* yam. The fructans have many potential uses in the food industry, mainly as a sweetener or dietary fiber. Yam belongs to the family *Dioscoreaceae*, it is characterized on the basis of a wide range of species of widely dispersed geographic origins around the world, which are vegetatively propagated through tubers.

Figure 1. Yam tuber (*Dioscorea alata*)

Yam tubers are used for human consumption, are formed internally by parenchymal tissues, high in starch and water, fiber, calcium oxalate and mucilage channels. By definition according to Bender, 2006; fructans is the general name to call the polysaccharides of fructose, this are part of the fiber and non-starch polysaccharides in plants. These compounds are also called polyfructosylfructoses. Fructans have linear, cyclic and branched structures. The fructosyl - glucose links are β-(2 ↔ 1) type, as the sucrose, but the fructosyl -fructose bonds are β-(1 → 2) or β-(6→ 2) types. For the branched fructans, the links tend to be β-(2 → 6) type. According to the type of structure, the fructans can be classified as inulin (branched), levan (linear). In dicotyledonous plants are mainly present the inulin type, but in monocots there is only a small part of this type.

Figure 2. Fructan structure, inulin type

Yam samples were obtained from San Carlos, Costa Rica; then was characterized and the fructans were extracted. In order to obtain the optimum conditions for fructans extraction, the extraction process was evaluated at three temperatures and five levels of time. The extracted fructans were separated by ultrafiltration and then were quantified. Quantification was carried out by the technique of HPLC; the samples were analyzed using a sugars determination column, using water as eluent, reading with a refractive index detector and using chicory inulin as standard. The fructans content obtained with the different method conditions were evaluated statistically, to determine the optimal conditions of extraction at a laboratory scale.

Consejo Nacional de Producción, Servicio de Información e Inteligencia de Mercados. 2010. Análisis de mercado de ñame. Datos sobre ñame. Recuperado en Abril 2010 de http://www.cnp.go.cr.

Segura, A.; Saborío, D.; Sáenz, M.V. Algunas normas de calidad en raíces y tubérculos tropicales de exportación de Costa Rica. Agronomía Costarricense 2003, volumen 27, número 1, pp 49-61.

Sandí, A.Y. ³Utilizaciòn del ñame (Dioscorea alata) y el tiquisque (Xanthosoma sagittifolium) de rechazo para la obtenciòn de adhesivos naturales en base acuosa.´. Tesis de Licenciatura. Universidad Nacional, Heredia, Costa Rica. 2008.

Bender, D.A. Bender's dictionary of nutrition and food technology. Eighth Edition. Woodhead Publishing Limited: Cambridge, England, 2006; pp. 203.

Roberfroid, M. Inulin-Type Fructans Functional Food Ingredients. CRC Press, 2005; pp. 60-63.

Ponce, J.; Macías, E.; Soltero, J.F.; Fernández, V.; Zuñiga, V.; Escalona, H. Physical-Chemical and non-linear rheological properties of aqueous solutions of agave fructans. e-Gnosis [Online]. 2008 volume 6, Art. 8. pp. 2,3.

Wang, H.; Zhang, Z.; Liang, L.; Wen, S.; Liu, Ch. A comparative study of High-performance liquid chromatography and colorimetric method for inulin determination. Eur Food Res Technol. 2010 volume 230. pp. 701-706.

Synthesis of Low Formaldehyde Emission Urea-Formaldehyde Resins and Their Application to the Manufacturing of Particleboards

P. Estévez, S. Vallejos, H. El Kaoutit, M. Trigo-López, F. Serna, F. García, J.L. de la peña, J.M. Pérez.

Departamento de Química, Grupo de Polímeros, Facultad de Ciencias, Universidad de Burgos, 09001 Burgos

e-mail: peb0002@alu.ubu.es

1.-Introduction

Urea-formaldehyde (UF) resins are the most used polycondensation resins for the manufacturing of particleboard panels due to their high reactivity, good performance and water solubility.[1] In spite of these advantages, they have two main disadvantages that are the formaldehyde emission from the panels and the poor resistance to water.

Response surface methodology (RSM) has being used as optimization procedure for low formaldehyde emission UF resins synthesis.[2] This work describes a central composite design methodology to optimize 3 selected variables (number of urea additions, pH and temperature) in the second urea addition, following three-stage process.

2.-Materials and Methods

Resins were synthesized from a precondensed formalin-urea solution and urea, following the traditional three stage process. Synthesis conditions of alkaline-acid step reactions were optimized in previous researches.[3] Central composite rotatable design was adopted for the experimental runs for response surface methodology, in the preparation of low formaldehyde emission UF resins.

Laboratory particleboards were prepared by using a standard mix of wood particles for the core and face layers. UF resins with additives and catalyst were sprayed on the wood particles and then were formed into a mat of dimensions 400 mm x 400 mm. The mat was prepressed at room temperature and further hot-pressed at 195 ºC for 2-3 minutes.

Perforator Method (European Standard EN 120) was used for measuring the formaldehyde content of wood-based panels.

3.-Results and Discussion

All resins were analyzed by standard methods. Differences in viscosity, gel time and free formaldehyde content were found depending on the synthesis conditions, but all of them were able to be used in the particleboard manufacturing process.

All particleboards were characterized according to European standard methods. Table 1 reports the main properties shown by the particleboards manufactured using the different UF resins synthesized. The formaldehyde content of the particleboards bonded with the modified process UF resins is well below the specified level of class E1 products (≤ 8 mg/ 100 g dry board) according to EN 13986, while maintaining good levels of internal bond strength, established in 0.35 Mpa (Particleboards Type P2, EN 312).

Table 1. Particleboards Characterization

Resin	Formaldehyde content (mg / 100 g dry board)	Internal Bond Strength (MPa)
1	2.6	0.46
2	2.8	0.46
3	3.2	0.62
4	2.3	0.52
5	2.6	0.66
6	3.9	0.67
7	3.2	0.50
8	3.1	0.57
9	2.5	0.66
10	2.2	0.56
11	2.1	0.53
12	4.0	0.50
13	4.3	0.47
14	3.3	0.56
15	3.6	0.58
16	3.6	0.55
17	3.0	0.69

Figure 1 shows: (a) Optimal response plot, with a minimum level of formaldehyde at a distance of 1,5; and (b) Optimal coordinate plot for the response in codified variables. These data transformed into natural variables are: pH: 7.4; Urea additions: 2 and Temperature: 50 ºC.

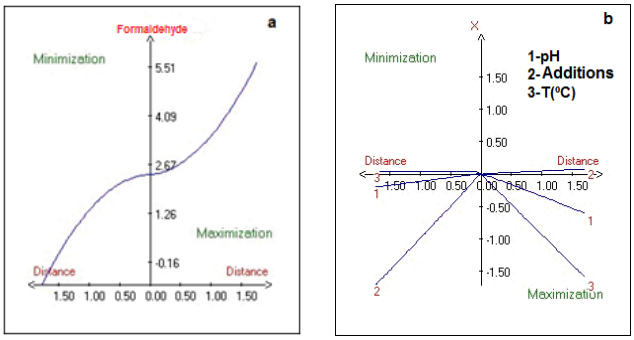

Figure 1. Ridge analysis (RSM).

4.-Conclusions

The effect of the number of second urea additions, pH and temperature was studied for the preparation of UF resins. The process was optimized on the basis of these studies. The results showed that the studied variables played a significant role in reducing the formaldehyde emission with a minor withdrawal of internal bond strength.

5.-References

1. A. Pizzi. Handbook of Adhesives technology, ed. Marcel Dekker, New York, 1994, 381-392.

2. J. M. Ferra et al. J. of Ad. Sci. and Tech., 2010, 24, 1455-1472.

3. P. Estévez, et al. XI Reunión del GEP. Libro de resúmenes. Ciencia de Polímeros: retos globales-nuevas estrategias, pp 236. Valladolid. 2009.

Controlled Free-Radical Copolymerization of 4-Vinyl Pyridine and *tert*-Butyl Acrylate via Reversible Addition-Fragmentation Chain Transfer (RAFT) Technique: Kinetics and Mechanism

Eugene Sivtsov[1], *Alexey Gostev*[1], *Elena Chernikova*[2]

[1] Saint-Petersburg State Institute of Technology, Plastics Technology Department, Saint-Petesburg, Russia
[2] Moscow State University, Department of Chemistry, Moscow, Russia

pjeka@yahoo.fr

The reversible addition-fragmentation chain transfer (RAFT) technique of free-radical polymerization was used to synthesize 4-vinyl pyridine (4VP)–tert-butyl acrylate (TBA) copolymers of gradient and block microstructure. Poly(4VP–TBA) can be easy transformed to copolymers of 4VP and acrylic acid, the self-assembling in acidic aqueous solutions of which was investigated by means of dynamic light scattering, turbidimetric and potentiometric titration. It was shown that microstructure strongly affected the size of the aggregates formed and the conditions of self-assembling.

Bulk copolymerization of 4VP and TBA was carried out in the presence of dibenzyl trithiocarbonate (BTC) as a RAFT agent and using the classic radical polymerization initiator N,N′-azobis(isobutyronitrile) (AIBN).

The gradient copolymers were obtained using monomers mixture in one-step process. Gradient structure was the result of the following:

– the monomers reactivity ratios difference (r_{4VP}=1.41 and r_{TBA}=0.04 as it was determined from NMR ^{1}H data of the monomers concentrations and the copolymer composition during the reaction);

– and a living character of the polymerization (a clear evidence of which is the copolymer molecular mass growing with the increasing of conversion, see Fig. 1).

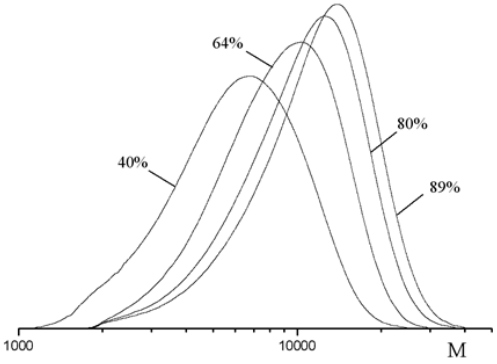

Figure 1. SEC traces of copolymers formed in bulk copolymerization of 4VP and TBA in the presence of BTC (80°C) at different conversions. [4VP]/[TBA]=58:42 mol.%.

As a result it leads to changing of the chain microstructure from both the tails of the macromolecules to their centres: the tails of the chains are enriched with 4VP units, while the middle of the chains – with TBA units. This gradient chain structure is formed due to 4VP higher reactivity and taking into account the mechanism of RAFT polymerization in the presence of trithiocarbonates (see the Table).

Table. Molecular mass and composition (concentrations of 4VP and TBA in copolymers) of the gradient poly(4VP-TBA) obtained from the monomers mixture 4VP:TBA=31:69, mol.% at different conversions C(%).

C, %	[4VP], mol.%	[4VP], units	[TBA], mol. %	[TBA], units	M_n
34	50	32	50	32	7700
56	45	38	55	46	10200
71	40	56	60	84	17000
81	36	59	64	105	20000

Kinetics and mechanism of 4VP and TBA RAFT copolymerization were studied by NMR ^{1}H spectroscopy. Thus, dynamics of benzyl protons concentration changing gives the information of comparative reactivity and effectiveness as a RAFT agent the initial BTC and polymeric trithiocarbonates formed in the course of the polymerization. The concentrations of BTC and mono substituted trithiocarbonate (polyRAFT$_1$) were registered during the polymerization. The data obtained in this study shows that polymeric radical is a better leaving group than benzyl radical. It is the reason that polyRAFT$_1$ concentration decreases slowly after its maximum, and polyRAFT$_1$ and polyRAFT$_2$ are present in the reaction mass together up to the high conversions. It is very important if the strictly definite gradient structure with composition changing from the tails to the middle of macromolecule must be synthesized.

Another useful information – concentration of 4VP units bound to the sulphur atom of trithiocarbonate fragment in polyRAFT$_1$ and polyRAFT$_2$, can be obtained from NMR ^{1}H spectra of the reaction mass. It was shown that after reaching the maximum at the early stage of reaction the concentration decreased slowly (see Fig. 2). It is a direct evidence of gradient microstructure poly(4VP-TBA) obtained.

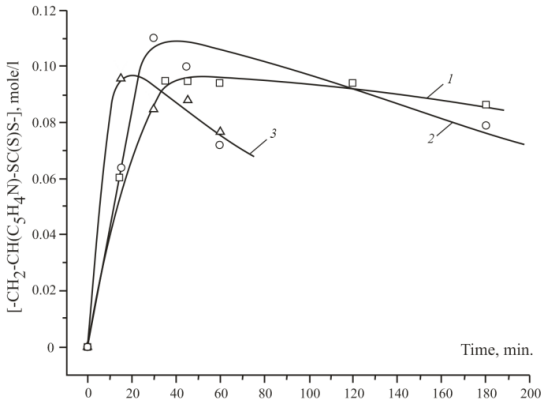

Figure 2. Time dependence of [-CH_2-CH(C_5H_4N)-SC(S)S-]. The monomers mixture composition, [4VP], mol.%: *1* – 25, *2* – 49, *3* – 75.

Conventional and RAFT Copolymerization of N-Vinyl Succinimide and 4-Vinyl Pyridine

Alexey Gostev, *Eugene Sivtsov*

Saint-Petersburg State Institute of Technology, Plastics Technology Department, Saint-Petesburg, Russia

pjeka@yahoo.fr

(Co)polymers based on N-vinylsuccinimide (VSI) cause intense interest due to possibility of application as hydrophilic non-toxic materials in medicine. Such copolymers can be easily modified by alkaline hydrolysis resulting in conversion of VSI units to the N-vinylsuccinimidic acid (VSA) units:

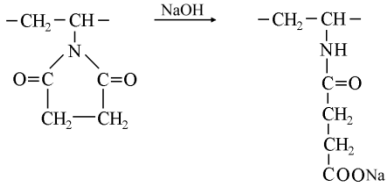

The carboxylic groups attached to the main chain via –NH–C(O)–CH_2–CH_2– spacer permit to bind low molecular compounds including medicinal products to the polymers, leading to various advantages of such polymeric drug conjugates, for instance, their prolonged action *in vivo*. However, a strong problem arises during production of VSI copolymers at high conversions: due to usual difference in reactivity ratios of VSI and other comonomers, which are most commonly used in copolymerization, the composition heterogeneous copolymers are formed that influences noticeably on the properties of the final product. Meanwhile the copolymer microstructure and composition heterogeneity are of great importance due to their influence on the reactions of addition of low molecular compounds to carboxylic groups of modified VSI copolymers and on macromolecules behavior in solutions.

Another problem arises when it is necessary to obtain soluble VSI polymers with high composition homogeneity by polymerization in bulk. This task cannot be achieved using conventional free-radical polymerization because of the chain transfer reaction to VSI cycle methylen protons leading to cross-linked unsoluble products. RAFT technique seems to be the most efficient way to solve both the problems of VSI polymerization denoted above.

Conventional and RAFT copolymerization of VSI and 4-vinyl pyridine (4VP) was studied in bulk and in solutions. Copolymers of VSI and 4VP can be used as precursors for obtaining zwitterionic copolymers by hydrolysis of VSI units and quaternization of 4VP units.

RAFT copolymerization of VSI and 4VP was carried out using dibenzyl trithiocarbonate (BTC) as a RAFT agent. The mechanism of the polymerization is shown on the Scheme below.

Monitoring of the reaction mixture components concentrations by NMR ^{1}H spectroscopy was used to study mechanism and kinetics of copolymerization and to calculate reactivity ratios of VSI and 4VP which were not described before in literature.

It was shown that poly(VSI-4VP) with various microstructures could be obtained using RAFT technique and BTC as a RAFT agent. Growing of MM in course of reaction is an evidence of pseudo-living character of the polymerization.

Scheme. Mechanism of copolymerization of VSI and 4VP in the presence of BTC (R= – $C_6H_5CH_2$).

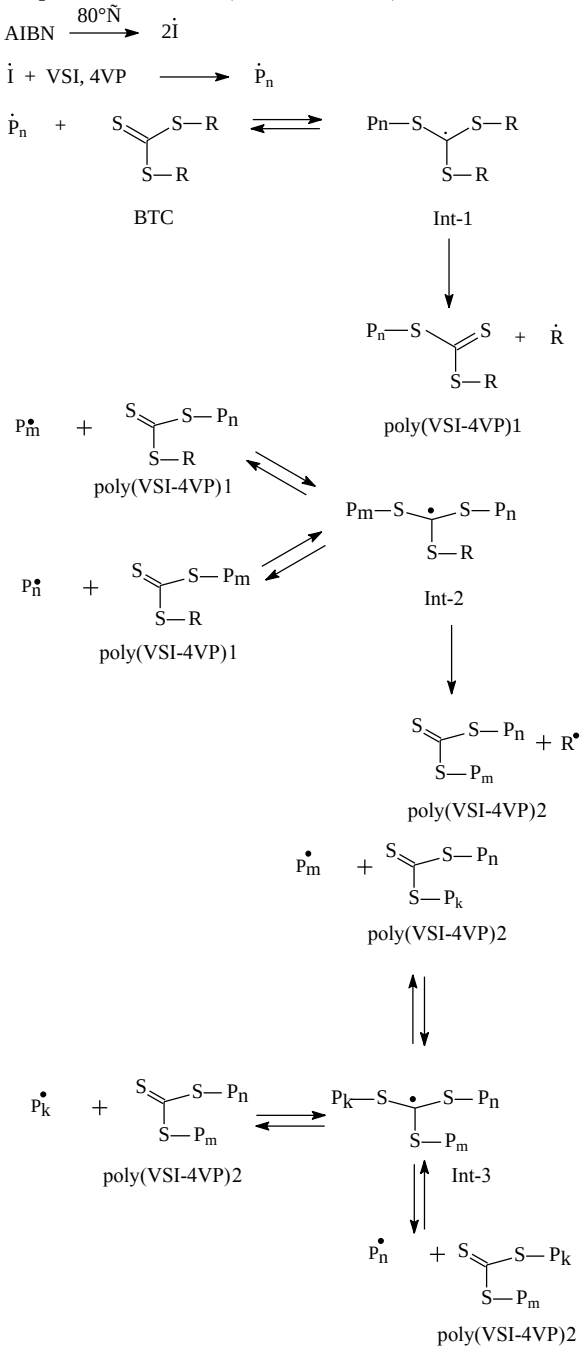

Copolymers synthesized according the Scheme have gradient structure in which CS_3-fragment is close to the middle of macromolecule and the composition of both the polymeric substituents P_n changes from the tails to the middle. The simplest gradient structure with the composition changing from one tail to another can be obtained by the reaction with a big excess of free radicals (e.g. AIBN, 80°C) in inert solvent.

Aromatic Copolyesters Containing Cyclic Diacetalized D-Glucitol

C. Japu,[a] A. Martínez de Ilarduya,[a] A. Alla,[a] E. Benito,[b] M.G. García-Martín,[b] J.A. Galbis[b] S. Muñoz-Guerra[a]

[a]Dept. d'Enginyeria Química, Universitat Politècnica de Catalunya, ETSEIB, Diagonal 647, 08028 Barcelona
[b]Dept. de Química Orgánica y Farmacéutica, Universidad de Sevilla, Profesor García González 2, 41012 Sevilla

cristina.japu@upc.edu

Introduction

The development of polymers based on monomers from renewable feedstocks is a steadily growing field of interest, especially from carbohydrates because of the unique structure and properties that can be generated in this case.[1] 2,4:3,5-Di-*O*-methylene-D-glucitol (Glux) is a carbohydrate-based diol suitable for the preparation of linear polycondensates.[2] The fused bicyclic dioxolane rings provide rigidity to the molecule making it an interesting candidate for replacing aromatic rings in conventional aromatic polyesters.

Materials and Methods

The ^{1}H and ^{13}C NMR spectra were recorded on a Bruker AMX-300 spectrometer. DSC experiments were performed at heating/cooling rates of 10 ºC·min^{-1} and TGA analysis was carried out under inert atmosphere. WAXS was performed on a Siemens diffractometer using K_{α}(Cu) radiation. Molecular weight analysis was performed by GPC using HFIP. Glux was readily prepared by acetalization of 1,5-D-gluconolactone with paraformaldehyde, followed by esterification with methanol of 2,4:3,5-di-*O*-methylidene-D-gluconic acid, and subsequent reduction.[1]

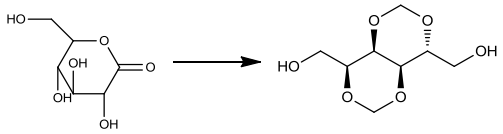

Results and Discussion

Copolyesters *co*PH$_x$Glux$_y$T (Figure 1) were synthesized by melt polycondensation from dimethyl terephthalate, 1,6-hexanediol and 2,4:3,5-di-*O*-methylene-D-glucitol using tetrabutyl titanate as catalyst. A series of copolyesters with Glux contents ranging between 5 and 32 mol-% was prepared. Synthesis results are displayed in Table 1.

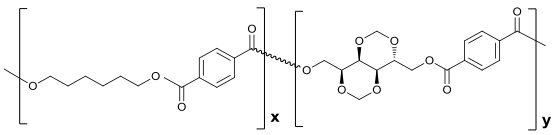

Figure 1. Structure of *co*PH$_x$Glux$_y$T copolyesters.

The ^{13}C NMR analysis showed that all the copolyesters had a random microstructure; the degree of randomness was determined from the signals of the non-protonated aromatic carbons of terephthalic units, which were split into nine peaks due to sequence distribution. The *co*PH$_x$Glux$_y$T copolyesters displayed optical activity according to what should be expected from the asymmetrical constitution of Gulx; specific optical rotations were found to span in the range from 1 to 10º.

Table 1. PH$_x$Glux$_y$T copolyesters: Synthesis results

Polyester	Reaction			Molecular size			
	Yield (%)	HD (mol %)	Glux (mol %)	M_n (g·mol^{-1})	M_w (g·mol^{-1})	PD	[η] (dL·g^{-1})
PHT	88	100	0	17 700	46 000	2.3	0.83
PH$_{95}$Glux$_5$T	80	95.4	4.6	15 500	41 000	2.4	0.72
PH$_{90}$Glux$_{10}$T	76	90.3	9.7	14 800	31 400	2.1	0.68
PH$_{80}$Glux$_{20}$T	68	81.6	18.4	13 900	33 000	2.2	0.65
PH$_{74}$Glux$_{26}$T	60	73.9	26.1	6050	16 000	2.5	0.34
PH$_{68}$Glux$_{32}$T	57	68.2	31.8	5100	12 400	2.5	0.29
PGluxT	30	-	100	3000	10 100	3.3	-

The thermal behaviour of *co*PH$_x$Glux$_y$T was evaluated by DSC and TGA and compared with that of poly(hexamethylene terephthalate) (PHT). The incorporation of Glux units in the chain of PHT decreased T_m and also T_d although the thermal stability of the copolyesters continued being satisfactory. Conversely, T_g increased significantly with the content in Glux so that a content of 5% in these units was enough to raise its value in 14 ºC.

The powder X-ray diffraction analysis of the copolyesters confirmed DSC data showing that all samples were semicrystalline. Nevertheless the cristallinity of *co*PH$_x$Glux$_y$T was lower than of PHT and decreased with increasing contents in Glux. The WAXS profiles revealed after annealing intense peaks corresponding to *d*-spacing characteristic of the β crystal form of PHT.[3]

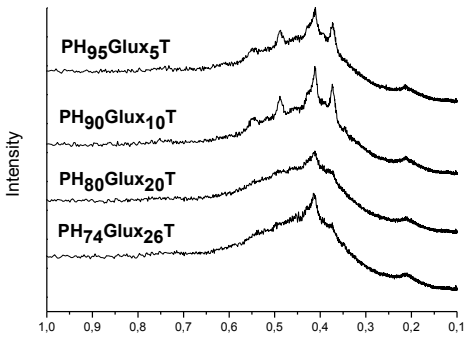

Figure 2. WAXS of annealed *co*PH$_x$Glux$_y$T.

Authors acknowledge the Spanish MICINN for financial support (MAT-2009-14053-CO2) and for the PhD grant awarded to C. Japu.

References

[1]Marín, R.; Muñoz-Guerra, S. *J Appl Polym Sci Part A: Polym Chem* **2008,** 46, 7996.
[2]Galbis, J.A.; García-Martín, M.G., *Monomers, Polymers and Composites from Renewable Resources*; Belgacem, M.N.; Gandini, A. Eds.; Elsevier: Oxford, UK, **2008**; pp 89-114.
[3]Wu, M.C.; Woo, E.M.; Yoshioka, T.; Tsuji, M. *Polymer* 47, **2006,** 5529.

Eco-Friendly Aliphatic Polyesters Containing 1,4-Cyclohexane Dicarboxylate Units: Effect of Diol Chain Length on Thermo-Mechanical Properties

Annamaria Celli[a], *Paola Marchese*[a], *Simone Sullalti*[a], *Justine Boyenval*[b], *Sophie Commereuc*[b]

[a] Department of Civil, Environmental, Materials Engineering, Via Terracini 28, 40131 Bologna, Italy
[b] Laboratoire de Photochimie Moléculaire et Macromoléculaire, Université Blaise Pascal & Ecole Nationale Supérieure de Chimie de Clermont-Ferrand, Les Cézeaux 63174 Aubière, France

annamaria.celli@unibo.it

Introduction

Aliphatic polyesters containing 1,4-cyclohexylene rings are an interesting class of materials, not yet fully investigated. They potentially have the good characteristics typical of biopolyesters (for example, polyalkylene dicarboxylates and polyhydroxy alkanoates), such as sustainability and biodegradability. Indeed, renewable biomass resources can be used as feedstock to prepare the monomers and some preliminary tests of biodegradation suggest that the aliphatic rings do not hinder the microorganism attack.[1] Moreover, the presence of cyclohexyl groups into the main chain provides rigidity to macromolecular chains, raises T_g, and imparts desirable physical-mechanical properties. In this way, the problem of the poor mechanical properties generally found in aliphatic polyesters can be solved. Finally, the 1,4-cyclohexylene unit shows the other remarkable peculiarity that it can have two possible configurations, *cis* and *trans*. In a polymer containing the 1,4-cyclohexylene rings, it will suffice to slightly modify the *cis*/*trans* isomeric ratio to obtain materials whose phase behavior changes from fully amorphous to semicrystalline.[2] Therefore, the final properties of these materials can be easily tailored according to the specific applications.
In this work diols with different chain length were tested as monomers for novel polyesters and the effects of the molecular characteristics on final properties were analyzed.

Materials

Two commercial samples of 1,4-dimethyl cyclohexanedicarboxylate (DMCD) with 22% and 100% of trans isomer, ethanediol, 1,3-propanediol, 1,4-butanediol, 1,5-pentanediol, 1,8-octanediol, and titanium tetrabutoxide (TBT) (all from Aldrich chemicals) were high purity products , used as received.

Results and Discussion

Polyesters from dimethyl 1,4-cyclohexane dicarboxylate (DMCD) and linear diols, containing from 2 to 8 $-CH_2-$ units, were synthesized (see Scheme 1). The *cis*/*trans* isomeric ratio of the aliphatic rings in the final polyesters is 90 or 50 mol%. Thermal and mechanical properties were investigated by DSC and DMTA. By comparing polymers having an odd or even number of $-CH_2-$ in the diol, to exclude odd/even effects, T_g significantly decreases with the increment of the chain length. For example, T_g, changes from 24 to -34°C by passing from ethanediol to 1,8-octanediol as monomers, when DMCD is 90 mol% *trans*. This large difference of 50°C is due to the increment of chain flexibility of the $-CH_2-$ sequences derived from the diol. Correspondently, melting temperature decreases from 146 to 94°C by passing from 1,4-butanediol to 1,8-octanediol. On the other hand, the mechanical properties are always good, independently of the diol chain length: the elastic modulus before T_g is about 10^9 Pa for all the semicrystalline samples prepared from DMCD 90% *trans*.
By decreasing the *trans* content of the DMCD monomer the materials generally lose the capability to crystallize, even if for the polymer from 1,8-octanediol the long flexible chain of the diol favours the formation of a low crystallinity level.

Conclusions

Novel polyesters have been successful prepared by using DMCD and different aliphatic diols as monomers. Significant relationships between the diol chain length, the *cis/trans* ratio of the cycloaliphatic units, and the solid-state properties were found.

References

[1] C. Berti, A. Celli, P. Marchese, G. Barbiroli, F. Di Credico, V. Verney, S. Commereuc, *Europ. Polym. J.* **2009**, *45*, 2402.
[2] C. Berti, A. Celli, P. Marchese, E. Marianucci, G. Barbiroli, F. Di Credico, *Macromol. Chem. Phys.* **2008**, *209*, 1333.

Scheme 1: Scheme of the synthesized novel polyesters

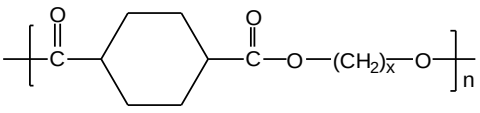

x = 2, 3, 4, 5, 8

Synthesis and Modification of Biopolymers with Unsatured Terminal Groups

C. Berti, A. Celli, L. Cruciani, P. Marchese, L. Sisti, M. Vannini

Dept. of Civil, Environmental and Materials Engineering, University of Bologna, Via Terracini 28, 40136 Bologna (Italy)

e-mail: laura.sisti@unibo.it

Introduction

Many countries nowadays are putting effort and emphasis on recycling plastic waste and, at the same time, on developing alternative degradable materials and materials from renewable resources. Several synthetic polymers have been identified as degradable in the natural environment, and, among them, aliphatic polyesters appear very attractive and promising. Despite their utility there remains a need to design materials with more variation in, for example, crystallinity, polarity, solubility, mechanical properties, etc. This need for an expanded set of properties has driven research in the area of preparing aliphatic polyesters with tunable properties. In this study the modifications of poly(lactic acid) (PLA) by reactive blending with citronellol (CL) and cardanol (CD) are reported. CL is a natural monoterpenoid, known as bioactive molecule with disinfectant and odor properties. CD (3-pentadecenyl phenol) instead, the main component obtained by thermal treatment of cashew nut shell liquid (CNSL), is a phenol derivative mainly having the meta substituent of a C15 unsatured hydrocarbon chain with mostly 1-3 double bonds. Only a small part of CD obtained in the production of the cashew kernel is used in the industrial field, though it has various potential industrial uses. Therefore, development of new applications for CD is strongly desiderable. CL was also employed in the synthesis of novel aliphatic polyesters based on dimethyl succinate (DMS) and 1,3-propanediol (PD). The aim was the production of linear and unsatured materials, without the addition of cross-linking inhibitors, and that can be further easily modified through several reactions techniques.

Materials and Methods

DMS, PD, CL, tin octanoate ($Sn(Oct)_2$) were furnished by Aldrich. CD was a gift from Satya Cashew Chemicals and PLA was supplied by NatureWorks.

Reactive blending: 0.200 mol (14.4 g) of PLA, 0.0100 mol of CL (1.64 g) or CD (8.95 g) and 175 ppm of $Sn(Oct)_2$ as catalyst were reacted for 2 hours at 170 °C in a 250 ml round bottomed flask equipped with a mechanical stirrer and a condenser.

Polymerization: 0.0950 mol (7.22 g) of PD, 0.0730 mol (10.7 g) of DMS and $3.60 \cdot 10^{-3}$ mol (0.560 g) of CL were reacted following a standard two stages polycondensation process with $Sn(Oct)_2$ as catalyst.

Results and Discussion

In Fig. 1. it is reported the reaction scheme between PLA and CL or CD. As can be seen in Table 1 the unsatured molecules covalently attached to PLA resulted to be around 1 and 2 mol%, as measured by ^{1}H-NMR. The molecular weights of the final products and the T_g were drastically lowered respect to the starting material, probably because of transesterification reactions occurring with the functional groups in the chain.

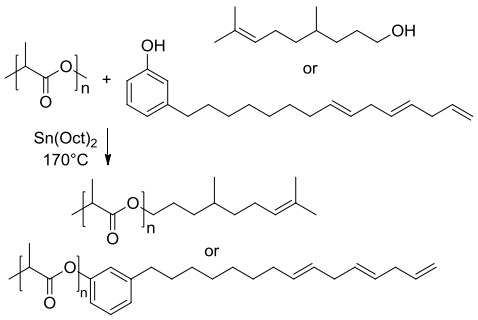

Fig. 1. Reactive blending scheme

In Fig. 2. The direct polymerization reaction scheme and conditions are reported. By ^{1}H-NMR it resulted that 2 mol% of unsaturation is present and that both molecular weights and thermal properties of the reference (poly(propylene succinate) – PPS) and telechelic unsatured material are comparable.

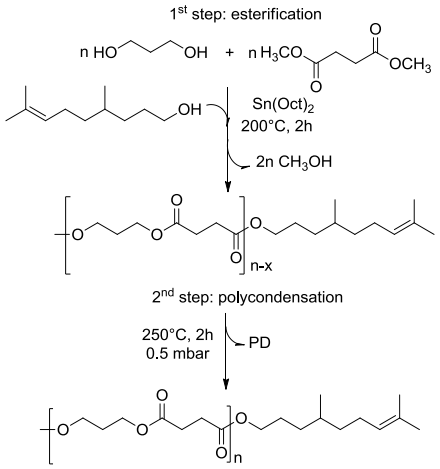

Fig. 2. PPScitronellol polymerization scheme

Tab. 1. Samples characterizations

Sample	Unsaturation[a] (mol %)	M_w[b]	T_g[c] (°C)
PLA	-	170000	62
PLA_citronellol	2	22000	49
PLA_cardanol	1	30000	45
PPSref	-	71000	-32
PPScitronellol	2	68000	-31

[a] ^{1}H-NMR analysis; [b] GPC analysis; [c] DSC 2nd heating scan

Conclusions

Telechelic unsatured aliphatic polyesters have been prepared by reactive blending and by direct polymerization. In particular direct polymerization permits to get a final material with a relatively high molecular weight. CL and CD were covalently bonded to the polymer allowing for further modifications of the polymeric structure.

Synthesis and characterization of lactide-graft-poly(vinyl alcohol) and miscibility study with poly(ethylene oxide)

A.Lejardi[1], *A.Etxeberria*[2], *E.Meaurio*[1], *J.Fernandez*[1], *J.R.Sarasua*[1]

[1]School of Engineering, University of the Basque Country (EHU-UPV)
Alameda de Urquijo s/n. 48013 Bilbao, Spain.
[2] Department of Polymer Science and Technology, Institute of Polymer Materials, University of the Basque Country (EHU-UPV), M. de Lardizabal, 3. 20018 Donostia, Spain.

E-mail: ainhoa.lejardi@ehu.es

Introduction. Poly(vinyl alcohol) (PVA) is a well known water-soluble polymer with widespread commercial applications. The repeating unit of PVA contains reactive hydroxyl groups that can be converted to ester groups through ring opening reactions. On the other hand Poly(ethyelene oxide) (PEO) is a highly crystalline polymer that exhibits miscibility with chemically dissimilar polymeric materials.[1] According to the Flory-Huggins model, attractive interactions between the components of a polymer blend are necessary to obtain a miscible polymer blend. The most commonly used method for establishing miscibility in polymer blends is through the determination of the glass transition temperature (T_g). A miscible polymer blend possesses a homogeneous amorphous phase and hence will exhibit a single glass transition temperature between the Tg´s of the pure components. In the case of blends in which one of the components is semicrystalline, the miscibility of the system involves a decrease in the equilibrium melting point of the crystalline polymer as a function of the blend composition. The presence of this depression is often considered to be a miscibility criterion.[2]

In this work we have selected a semicrystalline/amorphous pair to prepare blends: poly(ethylene oxide), PEO, and lactide-graft-poly(vinylalcohol),VA-g-LA. Although it is known in advance that PEO/PVA blend is immiscible and PEO/PLLA blend is partially miscible,[3,4] grafting is expected to favor miscibility in the PEO/VA-g-LA system, since it should decrease the OH self-association.

Materials and methods. PEO with weight-average molecular weight of 70,000 and PVA with weight-average molecular weight in the range of 13,000-23,000 and a degree of saponification of 98% were supplied from Sigma Aldrich. The monomer L-lactide was obtained from Purac.

The chemical characterization of the graft copolymers obtained was carried out by ^{1}H NMR, ^{13}C NMR and IR spectroscopy. The composition, the degree of substitution (DS) and the degree of polymerization (DP) were determined by means of ^{1}H NMR spectroscopy. The thermal properties of copolymers and the miscibility study were investigated by differential scanning calorimetry (DSC), IR spectroscopy (FTIR) and scanning electron microscopy (SEM).

Films of pure PEO and blends of PEO/VA-g-LA were prepared by casting the chloroform solutions of the polymers, followed by drying at room temperature.

Results and discussions. Ring-opening graft polymerization of L-lactide (LA) was carried out with poly(vinyl alcohol) in the presence of tin(II) 2-ethyl hexanoate catalyst in dimethyl sulfoxide (DMSO) in nitrogen atmosphere at 100º C. The desired graft copolymers, lactide-graft-poly(vinyl alcohol) were obtained using different feed compositions, and ^{1}H NMR shows that the length of the lactide side chain increases with the monomer feed composition.

The analysis of the PEO/VA-g-LA blends by DSC, FTIR and SEM suggests miscibility in the whole range of compositions. Due to the high crystallinity of PEO, the DSC curves for the PEO rich systems did not show a discernable glass transition temperature. However, the value obtained for polymer-polymer interaction parameter χ_{12}, was -0,22. The negative value of the interaction parameter confirms a thermodynamically miscible blend.

On the other hand, FTIR spectroscopy reveals that the hydroxyl stretching region shifts to lower wavenumbers as the content of PEO in the blend increases. This behavior is attributed to the presence of a new band, attributed to hydrogen-bonded species, indicative of the intermolecular interaction involving the PEO ether group and the VA-g-LA hydroxyl group.

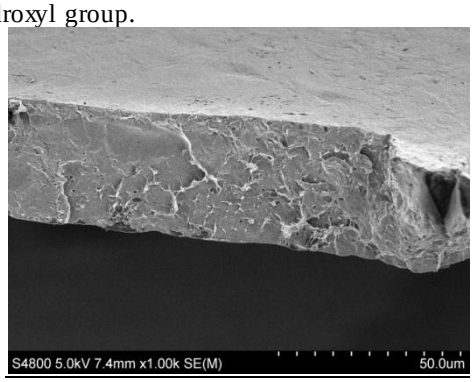

Figure1. SEM micrograph of PEO/VA-g-LA (50/50)

Figure 1 shows the SEM micrograph for the PEO/VA-g-LA 50/50 blend in which there is no observed phase separation. These micrographs support the results obtained by DSC and FTIR and indicate that the PEO/VA-g-LA blend is miscible.

Acknowledgements. The authors are thankful for funds from MICINN (BIO-2010-21542-CO2-01) and from the Basque Government, Department of Industry, Innovation and Commerce (Etortek IE10-276). A.L. thanks to the University of the Basque Country a pre-doctoral grant and SGIker (UPV/EHU) technical support for SEM measurements.

References

1.- E. Chiellini, A.Corti, S. D'Antone, R.Solaro, Prog. Polym. Sci. 28, 963–1014 (2003)

2.- E.Meaurio,E.Zuza, J.R.Sarasua, Macromolecules,38, 1207-1215 (2005)

3.- W.C. L, W.B L, Journal of Applied Polymer Science, 92, 1562-1568 (2004)

4.- Y.Agari, K.Sakay, Y.Kano, R. Nomura, Journal of Polymer Science, 45, 2972-2981 (2007)

Oleic and Undecylenic Acids-based diols and derived polyurethanes *via* thiol-ene coupling

González-Paz, R.J; Lligadas, G.; Ronda, J.C.; Galià, M.; Cádiz, V.

Department of Analytical Chemistry and Organic Chemistry, Rovira i Virgili University, Marcel.li Domingo s/n, 43007 Tarragona (Spain)

rodolfojesus.gonzalez@urv.cat

Introduction

Nature offers an abundance of opportunities for designing novel monomers and shaping structural and functional polymers in its wide variety of raw materials. Presently their relative use for monomers and polymers synthesis compared to petrochemicals is small. Natural oils, such as vegetable oils provide interesting feedstock - triglyceride fatty acids- that beyond their use in food allow additional chemistry that yields either opportunities for replacing petrochemicals or may be directly used to synthesize bio-inspired materials.[1]

Vegetable oils are becoming extremely important as renewable resources for the preparation of polyols required for the polyurethane industry.[2]

Classically the reaction between a thiol and a double bond has received significant attention as candidate for many applications. Resurgence over the past decades has occurred in response to the many benefits that thiol-ene coupling presents for polymer synthesis: tolerance to many different reaction conditions/solvents, clearly defined reaction pathways/products, and facile synthetic strategies from a range of easily obtained starting materials.[3]

In particular, thiol-ene click chemistry of fatty acid derivatives, obtained from plant oils, is a promising route that can be used for the synthesis of novel chemical intermediates from renewable resources.[4,5,6]

Results and Discussion

Our research applies the photoinitiated thiol-ene click chemistry of unsaturated oleic and 10-undecenoic acid methyl and allyl esters with hydroxyl-functionalized thiol (2-mercaptoethanol) for its ability to add hydroxyl functionality in lieu of double bonds. Due to terminal enes are significantly more reactive towards hydrothiolation compared to internal enes, thiol-ene addition to oleic acid derivatives required longer reaction times and higher amounts of radical photoinitiator, 2,2-dimethoxy-2-phenylacetophenone (DMPA). This methodology provides a green approach toward four novel plant-derived diols: UDM-diol, UDA-diol, OLM-diol and OLA-diol. The chemical structures of these products were confirmed by NMR and FTIR.

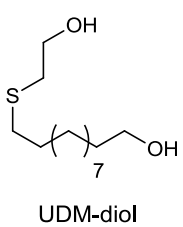

UDM-diol

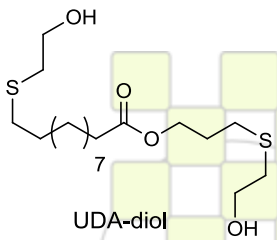

UDA-diol

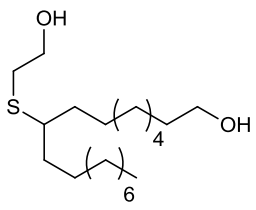

OLM-diol

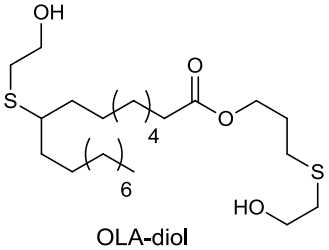

OLA-diol

The synthesized undecylenic and oleic acids based diols were polymerized with 4,4′-methylenebis (phenylisocyanate) (MDI), in DMF solution at 50 ºC for 24 h using tin (II) 2-ethylhexanoate as catalyst, to produce the corresponding thermoplastic polyurethanes (TPUs). Also, ultrasound irradiation has been tested to improve the polyurethane synthesis. Under these conditions TPUs were obtained in high yields (80-99%) with weight-average molecular weights in the 36-83 KDa range. Polydispersity degrees oscilated between 2.2 and 1.9 with perceivable differences between those with and without ester groups in the polymer chain. In the case of polyurethanes obtained with ultrasound irradiation weight-average molecular weight was higher and polydispersity was lower.

The chemical structures of polyurethanes were assessed by FTIR and NMR spectroscopy. The thermal and mechanical properties of the synthesized TPUs have been studied and show a clear dependence on the structure of the parent diol. MTT test was carried out to asses the potential citotoxicitity of the prepared polyurethanes. All thermoplastic polyurethanes scored 0, indicating no cytotoxic response, in spite of some evidences indicating that aromatic-based polyurethanes are cytotoxic.

References

1. Gandini, A.; Belgacem, M. N. Monomers, Polymers and Composites from Renewable Resources; Elsevier: Oxford, UK, 2008.
2. Lligadas, G.; Ronda, J. C.; Galià, M; Cádiz V. Biomacromolecules, 2010, 11, 2825-2835.
3. Hoyle, C. E.; Lowe, A. B.; Bowman, C. N. Chem. Soc. Rev., 2010, 39, 1355-1387.
4. Samuelsson, J.; Jonsson, M.; Brinck, T.; Johansson, J. Polym. Sci., Part A: Polym. Chem. 2004, 42, 6346-6352.
5. Lluch, C.; Ronda, J. C.; Galià, M; Lligadas, G.; Cádiz V. Biomacromolecules, 2010, 11, 1646-1653, 2010
6. Türünç, O.; Meier M. A. R. Macromol Rapid Commun. 2010, 31, 1822-1826

Synthesis and microbiologic assays of new polymers based on antibacterial biomolecules

Bénédicte Lepoittevin,[1] *Jessie Casimiro*,[1] *Corentin Rinfray*,[1] *Jean-Marie Herry*,[2] *Marie-Noëlle Bellon-Fontaine*,[2] *Philippe Roger*[1]

[1]Laboratoire de Chimie Organique Multifonctionnelle, Equipe Glycochimie Moléculaire et Macromoléculaire, Institut de Chimie Moléculaire et des Matériaux d'Orsay (ICMMO), UMR 8182, Bâtiment 420, Univ Paris-Sud, Orsay F-91405, France
[2]UMR 763 BHM, INRA-AgroParisTech, 25, avenue de la République, Massy F-91744, France
benedicte.lepoittevin@u-psud.fr; philippe.roger@u-psud.fr

Preparation of new surfaces to fight against microbial contamination is a subject of major interest nowadays in different areas such as household, industry, hospital, etc. Polymer surfaces with anti-adhesive or antibacterial properties would be of great interest for example to manufacture sheets and clothes as protections against nosocomial infections.

The aim of this study is to prepare new polymers based on biomolecules with a known antibacterial activity.

These polymers were prepared by conventional and controlled radical (Atom Transfer Radical Polymerization) polymerizations.

Natural biocide molecules are numerous but we will focus on some of them: gaïacol, myrtenol and D-glucosamine (Figure 1).

Gaïacol (2-methoxyphenol) **1** is a natural biocide molecule obtained from beechwood. Gaïacol is isolated from the gaïac resin. Gaïacol and derivatives are known and used for more than a century. Their main uses are antiseptics, gastric sedatives, flavorings, deodorants, fungicides and parasiticides.

Myrtenol **2** is an essential oil obtained from the myrtle (*Myrtus communis L.*). The benefits of myrtle are various. Different parts of the plants are used in cosmetics and medicine (antibacterial and antifungal activity).

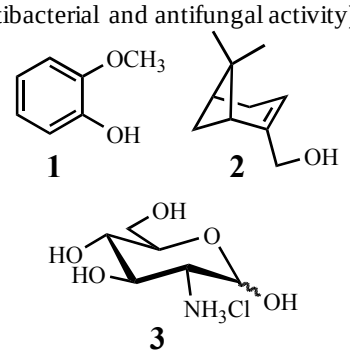

Figure 1. Gaïacol, myrtenol and D-glucosamine

Chitosan is a linear copolymer of β-(1→4)-linked D-glucosamine and *N*-acetyl D-glucosamine units in varying proportions. Among its various bioactivities, the antimicrobial activity of chitosan has been pointed out as one of its most interesting properties. Chitosan has exhibited high antimicrobial activity against a wide variety of pathogenic and spoilage microorganisms, including fungi, Gram-positive and Gram-negative bacteria. D-glucosamine **3**, monomer unit of chitosan was used in our study.

Methacrylate and acrylamide monomers were prepared using these biomolecules and their radical polymerization was studied.

For example, *N*-(4-hydroxy-3-methoxy-benzyl)-acrylamide monomer was prepared from gaïacol by Friedel-Craft reaction and polymerized using AIBN as thermal initiator (Scheme 1).

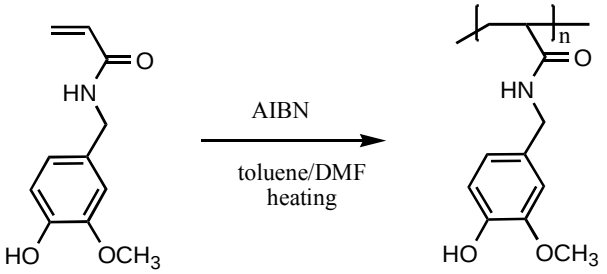

Scheme 1. Conventional radical polymerization of *N*-(4-hydroxy-3-methoxy-benzyl)-acrylamide

Anti-adhesive activity is tested after adsorption of polymer derived from gaïacol on glass slides. It is evaluated with different kind of bacteria (*H. alvei*, *S. epidermidis*, *E. coli* and *B. subtilis*).

Combination of ammonium groups and biomolecule-derivatives in the same polymer was performed to enhance the antibacterial activity.

For example, brominated compounds derived from gaïacol were prepared and used for quaternization reaction with poly((2-dimethylamino)ethyl methacrylate) (Scheme 2).

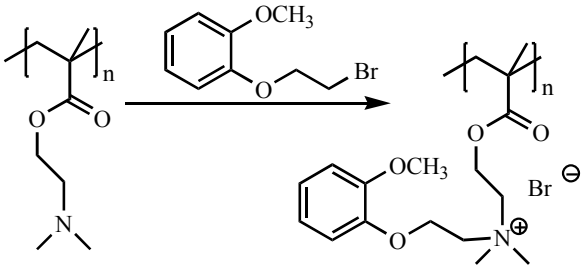

Scheme 2. Preparation of antibacterial polymer with both ammonium and gaïacol-derivatived groups.

References

1. Kenawy ER, Worley SD, Broughton R. Biomacromolecules, 2007, 8, 1359.
2. Xu FJ, Neoh KG, Kang ET. Progress in Polymer Science 2009, 34, 719.
3. Burt S. International Journal of Food Microbiology 2004, 94, 223.

Carbohydrate-based Polyurethanes: A Comparative Study of Polymers Made from Isosorbide and 1,4-Butanediol

R. Marín, A. Alla, A. Martínez de Ilarduya and S. Muñoz-Guerra

Dept d'Engingería Química, Universitat Politècnica de Catalunya, ETSEIB, Diagonal 647, 08028 Barcelona

sebastian.munoz@upc.edu

Introduction

Although some polyurethanes (PUR) containing isosorbide were described at the beginning of the nineties,[1] the knowledge on these compounds is very limited. Recently we have reported on segmented poly(ester-urethane)s in which 1,4-butanodiol (BD) was replaced by isosorbide (Is) as chain extender.[2] The main purpose of this work was to make a comparative study of non-segmented Is containing polyurethanes with their analogues made from BD. Hexamethylene diisocyanate (HDI) and 4,4'-methylene-bis(phenyl isocyanate) (MDI) are used for this synthesis.

Materials and Methods

Isosorbide was a gift from Roquette Freres S.A. Molecular sizes of PUR were estimated by both viscosimetry in dichloroacetic acid and GPC. NMR spectra were recorded on a Bruker AMX-300 in DMSO-d_6. DSC experiments were performed at heating/cooling rates of 10 ºC·min^{-1} and TGA analysis was carried out under inert atmosphere. Wide angle X-ray scattering (WAXS) was performed on a lab diffractometer or at the A2 beamline of the HASYLAB synchrotron (DESY, Hamburg).

Results and Discussion

The chemical structures of PUR studied in this work are depicted in Figure 1.

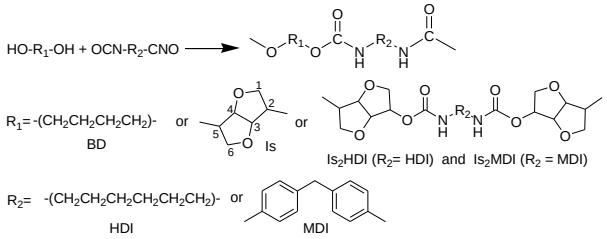

Figure 1. Chemical structures of polyurethanes studied in this work.

The selected diol or combination of diols (BD, Is, Is_2HDI or Is_2MDI) were made to react with the selected diisocyanate using dibutyltin dilaurate catalyst. The use of diol-urethane compounds as monomers ensured the incorporation of the Is units as dyads in the PUR chain and contributed to minimize the decomposition of isosorbide during polymerization. Synthesis results are compared in Table 1. The ^{1}H NMR spectra showed that PUR were enriched in BD units and all them displayed predominance of isosorbide end groups, mostly with the unreacted hydroxyl in *exo* position. This result is contrary to the relative reactivity of the hydroxyl groups observed in the synthesis of polyesters.[3]

The thermal properties and stability of PUR containing Is were evaluated and compared with those of PUR entirely made of BD. Incorporation of Is produced significant changes in T_g, T_m and T_d but no noteworthy differences were found between copolymers made from

Is or Is_2 monomers. In general the insertion of the Is units in the PUR chain increased the T_g and depressed the crystallinity.

WAXS revealed that the triclinic structure of PUR-(BD-HDI) was essentially retained in PUR-(BDIs-HDI), whereas the aromatic PUR gave profiles typical of disordered material. Annealing of PUR-(Is-HDI) induced the split of the 0.43 nm peak indicating that a new crystal structure was adopted.

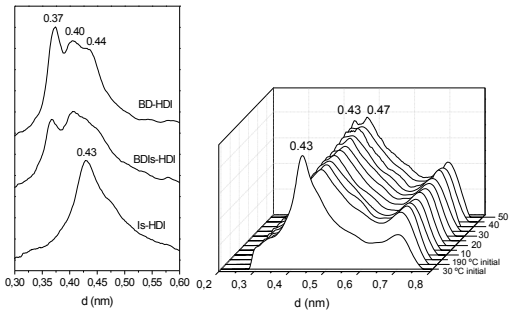

Figure 2. WAXS of PUR (left) and evolution of the PUR-(Is-HDI) profile with annealing time at 190 ºC (right).

The degradation in aqueous buffers (pH 2, 7.4 and 10, at 37 and 60 ºC for 40 days) of the pair PUR-(BD-HDI) and PUR-(Is-HDI) showed that the replacement of BD by Is weakens the resistance of PUR to water. This result is in agreement to previously reported work on polyamides and polyesters and confirm that the hydrodegradability enhancement in polycondensates made of carbohydrate-based units is a general fact.

Financial support given by MICINN with grant MAT-2009-14053-CO2-01 and HASYLAB technical support is acknowledged.

References

[1] Braun B.; Bergmann, M. *J Prakt Chem* **1992**, *334*, 298.

[2] Marín, R.; Muñoz-Guerra, S. *J. Appl. Polym. Sci.* **2009**, *114*, 3723.

[3] Noordover, B.A.J.; van Staalduinen, V.G.; Duchateau, R.; Koning, C.E.; van Benthem, R.A.T.M.; Mak, M.; Heise, A.; Frisen, A.E.; van Haveren, J. *Biomacromolecules* **2006**, *7*, 3406.

Thermal and Hydrolytic Degradability of Polyesters Containing Cyclic Acetalized Carbohydrate Units

C. Lavilla,[a] *C. Japu,*[a] *M.G. García-Martín,*[b] *J.A. Galbis,*[b] *S. Muñoz-Guerra*[a]

[a]Dept. d'Enginyeria Química, Universitat Politècnica de Catalunya, ETSEIB, Diagonal 647, 08028 Barcelona
[b]Dept. de Química Orgánica y Farmacéutica, Universidad de Sevilla, Profesor García González 2, 41012 Sevilla

graciagm@us.es

Introduction

The development of biobased polymers obtained from carbohydrates is a field of interest because of the unique structure and properties that can be generated in this case.[1] Cyclic acetalized diacids and diols, *i.e.* dimethyl 2,4:3,5-di-*O*-methylene-galactarate (Galx) and 2,4:3,5-di-*O*-methylene-D-glucitol (Glux) have been recently proven to be suitable monomers for the preparation of linear polyesters. One major problem associated to polyesters made from cyclic carbohydrate derivatives is their susceptibility to heat, which may limit the synthesis work and give rise to undesirable discoloration of the final polymer. On the other hand, it is of interest to evaluate the influence of the carbohydrate units on the hydrolytic degradability of the polyesters. In this communication, the degradability of a set of polyesters and copolyesters containing either Glux or Galx is preliminary evaluated.

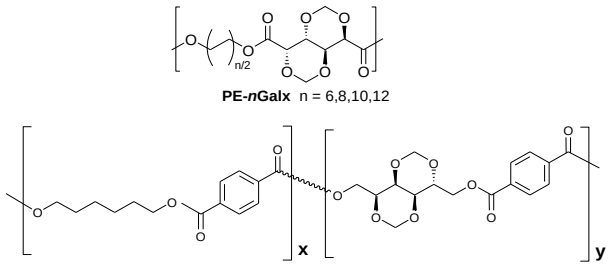

Scheme 1. Chemical structure of PE-*n*Galx polyesters (top) and *co*PH$_x$Glux$_y$T copolyesters (bottom).

Materials and Methods

PE-*n*Galx polyesters of M_w in the 30,000-40,000 range were obtained by melt polycondensation of Galx with aliphatic α,ω-alkanediols. Random copolyesters *co*PH$_x$Glux$_y$T with Glux contents ranging between 5 and 32 mol-% were synthesized by melt polycondensation of dimethyl terephthalate with mixtures of Glux and 1,6-hexanediol. The ^{1}H and ^{13}C NMR spectra were recorded on a Bruker AMX-300 spectrometer and the TGA analysis was carried out in the 30-600 ºC range under inert atmosphere. ATR-FT-IR was performed in a Jasco 4100 instrument.

Results and Discussion

The TGA traces of PE-*n*Galx polyesters reveal that PE-*n*Galx polyesters lost 5 % of mass at temperatures higher than 320 ºC. Comparison of the TGA traces of PE-*n*Galx polyesters with their homologues PE-*n*Ad made from adipic acid revealed that the introduction of ring acetal groups improves the thermal stability. The analysis by NMR of volatile generated upon heating a sample of PE-8Galx at 300 ºC indicated the presence of aldehydic, formiate and methylol groups. The ATR-FTIR of the residue revealed that the structure of the cyclic acetals might have been modified during the thermal treatment. On the other side the replacement of the 1,6-hexanodiol by Glux give rises to a decreasing in the thermal stability of the resulting copolymers that is more accentuated with increasing contents in the sugar units.

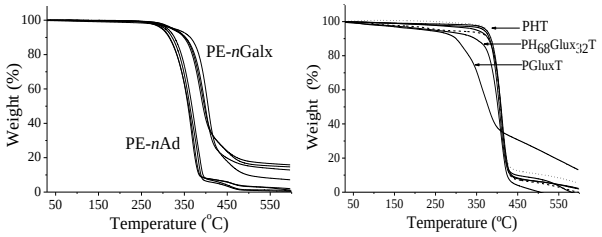

Figure 1. Compared TGA traces of polyesters.

The hydrolytic degradability of PE-8Galx and PE-8Ad was compared by incubating them in parallel in aqueous buffer under different conditions. Significant weight losses were detected for PE-8Galx, which apparently hydrolysed into low molecular water-soluble monomers and oligomers. The hydrolysis study of *co*PH$_x$Glux$_y$T was made comparing with the aromatic homopolyester PHT. In this case, it was also found that the incorporation of the Glux units slightly increased the degradability although the loss of weight only reached a few %.

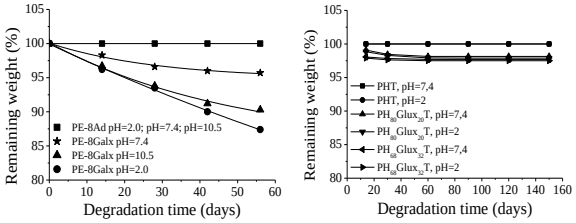

Figure 2. Evolution of the sample weight of polyesters incubated in aqueous buffer at room temperature at the indicated pH.

Conclusions

The replacement of alkylene diols by cyclic carbohydrate units, in both aliphatic and aromatic polyesters, increases slightly their susceptibility to the hydrolytic degradation. The effect of the replacement on the thermal stability seems to be opposite in each case.

References

[1]Galbis, J.A.; García-Martín, M.G. In *Synthetic Polymers From Readily Available Monosaccharides, Topics in Current Chemistry* **2010**, *295*, 147-176.

Acknowledgements

Authors acknowledge the MICINN Spanish for project grant MAT-2009-14053-CO and for the FPU and FPI grants awarded to C. Lavilla and C. Japu, respectively.

Polyhydroxybutyrate Nanocomposite Microcapsules with Brazilian Smectitic Clays

Maria das Graças da Silva Valenzuela, Wang Hui Shu, Hélio Wiebeck, Francisco Rolando Valenzuela Díaz

Departamento de Engenharia Metalúrgica e de Materiais, Escola Politécnica da Universidade de São Paulo, Brazil

mdgdsval@yahoo.com

Introduction: The search for better materials has placed the polymer/clay nanocomposites in the center of attention, especially because their considerable increasing of material properties in function of the nanoscale reinforcement. Biopolymer-based nanocomposites as polyhydroxybutyrate (PHB), due to the current concern over environmental problems and biomedical use, can be a good alternative to produce microcapsules with application in drug delivery systems. Polymeric microcapsules are microparticles such as can be loaded with biological or chemical substance at the sphere surface or encapsulated within the particle and be used as a drug delivery systems. The drug delivery systems based on polymeric microcapsules has witnessed tremendous progress in recent years due to their unlimited potential to improve human health [1]. It can be used in several industrial sectors, especially medical, pharmaceuticals and cosmetics to allow the developing of better therapies. PHB has been described as a good candidate for fabricating prolonged-action drug in the form of polymeric microcapsules [2]. This biopolymer offers many advantages over traditional petrochemically derived plastics. It is a linear homopolymer biosynthesized by various strains of bacteria by condensation of D(-)-B-hydroxybutyric acid and used as an energy and carbon source. PHB can be obtained by extraction from bacteria or by chemical synthesis. It is biocompatible and biodegradable, and completely nontoxic in the environment [2]. In this work, we describe the preparation of microcapsules from two PHB nanocomposite systems: a) PHB/OMMT (Cloisite 20A), (PHB1) and b) PHB/montmorilonite (MMT), natural Brazilian green policationic clay, (PHB2).

Materials and Methods: The PHB used for the nanocapsule preparation was obtained from PHB Industrial S.A. (São Paulo, Brazil). The organophilic clay (Cloisite 20A) with positively charged quaternary ammonium (dimethyl hydrogenated tallow 2-ethylhexyl quaternary ammonium chloride) was obtained from Southern Clay. The MMT clay, Brazilian green clay, a natural clay, was obtained from Bentonisa do Nordeste S.A. (Paraíba, Brazil). Firstly, the polymer PHB was dissolved in chloroform (25/1) at 40°C for 10 min, while the Cloisite 20A and Brazilian green clay were dispersed in chloroform (250/1) at room temperature, for 10 min. The organoclay and the polycationic clay dispersions were added separately to two PHB solutions and then mixed by stirring for 1 hour. After this time, 2 mL of each mixture were placed in glass dishes and leaved in a hood, overnight. After the solvent was evaporated, the two samples were dried in a vacuum oven for 1 day at 25°C. The microcapsules PHB/OMMT and PHB/MMT nanocomposite (NCN) were prepared by solvent evaporation technique from the resulting organic solutions.

Results: The XRD of films and microcapsules do not show $d_{(001)}$ peak, evidencing an exfoliated structure in the nanocomposites. The films have shown by SEM a homogeneous distribution of the claymineral particles spread uniformly in the PHB film matrix, Figure 1

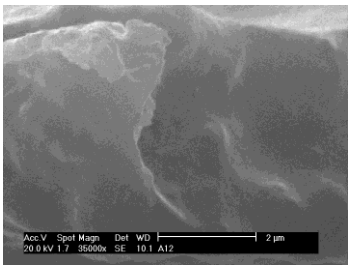

Figure 1. SEM, PHB film with green clay.

The nanocomposite microcapsules when analyzed by SEM revealed spheric particles with a porous surface structure very similar to a “hydrangea”, Figure 2.

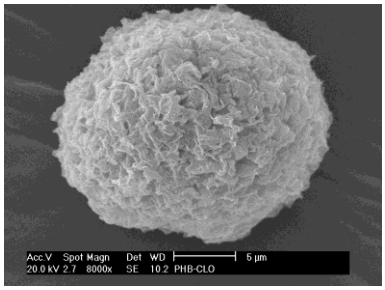

Figure 2. SEM PHB microcapsule with Cloisite clay.

Conclusions: PHB has been described as a good candidate for the manufacture of medicines with prolonged action in the form of polymeric microspheres. This biodegradable polymer, member of the polyhydrixyalkanoates family, offers many advantages over traditional plastics derived from petrochemicals. The properties of PHB can be improved by adding clay to form a compound. In this work were obtained nanocomposite microcapsules PHB / clay, using both hydrophilic and organophilic smectitic clays.

References:

1) Goldberg M, Langer R, Jia X. J. Biomater Sci. Polymer Edn 2007, 18:241-268.

2) Shishatskaya EI, Voinova ON, Goreva AV, Mogilnaya OA, Volova TG. J Mater Sci: Mater Med 2008, 19:2493-2502.

Structural features of copolymers of styrene and macromers of a vegetable oil

Sebastián Gómez Robles[1] and Maria I. Felisberti[2]

Physical-Chemistry Department, Chemistry Institute, State University of Campinas (UNICAMP), P.O. Box 6154, Zip Code 13083-970, Campinas - SP, Brazil

[1] sebrobles@iqm.unicamp.br, [2] misabel@iqm.unicamp.br

Introduction

The search of new polymeric materials from renewable resources is of great technological, scientific and environmental importance, since they can replace petroleum based polymers, and contribute to reducing greenhouse gases and the accumulation of plastic waste. Vegetable oils are renewable resources that mainly consist of triglycerides, whose structural features provide a wide range of synthetic possibilities to obtain several polymers that have shown similar properties to those of conventional polymers from petroleum, as well as the interesting properties such as mechanical damping and shape memory[1, 2]. The rubber seed oil (RSO) is a vegetable oil produced in large quantities in some countries like Brazil and Nigeria, and it does not compete with the food industry. Therefore, this vegetable oil is a very valuable alternative to produce new polymers with significant economic and environmental benefits. In this work we synthesized a series of copolymers of styrene (St) and vinyl macromers of RSO (monomers of high molecular weight).

Material and Methods

Macromers were obtained by synthetic route in two steps: glycerolysis oil followed by maleinization[3, 4]. This route affords macromers with functionality ranging from 2 to 4, which can generate crosslinked polymers useful to design biocomposites[5]. Macromers were characterized by thin layer chromatography (TLC), ^{1}H and ^{13}C NMR, infrared spectroscopy (FT-IR) and Raman Spectroscopy. Copolymers with different compositions were obtained by radical polymerization and characterized by swelling measurements and extraction in toluene, ^{1}H NMR and GPC of soluble fraction, dynamic mechanical analysis (DMA) of the whole materials and thermogravimetric analysis (TG/DTG) (before and after extraction of soluble fraction).

Results and Discussion

The macromers are mainly constituted by monoglyceride bis-maleate half-esters, as determined by spectroscopic characterizations.

Swelling and extraction of soluble fraction experiments of the copolymers show that the increase in St amount in the copolymers favors the incorporation of both monomers in the polymeric network, reducing the soluble fraction. However, the soluble fraction of the copolymer containing 90 % of St increases dramatically.

DMA analysis indicate that this copolymer is heterogeneous and presents at least two phases: one richer in St segments presenting Tg at 70°C and another poor in St at 48°C (Figure 1a).

Moreover, the width of peaks in the tan δ x T curves indicates that these copolymers are capable of absorbing a wide range of frequencies and thus are potentially applicable for soundproofing.

TG/DTG analyses of the copolymers allow concluding that both soluble and insoluble fractions of copolymers have macromers and St units, however a soluble fraction of copolymers with low content of St is richer in macromers.

The global composition of the soluble fraction approaches the structure of polystyrene as St content increases, as determined by ^{1}H NMR (Figure 1b) and GPC. The drastic increase in the soluble fraction of the copolymer containing 90 % St can be explain by the solubilization of the phase riche in St.

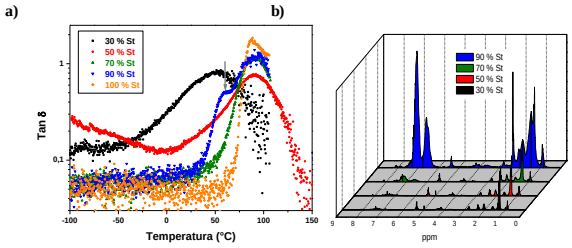

Figure 1. a) Tan δ as a function of temperature for RSO-macromers/styrene copolymers of different compositions. b) ^{1}H NMR spectra for soluble fraction of RSO-macromers/styrene copolymers of different compositions.

Copolymers with St content up to 50 % hydrolytically degrade easily, and copolymers with higher amounts are resistant to hydrolytic degradation. For this reason, the latter polymers are suitable for long term applications such as construction.

Conclusions

The synthesized copolymers possess a complex structure dependent on the composition characterized by a three-dimensional network with oligomers and/or polymers inside it. Phase segregation was observed for copolymers with high content of St. Copolymers have significant differences in their capacity to hydrolytic degradation.

References

1. Güner, F.S.; Yagci, Y.; Erciyes, A.T., Prog. Polym. Sci., **2006**, 31, 633-670.
2. Lu, Y.; Larock, R., ChemSusChem, **2009**, 2, 136-147.
3. Can, E.; Küsefoğlu, S.; Wool, R.P., J. Appl. Polym. Sci. **2002**, 83, 972-980.
4. Mosiewicki, M.; Aranguren, M.I.; Borrajo, J., J. Appl. Polym. Sci., **2005**, 97, 825-836.
5. Raquez, J.-M.; Deléglise, M.; Lacrampe, M.-F.; Krawczak, Prog. Polym. Sci., **2010**, 35, 487-509.

Synthesis and characterization of poly(L-lactide-co-ε-caprolactone) random copolymers

J. Fernández[1], *A. Etxeberria*[2], *E. Zuza*[1], *E. Meaurio*[1], *S. Petisco*[1], *J. R. Sarasua*[1]

[1]School of Engineering, University of the Basque Country (EHU-UPV)
Alameda de Urquijo s/n. 48013 Bilbao, Spain.
[2] Department of Polymer Science and Technology, Institute of Polymer Materials, University of the Basque Country (EHU-UPV), M. de Lardizabal, 3. 20018 Donostia, Spain.

E-mail: covi_bryant@hotmail.com

Introduction. Poly(L-lactide) (PLLA) is one of the most intensively studied biodegradable polymers[1]. However, its high stiffness and rather low deformability limits its potential for numerous clinical uses where elastomeric and shape memory biodegradable materials may be required. This unsuitability might be overcome by blending or copolymerization of PLLA with lower glass-transition temperature polymers such as poly(ε-caprolactone) (PCL). Hence, the synthesis of diblock, triblock, multiblock or random poly(L-lactide-co-ε-caprolactone) (PLCL) copolymers is of great interest.

In this work, random PLCL copolymers at variable temperatures are synthesized by ring-opening polymerization with tin (II) octoate as catalyst/initiator. The reaction by simultaneous addition of the L-LA and ε-CL at different comonomer ratio appears to be a suitable method for the preparation of copolymers with mechanical properties ranging from rigid to elastomeric[2].

Materials and methods. L-lactide monomer (assay > 99,5%) was obtained from Purac (The Netherlands). ε-CL monomer (99% assay) and stannous octoate were supplied by Sigma Aldrich.

The polymerization was carried out in a 50mL flask with magnetic stirring immersed in a controlled temperature oil bath. In each synthesis, predetermined amounts of L-La and ε-CL were simultaneously added and melted. The flask was purged for 30 minutes with a nitrogen stream under the surface of the melt. Then, the stannous octoate was added using a 2000:1 comonomers/catalyst molar ratio. After 24 hours, the product was dissolved in chloroform, precipitated pouring the polymer solution into excess of methanol and then dried under vacuum.

The average molecular weights and polydispersity were determined by Gel Permeation chromatography (GPC). Thermal properties were analysed by differential scanning calorimetry (DSC) at heating rate of 20ºC/min from -90ºC to 210ºC. The composition and microstructure of the copolymers were determined by means of Nuclear Magnetic Resonance spectroscopy[3] (^{1}H –NMR and ^{13}C NMR).

Tensile tests were performed with an Instron testing machine at a crosshead displacement rate of 5mm/min. The specimens for tensile tests were obtained from films of the synthesized PLCL. 250µm films were obtained by casting the chloroform solutions of the polymers followed by pressure melting at 175ºC and water quenching in order to achieve an amorphous state.

Results and discussions. Stannous octoate catalyst in cyclic esters polymerization is considered more effective at 120-150ºC. Therefore, ring-opening polymerization was carried out at 120ºC, 130ºC, 140ºC and 150ºC. On the other hand, feed monomer composition of the synthesized copolymers was 90:10, 80:20, 75:25 and 70:30 (mass:mass ratio of LA to CL) on several mixtures.

From the experiences developed varying the added catalyst it can be concluded that the highest conversions and molecular weights were obtained for a 2000:1 comonomers/catalyst molar ratio. As observed, the synthesis of random PLCL using stannous octoate follows the mechanism proposed by Kowalski et al[4].

Increasing the LA content in the feed, the glass transition temperature (T_g) and the melting temperature (T_m) approached to that of PLLA homopolymer. The crystallinity degree was also increased. The mechanical properties evolved in the same way towards the PLLA character, observing an increase in elastic modulus increase and a decrease in deformation at break.

Higher molecular weights were obtained at 130ºC and 140ºC. Furthermore, both the number and weight average molecular weights of synthesized PLCL copolymers increased at higher LA:CL ratio, probably due to the higher reactivity of LA units during copolymerization.

At lower temperatures a predominant formation of copolymers with moderate block character (multiblock character) was found; the number average sequence lengths were longer and the randomless character was closer to 0, the value corresponding to a pure block copolymer.

Acknowledgements. The authors are thankful to the Basque Government, Department of Education, Universities and Research for funds (GIC10/152-IT-334-10) and to the MICINN (BIO2010-21542-C02-01).

References

1.- R. Auras, B. Harte, S. Selke, Macromolecular Bioscience, 4, 835-864 (2004)
2.- X. L. Lu, W. Cai, Z. Y. Gao, Journal of Applied Polymer Science, 108, 1109-1115 (2008)
3.- J. Kasperczyk, M. Bero, Makromol. Chem, 192, 1777-1787 (1991)
4.- W.C. L, W.B L, 4.- A. Kowalski, A. Duda, S. Penczek, Macromolecules, 33, 7359-7370 (2000)

Thermosets from methyldiphenolic acid-based benzoxazine and diphenolic acid mixtures

Zuñiga, C.; Lligadas, G.; Ronda, J.C.; Galià, M.; Cádiz, V.

Department of Analytical Chemistry and Organic Chemistry, Rovira i Virgili University, Marcel.li Domingo s/n, 43007 Tarragona (Spain)

virginia.cadiz@urv.cat

Introduction

Over the last decade, an interesting addition cure phenolic resin, namely benzoxazine, has attracted much attention of the research community because of its unique advantages over most of the known polymers.

The chemistry of benzoxazines is responsible for a number of inherent processing advantages, including low melt viscosity, no harsh catalyst required, no volatile release during cure and minimal cure shrinkage. They also have a good thermal stability that is demonstrated by their high glass transition temperatures, degradation temperatures, and char yields. A unique combination of intramolecular and intermolecular hydrogen bonding also contributes to the properties of polybenzoxazines.

Although, polybenzoxazines offer a variety of advantages, pure polybenzoxazine-based polymers also suffer number of disadvantages too. The disadvantages of the typical polybenzoxazines are the high temperature needed for complete curing and the brittleness of the cured materials that can sometimes limit their potential applications. To properly address these issues and overcome the associated disadvantages, one of the most succesful strategies is the preparation of monomers with one additional functionality.[1] The crosslinking densities of polybenzoxazine homopolymers are believed to be considerably lower than those of ordinary thermosetting resins. The tightening of the network structure has been achieved by introducing additional crosslinkable sites.

Until now, benzoxazine monomers are synthesized either in solution or by a melt-state reaction using a combination of petroleum-based phenolic derivatives, formaldehyde and primary amines. The scarcity of nonrenewable resources encouraged the scientific community to develop and commercialize new biobased products that can alleviate the wide-spread dependence on fossil fuels and, enhance security, the environment and the economy.[2]

In this work, we studied the thermal behaviour of mixtures of renewable diphenolic acid (DPA) and its methylesterbenzoxazine derivative (MDP-Bz). The presence of a carboxylic group in DPA monomer should lower the high temperature needed to complete curing of these benzoxazines and serve as additional crosslinking site.

Results and Discussion

Recently, we have synthesized the ester derivative based benzoxazine, MDP-Bz, from renewable DPA, with a similar structure to bisphenol A (BPA), by traditional approaches.[3] Polybenzoxazines from MDP-Bz showed higher Tg 270 ºC, and higher crosslinking density compared to BPA-Bz, due to the transesterification that extensively takes place during the curing reaction.

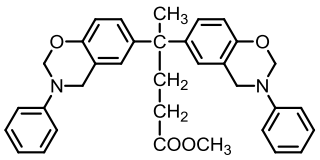

MDP-Bz

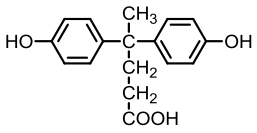

DPA

The curing behaviour of mixtures of MDP-Bz and 0, 1, 5, 10 y 25% (w/w) of DPA has been studied by DSC. A decrease of up to 80 ºC was observed for the mixture with higher DPA content. This catalytic effect can be related to the presence of free carboxylic acid groups, as using the methyl ester of DPA instead of DPA the decrease in the curing temperature is much lower.

To evaluate the thermal and mechanical properties of the resulting materials, rectangular samples with dimensions of 30 x 7 x 0.5 mm^3 were prepared by compression molding using either the free resin mixture or a glass fiber embeded mixture. The curing cycle was fixed according to DSC data. The resulting materials were orange rigid solids. In the case of free resin mixtures brittle materials were obtained but not in the glass fiber reinforced composites.

The dynamic mechanical and thermogravimetric properties of the polybenzoxazines were investigated.

The dynamic mechanical behaviour of the cured benzoxazine resins was obtained as a function of the temperature beginning in the glassy state of each composition to the rubbery plateau of each material. The crosslinking density of the polybenzoxazines can be estimated from the plateau of the elastic modulus in the rubbery state. The results indicate a similar crosslinking density and Tg's above 270ºC.

To determine the thermal stability and the decomposition behaviour, thermogravimetric analysis were carried out under nitrogen and air atmosphere. Materials showed thermal stability below 300 ºC and the degradation takes place in one main step. Samples have char yields, at 800 ºC, under nitrogen of ca. 30%.

References

1. Yagci, Y.; Kiskan, B.; Ghosh, N.N. J Polym Sci Part A: Polym Chem 2009, 47, 5565-5576.
2. Gandini, A.; Belgacem, M. N. Monomers, Polymers and Composites from Renewable Resources; Elsevier: Oxford, UK, 2008.
3. Zuñiga, C.; Larrechi, M.S.; Lligadas, G.; Ronda, J.C.; Galià, M.; Cádiz, V. J Polym Sci Part A: Polym Chem 2011, 49, 1219-1227.

Polybenzoxazine foams from renewable diphenolic acid

Zúñiga, C.; Lligadas, G.; Ronda, J.C.; Galià, M.; Cádiz, V.

Department of Analytical Chemistry and Organic Chemistry, Rovira i Virgili University, Marcel.li Domingo s/n, 43007 Tarragona (Spain)

camilojavier.zuniga@urv.cat

Introduction

Polymeric foam is a two-phase material consisting of gas dispersed in a continuous polymer matrix. This material is important and useful due to its strength-to-weight ratio. Furthermore the chemical resistance, cushioning performance, shock absorption, and thermal insulation are also prominent characteristics of this type of material.[1]

In many specific applications the fire resistance properties have to be considered. Although polyurethane, polyethylene and polystyrene foams have good mechanical and thermal properties they are not appropriate as they are easily burned. Among the inexpensive commercial polymeric foams, phenolic foam is the preferred material when fire resistance is critical. Phenolic foam also has low flammability, a low peak heat release rate, no dripping during combustion, and low smoke density, so they are suitable in these applications.

Polybenzoxazine is a newly developed class of phenolic resins derived from ring opening polymerization. Polybenzoxazine can overcome the drawbacks of conventional phenolic resin synthesis by eliminating the release of any byproducts during the curing reactions, the need of strong acid as catalyst and for toxic materials. Furthermore, polybenzoxazine has many advantageous characteristics compared with the traditional phenolic resin, such as high thermal stability, an excellent mechanical properties, easy processibility, low water absorption and near zero shrinkage after polymerization.[2]

This study deals with a new type of phenolic foams derived from a polybenzoxazine obtained from the non-toxic renewable diphenolic acid (DPA).

Results and Discussion

Recently, we have synthesized the benzoxazine monomer DPA-Bz, from renewable DPA by the traditional approach.[3]

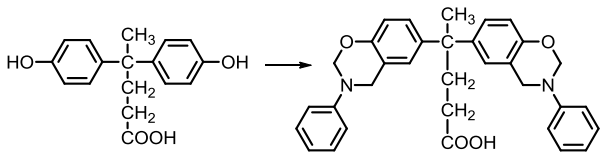

DPA DPA-Bz

Curing studies of this DPA-Bz showed the existence of esterification reaction between the carboxylic groups and the phenolic OHs, formed during the ring opening of oxazines. Thus, a highly crosslinked system with Tg of 208 ºC was obtained. These studies also showed that when curing was carried out without pressure a extensive foaming process occurred, probably due to the partial decarboxylation of the sample.

According to this behaviour, in a first step DPA-Bz was partially polymerized under pressure 6 h at 140 ºC and 2 h at 160 ºC, and further heated up to 220 ºC in air atmosphere to obtain a rigid foam. The sample incompletely cured showed by DSC a Tg at 145 ºC followed by an endothermic peak at 211 ºC that could be attributed to a decarboxylation reaction that promotes the foaming. Both thermal processes were also detected by DMTA as two different slopes in the loss of storage modulus plot versus temperature. This can be also observed in the Tan δ plot which showed two maxima at 178 ºC corresponding to the Tg, and at 206 ºC corresponding to the foaming process.

The Tg's of the completely cured polybenzoxazines were similar, with values of 207 ° C for the unfoamed polybenzoxazine and 200 ºC for the foam polybenzoxazine respectively, indicating a similar final crosslinking degree. However the density of the completely cured material was 1221 ± 0.6 Kg/m^3 whereas the density of the foam material was 48.6 ± 0.9 Kg/m^3. The decrease of the density corresponds to the resulting gases developed during the foaming process which increase the volume of the original sample around 25 times under the studied conditions.

The visual examination of a cross-section of the foam was carried out using ESEM. An examination of the foam revealed well-foamed structure. The foam showed a fine heterogeneous structure of relatively cell roundness with interconnected pores. The image analysis showed the cell size distribution of the foam which reveals that the most of the cells have a size between 20 and 100 μm. These results indicate that the obtained benzoxazine foam is much lighter than those obtained from similar benzoxazines where a foaming agent was added.[4]

It was observed that temperature and heating rate are significant parameters to control the foam morphology. As the higher these parameters the lower foam density.

References

1. Rodríguez-Perez, M.A. Adv. Polym. Sci. 2005, 184, 97-126.
2. Yagci, Y.; Kiskan, B.; Ghosh, N.N. J Polym Sci Part A: Polym Chem 2009, 47, 5565-5576.
3. Zúñiga, C.; Larrechi, M.S.; Lligadas, G.; Ronda, J.C.; Galià, M.; Cádiz, V. J. Polym. Sci. Part A: Polym Chem 2011, 49, 1219-1227.
4. Lorjai, P.; Wongkasemjit, S.; Chaisuwan, T. Mat. Sci. Eng. A 2009, 527, 77-84.

Aminoalkylphosphonic Acids And Glycylaminoalkylphosphonic Acids As Antibacterial Additives In Textile Chemistry

Marcin H. Kudzin,[a] *Zbigniew H. Kudzin*[b] *and Jozef Drabowicz*[c,d]

[a]Textile Research Institute, Brzezinska 5/15, Lodz 92-103, Poland;
[b] Faculty of Chemistry, University of Lodz, Tamka 12, Lodz 91-403, Poland;
[c]Centre of Molecular and Macromolecular Studies, Polish Academy of Sciences, Sienkiewicza 120a, Lodz 90-363, Poland;
[d]Jan Dlugosz University, Department of Chemistry and Environment Protection, Armii Krajowej 13/15, Czestochowa, Poland

E-mail: marcinkudzin@O2.pl.

Introduction

Aminoalkylphosphonic acids (AA^P) belong to the class of phosphoroorganic compounds of multidisciplinar importance due to their biological activity and chelating ability [1].

Materials and Methods

Recently we have published on the *N*-acylation [2] and chloroacetylation [3] of 1-aminoalkylphosphonic acids AA^P ($AA^P \rightarrow$ Mca-AA^P) and conversion of Mca-AA^P into glycylo-phosphonic peptides (Scheme 1: routes ***B1-B4***) [4].

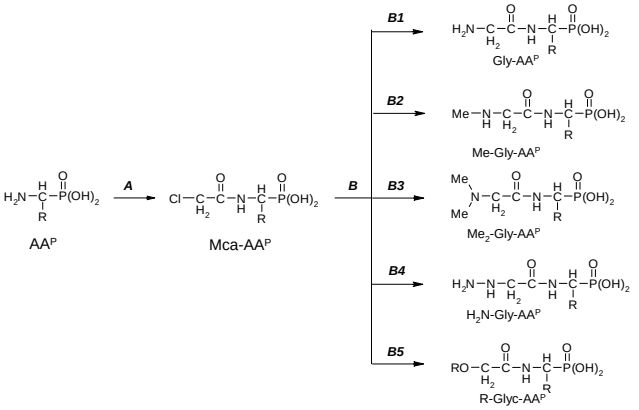

In this communication we would like to present our results on the biological properties of representative phosphonopeptides depicted on the Scheme 1.

Conclusions

Since compounds Mca-AA^P react also with alcohols (Scheme 1, route ***B5***), they can be consider as reagents for cotton modification.

References

[1] Kukhar, V.P.; Hudson, H.R. (eds.) In Book: *Aminophosphonic and aminophosphinic acids. Chemistry and biological activity*. Wiley& Sons Ltd: Chichester, New York, Weinheim, Brisbane, Singapore, Toronto, **2000**.

[2] Kudzin, Z. H.; Depczyński, R.; Andrijewski, G.; Drabowicz, J. Aminoalkanephosphonates. 1-(*N*-acylamino)alkanephosphonates. The synthesis via *N*-acylation of 1-aminoalkane-phosphonic acids. *Pol. J. Chem.* **2005,** *79***,** 529-539.

[3] Kudzin, Z. H.; Depczyński, R.; Kudzin, M. H.; Drabowicz, J.; Łuczak, J. 1-(*N*-Trifluoroacetyl-amino)alkylphosphonic acids. Synthesis and properties. *Amino Acids* **2007**, *33*, 663-667.

[4] Kudzin, Z. H.; Depczyński, R.; Kudzin, M. H.; Drabowicz, J. 1-(*N*-Chloroacetylamino)alkyl-phosphonic acids - synthetic precursors of glycylophosphono-peptides and related compounds. *Amino Acids* **2008**, *34*, 163-168.

[5] Kudzin, M. H.; Kudzin, Z. H.; Drabowicz, J. Thioureidoalkanephosphonates in the synthesis of 1-aminoalkylphosphonic acids. The Ptc-Amino-phosphonate method. *Arkivoc*, **2011** (in press).

Amphiphilic Poly(4-vinylpyrine) (P4VP) Block Copolymer Micelles for Metal Binding

Nurulsaidah Abdul Rahim, Fabrice Audoin, Johannes G.Vos, Andreas Heise

Dublin City University, School of Chemical Sciences, Polymer Chemistry Group, Glasnevin, Ireland

nurulsaidah.abdulrahim2@mail.dcu.ie

INTRODUCTION

Block copolymers (BC) with metal binding capability have a great potential as template for nanoparticles and catalytic process. Due to their potential to control molecular weight (Mn) and polydispersity index (PDI) controlled radical polymerisation is often applied in synthesis block copolymer.[1] For example, nitroxide mediated polymerisation (NMP) is effective method in controlled radical polymerisation of amine-containing vinyl monomers such as 4-vinylpyridine.[2] Here, we used SG1-alkoxyamine as unimolecular initiator in the synthesis of poly(4-vinylpyridine) (P4VP) and further chain extension with methyl methacrylate (MMA).

EXPERIMENTAL METHODS

P4VP was synthesised in DMF solution at 110°C with BlocBuilder (MAMA-SG1). Then, P4VP was used as macroinitiator for polymerization of MMA to produce block copolymer (P4VP-*b*-PMMA) at 90°C (Scheme1). Polymers were characterized by NMR, GPC in DMF and IR. For micelle formation, P4VP-b-PMMA was dissolve in THF solution and the size particles was analysed by dynamic light scattering.

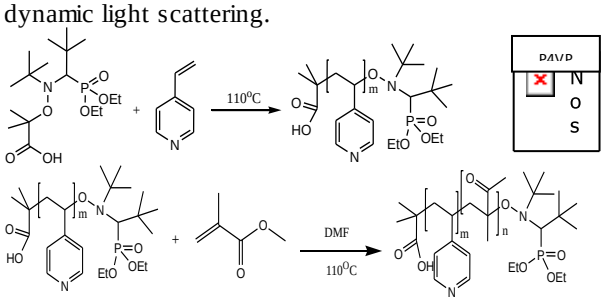

Scheme 1: Polymerisation of P4VP (*top*). Polymerisation of P4VP-*b*-PMMA (*bottom*).

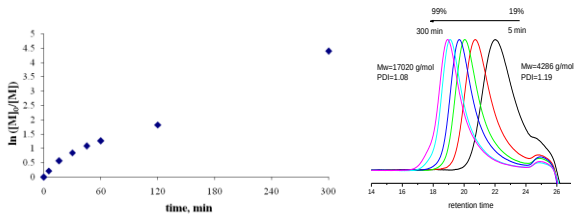

Figure 1. Evolution of ln ($[M]_0/[M]$) vs time of P4VP (*left*). SEC chromatograms of P4VP (*right*).

RESULTS AND DISCUSSION

P4VP was synthesised successfully by MAMA-SG1 as initiator with high monomer conversion to controlled molecular weight (17000 g/mol) and narrow polydispersity index (1.08). The kinetic plot ln ($[M]_0/[M]$) vs. reaction time shows a linear increase. (see Figure 1). Block copolymer were synthesised from the P4VP macroinitiators by chain extension with PMMA with and without addition of 10 % styrene (Table 1). The latter improved the monomer conversion.[3]

$P4VP_{200}$-$PMMA_{95}$ spontaneously associates into spherical inverse micelles in THF consisting of soluble PMMA shell and insoluble P4VP core at critical micelle concentration (CMC) of 0.1mg/mL with average diameter, 70 nm (Figure 2).

Table 1. Molecular weight, Mn and Polydispersity index (PDI) of P4VP-b-PMMA

Sample	Mn NMR g/mol	Mn GPC[a], g/mol	PDI[a]
P4VP-b-PMMA	26000	33000	1.14
P4VP-b-PMMA + 10% styrene	22000	28000	1.10

[a] measured by DMF GPC with Multy angle light scattering detection.

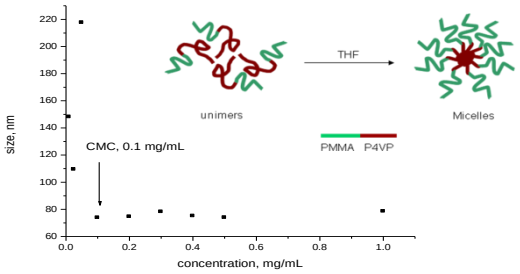

Figure 2. Plot of hydrodynamic diameter versus the concentration of $P4VP_{200}$-$PMMA_{95}$measured by dynamic light scattering at 90°C

CONCLUSION

In this work we successfully synthesised P4VP in high conversion with controlled Mn and narrow PDI by NMP. These macroinitiators were extended by PMMA to yield amphiphilic block copolymers capable of micelle formation in THF. Future work will emphasise on metal binding of the micelles.

REFFERENCES

1. Braunecker, W. A; Matyjaszewski, K. *Prog. Polym. Sci.* **2007**, *32*, 93–146.

2. Mather, B. D.; Baker, M. B.; Beyer, F. L.; Berg, M. A. G.; Green, M. D.; Long, T. E. *Macromolecules* **2007** *40*, 6834-6845.

3. Nicolas, J.; Mueller, L.; Dire, C.; Matyjaszewski, K. Charleux, B. *Macromolecules* **2009**, *42*, 4470-4478.

ACKNOWLEDGEMENT

This work was conducted under the Science Foundation Ireland (SFI) funded Principle Investigator Award 07/IN1/B1792. AH is a SFI Stokes Senior Lecturer (07/SK/B1241). N.A.R. acknowledges the financial support under MOHE and UPSI, Malaysia.

Sunflower Oil-modified Polyester Synthesis by Ring Opening Polymerization and Its Use in Organic Coatings

Çiğdem Taşdelen-Yücedağ, *A. Tuncer Erciyes*[*]

Istanbul Technical University, Faculty of Chemical and Metallurgical Engineering, Chemical Engineering Department, 34469, Maslak, Istanbul / Turkey

e-mail: erciyes@itu.edu.tr

Introduction

Triglyceride oils are the most important class of renewable sources since they have been used in the production of biodegradable polymer products[1]. In this study a sunflower oil-modified polyester (SOMPE) was prepared by the ring opening polymerization of ε-caprolactone in the presence of partial glyceride which is used as an initiator. Thus the obtained polyester was combined with benzoxazine monomer and the resulting product was examined in view of film properties.

Materials and Methods

SOMPE was synthesized by ring opening polymerization of ε-caprolactone (ε-CL) (Aldrich, 97%) initiated with partial glycerides of sunflower oil in the presence of tin (II) 2-ethylhexanoate (Aldrich, 95%) as catalyst (Scheme 1). The reaction was carried out at 130°C and then stopped after 24 h, by cooling. The product was isolated by precipitation of the reaction mixture from methanol and dried under vacuum at 30°C for 24 h.

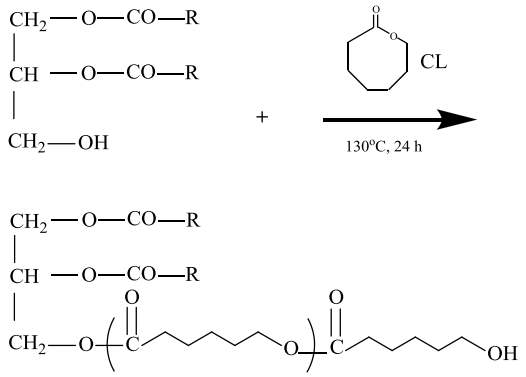

Scheme 1. The ring opening polymerization of ε-caprolactone initiated by partial glyceride.

The hydroxy-functional 1,3-benzoxazine (HFB-a) (Scheme 2) was synthesized according to the reported method[2].

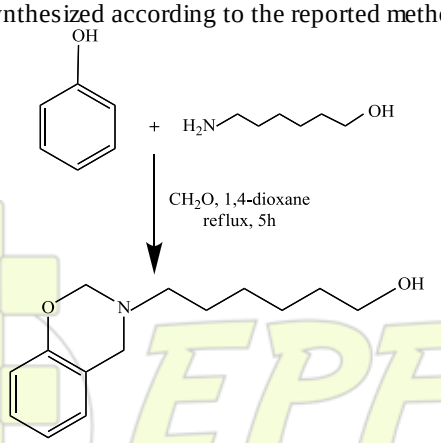

Scheme 2. Synthesis of hydroxy-functional 1,3-benzoxazine.

Results and Discussion

In the applied approach for the oil modification, the polyester chains were combined with the oil moieties through the hydroxyl groups of the partial glycerides. In order to confirm that partial glycerides were linked to the polyester segments, a reference homopolyester sample was prepared by water initiated ring opening polymerization of ε-caprolactone. The structure of SOMPE was well evidenced by comparing its ^{1}H-NMR spectrum with that of reference homopolyester sample. In the characterization studies together with ^{1}H-NMR measurements, FT-IR and GPC analysis were carried out. Since the film of SOMPE was found to be soft, SOMPE and HFB-a were combined with 2,4-toluene diisocyanate (TDI) through their hydroxyl groups (SOMPE/HFB-a). SOMPE/HFB-a was mixed with HFB-a in various weight ratios and cured. The cured film properties were investigated in order to find the optimum SOMPE/HFB-a ratio.

Conclusions

In the present study, a polyester modified with triglyceride oil was obtained by the ring opening polymerization of ε-caprolactone. The advantage of this process is the combining of oil and polyester segments during the ring opening polymerization without any additional application. It was understood that SOMPE could be used in order to improve the film properties of benzoxazine which can be used as a organic coating material.

References

[1]Güner, F.S., Yağcı, Y., and Erciyes, A.T., 2006. Polymers from triglyceride oils, *Progress in Polymer Science*, **31,** 633-670.

[2]Tüzün, A., Kışkan, B., Alemdar, N., Erciyes, A.T., and Yağcı, Y., 2010. Benzoxazine containing polyester thermosets with improved adhesion and flexibility, *Journal of Polymer Science: Part A: Polymer Chemistry*, **48,** 4279-4284.

Keywords: Sunflower oil-modified polyester, Poly(ε-caprolactone), ring opening polymerization, benzoxazine

Synthesis and optical, electrochemical and electroluminescence properties on new series of copoly-2,7-fluorene-1,4-(2/3-amino)benzene

A. Calero[a],*[a] R. Vazquez-Guilló[a], A. Salinas-Castillo[a], F. Montilla[b], C. Coya[c], A.L. Alvarez[c]

C. R. Mateo[a] and R. Mallavia[a]

r.mallavia@umh.es

[a]Instituto de Biologia Molecular y Celular, Universidad Miguel Hernández, Elche, 03202, Spain
[b]Departamento de Química Física, Universidad de Alicante, 03080. Alicante. Spain
[c]Depto. Tecnología Electrónica, Universidad Rey Juan Carlos, Mostoles, 28933, Spain.

Introduction

Conjugated polymers bearing reactive functional groups have been attracting interest and significant attention as promising components in luminescent optoelectronic devices and optical sensor (1-3). The great synthetic versatility of organic polymers makes them excellent candidates for studying the effects of structural modifications in the material properties. For example, π-conjugated polymers having a sulfo group, carboxylic group or hydroxy group have been reported. However, π-conjugated polymer having a $-NH_2$ side group has received less attention (4, 5), in spite of the presence of a tremendous number of reports about polyanilines. In this work, aniline units were introduced into polyfluorene backbone; by adjusting the monomer feed ratios (**Scheme 1**).

Results and Discussion

Synthesis and polymer characterization of **P1-P6** was done by conventional techniques, previously used in our lab (6). Stoichiometric copolymers poly[9,9-bis(hexyl-fluoren-2,7-diyl)-alt-co-(2/3-aminobenzen-1,4-diyl)] were synthesized via Suzuki coupling with air stable palladium (II) catalyst. All data were collected according to the typical co-polyfluorene structures and the results obtained in the polymer composition have been compared and contrasted by NMR and FTIR. Molecular weights were obtained by GPC calibration based on polyfluorene following the procedure described above (6). Special attention has been performed in the optical and electrochemical characterization of these polymers, in solution and solid films. Significant changes have been noted in the physicochemical parameters (wavelength absorption and emission, quantum yields and, also, redox potential) due to the presence of acceptor groups. It has been established electrochemical behavior acceptor ring in terms of its content in the final polymer. Stabilized cyclic voltammograms of **P1-P6** polymers deposited onto ITO glasses were obtained for cathodic (p-doping) and anodic branches (n-doping).

All the polymers present reversible p and n doping processes, except for polymer **P1**, where we observe only p-doping. Devices were fabricated using the following configuration: ITO/ PEDOT: PSS (50 nm)/ active polymer (~100 nm)/ Ca (20 nm)/ Al. Electroluminescence (EL) and current−voltage (I−V) characteristics of the synthesized polymers **P3** and **P5** into luminescent devices are encouraging. Thus, **P5** present maxima efficiency of 0.084 Cd/A (600 μA, 5,2 V), brightness of 6.38 Cd/m^2, and CIE coordinates (0.1758;0.1059) , without degradation colour while **P3** present change in CIES coordinates, low colour stability (0.2003;0.2011)→(0.1915;0.1725), as show in **figure 1**.

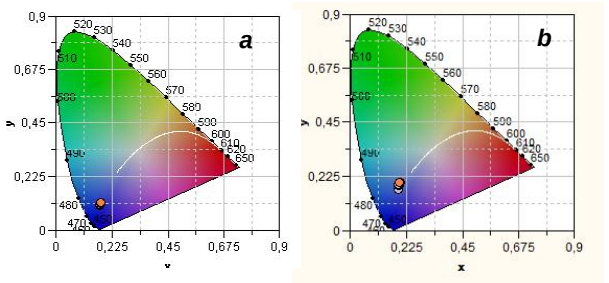

Figure 1. Colour evolution of two copolymer devices a) **P5** (1%-NH_2) and **P3** (10%-NH_2).

Acknowledgments: This work was supported by research project MAT-2008-05670 and PT2009-002 of MICNN.

References:

(1) Muller, C. D.; Falcou, A.; Reckefuss, N.; Rojahn, M.; Wiederhirn, V.; Rudati, P.; Frohne, H.; Nuyken, O.; Becker, H.; Meerholz, K. *Nature* **2003**, 421 (6925), 829−833.
(2) Duarte, A., Pu, K-Y, Liu, B. and Bazan, G.C. *Chem. Mat.* **2010**, *22*, 6736-6741.
(3) Thomas, S.W., Joly, G.D. and Swager, T.M. *Chem. Rev.* **2007**, *107*, 1339-1386.
(4) Zhang, Q. T.; Tour, J. M. *J. Am. Chem. Soc.* **1998**, 120, 5355.
(5) Yamamoto, T.; Muramatsu, Y.; Lee, B.-L.; Kokubo, H.; Sasaki, S.;Hasegawa, M.; Yagi, T.; Kubota, K. *Chem. Mater.* **2003**, 15, 4384.
(6) R. Molina, S. Gomez-Ruiz, F. Montilla, A. Salinas-Castillo, S. Fernandez-Arroyo, M. Ramos, V. Micol and R. Mallavia. *Macromolecules*. **2009**. 42 (15): 5471-7.

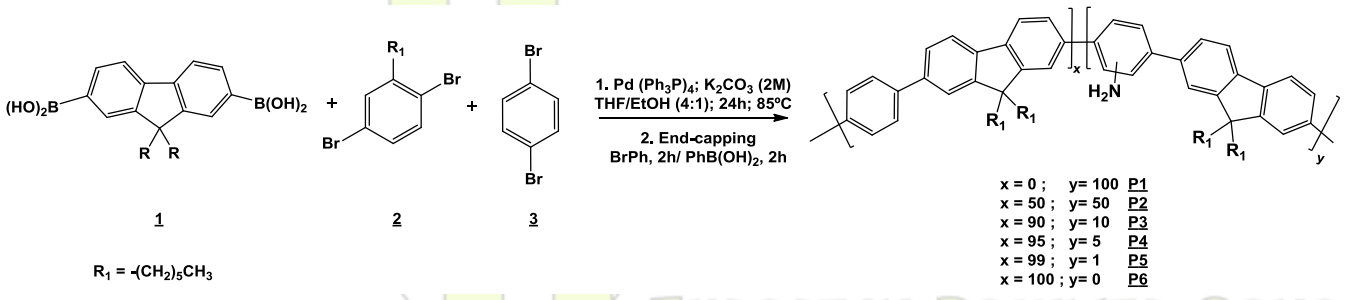

Scheme 1 Synthesis and representative structure of the copoly-2,7-fluorene-1,4-(2/3-amino)benzene.

Metathesis degradation of natural rubber in the presence of avocado and mandarin oils using ruthenium alkylidene catalysts

Araceli Martínez[1], *Mikhail A. Tlenkopatchev*[1]

[1] Instituto de Investigaciones en Materiales, Universidad Nacional Autónoma de México, Apartado postal 70-360, CU, Coyoacán, México D.F. 04510, México

tma@servidor.unam.mx

Introduction

In recent years, bio-based products have attracted much attention since these resources are renewable and can be used for energy, chemicals and other important materials production [1]. Thus, bio-based products such as *D*-limonene from citrus peel, soybean and avocado oils, can undergo metathesis reactions due to they contain carbon-carbon double bonds in their structures.

It has been reported that D-limonene and β-pinene have been used as chain transfer agents (CTAs) in order to obtain telechelics via ring opening metathesis polymerization (ROMP) of cycloolefins as well as cross metathesis degradation of natural rubber (NR) using ruthenium alkylidene catalysts[2-4].

The main aim of this research is focused on the metathesis degradation of natural rubber in the presence of avocado and mandarin oils as CTAs and using well-defined alkylidene ruthenium catalysts $(PCy_3)_2(CI)_2Ru{=}CHPh$ (**I**) and (1,3-dimesityl-4,5-dihydroimidazol-2-ylidene) $(PCy_3)CI_2Ru{=}CHPh$ (**II**).

Materials and Methods

NR was obtained from fresh field latex of AGROS (Guatemala) and used without further purification (M_n = 1.7x10^6, *MWD* = 1.5). Avocado and mandarin oils (NATURAL OILS & CHEMICAL) and alkylidene ruthenium catalysts **I** and **II** were used as received. 1,2-dichloroethane (Baker > 97%) was distilled over CaH_2 prior to use.

Metathesis degradations of NR (3.0 g) using avocado and mandarin oils as CTAs (***Scheme 1***) were carried out under a dry nitrogen atmosphere, in a reactor stirred magnetically, at 45°C. Avocado and mandarin oils (CTAs) were used in molar ratios of NR/CTA = 3:1 and 1:1 respectively. The catalyst **I** or **II** was added in molar ratios ranging from NR/catalyst = 250 to 1,000. Adding ethyl vinyl ether (0.3 mL, 3 mmol) under a nitrogen atmosphere terminated the reactions. The products were dried under a vacuum and characterized by ^{1}H-NMR and GPC.

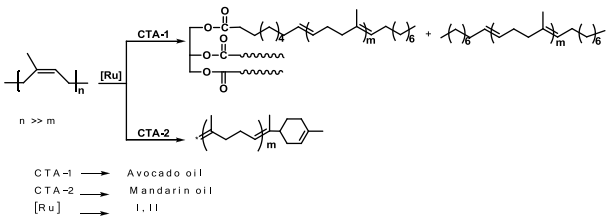

***Scheme 1*. Metathesis degradation of NR using avocado and mandarin oils as CTAs.**

Results and Discussion

Isolated oligomers were obtained in yields ranging from 50 to 80% when catalyst **I** was used whereas catalyst **II** produced oligomers in high yields (80-95%). Molecular weights were controlled primarily by the NR/CTA molar ratios giving values around M_n x 10^3 when molar ratios of 3:1 and 1:1 were used for avocado and mandarin oils, respectively.

Conclusions

Both, avocado and mandarin natural oils were successfully used as chain transfer agents in the metathesis degradation of natural rubber leading to the formation of oligomers with molecular weight distributions close to two. Catalyst **II** was able to depolymerized NR completely in comparison with catalyst **I** when the reactions were conducted in the same period of time.

Acknowledgements.

Financial support from the National Council for Science and Technology of Mexico (CONACYT) (PhD Scholarship to S.G.) is gratefully acknowledged. We thank CONACyT-SEMARNAT (contract 23432) and ICyTDF (contract 4312) for generous support to this research. We are grateful to Alejandrina Acosta, Gerardo Cedillo and Salvador López Morales for their assistance in NMR and GPC.

References

[1]- P. Gallezot, *Catal. Today* **2007**, 121, 76-91

[2]- R.T. Mathers, K.C. McMahon, K. Damodaran, C.J. Retarides and D.J. Kelley *Macromolecules* **2006**, *39*, 8982-8986.

[3]- R.T. Mathers, K. Damodaran, M.G. Rendos and M.S. Lavrich, *Macromolecules* **2009**, *42*, 1512-1518

[4]- S. Gutiérrez and M.A. Tlenkopatchev, *Polym. Bull.* In press.

Thiol-yne coupling to undecylenic acid derivatives. Synthesis of polyurethanes.

Beyazkilic, Z.; González-Paz, R.J; Lligadas, G.; Ronda, J.C.; Galià, M.; Cádiz, V.

Department of Analytical Chemistry and Organic Chemistry, Rovira i Virgili University, Marcel.li Domingo s/n, 43007 Tarragona (Spain)

zeynep.beyazkilic@urv.cat

Introduction

Plant oils and thereof derived fatty acids are important renewable raw materials for polymer chemistry.[1] Especially, castor oil is a very versatile renewable feedstock for all kinds of polymeric materials. One of the commercially available castor oil derived platform chemicals, undecylenic acid, was recently used to prepare a great variety of polymers, thus demonstrating its broad range of application possibilities. [2]

Whilst alkenic fatty acids occur abundantly in nature, alkynic fatty acids are rare. However, alkynic fatty acids are accessible in good yield by bromine addition and dehydrobromination from alkenic fatty acids. Alkynic fatty acids are furthermore prepared and used as intermediates in fatty acid synthesis, because the acetylene unit allows the easy assembly of building blocks and the stereospecific hydrogenation to *cis*- or *trans*-double bonds. The triple bond in alkynes allows C-C bond formations and functional group interconversions that supplement those at the double bond. [3]

In recent years, the radical mediated thiol-yne coupling procedure was introduced. The beauty of this thiol-yne coupling procedure is that it combines the readily available building blocks of the copper (I) azide-alkyne click reaction and the thiol-ene chemistry to create multifunctional materials under mild reaction conditions: two thiols are coupled to one alkyne using either a chemical radical source, UV irradiation, or sunlight at ambient temperature. The radical mechanism of the thiol-yne reaction makes it very robust and versatile method that tolerates a variety of functional groups. [4,5]

In this work, we take advantage of this reactivity to synthesize 10-undecinoic acid based diols as polyurethane precursors.

Results and Discussion

10-methyl undecynoate was obtained in moderate yield from the corresponding fatty acid by bromination, dehydrobromination, and esterification using well established procedures.

Our research applies the photoinitiated thiol-yne click chemistry to this alkine using mercaptoethanol and 2,2-dimethoxy-2-phenylacetophenone (DMPA) as initiator to obtain the ester-containing diol **1**. Moreover, the reduction of ester group yields a triol **2**. The chemical structures of these products were confirmed by NMR and FTIR.

To prepare a reactive vinylsulfide-containing diol **3**, we studied the mono thiol-yne addition. Thus, 1- hexyne, 1-octyne thiol and benzene thiol were used as model compounds. It was observed that an excess of alkyne is necessary to obtain the vinylsulfide in high yields.

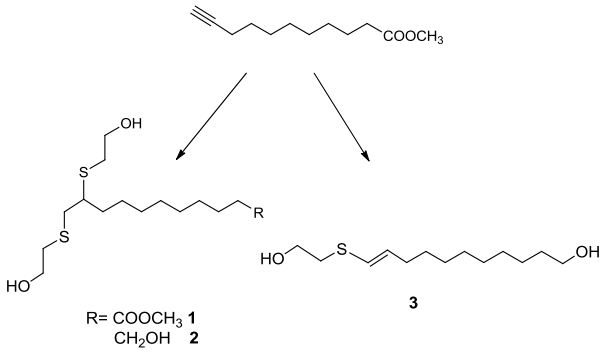

Functionalized linear polyurethanes have been obtained from **1** and **3** and thermosetting polyurethanes have been obtained from **2**. Linear polymers were characterized by NMR spectroscopy and molecular weights could be determined by SEC**.** The thermal and mechanical properties of linear and thermosetting polymers have been investigated. Preliminary studies on the functionalization of vinylsulfide containing linear polymers are also reported.

References

1. Xia, Y.; Larock, R.C . Green Chem, 2010, 12, 1893-1909
2. Mutlu, H.; Meier M.A.R. Eur. J. Lipid Sci. Technol. 2010, 112, 10-30
3. Augustin, K.E., Schäfer, H.J. Eur. J. Lipid Sci. Technol. 2011, 113, 78-82
4. Hoogenboom, R. Angew. Chem. Int. Ed. 2010, 49, 3415-3417.
5. Lowe, A.B.; Hoyle, C.E.; Bowman, C.N. J. Mater. Chem, 2010, 20, 4745-4750.

Phosphorus-containing high oleic sunflower oil flame retardant thermosets

Moreno, M., Lligadas, G, Ronda, J.C.; Galià, M.; Cádiz, V.

Departament de Química Analítica i Química Orgànica, Universitat Rovira i Virgili, Carrer Marcel·lí Domingo s/n, Campus Sescelades, 43007 Tarragona, Spain

e-mail: maryluz.moreno@urv.cat

Introduction

Recently, the use of plant oils as renewable feedstock for the development of designed polymeric materials has received particular attention due to environmental and economic concerns.[1] Synthetic polymeric materials are used in many areas and thus the fire hazards associated with the use of these materials are of great concern for both users and manufacturers. Plant oil based materials, just than many other currently used polymeric materials, are flammable, being this flammability a shortcoming in some applications. According to the sustainability issues, the design of a flame retardant material must preserve the efficacy of function while reducing risk and toxicity to human health and environment. Phosphorus based polymers are a well established class of flame retardant material which are preferred to the widely applied halogenated flame retardants due to health and environment reasons.[2]

The main component of the triglyceride vegetable oils are saturated and unsaturated fatty acids. The reactivity of the internal double bonds is limited and much work has been done on the functionalization of triglycerides to obtain useful monomers.[3] We described a new environmentally friendly route to obtain a enone-containing triglyceride from high oleic sunflower oil. [4] This derivative can react with aromatic primary amines via aza-Michael addition. We reported the formation of quinoline-containing triglyceride-based thermosets when this reaction is carried out at high temperatures. [5]

The aim of this work is to synthesize new phosphorus-containing plant oil derived thermosets with flame retardant properties. The previously mentioned enone-containing high oleic sunflower oil derivative has been partially modified via phospha-Michael addition and crosslinked through aza-Michael amine addition to the remaining double bonds.

Results and Discussion

The phospha-Michael addition has been studied by using diphenylphosphine oxide and the enone derivative of methyl oleate as model compounds. ^{1}H NMR kinetic experiments allow to establish the best reaction conditions and BF_3 as the most effective catalyst.

High oleic sunflower oil has been modified by applying these reaction conditions. The reaction has been done taking into account the average number of double bonds in the starting materials and designing a final thermoset with a phosphorus content of 2,5% weight. The chemical structure of the phosphine oxide containing triglyceride was assessed by FTIR and NMR spectroscopy, supporting the complete addition of the phosphine oxide. In a further step, the remaining double bonds have been reacted with 4,4'diaminodiphenylmethane to obtain crosslinked thermosets. The materials were also obtained in a one pot procedure by carring out the phospha-Michael and the aza-Michael addition in one step.

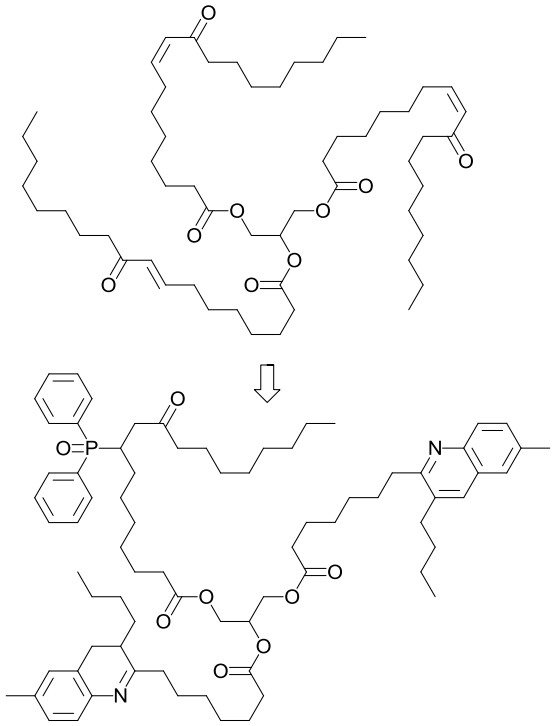

The thermal, mechanical and flame retardant properties of the synthesized polymers were evaluated, showing that the incorporation of phosphorus improves the flame retardant behaviour of these materials.

References

[1] Gandini, A.; Belgacem, M. N. Monomers, Polymers and Composites from Renewable Resources; Elsevier: Oxford, UK, 2008

[2] Lu, S.Y.; Hamerton, I. Prog Poly Sci 2002, 27, 1661-1712

[3] Meier, M. A. R.; Metzger, J. O. ; Schubert, U. S. Chem Soc Rev 2007, 36, 1788-1802.

[4] Montero de Espinosa, L.; Ronda, J.C.; Galià, M.; Cádiz, V. J Polym Sci Part A Polym Chem 2008, 46, 6843-6850.

[5] Montero de Espinosa, L.; Ronda, J.C.; Galià, M.; Cádiz, V. J Polym Sci Part A Polym Chem 2010, 48, 869-878.

Amphiphilic triblock copolymers of poly(ethylene glycol) and l-lactide: a possible mechanism of polymerization for coordination/insertion catalysts.

Rafael Bergamo Trinca[1], *Heitor Fernando Nunes de Oliveira*[2], *Maria Isabel Felisberti*[3]

Chemistry Institute, University of Campinas (UNICAMP), P.O. Box 6121, Zip Code 13083-970, Campinas - SP, Brazil

[1]rafaeltrinca@gmail.com, heioliveira@iqm.unicamp.br, [3]misabel@iqm.unicamp.br

Introduction

Amphiphilic polymers are macromolecules which simultaneously presents hydrophilic and lipophilic segments. This property may be reached by the synthesis of block copolymers, and in this case the choice of the blocks will lead to the final properties of the materials.

The synthesized copolymers, PLLA-*b*-PEG-*b*-PLLA, combine the characteristics of PLLA, such as biodegradability and lipophilicity, with the PEG biocompatibility and hydrophilicity. In other words, this triblock copolymer is a suitable candidate to use in pharmaceuticals, medical and biomedical engineering field.

There are many proposals to the catalytic mechanism of coordination/insertion ROP used to produce these copolymers. In order to study the mechanism of catalysis of tin 2-ethylhexanoate, two reactions conditions were proposed.

Materials and Methods

General synthesis of PLLA-b-PEG-b-PLLA copolymers

The copolymers were synthesized by Ring Opening Polymerization in toluene solution using 2-ethyl-hexanoate Sn(II) as catalyst. The macro initiator PEG is pre added to the reaction media with the catalyst to pre activation and then the monomer is added.

Catalyst Study

In order to study the catalyst action, two different ratios of the catalyst where used:

Method A: an equimolar ratio of catalyst and PEG hydroxyls groups was used.

Method B: the amount of catalyst used was related to the monomer LLA. The average LLA/ $Sn(oct)_2$ molar ratio was $n_{LLA}/n_{Sn(oct2)}$= 5000 This method is the most common on literature. [1,2,3,4]

Five different molar ratios of LLA and EG were used (n_{LLA}/n_{EG} = 0.3; 0.5; 1.0; 1.5 and 2.0).

Results and Discussion

The synthesized copolymers were characterized by ^1H NMR, DSC, TGA and GPC techniques. *Figure 1a* and *1b)* show the molar fraction of LLA in the copolymers obtained by using *Method A* and *Method B*, respectively. While copolymers obtained by using *Method A* kept the molar ratio of the reactants, in a very close agreement, the products from the *Method B* were richer with PEG in comparison with the reaction medium, an indicative of poor LLA monomer conversion.

DSC results showed a depression of the melting point of PEG crystalline phases, which were more pronounced in the *Method A* copolymers.

GPC analysis showed that the *Method A* materials present only a molar mass distribution while the *Method B* materials present a bimodal molar mass distribution, which means that side reactions are took place, like such as homopolymerization.

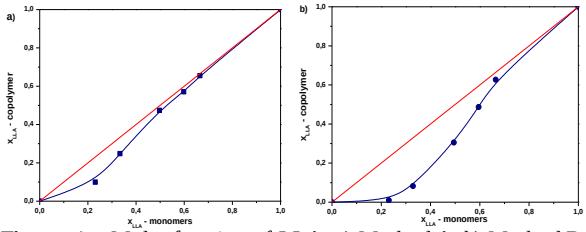

Figure 1 – Molar fraction of LLA: a) Method A, b) Method B;

The table bellow show the M_n molar mass obtained by GPC technique for these copolymers.

Method A	M_n (kDa)	Method B	M_n (kDa)
LP-8A-0.3	6.6	LP-8B-0.3	6.0
LP-8A-0.5	9.3	LP-8B-0.5	6.0
LP-8A-1.0	14.8	LP-8B-1.0	8.7
LP-8A-1.5	15.7	LP-8B-1.5	11.6
LP-8A-2.0	14.9	LP-8B-2.0	16.6

The molar mass M_n of PEG used as macro initiator was 5,8 kDa. Therefore, the molar mass of the *Method B* copolymers monomer molar ratios from 0.3 to 1.0 corresponds to a insertion of around 3 to 10 LLA units in the PEG macro initiator; this means these copolymers contain small PLLA block, which does not affect the PEG blocks crystallization.

Moreover, the *Method A* materials showed a noticeable growth of PLLA blocks, leading to the desired copolymers with best monomer conversion and reaction control.

Conclusion

The results presented in this work allow us to conclude that the hypothesis assumed in *Method A* is true. The coordination of each reactive PEG hydroxyl group leads to better results; in other words, the growing chains keep the coordination with the catalyst until a chain termination agent is added. *Method B* conditions, which use a small amount of catalyst, leave an excess of unreacted PEG and LLA monomer. This is due to absence of uncoordination of growing chains, as well as PEG chains, leading to a low conversion of monomer.

Acknowledgements

We thank FAPESP and CNPq for the financial support to the project.

References

1. Xiuli Hu, Shi Liu, Xuesi Chen, Guojun Mo, Zhigang Xie, Xiabin Jing; *Biomacromolecules*, *9*, 553–560 **(2008)**

2. Kataoka K, Harada A, Nagasaki Y, *Advanced Drug Delivery Reviews*, *47*, 113–131. **(2001)**

3. Castro ML, Wang SH; *Polymer Bulletin*, Berlin, v.51, n.2, 151-58 **(2003)**

4. Watanabe J, Kotera H, Akashi M; *Macromolecules*, *40*, 8731-8736 **(2007)**

Styrenated Oil Synthesis by "Click" Chemistry Approach

Pelin Yazgan[a], *A. Tuncer Erciyes*[a], *Neslihan Alemdar*[b], *Yusuf Yagci*[c]

[a] Istanbul Technical University, Department of Chemical Engineering, 34469 Maslak, Istanbul, Turkey
[b] Atatürk University, Department of Chemical Engineering, 25240 Erzurum, Turkey
[c] Istanbul Technical University, Department of Chemistry, 34469 Maslak, Istanbul, Turkey

erciyes@itu.edu.tr

Introduction

Numerous methods have been explored for the modification of existing materials or synthesis of new types of organic materials containing triglyceride oil. These materials play important role in industrial applications in the production of coating materials, lubricants, printing inks, soap, and surface active materials. Without any advancing modification as a coating material, film characteristics of a coating material reflected by triglyceride oils can not provide the desired properties such as drying time, flexibility, adhesion, hardness, resistances to water, alkali and acid. For the chemical modification various types of vinyl monomers are used. Among these monomers, styrene is the most widely used to improve the film properties [1].

In our laboratory, several studies from our laboratory were reported for the modification of oils in order to obtain oil-based binders [1-5]. As a continuation of these studies, in the present study, "click" chemistry strategy was applied as a new route for the preparation of styrenated oil. In the modification, polystyrene (PS) samples with controlled molecular weight and narrow polydispersity index, which were prepared by nitroxide mediated radical polymerization (NMRP) technique, were used [2, 3].

"Click" chemistry strategy provides quantitative yields, high tolerance of functional groups, insensitivity of the reaction to solvents, moderate reaction temperatures, possibility of working under both homogeneous and heterogeneous systems, short reaction times and high selectivity [6]. These mentioned benefits will be valid in this new styrenated oil production by "click" chemistry approach.

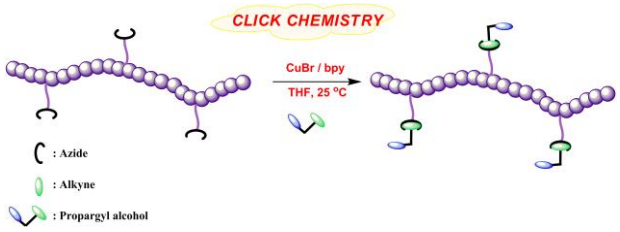

Scheme-1: Hydroxyl functionalized P(S-*co*-CMS) by "Click" chemistry.

Materials and Methods

The copper (I) catalyzed azide-alkyne cycloaddition (CuAAC) between terminal alkynes and azide were performed in the styrenated oil preparation. Copolymers of styrene and 4-chloromethyl styrene (P(S-*co*-CMS)) were prepared by NMRP technique and the chloromethyl groups were converted to azido groups by using NaN_3 and these azido groups were coupled with propargyl alcohol to result in hydroxyl groups on the PS chain by "click" chemistry (Scheme-1). In the next step these alcohol groups (PS-OH) were combined with the partial glyceride (PG) hydroxyls by the reaction of 2,4-toluene diisocyanate (TDI) (Scheme-2). The structures of the products were confirmed by FTIR and H^1-NMR. Thermal properties were determined by DSC and TGA analyses. In the end the sample was investigated in view of the film properties.

Results and Discussion

In this study, main goal is to modify triglyceride oils by using "Click" chemistry approach. For this purpose hydroxyl functionalized PS was prepared by "click" reaction and then PG's were incorporated to the PS chain. The usual benefits of the "click" reaction were also noted in the styrenated oil process. The obtained styrenated oil samples showed good film properties.

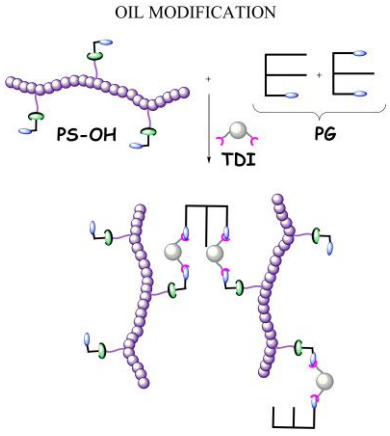

Scheme-2: Oil modification step.

Conclusion

The results showed that the "click" chemistry could be applied successfully for the modification of triglyceride oil through styrenation. It should be noted that the advantages of the "click" reaction was reverberated to this new process.

References

[1] Guner FS, Yagci Y, Erciyes AT., *Prog. Polym. Sci.* **2006**, 31(7), 633.
[2] Alemdar N, Erciyes AT, Yagci Y., *Prog. Org. Coat.* **2010**, 67, 55.
[3] Alemdar N, Erciyes AT, Yagci Y., *Prog. Org. Coat.* **2009**, 66(2), 99.
[4] Eksik O, Tasdelen, MA, Erciyes AT, Yagci Y. *Composite Interfaces* **2010**, 17, 357.
[5] Eksik O, Erciyes AT, Yagci Y., *J. Macromol. Sci. Part A-Pure Appl. Chem.* **2008**, 45(9), 698.
[6] Ergin M, Kiskan B, Gacal B, Yagci Y. *Macromolecules* **2007,** 40(13), 4724.

Effect of organoclay preparation and the processing conditions on the extent of exfoliation in nylon 6/ modified clay nanocomposites

E. Erdmann[1], M. A. Toro[2], H. A. Destéfanis[1], Michele Modesti[3]

[1]Instituto de Investigaciones para la Industria Química - INIQUI-CONICET, Consejo de Investigaciones- CIUNSa, Facultad de Ingeniería- UNSa, - 4400, Salta, Argentina;
[2]Instituto de Investigaciones para la Industria Química - INIQUI-CONICET, Consejo de Investigaciones- CIUNSa, Facultad de Ciencias Exactas- UNSa, Av. Bolivia 5150, 4400, Salta, Argentina);
[3]Department of Chemical Process Engineering, University of Padova, via Marzolo 9, 35131 Padova, Italy.

e-mail eleonora@unsa.edu.ar

Abstract: Polymer layered silicate nanocomposites have been studied for nearly 50 years, but many papers focus only on the importance of the chemistry used to modify the surface of the filler, without including considerations about the role of processing conditions. Nanocomposites synthesis by conventional polymer processing operations requires strong interfacial interaction between the polymer matrix and the clay to generate shear forces of sufficient strength in order to improve clay exfoliation[1]. Nylon 6 (N6) /clay nanocomposites have gained particular attention since the earliest researches, but studies have been concentrated mainly on preparation methods involving in situ polymerization[2]. Although the increase in barrier properties is claimed for this type of materials, there are very few papers about the improvement of barrier performances. Starting from these considerations the aim of this work was to show that the degree of clay delamination and dispersion depends on a combination of effective chemical treatment and optimized processing conditions. In this study the clay has been intercalated with organic species such as hexadecyltrimethyl ammonium chloride according Valenzuela et al.[3] (MMTAO2) and ε-caprolactam in HCl medium[4] (MMTA2). Polymer/clay nanocomposites were then prepared by two techniques. . The first was a melt intercalation process in a mixer chamber at 240°C for 10 min and 60 rpm with a 3% fill factor obtained from intercalated clays and commercial Nylon 6 (Nylodur) called N6/MMTA2 and N6/ MMTAO2.The other was an in situ polymerization process from intercalated material using the Kojima et al. techniques[4] for mixture of MMTAr2 and MMTAO2 with ε-caprolactam and 6-aminocaproic acid, as accelerator. A polymerized nylon "in situ" has been obtained, called MMTA3 and MMTAO3. Films for characterization were manufactured by compression molding in a Carver press, heating at 240°C and cooling the film in a cold press at room temperature. Barrier properties of N6/clay nanocomposites were studied by cyclohexane pervaporation. The influence of exfoliation and/or intercalation of clay platelets on barrier properties were then examined. In addition, the morphologies of N6/modified clay nanocomposites were studied by X-ray diffraction (XRD), scanning electron and transmission electron microscopy (SEM and TEM) and thermal gravimetric analysis (TGA). In figure 1 and figure 2 it can be observed that intercalation occurs for MMTA3 and N6/MMTA2, but a substantial reduction in the intensity of the diffraction peak derived from the interlayer spacing of the clay, evident in the MMTAO3 and N6/MMTAO2 composites, indicates that almost complete exfoliation of the silicate layers took place and the nanocomposite structure was obtained.

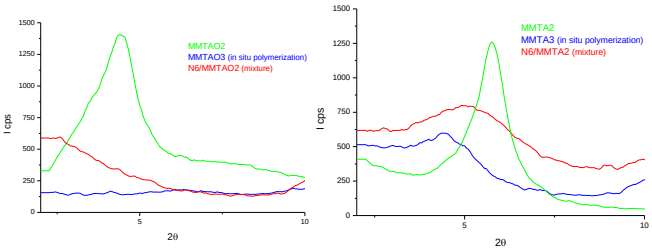

Figure 1 and Figure 2: XRD patterns for modified clays and the composites for two types of processing, mixture and "in situ" polymerization.

Results of TEM show that the addition of modified clay changes the material morphology and that the obtained materials present an intercalated and/or exfoliated nanocomposite structure (Figure 3 and 4).

Figure 3 and Figure 4: TEM images of a) N6/MMTA2 and b) MMTA3

All thermal degradation profiles were obtained from TG and DTG curves, with the course of the decomposition has that has been affected by the structure of the organoclay.
The decrease in the pervaporation values of nanocomposites, considering pure nylon 6 as reference, is associated with a reduction of free volume and mobility of polymer chains resulting in lower permeated flows. Hence it has been concluded that chemical modification of the montmorillonite clay and an adequate processing of polymer clay composites are necessary to generate polyamides with enhanced barrier properties without losing the properties of pure polymer.

References

1. Ray S.S. and Okamoto M.; Progress in Polymer Science 28, 2003, 1539-1641.
2. Erdmann E. et al. Materials Science Forum 570, 2008, 78.
3. Valenzuela Diaz F. Key Engineering Materials, 189(191), 2001, pp.203-207.
4. Kojima Y. et al. J. Polym. Sci., Polym. Chem., 31, 1993, 983-986.

Thermoplastic Polyurethanes with Undecylenic Acid-based Soft Segments: Synthesis and Properties

Lluch, C.; Lligadas, G.; Ronda, J.C.; Galià, M.; Cádiz, V.

Department of Analytical Chemistry and Organic Chemistry, Rovira i Virgili University, Marcel.li Domingo s/n, 43007 Tarragona (Spain)

marina.galia@urv.cat

Introduction

The popularity of polyurethanes (PUs) for biomedical applications stems from their excellent physical properties and good biocompatibility. Plant oils incorporation into PUs is known to provide flexibility, low melting temperature, hydrophobicity and pliability. Most importantly, it's degradation into naturally occurring compounds expands its utility in various medical applications like drug delivery and temporary implantable devices. Nowadays, the design of novel biobased polyols derived from plant oils is an active area of research.[1] By taking advantage of the wide variety of possibilities for chemical modification of plant oils, there is a broad palette of strategies to functionalize its structure with hydroxyl groups. Here, we report the preparation of novel thermoplastic PUs based on undecylenic acid, a major product of castor oil pyrolysis. The materials were characterized for properties relevant to biomaterial applications.

Materials and Methods

Soft segments used in this study were prepared from potentially 100% biomass-derived monomer, allyl ester of 10-undecenoic acid (UDA) via two one-pot thiol-ene click reactions.[2] The general chemical structure of these telechelic diols is shown in Figure 1a. PUs with 0, 40, and 60% hard segment content were synthesized in two-steps from UDA-based diols with M_n of 1000, 2000, and 3000 Da, diphenylmethane diisocyanate, and 1,4-butanediol in DMF solution at 70ºC. Polymers were analyzed by DSC, FTIR, SEC, DMTA, TGA and tensile tester. In addition, given the potential use of these materials for biomedical applications, hydrolytic degradation, biocompatibility, and performance as drug carriers have been evaluated.

Results and Discussion

As mentioned above, three series of PUs based on renewable oligomeric diols of different molecular weight as soft segment, and 1,4-butanediol, as chain extenders, in the hard segment structure have been synthesized via two-step polymerization to produce materials with distinct microstructures and properties. DSC and DMTA analysis showed several transitions associated with soft and hard segments in the low and high temperature range, respectively. Segmented PUs posses a nearly constant soft segment Tg values with the increase of hard segment content, as a result of the chain extension occurring during the first step of polymerization. However, when UDA-based diol with M_n of 1000 Da was used small amount of hard segment mixed in the soft domains. FTIR analysis confirmed the formation of disordered hard segment domains at high hard segment contents which were imaged by using tapping mode AFM. The thermal degradation follows the same trend in all synthesized PUs showing three main degradation steps, whereas mechanical properties were found to be governed by hard segment content.

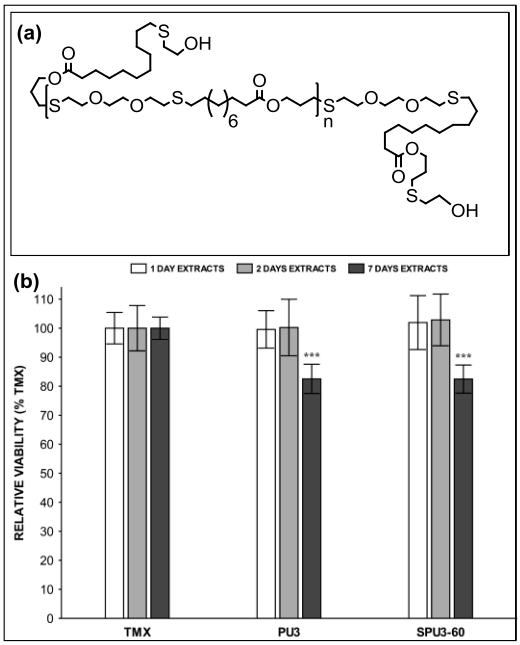

Figure 1. (a) Chemical strucucture of undecylenic acid-based soft segment. (b) MTT cytotoxicity results for control TMX, PU3, and SPU3-60.

Hydrolytic degradation of these materials was studied by placing individual samples in a phosphate buffer solution at 37 and 60ºC. Over a period of 3 months no significant mass loss of the polymer was detected. The biocompatibility of PUs and their parent diols was tested using a standard MTT cytotoxicity assay. The data in Figure 1b indicates that PUs extracts are not statistically toxic to human fibroblasts. Finally, drug-delivery experiments using rhodamine B showed that synthesized PUs provide a prolonged diffuse-controlled release and therefore could be suitable in applications where prolonged drug action over some days is required.

Conclusions

The suitability of the UDA-based telechelic diols as components for the synthesis segmented PUs with promising applicability as biomaterials has been demonstrated.

References

1. Lligadas, G.; Ronda, J.C.; Galià, M.; Cádiz, V. *Biomacromolecules* **2010**, *11*, 2825-2835
2. Lluch, C.; Ronda, J.C.; Galià, M.; Lligadas, G.; Cádiz, V. *Biomacromolecules* **2010**, *11*, 1646-1653.

Polybenzoxazine Prepolymers from Renewable Fatty Acid Derivatives

Tüzün A.; Lligadas, G.; Ronda. J.C.; Galià, M.; Cádiz, V.

Department of Analytical Chemistry and Organic Chemistry, Rovira i Virgili University, Marcel.li Domingo s/n, 43007 Tarragona (Spain)

alev.tuzun@urv.cat

Introduction

Polybenzoxazines are a new class of phenolic resins that can be prepared easily from phenols, primary amines and formaldehyde. The wide variation of raw materials allows considerable molecular-design flexibility for these monomers. The properties of polybenzoxazines are comparable or even superior to traditional phenolic resins, but polybenzoxazines also overcome many of the problems associated with phenolic resins. Benzoxazine polymerization exhibits negligible volumetric shrinkage, does not require any harsh acid catalyst, and has no reaction byproduct. Furthermore, polybenzoxazines posses excellent mechanical properties as well as thermal stability.[1]

However, there are some shortcomings for polybenzoxazines. The cured materials are brittle and relatively high temperature is needed for the ring-opening polymerization. Also, processing into thin film from the typical monomers is difficult because most monomers are powder and the polymers are brittle due to the short molecular weight of the network structure. In this way, extensive research has been done to address these specific drawbacks.

Traditionally, only low molecular weight benzoxazine monomers have been used as precursors of polybenzoxazines but in the last years linear polymeric benzoxazines have been developed by replacing the monofuncional amines and phenols by difunctional compounds. The resulting polymers contain benzoxazine units in the main chain and behave as a conventional thermoplastic which has good solubility, processability and film formation. This thermoplastic polymer can be crosslinked upon thermal treatment at elevated temperatures. Until now,[2,3] the approaches to prepare these useful low viscosity thermosetting polybenzoxazine precursors are based on the reaction of diamines of variable length and diphenols, thus producing polymers with uncontrolled molecular weight and high polydispersity.

We have recently demonstrated that thiol-ene click addition of difunctional thiols to α,ω-dienes is a straightforward methodology to prepare well-defined telechelics with controlled molecular weight.[4] Thus, in this work we have applied this methodology to two dienic benzoxazine monomer obtained from renewable unsaturated fatty acid derivatives.

Results and Discussion

Two α,ω-dienic benzoxazine monomers were prepared following conventional synthetic approach using formaldehyde, allylamine and two p-substituted phenols derived from 10-undecenoic acid, a pyrolysis derivative of castor oil. The parent phenols were synthesized from 4-benzyloxyphenol by reaction with 10-undecenyl bromide or 10-undecenoyl chloride and further hydrogenolytic deprotection of the benzyl groups. In this way the 3-allyl-6-(10-undecenoyl)-3,4-dihydro-2H-benzoxazine (Bz-A)

and the 3-allyl-6-(10-undecenyl)-3,4-dihydro-2H-benzoxazine (Bz-b) were obtained in good yield and purity as colourless oils.

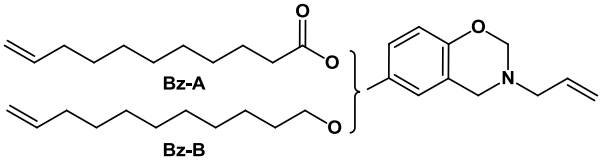

NMR structural characterization confirmed the formation of the benzoxazine ring and the absence of phenolic by-products. The thermal curing behaviour of these benzoxazines was studied by DSC showing the polymerization activating effect of the N-allyl group described by some authors. Bz-A or Bz-B and 3,6-dioxa-1,8-octanedithiol (DODT) were "clicked" to prepare benzoxazine-containing linear polymers with variable molecular weight by thiol-ene step–growth polymerization. The obtained low to medium molecular weight polymers were characterized by NMR, SEC and MALDI-TOF-MS which confirmed the high efficiency of this methodology.

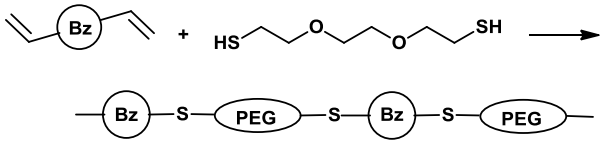

Kinetic studies by NMR allowed establishing the different reactivity of both ene groups, which leads to polymers predominantly ended by the less reactive allyl groups. Finally the curing behaviour of these low viscosity benzoxazine prepolymers was studied by DSC and the thermal and mechanical properties evaluated by TGA and DMTA.

References

1. Yagci, Y.; Kiskan, B.; Ghosh, N.N. *J Polym Sci Part A: Polym Chem* **2009**, *47*, 5565-5576.
2. Takeichi, T.; Kano, T.; Agag, T. *Polymer* **2005**, *46*, 12172-12180.
3. Agag, T.; Geiger, S.; Alhassan, S.M.; Qutubuddin, S.; Ishida, H. *Macromolecules 2010*, **43**, 7122-7127.
4. Lluch, C.; Ronda, J.C.; Galià, M.; Lligadas, G.; Cádiz, V. *Biomacromolecules* **2010**, *11*, 1646-1653.

Molecularly Imprinted Nanoparticles Prepared by Non-aqueous Emulsion Polymerization

Gita Dvorakova[1,2], Robert Haschick[3], Khalid Chiad[3], Markus Klapper[3], Klaus Müllen[3], Jiri Vohlidal[1], Andrea Biffis[2]

[1]Department of Physical and Macromolecular Chemistry, Faculty of Science, Charles University inPrague, Hlavova 8, 12843 Prague, Czech Republic

[2]Department of Chemical Sciences, University of Padua, via Marzolo 1, 35131 Padua, Italy

[3]Max-Planck Institute for Polymer Research, Ackermannweg 10, 55128 Mainz, Germany

gituchia@gmail.com

Molecular imprinting is an approach to study and/or mimic nature. In this technique a target molecule acts as a template around which monomers and cross-linking agents are arranged and copolymerized. After the template removal, binding sites complementary to the template are left in the resulting polymer. These binding sites are stabilized by the cross-linked structure and, like binding sites of biological receptors, are able to rebind the template selectively. [1]

In this contribution we present a preparation of molecularly imprinted polymer nanoparticles (NP) via polymerization in oil-in-oil emulsion [2, 3]. The biggest advantage of the presented method is the absence of water which can hamper the stability of monomer-template assembly during non-covalent imprinting thus decreasing the efficiency of the imprinting process. This problem is avoided here since polymerization occurs in droplets of acetonitrile (ACN) or dimethylformamide (DMF) dispersed in an immiscible non-polar phase such as cyclohexane or *n*-hexane. In this way, it is possible to prepare monodisperse molecularly imprinted polymer nanospheres of around 100 nm in size.

Imprinted (MIP) as well as non-imprinted nanoparticles (NIP) were synthesized using methacrylic acid (MAA) and ethylene glycol dimethacrylate (EDMA) as a functional monomer and cross-linker, respectively. Molecularly imprinted nanoparticles were prepared using different MAA:template ratio to study the effect of template present during the polymerization on rebinding properties of nanoparticles. All NP were characterized using dynamic light scattering and scanning electron microscopy (SEM) (Fig.1).

The efficiency of template removal and the rebinding properties of NP were studied by UV-Vis spectroscopy. Interactions between the template and the polymer were studied using Isothermal Titration Calorimetry (ITC).

Successful molecular imprinting of these nanoparticles was proved, and the resulting imprinting efficiency was indeed found to be superior to that obtained through related emulsion polymerization approaches using water.

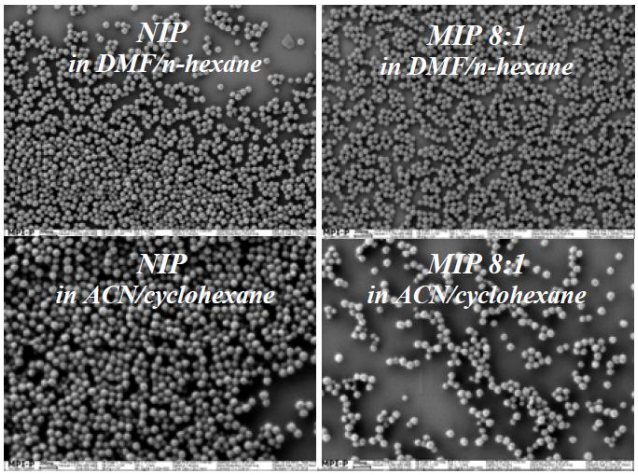

Fig.1: Representative SEM images of the synthesized polymers

References:

[1] a) B.Sellergen, Ed., Elsevier, Amsterdam 2001: Molecularly Imprinted Polyemrs; b) M.Komiyama, T.Takeuchi, T.Mukawa, H.Asanuma, Wiley-VCH, Weinheim 2003: Molecular Imprinting from Fundamentals to Applications; c) S.Piletsky, A.Turner, Eds., Landes Bioscience, Austin 2004: Molecular Imprinting of Polymers; d) M.Yan, O.Ramström, Eds., Marcel Dekker, New York 2005: Molecularly Imprinted Materials. Science and Technology.

[2] a) K.Müller, M.Klapper, K.Müllen, Macromol. Rapid Commun. 2006, 27, p.586; b) K.Müller, M.Klapper, K.Müllen, J. Polym. Sci. Part A: Polym. Chem. 2007, 45, p.1101; c) M.Klapper, S.Nenov, R.Haschick, K.Müller, K.Müllen, Acc. Chem. Res. 2008, 41, p.1190.

[3] For a preliminary account of our results see G.Dvorakova, R.Haschick, K.Chiad, M.Klapper, K.Müllen, A.Biffis, Macromol. Rapid Commun. 2010, 31, p.2035.

Acknowledgements: Financial support from the European Community through the Marie Curie RTN "NASCENT" (contract no. MRTN-CT-2006-033873) is most gratefully acknowledged.

Synthesis of Functionalized Polyesters via Ring-Opening Polymerization of ε-Caprolactone Initiated by Al-Based Catalysts

Yulia A. Piskun,[1] Irina V. Vasilenko,[1] Sergei V. Kostjuk,[1] Kirill V. Zaitsev,[2] Sergei S. Karlov[2]

[1]Research Institute for Physical Chemical Problems of the Belarusian State University
[2]Chemistry Department, Moscow State University, B-234 Leninskie Gory, 119899 Moscow, Russia

vasilenkoi@bsu.by

Introduction. Polyesters like poly-ε-caprolactone, polylactide and its copolymers have a great importance because of their biodegradability, biocompatibility and good compatibility with many other polymers. They are widely used in medicine, pharmacology, in the production of environment friendly polymer materials etc. Recently, considerable attention has been paid to the synthesis of functionalized polylactones due to the possibility to use them as building blocks, macromonomers or macroinitiators. This work is devoted to the investigation of ε-caprolactone polymerization initiated by simple functional aluminum alkoxides (**kt1**–**kt3**, Scheme 1) as well as new Al complexes with phenoxy-imine ligands (**kt4**, **kt 5**, Scheme 1).

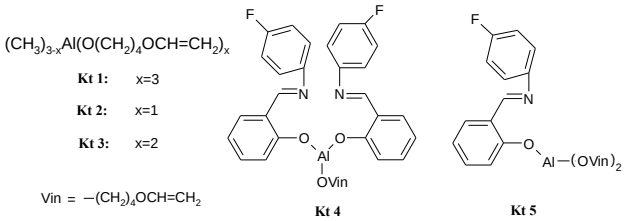

Scheme 1. Structures of catalyst used in this work

Results and Discussion. The main results of ring-opening polymerization of ε-caprolactone in the presence of aluminum alkoxides as catalysts are summarized in Table 1.

Table 1. Polymerization of ε-caprolactone in bulk initiated by functional aluminum-based catalysts

kt	T (°C)	time (min)	conv (%)	M_n[a]	PDI	F_n[b]	N[c]
1	40	40	69	16800	1.28	90	1.0
2		180	45	18870	1.36	100	1.0
3		545	55	21320	1.22	105	0.9
2	80	120	99	35600	1.62	95	1.0
3		120	97	20400	1.57	112	1.7
4		20[d]	15	4660	1.81	37	1.0
5		20[d]	60	14820	1.16	70	1.3
4	130	60	94	19380	1.45	65	1.4
5		60	93	24000	1.63	75	1.2

Conditions: [Al]=31.5 mM; [M]/[Al]=300. [a] Calculated according to following equation: M_n=0.52×M_n(SEC). [b] Calculated from ^{1}H NMR spectra as follows: F_n=2I(-O-C<u>H</u>=CH$_2$)/I(-C<u>H$_2$</u>-OH)×100. [c] N-number of chains per catalyst molecule, calculated as N=M_n(theor)/M_n(exp), where M_n(theor)=[M]/[kt]×114×Conv. [d] Time in hours.

As shown in Table 1, all aluminum alkoxides (**kt1**–**kt3**) studied in this work exhibited low activity at 40 ºC, although polyesters with high molecular weight (M_n up to 20,000 g mol^{-1}) and narrow molecular weight distribution (M_w/M_n≤1.36) could be obtained under these conditions (see Table 1). Among aluminum alkoxides studied, the highest activity showed **kt1**. Importantly, all polymers synthesized at 40 ºC are characterized by excellent functionality at the ω-end. The number of vinyl group per Al atom (N) equals 1.0 for all investigated catalysts at 40 °C despite the fact that di- and trialkoxyaluminum have two and three reactive groups, respectively. This is likely due to the aggregation of catalysts at low polymerization temperature, that is in agreement with data obtained earlier in ε-caprolactone polymerization with Al(O^{i}Pr)$_3$ as catalyst by Duda and Penczek [1].

The increase of the polymerization temperature up to 80 ºC led to increase of the catalyst activity of functional aluminum alkoxides (full monomer conversion less than for 2 h) keeping a high functionality of synthesized poly-ε-caprolactones (F_n~100%). However, some broadening of MWD was observed (see Table 1). The Al complexes with phenoxy-imine ligands (**kt4**, **kt 5**) exhibited low activity in comparison with aluminum alkoxides, although **kt5** afforded polymers with low polydispersity (M_w/M_n=1.16) and acceptable functionality (F_n=70). These complexes showed a good activity only at 130 ºC affording polymers with relatively broad MWD (M_w/M_n=1.45–1.63) and acceptable functionality in the case of **kt5** (Table 1).

Conclusions. In this work, we demonstrated that simple functional aluminum alkoxides are very effective catalyst for the synthesis of perfectly functionalized polyesters (F_n~100%) with M_n up to 20,000 g mol^{-1} and relatively narrow MWD (M_w/M_n<1.6) at elevated temperatures (40–80 ºC). The Al complexes with phenoxy-imine ligands exhibited high activity only at 130 ºC affording polyesters with acceptable functionality (F_n~75%) and MWD (M_w/M_n<1.6).

References

1. Biela T., Kowalski A., Libiszowski J., Duda A., Penczek S. *Macromol. Symp.* **2006**, *240*, 47-55.

Styrenated Oil Production by RAFT Method

Nazli Caglar[a], *A. Tuncer Erciyes*[a], *Neslihan Alemdar*[b], *Niyazi Bicak*[c]

[a] Istanbul Technical University, Department of Chemical Engineering, 34469 Maslak, Istanbul, Turkey
[b] Atatürk University, Department of Chemical Engineering, 25240, Erzurum, Turkey
[c] Istanbul Technical University, Department of Chemistry, 34469 Maslak, Istanbul, Turkey

erciyes@itu.edu.tr

Introduction

Triglyceride oils as natural sources are widely used in organic coating materials. In order to improve the film properties, modification processes are applied. For this purpose, styrenation is the well known modification method. In classical styrenation due to the homopolymer formation, the film properties of resulting product are not at the desired level. In order to eliminate the homopolymer formation, previously several studies were carried out in our laboratory [1-6]. Very recently the styrenation of triglyceride was carried out by the living/radical polymerization techniques [1, 3]. In a continuation of these studies, in the present study styrenated oil was prepared by RAFT technique using carboxylic acid functionalized RAFT agent (S-1-Dodecyl-S'-(α,α'-dimethyl-α"-acetic acid)-trithiocarbo-nate) [7].

Materials and Methods

Styrene (St) and 2,4-toluene diisocyanate (TDI) were purchased from Aldrich chemicals. As mentioned before, styrenated oil was prepared by the RAFT method. For this purpose polystyrene (PS) was prepared by the acid functionalized raft agent. The obtained PS chains were combined with partial glyceride (PG) by the reaction of TDI.

Results and Discussion

The applied styrenation process was explained in Scheme 1.

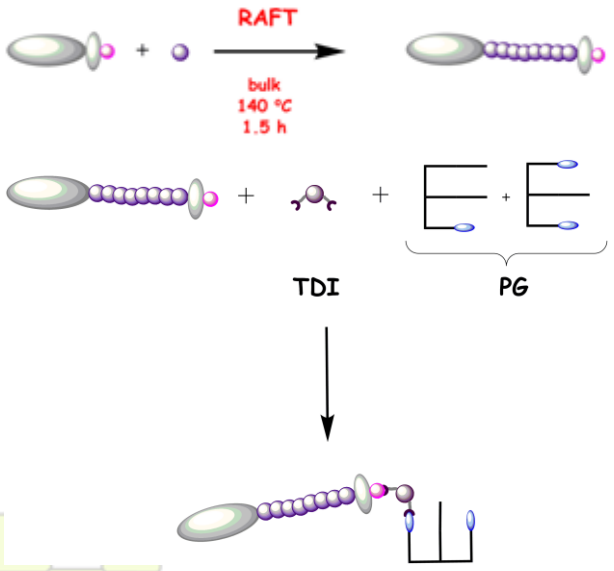

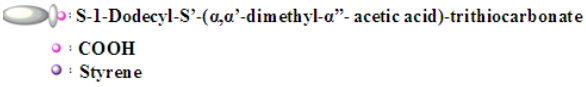

Scheme 1: The production of styrenated oil

In order to obtain a styrenated oil sample with good film properties, the PS/PG ratio and the molecular weight of PS were determined. Optimum PS/PG molar ratio and the molecular weight of PS were found to be 1/0.125 and 6589 Daltons, respectively. The obtained product showed good film properties.

Conclusion

In the present study, the styrenated oil was prepared by RAFT technique using acid functional RAFT agent. This new route provided the styrenated oil with good film properties.

References

[1] Alemdar N, Erciyes AT, Yagci Y., *Progress in Organic Coatings* **2009**, 66(2), 99.
[2] Guner FS, Yagci Y, Erciyes AT., *Progress in Polymer Science* **2006**, 31(7), 633.
[3] Alemdar N, Erciyes AT, Yagci Y., *Progress in Organic Coatings* **2010**, 67, 55.
[4] Alemdar N, Erciyes AT, Yagci Y., *Progress in Organic Coatings* **2009**, 66(2), 99.
[5] Eksik O, Tasdelen, MA, Erciyesl AT, Yagci Y. *Composite Interfaces* **2010**, 17, 357.
[6] Eksik O, Erciyes AT, Yagci Y., *J. of Macromol. Sci. Part a-Pure and Applied Chem.* **2008**, 45(9), 698.
[7] Lai JT, Filla D, Shea R., *Macromolecules* **2002**, 35, 6754.

Starch containing polyurethanes: structure and biodegradability

Travinskaya T., Mishchuk E., Savelyev Yu.

Institute of macromolecular chemistry, NAS of Ukraine, Kharkovskoe shosse, 48, o2160, Kiev, Ukraine

travinskaya-tamara@rambler.ru

Introduction. The increasing problem of accumulative plastic wastes and exhaustion of mineral oil have stipulated for the creation of biodegradable polymer materials on the basis of renewable recourses. Natural compounds based biodegradable waterborne polyurethanes are of increasing interests due to combination of their pollution free status and high performance properties.

Materials and Methods. In this work starch (1,5-35 wt%) containing aqueous polyurethane dispersions (IPU/St) with tailorable susceptibility for acid and alkaline hydrolysis, microorganisms' attack (*Bacillus subtilis*), temperature, UF radiation, and soil microflora have been obtained by dispersing of anionic oligourethane (based on hexamethylene diisocyanate and polyoxytetramethylene glycol) with starch water solution on the stage of chain extension. Supramolecular structure and degree of phase separation of the based film materials were evaluated by infrared spectroscopy (FTIR) and small X-ray scattering (SAXS). Relaxation behavior of IPU/St was studied by dynamic mechanical analysis; thermal-physic and viscoelastic properties were studied by DSC. Thermodestructive processes were evaluated by pyrolytic mass-spectroscopy.

Results and discussion. Obtained materials combine high physic-mechanical characteristics (tensile strength 8-13 MPa, elongation at the break point 875-2000%) and susceptibility to biodegradation: the adhesion of microorganisms (*B. sub*). to the film surface is one order higher in comparison with initial IPU. Besides, IPU/St samples are more exposed to acid and alkaline hydrolysis compared to IPU. Thermostability of the hydrolyzed films decreases drastically. Introduction of the St essentially changes the viscoelastic behavior of IPU material: the height of α-transition has been changed at low St content due to decrease of the part of flexible component and it localization during the hydrogen bonds formation. The further increase of St content leads to the formation of more ordered periodic structure. The IR-spectroscopy and dynamic thermal mechanical analysis data testify to the formation of intermolecular hydrogen bonds between urethane linkages of IPU and hydroxyl groups of St, and the analysis of pyrolysis mass spectra (after storage the samples in the soil during 6 month) allows to conclude the existence of chemical interaction between NCO groups of IPU precursor and hydroxyl groups of St. In accordance with pyrolysis data it should be noted that among native St destruction products', only a few have been observed among the pyrolysis products of starch-containing polyurethane dispersions. The formation of polymer-polymer amorphous micro areas in the composites' volume as the result of strong intermolecular interaction between components has been shown. All studied IPU/St systems are structurally heterogeneous. The higher the St content, the lower the
degree of microphase separation between the soft and hard blocks. Correspondingly, the degree of ordering of the hard blocks in domains as well as the domains in composites' volume becomes lower.

Conclusions. Thus, the novel biodegradable polyurethane-starch containing materials have been developed. The structural organization of the obtained IPU/St systems, and therefore their properties and ability to biodegradation are determined by their composition.

Preparation of Ordered Au/PEO-*b*-PFOMA Hybrid Films Through Phase Transition of Micellar Thin Films

Eun Jin Yoon, Nguyen Thi Hoai An, Do Hoon Kim, and Kwon Taek Lim

Department of Imaging System Engineering, Pukyong National University, Busan 608-739, Korea.

E-mail: ktlim@pknu.ac.kr

Introduction

Gold nanoparticles (NPs) have attracted much interest for applications as catalysts, chemical sensing and as well as building blocks for electronic devices that operate at the single-electron level. Semifluorinated block copolymers (BCPs) are amphiphilic materials that combine the unique self-assembly characteristics of block copolymers and the unparalleled properties of fluorinated polymers. Fluorinated blocks have attracted much attention due to their unique properties such as low surface energy, excellent chemical and thermal stability, low refractive index and dielectric constant, which cannot be achieved by the corresponding non-fluorinated materials. This paper reports a simple *in situ* synthesis of gold NPs in semifluorinated BCP thin films and size change of the NPs through a phase transition of the BCP thin films. Three different annealing modes of $LiAuCl_4$-load block copolymeric thin films were employed: in solvent vapor annealing at 70 ^{0}C, in supercritical CO_2 at 70 ^{0}C and in a vacuum oven at 100 ^{0}C. $LiAuCl_4$, gold precursor complexed with BCP consisting of semifluorinated and PEO blocks were reduced to Au nanoparticles that were well dispersed in the PEO phase of the disordered BCPs micellar thin films. The same sample after annealing, the formation of larger single gold particle per PEO domain with a small variation in size was observed.

Experimental

The semifluorinated BCPs, poly(ethylene oxide)-block-poly(1H,1H-perfluoro octyl methacrylate) (PEO-*b*-PFOMA) were synthesized by ATRP of FOMA using PEO-Br as the macroinitiator in the mixed solvent of TFT and benzene as described previously. For this study, 10k was utilized to make PEO_{10k}-*b*-$PFOMA_{12k}$.

PEO_{10k}-*b*-$PFOMA_{12k}$ was dissolved in $CHCl_3$ to yield 0.5 wt% solutions. $LiAuCl_4$ loaded micellar solutions were prepared by adding 0.1 wt% of $LiAuCl_4$ (99.995%, Aldrich) into the pre-prepared copolymeric micellar solutions. The thin films were prepared on mica substrates by spin-coating of the BCPs micellar solutions and $LiAuCl_4$ treated micellar solutions. Such the thin film was annealed in a vacuum oven at 100 ^{0}C for 24 h, $scCO_2$ annealing and PF-5080 vapor annealing at 70 ^{0}C.

Results and Discussion

Amphiphilic BCPs self-assemble into micelle-like objects when dissolved in solvents that are selective good solvents for one of the blocks. When the soluble block is much shorter than the insoluble block, the aggregates form a crew-cut morphology. $LiAuCl_4$ loaded micellar solutions were prepared by adding 0.1 wt % of $LiAuCl_4$ into the pre-prepared copolymeric micellar solutions. In TEM image, the gray regions are the PFOMA phase in accordance with the higher electron density of the fluorinated blocks, the bright color of the PEO phase is marked by dark dots, which are gold nanoparticles resulting from the reduction of tetrachloroaurate ions due to an interaction with PEO chains. It is clear that gold nanoparticles are well dispersed in the PEO phase and were not located in the entire PFOMA phase; and it showed a denser array of NPs. In the thin films, the average diameter of the gold nanoparticles was 6 nm. For phase transition, the thin films were annealed under saturated PF-5080 at 70 ^{0}C, in a supercritical fluid ($scCO_2$) environment at 70 ^{0}C, or thermally at 100 ^{0}C in a vacuum oven. Each treatment imparts mobility to the BCP thin films, allowing them to reach the equilibrium morphology. During phase transition, the nanoparticles were moved together with the PEO blocks, leading to the formation of a larger single particle in each domain. The particle size distribution of the gold nanoparticles from annealing at 100 ^{0}C was smaller than that from annealing in $scCO_2$ at 70 ^{0}C but broader than that from annealing in PF-5080 vapor at 70 ^{0}C. But in the case of $scCO_2$ annealing, many gold nanoparticles were observed. It is most likely that all nanoparticles locating in the PEO phase were constrained to follow the morphological change more easily than in the case of thermal and solvent treatment.

Conclusions

This study demonstrated the formation of larger single gold NPs in each phase PEO domain from a number of well dispersed smaller gold NPs within the self-assembled copolymeric thin films after annealing. PEO_{10k}-*b*-$PFOMA_{12k}$ diblock copolymers provide an excellent means of producing well dispersed gold NPs in the PEO phase with an average particle diameter of 6 nm. While the phase transitions that enable control of the size and location of the nanoparticles within a bulk BCP can be accomplished by exposing a BCP to any selective solvent, the use of supercritical fluids offers the possibility of tuning the morphology of the polymer in a very controlled manner. Sintering of NPs using phase transition of semifluorinated BCP is a simple and versatile method that can be extended to other particles.

Acknowledgment

This work was supported by the Korea Science and Engineering Foundation (KOSEF) grant funded by the Korean government (MEST) (R01-2008-000-21056-0).

References

1. Ae Jung Jang, Seung-kyu Lee, Seung Hyun Kim, Polymer 51, 3486-3492 (2010).
2. L. Meli, Y. Li, K. T. Lim, K. P. Johnston, P. F. Green, *Macromolecules* 40, 6713 (2007).
3. K. T. Lim, M. Y. Lee, M. J. Moon, G. D. Lee, S. S. Hong, J. L. Dickson, and K. P. Johnston, *Polymer* 43, 7043 (**2002**).

In Situ Micelle Formation and Inter-Block Crosslinking of PAA-b-PS via RAFT Polymerization

Eui Sang Lim, Le Thi Bao Tran, and Kwon Taek Lim

Department of Imaging System Engineering, Pukyong National University, Busan 608-739. Korea

E-mail: ktlim@pknu.ac.kr

Introduction

Poly(acrylic acid) is typical hydrophilic polymer and known as a weak polyelectrolyte. It can form complexes with some metal ions or organic compounds.[1] Block copolymers containing polyelectrolyte segment have structural features of polyelectrolytes, block copolymers and surfactants. The self-assembled nanostructures lack stability and tend to spontaneously dissociate into unimers under various factors such as temperature, high dilution or changes in ionic strength, which results in decreasing their efficiency in role as vehicles for drug and gene delivery. A variety of strategies have been explored to enhance the structural integrity of polymeric micelles of block copolymers. The cross-linking reaction performed within core domain[2] or through shell layer[3] was often employed for this purpose. Here, we reported the preparation of stable micelles by core-surface crosslinking.

Two types of amphiphillic PAA-b-PS diblock copolymers of different lengths of PS segment were prepared by reversible addition fragmentation chain transfer (RAFT) radical polymerization. Subsequently, the micelles of the block copolymers were subjected to *in situ* inter-block crosslinking by RAFT of divinyl benzene.

Experimental

Two types of amphiphilic diblock copolymer poly(acrylic acid)-*b*-polystyrene (PAA-*b*-PS) were synthesized by (RAFT) polymerization in dioxane by using trithiocarbonate-terminated PAA as a macroinitiator. The aggregates, star-like micelles and crew-cut aggregates, consisting of PS cores and PAA coronas, were prepared by direct dissolution of the copolymer in a selective solvent, ethanol. Subsequently, core-shell interface cross-link was governed by RAFT polymerization using divinylbenzene as a crosslinking agent.

Results and Discussion

The chemical structures, compositions of block copolymers, morphology and the size of the core-cross-linked micelles were characterized by NMR, FTIR, GPC, TEM, SEM. TEM images of the block copolymeric micelles before and after crosslinking reaction indicated that most of structures of star-like micelles were found to be globular aggregates with diameter ranging from 30 nm to 50 nm. Unlike the star-like micelles which is existing in solution as discrete spherical micelles, a large number of compound crew-cut micelles with diameter range from 50 nm to 120 nm were observed for larger PS block copolymers. Cross-linked micelles were found to have diameters much larger than those of initial micelles. There was a remarkable change in the structure of micelles after crosslinking reaction. The necklace-like compound nanoparticles were obtained after crosslinking crew-cut aggregates. The decrease of the cross-linking agent led to the formation of discrete cross-linked star-like micelles with average diameter of 80 nm.

Conclusions

Cross-linked spherical micelles from two types of PAA-*b*-PS diblock copolymers with the same PAA block length but different length of PS segment were prepared by RAFT technique. The self-assembly of the block copolymers in ethanol, followed by the inter-block crosslinking reaction with divinyl benzene which was occured *in situ*, provided an efficient method for the preparation of stable nanosized micelles.

Acknowledgment

This work was supported by Mid-career Researcher Program through NRF grant funded by the MEST (No. R01-2008-000-21056-0) and financially supported by the grant from the Industrial Source Technology Development Program (Project No. 10035163) of the Ministry of Knowledge Economy (MKE) of Korea.

References

1. Mori H.; Muller A. H. E.; Klee J. E. J Am Chem Soc 2003, 125, 3712-3713.
2. Kakizawa Y.; Harada A.; Kataoka K. J Am Chem Soc 1999, 121, 11247-11248.
3. Thurmond II K. B.; Kowalewski T.; Wooley K. L. J Am Chem Soc 1996, 118, 7239-7240.

Ethylene/1-Octene Copolymerization with Supported Salen-Type Complexes. Effect of Metal Type

Anna Pietruszka, Marzena Białek, Krystyna Czaja

Opole University, Faculty of Chemistry, Oleska 48, 45-052 Opole, Poland

krystyna.czaja@uni.opole.pl

Introduction

Linear low-density polyethylene (LLDPE) synthesized by copolymerization of ethylene with 1-olefins is among the polymers with highest production capacity. The structure and properties of such copolymer, for example its molecular weight, microstructure, density, melting point, and crystallinity depends on polymerization conditions, especially comonomer concentration, and are also influenced by catalytic system composition [1,2]. The subject of this work is the study of ethylene copolymerization with 1-octene over salen type complexes of titanium, zirconium and vanadium (Fig.1) supported on $MgCl_2(THF)_2$ modified by Et_2AlCl. The studies included the effect of transition metal type in catalyst as well as the effect of 1-octene concentration in the feed on catalyst productivity, comonomer reactivity and on copolymer composition and other properties of ethylene/1-octene copolymers produced. Moreover, the obtained results were compared with those obtained for appropriate salen complexes not immobilized on the carrier.

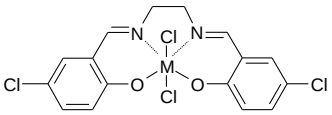

Fig. 1. Structure of salen complexes (M=Ti, V, Zr)

Materials and Methods

Materials. Ethylene (3.0 grade, Linde Gas) was purified by passing it over a column of sodium metal supported on Al_2O_3. Hexane was distilled from sodium/benzophenone. 1-Octene (Aldrich) was dried over molecular sieves. MAO (Witco, 10.0 wt %), Me_3Al (Witco, 2 M), argon (5.0 grade, Linde Gas) were used as received.

Catalyst synthesis. The supported precatalysts were synthesized according to the procedure described in ref. [3]. The carrier material (2.19g) obtained by the reaction of $MgCl_2(THF)_2$ with the Et_2AlCl (Mg/Al = 1/2 mol/mol) was co-milled with appropriate salen complex (0.2309mmol) in hexane/toluene at room temperature overnight. The resulting solid was separated, washed several times with toluene and hexane and dried.

Ethylene/1-octene copolymerization. The reactor was filled with hexane (0.15L), the required amounts of cocatalyst and 1-octene and then the catalyst precursor was added. The copolymerization was initiated by the introduction of ethylene. The monomer pressure was kept constant during polymerization (0.5 MPa). The reaction was stopped after 0.5 hr by the addition of acidic methanol solution. The polymer was subsequently filtered off, washed with methanol and dried.

Characterization. Molecular weight and molecular weight distribution were determined by gel permeation chromatography (using the Alliance 135 GPCV 2000 apparatus from Waters) at 135°C. Trichlorobenzene was used as a solvent, at the flow rate of 0.6 mL/min. DSC analyses were carried out using the 2010 DSC calorimeter from TA Instruments. The heat of fusion (ΔH_f) and the melting temperature (T_m) were measured for samples which had been previously melted and re-crystallized at the heating rate of 10°K/min. The comonomer content in copolymer was determined by FT-IR with the use of the Nicole Nexus 2002 FT-IR spectrometer.

Results and Discussion

Salen type complexes, both supported and unsupported, proved to be active in ethylene/1-octene copolymerization. However, it was found that supported complexes are more active then their unsupported counterparts. Activity of all investigated catalysts, independently on their composition, decreases with the increase of the concentration of the comonomer in the feed.

The compositions of the copolymers were determined by the IR method. It was found that the 1-octene incorporation rises with the increase of the comonomer concentration in the feed for all studied catalysts. Nevertheless, the amount of comonomer incorporated meaningly depends on the type of catalytic system used. First of all, immobilization of salen complexes on a magnesium carrier reduced their copolymerisation ability. This mean that the high steric hindrance brought about by the presence of the support. Secondly, the type of transition metal also determined 1-octene incorporation. Copolymers with clearly higher comonomer content were obtained over vanadium complex then over its titanium counterpart.

As it was observed for ethylene/1-olefin copolymers obtained with different catalysts, melting point and crystallinity of obtained products decrease with an increase of comonomer content in the copolymer.

Conclusions

It has been demonstrated that postmetallocene catalysts containing salen type complexes of early transition metals can effectively copolymerize ethylene with 1-octene and that their copolymerisation behaviour is significantly influenced by presence of the support and type of transition metal.

References

[1] Lehmus, P.; Kokko, E.; Härkki, O.; Leino, R.; Luttikhedde, H. J. G.; Näsman, J. H.; Seppälä, J.V. Macromolecules 1999, 32, 3547

[2] Huang, J.; Lian, B.; Qian,Y.; Zhou, W.; Chen, W.; Zheng, G. Macromolecules 2002, 35, 4871

[3] Białek, M.; Pietruszka, A. J Polym Sci Part A: Polym Chem 2009, 47, 3480

Anna Pietruszka is a recipient of a Ph.D. fellowship from a project funded by the European Social Fund.

ABSTRACTS

POSTER PRESENTATIONS

Topic 2: New Analytical and Characterization Tools

Fractionation Analysis Techniques for the Characterization of Copolymers with Bimodal Chemical Composition Distribution

Beatriz Paredes[1], Alicia Carrero[2], Rafael van Grieken[1], Inmaculada Suarez[2]

[1]Department of Chemical and Environmental Technology
[2]Department of Chemical and Energy Technology
ESCET, Universidad Rey Juan Carlos, c/ Tulipan s/n, 28933 Mostoles, Madrid, Spain

beatriz.paredes@urjc.es

Copolymers of ethylene and α-olefin such as 1-hexene ($C_6^=$) are very important commercial products classified as linear low density polyethylene (LLDPE). Because of the short chain branches that 1-hexene introduces onto the polymer backbone, the copolymers have lower melting point, crystallinity and density than the corresponding homopolymers; therefore, they can find applications in packaging, shrink films and cable coatings.[1] In the case of the characterization of copolymers, it is very important to measure the chemical composition distribution (CCD) in order to get a more complete understanding of the catalysts active sites and polymer properties.[2] Typically, temperature rising elution fractionation (TREF) or crystallization analysis fractionation (Crystaf) are used to determine CCD.

Ethylene-1-hexene copolymers synthesized with several comonomer contents were analyzed by GPC, DSC, ^{13}C-NMR, Crystaf and TREF. The catalytic system $(nBuCp)_2ZrCl_2$/MAO was supported on SBA-15 mesoporous materials with different pore sizes (8.8, 11.3 and 22.7 nm). Crystaf and TREF profiles show a bimodal chemical composition distribution, suggesting two different contributions in the same copolymer in spite of using a single site metallocene catalyst.

In order to study the influence of this bimodal character on the copolymer properties, fractionation techniques were used with the purpose of obtaining fractions to be analyzed off-line and correlate their properties with the characterization of the overall copolymer. These fractionation techniques are based on crystallinity differences and they are performed by precipitation or dissolution through temperature changes. In this context, the aim of this work was the analysis of support pore size on ethylene-1-hexene copolymers properties at different comonomer contents.

Figure 1 shows TREF results. An increment on support pore diameter increases the comonomer incorporation, perhaps due to the lower steric hindrance for the 1-hexene molecules in supports with larger pores. Bimodality can be attributed to the parallel channels' structure of SBA-15 materials; there must be sites located deep inside the pores while other sites may be placed outer and exposed to higher comonomer concentrations. TREF profiles of the obtained fractions demonstrate that separation by preparative TREF was done properly and their characterization reveals that the two copolymers fractions have distinct 1-hexene contents, which determines their properties. Chemical composition distribution of F2 is wider than F1 as a there is more heterogeneity for external sites leading to a copolymer with wider CCD. So, each copolymer has two populations of polyethylene chains related with the textural properties of the support and both influencing in the final properties of the copolymer.

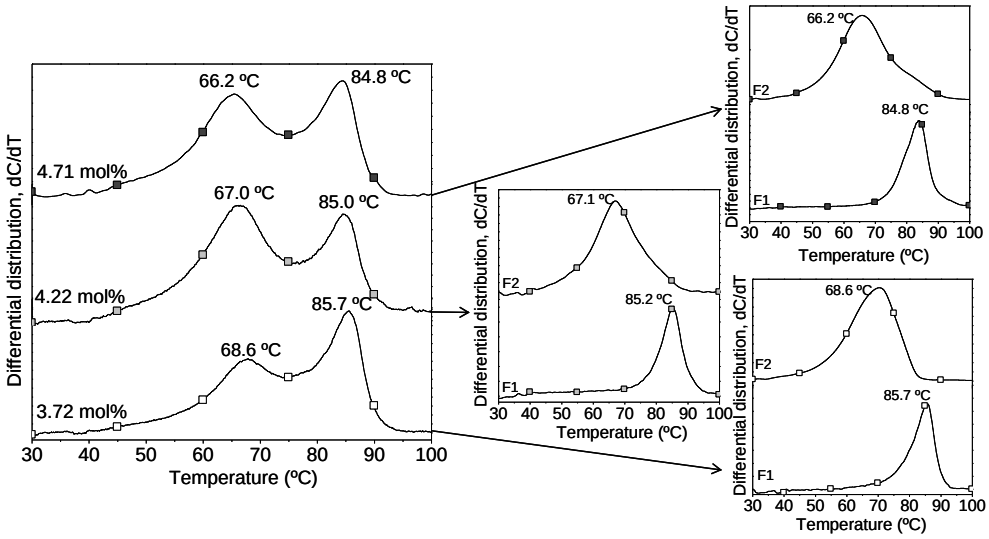

Figure 1. TREF profiles of ethylene-1-hexene copolymers and its fractions. Copolymers synthesized with MAO/$(nBuCp)_2ZrCl_2$ supported over SBA-15 materials with pore sizes 8.8 nm (□),11.3 nm (▣) and 22.7 nm (■).

References:

1. Peacock, A. J. Handbook of polyethylene. Structures, properties and applications. Marcel Dekker Inc., New York, 2000.

2. Kim, J. D.; Soares, J. B. P. Macromol Rapid Commun 1999, 20(6), 347-350.

Novel method for the in-situ estimation of curing shrinkage using FTIR/ATR spectroscopy and refractive index measurements

Xavier Fernández-Francos[a,b], Xavier Ramis[c], Àngels Serra[b], Marco Sangermano[a]*

[a]Dipartimento di Scienza dei Materiali e Ingegneria Chimica, Politecnico di Torino
[b]Departament de Química Analítica i Química Orgànica, Universitat Rovira i Virgili
[c]Laboratori de Termodinàmica ETSEIB, Universitat Politècnica de Catalunya

e-mail: chabyfer@yahoo.es

Introduction

Curing shrinkage is an important issue in the processing of thermosets because of the generation of internal stresses, microcracks and microvoids that reduce the durability of the material. There are several methods described in the literature for the measurement of shrinkage, among which rheometric,[1,2] gravimetric[1,3,4] and laser dilatometry[3] methods seem to be the most reliable and meaningful in comparison with indirect estimation using densities measured at room temperature.[4] However, these methods have some disadvantages, such as that they can only measure shrinkage above gelation,[2] a fairly high amount of sample is necessary[4] and temperature overshoots can take place in the sample,[1,3] thus limiting the method to somewhat slow processes.

We propose a novel method for the in-situ determination of degree of curing and curing shrinkage using FTIR/ATR and refractive index measurements at the curing temperature that overcomes some of the aforementioned drawbacks.

Materials and Methods

The dimethacrylates BisGMA and TEGDMA (Aldrich) were cured with Luperox AFR40 (Aldrich). DGEBA (Epikote 828, Hexion) was cured with ethylenediamine (Aldrich), ytterbium triflate (Aldrich) and 1-methylimidazole (Aldrich). DGEBA (Araldite CY 228-1, Huntsman) and anhydride (Aradur HY 918, Huntsman) were cured with a tertiary amine (DY 062, Huntsman).

Density measurements are based on the Lambert-Beer law. Considering that the path length in ATR devices is related to the penetration depth which, in turn, depends on the refractive index of the polymers, the degree of shrinkage can be calculated as

$$\frac{\Delta V_t}{V_0} = \frac{A_0}{A_t} \cdot C - 1$$

Where the absorbance *A* corresponds to that of a reference species that should not change during the curing process, C is a factor that depends on the refractive index change of the reference wavelength during curing and the subindexes *t* and *0* indicate the reaction time and the beginning of reaction. The degree of curing *x* can be calculated as

$$x = 1 - \frac{\left(A_{spec}/A_{ref}\right)_t}{\left(A_{spec}/A_{ref}\right)_0} \cdot B$$

Where the subindexes spec and ref correspond to the reactive and the reference species respectively and the factor B depends on the refractive index change of both species during curing. In order to simplify the determination, the refractive index changes can be directly related to the degree of curing[5] and the factor *B* can be approximately made equal to 1.

An FTIR Bruker Vertex 70 equipped with an attenuated total reflection accessory with thermal control and a diamond crystal (Golden Gate Heated Single Reflection Diamond ATR, Specac-Teknokroma) was used to determine the FTIR spectra. Refractive indexes of cured samples were measured with a Metricon device using 632 nm wavelength laser. Refractive indexes of uncured formulations were analyzed with an Abbé refractometer. An ARG2 rheometer with an EHP temperature device was used to determine gelation and monitor the shrinkage after gelation. A Mettler DSC822e was used to determine conversion at the gel point.

Results and Discussion

Preliminary results show a good linear relationship between degree of curing and the degree of shrinkage calculated with the FTIR/ATR and refractive index technique for all the systems, with similar results at the different curing temperatures. The results are comparable to those obtained with the rheometer, thus validating the proposed technique, which can be used to assess the real curing shrinkage of existing and novel systems.

References

1. Khoun, L.; Hubert, P. Polymer Composites 2010, 31, 1603-1610.
2. Lange, J.; Toll, S.; Manson, J. A. E.; Hult, A. Polymer 1995, 36, 3135.
3. Holst, M.; Schanzlin, K.; Wenzel, M.; Xu, J.; Lellinger, D.; Alig, I. Journal of Polymer Science, Part B: Polymer Physics 2005, 43, 2314-2325.
4. Li, C.; Potter, K.; Wisnom, M. R.; Stringer, G. Composites Science and Technology 2004, 64, 55-64.
5. Cusano, A.; Breglio, G.; Giordano, M.; Calabro, A.; Cutolo, A.; Nicolais, L. Journal of Optics A: Pure and Applied Optics 2001, 3, 126-130.

Acknowledgments

The authors would like to thank MICINN, FEDER and Generalitat de Catalunya (MAT2008-06284-C03-01, MAT2008-06284-C03-02, 2009-SGR-1512, FPI-2009). Huntsmann is acknowledged for kindly supplying the samples, and Carlos Escusa from Brenntag Quimica is also acknowledged for providing Hexion Epikote resin.

Raman Evaluation of the Structure of Organic Materials by Analyzing the Region of Stretching Vibrations of CH_2 and CH_3 Groups – Benefits and Limitations

P. Donfack,[1] K. Prokhorov,[2] E. Sagitova,[1,2] Yu.V. Zavgorodnev,[2] G. Nikolaeva,[2] M. Guseva,[3] V. Gerasin,[3] A. Materny,[1] E. Antipov,[3] and P. Pashinin[2]

[1]Jacobs University, School of Engineering & Science, Campus Ring 1, Bremen, 28759 Germany
[2]A.M. Prokhorov General Physics Institute, 38 Vavilov St., Moscow, 119991 Russia
[3]A.V. Topchiev Institute of Petrochemical Synthesis, 29 Leninsky Pr., Moscow, 119991 Russia

nikolaeva@kapella.gpi.ru

The region of the stretching vibrations of CH_2 and CH_3 groups is very interesting for structural analysis of polymers due to the very strong dependence of the corresponding Raman spectra on the material structure. For many polymers, Raman lines in this region are significantly more intense as compared with the lines in other spectral regions. This can be advantageous in examining substances in a small amount and/or in the presence of intense background. However, the analysis of Raman spectra in the region of the stretching vibrations of CH_2 and CH_3 groups usually faces the problem of the overlapping of a large number of unresolved lines. The deconvolution of the spectra cannot be unequivocally proven from the mathematical point of view. As a consequence, spectral characteristics of individual lines cannot be accurately determined.

In this work we discuss different procedures for the analysis of polarized Raman spectra of a number of materials including liquid n-alkanes, polyethylene (PE), isotactic polypropylene (PP), random ethylene/olefin and propylene/olefin copolymers, PE/clay and PP/clay nanocomposites, and PE/PP blends. These materials have common spectral features: The comparison of their Raman spectra allows us to develop new approaches for structural analysis of olefins and their derivatives.

As an example, we have considered neat PP and nanocomposites of PP with modified clay (Fig. 1). The presence of the clay leads to the appearance of intense luminescence background in the Raman spectra and to low signal-to-noise ratio which is especially lower in the spectra measured with crossed polarizations of the laser and scattered radiations. Therefore, the standard approach of the evaluation of molecular orientation, based on the measurements of depolarization ratios of certain Raman lines, is not feasible. Noteworthy, the qualitative analysis of the degree of macromolecular orientation in the nanocomposites can also be based on the intensity ratio of the lines peaking at 2963 and 2885 cm^{-1}. These lines are assigned to the asymmetric and symmetric vibrations of the CH_3 groups, respectively.

Fig. 2 shows the ratio of the peak intensities of the 2963 and 2885 cm^{-1} lines as a function of the draw ratio for PP/clay nanocomposites with different filler content. The spectra were measured with parallel polarizations of the laser and scattered radiations. The intensity ratio sharply increases with the draw ratio "λ" until $\lambda \approx 5$, corresponding to the formation of the neck region. Then it exhibits substantially slower variations. Interestingly, the rate of increase in the intensity ratio, and therefore the orientational ability of the PP macromolecules, decreases with the growth of the filler content.

Both lines with peaks at 2963 and 2885 cm^{-1} correspond to PP isotactic chains localized in the crystalline and noncrystalline phases. Our X-ray data indicate that the presence of the filler does not affect the orientational ability of the macromolecules localized within PP crystallites. Therefore, the decrease in the degree of molecular orientation in the PP/clay nanocomposites is due to the decrease in the orientational ability of the isotactic chains localized in the noncrystalline regions of the polymer matrix.

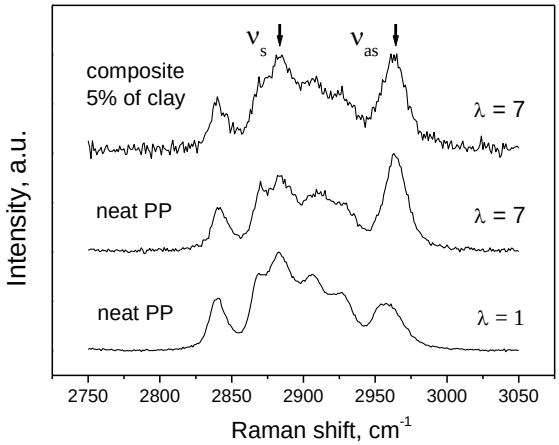

Fig. 1. Raman spectra of the neat PP and PP/clay nanocomposite with 5% of clay (λ is the PP draw ratio).

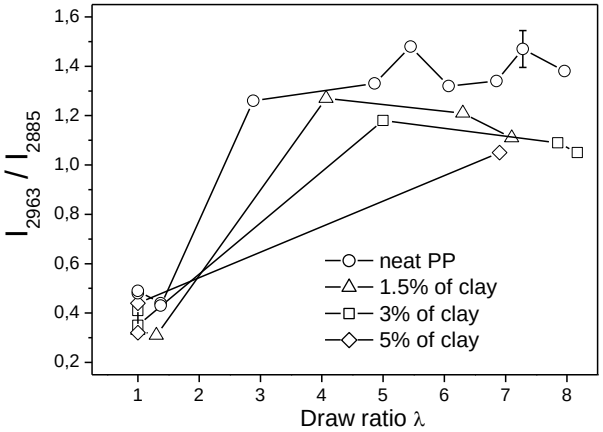

Fig. 2. Ratio of the peak intensities of the asymmetric and symmetric stretching vibrations of CH_3 groups as a function of the draw ratio for PP/clay nanocomposites.

This work is supported by the Russian Foundation for Basic Research (project code 09-02-00587-a) and the Grant of the President of the Russian Federation for the Support of Leading Scientific Schools (3675.2010.2).

Polymer Film Analysis

Ruth M. Zacur, Daniel R. Ercoli, Graciela S. Goizueta
Planta Piloto de Ingeniería Química, PLAPIQUI (UNS-CONICET)
Camino la Carrindanga Km 7 – (8000) Bahía Blanca – Argentina

rzacur@plapiqui.edu.ar

Introduction: Polymer films play a substantial role in the packaging of many consumer goods including perishable and non-perishable food items, medical instruments and supplies, and electrical components (1).
Among polyolefins, Polypropylene (PP) is a thermoplastic with a number of desirable properties such as high melting temperature, low density and high chemical inertness. In addition, its low cost places PP in an advantageous position with respect to most other plastic materials. Also, adequate properties are achieved commercially through a biorientation process that enhance toughness and gas barrier of films. So, the biaxially oriented PP (BOPP) is one of the most used film for packaging applications (2).
The complex technologies involved in the production of these films of thickness about 15-20 µm, justify the application of sophisticated analytical tools to solve processing troubles that could arise in some of the different manufacturing steps.
The present work focuses on the study of the structural characteristics of defects of about 50 µm on commercial BOPP films by Optical Microscopy (OM), Infrared Micro-Spectroscopy (IMS) and Scanning Electron Microscopy with Energy-Dispersive X-ray Spectroscopy (SEM/EDX).

Materials and Methods: Samples of about 2 µm thickness containing the imperfection were microtomed with a LEICA UCT at - 40 °C. They were observed under polarized light using an Optical Microscope Zeiss Phomi III POL and a video camera. Then samples were observed in the microscope while they were heated to 280 °C in a Mettler FP5 hot stage. Images were recorded and processed with the software AnalySIS 3.
IMS analysis was performed on microtomed samples of about ≅ 5 µm thickness using a Nicolet Nexus FTIR spectrometer with a Continuum Microscope. The number of scans was 200 and the digital spectral resolution was 4 cm^{-1} for each sample. The analyzed area was about 20 x 20 µm.
The morphological aspects and elemental composition of the microtomed surfaces containing the defects were studied by SEM/EDX using a JEOL 35 CF microscope equipped with a secondary electron detector and x-ray dispersive system EDAX DX-4. The samples were gold coated and the incident beam was perpendicular to the surfaces (voltage used was 10 kV).

Results and Discussion: Figure 1a shows an optical micrograph of the microtomed sample showing a defect in the central region. The defect appeared dark due to a lower light transmission in this region and remained without morphological modification after being heated to 280 °C. Figure 1b shows a SEM micrograph of the defect which was easily detected because a clear topographic contrast with the surroundings was obtained.

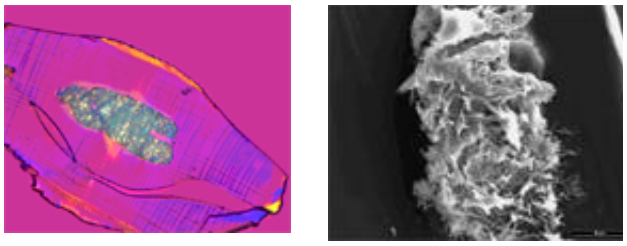

Figure 1: a) MO (x 400), b) SEM (x 1100)

Figure 2a shows an EDX spectrum obtained in the defect region where C, O and Na peaks appeared. In the rest of the film only the C peak was observed. The infrared spectrum of the defect region is shown in figure 2b. It was observed the presence of an aromatic compound. Additionally, absorption in the 1550-1610 cm^{-1} and 1300-1420 cm^{-1} region could be detected which are characteristics of stretching asymmetric and symmetric vibrations of CO_2^- groups present in salts of carboxylic acid (3).

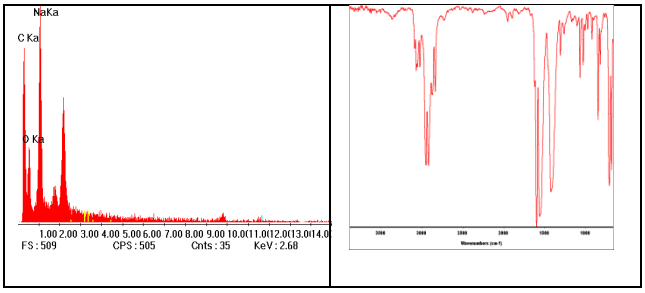

Figure 2: (a) X Ray, (b) IMS

Conclusions: The results showed that the defects on BOPP film were due to the presence of sodium benzoate.

References:

1. Brody A. L., Marsh K. S., Encyclopedia of Packaging Technology, Second Ed.; Wiley- Interscience, New York, 1997, 693-704.
2. Phillips R. A. , Nguyen T., App. Polym. Sci., 80, 2400-2415, 2001
3. Silverstein,R., Spectrometric Identification of Organic Compounds. *John Wiley & Sons, NY* ,1991.

Interplay between Raman Scattering and Atomic Force Microscopy in Characterization of Polymer Blends

P.Dorozhkin[1], A. Shelaev[2] and S. Magonov[3]

[1,2] NT-MDT, Zelenograd, Russia, [3]NT-MDT Development Inc., Tempe AZ 85284 USA

Atomic force microscopy (AFM) is routinely applied to compositional mapping of heterogeneous polymer materials. Recognition of the individual components in these materials is usually based on their specific morphology and differences of their local mechanical and electric properties. Nowadays a deficit of local chemical or spectral information in AFM can be overcome by combining it with confocal Raman microscopy. Such applications to polymer blends are fast developing and can be substantially enhanced with the use of multi-frequency AFM techniques which allow the simultaneous recording of surface morphology, local mechanical, dielectric and chemical (Raman spectra) response from the same sample area. Initial efforts in this direction will be presented in our work, which was focused on studies of films of immiscible blend of polystyrene (PS) and polyvinyl acetate (PVAC). The constituents of this blend have different local electric properties (surface potential, dielectric permittivity) that is well documented in single-pass Kelvin force microscopy and dC/dZ studies. The Raman spectra of PS and PVAC are characterized by specific individual bands of these components that provide their direct recognition in confocal Raman maps obtained on the surface of the blend films. A comparison of the KFM and dC/dZ images with Raman maps recorded at the same locations offers useful information about sensitivity as well as spatial and in-depth resolution of such characterization.

Characterization of Different Polymer Systems via Asymmetric Flow Field-Flow Fractionation (AF4)

Esra Altuntaş,[1] *Nicole Fritz,*[1,2] *Martin Hager*[1,2] *and Ulrich S. Schubert*[1,2*]

[1]Laboratory of Organic and Macromolecular Chemistry (IOMC) and Jena Center for Soft Matter (JCSM), Friedrich-Schiller-Universität Jena, Humboldtstrasse 10, 07743 Jena, Germany, Fax. +49 3641 948 202
[2]Dutch Polymer Institute (DPI), P.O. Box 902, 5600 AX Eindhoven, The Netherlands.

E-mail: ulrich.schubert@uni-jena.de; www.schubert-group.com

Introduction

The field of polymer science advances continuously due to the new emerged polymerization techniques and a need for new materials. In this context it is highly important to characterize different types of polymers to analyze their chemical structure and morphology. Therefore, there is a need for different separation methods to characterize various polymeric materials. The field flow fractionation (FFF)[1] technique is a fast emerging technique that can provide good separation for many different polymers, proteins, and particles using a single channel without any packing material inside. Recent progresses in the development of asymmetric flow field-flow fractionation (AF4) open new opportunities for the characterization of various polymers.

Materials and Methods

Asymmetric flow field-flow fractionation (AF4) system (AF2000 MT from Postnova) has been used to characterize different polymer systems. A mixture of poly(styrene sulfonate)s with different molar masses has been used as a model system with a broad molar mass distribution. A complete polymer separation and analysis was performed. A range of poly(2-ethyl-2-oxazoline)s and poly(ethyleneimine)s have been synthesized to measure with this system.

Results and Discussion

In this contribution, asymmetric flow field-flow fractionation (AF4) is used as an analytical separation technique for the characterization of different polymer systems such as poly(styrene sulfonate)s, poly(2-ethyl-2-oxazoline)s, and poly(ethyleneimine)s. Detailed information on the polymers is available on radii of gyration, polymer contour lengths, molar masses and coil conformation. This method is expected to be applicable for a wide range of water soluble synthetic and natural polymers.

References

[1] Giddings J. C. *Science* **1993**, *260*, 1456–66.

Thermogravimetric Analysis of an Acrylic Copolymer

Oberti T. G.[1], *Cortizo M. S.*[1], *Alessandrini J. L*[2]

[1] Instituto de Investigaciones Fisicoquímicas Teóricas y Aplicadas (INIFTA), Dpto. de Química, Fac. Cs. Exactas, UNLP,CCT-La Plata, CONICET CC 16, Suc. 4.

[2] Departamento de Física, Instituto de Física de La Plata (IFLP), CIC-PBA. Facultad de Ciencias Exactas, Universidad Nacional de La Plata (UNLP), Argentina.

E-mail: toberti@hotmail.com

Introduction

Known that the molecular properties, such as, chemical composition, stereochemical, molecular weight and molecular weight distribution are directly related with polymer properties and which in turn, are a reflection of the kinetic history of the reaction occurred during its formation. For this reason, when we think about the design of homopolymers, a blend of polymers or copolymers, glass transition temperature (Tg) is a very important parameter to consider as it defines in a way its flexibility, which influence on final properties of the material[1].

In this work is present the thermogravimetric analysis (TGA) for different composition of poly(diisopropil fumarate -co- p-nitrobenzyl acrylate) [P(DIPF-NBA)] and degradation activation energies were calculated for each composition.

Materials and Methods

The copolymers were synthesized under microwave energy using different amounts of both monomers. The mole fractions of the monomers in the copolymers were determinate by ^{1}H-RMN (see table).

To assess the transformation as well as the thermal stability of the resulting copolymers, thermogravimetry analysis was carried out using a 51 Shimadzu thermogravimetric Analyzer under nitrogen flow (25 mL / min) between 25 to 700 °C and heating rate 10 °C / min. The analysis of the glass transition temperature (Tg) was carried out in a differential scanning calorimeter Shimadzu-TA60. To that end, 5 mgr samples were introduced in sealed aluminum pans and analyzed with a flow of N_2 of 30 ml / min. To erase the thermal history were made heating / cooling ramps: 150 °C to 30 °C / min -100 °C to -30 °C / min to 250 °C to 10 °C / min. The degradation activation energies (E) of the sample were calculated from non-isothermal TG curves using Freeman and Carroll equation[2], assuming a first order reaction kinetic.

Results and Discussion

All copolymers appear to decompose in two-stage process and show higher initial decomposition temperatures (IDT) than corresponding homopolymers. PDIPF is degraded in single-step, starting to 250 °C, according to previously reported[3]. Although the maximum rate of degradation is similar for all polymers (320-330 °C), the degradation activation energy (E) was different. The Figure and Table shows that PNBA decompose more easily than the other polymers. An increase in thermal stability of copolymers, when the NBA content increases up to 0.66, was observed. Can not establish an order of stability only based on the composition copolymer, probably due to different average molecular weights of samples. In fact, the last two polymers exhibit M_w which are an order of magnitude lower than the others M_w.

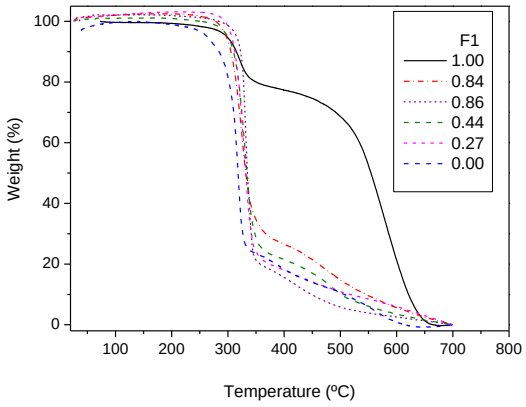

Figure: TGA curves of DIPF-pNBA copolymers under nitrogen at heating rate of 10 °C/min. F_1 is the mole fraction of pNBA in the copolymer.

Polymer	F_1	T_g (°K)	IDT	T_{max1}	T_{max2}	E (kJ/mol)	r^2
PDIPF	0.00	348	250	318(53.9)	-	228.6	0.94
(DIPF-NBA)	0.27	337	280	332(51.3)	616(95)	226.8	0.97
	0.44	331	272	332(46.5)	490(88.5)	254.6	0.99
	0.66	324	290	331(35.9)	452(90.3)	362	0.95
	0.84	321	290	327(41.7)	475(81.9)	189.6	0.97
PNBA	1.00	316	220	320(14.7)	580(67.3)	142.3	0.94

F_1 is the mole fraction of NBA in the copolymer
IDT is the initial decomposition temperature
T_{max} temperature at which the degradation rate reached a maximum (from DTG curves). Value in parentheses indicates the total weight loss (%) up to the temperature stated.

Conclusions

Since no melting peaks observed in DSC curves, these copolymers do not have crystalline regions.

The presence of ANB increases the thermal stability of the material.

References

1-M. Fernandez García, et al. Polym. Bull., 2000, 45: 397-404.
2- E. S Freeman, B. Carroll. J. Phys. Chem., 1958, 62: 394-397.
3- T. Otsu, et al. Makromol. Chem. Suppl., 1985, 12: 133-142.

Structural analysis of synthetic polymer by high-energy CID using MALDI SpiralTOF-TOF

Takaya Satoh[1], Ayumi Kubo[1], Yoshiyuki Ito[1], Masahiro Hashimoto[1], Masaaki Ubukata[2], Takafumi Sato[1], Jun Tamura[1] and Akihiko Kusai[3]

1. JEOL Ltd., 2. JEOL USA, Inc., 3. JEOL (Europe) SAS

kusai@JEOL.fr

[Introduction]

Recently, a tandem time-of-flight mass spectrometer (TOF-TOF) is used for structural analysis of synthetic polymer. A high-energy collision-induced dissociation (HE-CID) is mostly used method to make a fragmentation. There are two factors which make interpretation of a HE-CID product ion spectrum difficult: i) overlap of fragment pathways of HE-CID and post-source decay (PSD) on a product ion spectrum, ii) insufficient separation of fragment peaks caused by low precursor ion selectivity and low mass resolution.

The MALDI TOF-TOF combined a SpiralTOF [1] and an offset parabolic reflectron [2] for first and second TOFMS, respectively has been developed. The SpiralTOF, which has 17 m flight path, can select a monoisotopic ion so that each fragment pathway is observed as single peak on product ion spectrum. Furthermore, PSD ions are eliminated by electrostatic sectors inside the SpiralTOF. As a result, fragment pathways of HE-CID are preferentially observed on product ion spectrum.

In this study, some synthetic polymers were investigated for structural analysis using HE-CID spectrum acquired by the MALDI SpiralTOF-TOF.

[Experimental]

Poly(propylene glycol) average Mn ca. 1000 (Sigma-Aldrich), α-cyano-4-hydroxycinnamic acid (HCCA) (Wako) and sodium iodide were used as an anlayte, a matrix and a cationic compound, respectively. HCCA was dissolved in acetonitrile/deionized water solution (1:1) at a concentration of 10 mg/mL. PPG and sodium iodide were prepared by diluting in deionized water solution at concentrations 10 mg/μL and 1 mg/μL, respectively. PPG, HCCA and sodium iodide solutions were mixed in the ratio of 1:2:1, and 1 μL of the mixture was deposited on a MALDI target plate made of stainless steel by the dried-droplet method. JMS-S3000 with TOF-TOF option (JEOL Ltd., Japan) was used for data acquisition.

[Results and discussion]

Figure 1(a) shows the product ion spectrum of $[M+Na]^+$ whose m/z value was 1085. Repeat structure of propylene glycol monomer (58 u) was clearly observed of only selected precursor ion. There were no PSD ions on the product ion spectrum. Figure 1(b) shows enlarged spectrum of m/z < 190. In this region, fragment pathways related to near end-group were observed as single peaks.

[Conclusion]

The precursor ion was selected as a monoisotopic ion using the SpiralTOF. Also, a product ion spectrum was obtained by HE-CID using the SpiralTOF-TOF without any PSD ions. The expected fragmentation pathways were clearly observed.

[References]

[1] T. Satoh, T. Sato, J. Tamura, *J. Am. Soc. Mass Spectrom.* **2007**, *18*, 1318.

[2] E. N. Nikolaev, Á. Somogyi, D. L. Smith, C. Gu, V. H. Wysocki, C. D.Martin, G. L. Samuelson, *Int. J. Mass Spectrom.*, **2001**, *212*, 535

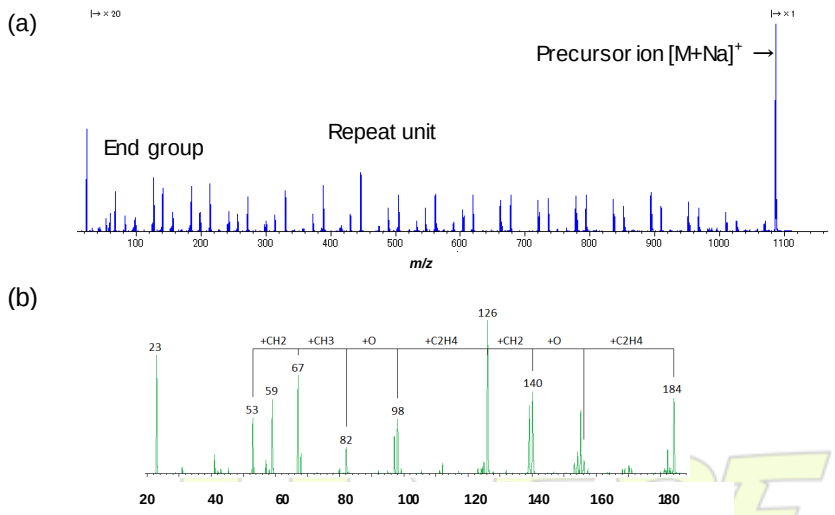

Fig. 1 (a) the product ion spectrum of PPG, and (b) enlarged product ion spectrum at m/z <190

Mechanical characterization of a linear polyethylene by means of Depth Sensing Indentation (DSI) measurements.

Vicente Lorenzo[1], *María Ulagares de la Orden* [1,2], *Rafael Claramunt*[3] *and Joaquín Martínez-Urreaga*[1]

[1] "POLímeros: Caracterización y Aplicaciones", Universidad Politécnica de Madrid (UPM), José Gutiérrez Abascal 2, 28006, Madrid, Spain
[2] Depto. "Química Orgánica I", Universidad Complutense de Madrid
[3]Depto. "Mecánica Estrcutural y Construcciones Industriales", UPM

vicente.lorenzo@upm.es

INTRODUCTION

Vickers microhardness (MH) is a well established experimental technique for the mechanical characterization of polymeric materials. Depth Sensing Indentation (DSI) is a method closely related to MH determination that yields a more detailed information about the indentation process because the load-penetration curve is continuously monitored. However, DSI has been scarcely applied to the mechanical characterization of polymers.

The aim of this paper is to present some preliminary results about characterization of polyethylene, PE, samples using DSI

MATERIALS AND METHODS

A linear polyethylene was used for this study. The melt flow index of this polymer is 0.6 g/min, its nominal density is 0.958 g/cm^3 and its viscosity average molecular weight is 1.25x10^5. The samples were molten and then pressed between the plates a hydraulic Collin press. Two different cooling rates were used, either slow cooling between the press plates (~ 1ºC/min) or quenching in ice-water (~ 100ºC/min). Former sample was labeled as S and later, as Q.

Table 1: degree of crystallinity, f_c^d, elastic modulus, E, and Vickers microhardness, MH, of the samples (these values were reported previously)

Sample	f_c^d	E (MPa)	MH (MPa)
Q	0.66	625	47
S	0.78	795	66

A Berkovich indentor attached to a Shimadzu Dynamic Hardness Tester DUH-211S was used for DSI measurements at 20ºC. A 20 mN maximum load, P_0, was applied with a loading speed of 13.3 mN/s, this load was hold for 5 s. before unloading (Figure 1).

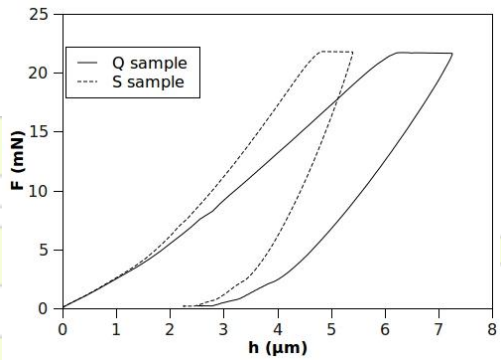

Figure 1: load (F) – penetration (h) depth curves

RESULTS AND DISCUSSION

The different hardness values that can be obtained from DSI experiments have been evaluated according to the standard methods (EN-ISO 14577-1). These methods has also been used for calculating the elastic moduli, E^*, from the initial part of the unloading curve.

The creep deformation under the indentor has been explained satisfactorily by using a four elements Maxwell-Voigt model and the correspondence principle to modify contact Hertz equation [1].

The delayed elastic-recovery has been analyzed by using the same equation that has been reported after studying Vickers indentation recovery by means of a Michelson-Morley interferometer[2].

Table 2: values for creep reduced modulus, E^*_1 (MPa), unloading modulus, E^* (MPa), Martens hardness, HT115 (MPa), indentation hardness, Hit (MPa), and retardation time for delayed elastic recovery, τ (s).

Sample	E^*_1	E^*	HT115	Hit	τ
Q	410	217	56	27	0.48
S	673	420	65.5	42.5	0.46

The comparison of the results in Table 2 with those obtained by using other experimental techniques (Table 1) shows a reasonable agreement between hardness values obtained from residual impressions, HT115 and MH, and between the different types of moduli.

Even more, it has been found that the short-term retardation time for delayed elastic-recovery under zero load does not depend on the degree of cristallinity. The same behaviour has been previously reported for the long-term delayed elastic recovery of Vickers indentations in PE [2].

CONCLUSIONS

These results show that DSI measurement can be an adequate and straightforward technique for the characterization of some aspects of the mechanical behaviour of polymeric materials

REFERENCES

[1] Fischer-Cripps, A. C., "A simple phenomenological approach to nanoindentation creep", *Mater. Sci. Eng., A*, **2004**, *385*, 74-82

[2] Lorenzo, V., Pereña, J.M., Fatou, J.G., Méndez Morales, J.A. and Aznarez, J.A., "Delayed elastic-recovery of hardness indentations in polyethylene", *J. Mater. Sci.*, **1988**, *23*, 3168-3172

Characterization of different varieties of cassava flour by solid state NMR spectroscopy

Gisele C. V. Iulianelli, *Maria Inês B. Tavares*

Instituto de Macromoléculas - Universidade Federal do Rio de Janeiro / Brazil

gisele@ima.ufrj.br

Introduction

Cassava (*Manihot esculenta Crantz*), known in Brazil as "mandioca", "macaxeira" or "aipim", is the main crop cultivated in several farming in Brazil and, also, in other areas in tropical América [1]. Cassava flour is mainly constitutes by starch, fiber, proteins, lipids and minerals [2,3]. However, it is known that the percentage of these components may differ substantially between the varieties, resulting in differences in their nutritional aspect. The focus of this paper was to investigate six varieties of cassava with respect to chemical composition and molecular dynamic behavior, employing nuclear magnetic resonance spectroscopy (NMR).

Materials and Methods

The samples were characterized by different solid-state NMR techniques, such as cross polarization magic-angle spinning (CPMAS), variable contact time (VCT), and proton spin-lattice relaxation time in the rotating frame ($T_1\rho H$). The ^{13}C NMR spectra were obtained on a Varian INOVA 300 spectrometer operating at 75.4 MHz for ^{13}C. For the VCT experiment, a range of contact time was established from 200 to 8,000 μs, and $T_1\rho$ values were determined from the intensity decay of ^{13}C peaks with increasing contact times.

Results and Discussion

^{13}C CPMAS NMR spectra (Fig. 1) showed three NMR signal located in a particular region that is assigned as polysaccharides, indicating that these samples consist mainly of starch. Comparing the ^{13}C CPMAS spectra of M1, M2 and M3 cassava samples they present a different structural organization in relation to the other samples, since NMR signals are located at lower chemical shifts, suggesting that those samples are more amorphous, probably due to the higher quantity of amylose ratio in starch composition.

From VCT experiment (Fig 2), it was observed a simple decay for all resolved ^{13}C signals. This molecular behavior shows that these samples have molecular rigidity. The best contact-time for the polarization transfer between ^{1}H and ^{13}C was 800 μs for all cassava flour samples, excluding M1 in which 400 μs was detected as a best contact-time. This result shows that M1 sample is more rigid than the others, due to its stronger intermolecular interactions, indicating that M1 sample probably has differences in its chemical composition.

The VCT experiment permits us to determine the $T_1\rho H$ relaxation time (Table 1). It can be seen that M2, M3, M4 and M6 samples are more homogeneous, since $T_1\rho H$ values are more uniform, while M1 and M5 samples show some heterogeneity in their composition and/or molecular organization. It was also observed, that M4 sample present a slightly lower molecular mobility. The $T_1\rho H$ behavior is related to chains interaction/proximity, which may be understood as indicating that M4 sample have higher amylopectin proportion, since this component is responsible for the crystallinity in starch granules [4].

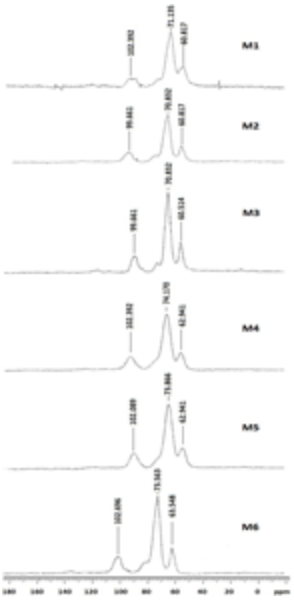

Figure 1- 13C CPMAS spectra for

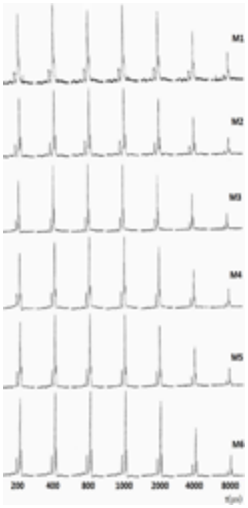

Figure2- VCT experiment

Table 1 - Proton spin-lattice relaxation parameter from cassava samples, determined during the VCT experiment

	Cassava Samples					
	M1	M2	M3	M4	M5	M6
δ(ppm)	102	99	100	102	102	103
	71	71	71	74	74	74
	60	61	61	63	63	64
$T_1\rho H$ (ms)	4	4	6	3	4	5
	11	6	5	3	6	5
	13	6	7	3	11	6

Conclusions

Solid state NMR techniques provided important information on chemical and structural characteristics of different cassava varieties. From the NMR data obtained in this study, it appears that the cassava samples studied showed variations on nutritional aspects based on their molecular structure and chemical composition, serving as markers for specific diets.

References

[1]-Siqueira, M.V.B.M., *et al. Genetics and Molecular Biology*, 32 (1), 104-110, 2009.

[2]-Chijindu, E.N., & Boateng, B.A.. *World Journal of Agricultural Sciences*, 4 (3), 404-408, 2008.

[3]-Dias, L.T., & Leonel, M. *Ciência agrotécnica, Lavras*, 30 (4), 692-700, 2006.

[4]-Corradini, E., Lotti, C., & Medeiros, E.S. *Polímeros: Ciência e Tecnologia*, 15 (4), 268-273, 2005.

Kinetic investigation of thermal degradation for low molecular weight 1,2-polybutadiene

Mohamad Ronagh Baghbani[1], *Farshid Ziaee*[1], *Hosein Bouhendi*[1], *Farhood Ziaie*[2]

1: Iran Polymer and Petrochemical Institute. Postal Code: 1497713115
2: Nuclear Science and Technology Research Institute.

E-mail: Mb_ronaghi777@yahoo.com

Introduction

Degradation of polybutadiene has been studied in recent years. These studies were investigation of environmental condition effects and undesired situation on degradation of polybutadiene. The main degradation mechanisms are cyclization, crosslinking and chain scission [1, 2]. In this study, thermal degradation of low molecular weight 1,2-polybutadiene (1,2-PBD) with different contents of 1,2-vinyl isomers by Nuclear magnetic resonance (^{13}C-NMR) method was investigated. Also, kinetic parameters of degradation reaction have been calculated.

Experimental

Low molecular weight (1,2-PBD) with 12%, 25%, 85% of 1, 2-vinyl isomers (A, B, C respectively) were purchased from Aldrich. About 2 g of (1,2-PBD) were placed into glass tubes (Diameter= 20mm) and nitrogen gas was purged. After that, tube was vacuumed and placed in oil bath during different times and temperatures. Finally, degraded (1,2-PBD) was solved in $CDCl_3$ and ^{13}C-NMR Spectrum was obtained.

Result and discussion

NMR Spectra of degraded samples at different temperature (235, 250 and 265° C) and times are shown in Figure1. Results show that crosslinking was occurred with two different mechanism, the first is reaction between 1,2-vinyl isomers of two different chains, and the other is reaction between 1,2-vinyl isomer from one chain and cis or trans isomers of another chain. Chain scission is also occurred in two mechanisms. One of them is chain scission at two adjacent 1,2-vinyl isomers and another one is chain scission at adjacent 1,2-vinyl with cis or trans isomers. Furthermore, kinetic of first mechanism of crosslinking and chain scission have been studied. Kinetic parameters such as degree of reaction, activation energy and K_0 (kinetic rate constant at ambient temp.) at first stages of reaction were obtained from integration of NMR Spectra. Rate of first crosslinking and chain scission mechanism against of 1,2-vinyl contents at different 1,2-PBD samples shows in Figure2. The kinetic equations of degradation mechanisms are presented in equation 1 and equation 2.

Equation1:

$$R_{Crosslinking1} = k_{01} \times e^{-E_{a1}/RT}[1,2-vinyl]^{\propto}$$

Equation2:

$$R_{Chain\ scission1} = k_{02} \times e^{-E_{a2}/RT}[1,2-vinyl]^{\beta}$$

We calculated α = 2.13, E_{a1} = 166.01 kJ/mol k and K_{01} = 1.44×10^{15} $lit^{1.134}/mol^{1.134}$k for first crosslinking mechanism. Also calculated β = 1.67, E_{a2} = 195.5 kJ/mol k and K_{02} = 4.59×10^{17} $lit^{0.67}/mol^{0.67}$k.

Conclusion

^{13}C-NMR Spectra of low molecular weight (1,2-PBD) showed that crosslinking and chain scission occurred in two different mechanisms, individually. Kinetic parameters of crosslinking and chain scission mechanisms were obtained.

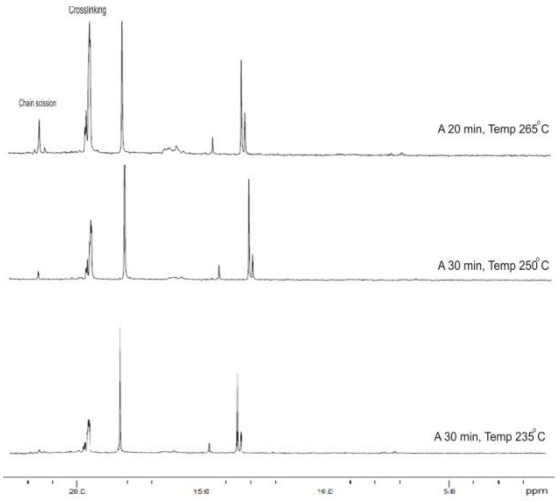

Figure1: ^{13}C-NMR spectra of degraded 1,2-PBD (sample A) in different time and temperatures

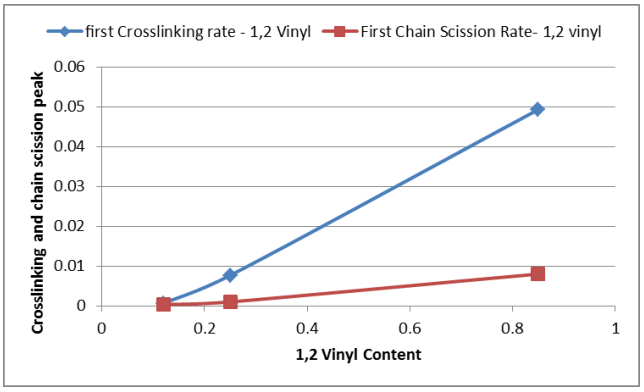

Figure 2: Rate of First Crosslinking and chain scission mechanism against of 1,2-vinyl contents at different 1,2-PBD samples

References

1- Coquillat M, Verdu J, Colin X, Audouin L, Neviere R. Polymer Degradation and Stability 92 (2007) 1326–33.
2- Ziaee F, Salehi Mobarakeh H, Nekoomanesh H. Polymer Degradation and Stability 94 (2009) 1336–1343.

Three-dimensional modeling of mold filling process in injection process using OpenFOAM

Narjes Jafari Esfad, Bahareh Azinfar, Ahmad Ramazani S.A.

Chemical and Petroleum Engineering Department, Sharif University of Technology, Tehran, Iran

narges_jafariesfad@yahoo.com

Introduction

Process of filling in the procedure of injection forming process is so important. Our goal in this research is to model the process of filling the mold in the injection molding process with using OpenFOAM.

Material and Methods

In this research Two-phase model concerning two-phase fluid including Viscoelastic and Newtonian (Air) was applied. Giesekus model was used for Viscoelastic phase which the studied phase was considered as a combination of the polymer and solvent. The viscosity of polymer fluid was assumed 1.2 Pa.s which is about 1000 times greater than water viscosity. The applied pressure difference was considered 8000 Pa. To improve the pressure distribution in the mold, two symmetrical vents on either side of mold were designed.

The dimensions of applied mold and its entry are designed100cm×100cm×1cm and 250cm×10cm×1cm consequently.

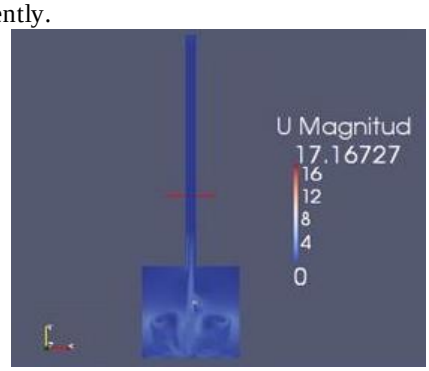

Figure 1: Velocity variation during filling process at t=1.5 for Viscoelastic fluid without vent.

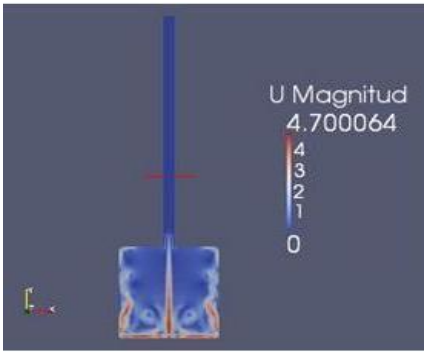

Figure 2: Velocity variation during filling process at t=1.0 for Newtonian fluid with vent.

Results and Discussion

Maximum observed flow rate for Newtonian fluid without vent is -0.0037 m/s while the applied velocity to the fluid in the program was -0.06 m/s that the velocity reduction can be considered by raising the cavity pressure during filling the mold because the upward force of air into the fluid reduces the fluid velocity. With applying a vent to the model, the problem of pressure built up in the cavity was solved and, the maximum flow rate obtained about-0.06 m/s. For viscoelastic fluid as can be observed in figure 3, when the vent not applied, the maximum flow rate is equal to -0.022 m/s which is due to the pressure rising into the cavity and therefore the upward force to the fluid decreases the velocity dramatically.

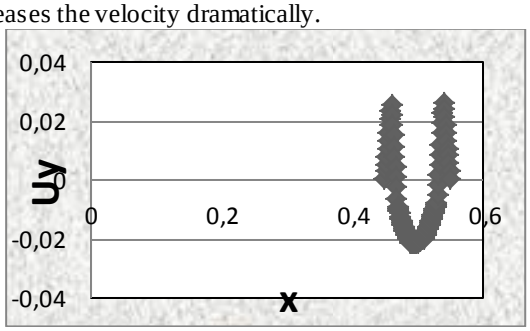

Figure 3: Velocity variation as a function of distance for viscoelastic Fluid without vent at entry point.

Two parts near the beginning and the end wall, encountered the upward velocity. To justify this phenomenon can be said, viscoelastic fluid on the walls due to non-slip condition, is trapped, while the upward air force raises the fluid near the wall which has less velocity. Thus, the attached fluid to the wall is not moving and the fluid resides in the center, finds the maximum velocity to the down direction.

Conclusions

A logical velocity gradient and pressure has been obtained. Die-swell phenomenon in viscoelastic fluid flow was observed well. When vent was not embedded, due to increase of pressure in the cavity, an upward force would be applied to the fluid which reduces the fluid velocity. When the vent is fitted, there is no upward force and the inputted fluid will be gain a greater velocity.

References

[1] Rudert, Schwarze; Experimental and numerical investigation of a viscoplastic carbopol gel injected into a prototype 3D mold cavity, 2009.

[2] Subbiah; Non-isothermal flow of polymers into two dimensional, thin cavity molds: a numerical grid generation approach,1988.

[3] Sanjay K.Mazumdar, Composites manufacturing materials product and process engineering, CRC press 2002.

[4]R.Byron,Bird,Robert,C.Armstrong,Ole,Hassager,Dynamics of polymeric liquids,Volume 1,second Ed.,A wiley – Interscience publication,1987.

[5] OpenFOAM 1.6 user Guide, 2009.

[6] Chen; Least-squares finite element methods for generalized Newtonian and viscoelastic flows, 2010.

Derivatives of Coumarin as Fluorescent Probes for Monitoring Photopolymerization Processes by Fluorescence Probe Technology

J. Ortyl, R. Popielarz

Cracow University of Technology, Faculty of Chemical Engineering and Technology,
Institute of Organic Chemistry and Technology, Warszawska 24, 31-155 Krakow , Poland.

jortyl@chemia.pk.edu.pl

Introduction.

Fluorescence Probe Technology (FPT) is a new method, applicable for monitoring of polymerization processes. The FPT method relies on measurement of changes in fluorescence characteristics of specially designed fluorescent molecular probes upon changes occurring in the probe environment.[1] Most of known fluorescent probes suitable for monitoring free radical polymerization, usually do not perform well in cationic polymerization systems. Only a few fluorescent probes suitable for cationic polymerization have been reported so far [2]. In this communication, we report the performance of the following coumarin derivatives (Fig. 1) in cationic photopolymerization of a monomer, in comparison to commercial Coumarin-1 probe, which is used for monitoring free radical polymerization:

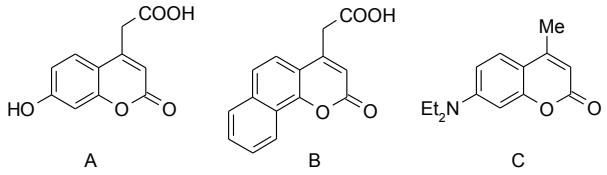

Fig.1. The fluorescent probes studied.

Materials and Methods

The compositions contained triethylene glycol divinyl ether (TEGDVE monomer, Aldrich), diphenyliodonium hexafluorophosphate (photoinitiator, $2.3 \cdot 10^{-2}$ mol dm^{-3}, Alfa Aesar) and a probe ($6.1 \cdot 10^{-3}$ mol dm^{-3}). (7-Hydroxycoumarin-4-yl)acetic acid (A) and (benzo[*h*]-coumarin-4-yl)acetic acid (B) were synthesized from 2-ketoglutaric acid and resorcinol or α-naphtol respectively, in sulfuric acid (95%). The cure monitoring system used in this study was described previously.[3]

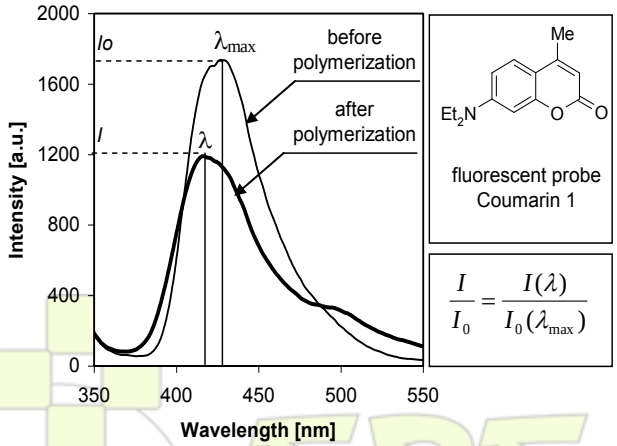

Fig.2. Fluorescence spectra of probe **C**.

Results and Discussion

The normalized fluorescence intensity (I/I_o) was applied as an indicator of the polymerization progress. The (I/I_o) was defined as the ratio of maximum fluorescence intensity at any given polymerization time to the maximum intensity at the beginning of polymerization (Fig. 2). Figure 3 shows the kinetic profiles of the photopolymerization process, obtained using (I/I_o) as the polymerization progress indicator. The coumarins A-B exhibit increase of the I/I_o upon monomer polymerization. While the I/I_o of Coumarin 1 probe, used as a reference, first decreased and then slightly increased during the polymerization of monomer. This indicates that Coumarin 1 response is strongly affected by protonation with hexafluorophosphoric acid generated in the system, while the response of the probes A-B is not sensitive to the acidic environment. Hence, the coumarins A-B are suitable for monitoring cationic polymerization processes by FPT, while Coumarin 1 is not.

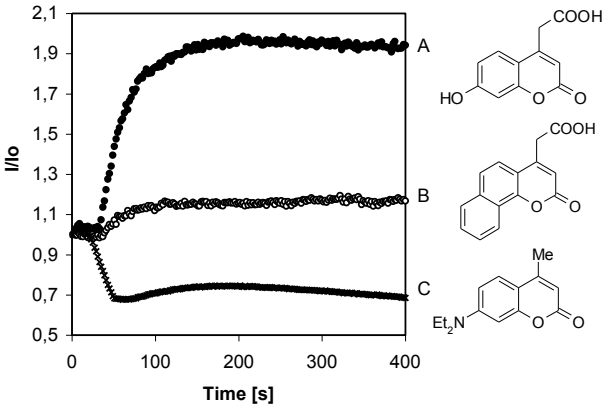

Fig.3. Kinetic profiles of cationic polymerization of TEGDVE, obtained by FPT method using the probes studied.

Conclusions

The coumarins (A-B) are applicable for use as new fluorescent probes for cure monitoring of cationic polymerization processes by FPT, using I/I_o as the polymerization progress indicator. The response of probe A is more sensitive to changes occurring in its environment than that of probe B. Regular kinetic profiles of cationic polymerization of a monomer are obtained with these probes. On the other hand, the I/I_o response of Coumarin 1 is strongly affected by the acidic polymerization catalyst, which makes it not good fore the cationic polymerization systems.

Acknowledgement

This work was supported by Foundation for Polish Science within the VENTURES project.

References

[1] Z.J. Wang, J.C. Song, R. Bao, D.C. Neckers, *J. Polym. Sci.: Part B: Polymer Physics* 1996, 34, 325.
[2] B. Strehmel, J.H. Malpert, A.M. Sarker, D.C. Neckers, *Macromolecules* 1999, 32, 7476.
[3] J. Ortyl, K. Sawicz, R. Popielarz. *J. Polym. Sci., Part A: Polym. Chem.*, 48 (2010) 4522.

Study of Thermo-mechanical and Thermo-oxidative Degradation of Polylactide by MALDI-TOF-MS . A Statistical Design of Experiments to Optimize the Sample Preparation Procedures.

J.D. Badía [1], *E. Strömberg* [2], *A. Ribes-Greus* [1], *S. Karlsson* [2,*]

[1] Institut de Tecnología de Materials (ITM), Universitat Politècnica de València (UPV)
[2] School of Chemical Science and Engineering, Fibre and Polymer Technology, Royal Institute of Technology (KTH)

*corresponding author: S. Karlsson (sigbritt@kth.se)

Introduction: Multiple processing by means of successive injection cycles was used to simulate the thermo-mechanical degradation effects on the oligomeric distribution of PLA under mechanical recycling. Likewise, an accelerated thermal ageing over PLA glass transition was performed in order to simulate its service life. MALDI-TOF MS was used for the analysis. The difficulty of performing good-quality and reliable MALDI measurements depends on many factors[1-2] such as the molar mass of the polymer, the choice of solvent, the choice of matrix, the ratio analyte/matrix, the use of cationization agent, the laser energy or the mode of detection (linear or reflector), among others . The sample preparation procedure was thus assessed by means of a statistical Design of Experiments (DoE).

Materials and Methods: Polylactide (PLA) 2002D from Natureworks LLC (Minnetonka, MN), was analyzed. MALDI matrixes, namely 1,8,9-anthracenetriol (dithranol), 2-(4-hydroxyphenylazo) benzoic acid (HABA), 2,5-dihydroxybenzoic acid (s-DHB) were tested as matrixes, as well as sodium trifluoroacetate (NaTFA) was used as cationization agent. Preparations were carried out in tetrahydrofurane (THF). Successive 5 processing steps (RPLA-i, with i: 1-5) by injection moulding employing an Arburg 420 C 1000-350 injector were applied. Temperature gradient set from hopper to die was 160, 170, 190, 200 and 190ºC. Moulds were set at 15 ºC. Cooling time residence was 40 s and total residence time ca. 60 s. After injection, a fraction of the samples was kept as test specimen and the rest was ground by means of a cutting mill Retsch SM2000, which provided pellets of size $\Phi < 20$ mm to be fed back into the recirculation process. Thermo-oxidative aging was performed on dehumidified virgin PLA by means of a Heraeus UT 6060 forced-ventilation oven under air atmosphere at 60 ºC. Samples were removed for analysis after the exposure times of 1, 3, 6, 10 and 12 weeks. MALDI-TOF/MS experiments were conducted in the 200-6000 Da *m/z* range by means of a Bruker UltraFlex MALDI-TOF mass spectrometer with a SCOUT-MTP ion source, in the reflector positive mode.

Results and Discussion / Conclusions: The application of DoE for the improvement of the MALDI analysis of PLA, on the basis of main effects plots, interaction effects plots and analysis of variance, stated that the best resolution was obtained with mixtures prepared with s-DHB as matrix, in a proportion analyte/matrix (V/V 1/5), without cationization agent.

Sample plate of samples for MALDI analysis

Degradation primarily affected the initially predominant cyclic $[LA_C]_n$ and linear H-$[LA_L]_n$-OH species. Intramolecular and intermolecular transesterifications as well as hydrolytic reactions occurred during the formation and disappearance of oligomeric species. In both degradation mechanisms induced by thermo-oxidative and thermo-mechanical degradation, the formation of H-$[LA_L]_n$-O-CH_3 is highlighted, although a different behavior was observed. Thermo-oxidative ageing presents a two-stage performance, governed by intramolecular transesterifications during the first stage and scission reactions during the second stage, when over-exposure to temperature conditions triggered the depolymerization of cyclic species. On the other hand, thermo-mechanical degradation seems to occur mainly via hydrolytic reactions and intermolecular transesterifications, giving rise to a noticeable major abundance of H-$[LA_L]_n$-O-CH_3 groups, especially after the third recyclate.

References: [1] Montaudo G., Montaudo M. S., Samperi F. Matrix-Assisted Laser desorption Ionization/Mass Spectometry of Polymers (MALDI-MS). In: Lattimer R. P. Montaudo G. *Mass Spectometry of Polymers.* Boca Raton, Florida : CRC Press LLC, 2001, pág. 422.
[2] Hoteling A J, Kawaoka K, Goodberlet M C, Yu W M, Owens K G. *Optimization of Matrix-Assissted Laser Desorption/Ionization Time-of-flight Collision-Induced Dissociation using Poly(ethylene glycol).* Rapid Communications in Mass Spectrometry 2003; 17: 1671-1676.

Acknowledgements: Spanish Ministry of Science and Innovation (Research Project UPOVCE-3E-013). Spanish Ministry of Education (FPU to J.D. Badía). UPV and KTH for additional economical support.

Diffusion during Radical Bulk Polymerization of Styrene and Metyl Methacrylate

Stempfle, B. K.; Dorfschmid, M.; Wöll, D.

Universität Konstanz, 78457 Konstanz, Germany

Beate.Stempfle@uni-konstanz.de

Diffusional changes during radical bulk polymerizations play a significant role for polymerization kinetics and the properties of the synthesized polymers. We investigated molecular diffusion of fluorescent perylene diimide molecules during the polymerization of methyl methacrylate (MMA) and styrene using fluorescence correlation spectroscopy (FCS) and single molecule widefield fluorescence microscopy (WFM). The combination of both methods allows for a detection of the diffusion of single fluorescent probe molecules from the initiation of polymerization up to high conversions.

In FCS, the detection range for the translational diffusion coefficient D reaches from 10^{-9} to 10^{-13} m^2s^{-1}, whereas WFM covers a range between 10^{-12} and 10^{-18} m^2s^{-1}. In contrast to ensemble methods, single molecule observation in WFM allows for the detection of heterogeneities of translational diffusion.[1] The fluorescent molecule acts as probe for the local microviscosity within the polymerization mixture. This microviscosity is determined by the local structure of the polymer-monomer mixture and its dynamics. With increasing conversion this structure changes and, due to a increasing polymer content, diffusion becomes more restricted.[2]

Our measurements show that translational diffusion becomes more restricted during the polymerization of MMA compared to the polymerization of styrene. Additionally, during the polymerization of MMA, an increased amount of immobile molecules was detected at conversions higher than 0.25. In styrene polymerization, this phenomenon can be also observed, but appears at much higher conversion and less pronounced. We assume that this is due to a more heterogeneous network with areas of higher density evolving during the polymerization of MMA. The size of the meshes is determined by entanglements of the polymer chains.

The conversion from monomer to polymer was monitored using RAMAN spectroscopy.[3] Compared to our earlier studies, our new set-up provides the possibility to measure RAMAN spectra and single molecule widefield movies in quick succession. Thus, even periods of rapidly changing converison, e.g. during the self-acceleration period, can be measured with high temporal accuracy.

[1] D. Wöll, H. Uji-i, T. Schnitzler, J.-i. Hotta, P. Dedecker, A. Herrmann, F. C. De Schryver, K. Müllen, J. Hofkens, *Angewandte Chemie International Edition* **2008**, *47*, 783.

[2] M. Dorfschmid, K. Müllen, A. Zumbusch, D. Wöll, *Macromolecules* **2010**, *43*, 6174.

[3] B. Chu, G. Fytas, G. Zalczer, *Macromolecules* **1981**, *14*, 395.

PVT Analysis of Chemical Reactions: Polymerization, Transesterification, Crosslinking

Jürgen Pionteck

Leibniz Institute of Polymer Research Dresden, Dept. Polymer Reactions and blends
Hohe Str. 6, 01069 Dresden Germany

pionteck@ipfdd.de

Introduction: Each material changes its specific volume (V_{sp}), the inverse of the density, in dependence on outer conditions like pressure (P), temperature (T) and others, i.e. V_{sp} = f (P, T, atmosphere, etc.).
However, not only these factors determine the material density but also chemical reactions which occur within the material. So, the analysis of changes in the specific volume over time can give valuable information about degree and kinetics of polymerisation, crosslinking, degradation, transesterification and other chemical and physical processes, for which typical examples will be presented.

Method: Changes in the specific volume were measured by means of a fully automated GNOMIX high pressure mercury dilatometer, which works in the temperature range between RT and 400°C and at pressures between 10 and 200 MPa. Below 200°C the absolute accuracy of the instrument is 0.002 cm^3/g, above 200 °C 0.004 cm^3/g. In practice, changes in specific volume as small as 0.0002 cm^3/g can be resolved reliably. Typically, ca. 1.5 mL of the material are loaded into the measuring cell which then becomes completely filled with mercury ensuring permanent hydrodynamic pressure to the sample. To hinder sticking of the sample to the cell wall the samples were embedded in a nickel foil cup. Depending on the tasks, different modes for the measurement are possible: isothermal pressurization, isobaric heating and cooling, following V_{sp} at constant P and T, or mixed modes. In the standard isothermal (ITS) mode at constant temperature the sample was pressurised from 10 MPa to 200 MPa and the data were collected in steps of 10 MPa. The values for ambient pressure (0.1 MPa) were obtained by extrapolating the V_{sp} values between 30 MPa and 10 MPa in steps of 1 MPa according to the Tait equation by means of the internal PVT software. A detailed description of the instrument is given in [1].

Example: When curing epoxy resins shrinkage of > 10 % may occur limiting the applicability of the resins due to stress formation. The shrinkage can be reduced by the addition of fillers or reactive components. Figure 1 shows as example the influence of the reactive rubber poly(butadiene-co-acrylonitrile) with two terminal carboxyl units (CTBN) and of its non-reactive di-n-butyl ester (CTBN-ester) on the shrinkage of an catalysed and non-catalysed epoxy systems consisting of diglycidylether of bisphenol A (DEGBA) and diaminodiphenylsulfone (DDS). The curing was done in-situ at 10 MPa and 157°C (details see [2]). In the catalysed reactive rubber-containing system the shrinkage is reduced to less than 1 %, while the pure resin shrinks by 6.1 %. While the CTBN-ester is inert and acts just like a diluting filler, the CTBN becomes incorporated within the formed epoxy network reducing its network density. Furthermore, the catalyst (di-n-butyl benzyl amine) causes increased ether formation resulting in linear polymer structures. Both effects are responsible for the reduced shrinkage.

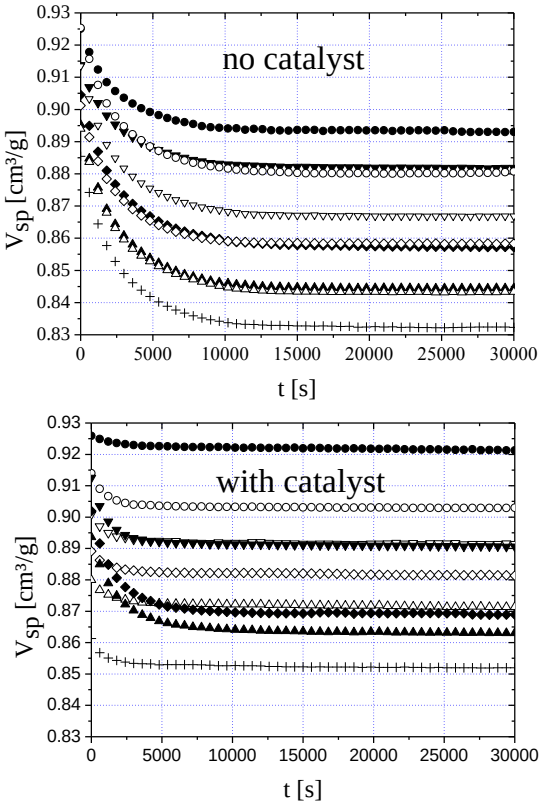

Figure 1. Influence of the rubber content and rubber reactivity on the shrinkage during curing of DGEBA/DDS. Rubber content: 0 (+), 5 (△), 10 (◇), 15 (▽), and 20 wt.% (○); full symbols CTBN, open symbols: CTBN-ester.

Further examples of PVT studies for the analysis of phase transitions, transesterification reactions, polymerisation, and physical swelling will be presented.

Acknowledgements: I am grateful for the long-time cooperation with the group of Prof. S. Thomas, Kottayam, Prof. G. Dlubek, Lieskau, and for the general technical assistance of H. Kunath, Dresden.

[1] P. Zoller, P., D. Walsh, *„Standard Pressure-Volume-Temperature Data for Polymers”,* Technomic Publishing, Lancaster: Chicago, IL, 1995.
[2] J. Pionteck, Y. Müller, L. Häußler, *Macromol. Symp.* (in press).

In situ Studies of Phase Structure and Crystalline Development of Poly(L-lactide/ε-caprolactone)/Poly(ethylene glycol) Blends by Atomic Force Microscopy

N. Hernandez-Montero[1], *J. M. Ugartemendia*[1], *T. Suárez*[2], *J.R. Sarasua*[1]

[1]University of the Basque Country (EHU-UPV). School of Engineering, Alameda Urquijo s/n, Bilbao 48013, Spain
[2]Bioftalmik S. L. Parque Tecnológico Ed 800 2ª planta. Derio 48060, Spain

natalia.hernandez@ehu.es

Introduction: Polylactides are gaining interest as biodegradable plastics for ecological packaging and biomedical applications. Poly(L-lactide/ε-carpolactone) (PLCL) and poly(ethylene glycol) (PEG) are both considered medical plastics. PLCL is an elastomer thermoplastic used in tissue engineering.[1] PEG is a semicrystalline polymer suitable for clinical applications such as chemical coating and vehicles for drug delivery[2].The aim of this work is to study the phase structure and PEG crystalline development in PLCL/PEG blends by using a hot-stage atomic force microscopy (AFM).

Materials and Methods: PEG was purchased from Sigma-Aldrich, Spain (Mn=35,000 g/mol) and PLCL (70/30 %mol) was supplied from Purac Biochem, the Netherlands (Mn=, 121,433 g/mol, PI=1,6). Blends of PLCL/PEG of different weight ratios, 50/50, 20/80 were prepared for AFM by spin-coating some drops of the blend solution (60 mg/mL) onto a mica substrate. AFM measurements were carried out with a Nanoscope III Multimode scanning probe microscope (Veeco). In order to analyse the phase structure and PEG crystalline morphology, isothermal crystallization experiments were performed by heating the samples in the AFM apparatus to approximately 80ºC for 5 min in order to erase the prior state and quenched to a crystallization temperature at 45ºC. After completion of PEG crystallization, the re-melting process of PEG crystallites in the blends was programmed and monitored by AFM.

Results and Discussions Polarized Light Optical Microscopy (PLOM) measurements were initially performed to study the crystallization kinetics and spherulitic morphology of PEG in PLCL/PEG blends. Larger and more perfect spherulites were found in blends containing higher amounts of PEG. PLCL is observed within the inter-lamellar amorphous regions of spherulites intimately mixing with PEG, suggesting a good miscibility (Figure 1).

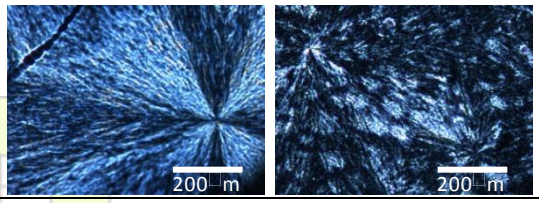

Figure 3. PLOM images of PLCL/PEG 20/80 with r_{esp}= 500µm (left) and PLCL/PEG 50/50 with r_{esp}= 277 µm (right).

For a more detailed analysis AFM was conducted. Figure 2 shows the on time phase structure and crystalline morphology of PLCL/PEG 50/50 and 20/80 blends during their isothermal crystallizations at 45 ºC. As can be observed in due course of crystallization of PLCL/PEG 50/50, PEG lamellae grow randomly from an amorphous darker phase. The arrows in the figures point to locations where amophous material, rich in PLCL, is located.

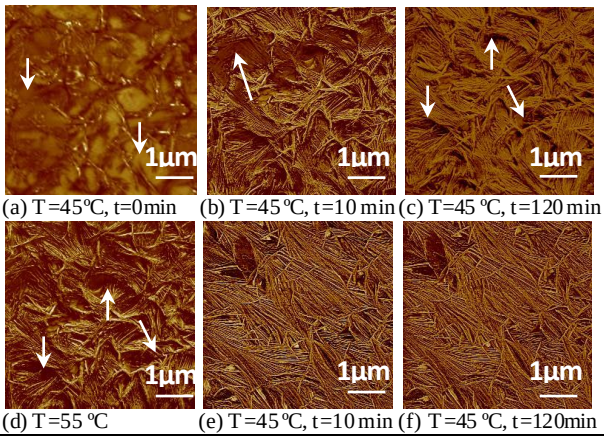

Figure 4. AFM phase images of PLCL/PEG 50/50 (a, b, c, d) and PLCL/PEG 20/80 (f,g).

With regard to PLCL/PEG 20/80 growth kinetics of PEG crystallites is much faster than in its 50/50 counterpart. PEG crystalline morphology is characterized by tightly packed well oriented stacks of lamellae of thickness within a 20-40 nm range. In addition the measured mean roughness parameter (Ra) is 11 nm after completion of the crystallization process whereas in PLCL/PEG 50/50 increases during crystallization from 6,5 nm to 20 nm.

Conclusions: PLCL content plays a key role in the organization of PEG lamellae in PLCL/PEG blends. High contents of amorphous PLCL (50/50) placed between PEG lamella stacks break the uniformity and linear growth of them. This phenomenon could be indicative of a good miscibility of both polymers.

Acknowledgements: The authors are thankful to the Basque Government, Department of Education, Universities and Research for funds (GIC10/152-IT-334-10) and for a pre-doctoral grant for J.M.U. MICINN (project BIO2010-21542-C02-01) and UPV-EHU for a pre-doctoral grant for N.H-M. are also gratefully acknowledged.

References:

1. Jeong,S.I., Kim,B.-S., Lee,Y.M., Ihn,K.J., Kim,S.H., and Kim,Y.Ha.. Biomacromolecules 2004, 5, 1303-1309.
2. Sheth, M., Kumar, A., Davé, V., Gross, R.A., McCarthy, S.P.1996.66:1495-1505.

SEC-DAD as a Powerful Tool for Characterization of Conjugated Polymers

Olga Trhlíková, Dmitrij Bondarev, Jan Sedláček, Jiří Vohlídal

Department of Physical and Macromolecular Chemistry, Faculty of Science, Charles University in Prague, Hlavova 2030, Prague 2, 128 43, Czech Republic

OlgaTrhlikova@seznam.cz

Nowadays conjugated polymers are materials of permanent interest because of large spectrum of potential applications such as construction of polymeric electroluminescence diodes, polymeric or composite photovoltaic solar cells, as sensors for ions, organic molecules as well as biomolecules. Conjugated polymers could be also used as an active component in the gas-separation and storage.

Substituted polyacetylenes as the fundamental conjugated polymers belong to the most studied materials of this class. Nevertheless, these polymers undergo oxidative degradation when exposed to atmosphere and in some cases the degradation is followed by cis-to-trans isomerisation. These processes affect the covalent and electronic characteristics of polyacetylenes and detailed study of changes during the ageing is important due to the fact that above mentioned properties are key features for potential functional applications in optoelectronic devices. Size exclusion chromatography (SEC) is very efficient method for study of molecular-weight characteristics and their changes during ageing. When equipped with diode array detector (DAD) it allows to obtain UV-vis spectra in selected retention times which correspond to apparent molecular weights according to the calibration. The differences in spectra allowed us to determine the cis-to-trans isomerisation proceeding during the ageing and also to propose detailed mechanism of the ageing processes (ref. 1).

Polyparaphenylenevinylene (PPV) and its various derivatives are promising materials for construction of light emitting diodes and polymer based solar cells. Also for this class of materials the stability is crucial. There are numerous studies dealing with the stability of PPVs in the solid state. We showed that the degradation of MEH-PPV proceeds also in the solution and the degradation processes depend on the solvent used and illumination conditions. Differences in UV-vis spectra for selected SEC retention times (molecular weights) in dependence on the conditions of ageing allow us to compare the extent of two processes accompanying the ageing, the degradation manifested by decrease in molecular weight and additions on the main-chain double bonds causing the decrease of conjugation without the decrease of molecular weight. In combination with other spectroscopic methods it is probable that we could be able to propose the mechanism of degradation and compare with the mechanisms proposed for degradation in the solid state.

SEC-DAD was also exploited in the study of preparation of composites MEH-PPV with gold nanoparticles (ref. 2). It was revealed that two methods used for preparation of nanocomposites affect MEH-PPV differently. The extent of degradation and additions on the double bonds were investigated. It was also showed that SEC-DAD technique is possible to use for monitoring of formation of nanocomposite aggregates during its preparation. The character of the spectra at different retention times allow us to distinguish between the polymer not participating in the interaction with nanoparticles and the formed nanocomposite.

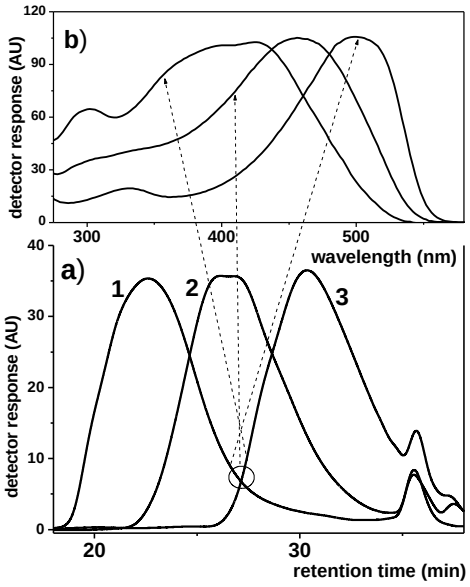

Fig. 1: Chromatograms obtained in the course of degradation of MEH-PPV in THF solution (a) and UV-vis spectra belonging to the macromolecules with apparent molecular weight 40000 which are present in all depicted stages of the degradation (b).

References:
1) Trhlíková O., Zedník J., Vohlídal J., Sedláček J., Polymer Degradation and Stability, 2010, submitted
2) Dammer O., Vlčková B., Procházka M., Bondarev D., Vohlídal J., Pfleger J., Materials Chemistry and Physics, 2009, 115, 352–360

Acknowledgements: Financial support of the Ministry of Education of the Czech Republic, projects MSM 0021620857 and KAN 100500652, the Czech Sience Foundation (project No. 203/09/0803) and the Science Foundation of Charles University (projects No. 315/2008 B-CH and 166410). O. Trhlíková and D.Bondarev are indebted to the Czech Science Foundation for fellowship (project No. 203/08/H032)

Heterogeneity during Controlled Radical Polymerization – a Single Molecule Fluorescence Microscopy investigation

Jan Martin Nölle,[1] *Karel Goossens*,[2] *Wim van Camp*,[3] *Dominik Wöll*[1*]

[1]Universität Konstanz, Zukunftskolleg/Fachbereich Chemie, Universitätsstraße 10, D-78464 Konstanz, Germany.
[2]Katholieke Universiteit Leuven, Department of Chemistry, Celestijnenlaan, 200F (PO box 2404), 3001 Heverlee, Belgium.
[3]Universiteit Gent, Polymer Chemistry Research Group, Krijgslaan 281 S4-bis, 9000 Gent, Belgium.

[*]Email: dominik.woell@uni-konstanz.de

Controlled radical polymerization has become an essential technique to produce polymers combining the advantages of free radical polymerization (inexpensive and tolerant to impurities) with those of ionic polymerization: it offers control over many key properties such as molecular weight, polydispersity and end groups. Even network properties such as network densities and homogeneity can be adjusted. These properties have great influence on the diffusion processes of particles during polymerization and in the synthesized networks. For example, many applications such as highly selective membranes demand a minimization of heterogeneities.

In our investigations on heterogeneities in polymer networks we go beyond the bulk measurements commonly performed using techniques such as Dynamic Light Scattering (DLS), Nuclear Magnetic Resonance Spectroscopy (NMR), and Positron Annihilation Lifetime Spectroscopy (PALS). Our project focuses on the observation of single molecule dynamics. Using Widefield Fluorescence Microscopy (WFM), the diffusion of single perylene diimide dye molecules which are introduced as probes for translational motion is detected and analyzed[1-2]. Recent results on local heterogeneity formation of linear and crosslinked polystyrene during the Nitroxide Mediated Polymerization (NMP) will be presented and compared with the behavior during free radical polymerization.
To follow the conversion during the polymerization process, Raman spectroscopy, a very powerful, fast and non-invasive tool was used. Combining Raman spectroscopy with widefield fluorescence microscopy on one setup offers the possibility to determine conversion and single molecule mobility almost simultaneously. This is of special interest in rapidly developing systems such as fast polymerizations or radical polymerizations at the gel point.

[1] D. Wöll, H. Uji-i, T. Schnitzler, J.-i. Hotta, P. Dedecker, A. Herrmann, F. C. De Schryver, K. Müllen, J. Hofkens, Radical Polymerization Tracked by Single Molecule Spectroscopy, *Angew. Chem. Int. Ed.* **2008**, *47*, 783-787.

[2] D. Wöll, E. Braeken, A. Deres, F. C. De Schryver, H. Uji-i, J. Hofkens, "Polymers and Single Molecule Fluorescence Spectroscopy, what can we learn?", *Chem. Soc. Rev.* **2009**, *38*, 313-328.

Continuous-Flow Off-Line Pyrolysis-GC/MS for Detection of Poly(vinylpyrrolidone)

Mališa Antić[1)], *Vesna Antić*[1)], *Alexander Kronimus*[2)], *Katja Oing*[2)] *and Jan Schwarzbauer*[2)]

[1)]University of Belgrade, Faculty of Agriculture, Serbia;
[2)]RWTH Aachen University, Institute of Geology and Geochemistry of Petroleum and Coal, Germany

e-mail: mantic@agrif.bg.ac.rs

Introduction: In contrast to the very intensive study of low molecular weight organic pollutants occurring in waste waters and river waters, the pollution with high molecular weight synthetic polymers has received by far less attention. Poly(vinylpyrrolidone) (PVP) is a widely used water soluble polymer whose occurrence in waste waters is likely. PVP is intensively used in the pharmaceutical industry as a binder in many tablets and in the production of one of the most important disinfectants, PVP-iodine. PVP also has application in adhesives, paper manufacturing, the food industry, detergents (as a dye transfer inhibitor) and in personal care products such as shampoos and hair gels [1]. The PVP is presumed to be detected in the polluted water samples as a result of its very frequent usage and suggested environmental stability [2]. However, an appropriate method for its identification and quantification in environmental samples is still lacking. The aim of this work was to develop an efficient analytical method for detecting trace levels of PVP in waste waters and surface waters by applying continuous-flow off-line pyrolysis-GC/MS.

Materials and Methods: Pyrolysis of commercial PVP, of some personal care products, of spiked water samples as well as of waste water samples and river water samples was performed in a tube furnace at 500°C under a continuous nitrogen flow. Two waste water samples were derived from the outlets of the municipal waste water treatment plants of Aachen and Düren, Germany. One sample was obtained from the industrial waste water canal in Pančevo, Serbia. Surface water samples from the Rur River were taken in November 2008 in the vicinity of the effluent from the waster water treatment plant of Düren. One sample was taken upstream of the effluents and two further samples downstream, at distances of 10 m and 50 m, respectively. Degradation products were trapped in dichloromethane and identified by GC/MS. The concentration of PVP was calculated on the basis of the main pyrolytic product, *N*-vinyl-2-pyrrolidone (NVP). The amount of NVP in pyrolyzates was determined by GC-FID analysis, based on calibration curve which was constructed using commercial NVP and corrected by an internal standard, 4-*tert*-butylcyclohexanone. Very good linear correlation between initial amounts of PVP and released amounts of NVP was obtained and used as external calibration.

Results and Discussion: Specific fragments of pyrolyzed polymers can reflect its original structure and, therefore, be used for polymer identification. In this work, commercial PVP was pyrolyzed at seven different quantification levels (20-1000 µg). When higher initial amounts of PVP were degraded (250-1000 µg), only NVP was identified as a degradation product. However, in experiments with lower initial amounts of PVP (20-125 µg), a second pyrolytic product, identified as pyrrolidone, 2-Py, appeared. Fig. 1 gives the molecular structure of PVP as well as of the main degradation products, NVP and 2-Py. Both products can unambiguously be related to the former polymeric structure; however, in our study only NVP was used for quantitative determination of PVP.

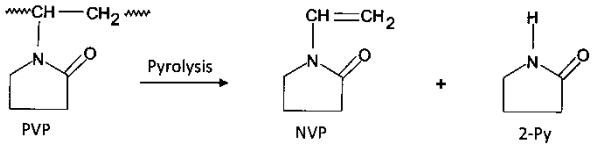

Fig. 1. Pyrolytic products of PVP

Two standard curves were used for calibration – the first which correlated the weight of NVP with the ratios of the areas of NVP peak and internal standard peak, and the second, "pyrolytic curve", which correlated amount of produced NVP with initial amount of PVP. The described pyrolytic method was applied to personal care products which contained PVP. The detected level of PVP was 6.4 (hair gel), 0.8 (laundry detergent) and 1.4 wt.% (tablets for throat disinfection). Spiked water samples, waste water samples and river water samples were pre-extracted with hexane and diethyl ether prior to pyrolysis. It was found that the recovery of spiked samples was 94.6±1.6 %, which indicated that pre-extraction did not provoke significant loss of polymer. These results also showed that "pre-extraction" can be used for environmental samples, in order to decrease the amount of organic substances which are also capable to be pyrolyzed, without significant loss of PVP. Finally, application of the developed method on real environmental samples revealed that PVP was present in effluents from waste water treatment plants in concentrations between 0.9 and 7 mg/L, as well as in river water affected by municipal sewage emissions with concentrations around 0.1 mg/L.

Conclusions: Continuous-flow off-line pyrolysis-GC/MS allowed very reliable quantification of PVP in complex environmental samples, even at trace levels. Furthermore, off-line method is very suitable for polymer detection in environmental samples because the optimal size of the sample can be easily adjusted prior to GC analysis, and the internal standards can be used in order to improve accuracy of quantitative determination of pyrolytic products.

References:

1. E.S. Barabas, *Encyclopedia of Polymer Science and Engineering*, John Wiley, New York, **17** (1987) 198-257.
2. S. Trimpin, P. Eicshhorn, H.J. Räder, K. Müllen, T.P. Knepper, *J. Chromatogr. A*, **938** (2001) 67-77.

Investigation of the Miscibility (Solubility) of Molten Polypropylene-Polyethylene Blends by means of Rheometry

Matthias Mihalic, Alois Schausberger

Institute of Polymer Science, Johannes Kepler University Linz,
Altenberger Straße 69, A-4040 Linz

E-mail: matthias.mihalic@jku.at

Rheometry is a powerful tool for the detection of phase separation in molten polymers and thus for the investigation of solubility of the components of a mixture.
An experimental set-up was designed in such a way that blends of polypropylene and polyethylene are produced in a small-scale laboratory extruder and the melt is subsequently injected directly into the measuring cell of a rheometer, where the dynamic moduli are determined. The reason for this procedure is that crystallisation, as it occurs during conventional sample preparation, always induces phase separation in a blend. This may negatively affect the measurement results, because neither will this separation be balanced out by diffusion in the melt, nor is the rheometer suitable to be used as a compounder.
The viscoelastic behaviour of soluble polymer blends is dominated by the main fraction which acts as a solvent, but it is modified by the properties of the dissolved component. In the case of solubility, the relaxation time spectrum of a blend can be gained from a simple weighted addition of the spectra of the pure components. Otherwise, phase separation will be reflected in the spectrum of the mixture obtained from dynamic mechanical data. This allows the calculation of the degree of solubility using the model of Gramespacher and Meissner.

References

Gramespacher H, Meissner J (1992) J Rheol 26:1127-1141
Schausberger A (1986) Rheol Acta 25:596-605
Baumgärtel M, Schausberger A, Winter HH (1990) Rheol Acta 29:400-408
Schausberger A (1991) Rheol Acta 30:197-202

Comparative Study Of Various Grades Of Polyethylene By Raman Spectroscopy: microstructural attribution of bands

Richard Jumeau[a,b], *Patrice Bourson*[a], *Michel Ferriol*[a], *François Lahure*[b]

a Laboratoire Matériaux Optiques, Photonique et Systèmes E.A.4423 - SUPELEC, Université Paul Verlaine de Metz, 2 rue Edouard Belin 57070 METZ, France

b Total Petrochemicals France, Usine de Carling – Saint-Avold, RN 33 - BP 61005 57501 SAINT AVOLD, France

richard.jumeau@supelec.fr, bourson@univ-metz.fr, mferriol@univ-metz.fr, francois.lahure@total.com

INTRODUCTION

In 2008, almost 30% of the world plastics production was dedicated to the polyethylene (70 million tons). So, polyethylene is a consumer polymer material because of its moderate cost of manufacturing and its physical and mechanical properties which are compatible with various applications of everyday life. Indeed, this polymer allows generally speaking an easy processing (extrusion, injection), it has an excellent electric insulation and shock resistance and presents a great chemical and biological inertia (food contact). To each application corresponds a grade, that is to say a polyethylene with different rheological properties. It is then essential to know how to differentiate these products by adapted methods of characterization.

EXPERIMENTAL

The knowledge of characteristic temperatures of the polyethylene such as the melting point, the recrystallization point or the glass transition temperature gives indications onto the viscosity and thus on the grade of the polymer. Raman spectroscopy is a technique of polymer analysis which is nowadays is growing fast given its advantages. It is a non-destructive technique and it gives deepened information about the morphology of the polymer, the viscosity and its cristallinity. Moreover, this technique can be perfectly used in the industry by means of adapted sensors and of more and more miniaturized devices.

Spectroscopic study was realized with a Raman spectroscope Aramis® from Horiba Jobin-Yvon fit with a laser in 785 nm and a network in 1200 lines/mm. An extract of the studied spectral range is presented in figure 1 with in blue a flowing Low Density PolyEthylene (LDPE) grade and in red a viscous LDPE grade.

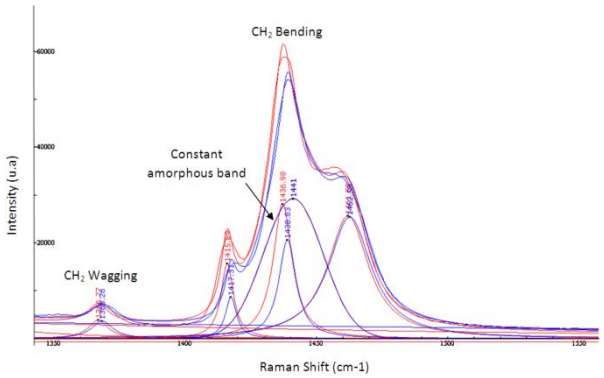

Figure 1: Raman spectroscopy of two LDPE grades

The Differential Scanning Calorimetry (DSC) and X-Ray Diffraction (XRD) will also be helpful to correlate our results. The calorimetric tests were made with DSC 200 F3 Maia® from Netzsch. It is a heat flux apparatus allowing working down to -170°C thanks to a supply in liquid nitrogen at the level of the thermostated chamber swept by nitrogen and regulated with an Intracooler at the rate of 10 K/min. Some DSC results are presented in an original shape on the radar graph of figure 2.

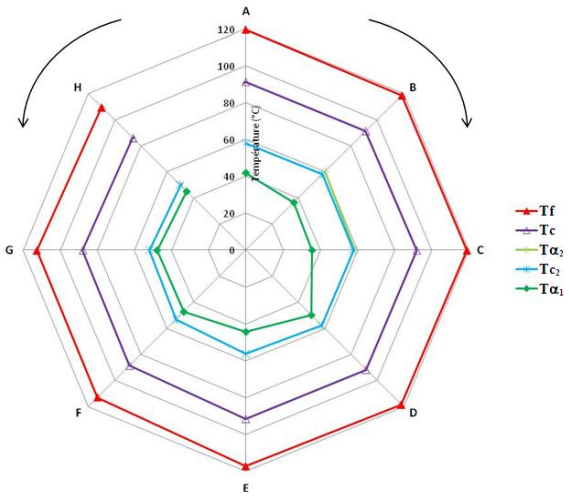

Figure 2: DSC results of 8 PE grades.

CONCLUSIONS

The object of this paper is not only to obtain the typical temperatures of polyethylene by Raman spectroscopy and to differentiate grades of polyethylene but also to get information on the structure of the polymer and of its cristallinity. In fact, with a detailed attribution of the bands, we are able to know to which bond each band corresponds[1,2] and its position in the crystalline structure. The final goal is to establish the possibilities of on-line analysis for quality control at the industrial scale. The determination of the polymer structure represents a major challenge in the industrial world of polymers.

REFERENCES

1 M. Pigeon and al., *Characterization of molecular Orientation in Polyethylene by Raman spectroscopy*, Macromolecules, **24**, 5687-5694, 1991

F.J. Boerio, J.L. Koenig, *Raman Scattering in Crystalline Polyethylene*, The journal of chemical physics, **52,7**, 3425-3431, 1970

Characterisation of morphology of uniaxial oriented PET – films and pressure-induced i-PP via confocal and polarised μ-RAMAN Spectroscopy

Krisztina Vincze-Minya[a], *Sabine Hild*[a], *Tobias Keplinger*[a], *Sibylle Jilg*[b], *Wolfgang Stadlbauer*[b], *Michael Aigner*[c], *Jürgen Miethlinger*[c]

[a]Institute of Polymer Science, Johannes Kepler University, Altenbergerstr.69, 4040-Linz, Austria
[b]TCKT – Transfercenter für Kunststofftechnik, Franz-Fritsch Str. 11, 4600-Wels, Austria
[c]Institute of Polymer Extrusion and Building Physics, Johannes Kepler University, Altenbergerstr.69, 4040-Linz, Austria

e-mail: krisztina.vincze-minya@jku.at

Introduction: The morphology of a polymer has a great bearing on its mechanical strength and stability and hence is of a great interest. For semicrystalline polymers, the ratio of crystalline and amorphous phases, and molecular orientation in these phases are essential to understand this relationship and to optimise physical properties and production conditions of the materials.

Methods: Since the discovery of Raman scattering effect in the late 1920s, several research articles, review papers, books and industrial patents have been published on the application of Raman spectroscopy for polymers. Typically, the technique is used to determine the polymer type and content, polymerization reaction kinetics, amount of pigment additives, amount of degradation. The change of morphology of the polymer such as crystallinity, and molecular orientation can also be characterized by Raman spectroscopy. A typical Raman spectrum has a few peaks of interest that describe orientation and crystallinity quantitatively and qualitatively.

Polarized Raman spectroscopy is a vibrational spectroscopic technique used to determine the molecular orientation[1]. This characterisation method has a few advantages compared to other analytical techniques: quantitative and precise measurement of molecular orientation distributions, and study of these distributions on both the crystalline and amorphous phases.

Materials: The crystallinity and orientation of pressure induced polypropylene (PP) and of films of uniaxial oriented poly(ethylene terephthalate) PET were characterized via confocal and polarised Raman spectroscopy. The samples were produced in similar conditions and they differ only in the induced pressure (in case of PP) and film thickness (in case of PET). The preparation of the samples simulates the production conditions.

Results and Discussion: In case of PP the ratio of the peaks at 841 and 809 cm^{-1} is sensitive to the molecular anisotropy. The crystallinity values of PP are calculated by dividing the integrated intensity of the 809 cm^{-1} peak (helical chain conformation) by the total integrated intensity under the 809 cm^{-1} to 841 cm^{-1} band (Nielsen method[2]). The frequency bands due to longitudinal acoustic vibrations which are not observed by infrared spectra but occur in Raman spectra, are related to chain length and lamella thickness.[3,4] The longitudinal acoustic vibration is dependent on the force constant (dependent on the chain's Young modulus), the interlamellar forces, structure of the chain folding sequence, the proportions of the amorphous and crystalline components and the density of the polymer.

PET gives strong, well-defined Raman spectra with sharp intense peak at 1616 cm^{-1}, which has been assigned to the symmetric stretching vibrational mode of the phenylene ring. The polarisability tensor for this vibrational mode is treated with cylindrical symmetry, and the ratios of the diagonal components are estimated. The spectrum also contains a band due to the carbonyl group near 1740 cm^{-1} and two strong bands, typical of aromatic esters, near 1260 cm^{-1} and 1130 cm^{-1}, due to the asymmetric and symmetric stretching vibrations of the C-O-C functional group. PET has a very strong band due to the aromatic component near 1000 cm^{-1}. In addition, bands due to the aliphatic and aromatic portions of the polymer are present in the spectrum, most which are in their normal positions. The strong band due to the aromatic ring out-of-plane deformation is not in ist normal position for para-substtituted aromatics, instead it is found at slightly higher wavenumbers, 730 cm^{-1}. This shift is attributed to an interaction of the ester group with the aromatic ring. The OH and COOH groups absorb near 3450 cm^{-1} and 3260 cm^{-1} respectively.

Conclusions: As seen in crystalline and amorphous materials, the degree of molecular orientation can be regarded as one of the most crucial parameters defining the macroscopic properties of the material. The vibrational spectra of the PP and PET are greatly influenced by both the crystallinity and molecular orientation of the polymer. Confocal and polarised Raman spectroscopy is a useful method to obtain exact information about crystallinity and orientation of polymers.

References:

[1]Tanaka M, Young R.J., *Journal of Materials Science*, 41 (2006) 963-991

[2]Nielsen A.S., Batchelder D.N., Pyrz R (2002) *Estimation of crystallinity of isotactic polypropylene using Raman spectroscopy*. Polymer, 43(9), 2671-2676

[3]Atkinson G.A., *Time resolved vibrational spectroscopy*, 1983

[4]Bellamy L.J. *The infrared spectra of complex molecules*, 1975

A Thermoset-Thermoplastic Blend: Spectroscopy Characterization

F.A. Mesa-Rueda[a], , A. Cuellar-Burgos[a], C. Vargas-Hernandez[b], J.E. Perilla[c]

[a]Departamento de Ingeniería Química, Universidad Nacional de Colombia, Manizales, Colombia.
[b]Laboratorio de Propiedades Ópticas de los Materiales, Universidad Nacional de Colombia, Manizales, Colombia.
[c]Departamento de Ingeniería Química y Ambiental, Universidad Nacional de Colombia, Bogotá D.C., Colombia

famesar@unal.edu.co

Upon processing of thermoset-thermoplastic blends, a cure-induced phase separation can take place. Although the developed morphologies can be easily observed and have been much studied, only limited information on the phase characteristics, like their composition and the degree of crosslinking, was reported in the literature. This study aimed at using micro-Raman spectroscopy for a direct and local characterization of the thermoplastic content and of the epoxide conversion within phase separated epoxy resins - polystyrene (PS) blends.

The performance of thermoplastic/thermoplastic blends is reasonably well studied and a number of their properties can be obtained as a function of their composition and of the processing conditions. In thermoset/thermoplastic blends, challenging issues remain, however, to be addressed. These include developing an understanding of the complexity of the combined curing and phase separation phenomena and the resulting blend properties. However, fewer studies have been reported concerning the chemical characteristics of the phases, such as the thermoplastic content and the epoxide conversion. Up to now, only indirect measurements of these properties have been carried out on thermoplastic-modified epoxy networks. Phase composition and partial miscibility of the components have been qualitatively assessed in cured blends on the basis of the number and values of the glass transition temperatures (T_g). Macroscopic determinations of the T_{gs} were performed by differential scanning calorimetry (DSC), temperature modulated DSC or dynamic mechanical analysis (*DMA*). In phase separated blends, most authors concluded that, at the end of cure, the epoxy-rich phase contained a low concentration of thermoplastic whilst a larger proportion of epoxy-curing agent species was dissolved in the thermoplastic-rich phase.

In brief, the above mentioned experiments did not allow the quantitative determination of the chemical characteristics of the phases. Moreover, it seems that no method has been reported to provide direct local measurements of the phase features. With the aim of filling this gap, this paper describes the use of micro-Raman spectroscopy as a direct method for characterising locally the phase chemical features in thermoplastic-modified epoxy systems. The combination of Raman spectroscopy and confocal microscopy is increasingly used for spatially resolved investigation of heterogeneous materials. In thermoplastic-thermoplastic blends, local qualitative or quantitative determination of phase composition has been performed (Overbeke et al. 2001). However, micro-Raman spectroscopy has not yet been significantly used for the characterisation of epoxy-thermoplastic blends.

In this study, one type of blend was mainly examined, composed of *trimethylene glycol di-p-aminobenzoate (TMAB)*, *diglycidyl ether of bisphenol-A* (*DGEBA*) and *polystyrene* (*PS*) identifying the most representative vibrational normal modes.

The technique is of both academic and industrial interest to study epoxy/amine systems in the production of thermosetting polymers and is demonstrated by practical applications in this paper including a study and identification of vibrational normal modes in the epoxy oligomer Diglycidyl ether of bisphenol-A (DGEBA) and trimethylene glycol di-p-aminobenzoate (TMAB) system. By micro-Raman spectroscopy, the principal vibration modes around 1626, 3333 y 3436 cm^{-1} were determined for amine groups of TMAB, and 915, 933, 1131, 1249-1252, 1407, 2713, 2760 y 3006 cm^{-1} for epoxy rings of DGEBA.

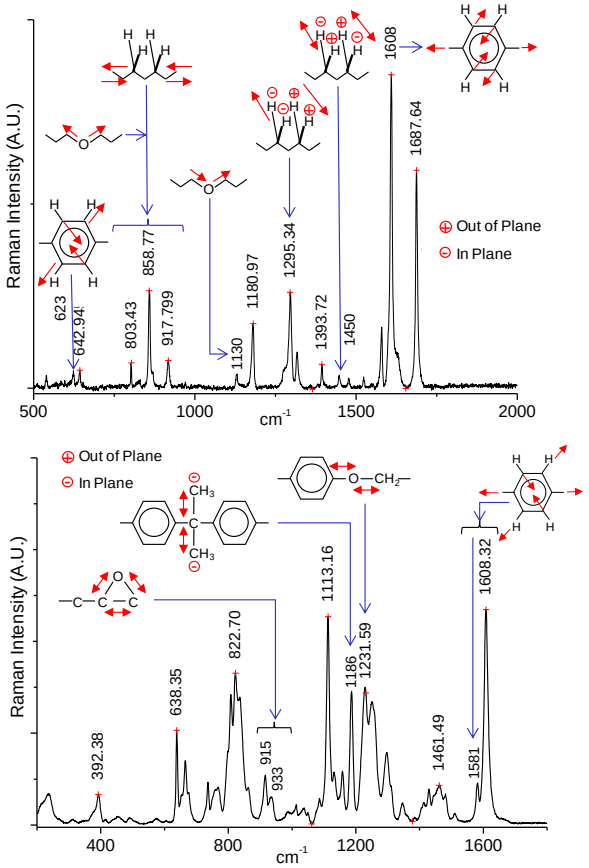

Figure 1. Some vibrational normal modes using micro-Raman spectroscopy of trimethylene glycol di-p-aminobenzoate-TMAB (up) and diglycidyl ether of bisphenol-A DGEBA (down).

References:

Overbeke et al (2001). Raman Spectroscopy Determination of the Thermoplastic Content within Epoxy Resin-Copolyethersulfone Blends. *Applied Spectroscopy*, 55, 1514-1522.

Characterization of the Mechanical Properties of EVA Foams by TMA

M.I. Beltrán[1], A. Marcilla[1], I. Pelaez[1], A. Otero[2]

[1]Chemical Engineering Department, Alicante University, Spain
[2]Cauchos Karey, Alicante, Spain

e-mail:maribel.beltran@ua.es

Introduction: Crosslinked EVA foams have been increasingly used in a great variety of applications. As a shock absorber, they are commonly present in footwear and sport floorings. The mechanical properties and, especially, the softness, resilience and compression set, together with the light weight (low density) are the key feature in these materials (1). Compression test to measure the permanent deformation of foam is normally carried out according the corresponding ASTM, compressing the foam by 50% for a relatively short period of time (by 6 hours) and then allowing the foam to recover for 30 min. It is known that these test may not be representative of the recovery and resilience performance of materials under intermittent forces or at longer terms, for example as those suffered by floorings or footwear (2).
In this work, EVA crosslinked foams with different type and concentration of filler have been prepared and characterized by termomechanical analyses (TMA) in order to obtained their permanent deformation under intermittent forces. Moreover, the density, hardness and morphology of the cellular structure have been measured.

Materials and Methods: A commercial EVA copolymer with 18% of VA provided by Trithene was employed. Formulations include calcium carbonate (Rocio-3), silica (Ebrosil), stearic acid (Croda), zinc oxide (Asturiana de Zinc), azodicarbonamide (Cellcom H919) as a foaming agent and peroxide (Luperox F40) as a crosslinking agent. The composition of the blends with different silica and calcium carbonate content are shown in Table 1.
To obtain the foams, all the components were blended in a Banbury plasticorder Guix-2P at 90º C for 8 minutes, and roll milled in a two roll mill Guix-2403. The obtained sheets were compression moulded in a hot press Mecamaq DE-200 at 160º C for 20 minutes. The final thickness of the sheets was roughly 2 cm. Foams characterization included density measurement in a Metler Toledo XS205 balance. Hardness was obtained by the ShoreA method using a Baxlo durometer. TMA was carried out in a Q400 model of TA Instruments performing 8 cycles of stress (at 1N and 40º C for 30 minutes)-relaxation (at 0.01 N and 40º C for 30 minutes). The bubbles distribution was obtained from SEM photographs (JEOL JSM-840).

Results and Discussion: The presence of calcium carbonate in the blends involves higher densities whereas the hardness increases with the higher amount of silica (Table 1). Moreover, the bubble size distribution of the foams is lower and more homogeneous in the blends that contain greater amounts of filler, especially silica.

Table 1. Foams composition and results.

	Content (phr)		Results	
Blend Name	Silica	Calcium carbonate	Density (g/cm^3)	Hardness (ShA)
R	25	15	0,122	30
S	40	0	0,103	27
C	0	40	0,143	20
N-F	0	0	0,151	15

From the TMA analysis, a time-stain curve for repeated cycles was obtained for each blend, as it can be seen in the Figure 1 for the R sample. The repeated cycles carried out in TMA may represent more adequately the forces applied to these materials in their daily uses than those applied in continuous compression tests, while the permanent deformation values obtained form TMA are in the order of those found in the bibliography. The previous study carried out showed than no further deformation occurs from the eighth cycle on.

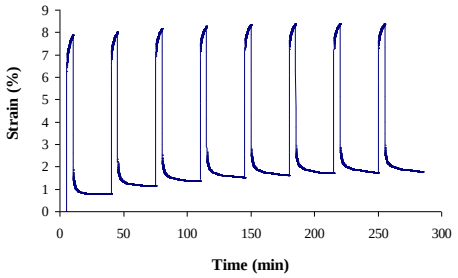

Figure 1. Strain curve of the R blend obtained in TMA.

The highest strain (last cycle) and the remaining strain of each curve have been obtained, and are shown in Table 2.

Table 2. Highest and remaining strain results.

	R	S	C	N-F
Highest strain (%)	8,09	9,34	12,14	20,64
Remaining strain (%)	1,55	1,71	2,63	4,71

Foams C and, specially, N-F, present higher values of strain than foams R and S, which present similar and low values of both parameters, showing the suitability of silica to improve resilience.

Conclusions: TMA has been employed to measure the mechanical properties of different foams, and a reasonably value of the permanent deformation has been obtained. The higher concentration of silica in the EVA foams reduces the permanent deformation of foams subjected to intermittent forces.

References:

1. Dubois, R., Karande, S., Wright, D.P. and Martinez, F. Journal of Cellular Plastics 38 (2002) 149-161.
2. Rodriguez-Perez, M.A., Velasco, J. I., Arencon, D., Almanza, O. and De Saja, J. A. Journal of Applied Polymer Science 75 (2000) 156-166.

Molecular Weight Distribution Changes in Irradiated Films of Vinyl Ketone Copolymers

S. Sánchez-Ballester[1], *J.D. Badia*[2], *A. Martinez-Felipe*[2], *A. Ribes-Greus*[2] *V. Soria*[1,*] *Institut de Ciència dels Materials* (ICMUV), Universitat de València[2] Institut de Tecnología de Materials (ITM), Universitat Politècnica de València (UPV)

corresponding author: V. Soria (vicente.soria@uv.es)

Introduction

The characterization of polymer degradation through the chain scission mechanisms is difficult in polydisperse samples because it needs to account for the diversity of chain sizes. The sequence of chain fragmentation can be detailed in the gradual changes in the form of the molecular weight distribution functions (MWD). Progressive changes in the MWD functions could only be determined by inspecting a set of SEC chromatograms obtained from the initial or zero degradation to final molecular chain scission. The molecular interpretation of the lateral shift pattern in the evolved MWD curve sequences is critical for gaining insight into the decay trajectory. The above is clearly confirmed by the gradual temporal movement from high MW to low MW zone on the left-hand side of the chromatogram. However, the chromatograms only provide data in terms of discrete average values, e.g. degree of polymerization and various statistical moments or average molecular weights, including polydispersity index. The differences in characteristic lateral movements of SEC traces or changes in their MWD shapes were analysed and assessed in terms of a distribution function model. Complementary FTIR measurements of virgin and degraded films served to confirm the extent of degradation.

Materials and methods

Preparation and characterization details for poly(methyl methacrylate-co-methyl isopropenyl ketone), PMIK films,were reported in a previous paper [1]. Samples of all copolymers were irradiated with a Ultravitalux (Osram) sunlamp in our lab. The IR spectra were recorded by NEXUS Spectrometer, ThermoNicolet Corp. (Madison WI, USA) in all cases at least 64 scans with an accuracy of 2 cm^{-1} were signal-averaged. The frequency scale was internally calibrated with a He-Ne reference to accuracy of 0.2 cm^{-1} and externally with polystyrene. The PMIK samples were placed on a horizontal holder for beam exposure, according to the ATR (alternative total reflection) spectroscopy technique, and data processed data with OMNIC software.

Results and Discussion/Conclusions

The Average Molar Masses of neat and degraded samples, extracted from SEC-RI traces, are shown below. The degradation observed over a 2-year period in the buried specimens (9 cm soil depth) was negligible. However photo-degradation effects, as expected, increased with the copolymer MIK content. . In the more extreme deterioration step, changes from 2.4 $\times 10^5$ to 6.5 $\times 10^3$ (g/mol) in M_n and from 1.8 to 2.2 in the polydispersity index were observed. Nevertheless, in all cases, the shapes of experimental SEC traces were unimodal, revealing the absence of recombination or cross-linking reactions during the chain scission process. A mathematical model was applied to assess the time-evolution of the MWD functions of sunlight

	$M_w \times 10^5$	$M_n \times 10^5$	PDI
0 h-Irradiation			
PMIK.00	4.96	2.99	1.7
PMIK.04	4.90	3.15	1.6
PMIK.07	4.58	2.47	1.8
PMIK.10	4.55	2.32	1.9
PMIK.15	4.24	2.41	1.8
100 h-Irradiation			
PMIK.00	4.73	2.94	1.6
PMIK.04	6.66	0.31	2.1
PMIK.07	0.53	0.25	2.1.
PMIK.10	0.54	0.25	2.2
PMIK.15	0.53	0.22	2.4
500 h- Irradiation			
PMIK.00	4.70	2.72	1.7
PMIK.04	0.32	0.15	2.1
PMIK.07	0.31	0.14	2.2
PMIK.10	0.24	0.11	2.2
PMIK.15	0.14	0.065	2.2

irradiated specimens. We also present a result of the numerical simulation for the transition of the weight distributions from the initial state to the degradated one.

Reference:

[1] Soria V. Celda B. Tejero R Figueruelo J.E Polymer Degradation and Stability 1985.10, 2871.

Acknowledgements: Spanish Ministry of Science and Innovation (Research Project UPOVCE-3E-013). Spanish Ministry for Education for the predoctoral research FPU position to J.D. Badía, Generalitat Valenciana for the Grisolia research Grant to A. Martinez Felipe and Research Project UPOVCE-3E

013. Universitat de València and Universidad Politécnica de València are acknowledged for additional funding.

Study of the Thermal Behavior of Syndiotactic and Atactic Polystyrene By Raman Spectroscopy

Nadège Brun[1,2], Patrice Bourson[1], Samuel Margueron[1], Michel Duc[3]

[1] Laboratoire Matériaux Optiques Photonique et Systèmes, SUPELEC, 2 rue Edouard Belin, 57070 Metz, France.
[2] Total Petrochemicals France, Usine de Carling, BP 90290, 57508 St Avold.France.
[3] Total Petrochemiclas France, Zone Industrielle Feluy , B-7181 Seneffe Belgium.

A lot of properties electrical, chemical, optical or physical can be explained by the chemical structure of polymer. For example, atactic polystyrene and syndiotactic polystyrene present differences about the regularity of their hydrocarbon chain. If the first has phenyl groups randomly distributed on both sides of the chain, the second has got a regular arrangement which the group has alternate positions along the chain. The amorphous or semi-crystalline character depends on reaction of polymerization. Actually, if reaction of polymerization is a radical polymerization, polymer will be amorphous. Whereas, polystyrene made by Ziegler-Natta polymerization is semi crystalline.

In the study of polymer, it is more important to measure of the glass transition temperature, Tg, and melting temperature Tm. Also, between the glass transition and the melting point, part of the hydrocarbon chain has enough energy to fall into crystalline arrangements. The temperature allowing this crystallisation phenomen is noted Tc. The polymer behaviour is fonction of the temperature of treatment.

Futhermore, the litterature of syndiotactic polystyrene index four polymorphs, α, β, γ et δ, can be grouped by pairs, according to the backbone conformation , the (α, β) has a planar all-trans "zigzag" conformation whereas the other pair (γ, δ) have a helical trans-trans, gauche-gauche conformation 1, illustrate the two types of conformation that literature gives. Using Raman spectroscopy, Kobayashi et al 2 observed that the ν1 vibration is very sensitive to the local backbone conformation resulting in the presence of two distinct peaks at 770-773 and 796-802 cm-1 corresponding to all-ltrans conformations and mixed trans/gauche conformations, respectively.

A preliminary work consist in comparison of Raman spectra of atactic polystyrene and syndiotactic polystyrene were investigated, in order to determine signature of crystallinity. The Raman spectrum of atactic polystyrene shows peaks which are different compared to Raman spectrum of syndiotactic polystyrene, as shows in figure 1:

The second study is function on the temperature and tries to correlate Raman spectroscopy with DSC. In figure 2, we focus on the spectra part from 700 to 800 cm-1. The peak observed at 770 cm-1, which is relating all-trans conformation, increases with temperature. Whereas the peak at 797 cm-1, which is associated trans-gauche conformation, reduces with temperature:

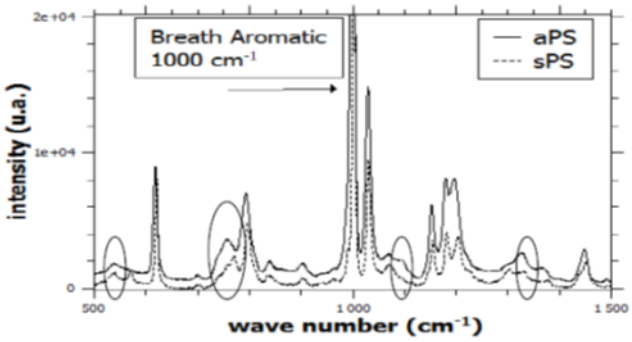

Figure 1: Raman spectrum of aPS (black) and sPS (dash line). Circles show the main differences between aPS and sPS spectra

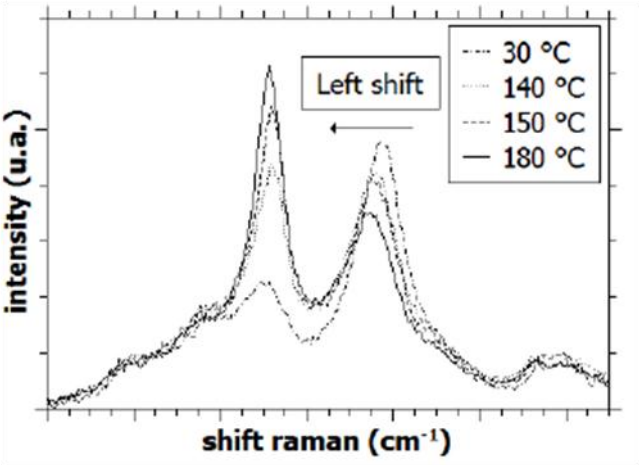

Figure 2: Raman spectrum of sPS at 30 °C, 140 °C.

As a polymer is characterized by phase transitions, observable by X-ray diffraction by DSC, XRD and vibrational spectroscopy. We propose to use Raman spectroscopy to characterize the crystallinity of polystyrene, in particular, amorphous and semi-crystalline phase, in order to correlate this method with DSC and XRD.

1. *Corradini, P.; Guerra, G.* Adv. Polym. Sci. **1992**, 100, 183.

2. *Kobayashi, M.; Nakaoki, T.; Ishihara, N.* Macromolecules 1989, 22, 4377.

Study, by Raman Spectroscopy, of the microstructure evolution of isotactic polypropylene during tensile test and relaxation: Measuring the chains orientation.

Chaudemanche S.a, Ponçot M.a, Martin J.a, Hiver J.M.a, Bourson P.b, Dahoun A.a

aInstitut Jean Lamour, UMR 7198 CNRS – Nancy University, Department SI2M (France)
bLaboratoire Matériaux Optiques, Photoniques and Systèmes, University Paul Verlaine Metz (France)

bourson@univ-metz.fr

Introduction During the forming process, by plastic deformation, of semi-crystalline polymers, the mechanisms of macromolecular chain orientation have an important role. It is the same during the relaxation after plastic deformations, which have a direct influence on the final product. The knowledge of these mechanisms is essential for good process control.

Therefore it conducted a study of the chains orientation of isotactic polypropylene during the elastic recovery.

Today the techniques used to study the chains orientation are heavy and long : X-ray and other light methods. In our experience using a Raman spectrometer to determine the chains orientation, the measurement takes a few seconds, which is much faster, and could allow in line measurements.

Material The semicrystalline isotactic polypropylene (noted IPP) investigated in this work was produced by ATOCHEM (Reference 3050 MN1).The density, determined by hydrostatic weighing is $\rho = 0.946$ g.cm^{-3}.

The crystallinity in weight is Xc = 0.67. The glass transition temperatures, Tg, and the melting temperature, Tm, determined by differential scanning calorimetry are respectively -5°C and 165°C [1-2].

Analyses by X-ray diffraction revealed the exclusive presence of the α-monoclinic crystal of isotactic polypropylene.

Mechanical Tests The experimental setup consists of a system VidéoTraction™[3] coupled to a Raman spectrometer. The traction machine is equipped with a camera that closely follows the movement of dots markers placed on the surface of the specimen. A computer calculates the strain from video images and control the traction machine accordingly to ensure a constant strain rate. The Raman scattering spectra are performed in a backscattering configuration. The laser has a wavelength of 785 nm. A polarizer is placed in the spectrometer; its polarization axis is parallel to the axis of the tensile test. The acquisition time is set to 5seconds. In this work, the mechanical tests were run at the strain rates $d\varepsilon/dt = 5.10^{-4}$ s^{-1}. We applied on the specimens a constant cycling deformation with increasing strain until $\varepsilon = 0.3$ (Figure 1). Then unloading it to the stress $\sigma = 0$. And a new round of tension began following up the deformation $\varepsilon = 0.6$. The strain step is $\Delta\varepsilon = 0.3$.

Spectral Signature Ponçot et al, [4] and J.Martin and al [5] have developed spectral signature to study the chain orientation of IPP during the uniaxial stain test. It uses two Raman bands located at 973 and 998cm-1. The first one is principally assigned to the asymmetric stretching mode of the C-C skeletal backbones while the second is referred to the rocking mode of the CH3 lateral alkyl groups. The CC bonds and alkyl groups which they are attached are in orthogonal positions. So when using a Raman polarized in the direction of CC bonds, must have observed an increase in the band at 973 cm^{-1} and a decrease of the band at 998cm^{-1}. Based on this observation, a simple criterion was developed, for measuring the orientation of carbon chains of the crystalline. The measure consists of calculating the intensity ratio between the 973cm^{-1} band intensity and the 998cm^{-1} band intensity. This Raman criterion correlated by X-ray diffraction, allows the measurement of orientation during the deformation. We call $R_{orient,c}$ the ratio of two bands of intensity. $R_{orient,c}$ = J(973cm^{-1}) / J(998cm^{-1}).

RESULTS AND DISCUSSION

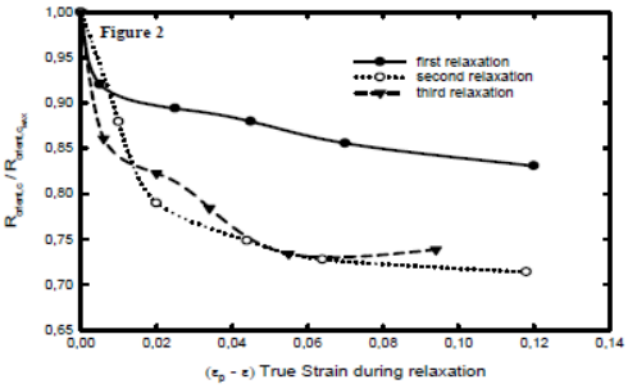

And it is interesting to link it to the reorientation of the chains of the crystalline phase. It is found that initially the reorientation is small, then to larger deformations, the reorientation decreases consistently Figure 2, we can compare the three relaxations. For the first at small strain, reorientation is low, and takes place from the beginning. For the two others relaxations reorientation is taller and has also held mainly at the beginning of relaxation. Experience shows that in the elastic phase and the early of plastic deformation, the phenomenon of crystalline chain orientation is not predominant. But once the amorphous phase disentangled, the chains orientation becomes a dominant mechanism. And during the elastic recovery the reorientation becomes increasingly large.

CONCLUSIONS

The technique coupling a spectrometer Raman with the VideoTraction™ allows in situ measurements during tensile tests. It was able to follow the macromolecular chains orientation during load and unload. Thus the microstructure evolution during relaxation could be studied. Dahoun [8] showed the evolution of the viscoelastic coefficient w/w0 load after load. The convergence of behavior at large strains has showed. In our experience the evolution of reorientation of the macromolecular chains follow the behavior of w. This knowledge of chains orientation is important in the drawing process; the mechanical properties depend on the preferred orientation of the chains. And others share the Raman Spectra can provide other information such as crystallinity and volume damage. It is therefore an inexpensive and rapid technique with a promising future.

Chromatographic characterization of PS-block-PEO

Monika Grabowsky, Muhammad I. Malik, Pritish Sinha, Harald Pasch

Department of Chemistry and Polymer Science, University of Stellenbosch, South Africa

Fax: +27218084967, e-mail: monikag@sun.ac.za, imran@sun.ac.za

Block copolymers are a promising group of materials used for many different applications such as surfactants, compatibilizers, detergents among many others. Block copolymers of polystyrene (hydrophobic in nature) and polyethylene oxide (hydrophilic) make them amphiphilic materials. The amphiphilic property of these block copolymers is exploited for above mentioned applications of these materials.

Block copolymers are complex materials with distributions in many properties like chemical composition distribution, molar mass distributions etc. Along with the block copolymers, the presence of homopolymers of both types in the sample is very difficult if not impossible to avoid. Specifically block copolymers of PS-b-PEO have not been investigated for above raised questions. Baran et. al.[1] used critical conditions for PS to get information about the PEO block but they have used only very lower molar mass products without facing big problems in solubility. In contrary to their study, we are investigating PS-b-PEO block copolymers with a wide range of molar masses of both blocks from several thousands to hundred thousands.

Liquid chromatography at critical conditions is used in this study to separate homopolymer fractions from the block copolymers. At critical conditions the block copolymer is separated according to the molar mass of the non-critical block which is excluded from the pores of the stationary phase.

The selection of a suitable solvent system was a real challenge for this study as both blocks are exceedingly incompatible with each other as well as with good solvents of the other block.

The block copolymer and homopolymer fractions are collected from LCCC and subjected to FTIR for further qualitative as well as quantitative analysis.

1. Baran, K.; Laugier, S.; Cramail, H. J Chromatogr B 2001, 753, 139-149.

Nanoparticle Characterisation by Field-Flow Fractionation

Werner van Aswegen[1], Imran Malik[1], Tino Otte[2], Harald Pasch[3]

[1]Department of Chemistry and Polymer Science, University of Stellenbosch, South Africa

[2]Postnova Analytics GmbH; Max-Planck-Strasse 14, Landesberg/Lech, D-86899, Germany

[3]SASOL Chair of Analytical Polymer Science, Department of Chemistry and Polymer Science; University of Stellenbosch, South Africa

Fax: +27218084967, e-mail: wvanaswegen@sun.ac.za , imran@sun.ac.za

The increasing interest and new developments in the fields of nanomaterials, medicine and biology have highlighted the extraordinary properties and the potential of nanoparticles (such as carbon nanotubes, quantum nanodots, gold and silver nanoparticles and micelles but to name only a few).

The analysis and quantification of these particles are therefore becoming of increasing importance and a range of separation techniques are therefore required.

Field-flow fractionation will play an essential role in the separation and analysis of these compounds as it is a powerful separation technique and has the advantage of overcoming most of the limitations associated with traditional chromatographic techniques such as size exclusion chromatography, gradient elution chromatography, Liquid chromatography at critical conditions etc.(1).

In this study we will investigate the characterisation and separation of various nanoparticles by two Field-Flow Fractionation sub-techniques.

The first being Asymmetrical Flow Field-Flow Fractionation (AF4) in which the separation is governed by an cross-flow that is perpendicularly applied to the main flow and results in a separation according to the diffusion coefficient of the particles and therefore the hydrodynamic size of the particles.

The second sub-technique is Centrifugal Field-Flow Fractionation (CF3). In this technique the separation field is generated by rotating a ring-type centrifugal channel. This rotation (spinning) generates a differential acceleration force on different particles resulting in a separation according to the size and mass (2).

We aim to compare both AF4 and CF3 and show the capability of both sub-techniques to address the analytical challenges posed by nanoparticles.

References:

(1) F. A. Messaud, R. D. S., J. R. Runyon, T. Otto, H. Pasch, S. K. Ratanathanawongs Williams. *Progress in Polymer Science* **2009,** 34, 351-368.

(2) S. K. Ratanathanawongs Williams, J. R Runyon, A. A. Ashames. *Anal. Chem.* 2011, 83, 634-642

Predicting the slow crack growth resistance of polyethylene resins using alternative short-time performance tests

C. Domínguez[a,*], A. Adib[b], J. Rodríguez[b], C. Martín[c], R. A. García[d]

[a] Polymer Technology Laboratory (LATEP). Rey Juan Carlos University, Móstoles (Madrid), Spain
[b] Department of Materials Science and Engineering. Rey Juan Carlos University, Móstoles (Madrid), Spain
[c] Repsol Technological Center. Móstoles (Madrid), Spain.
[d] Department of Chemical and Environmental Technology. Rey Juan Carlos University, Móstoles (Madrid), Spain

* E-mail: carlos.dominguez@urjc.es

High density polyethylene (HDPE) is the most commonly used material for the transportation and distribution of water and natural gas from nearly 40 years ago. For this application the resin has to fulfil certain mechanical properties, being one of the most critical the resistance to the Slow Crack Growth (SCG) process. This failure mechanism involves the formation of a craze at a point of stress concentration (fittings, welds, defect within the surface wall, surface flaws) and the subsequent growth and final fracture of the material in a brittle way [1].

SCG resistance is generally measured using the PENT test (Pennsylvania Notched Tensile test - ASTM F1473) in North America, whereas in Europe the FNCT (Full Nochted Creep Test – ISO 16770) is more usual. Another alternative test, currently under investigation, is the CDNT (Circumferentially Deep Notched Tensile test), which permits high degree of triaxial stress on ligament, which favours the brittle failure by SCG[2]. For any of these methods, the main problem is the long time that the new polyethylene grades need for being tested. For instance, PE100 or higher grades require hundreds (even thousands) of hours to finish the SCG test.

From mid-nineties to nowadays different groups have studied quicker methods for estimating the SCG resistance using a tensile test (mode I), drawing a polyethylene specimen to its natural draw ratio or further away to the strain hardening region. In this last method, the slope of the strain-hardening part (called strain hardening modulus $<G_p>$) in the true stress-true strain curve at elevated temperatures (~80ºC) correlates well with the data obtained by a classical accelerated ESCR test [3], being this method quite sensitive to subtle molecular differences between different polyethylene samples.

Another method for estimating the SCG resistance is based on the fact that the tie molecules density is the most important parameter which controls the SCG resistance of the resin [4]. The tie molecules density could be estimated from the molecular weight and short chain branching distributions experimentally obtained by GPC-FTIR, using a primary structural parameter (PSP2) [5]. This parameter is calculated using densities estimated from GPC-FTIR data and probability equations for tie molecules formation developed by Huang and Brown [6], showing a good correlation with the SCG resistance when a broad range of materials of different structure are analysed [7].
In the present work the SCG results obtained from different tests for evaluating the SCG resistance in polyethylene pipes have been compared with the PSP2 value and strain hardening modulus $<G_p>$ at 80ºC. With regard to the PSP2 value, the correlation is reasonably good when materials with a broad range of PSP2 values are analysed. However materials with very similar molecular and structural characteristics present lower sensitivity to the method. On the other hand, the SCG results showed in Figure 1, exhibit a good correlation with $<G_p>$, which open the possibility of using this method for a quick estimation of the resin SCG resistance, or at least, to discriminate materials with inadequate properties.

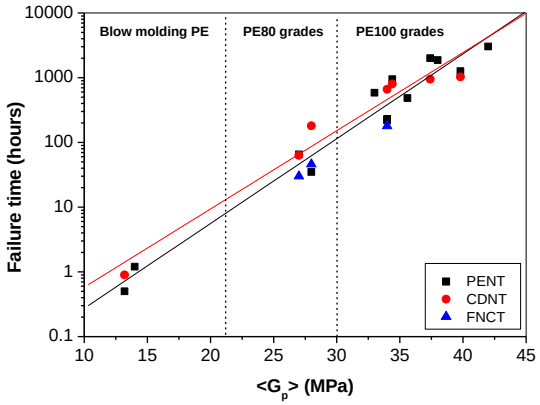

Fig.1 Failure time of different SCG tests vs <Gp>

1. Brown N. Polym. Eng. Sci. 2007, 47, 1951-1955.
2. Duan D. M., Williams J. G. J. Mat. Sci. 1998, 33, 625-638.
3. Kurelec L., Teeuwen M., Schoffeleers H., Deblieck R. Polymer 2005, 46, 6369-6379.
4. Seguela R. J. Polym. Sci. Part B: Polym. Phys. 2005, 43, 1729-1748.
5. DesLauriers P. J., Rohlfing C. Macrom Symp 2009, 282, 136.
6. Huang Y. L., Brown N. J Polym Sci Part B: Polym Phys 1991, 29, 129.
7. García R. A., Carrero A., Martín C., Domínguez C. J. Appl. Polym. Sci. 2011, *In press.*

ABSTRACTS

POSTER PRESENTATIONS

Topic 3: Advanced Processing and Recycling Technologies

Phase Behaviour of Blends of Poly(4-vinylphenol-co-methyl methacrylate) /Poly(styrene-*co*-4-vinylpyridine).

*Z. Benabdelghani**[1], *A. Etxeberria*[2]

[1]Laboratory of Storage and Valorization of Renewable Energies, Faculty of Chemistry, USTHB, P.O.Box 32,El Alia, Algiers 16111, Algeria.
[2]Departamento de Ciencia y Tecnologia de Polimeros and Instituto de Materiales Polimericos (POLYMAT). Universidad del Pais Vasco UPV/EHU. P.O. Box 1072. 20080 San Sebastian (Spain).

* To whom all correspondence should be addressed to e-mail address: Ben_Zit@yahoo.fr.

Introduction:

The research of new polymer materials with improved properties has been received considerable attention in both the academic and industrial points of view. In this way, the polymer blending is an attractive approach to obtain new polymeric materials with large scale proprieties. It has been demonstrated to be an effective alternative in achieving enhanced material properties such as better processability, lowered cost, etc. Thermodynamically, the miscibility of polymer blends is mainly dependent on the value of mixing enthalpy because the contribution of mixing entropy is negligible [1].

In the present contribution, we report in the first part the results of an investigation of the effect of introducing increasing amounts of specific group 4-vinylpyridine by copolymerization within the polystyrene (PS4VPy) matrix on Poly(4-vinylphenol-co-methyl methacrylate) (P4VPhMMA). The miscibility and phase behaviour in blends of poly(4-vinylphenol-co-methy methacrylate) (P4VPhMMA50) containing 50 % of methy methacrylate with random copolymers of poly(styrene-co-4-vinylpyridine) (PS4VPy) containing various amount of 4-vinylpyridine were investigated by differential scanning calorimetry (DSC), Fourier transform infrared spectroscopy (FTIR) and scanning electron microscope (SEM).

Results and discussion

2.1. DSC Study

The miscibility of the polymer blend can be studied by many techniques. Among them, thermal analysis is mainly used in this area. In general, the DSC is the most convenient method to elucidate the miscibility of polymer blends [2]. It well known that the binary polymeric system of poly(4 vinylphenol) (P4VPh), poly (methy methacrylate) (PMMA) and their copolymers with polystyrene (PS) have been found to be immiscible over the whole range of compositions and accessible temperatures [3].

As displayed in Figure 1, the inclusion of 5 mol % of vinylpyridine into the homopolymer PS is not sufficient to obtain the miscibility between PS and P4PhMMA50. The thermograms corresponding to blends of PS4VP05, P4VPhMMA50 and their blends reveal two Tg´s for each composition. As can be seen, these glass transition temperatures are similar to those of the pure constituents, respectively. This result indicates that the enhancing, respectively, of the repulsive interactions between comonomers styrene and 4-vinylpyridine and attractive interactions between 4-vinylphenol and 4-vinylpyridine are not sufficient to provide the miscibility between the blends of PS4VP05 and P4VPhMMA50.

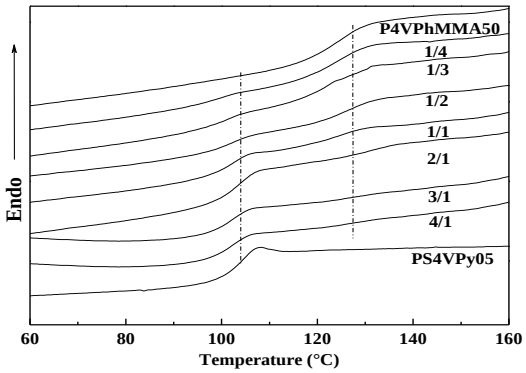

Figure 1: DSC thermograms of PS4VPy05, P4VPhMMA50 and their blends with different ratios.

2.2. SEM Study

The morphology of blends of PS4VPy05, PS4VPy15 and PS4VPy30 with P4VPhMMA50 in ratio 50/50 was also examined by SEM. In agreement with the DSC results presented earlier, the scanning electron micrographs of the fractured surfaces shown in figure 2 confirmed the immiscibility of these blends

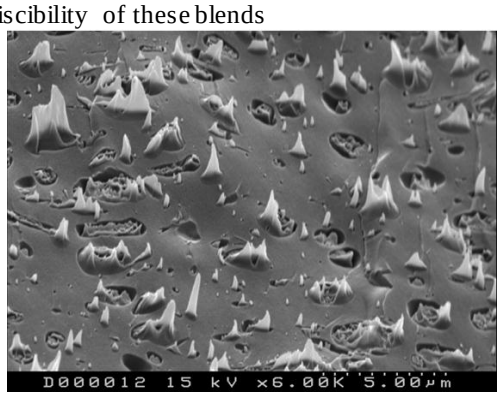

Figure 2: SEM photomicrograph of PS4VPy15/P4VPhMMA with ratio 50/50

However, above 20 % mol 4VP in PS4VP, blends of PVPhMMA50 and the random copolymers of PS4VP were found to be miscible. A single Tg intermediate between these constitutions is observed for each composition. When the amount of vinylpyridine exceeds to 40 % in PS4VPy, the obtained Tg's of P4VPhMMA50/PS4VPy blends were found to be significantly higher than those observed for each individual component of the mixture indicating that these blends are able to form interpolymer complexes. FTIR analysis reveals the existence of preferential specific interactions via hydrogen bonding between the hydroxyl and pyridine groups and intensifies when the amount of 4VPy is increased in PS4VP copolymers.

References

1. Paul D R, Barlow J W. Polymer 1984; 25: 487-494.
2. Benabdelghani Z, Etxeberria A, J of Appl Polym, in Press.
3. Kuo.S K; Polymer 2008,49:4420-4426.

Chemical characterization of organic-inorganic coating for dental applications

M.J. Juan-Díaz[1]. M. Martinez[1], M. Hernández-Escolano[2], J. Suay[3] M. Gurruchaga[1], I. Goñi[1]

[1] Polymer Science and Technology Department, Faculty of Chemistry of San Sebastian, UPV/EHU (Spain)
[2] Ctr. Biomaterials & Tissue Engineering, University Politecnic of Valencia, UPV (Spain)
[3] Jaime I University, Castellon, UJI, (Spain)

isabel.goni @ehu.es

Introduction

Titanium and its alloys are widely used implant materials in orthopaedic and dental field due to their excellent corrosion resistance and mechanical properties.[1] However, titanium can not directly bond to bone, and osseointegration via the natural oxide (TiO_2) is a long-term process. Moreover, titanium is not completely inert so it could release titanium particles that could finally result in the removal of the implant.[2] One way to avoid these effects is to protect the metallic implant with a biocompatible and bioactive coating.[3] Furthermore, these coatings can be used as drug delivery system for the prevention of infections.

The sol-gel process, one of the fastest growing field in materials chemistry is a technique suitable for coating the surface of a metal. This process consists in a creation of an oxide network by progressive condensation reactions of molecular precursors in a liquid medium.[4]

In the present work, an organic-inorganic hybrid coating from methyltrimethoxysilane (MTMOS) and 3-glycidoxypropyl trimethoxysilane (GPTMS) has been produced via the sol-gel route that could be recognized by biomolecules and also allow the development of a novel process on drug delivery systems. Materials with different ratios of MTMOS and GPTMS have been synthesized to study the effect of the precursors on the final material. Different curing processes have been used in order to obtain coatings with different condensation grades.

This paper is focused on the chemical characterization of the hybrid coating. The knowledge of the chemical structure of the formed network will facilitate the understanding of the material as an osseoinductor coating and as a drug delivery system.

Materials and Methods

Synthesis of the sols

The MTMOS/GPTMS sol was prepared by acid catalysis method, using MTMOS and GPTMS as silica precursors, isopropanol as solvent and 0.1M nitric acid (HNO_3) in order to obtain an acidic pH. Water was incorporated with the nitric acid solution in stoichiometric ratio. The molar ratios of MTMOS/GPTMS were 4:1; 1:1; and 1:4. The sol solutions were stirred for about 1h and kept for another hour at room temperature before use.

Curing process of the sol

Two different curing processes have been applied to the sols: (a) 15 min. 50ºC, 15 min. 100ºC, 90 min. 140ºC and (b) 15 min. 50ºC, 15 min. 100ºC, 45 min. 140ºC.

Characterization of the coatings

The chemical composition of the coating was investigated by Fourier Transformed Infrared spectrometry (FT-IR) and ^{29}Si nuclear magnetic resonance (^{29}Si-NMR) in liquid and solid state.

Results and Discussions

The ^{29}Si-NMR study of the sols was carried on for 5 hours, with sample analyzing every hour. It was, therefore possible to identify and follow the species forming during the hydrolysis and condensation reactions. In all the cases, the intensity of T_1 species decreases while T_2 and T_3 increase.

The characteristic peaks that indicates the formation of an inorganic network are found in FT-IR spectra: ν_{as} Si-O-Si at 1115 and 1090 cm^{-1}, ν Si-OH at 900 cm^{-1} and ν_s Si-O-Si at 780 cm^{-1}. Besides these bands characteristic of the inorganic network the presence of the organic groups was registered in all spectra. In the case of the MTMOS, the band at 1275 cm^{-1} confirms the presence of Si-CH_3, whereas for the GPTMS the band at 1730 cm^{-1} is assigned to C-O vibration of the γ-glycidoxypropyl group.

The identification of the final chemical structure of coatings with different curing processes was performed via ^{29}Si MAS-NMR. The presence of condensed species confirms the formation of a well-structured Si-O-Si network.

Conclusions

This study demonstrates that the sol-gel technology is an appropriate method to obtain hybrid organic-inorganic coatings. It was possible to follow the formation of the Si-O-Si network and to identify the final structure. Further studies that provide an insight on the influence of this structure on the material properties are underway.

Acknowledgements

The authors would like to thank the financial support of the Basque Government (SAIOTEK), Spanish Government (Ministerio de Ciencia e Innovación, Programa Impacto 2010) and University of the Basque Country (GIC 07/48-IT-234-07).

References

[1]E. De Giglio, M.R. Guascito, L.Sabbatini, G.Zambonin. Biomaterials. 2001, 22, 2609

[2]G.A. Crawford, N. Chawla, K. Das, S. Bose, A. Bandyopadhyay. Acta Biomaterialia. 2007, 3, 359.

[3]W. Khan, M. Kapoor, N. Kumar. Acta Biomaterialia. 2007, 3, 541.

[4]D. Wang, G.P. Bierwagen. Progress in Organic Coatings. 2009. 64, 327.

Low-temperature polymerization of vinyl monomers controlled by metallocomplexes based on C_2B_8-carborane ligand

Ivan Grishin[a], *Andrey Ohapkin*[a], *Igor Chizhevsky*[b], *Dmitry Grishin*[b]

[a]Research Institute of Chemistry of Nizhny Novgorod State University,
[b]A.N.Nesmeyanov Institute of Organoelement Compounds Russian Academy of Sciences

grishin_i@ichem.unn.ru

Introduction

Nowadays Controlled Radical Polymerization **(CRP)** is one of the most developing areas in the modern polymer chemistry as it is very promising tool for obtaining polymer materials with necessary properties. The development of new systems for CRP is a very challenging task. Using organometallic compounds for conducting CRP is a very effective way due to the unique properties of these systems, namely the possibility of its fine tuning by changing ligand environment of a transition metal atom. In this work we report about the use ruthenium carborane complex based on C_2B_8 ligand for CRP.

Materials and Methods

Complex **1** was synthesized according the literature[1]. Monomers were dried over CaH_2 and distilled under reduced pressure prior to use. The polymerization was conducted at 80°C in sealed glass tubes under reduced pressure in monomer bulk. The obtained polymer samples were purificated from monomer and catalyst by dissolving in chloroform and precipitating in petroleum ether. The molecular-weight distributions of the polymers were analyzed by size-exclusion chromatography.

Results and Discussion

In this work the system based on ruthenium carborane complex **1** containing C_2B_8-dicarbollide ligand was used for providing CRP:

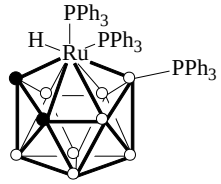

1

This is the first attempt to use *iso-nido*-metallocarboranes (0.125% mol.) for controlled synthesis of polymers. The carbon tetrachloride was used as an initiator (0.25% mol.).

The results of our experiments show that system based on **1** and carbon tetrachloride is capable to initiate polymerization of methyl methacrylate (MMA) even at 25°C. The polymerization proceeds up to high conversion of the monomer. The molecular weight of the obtained samples linearly increases with the conversion growth, what is typical for CRP. At the same time the curves of molecular weight distribution are not unimodal and have shoulders into the area of high molecular weights (fig.1.). The obtained polymer samples have rather broad molecular-weight distribution (M_w/M_n>1.5).

The polymerization can be resumed after addition of new portion of a monomer. The obtained post-polymer has a higher molecular weight indicating the living nature of the process.

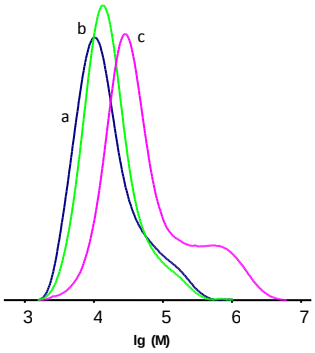

Fig 1. The curves of molecular-weight distribution of polyMMA obtained in the presence of **1** and CCl_4 at 25°C. Conversion, %: a – 20%, b – 30%, c – 95%.

The increase of temperature up to 40°C slightly improves a control over process allowing to obtain polyMMA samples with M_w/M_n=1.2-1.4. The molecular weight increases with conversion (fig. 2). The isolated polymer may be used as an initiator for post-polymerization.

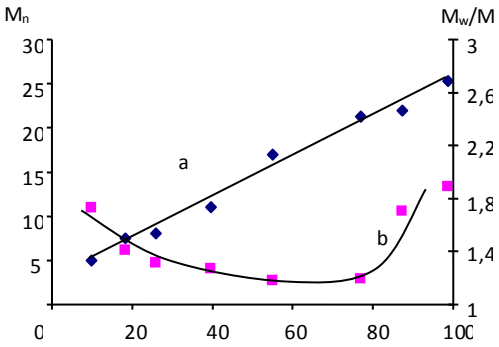

Fig 2. The dependences of molecular weight (a) and M_w/M_n (b) on conversion for MMA polymerization in the presence of **1** and CCl_4 at 40°C

It was established that the tested systems based on **1** and CCl_4 are capable to initiate polymerization of styrene and acrylates at 25°C. Unfortunately polymerization of buthyl acrylate is not controlled.

Conclusions

So, the ruthenium carborane complex **1** is a promising catalyst for CRP. Systems based on it capable to conduct polymerization of MMA even at room temperature and above, indicating it high activity.

References

1. Jung C.W., Hawthorne M.F. *JACS*, **1980**, *102*, 3024.

Acknowledgements: This work was supported by Russian foundation for basic researches (project №11-03-00074) and Russian Ministry of Education and Science ("Federal target program of scientific and scientific-pedagogical personnel of innovation of Russia on 2009-2013").

Morphological Characterization of PP for different Foam Injection Molding Processes with Chemical Blowing Agents.

V. Contreras [1,3], *N. Villarreal-Bastardo* [2], *J.C. Merino* [2,3], *J.M. Pastor* [2,3]

[1] Universidad Simón Bolívar, Departamento de Mecánica, Sección de Polímeros, Caracas 1080-A, Venezuela.
[2] Fundacion CIDAUT, Parque Tecnológico de Boecillo, Valladolid 47151 - España.
[3] Universidad de Valladolid, EII Paseo del Cauce 59, Valladolid 47011 - España.

email: vcontreras@usb.ve

INTRODUCTION.

Modification on conventional injection molding process of foaming thermoplastic polymers has raised much interest recent years because of its numerous advantages over conventional injection molding. However, compared to extrusion and other processes, the control of the injection foaming process appears more challenging because it deals with many additional controlling parameters such as injection speed, shot size and back pressure (1). In addition, good melt strength is fundamental to produce a foamed plastic, using either a physical or chemical blowing agent. Semicrystalline polymers like polypropylene (PP), have low melt strength, because they have linear structures with low content of branching. While resins like high melt strength polypropylene have been re-designed to improve melt strength, others may use additives or chemical modification that improve melt strength and thus enhance foaming (2-3). In this study, the feasibility of using two types of PP by different injection molding processes with a chemical blowing agent was evaluated.

MATERIALS AND METHODS.

Rheological and thermal behavior of a PP and a reinforced PP were analyzed by capillary rheology, DSC and SSA. Two ways of injection molding were used; conventional and core back injection molding. First of all, the cell structure and properties of foamed PP injected in both processes with different condition such as chemical foaming agent concentration, injection speed, as well as melt temperature were analyzed by microscopic techniques, flexural and impact properties.

RESULTS AND DISCCUSION.

The foamability of the reinforced PP was intrinsically good due to its rheological properties and material morphology, that was evaluated from SSA results and viscosity curves from Capillary rheology. Cell structure of these polymers may depend on the type of the foaming process and crystal structure, as well as the injection process used, which is clearly observed on the cell size and distribution found on the microscopy test (Figure 1). In the other hand, the skin layer of the pieces obtained on the both process could be an important factor for the flexural behavior. Although impact strength behavior is dominated by the relative density of the foam.

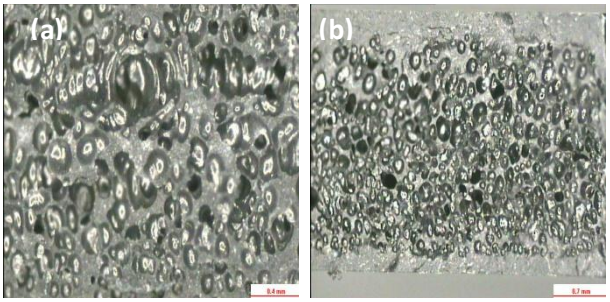

Figure 1. Optical Microscopy micrographs of (a) reinforced PP and (b) neat PP, foamed by core back injection molding

REFERENCES.

(1) Ming-Cheng Guo, Marie-Claude Heuzey, Pierre J. Carreau. Polym. Eng. Sci. 47, 1070–1081 (2007).
(2) Seyed H. Tabatabaei, Pierre J. Carreau, Abdellah Ajji. Polym. Eng. Sci. 50, 191–199 (2010).
(3) Markarian, Jennifer. Plast. Addit. Compd.. 28-30. (2009)

Development of Glass Reinforced PVC Composite - POSTER

1 - Ms. Daniela Gomes de Araujo

Graduate Program in Materials Science and Engineering – PPG-CEM / UFSCAR
daniela.gomes@owenscorning.com

2 - Prof. Dr Elias Hage Jr.

DEMa- Materials Engineering Departament/UFSCar
elias@power.ufscar.br

3 - Me Leandro Henrique Grizzo
Graduate Program in Materials Science and Engineering – PPG-CEM / UFSCAR
leandrogrizzo@gmail.com

The objective of this project is present a glass fiber reinforced PVC composite, that can be used in technical application due to better mechanical properties than unreinforced rigid PVC compound. This project presents a method to produce fiber glass reinforced PVC composite.

The concept is developing a fiber glass with a new sizing compatible with PVC matrix and a process to incorporate the long fibers in the PVC compound.

The method is through incorporating continuous glass fibers with vinyl matrix prepared by wire coating process and pelletizing the coated roving (by cutting in the range 13 to 14 µm in length). The pellets are mixed with granulated rigid PVC and this blend is fed directly into the injection-molding process machine. The direct injection molding is an excellent option because it reduces the number of processing, reduces the deterioration of the glass fibers length and reduces the possibility of PVC resins degradation.

In summary, long glass fiber reinforced PVC compound through incorporating by wire coating process is possible and it created an innovating process of reinforcement into the vinyl area, in addition to the better mechanical properties achieved that allow PVC can be used in a unrecognized high-performance applications that was not possible before.

New Copolymer of Tautomerizable Monomer

Giussi, Juan M.[1,2]*; Allegretti, Patricia E.*[1]*; Cortizo, M. Susana*[1,2]

[1] Laboratorio de Estudio de Compuestos Orgánicos
[2] Instituto de investigaciones Fisicoquímicas Teóricas y Aplicadas
[1,2]Departamento de Química - Facultad de Ciencias Exactas – Universidad Nacional de La Plata
Calle 47 y 115. La Plata – Buenos Aires – Argentina

jmgiussi@quimica.unlp.edu.ar

Introduction.

Although there are a lot of papers published on tautomeric studies of different organic compounds [1], no much works are related with tautomerics equilibria in polymers. For example, Czech studied metal chelate zirconium acetylacetonate (ZrACA) added into acrylic polymers with self-adhesive properties [2]. These acrylic polymers, known as acrylic pressure-sensitive adhesives (PSA), were crosslinked with ZrACA to obtain acrylic self-adhesives and to study the crosslinking reaction between carboxylic groups of the polymer chain and metal chelate crosslinking agent. The tautomeric equilibrium in this reaction is very important because these reactions occur through tautomeric forms.

We consider that tautomerics equilibria in polymers could be responsible for important properties and applications. That is why the aim of our work was the study of tautomerics equilibria in styrenic copolymer including a comonomer with tautomeric β-ketonitriles form.

Materials and Methods.

5-phenyl-3-oxo-4-pentenonitrile (CM_3) was obtained through an adaptation of a literature method [3]. The tautomerics equilibria in this monomer was study by mass spectra-gas chromatography (GC-MS) in gas phase, Nuclear Magnetic Resonance (NMR) in solution and Infrared (IR) spectroscopy in solid state. These experimental results were compared with DFT calculations[4].

CM_3 was copolymerized with styrene in thermal conditions at 60°C using azobisisobutyronitrile (AIBN) as initiator. The polymerization reactions were carried out in closed reaction tubes in vacuum. The reactions was quenching by precipitation with cold methanol. The polymer isolated was purified by dissolving in chloroform and precipitation on methanol. We repeated this procedure until only the peak of the polymer was seen in the size-exclusion chromatography (SEC). The weight average molecular weight (M_w) and the polydispersity index ($PI=M_w/M_n$) were determined by SEC using a series of four Waters columns and Cl_3CH as eluent. Polystyrene standard was used as calibrant.

Results and Discussion.

The tautomeric form of CM_3 is shown in the figure below. The tautomerisms nitrile-ketenimine monomer only was seen by GC-MS, while the tautomerism keto-enol was seen by NMR and IR spectra only [4].

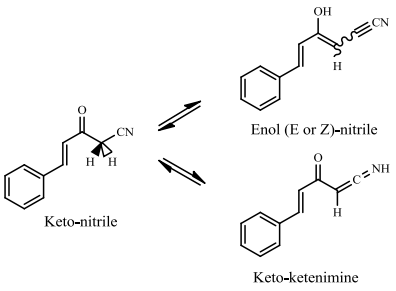

We expected that this type of behavior can be observed in the corresponding copolymers.

The table below shows the experimental condition and results obtained for copolymerization reactions.

Name	Time (hs)	Concentration AIBN*	f_{CM3}	Conversion (%)	Mw	Ip
$CoStCM_3^1$	14	0.50	0.67	14.5	34660	1.65
$CoStCM_3^2$	23	0.25	0.67	16.5	32580	1.80
$CoStCM_3^3$	24	0.25	0.2	34.3	82395	1.99
$CoStCM_3^4$	24	0.25	0.5	22.1	52520	1.88
$CoStCM_3^5$	24	0.25	0.75	14.5	33175	2.07
$CoStCM_3^6$	24	0.25	0.9	18.7	-	-

* (% p/p)

$CoStCM_3^6$ and $CoStCM_3^7$ were not determinate yet.

The polymers were characterized by IR spectroscopy. We could asignated picks for both monomers and also for tautomeric forms. Nitrile band at 2230 cm-1 and carbonyl band at 1685 cm-1. We assigned a band at 1620 cm -1 for double bound C=C for enolics forms in the polymers obtained. There is an increase of the reaction conversion when the content of CM_3 decrease, which suggest a lower reactivity of this monomer. Accordingly, an increase in the M_w was observed. Actually, we are carrying out determinations by NMR spectroscopy in order to determinate the copolymer composition (F) and then the reactivity ratio.

Conclusions.

New copolymers styrene-5-phenyl-3-oxo-4-penteno-nitrile was synthetized and characterized whose tautomeric equilibria study is been conducted.

References.

[1] Terent'ev et al; Mass Spectr. Rev. 15 (1996) 339.
[2] Czech et al; European Polymer Journal, 42 (2006) 2153.
[3] Coan et al; Organic Syntheses, 3 (1963) 30.
[4] Giussi et al; . Acta A: Mol. Biomol. Spectrosc. 78 (2011) 868.

"Smart Pellet" Additives for Reinforcement in Polypropylene Composite

Yuxin Wang, *David A. Schiraldi*

Department of Macromolecular Science and Engineering, Case Western Reserve University, Cleveland, OH-44106, United States.

Das44@case.edu

Introduction

The "smart pellet" method is based on production of an alternating, micro-scale multilayer film comprised of a matrix polymer and a fiber-filled polymer, followed by cutting this film into pellet size masterbatch particles. These multilayered pellets with the corresponding polymer matrix form a smart pellet system. Two such approaches described in the present work are: (1) use of polypropylene/inorganic fiber platelets as a means of delivering spatially-aligned inorganic fibers to polypropylene; (2) use of polysulfone /inorganic fiber platelets as both reinforcing agent and spatially-aligned inorganic fiber carrier for polypropylene.

Materials and Methods

Domolen 2300K polypropylene copolymer (PP) and a masterbatch of the same PP reinforced by 30 wt% magnesium-based inorganic whisker (Hyperform® HPR-803, Milliken Chemical) referred to as Fiber-PP (FP) were coextruded at 195°C,employing layer-multiplying technology. Basell Profax 8623 polypropylene copolymer (PP*) was also chosen as a matrix polymer. A masterbatch of PSF (Udel-3703) was reinforced by 30 wt% HPR-803; this masterbatch was referred to Fiber-PSF (FPSF). The multilayer strand of alternating PP and FPSF was melt extruded at 320°C for FPSF and at 275°C for PP while the thickness of individual PP and FP layer was targeted at 1.2 µm. The individual PP and FPSF layer thickness was designed at 4 µm. These two multilayer products were cut into pellet size by a flexible plastic blade.

These smart pellets were molded with corresponding polymer resins respectively on a Boy 22-S injection molding machine. The SEM/EDX experiments were performed on a Philips XL scanning electron microscope, operating at 15 or 20 kV. Tensile tests were conducted using an Instron 5566 Universal testing machine at a crosshead speed of 40 mm/min. Izod impact tests were conducted on specimens using a QC-63 universal impact testing machine on the half length flex bars with a V notch in the middle.

Results and Discussion

The fibers within FPP/PP "smart pellet" in the FP layers appear to be well oriented (Figure 1) in the melt flow direction. Injection molded FP/PP-PP composite exhibited greater improvement in the flexural modulus of PP than injection molded FP-PP which could be attributed to the fiber continuous dispersion in FP/PP-PP composite; though they shared similar morphology that fibers were aligned in flow direction, as well as final fiber length, which supports that no obvious difference was found in tensile and Izod strength tests.

The fibers were found to be located only in the PSF layers in FPSF/PP* smart pellet which was identified using element mapping (Figure 2).The mechanical tests of FPSF/PP*-PP* composite demonstrated that FPSF/PP* smart pellets improved the total mechanical properties more than PSF/PP* smart pellet with fiber as one more reinforcing agents. Higher flexural modulus and tensile properties of FPSF/PP*-PP* were achieved over PSF/PP*-PP*, indicating that fiber could work as an effective reinforcing agent incorporation with PSF.

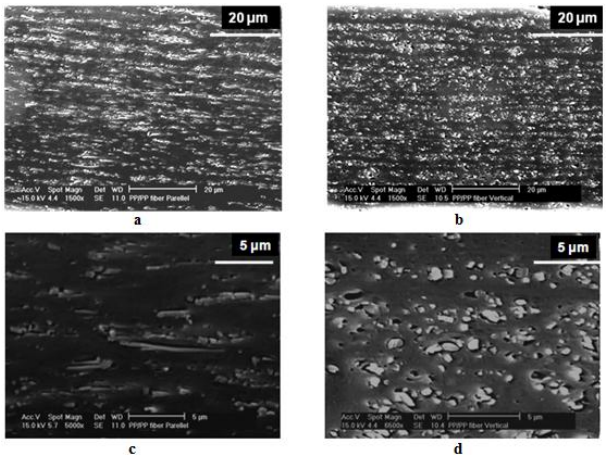

Figure 1. SEM images of the cross-section of FP/PP multilayer film. a/c: flow direction; b/d: transverse direction.

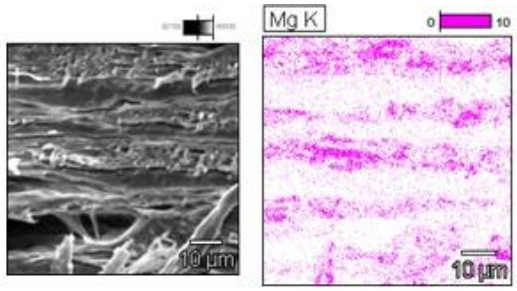

Figure 2. Element mapping graphs of the cross-section of FPSF/PP* multilayer strand in flow direction

Conclusions

"Smart pellet" method provides an effective way to improve the mechanical properties by introducing alternating polymer/fiber-filled polymer layered additives. Both a second polymer and fibers can work as reinforcing agents in the polymer system described in the paper.

References

Y. Liu, Y. Jin, A. Hiltner, E. Baer. *Macromol. Rapid Commun.*, **2003**,*24*,943-8.

H. Deng, R. Zhang, C. T. Reynolds, E. Bilotti, T. Peijs. *Macromol. Mater. Eng.*, **2009**,*294*,749-55.

Carbon Nanotube Imprinting Technique Using Brownian Motion in Polymer Melt

Masayuki Yamaguchi, *HoWon Yoon*

Japan Advanced Institute of Science and Technology

m_yama@jaist.ac.jp

ABSTRACT Localization method of multi-walled carbon nanotubes (CNTs) on the surface of a polymer sheet was demonstrated using interphase CNT transfer from one polymer to another. It was found that CNTs move from the polypropylene (PP)/CNT composite to polycarbonate (PC) during annealing procedure in the molten state of both polymers. The sheets of PP/CNT and PC were easily separated because of the large interfacial tension between PP and PC. The formation of a thin CNT-rich layer on the surface of the separated PC sheet produces electrical conductivity. Consequently, a conductive sheet is obtained with significantly small amounts of CNTs. Since the CNT transfer is attributed to Brownian motion, the annealing conditions such as temperature and time are responsible for the diffusion.

Introduction

As increasing the demand for electronic application of polymeric materials, a polymer with good electrical conductivity has been desired and investigated intensively these days. Carbon nanotubes (CNTs) are widely used as one of the high-performance modifiers because of the unique properties such as high stability, high electric and thermal conductivity, and large aspect ratio. Therefore, the properties of polymer composites containing CNTs have been studied intensively over the last decade for applications in electrostatic dissipation, electromagnetic interference shielding, and radio frequency interference shielding.

It was demonstrated by our previous work that CNT shows Brownian motion in a molten polymer. Hence, reorganization of CNT dispersion state in a molten polymer occurs at high temperature, leading to the formation of a conductive path [1].

In this paper, a new method of imprinting CNT by means of Brownian motion is demonstrated.

Experimental

Polycarbonate (PC) and polypropylene (PP) were used as polymer matrices. The composite of 20 wt% multi-walled carbon nanotubes (CNT) in a PP matrix was obtained from Hodogaya Chemical (Japan) as a pellet form. Typical diameters of employed CNT are from 40 to 80 nm, while the lengths are between 10 and 20 μm. The density is approximately 2.3 g/cm^3.

PP/CNT and PC were compressed into flat sheets using a compression-molding machine. Using them, the thermally activated transfer process of CNTs between surfaces of immiscible polymer pairs is investigated by the procedure illustrated in Figure 1. The laminated sheets were prepared by placing the pure PC sheet on the PP/CNT sheet. Then, annealing operation was performed in the compression-molding machine at various conditions [2].

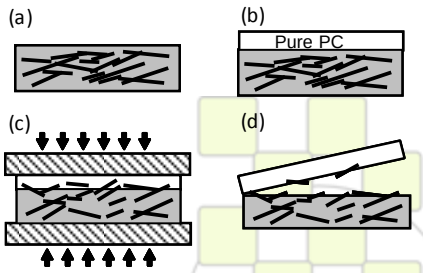

Figure 1.
Experimental procedure of CNT transfer; (a) a CNT-filled PP sheet, (b) place a pure PC sheet on the CNT-filled PP sheet, (c) anneal the laminated sheet in various conditions, and (d) separate the sheets after cooling.

Results and Discussion

Since PP is immiscible with PC, the piled sheets were separated without any difficulty after annealing operations. Then, the separated surface of the PC sheet was examined in detail.

As seen in the SEM picture of the cross-section of the PC sheet after annealing at 300 °C for 5 min, CNT-rich region is generated in the surface of PC. These CNTs were immigrated from PP/CNT during the annealing operation. Because of the concentrated layer, the surface resistivity decreases greatly to 10^3 [ohm/sq.]. This is significantly lower than the surface resistivity of a conventional polymer (> 10^{15} [ohm/sq.]).

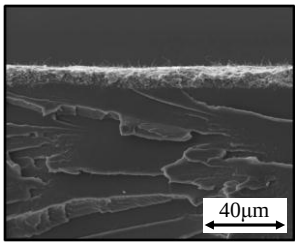

Figure 2. SEM picture of the cross-section of the PC sheet after annealing procedure at 300 ºC for 5 min with the PP/CNT sheet.

Since CNT transfer is attributed to Brownian motion, heating conditions such as temperature and duration time are responsible for the amount of transferred CNTs. For example, the thickness of CNT layers, as exemplified in Figure 2, is proportional to the square of the applied annealing time [2]. Moreover, the transfer phenomenon is influenced by the dispersion state of CNTs in the composite, the size of CNTs and their compatibility, and the chemical structure of the second polymer [2]. Finally, this method can be used to improve surface properties while minimizing CNT content in the bulk of the polymer composite and could be a feasible process to integrate CNTs into various devices.

Conclusions

Localization of CNT at the surface of a PC sheet is attained using the CNT transfer phenomenon from a PP/CNT sheet during annealing procedure at 300 °C. This result suggests that CNT prefers PC to PP. Since the technique gives a conductive polymer sheet with a small amount of CNT, it will be applicable in the industry.

References

1. H. Yoon, K. Okamoto, K. Umishita, M. Yamaguchi, *Polym Comp*., **32**, 97 (2011).
2. H. Yoon, K. Okamoto, M. Yamaguchi, *Carbon*, **47**, 2840 (2009).

Polymerisation of Pyrrole with Phenyliodine bis(trifluoroacetate)

Esin Ateş and Nilgün Kızılcan

Istanbul Technical University, Department of Chemistry, Istanbul 34469, Turkey

esinatess@gmail.com

Various types of inorganic or organic catalysts are used for chemical synthesis of polypyrroles. In the case of conducting polypyrroles halogens and salts of transition metals (eg. Ag^{+}, Cu^{2+}, Fe^{3+}, Ce^{4+}) are common catalysts that are able to serve both as an oxidizing agent for monomer and a doping agent for polymer chains.

Structure, size and concentration of oxidizing agent effect solubility, morphology, processibility and conductivity of resulting polymer. Large organic molecules or ions (eg. surfactants such as aryl sulfonates and their acids) are prefered to keep polypyrrole chains in a distance and interact with solvent. Thus the solubility of polypyrrole increases in organic solvents. Regulating concentration of the oxidant gives control over crosslinking and number of defects of π-conjugation located on polypyrrole chains. High overoxidation of pyrrole rigns lead to lower conductivity of resulting polymer.

Hypervalent iodine reagents provide an alternative synthetic route to classic reagents including heavy metals such as Hg^{2+}, Tl^{3+}, Cd^{4+} and Pb^{4+}. Low toxicity, good stability, easy handling and good reactivity are attractive properties of these reagents. Most known trivalent and pentavalent iodine reagents are phenyliodine (III) bis(trifluoroacetate) (PIFA), phenyliodine (III) diacetate (PIDA), [hydroxy(tosyloxy)iodo]benzene (Koser's reagent), iodosyl benzoic acid (IBA) and 2-iodoxybenzoic acid (IBX).

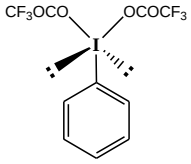

(PIFA)

PIFA is a tool to generate radicals from alohols, amines and azides[1]. Besides it is used in applications to generate radical cation from aryl compounds via single-electron-transfer(SET) mechanism. The latter provides further reactions with nucleophiles. When nucleophile is an aromatic ring then biaryl compounds are synthesized[2,3]. PIFA is able to assist oxidative coupling of phenolic compounds [4-6] and reactions of heteroaromatic compounds, eg. synthesis of pyrrole derivatives[7] and thiophene oligomers[8,9], however PIFA is not a usual catalyst for polymerisation process of these species.

In present study PIFA mediated synthesis of polypyrrole was performed. Experimental parameters such as oxidant/monomer molar ratio, concentration of PIFA, temperature and solvent were investigated. Although molar ratio of PIFA/pyrrole was 1/7, vigorous exothermic reaction occured. Effect of the reaction conditions on yield, solubility, thermal properties and conductivity of resulting polymer was determined. Polypyrrole synthesized in acetonitrile at 0°C has conductivity of 0.16 S/cm.

References

[1] T. Dohi, M. Ito, N. Yamaoka, K. Morimoto, H. Fujioka, Y. Kita, Tetrahedron 65 (2009) 10797–10815.

[2] N. K. Downer-Riley, Y.A. Jackson, Tetrahedron 64 (2008) 7741–7744.

[3] I. Moreno, I. Tellitu, J. Etayo, R. SanMartin, E. Dominguez, Tetrahedron 57 (2001) 5403-5411.

[4] H. Tohma, H. Morioka, S. Takizawa, M. Arisawa and Y. Kita, Tetrahedron 57 (2001) 345-352.

[5] H. Eickhoff, G. Jung and A. Rieker, Tetrahedron 57 (2001) 353-364.

[6] H. Tohma, M. Iwata, T. Maegawa and Y. Kita, Tetrahedron Lett. 43 (2002) 9241–9244.

[7] C. Alp, D. Ekinci, M.S. Gültekin, M. Şenturk, E. Şahin, Ö. İ. Kufrevioğlu, Bioorgan. Med. Chem. 18 (2010) 4468–4474.

[8] G. Saini, N.T. Lucas, J. Jacob, Tetrahedron Lett. 51 (2010) 2956–2958.

[9] A.K. Mohanakrishnan, P. Amaladass and J.A. Clement, Tetrahedron Lett. 48 (2007) 779–784.

Performance improvement of silicone rubber/carbon fiber composites

Eung Soo Kim, Young Ho Jeon, Mi Yeong Jo, Jin San Yoon

Department of Polymer Science and Engineering, Inha University, Incheon, Korea

jsyoon@inha.ac.kr

Introduction

Silicone rubber is one of the most important inorganic polymers. However, most applications require that PDMS be reinforced by solid fillers.[1] The most widely used fillers for reinforcing PDMS are silica, carbon black and fibrous fillers.[2]

Carbon fiber (CF) is an attractive reinforcing material due to its superior specific strength, specific modulus and low linear coefficient of thermal expansion.[3] Usually the interfacial interaction between CF and the polymer matrix is not strong enough to cause easy failure.[4] Therefore, surface-treatment of CF is required to raise the interfacial interaction enhancement.

In this study, silicone rubber composites were prepared with a room temperature vulcanized (RTV) type silicone rubber, carbon black, and CF. CF was modified by treating with nitric acid followed by grafting of the silane compound containing isocyanato group to the CF surface. The effects of the surface modification of CF on the mechanical and thermal properties were explored for the RTV/CF composites.

Results and Discussion

CF containing hydroxyl and carboxyl groups (Acid-CF) was prepared by treating neat CF with nitric acid under nitrogen flow. The surface of Acid-CF was then grafted with IPTS by having the isocyanate group of the IPTS residue on the surface of Acid-CF reacted with the hydroxyl and carboxyl groups of Acid-CF. The IPTS grafted CF was named as I-CF.

Condensation reaction between the alkoxy groups of I-CF and the silanol groups of RTV is feasible so that the RTV molecules grafted to I-CF should increase the interaction between the RTV silicone rubber and I-CF.

Chopped CF is usually supplied in bundles through the surface coating with organic matters because uncoated CF provokes dust scattering problems. Therefore, the coating agent needs to be removed from the CF surface in order to well disperse the chopped fiber in the rubber matrix.

The cross section morphologies of the RTV/CF composites are displayed in Fig. 1. The CF fibers in the RTV/CF composite exhibit a comparatively clean surface. On the other hand, I-CF in the RTV/I-CF composite is blotted with RTV debris, indicating that the wettability of I-CF to the RTV matrix was greatly enhanced.

The degree of cross-linking of RTV/CF and RTV/I-CF composites was estimated from the swelling properties of the composites in toluene. The swelling ratio (S_R) of the composites was determined by using Eq. (1).[5]

$$S_R = \frac{[m_s - (\alpha_{filler} m_d)]}{(\alpha_{pol} m_d)} \quad (1)$$

The RTV/carbon black/I-CF composites exhibited the lowest equilibrium swelling ratio, confirming the occurrence of the extra curing of RTV by I-CF.

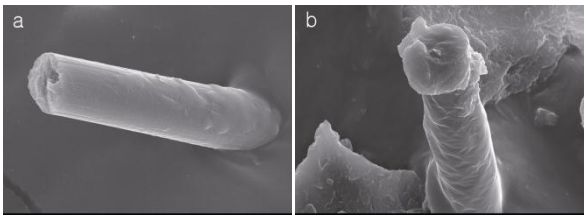

Fig. 1: SEM image of the fractured surface of (a) RTV/N774/CF (b) RTV/N774/I-CF

The tensile properties of the RTV composites are summarized in Table 1. The addition of CF to RTV/N774 did not raise the tensile strength, and the tensile strength of RTV/MA100/CF was marginally higher than that of RTV/MA100. In contrast, incorporation of I-CF to RTV/N774 and RTV/MA100 enhanced considerably the tensile strength of the respective composites. Moreover, the decrease in elongation at break of the composites was more significant when I-CF was incorporated into the composites instead of CF. These results confirm again the occurrence of the extra curing of RTV due to I-CF and the enhanced interfacial interaction.

Table 1: Tensile properties of the RTV/CF composites

	Tensile Strength (MPa)	Elongation (%)
RTV/N774	1.6	245
RTV/N774/CF	1.6	63
RTV/N774/I-CF	4.1	18
RTV/MA100	1.4	118
RTV/MA100/CF	1.7	41
RTV/MA100/I-CF	4.3	15

Acknowledgement

Authors are gratefully acknowledging the support by Defense Acquisition Program Administration and Agency for Defense Development..

References

[1] Mark JE, Allcock HR and West R, Inorganic Polymers. New Jersey: Prentice Hall, 1992.

[2] Morton M. Rubber technology. 3rd ed. New York: van Nostrand Reinhold; 1987.

[3] Choi MH, Jeon BH, Chung IJ. Polymer 2000; 41: 3243-52.

[4] Lang RW, Manson JA, Hertzberg RW. Polym Eng Sci 1982; 22: 982-7.

[5] Kaneko MLQA, Yoshida IVP. J Appl Polym Sci 2008; 108: 2587-96.

Novel mechanochemistry reactor and its use for rubber degradation studies in presence of stabilizers under controlled reactive gas atmosphere

Daniele Dondi, Armando Buttafava, M.Bianchi, Alberto Zeffiro, Antonio Faucitano

[1] Dipartimento di Chimica, Universita' di Pavia, V.le Taramelli 12, 27100 Pavia (Italy)

antonio.faucitano@unipv.it

Introduction

A lab reactor has been developed suited for investigating the mechanical degradation of polymeric materials in controlled gas atmosphere and with the possibility of on line monitoring of key chemical and viscosity parameter. The apparatus was then used to study the mechanical degradation of SBR rubber under inert and oxygen atmosphere and the effect of antioxidant and stabilizers belonging to the class of tetralkyl piperidine (HALS), guanidine and aromatic amines.

Materials and Methods

Fig 1 *Scheme of the lab reactor used for the mechanochemical degradation experiments.*

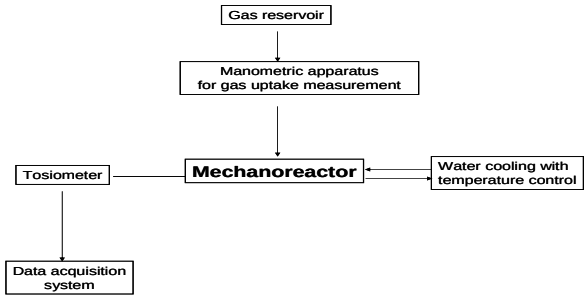

The tritor was made of two disks bearing interpenetrating blades one of which was kept rotating. The fixed disk was connected to a dynamometer for torque measurement. The reactor chamber was double jacket for thermostated water circulation and connected to a reservoir and a manometric apparatus for gas feed and uptake measurement . EPR and reduced viscosity measurements during the reaction were made by time to time sampling the material after stopping the apparatus.

SBR copolymer (23.5% styrene) was used as received. 2,2,6,6-tetramethyl piperidinyl sebacate (Tinuvin 770), Diphenyl guanidine (DPG) and di-tolyl paraphenylene ammine (DTPD) were used as antioxidant and stabilizers. The yield of mechanoradicals $R^{\bullet}$ was determined by carrying the reaction in presence of a known concentration of 2,2,6,6-tetramethyl piperidine-N-Oxyl stable radicals (TEMPO) and measuring its concentration decrease induced by the spin trapping reaction: $R^{\bullet} + >N\text{-}O^{\bullet} \rightarrow >N\text{-}O\text{-}R$

The reduced viscosity measurements were made with an Ubbelhode apparatus using tetraydrofurane as solvent.

Results and Conclusions

The kinetics of SBR degradation under nitrogen atmosphere is characterized by an initial stage where the viscosity decreases as a consequence of the prevalence of chain scission ; this trend is reversed in the later stages of the reaction because of the progressive taking over of the crosslinking mechanism.

.

The overall yield of mechanoradicals increases steadily with the machination time attaining magnitudes greater than 1.5×10^{-2} moles/kg after 4 h. The tendency of the radicals buil up curve to level off with the reaction time (fig 2) is to be reckoned with the decrease of mechanical stress due to the chain scission.

Under oxygen atmosphere a chain oxidation of the SBR matrix takes place which is characterized by an average oxygen uptake of 2×10^{-2} mole/h and a kinetic chain length λ ranging from 3.1 to 6.1 (moles of oxygen absorbed)/(moles of mechanoradicals) (Fig 3)

Oxygen acts as inhibitor of the crosslinking reactions so that a continuous decrease of the torque and the viscosity are observed in the whole reaction range. Similar effects are obtained when the reactions are performed under nitrogen atmosphere in presence of DTPD and DPG injbitors. The HALS T 770 acts as inhibitor of both the oxidation and the crosslinking process through the formation of the intermediate nitroxyl radicals, as a consequence, despite the difference in the reaction mechanisms, the kinetics of the SBR viscosity changes under O_2 and O_2 + HALS are similar .Reaction mechanisms are proposed for the rationalization of the observed results

Fig 2 *Mechanochemical degradation of SBR under N_2 atmosphere: Kinetics of build up of the overall yield of mechanoradicals as a function of the machination time*

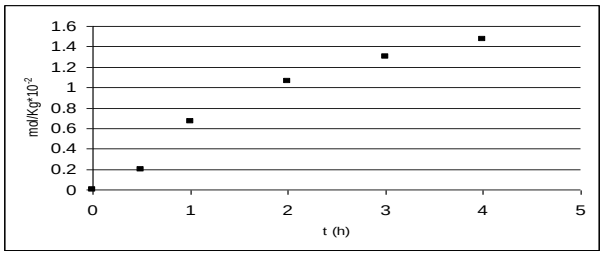

Fig 3 *Mechanochemical degradation of SBR under O_2 atmosphere: kinetics of the O_2 uptake and effect of HALS*

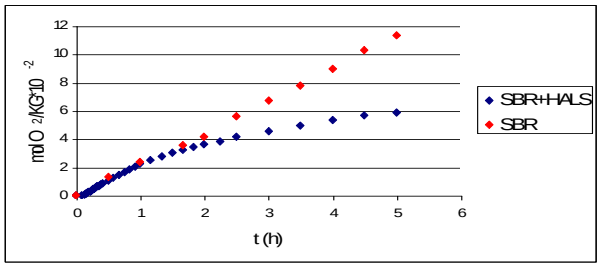

Bibliography

1) A.Buttafava, D.Dondi, M.Bianchi, F.Negroni, A.Faucitano, Abstracts European Polymer Congress Portoroz July 2007

2) D.Dondi, A.Buttafava, M. Bianchi A.Faucitano *Polymer Degrad. Stab*, to be submitted

Ion-imprinted Silsesquioxane Polymers: Synthesis and Structure

Mariusz Barczak[1)], *Katarzyna Michalak*[1)], *Yuriy L. Zub*[2)]

[1)] Faculty of Chemistry, Maria Curie-Sklodowska University, M. Curie-Sklodowska Sq. 5, Lublin 20-031, Poland
[2)] Chuiko Institute of Surface Chemistry, Ukrainian National Academy of Sciences, General Naumov Street 17, Kiev 03-164, Ukraine
e-mail: mbarczak@umcs.pl

Introduction: Typical molecular imprinting approach involves arranging monomer molecules during polymerization around a template moieties, usually accompanying by complex formation between the monomer and template [1,2]. Extraction of the template molecules leads to final material with predetermined arrangement of ligands.

Apart the adsorption sites, also pore structure can be controlled by employing surfactants with different chain lengths, e.g. quaternary ammonium compounds or block-copolymers [3-6]. If, these two template approaches are applied in one-pot synthesis the resulting materials have two different imprint arrangements on different-length scales; each with a specific function [7]. This approach is known as double impregnation method [8].

Here we describe the synthesis and characterization of copper ion-imprinted silsesquioxane polymers with fine porous structure obtained by aforementioned double impregnation method. Several different silica-monomers were used to investigate type and relative content of these monomers on final porous structure of the materials studied.

Materials and Methods: The following reagents have been purchased and used as received: tetraethoxysilane, TEOS (Aldrich), bis(triethosysilyl)ethane, BTSE (ABCR), bis(triethosysilyl)benzene, BTSB (ABCR), aminopropyltriethoxysilane, APES (ABCR), cetyltri-methylammonium bromide, CTAB (Aldrich), sodium hydroxide, NaOH (POCH), hydrochloric acid (37%, POCH), ethanol (99.8%, POCH).

The typical synthesis scheme was as follows. TEOS/BTSE/BTSB, APES, CTAB, NaOH, $CuCl_2$ and H_2O have been mixed in different molar ratios. The mixture was stirred for 24h and the solid blue product was recovered by filtration and extracted three times with acidic solution of ethanol to remove surfactant template and after was washed with HCl to strip copper ions

Obtained materials were characterized by several instrumental techniques to obtain detailed description of the structure, porosity and chemical composition. Powder X-ray diffraction (XRD) patterns were recorded using a Seifert RTG DRON-3 diffractometer (CuKα radiation) with 0.02º step size and 10s step time over a range 0.5º<2θ<5.0º at room temperature. Nitrogen adsorption isotherms were measured at -196ºC by using an ASAP 2405N adsorption analyzer (Micromeritics). Contents of the amine groups in the obtained samples were determined quantitatively by elemental analysis using Perkin-Elmer CHN 2400 analyzer. AFM images were received using MultiMode Scanning Probe Microscope "Nanoscope III" (Digital Instruments). The imaging technique was TappingMode and the scan size was 500nm×500nm. FT-IR/PAS spectra were recorded by means of a Bio-Rad Excalibur 3000MX spectrometer with photoacoustic detector MTEC300 over the 4000-400 cm^{-1} range at the resolution of 4 cm^{-1}.

Results and Discussion: The obtained materials are uniformly porous systems with specific surface areas in range of 140-750 m^2/g. The porous structure depends on the types of monomers used in synthesis and their molar ratios. XRD data testify about the good degree of ordering of the porous structure created after removal of the CTAB micelles.

FT-IR/PAS spectroscopy confirms successful co-condensation between functional groups carrier (APES) and structure forming agents (TEOS, BTSE, BTSB); thus the preferentially oriented $–NH_2$ groups are present in final materials (what is also supported by elemental analysis data).

Conclusions: Copper ion-imprinted silsesquioxane polymers have been synthesized using double impregnation method. Obtained materials have well developed specific surface areas, accessible pore sizes and can be potentially used as effective and selective sorbents or solid-phase extraction agents

Literature:

[1] K.J. Shea, *Trends. Polym. Sci.* **2** (1994) 166.
[2] H. Shi et al., *Nature* **398** (1999) 593.
[3] C.T. Kresge et al., *Nature* **359** (1992) 710.
[4] J.S. Beck et al., *J. Am. Chem. Soc.* **114** (1992) 10834.
[5] D.Y. Zhao et al., *Science* **279** (1998) 548.
[6] D.Y. Zhao et al., *J. Am. Chem. Soc.* **120** (1998) 6024.
[7] W. Genhua et al., *Anal. Chim. Acta* **582** (2007) 304.
[8] S. Dai et al., *J. Am. Chem. Soc.* **122** (2000) 992.

Acknowledgement: The research leading to these results has received funding from the European Community's 7th Framework Programme (FP7/2007-2013) under a Marie Curie International Research Staff Exchange Scheme, Grant Agreement No PIRSES-GA-2008-230790.

Free Radical Melt Grafting of Polyolefins by Using Nitroxide Radicals

D. Bélékian[1], *P. Chaumont*[1], *E. Beyou*[1], *P. Cassagnau*[1], *S. Quinebèche*[2], *J.J Flat*[2]

[1]Université de Lyon, F-69361, Lyon, France; CNRS, UMR 5223, Ingénierie des Matériaux Polymères, F-69622, Villeurbanne, France; Université Claude Bernard Lyon 1, F-69622, Villeurbanne, France
[2]ARKEMA, Centre d'Etude de Recherche et de Développement, 27470 Serquigny, France

denis.belekian@orange.fr

The more convenient route for a chemical modification of polyethylene in an internal mixer is to use free radical initiators such as peroxides [1,2]. The "grafting from" reaction starts with hydrogen abstraction on the polyethylene by alkoxyl radical generated from thermal decomposition of the peroxide. Then, the active species generated onto the hydrocarbon backbone may react with unsaturated monomers like maleic anhydride in order to form the graft copolymer (Figure 1).

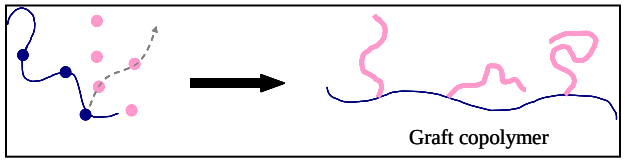

Figure 1: *Graft copolymer synthesis by using the "grafting from" process*

However, the main drawback of the free radical grafting is the low selectivity of the radical center leading to side reactions such as coupling for PE backbone, chain scission for PP backbone and homopolymer formation when using unsaturated monomers in the reaction media. This phenomenon is intensified at elevated temperature in the melt.
The main objective of our work (ANR MODEM/Arkema) is to chemically modify molten polyolefins (PH) by using nitroxide radicals ($NO^{\bullet}$) as hydrogen abstractors instead of peroxide-based radicals (Figure 2).

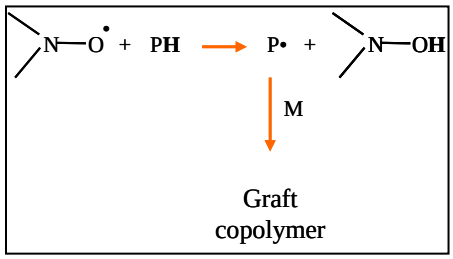

Figure 2: *Reactive pathway of free radical grafting by using nitroxyde radicals as hydrogen abstractor*

An extruder and/or a Haake rheomix can be used as internal mixer. Aspects of reactions, coupling/crosslinking and scission are determined by rheological measurements in a parallel plate geometry rheometer and discussed both in terms of the mechanism under different experimental conditions. Spectroscopy techniques (IR and UV spectroscopy) and gas chromatography-mass spectroscopy (GC-MS) allow us to highlight the grafting reaction.
However, we do not observe any polyethylene crosslinking in presence of nitroxyde radicals suggesting that these latter radicals are not efficient hydrogen abstractors. Thus, to ensure the grafting reaction, nitroxide radicals have been used in presence of peroxides (RO-OR) (Figure 3).

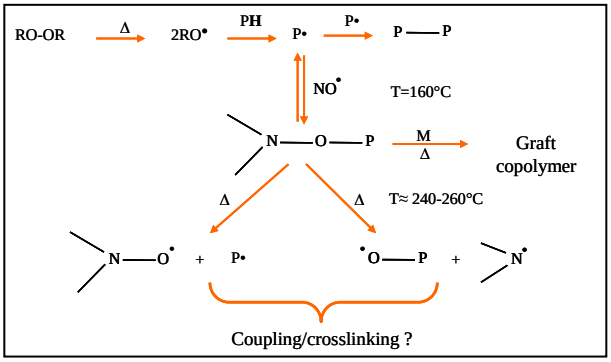

Figure 3: *Reactive pathway of free radical grafting by using a blend of the nitroxyde radical with a peroxide*

By controlling experimental conditions (peroxide/nitroxyde radical molar ratio, mixing efficiency and temperature), it allows us to prevent the polyethylene crosslinking and to form the graft copolymer.
Future work will consist in the use of a model compounds approach in order to predict the polyethylene grafting reaction. This approach will be based on a radical grafting reaction between peroxide-derived alkoxyl radicals, nitroxide radicals and a low molecular-weight alkane and/or polyethylene oligomers.

[1] M.K. Naqvi, M.S. Choudary, *J Macromol Sci Part C Rev Macromol Chem Phys*, C36, 601-629, **1996**
[2] T. Badel, E. Beyou, V. Bounor-legaré, P. Chaumont, J.J. Flat, A. Michel, *J. Polym. Sci, Part A*, 45, 5215-5226, **2007**

Polyvinylchloride: Synthesis And Modification Of Properties By Copolymerization

Elena Kotlova, Marina Pavlovskaya, Mariya Filippova, Dmitry Grishin

Research Institute of Chemistry Nizhny Novgorod State University

pavlovskaya@ichem.unn.ru

Introduction

Polyvinylchloride (PVC) is a thermoplastic synthetic material which scales of production rank second place after polyolefin's. PVC - universal polymer which depending on method of producing, compounding and technologies of processing gives the big assortment of materials with various physical and chemical properties: rigid, soft, transparent and opaque, maintained in the range of temperatures from -80 to +90÷110˚C. In consequence controlled radical polymerization of vinylchloride has not only scientific interest, but also a practical one.

Materials and Methods

All monomers - vinyl acetate (VA), acrylonitrile (AN), methylmethacrylate (MMA) and styrene (St) were dried and distilled before application. In a typical example monomer, initiator, iron complex were added to a reaction tube. Three freeze–pump–thaw cycles to remove oxygen were carrying out; the reaction tube was sealed under vacuum and then immersed in an oil bath thermostated. Polymer yields were determined by gravimetry. The number-average molecular weight (M_n) and molecular weight distribution (MWDs) of the (co)polymer were determined by gel permeation chromatography. Temperature of glass transition ($\mathbf{T_g}$) of synthesized polymers was measured by Differential Scanning Calorimetry.

Results and Discussion

As the initiating system in VC polymerization was offered iron carbonyl complex $[CpFe(CO)_2]_2$ in combination with organohalide compounds of the various nature (CCl_4, ethyl-α-bromoisobutyrate, *iso*-amyl iodide) at different temperatures (50-70˚C). It was shown that the initiating systems allow to spend polymerization VC without self-excited acceleration before high conversion (fig. 1).

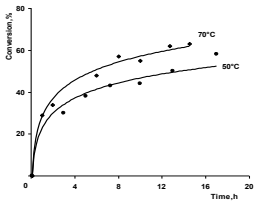

Fig. 1 Time-conversion curves for the polymerization of VC with $CCl_4/[CpFe(CO)_2]_2$ (0.25/0.125 mol.%) at various temperature

The M_n synthesized PVC increase in direct proportion to monomer conversion and also gave relatively narrow MWDs (~2.0). It was established that in the presence of the bromide initiator PVC samples are characterized by M_n=5100-6000, as well as PVC synthesized in the presence CCl_4. All polymer samples obtained have unimodal molecular weight distributions. Moreover, maximum VC conversion doesn't exceed 40% in case of injection of PPh_3 (0.125 mol. %) into initiating system and MWDs greatly increase (PDI~2.8).

The synthesized PVC used as the macroinitiator leads to formation of post-polymer and block-copolymers with monomers of various activity – MMA, St, AN, VA was investigated (fig.2). The temperatures of glass transition of the obtained block-copolymers were characterized.

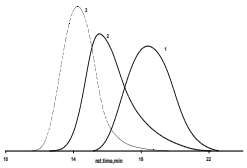

Fig. 2 Gel permeation chromatography traces of 1- initial PVC, $\mathbf{T_g}$= 78˚C , 2- PVC-b-PVA, $\mathbf{T_g}$= 43˚C, 3-PVA obtained at 70˚C, $\mathbf{T_g}$= 29˚C.

It was shown that depending on the substance content of PVC as an initiating component of system on the based iron carbonyl complexes and temperature synthesis at regulation composition and structure of obtained copolymer is possible.

By the method of the free-radical grafting in the presence of benzoyl peroxide (0.1 mol %) in butyl acetate as solvent the synthesis of the graft-copolymers on the based of obtained PVC was carrying out. The efficiency of a grafting depending on the nature of initial polymer (PVC/PVA) was estimated. Using PVC as initial polymer of it makes 36 % while for PVA - 7-10 % and not depending on temperature of synthesis. It is established that with increasing time of synthesis of copolymer PVC-PVA on the basis of PVA there is a change of structure of obtained copolymer that is reflected in change of temperature of glass transition copolymer samples (table).

Table Temperature of glass transition of synthesized copolymers

T, °C	Time, h	Tg, °C
50	10.5	40.5
	12.5	39.8; 82.5
70	12.5	50.0
	36.0	39.4; 60.9

Besides, using bromide functional polystyrene (PSt-Br) as organohalide initiator in the presence of 0.125 mol % $[CpFe(CO)_2]_2$ allows to receive copolymers with VC, AN, VA and MMA onto polystyrene.

Conclusions

Thus the system based on dicarbonylcyclopentadienyliron dimer and organohalide compounds allows to synthesize PVC in soft temperature conditions and to modify its properties. It was shown that the way of synthesis of copolymers VC influences on its physical-mechanical properties, in particular on temperature of glass transition.

Acknowledgements: This work was supported by Russian foundation for basic researches (project №11-03-00074) and Russian Ministry of Education and Science ("Federal target program of scientific and scientific-pedagogical personnel of innovation of Russia on 2009-2013").

Photodegradation and bacterial biodegradation of Polyethylene-Vinyl acetate (EVA) mulching films. Effect of calcium and iron stearates as pro-oxidant additives.

J. L. Pablos[a], *C. Abrusci*[b], *I. Marín*[b], *E. Espi*[c], *T. Corrales*[a], *F. Catalina*[a]

[a] Departamento de Fotoquímica, Instituto de Ciencia y Tecnología de Polímeros, CSIC, C/Juan de la Cierva 3, 28010-Madrid, Spain

[b] Departamento de Biología Molecular, Facultad de Ciencias, Universidad Autónoma de Madrid, Cantoblanco, 28049-Madrid, Spain

[c] Centro de Tecnología REPSOL, Autovía A-5, Km 18, 28935 Móstoles, Madrid

Jesusl@ictp.csic.es

Introduction.

Polyethylene and copolymer films are materials that persist in the environment for a long time. The problems with the disposal of agricultural plastic wastes become more and more severe. Nowadays, *plasticulture* (use of plastics in agriculture) results in increased yields: Agricultural films, mainly based on polyethylenes and copolymers of polyethylene-vinyl acetate, are used as coverings of greenhouses or tunnels over crop rows, as silage covers, as bale-wrap films, and as mulching films to cover soil. In this work we have compared the biodegradation of highly photodegraded polyethylene-vinyl acetate (EVA) copolymers and containing calcium and iron stearates as pro-oxidant additives in their formulations.

Materials and Methods.

In this work EVA films of 25 microns of thickness were prepared by Repsol containing iron and calcium stearates as pro-oxidant additives (at 0.2 % w/w).

The artificially simulated weathering (432 hours) was carried out in an ATLAS/ SUNTEST XLS-2500W Xenon lamp using a solar filter of borosilicate and fixing the incident energy at 550 W/m^2 in the interval 300-800 nm. EVA films degradation [1,2,3] was studied by FTIR to analyze structural changes in carbonyl region[4] (peak at 1738cm^{-1}/1715cm^{1}), and Chemiluminescence to follow the formation of hydroperoxides as oxidative species. Also, biodegradation was evaluated by measurement of the carbon dioxide produced in the bacterial metabolism using a Bac-Trac 4300 (SY-LAB Geräte GmbH, Neupurkerdorf, Austria). Biodegrading bacteria were a mixture *Bacillus* strains (MIX) isolated and identified[3] from samples exposed to agricultural soils in Murcia, Spain and a strain of *Brevibacillus borstelensis* as reference[5]. Biodegradation tests were carried out with controlled inoculums of the bacteria at 45ºC during 90 days. This temperature was selected since previous results[3] confirmed a more efficient biodegradation on the bioassays carried out at higher temperature.

Results and Discussion.

- *Photodegradation*

The analysis of non-isothermal chemiluminescence under nitrogen atmosphere provides a useful tool to evaluate the activity of stearates as pro-oxidants. The CL-temperature curves for EVA films showed the increase of intensity above ~100ºC with the degradation time and peaks at 110ºC in materials with pro-oxidant additives were observed. The activity of pro-oxidants on thermal oxidation of EVA films was also observed on CL intensity-time runs under oxygen.

Several changes in infrared absorption peaks can be seen in EVA films with irradiation time, decrease of the band at 1735 cm^{-1} (C=O of ester) and the growth at the absorption shoulder at 1715 cm^{-1} (Ketone carbonyl). After accelerated photodegradation of EVA films the effect of pro-oxidant additives was studied by different carbonyl index determinations.

- *Biodegradation.*

After biodegradation, the onset of the CL emission shifted towards lower temperature on the biodegraded samples and in general the intensity of the low temperature peaks increase. CL emission allows the evaluation of the metabolic activity of microorganisms on the polymer surface though the oxidation induced by reactive oxygen species (ROS) generated, such us peroxide radical, hydroperoxides, hydrogen superoxide and radical anion.

Incubation of the photo-oxidized polyethylene with *B. borstelensis* and *MIX* for 90 days showed a marked reduction in the amount of carbonyl peaks and estimated in terms of carbonyl index. Mineralization of the photodegraded EVA films was study by determination of the carbon dioxide produced in the metabolic action of the bacteria, using indirect impedance technique. The percentage of biodegradation reached was higher in the photodegraded materials containing Ca and Fe stearates (25-30%) that in the pure EVA films (15%)

Conclusions.

Biodegradation at 45ºC of photodegraded EVA films by bacteria: *Brevibacillus borstelensis* and the mixture of *Bacillus MIX (B.cereus, B.megaterium* and *B.subtilis*.) was efficient after 90 days of incubation and in particular when Ca and Fe stearates are present in the formulation. Photodegradation increases the rate of biodegradation of the EVA films by the bacteria studied in this work and the use of pro-oxidant in the formulations could be an interesting way to prepare more efficient biodegradable materials.

References.

1. J.L.Pablos, C.Abrusci, I.Marin, J.López-Marín, F.Catalina, E.Espí, T.Corrales. Polym Degrad Stabil 95 (2010) 2057-2064.

2. C.Abrusci, D.Marquina, A.Santos, A.Del Amo, T.Corrales, F.Catalina, Int Biodeter Biodegr (2009) 63, 759-764.

3. C.Abrusci, J.L.Pablos, T.Corrales, J.López-Marín, I. Marín, F.Catalina. Int. Biodeter Biodegr. In press.

4. J.Jin, S.Chen, J.Zhang. Polym Degrad Stabil 95 (2010) 725-732

5. D.Hadad, S.Geresh, A.Sivan, 2005. J.Appl Microbiol 98, 1093-1100.

Evaluation of photodegradation of polyethylene films with pro-degradant agents II.Morphological analysis

Jalma M. Klein[1], Ana M. C. Grisa[1], Rosmary N. Brandalise[1], Mara Zeni[1]*

[1] Centro de Ciências Exatas e Tecnologia – Caxias do Sul University, 95070-560, Caxias do Sul/RS – Brazil
(mzandrad@ucs.br)

Abstract

Polyethylene films, in general, are used by a short time and often only once, with further discard [1,2]. Its saturated chain without functional groups make it resistant to oxidation processes by light and heat action and, consequently, to biodegradation processes. Polymer oxidation processes can be accelerated by the use of pro-degradant agents, whose function is to promote the fragmentation. In this work we analyzed polyethylene films with different pro- degradant agent concentrations, after exposure to UVB radiation chamber (λ_{max} =313nm) for a period of up to 480 h. Polyethylene films extruded from the mixture of high density polyethylene (HDPE) and linear low density polyethylene (LLDPE) (60/40), were supplied by METALLYN Co., Brazil, ($PEOX_1$ e $PEOX_2$) and without pro-degradant agent (PE), both with 5 µm of thickness. Carbonyl and vinyl index were evaluated by FTIR Spectroscopy; crystallinity degree, by DSC. The evidence of photodegradation of the polyethylene film was evaluated by the increase in the CI (85 – 100%), in the VI (4 – 5%) and in the crystallinity degree (60 – 68%). From PE, $PEOX_1$ and $PEOX_2$ spectrum, performed before and after the UV irradiation exposure process (Fig. 1).

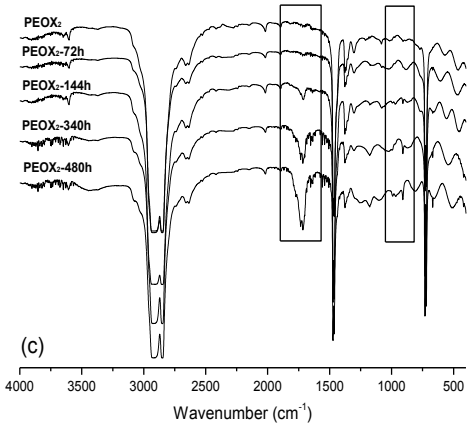

Figure 1 – FTIR spectrum showing the differences in the carbonyl and vinyl absorption peaks from samples before and after exposure to irradiation for a period of 480h.

The Figure 2 presents the vinyl index (VI) based on the absorption band at 908 cm^{-1}, measured during different exposure times[3].

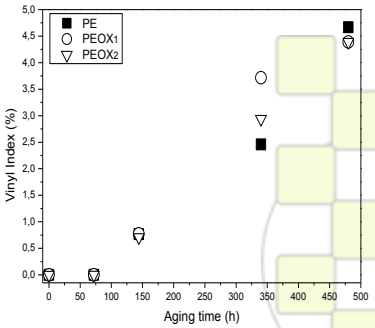

Figure 2 – Vinyl index of the samples PE, $PEOX_1$ and $PEOX_2$ as a function of UV irradiation exposure time.

The crystallization time as a function of the UV irradiation exposure time can be seen in Fig. 3.

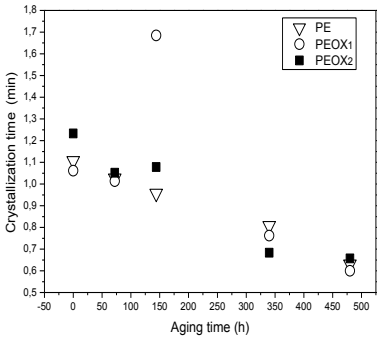

Figure 3 – Crystallization time for the samples PE, $PEOX_1$ and $PEOX_2$, before and after exposure to UV irradiation, for a period of 480h.

The photodegradation by UV irradiation of polyethylene films, with and without pro-degradant agent, was evidenced: by the increase in carbonyl index resulted from *Norrish* I reaction mechanism; and by the increase in vinyl index , resulted from *Norrish* II reaction mechanism. The chain scission reaction due to polyethylene irradiation promoted an increase in the crystallinity degree of the samples. The structure stabilization is evidenced by the crystallinity degree of samples with agent, after 480 h of exposure, and it is possible to states that the chain scission was the predominant mechanism. May be during the process of photodegradation occurred crosslinking reactions, according to *Norrish* III mechanism[4,5].

References

1. D.S. ROSA, R. PANTANO FILHO, *Biodegradação: um ensaio com polímeros*. Moara, Doctoral Tesis, São Paulo, 2003
2. I. Jakubowicz. *Polym. Degrad. Stab.* 2003, 80, 99.
3. M. Weiland, A. Daro, C. David *Polym. Degrad. Stab.* 1995, 48, 275.
4. A. Corti, S. Muniyasamy, M. Vitali, S.H. Imam, E. Chiellini *Polym. Degrad. Stab,2010, 93-110*.
5. A.C. Albertsson, C. Barenstedt, S. Karlsson *Acta. Polym.* 1994, 45, 97.

Chemical modification of Ethylene Butyl Acrylate copolymer with Hindered Amine Light Stabilizer HALS. Photostabilization study.

L. López-Vilanova[1], *E. Espí*[2], *A. I. Real*[2], *M. Calvo*[2], *A. Fontecha*[2] *J. L. G. Fierro*[3] *C. Peinado*[1] *F. Catalina*[1]

[1] Instituto de Ciencia y Tecnología de Polímeros – CSIC, Juan de la Cierva 3, Madrid, Spain
Centro de Tecnología Repsol, Autovía A-5, km. 18, 28935 Móstoles, Spain
[3]Instituto de Catálisis y Petroleoquímica-CSIC, M-607, km .15, Campus Cantoblanco, UAM, Spain

levil@ictp.csic.es; fcatalina@ictp.csic.es

Introduction

Low-density polyethylene (LDPE), ethylene-vinyl acetate copolymers (EVA) and ethylene-butyl acrylate copolymers (EBA) are the most common plastic materials used for greenhouse cover films. The lifetimes required for these films vary from one agricultural season to several years, depending on the geographical area where they will be used, the type of greenhouse, the crop, the use of pesticides, etc. To increase efficiency in long-term applications the polymeric HALS are the most efficient structures reaching a high price. The term `reactive processing of polymers´ has emerged in the polymer science and engineering community, and intense activity both in academia and in industry largely testifies to its ever-increasing importance. This work investigates the transesterification reaction of molten EBA copolymer in presence of low molecular weight HALS and organometallic catalyst.

Materials and Methods

A poly(ethylene-co-butyl acrylate) (EBA) containing 8% w/w of butyl acrylate (PA-805) from Repsol was used in this work. Two HALS with hydroxyl groups, 1,2,2,6,6-pentamethylpiperidin-4-ol, (HALS-NMe) and 1-methoxy-2,2,6,6-tetramethylpiperidin-4-ol (HALS-NOMe) were used as reactive structures. Also, HALS-NOR-371 from BASF was used as reference. Dimethyl tin oxide (DBTO) was used as catalyst in the reactions of EBA in the molten state[1]. Reactions were carried out in an internal mixer Haake Rheocord 9000 at 190 °C and the mixing speed of 64 rpm. In all cases, concentrations were fixed at 1% w/w of HALS, and 0.05 % w/w of catalyst (DBTO). The time for the reactions was 5,10,15,30 min and as reference, the reactions were also made in the absence of catalyst. All reaction products were cooled at room temperature and then carefully treated to eliminate unreacted HALS. Films of 100µm were prepared by compression molding using a Collin P-200-P press. In the present work, X-ray photoelectron spectroscopy (XPS) has been used to study the degree of modification for the transesterification reaction. The XPS was VG Escalab 200R spectrometer. Photostability was studied by FTIR from the formation of oxidized species formed during the accelerated aging in a climate chamber (Atlas Weather-OMeter Ci4000 (WOM)) under standard ISO 4892-2:1994 cycle at 0.47 W/m2 (340nm) and applying pesticides (*metam-sodium and cypermethrin*, 1:3) each 525h.

Results and Discussion

The N1s core-level spectra for films prepared at different reaction times showed a peak at ca. 400eV associated with the HALS incorporated in the material. The modification reached in the reaction was monitored by calculating the N/C atomic ratio. There is no clear correlation between reaction time and degrees of modification obtained (0.17-0.63%). For the reaction performed in absence catalyst, no nitrogen peak was detected. This indicates that unreacted low molecular weight HALS was removed in the extraction step. To assess the photostabilization efficiency of the samples the study was focused on the infrared band at 908 cm^{-1} due to acid groups formed during the accelerated aging. Modified EBA with HALS-NMe was better photostabilized with increasing reaction time. Also, the photostabilization behavior was excellent for EBA modified with HALS-NOMe remaining carbonyl formation in stationary phase until 3200 h (see Fig 1), this may be due to increased pesticide resistance of the HALS-NOMe.

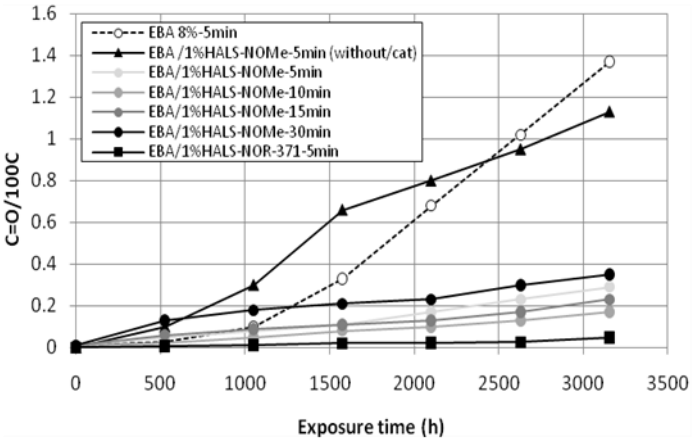

Figure 1 C=O/100C versus exposure time for the EBA, EBA/HALS-NOR-371, EBA/HALS-NMe, EBA/HALS-NMe/DBTO, EBA/HALS-NOMe, EBA/HALS-NOMe/DBTO.

Conclusions

EBA copolymer contained 8% w/w of butyl acrylate, has been modified in the molten state with HALS-NOR functionalities resulting in a very efficient polymeric light stabilizers with a large industrial interest.[2]

References

1. Hu, G. H.; Lambla, M. *Polymer 35*, 3082, 1994.
2. Moad, G., *Progress in Polymer Sci.* 24, 81, 1999.

Synthesis of Low Formaldehyde Emission Urea-Formaldehyde Resins and Their Application to the Manufacturing of Particleboards

P. Estévez, S. Vallejos, H. El Kaoutit, M. Trigo-López, F. Serna, F. García, J.L. de la peña, J.M. Pérez.

Departamento de Química, Grupo de Polímeros, Facultad de Ciencias, Universidad de Burgos, 09001 Burgos

e-mail: peb0002@alu.ubu.es

1.-Introduction

Urea-formaldehyde (UF) resins are the most used polycondensation resins for the manufacturing of particleboard panels due to their high reactivity, good performance and water solubility.[1] In spite of these advantages, they have two main disadvantages that are the formaldehyde emission from the panels and the poor resistance to water.

Response surface methodology (RSM) has being used as optimization procedure for low formaldehyde emission UF resins synthesis.[2] This work describes a central composite design methodology to optimize 3 selected variables (number of urea additions, pH and temperature) in the second urea addition, following three-stage process.

2.-Materials and Methods

Resins were synthesized from a precondensed formalin-urea solution and urea, following the traditional three stage process. Synthesis conditions of alkaline-acid step reactions were optimized in previous researches.[3] Central composite rotatable design was adopted for the experimental runs for response surface methodology, in the preparation of low formaldehyde emission UF resins.

Laboratory particleboards were prepared by using a standard mix of wood particles for the core and face layers. UF resins with additives and catalyst were sprayed on the wood particles and then were formed into a mat of dimensions 400 mm x 400 mm. The mat was prepressed at room temperature and further hot-pressed at 195 ºC for 2-3 minutes.

Perforator Method (European Standard EN 120) was used for measuring the formaldehyde content of wood-based panels.

3.-Results and Discussion

All resins were analyzed by standard methods. Differences in viscosity, gel time and free formaldehyde content were found depending on the synthesis conditions, but all of them were able to be used in the particleboard manufacturing process.

All particleboards were characterized according to European standard methods. Table 1 reports the main properties shown by the particleboards manufactured using the different UF resins synthesized. The formaldehyde content of the particleboards bonded with the modified process UF resins is well below the specified level of class E1 products (≤ 8 mg/ 100 g dry board) according to EN 13986, while maintaining good levels of internal bond strength, established in 0.35 Mpa (Particleboards Type P2, EN 312).

Table 1. Particleboards Characterization

Resin	Formaldehyde content (mg / 100 g dry board)	Internal Bond Strength (MPa)
1	2.6	0.46
2	2.8	0.46
3	3.2	0.62
4	2.3	0.52
5	2.6	0.66
6	3.9	0.67
7	3.2	0.50
8	3.1	0.57
9	2.5	0.66
10	2.2	0.56
11	2.1	0.53
12	4.0	0.50
13	4.3	0.47
14	3.3	0.56
15	3.6	0.58
16	3.6	0.55
17	3.0	0.69

Figure 1 shows: (a) Optimal response plot, with a minimum level of formaldehyde at a distance of 1,5; and (b) Optimal coordinate plot for the response in codified variables. These data transformed into natural variables are: pH: 7.4; Urea additions: 2 and Temperature: 50 ºC.

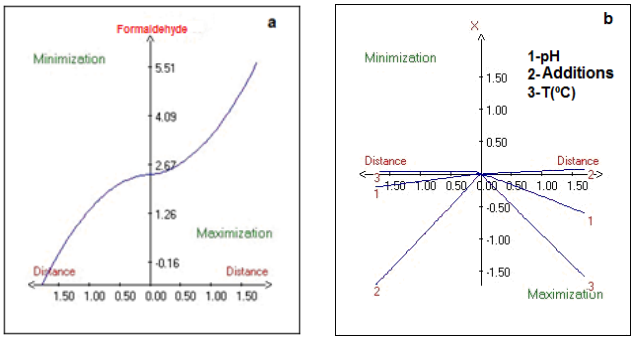

Figure 1. Ridge analysis (RSM).

4.-Conclusions

The effect of the number of second urea additions, pH and temperature was studied for the preparation of UF resins. The process was optimized on the basis of these studies. The results showed that the studied variables played a significant role in reducing the formaldehyde emission with a minor withdrawal of internal bond strength.

5.-References

1. A. Pizzi. Handbook of Adhesives technology, ed. Marcel Dekker, New York, 1994, 381-392.

2. J. M. Ferra et al. J. of Ad. Sci. and Tech., 2010, 24, 1455-1472.

3. P. Estévez, et al. XI Reunión del GEP. Libro de resúmenes. Ciencia de Polímeros: retos globales-nuevas estrategias, pp 236. Valladolid. 2009.

Modeling of butadiene polymerization using neodymium catalyst complex

Gumerov A.M., Davletbaeva I.M.

Kazan State Technological University, Kazan, Russia

gumerov_a@mail.ru

The problems of obtaining and using neodymium polybutadiene are connected with structural features of the neodymium catalyst system. First of all, it is polycentricity of a catalyst, which contains several points of anionic coordination polymerization differing by their activity. Therefore, to investigate the possibility of rubber properties regulation by controlling the molecular structure is an important scientific and practical issue.

In recent years, many researchers believe that most of the Ziegler-Natta catalysts have active centers of polymerization differing from one another by their kinetic parameters. In this study the mechanism of polymerization kinetics of 1,4-butadiene initiated by neodymium metal-complex system was identified.

The paper presents the kinetic scheme of the polymerization process. When developing the mathematical model the following assumptions were adopted. The rate constants of elementary stages do not change their values during the process and the active centers are formed simultaneously and instantaneously at the beginning of polymerization.

The consumption of monomer in chain transfer reactions is negligible compared with the monomer consumption in the reactions of chain growth.

The model polymerization kinetics is represented by differential equations of material balance of reagents involved in the process and shows the changes in their concentrations over time. The system of equations of the model can essentially be solved for known kinetic constants for polymers of length r = 1, 2, 3. . . n. It is obvious that for the considered set of polymers the investigated system has large dimensionality.

At the same time, there are efficient algorithms for solving systems of differential equations, which can reduce the order of the system. For the compact representation of the system of equations of polymerization kinetics, the method of moments is used. When the method of moments is used the system of differential equations is transformed into a closed form.

As a results of modeling the kinetic constants were found and the distribution curves of mean and average molecular weight were obtained. The solving of the direct problem describes satisfactorily the values of monomer conversion (Fig. 1), but there is a considerable discrepancy between the values of mean and average MW.

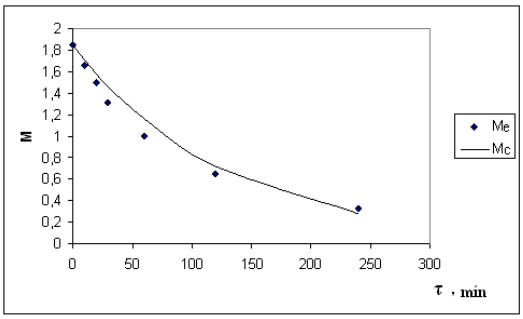

Fig. 1. The temperature dependence of monomer consumption; points - experimental data, solid line - calculation results

It was found that under the selected conditions the existence of three different activity centers for polymerization in the catalytic system is most likely.

Table 1. Kinetic parameters of polymerization of butadiene (l·min/mol) for the catalyst system, calculated with a three-center model of the active center. T_p=25 ° C; C_{but}=1,85 mol/l; $C_{Nd}=0{,}6\cdot10^{-4}$ mol/l; [Cl/Nd]=2,5

Constants	Value	Constants	Value	Constants	Value
k_{i1}	9.9132	k_{i2}	10.1016	k_{i3}	10.0116
k_{p1}	196.725	k_{p2}	21.1617	k_{p3}	98.1054
k_{m1}	0.0606	k_{m2}	0.1238	k_{m3}	0.0578
k_{Al1}	12.9915	k_{Al2}	13.1491	k_{Al3}	12.9854
k_{d1}	0.00040	k_{d2}	0.00040	k_{d3}	0.00039

where C_d is an deactivated center, k_i, k_m, k_{Al} and k_d are the rate constants of reactions of initiation, chain growth, transfer of kinetic chain onto hydrogen, the monomer, the organoaluminum compound and deactivation of the active center.

The presence of different types of active centers in the considered system, established by mathematical modeling, is confirmed by the presence of three unshared peaks at the curve of molecular weight distribution (MWD) of polybutadiene obtained at the initial stage of polymerization.

With increasing degree of monomer conversion the proportion of low molecular weight fractions decreases, while an increase of the undivided peak at the MWD curve in the region of high molecular masses is observed. Apparently, this is associated with the lower kinetic activity of the polymerization center, responsible for the formation of low molecular weight polymer.

Effects of incorporating waste rigid polyurethane foam in polymer compounds based on Polypropylene

Federal University of São Carlos

Simone Fontana Pereira; Elias Hage Junior

Introduction: The refrigeration industry widely uses the rigid polyurethane foam (PUR) as insulation in the cabinets and refrigerator's doors. Due to the large volume of industrial waste generated by this material (process, quality control and waste from end-users), it's needed to take environmental measures to avoid improper disposal of this material, what represents an environmental problem. Some alternatives to re-use this material has been studied over the past few years aimed to find an alternative for recycling rigid polyurethane foam and, if possible, with economic advantage. Materials and Methods: rigid polyurethane foam, polypropylene,PP-*g*-MA. The objective of this project is present a composite based on mixture of PP/PUR residues that can be used in a technical application showing not only a recycling alternative for the solid waste as well as improvements in mechanical properties. The method consists in incorporating residues of PUR in a matrix of PP by using PP-g-MA as a coupling agent and extrude the material. The pallets are then fed into an injection molding machine and the specimens are obtained.

Results and Discussions: Preliminary analysis shows that the incorporation of PUR residues in a thermoplastic material (PP) is feasible and the formed composite material shows good mechanical properties.

Conclusion: Automotive market is a potential end-user of this material once this industry has been gradually replacing traditional materials by plastics and composite materials over the years and mainly because both materials (PUR and PP) have a very low density what refers economy to the automotive market because a lighter car leads to lower fuel consumption.

Parallel versus perpendicular lamellar-within-lamellar self-assembly of A-b-(B-b-A)$_n$-b-C and (B-b-A)$_n$-b-C ternary multiblock copolymer melts: SSL theory, DPD, SCFT investigation.

V.A. Markov[1], Y.A. Kriksin[3], A.V. Subbotin[1,2] and G. ten Brinke[1]

[1]Department of Polymer Chemistry and Zernike Institute for Advanced Materials, University of Groningen, Nijenborgh 4, 9747 AG Groningen, The Netherlands
[2]Institute of Petrochemical Synthesis, Russian Academy of Sciences, Moscow, 119991,
[3]Institute for Mathematical Modeling, RAS, Moscow 125047, Russia
v.a.markov@rug.nl

One of the specific features of multiblock copolymers is the possibility of self-assembling in the form of periodical hierarchical structures involving different length scales. Such structures were first observed for comb-shaped supramolecules consisting of polystyrene-block-poly(4-vinylpyridine) (PS-*b*-P4VP) diblock copolymers and hydrogen-bonded pentadecylphenol (PDP) side chains attached to the P4VP blocks.[1] Subsequently it was found that undecablock copolymers PS-*b*-(PI-*b*-PS)$_4$-*b*-PI-*b*-PS and P2VP-*b*-(PI-*b*-PS)$_4$-*b*-PI-*b*-P2VP also formed double periodic lamellar-*within*-lamellar structures.[2] Here P2VP, PI and PS denote poly(2-vinylpyridine), polyisoprene and polystyrene, respectively. In contrast to the supramolecules systems, here the different lamellae are parallel In both cases the hierarchical structure formation results from the molecular architecture involving two different intrinsic length scales. Recently Fleury and Bates demonstrated[3] that a terpolymer C-E-C-E-C-P, consisting of cyclohexylethylene (C), ethylene (E) and propylene (P) blocks, self-assembled in the form of a perpendicular lamellar-*within*-lamellar structure when the copolymer chain length exceeded some critical value. Self consistent field theory investigations [?] showed that a transition from parallel lamellar-*within*-lamellar to perpendicular lamellar-*within*-lamellar structure will occur when the Flory-Huggins interaction parameter χ_{AB} is sufficiently large. A theoretical approach in the strong segregation limit further showed that the perpendicular lamellar-within-lamellar state becomes stable when the interaction parameters satisfy the relation

$0 < \chi_{EP} < 0.22\chi_{CP}$.[5]

For a next step the self consistent field theory approach was implemented and it was shown that the stable perpendicular lamellar-*within*-lamellar structure involved secondary structure layers that are shifted with respect to each other over half a period (see Figure 1). It can be easily understood by considering the C tail contributions. It was also found that the known methods to solve the SCFT equations suffer from unnecessary restrictions in case of ternary systems. For the existing methodology the system of equations can be only solved when the χ parameter values are beyond the Hildebrandt approximation surface. A new method was developed to solve the SCFT equations near and on the Hildebrandt approximation surface.

In order to cover all phase space dissipative particle dynamics was used. Transition from ternary to binary systemwas investigated by changing $N\chi_{BC}$ from 0 to 100.

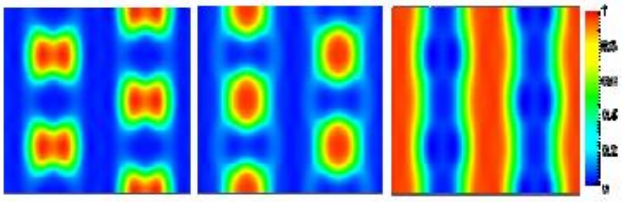

a) b) c)

Fig. 1. Volume densities profiles for perpendicular lamellar-*within*-lamellar structure a) A blocks; b) B blocks; c) C blocks. Red indicates largest concentration.

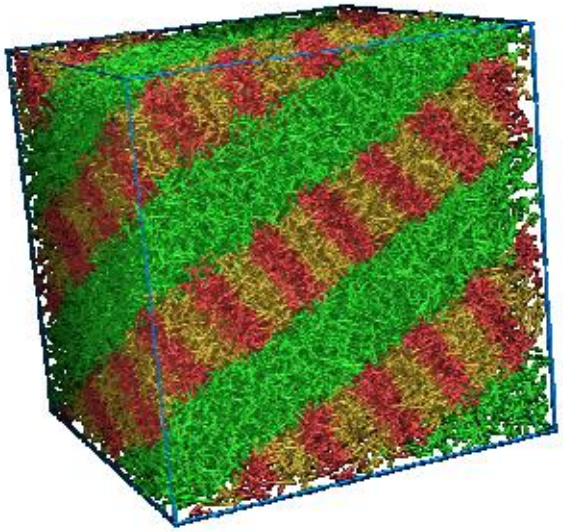

Fig. 2. Perpendicular lamellar-*within*-lamellar structure presented by a snapshot from DPD simulations.

1. Ruokolainen, J.; Mäkinen, R.; Torkkeli, M.; Mäkelä,T.; Serimaa, R.; ten Brinke, G.; Ikkala, O. Science 1998, 280, 557.
2. Masuda, J.; Takano, A.; Nagata, Y.; Noro, A.;Matsushita, Y. Phys. Rev. Lett. 2006, 97, 098301.
3. Fleury, G.; Bates, F.S. Macromolecules, 2009, 42, 1691
4. Wang L., Lin J. and Zhang L., Macromolecules, 2010, 43 (3), 1602.
5. Subbotin A, Markov V, and ten Brinke G. The journal of physical chemistry. B, 2010, 114(16):5250.

Aminoiminophosphoranate Complexes of Platinum and Palladium in Radical Polymerization of Vinyl Monomers

Elena V. Kolyakina,[*] *Marina V. Pavlovskaya*,[*] *Nikolay A. Ustynyuk*,[**] *Dmitry F. Grishin*[*]

[*]Research Institute of Chemistry of Nizhny Novgorod State University,
Gagarin Ave. 23/5, 603950, Nizhny Novgorod, Russia
[**]A.N.Nesmeyanov Institute of Organoelement Compounds Russian Academy of Sciences,
Vavilova str. 28, 119991, Moscow, Russia

E-mail: kelena@ichem.unn.ru

Introduction. Metal-catalyzed polymerization is one of the most rapidly developing areas of organometallic chemistry and polymer science. This technique allows the synthesis of polymers with well-defined compositions, architectures, functionalities and nanomaterials. In these few decades, new classes of molecular catalysts were found for the olefin and vinyl polymerization. Especially, half-metallocenes and non-metallocenes, complexes of transition metals promote formation of polymers in high efficiency and unique selectivity.

Materials and Methods. Vinyl monomers were washed with aqueous alkaline solution and water, dried over calcium chloride and then distilled. Initiators and solvents were purified by recrystallization and distillation. Reagents were placed in an ampoule. After degassing the content, the ampoule was sealed in vacuum. The polymerization was carried out at 50-70°C. Molecular weights were determined by SEC calibrated with polystyrene and polymethyl methacrylate standards. Topography of a polymer film was studied by AFM.

Results and Discussion. The influence of platinum and palladium complexes of various structures (see scheme) on the polymerization of a wide range of monomers (methyl methacrylate - MMA, butyl methacrylate - BMA, methyl acrylate – MA, butyl acrylate – BA, styrene – St) at temperatures 25-90°C was investigated.

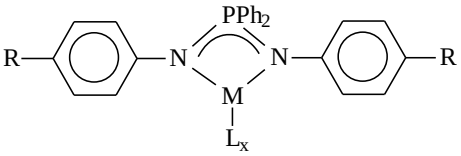

(M – Pd or Pt; x=1: L - allyl or aminoiminophosphoranate, x = 2: L_1 – Cl and L_2 - ethylene or PPh_3; R – ^{i}Pr, MeO, EtO_2C).

Scheme

It was shown, that these metal complexes are capable of initiating the vinyl polymerization in the presence of CCl_4. The influence of the central atom of a metal and ligands on the rate of polymerization and molecular-weight characteristics of polymers was established. For instance, the addition of the palladium complexes causes polymerization of vinyl monomers that proceeds to high conversions for 20-30 hours. The rate of polymerization in the presence of platinum complexes was essentially less than that of palladium complexes, and in some cases only small quantities of polymers were isolated. The obtained polymers with participation of the catalytic systems on the basis of the given complexes and CCl_4 are characterized by high molecular weights (MW) and index of polydispersity (2.0 - 2.5). It is necessary to note, that these metal complexes practically do not influence the process of the polymerization of MMA and St in the absence of CCl_4. In the most cases the rate of polymerization was comparable with the rate of autopolymerization.

The influence of ligand environment on the vinyl monomer polymerizations was revealed on the example of the palladium complexes. It was established, that the most effective catalysts are the complexes containing chlorine atom in the structure. The rate of polymerization of some studied monomers considerably rises when the electron donated groups (^{i}Pr, MeO) in the structure of the aminoiminophosphoranate ligand are presented in comparison with the complexes containing the electron accepting group EtO_2C. The MW of the samples synthesized in the presence of the studied catalytic systems depends on the rate of polymerization, similarly to that in the presence of traditional initiators.

The offered catalytic systems for polymerization can be used as an elegant way to incorporate nanodimensional particles of Pd to the polymeric matrix. The given complexes are thermally unstable at high temperatures and decay with formation of Pd particles *in situ*. In this case the macromolecules formed in the presence of the given systems play a role of the stabilizing ligand. Particles having size of 65 nanometers and less in the synthesized polymers are found out by atomic-force microscopy. These particles are fixed both on surface and in volume of the polymer film (figure).

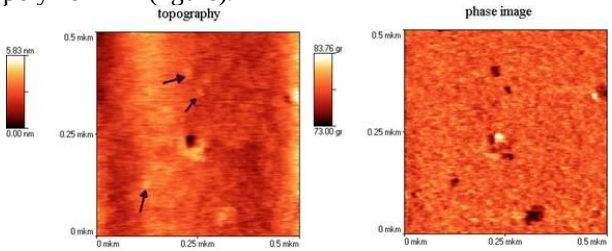

Figure. AFM images of film of polySt prepared in the presence of CCl_4 and Pd complexes.

Conclusions. It was established, that aminoiminophosphoranate platinum and palladium complexes show different properties. These complexes can simultaneously act as catalysts for polymerization of wide range of monomers and also serve as sources of nanoparticles.

Acknowledgements. This work was supported by the Russian Ministry of Education and Science (project of "Analytical program of development of higher school").

Atom Transfer Radical Polymerization of Methyl Methacrylate in the Presence of Four-Coordinated Cobalt Complex with Sterically Hindered o-Iminobenzoquinone Ligand

Elena V. Kolyakina,[*] *Andrey A. Poddel'sky*,[**] *and Dmitry F. Grishin*[*]

[*]Research Institute of Chemistry of Nizhny Novgorod State University,
603950, Gagarin Ave. 23/5, Nizhny Novgorod, Russia
[**]G. A. Razuvaev Institute of Organometallic Chemistry of Russian Academy of Sciences,
603950, Tropinina str, 49, Nizhny Novgorod, RUSSIA

E-mail: kelena@ichem.unn.ru

Introduction. The controlled/living radical polymerization technique has become a very powerful tool in the field of modern polymer science and engineering. Atom transfer radical polymerization (**ATRP**) is now one of the most rapidly developing areas in the past several years. Many novel polymers have been synthesized by the ATRP method. Through ATRP, it became possible to control over the molecular weight (**MW**), and to prepare polymers with the chain end reactivity. Traditionally ATRP is based on the catalysis of transition-metal halide/ligand complexes, which is the key point in ATRP. Up to now, various catalytic systems based on Cu, Fe, Ni, Ru, Mo and so forth, have been employed in ATRP. However, it is still challenge to develop new ATRP catalytic systems, especially cheap ones. Only few examples were reported using cobalt complexes as catalysts, which reduced initiator and were oxidized from Co(II) to Co(III) to initiate the controlled radical polymerization [1-4].

Materials and Methods. Methyl methacrylate (**MMA**) was extracted with 5% sodium hydroxide to remove the stabilizing agents, washed with water, dried over calcium hydride and distilled under reduced pressure before use. Initiators and solvents were purified by distillation. Reagents were placed in an ampoule. Oxygen was removed using three freeze-pump-thaw cycles. After degassing the content, the ampoule was sealed in vacuum. The polymerization was carried out at 50-90°C. MW were determined by SEC calibrated with polystyrene and polymethyl methacrylate standards.

Results and Discussion. The polymerization of MMA was conducted with bis-[4,6-di-*tert*-butyl-*N*-(2,6-dimethylphenyl)-*o*-iminobenzosemiquinonato]cobalt(II) (**Co(ISQ-Me)$_2$**)/amines (t-BuNH$_2$ or pyridine) as catalyst and with ethyl-2-bromoisobutyrate - **(EiB)Br** and CCl_4 as the initiators in bulk at 50-90°C. The results of experiments in **Table** show that the cobalt–mediated polymerization proceeds rapidly.

Table. The results of the polymerization catalyzed by Co(ISQ-Me)$_2$- 0.025 mol.%/t-BuNH$_2$ – 0.05 mol.%

Initiator	T,°C	*t*, (h)	Conv., %	$M_n \times 10^{-3}$	M_w/M_n
CCl_4	50	80	73	40	1.76
	70	30	94	46	1.50
	90	20	97	47	1.55
(EiB)Br	50	36	91	62	1.56
	70	24	95	51	1.48
	90	12	98	47	1.57

When the cobalt complex did not coordinate by amines no high conversion was observed, which indicate that the complex was an effective catalyst for ATRP and amines have a strong affinity to Co(ISQ-Me)$_2$. Dependence of MW of polyMMA on conversion is linear at 70°C (**Figure**).

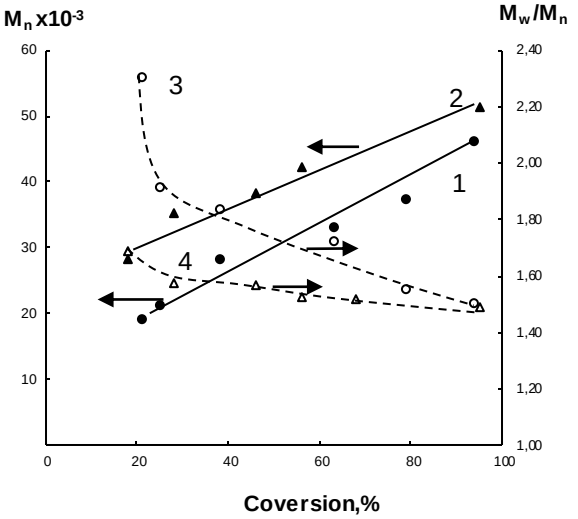

Figure. Evolution of M_n and M_w/M_n with conversion of poly MMA. *1*, *3*- CCl_4; *2*, *4* - (EiB)Br

However, the control over the polymerization was not ideal, the molecular weight distribution of the resulting polymer was relatively broad (M_w/M_n= 1.48-1.76).

In order to confirm the realization of ATRP mechanism of MMA polymerization in the presence of the cobalt catalyst system, the synthesis of block copolymers of MMA with St was performed on the basis of the macroinitiators obtained with participation of the studied complex. These results indicate the possibility of re-initiation of polymerization and the direct functionalization of polymers.

Conclusions. A new ATRP catalyst system, Co(ISQ-Me)$_2$/amines, was successfully used to catalyze the polymerization of MMA through ATRP mechanism.

Acknowledgements. This work was supported by the Russian Ministry of Education and Science (project of "Analytical program of development of higher school").

References.

1. B. Wang, Y. Zhuang, X. Luo, S. Xu, X. Zhou, *Macromolecules*, **2003**, *36*, 9684-9686.
2. Z. Li, Y. Zhang, M. Xue, L. Zhou, Y. Liu, *J. Polym. Sci., Part A: Polym. Chem.* **2005**, *43*, 5207-5216.
3. K. Matsubara, M. Matsumoto, *J. Polym. Sci., Part A: Polym. Chem.* **2006**, *44*, 4222-4228.
4. Z-X. Huang, Y-M. Zhang, H. Li, Y-G. Liu, *Macromol. Chem. Phys.* **2008**, *209*, 825-831.

Nitroxide-Mediated (Co)Polymerization of Vinyl Monomers with High-Molecular-Weight Alkoxyamines, Derived from C-Phenyl-N-tert-butylnitrone

Alexander Shchepalov, *Dmitry Grishin*

Scientific Research Institute of Chemistry, Lobachevsky State University of Nizhniy Novgorod
Gagarin Ave. 23/5, Nizhniy Novgorod, 603950, Russia

E-mail: sasha@ichem.unn.ru

Introduction. Development of novel methods for syntheses of nanomaterials and nanostructures possessing unique properties is one of the most promising and rapidly growing areas of modern chemistry. Block-copolymers, involving monomers of different nature, represent a basis for such highly-organized structures. Because of specific chemical nature, these molecules can self-assemble in strictly ordered systems.

Controlled radical polymerization in the presence of nitroxide radicals is one of the techniques, widely applied for design of block-copolymers incorporating various monomers and having strictly-determined structures. While, a convenient method for nitroxide radicals synthesis is based on the use of spin-traps, such as nitrones and nitroso compounds being commercially available. In particular, under conditions of vinyl monomers polymerization in the presence of nitrones or nitrozocompounds thus obtained polymer is a high-molecular-weight alkoxyamine. This alkoxyamine is capable to reinitiate polymerization upon the introduction of a new portion of a monomer. In the case of introduction of a monomer, different from a starting one, formation of a three-block copolymer of the type ABA occurs.

Results and Discussion. The processes occurring at vinyl monomers polymerization in the presence of alkoxyamines (derived from the spin-traps: C-phenyl-N-tert-butylnitrone (PBN) and nitrobenzene) were simulated with quantum-chemical methods. Effects of electronic and steric factors on **C-ON** bond energy in the alkoxyamines of interest were deduced. The calculations were carried out with the use of the density functional theory method (hybrid functional B3P86 and the basis set 6-31G(d)). On the basis of our simulations, possibility for radical polymerization of vinyl monomers to occur in the controlled regime in the presence of alkoxyamines was suggested for a wide temperature range. Meanwhile, temperature for the process to run in the controlled regime was revealed to depend largely on steric hindrance of the corresponding nitroxide radical, among all, on the chain length of a macroradical, attached to a spin-trap.

Our simulation results appear in good correspondence with the experimental data on the polymerization of styrene in the presence of alkoxyamines, *ex situ* generated from PBN, 2,2`-azobis(isobutyronitrile), and vinyl monomers. It was demonstrated that kinetic parameters of the process and molecular-weight characteristics of thus obtained polystyrene depend not only on the polymerization temperature, but also on alkoxyamine synthesis conditions. This is due to the fact that the presence of high-molecular-weight alkoxyamines leads to the controlled styrene polymerization with relatively high rates already at 80–90°C (in contrast, in the case of low-molecular-weight alkoxyamines, the controlled regime requires higher temperatures). Thus obtained polystyrene is characterized by the linear dependence of molecular weight on conversion and also by low polydispersity, decreasing in the course of polymerization (see: Figure).

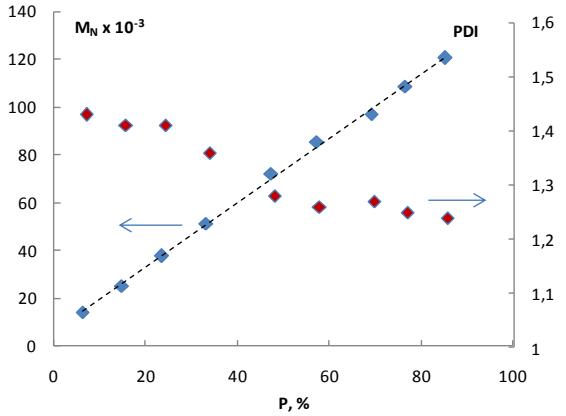

Figure. Molecular-weight characteristics of polystyrene obtained in the presence of a high-molecular-weight alkoxyamine (0.1 mol.%, 90°C).

Based on the obtained polystyrene, post-polymerization and synthesis of block-copolymers of acrylic and methacrylic monomers were conducted as well.

Upon methyl methacrylate polymerization at 90°C, "living" chains are being deactivated due to the formation of hydroxylamine derivatives from nitroxyl radicals. The polymer, derived under such conditions, has reduced initiating activity.

Upon synthesis of block-copolymers based on butylacrylate, deactivation of alkoxyamins is not observed.

Copolymerization of styrene and methyl methacrylate in the presence of high-molecular-weight alkoxyamines allows design of gradient copolymers. Meanwhile, the content of styrene chains in the copolymer is revealed to drop in the course of the process. Curves of the molecular-weight distribution corresponding to conversion higher than 20-30 % are unimodal. Polydispersity index of the copolymer samples decreases with the conversion growth from 2.2-2.4 to 1.2-1.3.

Summary. Therefore, the high-molecular-weight alkoxyamines, derived from PBN, allow controlled polymerization of styrene and butyl acrylate under moderate temperature and result in the formation of block-copolymers.

Acknowledgements. The work was financially supported by "Federal target program of scientific and scientific-pedagogical personnel of innovation of Russia on 2009-2013".

Synthesis and singlet-singlet energy transfer studies of copolymers involving fluorene-carbazole units as energy donor and porphyrin as pendant acceptor group

Sara M. A. Pinto[*a], *Mário J.F Calvete*[a], *Hugh D. Burrows*[a], *Mariette M. Pereira*[a], *Alfonso Salinas-Castillo*[b], *Ricardo Mallavia*[b]

[a]Departamento de Química, Universidade de Coimbra, 3004-535 Coimbra, Portugal
[b]Instituto de Biologia Molecular y Celular, Universidad Miguel Hernández, Elche 03202, Spain

email: smpinto@qui.uc.pt

Over the past two decades, conjugated polymers have become an important group of electronic and optoelectronic materials. Their attractive properties, such as electrical conductivity and electroluminescence, together with their high thermal stability and good mechanical properties allow them to find applications as photoconductors or in thin film transistors, organic light-emitting diodes and photovoltaic systems.[1] Polymers containing carbazole units are particularly good hole-transporting materials due to the electron-donating capabilities associated with nitrogen in carbazole which only can substituted by one chain enhancement the control of pendant groups. Also, it has been demonstrated that the incorporation of 3,6-carbazole units into fluorene-based polymer chains will improve the luminescent stability by interrupting the linear conjugate structures of polymers.[2]

In recent years, electronic energy transfer has experienced a resurgence of interest due to the fact that it is a very attractive method to modulate optical and electronic properties of conjugated polymers. Fluorene based copolymers are particularly attractive as energy donors in Förster Resonance Energy Transfer (FRET) because of their high fluorescence quantum yields and blue emission[3] that allow efficient transfer to acceptors emitting over the whole visible and near infrared spectrum. With appropriate heavy-metal acceptors, it is possible to capture both singlet and triplet state energy. However, blends of luminescent conjugated polymers with electronic energy acceptors tend to phase separate,[4] which can lead to losses in efficiency. This can be avoided by attaching the acceptor covalently to the polymer,[5] or by forming self-assembled systems.[6]

We report the synthesis and characterization of a novel group of polymers, incorporating fluorene-carbazole units as energy donor and porphyrin as pendant acceptor group. Also, a comparative study will be presented of singlet-singlet energy transfer between a system involving a covalent attachment of the acceptor to the polymer and a self-assembled system.

Acknowledgments: Financial support from Portuguese Science Foundation (POCI/QUI/58291/2004) and Spanish Ministry (MAT-2008-05670 and PT-2009-0002). Sara M.A. Pinto also thanks FCT for a PhD grant (SFRH/BD/47022/2008).

References:

[1] Li C., Bo Z., *Polymer*, **2010**, *51*, 4273; [2] Ostrauskaite J., Strohriegel P., *Macromol. Chem. Phys.*, **2003**, *204*, 1713, [3]Knaapila M., Winokur M. J., *Adv.Polym.Sci.*, **2008**, *212*, 227; [4] Xia Y., Friend R. H. *Adv.Mater.*, **2006**, *18*, 1371 ; [5]Montes V. A.; Pérez-Bolívar C.; Estrada L. A.; Shinar J.; Anzenbacher P., *J. Am. Chem. Soc.*, **2007**, *129*, 12598; [6] Pinto S. M., Burrows H.D., Pereira M.M., Fonseca S.M., Dias F.B., Mallavia R.; Tapia M.J., *J. Phys. Chem. B*, **2009**, *113*, 50, 16093.

Degradation Kinetics of Electron Beam Irradiated Poly (propylene-co-ethylene) Heterophasic Copolymer

Mojtaba Koosha[1], Nastaran Ebrahimi [2], Yousef Jahani [3], Seyed Abolfazl Seyed Sajadi [2]*

1* Department of Polymer Engineering and Color Technology, Amirkabir University of Technoology, Tehran, Iran; +982144580159; mkoosha@aut.ac.ir

2 Department of chemistry, Iran University of Science & Technology, Tehran, Iran; nebrahimi61@chem.iust.ac.ir

3 Faculty of Processing, Iran Polymer and Petrochemical Institute, Tehran, Iran; y.jahani@ippi.ac.ir

Introduction:

Polypropylene (PP) is a linear, high melting point polyolefin with excellent chemical resistance and acceptable range of mechanical properties[1]. There are various grades of polypropylene available in the market to cover wide range of applications. Heterophasic ethylene-propylene copolymers (HECO) were developed by in situ sequential homo-polymerization of propylene monomer and copolymerization of propylene and ethylene monomers to improve low temperature impact resistance of polypropylene homopolymers[2].

The modification of PP by high energy beams has been used widely to introduce desirable changes in its molecular architecture. The effect of irradiation on thermal stability of PP was the subject of some researches [4]. In this work, irradiated PP heterophasic copolymers were prepared by electron beam irradiation in different doses and the kinetic methods are applied to the thermogravimetric analysis data in order to determine the non-isothermal degradation kinetics and the results of these methods are compared.

Materials and Methods:

The polypropylene copolymer used in this study was the commercial grade Irapol EP-D60R. The samples were irradiated by a high power industrial electron beam accelerator [5] under nitrogen atmosphere. After irradiation the samples were annealed under nitrogen atmosphere for 30 min at 80°C, to enhance the mobility of free radicals and then 60 min at 130°C to deactivate the residual free radicals. Gel content of the samples was measured in boiling toluene solvent. Thermal properties of heterophasic PP copolymer were investigated by TGA.

Results and Discussion:

The main reactions that take place during irradiation are crosslinking and chain scission [3]. Gel content values correspond with the network structure formed in amorphous region of PP which is not soluble in the solvents. In TG curve of heterophasic PP copolymer, the initial weight loss occurred at 300 ^{o}C is related to the thermal decomposition of bond of polymer. Results also show that there is a shift in the decomposition process to higher temperatures at higher heating rates. The activation energies (*Ea*) of the samples are calculated by three methods [6]: the Kissinger method, the Flynn–Wall–Ozawa method and the Coats-Redfern method. It is clearly observed that the activation energy values computed using the Kissinger and Flynn–Wall-Ozawa methods are in good agreement. The trend observed here for the activation energies is possibly related to the competition of the chain scission and crosslinking reactions occurring in the copolymer during irradiation. The results show that crosslinking reactions are increased in the samples by increasing the irradiation dose, leading to a high molecular weight fraction and increased activation energy. There is a big difference between the *Ea* values of the samples computed by Coats-Redfern method and those computed by Kissinger and Flynn-Wall-Ozawa methods, and the trend is not similar. This discrepancy is possibly related to the fact that the Coats-Redfern method for the kinetic analysis of non-isothermal TGA data is unsuitable and inconsistencies exist in published kinetic results obtained using this approach

Conclusions

It can be concluded that there is a competition between crosslinking and chain scission reactions during irradiation of polypropylene heterophasic copolymer. The polypropylene homopolymer phase is more likely to undergo chain scission and the ethylene propylene rubbery phase is more likely to undergo crosslinking.

The values of activation energies calculated by Kissinger and Flynn-Wall-Ozawa methods were in good agreement and followed a similar trend. But the values obtained from Coats-Redfern method were different and did not show the same trend as the other methods.

References

[1] Cleland M. R., Singh A. , Silverman J., Radiation processing of polymers Munich:Hanser Publishers., 1992.

[2] Spisakova N., Ratzsch M. , Reichelt N. Partial crosslinking of the heterophasic ethylene-propylene copolymer in the solid phase. J. Macromol. Sci., Pure Appl. Chem. 2000;37(1-2):15-35.

[3] Schulze D., Trinkle S., Mülhaupt R. , Friedrich C. Rheological evidence of modifications of polypropylene by ß-irradiation. Rheol. Acta 2003;42(3):251-258.

[4] Dawood A. , Miura K. Pyrolysis kinetics of [gamma]-irradiated polypropylene. Polym. Degrad. Stab. 2001;73(2):347-354

[5]Bassaler J. M., Capdevila J. M., Gal O., Lainé F., Nguyen A., Nicolaï J. P. , Umiastowski K. Rhodotron: an accelerator for industrial irradiation. Nucl. Instrum. Methods Phys. Res., Sect. B 1992;68(1-4):92-95.

[6] Zong R., Hu Y., Wang S. , Song L. Thermogravimetric evaluation of PC/ABS/montmorillonite nanocomposite. Polym. Degrad. Stab. 2004;83(3):423-428.

Effect of Process Conditions on the Compatibilization of In-Reactor Alloys

H. Bagheri[1], M. Nekoomanesh[1], S. Hakim[1], Y. Jahani[1], Z. Q. Fan[2]*

1. Iran Polymer & Petrochemical Institute, P. O. Box 14965/115, Tehran, Iran

2. Department of Polymer Science and Engineering, Zhejiang University, Hangzhou, 310027, PR China

Introduction

The versatility of an in situ copolymerization of an alloy in a process known as "in-reactor alloy" facilitates the production of an immiscible alloy in one single reactor.[1] In this way, alloys with high ethylene-propylene rubber content are produced in two steps. In the first step, propylene is polymerized into a polypropylene homopolymer by a stereospecific catalyst system. In the second step, a mixture of ethylene and propylene are copolymerized using the same catalyst.

Materials and methods

PP/EPR in –reactor alloy was produced via multi-stage sequential gas-phase polymerization of propylene and gas-phase ethylene-propylene copolymerization in circular mode.[2] In this way, three samples were produced, named EP20, EP10, EP5. The sample EP20 was synthesized by ethylene-propylene copolymerization for 20 min and then propylene homopolymerization was carried out for 60 min. The switching number of this sample was designated as 1. The sample EP10, as switching number 2, was synthesized by ethylene propylene copolymerization for 10 min followed by propylene homopolymerization for 30 min. Overall, the total copolymerization time was 80 min. Analogically, the switching number 4 for EP5 was proceeded as above. The samples were studied with respect to the rheological behavior and final properties of the alloy. The polymer alloys based on different structural morphologies were characterized by SEM, GPC, ^{13}C NMR, DSC, rheological analysis, and mechanical testing.

Results and discussion

The results indicated that altering switch frequency has no effect on the microstructure and molecular weight distribution of the polypropylene with very low effect on the synthesized EPR phase Fig. 1. However, the morphological studies combined with rheological and mechanical investigations showed that increasing the switch frequency, reduces the size of the dispersed EPR leading to increase in mechanical performance due to increased interfacial adhesion and partial enhancement of crystalline content Fig. 2

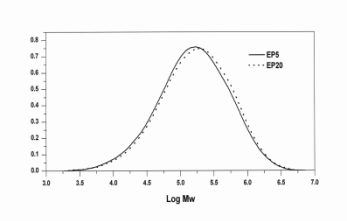

Figure 1. GPC curves of fractions part of samples, insoluble parts

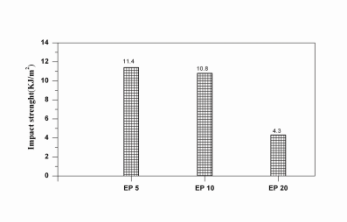

Figure 2. Mechanical properties of EP5, EP10 and EP20

References:

1- Mei, G.; Herben, P.; Cagnani, C.; Mazzucco, A. Macromol Symp 2006, 51395, 677.

2- Dong, Q. ; Wang, X. ; Fu, Z. S.; Xu, J.T.; Fan, Z.Q. Polymer 2007,48,5905.

Investigation of Expanded Graphite Nanoplatelet Its Properties and Composites Applied in EMI Shielding

NSC 99-2221-E-036-002-MY3

Chien-Pang Chang[1], *Ching-Shan Tsai*[1], *Jian-wei Lu*[1], *Chi-Yuan Huang*[1]*

[1]Department of Materials Engineering, Tatung University, Taipei, Taiwan

E-mail: cyhuang@ttu.edu.tw

Abstract

In this investigation, the expanded graphite (EG) was prepared by graphite intercalation compound (GIC) and thermal shock treatment (TST). Results indicated that the effect of thermal treatment caused the expansion degree of EG. By the TST, the EG owned high aspect ratio, and the electrical conductivity was no change that compare with the original nature graphite (NG). The EG were treated by ultrasonic method to get the expanded graphite nanoplatelet (EGP). In order to improve the conductivity of EGP, the key of modification was used acid treatment. The NG, EGP and Carbon Black (CB) were added to EVA (ethylene–vinyl acetate) for preparing the conductive composite, and analysis in EMI shielding.

Experimental

The EG were manufactured by GIC at 350, 650, 950, 1050 ℃ for 1 min. The EG were immersed in a 70% of aqueous alcohol solution and subjected to powdering in an ultrasonic bath for various hours. The resulting dispersion then was filtered and dried to get EGP. The 10g EGP were added in 500ml acid bath (3M HNO_3) with stirring (washing) for 2 hours and washed by distilled water until the filtering solution reached the pH value of original distilled water. The NG, EGP and CB were used as conductive fillers which were blended in the polymeric matrix. The polymeric composites possessed the EMI shielding effectiveness.

Results and discussion

Graphite is a form of carbon with the carbon atoms bonded in layer held together by the weak Van Der Waals force, allowing intercalation atoms or molecules that occupy spaces between the graphite sheets to form graphite intercalation compound GIC [1] which by TST method to form the EG. Tab. 1 showed the effect of TST related the expanded volume (EV) with the high aspect ratio.

Tab. 1 showed the EV of EG with various TST conditions.

TST(℃)	350	650	950	1050
EV(cm^3/g)	13.8	26.1	33.8	33.8

Fig. 1 showed the composites with the TST in 950℃ and 1050℃ of EG displayed the better EMI SE, and that of enhanced the EG dispersal to form the conductivity path in the polymer matrix [3].

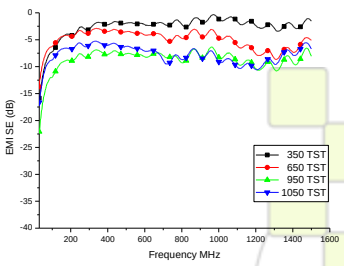

Fig. 1 EMI SE of EVA/EG (100/40) composites with various EG of TST conditions.

Fig. 2 showed the surface resistance of NG, EGP and acid treatment EGP (ACT-EGP). By the acid treatment of EGP, the surface resistance of ACT-EGP was decreased from 8.52 mΩ to 6.50 mΩ and possessed good electrical behavior. In summary, the acid treatment is inevitable for the purposes of purification [4], and modification of EGP increased the conductive properties.

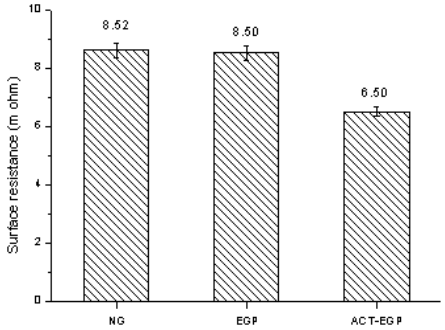

Fig. 2 The surface resistance of NG, EGP and ACT-EGP.

Fig. 3 showed the EMI SE of 40, 60 phr EGP and 40 phr EGP/20 phr CB composite. When the contents of 2D-nanaplate of EGP were added the 40 to 60 phr, it has no obvious that the EMI SE (10 dB-15dB). Therefore, the CB was extra added in the composite to improve the conductivity path between the EGP. In the same volume percent (60%), the composite of 40 phr EG/20 phr CB was exhibited the better EMI SE (25 dB). In this study, the carbon black were used for the bridge to conduct the 2D-graphite nanoplatelet forming continue conductive network in the polymer matrix,it enhanced the EMI SE from 8 to 25dB.

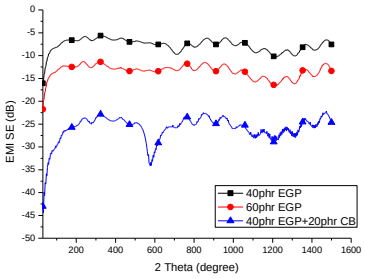

Fig. 3 The EMI SE of 40 phr EGP, 60 phr EGP and 40 phr EGP/20 phr CB composites.

References

[1] W. Lu, J.X Weng , D.J Wu, C.L Wu, G.H Chen, *Materials and Manufacturing Processes*, 21, 167, (2006).

[2] G.H Chen, D.J Wu, W.G Weng, W.L Yan, Journal of *Applied Polymer Science*, 82, 2506, (2001).

[3] P.G Jang, k.S. Suh, M. Park, J. K. Kim, W. N. Kim, H. G Yoon, *Journal of Applied Polymer Science*, 106, 110, (2007).

Electrosedimentation thromboresistant polymeric coverings on purely iron electrode

S.H. Sargsyan, A.S. Sargsyan, K.S. Margaryan

State Engineering University of Armenia, Teryan str. 105, Yerevan, 0009, Armenia
Yerevan State Medical University after M. Heratsy, 2 Koryuni str., Yerevan 0025, Armenia

artsar@web.am

One of prominent aspects of use of polymers in medicine is working out thromboresistant polymeric materials and coverings on their basis of metal implants(stents).

By us possibility of electrosedimentation of composite polymeric coverings on purely iron electrode on the basis of a copolymer vinilacetat-krotonic acid both flouroplast marks F-40D and F-4D in a water-alkaline solution is shown.

Level-by-level heterogeneity composite flouroplast fully coverings that is connected with the mechanism of their formation is established. The analysis of coverings on the flourine maintenance has shown that in the first seconds electrolysis on a metal surface is formed the coverings, not containing flourine, i.e. the covering on an electrode is formed at the expense of electrosedimentation.

Then covering formation follows the account electroforetics the mechanism for which the induction period is characteristic. Research of dependence of change of potential of the anode from time for various compositions in the course of electrochemical sedimentation in galvanostatic a mode confirms the prospective mechanism of formation of composite polymeric coverings.

Have been studied thromboresistant properties of coverings, interaction with modeling solutions fibrinogen and thrombocyte in vivo, and also with integral blood.

On the basis of medical and biologic researches it has been shown that the synthesized polymeric coverings are biocompatible, biodegraded and thromboresistant materials, suitable for use as coverings metal stents.

Temperature Effects in the Dynamics of Bipolaron in Polymer Chains

J. F. Teixeira, W.F da Cunha, P.H.O. Neto, L. F. Roncaratti,

R. Gargano and G. M. e Silva
Institute of Physics, University of Brasilia
jonathanteixeira.fis@gmail.com

Introduction

Conjugated polymers have been receiving increasing attention as suitable materials for electronic applications because of their flexibility and amenability to solution processing [1]. These materials for example can be used as the active layer of organic TFTs (thin-film transistors) and are great for the design of Organic Light Emitting Diodes (OLEDs). OLEDs promises superior performance in brightness and color resolution, thin aspect ratio and better physical characteristics. In its turn organic TFTs has various advantages over inorganic amorphous silicon TFTs and low-cost processing.

Defects in the chain are responsible for charge transport. These quasi particles can be polaron, bipolaron and exciton. Bipolarons and Polarons are self-localized particle like defects associated with characteristic distortions of the polymer backbone and with quantum states in the energy gap due to strong electron-lattice coupling.

Recently it was verified that interchain bipolaron transport is impossible with electric field typically used in conjugated polymer based devices. However, a recent work [2] has shown the importance of considering temperature effects in the charge transport for both intra and interchain process. It was obtained that the temperature raise increases inter and intrachain mobility of polarons. In this work we study the temperature effects over the dynamics of bipolarons on two coupled pi conjugated polymer chains.

Model

The systems are studied combining the one-dimensional tight-binding Su-Schrieffer-Heeger (SSH) model and the Langevin equation to include temperature effects. The SSH Hamiltonian is written as

$$H = \frac{1}{2}M\sum_i |\dot{u}|^2 + \frac{1}{2}K\sum_i (u_i - u_{i+1})^2 + \\ + \sum_{ij}[t_{i,i+1}|i><i+1| + t^*_{i,i+1}|j+1><j|]$$

The first term is the kinetic energy of motion of the sites in the chain. The second is the bond energy of the lattice atoms. $T_{i,i+1}$ in the last term is the hopping integral, which can be expanded to first order as $T_{i,i+1} = T_0 + \alpha(u_{i+1} - u_i)$. We study the dynamics performing numerical calculations within the time-dependent Approximation.

Results and Discussion

In the simulations we considered a system composed of a single and two coupled chains with 100 sites and periodic bond conditions of cis polyacetylene. The figure shows the result of a simulation with the previous described system under a 100K temperature regime. It was observed a greater charge delocalization compared with the 0K regime. This result suggests that thermal effects increase the charge carrier mobility [3]. When both temperature and electric field are present a level of bipolaron mobility even higher is achieved.

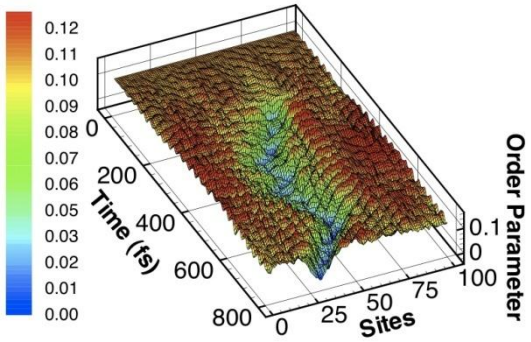

Conclusions

It was studied the dynamics of bipolarons in pi-conjugated polymers chains under several temperature regimes within the time-dependent Approximation.

We observed that the temperature effects are very important to the charge transport in conjugated polymers. Similar to the polaron equivalent simulation performed in [2], the temperature increase causes bipolaron delocalization and this fact leads to rise in its mobility, improving thereby the inter and intrachain charge transport.

References

[1] E.Lim, B.Jung, M.Chikamatsu, R.Azumi, K.Yase, L. Do and H.Shim. Organic Electronics Volume 9 (2008), 952

[2] P.H.O. Neto, W.F. da Cunha and G.M. e Silva. EPL, 88 67006 (2009)

[3] Dae Sung Chung et al., Appl. Phys. Lett., 93 (2008) 033303.

Excitons Dissociation in Semiconducting Polymers PN Junctions

W. F. da Cunha, P. H. O. Neto, L. F. Roncaratti, F. V. Moura, R. Gargano and G. M. e Silva*

Institute of Physics University of Brasilia

* wiliam@unb.br

Introduction

Conjugated polymers are central structures in the recently increasing field of molecular electronics. As the technology employed to design systems based in these molecules reached the current level, the interest in these devices increased drastically due both to the low cost of the processing techniques and to interesting features of the devices itself, such as low weight, controlled charge carriers concentration, etc.

A simple, yet very useful device concerning molecular electronics is the so called PN junction. These structures are obtained when different kinds of semiconductors are mechanically joined. A PN junction is actually the basic kind of device in electronics for many other devices derive from it. As examples of devices created out of PN junctions we have organic diodes, bipolar junction transistors and OLEDs [1].

Also, it is a well known fact that devices made from semiconductor polymers usually employ several types of polymer in order to achieve higher efficiency [2]. The reason for doing it so lies essentially in the dissociation process of the structures responsible for charge supply, i.e. excitons.

In this sense, the present work is devoted to the study of exciton dissociation as the result of the structure interaction with the junction potential. We also investigated how temperature affects the exciton lifetime and obtained a pair of polarons as resulting charge carriers.

Simulation

Numerical simulations were performed to investigate excitons dynamics and their subsequent dissociation. Our code consists on a modified version of the SSH model [3]. Within the Unrestricted Hartree-Fock Approximation we included electric field through the inclusion of a vector potential. Electron-electron interaction was taken into account via a Parr-Pariser-Pople mean field Hamiltonian and the temperature effects were considered in the lattice by applying the Langevin formalism on the equation of motion. Finally, we used a Brasovskii-Kirova type symmetry breaking parameter to simulate a cis-symmetry polymer.

The lattice and electronic equations of motion are simultaneously solved. The latter was traditionally carried out through the consideration of the time dependent Schrödinger equation via the UHF approximation. As for the former, we considered the Euller-Lagrange formalism modified to include a white noise in order to simulate thermal excitations [4].

Starting from a typical cis-polyacetylene chain, the used model parameters were suddenly modified in a particular site of the chain to simulate the heterojunction. We, then, prepared an initial state consisting of an exciton in the neighborhood of the PN junction.

Results and Discussion

We simulated two different chains of conjugated polymer by changing the model parameters of the molecule at a specific point defined as the PN junction. It was then considered an exciton in the neighborhood of the PN junction subjected to thermal effects implied through a classical Langevin equation.

The temperature behavior investigation has shown that exciton stability is critically decreased with temperature. The left figure shows the energy levels of a stable exciton at 0K. In the right, it can be noted the exciton dissociation into a pair of polarons when submitted to a 300K temperature regime.

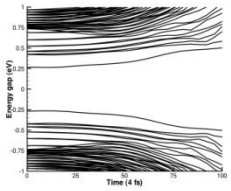

Stable exciton at 0K

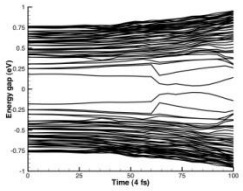

Exciton dissociation at 300K

The random walk imposed to the exciton subjects the structure to the action of the junction potential thus dissociating it into a pair of oppositely charged polarons. The external electrical field applied throughout the molecule accelerates the polarons in opposite directions, giving rise to the electrical current in the device.

Conclusions

We numerically obtained the experimentally observed fact of exciton dissociation in a pair of oppositely charged polarons [5].

It was observed that thermal effects are of major importance in the dissociation process as excitons subjected to the higher thermal regimes tends to dissociate faster, thus giving a more efficient contribution to the charge transport mechanism in PN junctions.

References

[1] A.P. Kulkarni; C.J. Tonzola; A. Babel; S.A. Jenekhe, Chemistry of Materials **16**, 4556 (2004).

[2] Y. Cao, I. D. Parker, G. Yu, C. Zhang, and A. J. Heeger, Nature (London) **397**, 414 (1999).

[3] W.P. Su; J.R. Schrieffer; A.J. Heeger, Physical Review Letters **42**, 1698 (1979).

[4] P.H.O. Neto; W.F. da Cunha; G.M. e Silva, Euro Physics Letters **88**, 67006 (2009).

[5] C. Arne; A. Morteani; R.H. Friend; C. Silva, The Journal of Chemical Physics **122**, 244906 (2005).

Modification of linear low-density polyethylene in single-screw extruder

Kazuya Ono[1], *Masayuki Yamaguchi*[2]

[1] Research and Development Division, Nihon Tetra Pak K. K.
[2] Japan Advanced Institute of Science and Technology

Kazuya.ono@tetrapak.com

Introduction

Linear low-density polyethylene (LLDPE) has been widely used in flexible packages as a sealant layer material owing to better low-temperature heat sealability, hot tack, and transparency than low-density polyethylene (LDPE). Further, LLDPE synthesized by metallocene catalyst are known to have better mechanical properties than LLDPE by Ziegler catalyst. However, it is generally said that the processability of LLDPE is inferior to that of LDPE. For instance, LLDPE tends to cause surface melt fracture phenomenon at lower shear rate in the extrusion processing.[1] The underlying cause of poor processability in LLDPE is considered to be lesser existence of long relaxation time components compared to LDPE. Therefore, the approaches to improve processability of LLDPE are focused on the control of MWD[2] and incorporation of LCB in the polymer. When LLDPE is extruded, the polymer undergoes structural change by heat and shear. It is very important to know the influence of processing conditions on thermal and rheological properties as the LLDPE is responsible for heat sealability in packages.

Materials and Methods

Two types of commercial ethylene-1-hexene copolymer, synthesized by metallocene catalyst; LLDPE-1 (MFR is 7.6 [g/10min], density is 912 [kg/m^3], M_n is 1.7 x 10^4, and M_w is 7.4 x 10^4) and LLDPE-2 (MFR is 3.8 [g/10min], density is 913 [kg/m^3], M_n is 3.0 x 10^4, and M_w is 7.1 x 10^4) were used. No additives were compounded in the materials. The extrusion tests were carried out by laboratory 20mm single-screw extruder with a circular strand die mounted on the head. The temperature of barrel and die was varied from 170 °C to 350 °C in increments of 30 °C. The extruded strands were trapped and quenched in a water bath. The SEC measurements were carried out to obtain the average molecular weights. The linear and non-linear rheological properties were evaluated by rotational and capillary rheometer, respectively. The shreds of strand were compression molded into sheet for FT-IR measurement and thermal analysis.

Results and Discussion

In the SEC measurement of extruded samples, the reduction of molecular weights at 350 °C extrusion indicates that the chain scission reaction is predominant at this temperature. When the extrusions are carried out at 320 °C or lower, however, the molecular weights and M_w/M_n ratio are not largely influenced by the extrusion processing. The SCB peaks in the FT-IR spectra and the melting points in the DSC curves are not affected by the extrusion processing, indicating that the number of SCB is unchanged. In regard to the rheological properties, the linear viscoelastic response sensitively describes modification of LLDPE by extrusion when the MWD is narrow. The van Gurp-Palmen plot of extruded LLDPE-2 samples, shown in Fig. 1, indicates that long relaxation time components are created by extrusion processing and the development is processing temperature dependent. Further, the relation of zero share visosity η_0 and M_w reveals that the increase of η_0 with increase in the temperature is due to branching caused by cross-linking reaction. On the other hand, the non-linear measurement can only depict the change in the LLDPE-1, which is supposed to contain long relaxation time components. The drawdown force measurement indicates that the polymer shows shear modification when extruded at 200 °C or lower. On the contrary, the strain-hardening in uniaxial elongation is enhanced to some extent when extruded at higher temperatures.

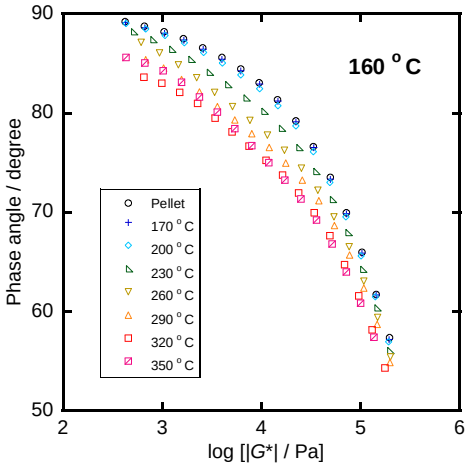

Fig. 1 van Gurp-Palmen plot of extruded LLDPE-2.

Conclusions

Influence of extrusion processing on structure and rheological properties of LLDPE were investigated by employing commercial polymers in which additives were not compounded. The FT-IR measurement and thermal analysis indicates that the SCB is not changed by extrusion. Further, the molecular weights obtained by SEC measurement are not drastically altered except for samples extruded at 350 °C. On the other hand, the rheological measurement reveals the development of long-chain branching structure by extrusion processing. The non-linear measurement is particularly important to evaluate modification of LLDPE in which long relaxation time components are involved.

References

1. K. K. Dohrer, D. H. Niemann, J. Plast. Film Sheet., *6*, 225 (1990)
2. E. Laiho, Polymers, Laminations and Coatings Conference 1998 Proceedings.

PET modification using PLA and chitosan

Diana Palma Ramírez, Aidé Minerva Torres Huerta, Miguel Antonio Domínguez Crespo, Edgar Onofre Bustamante

Instituto Politécnico Nacional, CICATA-Altamira, km 14.5 Carr. Tampico-Puerto Industrial Altamira, Altamira, Tamps. México 89600

atohuer@hotmail.com

Introduction. Polyethylene terephthalate (PET), a thermoplastic polyester is widely used in soft drink and mineral water bottles which constitute the third largest food packaging that is being regularly consumed after packaged tea and biscuits [1]. In order to reduce PET contamination, polymer blending, mechanical and chemical recycling are used [2]. Particularly, solid state mechanochemistry is applied to enhance the compatibility and control the molecular weight and morphology of polymers [3]. It has been reported that PET powders, when are processed by high-energy ball milling, showed a reduction of the average particle size, local orientation of the polymer molecules due to the stress, and a decrease in crystallinity [4]; and PET treated by vibratory milling in inert atmosphere, generated active particles sensitive to the radical acceptors and able to initiate the grafting of vinyl monomers whenever they present in the reaction medium [5]. In this work, the synthesis of PET-polylactic acid (PLA), PET-chitosan and PET-PLA-chitosan blends are reported, as well as the results of FT-IR, DRX and SEM analyses.

Materials and methods. PET from bottles, PLA and chitosan (Sigma Aldrich) were used to produce polymer blends by ball milling at 300 rpm. Cylindrical stainless steel grinding jar of 50 cm^3 and balls made of the same material in a 50:1 ratio was used. The proposed proportions were 5, 10, 15 wt% chitosan and 5 wt% PLA, samples were taken every 10 hours with a total time of 50 hours. The mixtures were analyzed using a PerkinElmer Spectrum one infrared spectrophotometer (range 4000-650 cm^{-1}), X-Ray Diffractometer D8 Advance type (range 5-60 θ (º)) and a SEM (JSM-6300) operating at 15kV.

Results and Discussion. Figure 1 shows the FT-IR results of PET, PET-chitosan in different proportions and PET-PLA for a milling time of 50 h. There were no changes in the signals, suggesting that the bonds in PET do not react or form secondary bonds with the PLA and chitosan biopolymers.

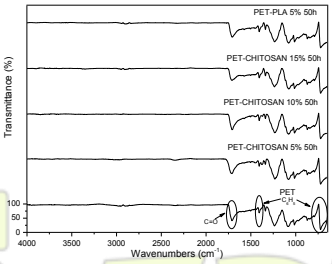

Figure 1. FT-IR Spectra of PET, PET-Chitosan (5, 10, 15 wt%) and PET-PLA (5 wt%).

From XRD spectra (Figure 2) it is confirmed the PET triclinic structure which is modified with the biopolymer type and milling time.

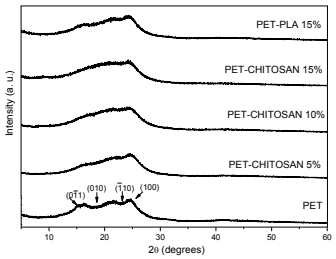

Figure 2 XRD patterns of PET, PET-Chitosan and PET-PLA for milling time of 50 h.

The slightly rounded particles are flattened into flakes because PET has a high impact resistance (Figure 3), and maybe more energy is required to reach a better blending.

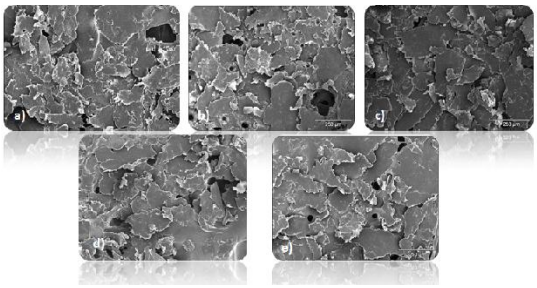

Figure 3. SEM micrographs of PET-PLA powder: a) PET; milling time of b) 20 h; c) 30 h; d) 40h, e) 50h.

Conclusions. PET-chitosan and PET-PLA blends were obtained by ball milling technique. Results suggest that there are no new bonds between PET and chitosan or PET and PLA, the biopolymer type and milling time greatly influences the crystallization of PET phase.

References.

[1] F. Mahdi, A. A. Khan, H. Abbas. Physiochemical properties of polymer mortar composites using resins derived from post-consumer PET bottles. Cement & Concrete Composites 29 (2007) 241–248.

[2] J. Font, J. Muntasell, E. Cesari, Poly(butylene terephthalate) poly (ethylene terephthalate) mixtures formed by ball milling, Materials Research Bulletin, 34 (1999), 157-165.

[3] R. Chen, Y. Chanbin, W. Hong, G. Shaoyun, Degradation kinetics and molecular structure development of hydroxyethyl cellulose under the solid state mechanochemical treatment, Carbohydrate Polymers, 81(2010), 188-195.

[4] C. Bai, R.J. Spontak, C.C. Koch, C.K. Saw, C.M. Balik, Structural changes in poly(ethylene terephthalate) induced by mechanical milling, Polymer 41(2000) 7147-7157.

[5] C. Vasiliu, D. Florin, Macromolecular Mechanochemistry, CISP, 2006, 217-221.

Mechanical Properties of Postconsumer Agave/Polyethylene Biocomposites

R.Jiménez-Amezcua[1], I .Reyes-González [1,2], S.Garcia-Enriquez[2], R. Gonzalez-Nunez[1]

(1)Dpto. de Ingeniería Química
(2) Dpto. de Química,
Centro Universitario De Ciencias Exactas E Ingenierías, Universidad de Guadalajara Jalisco,
Blvd. Marcelino García Barragán 1421. 44430 Guadalajara MEXICO

E-Mail: rubenglz@cencar.udg.mx,rosamjimenez@hotmail.com

Abstract: Composites of postconsumer high-density polyethylene with agave fiber (*Agave tequilana*) were prepared by singlescrew extrusion; Composites of natural fibers with thermoplastic materials provide engineers with new options for novel product development. One of the principal purposes of composite production is to improve matrix mechanical properties, for example, by reinforcing its toughness and strength. The low cost of fillers from recycled material makes them attractive for the production of these solids. Among other desirable properties, the composites should possess enhanced biodegradability and should be reusable. It was found that tensile and flexural moduli increased with fibre concentration while they decreased for impact strength.

Introduction

Pollution due to waste materials has been an important issue in the last decades. Millions of tons of synthetic polymers are discarded each year. For example, the European Union discards more than 13 million tons of plastic waste per year, mainly polyethylene, polypropylene, polystyrene, polyethylene terephthalate and polyvinyl chloride (Williams and Slaney, 2007). Unfortunately, these synthetic polymers are not biodegradable, remaining in the environment almost indefinitely (Friedrich et al., 2007; Gu, 2003). Another specific pollution problem taking place in South-west Mexico is the fiber wasted throughout the process of Tequila production, which is an alcoholic drink produced in some states of Mexico (90% in the state of Jalisco); it is obtained from distilled must prepared from juice extracted from Agave Tequilana Weber var. Azul(Consejo Regulador del Tequila, http://www.crt.org.mx). After the juice extraction process is carried out, fibers from Agave are disposed and they become a serious waste problem. Several research groups have proposed different alternatives to employ these fibers; however, these applications are not enough to dispose of the enormous amount of agave-fibers produced each year (during 2005 alone the production of agave-fibers was 711,000 tons; Iniguez et al., 2001a, 2003; Leduc et al., 2008). Natural fibers are abundant, with low cost, low density, high specific properties and non-abrasive (Saheb and Jog, 1999). Thus, the recycling of polymers and fibers is a very important aspect and it is necessary to find alternatives for the reprocessing of these materials. One of these alternatives is the production of natural fiber composites which is an emerging area in polymer science. Nowadays the main application of natural fiber composites is the production of materials for construction like panels, doors, windows, furniture and decorative pieces (Saheb and Jog, 1999). In this research, we studies the mechanical properties of postconsumer agave/polyethylene composites

Methods

Composite components

The materials used to produce the composites were recycled high-density polyethylene (HDPE) from scrapped milk bottles originally prepared using Paxon AD60-007 (Exxon Chemical, Houston,TX) with a medium molecular weight homopolymer, melt index 0.7 g/10 min and density 0.960 g/cm3, and fibers of *A. Tequilana* Weber var. Azul, obtained from residues of a local tequila company.

Fiber treatment

Fibers from *A. Tequilana* Weber var Azul were treated mainly in two steps: First, they were cleaned and second they were chemically treated (digestion). To clean the fibers, a sifting was made to eliminate the solids, later the pithy fibers were soaked in a container with tap water for 24 h, to hydrate the fibers and to facilitate pith separation. This separation was made in a Sprout–Waldron refiner(D2A509NH) with two 30 cm diameter discs, one fixed and the other rotating at 1770 rpm. Using centrifugation, the excess water in the fibers was eliminated and they were dried outdoors. The digestion of the fibers is performed to eliminate the lignin present in the fibers (Iniguez et al., 2001b). A lab scale digester was used with a 20% (wt/wt) NaOH solution and a temperature of 170 ^{0} C during 90 min.

2.3. Composite preparation

Once the fibers were treated, composite preparation was the next step. Foamed composite extrusion was carried out in a single-screw extruder Haake Rheomex 254 controlled by a Haake Rheocord 9000 control system (Thermo Fisher Scientific Inc.,USA). An amount of 0.5% of ACA (wt/wt) was added to a blend of

30% fiber and 70% recycled polymer and extruded with a screw speed of 30 rpm. The temperature profile from the hopper to the die of the extruder was set to 150/160/170/180 ^{0}C. After the extrusion process, the foamed composites were pelletized.

Conclusions: It was found that tensile and flexural moduli increased with fibre concentration while they decreased for impact strength.

References:

Friedrich, J., Zalar, P., Mohorc˘ic˘, M., Klun, U., Krz˘an, A., 2007. Ability of fungi to degrade synthetic polymer nylon-6. Chemosphere 67, 2089–2095. Gemeiner, P., Stefuca, V., Baies, V., 1995. Biochemical engineering of biocatalysts immobilized on cellulosic materials. Enzyme Microb. Technol. 15, 551–556.

Iniguez, G., Lange, S.E., Rowell, R.M., 2001a. Utilization of by-products from the tequila industry. Part 1: agave bagasse as a raw material for animal feeding and fibreboard production. Bioresour. Technol. 77, 25–32.

Iniguez, G., Diaz-Teres, R., Sanjuan-Duenas, R., Anzaldo-Hemandez, J., Rowell, R.M.,2001b. Utilization of by-products from the tequila industry. Part 2: potential value of Agave tequilana Weber azul leaves. Bioresour. Technol. 77, 101–108.

Iniguez, G., Vaca, P., Rowell, R.M., 2003. Tequila, slaughterhouse wastes and composting. Biocycle 44, 57–60.

Leduc, S., Galindo, J.R., Gonzalez-Nunez, R., Ramos-Quirarte, J., Riedl, B., Rodrigue, D., 2008. LDPE/agave fibre composites: effect of coupling agent and weld line on mechanical and morphological properties. Polym. Polym. Compos. 16, 115–123.

Saheb, D.N., Jog, J.P., 1999. Natural fiber polymer composites: a review. Adv. Polym.Technol. 18, 351–363.

Williams, P.T., Slaney, E., 2007. Analysis of products from the pyrolysis and liquefaction of single plastics and waste plastic mixtures. Resour. Conserv.Recyc. 51, 754–769..

Study of conductivity of PANI compounds processed by extrusion and compression

J.Ruiz[1], *B.Gonzalo*[1*], *J.L.Vilas*[2], *J.M.Laza*[2], *L.M.León*[2].

[1] GAIKER Technology Centre, Parque Tecnológico de Zamudio, Edificio 202,48170 Zamudio (Spain)
[2] Laboratorio de Quimica Macromolecular (Labquimac),Dpto. Química-Física, Facultad de Ciencia y Tecnologia, Universidad Del Pais Vasco, Apdo. 644 48080 Bilbao (Spain)

*Email: gonzalo@gaiker.es

Introduction

Conductive polymers have numerous applications in biomedical industry or in electrocromic applications (smart windows, optical filters…). In particular, the polyaniline (PANI) is one of the most used conductive polymers owing to its ease of synthesis[1] and their good electrical properties. However, its low processability and solubility as well as their poor mechanical properties limit their applications. To solve these problems, conductive compounds were made mixing the synthesized PANI with different thermoplastic polymers[2]. In this way, an improved processability was obtained at the expense of decreasing the conductivity of the synthesized PANI. Therefore, it is necessary to establish a commitment between conductivity and processability.
In this work, we study the effect of conductivity on the type of processing (compression and extrusion).

Materials and Methods

Ammonium peroxydisulfate (APS) and aniline chloride were used for the synthesis of PANI. Both products were supplied from Aldrich. This polymer was characterized chemically by Elemental Analysis (EA) and Fourier Transform Infrared Spectroscopy (FTIR), thermally by Differential Scanning Calorimetry (DSC) and Thermogravimetry (TG) and electrically (Van Der Paw method).
The used thermoplastic matrixes were polycaprolactone (PCL, melting point 75 ºC, from Union Carbide) and polybutylentherfthalate (PBT, mp=235 ºC, from BASF Chemical Company). Both matrixes were dried before use.
Compounds were processed by extrusion using a miniextruder with two conical and contrarotary screws (Haake MiniLab II). The optimum conditions of the processing were 100rpm for 10min. The compounds were also processed by extrusion using a hydraulic press (Telergon Hydraulic Press 40 Tn) applying 40 Tn of pressure for 30 min. For both processes, the processing temperature was slightly higher than the melting point of the thermoplastic polymer, respectively.

Results and Discussion

The chemical structure of the PANI was checked by EA and FTIR and was obtained a conductivity of 8 S/cm.
The compounds were processed at a 20 % and 40 % (percolation threshold)[3] from conductive polymer.

The aspect of the obtained compounds by compression and extrusion are shown in the following Figure:

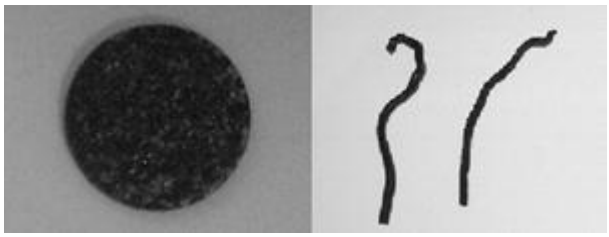

Figure 1: Pressed pellets and threads of conductive compounds.

The threads obtained with PCL are more flexible than the extruded with PBT. However, the pressed pellets have a similar aspect for both cases.

Comparing the results obtained for both processing, the values of conductivity decrease more notably for the compounds obtained by extrusion. This can be related to the shear speed because the channels of electron circulation can be broken.

The study of thermal properties exhibits that the melting point of PCL increases dramatically up to 120ºC (mp= 75ºC for pure PCL) when the compounds are processed. For the case of PBT, the melting point remains constant, due to the rigidity of that polymer.

Conclusions

- New conductive compounds have been obtained using PANI as the conductive filler.
- The samples processed by compression have much higher conductivities than the obtained by extrusion.
- The compounds obtained with PCL are much more flexible and homogeneous.

References

[1] Stejskal, J; Gilbert, RG; Pure Application Chemistry, 74(2002) 857.
[2] Cote, M; Cortes, MT; Beltran, D, et al. Polymer Composite, 30, 1(2009) 22.
[3]Ravati, S; Favis, BD
Polymer, 51, 16(2010) 3669.

Rheological Modeling of Single-Screw Extruders

Hossein Hosseini[1] *and Faezeh Aghazadeh*[2]

[1] Department of Chemical Engineering, University of Tabriz, Iran
[2] Tabriz petrochemical Company, Tabriz, Iran

h_hosseini@tabrizu.ac.ir

Polymer processing for production of all forms of polymeric articles has found a great place in chemical industries. One of the most widespread practical methods of polymer processing is the extrusion method that is based on pressing a polymeric melt through channels of the molding tool which have different geometrical cross-sections. The principal technical characteristic of extruders, named flow /pressure balance, and also modeling of deformation processes permit to evaluate their practical output in processing various polymers as a function of the hydraulic resistance which depends on the flow of an extruded polymeric material through the channels of the forming tool. The validity of obtained and presented results permits to recommend them reasonably not only for estimation of extruder output, but also for making calculations necessary in extruder equipment design: checking calculation of strength and stability of a screw; calculation of driving power of the equipment being designed; strength calculation of a plasticizing cylinder, etc.

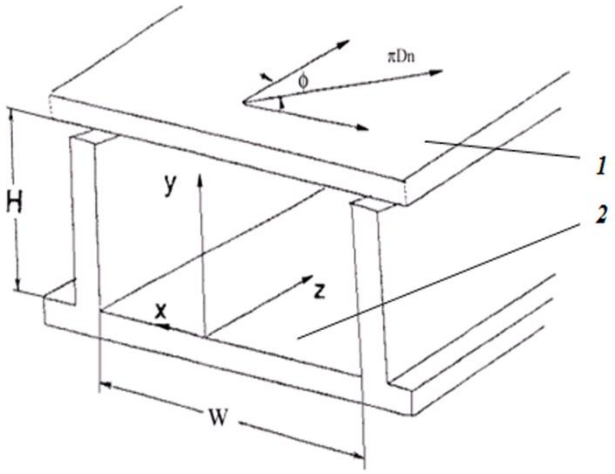

Figure 1. The Scheme of inverse motion of the working parts of a extruder:1 – cylinder wall; 2 – screw channel.

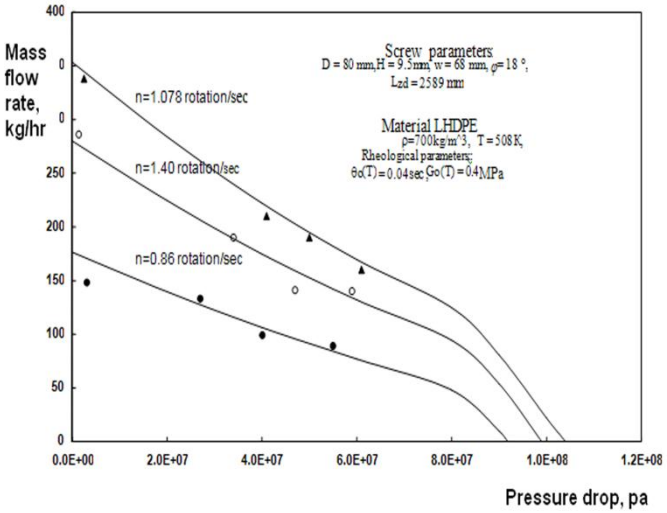

Figure 2. Flow/Pressure characteristics of the extruder at different screw rotation frequency.Lines: equation 19; Points: experimental data.

References

[1] P. Elkouss, D.I. Bigio, M.D. Wetzel and S.R. Raghavan, AIChE J., 52 (2006) 1451-1455.

[2] C. Rauwendaal, Polymer Extrusion, Fourth Edition, Hanser Gardner Publisher (2001).

[3] B. Elbirli, J. T. Lindt, S. R. Gottgetreu and S. M. Baba, Polym. Eng. Sci., 24 (1984) 988-993.

[4] E. E. Acur and J. Vlachopoulos , Polym. Eng. Sci., 22 (1982) 1084-1090.

Preparation of Core-Shell, Organic-inorganic, Hybrid Latexes via a New Single-step Pickering Emulsion Polymerization Method

A. Pakdel[a,*], *H. Eslami*[a,b], *S. Pourmahdian*[a,b]

[a]Polymer Engineering Department, Amirkabir University of Technology, Tehran, Iran.
[b]Chemistry Department, Amirkabir University of Technology, Tehran, Iran

* Corresponding Author's E-mail: Amir.pakdel@aut.ac.ir

Introduction: Nanocomposites have been increasingly studied because of their unique characteristics. Many processes have been envisaged to overcome the resulting problems like phase dispersion and agglomeration. We used a new single step process to produce inorganic nanoparticles of silica fixed on polymer particles and to reduce their agglomeration. In this novel process, simultaneous polymerization prevents the agglomeration of surface active, nano-sized silica particles. We used methyl methacrylate as monomer and silica as mineral emulsifier to produce these structures. In this study, we show that a single step process of precipitation and polymerization can be used under controlled process conditions e.g. amount of water soluble initiator and silica. Moreover, we studied the effect of added cationic surfactant on the morphology of final hybrid nanostructures.Emulsion polymerization is a routine commercial route for production of nano size polymer particles. A typical recipe consists of monomer, water, organic surfactants, initiator, and minor other additives. Inorganic emulsifiers, howevrer, are particles in nano to micrometer range that can be absorbed on the oil/water interface, minimize their surface energy and as a result, stabilize droplets and/or particles in their inevitable continuous collisions with each other [1]. Up to now, myriads of chemists have studied different aspects of such inorganic emulsifiers [2, 3].

Material and methods:

Materials: Methyl methacrylate was provided by Acros Organics. Sodium silicate (solid content of 35% wt. by carbon dioxide precipitation method) was technical grade and used as received. Cetyl trimethyl ammonium bromide (Merck) as catonic surfactant and Ammonium persulphate (Fluka) as water soluble initiator was used without prior treatment.

Typical Polymerization run: A conventional emulsion polymerization method with minor modification to generate silica nanoparticles at the interface of oil/water hybrid particles was used. At first, 1g catonic surfactant was dissolved in 30ml water from which 1ml was added to completely sealed container during the reaction process. Vacuum and argon purge was applied to the system three times. MMA and Sodium silicate solution were added to a round-bottom reactor and then agitated by an egg-shaped magnet at 1000 rpm. The temperature of the solution was raised to 70 °C and then initiator solution was added to the reactor. CTAB solution and Carbon dioxide were added to the reactor through 11 steps during the polymerization process.

Results: As mentioned in the experimental section, the procedure was performed through a one-pot polymerization system. At first, it was turned out that this one-step precipitation/ polymerization method is a reliable method in order to prepare hybrid particles. Our results demonstrate that, the precipitation of silica nanoparticles takes place in the presence of carbon dioxide. Freshly produced inorganic nanoparticles sit at the oil-water interface and can also stabilize emulsions of oil in water. Figure1shows SEM and TEM images of inorganic particle stabilized latex of Poly methyl methacrylate, produced via in-situ emulsion polymerization.

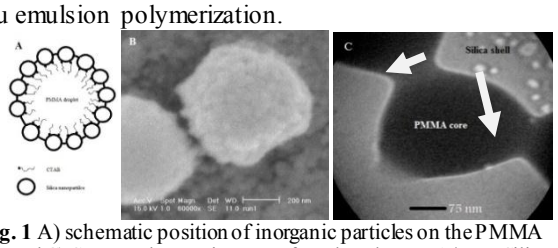

Fig. 1 A) schematic position of inorganic particles on the PMMA core, B and C) SEM and TEM images of produced PMMA/nano Silica latex via a new single step precipitation/polymerization method

Anchoring process of nano-silica particles happens spontaneously and decreases the interfacial tension of oil in water emulsion, and as a result, makes them thermodynamically stable. Stabilizing silica particles on the surface of polymeric core are in the range of 30-45(Fig.1 A). Energy dispersive X-ray microanalysis (EDX) clearly proves the presence of silica particles on the surface of hybrid latex (Figure 2).

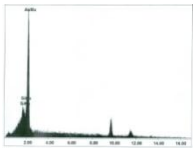

Fig. 2 EDAX spectrum for the surface of hybrid latex.

This proves the ability of oil-water surface to trap freshly produced silica nuclei. Trace amount of cationic surfactant simplify the generation of hybrid microspheres. As a result, CTAB molecules can be considered as a binder between organic and inorganic parts of final hybrid structures.

Conclusion:A facile and effective approach has been developed to prepare hybrid organic-inorganic microsphere via the one-pot emulsion polymerization. These hybrid microspheres would find applications in catalysis, cosmetics, and drug delivery. This method can be extended in order to prepare hybrid latexes from other organic monomers and inorganic particles.

References:

[1]S. U. Pickering: *J. Chem. Soc.* **1907**, *91*, 2001.
[2]S. Sacanna, W. K. Kegel, & A. P. Philipse: *Physical Review Letters*, **2007**, *98*, 158301.
[3]S. Sacanna, A. P. Philipse: *Advanced Materials*, **2007**, *19*, 3824.

Influence of crosslinker and stabilizer additives on the mechanical and the rheological properties of recycled plastic mixtures

J. Acosta García[1], C. Fonseca Valero[1], T. Aguinaco Castro [1], M.U. de la Orden[1], J. Martínez Urreaga[1], C. González Sánchez[2]

[1] POLca (Polímeros, caracterización y aplicaciones), UPM
[4] Departamento de Ingeniería Química y Tecnología del Medio Ambiente. Universidad de Oviedo. C/ Julián Clavería s/n.33071-Oviedo

Introduction

In order to reduce the environmental impact of plastic wastes, there is necessary to look for new ways of recycling and new fields of application for these recovered materials. In this work, mixtures of residual plastic of different origin, underwent different percentages of peroxide treatment in order to increase their compatibility and improve their behaviour as matrices of composite materials.

Materials and Methods

There were prepared different mixtures from agricultural waste recycled plastic (AF, BEFESA), and urban residual plastic wastes (RU), using a roll mixing machine, and adding different percentages of stabilizer (Irganox B900, Ciba) and crosslinker additives (Trigonox 145-E85 and Trigoniox 145-45B, Azko Nobel)

The different mixtures named as AFxx in function of the added percentage of AF and RU, were characterized, before and after the treatments, by means of spectroscopy techniques, thermal, mechanical and rheological measurements. MI measurements were made according to UNE-EN-ISO 1133 standard, working at 190 ºC with 2, 15 kg piston weight .

Results and discussion

Figure 1 shows the variation of the vinyl index, giving by the relationship between two absorbing bands in Infrared spectroscopy (VI= I908/I1461) in relation to the peroxide percentage addition for the AFRU64 mixture. There is observed that VI decreases as the percentage of peroxide increases due to a crosslinking process through the double bonds, mainly, of the HDPE macromolecular chains.

This figure also shows that the addition of 0, 3 wt-% stabilizer inhibits the peroxide action and the following disappearance of the double bonds.

On the other hand, the rheological characterization of the different mixtures is really important considering that these materials are going to be processed by extrusion and/or injection. An excess of peroxide added to the residual plastics mixtures, can cause an excessive increase of their viscosity, even avoiding their processing.

The MI values were lower for the peroxide treated mixtures and those decreased as the peroxide content increased. There were added to the AFRU64 mixture, from 0,10 to 0,20 wt-% liquid and solid peroxides, obtaining the highest MI mixture value for 0,12 wt-% solid peroxide added formulation, and so that, the least viscosity, making the processing easier.

The addition of 0, 3 wt-% antioxidant does not produce a significant change in the rheological properties of AFRU64 sample treated with 0,12 wt-% peroxide.

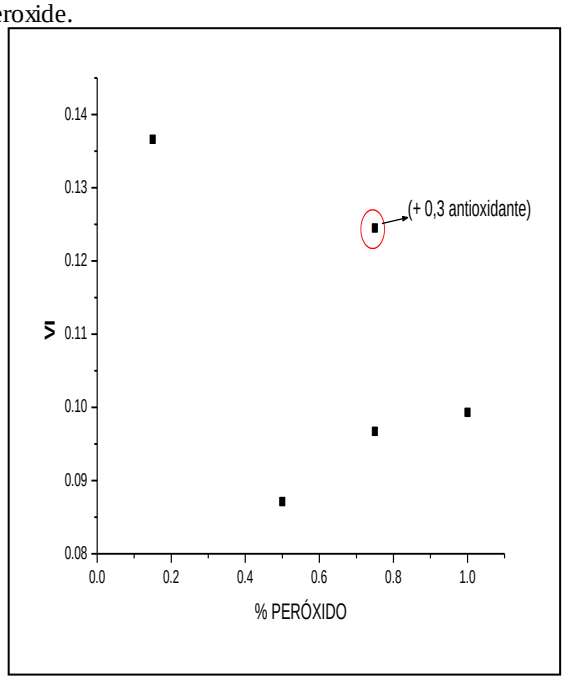

Fig 1. Variation of AFRU64 mixture residual double bonds by addition of liquid peroxide

Moreover, Young modulus and impact strength of the residual plastic mixtures increased with the percentage of added peroxide.

Acknowledgements

The financial support of the Secretaría General para la Prevención de la Contaminación y el Cambio Climático del Ministerio de Medio Ambiente through the. MMA07–A462–2007–2–02.7 project.

References

[1] Basfar A, Idriss, K.M., Mofti, S.M., "UV stability and radiation crosslinking of linear low density polyethylene for greenhouse applications", Polym. Degr. and. Stab., 82, (2003), 229-234

The Effect of Oil Content on the Grinding EPDM Elastomers and on the Structure of Rubber Powders

D. V. Solomatin, O. P. Kuznetsova, E. V. Prut

Semenov Institute of Chemical Physics, Russian Academy of Sciences,
4Kosygin str., Moscow, 119991 Russia

e-mail: evprut@center.chph.ras.ru

Introduction

The recovery and recycling of rubber waste is a very urgent problem that is related to their high resistance to biodegradation when they are buried and the evolution of toxic gaseous products upon their combustion [1]. In the same time the waste rubber articles are an enormous source of starting materials and their using makes it possible to extract and recycle valuable polymer materials. Previous recycling methods of rubber waste such as landfill disposal, incineration, and recycling have failed to provide opportunities for the complete reuse of plastic waste.

An application that has potential to utilize large volumes of waste rubbers is the use of this material as a filler in plastic compounds which retain processability and physical properties after incorporation of significant proportions of rubber.

The preparation of rubber powder (RP) by grinding is a general trend of rubber wastes treatment. The method of high-temperature shear deformation (HTSD) is based on the grinding of a material in a complex strained state by the action of uniform compression pressure and shear forces under elevated temperatures. This method is available for the production of finely rubber powder.

Materials and Methods

The polymers used in this study were iPP, commercial oil-free ethylene-propylene-diene rubber EPDM Dutral TER 4044 and oil-extended EPDM Dutral TER 4334 (Polimeri Europa, Italy).

Rubber vulcanizates of different crosslink densities were obtained by varying the amount of sulfur in the recipes, changing the ratio of sulfur to accelerator system. Blends were prepared in a Brabender plasticorder mixer at room temperature.

Using high-temperature shear deformation technique, the rubber powder (RP) was obtained from model vulcanized rubbers based on ethylenepropylenediene monomer (EPDM) with different content of vulcanizing agent (sulfur).

Results and Discussion

The particle size distribution of the rubber powders was determined by the method of vibratory sieving. Sieve analysis showed that for all types of RP had a majority of particle size of $0.315<d<0.63$ mm. The increasing of sulfur concentration in the rubber vulcanizate decreased percent of particles size of $d>0.63$ mm, while percent of particles size of $d<0.315$ mm increased. The RP particles have an asymmetrical shape. Two characteristic regions with a distinct boundary are observed at the surface of particles: a region of plastic fracture with highly developed surface and the region of brittle fracture with a smooth surface. The increasing of sulfur concentration in the original rubber vulcanizates leads to a decrease in the plastic fracture on the RP surface.

The rheological behavior of TPEs and dynamically cured TPVs with RP was determined by capillary rheometer. It is found that the addition of rubber powder into rubber phase of TPE increases its viscosity, and a partial replacement of EPDM on RP results in a significant decrease in the viscosity of blends in TPV. The viscosities of TPE and TPV depend on the content of rubber powder and crosslink density of vulcanized EPDM.

Blends EPDM/rubber powders, PP/rubber powders were also studied. It is shown that the performance of rubber powder in TPE and TPV depends on particle size, surface area, and composition.

References

1. Adhikari B., De D., Maiti S. *Prog Polym. Sci*. **2000**; 25: 909–48.

Characterization of Induced Thermo-mechanical Degradation on Poly (ethylene terephthalate)

J.D. Badía [1], *E. Strömberg* [2], *S. Karlsson* [2], *A. Ribes-Greus* [1,*]

[1] Institut de Tecnología de Materials (ITM), Universitat Politècnica de València (UPV)
[2] School of Chemical Science and Engineering, Fibre and Polymer Technology, Royal Institute of Technology (KTH)

*corresponding author: A. Ribes-Greus (aribes@ter.upv.es)

Introduction: The effects of thermo-mechanical degradation on poly(ethylene terephthalate) induced by mechanical recycling were simulated by successive injection molding cycles, and assessed in terms of a three-phase model involving crystalline, mobile amorphous fraction (MAF) and rigid amorphous fraction (RAF). The effects on the segmental dynamics and on the macroscopic mechanical performance were analyzed.

Materials and methods: Commercial bottle-grade poly (ethylene terephthalate) (PET) SEDAPET SP04 from Catalana de Polimers S.A., Grup LaSeda (Barcelona, Spain), in the form of pellets, was used. Successive 5 processing steps (RPET-i, with i: 1-5) by injection moulding employing an Arburg 420 C 1000-350 injector were applied. Temperature gradient set from hopper to die was 270, 275, 280, 285 and 280 ºC. Moulds were set at 15 ºC. Cooling time residence was 40 s and total residence time ca. 60 s. After injection, a fraction of the samples was kept as test specimen and the rest was ground by means of a cutting mill Retsch SM2000 (UK), which provided pellets of size $\Phi < 20$ mm to be fed back into the recirculation process.
Fourier-Transform Infrared Analysis with Attenuated Total Reflection (FTIR-ATR), Differential Scanning Calorimetry (DSC) and Scanning Electron Microscopy (SEM) were used for structural, morphological and thermal characterization. Dynamic-Mechanical-Thermal Analysis (DMTA) was performed for assessing the segmental dynamics and dynamic fragility of reprocessed PET. Tensile testing and Charpy Impact testing was carried out to determine the influence of morphological changes on the macroscopic mechanical performance of PET recyclates.

Results and Discussion/Conclusions: The application of the three-phase model to assess the evolution of the ratios of crystalline (X_C), mobile amorphous (X_{MAF}) and rigid amorphous (X_{RAF}) fractions is shown in the table. An initial (X_C, X_{MAF}, X_{RAF}) distribution of ~(29, 53,18) % was found for virgin PET. The crystalline fraction showed a slight overall increase, whereas MAF and RAF suffered the main effects of reprocessing, differing at RPET-5. Interestingly, the major change happened from the first to the second recyclate, involving a marginal modification close to a 10 % for X_{MAF} and X_{RAF}. The results suggest that the MAF is principally attacked due to thermo-mechanical degradation, releasing shorter chains that may fold among themselves and rearrange into inter-crystalline domains (RAF) with each reprocessing cycle, which may affect the mechanical performance of the material.

	X_{MAF} (%)	X_C (%)	X_{RAF} (%)
VPET	53,7 ± 0,6	29,0 ± 0,8	18,4 ± 1,1
RPET-1	52,8 ± 0,9	27,7 ± 0,9	20,3 ± 0,2
RPET-2	44,3 ± 0,8	24,9 ± 0,3	28,8 ± 0,7
RPET-3	41,1 ± 0,1	29,6 ± 0,4	32,0 ± 0,8
RPET-4	40,5 ± 1,9	29,0 ± 2,3	32,6 ± 2,4
RPET-5	35,2 ± 0,4	30,3 ± 0,3	36,9 ± 0,6

Evolution of crystalline (X_C), and rigid (X_{RAF}) and mobile (X_{MAF}) amorphous phases along the reprocessing cycles.

FTIR-ATR experiments showed that degradation reactions were mainly driven by the reduction of dyethylene glycol to ethylene glycol in the flexible part of the PET backbone, and chain scission processes that produced –OH terminated species with shorter chain length, which increased the yellowish aspect of PET recyclates. The packing behavior after rearrangement of shortened chains by thermo-mechanical degradation showed important variations in thermal, viscoelastic and mechanical properties. After each reprocessing step, the crystalline fraction was formed earlier and steeper during cooling, thus altering PET processability. Despite the overall crystallinity fraction scarcely changed, a deep characterization of the bimodal melting behavior indicated the segregation of the crystalline phase into populations with smaller lamellar thickness. The role of the MAF reveals that reprocessing affects the dynamic fragility of PET, as drawn from the study on the segmental dynamics of the glass-rubber relaxation, converting it into a stronger glass-former. The reduction of the MAF, which is mainly converted into RAF, and the shortening of chain lengths in the MAF might increased the free volume and had produced new conformations in which the change from a glassy to a rubbery state was overcome easier and involving less activation energy. The role of RAF is relevant in the behavior at break during macroscopic mechanical testing, due to it might act as precursor of crystallinity and/or vitrify, thus promoting a strain-induced crystallization during tensile drawing and enhance the embrittlement of PET.

Acknowledgements: Spanish Ministry of Science and Innovation (Research Project UPOVCE-3E-013). Spanish Ministry for Education (predoctoral research FPU position to J.D. Badía). UPV and KTH for additional economical support.

Influence of the multi-walled carbon nanotubes on morphology and material properties of PC/ABS nanocomposites obtained by extrusion.

Marcin Wegrzyn[†], *Ignacio Buezas*[†], *Enrique Giménez*[‡]

[†] AIMPLAS, Instituto Tecnológico del Plástico, Calle Gustave Eiffel 4, 46980 Paterna (SPAIN)
[‡] Instituto de Tecnología de Materiales, Universidad Politécnica de Valencia, 46022 Valencia (SPAIN)

marcin@aimplas.es[†], **nbuezas@aimplas.es**[†], **enrique.gimenez@mcm.upv.es**[‡]

Introduction

Carbon nanotubes (CNT) – one of the most promising materials in recent years is constantly the object of doubts and disputes, starting from the issue of good dispersion in composites [1-3]. The outstanding mechanical and electronic properties are dumped down by non-uniform CNT distribution – problem party solved by chemical or physical modification of carbon nanotubes. In context with industrial applications of polymer–carbon nanotubes systems, melt mixing is the preferred method of composite preparation. The aim of our work was to investigate the influence of carbon nanotubes modification on the final properties of nanocomposites produced by melt-mixing with various nanofiller addition methods and extrusion conditions.

Materials and Methods

The matrix polymer PC/ABS used in this study (T85) was supplied by Bayer Material Science. The MWCNTs were produced by catalytic carbon vapor deposition and purchased from Nanocyl (Belgium). The nanotubes were NC-7000 (Thin MWCNTs) and NC-3101 (COOH functionalized MWCNTs).

Nanocomposites with different content of MWCNT were produced by melt-mixing with a co-rotating twin-screw extruder. In this work, two ways of introducing nanotubes into the polymeric matrix were used. In the first case, nanotubes in powder were directly incorporated through the first or second extruder feeding gate. In the other case, MWCNT were previously dispersed in EtOH (with and without surfactants), and added into the extruder. Various screw speed of 400 rpm and 600 rpm and barrel temperatures in a range of 220-280 °C were applied.

Results and Discussion

Among the extensive characterization, optical and electronic microscopy (SEM, TEM) supported by Raman spectroscopy were used to confirm structure and morphology of the final material. Thermal and mechanical properties were evaluated by DSC, TGA, DMA, tensile testing. The study was completed by rheology and electrical conductivity tests.

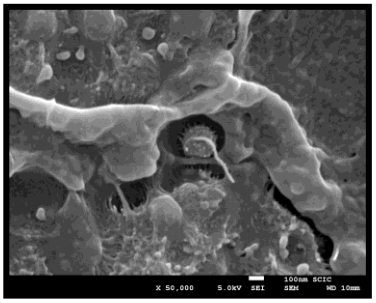

Fig. 1. *SEM micrograph of MWCNT (NC-7000) in the polybutadiene phase*

The dispersion of nanotubes in not homogeneous and tends to concentrate in polycarbonate phase. There is nanotubes appearance in terpolymer poly(acrylonitrile-butadiene-styrene) – ABS accepts nanofiller in polybutadiene spheres (Fig. 1).

Acknowledgements

The authors acknowledge the CONTACT project (FP7/2007-2013) for financial support.

References

[1] D. H. Park, K. H. Yoon, Y.-B. Park, Y. S. Lee, Y. J. Lee and S. W. Kim, *J. Appl. Polym. Sci.*, 2009, **113**, 450.

[2] A. Chandra, A. J. Kramschuster, X. Hu and L.-S. Turng, *ANTEC 2007*, 2184.

[3] Z. Spitalsky, D. Tasis, K. Papagelis and C. Galiotis, *Progres in Polymer Science*, 2010, **35**, 357.

Effect of Nano particles on Mechanical Properties of Biodegradable LDPE/ Starch/Nanoclay Composite

Abdulrasoul Oromiehie[1]*and Pegah Gusheh*[2]

1- Iran Polymer and Petrochemical Institute, Tehran, Iran
*a.oromiehie@ippi.ac.ir
2- Azad University, science & Research Unit, Tehran, Iran

Abstract
In this work the effect of nano particles on the properties of LDPE/starch/nanoclay were studied. Nanclay can be used to improve the mechanical, barrier and thermal properties of biodegradable composites.
The composites were prepared by varying starch content from 30 to 50% and 5% of nanoclay
The result showed that the mechanical properties were improved in the presence of nanoclay with increasing the starch content

Introduction:
Biodegradable polymers are materials that can be degraded by microorganisms and enzymes.
Application of biodegradable polymers includes disposable food service items food packaging, foams and agricultural mulch film. Increasing public concern over dwindling landfill space and accumulation of surface litter has promoted the developed of degradable plastics [1]. Nan clay was added to the blends in order to improve the interfacial strength of LDPE/Starch blends by exploiting the concept of nanocomposites [2,3]. Nan clay have antimicrobial properties as well. This article describes the effect of nanoclay on the in biodegradable composites (LDPE/Starch biopolymer) such as mechanical properties.

Experimental:
Materials:
Corn starch, low density polyethylene(LDPE), glycerol, nanoclay, Polyethylene grafted malice anhydride(PE-g-MA) and Polypropylene(PP).

Methods:
LDPE/Starch/Nan clay composites were prepared by mixing varying starch (plasticized with glycerol) content from 30 -50 wt% and 5 wt% of nanoclay in Brabender twin screw extruder at the following condition: 160/165/170/175/170/165^{0}C and 100rpm.

Results:
The result showed that the mechanical properties were improved in the presence of nanoclay when the starch percentage was increased, (table1) (table2). So this condition helps to have nanocomposites with high biodegradability this result of showed into fig(1,2.3).

Conclusion:
The effect of nanoclay in LDPE/Starch biocomposites improved the mechanical, barrier, thermal properties of the composites and biodegradability of nanocomposites.

Table(1)mechanical properties of LDPE/Starch/nano clay Composites

Samples / Mechanical properties	Starch/PE +5% PP 30/70	Starch/PE +5% PP 40/60	Starch /PE +5% PP 50/50
Strain at break (%)	12.07	17.23	25.22
Stress (MPa)	12.95	12.61	11.83
Young modulus MPa	335.2	318.2	273.00

Table(2)mechanical properties of LDPE/Starch composites(without nanocly)

Samples / Mechanical properties	Starch/PE+5%PP 30/70	Starch/PE +5%PP 40/60	Starch/PE +5%PP 50/50
Strain at break %	25.2	16.17	15.84
Stress (MPa)	13.82	14.23	14.35
Young modulus MPa	252.6	289.2	317.3

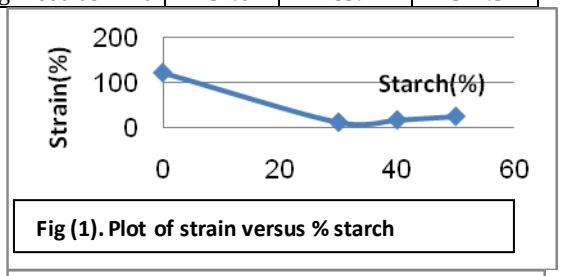

Fig (1). Plot of strain versus % starch

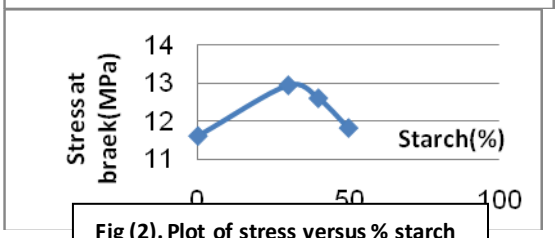

Fig (2). Plot of stress versus % starch

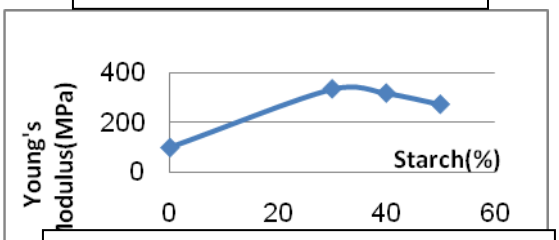

Fig (3). Plot of young modulus versus% starch

References:
[1] Johnson, K. E.;Pometto, A.L., Somasundaram , L.; Coats, J. J Environ Polym Degard 1993, 1,111,-116
[2] Giannelis EP. Polymer Layered silicate nanocomposites , ADV Mater 1996; 8:29-35.
[3] Okaya, T.; Kohno, H.;Terada, K.; Sato, T,; Maruyama, H.;Yamanchi, J.J Appl Polym Sci 1992, 45,1127-1134.

Antimicrobial gluten-gelatin films containing fatty-acids

Farayde Fakhouri [1], Silvia Maria Martelli[2], Angela Teixeira[3], Fábio Yamashita[1], Lúcia Helena Inocentinni Mei[3], Fernanda Paula Collares Queiroz[3]

1–Londrina State University. Department of Food Technology, Faculty of Agricultural Sciences, Londrina, Brazil
2 – Department of Biochemical and Microbial Technology, Faculty of Bioscience Engineering, Ghent University Coupure Links 653, B-9000 – Ghent, Belgium
3- Faculty of Chemical Engineering, Campinas State University, Cidade Universitária Zeferino Vaz, 13083- 852 - Campinas, Brazil

farayde@gmail.com

After processing, contamination by microorganisms is the major reason of food spoilage (*1*). Active packaging is an innovative food-packaging concept, particularly antimicrobial films or coatings (*2*). Edible films containing natural antimicrobials can minimize post-packaging contamination, reducing product lost and increasing food safety (*3*). It is well established that fatty acids and their corresponding esters are one group of compounds with antimicrobial activity and little or no toxicity (*4, 5*).

In this work, antimicrobial fatty acids (FA) were incorporated into gluten-gelatin films (5 wt-% to 50 wt-%) with the aim to improve their barrier properties and check their physical properties to be used in food packaging applications.

The fatty acids chosen were caproic, caprilic, capric, lauric, miristic and palmitic fatty acids. A 10 % solution of GLU/GEL (1:1) was used to obtain films by the traditional solvent casting technique. They were homogeneous and easy to handle. For all cases, the film thickness increased with an increase in FA amounts. Films containing palmitic acid had a thickness increment of 179 % while films containing miristic, lauric and caprilic acid had the thickness value increased by 104, 137 and 34 %, respectively. The biggest variation in thickness was obtained for films containing capric acid (from 0.036 mm to 0.146 mm).

The water vapor permeability (WVP) of samples is showed in Figure 1.

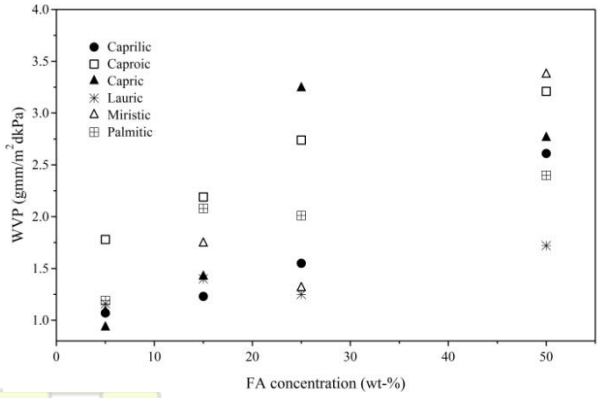

Figure 1. WVP of GLU/GEL/FA films

The WVP containing capric acid, decreased up to 15 % of FA in the film composition in relation with films without FA (data not shown), while for other FAs, the WVP decreased up to 25%. The values of WVP obtained for GLU/GEL/FAs are comparable with the values obtained for hydroxypropyl methyl cellulose and methyl cellulose, which presented values of 1.92 e 1.48 gmm/m^{2}dkPa, respectively. However, they are lower than 7.27 gmm/m^{2}dkPa, the value found for cellophane.

The water solubility of samples containing palmitic and caprilic FA increased from 29.0 % to 34.6 % and from 37.2 % to 41.0 %, respectively, which could be caused by the FA release in water. The addition of other fatty acids did not cause any change in the water solubility of samples. The opacity of films increased with the increase in the FA concentration. Among all, the films containing caproic acid, in the range of 5 % – 30 %, showed the lowest opacity values.

The results showed that the antimicrobial FA addition improved the barrier properties and the performance of GLU/GEL/FA films.

References

1. T. Padgett, I. Y. Han, P. L. Dawson, *Journal of Food Protection* **61**, 1330 (1998).
2. I. Sebti, F. Ham-Pichavant, V. Coma, *Journal of Agricultural and Food Chemistry* **50**, 4290 (2002).
3. T. Sivarooban, N. S. Hettiarachchy, M. G. Johnson, *Food Research International* **41**, 781 (2008).
4. P. Nobmann, A. Smith, J. Dunne, G. Henehan, P. Bourke, *International Journal of Food Microbiology* **128**, 440 (2009).
5. P. Nobmann, P. Bourke, J. Dunne, G. Henehan, *J. Appl. Microbiol.* **108**, 2152 (Jun, 2010).

The Development of a New Co-Polymer for Immobilizing an Optical Hg^{2+}-Sensitive Probe

F. J. Orriach-Fernández[1*], *A.L. Medina-Castillo*[1], *J.F. Fernández-Sánchez*[1], *A. Muñoz de la Peña*[2], *A. Fernández-Gutiérrez*[1]

[1]Department of Analytical Chemistry, University of Granada, Avd. Fuentenueva s/n, 18071 Granada, Spain
[2]Department of Analytical Chemistry, University of Extremadura, 06071 Badajoz, Spain

*fjorrifer@ugr.es

Introduction: Mercury pollutant poses a huge threat because of the lethal effects that it cause on the environment and living organisms due to its long residence, bioaccumulation and permanent damage in central nervous and endocrine systems[1]. Thus, highly sensitive and selective detection of Hg^{2+} in the environmental and biological milieus is an important goal. There are many studies in the literature dealing with mercury chemosensors in aqueous phase; however, with regard to the immobilization of chemosensors in solid phase, for our knowledge, little information is available. The main problem for the immobilization of Hg^{2+}-probes is due to the hydrophilic character of these dyes. There are not many polymers which can be used and which can be chemically compatible with these dyes. One promising Hg^{2+}-chemosensor (FC1) was developed by Bohoyo et al.[2]. It is based on a spirocyclic Rhodamine 6G phenylthiosemicarbazide derivative. The reagent shows a highly selective and sensitive colorimetric and fluorimetric reaction with Hg^{2+}. The obvious color change of the solution from colorless to pink upon the addition of Hg^{2+} demonstrates that FC1 can be used for ''naked-eye'' detection of Hg^{2+} in water effluents. The fluorescence intensity is proportional to the amount of Hg^{2+} at $ng{\cdot}mL^{-1}$ levels. In this work, we have synthesized a water-insoluble copolymer by Reverse Atom Transfer Radical Polymerization (ATRP) to immobilize the mercury chemosensor FC1, in order to develop an optical Hg^{2+}-sensing film.

Materials and Methods: An HEMA-co-MMA copolymer was synthesized by Reverse ATRP technique. It was obtained by dissolving MMA (168 mmol) and HEMA (66 mmol) in 15 ml DMSO and adding $CuBr_2$/PMDETA catalyst system. The mixture was stirring at room temperature and then 12 ml m-xylene and AIBN (0.27 mmol) were incorporated. The mixture was purged with highly pure nitrogen stream and then it was heated with continuous stirring. The polymerization was carried out at 80 ºC for 3 h. After that, the copolymer was recovered and purify by precipitation in distilled water at pH 6.6.

The cocktail used for developing the Hg^{2+}-sensing film was done by dissolving 60 mg of HEMA-co-MMA with 1.5 mg of FC1 and 1.5 mg of potassium tetrakis(4-chlorophenyl)borate salt (KTCPB), which was used to maintain the electroneutrality of the polymeric film. The membrane support was Polyethylene terephthalate (PET). The spin-coating technique was applied to obtain the membranes.

Results and Discussion: There are a variety of chemosensors based on Rhodamine 6G which are hydrophilic, but there is no information in the literature of this kind of chemosensors in solid phase.

Initially none of the polymers studied (PVC, Nafion, etc…) were successful for the FC1 immobilization due to the chemosensor is hydrophilic, and its luminescent characteristics are affected with the pH; emitting fluorescence below pH 4. Therefore we proposed the design of a new neutral copolymer which does not modify the properties of the chemosensor after its immobilization. This copolymer should have hydrophilic groups, it has to provide a neutral or basic media, and its optical properties do not overlap which the FC1 ones. Thus, we designed a copolymer based on the copolymerization of MMA and HEMA: HEMA was used to increase the hydrophilic character of the copolymer; none MMA nor HEMA provide acid media; and the optical properties of these co-monomers are different than those of FC1.

In order to demonstrate the applicability of this copolymer for the immobilization of FC1, we developed a sensing film by dissolving the copolymer and the Hg^{2+}-probe in a volatile solvent, in order to generate a polymer liquid membrane. In addition, KTCPB was added in order to maintain the electroneutrality of the film and glycerol was used as plasticizer to decrease the response time. This polymeric membrane was tested by immersing in an Hg^{2+} aqueous solution for 50 min and measuring and comparing its fluorescence and absorbance with other membrane which was immersed just in clean water (control). Satisfactory results were obtained; the proposed copolymer can be used for immobilizing FC1 without missing their properties against Hg^{2+}.

Conclusions: We have achieved the immobilization of the mercury chemosensor FC1 into a polymeric membrane. This copolymer has been synthesized by Reverse ATRP, and it is constituted by HEMA (28%) and MMA (72%). Currently we are optimizing the milieus conditions to improve the signal intensity. This work is a preliminary step for the development of a new optical Hg^{2+}-sensing film.

This copolymer opens a wide range of possibilities for the immobilization of these chemosensors and their application in optical sensors.

References:

1. Clarkson T.W., Magos L., Myers G.J.N. Engl. J. Med. 2003, 349, 1731– 1737.

2. Bohoyo-Gil D., Rodríguez-Cáceres, M.I., Hurtado-Sánchez M.C., Muñoz-De la Peña A. Appl. Spectros. 2010, 64, 520-527.

Acknowledgments: The authors thank to Spanish Ministry of Education (Projects CTQ2008-01394 and CTQ2008-06657) and the Regional Government of Andalucía (Excellence Projects P07-FQM-2738 and P07-FQM-2625) for their financial support.

Study of Structural Features of Fluorinated Paraffins

V.M. Bouznik[1], Yu.E. Vopilov[2], M.V. Doroshkevich[3], L.N. Ignatieva[4],M.D. Nivikova[5], M.A. Smirnov[6], V.P. Tarasov[6], A.N. Toropov[3], E.P. Kharitonova[2], A.V. Chernyak[6], G.Yu. Yurkov[1]*

[1] A.A. Baikov Institute of Metallurgy and Materials Science, RAS, Moscow, Russia
[2] M.V. Lomonosov Moscow State University, Moscow, Russia
[3] "HaloPolymer" JSC, Moscow, Russia
[4] Institute of Chemistry, FEBRAS, Vladivostok, Russia
[5] B.P. Konstantinov Kirovo-Chepetsk Chemical Industries, Kirovo-Chepetsk, Russia
[6] Institute of Problems of Chemical Physics, RAS, Chernogolovka, Russia

*e-mail: bouznik@ngs.ru

Fluoroparaffins are attractive as materials capable of enhancing tribological properties of objects they are applied to. Fluoroparaffins are superior to hydrocarbon lubricants in some aspects: they are generally more hydrophobic, more liophobic, and have smaller friction coefficient. The method used in this study for preparation of fluoroparaffins is based on fluorination of gaseous paraffin hydrocarbons of a specific molecular weight (ranging from C_{12} to C_{36}). A sequence of technological processes was used for extraction of perfluorinated paraffins which were later studied using a number of physical methods in order to reveal their morphological, topological, and molecular structure. The parameters of the fluorination process were identical for samples with different molecular weights of the initial paraffin hydrocarbons.

All the samples prepared are wax-like materials with no marked morphological structure, but SEM micrographs reveal the presence of layered formations in them. XRD studies of the pristine paraffins and perfluorinated samples confirm the presence of those structures, which is indicated by reflections at small angles. According to the experimental data, the perfluorinated paraffins also contain topologically unordered formations, which is indicated by two halos in XRD patterns at 2θ = 30-50° and 72°. Such halos are specific for low molecular weight fractions of polytetrafluoroethylene. Peaks attributable to crystalline components (the most prominent of them is at 2θ = 18°) which are specific for high molecular weight fractions of polytetrafluoroethylene are observed in patterns of high molecular weight paraffins.

A prominent dependence of thermal properties (weight loss onset temperature and melting temperature) of the perfluoroparaffins as function of their molecular weight was observed. Thermogravimetric curves of low molecular weight paraffins revealed smaller dispersion of molecular weights in them.

Infrared spectra of the fluoroparaffins studied generally resemble the IR spectrum of polytetrafluoroethylene but have some distinctive features. Specifically, the main bands (1228, 1154 cm^{-1}) are narrower than those in the spectrum of polytetrafluoroethylene, which unmasks some other bands. The fluoroparaffins' spectra do not contain bands attributable to amorphous formations. Besides the bands attributable to CF_2 groups of the molecular helix, the spectra also contain components at 1371 and 986 cm^{-1} which correspond to the terminal and lateral trifluoromethyl groups (CF_3), respectively, as follows from quantum chemical calculations for fluorocarbon conformer models. There are also bands which can be ascribed to hydrocarbon groups.

The samples were studied using high resolution magic angle solid state nuclear magnetic resonance (MAS NMR) on ^{1}H, ^{13}C, and ^{19}F nuclei. Attribution of peaks in the experimentally acquired NMR spectra was performed via comparison of the experimental data with the values of chemical shifts calculated using quantum chemistry. The studies revealed that the fluorination process does not result in complete substitution of hydrogen atoms by fluorine, and the spectra of all the samples contained peaks attributed to protons. The observed resonance lines indicate the presence of CH_2-, CFH-, CH_2F-, and CHF_2 groups. The ratios of functional groups in the samples prepared from paraffin hydrocarbons of different molecular weights were determined based on the intensities of the respective NMR peaks. These data are confirmed by ^{13}C spectra. ^{19}F NMR spectra reveal the presence of CF_3 groups in the samples; concentration of these groups depends on molecular weight of oligomers which comprise the fluoroparaffins.

The solubility of fluoroparaffins in supercritical carbon dioxide has been measured at temperatures of 318 - 383 K in the pressure range of 10 - 80 MPa and it was not lower than 50 g/L.

This work was partially supported by the Russian Foundation for Basic Research (grant nos. 11-08-00015 and 11-08-90436_Ukr), the basic research program of Russian Academy of Sciences.

Bioactive Textile Materials Covered with Polymers as Continuous Layers, Microparticles or Microcapsules

Georgeta Mocanu[1], *Marieta Nichifor*[1], *Doina Mihai*[1] *and Loti Cornelia Oproiu*[2]

[1]"Petru Poni" Institute of Macromolecular Chemistry, Iasi, Romania e-mail
[2]National Research&Development Institute for Chemistry & Petrochemistry, Bucharest, Romania

gmocanu@icmpp.ro; nichifor@icmpp.ro

Introduction

The increasing demand for textile with improved properties led to new fabrics called "multifunctional" "active" or "smart" with large application in technical, domestic or medical fields. The purpose is realized mainly by covering a textile material with a functional layers able to include, retain or reject different chemical compounds.[1] Materials or clothes containing antibacterial agent or other compound providing care and comfort are already on markets.

The aim of the present work is the coverage of textile materials with multifunctional polymer layers able to provide simultaneous protection and treatment to sensitive and allergic skins. For this goal the cotton fabric was covered with cationic polymers, which have by themselves antibacterial properties, or with polymer microparticles containing plant extract with antibacterial, antioxidant and antiallergenic activity.

Materials and Methods

Chitosan (CH) of medium MW, poly(vinyl alcohol) (PVA) of MW 100000 and 98% hydrolysis, glutaraldehyde (GA) (25% in water), 1,1-diphenyl-2-picrylhydrazyl (DPPH), acid orange (AO) and tripolyphosphat (TPA) were from Aldrich. A cotton fabric (200 g/m^2) was purified by treating it with an aqueous solution of sodium carbonate, followed by distilled water and ethanol. An extract of Viola Tricolor (VT) (3.5 % solution in water/ethanol mixture) was used as a biologically active compound. Dextran carrying pendant N.N(dimethyl)-N-benzyl-N-(2-hydroxypropyl) ammonium chloride groups (Dex-Q) was prepared as previously described.[2]

Binding of cationic polysaccharides (CH and Dex-Q) to the cotton surface was performed in aqueous medium, using GA as a crosslinker. The amount of polymer bound was determined with AO method (for CH), and by chloride ion titration (Dex-Q). The coated fabrics were immersed in VT solutions, and then dried to constant weight. Microparticles of CH crosslinked with TPA were prepared in aqueous solutions of pH 6. .PVA microcapsule containing VT were obtained by water-in-oil emulsion, followed by PVA crosslinking with GA. Cotton fabric was covered with a layer of microparticles, in the presence of a binder. Polymer and coated fabrics were characterized by FT-IR, UV, and SEM. The amount of VT released from microparticles or coated fabrics was quantified by UV analysis (330 nm) or reverse phase HPLC. Antioxidant activity of bound VT was determined by DPPH method, and antibacterial activity by specific tests on cell cultures.

Results and Discussion

Antibacterial properties of CH are well known, and those of Dex-Q have been previously demonstrated.[2] Cotton fabric were coated with various amounts of cationic polysaccharides (5-20 g %) (Fig. 1), but the original textile touch could be preserved only when the polysaccharide content was lower than 8 g%. Preliminary antibacterial tests showed promising activity of the treated cotton against some bacterial strains. Cotton coated with crosslinked CH and impregnated with VT presented also antioxidant activity, which was proportional to VT content. Microparticles of CH containing VT (10 g%) were fixed on the cotton fabric with a binder. The release rate of VT from these fabrics (Fig. 2) was lowest in the case of microparticles (curve 4) and increase with increasing crosslinking degree (curves 1-3). Microcapsules of PVA had a spherical shape and a size of 20-60 μm (Fig. 3a) and contained about 12 g % VT. The release of VT from these particles was slow, and they preserve the shape after the complete release (Fig. 3 b) suggesting the diffusion as the main release mechanism, with low contribution of erosion.

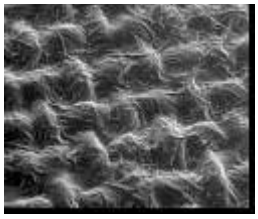

Fig. 1. SEM image of a cotton sample covered with CH layer

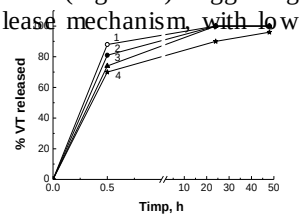

Fig. 2. Release profile of VT from cotton covered with CH formulations

a **b**

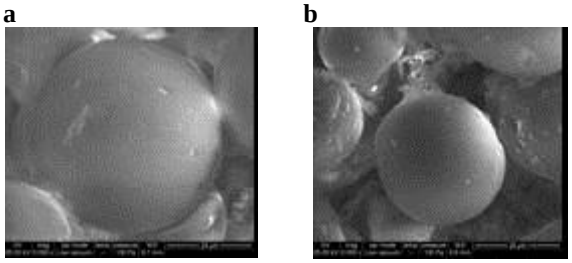

Fig. 3. SEM images of PVA microcapsule containing VT extract, before (a0 and after (b) complete release of the active compound.

Conclusion

Cotton fabrics were covered with different polymeric formulation (continuous layer, microparticles or microcapsules) with or without a bioactive compound (extract of Viola Tricolor). The results showed that these new functionalized textile have antibacterial and antioxidant activity and might be used as new biomaterials for medical or domestic applications.

References

1. U. Wollinaa, M. Heideb, W. Müller-Litzb, D. Obenauf, J. Ash, in Elsner P, Hatch K, W. Wigger-Alberti (eds): *Textiles and the Skin.Curr Probl Dermatol.* Basel, Karger, 2003, vol 31, pp 82–97.
2. M. Nichifor, M. C. Stanciu, B. C. Simionescu, *Carbohydr. Polym.* 2010, **82**, 965-975

Rheology Applied to the Study of Processing Behaviour of PVC-PBA Block Copolymers Obtained by LRP

[b]*Miren Itxaso Calafel*, [a]*Belen Pascual*, [a]*José Ignacio Conde*, [a]*Miquel Boix*, [b]*Antxon Santamaría*, [b]*María Eugenia Muñoz*

[a]ERCROS, S.A. Ctra. Tarragona-San Sebastián, km. 147, 22400 Monzón (Huesca)
[b]Departamento de Ciencia y Tecnología de Polímeros y POLYMAT, Universidad del País Vasco (UPV/EHU)
Centro Joxe Mari Korta, 20018 San Sebastián (SPAIN)

mariaeugenia.munoz@ehu.es

Introduction

Living radical polymerization (LRP) represents nowadays a reliable alternative to usual synthesis routes based on free radical polymerization, because its capacity to effectively control the molecular architecture of the polymer. A punctual, but very interesting success of this technology concerns to the synthesis of block copolymers of Poly-vinyl chloride-b-poly-butyl acrylate (PVC-b-PBA)[1,2]. Since PBA has a low glass transition temperature (-41ºC)[2], these copolymers open new ways in the effort to develop flexible PVCs processed without any plasticisers, such as di ethyl-hexyl phthalate (DEHP), more known as DOP[3].

Materials and Methods

In this contribution, basic and applied rheological properties of PVC-b-PBA block copolymers obtained by LRP are investigated, within the framework of the correlation *Structure-Rheology-Processing*. All the samples show a molecular weight close to Mw= 100000 g/mole with a polydispersity index around 2.5, being the main difference the PVC/PBA ratio of each sample. Dynamic viscoelastic measurements in the linear regime have been carried out in a AR G2 (TA Instruments) rheometer. An extrusion capillary rheometer, Gotffert 2002, has been employed to determine the viscosity as a function of shear rate and temperature.

Results and Discussion

The effect of the microstructure of the copolymer on the linear dynamic viscoelastic results (in the terminal zone) is linked to the morphology developed as a consequence of the micro(nano) phase separation. The transition from an ordered state (or self-assembled phases) to a disordered or homogeneous melt is investigated using viscoelastic methods. The non-linear rheological results, obtained in an extrusion capillary rheometer in conditions similar to industrial processing, are discussed considering the eventual order or disorder state of the melt. The viscosity data extending over a wide range of temperatures, shear rates and pressures give significant information on the processing feasibility of the different samples. As an example, the viscosity curves of Etinoflex-20 (PVC-PBA block copolymer with 20% BA) determined at three different temperatures are depicted in Fig.1. A comparison with plasticised PVC is also shown.

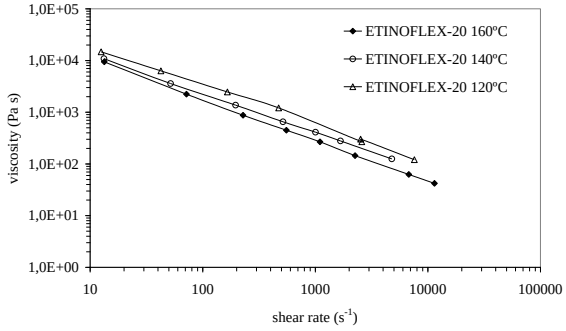

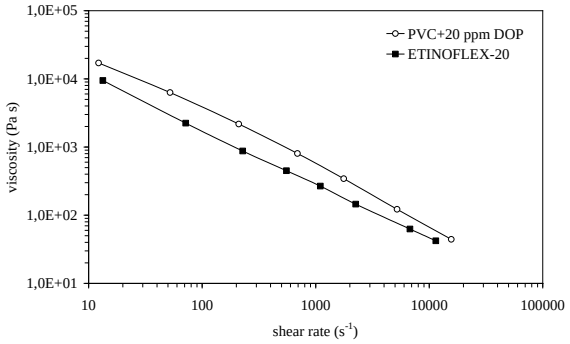

With the aim of linking basic and applied rheology, the extrusion results are interpreted considering the evolution of the copolymers morphology during flow.

References

[1] J. F. J. Coelho, A. M. F. P. Silva, A. V. Popov, V. Percec, M. V. Abreu, P. M. O. F. Gonçalves, M. H. Gil, *J Polym Sci: Part A: Polym Chem*, 44, 2809 (2006).
[2] J. F. J. Coelho, M. Carreira, A. V. Popov, P. M. O. F. Gonçalves, M. H. Gil, *Eur Polym J*, 42, 2313 (2006).
[3] J. F. J. Coelho, M. Carreira, P. M. O. F. Gonçalves, A. V. Popov, M. H. Gil, *J Vinyl Addit Technol*, 12, 156 (2006).

Acknowledgements

Financial support is acknowledged from GIC IT-441-10 (Basque Government).

Effects of Reprocessing Cycles on the Structure and Properties of Polypropylene/Cloisite 15A Nanocomposites

Stéphane Bruzaud[1], *Naima Touati*[2], *Mustapha Kaci*[2], *Yves Grohens*[1]

[1]Laboratoire d'Ingénierie des Matériaux de Bretagne, Université de Bretagne Sud
Rue de Saint Maudé, 56321 Lorient Cedex, France.
[2]Laboratoire des Matériaux Organiques, Faculté de la Technologie,
Université Abderrahmane Mira, Bejaia 06000, Algeria.

E-mail : stephane.bruzaud@univ-ubs.fr

The effects of reprocessing cycles on the structure and properties of isotactic polypropylene (PP)/Cloisite 15A (OMMT) (5 wt. %) nanocomposites was studied in presence of maleic anhydride grafted polypropylene (PP-*g*-MA) (20 wt. %) used as the compatibilizer to improve the clay dispersion in the polymer matrix. The various nanocomposite samples were prepared by direct melt intercalation in an internal mixer, and further they were subjected to 4 reprocessing cycles. For comparative purposes, the neat PP was also processed under the same conditions. The nanocomposite structure and the clay dispersion have been characterized by wide angle X ray scattering (WAXS), transmission electron microscopy (TEM) and rheological measurements. Other characterization techniques such as Fourier transform infrared spectroscopy (FT-IR), tensile measurements, differential scanning calorimetry (DSC) and thermogravimetric analysis (TGA) have also been used to evaluate the property changes induced by reprocessing. The study showed through XRD patterns that the repetitive reprocessing cycles modified the initial morphology of PP/OMMT nanocomposites by improving the formation of intercalated structure, especially after the fourth cycle. Further, the addition of PP-*g*-MA promoted the development of intercalated/exfoliated silicate layers in the PP matrix after the second cycle. These results are in agreement with TEM observations indicating an improved silicate dispersion in the polymer matrix with reprocessing cycles displaying a morphology with both intercalated/exfoliated structures. The initial storage modulus (G') of the nanocomposites, which was highly improved in presence of PP-*g*-MA seems to be less affected by reprocessing cycles at very low frequencies exhibiting a quasi-plateau compared to pristine PP/OMMT and PP. In contrast, the complex viscosity was found to decrease for the whole samples indicating that the main effect of reprocessing was a decrease in the molecular weight. Moreover, the thermal and mechanical properties of the nanocomposites were significantly reduced after the first cycle; nevertheless they remained almost unchanged during recycling. No change in the chemical structure was observed in the FTIR spectra for both the nanocomposites and neat PP samples after 4 cycles.

These results demonstrate that the recyclability of PP-OMMT/PP-*g*-MA nanocomposites is more complex because the resulting structure affects strongly the performance of the nanocomposites. Many factors should be considered mainly: the interaction filler-matrix, the type and loading rate of organoclay, the amount of PP-*g*-MA compatibilizer and the processing conditions.

Obtaining Porous Polyimides with controlled Pore Size

Elizabeth Rangel-Rangel, Eva M. Maya, Javier de Abajo, Angel E. Lozano, José G. de la Campa

Departamento de Química Macromolecular, Instituto de Ciencia y Tecnología de Polímeros (CSIC)

erangel@ictp.csic.es

Introduction and objectives

Lately, increasing research has been focused on obtaining new organic covalent microporous materials, resembling zeolites, zeotypes, activated carbons, and metal organic frameworks (MOF), for diverse applications such as supporting metal catalysts. While the covalent bonds in such networks provide high thermal and chemical stability, especially compared to MOFs, the organic structure allows tailor-made incorporation of multiple chemical functionalities into the networks, which is not possible for zeolites or activated carbons. Also, some physical properties, such as ductility and light weight, add value to such materials.[1] Porous shape and porous size of the material are very important requirements to achieve a large volume fraction accessible to anchor the functionality and consequently the metallic catalyst.

This work describes the synthesis and characterization of new porous polyimides (**PPIs**) with controlled porosity by using a rigid aromatic triamine and dianhydrides with different length.

Results and Discussion:

The synthesis of the 3,5-diamino-N-(4-aminophenyl) benzamide (**DAPBA**), was carried out in two steps with good yield (Figure 1); a) acylation of 4-nitroaniline with 3,5 dinitrobenzoyl chloride and b) reduction of nitro groups with hydrazine hydrate using Pd/C as catalyst.[2]

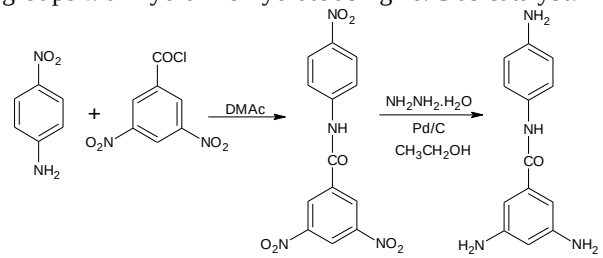

Figure 1. Synthetic route for obtaining **DAPBA**

The structure of **DAPBA** was confirmed by ^{1}H-NMR and FTIR.

The novel **PPIs** (Figure 2) were synthesized by reacting **DAPBA** with commercial dianhydrides (**PMDA, BPDA** and **BKDA**) and also with the dianhydride **IPPDA**, which has been previously described by our group.[3] The one-step polycondensation reaction was carried out in *m*-cresol at 180ºC for 6 hours following the procedure described elsewhere.[4]

ATR FTIR spectra of all porous polymers showed the characteristic bands of polyimides a 1773, 1713, 1348 and 731 cm^{-1} and the –NH- stretching band of the amide linkages at 3500 cm^{-1}. **PPIs** showed high thermal stability by thermogravimetrical analysis, with decomposition temperatures above 550ºC and one stage degradation pattern. DSC curves did not show any thermal transition below 400ºC. In Figure 3, an idealized structure of **DAPBA** with **PMDA** (dianhydride **1)** is depicted to show how pore is formed.

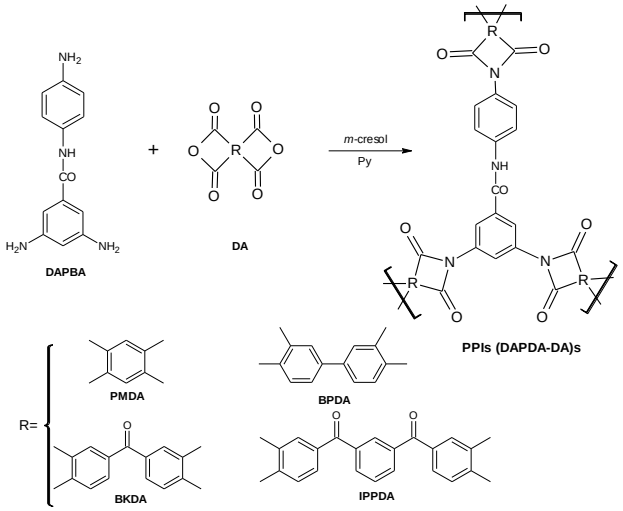

Figure 2. PPIs obtained in this work.

Pore size and pore distribution of the new materials by N_2 gas adsorption/desorption (BET) technique are in progress. Besides, CO_2 and CH_4 sorption experiments are being carried out.

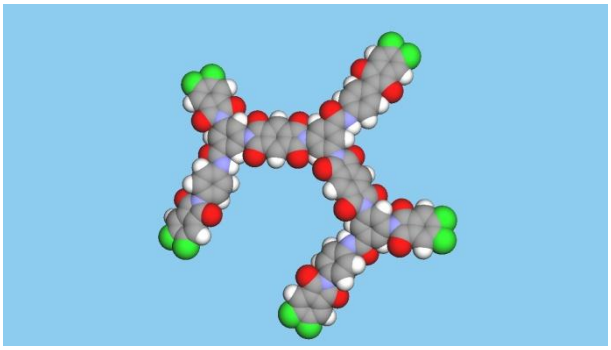

Figure 3. Molecular modeling of the reaction of **DAPBA** and **PMDA** anhydride. Green atoms mean points from where polymer network is growing.

Other **PPIs** with functional groups such as amino ones are being obtained to anchor metallic catalysts.

References:

[1] Schmidt J.; Werner M.; Thomas A.; *Macromolecules* **2009**, 42, 4426-4429.

[2] Wang H.; Li L.; Zhang X.; Zhang S.; *J. Membr. Sci.* **2010**, 353, 78-84.

[3] Ayala D.; Lozano A.; de Abajo J.; de la Campa J.G.; *J. Polym. Sci. Part A: Polym. Chem.* **1999**, 37, 805-814.

[4] Weber J.; Antonietti M.; Thomas A.; *Macromolecules*. **2008**, 41, 2880-2885.

Acknowledgments:

The financial support provided by MULTICAT project and MAT 2010-20668 is gratefully acknowledged. ERR thanks CSIC for a JAE-Pre grant.

Advanced Polymeric Composites for Self-healing Structural Materials

M. Raimondo[1], R. Corvino[1], L. Guadagno[1], P. Longo[2], C. Naddeo[1], A. Mariconda[2]

[1] Dipartimento di Ingegneria Industriale, Università di Salerno, Via Ponte Don Melillo-84088 Fisciano (SA) Italy;
[2] Dipartimento di Chimica, Università di Salerno, Via Ponte Don Melillo-84088 Fisciano (SA) Italy

rcorvino@unisa.it

Introduction: Thermosetting polymers are susceptible to damage induced by mechanical, chemical, thermal, UV radiation, or a combination of these factors. This could lead to the formation of microcracks within the structure where detection and external intervention are difficult or impossible. The microcracks can lead to substantial delamination and fiber-matrix debonding. To overcome the drawbacks related to the composite materials we have developed self-healing materials that allow us to obtain a material with the ability to autonomically heal cracks without any manual intervention or application of a specific stimulus (e.g. heat, radiation etc.). The design of our composite was already proposed in literature [1]. It includes monomer-filled microcapsules and a solid catalyst embedded in a thermosetting polymeric matrix. In this system, the crack ruptures the microcapsules, releasing the healing agent into the crack plane through capillary action; the healing agent contacts the catalyst, triggering polymerization that bonds the crack faces closed. The metathesis product (in the crack) obtained by Ring-opening Metathesis Polymerization (ROMP) shows high cross-linked fraction. The results on the cure behavior of this material and the influence of the components related to self-healing function on the dynamic-mechanical properties were investigated in a previous paper [2]

Materials and Methods: The catalyst used in the matrix was Hoveyda-Grubbs'catalyst (HG1). The epoxy matrix used was a blend of diglycidyl ether of bisphenol A (trade name EPON 828 – Acronym DGEBA) and a high molecular- weight epoxy flexibilizer, Dimer Acid Diglycidyl Ester (trade name HELOXY 71 – Acronym DADGE) which was used in small percentages to improve the toughness of the material and consequently crack growth stability. Microcapsules containing 5-ethylidene-2-norbornene (ENB) were prepared by *in situ* polymerization in an oil-in-water emulsion.
Scanning electron microscopy (SEM) pictures were obtained with a LEO 1525 microscope. The samples were covered with a 250-Å-thick gold film using a sputter coater (Agar mod. 108 A). The fracture toughness and healing efficiency of the formulated composites were measured using a tapered double–cantilever beam (TDCB) test [3]. The experiments were conducted with an Instron 4301 tensile and compression tester 1kN load cell.

Results and Discussion:
Figure 1 shows the sample geometry (TDCB) used to obtain quantitative results on the self-healing functionality. The figure also reports the image of a healed sample after a controlled damage.

Fig 1. Samples for getting quantitative results on the self-healing functionality (a-b); healed crack faces closed by means of the metathesis product inside a crack after a (TDCB) test (c).

Crack healing efficiency, η, is defined as the ability to recover fracture toughness and for the TDCB [4] geometry, is simply calculated as the ratio of critical fracture loads for the healed and virgin samples.

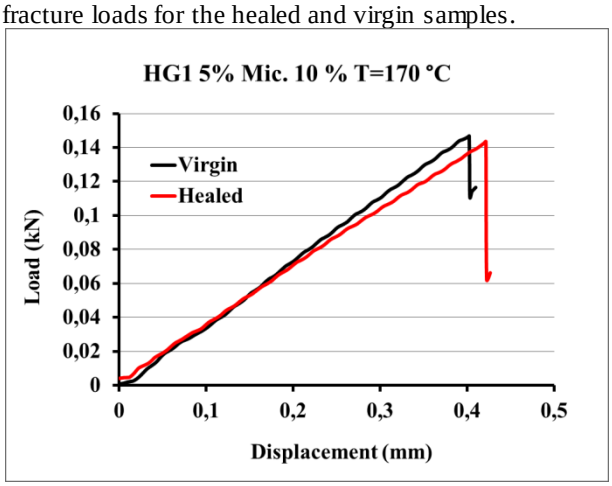

Fig 2. Load-Displacement curves for Virgin (black curve) and Healed (red curve) samples.

Figure 2 shows the Load-Displacement curves for a sample with 5% of Hoveyda-Grubbs I Catalyst and 10% of microcapsules ENB filled, cured up to 170 °C. The obtained efficiency is 97.75% .

Conclusions: We have formulated, prepared and characterized a multifunctional autonomically healing composite with a self-healing efficiency higher than 90%. The industrial scale production of this material is finalized to producing a new advanced structural composite with competitive advantage in the ratio cost/weight, product/process and performance/safety.

References:

[1] S.R. White, N.R. Sottos, P. H. Geubelle, J.S. Moore, M. R. Kessler, S. R. Sriram, E.N. Brown & S. Viswanathan, Nature 409 (2001) 794.
[2] L. Guadagno, P. Longo, M. Raimondo, C. Naddeo, A. Mariconda, A. Sorrentino, V. Vittoria, G. Iannuzzo, S. Russo, Journal of Polymer Science Part B: Polymer Physics, 48 (2010) 2413.
[3] E. N. Brown, N. R. Sottos and S. R. White, Experimental Mechanics, 42 (2002) 372.
[4] Mostovoy, S., Croseley, P. B. & Ripling, J. Mater. 2, 661–681 (1967).

Relationships between structures and physical properties of PVDF/MWNT composite

Soon Man Hong, *Jong Min Koo*

Polymer Hybrids Research Center, Korea Institute of Science and Technology
39-1 Hawolgok Seongbuk, Seoul 136-791, Korea

smhong@kist.re.kr

In recent years, carbon nanotubes (CNTs)-reinforced polymer composites are attracting much attention due to their excellent electrical conductivity. The incorporation of CNTs with very high aspect ratio into the polymer matrix is expected to produce unique physical properties in comparison with those of composites with three-dimensional structured nanoparticle. Poly(vinylidene fluoride) (PVDF) has been extensively studied because of its potential applications as piezoelectric and pyroelectric materials.

WAXD was used to observe the effect of MWNT content on the microstructure of thin PVDF composite films. Figure 1 describes the WAXD patterns for these composite films. Within a given range of scattering angles, three characteristic diffraction peaks appear at 2θ = 17.7, 18.4, and 19.9°, which correspond to (100), (020), and (110) reflections, respectively. This is assigned to the α–phase crystal which has a non-polar trans-gauche-trans-gauche (TGTG) conformation. PVDF composites exhibit decreased peaks for α–phase crystal from 0.5 wt% content. In addition to the features associated with α–phase crystal, the introduction of MWNT produces a shoulder at a 2θ value of 20.7° and it is clearer with increasing the MWNT content. This is attributed to the formation of β–phase crystal, the most polar among other crystals. This exhibits piezoelectric and pyroelectric properties of PVDF matrix.[1] We investigated the effect of MWNT content on the permittivity, electrical conductivity and thermal conductivity of PVDF. As shown in Figure 2, The permittivity of the PVDF composite was proportionally dependent on the content of MWNTs. Permittivity is improved with increasing the content of MWNT. However, permittivity is decreased with increasing the frequency in the range from 10^{-1} to 10^{4} KHz. Ionic conduction phenomena are slightly observed above 5wt% of MWNT. These results implied obviously that the PVDF filled with MWNTs could be prospective EMI shield material since we can enhance the permittivity and conductivity by controlling the content of MWNT. Figure 3 shows the variation of the electrical conductivity of PVDF composites with the MWNT content (conductivity of MWNT : 75 S/cm, conductivity of PVDF : 10^{-14} S/cm). The electrical conductivity was increased from 10^{-14} to 10^{0} S/cm with increasing the content of MWNT from 0 to 5wt%. However, when the content of MWNTs went over 5wt%, the electrical conductivity was almost independent of the MWNTs content. This indicates that there is conductivity saturation from a critical content because of formation of an infinite cluster.[2] Similar tendency was also observed in thermal conductivity above 3wt% of MWNT, as shown in Figure 4. In addition, the ferroelectric properties of PVDF composites will be discussed in this paper.

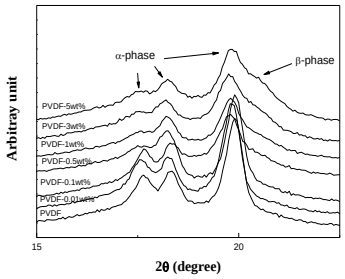

Figure 1.WAXD patterns of thin PVDF and PVDF/MWNT composite films.

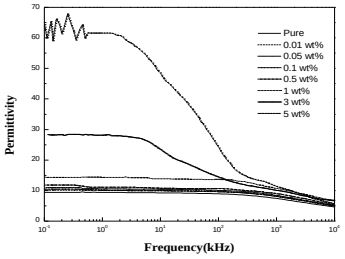

Figure 2. Variation of the permittivity of thin PVDF and

PVDF/MWNT composite films with MWNT content.

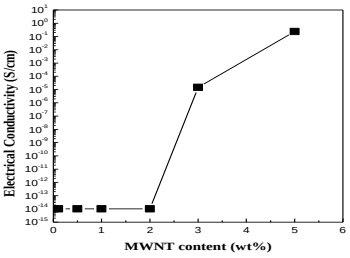

Figure 3. Variation of the electrical conductivity of thin PVDF and PVDF/MWNT composite films

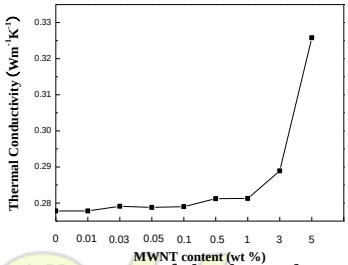

Figure 4. Variation of the thermal conductivity of thin PVDF and PVDF/MWNT composite films with MWNT contents

Thermoplastic Composites Reinforced with Keratin Fibers

F. Giunco[1a], L. Conzatti[1a], P. Stagnaro[1a], A. Aluigi[1b], E. Marsano[2], M. Castellano[2], C. Marano[3]

[1a] CNR-ISMAC, UOS Genova, via de Marini 6, 16149, Genova, Italy
[1b] CNR-ISMAC, UOS Biella, corso G. Pella 16, 13900, Biella, Italy
[2] DCCI, Università di Genova, via Dodecaneso 31, 16146, Genova, Italy
[3] Dip. CMIC, Politecnico di Milano, piazza Leonardo da Vinci 32, 20133, Milano, Italy

giunco@ge.ismac.cnr.it

Introduction

In recent years, there has been a growing interest in preparing polymer composites containing renewable organic reinforcements, such as lignocellulosic or protein fibers. Natural fibers provide several advantages since they are renewable and biodegradable, lighter than glass fibers while presenting reasonable strength and elastic modulus.[1-2]

Among these, keratin fibers, which are the major component of hair, wool and feathers, are abundantly present in wastes from textile industry, stock-farming and butchery. However, their compatibility with hydrophobic polymers like polyolefins is low. In fact, wool fibers have a hydrophilic character due to the presence of about 70 % of hydrophilic amino acids in the amino acidic sequence of keratin.[3] The treatment of the fiber surface with coupling agents, such as alkoxysilanes, or the use of maleated polyolefins as compatibilizers can improve the interface between fibers and matrix. Otherwise, better compatibility can be obtained with biodegradable polymer matrices with high hydrophilic character.

In this work, composite materials based on wool fibers, raw or chemically modified, and thermoplastic matrices, either polyolefins or biodegradable polyesters, were prepared and thoroughly characterized in terms of morphology, thermal properties and mechanical performances.

Materials and Methods

Composites based on polypropylene (PP) or biodegradable polyesters containing different amounts (up to 60 wt%) of wool fibers were prepared. In order to enhance the compatibility between fibers and matrix, maleated polypropylene (PP-*g*-MA) or wool fibers modified with 3-(trimethoxysilyl)propyl methacrylate were used. Composite materials were obtained mixing thermoplastic matrices with wool fibers using an internal batch mixer. In order to limit wool degradation, that occurs at around 200 °C, the mixing conditions, such as temperature, rotor speed and mixing time, were optimized.

Fiber surface modification was performed by hydrolyzing the silane in methanol - water (90/10 v/v) at 25 °C and adjusting the pH at 3.5 with acetic acid. The fibers were bathed in this solution, dried first at 60 °C for 24 h and then kept up at 120 °C for 2 h to complete the reaction. In order to remove unreacted silane, the treated fibers were finally extracted with acetone for 2 h.

Results and Conclusions

The FTIR spectrum of treated wool fibers indicates the presence of the C=O band at 1720 cm^{-1} relative to the chemically linked silane moieties. Chemical anchoring of the alkoxysilane on the fiber surface was confirmed and the amount of the grafted silane calculated by using thermogravimetric analysis.

Composite materials with up to 60 wt% of wool fibers were prepared. A thorough characterization of the samples was conducted by SEM, tensile tests, dynamic-mechanical, thermogravimetric and calorimetric analyses in order to understand the effects of fiber loading and compatibilizing agents on the final properties of the composite materials.

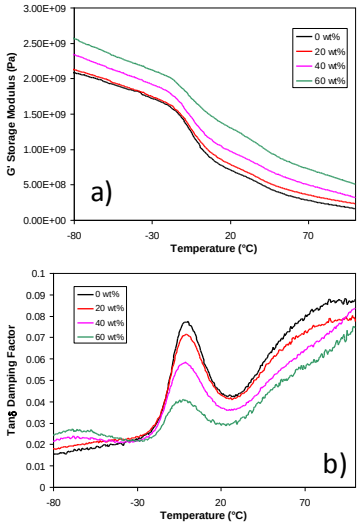

Fig. 1. Temperature dependence of G' (a) and tanδ (b) for compatibilized PP/wool fibers composites.

The adhesion between wool fibers and polymer, investigated by SEM, depends on the matrix, the presence of compatibilizer and the surface modification of the fibers. In general, the modulus of the composites (Fig. 1) increases with fiber loading, while the tensile strength of the composites decreases with increasing the fiber content. In particular, for the PP-based composites, the tensile strength was less reduced using maleated PP.

Research supported by CARIPLO Bank Foundation Project KEBAB 2009-2011

References

[1] Belgacem, M. N.; Gandini, A.; Monomers, Polymers and Composites from Renewable Resources, **2008**.
[2] Barone, J. R.; Schmidt, W. F.; Liebner, C. F. E.; *Compos. Sci. Technol.*, **2005**, *65*, 683-692.
[3] Tonin, C.; Zoccola, M; Aluigi, A.; Varesano, A.; Montarsolo, A.; Vineis, C.; Zimbardi, F.; *Biomacromolecules*, **2006**, *7*, 3499-3504.

Interfacial interactions in Flax fibre/PLA biocomposite: from model surfaces to real fibres

Eric Balnois, Gijo Raj, Christophe Baley, Yves Grohens

The overall mechanical properties of natural fibre reinforced biocomposites are largely governed by the intrinsic strength of reinforcement fibres as well as by the level of adhesion between the fibres and the matrix polymer. In order to gain a better understanding on the nature of the complex interactions between the fibre and the PLA matrix, Colloidal force microscopy (CFM) was adapted to this specific system to probe direct interaction forces between model surfaces and the PLA matrix. We develop the CFM set up to build a *layer model* that systematically allows to probe interactions between the main polysaccharides within the flax fibre, cellulose, hemicellulose and pectin and the PLA matrix to identity the weakest interaction system in a biocomposite. The results highlight important interactions of PLA with the hydrophilic pectin, even at low humidity rate, thus underlying the presence of several adhesion mechanisms, such as the presence of hydrogen bonds, capillary forces or interdiffusion processes. In parallel, adhesion force mapping of the flax fibre's surface by AFM force-volume technique revealed complementary results and highlight an important adhesion of the AFM probe with pectin materials on raw flax fibre.

Valorisation of Maghnite-H$^+$ as a catalyst for the synthesis of various biodegradable polyesters and polyacetals

Souad Bennabi[1,2], Nabahat Sahli[1], Mohamed Belbachir[1], Claire-Hélène Brachais[2], Jean-Pierre Couvercelle[2]

[1]LCP, Université d'Oran. BP 1524. El-Menouar, 31000 Oran, Algérie
[2]ICMUB - UMR CNRS 5260, 9 avenue Alain Savary, BP 47870, 21078 Dijon Cedex, France

e-mail: souad_bennabi02@yahoo.fr

In our laboratory, we were interested in the synthesis of biodegradable polymers by cationic way, by using an ecological catalyst : Maghnite-H$^+$. Maghnite-H$^+$ is a nontoxic catalyst issued from the proton exchange of Algerian Montmorillonite clay. Our results show that Maghnite-H$^+$ is active for the synthesis of polyesters upon heating and polyacetals at room temperature.

Introduction :

Biodegradable polymers have attracted rising attention because of their numerous applications in the medical materials (sutures, pins, surgical implants) or for pharmaceutical uses (matrix with controlled release of active ingredient). Many other uses are planned in order to replace polymers with high industrial tonnages (polyethylene, polyvinyl chloride) and limit their significant harmful effects on ecology. Maghnite-H$^+$ is a new catalyst based on Montmorillonite which was developed at the Chemistry Laboratory of the Polymers (LCP) and showed remarkable catalytic capacities in the reactions of polymerization of several vinyl and heterocyclic monomers[1-4]. The aim of this work is first, to study the structure of the H$^+$ activated Maghnite and then to compare the activity of this natural initiator towards various monomers yielding to biodegradable polymers.

Materials and Methods :

Maghnite, Algerian Montmorillonite clay, is provided by BENTAL (Algerian Society of Bentonite). The preparation of the Magnite-H$^+$ was carried out by using a method similar to that described by Belbachir and coworkers[1]. Indeed, the raw-Maghnite (20 g) was crushed for 20 min using a Prolabo ceramic balls grinder. It was then dried by baking at 105°C for 2 h. The Maghnite was then weighed and placed in an erlenmeyer flask together with 500 mL of distilled water. The Maghnite/water mixture was stirred using a magnetic stirrer and combined with 0.25M sulfuric acid, until saturation was achieved over 2 days at room temperature. The mineral was washed with water until it became sulfate free, and then dried at 150°C. Monomers were purchased from Aldrich, except ethyl glyoxylate (aldehyde monomer) kindly supplied by Clariant.

Results and discussion :

Maghnite-H$^+$ was characterized by XRD and IR. The results showed that the acid treatment of Maghnite involves the substitution of the intercalated cations by H$^+$. This phenomenon results in the increase in interlayer distance of 12 A° corresponding to a single layer water intercalated in Maghnite untreated, towards 15 A°, distance attributed to two layers water intercalated in Maghnite-H$^+$ [5].The Elemental Analysis (EA) of Maghnite-H$^+$ also shows decreased levels of impurities such as calcite, iron oxide, but enrichment in silica.

The following table summarizes the polymerization ability of Maghnite-H$^+$ clay towards e-caprolactone[a] [6], 1,3-dioxolane[c][2] ,D,L-Lactid[b] and ethyl glyoxylate[d]:

monomer	Conversion of monomer	Mn (g/mol)	Mw/Mn
e-Caprolactone	97.86%	3600	2,12
1,3-Dioxolane	85.8%	5 922	2.16
D,L-Lactide	94%	1890	1.70
Ethylglyoxylate	76%	17 016	1,17

[a]Maghnite-H$^+$/e-Caprolactone, weight ratio = 10%. (Reaction temperature 80°C and time 18h)
[b]Maghnite-H$^+$/D,L-Lactid, weight ratio = 5%. (Reaction temperature 120°C and time 20h)
[c]Maghnite-H$^+$/1,3-Dioxolane, weight ratio = 5%. (Reaction temperature 25°C)
[d]Maghnite-H$^+$/Ethyl glyoxylate, weight ratio = 5%. (Reaction temperature 25°C and time 18h)

Conclusion :

Maghnite-H$^+$ is able to convert in high yields various monomers leading to biodegradable materials. Molar masses arise between 3600g/mol and 17000g/mol. Moreover, this initiator seems to be very active even at room temperature for the synthesis of polyacetals. From these results it is clear that proton exchanged Montmorillonite clay, is an effective initiator for cationic polymerizations of cyclic esters, ether and aldehyde monomers .

References :

[1] M.Belbachir, A.Bensaoula ; US Patent.; 7, 094, 823, (2006).

[2] Fatiha. Reguieg, Nabahat. Sahli,Mohamed. Belbachir, P J. Lutz, One-Step Synthesis of Bis-Macromonomers of Poly(1,3-dioxolane) Catalyzed by Maghnite-H+,Journal of Applied Polymer Science, Vol. 99, pp3147–3152 (2006)

[3] A.Belmokhtar, N. Sahli, A. Yahiaoui,, M. Belbachir, Polycondensation of pyrrole and benzaldehyde catalyzed by Maghnite–H+, eXPRESS Polymer Letters Vol.1, pp7 443–449(2007)

[4] Kadidja. Beloufa, Nabahat. Sahli, Mohamed.Belbachir, Synthesis of Copolymer from 1,3,5-Trioxane and 1,3-Dioxolane Catalyzed by Maghnite-H$^+$, Journal ofAppliedPolymer Science,Vol. 115, pp2820–2827 (2010)

[5] Breen C.;Madejovà J.; Komadel P., High-pH alteration of argillaceous rocks: An experimental and modeling study. J.Mater.Chem, 5(3), 496-474, (1995).

[6] Amine Harrane, Rachid Meghabar, Mohamed Belbachir, Kinetics of the ring opening polymerization of–caprolactone catalysed by a proton exchanged montmorillonite clay, Reactive & Functional Polymers 66, pp 1696–1702(2006).

Thermal Decomposition of PVC Plastisol Foams. Influence of the concentration of plasticizer

A. Marcilla, A. Zoller and M.I. Beltrán

Chemical Engineering Department. University of Alicante (Spain)
PO Box 99 Alicante

antonio.marcilla@ua.es

Thermal decomposition of flexible PVC foams prepared with mixtures of two commercial plasticizers has been studied. Five PVC plastisols were prepared by mixing 100 phr (parts per hundred resin) of the ETINOX 400 from AISCONDEL (a poly vinyl chloride-vinyl acetate copolymer), 100 phr of a mixture of DEP (diethyl phthalate) and DIDP (di-isodecyl phthalate) of DEP concentration of 0, 25, 50 75 and 100%, respectively. Each formulation also included 2 phr of Reagens CL4 commercial Zn/Ca-stearate stabilizer, 6 phr of Lankroflex 2307 epoxidized soybean oil as co-stabilizer, and 2 phr of zinc oxide. After mixing, the pastes were subjected to a degassing process for 15 min with a maximum vacuum of 1 mbar for air removal. These plastisols were cured in an open mould at 180ºC during 10 min.

Approximately 6 mg of each sample, were subjected to TGA in a nitrogen atmosphere at heating rates of 5 K/min from room temperature to 873 K in a Termobalance METTLER TOLEDO, model TGA/SDTA 851e/SF/1100. A high purity nitrogen gas was fed at constant flow rate of 50 mL/min as an inert purge gas, thus avoiding unwanted oxidation of the sample. The continuous on-line records of weight loss and temperature were obtained to plot the thermogravimetric (TGA) curve and the derivative thermogravimetric analysis (DTG) curves.

Figure 1 shows the DTG curves obtained for the five plastisols studied. The DTG of the resin E400 has been included in both figures for comparison.

Figure 1. DTG of the plastisols prepared with the five mixtures of plasticisers studied and the resin E400.

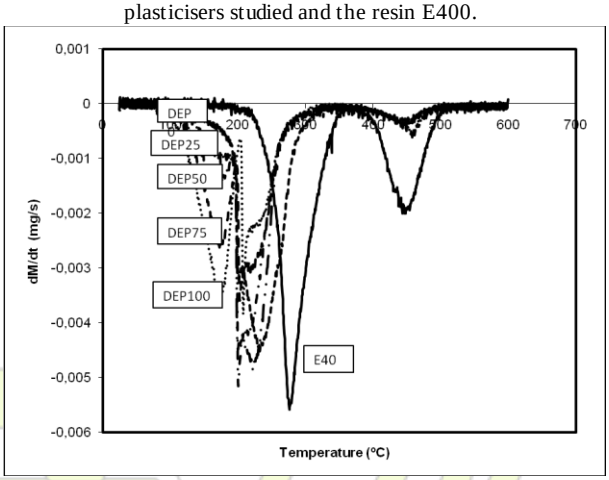

The thermograms obtained show the presence of four weight loss steps. The first one corresponds to the evolution of the DEP, the second one correspond to a sharp peak that may be ascribed to the decomposition of the stabilizer and co-stabilizer used, the third peak corresponds to the overlapping of the evolution of the DIDP plasticizer and the first decomposition step of the resin, including the dehydrochorination[1,2,3,4] and the loss of acetic acid from the vinyl acetate dominies of the resin. The third one corresponds to the final carbonization of the residue formed in the first step of the resin decomposition.

The area of the first peak is, as expected correlated with the concentration of DEP but its quantification reveals that this plasticisers has been partly volatilized during the curing of the paste, consequently the foams obtained have plasticizer concentration lower than the 100 phr programmed. Figure 2 shows the phr of plasticizer remaining in the foam obtained considering that the plastisol with 100% has lost no plasticizer.

Figure 2. Plasticizer remaining as a function of the concentration of DEP in the plasticizer mixture.

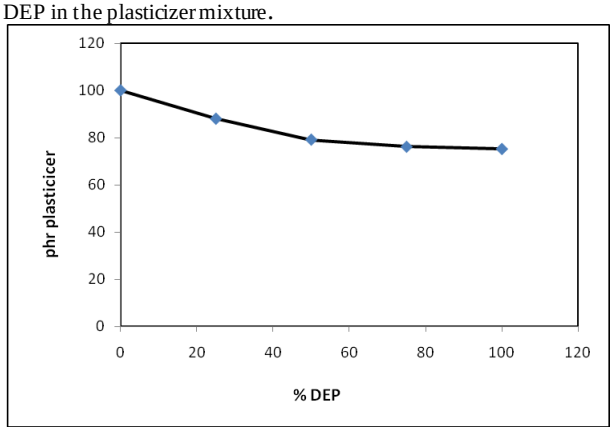

The peak corresponding to the first decomposition step of the resin shifts to lower temperatures as the amount of DEP in the plasticizeer increases, showing a type of destabilizing effect of the more compatible palsticizer.

References:

1. Marcilla, A. and Beltrán, M.I., Polymer Degradation and Stability 60 (1998) 1–10.
2. Jiménez A. et al., Polymer Degradation and Stability, 73 (2001) 447-453.
3. Beltrán, M.I. and. Marcilla, A, Polymer Degradation and Stability 55 (1997) 73–87.
4. Beltrán, M.I. and Marcilla, A, European Polymer Journal, 33, 8 (1997) 1271-1280.

Waste Recycling And Public Awareness "The Case Of Plastic Waste"

Ali Rıza Abay[1], *Mustafa Öksüz*[2]

[1]Social Work Department, Yalova University Yalova 77100, Turkey
[2]Polymer Engineering Department, Yalova University Yalova 77100, Turkey

aabay@yalova.edu.tr

Plastics became indispensable items within our daily lives as well as other technological advances. On the other hand, these tecnological advances pose threats in an increasing manner even if they serve us via vast number of applications. One of these threats comes from chemical wastes that are disposed to environment in an uncontrolled fashion. Environmental pollution has become a major concern for all developed nations as a consequence of continious advancement in technology which is closely related with the increasing demand in industrial production. Plastic wastes are the most persistent chemical wastes in nature. Due to the extremely slow decomposition rates, plastic wastes generate a significant environmental problem. Thus, in Turkey as well as advanced societies, plastic wastes play an important role within total environmental pollution. Lack of environmental concerns such as sustainability combined with the misusage and uncontrolled use of technology increases the rate of pollution day by day. Plastic and other waste problem peaked in recent years and public awareness has formed due to the tremendous efforts of governmental, academic and media institutions. Thus recycling of plastic wastes has an extreme importance in preventing the chemical wastes as well as economical benefits. This report will primarily emphasize on the nationwide impacts of plastic wastes and discuss the alternative ways to achieve recycling and improving the public awareness

Keywords: plastics, waste recycling, public awareness

Thermal Decomposition of PVC Plastisol Foams. Influence of the type of plasticizer

A. Marcilla, A. Zoller and M.I. Beltrán

Chemical Engineering Department. University of Alicante (Spain)
PO Box 99 Alicante

antonio.marcilla@ua.es

Thermal decomposition of flexible PVC foams prepared with commercial plasticizers has been studied. Twenty PVC plastisols were prepared by mixing 100 phr (parts per hundred resin) of the ETINOX 400 from AISCONDEL (a poly vinyl chloride-vinyl acetate copolymer), 100 phr of one of the twenty commercial plasticizers studied(see table 1), 2 phr of Reagens CL4 commercial Zn/Ca-stearate stabilizer, 6 phr of Lankroflex 2307 epoxidized soybean oil as co-stabilizer, and 2 phr of zinc oxide. After mixing, the pastes were subjected to a degassing process for 15 min with a maximum vacuum of 1 mbar for air removal. These plastisols were cured in an open mould at 180ºC during 10 min.

Table 1. Commercial plasticizers studied

acronym	Mw (g/mol)	Density ($g/cm^{3)}$	Provider
HNUP	418	0.971	BASF
NUP	450	0.958	BASF
DUP	475	0.953	BASF
DEP	222	1.118	BASF
DINP	421	0.973	BASF
DIDP	447	0.966	PHANCORP
DOP	391	0.983	BASF
DIBP	278	1.039	BASF
DIHP	362	0.991	EXXON MOBIL
DHA	314	0.935	BASF
DNA	398	0.922	BASF
PM632	7000	1.145	BASF
PM 652	3300	1.050	BASF
ATBC	402	1.050	MORFLEX
ATHC	486	1.050	MORFLEX
DINCH	425	0.949	BASF
EASTMAN	391	0.984	EASTMAN
H 600	604	1.000	HÉRCULES
H 707	750	1.000	HÉRCULES
MESAMOLL	368	1.055	BAYER

Approximately 6 mg of each sample, were subjected to TGA in a nitrogen atmosphere at heating rates of 5 K/min from room temperature to 873 K in a Termobalance METTLER TOLEDO, model TGA/SDTA 851e/SF/1100. A high purity nitrogen gas was fed at constant flow rate of 50 mL/min as an inert purge gas, thus avoiding unwanted oxidation of the sample. The continuous on-line records of weight loss and temperature were obtained to plot the thermogravimetric (TGA) curve and the derivative thermogravimetric analysis (DTG) curves.

Figure 1 and 2 show the DTG curves obtained for the linear and branched phthalates studied. The DTG of the resin E400 has been included in both figures for comparison.

Figure 1. DTG of the plastisols prepared with the 4 linear phthalates studied and the resin E400.

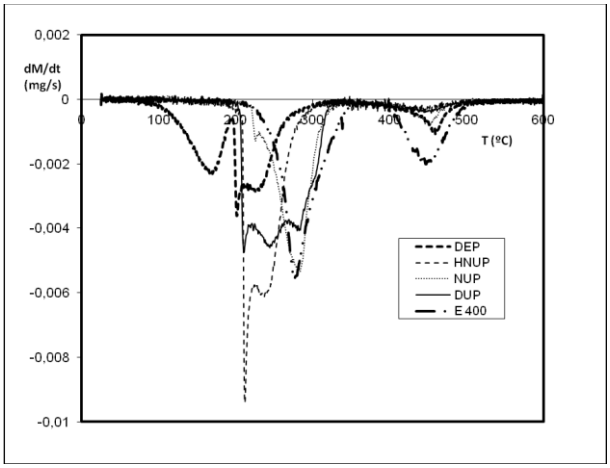

Figure 2. DTG of the plastisols prepared with the 5 branched phthalates studied and the resin E400.

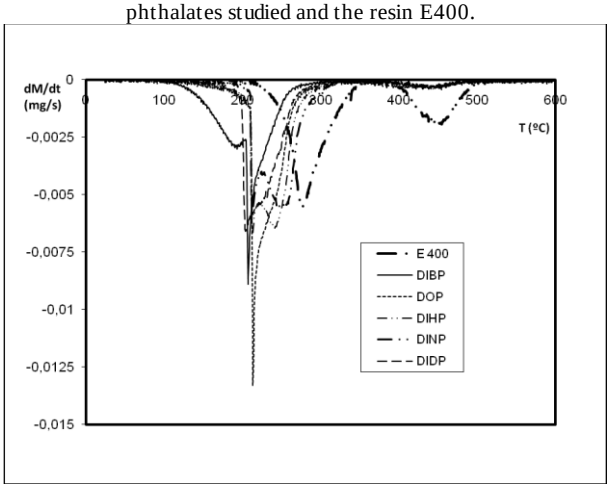

The thermograms obtained clearly show the presence of up to four weight loss steps. The first one corresponds to the evolution of the plasticizer in clear correlation with its corresponding boiling point. The rest are related with the dehydrochlorination and loss of acetic acid of the copolymer resin and the products of decomposition of the stabilizer and co-stabilizer, and the last one, at temperatures higher than 400 °C corresponding to the carbonization of the residue of this first step [1,2]. It can be observed that the lower the molecular weight of the plasticizer the lower the temperature of the first decomposition process of the resin.

References:

1. Jiménez, A. et al, Polymer Degradation and Stability, 73 (2001) 447-453.
2. Marcilla, A. and Beltrán, M.I., Polymer Degradation and Stability 60 (1998) 1–10.

Monitoring of Recycled AAO Templates. An Exhaustive Characterization after Polymer Extraction.

Iwona Blaszczyk-Lezak, Jon Maiz, Javier Sacristan, Carmen Mijangos*
Instituto de Ciencia y Tecnología de Polimeros, CSIC
*iblezak@ictp.csic.es

Introduction

Over the last decade one-dimensional (1D) nanostructures have attracted much attention due to their useful properties and many potential applications. One of the ways to prepare 1D polymer nanostructure is by use the porous anodic aluminum oxide (AAO) template and subsequent infiltration of the polymer into the nanocavities of the AAO templates [1-5]. Templates of this type are prepared electrochemically from aluminum metal. AAO templates are characterized by uniform tailored pores with hexagonal symmetry and long-range ordered architecture.

In order to exp and the use of nanostructured polymers it is mandatory to improve and scale-up the fabrication process from laboratory to an industrial level. But because of the time needed for preparation and the price of aluminum, it is first necessary to try to recover used AAO templates. Our group has chosen controlled high temperature treatment of infiltrated AAO membranes in an oven to eliminate the polymer from the template pores by thermal decomposition of the compound.

Materials and Methods

In order to investigate the possibility of thermal elimination of infiltrated PEO from AAO templates, several analytical techniques and procedures have been employed such as: thermogravimetric analysis (TGA), Raman microspectroscopy, wide angle X-ray diffractometry (WAXD), scanning electron microscopy (SEM). AAO templates with pore sizes of 35 nm and pore thickness of 110 mm have been used in this study. The infiltration of polyethylene oxide (PEO, M_W = 100 000 g/mol) was carried out by melt precursor film wetting method.

Results and discussion

Thermal properties of PEO nano rods into the AAO templates were investigated by means of TGA to select the temperature and time range where the thermal decomposition of infiltrated PEO takes place. From these results it is concluded that there is only small window that allows the total PEO elimination from the AAO nanopores in a reasonable time. The preferred conditions are T = 450^{O}C and 3 h long treatment.

In order to identify if some polymer still remains inside AAO template pores, the presence of characteristically PEO bonds has been investigated by means of Raman spectroscopy (Fig.1). Looking at the spectra corresponding to the AAO template infiltrated with PEO and subjected to a 3 hours of thermal treatment at 450ºC (spectra *c* and *d*), it seems clear that no one of the characteristic PEO Raman bands can be observed in this spectrum. It means that PEO have been successfully eliminated from the template.

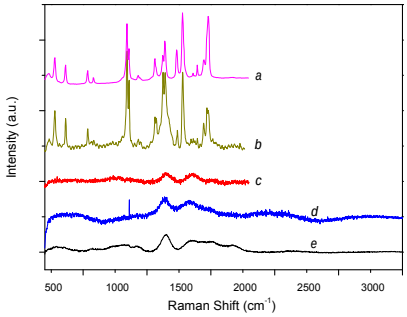

Figure 1. Raman spectra of: *a)* PEO in bulk, *b)* AAO with infiltrated PEO, *c)* recuperated AAO at T = 450 ^{O}C at 10 mm inside the pores, *d)* recuperated AAO at T = 450^{O}C and *e)* AAO template as reference.

The spectra WAXD corresponding to the thermally treated AAO samples does not show any character peak of the PEO, only amorphous halo of the alumina is observed. This is in agreement with results obtained by Raman spectroscopy. What is more, from the results of SEM, the hexagonally close-packed structure of AAO templates has not been changed during the high temperature process and even the shape of pores is maintained.

Conclusions

Results from this work highlight the importance of selecting appropriate conditions; temperature and time to successfully eliminate PEO from AAO template nanopores. The preferred conditions are T = 450 ^{O}C and 3 h long treatment. This methodology seems to be a promising route to re-use AAO templates especially for infiltration of new polymers under different experimental conditions.

References

[1] C.R. Martin, Science 266 (1994) 1961
[2] M. Steinhart, J.H. Wendorff, A. Greiner, R.B. Wherspohn, K. Nielsch, J. Schilling, J. Choi, U. Gösele, Science 296 (2002) 1997
[3] M. Zhang, P. Dobriyal, J.-T. Chen, T.P. Russell, J. Olmo, A. Merry, Nano Lett 6 (2006) 1075
[4] J. Martín, C. Mijangos, Langmuir 25(2) (2009) 1181
[5] J. Martin, M. Krutyeva, M. Monkenbusch, A. Arbe, J. Allgaier, A. Radulescu, P. Falus, J. Maiz, C. Mijangos, J. Colmenero, D. Richter, Phys Rev Letters 104 (2010) 197801

ABSTRACTS

POSTER PRESENTATIONS

Topic 4: Polymers for Advanced Applications Including Energy, Transport, Packaging and Environmentally Friendly Activities

Fluoropolymer dispersions: new environment-friendly products and technology

S.Musio, V. Kapeliouchko, T.Poggio*

Solvay Solexis S.p.A., p.le Donegani 5/6, 15047 Spinetta Marengo (AL), Italy

stefana.musio@solvay.com

Polytetrafluoroethylene (PTFE) has seen increasing demand in sophisticated industrial applications since 1938, due to its thermal and chemical inertness, release properties, and outstanding dielectric characteristics[1]. Aqueous dispersions of PTFE are particularly suitable for cookware antistick coatings and endless conveyor belts for the food industry: such dispersions are commonly obtained via emulsion polymerization in the presence of a non-telogenic perfluorinated anionic emulsifier, leading to 150-300 nm particles. Alternatively, a proprietary Solvay Solexis technology[2,3,4] using microemulsion polymerization allows the synthesis of 10-60nm particles, which are advantageously exploited in bimodal dispersions. This results in a more compact and less porous PTFE film structure leading to better application performances in terms of coating appearance, mechanical strength, and durability.

Recent developments in PTFE dispersions combine knowledge on new fluorosurfactants developments with yet available processes to reduce the content of fluorosurfactant in the dispersions[5] and with appropriately selected phenol-free non-ionic surfactant to eventually obtain environmentally friendlier PTFE dispersions that match or even improve the processing performance compared to standard products.

The formulation of fluoropolymer dispersions, purified from anionic fluorinated surfactants used in polymerization, requires re-design of specific ingredients in order to maintain the performance profile of the product in the whole range of applications, e.g. coating, impregnation, etc.

Starting from the colloidal properties of the initial systems, this presentation discusses in particular stability to shear and sedimentation as well as rheological behavior of PTFE dispersions.

In particular the environmentally friendly fluoropolymer dispersions obtained by substituting APE surfactants with "Green" Ethoxylated Alcohols and by extracting perfluorinated surfactants are discussed, which impart the following features:

- More newtonian rheological behavior resulting into better properties under a wider range of applicative conditions of temperature and shearing.
- Lower surface tension, both static and dynamic values, which imparts outstanding wetting ability especially under critical high-speed impregnation conditions.
- Excellent stability to shear and sedimentation due to better interaction of the surfactant with the polymer surface: the adsorption behavior is very similar to that of APE surfactants

Cleaner thermal degradation of the surfactant system resulting in higher quality of the final objects.

Reference:

1. Kirk-Othmer, Encyclopedia of Chemical Technology- 3rd Ed., John Wiley & Sons, New York, 1980, 11, p.1.
2. Visca M and E Giannetti, US Patent 4,864,006, 1987
3. Visca M and A Chittofrati, US Patent 4,990,283, 1988
4. Kapeliouchko V, E Marchese and P Colaianna, US Patent 6,297,334, 2001
5. Kuhls J and E Weiss, US Patent 4,369,266, 1983.

Properties enhanced PU coating using (Desmodure Z 4470) as isocyanate and the different Desmophens as polyalcohols

A. Shokuhi Rad

Chemical engineering group, Department of Engineering, Islamic Azad University, Ghaemshahr Branch, Ghaemshahr, Iran

Ashokuhirad@yahoo.com

Polyurethanes (PU) are engineering polymers since they show unique physical and mechanical properties. An isocyanate agent (Desmodure Z 4470) and three polyalchol agents (Desmophen 670BA, 1800 and A665, respectively) were used for formulation of the polyurethane coating with considering to self-healing property. The effect of the chain extender agent (ethylene glycol) and the optimum ratio of the isocyanate to polyalchol agent were studied. The attained results show that a hard polymer coating is obtained using Desmophen A665 polyalcohol in the absence of any chain extender, however a corrosion resistant and transparent coating is obtained using Desmophen 1800 and a ratio of NCO/OH=2 for pre-polymer formation stage and NCO/OH=0.85 in polymerization stage by adding proper amount of ethylene glycol. This obtained PU shows the best self-healing properties.

References:

[1] Bayer O. 1947, Angew Chem; 71:26

[2] Sonntag M. 2009, Surface Coatings International Part B: Coatings Transactions 82(9), 456-459

New epoxy thermosets obtained from DGEBA and hyperbranched polyesters having reactive/ unreactive chain ends using adipic dihydrazide as latent curing agent

Adrian Tomuta[1], *Xavier Ramis*[2], *Francesc Ferrando*[3], *Àngels Serra*[1]

[1] Departament de Química Analítica i Química Orgànica, Universitat Rovira i Virgili
[2] Lab. Termodinàmica, ETSEIB, Dept. Màquines i Motors Tèrmics, Universitat Politècnica de Catalunya
[3]Departament d'Enginyeria Mecànica, Universitat Rovira i Virgili

e-mail: adrianmarius.tomuta@urv.cat

Introduction

Epoxy resins are widely employed in technological applications, among them they are applied as electric insulating materials, adhesives or coatings. Epoxy resins can be considered as versatile materials because in addition of their structure and/or molecular weight they can be cured in different conditions depending on the curing agent selected. Epoxy resins can be cured by stoichiometric curing agents as for example aromatic or aliphatic amines, acid anhydrides, or isocyanates. Curing agents that show no activity under normal conditions but show activity by external stimulation, like temperature, can be called "latent curing agents". In this way, curing temperature can be conveniently selected by using the proper latent curing agent.

The versatility of epoxy thermosets can be broadened and some improvement in their characteristics can be accomplished by the use of hyperbranched polymers (HBPs) as modifiers. Generally, they have been used as tougheners[1] but some other characteristics such as the reduction in the shrinkage on curing and reworkability have been also improved.[2]

Depending on the hyperbranched structure and the reactivity of the end-groups, the HBP can be chemically incorporated to the network structure or lead to micro or nanophase separation. Also, the chemical nature of the final chains affects the kinetics of the curing and even the conversion at the gelation.

Materials

DGEBA epoxy resin (EPIKOTE™ 828, 187 g/eq, HEXION). 4,4-Bis(4-hydroxyphenyl)valeric acid, N,N'-dicyclohexyl carbodiimide, diethyl adipate, 10-undecenoil chloride, allyl bromide, hydrazine hydrate and m-chloroperbenzoic acid (Aldrich) were used as received. 4-(N,N-dimethylamino)pyridinium p-toluene sulfonate (DPTS) was prepared as described in the literature.[3]

Adipic dihydrazide was prepared by reaction of diethyl adipate with hydrazine hydrate in ethanol. This product was recrystallized in ethanol

Synthesis of the hyperbranched polymers

The hyperbranched polyester ($HBPE_{ol}$) was synthesized according to a previous procedure.[4] The structures of the modified HBPs are shown in the scheme.

$HBPE8_{vin}$ was synthesized by acylation reaction of $HBPE_{ol}$ with undecenoyl chloride in the presence of triethylamine as hydrochloric acid acceptor. This polymer was converted into $HBPE8_{epo}$ by epoxydation with m-chloroperbenzoic acid in CH_2Cl_2. $HBPE1_{vin}$ was obtained by modification of $HBPE_{ol}$ with allyl bromide in the presence of K_2CO_3. The allylated polymer was epoxydated to obtain $HBPE1_{epo}$. All these polymers were characterized by GPC and NMR measurements.

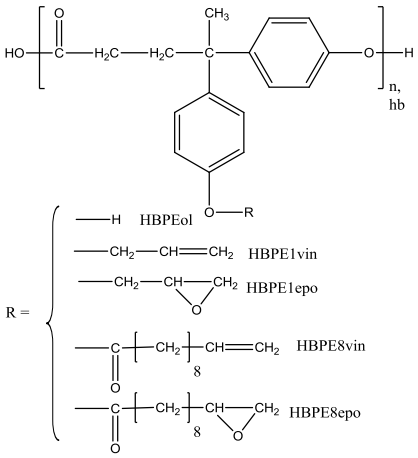

By differential scanning calorimetry the kinetics of the curing process was studied. The curing of neat DGEBA with adipic dihydrazide takes place by heating at 170 ºC in a latent manner. The addition of $HBPE_{ol}$ to the formulation accelerates the curing much more than when the other HBPs were added to the formulation and the latent character was not much affected.

The addition of $HBPE_{ol}$ to the formulation leads to an increase in the Tg of the thermosets without affecting the thermal stability, determined by TGA. However, the addition of a 10% wt. of the polyesters having vinyl groups as chain ends reduces the Tg of the final thermosets.

The materials obtained have better mechanical characteristics than the neat materials, which confirms the goodness of the modification proposed in this communication.

References

1. Varley RJ, Tian W. Polym Int 2004;53:69-77
2. Foix D, Erber M, Voit B, Lederer A, Ramis X, Mantecón A, Serra A. Polym Degrad Stab 2010;95:445-52
3. Moore JS, Stupp SI. Macromolecules 1990;23:65-70
4. Schallausky F, Erber M, Komber H, Lederer A. Macromol. Chem. Phys. 2008;209: 2331-8

Acknowledgments

To MICINN, FEDER and Generalitat de Catalunya (MAT2008-06284-C03-01, MAT2008-06284-C03-02, 2009-SGR-1512). A.T. to the Generalitat de Catalunya for his FPI grant.

Inhibition of the migration of low molecular weight moieties to rubber-polyurethane coating interface by incorporating filler

Rafael Torregrosa-Coque, José Miguel Martín-Martínez

Adhesion & Adhesives Laboratory. University of Alicante. 03080 Alicante (Spain)

jm.martin@ua.es

Introduction

One of the causes of poor adhesion of vulcanized rubbers to polyurethane adhesives is the existence of surface layers of antiadherent moieties, mainly antiozonants [1]. These weak-boundary layers are generally produced by migration of low molecular moieties (mainly paraffin wax) from the bulk to the rubber surface [2-4]. After coating application, the adhesion can be deteriorated by migration of the paraffin wax to the rubber-coating interface.
Fillers cause crosslinking of polymeric chains. Therefore, it could be feasible that the addition of fillers produces a change in the diffusion of low molecular weight moieties throughout the polymer, and therefore our hypothesis is that the addition of fillers in the polymeric coating can retard or even inhibit the migration of paraffin wax to rubber-polyurethane interface.

Materials and Methods

A vulcanized styrene-butadiene rubber was coated with unfilled and 2wt% nanosilica filled polyurethane solutions; their thicknesses were about 2 µm. The evolution of wax migration to the rubber-polyurethane interface was monitored by contact angle measurements and ATR-IR spectroscopy of the polyurethane coating with time after coating application.

Results and Discussion

Figure 1 shows the methylene groups of the wax bands in the ATR-IR spectra obtained with the two prisms, whereas the rubber bands (butadiene and styrene) appear only when the ZnSe prism is used. Therefore, the paraffin wax appears in a depth of about 2 µm from the external surface of the as-received rubber.

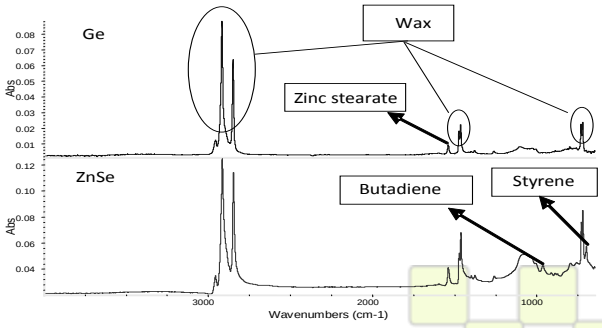

Figure 1. ATR-IR spectra of the as-received R2 rubber.

By increasing the time after PU coating application up to 14 days (Figures 2 and 3), the ATR-IR/Ge spectra show an increase in the intensity of the wax bands whereas the intensity of these bands does not change in the ATR-IR/ZnSe spectra. Therefore, the wax migrates mainly into the PU surface throughout the two PU coatings on the rubber.

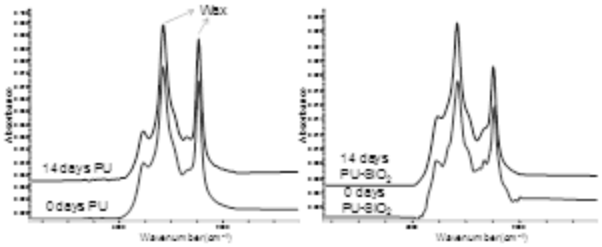

Figure 2. 3100-2700 cm^{-1} region of the ATR-IR spectra of the unfilled and nanosilica filled PU coatings on rubber with time. ZnSe prism.

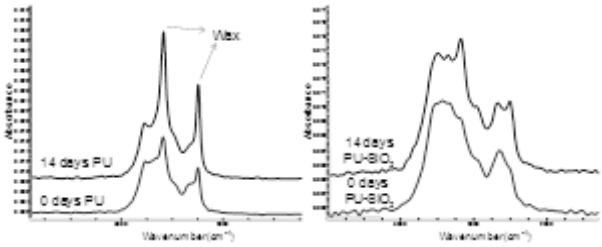

Figure 3. 3100-2700 cm^{-1} region of the ATR-IR spectra of the unfilled and nanosilica filled PU coatings on rubber with time. Ge prism.

Addition of nanosilica filler inhibits the extent of wax migration to the polyurethane coating. Because of the interactions by hydrogen bonds between the silanol groups on the nanosilica and the urethane groups in the polyurethane coatings, the degree of crosslinking increases avoiding the diffusion of the low molecular weight additive into the polyurethane coating.

Conclusions

A layer of about 2 µm of paraffin wax exists in the as-received rubber surface. By increasing the time after polyurethane coating application up to 14 days, an increase in the intensity of the paraffin wax bands was obtained, less markedly in the nanosilica filled coating.

References

1. Romero-Sánchez MD, Martín-Martínez JM. J Adhes 79 (2003) 1111-1133.S.H. Nah, A.G. Thomas, Rubber Chem Technol 54 (1981) 255-265.
2. P.J. Diamuro, H.L. Paris, M.A. Fath, Rubber Chem Technol 52 (1979) 973-984.
3. F. Cataldo, Polym Degrad Stabil 72 (2001) 287-296.

Epoxy Polymers and Composites for Advanced Applications

Roberto J. J. Williams

Institute of Materials Science and Technology (INTEMA), University of Mar del Plata and National Research Council (CONICET), Av. J. B. Justo 4302, 7600 Mar del Plata, Argentina

e-mail: williams@fi.mdp.edu.ar

Introduction: Due to their excellent properties epoxy polymers are extensively used in traditional applications such as adhesives, coatings and composites. In recent years there has been an increasing use of epoxies in the development of advanced functional materials.[1] Some examples will be given in this presentation.

Reversible Epoxy Networks: The reaction of diglycidylether of bisphenol A (DGEBA) with an *n*-alkylamine leads to a linear epoxy polymer. However, linear chains can be assembled by tail-to-tail associations between *n*-alkyl groups leading to a network with physical crosslinks. The strength of the physical bonds decreases with temperature and with the length of the *n*-alkyl group.[2] By increasing temperature the material reversibly transforms from a gel to a liquid, a fact that may used to develop self-healing epoxies.

Shape Memory Epoxies: When epoxies are heated above their glass transition temperature (T_g) they can be deformed to a temporary shape by applying a relatively small stress. By fixing the deformation and cooling below T_g, a glass is obtained that stores elastic energy in chain conformations removed from their equilibrium values. When the material is released from any constraint and is heated again above T_g, a rapid recovery of the initial shape is obtained as chains recuperate their equilibrium conformations. But if the heating step is performed keeping the initial deformation, the material develops a recovery stress. Actuators based on epoxies can make use of the shape recovery or the stress recovery. They can be designed for large tensile elongations (e.g., 75 % or higher) or large recovery stresses (e.g. 3 MPa or higher). However, meeting both requirements simultaneously is a difficult task because changes in the crosslink density affect both variables in opposite ways. An epoxy formulation based on the reaction of DGEBA with *n*-dodecylamine (DA) and *m*-xylylenediamine (MXDA) gives a network with both chemical and physical crosslinks that can be used for a shape memory material verifying both requirements.

Epoxy Networks Containing Silver Nanoparticles (NPs): Ag NPs can be introduced into epoxy coatings to obtain specific electrical or antimicrobial properties. Different methods can be employed to obtain a uniform dispersion of NPs. A DGEBA/DA gel was swollen with a 6mM solution of $AgNO_3$ in THF/H_2O (90:10). After rinsing with THF and drying in vacuum, the epoxy network was heated at 100 °C for 1 h, generating a uniform dispersion of Ag NPs with an average size close to 10 nm.[3] The reduction was performed by the secondary alcohols present in the epoxy backbone. The T_g increased from 20 °C (neat epoxy) to 28 °C (nanocomposite). A different strategy to obtain a uniform dispersion of Ag NPs in an epoxy matrix was to introduce reactive groups in the organic chains stabilizing the NPs. Silver NPs with an average size of 4nm and stabilized with an organic group containing secondary hydroxyls, were synthesized and dissolved in DGEBA. The epoxy was polymerized using a tertiary amine as initiator. Ag NPs were covalently bonded to the epoxy network through chain transfer reactions to the secondary hydroxyls of the organic ligands. The nanocomposites were strongly colored and showed a dependence of T_g on the concentration of NPs.[4]

Epoxy Networks Containing Single-Wall Carbon Nanotubes (SWCNT): Epoxy nanocomposites containing SWCNT exhibit significant improvements in mechanical, thermal or electrical properties. Surface functionalization of SWCNT enables to obtain an adequate dispersion of the nanotubes in the epoxy formulation. A problem that is present in some formulations is the different partition of the epoxy monomer and the hardener in the interphase, a process favored by the large specific area per unit volume. This leads to a heterogeneous network characterized by two relaxation peaks and a significant decrease of the glass transition temperature. This problem was avoided by a convenient functionalization of the SWCNT, producing a localized formation of bundles of nanotubes in the course of polymerization. The T_g of the nanocomposite was the same as the one of the neat epoxy.[5]

Epoxy Networks Containing POSS Crystalline Platelets: The dispersion of intercalated/exfoliated clays in polymers decreases their permeability due to geometrical effects. However, processing is difficult due to the initial high viscosity. An alternative is to produce the crystallization of an initially soluble precursor during polymerization. The feasibility of this idea was proved using a polyhedral oligomeric silsesquioxane (POSS) dissolved in the epoxy precursors.[6]

References

1. Pascault, J.P.; Williams, R.J.J.; Eds., Epoxy Polymers: New Materials and Innovations, Wiley-VCH, Weinheim, 2010.
2. Puig, J.; Zucchi, I.A.; Hoppe, C.E.; Pérez, C.J.; Galante, M.J.; Williams, R.J.J.; Rodríguez-Abreu, C. Macromolecules 2009, 42, 9344-9350.
3. Ledo-Suárez, A.; Puig, J.; Zucchi, I.A.; Hoppe, C.E.; Gómez, M.L.; Zysler, R.; Ramos, C.; Marchi M.C.; Bilmes S. A.; Lazzari, M.; López-Quintela, M.A.; Williams, R.J.J. J. Mater. Chem. 2010,20, 10135-10145.
4. dell'Erba, I.E.; Hoppe, C.E.; Williams, R.J.J. Langmuir 2010, 26, 2042-2049.
5. Auad, M.L.; Mosiewicki, M.A.; Uzunpinar, C.; Williams, R.J.J. Polym. Eng. Sci. 2010, 50, 183-190.
6. Di Luca, C.; Soulé, E.R.; Zucchi, I.A.; Hoppe, C.E.; Fasce, L.A.; Williams, R.J.J. Macromolecules 2010, 43, 9014-9021.

Development of Flexible Temperature Sensors - Realization and Characterization of Multifilaments based on Immiscible Polymers loaded with Carbon Nanotubes

A. Cayla[1,2], *C. Campagne*[1,2], *M. Rochery*[1,2], *E. Devaux*[1,2]

[1] Univ. Lille Nord de France, F-59000 Lille, France ; [2] ENSAIT, GEMTEX, F-59100 Roubaix, France.

aurelie.cayla@ensait.fr

Introduction

These works fall under the European research project Inteltex (FP6), which is created of the relationship between the use of nanotechnology and the need for textile innovation. One objective was to develop a flexible temperature sensor to be integrated in the Personal Protective Equipment (PPE) to prevent the pain threshold by firefighters. This sensitivity is ensured by the use of biphasic Conductive Polymers Composites (CPC) loaded with Carbon NanoTubes (CNT) in the form of multifilaments. These conductive fillers are introduced in the phase which is sensible to the temperature elevation (Polycaprolactone (PCL)) and protected by the second polymer whose melting temperature is higher (Polypropylene (PP)). For our application, an interpenetration of two phases (co-continuous morphology) and a selective localization of CNT in the PCL are privileged to obtain a good electrical conductivity at relatively low CNT contents [1]. But this one should be adapted to succeed to observe a Positive Temperature Coefficient (PTC) effect to detect the critical temperature. The main difficulty is to combine detection properties with mechanical properties to support the melt spinning process and the implementation of weaving textile).

Materials and methods

Poly(ε-caprolactone), namely CAPA 6400 from Solvay, is a biodegradable polymer with a relatively low melting temperature of about 58°C. Polypropylene (PP) was supplied by DOW under the reference H777-25R, which presents an appropriate spinning grade to lead to a good spinning ability of the blends with PCL. Multi-wall carbon nanotubes (MWNTs) were supplied by Nanocyl (Belgium) under the reference Nanocyl®-7000 and present a purity equal to 90%. The realization of multifilament composite is made in two main steps. The first one is to load the PCL with 4wt% of CNT using a Thermo-Haake co-rotating intermeshing twin-screw extruder with a screw diameter of 16 mm and a length to diameter ratio of 25. In a second step, the pellet issued from the first extrusion are blend with the matrix PP directly in the feed hopper of the melt spinning machine (driver SPINBOY I, Busschaert Engineering in Belgium). A spun multifilament contained 80 monofilaments (2 dies*40 holes) is obtained, and he is rolled up on two heated rolls with varying speeds (S1 and S2) to ensure a draw. The theoretical drawing of multifilament is given by the ratio DR = S2/S1. All characterizations: electrical, mechanical, and detection were made in this twisted multifilament (81tr/m).

Results and discussion

Electrical properties for temperature detections

In *Fig.*1, we can observe that the resistance decrease when we introduce the filled PCL. We can check by selective extraction that the morphology of the biphasic system became co-continuous with 50% of filled PCL. We see on Fig.1 that this content is necessary to obtain an interesting the conductivity became interesting for detection application.

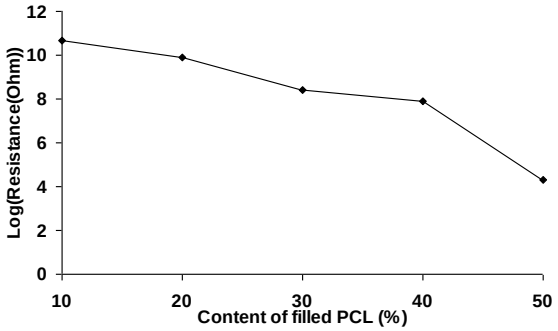

Fig. 1: Electrical resistance of PP/PCL+4%CNT (DR=1.06) measured on 1cm length of multifilament

In this study, to obtain good properties of detection a low DR was applied (S1= 80m/min, S2=90m/min and DR=1.12) to keep a satisfactory electrical conductivity. If the DR is too high the conductivity decreases due to depercolation of CNT and reduction of continuity of filled PCL.

Mechanical properties

Introduction of filled PCL decreases the mechanical properties of multifilament: Young modulus (*Fig.2*) and also stress at break decrease due to the low cohesion between PP and PCL but also by the presence of CNT leads defects due to agglomerates.

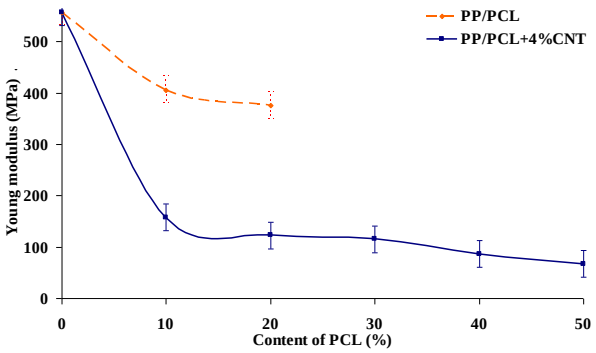

Fig. 2: Young modulus of PP/PCL with and without CNT measured on multifilaments (DR=1.06)

Conclusions

The presence of a PTC effect can be observed on the multifilament bit stretched with a content of 50% of filled PCL. Indeed, we observed a depercolation CNT due to volume expansion when the temperature reaches the melting temperature of PCL (58 ° C). However the low cohesion between the phases (PP and PCL) causes a sharp decrease of Young's modulus and stress at break. However these values are sufficient to support the steps of textile implementation.

References

[1] M. Sumita, K. Sakata, Y. Hayakawa, S. Asai, K. Miyasaka, M. Tanemura. Colloid Polym. Sci. 270 (1992) 134-139.

New Polytricyclnonenes and Polytricyclononadienes: from Monomer Synthesis to Polymer Gas Permeability

B.A. Bulgakov, M.V. Bermeshev, L.E. Starannikova, E.Sh. Finkelshtein

A.V.Topchiev Institute of Petrochemical Synthesis RAS

bbulgakov@gmail.com

Introduction. In our previous researches we have shown Me_3Si-substituted tricyclononenes to be active in ring-opening metathesis polymerization (ROMP) and addition polymerization. Resulting polymers demonstrated prospective gas-transport parameters comparable to known the highest-permeable polymers [1]. For example, permeability of addition poly(3,4-bis(trimethylsilyl)tricyclononene-7) is more than 2000 Barrers. So the structure of substituted tricyclononene appeared to be attractive basis for macromolecular design of new highly permeable polymers. The way to obtain substituted tricyclononenes is [2+2+2] cycloaddition between quadricyclane and corresponding olefins leading to only *exo*-products [2].

Results and Discussion. In this work we decided to expand range of "dienophiles" with, germanium- and tin-containing ethylenes and various acetylenes including sinlicon-containing ones:

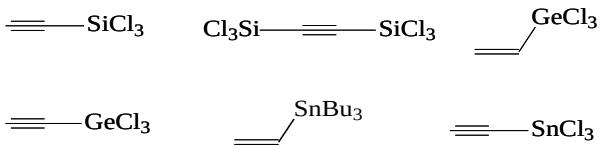

The main aim of this work was to study and compare behavior of monomers obtained in polymerization following by the comparison of gas-pemeability of corresponding polymers.

We have synthesized several new trichlorosilyl- and trichlorogermylsubstituted tricyclononenes and tricyclononadienes according to the scheme:

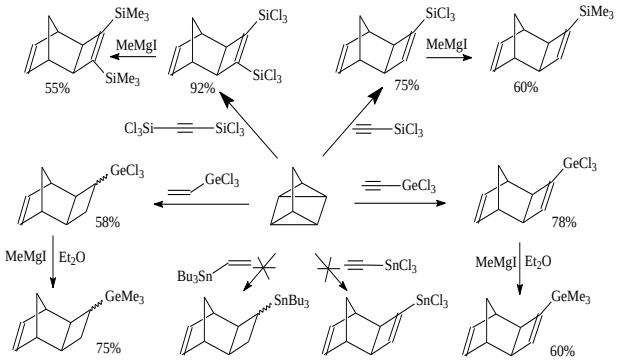

It should be noted that in contrast to $GeCl_3$- or $SiCl_3$-containing olefins interaction between Cl_3Sn-substituted ethylenes or acetylenes and quadricyclane does not result tricylononenes or tricyclononadienes. A presence of chlorostannanes induces immediate isomerization of quaricyclane into norbornadiene.

Products of condensation were methylated by use of common Grignard procedure to reach desired monomers. They were isolated as individual compounds -and characterized with NMR-spectroscopy and GC-MS. The relative activities of "dienophiles" in [2+2+2] cycloaddition were measured and some structure-activity correlations were considered.

We involved the monomers obtained into addition polymerization and ROMP:

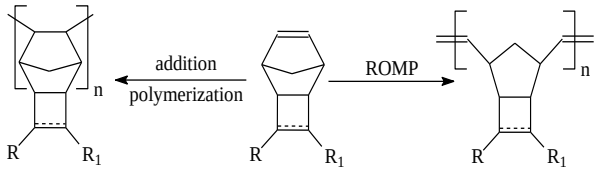

R = $SiMe_3$, $GeMe_3$ R_1 = H, $SiMe_3$

Addition polymerization was performed using a Pd-based catalytic system. We utilized $B(C_6F_5)_3$ and MAO as activators. Yields of polymers were up to 70% and M_w up to 450 000. For all addition polymers glass transition temperatures were not observed till decomposition.

ROMP was performed using the 1st generation Grubbs catalyst with yields up to 98% and M_w up to 800 000. T_g of polymers obtained are in the range from 99 to 127°C depending on nature of a substituent in monomer unit.

The polymers demonstrated high gas-transport characteristics. For example, carbon dioxide permeability of addition poly(3-(trimethylgermyl)tricyclononene) is more than 3800 Barrers. Selectivity coefficient for a pair of butane/methane is about 17,5.

Conclusions. Behavior of various substituted ethylenes and acethylenes in the reaction of [2+2+2] cycloaddition with quadricyclane was studied. Addition and metathesis polymers were obtained from monomers presented above with yields up to 98%. Gas-transport characteristics of these polymers were measured and correlations were discussed. The polymers concerned could be attributed to a class of the highest permeable polymers.

References.

1. Gringolts M., Bermeshev M., Yampolskii Yu., Starannikova L., Shantarovich V. and Finkelshtein E.// Macromolecules, 2010, *43* (17), pp 7165–7172

2. Petrov V.A. // Curr. Org. Synth., 2006, v.3 , pp.175-213

Acknowledgement. The authors gratefully acknowledge the support of the Russian Foundation of Basic Research (Grant No. 09-03-00342-a) and the Ministry of Education and Science of the Russian Federation (GK No.16.740.11.0338).

Enhancement of epoxy thermosets by modification with commercially available hyperbrached poly(ethyleneimine)s (LUPASOL™) as polymeric modifiers

Xavier Ramis[1], David Santiago[1], Xavier Fernández-Francos[2,3], Josep M. Salla[1], Ana Cadenato[1], Josep M. Morancho[1], Àngels Serra[3]

[1] Lab. Termodinàmica, ETSEIB, Dept. Màquines i Motors Tèrmics, Universitat Politècnica de Catalunya
[2]Dipartimento di Scienza dei Materiali e Ingegneria Chimica, Politecnico di Torino
[3]Departament de Química Analítica i Química Orgànica, Universitat Rovira i Virgili

e-mail: ramis@mmt.upc.edu

Introduction

In the recent years, the use of hyperbranched polymers (HBPs) as polymeric modifiers has gained attention due to their advantages in comparison with their linear counterparts: low melt viscosity and high concentration of functional end groups.[1] Depending on the hyperbranched structure and the reactivity of the end-groups, the HBP is either incorporated into the network structure or phase-separates, producing a significant enhancement in toughness.[2]

In this work it is proposed the use of a commercial hyperbranched, poly(ethyleneimine) (LUPASOL™, BASF) as a reactive polymeric modifier for epoxy thermosets. To the best of our knowledge, the use of poly(ethyleneimine)s as curing agent has been hardly explored so far.[3,4] Our aim is to investigate in detail the curing process and properties of the resulting thermosets.

Materials and Methods

DGEBA epoxy resin (EPIKOTE™ 828, 187 g/eq, HEXION) and LUPASOL™ PR 8515 (BASF), ethylenediamine (EDA, Aldrich) and 1-methylimidazole (1MI, Aldrich) were used as received. The following scheme depicts an idealized structure of LUPASOL.

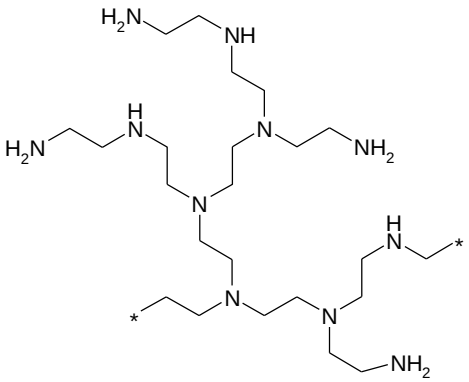

The following formulations were studied:

epoxy/amine eq ratio	1MI
1:1 (LUPASOL)	-
1:0.5 (LUPASOL)	1 phr
1:0.25 (LUPASOL)	1 phr
1:1 (EDA)	-

The curing kinetics was studied by DSC in non-isothermal experiments at different heating rates and isothermal experiments at different temperatures, and isothermal FTIR/ATR. Gelation was determined using TMA, rheometry and DSC. Thermal-mechanical properties were studied using DSC and DMA. Thermal stability was determined using TGA. Curing shrinkage was evaluated by density measurements of the uncured and cured formulations and dilatometric measurements using TMA. The curing of these systems was modelled by simple phenomenological and more complex mechanistic models taking into account the effect of vitrification and volume changes.

Results and discussion

The curing of DGEBA and LUPASOL takes place by an epoxy-amine condensation mechanism. The resulting tertiary amines are unable to promote the etherification of DGEBA epoxy groups. As a consequence, addition of an active tertiary amine such as 1MI is necessary for the complete curing of under-stoichiometric LUPASOL formulations. The curing takes place then in two overlapping processes: epoxy-amine condensation and alkoxide-propagated epoxy polyetherification initiated by 1MI. The epoxy-amine reaction generates a high number of hydroxyl groups which favours initiation of polyetherification by 1MI, which can be used in very low amounts. Combination of LUPASOL and 1MI has thus a synergistic effect in the completion of cure using small amounts of both components. Significant changes in the network development and final network structure are observed between LUPASOL- and EDA-stoichiometric mixtures. Also, important differences are observed between LUPASOL-stoichiometric and under-stoichiometric formulations.

References

1. Voit, B. Journal of Polymer Science, Part A: Polymer Chemistry 2000, 38, 2505-2525.
2. Boogh, L.; Pettersson, B.; Manson, J.-A. E. Polymer 1999, 40, 2249-2261.
3. Cortigene, L. R.; Sherman, W. R.: United States, 1971.
4. Nguyen, F. N.; Saks, A. M.; Berg, J. C. Journal of Adhesion Science and Technology 2007, 21, 1375-1393.

Acknowledgements

To MICINN, FEDER and Generalitat de Catalunya (MAT2008-06284-C03-01, MAT2008-06284-C03-02, 2009-SGR-1512, FPI-2009) and to Dr. Bruchmann of BASF AG for LUPASOL samples

Preparation of L-Arabinitol-Based Functional Polyurethanes

Cristina Ferris, M. Violante de Paz, Francisca Zamora, Belén Begines, Juan A. Galbis

Organic and Pharmaceutical Chemistry Dept., University of Seville, Spain

cferris@us.es

The use of polyurethanes in medical applications is being widely investigated due to their low toxicity, potential biodegradability, biocompatibility, and versatile structures, which make them useful for different applications [1].

Various hydroxyl-containing polymers have been synthesized for biomedical applications: for example, drug release systems based on poly(2-hydroxyethyl methacrylate) and poly(2-hydroxy-propyl methacrylate) hydrogels were recently reported for use in ophthalmology [2]. In addition, Harada *et al*. reported the synthesis of a polyethylene glycol and polyaspartic acid *block*-copolymer which can be used as drug carrier of the anticancer Docetaxel, covalently attached by ester bonds to the polymer chains [3].

Three new polymerizable diols — based on mono-, di-, and tri-*O*-allyl-L-arabinitol derivatives — were prepared from L-arabinitol as versatile materials for the preparation of tailor-made polyurethanes with varied degrees of functionalization (Figure 1). Their allyl functional groups can take part in thiol-ene reactions, to obtain greatly diverse materials.

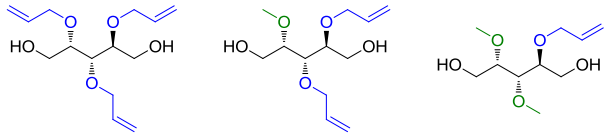

***Figure 1**: Chemical structures of allyl-containing L-arabinitol-based diol monomers.*

This "click" reaction with 2-mercaptoethanol was firstly studied on the highly hindered sugar precursor 2,3,4-tri-*O*-allyl-1,5-di-*O*-trityl-L-arabinitol, in order to apply it later to macromolecules. A polyurethane with multiple pendant allyl groups was synthesized by polyaddition reaction of 2,3,4-tri-*O*-allyl-L-arabinitol ($ArAll_3$) with 1,6-hexamethylene diisocyanate (HMDI), and then functionalized by thiol-ene reaction (Scheme 1). The coupling reaction took place in every allyl group, as confirmed by standard techniques.

The thermal stability of the novel polyurethanes was investigated by thermogravimetric analysis (TGA) and differential scanning calorimetry (DSC). This strategy provides a simple and versatile platform for the design of new materials whose functionality can be easily modified.

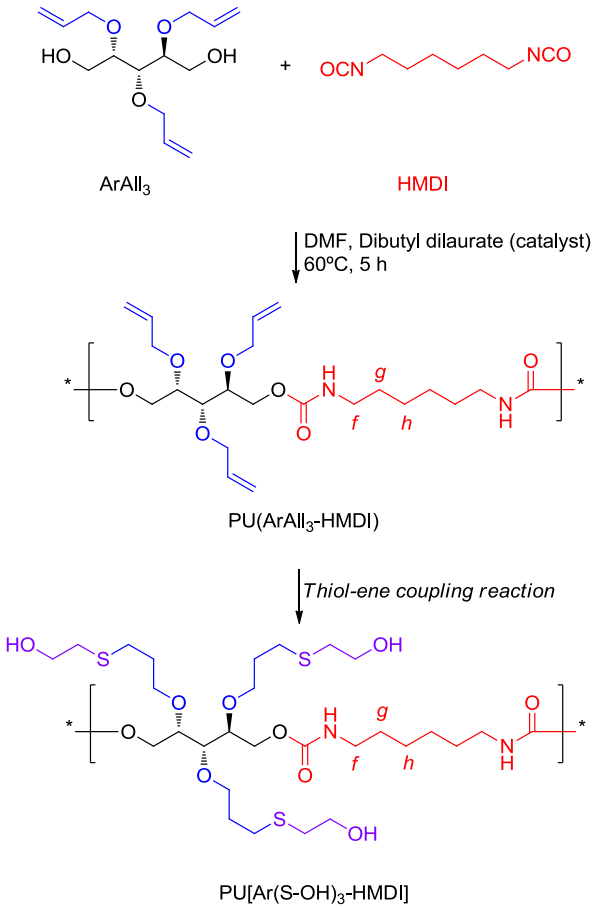

***Scheme 1**: Polymerization reaction of compound $ArAll_3$ with HMDI and subsequent thiol-ene coupling reaction with 2-mercaptoethanol.*

ACKNOWLEDGEMENTS

We thank the MICINN (Ministerio de Ciencia e Innovación, Grant MAT2009-14053-C02-02) and the Junta de Andalucía (Grant P07-FQM-02648) of Spain for financial support.

REFERENCES

[1] B. A. Weisenberg, D. L. Mooradian, *J. Biomed. Mater. Res.* **2002**, *60*, 283-291.

[2] Chauhan, A.; Kapoor, Y. WO Patent 2009032267, 2009.

[3] Harada, M.; Saito, H.; Kato, Y. WO Patent 2009142326, 2009.

Thiol-ene Coupling Reactions: A new Approach to Functionalized Polyurethanes

M. Violante de Paz, Cristina Ferris, Juan A. Galbis

Organic and Pharmaceutical Chemistry Dept., University of Seville, Spain

vdepaz@us.es

The rational design of polymers tailored to exert distinct biological functions plays an important role in the development of controlled drug delivery systems. Thus, the controlled release of therapeutic molecules of both, hydrophilic and hydrophobic drugs, is achieved by anchoring the active agent to polymer structures by means of physical interactions or by covalent linkages.

The thiol-ene reaction shows all the desirable features of a click reaction, i.e., it is highly efficient, simple to execute with no side products, and proceeds rapidly to high yields [1]. The thiol-ene method was applied to the preparation of highly functionalized linear polymers through the combination of different thiols and multi-ene polymers with enhanced properties namely, higher hydrophilicity, increased wettability, and improved biodegradation behavior. As far as we are aware, this method was first used by us in polyurethane chemistry to get a highly hydroxylated material [2].

The aim of the present work is the preparation of aliphatic and aromatic polyurethanes with varied degree of allyl groups and analyze the scope and limitations of click chemistry (CC) in the preparation of polyanionic, polycationic and polyolic linear PU for diverse applications. Consequently, its development may be a new approach to well-defined reactive polyurethanes useful for a variety of biomedical and nanotechnological applications.

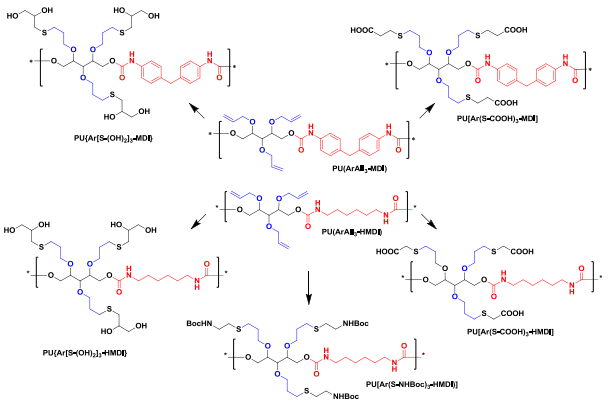

***Scheme 1**: Synthesis of polyanionic, polycationic and polyolic linear PU via click chemistry.*

1-Thioglycerol, thioglycolic acid and the freshly prepared *tert*-butyl (2-mercaptoethyl)carbamate were the thiols of choice in the present study because of their simple and convenient chemical structure. Complete coupling of thiol fragments to every allyl group was achieved in every experiment. With illustrative purpose, Figure 1 displays the reaction scheme and the ^{1}H-NMR spectra of both, the starting polymer PU(ArAll$_3$-MDI) and the final functionalized polyurethane PU{Ar[S-(OH)$_2$]$_3$-MDI}. Of note in the upper spectrum is the complete disappearance of signals from the vinyl protons (4.95 to 5.88 ppm) and the appearance of the peaks corresponding to the –OH groups (3H, 4.50-4.92 ppm) and to the *d*, *e*, *f*, *g*, and *i* methylene groups as well as the *h* methylidyne group present in the final compound.

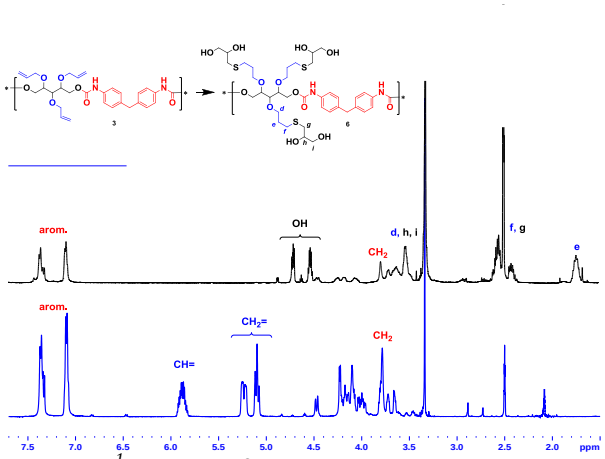

***Figure 1**: ^{1}H NMRs of PU(ArAll$_3$-MDI) (bottom spectrum) and PU{Ar[S-(OH)$_2$]$_3$-MDI} (upper spectrum) synthesized by thiol-ene reaction with 1-thioglycerol.*

All the new polymers were fully characterized by FTIR, NMR, GPC and elemental analysis, and their thermal properties were also studied. The DSC analysis of the polyurethanes studied in this work revealed that most of them are essentially amorphous polymers and the allyl MDI-based polymers are stiffer than the HMDI-counterparts, as come be deduced from their Tg values. Most of the polymers functionalized via CC exhibit a lower Tg value than the starting materials, with a marked increase in flexibility. The thermal stability of the polyurethanes was evaluated by thermogravimetry under an inert atmosphere. The presence of the hydroxyl, carboxylate and amine moieties in polyurethanes had a marked effect on the degradation profile compared with allyloxy pendant groups in PU.

Hydrolytic degradation studies under physiological conditions and the anchorage of an anticancer agent was also tested.

ACKNOWLEDGEMENTS

We thank the MICINN (Ministerio de Ciencia e Innovación, Grant MAT2009-14053-C02-02) and the Junta de Andalucía (Grant P07-FQM-02648) of Spain for financial support.

REFERENCES

[1] Dondoni, A. *Angew Chem Int Ed* **2008**, 47, 8995-8997.
[2] Ferris, C; de Paz, M. V.; Galbis, J. A. *J Polym Sci, Part* **2010**, *in press.*

Biodegradable linear sulfur-containing polyurethanes derived from carbohydrates

Belén Begines, Francisca Zamora, Violante de Paz, Cristina Ferris y Juan A. Galbis

Departamento de Química Orgánica y Farmacéutica. Facultad de Farmacia. Universidad de Sevilla. C/ Prof. García González nº 2, 41012, Sevilla. España. Fax: +34 95 455 6737; Tel: +34 95 455 6739

E-mail: bbegines@us.es

Polyurethanes are widely used in many different fields, such as engineering, construction, textiles, and for various applications, such as insulating, elastomers, adhesives, fibres, etc[1]. However, homogeneus polyurethanes obtained from alkanediols and diisocyanates are chemically stable polymers with and outstanding resistance to hydrolytic degradation[2]. The incorporation of sugar units into tradicional condensation polymers such as polyamides, polyesters and polyurethanes is considered as an interesting method for the preparation of new biodegradable and biocompatible materials for use in biomedical applications.[3-4]

In this article, we investigate the preparation of new aliphatic and aromatic polyurethanes from sugar-based monomers with cystamine dihydrochloride and cystine dihydrochloride by interfacial polycondensation.

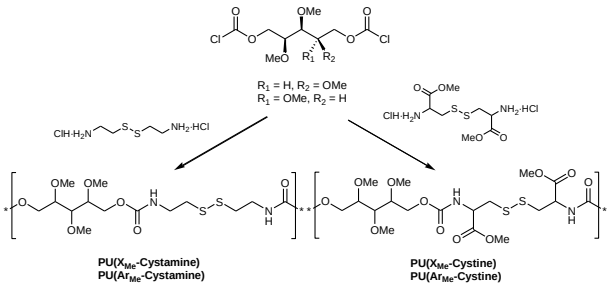

Polyurethanes were obtained with weight-average molecular weights between 6700 and 29000. The chemical structure of the resulting polymers were analysed by NMR and elemental analysis. The TGA studies demostrated that they are stable up to temperatures of about 240 ºC. The new polyurethanes were hydrolytically degradated in buffer solutions at pH 7.02 or pH 8.0 and 37 ºC and in the presence of glutathione under physiological conditions.[5]

Acknowledgements

We take this opportunity to express our gratitude to the MICINN (MAT2009-14053-C02-02) and Junta de Andalucía (Proyecto de Excelencia P07-FQM-02648) for their economic support.

References

1. Edwards, K. N., Ed.; Urethane Chemistry and Applications; ACS Symposium Series 172; American Chemical Society: Washington, DC, 1981.
2. Chapman, T. M. J Polym Sci, Part A: Polym Chem 1989, 27, 1993.
3. Galbis, J. A.; García-Martín, M. G. In Monomers, oligomers, polymers and composites from renewable resources; Gandini, A.; Belgacem, M. N. Eds.; Elsevier: Oxford, 2008; Chapter 5, pp 89-114.
4. Galbis, J. A.; García-Martín, M. G. In Carbohydrates in sustainable development II; Rauter, A. P.; Queneau, Y.; Vogel, P. Eds.; Topics in Current Chemistry, Vol 295; Springer: Heidelberg, 2010; Chapter 6, pp 147-176.
5. de Paz, M.V.; Zamora, F.; Begines, B.; Ferris, C.; Galbis, J.A. Biomacromolecules 2010, 11, 269-276, and references therein.

Sugar-based Polyurethanes and Polyureas

Francisca Zamora, Belén Begines, Isaac Roffé, Manuel Mancera and Juan A. Galbis

Departamento de Química Orgánica y Farmacéutica. Facultad de Farmacia. Universidad de Sevilla. C/ Prof. García González nº 2, 41012, Sevilla. España. Fax: +34 95 455 6737; Tel: +34 95 455 6739

E-mail: khfz@us.es

Polyurethanes are presented as linear, branched, cross-linked polymers, block copolymers, etc. showing multiple industrial applications[1] such as fibres, foams, elastomers, coatings, and biomedical applications due to its biocompatibility and low toxicity. So, among other uses, they have been used as drug carriers in controlled release systems[2]. The polyureas present a great resistance to abrasion, UV radiation, fats, oils, and solvents so they are used in the agri-food industry as coatings, etc. Likewise, polyureas-urethanes with possible biomedical applications have been obtained[3].

Both the polyurethanes and the polyureas are very resistant to degradation what makes impossible their use in applications in which the material is aimed to be destroyed after the use. For this reason, we have included hydrophilic units in these polymers with the aim of making them more sensitive to hydrolytic degradation. In this way, we have used monomers derived from attainable carbohydrates[4,5] with free or protected hydroxyl groups[6].

In this communication, we report on the synthesis and characterization of new aliphatic and aromatic xylitol-based polyurethanes by polymerization in solution or in bulk by using diisocyanates or dicarbamates as co-monomers. In this way, a series of polyurethanes were prepared by polyaddition reaction of xylitol to hexamethylene diisocyanate (HMDI), 4,4´-methylenebis(phenylisocyanate) (MDI), and by polycondensation reaction of xylitol with dimethyl hexamethylen dicarbamate or di-*tert*-butyl-4,4´-diphenyl methyl dicarbamate. We also describe the preparation of sugar-based polyureas by polyaddition reaction of 1,6-diamino-1,6-dideoxy-D-mannitol and 1,6-diamino-1,6-dideoxy-3,4-*O*-isopropylidene-D-mannitol with HMDI and MDI. As far as we are aware, this kind of polyhydroxilated polyureas has not previously been described in the bibliography. The new polymers were characterized by standard methods (Elemental analyses, GPC, IR, NMR). Polyurethanes were hydrolytically degradable under physiological conditions in contrast with less hydrophilic linear polyurethanes previously described[6]. The thermal properties of the novel polymers were investigated by thermogravimetric analysis and differential scanning calorimetry.

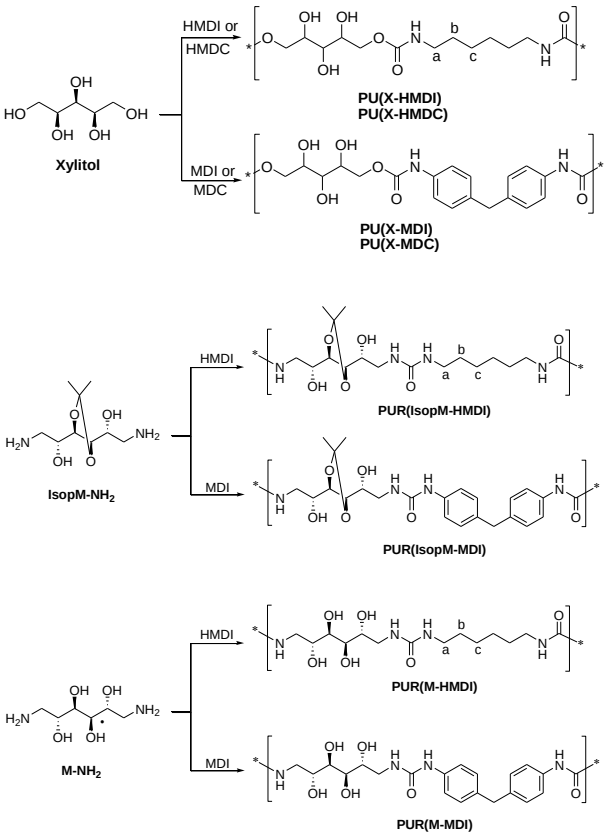

Acknowledgements

We take this opportunity to express our gratitude to the MICINN **(**MAT2009-14053-C02-02) and the Junta de Andalucía (Proyecto de Excelencia P07-FQM-02648) for their economic support

References

1. G. A. Howarth, *Surf. Coat. Int. Part B-Coat Trans.*, 2003, **86**, 111-118.
2. R. V. Sparer, C. M. Hobot, S. Lyu, K. Dang, CAN Patent 2004014449 A1 20040219, 2004.
3. M. Jayabalan, P. P. Lizymol, V. Thomas, *Polym. Int.*, 2000, **49**, 88-92.
4. J. A. Galbis, M. G. García Martín, *Sugars as Monomers*. In: Gandini, A., Belgacem, M. N., Eds.; *Monomers, Oligomers, Polymers and Composites from Renewable Resources*. Amsterdam: Elsevier, 2008 (chapter 5), pp. 89-114.
5. J. A. Galbis, M. G. García Martín. In Carbohydrates in sustainable development 11; Ranter, A. P.; Quenean, Y.; Vogel, P. Eds.; Topics in Current Chemistry, vol 295; Springer: Heidelberg, 2010; Chapter 6, pp 147-176.
6. M. V. de Paz, F. Zamora, B. Begines, C. Ferris, J. A. Galbis, *Biomacromolecules*, 2010, **11**, 269-276, and references therein.

Synthesis and Properties of Aromatic Polyamides derived from isomeric biphenyldicarboxylic acids. Theoretical Study of the Polycondensation Reaction.

Guiomar Hernández[2], José M. García, Félix García[1], Ángel E. Lozano[2], José G. de la Campa[2], Javier de Abajo[2].

[1] Departamento de Química Orgánica, Universidad de Burgos, Burgos, Spain.
[2] Instituto de Ciencia y Tecnología de Polímeros, C.S.I.C., Madrid, Spain.

guiomar@ictp.csic.es

Introduction

In order to achieve materials with good properties, for advanced applications, polymers with high enough molecular weight have to be synthesized. Even though diacid chlorides are condensation monomers considered highly reactive species for the properties of aromatic polyamides, there are big differences of reactivity between monomers structurally related. It has been demonstrated that geometrical and electronic parameters can greatly affect the reactivity of diacid chlorides of varied structure against the attack of nucleophiles such as aromatic diamines.

Herein, we report the synthesis and characterization of two sets of aromatic polyamides derived from two isomeric diacid chlorides, which distinguish from each other only in their geometry: 2,2'-biphenylenedicarbonyl chloride (22BPC) and 4,4'-biphenylenedicarbonyl chloride (44BPC).

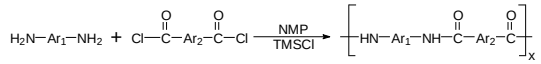

1a, 1b, 2a, 2b, 3a, 3b

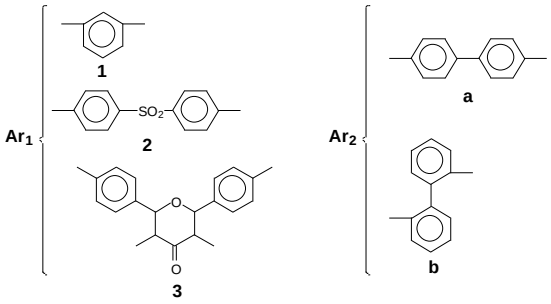

Materials and Methods

2,2'-BPC and 4,4'-BPC were prepared by treating the dicarboxylic acids with thionyl chloride according to the classical procedure. Aromatic diamines were thoroughly purified. Anhydrous aprotic polar solvents and all other materials and solvents were commercially available and used as received.

A typical polymerization reaction is as follows: a double-walled glass flask was charged with diamine and DMA under a blanket of nitrogen. After diamine dissolved, the stirred solution was cooled to 0ºC and diacid chloride was added. The mixture was allowed to react under nitrogen for 1h at 5 ºC, and then at 20 ºC for 3h. Yields were quantitative for polymers from 44BPC and over 90% for those from 22BPC.

Results and Discussion

On using the general synthetic method of solution polycondensation at low temperature, the monomers 22BPC and 44BPC were combined with three aromatic diamines, with very different chemical composition and reactivity, to obtain model polyamides.

It is also observed that the viscosities of polyamides from 22BPC were very low when compared with 44BPC.

As the formation of a condensation polymer starts with a first reaction on one edge, which could modify the reactivity of the remaining reactive group on the other one, models formed by reaction of aniline with one and two reactive group of the monomers were studied.

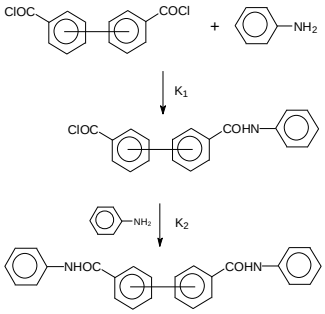

The charge values of the chloroformyl carbons were very similar for all the molecules. The 22DAC_aniline model showed the highest charge value.

LUMO energy differences permitted to state that 44DAC was a little more reactive than 22DAC. Also, the monoreaction process also slightly lessened the reactivity. Anyway, the LUMO energy value did not seem to give a good explanation for the low molecular weight of polymers obtained from 22DAC.

A molecular simulation using the AM1 semiempirical method was employed in order to figure out how the polycondensation reaction proceeded. It was observed that the existence of steric effects in the case of of 22DAC was the main responsible of the decrease of reactivity.

Conclusions

The molecular weight achieved in for these polyamides is strongly dependent on the geometry of the isomeric diacid used as monomer. Thus, 44BPC gave higher molecular weight polymers than 22BPC. It has been found that there are no critical electronic differences between the monomers 22BPC and 44BPC, both of them showing similar values for the energy of the lowest LUMO, however, the existence of important sterical factors affecting the amidation process seems to account for the high different reactivity against diamines experimentally found.

References

J M Garcia, F C Garcia, F Serna, J L de la Peña (2010). High-performance aromatic polyamides. *Progress in Polymer Science* **35**: 623–686 (2010).

P.W. Morgan. *Condensation Polvmers bv Interfacial and* Solution *Methods;* Interscience: New York, **1965.**

Acknowledgements

The authors gratefully acknowledge the financial support provided by MICINN project MAT2010-20668. G.H kindly acknowledges to CSIC a grant JAE-Intro.

Silarylene –containing poly(amide)s based on 4-(4-((4-(4-aminophenoxy)phenyl)dimethylsilyl)phenoxy)benzenamine. Effect of dicarboxylic acid structure used

Claudio A. Terraza, *Luis H. Tagle*, *Alain Tundidor*, *Deysma Coll*

Facultad de Química, Pontificia Universidad Católica de Chile, P.O. Box 360, Santiago, Chile

cterraza@uc.cl

INTRODUCTION

The poly(amide)s use (PAs) in industrial applications, it depends largely on their properties. Special attention presents the glass transition temperature (Tg) and the solubility, this last one related to the formation of films.

In this work, diverse properties of two PAs that differ in the presence of an oxyarene unit in their structure are compared.

EXPERIMENTAL PART

Two new monomers were synthesized according to the figure 1. In this way, starting from bis(4-hidroxyphenyl)dimethylsilane (1)[1], a dinitro derivative (2) was prepared, which was reduced to the diamine respective (3)[2]. Likewise, the compound (1) originated the dicarboxylic acid (3), which presents two oxiarene units if it is compared with the monomer (4).

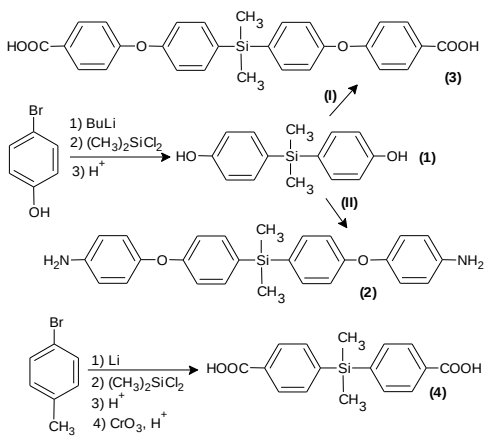

Fig. 1. Synthesys of silarylene-containing monomers.

These monomers were employed in the synthesis of two PAs, which were obtained by direct polycondensation methodology (Fig. 2). For this last, the system triphenylphosphite (TPP), $CaCl_2$, pyridine, and NMP was used.[3] Monomers and polymers were characterized spectroscopically (1H, ^{13}C, ^{29}Si NMR and FT-IR). Additionally, thermal, optic and solubility analysis to the PAs were developed.

RESULTS

Our group has published diverse works where the synthesis of condensation polymers derived from bis(4-aminofenil)difenilsilano is shown.[4] This diamine has been obtained with a yield of 40-50% and it corresponds to a stable solid of high melting temperature. However, when the phenyl groups are substituted by methyl, the obtained product is highly unstable.[5] In this work, we have obtained and characterized (Fig. 3) a derivative with the unit -$PhSi(Me)_2Ph$ - highly stable (yield = 45%, m.p. = 83-85 °C). The incorporation of the -OPh - moiety as much in the diamine as in the prepared dicid, it allowed to maintain the conjugation in the polymeric chain and to improve thermal and solubility parameters among others.

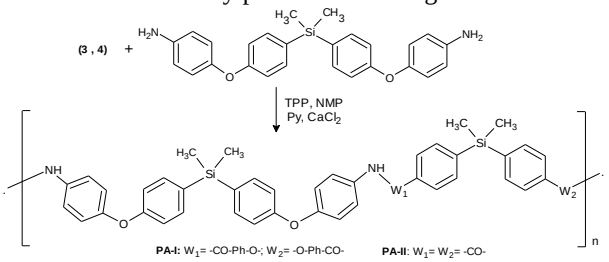

Fig. 2. Preparation of poly(amides)s.

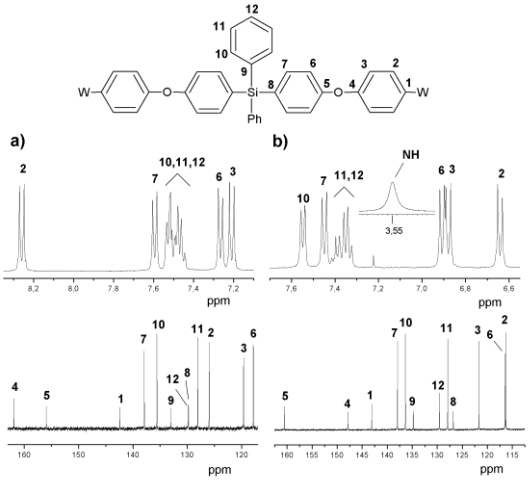

Fig. 3. NMR spectra of (a) dinitro and (b) diamine (2) compounds.

ACKNOWLEDGEMENTS

We thank to Fondo Nacional de Investigación Científica y Tecnológica, FONDECYT, through Project 1095151.

REFERENCES

[1] Davidsohn, W.; Laliberte, B.R.; Goddard, C.M.; Henry, M. C. *J Organomet Chem* 1972, 36, 283.

[2] Tundidor-Camba A.; Terraza C.A.; Tagle L.H.; Coll D. *J. Appl. Polym. Sci.*, DOI: 10.1002/app. 33443, 2010.

[3] Yamazaki, N.; Matsumoto, M.; Higashi, F.; *J Polym Sci Polym Chem Ed* 1975, 13, 1373.

[4] a) Tagle L.H.; Terraza C.A.; Leiva A.; Alvarez P. *e-Polymers*, 34, 2009. b) Terraza C.A.; Tagle L.H.; Leiva A.; Poblete L.; Concha F.J. J. Appl. Polym. Sci., 109, 303, 2008.

[5] Pratt J.R.; Massey W.D.; Pinkerton F.H.; Thames S.F. *J. Org. Chem.* 40, 1090, 1975.

Thermal Rearrangement in poly(*o*-hydroxyimide)s. Isomeric Effects on Physical and Gas Separation Properties.

Bibiana Comesaña[1], *Purificación Cuadrado*[2], *Cristina Álvarez*[1], *Antonio Hernández*[3], *Mariola Calle*[4], *Young Moo Lee*[4], *José G. de la Campa*[1], *Javier de Abajo*[1], *Angel E. Lozano*[1]

[1] Department of Macromolecular Chemistry, Institute of Polymer Science and Technology, CSIC, Madrid, Spain
[2] Department of Organic Chemistry, Faculty of Sciences, University of Valladolid, Valladolid, Spain
[3] Department of Applied Physics, Faculty of Sciences, University of Valladolid, Valladolid, Spain
[4] WCU Department of Energy Engineering, College of Engineering, Hanyang University, Seoul, Korea

bibicg@ictp.csic.es

The need of maintaining human welfare in developed countries and a moral duty to increase it in developing and third world ones, has forced to our society to improve in a large scale its industrial efficiency. Thus, with regards to gas separation processes by membranes, new materials with much better productivity are greatly sought.

It is well known the existence of a trade-off between the main two parameters defining gas productivity: permeability and selectivity[1]. Albeit not many structures have been able to circumvent that limitation, in this decade the development of the as-known PIMs materials [2] and principally the thermally rearrangement, TRs, polymers have marked a milestone giving materials with outstanding properties for gas separation applications. TRs polymers are materials where a solid state thermal rearrangement from a rigid structure to another rigid one, is carried out. Thanks to this conversion, materials with very high permeability and good selectivity have been obtained[3-5].

In particular, Park et al has developed a set of new gas separation membranes based on polyimides with o-hydroxy groups which undergo a thermal change to polybenzoxazole, PBOs[3]. These new membranes are extremely efficient on separate condensable gases and CO_2. These materials are so efficient that can be compared with carbon molecular sieves but having much better mechanical properties.

However, the relationship between chemical structure and its properties as a membrane for gas separation has only been insufficiently explored up to now. In this context, this work tries to figure out the effect of isomeric monomers on the final physical and gas separations properties (Figure 1). Thus, two nucleophilic aromatic biphenyl diamines with o-hydroxy groups have been used to make polyimides with o-hydroxy groups which were characterized by a wide variety of techniques (Figure 2). Furthermore, gas separation properties were also measured.

Thermal treatment processes were carried out in order to attain TR structures and properties were compared with the goal of achieving relationships to design in a controlled way new materials with enhanced properties.

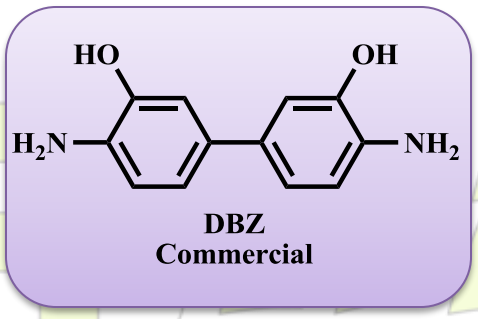

Figure 1

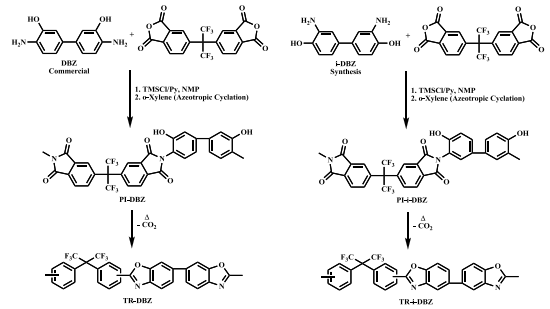

Figure 2

Also, another target of this work has consisted of finding out the differences on properties obtained by synthesizing PBOs from 3 different methods (Figure 3). It is important to assert that PBOs are mostly formed during this thermal process, and it is critical as well to explore how the rearrangement affects the material. This study could give us clues to search new structures suitable to undergo TR processes.

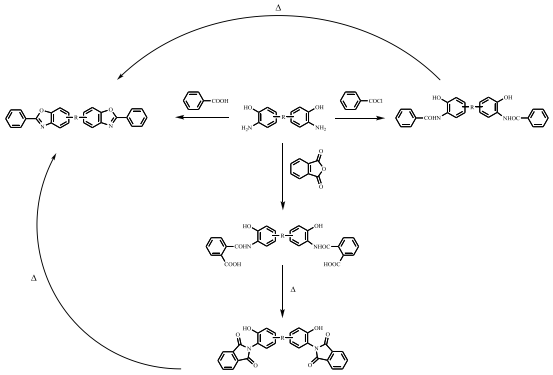

Figure 3

Bibliography

[1] Freeman BD. *Macromolecules* **32** (1999) 375-380

[2] Budd PM, Msayib KJ, Tattershall CE, Ghanem BS, et al. *J. Membr Sci* **251** (2005) 263-269.

[3] Park HB, Jung CH, Lee YM, Hill AJ, Pas SJ, Mudie ST, et al. *Science* **318** (2007) 254-258.

[4] Ha YM. *J Membr Sci*

[5] Hill AJ. *J Mem*

Ack

Autl rovided by MIC MAT2010-206 fellowship rece to Tratasa 2000 cknowledges Prof. Y.M. Lee and M. Calle the training obtained during a short stay in Hanyang University.

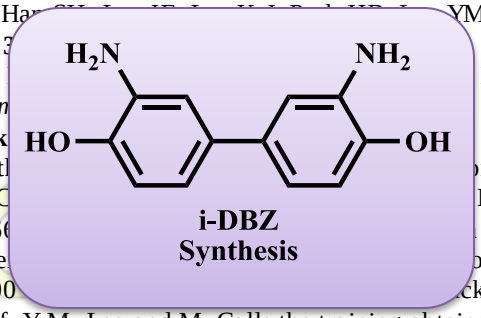

Peculiarities of water emulsion copolymerization of tetrafluoroethylene with perfluoro(3,6-dioxa-4-methyl-7-octene)sulfonyl fluoride to obtain proton conducting copolymers

S.S.Ivanchev[1], *V.S.Likhomanov*[1], *A.Yu.Menshikova*[2], *O.N.Primachenko*[1], *S.Ya.Khaikin*[1]

[1] St-Petersburg Department of the Boreskov Institute of Catalysis of the Siberian Branch of the Russian Academy of Sciences, 14 prospect Dobrolubova 197198 St-Petersburg, Russia
[2] Institute of High Molecular Compounds of the Russian Academy of Sciences, 31 Bolshoi prospect V.O. 199004 St-Petersburg, Russia

e-mail: ivanchev@SM2270.spb.edu

The copolymerization of tetrafluoroethylene with functional perfluorinated comonomers in aqueous emulsions was attempted in a series of recent studies [1-3].

In this report we present the analysis of kinetic features and mechanistic study of the copolymerization of these monomers in water emulsion systems.

An important condition providing a water emulsion copolymerization of the considered monomers is their preliminary dispersing according to various procedures. A conventional pre-emulsification method is found to provide copolymers with the composition remaining almost constant up to high (~85%) conversions of a functional comonomer featuring with a low reactivity.

We studied the changes in the dispersity of the initial monomer droplets and resulting polymer particles in the latex at different monomer conversions by light scattering using a Malvern Zetasizer Nano-ZS analyzer.

The dispersing of monomer droplets and polymer-monomer latex particles are found to proceed during the copolymerization.

A mechanism of elementary reactions at copolymerization is suggested upon the analysis of the solubility of the polymerization system components and the resulting copolymer in the water emulsion system.

The obtained data indicate a promising potential of water emulsion copolymerization of these monomers for obtaining a high quality copolymer useful for the production of proton conducting membranes.

References:

1. US Pat. 6602968 (2003).
2. RU Pat. 2348649 (2009).
3. WO Pat. Appl. 2009/082264 PCT (2009).

Application of Pulverized concrete cement powder as filler in PVC pipe

*Muralisrinivasan Natamai Subramanian**, *Arunachalam Thamaraichelvan***

*Plastics Technology consultant
** Head, Department of Chemistry, Thiagarajar College, Madurai.

plasconsultant@hotmail.com

The use of pulverized concrete powder for the production of rigid PVC pipes has been evaluated in comparison with calcium carbonate as filler. The powdered concrete powder is formulated with PVC at rate of 2, 4, 6, 8, and 10% with other additives for processing purpose. In this article, the focus is on understanding the pulverized concrete cement powder as a substitute for calcium carbonate used in PVC formulations. Short term hydraulic, impact, tensile and elongation tests are used as techniques of choice for the evaluation of PVC pipe and concrete cement blends for mechanical and processing properties. The results are very encouraging with powdered concrete cement in comparison to calcium carbonate.

New Copolymers of Norbornene and vinyl Monomers

Popov D.S., Bykov V.I., Makovetskii K.L., Bermeshev M.V., Butenko T.A., Finkelshtein E.Sh.

Topchiev Institute Of Petrochemical Synthesis RAS

del87@yandex.ru

Introduction. Interest in amorphous saturated norbornene polymers is due to a complex of useful properties, including chemical and thermal stability, high transparency, low water absorption. However, additive norbornene polymers have a very rigid chain, which leads to high glass transition temperature - close to the decomposition temperature (~ 410 °C). This prevents to the possibility of their processing by conventional methods. For the same reason its films are very brittle. To reduce the chain rigidity it is necessary to introduce flexible units, such as ethylene [1, 2]. The obtained copolymers contain 45-55% of norbornene units, have a structure close to the alternant, high molecular weight and glass transition temperature, which enable their processing. They have also high transparency, low birefringence, and have good film-forming properties. Later it was shown that as a flexible link you can use the available acrylic monomers [3]. These copolymers are of interest as a matrix stabilizing semiconductor nanoparticles, and can also be used for photo-and electroluminescent devices (diodes, flexible displays, optical devices with low power consumption, solar energy converters, etc).

Results and discussion. This work provides new data on the double and triple-norbornene radical copolymerization with cheap vinyl monomers (tert-butyl acrylate, methyl acrylate and decylacrylate). Introduction of polar groups to polymers cause the range of useful properties such as increased impact strength, rheological, adhesive and barrier properties, the ability to coloring and blending with other polymers. Norbornene and its derivatives increase the rigidity of the main chain, which allowed, in particular, to obtain copolymers with higher glass transition temperatures 116-62 °C than homopolymers of tert-butyl acrylate (T = 52 °C) and methyl acrylate (T = 10 °C). The main objectives of this work were the synthesis of macromolecular copolymers (Mw> 300000) with controllable composition. As vinyl monomers have been investigated tert-butyl acrylate, acrylic acid, decyl acrylate and methyl acrylate. The synthesis of high molecular weight samples of copolymers of specified composition succeeded in carrying out the copolymerization at 30 °C by a radical mechanism, using as the initiator benzoyl peroxide. To determine the effect of the molar composition of the feed mix on a molecular weight of polymer and its composition, the copolymerization of norbornene and vinyl monomers were carried out at a ratio of 10:1, 5:1, 3:1 and 1:1.

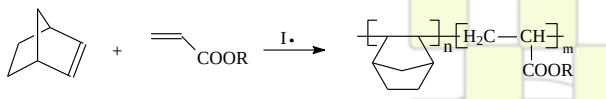

R = H, COO^{t}Bu, CH_3, $C_{10}H_{21}$

It was found that the decrease at this ratio leads to an increase in molecular weight, but it reduces the percentage of occurrence of norbornene in the chain. The composition of the copolymers was determined by elemental analysis, in the case of methyl acrylate addition 1H NMR spectroscopy. One of the possible applications of these copolymers with functional groups are materials (photoresists) for microlithography. The use of lasers operating at 193 or 157 nm wavelengths, allows to give specified surface nanoscale relief. Photoresists in its composition must contain a readily leaving under the action of the laser beam group, usually tert-butyl.

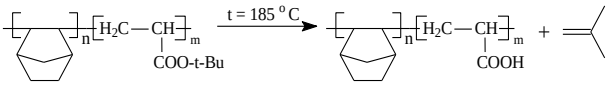

On the example copolymer of norbornene with methyl acrylate 3:1 (choice is the ability to easily determine the content of norbornene by 1H NMR spectroscopy) were obtained the dependence yield of copolymer and content of norbornene on time and temperature of the reaction and the dependence of molecular weight on temperature.

Conclusions. A new method of radical copolymerization was successfully used to obtain copolymers with high molecular weight. Norbornene copolymers with vinyl monomers were obtained and characterized by methods of elemental analysis, 1H NMR spectroscopy, DSC, GPC and laser light scattering. Also described its's potential application as photo-and electroluminescent devices.

References.

1. Makovetskii K.L., Finkelshtein E.Sh., Bykov V.I., Bagdasaryan A.Kh., Goodall B.L., Benedict G.M. US Patent 5929181, 1999.

2. Makovetskii K.L., Finkelshtein E.Sh., Bykov V.I.,. // Kinetics and catalysis, 2006, t. 47, № 2, pp. 241-244.

3. Makovetskii K.L., Finkelshtein E.Sh., Bykov V.I.,. Copolymerisation of norbornene and its derivatives with vinyl monomers. Russian conference "Current status and trends of organometallic catalysis of olefin polymerization", abstracts, Chernogolovka, 2008, p. 38.

Acknowledgement. The authors gratefully acknowledge the support of the Russian Foundation of Basic Research (Grant No. 11-03-00436-a).

Macromolecular Design of Energetic Tetrazole-containing Olygomers and Polymers

Kizhnyaev V.N., Pokatilov F.A., Vereschagin L.I., Smirnov A.I.

Department of Chemistry, Irkutsk State University

kizhnyaev@chem.isu.ru

Relative simplicity of the tetrazole fragment formation, its high reactional ability open great possibilities to the synthesis and macromolecular design of tetrazole-containing polymers. In the present work, the problems of synthesis and modification both carbon chain and hetero chain olygomers and polymers with tetrazole cycle are considered.

Polymerization method of the synthesis and macromolecular design of carbon chain tetrazole-containing polymers offer no difficulties owing to the combination of relative accessibility of tetrazole vinyl derivatives on the one part and high vinyltetrazole activity in radical homo- and copolymerization on the other part.

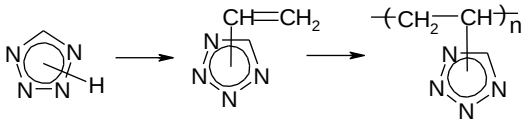

Another approach to the formation of tetrazole-containing high molecular compounds is application of azide/nitrile-"click" reaction with participation of the polymers already obtained. Apart from a well-known method to obtain poly-5-vinyltetrazole by polyacrylonitrile azidation, a wide range of low or high molecular hydroxyl-containing compounds may serve as starting substances to the method mentioned. This method includes two reactions: cyanoethylation of hydroxyl-containing compounds by acrylonitrile and azidation of the synthesizing compounds with nitrilic groups.

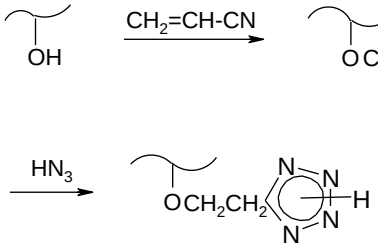

As the result monomer and polymer substances, containing N-H unsubstituted tetrazole fragment can be obtained.

Last circumstance gives possibility to formed olygomeric and polymeric substances of different architecture obtained by the condensable way from low molecular polytetrazoles. In case of high molecular compounds the branch and bloc polymers are formed. Alkylation reaction of N-H unsubstituted tetrazole cycle by compounds, containing halogenalkyle reactional centers is in base of these transformation. On dependence of tetrazole-containing compound functionality by polycondensed way, one can synthesize linear, branch, hyperbranch olygomeric and polymeric structures.

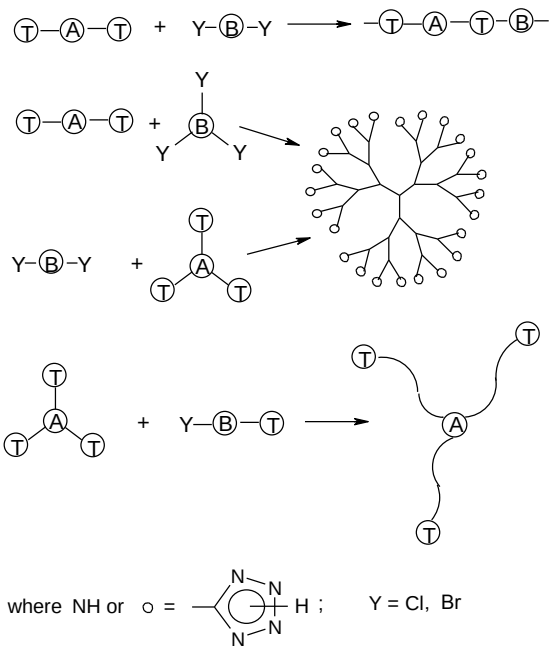

When using alkylation reaction various explosive groups may be inserted into tetrazole-containing polymers. It promotes to essential rise energy capacity given class of high molecular compounds.

The effect of fiber orientation on the thermal behavior of polypropylene fibers

Parviz, A. , *Dadashian, F.*

Department of Textiles,Islamic Azad University- South Tehran Branch, Tehran, Iran
Department of Textiles, Amirkabir University of Technology, Hafez Ave, Tehran, Iran

az.parviz@gmail.com

ABSTRACT: Polypropylene fibers(PP) as one of the most used synthetic fibers are treated under thermal conditions in different stages, such as production, texturizing and in some final uses.In this paper,the orientation is considered as a function of draw ratio ,they increase simultaneously. The effect of orientation on thermal behavior of PP fibers, by using Thermo Mechanical Analysis (TMA) and Differential Scanning Calorimetry (DSC) are studied.TMA results show that increase in orientation, causes increase in thermal range in which fiber has dimensional stability, although this range differs for fibers with different orientation and the best is about 104-139 ° C. DSC curve show that melting point is 161 °C for all of samples and not affected by orientation . An endothermic peak in this curve refers to the second melting point or the equilibrium melting point located around 221 ° c for fiber with most orientation and 223° C for two other samples with less orientation .

Generation of conductivity through transfer charge properties in flourene and diphenylsilane-containing poly(ester)s and poly(amide)s.

C. González-Herríquez[1], Luis H. Tagle[1], Claudio A. Terraza[1], Andrés Barriga[2], Alejandro Cabrera[2], Ulrich Volkmann[2]

Pontificia Universidad Católica de Chile, P.O. Box 360, Santiago, Chile: [1] Facultad de Química, [2]Facultad de Física

cgonzalen@puc.cl

INTRODUCTION

Poly(silylene)s are compounds very important due to their potential applications and photochemical properties, which have lead to additional applications as semiconducting polymers, as photoreceptors in electrophotography and as devices that require nonlinear optical material.[1,2] Their electronic properties are associated with electron conjugation in the silicon atom. Likewise, the incorporation of a Si atom in the main chain of a polymer increases the solubility due to the reduction of the packing force and the increase of the free volume of the system. Most of the silicon-containing aromatic polymers maintain a high thermal stability due to the ionic character of the Si-C bond.[3]

EXPERIMENTAL PART

Dicarboxylic acid (3) was synthesized by hydrolysis of the dinitrile derivative (2) which was obtained from 2,7-dibromo-9*H*-fluorene (1), CuCN and $FeCl_3$ system (Fig. 1). Diacid reacted with bis(4-aminophenyl)diphenyl silane and bis(4-hydroxyphenyl)diphenylsilane for obtaining PAF and PEF respectively (Fig. 1).

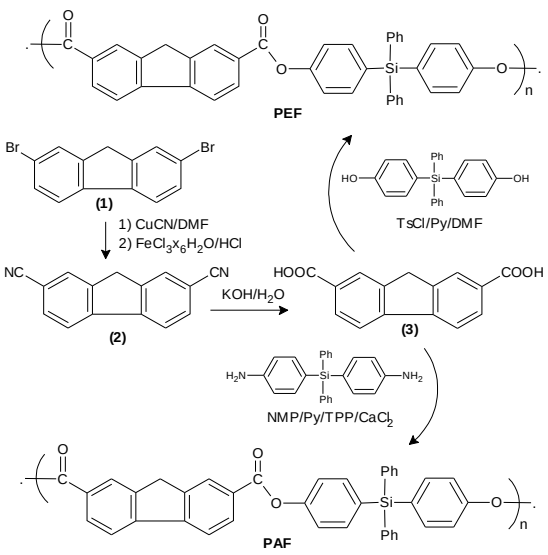

Fig. 1. Preparation of PEF and PAF.

The polymers were obtained in good yields and were characterized by IR, NMR, ESI, Raman, UV (*optical gap*), fluorescence spectroscopy, SEM-EDX, DSC and TGA. Electrical conductivity was evaluated after and before exposure to iodine vapor, utilizing polymeric films. Ellipsometric studies were used for the determination of the film thickness.

RESULTS

All polymers were successfully prepared by the direct polycondensation of the monomers. Diacid (**3**) and bisphenol was polymerized using thionyl chloride/DMF/pyridine as condensing agent to prepare PEF, and the reaction of diacid (**3**) and diamine, using TPP and pyridine, as condensing agent to prepare PAF. The influence of the reaction time on the physical and electrical properties of the polymer was studied. These compounds were soluble in various polar aprotic solvents and have moderate thermal stability. The incorporation of amide group in the chain reduces the Tg based on free surface effect. The time and temperature of crystallization was related with the morphology assumed by the polymeric chain.

Preliminary conductivity measurements showed adverse effects when oxidation of the polymer films is induced, these effects being related to a certain grade of disorder within of the systemor due to a structural change.

Table I. Conductivity of the polymers with and without doping to different reaction time and thickness.

	Time[a]	Film[b]	Without[c]	With[d]
PEF	2	2744 (±) 250	2.15	1.30
PEF	12	2805 (±) 250	3.30	1.44
PAF	3	2763 (±) 250	4.63	1.54
PAF	12	5877 (±) 250	1.90	7.70
PAF	12	2576 (±) 250	2.38	1.90

[a] Polymerization time (h), [b] Thickness of film (Å), [c,d] conductivity without and with doping respectively.

ACKNOWLEDGEMENT

C.M. González-Henríquez acknowledges a scholarship from MECESUP UCH 0601. Authors thank to FONDECYT: 1100015,1095151 and 1100882. Thanks to M. Soto, M. Pino and R. Trabol for SEM, XRD and conductivity characterization.

REFERENCES

[1] Miller R.D.; Wilson C.G.; Wallraff G. M.; Clecak N.; Sooriyakumaran R.; Michl R.; Karatsu J.; McKinley A.J.; Klingensmith A.J.; Downing *J. Polym. Eng. Sci*. 1989, 29, 882.

[2] Blazsó M.; West R.; Székely T. *J. Anal. Appl. Pyrolysis* 1989, 15, 175.

[3] a) Tagle L.H.; Terraza C.A.; Alvarez P.; Vega J.C. *J. Macromol. Sci. Part A: Pure Appl. Chem.* 2005, 42, 301. b) Terraza C.A.; Tagle L.H.; Leiva A. *Polym. Bull.* 2005, 55, 277. c) Tagle L.H.; Terraza C.A.; Alvarez P. *Phosph. Sulfur Silicon Related Elements* 2006, 181, 239. d) Terraza C.A.; Tagle L.H.; Leiva A.; Poblete L.; Concha F.J. *J. Appl. Polym. Sci.* 2008, 109, 303. e) Tagle L.H.; Terraza C.A.; Leiva A.; Devilat F. *J. Appl. Polym. Sci.* 2008, 110, 2424. f) Tagle L.H.; Terraza C.A.; Leiva A.; Yazigi N.; López L. *J. Appl. Polym. Sci.*, 2009, 117, 1526. g) A. Tundidor-Camba, C.A. Terraza, L.H. Tagle, D. Coll, *J. Appl. Polym. Sci.*, DOI: 10.1002/app. 33443, 2010.

Barrier Performance of Gelatin Coated PLA Films

Mercedes Leobono, Cristina Frova, Ruth Zacur, Daniel Ercoli, Graciela Goizueta

Planta Piloto de Ingeniería Química, PLAPIQUI (UNS-CONICET)
Camino La Carrindanga Km 7 – Bahía Blanca (8000) - Argentina

dercoli@plapiqui.edu.ar

Introduction: Most commercial films for food packaging applications requiring high barrier to oxygen and water vapor are made of multilayer structures of oxygen barrier polymers such as poly(ethylene-co-vinyl alcohol) and other polymers which provide useful mechanical properties and moisture-proof layers (polypropylene, polyethylene, polystyrene, etc.) (1,2). Due to the increasing need of minimizing environmental effects associated with polymers from fossil fuels, the development of environmentally benign plastics has attracted much of attention. One of the most promising candidates for this purpose is Poly(lactic acid) (PLA), a linear thermoplastic polyester produced from renewable resources (whey or corn) and biodegradable in compost (3). Particularly among proteins gelatin is cheap and abundant. Its good film forming characteristics, extremely high barrier to oxygen and inherent biodegradability make it a very attractive candidate to be considered as a coating material for PLA. Performance of PLA films coated with pure and glycerol plasticized gelatin are presented in this work in terms of their Oxygen (OP) and Water Vapor Permeability (WVP), mechanical and friction properties.

Materials and Methods: PLA (Mw≈140000, D% <1.5 wt %), Gelatin (practical grade) and Glycerol (analytically pure) were used as raw materials. Dried PLA was press moulded and films (≈100 μm) were obtained. Gelatin solutions were prepared dissolving 10 g of gelatin in 100 ml of water. For plasticized gelatin coatings 5 g of glycerol was also added. Coatings of PLA with pure and plasticized gelatin were obtained using a Bird applicator and allowing further evaporation of water at ambient conditions. Before proceeding with properties characterization the films were stored in a controlled-environmental chamber at 25ºC and 50%RH for several days. Table 1 shows the composition of each sample prepared. The thickness of films before and after coating was measured at different points with an inductive probe (Millimar) and the average was taken. Wetting tension of PLA films was determined using ASTM D2578. Films OTR were measured in an Ox-Tran 2/21 (Mocon) at 23ºC and 0%RH exposing PLA side of coated samples to the carrier gas (nitrogen) and the gelatin side to the test gas (oxygen). The WVTR was measured according to the desiccant method detailed in ASTM E96. Samples were sealed to the open mouths of acrylic test dishes containing dried calcium chloride and placed in a chamber under controlled atmosphere at 50 %RH and 25ºC. The weight of cells against elapsed time was plotted for at least 7 days. The slope of the linear portion of this curve is the rate of water vapor transmission (w/t). All tests were carried out in at least three repetitions for OTR and WVTR determinations. Static coefficients of friction (COF) and tensile stress-strain behavior at 25 mm/min were assessed in an Instron 3369. A minimum of ten samples were tested and the average values of Elastic Modulus (E) and Elongation at Break (Elb) were calculated.

Results and Discussion: Films of PLA showed good transparency and a high wetting tension ≈42 dyn/cm. It resulted in a very good adhesion and uniformity of gelatin coatings onto PLA surface. The average thickness of coatings was about 3–4 μm and did not affect optical properties of base PLA films. The use of glycerol as a plasticizer for gelatin improved its processability onto PLA surface and reduced its brittleness when dried. Static COF and mechanical properties of PLA with and without coatings are included in Table 1. COF values of coated films increased 2.5 times from that of uncoated PLA which could also be related to the greater surface rugosity observed. Elastic modulus (E) and Elb values of coated and uncoated films did not differ significantly from each other, meaning that the thin coating did not affect the base film mechanical performance. Moreover PLA films were fragile and would need to be plasticized in order to improve its ductility.

Table 1.Samples, Friction and Mechanical Properties

Film Sample	Coating		COF	E [MPa]	Elb [%]
	Gelatin	Glycerol			
PLA	NO	NO	0.13	2666	2.8
PLA/G	YES	NO	0.35	2700	3.6
PLA/GG	YES	YES	0.32	2640	3.5

OP and WVP results are shown in table 2. In earlier studies we have shown that OP for pure and plasticized gelatin films was ≈1 and 1.4 cc.mil/m^2.day respectively (4). The application of such an excellent oxygen-barrier coating led to a significant improvement of ≈75% in oxygen barrier performance of PLA base films. Meanwhile WVP values of PLA films were not significantly affected when coated.

Table 2.Oxygen (OP) and Water Vapour Permeabilities (WVP)

Film Sample	OP [cc.mil/m^2.day]	WVP [ng.m/m^2.s.Pa]
PLA	1036	0.015
PLA/G	228	0.017
PLA/GG	273	0.015

Conclusions: Pure and plasticized gelatin coatings onto PLA films produced a significant improvement in its oxygen barrier without modifying the WVTR. Although mechanical performance of PLA films is not affected by the presence of coatings, the coefficient of friction of coated films increased significantly.

References:

1. S. W. Hwang, J. K. Shin, S. B. Lee, R. Auras, *J. App. Pol. Sci*, 116, 5, 2010, 2846-2856
2. E. C. Chow, K. K. Mokwena, J. Tang, C. P. Dunne, T. C. S. Yang, *J. Food Engineering*, 92,3,2009, 291-296
3. G. Stoclet, R. Seguela, J. M. Lefebvre, S. Elkoun, C. Vanmansart. *Macromolecules*, 2010, 43 (3), 1488-1498
4. *"Barrier and Mechanical Properties of Edible Gelatin Based Films"*.D.Ercoli, G.Goizueta and N.Andreucetti, *PPS23*, Salvador, Brasil, 27-31/05/2007

Polypropylene Films of High Oxygen and Water Vapor Permeability for MAP Applications

Mariela Acosta, Daniel Ercoli, Graciela Goizueta, Jorge Lozano, Numa Capiati

PLAPIQUI – UNS – CONICET, Bahía Blanca, Argentina

dercoli@plapiqui.edu.ar

Introduction: Harvested plant products respire and transpire continuously, consuming oxygen (O_2) from the surrounding environment and producing carbon dioxide (CO_2) and water vapor [1]. The aim of modified atmosphere packaging (MAP) is to reach the most suitable storage atmosphere of a given product minimizing the time required to achieve it. This objective can be reached by matching the respiration rate of the packaged produce and the gas exchange through the plastic film [2]. An attractive way to obtain new materials with tailored properties for MAP applications is the blending of different polymer species [3].

The objective of this work was to develop Polypropylene (PP) based films for packaging of fresh produce. Particularly, we were interested in studying the effects of the addition of an elastomeric Polyethylene co-octene (POE) of high permeability to oxygen and water vapor to PP. The effects of blend composition as well as the mixing and processing conditions on blend permeabilities, mechanical properties and morphology were analyzed.

Materials and Methods: A commercial grade of PP (MFI 8 g/10min) and POE (MFI 1.0 g/10min) were used to obtain press molded and blown films. Blends of PP with 20, 30 and 40 wt% of POE were prepared in a counter rotating batch mixer (Brabender) at 205 or 215 °C and at 50 or 80 rpm. Films samples were obtained by two different procedures: in a hydraulic press at 205 °C (thickness ≈100 μm) and in a PP blowing machine (thickness ≈35 μm). The morphological aspects of the press and blown films were studied by scanning electron microscopy (SEM) using a LEO EVO 40XVP microscope. The oxygen permeability coefficient (OP) was measured in a Mocon Ox-Tran 2/21 at 23 °C and 0 %RH using a standard method (ASTM 3985). The water vapor permeability coefficient (WVP) was measured gravimetrically according to the desiccant method detailed in ASTM E96 at 25 ºC and 50 %RH. Tensile stress-strain behavior of film samples was determined in an Instron 3369 machine at 23 °C and 50 %HR for elastic modulus (E) and tensile elongation at break (%El_b) determinations.

Results and Discussion: SEM micrographs of press molded films showed a spherical and homogeneous POE phase distribution in the PP matrix through the whole transverse area of the film, irrespectively of the composition or blending conditions. Figure 1a shows as an example, a micrograph of a blend with 20 wt% of POE. Moreover, the sizes of domains increased when the content of POE in the blends increased. Blown films micrographs showed that the POE domains had different sizes when the surface of fracture was made in the machine (MD) or transverse direction (TD). For TD fractures domains were spherical, meanwhile MD fractures showed elongated domains (Figure 1b). These effects indicated that forces in MD and TD were unbalanced, being higher along MD.

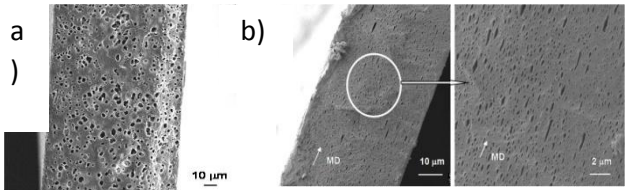

Figure 1. SEM micrographs of press molded film (a) and blown film (b) with 20 wt% of POE

It was found that in both series of blends OP and WVP increased mainly with POE content. This behavior could be directly attributed to the more permeable characteristics of POE.

For a given amount of POE, the OP or WVP of press molded films were higher than those of the corresponding blown films. For example, OP for a press moulded film of a blend with 40 wt% POE was about 175 % higher than that of pure PP film, meanwhile for the blown film the increase was about 55 %. These results could be mainly assigned to the morphological differences observed between blends obtained by both procedures.

All the blends studied showed E values lower than pure PP and a higher %El_b due to the elastomeric characteristics of POE. For example, blends with 40 wt% of POE exhibited the maximum decrease in E, being almost half the value for neat PP.

Conclusions: The addition of POE to PP is a valuable way for obtaining PP based blends with higher oxygen and water vapor transmission rates. Both permeabilities were found to be dependent mainly on the POE content and the morphology of the blends. Moreover, press molded and blown films exhibited good mechanical properties which were in the range of commonly used flexible packaging materials.

References:

1. P.V. Mahajan, T.K. Goswami. Enzyme kinetics based modeling of respiration rate for apple. *J Agric Eng Res*, 2001; 79(4):399.

2. A. Exama, J. Arul, R.W. Lencki, L.Z. Lee, C. Toupin. *J Food Sci*, 1993; 58(6):1365.

3. D.R. Paul, C.B. Bucknall. *Polymer Blends*. Wiley. 2000.

Studies on Preparation and Properties of Novel Photoluminescence Hydrogels

*Wen-Fu Lee * 、Han-Hsueh Tsai*

NO. 40, Sec. 3, Jhongshan North Rd. Jhongshan District, Taipei City 10451 TAIWAN, R. O. C.

E-mail:wflee@ttu.edu.tw

Abstract

Triphenylamine has a good electron-hole conductive property; so many scholars used triphenylamine derivatives as a hole-conductive material. The structure of triphenylamine has characteristics of photoluminescence or electroluminescence through intermolecular charge transfer, it can be combined with other materials to form a novel photoluminescence (fluorescent) material [1-2].

Hydrogel, a 3-D crosslinked network, can swell but does not dissolve in aqueous solutions [3]. Hydrogels have stimuli-responsive properties, which would be affected by the change of surrounding conditions such as temperature, pH value, ionic concentration, or electric field, etc. All of these can alter their swell ratio, volume, and drug release behavior [4]. When a hydrogel is introduced into a triphenylamine structure, the hydrogel can exhibit photoluminescence or electroluminescence characteristics. These functional polymers or their devices can be used in many practical applications such as light-emitted tracer or synthetic chemical sensors.

A novel photoluminescence monomer as crosslinker, dimethacryloyloxy ethylene oxycarbonyl triphenylamine (DMETPA), was synthesized firstly. Then, the composition and yield of two series of thermosensitive hydrogels based on NIPAAm using different crosslinkers DMETPA (N-TPA series) and EGDMA (N-EGDMA series) as Table 1 were prepared by UV-irradiation polymerization.

The appearance of the N-TPA series hydrogels shows yellow turbid opaque, but the N-EGDMA series hydrogels shows white translucent as Figure 1. Under UV irradiation, the hydrogels crosslinked with DMETPA exhibit blue fluorescent, but the hydrogels crosslinked with EGDMA does not have a photoluminescence effect as Figure 1. Moreover, the maximum PL emission of N-TPA hydrogels appeared around 458nm, the fluorescence intensity increase with increasing DMETPA content, but for the gels crosslinked with EGDMA exhibits no fluorescence.

The swelling ratios decreased with increased amount of crosslinker in the hydrogel. This is because the crosslinking density of the hydrogel increases with increasing amount of crosslinker, resulting in denser structure in the hydrogels, so the water does not easily enter into the hydrogels. However, comparing N-TPA3% gel and N-EGDMA3% gel, we find that the swelling ratios of the hydrogel containing DMETPA is significantly lower than the hydrogel containing EGDMA. This is because DMETPA bears triphenylamine structure; its hydrophobic property is stronger than the EGDMA structure. So the swelling ratios for the N-TPA series hydrogels are lower than those of the N-EGDMA series hydrogels, that is, the trend of swelling ratios for the hydrogels is N-EGDMA3% > N-EGDMA6% > N-TPA3% > N-TPA6%.

When the hydrogels were attained to equilibrium swelling ratio, the mechanical properties were measured with uniaxial compression by Universal Tester. The results indicate that the shear modulus (*G*), Young's modulus (*E*), and the effective crosslinking densities (ν_e) of the hydrogels increase with an increase of the content of crosslinker. The reason is that the gel structure becomes denser when the crosslinker amount increases, that results from effective crosslinking densities increase, hence, the values of *G*, *E*, ν_t and ν_e all increase. But the molar mass per crosslinked unit (M_c) decreases due to $M_c \propto 1/\nu_e$. Hence, M_c values decrease with increasing of the crosslinker amount.

References

[1] A. K. Bansal, A. Penzbofer, Chemical physics, No. 1-3, pp.48-56, 9-2008.

[2] K. Y. Chiu, T. X. Su, J. H. Li, T. H. Lin, G. S. Liou and S. H. Cheng, Journal of Electroanalytical Chemistry, Vol.575, No. 1, pp.95-101, 1-2005.

[3] J. Ricka and T. Tanaka, Macromolecules, Vol.17, No. 12, pp.2916-2921, 12-1984.

[4] J. Hrouz, M. Ilvasky, K. Ulbrich, and J. Kopecek, Eur Polym J, Vol.17, No. 4, pp.361-366, 5-1981.

sample code	NIPAAm (mol%)	TPA (mol%)	EGDMA (mol%)	Yield (%)
N-TPA3%	100	3		84.55
N-TPA6%		6		82.89
N-EGDMA3%			3	78.89
N-EGDMA6%			6	82.13

Table 1 Feed composition, and yield of the poly(NIPAAm) hydrogels

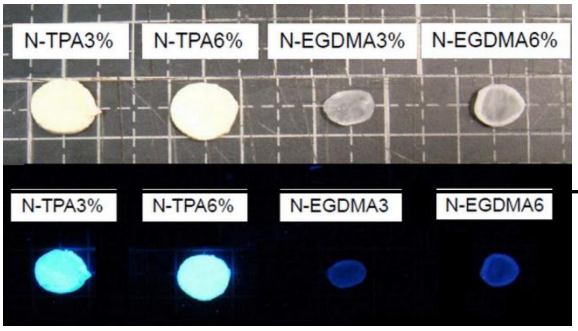

Figure 1 Appearance of a series of hydrogels based on N-series and under UV irradiation.

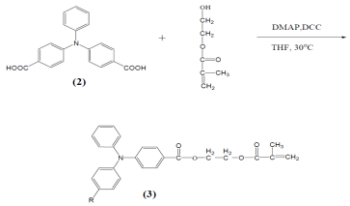

Scheme 1 Synthesis of dimethacryloyloxy ethylene oxycarbonyl triphenylamine (DMETPA).

Photovoltaic Cell Based on Lead sulfide\Conjugated Polymer Bilayer Heterojunction

F. Mighri [1,2], *J. Patel* [1,2], *A. Ajji* [1,3]

[1] Center for Research on Polymers and Composites, CREPEC

[2] Dep. of Chem. Eng., Laval University, Quebec, QC, G1K 7P4 Canada.

[3] Dep. of Chem. Eng., Ecole Polytechnique of Montreal, , Montreal, Quebec, QC, H3C 3A7 Canada

Frej.mighri@gch.ulaval.ca

Introduction: Recently, there has been a surge of interest in lead sulfide (PbS) nanostructured films because of their potential applications in optoelectronic devices. PbS has a large exciton Bohr radius of 18 nm and hence it exhibits strong quantum size effects. Their absorption edge can be tuned to anywhere from nearinfrared to visible [1]. For this reason, nanostructured PbS films are emerging materials for multilayer photovoltaic devices [2]. The objective of the present work is to develop an inorganic/organic heterojunction photovoltaic cell composed of size-quantized PbS and poly[2-methoxy-5-(2'-ethylhexyloxy)-p-phenylene vinylene] (MEH-PPV) layers deposited on indium tin oxide (ITO) coated glass substrate. PbS is used as an electron-transporting layer and MEH-PPV conjugated polymer is used for hole transport. **Experimental:** Aqueous solutions of lead acetate trihydrate (PbAc) and triethanolamine (TEA) were mixed in order to prepare PbAc-TEA complex. An aqueous solution of thiourea was then added into the PbAc-TEA complex solution and liquid ammonia was added into the resulted solution for complex decomposition. The ITO substrate was then inserted vertically and after 1 hour, a thin layer was deposited on the ITO surface. A viscous solution of MEH-PPV was prepared in toluene then deposited on this PbS layer using spin coating technique. Aluminum cathode was finally deposited on the heterojunction by thermal evaporation. **Results & Discussion:** Thickness and surface parameters of PbS nanostructured layers were characterized by AFM. It was found that these layers were highly uniform and show a porous network of PbS nanoparticles of around 11nm in size (Figure 1(a)). Film thickness (measured from Figure 1(b)) was uniform and was around 400nm. The composition of PbS film layer was characterized by XRD. The peaks shown in Figure 2 were identified to be those of cubic PbS. The average grain size estimated by the 'Scherrer equation' was around 11 nm, approximately the same as that measured by AFM. XPS was carried out in order to study the surface stability of PbS layer (Figure 3). It was observed that the surface of PbS layer is highly stable and there is no evidence of PbO phase (no surface oxidation). Figure 4(a) shows the optical absorption spectrum of the heterojunction. MEH-PPV layer absorbs strongly around 589 nm and after formation of junction with PbS layer, the total absorption shifted more towards the visible region. Total absorption of the device cell shows a band gap of around 1.65eV (Figure 4(b)). Figure 5 shows the voltage/current (I-V) characteristics of the developed heterojunction ITO\PbS\MEH-PPV\Al cell. Light power conversion under AM1.5 spectral conditions at 100 mW/cm^2 was around 0.39%.

References:

[1] Y. Wang et al., Chem. Phys. 87, 7315 (1987)

[2] R. Hawaldar et al., Mater. Sci. Eng. B. 132, 170 (2006)

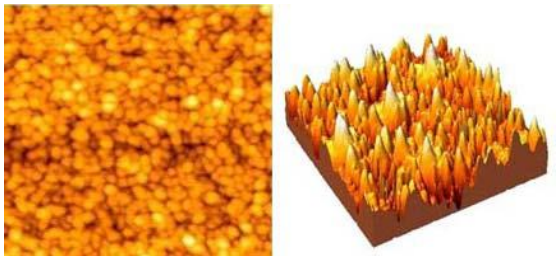

Figure 1: AFM of PbS layer **(a)** 2D and **(b)** 3D views.

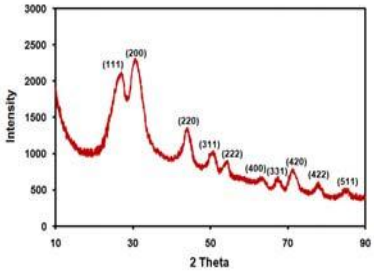

Figure 2: XRD of Pbs Layer.

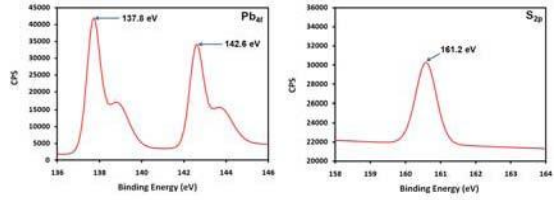

Figure 3: XPS of PbS Layer.

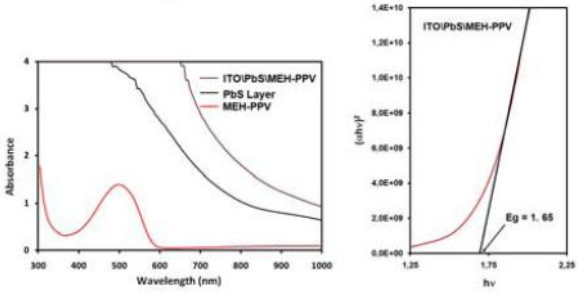

Figure 4: (a) Optical absorption spectra and (b) heterojunction band gap.

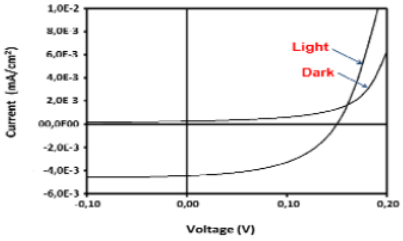

Figure 5: I-V Charactristrics of a bilayer heterojunction device.

Photoinduced Electron Transfer in an oligo-meta-phenylene ethynylene Donor-Bridge-Acceptor Complex

Bahar Bingöl†, Alec C. Durrell‡, Angel J. Di Bilio‡, Robert H. Grubbs†, Harry Gray‡

†The Arnold and Mabel Beckman Laboratory of Chemical Synthesis, Division of Chemistry and Chemical Engineering, ‡Beckman Institute, California Institute of Technology, Pasadena, California 91125.

bingol2@yahoo.com

Introduction.

Photoinduced long-range electron transfer (ET) plays a key role in artificial photosynthesis,[1-4] and optoelectronic devices.[5] The design of molecular systems for artificial photosynthesis and optoelectronic devices, that are capable of moving charge efficiently over long distances through molecular bridges, requires a fundamental understanding of ET in donor–bridge–acceptor (D-B-A) systems. Critical to all of these systems is the precise control of ET rates of long distances.

D-B-A complexes allow systematic investigation of parameters that control these ET processes. Previous studies of ET in D-B-A complexes showed that highly π-conjugated systems such as oligo(phenylene vinylenes),[7] oligo(fluorenes),[8] and oligo(para-phenylene ethynylenes)[9,10] as attractive materials. While there are numerous studies on D-B-A complexes para-phenylene ethynylene systems, [9,10] to the best of our knowledge, there is only one report of ET through conjugated chains of oligo(meta-phenylene ethynylenes) where organic compounds are used as electron acceptor and donor.[11] This is likely due to a combination of their time-consuming synthesis as well as a less conjugated structure that disfavors wire-like behavior. Despite these potential drawbacks, these systems possess many attractive qualities. Their relative flexibility allows for ET *via* through-space contacts and may favor efficient forward ET over charge recombination.

Here we report the synthesis and photophysical properties of the first D-B-A complex based on a transition metal derivative, rhenium tricarbonyl diimine, linked *via* oligo(meta-phenylene ethynylene) bridge to phenothiazine.

Materials and Methods.

Synthesis and Characterization. D-B ligand was constructed in a stepwise approach using zinc-mediated palladium-catalyzed cross-coupling reactions in a microwave reactor and protecting group strategies. The D-B-A complex (Scheme 1) was obtained by metalating the D-B ligand. The chemical structure of the complex was confirmed by nuclear magnetic resonance and mass spectroscopy. Steady-state and transient emission spectroscopy were employed to investigate the photoinduced electron transfer properties of the D-B-A.

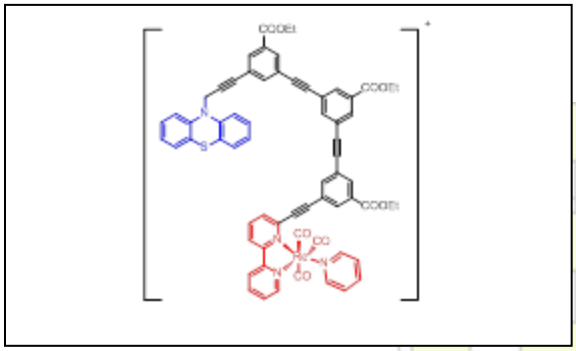

Scheme 1. Chemical structure of D-B-A

Results and Discusion.

Emission Properties. The steady-state emission spectrum of the D-B-A complex in dichloromethane solution has a broad band centered at 575 nm, which is characteristic of metal-ligand-charge-transfer emission of Re(I) complexes. Time-resolved emission spectroscopy was used to characterize the metal-to-ligand charge-transfer excited state of the D-B-A complex. The luminescence showed monoexponetial decay with reduced lifetimes compared to the reference compound, Re (I) $(CO)_3$(bipyridine)(pyridine). This suggests quenching attributed to phenothiazine → *Re ET. Rate constant for the electron transfer reaction is calculated as 1.8×10^5 s^{-1}.

Excited-state Electron Transfer. Deactivation of the D-B-A likely occurs through a combination of intermolecular and intramolecular ET processes. The rate of intermolecular ET and intramolecular ET were determined as 1.1×10^6 M^{-1} s^{-1} and 6×10^4 s^{-1}, respectively.

Conclusions.

A new D-B-A complex, where a rhenium tricarbonyl electron acceptor is linked *via* an oligo-*m*-phenylene-ethynylene bridge to a phenothiazine donor, was prepared. A combination of steady-state and transient emission spectroscopy indicate the D-B-A undergoes photoinduced long range ET.

References.

(1) Dempsey, J. L.; Winkler, J. R.; Gray, H. B. *Chem. Rev.* **2010**, *110*, 7024.
(2) Lewis, N. S.; Nocera, D. G. *PNAS* **2006**, *103*, 15729.
(3) Gray, H. B. *Nature Chemistry* **2009** *1*, 7.
(4) Eisenberg, R.; Gray, H. B. *Inorg. Chem.* **2008**, *47*, 1697.
(5) Saragi, T. P. I.; Spehr, T.; Siebert, A.; Fuhrmann-Lieker, T.; Salbeck, J. *Chem. Rev.* **2007**, *107*, 1011.
(7) Wasielewski, M. R. V.; Davis, W. B.; Svec, W. A.; Ratner, M. A. *Nature* **1998**, *396*, 60.
(8) Goldsmith, R. H.; Sinks, L. E.; Kelley, R. F.; Betzen, L. J.; Liu, W. H.; Weiss, E. A.; Ratner, M. A.; Wasielewski, M. R. *Proc. Natl. Acad. Sci. USA* **2005**, *102*, 3540.
(9) Eng, M. P.; Martensson, J.; Albinsson, B. *Chem. Eur. J.* **2008**, *14*, 2819.
(10) Creager, S.; Yu, C. J.; Bamdad, C.; O'Connor, S.; MacLean, T.; Lam, E.; Chong, Y.; Olsen, G. T.; Luo, J. Y.; Gozin, M.; Kayyem, J. F. *J. Am. Chem. Soc.* **1999**, *121*, 1059.
(11) Molina-Ontoria, A.; Fernandez, G.; Wielopolski, M.; Atienza, C.; Sanchez, L.; Gouloumis, A.; Clark, T.; Martin, N.; Guldi, D. M. *J. Am. Chem. Soc.* **2009**, *131*, 12218.

Synthesis and Photopolymerizations of New Hydrolysis-Stable Dental Monomers Containing Phosphonic Acids

Burçin Akgün, *Duygu Avci*

Department of Chemistry, Bogazici University 34342 Bebek Istanbul Turkey

avcid@boun.edu.tr

Introduction:

Monomers with phosphonic, mono- or dihydrogenphosphate or carboxylic acid groups have been synthesized and used in dental composites and dentin adhesives (1,2). These groups increase biocompatibility and adhesion to tooth by chelating with calcium in the tooth. However, monomers generally contain ester linkages which causes a serious problem due to hydrolysis under acidic conditions (3,4).

In this study, new phosphonated monomers that do not contain hydrolytically instable ester bonds have been designed to improve stability of dental materials. Besides hydrolytic stability, the synthesized monomers are expected to have other properties such as high rate of homo- and copolymerization, low polymerization shrinkage and high mechanical properties.

Materials and Methods:

Monomer and polymer characterization involved FTIR, ^{1}H-, ^{13}C-, ^{31}P-NMR. The photo-polymerizations were performed using a photo differential scanning calorimeter. Representative monomer synthesis is given below.

Synthesis of monomer **1a**

To a solution of diethyl 1-aminomethylphosphonate (0.099 g, 0.59 mmol) and anhydrous pyridine (0.047 g, 0.59 mmol) in 1.13 mL of dry dichloromethane, 2-(2-chlorocarbonyl-allyloxymethyl)-acryloylchloride (0.0598 g, 0.268 mmol) was added dropwise in an ice bath under N_2. After stirring overnight at room temperature, 5 mL of chloroform was added and the solution was extracted with water (2x2 mL), 2M HCl (2x3 mL), 2M NaOH (2x 3 mL) and brine (3 mL). After drying the organic phase with anhydrous Na_2SO_4, the solvent was evaporated. The yellowish viscous product was obtained in 67% yield.

Synthesis of **2a**

TMSBr (0.43 g, 2.78 mmol) was added dropwise to a solution of monomer **1a** (0.2245 g, 0.463 mmol) in 2 mL dry dichloromethane in an ice bath and under N_2. Then the solution was refluxed for 4 hours at 40 ^{0}C. After evaporation of the solvent, methanol was added and the mixture was stirred at room temperature overnight. The methanol was evaporated and the residue was washed with chloroform.

Results and Discussion:

The monomer synthesis involved the following steps: i) synthesis of TBEED from the reaction of t-butyl acrylate and paraformaldehyde in the presence of 1,4-diazobicyclooctane as catalyst, ii) conversion to acid by cleavage of t-butyl groups using trifluoroacetic acid, iii) conversion to acid chloride by using oxalyl chloride iv) reaction of the acid chloride and diethyl 2-aminoethylphosphonate and diethyl 1-aminomethylphosphonate to give monomers **1a** and **1b**, v) hydrolysis of phosphonate groups using trimethylsilyl bromide to give monomers **2a** and **2b** (Figure 1).

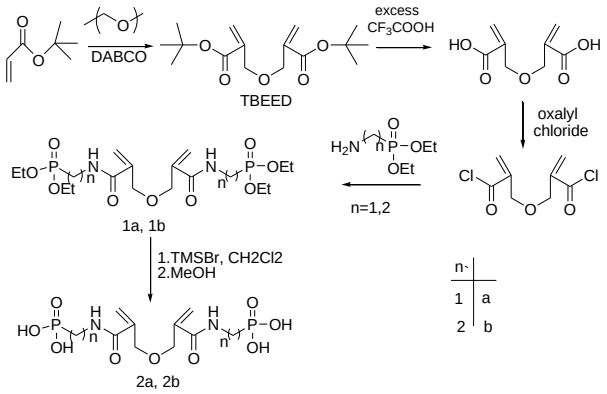

Figure 1. Synthesis of phosphonated-monomers.

Monomers were obtained in good yield as pure products. ^{1}H-, ^{13}C-, ^{31}P-NMR spectra confirmed the structure of the monomers. Phosphonated monomers **1a** and **1b** showed high crosslinking tendencies during thermal bulk and solution polymerizations. The homopolymerization and copolymerization behaviors of these monomers were also investigated with ethyl 2-hydroxy methacrylate (HEMA) using photo differential scanning calorimeter at 40 ^{0}C with 2,2'-dimethoxy-2-phenylacetophenone as initiator. Rate of polymerization of these monomers were found to be higher than TBEED.

Monomers **2a** and **2b** were found to be soluble in water and ethanol which is important for dental applications.

Conclusions:

Four novel monomers containing phosphonate or phosphonic acid groups have been prepared. The hydrolytic stability, binding efficiency and copolymerization studies of these monomers with HEMA and Bis-GMA are continuing.

Acknowledgements: Financial support of this research was provided by TUBITAK (109S382).

References:

1. Moszner, N.; Salz, U. Macromol Mater Eng 2007, 292, 245-271.

2. Moszner, N.; Salz, U.; Zimmerman, J. Dent Mater 2005, 21, 895-910.

3. Nishiyama, N.; Tay, F. R.; Fujita, K.; Pashley, D. H.; Ikemura, K.; Hiraishi, N.; King, N. M. J Dent Res 2006, 85(5), 422-426.

4. Inoue, S.; Koshiro, K.; Yoshida, Y.; De Munck, J.; Nagakane, K.; Suzuki, K.; Sano, H.; Van Meerbeek, B. J Dent Res 2005, 84(12), 1160-1164.

Nanocomposite Membranes Based on Nafion and $TiSiO_4$ nanoparticle

Yılser Devrim[a], Nurcan Baç[b], İnci Eroğlu[a]

[a]Chemical Engineering Department, Middle East Technical University, 06531, Ankara, Turkey
[b]Chemical Engineering Department, Yeditepe University, 34755, Istanbul, Turkey

yilser@gmail.com

Fuel cells are one of the most promising alternative power sources, with efficiencies of up to 60%, higher energy densities relative to batteries, and the ability to operate on clean fuels while producing no pollutants. Among fuel cells, Proton Exchange Membrane (PEM) Fuel Cells have received particular attention as a possible mobile electrical power source with high energy density. Proton exchange membrane is the key component of the PEM fuel cell for transferring protons from the anode to cathode as well as providing a barrier to the fuel gas cross-leaks between the electrodes.

Nafion is the PEM material most frequently used for this type of application because of its high proton conductivity, excellent mechanical properties, good chemical stability and commercial availability. However, the high cost, low stability at high temperatures, low conductivity at low humidity or high temperature limits the extent of its further application. Several approaches have been used to overcome this problem, such as the use of nanometer size inorganic filler in the Nafion matrix. The results showed that the modification of the polymer host membrane by the incorporation of hygroscopic oxides, such as ZrO_2, SiO_2, and TiO_2 particles, into Nafion has effectively extended the working temperature range. The inclusion of inorganic fillers improves the mechanical properties, the membrane water management and also contributes to inhibiting the direct permeation of reaction gases by increasing the transport pathway tortuousness.

Among the inorganic materials used in this field, TiO_2 and SiO_2 nanoparticles is good candidate as hydrophilic filler for the polymer membranes because it helps to maintain a suitable hydration of the membrane under fuel cell operating conditions, and the mechanical properties are improved.

In the present study, Nafion/Titanium Silicon Oxide ($TiSiO_4$) nanocomposite membranes for use in PEM fuel cells were investigated. Composite membranes were prepared using the recasting procedure and membrane thickness around 80µm was obtained from 10 wt.% $TiSiO_4$ loading. Nafion/$TiSiO_4$ nanocomposite membranes characterized by FTIR, thermal analysis, water uptake, XRD, SEM, EDS analysis and single cell performance. The introduction nanometer size $TiSiO_4$ supplies the composite membrane with a good thermal resistance and electrochemical performance. The physico-chemical properties studied by means of scanning electron microscopy (SEM) and X-ray diffraction (XRD) techniques have proved the uniform and homogeneous distribution of $TiSiO_4$ and the consequent enhancement of crystalline character of these membranes.

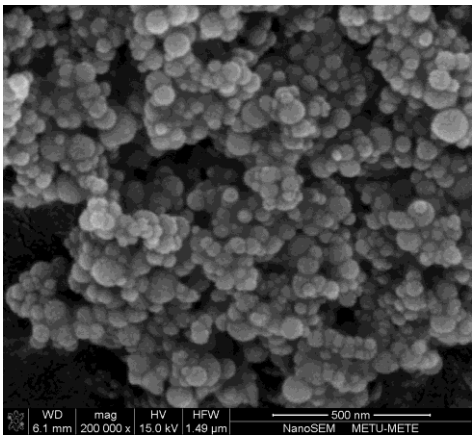

Figure 1. SEM image of $TiSiO_4$

The energy dispersive spectra (EDS) analysis indicated that the distribution of $TiSiO_4$ on the surface of the composite membrane was uniform. The membranes were tested in a single cell with a 5 cm^2 active area operating at 70 to 120°C. The results show that Nafion/ $TiSiO_4$ are promising membrane material for possible use in proton exchange membrane fuel cells.

Effect of processing conditions on the performance of polymer-based materials for biomedical applications.

Jimena Soledad Gonzalez, Leandro Nicolás Ludueña and Vera Alejandra Alvarez

Research Institute of Material Science and Technology (INTEMA), Engineering Faculty, National University of Mar del Plata, Juan B Justo 4302 (7600), Mar del Plata, Argentina.

jimena.gonzalez@fi.mdp.edu.ar

Introduction: Biocompatible polymers like polycaprolactone (PCL) and polyvinylalcohol (PVA) have several interesting properties that make them very interesting for biomedical applications; nevertheless many of them depend of the processing method.

In the case of wound dressing, the incorporation of nancoclays into PCL improves mainly the barrier [1] and mechanical properties [2]. This enhancement is strongly related with the clay dispersion degree [3]. The properties of PVA cryogels mostly depends on the crosslinking [4] and crystallinity degree [5]. On the other hand, it is still unclear the role that processing variables, such as the numbers of freezing/thawing (F/T) cycles, the cycle extent, the freezing temperature, , the polymer concentration and its molecular weight (*Mw*) play on the significant properties of the material.

The aim of this work was to analyze the effect of processing variables on the improvement of specific properties of of PCL-clay and PVA-hydrogel to be used as wound healing.

Materials and Methods: PCL-clay nanocomposites with 5 wt.% of organo-modified clay (Cloisite 20A, C20A, Southern Clay Inc.) were prepared by melt-intercalation in a micro-double-screw extruder DSM Xplore. The effect of processing conditions was analyzed by changing the residence time (2, 3 and 4 min), the temperature profile along the barrel ([60,80,100]°C; [60,90,120]°C; [70,100,130]°C) and the screw rotation speed (50, 100 and 150 rpm) . Materials were characterized by Differential Scanning Calorimetry (DSC): crystallinity (X_{cr}) and melting temperature (T_m) and by Gas Permeation Chromatography (GPC) to study the possible reduction of *Mw*. Then, films 0.5 mm thick were prepared by compression moulding and characterized by static tensile tests.

PVA-hydrogels were obtained from a aqueous solutions of 5, 10 and 15wt.% of PVA with different *Mw* (18000, 40500, 93500 and 155000) purchased by Sigma-Aldrich were prepared in distilled water at 85ºC for 4 h under constant stirring. Once the solutions were at room temperature, they were placed in ant adherent container and frozen (-18ºC) for 1, 12 or 24 h, then left at room temperature (25ºC) for the same times; cycle was performed 1 to 4 times. These obtained hydrogels were characterized by Thermogravimetric Analysis bound water content and degradation temperature and DSC: X_{cr} and T_m . Moreover, swelling behaviour, gel fraction (*GF*) and tensile properties were also determined.

Result and Discussion: The stiffness as well as the tensile strength and the deformation at break, of PCL and nanocomposites, were not substantially affected by processing conditions. Changing the extrusion parameters also had a negligible effect on the *Mw* and the X_{cr} of the matrix. It has been found [6] that shear forces in the melt-preparation of polymer layered silicates nanocomposites facilitate the brake-up of large sized agglomerates, whereas the extent of further exfoliation of the mineral layers is determined by the compatibility between the matrix and the mineral layers rather than by shear forces.

The strength and swelling ratio of the PVA-hydrogels were a function of the PVA concentration, the number of F/T cycles and *Mw*. As the number of F/T cycles, *Mw* and polymer concentration increased; the X_{cr} and *GF* increased too.

Conclusions: In the case of PCL-nanocomposites, the final properties will be strongly dependent on the clay dispersion degree. Once good polymer/clay compatibility is achieved, intense shear forces during processing (avoiding polymer matrix degradation) may accelerate the formation of the final clay morphology by breaking up large sized agglomerates but changing processing parameters will not modify the extent of clay dispersion.

For PVA-hydrogels an increment on the mechanical properties as a function on F/T cycles, *Mw* and polymer concentration were found. The results can be attributed to higher X_{cr} and crosslinking density. The repeated cooling and thawing back the hydrogel results in the formation of a stable three-dimensional network held together by crystals; the stability of the structure is reinforced by an increasing number of F/T cycles [7-8].

The obtained results suggest that it is possible to obtain polymers with controlled properties and to be optimist about their future use as wound dressing.

References:

[1] P. Messersmith and E. Giannelis. J. Polym. Sci. Part A: Polym. Chem. 33 (1995) 1047-1057.

[2] L. Ludueña, V. Alvarez, A. Vazquez. Mater. Sci. and Eng. A 460–461 (2007) 121–129.

[3] A. Ranade, K. Nayak, D. Fairbrother and N. D'Souza. Polymer 46 (2005) 7323–7333.

[4] R. Hernández, D. López, C. Mijangos,J.M. Guenet. Polymer 43 (2002) 56-61.

[5] R. Ricciardi, F. Auriemma, C. Gaillet, C. De Rosa, F. Laupretre. Macromol. 37 (2004) 9510-9516.

[6] D. Homminga, B. Goderis, S. Hoffman, H. Reynaers, G. Groeninck, Polymer 46 (2005) 9941–9954.

[7]N.A. Peppas, N. K. Mongia, Eur. J. Pharm. Biopharm. 43 (1997) 51-58.

[8]A. S Hickey, N.A Peppas, J. Membrane Sci. 107 (1995) 229-237.

Changing essential characteristics of Poly(vinylalcohol) cryogels by thermal treatments.

Jimena Soledad Gonzalez and Vera Alejandra Alvarez

Research Institute of Material Science and Technology (INTEMA), Engineering Faculty, National University of Mar del Plata, Juan B Justo 4302 (7600), Mar del Plata, Argentina.

jimena.gonzalez@fi.mdp.edu.ar

Introduction: The crosslinking method, based on freeze and then thaw (F/T) solution of Poly vinyl alcohol (PVA) several times, results in the formation of crystallites that serve as physical crosslinks making a three-dimensional network [1-2] that become the material insoluble in water. PVA molecules are aggregated during ice formation and hydrogen bonding is established between molecular chains. By increase the number of F/T cycles, residual free molecular chains are successively included in linking zones [3]. On the other hand, the glass transition temperature (T_g) of these kind of materials sharply decreases with the water content [4].

Heat treatments above the T_g [1-2] as well as repeated F/T cycles, are also used to achieve the same results mainly by increasing the amount of crystals of the polymer, which act as a physical crosslinkers of the network. When PVA films are annealed at constant temperature (between T_g and the melting temperature; T_m), the macromolecular chains have enough mobility to align themselves and fold to form crystals [2]. It is well known that the increasing in the polymer crystallinity degree (X_{cr}), results in a more resistant material [5].

The aim of this work was to investigate the effect of the annealing temperature over the structural and swelling characteristics of the PVA hydrogels obtained by F/T technique.

Materials and Methods: PVA hydrogels were obtained from a aqueous solutions of 10 wt.% of PVA (Mw 40500 g/mol, Sigma-Aldrich) were prepared in distilled water at 85ºC for 4 h under constant stirring. Once the solutions were at room temperature, they were placed in ant adherent mold and frozen (-18ºC) for 12 h, then left at room temperature (25ºC) for the same time; this cycle was repeated for 3 times. Then, dried (37ºC, 24 h) PVA hydrogel samples were annealed at different temperatures: 100, 110, 120, 130 and 140ºC in an oven for 1 h. These temperatures were selected because they were over the water evaporation temperature, and between the T_g and the T_m of the polymer. Hydrogels were characterized by Differential Scanning Calorimetry (DSC), to obtain T_g , T_m and X_{cr}; Scanning Electron Microscopy (SEM) to observe the porous structure, Thermogravimetric Analysis (TGA) to obtain the bound water content (*BW*). Moreover, swelling behavior (Equilibrium swelling degree, M_t and Thickness change, *TC*) in saline solution and gel fraction (*GF*) were also studied.

Results and Discussion: The porous of PVA hydrogles showed a wide distribution; the average size was 0.51± 0.22 µm. **Figure 1** shows the changes on T_g as a function of annealing temperature (AT). **Table 1** displays the main characteristics of hydrogels as a function of the heat treatment applied.

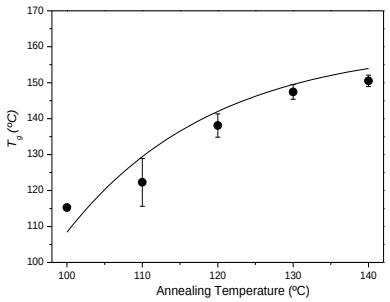

Figure 1. Effect of AT on the T_g

Table 1: Main characteristics of PVA hydrogels as a function of AT.

AT ºC	X_{cr} %	M_∞ %	BW %	GF %	TC %
none	28.8±8.9	186.2±2.2	9.5	44.7±0.1	142.3±32.8
100	33.2±4.1	194.6±9.4	7.8	63.9±1.4	100.3±6.7
110	52.2±1.9	177.7±10.2	*	77.3±1.7	*
120	34.7±3.6	146.3±5.2	7.2	83.5±2.1	85.57±13.9
130	38.6±1.9	109.6±9.4	6.9	96.3±4.4	*
140	42.7±5.2	70.7±6.0	7	98.1±1.0	43.6±10.2

* It was not possible to measure

T_g increasing exponentially with annealing temperature. T_g is related to the crosslinking degree and with the plasticize content, so that, the previous result can be attributed to a raise on the crosslinks and a decrease on water content (bound and unbound) [6]. According to that, GF increases and BW decreases.

It can be observed that the thermal annealing of PVA hydrogels have a direct influence on relevant hydrogels characteristics. Both, the X_{cr} and the T_g, which are measurements of crosslinking degree, increased as a function of the annealing temperature. Moreover all the most important properties of the hydrogels were influenced by these changes: the maximum swelling degree, the *TC* and the *BW* decreased whereas the *GF* increased as a function of AT. An exponential relationship between the main characteristics *GF* and X_{cr} was found. All these result were independent of the polymer concentration.

Conclusions: The obtained results indicate that PVA-hydrogels with desired characteristics can be obtained by means of a thermal treatment.

References:

[1]C.M. Hassan, N.A. Peppas, Adv. Polym. Sci. 153(2000) 37- 65.

[2]S.K. Mallapragada, N.A. Peppas, J. Polym. Sci. Part B: Polym. Phys. 34 (1996) 1339-1346.

[3]T. Hatakeyemaa, J. Unoa, C. Yamadaa et al. Thermochim. Acta 431 (2005) 144–148.

[4]J. Rault, Z.H. Ping, Q.T. Nguyen, J. Non-Cryst. Solid 172–174 (1994). 733–736.

[5]P.J. Willcox, D.W. Howie Jr, K. Schmidt-Rohr et al, J. Polym. Sci. B: Polym. Phys. 37 (1999) 3438-3454.

[6]J.L. Holloway, A. M. Lowman, G.R. Palmese, Acta Biomateriala 6 (2010) 4716-4724.

Highly-Ordered Nanoporous TiO_2 Films with Hierarchical Order directed by Self-Assembly

*Wonho Kim, Su Yeon Choi, Young Chan Kim, Seung Hyun Kim**

Division of Nano-Systems Engineering, Inha University, Incheon 402-751, South Korea

shk@inha.ac.kr

Introduction: Self-assembly has well been established as promising alternative to fabricate well-ordered nano-structures and nanoscale devices. Block copolymers, one class of self-assembling materials, have shown that they can be effectively utilized as templates and scaffolds for nanofabrication.[1] Furthermore, combining with chemical contrast between components enables block copolymer self-assembly to guide the formation of inorganic nanomaterials with well-defined structure that otherwise would be hardly produced. On the other hand, colloidal particles are also well-known to spontaneously produce crystal arrays with two- or three-dimensionally periodic lattices of monodisperse colloidal spheres,[2] providing opportunity for wide range of applications including photonic/electronic devices, nanoporous materials for catalyst supports, sensors, data storage media, and nanolithography.[3] However, self-assembly of one class can only produce simple pattern with regular periodicity, and highly-ordered colloidal crystals composed of particles of sub-100 nm diameter are very difficult to achieve via self-assembly.[4] In our work, two self- assembling materials are sequentially combined to produce nanoporous TiO_2 films with well-defined yet hierarchical order.

Materials and Methods: Polystyrene-*b*-poly (ethylene oxide) (PS-*b*-PEO) diblock copolymer having the molecular weight of 30,000 g mol^{-1} with 77 wt% PS was purchased from Polymer Source Inc., and used as a structure-directing agent. Titanium isopropoxide, hydrochloric acid and isopropyl alcohol were used for inorganic precursor solution. Suspensions of polystyrene (PS) spheres with 100 nm (4.5 nm Std Dev; 4.6 % CV) and 50 nm (7.2 nm Std Dev; 15.7 % CV) diameter were purchased from Duke Scientific. For preparation of template, PS-*b*-PEO diblock copolymer was first dissolved in 1,4-dioxane. As an inorganic precursor, titanium isopropoxide and hydrochloric acid was added into isopropyl alcohol and then stirred for 2 hours. Polymer solution and inorganic precursor were mixed at various volume ratios and stirred 1 hour. Organic/ inorganic hybrid film were deposited by spin-coating onto Si wafer substrate and were calcination at 500 °C for 1 hour or exposed to UV irradiation for overnight to remove PS-*b*-PEO. Titania films obtained so were used as a template for fabrication of colloidal crystals. Titania templates and colloidal crystals were characterized with multimode V scanning probe microscope (AFM, Digital Instruments/Veeco), and FE-SEM (Hitachi S-4300SE).

Results and Discussion: PS-*b*-PEO block copolymers used in this work can act as a structure-directing agent since titanium precursor is selectively incorporated into hydrophilic PEO domains through the coordination bonds. Figure 1 exhibits such results where different TiO_2 nanostructures including hole, line and cup patterns were directed by block copolymer self-assembly, depending on the amount of precursor added to block copolymer solution. As second step, nanoporous TiO_2 films shown in Figure 1 were used as a template for colloidal crystallization, and

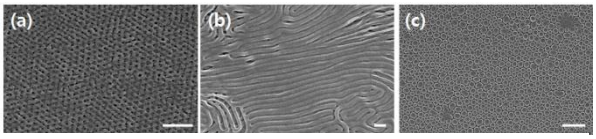

Fig. 1 SEM images on TiO_2 films after calcination for PS-*b*-PEO/ TiO_2 precursor 100/200 (a), 100/30 (b), and 100/10 (c).

the results are presented in Figure 2. Generally colloidal particles with 50 nm in diameter are very difficult to generate regular crystal arrays due to polydispersity in size. However, as seen in Figure 2(a), when the template with highly-ordered nanostructure was used, small nanoparticles can produce well-order arrays along template pattern. Small colloidal particles were also found to be guided by cup pattern, where PS nanoparticles sit on the cup template as well as between cups, as shown in Figure 2(b). When titanium precursor was applied for PS colloidal crystals and then calcined, inverted and nanoporous structure was generated, as seen in Figure 2(c). Nanopores are highly ordered according to PS colloidal crystals. Their size in Figure 2(c) is different from that produced from block copolymer self-assembly, and consequently, hierarchical nanoporous TiO_2 films with two different lengths was produced successfully.

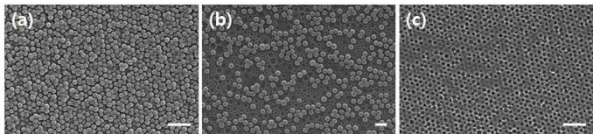

Fig. 2 SEM images on colloidal crystals and their inverted structure guided by TiO_2 nanoporous films shown in Figure 1.

Conclusions: It has been here demonstrated that nanoporous TiO_2 films with hierarchical order can be produced by combining self-assembly of two different systems, block copolymers and colloidal particles. These films with well-ordered, hierarchical structure can potentially be utilized for energy-conversion/energy-storage devices with enhanced efficiency.

Acknowledgements: This work was financially supported by the National Research Foundation of Korea (NRF) grant (No. 2010-0015541) funded by the Ministry of Education, Science and Technology (MEST).

References

1. Kim, D. H.; Sun, Z. C.; Russell, T. P.; Knoll, W.; Gutmann, J. S., *Adv. Funct. Mater.* **2005,** 15, 1160.
2. Chung, Y. W.; Leu, I. C.; Lee, J. H.; Hon, M. H., *Langmuir* **2006,** 22, 6454.
3. Kim, M. H.; Im, S. H.; Park, O. O., *Adv. Funct. Mater.* **2005,** 15, 1329.
4. Schumann, S.; Bon, S. A. F.; Hatton, R. A.; Jones, T. S., *Chem. Commun.* **2009**, (42), 6478.

Synthesis of Regioregular Poly(3-hexylthiophene) with Low Polydispersity Using Zincate Complex: Toward a Purification-Free System

Tomoya Higashihara and Mitsuru Ueda

Department of Organic and Polymeric Materials, Graduate School of Science and Engineering, Tokyo Institute of Technology, 2-12-1-H-120, O-okayama, Meguro-Ku, Tokyo 152-8550, Japan

e-mail: thigashihara@polymer.titech.ac.jp

There has been growing attention paid to poly(3-alkylthiophene)s (PATs) in many fields of polymer electronic devices, because PATs are the best class of balanced high-performance materials as *p*-type semiconductors in terms of solubility, chemical stability, charge mobility, and commercial availability. Since the quasi-living GRIM polymerization system based on chain-growth polymerization has been discovered by McCullough et al.,[1] followed by the improvement by Yokozawa et al.[2], it becomes possible to yield head-to-tail (HT)-PATs with controlled molecular weights (MWs) and low polydispersity indices (PDIs). However, thorough purification steps of monomers and solvents are often necessary in this system, because highly-reactive and moisture-sensitive Grignard agents are employed.

Herein we report the first demonstration of quasi-living catalyst-transfer polycondensation for the synthesis of high-MW regioregular HT-poly(3-hexylthiophene) (P3HT) using a dianion-type zincate complex, dilithium tetra(*tert*-butyl) zincate (^{t}Bu$_4$ZnLi$_2$), toward a purification-free polymerization system.

We first investigated the halogen-metal exchange reaction of 2-bromo-3-hexyl-5-iodothiophene (**1**) with an equivalent molar of ^{t}Bu$_4$ZnLi$_2$ in THF at 0 °C. After quenching the reaction with HCl solution or allyl bromide, 2-bromo-3-hexylthiophene or 5-allyl-2-bromo-3-hexylthiophene, respectively, was obtained quantitatively, which indicates that the halogen-metal exchange reaction took place quantitatively and selectively at 5-position to afford a zincate complex of thiophene monomer, dilithium tris(*tert*-butyl)-(2-bromo-3-hexyl-5-thienyl) zincate (**2**) (see Scheme 1). Based on these successful results, the catalyst-transfer polycondensation of **2** was performed with a Ni catalyst in THF (see also Scheme 1). The results are summarized in Table 1.

Scheme 1. Halogen-Metal Exchange Reactions and Catalyst-Transfer Polycondensation for Synthesis of Regioregular HT-P3HT Using ^{t}Bu$_4$ZnLi$_2$

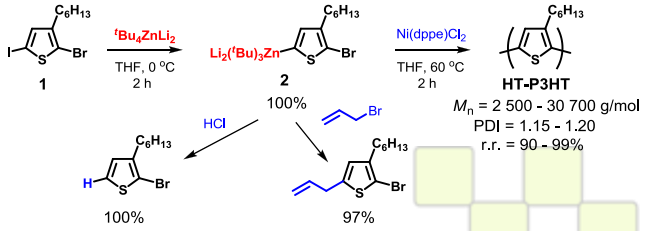

The polymerization of **2** proceeded in a controlled manner using 1,3-bis(diphenylphosphino)ethanenickel dichloride (Ni(dppe)Cl$_2$) as the catalyst in THF at 60 °C to afford HT-P3HTs with predicted M_n values (2.50 to 30.7 kDa) and low PDIs (<1.2) in high yields (run 1-5).

Table 1. Characterization Results of P3HT Obtained by Catalyst-Transfer Polycondensation of **2** Using ^{t}Bu$_4$ZnLi$_2$ in THF[a]

The regioregularity (r.r.) of high-MW P3HT (>10 kDa) was more than 97%, as determined by ^{1}H NMR.

run	Additive[b]	Yield[c]	[**1**]$_0$/[Ni]$_0$	M_n[d] (kDa)	PDI[d]	r.r.[e]
1		90	15	2.50	1.20	90
2		88	30	5.40	1.18	94
3		90	60	10.2	1.15	97
4		85	120	21.7	1.15	98
5		80	180	30.7	1.19	99
6[f]		75	60	11.5	1.17	97
7	^{i}PrOH	60	60	10.9	1.15	97
8	H_2O	50	60	16.8	1.72	97

[a]The polymerization was carried out using Ni(dppe)Cl$_2$ at 60 °C for 2 h. [b]Additives ([Additive]$_0$/[**1**]$_0$ = 1.0) were placed before the halogen-metal exchange reaction. [c]The yields of P3HT were determined by gravimetry after precipitation. [d]M_n and PDI were determined by SEC using polystyrene standards without soxleht extraction. [e]The regioregularity (r.r.) was determined by comparing the peak intensities of thienyl methylene protons in ^{1}H NMR spectra after soxleht extraction with methanol, acetone, and chloroform. [f]Undistilled THF (dehydrated, stabilizer-free, Wako Pure Chemical Industries Ltd., 99.5%) was used.

We next intended to apply the developed polymerization system to purification-free media, such as undistilled THF or THF containing protic impurities, toward low-cost mass production of HT-P3HT. The halogen exchange reaction of **1** with ^{t}Bu$_4$ZnLi$_2$ followed by polymerization of **2** with Ni(dppe)Cl$_2$ was carried out in undistilled THF (dehydrated, stabilizer-free, Wako Pure Chemical Industries Ltd., 99.5%) (run 6). As a result, HT-P3HT with controlled MW and low PDI could be obtained. Surprisingly, a similar experiment in THF containing a protic impurity of ^{i}PrOH ([^{i}PrOH]$_0$/[**1**]$_0$ = 1.0, [^{i}PrOH]$_0$/[Ni(dppe)Cl$_2$]$_0$ = 60) was also successful (run 7). Furthermore, high-MW HT-P3HT could be obtained in 50% yield in THF containing 1000 ppm water ([H_2O]$_0$/[**1**]$_0$ = 1.0, [H_2O]$_0$/[Ni(dppe)Cl$_2$]$_0$ = 60), although PDI increased to 1.72 (run 8). As a comparison, the GRIM polymerization system was attempted in purification-free media of THF. However, no polymerization took place at all in undistilled THF or in THF containing ^{i}PrOH or water under typical conditions, probably due to the termination of highly-sensitive Grignard agents toward impurities.

In conclusion, the selective halogen-metal exchange reaction of **1** with ^{t}Bu$_4$ZnLi$_2$ and quasi-living catalyst-transfer polycondensation of **2** with Ni(dppe)Cl$_2$ have been first demonstrated for the synthesis of high-MW regioregular HT-P3HT in high yields. This system was also realized in a purification-free polymerization media of THF, even in the presence of water.

References: (1) Iovu, M. C.; Sheina, E. E.; Gil, R. R.; McCullough, R. D. *Macromolecules* **2005**, *38*, 8649.
(2)Miyakoshi, R.; Yokoyama, A.; Yokozawa, T. *J. Am. Chem. Soc.* **2005**, *127*, 17542.

Improvement of Mechanical Properties of Soy Protein-Based Films

Pedro Guerrero, Tania Garrido, Sara Cabezudo, Koro de la Caba

Escuela Universitaria Politécnica. Plaza Europa 1. 20018 Donostia-San Sebastián, Spain

koro.delacaba@ehu.es

Introduction

Plastics are one of the most important materials employed in daily life. However, environmental pollution from their consumption has become a serious issue, particularly when they are used as one-time use packaging materials. To overcome this problem, biopolymers produced from natural resources are regarded as an attractive alternative since they are abundant, renewable, inexpensive, environmentally friendly and biodegradable. Among biopolymers, soy protein is a potential replacement for petroleum-based products due to its low cost, easy availability and biodegradability (1). Moreover, soy protein is extracted from soybeans used to obtain soy oil. During this process, soy flour is obtained as a secondary product and it can be purified to obtain soy protein concentrates (SPC) and soy protein isolates (SPI), which would add value to agricultural by-products. Although optimization in processing methods is required, this kind of proteins could offer significant opportunities to develop improved packaging materials in the future. These soy-based plastics could be employed as sort-term use or one-time use plastic products in place of the non-biodegradable materials currently used. Once disposed of, soy-based plastic does not take long to biodegrade and is safer for the environment than more durable petroleum based plastics. Furthermore, soy protein could be used for food packaging purposes since it meets food grade standards.

Materials and Methods

Soy protein isolate PROFAM 974 was supplied by Lactotecnia, S.L. (Barcelona, Spain). The commercial bovine gelatin type A (bloom 200/220) was obtained from Sancho de Borja S.L. (Zaragoza, Spain). Glycerol used in this study was food grade reagent obtained from Panreac.

SPI-based films with different gelatin contents (5, 10, and 15% by weight on SPI dry basis) were prepared by dispersing SPI and gelatin in distilled water. Dispersions were heated at 80 ºC and stirred. The pH of the dispersions were adjusted to the desired values (pH 1.4, 4.6, 7.5 and 10.0) with 0.1 M HCl or NaOH solutions. Then, glycerol was added as plasticizer at SPI/glycerol ratio: 70/30 (w/w), which was chosen on the basis of previous experiments (2). After that, dispersions were maintained at 80 ºC under stirring. Subsequently, these samples were dried at room temperature or freeze-dried and hot-pressed at 150 ºC and 12 MPa.

SPI-based films were designed as a function of gelatin content (5, 10, or 15%). Gelatin-free films were also prepared as control films and designed as SPI30.

Samples for tensile tests were bone shaped with a thickness of about 70-100 µm. Before testing, the samples were maintained for 48 h in a relative humidity of 50% at 25 ºC in a climatic chamber.

An electromechanical testing system (MTS Insight 10) was used to determine mechanical properties. Elastic modulus (E), tensile strength (σ) and elongation at break (ε) were determined according to ASTM D1708-93. Bone-shaped specimens (4.75 mm wide and 22.25 mm long) were cut. Five replicates were tested for each composition.

Results and Discussion

Soy protein is a polymer with polar and non-polar side chains, which present strong intra- and inter-molecular interactions, and restrict segment rotation and molecular mobility, leading to brittle films. The addition of glycerol makes them easy to handle because glycerol molecules reduce the strong interactions among the protein chains, so thus increasing elongation at break, but also decreasing tensile strength. However, this effect is greater for the films processed by casting than for the ones obtained by compression due to the natural plasticization effect of water, so it can be said that compression molded films present better balanced mechanical properties. Taking the above in consideration, the effect of pH on mechanical properties has been studied for the compression molded films. Increasing pH increases elongation at break because the grade of protein denaturation is favored at basic pHs, at which protein polar groups are exposed and can interact with glycerol molecules, so thus the strong hydrogen bonding among the protein chains is reduced, and the extensibility of the films is increased.

The highest tensile strength with a similar elongation at break, were obtained when 15% of bovine gelatin was added in the system plasticized with 30% of glycerol at pH 10. This improvement could be due to the high proline and hydroxyproline content in bovine gelatin, which could promote the formation of more ordered networks.

Conclusions

Experimental results reveal that films obtained by compression exhibit better mechanical properties than the ones processed by casting, allowing the processing of soy proteins by the methods employed for conventional plastics. On the other hand, films prepared at pHs higher than the one corresponding to the SPI isoelectric point (pH 4.6) exhibit much better strength and elongation at break than the ones processed at lower values. In all the cases, the films were transparent, and in the case of pH 10.0, apart from the best mechanical properties, the films present less yellow colour.

Mechanical properties of the gelatin-incorporated SPI-based films were affected by gelatin concentration. When gelatin was added, SPI-gelatin interactions were induced, leading to a great reinforcement of the film.

Acknowledgments

The authors thank MICCIN (project MAT2009-07735) for their financial support.

References

1. A. Gennadios, *Protein-based films and coatings*, Florida: CRC Press (2002).
2. P. Guerrero, A. Retegi, N. Gabilondo, and K. de la Caba. *J. Food Eng.*, **100**, 145 (2010).

Polyaniline–silver composites: Oxidation of aniline with silver nitrate accelerated by *p*-phenylenediamine

Patrycja Bober, Miroslava Trchová, Jaroslav Stejskal

Institute of Macromolecular Chemistry, Academy of Sciences of the Czech Republic, 162 06 Prague 6, Czech Republic

bober@imc.cas.cz

Polyaniline is one of the most famous conducting polymer, on account of its high electrical conductivity, environmental stability, ease of preparation from common chemicals, good processibility, and relatively low cost. In the last years, the interest in polyaniline–silver composite is growing; the presence of silver still improving their conductivity. Such materials may also potentially be useful in applications, such as water treatment, noble-metal recovery, antibacterial substances, electrode materials, electrocatalysis, *etc.* [1].

Aniline, *p*-phenylenediamine, or their mixtures of various compositions were oxidized with silver nitrate in 1 M nitric acid or 1 M acetic acid at room temperature. Products, the composites of polyaniline or poly(aniline-*co*-*p*-phenylenediamine) and silver, were characterized by Fourier-transform infrared, UV–visible spectra, conductivity and density measurements, and transmission electron microscopy.

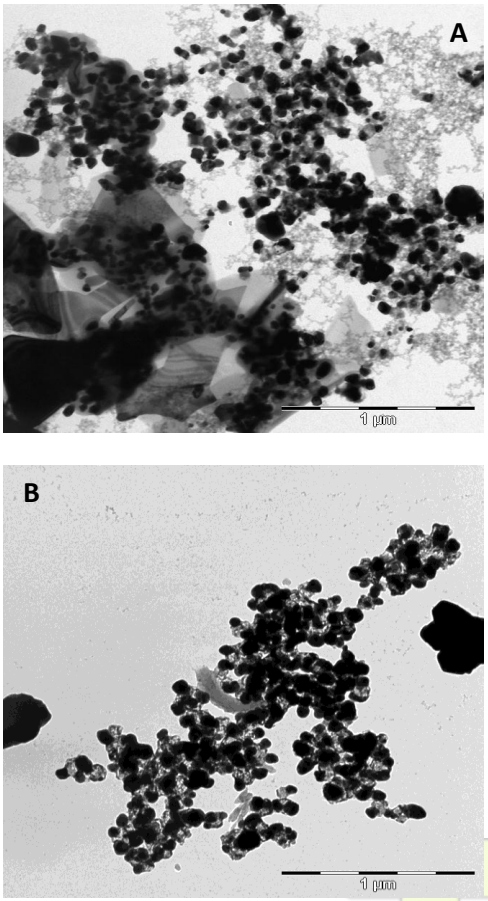

Figure 1. Micrographs of composites prepared with (A) 5 mol% *p*-phenylenediamine and (B) 60 mol% *p*-phenylenediamine mixtures with aniline in 1 M acetic acid, using silver nitrate as oxidant.

The oxidation of aniline with silver nitrate in is slow and takes over several months [2,3], an addition of a small amount of *p*-phenylenediamine, even 1 mol. % relative to aniline, shortens the reaction time to several hours or even minutes. Higher concentration of *p*-phenylenediamine produces conducting copolymer composites. Also *p*-phenylenediamine alone is similarly able to be oxidized to poly(*p*-phenylenediamine) and produce a composite with silver. Silver is present in the composites as nanoparticles of ~50 nm size (Figure 1) and as larger objects. The composites had conductivity in the range of the order of 10^{-3} to 10^{3} S cm^{-1} at comparable content of silver, which was close to the theoretical expectation, 68.9 wt.%. The composites prepared in 1 M acetic acid always have a higher conductivity, compared with those resulting from synthesis in 1 M nitric acid [4].

The acceleration of aniline oxidation with silver nitrate by small amounts of *p*-phenylenediamine is one of new ways to the preparation of polyaniline–silver composites. The composites are produced in short time with relatively high yield and very good conductivity.

References

1. I. Sapurina, J. Stejskal; *Polymer International* **2008**, 57, 1295.
2. N.V. Blinova, P. Bober, J. Hromadková, M. Trchová, J. Stejskal, J. Prokeš; *Polymer International* **2010,** 59, 437.
3. P. Bober, J. Stejskal, M. Trchová, J. Hromadková, J. Prokeš; *Reactive & Functional Polymers* **2010,** 70, 656.
4. P. Bober, J. Stejskal, M. Trchová, J. Prokeš, I. Sapurina; *Macromolecules* **2010,** 43, 10406.

Light Triggered Solutes Release from Covalent DNA Gels

Diana Costa[1], *A. J. M. Valente*[2], *M. Miguel*[2] *and B. Lindman*[3]

[1] Health Sciences Center, University of Beira Interior, Covilhã, Portugal
[2] Chemistry Department, Coimbra University, Coimbra, Portugal
[3] Physical Chemistry 1, Centre for Chemistry and Chemical Engineering, Lund University, Sweden

dcosta@fcsaude.ubi.pt

Introduction. We gained a deeper understanding of the release of different molecular weight solutes from photodegradable cross-linked DNA gels. In a first approach, the gel mesh size was determined and the ultraviolet range that causes the maximum network degradation was characterized. Then, we investigated how the disruption-dependent network swelling relates to the mesh size and the latter to the solute release behaviour.
Results and Discussion. Different cross-linker densities (0.5 %, 1 %, 3 % and 5 % ethylene glycol diglycidyl ether) DNA gels were studied as photodegradable systems, by ultraviolet light exposure, to control the release of DNA and high molecular weight, hydrophilic solutes. Network mesh size and the extent of swelling during degradation have been determined to characterize the effect of hydrogel degradation kinetics and simultaneous changes in gel structure on solute release profile. Modelling release kinetics, using Weibull function, can predict the DNA release pattern, which are dependent on both wavelength radiation and cross-linker concentration, and its mechanism of desorption, rather complex. Moreover, concerning the solutes release it can be inferred that not only hydrated radii play an important role, but other effects are also involved in the release mechanism and there is a clear difference between the mechanism for lysozyme and BSA and FITC-dextran. Conclusions. The Weibull function can describe the DNA release profiles and shows that they are dependent on both radiation wavelength and cross-linker concentration; the mechanism of DNA desorption is rather complex. There is no effect on the gel matrix with low energetic radiation and the diffusion of DNA is controlled by its concentration, whereas, by increasing radiation energy some interaction with DNA and/or EGDE takes place at the surface acting as an obstacle. Solute release from DNA gels is strongly affected by the relative value of the network mesh size and the hydrodynamic radius of the solute. In the presence of light, the release mechanism for lysozyme and BSA follows a Fickian diffusion, while FITC-dextran release presents a sigmoid curve indicating a more complex mechanism. In the absence of light, the solute release behaviour is significantly different. Although, lysozyme release is quite analogous to that occurring in the presence of light, BSA and FITC-dextran show a three-step released mechanism. The latter two steps are similar for both molecules, presenting a Super Case II transport, while the initial step indicates a different behaviour, probably related to the size of the desorbed particles.

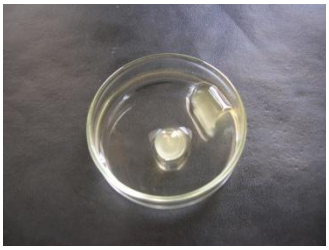

Figure 1. Picture from a ds-DNA gel prepared with 1% cross-linker density.

Surface properties of cationic polyelectrolytes hydrophobically modified

Hernán E. Ríos, Javier González and Marcela D. Urzúa.*

Department of Chemistry. Faculty of Sciences. University of Chile

hrios@uchile.cl

Amphipathic hydrophilic polyelectrolytes display in water solution two kinds of behavior depending on their hydrophobic/hydrophilic balance. The stabilization in the water phase is related with the trend of these systems to hypercoiling by hydrophobic interactions adopting a micelle-like structure. These polymers can eventually migrate spontaneously at the air-water surface or to a liquid-liquid interface. Works considering surface properties of polyelectrolytes have been focused to anionic systems. Therefore, poly (N,N-dimethyl-N,N-diallyl ammonium) chloride, a highly hydrophilic cationic polyelectrolyte, was hydrophobically modified and the surface properties of the resulting amphipathic polyelectrolytes were determined. The chemical modification was performed according to the method of Quina[1] et al., as follows:

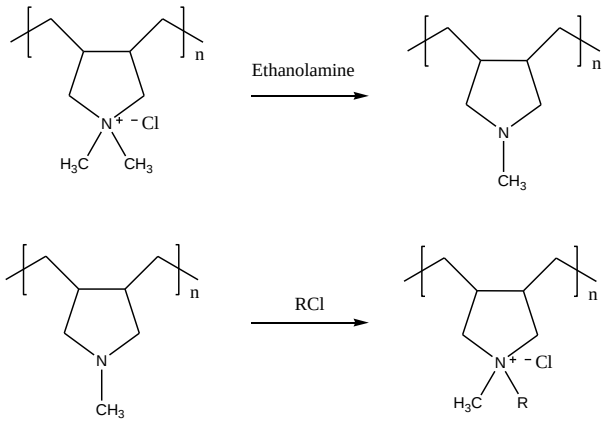

Figure 1. Surface tension behavior of PC12 (∇), PC10 (O), PC8 (Δ) and PC6(□) at 298 K

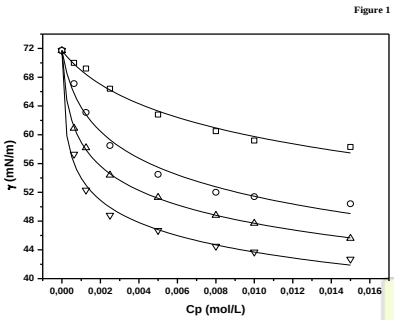

The surface tension curves were treated according to the Gibbs-Szyszkowski equation[2] and the results are summarized in the following Tables

Table 1. Limiting excess surface concentration, areas covered by monomer and PC_{20}

T(K)	*PCn*	$\Gamma^{\infty} x10^{10}$ $(mol\ cm^{-2})$	$\sigma x10^{16}$ (cm^2)	pC_{20}
283	PC6	3.46	48.0	1.09
	PC8	2.86	58.0	1.92
	PC10	2.34	71.0	2.26
	PC12	2.17	76.4	2.77
298	PC6	2.38	69.8	1.28
	PC8	2.32	71.5	2.05
	PC10	2.18	76.1	2.36
	PC12	2.02	82.3	2.78
308	PC6	2.20	75.6	1.25
	PC8	2.10	79.0	2.06
	PC10	2.01	82.6	2.57
	PC12	1.86	89.4	2.88

Table 2. Standard free energy adsorption contributions

T(K)	*PCn*	$-\Delta G^{o}_{ads}$ $(kJ\ mol^{-1})$	$-\Delta G^{o}_{tr}$ $(kJ\ mol^{-1})$	$-\Delta G^{o}_{int}$ $(kJ\ mol^{-1})$
283	PC6	21.2	15.4	5.8
	PC8	26.9	19.9	7.0
	PC10	30.3	21.7	8.6
	PC12	33.7	24.5	9.2
298	PC6	25.6	17.2	8.4
	PC8	30.3	21.7	8.6
	PC10	32.6	23.4	9.2
	PC12	35.7	25.8	9.9
308	PC6	26.8	17.7	9.1
	PC8	32.0	22.5	9.5
	PC10	35.4	25.4	10.0
	PC12	38.1	27.3	10.8

Table 4.Standard entropies and enthalpies of adsorption.

PCn	$T\Delta S^{o}_{ads}$ $(kJ\ mol^{-1})$	ΔH^{o}_{ads} $(kJ\ mol^{-1})$
PC6	68.6	44.9
PC8	61.4	32.1
PC10	59.6	26.9
PC12	51.5	15.5

The standard free energy of the adsorption process, ΔG^{o}_{ads}, was a linear function of the number of carbon atoms in the lateral chain as well as their transfer and interfacial contributions to the adsorption process with a -1.73 $kJmol^{-1}$ of methylene group to ΔG^{o}_{ads}. From the dependence of the surface tension with the temperature the ΔS^{o}_{ads} was determined. The latter parameter was always positive regardless the polyelectrolyte side chain length, thus the main driving force to ΔG^{o}_{ads} arises from the large positive ΔS^{o}_{ads} values.

References

1.Bazito RC, Cassio FL and Quina FH, *Macromol. Symp* **229:** 197-202 (2005)

2. Ríos HE, Fonseca CK, Brito C, Urzúa MD and Cabrera WJ, *J. Macromol. Sci. Part B. Physics* **45:** 335-342 (2006).

Acknowledgements. The financial support of Fondecyt (1090092) is recognized

Release of amoxicillin embedded in cellulose acetate-poly(vinyl pyrrolidone) fibers by coaxial electrospinning

M.M. Castillo-Ortega[1], A.L. Nájera-Luna[1], D.E. Rodríguez-Félix[1], F. Rodriguez-Félix[1], J. Romero-García[2], P.J. Herrera-Franco[3]

[1]Universidad de Sonora, C.P. 83 000, Hermosillo, Sonora, México
[2]Centro de Investigación en Química Aplicada, Saltillo, Coahuila, México
[3]Centro de Investigación Científica de Yucatán, calle 43 No. 130 Col. Chuburná de Hidalgo, C.P. 97200, Mérida, Yucatán, México

monicac@guaymas.uson.mx

Introduction

Electrospinning is a method that has been widely used in recent years, because of its simplicity and versatility and it can be used to prepare polymeric fibers with diameters ranging from a nanometer to a micrometer scale, for any polymer soluble in a volatile solvent. Electrospun scaffolds prepared from biodegradable polymers have great potentials in tissue engineering, drug delivery, and gene therapy [1]. According to a literature review, in the last years the number of related publications has increased. In these publications, a large number of different materials have been reported, including cellulose acetate and poly(vinyl pyrrolidone) [2], and other materials. Appropriate materials to produce nano and micrometric fibers with possible applications in tissue engineering, controlled release of drugs and as a bactericide are cellulose acetate (CA) and poly(vinyl pyrrolidone) (PVP) [3,4]. There exists the possibility of producing in a co-extrusion fashion both the CA and the PVP, with embedded amoxicillin, and then, after dissolving one of the polymers, PVP, to study amoxicillin release. The main goal of this work is to show the feasibility and to determine the optimal conditions for the preparation of fibrous composite membranes of CA and PVP with embedded amoxicillin, via coaxial electrospinning, and their use for the release of this drug at both pH 3 and 7.2.

Materials and Methods

For the preparation of the fibers, a careful study of all the variables was performed. The variables studied were, the concentration of the polymer solution, the applied voltage, the flow of the solution, and the distance between the needle and the collector plate. In the case of CA solution, an acetone-water mixture was used as a solvent with a polymer concentration of 8% W. For the PVP solution an ethanol-water mixture was used, with a polymer concentration of 8% W, containing 2 ml of an amoxicillin aqueous solution 1M. The solutions were transferred to plastic syringes of 10 ml capacity together with a syringe pump kds Cientific, whose flow velocity was varied in the range of 0.1-1.0 mL h^{-1}. A high voltage of 15-30 kV was applied to the polymer solution, using a high-voltage power supply Spellman, model CZE 1000R. Finally the distance between the needle and the collector plate was set at 15 cm. A square plate of aluminum (10 cm x 10 cm) was used as a collector. In order to study the drug release kinetics, the membrane samples containing amoxicillin were immersed in 400 ml of a buffer solution and were maintained in magnetic agitation at 25 °C. The release at both pH 3 and 7.2 was investigated. At certain time intervals, 50 µl of the buffer solutions were taken out from each release system and were diluted to a final volume of 3 ml (dilution factor of 60). The amount of amoxicillin released at that time was determined by UV-vis spectroscopy to 273 nm using a Perkin Elmer Lambda 20 UV-vis spectrophotometer system. This experiment was repeated until the absorbance values were constant, that is, when the equilibrium of released drug was reached. The amounts of amoxicillin released were determined by interpolation of absorbance values in a calibration curve previously developed. The IR characterizations were done using a Perkin-Elmer Spectrum GX FTIR spectrometer by the KBr pellet technique.

Results and Discussion

The optimal conditions for the preparation of cellulose acetate-poly(vinyl pyrrolidone) fibers with embedded amoxicillin, CA/PVP-amoxicillin/CA, were found to be: the flow rate was 0.2 mL h^{-1}, applied voltage value and the distance between the needle and the collection plate were found, 25 kV and 15 cm respectively. The FTIR spectroscopy of the fibers was performed in order to corroborate the existence of amoxicillin in CA/PVP-amoxicillin/CA. The following characteristic peaks were observed: for CA, ester stretching peak at around 1750 cm^{-1}; for PVP, the band at 1662 cm^{-1} is attributed to C=O stretching vibration of the amide group; for amoxicillin, amide stretching wide band at 3456 cm^{-1}.

The effect of the pH on the amoxicillin release (pH 3.0 and pH 7.2) was analyzed through the kinetics of release, the release at pH = 7.2 is higher than at pH = 3.0.

Conclusions

The optimal conditions for the preparation of fibers of cellulose acetate, poly (vinyl pyrrolidone) containing amoxicillin were found; FTIR spectroscopy characterization of fibers was performed. The effect of the pH on the release of amoxicillin was also studied. These materials have the potential application in both oral administration and fabrication of release transdermal patch administration of amoxicillin.

References

[1] H. Jiang, Y. Hu, Y. Li, P. Zhao, K. Zhu, W. Chen, J. Control. Release 108 (2005) 237-243.

[2] M.M. Castillo-Ortega, J. Romero-García, F. Rodríguez, A. Nájera.Luna, P.J. Herrera-Franco, J Appl Polym Sci (2010), 116, 1873-1878.

[3] Keun Son, Ji Ho Youk, Won Ho Park, Carbohydr Polym (2006), 65, 430-434.

[4] I. S. Chronakis, S. Grapenson, A. Jakob, Polymer (2006), 47, 1597-1603.

Effect of Fatty Acids on the Functional Properties of Biofilms for Packaging Applications

Pedro Guerrero, Itsaso Leceta, Nagore Gabilondo, Koro de la Caba

Escuela Universitaria Politécnica. Plaza Europa 1. 20018 Donostia-San Sebastián, Spain

pedromanuel.guerrero@ehu.es

Introduction

Many methods have been investigated to modify properties of biofilms, including physical, chemical and enzymatic treatments. An alternative to improve water barrier properties could be the combination of the biofilm with lipids, polysaccharides or proteins which could give rise to synergistic effects between the components and make the properties of the film suitable for use in packaging applications: reduced water vapour permeability, optimum flexibility, transparency and gloss.

The combination of soy protein with lipids is an interesting alternative to optimise film properties since some components, such as oleic acid, impart flexibility, whereas others, like beeswax can enhance the efficiency of the water vapour barrier properties. Gloss and transparency of the films, which are very relevant to the appearance of the coated product, are also modified by the incorporation of different lipids, to a different extent depending on the kind of lipid and the development of the film structure during the film drying (1).

Materials and Methods

Soy protein isolate (SPI) PROFAM 974 was supplied by Lactotecnia, S.L. (Barcelona, Spain) and commercial bovine gelatin type A (bloom 200/220) by Sancho de Borja S.L. (Zaragoza, Spain). Lactic acid was obtained from Panreac, epoxidized soybean oil from Hebron S.A. (Barcelona, Spain), and olive oil from Cooperativa La Carrera (Jaen, Spain). Glycerol used in this study was food grade reagent obtained from Panreac.

SPI-based films with gelatin content (15% by weight on SPI dry basis) and different contents of fatty acids (5, 10 and 15% by weight on SPI dry basis) were prepared by dispersing SPI, gelatin and fatty acid in distilled water. Dispersions were heated at 80 ºC under stirring. The pH of the dispersions was adjusted to 10.0 with 0.1 M NaOH (2). Then, glycerol was added as plasticizer at 70/30 (w/w) SPI/glycerol ratio. After that, dispersions were maintained at 80 ºC under stirring. Subsequently, these samples were freeze-dried and hot-pressed at 150 ºC and 12 MPa. Fatty acid-free films were also prepared as control films.

A contact angle meter (model Oca20, dataphysics instruments) was used to perform contact angle measurements on the surface of films and image analyses were carried out using SCA20 software.

Fourier transformed infrared (FTIR) spectra of the films were carried out on a Nicolet Nexus FTIR spectrometer using ATR Golden Gate (Specac).

Total soluble matter (TSM) expressed as the percentage of film dry matter solubilized after 24 h immersion in distilled water and moisture content (MC) of films were measured.

The light-barrier properties of films were determined by measuring their light absorption at wavelengths ranging from 200 nm to 800 nm, using a UV-Jasco spectrophotometer (Model V-630).

Color values of films were measured using a portable colorimeter (CR-400 Minolta Croma Meter) and CIELAB color scale.

Results and Discussion

Water contact angle values are good indicators of the degree of hydrophilicity of films, being higher when hydrophilicity is lower, so thus the final state of the water drop on the film surface can be taken as an indication of surface wettability. To understand the effect of fatty acids on film wettability, contact angles were measured for films with different content and type of acid and were related to control films. In this study, contact angle increased with the addition of lactic acid. This behavior indicates that SPI-lactic acid interactions could result in a decrease of hydrophilic groups of SPI, increasing hidrophobicity of the films. However, lower contact angles were obtained for films with olive and soybean oils due to the estherification reaction observed by FTIR spectroscopy. These values were in agreement with the decrease of TSM values for these systems.

Packaging films should maintain moisture levels within the packaged product. Therefore, the knowledge of water solubility and moisture content of the film is very important for food packaging applications. MC values were similar for all systems, and did not depend on the type or concentration of acid used in this study.

Control films showed excellent barrier properties to UV light in the range of 200-280 nm, which were not affected by the addition of fatty acids, regardless acid content and type. In the case of transparency values, the addition of olive or soybean oils diminished transparency, whilst the addition of lactic acid slightly affected transparency values. There was no change in lightness (L) when fatty acids were added, whilst redness (a) increased, independent of acid content, and yellowish (b) diminished, which showed that the addition of fatty acids improved the visual aspect of films, diminishing the typical yellowish of SPI films.

Conclusions

Contact angle values, indicators of surface wettability, increased with the addition of lactic acid. The best results on the outer surface were obtained when the content of lactic acid was 15%. Transparency and colour values of the films modified with lactic acid also showed the improvement of the properties of the SPI-based films for packaging applications.

Acknowledgements

The authors thank MICCIN (project MAT2009-07735) and Plan E for their financial support.

References

1. M.J. Fabra, P. Talens, and A. Chiralt, *Food Hydrocolloids*, **23**, 676 (2009).
2. P. Guerrero and K. de la Caba, 2010, *Journal of Food Engineering*, **100**, 261 (2010).

Block Copolymers of Polypyrrole with 4-Vinylaniline Modified Cyclohexanone Formaldehyde Resin

Esin Ateş and Nilgün Kızılcan

Istanbul Technical University, Department of Chemistry, Istanbul 34469, Turkey

esinatess@gmail.com

Homopolymers, copolymers, composites and blends of polypyrrole prepared in the presence of persulfate have been studied widely. Persulfate chemistry was applied in copolymerzation of polypyrrole with monomers such as aniline, o-toluidine, styrene, 2-ethylaniline and o-anisidine [1-5].

Persulfate initates emulsion poliymerization for several unsaturated monomers as styrene, acrylonitrile, allyl acetate, methyl vinyl ketone, methacrylonitrile, butadiene, vinyl acetate, acrylamide and vinyl chloride. Initiation mechanism of vinyl polymerisation by persulfate and aliphatic amine systems was proposed by several authors [6-9]. It was demonstrated that in these initiation systems the aliphatic amine component also took part in the initiation reaction of vinyl polymerization. Type of free radicals coming from aliphatic amines depends on number of alkyl groups bounded to nitrogen atom [7].

In the case of aromatic amines, persulfate is able to oxidize amine group and generates radical cation which reacts with another aromatic ring and in leads to form polymer [8].

In present study, block copolymers of polypyrrole with 4-vinylaniline modified cyclohexanone-formaldehyde resin(CFVAn) were synthesized in presence of $K_2S_2O_8$.

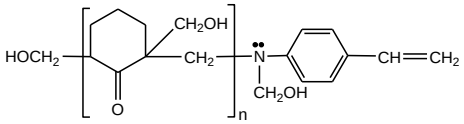

(CFVAn)

Solutions of resin and oxidant were prepared in dimethylsulfoxide and mixed together. Pyrrole was added to the mixture; a) at the beginning of stirring (t=0min.) and b) 15min. later (t=15min.). Reaction was carried out at 35°C for 1h. Reaction mixture was poured into water and polymer was precipitated slowly. Block copolymers were prepared with different molar ratios of pyrrole/modified resin to obtain solubility for copolymers. ESEM analysis indicates clearly that time of inserting pyrrole to reaction media is important and effects morphology of copolymers. Copolymers have particles with average size of 65-80nm. Conductivity value for copolymers is 1-3 S/cm.

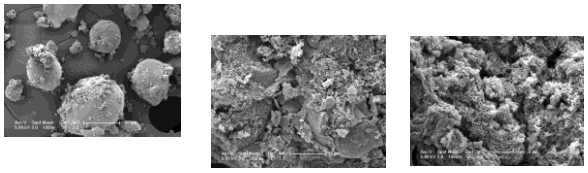

(a) **(b)** **(c)**

Fig. ESEM micrographs of modified resin CFVAn (a) and copolymers of polypyrrole with CFVAn, pyrrole added at t=0min. (b) and pyrrole added at t=15min. (c).

References

[1] N.V. Blinova, J. Stejskal, M. Trchova, J. Prokes, M. Omastova, Eur. Polym. J. 43 (2007) 2331–2341.

[2] X-G. Li, L-X. Wang, Y. Jin, Z.-L. Zhu, Y-L. Yang, J. Appl. Polym. Sci. 82 (2001) 510–518.

[3] X-G. Li, L-X. Wang, M-R. Huang, Y-Q. Lu, M-F. Zhu, A. Menner, J. Springer, Polymer 42 (2001) 6095-6103.

[4] X-G. Li, M-R. Huang, M-F. Zhu, Y-M. Chen, Polymer 45 (2004) 385–398.

[5] H. Eisazadeh, World Appl. Sci. J. 3 (2008) 14-17.

[6] G.S. Whitby, Synthetic Rubber, John Wiley&Sons, New York, 1954.

[7] P. Sepulveda and J. G. P. Binner, Chem. Mater. 2001, 13, 4065-4070

[8] C. Sivakumar, A. Gopalan, T. Vasudevan, Ten-Chin Wen, Synthetic Met. 126 (2002) 123-135.

[9] M. Campos, F.R. Simões, E.C. Pereira, Sensor Actuator, B 125 (2007) 158–166.

Sustainable Anaerobic Adhesive Technology Development

Dr David Birkett

Henkel Adhesive Technologies, Dublin, Ireland

david.birkett@henkel.com

Introduction: Anaerobic adhesives are one-part methacrylate ester formulations that polymerize in the presence of transition metals (notably ferrous substrates) and the absence of oxygen. Being solvent-free and non-flammable, curing at room temperature and allowing weight reduction in many engineering applications they already have good sustainability credentials, but there is nevertheless room for improvement in terms of health and safety and the use of renewable raw materials. This paper summarizes recent developments in these areas.

Materials and Methods: Most of the work centres around commercially available Loctite™ adhesives and modifications thereto. Nuts and bolts testing is according to ISO 10964.

Results and Discussion: Common accelerators for anaerobic polymerisation include the hazardous aromatic amines acetylphenylhydrazine and dimethyl-o-toluidine. We have shown that these can be suitably replaced by:

- Higher molecular weight acylphenylhydrazines such as succinylphenylhydrazine.[1]
- Polymers containing pendant acylphenylhydrazine groups.[2]
- Urethane methacrylate oligomers containing toluidine groups in the main chain.[3]
- A wide range of bicyclic aromatic amines, including the reaction product of tetrahydroquinoline and glycidol. [4]

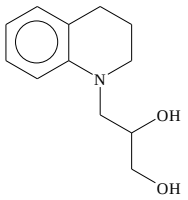

This in turn can be built into a urethane methacrylate oligomer as in reference 3. [5]

The main initiator for anaerobic polymerisation is the toxic cumene hydroperoxide. This can similarly be replaced by:

- Polymer bound peresters.[6]
- Complexes of hydrogen peroxide with amides such as urea or the monomer "diacetone acrylamide"[7]:

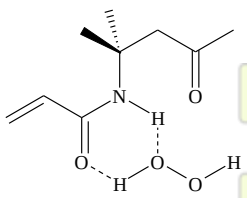

In line with our sustainability focus we endeavour to keep animal testing down to a minimum. We are initiating a project to calibrate non-mammalian test result with previous animal studies on aromatic amines, and we have tested full low hazard formulations on human volunteers and proved them to be non-irritant. Finally, monomers and urethane methacrylate oligomers with a significant renewable carbon content can readily be incorporated into anaerobic adhesive formulations.

Conclusions: Using some of the techniques outlined here our Product Development colleagues have been able to develop Loctite™ 2400 and 2700 threadlockers that have no hazard classification and in which there are no hazardous raw materials listed in Section 3 of the MSDS. Efforts in both Technology Development and Product Development continue to repeat this success for gasketing and retaining applications and to increase the use of renewable raw materials.

References: (Patent literature only)

1. U.S. 6,835,762
2. US20090025874 A1 and WO2009014688 A3
3. WO2009137448 A2, WO2009137455 A3 and WO2009137444 A2
4. WO2010127053 A2
5. WO2010127055 A2
6. US20090025874 A1 and WO2009014688A3
7. WO2010080795 A2 & A3

Nanoporous membranes with controlled pore dimensions

Y. González – Lemus[1] *and Dirk J. Broer*

[1] *Department of Chemical Engineering and Chemistry, Eindhoven University of Technology, Den Dolech 2, Eindhoven, Netherlands*

Nanoporous membranes are of interest for a wide range of applications: separation processes for liquid and gaseous mixtures, catalysis (including fuel cell systems) or lab-on-a-chip technologies [1]. We present a new fabrication process for nanoporous systems based on the self-organization of reactive liquid crystals containing hydrogen bridges. Photo-polymerization in the smectic phase of a reactive monomer forms a layered polymer network [2]. The nanopores are formed by breaking the bridges by heat (>170°C) or by a dip in an alkaline solution [3]. The process and an example of materials are shown in Figure 1.

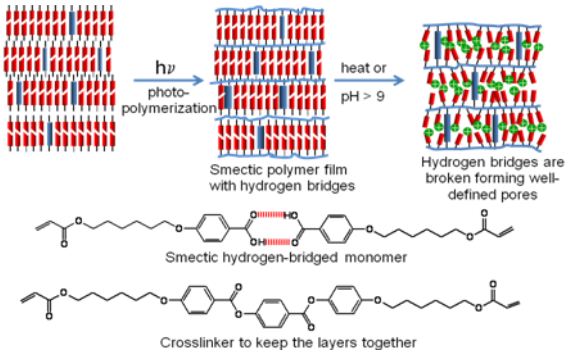

Figure 1 Schematic representation of the rupture of a hydrogen bonded smectic network under heat or high pH condition leading to sub-nanometer porous channels.

Upon breaking of the hydrogen bridges the integrity of the film is maintained by the presence of fully covalent cross-linkers connecting the smectic layers. These units are created by adding a small concentration of liquid crystal diacrylates to the monomer mixture prior to polymerization. This method allows for the creation of an organic nanoporous material that distinguishes itself from current nanoporous materials by its ease of manufacture, its ability to be formed only locally in a device, and its control over the pore dimensions down to or even below one nanometer [3].

The pores have a two-dimensional (sheet-like) shape. Figure 2 presents a cryo-TEM picture of the nanopores in cross-section, demonstrating a periodicity within the layers of 3 nm and a pore size in one direction of around 1 nm. The pores have been made visible by filling them with barium ions. It is the subject of our study to control this pore size by the choice of the crosslinker unit.

Critical step in the process is the breaking of the hydrogen bridges. We have studied this by various analytical tools such as FTIR, X-ray diffraction and DSC. As example we present here birefringent analysis which provides information on pH dependence of the bond rupture as well as on the local molecular order during and after this process (figure 3).

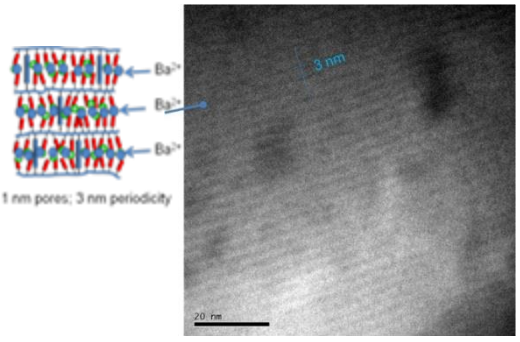

Figure 2. Cryo- TEM photograph of a cross-section of membrane film filled with $BaCl_2$ under alkaline.

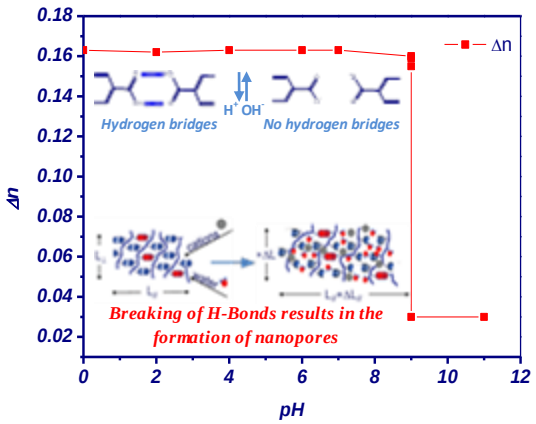

Figure 3. Birefringence of a planar oriented film as a function of pH. The film is immersed in low-pH buffer after which the pH is gradually increased by adding ammonia while recording the pH.

Figure 3 demonstrates that the hydrogen bonds rapidly rupture as soon as the pH > 9. Upon rupture the smectic layers are preserved but the order within the layers is largely lost. The small remaining birefringence above pH 9 points to the remaining orientation of the crosslinker units.

In conclusion, we form well-ordered polymer network containing hydrogen bridges by *in-situ* photo-polymerization of smectic monomers. The hydrogen bridges can (reversibly) break by temperature or by treatment with an alkaline solution. When the hydrogen bridges are broken the smectic order within the layers is lost; but the layer structure is maintained by the presence of crosslinking molecules.

References:

[1] Mathias Ulbricht. Polymer 47 (2006) 2217–2262.
[2] E. Peeters, J. Lub, J.A.M. Steenbakkers, D.J. Broer, Adv. Mat. 2006, 18, 2412
[3] Carmen Luengo González, Cees W. M. Bastiaansen, Johan Lub, Joachim Loos Kanbo Lu, Harry J. Wondergem, and Dirk J. Broer. Adv. Mater. 2008, 20, 1246–1252.

Incorporation of bioactive molecules in polymer matrix for food packaging.

Christelle Nguimjeu[1,2], M Kurek[3], F Sadaka[1], L Tighzert[2], I Vroman[2], C-H Brachais[1], J-P Couvercelle[1]

[1]ICMUB - UMR CNRS 5260, 9 avenue Alain Savary, BP 47870, 21078 Dijon cedex.
[2]GRESPI / MF – EA 4301 - ESIEC, Esplanade Roland Garros - Pôle Henri-Farman, B.P.1029 - 51686 Reims Cedex 2, France.
[3]AGROSup Dijon, 1 Esplanade Erasme, 21000 Dijon

E-mail : christelle.nguimjeu@gmail.com

Introduction:

For a large majority of foodstuff, development of micro organisms begins in the material surface, before spreading to the whole of the food [1-6]. The best way to prevent such microbial growth is introduce antimicrobial agents into polymer matrix. This antimicrobial film is a kind of active packaging that increases the display life of contained products, and maintains their quality, safety and sensor properties [2].

Antimicrobial films have gained an increasing interest in food packaging application in recent years [2-5].

The aim of this work is to investigate and compare the effect of two antimicrobial biomolecules incorporated into polymer and compounds.

Materials and methods:

The active films were prepared through three steps.

Step 1 : Masterbatch in internal mixer
Rotation speed : 60 rpm to 100 rpm
Cycle time : 5 min to 10 min
Temperature : 150°C to 220°C

Step 2 : Grinding the mixture
Pellets suitable for extrusion

Step 3 : Production of film
laboratory twin-screw extruder
1% to 4% of active agent

Fig 1: Preparation of active film

Gas chromatography (GC-MS), Fourier transform infrared spectroscopy (FTIR) and thermal analytical techniques (TGA and DSC) were used to characterize the active films and to determine their retention ability and the release of antimicrobial agent. Overall migration analysis method was used to determine the total of bioactive molecules migrated into the extraction media [4].

In order to evaluate the antimicrobial activity of the bioactive packaging, *B. Subtilis*, *E. coli*, *L. Plantarum* and *P. Camemberti* were used for microorganism test [5]. The tests were carried out without contact with the microorganisms. The whole was incubated in an oven at 37 ° C except for *P. Camemberti* at 25°C. The cultures were analyzed by counting and observing the growth of colonies after 0, 4, 19, 24 and 48 h.

Results and discussion:

The homogeneous dispersion of the bioactive molecules into the polymer matrix was verified using optical microscopy, and Scanning Electron Microscopy (SEM).

No changes in glass transition and melting temperature of antimicrobial films were observed, suggesting that little or no effect of thermal processing and, moreover plasticising effect by the addition of antimicrobial agents have been occurred.

The results of TGA-IR and GC-MS confirmed the presence of the active biomolecules in the films thus the processing conditions did not deteriorate them *(Fig 2)*.

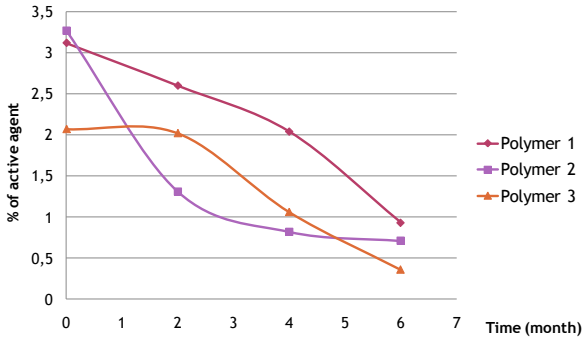

Fig 2: Release rate of active agent over time

Microbiological analysis confirmed the delay or the inhibition in growth or even no growth of bacteria in presence of active film *(Fig 3)*.

After six months of storage, the quantification tests have shown that some polymers retained better antimicrobial agent than the others and biomolecules were still active.

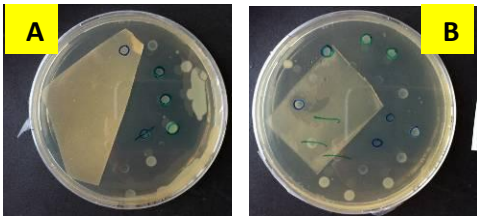

Fig 3: Test on Bacillus subtilis after 2 months of storage. A Polymer 1; B Polymer2 (2 day of incubation).

Conclusion:

In this work we developed antimicrobial films based on different polymers and compounds with two kinds of natural antimicrobial agents.

The processing data were optimized and the antimicrobial activities were validated after six months of storage. The release of active agents was influenced by the chemical structure of polymers.

The promising results obtained in this work are the basis for further study to be focus on the optimization of the active agent quantity in films.

The result of this study will be the subject of a patent.

References:

1. P.D; Warriss. Meat Science: An Introductory Text. Cabi Publishing, 2nd edition 9 (2009) 130 – 138.
2. P. Appendini, J.H. Hotchkiss. Innovative Food Science & Emerging Technologies 3 (2002) 113 – 126.
3. L. Frangos, N. Pyrgotou, V. Giatrakou, A. Ntzimani, I.N. Savvaidis. Food Microbiology 27 (2010) 115–121
4. V. Coma. Meat Science 78 (2008) 90–103.
5. V. Giatrakou, A. Ntzimani, I.N. Savvaidis. Food Microbiology 27 (2010) 132–136
6. J. Kaloustian, J. Chevalier, C. Mikail, M. Martino , L. Abou1 , M.-F. Vergnes. Phytothérapie 6 (2008): 160–164.

Modeling migration of colored food compounds into thermoplastic polymers: application to food cooking in reusable polymer bags

Sébastien Narses, Nadège Lautard, Thomas Fichu, Faten Sadaka, Claire-Hélène Brachais, Jean-Pierre Couvercelle

ICMUB, UMR 5260, Université de Bourgogne - 9 Av. Alain Savary – 21000 DIJON - FRANCE

Introduction

In the food packaging industry, commodity polymers like polyethylene (PE), polypropylene (PP) or technical polymers like polyamide (PA) are used in the form of films, and are generally in contact with food for short durations. When they are used as disposable films staining and absorption of aroma compounds into the polymer matrix is not a problem. Currently, sustainable development represents a growing challenge for both science and industry. In this purpose, a new method of steam cooking is under consideration. The major axis of this study is to use plastic reusable bags. In this case, staining and absorption of aroma compounds into polymer matrix can lead to aesthetic and flavor problems, resulting in a reduced consumer acceptance. [1] In some cases, like silicone pie moulds, inorganic mineral colorants are added to the polymer matrix to hide the transfer of coloring molecules from food. This solution cannot be used here because the film has to be transparent to allow the consumer to see the cooking evolution.

The aim of this work is to find a transparent polymer unaffected by long time exposure to coloring substances. In this purpose, a large variety of polymers have been studied; this abstract will only focus on three films:

- a multilayer film made from polypropylene and polyamide,
- a film made from polypropylene only,
- a fluorinated film made from FEP (Fluorinated-Ethylene-Propylene).

For the tests, curry sauce and ketchup, containing respectively curcumin and lycopene as their main coloring molecules were selected.

Materials and Methods

Multilayer PP-PA (Combitherm Flex, thickness 100 µm) and PP (Borclear RB707CF copolymer, thickness 100 µm) film samples were supplied by Wipak Gryspeert S.A.S. France, and FEP film samples (Norton FEP, thickness 25 µm) were obtained from Saint-Gobain Plastics France. Curry sauce and Ketchup were purchased in a supermarket and pure curcumin comes from Aldrich Chemical. Samples were dipped in the coloring substance, placed 24h in an oven at 60°C, washed with distilled water and dried with absorbing paper. Staining was evaluated by UV-visible spectrometry (Varian Cary 1E) and by colorimetry (Konica Minolta CR 400 colorimeter).

Results and discussion

Before each test, calculations of solubility parameters of polymers and coloring molecules with the Hoftyzer-Van Krevelen method [2] were performed. A summary of the expected interaction is reported in Table 1. In order to experimentally evaluate curcumin transfer into polymers, a first UV-visible calibration curve was made using curcumin dispersed in ethanol. According to Beer-Lambert's law, results on tested film samples showed that curcumin can be well quantified when it migrates from curry sauce to polymer matrix. It has been shown that PA is able to extract curcumin: its concentration in PA matrix is much higher than in curry sauce, which is coherent with previous calculations. ΔE values calculated with L*a*b coordinates measured by the colorimeter were also in accordance with interaction calculations, as shown in Table 1.

For the evaluation of polymers colored by ketchup, UV-visible spectrometry is not sensitive enough to perform quantifications. On the other hand, colorimetry always provides a good evaluation of coloration [3], and thus measurements were possible. The ΔE values measured in the case of ketchup coloring do not fit with the calculations since PP and FEP are not affected by ketchup (see below).

		PA layer of PP-PA	PP	FEP
Interaction calculation	Curcumin	High	Low	Low
	Lycopene	Low	High	High
ΔE values	Curcumin	High	Low	Low
	Lycopene	High	Low	Low
Theory-experiment accordance ?		Yes for curcumin, no for lycopene		

Table 1: Summary of expected interactions and experimentations on films with curry sauce and ketchup.

The structure-properties relationships of materials and coloring molecules are not taken into account in the empirical calculations of solubility parameter. Precisely, glass transition (which modifies the mobility of chains) and crystallinity level (which modifies the migration ability of colored compounds) are important but not considered parameters. Thus, as sorption modeling is not sufficient, experiments are essential to evaluate the migration of coloring molecules into polymer matrices.

Conclusion

A large variety of polymers, from commodity to highly technical polymers could be used for this application of steam cooking, but some of them are affected by coloration. Polymers generally used for kitchenware manufacturing such as PE, PP, PA, do not fit with the requirements. Other polymers used for cooking devices such as PET and polycarbonate are not affected by coloration but cannot be employed in manufacturing reusable bags. Only fluorinated or chlorofluorinated polymers and technical polymers remain in the purpose of manufacturing durable polymer bags for steam cooking.

References

[1] T.J. Nielsen, G.E. Olafsson, Food Chemistry (1995) 54, 255-260.

[2] D.W. Van Krevelen, *Properties of Polymers*, Third Rev., 189-225, Elsevier.

[3] R. Bagheri, M.F. Burrow, M. Tyas, Journal of Dentistry (2005) 33, 389–398.

Poly Lactic Acid Active Packaging: Migration of Natural and Synthetic Antioxidants

Majid Jamshidian, Elmira Arab-Tehrany, Stéphane Desobry

École nationale supérieure d'agronomie et des industries alimentaires, Institut National Polytechnique de Lorraine, 2 avenue de la Forêt de Haye, 54501 Vandoeuvre, France

Majid.jamshidian@ensaia.inpl-nancy.fr

Introduction:

The concept of antioxidant's controlled release has been well examined in polymer food packaging for active compounds such as antimicrobials, antioxidants, enzymes, flavors and nutraceuticals. Traditionally, antioxidants are added into initial food formulations which have some limitations during the shelf-life of products. Active packaging provides active protection by continually releasing active compounds such as antioxidants, antimicrobials, enzymes, flavors and nutraceuticals to package content, thus generating longer shelf-life foods, lower usage of additives and preservatives in food formulations, higher protection of flavors and higher food qualities.

Poly-lactic acid (PLA) is highly versatile, biodegradable, aliphatic polyester made from 100% renewable resources which offers great promise in a wide range of commodity applications and strongly competes with polystyrene for many food packaging applications. Antioxidant-PLA active packaging has not well been studied in various food simulating solvents, so the aim of this study is to determine the migration parameters (diffusion and partition coefficients) of natural and synthetic phenolic antioxidants (SPAs) including α-tocopherol, butylated hydroxyanisole (BHA), butylated hydroxytoluene (BHT), propyl gallate (PG), and tert-butylhydroquinone (TBHQ) from PLA films to three food simulating solvents at tow temperatures.

Materials and Methods:

Pre-weighed PLA films (3cm×2cm×~100µm) containing 1% w/w of antioxidants made by solvent-casting method were placed in contact with 10 mL of three food simulating solvents including 95% ethanol, 50% ethanol, and 10% ethanol in distilled water and at tow temperatures of 20°C and 40°C for 60 days. Migrated antioxidants were regularly measured by high performance liquid chromatography (HPLC) until equilibration points. Food simulants in contact with PLA films containing BHA, BHT, PG and TBHQ were analyzed using isocratic mode of acetonitrile-0.1% trifluoroacetic acid (TFA) (90%) and H_2O-0.1% TFA (10%) at pH 3.0 (acidified with acid acetic 1% v/v) at a flow rate of 0.5 $mL.min^{-1}$. For PLA films containing α-tocopherol, pure methanol was used in isocratic mode at a flow rate of 0.5 $mL.min^{-1}$. The final antioxidants concentrations in PLA films were analyzed by nuclear magnetic resonance spectroscopy (NMR). The Diffusion coefficients of antioxidants (D) were determined from the experimental data using a relationship derived from the Fick's second law for a plane sheet with constant boundary condition and uniform initial concentration. The partition coefficients (K) of equilibrated antioxidants were calculated on the basis of suggested formulas.

Results and Discussion:

The results show that there is a high relationship between simulant's physicochemical properties and migration temperature, and antioxidants release. At 20°C, equilibration days for 95% ethanol ranged from 16 to 60 days, for 50% ethanol, 50 days and for 10% ethanol, from 38 to 60 days; the corresponding equilibration ratios (M_t/M_0) ranged from 0.25 to 0.75, from 0.003 to 0.067 and from 0.0 to 0.003, respectively.

At 40°C, equilibration days for 95% ethanol ranged from 2 to 4 days, for 50% ethanol from 8 to 40 days and for 10% ethanol, from 24 to 60 days; the corresponding equilibration ratios ranged from 0.67 to 0.91, from 0.14 to 0.90 and from 0.0 to 0.24, respectively. PLA-α-tocopherol in 50% ethanol and PLA-TBHQ in 95% ethanol showed antioxidant degradation causing antioxidant concentration reduction at consequent days. Liquid chromatography mass spectroscopy (LC/MS) showed new-formed compounds for α-tocopherol and TBHQ in these simulants. As be seen, the migration rates at 20°C are slower than at 40°C and antioxidants concentrations at equilibration point are totally different for these two temperatures. Migration of all antioxidants was in accordance with Fick's second law.

Conclusion:

A successful active packaging against oxidation can be achieved by continuous antioxidant release during designed product shelf-life. Three food simulating solvents used in this study mimiced the leaching action of aqueous, alcoholic and fatty foods which are more in risk of oxidation. The results show that by decreasing simulant polarity and increasing the migration temperature, the antioxidant release rates are accelerated which is confirmed by zero release of BHT after 60 days in contact with 10% ethanol and near all of α-tocopherol release after 2 days in contact with 95% ethanol. Different migration rates of natural and synthetic antioxidants from PLA into various simulants and temperatures suggests the possibility to provide suitable antioxidants concentrations in PLA matrix for an effective antioxidant controlled release to a wide range of foods with different physicochemical properties. As the antioxidants involvement and their distribution in PLA matrix are significantly changed by the polymer processing method type, this research study will be completed with extruded PLA films containing these antioxidants.

New Polyester Obtained From Ethylketene

Najib Hayki, Nicolas Desilles, Fabrice Burel

INSA de Rouen, Laboratoire Polymères Biopolymères Surfaces, CNRS UMR 6270 & FR 3038
avenue de l'Université BP8, 76801 Saint-Etienne du Rouvray Cedex, France

najib.hayki@insa-rouen.fr

Introduction:

Ketenes are derivatives of carboxylic acids which contain two consecutive double bonds (RR'C=C=O). This family begins with the parent ketene CH_2=C=O and can be divided into aldoketenes (monosubstituted) and ketoketenes (disubstituted) monomers. The presence of two double bonds in an adjacent position makes them highly reactive. One of the most interesting properties of these compounds is their ability to be used as monomers.

The first ketenes that were prepared and characterized are diphenylketene, dimethylketene, and dibenzopentafulvenone[1]. The reaction involves the dehalogenation of the corresponding α-halo carboxylic derivatives by zinc according to the Staudinger's procedure. This method was modified by McCarney in 1975, carrying out the reaction under vacuum, at room temperature, in various solvents such as ether, ethyl acetate or tetrahydrofuran (THF). In this updated procedure, ethylketene was formed in 60% yield (Scheme 1)[2].

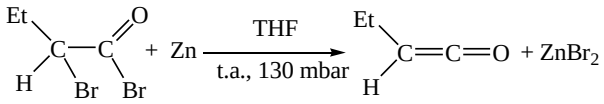

Scheme 1: Preparation of ethylketene

However, ethylketene and more generally aldoketenes, have never been polymerized successfully.

Materials and Methods:

In this work, we chose the Staudinger's procedure modified by McCarney for the synthesis of ethylketene. This latter was prepared in THF by reacting 2-bromobutyryl bromide with activated zinc, and the pressure in the apparatus was reduced to 130 mbar. This allowed THF to boil gently at room temperature. 2-bromobutyryl bromide diluted in THF was then added dropwise. Ethylketene was immediately formed and co-distilled with THF. The distillate was collected in the polymerization reactor cooled in liquid nitrogen (–180°C). The distillate was allowed to warm to –78°C, giving a green lime solution. Then, ethylketene was polymerized with various anionic initiators, at low temperature (Scheme 2).

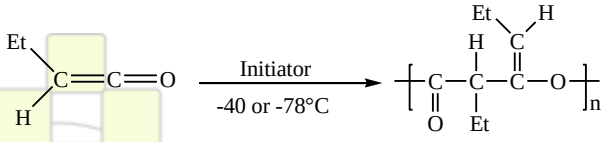

Scheme 2: Polymerization of ethylketene

Results and Discussion:

The influence of temperature and initiator on the polymerization of ethylketene was studied, with a monomer/initiator ratio close to 250 for every synthesis.

When the reaction was conducted at –40°C, $\overline{Mn}$ ranging from 6 500 to 11 300 g.mol^{-1} and low polymer yields were obtained. Conversely, good polymer yields were obtained at –78°C, indicating that the polymerization is better controlled at this temperature. Except for naphthalene sodium, high $\overline{Mn}$, between 14 700 g.mol^{-1} and 24 000 g.mol^{-1}, were obtained. All alkyl lithium initiators such as BuLi and sec-BuLi, and alkoxy lithium initiators such as ter-BuOLi afforded reactive systems with elevated polydispersities (I >1.5).

Initiation by the LDA/BuLi aggregate was also studied; this system led to a polymer not only with a high molecular weight $\overline{Mn}$ = 24 000 but also with a lower polydispersity (I ≈ 1.50).

The influence of monomer/initiator feed ratio was evaluated in terms of molecular weights and polydispersities, with sec-BuLi and the LDA/BuLi aggregate as initiator at –78°C. No strong evolution of the polydispersity index could be highlighted. This behaviour tends to indicate that the anionic polymerization of ethylketene is not free from chain transfer reactions.

Making chain extension experiments is a convenient way to study a living polymerization. Thus, block copolymerization with tert-butyl methacrylate was undertaken. The block copolymer was not formed, and attested the presence of termination reactions.

FTIR-ATR and NMR (^{1}H, ^{13}C) analysis showed that the obtained polymers are polyesters. This result is consistent with the cleavage of the obtained polymer chains in contact with $LiAlH_4$[3]. The thermal properties of these polymers were studied by TGA and DSC. All polymers exhibited a negative glass transition temperature (around – 18°C) and were thermally stable up to 160°C.

Conclusion:

New polyesters were successfully synthesized via the anionic polymerization of ethylketene at –78°C in THF, with yields up to 91%, molecular weights up to 24 000 g.mol^{-1} and polydispersity index close to 1.8.

References:

1. Staudinger, H., Berichte der Deutschen Chemischen Gesellschaft **1906,** 39, 968.
2. McCarney, C. C.; Ward, R. S., J. Chem. Soc., Perkin Trans. **1975**, 1600.
3. Sugimoto, H.; Kanai, M.; Inoue, S., Macromol. Chem. Phys. **1998,** 199, 1651.

Synthesis of cyclo-aliphatic polyamide precursors by polycondensation of diamines with ketene symetric dimers.

Nasreddine Kébir, Magda Ben Haddi, Najib Hayki, Fabrice Burel

INSA de Rouen, Laboratoire Polymères Biopolymères Surfaces (PBS), UMR 6270 CNRS FR 3038, avenue de l'université, 76801 Saint-Etienne-du-Rouvray, France.

e-mail: nasreddine.kebir@insa-rouen.fr

Introduction

Polyamides are an important class of versatile polymers and are used in various life fields. They combine excellent mechanical properties with good thermal stability and high melting temperatures. Usually, polyamides exhibit aliphatic and/or aromatic chemical structures. There are a number of articles in the literature that discuss the synthesis of polymers with cycloaliphatic units in the main chain, but they are principally concerned with the synthesis of such polymers bycycloolefin polymerization or cyclophotoaddition of bisolefinic derivatives.[1] Only a few works contain information on polycondensation polymers using cyclohexyl moieties.[2,3] Replacement of an aliphatic section of a polyamide by cyclic segment reduces chain flexibility, but rises the T_m because of a decrease in the entropy of melting. Generally, cycloaliphatic polyamides possess intermediate properties between aliphatic and aromatic ones.

Materials and Methods

Reagents: Tetramethyl-1,3- cyclobutanedione, p-phenylene diamine, hexamethylene diamine, dodecamethylene diamine, p-toluene sulfonyle, Sodium triacetoxyborohydride.

Characterisations: NMR, IRTF-ATR (Diamond), Size Exclusion Chromatography (SEC), TGA and DSC.

Results and discussions

Dimer of dimethyl ketene (DMK) (Tetramethyl-1,3-cyclobutanedione) is a commercially available product. It is also the main under product formed during ketene preparation by Staudinguer method.[4] This compound possesses two ketone functions which can be chemically modified.

This work aims to study the reactivity of DMK dimer towards aliphatic and aromatic diamines in several operating conditions.

Reductive amination was first conducted in classical conditions, i.e. presence of sodium triacetoxyborohydride as reductive agent, acetic acid as catalyst, dichloroethane as solvent and temperature range of 25 to 50°C. Unfortunately, slight carbonyl conversion and chain extension were obtained although the increase of concentration, diamine excess, and time reactions. This suggested a very weak reactivity of the sterically encumbered carbonyl groups. Aromatic diamine (p-phenylene diamine) was more reactive than aliphatic ones and afforded (when 5% excess of diamine) oligomers of Mn around 1000 g/mol with cycloaliphatic structure (scheme 1).

Therefore, the reaction was conducted in toluene at reflux (110°C) using p-toluene sulfonyle as catalyst for 24h. The reaction with aliphatic diamines afforded oligomers with Mn~400 to 800 g/mol depending on amine excess (5 to 100%). The spectroscopic data showed a 25-30 % of ring opening leading to heterogeneous structure.

The reaction with aromatic diamines afforded oligomer of Mn~1000 g/mol (100% excess) and polymer of Mn~50000 g/mol (5% excess) with totally cycloaliphatic structure.

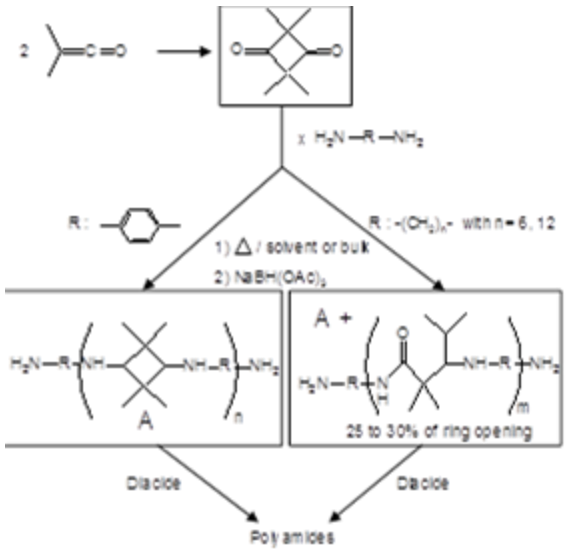

Scheme 1. Reaction of DMK dimer with diamines.

The reactions were also conducted in bulk at melt temperatures (100 to 150°C) using p-toluene sulfonyle as catalyst. Same results were obtained in terms of chemical structures (scheme 1). The molecular weights increased of about 40 to 50%.

The imine functions of these compounds were then reduced by reaction with $NaBH(OAc)_3$ (Scheme 1) to increase their chemical and thermal stability.

The thermal properties study of theses compounds showed Tg range values of 35-45°C for aliphatics and between 65 to 75°C for semi-aromatics. Aliphatic and semi-aromatic compounds were thermally stable until about 200 and 250°C, respectively.

Conclusion

Polycondensation of symmetric dimer of dimethyl ketene with excess of aromatic and aliphatic diamines afforded amino telechelic oligomers and polymers with partially and totally cycloaliphatic structures. These new compounds could be used for synthesis of new polyamides.

1. Hashimoto K. Prog. Polym. Sci. **2000**, 25, 1411-1462.
2. Osman M.A. Macromolecules. **1986**, 19, 1824- 1827.
3. Bulacovschi V, Simionescu. Macromol. Scl-Chem. **1985**, A22 (5- 7), 561- 577.
4. Staudinger H, Ber. Dtsch. Chem. Ges. **1906**, 39, 968.

Self-assembling Waves in Nanocomposites on Hydrophilic Polymer Base and their Advanced Applications

Ibragim E. Suleimenov

Almaty University of Power Engineering and Telecommunications, Almaty, Kazakhstan

Esenych@yandex.ru

Introduction

Research of the waves spontaneously arising in solutions of polymers and nanocomposites on this base is of not only academic, but also practical interest. In present report, particularly, it is shown that such waves can be used for the recording of data into the distributed environments. The basis for this purpose is the earlier observed hysteresis phenomena occurring in solutions of some stimulus-sensitive polymers [1].

Experimental

The (poly)-N-isopropylacrylamide (PNIPA) solutions containing silver nanoparticles obtained by photochemical reduction at various concentrations of components have been researched. Investigated solution is characterized by the apparent hysteresis that accompany the phase transition (from transparent to the nontransparent media) at temperature rise up to 35^0C [1]. Namely, dependences of the optical density of the solution at its heating and cooling differ and are shifted in temperature up to 3-5^0C. The solution was heated by electrical current in the galvanostatic mode directly. Dependences of the intensity of light passed through the solution on time were registered.

Results

It is shown, that there are definite conditions when heating of the solution by the electrical current leads to occurrence of fluctuations of optical density that can convert into a wave mode (fig. 1). The curve corresponds to the conditions of transition from the transparent to the turbid media. One can see, that there are regular fluctuations in the transition region. The occurrence of such fluctuations depends both on concentration of low-molecular component and on concentration of nanoparticles.

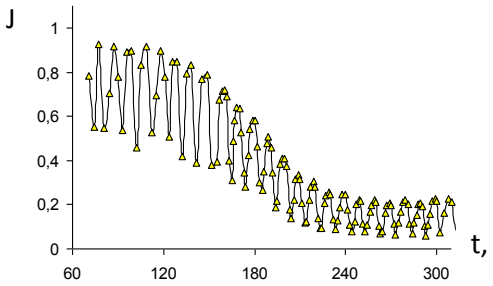

Fig. 1. Observed oscillations in PNIPA solution.

Discussion

The mechanism of occurrence of fluctuations is illustrated by Fig. 2. The S-like curve of dependence of optical density on temperature corresponds to occurrence of the hysteresis phenomena. Transition from one condition of the solution to another occurs at various temperatures (T_1, T_2).

It is shown, that oscillation takes place in such system according to the following mechanism. At the first stage the heating up to the temperature of phase transition occurs. It causes change of electrical conduction of the environment by jump, which is connected presumably with change of the state of the nanoparticle surface. Accordingly the electric power dissipated by the local region of the solution decreases, which results in its cooling and the subsequent transition to the initial condition (the second stage of oscillation). The hysteresis results in delay that provides for the stability of value of the registered fluctuations period.

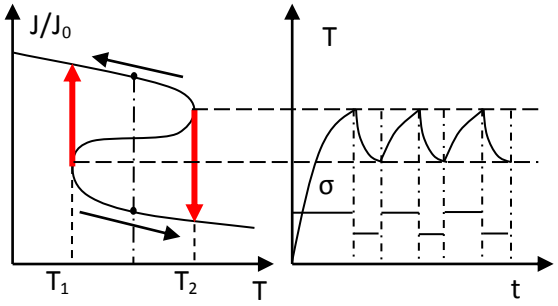

Fig. 2. Scheme of occurrence of oscillations.

It is shown also that in various points of the solution fluctuation occur in various phases, i.e. in the considered system the wave modes can be realized as well. Such waves can be used for recording of data in the distributed environment. Namely, with focusing waves in a certain point of the solution it is possible to achieve irreversible phase transition.

The design of the device is suggested in present report that provides stimulation of the waves of considered type. A set of equidistant point-electrodes is used that are arranged on the perimeter of an area filled with the polymer solution containing nanoparticles. It is shown, that artificial alteranting of phases between various sources allows synthesis of waves with arbitrary configuration of front (spacing between the electrodes should to be less than a half of the wavelength).

Conclusion

The phase transition in the thermosensitive polymer solutions containing nanoparticles is accompanied by the change of conductivity of the hysteresis character. The heating of such solution by electrical current results in the occurrence of steady fluctuations. They can convert into the waves. Such waves can be used for recording of data in the continuous media. It gives possibility for development of the display screens that do not require physical splitting into separate image elements (pixels).

References

1. Suleymenov I.E., Mun G. A, Guven O, et. al. *The Hysteresis Phenomena at Phase Transition in Solutions of Thermosensitive Polymers* // The Almaty University of Power and Communication Bulletin, №3/2, 2010, pp. 82-87.

Effect of Poly(amic acid)-treated $BaTiO_3$ on the Dielectric and Mechanical Properties of $BaTiO_3$/polyimide Composites

Jinhwan Kim

Department of Polymer Sci. and Eng., Polymer Technology Institute, Sungkyunkwan University, 300 Cheoncheon-dong, Jangan-gu, Suwon, Gyeonggi-do 440-746, Korea (South)

jhkim@skku.edu

A lot of attention has been paid to develop organic/inorganic composites utilized in electronics applications such as circuit board, packaging material, dielectrics, and passive protection materials. Among them, many efforts have been attempted to develop the embedded capacitor which can replace traditional discrete components. For this application, key materials are polymer/inorganic filler composites by taking advantages of polymers (processability) and inorganic fillers (high dielectric property and thermal stability). Incorporation of inorganic fillers having high dielectric constant (K) into a easily processable organic polymer matrix enables the resulting composite to retain the advantages of both materials.

For this purpose, barium titanate ($BaTiO_3$) is most widely employed among various inorganic fillers available commercially. On the polymer side, polyimide (PI) is widely used due to its excellent thermal stability and high mechanical strength not only in embedded capacitors but also in general purpose insulating materials. Therefore, combination of $BaTiO_3$ and PI would be a good choice for the above mentioned polymer/inorganic filler composite and thus many researches have been carried out to investigate various aspects of composites. One faces the difficulty of dispersing $BaTiO_3$ particles in PI precursor, which is a typical problem encountered in processing the polymer/inorganic filler composite. Since the properties of polymer/inorganic filler composites are significantly influenced by the dispersion of the filler particles, in addition to inherent properties of the polymer and inorganic fillers, the dispersion control is the key technology for obtaining the desired properties of polymer/inorganic filler composites.

Most common approach to control the dispersion of $BaTiO_3$ particles in PI matrix is to treat $BaTiO_3$ particles with a silane coupling agents. However, Chang et al. claimed very recently that as-received $BaTiO_3$ particles lack reactive functional groups on their surfaces and thus it is difficult to form chemical bonds with organic modification agents. They also showed that the treatment of $BaTiO_3$ particles with hydrogen peroxide (H_2O_2) can produce –OH groups on the surfaces.

In this presentation, we first modify the surfaces of as-received $BaTiO_3$ by adopting Cheng's method to induce –OH groups that will be further reacted with a coupling agent. If this approach is valid, the surfaces of $BaTiO_3$ particles would have significantly increased numbers of –OH groups, which enables further reaction with a coupling agent. Then, with the proper choice of a coupling agent, we may induce the reaction of coupling agent. Thus, modified $BaTiO_3$ particles are able to react with the PI precursor (poly(amic acid)) even at low temperature such as below 100 ^oC and are able to obtain poly(amic acid)-wrapped $BaTiO_3$ particles can be obtained. The schematic diagram of this sequential treatments is presented in Scheme 1. By employing this approach, we hope to obtain improved dispersion and consequently better electrical and mechanical properties.

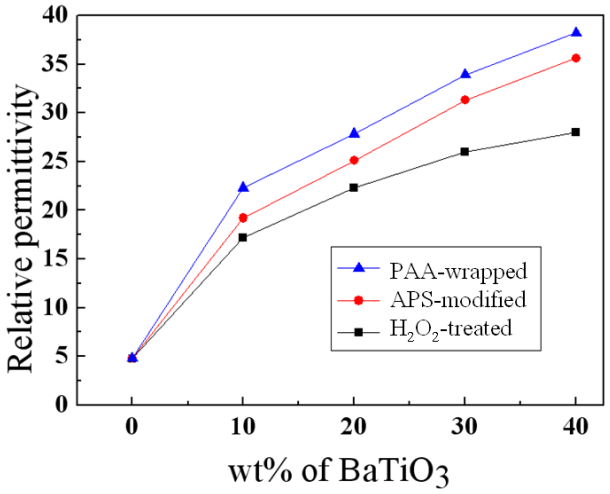

Figure 1. Relative permittivity at 1 MHz various surface modified $BaTiO_3$/PI composites as a function of $BaTiO_3$ concentration: (a) H_2O_2-treated, (b) APS-modified, and (c) PAA-attached $BaTiO_3$.

New Phenolic Resins for Advanced Materials

Gen-ichi Konishi

Tokyo Institute of Technology, Department of Organic and Polymeric Materials

konishi.g.aa@m.titech.ac.jp

Phenolic resins and related polymers are a very important class of common organic polymers, and they have numerous applications in the development of materials such as thermosetting resins, adhesives, photoresists, and polymer composites. The main characteristics of phenolic resins, such as heat stability and mechanical properties, are attributed to their rigid rod-like polymer backbone of *poly(phenylenemethylene)*. From this viewpoint, we have synthesized a wide variety of aromatic polymers from alkoxylated phenol derivatives such as anisole, phenethol, and diphenyl ether *via* a method similar to acid-catalyzed phenol-formaldehyde condensation. The obtained polymers exhibit good solubility in organic solvents and they are more resistant to heat and oxidation than phenolic novolacs. Furthermore, using hydroxyl-group-functionalized phenol derivatives, a functional novolac can be prepared via a one-step procedure. Therefore, a desired polymer can be designed using this methodology (Scheme 1).[1,2] It is very important to extend the use of this methodology to a wide variety of applications in the field of materials science.

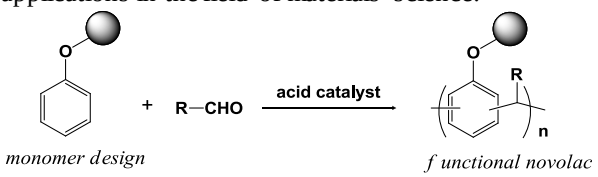

Scheme 1

In this presentation, we report the direct synthesis of a functional novolac having allyl ether in the side chain by the addition-condensation of designed phenol derivative with formaldehyde and the polymer reactions of the obtained polymers are also described.

We attempted the preparation of an allylated novolac. The addition-condensation of allyl phenyl ether (**1**) with formaldehyde was carried out; however, a novolac having allyl ether and phenolic hydroxyl groups was obtained *via* simultaneous phenol-formaldehyde condensation and Claisen condensation processes. In order to suppress the Claisen rearrangement, the addition-condensation of **1** with formaldehyde was carried out by using aqueous sulfuric acid and stirring at room temperature (25°C).

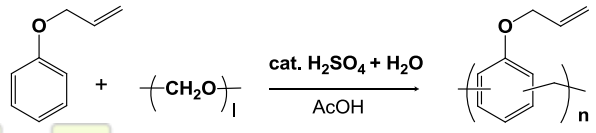

Scheme 2

The obtained novolac **2** had good solubility in common organic solvents. From the viewpoint of the procedure for preparing novolac, an advantage of this polymerization method is that it is quite easy to obtain a high-purity polymer. The ^{13}C-NMR spectrum provided details of the polymer structure of **2**. In particular, we focused on the zone at around 150 ppm of the aromatic carbon attached to the allyloxy group. The mono- (terminal moiety), di- (linear moiety), and tri-substituted (branch moiety) moiety can be identified by chemical sifts such as 153 (-CH_2-Ar), 156 (-CH_2-Ar CH_2-), and 150 (-CH_2-Ar-CH_2-(-CH_2-)-), respectively. The ratio of terminal, linear, and branch were 20%, 80%, and ~0%, respectively. It is noted that the main-chain structure of the obtained novolac was different form that of conventional novolac having a branch moiety. *The allylated novolac was linear structure*.

In order to investigate the applicability of the obtained allylated novolac for the curing reaction of thermosetting resins such as epoxy and phenolic resin, we examined the thermal Claisen rearrangement of the allylated novolac (**2**) by using DSC apparatus. From the DSC chart, large endotherms (88.9 and 153.6°C) and exotherms (140.1 and 217.5°C) were observed. The Claisen rearrangement is exothermic. At 150°C, ca. 40% of hydroxyl group have been generated; therefore, this allylated novolac can potentially be used as a thermal latent curing system (**Scheme 3**).

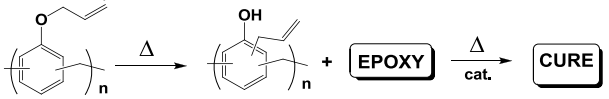

Scheme 3

In addition, we reported a novel optical materials based on lignin as a new phenolic polymer.[3] We successfully prepared lignophenols (**LP**) having hydroxyl groups alkoxylated with different types of alkyl halides via Williamson ether synthesis. We found that hydroxyl-group-alkoxylated **LP**s can be used as optical materials because the refractive indices and birefringences of these **LP**s are comparable to those of **PC**. The obtained polymers exhibited good film-forming abilities with transparency. These results suggest that natural polymer **LPs** are highly advantageous in that they have very good material properties and they can be produced from biomass.

Acknowledgement This work was mainly supported by the Industrial Technology Research and Development Grant (09C46222) from NEDO of Japan

References

(1) Kimura, T.; Nakamoto, Y.; Konishi, G. *Polym.* J., 2006, **38**, 606.
(2) Nemoto, T.; Konishi, *Polym.* J., 2010, **42**, 185.
(3) Nemoto, T.; Konishi, *Polym.* J., 2010, **42**, 896.

Covalent Attachment of Cholesterol Oxidase on Transparent Polyaniline Film for Cholesterol Sensing

T. Del Castillo-Castro, M.M. Castillo-Ortega, A. Ortiz Rascón, E.F. Placencia Fontes

Departamento de Investigación en Polímeros y Materiales, Universidad de Sonora, Apartado Postal 130, Hermosillo, Sonora CP 83000, México

e-mail: terecat@polimeros.uson.mx

Introduction:

The immobilization of biomolecules, such as proteins and peptides, is quite useful for practical applications due to their potential to improve the stability of enzymes [1,2]. The immobilization of enzymes can allow repeated use, facile separation from reaction mixtures, and prevent enzyme contamination in products [3].

In this work, a potential optical biosensing system composed by a poly(methyl methacrylate) (PMMA) support, a transparent thin film of polyaniline (PANI) and a covalent immobilized cholesterol oxidase (ChOx) is presented (Figure 1).

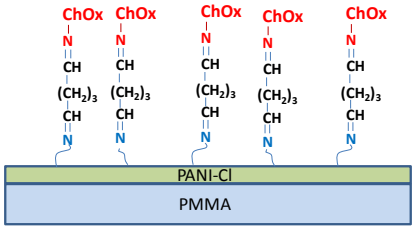

Figure 1. PMMA/PANI-ChOx system.

Materials and Methods:

Transparent and conductive thin films of PANI on PMMA support were obtained by the chemical bath method. PMMA substrates were introduced into a freshly prepared chemical bath of HCl, doubly distillate aniline and $(NH_4)_2S_2O_8$ at room temperature. The deposition of PANI was carried out at different reaction times and the resulting films were characterized by electrical measurements (multimeter Agilent 34410A), FTIR (Perkin Elmer, Spectrum GX), UV-vis spectroscopy (Perkin Elmer, Lambda 20) and atomic force microscopy (JSPM-4210).

Cholesterol oxidase was immobilized onto PANI films using covalent linkage through glutaraldehyde. First, 5 µL of 0.1% glutaraldehyde was spread over 1cm^2 surface of PANI film and allowed to dry. Later, 15 µL of cholesterol oxidase was added onto the same surface and left overnight. After immobilization, the PANI-ChOx films were rinsed with deionized water to remove any unbound enzyme molecule.

Results and Discussion:

The electrical measurements showed that the superficial conductivity of PANI film increased with the deposition time up to the 30 min, afterwards the value remained constant till the 80 minutes. The monitoring of the characteristic absorption band of *–NH-* group by FTIR confirmed the PANI deposition since the 5 min of chemical bath. Figure 2 depicts the UV-vis spectra of PMMA/PANI films as function of deposition time.

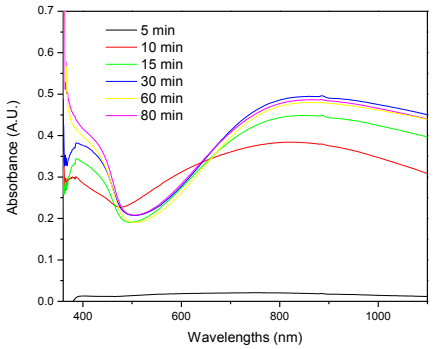

Figure 2. UV-vis spectra of PMMA/PANI system.

The UV spectra are characteristic of PANI salt in extended coil conformation: (*i*) band at 430 nm associated to π-polaron transition and (*ii*) broad free-carrier tail in the NIR. The intensity of absorption increases up to 30 min of deposition that can be attributed to the increase of PANI film thickness. Further deposition time does not produce significant optical changes. The AFM analysis showed that the PANI homogeneously deposited in globular form and this morphology persists up to 80 minutes of chemical bath.

The PMMA/PANI system obtained at 30 minutes of reaction was selected for the enzyme immobilization on the basis of its electrical, optical and morphological properties.

The immobilization of ChOx onto the PANI film produced a decrease of the superficial electrical conductivity as well as changes in FTIR and UV-vis spectrum.

Conclusion:

A potential biosensing platform of PMMA/PANI-ChOx was obtained by the PANI deposition using chemical bath and the subsequent covalent immobilization of the enzyme on the electroconductive polymer. The detailed studies of the effect of the pH and the temperature on the activity of the immobilized ChOx and the use of the PMMA/PANI-ChOx system for estimation of free cholesterol by optical methods are in progress in our laboratories.

References:

1. Miguel Arroyo; *Ars Pharmaceutica*, 39:2, 1998, 23-39.
2. Gülay Bayramoğlu, Meral Karakışla, Begum Altıntaş, Ayşegül U. Metin, Mehmet Saçak, M. Yakup Arıca; *Process Biochemistry*, 44:8, 2009, 880-885.
3. Ephraim Karchalski-Karzir, *Trends in Biotechnology*, 11:11, 1993, 471-478.

Synthesis of New Two-Dimensional Thiophene-Based Conjugated Copolymers and Their Applications to Thin Film Transistors and Photovoltaic Cells

Hsiang-Wei Lin,[a] *Jung-Hsun Tsai,*[b] *Chih-Jung Lin,*[b] *Hung-Chin Wu,*[b] *Chien Lu,*[b] *Yu-Wei Lin*[a] *Yi-Cang Lai,*[a] *and Wen-Chang Chen,*[a,b,*]

[a] Institute of Polymer Science and Engineering, National Taiwan University, Taipei 106 Taiwan;
[b] Department of Chemical Engineering, National Taiwan University, Taipei 106 Taiwan

e-mail: chenwc@ntu.edu.tw

Two-dimensional 4T-acceptor conjugated polymers have been shown to have excellent charge-transport characteristics and solar cell performances.[1] In this study, new two-dimensional conjugated homopolymer poly(5,5'''-di-(2-ethylhexyl)[2,3';5',2'';4'',2''']quarterthiophene) (P4T) and their copolymers, P4TT, P4TSe, P4TFT, P4TBDT, and P4TDTS, were synthesized by Stille coupling reactions under microwave heating. The effects of chemical structures on the electronic energy level, charge transport, and photovoltaic properties were explored systematically. Among these copolymers, P4TFT showed the highest organic field effect transistor (OTFT) hole mobility of 0.12 $cm^2 V^{-1} s^{-1}$ due to its highly crystalline packing structure. The performances of bulk heterojunction polymer solar cells based on the blends of these 4T-based copolymers and 1-(3-methoxycarbonyl) propyl-1 - phenyl-[6,6]-C-71 ($PC_{71}BM$) were also characterized. P4TSe/ $PC_{71}BM$ based photovoltaic device showed the highest power conversion efficiency (PCE) of 2.6% under AM 1.5 illumination (100mW/cm^2). The above results exhibited that two-dimensional conjugated copolymers emerged as a promising candidate for organic electronics.

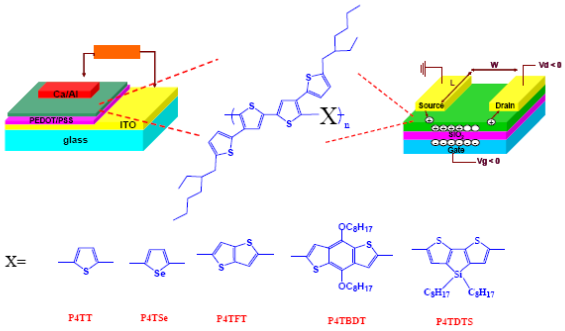

1. C. Y. Yu, B. T. Ko, C. Ting, and C. P. Chen, *Sol. Energy Mater. Sol. Cells*, **93**, 613 (2009).

Obtaining and stability of iodine-cationic starch complexes

Rima Klimaviciute, Joana Bendoraitiene, Ramune Rutkaite, Algirdas Zemaitaitis

Kaunas University of Technology, Radvilenu pl. 19, LT-50254 Kaunas, Lithuania

rima.klimaviciute@ktu.lt

Iodine has traditionally been available in solutions or tinctures but shows a high degree of instability. This problem was overcome by the development of iodophores (iodine carriers or iodine releasing agents). In the presence of potassium iodide iodine crystals dissolve in aqueous solution forming triiodide ions (I_3^-). One of the possibilities to obtain iodophores is the formation of complexes between I_3^- and cationic groups of polymer.

Starch is a low-cost natural renewable polymer that can be cationized with 2,3-epoxypropyltrimethylammonium chloride by reaching a high reaction efficiency [1]. Obtained cationic starches (CS) can interact with anionic iodine compounds and form ionic iodine-CS complexes possessing antimicrobial activity:

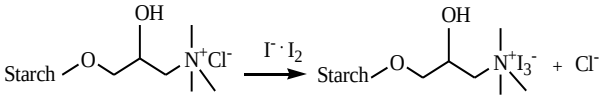

Depending on the conditions of cationization reaction and source of starch the CS with different properties have been obtained (see Table).

Table. CS used for iodine-CS complexes formation

Source of starch	Cationic starches (CS)	
	Solubility	Abbreviation
Hydroxyethyl starch (HOES)	Water soluble	CHOES
	Nanoparticles in water	Nano-CHOES
Native starch	Paste in cold water	PCS
	Water soluble	SCS
Cross-linked starch	Microparticles	CCS

Nano-CHOES were obtained by aqueous polyelectrolyte complex formation between water soluble CHOES and sodium tripolyphosphate. The formation of CHOES nanoparticles of spherical shape was verified by dynamic light scattering and scanning electron microscopy measurements. The nano-CHOES of different constitution and containing various amount of free quaternary ammonium groups were produced.

For formation of iodine-CS complexes nano-CHOES, CHOES, SCS or CCS with degree of substitution (DS) from 0.14 to 0.85 were used. The nano- or microparticles of iodine-CS complexes or water soluble complexes were formed. The iodine content introduced into iodine-CS complexes depended on the amount of free cationic groups in nano-CHOES, DS of SCS or CCS and the concentration of iodine in the aqueous iodine-potasium iodide solution used in the experiment. The maximum amount of iodine attached to CCS with DS=0.85 was 6.5 mmol/g and supported the presumption that more than two molecules of iodine could be attached to one cationic group of CCS.

Both the thermal stability and the ability to release iodine into the water or aqueous solution of HOES were assessed for iodine-CS complexes containing different content of incorporated iodine. The thermal stability of iodine-CCS complexes depended on the DS of CCS, the counter-ion of quaternary ammonium group and the amount of attached iodine. The thermal stability of nano-CHOES complexes increased with the introduction of polysalt into polyelectrolyte complex. The amount of released iodine into the water and aqueous solution HOES was lowest in the case the CCS-iodine microgranules or nano-CHOES-iodine were used.

The main advantage of the use of iodine-CS complexes as antimicrobial agents is the biodegradability of the polymeric matrix. As could be seen from the photographs presented in Fig. the CCS microgranules were easily destroyed during enzymatic treatment. Thus after the iodine consumption for antibacterial actions the remaining matrix of CS will be biodegradable.

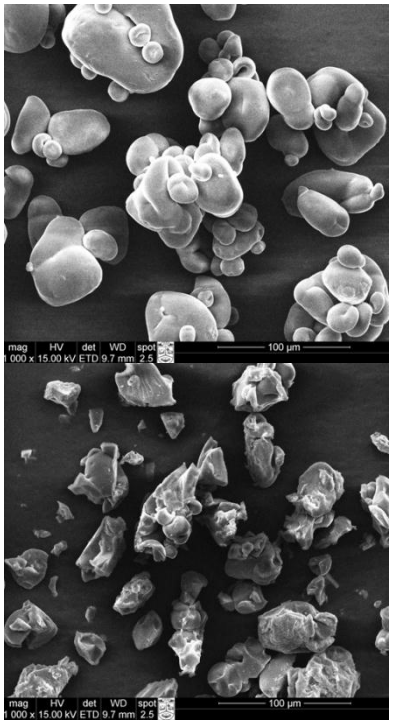

a)

b)

Fig. Microphotographs of CCS microgranules before (a) and after (b) treatment with *α-amylaze*

References: 1. R. Kavaliauskaite, R. Klimaviciute, A. Zemaitaitis. Factors influencing production of cationic starches. Carbohydr. Polym. 2008, vol. 73, p. 665–675.

Stabilization of Liposomes by Multilayer Films of Modified Polysaccharides

Anna Karewicz, Dorota Bielska, Anna Socha, Maria Nowakowska

Nanotechnology of Polymers and Biomaterials Research Group, Faculty of Chemistry, Jagiellonian University, 30-060 Cracow, Ingardena 3, Poland

karewicz@chemia.uj.edu.pl

Introduction: Liposomes are widely used as effective carriers of the biologically active agents, especially those of low bioavailability or low stability. Despite their many advantages (easy penetration of the cell membranes, low size, biocompatibility) liposomal vesicles suffer from their tendency to aggregate, significant leaking of the encapsulated drug and fast elimination by the reticuloendothelial system. The presented results illustrate our approach to limit these disadvantages and to enhance the efficiency of the carrier. Our method is based on coating of the liposomes with ultrathin films of biocompatible polyelectrolytes using layer-by-layer technique. The previous studies conducted in our group proved the supremacy of so-called "one-component" multilayer films, where polycation and polyanion chains possess the same backbone. Such films are more easily built and are more stable [1]. We have chosen three different natural polysaccharides and modified them in order to form stable coatings on the liposomes. Nanocarrier systems composed of liposomal vesicles coated with various mono and multilayer ultrathin polymeric films are discussed and compared.

Materials and Methods: To characterise modified polysaccharides ^{1}H NMR, elementary analysis and IR spectroscopy were used. The formation process and properties of the multilayered polymeric films were followed by UV/Vis absorption spectroscopy and AFM measurements. Stability of the obtained nanocarrier systems was tested using DLS, zeta potential and Cryo-TEM measurements, as well as the spectroscopic and conductometric titration.

Results and Discussion: Chitosan, dextran and hydroxypropylcellulose were modified by introducing the ionic groups and hydrophobic chains to their backbones. 2-Hydroxypropyl-1-trimethylammonium unit was introduced to obtain cationic derivatives while the anionic ones was obtained by the modification with sulfate moieties. Both groups were chosen in a way to assure the stable charge of the chain (positive or negative, respectively) for the wide range of pH values. All derivatives were characterized to confirm the successful modification of the initial polymer and the properties of the obtained compounds were determined. The ability of the obtained derivatives to form stable multilayer films was studied in detail. For all the "one-component" films an effective growth of the film thickness upon addition of subsequent layers was observed. However, while for the chitosan film a monotonous growth of the film was found up to ten bilayers, in the case of dextran the distinct substrate effect was observed. The coating procedures were developed and the effective coating of the liposomal vesicles by all the multilayer films studied was confirmed by following the size and zeta potential changes. Finally the efficacy of obtained films to stabilize liposomes was tested. Triton X-100, the non-ionic detergent causing disintegration of the liposomal bilayer was used to study the stabilizing effect of the coating. It was found that already a single monolayer increases the vesicle's stability for all polymers studied, provided that it is additionally anchored into the liposome's bilayer by the alkyl chain. Additional layers tend to increase further the stability of the liposome-polymer systems.

Conclusions: A series of ionically modified polysaccharides was obtained and they properties were characterised. Additional derivatization of the cationic chains was done in order to introduce the anchoring alkyl chains. All three polysaccharides used for further modifications can form stable multilayer systems. Chitosan-based "one-component" films, unlike the dextran-based ones, do not show the substrate effect during formation. Several polymer-coated liposomal carriers differing in the type of the coating and the number of the layers deposited on the vesicle's surface were studied. Already a monolayer polymer coating increases vesicle's stability, provided it is additionally anchored to the liposomal bilayer by the covalently attached alkyl chain, but multilayer coatings are even more promising.

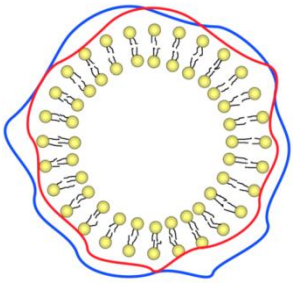

Figure 1. Schematic representation of liposome coated with polysaccharide layers

References:

1. Bulwan, M., Zapotoczny, S., Nowakowska, M., Soft Matter (2009) 5 (23), 4726-4732

Acknowledgements: Project operated within the Foundation for Polish Science Team Programme co-financed by the EU European Regional Development Fund, PolyMed, TEAM/2008-2/6. We thank the Polish Ministry of Science and Higher Education for the financial support in the form of the grant N N 209 118937

Polysaccharide coating of liposomes via layer-by-layer self-assembly as novel delivery system for proteins

Sergio Madrigal-Carballo [1], *Marianelly Esquivel* [1], *José Vega-Baudrit* [2], *María Sibaja* [1], *Amparo O. Vila* [3]

[1] School of Chemistry, National University, Heredia, Costa Rica.
[3] Nanotechnology Laboratory, CeNAT, San Jose, Costa Rica.
[2] Department of Physical Chemistry, University of Valencia, Spain.

smadriga@una.ac.cr

Instroduction: Natural polysaccharides, due to their outstanding merits, have received more and more attention in the field of drug delivery systems. The present work is focused on the formulation of multilayered polysaccharide-coated liposomes based on layer-by-layer (L-b-L) self-assembly via electrostatic deposition technique as a novel drug carrier for delivery of macromolecules, such as proteins. The building up of the polysaccharide-coated liposomes was achieved through the alternate adsorption of several layers of anionic (dextran sulfate or alginate) and cationic (chitosan) polysaccharides on a core composed by anionic nanosized soybean lecithin vesicles. The resulting nanoparticles were characterized according to their size, surface charge, morphology, encapsulation efficiency, loading capacity, as well as their protein release profiles.

Materials and Methods: *Formulation of liposomes:* Soybean lecithin liposomes were prepared from concentrated soy lecithin dispersions (250 g/L) according to procedures previously described. *L-b-L self-assembly of polysaccharide-coated liposomes by electrostatic deposition:* Fresh solutions of chitosan (CHT), alginate (ALG) and dextran sulfate (DXS) in concentrations ranging 0.01-0.25% w/v were prepared, in acetic acid (HOAc) 0.5% v/v for chitosan biopolymer and sodium chloride 10^{-5} mol/L for dextran sulfate and alginate, respectively. For the L-b-L build-up, the anionic liposomes from soybean lecithin were coated with alternating layers of positively charged CHT and negatively charged DXS or ALG (volume ratio of 1:1, respectively) until the desired number of polysaccharide layers was achieved. Addition of the newest layer was always carried out by adding the previous formulation dropwise, under continue stirring, into the coating solution, in order to avoid flocculation depletion and potential cross-linking caused by the lacking of the coating polysaccharide.

Results: Stable polysaccharide-coated liposomes were formed within only a narrow concentration range ($c_{min} < c < c_{max}$), and below and above this optimal range the liposomal system aggregated and eventually phase separated from solution. The minimal concentration required to form stable multilayered coated liposomes can be estimated from the change in ζ-potential with addition of each biopolymer layer. The L-b-L self-assembly electrostatic deposition technique succeeded in building a nanosized, spherical, monodisperse and stable hybrid protein delivery system (Figure 1) with a cumulative apparent hydrodynamic diameters between 357.3 ± 25.3 and 498.2 ± 69.6 nm and surface charges (ζ-potential) between -30.66 ± 1.55 and -26.74 ± 1.04 mV for the liposomal systems coated with 8 alternating monolayers of chitosan and dextran sulphate or alginate, respectively.

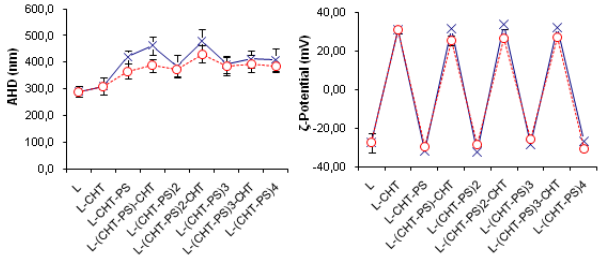

Figure 1. Apparent hydrodynamic diameter (AHD) and ζ-potential change with the adsorption of alternate polysaccharide layers onto soybean lecithin liposomes.

The systems offer good properties for encapsulation on its liposomal aqueous core and sustained release of a model protein, *in vitro* (Figure 2).

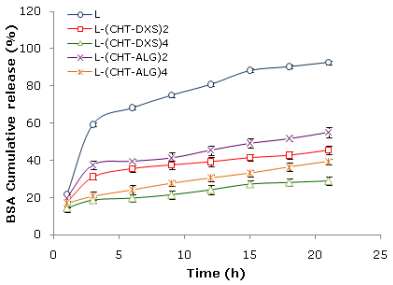

Figure 2. Bovine serum albumin (BSA) cumulative release from liposomes and polysaccharide-coated liposomes assembled with 2 and 4 polymeric bilayers. (L, uncoted liposomes; CHT, chitosan; DXS, dextran sulfate; ALG, alginate).

Conclusions: This study has shown that L-b-L self-assembly of polysaccharide-coated liposomes can be achieved by adding cationic (chitosan) and anionic (dextran sulfate or alginate) polysaccharides to a suspension of anionic liposomes (soybean lecithin) under carefully controlled solution compositions. The polysaccharide-coated-liposomes exhibited better release properties of a model protein, bovine serum albumin, than uncoated liposomes during cumulative release studies. Polysaccharide-coated liposomes may subsequently be of significant interest as novel biomaterial for the improved delivery of macromolecules such as, polymeric drugs or vaccines.

Acknowledgements: Authors dedicate this paper *in loving memory* to Prof. Dr. Francisco Molina Lucas (1952-2009), thank you professor for the gift of knowledge. This research was funded by Consejo Nacional de Rectores (CONARE), Government of Costa Rica.

Microparticles of the natural polymer Chitosan in aqueous suspension: stability of particle size distribution

Barboza, Ana Claudia R. N.[1,2]*; Pessine, Francisco B. T.*[1]

1. University of Campinas (Unicamp); 2. 3M Company

anabarboza@iqm.unicamp.br

Introduction: Polymers have proved to be effective carrier systems for sustained release of active substances. Biocompatibility and biodegradability in physiological conditions, generating innocuous degradation products, as well as safe formulations, are essential for this end use. The use of Chitosan (CTS) for that purpose has been extensively described in scientific literature and patents[1].
Preparations free of organic solvents help assure safety and avoid costly purification steps. Investigation and optimization of ionic crosslinking processes to obtain Chitosan micro and nanoparticles in water[2,3] are required to enable release profiles of actives suitable to various physiological media and administration routes, meeting a wide applications range. Stability of microparticles suspensions is also a critical feature.
This study aims to verify the stability of Chitosan microparticles aqueous suspensions ionically crosslinked by sodium triphosphate (TPP), in the presence of a polysorbate to avoid microparticles aggregation over time.

Materials and Methods: Chitosan (Chitopharm S) was kindly supplied by Cognis Brasil. Sodium Triphosphate (TPP) was acquired from Sigma Aldrich. Polysorbate (PS, Alkamuls 80) was kindly supplied by Rhodia.
Microparticles were prepared according to methodology[4] modified at our laboratory[5]. TPP solution at pH 5 was dropped on aqueous CTS solution at pH 4.5 with 1% PS during agitation using a high shear mixer at 5000 rpm for 12 min., and magnetic agitation for 6h.
Particle average diameter and particle size distribution (PSD) were measured by laser scattering with HORIBA LA-900 equipment on days 1, 13, 30 and 63.

Results and Discussion: Average particle diameters are summarized in the following table. For each sample, median particle diameter(µm), mean and standard deviation are presented; * values are averages of replicates.
Variation of initial (Day 1) particle diameter from one sample to another is inherent to the preparation process and can possibly be improved by a steadier dropping of TPP on the chitosan solution.
Particle size distributions (PSD) of Sample C are shown in the following figure; other samples behaved similarly. Analyzing the slight variations in PSD from Day 1 to Day 63, one sees a trend towards higher number of average-size particles and lower number of larger particles. Possible interpretation of this trend is that large ionically crosslinked microparticles are less stable and break apart into smaller particles.
When the section of the curve corresponding to smaller particles (< 5 µm) is looked closer, a slight decrease in the number of those particles is also seen. This gives indication of successful stabilization by PS, since only a small number of particles tend to aggregate into larger ones.

	Day 1			Day 13		
Sample	median	mean	std dev	median	mean	std dev
A	7,2*	11.3*	9.7*	7.7*	15.8*	14.4*
B	3.1	7.9	7.4	7.5*	10.6*	8.9*
C	6.9	12.9	11.5	5.9*	13.0*	12.0*

	Day 30			Day 63		
Sample	median	mean	std dev	median	mean	std dev
A	14.1	17.2	25.0	14.3	16.9	9.9
B	8.8	10.1	5.6	8.4	9.1	4.2
C	11.8	12.7	5.6	11.8	12.6	5.3

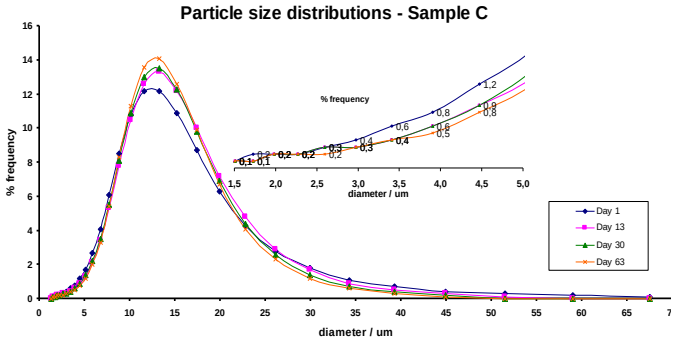

Conclusions: Chitosan microparticles obtained by direct ionic crosslinking with TPP in aqueous media showed to be adequately stabilized by PS on a 2 months time range, encouraging further studies of sustained release formulations using these particles as carriers.

References:

1 Agnihotri S.A., Mallikarjuna N.N., Aminabhavi T.M., *J. Control. Rel.* 2004, 100, 5-28.
2 Srinatha A., Pandit J.K., Singh S., *Indian J. Pharm. Sci.* 2008, 70(1), 16-21.
3 Gan Q., Wang T., Cochrane C., McCarron P., *Col. Surf. B: Biointerfaces* 2005, 44, 65-73.
4 Calvo P., Remuñán-López C., Vila-Jato J.L., Alonso M.J., *J. App. Polym. Sci.* 1997, 63, 125-132.
5 Barboza A.C.R.N., Pessine F.B.T., *33rd Annual Meeting of the Brazilian Chemical Society*. Águas de Lindóia-São Paulo/Brasil, 2010.

Acknowledgements:
- Profa. Dra. Maria H. A. Santana/UNICAMP, for the use of HORIBA LA-900 laser scattering equipment.
- Cognis Brasil, for donating Chitopharm S.
- Rhodia Brasil, for donating Alkamuls 80.
- This study is sponsored by 3M Company through Discover Grant 0049/2009.

Preparation and Evaluation of Novel Absorptive and Antibacterial Polyurethane Membranes for Wound Dressing Application

Abbas Yari, Hamid Yeganeh, Hadi Bakhshi*

Polyurethane Department, Iran Polymer and Petrochemical Institute, P.O.Box: 14965/115, Tehran, Iran

E-mail: h.yeganeh@ippi.ac.ir

Introduction

The skin is the first barrier of body against bacteria that cause infections. Thus, when skin damage the protection of the skin is a vital problem. Wound dressings can be used as a barrier against bacterial contamination and provide condition for wound healing [1]. An ideal wound dressing should has some specific characteristics such as hydrophilicity, permeability to water vapor, oxygen permeability, transparency for follow up wound healing, ability to absorb body fluids, good handling, proper adhesion, sufficient resilience, and antibacterial activity [2]. Due to excellent mechanical and physical properties as well as promising blood compatibility, polyurethanes have been widely used for biomedical applications. Additionally, because of their good barrier properties and oxygen permeability they are often used in wound dressings [3]. Functionalization of polymers by proper quaternary ammonium components, is an effective route for the induction of antibacterial activity [4] In the current study, wound dressing polyurethane membranes with strong antibacterial activity against both gram positive (Staphylacoccus aureus) and gram negative (Escherichia coli) bacteria as well as promising physical properties were prepared.

Experimental

The crosslinked membranes were synthesized by co-curing of epoxy terminated polyurethane prepolymers (EPUs) and glycidyltriethylammonium chloride (GTEACl) at different molar ratios with proper amount of 1,4-tetramethylenediamine as curing agent.

EPUs were prepared from polyethylene glycol at M_n= 1000 and 2000 g/mol, hexamethylene diisocyanate and glycidol. GTEACl was also synthesized from the reaction of epichlorohydrine with triethyl amine.

Results and discussion

The structure of prepared membranes was evaluated by FTIR spectroscopy and uniform incorporation and distribution of quaternary ammonium chloride groups in the polymers matrix was proved via Energy-Dispersive X-ray Spectroscopy and following the concentration of chloride ions.

The mechanical properties of membranes were evaluated from stress-strain curves. The molecular weight of EPU and GTEACl content were influenced the crosslink density (υ_c) and consequently the tensile properties of membranes. As it was expected, the υ_c decreased with increasing molecular weight of EPU and increasing of GTEACl content (because it was a monofunctional reagent). Depend on aforementioned variables the tensile strength and elongation at break of membranes were in the range of 1.0-10 MPa and 70-400% respectively.

It is well known that surface drying not only impedes delivery of nutrients and immune defenses to the wound surface but also markedly impedes the ability of cells to migrate across the wound surface. Therefore, among major parameters of the ideal wound dressing, water vapor transmission rate (WVTR) and equilibrium water absorptive capacity (EWA) of the dressing, which control the fluid balance are important parameters. The measured data are collected in Table 1, which showed direct dependence of these parameters to both υ_c and GTEACl content. For QPN-2000 samples, WVTR is much better than commercially available wound dressings, Tagaderm and Opsite. The water absorption data of prepared films clearly showed that these wound dressings are absorptive, so they can be employed for high exudative wounds.

The biocompatibility of membranes was evaluated by their cell culture with both L929 Fibroblast and MCA-3D Keratinocyte cell lines. As well, MTT assay showed excellent cells viability for all of the prepared membranes. Therefore, these membranes displayed good level of biocompatibility for wound dressing application. The antibacterial activity of membranes was evaluated by shaking flask and Agar plate methods (Table 1). All of membranes containing GTEACl showed good antibacterial properties. The bacteria reduction (BR%) increased with increasing the quaternary ammonium groups' content.

Conclusion

Due to acceptable tensile properties, excellent biocompatibility and antibacterial properties as well as optimum WVTR and EWA these membranes are promising candidates as wound dressing for high exudative wounds.

Table 1

Sample*	EWA (%)	WVTR (g/day/m^2)	BR%	
			E.coli	S.uareus
QPN-1000-0	144	650±20	0	0
QPN-1000-30	182	700±10	94.1	100
QPN-1000-40	205	720±10	100	100
QPN-1000-50	245	740±10	98.4	100
QPN-2000-0	497	1800±60	0	0
QPN-2000-30	253	2100±20	21.6	66
QPN-2000-40	368	2500±30	90.9	100
QPN-2000-50	550	2700±50	100	100

* **Q**uaternized **P**olyurethane **N**etwork (molecular weight of PEG=1000 or 2000-mol% of GTEACl

References

1. D. Queen, Int. Wound J. 1, 59, 2004.
2. J. M. Rosiak, Nuclear Instruments and Methods in physics Research B 151, 56, 1999.
3. M. U. Ozkaynak, Macromol. Symp 228, 177, 2005.
4. E. Kenawy, Biomacromolecules 8, 1359, 2007.

Swelling Behavior of Macroporous Polymer Networks

Cesar G. Gómez[1], Gustavo Pastrana[2], Daniel Serrano[2], Estanislao Zuzek[2], Marcelo A. Villar[3], Miriam C. Strumia[1]

[1]Departamento de Química Orgánica, Facultad de Ciencias Química, (IMVIB-CONICET) Universidad Nacional de Córdoba, Haya de la Torre y Medina Allende, Edificio de Ciencias II, Ciudad Universitaria, (5000) Córdoba.
[2]Grupo Nuevos Materiales y Dispositivos, Comisión Nacional de Energía Atómica, Centro Atómico Bariloche, (8400) San Carlos de Bariloche, Argentina.
[3]Planta Piloto de Ingeniería Química, PLAPIQUI (UNS-CONICET), Departamento de Ingeniería Química, Universidad Nacional del Sur, Camino "La Carrindanga" Km. 7, (8000) Bahía Blanca, Argentina.

gom@fcq.unc.edu.ar, mvillar@plapiqui.edu.ar, mcs@fcq.unc.edu.ar

Introduction: Macroporous polymer beads containing a permanent well-developed porous structure in dry state have a wide range of applications such as catalyst,[1,2] immobilization of enzymes,[3] HPLC supports, liberation of active substances, adsorbents,[4] among others. Their porous structure facilitates the diffusion of different solutes through the polymeric network.[5] Since these networks have particular properties such as a high crosslinking degree and a rigid structure in both swollen and dry state,[6] the study of their synthesis is therefore of considerable interest.[7] The influence of crosslinking agent content and stirring speed on the structure of the polymer network obtained for the system 2-hydroxyethyl metacrylate (HEMA) and ethylene glycol dimetacryclate (EGDMA) by suspension polymerize-tion was studied. The matrix pore system and its crosslinking degree were evaluated, principally, from their swelling in water. Characteristics parameters of the porous network were also obtained from a simple mathematical model.

Results and discussion: The water distribution between empty spaces of the network (w_{abs}^{water}) and the water adsorbed by polymer chains (w_{ads}^{water}) were obtained from water evaporation kinetics of swollen samples (Figure 1).

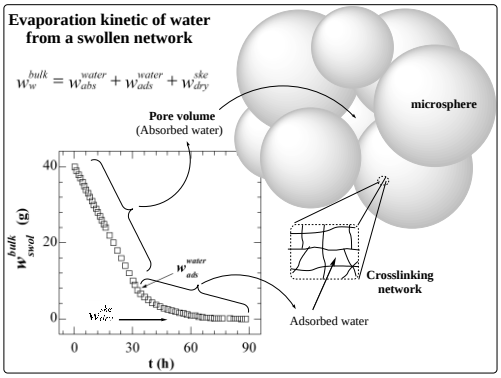

Figure 1. Evaporation kinetics of water from a swollen network indicates that water is retained by the matrix through the adsorption phenomenon and between empty spaces by absorption into the pores.

The development of a simple mathematical model for swollen networks allowed us to achieve relevant parameters such as the porosity (Eq. 1), and the volume increase of both pore and network.

$$\varepsilon_{swollen} = 1 - \left[\frac{(Q_{w_{ads}}^{water} - 1)}{\delta^{water}} + \frac{1}{\delta_{dry}^{ske}} \right] \cdot \frac{\delta_{dry}^{bulk}}{Q_v^{bulk}} \qquad (1)$$

Where the equilibrium water content, $Q_{w_{ads}}^{water}$, represents the fraction of water adsorbed by the network and the swelling volume degree, Q_v^{bulk}, corresponds to the network expansion. On the other hand, the true, δ_{dry}^{ske}, and apparent density, δ_{dry}^{bulk}, were determinated by pycnometric measurements.

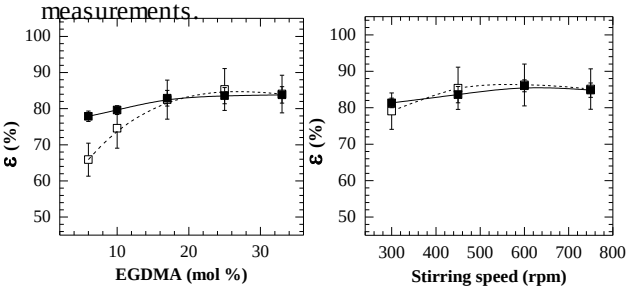

Figure 2. Porosity of the network in dry (filled symbols) and swollen state (open symbols).

Macroporous polymer networks synthesized with an EGDMA content higher than 10 mol% or using a stirring speed above 300 rpm exhibited a stable pore architecture (Figure 2). This behavior agrees with a high crosslinking density of the network formed, which depends, principally, on the crosslinker content.

Conclusions

The kinetics of water evaporation from swollen networks and the mathematical model proposed were used to describe the morphology of macroporous polymer networks. Water distribution into the network was used to determine parameters of interest such as porosity and volume increase of both pore and network. Results shown that samples with higher degree of crosslinking have stable pore architecture.

Acknowledgements

Authors thank CONICET, FONCYT, and SECYT-UNC for their financial support.

References

1. Kristensen T.E., Vestli K., Fredriksen K.A., Hansen F.K., Hansen, T. *Org. Lett.* **2009**, *11*, 2968-2971.
2. Liu C., Tang T., Huang B. *J. Polym. Sci. Part A: Polym. Chem.* **2003**, *41*, 873-880.
3. Mileti N., Vukovi Z., Nastasovi A., Loos K. *J. Mol. Catal. B Enzym.* **2009**, *56*, 196-201.
4. Bedair M, El Rassi Z. *J. Chromatogr. A* **2005**, *1079*, 236-245
5. Krajnc P., Štefanec D., Brown J., Cameron N. *J. Polym. Sci. Part A: Polym Chem* **2005**, *43*, 296-303.
6. Svec F., Frechet J. *Macromolecules* **1995**, *28*, 7580-7582.
7. Gomez C.G., Strumia, M.C. *J. Polym. Sci. Part. A: Polym. Chem.* **2008**, *46*, 2557-2566.

On the Morphology of Drawn UHMWPE Gel Films and PTFE Extrudates

H. M. Shabana

Prof. of Experimental Physics, Applied Science Dept., College of Technological Studies, PAAET, P. O. Box 42325, Shuwaikh 70654, KUWAIT.

e-mail: hmshabana@hotmail.com

Abstract

Two high performance polymers, polytetrafluoroethylene (PTFE) and Ultra high molecular weight polyethylene (UHMWPE) are investigated using several tools. The failure behavior exhibited by both polymers at different extrusion rates are discussed as a function of the time factor. The time at which both polymers failed is shown to be constant. These results reflect that the failure is independent on the rate of stretch, at least in specific range of stretching rates. The change of the maximum attainable draw ratio with the initial polymer concentration is investigated at different temperatures. At 130 ºC, the maximum attainable draw ratio increases as the initial polymer concentration decreases. The effect of drawing on the melting endotherm at different rates is also demonstrated for the drawn UHMWPE. Two peaks are observed, and may represent two components of morphology within the film and not a reorganization phenomenon. The second peak starts to disappear at draw ratio 4 and completely disappear at draw ratio 7. The melting point of the drawn gel films is shown to be nearly the same. The changes in morphology of the stretched UHMWPE are investigated by the scanning electron microscopy. The morphological changes in relation to specimens with different concentrations are given. Disentangled network and fibril structure are formed at the final stage. Several attempts are made to etch and to replicate UHMWPE to reveal the internal microstructure using the transmission electron microscope. Permanganic etching and both one and two-stage replication methods are used for this purpose.

Keywords: PTFE, UHMWPE, mechanical drawing, DSC, electron microscopy

Nonvolatile Memory Transistors using Ferroelectric P(VDF-TrFE) and Printed Semiconducting Channel

Soon-Won Jung, Kang-Jun Baek, Sung-Min Yoon, Jae Bon Koo, Yong Suk Yang, Kang Dae Kim, and In-Kyu You

Electronics and Telecommunications Research Institute (ETRI)

jungsoonwon@etri.re.kr

Organic non-volatile memories are the emerging research field due to its unique characteristics in charge storage properties and a relatively low manufacturing cost. Conjugated molecules and solution processable charge storage materials enable to realize the memory device by simple and cost-effective solution processes such as spin coating or various graphic art printing techniques. Among the many possible configurations for ONVMs, organic field effect transistors (OFETs)-based memory has many advantage including non-destructive read-out, complementary integrated circuit architectural compatibility, and single transistor realization.

To realize high performance ferroelectric OFET memory, ferroelectric polymer materials must show both robust mechanical properties as a gate dielectric and large dipole polarization as a memory element. Poly(vinylidene fluoride-trifluoroethylene) [P(VDF-TrFE)] copolymer is one of the promising materials to fulfill both properties at once.

There have been many reports on the memory characteristics of P(VDF-TrFE) with metal-ferroelectric-metal, metal-ferroelectric-insulator-semiconductor capacitors, or OFETs. Although these results clearly suggest a high feasibility of P(VDF-TrFE) for nonvolatile memory, there are a few challenges must be addressed such as a high programming voltage, low switching speed, and insufficient data retention time and various approaches including modifications of material and/or device structure have been proposed.

In this study, we demonstrate a low voltage operated top gated ferroelectric polymer transistor memory with a inkjet-printed organic semiconductor active channel and a poly(vinylidene fluoride-trifluoroethylene) ferroelectric gate insulator. Key features of our ferroelectric memory devices are all-solution process and a relatively low operating voltage. The low operating voltage was achieved by single P(VDF-TrFE) dielectric layer and the memory device typically operated a low gate and source-drain bias below 15 V.

[1] Q.-D. Ling, D.-J. Liaw, C. Zhu, D. S.-H. Chan, E.-T. Kang, K.-G. Neoh, Progress in Polymer Science 33 (2008) 917

[2] Y.-Y. Noh, N. Zhao, M. Caironi, H. Sirringhaus, Nat. Nanotechnol. 2 (2007) 784

[3] K.-J. Baeg, Y.-Y. Noh, J. Ghim, S.-J. Kang, H. Lee, D.-Y. Kim, Adv. Mater. 18 (2006) 3179

This project was supported by the IT R&D program of MKE (2008-F052-01, Development of Next Generation RFID Technology for Item Level Applications)

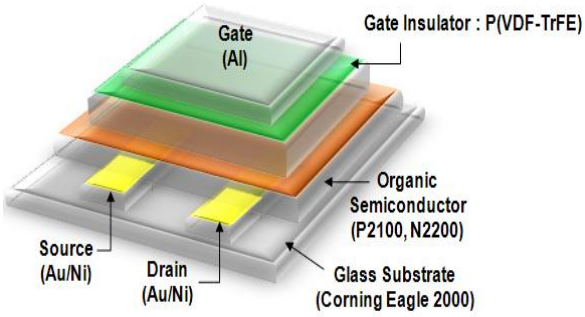

Figure 1. Schematic representation of the device configuration of a top-gate/bottom-contact polymer field-effect transistor.

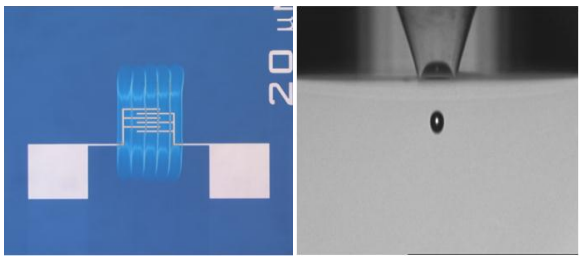

(a) (b)

Figure 2. (a) Optical image of inkjet-printed nonvolatile memory TFTs. (b) High speed CCD camera images of inkjet droplet formation.

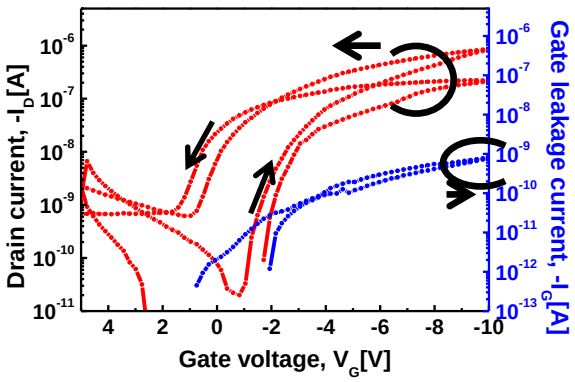

Figure 3. Transfer curves of top-gate and bottom-contact memory transistors with P(VDF–TrFE) film.

Drawing and Tensile Properties of Polyamide 6 / Calcium Chloride Composite Fibers

Jen-Taut Yeh[1*,2], *Yu-Ching Lai*[1], *Hong-Ping Chen*[2], *Liang Qiu*[2], *Fang-Chang Tsai*[2] *and Chien-Yu Yeh*[3]

1 Graduate School of Material Science and Engineering, National Taiwan University of Science and Technology, Taipei, Taiwan

2 Ministry of Education, Key Laboratory for the Green Preparation and Application of Functional Materials, Faculty of Materials Science and Engineering, Hubei University, Wuhan, China

3 Department of Chemical Engineering, National Taiwan University, Taipei, Taiwan

e-mail: jyeh@mail.ntust.edu.tw

Abstract Body: The intra- and inter-chain interactions in polyamide 6 (PA6) molecules are responsible for their thermal stability, high toughness and tensile properties that make PA6 possess bright perspective and advantage in developing high tensile strength with superior performance in textile field [1]. Several attempts have been made to improve the draw ratio and tensile strength values of polyamide fibers by disrupting the strongly interacted hydrogen bondings present in melt-crystallized PA6 fibers by adding crystallization inhibitors [2-5]. However, as far as we know, no investigation has ever been reported regarding the effects of $CaCl_2$ contents on the drawing and tensile properties of PA6 composite fibers. In this study, the beneficial effect of crystallization inhibitors on the drawing properties of the PA6 fibers was investigated using PA6/$CaCl_2$ composite fibers prepared at varying compositions. The compositions of the PA6/$CaCl_2$ specimens prepared in this study are summarized in Table 1. The influence of calcium chloride ($CaCl_2$) contents on the drawing and tensile properties of polyamide 6 (PA6) /$CaCl_2$ composite fibers prepared at varying drawing temperatures were investigated. At any fixed drawing temperature, the achievable draw ratio (D_{ra}) values of $PA6_x(CaCl_2)_y$ as-spun fiber specimens approach a maximum value, as their $CaCl_2$ contents are close to the 3 wt% optimum value. The maximum D_{ra} values obtained for $PA6_x(CaCl_2)_y$ as-spun fiber specimens prepared at the optimum $CaCl_2$ content reach another maximum as their drawing temperatures approach the optimum drawing temperature at 120 °C. The initial modulus, tenacity and birefringence values of the PA6 and $PA6_x(CaCl_2)_y$ fiber specimens were found to improve consistently with D_{ra} or with drawing temperatures when they were stretched to a fixed D_{ra}. Similar to those found for their achievable drawing properties, the ultimate modulus, tenacity and birefringence values of $PA6_x(CaCl_2)_y$ fiber specimens approach a maximum value, as their $CaCl_2$ contents and drawing temperatures approach the 3 wt% and 120 °C optimum values, respectively. The above interesting thermal and tensile properties of $PA6_x(CaCl_2)_y$ fiber specimens are attributed to the complex interactions between Ca^{2+}, Cl^-, carbonyl and amide groups of PA6 molecules during their preparation processes.

Table 1 Compositions of PA6 and $PA6_x(CaCl_2)_y$ as-spun fiber specimens.

Samples	PA6 (wt %)	$CaCl_2$ (wt %)
PA6	100	0
$PA6_{99.5}(CaCl_2)_{0.5}$	99.5	0.5
$PA6_{99}(CaCl_2)_1$	99	1
$PA6_{98}(CaCl_2)_2$	98	2
$PA6_{97}(CaCl_2)_3$	97	3
$PA6_{96}(CaCl_2)_4$	96	4
$PA6_{94}(CaCl_2)_6$	94	6
$PA6_{92}(CaCl_2)_8$	92	8

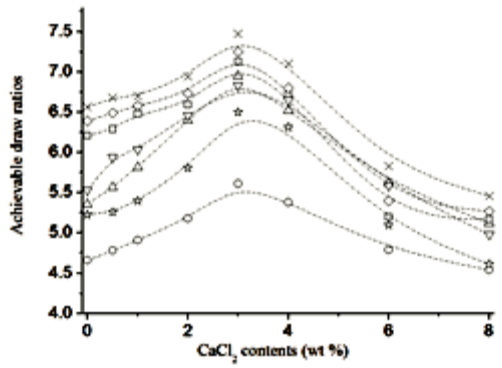

Figure 1 The achievable draw ratios of $PA6_x(CaCl_2)_y$ as-spun fiber specimens drawn at 60 °C (○), 80 °C (△), 100 °C (□), 110 °C (◇), 120 °C (×), 130 °C (▽) and 140 °C (☆), and a drawing rate of 50 mm/min.

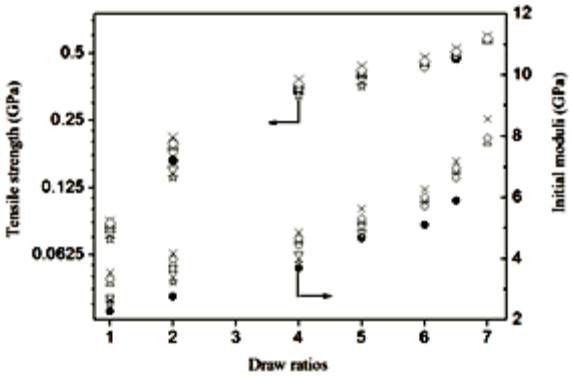

Figure 2 Tensile strengths and initial moduli of as-spun and drawn PA6 (●), $PA6_{99}(CaCl_2)_1$ (○), $PA6_{98}(CaCl_2)_2$(△), $PA6_{97}(CaCl_2)_3$ (×), $PA6_{96}(CaCl_2)_4$ (◇), $PA6_{94}(CaCl_2)_6$ (▽) and $PA6_{92}(CaCl_2)_8$ (☆) fiber specimens drawn at 120 °C and 50 mm/min.

References

1. Ito M, Takahashi A, Araki N, Kanamoto T (2001) Polymer 42:241.
2. More AP, Donald AM (1992) Polymer 33:4081.
3. Wyzgoski MG, Novak GE (1987) J Mater Sci 22:1715.
4. Dhevi DM, Choi CW, Prabu AA, Kim KJ (2009) Polym Compos 30:481.
5. Kotek R, Jung D, Tonelli AE, Vasanthan N (2005) J Macro Sci Poly Rev C45:201.

Drawing Properties of Modified Polyamide 6 fibers

Jen-Taut Yeh[1,2*,3], *Fang-Chang Tsai*[1], *Zhi-Wei Liu*[1], *Dong-Rui Wu*[1], *Yu-Ching Lai*[2], *Chien-Rong Yeh*[4] *and Kuo-Huang Hsieh*[5]

[1] Ministry of Education, Key Laboratory for the Green Preparation and Application of Functional Materials, Faculty of Materials Science and Engineering, Hubei University, Wuhan, China
[2]Graduate School of Material Science and Engineering, National Taiwan University of Science and Technology, Taipei, Taiwan, e-mail: jyeh@mail.ntust.edu.tw
[3] Key Laboratory of Green Processing and Functional Textiles of New Textile Materials, Wuhan University of Science and Engineering, Ministry of Education, Wuhan, China
[4] Department of Textiles and Clothing, Fu Jen Catholic University, New Taipei City, Taiwan
[5] Department of Chemical and Engineering, National Taiwan University, Taipei, Taiwan

Abstract The drawing properties of the modified PA 6 (MPA) fiber specimens prepared at varying drawing temperature were systematically investigated, wherein the MPA resins were prepared by reactive extrusion of PA 6 with the compatibilizer precursor (CP). At any fixed drawing temperature, the achievable draw ratio (D_{ra}) values of MPA as-spun fiber specimens increase initially with increasing CP contents, and then approach a maximum value, as their CP contents are close to the 5 wt% optimum value. The maximum D_{ra} values obtained for MPA as-spun fiber specimens prepared at the optimum CP content reach another maximum as their drawing temperatures approach the optimum drawing temperature at 120 °C. The tenacity and birefringence values of PA 6 and MPA fiber specimens improve consistently as their draw ratios increase. Similar to those found for their achievable drawing properties, the ultimate tenacity and birefringence values of MPA fiber specimens approach a maximum value, as their CP contents and drawing temperatures approach the 5 wt% and 120 °C optimum values, respectively. Investigations including Fourier transform infrared, melt shear viscosity, gel content, thermal and wide angle X-ray diffraction experiments were performed on the MPA resin and/or fiber specimens to clarify the optimum CP content and possible deformation mechanisms accounting for the interesting drawing and ultimate tensile properties found for the MPA fiber specimens prepared in this study.

Experimental The polyamide 6 (PA 6) and compatibilizer precursor (CP) used in this study were obtained from Zig Sheng Industrial Corporation and Formosa Chemicals and Fiber Corporation, Taipei, Taiwan, wherein PA 6 (Zisamide HP1101) is nylon 6 and CP is a 40% zinc-neutralized ethylene/acrylic acid copolymer (95:5). The Irganox B225 antioxidant was purchased from Ciba-Geigy Corporation, Basel, Switzerland. Before melt blending, PA 6 was dried at 80 °C for 16 hours. The dry-blended PA 6/ CP resins with 1000 ppm antioxidant were then fed into atwin-screw extruder (SHJ-20, Nanjing Jiant Corp., Nanjing, China) at varying weight ratios to make MPA resins. The extruder was operated at 210 °C in the feeding zone and at 230 °C towards the extrusion die with a screw speed of 100 rpm. The CP modified polyamide (MPA) resins obtained from the twin screw extruder was quenched in cold water at 15 °C and cut into pellet form. The compositions of the MPA specimens prepared in this study are summarized in Table 1.

Table 1 Compositions of PA 6 and MPA specimens.

Samples	PA 6 wt %	CP wt %	Samples	PA 6 wt %	CP wt %
PA 6	100	0	MPA_{10}	90	10
$MPA_{2.5}$	97.5	2.5	MPA_{15}	85	15
MPA_5	95	5	MPA_{20}	80	20
$MPA_{7.5}$	92.5	7.5			

Results and discussion

Fig. 1 summarized the values of achievable draw ratio (D_{ra}) of PA6 and MPA as-spun fiber specimens drawn at varying temperatures but at a fixed drawing rate of 50 mm/min. In a way similar to those found for their birefringence properties, at any fixed drawing temperature, the D_{ra} values of MPA as-spun fiber specimens increase initially with increasing CP contents, and then approach a maximum value, as the CP contents are close to the 5 wt% optimum value.

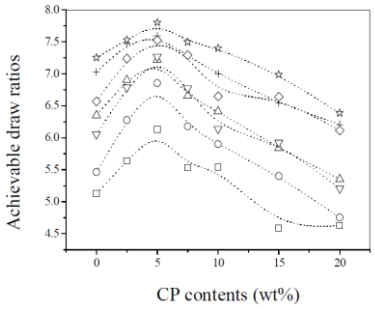

Figure 1 The achievable draw ratios of MPA_x specimens drawn at 25 °C (□), 60 °C (○), 80 °C (△), 100 °C (◇), 110 °C (+), 120 °C (☆) and 140 °C (▽) drawing rate 50 mm /min.

References

[1] N. Vasanthan and D. R. Salem, *J. Polym. Sci. Part B : Polym. Phys*., 39, 536 (2001).
[2] M. Robert and E. Arno, U.S. Patent, 6426, 128 (1998).
[3] F. Ide and A. Hasegawa, *J. Appl. Polym. Sci.* , 18 , 963 (1974).
[4] S. Cartasegna and W. Heider, *Intern. Polym. Sci. Tech*., 15, 85 (1988).
[5] R. Multhavpt, T. Duschek, and J. Rosch, *Polym. Adv. Tech*., 47, 465 (1993).
[6] J. Duvall, V. Topolkaraev, E. Bear, and C. Sellitti, *Polymer*, 35, 3948 (2004).
[7] J.T. Yeh, C.C. Fan-Chiang, and M.F. Cho, *Polym. Bull*., 35, 371 (1995).
[8] J.T. Yeh, C.C. Fan-Chiang, and S.S.Yang, *J. Appl. Polym. Sci*., 64, 1531 (1997).

Ultradrawing Properties of Ultra-high Molecular Weight Polyethylene/Functionalized Carbon Nanotube Fibers

Jen-Taut Yeh[1*,2,3], *Chi-HuiTsou*[1], *Yu-Ching Lai*[1], *Wen-Hung Wang*[1], *Huo-Peng Zhou*[2] *and Chien-Yu Yeh*[4]

[1]Graduate School of Polymer Engineering National Taiwan University of Science and Technology, Taipei, Taiwan
[2] Ministry of Education, Key Laboratory for the Green Preparation and Application of Functional Materials, Faculty of Materials Science and Engineering, Hubei University, Wuhan, China
[3]Key Laboratory of Green Processing and Functional Textiles of New Textile Materials, Wuhan University of Science and Engineering, Ministry of Education, Wuhan, China
[4]Department of Chemical Engineering, National Taiwan University, Taipei, Taiwan

e-mail:jyeh@mail.ntust.edu.tw

Abstract. Systemic investigation of the influence of the plain and functionalized carbon nanotube (CNT) contents on the ultradrawing properties of ultrahigh molecular weight polyethylene/carbon nanotubes and UHMWPE/functionalized CNTs as-prepared fibers are reported. In a way similar to those found for the orientation factor values, the achievable draw ratios (D_{ra}) of the FC_y and FC_{fx-y} as-prepared fibers approached a maximum value as their CNT and/or functionalized CNT contents reached their corresponding optimum values. The maximum D_{ra} values obtained for $FC_{fx-0.001}$ as-prepared fiber specimens prepared at varying maleic anhydride grafted polyethylene (PE_{-g-MAH})/modified CNTs weight ratios were significantly higher that of the $FC_{0.0015}$ as-prepared fiber specimen prepared at the optimum plain CNT content. Tensile property analysis further suggested that excellent orientation and tensile properties of the drawn FC_y and FC_{fx-y} fibers can be obtained by ultradrawing the fibers prepared at their optimum plain CNT and/or functionalized CNT contents. To understand the interesting orientation, ultradrawing and tensile properties of FC_y and FC_{fx-y} fiber specimens, FTIR, specific surface area, and SEM morphology analysis of the plain and functionalized CNTs were performed in this study.

Experimental. The UHMWPE resin used in this study is associated with a weight-average molecular weight (Mw) of 7.6 x 10^6, which will be referred to as resin U in the following discussion. The carbon nanotubes (CNTs) used in this study will be called C. Maleic anhydride grafted polyethylene (PE_{-g-MAH}) resin with a grafting ratio of 1.5 wt% was used to modify and functionalize CNTs for well-dispersing in UHMWPE/CNTs gel solutions. The sample designations of functionalized CNTs and weight ratios of modified CNT/ PE_{-g-MAH} used in the functionalizing experiments are summarized in Table 1. The ultrasonicated plain CNT or functionalized CNT solutions were then mixed with U resin at varying weight ratios and concentrations at 150 °C for 4 hours, during which 0.1 wt % of di-*t*-butyl-*p*-cresol was added as an antioxidant.

Table 1 Designations of functionalized CNT specimens and weight ratios of modified CNT/PE_{-g-MAH} used in the functionalizing experiments.

Functionalized CNT specimens	Weight ratios of PE_{-g-MAH}/ modified CNT
C_{f1}	5
C_{f2}	10
C_{f3}	15
C_{f4}	20

Results and discussion. The plain CNT specimens had a large specific surface area of 100.5 m^2/g. After oxidation by acid, the specific surface areas of the modified CNT specimens increase significantly to 184.7 m^2/g. The specific surface areas of the functionalized CNT specimens are even higher than those of the plain and modified CNT specimens. The specific surface areas of the functionalized CNT specimens increase significantly and reach the maximum value at 272.7 m^2/g as their weight ratios of PE_{-g-MAH} to modified CNTs increase to the optimum value at 10. Fig. 1 summarized the achievable draw ratios (D_{ra}) of the FC_y and FC_{fx-y} as-prepared fibers prepared at varying CNT and functionalized CNT contents. After addition of the plain and/or functionalized CNTs in UHMWPE, the D_{ra} values of both FC_y and FC_{fx-y} fiber series specimens increase significantly with the initial increase in plain and/or functionalized CNT contents. Note that the D_{ra} values of both FC_y and FC_{fx-y} fiber series specimens reach a maximum as their plain and/or functionalized CNT contents approach the optimum value at 0.0015 and 0.001 wt%, respectively.

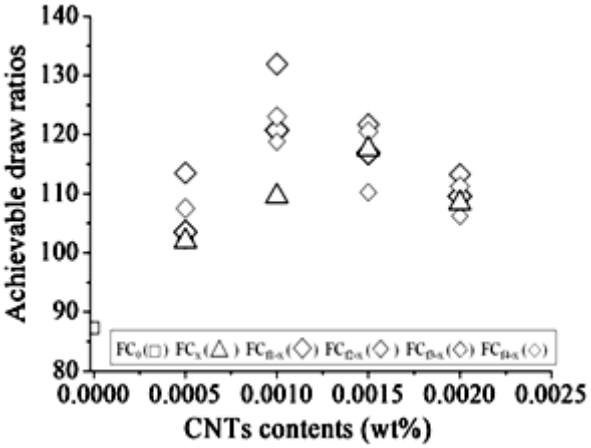

Fig. 1 The achievable draw ratios of FC_0, FC_x, FC_{f1-x}, FC_{f2-x}, FC_{f3-x} and FC_{f4-x} as-prepared UHMWPE fiber specimens prepared at varying CNTs contents.

References

1. S. Iijima, *Nature*, 354, 56 (1991).
2. R. Andrew, D. Jacques, A. M. Rao, T. Rantell, F. Derbyshire, and Y. Chen, *J. Appl. Polym. Sci.* , 75, 1329 (1999).
3. E. Kymakis, I. Alexandrou, and G.A.J. Amaratunga, *J. Appl. Phys.*, 93 ,1764(2003).
4. B. Vigolo, A. Penicaud, C. Coulon, C. Sauder, R. Pailler, C. Journet, P. Bernier, and P. Poulin, *Science*, 290, 1331 (2000).

Investigation of Argon Plasma Modification on Peel Strength of Woven Type Ultra High Molecular Weight Polyethylene

Chi-Yuan Huang[1*], *Jen-Taut Yeh*[2], *Kan-Nan Chen*[3], *Ching-Shan Tsai*[1], *Sheng-Kai Lin*[1], *Keng-Yu Tsao*[1], *Jing-Yi Wu*[1] *and Chien-Pang Chang*[1]

[1]Department of Materials Engineering, Tatung University, Taipei, Taiwan

[2]Graduate School of Material Science and Engineering, National Taiwan University of Science and Technology, Taipei, Taiwan

[3]Department of Chemistry, Tamkang University, Taipei, Taiwan

e-mail: cyhuang@ttu.edu.tw

Abstract

In the investigation, effects of surface modification by argon plasma on peel strength of woven type ultra high molecular weight polyethylene (UHMWPE) were studied. After plasma treated, the free radicals were generated on woven type UHMWPE surface and then converted to peroxide offer exposed to air. The concentration of peroxides were estimated by the 1,1-dipphenyl-2-picrylhydrazyl (DPPH·) method. From the results, the optimum free radical content for offering high T-peel strength was 1.27×10^{-9} mol/mm^2 at 40 W plasma-treated for 4 min. The plasma treated woven type UHMWPE possessed the hydrophilic property and introduced the number of anchors. The 3M 4475 adhesive possessed functional groups of N-H stretching vibrations (3333.36 cm^{-1}) and carbonyl stretching vibrations (1731.76 cm^{-1}). As it reacted with plasma treated UHMWPE, the chemical bonding significant increased in the adhesion strength between woven type UHMWPE and adhesive. This fibrils peel mechanism can offer peel strength as T-peel testing. As Surface modification by plasma treatment, the peel strength of UHMWPE fiber with adhesive 4475 composites was increased from 1.17 to 2.26 kgf/in.

Experimental

The woven type ultra high molecular weight polyethylene (UHMWPE) fiber was used as matrix, in which Spectra® fiber made by Honeywell, USA. 3M™ Scotch-Weld™ Nitrile High Performance Plastic Adhesive 4475 made by 3M Adhesives Division, USA. 1,1-dipphenyl-2-picrylhydrazyl (DPPH·) made by Tokyo Kasei, JAPAN. The UHMWPE fibers just were put into the cylinder and subjected to Ar plasma treatment. Ar plasma treatment was carried operating at 40 Watt and time of 4 min. The sample was cut into 100 × 25 mm by length and width. T-peel test was carried out using a tensile machine at room temperature in velocity of 10mm/min provided by ISO. The woven type UHMWPE fiber (25×50 mm^2) was immersed in a 1.0×10^{-4} M benzene solution of 1,1-diphenyl-2-picryhydrazyl (DPPH·) and kept at temperature 70 °C for 24 h to decompose the peroxide formed on the UHMWPE fiber surfaces. The DPPH· consumed was measured by the change of absorbance at 521 nm of UV–VIS spectra. The characteristic absorption peaks of functional groups of plasma-treatment UHMWPE fiber or UHMWPE fibers/adhesive composite were detected by a JASCO FT/IR-6200 IR (infrared) spectrometer.

Results and discussion

Fig. 1 showed that the optimum free radical content was 1.27×10^{-9} mol/mm^2 in plasma (40 W, 4 min) [1].

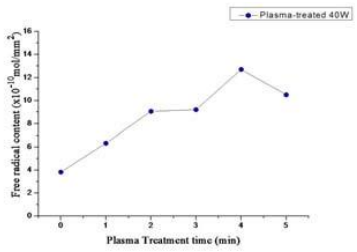

Fig. 1 Free radical content vs. times of various plasma treatments for woven type UHMWPE fiber.

Adhesive 4475-treated UHMWPE fiber and untreated UHMWPE fiber (Fig. 2) showed a new absorption appearing at 3341 and 1733 cm^{-1}, which had been assigned to amide groups and carbonyl groups. These new absorptions suggest that amide groups and carbonyl groups were formed on the adhesive 4475 surfaces [2].

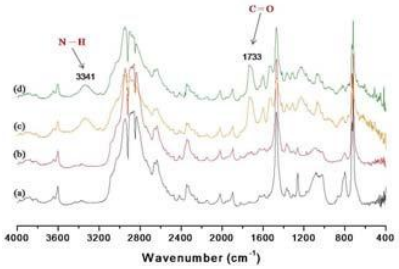

Fig. 2 The FTIR spectum of UHMWPE fibers using PR method in 60º (a) Un-treated fiber (b) Plasma-treated fiber (c) Fiber/Adhesive4475 (d) Plasma treated fiber/Adhesive 4475.

Fig. 3 showed that the optimum plasma treatment that could be induced at the UHMWPE fiber/adhesive 4475 peel strength was increased to 2.26 kgf/in [3].

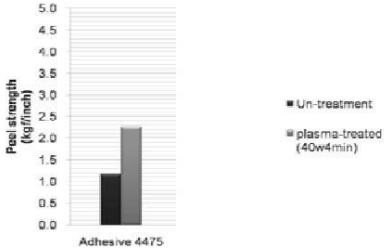

Fig. 3 Peel strength of woven type UHMWPE bonded by adhesive and after woven type UHMWPE fiber surfaces treatments (plasma 40w 4min).

References

[1] Rodrigo Scherer, Helena Teixeira Godoy, *Food Chemistry*, 112, 654 (2009).

[2] Michael Nase, Beate Langer, Hans Joachim Baumann, Wolfgang Grellmann, Gordon Geisler, Michael Kaliske. *J. Appl. Polym. Sci.*111,363 (2009).

[3] 3M™ Scotch-Weld™ Industrial Plastic Adhesive 4475 Material Safety Data Sheet.

Design and Synthesis of Low Refractive Index, Organosoluble, and Thermally Stable Fluorinated Polyamides Having *Ortho*-Linked Aromatic Units in the Main Chain

Ali Javadi, *Abbas Shockravi*

Faculty of Chemistry, Tarbiat Moallem University, No. 49, Postal Code 1571914911, Tehran, Iran

a.javadi@hotmail.com

Introduction

Wholly aromatic polyamides (PAs) are considered to be high-performance materials due to their high thermal stability, chemical resistance and outstanding mechanical properties, which make them useful for advanced technologies. However, most PAs are usually difficult to process due to their limited solubility in common organic solvents and high glass-transition temperatures. Therefore, many efforts have been made to improve the processing characteristics of these relatively intractable polymers. It has been demonstrated that incorporation of both flexible ether linkages and bulky naphthalene units into the polymer backbones can enhance the solubility and processability of aromatic polyamides without any significant reduction in thermal stability [1]. Another attractive approach employed to increase the solubility of polyamides is the incorporation of less symmetric units such as *ortho*-catenated aromatic rings in the main chains which leads to a reduction in crystallinity [2]. Recently, considerable attention has been devoted to the synthesis of fluorinated aromatic polyamids, especially the trifluoromethyl (CF_3)-containing poly(ether amide)s (PEAs) [3]. It has been recognized that the incorporation of bulky $-CF_3$ groups into PA backbones resulted in an enhanced solubility and optical transparency together with a lowered refractive index and dielectric constant, which was attributed to the low polarizability of the C–F bond and the increase in the free volume [4]. As part of our recent efforts to develop high-performance fluorinated polymers with excellent solubility and high thermal stability, as well as low refractive index and low birefringence for advanced optical and electronic applications, the current work reports the synthesis and characterization of a series of fluorinated PEAs from a high-purity CF_3-containing diamine, (DA), with various commercially available aromatic dicarboxylic acids.

Materials and Methods

The new CF_3-containing bis(ether amine), 1,1'-sulfide-bis-[(2-trifluoromethyl)4-aminophenoxy) naphthyl ether], was prepared in a two-step process. The first step is the chloro-displacement reaction of 2-chloro-5-nitrobenzotrifluoride with the potassium phenolate of 1,1'-thiobis(2-naphthol) formed in situ by the treatment with potassium carbonate in DMSO. The target bis(ether amine) was readily obtained in high yields by the Pd/C-catalyzed reduction of the intermediate dinitro compound (DN) with hydrazine hydrate in refluxing ethanol. The direct polycondensation was adopted here to prepare aromatic poly(ether amide)s.

Results and Discussion

All of the polymers were amorphous in nature, showed good solubility and could be readily dissolved in amide-type polar aprotic solvents (e.g., NMP, DMAc, DMF, and DMSO) and even dissolved in less polar solvents (e.g., *m*-cresol, THF, pyridine, and chloroform). The amorphous nature and good solubility of these PEAs can be attributed to the effect of the packing-disruptive $-CF_3$ and naphthyl groups and the *ortho*-linked structure, which could inhibit close packing and reduced the interchain interactions to enhance solubility. The presence of flexible ether and thioether linkages in the bis(ether amine) moiety also contributed to the enhancement in solubility. The thermal properties of the PEAs were evaluated by thermogravimetry analysis (TGA) and differential scanning calorimetry (DSC). The T_g values of aromatic PEAs were in the range of 221–263 °C, which follows the decreasing order of the chain flexibility and steric hindrance of the polymers backbones. The temperatures at 10% weight loss (T_{10}) values of the PEAs were in the range of 483–537 °C in nitrogen and in the range of 461–527 °C in air, respectively. The amount of residue of all PEAs at 700 °C in nitrogen atmosphere was higher than 50%. The data from thermal analysis showed that the resulting PEAs had fairly high thermal and thermooxidative stability. The in-plane (n_{TE}) and out-of-plane (n_{TM}) refractive indices of the PEA films measured at 1320 nm range from 1.5633 to 1.5844 and 1.5578 to 1.5754, respectively. In general, the low refractive indices of the resulting polymers are obviously attributed to the introduction of flexible ether and thiother linkages and large free volume of the C–F bond that interrupts chain packing and increase free volume. In this work, all the PEA films exhibited positive birefringence (Δn =0.0055–0.0097), indicating that the molecular chains were preferentially aligned in the film plane. The low birefringence of the PEAs can be mainly attributed to the flexible linkages, which effectively reduce the in-plane orientation of the PA main chains. The dielectric constants (ε) of the polymers can be estimated from the refractive index according to Maxwell's equation ($\varepsilon = n_{AV}^2$). All the synthesized PEAs had relatively low ε (2.44–2.50).

References

[1] Hsiao SH et al. *J Polym Sci A: Polym Chem* 42 (2004) 2377–2394.
[2] Yang CP et al. *J Polym Sci A: Polym Chem* 33 (1995) 2209–2220.
[3] Maji S et al. *J Appl Polym Sci* 108 (2008) 1356–1364.
[4] Qingming Z et al. *Polym Bull* 61 (2008) 569–580.

Multiple bicolor fluorescent micropattern formation on a single polymer film based on the polymeric photobase generator containing oxime-urethane and anthracene groups

Kyu Ho Chae and Hak Soo Kim

Department of Polymer Engineering, Chonnam National University, Republic of Korea

khochae@chonnam.ac.kr

Introduction

The formation of fluorescent micropattern on a thin polymer film has attracted considerable interest due to their possible application to the areas of photonic/ elctronic devices such as displays, optical memory devices and molecular switches, as well as the biosensor chips and imaging industries. Several methods for preparing fluorescent micropatterns in polymer films have been reported. Most of these preparation methods are based on photogenerated acids. Recently, photogenerated free radicals and photobleaching of fluorescent polymers were also applied to obtain fluorescent micropattern in polymer films.

In previous work, we have reported on fluorescence imaging based on a polymeric photobase generator containing oxime-urethane groups through the use of a prefluorescent dye for amino group.[1] Another study described the polymer containing phthalimido carbamate groups as a bicolor fluorescent imaging material.[2]

Here, we report on the multiple bicolor fluorescent micropattern formation on a single polymer film through the use of the photobase generation of oxime-urethane groups and photobleaching reaction of anthracene groups. The formation of bicolor micropatterns in a polymer film is of potential interest for the incorporation of photonic/electronic polymers in optical data storage devices or displays.

Materials and Methods

Polymerization: Typical polymerization conditions were as follow. A solution containing methyl methacrylate (0.2 g, 2.0 mmol), 9-anthracenylmethyl methacrylate (0.19 g, 0.7 mmol), benzophenone oximinocarbonylaminoethyl mehacrylate (0.23 g, 0.7 mmol) AIBN (3.1 mg) in 5 mL of THF was charged into a cap tube and purged with nitrogen for 15 min. After sealing the cap tube containing the reaction mixture, polymerization was carried out at 60 ^{o}C for 20 h. The polymer was isolated by double precipitation from THF into methanol.

Fluorescence micropatterning: A polymer film on the silicon wafer was covered with a photomask and irradiated with 310 nm UV light (6.0 J/cm^2). The irradiated film on the silicon wafer was dipped in rhodamine B solution for 10 s and subsequently washed in methanol. The dyed film on the silicon wafer was dried at room temperature under reduced pressure. The fluorescence micropatterns were observed by confocal microscopy.

Results and Discussion

Scheme 1 shows the photochemical reaction of terpolymer containing anthracene and oxime-urethane groups. The terpolymer bearing anthracene groups is fluorescent, but it became no fluorescencent upon irradiation due to the dimer or endoperoxide formation. Concomitantly, the oxime-urethane groups in the terpolymer photodecomposed to form amino groups. Treatment of the amino groups with rhodamine B led to the formation of amine and rhodamine adduct. Thus, the non-irradiated part of the terpolymer film has blue fluorescence, while the irradiated part became fluorescent through the formation of rhodamine-amine adduct.

Scheme 1.

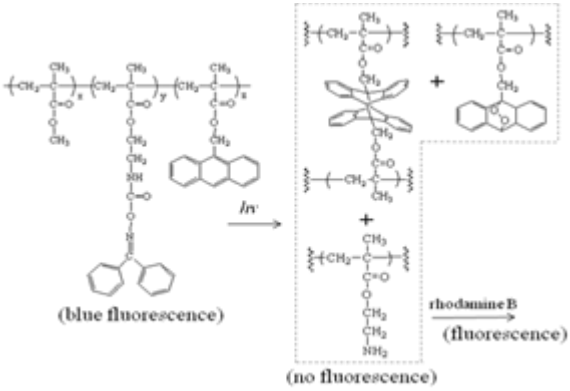

Figure 2 shows bicolor fluorescent micropatterns observed by the conforcal microscopy. Various bicolor micropatterns in a single polymer film were observed depending on the excitation wavelength.

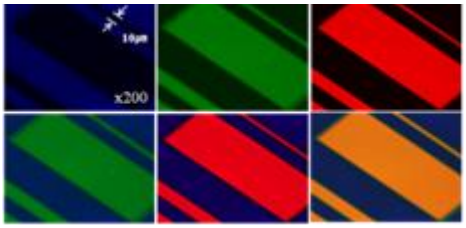

Figure 1. Fluorescent micropattern images obtained for a thin film of terpolymer on a silicon wafer.

In conclusion, we can create multiple bicolor micropatterns on a single polymer film through the use of photobleaching reaction of anthracene groups and photobase formation of oxime-urethane groups. This multiple bicolor micropatterning method may potentially be useful for the development of full-color displays or multiple optical data storage media.

References

[1] W. S. Choi, Y. –Y. Noh, and K. H. Chae, *Adv. Mater.*, **17**, 833, (2005).

[2] K. H. Chae and Y. H. Kim, *Adv. Func. Mater.*, **17**, 3470 (2007).

Starburst Triarylamine-Containing Electroactive Aramids with Ultra-Stable Near-Infrared and Multicolor Electrochromism

Guey-Sheng Liou, Hung-Ju Yen, and Hung-Yi Lin*

Functional Polymeric Materials Laboratory, Institute of Polymer Science and Engineering, National Taiwan University, 1 Roosevelt Road, 4th Sec., Taipei 10617, Taiwan

E-mail: gsliou@ntu.edu.tw (Liou, G.-S.)

Electrochromic materials exhibit a reversible optical change in absorption or transmittance upon electrochemically oxidized or reduced, such as transition-metal oxides, inorganic coordination complexes, conjugated polymers, and organic molecules.[1]

Intramolecular electron transfer (ET) processes were studied extensively in the mixed-valence (MV) systems,[2] and usually employed one-dimensional MV compounds contain two or more redox states. According to Robin and Day,[3] the *p*-phenylenediamine (PD) (cation radical)s have been reported as a symmetrical delocalized class III structure with a strong electronic coupling (the electron is delocalized over the two or more redox centers), leading an intervalence charge transfer (IV-CT) absorption band in the NIR region.[4]

Our strategy in this work is to design and synthesize the electroactive NIR and multi-electrochromic starburst triarylamine-based materials with the incorporation of electron-donating substituents at the *para*-position of phenyl groups, thus could greatly prevent the coupling reactions by affording stable cationic radicals and lowering the oxidation potentials.[5] The advantage of more electroactive sites and better processability than the conventional linear polymer was due to the introduction of starburst triarylamine derivatives into polymer system.

In this contribution, we therefore synthesized the diamine monomer, *N*,*N*-bis[4-(4-methoxyphenyl-4'-aminophenylamino)phenyl]-*N'*,*N'*-di(4-methoxyphenyl)-*p*-phenylenediamine, and their corresponding aromatic polyamides containing starburst triarylamine units with *para*-substituted methoxy groups. The incorporation of electron-donating methoxy substituents is expected to reduce the oxidation potential associated with increasing electrochemical and electrochromic stability of the result polyamides. Thus, we anticipate that these novel polyamides should be excellent in many aspects such as electrochemical stability with multiple electrochromic switchings, optical response times, coloration efficiency, and high optical contrast in both NIR and visible light regions.

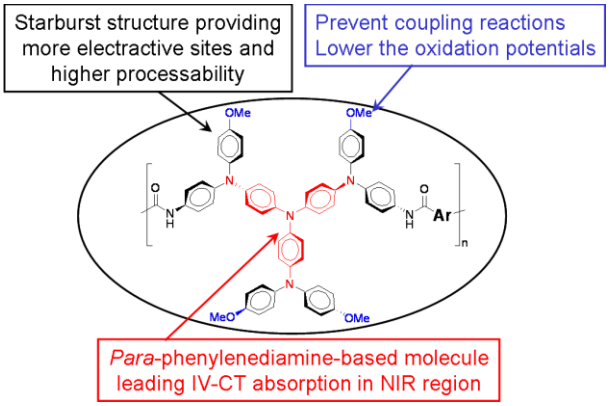

References and Notes

1. (*a*) P. M. S. Monk, R. J. Mortimer and D. R. Rosseinsky, *Electrochromism and Electrochromic Devices*; Cambridge University Press, Cambridge, UK, 2007; (*b*) P. M. Beaujuge and J. R. Reynolds, *Chem. Rev.*, 2010, **110**, 268.
2. (a) Creutz, C.; Taube, H. *J. Am. Chem. Soc.* **1973**, *95*, 1086. (b) Lambert, C.; Noll, G. *J. Am. Chem. Soc.* **1999**, *121*, 8434.
3. Robin, M.; Day, P. *Adv. Inorg. Radiochem.* **1967**, *10*, 247.
4. Szeghalmi, A.V.; Erdmann, M.; Engel, V.; Schmitt, M.; Amthor, S.; Kriegisch, V.; Noll, G.; Stahl, R.; Lambert, C.; Leusser, D.; Stalke, D.; Zabel, M.; Popp, J. *J. Am. Chem. Soc.* **2004**, *126*, 7834.
5. (a) Chang, C. W.; Liou, G. S.; Hsiao, S. H. *J. Mater. Chem.* **2007**, *17*, 1007. (b) Liou, G. S.; Chang, C. W. *Macromolecules* **2008**, *41*, 1667. (c) Hsiao, S. H.; Liou, G. S.; Kung, Y. C.; Yen, H. J. *Macromolecules* **2008**, *41*, 2800. (d) Chang, C. W.; Chung, C. H.; Liou, G. S. *Macromolecules* **2008**, *41*, 8441. (e) Chang, C. W.; Liou, G. S. *J. Mater. Chem.* **2008**, *18*, 5638. (f) Chang, C. W.; Yen, H. J.; Huang, K. Y.; Yeh, J. M.; Liou, G. S. *J. Polym. Sci. Part A: Polym. Chem.* **2008**, *46*, 7937. (g) Yen, H. J.; Liou, G. S. *Chem. Mater.* **2009**, *21*, 4062. (h) Yen, H. J.; Liou, G. S. *Org. Electron.* **2010**, *11*, 299. (i) L. T. Huang, H. J. Yen, C. W. Chang, G. S. Liou, *J. Polym. Sci. Part A: Polym. Chem.* **2010**, *48*, 4747.

Synthesis of copolymer based on polydimethylsiloxane and alkylamine

Ludovic Leymarie[1], *Philippe Chaumont*[1], *Etienne Fleury*[2], *Nathalie Sintes*[1]

[1] Université Lyon 1, IMP/LMPB Laboratoire des Matériaux Polymères et Biomatériaux, Villeurbanne, F-69622, France ;
[2] INSA de Lyon, IMP/LMM Laboratoire des Matériaux Macromoléculaires, Villeurbanne, F-69621, France ;

ludovic_leymarie@yahoo.fr

Abstract:
The reaction between epoxy and amine groups is one of the most efficent and studied reactions in the literature, especially for the synthesis of thermosetting polymers from α, ω functionalized reagents as diglycidyl ether of bisphenol A (DGEBA) with primary diamines. In the past, interesting researches have allowed to understand the mechanisms and the kinetics involved in the epoxy-amine reaction [1]. However, the reaction between α, ω functionalized-epoxy reagents and a monoamine was much less studied, especially with functionalized epoxy polydimethylsiloxane (PDMS-epoxy). Generally, these siloxanes are used for either cationic polymerization or photopolymerization [2].
Our work deals with the synthesis between a short functionalized glycidyl PDMS (PDMS AGE) and a long alkyl chain terminated primary amine without catalyst (Figure 1). All experiments have been carried out in a flask of 100mL using the same amount of reagents. The reaction has been studied for the molar ratio 1:1. We would like combining the good properties of PDMS such as wide temperature range use, flexibilty, good gas permeability, resistance to UV radiation with those of alkylamine in order to develop a product leading to a $(A_2B_2)_n$ copolymer structure with promising properties.

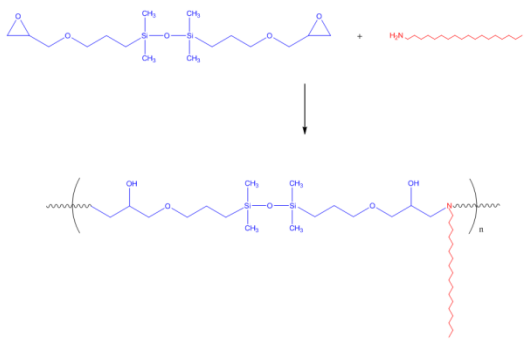

Figure 1: Reaction scheme between PDMS AGE and octadecylamine

First, the kinetic of the reaction was determined from PDMS AGE model compounds at different temperatures, evaluated by ^{1}H NMR. The reaction was efficient at low temperature (80°C) and the conversion of glycidyl groups reached at least 95% in all cases.

Then modelisations were performed using existing kinetic model. The adjustment between experimental data and Kamal and Sourour's model was excellent. Thefore the energy of activation could be determinated. The properties were studied by ATG and DSC. No residual alkylamine was observed by ATG. The structure was characterized by MALDI-TOF spectrometry and confirmed by GPC. We perfectly obtained the expected copolymer structure which is $(A_2B_2)_n$.

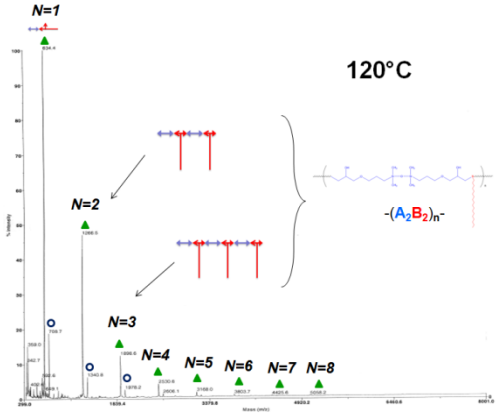

Figure 2: MALDI-TOF spectrum of copolymer obtained from PDMS AGE and oactadecylamine at 120°C.

We were able to prepare a copolymer based on polydimethylsiloxane and alkylamine using no catalyst. We reached the targeted copolymer structure which gave good stability properties. Finally, increasing the length of the "hard" part into the copolymer (like amino-functionalized polymers), we could imagine that the new product could be included to the thermoplastic elastomers class.

1. Sourour, S. and M.R. Kamal, Thermochimica Acta, 1976. **14**(1-2): p. 41-59.
2. Crivello, J.V. and G. Löhden, Macromolecules, 1995. **28**: p. 8057-8064.

Ion conducting solid electrolytes based on different macromolecular architecture containing PEO

David Glé, Didier Devaux, Trang Phan, Renaud Bouchet, Michael Robinet, Denis Bertin and Didier Gigmes

UMR 6264 Laboratoire Chimie Provence, Université de Provence, Marseille, France

david.gle@univ-provence.fr

Since the first Armand's discovery of polyethylene oxide (PEO) containing a lithium salt as ion conductive solid polymer[1], the solid polymer electrolytes based PEO have been extensively studied and applied to lithium rechargeable batteries[2-3]. However, the ideal electrolyte material with the ionic conductivity of a liquid and the mechanical strength of a solid remains somewhat elusive. To satisfy the performance requirements which are quite contradictory, new solid polymer electrolytes based block copolymers have been prepared. Because of the net repulsion between the polymer blocks which are covalently bonded end-to-end, block copolymers segregate into periodically spaced, nanoscale domains. The PEO and their derivatives, a lithium-salt solvating polymer, are usually chosen as one block component providing ionic conductivity. The ordered morphology meanwhile confers global mechanical rigidity to the material. By this way, polymer electrolytes with microphase separation structures have been proposed by several groups. Sadoway and al.[4-5] have developed a Li^+ ion conductive polymer electrolyte based on a similar concept; a lithium polymer battery exhibits an ionic conductivity of 10^{-5} $S.cm^{-1}$ at room temperature was successfully fabricated. Niitani and al.[6-7] used a block copolymer consisting of a poly(ethylene glycol) methyl ether methacrylate (MAPEG) and polystyrene as solid polymer electrolyte; this polymer electrolyte exhibits a high conductivity 10^{-4} $S.cm^{-1}$ at room temperature.

In this study, the concept of microphase separation structure was used to prepare our solid polymer electrolytes (SPE). These SPE are block copolymers consisting of a glassy mechanical block (Tg≥ 100°C) and a linear (scheme 1) or (scheme 2) branched PEO moiety to provide ionic conductivity synthesized by controlled polymerization technique called Nitroxide Mediated Polymerization (NMP).

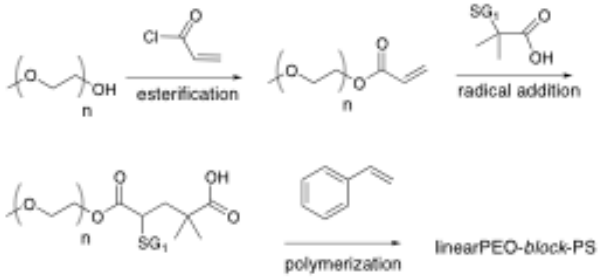

Scheme 1: Synthesis of SPE with linear PEO

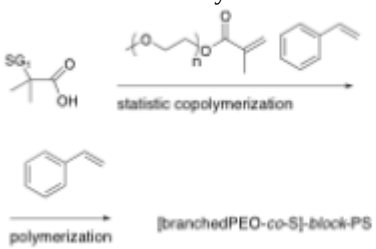

Scheme 2: Synthesis of SPE with branched PEO

Various copolymers with different composition or architectures (di or triblocks, linear or branched PEO (figure 1)) were synthesized and characterized by Size Exclusion Chromatography (SEC) and Liquid Chromatography at Critical Conditions (LCCC). The SPE performances for ionic conductivity and mechanical strength were evaluated by Electrochemical Impedance Spectroscopy (EIS) and Dynamic Mechanical Analysis (DMA) respectively.

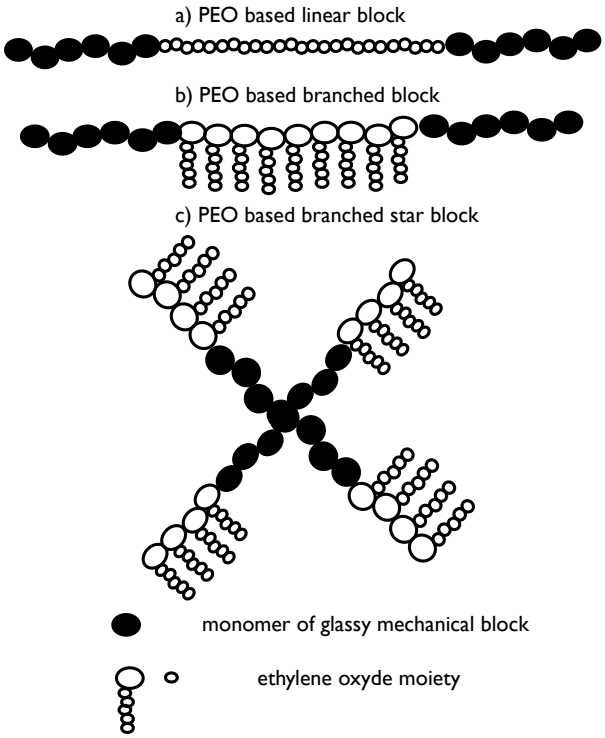

Figure 1: Architectures of SPE from linear or branched PEO

References

1- Armand M., Chabagno J., Duclot M. *2nd Inter. Meeting on Solid Electrolytes, Scotland*, 20-22, Sept, **1978**.

2- Scrosati B., Croce F., Panero S., *J. Power Sources*, **2001**, 100, 93.

3- Buriez O., Han Y., Hou J., Kerr J.B., Qiao J., Sloop S., Tian M., Wang S. *J. Power Sources*, **2000**, 89, 149.

4- Trapa, P. E.; Huang, B.; Won, Y.-Y.; Sadoway, D. R.; Mayes, A. M. *Electrochim. Solid-State Letters* **2002**, 5, A85-A88.

5- Soo, P. P.; Huang, B.; Jang, Y.-I.; Chiang, Y.-M.; Sadoway, D. R.; Mayes, A. M., *J. Electrochemi. Soc.* **1999**, 148, 32-37

6- Niitani, T.; Shimada, M.; Kawamura, K.; Dokko, K.; Rho, Y. H.; Kanamura, K.,. *Electrochemi. Solid-State letters* **2005**, 8, A385-A388.

7- Niitani, T.; Shimada, M.; Kawamura, K.; Kanamura, K., *J. Power Sources* **2005**, 146, 386-390

Block Copolymers via Macromercaptan Initiated Ring Opening Polymerization

David Glé,* Catherine Lefay,* Marion Rollet,* Didier Gigmes,* Denis Bertin,* Christina Schmid** and Christopher Barner-Kowollik**

*UMR 6264 Laboratoire Chimie Provence, Université de Provence, Marseille, France
**Institut für Technische Chemie und Polymerchemie, Karlsruhe Institute of Technology, Karlsruhe, Germany

david.gle@univ-provence.fr

Polylactide (PLA) is one of the most studied polymers for biomedical applications and also as an alternative for petroleum based materials.[1,2] However, depending on the targeted applications, homoPLA can be brittle or ill-equiped to serve as a processable material.[3] To improve the mechanical properties, block copolymers have been studied and among the various potential architectures diblock copolymers with a PLA-based block synthesized via Ring Opening Polymerization (ROP) and a second block prepared via living/controlled radical polymerization (CRP) methods are an attractive option. Among these methods, Reversible Addition Fragmentation Chain Transfer (RAFT) is probably the most versatile due to the large range of functional monomers that can be polymerized.[4] To combine ROP and RAFT techniques, several main approaches exist. One of the most employed is based on a dual initiator, such as a RAFT agent bearing a functional group that is capable of initiating the ROP of lactides.[5] Alternative strategies have been developed as well, such as introducing the RAFT agent after the ROP[6] or combining silmultaneous RAFT and ROP to produce grafted copolymers.[7] However all those methods keep the RAFT agent intact either at the end or in the middle of the polymer chain, introducing potential problems with regard to block stability and/or toxicity.

The present work details our efforts in preparing diblock copolymers based on PLA and polystyrene (PS) or polyethylene (PE), where the two blocks are linked by a covalent sulfur bond. The key idea is to transform the dithioester/trithiocarbonate end group into a thiol function by aminolysis and to subsequently use it as the initiator of the ROP of lactide (see Scheme 1).

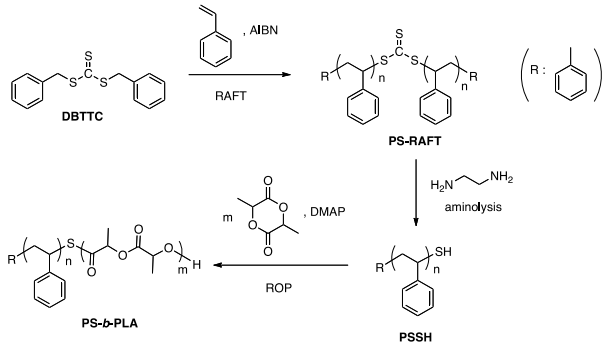

Scheme 1 Synthetic strategy for the synthesis of PS-*block*-PLA diblock copolymers

We initally present a model study employing styrylmercaptan as initiator for the ROP of lactide to prove the ability of thiols to ring-open the lactide in the presence of an organocatalyst. Subsequently, the synthesis of several PS-*block*-PLA copolymers with various PS/PLA length ratios is described.

The analyses of the polymeric material via multiple detector Size Exclusion Chromatography (SEC) and Liquid Chromatography under Critical Conditions (LCCC) as well as Diffusion Ordered NMR Spectroscopy (DOSY-NMR) evidences the formation of the desired block copolymer structures alongside residual macromercaptane and homopoly(lactide) in minor quantities. In addition, it was possible to prepare a thiol-capped poly(ethylene), which was subsequently employed to initiate the ROP of a lactide and to prepare a polyethylene-*block*-poly(lactide) copolymer, which formation was evidenced via NMR as well as SEC. The current study has demonstrated that it is indeed possible to employ RAFT derived macromercaptanes as initiating species in the organo-catalyzed ROP of lactides, thus providing an alternative platform for the generation of block copolymers with degradable and nondegradable strands.

References

1. Dechy-Cabaret, O.; Martin-Vaca, B.; Bourissou, D. Chem. Rev. 2004, 104, 6147-6176.
2. Uhrich, K. E.; Cannizzaro, S.M.; Langer, R.S.; Shakesheff, K. M. Chem. Rev. 1999, 99, 3181-3198.
3. Anderson, K.S.; Schreck, K. M.; Hillmyer, M. A. Polym. Rev. 2008, 48, 85-108.
4. Barner-Kowollik, C.; Perrier S. J. Polym. Sci. Polym. Chem. 2008, 46, 5715-5723.
5. Barner, L.; Perrier, S.; In Handbook of RAFT Polymerization; Barner-Kowolik, C., Ed.; Wiley-VCH: Weinheim, 2008; p 467.
6. Li, J.; REn, J.; Cao, Y.; Yuan, W. Polymer 2010, 51, 1301-1310.
7. Le Hellaye, M.; Lefay, C.; Davis T.P.; Stenzel, M. H.; Barner-Kowollik, C. J Polym Sci Polym Chem 2008, 46, 3058-3067.

Batch Anionic polymerization of octamethylcyclotetrasiloxane in emulsion using cationic and nonionic emulsifiers

Ines Mohorič[a] *and Urška Šebenik*[b]

[a]Hidria Institute for Materials and Technology, Sp. Kanomlja 23, 5281 Sp. Idrija, Slovenia
[b]University of Ljubljana, Faculty of Chemistry and Chemical Technology, Aškerčeva cesta 5, 1000 Ljubljana, Slovenia

urska.sebenik@fkkt.uni-lj.si

Introduction: In 1959, Hyde and Wehrly demonstrated a possibility of carrying out ring-opening polymerization of cyclosiloxanes in water emulsion[1]. Since then, anionic ring-opening polymerization (AROP) has been one of the most promising methods for preparing polysiloxane emulsions. D_4 (octamethylcycotetrasiloxane) has been the most widely used cyclosiloxane monomer in academic researches[1-8], patents[9-10] and in organosilicone industry.
In this work, batch AROP of D_4 in emulsion was investigated. Cationic and nonionic emulsifier were used. The concentration of emulsifiers was above their critical micelle concentration. Effects of emulsifier mixture concentration, nonionic/cationic emulsifier ratio and cationic emulsifier/initiator ratio on the kinetics and on the evolution of average molecular weight and distribution with time were studied and discussed[11].

Materials and Methods: Cationic emulsifier (hexadecyltrimethylammonium bromide - CTAB), nonionic emulsifier (secondary alcohol ethoxylate, Tergitol, Type 15-S-9), octamethylcyclotetrasiloxane (98%, Aldrich), KOH (p.a., Merck), deionized water.
Polysiloxane emulsions were synthesized isothermally at 80 °C in a 250 ml glass reactor equipped with a reflux condenser, a mechanical stirrer, a digital thermometer, and a nitrogen gas inlet. Monomer was added to the emulsifier solution and the pre-emulsion was stirred at 1000 rpm for 15 minutes. After 15 minutes, the mixture was heated and the stirring speed was lowered to 500 rpm. To initiate the polymerization KOH was added. The reactor content was sampled during the polymerization. To stop the polymerization HCl (0.5 M) was added to the withdrawn samples.
The conversion was determined by gravimetric analysis, by which the amount of monomer converted to large non-volatilizable polymeric chains was determined. Here, all volatile oligomeric cycles, which are formed during polymerization, were treated as monomer in conversion calculations. Average molecular weights were determined by gel permeation chromatography.

Results and Discussion: Monomer conversion and therefore polymerization rate increased with increasing overall emulsifiers' concentration, cationic/nonionic emulsifier ratio and cationic emulsifier/initiator ratio. KOH concentration affected polymerization kinetics only when the ratio KOH/CTAB was lower than equimolar ratio. Observations may be explained by polymerization mechanism proposed by Zhang[3] and De Gunzbourg[6]. During AROP in emulsion, different chemical reactions take place on the polymer particle surface and inside the particle. Main chemical reactions by which polymer is formed (initiation, propagation and termination) occur on the particle surface, where the cationic emulsifier is associated to the active centre (hydroxide anion). Therefore, it may be concluded that the polymerization rate is increased by increasing the specific particle/water interface and the number of active centres, which are defined also by the concentration of cationic emulsifier.
Average molecular weight and PDI increased with monomer conversion, what may be explained by polymer chain growth by successive polyaddition of D_4 and reversible termination at the particle surface and by chain growth by condensation reactions in the particle interior. By raising the amount of emulsifiers, the number of initiation sites increased what resulted in an increased number of polymer chains (N). Hence, at a given conversion, i.e. when an explicit part of monomer was consumed, the average length of chains was smaller while their number was larger. However, the initiation is not the only reaction that affects the N value. At higher conversions, condensation reactions become important as well. Each initiation reaction leads to the formation of one chain and each condensation reaction leads to the disappearance of one chain. Although the rate of N growth slowed down with time and conversion (N increased during the entire time (4 h) and conversion interval (up to 68%)), it may be concluded that initiation reactions prevailed over the condensation reactions during the period under investigation.

References:

[1] Zhang Z, Zhou N, Xu C, Xie Z. Chin J Polym Sci 2001;19:7-11.
[2] Hyde JF, Wehrly JR. U.S. Patent 2,891,920, June 23, 1959.
[3] Zhang X, Yang Y, Dai D. Polym Comm (China) 1982;2:154-157.
[4] Zhang X, Yang Y, Liu X. Polym Comm (China) 1982;2:104-111.
[5] Zhang X, Yang Y, Liu X. Polym Comm (China) 1984;4:226-232.
[6] De Gunzbourg A, Favier J-C, Hémery P. Polym Int 1994;35:179-188.
[7] Barrère M, Ganachaud F, Bendejacq D, Dourges MA, Maitre C, Hémery P. Polymer 2001;42,7239-7246.
[8] Zhuang Y-Q, Ke X, Zhan X-L, Luo Z-H. Powder Technol 2010;201:146-152.
[9] Gee RP. U.S. Patent 5,925,469, Jul 20, 1999.
[10] Ferritto MS, Schulz WJ. U.S. Patent 6,294,634 B1, Sep 25, 2001.
[11] Mohorič I, Šebenik U. Polymer, in press.

Kinetic Study of Aqueous Free- Radical Polymerization of 2-Acrylamido-2-methyl-1-propanesulfonic Acid via On-line ^{1}H NMR Technique

E. Nadim, H. Bouhendi, F. Ziaee, A. Nouri*

Iran Polymer and petrochemical Institute, P.O.BOX 14965/115, Tehran, Iran.

*Boouhendi@yahoo.com

Introduction

In recent years, Poly 2-acrylamido-2-methylpropanesulfonic acid, poly (AMPS), and its derivatives are often used as water- soluble polymers with various applications. Hence, according to the industrial application of poly AMPS, it is necessary to study its polymerization kinetic precisely to optimize the polymerization process and control characteristics of final product [1]. At this article, for the first time, the kinetic of AMPS polymerization in the presence of potassium persulfate in D_2O by ^{1}H NMR spectroscopy was investigated.

Materials and Methods

AMPS and potassium persulfate (KPS) were purchased from Fluka and Merck, respectively, Deuterium oxide (D_2O) as solvent was obtained from ARMAR Chemicals, Switzerland. H NMR experiments were carried out on a Bruker Avance 400 MHZ, Germany. At first a sample containing reaction mixture, solvent, monomer and initiator which was purged with nitrogen to remove dissolved air, was introduced into sample cavity and allowed to calibrate. Then, the sample tube was sent out. After setting the cavity at desired temperature, sample tube was inserted in to the sample chamber and the start time was recorded. The spectra were recorded at each 30-60 time interval up to high conversions (more than 75%).

Result and Discussions

Among different NMR techniques, ^{1}H was preferred over ^{13}C because of its greater sensitivity, higher rate of data collection and ability to use smaller diameter tubes, which helped maintaining isothermal conditions [2].

In order to estimate order of reaction the following equation was applied [2].

$$R_p = -\frac{d[M]}{dt} = \frac{d\Pi}{dt}[M_0] = k[M]^n[I]^p \qquad (1\text{-a})$$

or

$$R_p = k_0[M]^n[I]^p e^{\frac{E_a}{R}\frac{1}{T}} \qquad (1\text{-b})$$

Where R_p, [I], [M], [M_0] and E_a are polymerization rate, initiator and monomer concentrations, initial concentration of monomer, and activation energy respectively. In constant initial monomer content, slope of *-logR_p vs.-log [I]* shows the order of reaction with respect to the initiator concentration. Calculated amount of *p* was 0.48. *n* value determined by slope of *-logR_p vs.-log [M]* was 1.94. In a constant amount of monomer and initiator, slope and intercept of *-lnR_p vs.1/T* plot represent E_a and k_0, respectively. Calculated amount of E_a was 92.7kj/mol.K and k_0 determined by intercept of mentioned plot was 3.385×10^{13} mol.lit^{-1}.sec^{-1}.

As typical ^{1}H NMR spectra of a sample are illustrated in Figure 1.

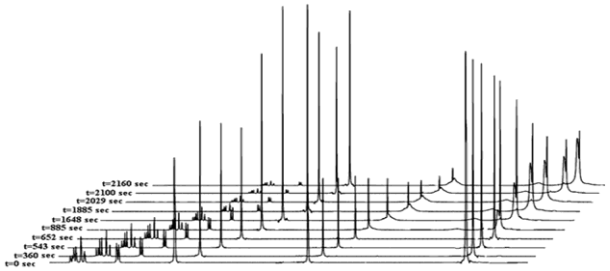

Figure 1: Typical ^{1}H NMR spectra at constant amount of initiator

Mechanistic study

The general rate of polymerization, with respect to usual assumption, is given by Equation (3);

$$R_p = k_p\left(\frac{2k_3}{k_t}\right)^{1/2}\left(\frac{K_c}{1+K_c[M]}\right)^{1/2}[S_2O_8^{-2}]^{1/2}[M]^{3/2} \qquad (3)$$

Order of reaction with respect to monomer from 1.5 to 1 would be described by above equation. But it is crucial to mention that for monomolecular termination, involving the reaction between the propagating radical and fragment of persulfate, order of reaction would reach to 2.

If R_{pm} represents polymerization rate by monomolecular termination (eq.4) and $\alpha = \frac{k_{tb}}{k_{tb}+k_{tm}}$ (in which k_{tb} and k_{tm} represent bimolecular and monomolecular termination constants respectively);

$$R_{pm} = k_p\left(\frac{K_c}{1+K_c}\right)\frac{2k_3}{k_{tb}}[M] \qquad (4)$$

Then R_p could be adjusted to Equation (5);

$$R_p = \omega[S_2O_8^{-2}]^{1/2}[M]^2\left\{\alpha\frac{1}{k_{tm}}\left(\frac{K_c}{1+K_c[M]}\frac{2k_3}{[S_2O_8^{-2}]}\right)^{1/2} + \left(\beta\left(\frac{1}{k_{tb}[M]}\right)^{1/2}\right)\right\} \qquad (5)$$

Where $\omega = (2k_3)^{1/2}k_p\left(\frac{K_c}{1+K_c[M]}\right)^{1/2}$ and $\beta = 1-\alpha$

Here, considering to monomer and initiator concentration and also initiation type, the power dependency of polymerization rate to monomer would change up to 2.

Conclusion

Determined order of reaction based on monomer and initiator resulted n=1.94 and p=0.49 with excellent deviations. Also, activation energy and k_0 over range of 35-47°C were determined and resulted E_a=92.7kj/mol.K and $k_0=3.385\times10^{13}$ mol. lit^{-1}.sec^{-1}.

References

1. P. A. Williams, Ed. *Handbook of Industrial Water Soluble Polymers*, Blackwell, 2007.

2. A. R. Mahdavian, M. Abdollahi and H. R. Bijanzadeh, *Journal of Applied Polymer Science*, **93**, 2007–2013, (2004).

Continuous Synthesis of Polyesteramides via a Reactive Extrusion Process.

Gupta, Manisha[1]; *Siegmund, Felixine*[2]; *Zhu, Xiaomin*[1]; *Möller, Martin*[1]; *Haberstroh, Edmund*[2]; *Fijten, Martin*[3]

[1]DWI at RWTH Aachen University, Aachen, Germany, [2]LFK RWTH Aachen University, Aachen, Germany, [3]Eindhoven University of Technology, Eindhoven, The Netherland

Email: gupta@dwi.rwth-aachen.de, siegmund@lfk.rwth-aachen.de, zhu@dwi.rwth-aachen.de, moeller@dwi.rwth-aachen.de, haberstroh@lfk.rwth-aachen.de, M.W.M.Fijten@TUE.NL

Introduction: The problem of environment pollution has created an urgent need for the production of new biodegradable polymers. In addition, such materials have also found a wide variety of applications in the field of medicine, and aliphatic polyesters such as polylactide and polyglycolide are the state-of-the-art examples. Polyesters, however, suffer from weak mechanical strength and during their degradation the release of acidic products leads to a local acidic microenvironment due to bulk erosion, hindering cell growth and hence provoking inflammatory responses [**1**]. Polyesteramides (PEAs) include both ester and amide groups in the main polymer chain and thus combine the good mechanical and processing properties of technical polyamide with good biodegradability of aliphatic polyesters. At the same time, introduction of amide groups is also an approach to solve the problem of acidic degradation of polyesters due to surface erosion mechanism [**2-4**]. PEAs are mainly produced by batch synthesis, a well known example is the former commercial product from Bayer AG - BAK 1095 that is based on 1,4-butanediol, adipic acid and 1,6-aminohexanoic acid [**5**]. In literature the preparation of block and statistic polyesteramide on a twin-screw extruder from ε-caprolactam and ε-caprolactone was reported, however, it has never become an industrial process. In this work, we report a new reactive extrusion continuous process for the preparation of PEAs, which is based on the anionic ring opening polymerization of ε-caprolactam in the melt of commercially available polyester – polycaprolactone (PCL).

Materials and Methods: Sodium caprolactamate and hexamethylene-1,6-dicarbamoylcaprolactam were used as initiator and activator, respectively. The reactive extrusion was carried out on a twin-screw microcompounder (15 ml, DSM Xplore) combined with a mini injection molding machine (5 ml, DSM Xplore). The reaction conditions were optimized regarding the yield and molecular characteristics. The polymers synthesized in the microcompounder were stirred with water to remove the rest of monomer and to deactivate the initiator. The chemical composition of the synthesized PEAs was determined by means of elementary analysis. Differential scanning calorimetry (DSC) and thermogravimetric analysis (TGA) were employed to study the thermal behavior of the polymers. Size-exclusion chromatography (SEC) was performed using hexafluoroisopropanol with potassium trifluoro acetate (3 g/L) and toluene (2.5 mL/L) as eluent. The molecular weight was calculated against polymethyl methacrylate standards. The mechanical properties of PEAs were studied on a standard Zwick tensile tester (type Z010) using the specimens prepared on the mini injection molding machine.

Results and Discussion: PEAs of different chemical compositions were successfully prepared with almost quantitative yield. Monomodal molecular weight distribution was observed by SEC. The amide fragments were incorporated into the polyester backbone via the chain transfer reaction. Because of comparable melt viscosity before and after the polymerization reaction, the process design was significantly simplified. DSC curves of synthesized PEAs showed two melting and crystallization peaks upon heating and cooling, respectively. The position of these peaks is quite close to the phase transition temperatures of PCL and polycaprolactam, indicating the block structure of these PEAs. According to TGA measurement the PEAs exhibited a two-step degradation profile with weight losses occurring at lower temperature than both pure PCL and polycaprolactam. It was shown by tensile test that these polymers possessed quite good mechanical properties.

Conclusions: Block-structured PEAs were successfully prepared with almost quantitative yield by a new reactive extrusion continuous process that was based on anionic polymerization of ε-caprolactam in the PCL melt. The influence of initiator and activator concentrations as well as the ratio of two monomer units on the physico-chemical properties of synthesized PEAs was studied. Due to its simplicity this procedure can easily be up-scaled to an industrial process.

References:

[**1**] Li, S. *J. biomed. Mater. Res. B* **1999**, *48*, 342.
[**2**] Liu, C.B.; Jia, W.J.; Qian, Z.Y.; Huang, M.J.; Gu, Y.C.; Chao, G.T.; Gou, M.L.; Gong, C.Y.; Deng, H.X.; Lei, K.; Huang, A.L.; Tu, M.J. *J. Polym. Res.* **2007**, *14*, 31.
[**3**] Qian, Z.; Li, S.; He, Y.; Li, C.; Liu, X. *Polym. Degrad. Stab.* **2003**, *81*, 279.
[**4**] Qian, Z.; Li, S.; He, Y.; Li, C.; Liu, X. *Polym. Degrad. Stab.* **2004**, *84*, 41.
[**5**] Grigat, E.; Koch, R.; Timmermann, R. *Polym. Degrad. Stab.* **1998**, *59*, 223.

Electromagnetic properties of Polyaniline hybrid nanocomposite Application to gas sensing and EMI shielding

N.El kamchi[1], *J-L.Wojkiewicz*[1], *N.Redon*[1], *T.Lasri*[2]

1 Université Lille Nord de France, Ecole des Mines de Douai, Dpt Chimie Environnement, 59500 Douai, France
2 Institut d'Electronique, de Microélectronique et de Nanotechnologies, Groupe MITEC, UMR 8520, 59652 Villeneuve d'Ascq, France

Email: noureddine.el.kamchi@mines-douai.fr

In this work, two types of hybrid nanocomposite samples were prepared, based on an addition of carbon coated cobalt (ccco) nanoparticles in a miscible blend of conducting Polyaniline (Pani) and polyurethane (Pu) matrix. The physical properties of the nanocomposites were studied in function of the doping rate and the mass fraction of polyaniline in the blend, from DC two microwave frequencies. Then two applications were treated; The first was the use of a polyaniline- polyurethane composite as an organic electronic ammonia sensor. The second application was relative to electromagnetic shielding in the microwave region.

The first nanocomposite was made with Pani in its insulating form (PaniEB) doped with Camphor Sulfonic Acid (CSA) and blended with Pu in solution. The doping transform the Pani from the insulating form (Pani EB) to a conductive form (PAni ES), and increase drastically the conductivity[1]. Pani-Pu composite showed a very low percolation threshold (<0.2%) with a maximum of conductivity of 10^4 S/m . Three doping rates were made : 10%, 25% and 50%; the latter correspond to the maximum of conductivity. Then we investigated the effect of doping rate on the reactivity of Pani-Pu composites with several concentrations of ammonia. The result showed that the reaction between ammonia and Pani-Pu composites depend on the doping rate. Moreover, the composite doped at 25% showed a detection threshold below 20ppb [Fig1].

The second nancomposite was obtained with the same components, adding magnetic carbon cobalt nanoparticles for EMI applications. We investgated the effect of doping and magnetic nanoparticles concentration (varies from 5 to 20%) on the electromagnetic properties (permitivity and permeability), shielding effectiveness (SE) and the absorption coefficient at microwave frequency [8-18GHz].

The results obtained showed a high shielding effectiveness (up to 80dB) and an absorption coefficient up to 10 dB [fig2]. The experience showed that we can adjust these characteristics by modifying the composition of the nanocomposite, to increase either the absorption (by increasing the magnetic charges concentration) or the reflexion (by increasing the Pani concentration).

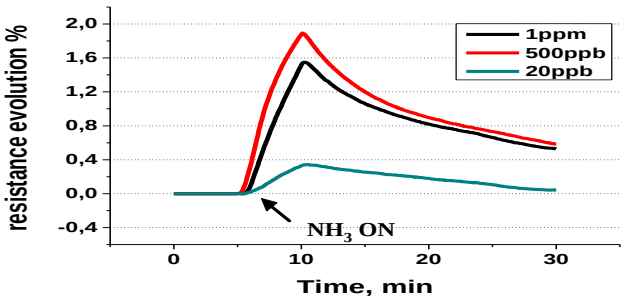

Fig1: resistance evolution of Pani-Pu composite exposed to ammonia

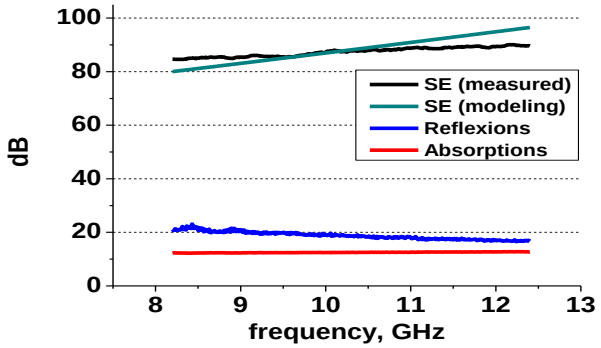

Fig2: Shielding effectiveness of a Pani-Pu-ccco three layers nanocomposite

[1] Cao Y., Smith P., Heeger A.J., *« Counter-ion induced processibility of conducting polyaniline»* Synthetic Metals, 55-57 (1993) pp 3514-3519

Graft Copolymers via ROMP and Diels–Alder Click Reaction Strategy

Nese Cerit, Hakan Durmaz, Aydan Dag, Okan Sirkecioglu, Gurkan Hizal, Umit Tunca

Istanbul Technical University

nesem_83@hotmail.com

Abstract

Anthracene-functionalized oxanorbornene monomer and oxanorbornenyl polystyrene (PS) with ω-anthracene end functionalized macromonomer were first polymerized via ring opening metathesis polymerization using the first-generation Grubbs' catalyst in dichloromethane at room temperature and then clicked with maleimide end-functionalized polymers, poly(ethylene glycol) (PEG)-MI, poly(methyl methacrylate) (PMMA)-MI, and poly(tert-butyl acrylate) (PtBA)-MI in a Diels–Alder reaction in toluene at 120^{0}C to create corresponding graft copolymers, poly(oxanorbornene)-g-PEG, poly(oxanorbornene)-g-PMMA, and graft block copolymers, poly(oxanorbornene)-g-(PS-b-PEG), poly(oxanorbornene)-g-(PS-b-PMMA), and poly(oxanorbornene)-g-(PS-b-PtBA), respectively. Diels–Alder click reaction efficiency for graft copolymerization was monitored by UV–vis spectroscopy. The dn/dc values of graft copolymers and graft block copolymers were experimentally obtained using a triple detection gel permeation chromatography and subsequently introduced to the software so as to give molecular weights, intrinsic viscosity ([g]) and hydrodynamic radius (Rh) values.

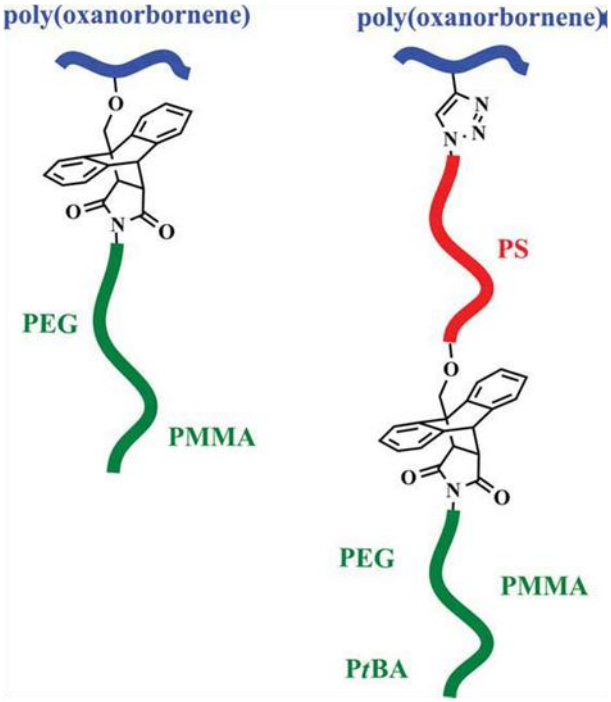

Branching Polyethylenimine Functionalized with Methylbenzimidazole: An Approach to Enhance Proton Conductivity via Multi-direction of Heterocycles

Autchara Pangon[1], *Kohji Tashiro*[2], *and Suwabun Chirachanchai*[1,3,*]

[1]The Petroleum and Petrochemical College, Chulalongkorn University, Soi Chula 12, Phyathai Road., Pathumwan, Bangkok 10330, Thailand

[2]Department of Future Industry-oriented Basic Science and Materials, Graduate School of Engineering, Toyota Technological Institute, Hisakata 2-12-1, Tempaku, Nagoya 468-8511, Japan

[3]Center for Petroleum and Petrochemicals, and Advanced Materials, Chulalongkorn University, Bangkok 10330, Thailand

e-mail: csuwabun@chula.ac.th

Heterocycles, for example imidazole, pyrazole, and benzimidazole have received much attention as proton conductive species in water-free polymer electrolyte membrane (PEM) for fuel cell due to their high thermal stability and amphoteric structure which can either donate or accept protons initiating proton transferring through hydrogen bond network.[1,2] The key point is to enhance the proton transfer efficiency of the heterocycles in the membrane. Up to the present, acid doped polybenzimidazole or blending imidazole derivatives, for example, have been reported.[3,4] The present work proposes the use of multi-benzimidazole branching to produce the proton transfer route in multi-direction in order to enhance the proton conductivity in PEM.

Polyethylenimine (PEI) is a flexible polymer which is available in linear and branch forms. Due to its high density and multi–direction of reactive amine functional groups of the branch PEI (*b*PEI) as compared with the linear one, *b*PEI was selected as a polymer core for functionalization with benzimidazoles as proton conductive molecules by a simple reaction of *b*PEI and 2-(chloromethyl)benzimidazole (CB) under basic condition as shown in Scheme.

Scheme

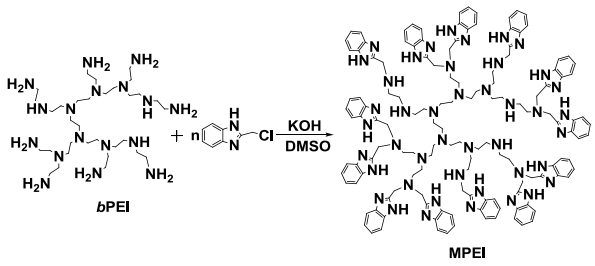

The MPEIs with a different degree of methylbenzimidazole substitution (DS) were prepared by varying the molar ratios of *b*PEI:CB. The polymer structure was proven by Fourier transform infrared spectroscopy (FTIR) Nuclear magnetic resonance (NMR) and elemental analysis. Edited-HSQC (Heteronuclear single quantum correlation) experiment was used to determine the proton and carbon connectivity. As shown in Figure, the peaks at F and G represent the methylene protons between benzimidazole and amine functional groups confirming the attachment of methylbenzimidazole on *b*PEI chain.

The modified MPEIs are appropriate for the use in high temperature PEM fuel cell due to their high thermal stability up to 280 °C as confirmed by TGA. The MPEIs showed a significant change in glass transition temperature (T_g) as observed from an increase of T_g along with an increase of DS. The hydrogen bond network and morphology changes related to temperature analyzed by temperature dependence FTIR and WAXD suggested the role of heterocycles and their favorable hydrogen bond for proton transfer efficiency.

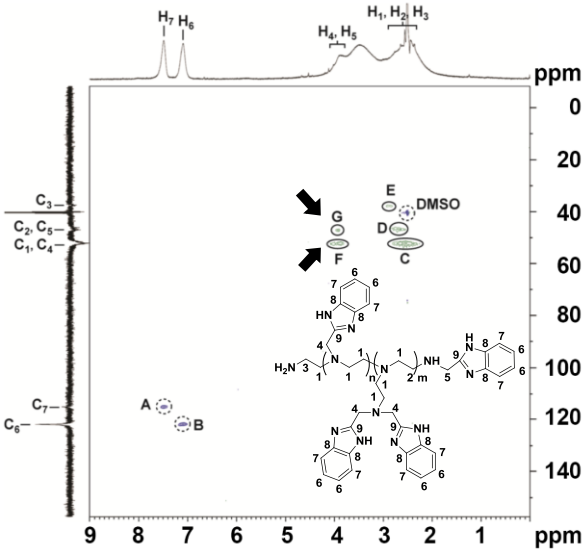

Figure Edited-HSQC spectrum of MPEI (solid line = negative phase peak, broken line = positive phase peak).

A systematic variation of benzimidazole units on the polymer chain conjugated on *b*PEI leads to an understanding of the structure-temperature-proton conductivity relationship and this will be clarified in the presentation.

Acknowledgement

A. Pangon would like to acknowledge the scholarship from the Development and Promotion of Science and Technology Talents Project, (DPST), Thailand and **Japan Student Services Organization, (JASSO), Japan.**

References

1 M. Münch, K.D. Kreuer, W. Silvestri, J. Maier, G. Seifert, Solid State Ionics, 145 (2001) 437-43.

2 M. Münch, K.D. Kreuer, W. Silvestri, J. Maier, G. Seifert, Solid State Ionics 145 (2001) 437-443.

3 M. Yamada, I. Honma, Polymer 46 (2005) 2986–92.

4 R. Bouchet, E. Siebert, Solid State Ionics 118 (1999) 287–299.

Preparation and Characterization of Impregnated PVA/PSSA_MA/THS-PSA Membranes into Porous Polyethylene Membranes for Fuel Cell Applications

Chan Jong Park, Il Hyung Kim, Sung Pyo Kim, Hak Min Lee, Ji Won Rhim

Department of Chemical Engineering, Hannam University, 461-6 Jeonmin-dong, Yuseong-gu, Daejeon 305-811, Korea

jwrhim@gmail.com

In our laboratory, the poly(vinyl alcohol) (PVA) membranes, crosslinked with poly(styrene sulfonic acid-*co*-maleic acid) (PSSA_MA), was developed for fuel cell application[1]. 3-(trihydroxysilyl)-1- propanesulfonic acid(THS-PSA), which contains both the silica compound and the sulfonic acid group, was added into PVA/PSSA_MA membranes to enhance the proton conductivity and to reduce the methanol permeability simultaneously[2]. However, the resulting membranes of PVA/PSSA_MA/THS-PSA membranes showed very brittle when the PSSA_MA and THS-PSA contents were over 7 wt%. Then, to maintain the mechanical strength and the stability of the dimension at medium high temperatures, and also to enhance the proton conductivity, the impregnation methods were considered.

The PVA/PSSA_MA/THS-PSA was impregnated into porous polyethylene membranes. The contents of PSSA_MA over 10 wt% were possibly impregnated into PE membranes, and the dimensional stability was obtained through crosslinking.

This study focuses on the investigation of the impregnation of the poly(vinyl alcohol)(PVA) crosslinked with poly (styrene sulfonic acid-co-maleic acid)(PSSA-MA) to porous polyethylene membrane for the fuel cell application. In order to characterize the prepared membranes, the meaurements of the water content, contact angle, FT-IR spectra, thermal gravimetric analysis, ion exchange capacity, proton conductivity, methanol permeability and elastic modulus were carried out. The contents of PSSA_MA in the impregnated membranes could be increased up to 25% without the membrane brittleness which was the defect of the dense PVA/PSSA_MA membranes. The impregnated PVA/PSSA_MA(90:10) membrane exhibited a higher ion exchange capacity (1.2 meq./g dry membrane) than Nafion membrane (0.91 meq./g dry membrane). Through the elastic modulus measurement, the dimensional stability of the resulting membranes was expected to be increased higher than the dense membranes. The methanol crossover and water content were decreased even if the PSSA_MA content increased due to the reduction of the free volume.

The following figure shows the expected reaction scheme between PVA and PSSA_MA.

And the next figure describes the proton conductivities with increasing the PSSA_MA contents. The proton conductivity increases close to 0.02 S/cm at 25% PSSA_MA content.

Details will be discussed at the conference.

References

[1] D. S. Kim, M. D. Guiver, S. Y. Nam, T. I. Yun, M. Y. Seo, S. J. Kim, H. S. Hwang, J. W. Rhim, Preparation of ion exchange membranes for fuel cell based on crosslinked poly(vinyl alcohol) with poly(styrene sulfonic acid-*co*-maleic acid), J. Memb. Sci. 281 (2006) 156-162.

[2] D. H. Kim, B. S. Lee, B. S. Lee, S. W. Yoon, J. W. Rhim, and H. S. Byun, Preparation and Characterization of PVA/PSSA-MA Electrolyte Membranes Containing Silica Compounds for Fuel Cell Application, Membrane J. 18 (2008) 1-8.

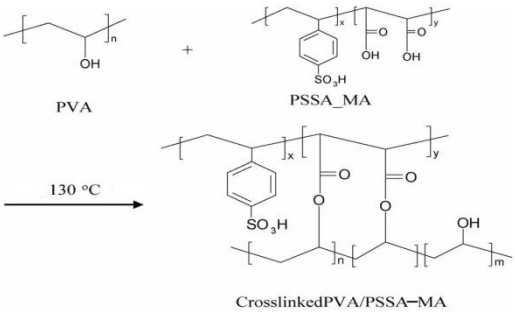

Fig. 1 Possible reaction mechanism of PVA and PSSA_MA

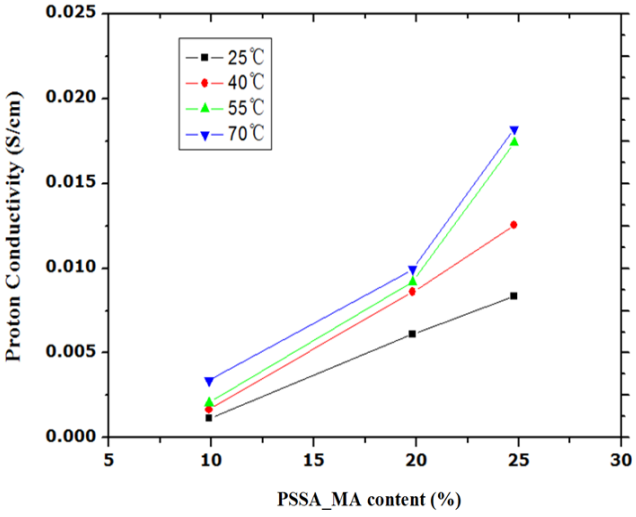

Fig. 2 Proton conductivity of PVA/PSSA_MA/THS-PSA membranes

Dual 'Stimuli' Responsive Hydrogel: Effect of Ionizable Monomer on the Swelling Behavior

G. Roshan Deen[1], *Vivien Chua*[1] *and Xian Jun Loh*[2]

[1]Soft Materials Laboratory, Natural Sciences and Science Education, NIE, Nanyang Technological University, Singapore 637616.

[2]Institute of Materials Research and Engineering, Singapore 117602.

Introduction

In recent years, new research emphasis has been directed towards integrating multiple functions into a single polymeric material. Among the new advances in materials science are functional polymers with structural designs intended to produce a specific function. 'Stimuli' responsive polymers are polymeric materials which change their physical properties in response to external stimuli such as pH, temperature, electric field, illumination, pressure, magnetic field etc [1,2]. The potential responses to these stimuli can be changes in phase, shape, volume and optical properties. These interesting materials find applications in controlled drug delivery systems, skin care products, enzyme immobilizations, chemical sensors etc. When these polymers are chemically crosslinked using a suitable crosslinking agent, materials called hydrogels are obtained.

In this work, new hydrogels composed of *N*-isopropyl acrylamide (NIPAM) and *N*-acryloyl-*N*'-ethyl piperazine (AcrNEP) were prepared by free-radical solution polymerization at room temperature. The swelling behavior of the hydrogel and the effect of AcrNEP (a ionizable monomer) on the swelling was studied in detail.

Materials and Method

The monomer AcrNEP was synthesized by the method described earlier[3]. NIPAM (Aldrich), *N*,*N*'methylene bisacrylamide (MBA, Aldrich)), potassium persulfate (Aldrich), and *N,N,N',N'*-tetra methylene ethylene diamine (TEMED, Aldrich) were used as received. 1.0 M HCl and 1.0 M NaOH were used to prepare solutions of various pH (2-12).

Copolymer hydrogels of AcrNEP and NIPAM were synthesized by free-radical solution polymerization. Hydrogels containing various monomer feed ratios with a fixed crosslinker content of 2 wt% were prepared. The monomer feed ratios are summarized in Table 1. The chemical structure of the monomers and the crosslinker is shown in Figure 1.

Table 1 Monomer feed ratios used in the preparation of hydrogels.

Hydrogels	Feed compositions		Appearance after polymerization
	NIPAM (g)	AcrNEP (g)	
NA 90-10	0.9006	0.1098	Transparent soft solid
NA 70-30	0.7052	0.3382	Transparent soft solid
NA 50-50	0.5058	0.5106	Transparent soft solid
NA 20-80	0.2048	0.8083	Transparent soft solid

Silver nanoparticles were fabricated in the matrix of the hydrogel by the method of diffusion and *in-situ* chemical reduction.

Results and Discussion

All the hydrogels prepared in this showed excellent response to changes in pH. Figure 2 shows pH responsive character of the gels as function of AcrNEP content. The gels swell in acidic solution and de-swell in basic solution owing to protonation and de-protonation of the tertiary amine moiety of AcrNEP. The gels also exhibited temperature response and deswelled above the critical solution temperature of PNIPAM (32 °C).

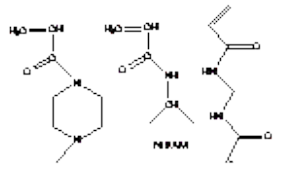

Figure 1. Chemical structure of

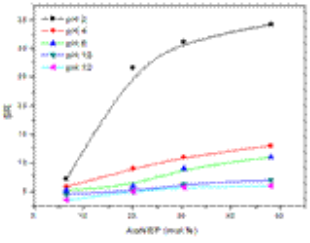

Figure 2. pH responsive swelling.

The presence of silver nanoparticles in the gel matrix was confirmed by UV-Vis spectrophotometry and scanning electron microscopy. A distinct absorption maximum was observed at a wavelength of 406 nm. The average size of the silver nanoparticles was around 50 nm. Water sorption of these gels followed non-Fickian behavior in acidic solution and Fickian behavior in basic solution. The penetration velocity of solvent (water) into the gel matrix increased with increasing ionic monomer in the hydrogel. Table 2 shows the water sorption parameters in solution of pH 2.

Table 2. Water sorption parameters.

Hydrogel	*n*	*k*	$D \times 10^8$ (cm^2 s^{-1})	$v \times 10^3$ (cm g^{-1})
NA 90-10	0.64	0.02	4.98	1.95
NA 70-30	0.67	0.03	6.63	2.06
NA 50-50	0.58	0.03	11.3	2.36
NA 20-80	0.49	0.07	13.8	2.76

Conclusions

A new type of pH and temperature responsive crosslinked hydrogel of NIPAM and AcrNEP was successfully synthesized. The presence of ionizable monomer played a vital role in tuning the pH responsive character of these gels. Swelling and de-swelling profile of the gels in solution of pH 2 and pH 12 showed a response time of about 60 min with good reversibility. Silver nanocrystals of size range 50 nm were fabricated in the matrix of these hydrogels.

References

1. J.K. Oh, D.J. Siegwart and K. Matyjaszewski, *Biomacromolecules* 2007, 8, 3326.

2. N.A. Peppas, J.Z. Hilt, A. Khademhosseini and R. Langer, *Adv. Mater.* 2006, 18, 1345.

Copolymerization of 2,2-Diallyl-1,1,3,3-tetraethylquanidiniumchloride with Maleic and Fumaric Acides

Gorbunova M.

Institute of Technical Chemistry, Ural Branch of Russian Academy of Sciences

mngorb@newmail.ru

A range of nitrogen-, phosphorous-containing allyl compounds for the synthesis of linear high molecular weight polymers via reaction of radical homo- and copolymerization to be carried out is rather narrow. Actually, among allyl monomers only quaternary salts of diallylammonium have found an application as monomers for the synthesis of polyfunctional polymers [1]. Moreover, the breadth of useful properties spectrum makes polymers based on them unique, so searching and studying of *N*-containing allyl monomers of new structural types is quite advisable. It is well known containing guanidine group compounds possess wide spectrum of antibacterial activity and use as medicine and fungicides [2]. That is why guanidine group introduction into high molecular compounds is undoubtedly of present interest.

Activity of 2,2-diallyl-1,1,3,3-tetraethylguanidiniumchloride (AGC) in reactions of radical copolymerization with maleic and fumaric acides has been studied. 2,2-Diallyl-1,1,3,3-tetraethylguanidiniumchloride was found to be copolymerized with fumaric acide in the conditions of free-radical initiation, the copolymers being characterized by statistical distribution of monomer units. AGC copolymerizes with maleic acid, the peculiarity of the system is a high tendency of the comonomer units toward alternation in the polymer chain (figure 1).

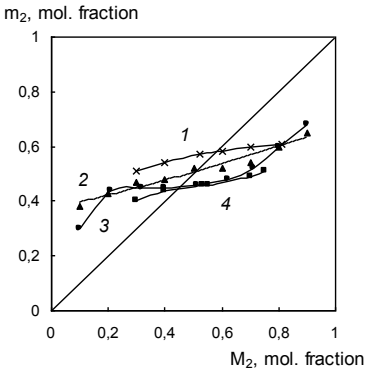

Figure 1. Dependance of composition of AGC copolymer with MA (M_2) on the monomer ratio at polymerization in methanol (*1*), in chloroform (*2*), in ethanol (*3*) and at bulk (*4*). $[M_1 + M_2] = 6$ mol/l, [AIBN] = 3 mass. %, T = 80°C.

AGC is less active if compared with maleic and fumaric acides. The rate of copolymerization of AGC with maleic and fumaric acides reduces with increasing molar fraction of acid in initial monomer mixture (figure 2).

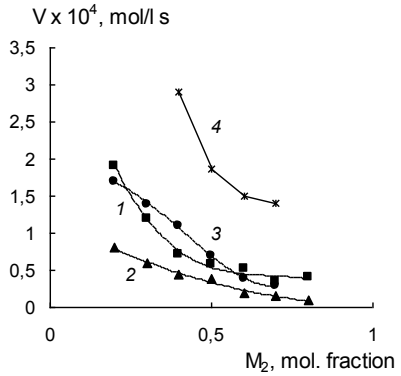

Figure 2. The rate of copolymerization of AGC with MA (M_2) vs. the monomer ratio. $[M_1 + M_2] = 6$ mol/l, $[M_1]/[M_2] = 0.5/0.5$, [AIBN] = 3 mass. %, T = 80°C. *1* – ethanol, *2* – methanol, *3* – chloroform, *4* – in bulk.

As a result of kinetic investigations at initial conversions it was determined that a usual for radical polymerization reaction half order with respect to initiator is observed indicating bimolecular mechanism of the growing chain failure, as well as deficiency of degradative chain transfer to the monomer intrinsical to allyl monomers.

The structure of the polymers obtained was identified by NMR ^{13}C. Analysis of the values of chemical shifts of the signals and their multiplets shows AGC to copolymerize with maleic and fumaric acides both double bonds participating.

The copolymers of AGC with maleic and fumaric acides are nontoxic, have a notable antibacterial activity and can be used for medicine aims.

Financial support by the Russian Foundation for Basic Reseach (grant № 09-03-00220) is gratefully acknowledged.

References

1. Vorob'eva, A.I., Prochuhan, Yu.A., Monakov, Yu.B. 2003. Polymer sci. 45: 2118-2136.
2. Topchiev D.A., Malkanduev Yu.A.. Cationic polyelectrolytes: obtaining, properties and using. M.: Akademkniga, 2004.

Influence of microcrystalline cellulose on thermal properties of polypropylene composite nonwovens

Katarzyna Bujnicka, Jolanta Kałużka

The Textile Research Institute Lodz, 5/15 Brzezińska Str., Poland

kbujnicka@iw.lodz.pl

Introduction

Properties of many polymers can be modified by adding other substances including the various nucleating agents[1]. The polypropylene is a cheap and very popular polymer. Nowadays when the public awareness and the concern for the environment is increasing the practical use of polypropylene is limited due to its chemical resistance and the slow degradation of products made of it. In order to increase susceptibility of polypropylene to degradation its degradable composites with natural additives are formed. Studies on the influence of these additives on hydrolytic and photolytic degradability of polypropylene composite nonwovens, showed that microcrystalline cellulose (3%wt) increases degradation capability (hydrolytic and photolytic)[2]. In this paper the influence of degradable microcrystalline cellulose on the thermal properties and crystalline structure of processed polypropylene composite nonwovens by melt-blown technique is presented.

Materials and Methods

The granulate polypropylene (melting flow index MFI = 1200 g/10min) its polypropylene matrix and polypropylene composite nonwovens with 1, 2 i 3 % wt of the microcrystalline cellulose have been tested. The average diameter of cellulose granule has been 20 µm (Sigma–Aldrich). The study has been carried out using differential scanning calorymetry (DSC). The thermal analysis measurement were performed using DSC 6220 Exstar SII Nano Technology by Haas. The samples of about 5 mg were heated to 260 °C in the aluminum melting-pots. The experiments were carried out in nitrogen atmosphere and the scans were obtained at 20°C/min. Thus, a melting endotherm of all samples with melting point (T_m) and melting enthalpy ($\Delta H_{exp\ (w)}$) was obtained. The thermal characteristics of polypropylene composite nonwovens for components in anisotropic and isotropic system was determinated. On the basis of the crystallization exotherm the crystallization temperature (T_c) of the polymer was calculated. The degree of crystallinity (X_c) of the each investigated sample was determinated based on DSC measurements using the by equation:

$$X_c = \frac{\Delta H}{\Delta H_m^0} \cdot 100\,\%$$

where: ΔH – actual melting enthalpy of nonwovens sample [J/g]; $\Delta H_m{}^0$ – theoretical value of enthalpy for 100 % crystalline polypropylene, for polypropylene $\Delta H_m{}^0$ = 209 J/g[3]. $\Delta H = \Delta H_{exp(w)}/w$; where: w- weight fraction of polypropylene; $\Delta H_{exp(w)}$ - melting enthalpy of polypropylene obtained graphically from the area of the endothermic peaks of the DSC thermograms.

Results and Discussion

The effect of adding cellulose on the degree of crystallinity and thermal properties of polypropylene composite nonwovens has been examined. The changes in melting point, melting enthalpy and crystallization temperature of polypropylene composite nonwovens were observed. The melting point of polymer in the composites decreases slightly and proportionally to the content of the degradable additives (Fig. 1).The similar trend was observed for isotropic system.

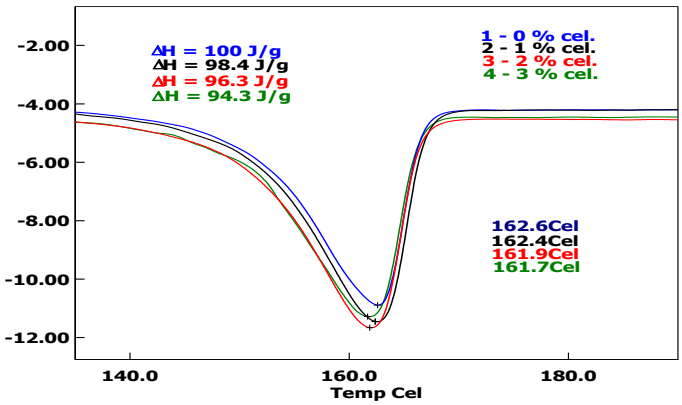

Fig.1 DSC thermograms – melting curves for anisotropic system: 1- 0 % wt of cellulose, 2 - 1 % wt of cellulose, 3- 2 % wt of cellulose, 4- 3 % wt of cellulose.
ΔH- actual melting enthalpy of nonwovens sample.

The cellulose used as biodegradable fillers in polypropylene composite nonwovens reduced homogeneity of the system and at the same time the melting enthalpy of polypropylene nonwovens sample was decreased. The minimal value of the melting enthalpy of 94,3 J/g was determined for nonwovens with 3 % wt of the microcrystalline cellulose. On the basis of the analysis of actual melting enthalpy (ΔH) of nonwovens samples, it was found that the degree of crystallinity of composites decreases proportionally with the cellulose content. The microcrystalline cellulose in polypropylene nonwovens did not form a nucleation center leading to a decrease of crystal growth in the crystallization process of the polymer. Cellulose has a hydrophilic character. Thus the hydrophobic polypropylene molecules are not adsorbed on the nucleation surface.

Conclusions

Addition of cellulose to the polypropylene nonwovens hinders the crystallization process of polymer. Low degree of crystallinity causes visible increased fragility and susceptibility of composite nonwovens. Thus, the biodegradable additive shows to enhance the degradability of new nonwovens.

References

1. M. Mucha, Z. Królikowski, *Journal of Thermal Analysis and Calorimetry* 2003, **74**, 549.
2. J. Kałużka, K. Bujnicka, M. Łatwińska, J. Sójka – Ledakowicz, M. Kudzin, *Przemysł Chemiczny* 2010, **89** (12), 1654.
3. R. Sobczak, Z. Nitkiewicz, J. Koszkul, *Composites* 2003, **2** (8), 343.

The study was financed by the Polish Ministry of Science and Higher Education. Grant No.:PBZ-MNiSW-01/II/2007 (2007-2011)

Contact Polymerization of the Composition on the Basis of Acrylamide and Formaldehyde on Metal Surfaces

Lidia Kolzunova, Maxim Karpenko

Institute of Chemistry, Far Eastern Branch of Russian Academy of Sciences. Vladivostok. Russia

kolzunova@ich.dvo.ru

Introduction.

Recently, a substantial body of work has been performed on the search of polymerization compositions (PC) which would enable one to form, by means of the electropolymerization process, polymer films on electroconductive substrates. These films could, on one hand, find an independent application or, on the other hand, be used as special-purpose coatings. Among such PC one should mention as prospective the composition containing acrylamide (AA), N,N'-methylenebisacrylamide (MBAA), formaldehyde (F) and zinc chloride. The films produced on the basis of the above PC were suggested to use as protective and electrical insulating coatings or ultrafiltration and reverse-osmosis membranes [1]. For the monomer composition under study we revealed and recorded the post-polymerization effect by video microscopy and gravimetric methods. It was shown that principal reason of post-polymerization origin could be the phenomenon we found that consists in the fact that in the absence of external current regular zinc metal is capable to initiate polymerization in solutions of the same PC which was used for electropolymerization. Such a process would result in formation of a uniform polymer film. Since the formed polymer film, at least during the first minutes of synthesis, has a sufficiently high porosity, it allows low-molecular components participating in electropolymerization passing freely through the film to the zinc sub-layer (which was produced on a cathode during electrolysis process) and polymerize on it in accordance with the found effect in the absence of the external current source.

So the objective of this work was to study the process of initiating polymerization of acryl monomers by metal zinc and other metals under no-current conditions.

Results and Discussion.

Comparative studies of the kinetics of electropolymerization and zinc-initiated polymerization by the gravimetric method showed that zinc initiation is more efficient for this purpose. The course of the plots showing the dependence of the polymer deposit mass on time results from the fact that the formed polymer gradually seals the electrode surface which, thereafter, suppresses the supply of the electrolysis solution components to metal. As a result, the polymerization initiation process becomes attenuated. That is why it is impossible to grow a polymer film of a thickness more than 500-600 micrometers. It is clear from the above observations why post-polymerization does no prevail over electropolymerization, although the initiation by zinc is more efficient. It is evident that electropolymerization results in formation of sufficiently fine-porous film, so that subsequent polymer deposit mass growth is limited by the porous blockage in the same manner as at switched-on current.

Further studies were directed to revealing the mechanism of the polymerization initiation by zinc. We suggest that at zinc-initiation the formation of active particles inducing polymerization is the result of the zinc-acrylamide complex electroreduction. The point is, after putting the zinc rod into the polymerization composition under study it gains the potential about -(0.95-1.00) V. This value is sufficient to induce the reduction of the complex with formation of active particles and efficient electropolymerization. The cathode potential gradually decreases in the course of $[Zn^{2+}]$ increase. The polymerization rate (polymer product yield) is the higher when the higher is the potential).

It was established that it is possible to initiate polymerization not only by Zn, but also by other metals. The main criterion should consist in emerging of a sufficient (at least -(0.90-0.95 V) electrode potential in the PC under study. One could use, for example, Mg and Al, since both are more active that Zn. However, the polymer yield on Mg is too small because at excessively high potentials (E_{Mg} = -1.80 V) the rate of polymer deposition on the metal surface tends to drop, since the concentration of formed radicals increases resulting in their recombination with each other rather than initiation of regular polymerization. Besides, low polymer yield on the metal surface results from active gas emission due to water decomposition in the specified potential range and removal of polymer chains into bulk solution. Use of Al is characterized by its passivation in the polymer composition under study resulting in the fact that the potential value does not exceed -0.60 V, which is insufficient for discharge of the zinc-monomer complex with formation of active particles initiating polymerization. For low-active metals (Fe, Cu), whose electrode potentials are even lower, no polymer formation was observed as well.

Conclusion.

The previously unknown polymerization method based on initiating the film formation process by metal zinc (other active metals), which we developed for the polymerization composition on the basis of acrylamide, its derivatives and formaldehyde, can be competitive as compared to electropolymerization for the following reasons. On one hand, the method enables one to produce the same deposits as the latter one under technologically more advantageous no-current conditions. On the other hand, since polymerization proceeds on the metal surface in the absence of external current source, it becomes possible to produce, with using the suggested method, hollow polymer spheres, if the process is conducted on micro-powders of respective metals followed by their solution.

References.

1. L.G. Kolzunova, Russ. J. Electrochem. 40 (2004) 337.

Synthesis and characterization of poly(L-lactic acid) nanocomposites with vermiculite of different modification

I. Aranburu, M.D. Fernández, M.J. Fernández

Department of Polymer Science and Technology, Faculty of Chemistry, University of the Basque Country, San Sebastian, Spain

ibai.aranburu@ehu.es

Polymer-layered silicate nanocomposites have received special attention in the recent years owing to their hybrid properties synergistically derived from two components when they are mixed intimately [1, 2]. The nanoscale incorporation of layered silicate materials in the polymer matrices is not straightforward and in most of the instances, surface modification of these materials is required to obtain organically modified silicates or clay which then is more compatible with the organic polymer matrices. The most widely used method is the treatment of the clays with quaternary ammonium salts, which allows the substitution of some metal ions present in the structures of the clay by quaternary ammonium ions with large organic groups. Another modification procedure includes the grafting of silanes containing a functional group, which can specially interact with the polymer matrix. Clay minerals have reactive hydroxyl groups at the surface and at the edge of the layers that can react with silanol (Si–OH) groups of the hydrolyzed silane to form siloxane (Si–O–Si) bonds.

Poly(L-lactide) (PLLA), one of the most popular and important biodegradable polymers, is a linear aliphatic thermoplastic polyester that exhibits excellent properties which are comparable to many petroleum-based plastics. Moreover, the properties of PLLA can be modified in a controlled manner through filling with inorganic nanoparticles. Nanocomposites can be synthesized by melt/solution blending and in-situ polymerization. The particular blending process which is used have a significant influence on the structure, and hence the properties of the nanocomposite.

The present study focuses on synthesis and characterization of different organically modified vermiculites (VMTs) and PLLA-modified VMT nanocomposites produced using melt compounding and solution blending. Three organoclays were prepared: OVMT, through the cationic exchange reaction of NaVMT with hexadecyltrimethyl-ammonium bromide (HDTMAB), VMTS and OVMTS by grafting glycidoxypropyltrimethoxysilane (GPMS) with the SiOH groups of VMT and OVMT respectively, to introduce epoxy functional groups on the silicate layers.

The organo-clays were characterized by ^{13}C and ^{29}Si solid-state nuclear magnetic resonance (NMR), X-ray diffraction (XRD), Fourier transform infrared spectros-copy (FTIR), high-resolution thermo-gravimetric analysis (HRTGA), and scanning electron microscopy (SEM). With the cation exchange of Na^+ for the cationic surfactant, expansion of the VMT layers takes place. Basal spacing value of OVMT indicates bilayer arrangement in the galery. The interlayer spacing of the VMT is the same as the VMTS, confirming that the grafting reaction occurs mainly outside the clay layers, onto the edge of clay platelets. HRTGA allows identification of two kinds of organic species on clay, physically and chemically adsorbed species, and demonstrates that the external-surface physically adsorbed surfactant can be removed after washing treatment, resulting in an increase in thermal stability and a slight decrease in the interlayer spacing of the resultant organoclays. OVMT and OVMTS display the lowest onset temperature decomposition compared with that of NaVMT, and VMTS due to the ammonium cation incorporation.

PLLA nanocomposites containing 2, 5 and 10 wt% of modified VMTs prepared by different procedures were characterized by XRD, HRTGA, and transmission electron microscopy (TEM). The PLLA/OVMT and PLLA/OVMTS nanocomposites increase the basal spacing value of modified VMTs. The increase in the interlayer spacing of the composites with OVMT and OVMTS, compared with that of the corresponding neat organoclay, indicates that intercalation of the PLLA chains inside the clay galleries occurs. The intensity of the peak related to the interlayer spacing value of the clay gradually increases with the mineral content rise, due to the increase of the diffracted X-rays by the additional intercalated oganoclay. The broadening of this peak is also observed due to partial disruption of parallel stacking or layer registry of the pristine organoclay, which reveals the existence of some exfoliated clay platelets. This intercalation/exfoliation coexistence is in agreement with the TEM data. The XRD reflections of the PLLA/VMTS material are close to that of VMTS, indicating that this sample is in fact a mixture of polymer and unintercalated clay particles. For the composites prepared from solution, the introduction of organophilic inorganic material improves the thermal stability of the polymer increasing the onset decomposition temperature, in oxidant atmosphere. The dispersed inorganic platelets assist the formation of a protective layer on the surface of the polymer, which acts as an insulator and a mass transport barrier retarding the decomposition rate of the polymer matrix. On the contrary, the melt prepared nanohybrids exhibit a lower thermal stability compared to PLLA and the solution cast ones, due to the polymer and surfactant degradation associated with melt processing.

Acknowledgement. The authors gratefully acknowledge the financial support by the Excma. Diputación Foral de Gipuzkoa (project 2009-2011), the European Union, and the Gobierno Vasco (SAIOTEK project 2010-2011 and Subvención a Grupo Consolidado IT330-10).

Bibliography

1-Ray S.S., Okamoto M. *Prog. Polym. Sci.* 28, 1539 (2003)

2-Paul, D.R., Robeson, L.M. *Polymer* 49, 3187 (2008)

Upon the Synthesis Possibilities of 2 - Hydroxyethyl Methacrylate Copolymer with a Comonomer with Spiroacetal Moiety

Aurica P.Chiriac, Loredana E. Nita, Manuela T. Nistor

"Petru Poni" Institute of Macromolecular Chemistry, Grigore Ghica Voda Alley No. 41-A, 700487 IASI, Romania

e-mail: achiriac1@yahoo.com

Introduction: The copolymerization processes between hydrophilic and hydrophobic monomers present interest in the design and synthesis of different compounds such as hydrogels and biocompatible materials. A large number of studies were devoted to the homopolymerization and copolymerization of 2-hydroxyethyl methacrylate (HEMA) owing to the multiple application fields of the poly(HEMA) and its copolymers. The incorporation of spiroacetal groups in the polymers structures improves the solubility and the adhesive properties. More than that, these polymers induce good oxidative and thermal stability, are good fiber formers, and films prepared from some of polymers that include this structural unit present good flexibility and tensile strength. These characteristics are attributed to the properties inherent into the spiroacetal ring: stiffness, which is higher than cycloaliphatic rings but lower than aromatic rings; interactions on ether oxygen such as hydrogen bonds or coordinate bonds with other functional groups, and bulkiness. The present study reports the synthesis of a copolymer based on HEMA and 3, 9-divinyl-2, 4, 8, 10-tetraoxaspiro(5.5) undecane (U) acquired through radical aqueous dispersion polymerization in the presence of AIBN.

Methods: The prepared dispersions were characterized from the viewpoint of the hydrodynamic radius, zeta potential and conductivity evolution during syntheses. The mean particle size and size distribution, as well as zeta potential and conductivity were also evaluated for the synthesized polymeric particles. The polymers compositions were confirmed by FTIR and ^{1}H-NMR spectra. Also, the thermal stability of the polymeric compounds was evaluated. SEM and AFM investigations of the polymer morphology are also presented.

Results and Discussion: The reactions taken into study refer to the heterogeneous free radical polymerization processes which involve the emulsification of a hydrophilic monomer (HEMA) and another hydrophobic (U) in water by an oil-in-water emulsifier (SLS), followed by the initiation reaction with an oil-soluble initiator (AIBN). In parallel with this variant of synthesis two other alternatives have been performed, respectively surfactant-free, but in the presence of protective colloid – cyclodextrin (CD) and poly(aspartic acid) (PAS) – which can prevent the interactive latex particles from coagulation. They may assure the colloidal stability via electrostatic stabilization mechanism or steric stabilization mechanism, or both. Also, the homopolymer poly(2-hydroxyethyl methacrylate) was prepared just to compare it with the synthesized copolymers. The presence of the comonomer positively affects the thermal behavior of the copolymer. As it was expected, the comonomer improves the overall thermal stability of the polymers. Also, the acquired type of network structure confers an increased thermal stabilization to the polymer. The inclusion of the oligosaccharides in the synthesis, like cyclodextrin, leads to the decrease of the initial decomposition temperature, because of the hydroxyl groups that are bordered outside of the ring. The same behavior is experienced for the other used dispersing agent, respectively PAS. This slight decrease of T_{onset} did not significant affect the system thermal stability, offset by the other improved properties conferred by achieving a network structure. SEM micrographs show that the polymers prepared with different stabilizers possess a distinct structure. The homopolymer seems to be with a lamellar structure instead of the copolymers that appear with an internal structure more homogeneous and dense.

Conclusions: The study presents the possibility to prepare a copolymer based on HEMA and 3, 9-divinyl-2, 4, 8, 10-tetraoxaspiro(5.5)undecane (U) through radical polymerization in the presence of AIBN, with a solid content of 10 wt.-% in the presence of a classic ionic surfactant – sodium lauryl sulfate (SLS) – and comparatively just using two variants of protective colloid: cyclodextrin and poly(aspartic acid). It is concluded on the proper critical micellar concentration for used surfactants, respectively attributing a mixed mode of particle nucleation (micellar and homogeneous nucleation) in case of synthesis with SLS and an entropic mechanism of stabilization with CD and PAS as stabilizers. The mean particle size and size distribution, as well as zeta potential and conductivity determination on the prepared polymeric particles attest: a relatively monodisperse distribution for the particle size; particles with negatively charged surfaces and copolymers conductivity prepared in the presence of PAS or CD increased by several orders against homopolymer. The thermal stability of the polymeric compounds was evaluated. As it was expected the comonomer improves the overall thermal stability of the polymers.

Taking into account the special effects which may be generated by both comonomers – network formation, biodegradability and biocompatibility, gel formation capacity, binding properties, amphilicity, good oxidative and thermal stability, good films formers, acid pH sensitivity – the interest in the development of these new polymeric structures with emphasis on theoretical aspects is thoroughly justified.

The Temperature Influence upon the Complexation Process between Poly(aspartic acid) and Poly (ethylene glycol)

Loredana E. Nita, Aurica P. Chiriac, Maria Bercea, Iordana Neamtu

"Petru Poni" Institute of Macromolecular Chemistry Grigore Ghica Vodă Alley No. 41 A, 700487, Iaşi ROMANIA

lnazarie@yahoo.co.uk

Introduction:

As it is well known, polymer blends, as physical mixtures between structurally different polymers that interact through secondary forces with no covalent bonding, constitute a useful approach for preparing materials with tailor made properties different from those of the constituent polymers. Blending polymers may result in reducing their basic cost, improving their processing, and maximizing their specific properties. Progressive elucidation of the effect of specific interactions on the miscibility in polymer blends has been one of the most noticeable achievements in the study of polymer blends in the last two decades.

In the present study the temperature influence on the formation of an interpolymer complex (IPC) based on poly(aspartic acid) (PAS) and poly(ethylene glycol) (PEG), it was investigated. The temperature influence during IPC formation was investigated onto the temperature range between 22^{o}C – 37^{o}C. The chosen domain of temperature corresponds to the storage temperature of the samples up to human body temperatures, owing to the final purpose the IPC utilization as biomaterials. The influence of the PEG molecular weight as well as the composition – the ratio between PAS and PEG – of the blends on the IPC formation was investigated. The directions of analysis have in view (1) to confirm the intervened interpolymer interactions based between others on the hydrogen-bonds evidenced by FT-IR spectroscopy, (2) to estimate through the dynamic viscosity the miscibility between PAS and PEG macromolecular chains and also, to find the best conditions in order to achieve the intermolecular complex related on the PAS/PEG domain of composition, temperature, and PEG molecular weight.

Materials and methods

Materials: Poly(aspartic acid) was synthesized in our laboratory through a reaction in two steps. The prepared homopolymer has the molecular weight of about 15,110 and the polydispersity index of 1.317. Poly(ethylene glycol)(PEG), Fluka Germany provenience, was used without further purification. PEG of four different molecular weights (Mw), respectively 2000 Da ([η] = 0.0935 dL/g), 4000 Da ([η] = 0.1211 dL/g), 10,000 Da ([η] = 0.2348 dL/g), and 35,000 Da ([η] = 0.5134 dL/g) (denoted in the present paper as PEG 2000, PEG 4000, PEG 10000 and PEG 35000) in order to cover several orders of weight extent was taken into study

IPC preparation: Briefly, the PAS/PEG complex was prepared by direct mixing the stock aqueous solutions of 1% concentration for 60 min, in the different PAS/PEG ratios (vol.%) respectively 0/100, 20/80, 50/50, 80/20 and 100/0. Thus, the total polymer concentration in the mixture was maintained constantly during each experiment. The solution of the polymer mixtures was then poured into Petri dishes and the films were obtained after drying at the room temperature.

Results and discussion

The importance of blending has increased in recent years because it has become a useful approach for preparing materials with tailor made properties different from those of the constituent polymers. The electrokinetic and rheological properties of the PAS/PEG blends are important parameters for the estimation of the behavior of blends under different conditions (temperatures and compositions). In the present paper, the influence of the temperature on the IPC formation was investigated in the temperature range of 22^{o}C to 37^{o}C. The observed behavior was discussed as a function of the molecular weight of PEG and the ratio between PAS and PEG during blends preparation. The intra-association (self-association) of the carboxyl groups in PAS and inter-association (intermolecular interactions) between PAS and PEG constituent components influence the frequency dependence of the dynamic moduli in the terminal region of the miscible blend systems investigated. Thus, the local polymer–polymer interactions by FT-IR spectroscopy, confirming hydrogen-bonding interactions, they were put into evidence. The miscibility and the polymer-polymer interactions were proved from the dynamic viscosity. Zeta potential and electrical conductivity of the blends were used to obtain the optimum conditions of temperature, PEG molecular weight and ratio between PAS and PEG, to have intermolecular complexes.

The corroborated data evidence the interpolymer complex formation using macromolecular compounds with closely molecular weights or the preparation of an interpolymer association with compact structure based on attractive forces between poly(aspartic acid) and poly(ethylene glycol) in the case of the compounds with different molecular weight.

Acknowledgments

This work was supported by CNCSIS-UEFISCSU, project number PN II-RU No. 53/10.08.2010, code 656, entitled: **New hydrogel with biomedical aplication.**

Light-Driven Wettability Changes on a Photoresponsive Electrospun Mat

Menglin Chen[1] and Flemming Besenbacher[1,2]

[1]Interdisciplinary Nanoscience Center (iNANO), [2]Department of Physics and Astronomy (IFA), Aarhus University, DK-8000 Aarhus C, Denmark.

E-mail address: menglin@inano.au.dk

Functional surfaces with controllable wettabilities upon external stimulus have come to the forefront of research providing many new possibilities for biological and industrial applications.1 A particularly intriguing possibility is offered by light-responsive materials based on the photoisomerization of constituent molecules that undergoes a large conformational change between two states in response to the absorption of light at two different wavelengths,2 eg. *trans–cis* isomerisation of azobenzene chromophores.3

Electrospinning, a remarkably robust and versatile method for fabricating nanofibers, has become particularly powerful when its intrinsical nanoscale topography is combined with easy add-on functions. Herein we report the first study of light-responsive electrospun azobenzene modified polycaprolactone (PCL-azo) nanofibers (Figure 1).4 Surface chemistry of the nanofibers was probed with X-ray photoelectron spectroscopy (XPS) and Time-of-flight secondary ionmass spectrometry (ToF-SIMS). The light-responsive wettability of the fibers was subsequently investigated using contact angle (CA) measurements.

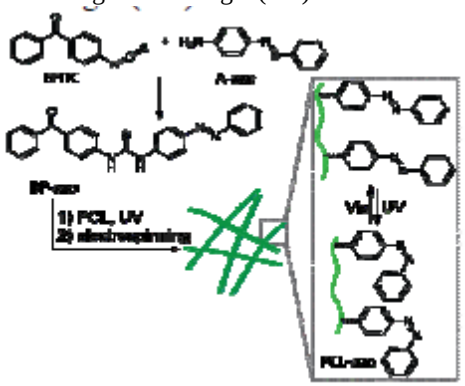

Figure 1. Schematic illustration of electrospinning of PCL-azo and the produced light-responsive nanofibers.

The conjugation of azobenzene with PCL was performed in a one-pot reaction (Figure 1). The heterobifunctional, photoactive crosslinker, BPITC, with isothiocyanate group reactive to aromatic amines and benzophenone species ready for C-H insertion in PCL upon UV illumination, was reacted with excess of A-azo first to form BP-azo and subsequently PCL. Thus the modified polymer PCL-azo having PCL as the linear main chains and BP-azo as the branch side chains was formed. XPS provides quantitative information of azobenzene present in the outer molecular layers, and BP-azo was proved to be successfully conjugated with PCL with nearly 90% yield in the one-pot reaction. ToF-SIMS was applied to identify the chemical species and to map their distribution on the surfaces of individual nanofibers with a depth resolution of 1–2 nm. The unique nominal m/z values from PCL main chains and BP-azo side chains were used to obtain chemical maps of the distribution of BP-zao side chains and PCL main chains on the fiber surfaces. (Figure 2)

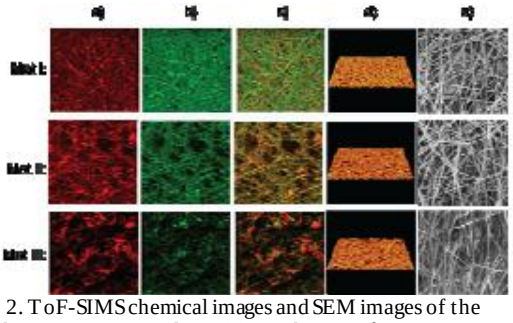

Figure 2. ToF-SIMS chemical images and SEM images of the nanofibrous mats I-III. Column (a): Azobenzene fragment ion images; column (b): PCL fragment ion images; column (c): Overlay images of column (a) and column (b); column (e): 3D images of total ions; column (e): SEM images. Area: 20μm • ~20μm.

The photo-responsibility of azobenzene is found to be retained in the electrospun fibers by water contact angle (CA) measurements. All the mats turned from hydrophobic to hydrophilic upon UV irradiation (365nm, I_{UV}=15 mWcm^{-2}, 1 h) and switched back upon visible light irradiation, where the Mat III showing the most significant changes. (Figure 3)

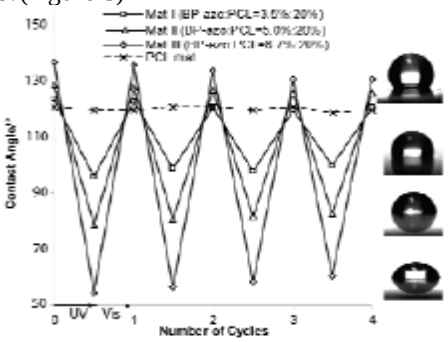

Figure 3. Reversible photo-response switching between hydrophobicity and hydrophilicity upon UV/vis irradiation.

The exhibited large, reversible and light-responsive wettability changes, arising from both the azobenzene functionalization and the roughness intrinsically offered by the electrospun nano/microscale hierarchical structures, allow us to control the properties and the function of the nanofibers with light, which open up for a lot of interesting and visionary applications in drug delivery, tissue engineering, sensors and optical storage.

ACKNOWLEDGMENT

We gratefully acknowledge the funding to the current project NanoNonwovens from The Danish National Advanced Technology Foundation, the collaboration with Fibertex A/S, the Danish Research Agency for the funding to the iNANO Center and the Lundbeck and the Carlsberg Foundations for their financial support.

1. Russell, T. P., *Science* **2002,** *297*, 964-967.
2. Ercole, F.; Davis, T. P.; Evans, R. A., *Polym. Chem.* **2010,** *1*, 37-54.
3. Sudesh Kumar, G.; Neckers, D. C., *Chem. Rev.* **1989,** *89*, 1915-1925.
4. Chen, M.; Basenbachor, F., *ACS Nano*, **2011**, accepted.

Polymeric Nanocomposites Produced From Polypropylene and Nanocellulose Whiskers

H.Ayşen Önen, Istanbul Technical University, Department of Chemistry, Maslak, Istanbul, Turkey
onen@itu.edu.tr
Nuray Ucar, Istanbul Technical University, Deparment of Textile Engineering, Taksim, Istanbul, Turkey
ucarnu@itu.edu.tr
Elif Bahar, Istanbul Technical University, Institute of Science&Technology, Department of Polymer Science&Technology, Maslak, Istanbul, Turkey
elifrafiye@gmail.com
Mustafa Oksuz, Yalova University, Department of Polymer Engineering, Yalova, Turkey
muoksuz@gmail.com
Youjiang Wang, Georgia Insitute of Technology, School of Material Engineering, Atlanta, USA
youjiang.wang@ptfe.gatech.edu
Mehmet Ucar, Kocaeli University, Mechanical Education Department, Izmit, Turkey
ucarm@kocaeli.edu.tr
Onur Ayaz, Istanbul Technical University, Institute of Science&Technology, Department of Polymer Science&Technology, Maslak, Istanbul, Turkey
onur.ayaz@yahoo.com
Ali Demir, Istanbul Technical University, Textile Engineering Deparment, Taksim, Istanbul, Turkey
ademir@itu.edu.tr

Recently, studies which are made for the nanocomposite materials increase, since nanocomposite materials usually have better properties than composite materials containing micron or larger sized reinforcing materials. As can be seen from the literature, some nanomaterials such as carbon black, carbon nanotube, silica and clay have been widely studied and they have been used to make nanopolymer composite materials, which can be used for technical textile, aerospace, automotive industries and building, defence etc. Although some studies on cellulose nano whiskers (CNW) have been carried out in the last two decades, considerable effort has been devoted in recent years to the research and development of materials that utilize CNW, in order to reinforce different polymeric composites. Cellulose one of the most abundant natural polymers, has many advantages such as renewability, biodegradibility, nontoxicity, high specific strength and stiffness, low cost and also providing thermal stability, rigidity and strength to the polymer matrix.

Most of the previous studies were made on incorporation of hydrophilic CNW into polar polymer matrix solved with polar solvent (such as PVA solved with water) or into apolar polymer matrix solved with polar solvent such as DMF-Latex (1-6). From these studies, it has been seen that the CNW improved the thermal stability and mechanical properties of the composite materials. Due to the incompatibility with the hydrophilic CNW, it is necessary to develop new techniques to efficiently incorporate the CNW into the apolar polymer matrixes which is solved with apolar solvents.

The aim of the present study was to develop a nanocomposite materials made from apolar matrix solved with apolar solvent and hydrophilic CNW. For this purpose, one of the most widely used polyolefin polymer,polypropylene, was selected as a representative apolar matrix, since very few number of studies have been devoted to its reinforcement with CNW (7).

To compatibilize the hydrophilic CNW into apolar polymer matrix , Maleic Anhydrite grafted polymers such as MAH elastomer (Polystyrene-block-poly(ethyleneran-butylene)-block-polystyrene graft-maleic anhydride) were included into the formulations. The effects of the amount of CNW on the overall properties of the final polymeric nanocomposite product (especially thermal and mechanical properties) have been investigated.

References

1- Dufresne, A., Kellerhals, M.B., Witholt, B., Macromolecules, 32, 7396-7401, 1999
2-Petersson, L., Kvien, I., Oksman, K., Composite Science and Technology, 67, 2535-2544, 2007
3-Favier, V., Chanzy, H., Cavaille, J.Y., Macromolecules, 28, 6365-6367, 1996
4- Marcovich, N.E., Auad, M.L., Bellesi, N.E., Nutt, S.R., Aranguren, M.I., J. Mater. Res., Vol 21, No 4, April, 870-890, 2006
5- Favier, V., Canova, G.R., Cavaille, J.Y., Chanzy, H., Dfresne, A., C. Gauthie, C., Polymers for Advanced Technologies, 6, 351-355, 1995
6-Hajji, P., Cavaille J.Y., Favier V., Gauthier C., Vigier G., Polymer Composites, 17, 4, 612-619, 1996
7- N.Ljungberg, C.Bonini, F.Bortolussi, C.Boisson, L.Heux, J.Y.Cavaille, Biomacromolecules, 2005,6,2732-2739

High Molecular Weight Polymers for Gas Separation Applications

Lucía Escorial[a,c], *Alberto Tena*[a,c], *Angel E. Lozano*[b,c], *Javier de Abajo*[b,c], *Antonio Hernández*[a,c], *Pedro Prádanos*[a,c], *Laura Palacio*[a,c]

[a] Departamento de Física Aplicada, Universidad de Valladolid, Valladolid
[b] Instituto de Ciencia y Tecnología de Polímeros,CSIC, Madrid
[c] Surface and Porous Materials (SMAP), UA CSIC-UVA,R&D Building, Valladolid

lucia.escorial@uva.es

The use of polymeric membranes for gas separation in industrial applications is growing up in a very fast pace. Some of these applications are: CO_2/CH_4 separations in natural gas processing, CO_2 separations for enhanced oil recovery, alkene/alkane separations, etc. For polymers employed as gas separation membranes, high permeability and high selectivity are essential to minimize capital and operating costs. However, the separation performance at industrial operation conditions is compromised by plasticization-induced permselectivity losses. Plasticization is an increase in the diffusivity of a penetrant due to the facilitation of local polymer segmental motion caused by the presence of another penetrant molecule. [1][2]

In figure 1 the most typical behaviors experienced by passage of plasticizer gases as a function of pressure are shown. For type 3, permeability increases with pressure, but selectivity decreases significantly. For type 2, the most common behavior for glassy polymers, a minimum in the relationship between the permeability and the feed pressure (plasticization pressure) is observed; subsequently an increase in pressure produces an augment of permeability and a decrease of selectivity. For type 1, permeability decreases when pressure is high but selectivity is maintained. Therefore, the most interesting behavior for working with membranes at high pressure, would be the type 1.[3][4][5]

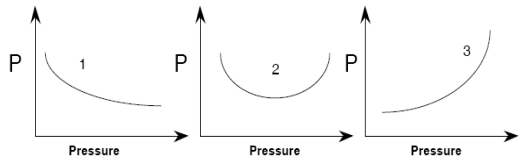

Figure 1

Our group is very interested on the development of plasticization-resistant polymer membranes using diverse approaches. Several methods to reduce the plasticization have been described but not too many are able to entirely remove it. In that way, some of these methods are physical and chemical crosslinking by heat treatment, chemical crosslinking by use of difunctional or polyfunctional compounds, or crosslinking by exposure to UV. However, most of the preceding crosslinking methods involve procedures difficult to apply in commercial membranes, increasing the cost or the manufacturing process. Also, some of them significantly reduce permeability.

Our group has demonstrated recently that some prefluoro polyimides, as 6FDA-6FpDA, with very high molecular weight, are more resistant against plasticization[6]. Thus, this study tries to figure out whether that result is universal and can be extended to other aromatic polyimides.

Thus, two polymers widely used in the industry, Matrimid® and P84®, Figure 2, along with other conveniently chosen ones, have been synthesized . After optimization of the polycondensation reaction, a methodical gas separation study at different feed pressures and temperatures has been carried out and results compared in order to establish relationships between Mw and properties.

Preliminary results denote that when the molecular weight of polymer reaches a threshold value, the plasticization is reduced and the capability to bear high pressures of real gases, as CO_2, is increased.

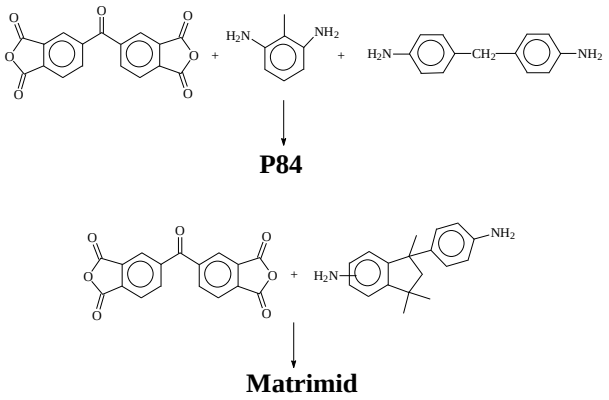

Figure 2

Results seems point out that in order to achieve materials with good capability to be employed in advanced industrial applications, a control of the molecular, in the sense of using high or very high molecular weight, should be considered.

Bibliography

[1] J.D. Wind, C. Staudt-Bickel, D.R. Paul and W.J. Koros. *Ind. Eng. Chem.*, 41 (2002) 6139-6148.
[2] A. Taubert, J.D. Wind, D.R. Paul, W.J. Koros and K.I. Winey. *Polym.*, 44 (2003) 1881-1892.
[3] A. Bos, I.G.M. Pünt, M. Wessling, H. Strathmann. *J. Memb. Sci.*, 155 (1999) 67-78.
[4] K. Okamoto, K., N. Kenji, H. Jinaqiang, T. Kazuhiro, and K. Hidetoshe, *J. Memb. Sci.*, (1997) 134-171.
[5] A. Bos, I.G.M. Pünt, M. Wessling, H. Strathmann. *Sep. Purif. Tech.*, (1998) 12-27.
[6]D.M. Muñoz, M. Calle, J.G. de la Campa, J. de Abajo and A.E Lozano, *Macromol.*, 42 (2009), 5892-5894.

Acknowledgements
Authors gratefully acknowledge the financial support provided by Spanish MICINN (projects MAT2007-62392/MAT and CIT-420000-2009-32) and to Junta de Castilla y León through the GR-18 Excellence Group

Synthesis of poly(o-acyloxyamide)s for gas separation applications

Blanca Díez[a], Angel Marcos-Fernández[b], Purificación Cuadrado[c], Antonio Hernández[a], José G. de la Campa[b], Javier de Abajo [b], Angel E. Lozano[c].

[a]Dpto. Física Aplicada, Facultad de Ciencias, Universidad de Valladolid, Valladolid, Spain.
[b]Dpto. Química Macromolecular, Instituto de Ciencia y Tecnología de Polímeros, CSIC, Madrid, Spain.
[c]Dpto. Química Orgánica, Facultad de Ciencias, Universidad de Valladolid, Valladolid, Spain.
blancad@termo.uva.es

Introduction

The use of polymer membranes for gas separation is increasing in the industry for a wide variety of applications. This technology is competing with consolidated operations such as pressure swing and cryogenic distillation. In this context, there is an increase need for gas separation processes involving the purification or removal of condensable and/or acid gases by economical and environment reasons. In order to develop a *state of the art* technology for these applications, new efforts have to be carried out in order to obtain materials with high rigidity, high and controlled fractional volume and extension of the separation through the time. In the last 5 years, two main approaches dealing with these requirements have been divulged on this topic. Thus, Budd developed the polymers with intrinsic microporosity (PIMs) that showed very high permeabilities even though their selectivity was rather low. Later, a new approach involving a thermally driven rearrangement of poly(*o*-acyloxyimide)s was developed by Park et al (2). By using this methodology, authors were able to make polymer membranes with outstanding gas separation properties (very high permeability and excellent permselectivity) for condensable gases as CO_2.

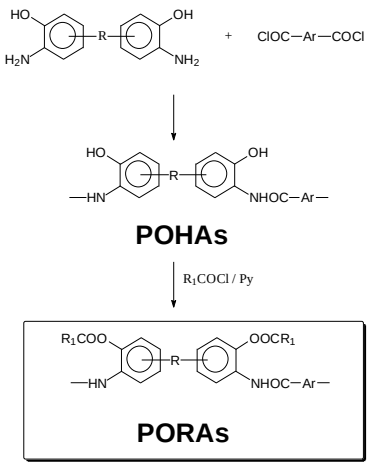

Figure 1. Synthesis of POHAs and PORAs

This work has been designed for the preparation of poly(*o*-acyloxyamide)s (PORAs) by reaction of bis-*o*-hydroxydianilines with diacid chlorides and subsequent derivatization of formed poly(*o*-hydroxyamide)s (POHAs). The ultimate target is attaining processable polymers with good gas productivity (Figure 1). Also, a thermal degradation study has been set out in detail in order to evaluate the ability of these systems to undergo thermal rearrangement processes to polybenzoxazoles.PORAs were characterized and evaluated as gas separation systems and their properties were compared both with POHAs and with related polyamides.

Results and Discussion

On using an *in situ* silylation methodology developed in our group (3), poly(*o*-hydroxyamide)s with very high molecular weight and good mechanical properties have been attained. These polyamides showed a weight loss at around 450 ºC, consistent with the formation of polybenzoxazoles. The $OOCR_1$ substituted polymers showed weight losses at lower temperature than those of their homologous POHAs. However, degradation processes were also observed.

All the polymers, regardless they were derivatized (PORAs) or not (POHAs), were amorphous.

Concerning gas separation properties, POHAs had low permeability and high selectivity, as it is usual for polymers with low FFV. However, derivatized polymers showed much better gas permeation properties. In particular, the polymers derivatized with pivaloyl chloride had a permeability-selectivity balance much better than other polymers widely used in the gas industry ($P(O_2) > 10$ barrer and $\alpha(O_2/N_2) > 4.5$).

PORAs underwent, for the polymer structures, an unavoidable degradation of the molecule during the conversion to PBOs. When the reaction was carried out using the classical method between acid chlorides and 2-aminophenol monomers, the presence of the *ortho*-hydroxy group lessened the reactivity of the amino group for monomers having electron-withdrawing groups.

Conclusions

A set of new polyamides having o-acyloxy groups has been developed. These polymers showed high film-forming ability and good gas separation properties. Relationships between substituted group size, gas permeability and X-ray diffraction patterns could be outlined. A theoretical and experimental study to figure out how these structures evolve to thermally rearranged materials (TR) was carried out. By means of this study, a relationship between groups attached to the aromatic rings, and ability to undergo a thermal rearrangement could be established.

Acknowledgements

Authors are indebted for their economic support to MICINN (projects MAT2010-20668 and MAT2008-00619) and to Junta de Castilla y León through the GR-18 Excellence Group.

References

(1) Budd, P.M.; Ghanem, B.S. *Chem. Comm.*, **2004**, *2*, 230.
(2) Park, H.B.; Jung, C.H.; Lee, Y.M.; Hill, A.J.; Pas, S.J.; Mudie, S.T.; Van Wagner, E.; Freeman, B.D.; Cookson, D.J. *Science*, **2007**, *318*,254.
(3) Muñoz, D.M.; Calle, M.; de la Campa, J.G.; de Abajo, J.; Lozano, A.E. *Macromolecules.*, **2009**, *42*, 5892.

Design of experiment - versatile tool for structure-property relationship investigations

Andrey Buryak Borealis Polyolefine GmbH,

Innovation & Technology, St.-Peter- Strasse 25, 4021 Linz, Austria

andrey.buryak@borealisgroup.com

Introduction: Even though the basic relationships between polymer structure and final application properties of polyethylene are already established in the literature [1-3], continuous material improvement is still ongoing. In this work a systematic investigation of structure-property relationships in bimodal polyethylene was carried out with the help of design of experiment. Applicability of the approach for the structure-property investigation studies and material optimization is discussed.

Materials and Methods: A series of bimodal polyethylene resins consisting of high and low molecular weight fractions were produced in a multistage polymerization process using a Ziegler-Natta catalyst. Four polymer design parameters were varied: 1st component melt flow rate, final melt flow rate, final resin density and the split between the two fractions.

Vertical: Final melt flow rate (5.0 kg), g/10 min
Horizontal: 1st component melt flow rate (2.16 kg), g/10 min

Tensile and impact (V-notched Charpy) properties of the produced resins were measured on specimens prepared

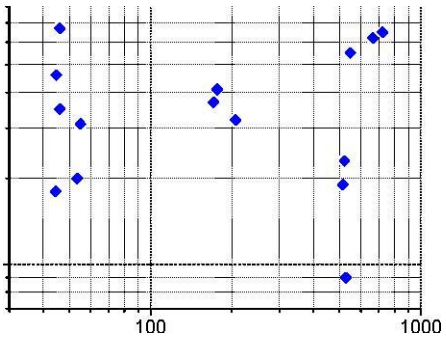

from compression moulded plates and correlated to the polymer design parameters.

Results and Discussion: The results of V-notched Charpy impact at 0°C can be reliably predicted from the polymer design variables (R^2 = 0.94) as can be seen from the graph below. The same is true for the impact measured at -20 °C. In both cases, high molecular weight of the first and the second components, higher amount of the high molecular weight component as well as lower final density were found to be favourable for high impact resistance.

An equally good model (R^2 = 0.94) was derived to predict the yield stress of the investigated bimodal HDPE resins. Along with the expected density influence, a statistically significant contribution from the final polymer melt flow rate was detected, indicating the influence of melt viscosity on the final crystallinity of compression moulded specimens.

Conclusions: The presented results show that design of experiment is a very convenient and versatile tool for systematic investigation of structure-property relationships in complex polymer systems. In a single series of experiments the influence of several polymer design parameters on the properties of interest can be evaluated

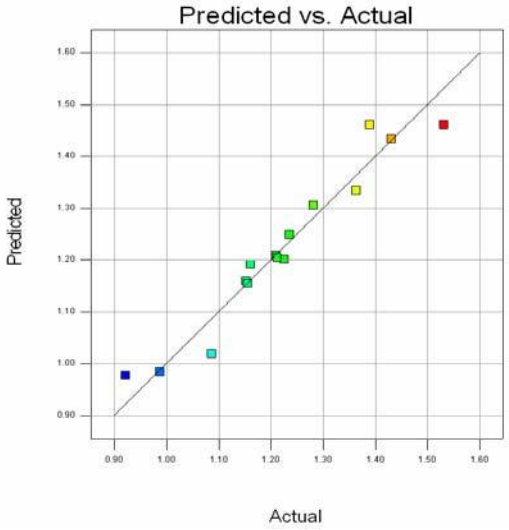

while minimizing the number of experiments and improving the efficiency of research work.

References:

[1] R. Nunes et al., Polym. Eng. Sci. *22* (1982), 205-228
[2] L. Mandelkern et al., Macrocolecules *27* (1994), 5297-5310
[3] R. Krishnaswamy et. al., Macromolecules 41 (2008), 1693-1704

Synthesis and characterization of star-shaped conjugated systems with Triphenylamine core for photovoltaic applications

N. Metri, X. Sallenave, C. Plesse, L. Beouch, P.H. Aubert, G. Sini, F. Goubard, C. Chevrot

Laboratoire de Physicochimie des Polymères et Interfaces (LPPI), Cergy-Pontoise University. 5 mail Gay Lussac, 95031 Cergy-Pontoise Cedex, France

noura.metri@u-cergy.fr

The objective of this work concerns the synthesis and characterizations of novel conjugated organic molecules which were subsequently designed as hole-transporting materials in DSSCs based on TiO_2. These molecules must have the following properties: (i) a high hole mobility, (ii) an excellent pore-filling in TiO_2, and finally (iii) a weak trend to crystallization.

Currently, the reference molecule, Spiro-MeOTAD (2,2',7,7'-tetrakis-(N,N-di-p-methoxyphenyl-amine)-9.9'-SPIROBIFLUORENE) developed by Grätzel, has achieved photovoltaic conversion efficiencies around 5.1%.[1]

The approach developed in our laboratory involves the synthesis of five star-shaped molecules (**1-5**) with triphenylamine (TPA) core and Thieno[3,2-*b*]Thiophene (TTh) derivates which lead to amorphous materials with isotropic optical and charge carrier properties. We will present the synthesis methods used for these compounds and their thermal, optical and electrochemical characterization. Particular attention will be focused on determining the HOMO and LUMO energy levels of these new materials and their optical gap, which must remain high enough to limit any competition for absorption with the sensitizing dye. Finally, molecular engineering will be discussed in order to adjust ideally these properties for the photovoltaic application.

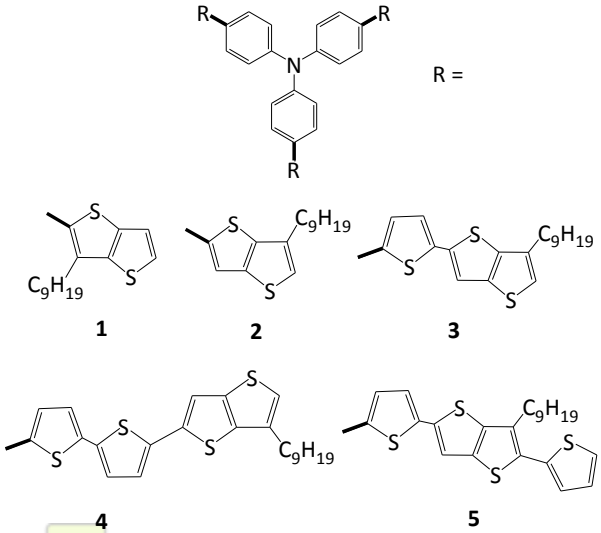

Five star-shaped molecules

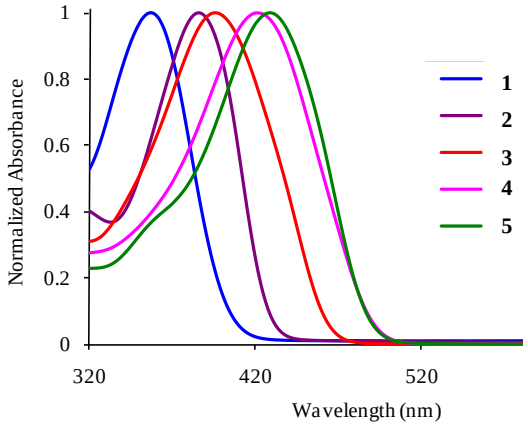

Absorption Spectra of compounds **1-5**

[1] Snaith, H.J.; Moule, A.J.; Grätzel, M. *Nano Lett.*, **2007**, *7*, No. 11, 3372

Functionalization of Polystyrene Surfaces

A. del Prado-Abellán, N. Briz, A. Gallardo, C. Elvira, H. Reinecke ICTP-CSIC, Madrid, Calle Juan de la Cierva, 3.

hreinecke@ictp.csic.es Introduction

One of the polymer most commonly used as a support for microessays is polystyrene (PS) due to its easy processability, low costs and, more importantly, its transparency. This work is focused on the controlled chemical modification of PS surface, creating thus functional groups for the insertion of molecules for the use in clinical essays or for separation of compounds. The functionalization of PS surfaces with SO2Cl groups, recently patented in our group, can be performed by a wet-chemical treatment in solution of concentrated chlorsulfonic acid at different times. The transparency of the modified surfaces is completely maintained upon this reaction. Being strong electrophiles the created functional groups are capable of reacting in a second step with nucleophiles such as amines, alcohol and thiols. The use of bifunctional nucleophiles allows binding of a huge number of different functional groups to the surface. These modifications where observed by spectroscopic techniques such as RAMAN and ATRIR. A concentration gradient on a nanometer scale of functional groups along the cross section of the polymer is formed. The aim of the present work is to study in more detail the distribution of these groups. Therefore, model compounds of well defined polymer-substrate systems have been prepared using a bottom-up approach.

Materials and methods

Monomer, p-vinylphenylsulfonyl chloride, was obtained using sodium p-vinylphenylsulfonate and thionyl chloride with catalytic amounts of DMF [1] (figure 1).

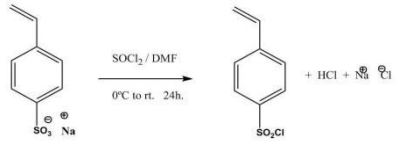

Figure 1: Synthesis of p-vinylphenylsulfonyl chloride.

The polymerization of this monomer was performed through radical polymerization in dissolution using the thermal initiator 2,2'-azobis-isobutyronitrile (AIBN) in toluene. Homopolymer and copolymers with different amounts of pure styrene were synthesized (figure 2).

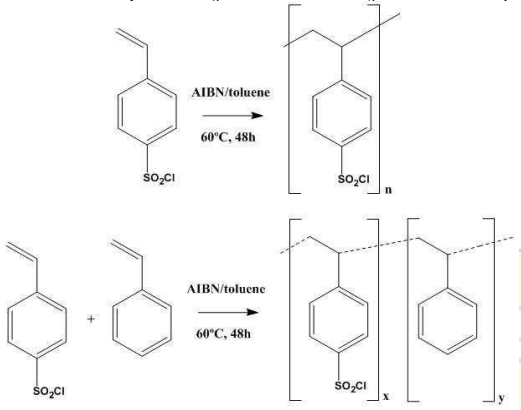

Figure 2: Polymerization in disolution of the modified monomer with and without comonomer.

Results and discussion

In order to establish a regular, structurally homogeneous surface with known number of chlorsulfonyl groups the most appropriate method is a bottom-up approach. In contrast to the chemical modification of PS by chlorosulfonic acid one starts here with a monomer (p-vinylphenylsulfonyl chloride) and obtains the corresponding polymer with the same functional group by radical polymerization. The obtained polymeric materials were studied by ATR-IR. Peaks at 1170 and 1370 cm^{-1} indicate the presence of SO2Cl units. In order to compare the ATR-IR spectra of homopolymer and copolymers of different compositions (figure 3), the spectra are normalized with respect to the signal at 1450 cm^{-1} that corresponds to C-H bonds of the polymeric chains and should not be affected by the substitutent in para position of the aromatic ring. After normalization one can correlate the intensity of the signals corresponding to SO2Cl groups to their quantity in the polymer. Comparing these IR spectra with those measured on PS surfaces functionalized by chemical modification with chlorosulfonic acid one can state an excellent concordance. This is an indication that the functionalization with SO2Cl takes place in a controlled and selective way without detectable side-reactions.

Conclusion

In this contribution a detailed characterization of the modified surfaces is given and possible applications of the modified surfaces are discussed.

Reference

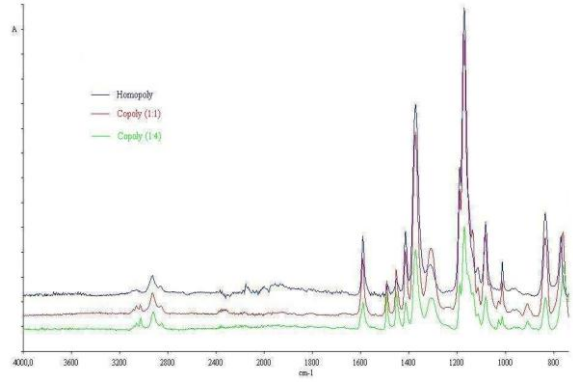

[1] H. Kamogawa, A. Kanzawa, M. Kadoya, T. Nayto, M. Nanasawa. Bull. Chem. Soc. Jpn, **1983**, (56) 762-765.

Acknowledgment

Authors gratefully acknowledge support from MAT-2010-20001. A. del Prado-Abellán acknowledges MEC the scholarship provided by MEC

Enhancing the Formation of the New Trigonal Polymorph in iPP-1-Pentene Copolymers

Ernesto Pérez, María L. Cerrada, Rosario Benavente and José M. Gómez-Elvira

Instituto de Ciencia y Tecnología de Polímeros (CSIC), Juan de la Cierva 3, 28006-Madrid (Spain) e-mail: mlcerrada@ictp.csic.es

Isotactic polypropylene, iPP, and its copolymers with other alpha-olefins are attracting an enormous interest, both industrially and academically, since a long time ago. One of the most striking reasons for the academic interest is the amazing polymorphism exhibited by these materials. Thus, depending on microstructural features, crystallization conditions and other factors like the use of specific nucleants, three different polymorphic modifications, α, β and γ, all sharing a three-fold conformation, have been reported [1,2]. Moreover, fast quenching of iPP leads to a phase of intermediate or mesomorphic order, which, on heating, undergoes a transformation into the α form.

In addition to those four modifications, a new trigonal form has been recently described [3-6] in the case of copolymers of iPP with high contents of 1hexene or 1-pentene as comonomers, named as δ form. In those reports, the new trigonal δ modification is the only one obtained for comonomer contents above around 14 mol-%, while variable proportions of it with the α modification were found in the comonomer range from around 8 to 13 mol-%. For these intermediate contents, it has been recently established [5] that the mesomorphic modification, as well as the α crystals, are competitors in the formation of the new trigonal modification.

One of the most interesting characteristics of those copolymers exhibiting the δ form is the surprisingly high degrees of crystallinity attained, reported to be on the order from around 25 to 40% for comonomer contents ranging from 15 to 30 mol-% of counits. The thermal history imposed to these samples is generally a cooling from the isotropic melt to room temperature, and the ageing at ambient conditions for long times (months).

With these considerations, a plausible question arises immediately: is it possible to enhance even more those unexpectedly high crystallinities? This is precisely the aim of the present communication, by imposing different crystallization conditions to a copolymer of iPP and 1-pentene.

The copolymerization of propylene and 1-pentene was carried out in toluene, with rac-dimethylsilylbis(1-indenyl)zirconium dichloride/MAO as the catalyst/co-catalyst system. This presentation deals with a copolymer, named as cPPe13, with the following characteristics: 1-pentene content in the copolymer:

13.0 mol-%, M_w: 103000 g/mol, M_n: 49900 g/mol, *mmmm* content: 90.3%.

Film samples of copolymer cPPe13 were obtained from the reactor powder by compression molding in a Collin press between hot plates, and subsequently cooled down to room temperature under two different thermal treatments: a relatively fast cooling between plates refrigerated with cold water after the melting of the material in the press (sample cPPe13Q, cooling rate around 80 °C/min), and a slow cooling at the inherent cooling rate of the press, after the power was switched off (sample cPPe13S, cooling rate around 1.5 °C/min).

A sample cast from hexane (cPPe13cast) and a specimen annealed at 65 °C (cPPe13ann65) were also prepared and analyzed.

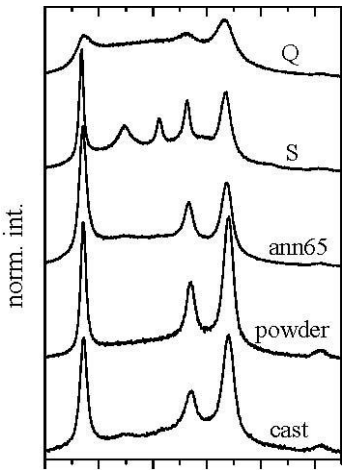

Fig. 1. Room-temperature X-ray diffractograms of the indicated specimens of copolymer cPPe13.

The X-ray diffraction results indicate a very interesting polymorphism in this copolymer, and, when crystallized from solution, amazingly high degrees of crystallinity are obtained, which can be as high as 65%, on the order of those ones obtained for iPP homopolymer.

References:

1) Brückner S, Meille SV, Petraccone V, Pirozzi B. Prog Polym Sci 1991;16: 361. 2) Phillips P. J., Mezghani K., In Salamone JC, editor. The Polymeric Materials Encyclopedia, CRC Press: Boca Raton, 1996. Vol. 9, p. 6637. 3) a) Poon B, Rogunova M, Hiltner A, Baer E, Chum SP, Galeski A, Piorkowska E. Macromolecules 2005;38:1232; b) Lotz B, Ruan J, Thierry A, Alfonso GC, Hiltner A, Baer E, Piorkowska E, Galeski A. Macromolecules 2006;39:5777. 4) a) De Rosa C, Dello Iacono S, Auriemma F, Ciaccia E, Resconi L. Macromolecules 2006;39:6098 b) De Rosa C, Auriemma F, Corradini P, Tarallo O, Dello Iacono S, Ciaccia E, Resconi L. J Am Chem Soc 2006;128:80. 5) Cerrada ML, Polo-Corpa MJ, Benavente R, Pérez E, Velilla T, Quijada R. Macromolecules 2009;42:702. 6) Stagnaro P, Boragno L, Canetti M, Forlini F, Azzurri F, Alfonso GC. Polymer 2009;50:5242.

Acknowledgements

The financial support of MICINN (Projects MAT2007 65519-C02-01, MAT2010-19883 and PET2008-0108) is gratefully acknowledged.

Persistence of order in liquid crystalline copolymers

V. Rodríguez-Amor, J. P. Fernández-Blázquez, M. L. Cerrada, A. Bello and E. Pérez

Instituto de Ciencia y Tecnología de Polímeros (CSIC), Juan de la Cierva 3, 28006-Madrid (Spain)

e-mail: ernestop@ictp.csic.es

There has been in the last decades an intensive research dedicated to study the crystallization of liquid-crystalline (LC) copolyesters (1-3). In principle, the different chemical units of a random copolymer are not able to contribute fully to the three-dimensional periodicity of the crystal lattice (1), but yet they can crystallize by segregation and lateral matching of identical sequences. It can be anticipated that the tolerance of counits will be even easier for LC phases, due to their lower packing requirements.

For instance, in the SmA phase the molecules are arranged in layers so that their long axes are on average perpendicular to the layer planes, displaying one-dimensional (quasi) long-range order, but there is no translational periodicity in the planes of the layers or between the layers. This layering leads to a number of equally-spaced low-angle pseudo-Bragg peaks, although the tendency for layering is usually rather weak. The implication is that only the first one or two pseudo-Bragg peaks have observable intensity.

However, it has been reported (4) that the X-ray diffraction patterns of some polymeric SmA phases show more than one order of reflection from the layers, and that the first order is not necessarily the strongest.

Besides the introduction of flexible spacers, the copolymerization with non-mesogenic monomers is a widely used strategy in LC polymers in order to tailor the transition temperatures and the final properties (3,5).

This work presents the results about the persistence of order in main-chain LC copolyesters of bibenzoate (B) and terephthalate (T) units.

The copolymers and the homopolymers have been synthesized by melt transesterification of different proportion of diethyl *p,p'*-bibenzoate and dimethyl *p,p'*-terephthalate with diethylene glycol. The chemical composition of the sample was analyzed by ^{13}C-NMR spectroscopy, and the molecular weights were obtained by SEC. The results are the following:

Sample	mol % T	M_n (g/mol)	M_w (g/mol)
PDEB	0	15800	31200
CDETB8	8	23700	45200
CDETB18	18	17800	33300
CDETB27	27	14800	28300
CDETB38	38	20100	41300
PDET	100	50400	156000

Variable temperature X-ray diffraction experiments were performed by employing synchrotron in beamline A2 at HASYLAB (Hamburg, Germany).

The X-ray diffractograms of these samples cooled from the melt to room temperature show a broad amorphous-like diffraction in the wide-angle region, and a narrow diffraction in the middle-angle region (and several orders), corresponding to the layer spacing. This layer spacing shifts slightly to higher angles (lower *d* values) as the T content increases.

But more interesting is the behavior of the intensity of these smectic layer orders. Thus, and contrary to the case of other reported polybibenzoates, up to 4 orders are observed for the homopolymer PDEB, and, interestingly, the second order is slightly more intense than the first one. For the copolymers, besides the slight change of the layer spacing, a more important variation is observed in the relative intensities of the different orders, the intensities of the higher orders decreasing very much with the T content in the copolymer.

By subtracting the corresponding amorphous-like broad diffraction, the different orders of the layer spacing can be isolated, and a kind of electron density profile has been obtained by appropriate Fourier transformation. These profiles are shown below:

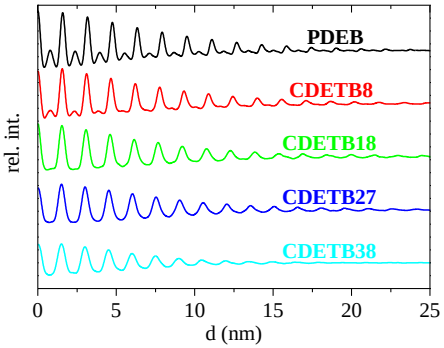

It can be observed that the correlation length decreases slightly with the T content, and, more importantly, they display a pseudoperiodicity *d*/2 which is very evident in the homopolymer PDEB, but undergoes a continuous vanishing as the T content increase, in such a way that the profile for copolymer CDETB38 is close to the one arising from a single sinusoidal function.

In conclusion, the persistence of liquid-crystalline order is well evident in these copolymers.

References

1) S. Hanna, A. Romo-Uribe, A. H. Windle, Nature (London) 1993, 366, 546.

2) A. Biswas, J. Blackwell, Macromolecules 1988, 21, 3146.

3) H. Ma, T. Uchida, D. M. Collard, D. A. Schiraldi, S. Kumar, Macromolecules 2004, 37, 7643.

4) P. Davidson, Prog. Polym. Sci. 1996, 21, 893.

5) J. Pérez-Manzano, J. P. Fernández-Blázquez, A. Bello, E. Pérez, Polymer Bull. 2006, 56, 571.

Acknowledgements

The financial support of MICINN (Projects MAT2007 65519-C02-01 and MAT2010-19883) is gratefully acknowledged. The synchrotron work at Hasylab was supported by the European Community (FP7/2007-2013, grant agreement 226716). We thank the collaboration of the Hasylab personnel.

Mineralization Ability Of HEMA-AMPSA Copolymers Incubated In Simulated Body Fluid

Paul Stanescu, Catalin Zaharia, Corneliu Cincu, Florin Miculescu

Politehnica University of Bucharest, Department of Science and Engineering of Polymers, Calea Victoriei 149, 010072 Bucharest, Romania

paul_stanescu@yahoo.com

INTRODUCTION: Preparation of new biocompatible materials for bone reconstruction has consistently gained interest in the last few decades. Wide ranges of materials were used as synthetic bone grafts. The design of osteoconductive behaviour is considered one of the most important characteristics of natural grafts, consisting especially in apatite-type content. The use of polymers for bone repair allows the synthesis of numerous biomaterials with specific structure and properties. Polymers are used in osseous applications due to their wide chemical composition, to their different mechanical behaviour and because the organic bone matrix are mainly formed by macromolecules [1]. In order to form apatite deposits in/on the implant, after implantation, polymer must contain negative chemical groups, in order to mimic the activity of bone proteins responsible for mineralization. The present research focuses on the preparation and characterization of 2-hydroxyethyl methacrylate (HEMA) and 2-acrylamido-2-methylpropane sulphonic acid copolymers as scaffolds for bone pathology.

MATERIALS AND METHODS: The polymeric matrices were synthesized by bulk radical polymerization using benzoyle peroxide as initiator and ethylene glycol dimethacrylate as cross-linking agent. Various increasing molar concentrations of AMPSA were used to obtain copolymer pellets (3 %, 5 %, 10 % molar content of AMPSA in feed). Polymerizations were conducted at 80 °C for 12 h. There were obtained polymeric pellets with flat shape and maximum surface, which were extracted in Soxhlet for 12 h with distilled water to remove any traces of the residual monomer that could negatively influence the in vitro assays. ATR-FTIR spectra of the copolymers were obtained at 20 °C and constant 40 % relative humidity. For mineralization tests, three samples of copolymer were incubated in synthetic body fluid (SBF1x, protocol of Professor Kokubo T.) at pH 7.45, adjusted with tris(hydroxy-methyl) aminomethane (Tris) and hydrochloric acid HCl, for 14 days, under sterile conditions, in containers with 50 mL of the incubation medium at 37 °C. The surface morphology after incubation was examined using scanning electron microscopy (SEM) coupled with energy dispersive X-rays spectroscopy (EDX). Polymers biocompatibility was verified by testing their in vitro cytotoxicity and viability on J774.2 cell line.

RESULTS AND DISCUSSION: Series of p(HEMA-co-AMPSA) copolymers with increasing molar concentrations of AMPSA were synthesized by bulk polymerization procedure. FTIR-ATR spectra showed absorbance wavelengths of the specific bonds which appeared in the polymers obtained (tertiary C atom at 1539.1 cm^{-1} from AMPSA), confirming the structure of the new materials (spectra not shown here). During incubation in SBF, several micro-cracks appeared on all polymeric surfaces. Scanning electronic microscopy (SEM) and energy dispersive X-rays (EDX) showed the presence of apatite deposits onto the surfaces of p(HEMA-co-AMPSA) copolymers incubated in SBF 1x. Best results were observed onto surface of p(HEMA-co-AMPSA) polymers with 10 and 15 % (molar) AMPSA (figure 1). This sustains the idea that negatively-charged sulphonic groups have a major influence upon the mineralization process of biomaterials. EDX spectra proved also the presence of nice HA crystals onto polymeric surfaces (Ca/P molar ratio of 1.68 and 1.7). The most promising polymers for mineralization potential having 5 and 10 % AMPSA molar content were then submitted to cytotoxicity and viability tests. Most of the cells retained their typical morphology of J774.2 cells with more and more extensions. A lot of cells could be evidenced at the polymer surface. Slightly toxic effects were noticed for polymers with 10 % AMPSA molar content in the feed. Probably the toxic limit concentration of AMPSA for the cells was achieved.

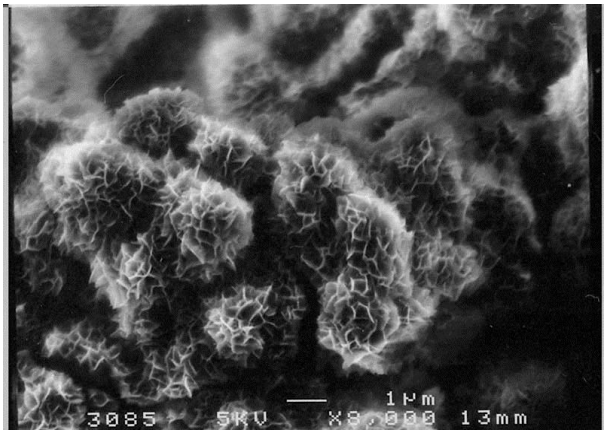

Fig.1. SEM microphotographs for p(HEMA-co-AMPSA) with 10 % AMPSA molar content in the feed incubated in SBF 1x

CONCLUSIONS: This research work offers an interesting perspective of the mineralization process of HEMA-based copolymers with sulphonic groups incubated in SBF 1x. Therefore, the new synthesized materials represent potential scaffolds for apatite crystal growth stimulation in bone tissue engineering.

ACKNOWLEDGEMENTS:

Authors recognise financial support from the European Social Fund through POSDRU/89/1.5/S/54785 project: "Postdoctoral Program for Advanced Research in the field of nanomaterials".

REFERENCES:

[1]. D.Puppi, F. Chiellini, A.M. Piras, E. Chiellini, *Polymeric materials for bone and cartilage repair*, Progress in Polymer Science, 35(4), 2010, pp. 403-440.

Experimental Investigation of Crosslinked Polymer Formulation for Drilling Fluid Approach to Modified Rheological Properties in Carbonate Wells

*Yousef Tamsilian, Ahmad Ramazani S.A**

Sharif University of Technology, Department of Chemical and Petroleum Engineering, Tehran, Iran

*Email: ramazani@sharif.edu

Abstract

To modified rheological properties of drilling mud, preparation of appropriate hydrogels from Chitosan N-Isopropylacrylamide hydrogels by thermal and gamma radiation have been considered. In the thermal method, initiator and crosslinking agent have been used where gamma radiation process have been done in absence of any kind of initiator and crosslinking agents. Presented results illustrate that the gamma radiation method produced hydrogel with higher water swelling ratio. Rheological properties of modified hydrogel drilling fluid, such as apparent viscosity, plastic viscosity, gel strengthen, and yield point were investigated and compared with those of Cellulosemethylcarboxyl (CMC) and Xanthenes (XC) resins prepared drilling fluids which are widely used in drilling fluids. The hydrogel synthesized by gamma radiation showed improving rheological properties for drilling fluid comparing to CMC, XC, and thermally prepared hydrogel. Obtained results depict that increase in gamma radiation dose and monomer concentration which rendered high swelling hydrogels, were more suitable for improving drilling mud application. In other words, presented results demonstrate that whereas linear polymer effects on mud properties are more significant in polymer low concentration, prepared crosslinked hydrogel effects are more significant at high concentrations.

Key words: polymer, hydrogel, chitosan, drilling fluid, rheological properties

Hybrid composites based on Polypropylene (PP): Mechanical Properties of PP/Talc Composites Reinforced with different Calcium based Inorganic Fillers

M. Yazdani-Pedram [1], H. Aguilar [1], P. Toro [2], R. Quijada [2]

[1]Facultad de Ciencias Químicas y Farmacéuticas, Universidad de Chile, S. Livingstone 1007, Santiago, Chile.
[2]Facultad de Ciencias Físicas y Matemáticas, Universidad de Chile, Santiago, Chile.

mypedram @gmail.com

Introduction: Recently, it has been observed that by incorporating filler particles into the matrix of talc reinforced polymeric composites, synergistic effects may be achieved in the form of higher modulus and reduced material costs, yet accompanied with decreased strength and impact toughness [1]. Such multicomponent hybrid composites based on poly (butylene terephtalate) (PBT) [2], acrylonitrile–butadiene–styrene copolymer (ABS) [3] and polypropylene (PP) [4] matrices have been studied. The aim of this work was to study the effect, on the mechanical properties, of the addition of second reinforcing filler such as mineral calcium carbonate (CC) or biomineralized calcium carbonate from eggshells (BCC) or a synthetic calcium silicate (SiCa) to the PP/talc composite.

Materials and Methods: The PP used was an isotactic homopolymer with melt flow index of 13 g/10 min, 230 °C, 2.16 Kg. The fillers used was: talc (TA) from Reverte with particle size d(50)=2.4 µm and surface area (SA) of 6.3 $m^2 g^{-1}$; CC from Reverte with d(50)=0.7 µm and SA of 9.1 $m^2 g^{-1}$; BCC with d(50)=8.4 µm and SA of 18.0 $m^2 g^{-1}$ and SiCa was kindly donated by professor T. Borrmann, Victoria University of Wellington, New Zeland with d(50)=12.0 µm and SA of 243.1 $m^2 g^{-1}$. The composites were prepared by melt mixing of the PP with one filler (reinforced composites) or a 1/1 mixture of fillers such as TA/CC or TA/BCC or TA/SiCa (hybrid composites). These composites were obtained by using a Brabender-Plasticorder batch mixer at a constant temperature of 190 °C during 15 minutes at a rotor speed of 75 rpm and under nitrogen atmosphere to prevent polymer oxidation. After the melt mixing, the tensile mechanical tests were performed according to the ASTM D 638-95.

Results and Discussion: Our study showed that the tensile modulus of PP/TA composites was improved by adding other inorganic fillers such as CC or BCC or SiCa. It was shown that the addition of any calcium-based inorganic reinforcements in PP/TA composites increased the stiffness according to the filler contents up to 20 wt.-%. On the other hand, the strength and toughness were decreased and the elongation at break is simultaneously reduced according the filler content. This effect could be attributed to the fact that reinforcing calcium based inorganic fillers strongly restrain the deformation of the polymer matrix as demonstrated in previous studies [5].

As shown in Figure 1, the enhancement of Young modulus of PP/TA reinforced composites compared with PP/calcium based inorganic filler composites and hybrid PP/TA reinforced composites depend on both compositions and surface areas of the filler. In particular, the BCC filler represent a new natural alternative reinforcing filler for PP and show a higher stiffness than the similar PP/CC composites. The better reinforcing effect of the BCC could be attributed to its higher surface area than the CC or talc filler. In the case of hybrid composites, it was observed that up to 50 wt.-% replacement of talc by CC or BCC or SiCa did not affect the Young modulus. This replacement of talc filler depend on the type and filler content and showed a higher modulus for PP/TA-BCC or PP/TA-SiCa hybrid composites than the PP/TA composite up to 20 wt.% of filler content. The addition of filler with higher surface area could promote a better dispersion of filler in the polymer matrix. Beside, a more phase homogeneity could be the explanation of this enhancement of the stiffness in the hybrid PP composites with TA-BCC or TA-SiCa fillers.

Conclusions: The mechanical properties of PP/talc composite could be improved by the addition of second micrometric filler based on calcium with higher surface area than talc.

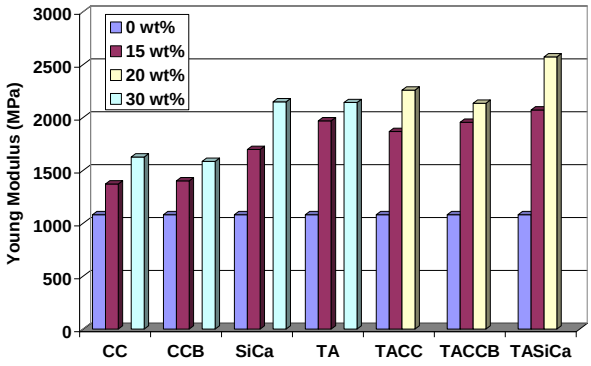

Figure 1. Young modulus of mineral filled composites: (CC =PP/CC; BCC = PP/BCC; SiCa = PP/SiCa; TA= PP/TA composites) and hybrid PP/talc (TACC= PP/TA-CC; TA-BCC=PP/TA-BCC; TASiCa=PP/TA-SiCa).

References:

1. Y.W. Leong, Z.A.Mohd Ishak, A.Ariffin, J. Appl. Polym. Sci., 91, 3327-3336 (2004)
2. N. Hargarter, K. Friedrich, P. Catsman, Compos. Sci. Technol., 46, 229–44 (1993)
3. S-Y Fu, B. Lauke, Composites: Part A, 29, 575–83 (1998)
4. Y. W. Leong, M. B. Abu Bakr, Z. A. Mohd Ishak, A. Ariffin, J. Appl. Polym. Sci., 98, 413–426 (2005)
5. J. S. Szabo, T. Czigany, J. Macromol. Sci., Phys. B, 41, 1191–204 (2002)

Acknowledgements: Financial support of Conicyt through Project FONDECYT 1090260 and Vicerectoria de Investigación y Desarrollo (VID), Universidad de Chile are greatly appreciated

Hot melt poly-ε-caprolactone/poloxamine implantable blends that sustain the release of ciprofloxacin

Ana M. Puga1, Carmen Alvarez-Lorenzo1, Beatriz Magariños2, Ángel Concheiro1

1Dept. Farmacia y Tecnología Farmacéutica. 2 Dept. Microbiología, Facultad de Farmacia, Universidad de Santiago de Compostela, 15782-Santiago de Compostela, España

e-mail: anapuga.azcarate@gmail.com

Introduction

Implants that serve as cell scaffolds and as drug delivery systems to prevent infections enable a faster healing of the tissues. This is particularly useful for the management of osteomyelitis, since the local administration of antimicrobials reduces adverse effects of the systemic treatment (1). Poly-ε-caprolactone (PCL) is a common component of biodegradable implants that erodes slowly due to its high hidrophobicity. Blending with other polymers may accelerate its degradation (2). On the other hand, injectable implants are attracting raising interest. Poloxamines (Tetronic®) are pH- and temperatureresponsive block copolymers that render *in situ* gelling solutions (3). The aim of this work was to prepare implants based on blends of PCL and poloxamines, applying hot melting without organic solvents, that are able to control the release of ciprofloxacin.

Materials and methods

Materials

Poloxamines Tetronic® 908, 1107, 1301 and 1307 were from BASF (New Milford, CT, USA). Ciprofloxacin was from Fagron (Spain) and PCL from Sigma-Aldrich (Mn 42500 Da, St. Louis MO, USA).

Preparation of implants by hot melting

Implants containing PCL and poloxamine in different ratios (0:1, 0.25:0.75, 0.50:0.50, 0.75:0.25, 1:0) and ciprofloxacin (10 mg/g) were obtained by melting at 80ºC under stirring. Then, implants were cooled in a water-ice bath and stored protected from light.

Ciprofloxacin release

Phosphate buffer pH 7.4 (10 ml) at 37ºC was added to test tubes containing the implants prepared at 80ºC. Ciprofloxacin release was monitored spectrophotometrically at 271 nm (Agilent 8453, Germany) while keeping the systems under oscillation movements (25 osc/min).

In vitro degradation assay

PCL:poloxamine implants were weighted and pretreated with NaOH 5M (10 ml) for 72 h at 20ºC. The medium was then replaced by phosphate buffer pH 7.4 (10 ml) at 37ºC. At prestablished times implants were removed, washed with water, dried for 12 h at 37ºC and weighted. Finally they were immersed again in phosphate buffer.

In vitro microbiological study

Staphylococcus aureus ATCC25923 was inoculated in Falcon® tubes containing Mueller-Hinton broth at a concentration of 3.2 x 106 CFU/ml. Implants, with and without drug, were incubated in this suspension at 37ºC for 24 h and the resistence of *S. aureus* to the drug was monitored by colony counts.

Results and discussion

Ciprofloxacin release

Implants containing solely PCL released ciprofloxacin very slowly; increasing the poloxamine ratio, the drug release rate accelerates.

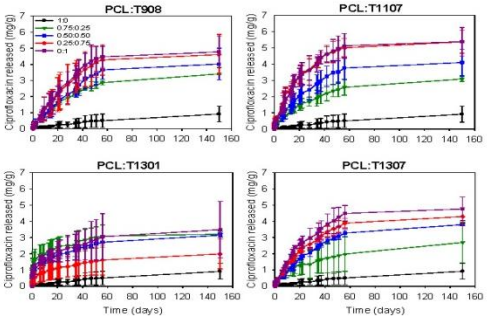

Figure 1. Ciprofloxacin release in phosphate buffer pH 7.4 from PCL:poloxamine implants prepared at 80ºC.

In vitro degradation assay

PCL implants eroded very slowly; as poloxamine content increases, erosion process turns faster.

In vitro microbiological study

In vitro microbiological assays confirmed the effectiveness of the implants with drug against *Staphylococcus aureus*. Although after 24 h some colonies could be observed in the test tubes, after 48 h bacterial growth was almost negligible.

	24h	48h	72h
T908:PCL			
0.5:0.5	$1{,}6 \times 10^{1}$	<10	<10
1:0	$4{,}9 \times 10^{2}$	<10	<10
T1107:PCL			
0.5:0.5	<10	<10	<10
1:0	<10	<10	<10
T1301:PCL			
0.5:0.5	$3{,}1 \times 10^{2}$	<10	<10
1:0	$3{,}7 \times 10^{2}$	<10	<10
T1307:PCL			
0.5:0.5	<10	<10	<10
1:0	$2{,}8 \times 10^{1}$	<10	<10
T:PCL			
0:1	<10	<10	<10

Table 1. *Staphylococcus aureus* CFU/ml in Mueller-Hinton broth containing PCL:poloxamine implants with ciprofloxacin (10 mg/g).

Conclusions

PPCL:poloxamine implants can be easily obtained by hotmelting without using organic solvents. Drug releaseand erosion profiles can be tuned varying the ratio ofeach component in the blend composition.Microbiological tests indicate that the implants arepotentially useful for the osteomyelitis treatment.CL:poloxamine implants can be easily obtained by hot melting without using organic solvents..

.

References

(1) Leprere et al., Biomaterials 30:6086-6093 (2009)
(2) Lam et al., Biomed. Mater.Res. 90A:906-919 (2009)
(3) Alvarez-Lorenzo et al., Front. Biosci. E2:424-440 (2010)

Monomers *vs* Polymers of Cu(III) Corroles on Reduction of O_2

Jorge Vélez, *F. Isaacs*, *M. J. Aguirre*

Dpto. de Química de los Materiales, Facultad de Química y Biología, Universidad de Santiago de Chile, Casilla 40, Correo 33, Santiago, Chile.

Jorge.velez@usach.cl

Introduction:

Corroles, macrocycles belonging to the porphyrinic family (1,2), stabilize transition metals of in high and unusual oxidation states due to the contraction of the ring originated by the loss of one of the meso carbons. Metalocorroles are of special interest since there can achieve displacements of potential and valuable increases of current in the reaction of O_2 reduction (3) simulating enzymatical reactions of this type. In this work we present the characterization of two Cu(III) corroles (Fig. 1) and their behavior in the electrorreducción of O_2 in aqueous solutions at different values of pH.

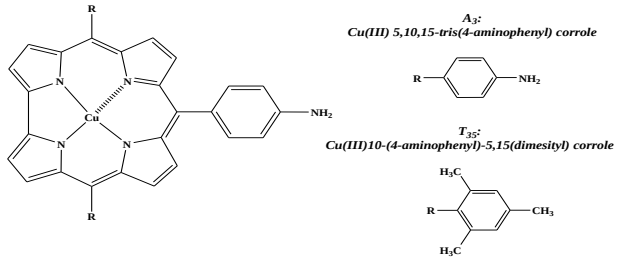

Fig.1. Structure of Cu(III) corroles studied.

Experimental

Glassy carbon electrodes were modified by evaporation of a drop and by electropolymerization of the corrolic solution in DMF. The electrochemical experiments were performed with CH-Instruments (Austin, TX, USA) Model 600B. A three-electrode system was used and consisted of a glassy carbon working electrode, a platinum wire counter electrode, and Ag/AgCl reference electrode. The activity of the modified electrodes for the oxygen reduction were performed in aqueous solutions at different pH values (3, 7 and 12) in N_2 athmosphere.

Results and Discussion

In the electrochemistry characterization of the corroles in DMF's solution (Fig. 2) three reversible waves are observed for the A_3 complex, whereas the complex T_{35} presented two reversible waves and a cathodic irreversible peak. The waves showed as II for both complexes centred to $E_{1/2}$ -0.22 and -0.12 V might correspond to the metallic couple Cu the (III)/ (II).

Knowledges

- Fondecyt 3100066
- Beca Apoyo termino de tesis Conicyt 24081014

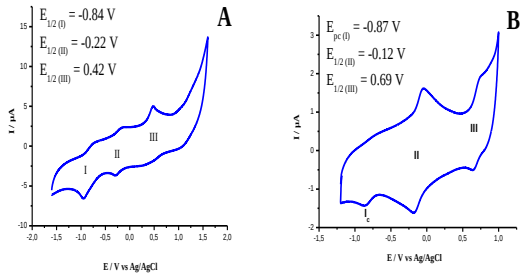

Fig. 2: Cyclic voltammograms of the corrolic solutions in DMF/TBAP 0.1M. 0.1 Vs-1, N2. A: Corrol A3, B: Corrol T35.

The electrocatalysis of O_2 reduction hows, in general, that the electropolymerized complexes on CV are more efficient for this reaction, and that of both compounds, which delivers better results to any pH turns out to be the one that possesses three aminophenyl groups in the periphery of the macrocycle, that is to say, the corrol A_3, having the starting wave for this reaction near to the -0.15 V.

In addition, at pH 3 for the complex A_3 (is observed a phenomenon that does not appreciate to any other value of pH worked. As much for the modification realized with drop as well as with electropolymer, there are seen two waves of reduction and one of oxidation. This gives a clear indication that the corrol A_3 in this way is capable of reducing O_2 to H_2O by four electrons.

Conclusions

- The characterization studies of this Cu corroles by NMR ^1H (not showed spectrum) indicate that in these complexes the dominant basal state is the diamagnetic Cu(III).
- In almost all the cases, the system A_3 showed to be more electrocatalytic in the O_2 reduction presenting the potential wave for this reaction near to -0.15 V.
- The number of electrons transferred in the O_2 reduction is four, indicating the reduction from O_2 to H_2O.

References

1. Tezuka, M.; Iwasaki, M. *Chem. Lettrs*. 1998, 27, 1017.
2. Tezuka, M.; Iwasaki, M. *Chem. Letts*. 1993, 22, 427.

Collman, J.P.;Kaplun, M.;Decréau, R.A. *Dalton Trans*. 2006, 4, 554.

Electrical resistance behavior under strain of in situ polymerized polyaniline in swollen NBR

J. C. Encinas[1], *M. M. Castillo-Ortega*[1], *T. Del Castillo-Castro*[1], *P. J. Herrera Franco*[2]

[1]Departamento de Investigación en Polímeros y Materiales, Universidad de Sonora
[2]Centro de Investigación Científica de Yucatán, A.C.

carmelo@polimeros.uson.mx

Introduction

Limitations such as fragility and impact resistance are some of the major problems associated with practical applications of conductive polyaniline. An effective method to overcome some of these problems is by preparing composite materials containing the intrinsically conductive polymer as filler dispersed in thermoplastic matrices [1].

Conducting polymers widely used as sensors are inherently rigid. An effective method to overcome this problem is by preparing composite materials containing the intrinsically conductive polymer as filler dispersed in elastomers such NBR. The preparation methods used has big influence on the electrical and mechanical properties of the composite material. Different blending methods has been studied with the objective of resolve this problems.

Materials and Methods

The fabrication technique is key component to optimizing the properties of the strain sensor. For this work composite material of acrylonitrile butadiene rubber (NBR) and polyaniline was prepared by in situ polymerization of aniline swollen in NBR film. The quantity of absorbed aniline was increased using an organic solvent to swell the NBR. The polymerization was carried out by immersing the swollen NBR films in a solution of copper(II) perchlorate hexahydrate. The resulting films were characterized by SEM, DTA, electrical conductivity, surface resistivity, and mechanical properties with the aim to use as a mechanical stress sensor.

Results and Discussion

Some indication of the high-temperature miscibility of PANI with NBR in their blends may also be gained from the onset temperatures [2]. We measured the thermal properties of the composites using a Perkin Elmer DTA-7. Only small shifts in the onset temperature of the major exotherm are observed indicating that the miscibility is limited in this blend at room temperature.

Uniaxial stress-strain measurements were performed on a universal testing machine. The mechanical properties of the NBR are affected by blending with PANI mainly decreasing the ultimate elongation at break. However composites with the highest content of polyaniline have enough elasticity (199 %) to be used as elastomeric sensor.

The electrical conductivities of composite films were measured by the standard two-point probe method with the electrodes in a sandwich configuration and also by evaluating the surface resistance in one side of the film.

We found that composites have surface conductivity but also have a bulk conductivity indicating presence of polyaniline inside the elastomer not only over the surface like many composites prepared with similar methods of in situ polymerization.

Some samples were subjected to repeated stress-strain cycles in a Universal Testing Machine and the change in electrical resistance was measured. Two electrodes were settled on the grips of a mechanical universal testing machine to measure the change in electrical resistance of the sample during a strain-stress testing. A cycle of elongation at a rate of 44 mm / min was carried out and a graph of the resistance of the sample during the test was obtained.

Repeated cycles displayed a similar behavior showing that the sample could have a use as deformation sensor.

Conclusions

A reversible dependence of electrical resistance at stretch has been only observed in case of nano-size conductive particles [3] while a irreversible tenso-resistive effect is obtained in micro-size particles.

Our results suggest that PANI distribution in NBR matrix plays an important role in tenso-resistive behavior. A stress sensor is proposed using this composite material

References

1. Castillo-Ortega, M. M.; Del Castillo-Castro, T.; Encinas, J. C.; Perez-Tello, M.; De Paoli, M. A.; Olayo, G., *Journal of Applied Polymer Science* **2003,** *89* (1), 179-183.

2. Yong, K. C.; Foot, P. J. S.; Morgan, H.; Cook, S.; Tinker, A. J., *European Polymer Journal* **2006,** *42* (8), 1716-1727.

3. Knite, M.; Teteris, V.; Kiploka, A.; Kaupuzs, J., *Sensors and Actuators a-Physical* **2004,** *110* (1-3), 142-149.

Ultra-thin Electronic Nanocomposites of Carbon Nanotubes and Self Assembled Block Copolymers

Cheolmin Park, *Jinwoo Sung*, *Yeon Sik Choi*, *Sung Hwan Cho*

Department of Materials Science and Engineering, Yonsei University, Seoul, Korea

e-mail: cmpark@yonsei.ac.kr

Introduction

The nanostructures of block copolymers are of great importance due to their capability of fabricating nanocomposites with the functional materials such as quantum dots and single-wall carbon nanotubes (SWNTs). In this presentation, our current efforts will be discussed to develop ultra-thin electronic composite sheets of networked SWNTs self-assembled with various types of block copolymers such as amphiphilic and conjugated block copolymers which have versatile potential applications of low electric resistance sheets for transparent electrodes,[1] semi-conducting channel layers for organic transistors[2] and bipolar hole-electron carrier channel network for high performance electro-luminescence devices.

Results and discussion

The versatile application of the electronic composite sheets is mainly attributed to (1) the efficient dispersion of SWNTs with a conjugated block copolymer, poly(styrene-*block*-paraphenylene) (PS-*b*-PPP), in solution, (2) the control of the number of nanotubes by centrifugation, and (3) the individually networked deposition of SWNTs embedded in the conjugated block copolymer on the target substrate by spin coating as shown in Figure 1.

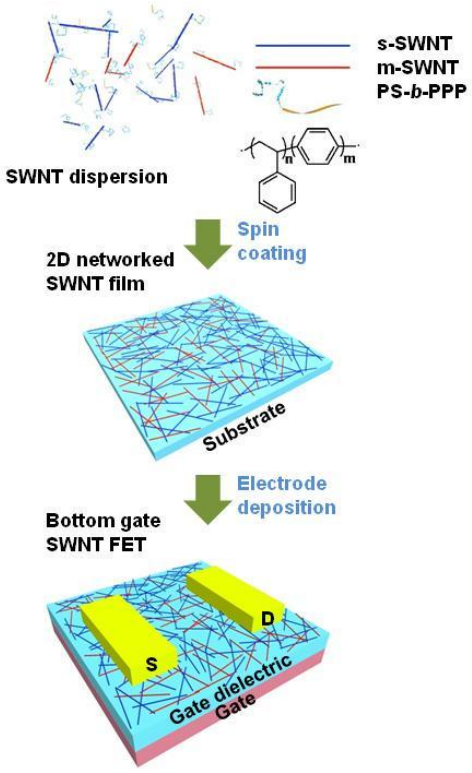

Figure 1. Schematic of field effect transistors fabricated with SWNTs/block copolymer nanocomposites

The individually deposited SWNTs are also visualized in under-focused phase contrast in TEM as shown in Figure 2. A single nanotube is apparent with the characteristic granular domains of approximately 7 nm in diameter in the inset of Figure 2.

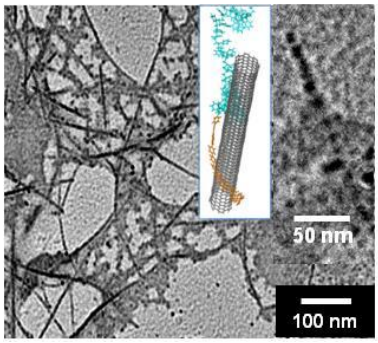

Figure 2. TEM micrograph of a SWNTs/PS-b-PPP nanocomposite

A highly reliable bottom gate/top contact field effect transistor with a networked composite film was realized with a specific range of tube density and a high on/off current ratio of approximately 10^5 which resulted from the Schottky barriers evolved between the individual m- and s-SWNTs in the network.

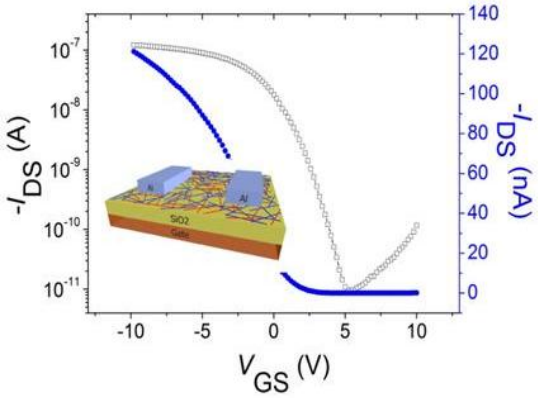

Figure 3. Transfer characteristics of SWNT transistor with Al contact and SiO_2, insulator.

Furthermore, the fabricated electronic nanocomposites are highly transparent, flexible, and chemically robust and thus, they can be conveniently micro and nano-patterned by nanoimprinting techniques.

References

1. J. Sung *et al. Adv. Mater.* **2008** 20, 1505.
2. J. Sung *et al. Adv. Funct. Mater.* **2010** 20, 4305.

Polymer Electrolyte Membranes Based on Poly(phenylene ether)s with Pendant Perfluoroalkyl Sulfonic Acids

Kazuhiro Nakabayashi, Tomoya Higashihara, and Mitsuru Ueda

Department of Organic and Polymeric Materials, Tokyo Institute of Technology, 2-12-1-H120, O-okayama, Meguro-ku, Tokyo 152-8552, Japan

ueda.m.ad@m.titech.ac.jp

Development of polymer electrolyte membranes (PEMs) based on aromatic polymers have been investigated over the past decades to realize alternatives of sulfonated perfluoropolymers (e.g., Nafion® and Flemion®). For example, PEMs based on sulfonated multiblock copolymers have been widely studied as the promising polymer architecture for high-performance PEMs.[1] Recently, the introduction of perfluroalkyl sulfonic acids into aromatic polymers also demonstrated drastic improvement of proton conductivity due to its high acidity (pK_a~ –6).[2] Thus, as well as sulfonated multiblock copolymers, this approach can be a promising way to improve performances of aromatic PEMs.

Hence, in this work, novel poly(phenylene ether)s containing pendant perfluoroalkyl sulfonic acids with ion exchange capacity (IEC) of 1.17–1.83 mequiv/g (**4a–5a**) were synthesized by the aromatic nucleophilic substitution reaction of a perfluoro monomer (decafluorobiphenyl or hexafluorobenzene) with 2,5-bis(4'-iodophenyl)hydroquinone, followed by the Ullman coupling reaction with potassium 1,1,2,2,-tetrafluoro-2-(1,1,2,2-tetrafluoro-2-iodoethoxy)ethanesulfonate (**PTES**). These poly(phenylene ether)s consist of the rigid polymer backbones with the high fluorine content and the flexible perfluoroalkyl sulfonic acid side chains, that is, the structure mimics that of the sulfonated perfluoropolymers (Figure 1). Their IEC values could be readily controlled by changing the equivalent of **PTES** in the Ullman coupling reaction. The structure of polymers was confirmed by ^{1}H and ^{19}F NMR spectra.

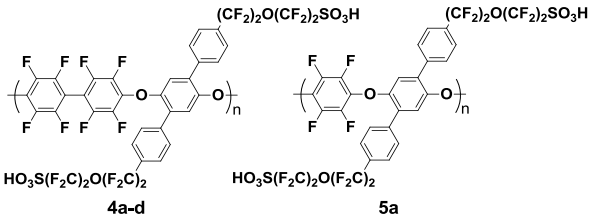

Figure 1. Structure of **4a–5a**.

The **4a–5a** membranes prepared by solution casting showed significantly low water uptake (19.3–28.0 wt %) and excellent dimensional stability even in the hydrated state, which were due to the strong hydrophobicity of the polymers (i.e., the high fluorine content). Besides, the high oxidative stability against hot Fenton's reagent (3% H_2O_2 aqueous solution containing 2 ppm $FeSO_4$ at 80 °C) was achieved. Humidity dependence of water uptake was evaluated in the **4a–5a** membranes at 80 °C. The **4a** and **4b** membranes with IEC = 1.17 and 1.38 mequiv/g showed low water uptake comparable to the Nafion 117 membrane in a whole range of relative humidity. The **5a** membrane with IEC = 1.83 mequiv/g showed the highest water uptake (24.0, 20.1, 12.6, and 8.8 wt % at 95, 80, 50, and 30% RH, respectively), which corresponded to λ (the number of water molecules per a sulfonic acid) = 7.3, 6.1, 3.8, and 2.7, respectively. These λ values are as high as those of the Nafion 117 membranes. Figure 2 shows humidity dependence of proton conductivity of the **4a–5a** membranes at 80 °C. All membranes show high proton conductivity comparable to the Nafion 117 membrane at 95% RH. The proton conductivity of the **4a–d** membranes, however, decreases rapidly with decreasing relative humidity from 95 to 30% RH. On the other hand, the **5a** membrane with IEC = 1.83 mequiv/g maintains high proton conductivity comparable to the Nafion 117 membrane to 30% RH. The high λ values of the **5a** membrane should contribute to high proton conductivity. As for sulfonated aromatic polymers with the same IEC values, high proton conductivity like the **5a** membrane has never been achieved, which obviously indicates that the high acidity of perfluoroalkyl sulfonic acids contributes to drastic improvement of proton conductivity.

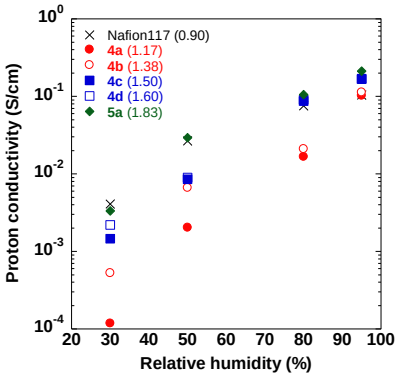

Figure 2. Humidity dependence of proton conductivity of **4a–5a** and Nafion 117 membranes at 80 °C.

In summary, novel poly(phenylene ether)s containing pendant perfluoroalkyl sulfonic acid with IEC = 1.17–1.83 mequiv/g (**4a–5a**) were successfully synthesized. All membranes showed high dimensional and oxidative stability. Among them, the **5a** membrane with IEC = 1.83 mequiv/g accomplished high proton conductivity comparable to the Nafion 117 membrane in the range of 30–95% RH, which resulted from the strong acidity of perfluoroalkyl sulfonic acids.

References: (1)(a) Yu, X. et al. *Macromol. Symp.* **2006,** *245*, 439-449. (b) Nakabayashi, K. et al. *J. Polym. Sci. Part A: Polym. Chem.* **2010,** *48*, 2757-2764. (2)(a) Miyatake, K. et al. *Chem. Commun.* **2009,** 6403-6405. (b) Yoshimura, K. et al. *Macromolecules* **2009,** *42*, 9302-9306.

Study of the new functionalized dimethacrylate copolymers for biochemical applications

Beata Podkościelna, Barbara Gawdzik and Andrzej Bartnicki

Faculty of Chemistry, MCS University, pl. M. Curie-Skłodowskiej 5,
20-031 Lublin, Poland; tel/fax: +48 81 524 22 51

*email: beatapod@poczta.umcs.lublin.pl

Introduction

In recent years, copolymers based on GMA have attracted increasing interest. The attention focused on these copolymers is largely due to the ability of pendent epoxide groups to enter into a large number of chemical modifications of the initial polymer. Copolymers based on GMA have been used as supports for enzymes and as sorbents for chromatography, they can also be used in removing metal ions (eg. mercuric ions) or even as biomaterials [1-2]. Immobilization on polymers is most important in the industrial application of enzymes, which as immobilized biocatalysts offer unique advantages in terms of better process control, increased stability etc.[3]

Materials and Methods

Copolymers containing glycidyl methacrylate and bis[4(2-hydroxy-3-methacryloyloxypropoxy)phenyl]-sulfide (BES.DM) were obtained in a suspension-emulsion copolymerization procedure [4]. The initiator AIBN (1 wt %) was dissolved in monomers, and then the mixture was diluted with a mixed solvent (toluene/decan-1-ol) taken in different proportions. Different concentrations of toluene in the mixture with decan-1-ol were used to qualify the effect of the diluent character on the microsphere properties. The dispersion medium was prepared through the dissolution of 1 wt% bis(2-ethylhexyl)sulfosuccinate sodium salt (DAC, BP) in deionized water, and it was used in a 1/5 (w/w) ratio according to the organic phase. The reaction mixture was stirred at 600 rpm for 18 h at 80 ^{o}C.

After cooling a purification procedure was applied to remove the diluents and unreacted monomers from the products. The obtained copolymers were washed with distilled water, filtered off, dried and then extracted in a Soxhlet apparatus by different solvents. Microscopic examination showed that in most cases particles of perfectly spherical shapes with diameters in the range 5-30 µm were obtained. Uniform particles (5-15µm) used in further studies. Chemical structure of the obtained copolymers was confirmed by spectroscopic method.

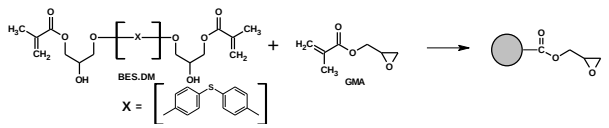

Scheme of copolymerization

The selected copolymers were modified with some amines in the epoxide ring opening reaction. 10 g of selected microspheres were placed together with diethylenetriamine (DETA) or triethylenetetramine (TETA) (10 excess to epoxide groups) and 200 mL of toluene. The whole content was heated over a water bath at 80^{o}C for 24 h. Their FTIR and elemental analyses were carried out. Next, the obtained microspheres were tested as matrices in immobilization proceses of selected enzymes.

Results and Discussion

New copolymers of different degrees of crosslinking obtained from glycidyl methacrylate (GMA) and bis[4(2-hydroxy-3-methacryloyloxypropoxy)phenyl]-sulfide (BES.DM) as crosslinkers were obtained according to reaction shown in Scheme 1 [5]. The obtained copolymers have different number of epoxy groups ranging from 0.73 to 2.79 mmol/g. The closest epoxy groups numbers to theoretical values are characteristic for microspheres containing 1:1 and 1:2 (mol%) GMA:BES.DM.

The monomers were used for the synthesis of porous microspheres in the presence of pore-forming diluents, decan-1-ol and toluene. Influence of diluents composition on their structures was studied. Porous structure of the obtained microspheres in dry (from nitrogen adsorption-desorption measurements) states, their thermal properties (thermogravimetric analysis), and swelling characteristics in 10 solvents of different chemical nature were examined.

A selected microspheres with hanging epoxide groups are tested in reactions with biological active compound (e.g enzymatic proteins) to develop effective procedures for the immobilization of selected enzymes in these media.

Conclusions

Synthesis, copolymerization, and properties of the new copolymers of bis[4(2-hydroxy-3-methacryloyloxy-propoxy)phenyl]sulfide (BES.DM) and glycidyl methacrylate (GMA) of different cross-linking degree in the form of microspheres are presented. Thermal resistance of the studied copolymers increased with increase of BES.M concentration. Swelling characteristics and the epoxide content around 0.73 - 2.79 mmol of epoxy groups per gram make these copolymers very interesting for their chemical modification.

References

[1] Blondieau D. Bigan M. Despres P. React Funct Polym 1995, **27**, 175.

[2] Onjia A. Milonjić S.K. Jovanović N.N. React Funct Polym 2000, **43**, 269.

[3] Panzavolta F. Soro S. D'Amato R. Palocci C. Cernia E. Russo M. V. J. Mol. Catal. B: Enzym. 2005, **32**, 67.

[4] Podkościelna B. Gawdzik B. Bartnicki A. J Polym Sci Pol Chem 2006;**44,** 7014.

[5] Podkościelna B. J. Appl. Polym. Sci. DOI: 10.1002/app.33420

Rheologhical properties of poly (Acryl amide with 2-Acrylamido-2-methyl-1-propane sulphonic acid) microgel via precipitation polymerization.

M.Fathollahi,H.Bouhendi[2],M.J.ZohurianMehr[2],K.Kabiri[2],Sh.Roostamizadeh[1],*

.[1]*DepartmentofChemisry, K. N. Toosi University of Technology, P.O. Box 15875-4416, Tehran, Iran.*
[2] Iran polymer and Petrochemical institute (IPPI), P.O.Box 14965-115 Tehran, Iran.

[*]Correspondingauthor,Emailaddress:H.Boouhendi@ippi.ac.ir

Abstract Body: Cross-linked Copolymer of Acrylamide (AM) and 2-acrylamido-2-methyl-1-propane sulfonaic acid (AMPS) were prepared via thermally initiated free – radical precipitation polymerization in an organic solvent. 1-6 Hexa diol di acrylate And 2,2 azobis isobutyronitrile were used as cross-linker and initiator respectively. The effect of (HDDA) concentration on different features of sample(i.e., spectral characteristics, glass transition temperature, equilibrium swelling, gel content rheological properties) was investigated. The Flory-Rehner equation and rubber elasticity theory were used to discuss the network structure of polymer. Apparent and rotational viscosities were used to determine the optimal cross-linker concentration. The sample maximum with value of viscosity was obtained using 0.9 mmol/L of the cross-linker. In addition the m and n parameter of Ostwald equation were investigated as well

A feasible route to disperse bacterial cellulose nanowhiskers in polymers by melt compounding of interest in packaging applications and physical characterization of the optimized nanocomposites

Martinez-Sanz Marta, Lopez-Rubio Amparo And Lagaron Jose Maria

Novel materials and nanotechnology group, iata, csic, apdo. Correos 73, 46100 burjassot, spain

E-mail: lagaron@iata.csic.es

Abstract Body:

The present work reports on the development and physical characterization of novel nanocomposite materials obtained through melt compounding consisting of an EVOH matrix reinforced with bacterial cellulose nanowhiskers (BCNW). Cellulose-based fillers are in general very difficult to disperse via melt blending processing routes and hence most of the existing studies relate to composites obtained by solvent casting. With the overall aim of enhancing the nanofiller dispersion in melt compounding processes, several methodologies have been developed and optimized for the efficient incorporation of bacterial cellulose nanowhiskers and in general of cellulose nanowhiskers into polymeric matrixes (1).

Bacterial cellulose was selected as the reinforcing agent due to its structure and unique properties, such as high crystallinity, high degree of purity, low density and biocompatibility. Furthermore, while plant cellulose is associated with other kinds of natural biopolymers like lignin and hemicellulose, bacterial cellulose is obtained with a high degree of purity. These outstanding properties have made bacterial cellulose an interesting filler to reinforce nanocomposite polymeric and biopolymeric materials (2-5).

Highly crystalline bacterial cellulose nanowhiskers (BCNW) were first incorporated into an EVOH carrier by means of both high voltage spinning and solution precipitation in liquid nitrogen and, subsequently, melt-mixed with the pure EVOH matrix, generating diluted nanocomposite compression moulded films with a final concentration of 2 wt.-% BCNW (6). The morphology of these materials was studied by optical microscopy with polarized light, TEM and cryo-SEM, revealing a significant improvement in the dispersion of BCNW through the developed methods as compared to direct melt-mixing of the freeze-dried material with the polymeric matrix. Furthermore, for the precipitation method, it was possible to incorporate up to 4 wt.-% BCNW without significant aggregation of the nanoreinforcement.

While the direct addition of freeze-dried BCNW had a negative effect on the water permeability and mechanical properties of the material, reductions of more that 50% in water permeability and increased elastic modulus and tensile strength were measured for the nanocomposites with enhanced dispersion.

Thus, a full morphological and physical properties characterization of the optimized nanocomposites were carried out relating their particular structure to specific properties relevant to the high barrier application in packaging.

References :

(1) Lagaron, J.M.; Martinez-Sanz, M.; Lopez-Rubio, A.; Patent Application P201030663

(2) Millon, L.E.; Wan, W.K. *J. Biomed. Mater. Res. Part B*, **2006**, *79B*, 245–253.

(3) Gindl, W.; Keckes, J. *Compos. Sci. Technol.*, **2004**, *64*, 2407–2413.

(4) Park, W. I.; Kang, M.; Kim, H. S.; Jin, H. J. *Macromol. Symp.*, **2007**, *249-250*, 289–294.

(5) Wan, Y.Z.; Luo, H.; He, F.; Liang, H.; Huang, Y.; Li, X.L. *Compos. Sci. Technol.*, **2009**, *69*, 1212-1217.

(6) Martinez-Sanz, M.; Olsson, R..; Lopez-Rubio, A.; Lagaron, J.M., Cellulose, Online First, 24 November 2010

Synthesis of Novel Oligoimides and Their Applications to Non-volatile Memory

Tadanori Kurosawa[1], *Wen-Ya Lee*[2], *Tomoya Higashihara*[1], *Mitsuru Ueda*[1], *and Wen-Chang Chen*[2,3]

1: Department of Organic and Polymeric Materials, Tokyo Institute of Technology, 2-12-1-H-120, Ookayama, Meguro-ku, Tokyo 152-8552, Japan
2: Department of Chemical Engineering, National Taiwan University, Taipei, Taiwan 106
3: Institute of Polymer Science and Engineering, National Taiwan University, Taipei, Taiwan 106

E-mail: kurosawa.t.ab@m.titech.ac.jp

Introduction

Memory devices based on organic materials have been receiving interests because of simplicity in device structure, good scalability, low-cost potential, and low-power operation compared to silicon-based memories[1]. From the molecular designing point of view, donor (D)-acceptor (A) structure is known to be very important for the expression of memory characteristics[2, 3]. In this study, we report the synthesis and memory characteristics of two novel oligoimides (OIs) with D-A-D structure, which were derived from 4,4'-(hexafluoroisopropylidene)diphthalic anhydride (6FDA) and 4-aminotriphenylamine (ATP), or *N*-(4-aminophenyl)carbazole (AC), respectively. In addition a novel A-D-A type OI derived from 4,4'-diaminotriphenylamine (DATP) and 4-(trifluoromethyl)phthalic anhydride (3FA), is also reported. The role of D and A moiety and their sequence in memory characteristics were investigated.

Results and discussion

Synthesis of OIs. OI (ATP-6FDA) and OI(AC-6FDA) were synthesized by the condensation reaction of amines (ATP or AC) with dianhydride (6FDA), followed by chemical imidization as shown in scheme 1. On the other hand, OI(DATP-3FA) was obtained from DATP and 3FA via thermal imidization due to its high solubility (Scheme 2). The desired structures of the three OIs were confirmed by ^{1}H NMR, ^{13}C NMR, IR, and elemental analysis. All the OIs were readily soluble in common organic solvents which might be originated from the introduction of hexafluoroisopropyl or trifluoromethyl units. In addition, it was possible to prepare a smooth thin film by vacuum evaporation and deposition.

Scheme 1. Synthetic route of OI(ATP-6FDA) and OI(AC-6FDA)

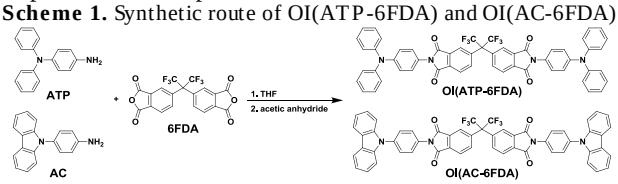

Scheme 2. Synthetic route of OI(DATP-3FA)

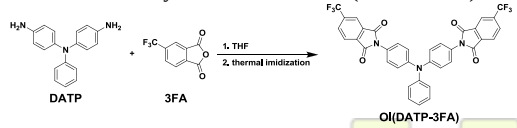

Thermal, optical, and electrochemical properties of OIs. The thermal, optical and electrochemical properties were evaluated by using TGA, UV-vis spectroscopy, and CV. These data are summarized in Table 1. All OIs showed excellent thermal stability such as high 5% weight loss temperature ($T_{d5\%}$) over 380 ˚C, which are expected to meet the requirement of heat resistance in electronics industry. The optical band gaps (E_g^{opt}) of OI(ATP-6FDA), OI(AC-6FDA), and OI(DATP-3FA) were 3.28, 3.51, 3.11 eV, respectively. The largest band gap of OI(AC-6FDA) indicates that this OI takes the most twisted conformation of the three.

Table 1. Thermal, optical, and electrochemical properties of OIs

	$T_{d5\%}$ (˚C)	E_g^{opt} (eV)	HOMO (eV)	LUMO (eV)
OI(ATP-6FDA)	459	3.28	-5.21	-2.10
OI(AC-6FDA)	526	3.51	-5.53	-2.02
OI(DATP-3FA)	381	3.11	-5.32	-2.21

Memory properties. The memory effects of the OIs were demonstrated by the current-voltage (I-V) characteristics of an ITO/OI/Al sandwich device. Thin films of OIs were deposited onto ITO. Figure 1 shows the representative memory properties of OI(ATP-6FDA). OI(ATP-6FDA) shows non-volatile negative differential resistance (NDR) behavior with a threshold voltage around 4 V and a high ON/OFF ratio in the range of 10^3~10^4 (Figure 1(a)). Also, OI(ATP-6FDA) exhibits good response to the write-read-erase-read (WRER) voltage bias more over than 30 cycles (Figure 1(b)). These results indicate that OI(ATP-6FDA) has the potential for being the alternative material of current memory devices.

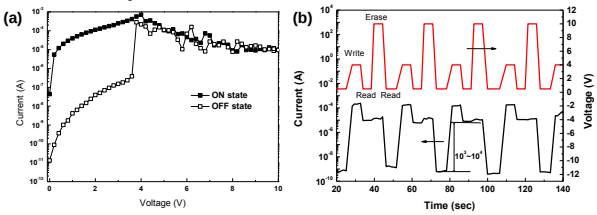

Figure 1. (a) I-V characteristic and (b) current response of OI(ATP-6FDA)

Conclusions

New three OIs containing D and A units in the arrangement of D-A-D or A-D-A were designed and synthesized in order to investigate the role of D and A moiety and their sequence in memory characteristics. All OIs showed high thermal stability. OI(ATP-6FDA) showed NDR behavior with a high ON/OFF ratio. The memory properties of other OIs will be further investigated.

References

(1) Ling, Q. D.; Liaw, D. J.; Zhu, C. X.; Chang, D. S. H.; Kang, E. T.; Neoh, K. G. *Prog. Polym. Sci.* **2008**, 33, 917
(2) Ling, Q. D.; Chang, F. C.; Song, Y.; Zhu, C. X.; Liaw, D. J.; Chang, D. S. H.; Kang, E. T.; Neoh, K. G. *J. Am. Chem. Soc.* **2006**, 128, 8732
(3) Ma, Y.; Cao, X.; Li, G.; Wen, Y.; Yang, Y.; Wang, J.; Du, S.; Yang, L.; Gao, H.; Song, Y. *Adv. Funct. Mater.* **2010**, 20, 803

Click Chemical modifications of PVC surfaces for antibacterial applications.

Jérôme Lafarge, Nasreddine Kébir, Fabrice Burel

INSA de Rouen, Laboratoire Polymères Biopolymères Surfaces (PBS), UMR 6270 CNRS FR 3038, avenue de l'université, 76801 Saint-Etienne-du-Rouvray, France.

e-mail: nasreddine.kebir@insa-rouen.fr

Introduction

Polymers are a class of materials which are very used in the biomedical field. However, their applications are limited by the bacterial infection phenomenon which is a very serious problem. Indeed, approximately 65 % of the hospital infections are related to implants and biomedical materials. This phenomenon is responsible of big economic cost and of significant mortality.[1,2] To prevent this problem, several strategies were proposed, especially the impregnation of the biomaterial with antibiotics. Unfortunately, this strategy can not be used for long times and would exhibit appearance of resistance phenomena. On the other hand, the grafting of bioactive polymers on biomaterial surfaces is considered as a very recent strategy and a promising solution. [2,3]

The major challenge in the conception of a new antibacterial biomaterial consists in finding the chemical structure which gives the widest spectrum activity towards microorganisms and a maximum time durability of this activity.

Materials and methods

Reagents: PVC (sigma-Aldrich), NaN3, propargyl amine, PVBC.

Characterizations: NMR, FTIR-ATR (diamond), fluorimetry, Size Exclusion Chromatography (SEC), AFM, XPS, TGA, DSC, contact angle measurements.

Results and discussions

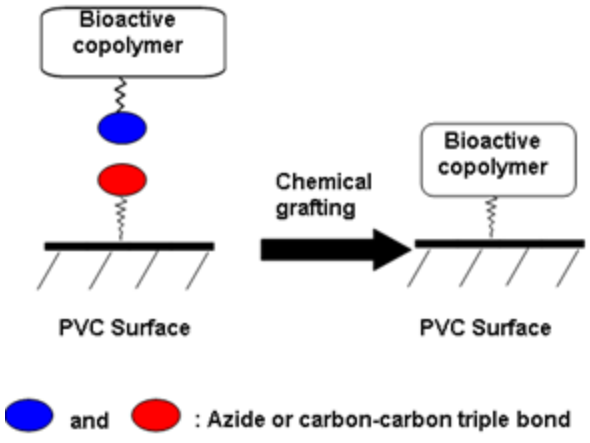

Scheme 1. chemical grafting of antibacterial polymers on PVC surfaces.

eral
h is
The chemical pathway consisted on click addition between azide groups and carbon-carbon triple bond. PVC surfaces as well as a serial of antibacterial copolymers bearing these two anchorage groups were successfully prepared and characterized.

Two strategies in terms of antibacterial properties were envisaged, namely the bactericidal and the anti-adhesive (bacteriophobe) ones.

In the case of the bactericidal strategy, copolymers bearing various bactericidal groups (quaternary ammoniums, guanidinium…) and chemical backbones (polystyrene, polymethacrylate…) were synthesized and characterized by spectroscopic techniques. The thermal properties of these copolymers were assessed by TGA and DSC, which particularly showed a decrease of thermal stability and increase of Tg after quaternization of tertiary amines. The copolymers were then chemically grafted onto PVC surface by click addition for which the operating conditions were optimized. The surface density of the quaternary ammoniums was quantified by colorimetric titration using fluorimetry.[4] This study showed densities higher than 10^{14} charge/cm^2 which is characteristic of bactericidal surfaces. Surface energy as well as surface hydrophilicity were assessed by contact angle measurements in static and dynamic modes, using different liquids especially water. This study mainly showed an increase of surface hydrophilicity and energy after copolymers grafting. Besides, the influence of the chemical grafting on the thermo-mechanical properties of the PVC material was also studied. No significant changes were observed. AFM study showed changes of topography.

Finally, preliminary study using epifluorescence microscopy (LIVE and DEAD test) and zone of inhibition experiment showed bactericidal properties of the PVC surfaces against Pseudomonas aeruginosa and staphylococcus aureus. The anti-adhesive strategy is under investigations.

Conclusion

In this work, antibacterial copolymers were successfully grafted on PVC surfaces by click addition.

1. a) Costerton JW, Stewart PS, Greenberg EP, Science 1999; 284, 1318-1322. b) Chicurel M, Nature **2000**; 408, 284-286.
2. Pavon-Djavid G, Hélary G, Migonney V. ITBM-RBM **2005**; 26:183-191.
3. Arnt L, Nüsslein K, Tew GN, Journal of Polymer Science: Part A: Polymer chemistry **2004**; 42:3860-3864.
4. Kébir N, Semetey V. Curie Institute and CNRS patent, WO/**2008**/041187.

Sensory Coumarin-Containing Polymers

S. Vallejos, P. Estévez, H. El Kaoutit, M. Trigo, F. Serna, F. García, J.L. Peña, J.M. García

Departamento de Química, Facultad de Ciencias, Universidad de Burgos, 09001 Burgos, Spain

svallejos@ubu.es

Introduction

Coumarins establish a family of dyes (Scheme 1), which are applicable in different fields of science and technology.

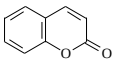

coumarin (2*H*-chromen-2-one)

Scheme 1

They exhibit strong fluorescence in the UV and VIS region, which makes them suitable to use as a colorants, dye laser media and as nonlinear optical chromophores. In medicine coumarin derivatives are used as anticoagulants, as a fluorescent indicators for the physiological pH region and as fluorescent probes to determine the rigidity and fluidity of living cells and its surrounding medium. Coumarins and its derivatives has been a subject of considerable interest in numerous fields.

Due to the interesting properties associated with coumarins, we are studying the fluorescence enhancing or quenching phenomenon and chromogenic behaviour of coumarin-derivatives containing polymers upon interaction with different chemicals. Regarding this point, we are applying our previously developed technique to put these organic molecules in water solution by incorporating as comonomers in water soluble polymers. Furthermorne, the incorporation as comonomers in bulk polymerization to give crosslinked hydrophilic dense films, gave rise to handle sensory materials to be uses as naked eye cromogenic sensor

Materials.

We follow conventional organic reactions, starting with the commercial 2*H*-chromen-2-one (coumarin), to prepare the chemosensory coumarin-containing motifs (see monomers structure on Scheme 2). The solution radical copolymerization of the sensory monomers with a set comonomers renders water soluble polymers (Scheme 2) with the sensory comonomer in a molar ration lower than 5%, and, preferably lower than 2%. In the same vein, the bulk copolymerization of the comonomers using a cross-linking agent, e.g., 1,2-ethanedioldimethacrylate, gives hydrophilic dense membranes with gel behavior (water swelling percentage ranging 50-200%). The membranes as easily handle materials, with good mechanical properties, even after water or organic-solvents swelling.

The membrane will be used to prepare naked eye sensory strips for the detection of different chemicals. As an illustrative example, Figure 1 depicts the chromegenic sensing of cyanide in water using one of our previously prepared sensory membranes.**¡Error! Marcador no definido.** The water soluble polymers will be use to characterize the observed sensing phenomena, from a chemical and physical viewpoint. The chemosensing phenomena may arise from feeble reversible interactions (binding site-signalling and displacement approach) or from irreversible chemical reactions (chemodosimiter approcach).

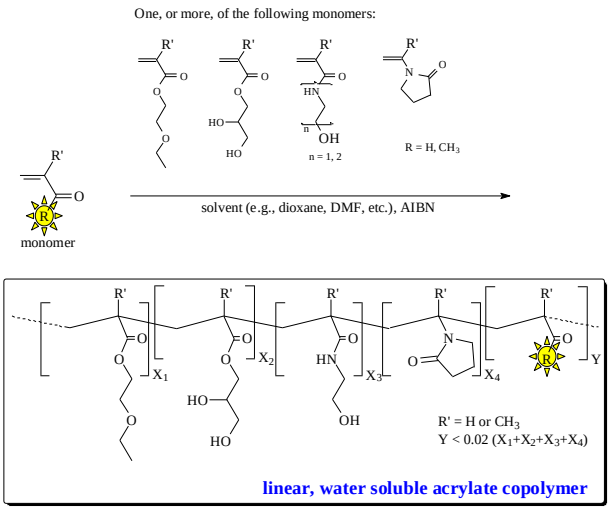

Scheme 2

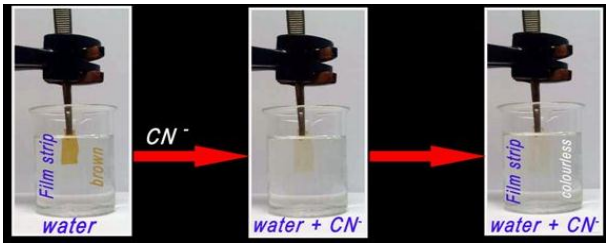

Figure 1

References

. Voutsadaki, G.K. Tsikalas, E. Klontzas, G. E. Forudakis, H. E. Katerinopoulos. *Chem. Commun.* **2010**, *46*, 3292.

[1] R. O'Kennedy, R.D. Thornes, *Coumarins: biology, applications, and mode of action*, Wiley, Chichester: 1997.

[1] F. García, J.M. García, B. García-Acosta, R. Martínez-Mañez, F. Sancenón, N. San-José, and J. Soto, J. *Chem. Commun.* **2005**, 2790.

[1] B. García-Acosta, F. García, J.M. García, R. Martínez-Mañez, F. Sancenón, N. San-José, and J. Soto, *Org. Lett.* **2007**, *9*, 2429.

[1] S. Vallejos, P. Estévez, F.C. García, F. Serna, J.L. de la Peña, J.M. García, *Chem. Commun.* **2010**, *46*, 7951

High Performance Gas Separation Membranes with Aging and Plasticization Resistance

Alberto Tena[1], *Ángel E. Lozano*[1,2], *Ángel Marcos-Fernández*[1,2], *Jose G de la Campa*[1,2], *Javier de Abajo*[1,2], *Laura Palacio*[1], *Pedro Prádanos*[1], *Antonio Hernández*[1]

[1]SMAP UA-UVA_CSIC, Universidad de Valladolid, Facultad de Ciencias, Real de Burgos s/n, 47071 Valladolid, Spain
[2]Instituto de Ciencia y Tecnología de Polímeros, CSIC, Juan de la Cierva 3, 28006 Madrid, Spain

albtena@ictp.csic.es

There is a commanding economical and social need of improving the gas purification of mixtures including carbon dioxide as a component. The separation of this gas can be carried out by diverse methods including chemical absorption, pressure swing sorption, PSA, carbon molecular sieves and so on. However, these systems suffer from diverse limitations.

It is well known that many polymeric compounds show excellent processability, good mechanical properties and high thermal stability, and that some aromatic polymers and polyheterocycles having high fractional free volume are excellent candidates for gas separation applications. However, polymer membranes have some limitations when they are applied in industry, since their separation productivity (balance between permeability and selectivity) is not preserved when the feeding pressure is high or when the process involves a gas able to interact with the polymer matrix [1]. Thus, many polymers show a minimum in the perrmeabilty *vs* applied pressure plot. This pressure is named the plasticization pressure and denotes the maximum pressure at which the material can be employed throughout the operative (industrial) life. In addition, when the polymeric materials reach the plasticization point, there is a drastic decrease in selectivity lessening the ability of the membrane to discriminate a mixture of gases in their components [2].

The need of new materials with a lower capability of undergoing plasticization processes has moved to investigate new ways of making polymeric materials. Our approach includes the use of polymers with good separation properties having very high molecular weight. Specifically, polyimide **6FDA-6FpDA** has been used (Figure 1), which features outstanding gas separation for various pairs of gases when the supply pressure is low [3].

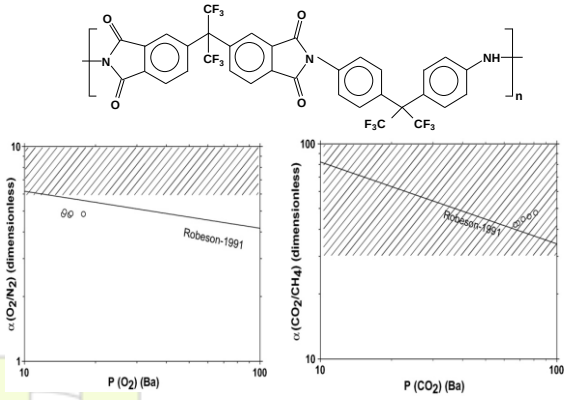

Figure 1. Structural unit and gas separation properties of 6FDA-6FpDA

Properly, on using a specific method of synthesis, polymers of high or very high molecular weights have been obtained in a controlled way [4]. These polymers, that were cast on films and evaluated for CO_2 and other gases at different pressures, showed a dazzling ability to resist plasticization (Figure 2).

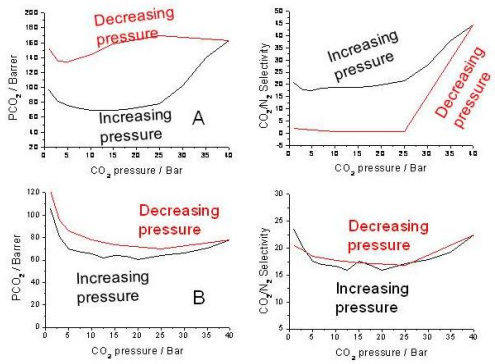

Figure 2. Variation of CO_2 permeability and CO_2/N_2 selectivity with the supply pressure to samples heated at 180ºC (A) and T above to Tg (B)

For industrial applications, this behavior must be constant over time.

In this paper, we also present a study of how permeability and selectivity for a 6FDA-6FpDA membrane evolves, at a constant pressure, as a function of exposure time.

Results permit to state that very high molecular weight combined with a thermal treatment can prevent both the plasticization and the aging processes.

Up to date, no many references have narrated that behavior. Thus, only chemical treatments, as crosslinking, and use of IPNs systems have been efficiently employed to decrease the plasticization.

Aknowledgements

We are indebted to the Spanish Junta de Castilla y León for the financing of this work through the GR-18 Excelence Group Action and to the Ministry of Science and Innovation in Spain for their economic support (projects MAT2007-62392/MAT and MAT2008-00619/MAT). A. Tena thanks CSIC for a predoctoral JAE fellowship received to carry out this work.

References

[1] Okamoto, K.; Noborio, K.; Hao, J.; Tanaka, K.; Kita, H. *Permeation and Separation Properties of Polyimide Membranes to 1,3-Butadiene and n-Butane.* J. Membr. Sci., 1997, **134**, 171.

[2] Coleman, M.R.; Koros, W.J. *Conditioning of Fluorine-Containing Polyimides. 2. Effect of Conditioning Protocol at 8% Volume Dilation on Gas-Transport Properties.* Macromolecules, 1999, **32**, 3106

[3] Recio, R.; Palacio, L.; Prádanos, P.; Hernández, A.; Lozano, A.E.; Marcos, A.; de la Campa, J.G.; de Abajo, J. *Permeability and selectivity of 6FDA-6FpDA gas membranes prepared from different solvents* J. Membr. Sci., 2007 **293** 22

[4]Muñoz, D.M. de la Campa, J.G. de Abajo, J.. Lozano, A.E. *Experimental and Theoretical Study of an Improved Activated Polycondensation Method for Aromatic Polyimides,* Macromolecules, 2007 **40** 8225.

Gas Separation Membranes Derived From Rigid, High-Free-Volume, Fluorinated Polyimides.

Marta Juan-y-Seva, Cristina Álvarez, Ángel E. Lozano, Javier de Abajo and José G. de la Campa

Instituto de Ciencia y Tecnología de Polímeros, Consejo Superior de Investigaciones Científicas, CSIC
Juan de la Cierva 3. 28006 Madrid, Spain

martajys@ictp.csic.es

Introduction

In the last decades, a huge research effort has been employed to prepare polymer membranes for gas separations that improve the well-established trade-off between permeability (gas flux) and selectivity (separation capacity), also known as Robeson's upper bound [1]. Aromatic fluorine-containing polyimides, mainly those having the group hexafluoroisopropylidene, are some of the most attractive and promising gas-separation materials. They do not only present a favorable balance of gas permeability and selectivity but also excellent thermal, chemical and mechanical properties.

Recent research in this subject [2, 3] has shown that the simultaneous increase in main chain rigidity (strongly hindered ring rotation) and fractional free volume, FFV, (low packing density) provides polyimides with high permeability and good selectivity.

This work shows the synthesis of a series of polyimides derived from the twisted, non-coplanar diamine 1,4-bis(4-amino-2-trifluoromethylphenoxy)2,5-di-*tert*-butyl benzene (CF_3TBAPB). The effect of trifluoromethyl (CF_3) groups on the transport properties has been studied by comparing with analogous polyimides without CF_3 moieties (TBAPB) [2].

Materials and Methods

A series of polyimides was synthesized from diamine CF_3TBAPB and three commercial dianhydrides following the classical one-step polyimidation methods. The structures are shown in Fig.1. Polyimides were obtained by both thermal **(H)** and chemical **(C)** imidization of the polyamic acid precursor. The chemical structure of polyimides was confirmed by conventional techniques such as ^{1}H-NMR, ^{13}C-NMR and FTIR.

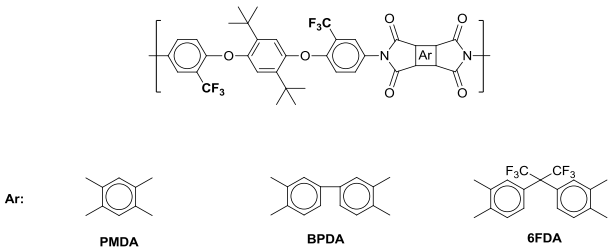

Fig.1. Chemical structure of polyimides

Polymer films were heated above their glass transition temperature, Tg, under a nitrogen atmosphere to strip off the residual solvent. Structural characterization of films was performed by WAXS. FFV was calculated from density data obtained by a buoyancy method [2].

Thermal stability and Tg, were determined by TGA and DSC, respectively.

Pure gas permeability coefficients (P) were determined by using a barometric permeation method at 30 °C and 3 bar pressure. Ideal selectivity for two pure gases was defined as $\alpha(A/B) = P_A/P_B$. For permeation experiments, O_2, N_2, CH_4 and CO_2 were used.

Results and Discussion

All polyimides showed high thermal stability, with decomposition temperatures above 480 °C, and Tgs higher than 270 °C. The reaction of diamine CF_3TBAPB with rigid dianhydrides yielded polyimides with much higher FFV than the analogous TBAPB series.

The performance of these membranes for gas pair CO_2/CH_4 is shown in Fig. 2. In general, the new polyimides exhibited higher permeability to specific gases, with good selectivity, than those analogous without CF_3 groups.

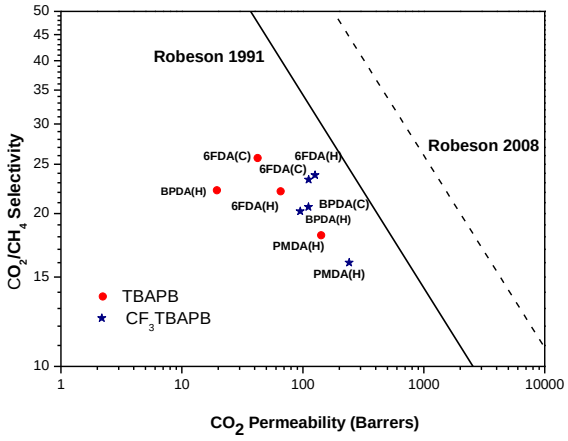

Fig.2 CO_2/CH_4 Selectivity versus CO_2 Permeability

No clear relationships between membrane properties and imidization method were found.

Conclusions

Novel polyimides having high FFV and high molecular chain rigidity have been obtained by a right combination of CF_3 and *tert*-butyl pendent groups on a diamine moiety. These fluorinated polyimides showed an excellent balance for gas separation, particularly for O_2/N_2 and CO_2/CH_4.

References

[1] L.M. Robeson, *J. Membr. Sci.* **62** (1991) 165-185 and **320** (2008) 390-400.

[2] M. Calle, A. E. Lozano, J. G. de la Campa, J. de Abajo, C. Álvarez, *J. Membr. Sci.* **365** (2010), 145-153.

[3] M. Calle, A. E. Lozano, J. G. de la Campa, J. de Abajo, *Macromolecules* **43** (2010) 2268-2275.

Acknowledgements

Authors gratefully acknowledge the financial support provided by MICINN project MAT2010-20668. M. JyS. would like to thank MICINN for a PhD scholarship.

Direct Patterning of Regioregular Poly(3-hexylthiophene)

Yuta Saito, *Tomoya Higashihara*, *Mitsuru Ueda*

Department of Organic and Polymeric materials, Tokyo Institute of Technology

ueda.m.ad@m.titech.ac.jp

Introduction. Recently, semiconducting π-conjugated polymers (πCPs) have become the subject of great interest in electronic device application such as organic solar cells and organic thin film transistors (OFETs). Semiconducting πCPs should be simple, low cost and large area patternable to simplify the fabrication of the electronic devices. Although the patterning processes of πCPs by ink-jet printing and microcontact printing methods have been reported, their processability and resolution are still not enough for the practical device fabrications. [1] Thus, micro-fabrication of πCPs by photolithography method, which allows using conventional equipments for semiconductor manufacturing, has recently been reported. [2] However, complicated synthetic routes are required for obtaining such materials and those are not favorable in terms of environmental and industrial issues.

Previously, we reported the simple photolithographic patterning method of poly(3-hexylthiophene) (P3HT), which is a representative πCP. [3] However, the head-to-tail (H-T) regioregularity of P3HT used as a matrix polymer was only 85 %, and it may result in low OFET properties because of low crystallinity and less chain packing.

Here, we report a simple patterning process of H-T regioregular P3HT (rr-P3HT) with a regioregularity of 95 %. The photosensitive rr-P3HT was prepared by combining 4,4'-methylenebis [2,6-bis(methoxymethyl) phenol] (MBMP) as a cross-linker and diphenylidonium 9,10-dimethoxyanthracene-2-sulfonate (DIAS) as a photoacid generator.

Materials and Methods. rr-P3HT and MBMP were synthesized according to a previous report. [4,5] Other reagents and solvents were used as received.

Photolithographic properties of rr-P3HT resists were evaluated as following methods. rr-P3HT was dissolved in 1,1,2,2-tetrachloroethane, followed by addition of MBMP and DIAS. The 100 nm thickness of polymer films were obtained by spin-casting from the solution on a silicon wafer. These films were pre-baked at 80 °C for 1 min, and then exposed by non-filtered ultra-high pressure mercury lamp, followed by post-exposure baking (PEB) at temperature (120-170 °C) for 1 min. The dissolution rate (Å/sec) of the film was determined from the changes in the film thickness before and after development with chloroform.

Results and Discussion. In this patterning process, the PEB temperature is crucial because the diffusion of photo-generated acids from PAG after UV exposure is an important key factor (Scheme 1). Thus, the effect of the PEB temperature on the dissolution rate in chloroform was investigated. Very high dissolution contrast was obtained at a PEB temperature between 140 and 170 °C. This result indicates that the cross-linking reaction is promoted effectively under these PEB conditions.

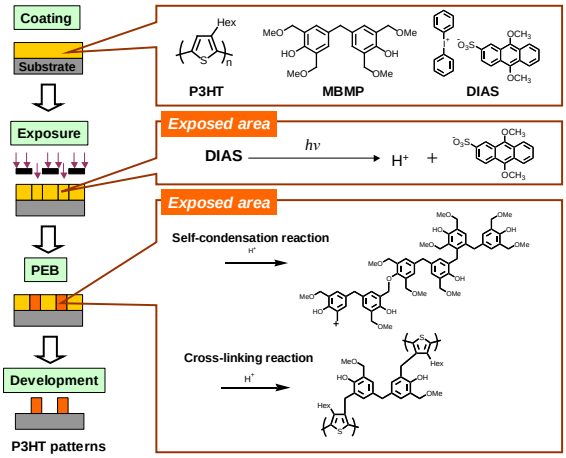

Scheme 1. Patterning process of P3HT resist

The loading weight contents of MBMP and DIAS were optimized for the dissolution rate. It is expected that MBMP and DIAS may inhibit carrier transportation in the semiconductive layer of OFETs, so the amounts of MBMP and DIAS should be minimized. Large dissolution contrast between exposed and unexposed area was obtained in the case of 5 wt% MBMP and DIAS loadings.

Based on these preliminary optimization studies, optical images of the contact-printed pattern were obtained using the P3HT resist consisting of rr-P3HT (90 wt%), MBMP (5wt%), and DIAS (5 wt%) (Figure 2). A clear negative pattern was successfully obtained with 15 μm features on a 100 nm thick film.

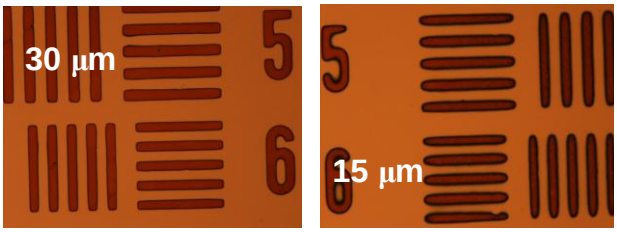

Figure 2. Optical images of the patterned P3HT resist

Conclusion. A simple patterning method of rr-P3HT by photolithography has been developed. A clear 15 μm lines were fabricated on a film containing rr-P3HT, MBMP, and DIAS. OFET using this patterned rr-P3HT is expected to show high transistor properties.

References.

[1] S. Holdcroft, *Adv. Mater.* 2000, 13, 1753
[2] K. Lu, Y. Guo, Y. Liu, C. Di, T. Li, Z. Wei, G. Yu, C. Du, S. Ye, *Macromolecules* 2009, 42, 3222
[3] K. Endo, T. Higashihara, M. Ueda, *Polym. J.* 2009, 41, 808
[4] R. Miyakoshi, A. Yokoyama, T. Yokozawa, *J. Am. Chem. Soc.* 2005, 127, 17542
[5] K. Mizoguchi, T. Higashihara, M. Ueda, *Polym. J.* 2008, 40, 645

Asymmetric Porous Membranes from PEG Modified Aromatic Polyamides

Serena Molina, Aránzazu Martínez-Gómez, Ángel E. Lozano, José G. de la Campa and Javier de Abajo

Instituto de Ciencia y Tecnología de Polímeros, Consejo Superior de Investigaciones Científicas, CSIC
Juan de la Cierva 3. 28006 Madrid, Spain

smolina@ictp.csic.es

Introduction

In recent years, water consumption has exponentially increased due to the global population growth, so that the development of different technologies for obtaining and optimizing its use is essential.

Although evaporation processes are still used considerably, ultrafiltration, nanofiltration and reverse osmosis membrane processes are predominantly used at present in the purification and desalination of water. For this reason, the research and development on novel polymer materials is important to fabricate membranes more permeable, more selective and more durable [1].

Biofouling is one of the most important problems in these technologies because it causes the flow through the membrane to decrease significantly with time and gives way to shorter lifetime. Biofouling could be minimized by periodical washing with aggressive chemical products, which on turn can degrade the polymeric membranes. This problem can be solved by using hydrophilic polymers because it has been found that microorganisms and biological substances are weakly adsorbed on hydrophilic membranes [2].

The aim of the present work has been to prepare novel aromatic polyamides with improved hydrophilicity, and the fabrication of asymmetric porous membranes from them. The approach chosen to achieve this target has been to incorporate highly hydrophilic groups, such as sulfonyl, phenolic, amide and oxyethylene within the same polymer. This modification is justified by the results of a previous work, where it has been possible to confirm the great ability of PEG to absorb water [3].

Materials and Methods

Polyamides shown in Figure 1 were synthesized by partial or total nucleophilic substitution with Cl-PEG on the phenolic starting polymer. The chemical structure and modification degree of modified polyamides were confirmed by conventional techniques such as ^{1}H-NMR, ^{13}C-NMR and FTIR, and they were characterized by GPC, contact angle, TGA, DSC, and X-ray diffraction.

Asymmetric porous membranes were prepared by the conventional method of phase inversion using DMF as solvent and water as coagulation medium. Then, they were evaluated as ultrafiltration membranes at laboratory scale (P=3 bar).

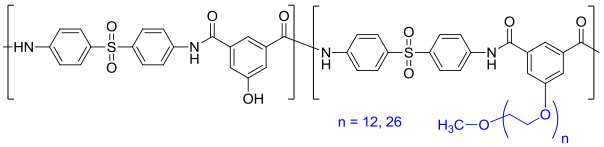

Figure 1. PEG containing aromatic polyamides

Results and Discussion

Hydrophilicity of the novel polymers were investigated first by contact angle measurements. It was observed that the greater the content of PEG the higher the contact angle, what indicated higher hydrophilicity. The membranes were then characterized by their molecular weight cut-off as a function of pore size and distribution.

The introduction of PEG chains allowed increasing membrane permeability respect to the unmodified polyamide and commercial polyamides. Thus, on increasing the modification degree and the length of PEG side chains the water uptake increased and the water flux became higher.

Therefore, a lower biofouling is to be expected in the modified polymeric membranes and works are at present being carried out to evaluate this improvement.

Conclusions

Aromatic polyisophthalamides bearing free –OH groups can be conveniently modified by incorporating PEG side chains by a nucleophilic displacement reaction. The hydrophilicity of these novel materials can be tuned by controlling the molecular weight of PEG and the modification degree. Higher hydrophilicity should give way to higher biofouling resistance, which would allow a longer lifetime of membranes.

References

[1] Richard W. Baker. *Membrane Technology and Applications*. 2nd Edition, Wiley, New York, 2004.

[2] D. Rana, T. Matsuura. *Chem. Rev*. 2010, **110**, 2448–2471.

[3] J.J. Ferreiro, J. G. de la Campa, A. E. Lozano, J. de Abajo, J. Preston. *J. Polym. Sci., Part A: Polym. Chem*. 2007. **45**, 4671-4683.

Acknowledgements

Authors gratefully acknowledge the financial support provided by the MICINN (MAT2010-20668).

Photophysical properties of some copoly(1,3,4-oxadiazole-ether)

A. Airinei[1], R. I. Tigoianu[1,2], M. Homocianu[1], C. Hamciuc[1], E. Hamciuc[1]

[1]"Petru Poni" Institute of Macromolecular Chemistry, Aleea Grigore Ghica Voda, 41A, Iasi -700487, Romania
[2]"Al. I. Cuza" University, Faculty of Physics, 11 Bdv. Carol I, Iasi-700506, Romania

airineia@icmpp.ro

Introduction: Poly(1,3,4-oxadiazole)s and their derivatives have been widely utilized in electronic devices as electron-transporting and hole-blocking materials or in obtaining polymer light-emitting diodes and photovoltaic cells [1, 2]. Copolymerization with solubility-enhanching units, such as fluorene or phenolphthalein led to materials with improving properties and solubility [3, 4].

Materials and Methods: Copolymers Ia-e were prepared using reported procedures [3,4]. Ultraviolet-visible and fluorescence spectra were recorded on an Analytik Jena SPECORD 200 spectrophotometer and PerkinElmer LS55 luminescence spectrometer using 10 mm quartz cells.

Results and Discussion: Aromatic copolyethers containing 1,3,4-oxadiazole rings **Ia-e** were obtained by nucleophilic substitution polymerization technique of 2,5-bis(p-fluorophenyl)-1,3,4-oxadiazole with 9,9-bis(4-hydroxylphenyl)fluorene or a mixture of latter in different amounts with 4,4'-isopropylidenediphenol [1,4]. Their properties were investigated by electronic absorption and photoluminescence spectroscopy. The copolymers in dimethyl sulfoxide (DMSO) solution emitted in the range of 360-370 nm depending on the copolymer structure. The emission band can be assigned to the oxadiazole moiety.

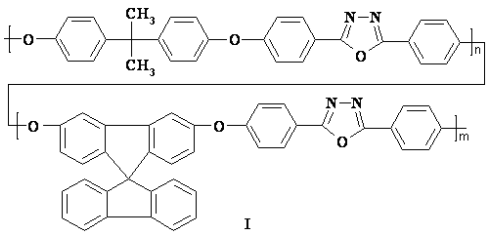

I

Ia: n=1, m=0; **Ib**: n=0.75, m=0.25; **Ic**: n=m=0.5; **Id**: n=0.25, m=0.75; **Ie**: n=0, m=1

The sensing capability of copolymers **Ia-e** to different nitroaromatic compounds such as nitrobenzene (NB), picric acid (PA), 1,3-dinitrobenzene (1,3- DNB), 2,4-dinitrotoluene (2,4-DNT), 2,6-dinitrotoluene (2,6-DNT) or fluoride ion was analyzed in $9 \cdot 10^{-4}$ M DMSO solutions. These nitroderivatives were chosen because they are structurally similar to well-known explosive 2,4,6-trinitrotoluene. Upon addition of picric acid as quencher, the emission intensity of **Ib** decreased dramatically with a blue shift of the emission maximum and a fluorescence quenching up to almost 30-fold (Fig. 1). In contrast, only about 4-fold decrease of fluorescence intensity was found for **Ia** or **Id** using 2,6-DNT as quencher. The Stern-Volmer plots of copolymers **Ia-e** were linear at low concentrations of nitroaromatics but deviated from linearity for higher concentrations of quencher, showing a positive curvature. The Stern-Volmer constants for **Id** estimated from the initial linear parts of S-V curves are 54160, 5540, 6870 and 5360 M^{-1} for PA, DNB, 2,4-DNT, 2,6-DNT, respectively. The K_{SV} data suggest that picric acid is the most efficient quencher, followed by 2,4-DNT and 1,3-DNB.

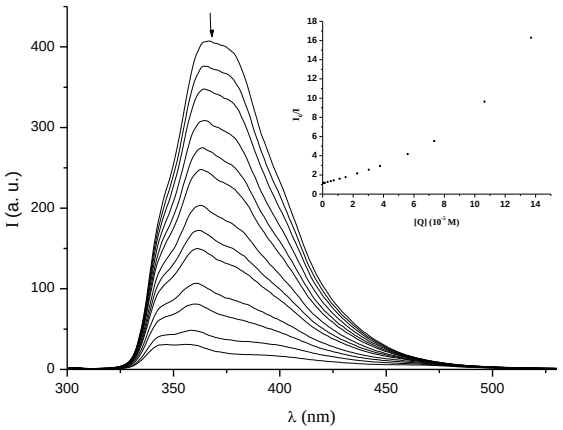

Fig. 1. Fluorescence spectra of **Ic** in DMSO upon addition of picric acid, excitation wavelength 298 nm. Stern-Volmer plot is shown as inset

The influence of the solution on the spectral characteristics of copoly(1,3,4-oxadiazole-ether)s was studied in solvents having different polarities. The emission intensity decreased from a highly polar solvent to a less polar one. However, the solvatochromic effect on the electronic absorption bands (λ_{max}) was less significantly for copolymers **Ia-e**.

Conclusion: Oxadiazole copolymers exhibit good fluorescence-emitting ability especially the polymers containing fluorene units and their emission can be efficiently quenched on the addition of nitroaromatic compounds.

References:

1. Y. Shirota, H. Kageyama, Chem. Rev., 107, 953-1010 (2007)
2. H. H. Sung, H. C. Lin, Macromolecules, 37, 7945-7954 (2004)
3. C. Hamciuc, E. Hamciuc, A. M. Ipate, M. Cristea, L. Okrasa, J. Appl. Polym. Sci., 113, 383-391 (2009)
4. C. Hamciuc, E. Hamciuc, A. M. Ipate, L. Okrasa, Polymer, 49, 681-690 (2008).

Spectral-Luminescent Properties of Polyurethanesiloxane Polymers Doped by Rhodamine 6G

[1]Akhmetshina A.I., [1]Davletbaeva I.M., [1]Gumerov A.M., [2]Kopylova T.N., [2]Samsonova L.G.

1 Kazan State Technological University, Kazan, Russia
2 Tomsk State University, Tomsk, Russia

aai-89@mail.ru, davletbaeva09@mail.ru, slg@phys.tsu.ru

The problem of low photochemical stability of organic dyes in polymeric media leads to the search for new optically transparent polymers for dye lasers. Their use contributes to the miniaturization of lasers and lower their costs.

In the course of research the mesoporous polymers based on polyether (PEG), 2,4-toluene diisocyanate (TDI) and octamethylcyclotetrasiloxane (D4) were synthesized. The formation of mesopores occurs as a result of microphase separation. The detection of cavities in the polymer was the premise for the study of polyurethanesiloxsane polymers as the polymer backbone for the organic dyes introduction. The introduction of xanthene dye Rhodamine 6G into polymer system was carried out by its adsorption from the solution in ethanol in the pores of the polymer.

The range of transparency of polyurethanesiloxsane samples was determined by the spectral method. It was established that in the case of doping polymers with Rhodamine 6G, the absorption band characteristic for this dye appears in the electronic absorption spectrum.

Fluorescence intensity for various samples correlates with the value of the optical density at the excitation wavelength. The bands have average half-width equal to 60 nm. Fluorescence intensity, as well as in the case of the electronic absorption spectrum, is maximal for the samples obtained at molar ratio [PEG]: [TDI]: [D4] = 1:15:15, [PEG]: [TDI]: [D4] = 1:10:20 and [PEG]: [TDI]: [D4] = 1:10:15.

It was found that when polymer obtained with the high content of 2,4-toluene diisocyanate organic dye (Rhodamine 6G) being doped, the line of stimulated luminescence spectrum narrows tenfold. The operational life of the sample on the basis of [PEG]: [TDI]: [D4] = 1:15:30 was more than 10,000 laser pulses at the pump power density 27 MW/cm2. For this sample, there was the smallest half-width of the lasing spectrum at excitation power density of 23.3 MW/cm^2 (Figure 1)

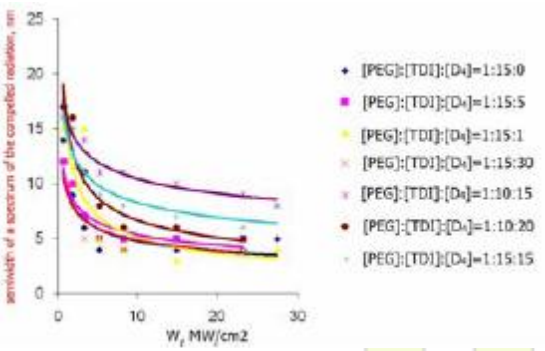

Fig. 1. Dependence of semiwidth of a spectrum of the compelled radiation of Rhodamine 6G (5•10-3 mol/l) from intensity of excitation IAG-Nd3 + the laser (532 nm).

(Fig.

The normalised spectra of laser generation and fluorescence of Rhodamine 6G in polymer are presented [PEG]:[TDI]:[D4] =1:15:30. For this sample the least semiwidth of a spectrum of generation was observed at excitation power density 23.3 MW/cm^2 (Fig. 2).

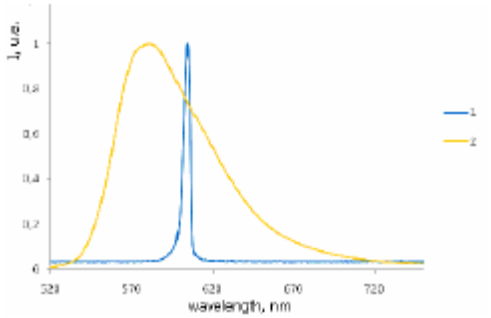

Fig. 2. Spectra of the spontaneous and compelled radiation of Rhodamine 6G in the sample [PEG]:[TDI]:[D4] =1:15:30 (excitation power density 23.3 MW/cm^2): 1 – a spectrum of the compelled radiation, 2 – a fluorescence spectrum.

It was established that the photostability of rhodamine 6G molecules largely depends on the content of dimethylsiloxsane component in the polymer (Fig. 3).

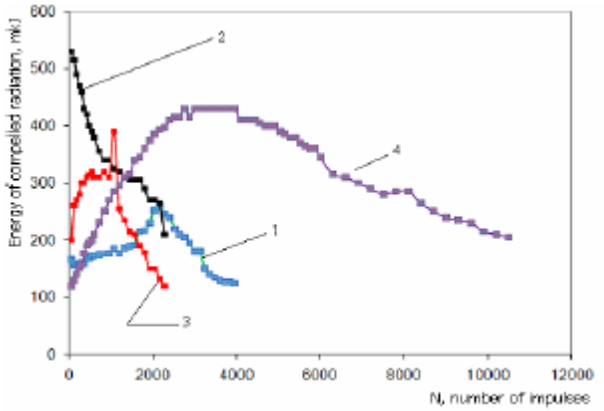

Fig. 3. Photostability of polymeric matrixes, doped by Rhodamine 6G (5•10-3 mol/l) at energy of an impulse a rating 30 mJ
1 - [PEG]:[TDI]:[D4] =1:15:0,
2 - [PEG]:[TDI]:[D4] =1:15:5,
3 - [PEG]:[TDI]:[D4] =1:15:10,
4 - [PEG]:[TDI]:[D4] =1:15:30

The photostability of the polymer obtained at high content of dimethylsiloxsane component increases more than threefold.

Acrylates Block Copolymers with N-trityl-L-serine methyl ester and Pyrene Prepared by ATRP

E.C. Buruiana, V. Podasca, T. Buruiana

Petru Poni Institute of Macromolecular Chemistry, 41 A Gr. Ghica Voda Alley, 700487, Iasi, Romania

e-mail: emilbur@icmpp.ro

In recent years, the strategy for designing and producing synthetic polymers containing appropriate amino acids has attracted a great interest because these materials can display novel and improved properties (e.g. biodegradation, biocompatibility, chirality, etc). Most of the prior work has been focused on the production of polypeptides [1], polyesters polyamides, and polysulfides having (L-) glutamate, lysine, proline, tyrosine or cysteine units in their backbone,which are intended for applications in the pharmaceutical field, molecular separations, tissue engineering,. microchips or stimuli-responsive materials. For achieving such functional polymers with controlled molar mass, narrow molecular weight distribution, and well-defined architecture, new synthesis methodologies were used, like ring-opening polymerization, atom transfer radical polymerization [2,3], reversible additionfragmentation chain and transfer polymerization. Within the family of amino acids-based copolymers, our group has been reported data concerning the oligoconjugates based on dipeptide and poly(3-hydroxybutyrates)[4], or poly(N-acryloyl chloride) functionalized with (S)-phenylalanine and pyrene units [5] obtained by classical procedures (anionic ring opening polymerization, radical polymerization, grafting).

The objective of the present work is to investigate the preparation of novel acrylates diblock copolymers with Ntrityl-L-serine methyl ester and Pyrene derivative used as initiator in atom transfer radical polymerization (ATRP). Furthermore, the presence of luminescent fluorophore, covalently linked on the end of polymer backbone, could be exploited for development of optically active and photo luminescent polymers, suitable for applications in biomedicine, biology, analytic techniques, and optical devices.

Materials and Methods

Metyl methacrylate (MMA); CuBr; 1-**(**Bromoacetyl**)**-pyrene, N,N,N',N",N"-Pentamethyldiethylenetriamine (PMDETA), 1,4-Dioxan, N-Trityl-L-serine methyl ester and 2-Methacryloyloxyethyl isocyanate were purchased from Aldrich. As polymerization method, ATRP was used for preparing diblock copolymer.

Results and Discussion

First, methacryloyloxyethylcarbamoyloxy-N, trityl serine methyl ester **(MTS)** was synthesized and characterized to be used as co-monomer for the preparation of diblock copolymer. The polymerization of this monomer was initiated of a macroinitiator based on acetyl pyrene- and bromine-terminated poly(methylmethacrylate). The structure of the resulting copolymer is given in Figure 1.

The spectral analysis ($_1$H NMR, FTIR, UV/vis) confirmed the structure of block copolymer, and GPC measurements showed that the molecular weight of this polymer was about 13610 (polidispersity index: 1.1), in agreement with NMR data. In the UV spectrum, both macroinitiator and block copolymer presented absorption bands at 310 and 348 nm, due to π-π*transition of the pyrene ring., while in the fluorescence spectrum they emits at 389 nm, 410 nm and 432 nm, all corresponding to the pyrene monomer fluorescence.

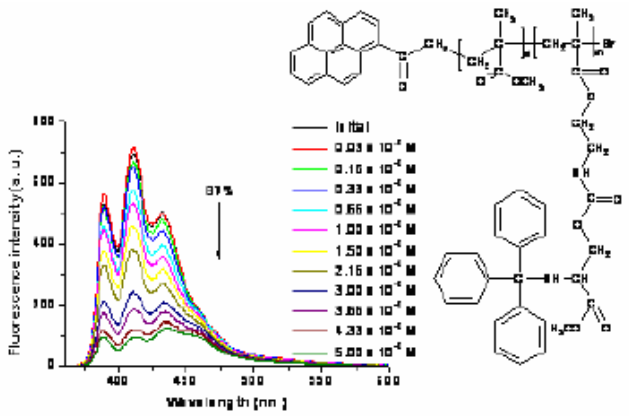

Figure 1. Structure of diblock copolymer based on MMA and MTS, and its photobehavior by the addition of TCNQ in DMF solution.

Quenching experiments were performed in the presence of various aromatic nitroderivatives and amines, KI, tetracyanoquinodimethane (TCNQ), the minimum concentration detected being 3x10 $^{-7}$ M/L for the latter.

Conclusions

In conclusion, the formation of diblock copolymer of **(MMA)**$_{40}$–b-**(MTS)**$_{18}$ containing pyrene molecule on the end of macromolecular chain was investigated using ATRP, the results obtained by the fluorescence study suggesting possible applications as chemosensors.

References

1. H.A. Klok, J.F. Langenwalter, S. Lecommandoux, *Macromolecules* 33 (2000) 7819
2. R.E. Richard, M. Schwartz, S. Ranade, A.K. Chan, K. Matyjaszewski, B. Sumerlin, *Biomacromolecules* 6 (2005) 3410
3. E.C. Buruiana, M. Murariu, T. Buruiana, J. Lumin. 130 (2010) 1794
4. E.C.Buruiana, M. Kowalczuk, G. Adamus, Z. Jedlinski, *J. Polym .Sci.: Part A: Polym .Chem*. 46 (2008) 4103
5. E. Buruiana, T. Buruiana, L. Hahui, *J. Photochem. Photobiol. A: Chem*. 189 (2007) 65.

Hybrid Composites based on Photopolymerizable Urethane Dimethacrylates and Silver Nanoparticles

Tinca Buruiana[1], *V. Melinte*[1], *F. Jitaru*[1], *L. Balan*[2] *and E.C. Buruiana*[1]

[1]Petru Poni Institute of Macromolecular Chemistry, 41 A Gr. Ghica Voda Alley, 700487, Iasi, Romania
[2]Institute de Sciences des Materiaux de Mulhouse, France

e-mail: tbur@icmpp.ro

Introduction

Nowadays, there is a considerable interest focused on the concept of using light in the development of multifunctional materials with novel or improved properties targeting a wide range of applications. Acrylates, methacrylates and urethane (di)methacrylates with controlled design and functionality are among the most investigated structures, because the resulting crosslinked materials find applications in various fields such as coatings, adhesive, microlithography, dental materials tissue engineering, orthopedic surgery, drug delivery systems, and many others [1]. For the majority practical purposes UV photocurable resins consist of a combination of multifunctional acrylates (mono-, di-, tri-) that form very complex polymeric networks. One of the goals of polymer science is to understand the nature and the state of the formed polymer in its application, for which is useful knowing and correlating the structure, properties and kinetics of a given process that take place in such materials.

For modern applications of some biomaterials, the chemistry of hybrid nanocomposites has also been explored to establish if the structural order within the material can be controlled on nanometer/submicron scale. In particular, the dispersion of nanosized inorganic particles into a polymer matrix open the possibility of generating new types of nanostructured materials (nanodevices) with designed surface and structural properties, which can be used in physical, biological, biomedical, and pharmaceutical applications [2]. Thus, the incorporation of inorganic particles like silica [3], hydroxyapatite [4] or nanometer silver particles [5] in some photopolymerizable monomers led to materials for applications in catalysis, drug and wound dressing, optical information storage, surface-enhanced Raman scattering, and others.

In this study, we synthesized a series of multifunctionalized urethane dimethacrylates to be further used for preparing of hybrid nanocomposites, where the impact of nanosized silver particles on the properties and morphology of the final crosslinked nanomaterials by UV-irradiation, is discussed.

Materials and Methods

Poly(dimethyl siloxane) (M_n = 5600), PEG (Mn = 1000), L-tartaric acid (TA), isophorone diisocyanate (IPDI), 2-hydroxyethyl methacrylate (HEMA) were purchased from Sigma Aldrich Chemical Co. and used without further purification. The initiators used were Irgacure 651 and Irgacure 819 (from Sigma-Aldrich Chemical Co.).

Results and Discussion

A series of photopolymerizable urethane dimethacrylates with different functionalities (eg. siloxane, carboxylic groups, etc) incorporating a small quantity of silver nanoparticles (1-2.5 wt.%) were subjected to photopolymerization experiments using suitable photoinitiators. In tandem, hybrid composites with nanosilver particles were also prepared by in situ procedure. ^{1}H NMR and FTIR spectroscopies confirmed the structure of the urethane dimethacrylates. Subsequently, the progress of photopolymerization of these monomers under UV irradiation was investigated by FTIR spectroscopy and photoDSC with respect to conversion and polymerization rate using Irgacure as an initiator. Combined analyses of UV spectroscopy and scanning electron microscopy (TEM) confirmed the existence of nanosized silver uniformly distributed in the polymer matrix (Fig. 1). Other specific properties of the synthesized hybrid nanocomposites will be presented, too.

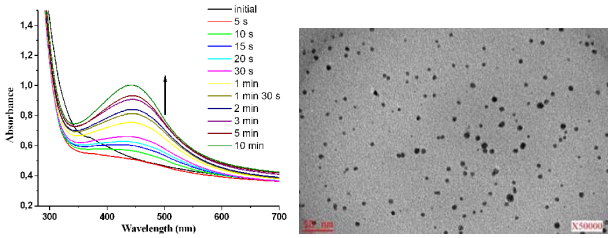

Figure 1. UV spectrum of the hybrid composite and TEM bright field image of the silver nanoparticles (2.5 wt.%) dispersed into a polymer matrix after UV irradiation.

Conclusions

In summary, we have described novel hybrid materials composed of polymeric networks formed by photopolymerization of various urethane dimethacrylates and silver nanoparticles (1-2.5 wt.%) incorporated before UV curing or by in situ synthesis. The UV-curing behaviour of all monomers with respect to conversion and polymerization rate showed that there are small differences in function of structural and compositional factors.

References

1. X. Cheng, S. Liu and W. Shi, *Progr.Org.Coat.* 65, 1 (2009)
2. B. A. Rozenberg and R. Tenne, *Prog. Polym. Sci.* 33, 40 (2008)
3. T. Buruiana, V. Melinte, L. Stroea and E. C. Buruiana, *Polym. J.* 41, 978 (2009)
4. Z. Zhou, D. Yang, J. Nie, Y. Ren and F. Cui, *J. Bioact. Compat. Polym.* 24, 405 (2009)
5. L. Balan, R. Schneider and D. J. Lougnot, *Progr. Org. Coat.* 62, 351 (2008).

Organic-Inorganic Gels for Heterochain Polymers Modification

[1]Gumerova O.R., [2]Davletbaev R.S.

[1]Kazan State Technological University, Kazan, Russia
[2]Kazan State Technical University, Kazan, Russia

olese4ka85@mail.ru

The synthesis of organic-inorganic gels based on the tetraethoxysilane and thermodynamically incompatible olygomers - oligooxyethylene glycol and oligodimethyl siloxane - is worked out.
The experimental research was aimed at overcoming incompatibility of inorganic and organic components, that is the main problem of obtaining materials based on the sol-gel technology.
The estimation of probability of cross-link density formation showed that as a result of tetraethoxysilane hydrolysis and following polycondensation the fractal clusters of silica are formed in the bulk of the oligomer matrix. Silica network in the bulk of oligomer is formed by orientation of fractal interconnected clusters as well as interfacial formation of associates of potassium-siloxanolate groups. Owing to the associates lability silica gel is spread in polymer melts or reactive oligomers with the subsequent forming of silica network in the bulk of polymeric matrix:

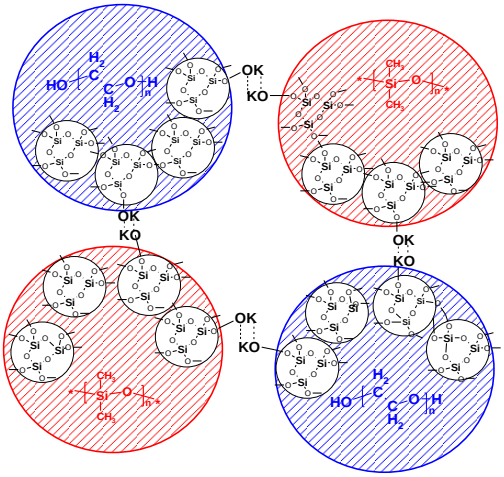

The silica fractal clusters were researched as nanostructure forming modifiers of polymers based on aromatic isocyanates in order to improve their performance properties. It was determined that gel did not interreact with isocyanate groups and produced no catalytic effect on the reaction of isocyanate groups with hydroxyl ones.
It was established that the modification of heterochain polymers on the base of aromatic isocyanates by organo-inorganic gels led to the formation of additional intermolecular interactions. As a result the significant increase of tensile strength and Young's modulus in the area of very low concentrations was observed. This effect is evident in Fig. 1.

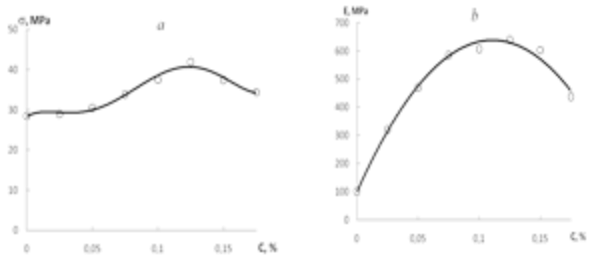

Fig. 1 Tensile strength (*a*) and Young's modulus (*b*) as functions of concentration organic-inorganic gel in heterochain polymer

It was shown that the structural modification of block-copolymers based on polyethers, aromatic isocyanates and organocyclosiloxanes by gel led to the enhancement of microphase separation and adsorption ability of polymer, caused by interfacial formation of mesopores. Temperature dependence of dielectric loss tangent is shown below in Fig. 2 for the polymer, modified with organic-inorganic gel in amount of 0.01 mass %.

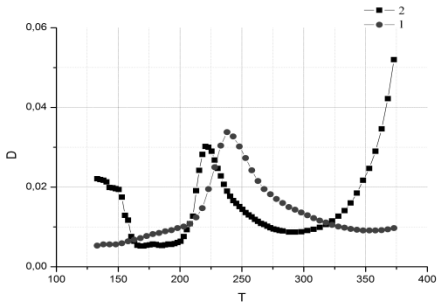

Fig. 2 Temperature dependence of dielectric loss tangent for the polymers: 1 – unmodified, 2 – modified

The addition of organic-inorganic gel into the polymer matrix resulted in significant changes in surface relief that was obtained with the help of atomic-force microscopy.
It was determined that the modification of heterochain polymers by organic-inorganic gels caused the formation of additional intermolecular interactions. Consequently the significant increase of physical-mechanical properties in the area of very low concentrations was observed.
Temperature dependence of dielectric loss tangent and atomic-force microscopy results showed the significant effect of the organic-inorganic gel modification on the microphase separation process.

Novel Polymetacrylamides Containing a Triazole Moiety. Application to the Extraction/Elimination of Metal Cations from Aqueous Media

M. Trigo, A. Gómez, P. Estévez, S. Vallejos, H. El Kaoutit, F. Serna, F. García, J.L. de la Peña, J.M. García

Departamento de Química, Facultad de Ciencias, Universidad de Burgos, 09001 Burgos, Spain

mtl0005@alu.ubu.es

Introduction

The properties and characteristics of the triazole heterocycle are expected to be retained by the polymer containing it. In this regard, the triazole derivatives are well-known binding sites for metals, and can be used for the removal of cations as well as sensing and molecular recognition.[1-4]

Due to the general interest of the elimination of environmentally polluting metals, we describe the synthesis of a metacrylamide monomer containing a triazole moiety and the preparation of related novel polymethacrylamides with this aim.

Materials

Three different copolymers (**I**, **II** and **III**) were prepared by radical copolymerization of mixtures of the three different co-monomers (Scheme 1, Table 1) using ethylene glycol dimethacrylate as cross-linking agent (**II** and **III**) and AIBN as a radical thermal initiator.

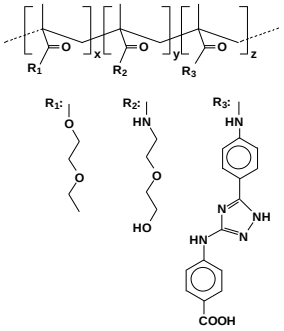

Scheme 1. Chemical structure of copolymers

Table 1. Materials

Copolymer	Appearance	$R_1(x)^a$	$R_2(y)^a$	$R_3(z)^a$	CLA [b]	WSP [c]
I	Powder-lineal water soluble	-	95	5	-	-
II	Powder - crosslinked	-	95	5	5	-
III	Film-crosslinked	29.7	69.3	1	1	167

[a] Molar composition ratio of the monomers. [b] Cross-linking agent (1,2-ethanedioldimethacrylate) molar percentage [c] Water-swelling percentage: weight percentage of water uptake by the films upon soaking until equilibrium, in pure water.

Cation elimination/extraction and recognition

Cross-linked copolymethacrylamide **II** was employed as a solid extraction phase. In order to study the influence of the electron environment in triazol moiety on extraction effectiveness, cross-linked copolymer **II** and polymethacrylamide **I** were treated to deprotonate carboxylic acid moiety.

Cation extraction experiments of several cations from aqueous solution using copolymethacrylamide **II** and deprotonated methacylamide **II** as extractant phase show that the best results in terms of extraction percentage, distribution coefficient and selectivity are obtained with Pb^{II}, Hg^{II} and Ag^{I}, reaching extraction percentages between 90 and 97%.

A cation sensing ability of the membrane **II** towards cation Fe^{III} was observed in extraction experiments, changing from colorless to reddish upon soaking in aqueous solution. In contrast, the polymer remained completely silent in the presence of the other cations tested.

The colorimetric cation sensing ability of film **III** was studied by UV-visible spectrometry (Figure 1), resulting in a gradual increment of the absorbance of the 455 nm band with the Fe^{III} concentration.

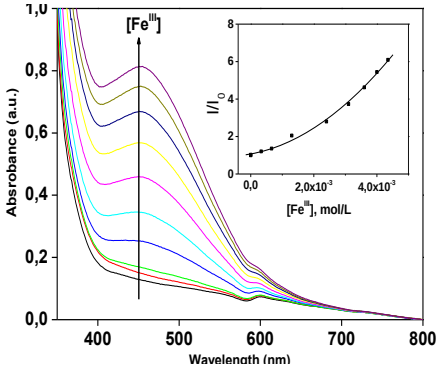

Figure 1. UV/Vis titration curve of film **III** with Fe^{III} in water (inset: I/I_0 vs. Fe^{III} concentration at 455 nm).

A. Gómez-Valdemoro, N. San-José, F. García, J.L. De La Peña, F. Serna, J. M. García. *Polym. Chem*. **2010**, *1*, 1291-1301

[2] (a) S. Elshani, P. Apgar, S. Wang and C. M. Wai, *J. Heterocycl. Chem*. **1994**, *31*, 1271–1274; (b) L. Uzun, A. kara, B. Osman, E. Yilmaz, N. Besirli and A. Denizli, *J. Appl. Polym. Sci*. **2009**, *114*, 2246–2253; (c) A. Kumar and P. S. Pandey, *Tetrahedron Lett*. **2009**, *50*, 5842–5845; (d) J. Zhan, D. Tian and H. Li, *New J. Chem*. **2009**, *33*, 725–728.

[3] H. C. Hung, C. W. Cheng, I. T. Ho and W. S. Chung, *Tetrahedron Lett*., **2009**, *50*, 302–305.

[4] (a) B. Liu, G. C. Guo and J. S. Huang, J. Solid State Chem. **2006**, *179*,3136–3144; (b) G. Mahmoudi, A. Morsali and L. G. Zhu, Z. *Anorg. Allg. Chem*. **2007**, *633*, 539–541; (c) K. C. Chang, I. H. Su, A. Senthilvelan and W. S. Chung, *Org. Lett*. **2007**, *9*, 3363–3366

Polyurethanes Based on Sterically Hindered Esters of Boric Acid

[1]*Emelina O.Y.*, [2]*Davletbaev R.S.*

[1]Kazan State Technological University, Kazan, Russia
[2]Kazan State Technical University, Kazan, Russia

emelina_oy@mail.ru

One of the promising directions in polymer chemistry is synthesis of polymers with fire resistance and high strength. Preparation of strong and heat-resistant polymer materials is achieved by adding into the polymer matrix such elements as boron, silicon, fluorine, etc.

Use limitation of organoboron polymers is primarily caused by their hydrolytic instability. The hydrolytically stable esters of boric acid are performed by creating steric hindrance around the boron atom.

It was determined by the method of NMR ^{1}H-spectroscopy that intermolecular complexes are formed in boric acid ethers with the participation of borate anions and tertiary amines. Viscosimetric analysis of sterically hindered esters of boric acid indicated the presence of intermolecular ionic complex interactions as well. The data of infrared spectroscopy and titration analysis on the consumption of hydroxyl groups indicated that all the initial reagents had reacted completely forming sterically hindered ether.

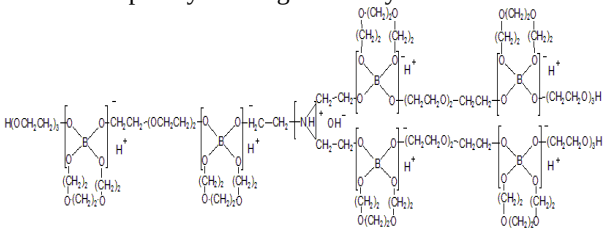

The sterically hindered esters of boric acid were produced by di- and trisubstituted glycol. The structure of esters of boric acid suggests the presence in his part of the terminal hydroxyl groups able to interact with isocyanate groups.

Polyurethanes derived from sterically hindered esters of boric acid, have high physical and mechanical properties.

Thermal properties of organoboron polymers were studied using thermogravimetric analysis. It was established that the beginning of thermal oxidative degradation observed in the range from 240 to 311°C and a maximum speed of thermal oxidative degradation was achieved at temperatures of 351 to 412°C depending on the percentage of boron (Fig. 1, 2).

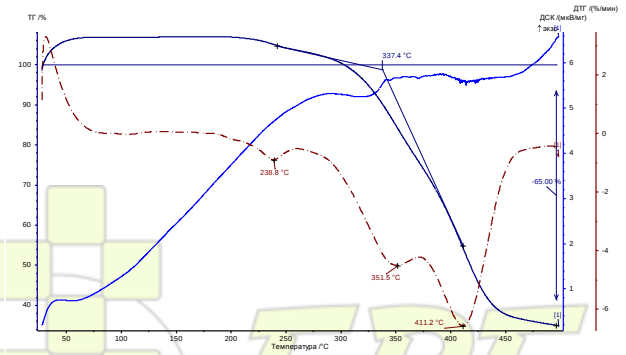

Fig. 1 Curves of differential thermal analysis for polymer obtained on the basis of sterically hindered ester of boric acid (5.0% boron)

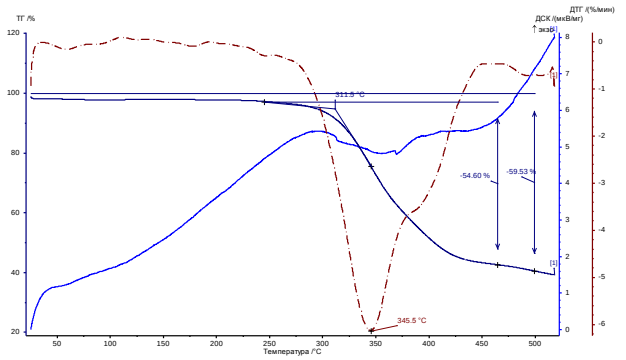

Fig. 2 Curves of differential thermal analysis for polymer obtained on the basis of sterically hindered ester of boric acid (7.5% boron)

The data of infrared spectroscopy, NMR ^{1}H-spectroscopy and viscosimetric analysis showed the presence of intermolecular ionic complex interactions in sterically hindered esters of boric acid. The contribution of organoboron part in the polymers caused increasing their thermal stability and physical and mechanical properties.

Epoxy Polymers for Medical Applications. In vitro Biological Properties

Filiberto González Garcia1, Maria E. Leyva1, Alvaro A. A. de Queiroz1, Olga Z. Higa2

1Institute of Exact Sciences, Federal University of Itajubá, Brazil.
2Institute of Nuclear and Energy Research, University of São Paulo, Brazil.

e-mail; fili@unifei.edu.br

Introduction

Today, polymers represent the most important and largest family of materials being used in medical technology. Applications of polymers in medicine and surgery include temporary, permanent devices and complex devices simulating the physiological function.

In the literature there are some studies related to epoxy formulations for orthopedic and dental applications. Many studies have examined the cytotoxicity *in vitro* of epoxy networks[1-2] as well as their monomers precursors.[3-4] However, to our knowledge, only one work has been undertaken about the blood compatibility of epoxies materials.[5] The requirement of materials to medical applications varies markedly according to the application being considered. One of the major problems encountered in medical applications is blood compatibility since many of these devices either handle blood directly or come into contact with blood in subcutaneous or implantable devices. The purpose of the present study was to examine the blood compatibility and cytotoxicity properties of four epoxyamines networks.

Materials and Methods

The epoxy prepolymer used was a diglycidyl ether of bisphenol-A (DGEBA; DER 331 from Dow Chemicals, Brazil), with an epoxide equivalent weigh 187 g eq.$^{-1}$.

The aliphatic amines used were triethylenetetramine (TETA; DEH 24 from Dow Chemical, Brazil), diethylenetriamine (DETA), 1-(2-aminoethyl)piperazine (AEP) and isophorone diamine (IPD) from Aldrich, Brazil (99 % purity). The epoxy polymers were prepared using stoichiometric amounts (ratio epoxy to amino-hydrogen, e/a = 1). The cure schedule chosen for each formulation were optimized by previous calorimetric studies in order to obtain the cured-fully networks.[6] In this work, the *in vitro* blood compatibility of the epoxy networks was studied by four *in vitro* bioassays: protein adsorption, blood platelet adhesion, thrombus formation and cytotoxicity. The cytotoxicity was evaluated against Chinese hamster ovary (CHO) cells, ATCC CHO k1 (American Type Culture Collection, ATCC). Details of all tests using in this work were previously published.[5]

Results and Discussion

For the epoxy materials surfaces studied in this work was observed a higher human albumin adsorption when compared to the human fibrinogen adsorption suggesting a nonthrombogenic behavior for these surfaces. The results about platelet adhesion and thrombus formation indicated that DGEBA-IPD and DGEBA-AEP epoxy networks exhibits better hemocompatible behavior. It is well known that the biocompatibility is certainly controlled by the cellular activity at the interface of the synthetic material. The cytotoxicity level of epoxy specimens was relatively low for all materials studied (Fig. 1). The materials revealed no signs of cytotoxicity to Chinese hamster ovary cells, showing a satisfactory cytocompatibility.

For this reason it is possible to consider that the epoxy polymers studied are biocompatible materials.

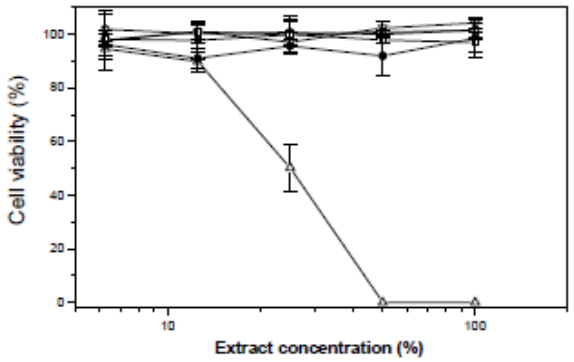

Fig. 1 Cytotoxicity of the DGEBA-DETA (□), DGEBA-TETA (■), DGEBA-AEP (●) and DGEBA IPD (○) epoxy networks extracts, negative control (UHMWPE) (∇), and positive control (phenol) (Δ) against Chinese hamster ovary cells.

Conclusions

The protein adsorption assays onto polymeric surfaces showed that the epoxy polymers adsorbed more human albumin than human fibrinogen. The results about platelet adhesion and thrombus formation indicated that DGEBA-IPD and DGEBA-AEP epoxy networks exhibits better hemocompatibility. The cytotoxicity results indicate that every studied epoxies materials are biocompatible with Chinese hamster ovary cells.

Studies of these materials using animal models, drug release and adhesion assays using bone-titanium joints for use as orthopedic cement are currently being investigated in our laboratories and the results will be reported elsewhere.

References

1. Geckeler, K.; Wacker, R.; Martini, F.; Hack, A.; Aicher, W. Cell Physiol Biochem 2003, 13, 155.
2. Kostoryz, E. L.; Tong, P.Y.; Chappelow, C. C.; Eick, J. D.; Glaros, A. G.; Yourtee, D. M. Dental Materials 1999, 15, 363.
3. Hyoung, U. J.; Yang, Y. J.; Kwon, S. Y.; Yoo, J. H.; Myoung, S. C.; Kim, S. C. J Prev Med Public Health 2007, 40, 155.
4. Hashimoto, Y.; Moriguchi, Y.; Oshima, H.; Kawaguchi, M.; Miyazaki, K.; Nakamura, M. Toxicology in vitro 2001, 15, 421.
5. González Garcia, F.; Leyva, M. E.; de Queiroz, A. A. A.; Higa, O. Z. J Appl Polym Sci 2009, 112, 1215.
6. González Garcia, F.; Soares, B. G.; Pita, V. J. R. R. Pita.; Sánchez, R.; Rieumont, J. J Appl Polym Sci 2007, 106, 2047.

Polymer Chemosensoring Materials with Crown-Ether Derivatives for Advanced Application in Environmental Monitoring

D.O. Soloveva, I.S. Zaitsev, M.S. Tsarkova, A.N. Timonin, S.Yu. Zaitsev, S. K. Sazonov, A.I. Vedernikov*, S.P. Gromov**

Moscow State Academy of Veterinary Medicine and Biotechnology;
*Photochemistry Center of Russian Academy of Science

e-mail: d.solovieva@mail.ru

Introduction

Design and preparation of the ultrathin films based on crown-containing dyes is currently one of the most interesting and rapidly developing areas of research at the "junction" of polymers and colloids, physical-organic and biological chemistry, bio- and nanotechnology [1]. The properties of a new class of photochromic materials synthesized at the Photochemistry Center of the Russian Academy of Sciences [2], such as crown-containing dyes, have recently become the subject of intense studies. The presence of a crown ether fragment in the dyes facilitates their selective bonding to metal cations. Spectral measurements taken in organic and water-organic media have shown cation influences on the physico-chemical properties of the sensor molecule [2]. There are three functional parts in the structure of the amphiphilic pyridinium benzodithia-18-crown-6 dye (**1**) (Figure 1): an ion-selective part of the dithia-containing macrocycle, a photosensitive benzo-C=C-pyridinium part, and a lipid-like hydrophobic "tail" (C18).

Figure 1. The structure of the amphiphilic pyridinium benzodithia-18-crown-6 dye (**1**).

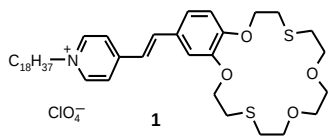

1

Materials and Methods

The polymer films with the dye **1** (total thickness of 10 μm) were prepared by modified spreading technique on the medical glass substrate from 10% polymer solutions in chloroform. The spectra of the polymer-dye films were recorded in the range 300–800 nm using absorption and fluorescence spectrophotometers. The absorbance of the polymer films without dye was below 300 nm. The influence of heavy cations on these films was studied using 10^{-3}, 10^{-4}, 10^{-5} and 10^{-6} M $Hg(ClO_4)_2$ or $AgClO_4$ aqueous solutions. The spectra of the dye-polymer films in all cases showed a strong band with an absorption maximum at 400–450 nm, which was assigned to the dye *trans*-form according to published data on the pure dye in some organic solvents [2].

Results and Discussion

Applying various salts to the polymer-dye film, it was possible to directly obtain changes in the dye **1** spectral parameters (the wavelength maximum and its shift). For example, the absorption wavelength maximum for the polymer-dye film based on poly(vinyl chloride) (PVC) was at 419 nm and absorption intensity about 0.160 arbitrary units. The maximal shifts of absorption on about −26 nm for the polymer-dye film were found in the case of 10^{-3} M $Hg(ClO_4)_2$ aqueous solutions. There were no linear dependences between salt concentration in solution and the wavelength shift for the absorption maximum in the case of $Hg(ClO_4)_2$. The same polymer-dye films were used for detection of silver cations in aqueous solutions and showed better results. The maximal shifts of absorption on about −25 nm for the polymer-dye film were found in the case of 10^{-3} M $AgClO_4$ aqueous solution (Table 1).

Table 1. The wavelength for the absorption maximum (nm) for the polymer-dye film based on PVC before (λ_0) and after (λ) treatment with $AgClO_4$ solutions.

Ag^+ M	λ_0, nm	λ, nm	$\Delta\lambda$, nm
10^{-3}	419 ± 1	394 ± 1	−25
10^{-4}	419 ± 1	405 ± 1	−14
10^{-5}	419 ± 1	412 ± 1	−7
10^{-6}	419 ± 1	418 ± 1	−1

Linear dependence between salt concentration in solution and the wavelength shift for the absorption maximum was found in the case of $AgClO_4$ solutions which could be promising for the quantitative detection of the silver cations in aqueous solutions.

The fluorescence wavelength maximum for the polymer-dye film based on PVC was at 502 nm and fluorescence intensity about 450 arbitrary units. The maximal shifts of fluorescence on about −15 nm for the polymer-dye film were found in the case of 10^{-3} M $Hg(ClO_4)_2$ aqueous solutions. It is important to underline the almost linear dependence between salt concentration in solution and the wavelength shift for the fluorescence maximum in the case of $Hg(ClO_4)_2$ **solutions. This could be promising for the quantitative detection of the mercury cations in aqueous solutions. On the other hand, the maximal shifts of fluorescence on about** −19 nm for the polymer-dye film were found in the case of 10^{-3} M $AgClO_4$ aqueous solutions.

Conclusions

Thus, the wavelength shift for the absorption maximum in the case of $AgClO_4$ solutions and wavelength shift for the fluorescence maximum in the case of $Hg(ClO_4)_2$ indicated the most promising materials for novel optical chemosensor for quantitative detection of the silver and mercury cations in aqueous solutions that is important for environmental monitoring.

References

1. Zaitsev, S.Yu. Supramolecular nanodimentional systems at the interfaces: concepts and perspectives for bio nanotechnology. LENAND: Moscow, Russia, 2010, P. 208.
2. Ushakov, E.P.; Alfimov, M.V.; Gromov, S.P. Russian Chemical Reviews 2008, 77 (1), 39–59.

Gradient in Viscoelastic Properties of Polymers to Control Adhesion

François Tanguy[1], Ralph Even[2], Isabelle Uhl[2], Anke Lindner[3], Costantino Creton[1]

[1] Laboratoire de Physico-chimie des Polymères et des Milieux Dispersés (PPMD), ESPCI
[2] The Dow Chemical Company
[3]Laboratoire de Physique et Mécanique des Milieux Hétérogènes (PMMH), ESPCI

francois.tanguy@espci.fr

In order to obtain polymers showing good adhesive properties, materials having both a liquid-like behavior (to create easily a molecular contact and dissipate energy upon debonding) and an elastic behavior (to resist shear forces) are necessary.
Efficient bonding to rougher low energy surfaces requires however a low elastic modulus and a high degree of viscoelasticity. Such a very soft adhesive will then possess a low resistance to stress during debonding. We believe that an innovative solution to this problem is to create a gradient in the viscoelastic properties of the adhesive to obtain a more dissipative behavior near the adhesive/adherend interface and a more elastic behavior in the bulk. Multi-layer materials can offer these properties. Bi-layer adhesives have already been studied and show some interesting properties [1].

Materials and Methods:

We focus here on model acrylate polymers (PolyBA-co-AA) prepared by emulsion polymerization for applications as Pressure Sensitive Adhesives (PSA).
Different molecular weights (Mw) and architectures were studied. All polymers were nearly linear and uncrosslinked with a relatively high average Mw (300k-1570k).
In order to create a gradient in viscoelasticity through the thickness, multi-layer materials were made, using the different latexes at our disposal. Thin films of homogeneous polymers were dried with a final thickness of 25µm. Once prepared, films with different properties were assembled to obtain multi-layer materials. In order to ensure good adhesion between the layers, the films were subsequently annealed at 80°C under load for 10 hours.
Probe-tack tests were carried out on these films on glass slides. The analysis of the stress – strain curves and real-time movies obtained through this experiment provide the information to evaluate the adhesive properties of the sample [2].
Adhesive properties were completed with detailed rheological characterizations. The linear viscoelastic properties and the large strain properties of the films were measured in the standard parallel plate shear geometry, and in the uniaxial extensional geometry.

Results and Discussions:

Bi-layer adhesives show interesting synergetic properties lying in between the properties of homogeneous layers of the two materials. Adding a viscous layer to an elastic backing layer, leads for example to a slightly increased adhesion, especially on a polyethylene substrate. Due to the elastic backbone, an interfacial debonding is obtained, with a higher level of dissipation at the interface due to the viscous layer.
Note that the viscoelastic properties of the two layers have to be relatively close: if the layers are too different, only the softer viscous layer is deformed, resulting in a cohesive debonding.

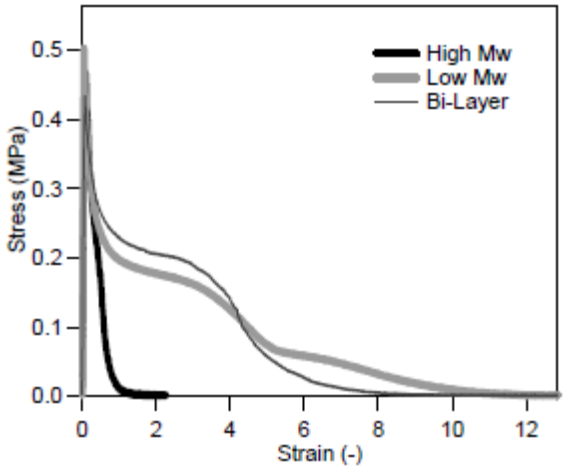

Fig. 1: Tack curves for homogeneous materials (thick lines) and bi-layers (thin line); Vdeb = 10 µm/s

When changing the thickness of the two layers, we observed a strong variation of the overall adhesive properties. This can be explained by the formation and growth of fibrils inside the material, sensitive to the thickness of the viscous layer and to the position of the interface.

Conclusions:

We have successfully prepared multi-layer adhesives from acrylic polymers made from model latexes. We have shown that their adhesive properties are enhanced compared to homogeneous adhesives, especially on polyolefins. Thickness and viscoelastic properties of each layer are two important parameters and need to be finely tuned.

Acknowledgements:

We acknowledge funding from an FP7 EU collaborative project (MODIFY- 228320). We also acknowledge fruitful discussions with the polymer rheology group at UCL (L. Mohite, C. Bailly).

References:

[1] Carelli, C.; Deplace, F.; Boissonnet, L.; Creton, C. Journal of Adhesion, 83 (2007), 491-505.
[2] Lakrout, H.; Sergot, P.; Creton, C. Journal of Adhesion. 69 (1999), 307-359.

Comparative Study for Tin and Zinc Catalysts for Lactide Polymerization

Jakub Wojtaszak, Jolanta Ejfler, Izabela Czeluśniak

Faculty of Chemistry, Wroclaw University, 14 F. Joliot-Curie 50-383 Wroclaw, Poland

DRWHO@eto.wchuwr.pl

Introduction:

In recent years, there has been increasing interest in biodegradable and bioassimilable polylactide (PLA) due to their pharmaceutical and biomedical applications. The low-molecular-weight PLA has been recently proposed as materials in drug delivery systems.[1] With those type of applications, it is critical that polymers decomposition profile has to be precisely matched to the needs of the application. In practice, PLA is prepared industrially via the ring-opening polymerization (ROP) of L-lactide (LA) using bis(2-ethylhexanoate)tin(II), $Sn(Oct)_2$.[2] This initiator is widely used in preparing of various graft and block copolymers starting from any hydroxyl derivatives as co-initiators and using cyclic esters as monomers.[3]

Much interest have been devoted also to zinc complexes as potential nontoxic catalysts. Recently, the zinc initiator/alcohol system has been demonstrated high activity in ROP of LA and allow for better control of the polymerization, as in the case of $Sn(Oct)_2$.[4] Among known Zn complexes the zinc initiators with aminophenolate ligands have been found as excellent initiators for LA polymerization in the presence of alcohol as co-initiator.[5]

The aim of this study was to compare the widely used $Sn(Oct)_2$ catalyst with $[Zn(\eta^2\text{-}L^2)_2]$ initiator (L= N-[methyl(2-hydroxy-3,5-di-tert-butylphenyl)]-N-methyl-N-(1,3-dioxolan-2-yl-methyl) for synthesis of low-molecular PLA with acetylene end-group.

Materials and Methods:

The polymerizations were carried out under nitrogen using the conventional vacuum/nitrogen line or glove-box techniques. NMR spectra were recorded using a Bruker AMX-300 and 500 spectrometers. Gel Permeation Chromatography (GPC) data were obtained using a Viscotek GPC max equipped with a refractive index detector Viscotek VE 3580 and 2x 300 mm Shodex GPC 6 µm KF-802.5 columns. Tetrahydrofuran (THF) was used as the eluent at a flow rate of 1.0 mL/min at 30°C. Polystyrene standards were used for calibration.

Results and Discussion:

The low-molecular-weight PLA polymers terminated with an acetylene group were synthesized by ROP of LA in the presence of $Sn(Oct)_2$ and $[Zn(\eta^2\text{-}L^2)_2]$ initiator and propargyl alcohol as co-initiator (Scheme 1). The degree of LA polymerization (DP) value was calculated from the LA-to-alcohol-to-complex ratio and from ^1H NMR spectra. For presented polymers, theoretical DP was in good agreement only in the case of using Zn initiator. Generally, the tin initiator gave higher DP value than calculated. Moreover, the polydispersity indexes of PLA were higher than those observable for Zn complex.

In order to confirm the structure of synthesized PLA the ^1H NMR spectra have been analyzed. The main evidence for present of the propynyl end-group is the chemical shift of methylene protons of propynyl group attached to polymer chain, observable in spectra of PLA synthesized using both initiators. However, ROP of LA by Zn initiator gave polymer with higher tacticity.

The ROP of LA by both initiators was carried out in NMR probe. In the case of Sn initiator, beside ROP of LA

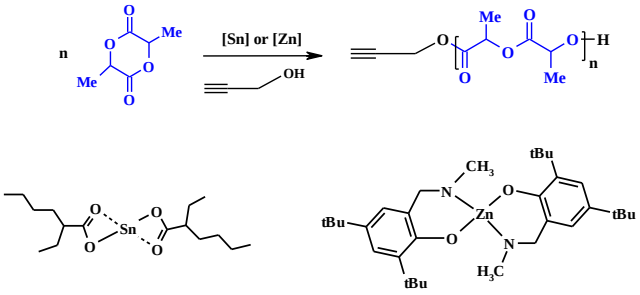

Scheme 1

reaction LA estrification occured giving propynyllactyllactace as side product.

Conclusion:

The presented results lead to the conclusion, that in the ROP of LA initiated by $Sn(Oct)_2$ esters of LA formed besides PLA. In order to obtain desired product, PLA or LA ester, the initiator-to-alcohol-to-LA molecular ratio must be precisely selected.

References:

1) Mauduit J., Bukh N., Vert M. *J. Controlled Release* 23 (1993) 209.; Bodmeier R.; Chen H. J. Pharm. Sci. 78 (1991) 819.

2) Nijenhuis A.J., Grijpma D.W., Penning A.J. *Macromolecules* 25 (1992) 6419.; Kricheldorf H.R., Kreiser-Saunders I., Boettcher C. *Polymer* 36 (1995) 1253.; Kowalski A.; Duda A., Penczek S. *Macromolecules* 33 (2000) 689.

3) Mecerreyes D., Jerome R., Dubois P. *Adv. Polym. Sci.* 147 (1998) 1.; Czelusniak I., Khosravi E., Kenwright A. M., Ansell C. W. G. *Macromolecules* 40 (2007) 1444.

4) Wu J., Yu T-L., Chen C-T., Lin C-C. *Coordination Chem. Rev.* 250 (2006) 602.

Ejfler J., Szafert S., Mierzwicki L., Jerzykiewicz L. B., Sobota P. *Dalton Trans.* (2008) 6556.

Magnesium Catalysts Design for Ring-Opening Polymerization of Lactides

Jolanta Ejfler, Slawomir Szafert, Krzysztof Mierzwicki, Piotr Sobota

Department of Chemstry, University of Wrocław, 14 F. Joliot-Curie, 50-383 Wrocław, Poland

e-mail: je@wchuwr.pl

Introduction

Polylactide (PLA) is the most prominent examples among the biodegradable polymers due to its wide application in biomedical and pharmaceutical fields.

Although many developed strategies for the preparation of PLAs, the most effective remains ring-opening polymerization (ROP) initiated by metal alkoxides and among them candidates of primary importance are monomeric complexes with nontoxic and essential for life metals such as magnesium. Up to now only few examples of magnesium compounds that are active as initiators in ROP of cyclic esters have a structure proven by X-ray analysis, which is highly desirable to design well-defined "single-site" initiators. Herein, we report the preparation and the detailed structural discussion of a series of homoleptic magnesium complexes with aryloxo and aminaphenolate ligands.

Results of the compounds' activity in ROP of lactides are also reported.

Results and Discussion

For the synthesis of magnesium compounds we utilized variety of oxo ligands including commercially available 2,3-dihydro-2,2-dimethyl-7-benzofuran alcohol (ddbfo-H; **1a**-H) and tetrahydrofurfuryl alcohol (thffo-H; **1b**-H) as well as aminaphenolate ligands: tbabp-H (**1c**-H_2), tbpca-H (**1d**-H), tbpmpa-H (S-**1e**-H) and tbpoa-H (**1f**-H), obtained by route previously reported by our group (Scheme 1).1

The reactions of not sterically demanding bidentate **1a**-H or **1b**-H with $MgBu_2$ yield tetranuclear compounds $[Mg(ddbfo)_2]_4$ (**2a**) and $[Mg(thffo)_2]_4$ (**2b**) with open dicubane geometry. Higher dentate or more bulky bidentate ligands like the chiral and racemic amino-*bis*-phenolate ligands *R*-**1c**-H_2 and *rac*-**1c**-H_2 form much less aggregated structures, the dimeric magnesium complexes $[Mg(R\text{-bpthfa})]_2$ (*R*-**2c**) and $[Mg(rac\text{-bpthfa})]_2$ (*rac*-**2c**) as presented in Scheme 1.

The aminophenolate bidentate ligands **1d**-H and *S*-**1e**-H appear to be well suited for the synthesis of monomeric tetrahedral magnesium compounds $[Mg(tbpca)_2]$ (**2d**) and $[Mg(tbpmpa)_2]$ (*S*-**2e**). The hemilabile **1f**-H ligand in the reaction with $MgBu_2$ gave six-coordinate complex $[Mg(tbpoa)_2]$. **2f**. The structures of all magnesium complexes were confirmed by NMR spectroscopy as well as X-ray study.

Lactide Polymerization

The monomeric hexacoordinated magnesium **2f** proved to initiate polymerization L-LA (**2f**/L-LA = 1/50) in high conversion within 30 min to afford PLA with moderate Mw = 8600 and PDI = 1.12. In this case, the NMR end group analysis of isolated PLA indicated the presence of hydroxyl and aminophenolate ester end groups. Monomeric tetrahedral compounds **2d** and *S*-**2f** were next tested.

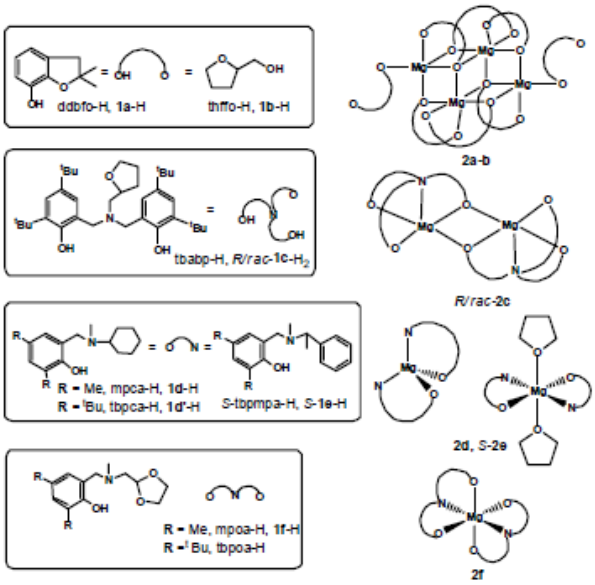

Scheme 1. The magnesium compounds with aryloxo and aminaphenolate ligands.

Although they both showed no activity they become extremely active when external donor was added as described in Table 1. All of the initiator systems exhibit molecular weights in close agreement with calculated values and narrow PDI characteristic for well controlled living propagation.

Table 1. Polymerization of L-LA with initiators (I) **2d**, *S*-**2e**, **2d**/BnOH, *S*-**2e**/BnOH

(I)	[I]:[L-LA]: BnOH	t min	$10^{-3}M_n$[b]	$10^{-3}M_n$[c]	C %	PDI[c]
2d	1/100/0	5d	-	-	-	-
2d	1/50/1	1	6.88	7.02	96	1.09
2d	1/100/1	5	15.58	13.37	92	1.10
S-2e	1/100/0	5d	-	-	-	-
S-2e	1/50/1	1	7.20	6.59	90	1.02
S-2e	1/100/1	10	14.82	13.80	95	1.08

General polymerization conditions: solvent toluene (10 mL), T = 25 °C, [I] = 0.025; a conversion determined by 1H NMR spectroscopy; b determined by GPC, PDI calibrated with polystyrene standards.

Conclusion

We have synthesized and characterized new magnesium aryloxides. The results clearly support the adventage of monomeric magnesium species over polynuclear analogos in lactide polymerization. The dynamic behavior in solution involve by hemilabile aminophenolate ligands may be an important factor for catalytic applications.

References

[1] J. Ejfler, K. Krauzy-Dziedzic, S. Szafert, L. Jerzykiewicz, P.Sobota, *Eur. J. Inorg. Chem. 2010,3602.*

Fluorene-Derivative Containing Polymers as Sensory Materials for the Colorimetric and Fluorogenic Sensing of Analytes.

H. El Kaoutit, P. Estévez, S. Vallejos, M. Trigo-López, F.C García, F. Serna, J. de la Peña, J.M García

Departamento de Química, Facultad de Ciencias, Universidad de Burgos, Plaza de Misael Bañuelos s/n, 09001 Burgos, Spain

hamidkat2000@yahoo.fr

Introduction

Due to the outstanding mechanical properties of aromatic polyamides (aramids), we have used the aramid backbone to prepare advanced functional materials. Thus, we have synthesized chemically modified copolyamide consisting of 90% of structural units of poly(*m*-phenylene isophthalamide) (NOMEX®) and 10% of structural units containing pendant fluorene derivatives. Following this strategy, the excellent mechanical and thermal properties of NOMEX® were maintained, and the materials gave rise to creasable films or dense membranes to be used as colorimetric or fluorescence sensory materials.1 Moreover, a 10% mole content of the structural units with the urea binding site and fluorescent fluorene group is especially adequate for measuring changes in the fluorescence behavior upon interaction with analytes and, sufficient for giving rise to perceptible ‘‘naked eye’’ colorimetric variations.

Results and discussion

The copolymer **CP1** was firstly prepared and then chemically modified to render copolymers **CP2** to **CP6** (Scheme 1).[2] These modifications were carried out following orthogonal and high yielding reactions and were previously studied using model compounds. This synthetic approach has proven to be a really adequate strategy to prepare new functional soft materials. The reaction conditions were optimized with the model compounds and then applied to the polymers. These model compounds were also used to study the chromogenic and fluorogenic behaviour of the polymers in solution, supposing that each model mimics the behaviour of its corresponding polymer, but with a defined molecular weight and higher solubility.[3,4]

Chromogenic and fluorescence behavior

As previously outlined, the chromogenic and fluorescentbehaviors of high-performance polymers are key properties for many novel applications, such as for chromogenic and fluorogenic sensing materials or for hybrid LUCO/LED emitting devices. The copolymers (Scheme 1) give rise to fluorescent and colored solutions in organic solvents. Upon addition of different anions, a fluorogenic and chromogenic response is observed, as depicted for CP2 in Figures 1 and 2. Thus, the addition of CO3 2- gives rise to a selective color change and to the fluorescence quenching.

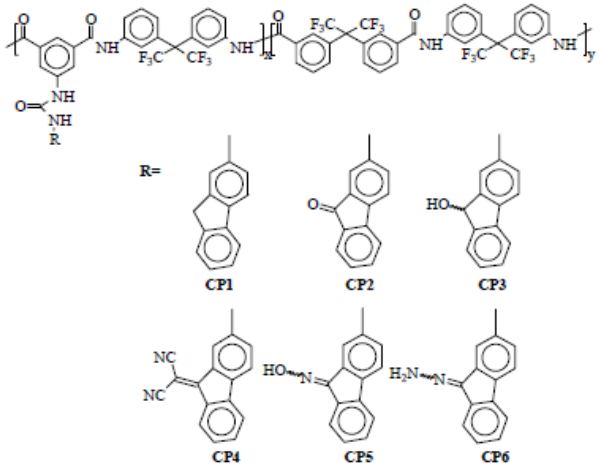

Scheme 1. Chemical structure and codes of the modified copolyamides.

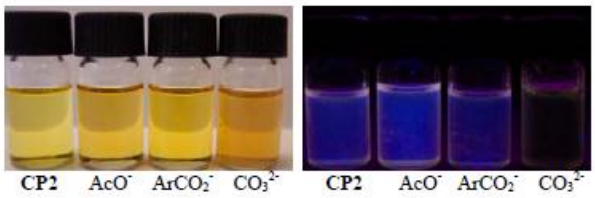

Figure 1. Chromogenic (left) and fluorescence (right) images of solutions of copolyamide **CP1**, **CP2**, **CP3**, **CP4**, **CP5** and **CP6** (from left to right) in DMSO (8x10-3M). The anions have a concentration of 2x10-2M. The right photograph was taken under irradiation with UV (365nm).

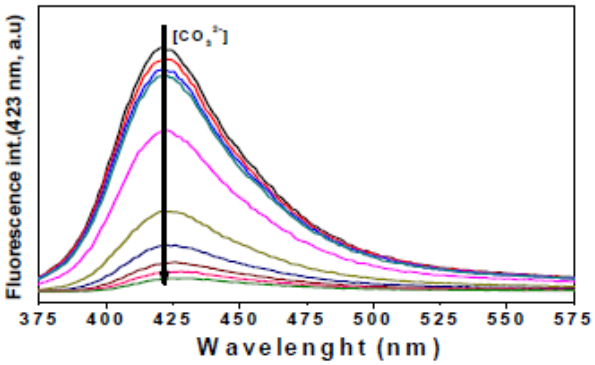

Figure 2. Fluorescence titration curves of a DMSO solution of the copolyamide **CP2** with potassium carbonate (fluorescence intensity at 423 nm).

References

1 García, J. M.; García, F. C.; Serna, F.; de la Peña, J. L. Prog Polym Sci 2010, 35, 623.
2 Estévez, P.; El-Kaoutit, H.; García, F.C.; Serna, F.; de la Peña, J.L.; García, J.M. J Polym Chem Part A: Polym Chem 2010, 48, 3823.
3 San-José, N.; Gómez-Valdemoro, A.; Calderón, V.; de la Peña, J.L.; Serna, F.; García, F. C.; García, J. M. Supramol Chem 2009, 21, 337.
4 San-José, N.; Gómez-Valdemoro, A.; Ibéas, S.; García, F. C.; Serna, F.; García, J. M. Supramol Chem 2010, 22, 325.

Study Of Surface Energy Of Polypropylene Films Treated By Corona At A Ambient Temperature And Above.

H. C. de Sena1 and J. S. C. Campos1

1DTP, FEQ, State University of Campinas, Campinas, SP, Brazil

hildosena@feq.unicamp.br

Introduction: This work examines the critical surface tension and the surface free energy of polypropylene films (PP) under three different conditions: corona treatment at room temperature, corona treatment above ambient temperature and without treatment. The objective is to modify the surface of PP films raising the surface free energy and evaluate the temperature influence on the surface energy of these films.

Materials and Methods: The material was PP isotactic produced by the Policast company with 28µm average thickness. Corona's generator geometry is point-plan type with 5000 volts potential between the electrodes [1]. The critical surface tension and the surface free energy of PP films were obtained by measuring the contact angle between a drop of deposited liquid on the PP surface against the parameters of corona treatment time (2s to 90s) and the distance between the electrodes (5mm). Films previously cleaned with ethanol were used to determine the contact angle without corona treatment, then treated with corona discharge at room temperature (25°C) and above (55°C). Measurements of contact angle were carried out with a Tantey Model CAM-MICRO goniometer under the sessile drop method at 23°C (3°C) in water, glycerol, formamide, diiodomethane and ethylene glycol. To determine the critical surface tension of the PP films in different treatments Zisman's approach was performed [2]. The surface free energy of the polymer is analyzed using the alternative formulation of equation of state (EQS) propose by Kwok and Neumann [3], the Wu and VCG (van Oss, Good and Chaudhury) approach derived from Young equation [4-7]. The form of EQS used in this work is as follows:

$$0 = -\gamma_{LV}(1+\cos\theta) + 2\sqrt{\gamma_{SV}\gamma_{LV}}\,(1-\beta_1(\gamma_{SV}-\gamma_{LV})^2) \qquad (1)$$

Where:

β is a constant which equals 1,057x10^{-4} (m/mN)^2.

Results and Discussion: The surface free energy values of PP films calculated from Zisman's approach, EQS, Wu and VCG approach are given in Table 1 and Fig. 1.

Table 1. The surface free energy (γ_{SV}) values reproduced from different approaches and treatments.

Approach	γ_{SV} (mN/m)		
	Without corona [a]	Corona at 25°C (2°C)	Corona at 55°C (2°C)
Zisman's	34,62	39,56	40,31
EQS	33,45	45,87	45,46
Wu [b]	42,23	62,63	61,35
VCG [b]	36,87	48,14	47,38

[a] Films previously cleaned with ethanol were used to determine the contact angle without corona treatment.

[b] Mean of the surface free energy of PP films treated with corona discharge above 10s of treatment.

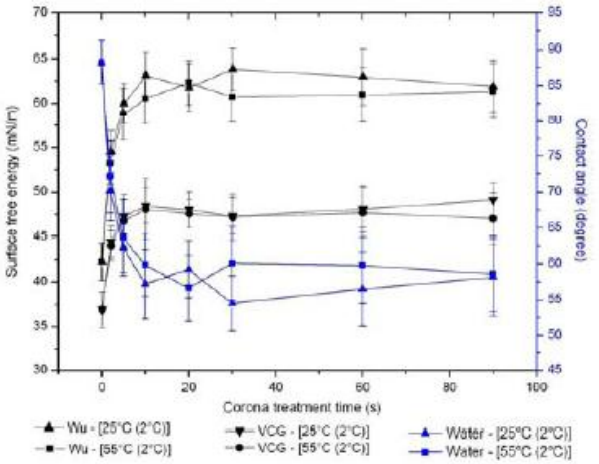

Fig. 1. Contact angle and γ_{SV} values of PP films determinate by Wu and VCG approach.

Conclusions: The results shows significant influence of corona treatment in order to increase the surface energy of PP films by decreasing the contact angle value between the sample and drop of water. Films treated by corona at room temperature and above ambient temperature did not show significant differences in the values of critical surface tension as well as for surface free energy.

Keywords: Polypropylene, Corona treatment, Critical surface tension, Surface free energy.

References:

[1]. Sinézio, J.C.C. Novo triodo corona e sua aplicação no estudo das propriedades elétricas do polímero PVDF. 1990, 102f. Thesis (Ph.D. in Physics and Materials Science) - University of São Paulo, USP-São Carlos, SP.

[2]. Zisman, W.A. Contact angle, wettability and adhesion, in: Advances in Chemistry Series, v.43, Washington, p.1-51, 1964.

[3]. Kwok, D. Y.; Neumann, A. W. Colloids and Surfaces A: Physicochem. Eng. Aspects. 161, 31-48, (2000).

[4]. Wu, S. J. Polym. Sci. C. 34, 19-30 (1971).

[5]. Ahadian, S.; Moradian, S.; Tehran, M. A. Appl. Surface Sci. 256, 1983-1991 (2010).

[6]. Biresaw, G.; Carriere, C. J. J. Polym. Sci. B: Polym. Phys. 39, 920-930 (2001).

[7]. Erbil, H. Y.; Hazer, B. J. Appl. Polym. Sci. 60, 1313-1320 (1996).

The authors thank A. C. L. Lisboa and L. A. P. Martins for reviewing on this manuscript. This work was supported by CAPES.

Background and New Opportunities with the Aromatic Thermosetting Copolyesters

Zeba Parkar and James Economy

Department of Materials Science and Engineering, University of Illinois, Urbana Champaign

jeconomy@illinois.edu

Work on aromatic thermosetting copolyesters (ATSP) was first announced via the issuance of a U.S. Patent (1995)[1] which describes the synthesis and properties of this novel family of polymers. In the present paper we provide a very brief review of the development of linear polyesters from 1881-1995. We then discuss our more recent work on ATSP. Finally, we consider four distinct areas of opportunity for commercial utility of the ATSP currently under development in our group, namely 1) a matrix for high performace composites, 2) a coating to achieve very high flame resistance, 3) design of outstanding ablation materials and 4) coatings which display outstanding wear resistant surfaces.

Early Work on the Aromatic Copolyesters: This work may represent some of the earliest published research in the field of polymers. In 1882, Klepl[2] reported the thermal polymerization of phydroxybenzoic acid (PHBA) to form a p-oxybenzid along with the dimer and trimer of the PHBA polymer. Schiff[3] reported on forming a similar polymer by reacting the acid chloride of PHBA with itself. In 1909 Emil Fischer[4] published a paper confirming Klepl's preparation of the dimer and trimer one year before Ostwald proposed his colloidal theory as an alternate interpretation for the nature of polymers. It wasn't until 1930 when the colloid interpretation was put to rest by Staudinger.

The next report on this family of materials was in 1959 when Gilkey and Caldwell[5] published a paper in which they reported that the homopolymer of p-acetoxy benzoic acid was unstable at 350°C producing a sublimate as a byproduct. We began our work in 1962 and by the spring of 1963 we had successfully prepared the homopolymer of PHBA which indeed was stable in air at 350°C. The Ekkcel or Xydar copolymer consisted of PHBA and BPT (bisphenol terephthalate) (molar ration 2:1 respectively) and was designed originally to melt at temperatures of 400°C. It could be extruded to temperatures above 400°C but under high shear conditions tended to fibrillate. One of the unique features of these aromatic copolyesters is their ability to undergo ordering and randomization reaction on heating at temperatures of 350°C and above.

Commercial Development of the Aromatic Copolyester of PHBA: In 1971 we announced the availability of the PHBA homopolymer[6] as a coating made by plasma spray for use primarily as an abradable seal in aircraft engines. This market in the ensuing years grew to a highly profitable $25 million per year by the early 1980's but began to fall off by the year 2004. In the case of the melt processable copolyester a 25 million lb/year plant was built by the late 1970's by Dart-Kraft to manufacture this polymer for use in high temperature kitchenware. This market has ceased in the USA but appears to continue in Europe. Work on a Kevlar-like fiber based on the aromatic polyesters has not been pursued even though it would have significant advantages over Kevlar including an LOI of 0.40 compared to 0.28 for Kevlar, very low moisture uptake compared to Kevlar and a much lower cost of manufacture. These fibers are melt spun compared to the need for H_2SO_4 as a spinning solvent for Kevlar.

ATSP: Thermosetting copolyesters of trimesic acid, acetoxybenzoic acid, isophthalic acid and hydroquinone diacetate have been prepared[7] and shown to display a number of important features with obvious commercial potential in the area of 1) ablative shields, 2) high temperature carbon reinforced composites,[8] 3) flame resistant coatings, and 4) highly wear resistant coatings. Progress in each of these four topics will be reviewed in this presentation. In addition, a number of key advantages of this novel system will be described including 1) Ease of consolidating molded structure to greatly reduce porosity by carrying out high temperature Interchain Transesterification Reactions (ITR) 2) Taking advantage of the liquid crystalline nature of the ATSP to match the negative CTE of the carbon fiber reinforcement 3) The unique flame resistance (LOI ~ 0.4) to greatly enhance the flame resistance of a wide variety of textiles 4) preparing ultra-low wear blends of ATSP/Teflon (1:1)[9].

From the above, it should be fairly evident that the ATSP resin will in the near future achieve significant commercial success.

References:

1 Economy, J. U.S. Patent 5,439,541, 1995.
2 Klepl, A. *J Prakt. Chem.* 1882, 25, 525.
3 Schiff, H. *Ber. Dtsch. Chem. Ges.* **1882**, 15, 2588-2592.
4 Fischer,E. Berichte 1909, 42, 215.
5 Gilkey, R.; Caldwell, J. R.; *J. App. Poly. Sci.* 1959, 2, 198-202.
6 Economy J,; Cottis, S. G.; Novak, B.E. U.S. Patent 3,962,314, 1972.
7 Frich, D.; Goranov, K.; Schneggenburger, L.; Economy, L. *Macromolecules* **1996**, 29, 7734-7739.
8 Abdul Samad, Z. F.; Economy, J. *Annual Technical Conference – ANTEC Conference Proceedings*, **2009**, 4, 2276-2280.
9 Zhang, J.; Demas, N.; Polycarpou, A. A.; Economy, J. *Polym. Adv. Technol.* **2008**, 19(8), 1105-1112.

Effect of Acrylic Copolymer Dispersants Bearing Epoxy Groups on Dielectric Properties of Carbon Black-filled Epoxy System

Bui Thanh Son, Jin-Young Bae

Department of Polymer Science and Engineering, Sungkyunkwan University, Suwon-si, Gyunggi-do 440-746, Republic of Korea

e-mail b521@skku.edu

Introduction

Material requirements for the commercial applications of embedded capacitor dielectrics include high dielectric constant (K) and low dielectric loss. Much effort has been made to achieve high-k and low-loss at low temperature by thin film deposition, anodization, sol-gel process, and polymer thick film composites. For the polymer thick-film methods, many attempts have been tried to increase the dielectric constant of polymers by employing conductive fillers such as carbon black for percolative high-k polymer composites. However, high dielectric loss (usually >100%) of carbon black-polymer composites was obtained due to the imperfect passivation of carbon black leading to the current leakage through carbon black near the percolation threshold. In this study, good dispersion (and passivation) of carbon black particles in polymer matrix is considered as a very effective way to lower dielectric loss.

Materials and Methods

Preparation of [carbon black/acrylic dispersant/epoxy] composites : A representative example of [carbon black/acrylic dispersant/epoxy] composites was prepared by mixing carbon black, acrylic dispersant, 3,4-epoxycyclohexylmethyl-3,4-epoxycyclohexanecarboxylate, hexahydro-4-methylphthalic anhydride, 1-methylimidazole in the presence of ethyl acetate solvent. The whole mixture was stirred using a high-speed homogenizer (3 min) and ultrasonicated (3 min), respectively. The process was repeated three times. Then, the solvent was removed using a rotary evaporator under a reduced pressure. The resulting carbon black-epoxy paste was used to form a dielectric which was coated onto a copper clad substrate with a single edge blade. Then the sample was cured at 160-190 ^{o}C for 2 hr in the furnace.

Results and Discussion

In this study, we describe the use of copolymeric dispersants with an acrylic backbone and epoxy side groups for formulating [carbon black/epoxy] composites. Six epoxy-containing acrylic copolymer dispersants were prepared from hexyl methacrylate (HMA), poly(ethylene glycol) ethyl ether methacrylate (PEGMA) and glycidyl methacrylate (GMA) via a group transfer polymerization (GTP) technique. The epoxy-containing acrylic copolymer of the highest concentration of PEGMA showed the desirable passivation effect on carbon black, and was found to lower the viscosity of [carbon black/epoxy] paste, leading to well-cured composite after heat treatment. The thick composite film prepared by employing the [carbon black/epoxy/acrylic dispersant] paste was built up on a Cu plate by a screen printing process followed by thermal curing. The dielectric properties of 3.1 vol. % carbon black-filled epoxy showed us high-k (Dk 4900) and rather low dissipation factor (Df 29%) @ 1 MHz.

In conclusion, the passivation of conducting CB by acrylic copolymer dispersants bearing epoxy groups was employed in order to make it possible to maintain the low dielectric loss (Df) which is normally increased by the current leakage through conducting CB. Well-defined acrylic copolymer dispersants synthesized by GTP method were incorporated into the epoxy matrix for controlling CB dispersion/ passivation. Among various dispersants, Dispersant 1 (HMA/PEGMA/GMA 1/1/1) with proper amounts of hydrophilic and hydrophobic moieties gives the best CB passivation effect with low viscosity in epoxy paste and high K/low loss in epoxy film

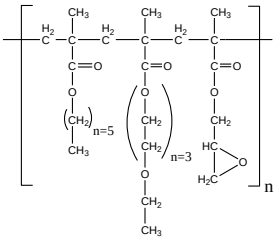

Figure 1. The typical structure of acrylic copolymer dispersants bearing epoxy groups

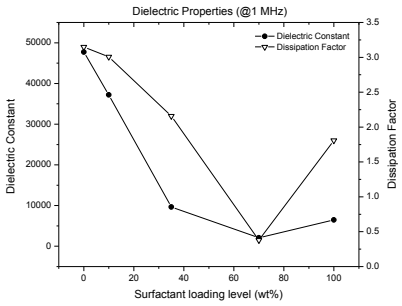

Figure 2. Dielectric properties of carbon black (3.1 vol%)-filled epoxy composite as a function of dispersant loading.

References

[1] Clyde F. Coombs, Jr. Printed Circuits Handbook, McGraw-Hill (2007), 6th Edn.

[2] Jiongxin Lu, C. P. Wong, Recent advances in high-k nanocomposite materials for embedded capacitor applications. IEEE Transactions on Dielectrics and Electrical Insulation (2008), 15(5), 1322-1328.

Synthesis and Characterization of Novel Graphited Polythiophene

Ayumi Takahashi, Kaoru Ohshimizu, Tomoya Higashihara, and Mitsuru Ueda

Department of Organic & Polymeric Materials
Graduate School of Science and Engineering, Tokyo Institute of Technology
2-12-1-H120, O-okayama, Meguro-ku, Tokyo 152-8552, Japan

ueda.m.ad@m.titech.ac.jp

Introduction. Graphenes have garnered significant attention because of their unique electronic properties, such as massless Dirac fermion behavior, half-integer quantum Hall effect, and high-carrier mobility (μ=10^5 cm^2/(Vs) or higher).[1,2] Graphene-based nanostructures are recognized as promising building blocks for an alternative to silicon-based mesostructures in future electronic nanodevices. Several methods have so far been reported to produce graphene sheets based on exfoliation or chemical oxidation of graphite or heat treatment of silicon carbide.[3] Recently, Müllen and co-workers reported the synthesis of linear two-dimensional graphene nanoribbons by the oxidation of polyphenylenes having phenyl side chains synthesized via Suzuki-Miyaura coupling.[4] They first succeeded in controlling the width of graphene nanoribbons. However, polydispersity indicies (PDIs) of graphene nanoribbons have not been controlled yet because the polyphenylene derivative was synthesized via conventional polycondensation. In this report, we report the synthesis of novel graphited polythiophene via oxidantion of polythiophene derivatives with low PDIs, which were obtained by the Grignard metathesis (GRIM) polymerization.[5,6]

Materials and Methods. The synthetic routes of polythiophene derivative are depicted in Scheme 1. The monomer, 2-bromo-5-chloromagnesio-3-(4'-(3",7"-dimethyloctoxy)phenyl)thiophene (**2**), was prepared by the stoichiometric Grignard exchange reaction of **1** with ^{i}PrMgCl at 0 °C for 30 min in the presence of LiCl in THF. (1,3-Bis(diphenylphosphino)propane)nickel(II) dichloride was then added and polymerization was carried out at room temperature for 1 h. The reaction was quenched with 5N-HCl aq. to generate poly (3-(4'-(3",7"-dimethyloctoxy)phenyl)thiophene) (P3PhT(**3**))(M_n 8900, PDI 1.05). Intramolecular Scholl reaction of the P3PhT was performed subsequently with $FeCl_3$ as an oxidative reagent at room temperature. P3PhT was dissolved in $CHCl_3$ under argon and a solution of $FeCl_3$ in CH_3NO_2 was added. The resulting solution was stirred for 72 h. The reaction was quenched with methanol and conc. HCl aq. to obtain graphited polythiophene of **4**. The synthetic route of **4** is shown in Scheme 2.

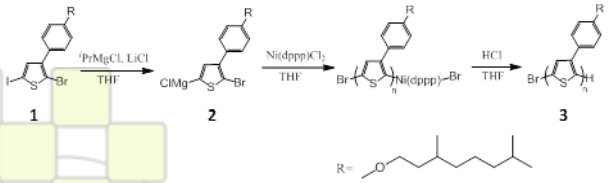

Scheme 1. Synthetic routes of P3PhT (3)

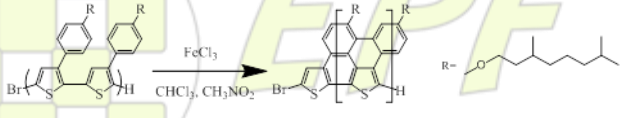

Scheme 2. Synthetic route of graphited polythiophene (4).

Results and Discussion.
The comparison of the ^{1}H-NMR spectra and UV-vis spectra of **3** and **4** is shown in Figure 1 and 2, respectively. In Figure 1, the signals of aromatic protons in **4** at 6.8-7.2 ppm slightly diminish after the oxidative reaction.

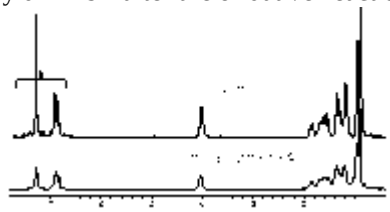

Figure 1. 1H-NMR spectra of 3 and 4.

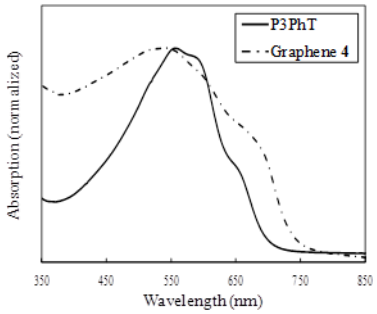

Figure 2. UV-vis spectra of 3 and 4 in the films.

Moreover, the UV-vis spetrum of **4** (λ_{onset} = 738 nm) shows a red shift by 50 nm compared to that of the precursor **3** (λ_{onset} = 696 nm) in the film state.
These results suggest that the intramolecular oxidation of **3** partially proceeds to result in more planer conformation.

Conclusions. Novel graphited polythiophene via oxidation of polythiophene derivatives could be synthesized. ^{1}H-NMR spectra and UV-vis spectra supported the formation of the partial graphited structures.

References.

[1] A. K. Geim and K. S. Novoselov, *Nat. Mater.*, **6**, 183-191 (2007).
[2] A. Bostwick, T. Ohta, T. Seyller, K. Horn and E. Rotenberg, *Nat. Phys.*, **3**, 36-40 (2007).
[3]H. Shinoyama, *J. Mater. Sci. Lett.*, **20**, 499-500 (2001).
[4] X. Yang, X. Dou, A. Rouhanipour, L. Zhi, H. J. Rader and K. Müllen, *J. Am. Chem. Soc.*, **130**, 4216-4217 (2008).
[5]M. C. Iovu, E. E. Sheina, R. D. McCullough, *Macromolecules*, **38**, 8649-8656 (2005).
[6]R. Miyakoshi, A. Yokoyama, T. Yokozawa, *J. Am. Chem. Sci.*, **127**, 17542-17547 (2005)

Synthesis and Characterization of Thianthrene-based Poly(phenylene sulfide)s with Very High Refractive Index over 1.8

Yasuo Suzuki, Kimiya Murakami, Shinji Ando, Tomoya Higashihara, Mitsuru Ueda

Department of Organic and Polymeric Materials, Tokyo Institute of Technology

ueda.m.ad@m.titech.ac.jp

Introduction

In recent years, high refractive index polymers have been developed for various optoelectronic applications.[1] Especially, in polymeric microlens for CMOS image sensors, very high refractive index (high-*n*) exceeding 1.7 or even 1.8, is frequently desired, even though typical refractive indices of conventional polymers are in the range of 1.30–1.65. The general approach to enhance refractive index in polymers is the introduction of substituents with high molar refraction or low molar volume, such as heavy halogens, sulfurs, and metal atoms, according to the Lorentz-Lorenz equation.

Poly(phenylene sulfide) (PPS) is one of the most promising high-*n* polymers because of its high sulfur content and well-packed structure. In a previous report, thianthrene-based PPS (TPPS) **1** and **3** were prepared from 2,7-difluorothianthrene (DFT) and 4,4'-thiobisbenzenethiol (TBBT) or sodium sulfide, respectively. However, TPPS **1** was poorly soluble and TPPS **3** was insoluble in organic solvents, and the reported refractive index of TPPS **1** (1.692 at 633 nm) was unexpectedly low despite of its high sulfur content.[2]

We report herein the synthesis of TPPSs with low to moderate molecular weights (MWs) to endow the solubility. These TPPSs were prepared from DFT and dithiols, including TBBT, *m*-benzenedithiol (*m*BDT), or sodium sulfide nonahydrate, by aromatic nucleophilic substitution reactions. Their refractive indices were extremely high, reaching 1.8020, which is the highest value in reported organic polymers with high transparency in the visible region.

Results and Discussions

The TPPSs were prepared by the polycondensation of DFT with dithiols, such as TBBT, *m*BDT, and sodium sulfide nonahydrate (**Scheme**). To increase the solubility of TPPSs, the molecular weights ($M_{n\ calc}$) were controlled by changing the molar ratios of monomers. TTPSs **1** and **2** ($M_{n\ calc}$=10,000) were soluble in *N*,*N*'-dimethylpropyleneurea (DMPU), 1,1,2,2-tetrachloroethane (TCE), and *N*-methylpyrrolidone (NMP), but insoluble in *N*,*N*-dimethylformamide (DMF), dimethylsulfoxide (DMSO), and $CHCl_3$ at room temperature. On the other hand, TPPS **3** with the most rigid structure among them was least soluble except for that with $M_{n\ calc}$=5,000 which was only soluble in DMPU.

Thermal stability of the TPPSs was evaluated with thermogravimetry (TG) and differential scanning calorimetry (DSC) (Table). All the TPPSs obviously exhibit good thermal stabilities without significant weight loss up to approximately 400 °C. The 5% weight loss temperatures ($T_{5\%}$) are higher than 430 °C. The T_g values are in the range of 143-147 °C, based on the DSC measurement. These results indicate that TPPSs have suitable thermal properties for optical materials.

Films of TPPS **1** ($M_{n\ calc}$=10,000), **2** ($M_{n\ calc}$=10,000), and **3** ($M_{n\ calc}$=5,000) were prepared by spin-casting from their TCE or DMPU solutions followed by heating up to 250 °C to remove the solvent. All films are tough and flexible enough to evaluate optical properties despite their low-to-moderate MWs. All TPPS films show good transparency in the visible region, and the transmittances of TPPSs **1**, **2**, and **3** at 400 nm are 93, 64, and 84%, respectively. The refractive indices of TPPSs were measured at 633 nm with a prism coupler (**Table**). The refractive index of TPPS **1** was reported as 1.692, which is too low judging from its sulfur content (34.65 wt%). In contrast, all TPPS films with low-to-moderate-MWs exhibit very high-*n* in the range of 1.7856-1.8020, which are in the highest class of organic polymers without inorganic components. To our best knowledge, this is the first report of a wholly colorless and transparent in the visible region with refractive indices over 1.80. Moreover, the very low in-plane/out-of-plane birefringences (Δn) of the TPPS films ranging from 0.0033 to 0.0039 is suitable for optoelectronic applications (**Table**).

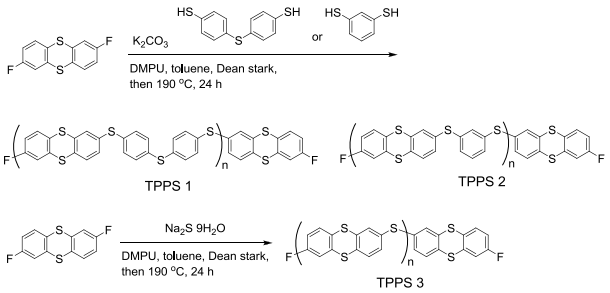

Scheme. Synthesis of TPPSs.

Table. Thermal and optical properties of TPPSs.

TPPS	Sc[a] (wt%)[a]	$T_{5\%}$ (°C)	T_g (°C)	$T_{400\ nm}$ (%)	Δn[b]	n_{av}[c]
1	34.65	471	143	93	0.0037	1.7856
2	36.18	438	142	69	0.0039	1.7966
3	39.04	430	145	84	0.0033	1.8020

[a]Sulfur content. [b]Birefringence. [c]Average refractive index: $n_{av} = [(2n_{TE}^2 + n_{TM}^2)/3]^{1/2}$.

Conclusions

The TPPSs with low to moderate MWs were prepared by the polycondensation of DFT with TBBT, *m*BDT, or sodium sulfide nonahydrate showed relatively high solubility, high transparency in the visible region, and high thermal stability. Furthermore, these polymers exhibited very high refractive indices of 1.7856–1.8020 at 633 nm while maintaining low birefringence values.

References

(1) Liu, J-G.; Ueda, M. *J. Mater. Chem.* **2009**, *19*, 8907.
(2) Robb, M. J.; Knauss, K. M. *J. Polym. Sci,. Part A: Polym. Chem.* **2009**, *47*, 2453.

Surface and Foam Characteristics of PPG-b-PDMS-b-PPG tri-block copolymer as an anti-foaming agent

Burcu Kekevi[1,2], *Hale Berber*[1], *Hüseyin Yıldırım*[1,3]

1) Yildiz Technical University, Department of Chemistry, Davutpasa Campus, 34220 Esenler-Istanbul, Turkey.
2) Yalova Community College, Department of Material and Material processing, Rubber & Plastics Technologies Program, 77100 Yalova, Turkey.
3) Yalova University, Department of Polymer Engineering, 77100 Yalova, Turkey.

brcsari@gmail.com

Polymers, which are produced by emulsion polymerization technique, are called latexes. These latexes have been largely used in adhesive, paint, paper coating and textile industries. In latexes, surfactants are used with different aims but besides they can cause some undesirable problems like formation of foam. Particularly, in processing of paper coating adhesives, foam, especially micro foam, which is tiny, often invisible bubbles, suspended to give rise to undesirable viscosity increases and cause various surface deformations. It can be regarded as the most troublesome to accomplish in processing because it is harder to recognize and eliminate. In order to eliminate these unfavorable problem, anti-foaming agents need to be used whether in synthesis or after synthesis.

In this study, PPG-b-PDMS-b-PPG tri block copolymers, having different molecular weights, were synthesized as anti-foaming agents in order to eliminate micro foams in fast process of paper coating of acrylic based latexes. PPG-b-PDMS-b-PPG tri block copolymers were synthesized by polycondensation reaction of a Cl terminated PDMS and PPG with different molecular weights. Surface tension of tri-block copolymers were determined by Du Nouy tensiometer. Foamability was analysed by Ross-Miles test method and foam characteristics were observed under Leica DMR microscope.

Synthesis of water-soluble Polyamide Dendrimers for DNA Sensors

Yumiko Ito [1], Ching-Yi Chen [2,3], Tomoya Higashihara [1], Wen-Chang Chen [2,3], Mitsuru Ueda [1]

1: Department of Organic and Polymeric Materials, Graduate School of Science and Engineering, Tokyo Institute of Technology, 2-12-1-H120 O-okayama, Meguro-ku, Tokyo 152-8552, Japan
2: Department of Chemical Engineering, National Taiwan University, Taipei, Taiwan 106
3: Institute of Polymer Science and Engineering, National Taiwan University, Taipei, Taiwan 106

ueda.m.ad@m.titech.ac.jp

Introduction

Recently, water-soluble conjugated polymers have received much attention because of their potential utilities in the field of sensitive chemical and biological sansors.[1] Especially, it was shown that water-soluble dendronized conjugated polymers could be strong candidates because they possess high quantum yield in water due to hydrophilic dendron segment effectively preventing the aggregation of conjugated polymer.[2] However, the synthesis of dendronized polymers requires multi step procedures via grafting-onto or macromonomer approaches. In this work, we synthesized simpler water-soluble polyamide G1, G2 and G3 dendrimers, which had a pyrene unit as a fluorescence group and ammonium periphery. DNA sensing behavior of the dendrimers would be investigated using UV-Vis absorption and Emission spectra.

Results and discussion

Synthesis of AB2 building blocks Scheme 1 shows the synthesis of AB2 building blocks. **2** was synthesized according to a previous paper.[3] 3,5-Dihydroxy benzoate was reacted with **2** under the presence of K_2CO_3 to obtain protected AB2 building block (**3**). AB2 building block (**4**) was obtained by the hydrolysis of the methyl ester group of **3**.[4]

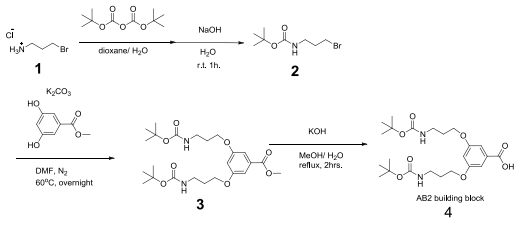

Scheme 1 Synthesis of AB2 building blocks

Synthesis of Dendrimers The dendrimers were grown from 1-aminopyrene by a divergent approach using diphenyl (2,3-dihydro-2-thioxo-3-benzoxazolyl) phosphonate (DBOP) as condensing agent.[5] Coupling reactions for the synthesis of protected-dendrimers (**5, 7, 9**) were conducted by a two-step method[6] consisting of (1) activation of carboxylic acids of AB2 building blocks by DBOP to generate an active amide and (2) condensation of the active amide with 1-aminopyrene, G1 or G2 dendrimers. *tert*-Butyl carbamate group of protected-G1, G2 and G3 dendrimers (**6, 8, 10**) were deprotected using trifluoroacetic acid to obtain cationic charged dendrimers. (Scheme 2) All products were characterized by IR and ^{1}H-NMR spectroscopy, and the MALDI-TOF MS spectrum of dendrimers and only showed signals attributed to the presumable MSs .

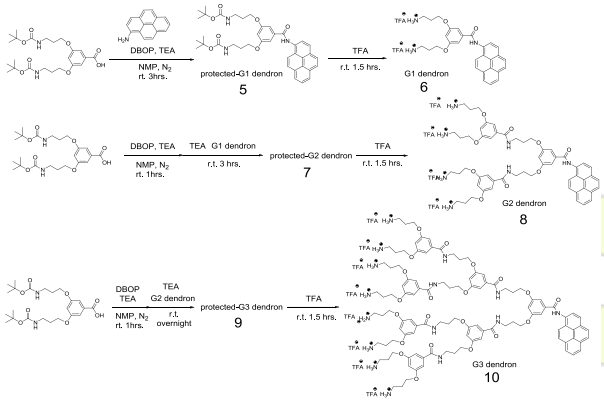

Scheme 2 Synthesis of polyamide dendrimers.

DNA sensing behavior of dendrimers The interactions between DNA and G1 dendrimers were investigated by the changes of G1 dendrons UV-Vis absorption and emission spectra. As shown in Figure 1a, UV absorptions of G1 dendrimers are red-shifted by adding DNA. Decrease in the emission of G1 dendrons upon adding DNA is also observed in Figure 1b. Because the maxima and shapes of emission spectra do not change and no new peaks appear, possible mechanism for the quenching of cationic G1 dendron is attributed to its aggregation near the negatively charged DNA, leading to self-quenching.

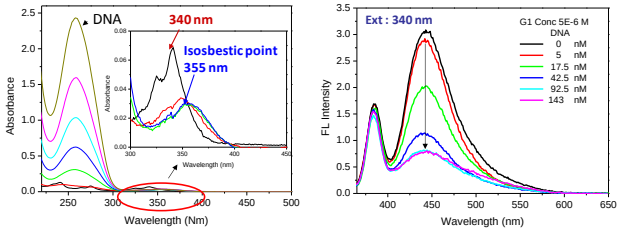

Figure 1 Absorption (a) and Emission (b) spectra of G1 dendrons in the presence of DNA in aqueous solution.

Summary

Cationic water soluble dendrimers that contain a fluorescence molecule pyrene at the core were successfully synthesized via divergent method using DBOP as the condensing agent. UV absorption and emission spectra of G1 dendron showed the DNA sensing behavior. DNA sensing behavior of G2 and G3 dendriers is now under investigation.

References

1 Feng, F., Liu, L., Yang, Q., Wang, S., *Macromol. Rapid Commun.* **2010**, 31, 1405.
2 Yu, M., Liu, L., Wang, S., *J. Polym. Sci., Part A. Polym. chem.* **2008**, 46, 7462.
3 Georgiades, S. N., Clardy, J., *Org. Lett.* **2005**, 7, 4091
4 Klopsch, R., Koch, S., Schüter, D., *Eur. J. Org. Chem.* **1998**, 1275.
5 Ueda, M., Kameyama, A., Hashimoto, K. *Macromolecules* **1988**, 21, 19..
6 Okazaki, M., Washio, I., Shibasaki, Y., Ueda, M. *J. Am. Chem. Soc.* **2003**, 125, 8120.

Synthesis and Characterization of Polyurethane-based Shape Memory Polymers with Low Transitional Temperature for Medical Applications

M. Ahmad[a], J.K. Luo[a], B. Xu[b], H. Purnawali[c], P.J. King[d], P. Chalker[d], Y.Q. Fu[b], W.M. Huang[c] and M. Miraftab[a]*

[a]Institute of Materials Research & Innovation, University of Bolton, Bolton, BL3 5AB, U.K
[b]Department of Mechanical Engineering, School of Engineering and Physical Sciences, Heriot-Watt University, Edinburgh, EH14 4AS, U.K
[c]School of Mechanical and Aerospace Engineering, Nanyang Technological University, 50 Nanyang Avenue, Singapore, 639798
[d]Department of Materials, University of Liverpool, L69 3BX, U.K

Corresponding author's email: J.Luo@bolton.ac.uk

Shape memory polymers (SMPs) are one type of smart materials, and have found tremendous applications in space exploration, engineering, and recently in medical devices [1,2,3] owing to their superior properties of large deformation, light weight, low density, low cost and easy processing etc [4]. Most commercially available SMPUs have a high elastic strength and high glass transitional temperatures, higher than the human body temperature, therefore are not particularly suitable for medical device applications. SMPs with a relatively low elastic strength and a near-body transitional temperature are desirable for medical devices such as the laser-activated cork screw surgical tool [5] and the SMP-based bandages [6]. Therefore it would be useful to develop low T_g and low elastic strength pure SMPs for medical applications, and further modifications can be made to change these SMPs into ones which can be activated by other mechanisms such as light by adding nanoparticles. In this research, different polyols and hard segments (MDI and IPDI at different molar ratios) were used to synthesize polyurethane-based SMPs (SMPUs) with tailored and controllable properties suitable medical device applications.

Various polyurethane-based shape memory polymers (SMPUs) were synthesized using five types of polyols (poly(caprolactone) (PCL), poly(ethylene adipate) 2200 (PEA), polyether-type polyols of poly(ethylene glycol) (PMTG), and two polyester-type polyols of poly(butylene adipate) (PBA) and (PBA-U)) as soft segments and two different diisocyanates: isophorone diisocyanate (IPDI) and 4,4′-diphenylmethane diisocyanate (MDI) as hard segments. The effects of the concentration of the diisocyanates, and polyols on material properties such as crystallinity, transition temperature, shape memory effect and tensile strength were investigated.

X-ray characterization revealed only polyol soft segments have crystalline structure, mixture of hard segments with polyols do not introduce additional crystalline structure but reduce the crystallinity of the polyols. The crystallinity of the SMPUs increases with IPDI content. The result showed that high concentration IPDI in polymers may prevent or restrict the reaction and crosslink between polyol and diisocyanate, and a large amount of soft polyol and diisocyanate hard segments may co-exist as separated "macrophases", not good for the formation of high quality SMPUs, in agreement with the shape memory effect obtained.

SMPUs with a maximum strain over ~1000%, recovery rate up to ~98%, fixity up to ~90% and near body transitional temperatures of 35~45°C were obtained that are suitable for the development of SMPU-based medical devices. The SME properties are summarized in table. A high content of MDI hard segment results in SMPUs with better shape memory effect, increase in IPDI content leads to deterioration of shape memory effect: reduced maximum strains and stress recovery rates, but increased shape fixity. The results indicate that high concentration IPDI prevents or restricts chemical reaction and crosslinks between polyols and hard segments, leading to large phase separation and coexistence of soft and hard segments in macrophases.

SR.NO	SAMPLE	PEAK TEMP. (*T*pm) (°C)	ΔH (J/G)	Stress at Break (MPa)	Strain at Break (%)
1	**PCL (P)**	**51.6**	**76.6**		
2	PCL-PU-1	40.3	8.6	6.99	930
3	PCL-PU-2	41.3	18.8	6.24	869
4	PCL-PU-3	44.3	23.4	5.64	790
5	PCL-PU-4	42.6	20.5	4.39	334
6	PCL-PU-5	43.3	27.2	3.06	192
7	PCL-PU-6	39.0	30.1	2.81	104
8	PCL-PU-7	39.3	32.6	2.21	37
9	**PMTG(P)**	**41.3**	**106.8**		
10	PMTG-PU-3	27.4	30.6	2.47	985
11	PMTG-PU-4	24.4	27.8	2.09	625
12	PMTG-PU-5	26.0	33.8	0.94	17
13	**PBA-U (P)**	**58.3**	**73.6**		
14	PBA-U-PU-3	44.6	23.6	8.55	796
15	PBA-U-PU-4	46.3	33.1	4.61	411
16	PBA-U-PU-5	47.3	40.0	3.44	63
17	**PEA(P)**	**55.3**	**63.2**		
18	PEA-PU-3	42.3	19.4	5.53	784
19	PEA-PU-4	41.3	26.7	4.43	328
20	PEA-PU-5	42.3	27.3	1.53	119
21	**PBA(P)**	**55.0**	**55.2**		
22	PBA-PU-3	48.6	35.8	7.32	631
23	PBA-PU-4	43.6	34.4	4.53	293
24	PBA-PU-5	46.6	38.0	3.23	61

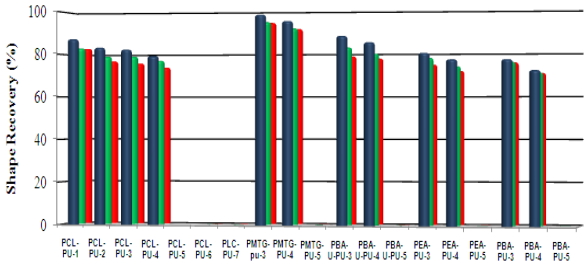

[1].Lan X, et al; Smart Mater. & Str. 2009; **18**: 024002.
[2].Lendlein A and Langer R; Sci. 2002; **296**: 1673.
[3].Yin W et al, 16th SPIE on Smart Str./NDE.2009: 7292.
[4].Sokolowski W et al. J; Biomed. Mater. 2007; **2**: S23.
[5]. Small W et al. Opt. Express, 2005; **13**: 8204.
[6]. J.K. Luo, et al. U.K Patent No. GB0908036:7.

Amphiphilic Multiarm Star Block Copolymer via Diels-Alder Click Reaction

Nese Çakır, Aydan Dag, Hakan Durmaz, Gurkan Hizal, Umit Tunca

Istanbul Technical University

cbu_nese_87@hotmail.com

Abstract

Multiarm star block copolymer: poly(caprolactone)$_m$-poly(divinylbenzene)-poly(ethylene glycol)$_n$,(PEG)$_n$ -PCL)$_m$-polyDVB, was successfully prepared via a combination of cross-linking and Diels-Alder click reaction based on "arm-first" methodology. For this purpose, multiarm star polymer with anthracene functionality as reactive periphery groups was prepared by a cross-linking reaction of divinyl benzene using α-anthracene end functionalized polycaprolactone (Anth-PCL) as a macroinitiator. Thus, obtained multiarm star polymer was then reacted with furan protected maleimide-end functionalized polymer: MI-PEG at reflux temperature of toluene for 48 h resulting in the corresponding multiarm star block copolymer via Diels-Alder click reaction. The multiarm star and multiarm star block copolymer was characterized by using ^{1}H NMR, SEC, Viscotek triple detection SEC (TD-SEC) and UV.

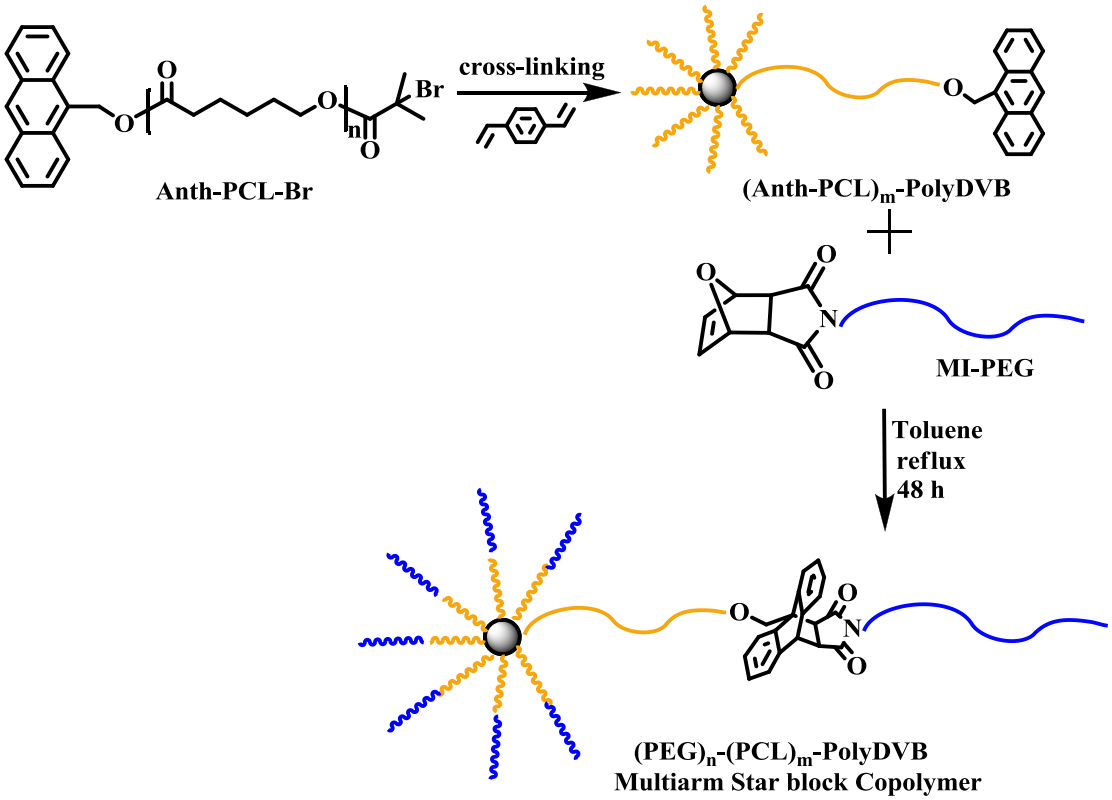

Synthesis and Characterization of Biodegradable Polyester Resins

Stefan Theiler, *Helmut Keul*[*], *Martin Möller*[*]

Institute for Technical and Macromolecular Chemistry, RWTH Aachen University and DWI an der RWTH Aachen e.V./Pauwelsstr. 8, D-52056 Aachen, Germany

E-mail: keul@dwi.rwth-aachen.de

Introduction: Chemical approach towards biodegra-dable polyester resins via Michael addition is presented. Star-shaped poly(caprolactone)s were prepared by means of chemically catalyzed ring-opening polymerization of ε-caprolactone with a multifunctional initiator followed by end capping with acrylate. Polyesters with pendant double bonds were used to form novel polyester resins by means of Michael addition using several polyether diamines as crosslinking agents (Figure 1). Variation of crosslinking agent, crosslinking density and the composition of the star-shaped functional poly(caprolactone) allows the adjustment of the resins hydrophilicity, thermal and mechanical properties.

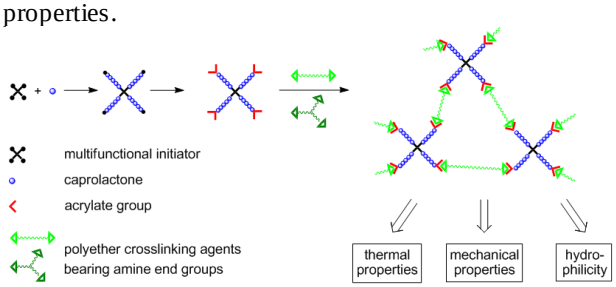

Figure 1. Biodegradable polyester resins: synthesis of star-shaped poly(caprolactone) and crosslinking with polyether crosslinking agents bearing amine end groups.

Materials and Methods. Star-shaped functional poly(ε-caprolactone)s (**1a-f**) used in this work were synthesized according to [1]. Characteristics of the prepolymers are shown in Table 1.

Table 1. Functional prepolymers: degree of functionalization, NMR and SEC analysis.

	Prepolymer	DF[a] %	$M_{n,NMR}$[b] g·mol^{-1}	$M_{n,SEC}$[c] g·mol^{-1}	M_w/M_n[c]
1a	s6PCL5-A[d]	99	3900	7400	1.23
1b	s4PCL5-A	93	2700	4300	1.42
1c	s4PCL10-A	95	4600	9000	1.40
1d	s4PCL20-A	90	9700	19400	1.23
1e	s4PCL50-A	94	23300	40200	1.13
1f	s4PCL100-A	100	46200	70600	1.11

[a] Degree of functionalization determined by NMR. [b] Number average molecular weight (M_n) determined by NMR. [c] M_n and molecular weight distribution (M_w/M_n) determined by SEC (PMMA standards). [d] s6PCL5-A indicates: star-shaped PCL with 6 arms and 5 CL repeating units per arm.

For the preparation of biodegradable polyester resins star-shaped acrylate functionalized poly(ε-capro-lactone)s (**1a-f**) and a crosslinking agent (ratio of acrylate to amine groups: 1:0.25 to 1:1.50) were dissolved in dichloromethane. The mixture was kept at room temperature in a stream of dry air until the solvent was evaporated (for ~30 min), followed by heating in an oven at 55 °C for 15 h.

Results and Discussion. Biodegradable polyester resins of all poly(caprolactone) prepolymers have been prepared with amino-telechelic poly(tetrahydrofuran), Jeffamines (PEO/PPO di-/triamines) and PEG diamines of different molecular weights as crosslinking agents. Determination of converted C,C-double bonds by means of Raman spectroscopy proves that the degree of crosslinking can be adjusted by the ratio of acrylate to amine groups in the feed (for acrylate:amine >1). At a molar ratio of 1:1 all C,C-double bonds were converted. Resins prepared with a ratio of acrylate:amine <1exhibit free amino groups which can be used for biofunction-alization.

Hydrophilicity of the polyester/polyether resins can be adjusted by using different crosslinking agents. Crosslinking with amino-telechelic poly(tetrahydro-furan) results in hydrophobic resins, while crosslinking with PEG diamines results in hydrophilic resins.

Thermal properties of the resins were investigated by means of DSC. Increasing crosslinking density results in a decrease of melting temperature and enthalpy. Using prepolymers with increasing CL chain length (**1a** to **1f**) and a 1:1 molar ratio of acrylate to amine groups, melting temperature and enthalpy increase.

Tensile strength of the resins was measured according to the ISO 37 norm. Resins with high crosslinking density show elastic behavior while resins with low crosslinking density show viscoelastic behavior. Increasing the CL chain length in the prepolymer results in resins with higher E moduli, Yield and breaking stress.

Conclusions. Starting from poly(ε-caprolactone), prepolymers biodegradable resins were prepared using amino terminated polyethers as crosslinking agents. Crosslinking density can be tuned by the ratio of prepolymer to crosslinking agent in the feed as well as by the composition of both components. Hydrophilicity, mechanical and thermal properties of these polyester/polyether resins can be adjusted in a wide range. The biodegradable polyester resins are promising candidates in biomedical applications, for example in the development of vascular prostheses.

References.

[1] Theiler S, Teske M, Keul H, Sternberg K, Möller M. Synthesis, characterization and in vitro degradation of 3D-microstructured poly(ε-caprolactone) resins. Polymer Chemistry 2010;1:1215-25.

[2] Theiler S, Mela P, Keul H, Möller M. Multifunctional Polyesters for Bioartificial Vascular Prostheses. Macromolecular Symposia 2010:296:453-6.

MWCNT- Epoxy Composite- Electrodes for Environmentally Friendly Detection of Pharmaceutical Compounds

A. Remes [1], F. Manea [1], A. Pop [1], N.K.K. Kowlgi [2], S.J. Picken [3], J. Schoonman [4]

[1] "Politehnica" University of Timisoara, Sqr. Victoriei no. 2, 300006 Timisoara, Romania

[2] Self-Assembling System, Department of Chemical Engineering, Delft University of Technology, Julianalaan 136, 2628BL, Delft, The Netherlands

[3] NanoStructured Materials, Department of Chemical Engineering, Delft University of Technology, Julianalaan 136, 2628BL, Delft, The Netherlands

[4] Materials for Energy Conversion and Storage, Department of Chemical Engineering, Delft University of Technology, Julianalaan 136, 2628BL, Delf, The Netherlands

adriana.remes@chim.upt.ro

Introduction

Carbon nanotubes (CNTs) have become the subject of intense investigation since their discovery [1]. Such considerable interest reflects the unique behavior of CNTs, including their remarkable electrical, chemical, mechanical and structural properties. Numerous advantages of CNTs as electrode materials have been attested for analysis of diversified chemicals of food quality, clinical and environmental interest [2,3].

Materials and Methods

Multiwall carbon nanotubes (MWCNTs) with a 90% purity, synthesized by catalytic carbon vapor deposition (CCVD) were provided by Nanocyl™ NC7000. The epoxy resin Araldite®LY5052 and the curing agent Aradur®5052 were produced by Hunstman Corporation. The MWCNTs and all the reagents were used as received. Different contents of MWCNTs (in the range between 0.1% and 30% wt.) were used to obtain composite electrodes using two-roll mill procedure (TRM). The dispersion and morphology of MWCNTs- epoxy composite- electrodes were characterized using different microscopic techniques, i.e., dynamic light scattering (DLS), atomic force microscopy (AFM), and scanning electron microscopy (SEM). Also, the electrical conductivities of these composites were investigated by DC conductivity measurements. The electroactive surface areas of the composite electrodes were determined through the electrochemical characterization using the classical potassium ferricyanide ($K_3[Fe(CN)_6]$ method. Cyclic voltammetry (CV), differential-pulsed voltammetry (DPV), square-wave voltammetry (SWV) and chronoamperometry (CA) techniques were applied to determine the electroanalytical performance of the electrode in order to detect salicylic acid (SA), which was chosen as model for the pharmaceutical compounds.

Results and Disscussion

Figure 1.a shows the SEM image of the composite electrode containing 20 %, wt. MWCNT (MWCNT20) with good dispersion of CNTs in the polymer matrix, forming a three-dimensional network.
The electrochemical characterization revealed a higher electroactive surface area of the MWCNT20 electrode, which was selected as optimum for further detection experiments. In figure 1.b the CVs of MWCNT20 composite electrode in the presence of SA are presented to characterize its electrochemical behavior in alkaline medium.

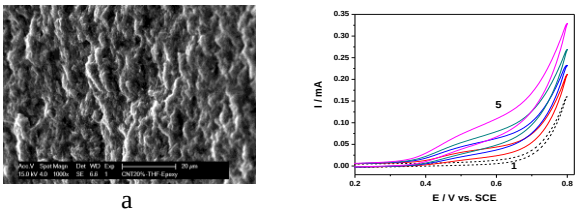

a b

Fig.1a- SEM image of MWCNT20 electrode; b- CVs of MWCNT20- electrode recorded in 0.1 M NaOH supporting electrolyte (1) with addition of: 1, 2, 3, 5mM SA (2-5). Scan rate: 50mVs^{-1}.

The good results regarding the electroanalytical parameters of the detection were achieved using CV, DPV, SWV and CA techniques. Additionally, the detection measurements were performed for the determination of acetyl salicylic acid (ASA) from real pharmaceutical samples (aspirin tablets). The obtained results are promising for practical application in drug testing.

Conclusions

The composite electrode containing 20 %, wt. MWCNT (MWCNT20) was selected as optimum for the detection experiments based on the correlation between morphology, electrical conductivity and electrochemical behavior.
The MWCNT20 composite electrode exhibited useful features as environmentally friendly sensor for the electrochemical determination of SA and ASA with respect to its mechanical resistance, very low cost, simple preparation and easy renewal of the active electrode surface.

References

[1] J.Wang, Electroanalysis, 2005, 17 (1), 7.
[2] K.V. Sandeep, D. Zheng, K. Al-Rubeaan, J.H.T. Luong , F.S. Sheu, Biotechnology Advances 2010, in press.
[3] W.D. Zhang, B.Xu, Y.X. Hong, Y.X. Yu, J.S. Ye, J.Q. Zhang, J. Solid State Electrochem., 2010, 14, 1713.

Electrospun nanofibers of a biodegradable poly(ester amide). Scaffolds loaded with antimicrobial agents.

Alfonso Rodríguez-Galán, Manuel Roa, Angélica Diaz, Jordi Puiggalí, Luis Javier del Valle

Dpt. Chemical Engineering. Universitat Politècnica de Catalunya. Av. Diagonal 647. 08028-Barcelona. Spain

alfonso.rodriguez-galan@upc.edu

Introduction. Biomedical applications such as preparation of scaffolds used for tissue engineering and drug delivery, have become one of the most interesting topics in the electrospinning field. The most used materials correspond to polyesters, polyamides and polyurethanes. However, only a few papers have been published reporting the elaboration of poly(esteramide)s (PEAs) nanofibers.
PADAS is a regular and biodegradable poly(ester amide) based on 1,12-dodecanodiol, L-alanine, and sebacic acid obtained by interfacial polymerization. Due to its biodegradable nature, it can be used like biomaterial that suppors and favours the cellular growth.

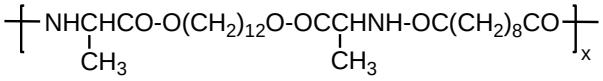

Chemical structure of PADAS

In this study, ultrafine PEA fibers containing antimicrobial compounds were prepared by electrospinning of a PADAS solution with small amounts of silver nitrate ($AgNO_3$) or Chlorhexidine.

Results and Discussion. Regular and homogeneous PADAS fibers could be obtained from hexafluoroisopropanol (HFIP) solutions at concentrations ranging between 1-10% (Figure 1). Experiments performed with other solvents rendered irregularly shaped fibers or mixtures of fibers and beads.

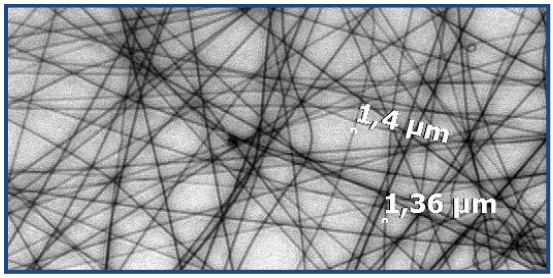

Figure 1. Optical micrograph of PADAS fibers electrospun from a 10% HFIP solution.

Fibers containing antimicrobial agents such as $AgNO_3$ or Chlorhexidine diacetate could be prepared from a 10% PEA/HFIP solutions. Because low solubility of the salt in HFIP, fibers with $AgNO_3$ were prepared from drug/polymer ratios of 0.001-0.24% while Chlorhexidine containing fibers were obtained at concentration of 0.3-4.2%.
The morphologies of the ultrafine PADAS fibers were observed on a scanning electron microscope after gold coating (Figure 2). The average diameters were determined by analyzing SEM micrographs with an image analysis program.

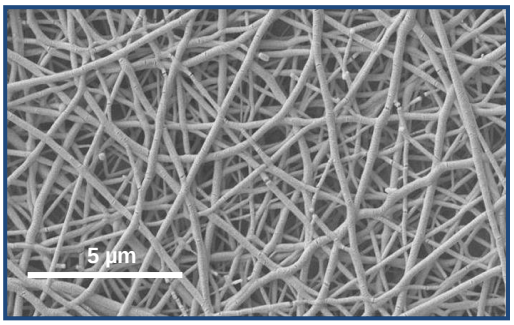

Figure 2. SEM image of ultrafine electrospun PEA fibers from 10 % PADAS/HFIP solution containing 0.16% of $AgNO_3$.

Our results showed that the diameter of fibers containing $AgNO_3$ decreased dramatically: when the conductivity of a polymer solution is increased by adding a salt, the diameter of the resultant fibers is significantly reduced.
Antibacterial activity of scaffolds made from nanofibers containing silver nitrate or Clorhexidine have been evaluated against Gram positive and negative bacteria. Fibers with silver salt are more effective than Chlorhexidine fibers inhibing the growing of both kinds of bacteria.

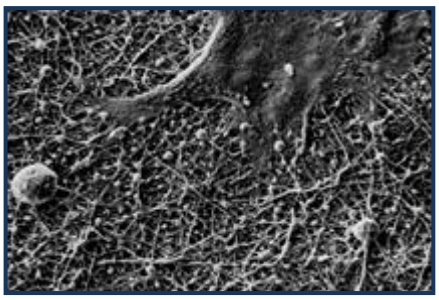

Figure 3. SEM image of Hep-2 cells on PADAS fibers.

The capability of scaffolds made from antimicrobial PADAS fibers to support cell attachment and proliferation was also evaluated (Figure 3).

Conclusions. Fibers of PADAS with diameters of 500-2000 nm can be prepared by electrospinning of 1-10% solution in HFIP. nanofibers with antimicrobial activity against *E. coli* and *M. luteus* are obtained when $AgNO_3$ or Chlorhexidine are added to the PEA/HFIP solutions,. These nanofibers are biocompatible with epithelial Hep-2 and MDCK cells.

Acknowledgement. This research has been supported by a grant from MCYT/FEDER (MAT-2009-11503).

Surface Modification of Titanium Dioxide by a modified emulsion/dispersion polymerization with an aid of ultrasonication

Jeong Ho An and MinJae Kim

Department of Polymer Science and Engineering
SungKyunKwn University
Chunchun-dong 300, Jangan-gu, Suwon, KOREA 440-746

Jhahn1us@skku.edu

Introduction: The encapsulation of titanium dioxide nano-powder has been attempted by a modified emulsion/dispersion polymerization using wall materials composed of methyl methacrylate (MMA), ethylene glycol dimethacrylate (EGDMA) and methacrylic acid (MAA). The nano hybrid composite particles diameters of 0.2um - 10um have received much interest in a wide range of industrial fields, such as diagnosis, electronics, toner, and dispersion stability properties. Moreover, inorganic core/organic shell hybrid composite particles may provide better electrical, optical and thermal properties and extend their range of industrial application. Encapsulation of inorganic particles by a polymer shell provides better mechanical properties such as strength, shape, and chemical resistance. Above all, the enhancement in dispersion stability of hybrid composite particle is most significant characteristics of inorganic core/polymer shell composite particles.

Materials and Methods

Using monomers took Methyl methacrylate (MMA, purity 99%), methacrylic acid (MAA), crosslinking agent used to Ethylene glycol dimethacrylate (EGDMA), Methyl alcohol (MeOH, SAMCHUN chemical), 2,2'-azobis(2-methylpropionitrile) (AIBN), and polyvinylpyrrolidone (PVP, Mw=55,000/360,000 g/mol) (Sigma Aldrich Co. Ltd.) were chemically pure grade and purified by reduce pressure distillation. Titanium dioxide (TiO_2) nano particles are offered from TRONOX™ (TR-HP-2). The TiO2 used in this study are a rutile crystal structure, hydrophilic surface property, below to 1.0um size. In the first step, 0.2% (w/v) of PVP was dissolved in a methanol in a 500ml customizing three necks round bottomed flask equipped with a ultra-sonicator, a thermometer, a reflux condenser, and a nitrogen gas inlet and outlet. TiO2 nano-particles were dispersed in the mixture of MMA and EGDMA by 15min ultra-sonication at room temperature. The TiO2 dispersion in the monomer mixture was done by ultra-sonication, mixture was poured into 0.2% (w/v) of PVP methanol solution and emulsified with ultra-sonication 15min again. Then a solution of AIBN was added into reactor. The vibrating power was changed from 50% to 40%. Then the flask was immersed into a 65◦C oil bath under a nitrogen atmosphere. In the second step, MAA was added slowly into the reactor to incorporate the composite particle surface. After adding the MAA, the reactions were carried out for 4 h at the same temperature. Cooling to room temperature terminated the reaction. After termination process ended, deionized water was added to the produced hybrid composite particle mixture for clean, didn't reaction monomers, and it was isolated from the mixture by centrifugation. Hybrid composite particles were washed with deionized water several times. Finally, the particles were drying at 60◦C in a convection vacuum oven.

Results and Discussion

The effect of sonication can be clearly shown in terms of the particle size. In Figure 1(RTMA; without sonication, UTMA and UHTMA; with sonication), the particle size results are summarized, showing that if sonication step is added during the polymerization, the particle size much reduced compared with that without sonication.

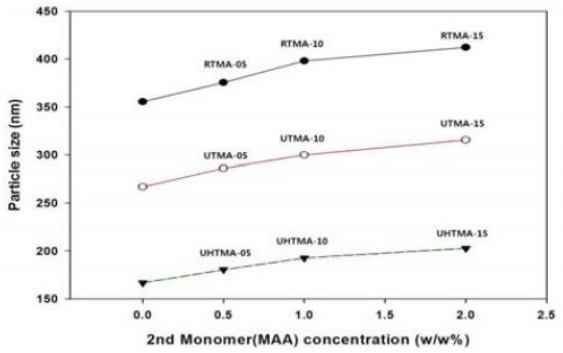

Fig.1 Particle size analysis by DLS.

Conclusions

In the current experiment, it has been attempted that the conventional emulsion/dispersion polymerization is modified to ensure the stability of nano-particle during the encapsulation process as well as the efficient encapsulation. With an aid of ultra-sonification it is found that the very thin wall is formed around the surface of titanium dioxide nano-particles and that the majority of the encapsulated particles contain single titanium dioxide particle.

References

[1] Haga Y, Inoue S, Sato T. Yosomiya. Angew. Makromol. Chem. 1986; 139:49.
[2] Man Sig Lee, Gun-Dae Lee, Seong-Soo Hong. J. Ind. Eng. Chem. 2003;9(5):55
[3] Gupta PK, Hung TC, Lam FC, Perrier DG. Int J Pharm 1998;43:167.
[4] Castellanos JR, Mendizabal E, Puig JEJ. Appl Polym Sci Appl Polym Symp 1991;49:91.
[5] Mendizabal E, Castellanos-Ortega JR, Puig JE. Coll Surf 1992;63: 209.
[6] MacGregor JF, Penlidis A, Hamielec AE. Polym Process Eng 1984;2: 179.

The sulfobetaine-type surfactants applied for Nafion 212 on PEMFC

Tzu Hsuan Chiang[1], Yu-Ming Hsieh[2], Li-Ming Chen[1]*

[1]Department of Energy and Resources, National United University, Taiwan
2Asia-Pacific Institute of creativity, Department of Health nutrition and biotechnology, Taiwan

thchiang@nuu.edu.tw

Authors Instructions:

This study focus on modified proton exchange membrane, Nafion 212, which hope enhance conductivity simultaneously decrease AC impedance by immersed sulfobetaine-type surfactants as N-Octyl-N,N-Dimethyl-3-Ammonio-1-Propanesulfonate (DAPS).

Introduction

This study surfactant as N-Octyl-N,N-Dimethyl -3-Ammonio-1-Propanesulfonate ($C_{13}H_{29}NO_3S$) is a zwitterionic surfactant that having a head group containing both a negatively charged chemical moiety and a positively charged chemical moiety. That can provide an improved stabilization mechanism than an ionic-type surfactant [1] simultaneously structure have SO^{-3} group can help proton conduction. There is not had any research to study the sulfobetaine-type surfactants as DAPS applied for Nafion 212 on PEMFC. Therefore, this investigate is very important.

Materials and Methods

The materials of investigation were include proton exchange membrane as Nafion 212 (thickness is 0.05mm), surfactant as N-Octyl-N,N-Dimethyl-3-Ammonio-1-Propanesulfonate ($C_{13}H_{29}NO_3S$) which chemical structure as

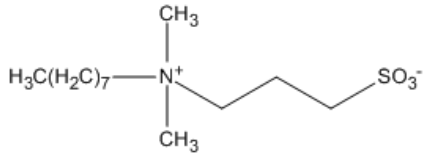

The experimentation that Nafion 212 (size is 5*5cm) was soke into 3% DAPS surfactant for 1,3,6 and 24hrs then dry on oven. It was employ AC impedance apparatus to analyze the property of membrane.

Results and Discussion

The Warburg impedance [2] was impedance of electrolyte (bulk resistance, Rb) as Nafion 212/ DAPS for ionic move. The which impedance of electric charge to transfer (charge transfer resistance, Rct) which was electric charge to transfer need reaction activation energy and parallel connection with capacitance (C) as shown in Figure 2 that can calculate conductivity of Nafion 212/ DAPS from σ=L/(Rb*A)

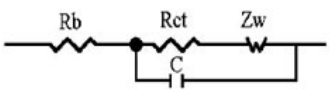

Figure 1 Simulate impedance of equivalent circuit.

Nafion 212 immersed into 3% DAPS surfactant for 1,3,6 and 24hrs that can obtain AC impedance as shown in Figure 2. The Rct had smallest when Nafion 212 immersed into 3% DAPS surfactant for 24hrs whcih mens electric charge to transfer need smaller reaction activation energy.

As Nafion 212 immersed 3% DAPS surfactant for 3hrs which had highest conductivity as shown in Figure 2.

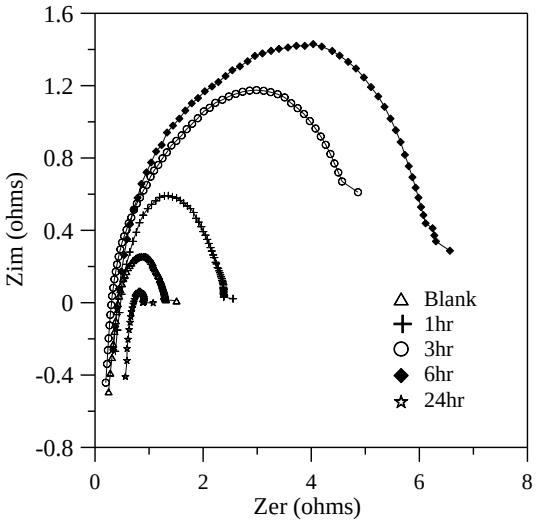

Figure 1 AC impedance of Nafion 212 immersed 3% DAPS surfactant on different time.

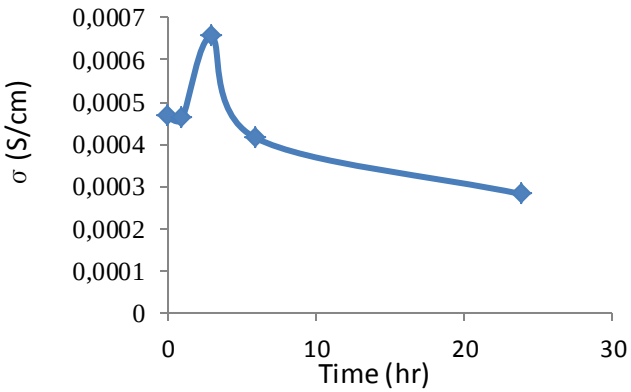

Figure 2 Conductivity of Nafion 212 immersed into 3% DAPS surfactant on different time.

Conclusions

Nafion 212 immersed into 3% DAPS surfactant for 24hrs whcih need smaller reaction activation energy but immersed 3hrs on 3% DAPS surfactant which had highest conductivity

References

1. C. Graillat, B. Dumont, P. Depraetere, V. Vintenon, C. Pichot, *Langmuir*, 1991, *7* (5), pp 872–877.
2. B. E. Conway, J. Electrochem. Soc., 1991, 138, 1539.

Semiconducting Properties of Irradiated Polyethylene Sheets

[1]Famiza Latif, [1]Mohd Hafiz Yaakob, [1]Rahmah Mohamed, [2]Khairul Zaman Mohd Dahlan

1. Faculty of applied Sciences, Universiti Teknologi Mara, 40450 Shah Alam , Selangor, Malaysia
2. Malaysian Nuclear Agency, Bangi, 43000 Kajang,Selangor, Malaysia.

famiza@salam.uitm.edu.my

1.0 Introduction :

Electronic conducting polymers are difficult to be synthesized because it involves meticuluos procedures and requires several chemicals. Other alternative is to radiate any polymers to form *trans*-vinylene (C=C) group [1]. Therefore, the conductivity of these irradiated conducting polymers is expected to occur through the delocalization of electrons of the conjugated bonds structure along the polymer chain [2]. In this study two types of polyethylene i.e. HDPE and LDPE were chosen to investigate how the different in the chain arrangement of the polyethelenes may affect the overall structure the polymers upon radiation hence their electrical properties. Furthermore, conjugated bonds are expected to be easily formed after irradiation due to their simple and straight polymer chains structure. There are several studies on irradiated HDPE [1] and LDPE [3] that had been done. However, most studies concentrated on the mechanical and thermal properties of these irradiated polyethylene. To date, there are no studies on electrical properties of HDPE and LDPE that have been reported.

2.0 Materials and Methods:

Both HDPE and LDPE sheets were prepared by compression moulding technique. The sheets were then Irradiated using electron beam accelerator, EPS-3000 at 100 to 800 kGy of irradiation dose with 2 MeV and 10 mA. The morphology of these irradiated HDPE and LDPE sheets were observed under FESEM, Quanta 200 F. The changes in the structure of both irradiated sheets were analyzed using ATR–FTIR Perkin Elmer Spectrum One FTIR spectrophotometer in the frequency range of 4000 – 400 cm^{-1}. The thermal properties of both samples were studied using TGA Pyris 1 and DSC Q200. The type of HDPE and LDPE semiconductor were carried out by hot-point probe measurement and the band gap energy for both irradiated samples were determined from the UV spectra obtained from Perkin Elmer Lambda 800 UV-vis spectrophotometer.

3.0 Results and Discussion:

Interestingly, it was found that LDPE was able to withstand higher irradiation dose up to 800 kGy without showing any degradation as compared to HDPE that started to degrade at 700 kGy. Both sheets became harder after irradiation due to the formation of interchain crosslinking in their polymer structures. This has been confirmed from their respective TGA and DSC analysis in which their decomposition and melting temperatures were higher than in their un-irradiated systems. The formation of crosslinking in these irradiated HDPE and LDPE system were further confirmed from the formation of interpenetrating structures which were observed from their electron micrographs (Figure 1). From the hot-point probe measurement, both irradiated HDPE and LDPE were *p*-type semiconductors. The presence of charge carriers in these systems were due to the delocalization of electrons from the conjugated C=C bonds that were formed in these irradiated systems. The formation of these conjugated C=C bonds in these irradiated HDPE and LDPE systems has been confirmed from their FTIR analysis in which the C=C bonds of *trans*-vinylene and *end*-vinyl were detected at 965 cm^{-1} and 888 cm^{-1} respectively. However, it was found that irradiated HDPE system exhibited higher concentration of conjugated bonds than LDPE due to the closer chain arrangement in the HDPE system that in turn enhance the electrons delocalization along the HDPE chain hence giving lower band gap energy of 2.75 eV compared to LDPE which was 3.97 eV. Interestingly, it was found that the band gap of irradiated HDPE was lower than the polyphenylene [4] and silicon carbide [5] semiconductor.

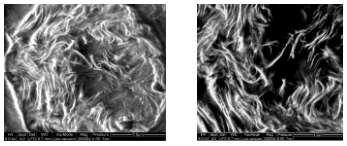

(a) (b)

Figure 1: FESEM micrographs for (a) HDPE and (b) LDPE sheets at 600 kGy of irradiation dose.

4.0 Conclusions

A p-type irradiated HDPE and LDPE semiconductor with band gap energy of 2.75 eV and 3.97 eV respectively can be obtained by Electron Beam irradiation

5.0 Acknowlegements

This study was funded by Fundamental Research Grant Scheme awarded by the Ministry of higher Education Malaysia.

References

1. McLaughlin W.L., Silverman J., Al-Sheikh M., Chappasc W. J., Liu Z. J., Millere A., Batsberg-Pedersen W. (1999). *Radiation Physics and Chemistry*, 56, 503-508.
2. Mishra R, Tripathy S.P., Sinha D., Dwivedi K.K., Ghosh S., Khating D.T., Muller M., Fink D., Chung W.H. (2000). *Nuclear Instruments and Methods in Physics Research B*, 168, 59 – 64.
3. Kumar V. S., Ghadei B., Chaudhuri S. K., Krishna J. B. M., Das D., Saha A. (2008). *Radiation Physics and Chemistry*, 77, 751–756.
4. Dai L. (2004). *Macromolecules*, 496, 291.
5. Unlu H. (1992). *Solid State Electronics*, Vol 35:9, 1343-1352.

Thermal Conductivity of Plastic Materials in Embedded Electronics Applications

J.Sarlin[1], *M.Koponen*[1] *and A.Sitomaniemi*[2]

[1] VTT Advanced Materials, Tampere, Finland
[2] VTT Photonic devices and measurement solutions, Oulu, Finland

Juha.Sarlin@vtt.fi

Introduction

Thermal conductivity is a crucial material property in novel plastic based products with embedded electronics containing dissipative components. Another application example is present small housing for transformers and battery chargers. Typically construction of these products doesn't include heat sinks. The dominating route for heat transport out from the product is radiation; usually forced convection is not applied. Although minimization of energy consumption in these small systems is an unconditional necessity local hot spots may be harmful and/or cause material degradation and structural defects. High temperatures are uncomfortable for skin contact and long term high local thermal expansion cause effects like delamination, etc. Today there exist commercial compounds with conductivity 5 - 10 W/Km, and many of them are electrically conductive. Such needs of mass production as low cost, excellent processability, high impact properties, etc, set needs of new heat conductive plastic compounds.

A lot of tomorrow's products with embedded electronics are based on injection molding technology, and a potential method to manufacture these smart products is in-mould labeling method where electronics is transferred by films containing this functionality. Both technologies, films and injection molding, require excellent processing properties of plastics.

Heat conductivity in composites is a complicated issue. Novel nanofillers are promising candidates to create high conductive materials, for example heat conductivity of CNT may be 3 - 6 kW/Km when the typical value of neat polymer is about 0.2 W/Km. Phonons plays the major role in heat transfer in plastics, but in some cases contribution of radiation may be essential. The crucial issue in heat conductive compounds is energy transfer over filler-matrix interface.

Modern numerical tools allow us to simulate heat transfer in realistic applications. These methods give us a strong support to study new constructions and material properties.

Simulation

According our simulation of some constructions in plastic embedded electronics with dissipative elements, careful constructions may allow using materials with quite low heat conductivity, typically 1 - 2 W/Km may allow to avoid undesired high temperatures in hot spots. Increased heat conductivity expands the area with higher temperature, but the maximum temperatures fall down to such values which are less harmful, i.e values with "comfortable" skin contact and without risk of chemical degradation of plastic material.

These results give a motivation to develop compounds characterized with good processability and mechanical properties, with moderate heat conductivity and with reasonable price.

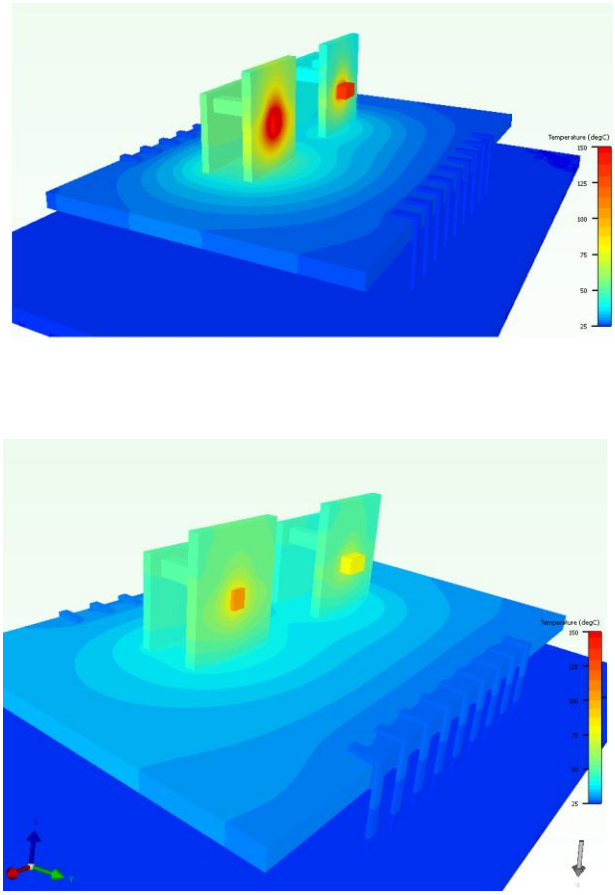

Figure: Simulation examples of an optoelectronic component with two hot spots. The thermal conductivities of materials are 0.27 W/Km (above) and 2 W/Km (below).

Experimental work

Polypropylene is used as a matrix material for composites. Different type of carbon base and mineral fillers in micro and nano scale were used.

Conclusions

To construct (non-conductive) plastic compounds with moderate thermal conductivity (1 - 2 W/Km) is a challenging topic. The requirement of good mechanical properties limits filler loadings, especially cases were fillers have strong reinforcing effects, a good example is CNT. Many mineral particles allow high loading levels. A route toward desired goal is hybrid systems with (at least) two different types of fillers.

Modification of Polysulfones by Click Chemistry: Amphiphilic Graft Copolymers and Their Protein Adsorption and Cell Adhesion Properties[1]

Lokman Torun,[1] Gorkem Yilmaz,[2] Hojjat Toiserkani,[2] Dilek Odaci Demirkol,[3] Serhan Sakarya,[4] Suna timur,[3] Yusuf Yagci[2]

[1]Chemistry Institute, TUBITAK Marmara Research Center, Gebze, Kocaeli 41470, Turkey
[2]Chemistry Department, Faculty of Science and Letters, Istanbul Technical University, Maslak, Istanbul TR 34469, Turkey
[3]Biochemistry Department, Faculty of Science, Ege University, Bornova, Izmir 35100, Turkey
[4]Department of Infectious Diseases and Clinical Microbiology, Adnan Menderes University School of Medicine, Aydin TR-09100, Turkey

Lokman.torun@mam.gov.tr

As part of our continuous interest in developing synthetic methods for the preparation and modification of various macromolecular structures, we present modification of polysulfunes (PSUs) by modular approach to yield amphiphilic graft copolymers. For this purpose, PSU was first chloromethylated using paraformaldehyde in the presence of $SnCl_4$ and $(CH_3)_3SiCl$. Subsequent azidation in the usual manner produced PSUs with side chain azide functions. Parallel to this, α-alkynefunctionalized poly(tert-butylacrylate) (alkyne-PtBA) was synthesized by ATRP. Then, alkyne-PtBA was successfully clicked to the PSU main chain. At the final stage, the ester groups were hydrolyzed in the acidic media to give polyacrylic polyacrylic acid-grafted polysulfone (PSU-g-PAA) (Scheme 1). The final structure was confirmed by H NMR, IR, UV-Vis and GPC.

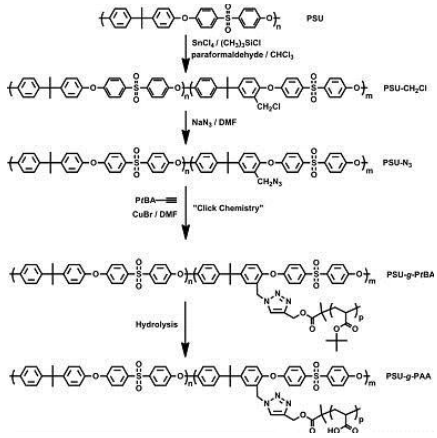

Scheme 1.

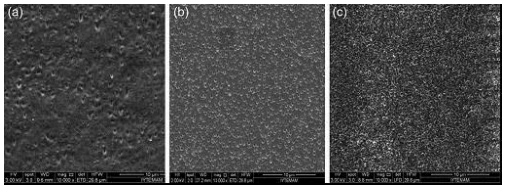

Figure 1 SEM images of PSU (a), PSU-g-PtBA (b) and PSU-g-PAA (c) membranes (magnification is10,000).

Protein adsorption experiments were carried out on the membranes with BSA. When the membranes were treated with 0.5 mg BSA, relative protein amounts on PSU, PSU-g-PtBA, and PSU-g-PAA were found to be as 41, 46, and 30%, respectively. As correlated with the contact angle measurements, the highest adsorption amount was observed for the most hydrophobic PSU-g-PtBA. After 24 h incubation, microscopic images of Caco-2 cells (as the model of eukaryotic cells) adhered on to the PSU (b) and PSU-g-PtBA (c), and PSU-g-PAA (d) membrane covered on the tissue culture plates (Figure 2). Prokaryotic cell adherence to the membranes was investigated by using both S. aureus and E. coli. Aureus cells were counted to be adhered than E. coli cells. The grafting of hydrophilic PAA on the PSU intensively decreases the adhesion of S. aureus cells. Hence, almost twofold reduction in the cell amount on the PSU-g-PAA surface was observed /Figure 3).

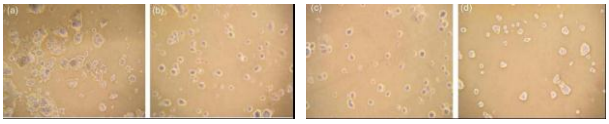

Figure 2. Microscopic images of Caco-2 cells adhered on the tissue plate for negative control (a), PSU (b), PSU-g-PtBA (c), and PSU-g-PAA (d) membranes

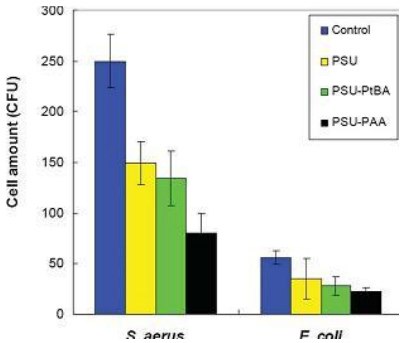

Figure 3. Amount of adhered bacteria on the PSU membranes.

In conclusion, this work demonstrated that click chemistry can efficiently be used for the synthesis of amphiphilic graft copolymers of PSUs. The strategy of combining controlled living polymerization and click chemistry methods provides fair control on the hydrophilic characteristics to be introduced to the PSU precursor. The obtained polyacrylic acidgrafted PSU displayed increased hydrophillicity characteristics, which reduced their protein fouling and cell adhesion properties with respect to the unmodified PSU precursor.

Istanbul Technical University and the State Planning Organization of Turkey (DPT, project no 2005K120920) are acknowledged for the financial support. H. T. thanks to Hormozgan to University, Iran.

[1]**a)** Toiserkani' Hojjat; Yilmaz, Gorkem; Yagci, Yusuf; Torun, Lokman. **Functionalization of Polysulfones by Click Chemistry.** *Macromol. Chem. Phys.* **2010**, *211*, 2389–2395. **b)** Yilmaz G, Toiserkani H, Demirkol DO, Sakarya S, Timur S, Yagci Y, Torun L, **Modification of polysulfones by click chemistry: Amphiphilic graft copolymers and their protein adsorption and cell adhesion properties.** *Journal of Polymer Science Part A: Polymer Chemistry*, **2011,** 49(1), 110–117.

Chalcone Modified Urethane Acrylates

H.Ayşen Önen[1], *Bahadır Güler*[2], *İ.Ersin Serhatlı*[1]

1.Istanbul Technical University, Department of Chemistry, Maslak, Istanbul, Turkey
2. Istanbul Technical University, Institute of Science&Technology, Department of Polymer Science&Technology, Maslak, Istanbul, Turkey

onen@itu.edu.tr, bahadirguler@live.com, serhatli@itu.edu.tr

UV curable coatings have gained more and more attention and are expected to substitute the conventional solvent-based coatings, because of their superior properties and processing advantages such as excellent chemical resistance, solvent-free technology, ultrafast polymerization, and good weathering characteristics.[1] Among the oligomers used for UV-curable coatings, polyurethane acrylate (PUA) oligomers have gained more and more attention and speedy development due to a wide range of excellent application properties, such as high impact and tensile strength, abrasion resistance and toughness combined with excellent resistance to chemicals and solvents.[2]

Photosensitive polymers with photocrosslinkable groups are used in a wide variety of applications in the field of macro- and microlithography, printing, liquid crystalline display, nonlinear optical materials , holographic head-up-display, integrated circuit technology, photocurable coatings, photoconductors, energy exchange materials, etc. Among the various photocrosslinkable groups, chalcone group containing α,β-unsaturated carbonyl unit has attracted particular attention due to its excellent photoreactivity at UV absorption wavelength.[3]

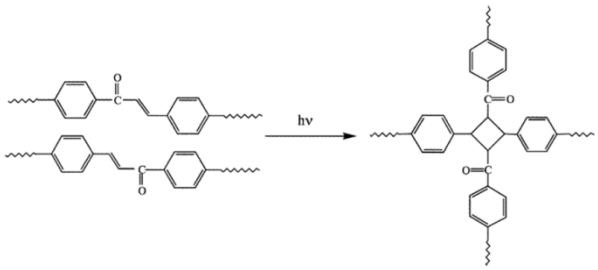

In this work, novel UV curable chalcone modified urethane acrylates (UA-C) containing isophorone diisocyanate and polyethyleneglycol segments were synthesized and employed in UV curable formulations. Crosslinking behaviour and film properties were investigated.

References

1 Jun Wei, Fang Liu, Zhimin Lu, Ling Song and Dongdong Cai, *Polym. Adv. Technol*, 2008, *19, 1763.*

2 F. Wang, J.Q. Hu, W.P. Tu, *Progress in Organic Coatings*, 2008, *62, 245.*

3 Dong Hoon Choi, Sang Joon Oh, Hyo Bok Cha, Joon Youl Lee, *European Polymer Journal*, 2001, *37, 1951.*

Usage of Grafted Chitosan Beads as Adsorbents for Copper(II) Ions Removal from Aqueous Solutions

Ayça Bal1, Bengi Özkahraman2, Işıl Acar1, Gamze Güçlü1, Mustafa Özyürek3

1 Istanbul University, Faculty of Engineering, Chemical Engineering Department, Avcılar, Istanbul, 34320, Turkey
2 Hitit University, Faculty of Engineering, Chemical Engineering Department, Çorum, 19030, Turkey
3 Istanbul University, Faculty of Engineering, Chemistry Department, Avcılar, Istanbul, 34320, Turkey

aycabal@gmail.com, bengiozkahraman@gmail.com, acar@istanbul.edu.tr, gguclu@istanbul.edu.tr

Introduction: Heavy metal ions contamination causes a serious environmental problem because of their increased discharge, toxic nature and other adverse effects on receiving waters [1]. The presence of Cu (II) ions in water is also a problem. Excessive intake of copper results in an accumulation in the liver [2-3] and become toxic to humans, causing cancer etc [4]. Therefore, there is a need to develop technologies that can remove excessive copper ions found in water [5]. The conventional methods for the removal of dyes and heavy metals from wastewater include coagulation and flocculation, oxidation or ozonation, membrane separation, and adsorption [6]. Among all the treatments proposed, adsorption is one of the more popular methods for the removal of pollutants. This process is preferred because of treating industrial effluents and it is a useful tool for protecting the environment [7]. The adsorbents may be of mineral, organic or biological origin. Activated carbons [8, 9], zeolites [10, 11], clays [12, 13], silica beads [14], biomass [15] and polymeric materials [16] are significant examples.Recently, the use of natural polymers such as cellulose, starch, chitosan, alginate has received great attention due to their biodegradability [17]. Chitosan is non-toxic, hydrophilic, biocompatible, biodegradable and anti-bacterial, which has led to various applications in different industries [18]. Chitosan is a β-(1,4)-linked polysaccharide of Dglucosamine derived from chitin, and it is a major component of the shells of crustacean organisms [19]. It is possible to significantly improve adsorption properties of chitosan by physical or chemical modification. Chemical modifications may include: chemical cross-linking (to increase polymer stability in acidic solutions), or grafting of new functional groups (to increase the adsorption sites) [20].

In this study, we studied the preparation of itaconic acid and crotonic acid grafted crosslinked-chitosan beads and their potential use as an adsorbent for removal of Cu(II) ions from aqueous solutions.

Materials and Methods: Chitosan-*g*-poly(itaconic acid) (Ch-g-IA) crosslinked beads and chitosan-*g*poly(crotonic acid) (Ch-g-CA) crosslinked beads were synthesized in two sequential steps. In the first step, chitosan beads were prepared by phase-inversion technique and then were crosslinked with epichlorohydrin under alkaline condition. In the second step, the graft copolymerization of itaconic acid or crotonic acid onto the chitosan beads was initiated by ammonium persulfate (APS) under nitrogen atmosphere.

Results and Discussion: Grafted chitosan beads were characterized by FT-IR analysis and grafting percentage determination. Grafting percentages values of Ch-g-IA and Ch-g-CA beads were determined as 18 % and 9 %, respectively. Then, their adsorption capacities were investigated in case of their usage in removal of Cu (II) from aqueous solutions. Adsorption capacities were determined as 0.25 and 0.3 mmol of Cu(II) per gram of croslinked chitosan beads for Ch-g-CA and Ch-g-IA, respectively. In addition, Cu (II) ions adsorbed on Chg- IA and Ch-g-CA crosslinked beads were regenerated effectively by 1 M HNO3 solution. The adsorption capacity of the recycled beads can still be maintained acceptable level at the 5th cycle. Grafted chitosan beads can be effective adsorbents for removal of Cu(II) ions from aqueous solution.

Conclusions: Grafted chitosan beads can be effective adsorbents for removal of Cu(II) ions from aqueous solution.

Keywords: Chitosan bead; Itaconic acid; Crotonic acid; Adsorption; Copper

References

[1] W.S. Wan Ngah, C.S. Endud, R. Mayanar (2002), *React. Funct. Polym.* 50, 181–190.
[2] Shengling Sun, Aiqin Wang (2006), *J Hazard Mater. B.* 131, 103–111.
[3] Gandhi MR, Kousalya GN, Meenakshi S (2011), *Int. J Bio. Macromol.* 48, 119–124.
[4] Wan MW, Kan CC, Lin CH, Rogel BD, Wu CH (2007), *Chia-nan Annual Bull.* 33, 96-106.
[5] R. Schmuhl, H.M. Krieg, K. Keizer (2001), *Water SA.* 27, 1-7.
[6] I. Acar, T.B.İyim, S.Özgümüş (2008), *J. Appl.Polym. Sci.* 109, 2774–2780,
[7] Gregorio Crini (2005), *Prog. Polym. Sci.* 30, 38–70.
[8] Hu Z, Lei L, Li Y, Ni Y (2003), *Sep Purif Technol.* 31, 13–18.
[9] Rivera-Utrilla J, Bautista-Toledo I, Ferro-Garcia MA, Moreno Castilla C (2003), *Carbon.* 41, 323–330.
[10] E. Erdem, N.Karapinar, R. Donat (2004), *J Coll. Inter. Sci.* 280, 309–314.
[11] T. Motsi, N.A. Rowson, M.J.H. Simmons (2009), *Int. J. Miner. Process.* 92, 42–48.
[12] Celis R, Carmen Hermosin M, Cornejo J (2000), Heavy metal adsorption by functionalized clays, *Environ Sci Techno.* 34, 4593–4599.
[13] Yavuz O, Altunkaynak Y, Guzel F (2003), *Water Res.* 37, 948–952.
[14] Xin Huang, Xuepin Liao, Bi Shi (2010), *J Hazard. Mater.* 173, 33–39
[15] Loukidou MX, Matis KA, Zouboulis AI, Liakopoulou Kyriakidou M (2003), *Water Res.* 37, 4544–4552.
[16] Azanova VV, Hradil J (1999), *React Funct Polym.* 41, 163–175.
[17] P. Miretzky, A. Fernandez Cirelli (2009), *J Hazard. Mater.* 167, 10–23
[18] W.S. Wan Ngah, S. Ab Ghani, A. Kamari (2005), *Bioresour. Technol.* 96, 443–450
[19] X.D. Liu, S. Tokura, M. Haruki, N. Nishi, N. Sakairi (2002), *Carbohyd. Polym.* 49, 103-108
[20] Shengling Sun, Aiqin Wang (2006), *Sep. Purif. Technol.* 49, 197–204

Effect of Glass Fiber and Glass Beads Content on Mechanical and Tribological Properties of Polyamide-6

A Mimaroglu, MSc, PhD and H. Unal, Msc, PhD

mimarog@sakarya.edu.tr, unal@sakarya.edu.tr

In this experimental study, two mineral fillers were selected on the basis of their shape and size which was spherical glass beads and fibrous glass fiber fillers. These fillers are added to polyamide-6 to produce composite materials with improved mechanical properties at lower production cost. Composites of polyamide-6 reinforced with glass beads and glass fibers were prepared in a twin-screw extruder, followed by injection moulding. The tensile, Izod, flexural and tribological properties of the injection moulded composites were investigated. Tensile measurements showed that the tensile strength and modulus of the composites increased with increasing filler content. The impact strength and elongation at break decreases with the increase in filler ratio. The results of single components were as aspected. The best mechanical properties were attained by the simultaneous use of two fillers. In addition, the content of glass beads partial replacement of glass fiber with glass beads resulted in reduced coefficient of friction and wearing rate of the materials.

The Influence of Nature of Nickel Complexes and Halide-Containing Initiators on the Polymerization of Vinyl Monomers

Natalya Valetova, Galina Malysheva, Ilya Ilitchev, and Dmitry Grishin

Research Institute of Chemistry, Lobachevsky State University of Nizhny Novgorod
Gagarin Ave. 23/5, Nizhny Novgorod, 603950, Russia

e-mail: nata-bor-2005@mail.ru

Introduction. Application of metal complexes for regulation of elementary stages of polymerization is one of the most developing area in synthetic chemistry of polymers.

Materials and Methods. $NiBr_2(PPh_3)_2$ was prepared according to literature [1] from $NiBr_2*3H_2O$ and triphenylphosphine in butanol-1 while 2,2'-bipy$NiBr_2$ was synthesized by mixing of the THF solutions of $NiBr_2$ and 2,2'-bipy at 50^0C [2]. Zinc dust activation was carried out by Clemmensen method [3]. The reaction was as follows: zinc dust, a nickel complex, a halide initiator and a monomer were charged into an ampoule with a magnetic stirring bar. The mixture was heated at 65^0C for 5h, after that the ampoule was opened and the mixture was poured into excess hexane.

Results and Discussion. The catalytic systems based on bis(triphenylphosphine)- or (1,2-diphenylphosphinoethane) nickel dibromide and iodobenzene with zinc dust were reported [4-6] to initiate polymerization of styrene and methyl methacrylate (MMA). Developing this area and searching new effective chain regulators, we study the activity of the catalytic system $NiBr_2(PPh_3)_2$/Zn/PhI in the polymerization of butyl acrylate (BA) and butyl methacrylate (BMA) as well as in the copolymerization of BMA with styrene. In addition, the influence of ligand structure in the nickel complex and that of organic halide initiators was estimated in MMA polymerization. It was established that polymerization of BMA in the presence of the $NiBr_2(PPh_3)_2$/Zn/C_6H_5I catalytic system results in the polymer with the yield about 80%. On the contrary to conventional radical polymerization, BMA reacts more actively than BA in this case. The study of dependence of styrene-BMA copolymer composition on the content of monomer mixture indicates that this catalytic system exerts no influence both the copolymer composition and the relative ratio of monomers r_{st}=0.68 and r_{BMA}=0.31. In the case of conventional radical copolymerization of BMA and styrene in the presence of AIBN the relative ratios of monomers are r_{st}=0.67 и r_{BMA}=0.34.

It was found that the presence of strong electronoaccepting groups in *para*-position of aromatic initiator – bromobenzene in the polymerization of MMA catalysed by $NiBr_2(PPh_3)_2$/Zn results in considerable growth in the yield of polymers compared with reaction in the presence of bromobenzene itself or other arylbromides containing electronodonating groups in the aromatic ring when the yield of polymers does not exceed 9 % in 5 h. For instance, PMMA was prepared with *para*-bromobenzonitrile or *para*-bromoacetophenone in the yield of 99 and 51 % in 17 and 36.5 h, respectively. MMA polymerization proceeded with phenyl iodine reaches 83 % polymer yield in 7 h [5]. The structure of initiators exerts a considerable influence of the yield of polymers: it grows in the row PhI<$(CH_3)_2C(Br)C(O)OC_2H_5$<$C_6H_5CH_2Cl$<$CHCl_3$. The structure of ligands attached to nickel atom is also crucial for the reaction. It was found that the use of 2,2'-bipy$NiBr_2$ catalyst results in higher yield of polymer than that of 4,4'-bipy$NiBr_2$ but lower yield than $NiBr_2(PPh_3)_2$.

Conversion smoothly grows with time of reaction in the polymerization of BMA and MMA catalyzed by $NiBr_2(PPh_3)_2$ and 2,2'-bipy$NiBr_2$, respectively. The number-average molecular weight of polymers also gradually increases with conversion. The MWD curves shift towards high molecular weight region. These features are characteristic of «living» radical polymerization.

Conclusions. The structure of both organic halide acting as initiator and the nickel complex influences the yield and molecular weight parameters of the polymers obtained. The most active nickel complex involving in the catalytic system was found to be $NiBr_2(PPh_3)_2$. P-bromobenzonitrile as aryl bromide shows the most initiating activity in MMA polymerization while the most active alkyl halide under similar conditions was found to be $CHCl_3$. The polymerization of vinyl monomers catalyzed by the system derived from these compounds proceeds via the controlled regime up to yield of 99%.

Acknowledgement. This work has been supported by the Russian Federal Agency for Education "Federal target program of scientific and scientific-pedagogical personnel of innovational Russia" on 2009-2013.

References.

1. L.Venanzi, *J. Chem. Soc*.1958. *V.2*. P.719.
2. S.Kurskov, I. Ivleva, I. Lavrent'ev, M. Khidekel, *Izv. Akad. Nauk SSSR, Ser. Khim.,* 1977. *V. 8*. p. 1708.
3. L.F. Fieser, and M. Fieser, *Reagents for Organic Synthesis*, John Wiley and Sons, Now York, 1969, 2.
4. D. Grishin, N.Valetova, I. Ilitchev, M. Prokhorova, and I.Beletskaya, *Russ.Chem.Bull*., 2006. *V.55*. No 11. p. 2106.
5. I. Ilitchev, N. Valetova, M. Moskalev, and D. Grishin, *Kinetics and Catalysis*, 2008. *V. 49*. No 4. p. 531.
6. N. Valetova, I. Ilitchev, and D. Grishin, *Russ. J. Appl. Chem*., 2010. *V. 83*. No 5. p. 843.

First Linear-Soluble Poly (*p*-phenylenemethylene) via Boron Ester of Benzyl Alcohol

Deniz Gunes, Yusuf Yagci, Niyazi Bicak

Istanbul Technical University, Department of Chemistry, Maslak 34469 Istanbul, Turkey

denizsun@gmail.com

Introduction: Poly(phenylene alkylene)s consisting of alkyl bridged phenyl rings are chemically inert and heat resistant polymers with low dielectric constant, high solvent resistance and good barrier properties.[1] Among those, poly (*p*-xylene) has found great interest as coating material. Structurally similar polymer, poly(*p*-phenylenemethylene) (PPM) has also found attention since the first report of Friedel and Crafts on the reaction of benzyl chloride with aluminum chloride in 1885.[2] Various Friedel-Crafts catalysts have been studied for polymerization of a wide variety of benzyl derivatives including benzyl halides, benzyl alcohol and benzyl ethers. However, all those attempts were failed in preparing soluble and linear PPM due to side reactions via *ortho* position of the phenyl ring.

Herein, we present the first report for the synthesis of entirely soluble PPM starting from boron ester of benzyl alcohol (tribenzylborate) (TBB) by an acid-catalyzed polymerization.

Result and Discussion: The structure of the polymer was confirmed by both ^{1}H and ^{13}C NMR analysis. The ^{1}H NMR spectrum of the isolated polymer represents a quite simple pattern in which intense singlets appearing at 7.1 and 3.8 ppm associated with aromatic and methylene protons respectively were noted. The ^{13}C NMR spectrum of the polymer shows aromatic carbon signals around 128 ppm and aliphatic carbon signal at 39-41 ppm, whereas the signal of the methylol carbon at the chain end is invisible. Another weak signal centered at 138 ppm must be due to aromatic quaternary carbons of the phenyl rings.

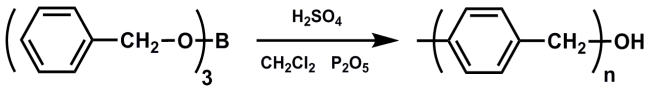

Notably, TGA analysis revealed reasonably high decomposition temperature (540 °C). It is important to note that TGA curve represents a single and sharp decomposition, suggesting one type of connection between the repeating units in the polymer. In view of the simplicity of the TGA pattern, the multiple peaks in the ^{13}C NMR spectrum of the polymer can hardly be ascribed to ortho and para isomerism.

DSC traces of the polymers showed no glassy transition within the 0-300°C temperature range. This must be due to absence of side chains in the polymer structure.

Interestingly, the XRD patterns of the polymers disclosed a completely amorphous structure.

The dielectric spectrum of the polymer presented in shows that, ε^{0} (real part of the dielectric constant) is extremely small (1.8 to 1.9) in the 10 kHz to 13 MHz range and almost independent of frequency, indicating the absence of polar or ionic groups in the polymer structure.

It is important to note that THF solutions of the light-yellow polymers exhibit green-yellow fluorescence, which is visually observable. A broad fluorescence emission band with a maximum at 422 nm is observed by excitation at 370 nm of wavelength. The broad and intense absorption band in the 320-410 nm range is associated with benzenoid transition of the polymer and implies reasonable UV filtering effect of the polymer.

Conclusion: Acid-catalyzed reaction of TBB at room temperature results in the formation of poly(1,4-phenylene methylene) with the molecular weight in the range of Mn = 1000-8600 Da.[4] The polymerization proceeds via carbocationic mechanism, with first-order kinetics with respect to TBB and 0.7th order with respect to proton concentration. The resulting amorphous polymers that consist of the ^{1}HNMR and ^{13}CNMR spectral analysis evidencing 1,4-phenylene methylene repeating units show high thermal stability (polymer degradation temperature: 540 °C) and very low dielectric constant ($\varepsilon^{'}$ = 1.8 to 1.9), as in the case for poly(para-xylene) and related poly(phenylene alkylene)s.

References

1- Greiner A. *Trends Polym. Sci*. 1997, 5, 12.
2- Friedel C, Crafts J.M. *Bull. Soc. Chim.* 1885, 43, 53.
3- *Brotherton, R. J.; Weber, C. J.; Guilbert, C. R.; Little, J. L.Ullmanns Encyclopedia of Industrial Chemistry, 5th ed.; VCH Publishers: Deerfield, FL, 1985; Vol. A4.*
4- Gunes D, Yagci Y, Bicak, N. *Macromolecules* 2010, 43, 7993–7997

Block-Brush Copolymers via Romp and Sequential Double Click Reaction Strategy

Hatice Sahin, Aydan Dag, Hakan Durmaz, Gurkan Hizal, Umit Tunca

Istanbul Technical University

haticesahin85@hotmail.com

Abstract

We report an efficient way, sequential double click reactions, for the preparation of brush copolymers with AB block-brush architectures containing polyoxanorbornene (poly(ONB)) backbone and poly(ε-caprolactone) (PCL), poly(methyl methacrylate) (PMMA) or poly(*tert*-butyl acrylate) (P*t*BA) side chains: poly(ONB-*g*-PMMA)-*b*-poly(ONB-*g*-PCL) and poly(ONB-*g*-P*t*BA)-*b*-poly(ONB-*g*-PCL). The living ROMP affords the synthesis of well-defined poly(ONB-anthracene)$_{20}$-*b*-poly(ONB-azide)$_5$ block copolymer with anthryl and azide pendant groups. Subsequently, well-defined linear alkyne end-functionalized PCL (PCL-alkyne), maleimide end-functionalized PMMA (PMMA-MI) and P*t*BA-MI were introduced onto the block copolymer via sequential azide-alkyne and Diels-Alder click reactions, thus yielding block-brush copolymers. The molecular weight of block-brush copolymers was measured via triple detection GPC (TD-GPC) introducing the experimentally calculated dn/dc values to the software

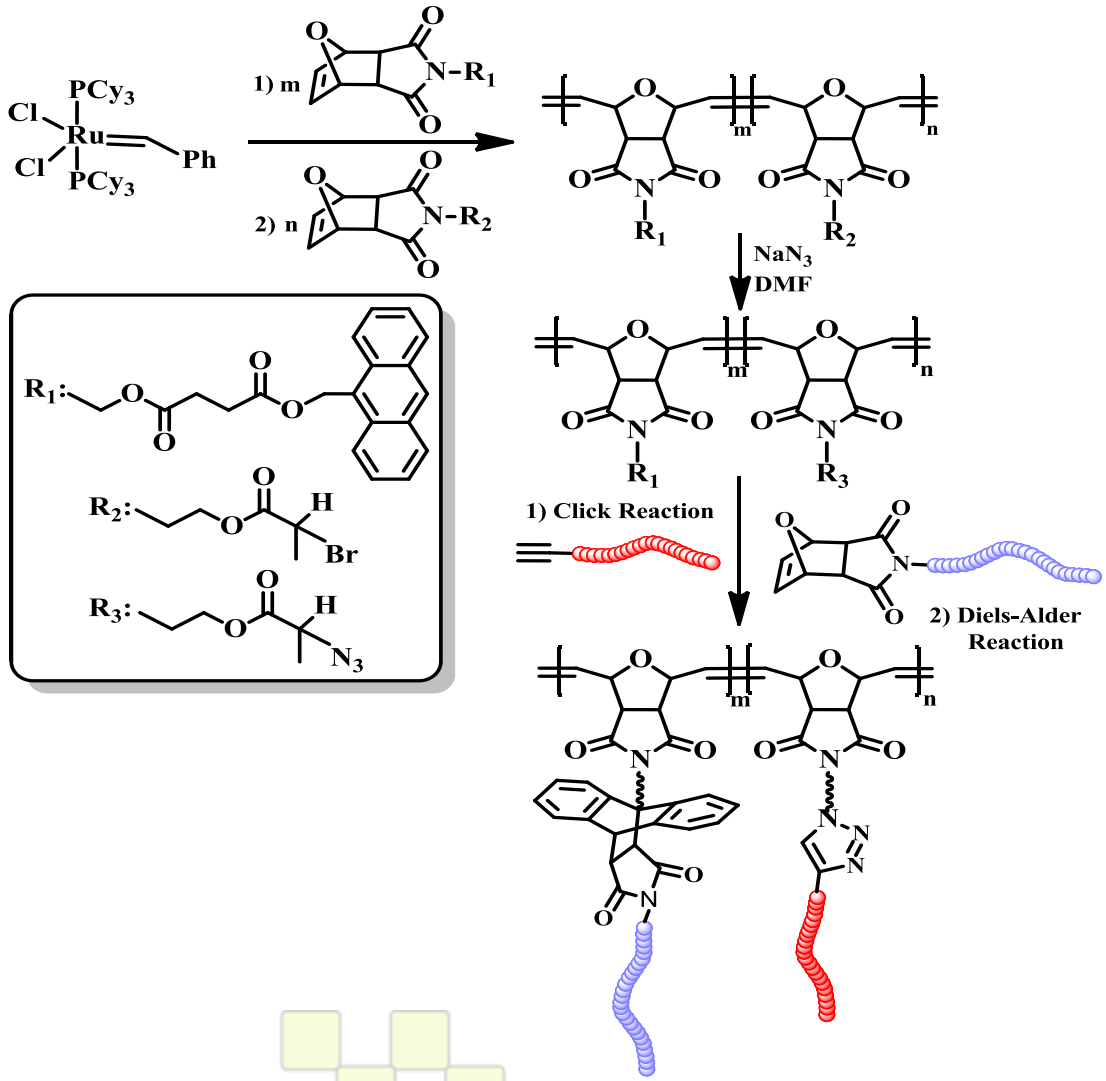

New mixed matrix composite membranes made from polymers able to undergo thermal rearrangement processes. Gas separation study.

Beatriz Bayón[1,2], Lucia Escorial[1,2], Angel E. Lozano[1,2], Young Moo Lee[3], Pedro Prádanos[1,2], Laura Palacio[1,2], Antonio Hernández[1,2]

1 Department of Applied Physics, Faculty of Sciences, University of Valladolid, Valladolid, Spain
2 Institute of Polymer Science and Technology, CSIC, Madrid, Spain
3 WCU Department of Energy Engineering, College of Engineering, Hanyang University, Seoul, Korea

laurap@termo.uva.es

Polymer membranes have served as a key element in many useful scientific and technological fields such as water purification, sensors, fuel cells and gas and vapor separation. Gases are among the most important commercial products, and their separation and purification have a high economical and environmental impact. In this regard, there is a growing interest in the development of novel polymeric materials with improved performance to be used as permselective membranes in the separation of gas and vapor mixtures.

Aromatic polyimides (PIs) have been traditionally considered to be efficient separation materials due to their good permeability and high selectivity for gas separation. They offer excellent thermal and mechanical properties, as well as good chemical resistance. Aromatic polymers interconnected with heterocycling rings, such as polybenzoxazoles (PBOs), possess superior thermal and chemical properties due to their rigid-rod structure having high-torsional energy barriers between two individual phenyleneheterocyclic rings. This restricted freedom of movement could lead to large differences in the mobility of penetrants according to their sizes, and, hence, to high gas selectivities.

Unfortunately, it is very difficult to dissolve PBOs in common solvents for membrane preparation. This fabrication challenge makes very difficult to report permeation and separation data for these materials.

To avoid the solubility drawback, Mathias et al. proposed a new and simple synthetic method using thermal conversion in solid state of *o*-hydroxyl-containing polyimides to polybenzoxazoles (PBOs) through a thermal treatment (TR method)[1].

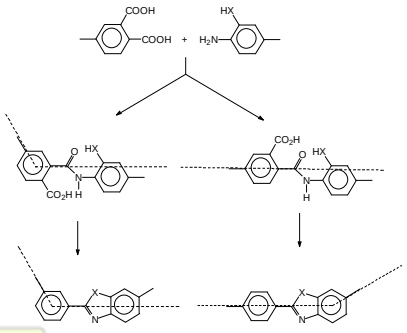

Fig. 1: Thermal transposition from *o*-OH-PI to PBO

Also, it is known that poly(*o*-hydroxyamide)s are able to evolve to PBOs under thermal treatments at temperatures near 350°C[2].

Thus, the thermal rearrangement (TR) method has been recently applied to aromatic polyamides (PAs) and poliimides (PIs) containing *o*-positioned functional groups (e.g. –OH, and –SH), producing materials with impressive permeation and selectivity values[3].

On the other hand, mixed matrix composite, MMC, membranes offer the potential of combining an easy processability and improved gas separation properties for many combination of polymer and particles. In this way, when the composite is well designed, the presence of inorganic or activated carbon particles in a polymer matrix may lead to increments of permeability and also to improvements of permselectivity what permits to exceed the gas productivity trade-off [4,5].

Here, a work dealing with new mixed matrix composite membrane having activated carbon particles and polymer matrix poly(*o*-hydroxyamide)s is presented. These MMCs-PAs have been characterized and their gas separation properties evaluated. Also, the membranes have undergone thermal treatments at temperatures higher than 350 °C, in order to achieve MMC-PBOs. Carbon load and temperature treatment have been optimized in order to achieve the best gas separation properties.

Finally, preliminary results using as polymer matrix poly(o-hydroxyimide)s and other inorganic particles have been accomplished.

Acknowledgements

Authors gratefully acknowledge the financial support provided by the Spanish MICINN (projects MAT2007-62392/MAT and CIT-420000-2009-32).

Bibliography

[1] G.L. Tullos, L.J. Mathias, Unexpected thermal conversion of hydroxy-containing polyimides to polybenzoxazoles, *Polym.* **40** 3463–3468, 1999

[2] J.H. Chang, K. M. Park, I. C. Lee, Thermal cyclodehydration of aromatic precursor polymers to polybenzoxazole and polyimide,their thermal and mechanical properties, *Polym. Bull.* **44**, 63–69 2000

[3] H.B. Park, S.H. Han, C.H. Jung, Y.M. Lee, A.J. Hill, Thermally rearranged (TR) polymer membranes for CO_2 separation, *J. Membr. Sci.*, **359** 11-24, 2010

[4] L. M. Robeson, The upper bound revisted, *J. Membr. Sci.*, Vol. **320**, 390-400, 2008

[5] M. Sadeghi, M. A Semsarzadeh, H. Moadel, Enhancement of the gas separation properties of polybenzimidazole (PBI) membrane by incorporation of silica nano particles, *J. Membr. Sci*, **331**, 21- 30, 2009

Effects of Types and Amounts of Plasticizer on the Curing Kinetics of Unsaturated Polyester

Zekeriya DOĞRUYOL[1], Mehmet Arif KAYA[2], Sevnur Keskin DOĞRUYOL[2], Hüseyin YILDIRIM[2,3], Nergis ARSU[2]

[1] Physics Department, Yıldız Technical University, Davutpaşa Campus, 34220 Istanbul, Turkey
[2] Chemistry Department, Yıldız Technical University, Davutpaşa Campus, 34220 Istanbul, Turkey
[2]Polymer Engineering Department, Yalova University, 77100 Yalova, Turkey

zekeriya41@yahoo.com, m_arif_kaya@yahoo.com, sevnurkeskin@yahoo.com, nergisarsu@gmail.com, husyil@gmail.com

Introduction

Unsaturated polyesters produced by polycondensation of saturated and unsaturated dicarboxylic acids with glycols have been introduced firstly by Vorlander in 1984 [1], and developed by Carlton Ellis with addition of liquid monomer such as styrene to unsaturated polyesters [2]. Unsaturated polyester resins are used in composites, sheet production, surface coatings and moulding processes.

Plasticizers are usually used to improve the thermomechanical quality of materials such as reducing the glass transition temperature. It is well known that plasticizer can act as a diluent by reducing the viscosity for polymerization process.

When unsaturated polyesters are cross-linked with a vinylic reactive monomer, such as styrene it is obtained very rigid, thermal and chemical resistant, film forming materials and coatings. Cross-linking process can be carried out via thermal or photoinitiation by using suitable catalyst and initiator pairs. Both of these ways have typical advantages and drawbacks but photocuring process is more preferable than thermalcuring process because of possessing control ability on the curing kinetics. Various parameters such as type of photoinitiator [3], light intensity [4], photoinitiator concentration [5], temperature and monomer functionality affect the kinetic reaction in the course of the photocuring.

Although several researchers have studied the effect of plasticizer type and amount on the polymerization kinetics, the kinetics of their photopolymerization have not been studied widely.

Materials and Methods

In this study, commercially available unsaturated polyester resins were cured with one component Type II initiator, namely 2-Mercaptothioxanthone (TX-SH) and different type and amounts of plasticizers (Dioctyl phthalate and Trioctyl Trimellilate) were added to the formulations and the effect of plasticizers on the curing kinetic of polyester resins were studied by Photo-DSC technique.

The values of curing kinetic parameters such as, the time (t_{max}) to reach the maximum value of the rate of polymerization (Rp_{max}) and final conversion (C_s) presented considerably variations depending on the effects of types and amounts of plasticizer.

Keywords: photopolymerization, curing kinetics, unsaturated polyester resin, plasticizer

References

1- H.V. Boenig, "Unsaturated Polyesters", Elsevier, New York (1964).
2- S.H. Goodman, "Handbook of thermoset plastics", Noyes Publication, New Jersey (1998).
3- Z. Doğruyol, F. Karasu, D.K. Balta, N. Arsu, Ö. Pekcan, Phase Transit. 81 (2008) 935–947.
4- Z. Doğruyol, N. Arsu, Ö. Pekcan, J. Macromol. Sci. Part B 48 (2009) 745–754.
5- Z. Doğruyol, F. Karasu, G. Temel, D.K. Balta, M. Aydın, S. Keskin, Ö. Pekcan, N. Arsu, In Basics and Applications of Photopolymerization Reactions, In Applied Polymer Science Series, J.P. Fouassier, X. Allonas, Ed., Research Signpost, Trivandrum, 2010, Chap. 11, 161–173.
6- L. Çokbağlan, N. Arsu, Y. Yağcı, et al., Macromolecules 36 (2003) 2649–2653.

Use of waste polymer as thickener agent in lubricating greases

J.E. Martín-Alfonso, C. Valencia, M.C. Sánchez, J.M. Franco, C. Gallegos

Departamento de Ingeniería Química. Facultad de Ciencias Experimentales. Universidad de Huelva. Campus Universitario del Carmen, 21071, Huelva. Spain.

Phone: +34 959 219985, Fax: +34 959 219983, E-mail: jose.martin@diq.uhu.es

Introduction

Nowadays, especially in the developed world, there has been a great interest the use of recycled resources for different industrial applications due to its positive effect on the environment. From a general perspective, there is a marked tendency to increase the use of recycled materials, as a result of government regulations or due to increasing public concern for a pollution-free environment. In general, lubricating greases are highly structured colloidal dispersions, consisting of a thickener dispersed in mineral or synthetic oil. In recent years, increasing attention has been directed towards polymers or biopolymers to development new thickener agents with suitable properties to substitute traditional thickeners [1, 2]. Some thermoplastics polymers exhibit the ability for swelling and gel formation in organic media and therefore they serve as the dispersion medium of greases. The overall objective of this work was to study the influence of plastic waste concentration on the rheological properties and microstructure of polymer based lubricating greases. With this aim, viscous and linear viscoelastic measurements, as well as morphological analysis and differential scanning calorimetry tests, have been performed on the samples.

Experimental

Materials

A naphthenic oil (SR-10) from crude distillation, kindly provided by Verkol Lubricantes (Spain), and waste polymer supplied in pellets by Eslava Plasticos, S.A (Spain) was used as the gelling agent.

Manufacture of lubricating greases

Processing of lubricating greases was performed in an open vessel, by stirring with an IKA RW-20 mixer (Germany) with a four-blade propeller to disperse the gelling agent. Batches of 600 g were processed for 60 min at 170 ºC and rotational speed of 150 rpm. Then, the solution was cooled down to room temperature in order to induce gelification. Cooling was carried placing the solution on steel sheet having the sample a thickness of 3-5 mm. A final homogenization treatment (rotational speed: 4000 rpm; homogenisation time: 5 min), using a rotor-stator turbine (Ultra Turrax T-50, Ika, Staufen, Germany), was applied at room temperature. Waste polymer contents in the blends were 4, 6.5, 9, 11.5 and 14 % (w/w).

Results

Figure 1 shows the mechanical spectra, in the linear viscoelasticity range of polymer based greases as a function of waste polymer concentration. As can be observed, the linear viscoelasticity response is qualitatively similar for all the greases studied and also to that found with other commercial lubricating greases [3].The evolution of the storage and loss moduli with frequency for these lubricating greases (higher values of the storage modulus and a minimum in the loss modulus at intermediate frequencies) is characteristic of polymeric systems with physical entanglements [4]. As can be observed in Figure 1a, a significant increase in both SAOS functions, and a shift of the minimum in G'' to higher frequencies, are noticed when increase waste polymer concentration. The above-mentioned increase in both linear viscoelasticity functions is similar in the low frequency range and, consequently, the relative elastic characteristics of these gel-like dispersions are not significantly affected, as can be observed in Figure 1b where the loss tangent (G''/G') is plotted versus frequency. In this sense, formulations containing high waste polymer concentration show minimum loss tangent values at large frequencies.

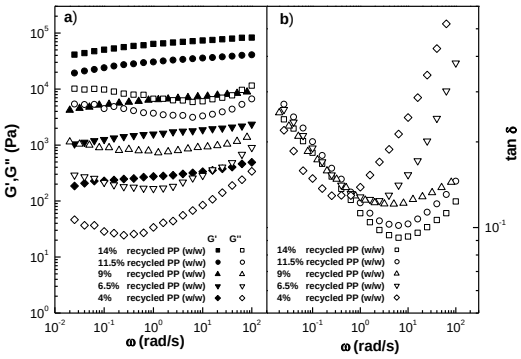

Figure 1. Frequency dependence of the storage and loss moduli (a) and tan δ (b) at 25ºC.

Conclusions

From the result obtained, it can be deduced that this waste polymer can be potentially used as an effective thickener agent for lubricating greases. The evolution of the linear viscoelasticity functions with frequency is qualitatively similar to that found for traditional lithium lubricating grease. It is observed that lubricating greases based on waste plastic show enhanced of viscoelastic modulis with respect to traditional lithium lubricating greases, which may represent an important advantage. In general, the studied formulations in polymer-based greases show lower mechanical stability tendency, mainly at lower plastic waste content, than traditional lubricating greases.

Acknowledgements

This work is part of a research project (CTQ2004-02706) sponsored by a MEC-FEDER program. The authors gratefully acknowledge its financial support.

References

[1] J. E. Martín Alfonso, R. Yañez, C. Valencia, J. M. Franco, M. J. Díaz, *Ind. Eng. Chem. Res.* **2009**, 48, 6765-6771.
[2] R. Sánchez, J.M. Franco, M.A. Delgado, C. Valencia, C. Gallegos, *Carbohydr. Polym.* **2011**, 83, 151-158.
[3] J.M Madiedo, J.M Franco, C. Valencia and C. Gallegos, *J. Tribol.* **2000**, 122, 590-596.
[4] J.D. Ferry, Viscoelastic Properties of Polymers, Wiley, New York, 1980.

Thermal properties of polymer composites containing ultrasonicated cellulose

Adriana N. Frone,[1] Denis M. Panaitescu,[1] Catalin I. Spataru,[1] Dan Donescu,[1] Paul Stanescu,[2] Michaela D. Iorga[1]

[1]National Institute for Research and Development in Chemistry and Petrochemistry, Polymer Department, 202 Spl. Independentei, 060021, Bucharest, Romania
[2]University Politehnica of Bucharest, Faculty of Applied Chemistry & the Materials Science, 1-7 Polizu Stret, 011061, Bucharest, Romania

panaitescu@icf.ro

Introduction

Polymer composites with cellulose fibers (with micro or nano size) are developed with the aim of substituting for glass-fiber-containing composites in some important applications like biomedicine, cosmetics, packaging industry, automotive, construction and other industrial fields [1-2]. Nano-scale cellulose fibers production and application in composite materials is a relatively new research field and has gained increasing attention in the past two decades [3-4]. Two directions could be detected: research studies which explore the development of nano-bio-plastics as fully biodegradable nanocomposites and studies aimed at dispersing cellulose nanofibers in non-biodegradable, petroleum derived polymers.

The main goal of this work is to employ different ultrasonic conditions in order to isolate nanofibers from microcrystalline cellulose (MCC) and to evaluate their influence on the thermal behavior of poly(vinyl alcohol) (PVA). PVA was chosen as a matrix because of the expected interaction of its hydroxyl groups with the hydrophilic surfaces of the cellulose nanofibers, leading to strong hydrogen bonding.

Materials and Methods

PVA 120-99, 1200 polymerization degree and 99% hydrolysis degree, was used as a matrix. Cellulose nanofibers were obtained from microcrystalline cellulose (MCC) using high power ultrasound technique, different power and time of sonication. Nanofibers isolated by applying different ultrasonication conditions were characterized by atomic force microscopy. AFM images were captured in tapping mode by a MultiMode 8 atomic force microscope equipped with a Nanoscope V converter from Bruker.

The obtained cellulose fibers (NF), 5wt. % were used as reinforcements in a poly(vinyl alcohol) (PVA) matrix. The thermal properties of PVA/NF cellulose fibers nanocomposite films were determined and compared with the thermal behavior of cellulose microfibrils (MF) containing PVA.

Differential scanning calorimetry (DSC) and thermogravimetric analysis (TGA) were performed on a SDT Q600 V20.9 from TA Instruments under helium flow (100 mL/min). The samples were dried for 24 h at 40 ^{o}C before characterization and were tested from the ambient temperature to 600 ^{o}C at a heating rate of 10^{o}C/min.

Results and Discussion

Several differences were observed in AFM images regarding the size and the aspect ratio of the nanofibers obtained in different ultrasonic conditions. When increased power and time of ultrasonication were used, the thickness of nanofibers decreased from an average of 50 nm to almost 20 nm. An AFM image (500 nm x 500 nm) of NF cellulose fibers obtained by ultrasonication is shown in the figure below.

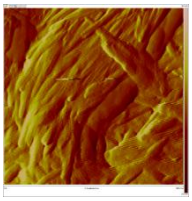

No significant changes for glass transition temperature (T_g) and melting point (T_m) of PVA composites with reference to neat PVA were observed in DSC diagrams of PVA/NF composites, only a slight increase in crystallinity was noted. In case of PVA/MF composites a significant decrease of both T_g and cristallinity was revealed by DSC. The stronger interactions between cellulose fiber surface and adjacent PVA chains in case of smaller size fibers and the influence of water were proposed to explain these results. TGA and DSC results pointed out that most of the water present in PVA composites was bound water, with a limited lubrication effect.

Thermogravimetric analysis (TGA) was used to investigate the effect of cellulose fibers on the thermal stability of the composites. Slightly higher onset degradation temperatures were obtained for PVA/NF composites in comparison to neat PVA, showing an increase of the thermal stability caused by the addition of cellulose nanofibers. No changes were detected in case of PVA/MF composites.

Conclusions

Nanofibers with valuable properties can be obtained using the method of ultrasonication. In contrast to common cellulose fibers with micrometer size, cellulose nanofibers can enhance the thermal stability of PVA.

References

1. Petersson, L., Kvien, I., Oksman, K. (2007) "Structure and thermal properties of poly(lactic acid)/cellulose whiskers nanocomposite materials," *Composite Science and Technology* 67(11-12), 2535-2544
2. Dong, S. P., and Roman, M. (2007). "Fluorescently labeled cellulose nanocrystals for bioimaging applications," *J. Amer. Chem. Soc.* 129(45), 2007, 13810-13811.
3. Eichhorn, S. J., Dufresne, A., Aranguren, M., Marcovich, N. E., Capadona, J. R., Rowan, S. J., Weder, C., Thielemans, W., Roman, M., Renneckar, S., Gindl, W., Veigel, S., Keckes, J., Yano, H., Abe, K., Nogi, M., Nakagaito, A. N., Mangalam, A., Simonsen, J., Benight, A. S., Bismarck, A., Berglund L. A., and Peijs, T. (2010). "Review: Current international research into cellulose nanofibres and nanocomposites," *Journal of Materials Science* 45(1), 1-33
4. Hubbe, M. A., Rojas, O. J., Lucia, L. A., and Sain, M. (2008). "Cellulosic nanocom-posites: A review," *BioResources* 3(3), 929-980.

Application of Microencapsulated Phase Change Materials to Improve Thermo-regulating properties of textiles

Luz Sánchez-Silva, Ana M. Borreguero, Juan F. Rodríguez, Paula Sánchez*

Department of Chemical Engineering, University of Castilla-La Mancha
Avda. Camilo José Cela, s/n, E-13004 Ciudad Real, SPAIN

marialuz.sanchez@uclm.es

Abstract

Textile industry shows a growing interest into the functionalization of textiles for innovative commercial applications. The emerging technologies based on microencapsulation are able to confer new properties and add value to the textiles that were not possible or cost-effective using other processes.

A thermoregulatory fabric is an intelligent textile that has the property of offering suitable response to changes in external conditions or to external and environmental stimuli. The level of thermal wellbeing depends on the heat exchange between the human body and the environment that surrounds it, many efforts have been devoted to induce a thermo-regulating effect into textiles. When the external temperature is higher than the material melting point, it produces a freshness sensation. However, when the external temperature is lower than material melting point it produces a warmness sensation. This behaviour is due to the presence of microcapsules containing phase change materials (PCM).

To apply these PCM microcapsules to fabrics, their thermal activity must work in a range of skin temperature and be harmless to the skin. When the body is at its normal temperature there are certain temperature ranges common to certain parts of the body. The core of the body, or the abdominal area, and the head normally maintain an average skin temperature higher than that associated with other areas of the body. Generally, the overall average comfortable skin temperature is 33.3ºC, and if this cannot be maintained, a person begins to feel uncomfortable.

In this study, polystyrene microcapsules containing phase change materials were synthesized by suspension like polymerization process. Thermal properties, surface morphology and structural stability of the PCM microcapsules were investigated using differential scanning calorimetry (DSC), thermogravimetric analysis (TGA), environmental scanning electron microscopy (ESEM) and infrared thermography (IR) techniques. The intactness of PCM microcapsules can be maintained up to approximately 135ºC according to TGA and DSC analyses. In addition, the fixation of microcapsules into textile substrate by means coating technique was tested. Different coating products, mass ratio of microcapsules to coating binder and different textile substrate were studied in order to get thermal comfort in fabrics. Furthermore, a comparison was made of the thermal insulating effect of the thermo-regulating textiles according to the used textile substrate.

PCM microcapsules were successfully incorporated into the textiles by using TEXPRINT ECOSOFT N10® and WST SUPERMOR® as polymeric binders without modifying the original properties of textile (Figure 1).

Microcapsules were successfully fixed into seven fabric substrates for different textile applications by a coating technique. Results also indicated that the presence of microcapsules containing Rubitherm® RT31 produces a significant thermal insulation effect during a cold to warm transition or vice versa (20-45ºC), as can be seen in Figure 2. Thus, this kind of microcapsules can be used to obtain textiles with comfort-related properties.

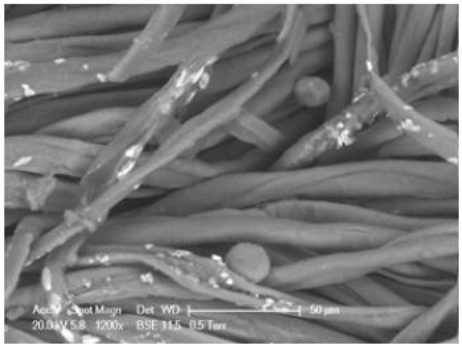

Figure 1. ESEM micrographs of a thermo-regulating textile.

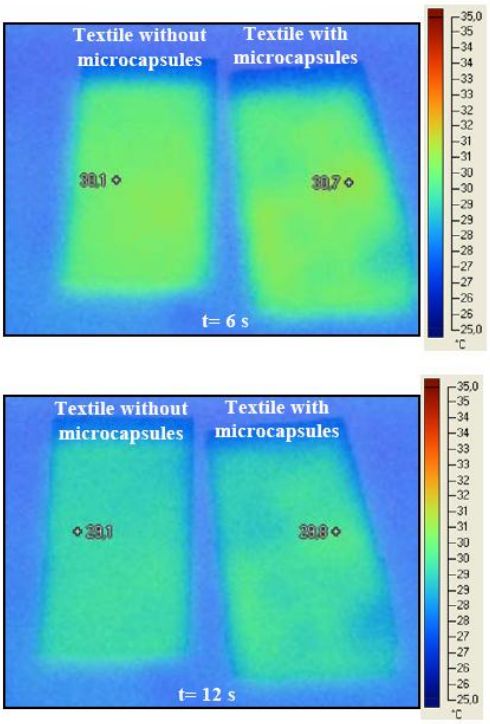

Figure 2. Infrared camera images of coated textile with and without PCM microcapsules at different times.

Removal of crystal violet from aqueous solution by thermosensitive hydrogels: Investigation the effect of hydrophilic comonomer amount

B. Özkahraman[a], *I. Acar*[b], *S.Emik*[b]

[a] Hitit University, Faculty of Engineering, Chemical Engineering Department, Çorum, 19030, Turkey.
[b] Istanbul University, Faculty of Engineering, Chemical Engineering Department, Avcilar, Istanbul, 34320, Turkey.

bengiozkahraman@hitit.edu.tr, acar@istanbul.edu.tr; s.emik@istanbul.edu.tr

Introduction: Residual synthetic dyes are the major contributors to color in wastewaters generated from textile and dye manufacturing industries [1]. Because of this reason, the removal of color from industrial effluents becomes environmentally important [2]. Synthetic dyes usually have a complex aromatic molecular structure and exhibit considerable structural diversity [3-4], which make them more stable and more difficult to biodegrade [5-7]. The conventional methods for the removal of dyes from wastewater include coagulation and flocculation, oxidation or osonation, membrane separation, and adsorption [8]. Among several chemical and physical methods, adsorption process is one of the most effective methods to remove dyes from wastewater [2]. Many kinds of adsorbents have been developed for various applications [9, 10]. Some low-cost materials have also been directly used as sorbents, such as chitosan, zeolites, clay, fly ash, coal, natural oxides, industrial wastes for dye adsorption [11].

Hydrogels are three-dimensional cross-linked polymeric structures which are able to swell in aqueous environments [12]. Some hydrogels are stimuli sensitive; they exhibit significant changes in their swelling and mechanical properties in response to changes in pH, ionic strength, or temperature of the external environment [13-14]. The best known temperature sensitive polymeric network is poly(N-isopropylacrylamide) [15-16] and has a lower critical solution temperature (LCST) at about 32°C [17]. Therefore, N-isopropylacrylamide monomer takes a wide and important place in synthesis of thermosensitive hydrogels [18-20].

The aim of this work is investigating the usage of p(N-isopropylacrylamide-co-itaconic acid) p(NIPAm-co-IA) temperature sensitive hydrogels for removal of cationic dye (crystal violet) from aqueous solutions. For this purpose, N-isopropylacrylamide was copolymerized with various amounts of sodium salt of itaconic acid in the presence of crosslinking agent N,N methylenebisacrylamide to obtain temperature sensitive hydrogels. The chemical structure, swelling and deswelling properties of these hydrogels were investigated. In addition, their adsorption properties (ie. adsorption capacities, kinetics, isotherms) were investigated in case of their usage in removal of crystal violet (CV) solution.

Materials and Methods: Monomers (NIPAAm and IA (10% wt.)) and the crosslinking agent (NMBA) (1% molar ratio of the total mixture) were dissolved in deionized water in glass tubes. The required amounts of PPS and PBS were added. The solution was purged with nitrogen gas for 30 min. to eliminate dissolved oxygen in the system. The polymerization reactions were carried out for 24 h at 10°C. At the end of the polymerization, the hydrogels were washed 1 L fresh water four times to remove any unreacted monomers and initiators. Then the hydrogels were dried under vacuum at 50°C during 24 hours for using dye adsorption experiments.

Dye adsorption experiments were carried out in 100 mL beaker flasks containing 50 mL of synthetic dye solution at room temperature. Hydrogel (0.05 g) was added to the CV solution (500 mg/L) for the determination of adsorption capacity. After desire treatment period (1., 3., 5., 7., 24., 48. and 96. hours) the residual dye concentration in the solution was determined colorimetrically with a spectrometer by the measurement of absorbance at the maximum absorption wavelength (590 nm for CV). All of the experiments were done at their natural pH value of dye solutions and were carried out in triplicate. The adsorption capacities (mg dye/g hydrogel) of hydrogels were calculated using the following equation:

$$q_e = (C_o - C_e)V/m$$

where q_e (mg/g) is the adsorbed amount of dye per gram hydrogel, C_o and C_e are the initial solution concentration (mg/L) and equilibrium concentration (mg/L), respectively; V is the volume of the solution; and m is the amount of the hydrogel used (g).

Results and Discussion: According to adsorbed dye amounts, the adsorption capacities of hydrogels, having different hydrophilic comonomer amount, were found in the range of 75 - 100 mg dye/g hydrogel. In addition, the results indicated that the pseudo-second-order kinetic model fitted better than the data obtained from pseudo-first-order model for the adsorption of CV on to hydrogels. Furthermore, according to effect of the initial dye concentration findings, it is concluded that, Freundlich isotherm explains the adsorption better than Langmuir isotherm.

Conclusions: The results showed that the synthesized hydrogel can be used as an adsorbent for important applications for removal of cationic dyes from wastewater.

References

[1] Ramakrishna KR, Viraraghavan T (1997) *Waste Manag* 17, 8, 483-488.
[2] Uzun I, Güzel F (2005) *J Haz Ma*. B118, 141-154.
[3] Forgacs E, Cserhati T, Oros, G (2004) *Environ Int* 30, 953-971.
[4] Gong R, Sun Y, Chen J, Liu H, Yang C (2005. *Dyes Pigments* 67, 175-181.
[5] Fewson CA (1988) *Trend Biotech* 6, 148-153.
[6] Seshadri S, Bishop PL, Agha AM (1994) *Waste Manag* 15,127-137.
[7] Nigam P, Armour G. Banat IM, Singh D, Marchant, R (2000) *Bioresour Technol* 72, 219-226.
[8] Acar I, İyim TB, Özgümüş S (2008) *J Appl Polym Sci* 109, 2774–2780.
[9] Weng CH, Pan YF (2006) *Coll Surf A Physicochem Eng Asp* 274, 154–162.
[10] Gupta VK, Mohan D, Saini VK (2006) *J Coll Interf Sci* 298, 79–86.
[11] Babel, S, Dacera, DM (2006) *Waste Manag* 26, 988-1004.
[12] Byrne ME, Park K, Peppas NA (2002) *Adv Drug Deliver Rev* 54, 149–161.
[13] Bernardo MV, Blanco MD, Olmo R, Teijon, JM (2002) *J App Polym Sci* 86, 327–334.
[14] Peppas NA, Bures P, Leobondung W, Ichikawa, H (2000) *Eur J Pharm Biopharm* 50, 27-46.
[15] Qiu Y, Park K (2001) *Ad. Drug Deliver Rev* 53, 321-339.
[16] Carillo F, Defays B, Colom X (2008) *Eur Polym* 44, 4020–4028.
[17] Schild, HG (1992) *Prog Polym Sci* 17, 163-249.
[18] Zhang XZ, Zhang JT, Zhuo RX, Chu CC (2002) *Polym Com* 43, 4823-4827.
[19] Jin S, Liu M, Chen S, Gao C (2008) *Eu. Polym J* 44, 2162-2170.
[20] Ling Y, Lu M, (2009) *J Polym Res* 16, 29-37.

The synthesis and physico-chemical properties of dextran phosphates

M. Zhyhala, N. Yurkshtovich*, N. Golub**, V. Alinovskaya**, T. Yurkshtovich**, R. Kosterova***

Institute Of General and Inorganic Chemistry Of The National Academy Of Sciences Of Belarus*
The Research Institute for Physical Chemical Problems of the Belarusian State University**

Margarita_Zh@tut.by

Introduction

The development of polymeric materials of medical use to posses prolonged and adjustable therapeutic effect is an actual and perspective direction in modern Macromolecular Chemistry. Natural polysaccharides and their derivatives, in particular the products of etherification of polysaccharides by phosphoric acid are of considerable interest among polymer mediums. Dextran phosphates are known to be referred to low-toxic substances that possess immunomodulatory activity, biodegradability and can be obtained in the form of stable viscous solutions and hydrogels [1,2]. In this work the samples of water-soluble dextran phosphates using melt H_3PO_4: $(NH_2)_2CO$ were obtained and the influence of the etherification reaction conditions on the functional composition and yield of the zol-fraction was studied.

Materials and Methods

The parent polymer was dextran with molecular weight $6 \cdot 10^4$ Da. Phosphorylation reaction of dextran was carried out in the melt H_3PO_4: $(NH_2)_2CO$ in the temperature range 100 - 135°C [3].The regularities of the etherification reaction of dextran, depending on composition of the mix, temperature and pressure of the reaction zone (0,15-1,0 bar) were studied. Chemical composition and physical and chemical properties of the reaction products were evaluated by IR spectroscopy, ^{31}P-nuclear magnetic resonance (NMR), Scanning Electron Microscopy, elemental analysis, viscometry, High-performance liquid chromatography and potentiometric titration.

Results and Discussion

Materials with the degree of substitution by phosphate (DS_P) and carbamate groups (DS_N) 0,27-0,69 and 0,13-0,48 respectively and zol-fraction of 23,5-100 % yield were obtained. The dextran phosphates were established to be mono-and dibasic mono-and diphosphates, which percentage depends on the system conditions.

It was shown, that increasing the quantity of phosphorous acid leads to the increase in DS_P and the decrease in the zol-fraction due to the formation of additional crosslinks in the structure of the modified polysaccharide. The decrease in urea content increases the yield of the zol-fraction of dextran phosphates, since with the decreasing of pH of the mixture the degree of degradation of macromolecules increases, as well as the formation of monobased phosphates is predominant. With the growth of the reaction temperature the medium molecular weight of the reaction products significantly increased and their solubility was sharply reduced. The yield of zol-fraction was established to decrease as the pressure of the system reduced.

SEM data showed structural changes of polysaccharide in consequence of the modification. Granules of dextran phosphates was shown to be broken into unhomogeneous pieces with loose and porous structure.

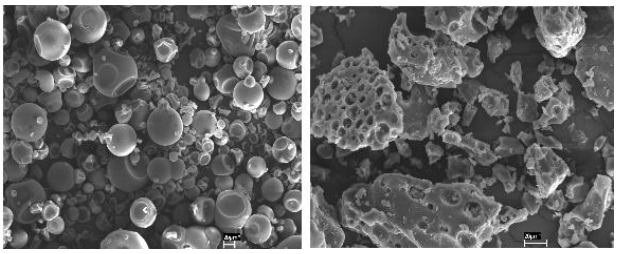

Figure 1 Electronic microphotos of initial (I) and modified dextrans (II) with DS_P = 0,67, DS_N = 0,20.

Conclusion

Thus, during the research optimum conditions for the obtaining of the stable viscous solutions of dextran phosphates, having large exchange capacity that allows to use them as polymers- mediums for drugs have been defined. The possibility of application of phosphate-dextran as a medium of anticancer drug, in particular, α-2b-interferon was established.

References

1. Granja, P.L. Cellulose phosphates as Biomaterials. II. Surfase Chemical Modification of Regenerated Cellulose Hydrogels // P.L. Granja, L. Ponysegu, D. Defficux, G. Daude, B.D. Jeso, C.Labrugere, M.A. Barbosa. - Cellulose Journal of Applied Polymer Science. - 2001. - V. 82. - P. 3354-3368.

2. Denizli, B.K. Preparation conditions and swelling equilibria of dextran hydrogels prepared by some crosslinking agents // B.K.Denizli, C.H. Kaplan, M.O. Zakir, Guner Ali. - Polymer. - 2004. - V.45. - P. 6431-6435.

3. Heinze, U. New starch Phosphate Carbamides of High Swelling Ability: Syntesis and Characterization // U.Heinze, D.Klemm, E.Under, F. Piescher. - Starch/ Stärke. - 2003. - V.55. - P. 55-60.

New Branched oligophenylenefluorenes for luminescent applications

Irina A. Khotina, Alexey I. Kovalev, Alexey V.Shapovalov, Natalia S. Kushakova

A. N. Nesmeyanov Institute of Organoelement Compounds RAS

khotina@ineis.ac.ru

Fluorenylene dendrimers - 1,3,5-tri (2-fluorenyl) benzene and 1,3,5-tri [2 - (9,9-dioctylfluorenyl)] benzene, which are model compounds for the branched oligophenylenefluorenes, synthesized by the cyclocondensation of unsubstituted and dioctylsubstituted acetylfluorenes respectively.

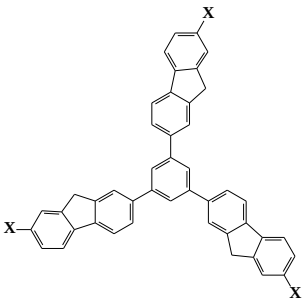

1

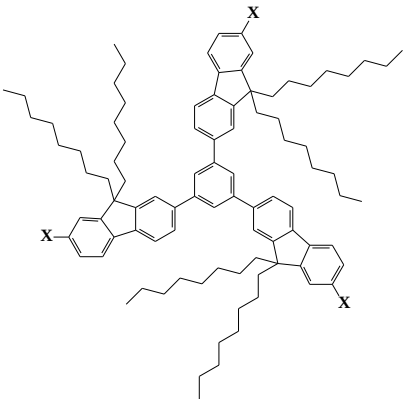

2

X = H, Br

Joint polycondensation of phenyl-bis-pinacoldiborate with tribromoarylenes in the presence of Pd complex in Suzuki reaction “A3 + B2” type led to the synthesis of branched oligophenylenefluorenes. The absorption and fluorescence spectra of model compounds and oligophenylenefluorenes recorded in solutions and interpreted. It was shown that the synthesized branched oligomers did not have the aggregation of fragments, which distinguishes them from known linear fluorescent polymers.

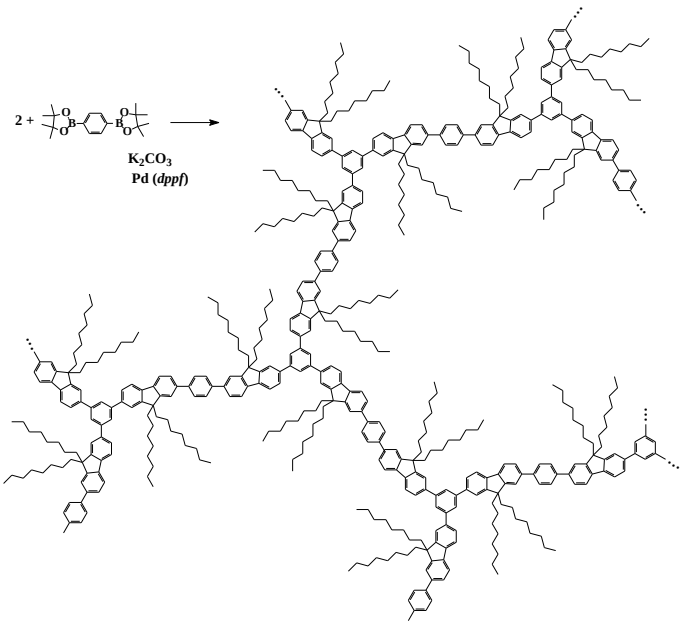

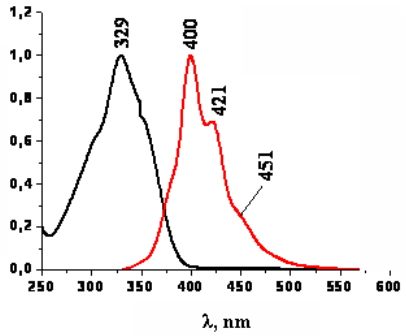

Comparative analysis of the fluorescence spectra of model compounds and oligofluorenes shows that the latter are more structural. A bathochromic shift of the main fluorescence bands at 25 nm and 35 nm and an increase in Stokes shift also observed. This, despite the great length of phenylene chains in the oligomer molecules, in comparison with similar chains in model compounds, may be associated with a decrease in the effective length of conjugation, the violation of planarity, such as occurs in hexaphenyl compared with terphenyl.

Synthesis, Morphological Characterization and Antimicrobial Application of Nanostructured Membranes of Cellulose Acetate

Silvia V. G. Nista[1], Karen Segala[1], Lívia Cordi[2], Osmar R. Bagnato[3], Nelson Duran[4], Liliana M. F. Lona[1], Lucia H. I. Mei[1]*

[1*]Faculdade de Engenharia Química – UNICAMP, Av. Albert Einstein, 500, C.P. 6066, 13083-970 Campinas/SP
[2] Instituto de Biologia – UNICAMP, Rua Monteiro Lobato, 255 CEP 13083-970 Campinas/SP
[3] Laboratório de Microscopia Eletrônica (LME) - LNLS – C. P. 6192, 13083-970 Campinas/SP
[4] Instituto de Química – UNICAMP, C.P. 6154, 13083-862 Campinas/SP

silnista@feq.unicamp.br ; ksegala@feq.unicamp.br; cordi@unicamp.br ; osmar@lnls.br ; duran@iqm.unicamp.br; liliana@feq.unicamp.br; lumei@feq.unicamp.br

Introduction

The electrospinning process is very attractive due to its low cost methodology and easily adaptable to industrial scale production of nanofibers, especially biomaterials, in a simple and repetitive method[1]. Cellulose acetate (CA) is an amorphous, nontoxic and odorless polymer most commercialized currently and soluble in various solvents[2]. The development of anti-septic[3], biocompatible and nanostructured membranes of CA, by electrospun method, with the incorporation of silver nanoparticles is an interesting option. This new materials are very promising in the helth area, because of its low cost compared to options available today.

Materials and Methods

The AgNPs were synthesized in a aqueous media by chemical reduction of $AgNO_3$ using $NaBH_4$ as reducing agent and sodium citrate as stabilizer. The nanometric dimension of the silver particles was monitored by UV–vis and confirmed through Transmission Electron Microscopy (TEM). Cellulose acetate (CA) membranes nanostructured, with AgNPs, were successfully prepared via electrospinning of CA in DMAc/Acetone/Water (32%/63%/5%) solvent mixture, and characterized using FEG and SEM microscopy. The antimicrobial action of the CA film impregnated with AgNPs was evaluated by the use of both *Gram* positive microorganisms, *Staphylococcus aureus* (*S. aureus*) ATCC 29213 and *Staphylococcus epidermides* (*S. epidermides*) ATCC 12228.

Results and Discussion

The Figure 1 shows the UV-vis spectrum of Ag nanoparticles sinthesized in aqueous medium.

The Figure 2a shows the images of SEM and 2b of FEG, for cellulose acetate nanoestructured membranes with Ag nanoparticles.

Microbiological analysis confirmed the antimicrobial activity of the films by the inhibition of bacterial growth for *S.epidermides* and for *S. aureus*.

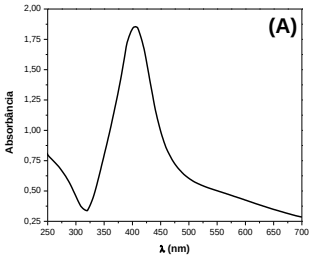

Figure 1- UV-vis spectrum to Ag nanoparticles sinthesized in aqueous medium

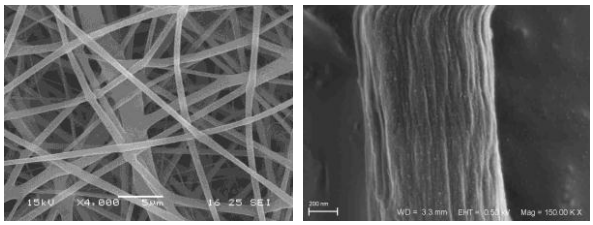

(a) (b)

Figure 2 – Images for cellulose acetate nanoestructured membranes with Ag nanoparticles, from:
(a)SEM (b) FEG

Conclusions

The silver nanoparticles impregnated in the cellulose acetate nanoestructures membranes, confer anti septic properties to this new material.

References

1.Ramakrishna, S.; Fujihara, K.; Teo, W.; Yong, T.; Ma, Z., Ramashesan, R. "Electrospun nanofibers: solving global issues", *Mater. Today* 2006, 9, 3.
2.Schiffman, J.; Schauer, C. "A Review: Electrospinning of Biopolymer Nanofibers and their Application", *Polymer Reviews* 2008, 48, 317-352
3.Son, W. K.; Youk, J. H.; Park, W. H. "Antimicrobial cellulose acetate nanofibers containing silver nanoparticle", *Carbohydrate Polym.* 2006, 65, 430-434.

Synthesis and Characterization of Silicon Containing Membranes for PEM Fuel Cells

Mehmet Arif KAYA[1], Huseyin YILDIRIM[1,2]

[1]Chemistry Department, Yıldız Technical University, Davutpaşa Campus, 34220 Istanbul, Turkey
[2]Polymer Engineering Department, Yalova University, 77100 Yalova, Turkey

m_arif_kaya@yahoo.com, husyil@gmail.com

Introduction

World have to find out new solutions to facing problems such as depletion of fossil fuel reserves, global warming and pollution of our planet. An alternative energy resource must overcome these problems and it must be renewable, economical and convenient for many applications.Proton Exchange Membrane Fuel Cell (PEMFC) is very promising new energy resource for humankind. PEMFCs have important advantages such as high energy conversion, environment friendly, low emission values in contrast to conventional fossil energy resources. Polymeric Proton Exchange Membranes are most important components of Fuel Cells. These membranes account for proton transfer and separation anod and cathode. Perfluorinated ionomers as Proton Exchange Membrane have been used for long times in Fuel Cells, recently new alternative structures have appeared in this area. Especially high performance polymers have outshined the other alternatives because of their resistance to application conditions and easily modification ability for membrane form. Sulfonated and/or phosphonated high performance polymers such as polysulfones, polyetherketones, polyimides, polyphenylenes have taken place in membrane applications.

Polysulfones (PSU) can dissolve many solvents and have high glass transition temperature, high thermal stability, good mechanical properties, and excellent resistance to hydrolysis and oxidation. Their outstanding properties have resulted several important advantages in Proton Exchange Membrane researches.

Polydimethylsiloxane (PDMS) has extremely low T_g (-125 °C) so PDMS is most flexible chain molecules known. PDMS has not only high thermal and chemical stability but also poor mechanical properties and high gas permeability.

Copolymerization of flexible, durable and mechanically poor PDMS blocks with relatively brittle, durable and mechanically good PSU blocks can improve drawbacks of each blocks.

Sythesis and properties of PSU-PDMS multiblock copolymers have been reported by many researches [1-5]. These multiblock copolymers exhibit multi-phase separation and high thermal and hidrolitic stability. Altough PSU-PDMS multiblock copolymers are suitable for Fuel Cell conditions (thermal and chemical stability etc.), they were not examined in this purpose by researchers.

Materials and Methods

In this study, firstly it is synthesized α,ω-difunctional telechelic polysulfone oligomers using 4,4'-dichlorodiphenyl sulfone (DCDPS) and different dihydroxyl compounds.

Commercially available α,ω-difunctional telechelic polydimethylsiloxane oligomers containing different functional end groups with different molecular weight were copolymerized with α,ω-difunctional telechelic polysulfone oligomers.

Multiblock PSU-PDMS copolymers were modified via electrofilic substation way in mild sulfonation reactions in order to obtain Proton Exchange Membranes.

Obtained Proton Exchange Membranes were characterized by ATR FT-IR, NMR, GPC and performance tests.

Keywords: polydimethylsiloxane, polysulfone, telechelic oligomer, multiblock copolymer, sulfonation, proton exchange membrane.

References

1- Noshay, A., Matzner, M. and Williams, T. C., "Silylamine-Hydroxyl Reaction in the Synthesis of Organo-Siloxane Block Copolymers", Ind. Eng. Chem. Prod. Res. Dev., (1973), 12 (4), 268-277.

2- Giurgiu, D., Hamciuc, V., Butuc, E., Cozan, V., Stoleriu, A., Marcu, M. and Ionescu, C.,"Synthesis and Characterization of Polysulfone-Poly(alkylene oxide) Block Copolymers Containing Poly(dimethylsiloxane)" Journal of Applied Polymer Science, (1996), 59, 1507-1514.

3- Hamciuc, V., Giurgiu, D., Butuc, E., Marcu, M., Ionescu, C.,and Pricop., L.,"Synthesis of polysulfone block copolymers containing polydimethylsiloxane", Polymer Bulletin, (1996), 37, 329-336.

4- Hamciuc, V., Giurgiu, D., Marcu, M., Butuc, E., Ionescu, C.,and Pricop., L.,", "Polysulfone-Polydimethylsiloxane Block Copolymers Containing Si-O-C Bonds", Journal of Macromolecular Science, Part A Pure and Applied Chemistry, (1998), 35(4), 563-575.

5- Di Pasquale, G., La Rosa, A., Marno, A.,"Synthesis and surface characterization of a new multiblock copolymer based on poly(dimethylsiloxane) and aromatic polysulfone", Macromol. Rapid Commun., (1997), 18, 267-272.

Optical and Transport Properties of Poly(thiophene-3-ylacetic acid) and Its Sodium Salt

J. Cerar,[b] D. Bondarev,[a] P. Nachtigall,[a] J. Vohlidal,[a] V. Vlachy[b]

[a]Charles University, Faculty of Sciences, Dept. of Phys. and Macromol. Chem., CZ-128 40, Praha 2;
[b]University of Ljubljana, Faculty of Chemistry and Chemical Technology, SI-1000 Ljubljana, Slovenia

vohlidal@natur.cuni.cz

Background & Methods: Unlike the structure and the ionic equilibria, the thermodynamic and transport properties of aqueous solutions of conjugated polyelectrolytes including PTAA are little known. Our work aims to partly fill this gap by examining the transport of ions in aqueous solutions of partially (34.6 %) neutralized regio-irregular PTAA (PTAA/Na). Aqueous solutions of PTAA/Na were carefully purified by dialysis. The conductivity of these solutions has been studied as a function of the concentration of ionized groups and temperature. The conductivity data were complemented by determination of the macropolyion constituent transport numbers at 25 °C using the indirect moving boundary method; coloring of PTAA anions enables easy monitoring the boundary movement, as well as easy determination of the polymer concentration in a solution. Combination of these results allowed us to estimate the fraction of so-called "free" counterions in the system. In addition, we studied the UV/vis spectra of PTAA/Na, PTANa and PTANa/Me to obtain new information on the solution behavior of PTAA derivatives. These results are extensively compared with the UV/vis data obtained by others groups and completed with the DFT calculations aimed at estimation of the preferred conformations of PTAA chains and electronic transitions in the chains.

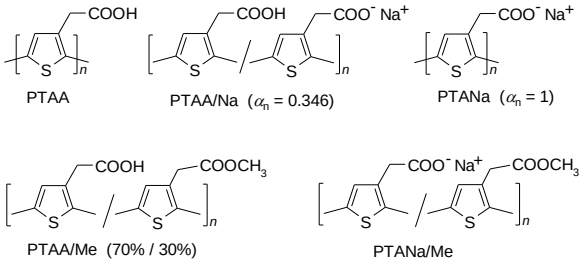

Results & Discussion: The transference numbers of PTAA/Na macropolyion constituent, T_p, showed only a small dependence on the polymer concentration. The fraction of "free" sodium counterions, *f*, obtained from the measured T_p and molar conductivity increased as the polymer concentration decreased. This behavior strongly contrasts with that of highly charged strong polyelectrolytes such as DNA or poly(styrenesulfonic acid) and its salts, for which *f* is a decreasing function of the solution dilution, which indicates an increase in the counterion-macropolyion association in highly diluted solutions. On the contrary, PTAA/Na obeys the concentration dependence observed typically for dilute solutions of spherical macropolyions and cylindrical oligopolyions.

The observed qualitative identity of the UV/vis spectra taken from a DMF solution and from a film of PTAA showed that π-stacking of thiophene rings in bulk PTAA does not occur, which strongly contradicts with the behavior currently observed for majority of polythiophenes. Strong intramolecular non-covalent interactions via hydrogen bond stabilizing distorted conformations of PTAA chains are proposed to be the main reason for this exceptional behavior, as well as for the slowness of conformational relaxations of PTAA/Na chains in solutions.

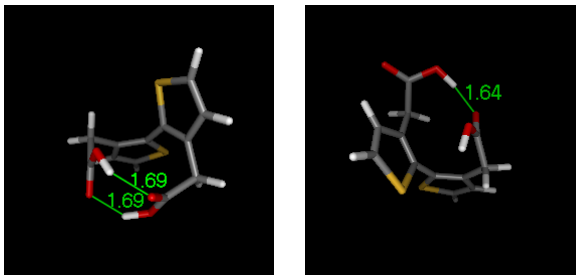

We demonstrated the validity of the Lambert-Beer law for PTANa and PTAA/Na but the non-validity of this law for PTANa/Me aqueous solutions; the latter system was instead found to exhibit an isosbetic point at 402 nm. This can be explained by the aggregation of the polymer chains due to the presence (ca. 1/3) of non-hydrolyzed ester groups in the chains. On the other hand, we did not observe any isosbestic point during acidobasic titrations of PTAA/Na solutions though two such points have been reported by another research group. Only continuous shifts of the absorption bands without their crossing have been observed during the latter titrations.

We have summarized and critically evaluated discrepancies between published spectroscopic data and those obtained in this work, as well as among the data on PTAA-based systems available in the literature. These discrepancies can be partly ascribed to certain differences in the chemical structure of the samples studied by various groups and partly to the history of the studied polymer solutions (owing to the slowness of conformational relaxation of PTAA/Na chains).

Conclusions: The main output of the present work is the first characterization of the transport properties of a weak anionic conjugated polyelectrolyte: partially neutralized PTAA. The second output is new knowledge on the unusual spectroscopic behavior of PTAA forms and the rational lying behind it.

Acknowledgments: Financial supports of the Slovenian Research Agency (0103-0201), Czech Science Foundation (104/09/1435 and 203/08/H032), Ministry of Education of the Czech Republic (MSM0021620857) and Grant Agency of the Charles University (D. B., project 166410) are acknowledged.

Influence of Type of Methacrylic Esters on Properties of Acrylic Core/Shell Dispersions

Klemen Burja[1], *Ema Žagar*[2], *Saša Skale*[3]

[1]PoliMaT, Tehnološki park 24, 1000 Ljubljana,
[2]Kemijski inštitut, Hajdrihova 19, 1000 Ljubljana
[3]Helios Group, Količevo 2, 1230 Domžale

klemen.burja@helios.si

The water-born resins in ecologically acceptable coatings represent advantageous materials in comparison to previously used solvent-born resins. Among the most widely used water-born dispersions are the polyacrylic ones. Since one of desired properties is the ability of the coating to repel water, the aim of our work was to elucidate the effect of the type of methacrylic ester side chain on hydrophobicity of polyacrylic dispersion.

For this reason we prepared acrylic dispersions of different chemical composition by a two step emulsion polymerisation.[1-3] The methacrylic part of the polymer was varied using methacrylic esters of different hydrophobicity, *i.e.*, methyl methacrylate, *n*-butyl methacrylate, *t*-butyl methacrylate, 2-ethylhexyl methacrylate and isobornyl methacrylate. In addition, acrylic acid monomer, which is used as a *co*-stabilizer for acrylic water dispersions, was replaced by two other type of monomers, *i.e.*, 2-hydroxyethyl methacrylate and maleic acid. The molar ratio between monomers, surfactant and initiator used in emulsion polymerization was in all cases constant. We evaluated various physical and chemical properties of the synthesized acrylic dispersions and their dried films, such as particle size distribution, molecular weight, rheology, glass transition temperature and surface tension.

References:
[1] C.S. Chern, *Prog. Polym. Sci.* **31** (2006) 443.
[2] S.C. Thickett, R.G. Gilbert, *Polymer* **48** (2007) 6965.
[3] M. Nomura, H. Tobita, K. Suzuki, *Adv. Polym. Sci.* **175** (2005) 1.

Synthesis and self-assembly of block copolymers bearing *o*-nitrobenzyl side groups

Olivier Bertrand, Jean-Marc Schumers, Charles-André Fustin and Jean-François Gohy

Université chatholique de Louvain, Institut de la matière condensée et des nanoscience/Bio et Soft Matter

olivier.bertrand@uclouvain.be

In the past decade, block copolymers have proved themselves to be powerful tools for preparing a wild range of nanostructured materials, either in the solid phase (thin films) [1-2] or in solution (micelles) [3-4] since they are able to self-assemble at the nanoscale into well-ordered morphologies. Moreover, the family of stimuli responsive block copolymers shows great potential for application in diverse fields due to their ability to change their properties when submitted to a stimulus (pH, temperature, light irradiation) [4]. Among all the existing stimuli light is particularly interesting [5] since it can be localized in time and space, it can be triggered from outside of the system, and it does not require particular reagents which limit byproducts.

We report on block copolymers containing *o*-nitrobenzyl photocleavable side groups. They are interesting precursors to trigger micellization by light. The block copolymers are composed of a polystyrene (PS) block and a poly(nitrobenzyl acrylate) or poly(dimethoxynitrobenzyl acrylate) block bearing photocleavable side-groups (PNBA-*b*-PS and PDMNBA-*b*-PS). The synthetic strategy consists in preparing block copolymer precursors by Atom Transfer Radical Polymerization (ATRP), and grafting the desired *o*-nitrobenzyl derivative in a post-modification step (**Scheme 1**)

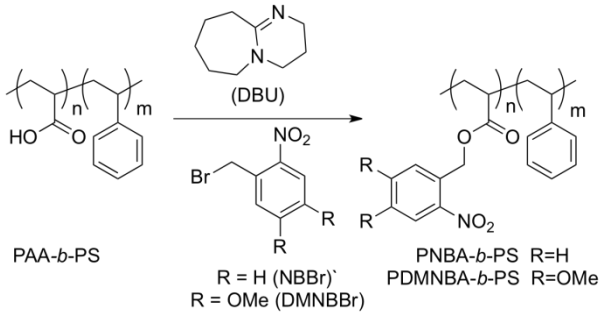

Scheme 1: synthesis strategy.

The copolymers will be used for light induced micellization. Starting from the copolymer dissolved in a non selective solvent like chloroform, a UV irradiation will be performed to cleave the *o*-nitrobenzyl moieties and generate COOH groups. Since the poly(acrylic acid) (PAA) block thus formed is insoluble in the solvent used, it will aggregate leading to the formation of micelles with a PAA core and a PS corona (**Figure 1**).

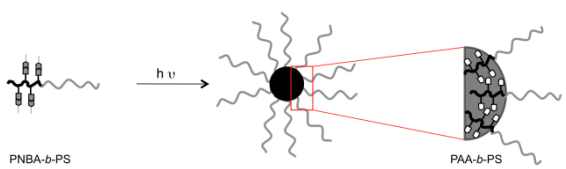

Figure 1 : light induce micellization.

[1] C. Park, J. Yoon, E. L. Thomas, *Polymer*, **2003**, 44, 6725-6760

[2] H-C. Kim, S-M. Park, W. D. Hinsberg, *Chem. Rev.*,**2010** ,110, 146-177

[3] J-F. Gohy, *Adv. Polym. Sci.*, **2005**, 190, 65-136

[4] N. Rapoport, *Prog. Polym. Sci.*, **2007**, 32, 962-990

[5] J-M. Schumers, C-A. Fustin, J-F. Gohy, *Macromol. Rapid Commun.*, **2010**, 31, 1588-1607

Zinc Metal as Catalyst for Direct Grafting of Vinyl Acetate from PVC

Gokhan Cankaya, *Niyazi Bicak*

cankayagok@gmail.com

Istanbul Technical University Department of Chemistry, Maslak 34469 Istanbul-Turkey

Introduction: Modification of PVC by grafting is desirable to attain materials with tunable mechanical properties. The earlier methods of PVC modification by grafting from approach are based on radiation grafting and photoiniferter techniques. ATRP has also been used in combination with telechelic approach for grafting of PVC. In the following works Percec *et. al*[1] and our group[2] demonstrated graft copolymerization of some acrylic monomers by ATRP method from labile chlorines of PVC. This process allows control of the grafting degree; however color of the graft copolymer is important drawback.

More recently we have developed activated zinc powder-alkyl halide initiation system for controlled/living polymerization of vinyl monomers, including vinyl acetate. In this presentation, this method was extented to prepare for graft copolymerization from chlorine atoms of PVC. Overall process is stirring monomer solution of PVC with activated zinc catalyst at 70 ^{0}C.

Result and Discussion

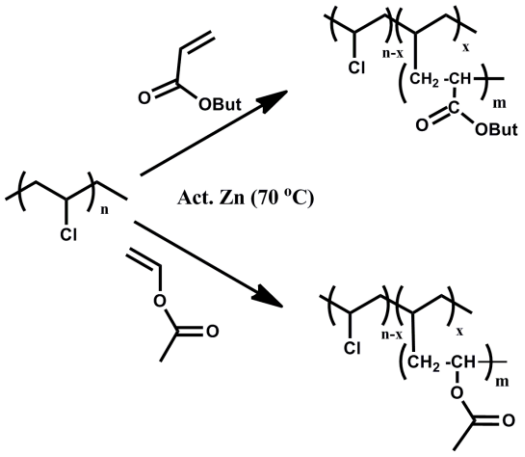

Scheme-1: Grafting of PVC with BA and VAc by Zn catalyst

Zinc activated grafting from approach was applied for the vinyl monomers, vinyl acetate and butyl acrylate. The ^{1}HNMR spectrum of the PVC-*g*-PVAc in fig-1 shows a sharp singlet at around 4.9 ppm, which arises from CH-O bond of Vac and 3.6 ppm corresponding CH-Cl bond implying unreacted chlorine groups of PVC.

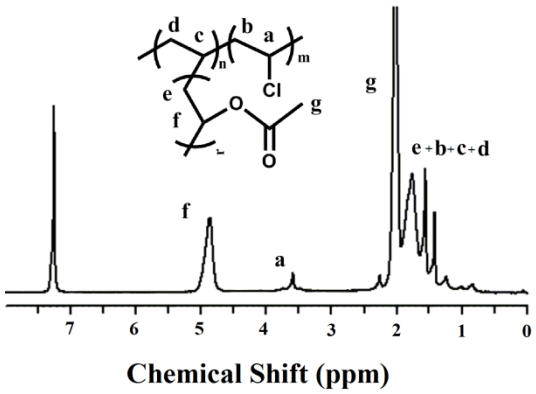

Figure 1: ^{1}HNMR spectrum of grafting of PVC with VAc by Zn catalyst

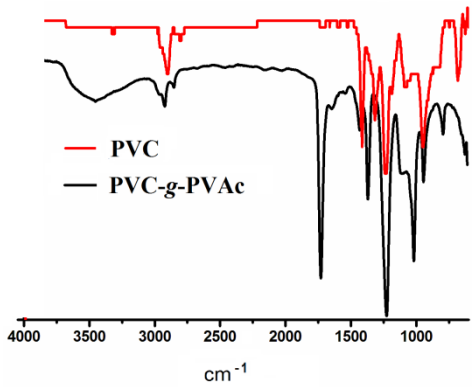

Figure 2: FT-IR spectrum of grafting of PVC with Vac by Zn catalyst

FT-IR spectrum of the graft copolymer is well agreement the NMR spectrum. Apart from the PVC, carbonyl groups of the grafted polymer appeas at 1731 cm^{-1} as seen in fig-2.

Conclusion: The results showed that the process allows direct grafting of PVC and high graft yields (up to 1400 %) are attained within reasonable periods.

References

(1) V. Percec, A. Cappotto, B. Barboiu, Macromol Chem Phys, 203, 1674 (2002)

(2) N. Bicak, B. Karagoz, D.Emre. J. Polym.Sci Polym Chem, 44, 1900 (2006)

Development of Stimuli-Responsive Polymers for Liposome Based Drug Delivery Systems

P. Alves, J.F. Coelho, M.H. Gil, P.N. Simoes

Department of Chemical Engineering, University of Coimbra, Pólo II, Phinhal de Marrocos, Coimbra 3030-790, Portugal

palves@eq.uc.pt

Introduction:

Liposomes are self-assembled vesicles that consist of an aqueous core domain entrapped by a lipid bilayer. They are attractive materials for drug delivery systems (DDS) due to their biocompatibility, non-immunogenicity, non-toxicity and ability to entrap both hydrophilic and hydrophobic compounds [1,2]. Despite the promising capabilities as DDS, liposomes have shown low transfection efficiency and low stability in the systemic circulation. To overcome these problems, functional polymers are being attached to the liposomes by means of a hydrophobic anchor, forming polymer-caged liposomes (PCL). This strategy also allows the preparation of PCL that can respond to environmental stimuli (pH and temperature), enhancing their usefulness as DDS.

The development of new polymers to be used in PLC is crucial in these systems. This work reports the tailored synthesis of macromolecules based on a LRP method, more specifically a metal catalyzed method, known as Single Electron Transfer (SET). This strategy presents several advantages over other methods, such as mild work conditions, fast kinetics and very high tolerance to different functionalities. It is a well established method and provides an effective tool for synthesizing advanced polymer materials with different architectures, topologies, compositions, and high degree of control over polymer microstructure.

Methods

In the present work, cholesterol (CHO) was used to anchor the polymer into liposome. The synthesis started with the esterification of the OH-end group of Cholesterol with bromocarboxylic acids, yielding an initiator structure, shown in scheme 1.

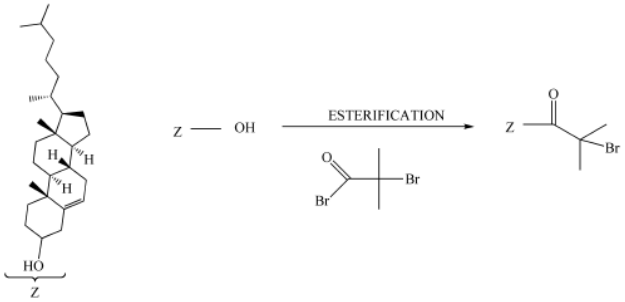

Scheme 1: Representation of cholesterol esterification.

This previously obtained CHO initiator with the terminal bromide was then used for the SET/LRP of tert-butyl acrylate (tBA) with Cu(0) and tris[2-(dimethylamino)ethyl]amine (Me6-TREN) in dimethylsulfoxide (DMSO) at 30ºC [3, 4]. The schematic reaction of this procedure is presented in scheme 2.

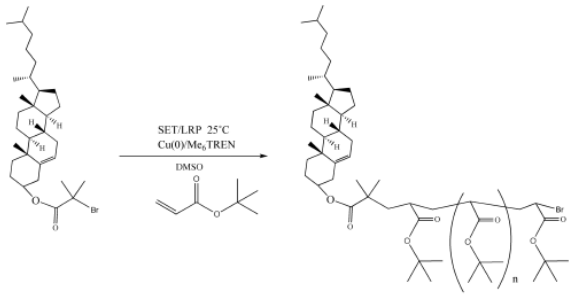

Scheme 2: Representation of the SET/LRP reaction.

The tBA units of CHO-PtBA were then deprotected with trifluoroacetic acid (TFA) to form CHO-PAA [5] (scheme 3).

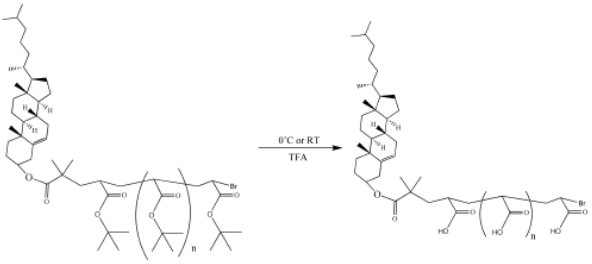

Scheme 3: Representation of the hydrolyses of tBA to acrylic acid.

Results

The synthesized polymers were completely characterized by H-NMR, FTIR, DMTA, mDSC, TGA and multiSEC. The behavior of the complexes liposome/polymer regarding polymers with different characteristics was investigated towards its application in DDS.

References:

[1] Paasonen L, Romberg B, Storm G, Yliperttula M, Urtti A and Hennink WE. Bioconjugate Chem. 18:2131–2136, 2007.

[2] Lee S-M, Chen H, Dettmer CM, O'Halloran TV and Nguyen ST. J. Am. Chem. Soc. 129:15096–15097, 2007.

[3] Coelho JF, Simões P, Mendonça PV, Fonseca, A and Gil, MH. J. Appl. Polym. Sci. 109:2729–2736, 2008.

[4] Percec V, Guliashvili T, Popov AV, Ramirez-Castillo E, Coelho JF and Hinojosa-Falcon LA. J. Polym. Sci. Part A 43:1649–1659, 2005.

[5] Rathfon J. M. and Tew G. N. Polymer 49:1761–1769, 2008.

Rapid Removal of Copper from ATRP Mixtures by Chemical Reduction with Wetted Zinc Powder

Fatma Canturk, Bunyamin Karagoz, Niyazi Bicak

Istanbul Technical University, Department of Chemistry, Maslak 34469 Istanbul, Turkey

fatoshh@gmail.com

Introduction: Copper mediated ATRP is an excellent controlled/living polymerization technique that allows creating various polymer architectures.[1] despite its peculiarities ATRP has not found application in mass production of polymers. This is due to color of the polymer products arising from the copper residues.
The use copper catalysts anchored to solid supports has been considered as useful for recovery and reuse the catalyst. The copper complexes physically adsorbed on silica supports were determined to be effective in preparing copper-free polymers at the end of the polymerization. However, heterogeneity of the process does not allow attaining narrow molecular weight distributions. The Schiff base ligand covalently linked to silica support[2] was reported to give copper-free polymers with relatively high polydispersities (PDI: 1.4-1.6). Shen group[3] and other groups introduced various amine ligands covalently attached to solid supports to attain better control of the molecular weights. Copper complexes immobilized on Janda gel resin was determined to give colorless polymers[4]. However, the resulting polymers showed broad polydispersities. Post purification after the polymerization was consired as useful to avoid loss of control of the chain growth.Despite those endovours in obtaining copper free polymers with low polydispersities is still a chalanging problem and needs further development.

Herein, we describe a quick method of the copper removal from ATRP mixtures, based on chemical reduction with zinc powder.

Result and Discussion: It was demonstrated that, simple mixing of an ATRP mixture with wetted zinc powder (i.e. 0.3 g per mmol copper) together with small amounts of silica gel as seeding material yields colorless solutions and the elemental copper precipitated at the bottom, in less than 5 min.

$$CuBr_2 \cdot L + Zn(0) \longrightarrow Cu(0) + ZnBr_2 \cdot L$$

Scheme 1: Chemical reduction of the copper complex by zero-valent zinc.

Table 1: Ligand and solvent effects on the chemical reduction of copper by zinc powder in ATRP solution.

Run	*[Zn] /[Cu] (mol/mol)*	*Ligand*	*Contact time for decolorization*
1	5	HTETA	3.5 min
2	5	PMDETA	1.3 min
3	5	Bipyridyl	2.7 min

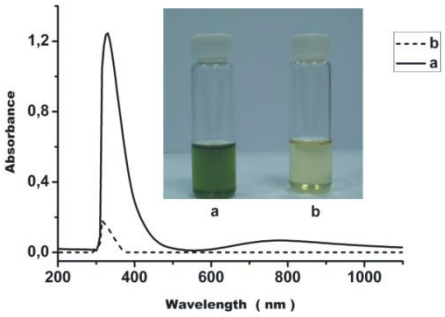

Figure 1: UV-Visible spectrum of ATRP solution of PMMA in toluene (diluted 1/ 250), before (a) and after (b) copper removal by zinc powder.

AAS and UV spectra of the filtered polymer solution showed no any trace of copper (Fig-1).

The polymer (PMMA) (Mn:12400) isolated from clear ATRP solution obtained by short contact with zinc powder was determined to be "still living" as confirmed by chain extension with styrene yielding block copolymer, PMMA-*b*-PS (Mn:15800) (Fig-2).

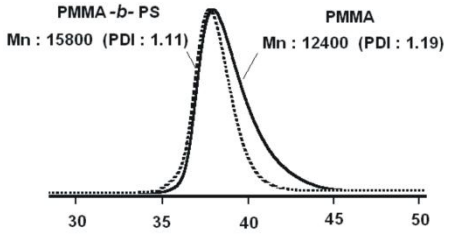

Figure 2: GPC trace of PMMA and PMMA-*b*-PS .

Prolonged stirring with zinc powder (*i.e.* 24 h) however, yields non-living polymer, due to reductive dehalogenation of the end-groups. Reduction of the bromoalkyl end-groups can be accelerated by adding few mL acetic acid and completed within 2 h.

Conclusion: Treatment of ATRP solutions by zinc powder provides rapid removal of the copper complex and the terminal halide groups remain unaffected.

References:

1- V. Coessens, T. Pintauer, K.Matyjaszewski ; Prog. Polym. Sci. 26 (2001) 337-377
2- Haddleton, D. M.; Kukulj, D.; Radigue, A. P, Chem Commun 1999, 99–100.
3- Shen, Y.; Zhu, S.; Pelton, R, Macromolecules 2001, 34, 5812–5818.
4- Honigfort, M. E.; Brittain, W. J, Macromolecules 2003, 36, 3111–3114.

Solid Supported Benzoquinone as a Click Component for Facile Immobilization of Amino Acids and Proteins

Kubra Yuksel, Gokhan Cankaya, Okan Sirkecioglu, Niyazi Bicak

Istanbul Technical University, Department of Chemistry, Maslak 34469 Istanbul, Turkey

yksel_kbra86@hotmail.com

Introduction: The term "click chemistry" has been coined by K. B. Sharples in order to define nearly quantitative reactions providing easy connection of two reagents having highly reactive groups. To date, the Cu(I)-catalyzed 1,3-dipolar cycloaddition of alkynes to azides, yielding triazole connection has been one of the most popular click reaction. This reaction proceeds in various media including aqueous solutions[1]. Another popular click reaction is Diels-Alder reaction based on cyclization of diene and dienophile at ambient temperatures[2].Altough other click reactions such as reaction of epoxides with amines or carboxylic acids are already being used extensively industry, this chemistry is less common in academia.Herein, we describe a forgotten compound, benzoquinone as a click component due to its exceptional michael addition capability. Benzoquinone is unique member of quinones having reversible redox behavior and a very reactive Michael acceptor for amines, thiols and hydrocyanic acid etc. This chemical behavior has been exploited in designing heat stable polymers and redox-active materials. In this work, we have studied preparation of solid supported benzoquinone for easy immobilization of proteins and amino acids.

Result and Discussion:

In this study, surfaces of micron size silica spheres were modified with 3-trimethoxy silyl 1-amino propane (Scheme-1).

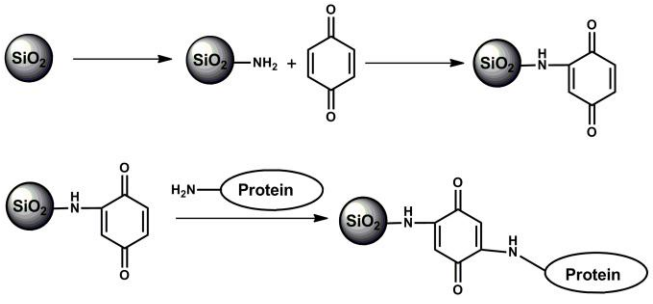

Scheme-1: Solid Michael receptor for amines, amino acids and thiol functional polymers.

TGA and acid titration methods revealed an amine content of 1.2 mmol per gram. The resulting material was reacted with benzoquinone in methanol solution.

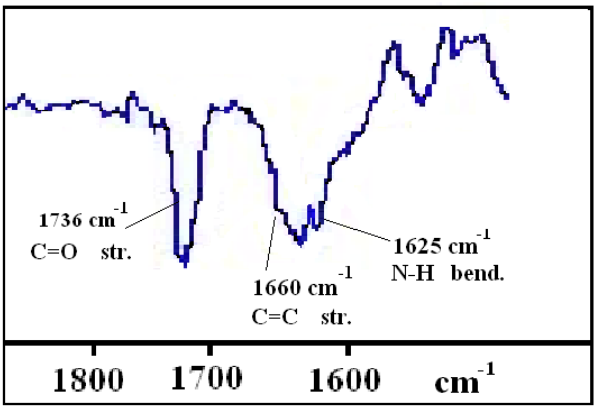

Figure-1: FT-IR spectrum of quinone functional silica microspheres.

FT-IR spectrum of this material showed (Fig-1) characteristic vibration bands of carbonyl groups of the quinone moiety at 1736 cm^{-1}. Stretching vibration of carbon-carbon double bands appeared at 1660 cm^{-1}. Another typical band, N-H bending vibration was observed at 1625 cm^{-1}, indicating incorporation of benzoquinone into the structure.

The resulting material was employed as efficient Michael acceptor for immobilization of amine functional compounds such as amino acids and proteins.

Two amino acids (glycine and alanine) were introduced to quinine functional surface of the silica microspheres in methanol solution using calcium hypochloride as oxidant.

The structures of the materials obtained in each step were confirmed by FT-IR andTGA analyses.

The results showed that addition of amino acids takes place in high yields which approches to the benzoquinone density of the microspheres. Ovalbumine was also studied for the surface modification in similar conditions.

Conclusion: The click chemistry with surface bound benzoquinone moieties is useful to generate amino acid functional micro beads. Although we have not studied yet, such materials might be used as chiral stationary phase for separation of amino acids and proteins.

References

1- F. Himo, T. Lovell, R. Hilgraf, V. V. Rostovtsev, L. Noodleman, K. B. Sharpless, V. V. Fokin, *J. Am. Chem. Soc.*, **2005**, *127*, 210-216.

2- Hartmuth C. Kolb, M. G. Finn, and K. Barry Sharpless *Angew. Chem. Int. Ed.*, 40, 2004 -2021 (2001)

Preparation and characterization of a polyetherimide/polyaniline composite

Evandro M. Alexandrino[1], *Maria I. Felisberti*[2]

Chemistry Institute, University of Campinas (UNICAMP), P.O. Box 6121, Zip Code 13083-970, Campinas - SP, Brazil

[1]evaalexandrino@iqm.unicamp.br, [2]misabel@iqm.unicamp.br

Introduction

Polyaniline (PAni) is one of the most interesting conductive polymers due to its excellent environmental stability, easy and cheap chemical synthesis and interesting electrical and electrochemical properties in the emeraldine form. On the other hand, it shows poor mechanical properties and processability. In the last three decades, since the work from MacDiarmid *et al.*[1], the combination of polyaniline with thermoplastics, elastomers and thermosetting polymers as composites and blends has been widely studied. However, the preparation of polymer composites with high thermal performance thermoplastic has been less explored due to the lower thermal stability of polyaniline in the doped state with usual dopants like HCl. Among the methods to improve the thermal stability of PAni, the use of organic acids with high molecular weight such as camphorsulfonic acid (CSA), dodecyl benzene sulfonic acid (DBSA) and *p*-toluene sulfonic acid (TSA) showed interesting results[2].

Polyetherimide (PEI) is an amorphous high thermal performance thermoplastic, with good mechanical and chemical resistance. In this work, a composite using polyetherimide as the matrix and doped polyaniline with *p*-toluene sulfonic acid as polymer filler was prepared by extrusion process, and their morphological, structural, mechanical and thermal properties were determined.

Materials and methods

Aniline (Vetec, 99%) was distilled under vacuum before use. Ammonium persulfate (Synth, 98%), HCl (Synth) and NaCl (Synth, 99,5%) were used without further purification. The polyetherimide (trade name Ultem®1001) was obtained from SABIC Innovative Plastics.

Polyaniline was synthesized by chemical oxidation, through the addition of a solution 3M $(NH_4)_2S_2O_8$/1M HCl/3M NaCl to a solution 0,4M aniline/1M HCl/3M NaCl, dropwise and under vigorous stirring. This reaction was kept between -10ºC and 0ºC. The green solid (PAni/HCl) was washed with a H_2O:EtOH solution (5:2 v/v) and dried under vacuum for 36h. The PAni/HCl was undoped by stirring in a NH_4OH 1M solution for 24h, washed and dried again, and then was doped with *p*-toluene sulfonic acid (PAni/TSA) by stirring in a TSA 1M solution for 24h. The composite with 10% of PAni/TSA were prepared in a double screw mini compounder at 330ºC and injection molded under pressure of 8 bar and temperature of 330ºC in bars for tensile tests according with ASTM D1708.

Samples were thermal characterized by TGA (Seiko EXSTAR6000 TG/DTA 6200 at 10ºCmin^{-1}) under oxidative atmosphere and DSC (TA Instruments 2910 at 10ºCmin^{-1}) under N_2 atmosphere. Structural characterization was made by FTIR (Bomem MB series B-100 from 4000 cm^{-1} to 400cm^{-1}) and morphological characterization was obtained by SEM (JEOL JSM6360-LV 10kV). The tensile test was realized in a EMIC DL 200 apparatus.

Results and discussion

The FTIR spectra of the synthesized polyanilines show the main absorptions of polyaniline in the emeraldine form. The ratio between "quinoid ring" (1580 cm^{-1}) and the "benzoid ring" (1460 cm^{-1}), confirms the emeraldine state in the obtained polyanilines[3].

TGA analysis shows that Pani/TSA presented a higher stability in comparison to PAni/HCl. The T_{10} (10% weight loss temperature) for PAni/TSA is approximately 310°C. The PEI-PAni/TSA composite with 10% of polyaniline shows T_{10} at 532°C, near the value for pure PEI. The differential thermogravimetric analysis (DTG) shows acceleration in the second loss event. DSC analysis of the composite shows no alteration in the T_g value in relation to the pure polyetherimide.

The tensile test shows a significant decrease (38%) of the tensile stress for the composite comparing to the value obtained for the polyetherimide. However, the value obtained for the composite is in the same range of the one of pure polycarbonate.

The polyaniline morphology shows the characteristic globular aggregates, which were related to the high superficial tension. The composite presented agglomerates of polyaniline throughout the polyetherimide matrix, with a good adhesion in the interfacial region. The micrographs of the fracture resulting from tensile test suggest different fracture mechanism for PEI and its composites (Figure 1).

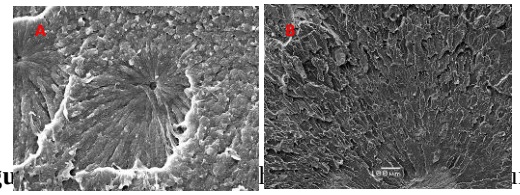

Figuures: (A) pure PEI; (B) PEI-PAni/TSA

Conclusion

Composites of PEI and PAni/TSA showed a decrease of the mechanical properties, probably due to the presence of aggregates of polyaniline. The SEM micrographs show a good interfacial adhesion and suggest changes in the fracture mechanisms.

References

[1] MacDiarmid, A. G. *et al.*; *Mol Crystall Liq Crystals*; **1985**; 121; 173-180

[2] De Paoli, M. A.; Mitzakoff, S.; *Eur Polym J*; **1999**; 35; 1791 - 1798

[3] Schetinni, A. R. A. *et al.*; *Synth Metals*; **2009**; 159; 1491-1495

Cationic Homo and Copolymerization of Indene and Other Olefins

Fábio José B. Brum[*], *Maria Madalena C. Forte, Felipe N. Laux*

Federal University of Rio Grande do Sul (UFRGS)/LAPOL/Engineering School, Brazil
[*]P.O. Box 15010 – Porto Alegre, 91501-970 /RS/Brazil – fjbrum@yahoo.com.br

Monomers such as indene (Ind), styrene (St) and limonene (Lim) can be polymerized by acid catalysis (1). Papers published in the last two decades have described the polymerization of indene at low temperatures using catalyst type Friedel-Crafts (2). The number-average molecular weight (Mn) of polymers produced by cationic polymerization depends on the type and amount of catalyst. The type or reaction mechanism varie according to the catalytic system employed (3). In this study, the effect of the comonomer type on the number-average molecular weight (M_n) and glass transition temperature (T_g) of the indene copolymers, using $AlCl_3$ as catalyst, were evaluated. The indene (Ind) cationic homo and copolymerization with styrene (St) and limonene (Lim) were performed at -20 °C under N_2 atmosphere. The resulting polymers were characterized by infrared (FTIR) and gel permeation chromatography (SEC). The Tg of the polymers was determined by calorimetry (DSC). The molar ratio monomers/catalyst of 100 was the same for all polymerization reactions.

Table 1 shows the reaction conversion, M_n, polydispersity (M_w/M_n) and T_g of the polyindene (Pind), polystyrene and polylimonene obtained. The indene polymerization conversion was higher than those with the other monomers. Lim present very low reactivity with $AlCl_3$ catalyst and thus the lowest conversion degree. As expected, the PInd presented the highest M_n (33,000 g mol) and it was obtained only oligomeres of limonene (M_n<500 g/mol). Although the styrene polymerization presented the highest reaction conversion the PS M_n was around 2,500 g/mol. The polymers polydispersity was quite different and that of PS was very anomalous, possibly due to a competition between initiation and termination reactions (3). The Pind T_g was approximately 207 ° C due to the chain stiffness, since the PInd has a semi-ladder structure. The limonene oligomer presented solidification temperature at around -7 ºC due to its very low M_n.

Table 1. Monomers homopolymerization* conversion and product characteristics

Polymer	Pind	PS	PLim
Conversion (%)	80.59	92.48	7.23
M_n (g/mol)	$33x10^3$	$2.5x10^3$	478
M_w/M_n	2.1	13.8	1.5
Tg (°C)	207	99	-7

*$AlCl_3$ = 2.42 x 10^{-3} mol; [Ind] = 1.95 mol/L; [St] = 2.15 mol/L; [Lim] = 1.71 mol/L T = -20°C; t = 5h.

Figure 1 shows the M_n, M_w/M_n and T_g values of Ind-co-St copolymers as function of the comonomer relative composition in the medium. The St caused a significant decrease in the copolymer M_n since it play as chain transfer agent through beta-elimination reaction. An increase in the Lim content up to 40% increased the M_w/M_n of the Ind-co-St copolymers due mainly to the M_n decrease. The Tg values of the copolymers stood between the homopolymers' Tg values according to the comonomer content.

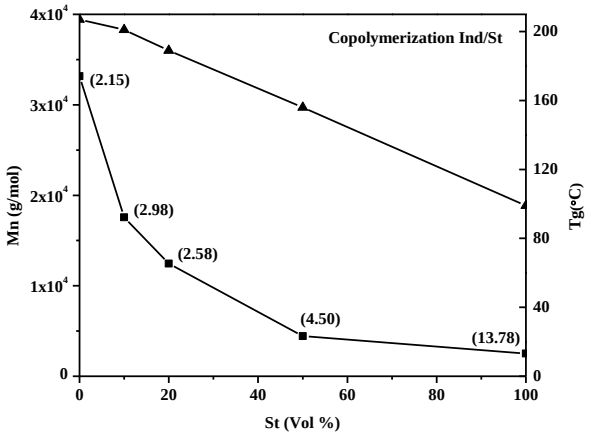

Figure 1. Mn and Tg of the Ind-St copolymers as function of St content (Tab.1).

Figure 2 shows the M_n, M_w/M_n and T_g values of indene-limonene (Ind-co-Lim) and styrene-limonene (St-co-Lim) copolymers as function of the relative composition in the reaction medium. The Lim caused a significant decrease in the M_n of the Ind-co-Lim copolymer since it play as chain transfer agent through beta-elimination reaction. The copolymer M_w/M_n values varied from 2 and 3. On the other hand, content until 20% of Lim increased the St-co-Lim copolymer M_n. The M_w/M_n of the St-co-Lim copolymers decreased as lower the copolymer M_n value.

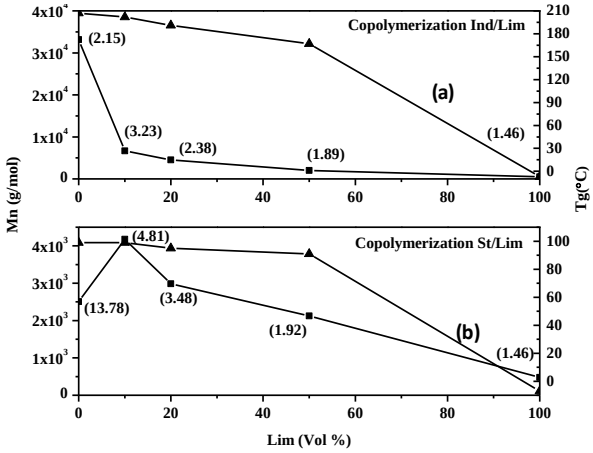

Figure 2. M_n (M_w/M_n) and T_g of the Ind-co-Lim (a) and St-co-Lim (b) copolymers in function of the St content.

St and Lim depressed significantly the M_n and have the same effect on the T_g of the Ind copolymers. This may be related to a higher effect of St and Lim as a chain transfer agent than Ind.

Acknowledgements

The authors thank the Agencies CNPq and CAPES.

References

1. K. Shokyoku, I. Nobuyuki, T. Akira, Y. Hitoshi, H. Toshinobu. Journal of Polymer Science Part A: Polymer Chemistry, 2002. 40(14): p. 2449-2457.
2. M. Givehchi, M. Tardi, A. Polton, P. Sigwalt. Macromolecules, 2000. 33(3): p. 710-716.
3. H. Wang, V. Bennevault-Celton, B. Cheng, H. Cheradame. European Polymer Journal, 2007. 43(3): p. 1083-1090.

Poly(ethylene imine) Tedhered Microspheres for Selective Extraction of Aldehydes from Organic Mixtures

Baris Gure, Deniz Gunes, Bunyamin Karagoz, Niyazi Bicak

Istanbul Technical University, Department of Chemistry, Maslak 34469 Istanbul, Turkey

gurebaris@gmail.com

Introduction: Selective separation of organic compounds by solid supported trapping agents is of importance due to its advantages over traditional separation-purification techniques such as distillation, fractional crystallization, derivatization, precipitation etc. Common techniques of aldehyde separation from organic mixtures need extreme care, due to their easy oxidation by air oxygen. Derivatization of aldehydes by bisulfite addition and hydrazone formation is mostly applicable in lab-scale processes, but not in industrial processes. Years ago, Wanzlick *et.al*. described dianilino ethane as efficient and selective reagent for selective extraction of aldehydes by forming pyrrolidine ring[1]. In the following works, diethylene triamine (DETA) and triethylenetetramine (TETA) immobilized to ST-DVB resin was demonstrated to be efficient and selective sorbent for removal of aldehydes from organic solutions, by our group[2].

In the present work, 1,2-diaminoethane-aldehyde chemistry was extended to poly(ethylene imine) (PEI) surface brushes tethered to crosslinked PBEMA microspheres prepared by suspension polymerization of 2-bromoethylmethacrylate, methyl methacrylate and ethyleneglycoldimethacrylate[3].

Result and Discussion: PBEMA was fabricated by SIP of 2-methyl-2-oxazoline from bromoethyl groups originating from BEMA co-monomer involved. (Scheme-1)

Polyoxazoline grafts so generated (62-133 %) generated were then converted to PEI by acid and base hydrolysis respectively (Scheme-1).

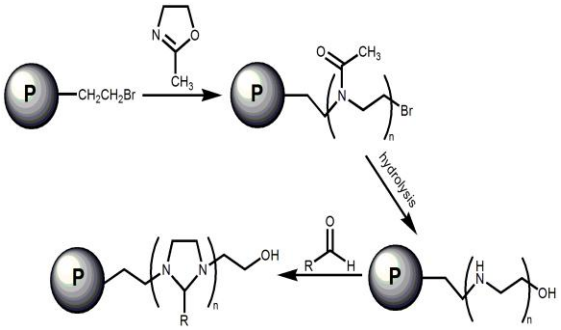

Scheme 1: Schematic illustration of grafting, hydrolysis and aldehyde separation.

The resulting PEI brushes were employed in extraction of various aldehydes from methanolic solutions. Experiments revealed that, aldehyde uptake capacities found (1.5-2.1 mmol.g^{-1}) were almost equal to the theoretical capacity (by assuming two nitrogen per aldehyde molecule). The aldehydes loaded were easily leached out by acid treatment and the resin material was recovered.

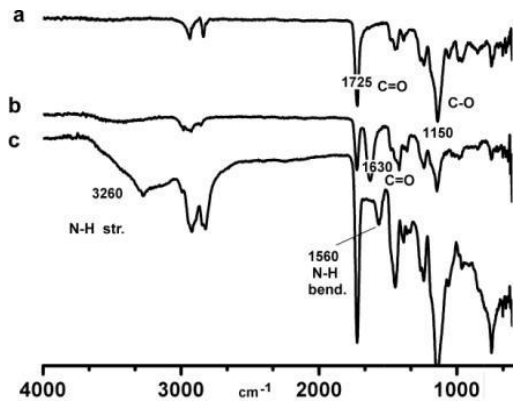

Figure 1: FT-IR spectrum of the a) BEMA beads b) Oxazoline grafted PBEMA and c) PEI grafted PBEMA

Table 1: Trapping capacities of PEI grafted PBEMA

Aldehyde	Capacity (mmolg^{-1})	Capacity after the regenaration (mmolg^{-1})
Benzaldehyde	2.2	2.0
Acetaldehyde	7.1	6.8
4-Hydroxy Benzaldehyde	2.26	2.1
Salicylaldehyde	4.52	4.1
Phtaldialdehyde	-	-

Conclusion: PEI brushes tethered to crosslinked PBEMA beads showed reasonably high trapping capacities for aromatic and aliphatic aldehydes. This material demonstrated to be approximately same results after the regeneration. Consequently, the resins described are cost effective sorbents for the removal and recovery of aromatic aldehydes from various mixtures.

References

1- Wanzlick H.W., *Chem. Ber*. 1953, 86, 1463.
2- Bicak N., B. F. Senkal, *Journal of Polymer Science: Part A: Polymer Chemistry*, 1997, 35, 2857–2864.

Sulfonated Polystyrene Brushes Tethered to PS-DVB Microspheres as New Generation of Ion Exchange Polymers

Ozlem Ozer, Ahmet Ince, Niyazi Bicak

Istanbul Technical University, Department of Chemistry, Maslak 34469 Istanbul, Turkey

ozlem.ozer86@hotmail.com

Introduction: Ion exchange resins are densely crosslinked macroreticular or macroporous polymers bearing ionic functional groups, readily capable of forming salts with metal ions in aqueous solutions. These materials have found extensive uses for large-scale producing of deionized water, which is of interest for processing of industrial and manucipal waters.

Advents of living polymerization techniques, such as ATRP, RAFT and NMP have made it possible to create new sophisticated polymer architectures. These techniques have enable also surface initiated polymerization (SIP) on inorganic or insoluble organic supports. There appear tremendous reports aimed at generating various functional polymer brushes on solid supports. These functional brushes may confer compatibility, selective binding of different organic species or biomolecules.

It was considered that, flexibility and partial mobility of the graft chains may provide rapid interaction of the functional groups located on these chains. Insoluble supports possessing ion exchange groups are expected to have rapid exchange of metal ions. One important limitation in their preparation is connection of the linear polymer brushes with solid support with hydrolytically stable linkages.

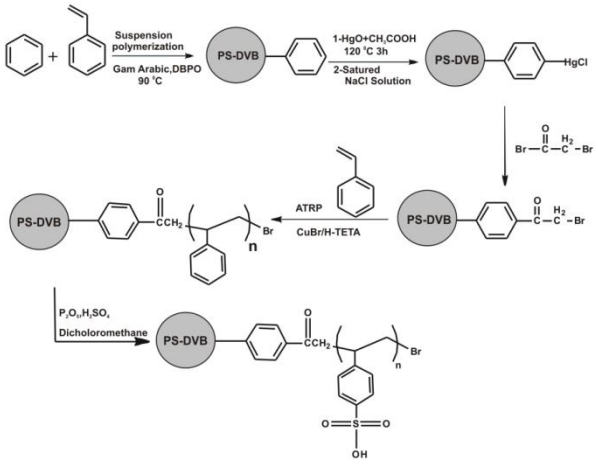

Result and Discussion: Ongoing studies in our lab we have developed a method for linking of surface brushes with various supports by hydrolytically stable bonds.

Taking advantage of this chemistry, in the present work surfaces of PS-DVB(10 %) microspheres[1] were decorated with linear PS brushes in high yields (540 %). Subsquent sulfonation of the brushes yielded sulfonic acid functional (4.1mmolg^{-1}) hairy beads (Scheme-1). The resulting material was demonstrated to have fast and high ion exchange capacities for metal ions in water.[2]

Metal ion	Theoretical capacity[1] (mmolg^{-1})	Capacity of the acid form (mmolg^{-1})	Capacity of the sodium form (mmolg^{-1})
Ca(II)	2.05	3.7±0.2	3.6±0.1
Mg(II)	2.05	0.9±0.1	1.8±0.1
Mn(II)	2.05	0.6±0.1	1.9±0.1
Fe(III)	2.05	1.1±0.2	1.2±0.1

(1) By assuming two sulfonic acid group per divalent metal ion.

It was found that the capacities of sodium form are equal or slightly higher than those of the acid form of the resin.

Conclusion: The sulfonated PS brushes tethered to solid PS-DVB microspheres showed high exchange capacities for the metal ions studied. The capacities approach to theoritical capacity when used as sodium form. Regenerability and recovery of this material is similar to those of commercial ion exchange polymers. Since the grafting degree is a adjustable parameter any desired capacity of resin material can be attained by the SIP methodology described.

References

1- G. F. D'Alelio, *U. S. Patent* 2,366,007 (1944).
2- R. H. Wiley and E. E. Sale, *The Journal of Physical Chemistry* **42,** 491 (1960).

Butyl Sulfonium Sulfate as Cationic Initiator for Synthesis of Poly(cyclohexeneoxide)-*b*- Poly(2-methyl-2-oxazoline) Copolymers

Ceren Elci, Okan Sirkecioglu, Niyazi Bicak

Istanbul Technical University, Department of Chemistry, Maslak 34469 Istanbul, Turkey

cerenelci@gmail.com

Introduction: Synthesis of block copolymers derived from the monomers polymerizing by different mechanisms is difficult to achieve. End-group transformation of the first block is one of the most common routes to attain such block structures. Various end-group transformation methods, cationic to radical, anionic to radical or radical to ionic have been developed for preparing block copolymers[1-2].

In this work, we have studied synthesis of poly(cyclohexeneoxide)-*b*-poly(2-methyl-2-oxazoline) (PCHO-*b*-POXA) copolymers using sulfonium sulfate as single initiator. Although, both monomers are polymerizable by cationic-ring-opening (CROP) mechanism, there is no living cationic initiation system initiating polymerization of both monomers.

Result and Discussion:

In this study a room temperature ionic liquid (butyl dimethyl sulfonium butyl sulfate) derived from dibutyl sulfate and dimethyl sulfide was demonstrated to be efficient "latent initiator" for CROP of cyclohexeneoxide (CHO) above 110 °C. Although the polymerization of CHO is slow, appreciable yields are attained within 24 h (72 %). Polymerization of the oxazoline monomer at the same temperature from sulfonate end-groups of PCHO simply gave well-defined block copolymers, poly(cyclohexeneoxide)-*block*-Poly(N-acetyl ethyleneimine). Subsequent hydrolysis of the second block yielded a chelating amphiphilic block copolymer, PCHO-*b*-PEI in good purities[3].
The structures of the polymer were confirmed by ^{1}H NMR, FT-IR, GPC analyses.

Conclusion: The initiator system described provides an easy access to amphiphilic block copolymer, (PCHO-*b*-POXA). Apparent advantage of this procedure is formation of the amphiphilic block copolymer without necessity of end group modification Having easy modification capability of the imino group, the resulting block copolymer might be of interest in diverse applications, i.e. construction of metal or metal oxide nanocomposites with unusual physicochemical behaviors.

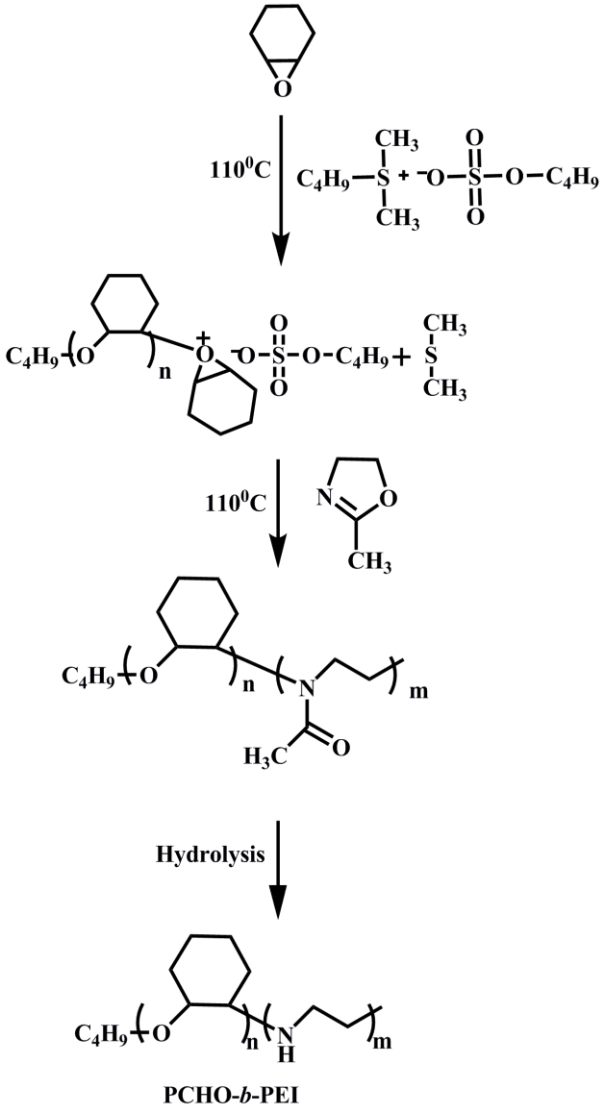

PCHO-*b*-PEI

References

1- Yagci Y, Tasdelen M.A. Prog. In Poly. Sci. 2006, 31, 1133-1170
2- Jingson J, Richard D. M., Macromolecules 2002 35 9882-9889
3- Karagoz B., Gunes D.,Bicak N., Macromolecules 2010 211 1999-2007

Modeling of precipitation co-polymerization of water-soluble polymers in organic solvent

Rosario Mazarro, Paolo Arosio, Giuseppe Storti, Massimo Morbidelli

Institute for Chemical and Bioengineering, ETH Zurich, Wolfgang-Pauli-Str. 10, 8093 Zurich, Switzerland

rosario.mazarro@chem.ethz.ch

Introduction: Several water-soluble polymers are industrially produced by solution polymerization. This operating mode is typically limiting the quality of the final product, in particular in terms of maximum molecular weight. In order to explore the potential of a heterogeneous process, the reaction can be carried out in organic solvent. Precipitation polymerization is generically defined as a heterogeneous polymerization in which the produced polymer is insoluble in the reaction medium.[1,2] Both the initiator and monomer are soluble in the solvent and the reaction starts as a homogeneous polymerization in the continuous phase. With the proceeding of the reaction, the polymer chains grow and precipitate thus nucleating a second, dispersed phase. Since monomer and initiator are soluble also in the newly formed, polymer-rich phase, from this point on - in terms of conversion, after a few percents - the reaction can occur in both phases. Since the difference in reactivity between the two phases can be significant, the properties of the final product can be largely different depending upon the reaction locus. Therefore, the identification of the specific contribution of each reaction locus is crucial for proper understanding and design of the process.

The aim of this work is to combine experimental and modelling activities to elucidate the main mechanisms regulating the product quality of the precipitation co-polymerization of two different systems, namely, the co-polymerization of vinylimidazole and vinylpyrrolidone in butylacetate, and the one of acrylic acid and vinylpyrrolidone in a mixture of ethyl acetate and cyclohexane.

Materials and Methods: Several reactions have been performed in well stirred, isothermal, glass reactor while changing operating parameters such as monomer mixture composition, monomer mixture holdup, initiator amount, stirring rate, presence of stabilizer, and temperature. Conversion and co-polymer composition have been measured by gravimetry and gas chromatography; the molecular weight distribution (MWD) by gel permeation chromatography; and the particle size distribution (PSD) by light scattering.

Results: A comprehensive model of the system has been developed based on the previous literature for homo-polymerization processes.[3,4] Two phases are considered: the continuous, solvent-rich, and the dispersed, polymer-rich phase. A simple kinetic scheme, typical of free radical polymerization, is considered in each phase, in order to account for the heterogeneous nature of the system. Notably, the diffusion of active chains from the continuous to the dispersed phase is accounted for. Finally, the model includes the population balance equations for active and dead polymer in order to describe the complete molecular weight distribution of the final product.

Even though the parameter evaluation problem was especially difficult due to the lack of values from the literature, the final model predictions in terms of kinetics, co-polymer composition and MWD are quite satisfactory (Figure 1).

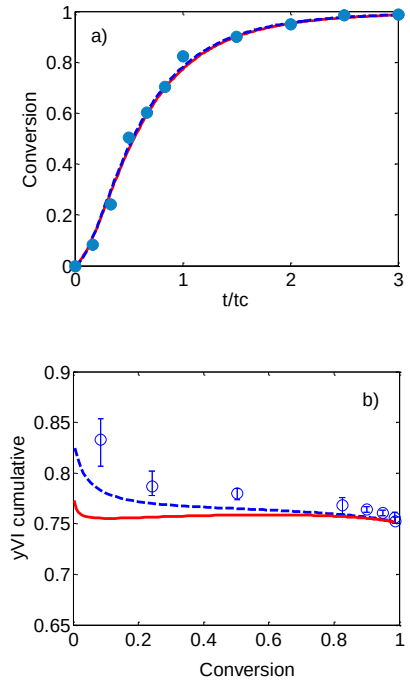

Figure 1. Conversion versus time (a) and cumulative composition versus conversion (b) for the co-polymerization of vinylimidazole and vinylpyrrolidone (75/25) in butylacetate. Symbols: experimental data. Line: model simulations in the two limiting cases: completed transport of the active chains from the continuous to the dispersed phase (—) and no transport (--).

Two completed different systems have been analyzed. In the co-polymerization of vinylimidazole and vinylpyrrolidone in butylacetate, the reaction is going on in two fully segregated phases, being the mass transport of active chains negligible. This way, the final polymer is a mixture of two types of macromolecules, each one reflecting the conditions of the phase originating them. In the co-polymerization of acrylic acid and vinylpyrrolidone in a mixture of ethyl acetate and cyclohexane and using a stabilizer, the inter-phase transport of active chains is found to play a crucial role in determining the reaction rate, even though most of the polymer is produced in the continuous phase.

References:

1. Arshady, R. Colloid Polym. Sci. **1992**, *270*, 717-732.
2. G. Odian, Principles of polymerization, Wiley-Interscience, Hoboken, N. J. **2004**.
3. Müller, P. A., Storti, G., Morbidelli, M. *Chem. Eng. Sci.* **2005**, *60*, 377–397.
4. Müller, P. A., Storti, G., Morbidelli, M. *Chem. Eng. Sci.* **2005**, *60*, 1911–1925.

Ultrafast Relaxation Dynamics of Exciton in Poly-*p*-phenylenevinylene Oligomers

F. V. Moura, P. H. O. Neto, W. F. da Cunha, L. F. Roncaratti, R. Gargano and G. M. e Silva

University of Brasilia

fabiomoura@fis.unb.br

Introduction

Polymer-based solar cells have recently been widely studied as a potential low-cost replacement for the conventional ones. Besides, organic solar cells have others advantages like low toxicity, mechanical properties and ease of fabrication. Despite continued interest in electronic properties of these materials, an understanding of the basic processes remains elusive. Particularly, the phenomenological reasons for the ultrafast relaxation of excitons, recently observed in organic based compounds [1], are lacking. The time to geometrical relaxation on a exciton transition was estimated in 90 *fs* by means of a ultrafast pump-probe spectroscopy technique. However, the heterogeneous morphology of conjugated polymers thin films makes difficult to separate the effects of chain conformation and interchain contacts from the intrinsic electronic properties. In this sense we investigated the excitons generation in poly-*p*-phenylenevinylene (PPV) oligomers with a fully dynamics atomistic description.

Model and Methods

Using a modified version of the Hückel model Hamiltonian [2] to include temperature effects and photoexcitation process we studied the dynamic of both triplet and singlet excitons in a PPV sample. We take into account a nearest-neighbor hopping term in which the distance between carbons was considered. The temperature are incorporated on the method in a classical approach by means of a Langevin equation. The photoexcitation was simulated changing the molecular-orbital occupation number. In order to time evolute the system we applied the Ehrenfest molecular dynamic [3]. Introducing an expansion in terms of the eigenenergies and eigenstates of the electronic hamiltonian, we obtain the following time evolved wave function:

$$\psi_{k,s}(n,t_{j+1}) = \sum_l \left[\sum_m \phi^*_{l,s}(m,t_j)\psi_{k,s}(m,t_j)\right] \times exp\left(-i\frac{\varepsilon_l \Delta t}{\hbar}\right)\phi_{l,s}(n,t_j).$$

Results and Discussion

Our system is composed of a single chain of poly-*p*-phenylenevinylene, consisting of 8 monomers. We performed a photoexcitation at approximately 200 fs. As a result, a non-linear excitation was observed to take place by means of lattice distortion. Analyzing the collective behavior presented by the structure, the electronic state and its order parameter, we concluded that it has properties of a triplet polaron-exciton.

In the figure bellow, we present the time evolution of energy levels for the system. The energy levels shrinkage at approximately 220 *fs* represents the electron level promotion caused by an photon absorption.

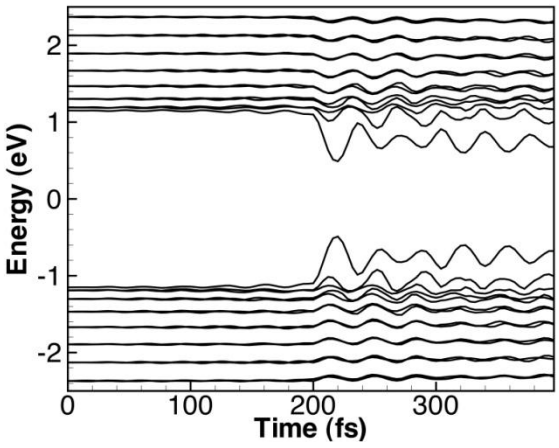

After the excitation, starting at approximately 240 *fs*, it is clear the presence of the energy level behavior of a exciton, that remains a consistent throughout the simulation. It is important to note that the creation time of this structure is consistent with experimentally obtained time[1].

Conclusions

In this work, we investigated the relaxation mechanism of a photoexcitated carrier into both singlet and triplet polaron-exciton. The remarkable agreement of the exciton creation time with experimental evidences for PPV allows us to conclude that our model [3] is, in many aspects, a fundamental tool when it comes to the phenomenological understanding of the charge behavior in this important molecule.

[1] Y. H. Lee, *et al*, Chem. Phys. Lett. 498 71 (2010)

[2] P. H. O. Neto, *et al*, J. Phys. Chem. A 113 14975 (2009)

Corrosion and Adhesion Study of Hybrid Coatings on 316 L Stainless Steel

D. del Ángel-López[1], M. A. Domínguez-Crespo[1], A. M. Torres-Huerta[1], A. I. Flores-Vela[1].*

IPN, CICATA-Altamira Km. 14.5 carretera Tampico - Puerto Industrial. Altamira, Tamaulipas. CP 89600

e-mail: mdominguezc@ipn.mx, adcrespo2000@yahoo.com.mx

Introduction. Organic coatings are effectively used for the protection of metals owing partly totheir capacity to act as a physical barrier between the metal surface and the corrosive environmentin which they perform their function [1,2]. Polyurethanesare very tough materials with high hardness and good chemical resistance.They can be tailor-made to gain properties which lead to versatile applications such ascoating systems for waterproofing and corrosion protection[3]. On the other hand, organic–inorganic hybrid coatingshas been received great attention due to its performance is much better than the single materials. In this way, this work is focused on the preparation and evaluation of ZrO_2-SiO_2 doped polyurethane films (2, 4, 6 and 8 wt-%) obtained on stainless steel 316L. The effect ofprocessing conditions was also analyzed including deposition time, different ZrO_2-SiO_2ratios and sintering treatments. In this paper, synthesis and characterization of ZrO_2-SiO_2 powders by sol-gel are reported.

Materials and Methods. Polyurethane (Desmodur E21®) provided by Bayer® (Mexico),N,N-dimethylformamide (DMF) as solvent, while ZrO_2-SiO_2nanoparticleswere prepared by sol-gel method (Figure 1) and zirconium n-propoxide (ZP;$Zr(OC_3H_7)_4$), acetylacetone (acac), tetraethoxysilane(TEOS), ammonium hydroxide (NH_4OH),ethyl alcohol (ethanol), deionized water and isopropyl alcohol(2-propanol) were utilized as starting materials. ZP (70 wt%in n-propanol solvent) solution was used withTEOS (>98%) and acac (99.5%) and isopropanol(99.7%)(solution 1). On the other hand, a second solution was prepared from TEOS diluted in ethanol and NH_4OH at vigorous stirring (solution 2); then, a solution 2 was added to the solution 1 and the resulting solution was stirred continuously for 15min., after that, deionized waterwas added and the obtainednanoparticles were subjected to heat treatment at 400, 600 and 800°C[7].The preparation of the PUR/ZrO_2-SiO_2 materials was as follows:the polymer solution at room temperature and a solution containing 10 mL of DMF and the designed amount of the ZrO_2-SiO_2 nanoparticles (2 wt%, 4 wt%, 6 wt% or 8 wt%) was added and stirred for 3 hours. The PUR/ZrO_2-SiO_2 films were obtained by casting the solution onto a glass plate and dried in a vacuum oven (10−2 Torr) for three days at 100°C.

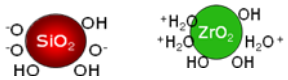

Figure 1. Sol-Gel Synthesis

Results and discussion. Different compositions of ZrO_2-SiO_2 nanoparticles were synthesized and heat treated (25:75, 50:50, 75:25wt%);representative XRD spectrafor 75:25 wt% composition are displayed in Figure 2. The oxide powders at 400 and 600°C areamorphous, while those at 800°C show the presence of tetragonal ZrO_2. Sol-gel-derived pure ZrO_2 preparedfrom a similar precursor system crystallizesat about 400°C, forming a metastable tetragonal phase. Then, the presence of SiO_2 could be inhibiting the tetragonal ZrO_2crystallization at low temperatures. On the other hand, 25:75 and 50:50 wt% compositions at the three different temperatures showed a similar behavior for 75:25 wt% composition at 400 and 600 °C.

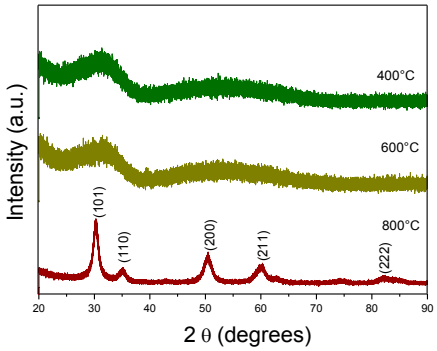

Figure 2. XRD of 75:25 wt% ZrO_2-SiO_2at 400,600,800°C

Conclusions. ZrO_2-SiO_2 powders by sol-gel were obtained. At low temperatures, an amorphous phase is observed and at higher temperature (800 °C), only tetragonal ZrO_2phase is detected. It is expected that these powders enhance the corrosion protection of polyurethane coatings.

References

1. H. Leidheiser Jr., Corrosion 38 (1982) 374–383.
2. G.W. Walter, Corros. Sci. 26 (1986) 27–38.
3. S.Mallakpour, Z.Rafiee,Polymer Bulletin 60(2008) 507–514.

Enhancement on Redox-Stability and Electrochromic Performance of Aromatic Polyamides Incorporating 3,6-Dimethoxycarbazolyl-substituted Triphenylamine Units

*Hui-Min Wang, Sheng-Huei Hsiao**

Department of Chemical Engineering and Biotechnology, National Taipei University of Technology, Taipei, Taiwan

shhsiao@ntut.edu.tw

Abstract: New series aromatic polyamides (**8a-d**) with main-chain triphenylamine and pendent 3,6-dimethoxy-carbazol-9-yl units were synthesized from 4,4'-diamino-4''-(3,6-dimethoxycarbazol-9-yl)triphenylamine (**6**) and various aromatic dicarboxylic acids (**7a-d**) via the phosphorylation polyamidation technique. These polyamides were amorphous with good solubility in many organic solvents and could be solution-cast into flexible and strong films. They showed well-defined and reversible redox couples during oxidative scanning, with a strong color change from colorless neutral form to green and blue oxidized forms at applied potentials scanning from 0.0 to 1.3 V. They exhibited enhanced redox-stability and electrochromic performance as compared to the corresponding analogs without methoxy substituents on the active sites of the carbazole unit.

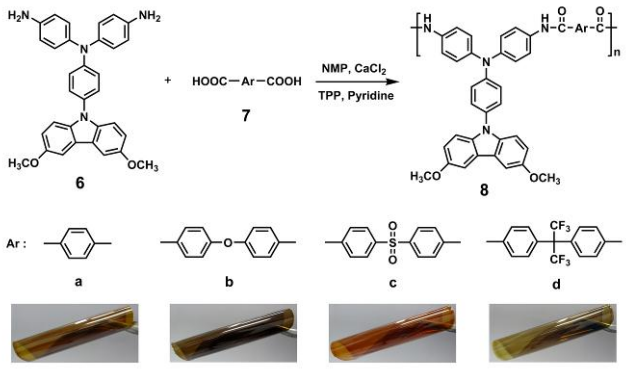

Scheme 2. Synthesis of polyamides **8a-8d**.

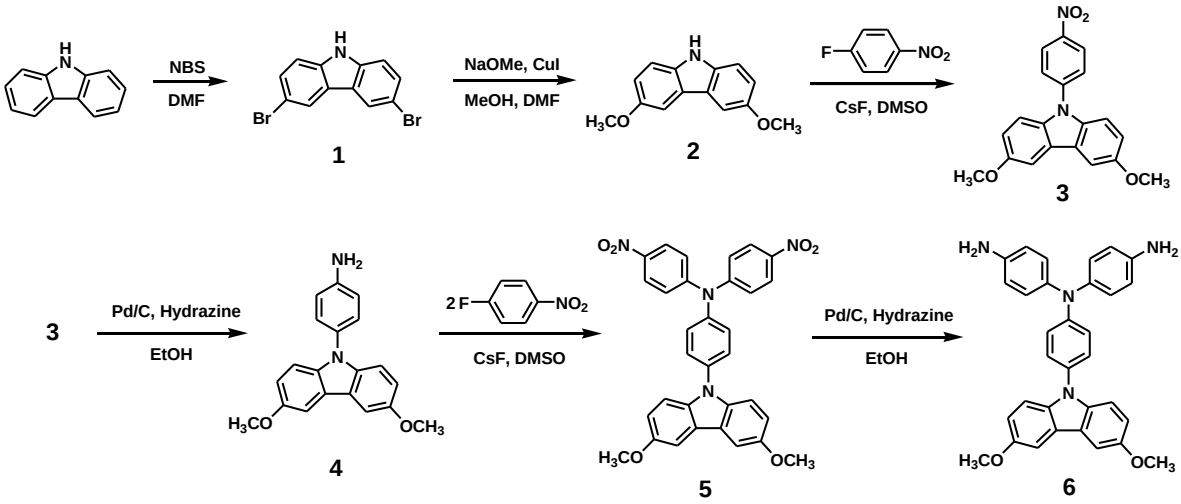

Scheme 1. Synthetic route to target diamine monomer **6**.

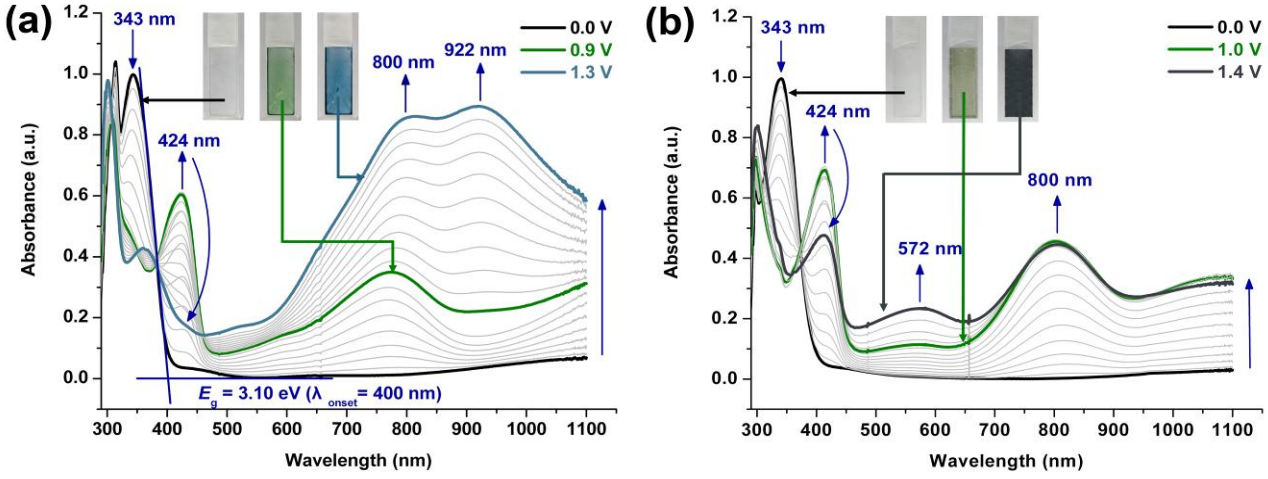

Figure 1. Spectral changes of the cast films of (a) polyamide **8b** and (b) polyamide **8'b** on an ITO-coated glass in 0.1 M Bu_4NClO_4/CH_3CN at various applied potentials (vs Ag/AgCl). The insets show the color changes of the polymer films at indicated electrode potentials

Synthesis and Properties of Novel Triptycene-Based Polyimides

*Hui-Min Wang, Sheng-Huei Hsiao**

Department of Chemical Engineering and Biotechnology, National Taipei University of Technology, Taipei, Taiwan

shhsiao@ntut.edu.tw

Abstract: Two new triptycene containing bis(ether amine)s, 1,4-bis(4-aminophenoxy)triptycene (**4**) and 1,4-bis(4-amino-2-trifluoromethylphenoxy)triptycene (**6**), were synthesized respectively from the nucleophilic chloro-displacement reactions of *p*-chloronitrobenzene and 2-chloro-5-nitrobenzotrifluoride with 1,4-dihydroxytriptycene in the presence of potassium carbonate, followed by palladium-catalyzed hydrazine reduction of the dinitro intermediates. The newly synthesized bis(ether amine)s were polymerized with six commercially available aromatic tetracarboxylic dianhydrides to obtain two series of novel triptycene-based polyimides **8a-f** and **9a-f** by using a conventional two-step synthetic method via thermal and chemical imidization. All the resulting polyimides exhibited high enough molecular weights to permit the casting of flexible and strong films with good mechanical properties. Incorporation of trifluoromethyl groups in the polyimide backbones improves their solubility without decreasing their physical properties. Most of the polyimides derived from the fluorinated monomer **6**, especially those prepared via the chemical imidization method, were soluble in aprotic polar solvents. In general, the trifluoromethyl-substituted **9** series polyimides showed a reduced color intensity, a slightly lowered glass-transition temperature (T_g), and comparable thermal stability as compared to the corresponding **8** series analogs. The fluorinated polyimides **9a-f** showed high T_g in the range of 272 – 335 °C and did not reveal significant decomposition before 500 °C in nitrogen or in air. The fluorinated polyimides **9d** and **9f** derived from diamine **6** with 4,4-oxydiphthalic anhydride (ODPA) and 4,4'-(hexafluoroisopropylidene)diphthalic anhydride (6FDA), respectively, could afford almost colorless thin films.

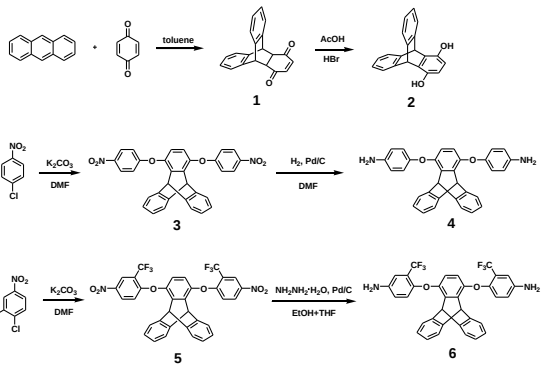

Scheme 1. Synthetic route to the triptycene-containing bis(ether amine)s.

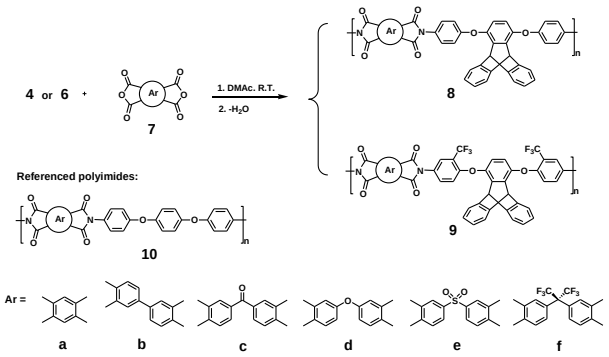

Scheme 2. Synthesis of triptycene-containing polyimides.

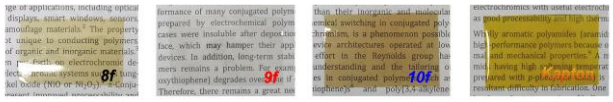

Figure 1. Photographs of the polyimides **8f**, **9f, 10f** and Kapton films (thickness ~50 mm).

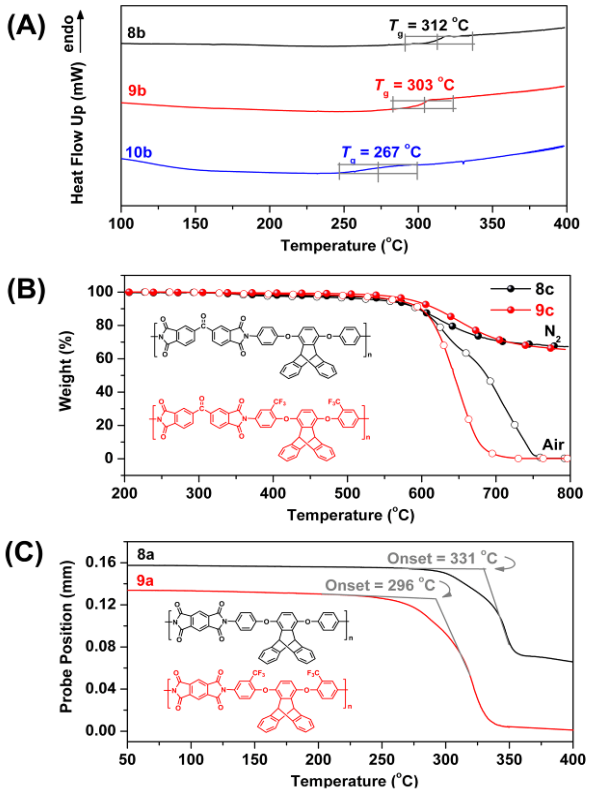

Figure 2. (a) DSC curves of polyimides **8b**, **9b** and **10b**. (b) TGA curves of polyimides **8c** and **9c** in both air and nitrogen atmospheres. (c) TMA curves of polyimides **8a** and **9a**.

References

1. Wilson, D.; Stenzenberger, H. D.; Hergenrother, P. M., Eds.; Polyimides; Blackie: Glasgow and London, 1990.
2. Yang, J.-S.; Yan, J.-L. Chem Commun 2008, 1501-1512..
3. Bartlett, P. D.; Ryan, M. J.; Cohen, S. G. J Am Chem Soc 1942, 64, 2649-2653.
4. Yang, J.S.; Swager, T. M. J Am Chem Soc 1998, 120, 11864-11873.
5. Hsiao, S. H.; Chung, C.-L., Lee, M.-L. J Polym Sci Part A: Polym Chem 2004, 42, 1008-1017.

PREPARATION OF CONDUCTING POLYPYRROLE/POLYTETRAMETHYLENE ETHER (PTME) COMPOSITES

W. M. de Azevedo, J. Batista and Eduardo H. L. Falcão

Departamento de Química Fundamental, Universidade Federal de Pernambuco, Cidade Universitária, 50670-901, Recife,PE, Brazil

Abstract

In the last decade intensive enforce has been done towards the development of new solid state devices based on conducting polymers, such as solar cells, flexible electronics, electrochromic displays, modified electrodes, organic light emitting diodes, field effect transistors, memory devices, chemical, gas, bio sensors and radiation detectors. However, in order to be used as a suitable material for applications in a variety of technological fields one has to overcome certain limitations such as poor mechanical properties and processibility, instability in ambient conditions. Several approaches have been developed up to now to improve these properties, and one technique that stands out among them is the development of conducting composites.

In this work, the preparation of a polypyrrol/ **Poly(tetramethylene ether)** composite in high yield with good mechanical and electric properties is described. The method consists of one pot reaction where the pyrrol monomer and tetrahydrofuran are mixed in a beaker in the presence of strong acid. Soon after the acid is added to the solution the reaction starts, and after 24 hours the polymerization process is finished. The materials obtained can be thin of thicker film with soft or hard mechanical properties depending on the ratio of pyrrol/THF and the amount of acid used. The composition, morphology and electrical properties has been characterized by FTIR, SEM and conductivity measurements.

Synthesis of new membrane of fuel cells based on sulfonated block copolyimide

Maryam Oroujzadeh, Shahram Mehdipour-Ataei

Iran Polymer and Petrochemical Institute, P.O. Box 14965/115

orujzadeh@yahoo.com

Nowadays, in modern world, energy consumption has become a necessity. At present, the major part of this energy, provide from combustion of fossil fuels and these resources has become an essential part of our modern life, but this consumption of fossil fuels has caused bad effects on the environment , so today there is an increasing interest on usage of alternative energy resources. Fuel cells are environmentally friendly devices for energy conversion and power generation. Proton exchange membrane fuel cells are one of the most promising classes of fuel cells and among these polymeric membranes aromatic polyimide is a suitable choice because of high decomposition temperature, high oxidative stability and good mechanical properties.

To produce a proton conductive and durable polymer electrolyte membrane for fuel cell applications, a series of sulfonated copolyimide containing flexible and aliphatic groups in the main chains were synthesized. Firstly, new sulfonated diamine 4,4'-bis(4-amino-3-methyl phenoxy)-benzhophenon-3,3'-disulfonic acid (BAMPBPDS) was synthesized by nucleophilic substitution reaction of 4-amino-3-methyl phenol with 4,4'-dichlorobenzhophenon-3,3'-disulfonicacid disodium salt (DCBPDS) in the presence of potassium carbonate and subsequent acidification with concentrated hydrochloric acid.(scheme 1) Then new sulfonated copolyimides with control degree of sulfonation were prepared via polycondensation reaction of sulfonated diamine BANBPDS in companion with two nonsulfonated diamines 4,4'-oxydianiline (ODA) and 1,8-diamino-3,6-dioxaoctane (DADO) and reaction with 1,4,5,8-naphtalene tetracarboxylic dianhydride (NTDA).

Scheme 1. Preparation of BAMPBPDS

IR-spectrum and H-NMR were used to confirm the structure of copolymers and the thermal properties of copolymers were investigated with TGA and DSC. Membranes were prepared by solution casting method. The physical properties such as ionic exchange capacity (IEC), water uptake and proton conductivity were investigated. These polymers showed promising properties for application as a proton exchange membrane for fuel cells.

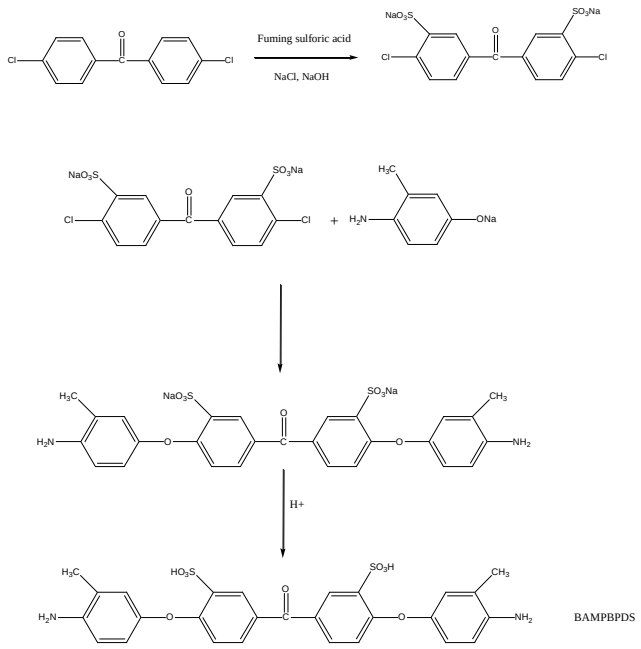

Scheme 1. Preparation of BAMPBPDS

Functional PolyHIPE Materials for Metal Adsorption

E. Hilal Mert[1], Mehmet Arif Kaya[2], Hüseyin Yıldırım[1,2]

[1]Yalova University, Faculty of Engineering, Polymer Engineering Department, 77100 Yalova, Turkey
[2]Yildiz Technical University, Department of Chemistry, 34220 Istanbul, Turkey

hmert@yalova.edu.tr, husyil@yildiz.edu. tr

High internal phase emulsion (HIPE) is a water-in-oil (w/o) emulsion, consisting of at least 74% of disperse phase of the total emulsion volume and the ratio of the disperse phase can reach up to 99%. Continuous phase of a HIPE contains monomers, a cross-linker, and a surfactant whereas aqueous phase usually contains an electrolyte[1]. Cross-linking of a HIPE results in the formation of highly porous, low-density material named poly(high internal phase emulsion) (polyHIPE).

Surface properties of polyHIPE monoliths can be varied according to their chemical composition and preparation conditions. Generally, surface area of polyHIPE materials obtained this way is around 5 $m^2 g^{-1}$ and their pore size is between 5 – 100 µm. However, their surface area could be increased by using a porogen or increasing the ratio of cross-linking[2].

The simplicity of the preparation of polyHIPE polymers and their structural properties enables them to use in many different areas. For instance polyHIPE materials can be used in industrial applications such as filtration technology and ion exchange systems. They can be used as scavengers in batch and flow-through processes and for removal of metals from contaminated water sources. However, synthesize of functional polyHIPE polymers are limited; because of the polar character of monomers that are suitable for modification.

In this study, a new synthetic approach to prepare functional polyester based polyHIPE materials by using a commercial unsaturated polyester resin was described. The originality of this research is based on the cross-linking of the HIPEs. Our study involves commercial unsaturated polyester resin curing process in HIPEs. Cross-linking was achieved through the double bonds of polyester by using monomer mixtures; consequently, polyester remained as the main chain in the polymer matrix.

HIPEs that contain 85% of water as internal phase were prepared by using unsaturated polyester, glycidylmethacrylate (GMA), divinylbenzene (DVB) and triethanolamine (TEA) as emulsion stabiliser. Macroporous low-density polyester based polyHIPE monoliths were obtained by removal of internal phase after the cross-linking of HIPEs with GMA-DVB mixtures via thermal initiation. Macroporous polyHIPE beads were prepared via suspension polymerization of the pre-obtained HIPEs. In such studies hydroxyl ethyl cellulose was used to stabilize dispersed droplets of HIPEs in the suspension medium.

The morphological structures of the polyHIPE materials were investigated by scanning electron microscopy (SEM) and Brauner-Emmet-Teller (BET) molecular adsorption method was used to determine the specific surface areas and average pore sizes.

Modification of the polyHIPE monoliths and microbeads was carried out with chelating ligands such as ethylenediamine (EDA), hexamethylenediamine (HMDA) and 4-aminosalysilic acid (ASA). Elemental analysis was used to confirm the modification of polyHIPE materials. The adsorption capacities of the modified polyHIPE materials for Ag(I), Cu(II) and Cr(III) were determined under non-competitive conditions at pH 3 at room temperature. The adsorption capacities of the modified materials were determined by atomic absorption spectroscopy (AAS).

1. N.R. Cameron, Polymer, 46 (2005) 1439-1449.
2. N.R.Cameron, A. Barbetta, J. Mater. Chem., 10 (2000) 2466-2471.

Development Of Gel-like Dispersions For Bio-lubricant Applications Using Castor Oil and Different Cellulose Pulp Samples

N. Núñez, J.E. Martín-Alfonso, J.M. Franco, C. Valencia, M.J. Díaz, C. Gallegos

Departamento de Ingeniería Química. Universidad de Huelva, Facultad de Ciencias Experimentales. Campus de "El Carmen", 21071, Huelva (Spain).

barragan@uhu.es

Introduction

Lubricating greases basically consist of a thickening agent, generally metal soaps or urea derivatives, dispersed in lubricating liquid, mineral or synthetic oil, forming a colloidal suspension (Sacchettini et al., 1985; NLGI, 1994). The performance of lubricating greases depends on the nature of its components and the microstructure achieved during processing (Delgado et al., 2005). The inclusion of polymers in grease formulations has been a common practice for many years. Polymers have played a significant role as additives in greases for modification of some performance characteristic such as dropping point, appearance, structure, tackiness, water resistance, and bleed. The rheological modification induced by polymeric additives affects the viscoelasticity of lubricating greases, which is important for preventing loss of lubricant or reinforcing sealing properties, but also the flow properties under working conditions (Martín-Alfonso et al., 2009). As the main components of lubricating greases are considered non-biodegradable materials, there is a general tendency to promote the replacement of these by renewable resources, increasing the use of eco-friendly consumer products.

Taking in account these considerations, in this work, the possibility of using different cellulosic polymers as bio-thickener agents to formulate gel-like dispersions in castor oil, potentially applicable as biodegradable lubricating greases, is explored. Cellulosic polymers from different raw materials and submitted to different pulping process and/or several acidic treatments were characterized and used to prepare these formulations.

Materials

Castor oil (211 cSt at 40ºC, Guinama, Spain) was selected as biodegradable lubricating oil. Ethyl cellulose (M_n 66000 g/mol; 49 % ethoxy content) from Sigma-Aldrich was used as gelling agent to modify the castor oil rheological properties, as previously described (Sánchez et al., 2010). Different industrial cellulosic pulps were used to prepare gel-like dispersions in the castor oil medium. Commercial grade Kraft cellulose pulp from *Eucalyptus globulus* was kindly supplied by ENCE, S.A. (Huelva factory, Spain) together with other two cellulose pulp samples obtained at different pulping process stages of the factory i.e. outflow of digesters and first process stage of bleaching (DPo), respectively.

Apart from the industrial pulps supplied by ENCE, other pulps produced in the laboratory such as Kraft and mechanical pulps from *Pinus radiata*; mechanical and semi-mechanical pulps from *Eucaliptus globulus* and a recycled pulp sample, were also used in this work.

Solvents and other chemicals employed were of reagent grade and used as received from Sigma-Aldrich.

Results, discussions and conclusions

The influence that cellulosic pulp characteristics and composition exert on the rheological properties and mechanical stability of the resulting gel-like dispersions was evaluated. From the experimental results obtained, it can be deduced that the rheological response of cellulosic polymer-based gel-like dispersions is mainly a consequence of the balance between the cellulose polymerization degree and lignin and α-cellulose contents. However, cellulosic pulp-based dispersions studied generally present poor mechanical stability or low consistency indexes, as well as higher leakage tendencies, at high temperatures, than that expected for lubricating greases.

References

Delgado M.A., Sánchez M.C., Valencia C., Franco J.M. and Gallegos C. *Chem. Eng. Res. Des.*, 83, 1085 (2005).

Martín-Alfonso J.E., Valencia C., Sánchez M.C., Franco J.M. and Gallegos C. *Ind Eng. Chem. Res.*, 48, 4136 (2009).

NLGI, In Lubricating Greases Guide; National Grease Institute: Kansas City, MO, (1994).

Sacchettini M., Magnin A., Piau J.M., Pierrard J.M. Caractérisation d´une graisse lubrifiante en écoulements viscosimétriques transitoires. J. Theor. Appl. Mech., 4, 165 (1985).

Sánchez, R.; Franco, J. M.; Delgado, M. A.; Valencia, C.; Gallegos, C. *Carbohydr. Polym.*, in press, 2010, DOI 10.1016/j.carbpol.2010.07.033.

Acknowledgements

This work is part of a research project (CTQ2007-60463) sponsored by a MEC-FEDER program. One of the authors (N. Núñez) has received a Ph.D. Research Grant from the "Ministerio de Ciencia e Innovación". The authors gratefully acknowledge its financial support. Thanks are also given to ENCE S.A. (Huelva factory) for the supply of industrial cellulose pulp samples.

Modification of High Ortho Novolac: A Novel Si/Acrylate Modified Resin and Its Surface Coating Properties

S. Emik, T.B. İyim, S. Özgümüş*

Istanbul University, Engineering Faculty, Chemical Engineering Department 34320 Avcilar, Istanbul / TURKEY

s.emik@istanbul.edu.tr

Introduction

Phenolic resins comprise a large family of oligomers and polymers, which are various products of phenols, reacted with formaldehyde. They are versatile synthetic materials with a large range of commercial applications such as thermal insulation materials, molding powders, laminating resins, adhesives, binders, surface coatings, impregnates, and composite material, because of their excellent ablative properties, structural integrities, thermal stability and solvent resistances [1-3]. On the other hand, in general, phenolic resins are inherently brittle due to their high cross-link density, and consequently, their application, especially in resin industry, has significantly been limited by inherent brittlenesss [4]. Long since, toughening and improving the thermal and mechanical properties of phenolic resins have been important and much attended research area. The main aim of this work is to improve the thermal resistance and brittleness of high ortho novolac resin (N), which is reactive than other novolac resins. For this purpose, firstly high ortho novolac resin was prepared according to the known procedure [5-7] and then modified in two stages. The first stage was the modification of N with a silicone containing vinyl monomer, trimethoxyvinylsilane. In the second stage, the silicone and vinyl modified novolac, (VSMN), was reacted with an acrylic monomer, methylmetacrylate. The modification reactions yield a novel resin, (VSMN-A), which should be easily used as a surface coating material; has higher thermal resistance, flexibility and better film properties than those of pure novolac resin.

Materials and Methods

Phenol (P), formaldehyde (FA) (37% aqueous solution stabilized with 10% methanol), trimethoxyvinylsilane (TMVS), methylmethacrylate (MMA), and the rest of materials that used in reactions were all purchased from Merck AG, and in analytical or synthesis grade. High ortho novolac resin was prepared according to a known procedure [5-7]. The first modification stage of N was performed by the reaction of TMVS and N in the presence of p-toluene sulfonic acid as catalyst, which yields a silicone and vinyl groups incorporated N resin, VSMN. In the second modification stage, to obtain an acrylic modified resin (VSMN-A), VSMN was reacted with MMA in the presence of benzoil peroxide as initiator.

The investigation of the surface coating properties of resins were performed according to related DIN or ASTM standards and thermal properties were investigated by TGA and DSC analysis. The thermal gravimetric analysis were carried out by Shimadzu TGA 50A instrument with a heating rate 10oC/sec, under air, and in DSC analysis Seteram DSC 131 instrument was used. FT-IR spectra of the all resins were recorded by Digilab Excalibur FTS 3000 MX instrument in the range of 400–4000 cm-1

Results and Discussion

The TGA results of the resins were given in Figure 1. As it seen from figure, after the modification reactions the modified resin VSMN-A exhibit higher thermal resistance than pure N.

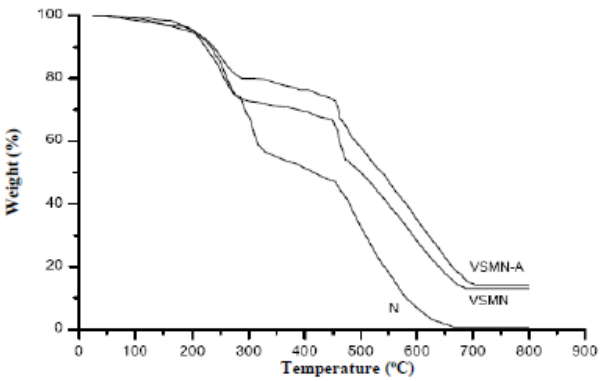

Figure1. The TGA curves of the resins.

Table 1 summarizes some surface coating properties of the resins, as it clearly seen that, by the modification reactions more flexible, and gloss resins were obtained.

Table 1. Surface coating properties of the resins.

Resin	Hardness (König s)	Adhesion (%)	Drying Degree	Gloss (at 45°)	Impact Res. (%)
N	230	<35	7	75	10
VSMN	220	85	7	80	20
VSMN-A	185	100	7	85	>60

Conclusions

In this work high ortho novolac resin was successfully modified with Si and acrylic moieties to obtain more thermal resistance and better surface coating properties than those of pure novolac.

Acknowledgments:This work was supported by Research Fund of the Istanbul University, Project Number T-802.

References

1. Synthetic methods in step-growth polymers / edited by Martin E. Rogers and Timothy Long. Hoboken, New Jersey, 2003. ISBN 0-471-38769-X.
2. Choi, M. H.; Chung, I. J.; Lee, J. D. Chem Mater 2000, 12, 2977.
3. Choi, M. H.; Jeon, B. H.; Chung, I. J. Polymer 2000, 41, 3243.
4. Ma, H.; Wei, G.; Liu, Y.; Zhang, X.; Gao, J.; Huang, F.; Tan, B.;Song, Z.; Qiao, J. Polymer 2005, 46, 10568.
5. Peer, H. G. Rec Trav Chim Part I 1959, 78, 631.
6. Peer, H. G. Rec Trav Chim Part II 1960, 78, 851.
7. Tuğtepe, M.; Özgümüş S. J Appl Polym Sci 1990, 39, 83.

Polyynic Benzoxazines. Synthesis and Polymerization.

Nurbey Guliaa and Sławomir Szafert,a,b*

a Department of Chemistry, University of Wrocław, 14 F. Joliot-Curie, 50-383Wrocław, Poland; b Wrocław Research Center EIT+ Ltd., 147/149 Stabłowicka, 54-066 Wrocław, Poland.

e-mail: szaf@wchuwr.pl

Introduction. Compounds with unsaturated elemental carbon chains constitute the most fundamental class of carbon-based molecular wires. Such one-dimensional assemblies are attracting a great deal of attention from the standpoints of fundamental, physical, and chemical properties and are potentially useful in the development of nano-scale electronic devices. These rod-like structures are also interesting for polymer science due to their ability to undergo topochemical 1,n-polymerization.1

On the other hand the benzoxazines are already known as valuable synthons in interesting group of commercially used polymers. Contribution will present synthesis and characterization of benzoxazine end-capped di and tetraynes. Initial tests on polymerization of these compounds will also be shown.

Materials and Methods. Solvents were treated by standard methods. Substrates were purchased from Aldrich and used as received. 1H and 13C NMR spectra were detected using Bruker ESP 300E or 500 MHz spectrometer.

Differential scanning calorimetry was conducted using a Perkin-Elmer DSC-7. Thermogravimetric analyses were determined with a SETARAM Setsys TG-DTA 16. IR analysis were recorded with a Bruker IFS 66/S. Mass spectrometric measurements were performed using a Bruker micrOTOF-Q electrospray mass spectrometer.

Preparation of initial 6,8-di-*tert*-butyl-3-(4-bromophenethyl)- 3,4-dihydro-*2H*-benz[1,3]oxazine. To a solution of 2,4-di-*tert*-butylphenol (2.77 g, 13.3 mmol) in 100 mL of MeOH *p*-bromophenethylamine (2.10 mL, 13.3 mmol) and formaldehyde (2.10 mL, 26.6 mmol) were added. Mixture was refluxed for 90 h. The solvent was evaporated and the oily residue was dissolved in 10 mL of MeOH and placed in a freezer (-30 °C). After 2 days white solid precipitated. It was filtered off and washed with a small amount of ice-cold MeOH. Yield 3.68 g (64%). mp 117 °C; NMR (500 MHz, CDCl3); 1H: δ = 7.39 (d, J = 8.4 Hz , 2H), 7.15 (d, J = 2.5 Hz, 1H), 7.09 (d, J = 8.4 Hz, 2H), 6.79 (d, J = 2.5 Hz, 1H), 4.86 (s, 2H), 4.02 (s, 2H), 2.99 (t, J = 7.7 Hz, 2H), 2.84 (t, J = 7.7 Hz, 2H), 1.37 (s, 9H), 1.28 (s, 9H). 13C: δ = 150.8, 142.3, 139.2, 136.8, 131.6, 130.7, 122.1, 122.0, 120.1, 119.1, 81.7, 53.1, 51.4, 35.0, 34.5, 34.4, 35.0, 34.5, 34.4, 31.7, 29.8. HRMS(ESI): calcd for C24H33BrNO 430.1740 [M + H]+; found 430.1702. EA: calcd for C24H32BrNO: C 66.97, H 7.49, N 3.25; found: C 67.03, H 7.73, N 3.17.

Results and Discussion. 2,4-Di-*tert*-butylphenol and *p*-bromophenethylamine were combined in MeOH under typical Mannich conditions to give benzoxazine **1** in 93% yield (Scheme 1). This has been modified *via* Sonogashira coupling into trimethylsilyl-substituted derivative **2** (78%), which after deprotection (**3**, 95%) and oxidative coupling gave diyne **4** in 97% yield as shown in Scheme 2.

Compounds **1-4** were characterized by spectroscopic methods and gave correct elemental analysis.

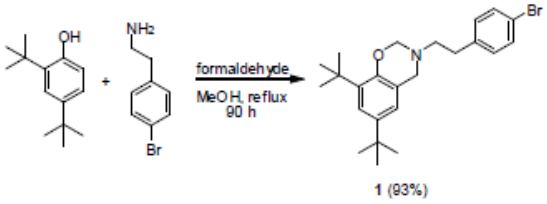

Scheme 1

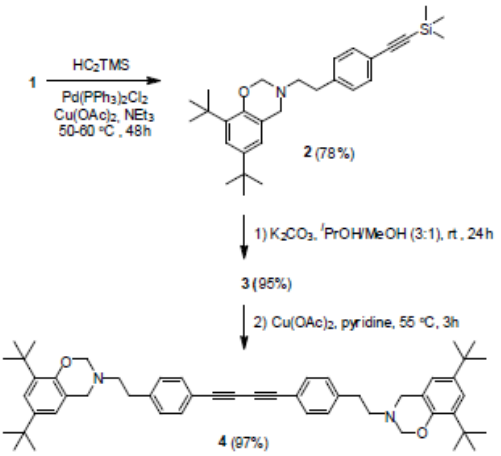

Scheme 2

Deprotected **3** could easily be transformed into diyne **5** (33%) which after *in situ* deprotection and dimerization gave octatetrayne **6** in 41% yield as shown in Scheme 3.

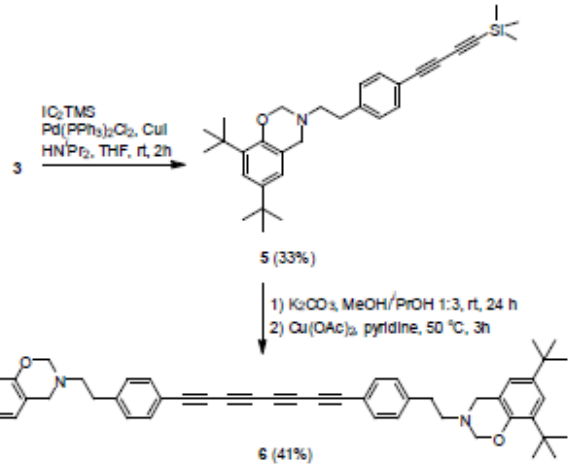

Scheme 3

Compounds 4 and 6 were polymerized under standard conditions using PCl5 as an initiator.

References.

[1] (a) Foley, J. L.; Li, L.; Sandman, D. J.; Vela, M. J.; Foxman, B. M.; Albro, R.; Eckhardt, C. J. *J. Am. Chem. Soc.* **1999**, *121*, 7262. (b) Carre´, F.; Devylder, N.; Dutremez, S. G.; Guérin, C.; Henner, B. J. L.; Jolivet, A.; Tomberli, V. *Organometallics* **2003**, *22*, 2014.

Investigation Long-Chain and short chain Crosslinkers on Microgel Networkd with precipitation polymerization Method

*H. Es-haghi[1], H. Bouhendi[*2], G. Bagheri Marandi[1], M.J. Zohurian-Mehr[2], K. Kabiry[2].*

1. Department of Chemistry, Islamic Azad University,Karaj Branch, PO Box 31485-313, Karaj, Iran
2. Iran Polymer and Petrochemical Institute (IPPI), P.O. Box 14965-115, Tehran, Iran
*Corresponding autor e-mail address: H.Boouhendi@ippi.ac.ir

Abstract Body: long chain crosslinkers, polyethylene glycol diacrylate 400 (PEGDA) and polyethylene glycol dimethacrylate330 (PEGDMA), and short chain crosslinker, *N*,*N*′-Methylenebisacrylamide (MBA), were utilized to prepare crosslinked poly(acrylic acid) microgels via precipitation polymerization. To investigation effect of crossslinkers chain length on properties and structure of polymer, FTIR spectra were used for elucidating the structure of samples (Fig. 1) and apparent viscosity was used to determine optimum crosslinker concentration (Fig. 2), also. Indeed, these microgels follow by closely packed hard sphere model and power low behavior too. The alcohol absorbency, gel content and T_g were improved by utilizing PEGDA as the crosslinker. Rheological measurements of the water-swollen gels showed superior storage modulus with the long chain crosslinker (Fig. 3). $\overline{M}_c$ was calculated by the Flory-Rehner equation [2] and rubber elasticity theory. In addition viscosity coefficient *(m)* and flow behavior index *(n)* of Ostwald equation were investigated as well.

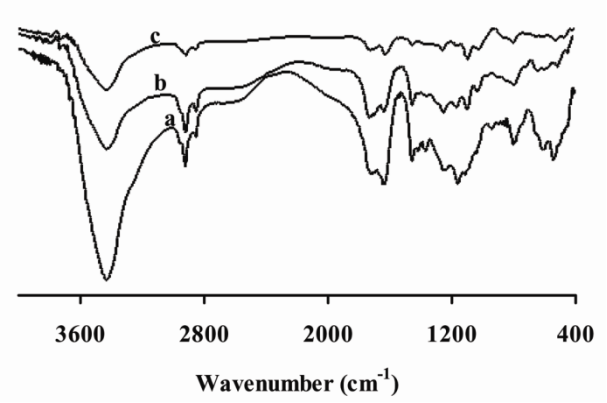

Fig. 1. FTIR spectra of crosslinked PAA.
(a) PAA-MBA, (b) PAA-PEGDMA, (c) PAA-PEGD

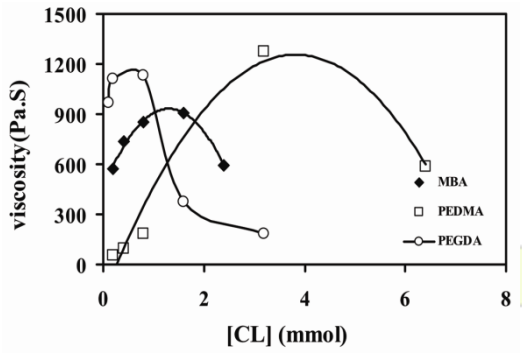

Fig. 2. Effect of crosslinker concentration on apparent viscosity at Various amounts and types of crosslinker.

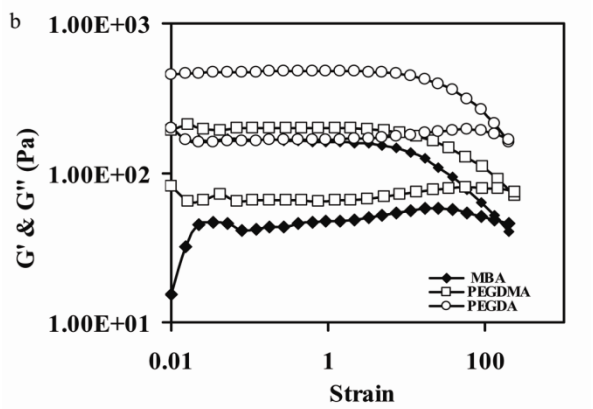

Fig. 3. G' & G'' at optimum crosslinker concentration.

[1]. Islam M. T., Rodrı´guez-Hornedo N., Ciotti S., and Ackermann Ch. (2004) *Pharma. Res*; **21**,1193-1199.
[2] Thomas J. B., Tingsanchali J.H., Rosales A. M., Creecy C. M., McGinity J. W.and Peppas N. A. (2007) *Polymer*; **48**: 5042-5048.

Synthesis and characterization of hybrid acrylic copolymers with and without (isobutyl)propylmethacrylate polysilsesquioxane (POSS)

Carvalho, A.[a, b], *Veludo, E.*[b], *Machado, J.*[b], *Gil, M. H*[a].

[a] Chemical Engineering Department, Faculty of Science and Technology of University of Coimbra, Pólo2 ,3030-290 Coimbra, Portugal.

[b] CIN – North Industrial Corporation, sa, Avenida Dom Mendo nº 831, Apartado 1008, 4471-909 Maia, Portugal.

Polymeric hybrid material and their specific functionalization, have attached great interest, due their chemical, thermal and mechanical properties performance, relative to their equivalent non hybrids. The organic and inorganic parts are combined by interactions such as hydrogen bonds and chemical covalent bonds. In this kind of system, the inorganic fraction acts as a reinforcing agent to improve hardness, strength and thermal stability of the organic polymeric fraction.[1, 2,3,4]

Siloxane based materials concentrate great interest because of their excellent chemical, physical and electric properties, but there the low interactions between molecules do not leave those materials to form fibers and films. In order to overcome this fact, the primary structure of the siloxane could be modified by side chain funcionalization or by changing the main chain, forming hybrid materials.[3]

Hybrid materials are used in several and diverse areas, such as medical products, fabrication of electronic devices, dielectric materials, protective and high performance coatings.

The enhancement of the hybrid material properties can be achieved by incorporating a variety of materials such as carbon nanotubes, layered silicates and polyhedral oligomeric silsesquioxanes (POSS) into common polymers.

In this work we would like to present two new hybrid polymers, the poly(methylmethacrylate – co - isobutyl acrylate – co - glycidyl methcrylate – co - vinyltriethoxysilane) and Poly(methylmethacrylate – co - isobutyl acrylate – co - glycidyl methcrylate – co – vinyltriethoxysilane – co – (isobuthyl) propylmethacrylate (POSS). These copolymers were prepared by a solution polymerization..[5]

The chemical structure of the hybrid co-polymers prepared was confirmed by Fourier transformed Infrared spectroscopy (FTIR) and proton nuclear magnetic resonance (^{1}H-NMR). These copolymers were used to prepare transparent films. Their surface morphology was evaluated by optical microscope analysis (OM). The hybrid co-polymer films free surface energy was determined using static contact angle determinations (CA). The dispersive and polar energy components for the free surface energy (SE) were also determined. The thermal stability of the hybrid materials prepared was also evaluated by termogravimetrical analysis (TGA).

From these results, it was possible to verify that we could prepare the proposed copolymers, using a solution polymerization methodology. It was possible to incorporate the POSS derivative monomer in the polymer structure. The synthesis and isolation methodology does not affect the functional groups integrity presented in the polymeric structure, as has been verified by the FTIR and ^{1}H-NMR analysis. The copolymers films prepared are transparent and presents a regular surface morphology (OM analysis). The incorporation of the POSS part increases the thermal resistance (verified by TGA analysis) of the final material and the hydrophobic character of the copolymer film surface (CA and SE analysis).

[1] Nair, M. B., Blum, F. D., Polymer Preprints, 2005, 46, 367;

[2] Wembo, L. et al, Prod. Eng. Chem. Tech., 2010, 18, 156-163;

[3] Abe, Y., Gunji, T., Prog. Pol. Sc., 2004, 29, 149-182;

[4] Sanchez, C., Rozes, L., Ribot, F., Laberty-Robert, C., Grosso, D., Sassoye, C., Boissiere, C., Nicole, L., C. R. Chemie, 2010, 13, 3-39;

[5] Guo, T.Y., Xi, C., Hao, G. J., Song, M. D., Zhang, B. H., Adv. Pol. Tech., 2005, 24, 288-295.

Synthesis, characterization and applications of N-vinyl pyrrolidone and itaconic acid based hydrogels

Mümin Evren[1], Işıl Acar[1], Gamze Güçlü[1], Kubilay Güçlü[2]

[1]Istanbul University, Faculty of Engineering, Chemical Engineering Department, Avcilar, Istanbul, 34320, Turkey.
[2]Istanbul University, Faculty of Engineering, Chemistry Department, Avcilar, Istanbul, 34320, Turkey.

acar@istanbul.edu.tr; gguclu@istanbul.edu.tr

Introduction: Hydrogels are three-dimensional cross-linked polymeric structures which are able to swell in aqueous environments [1]. The hydrophilicity of these materials is due to the presence of water compatible groups such as -OH, -COOH, -$CONH_2$, and -SO_3H [2] and the ability to swelling with water depends firstly on the type of polymers and on the degree of crosslinking [3]. Hydrogels are becoming increasingly important because of their potential applications in industry. They are used for preparation of membranes in water purification and separation, catheters, contact lenses, agriculture, food industry, medicine, and biotechnology [4-5]. Heavy metal ions contamination causes a serious environmental problem because of their increased discharge, toxic nature [6]. Today, high levels of heavy metals in water resources have been caused several acute and chronic illnesses in humans [7]. Therefore, there is a need to develop technologies that can remove excessive heavy metal ions found in water [8]. The conventional methods for the removal of heavy metals from wastewater include coagulation and flocculation, oxidation or ozonation, membrane separation, and adsorption [9]. Among all the treatments proposed, adsorption is one of the more popular methods for the removal of pollutants [10].

The aim of this work was to synthesis, characterization and applications of N-vinyl pyrrolidone (NVP) and itaconic acid (IA) based hydrogels. For this purpose, poly(N-vinyl pyrrolidone-itaconic acid) copolymeric hydrogels [poly(NVP-co-IA)] were obtained by free radical polymerization in aqueous media.

Materials and Methods: Hydrogel synthesis experiments carried out as follows: Monomer (IA) was dissolved in dissolved in deionized water in glass tubes. Then NVP, and crosslinking agent (N,N methylene bisacrylamide (NMBA)) was added to this tube. The required amounts of ammonium persulfate (APS) as initiator and tetramethylethylenediamine (TEMED) as accelerator were added. The solution was purged with nitrogen gas for 10 min. to eliminate dissolved oxygen in the system. The polymerization reactions were carried out for 20°C at 72 h. At the end of the polymerization reactions, the hydrogels were washed fresh water to remove any unreacted monomers and initiators. The hydrogel were dried under vacuum at 50°C during 24 h for using swelling and heavy metal adsorption experiments.

Water absorption (swelling) capacities of hydrogels were determined by tea bag method. To apply this method, a tea bag that was made of 250-mesh nylon screen, contains a known amount of dried hydrogel sample was immersed entirely in water and kept there to attain swelling equilibrium for a certain time (Q_t), then hung up for 1 min. to drain the excess solution, and weighed. The water uptake was calculated to the following equation.

$$Q_t = (W_{wet} - W_{dry})/W_{dry}$$

where Q_t is the swelling ratio for a given time, W_{wet} and W_{dry} are the weights of the swollen gel and the dry sample, respectively. In case of equilibrium swelling ratio, the Q_t symbol is given as Q_e.

Heavy metal adsorption experiments were carried out at ambient temperature. Stock solution containing Cu^{2+} and Pb^{2+} ions were prepared by dissolving metal acetate salts in distilled water and by using diluted HNO_3 pH of stock solution was adjusted to 4. A fixed amount of hydrogel (0.75 g) were immersed in 50 mL of stock solution (8 mmol metal ion/L), and the mixture was stirred with a magnetic stirrer. The amount of residual metal ions in the aliquots of withdrawn solution was followed by atomic absorption spectrometer (AAS) (Varian SpectrAA FS-220) up to 72 h. Metal ion removal capacities of the copolymers (mmol/$g_{copolymer}$) were calculated as follows:

$$(C_i - C_t) \times V / M_{copolymer}$$

where C_i, initial concentration of metal ions in the solution (mmol/L); C_t, the concentrations of metal ions in the solution after metal ion removal (mmol/L); V, volume of the solution (L); and $M_{copolymer}$, the weight of hydrogel (g).

The mechanical properties of hydrogels were also determined with Zwick/Roell universal tensile testing instrument. Stress-strain measurements were performed on poly(NVP-co-IA) hydrogel with differing crosslinker concentrations.

Results and Discussion: As expected, increasing the percentage of crosslinking agent content in feed composition from 0.5 to 4 decreases the equilibrium swelling ratios (Qe) from about 550 to 35 mg H_2O/g hydrogel, respectively. The adsorption capacities of poly(NVP-co-IA) hydrogels for Cu^{2+} and Pb^{2+} were increased with the increase of the adsorption time. In addition, increasing the percentage of crosslinking agent content in feed composition from 1 to 4, increases the values of elastic modulus for poly(NVP-co-IA) hydrogels from about 171 to 1831 kPa, respectively.

Conclusions: According to the results, the poly(NVP-co-IA) copolymeric hydrogels have better mechanical properties than NVP and IA homopolymers. And we can say that, poly(NVP-co-IA) hydrogels can be used as an adsorbents for removal of Cu^{2+} and Pb^{2+} ions from wastewater.

Keywords: N-vinyl pyrrolidone, Itaconic acid, Adsorption, Hydrogel, Heavy metal removal, Mechanical Properties.

References

[1] Byrne ME, Park K, Peppas NA (2002) *Adv Drug Deliver Rev* 54, 149–161.
[2] Özkahraman B, Acar I, Emik, S (2011) *Polymer Bulletin*, 2010, DOI: 10.1007/s00289-010-0371-1.
[3] Akkaya MC, Emik S, Güçlü G, Iyim TB, Özgümüs S (2009) *J App Polym Sci* 144 (2): 1150-1159.
[4] Rosiak JM, Olejniczak (1993), *J Radiat Phys Chem* 42, 903.
[5] Lin SH (1993) *J Chem Technol Biotechnol* 1993, 58, 159.
[6] Wan Ngah WS, Endud CS, Mayanar R (2002), *React Funct Polym* 50, 181–190.
[7] Sun S, Wang A (2006), *J Hazard. Mater B*. 131, 103–111.
[8] Crini G (2005), *Prog Polym Sci* 30, 38–70.
[9] Acar I, İyim TB, Özgümüş S (2008), *J Appl Polym Sci* 109, 2774–2780.
[10] Hu Z, Lei L, Li Y, Ni Y (2003), *Sep Purif Technol* 31, 13–18.

Removal of cationic dyes from aqueous solution by N-vinyl pyrrolidone and crotonic acid based hydrogels

Işıl Acar, Muharrem Akar, Gamze Güçlü

Istanbul University, Faculty of Engineering, Chemical Engineering Department, Avcilar, Istanbul, 34320, Turkey

acar@istanbul.edu.tr; gguclu@istanbul.edu.tr

Introduction: Hydrogels are three dimensionally cross-linked polymer network structures composed of hydrophilic homo- or hetero- copolymers, which are able to swell in aqueous environments [1]. The hydrophilicity of these materials is due to the presence of water compatible groups such as -OH, -COOH, etc. [2] and the ability to swelling with water depends firstly on the type of polymers and on the degree of crosslinking [3]. Today, hydrogels are used for preparation of membranes in water purification and separation, catheters, contact lenses, agriculture, food industry, medicine, and biotechnology [4-5].

Residual synthetic dyes are the major contributors to color in wastewaters generated from textile and dye manufacturing industries [6]. High levels of residual dyes in wastewaters have been caused several problems. Colored water is not only esthetically undesirable but also blocks sunlight which is essential for many chemical reactions which are necessary for aquatic life [7]. Therefore, there is a need to develop technologies that can remove excessive synthetic dyes found in an industrial effluent [8]. The conventional methods for the removal of dyes from wastewater include coagulation and flocculation, oxidation or ozonation, membrane separation, and adsorption [9]. Among all the treatments proposed, adsorption is one of the more popular methods for the removal of dyes [10].

The aim of this work was to synthesis, characterization and applications of N-vinyl pyrrolidone (NVP) and crotonic acid (CA) based hydrogels. In this case, firstly, poly(N-vinyl pyrrolidone-crotonic acid) copolymeric hydrogels [poly(NVP-co-CA)] were obtained by free radical polymerization in aqueous media. Then, swelling behaviours, adsorption properties and mechanical strengths of hydrogels were investigated.

Materials and Methods: Hydrogel synthesis experiments carried out as follows: Monomer (CA) was dissolved in dissolved in deionized water in glass tubes. Then NVP, and crosslinking agent (N,N methylene bisacrylamide (NMBA)) was added to this tube. The required amounts of ammonium persulfate (APS) as initiator and tetramethylethylenediamine (TEMED) as accelerator were added. The solution was purged with nitrogen gas for 10 min. to eliminate dissolved oxygen in the system. The polymerization reactions were carried out for 20°C at 24 h. At the end of the polymerization reactions, the hydrogels were washed fresh water to remove any unreacted monomers and initiators. The hydrogel were dried under vacuum at 50°C during 24 h for using swelling and cationic dye such as Safranine T (ST), Brilliant Green (BG) and Brilliant Cresyl Blue (BCB) adsorption experiments.

Water absorption (swelling) capacities of hydrogels were determined by tea bag method. To apply this method, a tea bag that was made of 250-mesh nylon screen, contains a known amount of dried hydrogel sample was immersed entirely in water and kept there to attain swelling equilibrium for a certain time (Q_t), then hung up for 1 min. to drain the excess solution, and weighed. The water uptake was calculated to the following equation.

$$Q_t = (W_{wet} - W_{dry})/W_{dry}$$

where Q_t is the swelling ratio for a given time, W_{wet} and W_{dry} are the weights of the swollen gel and the dry sample, respectively. In case of equilibrium swelling ratio, the Q_t symbol is given as Q_e.

Dye adsorption experiments were carried out in beaker flasks containing 50 mL of synthetic dye solution at room temperature. Hydrogel (0.05 g) was added to the cationic dye solution (500 mg/L) for the determination of adsorption capacity. After desire treatment period (1., 3., 5., 7., 24., 48. and 96. hours) the residual dye concentration in the solution was determined colorimetrically with a spectrometer by the measurement of absorbance at the maximum absorption wavelength, that is, 530, 618 and 622 nm for ST, BG, and BCB, respectively. All of the experiments were done at their natural pH value of dye solutions and were carried out in triplicate. The adsorption capacities (mg dye/g hydrogel) of hydrogels were calculated using the following equation:

$$q_e = (C_o - C_e)V/m$$

where q_e (mg/g) is the adsorbed amount of dye per gram hydrogel, C_o and C_e are the initial solution concentration (mg/L) and equilibrium concentration (mg/L), respectively; V is the volume of the solution; and m is the amount of the hydrogel used (g).

The mechanical properties of hydrogels were also determined with Zwick/Roell universal tensile testing instrument. Stress-strain measurements were performed on poly(NVP-co-CA) hydrogel with differing crosslinker concentrations.

Results and Discussion: As expected that increasing the percentage of crosslinking agent content in feed composition, decreases the Q_e values. The adsorption capacities of hydrogels for ST, BG, and BCB were increased with the increase of the adsorption time. In addition, increasing the percentage of crosslinking agent content in feed composition, increases the mechanical strength of poly(NVP-co-CA) hydrogels.

Conclusions: The results showed that, the poly(NVP-co-CA) copolymeric hydrogels have different mechanical strength due to percentage of crosslinking agent content in feed composition. In addition, synthesized poly(NVP-co-CA) hydrogels can be used as an adsorbents for removal of cationic dyes such as ST, BG, and BCB from wastewater.

References

[1] Byrne ME, Park K, Peppas NA (2002) *Adv Drug Deliver Rev* 54, 149–161.
[2] Özkahraman B, Acar I, Emik S (2011) *Polymer Bulletin*, 2010, DOI: 10.1007/s00289-010-0371-1.
[3] Akkaya MC, Emik S, Güçlü G, Iyim TB, Özgümüs S (2009) *J App Polym Sci* 144 (2): 1150-1159.
[4] Rosiak JM, Olejniczak (1993), *J Radiat Phys Chem* 42, 903.
[5] Lin SH (1993) *J Chem Technol Biotechnol* 1993, 58, 159.
[6] Ramakrishna KR, Viraraghavan T (1997) *Waste Manag* 17, 8, 483-488.
[7] Rauf MA, Qadri SM, Ashraf S, Al-Mansoori, KM (2009) *Chem Eng J, 150*, 90-95.
[8] Crini G (2005), *Prog Polym Sci* 30, 38–70.
[9] Acar I, İyim TB, Özgümüş S (2008), *J Appl Polym Sci* 109, 2774–2780.
[10] Hu Z, Lei L, Li Y, Ni Y (2003), *Sep Purif Technol* 31, 13–18.

Biodegradable Thermo-Sensitive Polyurethane-Based Foams for Tissue Engineering

J. Girones[a], *J.A. Mendez*[b], *J. San Roman*[a]

a) Instituto de Ciencia y Tecnologia de Polimeros, (CSIC), Biomateriales, C/Juan de la Cierva, 3, 28006 Madrid. b) Grup LEPAMAP, Universitat de Girona, Campus Montilivi, 17071 Girona

jgirones@ictp.csic.es

Introduction

Due to their availability in a wide range of physical properties and their excellent tissue compatibility, polyurethanes have found several biomedical applications, as implantable devices or as supporting material. Polyurethanes have been extensively studied as biodegradable and/or injectable porous scaffolds for tissue repair.[1] On the other side, since the mid-1990's lineal poloxamers, have been the subject of many studies and some have been approved by the FDA and the EPA for its use in controlled drug release and tissue engineering. Nevertheless, in spite of their large clinical potential, their poor mechanical properties, high permeability and limited stability rendered these biomaterials inappropriate for most biomedical applications.[2, 3]

In this work, we present novel thermosensitive biodegradable polyurethane scaffolds based on a star-shaped poloxamer. The hydrophylicity of the PUR, as well as it biodegradation kinetics, could be controlled by selecting the appropriate biodegradable polyester used as chain extender. In addition, the potential application of this material in tissue engineering was analyzed.

Materials & Methods

The star-shaped PEO-PPO-PEO copolymer, with a commercial code Bayfit 10WF15® was supplied by Bayer in purified form. PPO:PEO ratio was determined as 5:1 (PEO 12-13%wt) whilst the proportion primary: secondary hydroxyl groups was found to be 70:30 (NMR). Described as first electrostatic interactions, cloud point was 14ºC (Nano-DSC from 1% aqueous solutions). As chain extenders, homo- and copolymers of D,L-lactide (La) and ε-caprolactone (Cl) with Mw ranging from 500 to 4000Da were synthesized by ring-opening polymerization.

PUR scaffolds were prepared by the salt leaching method following the pre-polymer technique.[4] In short, the poloxamer was used as polyol and reacted with 1,6-hexamethyldiisocianate (HMDI). The resultant isocyanate-terminated prepolymer was mixed with the porogen and the chain extender and put into 8mm in diameter by 12mm thick Teflon molds to render the scaffolds. An NCO:OH ratio of 1.15 was targeted.

Results

Effect of porosity and porogen crystal size

The salt (sodium chloride) particles used as porogen were milled and sieved into fractions: 0-150, 150-200, 200-250, 250-400 and >400μm. Scaffolds with porosity between 80 and 95% were prepared. Leaching was verified by mass loss, thermogravimetric analysis and SEM. Polyurethane scaffolds prepared with porogen content below 80% wt did not loss all the salt, evidencing non-fully interconnected pore network. In absence of organic solvents, scaffolds with porosity above 90% were not possible to obtain since disintegrated during leaching.

Mechanical – Thermal properties

Scaffolds withstood the action of stress load and underwent an elastic recovery without detectable hysteresis. The PUR foams showed no appreciable thermal degradation untill 300ºC. After leaching, scaffolds preserved the original dimensions when placed in aqueous solutions at 20-40ºC. However, when cooled below the poloxamer cloud point, scaffolds swelled and absorbed water.

The amount and nature of the polyester chain extender had a big influence on the thermal swelling of the scaffolds. The swelling capacity of the scaffold diminished progressively with porosity and was directly related with poloxamer content. PEG chain extenders presented the higher swelling (over 10 fold). Nevertheless, scaffolds extended with PCL or P(CL-co-LA) copolymers presented increments above 300%.

Incubation in SBF

In order to study their biodegradation and to grow apatite, the polyurethane scaffolds were immersed in 1.5SBF (changed twice a week) at 37ºC. By changing the nature of the chain extender (composition, conformation, molecular weight…) we were able to obtain scaffolds that withstood structural integrity shape for less than a day or over 6 months.

Even after 60 days scaffolds no sign of apatite precipitation could be detected by SEM. In order to increase the bioactivity of the polyurethane-based scaffolds, these were dip-coated with Bioglass 45S5, rinsed and were immersed in 1.5SBF. PCL-extended scaffolds observed by SEM after 60 days showed the presence of large number of hydroxyl apatite microparticles (EDX) at the surface of the pore walls, suggesting the preservation of some osteoconductive character commonly assigned to PCL.

References

[1] Gorna, K; Gogolewski, S, *J Biomed Mater Res A,* **2006**, 79, 128-138

[2] Lippens, E; Vertenten, G; Girones, J; Declercq, H; Saunders, J; Luyten, J; Duchateau, L; Schacht, E; Vlaminck, L; Gasthuys, F; Cornelissen, M., *Tissue Engineering A,* **2010**, 16, 617-627.

[3] Fedorovich, NE; Swennen, I; Girones, J; Moroni, L; van Blitterswijk, CA; Schacht, E; Alblas, J; Dhertt, WJA, **2009,** 10, 1689-1696.

[4] Guelcher, SA, *Tissue Engineering B*, **2008**, 14, 3-17.

Development of green coatings made from biopolymers for environmental friendly packaging

Rullier, B. Bonino, J-P., Menu, M-J., Gressier, M., Ansart, F.

CIRIMAT, Université Paul Sabatier, 118 Route de Narbonne, 31062 TOULOUSE Cedex 9 - FRANCE

rullier@chimie.ups-tlse.fr

The preservation of our environment goes through the replacement of toxic and dangerous substances by new green environmental-friendly products and the improvement of products biodegradability. This context has as an immediate consequence the development of renewable resources. Especially, thanks to their biodegradable properties, biopolymers can constitute an answer to environmental issues. The food industry is one of the main users of plastics through the food packaging. The first role of a packaging is to protect its content. The preservation of food products required specific packaging with very efficient barrier properties towards especially oxygen and/or water. Our work aims at developing new coatings made from biopolymers such as proteins, polysaccharides or fatty acids. These coatings have been processed on a biodegradable plasticized-starch substrate. In order to study barrier properties to the oxygen and the water, oxygen permeability and contact angle measurements have been carried out. Our results show that the coatings made from fatty acids have a wettability lower than the one obtained directly for the substrate without coating, indicating a better barrier property to water, probably due to the hydrophobic feature of fatty acid. We observed also that contact angle measurements are not directly correlated to oxygen permeability but provide complementary information. Coatings can have equivalent oxygen permeability values, but different wettabilities.

Post-Curing of Photo-Polymeric Dental Composites - Effects on Mechanical and Dielectrical Performance

Johannes Steinhaus[1,2], *Bernhard Moeginger*[1], *Daniel Lyssek*[1], *Berenika Hausnerova*[2]

[1] Bonn-Rhein-Sieg University of Applied Science, Department of Natural Sciences, D-53359 Rheinbach, Germany
[2] Tomas Bata University in Zlin, Faculty of Technology, CZ-760 01 Zlín, Czech Republic
e-mail: Johannes.Steinhaus@h-brs.de

Introduction: Photo-curing dental filling materials are highly filled acrylic resins having a paste-like consistency. Immediately after light-curing for 40 to 60s the flexural modulus of such composites is in the order of 7 to 8 GPa. During the first days after curing their flexural modulus is increased up to 10-15 GPa due to the post-curing processes [1, 2]. Precise measurements of the evolution of the mechanical properties require elaborate methods, e.g. **D**ynamic **M**echanical **A**nalysis, **T**hermo-**M**echanical **A**nalysis, time dependent hardness testing, etc., and a thorough sample preparation [3]. For deeper insights into both the curing process and the long-term application properties of dental composites a real-time investigation during the first days after photo-curing is essential [4]. The aim of these investigations is to find a quantitative correlation of the changes of the ion viscosity measured by a dielectric analyzer (DEA) and the mechanical properties during the post-cure. Therefore, simultaneous DEA and DMA measurements were performed in the DMA oven using a single cantilever device. At the fixed end of the sample holder the DEA sensor was placed affirming both measurements at a single sample. Then the mechanical and dielectric properties were compared in a time range of some days. As the post-cure is driven by unreacted monomers the remaining increase of the crosslink density is determined by the shift of the glass transition temperatures after a heating run up to 200°C.

Materials: A nano-hybrid photo-curing dental filling composite consisting of acrylic resins (~11%), micro- and nano-scale glass particles (~ 88%), and additives (initiator, accelerator, stabiliser, colour, etc. (~1%).

Equipment and Methods:

DMA device: Netzsch DMA 242C, single cantilever bending mode at a frequency of 1Hz in the oven

DEA device: Netzsch DEA 230/1 and interdigitated Mini-IDEX sensors (sensor surface: 5x7mm², electrode distance: 100µm) at a frequency of 10Hz.

Sample: rectangular beam (1x5x34mm³), light-cured according to DIN ISO 2000

The sample was slightly pressed to 1mm thickness on the DEA-Sensor, light cured for 60s. The measurements started 5 minutes later.

All measurements were performed in 2 steps. In a first step the post-curing was monitored for 12, 24, 36, 48 or 72h at 36°C. In the second step the test chamber was heated with 5 K/min from 36°C to 200°C twice, in order to determine the glass transition temperatures of the post-cured and the annealed state.

Results and discussion: During the isothermal post-cure the DEA and DMA curves show the same time dependency which can be described in a zero order approach as logarithmic on time (Fig. 1). The DMA measurement shows a 30 to 40% increase of the flexural modulus during the first 24h of post-curing. The DEA curve shows the same time dependency although the ion viscosity is increased by approximately 70%.

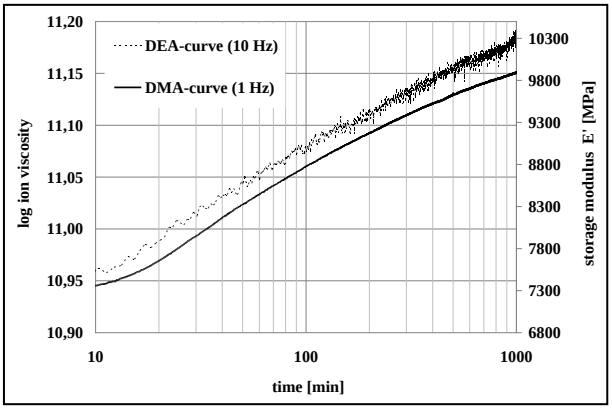

Fig. 1: DEA and DMA curves during isothermal post-curing at 36°C.

Between the 1st and 2nd heating run of the post-cured sample a shift of T_g to higher temperatures is observed due to curing processes taking place if the matrix mobility is significantly exceeded above T_g (Fig. 2). Evaluation of the inflexion points of the 1st and 2nd DMA curve shifts the T_g from 75 to 125°C. The DEA curves also show inflexion points at 73°C in the 1st heating run and at about 140°C in the 2nd heating run. It is found that the DEA indicates a slightly larger T_g-shift. This may be attributed to the fact that ions and dipoles are affected in a different way by the glass transition process.

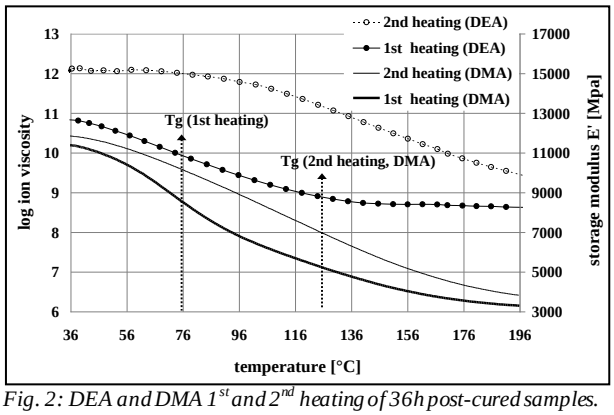

Fig. 2: DEA and DMA 1st and 2nd heating of 36h post-cured samples.

Conclusions: Simultaneous DEA and DMA measurements yield the same time dependency. This leads to the assumption that the mechanical properties of such composites may be determined using ion viscosity data and a calibration curve. Furthermore, it is shown that light curing at body temperature does leave unreacted molecules in the composites which lead to thermally stimulated post-curing processes if the temperature is raised above the actual T_g.

References:

[1] Moeginger et al., Macromol. Symp. Vol. 296 (2010)
[2] R. V. Mesquita et al., Dental Materials, Vol. 22 (2006)
[3] A. Maffezzoli et al., Thermochimica Acta 269/270 (1995)
[4] I. B. Lee et al., Dental Materials, Vol 23 (2007)

Hybrid chitosan-hydrolised collagen films for burn injuries. A preliminary study

Franco-Marquès E[1]., Méndez J.A[1]., Gironès J[2]., Pèlach M.A[1].

1. Lepamap group. University of Girona, Spain
2. Dept. of Biomaterials, ICTP, CSIC, Spain

e-mail: jalberto.mendez@udg.edu

Introduction

Skin is the biggest organ in the body representing by 15% of its weight and with an equivalent surface of 1.7 m^2 in an adult individual. This organ is responsible of the body isolation, stimuli perception and thermal protection.

Due to this external location of this organ, skin is always in contact with the extracorporeal environment, which can be extremely aggressive against him. One of the most incident aggressions against skin is that related with burn injuries, producing necrotic phenomena depending on the deep affectation. This effect is resulting from the thermophilic, hydrophilic and high thermal conductivity character of skin.

Current treatment of burn skin is based on rehydratation of the burnt area with antibiotic supply.

In this work the incorporation of hydrolised collagen has been studied as cell proliferation promoter [1] after disease, expecting a material capable to offer a palliative help in the treatment of such kind of patients.

Materials and methods

Hydrolised chitosan powder obtained from bovine muscular tissue has been kindly supplied by Proteïn, S.A. (Celrà, Spain) and was used without any prior purification. Chitosan, kindly provided by ICTP, CSIC (Madrid, Spain) was used as polymeric support of collagen. Chitosan was previously purified by solubilisation at low pH (acetic acid 1% w/v) and reprecipitation with a solution of NaOH (9 % w/v) until neutral pH. Moreover, partial deacetylation was carried out under alkali conditions. A solution of glutaraldehyde (40% w/v) (Aldrich) has been used as crosslinking agent for chitosan.

Hybrid chitosan-hydrolised collagen films (HCHCF) were prepared by casting. Chitosan, hydrolised collagen and glutaraldehyde were dissolved in a buffer solution (acetic acid/acetate 0.25 M). The solution was placed on Petri dishes and water was evaporated at room temperature for 72 h. Figure 1a shows HCHCF films after casting. Better formulations were chosen for making dressings using medical gauze as support.

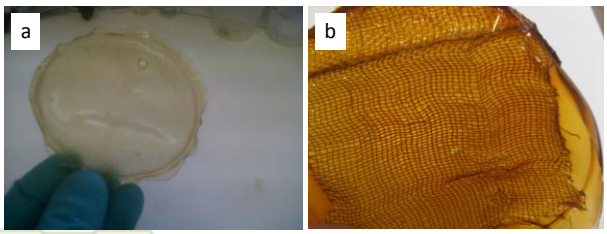

Figure 1. a) Hybrid chitosan-hydrolised collagen film obtained by casting. Chitosan-hydrolised collagen dressing oftained from formulation Col50-L

The films were characterized as follows: water absorption capacity, delivery of collagen, polymer-polymer interactions (FT-IR), thermal properties (DSC, TGA) and microscopic characterization.

Results and discussion

In terms of collagen composition, two different formulations were prepared: loaded with 30 and 50 wt% regarding chitosan content. Talking about glutaraldehyde (crosslinker) three compositions were formulated: 0.75, 2.0 and 5.0 wt% regarding chitosan content. The formulations prepared in this work are summarized in table 1.

Formulation	Collagen (wt%)*	Glutaraldeyde (wt%)*
Col30	30	0
Col30-L	30	0.75
Col30-M	30	2.0
Col30-H	30	5.0
Col50	50	0
Col50-L	50	0.75
Col50-M	50	2.0
Col50-H	50	5.0

Table 1. Compositions of hybrid chitosan-collagen films.

Plain chitosan has the capacity to absorb water until 76% (pH 7.4, T^a: 37ºC). Collagen induces an increase of water uptake until values close to 180% in just 15 min, attributed to its high hydrophilicity. Collagen is released in a very short time because it is not attached neither physically nor chemically to chitosan, confirmed by FT-IR.

The addition of glutaraldehyde induces chitosan crosslinking and an increase in T_g of chitosan. In order to have higher flexibility of the film lower values of glutaraldehyde (L) addition must be used to build the dressing. Figure 1b shows the dressing made with the formulation Col50-L. The dressing shows high flexibility, high water absorption capacity and total release of collagen in a short period of time.

Conclusion

Chitosan is a good support as collagen carrier to release it in a very short period of time to induce faster growing of cells in burn treatments.

References

[1] Oesser, S., Seifert, J. Cell. Tissue. Res. 311, 393-399 (2003).

Preparation of poly (norbornene) and poly-(dicyclopentadiene-co-norbornene) polyHIPEs

*Sebastijan Kovačiča, Christian Slugovc*b, Peter Krajnca**

a University of Maribor, Faculty of Chemistry and Chemical Engineering, Laboratory for Organic and Polymer Chemistry, Smetanova 17, Maribor, Slovenia
b Institute for Chemistry and Technology of Materials, Graz University of Technology, Stremayrgasse 16, Graz, Austria

peter.krajnc@uni-mb.si; slugovc@tugraz.at

Polymerisation of norbornene or mixtures of norbornene and dicyclopentadiene in the continuous phase of a high internal phase emulsion via ring opening metathesis (ROMP) was performed. The 2nd generation UMICORE initiator **(M2)** was used to start ROMP under high internal phase emulsion (HIPE) conditions1. Different norbornen base formulations (e.g. 20 mol% and 80 mol% dicyclopentadiene, or a 1:1 mixture) were investigated. Highly porous (up to 80%) open cellular monolithic materials with pores approximately 5 µm in diameter and with interconnecting pores approximately 2 µm in diameter were obtained (Figure 1, 2). Morphology of the resulting poly(norbornene) and poly(DCPD-conorbornene) polyHIPEs have been studied with Scanning Electron Microscopy analysis. The mechanical properties of copolymers were studied by tensile strength test. High E-modules of about 80 MPa characterized this novel class of polyHIPE materials.

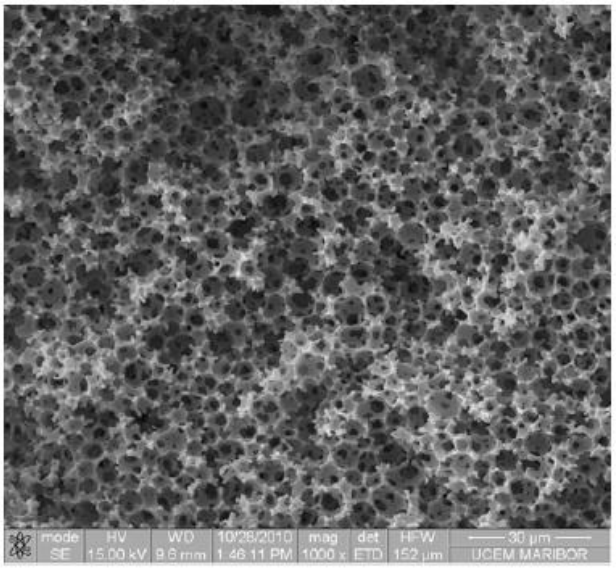

Figure 2. SEM image of DCPD-co-norbornene poly HIPE with 50 mol% of DCPD

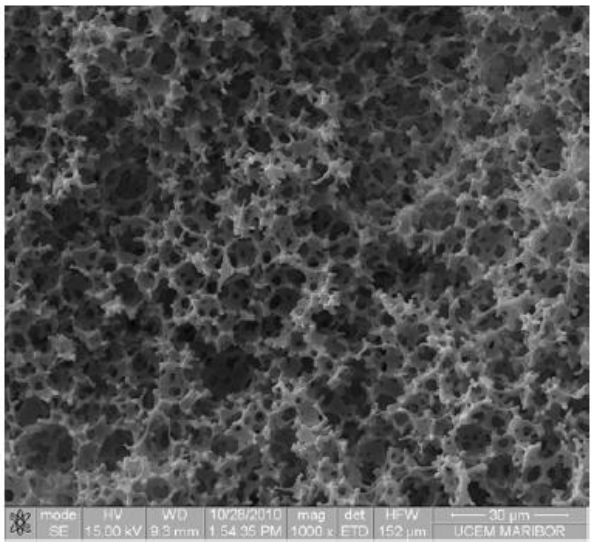

Figure 1. SEM image of norbornene polyHIPE

Influence of different cross-linking mechanisms on the material properties of a silicone-based TPA-functional polymer for optical waveguides

Sonja Feldbacher[1], Rachel Woods[1], Sabine Bichler[1], Valentin Satzinger[2], Volker Schmidt[2], Georg Jakopic[2], Gregor Langer[3] and Wolfgang Kern[4]

[1]Polymer Competence Center Leoben GmbH, Roseggerstraße 12, A-8700 Leoben, Austria
[2]Institute of Nanostructured Materials and Photonics, Joanneum Research, A-8160 Weiz, Austria
[3]AT&S AG, Fabriksgasse 13, A-8700 Leoben, Austria
[4]Institute of Chemistry of Polymeric Materials, University of Leoben, A-8700 Leoben, Austria

feldbacher@pccl.at

The lately in literature described use of two-photon based photo-processes for producing optical applications arises the need of development and investigation of suitable functional optical materials, especially for advanced applications in the field of optoelectronics and microelectronics such as optical waveguides on printed circuit boards (PCBs). In such materials the optical as well as the mechanical and thermal properties are very important, because functionality, stability and processability of the material depend strongly on these properties. Modification of the material usually influences more than one property and can change the processability of the material. In polymers, for example, the material properties are influenced by modification of the crosslinking reaction.

In this work the influence on the material properties of two newly developed optical silicone-based materials using a different cross-linking mechanism is described. The materials are photoreactive and three-dimensional waveguides can be inscribed by two-photon laser patterning (TPA). The crosslinking in the material occurs in one case through the vinyl terminated diphenylsiloxane-dimethylsiloxane copolymer and a hydride (Si-H) component, and in the other case through an epoxy terminated diphenylsiloxane-dimethylsiloxane copolymer and an amine component. For the TPA functionality different types of acrylate and methacrylate monomers were introduced in both materials and photo-polymerized by femto-second laser excitation using a selected photoinitiator.

Both materials were characterised by Fourier transform infrared spectroscopy (FTIR) and thermal gravimetric analysis (TGA). The optical waveguides were characterised by phase contrast microscopy. Optical transparency, thermal stability and processability as well as the quality of produced waveguides are compared.

Supramolecular Block Copolymers: Synthesis and Investigation of the Crystallization Behavior.

Elena Ostas[1], Klaus Schröter[2], Thomas Thurn-Albrecht[2], Gaurav Kumar Gupta[2], Ilja Gunkel[2], Mario Beiner[2] and Wolfgang H. Binder[1]

[1]Institute of Chemistry, Chair of Macromolecular Chemistry, Division of Technical and Macromolecular Chemistry, Faculty of Natural Science II (Chemistry, Physics and Mathematics), Martin-Luther University Halle-Wittenberg, Halle (Saale) D-06120, Germany.

[2]Institute of Physics, Faculty of Natural Science II (Chemistry, Physics and Mathematics), Martin-Luther University Halle-Wittenberg, Halle (Saale) D-06120, Germany.

e-mails: elena.ostas@chemie.uni-halle.de, wolfgang.binder@chemie.uni-halle.de

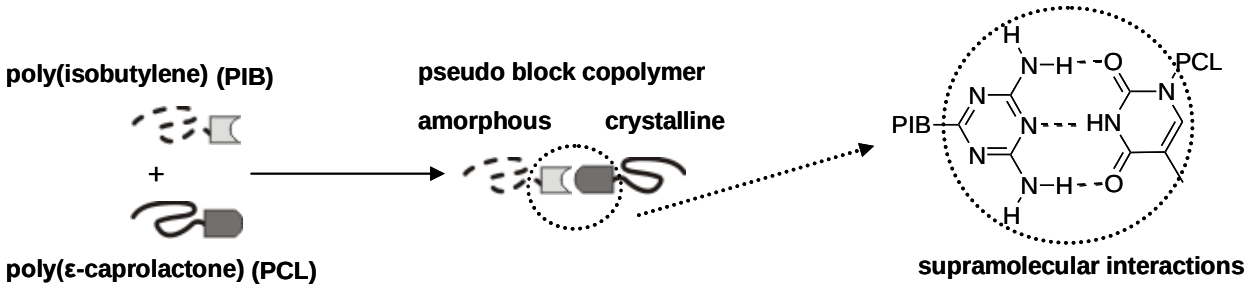

The crystallization in block copolymers under homogeneous- and heterogeneous nucleation is currently well understood revealing the strong influence of crystallisation in competition to micropahse separation[1]. We present synthetic strategy and investigations on crystallization processes in weakly interacting supramolecular pseudo-block-copolymers composed of poly(ε-caprolactone)-b-poly(isobutylene) (PCL-b-PIB) blocks, connected via specifically interacting hydrogen-bonds of thymine/2,6-diaminotriazine. Due to the presence of hydrogen bonds, acting as a partially reversible attractive force between polymer blocks, the presented systems should display a dynamic character during crystallisation. In order to obtain PCL modified with supramolecular receptors, acetylene telechelic PCL was synthesized in the first step, proceeding via ring opening polymerization using 5-hexyn-1-ol as the initiator. In the next step acetylene functionalized PCL was connected with an azide functionalized thymine using a copper (I) mediated 1,3-dipolar cycloaddition ("click" reaction[2]). In order to obtain PIB modified with supramolecular receptors, the azide functionalized PIB
was prepared and modified with 2,6-diaminotriazine via the "click"- reaction[3]. Covalent mixing of thymine functionalised PCL with the 2,6-diaminotriazine-substituted PIB generated the supramolecular pseudo-block copolymers. Investigations of the crystallisation behaviour via non isothermal DSC measurements revealed a strong decrease in the crystallisation temperature of the block copolymers in comparison to the homopolymers. The Avrami analysis of the block copolymers (via isothermal DSC measurements) showed Avrami-exponents close to 3, indicative of a confluence of the growing crystals during the crystallization process. SAXS-measurements revealed a strong Leibler-peak which is retained in the melt state is probably originating from the microphase separation of PCL and PIB blocks.
The presented pseudo-block copolymers represent the first of their kind, demonstrating the strong energy of crystallization in comparison to microphase separation.

1.- Nandan, B., Hsu, J-Y. Chen, H.-L. *J.Macromol.Sci*, C, **2006**,46,143-172.
2.- Binder, W. H.; Sachsenhofer, R., *Macromol. Rapid. Commun*. **2008,** 29, (12-13), 952-981.
3.- Herbst, F.; Schröter, K.; Gunkel, I.; Gröger, S.; Thurn-Albrecht, T.; Balbach, J.; Binder, W. H. *Macromolecules*, 2010, *43* (23), 10006-10016

New Thio-Click Hyperbranched Polymers as Macroinititators for the Dual Curing of Cycloaliphatic Epoxy Resins

D. Foix[1], *X. Ramis*[2], *A. Serra*[1], *M. Sangermano*[3]

1. Dept. of Analytical and Organic Chemistry, University Rovira i Virgili, Spain
2. Thermodynamics Laboratory, ETSEIB University Politècnica de Catalunya, Spain
3. Politecnico di Torino, Dipartimento di Scienza dei Materiali e Ingegneria Chimica, Italy

e-mail: david.foix@urv.cat

Introduction

Epoxy resins are among the most widely used materials in the coating of electronic devices. This is because they present good properties in terms of electrical insulation, adhesion to various components and thermal stability.

Hyperbranched polymers (HBPs) have been added to epoxy resins in order to improve some of their properties such as processability, reworkability or toughness.

In our case, we have synthesized a hyperbranched polymer with terminal hydroxyl groups to be able to link the HBP to the structure and long aliphatic chains that have proved to yield phase separation in similar systems.[1] In addition, the presence of sulfur in the structure of the polymer can lead to the formation of a macroinitiator by means of UV irradiation that can be further cured by thermal treatment.

Materials and Methods

Triethylamine, 1,1,1-tris(hydroxymethyl) propane (TMP), 10-undecenoil chloride, 1-thioglycerol and 2,2-dimethoxy-2-phenylacetophenone (DMPA) from Aldrich was used as received. THF was dried before using.

The cycloaliphatic resin 3,4 - epoxycyclohexyl- methyl-3',4'- epoxycyclohexyl carboxylate (CE) from Huntsman was used. Triphenylsulfonium hexafluoro- antimonate (PI, $Ph_3S^+SbF_6^-$, Aldrich) was added as an actual content of 4 phr with respect to the epoxy content. HBP, whose schematic structure is shown in **Scheme 1**, was added in a range between 5 and 15 phr.

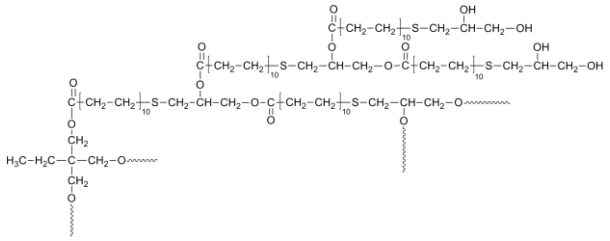

Scheme 1. Chemical structure of the HBP.

The HBP was synthesized as described by C. J. Hawker et al.[2] for a similar structure, which in their case was a dendrimer. TMP was first esterified with undecenoyl chloride by a classical methodology. The salts formed were removed by filtration and the product extracted with HCl and water. Then it was dissolved in the minimal amount of THF and 1-thioglycerol and DMPA (0.4%mol) were added. The mixture was irradiated for 2 hours with 365 nm UV light at room temperature. The product was precipitated in diethyl ether. These two steps were repeated twice until a 3rd generation HBP was obtained. The chemical structure was confirmed by ^1H and ^{13}C-NMR and the molecular weight and polydispersity were determined by GPC.

Results and Discussion

The synthesized HBP was blended with the epoxy resin (CE) and we studied its curing. We first irradiated the sample at room temperature with UV light in the presence of photoinitiator to generate the thermal initiator, because tioethers are converted into sulfonium salts.[3] It is worthy to point out that some UV curing of the epoxide also takes place. We were able to quantify this amount by means of photo-DSC experiments. As the amount of HBP was increased the percentage of epoxides reacted was reduced. Three hours of thermal postcuring at 150ºC was required to teach full cure.

In order to confirm if the OH groups of the polymer were chemically incorporated to the network we determined the gel percentage of the cured materials. In all cases this was quantitative. Hydroxyl groups can be incorporated in epoxy networks by the AM mechanism that takes place in cationic systems.

Dynamomechanical analysis (DMTA) was performed to the cured samples and in all cases high values for the maximum of tan δ were obtained but the highest one was for the sample containing 5 phr of HBP.

Thermogravimetric analysis was also carried out in the thermosets with no significant differences between samples.

Conclusions

A new hyperbranched polymer was synthesized by means of successive esterification with undecenoyl chloride and thiol-ene UV-assisted click reaction.

The obtained HBP was successfully copolymerized with CE in a dual process (UV plus thermal treatment).

We can assume that the HBP becomes incorporated to the network as the gel content was quantitative for all the samples.

The Tgs of all thermosets obtained are high (above 200ºC) and the thermal stability is not influenced by the amount of HBP.

References

1. X. Fernández-Francos, D. Foix, A.Serra, J. M. Salla, X. Ramis. React & Funct Polym. 2010, 70: 798-806.
2. K. L. Killops, L. M. Campos, C. J. Hawker. J Am Chem Soc. 2008, 130: 5062-4.
3. M. Sangermano, M. Cerrone, G. Colucci, I. Roppolo, R. Acosta-Ortiz. Polym Int. 2010, 59:1046-51.

Synthesis of new methacrylates bearing phosphonic acid groups for an application in dental materials

Catel, Y.; Fischer, U.; Moszner, N.

Ivoclar Vivadent AG, Research and Development, Bendererstrs 2, FL 9494 Schaan, Liechtenstein

Yohann.Catel@ivoclarvivadent.com

Introduction

Acidic monomers are of particular interest in the field of dental materials. They could either be phosphates, carboxylic or phosphonic acids. As key component in self-etching adhesives, they are able to etch enamel and dentin surfaces, promote the infiltration of the adhesive into the demineralised surfaces and mediate the formation of a bond to a composite.[1] It has also been demonstrated that some acidic monomers are able to chemically adhere to the dental tissues (hydroxyapatite).[2] These interactions may enhance sealing for the prevention of nano-leakage and thus extend bonding longevity. [2a]

Dental composites are made of an organic matrix (dimethacrylates, photoinitiator, additives) and inorganic fillers.[3] These materials do not provide an efficient bond to the tooth tissue. To overcome this drawback, it has been suggested that the incorporation of acidic monomers to the organic matrix may result in an adhesion of the composite to the tooth.[4]

To improve the efficiency of commonly used dental materials, the synthesis of new acidic monomers is highly desired. It has been demonstrated that phosphonic acids are good candidates for chemical adhesion.[2b,5] Hence, we focused on the preparation of various monomers (aliphatic, aromatic, fluorinated, etc.) bearing phosphonic acid groups. Both monomethacrylates and crosslinking monomers were selected. In this work, we described the synthesis and the applications of the new monomers **1-7** (Figure 1).

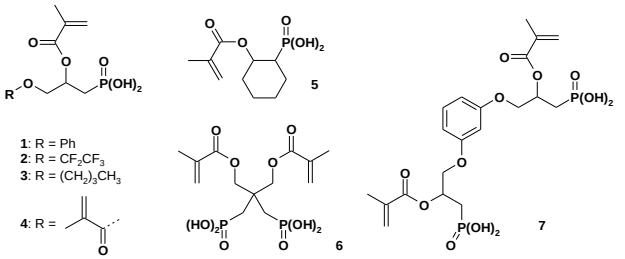

Figure 1: Structure of monomers 1-7

Results and discussion

Monomers **1-3**, **5** and **7** were easily prepared in 3 steps with good to moderate yields. The first step involved the preparation of hydroxyphosphonates by the opening of an epoxide ring with triethylphosphite in the presence of zinc chloride. The resulting hydroxyphosphonates were acylated by reaction with methacrylic anhydride, in the presence of triethylamine and a catalytic amount of 4-dimethylaminopyridine. The silylation of phosphonates with bromotrimethylsilane, followed by a methanolysis, provided the desired acidic monomers. Monomer **4** was synthesized in 5 steps, from glycidol, in a 38% global yield. First, the hydroxyl group of glycidol was protected using 3,4-dihydro-2H-pyran with a catalytic amount of pyridinium p-toluenesulfonate (PPTS). The resulting epoxide was then opened with triethylphosphite in the presence of zinc chloride. The deprotection of the tetrahydropyran group (THP) easily provided the corresponding diol. An acylation, followed by the mild deprotection of the phosphonate group, provided the monomer **4**. As for the crosslinking monomer **6**, it was synthesized in 5 steps from 2,2-bis(bromomethyl)-1,3-propanediol in a 27% global yield. The diol was first protected with 2,2-dimethoxypropane using a catalytic amount of PPTS. Then, the resulting acetal was subjected to a Michaelis-Becker reaction to provide the corresponding diphosphonate. In the third step, the diol was deprotected using Amberlyst H-15 in methanol. After an acylation and a deprotection of the phosphonate groups, monomer **6** was obtained.

In order to evaluate their acidity, each monomer was dissolved in a EtOH:water (1:1) solution (20 %wt) and the pH values were measured. The values were all bellow 1.5, showing the great ability of these monomers to etch the dental tissues. Furthermore, the ability of these phosphonic acids to demineralize HAP was investigated via a ^{13}C NMR spectroscopic study.

The reactivitiy of the synthesized monomers in photopolymerization was also studied. Thus, each monomer was copolymerized with N,N'-diethyl-1,3-bis(acrylamido)-propan (DEBAAP) (acidic monomer:DEBAAP = 1:9) and the rate of polymerization was investigated by photo-DSC.

In order to evaluate the adhesive properties of methacrylates **1-7**, new dental adhesive were formulated. Most of these adhesives showed high bond strength values and confirmed a strong bond between a restorative composite and dentin.

Conclusion

The new acidic monomers **1-7** were efficiently synthesized in 3 to 5 steps. It has been demonstrated that they are able to demineralize the dental tissues. Their reactivity in photopolymerization as well as their adhesive properties were also investigated. These new methacrylates are good candidates for applications in dental formulations.

References

1. Nakabayashi, N.; Pashley, D.H. "Hybridization of dental hard tissues". Tokyo: Quintessence; **1998**.

2.(a) Yoshida, Y. *et al. J. Dent. Res.* **2004**, *83*, 454-458. (b) Van Landuyt, K. L. *et al. J. Dent. Res.* **2008**, *87*, 757-761.

3. Moszner, N.; Salz, U. *Macromol. Mater. Eng.* **2007**, *292*, 245-271.

4. Hecht, R.; Ludsteck, M.; Raia, G. *J. Dent. Res.* **2002**, *81*, A-75.

5. Moszner, N.; Salz, U.; Zimmermann, *J. Dent. Mater.* **2005**, *21*, 895-910.

Resonance effect on conductivity of poly(esters)s containing silarylene and thiophene moieties after polarized by application of an external field

C. González-Herríquez[1], Luis H. Tagle[1], Claudio A. Terraza[1], Alvaro Cañete[1], Angel Leiva[1], Andrés Barriga[2], Ulrich Volkmann[3], Alejandro Cabrera[3], Esteban Ramos[3], Maximiliano Pavez[3]

Pontificia Universidad Católica de Chile, P.O. Box 360, Santiago, Chile: [1] Facultad de Química, [3] Facultad de Física, [2] Facultad de Ciencias Químicas y Farmacéuticas, Universidad de Chile, Av. Vicuña Mackenna 20, Santiago, Chile

cgonzalen@uc.cl

INTRODUCTION

Conjugated polymers.[1] composed of repeated small aryl ring molecules such as benzene, thiophene or others, are of broad interest due to their optical, electronic and magnetic properties.[2] These characteristics have been utilized in different devices such as: organic electronic and optoelectronic, including light emitting diodes (LED), field-effect transistors (FET) and photovoltaic cells.[3] For many of these applications the control of the band gap is essential, thus small values and broad absorption bands can be designed to facilitate the efficiency of photon harvesting. Electronic properties promote charge separation and transport.[4]

EXPERIMENTAL PART

The preparation of dicarboxylic acid monomer (3) was realized by two away from 2,5-dibromothiophene (Fig. 1). A Vilsmeier adduct prepared with tosyl chloride, pyridine and DMF was employed in the polycondensation between the new monomer and five different silicon-containing diphenols.

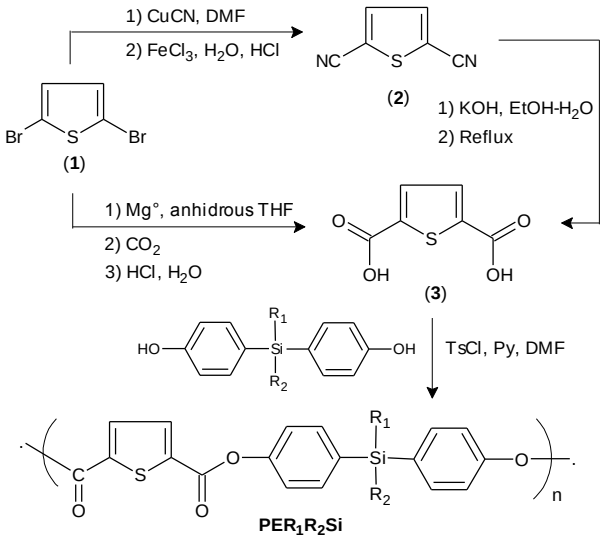

Fig. 1. Preparation of PER_1R_2Si.

RESULTS

Poly(ester)s by direct polycondensation of thiophene 2,5-dicarboxylic acid (**3**) and five different diphenols (**4a-e**), were synthesized using tosyl chloride/pyridine/dimethylformamide system as a condensing agent. The resulting polymers were obtained in good yields and were characterized by FT-IR, NMR (^1H, ^{13}C, ^{135}dept and ^{29}Si). These polymers were completely soluble in aprotic solvent, such as DMF, DMSO and NMP. The range of effective mass of the polymers is $1x10^5$ - $2x10^5$ m/z, which was determined by electrospray ionization mass spectrometry (ESI-MS). The factor of asymmetry and steric hindrance prevents a dense packing of the polymeric chains, showing a decrease in the glass transition temperature from -78 to -51 °C and loss of thermal stability (141-171 °C). Optical band gap of the polymers were 4.54 to 4.48 eV, related with an insulator behavior. The molecular arrangement was investigated with X-ray diffraction. All samples exhibited a degree of ordering, which was associated with two monoclinic lattices. Additionally, the electrical properties were studied by the two-point method with contacts on top of the films (Fig. 2). The samples were previously polarized in an external electric field, showing a better alignment of the dipoles in the direction of the field, resulting in an increase of conductance.

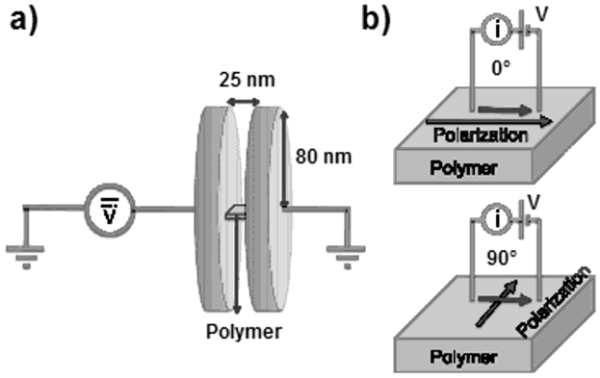

Fig. 2. (a) Experimental set up to polarize the polymers (voltage 2-16 V). (b) Once the polymer was polarized, the two-point method was used to measure the current parallel (0°) and perpendicular (90°) to the polarization.

ACKNOWLEDGEMENTS

C.M. González-Henríquez acknowledges a scholarship from MECESUP UCH 0601. Authors thank to FONDECYT: 1100015,1095151 and 1100882. Thank to M.J. Retamal for AFM characterization.

REFERENCES

[1] Park, S-M. Electrochemistry of *p*-Conjugated Polymers. In: Handbook of Organic Conductive Molecules and Polymers, Nalwa, H. S., Ed., Chichester, Wiley, 1997, Vol. 3, 429-469.

[2] Nagai, A.; Chujo, Y. *Macromolecules*. 2010, 43 (1), 193–200.

[3] Tsai, J-H.; Lee, W-Y.; Chen, W-C.; Yu, C-Y.; Hwang, G-W.; Ting, C. *Chem. Mater*. 2010, 22 (10), 3290–3299.

[4] Peng, Q.; Park, K.; Lin, T.; Durstock, M.; Dai, L. *J. Phys. Chem. B*. 2008, 112 (10), 2801–2808.

Poly(amide-imide)s containing silarylene and L-aminoacid moieties. Relation with electrical conductivity and Raman active vibrations

C. González-Herríquez[1], Luis H. Tagle[1], Claudio A. Terraza[1], Andrés Barriga[2], Ulrich Volkmann[3], Alejandro Cabrera[3], Esteban Ramos[3], Maximiliano Pavez[3]

Pontificia Universidad Católica de Chile, P.O. Box 360, Santiago, Chile: [1] Facultad de Química, [3] Facultad de Física, [2] Facultad de Ciencias Químicas y Farmacéuticas, Universidad de Chile, Av. Vicuña Mackenna 20, Santiago, Chile

cgonzalen@uc.cl

INTRODUCTION

Poly(amide-imides)s have been widely used like opto-electronic materials, adhesives, composite materials, fiber and film material.[1] Additionally, it have been developed as alternative materials offering a compromise between excellent thermal stability, good solubility in highly polar solvents, low Tg and easier processability with respect to poly(imide)s.

EXPERIMENTAL PART

Diphenylsilarylen and L-aminoacid-containing chiral dicarboxylic acid were prepared from *o*-bromoxylene (Fig. 1). These monomers were employed in a direct polycondensation with (4-aminophenyl)diphenylsilane using triphenylphosphite (TPP)/pyridine, $CaCl_2$ and NMP as condensating system.[2]

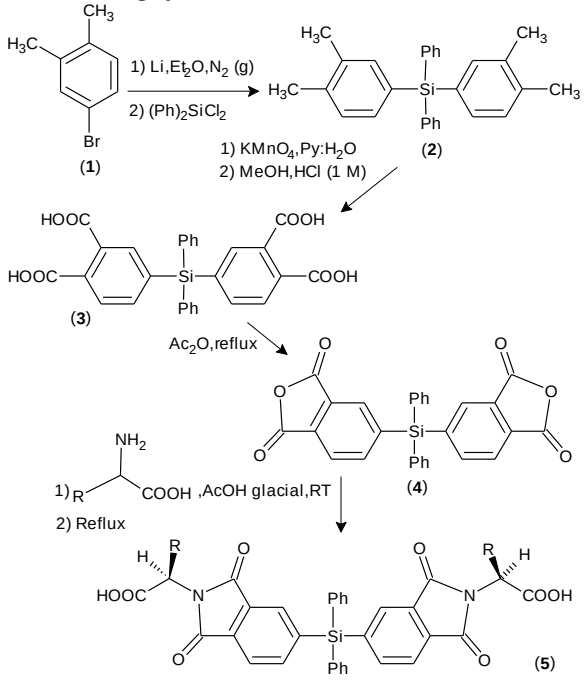

Fig. 1. Synthesis of chiral dicarboxylic acids. R= -CH_3, $(CH_3)_2CHCH_2$-, $(CH_3)_2CH$- and $PhCH_2$-.

RESULTS

Optically active poly(amide-imides)s were synthesized by direct polycondensation between an aromatic diamine and a dicarboxylic acid containing both the diphenylsilylene unit. Polymers were obtained in good yields and showed a high solubility in common aprotic polar solvent. The precursors were characterized by elemental analysis (EA), FT-IR and NMR spectroscopy (^1H, ^{13}C and ^{29}Si). Additionally, the main vibrations of the functional group (C=O, C=C or N-H) in the polymers with respect to the temperature, were characterized by Raman spectroscopy (Fig. 2).

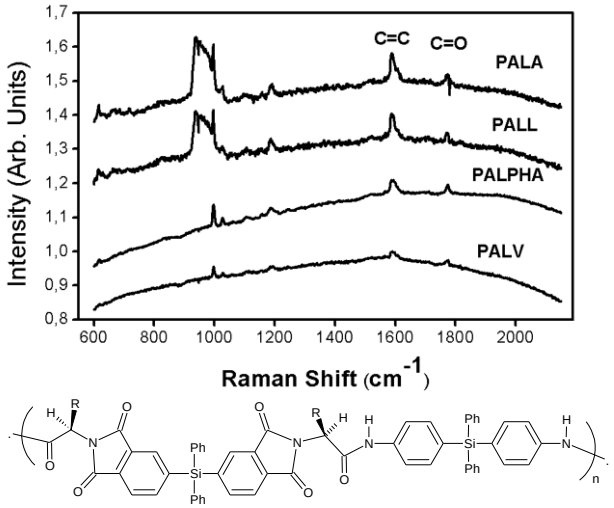

Fig. 2. Raman spectra at room temperature. R: PALA= -CH_3, PALL= $(CH_3)_2CHCH_2$-, PALV= $(CH_3)_2CH$- and PALPHA= $PhCH_2$-.

The glass transition temperature (T_g) was determined by studying the Raman peaks behavior and corroborated by DSC (Fig. 2). Thermal stability was studied by TGA. The molecular weight of the compounds was obtained by MALDI-TOF mass spectrometry and their optical properties were analyzed by UV/Vis diode array. On the other hand, the electronic properties of the polymers as well as the delocalization of charge carriers within of the structure have been analyzed by conductance-voltage curves showing that these materials are excellent candidates for integrated opto-electronic applications.

ACKNOWLEDGEMENTS

C.M. González-Henríquez acknowledges a scholarship from MECESUP UCH 0601. Authors thank to FONDECYT: 1100015,1095151 and 1100882.

REFERENCES

[1] a) D. Liaw, P. Hsu, B. Liaw, *J. Polym. Sci. Polym. Chem.* 2001, *39*, 63. b) K. Babooram, B. Francis, R. Bissessur, R. Narain, *Compos. Sci. Technol.* 2008, *68* (3-4), 617. c) D. Liaw, B. Liaw, *Polymer* 2001, *42*, 839. d) S.H. Hsiao, C.P. Yang, *J. Polym. Sci. Polym. Chem.* 1990, *28*, 1149. e) D. Liaw, W. Chen, *Polym. Degrad. Stabil.* 2006, *91*, 1731. f) M. Barikani, S. M. Ataei, *J. Polym. Sci. Polym. Chem.* 1999, *37*, 2245. g) Y. Wang, S. Goh, T. Chung, P. Na, *J. Membrane Sci.* 2009, *326* (1), 222. h) G. Ventura, E. Gottardi, I. Peroni, A. Peruzzi, G. Ponti, *Nucl. Phys.B.* 1999, *78*(1-3), 571.

[2] A. Tundidor-Camba, C. A. Terraza, L. H. Tagle, D. Coll, *J. Appl. Polym. Sci.* (DOI: 10.1002/app. 33443), 2010

Synthesis, characterization and thermal studies of halogenated poly(imide-diamides) containing silicon in the main chain

Luis H. Tagle, Claudio A. Terraza, Deysma Coll, Alain Tundidor-Camba and Angel Leiva

Facultad de Química, Pontificia Universidad Católica de Chile, P.O. Box 306, Santiago, Chile.

ltagle@uc.cl

INTRODUCTION

Poly(amides) and poly(imides) are high-performance polymers with thermal and mechanical properties, which made them useful for advanced technologies.[1] One of the main problems of this kind of polymers is the low solubility, which affects their processability. It is known in this sense that the polymer solubility is related to the presence of flexible and polar units, the meta-oriented aromatic rings and also the presence of several functional groups in the polymeric chain.[2-4] In this sense, it is possible to obtain soluble polymers with lower Tg values but maintaining the thermal stability. On the other hand, the presence of silylaromatic units in the polymeric chain, also can increase the solubility due to the ionic character of the C-Si bond.[5] In this work we described the synthesis, characterization and thermal properties of poly(imide-diamides) derived from diacids that contain both groups: imide and amide, which were synthesized from tetrachloro or tetrabromo phthalic anhydride and aminoacids as flexible units. These diacids were polymerized with an aromatic diamine containing the Si atom in the structure

EXPERIMENTAL PART

The chlorinated or brominated 2-phthalimidyl-R-acids were obtained from tetrachloro or tetrabromo phthalic anhydride and the following aminoacids: glycine, L-alanine, L-phenylalanine, L-valine, L-leucine, L-isoleucine and p-aminobenzoic. These chlorinated or brominated acids reacted with thionyl chloride and then with 5-amino-isophthalic acid in order to obtain the monomeric diacids.[6] The diamine bis(4-aminophenyl)diphenylsilane was obtained according to a described procedure.[7]

Poly(imide-diamides) were obtained from the diacids and the diamine with triphenyl phosphite, pyridine and $CaCl_2$ in N-methyl-2-pyrrolidone. The mixture was stirred a 120 ºC and precipited in methanol. Polymers were filtered, washed, dried until constant weight and characterized.

RESULTS

Poly(imide-diamides) were obtained according to the scheme showed in the figure.

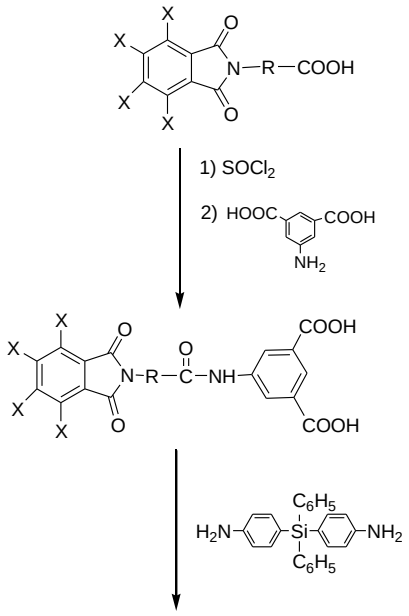

Poly(imide-diamide)

X: Cl, Br.

Where R: CH_2 (Cl-PIDA-I, Br-PIDA-I); $CH(CH_3)$ (Cl-PIDA-II, Br- PIDA-II); $CH(CH_2\text{-}C_6H_5)$ (Cl-PIDA-III, Br-PIDA-III); $CH\text{-}CH(CH_3)_2$ (Cl-PIDA-IV, Br- PIDA-IV); $CH\text{-}[CH_2\text{-}CH(CH_3)_2]$ (Cl-PIDA-V, Br-PIDA-V); $CH(CH\text{-}CH_3)\text{-}CH_2CH_3$ (Cl-PIDA-VI, Br-PIDA-VI); $p\text{-}C_6H_4$ (Cl-PIDA-VII, Br-PIDA-VII)

Poly(imide-diamides) were characterized by IR, ^{1}H, ^{13}C and ^{29}Si NMR, and the results were in agreement with the proposed structures. The η_{inh} values were obtained in order to estimate the molecular weights of the polymers. The thermal properties, glass transition temperature Tg, and the thermal decomposition temperatures TDT, were measured and the values related to the polymeric structures and the nature of the halogen atoms in the imide group.

ACKNOWLEDGEMENTS

The authors acknowledge the financial support to FONDECYT, through grant 1100015. D. Coll and A. Tundidor-Camba acknowledge their scholarships to CONICYT.

REFERENCES

[1] Cassidy, P.E., "Thermal Stable Polymers. Synthesis and Properties", Marcel Dekker, 1980.
[2] Mallakpour, S. and Kowsari, E., Polym. Adv. Technol., 2005, 16, 732.
[3] Liaw D.J. and Liaw, B.Y., Polymer, 2006, 42, 839.
[4] Sava, I. and Bruma, M., Macromol. Symp., 2006, 239, 36.
[5] Bruma, M. and Schulz, B., J. Macromol. Sci., Polym Rev, 2001, 41C, 1.
[6] Mallakpour, S. and Sepehri, S., Polym. Adv. Technol., 2008, 19, 1474.
[7] Pratt, J.R., Massey, W.D., Pinkerton, F.H. and Thomas, S.F., 1975, 40, 1090.

Inclusion of Cytidine in Nanoparticles as a Model for HIV Drugs

Ignacio Moreno-Villoslada[1], J.P. Fuenzalida Werner[2], Francisco M. Goycoolea[3] and Hiroyuki Nishide[4]

1 Instituto de Quımica, Facultad de Ciencias, Universidad Austral de Chile, Valdivia, Chile
2 Department of Pharmacy and Pharmaceutical Technology, Faculty of Pharmacy, University of Santiago de Compostela, 15782 Santiago de Compostela, Spain.
3 Department of Applied Chemistry, School of Science and Engineering, Waseda University, Tokyo, Japan

jpfuenzalidaw@gmail.com

The use of nanotechnology to improve the pharmacokinetics of drugs presents the challenge of the inclusion of hydrophilic low molecular-weight species (HLMWS) in nanoparticulate systems. Chemical modifications achieved to bind these molecules to nanoparticles affect significantly the structure activity relationships of the drugs.[1] In order to include non-modified HLMWS in nanoparticles, strong chemical interactions with the nanoparticle matrix are needed, such as Van der Waals forces, hydrogen bonds, hydrophobic forces, and aromatic-aromatic interactions.

Water-soluble polymers may be constituents of these nanoparticulate matrices. HLMWS containing aromatic charged groups may present strong interactions with polymers bearing aromatic groups in their structure. As an example, molecules such as methelyne blue, rhodhamine 6G, triphenyltetrazolium chloride, or chlorpheniramine maleate undergoe strong interactions with poly(sodium 4-styrenesulfonate) (PSS).[2]

Cytidine (CTDN) is a nucleoside chosen as model drug of Nucleoside / Nucleotide Reverse Transcriptase Inhibitors, used in antiviral treatment. CTDN presents aromatic character and high solubility. Is a molecule sensitive to environmental pH. The UV-Vis spectra of CTND (Figure 1) show a change on the local maximum by increasing the pH, and have an isosbestic point at 265 nm. PSS has the capacity of move to lower energy the isosbestic point and increase the pKa of CTDN. In consequence, PSS promote the formation of protonated CTDN[3]. Other polyanions such as poly(sodium vinyl sulfonate) (PVS), poly(styrene-alt-maleic acid) (P(S-alt-MA)), and poly(acrilyc acid) (PAA), only produce a discreet change on the pKa and did not affect the isosbestic point. Diafiltration experiments showed a higher ability of PSS to bind CTDN, and a high sensitivity to the addition of NaCl was found. H^1-RMN spectroscopy showed that PSS produces an upfield shift of CTDN aromatic signals, as a signal of the existence of aromatic-aromatic interactions between both species. This behavior is not observed in the presence of NaCl.

Nanoparticles were made by ionic complexation at pH 4 between the different anionic polymers and chitosan, a cationic polymer. The effect of varying molar ratios of charges (n+/n-) and total amount of charge in solution (n+ + n-) was evaluated. Nanoparticles with PSS, P(S-alt-MA) and PVS were prepared. The total amount of charge varied between 1 and 6 mM. It was found that the optimal conditions were 4 mM of total charges and n+/n- between 0.3 and 2.2 (Figure 2). However, n+/n- 1.5 was chosen since CTDN bound to the polyanions is expected to be located at the inner core of the nanoparticle. The nanoparticles were loaded with CTDN and the load efficiency analyzed by HPLC.

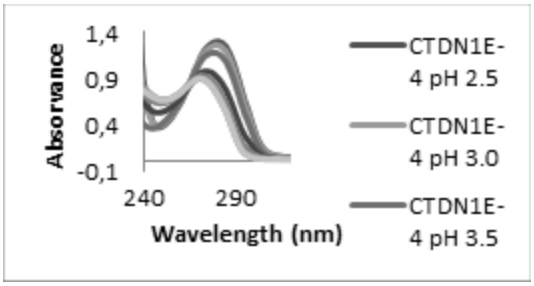

Figure 1: CTDN UV-Vis Spectra at 1E-4M at different pH conditions

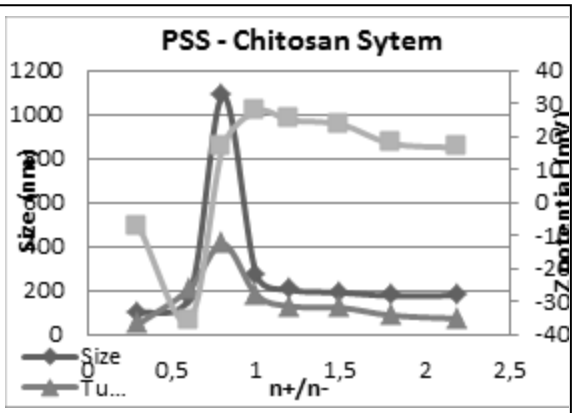

Figure 2: Nanopartide characteristic PSS-Chitosan System

Bibliography:

1.- V.J. Stella, K.W. Nti-Addae, Prodrug strategies to overcome poor water solubility, Adv. Drug Deliv. Rev. 59 677–694, 2007

2.- Ignacio Moreno-Villoslada, et al, Different Models on Binding of Aromatic Counterions to Polyelectrolytes. Mol. Cryst. Liq. Cryst., Vol. 522: 437-448, 2010

3.- Barbara S. Berlett, et al, Use of Isosbestic Point Wavelength Shifts to Estimate the Fraction of a Precursor That Is Converted to a Given Product, Analytical Biochemistry **287,** 329–333, 2000

Acknowledgements: The authors thank Fondecyt grant 1090341 for financial support.

Thioxanthone Containing Novel Dendritic Photoinitiators

Tezcan Parali[1], Zekeriya Dogruyol[2], Gokhan Temel[3], Nergis Arsu[4], Metin Tulu[4]

[1] Dept. of Chemistry Fatih University, Istanbul, 34500 Turkey
[2] Dept. of Physics Yildiz Technical University Istanbul, 34220 Turkey
[3] Polymer Eng. Yalova University, Yalova, 77100 Turkey
[4] Dept. of Chemistry Yildiz Technical University Istanbul, 34220 Turkey

e-mail:mtulu@yildiz.edu.tr

Dendrimers are highly branched and have well-defined architectures with a number of special chemical and physical properties [1, 2]. Their highly branched and uniform structures can be used in the field of coatings industry, chemical sensors and drug delivery systems [3].

Recently, the use of PPI dendrimers as co-initiators in photoinitiated radical polymerization, has been tested [4]. The photopolymerization was carried out with UV radiation employing benzophenone and thioxanthone as sensitizers. The investigation of the structure of the resulting polymers suggested the presence of stretched polymer chains around the dendrimer. In another study, macrophotoinitiators were prepared using DAB dendrimers and thioxanthone as sensitizer in the UV system[5]. These initiators were found suitable for use in aqueous systems. The use of dendrimers as co-initiators seems to be promising and it was therefore of interest to investigate the extension of their use to the visible zone of the spectrum. Additionally Poly(propylene imine) dendrimers were recently used as the hydrogen donor for type II photoinitiation of methylmethacrylate monomer in free radical polymerization [6].

There are two types of photoinitiators in free radical polymerization: an alpha type scission initiator (type I) and a hydrogen abstraction type photoinitiator (type II). Because the initiation is based on a bimolecular reaction, type II photoinitiators are generally slower than type I photoinitiators, which are based on a unimolecular formation of radicals. Benzophenone (BP) is a well known type II photoinitiator (PI) for the radiation curing of coatings printing inks, etc. After triplet state excitation, benzophenone is able to abstract hydrogen from ether, amine, alcohol or thiol functional co-initiators. Thus, reactive centers can be generated on
co-initiator molecules to initiate free radical polymerization

As a macrophotoinitiators, up to third generation of dendrimer was synthesized[7]. Initial core of all dendrimers was based on poly(propylene oxite) amine (Jeffamine®). At the second stage, previously synthesized 2-acryloyl thioxanthone was coupled to amine terminated dendrimers. All the reactions were performed by using microwave irradiation technique. The photophysical and photochemical properties of these photoinitiators were studied. Later absorption characteristics of Jeff-(3)-Thioxanthone (J-(3)-TX), Jeff-(6)-Thioxanthone (J-(6)-TX) and Jeff-(12)-Thioxanthone (J-(12)-TX) were determined in different solvents. The fluorescence emission spectra of Jeff-(3,6,12)-TX were also ivestigated by exciting at λ_{exc} = 395 nm.

In conclusion, BP/Me- β-CD water soluble photoinitiator was readily prepared in a conventional complexation procedure, and fully characterized by ^{1}H-NMR, UV and FT-IR. Laser flash photolysis and phosphorescence studies show that BP/Me-β-CD complex is similar to the parent benzophenone compound after the complexation reaction. However, these inclusion complexes could initiate polymerization of acrylamide in aqueous media.

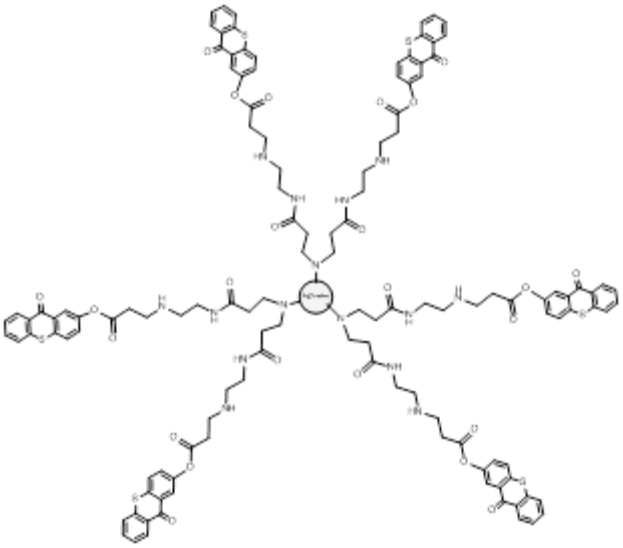

Scheme 1. Dendritic Photoinitiator

References:

1. M. Mammen, S.K. Choi, G.M. Whitesides, *Angew. Chem. Int. Ed.* 37 (1998) 2755–2794.
2. A.W. Bosman, H.M. Janssen, E.W.Meijer, *Chem. Rev.* 99 (1999) 1665–1688.
3. M.A. Tasdelen, A.L. Demirel, Y. Yagci, *Eur. Polym. J.* 43 (2007) 4423–4430
4. M.A. Tasdelen, A.L. Demirel, Y. Yaggi, *Eur. Polym. J* 43 (2007) 4423.
5. X. Jiang,W.Wang, H. Xua, J. Yin, J. *Photochem. Photobiol. A: Chem.* 181 (2006) 233.
6 G. Pistolis, A. Malliaris, *Langmuir* 18 (2002) 246–251.
8. Gokhan Temel, Tezcan Parali, Metin Tulu, Nergis Arsu, *Journal of Photochemistry and Photobiology A: Chemistry*, 213 (2010) 46–51

Characterization, Melting and Crystalline Properties of Isotactic (4,2)-Enchained Poly(1-Butene)

Carolina Ruiz-Orta, Rufina G. Alamo

FAMU-FSU College of Engineering, Chemical and Biomedical Engineering Department, 2525 Pottsdamer St., Tallahassee, FL 32310

Alamo@eng.fsu.edu, Carolina@eng.fsu.edu

Introduction. The availability of new crystalline polyolefins by control of catalyst "chain-walking" offers the opportunity to study crystalline properties of new polymer structures similar to the most common polyolefin commodities. Living polymerization of 1-butene with an α-diimine Ni(II) catalyst generates new crystalline polybutenes with unique chain microstructures.[1] A normal (1,2) insertion followed by a subsequent chain-walking to the fourth carbon results in a (4,2) addition. Conversely, a regio (2,1) inversion followed by chain-walking produces (4,1) linkages leading to a sequence of four consecutive methylenes in the backbone chain. In addition, when high selectivity for (4,2)-enchainment is exhibited a (4,2)-enchained poly(1-butene) is obtained. This polybutene is isostructural with poly(*trans*-2-butene). In this work we study crystalline properties of the novel polybutenes with a similar content of (4,2) and (4,1) additions and different content of stereo defects.

Materials and Methods. The molecular characteristics of the two polybutene samples studied are as follows. From ^{13}C NMR, (4,2) additions (~96 mol%), stereo errors (9 or 16 mol%); (4,1) additions (~ 4 mol%), and zero (1,2) additions in both samples. The combined (4,2) and stereo defects are 12, (4,2PB12) and 21 mol% (4,2PB21) for the most and the least crystalline samples studied. From GPC, Mw = 54,000 Dalton, Mw/Mn = 1.5.

The melting peaks, T_m, heat of fusion, ΔH, and overall crystallization kinetics were followed by DSC (Perkin Elmer DSC7). Wide and small angle x-ray diffractograms (SAXS, WAXD) were obtained at ambient temperature on samples that were previously isothermally crystallized either in the DSC or in thermostated baths. The degree of crystallinity derived by WAXD, X_c, was determined from the x-ray powder diffraction profiles of samples isothermally crystallized at different temperatures, T_c. The WAXS pattern of molten 4,2PB was used as amorphous halo. Crystal and interlamellar thicknesses were obtained from SAXS profiles via one-dimensional correlation function analysis. Spherulitic morphology and linear growth rates were analyzed by polarized optical microscopy and a Linkam hot stage, and lamellar morphology by AFM in non-contact AC mode. The densities were measured at room temperature in a water/isopropanol density gradient column calibrated with standards glass floats.

Results and Discussion. *Crystalline Structure*. In spite of a relatively low tacticity (mm <0.8), and a significant content of (4,1) defects, WAXD patterns exhibit two relatively sharp crystallographic reflections at 2θ = 16.9 and 19.7 degrees, consistent with high order chain-packing symmetry. Unlike *i*PP and poly(1-butene) that display polymorphism with increasing stereo defects or increasing crystallization temperature, the crystallographic phase of 4,2PB is maintained with increasing T_c or defects. The WAXD-derived degree of crystallinity (X_c) is low (<30 %) in 4,2PB21, and exhibits a modest 37 to 52 % increase in a large T_c range in the sample with 12 mol% defects.

Under isothermal crystallization, 4,2PB12 develops relatively thick lamellar crystallites (~ 95 Å thick by AFM) that aggregate in highly ordered spherulites. This feature and the relatively high crystallinity content for a copolymer with a high content of structural defects suggests co-crystallization of the stereo defects, similarly to the inclusion of stereo defects in *i*PP crystallites. With increasing chain defects the structural irregularities break down the spherulitic and lamellar habits.

Thermodynamic Parameters. Degrees of crystallinity of isothermally crystallized specimens were combined with density measurements, heat of fusion, and lamellar thicknesses to estimate the densities of the crystalline and amorphous phases, ρ_c = 0.9494 g/cm^3 and ρ_a = 0.8698 g/cm^3, respectively, and the heat of fusion per mole of crystalline unit (ΔH° = 132.6 J/g). Accounting for a re-structuring of crystallites during melting, the crystallites thicknesses and melting temperatures were analyzed with the simplified Gibbs-Thompson equation to extract values of the equilibrium melting temperature and the basal surface free energy of the crystallites. The value of $T_m°$ = 135 ± 4°C. The defects reduce the $T_m°$ value of 4,2PB in reference to expectations for the defect free chain and values. At a 12 mol% defect level, the $T_m°$ is similar to the value for form I of *i*poly(1- butene), and significantly lower than for *i*PP and *s*PP. However, the heat of fusion per mole of crystalline units (8670 J/mol) is similar to the values of *i*PP and *s*PP in spite of a larger repeat unit. From the Gibbs-Thompson relation, the interfacial free energy is σ_e = 77 erg/cm^2. This value is supported by a basically identical σ_e value obtained from an analysis of lamellar growth rates according to secondary nucleation theory. The σ_e value of 4,2PB is similar to values obtained for polyethylene and *i*PP homopolymers (~ 70 erg/cm^2), and lower than for *i*PP copolymers with about the same content of defects. This feature suggests a relatively flexible conformation that favours chain folding in the novel poly(butenes).

Conclusion. The thermodynamic and structural properties of 4,2PB synthesized with a α-diimine Ni(II) catalyst have been analyzed. Stereo and (4,1) regio are defects that hinder the crystallization, as given by the decreasing rates, decreased levels of crystallinity and lowered melting temperatures with increasing defect content.

Acknowledgment. We gratefully acknowledge G.W. Coates from Cornell University for synthesis, and the USA National Science Foundation for funding.

1.- J.M. Rose, A.E. Cherian, G.W. Coates. J. Am. Chem. Soc. 2006, 128, 4186-7.

Synthesis and Properties of a Self-Doped Polyacetylenes via the Activated Polymerization of Ethynylpyridines by the Ring Cleavage Reaction of Cyclic Compounds

Y. S. Gal[1], *S. H. Jin*[2], *J. W. Park*[3], *W. S. Lyoo*[4], *K. T. Lim*[5]

[1]Chemistry Division, Kyungil University, Gyeongsangbuk-Do, Korea, [2]Department of Chemistry Education, Pusan National University, Busan, Korea, [3]Department of Chemistry, The Catholic University of Korea, Bucheon, Korea, [4]School of Textiles, Yeungnam University, Gyeongsangbuk-Do, Korea, [5]Division of Image and Information Engineering, Pukyong National University, Busan, Korea

e-mail: ysgal@kiu.ac.kr

Introduction

Substituted polyacetylenes are highly desirable due to their greater oxidative stability compared with the polyacetylene itself. And also, the attachment of pendant groups can also add to the functional properties of the material.[1,2]

The conjugated polyelectrolytes such as poly(propiolic salt)s, triethylammonium salt of poly(6-bromo-1-hexyne), poly(dipropargylammonium salt)s, and poly(ethynylpyridine) were reported.[1] We have also reported the preparation of various ionic conjugated polymers having different functionalities.[1,2] Due to their extensive conjugation and ionic nature, these ionic polyacetylenes have potentials as materials for mixed ionic and electronic conductivity, energy storage devices such as batteries, permselective membrane, and light-emitting devices.[1]

Here, in a series of synthesis of conjugated polymers, we report the synthesis of a self-dopable ionic conjugated polyacetylene via the activated polymerization of 2- and 3-ethynylpyridines by the ring cleavage of designed cyclic compounds.

Experimental

2 and 3-Ethynylpyridines (Aldrich Chemicals.,) were used as receivesd. An ionic conjugated polymews were synthesized by the activated polymerization of 2 or 3-ethynylpyridines by using such ring-openable compounds as propiolactone, 1,3-propanesultone, 1,4-butanesultone, etc. As the polymerization reaction proceeded, the color of reaction mixture was changed from the light brown of the initial mixture into dark red solution. And the viscosity of reaction solution was also increased. After the polymerization time, the resulting polymer solution diluted with additional DMF was precipitated into an excess amount of ethyl ether, followed by filtration. The collected powder was dried under vacuum overnight at 40 ^{o}C for 24 h.

Results and Discussion

Ionic self-dopable conjugated polyacetylenes were easily prepared by the activated polymerization of 2- and 3-ethynylpyridine with the ring-cleavage reaction of designed cyclic compounds without any additional initiator or catalyst. As the reaction proceeded, the color of reaction mixture was changed from the light brown of the initial mixture into dark red solution. And the viscosity of reaction solution was also increased. This polymerization proceeded well in relatively mild reaction condition to give high yields of polymer.

The molecular structures of the resulting ionic polyacetylenes were characterized by such instrumental methods as infrared, NMR, and UV-visible spectroscopies. FT-IR spectra of 2-ethynylpyridine, cyclic compound, and resulting ionic polyacetylene were measured and compared. FT-IR spectrum of an ionic polyacetylene did not show the acetylenic C≡C bond stretching (2110 cm^{-1}) and acetylenic ≡C-H bond stretching (3293 cm^{-1}) frequencies of 2-ethynylpyridine. Instead, the C=C stretching frequency peak of conjugated polymer backbone around 1575-1670 cm^{-1} became relatively more intense than those of the C=C and C=N stretching frequencies of 2-ethynylpyridine. The electro-optical and electrochemical properties of ionic polyacetylenes were studied by using UV-visible and photoluminescence (PL) spectroscopies and cyclic voltammograms (CV). The absorption spectra of polymers exhibits characteristic absorption peak at visible region, which is due to the $\pi \rightarrow \pi^*$ interband transition of conjugated polymers. The photoluminescence spectrum of an ionic conjugated polymer with N-propylsulfonate functional group showed that the photoluminescence maximum peak is located at 552 nm corresponding to the photon energy of 2.25 eV. The cyclovoltammograms of polymer exhibited the irreversible electrochemical behaviors between the oxidation and reduction peaks. The oxidation current density of polymer versus the scan rates is approximately linear relationship in the range of 30 – 120 mV/sec. It was found that the the kinetics of the redox process of polymer is almost controlled by the reactant diffusion process from the oxidation current density of polymer versus the scan rates.

Conclusions

We synthesized various ionic conjugated polyacetylenes by simple activated polymerization of ethynylpyridine without any additional catalyst or initiator. These self-dopable polyacetylenes may be used as material candidates for chemical sensors, OLEDs, solar cells, etc.

Acknowledgment

This work was supported by a grant No. RTI04-01-04 from the Regional Technology Innovation Program of the Ministry of Knowledge Economy (MKE), Korea and KRF grant funded by the Korea government (No. R01-2008-000-21056-0).

References

1. S. K. Choi, Y. S. Gal, S. H. Jin, and H. K. Kim, *Chem. Rev*., 100, 1645 (2000).

2.. Y. S. Gal, S. H. Jin, J. W. Park, and K. T. Lim, *J. Polym. Sci.: Part A: Polym. Chem*., 47, 6153 (2009).

Porous polymer surfaces with superhydrophobic/superhydrophilic micropatterns: towards genome-on-a-chip cell microarrays

*Florian L. Geyer[1,2], Urban Liebel[1], Erica Ueda[1], Pavel A. Levkin[1,2]**

[1]Karlsruhe Institute of Technology, Institute of Toxicology and Genetics, Germany
[2]Heidelberg University, Department of Applied Physical Chemistry, Germany

Email: levkin@kit.edu

Living cells are extremely complex biological systems and a variety of cell assays have been developed to study these systems *in vitro*. In the last few years, cell microarrays have emerged as a promising technique that enables cell assays in a highly parallel and miniaturized manner.[1-3] However, due to cross-contamination and cell migration problems, the density of most current cell microarrays is still limited.

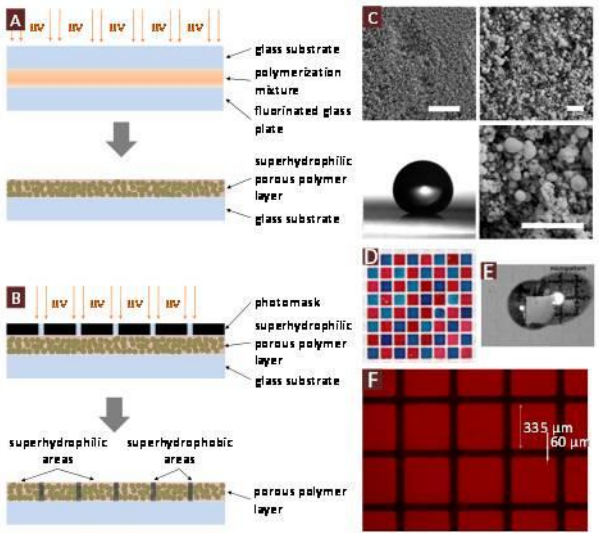

Figure 1. (A) Scheme of the preparation of a superhydrophilic porous polymer film on a glass substrate by UV-initiated free-radical polymerization. (B) Fabrication of the superhydrophobic grid-like pattern on the superhydrophilic surface by UV-initiated photografting. (C) Water droplet on the superhydrophobic polymer; SEM images of the same polymer. Scale bars: top left - 10 µm, top right and bottom - 1 µm. (D) The array with microspots filled with alternating water solutions of red and blue dyes. (E) A water droplet on a single superhydrophilic microspot. (F) Fluorescent microscope image showing the array with spots filled with Rhodamine 6G.

We discovered a way to overcome these problems using a porous superhydrophilic polymer, poly(2-hydroxyethyl methacrylate-*co*-ethylene dimethacrylate), coated onto a substrate and patterned with superhydrophobic barriers[4,5] using photografting - a surface modification technique. Cell experiments carried out with several commonly used cell lines confirmed preferential adhesion and proliferation of cells on the superhydrophilic spots and virtually no cell growth on the superhydrophobic barriers. In addition, the narrow superhydrophobic gaps between the spots proved to be highly efficient barriers against cell migration. Because of the extreme difference in wettability between the superhydrophilic and superhydrophobic areas, this method allows us: (1) to significantly reduce the distance between the microspots and (2) to achieve precise control over the size and (3) geometry of the microspots. Moreover, the transparency of the porous polymer inside the hydrophilic spots allows for microscopic investigation to be carried out. This allows us to increase the amount of spots on one 11 x 7 cm² area (standard microtiter plate size) to about 50000 square spots large enough to accommodate at least 100 cells to deliver statistically valid read-out data. Spotting solutions are adsorbed in the porous structure of the spots, while the superhydrophobic pattern prevents spreading to adjacent spots, thus also eliminating the serious problem of cross-contamination.

We envision that this technology based on a porous polymer coating will enable fabrication of "genome-on-a-chip" cell microarrays and will transform genome-wide cell screening experiments into a significantly more affordable and convenient biological tool.

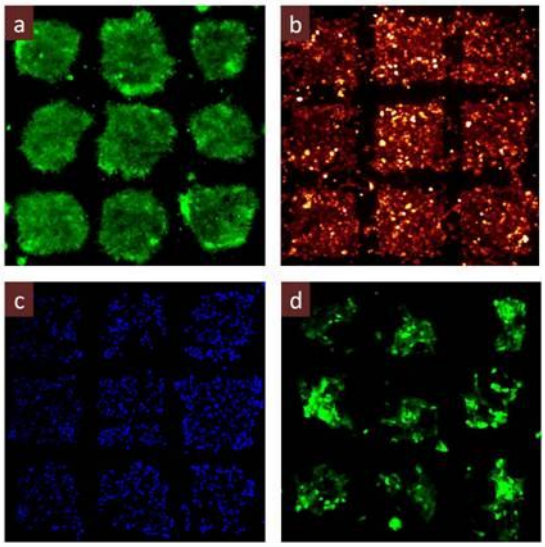

Figure 2. Different cell lines growing on the array for 48 hours. (a) Mouse mammary carcinoma cells with GFP expression vector. (b) Rat mammary carcinoma cells with mCherry expression vector. (c) HEK cells, DAPI stained. (d) Hepa cells with GFP-expression vector.

[1]D.B. Wheeler, A. E. Carpenter, D. M. Sabatini, *Nature Genetics* **2005,** *37*, 25-30.
[2] A. L. Hook, H. Thissen, N. H. Voelcker, *Trends in Biotechnology* **2006,** *24*, 471-477.
[3] H. Erfle, B. Neumann, U. Liebel, P. Rogers, M. Held, T. Walter, J. Ellenberg, R. Pepperkok, *Nature Protocol*, **2007**, 2, 392-399.
[4] P. A. Levkin, F. Svec, J. M. J. Fréchet, *Adv. Funct. Mater.* **2009**, 19, 1993–1998.
[5] F. L. Geyer, U. Liebel, E. Ueda, P. A. Levkin, submitted

Acknowledgements: We are thankful to the Helmholtz Association's Initiative and Networking Fund (grant VH-NG-621) for the financial support.

Photoelectrochemical Properties of Doped Polyaniline: Application to Hydrogen Production Upon Visible Light

Z. Benabdelghani[1], G. Rekhila[1], M. Trari[1], A. Etxeberria[2]*

[1]Laboratory of Storage and Valorization of Renewable Energies, Faculty of Chemistry, USTHB, P.O.Box 32,El Alia, Algiers 16111, Algeria.
[2]Departamento de Ciencia y Tecnologia de Polimeros and Instituto de Materiales Polimericos (POLYMAT). Universidad del Pais Vasco UPV/EHU. P.O. Box 1072. 20080 San Sebastian (Spain).

* To whom all correspondence should be addressed to e-mail address: Ben_Zit@yahoo.fr

Introduction:

Over the last years, the conducting polymers found a new interest from both academic and industrial points of view due to their interesting properties and possible applications, in the conversion of solar energy into electrical and/or chemical forms. In order to diminish the dependence of the fossil fuels and in this way the greenhouse gases, the solar power is considered as eco-friendly energy, an attractive alternative due its large abundance and consistency [1,2].
For this purpose, the use of polymer semiconductors as photoactive electrodes and photovoltaic devices attracts much attention of a large scientific community [3]. Such materials are not only able to function in a similar way to inorganic semiconductors but have additional advantages including environmental friendliness, low cost, light weight, easy fabrication, and potentially manufacturable as large-area coatings. They have been considered as promising materials for organic light conversion devices, in particular, for solar cells and photodetectors.

Our aim in this contribution was focused on a study of photoctalytic process in order to product the hydrogen using polymer semiconductor materials such as doped polyaniline (emeraldine salt).

2. Experimental

The powder was cold pressed into pellets under 1 kbar. In order to minimize the contact resistance, silver paint was deposited on the back pellet by spot welding a copper wire. The pellets were mounted in Teflon holders to give a projected surface area of 1.32 cm^2.
PEC measurements were done in NaOH (1 M) electrolyte under potentiostatic conditions using a three electrode cell with a large Pt counter electrode and a saturated calomel reference electrode (SCE). The electrode potential was monitored by a computer controlled potentiostat (Voltalab PGZ 301, Radiometer).
The electrode was illuminated through a flat optical window by a 200 W tungsten lamp.
Prior each run, A nitrogen stream was passed over the solution to remove dissolved oxygen, the purging rate was maintained constant at 10 mL mL^{-1} during 35 min.
50 mg of powder (PANI) was suspended by magnetic stirring in a double walled Pyrex reactor in 250 mL of aqueous Na_2SO_3 (0.1 M) solution.
The light source was an assembly of three tungsten lamps which are predominantly in the 400-900 nm (max. 650 nm), disposed around the reactor.

Hydrogen in the outgoing gas was identified by gas chromatography. The amount was collected volumetrically with a water manometer in an inverted burette via water displacement. Blank runs were carried out and no hydrogen was evolved in the dark.
The experiments were repeated three times with very reproducible results

Results and discussion:

The photoelectrochemical properties of polyaniline (emeraldine-salt) (PANI) doped was investigated by the photocurrent technique and capacitance measurements in various electrolytes. The volume evolved of H_2 as showed in Figure 1 reveals the applicability of this material for the photocatalytic conversion. The photocatalytic properties have been evaluated for the first time according to the H_2 evolution under visible light.

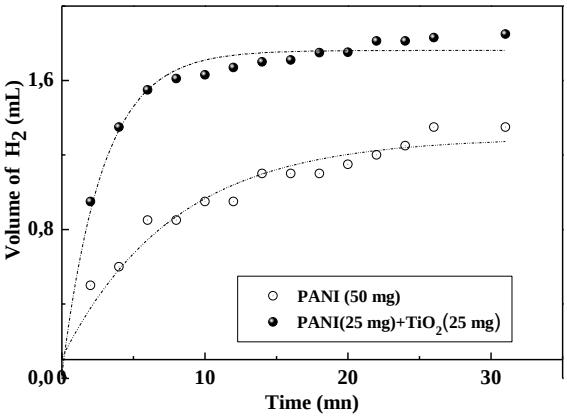

Figure 1: Volume evolved H_2 versus irradiation time on Na_2SO_4 solution (0,1 M)

Therefore, favorable valence band position for water reduction makes the PANI as an ideal photocathode. Our results indicate that the doped PANI is able to generate incident photon to chemical chemical efficiency of 4% under an intensity of 20 mW cm^{-2}.

References

1. Djellal L, Omeiri S, Bouguelia A, Trari M, J of Alloys and Compounds 2009, 476: 584-589.
2. Benabdelghani Z, Etxeberria A, J of Appl Polym, in Press.
3. Hsu C.W., Wang L.W, Su. F, J of Colloid and interface science 2009, 329: 182-187.

Poly(2-Isopropenyl-2-oxazoline): Hydrogel Formation and Potential Applications

*Verena Schenk,[1] Lisa Ellmaier,[1] Frank Wiesbrock[2];**

[1] Polymer Competence Center Leoben GmbH PCCL, Roseggerstrasse 12, AT-8700 Leoben, Austria.
[2] Graz University of Technology, Institute for Chemistry and Technology of Materials, Stremayrgasse 9/V, AT-8010 Graz, Austria.

e-mail: f.wiesbrock@tugraz.at

Introduction

Hydrogels or aquagels are solid, three-dimensional networks consisting of hydrophilic polymer chains that can be obtained from chemical or physical cross-linking processes. They are water-swellable, but not soluble. Due to their high water content, hydrogels are often highly biocompatible with minimal absorption of proteins. Hence, aquagels possess a wide range of potential applications, especially in the fields of tissue engineering and drug delivery,[1] which are closely related to the chemical structure of their components and the networks' morphologies.[2]

Given the FDA approval for poly(2-ethyl-2-oxazoline) and poly(2-phenyl-2-oxazoline), it is surprising that the group of poly(2-oxazoline)s has been scarcely considered for hydrogel formation so far (21 CFR 175.105).

Materials and Methods

Poly(2-oxazoline)s can be synthesized by living cationic ring-opening polymerization. Different functionalities are achieved through consumption of monomers with various side-chains. Moreover, the living nature enables a target-oriented synthesis of tailor-made block copolymers (Scheme 1).[3]

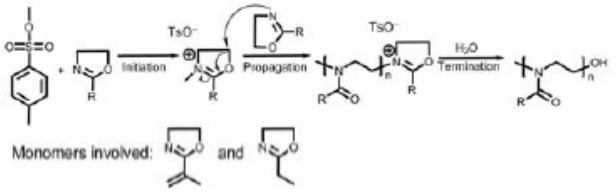

Scheme 1: Ring-opening polymerization of poly(2-oxazoline)s.

Results and Discussion

Microwave-assisted heating has enabled to shorten the reaction times of the polymerization of 2-oxazolines significantly by factors up to 400, while the living character of the polymerization is maintained (Figure 1).[4;5]

Under microwave irradiation, several hydrogels were synthesized to create sub-libraries of this novel material class (Figure 2). During the polymerization of poly(2-isopropenyl-2-oxazoline), cross-linking occurs, the mechanism of which was investigated thoroughly.

In this poster presentation, the mechanism of hydrogel formation and material characterizations of the synthesized hydrogels, in particular the correlation hydrogel composition - swelling degrees in different solvents will be shown.

Figure 1: Biotage Initiator 8.

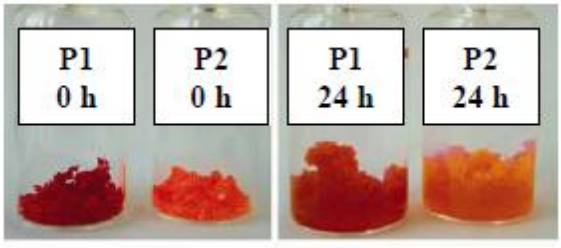

Figure 2: Poly(2-isopropenyl-2-oxazoline) (**P1**) and poly(2-ethyl-2-oxazoline)-co-poly(2-isopropenyl-2-oxazoline) (**P2**) with trapped Eosin Y in dry (left) and in swollen state (right; in water).

Conclusion

Poly(2-isopropenyl-2-oxazoline)- based hydrogels can easily be synthesized by microwave-assisted polymerization protocols. Swelling degrees can be tailor-fabricated by the copolymer composition.

References

[1] C. Hiemstra, W. Zhou, Z. Zhong, M. Wouters, J. Feijen, *J. Am. Chem. Soc.* **2007**, *129*, 9918-9926.

[2] J.C. Cuggino, C.I. Alvarez Igarzabal, J.C. Rueda, L.M. Quinzani, H. Komber, M.C. Strumia, *Eur. Polym. J.* **2008**, *44*, 3548-3555.

[3] F. Wiesbrock, R. Hoogenboom, M. Leenen, S.F.G.M. van Nispen, M. van der Loop, C.H. Abeln, A.M.J. van den Berg, U.S. Schubert, *Macromolecules* **2005**, *38*, 7957-7966.

[4] C. Ebner, T. Bodner, F. Stelzer, F. Wiesbrock, *Macromol. Rapid Comm.* **2011**, *32*, 254-288. [5] A. Hecke, A.M. Kelly, B. Wirnsberger, F. Wiesbrock, submitted.

Ionic liquid based membranes: water sorption properties

Kateryna Fatyeyeva[1], Sergiy Rogalskyy[2], Oksana Tarasyuk[2], Stéphane MARAIS[1]

[1] Université de Rouen, Laboratoire Polymères, Biopolymères et Surfaces, UMR 6270 & FR 3038 CNRS, Bd. Maurice de Broglie, 76821 Mont Saint Aignan Cedex, France
[2] Institute of Bioorganic Chemistry and Petrochemistry, National Academy of Sciences of Ukraine, Kharkivske chausse 50, 02160 Kyiv, Ukraine

kateryna.fatyeyeva@univ-rouen.fr

Ionic liquids (ILs) have received a great deal of attention in recent years and a diverse array of these materials has been synthesised. Much of the interest has been due to their unique solvent properties and low volatility that have been put to use in a wide range of synthetic applications in so-called "green chemistry". Attention has been mainly directed towards modifying ILs to manipulate solvent and electrochemical properties. ILs have excellent thermal stability, low volatility, they can also have wide electrochemical potential windows and in some cases they offer unique solubility properties.

The synthesis of a serie of imidazolium-based ILs (1-*n*-alkyl-3-methylimidazolium, where *n* = 4, 6-8, 12) was performed and their physicochemical properties were investigated. The water vapour sorption behaviour of ILs was examined. Equilibrium moisture content was determined as a function of the relative humidity at 25 °C by means of microgravimetric technique. The influence of the chemical structure, including the type of anion and length of the alkyl chain, on the water vapour sorption has been studied. The experimental results indicate the sorption capacity increase with the decrease of the alkyl chain length.

The synthesized ILs were immobilised in porous polymer membranes in order to study the potential of using supported ionic liquid membranes for gas and liquids separation. Different aspects were investigated, such as the evaluation of the membrane stability and the influence of the IL chemical structure on the permeability and gas selectivity.

Thermophysical, electrical and mechanical properties of ethylene-vinylacetate copolymer (EVA) filled with wollastonite fibers coated by silver

I. Krupa1, V. Cecen2, R. Tlili3, A. Boudenne3, L. Ibos3. J. Prokes4

1 Polymer Institute, Slovak Academy of Sciences, Dúbravská cesta 9, 845 41 Bratislava, Slovakia
2 Dokuz Eylul University Mechanical Eng. Department 35100 Bornova/Izmir, Turkey
3 CERTES EA 3481 - Centre d'Etude et de Recherche en Thermique, Environnement et Systèmes, Université Paris 12 Val de Marne, 61 Av. du Général de Gaulle, 94010 Créteil cedex, France
4 Charles University Prague, Faculty of Mathematics and Physics, V Holešovičkách 2, 182 00 Prague 8, CZECH REPUBLIC

Igor.Krupa@savba.sk

Common industrial polymers, in general, are materials with very low value of thermal and electrical conductivity. However, many industrial applications including circuit boards, heat exchangers, electronics protection, etc require an improvement the thermal conductivity of plastics. Similarly, plastics with improved electrical conductivity are used as heating elements, temperaturedependent resistors and sensors, self-limiting electrical heaters and switching devices, antistatic materials for electromagnetic interference shielding of electronic devices.

Metal-coated inorganic fibers are often as a substitute for metals in electrically and thermally conductive composites. The advantages are the easiness of metallization of convenient substrates, high conductivity, low density and lower prices when compared to metals. Among the most frequently metalized substrates are glass fibers, carbon fibers and mica.

Here we will present a preparation of composites filled with new type of conductive fibers based on silver coated wollastonite. SEM micrograph of silver coated wollastonite fibers is shown in Figure 1.

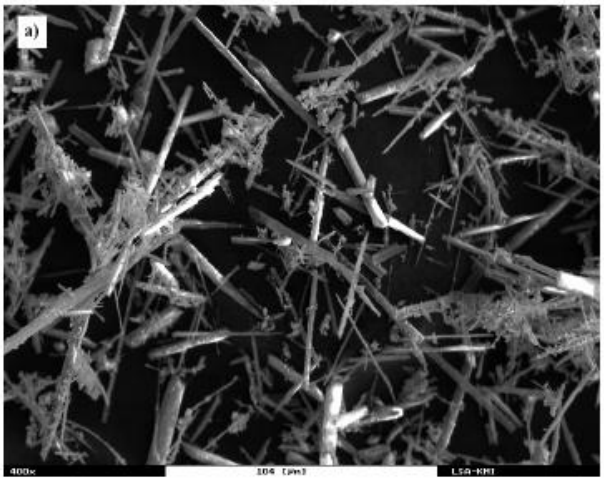

Fig.1 SEM micrograph of coated wollastonite.

The fibers were used for the preparation of elastic, highly electrically and thermally conductive polymeric composites based on ethylene-vinylacetate copolymer. It was shown that silver coated fibers significantly improved both the thermal and electrical conductivity of composites despite the low silver volume content. The electrical percolation threshold was found about 8 vol.% and the highly electrical conductivity value (1.8×105 S.m-1) is reached for 29 vol.% of filler fraction.

The experimental results were discussed and compared to various theoretical models.

Acknowledgement

The research was supported by the Scientific Grant Agency of the Ministry of Education of Slovak Republic and the Slovak Academy of Sciences (project No. 2/0063/09). This work is a part of the research plan MSM0021620834 that is financed by the Ministry of Education, Youth and Sports of the Czech Republic

Synthesis of Functionalised Polymer Microspheres with Ultra-High Specific Surface Areas and their Applications in Selective Chemical Extractions

P.A.G Cormack[1], A. Davies[1] and N. Fontanals[2]

[1]WestCHEM, Department of Pure and Applied Chemistry, University of Strathclyde, Thomas Graham Building, 295 Cathedral Street, Glasgow, G1 1XL, Scotland.
[2]Departament de Química Analítica i Química Orgànica, Universitat Rovira i Virgili, Campus Sescelades, Marcel·lí Domingo, s/n, 43007 Tarragona, Spain.

peter.cormack@strath.ac.uk; arlene.davies@strath.ac.uk

Introduction

Traditional solid-phase extraction (SPE) sorbents are silica-based, however polymeric sorbents are becoming increasingly popular due to their enhanced stability and sorption properties. In addition, recent advances in polymerisation techniques, which have allowed the facile synthesis of appropriately sized particles, and the ease with which polymer sorbents can be functionalised, make polymers ideal for use as SPE sorbents.[1] The retention properties of such materials can be enhanced further by carrying out Davankov-type hypercrosslinking reactions to yield sorbents with high specific surface areas.[2]

This work combines the concepts of polymeric sorbents, hypercrosslinking and functionalisation chemistry to produce novel polymeric materials tailored for use in ion-exchange SPE.

Materials and Methods

Swellable, micrometer-sized polymer particles were synthesised using precipitation polymerisation[3], with ultra-high specific surface areas being introduced subsequently into the particles through Davankov-type hypercrosslinking reactions.[4] Pendent ion-exchange groups were installed into the polymers with ease, either by the use of functional monomers or through post-polymerisation chemical modification reactions (Figure 1).

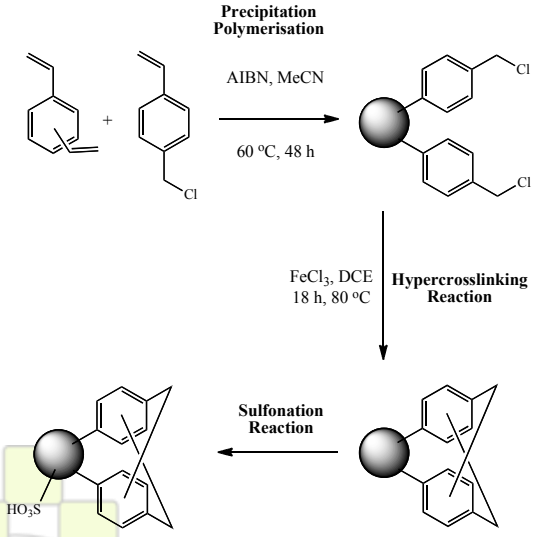

Figure 1 – Synthesis of ultra-high specific surface area strong cation-exchange sorbent.

Results and Discussion

Strong and weak anion- and cation-exchange sorbents, with specific surface areas in excess of 1,000 m^2/g, were all synthesised using this generic synthetic methodology. An example of the synthesis of a strong cation-exchange sorbent is presented in Figure 1.

The polymers were then exploited as sorbents in ion-exchange SPE. For example, the impressive performance of the strong cation-exchange (SCX) materials were demonstrated in the SPE of basic pharmaceuticals from environmental water samples. The novel sorbents were benchmarked against commercially available sorbents, and were found to compare favourably.

Conclusions

Ultra-high specific surface area polymer microspheres with ion-exchange functionality were prepared and successfully applied as sorbents in ion-exchange SPE.

References

(1) N. Fontanals, R. M. Marcé and F. Borrull, *Trends Anal. Chem.*, (2005), **24**, 394; N. Fontanals, R. M. Marcé, F. Borrull and P. A. G. Cormack, *Trends Anal. Chem.*, (2010), **29**, 765.

(2) V. Davankov, S. V. Rogoshin and M. P. Tsyurupa, *J. Polym. Sci.*, (1974), **74**, 95 and 189; N. Fontanals, M. Galia, P. A. G. Cormack, R. M. Marcé, Sherrington and F. Borrull, *J. Chromatogr. A.*, (2005), **1075**, 51; V. Davankov, L. Pavlova, M. Tsyurupa, J. Brady, M. Balsamo and E. Yousha, *J. Chromatogr. B.*, (2000), **739**, 73.

(3) H. D. H Stöver and K. Li, *J. Polym. Sci. Part A: Polym. Chem.*, (1993), **31**, 3257.

(4) N. Fontanals, P. Manesiotis, D. C. Sherrington and P. A. G. Cormack, *Advanced Materials*, (2008), **20**, 1298.

Synthesis and in vitro biocompatibility of copolymers, telomers, and hydrogels of polyvinylpyrrolidone with sulphonic and carboxylate groups

M. Gómez-Tardajos[1], C. Elvira[1], Y. Rochev[2], H. Reinecke[1], A. Gallardo[1].

[1]Instituto de Ciencia y Tecnología de Polímeros, Consejo Superior de Investigaciones Científicas, CSIC, Spain.
[2]National Centre of Biomedical Engineering Science, National University of Ireland, Galway, Ireland.

tardajos@ictp.csic.es

Introduction

Polyvinylpyrrolidone (PVP), a well known biocompatible polymer, is a water-soluble amphiphilic nontoxic polymer commonly used in a wide range of applications in the pharmaceutical and nutritional area, cosmetics, personal hygiene, paintings, etc.

However, PVP lacks reactive groups, which limits the possibility of adding new functions to the polymer in order to modify its physical and chemical properties. Our group has recently developed a strategy that allows preparing vinylpyrrolidone (VP) functionalized with sulphonic groups [1]. VP containing carboxylate groups was prepared based on the method described by Bencini et al. [2]. These two monomers were copolymerized with VP in order to obtain functionalized PVP by a bottom-up approximation.

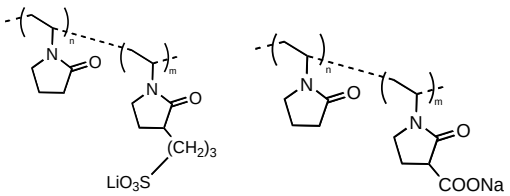

Fig1: Structure of the polymers.

Copolymer, telomers and hydrogels were prepared using these new compounds. The aim of the present work was to study their biocompatibility in order to check them for potential applications as biomaterials.

Materials and Methods

The copolymers were synthesized by free radical polymerization in water with AIBN as initiator. The molar amount of modified VP was ranging from 0 to 100%. Nitrogen was flushed through the polymerizing solution for 30 min. The polymers were purified by dialysis using membranes with pore-size of Mw cut-off 3500.

The telomers were synthesized by free radical polymerization in water with AIBN as initiator and isopropylmercaptan as transfer agent. The molar amount of modified VP was 5 and 10%. Nitrogen was flushed through the polymerizing solution for 30 min. The polymers were purified by dialysis using membranes with a pore-size of Mw cut-off 800.

The hydrogels were prepared by photopolymerization with Ciba-Geigy Irgacure 369 as initiator using the novel crosslinker shown in figure 2. Different hydrogels were obtained by changing the molar amount of modified VP and crosslinker.

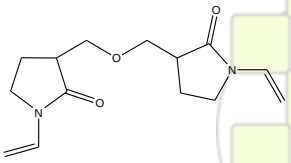

Fig 2: Structure of the new Crosslinker.

The biocompatibility was tested in vitro in fibroblasts 3T3 letting the cells grow for 24 hours and then adding the water soluble polymers and incubated them for another 24 hours. The results were analyzed by using the Alamarblue assay, based on the reduction of the reactive once it gets into the living cells, and the Picogreen assay based on the amount of remaining DNA after a few cycles of freezing and thawing of the cells.

Results and Discussion

Copolymers with Mn between 2.3-10x10^4 KDa, telomers with Mn between 8-1.5x10^3 KDa (calibration of SEC was carried out with PEG standars in water) and hydrogels with 1 and 10 molar % of crosslinker were obtained. The chemical structures were confirmed by conventional techniques such as ^{1}H-NMR and FTIR. All the copolymers and telomers show high level of biocompatibility in the range of concentration indicated in figure 3 for both assays and the difference between control and highest concentrations are not significantly different.

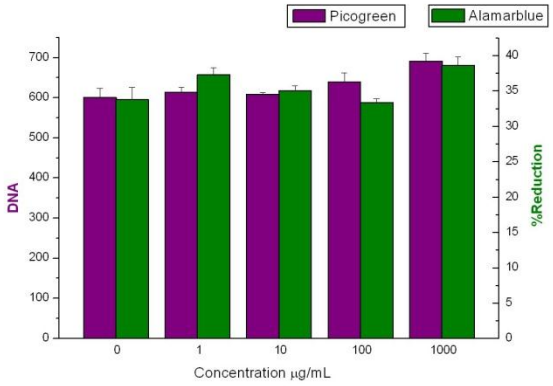

Fig 3: Alamarblue and Picogreen results of one copolymer.

The hydrogels also show no cell adhesion due to the hydrophilicity of the chemical structure.

Conclusions

The new copolymers, telomers and hydrogels were as biocompatible as PVP. The new functionalities of the PVP bases polymers can furthermore be safely used in biological environment.

References

[1] M. Pérez Perrino. European Polymer Journal 2010, 46, 1557-1562.

[2] M. Bencini. Macromolecules 2005, 38, 8211-8219.

Acknowledgements

Authors gratefully acknowledge MICINN the financial support provided by project MAT2007-63355 and for M. Gómez PhD scholarship.

Addition of Polymer to Viscoelastic Solutions of Living Micellar Chains

Pletneva V.A., Molchanov V.S., Philippova O.E.

Physics Department of Moscow State University

molchan@polly.phys.msu.ru

Introduction. Due to hydrophobic aggregation surfactant molecules are able to form enormously long wormlike micelles (also known as living chains) in water medium in the presence of salt. These surfactants are widely used to tune viscoelastic properties of solutions. It was demonstrated that in some cases the addition of polymer chains can increase significantly the viscoelasticity of the surfactant solution. The hydrophilic polymer having hydrophobic side groups can interact with wormlike micelles forming a common network in the system. The present paper is focused on the study of the influence of polymer structure and its concentration on the rheological properties of surfactant/polymer solutions.

Materials. Potassium oleate was used as the surfactant and hydrophobically modified polyacrylamide (HM PAAm) was used as the polymer. Living chains of the surfactant were obtained by adding salt (potassium chloride) screening repulsion on the surface of the micelles.

Method. Viscoelastic properties of the solutions were examined by means of Haake rheometer RS 150.

Results and Discussion.

It was shown that the addition of HM PAAm leads to the increase of the viscosity, the elastic modulus and the frequency range of elastic response of the system (G'>G''). To study the effect of molecular weight of polymer on the rheological properties of surfactant/polymer system we used two polymer samples of the same composition with the following molecular weights: $0.14 \cdot 10^6$ g/mol (short polymer) and $1.17 \cdot 10^6$ g/mol (long polymer). First, the effect of the addition of small amount (0.2 wt.%) of polymer was studied. This concentration is close to the overlap concentration of polymer chains C* estimated for the long polymer. At the same time, it is well below the C* for the short polymer. So, at this concentration the polymer chains interact only with micelles. As it could be expected the viscosity of surfactant/polymer solution with long polymer is higher than that for the system with short polymer. This result can be explained as follows. On the one hand, the long polymer links more micelles, on the other hand, it has a longer relaxation time. This explanation is confirmed by the increase of the elastic modulus (indicating to higher number of entanglements) and the increase of the frequency range of elastic response.

Next we studied surfactant/polymer system at higher concentration of polymer (1.2 wt.%), which is close to C* concentration of short polymer. At these conditions the effect of molecular weight of polymer on the rheological properties becomes more pronounced. This may be explained by the fact that at this concentration the chains of long polymer entangle with each other, which increases the total number of entanglements in the system. Thus, it was shown that the rheological properties of the surfactant/polymer solution depend essentially on the molecular weight of polymer.

At the next stage of the research the influence of the content of hydrophobic groups of the polymer on the rheological properties of the surfactant/polymer solution was examined. For this purpose two polymer samples with different number of hydrophobic groups 0.5 mol.% and 1.0 mol.% were used, other characteristics of the polymers being identical. The concentration of polymer was chosen close to C* value: 0.3 wt.%. It was shown that with increasing content of hydrophobic groups in the polymer the viscosity increases by one order of magnitude, the elastic modulus increases by a factor of 5 and the range of elastic response becomes much larger. All these effects may be explained by the formation of additional crosslinks due to penetration of larger number of hydrophobic groups in the micelles. Thus, it was proved that the number of hydrophobic groups directly controls viscoelastic properties of surfactant/polymer solutions.

Hereafter, the effect of polymer concentration was studied while surfactant content was fixed. The polymer concentration varied from 0.1 wt.% (below C*) to 1.5 wt.% (above C*). Above overlap concentration side groups of polymer chains can form hydrophobic domains. It was observed that the viscosity and the elasticity increase significantly with increasing concentration of polymer.

Conclusions. Thus, it can be concluded, that the addition of HM polymer into wormlike micelles solution can significantly change viscoelasticity, the effect being depending on the structure and the content of the polymer.

Acknowledgement. This publication was based on the work supported by Award No KUK-F1-034-13, made by King Abdullah University of Science and Technology (KAUST).

Copolymerization of Monomer Systems Based on N-vinylpyrrolidonefor Advanced Applications

[1]Soloveva D.O., [2]Zaitseva V.V., [2]Shtonda A.V., [2]Tyurina T.G., [2]Opeida I.A., [1]Zaitsev S.Yu.

[1]Moscow State Academy of Veterinary Medicine and Biotechnologies
[2] Institute of Physical - Organic and Coal Chemistry of the Ukraine National Academy of Sciences

e-mail: d.solovieva@mail.ru

Introduction:
Design of the polymer materials for advanced application is an actual problem of the polymer and physical chemistry, modern technology and chemical engineering. One of the ways of its decision is the copolymerization of various vinyl monomers and obtaining the materials with desirable properties [1, 2].

Materials and Methods:
Copolymerization of N-vinylpyrrolidone (VP) with maleic anhydride (MA) and methylmethacrylate (MMA) in bulk in the presence of benzoil peroxide (Fig.1, curves 1, 3, 4, 6-8) and in its absence (Fig.1, curves 3, 5, 9) was performed. The copolymer conversion was studied by ^{1}H NMR (Fig.1, curves 1, 3, 4) spectroscopy (DMSO d_6, TMS, 400 MHz), dilatometry (Fig.1, curves 2, 5, 6, 9) gravimetry (Fig.1, curves 7, 8) methods.

Results and Discussions:
Monomer interaction with each other and with benzoil peroxide was shown by UV-spectroscopy, ^{1}H- and ^{13}C-NMR methods. The structures of molecular complexes were calculated. Dilatometry curves (Fig.1) of the copolymerization procedure show the acceleration effect which is connected with participation of all monomers (especially N-vinylpyrrolidone) in the process. There are some formation of cooligomers in addition to copolymers were found. The numerous effects were found by gravimetry and the analysis of solutions after deposit allocation after clearing of the basic product [1,2]. According to a monomer expenditure through the set time intervals the reaction rates of the formation of copolymers and cooligomers were defined. The model of copolymerization, the description of the general rate of process and structure of copolymers was proposed.

Table 1. Parameters of copolymerization based on vinylpyrrolidone (VP), maleic anhydride (MA), methylmethacrylate (MMA).

τ, min	S_{summ},.%				Copo-lymer + cooli-gomer
	NMR	Dilato-metry	Gravi-metry	Oligo-mers (NMR)	
VP - MA					
0	0	0	0	0.000	0
20	3.63	2.56	0	0.24	0.24
52	5.22	7.59	5.62	0.95	6.57
69	7.19	9.2	6.06	1.90	7.96
126	10.65	12.93	7.54	3.91	11.95
VP - MMA					
0	0	0	0	0	0
30	2.53	0.84	0.80	0.99	1.79
71	5.75	5.36	4.07	1.74	5.82
94	7.11	6.92	4.96	2.86	7.92
144	10.98	9.12	7.02	4.84	11.86

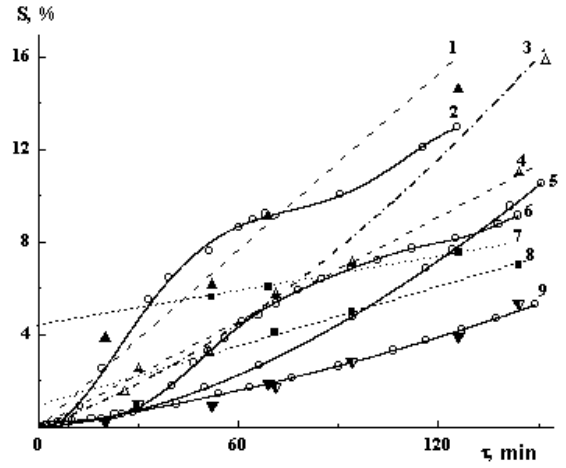

Figure 1. Dependence of copolymers and oligomers conversion (S) vs time (τ).

Conclusions:
Thus, preparation of special copolymers with some biological activity were obtained and studied. Such copolymers are promising for application in bioengineering and biotechnology, human and animal medicine.

References:
1. S.Yu. Zaitsev, V.V. Zaitseva. Supramolecular chemistry. Part 1. Molecular complexes in the radical copolymerization. Monograph. - Moscow – Donetsk: Moscow State Academy of Veterinary Medicine and Biotechnology, 2009. (in Russian)
2. S.Yu. Zaitsev, V.V. Zaitseva. Supramolecular chemistry. Part 2. Complex-radical copolymerization. Monograph. - Moscow – Donetsk: Moscow State Academy of Veterinary Medicine and Biotechnology, 2010. (in Russian)

A Study Of Cationic Polymerization Of 1-(2-Hydroxyethyl)aziridine

Asta Šakalytė[1], José Antonio Reina[2], Marta Giamberini[1]*

1. Departament de Enginyeria Química, Universitat Rovira i Virgili, Av. Països Catalans, 26 Campus Sescelades, 43007 Tarragona, Spain
2. Departament de Química Analítica i Química Orgànica, Universitat Rovira i Virgili, Carrer Marcel·lí Domingo s/n, Campus Sescelades, 43007 Tarragona, Spain

marta.giamberini@urv.cat

Introduction

Hydroxylated polymers can be regarded as powerful precursors in the preparation of new polymers through chemical modification, which can finally lead to properly functionalized macromolecules for specific applications. According to this approach, polymers like poly(vinyl alcohol) (PVA) and poly(glycidol) have been extensively used in order to get hydrogels, membranes, emulsifiers, stimuli-responsive materials, etc.

Polyamines can be prepared by ring opening polymerization of aziridines and azetidines, through a cationic mechanism, as only the three- and four-member rings contain enough ring strain to be polymerized. This polymerization reaction proceeds with the competition of many undesirable side reactions such as proton transfer termination, branching and macrocycle formation. Proton transfer termination can be avoided by using tertiary amines as monomers, but the other two undesirable reactions can be only reduced by means of an appropriate choice of the monomer structure and the polymerization conditions. For this reason, the polymerization of each aziridine and azetidine implies a deep optimization of the reaction conditions[1].

In this work we tackle the polymerization of a hydroxylated aziridine, 1-(2-hydroxyethyl)aziridine, which could lead to a suitable starting polymer in the preparation of more complex polyamines through its chemical modification. In particular, we are finally interested in the preparation of Side-Chain Liquid Crystalline polyamines (SCLCPs) by chemical modification with tapered groups.

Materials and Methods

All reagents (1-(2-hydroxyethyl)aziridine (95%), boron trifluoride diethyl etherate (46,5% BF_3 basis), boron trifluoride ethylamine complex, lanthanum trifluoromethanesulfonate (99,9%), scandium trifluoromethanesulfonate (99%), methyl trifluoromethanesulfonate (98%), ethylamine (2.0 M solution in THF) trimethylsulfonium iodide (98%), triphenylcarbenium hexachloroantimonate, triethyloxonium tetrafluoroborate, benzylamine (99%)) were supplied by Fluka or Aldrich and used as received.

Solvents (acetonitrile, N,N-dimethylformamide) were purified according to the literature[2].

The obtained polymers were characterized by viscosity determination, Infra-red spectroscopy (IR), Differential Scanning Calorimetry (DSC), Thermogravimetric Analysis (TGA) and ^{1}H and ^{13}C NMR. By taking advantage of the extremely regular structure of the main chain, we also recorded the ^{15}N NMR which, in this case, allowed us to detect end groups and branching points and to exclude side reactions arising from the hydroxyl groups.

Results and Discusion

The polymerization of 1-(2-hydroxyethyl)aziridine was reported by Rivas et al.[3] in the early 90's by using $BF_3 \cdot Et_2O$ but, though the reported ^{1}H and ^{13}C NMR spectra showed the expected signals as prevailing, they also showed small signals which were not discussed by the authors and which arise from end groups, branching or macrocycle formation, as well as side reactions which involve the participation of the hydroxyl group. In this study we deepened the cationic polymerization of this monomer by using several initiators ($BF_3 \cdot Et_2O$, $BF_3 \cdot EtNH_2$, $La(OTf)_3$, Methyl triflate, etc.) in order to obtain polymers with a variety of molecular weights and backbone macrostructures, since these features can strongly affect the mesomorphic behaviour of side-chain liquid crystalline polymers to be subsequently synthesized.

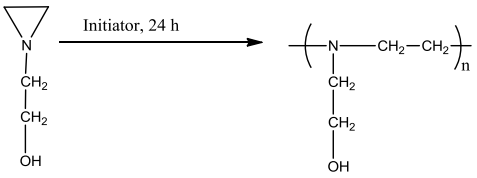

Conclusions

Polymerization with boron trifluoride amine complex gave the best results as far as the obtainment of a polyamine with linear structure and a moderate molecular weight is concerned. The obtained polymers will be used for further preparation of Side-Chain Liquid Crystalline polyamines containing mesogenic groups, which can lead to supramolecular columnar mesophases; in such structures, the polymer backbone is expected to form a helical structure, which gives the ability to transport proton ions by the channel mechanism.

References

1. E. J. Goethlas, J. M. Geeraert, in Plastics Engineering (New York), Macromolecular Design of Polymeric Materials, 1997, 40, 223-246.
2. B. S. Furniss and et. al Vogel's Textbook of Practical Organic Chemistry fith edition, Pearson Education, 1989, 395-412.
3. B. L. Rivas, K. E. Geckeler, E. Bayer, European Polymer Journal, 1991, 27, 1165-1169.

Aknowledgements

The authors would like to thank Ministerio de Ciencia e Innovación (MAT2008-00456) for providing financial support for this work.

Homeotropic Alignments of Nematic Liquid Crystals on Polar Substrates

Young Ju Kim, Mongryong Lee, and Kigook Song

Materials Research Center for Information Display, Kyung Hee University, Korea

ksong@khu.ac.kr

Introduction

The alignment of a liquid crystal molecule on a substrate depends on various interactions between liquid crystal and substrate, such as dispersion forces, dipolar interactions, steric interactions, and physical interactions due to distortion of orientation field of liquid crystals. These forces act oppositely sometimes and which interaction is dominant depends on the prevailing circumstances. Among those interactions, dispersion force (van der Waals force) is regarded as a long-range interaction and other interactions are regarded as short-range interactions which never go beyond a few tens of angstrom. In the present study, homeotropic alignment mechanisms of nematic liquid crystals on polar substrates were investigated. The relations between homeotropic alignment of liquid crystals and polarity of substrates were studied using polarized optical microscopy, conoscope, and FTIR spectroscopy.

Results and Discussion

Both positive LC (E7 Merck, $\Delta\varepsilon$=13.8) which is a mixture of cyano group liquid crystals and negative LC (LC-242 BASF, $\Delta\varepsilon\approx$-1.8) show homogeneous (planar) alignment on a glass substrate without any treatment. After glass substrates were treated with oxygen plasma, however, positive E7 were still aligned homogeneously whereas homeotropic (vertical) alignment was introduced for negative LC-242. After the plasma treatment, polarizability of the glass substrate along the surface increases by forming hydroxyl groups. In order to get more overlap areas in long-range van der Waals interactions between polarizability of liquid crystal molecules and that of the glass surface, positive E7 molecules (longitudinal dipole moment) prefer to align along the planar direction whereas vertical alignments are observed for negative LC-242 molecules whose polarizability direction is perpendicular to the molecular axis (transverse dipole moment).

As shown in Figure 1, FTIR absorption intensity of C≡N stretching mode (2226 cm^{-1}) of E7 decreases by changing its phase from isotropic to LC phase at 59°C. On untreated glass substrates, the C≡N stretching intensity of E7 becomes a maximum at near transition temperature (58.2°C). However, the peak intensity abruptly decreases and exhibits a minimum at near the transition temperature for E7 on a plasma treated substrate. These findings suggest the orientation changes of the LC director upon the phase change in which E7 momentarily shows homeotropic orientations. These results are good agreement with POM observations.

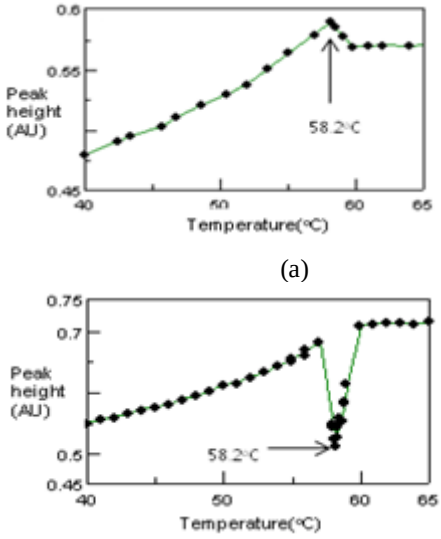

Figure 1. FTIR intensity of C≡N stretching mode (2226 cm^{-1}) of E7 with temperature. (a) for LC on untreated glass substrate, (b) for LC on plasma treated substrate.

Two competing temperature dependent forces are involved in determining the LC director orientation; one that prefers the homogeneous and the other homeotropic orientations. The long range van der Waals forces play an important role in deciding the orientation of LC director in a nematic temperature region, while the short range dipolar interaction becomes more important as the substrate becomes more polar with increased plasma treatments. At the transition temperature, highly polar nitrile group of E7 makes the long molecular axis aligned vertically by strong dipolar interaction with polar substrates. The orientation changes from vertical to planar alignments as further decreasing temperature can be explained by increasing van der Waals interaction due to increase dielectric anisotropy of liquid crystals.

Conclusions

The homeotropic alignment mechanisms for nematic liquid crystals were studied on polar substrates. The homogenous alignment was obtained for positive nematic liquid crystals while the homeotropic alignment for negative liquid crystals. These studies provide experimental evidences showing that there is competing forces to determine orientation of liquid crystals, and alignment can be controlled by adjusting substrate polarity.

Surface properties of silica modified by silane with polybutadiene oligomer tail

Maila Castellano[1], Antonio Turturro[1], Alessandro Bertora[1], Enrico Marsano[1], Lucia Conzatti[2], Giovanna Colucci[3]

[1] Dipartimento di Chimica e Chimica Industriale, Università di Genova- Via Dodecaneso, 31- 16146 Genova- Italy
[2] Istituto per lo Studio delle Macromolecole, ISMAC-CNR - Via de Marini, 6 - 16149 Genova- Italy
[3] Dipartimento di Scienza dei Materiali e Ingegneria Chimica, Politecnico di Torino - C.so Duca degli Abruzzi, 24 – 10129 Torino- Italy

maila.castellano@unige.it

Introduction

Chemical modification of surface of oxide powders by covalent attachment of organosilanes is a versatile technique to tune surface properties, on the grounds of different requirements and specific applications. In the polymer field such a modification plays an important role in promoting adhesion between powder and polymer, in improving the disperdibility of oxide powders into polymer matrix, etc.. The dispersion of silica in a rubbery matrix is an indispensable condition to obtain compounds with high physical-mechanical performance. However, the high hydrophilic character of silica makes it very difficult to spread it into an array of hydrophobic rubbery. Therefore, alkoxysilanes, like TESPT (bis(triethoxysilylpropyl)tetrasulfide) and NXT (3-octanoylthio-1-propyltriethoxysilane), are currently used to reduce the hydrophilicity of silica surface and to prevent the formation of particle aggregates. Alkoxy groups of silane condense with free silanols of silica surface, giving rise to Si-O-Si surface. The accessability and then the reactivity of silanols is probably not the same for all of them, and will also depend both on alkoxysilane molecule size and on the number of alkoxy groups present in the same silane molecule.

For several years, our research group has devoted research activity to investigate the influence of the silica modification on the rubber reinforcement (1,2,3).
In this communication, we discuss the surface thermodynamic properties of silica modified with two new alkoxysilanes, prepared by us, with a polybutadiene oligomer tail. The long hydrocarbon chain should facilitate the dispersion of silica into the rubber matrix, due to its high compatibility with the elastomer matrix, as shown in another communication (4). Moreover, polybutadiene tail would have an enhanced reactivity for a new technology of vulcanization of rubber in the tire industry, like irradiation or peroxides.

Materials and Methods

Two new silanes, sb1 and sb3, were prepared by grafting 3- mercaptopropyltrimethoxysilane onto poly-butadiene oligomers of about <Mn> = 900 and 5000 , respectively. Sylilation of precipitated silica Zeosil 1165 MP (Rhône Poulenc) with sb1 and sb3 was performed in accordance with the method described elsewhere (1).
Degree of grafting on the silica was determined by thermal gravimetric analysis (TGA) and elemental analysis (EA), ranging from 4 to 40 wt%. Modified silica was investigated as the stationary phase by inverse gas chromatography (IGC) (1,2). n-alkanes, 1-alkenes, and alkylbenzenes were used as probes for the determination of thermodynamic properties of silica surface. The IGC measurements were performed in the range 80-160°C. Thermodynamic quantities of adsorption, like $\Delta G°$, $\Delta H°$, and $\Delta S°$ were determined, together the dispersive component, γ_s^d , and the interaction parameter, I^{sp}, of surface tension of modified silicas.

Results and Discussion

To determine the real grafting degree onto silica, the loss weight by TGA and the C wt-% of grafted silane obtained by EA were considered. From the real grafting degree the residual OH silanol percentage was calcula-ted. This ranges from about 65 to 98%. The adsorption free energy on the silicas is heavily affected by the sylilation with sb1 and sb3, and then the surface free energy. Both the dispersive component γ_s^d and the interaction parameter are reduced to a half after the graft of about 10 wt% of sb1 or sb3 and do not change more on increasing the degree of grafting. By considering the number of grafted molecules /nm^2 the role of the polybutadiene tail length is clearly put into evidence; in other words, the long hydrocarbon tail acts as a shield, hindering interactions between probe and residual OH silanol groups of silica surface. This phenomenon permits a reduction in the amount of silane to be grafted to decrease the polar character of silica surface.

Conclusions

Silanes sb1 and sb3 are able to change the character of silica surface from hydrophilic to hydrophobic, as a result of very low silane grafts. Moreover, on increasing the length of silane tail decreases the number of silane molecules to be grafted. When sb3 is used , the sylilation of about 5% of OH silanol groups is enough to practically obtain the hydrophobic character of silica.

This work was supported by the Italian National Program MIUR-ELASTORAD FIRB 2006 and Pirelli Tyre S.p.A.

References

1) M. Castellano, L. Conzatti, G. Costa, L. Falqui, A. Turturro, B. Valenti, F. Negroni Polymer, 2005,46,695
2) M. Castellano, L. Conzatti, A. Turturro, G. Costa, G. Busca, J. Phys. Chem. B , 2007, 111, 4495
3) A. Bertora, M. Castellano, E. Marsano, M. Alessi, L. Conzatti, P. Stagnaro, G. Colucci, A. Priola, A. Turturro Macromol. Mater. Eng. 2011, 296,000
4) M.Castellano, A. Turturro, E. Marsano, A. Bertora, P. Stagnaro Abstract EPF 00829

Reinforcement of SBR with silica modified by silane with polybutadiene oligomer tail

Maila Castellano[1], *Antonio Turturro*[1], *Enrico Marsano*[1], *Alessandro Bertora*[1], *Paola Stagnaro*[2]

[1] Dipartimento di Chimica e Chimica Industriale, Università di Genova - Via Dodecaneso, 31- 16146 Genova- Italy [2] Istituto per lo Studio delle Macromolecole, ISMAC-CNR - Via de Marini, 6 - 16149 Genova- Italy

maila.castellano@unige.it

Introduction

The reinforcement of rubber means the pronounced increase of tear resistance, tensile strength, abrasion resistance and modulus far beyond the values predicted by the theory. It is generally accepted that this phenomenon depends, to a large extent, on physical and chemical characteristics of the elastomer, filler properties (loading, particle size, specific surface area, structure, surface activity, etc..), and processing.

It has been found that precipitated silicas improve performances of the tire tread, increasing wet grip and decreasing rolling resistance, and thus the fuel consumption. These improvements are achieved only if the silica is highly dispersed in the elastomeric matrix. This is obtained by reducing the highly hydrophilic character of silica particles preventing the phenomenon of aggregate formation. To do this some silanes, like bis(triethoxysilylpropyl)tetrasulfide (TESPT), and 3-octanoylthio-1-propyltriethoxysilane (NXT and NXT Z silanes) have been proposed and are currently applied. We have suggested that an interesting new modifier of silica could be an alkoxysilane with an oligomer polybutadiene tail (1). Such a modifier should facilitate the silica dispersion into SBR matrix, due to its compatibility with the elastomer matrix, and would have an enhanced reactivity for a radical process vulcanization to be performed by thermal initiators (for instance, peroxides) or irradiation. To this end, we have prepared two new modifiers by grafting 3-mercaptoprop-yltrimethoxysilane onto polybutadiene oligomers. Surface thermodynamic properties of a precipitated silica modified with such silanes are reported in another communication (2).

In this communication we present results concerning the curing kinetics, tensile, and dynamic-mechanical properties of compounds of e-SBR /silica modified with aforementioned new silanes.

Materials and Methods

The new alkoxysilanes coupling agents, sb1 and sb3, were prepared by grafting 3-mercaptopropyltrime-thoxysilane onto polybutadiene oligomers of about <Mn> = 900 and 5000 , respectively. Precipitated silica Zeosil 1165 MP (Rhône Poulenc) was modified with sb1 and sb3 according to a procedure previously described (3). e-SBR-based compounds were prepared by mixing e-SBR with 30 phr of carbon black , 30 phr of silica modified with several degrees of grafting, and all the ingredients used in tire production. Silica was used unmodified, modified with TESPT during mixing, modified with sb1 or sb3 during the mixing, and pre-modified with sb1 or sb3.

The compounds were characterized by vulcanization kinetics, tensile testing at low (10%) and high (300%) deformation, dynamic-mechanical behaviour (G*, G', G'', tanδ) as a function of temperature and strain , and morphological observation by transmission electron microscopy.

The results are compared with those of the compound loaded with silica modified with TESPT.

Results and Discussion

Silanes with long chains of polybutadiene act as a plasticizer of e-SBR matrix ; they, moreover, negatively affect the scorch time, but speed up the process of curing , leading to the same final crosslink density of compound loaded with TESPT-modified silica.

sb1 and sb3 silanes have hardly any effect on the tensile properties of compounds; however, they reduce the value of G' modulus at low deformation leading it to a practically constant value at 10% of strain . In other words, they facilitate the dispersion of silica into e-SBR matrix, reducing the Payne effect , i.e. the interactions filler-filler. The extent of such an effect depends on length of polybutadiene tail, on the degree of grafting of silica, and on the procedure of silica grafting.

Conclusions

These results indicate that the new silanes are technologically interesting coupling agents, that could be an alternative to currently used silanes. Work is still in progress to evaluate the minimum amount of sb1 or sb3 silane, sufficient to provide a hydrophobic silica to prepare rubber-based compounds, with high silica content for interesting technical developments in the future, for instance, vulcanization by irradiation or thermal initiators.

This work was supported by the Italian National Program MIUR-ELASTORAD FIRB 2006 and Pirelli Tyre S.p.A.

References

1) A. Bertora, M. Castellano, E. Marsano, M.Alessi, L. Conzatti, P. Stagnaro, G. Colucci, A. Priola, A. Turturro Macromol. Mater. Eng.
DOI: 10.1002/mame.201000335

2) M. Castellano, A. Turturro, A. Bertora, E. Marsano, L. Conzatti, G. Colucci , Abstract EPF 00828

3) G. Costa, G. Dondero, L. Falqui, M. Castellano, A.-Turturro, B. Valenti, Macromol. Symp. 2003,193,195

Modulation of the Charge Carrier Transport in Conjugated Polymers by Means of Polar Additives

Petr Toman,[1] Wojciech Bartkowiak,[2] Jiří Pfleger[1]

[1] Institute of Macromolecular Chemistry, Academy of Sciences of the Czech Republic, Heyrovský Sq. 2, 162 06 Prague 6, Czech Republic

[2] Institute of Physical and Theoretical Chemistry, Wrocław University of Technology, Wyb. Wyspiańskiego 27, 50-370 Wrocław, Poland

e-mail: toman@imc.cas.cz

Introduction

Recently, a great deal of the scientific interest was devoted to the research into different types of polymer-based photoswitching systems because of their potential use as elements of future logic and memory devices [1,2]. Conjugated polymers, like poly(phenylene vinylene) and polythiophene derivatives, possess excellent semiconducting and luminescent properties accompanied by relatively easy processing and low cost. Charge carrier transport in these materials proceeds predominantly along the conjugated polymer backbones with the participation of the inter-chain hopping. If the frequency of the external electric field is not too high, the slow inter-chain motion acts as a bottleneck determining the macroscopic charge carrier mobility. In this paper, a combined quantum mechanical / semi-classical model of the charge carrier transport in polymers doped by a polar additive is put forward.

Model and Methods

The proposed model involves the quantum mechanical description of the charge carrier states on the conjugated polymer chain segments, the charge carrier thermalization, and the semi-classical description of the charge carrier hops between different chain segments.

The conjugated chain segments are modeled as sequences of interacting sites corresponding to the repeat units. The charge carrier states on such a segment can be described by the tight-binding Hamiltonian. Taking the wave function as a superposition of the states located at individual sites, the time-independent Schrödinger equation can be solved and the stationary states can be found.

The model considers full charge carrier thermalization over all states of the given chain segment between two subsequent hops. This thermalization is usually accomplished within several picoseconds. Thus, it is much faster than the inter-chain hopping. Our model can assume alternatively the charge carrier thermalization either to the Fermi-Dirac distribution, or to the more simple Boltzmann distribution, that is appropriate for low charge carrier concentrations. While the former distribution is useful for the modeling of the charge carrier concentration dependence of the dc mobility, the latter one enables to calculate the frequency dependence of the ac mobility.

Description of the inter-chain charge carrier jumps is based on the Marcus theory. The use of the quasi-classical Marcus concept instead of the quantum mechanical one is justified by the fact that the inter-chain transfer integrals are much smaller than the charge carrier reorganization energy. Consequently, due to its interaction with the phonon reservoir the charge carrier residing on a given chain segment looses any quantum coherence before jumping to another segment. Finally, our model solves master equations determining the time evolution of the charge carrier distribution.

Results and Discussion

The hole transport in two conjugated polymers (poly(phenylene vinylene) and polythiophene) doped with a polar photochromic additive (spiropyrane derivative) was calculated. Upon irradiation with light of an appropriate wavelength, the admixed molecule undergoes a ring-opening reaction from the closed form to the open form, which is accompanied by a charge redistribution resulting in a two- or three-fold increase of the molecular dipole moment. It was found, that the photochromic transformation of the additive results in a broadening of the distribution of the local charge carrier site energies and, consequently, in the decrease of the inter-chain hole dc mobility by two or three orders of magnitude at the experimentally achievable concentrations of the additive. While the mobility in the polymer with a low value of the local energy disorder (low additive concentration or low additive dipole moment) is frequency-independent, for higher values of the local energy disorder there is a certain increase of the mobility with the frequency. The calculated temperature dependence of the mobility shows essentially Arrhenius–type behavior with a moderate sub-Arrhenius deviation at the low additive concentration and the low-temperature saturation at the high additive concentration.

Conclusions

The results confirm the possibility to construct an efficient optoelectrical modulator based on a polymer doped with a photochromic polar additive. The proposed model can be used for the selection of suitable molecular systems and finding the optimal conditions in order to improve the device performance.

Acknowledgement

This work was supported by the Czech Science Foundation (Project No. P205/10/2280), by the Ministry of Education, Youth, and Sports of the Czech Republic and the Polish Ministry of Science and Higher Education (Project No. MEB051010, Czech-Polish cooperation), and by the Wroclaw University of Technology.

References

[1] Carter FL, Siatkowski RE, Wohltien H (Eds.). *Molecular Electronic Devices*, 1988. North-Holland, Amsterdam.

[2] Kawai T, Nakashima Y, Irie M. *Adv. Mater.* 2005; 17: 309-314.

Thermal and mechanical properties of flexible bioplastics based on modified starch and gelatin

Farayde Fakhouri [1], Rodolfo C. de Jesus[2], Daryne L. Costa[3], Fabio Yamashita[1], Lúcia H. Innocentini-Mei[2], Fernanda P. Collares-Queiroz[2]

1 –Londrina State University. Department of Food Technology, Faculty of Agricultural Sciences, Londrina, Brazil
2- Faculty of Chemical Engineering, Campinas State University, Cidade Universitária Zeferino Vaz, 13083- 852 -Campinas, Brazil
3 – Departament of Chemistry and Enviromental Area, UNED Bela Vista, CEFET-MT, Cuiabá – MT, CEP 78000-000, Brazil- . 3 Department of Food Science and Technology

farayde@gmail.com

The use of edible and biodegradable films is a good alternative to replace part of those polymers made from non renewable raw material used in the market. In this work, we developed flexible bioplastic composites based on lipophilic corn starch and gelatin plasticized with glycerol (20% compared to the mass of starch), obtained by thermoplastic extrusion process, followed by blowing for film formation. Different concentrations of gelatin were added (0%, 10% e 20% w/w) to follow the behavior of mechanical properties. The mechanical (tensile strength and elongation) and thermal properties (Thermogravimetric analysis, Differential Scanning Calorimetry and Termodynamic mechanical analysis were characterized for all biofilms studied. Balloons of 12 to 14.5 cm in diameter were formed by blowing and, at nacked aye did not show insoluble particles or fractures (Figure 1).

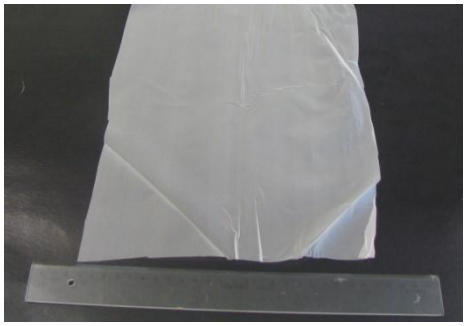

Figure 1. Biofilms

As expected, the addition of gelatin resulted in an increase of mechanical properties of the biofilms in longitudinal and transversal directions (Figure 2).

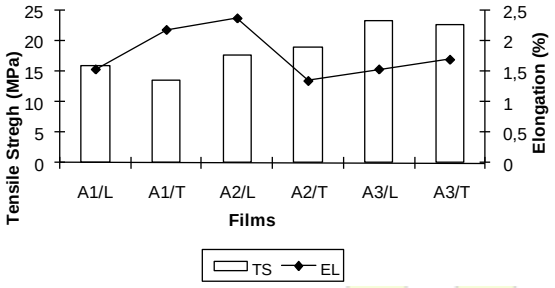

Figure2. Mechanical Properties

The thermal analyses showed that the behavior of the glass transitions of these bioplastics are very similar (Figure 3).

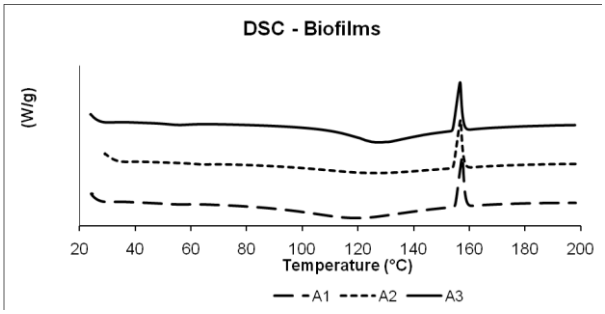

Figure 3. Differential Scanning Calorimetry

Desarrollo de una espuma polimérica atóxica con propiedades de resilencia

Julieta Heba[1], Cynthia García[1], Leonardo Warcok[1], María Gómez[2], Marta Calatayud[1], Omar Ferré[2]

Instituto Nacional de Tecnología Industrial (INTI), [1]INTI Química, [2]INTI Caucho, Bs. As., Argentina

martac@inti.gob.ar oferré@inti.gob.ar

Introducción: Las úlceras o escaras de la piel representan un grave problema que afecta a las personas inmovilizadas ya que se forman por la presión y el contacto prolongado de la piel con el material de apoyo. Para evitarlas se intenta que el material de soporte y apoyo actúe como un intercambiador de calor, enfriando y evitando el aumento de temperatura de la piel en contacto.
Con el objetivo de conocer la composición de este tipo de materiales de soporte para desarrollar un material polimérico similar, a base de materias primas nacionales y/o disponibles en el país, se estudió una espuma o masilla blanda que conforma el relleno de un almohadón "antiescaras" utilizado como asiento de automóviles para discapacitados. Según la bibliografía consultada el material investigado debería tener una composición atóxica y resistente al fuego, además de consistir en un material deformable ante la aplicación de presión externa y adaptable al contorno particular del cuerpo humano.

Materiales y métodos: La espuma polimérica original y fracciones de la misma, obtenidas aplicando diversas técnicas de separación, se analizaron por espectroscopía infrarroja (IR), resonancia magnética nuclear de protón (^{1}H RMN), de carbono (^{13}C RMN) y por correlaciones nucleares (COSY, HMQC y HMBC), así como por fluorescencia (XRF) y difracción de rayos X (XRD).

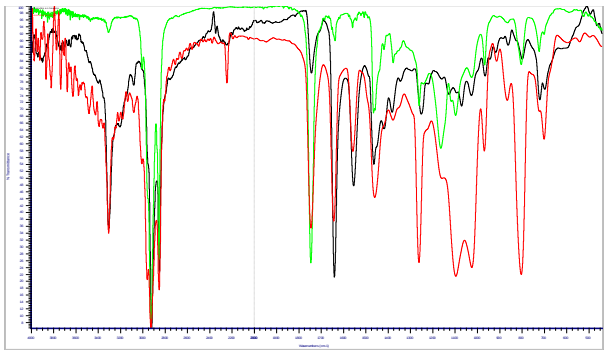

Figura 1. Comparativo por FTIR de la fracción de la muestra soluble en cloroformo (verde) vs. la fracción insoluble en hexano (negro) y vs. la fracción insoluble en etanol (rojo).

La identificación general se realizó por IR, utilizando un equipo FTIR Nicolet Impact 400D. La figura 1 muestra algunos de los espectros logrados.
Del análisis de las diferentes fracciones obtenidas, resulta útil y representativo realizar un examen comparativo entre los respectivos espectros ^{1}H RMN. Para estos registros se utilizó un equipo Bruker Avance DPX 400 con sonda multinuclear de gradiente.
La figura 2 muestra la comparación entre tres de las fracciones antedichas.

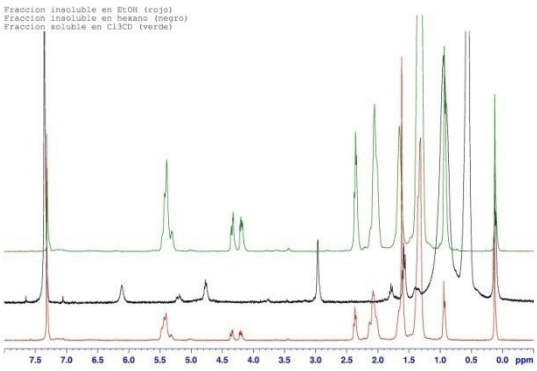

Figura 2. Comparativo ^{1}H RMN de la fracción de la muestra soluble en cloroformo (verde) vs. la fracción insoluble en hexano (negro) y vs. la fracción insoluble en etanol (rojo).

Las propiedades reológicas del producto desarrollado se midieron con un reómetro oscilatorio Anton-Paar MCR 300, obteniéndose curvas comparativas de módulo elástico (G') y módulo viscoso (G'').

Resultados y discusión: El estudio realizado fue un punto de partida para el desarrollo de un material polimérico similar. Se ensayaron varias formulaciones potenciales a escala laboratorio. Se estudió la influencia de las diferentes formas de incorporación de los componentes y posteriormente se evaluaron las propiedades reológicas y el desempeño de los materiales desarrollados.

Conclusiones: Se obtuvo un producto de propiedades similares al de referencia, empleando materias primas económicas y de fácil acceso en el mercado local.

Referencias:

[1] L. Nickerson, D. L. Howard, et al, Pressure-compensating compositions and pads made therefrom, US Patent 5,869,164 (1999).
[2] S. Smith, Method of preparing fire retardant siloxane foams and foams prepared therefrom, US Patent 3,923,705 (1975).
[3] H. Nishigaski, K. Watanabe, et al, Flame resistant oil, US Patent 4,556,511 (1985).
[4] Z. Yasuda, H. Koizumi, et al, Process for modifying rheological and suspension properties of nonaqueous suspension, US Patent 3,937,678 (1976).
[5] D. Colvin, J. C. Mulligan, et al, Method of using a PCM slurry to enhance heat transfer in liquids, US Patent 4,911,232 (1990).
[6] M. Kriesel, Multi-axially stretchable polymer shock absorbing pad, US Patent 20080026658 (2008).
[7] J. L. Sereboff, Gel filled deformable cushion and composition contained therein, US Patent 5,590,4308 (1997).
[8] D. L. Howard, Rubbery gels made from vegetable oils, US Patent WO 2006/063006 (2005).

Thermoplastic Elastomers Based on Graft Copolymers

Gözde Tuzcu[1,2], *Martin Van Duin*[1,3], *Bert Klumperman*[1,4]

[1]Eindhoven University of Technology (TU/e), Eindhoven, The Netherlands
[2]Dutch Polymer Institute (DPI), Po Box 902, 5600 AX Eindhoven, the Netherlands
[3]DSM research, Geleen, The Netherlands [4]Stellenbosch University, Private Bag X1 Matieland, 7602 South Africa

g.tuzcu@tue.nl

Abstract:

Styrenic thermoplastic elastomers (TPE-S) exhibit rubbery behavior without the need of chemical crosslinking. In these materials, the polystyrene blocks phase-separate from the rubber phase to form glassy domains that act as physical crosslinks. Upon variation of the copolymer topology or of the glass transition temperature of either one of the two phases, the characteristic thermo-mechanical behavior of the thermoplastic elastomers will also change. In this study, thermoplastic elastomers are synthesized that possess a graft copolymer topology. This is achieved by synthesizing chain end-functional polystyrene (PS) or chain end-functional poly(styrene-alt-phenylmaleimide) P(SMI) via reversible addition fragmentation chain transfer polymerization, atom transfer radical polymerization or nitroxide mediated radical polymerization and grafting these chain end-functional polymers onto functional elastomers. According to dynamic mechanical thermal analysis of the samples, elastomeric behaviour is observed for the synthesized graft copolymers. The width of the rubber plateau is increased in the examples of TPE-S synthesized with P(SMI).

This work is part of the research Programme of the Dutch Polymer Institute DPI, Eindhoven, the Netherlands, project nr. #649.

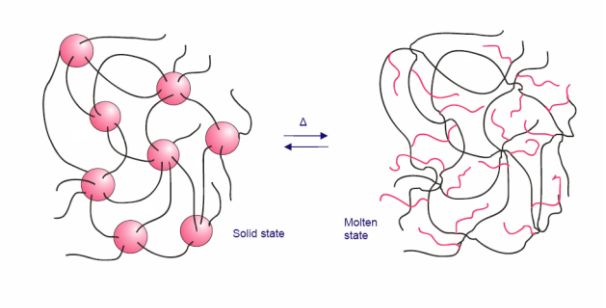

Fig.1 Thermal behaviour of the TPE-S in molecular scale

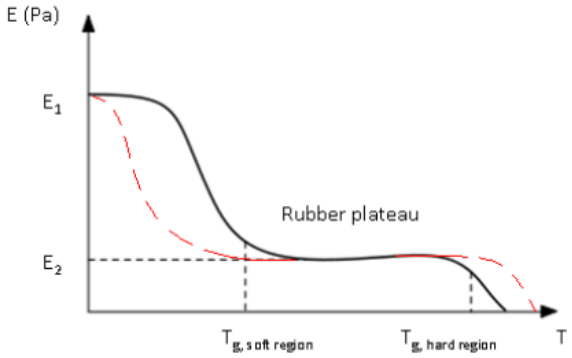

Fig.2 Thermal behaviour of TPE's in macro scale

Fluorescent Labeling of Calcium Alginate Beads with Rhodamine 6G Assisted By Polyaromatic-Anion.

Esteban Araya-Hermosilla[1], *Ignacio Moreno-Villoslada*[1], *Sandra Orellana*[1], *Felipe Oyarzun-Ampuero*[1], *Hugo Silva*[2], *Alejandro Yañez*[2].

Instituto de Química[1], Instituto de Bioquímica[2], Facultad de Ciencias, Universidad Austral de Chile. Isla Teja S/n, Casilla 567

esteban_araya84@yahoo.es

Alginate is a polysaccharide obtained from seaweed, it is a linear copolymer composed of 1,4-linked β-D-mannuronate (M) and α-L-guluronate (G). It has a carboxylate group in each M or G unit, and it is also a polyelectrolyte, highly negatively charged at neutral or basic pH[1]. Alginate is used in food products, cosmetics, drug formulation, and as an antigens coater for oral fish vaccines[2,3,4]. Therefore, evaluating the course of calcium alginate beads through digestive system of fishes, by labeling them, is very important from a pharmacokinetic point of view. Short-range aromatic-aromatic interactions between fluorescent dyes and polyelectrolytes bearing aromatic groups can help to retain the dye inside the calcium alginate microcapsules. It may also enhance the fluorescence of the system due to the dispersion of the dye when an excess of polymer is present[5].

Thus, Rhodamine 6G (R6G) has been included in calcium alginate beads in the absence and in the presence of poly(sodium 4-styrenesulfonate) (PSS). Solutions were injected in a microencapsulator (Biotech Encapsulator) and the shower of drops produced by the encapsulator's vibration was captured in flasks containing 200 ml of calcium chloride to form calcium alginate microcapsules. Microscopic photographs, using fluorescent and natural light, were taken, and the amounts of R6G analyzed by UV-Vis spectroscopy. A larger amount of microencapsulated R6G was obtained when PSS was present (Figure 1), due to a slower diffusion of the dye from the beads to the bulk.

The beads containing PSS and R6G were filtered and put in deionized water. Up to 40 % of the encapsulated R6G, is released. As deduced from spectroscopic measurements, the released R6G is bound to PSS, so that the dye serves to evaluate the diffusion of the polyelectrolyte from the beads (Figure 2). In the presence of NaCl 0.1 M up to 90 % of the encapsulated R6G is released, which is also bound to PSS.

With the aim to control the release of PSS/R6G complexes from the beads, the beads were filtered and incubated in solutions of different concentrations of chitosan. The beads coated with chitosan were put in NaCl 0.1 M aqueous solution. The release of PSS/R6G complexes diminished drastically when the chitosan concentration was higher or equivalent to the alginate concentration (Figure 2).

The short-range aromatic-aromatic interaction between the PSS and R6G favors the retention of the dye inside the calcium alginate beads. The release of PSS/R6G complexes in deionized water may be due to swelling produced by water absorption, and consequent diffusion until reaching equilibrium. In the presence of NaCl 0.1 M, sodium ions compete with the calcium breaking the crosslinking of the M blocks, increasing swelling[1] and pore aperture. Besides, the entrance of Na^+ and Cl^- ions into the beads may also increase the osmotic strength, thus favoring the swelling of the systems. The polycation chitosan may form a coating that produces a positive potential inhibiting the release of PSS/R6G complexes.

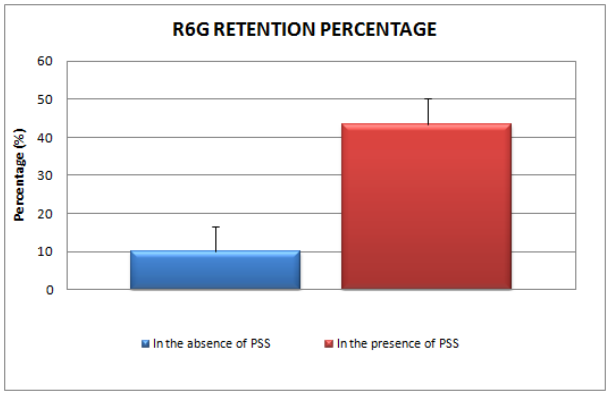

Figure 1.

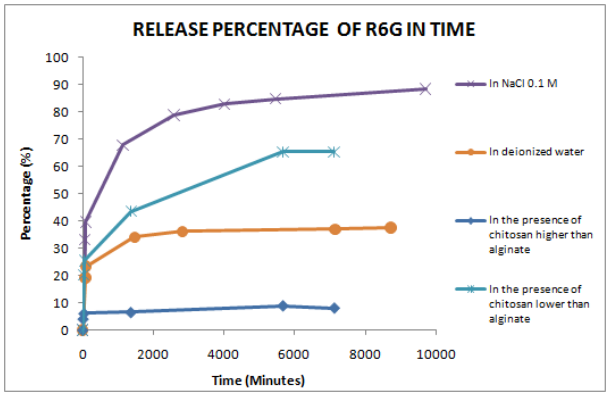

Figure 2.

References:

1.-Wang, X.; Spencer, H.G. Polymer.1998, 13, 2759-2764.
2.-Tonnesen, H.; Karlsen, J. Dr. Dev. Ind. Pharm. 2002 28(6), 621-630.
3.-Rodrigues, P.; Hirsch, D.; Figueiredo, H.; Logato, P.; Moraes, A. Process Biochemistry. 2006, 41, 638-643.
4.-Romalde, J.; Luzardo-Alvárez, A.; Ravelo, C.; Toranzo, A.; Blanco-Méndez, J. Aquaculture. 2004, 236, 119-129.
5.-Moreno-Villoslada, I.; Fuenzalida, J.; Tripailaf, G.; Araya-Hermosilla R.; Pizarro, G.; Marambio, O.; Nishide, H. J. Phys. Chem. B., 2010 114, 11983

Agradecimientos: Proyecto INNOVA CORFO 07CN13PPT256, Proyecto FONDECYT Nº 109034.

Structure, morphology and transport properties of nanocomposites films prepared from starch, montmorillonite and silver nitrate

M. Meyer, F. Gouanvé, E. Espuche

Université de Lyon, F-69003, Lyon, France; Université Lyon 1, F-69622 Villeurbanne, France;
CNRS, UMR5223, Ingénierie des Matériaux Polymères

Introduction

Renewable sources of polymeric materials offer an alternative to maintain sustainable development of economically and ecologically attractive technology. In the family of renewable sources based biodegradable polymeric materials, starch has been considered as one of the most promising materials because it is readily available and may form cost effective end products.[1,2] Starch-based materials have received great attention for packaging applications as they exhibit low oxygen permeability at dry state. Nevertheless, pure native starch films are brittle. Plasticizers are then often added to improve the polymer flexibility. Despite their enhanced mechanical properties, plasticized starch based films cannot meet all the requirements of packaging applications. In particular, these materials remain water sensitive and, therefore, loose their barrier properties upon hydration. In this context, the nanocomposites concept, with the introduction of lamellar fillers like nanoclays, can be a promising option as it could lead to decrease the initial gas permeability of the plasticized film as well as to keep a low oxygen flux upon hydration[3]. Beyond the degradability and the barrier properties, the development of materials that interact with the food, playing an active role in the preservation is more and more considered for packaging application. Antimicrobial active film can be obtained by incorporating an antimicrobial agent in the films. In the family of antimicrobial agent, metal nanoparticle such as silver is one of the most promising.[4] One method can be used to prepare such nanocomposites materials is to generate in situ silver nanoparticles in the starch polymer thanks to a silver complex.[5] Interactions between starch and the silver precursor are required to obtain a homogeneous dispersion of nanoparticles in the matrix. In this way, the aim of this work is to prepare biodegradable films based on potato starch, montmorillonite and silver nanoparticules as antimicrobial agents.

Materials and methods

Native potato starch (Sigma), glycerol, silver nitrate (Aldrich) and Nanofil® 757 (Süd Chemie) were used to films processing. Films were prepared by a solution/cast process of starch with different amounts of nanoclays and silver nitrate. The silver nanoparticles have been generated in situ by thermal treatment. The structure and the morphology of the films were characterized using different techniques: X-ray diffraction (XRD), transmission electron microscopy (TEM) and UV-spectroscopy. Thermal stability of the different films was studied by thermogravimetric analyses (TGA). Water sorption analysis and oxygen permeability measurements were performed at 25°C as a function of the film composition.

Results and discussion

The favorable interactions established between the nanoclays gallery and the hydroxyl groups of starch, were at the origin of the rather good clay dispersion state: a mixture of exfoliated and intercalated structures was indeed observed whatever the nanocomposites composition. Concerning the in situ generation of silver nanoparticles, a homogeneous dispersion of nanometer size was obtained.

The water sorption mechanism was studied as a function of the composition of the films and modeled by Park equation "Eq.1", considering three sorption modes.

$$C = \frac{A_L \cdot b_L \cdot a_w}{1 + b_L \cdot a_w} + k_H \cdot a_w + K_a \cdot a_w^n \qquad (1)$$

where, A_L the Langmuir capacity constant, b_L the Langmuir affinity constant, k_H the Henry's solubility coefficient, K_a the equilibrium constant for the clustering reaction, n the mean number of water molecules per cluster, C the water concentration in polymer, and a_w the water activity. By this fitting approach, it was shown that the water uptakes were the results of different contributions. The polar groups present in starch, in glycerol and at the clay surface could contribute to the sorption mechanism.

Oxygen permeability was studied for a wide range of relative humidity and the following general trends were observed. For all films, the permeability coefficient slightly increased in the range of relative humidity between 30 to 45% and highly increased at higher activities. Introducing clays led to decrease the gas permeability whatever the matrix.

Conclusions

In this work we showed the feasibility of making films based on starch biodegradable, montmorillonite and silver nanoparticules as antimicrobial agents. To obtain satisfactory mechanical properties, barrier properties and antimicrobial properties, it is important to have optimal concentration of different components in order to obtain a good dispersion of the nanoclays and also the silver nanoparticles in starch matrix.

References

[1] Averous L, Fauconnier N, Moro L, Fringant C, *J. Appl. Polym. Sci*. 2000; 76(7): 1117-1128

[2] Yilmaz G, Jongboom R O J, Van Soest J J G, Feil H, *Carbohydr. Polym.* 1999; 38(1), 33-39

[3] Zhang YC, Han J H, *J. Food Sci*. 2006; 71(6), 253-261

[4] Zheng M., Gu M.,Jin G., *Mat. Sci. Eng. B-Solid*., 2000; 77(1): 55-59

[5] Clemenson S., David L., Espuche E., *J. Polym. Sci. Pol. Chem.* 2006; 45(13), 2657-2672

Design of novel, fluorescent-tuneable, pH-sensing, water-insoluble, lineal copolymers synthesized by ATRP and its application in the development of pH-sensing nanofibres made by electrospinning

Antonio L. Medina-Castillo1, Jorge F. Fernández Sánchez1, Alberto Fernández-Gutiérrez1*

1Department of Analytical Chemistry, University of Granada, Avd. Fuentenueva s/n, 18071 Granada.

*antonioluismedina@ugr.es

Introductions: The pH monitoring is crucial on many (bio)chemical process. The ability to create a copolymer whose optical properties change with the microenvironmental pH can be useful for many applications, such as controlling the catalytic activity of immobilized enzymes or the binding affinities of ligands to metal ions. Furthermore, immobilization of these copolymers on multiple sites of an imaging fiber could give rise to the elaboration of a wide range pH optical sensor. In this work, Reverse Atom Transfer Radical Polymerization (ATRP)[1] were used for synthesizing novel fluorescent-tuneable, pH-sensitive, waterinsoluble lineal copolymers which were used for designing new pH-sensitive, nanostructured sensing films based on nanofibres made by electrospinning.

Materials ands Methods: The copolymers are based on the copolymerization of fluorescein o-acrylate (fluorescent pH-sensitive monomer) with methyl methacrylate and hydroxyl ethyl methacrylate (principal framework of the copolymers). 3- methacryloylaminopropyl-trimethylammoniumchloride (positively charged monomer) and 2-acrylamido-2- methylpropane sulfonic acid (negatively charged monomer) were used to introduced and modify the electrostatic properties of the copolymer synthesized.

Result and discussions: In order to obtain a fluorescent-tuneable pH-sensitive lineal copolymer, fluorescein o-acrylate (FOA) was selected as fluorescence pH-sensitive probe, MMA and HEMA were selected as the principal framework of the copolymers by their adequate reactivity ratios to provide statistical copolymers, and by their compatibility with a wide range of pure solvents and solvent mixtures, and MAPTAC and AAMPS were selected for modifying the electrostatic properties of the copolymers and therefore their microenvironmental pH because the quaternary ammonium groups ($R4N^+$) of MAPTAC remains cationic at all pH values and the sulfonate group ($SO3^-$) of AAMPS remains ionized even in highly acidic conditions. The electrostatic properties of these copolymers were investigated and perfectly adjusted to allow changes in the microenvironmental pH and to maintain their insolubility in aqueous media. The copolymers were characterized by Fourier Transform Infrared spectroscopy (FT-IR), nuclear magnetic resonance (^{1}HNMR) spectroscopy. Molecular weight and polydispersity (M_w/M_n) were calculated by triple detection gel permeation chromatography (GPC). The copolymers were used for providing highly fluorescent pH-sensitive nanofibres made by electrospinning. The selected flow rates and voltages within of the electrospinning configuration allowed the collection of dry fibers in non-wovenmats. The nanofibres were characterized by scanning electron microscopy (SEM) and fluorescence microscopy (see Fig.1.) and the fiber mats were successful used for pH-monitoring in two different pH ranges (6.5-8 and 8-10) showing reversibility, high sensitive and low response times (see Fig.2.)

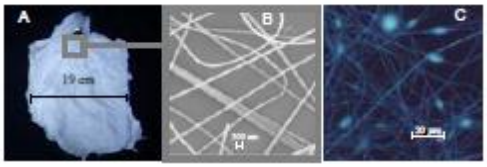

Fig.1. SEM Pictures of nanofibre mats at pH 9.5 and 7.8, respectively.

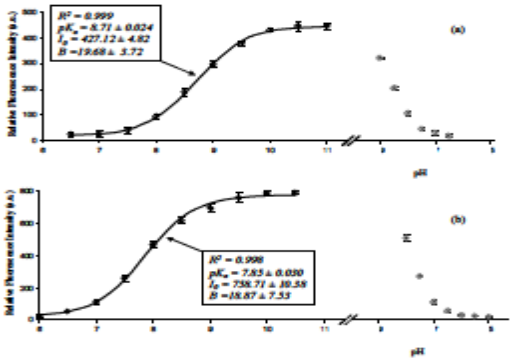

Fig.2. pH calibration of a) N-F-NP1 and b) N-F-NP1(X) fiber mats and reversibility of the optical signals.

Conclusions: Four novel lineal copolymers based on the copolymerization of FOA, as a fluorescence pHsensitive probe, were synthesised by reverse-ATRP. We demonstrate that the microenviromental pH of the water-insoluble lineal copolymers can be modified by a light modification of the electrostatic properties of the copolymers. In addition, the copolymers synthesized in this work are highly soluble in organic solvents (between 25-30 wt %) such as THF, acetone or DMF, but insoluble in water. Due to these facts, they can be considered as potential candidates for an easy preparation of novel, nanostructured optical pHsensitive sensing films with different structures, morphologies and geometries by several techniques (electrospinning, spin coating, layer by layer deposition by deep coating, spray dry, spray coating, etc…).

References: [1]K. Matyjaszewski and J. H. Xia, Chemical Reviews, 2001, 101, 2921-2990.

Acknowledgments:
The authors express their thanks to the Spanish Ministry of Education (FPU grant reference AP2006-01144 and Project CTQ2008-01394) and the Regional Government of Andalusia (Excellence projects P07-FQM-02738 and P07-FQM-02625). In addition, they thank the company Y-Flow S.L. for their collaboration in the development of the sensing films by electrospinning.

Block Copolymer Surfactants In Emulsion Polymerization: The Influence Of The Miscibility Of The Hydrophobic Block On Kinetics, Particle Morphology And Film Formation

Alexandra Muñoz-Bonilla,[‡] Syed Imran Ali,[†] Adolfo del Campo,[§] Marta Fernández-García,[‡] Alex M. van Herk,[†] Johan P.A. Heuts[†]

[‡]Instituto de Ciencia y Tecnología de Polímeros (CSIC), C/ Juan de la Cierva 3, 28006-Madrid, Spain.
[†]Laboratory of Polymer Chemistry, Eindhoven University of Technology, P.O. Box 513, 5600 MB Eindhoven, The Netherlands
[§]Instituto de Cerámica y Vidrio (CSIC), C/ Kelsen 5, 28049-Madrid, Spain.

sbonilla@ictp.csic.es

Introduction

The use of polymeric surfactants, mainly amphiphilic block copolymers, as stabilizer in emulsion polymerization has attracted attention because of the several advantages imparted to the properties of the resulting latex. Besides the low critical micelle concentration, amphiphic block copolymers exhibit low diffusion coefficient and can be anchored or adsorbed to the particles. Therefore the use of block copolymers as surfactants in emulsion polymerization can lead to the preparation of "hairy" particles. Whereas the hydrophilic segments of the block copolymer provide the colloidal stabilization of the polymer particles along with a specific surface functionality, the hydrophobic segments strongly adsorb or anchor to the polymer-water interface and therefore relatively long hydrophobic lengths are expected to be more efficient. In this sense the compatibility or miscibility between the hydrophobic block and the growing polymer particle is a very relevant parameter that determines how the amphiphilic block copolymer is anchored to the particle surface. We report the synthesis of hairy particles by the emulsion polymerization of methyl methacrylate using amphiphilic block copolymers of polystyrene-*b*-poly[poly(ethylene glycol) methyl ether methacrylate] (PS_{40}-*b*-$PPEGMA_{70}$) as stabilizer. In this case the hydrophobic PS segment is different from the polymer in growing latex particles, PMMA, and since PS and PMMA are immiscible, an incompatibility effect may occur and the mechanism of emulsion polymerization reaction could be affected.

Materials and Methods

Amphiphilic block copolymer (PS_{40}-*b*-$PPEGMA_{70}$) was synthesized via atom transfer radical polymerization (ATRP) as previously reported.[1] Methyl methacrylate, MMA, was purified by passing over a basic alumina column. Ammonium persulfate and sodium thiosulfate were used as received.

Preparation of micellar solution. The micellar solution was prepared by dissolving the block copolymer in a few drops of THF and subsequently distilled water was added dropwise with vigorous stirring. The sample was transferred to dialysis tubing and dialyzed against distilled water.

Emulsion polymerization of MMA using PS_{40}-b-$PPEGMA_{70}$ as surfactant. All the emulsion polymerizations of MMA (overall solids contents of 16.6 %) were carried out in batch. The micellar solution was added to the double-walled reactor. The monomer, MMA was added dropwise into the reactor and the mixture was purged with argon. Then, the mixture was heated at 35 °C. The redox initiator solution ammonium persulfate/sodium thiosulfate was injected to start the polymerization. At different reaction times, aliquots were extracted by syringe and the monomer conversion was determined by gravimetry.

Results and Discussion

It was shown that the incompatibility between the growing polymer particles of poly(methyl methacrylate) and the hydrophobic segment of the block copolymer surfactant (polystyrene) affects both the kinetics of the emulsion polymerization and the resulting particle morphology. Because of the incompatibility of the two polymers, phase separation occurs and the morphology of the particles changes from rough spherical core-shell particles to more irregular particles (see Figure 1) as the amount of block copolymer surfactant increases. This, in turn, has an effect on the film formation resulting in turbid films.

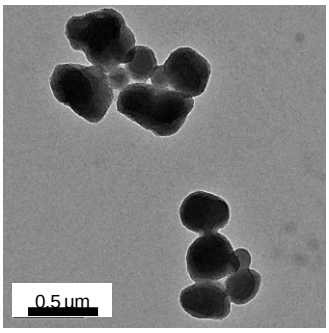

Figure 1. TEM image of PMMA latex stabilized with 5.5 wt% of PS_{40}-*b*-$PPEGMA_{70}$ copolymer surfactant.

The emulsion polymerization of methyl methacrylate, the obtained hairy latex particles and the film formation process were compared with the results obtained in the emulsion polymerization of styrene where both the core of the particles and the hydrophobic segment of the block copolymer are the same polymer. In this case spherical and monodisperse particles are obtained irrespectively of the block copolymer surfactant concentration, and transparent films are formed after annealing above the glass transition temperature.

Acknowledgment

This work was financially supported by the Stichting Emulsion Polymerization (SEP) and the Ministerio de Ciencia e Innovación (Project MAT2010-17016). A. Muñoz-Bonilla gratefully acknowledges CSIC for her JAE-doc contract.

References

1. Muñoz-Bonilla, A.; van Herk, A. M.; Heuts, J. P. A. Macromolecules **2010**, *43*, 2721–2731.

SIDE-CHAIN LIQUID-CRYSTALLINE COPOLYETHERS WITH TAPERED MESOGENIC GROUPS

*S.V. Bhosale1, M.A. Rasool2, M. Giamberini2, *J.A. Reina1*

1. Departament de Química Analítica i Química Orgànica, Universitat Rovira i Virgili, Carrer Marcel.li Domingo s/n, Campus Sescelades, 43007 Tarragona, Spain
2. Departament de Enginyeria Química, Universitat Rovira i Virgili, Av. Països Catalans, 26 Campus Sescelades, 43007 Tarragona Spain

*joseantonio.reina@urv.cat

The design, synthesis, and study of supramolecular assemblies capable of transporting ions across membranes by the channel mechanism have been the subject of increasing interest. Some of the authors[1-3] obtained liquid crystalline polyethers which selfassembled into columnar structures by grafting a tapered mesogenic group onto commercial poly(epichlorohydrin) (PECH). In this work, our objective was to prepare side-chain liquid crystalline columnar polyethers by chemical modification of the copolyethers, poly[epichlorohydrin-co-(ethylene oxide)] [P(ECH-co-EO)] 1:1, with tapered 3,4,5-tris[4-(*n*-dodecan-1-yloxy)benzyloxy]benzoate group. This class of polymers could be an alternative approach for the preparation of new proton conducting membranes to be applied, for instance, in Direct Methanol Fuel Cells (DMFCs)

Materials and methods

All organic and inorganic chemicals were supplied by Aldrich and used as such as received. Tetrahydrofuran (THF) was freshly distilled from sodium benzophenone ketyl under argon. Tetrabutylammonium bromide (TBAB) ≥99% (Fluka) was dried at 50 °C *in vacuo* for 1 day. The side-chain liquid-crystalline (LC) copolyethers were obtained by chemical modification of P(ECH-co-EO) with potassium 3,4,5-tris[4-(*n*-dodecan-1-yloxy)benzyloxy]benzoate[2] using different solvents like anhydrous THF, dimethylformamide (DMF), and N-methyl-2-pyrrolidone (NMP). It was heated at 65 °C in THF and in the case of NMP, it was heated at 80 °C. The DMF was used in catalytic amount. In case of TBAB, stoichiometric amounts were used. The structure and composition of the copolymers were characterized by NMR spectroscopy. Thermal characterization was carried out by differential scanning calorimetry (DSC) and thermogravimetric analysis (TGA). Mesomorphic behavior was characterized on the basis of DSC, polarized optical microscopy (POM) and X-ray diffraction.

Results and discussion

We have obtained co-polyethers bearing tapered 3,4,5-tris[4-(*n*-dodecan-1-yloxy)benzyloxy]benzoate group. The bimolecular substitution of the chlorine atom in P(ECH-co-EO) with these tapered potassium carboxylate gave the desired polymer with no substantial modification in either the backbone size or the polymer microstructure as shown in the given chemical reaction scheme.

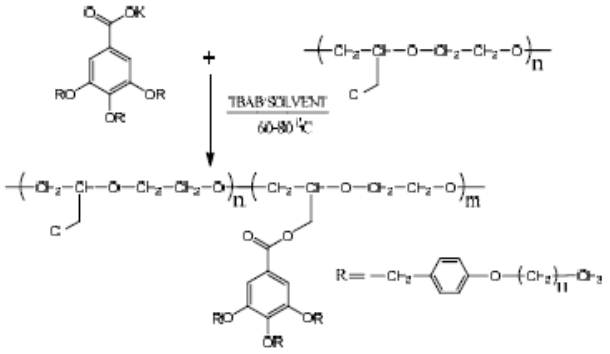

The composition of the copolymer was calculated by NMR spectroscopy. The average degrees of modifications ranging from 30-60% were estimated by ^{1}H NMR spectra and chlorine elemental analysis. On the basis of average degree of modification, the percentage yields ranging from 80-90% were calculated. The glass transition temperatures were determined by DSC and ranged from -20 ºC to 18 ºC; TGA showed maximum weight loss at around 550-600 °C. The materials were mesomorphically characterized on the basis of DSC, polarized optical microscopy, and X-ray diffraction experiments. In most copolymers a hexagonal columnar mesophase was recognized.

Conclusions

In this work, we prepared a family of side-chain LC copolymers by modification at different extent of poly[epichlorohydrin-co-(ethylene oxide)] 1:1 with tapered mesogenic potassium 3,4,5-tris[4-(*n*-dodecan-1-yloxy)benzyloxy]benzoate. Most copolymers exhibited a hexagonal columnar mesophase. The columnar organization should allow proton transport by the channel mechanism. Therefore, these copolymers will be used to prepare oriented membranes and tested for proton transport.

References

1. Ronda, J.C. Reina, J.A. Cadiz, V. Giamberini, M. Nicolais, L. *J. Polym. Sci. Polym. Chem.* **2003**, *41*, 2918-2929.

2. Ronda, J.C. Reina, J.A. Giamberini, M. *J. Polym. Sci. Polym. Chem.* **2004,** *42*, 326-340.

3. Giamberini, M. Ronda, J.C. Reina, J.A. *J. Polym. Sci. Polym. Chem.* **2005,** *43*, 2099-2111.

Acknowledgement

The authors would like to thank Ministerio de Ciencia e Innovacion (MAT2008-00456) for providing financial support for this work.

Hybrid Electrospun Fibres Showing Spin-Crossover Properties

D. López[1], G. Mitchell[2], M. Rubio[1], A. Roig[3]

[1]Instituto de Ciencia y Tecnología de Polímeros, CSIC, c/ Juan de la Cierva 3, 28006 Madrid, Spain
[2]Centre for Advanced Microscopy, Unviersity of Reading, Whiteknights RG6 6AF, UK
[3]Instituto de Ciencia de Materiales de Barcelona, CSIC, Campus de la UAB, 08193 Bellaterra, Spain

daniel@ictp.csic.es

Introduction: In this contribution we explore the possibility of preparing electrospun fibres containing the metallo-organic polymer [Fe(II) (4-octadecyl-1,2,4-triazole)$_3$(ClO$_4$)$_2$]$_n$ (PFe(II)), using an atactic polystyrene matrix. We evaluate the structure, morphology, phase transitions and properties of the fibres.

The metallo-organic polymer exhibits a thermally induced transition between two electronic states: a low-spin (LS) and a high-spin (HS) state which are dia- and paramagnetic, respectively. The spin-crossover is accompanied by a strong thermochromism that provides additional applications for the system as new materials with especial optical, magnetic and electronic properties.

The limiting step for the development of applications with these systems is the transfer of the bulk properties of the metallo-organic polymer in the solid state to systems suitable for technologic applications. The ability to isolate and preserve such linear metallo-organic polymers in fibres would provide as with a new way to obtain new functional materials.

Preliminary results showing the suitability of the electrospinning method to obtain hybrid fibres preserving the spin-crossover phenomenon of the metallo-organic polymer are shown here.

Materials and methods: Electrospinning was performed using a glass syringe mounted in a syringe pump fitted with a 22-gauge needle with an internal diameter of 0.41mm. A flow rate of 0.13 ml/min was employed. A Glassman High Voltage power supply was used which allowed defined voltages over the range of 15 kV. In this work we have used a flat aluminium collector placed 15 cm from the needle.

Fibres were electrospun from a DMF based solution containing 30% w/w of atactic polystyrene with variable proportions of PFe(II) of 0.0, 0.5, 1.0, 5.0 and 10 %.

Results and Discussion: During electrospinning, the electric field overcomes the surface tension of the droplet at the needle to produce firstly a Taylor cone and subsequently a jet producing fibres. These fibres were deposited chaotically on a flat electrode with no preferred orientation within the plane of the electrode.

It was not possible to prepare electrospun fibres from pure PFe(II), however, it was possible to prepare fibres using a range of PFe(II) concentrations dispersed in a polystyrene matrix. Generally, at the higher the concentration it was more difficult to prepare the fibres (see Figure 1).

The mean fibre diameter of the fibres varies with the level of the PFe(II). There appears to be a systematic reduction in diameter with increasing PFe(II) content at low concentration. Whereas at higher concentration the fibre diameter is invariant with compositions, and beads formation appears.

The magnetic properties of the fibres appear to be very similar to those exhibited by the pure PFe(II). DSC studies show a transition at ~60 ºC associated with a structural transition of the metallo-organic polymer, but which is not repeated during a second heating, whereas wide angle x-ray scattering studies show that the local structure of the atactic polystyrene matrix has been largely preserved. At the higher concentration of the PFe(II) there are some distinctive peaks at low angles which show that the basic structure of the PFe(II) is also preserved.

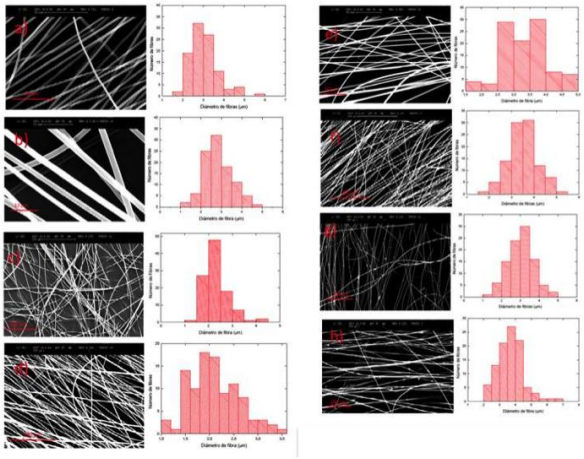

Figure 1 SEM images of aPS-PFe(II) fibres of different compositions and fibre size distribution

Conclusions: This study shows that microscale electrospun fibres of polystyrene containing PFe(II) can be prepared. The properties and structure of the PFe(II) appear to be largely retained, although the disappearance of the structural transition at 60 ºC during a second heating of the electrospun fibres suggests structural rearrangement on heating above the glass transition of the polymer.

References:

1.- M Rubio, R Hernández, A Roig, A Nogales, D López Eur. Polym. J. **47**, 52-60 (2011)
2.- M Rubio, D López Eur. Polym. J. **45**, 3339-3346 (2009)
3.- D López, M Rubio, G Mitchell, A Roig J. Mat. Chem (submitted)

Dissolution Modeling of Smart Nano-Scale Coated Polymer Particles in Polymer Flooding Process

M. Ashrafizade[a], *A. Ramazani*[a] *S. A.*, *S. Sadeghnejad*[a]

[a]Chemical and petroleum engineering Department, Sharif University of Technology, Tehran, Iran

* Corresponding Author's E-mail: ramazani@sharif.ir

Introduction

The main purpose of this paper is simulation of in-situ release of nano-size polyacrylamide (PAA) with water-insoluble coatings (i.e. Polystyrene, PS) (Fig. 1a) at the water-oil interface during the polymer flooding of oil reservoirs. Reaching at the water-oil interface, the oil soluble coat of PAA particles solves into the oil phase. Subsequently, the main polymer (i.e. PAA) which is not soluble in the oil phase starts to diffuse and solve into the water phase and increase the in-situ viscosity of water.

Using this method, the amount of polymer, used in flooding, will reduce. Moreover, because of the in-situ release of the polymer and consequently the viscosity reduction of the injected fluid, the driving force for polymer injection will reduce. In addition, using nano-size particles reduces the trapping of the polymer near the wellbore. Finally, smart coatings can decrease PAA degradation caused by salinity, pH, and high temperature of the reservoir. All of these effects together increase the polymer flooding efficiency and reduce the cost of EOR projects.

Physical Description and Modelling of the Process

The physical process of in-situ release can be considered under the term of controlled release in drug delivery systems [1-2]. However, this work is the first one that considers controlled release application in polymer flooding.

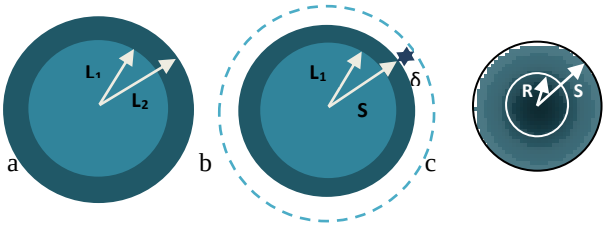

Fig.1. a) PAA core with radius of L_1 and PS coating with radius of L_2. b) Dissolution of PS into the oil phase c) Dissolution of PAA into the water phase

PS dissolution model is considered as a spherical diffusion followed by the polymer chain disentanglement through a diffusion boundary layer of thickness, δ (Fig. 1b):

$$\frac{\partial C_p}{\partial t} = \frac{D_p}{r^2}\frac{\partial}{\partial r}\left(r^2 \frac{\partial C_p}{\partial r}\right) \qquad (1)$$

where C_p is volume fraction of polymer, and D_p is polymer diffusion coefficient in the boundary layer. At initial condition as well as the exterior of the boundary layer $C_p = 0$. At the inner side of boundary layer, it is assumed that a polymer chain requires a minimum time to disentangle (i.e. $\frac{\partial C_p}{\partial r} = 0$). After this period, the rate of diffusion is sufficiently high and hence the flux is disentanglement-limited (i.e. $-D_p \frac{\partial C_p}{\partial r} = cte$) until the polymer concentration reaches an equilibrium value in the boundary layer. The interface, S, moves due to polymer chain disentanglement (i.e. $\frac{dS}{dt} = D_p \frac{\partial C_p}{\partial r}$).

A swellable-chain disentanglement model is considered for PAA dissolution into the water phase. Initially, the glassy polymer starts swelling due to water penetration and the simultaneous transition from the glassy to the rubbery state. Thus two distinct fronts are observed (Fig.1c), the swelling interface at position R and the polymer-water interface at position S. Initially, front R moves inwards whereas front S moves outwards as long as swelling prevails. When the water concentration exceeds critical value chain disentanglement begins and both R and S start to decrease.

Water transport can be expressed by Eq.1 but with the water properties (i.e. C_w, D_w). The moving boundary condition at the interface R is given by $C_w \frac{\partial R}{\partial t} = -D_w \frac{\partial C_w}{\partial r}$.

Besides, the PPA dissolution model is the same as PS dissolution model but with different boundary conditions. Finally, the interface S moves due to polymer swelling and subsequent chain disentanglement as: $\frac{dS}{dt} = D_w \frac{\partial C_w}{\partial r} + D_p \frac{\partial C_p}{\partial r}$

By defining proper dimensionless parameters and fixing the moving boundary condition of the governing equations [3], the governing equations are discretized using fully implicit finite difference scheme and solved with Broyden method [4].

The impact of different sensitivity parameters on dissolution time is analysed (e.g. Fig. 2).

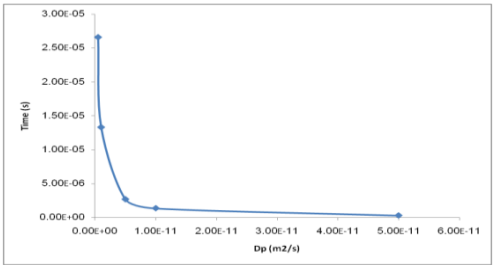

Figure 2: Impact of diffusivity coefficient on dissolution time

Summary

We have introduced a new state of the art methodology for improving polymer flooding efficiency. The polymer dissolution process is numerically modelled by finding the governing equation of the moving boundary problem. Consequently, the sets of governing equations are discretized using fully implicit finite difference scheme and solved with Broyden method.

References

[1] S. Kiil, K. D. Johansen, J. Controlled Release 90 (2003) 1–21.
[2] N. Wu, L.S. Wang, D.W. Tan, S.M. Moochhala, Y.Y. Yang, J. Con. Relea. 102 (2005) 569–581.
[3] T.C. Illingworth, I.O. Golosnoy, J. Comp. Phys. 209 (2005) 207–225
[4] C.D. Holland , Fundamentals of multicomponent distillation, first ed., McGraw-Hill, 1981.

Nanoclay Composite Barrier Coating for Plastic Substrate of Flexible Display

Sung Soo Kim and Hana Ra

Kyung Hee University, Korea

sungkim@khu.ac.kr

Introduction: Plastic substrates are gaining much interest for its application to flexible display, since it has several advantages over the glass substrate such as light weight, flexibility and transparency.[1] PES films had good clarity and a high thermal resistance to be operated at high temperature,[2] and it could be used as substrates for flexible devices, such as organic thin film transistor(OTFT),[3] liquid crystal display(LCD)[4] and OLED[5-7]. Flexible substrate should have comparable barrier properties to water vapor and oxygen comparable to those of glass. Therefore, additional layer should be formed on plastic substrate to achieve the requirements, and many technologies have been proposed including the thin oxide films, which were prone to mechanical damages and poor adhesion. Functional coating of nanoclay composite layer was proposed can solve the problems, and it can play a role to improve the mechanical properties and barrier properties due to large aspect ratio of nanoclay.[13]In this work, sodium montmorillonite nanoclay was modified with cationic surfactant to enhance the intercalation, and effects of alkyl chain length were examined by various methods such as treatments by cationic surfactant and coupling agent. Nanoclay was functionalized with isophorone diisocyanate- 2-hydroxyethyl acrylate (IPDI-HEA) for subsequent reaction with UV curable polymer. Improvement of mechanical and barrier property of composite layer was examined. Any deterioration in optical performances of substrate after composite layer formation was also examined.

Experimental: Sodium montmorillonite(Na^+-MMT) nanoclay was modified with cationic surfactants was conducted via a cationic-exchange process, and isophorone diisocyanate and 2-hydroxyethyl acrylate (IPDI-HEA) containing a catalyst, dibutyltin dilaurate(DBTDL), at 0.1 wt% and p-hydroxyanisole at 1000 ppm were added and stirred vigorously at 70 ℃ for 48 hrs. Thus obtained functionalized clays were added into the pre-polymer mixture consisted of PU acrylate to make composite solution. The polymer/functionalized nanoclay composite solution was spin coated on PES substrate and was UV-cured.

The X-ray diffraction (XRD) patterns were recorded and the Fourier transformed infrared (FTIR) spectra were obtained. The thermogravimetric analysis (TGA) was performed at a heating rate of 5 ℃/min from room temperature to 900 ℃ under N_2 atmosphere. The mechanical properties were measured using a pencil hardness tester and a falling ball impact testerThe light transmittance of the cured film was measured using a color filter spectral multi channel, and haze was determined. The barrier properties were determined oxygen transmission rate and water vapor transmission rate.

Results: The TGA curves for Na^+-MMT, modified and functionalized clays were compared Fig. 1(a). The weight loss of functionalized clays was increased due to the decomposition of organic groups adsorbed between the interlayer after grafting of IPDI-HEA. The XRD patterns in Fig. 1(b) show that the interlayer spacing of functionalized clays was more increased due to the grafting occurred inside the clay layers. From the XRD and TGA results, it could be found that the IPDI-HEA with reactive acrylate groups was successfully grafted on the nanoclay for the functionalization of clays.

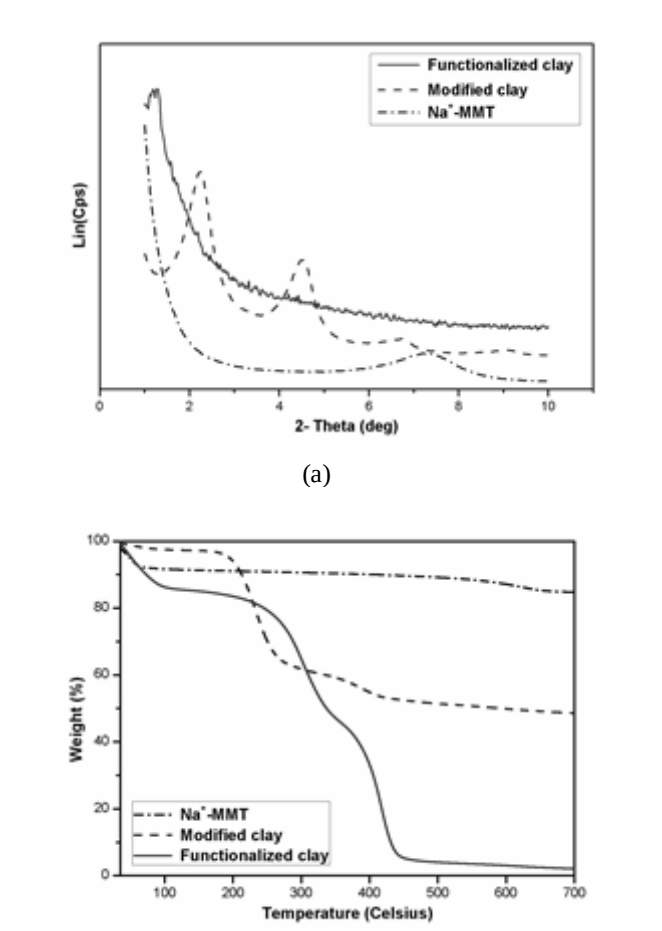

Figure 1. (a) XRD and (b) TGA analyses of nanoclay before and after grafting with IPDI-HEA.

References:

[1] S. Logothetidis, Mater. Sci. Eng. B, 152, 96, (2008).
[2] M. C. Choi, Y. Kim, C. S. Ha, Prog. Polym. Sci., 33, 581, (2008).
[3] S. C. Lim, S. H. Kim, J. H. Lee, H. Y. Yu, Y. Park, D. Kim, T. Zyung, Mater. Sci. Eng. B, 121, 211, (2005).
[4] H. Hah, S. J. Sung, M. Han, S. S. Lee, J. K. Park, Displays, 29, 478, (2008).

New phenol functionalized polyamides: a new polymer family for multiple applications

Stéphane Jéol[1], *Franck Touraud*[1], *Cécile Corriol*[1], *Jean-Pierre Marchand*[2]

[1] Rhodia Centre de Recherches et Technologies de Lyon, 85 avenue des frères Perret, 69192 Saint-Fons, France
[2] Rhodia Engineering Plastics, Avenue Ramboz – BP64, 69192 Saint-Fons, France

stephane.jeol@eu.rhodia.com

Since the discovery of polyamide more than 70 years ago, several industrial polyamides have been extensively studied and produced industrially to address well-known markets such as textile, industrial yarns, packaging, automotive, electric and electronic, industrial consumer goods, … Efforts to provide the right macromolecular structure to obtain the right properties were reported : the choice of monomers and comonomers, the molecular weight and its distribution or the architecture (linear, stars, branched, hyperbranched, …) are the classical levers. For some new applications of polyamides, it is not always possible to reach the desired properties by using these levers.

One particularity of polyamides is to have their properties (thermal, mechanical, …) more governed by the presence of inter-chains interactions (H-bond) than by the chain length or the nature of the monomers (aliphatic, cycloaliphatic, aromatic).

In this context, we have developed (Ref. A) a novel approach to bring new properties to polyamides, by modulating the inter-chain interactions of polyamides. We present here the development of new polyamides bearing pendant phenol functions, that provide new H-bond having high energy between phenol Ø-OH and amide -NH-(C=O)- groups.

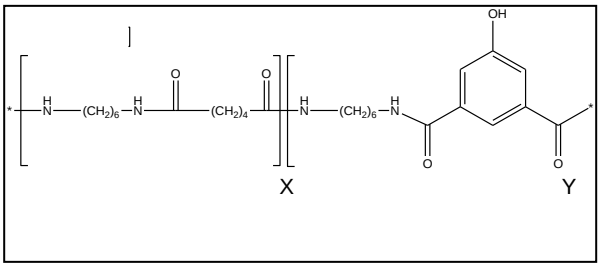

Figure 1. Molecular structure of copolyamides PA 66/6HIA X/Y, bearing pendant phenol groups.

The functional PA 66 named PA 66/6HIA X/Y (Figure 1) are presented. Chemical characterizations (NMR, SEC, end-group titration) of the bulk synthesized PA 66/6HIA indicate the desired structure is obtained.

Molecular modelling (Figure 2) and thermal properties of the functional polyamide are used to highlight the presence of new interactions and how they modify the chain mobility. Well-known copolyamide PA 66/6I (I=Isophthalic acid) having an aromatic structure but without any functionality are used as a comparison. Higher Tg was found by DSC for PA 66/6HIA than for the non functional PA 66/6I.

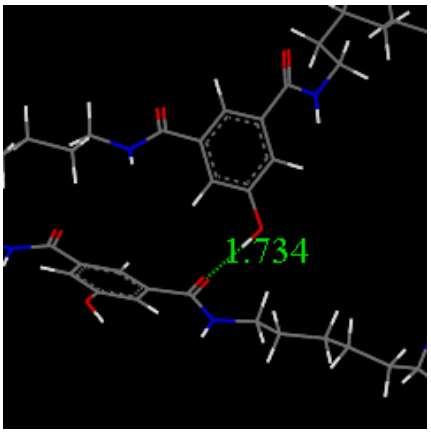

Figure 2. Example of molecular modelling of the H-bond happening in the functional PA.

These functional polyamides can address several new applications where the performances of standard polyamides are limited. Some example of applications are developed.

Acknowledgments

The authors thank the financial support of Rhodia business units Engineering Plastics and Polyamide & Intermediates and the people involved in this work.

References

A. Patent WO2010034805A1. Modified polyamide, method for preparing same, and article obtained from said polyamide. Stéphane JEOL, Franck TOURAUD.

Optical CO_2-Sensing Film for Clinical Applications based on a Fluorescent pH-Sensitive and Water-Insoluble Lineal Copolymer

P.K. Contreras-Gutierrez, A.L. Medina-Castillo, J.F. Fernandez-Sanchez, A. Fernandez-Gutiérrez

Department of Analytical Chemistry, University of Granada. C/Fuentenueva s/n 18071, Granada, Spain

jffernan@ugr.es

Introduction

The quantitative detection of CO_2 is important in such fields as environmental protection, food packaging and medical monitoring (breath-by-breath analysis).[1]

Many papers have been published on the development of optical CO_2-sensing layers and several patents have been filed. Nevertheless, the response and recovery times of these methods are often too slow for breath-by-breath analysis and also the number of fluorescent compounds that change in intensity in the presence of CO_2 is extremely limited and their useful lifetime tends to be short and unpredictable.

A suitable CO_2 sensor for clinical applications must provide a linear response function within a range of about 2% and 20% CO_2 vol/vol in air; it must not be very sensitive to humidity, should be stable for at least one month and easy to produce. In addition, luminescence properties are ideally required in order to avoid interferences.

In 1997 Mills et al.[1] developed an optical phase which was based on a ethyl cellulose containing the pH-sensitive hydrophilic indicator dye combined with a phase-transfer agent, tretraoctylammonium hydroxide (TONOH), and a plasticizer. In 2007, Fernandez-Sanchez et al.[2] optimized Mills's membrane. They determined that the CO_2-sensitive dye should have a $pK_a \geq 7.5$ and two types of functional groups, one that can to be deprotonated (e.g. a phenol) and one that can stabilize the negative charge (e.g. lactone, sulphite or diazo groups).

Our research group has recently synthesized a novel fluorescent pH-sensitive and water-insoluble lineal copolymer (NP1(x)) which has an apparent pK_a of 7.8, a phenol group and a lactone group thus it should be suitable for developing CO_2-sensing films. In this work, we analyze the potential application of this new polymer for the development of CO_2-sensing films for breath-to-breath analysis.

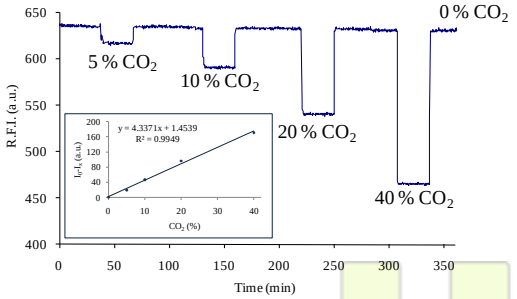

Fig. 1. Response of the proposed sensing layer with different concentrations of CO_2.

Materials and Methods

150 mg of NP1(X) and 375 mg of TONOH were dissolved in 3 mL of MeOH. 500µL of this solution were coated in a glass support with a spin coating at 700 r.p.m.

The sensing films were characterized by measuring the florescence signal (I_0-I_x) at $\lambda_{exc/em}$=480/520 nm, where I_0 is the fluorescence emission of the film in synthetic air (40% RH and flow-rate of 100 mL min^{-1}) and I_x is the fluorescence emission on exposure to different percentages of CO_2 (vol/vol) for 300 s at 40% RH and a flow-rate of 100 mL min^{-1}.

Results and Discussion

In order to test the applicability of NP1(X) in the development of CO_2-sensing films for medical applications, the concentration of NP1(X), the amount of TONOH, the effect of the flow-rate, the effect of the humidity and the study of interferences were developed.

We determined that the best cocktail composition for the determination of % CO_2 (vol/vol) at 40% relative humidity (RH) and a flow-rate of 100 mL min^{-1} is: 50 mg mL^{-1} NP1(X) and 125 mg mL^{-1} of TONOH in methanol.

The study of the effect of the flow-rate reveals that the (I_0-I_x) florescence signal is not influenced by the flow-rate thus it could be used for detecting CO_2 in flow-rates from 50 to 250 mL min^{-1}.

The study of the RH shows that the RH of the media has to be highest than 25% for a good recognition of CO_2. When the RH>25% the sensing film is not affected by the humidity.

Lastly, NO_x, CO and O_2 were tested as potential interferences. Any of them interfere significantly in the determination of CO_2.

Conclusions

The experiments and results described in this work show that the fluorescent pH-sensitive and water-insoluble lineal copolymer described by our research group can be used for developing optical CO_2-sensing films.

The stokes shift (40 nm), sensitivity to CO_2 (detection limit of 0.5 % CO_2 (vol/vol)), absence of relevant interference species, reversibility and short response time allow this sensing-films to be used in breath-by-breath CO_2 analysis (see Fig. 1).

Acknowledgment

The authors thank the Spanish Ministry of Education (Project CTQ2008-01394) and the Regional Government of Andalusia (Excellence projects P07-FQM-02738 and P07-FQM-02625) for their financial support.

References

1. A. Mills, A, Lepre, L Wild. Sens. Actuators B 419 (1997) 38-39.

2. J.F. Fernández-Sánchez, R. Cannas, S. Spichiger, R. Steiger, U.E. Spichiger-Keller. Sens. Actuators B 128 (2007) 145–153.

Properties of conductive layers printed by ink-jet printing.

Monika Rom, Jaroslaw Janicki, Stanislawa Przybylo, Ewa Sarna, Ryszard Fryczkowski

University of Bielsko-Biala, Institute of Textile Engineering and Polymer Materials, POLAND

mrom@ath.bielsko.pl

Introduction

There are numerous trials on application of conductive polymers in various areas from so called 'plastic electronics' through implantable biomedical scaffolds to sensors. Most of conductive polymers can be deposited on different surfaces by electrochemical deposition, self-assembly or spin-coating, but those methods have some restrictions such as rather small areas and require special conditions. Processability of conductive polyaniline (PANI) and polypyrrole (PPy) strongly depends on route of synthesis.

Among different methods of polymer deposition inkjet printing seems to be very attractive as it allows to obtain not only patterns of high resolution and high repeatability but also repeatable layer-by-layer deposition. Inkjet printing demands preparation of inks which despite of appropriate particle sizes (in order to avoid clogging of nozzles), must be stable in time. Moreover viscosity of inks has to be low enough to enable jetting and high enough to avoid wicking from the nozzle.

Materials and methods

Both polyaniline and polypyrrole were synthesized by oxidative polymerization in water at presence of ammonium persulfate (APS) and dodecylbenzylsulfonic acid (DBSA) as a micellar and simultaneously doping agent. Synthesis was performed at room temperature [1,2]. As synthesized polymers were subjected to dialysis for 48h [3].

Stability of PANI and PPy dispersions in water was checked at first by visual method. Viscosity measurements were done using rotational viscometer (Myr) equipped with device for low viscosity and small quantity samples. UV-Vis spectrophotometric analysis by was used to confirm conductive state of synthesized polymers.

„Inks" were deposited layer by layer on various substrates including textiles using Dimatix Fujifilm inkjet printer DMP-2831. Printings were observed using Scanning Electron Microscopy and printer's visualisation system.

Results and Discussion

Stable in time PANI and PPy dispersions were obtained by micellar polymerization. UV-Vis spectra indicated the conductive form of both PPy and PANI. Such a dispersions of PANI and PPy after dialysis did not need viscosity optimization, as they meet requirements. After deposition and during drying of inks phase separation occurred, as the result of phase separation polymers agglomerated and DBSA spots could be distinguished on the printed surfaces. That phase separation affected also rubbing fastnesses of printings.

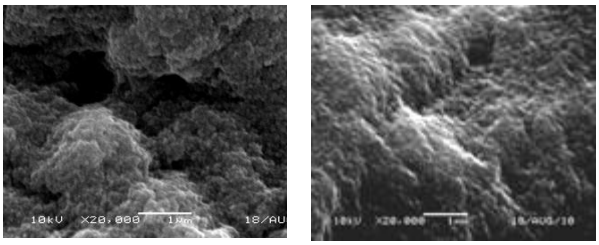

Fig.1. PPy (left) and PANI (right) – form ink, dried and extracted with ethanol.

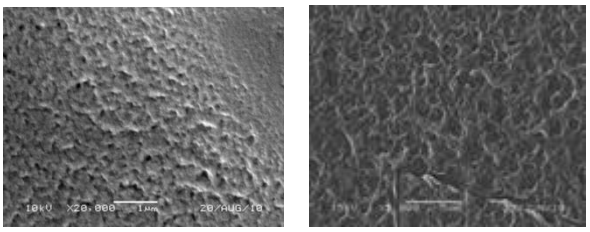

Fig.2. PPy (left) and PANI (right) printed layers, both on PET film.

Conclusions

The concentration of inks was not high enough to allow to obtain continuous printings after one layer deposition, on the other hand increasing of concentration was leading to higher viscosity of compositions which then agglomerated and were problematic for filtration indispensable before filling the cartridge with ink. One of the possible ways of improvement is layer by layer deposition, however phase separation and the excess amount of DBSA remaining in the ink is the challenge.

References

1. M. G. Han, Synthetic Metals 126 (2002) 53-60
2. Y.Q.Shen, M.X.Wan, J.Polym. Sci. Part A Polym. Chem. 35, 3689 (1997)
3. O. Ngamna, Langmuir 2007, 23, 8569-8574

Acknowledgments

This work was supported by Polish Ministry of Science and Higher Education Project No.: O N508 0510 35.

Polymethacrylamides´s synthesis. Dendronized Polymers

Nancy Alvarado, Deodato Radic´

Pontificia Universidad Católica de Chile

nlalvara@uc.cl

Introduction

A dendronized polymers is a linear polymer with highly branched substituents, where due to be presented tubular type polymers are also called "comb". It is interesting to study this type of structures where, due to the size of dendron interactions can be found on the type dendron / dendron, dendron / dendron main chain or / solvent [1]. Dendronized polymers have a spherical or cylindrical shape, depending on size and generation number of dendritic side chain due to the large size of individual chains [2,3]. These "molecular cylinders" can be adapted to a specific chemical composition, stiffness, surface functionalization, and properties of the chain as well as their counterpart spherical dendrimers [4]. The size of the cylinder depends on the degree of polymerization, which determines the length, and moreover dendron generation determines the diameter. Conventional polymers have a diameter in the range of angstroms, whereas the linear polymers dendronizados have diameters in the range of nanometers.

These well-defined architecture could then be used for applications at the nanoscale level, eg in catalysis or as carriers of chemical [5].

Materials and Methods

DEAEMA monomers (diethylaminoethylmethacrylamide) and 2.2 'DAEAEMA (diaminoethylaminoethylmethacrylamide) were obtained through the synthesis of methacrylic acid chloride with diethylethylenediamine in the case of the first monomer and tris (2-aminoetthylamine) for the second monomer both in THF and using triethylamine as acid acceptor. Figure 1

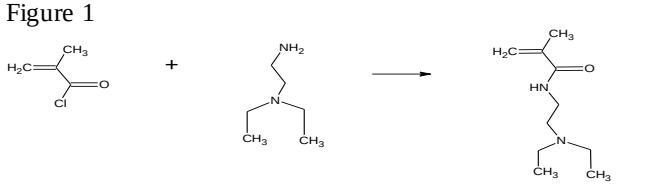

DEAEMA

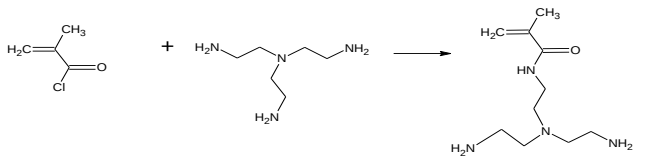

DAEAEMA

Figure 1. Synthesis of DEAEMA and DAEAEMA.

Meanwhile, polymerization was carried out as follows: the dendronized polymer PG0, shown in Figure 1 was obtained through bulk polymerization method using the following procedure: weighed 1.0 g of the corresponding monomer, was added 0.5% of AIBN under N_2 atmosphere, the balloon was left in a water bath at 65 °C for 48 hours. The solid obtained was dissolved in $CHCl_3$ and then was precipitated with petroleum ether. The dendronized polymer PG1-NH2 (Figure 1b) was obtained by polymerization in vacuum line, then left in a water bath at 65 °C for 16 hours. Viscous solution was obtained which was added acetone and got a yellow precipitate. The polymers were characterized by NMR-^{1}H, which ensures that we are in the presence of polymers. Figure 2.

Figure 2. Dendronized Polymers

Results and Discussion

Structures have been obtained dendronized polymers, which have been characterized by thermal analysis (TGA) and differential scanning calorimetry (DSC) values were obtained according to their structures, ie, the decomposition temperature increases with the dendrimeric structure. Is currently conducting a study of mixtures of dendronizedpolymers and polymers classics, to investigate the interaction between them, and mixes with small molecules among which include ibuprofen and thus study its possible inclusion as a guest on a host of dendronized polymer type.

Conclusions

Dendronized polymers are particular structures, whereby due to its unique shape may undergo various studies aimed at finding properties that are not present in their linear analogues. Another interesting approach is to insert small molecules into the cavities of these polymers. The scope for this type of structure is so varied ranging from material science to medical applications.

References

1) A.D. Schlüler and J.P. Rabe. Andew. Chem. Int. Ed. 2000, 39, 864
2) Yin, R., Zhu, Y., Tomalia, D., Ibuki, H., J. Am. Chem. Soc 1998, 120, 2678.
3) Teertstra, S., Gauthier, M., Macromolecules 2007, 40, 1657.
4) Helms, B., Mynar, J., Hawker, C., Fréchet, J., J. .Am. Chem. Soc. 2004, 126, 15020.
5) Cameron, L., Fréchet, L. Macromolecules 2006, 39, 476.

Zinc dithiocarbimates as accelerators for natural rubber vulcanization

Cunha, L. M. G.[a,*]; *Rubinger, M. M. M.*[b]; *Oliveira, M. R. L.*[b]; *Visconte, L. L. Y.*[a]

[a]Instituto de Macromoléculas Professora Eloisa Mano – Universidade Federal do Rio de Janeiro
[b]Departamento de Química – Universidade Federal de Viçosa

[*] leandromgc@ima.ufrj.br

Introduction

Metal complexes of dithiocarbamates are used worldwide in rubber vulcanization but are frequently criticized for their potential production of nitrosamines during the vulcanization processes [1].

The interest on metal complexes of dithiocarbimates is related to their similarity with the dithiocarbamate complexes (Figure 1), especially as far as the presence of the $Zn(S_2C{=}NR)_2$ moiety in the former structures is concerned.

Figure 1: Basic structure for: (a) dithiocarbamate; (b) dithiocarbimate

In this work the vulcanization efficiency of new compounds containing the anionic complex bis(alkylsulfonyldithiocarbimate)zincate(II) with the chemical structure $(Ph_4N)_2[Zn(RSO_2N{=}CS_2)_2]$, where Ph_4N = tetraphenylphosphonium cation, R = ethyl (**1**), or octyl (**2**), towards the vulcanization process of natural rubber compounds has been investigated and compared with the commercial accelerators TBBS and ZDEC. The presence of the R-sulphonyl group linked to the nitrogen atom of the dithiocarbimate moiety is important and may prevent the production of nitrosamines.

Experimental

The compounds were synthesized according to the methodology described in a previous work [2].

Natural rubber was compounded following the formulation: natural rubber, NR (100 phr), stearic acid (2.5 phr), zinc oxide (3.5 phr), sulfur (2.5 phr), Irganox® (1.0 phr), accelerator (3.2 mmol).

The mixture was carried out in a roll mill with 1:1.25 friction ratio, at room temperature. Rheometric parameters were determined in an oscillating disk rheometer from Tecnologia Industrial, at 150 °C and 1° arc, according to ASTM D 2084.

Results and Discussion

Figure 2 shows the rheometric curves obtained for compositions with the new accelerators as well as with TBBS and ZDEC. Considering that the increase in torque values is directly related to the amount of crosslinks formed during vulcanization process, it is possible to conclude that the new accelerators promote crosslink formation in the same magnitude as compared with TBBS. These results indicate that compounds 1 and 2 are effective in forming crosslinks during natural rubber vulcanization.

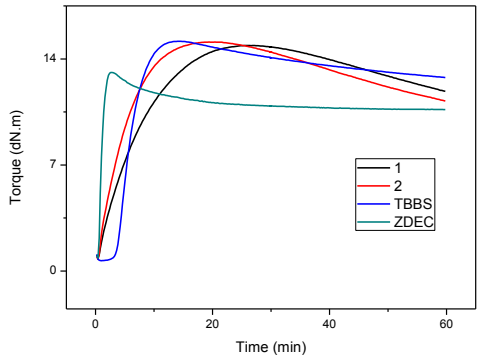

Figure 2: Rheometric curves for compositions with the new and commercial accelerators at 150ºC

Table 1 shows the values of the rheometric parameters for natural rubber compositions with the new and commercial accelerators.

Table 1: Rheometric parameters for natural rubber compositions with new and commercial accelerators

Accelerator	ts_1 (min)	ΔM (dN.m)	t_{90} (min)	R_{30} (%)
1	0.86	14.03	15.45	19
2	0.76	14.36	10.41	10
TBBS	0.68	14.49	9.10	9
ZDEC	0.80	12.32	1.71	18

ts_1 = scorch time; ΔM = maximum torque – minimum torque; t_{90} = optimum vulcanization time; R_{30} = reversion rate

The obtained values for t_{90} showed that accelerator **1** is slower than accelerator **2**. These results can be due to the size of the aliphatic chain. Longer aliphatic chains can improve the solubility of the vulcanization agent in the polymer matrix, making easier the access of the reaction site by the reactive species.

Conclusion

The new accelerators **1** and **2** are active in natural rubber vulcanization. New tests for mechanical properties and crosslink density are being conducted.

References

[1] Travas-Sejdic J, Jelencic J, Bravar M, Frobe Z (1996) Eur Polym J 32:1395-1401.

[2] Cunha LMG, Rubinger MMM, Sabino JR, Visconte LLY, Oliveira MRL (2010) Polyhedron 29: 2278–2282.

Characterization of Gas-Barrier Coated Polyethersulfone Substrate for Flexible Display Application

*Yeonseon Ahn, Mansu Kim, Sang-Hyon Paek, Young Chul Kim**

Department of Chemical Engineering, Kyung Hee University, Yongin-si, Gyeonggi-do 446-107, Korea

kimyc@khu.ac.kr

Introduction: Flexible displays, which can be rolled-up or folded for storage, have been at the focus of many research activities. To realize flexible displays, the development of high gas-barrier plastic substrates and encapsulation layers is recognized as one of key technologies. Researchers reported that the water vapor transmission rate (WVTR) of plastic substrates requires below 10^{-6} g/m^{2}day for flexible OLEDs (FOLEDs) [1]. However, the detection limit of the most widely used measurement system (MOCON Inc.) is 5×10^{-4} g/m^{2}day [2]. As the barrier property of plastic substrates is enhanced, the ultra-low water vapor permeation measuring system becomes required and useful for the study on the permeation mechanism and understanding of device lifetime and degradation phenomena [3].

In this study, we characterized the gas-barrier property of SiN_x- or SiO_x- coated polyethersulfone (PES) substrates by the calcium (Ca) cell test with time dependent quantitative permeation data and Fickian diffusion models, which can estimate the steady-state gas flux as well as the lag time for gas permeation.

Materials and Methods: In order to prepare gas-barrier plastic substrate specimens, 30 nm-thick SiN_x or SiO_x layer was deposited by plasma-enhanced chemical vapor deposition (PECVD) onto 200 μm-thick polyethersulfone (PES) substrates (i-Components Co., Korea).

And the Ca test cells employed for the barrier property characterization were fabricated as follows: On a carefully cleaned glass substrate, a 250 nm-thick Ag electrode was deposited and then the central 3 x 3 cm^2 area was covered with a 250 nm-thick Ca layer to contact with the electrode in a vacuum evaporator. A 4 x 4 cm^2 piece of a barrier substrate specimen, after cleaned with isopropyl alcohol and dried in vacuum for several hours, was attached to the Ca and electrode-coated glass substrate using UV-sealant.

Results and Discussion: We first obtained the time-dependent water vapor permeation data from the neat PES substrates in a 38 ℃ and 90% RH condition. By measuring the time taken until the steady-state water vapor concentration profile builds up across the cross section of the PES substrate, we could estimate the lag time which may be directly related to the shelf-life of the device made using the substrate. Also, The WVTRs of the neat PES substrates with 125 and 200 μm thicknesses were estimated by analyzing the electrical degradation rate of the Ca cells to be 29.3 and 34.1 g/m^{2}day, respectively. The WVTR of the 200 μm-thick neat PES substrate measured by the MOCON test at 38 ℃/100% RH was 54.1 g/m^{2}day. This confirms that the permeation rate measured by Ca cell test is fairly accurate.

We characterized the barrier properties of the two substrates, PES/SiN_x and PES/SiO_x. In the steady-state permeation region, the slop of water vapor fluence is directly related to the permeation rate, which was calculated to be 1.5×10^{-1} and 6.0×10^{-2} g/m^{2}day, respectively. Also, we could estimate the water vapor diffusivity and solubility of the each barrier layer by using a series resistance model and the lag time equation for a two-layer system. The PES/SiO_x substrate showed higher gas-barrier property with lower water vapor diffusivity and solubility than the PES/SiN_x substrate.

The lag times and WVTRs measured for the neat PES (200 μm), PES/SiN_x and PES/SiO_x substrates are shown in the table below.

Atomic force microscopic (AFM) observation on the PES/SiN_x and PES/SiO_x substrates revealed that the SiO_x surface was smoother than the SiN_x surface with the root mean square (RMS) roughness values of 0.70 and 1.43 , respectively. It is considered that the more densely packed layer of SiO_x with the smoother surface gave the better barrier properties.

	Lag time (hour)	Diffusivity (barrier layer) (cm^2/s)	WVTR (g/m^2 day)	
			Ca test	MOCON
PES	0.37		34.05	54.1
PES/SiNx	7.9	6.48×10^{-18}	1.5×10^{-1}	2.8×10^{-1}
PES/SiOx	122	3.45×10^{-18}	6.0×10^{-2}	7×10^{-2}

Environmental condition: 38℃, 90%RH (Ca test)

Conclusions: The course of degradation of Ca test cells via water vapor permeation could be divided into 3 regions; transient, steady-state, and saturated permeation. By determining the transient permeation region, where the concentration gradient across the substrate cross section is building up, we could estimate the lag time before degradation starts. From the time-dependent quantitative permeation data obtained by the Ca cell test, the water vapor diffusivity and solubility of each layer were estimated for the two layer systems. We propose that this approach for characterizing the barrier properties of polymer-based multilayer substrates can be utilized to design ultra-barrier substrates for flexible display application.

References

[1] Lewis, J. S.; Weaver, M. S. *IEEE J. Sel. Top. Quantum Electron.* **2004,** *10*, 45.

[2] MOCON-AQUATRAN®, Minneapolis, MN 55428.

[3] Kumar, R.S.; Mark, A. ; Eric, O.; Guenther, E.; Chua Soo, J. *Thin Solid Films* **2002**, *417*, 120-126.

Aromatic polyimides containing methyl substituents and study of their physical properties

Stefan Chisca, Ion Sava, Valentina Elena Musteata, Maria Bruma

„Petru Poni" Institute of Macromolecular Chemistry, Aleea Gr. Ghica Voda 41 A, Iasi 700487, Romania

e-mail: stefan.chisca@icmpp.ro

Introduction

Aromatic polyimides are unique due to their high thermal stability, chemical resistance, electrical characteristics, toughness, and dimensional stability. Therefore, they have gained much interest in many applications, such as insulating layers for semiconductor devices, microelectromechanical systems or substrates for flexible printed circuits, particularly owing to their relatively low dielectric constant [1,2].

The focus of this work is to investigate a series of polyimides having various structures by using dielectric spectroscopy to gain insight into the molecular mechanism determinning its dielectric properties and kinetic characteristics [3].

Materials and Methods

Aromatic polyimides were prepared by polycondensation reaction of two aromatic diamines, such as 4,4'-diaminodiphenylmethane (DDM) and 3,3'-dimethyl- 4,4'-diaminodiphenylmethane (MDDM), with aromatic dianhydrides, such as 4,4'-isopropylidene-diphenoxy-bis(phthalic anhydride) (6HDA), benzophenonetetracarboxylic dianhydride (BTDA) and hexafluoroisopropylidene-bis(phthalic anhydride) (6FDA) (scheme 1) [4].

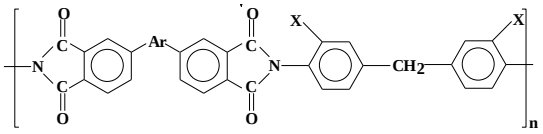

a: Ar = - O-C_6H_4- $C(CH_3)_2$ - C_6H_4- O -; X = H ;
b: Ar = - O-C_6H_4- $C(CH_3)_2$ - C_6H_4- O -; X = CH_3
c: Ar = CO; X = H ;
d: Ar = CO; X = CH_3
e: Ar = $C(CF_3)_2$; X = H ;
f: Ar = $C(CF_3)_2$; X = CH_3

Scheme 1. Structure of the aromatic polyimides

The structures of these polymers were determinated by FT-IR, and the thermal properties were investigated by thermogravimetric analysis (TGA) and differential scanning calorimetry (DSC). Dielectric parameters and molecular relaxations were characterized by dielectric relaxation spectroscopy (DRS).

Results and Discussion

These polyimides exhibited high thermal stability, with decomposition temperature being above 430 ºC in air, and high glass transition temperature being in the range of 200 – 287 ºC.

Dielectric properties of polyimides were evaluated on the basis of dielectric constant, dielectric loss and electric modulus, and their variation with frequency and temperature. These dependencies constitute very important factors to be considered for dielectric materials in their microelectronic applications. The polyimide films exhibited low dielectric constant values, being in the range of 2.88 - 3.48 at 1 Hz at room temperature.

The sub-glass relaxation processes were investigated and showed that for polymers based on 6HDA and 6FDA three relaxation processes (γ, β_1 and β_2) were observed, and for polymers based on BTDA only two (γ and β) relaxations were detected (figure 1).

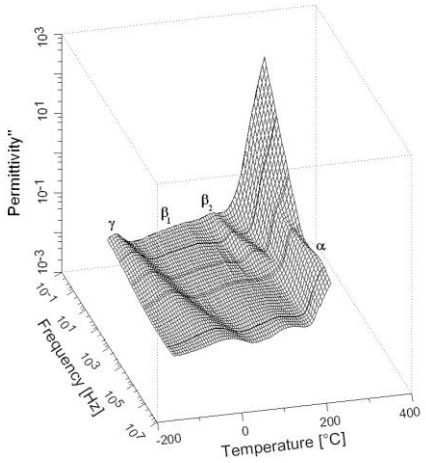

Figure 1. Dielectric loss vs. frequency and temperature, for polyimide **a**

The γ transition was correlated with water absorbed from atmosphere. β_1 relaxation was associated with motions in the diamine part and has a higher activation energy for polymers having methyl substituents on diamine segment. β_2 relaxation was attributed to the rotation of side groups (CF_3 and CH_3) in the dianhydride part and is dependent on local conformation.

Conclusions

All these characteristics make the present polymers potential candidates for applications as high performance dielectrics.

Acknowlegment:

This work was supported by CNCSIS-UEFISCU Project No. PN-II-RU, code TE_221/2010.

References

1. Hergenrother PM. The use, design, synthesis and properties of high performance/high temperature polymers: an Overview. High Perform Polym 2003;15:3-45.
2. Rebeiz GM, Tan GL. Introduction to RF MEMS for microwave applications, RF MEMS Theory, Design, and Technology. New Jersey: Wiley Interscience, Hoboken, 2003.
3. Chisca S, Musteata VE, Sava I, Bruma M. Dielectric behavior of some aromatic polyimide films. Eur Polym J DOI:10.1016/j.eurpolymj.2011.01.008.
4. Sava I, Chisca S, Bruma M, Lisa G. Comparative study of aromatic polyimides containing methylene units. Polym Bull 2010;65:363-375.

Synthesis and Photophysical Properties of Donor-Acceptor Block Copolymers

Erika Bicciocchi,[a,b] *Ming Chen*,[b] *Ezio Rizzardo*,[b] *Ken Ghiggino*[a]

[a]School of Chemistry, The University of Melbourne, Victoria, 3010, Australia
[b]CSIRO Materials Science and Engineering, Clayton Vic 3168, Australia

Erika.Bicciocchi@csiro.au

Introduction

The performance of an organic photovoltaic (OPV) cell is mainly determined by the properties of the active layer, which is generally composed of a blend of an electron donor and an acceptor. Since both, donor and acceptor materials tend to phase separate on a macroscopic scale the morphology of this active layer is of utmost importance. Block-copolymers have been known to exhibit the ability to stabilize polymer blends. Their use in OPV devices, however, has apart from a few examples,[1-3] been mainly neglected.

We thus embarked on a project which aims to develop a generic synthetic methodology for obtaining electron donor-acceptor (D-A) functionalized block copolymers with tailored properties, which will be used to fabricate stable and efficient OPV devices.

Results and Discussion

The aim of this project is to develop a generic synthetic approach for D-A block copolymers, where the donor and acceptor blocks are made from a conjugated polymer and a coil macromolecule with attached C60-pendant, respectively. So far the most promising polymers for the conjugated block are synthesized by polycondensation reactions such as Stille and Suzuki coupling. For the coil part, reversible addition fragmentation chain transfer (RAFT) technique was employed and a combination of those techniques was chosen for the synthesis of D-A block copolymers. As a proof of concept, it was decided to use poly(9,9-dihexylfluorene-alt-bithiophene) (F6T2) as a model system for the conjugated block because the monomers are commercially available and the polymer has been widely studied.

The coil polymer was obtained by copolymerizing styrene with benzoylbutyric acid functionalized vinylbenzyl chloride under the control of a trithiocarbonate RAFT-agent. The product so obtained contained pendant keto groups which were subsequently directly modified with tosylhydrazone to facilitate the C60 attachment. This direct modification, however, appeared to be problematic as the RAFT groups are easily cleaved by a nucleophilic attack by the tosylhydrazine yielding thiol end groups, which can couple through disulfide formation. A possible way around is the chemical removal of the RAFT end group using *N*-ethylpiperidine hypophosphite and a radical initiator, resulting in a complete disappearance of it.[4]

After removing the RAFT groups the polymer was converted to the corresponding polytosylhydrazone, which reacted further with fullerene to give the final coil block. The attachment of C60 to the polymer was confirmed by gel permeation chromatography analysis equipped with a photo-diode array detector (GPC-PDA) and ^{13}C-NMR.

The conjugated rod block was synthesized as reported in the literature by a Suzuki coupling reaction and in the presence of a small excess of diboronic acid to ensure the presence of terminal boronic ester end-groups, which were subsequently end capped with the coil polymer obtained after the RAFT group removal.[5] The further functionalization of the coil part with fullerene was carried out in a similar way as describe above yielding rod-coil D-A block copolymer **1**. The link between the rod and coil part was verified through GPC-PDA measurements and the presence of the polymer blocks was confirmed by IR and UV spectroscopy.

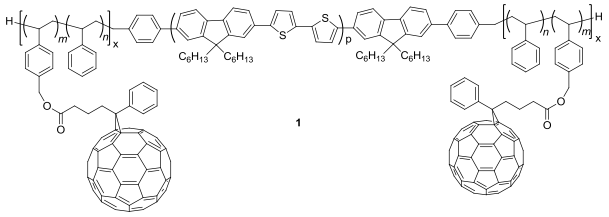

1

A further confirmation of the successful synthesis of block-copolymer **1** was inferred from fluorescence spectroscopy, where the presence of the C60 acceptor completely quenched the fluorescence of the conjugated polymer donor in a thin film due to an electron transfer process.

Conclusion

In this contribution we successfully developed a generic methodology for the synthesis of D-A block copolymers through a combination of Suzuki-coupling and RAFT polymerization. We found that it is essential to remove the trithiocarbonate end-groups in order to prevent disulfide formation through the nucleophilic attack of tosylhydrazine. The final structure of the D-A block copolymer was analysed and confirmed by spectroscopic analysis. The interaction of the donor and the acceptor block was verified by fluorescence quenching of a thin film of the polymer and as such it might find useful application in OPV devices.

References

1. U. Stalmach, B. de Boer, C. Videld, P.F. van Hutten and G. Hadziioannou, *J. Am. Chem.Soc.*, **2000**, *122*, 5464-5472.
2. M.H. van der Veen, B. de Boer, U. Stalmach, K.I. van de Wetering and G. Hadziioannou, *Macromolecules*, **2004**, *37*, 3673-3686.
3. C.Yang, J.K. Lee, A.J. Heeger and F. Wudl, *J. Mater. Chem.*, **2009**, *19*, 5416-5423.
4. Y.K. Chong, G. Moad, E. Rizzardo and S.H. Thang, *Macromolecules*, **2007**, *40*, 4446-4455.
5. G.L. Schulz, X. Chen and S. Holdcroft, *App.Phy. Lett.*, **2009**, *94*, 023302.

New Highly Thermostable Phthalonitrile-Containing Aromatic Polyamides and Poly(amide imide)s for High Performance Applications

Ionela-Daniela Carja, Corneliu Hamciuc, Elena Hamciuc, Tachita Vlad-Bubulac

"Petru Poni" Institute of Macromolecular Chemistry, Aleea Gr. Ghica Voda 41A, Iasi-700487, Romania

daniela.carja@icmpp.ro

Introduction

Aromatic polyamides and polyimides are well known due to their excellent thermal stability and electric insulation properties [1, 2]. However, their applications are limited because most of these rigid polymers are insoluble and infusible. Aromatic poly(amide imide)s have been developed as alternative materials offering a compromise between excellent thermal stability and processability. It has been shown that the introduction of voluminous pendant groups, such as phthalonitrile bulky group, into rigid polymer chain can impart a significant increase of glass transition temperature by restricting the segmental mobility while providing good solubility because of decreased packing and crystallinity. Also, the solvent resistance and thermal properties of the phthalonitrile-containing polymers were enhanced by thermal treatment around the glass transition temperature for an extended period of time due to the crossslinking site formation through the thermal polymerization of the nitrile groups on pendant phthalonitrile units [3].

Material and Methods

Monomer **1** was prepared by nucleophilic displacement reaction of 4-nitrophthalonitrile with 4,4′-diamino-4″-hydroxy-triphenylmethane, in the presence of anhydrous potassium carbonate. Aromatic polyamides **4** and poly(amide imide)s **5** were synthesized by low temperature solution polycondensation of terephthaloyl chloride or 2,2-bis[N-(4-chloroformylphenyl)phthalimidyl]hexafluoro-propane, respectively, with a mixture of **1** and other aromatic diamines **3**, in various ratios, using NMP as solvent and pyridine as acid acceptor (Scheme 1). The polymers were characterized by using different techniques: FTIR and ^{1}H NMR spectroscopy, GPC, AFM, ATG, DSC, DMA, BDS, WAXD.

Results and Discussion

A new diamine **1** was prepared and characterized and its self-promoted cure behavior was investigated. It exhibited a low melting point of 78.4°C and could be cured at temperatures of 230-250°C. The resulting resins had exceptional high thermal and thermo-oxidative stability, the 5% weight loss being above 500°C and the char yield at 700°C being over 62%, in air or inert atmosphere.

Based on diamine **1**, new aromatic polyamides **4** and poly(amide imide)s **5** containing phthalonitrile groups were synthesized. The molecular structure was identified by FTIR and ^{1}H NMR spectroscopy. The polymers exhibited good solubility in organic solvents and film forming properties. They showed high thermal stability, the decomposition temperature being above 400°C. Electrical properties of the polymer films were evaluated on the basis of dielectric constant and dielectric loss and their variation with frequency and temperature.

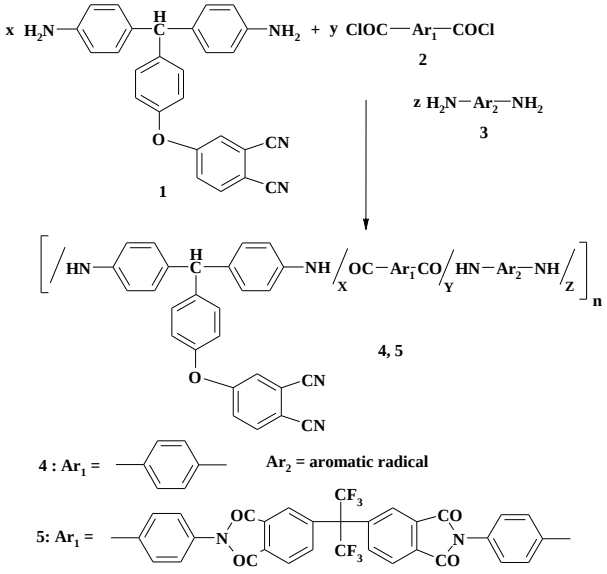

Scheme 1. Synthesis of the polymers.

The electromechanical properties of some poly(amide imide) films were investigated. Nanoactuation has been determined to be in the range of 300-400 nm, at 130-220 V, with plane flexible thin electrodes.

Conclusions

New polyamide and poly(amide imide)s were synthesized based on a new diamine containing phthalonitrile group. The polymers had good solubility in organic solvents and could be processed from solutions into thin flexible films having the thickness in the range of tens of micrometers. The presence of the phthalonitrile groups in the macromolecular chains increased the humidity absorption and dielectric constant of the polymers. By applying a thermal treatment an increase of the solvent resistance was observed. The polymers showed high thermal and thermo-oxidative stability. They exhibited flame retardancy, the chair yield at 700°C having high values both in air and inert atmosphere.

References

1. J. Gallini, *Polyamides, aromatic*, in *Encyclopedia of Polymer Science and Technology*, vol. 3, New York: John Wiley & Sons, 2005, pp. 558–584.
2. C.E. Sroog, *Prog. Polym. Sci.*, **16**, 561, 1991.
3. K. Zeng, H. Hong, S. Zhou, D. Wu, P. Miao, Z. Huang, G. Yang, *Polymer*, **50**, 5002, 2009.

Acknowledgements

This work was supported by *CNCSIS – UEFISCDI*, project number PNII – IDEI code ID_997/2008.

Polyaniline Synthesis Using Fenton Reagent: Effect of Substitution of Aniline

Michal Blaha, Jiri Zednik, Jan Svoboda and Jiri Vohlidal

Charles University in Prague, Faculty of Science, Department of Physical and Macromolecular Chemistry, Hlavova 2030, CZ-128 43 Prague 2

e-mail: Michal.Blaha@csop.cz

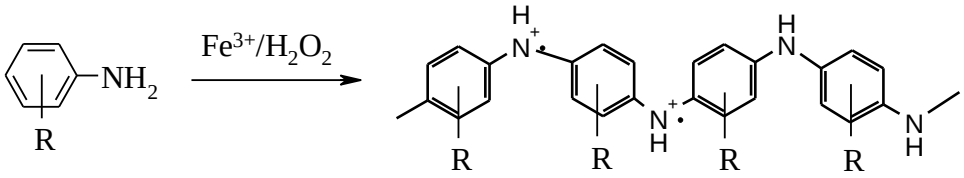

Polyaniline (PANI) is conjugated polymer that has already found practical applications in the construction of capacitors, analytical sensors, antistatic films and coatings, materials for electrostatic discharge protection, electrochromic windows, anticorrosion paints, etc. It is usually prepared by chemical oxidative polymerization. Its replacement by catalytic process can lower contamination of forming polymers by oxidant residues and it can reduce production of waste solvents (their recycling represents half of cost of polymer production). This aim can be achieved by using a catalyst system that mediates the oxidation of a monomer by oxidant such as hydrogen peroxide, which is transformed into water during the polymerization. Also other systems have been examined, but Fenton system (Fe^{3+}/H_2O_2 in acidic aqueous environment) is the most promising one.

Although few papers were published in last fifteen years in this field, no one of them was dealing with reaction course of polymerization and dependence of physical and chemical properties of resulting PANI on H_2O_2-to-aniline mole ratio, to which we paid attention in our previous work. We previously focused on dependence of spectral properties of PANI on H_2O_2-to-aniline mole ratio. While PANIs prepared with substoichiometric H_2O_2-to-aniline mole ratio exbibit spectral properties comparable to PANI prepared with ammonium persulfate, PANIs prepared with overstoichiometric H_2O_2-to-aniline mole ratio exbibit some differences in UV/vis, FTIR and Raman spectra, which is an evidence of structure defects. These differences compared to spectra of PANI prepared with ammonium persulfate indicate presence of protonized structures also in base (dedoped) forms of polymers, which is typical for self-doped PANIs. NMR spectra of oligomers resulting from polymerization done with high overstoichiometric H_2O_2-to-aniline mole ratio indicate presence of C–OH or C–O–C bonds in their structure.

To get information about the reaction course we used mainly combination of potential time profiling, capillary zone electrophoresis and also gravimetry of resulting polymer.

As already known, from our previous work, extent of structure defects does not depend only on H_2O_2-to-aniline mole ratio, but also on ring substitution of aniline. We recently studied polymerization of aniline, 2-methoxyaniline and 2-chloroaniline and we have found that extent of structure defects is high in case of electron donating methoxy group and is low in case of electron withdrawing chloro atom.

Nowadays, we present more detailed study of the effect of the substituent on properties of corresponding polyaniline. Potential time profiling measurements were done for all studied monomers (aniline, 2-methoxyaniline, 2-chloroaniline and 2-ethylaniline). Results obtained are discussed concerning to ionization energies (potentials) of these compounds, which were calculated by Gaussian using B3LYP method, and concerning to oxidation potentials of monomers measured on cyclic voltammetry instrumentation in acidic solutions having same concentrations of monomer and hydrochloric acid as in case potential time profiling measurements.

Acknowledgement:
Financial support of the Ministry of Education of the Czech Republic (MSM0021620857) is gratefully acknowledged; M. Bláha is indebted to the Czech Science Foundation for the fellowship (project No. 203/08/H032).

UV cured acrylic membranes reinforced by Cellulose MicroFibrils for Lithium Batteries

A.Chiappone[1], R.Bongiovanni[1], J.R. Nair[1], C. Gerbaldi[1], E.Zeno[2]

[1]Department of Materials Science and Chemical Engineering, Politecnico di Torino, Corso Duca degli Abruzzi 24, 10129 Turin, Italy

[2]Centre Technique du Papier (CTP), Domaine Universitaire, B.P. 251, 38044 Grenoble Cedex 9, France

annalisa.chiappone@polito.it

Introduction

Nowadays natural fibers are used as reinforcements for the production of polymer composites since they are low-cost, biodegradable, readily available and characterized by low density and high specific properties.[1] Microfibrillated cellulose (CMF) is obtained through an easy process that does not involve chemical reactions. The cellulose particles obtained have a diameter range of 10–100 nm, length in the microscale and show a web-like structure alternating crystals and amorphous strings[2].

Free radical photo-polymerisation is a successful approach for the production of composite thermo-set polymer membranes, the process takes place at room temperature under UV light, is easy, reliable and rapid[3]. Considering the interesting properties of CMF and the potentiality of photo-polymerisation this work describes a UV cured CMF-polymer composite membrane to be applied as electrolyte in Li batteries[4]. Studies on UV-cured methacrylic-based polymer membranes as gel-electrolytes have already been developed[5-7] and good performances in terms of electrochemical properties are reported, membranes are flexible, self standing and easy to handle. The use of a mechanical reinforcement such as CMF could lead to interesting results.

Materials and Methods

CMF nanoparticles were prepared by treating bleached cellulose fibres in a microfluidizer processor. A CMF aqueous suspension (1%wt) has been prepared. The reactive formulation for polymer membranes was based on a dimethacrylic monomer, bisphenol A ethoxylate (15 EO/phenol) dimethacrylate (BEMA, Mn: 1700, Aldrich), and poly(ethylene glycol) methyl ether methacrylate (PEGMA, Mn: 475, Aldrich) in 1:1 ratio. 2hydroxy-2methyl-1phenyl-1propanon (Darocur 1173, Ciba Specialty Chemicals) was the free radical photo-initiator (2%wt). The CMF suspension was added to the reactive formulation in different ratios in order to obtain nanocomposites containing 1, 3, 5% wt of microfibrils. The liquid mixture was left 12 hours in oven at 60°C to obtain the water evaporation and subsequently UV cured for 3 min. under N_2 flux by using a medium vapour pressure Hg lamp (30mWcm^{-2}). Later free, self standing films obtained after photopolymerisation were treated in vacuum at 70°C overnight. Membranes were then swelled with a liquid electrolyte solution containing a 1.0 M $LiPF_6$ in Ethylen-carbonate/Diethyl-carbonate (EC/DEC 1:1 w/w) solution (Ferro Corp., battery grade).

Results and Discussion

The polymer membrane obtained copolymerising the monomers BEMA and PEGMA with the in situ addition of CMF was a freestanding, extremely flexible and non-sticky membrane.

a

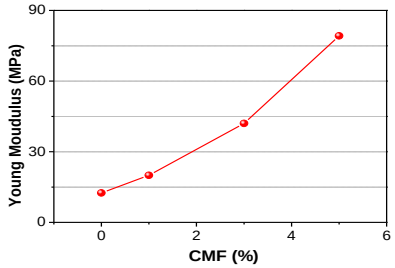

The addition of CMF to the polymer did not affect the Tg, slightly increased the thermal stability and enhanced remarkably the mechanical properties both before and after swelling in the liquid electrolyte. Tensile test performed on the composite membranes (figure a) and bending test performed on the swelled ones showed the enormous difference in the mechanical performances given by the use of CMF. The electrochemical characterisation showed that the membranes swelled in the liquid electrolyte present high values of ionic conductivity also in presence of CMF (Figure b), an appreciably high electrochemical stability window and good cyclability.

b

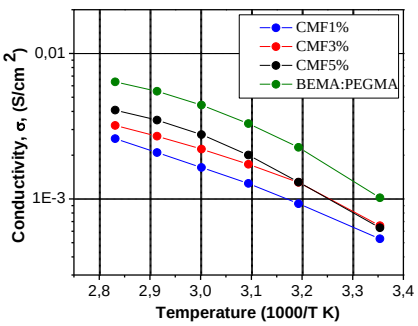

Conclusion

Microfibrillated cellulose was successfully used to reinforce methacrylic-based composite polymer membranes prepared by UV-curing for the application in the field of lithium batteries. The prepared membranes gave interesting results in terms of mechanical properties and electrochemical performances, therefore, these kinds of polymer electrolytes are particularly promising in the field of Li-based thin flexible batteries.

References

1.I.Sirò,D.Plackett (2010) Cellulose17, 3: 459-494(36)
2.J.Lu et al (2008) Composites:PartA 39 738–746
3.J.J. Decker C (1996) Prog Polym Sci 21:593
4.B .Scrosati (1995) Nature 373:557
5.J. Nair et al (2008) J.Power Sources 178 751.
6.C. Gerbaldi et al (2008)J. Appl. Electrochem. 38 :985.
7.C. Gerbaldi et al (2009) J. Appl.Electrochem., 39: 2199–2207.

Photoinduced Surface relief gratings of Azopolymers with rigid and flexible chains

Ion Sava[1], Nicolae Hurduc[2], Liviu Sacarescu[1], Victor Damian[3]

[1]„Petru Poni" Institute of Macromolecular Chemistry, Aleea Gr. Ghica Voda 41 A, Iasi 700487, Romania
[2]Technical University „Gh.Asachi" Iasi, Department of Natural and Synthetic Polymers, Bd. Mangeron 71, Iasi, Romania
[3]National Institute for Laser, Plasma and Radiation Physics, Atomistilor str. 409, Bucharest-Magurele, Romania

Email:isava@icmpp.ro

Azobenzene and many of its derivatives have been studied for a long time due to their properties that allow various applications triggered by light. Usually these applications are based on the, photoinduced isomerism of the azobenzene which result in significant conformational and dipole moment changes.[1-3]

This paper presents the UV photochromic response of azo-polyimide compared with azo-polysiloxane thin films for surface relief gratings.

Experimental

The structures of the investigated azo-polymer are shown bellow:

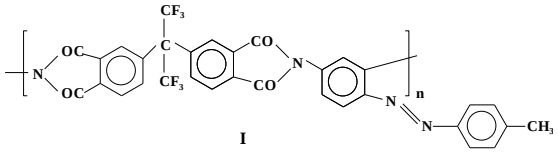

I

Azo-polyimide

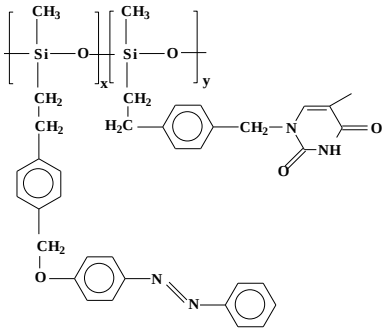

II

Tymine modified azo-polysiloxane

The azobenzene *trans-cis* isomerization and *cis-trans* relaxation photocromic process, was investigated both in solution and in solid state by UV spectroscopy with BOECO S1 UV spectrophotometer. The light source, was an Nd:YAG laser working on his third harmonic at 355 nm and with a pulse length at FWHM (full width half maximum) of 6 ns. The obtained structurated surfaces were characterized by optical microscopy and atomic force microscopy (AFM). AFM investigations were done using a Solver PRO-M, NT-MDT apparatus. The film topography was analyzed in *semicontact mode*, in air, using a rectangular cantilever NSG10/Au with a nominal elasticity constant K_N = 11.5 N/m.

Results and discussion

Both polymers present a high thermal stability with the initial decomposition temperature over 300°C, good solubility in different solvents and good film forming ability. An important difference concerning the glass transition temperature was observed. Therefore, the azo-polyimide shows a value of 228°C, higher than the azo-polysiloxane one (34 °C).

The time dependence of the photoisomerisation process shows that the maximum conversion degree of polyimide from *trans* to *cis* isomer in the solid state is lower (only 39%) compared with the modified azo-polysiloxane (55%). Also, it was observed that the time scale for the *cis-trans* relaxation activated by visible light is similar to the reverse UV induced *trans–cis* isomerization; this aspect is favourable to generate the photoinduced fluid state according to the conformational instability concept.[4]

The induced surface relief grating AFM profile evidenced the evolution of the surface structuration from disorder to order, up to a sinusoidal profile corresponding to the surface grating formation. The structuration time depends on the incident laser fluence / intensity and number of irradiation pulses. AFM profiles of the surface relief induced by an interference field with a medium fluency of 8.4 mJ/cm^2 and 100 subsequent laser pulses are similar for both azo-polymers.[5] The depth of the photoinduced structure is about 90 nm for the azo-polysiloxane film and 100-110 nm for the azo-polyimide film. The difference consists in the evolution of the structure with the number of incident laser pulses, respectively irradiation time. After only 10 irradiation pulses the height of the ''hills'' on the surface of azo-polyimide was half of those on the azo-polysiloxane surface. This should be the effect of the azo-polyimide main chain rigidity which slows down the molecular reorganization.

Conclusions

The SRG induced on the films surface of azo-polyimide and azo-polysiloxane modified with thymine have a very good time stability and a good contrast of the surface volume structuration.

Acknowledgement: The authors express their gratitude to STREAM, Grant agreement no.264115/2011 for the financial support.

References

1. A. Natansohn, P. Rochon, *Chem. Rev.*, **102,** 4139, 2002.
2. L. Ding, T.P. Russell, *Macromolecules*, **40**, 2267, 2007.
3. K.G. Yager, O.M. Tanchak, C. Godbout, H. Fritzsche, C.J. Barrett, *Macromolecules*, **39,** 9311, 2006.
4. N. Hurduc, R. Enea, D. Scutaru, L. Sacarescu, B. C. Donose, A. V. Nguyen, *J Polym Sci A1,* **45**, 4240, 2007.
5. I. Sava, L. Sacarescu, I. Stoica, I. Apostol, V. Damian, N. Hurduc, *Polym. Int.,* **58**, 163, 2009.

Heterocyclic polynaphthaleneimides containing siloxane groups in the main chain

Radu-Dan Rusu, Mariana-Dana Damaceanu, Maria Bruma

"Petru Poni" Institute of Macromolecular Chemistry, Aleea Gr. Ghica Voda 41A, Iasi-700487, Romania

Email: radu.rusu@icmpp.ro

Introduction

High-performance polymers are used in applications that demand service at enhanced temperatures, while structural integrity and an excellent combination of chemical, physical and mechanical properties are maintained. Some of the important polymers in this respect are polyimides and poly(1,3,4-oxadiazole)s [1,2]. However, these polymers have the common problem of being difficult to process owing to their infusibility and poor solubility in organic solvents. Therefore, much effort has been done to develop structurally modified aromatic polymers that have increased solubility without sacrificing their thermal stability. A combination of several structural modifications, that is, the incorporation of 1,3,4-oxadiazole rings, naphthalene units and flexible groups in the polymer backbones, minimizes the trade-off between the solubility and properties of wholly aromatic polyimides. This work describes the synthesis and characterization of a series of polynaphthaleneimides containing flexible siloxane bridges and oxadiazole moieties in the main chain.

Materials and methods

A series of new aromatic poly(1,3,4-oxadiazole-naphthaleneimide)s have been synthesized by two-step solution polycondensation reaction of three different aromatic diamines containing oxadiazole ring with a mixture of naphthalenetetracarboxylic dianhydride and 1,3-bis(4'-phthalic anhydride) tetramethyldisiloxane taken as 1:0.5:0.5 molar ratio. The general structure of these copolymers is presented in the scheme below.

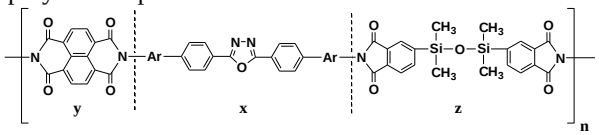

x : y : z = 2 : 1 : 1

Ar = PI 1 : - ; PI 2 : 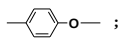 ; PI 3 : 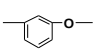

The polycondensation reaction was carried out in 1-methyl-2-pyrrolidinone (NMP) in the presence of benzoic acid as catalyst, under anhydrous conditions in nitrogen atmosphere, at high temperatures (200°C). The relative amounts of monomers and NMP were adjusted to maintain a solid content of 8%.

The solubility, inherent viscosity, thermal stability, glass transition temperatures, UV absorption and photoluminescence properties of these polymers have been evaluated with respect to their chemical structure.

Results and discussion

The poly(1,3,4-oxadiazole-naphthylimide)s are soluble in a convenient aprotic amidic solvent such as NMP, and, except for polymer **PI 2**, in N,N-dimethylacetamide and dimethyl sulfoxide, when slightly heated. Copolyimide **PI 3** containing *m*-catenated phenylene rings proved to be also soluble in N,N-dimethylformamide, and even in less polar solvents such as chloroform. The inherent viscosity values of these polymers are in the range of 0.15-0.2 dL/g.

The structures of the polymers were identified by means of elemental analysis, IR and ^{1}H NMR spectroscopy.

The thermal properties of these copolynaphthaleneimides were evaluated by means of DSC and TGA. The copolyimides exhibited Tg values in the range of 201-255°C. The polymers showed excellent thermal stability, as expected in case of aromatic polyimides: the initial decomposition temperatures were about 477-489°C and the temperatures of 10% gravimetric loss were in the range of 497-508°C. The temperature of the maximum decomposition rate of polymer **PI 1** is 515°C, while the decomposition of copolyimides **PI 2** and **PI 3** takes place in two steps as shown by DTG curves: the first step occurs in the range 512-516°C and the second in the range 520-525°C.

Since the 1,3,4-oxadiazole ring is known as a light emissive unit [3], we have also performed a study of the UV absorption and photoluminescence properties of these polymers. It was found that all the oxadiazole-containing copolyimides in NMP solutions show one strong UV absorption maximum around 302 nm, mainly determined by the diphenyl-1,3,4-oxadiazole unit [4], and two peaks at 360 nm and 380 nm, due to the naphthylimide chain segments [5], the spectra being quite identical. All three poly(oxadiazole-imide)s showed blue photoluminescence, in the range 410–445 nm, which makes them promising candidates for future use as high-performance materials in the construction of light-emitting devices.

Conclusion

The incorporation of naphthylimide units, oxadiazole rings and of flexible siloxane bridges in the main chain gave products with good solubility and satisfying properties, which would be useful for various high-performance applications, especially in electroluminescent devices with high stability.

Acknowledgements

The financial support provided by CNCSIS_UEFISCDI through the Project PN II-RU, code TE_221, no. 31/2010 is acknowledged with great pleasure.

References

1. Schulz B, Bruma M, Brehmer L, *Adv Mater*, **1997**, *9*, 601-613.
2. Hergenrother PM, *High Perform Polym*, **2003**, *15*, 3-45.
3. Akcelrud L, *Prog Polym Sci*, **2003**, *28*, 875-962.
4. Rusu RD, Damaceanu MD, Marin L, Bruma M, *J Polym Sci Part A: Polym Chem*, **2010**, *48*, 4230-4242.
5. Damaceanu MD, Rusu RD, Bruma M, Jarzabek B, *Polym J*, **2010**, *42*, 663-669.

Study on the Crystallization of Poly(nonamethylene azelate) and its Copolymers Incorporating Pimelate Moeities

A. Díaz, L. Franco, R. Díaz, M.T. Casas, J. Puiggalí

Departament d'Enginyeria Química, Centre de Recerca en Nanoenginyeria, Universitat Politècnica de Catalunya, ETSEIB, 08028-Barcelona

Jordi.Puiggali@upc.edu

Aliphatic polyesters play a significant role as biodegradable polymers due to their potentially hydrolyzable ester bonds. Polyalkylene dicarboxylates constitute a specific family of polyesters that is receiving great attention since the excellent mechanical and thermal properties of poly(butylene succinate) make feasible its commercialization. Many works have been focused on the structural study and degradation mechanism of different members of this family and particularly those derived from even diols and even dicarboxylic acids. On the contrary, scarce information is available on odd-odd derivatives. This point merits attention since both structure and properties should be sensitive to the so called odd-even effect. Specifically, the polyester constituted by 1,9-nonanediol and azelaic acid is interesting since the high methylene content of its repeat unit gives rise to a semicrystalline polymer with a higher melting point than polycaprolactone, one of the most applied biodegradable polymeric material. Properties can be easily modified by copolymerization with a second dicarboxylic acid. Thus, the effect of the incorporation of pimelic acid units on the crystallization process, crystalline structure and morphology has also been considered in this work.

Polyesters were synthesized from the appropriate mixture of dicarboxylic acids and an excess of 1,9-nonanediol (molar ratio 2.2/1) by thermal polycondensation. The reaction was first performed in a nitrogen atmosphere at 150 ºC for 6 h and then in vacuum at 180 ºC for 18 h. Titanium tetrabutoxyde was used as a catalyst. The polymer was dissolved in chloroform and precipitated with ethanol. The polymerization yield was always close to 70%. Calorimetric studies indicated that all samples were able to crystallize showing a eutectic point at the intermediate composition which also gave rise to a small decrease on the degree of crystallinity (Figure 1a). Crystallization from the melt rendered negative birefringent spherulites with ringed or fibrilar textures depending on the degree of supercooling and even on the composition (Figure 1b).

X-ray fiber diffraction patterns indicate that poly(nonamethylene azelate) crystallizes according to an orthorhombic unit cell with a large *b* parameter (i.e. close to 1.5 nm) and a practically all trans molecular conformation (Figure 2a). Patterns of copolymers showed similar trends although the intensity of some *hkl* reflections was enhanced (Figure 2b).

All copolymers crystallized from dilute 1,6-hexanediol solutions as lozenge crystals (Figure 3) with a degree of truncation that increased with the crystallization temperature as was also reported for other even-even polyesters. Electron diffraction patterns of the different samples were similar and compatible with rectangular unit cells of smaller dimensions than those deduced from fiber patterns. Crystalline structure is consequently defined by an arrangement of only two distinctive chain segments in chain axis projection.

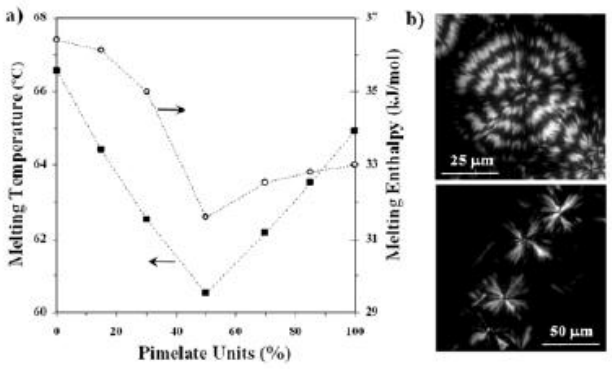

Figure 1. a) Variation of the melting temperature and enthalpy of poly(nonamethylene azelate-*co*-pimelate)s with the molar percentage of pimelate units. b) Spherulitic morphologies obtained by crystallization from the melt state of poly(nonamethylene azelate-*co*pimelate) containing 15% (up) and 50% (down) of pimelate units.

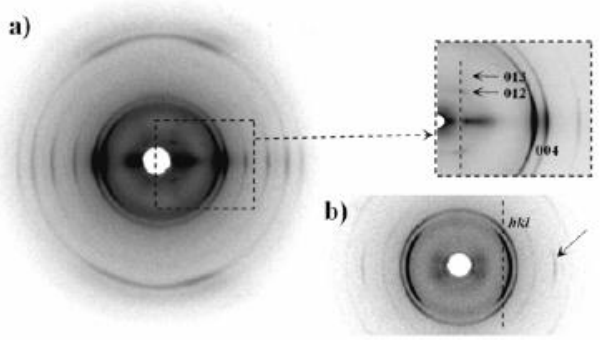

Figure 2. Fiber X-ray diffraction patterns of poly(nonamethylene azelate) (a) and the copolymer containing 15% of pimelate units (b).

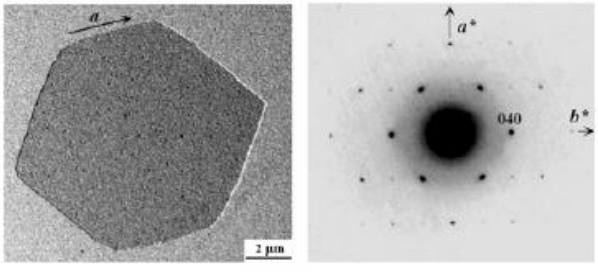

Figure 3. Lamellar crystal and electron diffraction pattern of poly(nonamethylene azelate-*co*-pimelate) (50% of pimelate units).

Acknowledgements: This research has been supported by a grant from CICYT/FEDER (MAT2009-11503).

Combination of ionic and covalent cross-links on elastomeric ionomers: Effect on the structure-properties relationship

M.A. Malmierca*, L. Ibarra, A. Rodríguez, I. Mora-Barrantes, J.L. Valentín.

Instituto de Ciencia y Tecnología de Polímeros (CSIC), c/ Juan de la Cierva, 3. 28006 Madrid, Spain

* *email:* malonso@ictp.csic.es

Introduction:

Conventional elastomers are characterized by a long-range elasticity obtained after the vulcanization process because of the creation of covalent cross-links between the polymer chains. These materials present many recycling problems because of the permanent character of the covalent cross-links.

Moreover, ionic elastomers have a thermo-reversible network structure that allows their recycling. Ionic elastomers are characterized by a strong physically crosslinked network resulting from a phase separation of ionic-rich nano-domains. The ionic domains are formed by the association of ionic groups that tend to aggregate forming multiplets and clusters that act as cross-links promoting the elastic behaviour of these polymers[1, 2]. In addition, the trapped glassy rubber around them improves the physical properties of these materials acting as reinforcement of the soft rubbery matrix.

However, the thermal lability of ionic cross-links leads poor mechanical properties at high temperatures, restricting their possible applications.[3, 4, 5] In order overcome these inconveniences, covalent cross-links on the thermo-reversible network structure of ionic elastomers have been formed.

The principal aim of this work is combining both types of cross-links in an elastomeric matrix to obtain thermo-reversible elastomers with enhanced properties at high temperatures.

Materials and Methods:

In order to study the effect of covalent crosslinks on the ionic network structure, we have used a polymer matrix based on carboxylated nitrile rubber (XNBR), with a carboxylic group content of 7 wt % which allows its crosslink via metallic oxides (MgO) resulting in a controlled ionic network. The covalent bonds between the polymeric chains were created by the addition of dicumyl peroxide.

The properties of the compounds have been obtained through uniaxial strain-stress tests and rheological measurements and the structure has been studied through dynamic mechanical measurements and low field NMR based on Multiple Quantum experiments.

Results and Discussion:

Formation of covalent cross-links provokes the increase on the number of ionic nano-domains that present smaller and more homogeneous size distribution. This variation in the network structure is closely related with the enhanced properties showed by these materials. The properties at high temperatures improve with low contents of covalent cross-links in the ionic elastomer but without altering their reversible thermoplastic nature (Figure 1).

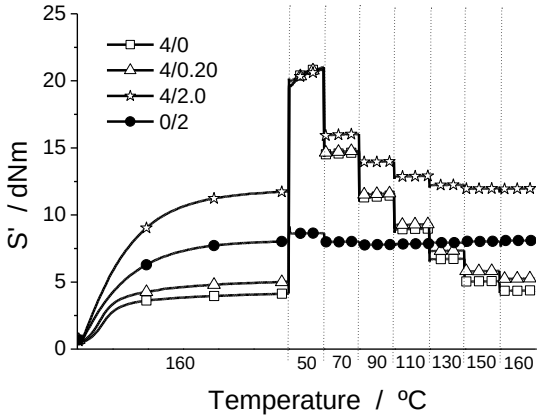

Figure 1. Variation of the elastic torque component with the temperature of different compounds with a MgO/Dicumyl peroxide ratio from the moving rheometer.

Conclusions:

According to the obtained results it is possible to conclude that the proper combination of covalent and ionic cross-links allows us to control the network structure of ionic elastomers in order to tune the properties of these materials.

Acknowledgements:

The authors thank CICYT (Comisión Interministerial de Ciencia y Tecnología) for financial support of this work through Project MAT 2008/02362. Marta Alonso Malmierca would also like to express her gratitude to the Consejo Superior de Investigaciones Cientifícas for predoctoral grant (JAEPre088) and Irene Mora-Barrantes for predoctoral grant (I3P BPD006) in Consejo Superior de Investigaciones Cientifícas. Juan López Valentín thanks Ministerio de Ciencia y Tecnología for his Ramón y Cajal fellowship.

References:

[1] Eisenberg, A.; Hird, B.; Moore, R. B. Macromolecules 23 (1990) 4098.

[2] Yarusso, D.C.; Cooper, S.L. Macromolecules 16 (1983) 1871

[3] L. Ibarra; M. Alzorriz Polymer International 49(1) (2000) 115-121

[4] L. Ibarra; M. Alzorriz J. Appl. Polym. Sci. 87 N1 5 (2003) 805-813.

[5] L. Ibarra; M. Alzorriz J. Apl. Polym. Sci. 103 (3) (2007)1894-1899

Preparation of HDPE/MMT$_{HDTMA/PVA}$ Nanocomposites: Morphology, Structure And Mechanical Properties

Maria C. Carrera [1], Eleonora Erdmann [1], Hugo A. Destéfanis [1] José M. Pastor Barajas [2]*

[1] Instituto de Investigaciones para la Industria Química - INIQUI-CONICET, Consejo de Investigaciones - CIUNSa, Facultad de Ingeniería- UNSa, Buenos Aires 177- 4400, Salta, Argentina.
[2] Dpto. Física de la Materia Condensada- Escuela de Ingenierías Industriales- Universidad de Valladolid, Centro de Investigación y Desarrollo en Transporte y Energía -CIDAUT, Paseo del Cauce 57, 47005- Valladolid, España.

jmpastor@fmc.uva.es

The enhancement of mechanical properties of polymer/clay nanocomposites over polymers is clearly obtained in most of the polymers [1, 2]. The aims of this study are to control the mechanical properties of nanocomposites and to design materials with better properties.

In this work nanocomposites of high density polyethylene with organoclay modified with polyvinyl (alcohol) by in situ polymerization, were prepared for the melt intercalation technique. It was used two different routes to prepare the modified organoclay. The clay MMT$_{HDTMA/PVA}$ (POH) was dispersed in propylic alcohol and the clay MMT$_{HDTMA/PVA}$ (AV) was dispersed in the monomer, vinyl acetate.

The morphology and structure of these materials were studied by X-ray diffraction (XRD), optic microscopy (OM), scanning and transmission electronic microscopy (SEM, TEM). The mechanical properties of traction were performed in an Instron universal machine (Model 5569). The results showed that the morphology changed with the route of organoclay preparation. In the figure 1 the material with HDPE/MMT$_{HDTMA/PVA}$ (POH) 0.6%, presented an agglomerated and intercalated clay morphology whereas the material with HDPE/MMT$_{HDTMA/PVA}$ (AV) 0.6%, presented the intercalated-exfoliated structure (figure 2)

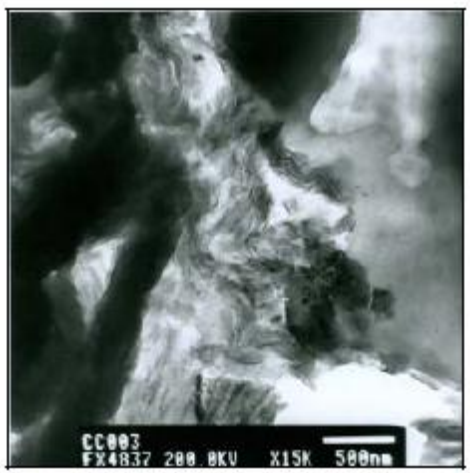

Figure 1. TEM of HDPE/MMT$_{HDTMA/PVA}$ 0.6% (POH)

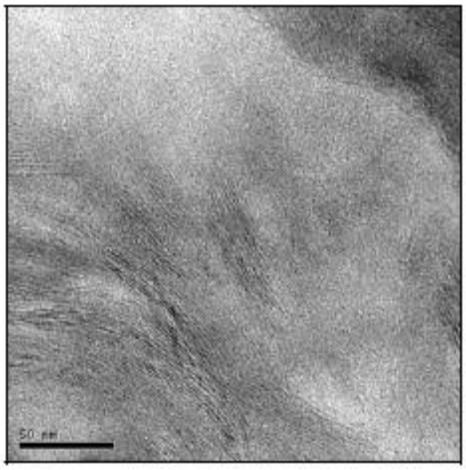

Figure 2. TEM of HDPE/MMT$_{HDTMA/PVA}$ 0.6% (AV)

The table 1 shows that the best Young modulus and break elongation values correspond to HDE/MMT$_{HDTMA/PVA}$ 0.6% (AV).

Table 1. Mechanical properties of: HDPE, HDPE/MMT$_{HDTMA/PVA}$ 0.6% (POH) and HDPE/MMT$_{HDTMA/PVA}$ 0.6% (AV).

Sample	Young Modulus (MPa)	Break strength (MPa)	Break elongation (%)
HDPE	745	20,4	431
HDPE/ MMT$_{HDTMA/PVA}$ 0.6% (POH)	657	18,8	365
HDPE/ MMT$_{HDTMA/PVA}$ 0.6% (AV)	824	19,9	503

A relationship between the mechanical properties and the clay morphology observed by TEM has been detected.

References

[1] Tjong S.C. Materials Science and Engineering R, Vol. 53, (2006), 73–197.
[2] Paul D.R., Robeson L.M.. Polymer, Vol. 49, (2008), p. 3187–3204.

Nitrate remove from drinking water using polymer/MWCNTs nanocomposites

Mohammad Reza Nabid[1], Roya Sedghi[1,2], Roghayye Sharifi[1] and Nayerehossadat Mousavi Rad[1]

[1]Department of Chemistry, Faculty of Science, Shahid Beheshti University, 1983963113 Tehran, Iran
[2]Department of Chemistry, School of Sciences, Alzahra University, Vanak, Tehran, Iran

m-nabid@sbu.ac.ir

Introduction:

The nitrate ion in groundwater is becoming an environmental problem of major concern due to its high toxicity that causing cancer and nethemoglobinemia [1,2]. The important sources of nitrate can be inorganic fertilizer, industrial and sanitary waste waters, vegetable residues and compost, as well as rainfall and spontaneous nitrification of atmospheric nitrogen by nitrification bacteria. The dissolved nitrates filtrate through the ground by rainfall or irrigation and contaminate phreatic waters that feed wells from which drinking water is taken. Nitrates consumed with drinking water can be converted into nitrites in human body and may cause health problem. The increasing rigorousity of the drinking water quality standard, 50 mg/L in the European Union or 25 mg/L in USA, generates the urgent need to develop a new technology for nitrate removal from aqueous solutions. Recently, the catalytic reduction of nitrate by platinum and palladium metals is attracting considerable interest [3]

Experimental and Methods:

The nanocomposites of polymers/MWCNTs were synthesized via in situ chemical oxidation polymerization method. These nanocomposites synthesized in different mass proportions of monomer to MWCNTs.

Results and Discussion:

In this research, we prepared nanocomposites of multiwalled carbon nanotubes (MWCNTs) with different polymers (such as: polyaniline (PANI), polypyrrole (PPY), poly(1,8-diaminonaphthalene) (poly(1,8-DAN)), poly (3,4-ethylenedioxythiophene) (PEDOT)) and poly (vinyl pyridine) (PVP), as effective and reusable nanocomposites for nitrate removal from drinking water. The nitrate removed from water with toxic concentration using ion-exchange mechanism with synthesized polymers counter ions without any toxic byproducts. We used different dopants as polymers counter ions and results shown that effective exchange of nitrate with Cl^- ions.

The different experimental parameters such as pH of the sample, polymers ion-pairs or dopants, temperature, nanocomposite loading, and ratio of polymer versus MWCNTs in nanocomposites, affect the amount of nitrate removal.

In order to examination of different nanocomposites in nitrate removal, every nanocomposite with different proportion in mass of polymer/MWCNTs was used. Results shown that effective nanocomposite with lower concentration of polyaniline is 3:1 and 4:1 nanocomposite. Since the pH of the aqueous solution is an important analytical factor in nitrate ions removal, the influence of pH on removation was examined in the pH range of 2-12 for each nanocomposite.

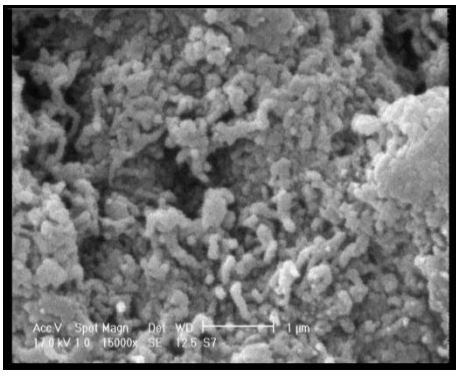

Fig. 1. SEM image of PANI/MWCNTs nanocomposite in 3:1 proportion.

In nanocomposite with higher concentration of PANI more remove percent has never been seen. For optimization of other factors that affecting nitrate removal the 3:1 portion selected because of higher physical stabilization in reusing for several times. In higher polymer concentration in nanocomposite the processability shows decrease.

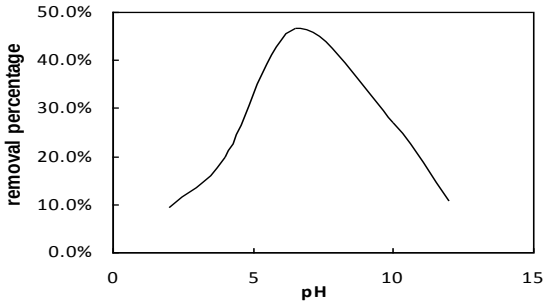

Fig. 2. Effect of water acidity on nitrate removal percent with PANI/MWCNTs.

Since the pH of the aqueous solution is an important analytical factor in the nitrate ions removal, the influence of pH on removing was examined in the pH range of 2-12 for each nanocomposite. The effect of solution acidity was investigated under prior found optimum condition. The results for PANI nanocomposite are shown in figure 2. It is obvious that the best removal of nitrate was done in pH= 6.5.

Conclusions:

The better performances explain by high degree of doping for PANI that allows the more exchange between nitrate and dopant anion of the conducting polymer.

References:

1. A. Pintar, Catal. Today 77(2003)451.
2. L.W. Canter, Nitrates in Groundwater, CRC Press, Boca Raton, 1996.
3. I. Dodouche, D. Pereira Barbosa, M. Rangel, F. Epron, Appl. Catal. B: 93 (2009) 50.

Influence of the swelling behavior on the electrochemistry of redox hydrogel gels

G.Osterwinter, C. Bunte, O. Prucker, J. Rühe

University of Freiburg Department of Microsystems Engineering Laboratory for Chemistry & Physics of Interfaces
Georges-Köhler-Allee 103 79110 Freiburg Germany

gregor.osterwinter@imtek.uni-freiburg.de

Introduction

Hydrogels for mediated electron transfer electrodes (MTE) are composed of redox units, potentially crosslinking units and monomer units[1]. In Bio Fuel Cells containing MTEs the diffusion of charge carriers is a crucial power factor which has an immense influence on the efficiency [2]. Based on Fick's law of diffusion the electron flow J_e can be described as follows [3]:

$$J_e = D_{ap}\frac{dC_B}{dx} = -D_{ap}\frac{dC_A}{dx} \quad (1)$$

At constant concentrations of the mediators J_e is influenced only by D_{ap} which is available via Blauche-Savéant equation:

$$D_{ap} = \frac{1}{6}k_{ex}(\delta^2 + 3\lambda^2)C_{A,B} \quad (2)$$

k_{ex} identifies the transfer rate of the mediator and δ the electron hopping distance. The variable λ is related to the flexibility of redox units and is of utmost importance, as λ is the only variable which can be influenced by variation of the chemical and physical environment of the mediator molecules.

By variation of the content of crosslinking molecules or by using different polymer backbones the influence of those parameters on λ can be discovered. Furthermore, the stability of MTEs at decreasing crosslinker concentration is of general interest.

Materials and Methods

A series of copolymers containing DMMA, MABP as the crosslinking unit and an active ester was synthesized and the crosslinker content was varied. In the subsequent step the polymer was converted to a redox gel by attaching a ferrocene unit to the active ester (see Figure 1). The chemical composition was verified by using FTIR and NMR. Molecular weights were examined using GPC.

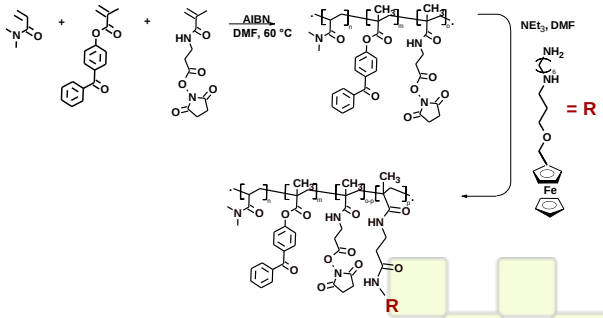

Figure 1: Reaction scheme for the polymerization and the incorporation of ferrocene moieties.

In order to characterize the swelling behavior of these films SPR measurements were employed (see Figure 2a). Substrates were dip coated in a polymer solution and were then crosslinked by UV irradiation (365 nm). The benzophenone unit reacted via CH insertion with other polymer chains to form a polymer network [4]. For CV measurements (see Figure 2b) the electrode tips were spin coated followed by a crosslinking step [5].

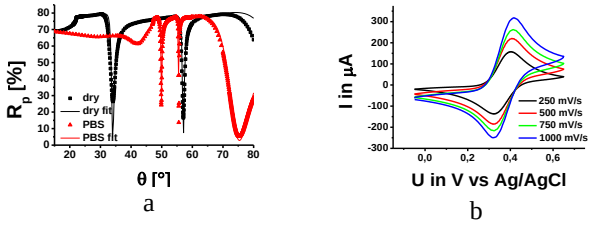

Figure 2: Graphs for SPR measurements in swollen and dry state (a) and cyclic voltammograms at different currents (b).

Results and Discussion

SPR measurements showed that the amount of the crosslinking unit has an influence on the swelling behavior of the hydrogel. A reduction of the benzophenone content from 12 to 1% causes an increase of the swelling of 59%, as shown in Figure 2a. CV measurements showed a better electron transport at smaller amounts of benzophenone. By using the Randles-Sevcik equation the diffusion of the electrons in the hydrogel was obtained.

Conclusion

In this work we show that the transport of electrons is directly related to the swelling behavior of the gel. By reducing the oncentration of the crosslinking unit the swelling of the hydrogel increases and the diffusion of electrons through the hydrogel is increased as well.

References

[1] Bunte C., Prucker O., König T., Rühe J., Langmuir, **2010**, *26*, 6019–6027.
[2] Mao F., Mano N., Heller A., *Journal of the American Chemical Society*, **2003**, *125*, 4951-4957.
[3] Blauche N., Savéant J.-M., *Journal of the American Chemical Society*, **1992**, *114*, 3323-3332.
[4] Schuh K., Prucker O. and Rühe, J. *Macromolecules* **2008**, *41*, 9284-9289.
[5] Toomey R., Freidank D., Rühe, J., *Macromolecules*, **2004**, *37*, 882-887.

Non Aqueous PolyHIPEs as Novel Polymer Separators for Lithium Ion Batteries

Natasha Shirshova[1], Emilia Kot[2], Alexander Bismarck[1], Joachim H.G. Steinke[2]

[1]Department of Chemical Engineering, Polymer and Composite Engineering (PaCE) Group, Imperial College London, South Kensington Campus, London, SW7 2AZ, U.K.

[2]Department of Chemistry, Imperial College London, South Kensington Campus, London, SW7 2AZ, U.K.

j.steinke@imperial.ac.uk; n.shirshova@imperial.ac.uk

Introduction

In today's information rich society the role of lithium ion batteries can not be overestimated, as their applications are ranging from mobile electronic devices to hybrid vehicles. Thus research needs to take into account not only improvements of their performance but also reduction of cost, environmental impact and improved safety [1]. The main areas of research are directed towards the key elements of a Li battery: electrode materials, electrolyte and separator (porous membrane). The latter being the focus of our research.

Using the existing organic electrolytes embedded into a polymer membrane as electrolyte/separator combination raises safety concerns due to the flammability of such electrolyte. In addition current manufacturing processes of separators involve several steps making the process costly. Our approach is to combine the benefits of existing printing technologies with an ink formulation which produces an electrolyte-filled separator in a single processing step. As ink we investigated high internal phase emulsions (HIPE) which can be polymerised in situ as a method of producing a porous thin film network. [2-3].

Experimental Part

Non aqueous high internal phase emulsions were prepared by dropwise addition of the dispersed phase (ionic liquid or mixture of propylene carbonate (PC) with ethylene carbonate (EC) doped with Li salt) into the external phase (thermal or UV radical polymerisation initiators, monomer, crosslinker and a surfactant) at constant stirrer speed. The emulsion was then cast as film and polymerised using thermal (at 70°C) or room temperature UV-activated radical initiation (larger polyHIPE monoliths were prepared in parallel).

Results and discussion

The choice of the internal phase was determined by a number of factors. A PC/EC doped with lithium salt is widely used as electrolyte for batteries and useful as baseline for our research. An ionic liquid was chosen because of their extremely low vapour pressure (simplifying printing), non-flammability and high conductivity.

Conditions to form stable HIPEs were identified and it was observed that content of an internal phase has a strong influence on the stability of HIPEs. Independent of content and polymerisation method, the obtained polymerised HIPEs (polyHIPEs) possess a highly porous interconnected structure. Figure 1 shows the morphology of the polyHIPE after removing the dispersed phase. As the polyHIPEs are already filled with electrolyte, they can be used as deposited and exhibit ionic conductivities in the range of 5-10 mS/cm as prepared. Details on the properties of the synthesised polyHIPEs and printing results of thin polyHIPE films will be presented at the meeting.

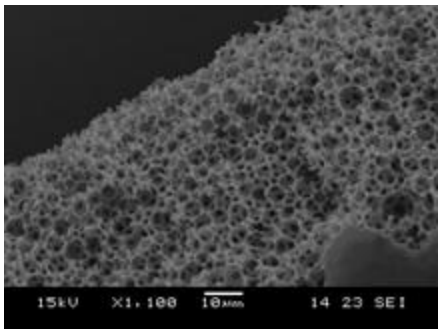

Figure 1. SEM micrographs of polyHIPEs after removing internal phase.

Conclusions

In conclusion, by selecting appropriate conditions and monomer/crosslinker/surfactant formulations we were able to produce a (highly porous) polyHIPE thin film prefilled with ionic liquid or a mixture of propylene and ethylene carbonates electrolyte with high ionic conductivity values. This is a key advance in the ability to realise more environmentally friendly and more cost effective thin film batteries via multi-layer printing with roll-to-roll compatibility.

Acknowledgements

Funding from the EU as part of the FP7 project "Greenbat" (Grant Agreement No. 224582) is gratefully acknowledged.

References

1. B. Scrosati and J. Garche, *Lithium batteries: Status, prospects and future.* J. Power Sources, 2010. **195**: p. 2419-2430.
2. H. Zhang and A.I. Cooper, *Synthesis and applications of emulsion-templated porous materials.* Soft Matter 2005. **1**: p. 107-113.
3. S.S. Manley, et al., *New insights into the relationship between internal phase level of emulsion templates and gas–liquid permeability of interconnected macroporous polymers.* Soft Matter, 2009. **5**: p. 4780-4787.

Natural antioxidants for polymer

Anna Masek, Anna Kosmalska, Marian Zaborski

Technical University of Lodz, Institute of Polymer and Dye Technology, Stefanowskiego 12/16, 90-924 Lodz, Poland

anna.masek@p.lodz.pl

Introduction:

Ozone is a strong oxidant agent and has an influence on the rate of rubber ageing. The degradation by ozone is characterised by the appearance of cracks on the polymer surface [1-2]. The aim of this work was the research on antioxidation activity of flavonoides towards ozone ageing of EPM rubber.

Materials and Methods:

The object of the study was *trans*-chalcone (1phr) and flavone (0,5phr) obtained from Aldrich. The compositions of the prepared mixes were as follows: ethylene-propylene rubber (EPM, Dutral CO-054, Mentedison Ferrara, Italy) 100 phr, dicumyl peroxide (DCP, Fluka) 2 phr - used as a cross-linking agent and hexadecyltrimethylammonium bromide (CTBA, Sigma Aldrich) 2 phr - as dispersing agent. Fumed silica Aerosil 380 (Degussa) was used as a filler (30 phr). Rubber blends were prepared by means of a laboratory mixing mill with rolls of the following dimensions: length L = 330 mm, diameter D = 140 mm. The speed of rotation of the front roll was V_p = 20 rpm, friction 1.1, the average temperature of rolls was about 40°C. The vulcanization of rubber blends was carried out with the use of steel vulcanization molds placed between the shelves of electrically heated hydraulic press. A teflon film was used as spacers preventing the adherence of blends to the press plates. Samples were vulcanized at a temperature of 160°C, under a pressure of 15 MPa for 30 min. The density of crosslinks in the rubber network of vulcanizates was determined by the method of equilibrium swelling. The vulcanizates were subjected to equilibrium swelling in toluene for 48 h at room temperature. The swollen samples were then weighed on a torsion balance and dried in a dryer at a temperature of 60°C to a constant weight and after 48 h they were reweighed. The cross-linking density was determined on the basis of Flory-Rehner's equation:

$$\vartheta_e = -\frac{1}{V_0} * \frac{\ln(1-V_r)+V_r+\mu V_r^2}{(V_r^{\frac{1}{3}}-\frac{V_r}{2})}$$

for the elastomer-solvent interactions amounting to $\mu = 0{,}501 + 0{,}273\ V_r$, where V_r is the volume fraction of the elastomer in the swollen gel. The tensile strength of vulcanizates was tested according to standard PN-ISO 37:1998 by means of a ZWICK tester, model 1435, for dumbbell w-3. Ageing characteristics were determined according to standard PN-82/C-04216. Ozone ageing was performed by means of an Anseros SIM 6300 apparatus from Anseros Klaus Nonnenmacher GmbH. The measurement lasted for 50 and 150 h, the ozone concentration was 300 pphm at 40°C.

Result and Discussion

After ozone ageing no significant changes in the mechanical properties and cross-link density were observed in the sample, when compared to the reference sample. The ageing coefficients, equal to 1,03 and 0,98, indicate considerable protection of vulcanizates against ozone ageing, provided by the applied natural antioxidants.

Table 1. Effect of flavonoids on the cross-linking density of EPM vulcanizates, $\nu_{(t)}$ – crosslinking density calculated on the basis of swelling in toluene.

	$\nu_{(t)}*10^5$, (mol/cm^3) Before ageing	$\nu_{(t)}*10^5$, (mol/cm^3) After ozone ageing (50h)	$\nu_{(t)}*10^5$, (mol/cm^3) After ozone ageing (150h)
EPM	3,46	1,72	0,70
EPM/ chalcone/ flavone	4,49	3,74	3,65

Table 2. Effect of flavonoids on the tensile strength of EPM vulcanizates. SE300% – stress at 300% of elongation, TS – tensile strength, Eb – elongation at break, TS_A - tensile strength after ageing, TS_B - tensile strength before ageing.

	SE_{300}, (MPa)	TS, (MPa)	Eb, (%)	TS_A/TS_{BA}
EPM	3,10	17,67	670	-
EPM/ chalcone/flavone	2,32	19,50	653	-
After ozone ageing (50h)				
EPM	2,92	6,39	557	0,66
EPM/ chalcone/flavone	3,09	20,10	562	1,03
After ozone ageing (150h)				
EPM	1,12	4,33	674	0,36
EPM/ chalcone/flavone	2,97	19,30	575	0,98

Conclusion:

Flavonoide derivatives improve the great resistance of elastomers to ozone ageing. Flavonoides can be pro-ecological alternative antioxidants for polymers.

Referneces

[1] Meijers G., Gijsman P. (2001) Polym. Degrad. Stab. 74,387-391.

[2] Cataldo F. (2001) Polym. Degrad. Stab. 72, 287-296.

Acknowledgement

This study was supported by the project No. POIG 01.01.02-10-123/09.

Polymers Silver Electrodes Plating

Eduardo Henrique Geraldo and [1]João Sinézio de Carvalho Campos

[1]Department of Polymer Technology, School of Chemical Engeneering, State University of Campinas, Av. Albert Einstein, 500, 13083-852, Campinas-SP-Brazil

ehgeraldo@gmail.com , sinezio@feq.unicamp.br

Introduction

Electroless plating is a process in which a metal salt is reduced to metal onto a surface from solution. This process has been widely utilized in coating many materials with metal films for numerous applications [1.2]. It allows to obtain uniformity thick coatings and gives the possibility to regulate physical-chemical properties of coatings (such as electrical conductivity). Dielectric substrates must be catalytically activated prior to the plating to provide a surface that can interact with silver ions in the solution causing their reduction on the surface and growth of a coating.

Experimental

In present study, we prepared silver films by electroless plating on PET poly (ethylene terephthalate) considering this approach in fabricating templates for DTR process nanostructures. We investigated the effects of the micro-struture surface and electrical properties on the growth of the electroless silver film,

the negative substrates used for silver films were initialy exposure by DLP (Digital light process) as interlayer method was verified by a metallization process following.

Electroless plating on the polymer

The plating bath was coposed as following: 80ml of NaCl, 658 ml water, 10ml of VDL ($AgNO_3$), 266 ml of Natriumthiosulfat ($Na_2S_2O_3$), 66 ml of EDTA (HO_2CCH_2), with incrise VDL concentration and decrise the water amount to comparation (deposited in freshly prepared solution in absence of additives the simplest conditions) other three types formulation solutions were carried out include (1 ml, 1%) of inhibitor VG (ethanol solution). The process of electroless deposition was divided in stages; firstly submersed vertically the samples in solution with carbon solid as cathode, electrical potential applied at 1.0 to 2.0 Volts range at 30 seconds and 1 minute of potetial exposure, secondly samples dried about 30 min in room temperature. After electrical properties analysis through multimeter connect in electrodes to defined area interpretation; scanning microscopy and microstruture steps analysis.

Electrical characterization of electroless Ag plating

The solution with 20 ml of VDL show up better than 10 ml or 30 ml to electrical resistivity as 1.3 or 1.5 (Ω/□) to 1.2V and 1.6V inputting potential when the exposured was 30 seconds. When the samples exposure to 1 minute inputting potential the three type of solution shows up lower electrical resistivity results as 0.7 and 0.4 (Ω/□) since 1.4 , 1.6, 1.8 and 2.0 V. The samples exposure in presence of VG inhibitor reach lower electrical resistivity since 1.2, 1.4, 1.6, 1.8 and 2.0 V inputting potential as 0.9 or 0.7 (Ω/□) not importance the VDL amount were observed.

Results and discussion

Most structural investigations were carried out using silver coating types: coatings obtained by fresh electroless plating solution, coating obtained in presence of an accelerator, coatings obtained by electroplating. The thickness of the coatings under inverstigation was approximately 4 μm.

Deposited in a freshly prepared solution in the absence of additives, the simplest conditions; the main part of coating is a uniformly growing layer.

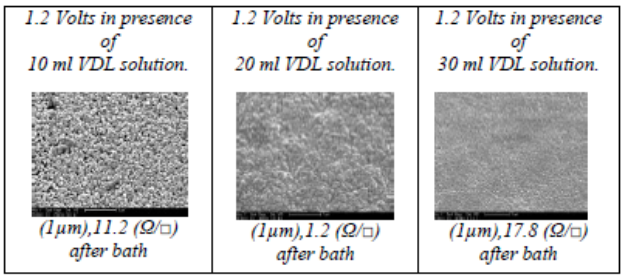

During 30 seconds of exposure to 1.2V in presence of 20 ml VDL type solution reach lower electrical resistivity without inhibitor.

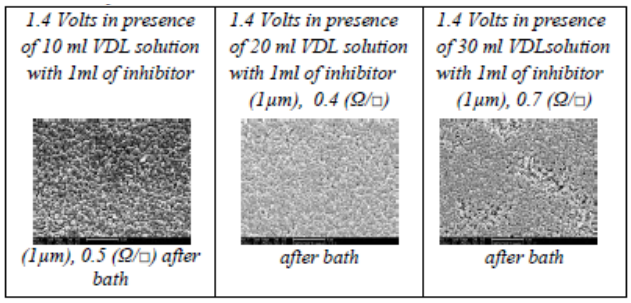

During 1 minute of exposure to 1.4 V in presence of 20 ml VDL type solution reach lower electrical resistivity inhibitor to 30 seconds of bath were the same values to electrical resistivity in presence of 1 ml of inhibitor.

Conclusions

Our investigation sought to obtain the greatest possible number of answer to Ag plating bath which were created patterns of some chemical and physical parameters that have been constant throughout the investigation. The three types of solutions that VDL amount were increase shows up interesting to reducion electrical resistence to range of voltages applied although the values are very close.

The use of inhibitor (1 ml, 1% VG) change the range of voltage applied induce the reduction of electrical resistence, the values are not less after bath plating but were crucial to obtaining homogeneous deposition. In presence of 20 ml of VDL and addition of inhibitor to 30 seconds or 1 minute exposure and 1.2, 1.4 and 1.6.

References

[1] J. B. Hajdu, Plating Surf. Finish. 83 (1996)29

[2] V.M. Dubin, Y. Shacham-Diamand, B Zhao, P.K Vasuder, H. Ting. J. Electrochel, Soc. 144 (1997) 898

[3] J. Wessel, J. Opt. Soc. Am 2 (1985 1538)

[4] I. Barsegova, A. Lewis, A. Khatchatouriants, A. Maevitch, A. Ignatov, N. Axelrod, Appl. Phys, Lett (2002) 3461.

Synthesis and Characterization of a Ionic Polymers Derived from Disubstituted Acetylenes

Radoslava Sivkova, Dmitrij Bondarev, Jiří Zedník , Jan Sedlaček and Jiří Vohlidal

Department of Physical and Macromolecular Chemistry, Faculty of Science, Charles University in Prague, Hlavova 2030/8, Prague 2, Czech Republic, CZ-12843

r.sivkova@gmail.com

In the last few decades there has been a permanent interest in the investigation of organic conducting and semiconducting polymers for applications in electronics, photonics, nonlinear optics, and related fields. Substituted polyacetylenes, as the fundamental conjugated polymers, belong to the most studied materials of this class.

Recently, variety of poly(monosubstituted acetylene)s and poly(disubstituted acetylene)s has been prepared and used in the fields such as liquid crystals, polymeric light-emitting diodes, chemo- and biosensors, gas separation membranes, etc. Poly(disubstituted acetylene)s have become more favorable as they were found to exhibit enhanced resistance to oxidative and thermal degradation.

Polyacetylene-based polyelectrolytes such as poly(propionic)acid, triethylammonium salt of poly(6-bromo-1-hexyne) had been reported. Also a new class of ionic polyacetylenes has been prepared via the activated polymerization of ethynylpyridines with alkyl halides.

In this contribution we report on the synthesis and transformation of several poly(disubstituted acetylene)s containing halogen atom in a pendant group and their modification to ionic polymers.

All monomers were synthesized by the means of Sonogashira coupling. Polymerization was carried out with $TaCl_5$ and $WOCl_4$ catalysts and polymers were purified by repeated precipitation in methanol with the aim to remove the catalytic residua. After careful drying all prepared polymers were characterized by means of SEC and standard spectroscopic methods. The resulting polymers had satisfactory molecular weight characteristics (M_w >50000). These polymers were further modified via two different approaches (i) by quaternization reaction with 1-methylimidazole or (ii) by combination of "click"-modification and quaternization (Fig.1)

The reaction of the parent polymers with 1-methylimidazole was carried out in mixture of methanol and THF for 24 hours at 80°C, then DMSO was added in order to increase the solubility of the polymer in the reaction mixture and the heating was continued for another 24 hours. The resulting product is soluble in polar solvents such as DMSO, acetonitrile and even water.

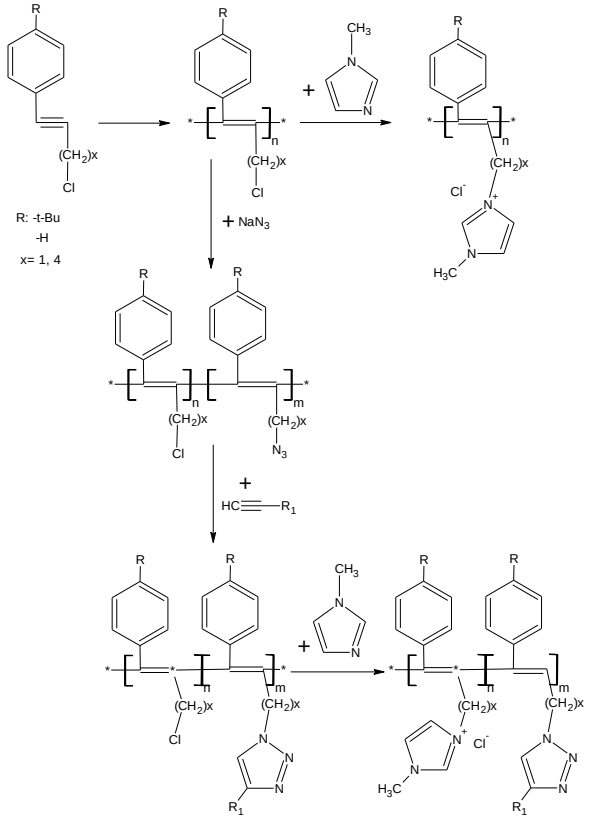

Scheme 1.: Synthetic route for polyacetylenes

The two step modification was applied as other approach including first transformation of part of the Cl-groups to azido-ones, and following "click" reaction with various terminal triple bond-containing compounds. The resulting modified polymers are still containing free Cl-groups which could be quarternized in the same manner described above.

Acknowledgement: Financial supports from Ministry of Education of Czech Republic (MSM002160857), Czech Grant Agency (Project No. 203/09/0803) and Charles Univ. Grant Agency (Project No. 166410) are gratefully acknowledged. R. Sivkova is indebted to the Czech Science Foundation for the fellowship No. 203/08/H032.

Polyacetylenes with Cyclopropyl Pendant Groups: Precursors for Polyacetylene-based Polymer Networks

Vladimíra Hanková, Eva Slováková, Jiří Zedník, Jiří Vohlídal, Jan Sedláček

Department of Physical and Macromolecular Chemistry, Faculty of Science, Charles University in Prague, Hlavova 8/2030, CZ-128 40 Prague 2-Albertov, Czech Republic

hankovavladimira@seznam.cz, http:www.natur.cuni.cz/~pm

Cyclopropylacetylene (cPrA) has been homopolymerized and copolymerized with arylacetylenes (phenylacetylene – PhA, 4-biphenylylacetylene – BPhA) into linear polyene-type polymers with cyclopropyl pendant groups (Scheme 1). Coordination polymerization induced with [Rh(NBD)acac] (NBD = norbornadiene) catalyst has been applied (Table 1).

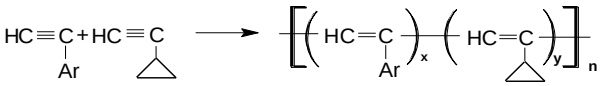

Scheme 1

Table 1: Results of homopolymerization and copolymerization of cPrA with PhA or BPhA on [Rh(NBD)acac]. [cPrA] = 2.4 mol/dm^3, [PhA] = [BPhA] = 0.6 mol/dm^3, [Rh] = 0.024 mol/dm^3. THF, room temperature, 24 h.

Comonomer	Yield (%)	10^{-3} M_w	cPrA units in copolymer (mole%)
-	10	6	100
PhA	24	27	49
BPhA	30	30	55

Table 2: Results of homopolymerization and copolymerization of cPrA with PhA on [Rh(NBD)acac] performed in bulk. [cPrA] = 12 mol/dm^3, [PhA] = 0.6 mol/dm^3, [Rh] = 0.024 mol/dm^3. Room temperature, 24 h.

Comonomer	Yield (%)	10^{-3} M_w	cPrA units in copolymer (mole%)
-	20	11	100
PhA	19	18	87

Various Rh(I) complexes (mainly of the $[Rh(diene)Cl]_2$ type) are well known as active catalysts of polymerization of monoaryacetylenes. In the case of alkyacetylenes either no or only very low polymerization activity of these complexes is being reported. Nevertheless, we succeeded in achievement polymer yields up to 30% (M_w up to 30 000) in homo- and copolymerization of cPrA. Applied catalyst, [Rh(NBD)acac], seems to be appropriate for this kind of polymerization since it does not require any cocatalyst for the activation and can be thus applied also in bulk polymerizations. Particularly, in bulk conditions the enhanced activity of [Rh(NBD)acac] was observed (TON values up to 100, Table 2). The activation of [Rh(NBD)acac] proceeds via acac-ligand liberation in the form of acetylacetone as we reported in [1].

We believe that by a proper optimization of cPrA polymerization systems (example given in Table 3) a broader variability in comonomeric composition can be achieved besides the enhancement of the yield and MW characteristics of products.

Table 3: Results of copolymerization of cPrA with PhA on [Rh(NBD)acac] of various concentration. [cPrA] = 2.4 mol/dm^3, [PhA] = 0.6 mol/dm^3. THF, room temperature, 24 h.

[Rh] in mmol/dm^3	Yield (%)	10^{-3} M_w	cPrA units in copolymer (mole%)
6	13	24	45
24	24	27	49
72	34	20	67

The thermal treatment (250° C, vacuum) of soluble cPr groups containing copolymers resulted in their crosslinking and gave rise to insoluble dark red powder products. The crosslinking proceeded via reaction of cPr pendants as indicated by IR spectroscopy. Research on the preparation, characterization and functional testing of this kind of conjugated polymer networks is now in progress in our laboratory.

Reference

[1] Svoboda J., Sedláček J., Zedník J., Dvořáková G., Trhlíková O., Rédrova D. Vohlídal J., Balcar H.: J. Polym. Sci. A: Polym. Chem. 46, 2776 – 2787 (2008)

Acknowledgement

Financial supports of the Ministry of Education of Czech Republic (MSM0021620857), Czech Science Foundation (project No P108/11/1661) and Grant Agency of Charles University (project No 1352/2010) are gratefully acknowledged. V. Hanková is indebted of the Czech Science Foundation for the fellowship No. 203/08/H032.

The studies of polymer nanocomposites based on thermoplastics and binary conductive nanofillers

V. Levchenko [1,2], Ye. Mamunya [1], G. Boiteux [2], E. Beyou [2], P. Alcouffe [2], E. Lebedev[1]

[1]Institute of Macromolecular Chemistry, NAS of Ukraine, 48 Kharkivske Chaussee, Kyiv 02160, Ukraine
[2] Université de Lyon, Université Lyon 1, Ingénierie des Matériaux Polymères, UMR CNRS 5223, 15 Boulevard Latarget, F-69622 Villeurbanne, France

beyou@univ-lyon1.fr

Nowadays the conductive nanofillers, such as carbon nanotubes (CNT) [1,2] or metal nanoparticles (MNP) [3], are widely used as conductive component for imparting the electrical conductivity and improving thermal conductivity of bulk polymers. Electrical characteristics of composites containing the conductive filler change dramatically when the filler content reaches a critical concentration, commonly known as a percolation threshold. The electrical properties of such conductive polymer composites depend on many reasons, namely the content, shape, size, spatial distribution, interaction with polymer matrix of fillers.

One can assume that combination of two types of the fillers (CNT and MNP), where fillers are interact between each other [4] or MNP decorated on CNT surface [5,6], enables to integrate their properties and even to gain the enhancement of characteristics owing to the mutual influence. To justify such an effect there were chosen the multi-walled carbon nanotubes (MWCNT) with the aspect ratio $l/d \approx 1000$ and nickel (Ni) nanoparticles with average size 60 nm in diameter as the fillers for polypropylene (PP) matrix. Direct current (DC) conductivity σ_{DC} of the PP/MWCNT, PP/Ni and PP/Ni/MWCNT composites as a function of the filler volume content was investigated by two-electrode method.

The PP/MWCNT composites due to high aspect ratio of the nanotubes reveal a low value of the percolation threshold, namely φ_c=0.7 vol.% (curve 2 on Fig.1), whereas the PP/Ni composites are nonconductive within the whole investigated range of filler content (up to 7.5 vol.%) (curve 3). The latter effect can be explained by spherical shape of Ni particles and the presence of polymer-metal interaction. The composites with binary Ni/MWCNT filler revealed a strong effect of enhancement of the DC conductivity. For all PP/Ni/MWCNT composites content of Ni filler was constant and equal to 2.5 vol.%, while content of MWCNT varied. In this case the value of percolation threshold of the PP/2.5%Ni/MWCNT composites decreases sharply and is equal to 0.2 vol.% (curve 1), i.e. it is more than three times lower in comparison with PP/MWCNT composites. Such shift of the percolation threshold to lower content of conductive filler MWCNT can be explained by the presence of bridging effect. Long carbon nanotubes can connect the Ni particles or Ni aggregates and form more conductive pathways in composites. Evidently, in this case considerably lower content of nanotubes is necessary to provide the appearance of conductivity, that results in the shift of the percolation threshold.

DSC results showed that addition of nanotubes into the polymer matrix provides shift of the crystallization peak from 114 °C for pure PP to 127 °C for the composite with 1.5 vol.% of MWCNTs that indicates nucleating action of MWCNTs. Adding of Ni particles into PP/MWCNT composites does not shift the crystallization peak maximum, i.e. the presence of Ni particles does not affect crystallization processes in PP that contains nanotubes. The crystallization behavior was found to be the same for both PP/MWCNT and PP/Ni/MWCNT composites, thus, the percolation threshold reducing caused solely by the bridging effect.

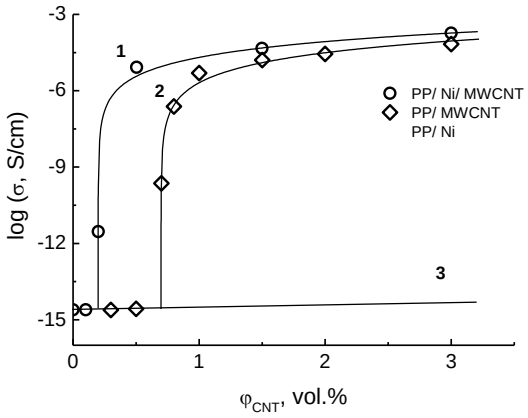

Fig. 1. DC conductivity of the PP/2.5%Ni/MWCNT (1), PP/MWCNT (2) and PP/Ni (3) composites depending on the MWCNT content.

Acknowledgements

V. Levchenko would like to acknowledge the EGIDE (France) for the financial support (Eiffel grant № 625674L).

References

1. Connell, M.O. Carbon Nanotubes : Properties and Applications, CRC Press, Boca Raton 2006.
2. Akbar S.; Beyou E.; Cassagnau P.; Chaumont P.; Farzi G. Polymer 2009, 50, 2535.
3. Wang, B.B.; Li B.; Zhao, B.; Li, C.Y. J Am Chem Soc 2008, 130, 11594.
4. Liang, G.D.; Bao, S.P.; Tjong, S.C. Mater Sci Eng Pt B 2007, 142, 55–61.
5. Georgakilas, V.; Gournis, D.; Tzitzios, V.; Pasquato, L.; Guldi, D.M.; Prato, M. J Mater Chem 2007, 17, 2679–2694.
6. Ma, P.Ch.; Tang, B.Z.; Kim, J.-K. Carbon 2008, 46, 1497-1505.

Synthesis and Complexation Properties of Terpyridine Derivatives: Building of Supramolecular Polymers

Tereza Vitvarova, Jiri Zednik, Pavla Stenclova, Jiri Vohlidal and Jan Svoboda

Department of Physical and Macromolecular Chemistry, Charles University in Prague, Faculty of Science, Hlavova 2030, CZ-128 40, Prague 2, Czech Republic

tereza.vitvarova@seznam.cz

Supramolecular polymers are polymers consisted of molecular building blocks, which are connected together by non-covalent intermolecular interactions. The length of their chain depends mainly on stability and character of that interaction. In coordination (or metallo-supramolecular) polymers, the interaction is realized between metal and ligand. Right choice of metal and ligand is the key to obtain polymer with demanding properties. By these we can tune for example magnetic properties, conductivity (thermal or electric). The most important property of complex, which can be used as building block for supramolecular polymers, is stability. One of the most suitable ligands is 2, 2‘: 6’, 2‘‘-terpyridine because of his high affinity to transitive metals and his octahedral geometry (reduced possibility of creating enantiomers). Terpyridine is easy to obtain and it’s not so hard to functionalize it. With different substituents we can expect different stability and also chemical properties (solubility, polarity).

Two terpyridines with thienyl and ethynyl substituent as a model compounds of bis(terpyridines) with all-conjugated bridge were prepared. Reaction with various metals was studied using methods of UV-VIS, photoluminescence and NMR spectroscopy. By these techniques we can observe the complexation and we are also able to calculate the stability constant. Kinetic of complexation was studied using 2D-NMR spectroscopy..

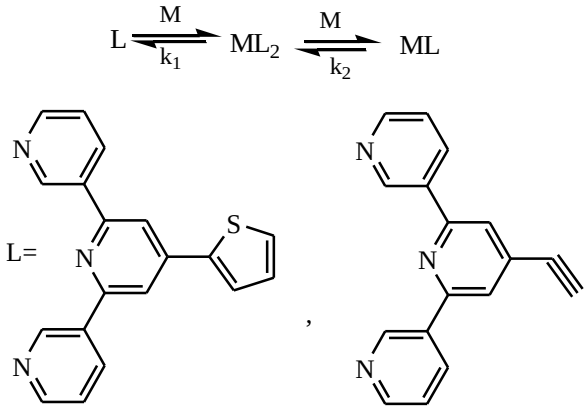

Fig.1: Scheme of complexation

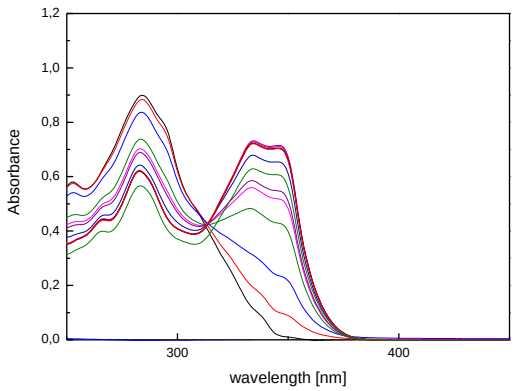

Fig.2: UV-VIS spectrometric study of complexation of 4’thien-2-yl-terpyridine with Zn^{2+}

The authors acknowledge the financial support from the Grant Agency of Czech Republic No.: 104/09/1435 and 203/09/0803, the Science Foundation of Charles University (project 157810) and the Ministry of Education of the Czech Republic No.: MSM0021620857.

Study on the Copolymerization of Potassium Chloroacetate and Potassium *n*-Chloroacetyl-6-aminohexanoate

S.K. Murase, A. Rodríguez-Galán, L. Franco, J. Puiggalí

Departament d'Enginyeria Química, Centre de Recerca en Nanoenginyeria, Universitat Politècnica de Catalunya, ETSEIB, 08028-Barcelona

Jordi.Puiggali@upc.edu

Alkali metal halogenoacetates lead to polyglycolide upon heating at temperatures higher than 100 ºC by a polycondensation reaction that has the formation of a metal halide salt as the driving force of the process. Thus, the reaction conduces to micrometer-sized metal halide crystals dispersed in a matrix of polyglycolide.[1] Despite the advantages derived from the simplicity of this method, its application is hindered due to the limited molecular weight that can be reached as a consequence of secondary reactions and thermal decomposition at the high temperatures required for the progress of the reaction. However, this method was successfully applied to get poly(ester amide)s constituted by an alternating sequence of glycolic acid and ω-amino acid units,[2] whose synthesis was previously proposed in base of high time consuming methods which involved selective protection and deprotection of reactive groups.

New monomers were easily synthesized, in this case, by the reaction of chloroacetyl chloride with the appropriated ω-amino acid and by a subsequent neutralization with the selected metal hydroxide. The proposed synthesis rendered high molecular weight samples when ω-amino acids had high methylene content (i.e. 6-aminohexanoic, 11-aminoundecanoic and 12-aminododecanoic acid derivatives). Polymerizations could take place in the solid phase, the liquefied phase, or both phases, depending on the number of methylene groups and the kind of salt. In fact, these two conditioning factors had an influence on the melting point of the monomer, which can be either higher or lower than the reaction temperature.

Copolymerization of chloroacetate (MGL) with a *N*-chloroacetyl-ω-aminoalkanoate is also an interesting topic since may render random copoly(ester amide)s with tuneable properties as a consequence of the control on the ester/amide ratio. This work is specifically focused into the study of the copolymerization with the 6-aminohexanoic acid derivative (MEA) (Figure 1). In order to favour copolymerization potassium salts were selected due to the low reactivity difference between the two involved monomers. Polymerization kinetics of different MGL/MEA mixtures was evaluated by the FTIR in-situ technique (Figure 2) since it is sensitive to formation and destruction of chemical bonds (e.g. carboxylate groups of the ester and the salt compounds). Calorimetric and spectroscopic observations indicated that polymerization proceeded faster when each monomer was mixed with the corresponding comonomer (Figure 3). The deduced Arrhenius parameters showed a decrease on the activation energy of the monomer mixtures respect to the neat monomers.

Calorimetric, thermogravimetric, chromatographic and NMR spectroscopic techniques were also applied to control polymerization and characterize the final reaction products. In general, promising results can be attained when reaction is performed with MEA content higher than 50%.

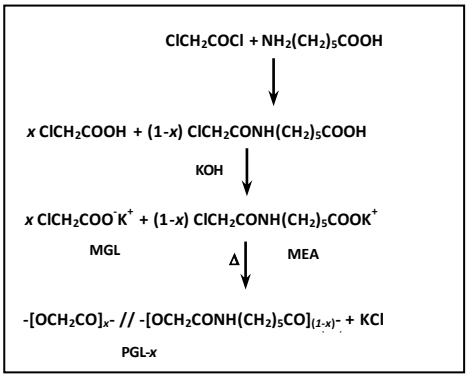

Figure 1 Synthesis of random copoly(ester amide)s by melt polycondensation with formation of a metal halide salt as a driving force.

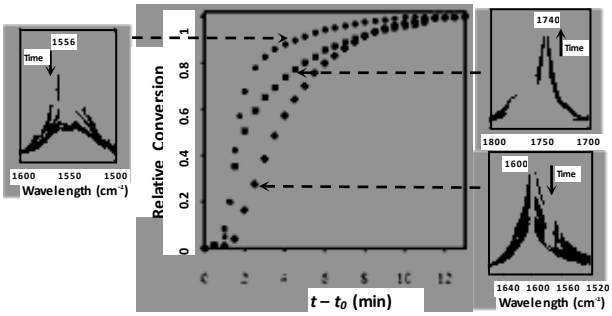

Figure 2. Conversion plots for the polymerization of a representative monomer mixture at 110 ºC determined from the time evolution of carboxylate FTIR absorption bands.

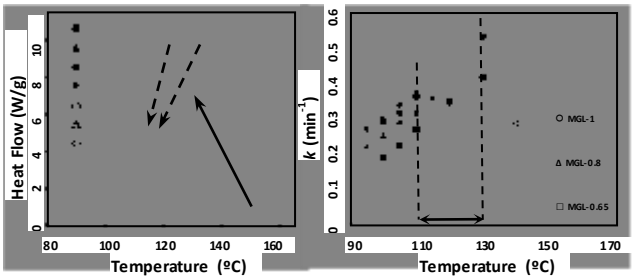

Figure 3. DSC polymerization exotherms (left) and temperature dependence of the polymerization kinetic constant (right) for different monomer mixtures.

Acknowledgements: This research has been supported by a grant from MCYT/FEDER (MAT2009-11503).

1. M. Epple, O. Herzberg, J. Mater. Chem. **1997**, 7, 1037.
2. M. Vera, A. Rodríguez-Galán, J. Puiggalí, Macromol. Rapid Commun. **2004**, 25, 812.

Solvent-free aqueous polyurethane dispersions

Isabel Fernandes[1], *Filomena Barreiro*[1*], *Mário Rui Costa*[2]

1. LSRE – Polytechnic Institute of Bragança, Campus de Santa Apolónia, Ap 1134, 5301-857 Bragança, Portugal
2. LSRE - Department of Chemical Engineering, Faculty of Engineering, University of Porto, Rua Dr. Roberto Frias, 4200-465 Porto, Portugal

(ipmf@ipb.pt, barreiro@ipb.pt and mrcosta@fe.up.pt)

Introduction

The industrial production of aqueous polyurethane dispersions (PUDs) is nowadays a well established technology. There are two main synthetic routes to produce PUDs: the acetone process (a former process developed by Bayer AG) and the pre-polymer process (developed as an alternative response to the patented acetone process). Comparatively to the acetone process, the pre-polymer process has one major advantage since it requires none or only small amounts of acetone.

The pre-polymer process, at present, is being forced to readapt due to ongoing developments, partly motivated by process constraints, raw materials restrictions and the need to obtain a true solvent-free product. Allied to this fact it is worth mentioning the European REACH legislation, which is having a considerable influence on the PUD industry.

Most of the industrially produced PUDs use dimethylol propionic acid (DMPA) as the internal emulsifier. DMPA is sparingly soluble in the reactive mixture and needs to be previously dissolved in an organic solvent, usually N-methyl-2-pyrrolidone (NMP). NMP is difficult to remove and will remain in the final product.

There are some alternatives to achieve the NMP-free concept. Among them we can refer the direct NMP replacement by an equivalent solvent, the DMPA replacement by an equivalent hydrophilising diol but with better solubility in the reactive mixture and the pre-neutralization of DMPA prior to reaction with isocyanates [1, 2].

Materials and methods

In this work we present a modified pre-polymer process that includes four main stages: (1) Pre-polymer synthesis, (2) Pre-polymer dispersion, (3) Chain extension and (4) Co-solvent removal, as described in Figure 1. Comparatively to the conventional pre-polymer process the hydrophilising diol was used in its salt form, i.e., after neutralization with a tertiary amine. The chemical system comprises a polyetherdiol (polytetramethylene glycol (PTMG) or polypropylene glycol (PPG)), an isocyanate (isophorone diisocyanate (IPDI)), a hydrophilising diol (DMPA), a neutralizing amine (triethylamine (TEA)), a chain extension agent (ethylenediamina (EDA) diethylenetriamine (DETA) or hydrazine monohydrate (HYD)), a catalyst (stannous octoate – SO) and acetone as the co-solvent for the DMPA salt solubilisation.

The obtained dispersions have been characterized in terms of pH, viscosity, solid content, particle size and stability (thermal and electrolyte presence).

Several samples have been synthesized and compared with a base formulation produced by the conventional pre-polymer process.

Results and conclusions

In this work it has been shown that the use of DMPA in its salt form can provide a way to readapt, with minor modifications, the conventional pre-polymer process to produce dispersions in accordance with the present PUD market requirements (NMP-free). By substituting DMPA through its salt form, NMP can be directly replaced by acetone that provides the possibility to obtain solvent free dispersions since acetone will be easily removed at the end of the synthesis and could be further recycled and reused in the process. Additionally, the developed process was facilitated in what concerns the pre-polymer dispersion stage and chain extension effectiveness. Table 1 shows the comparison between samples produced by the two processes.

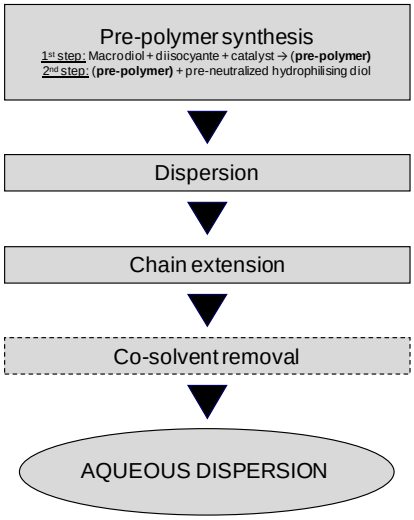

Figure 1. Schematic drawing of the modified pre-polymer process.

Table 1. Dispersion properties obtained by the conventional (A) and the modified (B) processes.

Process	pH	Solid content %(w/w)	Particle size(*) (nm)	Viscosity (mPa.s)
A	8.5	30.0	Volume: 74.0 (m) Number: 54.0 (u)	17.3
B	8.1	40.5	Volume: 139 (m) Number: 50.2 (u)	26.0

(*) Multimodal (m) and unimodal (u) distributions

References

[1].Gertzmann, R., Irle, C., Schmitt, P. (2007). Waterborne Polyurethane Coatings for Wood Floor-The Next Generation, *Bayer MaterialScience AG technical information*, Leverkusen, Germany

[2].Mestach, D., Goossen, J., (2007). *New* Approaches for Solvent-Free Waterborne Polyurethanes, *Polyurethane Magazine International*, 5, 313-318.

Thermoresponsive Polyether-Grafted Hyaluronan: Synthesis and Reversible Gelation Behavior

J. Aréguian[a,b], *R. Auzély-Velty*[a]

[a]Centre de Recherches sur les Macromolécules Végétales (CERMAV-CNRS), BP53, 38041 Grenoble Cedex 9, France, affiliated with Université Joseph Fourier, and member of the Institut de Chimie Moléculaire de Grenoble.
[b]ARD, Route de Bazancourt, 51110 Pomacle, France

julie.areguian@cermav.cnrs.fr; rachel.auzely@cermav.cnrs.fr

Introduction.

Over the last few decades, hydrogels have attracted considerable attention as biomaterials in the biochemical and biomedical fields. One of the most promising polysaccharides to design such biocompatible matrices promoting cell adhesion and growth is hyaluronan (HA). This linear anionic polymer has important biological properties but also unique viscoelastic properties in aqueous solution.[1] For some time now, we have performed alkylation of hyaluronan, allowing the formation of original physical gels in aqueous solution.[2] The gelation properties were related to the length of the grafted alkyl chains as well as to the density of grafting, but also to polymer and external salt concentration.

Furthermore, reversible hydrogels that can be formed in situ by phase transition (sol-gel transition) in response to a temperature change have become increasingly important because of their potential applications in non-invasive techniques.

Thus, by replacing hydrophobic alkyl chains by a thermosensitive polymer, as it was done on chitosan in previous work [3], it may be possible to control gelation with the temperature. Such a property can facilitate injections. In these systems, the formation of physical junctions required for gelation is generally due to the association of the grafted thermosensitive groups possessing a Lower Critical Solution Temperature (LCST) in aqueous solution. In this context, we grafted thermosensitive polyether groups on HA, consisting of Jeffamine® (or POEP) chains having a LCST close to 32 °C, i.e. near the body temperature.

In this presentation, the gelation properties as a function of environmental conditions and structural parameters of these new hydrogels will be discussed. Then, these properties will be compared to those of alkylated HA derivatives.

Moreover, preliminary studies on cell adhesion and growth within these both physical gels will be developed.

Materials and Methods.

Materials. The hyaluronan used was from A.R.D (Pomacle, France); two batches of a weight-average molecular weight M_w 200 000 g/mol and M_w 700 000 g/mol. POEP was obtained from Texaco Chemical (Austin, Texas, USA) and all other chemicals were purchased from Fluka (Buchs, Switzerland).

^{1}H NMR spectroscopy. Polymers dissolved in D_2O were characterized on a Bruker DRX400 spectrometer operating at 400 MHz.

Rheological experiments. Dynamic experiments were performed with a cone-plate rheometer (AR 2000 from TA Instruments). A cone with a diameter of 4 cm and an angle of 4° was used. Experiments were carried out with a film of silicone to avoid solvent evaporation. All the dynamic rheological data were checked as a function of strain amplitude to ensure that the measurements were performed in the linear viscoelastic region. The solutions of hyaluronan derivatives were prepared by dissolving them in PBS 1X buffer.

Results and Discussion.

According to previous works, alkylation of hyaluronan showed interesting thickening properties in aqueous solution, which were more important using a shorter hyaluronan.[4] By replacing the hydrophobic alkyl chains by chains of a thermoresponsive random copolymer of PEO and PPO (POEP), we obtained new derivatives exhibiting a remarkable thermogelling behaviour.

The resulting Jeffamine®-hyaluronan derivatives obtained have been perfectly characterized by ^{1}H NMR spectroscopy. The dependence of the elastic and viscous moduli as a function of temperature was obtained by dynamic rheology, as well as the study of the reversibility of these systems. Multiwave rheological experiments allowed us to define precisely the phase- transition temperature (or critical temperature).

The phase transition was shown to depend on the length of the hyaluronan chain, having a critical temperature closer to body temperature using a 700 000 g/mol hyaluronan instead of a 200 000 g/mol one. Furthermore, contrary to alkylated HA, better gelation properties were observed for the HA-POEP derivatives using a 700 000 g/mol hyaluronan, of which elastic moduli were significantly higher than those of alkylated HA derivatives.

As the preliminary studies on cell adhesion and growth are underway, the results obtained will be developed during the presentation.

Conclusion and perspectives.

Based on the interesting thermogelling properties of the HA derivatives, we plan to improve their synthesis methodology. This in particular will allow us to investigate deeply the potential of the thermoreversible gels as biomimetic substrates for the growth of various cell types.

References

[1] G. Kogan, L. Soltes, R. Stern, P. Gemeiner, *Biotechnol. Lett.*, **2007**, *29*, 17-25.
[2] C. Creuzet, S. Kadi, M. Rinaudo, R. Auzély-Velty, *Polymer* **2006**, *47*, 2706-2713.
[3] C. Creuzet, M. Rinaudo, R. Auzély, *L'actualité chimique* **2006**, *294*, 34-38.
[4] S. Kadi, D. Cui, E. Bayma, T. Boudou, C. Nicolas, K. Glinel, C. Picart, R. Auzély-Velty, *Biomacromolecules* **2009**, *10*, 2875-2884.

Electrochemical response of host-guest assemblies of polysaccharides immobilized on surfaces

J. Mergy[a], *G. V. Dubacheva*[b], *P. Labbé*[b], *L. Guérente*[b] *and R. Auzély-Velty*[a]

[a]Centre de Recherches sur les Macromolécules Végétales (CERMAV-CNRS), affiliated with Université Joseph Fourier, BP53, 38041 Grenoble cedex 9, France

[b]Laboratoire Ingénierie et Interactions Biomoléculaires (I2BM), Département de Chimie Moléculaire (DCM) UMR CNRS 5250, Université Joseph Fourier, BP 53, 38041, Grenoble, France

e-mail : rachel.auzely@cermav.cnrs.fr

Introduction

The supramolecular assemblies based on polymers modified by cyclodextrins (CDs) and/or hydrophobic guest molecules have inspired interesting developments in the biomedical, pharmaceutical and cosmetic fields. Over the last ten years, several works have thus been dedicated to the development of hydrogels, nano/microparticles, nano/microcapsules and thin films. In this context, we have been interested since several years in developing supramolecular assemblies taking advantage of the specific properties of natural polysaccharides. Chitosan (CHI) and hyaluronic acid (HA) were thus selectively modified by β-CD and adamantane (AD), leading to "guest" and "host" polysaccharides.[1,2] Interesting thickening properties or transparent gel formation due to the multivalent complexation between polysaccharide chains were observed in aqueous solution. In the next step, we extended the formation of such assemblies on surfaces. Multilayers based on host-guest complexation were prepared from the alternate deposition of chitosan derivatives bearing either β-CD or hydrophobic guest molecules, on a planar surface functionalized by guest molecules.[3] Such "host-guest" assemblies may be sensitive to various stimuli which can act either on the electrostatic interactions between the polymer chains or on the host-guest complexes stabilizing the multilayers. In this presentation, we will describe our recent studies aimed at better understanding the build-up of such multilayer assemblies and investigate their sensitivity to electrochemical stimuli.

Materials and Methods

Materials. Chitosan Protasan was provided by FMC BioPolymer AS, Novamatrix (Norway). Hyaluronic acid was kindly provided by ARD (France). β-Cyclodextrin (β-CD) was kindly supplied by Roquette Frères (France). All other chemicals were purchased from Sigma-Aldrich-Fluka. β-CD monoalkyne was synthesized from a β-CD monocarboxylic acid derivative as reported previously.[4]

Synthesis of host and guest polysaccharides. The covalent grafting of β-CD and ferrocene (Fc) molecules on the polysaccharides was performed according to procedures described previously.[1,2]

SAM-coated gold electrodes. Self-assembled monolayers (SAMs) of β-CD were prepared by a "click" reaction between the β-CD monoalkyne derivative and azide groups exhibited by SAM as reported previously.[4]

E-QCM-D. Combination of electrochemical and QCM-D measurements was performed using electrochemical QCM-D module (Q-Sense, Sweden), connected with CHI 440 potentiostat (CH-Instruments, Inc., USA).[4]

Results and Discussion

In this work, we investigated several assemblies of host and guest polysaccharides. Taking advantage that complexation between Fc and β-CD is strongly diminished upon electrochemical conversion of Fc to the ferrocenium cation, we functionalized polysaccharides with Fc moieties to make them "electroactive". Moreover, as the number of effective layer-by-layer deposition cycles seems to be strongly dependent on electrostatic repulsions between the layers,[5] we prepared neutral, positively charged and negatively charged polysaccharide derivatives starting from chitosan, hyaluronic acid and dextran.

Having the polymers in hands, we first verified the ability to detach a guest polysaccharide layer on a host surface in response to the electrochemical oxidation of the Fc groups. QCM-D monitoring of detachment process coupled with CV showed that all specifically attached Fc-grafted polymer can be irreversibly released from SAM-β-CD-coated gold surface by applying oxidizing potential. Next, we examined the stepwise construction of multilayer thin films based on host-guest interactions between Fc- and β-CD-functionnalized neutral or charged polysaccharides The multilayer build-up was indeed found to be strongly limited when charged host and guest polysaccharides were assembled.

Conclusion

In summary, the present work establishes the possibility to control the multilayer assembly driving force by switching the redox state of Fc guests grafted on polysaccharides. This appoach offers new opportunities for building at the nanoscale stimuli-responsive films with potential applications in the field of nanobiotechnologies.

References

[1] R. Auzély-Velty, M. Rinaudo, *Macromolecules* **2002**, *35*, 7955.

[2] A. Charlot, R. Auzély-Velty, *Macromolecules* **2007**, 40, 1147.

[3]A. Van der Heyden, M. Wilczewski, P. Labbé, R. Auzély, *Chem. Commun*. **2006**, 3220.

[4] G. V. Dubacheva, A. Van der Heyden, P. Dumy, O. Kaftan, R. Auzély-Velty, L. Coche-Guerente, P. Labbé, *Langmuir* **2010**, *26*, 13976.

[5] G. V. Dubacheva, P. Dumy, R. Auzély, P. Schaaf, F. Boulmedais, L. Jierry, L. Coche-Guerente, P. Labbé, *Soft Matter* **2010**, *6*, 3747.

Semiconducting Materials based on Block and Graft Copolymers having Donor and Acceptor Functionalities for Molecular Electronics

Joannis K. Kallitsis[1,2], *Souzana N. Kourkouli*[1,2], *Andreas A. Stefopoulos*[1,2], *Aikaterini Andreopoulou*[1], *Angeliki Siokou*[2]

[1]Department of Chemistry, University of Patras, Patras GR26504 Greece
[2]Foundation for Research and Technology Hellas, Institute of Chemical Engineering and High Temperature Processes (FORTH-ICEHT), Patras GR26504, Greece.

j.kallitsis@upatras.gr

Introduction

Control of the morphology, as well as the modulation of the electronic properties, are of utmost importance, in order to provide materials that can meet the prerequisites for application in molecular electronics. Despite the fact that significant improvements on the polymeric electron donors have been made during the last years, the morphology control and the development of proper polymeric electron acceptor remain a challenge. The most efficient electron accepting materials used so far in OPVs are based on modified fullerene species. However, further improvement is needed in order to achieve more efficient separation and transport of the separated charges to the respective electrodes. Attempts to this direction have been made either by influencing the miscibility between the donor and acceptor phases of by the development of more efficient electron donor or acceptor materials. In the case of the acceptors, and since polyquinolines are one of the most promising classes of electron accepting and transporting polymers[1], their combination with other electron active materials is expected to provide new materials with ideal characteristics for use in OPVs.[2,3] Moreover, the modification of the quinoline monomers with electron withdrawing groups can be a simple way to control the electronic properties of the final materials.

Results & Discussion

In our approach to develop polymeric or hybrid electron acceptors, we have used vinyl quinoline derivatives with different substituents.[1a,3] These materials have been combined with typical polymeric electron donor materials like polythiophene after proper modification in order to develop efficient electron donor-acceptor interphases, *Scheme 1*.

Starting from the modification of quinoline with various electron withdrawing groups, we then synthesized vinyl monomers based on modified quinolines applicable in controlled or free radical polymerizations. Thus we were able to synthesize homopolymers that can be used as electron accepting phases in OPVs since their LUMO level is as low as 3,65 eV.[3]

An additional advantage offered by these quinoline monomers is that they can be easily used in the preparation of more complex polymeric architectures. For example block or brush type rod-coil copolymers can be synthesized employing various properly modified rigid macromolecular entities acting as initiators. As rigid blocks we have selected well established and extensively used as polymeric donors regioregular poly(thiophene)s. Another exceptional case has been their combination with different carbon nanostructures leading to electron accepting hybrid materials.[3] The same approach has also been employed for the preparation of polymer electron donor carbon-based electron accepting hybrid materials.[4]

For the different copolymer architectures like block or brush-type copolymers the influence of the detailed polymeric architecture on the organization behaviour and subsequent phase separation phenomena has been examined.

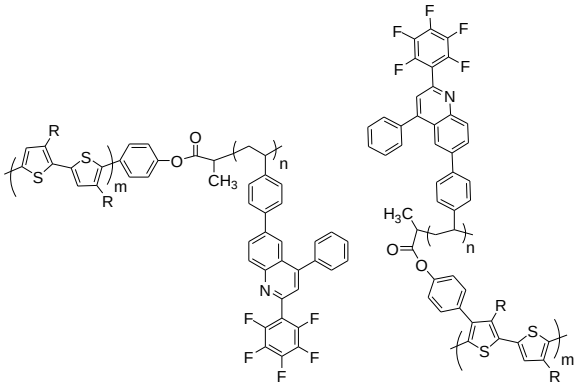

Scheme 1. Block and Brush-type copolymers of *rr*-poly(thiophene) and poly(vinyl-perfluorophenyl-quinoline).

Acknowledgement

The authors thank the European Social Fund (ESF), Operational Program for EPEDVM and particularly the Program Herakleitos II, for financially supporting this work.

References

[1] (a) M.M Alam, S.A. Jenekhe, *Chem. Mater.* **2004**, *16*, 4647–4656. (b) S.P. Economopoulos, A.K. Andreopoulou, V.G. Gregoriou, J.K. Kallitsis, *Chem. Mater.* **2005**, *17*, 1063-1071.

[2] S.P. Economopoulos, C.L. Chochos, V.G Gregoriou; J.K. Kallitsis, S. Barrau, G. Hadziioannou, *Macromolecules*, **2007**, *40*, 921-927.

[3] A.A. Stefopoulos, S.N. Kourkouli, S. Economopoulos, F. Ravani, A. Andreopoulou, K. Papagelis, A. Siokou, J.K. Kallitsis, *Macromolecules*, **2010**, *43*, 4827–4828.

[4] A.A. Stefopoulos, C.L. Chochos, M. Prato, G, Pistolis, J.K. Kallitsis, *Chem. Eur. J.* **2008**, *14*, 8715-8724.

Study on adsorbing chromium (VI) into hyperbranched copolymers from aqueous solution

M. Luzon[a], *T. Corrales*[a], *C. Peinado*[a], *V. San Miguel*[a], *F. Catalina*[a]

[a]Departamento de Fotoquímica, Instituto de Ciencia y Tecnología de Polímeros, CSIC, C/ Juan de la Cierva 3, 28006, Madrid, Spain

mluzon@ictp.csic.es

Introduction:

The presence of high concentrations of chromium in the wastewater is of concern due to the toxicity of this metal ion. Several processes are used to reduce chromium discharge by industry, ultrafiltration combined with water-soluble polymers has been shown to be a useful process for removing metal ions from pollutant wastewaters. In this work, a series of water soluble linear and hyperbranched (HBP) copolymers were synthesized via addition–fragmentation chain transfer polymerization (RAFT), by copolymerization of di(ethyleneglycol) methacrylate (DEGMA), oligo (ethyleneglycol) methacrylate (OEGMA) and ethyleneglycol dimethacrylate (EGDMA) used as crosslinker. The polymers were characterized by analysis of Gel Permeation Chromatography (GPC) and Nuclear Magnetic Resonance (RMN). The lower critical solution temperature (LCST) has been studied by UV-VIS spectroscopy and dynamic light scattering. Due to the properties of these polymers in solution they may be applied in the remediation of contaminated waters, and their capacity of adsorption of chrome has been studied.

Methods:

Normalized method for chromium (VI) determination.
The colorimetric method to determine chromium hexavalent[4] was used to know the concentration of chromium in solution. A calibration curve was done before the determination. Dissolved hexavalent chromium may be determined colorimetrically by reaction with diphenylcarbazide in acid solution. The reaction is very sensitive. Addition of an excess of diphenylcarbazide yields the red-violet product, and its absorbance is measured photometrically at 540nm.

Analysis of adsorption of chromium.
To determine the adsorption capacity dialysis experiments were performed.
A dialysis bag (MWCO = 6000-8000 Da) containing 6 mL of the polymer solution was sealed and immersed in ultra pure water solution (70 mL, pH 7) at 45 ºC in a thermostatically controlled oven. The copolymer concentration was 5 g/l for all the polymers, lineal and hyperbranched. Aliquots of 1 mL were withdrawn from the solution periodically. The volume of the solution was held constant by adding 1 mL fresh ultra pure water solution after each sampling to ensure sink conditions. The amount of chromium adsorbed by polymers was determined by a normalized method for chromium (VI) determination.

Results and Discussion:

As it is shown in the figure, the adsorption capacity for chromium (VI) was studied for the different polymers. Hyperbranched polymers adsorb more chromium (VI) than the linear polymer. That is because of the structure of the polymers, hyperbranched polymers form a network with nanocavities where the chromium can adsorb. Hyperbranched polymer with higher ratio of OEGMA/DEGMA is more efficient as adsorbent because there are more ethylene glycol side chains for adsorbing contaminant.

Polymer	%DEGMA[a]	%OEGMA[a]	%EGDMA[a]	LCST[b]
P 2 Lin.	74.4	25.6	-	56.6
P 3 HBP	84.6	12.2	3.2	40.3
P 4 HBP	72.7	23.7	3.6	53.4

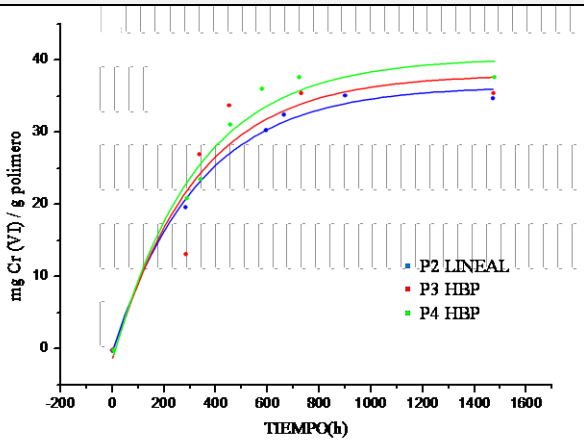

Conclusions

In this study, a series of linear and hyperbranched copolymers based in ethylene glycol methacrylate has been synthesized. It was determined its lower critical solution temperature and its capacity for the removal of chromium (VI) from aqueous solution. The values of chromium captured are close to 40 mg per gram of polymer, which means that these polymers could be used as an effective adsorbent[5].

References

1. Lutz, J.-F.; Hoth, A. Macromolecules 2006, *39*, 893-896.
2. Lutz, J.-F. J. Polym. Sci. PartA: Polym. Chem. 2008, *46*, 3459-3470.
3. Luzón, M.; Boyer C.; Peinado, C; Corrales, T.; Whittaker, M.; Tao, L; Davis, T. Journal Polymer Science, 2010, *48*, 2783-2792
4. APHA, AWWA, WPCF. Methods for the Examination of Water and Wastewater, 17 th ed, Madrid: Diaz de Santos, 1989, p.3-103
5. Kara, A. M. J. Appl Polym Sci 2009, *114*, 948-955.

Synthesis and Characterization of a Molecularly Imprinted Polymer Optosensor for TEXs-Screening in Drinking Water

Francisco J. Sainz-Gonzalo[*], *Antonio L. Medina-Castillo, Jorge F. Fernández-Sánchez, Alberto Fernández-Gutiérrez*

Department of Analytical Chemistry, Faculty of Sciences, University of Granada, Avda. Fuentenueva s/n, 18071 Granada, Spain

*franjaviersainz@ugr.es

Introduction: The acronym TEXs defines the mixture formed by toluene, ethylbenzene and the three xylene isomers (*o*-, *m*- and *p*- xylene). These compounds are widely used as solvents and raw materials in many industries and are present in many petroleum derivatives. Therefore, for public health reasons, it is necessary the monitoring of these contaminants in situ and in real time through the use of chemical sensors.

Molecularly imprinted polymers (MIPs) are made by synthesizing highly cross-linked polymers in the presence of "printing" molecules (templates). After removal of the template, the polymer can be used as a selective medium for the template molecule and structurally related compounds. The use of MIPs as optically active surfaces has proved to provide highly selective molecular recognition properties and some excellent physical–chemical and mechanical properties in the design of optosensors. This work describes the use of the semiempirical model[1] proposed by our research group for the synthesis and optimization of a toluene-imprinted polymer and its implementation in a luminescent optosensor for screening TEXs in drinking water.

Materials and Methods: The optimum MIP was prepared in a closed vial by mixing MMA and EDMA (80:20 mol% for a total number of moles of 0.0123) with 13.7 mg AIBN, which was used as radical initiator, 0.783 mL of toluene (molar fraction 0.18) which was used as template molecule, and 2.717 mL of chloroform (molar fraction 0.82). The polymerization was undertaken in an 80 ºC oil bath heated under a nitrogen flow. Non-imprinted polymer (NIP) for use as control was prepared and treated in the same manner.

A flow injection analysis (FIA) system was used for the analytical evaluation of the polymers. The luminescence measurements were developed at $\lambda_{exc/em}$ = 260/284 nm.

Results and Discussion: MIP/NIP ratio was the criterion used to evaluate the imprinting properties of the polymers. The synthesis and the optimization of the MIP were achieved evaluating the following chemical variables: polymer composition (80% MMA, 20% EDMA), solvent (chloroform), molar fraction of toluene (0.18), total reaction volume (3.5 mL) and reaction temperature (80 ºC). Fig. 1 shows the optimum fiagrams when 500 µg L^{-1} of toluene were injected into the flow system using MIP and NIP as sensing materials. The instrumental parameters as detector voltage (700 V) and excitation and emission slit widths (4/4 nm) were also optimized. Lastly, the flow injection variables: flow-rate (1.5 mL/min) and injection volume (2.0 mL) and the presence of organic solvent (absence), pH (7.0) and ionic strength (NaCl 1.0 M) were evaluated. The adjustment of the water samples at pH 11.0 eliminated the possibility of interferences.

Fig. 1. Response of the MIP (black line) and NIP (grey line).

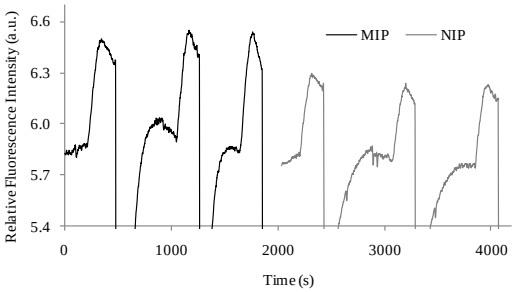

Ethylbenzene was selected as representative compound of TEXs for the establishment of the cut-off level because it provided the lowest signal. The cut-off level selected was established by the maximum contaminant level (MCL) of US-EPA in 700 µg/L. The reliability of the screening test was determined by the percentage of false positives (32%) and false negatives (0%) for a total of 50 samples. To demonstrate its applicability, 15 real water samples were analyzed obtaining 20% false positives and 0% false negatives.

Conclusions: A molecularly imprinted polymer was developed successfully for the TEXs compounds. The MIP/NIP ratio obtained for this type of compounds was acceptable. Response times were short and the reproducibility and repeatability obtained with the MIP was high. The elimination of interferences was performed with the adjustment of the water samples at pH 11.0. The optosensor, which was made up of the synthesized MIP, was used to develop a screening test. The test has been successfully used in the determination of TEXs in drinking water, and it could be an important alternative for using in routine laboratories.

Reference: [1]Medina-Castillo, A.L. et al., 2009. Biosens. Bioelectron. 25 (2), 442–449.

Acknowledgments: The Spanish Ministry of Education (Project CTQ2008-01394) and the Regional Government of Andalusia (Excellence projects P07-FQM-2738 and P07-FQM-2625) were thanked for the financial support of this work.

Synthesis and Properties of Aromatic Poly(disubstituted acetylene)s

Jiří Zedník, Zuzana Duchoslavová, Jan Svoboda, Radoslava Sivkova, Vladimíra Hanková, Jan Sedlaček, David Vrbata and Jiří Vohlidal

Dpt. of Physical and Macromolecular Chemistry, Faculty of Science, Charles University in Prague, Hlavova 2030/8, Prague 2, Czech Republic, CZ-12843

jzednik@centrum.cz

Introduction

Conjugated polymers attract great attention of polymer chemists in last few decades due to their unique properties which pave the way to new interesting application of those materials in new fields of modern research, e.g. photovoltaic cells, light-emitting diodes, field effect transistor etc. Poly(disubstituted acetylene)s belong to this interesting family of materials. Compared to their monosubstituted derivatives they exhibit strongly improved oxidative and thermal stability.

Materials and Methods

In this contribution we report synthesis of mostly new disubstituted acetylene based monomers (see Fig.1)

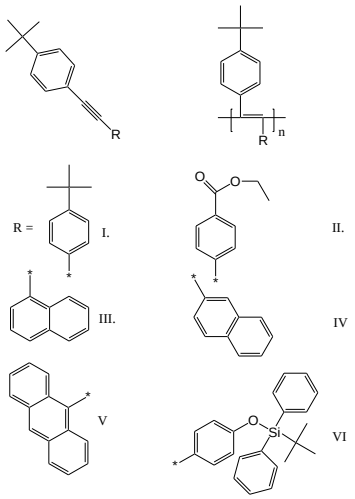

Figure 1. Synthesized monomers and polymers

All monomers were synthesized by the means of standard palladium catalyzed Sonogashira coupling using 4-*t*-butylphenylacetylene as acetylene bearing moiety, appropriate bromo/iodo derivatives and the piperidine as the solvent and base. After the purification by the column chromatography/crystallization all monomers were characterized by the means of standard spectroscopic methods. Also the luminescence properties of the prepared monomers have been studied. For better understanding of experimentally measured UV/vis and luminescence spectra TD-DFT calculation using Gaussian software has been performed.

Prepared monomers were polymerized using the metathesis catalyst based on $TaCl_5/SnPh_4$/toluene using the inert schlenk/glovebox technique. All polymers were purified by repeating dissolving in toluene and precipitation to methanol with a scope to get rid off the catalytic residua. After careful drying all prepared polymers were characterized by means of GPC and standard spectral methods. Also the luminescence study by the means of the time resolved and steady state fluorescence spectroscopy has been done.

Results and discussion

All monomers were prepared in moderate to good yield. Except for the monomer V, monomers do not exhibit absorbance in visible region. Yellowish cast of the monomer V is caused by the extended conjugation through the anthracene condensed aromatic ring. UV/vis spectra of monomers III and IV appear very similar, only the electronic transitions for monomer III are shifted to lower energies. Concerning the luminescence properties: Monomer I and and VI are not fluorescent. Monomer II shows only low quantum fluorescence yield (6 %). Monomers III and monomer IV exhibit very similar luminescence properties (quantum fluorescence yield around 30%). Monomer V exhibits high fluorescence yield (around 60 %) Measured trends in obtained spectra are in good agreement with TD-DFT calculation.

Polymers I and II are insoluble in common solvents. Insolubility of polymer I could be explained probably by the extended symmetry of resulting polymeric chains, which could lead to the enhanced regularity of packing of chains in the solid state. The insolubility of polymer II is caused by the loss of protective ethyl ester group which accompany the polymerization/isolation process. This fact has been proved by the means of NMR spectroscopy. Polymer III is red and non-fluorescent (MW around 10 000 and polymer yield 16 %). Polymer IV is yellow and highly fluorescent (MW around 50 000 and polymer yield 50 %). Consequently the sterical hindrance of 1- or 2- naphtyl pendant group causes dramatic change in the monomers reactivity and resulting polymer properties. Trials to polymerize monomer V ends up only with low molecular weight oligomers (dimers/trimers). Copolymerization of monomer V with monomer IV leads to decrease of the resulting polymer yield and molecular weight. However the yield of polymer VI is only moderate (19 %) the resulting polymer exhibits high MW (200 000) and very interesting luminescence properties. Contrary to the fact, that starting monomer is not fluorescent; prepared polymer exhibits quantum fluorescence yield around 70%. After deprotection, post-polymerization modification could be applied which paves the way for further improvement of polymer properties.

Acknowledgement: Financial supports of Ministry of Education of Czech Republic (MSM002160857) and Czech Grant Agency (Projec No 203/09/0803) and Charles Univ. Grant Agency project no 1352/2010 are gratefully acknowledged. R. Sivkova and V Hanková are indebted of the Czech Science Foundation for the fellowship No.: 203/08/H032.

Composite Polymer Materials for Stabilization of Washing Liquid of Oil and Gas Wells

Negmatova K.S., Sobirov B.B., Negmatov S.S. Isakov Sh.S., Kobilov N.S., *Negmatova M.I., Haydarov J.M.*

Tashkent State Technology University, State unitary enterprises "Fan va Taraqqiyot", Tashkent, Uzbekistan

email: polycomft2005@rambler.ru

Introduction. For high-quality drilling oil and gas wells it is required effective drilling fluids, and their quality depends on the used chemicals.

Existing chemicals both domestic and foreign manufacturers, such as the carboxymethylcellulose, K-4, K-9, hydrolyzed polyacrylonitrile, NaOH, CaC03, sulphanol, graphite, and others, which are costly and many of them are imported to Uzbekistan from abroad. Of these the most widely used and imported in large quantities, is the chemical reagent carboxymethylcellulose. However, these reagents do not always meet those requirements that apply to reagents used in complicated geological technical conditions of Uzbekistan.

In this regard, in a number of years scientific and pedagogical staff of State Unitary Enterprise "Fan va Taraqqiyot in conjunction with research staff of the Central Experimental firm "MEF", OOO "Kompozit" and OOO "Mehanokimiyo Tehnologiya" conducted research to develop effective composite polymeric reagents, using local and secondary natural resources of the country.

Materials and methods. In the development of composite polymer materials for the stabilization of drilling fluids used in drilling oil wells, we used mainly waste oil and fat production - gossypol resin, as well as carboxymethylcellulose, polyacrylamide, and the production of nitrogen fertilizers nedopal (waste based fertilizer). Gossypol resin consists of 52 to 64% of free fatty acids and their derivatives, and the rest - a product of condensation and polymerization of gossypol and its transformation, resulting from the extraction of cottonseed oil, mainly in the process of distillation of fatty acids from soapstok. In the gossypol resin found 12% of the nitrogen-containing compounds, 36% of the transformation products of gossypol fatty and oxidefatty acids. It is a homogeneous fluid mass from dark brown to black color [1]. Regarding nedopal it formed in process of cleaning of produced water of nitrogen fertilizers production from such salts, as NaCl, KCl, $CaCl_2$, Mg, Cl_2 and others. Wastes, called nedopal, with humidity 50-60% consist of $CaCO_3$, $MgCO_3$, $Ca(OH)_2$, NaOH and cation compounds KCOO Na, KCOOK [2].

It should be noted that gossypol resin before use has been previously transformed into a powder by physical and chemical processing [3, 4]. Nedopal was previously released and crushed to particle size of not more than 0,02 mm. All of these and other components in the ratio according to the developed formulations were mixed in a mixer with a z-shaped blade until smooth. To determine the physical and chemical properties of drilling fluids on the basis of the developed composite polymer chemicals samples were selected in sufficient amount to conduct a comprehensive analysis and prepare drilling fluids. By adjusting the ratio of the components included in the formula drilling fluids with appropriate technological properties were obtained. Physico-chemical properties of solutions were determined according to existing state standards.

Results and discussions. The table shows the physical and chemical properties of drilling fluids on the basis of the developed composite polymeric reagents.

1. M	2. Technological parameters				
ark of multiphase	3. ensity	4. isco-	5. ater	6. Crust-	7. H
8. C	9.	10. 3	11.	12.	13.
14. C	15.	16. 4	17.	18.	19.
20. C	21.	22. 4	23.	24.	25.
26. C	27.	28. 6	29.	30.	31.
32. C	33.	34. 8	35.	36.	37.
38. C	39.	40. 1	41.	42.	43.

As can be seen from the data muds have different physic-chemical parameters.

In this regard, drilling muds, prepared on the basis of composite chemicals CPM-1-1, CPM-1-2, a density from 0,80 to 0,95 g/cm3 recommended for use in drilling oil and gas wells, where the reservoir pressure below the hydrostatic and drilling fluids on the basis of CPM-2-1, CPM-2-2, having a density from 1.04 to 1.50 g/cm3 with an average hydrostatic formation pressure. Drilling fluids based on CPM-3-1 and CPM-3-2 having a density from 2.05 to 2,25 g/cm3 recommended for use in drilling wells under high reservoir pressures.

Conclusions. Thus, based on obtained results of research, we can say that by selecting appropriate ingredients and adjusting their ratio, we can obtain effective composite materials, like chemical reagents for stabilization of flushing water, used in drilling of oil wells.

References

[1] Fatkullaev E., Dzhalilov A.T., Minsker K.S., Marin A.P. Integrated use of secondary processed products of cotton in the production of polymeric materials. Tashkent, Publishing House "Fan" UzSSR. 1988. 144 p.

[2] Negmatova K.S. The research of the synepgistic of carbonate-polymer composition and posibilityof usingit in drilling mud. tashkent. Uzbek Chemical Journal. 2010. №4, p 46-49.

[3] Technological regulations for powdery gossypol compositions (PGC) for drilling fluids. TR-PGC: 2010. Negmatov SS, Lysenko AM, Rakhimov J.K, Negmatova K.S, Rakhimov H.YU.

Technological terms. TU Uz 10-90-2010. Gossypol powdered composition (ISC) for drilling fluids. 2010. Negmatov S.S., Lysenko A.M., Rakhimov J.K., Negmatova K.S., Rakhimov H.U.

Developing of Antifriction Wear-Resistant Polymer Composite Materials and Products from them for Working Bodies of Facilities of Mechanization of the Cotton Industry

Abed-Negmatova N.S., Musabekov D.Rh., Gulyamov G., Negmatov Sh.S., Negmatova M.I., Kodirov Sh.B., Sobirov A.B.

Tashkent State Technology University, State unitary enterprises "Fan va Taraqqiyot", Tashkent, Uzbekistan

email: polycomft2005@rambler.ru

Introduction. In the development of composite polymeric materials the most important is the choice of material and fillers. The choice is made by taking into account the purpose of the material: for anti-friction material – it is a low coefficient of friction with raw cotton in various operating conditions, for wear-resistant material - minimal wear and for anti-friction-resistant material - needed a low coefficient of friction and low wear of the material friction with raw cotton [1].

Materials and methods. In the developing of composite polymeric materials as an object of the research following thermoplastic polymers were chosen: high density polyethylene and polypropylene; and as fillers were used: graphite, carbon black, kaolin, talc, glass fibers, wollastonite, and cotton lint. But each of fillers has its shortcomings and good sides. Basic mechanical properties of samples (breaking stress in bending, flexural modulus, resilience, Brinell hardness) determined by standard methods – by state standards. The complex of tribological properties (coefficient of friction, wear-out rate) of composition interacting with raw cotton determined on disc tribometer, the equipment for measuring linear wear.

Results and discussions. Experimental studies have established that glass fibers, wollastonite, cotton lint increase coefficient of friction and decrease wear-out rate. Graphite, carbon black, talc and kaolin decrease coefficient of friction, but increase wear-out rate of composite materials, and also improve thermal conductivity and electrical conductivity, by what decrease the temperature and the charge of the statistical power. Efficiency of these fillers, especially fibrous, significantly appears with little content, that is, with less content of fiber glass the wear-out rate significantly decreases, but with increasing the content of fiber glass, the wear-out rate of composite materials decreases comparatively little, but the coefficient of friction increases highly. When graphite and carbon black are added to composite material, the coefficient of friction effectively decreases [2].

We have developed antifriction and antifriction-wear-resistant composite materials based on polyolefin – high density polyethylene and polypropylene on the established optimal ratios. They provide important physical-mechanical, tribological and operational properties [3].

The table shows strength and tribological properties of developed antifriction polyethylene (APEC) and polypropylene compositions (APPC), also antifriction-wear-resitant polypropylene compositions (AWPPC).

Strength and tribological properties of polyethylene and polypropylene compositions.

As we see from the table, the properties of polyolefin composite polymer materials meet the functional requirements, imposed to the materials for the details of friction parts working bodies of cotton processing machines. The main requirements are manufacturability and cost of used materials, effective damage decrease of cotton wool and cotton seeds, elimination of the accumulation of statistical power and winding fiber on top of the peg, elimination of sparks, appeared due to collision of working parts of machine and foreign bodies in cotton mass (such as pieces of metal, stones).

Index	APEC-1	APEC-2	APPC-1	APPC-2	AWPPC
Breaking stress in bending MPa	33,4	35,4	90,1	85,7	93,3
Toughness kJ/m²	17,5	21,0	97,3	91,3	103,7
Brinell hardness MPa	45,1	48,4	80,3	76,2	73,8
Flexural modulus GPa	0,62	0,65	1,85	0,75	1,7
Coefficient of friction (at P=0,01 MPa V=1,5 m/s W=8,2%)	0,36	0,34	0,27	0,29	0,29
Wear-resistant rate (at P=0,01 MPa V=1,5 m/s W=8,2%)	5,7	5,5	3,12	3,2	2,8

P - unit pressure, V- sliding speed, W- moistness of raw cotton

Conclusions. The produced the parts of friction pairs of working bodies of the cotton machines used for receiving, transportation, development and supply of raw cotton in the subsequent process units.

Using the developed composite polymer materials for the details of friction parts working bodies of cotton processing machines, we achieved the increase of machine productivity to 12-16% and decrease of expendable power to 7-18%, decreasing of cotton seed and cotton wool damage, and elimination of possible cotton fire.

References

1.Negmatov S.S., The basics of the processes of contact interaction of composite polymer materials with pulp. Tashkent, Fan, 1984, p.219-232

2.Gulyamov G., Negmatov N., Antifriction polypropylene composite materials for working bodies of cotton machines. Plastics, 2002, №4, p.40-41

3.Patent RUz;02649. Antifriction wear-resistant polymer composition. Negmatov S., Gulyamov G., Abed-Negmatova N., 2005, №2.

Developing of Wood Polymer Composite Materials and Sliding Bearing for Cotton Machines and Mechanisms

Musabekov D.Kh., Abed-Negmatova N.S., Gulyamov G., Negmatov S.S.,Shernaev A.N., Kodirov Sh.B., Sobirov B.B.

Tashkent State Technology University, State unitary enterprises "Fan va Taraqqiyot", Tashkent, Uzbekistan

email: polycomft2005@rambler.ru

Currently, in modern machines and mechanisms bearings in the friction are widely used. Operation of such sites in the dusty conditions of the atmosphere leads to premature wear of machines and mechanisms; and they fail. Possible regulatory clearance in rolling bearings and their maintenance is not available, but they can be replaced with new bearings, including sliding bearings.

Currently, the original technological principles of formation of composite polymer materials with desired properties are developed and implemented. Herewith, wood (poplar) and modified polymers (polyethylene of high density and polypropylene, filled with graphite and soot) can be used as antifriction material. Developed new composite wood-polymer materials are high wear-resistant, cheep, have production technology with little quantity of waste output, good dumping properties, low coefficient of friction, possible to work with little or no lubrication at all.

Current practice of use of wood-polymer composite materials in antifriction friction units requires exploratory work on the development of optimal construction of model sliding bearings.

Successful development of construction of sliding bearings from made of composite materials based on wood and modified polymers can done only with full analysis of work of friction units of cotton machines and mechanisms, analysis of features of their behavior in different operational conditions, technological abilities of construction.

There are different construction of sliding bearings made of wood-polymer materials based on wood and polymers. Efficient constructive method for improving shape stability of wood-polymer composite materials is to use them in friction units in squeezed condition, what achieved in the combined sliding bearings. The construction of sliding bearings made of wood-polymer materials based on poplar is shown on the picture. Bolster is made of round logs with an allowance for machining and sediment during compaction. Further, it is impregnated with ingredients. After impregnation bolster placed in the cowling and in this position placed in press-form for the further pressing. After the pressing the bearing has the shape as shown on the picture.

Polymer Reagents for Stabilization of Drilling Mud, Used in the Process of Drilling of Oil Wells

Negmatova K.S., Sharipov G.N., Isakov Sh.S., Negmatov S.S., Sobirov A.B., Rahimov Kh.K.

Tashkent State Technology University, State unitary enterprises "Fan va Taraqqiyot", Tashkent, Uzbekistan

email: polycomft2005@rambler.ru

For high-quality oil and gas well drilling require effective drilling fluids, good cleaning of the bottom hole drilled rock forming a thin crust with a smooth surface on the walls of wells, and thereby alert the collapse of rocks.

In turn, the quality of the drilling fluid depends on the used chemicals reagents. In most cases the chemicals for the stabilizer of mud applied carboxymethylcellulose, in Uzbekistan, mainly imported from abroad.

In this connection, in this paper, the physico-chemical properties of polymeric reagents -carboxymethylcellulose, derived from purified linter, poplar and cotton cellulose and their suitability to stabilize the drilling fluids.

It should be noted that in obtaining carboxymethylcellulose from poplar pulp, the degree of substitution of carboxyl groups in carboxymethylcellulose depends on temperature of the etherification process and molar state of cellulose with the sodium salt of monochloroacetic acid or monochloroacetate. So at 40 ^{0}C degree of substitution has a value of 0,60-0,65, and with increasing temperature, the reaction mixture to 80 ^{0}C, an increase of its value to 0,80-0,88.

Such a pattern is observed when obtaining carboxymethylcellulose of cotton cellulose and cellulose from the lint.

The results of preliminary studies of selected physical and chemical properties of the obtained reagents carboxymethylcellulose based on above types of cellulose differ significantly from each other. In this context, we studied the complex physical and chemical properties of the obtained polymeric reagents - carboxymethylcellulose. Studies have shown that physical and chemical properties of carboxymethylcellulose from the poplar and cotton cellulose and purified cotton fibers are within the following limits: the degree of polymerization, -970, 1370 and 1050, the degree of substitution of carboxymethyl group - 82.88 and 85, the content of the basic substance - 50%, 52% and 52%, viscosity 2% aqueous solution - 1200 cps, 1350 cps, 1250 cps, pH environments -10,8, 10,4 and 11,2 respectively.

Herewith high viscosity and high yield of the polymer main chemical reagent carboxymethylcellulose is derived based on cotton cellulose, and all indicators meet the technical requirements 88,2-2-2005. Solubility carboxymethylcellulose based on cotton cellulose is not inferior to foreign analogues.

In the enterprise NTTS "Kompozit" mastered the production of the technology of polymer reagent - carboxymethylcellulose. Currently, the reagent carboxymethylcellulose obtained from the poplar trees, cotton and cotton lint has been used successfully to stabilize the drilling fluids used in drilling oil wells in Uzbekistan.

Atom Transfer Radical Polymerization of Polymerization of MMA and Styrene Initiated by 3,5-bis(perfluorobenzyloxy)benzyl 2-bromopropanoate

Tuba Çakır Çanak, Mukaddes Selçukoğlu, Esin Hamuryudan, İ.Ersin Serhatlı

Department of Chemistry, Istanbul Technical University, Maslak 34469, Istanbul, Turkey

cakirtuba@itu.edu.tr, selcukoglu@itu.edu.tr, esin@itu.edu.tr ,serhatli@itu.edu.tr

Abstract: The synthesis of polymethylmethacrylate (pMMA) and polystyrene (pSt) were realized with newly synthesized initiator, 3,5-bis(perfluorobenzyloxy)benzyl 2-bromopropanoate (FBr) in the presence of copper bromide (CuBr) and N, N, N', N'', N''-pentamethyl-diethylenetriamine (PMDETA) at several temperatures by using atom transfer radical polymerization (ATRP). The perfluorinated aromatic group containing initiator was prepared by esterification of the (3,5-bis(perfluorobenzyloxy)phenyl)methanol (FOH).

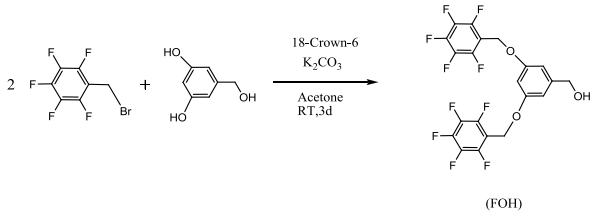

(FOH)

Both initiator and polymers were characterized by ^{1}H-NMR spectroscopy, gel permeation chromatography (GPC), differential scanning calorimetry (DSC) and thermogravimetric analysis (TGA).

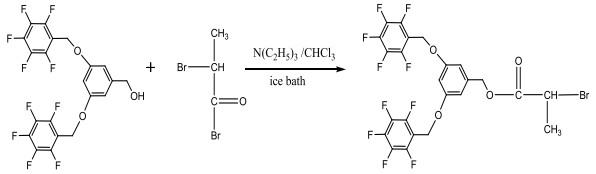

(FOH) (FBr)

The ATRP was supported by an increase in the molecular weight of the forming polymers and also by their monomodal molecular weight distribution. Contact angle measurements of water on films of synthesized polymers indicated higher degree of hydrophobicity than that of pure pMMA and pure pSt.

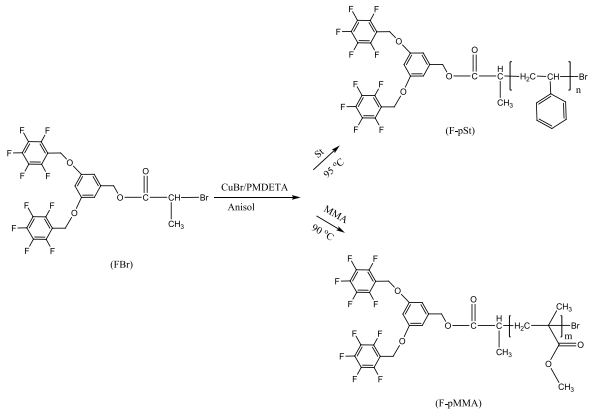

(FBr) (F-pSt) (F-pMMA)

The ATRP was supported by an increase in the molecular weight of the forming polymers and also by their monomodal molecular weight distribution. Contact angle measurements of water on films of synthesized polymers indicated higher degree of hydrophobicity than that of pure pMMA and pure pSt.

ATRP of St and MMA afforded perfluorinated aromatic group-terminated pSt and pMMA with narrow molecular weight distribution. A linear relationships between both $\ln[M]_o/[M]$ vs time and molecular weight vs conversion indicated controlled/living polymerization of St and MMA using FBr as ATRP initiator. The DSC results correlate well with the results of pure pSt and pMMA polymers. Introducing the fluorinated groups into the polymer gave higher residue in the TGA analysis. Contact angle measurements indicated that the surface wettability of the obtained films decreased significantly.

References:

1. Matyjaszewski, K., Davis, T.P., *Handbook of radical polymerization*, John Wiley & Sons, Inc. Third Avenue, New York, 2002

2. Wang, J., Matyjaszewski, K., *J.Am. Chem. Soc.* **117** (1995) 5614.

3. Tang, C.; Liu, W.; *J. Appl. Polym. Sci.* 117 (2010)1859.

4. Ameduri, B. ; *Macromolecules* 43 (2010) 10163.

5. Imae, T.; *J. Colloid Interface Sci.*, 8 (2003) 307.

6. Iyengar, D. R.; Perutz, S. M.; Dai, C.-A.; Ober, C. K.; Kramer, E. J. *Macromolecules*, 29 (1996) 1229.

7. Lou, L.; Koike, K.; Okamoto Y.; *J. Polym. Sci., Part A: Polym. Chem.* 48 (2010) 4938.

Release Behavior of Biodegradable Polyesters Reinforced with Triclosan Loaded Polylactide Micro/Nanofibers

L.J. del Valle, A. Díaz, M. Royo, A. Rodríguez-Galán, J. Puiggalí

Departament d'Enginyeria Química, Centre de Recerca en Nanoenginyeria, Universitat Politècnica de Catalunya, ETSEIB, 08028-Barcelona

luis.javier.del.valle@upc.edu

Polymeric micro and nanofibers are highly interesting materials for applications such as tissue engineering and drug delivery because the large surface area to volume ratio affords interesting new properties. Electrospinning is currently one of the most versatile processes for preparing such kind of fibers since it is applicable to a wide range of materials (e.g. synthetic and natural polymers) at a low cost and with high yield. Basically, electrospinning makes use of electrostatic forces (10-100 kV) to stretch a polymer diluted solution as it solidifies. Furthermore, electrospun fibers can be easily loaded with pharmacological active agents by adding the appropriate drug to the polymer solution before performing the electrospinning process.

Aliphatic polyesters constitute the main family of biodegradable polymers despite, in general, they lack of good thermal and mechanical properties. Polylactide (PLA) is one remarkable exception since has high melting point (173-178 ºC) and tensile modulus (2.7-16 GPa). Thus, it seems interesting to use electrospun polylactide micro/nanofibers as reinforcing materials of polyester matrices. In this work, polycaprolactone (PCL), poly(nonamethylene azelate) (P99) and poly(nonamethylene azelate-*co*-pimelate) (COP) were selected as matrices due to their different molecular weight and hydrophobicity. Samples were prepared by pressing the mixture of the powdered polyester (PCL, P99 or COP) and the polylactide fibers at a temperature 10 ºC above the melting point of the polyester matrix. Triclosan, a well demonstrated antimicrobial drug, was loaded in different ways (Figure 1) and the release behaviour studied.

Stress-strain tests demonstrated the improvement on mechanical properties which was more significant for the low molecular weight samples (P99 and COP) and by adding microfibers (M) instead of nanofibers (N). SEM micrographs of fracture surfaces indicated a detachment of fibers as shown in Figure 2 for representative samples.

The triclosan release percentage clearly increased when nanofibers were employed (i.e. PCL-N and PCL-M released 74% and 36% after 4000 min of exposure to a Sörensen/ethanol medium, respectively) and also when more hydrophobic polyester matrices were employed (Figure 3).

The film surface of the more hydrophobic polyesters (P99 and COP) supported the cellular adhesion (human laryngeal epidermoid carcinoma HEp-2 cells) better than polycaprolactone and the culture plate (TCPS). Cellular proliferation was also evaluated after 7 days of culture. It was found that the number of cells that colonized P99 and COP samples was significantly higher ($p < 0.05$) than observed over the control sample. Furthermore, proliferation was not influenced by the morphology of the reinforcing fibers (Figure 4).

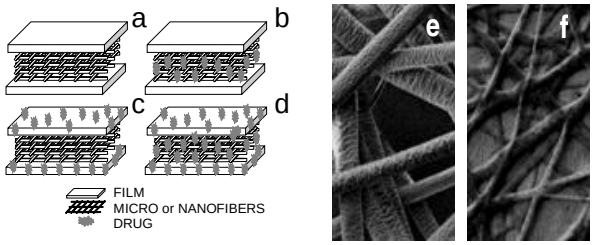

Figure 1. Schematic representation of the different triclosan loaded samples (left) and SEM micrographs showing electrospun micro and nanofibers of PLA (right).

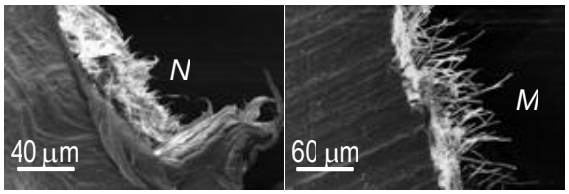

Figure 2. SEM micrographs showing the fracture surface of PCL reinforced with PLA nanofibers (left) and COP reinforced with PLA microfibers (right).

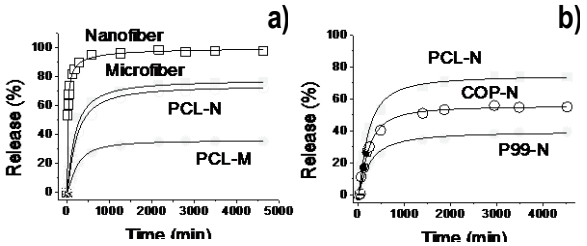

Figure 3. Comparison between cumulative triclosan release in a Sörensen/ethanol medium from samples incorporating micro or nanofibers of PLA (a), and from different polyester matrices incorporating PLA nanofibers (b).

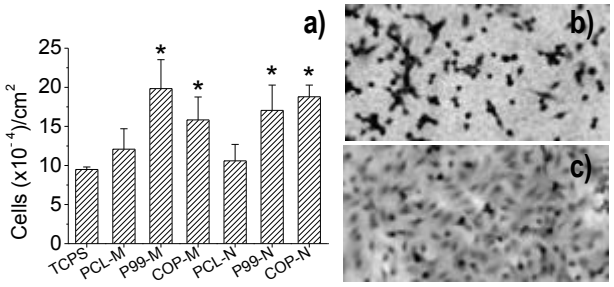

Figure 4. a) HEp-2 cell proliferation on the different studied substrates (asterisk denotes $p < 0.05$ versus control). b) and c) Optical micrographs showing the morphology of HEp-2 cells adhered to PCL and COP substrates, respectively.

Acknowledgements: This research has been supported by a grant from MCYT/FEDER (MAT2009-11503).

Adhesive Properties of Low T_g Polymers Bearing Hydrogen Bonding Moieties.

Sandrine Pensec[1], Jérémie Courtois[2], Hanbin Wang[1], Cécile Fonteneau[1], Guylaine Ducouret[2], Laurent Bouteiller[1], Costantino Creton[2]

[1] UPMC Univ. Paris 6, UMR 7610 CNRS, Chimie des Polymères, 3, rue Galilee, F-94200 Ivry, France
[2] Physico-Chimie des Polymères et des Milieux Dispersés, UMR 7615,UPMC-CNRS-ESPCI, 10 rue Vauquelin 75231 Paris Cedex 05 France

sandrine.pensec@upmc.fr

Supramolecular polymers are chains of small molecules held together through reversible non-covalent interactions. The dynamic character of such weak interactions is responsible for the appearance of new properties, as compared to those of usual covalently bonded polymers. For example, these materials can display thermoreversible polymer-like properties (such as viscoelasticity)[1], or even form self-healing elastomers.[2]

An interesting application of supramolecular chemistry is the combination of flexible polymers with hard domains containing self-assembled polar groups. A typical example of supramolecular polymer is a flexible polymer or oligomer functionalized with hydrogen bonding end-groups. The structure and the rheological properties of such systems have been reported and they typically show an increase in the long relaxation times and hence of the viscosity[3],[4]. The dissipation of energy upon deformation, corresponding to this increased viscosity, is precisely what is needed to manufacture self-adhesive materials also called pressure-sensitive-adhesives (PSA).

In this context, some low T_g polymers with a bis-urea moiety in the middle of the chain have been synthesized. For example, in solution in a non polar solvent, we have shown that one of them (PIBUT) readily associates in a comb-shaped polymer with a reversibly associating backbone[5]. The supramolecular structure of the bulk polymer[6], the rheological measurements and the promising adhesive properties both on steel surfaces and on typical low adhesion surfaces such as silicone will be reported.

1. J.H.K.K. Hirschberg, F.H. Beijer, H.A. van Aert, P.C.M.M. Magusin, R.P. Sijbesma, E.W. Meijer, *Macromolecules* **1999**, 32, 2696
2. P. Cordier, F. Tournilhac, C. Soulie-Ziakovic, L. Leibler, *Nature* **2008**, 451, 977
3. O. Colombani, C. Barioz, L.Bouteiller, C. Chanéac, L. Fompérie, F. Lortie, H. Montès, *Macromolecules* **2005**, 38, 1732
4. H. Kautz, D.J.M vanBeek, R.P. Sijbesma, E.W. Meijer, *Macromolecules* **2006**, 39, 4265
5. S. Pensec, N. Nouvel, A. Guilleman, C. Creton, F. Boué, L. Bouteiller, *Macromolecules* **2010**, 43, 2529.
6. J. Courtois, I. Baroudi, N. Nouvel, E. Degrandi, S. Pensec, G. Ducouret, C. Chanéac, L. Bouteiller, C. Creton, *Adv. Funct. Mater.* **2010**, 20, 1803.

Preparation of Cationic Polymer Brushes on Silicon Wafer Surface via RAFT Polymerization

Serkan Demirci[1], *Tuncer Çaykara*[2]

[1]Ahi Evran University, Faculty of Arts and Sciences, Department of Chemistry, 40100, Kırşehir, Turkey
[2]Gazi University, Faculty of Arts and Sciences, Department of Chemistry, 06500, Ankara, Turkey

srkndemirci@gmail.com

Abstract

Polymer brushes consist of ordered assemblies of polymeric chains that are terminally grafted or adsorbed onto a substrate surface at one or more anchoring points [1].

Generally, polymer brushes are prepared via two basic methods such as "grafting to" and "grafting from" [1]. The most widely used and versatile polymerization technique to prepare polymer brushes by the "grafting from" method are the various surface-initiated controlled living free radical polymerization (CLRP) methods, such as atom transfer radical polymerization [2], nitroxide-mediated polymerization [3], and reversible addition-fragmentation chain transfer (RAFT) polymerization [4].

The main advantages of RAFT polymerization when compared to other CLRP techniques include the ability to polymerize a wide variety of monomers; polymerizations may be conducted over a wide range of temperatures; it allows for the preparation of polymer brushes with functional end-groups [4,5].

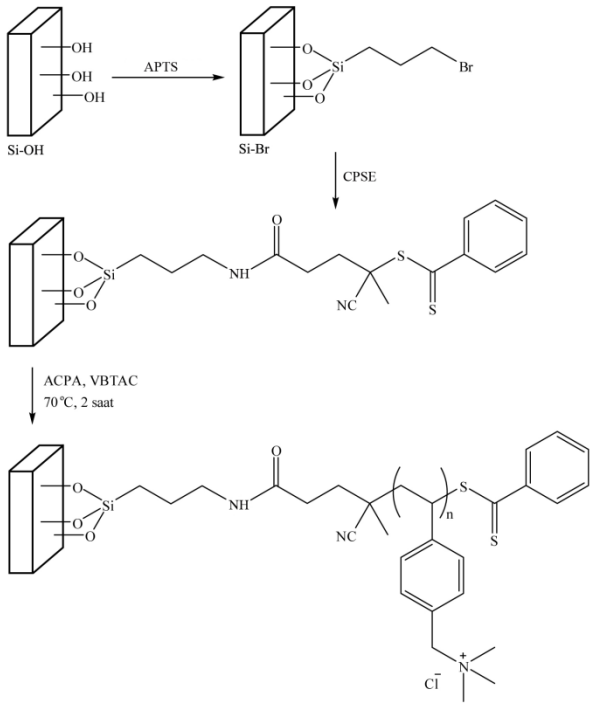

Scheme 1. The immobilization of RAFT agent onto silicon surface and the RAFT mediated synthesis of PVBTAC brushes.

In this study, RAFT polymerization technique has been used to synthesize cationic poly((*ar*-vinylbenzyl) trimethylammonium chloride) (PVBTAC) polymer brushes were prepared under RAFT conditions using silicon wafer surfaces that were modified with surface immobilized RAFT agent (4-cyanopentanoic acid dithiobenzoate).

The formation of homogeneous tethered PVBTAC brushes, whose thickness can be tuned by reaction time varying, is evidenced by using the combination of Fourier transform infrared spectroscopy, x-ray photoelectron spectroscopy, atomic force microscopy and water contact-angle measurements. The calculation of grafting parameters from the number-average molecular weight, $\overline{M}_n$ (g/mol) and ellipsometric thickness, h (nm) values indicated the synthesis of densely grafted poly((*ar*-vinylbenzyl)trimethyl ammonium chloride) films and allowed us to predict a polymerization time for forming a "brushlike" conformation for the chains.

The addition of sacrificial RAFT agent results in the formation of free polymer in solution, which was characterized and confirmed the formation of well defined polymers. The possibility to tune the surface properties (e.g., film thickness, grafting density, wettability, and surface morphology) by varying reaction time is also demonstrated.

References

[1] Advincula, R.C., Brittain, W.J., Caster, K.C., Ruhe, J. Polymer Brushes: Synthesis, Characterization, Applications; Wiley-VCH: New York, 2004.
[2] Turan, E., Demirci, S., Çaykara, T. Thin Solid Films 2010, 518, 5950-5954
[3] Husseman, M., Malmstrom, E.E., McNamara, M., Mate, M., Mecerreyes, D., Benoit, D. G., Hedrick, J.L., Mansky, P., Huang, E., Russell, T.P., Hawker, C.J. Macromolecules 1999, 32, 1424-1431.
[4] Gürbüz, N., Demirci, S., Yavuz, S., Çaykara, T. J Polym Sci Part: A Poly Chem 2011, 49, 423-431.
[5] Perrier, S. Takolpuckdee, P. J Polym Sci Part A: Polym Chem 2005, 43, 5347-5393.

Engineering of Magnetic Poly(ε-caprolactone) Nanomedicines Against Arthritis

Eva Sáez-Fernández[1], Visitación Gallardo[1], Mª Adolfina Ruiz[1], Ángel V. Delgado[2], José L. Arias[1]

[1]Department of Pharmacy and Pharmaceutical Technology, University of Granada, Spain.
[2]Department of Applied Physics, University of Granada, Spain.

evasaez@ugr.es

Introduction. Many of the diseases in the musculoskeletal system are characterized by local inflammatory processes which are currently treated with non-steroidal anti-inflammatory drugs (NSAIDs) or corticosteroids. Diclofenac sodium is a NSAID that has been shown to be effective in the treatment of acute pain and a broad variety of inflammatory processes including arthritis. Despite its efficient activity, this drug suffers from several drawbacks, e.g., a short plasma half life, a high percentage of protein binding, and a very high pre-systemic metabolism [1].
In this communication we describe a reproducible technique for the preparation of magnetically responsive polymeric nanoparticles (NPs) loaded with diclofenac sodium for arthritis treatment.

Materials and Methods. Superparamagnetic Fe_3O_4 NPs (mean size ≈ 10 nm) were prepared following the chemical co-precipitation method [2]. Poly(ε-caprolactone) (PCL) NPs were synthesized by an interfacial polymer disposition process (average diameter ≈ 100 nm) [3]. The method followed to formulate Fe_3O_4/PCL (core/shell) NPs (mean size ≈ 90 nm) was similar to that above mentioned for the preparation of PCL NPs, except that the aqueous phase was a Fe_3O_4 suspension. Inspection of the coating efficiency of the magnetic cores was done through analysis of HRTEM pictures. FTIR spectrometry data was used for the characterization of the chemistry of the three different types of NPs. The magnetic properties of Fe_3O_4 and magnetic nanocomposites were determined using a vibrating magnetometer at room temperature.
Diclofenac sodium loading to the NPs was achieved by: *i*) single drug surface adsorption onto preformed NPs; and, *ii*) entrapment procedure or drug absorption into the Fe_3O_4/PCL NPs. Drug release from core/shell NPs was performed *in vitro* following the dialysis bag method, where PBS of pH 7.4 was the release medium.
Spectrophotometry was validated and used successfully, at the maximum absorbance wavelength of diclofenac sodium (276 nm), as the analytical technique in the determination of drug loading and release. A qualitative estimation of the adsorption process was possible by electrophoresis. All the experiments were carried out in triplicate.

Results and Discussion. HRTEM photographs of the magnetic core/shell NPs established that the Fe_3O_4 nuclei were covered by a well-defined polymeric shell. The main feature of the infrared spectra of the three types of NPs was the presence of all the bands corresponding to PCL in the spectrum of the nanocomposites, thus confirming that the shell observed by HRTEM corresponded well to the polymeric coating. We determined the initial susceptibility of Fe_3O_4 (χ_i ≈ 0.15), and Fe_3O_4/PCL (χ_i ≈ 3.15) for the core/shell NPs.
A positive effect of NSAID concentration in the incubation medium on the adsorption efficiency onto Fe_3O_4/PCL NPs was observed. The entrapment efficiency of diclofenac sodium to NPs increased with the amount of drug in solution up to ≈ 11 % for the range of concentrations investigated. However, NSAID loading remained very low when using the surface adsorption procedure (maximum drug loading ≈ 4 %). Electrokinetic measurements qualitatively confirmed the conclusions based on adsorption determinations.
A thermodynamically favoured drug entrapment into nanocomposites led to high NSAID loading values: the hydrophobic drug kept in contact with the hydrophobic PCL when the NPs were formed, rather than as isolated molecules in water. Like the adsorption procedure, a positive effect of drug concentration on the absorption efficiency into the NPs was observed. Compared to surface adsorption, both the entrapment efficiency and the drug loading were significantly enhanced whatever the initial NSAID concentration fixed. For instance, when the initial drug concentration in the adsorption/absorption medium was 10^{-2} M, these parameters rise from ≈ 11 % and ≈ 4 % (after drug adsorption) to ≈ 49 % and ≈ 18 % (when the drug was absorbed into the matrix), respectively. The release of diclofenac sodium adsorbed onto the nanocomposites was a rapid desorption process from the polymeric surface. On the opposite, the release of drug absorbed into Fe_3O_4/PCL NPs was a biphasic process. The rapid first phase likely corresponded to the leakage of the surface-associated and/or poorly entrapped NSAID. Diclofenac release during the slower release phase may result from drug diffusion through the polymeric matrix.

Conclusions. The optimal preparation conditions to obtain diclofenac-loaded Fe_3O_4/PCL NPs suitable for parenteral administration have been determined. We put forward that such formulation hold very important properties (e.g., very suitable response to weak magnetic fields, high drug loading and sustained drug release), suggesting its potential application for efficient delivery of diclofenac sodium to inflammation.

Acknowledgements. Financial support from Junta de Andalucía, Spain, under Project PE-2008-FQM-3993.

References. [1] Carson, J., et al., N. Engl. J. Med. 323 (1989) 135. [2] Massart, R., IEEE Trans. Magn. 17 (1981), 1247. [3] Sinha, V.R., et al., Int. J. Pharm. 278 (2004) 1.

Development of a Poly(ε-caprolactone)-Based Magnetic Biodegradable Nanoplatform Against Cancer

Eva Sáez-Fernández[1], *Visitación Gallardo*[1], *Mª Adolfina Ruiz*[1], *Ángel V. Delgado*[2], *José L. Arias*[1]

[1]Department of Pharmacy and Pharmaceutical Technology, University of Granada, Spain.
[2]Department of Applied Physics, University of Granada, Spain.

evasaez@ugr.es

Introduction. One of the problems associated to chemotherapy is the inability to target a specific area of the body. To reach an acceptable therapeutic level at the desired site, high drug doses must be administered even though severe toxicity will occur. As an alternative, magnetically responsive nanoparticles (NPs) can specifically deliver anticancer drugs to targeted tumors under the guidance of magnetic gradients. Then, the magnetic force will focus the magnetic particle into the tumor interstitium (or tumor neovasculature) until the drug is completely released.

In order to increase the therapeutic activity of 5-fluorouracil (5-FU) along with an overcome of their important drawbacks, we investigated their formulation into a magnetic nanoplatform made of biodegradable poly(ε-caprolactone) nanoparticles (NPs) with a superparamagnetic core (magnetite, Fe_3O_4). It is expected that the polymeric shell will play the role of transporting the drug to the tumor tissue (controlling its release). Simultaneously, iron oxide cores will allow the magnetic guidance of the NPs towards the site of action.

Materials and Methods. PCL (mean size: 97 ± 7 nm) and superparamagnetic Fe_3O_4 (9 ± 2 nm) NPs were prepared following the interfacial polymer disposition method [2], and the chemical co-precipitation process [3], respectively. The method followed to synthesize Fe_3O_4/PCL (core/shell) NPs was similar to that followed for the preparation of polymeric NPs, except that the aqueous phase was a Fe_3O_4 suspension.

Particle size was determined by HRTEM photographs and PCS. Characterization of the internal structure of Fe_3O_4 and core/shell NPs was performed by X-ray diffractometry. Surface electrical properties of the NPs were analyzed by electrophoresis measurements as a function of both pH and KNO_3 concentration. Magnetic properties of Fe_3O_4 and Fe_3O_4/PCL NPs were determined with a vibrating magnetometer at room temperature.

Two possible routes can be thought of for 5-FU loading to the core/shell nanoplatform: surface adsorption onto NPs previously formed, after incubation in a drug solution; and, drug incorporation into the polymeric matrix, by its addition to the aqueous medium before the NP formation. Drug release from nanocomposites was performed *in vitro* following the dialysis bag method, using PBS (pH ≈ 7.4) as the release medium. UV-Vis spectrophotometry was validated and used successfully (maximum absorbance wavelength of 5-FU: 266 nm) to quantify drug loading and release. Electrokinetic determinations were used to qualitatively confirm the conclusions based on adsorption determinations. The experiments were done in triplicate.

Results and Discussion. The interfacial polymer disposition method followed for the preparation of Fe_3O_4/PCL NPs allowed the formation of a well-stabilized spherical nanocarrier with an average diameter of 86 ± 12 nm. HRTEM photographs further established that iron oxides were well-covered by the PCL shell. X-ray diffractograms of composite and Fe_3O_4 NPs showed excellent coincidence with the ASTM pattern of Fe_3O_4, an indication of the mineralogical purity and high crystalline nature of the synthesized Fe_3O_4 NPs. Since the ζ–pH and ζ–ionic strength trends of the core/shell NPs were almost identical to those of pure PCL and considering that, oppositely, pure Fe_3O_4 NPs displayed very different electrical profile, it was concluded that the deposition of the PCL coat onto Fe_3O_4 has effectively taken place. The enhancement of saturation magnetization when the magnetic nuclei were merged into a PCL layer was significant: ≈ 12 kA/m for Fe_3O_4, and ≈ 260 kA/m for Fe_3O_4/PCL.

5-FU adsorption efficiency onto Fe_3O_4/PCL NPs was positively influenced by the drug concentration in the incubation medium. Similar effect was also observed when the drug was entrapped into the nanocomposites. However, much higher 5-FU loading values were obtained by following the drug absorption procedure. For instance, when the initial drug concentration in the adsorption/absorption medium was 0.01 M, these parameters rise from ≈ 18 % and ≈ 2.5 % (after drug adsorption) to ≈ 51 % and ≈ 8 % (by 5-FU absorption into the nanocomposite matrix), respectively. Sustained drug release properties were only possible upon drug absorption. The release of drug absorbed into Fe_3O_4/PCL NPs was a biphasic process. The rapid first phase likely corresponded to the leakage of the surface-associated and/or poorly entrapped drug. 5-FU release during the slower release phase may result from drug diffusion through the polymeric matrix.

Conclusions. It was defined the optimal formulation conditions to obtain 5-FU-loaded Fe_3O_4/PCL NPs for parenteral administration. The nanocomposites are characterized by an unusually high drug loading, a significant magnetic susceptibility, and a low burst release. Consequently, the magnetic nanoplatform opens promising possibilities to improve the delivery of 5-FU to cancer.

Acknowledgements. Financial support from Junta de Andalucía, Spain, under Project PE-2008-FQM-3993.

References. [1] Arias, J.L., Molecules 13 (2008) 2340. [2] Sinha, V.R., et al., Int. J. Pharm. 278 (2004) 1. [3] Massart, R., IEEE Trans. Magn. 17 (1981), 1247.

Fabrication of pH Responsive Copolymer Brushes on Silicon Wafer Surface via Reversible Addition-Fragmentation Chain Transfer Polymerization

Selin Kınalı Demirci[1], *Serkan Demirci*[2], *Tuncer Çaykara*[1]

[1]Gazi University, Faculty of Arts and Sciences, Department of Chemistry, 06500, Ankara, Turkey
[2]Ahi Evran University, Faculty of Arts and Sciences, Department of Chemistry, 40100, Kırşehir, Turkey

srkndemirci@gmail.com

Abstract

Polymer brushes are generally defined as layers of polymer chains end-grafted to a solid surface and some of them show controlled dynamic behavior in response to external stimuli, such as temperature and pH [1].

Stimuli-responsive surfaces have a great potential in many technologically important areas such as bioanalysis, biomimetics, and nanoelectromechanical systems [2,3].

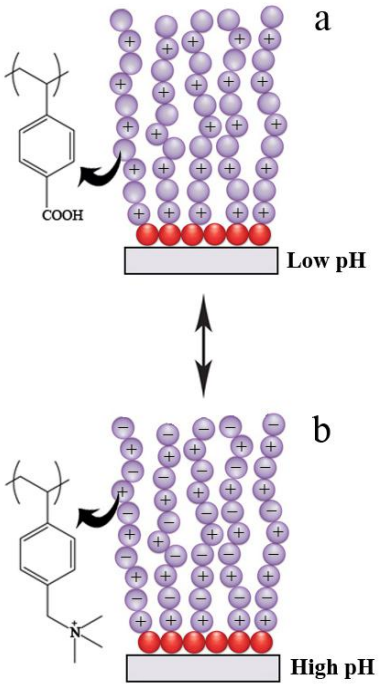

Figure 1. A surface switching from cationic to neutral in response to environmental pH change (a) in low pH solutions, (b) in neutral or higher pH solutions.

In this study, pH responsive copolymer brushes which contain positively-charged (*ar*-vinylbenzyl)trimethyl ammonium chloride (VBTAC) and negatively-charged 4-vinylbenzoic acid (VBA) on silicon wafer surface were synthesized by reversible addition-fragmentation chain transfer (RAFT) polymerization.

The azo initiator immobilized substrate, was prepared by the silanization of hydroxyl groups on silicon wafer with 3-aminopropylthriethoxysilane (APTS) and by the amide reaction of APTS with 4,4'-azobis-4-cyanopentanoil chloride; followed by the RAFT polymerization of VBTAC and VBA using a "free" initiator, that is, 4,4'-azobis-4-cyanopentanoic acid and RAFT agent, that is, 2-(2-carboxy-ethylsulfanylthiocarbonylsulfanyl) propionic acid.

The resulting polymer brushes were characterized by Fourier transform infrared spectroscopy, x-ray photoelectron spectroscopy, atomic force microscopy, water contact-angle measurements, gel permeation chromatography and ellipsometry techniques.

VBTAC and VBA were grafted from silicon wafer surface by combining the self-assembly and the RAFT technique, leading to highly pH responsive surface. The surface has charge neutrality under neutral and basic conditions, and is positively charged under acidic conditions due to the protonation of the carboxylic acid group.

References

[1] Duner, G., Anderson, H., Myrskog, A., Hedlund, M., Aastrup, T., Ramström, O. Langmuir 2008 24, 7559-7564.
[2] Turan, E., Demirci, S., Çaykara, T. Thin Solid Films, 2010 518, 5950-5954.
[3] Mi, L., Bernards, M.T., Cheng, G., Yu, Q., Jiang, S. Biomaterials, 2010 31, 2919-2925.

Microencapsulation of butyl stearate with melamine-formaldehyde resin: Effect of decreasing pH value on composition and thermal stability of microcapsules

Branko Alič, Urška Šebenik, Matjaž Krajnc

University of Ljubljana, Faculty of Chemistry and Chemical Technology, Aškerčeva cesta 5, 1000 Ljubljana, Slovenia

matjaz.krajnc@fkkt.uni-lj.si

Introduction:

Melamine-formaldehyde (MF) microcapsules with water-immiscible core material are prepared by *in situ* polymerization. Polymerization of MF resin occurs in the continuous water phase and as pre-polymer molecular weight increases, pre-polymer deposits on the surface of the dispersed phase. By further polymerization and crosslinking MF shell is formed.

In this work, microencapsulation of butyl stearate (a phase change material) with melamine-formaldehyde resin using different decreasing rates of pH value was investigated.

Materials and Methods:

Materials: Etherified MF resin (70 wt. %), butyl stearate (technical 40-60 %), sodium dodecyl sulfate (96%), 1 wt. % formic acid solution, deionized water.

Emulsion preparation: 25 g of butyl stearate, 2.5 g of sodium dodecyl sulfate, 15 g of MF resin and 458 g of deionized water were mixed at a rate of 1000 rpm using dispermat for 30 minutes.

Microencapsulation: The emulsion was poured into a 500 ml glass reactor equipped with a reflux condenser, a mechanical stirrer, a digital thermometer and a glass electrode for pH measurements. The pH value of reactor content was adjusted to 6.0 using 1 wt. % formic acid and heated to 70 °C at the stirring speed of 500 rpm. The pH value of reaction mixture was controlled and regulated during the whole microencapsulation process as presented in Fig. 1.

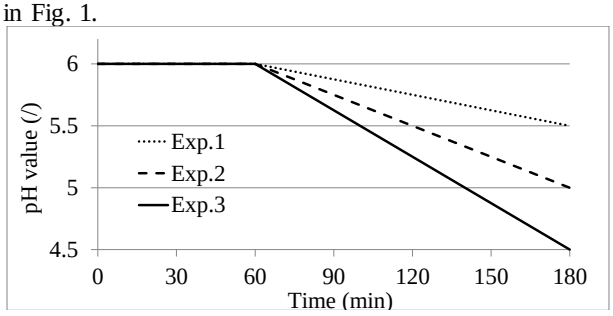

Fig. 1: pH value of reaction mixture during encapsulation process.

During the microencapsulation several samples were taken to investigate core/shell ratio, thermal stability of microcapsules and shell morphology. The core/shell ratio was determined by differential scanning calorimetry (from melting enthalpy of butyl stearate). Thermal stability of microcapsules was determined by thermogravimetric analysis. Shell morphology and its thickness were investigated by scanning electron microscopy.

Results and Discussion:

The wt. % of shell material increased during microencapsulation (Fig.2). Depositing of MF pre-polymer and pure MF particles on the microcapsules surface depended on pH value of reaction mixture. Lower pH value resulted in higher wt. % of shell material in microcapsules. The increase in wt. % of shell material was mainly due to the deposition of pure MF particles on the surface (Fig.3). However, the shell thickness also increased.

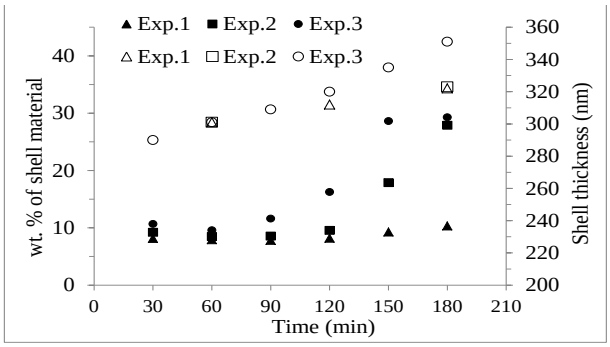

Fig. 2: The wt. % of shell material (plain symbols) and shell thickness (open) during microencapsulation.

As expected, thermal stability of microcapsules increased with the time of microencapsulation. For microcapsules containing over 70 % of core material (final products) only about 20 % mass loss was observed at temperatures where pure core material completely evaporates. The rest of core material (already decomposed) evaporated at temperatures above 340 °C when MF shell decomposed. From TGA and DSC analysis it was concluded that for a better thermal stability slow deposition of MF pre-polymer on the surface of the dispersed phase is necessary.

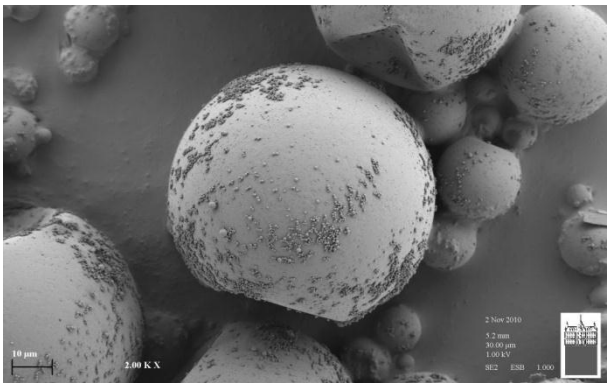

Fig. 3: SEM image of microcapsules obtained by experiment 1.

References:

[1]Salaün, F.; Devaux, E.; Bourbigot, S.; Rumeaud, P. Chem. Eng. J., 2009, 155, 457.

[2]Alič, B,; Šebenik, U.; Krajnc, M.; J. Appl. Polym. Sci., 2011, 119, 3687.

Polymerization of Octamethylcyclotetrasiloxane in a Microtube Reactor with Liquid-Liquid Slug Flow Pattern

Ervin Šinkovec and Matjaž Krajnc

University of Ljubljana, Faculty of Chemistry and Chemical Technology, Aškerčeva cesta 5, 1000 Ljubljana, Slovenia

matjaz.krajnc@fkkt.uni-lj.si

Introduction, Results and Discussion: A controlled hydrodynamic flow is an important feature of microstructured reactors. When two immiscible liquids in a microchannel are used, different flow patterns such as annular flow, parallel flow, drop flow or slug flow can be obtained. Circulation patterns in liquid-liquid microchannel flow vary with the physical properties of liquids as well as with operating parameters such as flow ratio of two immiscible liquids, mixing elements geometry, channel geometry and capillary dimensions[1]. In a microtube reactor with stable two-phase slug flow pattern a high degree of control over the slug size distribution can be achieved and the liquid-liquid interfacial surface-to-volume ratio may be strictly defined. A known specific interfacial area enables to investigate processes in heterogeneous systems, such as mass transport between two immiscible liquids and/or chemical reaction on the liquid-liquid interface.

Here as a case study anionic polymerization of octamethylcyclotetrasiloxane was chosen. Systematic studies of anionic ring-opening polymerization (AROP) in emulsion[2-4] showed that during AROP in emulsion, different chemical reactions by which polymer is formed (initiation, propagation and termination) take place on the polymer particle surface (organic-aqueous interphase) and inside the particle (organic phase). Chain growth is initiated by hydroxide anion of a water-soluble initiator, which is coupled with a cationic emulsifier on the particle surface. The emulsifier cation remains associated to the active center (hydroxide anion) of growing polymer chain during the propagation step. Termination occurs through protonation by water to give silanol end-groups. The reversibility of termination reaction is a key factor for long chain generation[3]. Backbiting reactions, also occurring at the interface, produce small oligomeric cycles accumulating on the particle surface, where the steric constraints imposed by the ion-pairing limit the size of the obtained rings. In the particle interior condensation and redistribution reactions take place, which do not affect the monomer conversion. In this work, an attempt was done to follow the extent of reactions occurring at the interface by varying surface-to-volume ratio of organic phase. The surface-to-volume ratio was controlled by varying organic and aqueous volumetric flow rate. Desired residence time was achieved by varying total flow rate and/or length of microtube reactor. Effects of emulsifier and initiator concentrations on the slug flow stability and on the kinetics were investigated as well. Monomer conversion was determined by gravimetric analysis, by which the amount of monomer converted to large non-volatilizable polymeric chains was determined. All volatile oligomeric cycles, which are formed during polymerization, were treated as monomer in conversion calculations.

It was observed that the composition of aqueous phase has a significant influence on the slug flow stability. Varying the emulsifier and initiator concentrations had a strong impact on the stability of the flow regime. Since microreactor studies request a stable and reproducible two-phase flow pattern, which allows a high control over the slug size distribution, chemical kinetics and mass transfer between phases were investigated only at stable operating regime. In a microtube reactor, a stable regime is characterized by a reproducible slug flow (Figure 1).

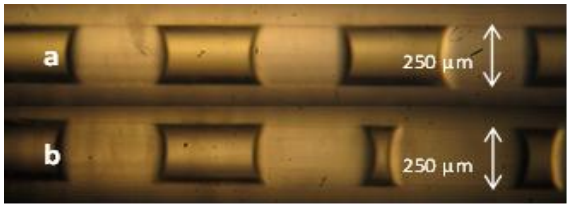

Figure 1. a) Stable two phase slug flow, b) unstable two phase slug flow

Materials and Apparatus: Cationic emulsifier (hexadecyltrimethylammonium bromide, benzalkonium chloride), potassium hydroxide (p.a., Merck), deionized water.

Microreactor experiments were carried out in the microtube reactor connected to high performance syringe pumps (Harvard Apparatus, Holliston, USA) with fluorinated ethylene propylene tubes (Vici AG, Schenkon, Switzerland). Syringe pumps ensured highly controllable flow rates. The reaction in the fluorinated ethylene propylene microtube reactor with an internal diameter of 250 µm was carried out at a slug-flow regime. The organic phase feed consisted of octamethylcyclotetrasiloxane. The aqueous phase consisted of aqueous solution of ionic, nonionic emulsifiers and initiator (potassium hydroxide) in various proportions. The mixing of phases was done in a poly-etheretherketone T-mixer (Vici AG, Schenkon, Switzerland) with an internal diameter of 250 µm.

References:

[1] Zhao, Y.; Chen, G.; Yuan, Q., *AIChE Journal*, (2006) **52**, 4052.

[2] De Gunzbourg, A.; Favier, J.-C.; Hémery, P., *Polymer International*, (1994) **35**, 179.

[3] Barrère, M.; Ganachaud, F.; Bendejacq, D.; Dourges, M. A.; Maitre, C.; Hémery, P., *Polymer*, (2001) **42**, 7239.

[4] Barrère, M.; Maitre, C.; Dourges, M. A.; Hémery, P., *Macromolecules*, (2001) **34**, 7276.

Conductive polymer composites obtained from urea–formaldehyde resin and copper powder

Gabriel Pinto[1], Abdel-Karim Maaroufi[2], Rosario Benavente[3], José M. Pereña[3]

[1]Departamento de Ingeniería Química Industrial y del Medio Ambiente, Escuela Técnica Superior de Ingenieros Industriales, UPM, Madrid, Spain.

[2]Laboratory of Composite Materials, Polymers and Environment, Department of Chemistry, Faculty of Sciences, Rabat Agdal, Morocco

[3]Instituto de Ciencia y Tecnología de Polímeros (CSIC). Madrid, Spain.

gabriel.pinto@upm.es; perena@ictp.csic.es

Introduccion

As well known, most polymers are thermally and electrically insulating. The increase of thermal and electrical conductivities of polymers opens large new markets. The advantages of conductive polymer composites when compared with typically used metals includes improved corrosion resistance, lighter weight, and the ability to adapt the conductivity properties to suit the application needs (1).

There is a critical composition (percolation threshold) at which the conductivity increases by some orders of magnitude from the insulating range to values in the semiconductive or conductive range.

This work is concerned with the preparation, characterization and study of the electrical conductivity of composite materials prepared by compression moulding of mixtures of copper powder and a commercial grade thermosetting resin of urea–formaldehyde filled with alpha-cellulose in powder form.

Materials

The matrix polymer used in our experiments was a commercial grade urea–formaldehyde embedded in alpha-cellulose (30 wt %) supplied in the form of powder.

The electrical conducting filler used was copper, average particle size of 150–200 µm, density of around 8.92 g/cm3, and electrical conductivity of the order of 6.3 x 10^5 S/cm. Both the polymer and the metal powders were dried before use at 60 ºC during 48 h.

Composite Fabrication

Composites of urea–formaldehyde embedded in alpha-cellulose powder filled with copper were fabricated by mixing the polymer matrix and the filler powders for 2 h in an internal mixer, followed by compression moulding in a specially designed mould with three cavities of 30.0-mm diameter and 3.0-mm thickness each one. The moulding parameters were 20 MPa and 150 ºC for 30 min (2).

The homogeneity of composites was controlled by morphological pictures obtained by optical microscopy. Furthermore, to check the void level within the samples, which influences remarkably the electroconductivity, the porosity rate has been calculated from the densities of the composites.

Results and Discussion

By comparison between experimental and theoretical densities of samples, the porosity of composites. was obtained Even though the average fraction voids in volume begins to increase for low values of filler concentration, for values higher than 12 vol % that fraction is almost constant, with a value of 11% ± 2%, thus assuring the good quality of the obtained composites.

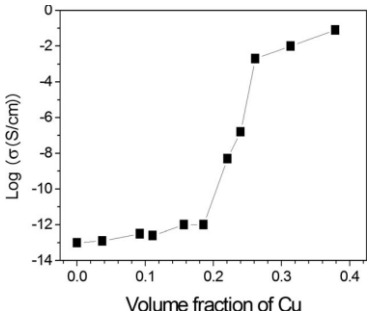

Figure 1. Variation of the electrical conductivity of urea-formaldehyde embedded in cellulose powder/Cu composites with Cu content

The electrical conductivity of the composites as a function of filler content for the samples shows the typical S shaped dependency (Figure 1) with three regions (dielectric, transition, and conductive). As expected, samples with low-filler content are almost nonconductive. However, the electrical conductivity of the composites increases dramatically as the copper content reaches the percolation threshold at 24.0 vol % of filler. The value of the percolation threshold is obtained from the maximum of the derivative of the conductivity as a function of filler volume fraction.

The electrical conductivity of the composites is $<10^{-12}$ S/cm, unless the metal content reaches the percolation threshold of 24.0 vol %, beyond which the conductivity increases markedly by as much as 11 orders of magnitude, indicating an insulator–conductor phase transition.

The obtained results on electrical conductivity have been well interpreted with the statistical percolation theory. The deduced critical parameters, such as the threshold of percolation, V_f*, the critical exponent, t, and the packing density coefficient, F, were in good accord with earlier studies. In addition, the hardness of samples remained almost constant with the increase of metal concentration.

References

1. J.A. King, K.W. Trucker, J.D. Meyers, E.H. Weber, M.L. Clingerman, and K.R. Ambrosius, Polym. Comp., 22, 142 (2001).

2. G. Pinto, A.-K. Maaroufi, R. Benavente, J. M. Pereña Polym. Comp., 32, 193 (2011).

Acknowledgments

We acknowledge the financial support from CSIC/CNRST-Morocco (project 2007MA0043) and Ministerio de Ciencia e Innovación (projects PET2008-0108, MAT2007-65519-C02-01 and MAT2010-19883).

Ruthenium olefin metathesis initiators bearing one or two N,O chelating coligands in the triggered polymerization of DCPD

Julia Wappel,[1] *Christian Slugovc*[1]*

[1] Graz University of Technology, Institute for Chemistry and Technology of Materials, Stremayrgasse 9/V, AT-8010 Graz, Austria.

e-mail: julia.wappel@tugraz.at

Over the last past decade olefin metathesis has emerged as an important tool for the formation of carbon-carbon double bonds. Particularly due to their good group, oxygen and moisture tolerance and the possibility of a controllable reaction progress, metathesis has gained more and more popularity.[1] In polymer chemistry, especially the ring opening metathesis polymerization (ROMP) has been a field of great interest.

The cheap industrial side product DCPD, an auspicious product for many commercial applications, is easily polymerized by the means of ROMP. Driven by the challenge to prepare well defined DCPD polymers under easy manageable processing conditions, latent initiator systems are desirable. These systems allow to store the initiator and the polymer together and to initiate the polymerization whenever requested. Feasible initiation mechanisms are thermal or acid activation.

Many ruthenium based complexes featuring an *O,N*-bidentate ligand exhibit such latency and olefin metathesis activity can be neglected.[2,3,4] Herein we present the influence of various initiators bearing *N,O*-chelating co ligands on the polymerization characteristics of DCPD. The catalysts vary in terms of their carbene and the *N,O* ligand(s), as well as of the steric arrangement of the N,O ligand(s). Different activation techniques are taken into account.
The new initiators are compared to well established commercially available metathesis catalysts.

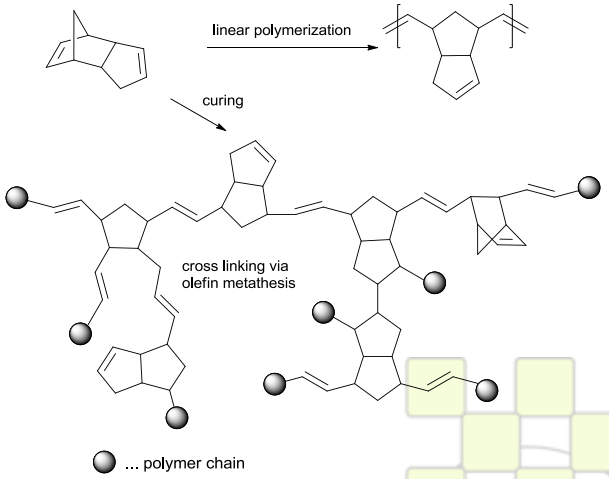

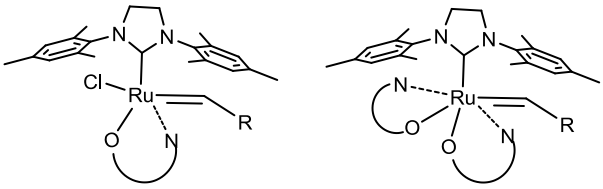

References:
[1] A. Leitgeb, J. Wappel, C. Slugovc; Polymer, **2010**, *51*, 2927.
[2] R. Drozdzak, N. Nishioka, G. Recher, F. Verpoort; Macromol. Symp. **2010**, *293*, 1.
3[1] J.S.M Samec, B.K. Keitz, R.H Grubbs; J.Organomet. Chem. **2010**, *695*, 1831.
[4] S. Monsaert, A.L. Vila, R. Drozdzak, P.Van der Voort, F. Verpoort; Chem. Soc. Rev. **2009**, *38*, 3360.

Biocide Finishing of poly(Isoprene) by Thiol-ene Click Chemistry

Julia Kienberger[1], *Nadja Noormofidi*[1], *Christian Slugovc*[1]*

[1] Graz University of Technology, Institute for Chemistry and Technology of Materials, Stremayrgasse 9/V, 8010 Graz, Austria.

e-mail: julia.kienberger@tugraz.at

In many fields of applications, the maintenance of high hygienic standards is of absolute necessity. Regarding medical devices, water pipe systems or food packaging facilities, biocide surfaces are partly inevitable or, at least, simplify and cheapen industrial processes. Conventional methods implement the use of low-molecular weight disinfectants, however, such particles often suffer from disadvantageous leaching or accumulation effects.[1] In order to circumvent such problems, high molecular weight materials like polymers with integrated biocidic properties are an attractive alternative. Moreover, the combination of hydrophobic backbone and hydrophilic attributes, which repulse destroyed bacteria cells, is an efficient and variable tool to obtain potent and long-term active antimicrobial polymers.

Thiol-ene click chemistry is a powerful and versatile tool, awakening more and more interest not only in the scientific community, but also for industrial applications.[2] The ability to combine a wide range of aliphatic and aromatic mercaptans with an endless possibility of double bonds accessible and nevertheless most simple and easy to handle conditions makes this reaction unique.

In our approach we apply thiol-ene reactions to functionalise poly(isoprene) with a high content of 1,2-linked repeating units with thiolamines. This polymer is perfectly applicable for biocide purposes, as it features hydrophobicity as an intrinsic property and by either alkylation or protonation of the amino functionality quaternary ammonium salts “QUAT”s[3] are introduced into the polymer.

A series of new polymers is synthesized and characterised in terms of thermal stability and antimicrobial activity, yielding very promising new materials suitable for compounding purposes.

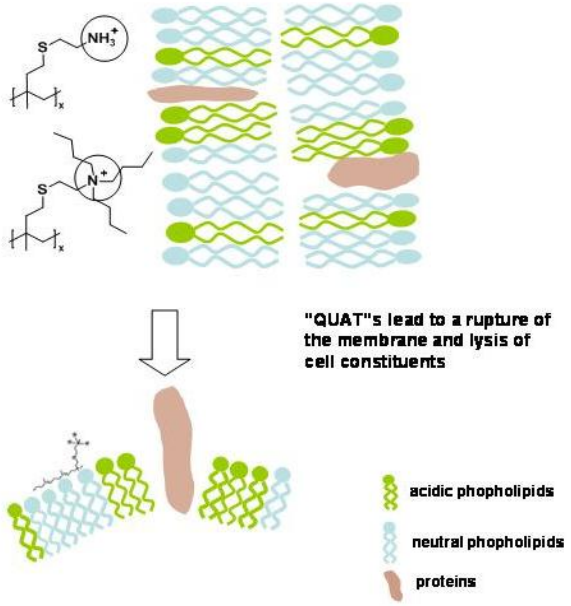

---

[1] E.R. Kenway, S.D. Worley, R. Broughton, *Biomacromolecules,* **2007**, *8*, 1359.

[2] S. Schlögl, A. Temel, W. Kern, R. Schaller, A. Holzner, *KGK-Kaut. Gummi Kunst.*, **2010**, *63*, 187.

[3] P. Ottersbach and B. Kossmann, *GIT Labor-Fachzeitschrift,* **2002**, *46*, 454.

From Emulsion Templating of Poly(cyclooctene) Towards Elastic, Porous Monolithic Materials

Florian Preishuber-Pflügl [1], *Peter Krajnc* [2], *Christian Slugovc* [1*]

[1] Graz University of Technology, Institute for Chemistry and Technology of Materials, Stremayrgasse 9/V, AT-8010 Graz, Austria.

[2] University of Maribor, Faculty of Chemistry and Chemical Engineering,Smetanova 17, SI-2000 Maribor, Slovenia.

e-mail: flo_pp@sbox.tugraz.at

Introduction

Porous polymers have gained a lot of attention in the last years due to their unique morphology that opens a wide field of possible applications. Materials with pore sizes ranging from a few to several hundred micrometers are successfully applied in tissue engineering, catalyst support materials, filtration media and chromatography.[1]

Results and Discussion

Successful preparation of high internal phase emulsions (HIPE) with a variety of monomers has been reported. Ring opening metathesis polymerization (ROMP) of DCPD (dicyclopentadiene) with initiator M2 was employed for the preparation of well defined poly-HIPE structures (Fig. 2, left).[2] A similar approach with cyclooctene (COE) led to a material with a different structure (Fig. 2, right) and distinctly different mechanical properties.

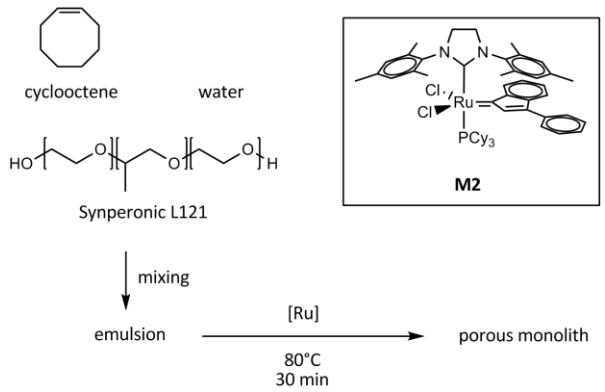

Fig. 1 – Preparation procedure.

Poly(cyclooctene) without any crosslinker is characterized by a low glass transition temperature (T_g) of about -80°C and a melting point of 65°C, depending on the *cis-trans*-ratio of the polymer. In contrast to norbornene-derived polymers, poly(cyclooctene) possesses secondary allylic carbons making it less sensitive to oxidation.[3] This is a valuable advantage that protects the polymer from aging and decomposition.

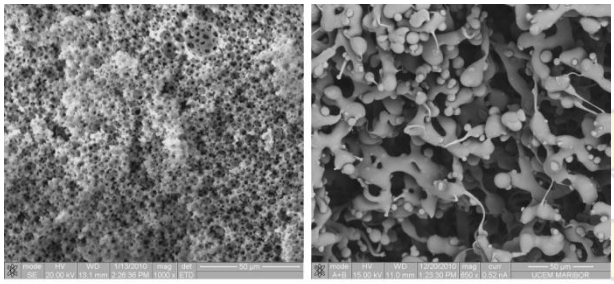

Fig. 2 - Structural differences between DCPD-polyHIPE material (left) and porous poly-COE monolith (right); scale bars 50 µm.

The low melting point of the polymer is a significant drawback for the synthesis of the material. For a proper handling of the emulsion, the initiator loading must be low; otherwise the mixture can not be transferred to the mold. As a consequence, the curing temperature has to be rather high to guarantee a complete conversion of the monomer. This high temperature may affect the inner structure of the monolith and it has turned out to be a difficult hurdle on the way towards a poly-HIPE structure in poly-COE.

Conclusion

The synthesis of highly porous polycyclooctene monoliths via ROMP has been shown. The good oxidation stability of the polymer compared to polynorbornenes makes it a promising candidate for further applications. Mechanical properties and chemical characterization will be disclosed in the contribution. Further modifications concerning morphology will be carried out.

References

1. (a) Cameron, N. R. *Polymer* **2005**, 46, 1439-1449. (b) Zhang, H.; Cooper, A.I. *Soft Matter* **2005**, 1, 107-113.
2. Kovačič, S.; Krajnc, P.; Slugovc, C. *Chem. Commun.* **2010**, 46, 7504-7506.
3. Schlemmer, B.; Gatschelhofer, G.; Pieber, T.R.; Sinner, F.M.; Buchmeiser, M.R. *J. of Chromatography* **2006**, 1132, 124-131.

Water-soluble polymers prepared by Ring opening metathesis polymerization

Katharina Gallas,[1] *Tanja Wrodnigg*,[2] *Christian Slugovc*[1*]

[1] Graz University of Technology, Institute for Chemistry and Technology of Materials, Stremayrgasse 9/V, AT-8010 Graz, Austria.

[2] Graz University of Technology, Institute for Organic Chemistry, Stremayrgasse 9/V, AT-8010 Graz, Austria.

e-mail: gallas@tugraz.at

There is a great demand for new and well defined water soluble polymers because of their broad variety of applications in fields like bioseparation, diagnostics, sensor applications or controlled release of bioactive agents.[1] An approach towards the release of substances is to make use of phase separation driven by increasing temperature. This effect is called the lower critical solution temperature (LCST)[2] which is a feature of, among others, polymers bearing oligo(ethylene oxide) groups in the side chain.[3] Recently, work on poly(norbornenes) bearing oligoglycol side chains was published.[4] In this case, the LCST is largely independent from the molecular weight and the macromolecular architecture. Only polymers prepared from *endo*,*exo*-bicyclo[2.2.1]hept-5-ene-2,3-dicarboxylic-acid, bis[2-[2-(2-ethoxyethoxy)ethoxy] ethyl] ester (**1**) showed satisfactory water solubility and a LCST of about 25°C.[4] Herein we aim at tuning the LCST by copolymerization with mannose (**2**) or alkyl amino hydrochloride (**3**) bearing monomers.

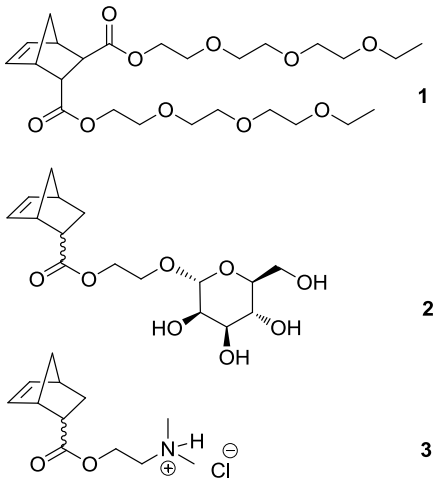

Figure 1: Water-soluble monomers *endo*,*exo*-bicyclo[2.2.1]hept-5-ene-2,3-dicarboxylicacid,bis[2-[2-(2-ethoxyethoxy)ethoxy]ethyl]ester (**1**), mixture of *endo*- and *exo*-bicyclo[2.2.1]hept-5-ene-2- methacrylate-2-(α-D-mannopyranosyloxy)ethyl (**2**), mixture of *endo*- and *exo*-bicyclo[2.2.1]hept-5-ene-2-carboxylicacid(2-dimethylaminoethyl)ester hydrochloride (**3**)

2 was prepared through an *O*-glycosylation reaction of the acetyl protected mannose with excellent α-anomer selectivity following the work of Obata et al. who prepared similar acrylates.[5] Ring opening metathesis polymerization has been chosen because of its high functional group tolerance, the reliability and the capability to synthesize a plenitude of different polymer architectures. Complex **M31** has been chosen as the initiator in this case.[6]

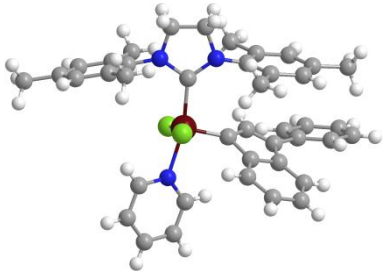

Figure 2: [(H_2IMes)(py)Cl_2Ru(3-phenylindenylid-1-ene)] (H_2IMes = N,N-bis(mesityl)-4,5-dihydroimidazol-2-yl, py = pyridine) (**M31**)

Homopolymers of **1**, **2** and **3** were prepared using initiator : monomer ratios of 1 : 100, 1 : 200 and 1 : 300 and their solubility in water as well as their LCST was determined. Furthermore, random copolymers consisting of different ratios of **1**, **2** and **3** as well as block copolymers were prepared and the properties of those copolymers were compared with those of the homopolymers. The contribution will display these data in detail.

References

[1] Langer, R.; Tirell, D.A. *Nature* **2004**, *428*, 487-492.
[2] Kohori, F.; Yokoyama, M.; Sakai, K.; Okano, T. *J. Control Release* **2002**, *78*, 155-163.
[3] Lutz, J.F.; *J. Polym. Sci. Part A: Polym.Chem.* **2008**, *46*, 3459-3470.
[4] Bauer, T.; Slugovc, C. *J. Polym. Sci. Part A: Polym. Chem.* **2010**, *48*, 2098-2108.
[5] Obata, M.; Shimizu, M.; Ohta, T.; Matsushige, A.; Iwai, K.; Hirohara, S.; Tanihara, M. *Polym. Chem.* **2011**, in press. DOI: 10.1039/C0PY00326C.
[6] Burtscher, D.; Lexer, C.; Mereiter, K.; Winde, R.; Karch, R.; Slugovc C. *J. Polym. Sci. Part A: Polym. Chem.* **2008**, *46*, 4630-4635.

Thermal Studies of Interpenetrating Methacrylate/Epoxy Resins

Nicoleta M. Florea, Adriana Lungu, Raluca Stan, Horia Iovu

Faculty of Applied Chemistry and Materials Science, University Politehnica of Bucharest, Romania

s_nicoleta2005us@yahoo.com

Introduction

Most thermosetting resins are used with reinforcing agents to produce a composite material with better mechanical and thermal properties. Optimisation of the properties of thermosetting polymers for a specific application has been achieved by blending of thermosets to form "Interpenetrating Polymer Networks" (IPNs). IPNs are blends of two or more crosslinking polymers and appropriate blending should allow their properties to be tailored to the application. Two types of IPNs may be formed, depending on the polymer components are crosslinked or not: full-IPNs (presence of crosslinks in both network polymers) and semi-IPNs (one of the components is crosslinked and the other is linear) [1-3].

In this study, full-IPNs composed of bisphenol A diglycidyl dimethacrylate (BisGMA) and diglycidyl ether of bisphenol A (DGEBA) epoxy resin were prepared by *in situ* polymerization. The presence of the bisphenol A diglycidyl structure in both the vinyl esters and epoxy resins respectively enhance miscibility in the formed IPN. Moreover, the OH groups from BisGMA can play a catalytic role in the epoxy cure.

Materials and Methods

An organic peroxide such as azobisisobutyronitrile (AIBN) was used as initiator for BisGMA, and an anionic polymerizing curing agent 1 methyl-imidazole (1-MeI) for DGEBA, respectively. Both, dimethacrylate and epoxy monomers were mixed separately at ambient temperature with their respective initiators before being combined in different ratios (75:25; 50:50; 25:75 wt%).

The polymerization process was done at 120°C for 2h and then post-cured at 160°C for 30 min. As references, BisGMA and DGEBA homopolymers were also prepared in the same conditions as the corresponding IPNs.

The obtained IPNs were characterized by ATR-FTIR, TGA, DSC and DMA techniques in order to investigate the properties of the IPNs which are dependent on the phase separation of the individual thermosseting components.

Results and Discussion

The ATR-FTIR spectra for initial blends confirm the presence of the C=C double bonds from methacrylic groups which appear at 1638 cm^{-1} and the epoxy groups at 915 cm^{-1}. These bands can be used to monitor the reaction and calculate the final conversion after the polymerization process.

DSC analysis was performed in order to obtain the individual heats of polymerization.

The DSC thermograms of the initial blends for IPN exhibit two distinct exothermic peaks, one at ~ 80°C, which corresponds to heat polymerization for methacrylic groups from BisGMA and anotherone at ~ 120°C assigned to the epoxy groups from DGEBA (Fig. 1). During the crosslinking process these peaks completelly dissapear due to the methacrylic and epoxy groups consumption during the polymerization process.

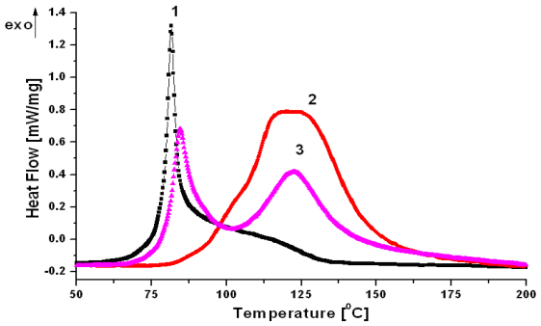

Fig.1. DSC thermograms for: 1)BisGMA, 2) DGEBA, 3) 50:50 wt% BisGMA-DGEBA before polymerization

The bisGMA and DGEBA curing exotherms are shifted to higher temperatures in the IPNs, which is consistent with the effects of dilution [2].

DMA tests was also performed for the final full-IPNs and homopolymers respectively (Fig. 2).

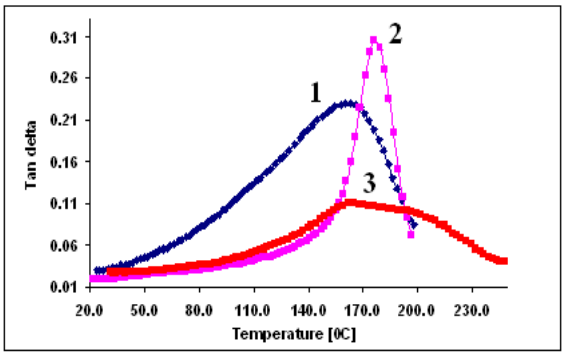

Fig. 2. DMA plots of: 1)BisGMA, 2) DGEBA, 3) 50:50 wt% BisGMA-DGEBA after polymerization

T_g of the neat BisGMA/AIBN is 160°C, while the T_g of the neat DGEBA/1-MeI is 176°C. The T_g of 50:50 full IPN is 169°C, which is an average between the two T_g values of DGEBA and BisGMA, suggesting a single phase morphology.

Conclusions

Mechanical properties will be also investigated to confirm if the bisphenol-A addition in IPNs increases the rigidity of the polymer backbone.

Further, nanocomposites with polyhedral oligomeric silsesquioxane (POSS) will be obtained for the IPN with highest thermal and mechanical properties.

References

[1] K. M., Dean, W. D., Cook, M. D., Zipper, P. Burchill, *Polymer*, **2001**

[2] K. M., Dean, W. D., Cook, *Polymer International*, **2004**

[3] K. M., Dean, W. D., Cook, M. Y., Lin, *European Polymer Journal*, **2006**

Acknowledgements

This work was supported by CNCSIS –UEFISCSU, project number PNII – IDEI 1718/2008 and by the Sectoral Operational Programme Human Resources Development 2007-2013 of the Romanian Ministry of Labour, Family and Social Protection through the Financial Agreement POSDRU/6/1.5/S/16.

Electromechcanical performance of epoxy/vapour grown carbon nanofiber composites for pressure sensor applications

A. Ferreira[1], *P. Cardoso*[1,2], *A. J. Paleo*[2], *D. Klosterman*[3], *J. A. Covas*[2], *F. W. J. van Hattum*[2], *S. Lanceros-Mendez*[1]

1- Center / Department of Physics, University of Minho, Campus de Gualtar, 4710-057 Braga, Portugal,
2- IPC/I3N – Institute for Polymers and Composites, University of Minho, Campus de Azurém, 4800-058 Guimarães, Portugal
3- Chemical & Materials Engineering, University of Dayton, 300 College Park, Dayton, OH 45469-0246, USA.

Armando.f@fisica.uminho.pt

Abstract

Epoxy resins have a wide range of applications in materials science. By incorporating high aspect ratio fillers like carbon nanotubes (CNT) or vapour grown carbon nanofibers (VGCNF), the epoxy mechanical and electrical properties are tailored and the range of applications extended. As both the electrical and mechanical, and therefore, the electromechanical response of the polymer composites depend of the filler content and dispersion, this investigation reports on the piezoresisitive response of epoxy/VGCNF composites prepared by four different dispersion methods. The composite response is investigated as a function of VGNNF loading and dispersion. Strain sensing by variation of the electrical resistance in the composites was tested by a four-point bending and the dependence of the gauge factor as a function of the deformation and velocity of deformation was calculated as well as the reproducibility of the electrical response. The experimental results showed that the composites have an overall appropriate response for being used as piezoresistive sensor. The applications limits will be also addressed.

Acknowledgements

The authors thank the Foundation for Science and Technology, Portugal, for financial support through projects PTDC/CTM/69316/2006, PTDC/CTM-NAN/112574/2009 and NANO/NMed-SD/0156/2007, and grants SFRH / BD / 69796 / 2010 (AF) and SFRH/BD/41191/2007 (PC). Joint Luso-American Foundation (FLAD) - NSF U.S. Research Networks Program research grant (FH and DK). We also thank Albermarle for the hardener, Hexion Specialty Chemicals for the epoxy resin, and Applied Sciences for providing their facilities.

Study of the Basalt Fibers' Damage Assessment due to Different Sizing Removal Processes

J. Kano-Ibarretxe, R. Hernandez, A.M. Zaldua, T. Guraya[a], I. Mondragon[b]

Leartiker, Research Centre, Polymer Department, Xemein Etorbidea 12A-1º, 48270 Markina-Xemein, Spain
[a]The University of the Basque Country, Mining and Metallurgy Engineering; and Materials Science Department, Plaza la Casilla 3, 48012 Bilbao, Spain
[b]The University of the Basque Country, Materials + Technologies Group, Chemical & Environmental Engineering Department, Pza. Europa 1, 20018 Donostia- San Sebastián, Spain

jcano@leartik.com

The basalt is a basic igneous effusive rock of mineral composition and is the result of cooling of lava at the surface of a planet, in contact with air or water. It is considered an attractive raw material for fiber production because of its relatively homogeneous chemical structure, its wide availability throughout the world, its great purity and its ability to form fibers in the molten state.

The inorganic nature of basalt fibers makes them unsuitable for mixing with carbon based polymers unless a coupling agent is added. These coupling agents or sizings are added by the comercializers of fibers, but the composition of the sizing and in some cases their nature may not be the best option for a specific matrix.

The present work tries to determine the less aggressive sizing removing process for basalt fibers (BASUD280, Basaltex, Belgium) measuring and controlling their morphological and mechanical changes. That must be taken into consideration in order to manufacture a polymeric composite material, since the mechanical properties of an unidirectional composite are mainly dependent on the behavior of the reinforcement.

Calcination is the most used sizing removing technique but this process results in a weakening of the fiber that is not often measured. In the present work different removing processes are used to take out the surface treatment of basalt fibers such as a partial elimination of the coating by sohxlet extractions in several solvents like acetone (PANREAC, 99.5 %,), tetrahydrofuran (PANREAC, 99.9 %,) or chloroform (PANREAC, 99.0 %,). The nonsoluble part is then removed by pyrolysis; and is compared with the results obtained by direct taking out the sizing by pyrolysis and calcination.

The effectiveness of all processes has been analyzed taking into account the loss of weight of the fibers after treatments and to check the partial or total sizing elimination after the different treatments thermogravimetric analysis (TGA) has been used.

Besides, the surface of treated and untreated (with original sizing) fibers and the extracts resulted from the extractions have been chemically analyzed by Fourier transform infrared spectroscopy (FTIR) and attenuated total reflection spectroscopy (ATR).

The fibers have been mechanically characterized using monofilament stress-strain test in a Rheometrics RSII analyzer. The results have been analyzed statistically using the Weibull two parameter distribution.

To determine the morphological changes suffered by the fibers in the surface scanning electron microscopy (SEM) tests have been performed for each sizing removing technique used. The chemical composition of the surface of the treated and untreated fibers has been also analyzed by energy dispersive spectroscopy (EDX).

Figure 1: a) basalt fibers with the original sizing; b) basalt fibers after acetone extraction

a)

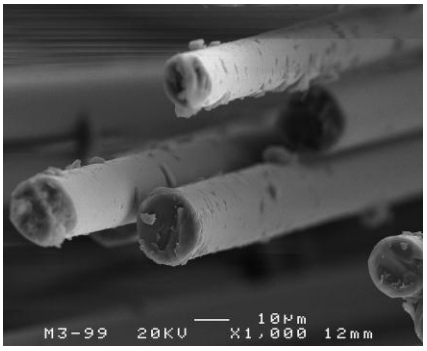

b)

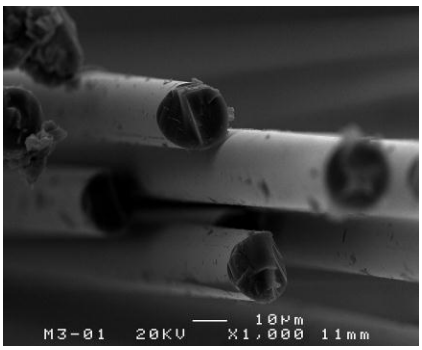

CONCLUSIONS:

Preliminary results have shown that with all the solvents used in the extractions part of the sizing is removed, being the acetone the most effective as can be observed in figure 1.

LITERATURE:

[1] D. Saravanan, Spinning the Rocks – Basalt Fibres, IE (I) Journal-TX, 86 (2006) 39.

[2] J. M. Park, S. Wae-Gyeong, Y. Dong-Jin, A study of interfacial aspects of epoxy-based composites reinforced with dual basalt and SiC fibres by means of the fragmentation and acoustic emission techniques, Compos. Sci. Technol., 59 (1999) 355.

[3] A.V. Knot'ko, A.V. Garshev, I.V. Davydova, V.I. Putlyaev. Chemical Processes during the Heat Treatment of Basalt Fibers, Prot. Met., 43 (2007) 694.

Synthesis and Study of New Poly(Amide Imide)s as Advanced Materials

Irina Bacosca, Elena Hamciuc, Valentina E. Musteata, Maria Bruma

"Petru Poni" Institute of Macromolecular Chemistry, Iasi, Aleea Grigore Ghica Voda, 41A, 700487, Romania

email: ibacosca@icmpp.ro

Introduction

Aromatic polyimides are high performance polymers used in applications which demand resistance at high temperature maintaining in the same time their structural integrity and a good balance between their chemical, physical and mechanical properties.[1] Particularly interesting is the potential use of polyimides in microelectromechanical systems (MEMS) devices due to their chemical and thermal stability necessary to withstand conventional MEMS processing. However, wholly aromatic polyimides, though thermally stable, do not always provide the optimum properties for many specialty applications because of deficiencies in processability and solubility. Poly(amide imide)s bring together superior mechanical properties associated with amide units and high thermal stability determined by the existence of imide rings.[2]

Materials and Methods

2,6-Bis(*p*-aminophenoxy)benzonitrile, **1a**, and 2,6-bis(*m*-aminophenoxy)benzonitrile, **1b**, were prepared by nucleophilic displacement of 2,6-dichlorobenzo-nitrile with *p*- or *m*-aminophenole using DMAc as solvent.[3] 1,3-Bis-2-cyano-3-(3-aminophenoxy)phenoxybenzene, **1c**, was prepared as reported earlier.[4] The new diacid chlorides, **2a** and **2b**, were synthesized by reflux with thionyl chloride of the corresponding diimide diacids resulting from the reaction of trimellitic anhydride with diamines **1a** and **1b**, respectively.

Results and Discussion

New poly(amide imide)s were synthesized by one step polycondensation reaction, at low temperature, of equimolecular amounts of diamines **1** and diacid chlorides **2** using NMP as a solvent and propylene oxide as acid acceptor. The structure of the diamine and diacid chloride monomers is presented in scheme 1.

Scheme 1. Structure of the monomers.

1a: 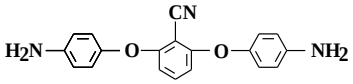

1b: 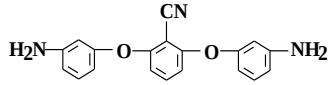

1c: 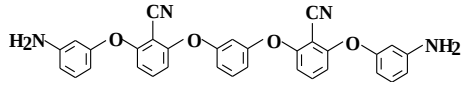

2a: 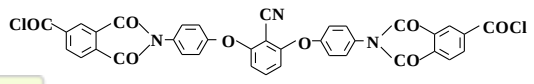

2b: 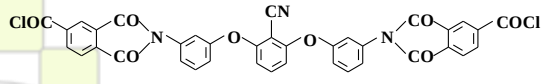

The structure of the poly(amide imide)s was identified by FTIR spectroscopy. Infrared spectra of all polymers showed strong absorptions at 1780, 1718, 1378 and 732 cm^{-1} which were assigned to the imide rings. Strong bands of absorbtion characteristic for the new formed amide linkage appeared at 3385 cm^{-1} assigned to the N–H stretching vibration, at 1688 cm^{-1} atributed to the C=O stretching vibration and at 1576 cm^{-1} due to the N–H bending vibration.

The good solubility of the poly(amide imide)s is due to the relatively high flexibility of macromolecular chains which was obtained by the introduction of ether and amide linkages into the structure of the polymers. All polymers were soluble in polar organic solvents such as NMP, DMAc, DMSO or DMF, at room temperature. Polymers containing more meta-catenation were soluble in less polar solvents such as THF.

Thermogravimetric analyses shows that the present poly(amide imide)s are highly thermostable: the temperature of 5% weight loss is situated in the interval of 315-510^{o}C and 10% weight loss in the domain of 430-520^{o}C.

Molecular relaxations of polymer film based on 4,4'-(1,3-phenylenedioxy)dianiline and diacid chloride **2a** were determined and the results evidenced two second order phase transitions γ and β and one primary transition α. A nano-actuation study of the same polymer film was performed using different dc voltage of 70, 100, 130 and 150 V. The best results were obtained at 150 V and an electric field of 833.33 Vm^{-1} when the nano-displacement had a value of -140 nm and a sensibility of 0.933 nm/V.

Conclusions

A new series of poly(amide imide)s containing various amount of CN groups was synthesized by one step polycondensation reaction of new diacide chlorides with different diamines containing flexible linkages. The polymers had a good solubility, high thermal stability and film forming ability. One polymer film exhibited a nano-displacement of -140 nm at 150 V. All these results make the present polymers potential candidates as advanced materials for high performance applications.

Acknowledgements: This work was supported by CNCSIS– UEFISCDI, project number PNII–IDEI code ID_997/2008. We thank Dr. M. Cristea at "Petru Poni" Institute of Macromolecular Chemistry, Iasi, and Dr. M. Igant at INCDIE ICPE-CA, Bucharest, Romania, for DMA and nano-actuation measurements, respectively.

References

1. J de Abajo, J.G. de la Campa, In „Progres in polyimide chemistry" H.R. Kricheldorf Ed, Berlin, Springer, pp. 23-61,1999.

2. C.P Yang, R.S. Chen, M.J. Wang, *J Polym Sci: Part A: Polym Chem*, **40**, 1092–1102, 2002.

3. I. Bacosca, E. Hamciuc, M. Bruma, I.A. Ronova; *High Perform Polym*, **22**, 703-714, 2010.

4. B. Gonzalo, J.L. Vilas, T. Breczewski, M.A. Perez-Jubindo, M.R. de la Fuente, M. Rodriguez, L.M. Leon, *J Polym Sci: Part A: Polym Chem*, **47**, 722–730 (2009).

Synthesis of Bimodal Polypropylene through Binary Metallocene Catalysts

Rafael van Grieken1, Alicia Carrero2, Beatriz Paredes1, Ester Lopez-Moya1

1Department of Chemical and Environmental Technology
2Department of Chemical and Energy Tecthe hnology ESCET, Universidad Rey Juan Carlos, c/ Tulipan s/n, 28933 Mostoles, Madrid, Spain

alicia.carrero@urjc.es

Metallocene catalysts together with aluminoxanes can polymerize olefins into polyolefins having narrow molecular weight distribution. This type of polyolefins is suitable for precision injection moulding, general injection moulding and fibre production. However, for numerous applications such as thermoforming, extrusion, blow moulding, production of polyolefin foams and films and in packaging such food packaging, wider or bimodal molecular weight distributions (BMWD) are required.[1] Traditionally the production of bimodal resins is carried out by a cascade process, using conventional Ziegler-Natta catalysts or by mixing together two polypropylenes of different molecular weight (M_w). A more attractive and economical route is to use two or more metallocene precursors simultaneously yielding a polypropylene mixture consisting of the polymer fractions produced by the different metallocenes individually[2]. Therefore, catalytic sites that have different kinetic responses, such as different propagation and termination rate constants, would produce a blend of polymeric chains with different predominant molecular masses.

The main driver for this development is the decrease in investment costs for a single reactor compared to a staged process. Also, as it is generally accepted that the high and low molecular weight fractions should be intimately mixed to obtain good product properties, the combination of two or more catalytic systems in the same reactor could lead to such efficient mixing.

As it is known, to replace the conventional heterogeneous Ziegler–Natta catalysts used in industrial slurry and gas-phase processes, metallocene catalysts have to be immobilized a carrier. In general, the heterogeneization of soluble metallocene catalysts implies an activity decrease although polymers produced with supported catalysts present higher molecular weights.

In this work, three metallocene catalysts with C_2 symmetry rac-Me_2Si $(Ind)_2ZrCl_2$ (CAT1), rac-$Et(Ind)_2ZrCl_2$ (CAT2) and rac-Me_2Si(2-Mebenzoind) $_2ZrCl_2$ (CAT3) have been evaluated in homogeneous propylene polymerization at 30, 50 and 70 °C in a 1.0 L stirred-glass reactor filled with 400 cm^3 of n-heptane as diluent and MAO/metallocene molar ratio = 900. The monomer consumption was followed by a mass-flow indicator in order to keep the reactor pressure at 5 bar during the polymerization. After 15 minutes, polymerization reaction was stopped by depressurization and quenched by addition of acidified (HCl) methanol. Polypropylenes obtained were characterized by gel permeation chromatography (GPC) to determine molecular weight and molecular weight distributions; differential scanning calorimetry (DSC) was used to obtain polymer melting temperature and crystallinity.

Table 1 shows the polymerization activity reached with each catalyst at 30 °C and 70 °C as extreme temperatures to show the maximum difference in molecular weights. Attending to molecular weight values, CAT3 can be combined at both temperatures with CAT1 or CAT2 since is one order of magnitude larger, which will allow to observe the high and low fractions of molecular weight that are appropriate for bimodal molecular weight distribution. It is important to remark that also at 70ºC the mixture of CAT1 and CAT2 could lead to a feasible bimodal product.

All the catalysts gave a polymer with a polydispersity index a little bit higher than 2.0, value expected for a single-site metallocene catalyst. Polypropylene samples presented a single melting peak in DSC analysis, showing the typical melting behaviour for metallocenebased isotactic polypropylene. that is a direct relationship between T_m and M_w, decreasing both factors when the polymerization temperature is increased because of the chain transfer reactions).

CAT3 produces PP with a slightly higher melting point value, which suggests an increment in stereo or regioregularity

Table 1. Polymerization activity and polypropylene characterization

Catalyst	Activity 30 ºC (kg PP/molM·h·bar)	M_w (g/mol)	T_m (ºC)	α (%)
CAT1	291	39593	150	58
CAT2	423	25638	144	57
CAT3	374	403876	155	53

.

Catalyst	Activity 70 ºC (kg PP/molM·h·bar)	M_w (g/mol)	T_m (ºC)	α (%)
CAT1	2360	10446	138	54
CAT2	2512	5567	128	53
CAT3	5500	380670	149	50

Based on the above results, it seems reasonable to prepare supported binary catalysts by the consecutive impregnation of CAT1 or CAT2 and CAT3 onto MAOmodified silica for obtaining reactor blends of isotactic polypropylenes with bimodal MWD. Besides, a comparison will be established with mixtures of individual supported catalysts in different proportions.

REFERENCES

1. Severn, J. R.; Chadwick, J. C. Tailor made polymers: via immobilization of alpha-olefin polymerization catalysts. Wiley-VCH Verlag GmbH & Co. KGaA Weinheim, 2008, 352 pp.
2. Tynys, A.; Saarinen, T.; Bartke, M.; Lofgren, B. Polymer 48 (2007), 1893-1902.

Ethylene-Propylene Copolymers Synthesized with Homogeneous and Supported Metallocene Catalyst in the Whole Range of Compositions

Javier Arranz-Andrés[1], Inmaculada Suárez[2], Rosario Benavente[1], Ernesto Pérez[1]

[1]Instituto de Ciencia y Tecnología de Polímeros (CSIC). Juan de la Cierva 3, 28006-Madrid, Spain.
[2]Escuela Superior de Ciencias Experimentales y Tecnología, Universidad Rey Juan Carlos, 28933 Móstoles-Madrid, Spain.

rbenavente@ictp.csic.es

Introduction

The polymerization of ethylene and propylene by organometallic catalysts is a subject of increasing interest for scientists and industry. This growth is lead by a new catalyst generation, the metallocene systems, which are able to tailor polymer microstructure and physical and mechanical properties.[1]

These characteristics are due to the control of the resulting average molecular weight and distribution, and of the comonomer content and tacticity by careful selection of the appropriate catalyst structure and polymer manufacturing conditions. These novel copolymers constitute a very interesting approach for stiffness/impact resistance optimization.[2,3]

Materials and Methods

Ethylene-propylene copolymers were synthesized in the whole composition range using a metallocene catalyst, both in homogeneous phase (*H* copolymers), and supported (*S* copolymers). Copolymerization reactions were carried out in a 1 liter Büchi stirred glass reactor. Copolymers were obtained with controlled feeding in the whole range of compositions.

The molecular weights and distributions were determined by gel-permeation chromatography (GPC). The experimental propylene and ethylene contents in the copolymers were calculated by ^{13}C NMR. The films obtained by compression molding were characterized from a morphological and thermal standpoint by WAXS and SAXS (with synchrotron radiation) and differential scanning calorimetry. In addition, mechanical properties have been evaluated.

Results and Discussion

Some differences were found between the two series. On the one hand, the amount of ethylene needed to obtain a certain proportion of γ form is lower in *H* than in *S* series. Moreover, the composition for obtaining the pseudo hexagonal form is also different for the two series. Figure 1 depicts the variation with the ethylene content of the spacings corresponding to the (110) and (200) diffractions of the orthorhombic unit cell of polyethylene, for the two series of copolymers, showing the eventual transformation into a pseudo hexagonal structure.

On the other hand, crystallinity degrees, crystal sizes and microhardness values all display a similar variation with the comonomer content for the two series. Consequently, in spite of the structural differences between the two series, from a macroscopic point of view, materials with similar macroscopic mechanical properties can be produced using both supported and homogeneous metallocene catalysts.

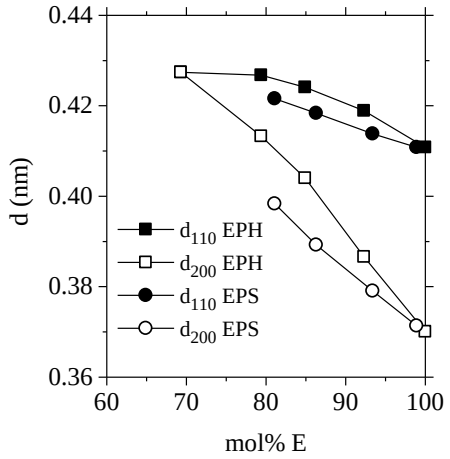

Figure1. Spacings corresponding to the (110) and (200) diffractions versus ethylene content.

Conclusions

Ethylene-propylene copolymers were synthesized in the whole composition range using a metallocene catalyst, both in homogeneous phase (*H* copolymers), and by supporting (*S* copolymers) with the same catalytic system. Although some structural differences have been found between *H* and *S* copolymers, from a macroscopic scale, materials with similar mechanical properties can be produced using both supported and homogeneous metallocene catalysts. And if the macroscopic properties are rather similar, it is evident that the supported catalyst production is the more appropriate choice from the industrial point of view.

References

1.- B. Löfgren and J. Seppälä, Metallocene-based Polyolefins. Preparation, properties and technology, Vol. 2, J. Scheirs, W. Kaminsky, Eds., New York: Wiley 2000, p. 143.

2.- J. Arranz-Andrés, I. Suárez, B. Peña, R. Benavente, E. Pérez, and M. L. Cerrada, Macromol. Chem. Phys., 208, 1510 (2007).

3.- S. P. Westphal, M. T. K. Ling, S. Y. Ding and L. Woo, Metallocene Catalyzed Polymers, Materials, Properties, Processing and Markets, G. M. Benedikt, B. L. Goodall, Eds., New York: PDL 1998, p. 135.

Acknowledgments

We acknowledge the financial support of REPSOL, and MICIIN (projects PET2008-0108, MAT2007-65519-C02-01 and MAT2010-19883). The synchrotron work was also supported by MICIIN through specific grants for the access to the CRG beamline BM16 of the ESRF. J. Arranz-Andrés thanks to the CSIC JAE-Doc Program for his financial support.

Microstructure characterization and influence on gamma form content of polypropylene copolymers and terpolymers

S. Caveda[1], *R. Benavente*[2], *E. Pérez*[2], *E. Blazquez*[2], *B. Peña*[1], *R. van Grieken*[3], *I. Suárez*[3]

[1]CTR Repsol, Móstoles, Madrid (España)
[2]Instituto de Ciencia y Tecnología de Polímeros, CSIC, Juan de la Cierva 3, 28006 Madrid (España)
[3]Escuela Superior de Ciencias Experimentales y Tecnología, Universidad Rey Juan Carlos, 28933 Móstoles-Madrid (España)

scavedac@repsol.com

Introduction

Isotactic polypropylene, iPP, can be conveniently modified by the introduction of comonomer units, randomly distributed. Polymer crystallinity is disturbed, thus being a powerful tool to modify macroscopic properties. Comonomer insertion interrupts the isotactic sequences, acting as a structural defect, and the formation of γ form is enhanced[1-4]. As a consequence, crystallinity decreases and crystal structure is modified. Comonomer type and concentration determine the extent of these modifications, resulting on important changes on macroscopic properties.

Materials and Methods

Table 1 shows comonomer contents together with molecular weights of the products being studied.

Polymers	Comonomer % mol	Mw (g/mol)	Mn (g/mol)	PI (Mw/Mn)
Homo	0	543,500	82,500	6,6
CPE2.5	2.5	323,000	90,000	3.6
CPE4.8	4.8	385,000	87,500	4.4
CPE8.9	8.9	617,000	124,500	5.0
CPB1.6	1.6	717,000	135,500	5.3
CPB5.0	5.0	523,000	122,000	4.3
CPB8.8	8.8	629,500	147,000	4.3
CPT2.0	1.0 + 1.0	261,500	89,000	2.9
CPT4.5	1.5 + 3.0	249,000	59,000	4.2
CPT9.8	4.2 + 5.6	638,000	173,000	3.7

Table 1. Structure characterization

Results and Discussion

X-ray diffraction is used to study the crystallization of copolymers and terpolymers. Figure 1 shows the diffraction patters obtained.

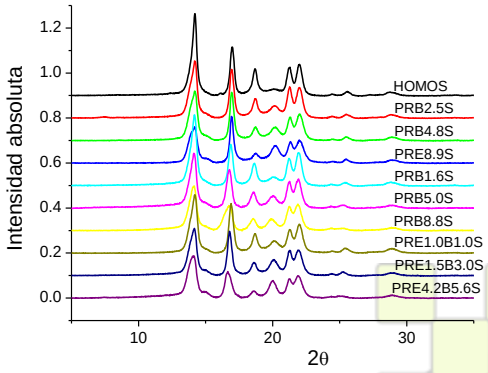

Figure 1. X-ray diffraction patterns.

1-Butene copolymers and terpolymers diffractions show a displacement to lower angles, as a result of a distortion of the crystalline cell, due to cocrystallization and/or by comonomer introduction. This phenomenon is greater in case of 1-butene copolymers than in terpolymers, and it is not observed in ethylene copolymers, showing that 1-butene is included in the crystalline structure in greater proportion than ethylene, and so expanding the crystal cell[5,6,7].

When these polymer samples are rapidly cooled from the melt, they display (Figure 1) the characteristic reflections of monoclinic cell α. This crystalline morphology is not the most favored kinetically, neither the most stable thermodynamically. Nevertheless, it reaches the best commitment between these two criteria, which is why it is the most commonly observed form of crystallization in polypropylene. However, if the cooling is slow, an additional diffraction appears at 20.0º, which is absent in the homopolymer, that corresponds to the orthorhombic form γ. This morphology thus favored by the introduction of defects in the chain and by slow crystallization conditions. Microstructure characterization is performed, using ^{13}C-NMR, to analyze type, content and comonomer distribution, and its influence on the γ-form content.

Conclusions

1-Butene copolymers show higher crystallinity and lower γ-form content than ethylene copolymers and terpolymers. Microstructure analysis shows a random distribution of 1-butene on the polypropylene chain.

Acknowledgements

We acknowledge the financial support of REPSOL, and MICIIN (projects PET2008-0108, MAT2007-65519-C02-01 and MAT2010-19883).

References

[1] Guidetti, G.; Busi, P.; Giulianelli, I.; Zanetti, R. Eur. Polym. J. 1983, 19, 757.
[2] Hosier, I. L.; Alamo, R. G.; Esteso, P.; Isasi, J. R.; Mandelkern, L. Macromolecules 2003, 36, 5623.
[3] Laihonen, S.; Gedde, U.W.; Werner, P.E.; Martínez-Salazar, J. Polymer 1997, 3, 361.
[4] Mezghani, K.; Philips P.J. Polymer 1998, 39, 3735.
[5] Monasse, B.; Haudin, J.M. Colloid Polym. Sci., 1998, 266, 679.
[6] Feng, Y.; Hay, J.N. Polymer 1998, 39, 6589.
[7] Hosoda, S.; Hori, H.; Yada, K.; Nakahara, S.; Tsuji, M. Polymer 2002, 43, 7451.

Synthesis and Analysis of Properties of Poly (vinyl alcohol) composites

Gulfam Nasar, Mohammad Saleem Khan, Uzma Khalil

National Center of Excellence in Physical Chemistry, University of Peshawar, Pakistan

gulfamnasar@yahoo.com

Introduction:

Material science is the trendiest field of today's research. During the recent years, lot of research is being conducted in search of more handy and cheaper materials. Polymer composites are adding a great deal of material which is more durable and useful as compared to the conventional material. Mechanical and thermal properties of composite materials greatly depend on the nature, proportion and compatibility of the components of the composite materials. In this paper we have tried to find the relationship of these properties i. e. thermal conductivity, tensile strength and Young's Modulus of the composite material. Polyvinyl alcohol has excellent film forming, emulsifying, and adhesive properties. It is also resistant to oil, grease and solvent[1]. It has excellent solubility in water. It also has greater compatibility with inorganic salts when composite materials are synthesized using inorganic salts as fillers[2]. Mechanical, thermal and structural properties of composite materials greatly depend on the nature, proportion and compatibility of the components of the composite materials[3].

Material:

PVA, Na_2SO_4, Li_2SO_4

Method:

For this work, two systems were studied; Poly vinyl alcohol/ Sodium sulphate composite, and Poly vinyl alcohol/ Lithium sulphate composite. Various concentrations of these salts were added to Poly vinyl alcohol, using triply distilled water as solvent. Films were caste, dried at room temperature and were subjected to mechanical, structural and thermal characterization. Thermal conductivity was found out at room temperature using Quick thermal conductivity meter. Polyethylene, silicon and quartz were used as reference. It was found out that the thermal conductivity of both the systems is highly dependent of the nature and the concentration of added salt in the polymeric composite.

Result and discussion:

Thermal conductivity of the Poly vinyl alcohol/ Sodium sulphate composite, and Poly vinyl alcohol/ Lithium sulphate composite, decreased with concentration of the salts in the polymer composite. These composites were also analyzed for their structure and the properties exhibited were explained on the bases of their structure. Similar trends were observed in mechanical properties of these composites, eg tensile strength elongation at break and Young's Modulus. The present study shows that there is a remarkable improvement in the properties in terms of mechanical and thermal properties of the polymeric material. These mechanical properties were studied using UTM (Universal Testing Machine). For morphological study, XRD(X-Ray diffraction\) was used and it was found that crystallinity of the composite decreases with addition of salts in the polymer composite studied.

References:

[1]Chawla K.K. **1987.** Composite Materials Science and Engineering; Springer- Verlag, New York,

[2]Kutsenko A. S.; Maloletov S. M.; Kuchmii S. Y.; Lyakhovetskii V. R.; Volkov V. I.**2002**. Vol. *38*, 3. *Theoretical and Experimental Chemistry.*

[3]Yudanova T. N.; Aleshina E. Yu.; Gal'braikh L. S.; and. Krest'yanova I. N. **2003**,*37*, 26 – 28.*Pharmaceutical Chemistry Journal*

Synthesis and Characterization of Conjugated Ionic Polymers with Potential Applications in Optolectronic Devices.

Dmitrij Bondarev[1)], Jiří Zedník[1)], Jiří Vohlídal[1)], Jiří Pfleger[2)], Samrana Kazim[2)], Veronika Slunečková[2)]

[1)] Department of Physical and Macromolecular Chemistry, Faculty of Science, Charles University in Prague Hlavova 2030, Prague, 128 43, Czech Republic

[2)] Institute of Macromolecular Chemistry, Academy of Sciences of Czech Republic Heyrovského nám. 2, Prague, 162 06, Czech Republic

dbondarev@email.cz

Conjugated polyelectrolytes belong to the class of polymers with potential applications in construction of optoelectronic devices. These polymers possess unique properties which arise from a combination of pi-conjugated main-chain and ionic pendant groups. Main-chain conjugation allows expecting active response to optical or electrical stimuli resulting in potential applications in electroluminescence or photovoltaic devices. Attached ionic groups cause the solubility in water-miscible, environmentally friendly solvents and can mediate specific interactions with ionic polymer carrying oppositely charged moieties, metal nanoparticles or metal oxide surfaces such as titanium dioxide structures which are widely used in construction of photovoltaic devices.

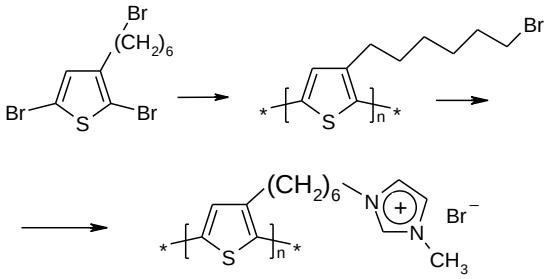

Scheme 1: Preparation of cationic, water soluble polythiophene with HT-regioregular backbone.

Conjugated polymers based on thiophene main-chain units seem to be the promising materials for construction of optoelectronic devices, especially polymer containing photovoltaic solar cells. Polythiopehenes exhibit increased stability contrary to the other conjugated polymers, e.g. polyparaphenylenevinylenes which are also widely used. Also sufficiently high charge (holes) mobility is an advantage. Incorporation of ionic groups on the polymer could produce some benefits such as combination of electronic conductivity provided by the conjugated polymer backbone and the ionic conductivity provided by the side groups. Ionic groups are also utilized for improving the injection of charges from electrodes into the active polymer layers. Polythiophene derivative (Ref. 1) shown in Scheme 1 was selected as a basic material. Described material shows interesting optical properties manifested by formation of micelle-like structures. Further work is aimed at modification of the material by changing the counteranions and incorporation of low band gap units either into the main chain or as a side group to improve optical absorption in the higher wavelength region.

Second class of ionic polythiophenes represents anionic conjugated polymers. Material shown in Scheme 2 is the basic anionic polythiophene. It was shown that interaction with TiO_2 surfaces is sufficient as well as interaction with cationic polythiophenes but the low regioregularity is the serious drawback of this polymer for its utilization as the active layer. Thus the HT-regioregular anionic polythiophene was prepared by catalytic polymerization and experiments described for irregular counterpart are in progress. Nevertheless, the sodium salt irregular anionic polythiophene exhibits interesting optical properties and electrochemical behavior (Ref. 3). All the materials studied are characterized by SEC chromatography and spectroscopic methods such as UV-is, FTIR, NMR a photoluminescence spectroscopy. Interaction of cationic polythiophene with Au nanoparticles also by the Raman spectroscopy.

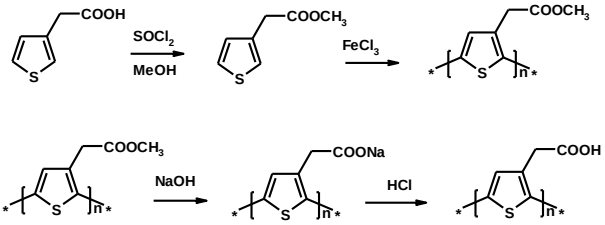

Scheme 2: Preparation of anionic polythiophene by oxidative polymerization.

References:

1) Bondarev, D.; Zedník, J.; Šloufová, I.; Sharf, A.; Procházka, M.; Pfleger, J.; Vohlídal, J. J. Pol. Sci: A - Polym. Chem., 2010, 48, 3073-3081

2) Kazim, S.; Pfleger, J.; Procházka, M.; Bondarev, D.; Vohlídal, J. J Colloid Int Sci, 2011, 354, 611-619

3) Cerar, J.; Bondarev, D.; Vohlídal, J.; Vlachy, V. submitted to Macromolecules

Acknowledgements: Financial support of the Ministry of Education of the Czech Republic, projects MSM 0021620857 and KAN 100500652, the Czech Sience Foundation (project No. 203/09/0803) and the Science Foundation of Charles University (projects No. 315/2008 B-CH and 166410). O. Trhlíková and D.Bondarev are indebted to the Czech Science Foundation for fellowship (project No. 203/08/H032)

Synthesis and FTIR analysis of nanocomposite UV crosslinkable acrylic pressure sensitive adhesives

J. Kajtna[1], *M. Krajnc*[2]

[1] Aero d.d., Ipavčeva ulica 32, 3000 Celje, Slovenia; jernej.kajtna@aero.si
[2] Faculty of Chemistry and Chemical Technology, University of Ljubljana
Aškerčeva cesta 5, 1000 Ljubljana, Slovenia; matjaz.krajnc@fkkt.uni-lj.si

Introduction:
Polymer/nanoclay nanocomposite materials are becoming increasingly popular also in the field of pressure sensitive adhesives (PSA). Due to the high surface area of clay particles, novel materials with improved properties can be synthesized at much lower amounts of clay as compared to traditionally used fillers. The nanocomposite material posses improved or novel properties, and often exhibit a balance of previously antagonistic properties. Due to increased environmental concerns a lot of interest is placed in the development of new radiation curable pressure sensitive adhesives (PSA), especially ultraviolet (UV) curable PSA. According to recent papers in this research field covers the synthesis and characterization of UV crosslinkable PSAs synthesized in organic solvents (solution polymerization) [1-3] or as solvent-free acrylic PSAs [4,5].
The improved properties, especially influence on cohesivity, of polymer nanocomposite materials would be also desirable in the field of PSA materials. However, it is highly important that the pressure sensitive character of the adhesive coating is not compromised.
The main research goal of the study was to synthesize 100% solid UV crosslinkable acrylic prepolymers with added modified montmorillonite (MMT) clays. The influence of different types and amounts of modified MMT clays on polymerization kinetics, prepolymer properties, on adhesive properties and on crosslinking process was determined.

Materials and methods: The 100 % solid, UV crosslinkable adhesives were synthesized in 1000 ml glass reactor using Mettler Toledo LabMax system equipped with ReactIR IC10 diamond composite probe which enables in-line monitoring of polymerization process. Different formulations were tested and the polymerizations were carried out at equal process parameters. The basic formulation was equal for all syntheses; the only difference was in type and amount of added MMT clays (amounts from 0.5 to 3 wt. %). MMT clays differ in their hydrophobic nature, which is changed from Cloisite 15A (the most hydrophobic), Cloisite 93A to Cloisite 10A.
Synthesized prepolymer mixtures were coated on siliconized glassine paper on pilot coating machine using a Mayer bar coating system. The pilot coating machine is equipped with UV light - medium pressure Hg vapor lamp, 400 W/in. All adhesive coatings were subjected to UV light for 30 sec, where the total UV exposure equaled 750 mJ/cm^2. Total UV exposure and residence time under UV source was measured with ILT 490 profiling belt radiometer (International Light Inc.). Duration of UV light exposure for successful crosslinking and for determination of the MMT addition influence on crosslinking process was determined by attenuated total reflectance-Fourier transform infrared (ATR-FTIR) spectroscopy with Perkin Elmer Spectrum One FTIR spectrophotometer. Viscosities of synthesized prepolymers were measured using Brookfield viscosimeter. Final conversion of monomers for all syntheses was determined gravimetrically by drying 2 g of PSA in vacuum dryer at 70 °C for 24 h. For the adhesive performance characterization three different test methods were used: the peel adhesion at 180° (FTM 1 – Finat test method 1), the probe test (Polyken test), and the shear resistance (FTM 8).

Results and Discussion:
Results of the study showed, that the addition of MMT clays has a significant influence on all of the measured properties. Viscosity of prepolymers increased with increasing amount of added MMT clay. In-line monitoring of polymerization process showed differences in overall monomer conversion time plots. It seems that polymerization reaction is inhibited in the initial stage when MMT clays 15A and 10A were used, while no differences in overall monomer conversion plots can be determined when MMT clay 93A was used. Monitoring of crosslinking process was based on observation of C=O group conversion upon exposure to UV light, which induces the loss of conjugation between the carbonyl group in the aromatic ring. Therefore, the kinetic profile of UV crosslinkable PSAs may be observed by evaluation of absorption band at 1600 cm^{-1}.
Results showed that the addition of MMT clays at high level (3 wt.%) hindered the crosslinking process. However, 30 sec of UV exposure was enough to achieve complete crosslinking of the prepolymers. The adhesive properties measurements, especially shear strength measurements, showed improved cohesivity of the adhesive coating as a result of nanocomposite structures formation.

References:
[1]Czech, Z., *Polym Bull*, (2004) **52**, 283.
[2]Czech, Z., *Int J Adhes and Adhes*, (2006) **26**, 414.
[3]Czech Z.; Martysz, D., *Int J Adhes and Adhes*, (2004) **24**, 533.
[4]Czech Z., *Int J Adhes and Adhes*, (2004) **24**, 119.
[5]Czech Z.; Wesolowska, M., *Eur Polym J*, (2007) **43** 3604.

Synthesis and Photo-responsive Behavior or Spiropyran End-functionalized Polymers by ATRP

Claudia Ventura[1], *Robert Byrne*[2], *Fabrice Audouin*[1], *Dermond Diamond*[2] *and Andreas Heise*[1]

[1]Dublin City University, School of Chemical Sciences, Glasnevin, Dublin 9, Ireland.
[2]Dublin City University, National Centre for Sensor Research, Glasnevin, Dublin 9, Ireland.

claudia.ventura2@mail.dcu.ie

INTRODUCTION

Photo-responsive polymers have been investigated intensively as important elements for the development of smart materials and devices. The ability of these materials to respond with a property transformation triggered by light can be utilized specifically in biomedical applications such as targeted drug delivery and sensing. Photo-responsive polymers have been reported in the literature using various chromophores.[1] Our interest is in polymers functionalized with benzospiropyran (BSP), a well-known photocromic molecule that has the ability to reversibly switch from an uncharged, colorless, spiropyran (SP) form, to a zwitterionic, planar, highly colored merocyanine (MC) form upon exposure to light.[2] Of particular interest is to determine the minimum number of BSP units in a polymer required to trigger a measurable response. In this work we report the synthesis of polymers (PMMA) with a single BSP terminal unit and the investigation of their light responsive.

RESULTS AND DISCUSSION

ATRP was chosen for the synthesis of BSP functional PMMA due to the high end-group fidelity of this technique. A BSP functional ATRP initiator (BSP-Br) was synthesized by the reaction of 2-bromo-2-methylpropionyl bromide with an OH functional BSP (BSP-OH) (Scheme 1).

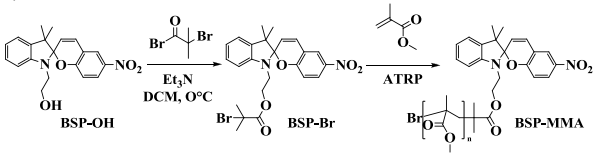

Scheme 1: Synthesis of benzospiropyrane ATRP initiator (BSP-Br) and benzospiropyrane functionalized poly(methylmethacrylate) (BSP-MMA).

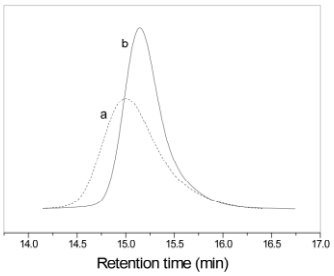

Figure 1: Size exclusion chromatograms of BSP-PMMA1 (a) and BSP-PMMA2 (b).

The polymerizations were carried out using the BSP-Br initiator and methylmethacrylate (MMA) monomer at two different ratios at 60˚C in THF in the presence of the heterogeneous ATRP catalytic system Cu(I)Cl/Cu(II)Cl/HMTETA (Scheme 1). Both polymerizations were stopped after three hours and not further optimized. The resulting number-average molecular weights of BSP-MMA-1 and BSP-MMA-2 were 3600 g/mol and 23800 g/mol, respectively with polydispersities of 1.3 and 1.1 (Figure 1). The polymer structure was confirmed by ^{1}H and ^{13}C NMR, MALDI ToF and UV-Vis spectrophotometry.

Both polymer exhibit conventional SP-MC photochromism in acetonitrile with the strong long-wavelength absorption band located at 568 nm associated with a change from a colorless to a pink solution (Figure 2). The position of the absorption maxima suggests that the SP endgroups experience a non-polar environment with little contact to solvent molecules.

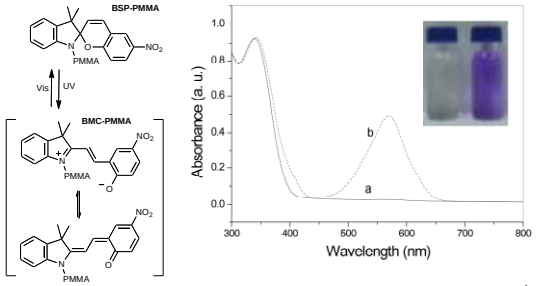

Figure 2:UV-vis spectra of BSP-PMMA1 (1 x 10^{-4} M in acetronitrile) before (a, non colored solution) and after (b, pink solution) 60 s of UV (365nm) irradiation.

Kinetic studies show that the MC to SP transition is increasingly faster with increasing temperature for the longer polymer. The thermodynamic reasons for this unexpected behavior are currently under investigation.

CONCLUSION

In the work presented new light-responsive polymeric methacrylates, bearing a single BSP terminal unit have been synthesized and their photocromic and photoinduced properties have been investigate We were able to show that a single unit is sufficient to obtain effects similar to the multi BSP copolymers and that the switching kintics in acetonitrile depend on the molecular weight.

REFFERENCES

1 F. Ercole, T. P. Davis, R. A. Evans *Polym. Chem.* **2010**, *1*, 37

2 R. Byrne, C. Ventura, F. B. Lopez, A. Walther, A. Heise, D. Diamond *Biosens. Bioelectron.* **2010**, *26*, 1392.

ACKNOWLEDMENTS

This work was conducted under the Science Foundation Ireland (SFI) funded Principle Investigator Award 07/IN1/B1792. AH is a SFI Stokes Senior Lecturer (07/SK/B1241).

Synthesis of Hybrid Materials via Photopolymerization of Benzoin Functionalized Silica Nanoparticles

Müfide D. Karahasanoğlu, Ayşen Önen, İ. Ersin Serhatlı

Istanbul Technical University

karahasan5@itu.edu.tr, serhatli@itu.edu.tr, onen@itu.edu.tr

Introduction

Organic–inorganic hybrids that combine the advantages of both kinds of materials, such as mechanical strength and thermal stability with the processability and flexibility of an organic polymer matrix, exhibit multifunctional characteristics.

Silica particles have attracted much interest due to their low toxicity, ease of formation in a wide range of sizes and morphologies, high stability, and the surface that can be further functionalized [1-4]

Some chemical agents with more active functional groups are usually employed to substitute the hydroxyl groups to form various functional groups on silica nanoparticle surface. Isocyanate group is considered to be an ideal activator for surface modification of silica nanoparticles. Reactive isocyanate groups of toluene-2,4-diisocyanate enable the reaction of silica nanoparticles with benzoin molecules[5]. Benzoin functionalized silica nanoparticles may be considered as good candidate for photopolymerization systems[6,7].

Materials and Methods

Spherical silica particles, according to Stöber process, were prepared by hydrolysis and condensation reactions of TEOS in an ammonia/absolute ethanol solution.

Synthesized silica nanoparticles were dispersed in toluen using ultrasonic sonicator at room temperature. The dispersion was reacted with excess toluene-2,4-diisocyanate (TDI) and catalytic amount of dibutyl tin dilaurate (DBTL) as shown in Scheme 1. The reaction mixture was stirred at 60 °C for 8 hours. In order to remove all the substances physically adsorbed on the surface of the silica nanoparticles, synthesized TDI functionalized silica nanoparticles were sequentially rinsed with toluene and benzene respectively and re-centrifuged.

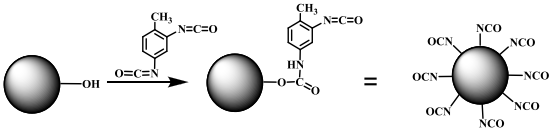

Scheme 1

TDI reacted silica nanoparticles were dispersed in dimethylformamide using ultrasonic sonicator. Into a three-necked round bottom flask Si-TDI dispersion, excess benzoin, catalytic amount of dibutyl tin dilaurate were charged. The reaction mixture was stirred at 60°C for 10 hours. In order to remove all the substances physically adsorbed on the surface of the nanoparticles, nanoparticles were sequentially rinsed with chloroform and re-centrifuged.

Benzoin functionalized silica nanoparticles were put into dimethylformamide in a tube to disperse in a sonicator under nitrogen atmosphere. Methyl methacrylate was added into the tube containing dispersion of nanoparticles. After UV exposure for photopolymerization, hybrid dispersion was precipitated into methanol. In order to remove homopolymer of polymethyl methacrylate (PMMA), hybrid polymer was dissolved in acetonitrile and centrifuged to obtain PMMA grafted silica nanoparticles as shown in Scheme2.

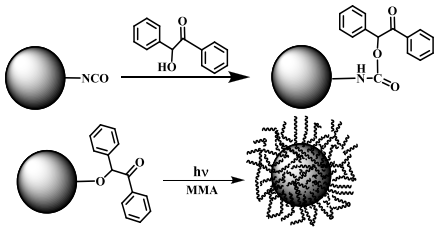

Scheme 2

Results and Discussion

Monodispersed silica nanoparticles were obtained in the size range of 40 nm-100 nm. The size, morphology and dispersity of prepared silica particles were determined by SEM characterization analysis. FTIR spectrums displays characteristic absorptions of synthesized bare, TDI and benzoin grafted silica nanoparticles.

SEM image analysis of Figure 1 shows that the average diameter of silica nanoparticles increases noticeably after the polymerization.

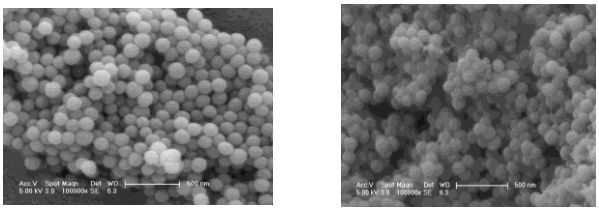

(a) (b)

SEM images of a) bare(60nm) silica nanoparticles and b) PMMA grafted silica nanoparticles (80nm).

Si-TB-PMMA and homopolymer of PMMA were heated up to 900°C by the 20°C/min rate. The residue increased significantly to % 56 for the %10 content of silica. It is obviously seen that silica nanoparticle has an increasing effect on the residue content.

References

1. Stober, W.; Fink, A.; Bohn, E. *J.; Colloid Interface Sci*., **1968**, *26*, 62
2. Costa, C. A. R.; Leite, C. A. P.; Galembeck, F.; *J. Phys. Chem*., **2003**, *107*, 4747-4755
3. Lin, J.; Siddiqui, J. A.; Ottenbrite, R. M.; *Polym. Adv. Technol*., **2001**, 12, 285-292
4. Sun, Y.; Zhang, Z.; Wong, C. P.; *Journal of Colloid and Interface Science*, **2005**, 292, 436–444
5. Che, J.; Xiao, Y.; Wang, X.; Pan, A.; Yuan, W.; Wu, X.; *Surface & Coatings Technology*, **2007**, 201, 4578-4584
6. Han, Y. H.; Taylor, A.; Mantle, M. D.; Knowles, K. M.; *J Sol-Gel Sci Technol*, **2007**, 43, 111–123

Kim, S.; Kim, E.; Kim, S.; Kim, W.; *Journal of Colloid and Interface Science*, **2005**, 292, 93-98

Hybrid Photosensitizers For the Removal of Trace Pollutants from Water

Anna Karewicz, Dorota Bielska, Marta Kumorek, Krzysztof Szczubiałka, Maria Nowakowska

Nanotechnology of Polymers and Biomaterials Research Group, Faculty of Chemistry, Jagiellonian University, 30-060 Cracow, Ingardena 3, Poland

karewicz@chemia.uj.edu.pl

Introduction: Industrial activity is one of the principal causes of water contamination. Large amounts of chemical compounds, which are not capable of degrading by themselves, are dumped into the rivers and lakes. Among them are alkylphenols - one of the most important endocrine disrupting groups of chemicals present in the environment. n-Nonylphenol, a widely used pesticide, belongs to this group. It enters the environment in large amounts, directly through waste waters or indirectly with nonylphenol polyethoxylates. It is stable in water and exhibits aquatic toxicity and estrogenic activity even at very low concentrations. One of the suitable ways to enable biodegradation of toxic water wastes, including n-nonylphenol, is by their photosensitized oxidation using a visible light. In our work we have studied two systems based on the visible light absorbing chromophores, characterized by the high yields of singlet oxygen production. Both chromophores, rose bengal (RB) and porphyrin (Po), are effective photooxidizing agents. However, the removal of sparingly water soluble toxic compounds requires a more complex system allowing efficient interaction between the oxidizing species and the molecules of the contaminant. It is also important to obtain the multiple use photosensitizer. To satisfy these requirements we have designed two hybrid materials where the chromophores are incorporated into the clay nanostructures: 1) water soluble 5,10,15,20-tetrakis(4-hydroxy-phenyl) porphyrin (THPPo) covalently bound to the poly(ethylene glycol) (PEG) chain, 2) molecular rose bengal. The performance of the low molecular weight chromophore and the polymer-modified one before and after their successful intercalation were studied and compared.

Materials and Methods: The porphyrin pegylation product was characterized by ^{1}H NMR and MALDI-TOF analysis. The incorporation of the chromophores into the clay was followed by UV/Vis absorption spectroscopy. Irradiation process was conducted in Rayonet system equipped with 8 lamps emitting at the wavelength of 575 nm. Photooxidation kinetics was followed using UV/Vis absorption and emission spectroscopy and GC-MS analysis.

Results and Discussion: The analysis of the ^{1}H NMR and MALDI-TOF spectra confirmed the attachment of 2000 Da PEG chains to THPPo. Two maxima appear in the spectrum, revealing that the product contains mono- and di-substituted THPPo. The content of the latter was below 9%, as was determined by ^{1}H-NMR analysis. The process of intercalation of THPPo-PEG and rose bengal into the clay was monitored by the UV/Vis absorption measurements. The maximum amount of THPPo-PEG inserted in the Cloisite 30B clay was determined to be 24%, while in the case of rose bengal 69% of the compound was inserted into the halloysite clay. For both chromophore-clay systems their photosensitizing performance was studied in comparison to the chromophore alone. RB or RB-clay sensitizer was added to the aqueous solution of n-nonylphenol (6 mg/l) and irradiated. During irradiation the samples were constantly saturated with oxygen. The oxidation kinetics was followed by UV/Vis absorption measurements. RB alone as well as RB-clay system effectively photosensitize the oxidative decomposition of n-nonylphenol. Within the first 80 minutes over 90% of the pollutant in the case of clay system and almost 80% in the case of the free RB was degraded. The hybrid material proved to be a better photosensitizer compared to the RB alone. The GC-MS allowed characterisation of the oxidation products. For the THPPo-PEG and THPPo-PEG-clay the experiment was performed in an aqueous solution containing anthracene-2-sulfonic acid sodium salt (ANS). ANS was used as a well-known acceptor of singlet oxygen. Using first the model acceptor was found necessary due to the complexity of the hybrid system. During irradiation the samples were constantly saturated with oxygen. Results of the experiment are illustrated below.

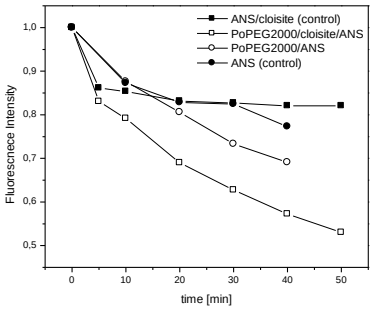

Conclusions: The new photoactive dye, THPPo-PEG, was obtained and characterised. The THPPo-PEG-clay system shows a better performance as a photosensitizer of the ANS oxidation in aqueous media compared to the THPPo-PEG alone. RB-clay is more effective in the photooxidation of n-nonylphenol, a widespread water pollutant, than free RB molecule.

Acknowledgements: Project operated within the Foundation for Polish Science Team Programme co-financed by the EU European Regional Development Fund, PolyMed, TEAM/2008-2/6. We thank the Polish Ministry of Science and Higher Education for the financial support in the form of the grant K/PBW/000487

Structure and Conductivity of the Copolymers of 2-Methoxyaniline with Aminobenzoic and Aminobenzenesulfonic Acids

David Pahovnik,[1] *Ida Mav-Golež*,[2] *Majda Žigon*,[1,3] *Jiří Vohlídal*[4]

[1]Laboratory for Polymer Chemistry and Technology, National Institute of Chemistry, Ljubljana, Slovenia; [2]Krka, d.d., Novo mesto, Slovenia; [3]Centre of Excellence PoliMaT, Ljubljana, Slovenia; [4]Department of Physical and Macromolecular Chemistry, Faculty of Science, Charles University, Prague, Czech Republic

david.pahovnik@ki.si

Polyanilines (PANI) are environmentally stable conducting polymers with excellent electric, magnetic, and optical properties that have attracted a considerable attention due to high application potential. The unsubstituted polyaniline is insoluble or sparingly soluble in almost all solvents, neither it can be processed thermally. Therefore, there is a permanent interest in development of better processable substituted PANIs though the substituents attached to main chains are known to decrease their conductivity.

PANIs carrying acidic side groups are of particular interest as these groups can also act as internal proton-doping agents; therefore, PANIs of this class are called self-doped PANIs. The emeraldine salt (ES) form of a self-doped PANI is usually doped internally, by the acidic side groups linked to PANI chains, as well as externally, by an added acid (mostly that one used in the preparation of the PANI).

The effect of reaction conditions: feed monomer ratio, oxidant/monomers ratio, reaction temperature, reaction time and concentration of HCl, on the structure and conductivity of copolymers of 2-methoxyaniline (OMA) with anilinic acids (ANIA): 2- and 3-aminobenzoic acids and 2- and 3-aminobenzenesulfonic acids, has been studied using the ICP-AES/elemental analysis, size exclusion chromatography, NMR, FT-IR and UV-vis spectroscopy, and impedance spectroscopy.

To prepare the PANIs the oxidant was dissolved in aqueous HCl and the solution formed was added to a stirred aqueous HCl solution of OMA and particular ANIA monomer of a given composition. The resulting copolymerization mixture was allowed to react under stirring for up to 20 h.

The molar fraction of OMA units in a resulting copolymer, F_1, has been always higher than the OMA fraction in the corresponding feed monomer mixture, f_1, because OMA carrying electron-donating methoxy group is much more reactive than any ANIA tested. Accordingly, the yield and molecular weight (MW) of the copolymers are increasing functions of f_1 and a use of an under-stoichiometric amount of oxidant and/or shortening the copolymerization time favor incorporation of OMA units into copolymer chains. An increase in the polymerization temperature causes a decrease in the content of OMA units (F_1) as well as a decrease in both the yield and MW of the copolymer while an increase in the reaction mixture acidity yields qualitatively opposite effects. The electrical conductivity, σ, of the copolymers prepared lies in the region typical of semiconductors (from 0.05 to 2.5 mS/cm) and, in the first approximation, it is an exponential-growth function of F_1. A good qualitative correlation of σ values with the relative intensity of the Q-band of UV/vis spectra is observed for all copolymers. The data obtained indicate that, in spite of the self-doping effect of ANIA acidic side groups, the incorporation of ANIA units into polymer chains deteriorates the copolymer conductivity and that this effect is caused by a decreased content of emeraldine form in copolymers containing more ANIA units (Fig. 1).

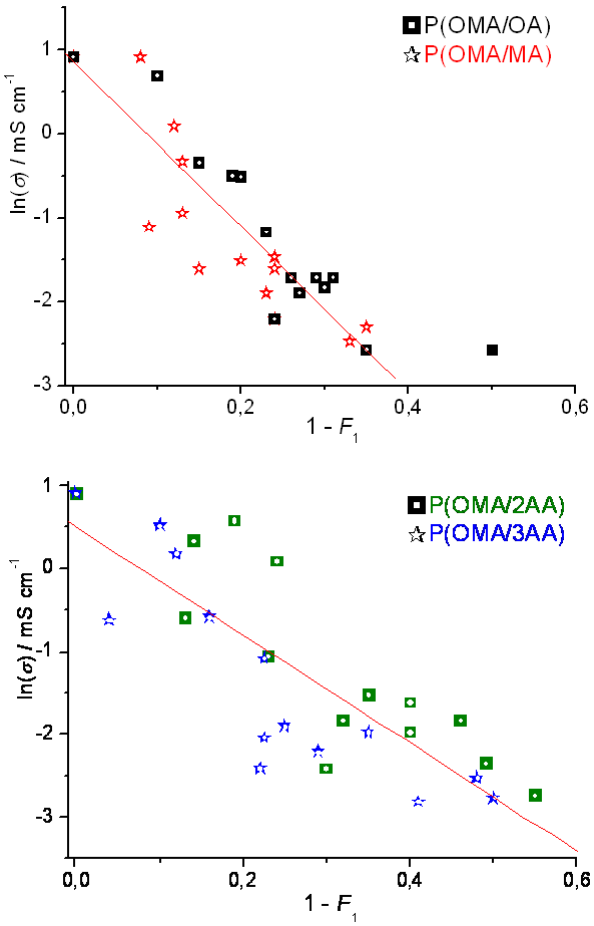

Fig. 1) Semilogarithmic dependences of the σ of P(OMA/ANIA) copolymers on the mole fraction of OMA units in the copolymer, F_1.

The results obtained show that a variation of the reaction conditions such as the feed monomer ratio, oxidant/monomers ratio, reaction time, or acidity and temperature of the copolymerization mixture primarily affects composition of P(OMA/ANIA) copolymers but only little their others structure features.

Morphological Characterization and Mechanical Properties of Poly(Lactic Acid) Blends

Márcia O. Taipina, Márcia M. F. Ferrarezi, Laura C. E. Silva, Maria C. Gonçalves

Institute of Chemistry, University of Campinas (UNICAMP), Campinas, Brazil

maria@iqm.unicamp.br

Introduction

Poly(lactic acid) (PLA) is a high modulus thermoplastic that can be easily processed by conventional techniques. However, PLA is very brittle under tensile and bending loads. PLA properties can be improved by addition of plasticizers, by blending PLA with other polymers or by adding specific fillers. Several research works investigating PLA/thermoplastic starch (TPS) blends have been done. However, the incompatibility between PLA and starch are responsible for formation of blends with poor mechanical properties [1,2]. In this work, the strategy to improve PLA properties and the compatibility between PLA and TPS was the addition of poly(ethylene glycol) (PEG), due to the partial miscibility between PLA and PEG as well as TPS and PEG. Therefore, the main objective was to evaluate the influence of PEG addition on the morphology and mechanical properties of PLA/TPS blends.

Experimental

Materials: PLA (M_W = 300 000 g/mol) was supplied by Nature Works and PEG (M_W = 4 000 g/mol) was obtained from Aldrich. Thermoplastic starch was prepared as described in an earlier work [3].

Processing of the blends: The blends were processed in a twin-screw DSM micro-extruder at 100 rpm for 1 min. Later, the blends were injection molded in a DSM micro-injector in order to prepare tensile and impact specimens (ASTM-D256 and ASTM-D1708). The mold and injection temperatures were 40 and 180°C, respectively. Table 1 shows the blend compositions.

Characterization: The morphologies of the samples were investigated in a field emission scanning electron microscope from JEOL, operating at an accelerating voltage of 3.0 kV. Differential Scanning Calorimetry analyses (DSC) were conducted on a DSC model 2910, TA Instruments.

Table 1: Compositions of the processed blends.

Samples	PLA (%wt)	TPS (%wt)	PEG (%wt)
PLA/TPS (2:1)	67	33	-
PLA/TPS (3:1)	75	25	-
PLA/PEG	75	-	25
PLA/TPS/PEG	56	19	25

Results and Discussion

Figure 1 presents the morphologies of the cryogenic fracture sample surfaces. PLA/TPS blends presented phase separation with cavities generated due to particles detachment during sample fracturing, due to the low adhesion between the phases. PLA/PEG showed continuous morphologies; no phase separation was detected. PLA/TPS/PEG blend showed smooth TPS domains as dispersed phase, rougher PLA phase domains and pores, which were concentrated in PLA phase.

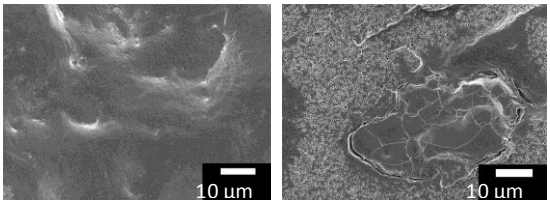

Figure 1: Micrographs (a)PLA/PEG (b) PLA/TPS/PEG.

DSC results are shown in Table 2. The TPS domains of the blends acted as nucleating agents, enhancing the PLA crystallization process. The addition of PEG also facilitated PLA crystallization, as it can act as a plasticizer.

Table 3 shows the mechanical properties of the materials. The presence of the TPS ductile phase resulted in the modulus decrease, but in the increase of the elongation at break and impact strength. Also, a significant increase of the elongation at break was observed for the PLA/PEG blend in relation to PLA. Lastly, the addition of PEG generated an increase of the impact strength, without significantly decreasing the modulus in relation of the values of PLA/TPS blend.

Table 2: DSC results of PLA and PLA blends.

Samples	T_{CC} /°C (PLA)	$\%X_C$ (PLA)
PLA	130	17.7
PLA/TPS (2:1)	109	28.9
PLA/TPS (3:1)	107	30.8
PLA/PEG	80	32.2
PLA/TPS/PEG	81	27.8

Table 3: Mechanical properties of the samples.

Samples	Impact strength (J/m)	Elasticity modulus (MPa)	Elongation at break (%)
PLA	22 ± 3	532 ± 43	13.7 ± 0.7
PLA/TPS (2:1)	52 ± 10	98 ± 25	ND
PLA/TPS (3:1)	55 ± 4	172 ± 34	22 ± 2
PLA/PEG	43 ± 11	9.2 ± 0.8	227 ± 29
PLA/TPS/PEG	119 ± 14	137 ± 17	ND

where: ND = not determined by the equipment.

Conclusions

The results showed that the addition of PEG probably allowed interactions between PLA and TPS phases, as the impact strength increased and the elasticity modulus was similar to the one of PLA/TPS blend.

References

1. Martin O., Averous L. Polymer 2001, 42, 6209
2. Arroyo OH., Huneault MA., Favis BD., Bureau MN. Polym Comp 2010, 31, 114
3. Favaro MM., Goncalves MC. Proceedings of 7th ISNAPOL, Gramado, Brazil, sept. 2010.

Acknowledgements: The authors would like to thank CNPq for financial support and Nature Works and Copagra for providing the materials for this research.

Photocatalytic activity of TiO_2 nanocomposites on degradation of water pollutions

Mohammad Reza Nabid[1], *Roya Sedghi*[1,2] *and Saeede Gholami*[1]

[1]Department of Chemistry, Faculty of Science, Shahid Beheshti University, 1983963113 Tehran, Iran
[2]Department of Chemistry, School of Sciences, Alzahra University, Vanak, Tehran, Iran

m-nabid@sbu.ac.ir

Introduction:

The carcinogenic dyes are the major constituents of the industrial effluents. Various approaches have been developed to remove organic dyes from the natural environment.

One of the important properties of the inorganic solid TiO_2 nanomaterials is its photocatalytic activity in many applications ranging from antibacterial surfaces to photocatalytic reactions [1,2]. In addition to TiO_2, there are a wide range of metal oxides and sulfides have been successfully tested in photocatalytic reactions [3]. Interaction of these semiconductors with photons having an energy comparable (equal or higher) to the band gap may cause separating the conduction and the valence bands. This event is known as electron–hole pair generation.

Photocatalytic properties of the surface modified TiO_2 catalyst was investigated by degradation of methyl orange (MO) in visible light as a model [4, 5].

Experimental and Methods:

The TiO_2/ZnO/Fe_3O_4/polyaniline (PANI) nanocomposite was prepared according to the following steps: for the preparation of TiO_2 NPs, a solution of 1.5 M ammonium sulfate which consisted of 0.75 M titanium (IV) chloride was used. The precipitated titanium hydroxide was calcined at 400 °C for 4 h. The ZnO nanoparticles prepared via Tang et al. method [6]. The magnetite nanoparticles were prepared by the conventional co-precipitation method with some modifications [7] and PANI synthesized by oxidation polymerization.

Results and Discussion:

The aim of this study is photodegradation of methyl orange in the presence of artificial UV and visible light and nanocatalysts, and then investigates the effectiveness of conducting polymer coated on semiconductor photocatalytic properties.

For degradation of MO, batch experiments were carried out by irradiating the aqueous solution of dye, in the presence of different magnetic nanocomposite such as ZnO/Fe_3O_4/polyaniline and TiO_2/ZnO/Fe_3O_4/PANI in the presence of UV and visible light. The rate of decolorization was estimated from residual concentration spectrophotometerically. For degradation of MO, batch experiments were carried out by irradiating the aqueous solution of dye, in the presence of different magnetic nanocomposite such as ZnO/Fe_3O_4/polyaniline and TiO_2/ZnO/Fe_3O_4/PANI in the presence of UV and visible light. The rate of decolorization was estimated from residual concentration spectrophotometerically. The structure and properties of synthesized photocatalysts were characterized by x-ray diffraction (XRD), UV-vis diffusive reflectance, Differential scanning calorimetry (DSC) and FT-IR spectroscopy.

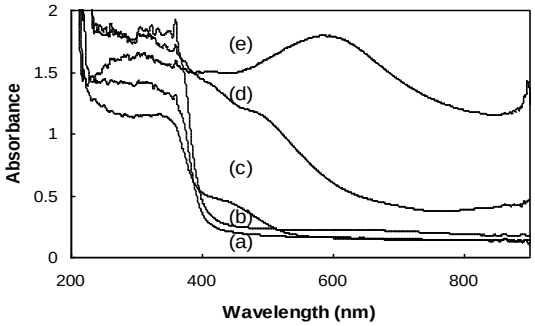

Fig. 1. UV-vis diffusive reflectance of (a) ZnO nanoparticles, (b) TiO_2/ZnO nanocomposite, (c) TiO_2 nanocomposite, (d) TiO_2/ZnO/Fe_3O_4 and TiO_2/ZnO/Fe_3O_4/PANI nanocomposites.

Figure 2 shown degradation of MO under visible light in 60 min. The effect of process parameter viz. pH, initial concentration of MO, and phtocatalyst loading on decolorization of MO solution has also been assessed.

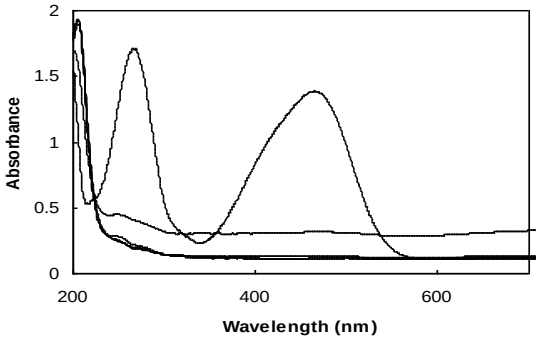

Fig. 2. UV-vis absorption of MO in 15, 30, 45, 60 min under visible light.

Conclusions:

This prepared photocatalyst had a better photocatalytic activity than that of either reported before and the experimental results indicated that 100% degradation of MO in the presence of visible source.

References:

1. S.K. Kansal, M. Singh, D. Sudc. J. Hazard. Mater. 141 (2007) 581.
2. C. Karunakaran, S. Narayanan, P. Gomathisankar. J. Hazard. Mater.181 (2010) 708.
3. Y. Li, Xi Zhou, X. Hu, X. Zhao, P. Fang. J. Phys. Chem. C 113 (2009) 16188.
4. C. Xu, L. Cao, G. Su, W. Liu, X. Qu, Y. Yu Micropor. Mesopor. Mat. 118 (2009) 210.
5. M. Zhang, T. An, X. Liu, X. Hu, G. Sheng, J. Fu. Mater. Lett. 64 (2010) 1883.
6. E. Tang, B. Tian, E. Zheng, C. Fu, G. Cheng. Chem. Eng. Comm., 195 (2008) 479.
7. Y.P. Guan, H.Z. Liu, Z.T. An, J.J. Ke, J.Y. Chen, CNPatent No. ZL 98124516.1, 1998.

Spectroscopic and Thermodynamic Study of Phase Transition in Solutions of Acrylamide/ *N*Isopropylmethacrylamide Copolymers

Julie Šťasntá[a], *Lenka Hanyková*[a], *Jiří Spěváček*[b]

[b]Faculty of Mathematics and Physics, Charles University, V Holešovičkách 2, 180 00, Prague 8, Czech Republic;
[a]Institute of Macromolecular Chemistry, Academy of Sciences of the Czech Republic, Heyrovsky Sq. 2, 162 06 Prague 6, Czech Republic;

chamky@seznam.cz

Introduction: Some polymers with amphiphilic character, including acrylamide-based polymers, exhibit in aqueous solution a lower critical solution temperature (LCST). They are fully soluble at low temperatures, but a small increase of temperature above the LCST causes a phase transition. The polymer precipitates from the solution and the solution gets milk-white turbid. On the molecular level, phase separation is a macroscopic manifestation of a coil-globule transition followed by aggregation and formation of so called mesoglobules
[1]. Their thermosensitivity makes these polymers interesting for biomedical and technological applications, e.g. as drug release polymers. In this work, we used NMR spectroscopy and Differential Scanning Calorimetry to investigate changes in the structure and dynamics during temperature-induced phase separation of the poly(acrylamide/*N*-isopropylmethacrylamide) p(AAm/IPMAm) copolymers.

Materials: *N*-isopropylmethacrylamide (IPMAm, Aldrich) and acrylamide (AAm, Fuka) were used to prepare PIPMAm homopolymer and P(AAm/IPMAm) copolymers by radical polymerization. The AAm mole fraction in the copolymers is 0.01, 0.06 and 0.16. The samples were dissolved in D2O, 5 wt.% for NMR and 10 wt.% for DSC.

Methods: The 1H NMR measurements were carried out with Bruker Avance 500 spectrometer operating at 500.1 MHz. The DSC measurements were performed in differential scanning calorimeter Pyris 1 (Perkin-Elmer).
From the temperature dependent integral intensities of NMR signals we calculated the p-factor [2], a fraction of phase separated polymer units. Temperature dependences of p-factor provide quantitative information on the critical temperature, width and extent of the phase separation. Further, using p-factor the van't Hoff's plot was constructed [3] and comparison of obtained thermodynamic parameters with DSC results was made.

Results and Discussion: Temperature dependences of p-factor measured for all samples showed significant increase in the range of the phase separation as the consequence of restricted mobility of polymer units involved in globular structures. From the analysis of these dependences and DSC characteristics (the onset temperatures and enthalpy changes) it follows that increasing fraction of AAm units in the copolymer significantly shifts the transition towards higher temperatures, broadens the transition interval and reduces the maximum value of phase-separated fraction. In contrast to IPMAm units, virtually all hydrophilic AAm units are directly detected in high-resolution NMR spectra of these systems even at temperatures above the phase transition. Because the AAm units are incorporated in polymer chains forming phase-separated globular structures, their rather high mobility suggests that they extensively interact with solvent molecules, i.e., they are hydrated in D2O. This fact results in dynamic heterogeneity of copolymer chains in mesoglobules where AAm sequences and surrounding short IPMAm sequences are hydrated and mobile, while the sufficiently long IPMAm sequences are dehydrated and their mobility is strongly reduced. All these results are consistent with the NMR relaxation experiments [2] showing that P(AAm/IPMAm) copolymer mesoglobules are rather porous and disordered.
The van't Hoff plot calculated from NMR data clearly showed an endothermic two-step process, which have different enthalpic and entropic components. The comparison of these values and the data obtained from the DSC thermograms enables us to estimate number of cooperative units involving in the phase separation as well as to discuss energetic contributions arising from the changes in hydrophilic and hydrophobic interactions.

Conclusion: The information about the critical temperature, degree of the transition and its graduality obtained by NMR and DSC methods corresponds to each other. The increasing fraction of hydrophilic AAm units in the copolymer significantly shifts the transition towards higher temperatures, broadens the transition interval and reduces fraction of phase–separated units.
Relatively high mobility of AAm units incorporated in globular structures results in heterogenity of chains in globules. This conception is consistent with results of relaxation experiments. With both used methods the thermodynamic quanitities of phase transition in the copolymer solutions were determined and compared.

Acknowledgement: Support by the Grant Agency of the Czech Republic (Project 202/09/1281) and Ministry of Education, Youth and Sports of the Czech Republic (Project SVV-2011- 263 305) are gratefully acknowledged.

References:

1. V. O. Aseyev, H. Tenhu, F. M. Winnik, *Adv. Polym. Sci.* 2006, *196*, 1-85.
2. H. Kouřilová, J. Šťastná, L. Hanyková, Z. Sedláková, J. Spěváček, *European Polymer Journal*, 2010, 46, 1299 – 1306.
3. C. V. Rice, *Biomacromolecules*, 2006, 7, 2923 - 2925

Innovative perfluoropolyether-based copolymers: another breakthrough in fluorine chemistry

M. Avataneo, P.A. Guarda and G. Marchionni

Solvay Solexis S.p.A., R&D Centre, V.le Lombardia, 20 - 20021 Bollate (MI) – Italy

Marco.avataneo@solvay.com

Solvay Solexis has always been engaged in answering to the most challenging needs of high technology markets by developing new and innovative fluorinated products in the field of fluoropolymers [1], fluoroelastomers [2] and fluorinated fluids [3]. Very recently, a new technological platform has been introduced for the synthesis of a pioneering class of perfluoropolyether (PFPE) based copolymers [4, 5] that will fill many of the gaps existing today in markets not currently served by PFPEs. This new chemistry, based on the radical reaction of peroxidic perfluoropolyethers [6] with unsaturated fluorocompounds, can be exploited for the preparation of a huge variety of copolymers not achievable with conventional techniques:

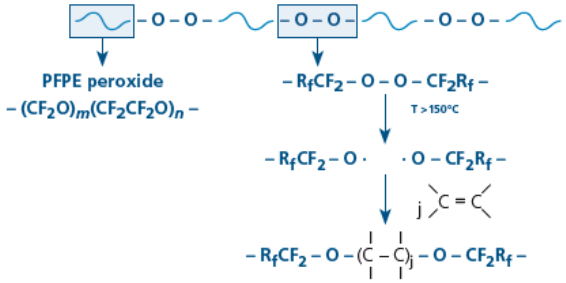

Due to the novelty of these materials, applications are endless, from thin film lubrication to gel based greases [4], to PFPE thermal stabilizer additives [5], polymer processing aids [7,8] and low Tg perfluoroelastomers [5], just to name a few. Many other applications are still under evaluation and development.

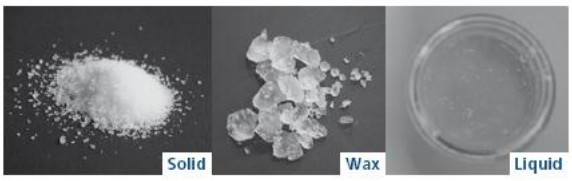

PFPE-TFE block copolymers: from solid to liquid

References:

[1] G. Brinati, A. Marrani, B. Goffaux, EP 2133370

[2] M.Apostolo, F.Triulzi, J. Fluorine Chem., 125, 2004, 303–314

[3] P. A. Guarda, F. Riganti, G. Marchionni, A. Di Meo; 20th ELGI Annual General Meeting , Lisboa (P), April 20-22, 2008.

[4] M. Avataneo, P.A.Guarda. G. Marchionni, P. Maccone, G. Boccaletti, US2010105584

[5] G. Marchionni, M. Avataneo, P.A.Guarda, EP2100909

[6] G. Marchionni,G. Ajroldi, G. Pezzin, in Comprehensive Polymer Science, S.L. Aggarwal and S. Russo Eds.; Second Supplement; Pergamon, London, 1996, 347-388.

[7] J. Abusleme, M. Avataneo, G. Perfetti, US2009326154

[8] Moore T. , Reichmann M., Avataneo Marchionni G., WO 2010/097363

Novel liquid crystal ionomers for Polymeric Electrolyte Membranes in Direct Methanol Fuel Cells

[1]A. Martínez-Felipe, [1]L. Santonja-Blasco, [1]R. Teruel-Juanes, [2]P.A. Henderson, [3]M. Giaccinti-Baschetti, [3]G. Sarti, [2]C.T. Imrie, [1,*]A. Ribes-Greus

[1]Institute of Materials Technology, Universidad Politécnica de Valencia
[2]Chemistry, School of Natural and Computing Sciences, University of Aberdeen
[3]Department of Chemical Engineering, Mineral and Environmental Technology, Università degli studi Bologna

*e-mail: aribes@ter.upv.es

Introduction

Ionomers are polymers containing a certain concentration of ionic groups. The combination of ionic and hydrophobic groups and residues in such materials usually leads to phase separated morphologies, induced by intra and intermolecular aggregation. The resulting aggregation state may be depending on the molecular structure, and can be somehow controlled by the nature and distribution of monomers units [**1**]. A possible strategy to obtain ionomers with controllable structures less depending on spontaneous phase separation is to introduce ionic groups in side chain liquid crystal polymers (**SCLCPs**), obtaining Liquid Crystal Ionomers, **LCIs**. SCLCPs consist of a polymer backbone, a flexible alkyl spacer and a mesogenic group [2]. SCLCPs combine macromolecular characteristics, such as mechanical integrity, with, for example, the electro-optic properties of low molar mass liquid crystals, on a much slower timescale. LCIs can be applied to obtain controllable membranes, since the morphology of the liquid crystal (LC) phases (mesophases) can be regulated by external stimuli. Controlling the resulting structure of the mesophases can also avoid the formation of random ordering morphologies caused by spontaneous phase separation in typical ionomers. We believe that the use of LCIs can be attractive to obtain electrolytes capable to discriminate the diffusion of ions and other molecules by the formation of defined transport pathways. Such is the case of Polymer Electrolyte Membranes used in Direct Methanol Fuel Cells, where high proton conductivities are required with low methanol crossover from the anode to the cathode.

Materials and methods

We have prepared a series of new membranes containing LCIs. The LCIs have been synthesised by radical copolymerization to yield a SCLCP structure, including azo-benzenic units (poly[10-(4-methoxy-4'-oxy-azobenzene) decyl methacrylate, 10-MeOAzB), as the mesogenic units, and sulfonated acrylamide groups (poly[2-acrylamido-2-methyl-1-propanesulfonic acid, AMPS) to provide the copolymers with the ionic sites and potential proton conduction. The structure of the resulting polymers is seen in **Figure 1**. The synthetic route allows for the introduction of other acrylate units as side groups to modify the thermal properties of the resulting LCIs. Thus, we have also investigated the effect of the attachment of methacrylate (MA) and methyl(methacrylate) (MMA) units as a way to obtain tailor made polymers

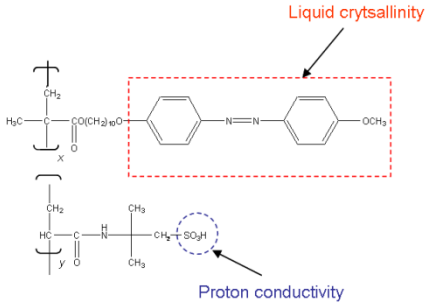

Figure 1. Chemical structure of the LCIs

Results and conclusions

The 10-MeOAzB/AMPS LCIs show mesomorphism in a broad range of compositions ($x_{10\text{-MeOAzB}} \geq 0.5$, molar), by the formation of stable Smectic A phases up to T~135ºC. The introduction of AMPS does not reduce the phase stability to a great extent, possibly by the incorporation of ionic interactions. The disappearance of the liquid crystallinity at higher ionic concentrations ($y_{AMPS} > 0.5$, molar) is possibly due to the formation of ionic aggregates and sudden increase of physical crosslinking. Some experimental results also suggest that the phase stability of the LCI can be easily reduced by the introduction of MA and MMA units in the backbone. Due to the high glass transition of the copolymers, the LCIs have been mixed with several polymers with low glass transitions (T_g) to obtain flexible membranes. Blends of Poly(vinyl acetate), Poly(methyl acrylate), Poly(ethylene oxide) and Poly(vinyl alcohol) are used to form homogeneous films containing the LCIs. The mesogenic behaviour of the membranes is investigated by thermal and spectroscopic analysis to determine the degree of phase separation in the membranes and the possible inhibition of the liquid crystallinity. The absorption properties of the resulting membranes are also studied as a function of their composition and morphology, and the results indicate the potential of the materials to control transport properties.

References

1. L.E. Karlsson, P. Jannasch, B. Wesslén, Macromol. Chem. Phys. 203 (**2002**) 686
2. Shibaev, V.P. Polym. Sci. Ser. A 51 (**2009**) 1131
3. DeLuca, N.W., Elabd, Y.A. J Polym. Sci. Part B: Polym. Phys. 44 (**2006**) 2201

Acknowledgments

The authors thank the financial support of the Generalitat Valenciana, through the Grisolia and Forteza programs, and the Spanish Ministry of Science and Innovation, through the Research Projects ENE2007-67584-C03 and UPOVCE-3E-013 and the awarding of two FPI and FPU pre-doctoral grants

Crosslinked PVA Membranes for Direct Methanol Fuel Cells

*A. Martínez-Felipe, L. Santonja-Blasco, M. Rosado-Gil, *A. Ribes-Greus*

Institute of Materials Technology, Universidad Politécnica de Valencia

* aribes@ter.upv.es

Introduction

Poly(vinyl alcohol) (PVA) has been proposed an a component in Polymer Electrolyte Membranes (PEM) for Direct Methanol Fuel Cells (DMFC), as a way to reduce methanol crossover through electrolyte, due to its high selectivity for water with respect to alcohols [1, 2]. Prior to be used in the cells, some modifications must be considered in PVA membranes:

- Introduction of ionic groups may be necessary to improve its proton conductivity.
- Physical or chemical crosslinking is required to avoid collapsing in water and to obtain stable films.

Crosslinking with sulfonate diacids combines the formation of stable structures with the introduction of ionic conducting groups [3]. In this work we present some results concerning the preparation and characterisation of PVA-crosslinked membranes, including the effect of the hydrolysis degree in PVA in films formation and the resulting water/methanol absorption properties.

Materials and methods

Samples of PVA with different hydrolysis degrees (HD = 89%, 96% and 99%, MW ~ 85,000 – 124,000 $g \cdot mol^{-1}$, Sigma Aldrich) were mixed with water to form 10%, wt. %, solutions by stirring at 90ºC for 6 hours. Corresponding amounts of a commercial sulfosuccinic acid (SSA) solution (70%, wt. % in H_2O, Sigma Aldrich) were added to the solution, followed with further stirring at room temperature for 24 hours. The resulting homogeneous transparent solutions were cast on a Teflon sheet, and solvent was evaporated at ambient conditions, until no further loss weight was observed. Different PVA-SSA films were obtained in the 0 – 30% SSA weight percentage range (dry weight). Some of the films were submitted to thermal treatment (2 hours, 100ºC) to promote chemical crosslinking by esterification between the OH groups of PVA and the COOH terminations of the di-carboxylic acid (SSA). The proposed mechanism for this esterification is shown in **Figure 1**. Additionally, non-woven Poly(propylene) was used as a substrate in order to enhance the consistency of some of the membranes.

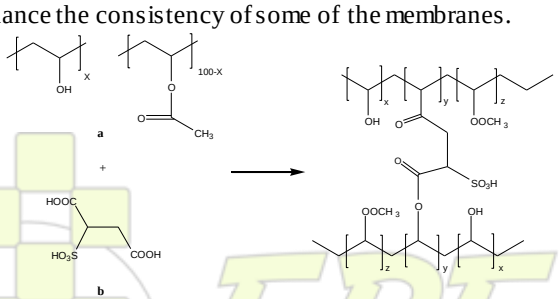

Figure 1. Esterification between PVA (a) and SSA (b)

The structural changes occurring during the formation of the membranes were studied by using Fourier Transform Infrared Spectroscopy (FTIR) and Thermogravimetric Analysis (TGA). Some of the transport properties of the membranes were determined by performing solvent absorption (swelling) and desorption tests. The ionic exchange capacity (IEC) of some of the membranes was also calculated.

Results and conclusions

The formation process of the PVA-SSA membranes was successfully monitored by analysing the IR bands of the OH ($\nu \sim 3000\ cm^{-1}$), C=O ($\nu \sim 1720\ cm^{-1}$) and SO_3 ($\nu \sim 1040\ cm^{-1}$) groups. The results suggest that chemical crosslinking could occur, to some extent, even prior to thermal treatment. On the other hand, HD promotes differences on the efficiency of the crosslinking process. In PVA membranes with low hydrolysis degrees it is possible to observe a threshold concentration at which further increases of SSA contents do not leave to higher crosslinking degrees.

The results also suggest that PVA with HD degrees of 96% are appropriate for the formation of PVA-SSA crosslinked membranes, thus, some of their transport properties were tested. The absorption and desorption tests show considerable differences on the transport mechanisms of water, methanol and their binary mixtures in the PVA-SSA crosslinked membranes. The reduction on the concentration of OH groups caused by crosslinking seems to be the main effect on the reduction of water absorption. On the other hand, methanol is mostly absorbed through non-polar regions, and appears to be unaffected by the crosslinking degree. Increasing the crosslinking degree causes two effects superimposed: increase on the ionic conductivity (as seen from IEC) and reduction of the water/methanol selectivity. Under this view, additional mechanisms to control the polar and non-polar phases of PVA membranes must be carried out to improve the water/methanol selectivity maintaining high ionic contents in the PVA-SSA membranes.

References

1. DeLuca, N.W., Elabd, Y.A. J Polym. Sci. Part B: Polym. Phys. 44 (**2006**) 2201

2. Pivovar, B.S.; Wang, Y.; Cussler, E.L. Journal of Membrane Science, 154 (**1999**) 155

3. Rhim, J.W.; Lee, S.W.; Kim, Y.K. J Appl Polym Sci 85 (**2002**) 1867

Acknowledgments

The authors thank the financial support of the Generalitat Valenciana, through the Grisolia and Forteza programs, and the Spanish Ministry of Science and Innovation, through the Research Projects ENE2007-67584-C03 and UPOVCE-3E-013 and the awarding of two FPI and FPU pre-doctoral grants.

Developing of Effective Multipurpose Polymer-Bitumen Compositions

Negmatov S.S., Rahmonov B.Sh., Sobirov B.B., Abdullaev A.X., Salimsakov Y.A., Negmatova M.I., Sobirov A.B.

Tashkent State Technology University, State unitary enterprises "Fan va Taraqqiyot", Tashkent, Uzbekistan

email: polycomft2005@rambler.ru

Known, that the bitumen used in road construction as binding materials of asphalt concrete pavements and as joints and cracks sealant, as well as in the production of waterproofing materials for civil and industrial construction.

One of the significant shortcomings of bitumen is their relatively high softening temperature, which does not exceed the 50-55 ^{0}C. For this reason, composite materials based on bitumen cannot be operated in conditions of high temperatures, and pavements are easily damaged and require frequent repairs. This also applies to roofing material, obtained by using bitumen.

Based on the above it follows that the increase of softening point of bitumen in some way would eliminate this disadvantage and increase the time of maintenance-free operation of roads and roofs with bitumen used as binders.

One way to improve the softening temperature of asphalt is the modification of bitumen with macromolecular polymer ingredients softening temperature of which is much higher than the softening point of bitumen. As such modifiers, we used secondary polyethylene, polyvinyl chloride, fine rubber powder.

Obtaining of the effective polymer-bitumen compositions was performed in a reactor heated to a temperature up to 150 ^{0}C.

At the beginning of the reactor was charged with bitumen in an amount of 75 kg, temperature was brought to 100 ^{0}C and was charged with powdered secondary polyethylene in an amount of 25 kg. The temperature was gradually raised to 150 ^{0}C. And a homogeneous mass was formed, i.e. mixture of bitumen with a secondary molten polyethylene (melting temperature of the secondary polyethylene equals 150 ^{0}C). Then the homogeneous bitumen-polymer composition unloaded onto pallets for cooling. After cooling, the softening point was determined by preparing a composition, which was 75 ^{0}C. In the same way bitumen-polymer compositions were obtained using recycled polyvinyl chloride and finely ground rubber powder.

It was revealed that the modification of bitumen with secondary polyvinyl chloride allows obtaining bitumen-polymer composition with a softening point of 75 ^{0}C and more.

Modification of asphalt rubber with finely crushed powder in an amount up to 25 massive particles allowed obtaining bitumen-polymer composition with a softening point at 65 ^{0}C.

Thus, based on the results of studies we can conclude that with the modification of bitumen with macromolecular compounds as the secondary polyethylene, polyvinyl chloride, fine rubber powder it is possible to obtain compositions with softening point in 65-75 ^{0}C, which is 15-20 ^{0}C higher than the softening point of bitumen.

Nanostructures, morphology and properties of Poly[N-(2-cyanoethyl)pyrrole]

Georgina Fabregat[1,2], *Elaine Armelin*[1,2] *and Carlos Alemán*[1,2]

[1]Departament d'Enginyeria Química, ETSEIB, Universitat Politècnica de Catalunya, Av. Diagonal 647, 08028, Barcelona, Spain.

[2]Centre for Research in Nano-Engineering, Universitat Politècnica de Catalunya, Campus Sud, Edifici C', C/Pasqual i Vila s/n, Barcelona E-08028, Spain

georgina.fabregat@estudiant.upc.edu, elaine.armelin@upc.edu and carlos.aleman@upc.edu

Introduction. In this study we compare the morphology and structure of poly[*N*-(2-cyanoethyl)pyrrole], abbreviated PNCPy, obtained by anodic and oxidative chemical polymerization of *N*-(2-cyanoethyl)pyrrole. In addition, the ability of PNCPy prepared by oxidative polymerization to generate hollow microspheres has been evaluated using the Layer-by-Layer (LbL) self-assembly method.[1] The construction of nanostructures is aimed to use the electrochemical properties of this material for the construction of drug delivery systems. On the other hand, films generated by chronoamperometry (CA) have been used for the detection of dopamine, a neurotransmitter involved in neurological disorders (*i.e.* Parkinson's disease is provoked by a deficiency of dopamine).

Materials and Methods. In all cases chemical polymerization processes were carried out in aqueous ethanol solution using an oxidant/monomer molar ratio of 4:1, the oxidant agent being ferric chloride. The reactants were stirred for 24h at 70 ºC. The fine brown powder obtained was purified washing with ethanol and water solutions. Sulfonated polystyrene microspheres were used as a template in the LbL self-assembly synthesis of PNCPy. Electrochemical polymerizations were carried out by CA using a constant potential of 1.40 V, a polymerization time of 3 s, and an acetonitrile solution with $LiClO_4$ as supporting electrolyte. Electropolymerizations were performed in a three-electrode cell with a working electrode of glassy carbon bare. Structural properties of chemically and electrochemically PNCPy synthesized were studied by Attenuated Total Reflection (ATR) and Specular Reflection (GATR) FTIR spectroscopy. The samples were also examined by ultraviolet-visible reflectance spectroscopy (UV-Vis). Morphological studies were performed using focuses ion beam/scanning electron microscopy (FIB/SEM) and transmission electron microscopy (TEM). The detection of dopamine was investigated by cyclic voltammetry (CV) in the potential range from -0.4 to 0.8 V, in phosphate buffer (pH=7.4), and using glassy carbon bare as working electrode.

Results and Discussion. FTIR studies evidence the loss of the cyano group band (2233 cm^{-1}) in the samples prepared by chemical polymerization. Thus, the cyano group converts into a primary amine, as is schematically represented in Fig. 1A) and 1B), which is expected to be very useful for the detection of biomolecules. In contrast, FTIR spectrum of PNCPy obtained by electrochemical synthesis retains the cyano group.

SEM micrographs of PNCPy showed a globular morphology in all cases, independently of the synthesis procedure. These observations are fully consistent with early studies on polypyrrole and poly(N-methylpyrrole), which described similar morphologies.[2] This globular growth was particularly apparent for powder PNCPy arising from chemical polymerization (*i.e.* in absence of PSS template), in which microspheres of uniform size distribution (2.1µm) and high roughness resulting from subunits aggregation (51nm) were surprisingly identified.

On the other hand, the production of hollow spheres under the experimental conditions described above was not satisfactory. The average layer thickness of some hollow PNCPy microspheres was below 50nm, even though an irregular and not uniform thickness distribution was observed.

The thickness of the PNCPy films generated by CA using a polymerization time of 3 s was around 78 nm. CV assays indicated that these films were useful to detect very small concentrations of dopamine in solution.

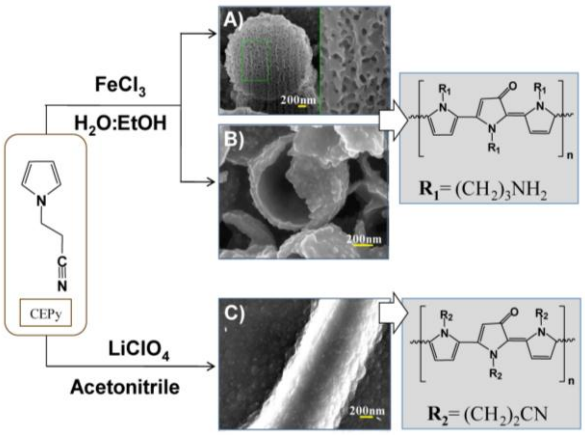

Figure 1. Scheme showing SEM images and chemical structures of: microspheres from oxidative chemical polymerization (A) and (B); and films obtained by electrochemical polymerization (C).

Conclusions. Results suggest that oxidative polymerization provides a simple and fast method to obtain microspheres, the use of PSS templates being not required. The electrochemical properties of the produced materials are currently under study. PNCPy generated by CA is a very useful material for the detection of small concentrations of dopamine.

References. [1] Wang, Y.; Angelatos, A.S., Caruso, F. *Chem. Mater*. 2008, *20*, 848. [2] Martí, M.; Fabregat, G.; Estrany, F.; Alemán, C.; Armelin, E. *J. Mat. Chem*. 2010, *20*, 10652.

Acknowledgements. Financial support for this work was provided by MICINN of Spain and FEDER with grant nº MAT2009-09138. G.Fabregat acknowledges FPI-UPC fellowship support. C.Alemán acknowledges "ICREA Academia" for excellence in research funded by the Generalitat de Catalunya.

Development of Effective Technologies of Heat and Frost Resistant Composite Materials for Sealing the Joints and Cracks of Asphalt Roads, Bridges and Airfields

Rahmonov B.Sh., Negmatov S.S., Sobirov B.B., Abdullaev A.X., Salimsakov Y.A., Soliev R.H. Mahkamov D.I., Bozorov A.N., Sobirov A.B.

Tashkent State Technology University, State unitary enterprises "Fan va Taraqqiyot", Tashkent, Uzbekistan

email: polycomft2005@rambler.ru

Durability and safety of the expansion joints of concrete pavement and the maintenance and elimination of cracking of asphalt concrete pavements is an important and urgent task. In solving this problem special emphasis on the use of sealing materials, which enhance effectiveness of joints with maintaining their durability, continuity during the annual cycle, and is not allowed to increase fracture over time.

In practice, this problem is solved by using different types of sealing materials. They can be prepared on the basis of rubber bitumen and gossypol resin which maintain flexibility at both extreme low and high temperatures. They are used to fill the joints of cement concrete pavement of the roads, for repair of chips, and selective termination of shells, as well as for crack repair of asphalt surfaces.

Technological process of obtaining of the bitumen compositions comprises the following steps: preparation of bulk ingredients (clearing of unwanted impurities, fine grinding, mechanical activation), preparation of bitumen, modification of gossypol resin and flow mixing the ingredients and feed for blending, mixing the ingredients for obtaining the bitumen compositions; unloading asphalt compositions on trays, cooled and transferred to a finished product warehouse.

The full technological process includes the following operations: preparation of bulk ingredients carried on the preparatory site. There committed to crushing ingredients such as waste tires, hydrolytic lignin, secondary polyethylene and polyvinyl chloride to a powder, basalt fibers, hydrated lime and wollastonite not only crushed, but mechanically activated as well.

Bitumen grade BN-90/10 comes as a roll, wrapped in a craft paper. First, it is freed from the paper and crushed to small sizes. Then weighed according to the formulary card and loaded into reactor equipped with an adjustable steam or electrically heated to maintain the temperature within 110-120 ºC.

Gossypol resin and modifying additives are loaded into another reactor with heating jacket to a temperature of 170-180 ºC, where gossypol resin is modified.

From the reactor melted to a flow able state modified bitumen BN-90/10 and gossypol resin flow into a third reactor through dispensers for mixing with other ingredients. In turn, the other ingredients are weighed according to the recipe and loaded into the same reactor.

Mixing of the components loaded into the third reactor lasts for 2.5 hours at a temperature of 180±10 ºC.

Then finished bitumen composition is unloaded onto 70 x 50 x 5 cm pallets and cooled to the room temperature on the shelves and sent to finished production storage.

Study of Composition and Technology of Highly Filled Composite Polymeric Materials for Asphalt Roads, Which Can Be Used in Hot Climates and Increasing Their Operation Life

Sobirov B.B., Rahmonov B.Sh, Negmatov S.S., Abdullaev A.X., Inoyatov K.M., Salimsakov Y.A., Mahkamov D.I., Soliev R.H.

Tashkent State Technology University, State unitary enterprises "Fan va Taraqqiyot", Tashkent, Uzbekistan

email: polycomft2005@rambler.ru

Our studies over the years have shown that the durability of composite polymer materials designed to cover the roads and sealing of joints and cracks in the first place depends on the heat resistance of the ingredients within the composition.

In these compositions, the least heat resistant ingredient is bitumen and gossypol resin, softening temperature and flow does not exceed 60-70 ^{0}C. In hot climates, as in Central Asia pavements are heated to 100-110 ^{0}C, which leads to a reduction in their longevity as a result of formation of corrugation on the road surface and cracks through which increases the penetration of rain water and intensifies the destruction of the all road bed.

To eliminate these deficiencies and improve the durability of highly filled composite polymeric materials designed to cover the roads we have carried out research into the modification of bitumen grade (bitumen) BN-90/10 BN-70/30 and secondary polyethylene. As a secondary polyethylene we used the used greenhouses' plastic film, domestic packages, bottles and waste polyethylene.

While obtaining a coating the composition temperature is brought up to 150-170 ^{0}C, and the sealing composition is obtained at 170-190 ^{0}C. If we consider that the softening temperature of low density polyethylene is in the range of 100-120 ^{0}C, and the melting temperature and flow at the level of 150-170 ^{0}C, can be expected in terms of production of paving and sealing materials the obtaining of a homogeneous molten mass, which will play the role of the combined polymer binder and determines the heat resistance and durability of the resulting compositions.

Given this assumption, we researched the effect of different amounts of recycled polyethylene on the softening point of bitumen and compositions based on them. In the current study found that the introduction of the bitumen 10-20% recycled polyethylene contributes to their softening temperature at 20-25 ^{0}C.

The composite materials for road paving and sealing of joints with bitumen containing 20% recycled polyethylene were obtained. They have been used in the construction of the road "Fargona Hulka Yuli".

Observations made during the years of the conditions of the roads, showed that on the road surface does not appear corrugation, and joints and cracks remain sealed for 3-3,5 years.

Thus, we conclude that the increase in longevity of highly filled composite polymeric materials designed to cover the roads can be achieved by increasing the softening point of bitumen by introducing to them 20-25% recycled polyethylene, which will lead to longer maintenance-free operation of roads by 2-2,5 times.

COMPATIBILITY STUDIES OF POLY(ETHER IMIDE) WITH LIQUID CRYSTAL MIXTURES

Fatih Çakar, Hale Ocak, Belkis Bilgin-Eran, Özlem Cankurtaran and Ferdane Karaman

Yildiz Technical University, Department of Chemistry, 34220, Istanbul-Esenler, Turkey

E-mail: fatih.cakar@gmail.com.

ABSTRACT

The liquid crystalline state of matter is a fascinating subject for both basic and technological reasons. Liquid crystalline compounds (LCs) have been developed into a very useful class of materials. They have found a variety of application such as display devices, optical and thermal sensors and stationary phases in chromatographic columns [1]. By introducing a chiral moiety into LC molecules, unusual physical properties can also be obtained [2]. In general, the mesomorphic properties of LCs are strongly affected by the type of molecular core, the structure of the chiral part as well as by the length and character of the non-chiral chain.

Mixing is very important in modern technologies for processing of materials composed of many different chemical components [3]. Polymer and liquid crystal mixtures are an important area of interest in science and engineering because of its many applications in industry. Miscibility can be detected by a number of techniques. Among these techniques, it is well known that determination of the viscometry of a dilute solution is a simple and quick method for determining the miscibility.

This study deals with the determination of the miscibility of poly (ether imide) (Ultem) and their mixtures with liquid crystalline compounds in dilute solutions. Mixtures of variable compositions from 0 to 100 wt% were prepared by solvent casting. Their miscibility was investigated by using viscometry.

REFERENCES

[1] H. Ocak, D. Sakar, F. Cakar, O. Cankurtaran, B. Bilgin Eran and F. Karaman, *Liquid Crystals*, 35, 1351, 2008.

[2] A. Bubnov, M. Kaspar, V. Novotna, V. Hamplova, M. Glogarova, N. Kapernaum and F. Giesselmann, *Liquid Crystals*, 35, 1329, 2008.

[3] R. Holyst, Solubility and mixing in fluids. *Encycl. Appl. Phys.*, 18, 573, 1997.

The research was supported by Scientific Research Projects Coordination Center of Yildiz Technical University (29-01-02-ODAP02)

Development of polyester coating using branched polymers and silanes.

J. Gamez-Perez[(1)], *M. Puig*[(1)], *J. J. Gracenea*[(2)], *A. Jiménez*[(3)], *J. Suay*[(1)]

(1) Polymers and Advanced Materials Research Group (PIMA), Universitat Jaume I (Castelló de la Plana)
(2) Medco, S.L. (Castelló de la Plana)
(3) Science Materials Department, Universidad Carlos III (Madrid)

jose.gamez@esid.uji.es

Introduction

Organic powder coatings are considered the best alternative for the reduction of volatile organic contents (VOCs) in the anticorrosive-coatings industry because they present VOC emissions lower than 4% [1] and [2], while solvent-based paints present more than 60% of VOCs. Despite this big advantage, organic powder coatings present some limitations like the difficulty to be applied on thermo-sensible substrates as wood, plastic or structural aluminum alloys (e.g. aeronautic industry) due to the high temperatures used on their curing. For this reason there is an interest on creating organic powder coating systems with low curing temperature and time together with good anticorrosive properties.
In many industrial applications such as industrial coatings, thermal and mechanical properties of the thermoset systems determine the quality of the final product. Moreover, in thermosetting coatings, curing at lower temperatures and/or shorter times and the strong adhesion to the metallic substrates are the main objectives to obtain good products to be used in the industry with energy saving. It has been reported that volume shrinkage during curing leads to poor adhesion to the substrate, warping, delamination, and the apparition of microvoids and microcraks, which reduce the durability of the paint [3]; thus, coatings obtained without shrinkage can be expected to have enhanced mechanical properties and longer service lives. Nevertheless, the main difficulty on developing new coatings is to combine fast curing with no shrinkage and maintaining their good mechanical properties.

Materials and Methods

In this study, we produced new polyester coatings using branched polymers and silanes to promote adherence to galvanized steel substrate. In order to have an overall idea of the influence of the silanes on the adhesion of the system, adhesion tests were carried out, in accordance to ISO 4587 (figure 1).

Results and Discussion

These coatings can show big advantages because of their mechanical properties combined with a very fast curing (thus improving the quality of the film and reducing curing costs). In addition, to prove the quality of the new systems, we compare the results to those obtained with a conventional polyester formulation. The study is completed showing the application of a new accelerated electrochemical cyclic test applied to obtain the anticorrosive properties of the coatings formulated, as schematized in fig. 2.

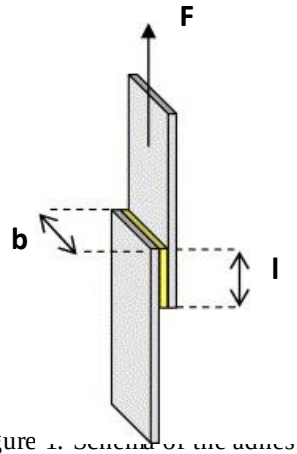

Figure 1. Scheme of the adhesion test

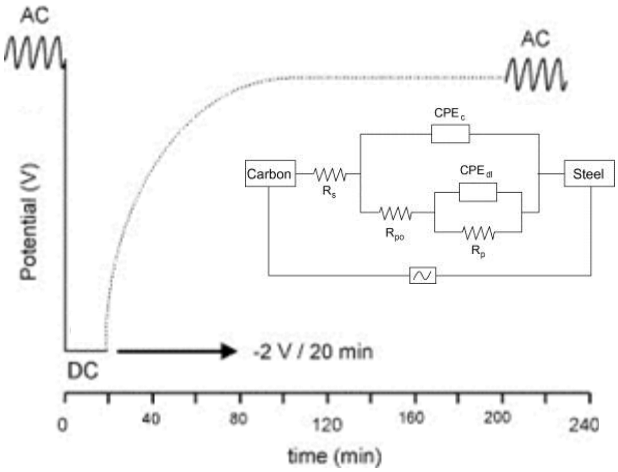

Fig. 2.AC/DC/AC test: schematic figure of Potential (V) vs. time and equivalent circuit used to model the electrochemical cyclic test [3].

References

[1] R.A. Dickie, D.R. Bauer, S.M. Ward and D.A. Wagner, *Prog. Org. Coat.* **31** (1997), p. 209.
[2] S.S. Lee, H.Z.Y. Han, J.G. Hilborn and J.-A.E. Manson, *Prog. Org. Coat.* **36** (1999), p. 79.
[3] J. Suay et al *Progress in Organic Coatings* 66 (3), pp. 306-313

Acknowledgements

The research work is taking place thanks to the public support provided by the Spanish Ministry of Science and Innovation (IPT-010000-2010-004).

Synthesis, Structure and Properties of Poly(urethane-urea-siloxane)s

Vesna Antić[1)], *Milica Balaban*[2)], *Marija Pergal*[3)], *Iolanda Francolini*[4)] *and Andrea Martinelli*[4)]

[1)]University of Belgrade, Faculty of Agriculture, Serbia; [2)]University of Banja Luka, Faculty of Science, Bosnia and Herzegovina; [3)]University of Belgrade, Institute of Chemistry, Technology and Metallurgy, Serbia; [4)]University of Rome "Sapienza", Dept. of Chemistry, Italy

e-mail: vantic@agrif.bg.ac.rs

Introduction: Poly(urethane-urea) copolymers (PUUs) represent an important subclass of segmented polyurethanes (PUs) in which diamines are used as the chain extenders instead of diols. Due to the stronger hydrogen bonding in the hard domains, the PUUs possess improved mechanical properties compared to conventional thermoplastic PUs. The soft phase (flexible and non-polar) is mainly made up of polyether, polyester or polysiloxane segments, while the hard phase is highly polar urethane and/or urea segments based on different isocyanates and chain-extenders [1]. Siloxane-based segmented PUs and PUUs have attracted much attention because of their properties such as water repellence, heat resistance, anti-adhesion (low surface free energy) as well as biological inertness. Poly(urethane-urea-siloxane)s (PUUSs), which are the subject of this work, have already found commercial applications as elastomers, solvent-based adhesives for automotive industry and biological implants, because of their elasticity, high mechanical stability and biocompatibility [2]. The present work is focused on the synthesis and characterization of PUUS copolymers based on hydroxypropyl terminated polydimethyl-siloxane (PDMS) as the soft segment and 4,4'-methylene diphenyl diisocyanate/ethylene diamine (MDI/ED) as the hard segment. A series of PUUSs with different hard segment content (from 43 to 61 wt.%) was prepared. The effect of the structure and composition of the copolymers on their thermal and morphological properties was investigated.

Materials and Methods: The PUUS copolymers were prepared by two-step polyadition method in the solution. The isocyanate-terminated prepolymer prepared from α,ω-dihidroxypropyl-PDMS (M_n=1000 gmol^{-1}) and MDI in the first reaction step, was further chain-extended by addition of ethylene diamine. The required amount of MDI was also added in the second step and reaction was continued for 3 h. The syntheses were carried out at 40°C with stannous octanoate as a catalyst (0.05 mol% based on PDMS). The concentration of the monomers was 25 wt.% in the mixture of tetrahydrofuran/N-methylpirrolidone (1/9). ^{1}H and ^{13}C NMR spectra were recorded on Varian Gemini-200 spectrometer at 25°C using DMSO-d_6 as solvent. The intrinsic viscosities, [η], were measured at 25°C in NMP. The copolymers were characterized by GPC in NMP as the mobile phase. Thermal analyses (DSC and TGA) were performed under nitrogen atmosphere, with a heating rate of 10 °Cmin^{-1}, over a temperature range of -150 to 200°C (DSC) and 25 to 600°C (TGA). Copolymers were also characterized by AFM measurements.

Results and Discussion: The general structure of the synthesized PUUSs was confirmed by NMR analysis. The ^{1}H spectra of copolymers showed characteristic signals of the NH urea and NH urethane protons. In the ^{13}C NMR spectra, a resonance signals at 153.8 and 155.7 ppm was observed, which indicates the presence of the carbonyl carbons from urethane and urea bonds, respectively. The lengths of the hard segments (L_n) were calculated from quantitative ^{13}C NMR spectroscopy [3] and were in range from 1.94 to 4.73. The samples with higher content of the hard segments generally showed higher [η] values and higher molecular weights (Table 1). The T_g of the soft segments was observed at -108°C, indicating that the PDMS was microphase separated from the hard segment. A broad endothermic peak, observed about 70 °C, can be related to disruption of short-range ordering of the hard segments or to their T_g. High temperature transitions were not detected, because the thermal degradation of the urea and urethane bonds occurs around 200°C, before melting of the copolymers (Table 1). Contact mode AFM images of the surface topology were used to characterize the PUUSs. The distribution of hard and soft phases on the polymer surface was analyzed by 3D- and 2D- mode contact error. The three-dimensional large-scale resolution images clearly showed spherulitic structure. It was also shown that the roughness coefficient varied with the content of the hard segments.

Table 1. Composition, [η], molecular weights (M_n) and thermal stability of the PUUSs

Sample	HS, wt.% (NMR)	L_n (HS)	[η], dL/g	M_n, g/mol	$T_{10\%}$, °C
PUUS1	43	1.94	0.29	19540	211
PUUS2	47	3.11	0.25	15600	262
PUUS3	59	4.35	0.33	23000	239
PUUS4	61	4.73	0.51	37200	249

Conclusions: A series of four samples of segmented PUUSs, with different hard to soft segment ratio, was prepared and characterized. The structure and composition of the PUUSs was confirmed by NMR spectroscopy. DSC analysis and AFM measurements revealed that the copolymers show a high degree of phase separation between hard and soft segments. TG analysis in nitrogen showed that PUUS copolymers were stable up to 200°C.

References:

1. J. T. Garrett, J. Runt, *Macromolecules* **33** (2000) 6353.
2. I. Yilgör, J. McGrath, *Adv. Polym. Sci.* **86** (1988) 1.
3. N. Luo, D. N. Wang, S. K. Ying, *J. Polym. Sci. Pol. Chem.* **34** (1996) 2157.

Physical aging of melt-blown PLA fibres

Jaroslaw Janicki, Monika Rom, Janusz Fabia

University of Bielsko-Biala, Institute of Textile Engineering and Polymer Materials, Poland

jjanicki@ath.bielsko.pl

Introduction

Due to new and more efficient methods of polylactide (PLA) synthesis its bulk production is possible so that the application of PLA to production of conventional materials is more probable and feasible, even though in the past it was restricted to mostly to specialty products such as medical.

PLA is the thermoplastic polyester and can be melt processed at the temperature range comparable with polypropylene's, however it requires careful drying prior to processing in order to avoid degradation during process [1].

Formation of PLA fibres can be carried out either by dry or melt spinning processes. Manufacturing of ultra-fine fibres, which are beneficial for specific applications such as filtration, is possible by electrospinning but also by melt-blown technology, which allows to obtain much better efficiency of the process[2].

Materials and Methods

Commercial grade crystalline NatureWorks®PLA 3051D was processed using lab-scale melt-blown equipment at CENARO Institute (Lodz, Poland). The equipment enables to adjust several parameters including temperatures at different sections, air pressure (velocity) used to attenuate the filaments and the distance between extruder die and collector and others. Polymer before processing was dried to the water content of 250ppm. Crystallinity of melt-blown PLA was analyzed by WAXS using URD-6 Seifert diffractometer. Observations of morphology were done by SEM (Jeol JSM 5500LV), and thermal analysis by DSC (TA Instruments 5100).

Results and Discussion

Classically PLA filament is formed in a two-stage melt spinning process, in which hot drawing enables for fiber orientation, and crystallinity is achieved as the result of stress-induced crystallization. In case of melt-blown technology drawing is realized by high velocity air which is used to attenuate filaments and there is no possibility of subsequent drawing step leading to crystallization and orientation, so that as-spun PLA melt-blown fibres are amorphous (Fig.1), however the cold crystallization process occurs as the effect of fibres' annealing at temperatures above T_g. Changes in supermolecular structure occurs also at temperatures below T_g as observed from DSC and WAXD of samples analyzed after one year of storage at room temperatures, and samples annealed at the temperature below T_g. Such changes are explained by physical ageing [3,4].

The process of fibres skin and core solidification is radial and uneven and the effects of uneven solidification resulting in shrinkage of outer layer are observed on fibres' surfaces (Fig.2.).

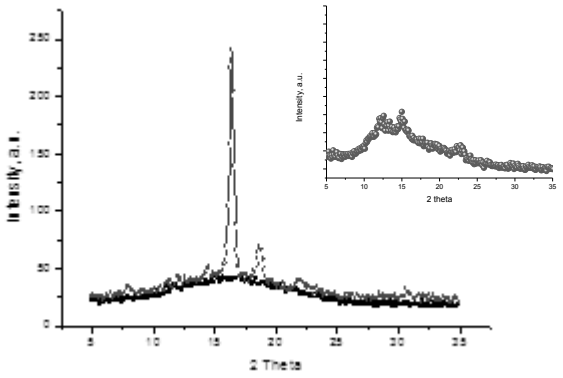

Fig.1. X-Ray scattering patterns of virgin polymer (gray), as-spun fibres (black) and fibres after one year storage (right top corner).

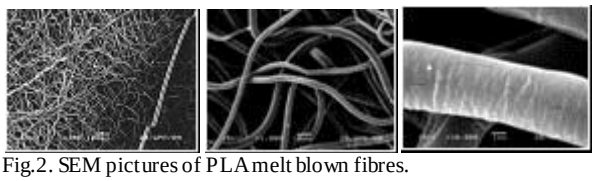

Fig.2. SEM pictures of PLA melt blown fibres.

Conclusions

Melt-blown technology enable to obtain ultra-fine fibrous structures which are of special importance in case of for example filtering materials. When planning production of such materials one need to consider the physical ageing effect, which is resulting with crystallization of materials' structure that may affect properties of final product during storage.

References

[1] L.-T. Lim, R. Auras, M. Rubino ; Prog. Polym. Sci. 33, 8, 2008, 820-852

[2] Patent No WO 2009152349 (A1)

[3] J.N.Hay, Pure&Appl. Chem., 67, 11, 1995, 1855-1858

[4] R. Acioli-Moura, X.S. Sun ; Polymer Eng. Sci. 48, 2008, 4, 829–836

Acknowledgments

Studies were carried on in the framework of project financed by Polish Ministry of Science and Higher education contract No PBZ-MNiSW-01/II/2007.

Recovery of Copper with Sulfonated Microcapsules Containing DEHPA

A. Alcázar, A.M. Borreguero, M. Carmona, A. de Lucas and J.F. Rodríguez

Institute of Chemical and Environmental Technology (ITQUIMA), Department of Chemical Engineering, University of Castilla-La Mancha, Avda. Camilo José Cela s/n 13004 Ciudad Real, Spain

Angela.Alcazar@uclm.es

A wide variety of aqueous waste solutions and the natural formation of acidic mine drainage are the most serious difficulties encountered in mining and metallurgy activities and this is a serious environmental problem. Furthermore, these solutions can also constitute a potential source of many valuable and scarce metals.

Solvent extraction and ion exchange technologies have been widely used for the recovery or removal of heavy metals from aqueous phases. However, different problems have been encountered on applying these techniques. Although the extractants are highly selective, this technique requires a high level of mechanical agitation to improve the kinetics of the process, a requirement that promotes leakage of the extractant from the aqueous/organic interface to the aqueous phase during the separation of the two phases (1, 2). On the other hand, ion exchangers can be easily regenerated but gel form resins have low selectivity and those with a high selectivity (chelating resins) have low diffusion coefficients, a characteristic that leads to low mass transfer rates (3, 4). An interesting alternative to overcome these limitations is the microencapsulation of extractants within a functionalizated polymeric shell. This new type of material would be expected to combine the advantages of the aforementioned methods and improve selective removal of heavy metals from an aqueous phase.

The material is formed by a shell of sulfonated poly(styrene-co-divinylbenzene) (P(St-DVB)) and di(2-ethylhexyl)phosphoric acid (DEHPA) as core. The microencapsulation was accomplished by suspension like polymerization technique at 80 ºC. The shell sulfonation was carried out using sulfuric acid at 50 ºC.

According to the TG analysis, a 34.86 % of DEHPA was encapsulated and this microcapsules exhibit a spherical shape with an average particle size in number of 340 µm, close to those reported in literature for commercial resins (5).

Kinetic and equilibrium studies were carried out in order to determine the behaviour of this new material and check the effect of the shell sulfonation in the ion exchange process. Experiments were generated for the H^+/Cu^{+2} system at 25 ºC using different synthesized materials: sulfonated particles without DEHPA (SND), sulfonated microcapsules (SD), non-sulfonated microcapsules (DNS); and Amberlite IR-120 as commercial resin reference material.

Equilibrium data were fitted to the Langmuir isotherm as a first approximation. As can be seen from Fig.1., SD microcapsules show a capacity of 1.702 meq/g, which is almost 13 times higher than that of DNS (0.134 meq/g). This indicates that sulfonation increases the mobility of metal ions up to the extractant agent. In addition, the capacity of the SD is also higher than that of SND (0.938 meq/g), which shows that the presence of DEHPA enhances the metal removal from the aqueous phase. Despite of that fact, SD capacity is still lower than that for the commercial resin (4.444 meq/g). Therefore the content of encapsulated DEHPA should be increased in order to obtain a competitive product for its industrial application.

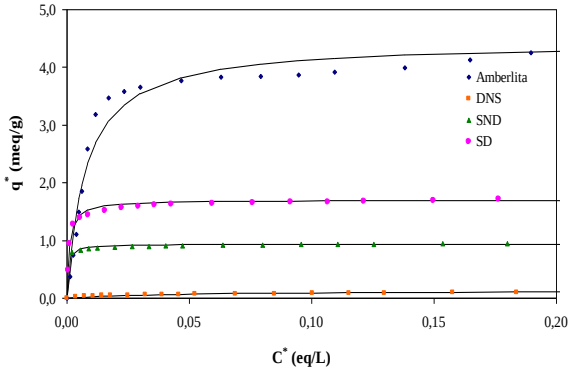

Fig.1. Equilibrium isotherms for the studied materials

Finally, kinetic studies allowed to determine the interdiffusion coefficients of copper for these materials by means of an homogeneous model, which assumes that a quasi-homogeneous phase exists inside the solid particles. Experimental data were perfectly fitted to this model and gave the following intediffusion coefficients: $2.90 \cdot 10^{-8}$, $1.86 \cdot 10^{-7}$, $2.50 \cdot 10^{-7}$ and $8 \cdot 10^{-7}$ cm^2/s for DNS, SD, Amberlite IR-120 and SND, respectively. These values indicate that sulfonated microcapsules have kinectics of the same order of commercial resins and much higher than that of non-sulfonated materials.

These results indicate that this material would be a suitable alternative for the extraction and separation of heavy metal ions from aqueous solutions since kinetic studies show that this kind of microcapsules could be used to remove copper from aqueous solutions, due to their high selectivity and the high rate of the separation process.

References:

(1) S. Nishihama, N. Sakaguchi, T. Hirai, I. Komasawa, Hydrometallurgy 64 (2002) 35–42.
(2) W.W. Yang, G.S. Luo, X.C. Gong. Separation and Purification Technology 43 (2005) 175–182.
(3) C.A. Sauer, Desalination 51 (1984) 313–324.
(4) K. Frederick, Ultrapure Water (1996) 53–56.
(5) H.W. Kauczor and A. Meyer, Hydrometallurgy 3 (1978) 65-73.

A comparison of the morphology and thermoresponsive switching behavior in thin films of cyclic and linear poly(N-isopropylacrylamide)

David Magerl[1], *Xing-Ping Qiu*[2], *Françoise Winnik*[2], *Monika Rawolle*[1], *Gerd Herzog*[3], *Stephan V. Roth*[3], *Peter Müller-Buschbaum*[1]

[1] Physik-Department, Lehrstuhl für Funktionelle Materialien, Technische Universität München, D-85747 Garching, Germany
[2] Université de Montréal, Faculty of Pharmacy and Department of Chemistry, CP 6128 Succursale Centre Ville Montréal QC H3C 3J7, Canada
[3] HASYLAB at DESY, D-22603 Hamburg, Germany

david.magerl@ph.tum.de

Introduction

Stimuli-responsive hydrogels are cross-linked networks built-up at the presence of water that expand or contract by the change of external stimuli. These so called intelligent hydrogels are of increasing interest because of their use in a variety of applications such as drug-delivery and sensors. One of the most studied polymers in this context is poly(N-isopropylacrylamide) (PNIPAM) with a lower critical solution temperature (LCST) around 32 °C in pure water. Below the LCST the PNIPAM chains are hydrophilic and dissolve well in water. Above the LCST the PNIPAM repels the stored water, forms globules and precipitates from water.

Most studies of PNIPAM only take a close look to the behavior in aqueous solutions, but thin film geometries are of special interest especially with regard to sensor application. Thin films of PNIPAM swell significantly by absorption of water molecules when exposed to water vapor [1]. When heated above the LCST a deswelling of the films is observed which is even apparent for model sensors with a metal top-layer [2].

There are only few studies of cyclic PNIPAM, although this topology is of great interest because of the absence of end-groups. End-groups have a significant impact on the LCST, as reported in comparative studies of cyclic and linear PNIPAM [3,4].

Materials, Methods and Results

In this study, we compare the properties of thin films of cyclic and linear PNIPAM with comparable molecular weights and a low polydispersity. Spin coating was used to create thin and homogenous film on silicon substrates that were pre-cleaned using a basic cleaning procedure to achieve a hydrophilic surface. For both polymers we prepared films of different thicknesses from chloroform solution and characterized them with optical microscopy and X-ray reflectivity.

For the investigation of the swelling behavior a small probe cell is used to create saturated water vapor and the film thickness is measured with white light interferometry. The time-dependent swelling when exposed to water vapor is investigated for both systems, the cyclic and the linear PNIPAM thin film, as well as the thickness changes upon heating of the samples above the LCST. The heating was done in steps with a waiting time at each temperature long enough to ensure equilibration of the thin PNIPAM films with the surrounding water vapor.

Interface correlation of the surface of the cyclic PNIPAM thin film with the roughness of the substrate is examined using grazing incidence small angle X-ray scattering (GISAXS). With this non-destructive method we are capable of investigating the correlated roughness not only on a limited spot on the sample surface but averaged statistically over the whole illuminated area [5]. Selected 2d GISAXS images are shown in **figure 1**.

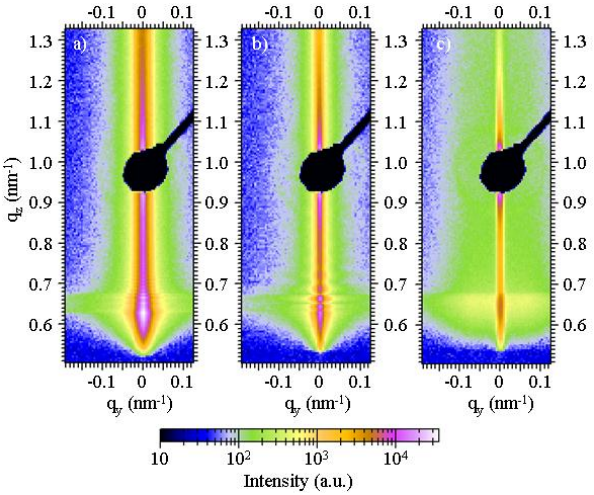

Figure 1. 2D GISAXS images of dry, cyclic PNIPAM films with different film thickness (decreasing from a) to c)). The specular beam is shielded with a beamstop to protect the detector.

Conclusion

By comparison of cyclic and linear PNIPAM thin films we get more detailed information of the influence of end-groups on the LCST as well as the thin film morphology.

References

[1] W. Wang, E. Metwalli, J. Perlich, C. M. Papadakis, R. Cubitt, P. Müller-Buschbaum, *Macromolecules* **2009**, *42*, 9041

[2] W. Wang, G. Kaune, J. Perlich, C. M. Papadakis, A. M. Bivigou Koumba, A. Laschewsky, K. Schlage, R. Röhlsberger, S. V. Roth, R. Cubitt, P. Müller-Buschbaum, *Macromolecules* **2010**, *43*, 2444

[3] X.-P. Qiu, F. Tanaka, F. M. Winnik, *Macromolecules* **2007**, *40*, 7069

[4] Y. Satokawa, T. Shikata, F. Tanaka, X.-P. Qiu, F. M. Winnik, *Macromolecules* **2009**, *42*, 1400

[5] P. Müller-Buschbaum, J. S. Gutmann, C. Lorenz, T. Schmitt, M. Stamm, *Macromolecules* **1998**, 31, 9265

Incorporating Nanostructured Polypyrrole Counter Electrodes into Dye-Sensitized Solar Cells

Sang Soo Jeon,[1] *Chulwoo Kim*,[2] *Jaejung Ko*,[2] *Seung Soon Im*[*1]

[1]Department of Fiber and Polymer Engineering, Hanyang University, Seoul 133-791, South Korea. [2]Department of Advanced Material Chemistry, Korea University, Jochiwon, Chungnam 339-700, South Korea.

Pillip76@empal.com

Introduction

Since the dye-sensitized solar cell (DSSC) was introduced in 1991,[1] it has shown great promise as low-cost, highly efficient power generator for green and renewable energy sources. In recent years, effort has been directed toward conducting polymers as potential counter electrodes (CEs) in DSSCs due to their advantages of high catalytic activity and low material cost.[2,3] Among the conducting polymers, polypyrrole (PPy) is of special interest due to its ease of synthesis, high conductivity, and low cost. Therefore, these advantages of PPy motivated us to explore its feasibility as an alternative material to Pt CEs. Here, we report on PPy nanoparticles coated on FTO glass as a highly efficient CE for DSSC applications.

Materials and Methods

Myristyl trimethyl ammonium bromide and decyl alcohol were dissolved in distilled water. Then, pyrrole monomer was added to the solution. $FeCl_3$ solution was added to the above solution. After polymerization, PPy nanoparticles were re-dispersed in methanol. The resulting PPy dispersions were then dropcast onto an FTO glass. To improve the conductivity of the PPy layers, the PPy/FTO CEs were treated with HCl vapor.

A transparent nanocrystalline layer was prepared on the FTO glass using TiO_2 paste. The TiO_2 electrodes were heated gradually up to 500°C. A paste containing 400-nm anatase TiO_2 particles was deposited using doctor blade printing. The TiO_2 electrodes were heated gradually up to 500°C. Then, the electrodes were immersed in N719 dye solution for 12 hr. The dye-adsorbed TiO_2 electrodes and various PPy CEs were assembled in a sealed sandwich-type cell. Then, the electrolytes were introduced into the cell.

Results and Discussion

The methanol-based PPy dispersions of 5.0 wt% were dropcast onto FTO glass. Fig. 1 shows SEM images of the surface and cross-section of the PPy layer on FTO. The surface of the PPy layer is a nanoporous structure of PPy particles. The porous structure increases the specific surface area, which might facilitate the electrocatalytic activity of the I_3^-/I^- redox reaction in the electrolyte solution. The thickness of the PPy layers coated using 5.0 wt% PPy dispersions was ~10 μm.

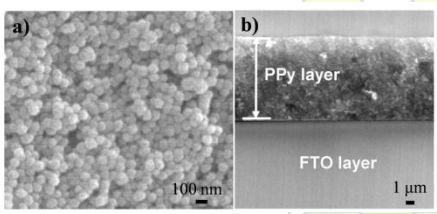

Fig. 1 SEM images of the (a) surface and (b) cross-section CEs coated with 5 wt% PPy on FTO glass.

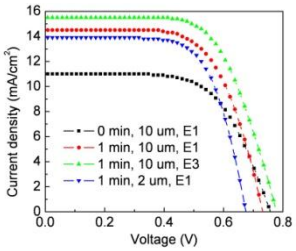

Fig. 2 *J-V* curves of the DSSCs using various PPy/FTO CEs.

The current density-voltage (*J-V*) curves for DSSCs based on various CEs and electrolyte compositions are presented in Fig. 2. When the HCl treatment time for 10-μm PPy-layered CE using electrolyte E1 was increased from 0 to 1 min, J_{sc} increased from 11.0 to 14.5 $mAcm^{-2}$, whereas V_{oc} and *ff* remained essentially constant, so that η = 6.83%. The enhanced photovoltaic performance might be due to the greater catalytic activity and lower surface resistivity of the PPy layer with HCl vapor treatment compared with as-prepared PPy CE. Increasing the HCl treatment time to 10 min reduced η to 5.39%. In addition, when the PPy layer thickness changed from 10 to 2 μm with a fixed HCl treatment time of 1 min and the same electrolyte (E1), V_{oc} and J_{sc} dropped to 675 mV and 13.8 $mAcm^{-2}$, respectively, whereas *ff* remained constant, affording a slightly lower η of 6.35%. When we changed the electrolyte composition from E1 to E4 with a fixed HCl treatment time (1 min) and a PPy layer thickness of 10 μm, the optimized cell gave J_{sc} = 15.5 mA cm^{-2}, V_{oc} = 778 mV, and *ff* = 0.64, corresponding to η = 7.73% using the E3 electrolyte composition.

Conclusions

PPy nanoparticles (~85 nm) were synthesized within micelles. PPy-layered FTO glass as the CE for DSSCs was fabricated by dropcasting a PPy-dispersed colloidal solution. By controlling the thickness and HCl vapor treatment time of the PPy layer on the FTO substrate and adjusting the electrolyte composition, the power conversion efficiency of the DSSC reached a maximum of ~7.73%. Although we obtained a reasonable DSSC performance compared with PEDOT or Pt electrodes, in principle, it is possible to improve the performance of the PPy-based CEs using the same simple approach if the particle size is controlled and the electrical conductivity is increased.

References

1 B. O'Regan and M. Grätzel, *Nature*, 1991, **353**, 737.
2 S. Ahmad, J. H. Yum, Z. Xianxi, M. Grätzel, H. J. Butt and M. K. Nazeeruddin, *J. Mater. Chem.*, 2010, **20**, 1654.
3 J. M. Pringle, V. Armel and D. R. MacFalane, *Chem. Commun.*, 2010, **46**, 5367.

The preparation of nanofiber composites of Poly(butylene succinate)/TS-1 zeolite for drug delivery system

SungYeon Hwang,[1] *EuiSang Yoo*,[2] *SeungSoon Im*[*1]

[1]Department of Fiber and Polymer Engineering, Hanyang University, Seoul 133-791, Republic of Korea. [2]KITECH Textile Ecology Laboratory, 1271-18 Sa 1 Dong, Sangrokgu, Ansan City, Gyungido, Republic of Korea.

Crerw75@hanyang.ac.kr

Introduction

There have been considerable interested in the development of nanofiber composites of biodegradable polymer as effective drug delivery vehicles over the past decade.[1-2] Among various biodegradable polymer, poly(butylene succinate) (PBS) is very promising materials to applied for biomaterials fields. However, nanofiber composites for PBS have not yet energetically studied due to the difficult processing control of PBS nanofiber. In this study, nanofiber composites of PBS/TS-1 zeolite were prepared. TS-1 zeolite is a inorganic ion exchanger with high ion exchange capabilities, resuting in cationic ions that can be easy to process the fine-nanofiber composites. We expected that the unique characteristics of TS-1 zeolite such as adsorption/desorption of polar molecules in pore would be lead to control the released drugs as well as enhanced biodegradability.[3]

Materials and Methods

PBS resins were supported by S-Enpol company. The TS-1 zeolite was kindly provided by the Korea Institue of Ceramic Eng. & Tech (KICET). The amount of Ti(IV) incorporated in the used TS-1 zeolite framework is consistent with a Si:Ti ratio of 62 based on X-ray fluorescence spectrometry. 2,2,2-Trifluoroethanol (TFE) solution (99.8%) was purchase from ACROS. Reagents were used without further purification.

The solutions were stirred at room temperature with magnetic bar for 24 hours to obtain the regular solutions. To investigate the effect of solution concentration on morphological appearance of the as-spun PBS fibers, PBS was dissolved in TFE solutions of varied concentration ranged from 5 to 20 wt% solution. As a result, we confirmed that 15 wt% concentration of PBS solution is suitable for electrospinning. The spinning solutions of PBS/TS-1 zeolite composites were prepared by mixing 15 wt% PBS in TFE solvents with various TS-1 zeolite contents. Table 1 shows the Electrospinning processing condition. The mixed solutions were poured into 10ml plastic syringe equipped with a nozzle (24gauge). An electrode connected with a high voltage supply capable of generating positive DC voltages (15 kV) was fixed to the syringe. An aluminum foil and the cylinder drum were used as collectors. The collected nanofibers were placed in vacuum oven overnight at room temperature to fully eliminate solvent residuals.

Table 1. Electrospinning condition

Processing conditions	Value
Voltage	15 kV
Tip to collector distance	15 cm
Needle gauge	24 gauge
Flow rates	1ml/h
Types of collector	Al foil on cylinder drum

Results and Discussion

Fig 1. Shows the N_2 adsorption-desorption isotherm (Fig 1(a)) and electron microscopic investigation of TS-1 zeolite (Fig 1(b) and (c)). TS-1 zeolite has a Brunauer-Emmett-Teller (BET) surface area of $334 m^2 g^{-1}$ and pore volume of 0.53mL/g. Fig 1 (b) shows SEM images of TS-1 zeolite particles. The particle size is in the range of 80-100 nm with uniformly globular morphologies. .

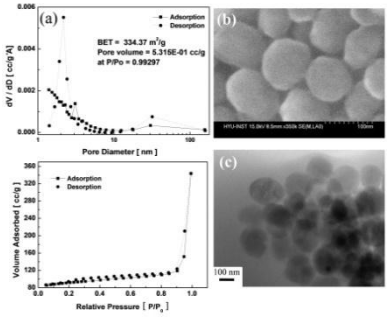

Fig. 1 The pore size distribution curves and N2 adsorption/desorption isotherms of TS-1 zeolite (b) SEM images of TS-1 zeolite at high magnification (c) TEM images.

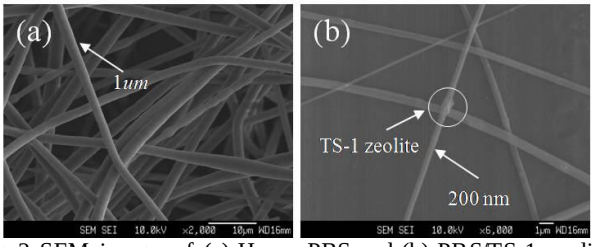

Fig. 2 SEM images of (a) Homo PBS and (b) PBS/TS-1 zeolite composites with 0.2 wt% zeolite contents.

Fig 2 shows SEM morphologies of PBS and PBS/TS-1 zeolite composites. In the case of PBS/TS-1 zeolite composites, the thickness of fiber was drastically decreased compared with Homo PBS. This result attributed that the electrostatic characteric of TS-1 zeolite lead to increase the flow rate of PBS molecular.

Conclusions

The nanofiber of PBS/TS-1 zeolite composites were prepared by electrospinning methods. TS-1 zeolite leads to decrease fiber diameter. The characteristic of molecular uptake for TS-1 zeolite can anticipate the control of released drugs.

References

1. Peresin MS, Habibi Y, Zoppe JO, Pawlak JJ, Rojas OJ *Biomacromolecules*, 2010, **11**, 674.
2. Asran AS, Razghandi K, Aggarwal N, Michler GH, Groth T *Biomacromolecules*, 2010, 11, 3413.
3. Hwang SY, Yoo ES, Im SS *Polymer*, 2011, Accepted.

Morphology Control of Poly(*p*-oxybenzoyl) Crystals using Direct Polymerization of *p*-Hydroxybenzoic Acid in the Presence of Boronic Anhydrides

Masahiro Kihara, Shin-ichiro Kohama, Shota Umezono, Kanji Wakabayashi, Shinichi Yamazaki, Kunio Kimura

Graduate School of Environmental Science, Okayama University

E-mail: polykim@cc.okayama-u.ac.jp

Introduction

Poly(*p*-oxybenzoyl) (POB) has received great attention as high performance materials [1] and morphology is of great importance to control the performance. It has been reported that aromatic polyamides could be prepared by the direct polymerization in the presence of 3,4,5-trifluorophenylboronic acid (TFB).[2] This study implies that TFB would work for the direct polymerization of *p*-hydroxybenzoic acid (HBA) to yield POB. This paper described the direct polymerization of HBA in the presence of various anhydrides of boronic acid such as TFB (TFBA), 4-methoxyphenylboronic acid (MPBA) and 4-biphenylboronic acid (BPBA) not only to develop a new procedure for the POB synthesis but also to control the morphology of the POB crystals.

Table Polymerization of HBA in the presence of boronic anhydride

Run no.	Polymerization condition [a]		Yield (%)	Mn (x10^3)	Morphology [b]
	Boronic anhydride	c_B (mol%)			
T-1	TFBA	1	0		
T-2	TFBA	5	21	4.7	needle
T-3	TFBA	10	25	3.8	needle
T-4	TFBA	50	28	4.4	SAS
T-5	TFBA	100	32	5.4	SAS
M-1	MPBA	1	0		
M-2	MPBA	5	13	3.5	slab
M-3	MPBA	10	15	1.9	FS
M-4	MPBA	50	30	5.8	needle
M-5	MPBA	100	19	6.9	SAS
B-1	BPBA	1	0		
B-2	BPBA	5	42	1.8	needle, slab
B-3	BPBA	10	33	2.9	FS
B-4	BPBA	50	44	14.4	FS
B-5	BPBA	100	48	14.7	fibril, SAS

[a] Polymerizations were carried out in DBT at a concentration of 1.0% at 300°C for 24 h. [b] SAS and FS stand for spherical aggregates of slab-like crystals and fibrillated slab-like crystals, respectively.

Experimental

HBA was purchased from TCI. Boronic acids purchased from Sigma-Aldrich were converted into anhydrides during recrystallization from toluene. An isomeric mixture of dibenzyltoluene (DBT) was obtained from Matsumura Oil (Barrel Therm 400) and distilled.

A polymerization of HBA in the presence of TFBA is described as an example. HBA (0.23g, 1.67 mmol) and 20 mL of DBT were placed into a cylindrical flask equipped with a mechanical stirrer and gas inlet and outlet tubes. Polymerization concentration was 1.0 %. The reaction mixture was heated under a slow stream of nitrogen up to 300°C with stirring. HBA was dissolved during heating. TFBA (0.26g, 0.56 mmol) was added into the solution at 300°C and stirring was stopped after TFBA was entirely dissolved. Concentration of boronic acid residue (c_B) was 100 mol%, defined as the molar ratio of boronic acid residue to the HBA, ([TFBA] x 3 / [HBA]) x 100. Temperature was maintained at 300°C for 24 h. The solution became turbid at an initial stage of the polymerization and then precipitates were formed with time. Precipitated POB crystals were collected by filtration at 300°C, and washed with *n*-hexane.

Results and Discussion

Table presents results of the polymerization. HBA was insoluble in DBT at 25°C but it became dissolved during heating. POB crystals were obtained as precipitates at c_Bs from 5 to 100 mol% with the yields from 21 to 32%. Some amounts of oligomers were left in the solution because of the solubility, and therefore the yield of the precipitated crystals was not so high. The POB crystals were formed as precipitates in the solution and the morphology was considerably influenced by not only the structure of the boronic anhydride but also the value of c_B. Needle-like crystals were firmed in the presence of TFBA at c_Bs of 5 and 10 mol% by the spiral growth of lamellae (Fig (a)). Spherical aggregates of slab-like crystals were formed at c_Bs from 50 to 100 mol% (Fig. (b)). The polymerization with MPBA and BPBA also yielded the needle-like crystals at c_Bs of 50 mol% and 5 mol%, respectively. The polymerization with TFBA at lower c_B was favorable to prepare the needle-like crystal. A WAXS intensity profile of the needle-like crystals showed that diffuse halo attributed to amorphous regions was hardly detected and the needle-like crystal possessed high crystallinity. From the morphological change of the crystals during polymerization, it was suggested that they were formed by the spiral growth of lamellae, resembling the POB whiskers prepared from *p*-acetoxybenzoic acid.[3] Molecular weight was also influenced by the structure of the boronic anhydride and c_B. Mn determined by the end-group analysis increased generally with c_B and BPBA gave the highest Mn of 14.7 x 10^3 at c_B of 100 mol%. The loose packing of the molecules in the crystal caused by the bulkiness of the end-groups made the polymerization more efficiently.

Conclusions

POB crystals were formed by the direct polymerization of *p*-hydroxybenzoic acid in the presence of boronic anhydrides. Morphology and molecular weight could be controlled by the chemical structure and the concentration of boronic anhydride.

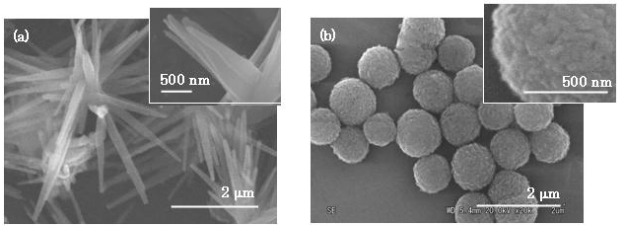

Fig. POB crystals prepared in (a) T-3 and (b) T-5.

References

[1] J. Economy, R. S. Storm, V. I. Matkovich, S. G. Cottis, B. E. Nowak, *J. Polym. Sci., Polym. Chem. Ed.* 14, 2207, 1976. [2] K. Ishihara, S. Ohara, H. Yamamoto, *Macromolecules*, 33, 3511, 2000. [3] K. Kimura, S. Kohama, S. Yamazaki, *Polym. J.* 38, 1005, 2006.

Selective Synthesis of Aromatic Copolyester Using Reaction-induced Crystallization under Shear Flow Influence of shearing on composition of copolyester

Toshimitsu Ichimori, Shinichi Yamazaki, Kunio Kimura

Graduate School of Environmental Science, Okayama University

E-mail: polykim@cc.okayama-u.ac.jp

Introduction

It had been previously reported that copolymers rich in a *p*-oxybenzoyl (*p*-OB) moiety were selectively synthesized from the copolymerization of *p*-acetoxybenzoic acid (*p*-ABA) and *m*-acetoxybenzoic acid (*m*-ABA) by using crystallization of oligomers during polymerization. [1,2] In the copolymerization of 4-(4-acetoxybenzoyloxy)benzoic acid (*p*-ABAD) which is the dimer of *p*-ABA and *m*-ABA, the selectivity became higher because *p*-OB homo-oligomers were more rapidly formed. [3] Furthermore, it was found that the selectivity became much higher by the application of shearing. [4]

In this study, the influence of the timing of shearing on the selectivity was examined in the polymerization of *p*-ABAD and *m*-ABA.

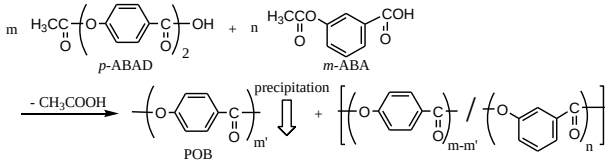

Scheme Copolymerization of *p*-ABAD and *m*-

Materials and Methods

p-ABAD, *m*-ABA and liquid paraffin (LPF) were purified according to the previous procedures[1,2,3]. LPF was placed into a cylindrical vessel equipped with a stir bar, mechanical stirrer and a gas inlet tube, and heated under a slow stream of nitrogen. *p*-ABAD and *m*-ABA were added into LPF at 330°C with varying the content of *p*-OB moiety (χ_f) in feed. The solution was stirred after a certain time with the share rate (γ) of 489s^{-1} and the polymerization was carried out at 330°C. The solution becomes turbid and then the polymers were precipitated. The precipitated polymers were collected by filtration at 330°C, and washed with *n*-hexane. The content of *p*-OB moiety in the precipitated polymers (χ_p) was determined by gas chromatograph after hydrolysis of polymers.

Results and Discussion

Results of the polymerization at χ_f of 40mol% were plotted in Fig. Although the yield of polymers became lower, the value of χ_p increased by shearing. The solution became turbid due to the precipitation of oligomers at 40min in this polymerization. Therefore, shearing was applied after 30 min (before turbid) and 70 min (after turbid). The value of χ_p of the polymers prepared without shearing was 82.5 mol% after 6 h. On the other hand, it prepared under shearing became much higher. The values of χ_p prepared under shearing before and after turbid were 93.4 mol% and 96.1 mol%, respectively. The mechanism of selective polymerization between *p*-ABAD and *m*-ABA is explainable as follows; *p*-OB homo-oligomers are more rapidly formed in the solution than co-oligomers due to the dimer effect and the difference in the reactivity. When the molecular weight of the *p*-OB homo-oligomers exceeds a critical value, they are precipitated *via* crystallization to form the crystals at the early stage in the polymerization. Co-oligomers are gradually formed, and they are also phase-separated. While co-oligomers containing a few *m*-oxybenzoyl (*m*-OB) moieties are precipitated *via* crystallization, they are excluded from the crystal by the segregation effect, and the *m*-OB moiety is not present in the crystals. At the middle stage of the polymerization, co-oligomers containing more *m*-OB moiety are formed in the solution, but they are unable to precipitate due to higher miscibility. Further polymerization proceeds between oligomers in the precipitated crystals, and the poly(*p*-oxybenzoyl) is selectively formed. When the shearing was applied before turbid, *m*-OB moieties were slightly incorporated because the reactivity was enhanced by shearing. Thus, co-oligomers containing a few *m*-OB moiety were gradually precipitated with time. In the case of shearing after turbid, the concentration of *m*-OB moiety in the solution became higher when shearing was applied, because the precipitation of *p*-OB homo-oligomers already started. While the reactivity of *m*-ABA was enhanced by the shearing, leading to the formation of co-oligomers containing more *m*-OB moiety, they could not be precipitated because the shearing increased the miscibility. As a result, shearing suppressed precipitating the oligomer rich in *m*-OB moiety and the selectivity was drastically enhanced.

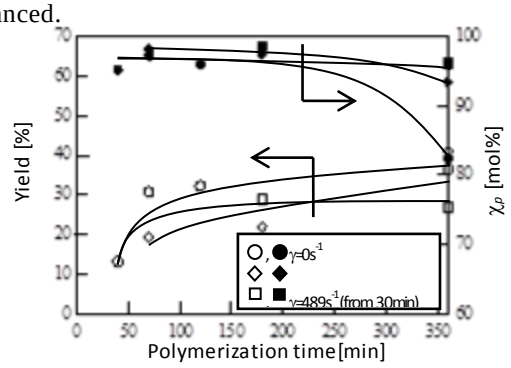

Fig. Time dependencies of yield and χ_p of precipitated polymers in copolymerization at χ_f of 40mol%.

Conclusion

Selectivity was drastically enhanced by the application of shearing after turbid due to the suppression of the precipitation of *m*-OB moiety.

References

[1] K. Kimura, Y. Yamashita, *J. Polym. Sci., Part A: Polym. Chem.*, **34**, 739, 1996. **[2]** K. Kimura, S. Kohama, J. Kuroda, Y. Shimizu, T. Ichimori, Y. Yamashita, *J. Polym. Sci., Part A: Polym. Chem.,* **44**, 2732, 2006. **[3]** K. Kimura, Y. Shimizu, T. Ichimori, S. Kohama, S. Yamazaki, Y. Yamashita, *J. Polym. Sci., Part A: Polym. Chem.,* **46**, 1598, 2008. **[4]** K. Kimura, T. Ichimori, K. Wakabayashi, S. Kohama, S. Yamazaki, *Macromolecules*, **41**, 4193, 2008.

Facile, single-step preparation of versatile, high surface area nanoporous hybrid materials

Ian Teasdale, Ivo Nischang, Oliver Brüggemann*

Institute of Polymer Chemistry (ICP), Johannes Kepler University Linz

ian.teasdale@jku.at

New, facile, porous hybrid polymeric materials based on polyhedral silsesquioxane nanohybrid building blocks are presented. A single-step molding process via a simple vinyl polymerization of the bulky precursors leads to an inherently nanoporous network with good thermal stability and extremely high surface areas for polymeric materials (BET 700-900 m_2g^{-1}). The significant amount of residual vinyl groups from the multi-vinyl precursor can be simply modified by thio-ene click chemistry for ready access to a wide range of surface properties and high loading capability. We also show how through simple solvent variations, hierarchically-structured porous materials with excellent flow-through properties and tailored macroporosity can be readily achieved and describe their preparation as monolithic materials, covalently anchored to a confining container. The versatile and mild chemistry facilitates spacial selectivity and the preparation of a wide range of forms, including microspheres and monolithic materials for micro-fluidic and chip-based applications for which the use of sol-gel processes is limited.

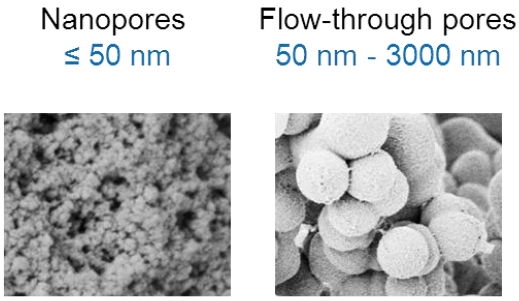

Emulsion Polymerization of Styrene: Simulation the effects of mixed ionic and non-ionic surfactant system in presence of coagulation

Samira Feiz, Amir H. Navarchian

Department of Chemical Engineering, Faculty of Engineering, University of Isfahan

Navarchian@eng.ui.ac.ir

1. Introduction: The end product properties in the emulsion polymerization are strongly correlated with particle size distribution (PSD) of the latex formed. The main factors that in turn affect the PSD are the composition as well as concentration of emulsifier used. These two influence also the average particles diameter, the total number of particles *(N_p)* and conversion. The ionic surfactants stabilize the particles by electrostatic repulsion, while the non-ionic surfactants cause the stabilization by steric hindrance mechanism [1].

Mixed surfactant system is applied to control the average particle size and PSD in industrial processes. The only available work on modeling this system is that published by Unzueta and Forcada (1997) using a monodisperse assumption for particle sizes [2].

In the current work we have modeled the effects of mixed surfactant systems (SDS as ionic and Brij35as nonionic surfactant) on PSD of particles for batch emulsion polymerization of styrene. A new model is developed to compute the rate of coagulation considering the polydispersity of the particle sizes.

2. Modeling:

Using the zero-one model [1] polymer particles are characterized by population density functions ($f(r,t)$). The particles that have a polymeric radical (f^P_1), particles that have no radicals *(f_0)*, and particles that have a monomeric radical (f^M_1) are given as [3]:

$$\frac{\partial f_0(r)}{\partial t} = \rho\left[f_1^P(r) + f_1^M(r) - f_0(r)\right] + k_{dM}.f_1^M(r) - f_0(r)\int_0^\infty \beta(r,r')\left[f_0(r) + f_1^P(r')\right]dr' + \int_0^\infty \beta(r', r-r')\left[f_0(r')\,f_0(r-r') + f_1^P(r')\,f^P_{1(r-r')}\right]dr' \quad (1)$$

$$\frac{\partial f_1^P(r)}{\partial t} = \rho_{init}.f_0(r) - \rho.f_1^P(r) - k_{tr}[M]_p\,f_1^P(r) + k_p[M]_p\,f_1^M(r) - \frac{\partial((dr/dt)\,f_1^P(r))}{\partial r} + R_{nuc}\delta(r-r_{nuc}) - f_1^P(r)\int_0^\infty \beta(r,r')\left[f_0(r') + f_1^P(r')\right]dr' + \int_0^\infty \beta(r', r-r')\left[f_0(r')f_1^P(r-r') + f_1^P(r')f_0(r-r')\right]dr' \quad (2)$$

$$\frac{\partial f_1^M(r)}{\partial t} = k_{tr}[M]_p\,f_1^p(r) - (k_p[M]_p + \rho + k_{dM})\,f_1^M(r) + e^0\,f_0(r)[P_w]^0 \quad (3)$$

Where ρ, k_{dM}, R_{nuc} and β are overall rate of radical entry, coefficient of desorption rate for monomeric radicals, and the nucleation and coagulation rates, respectively. The propagation growth rate is given in terms of monomer concentration in the particles $[M_p]$ [1,3]:

$$\frac{dr}{dt} = \frac{1}{4\pi r^2 \rho_p N_A}\,k_p[M]_p\,M_W \quad (4)$$

The critical micelle concentration of the surfactant mixture *(CMC_{12})* and the composition of micelles (α^m) was calculated according to the thermodynamic theory for non-ideal mixtures, using Rubingh expressions [2].

Micellar nucleation occurs when $[S]_w > CMC_{12}$ [3]:

$$\Re_{Micellar}(t) = \sum_{l=z}^{j_{cr}-1} e^l_{micelle}[P_w]^l\,C_{micelle} \quad (5)$$

In addition, upon reaching the critical chain length, j_{cr}, the oligomers in the aqueous phase precipitate out of the aqueous phase, and form a new particle [3]:

$$\Re_{homogenous}(t) = k_p^w[P_W]^{j_{cr}-1}[M]_w \quad (6)$$

The coagulation rate coefficient β_{ij} between two particles with radius r_{si} and r_{sj} is given by [1,3]:

$$\beta_{ij} = \beta_{ji} = c\,\frac{2k_BTN_A}{3\mu W_{ij}}\left(2 + \frac{r_{si}}{r_{sj}} + \frac{r_{sj}}{r_{si}}\right) \quad (7)$$

The Fuch's stability ratio is found from:

$$W_{ij} = (r_{si} + r_{sj})\int_{(r_{si}+r_{sj})}^\infty \exp\left(\frac{\Phi}{R^2}\right)dR \quad (8)$$

The total potential between the two particles, Φ, is a combination of attractive and repulsive potential of anionic and non-ionic surfactant molecules on the surface of particles.

3. Result and discussion

At the beginning of polymerization, the particle numbers increases, as a result of formation of new particles through nucleation. At high polymer volume fractions, the number of particles tends to decrease upon coagulation, because of collision of any two particles and increase due to secondary micellar nucleation. These two effects occurs with the same rate, so that the N_p remains constant. By increasing Brij35 in composition of the surfactant mixture, the average repulsive potential on the particle surfaces decreases, while the rate of coagulation increases. Hence, the total number of particles and conversion decreases (Fig. 1).

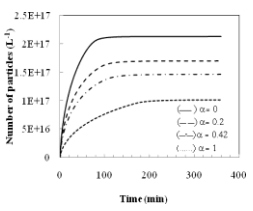

Fig.1. Effect of nonionic surfactant mole fraction in the feed (α) on N_p.

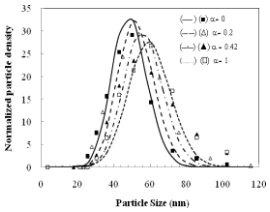

Fig. 2. Effect of nonionic surfactant mole fraction in feed (α) on final PSD

By using Brij35, because of the higher amount of $[S]_w$ in system and the longer time of nucleation [1-3], particles with different size are formed during the polymerization process and a broader PSD curve is obtained finally. Moreover, due to the less stabilization capability of non-ionic surfactant than that of anionic one and therefore increasing the rate of coagulation, the average particle radius increases. The model fits well the experimental data obtained in this work.

4. conclusion

Increasing the non-ionic surfactant in the emulsifier mixture led to a broader PSD with larger particle sizes, and less total particle number and conversion.

Refrences

[1]. Immanuel et al., 2003. AIChE, 49(6), 1492-404.
[2]. Unzueta and Forcada, 1997. J. Appl. Polym. Sci., 66, 445-458.
[3]. Coen et al.,1998. Polymer, 39,7099–112.

Wear Resistance Optimization of PU/TiO_2 Coatings on Aluminium Surfaces

Mehrdad Taheran[1], Amir H. Navarchian[1], Reza Shoja Razavi[2]

[1]Department of Chemical Engineering, Faculty of Engineering, University of Isfahan
[2] Department of Material Engineering, Malek AshtarUniversity of Technology, Shahin Shahr, Isfahan, Iran
navarchian@eng.ui.ac.ir

1. Introduction:

Polyurethane (PU) coatings used in many applications need to have enough wear resistance to satisfy the practical and economical aspects [1]. The aim of this work is to develop a coating on aluminum surface based on PU binder and TiO_2 pigment having maximum wear resistance. The influences of polyol molecular weight (A), diisocyanate type (B), surface pretreatment (C), NCO/OH ratio (D) and pigment volume concentration (E), on wear resistance of PU coatings have been statistically investigated.

Experimental:

To synthesize the prepolymer, 40 g of PTMG (MW = 1000 or 2000) was reacted with diisocyanate (Hexamethylene diisocyanate (HDI), isophorone diisocyanate (IPDI)) according to specified NCO/OH ratio (1.4, 1.6 or 1.8). The reactions were carried out at 80°C for 6 hrs in a three-necked flask. The prepared resin was dissolved in solvent (xylene /n-butyl acetate: 50/50, v/v) and the specified amount of TiO_2 was added to the mixture. TiO_2 pigments (particle size 10µm) were dispersed in resin with a pearl mill apparatus at 800 rpm [2]. Chemical (using alcoholic phosphoric acid cleaner) and anodic (sulfuric acid anodic) methods were used for surface pretreatment. A standard L_{16} Taguchi array was employed for experimental design, using S/N ratio as response.

2. Result and discussion

2.1 Analysis of variance

Table 1 shows the analysis of variance (ANOVA) statistical terms for wear resistance of PU/TiO_2 coatings. The critical F-values for two and three-level factors at confidence level of 95% are 5.33 and 4.46, respectively [3]. According to this table, the important contributors to variability of the results are polyol molecular weight (A), pigment volume concentration (E), diisocyanate type (B), and NCO/OH ratio(D), respectively. Factor C represents the lowest F-ratio in the ANOVA table which implies that surface pretreatment method does not affect the response significantly.

Table 1. ANOVA table for mass loss in wear test (M_L)

Factor	DOF	Sum of squares	Variance	F-ratio	Contribution%
A	1	85.371	85.371	117.884	41.005
B	1	18.534	18.534	25.592	8.627
C	1	2.184	2.184	3.016	0.707
D	2	14.557	7.278	10.05	6.350
E	2	79.987	39.993	55.225	38.046
Other/error	8	5.793	0.724		5.265
Total	**15**	**206.429**			**100**

3.2 Influence of operating variables

As observed in Fig. 1, the use of polyol with higher molecular weight results in higher elongation at break [4] that tolerates higher stresses before breaking and consequently gives higher abrasion wear resistance [5]. Pigment particles serve as reinforcing filler and increase the tensile strength and wear resistance of prepared coating [5]. Formation of allophanate or biuret crosslinks at higher NCO/OH result in also higher wear resistance. The wear resistance of coatings made from IPDI as diisocyanate is higher than those composed of HDI. This behavior can be justified by the structures of these two chemicals.

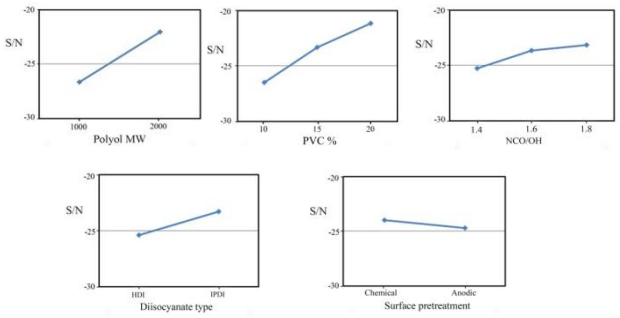

Fig. 1. The effect of factors on wear resistance

3.3 Optimum conditions

The optimum conditions to attain a PU/TiO_2 coating can be determined from maximum points in main effect plots (Fig.1). A new sample was prepared according to proposed factor levels. The predicted value for mass loss in optimum conditions (6.4 mg), was found reasonably in agreement with the experimental data (5.9 mg). The morphology of optimum sample was examined by SEM microscopy (Fig.2 and Fig. 3). The smooth surface of coating was worn and became rough and matt after wear test. These figures suggest that the adhesion mechanism is dominant in wear action [6,7].

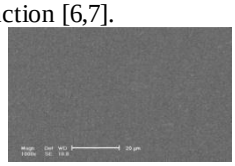

Fig. 2. SEM image of the optimized coating before wear

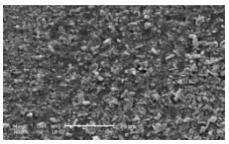

Fig. 3. SEM image of the optimized coating after wear

4. Conclusions

The higher wear resistance is obtained with higher polyol molecular weight, higher pigment volume concentration, with IPDI and at NCO/OH ratio = 1.8. Both the chemical and anodic methods give raise the same wear resistance in this work.

References

[1]. Chen et al., 2007. Eur. Polym. J., 43, 4151– 4159.
[2]. Taheran & Navarchian, 2010. 13th National Iranian Chemical Engineering Congress, Kermanshah, Iran.
[3]. Roy, K. R., 2001, John Wiley & Sons,New York.
[4]. Hepburn, C., 1999, Elsevier Science Publishing, New York.
[5]. Wicks, Z. W., 2007, John Wiley & Sons, New Jersey.
[6]. Ludema, K. C., 1992, ASM International, pp. 320-350
[7]. Li et al., 2002, Wear, 249, 877–882.

Changes of Supermolecular Structure and Selected Properties of Polymer Matrix of Polyamide Fibres Caused by Addition of LCO Modifier

M. Baczek, J. Janicki

Institute of Textile Engineering and Polymer Materials, University of Bielsko-Biała, Bielsko-Biała, Poland

mbaczek@ath.bielsko.pl

Keywords: Liquid Crystalline Oligoester, PA6/LCO blends, supermolecular structure, WAXS, SAXS, tensile strenght parameters

Polyamides have become essential materials in fibre production for textiles and technical uses.
However, such applications require extremely high strength parameters as well as excellent dimensional stability. In order to improve polymer properties they are reinforced with with very high strength and high modulus liquid crystalline polymers. Blending of thermotropic LCP with semicrystalline thermoplastic polymers to form in-situ polymer composites is very attractive because LCP acts as reinforcing elements in the blends and its addition to a polymer matrix has profound impact on its physical and mechanical properties of the final product [1-3]. Synthesized liquid crystalline oligoester was in this study applied as liquid crystalline polymeric component in fibre forming PA6/LCO blends. Thermotropic Liquid Crystalline Oligoester can be used as a proper compound

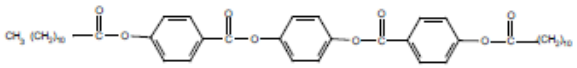

Figure 1. The macromolecular chain of synthesized liquid crystalline oligoester.

The objective of research presented in this work was to determine the influence of the LCO on the parameters of the supermolecular structure, thermal and mechanical properties of fibres obtained from PA6/LCO blends with 95% of PA6 and 5% of LCO by weight.
The relationship between supermolecular structure and mechanical properties of the obtained fibres was also presented.
The parameters of the supermolecular structure based on the the structural investigations using wide angle X-ray scattering (WAXS) and small angle X-ray scattering (SAXS) methods have been calculated.
The crystalline structure of PA6/LCO fibres was investigated by WAXS methods. The results of measurements were analyzed in the aspect of the structure of PA6 matrix changes caused by addition of LCO modifier. The degree of crystallinity was calculated using a modified Hindeleh & Jonson method [6-7] and a computer program WAXSFIT [8]. Sizes of crystallites were estimated using the Sherrer equation.
The lamelar structure of PA6/LCO fibres was investigated by small angle X-ray scattering methods and the results of measurements were analyzed in the aspect of the lamellar structure of PA6 matrix changes caused by addition of LCO modifier. The parameters of lamellar structure (long period, the lamellar and the amorphous layer thickness) were obtained using the linear correlation function approach
The results of 2D-SAXS measurements have additionally allowed to obtain information concerning the location of for processing with semicrystalline PA6 due to relatively low melting temperature and wide temperature of mesophase [4-5]

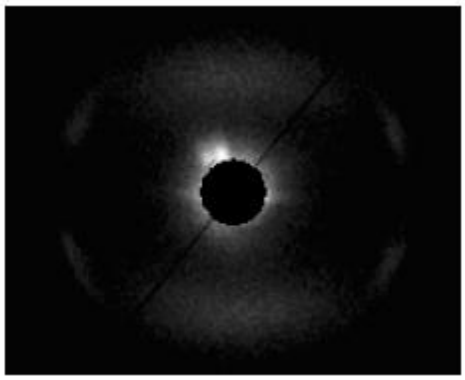

oligoester domains in the polyamide matrix of the obtained fibres.

Figure 2. 2D-SAXS pattern for PA6/LCO 95/5 fibres

Based on the results of SAXS investigation, model of the structure of PA6/LCO fibres was proposed. Liquid crystalline oligoester domains which are situated into interfibrillar area of polyamide matrix with lamellar structure is characteristic of these fibres
Specific dispersion of the LCO domains in polymer matrix mentioned before has profound impact on mechanical properties of modyfied fibres. Figure 4 summarized the results of the mechanical tests obtained for both modified and unmodified polyamide fibres.
The comparative analysis shows that presence of liquid crystalline oligoester has positive influence on the tensile strenght parameters.

References

[1] Ho, J.C.; Wei, K.H. *Macromolecules*, **2000**, 33, 5181.
[2] Hakeni, H. *Polymer*, **2000**, 41, 6145.
[3] Liang, B.; Pan, L.; He, X. *J. Appl. Polym. Sci*. **1997**, 66, 217.
[4] Janicki, J. *Acta Phys. Pol. A*, 2002, 101, 761-766.
[5] Bączek M, *Nanostruktura i wybrane własności włókien formowanych z polimerowych kompozytów molekularnych*, Bielsko-Biała 2009.
[6] Hindeleh, A.M.; Johnson D.J. *J.Phys (D)* **1971**, 4, 259
[7] Hindeleh, A.M.; Johnson, D.J. *Polymer* **1978**, 19, 27.
[8] M.Rabiej, *Polimery* **2002**, 47, 423.

Kinetic Study on Photopolymerization of Acrylates by Photo-DSC and RT-FTIR: The Effect of Thioxanthone based Dendritic Photoinitiators and Light Intensity

Zekeriya DOGRUYOL[1], Tezcan PARALI[2], Mehmet Arif KAYA[3], Metin TULU[3], Nergis ARSU[3]

[1]Yildiz Technical University, Physics Department, Davutpasa Campus, 34220 Istanbul, Turkey
[2]Fatih University, Chemistry Department, Buyukcekmece Campus, 34500 Istanbul, Turkey
[3]Yildiz Technical University, Chemistry Department, Davutpasa Campus, 34220 Istanbul, Turkey

e-mail:m_arif_kaya@yahoo.com

Introduction

Photopolymerization has been the basis of numerous conventional applications in coatings, adhesives, inks, printing plates, optical waveguides, and microelectronics. Some other less traditional but interesting applications, including production of laser videodiscs, curing of acrylate dental fillings, and fabrication of 3D objects [1].

Photoinitiators for radical photopolymerization are classified as cleavage (type I) and H-abstraction type (type II) initiators [2]. Although alkylamines are very efficient hydrogen donors, high usage of volatile and odorous compounds generate some disadvantages to type II systems [3]. Dendritic photoinitiators may overcome these problems, since dendrimers are unique macromolecules having highly branched, well-defined architectures with a number of interesting characteristics. Their nanoscale structures have a variety of potential applications in the fields of coatings, chemical sensors, catalytic nanoreactors, drug delivery systems and liquid crystalline dendrimers. The introduction of thioxanthone into dendrimers can lead to the novel dendritic macrophotoinitiators, which have obvious advantages; such as intramolecular reactions because of the formation of more reactive species and protecting the active species by macromolecular chain due to the macromolecular effect [4].

Polymerization reaction kinetics are affected with various parameters such as type of photoinitiator [5], light intensity [6], photoinitiator concentration [7], temperature and monomer functionality during the photocuring. In this study, new dendritic macrophotoinitiators (Jeff-(3,6,12)-TX) through introducing thioxanthone moieties were synthesized and the kinetics of polymerization reaction of mono and multifunctional acrylates in the presence of these new dendritic photinitiators with MDEA were studied by means of photo-DSC and RT-FTIR. The effect of light intensity on the photopolymerization of Lauryl acrylate (LA) was also investigated for these new three dendiritic photoinitiators (Jeff-(3,6,12)-TX) by Photo-DSC. The photopolymerization kinetic parameters, the time (t_{max}) to reach the maximum value of the rate of polymerization (Rp_{max}) and final conversion (C_s) were determined by depending on the effects of amounts of thioxanthone group (3,6,12) and the light intensity.

Methods

IR spectra were taken ATI Unicam Mattson 1000 FTIR Spectrophotometer. JOBIN YVON HORIBA FluoroMax-P Fluorescence Spectrophotometer was used to take fluorescence spectra. The photolyzing light was generated by a medium pressure mercury lamp (Flexicure UV system) and was conducted through a flexible fiber optic for the photolysis. DSC spectra were taken on a TA Q Series DSCQ100 with PCA photo unit. The mass of the samples were 2.6 ± 0.1 mg into the aluminum DSC pans and the measurements were carried out in an isothermal mode at 25 °C under a nitrogen atmosphere by UV light with intensities of 30, 40 and 60 mW/cm^2.

Result and Discussion

Increasing light intensity from 30, 40 and 60 mW/cm^2, heat flow of polymerization reaction and the rate of polymerization increased with decreasing order of TX moieties in the dendritic macrophotoinitiator except Jeff-12TX. Jeff-12TX worked well with the 40mW/cm^2 light intensity value. Further increasing of light intensity adversely affected both heat flow and the rate of polymerization for Jeff-6TX and Jeff-12TX. An increase of the light intensity leads to a higher maximum polymerization rate, and the maximum is achieved more rapidly after the start of the reaction.

Conclusion

Dendritic macrophotoinitiators were used in RT-FTIR and Photo-DSC formulations without MDEA and polymerization was not occurred in air atmosphere. Therefore, the initiation mechanism of these three dendritic macrophotoinitiators is similar to thioxanthone itself. The initiating radicals are aminoalkyl radical which obtained from MDEA and ketyl radicals are usually not reactive toward to TMPTA due to steric hindrance and the delocalization of unpaired electron.

References

1. Yagci Y., Jockusch S. and Turro N.J. Macromolecules 2010, 43, 6245–6260.
2. Hageman H.J. Prog. Org. Coat. 1985, 13, 123–150.
3. Kloosterboer, J.G. Adv. Polym. Sci. 1988, 84, 1–61.
4. Jiang X. and Yin J. Macromolecules 2004, 37, 7850–7853.
5. Dogruyol Z., Karasu F., Balta D.K., Arsu N., Pekcan O. Phase Transit. 2008, 81, 935–947.
6. Dogruyol Z., Arsu N., Pekcan O. J. Macromol. Sci. Part B 2009, 48, 745–754.
7. Dogruyol Z., Karasu F., Temel G., Balta D.K., Aydın M., Keskin S., Pekcan O., Arsu N. In Basics and Applications of Photopolymerization Reactions, In Applied Polymer Science Series, J.P. Fouassier, X. Allonas, Ed., Research Signpost, Trivandrum, 2010, Chap. 11, 161–173.

Effect of Nanofillers on Curing Kinetics and Thermal Properties of Epoxy Amine Thermosets

Amit Kumar Ghosh, Guy Van Assche, Bruno Van Mele

Vrije Universiteit Brussel, Pleinlaan 2, 1050 Brussels, Belgium

e-mail- aghosh@vub.ac.be

Abstract: The effect of nanoclay (Cloisite 30B) and MWNT (multi-walled carbon nanotube) on the curing kinetics of an epoxy-amine system were studied.

In this work, diglycidyl ether of bisphenol A (DGEBA) epoxy resin was used in combination with 4,4'-methylene dianiline (MDA) and aniline. MDA and aniline were combined to improve the mixing process of resin and hardener, and to improve the dispersion of nanofillers in the nanocomposite samples. The nanofillers were premixed with the epoxy resin by a high speed stirring process. The final samples were prepared by mixing the filled epoxy resin and the mixture of MDA and aniline.

The quality of dispersion of nanofillers (intercalation/exfoliation) was analysed by atomic force microscopy and by X-ray diffraction method. Modulated temperature differential scanning calorimetry (MTDSC) was used to study the cure kinetics of both pure resin and resins with fillers. The reaction enthalpy, the initial and final glass transition temperature (T_g) of the materials and the reaction kinetics were determined for all samples by isothermal and non-isothermal cure measurements. Rheological studies were carried out to determine the point of gelation and vitrification of different samples.

It was found that there is an accelerating influence of nanofillers on the curing kinetics of the system. This effect is more pronounced with nanoclay. Both nanocaly and MWNT showed that the accelerating effect is more pronounced if the nanofillers are dispersed properly in the matrix. The final T_g of the cured samples were significantly higher for nanocomposite than the pure resin.

Reference:

1. J. D. Menczel, R. B. Prime, Ed. (2009). Thermal Analysis of Polymers, WILEY - A John Wiley & Sons, Inc., Publication: 130-203.
2. T. D. Ngo, M.-T. Ton-That., S.V. Hoa, K.C. Cole (2007). "Curing kinetics and mechanical properties of epoxy nanocomposites based on different organoclays." Polymer Engineering and Science 47(5): 649-661.
3. D. Puglia, L. Valentini, I. Armentano, J. M. Kenny (2003). "Effects of single-walled carbon nanotube incorporation on the cure reaction of epoxy resin and its detection by Raman spectroscopy." Diamond and Related Materials 12: 827-832

Preparation of Organometallic Polymers with Conjugated Building Blocks

Pavla Stenclova, Jiri Zednik, Tereza Vitvarova, Jiri Vohlidal and Jan Svoboda

Department of Physical and Macromolecular Chemistry, Charles University in Prague, Faculty of Science, Hlavova 2030, Prague 2, CZ-12843

st.pavla@centrum.cz

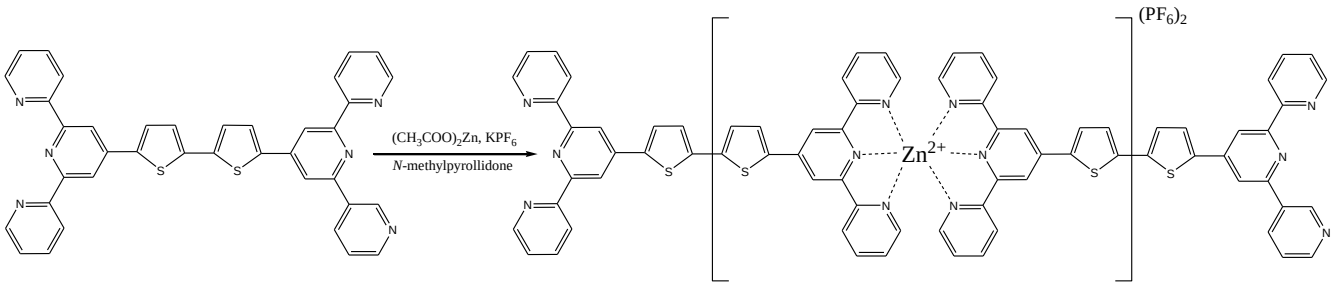

Fig.1: Synthesis of supramolecular polymer

Terpyridines have recently evoked great interest as ligands for preparation of supramolecular systems with diverse chemical properties. Positions of nitrogen atoms of terpyridine ligands allow easy tridentate facial and meridian coordination to various metal atoms (for example Ru, Os, Ir, Fe, Zn, Co) and a formation of metallo-supramolecular assemblies with well-defined stereochemistry (in contrast to many other modules) which is important for reproducible preparation of functional materials.

Among the unique properties of terpyridine compounds, their luminescent behavior upon complexation with metal ions is attractive due to high application potential as light-emitting devices and probes. It has been demonstrated that the ligand choice affects the luminescence properties of a resulting supramolecular assembly. That is the reason why the synthesis of tailored terpyridine ligands has become a fundamental step for preparation of high performance metal-coordination functional materials. The main interest was focused to monotopic terpyridines, but bis-terpyridines with all-conjugated chain between terpyridine units were investigated, too.

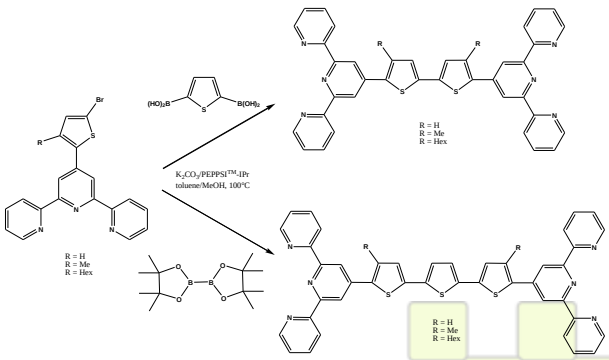

Fig.2: Preparation of ligands using Suzuki-Miyaura reaction.

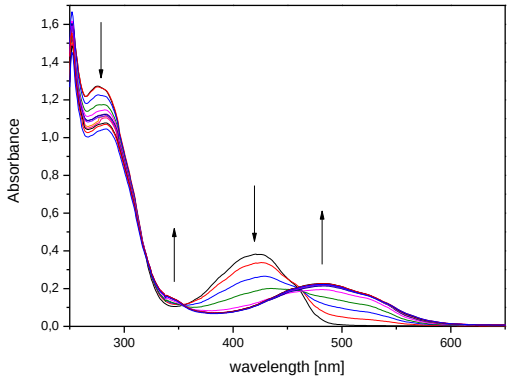

Fig.3: Absorption spectra of titration bis(terpyridyl)terthiophene with zinc (II)

Six novel bis-terpyridines were prepared using palladium-catalyzed Suzuki-Miyaura type cross-coupling reactions and their photophysical properties were investigated.

Complexation of ligands with different metals was studied using UV/vis and emission luminescence spectroscopy.

Supramolecular polymers were prepared from soluble ligands with zinc (II) and iron (II) and their properties were also studied.

Acknowledgement:

The authors acknowledge the financial support from the Grant Agency of Czech Republic No.: 104/09/1435 and 203/09/0803, the Science Foundation of Charles University (project 157810) and the Ministry of Education of the Czech Republic No.: MSM0021620857.

Synthesis of Porous Polymeric Organic Frameworks (POFs) with C_{3v} symmetry and controlled pore size

Ester Verde , Eva M. Maya , José G. de la Campa , Javier de Abajo , Ángel E. Lozano

Departamento de Química Macromolecular, Instituto de Ciencia y Tecnología de Polímeros (CSIC)

ester@ictp.csic.es

Introduction and objectives

There is a growing interest in porous organic polymers having anchored metal catalysts, due to their simplicity of synthesis, low density and high selectivity relative to inorganic systems[1]. Recently, Pandey et al. reported a facile, one-pot, quantitative synthesis of imine-linked microporous polymer organic frameworks (POFs) having surface areas up to 1500 m^2/g^{-1} and high H_2 and CO_2 sorption, converting these polymers into good candidates for gas storage and gas separation. These novel polymers can be considered wholly organic analogues of porous materials like metal-organic frameworks[2] (MOFs) and zeolites in terms of pore properties. The highly cross-linked nature of POFs confers them high thermal stability and they also have the ability, depending on the monomer used, to incorporate diverse groups on the pores, which, if they are conveniently modified, permits to tune the surface to interact with different types of guest molecules.

The aim of this work is focused on the preparation and characterization of new POFs with C_{3V} symmetry based on aromatic polyamides with controlled porosity by varying the length and geometry of employed monomers.

Results and Discussion:

In order to optimize the reaction conditions, a model compound was synthesized in a one step reaction using trimesic acid and 4-*tert*-butylaniline by means of the Yamazaki polycondensation reaction[3] (Figure 1). The model compound was obtained with high yield and purity as was checked by DSC, and by elemental analysis. The structure was also confirmed by ^{1}H-NMR, ^{13}C-NMR and FTIR-ATR.

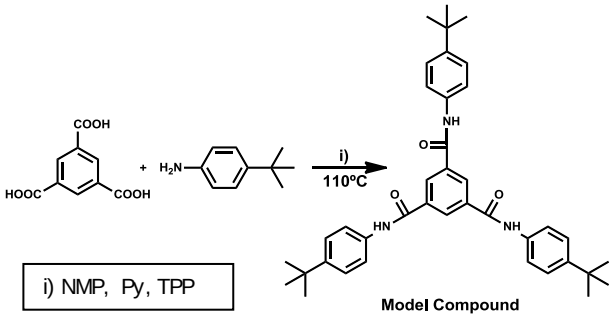

Figure 1: Synthesis of model compound

The synthesis of POFs was carried out by combination of trimesic acid and diamines of different length and geometry (*p*-diamines or *m*-diamines) (Figure 2) using the reaction conditions depicted in Figure 1.

Thermogravimetrical analysis of these POFs revealed high thermal stability, with decomposition temperatures above 450ºC and only one step degradation pattern. DSC curves showed no Tg below 400ºC.

Pore size and pore distribution of these new materials using the BET technique (N_2 gas adsorption/desorption) and also CO_2 and CH_4 sorption at diverse temperatures have been carried out.

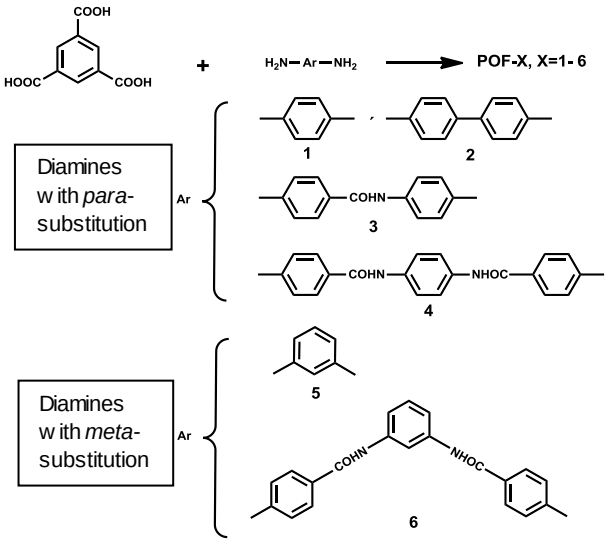

Figure 2: POFs obtained in this work

Finally, diamines having nitro groups have been used to make new POFs. Those nitro moieties will be reduced to amino ones and functionalized with organic moieties able to anchor metals with ability to catalyze organic reactions. In Figure 3, a schematic representation of these new materials is depicted. Reduction reactions and functionalization with designed groups are on the way.

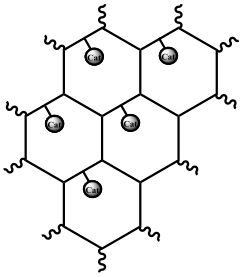

Figure 3: Schematic representation of new POFs with functional groups.

References:

[1] Pandey, P.; Katsoulidis A. P.; Erayice, I.; Wu,Y.; Kanatzidis, M. G.; Nguyen, S. T.; *Chem. Mater.* **2010**, *22*, 4974.

[2] Corma, A.; García, H.; Llabrés i Xamena, F. X.; *Chem. Rev.* **2010**, *110*, 4606.

[3] Yamazaki, N.; Niwano, M.; Kawabata, J.; Higashi, F.; *Tetrahedron*, **1975**, *31*, 665.

Acknowledgments:

The financial support provided by MICINN through projects MULTICAT and MAT2010-20668 is gratefully acknowledged.

Enhancing Properties of Piezoelectric Polyimides by Copolymerization

M. San Sebastián[1], A. Maceiras[1], J.L. Vilas[1], T. Breczeswki[2], M. A. Pérez-Jubindo[2], M. R. de la Fuente[2].

[1] Laboratorio de Química Macromolecular (Labquimac), Dpto. Química-Física
[2] Dpto. Física Aplicada II Facultad de Ciencia y Tecnología, Universidad del País Vasco, Apdo 644, 48080, Bilbao, Spain.

maria.sansebastianh@ehu.es

Introduction

The piezoelectricity in amorphous polymers is mainly due to the orientation polarization of the molecular dipoles. Aromatic polyimides are high-performance polymeric materials possessing an exceptional array of properties. The thermal stability, chemical resistance and excellent mechanical and electrical properties makes them able to be used as sensors and actuators(1).
An improvement of piezoelectric response of these polymers can be obtained by adding dipoles in the chain. Previously, piezoelectric polyimides have been synthesized containing –CN dipolar groups in the polymer chain(2). Although the obtained polyimides present interesting mechanical and piezoelectric properties, it has not been possible to combine both properties in the same material.
In order to obtain a material with the best mechanical and piezoelectric response, copolyimides have been synthesized using a mixture of the diamines.

Materials and Methods

The commercial products used for the copolymer synthesis were 1,3-Bis(3-aminophenoxy)benzene, supplied by Acros Organics Ltd, 2,4 dichlorobenzonitrile supplied by Merck., 4,4'-oxydiphthalic anhydride (ODPA), 2,6-dichloro-benzonitrile, and dimethylacetamide (DMAc), supplied by Aldrich. The diamines were recrystallized from EtOH/H_2O(1:1). The dianhydride was dried at 453K in a vacuum chamber, and the solvent was used as received.
Copolyimides were obtained by reaction between the dianhydride ODPA and two aromatic diamines(2), in two-step reaction.
The copolymer films were prepared by thermal treatment of a solution of poly(amic acid) in N, N-dimethylacetamide. For polarization and dielectric measurements, the samples were prepared and poled by standard poling method, using a supply source HITEK Power Series 4000, and the temperature was raised up to 505K during 15 minutes. Then the temperature was decreased to room temperature maintaining the applied electric field to freeze the polarized state. The frozen-in polarization, P_r, of the poled samples was measured by the Thermally Stimulated Depolarization Current (TSDC) method(3) by a Keithley 6517 electrometer.

Results and Discussion

Several copolyimides were synthesized by the conventional two-step method starting with diamines and aromatic dianhydride through ring-opening polyaddition and subsequent thermal cyclodehydration imidization. All of them have been characterized.
Copolymers exhibited only one Tg, indicating that the repetitive units are randomly distributed along the polymer chain. In addition, no endothermic peaks above their glass transition temperatures were observed in DSC measurements which may be attributed to the amorphous molecular structure for all polymers.
The results of the TSDC method show that the temperature dependence of the depolarization current for copolymers is slightly lower than the pure polyimide with higher Pr. The value of this parameter is associated with the composition of the copolymer and increase if the amount of polyimide with higher Pr in the copolymer increases. It is not clear from these initial results if there a direct dependence with copolymer composition exists, or whether it should be considered in terms of sequence distributions.
The obtained copolymers have improved the mechanical properties of the polymers with higher Pr, but have decreased slightly mechanical properties for polymers with low Pr.

Conclusions

Different series of aromatic piezoelectric copolyimides have been obtained and characterized.
The mechanical properties of the piezoelectric polyimides have been improved by means of copolymerization, the value of the polarization being maintained.
A new way to study and control the influence of sequences distribution over mechanical and electrical properties is open.

Acknowledgements

This work has been supported by the Basque Government, ETORTEK program project ACTIMAT.
Technical and human support provided by SGIker (UPV/EHU, MCINN, GV/EJ, ERDF and ESF) is gratefully acknowledged.

References

(1) Ghosh, M.K., Mittal, K.L., Eds.; Polyimides: Fundamentals and Applications; Marcel Dekker, Inc.: New York, 1996
(2) Gonzalo, B.; Vilas, J. L.; Breczewski, T; Pérez-Jubindo, M. A.; De La Fuente, M. R.; Rodriguez, M.; León, L. M. J. Polym. Sci., Part A: Polym.Chem. 2009, 47, 722.
(3) Ramos, M.; Mano, J. J. J. F. Thermochim Acta 1996, 285, 347.

Plastics with reduced flammability, containing graphite halogen-free additives

Piotr Jankowski, Michał Kędzierski

Industrial Chemistry Research Institute, 8 Rydygiera str., 01-793 Warsaw, Poland.

piotr.jankowski@ichp.pl

Introduction: One of the most important problems related to the production of polymeric materials is their flammability. European regulations for the use of flame retardants demand the development of halogen-free additives for different kind of plastics. Investigations involve reduced flammability of plastics concentrate to replace halogen antipyrene by halogen-free additives. A significant disadvantage of halogen additives is the emission of very toxic and corrosive fumes from the field of the fire to the environment during combustion. On the other side the halogen-free additives characterize usually minor effectiveness than halogen compounds. Graphite is neutral to the environment. Various kind of graphite additives are attractive substitutes for halogen antipyrene. Moreover graphite flame retardants produce less toxic gases and smokes compared to halogen-containing flame retardants. However application of graphite alone, in many cases (for example polystyrene - easy flammable polymer), does not warrant sufficient reduction of fire. In this case halogen additives are commonly utilized [1-3]. Numerous publications emphasize increasing electrical properties of polystyrene modified by graphite, but skeptically assess its resistance to flame [4,5]. In the other side some articles positively refer application of graphite as an antipyrene for the polystyrene [6,7].

The main purpose of our investigations was preparation of effective flame retardant containing modified graphite or its compositions with additional supportive flame retardants – phosphorus compounds.

Materials and Methods: Expanded graphite (**EG**) (Sinograf SA). For graphite modification: melamine (Aldrich), cyanuric acid (Aldrich). Unsaturated polyester resin Polimal-109 („Organika-Sarzyna" Inc.). Dian epoxy resin Epidian 5 („Organika-Sarzyna" Inc.). Phosphorus compounds: triphenyl phosphate (**TP**) (Aldrich), tritolyl phosphate (**TTP**) (Aldrich), triphenylphosphine (**TPP**) (Aldrich). Styrene (POCh).

The flammability of polyester, epoxy and polystyrene compositions has been determined by the oxygen index test (OI) according to ASTM D 2863-97 standard and horizontal and vertical flammability according to PN-EN-60695-11-10:2002 standard. Thermogravimetric analysis were made on Mettler Toledo equipment TGA/SDTA851 in the air environment. Microscopic analysis were made on Scanning Electron Microscope with EDS analysis – JEOL JSM – 6490LV.

Results and Discussion: The method of obtaining additives containing expanded graphite modified by melamine cyanurate was worked out. Synthesis of melamine cyanurate was lead in the presence of expanded graphite [8]. This compound was used as a additive for suspension polymerization of styrene [9]. Epoxy and polyester compositions with this modified expanded graphite were made. Moreover the composition of expanded graphite with phosphorus compound or different type of modified graphite were utilized as a flame retardant for polystyrene, polyester and epoxy resins. It has been observed that the presence of expanded graphite modified by melamine cyanurate in the polystyrene increases the OI from 17 % to 24,5 %. The highest parameters of horizontal and vertical flammability FH-1, V-0 has been received (*tab. 1 p. 1*). The presence of the same type of modified expanded graphite in the epoxy resins increases the OI from 22 % to 26,9 % (*tab. 1 p. 2*). The composition of expanded graphite with phosphorus compound turned out to be effective additive for polystyrene and epoxy resins. In the polystyrene the OI increases from 17 % to 25,5 %. The highest parameters of horizontal and vertical flammability FH-1, V-0 has been received (**EG** with **TP, TPP, TTP**) (*tab. 1 p. 3-5*). The presence of phosphorus expanded graphite composition in the epoxy resins increases the OI from 22 % to 29,8 % (**EG** with **TP, TPP, TTP**) (*tab. 1 p. 6-8*). Different types of modified graphite (graphite oxide modified by melamine formaldehyde resins) turned out to be effective additive for polystyrene and polyester resins. In the polystyrene the highest parameters of horizontal and vertical flammability FH-1, V-0 has been received (*tab. 1, p. 9*). The presence of the same modified graphite in the polyester resins increases the OI from 21 % to 27,3 % (*Tab. 1, Pos. 10*).

	amounts of additives (portion weights)	OI (%)	horizontal flammability	vertical flammability
1	15	24,5	FH-1	V-0
2	10	26,9	FH-1	V-0
3	15	25,5	FH-1	V-0
4	15	-	FH-1	V-0
5	15	-	FH-1	V-0
6	10	27,7	-	-
7	10	28,8	-	-
8	10	29,8	FH-1	V-0
9	15	-	FH-1	V-0
10	10	27,3	-	-

Tab. 1 Flammability analysis

Conclusions:

Modified graphite or its compositions with phosphorus compounds can be effective flame retardants for polystyrene as well as for polyester and epoxy resins. Decreasing flammability of polystyrene by graphite modified by melamine cyanurate is particularly important because of pro-ecological character this type of flame retardants.

References:

1. *Pat USA* 4 699 943 (1987).
2. *Pat USA* 5 302 625 (1994).
3. *Pat USA* 6 271 272 (2001).
4. Goyal R.K., Mulik U.P., Jagadale P.A.: *Journal of applied polymer science* 2009, **111(4)**, 2071.
5. Chen G., Wu C., Weng W., Wu D., Yan W.: *Polymer Communication* 2003, **44**, 1781.
6. Uhl F.M., Wilkie C.A.: *Polymer Degradation and Stability* 2004, **84**, 215.
7. Ding R., Hu Y., Gui Z., Zong R., Chen Z., Fan W.: *Polymer Degradation and Stability* 2003, **81**, 473.
8. Pol. pat. appl. P-393346 (2010).
9. Pol. pat. appl. P-393345 (2010).

Water transport properties in biodegradable copolyesters

Nadège FOLLAIN[1], *Eric DARGENT*[2], *Frederic Chivrac*[3], *Florent GIRARD*[3], *Stéphane MARAIS*[1]

[1] Université de Rouen, Laboratoire Polymères, Biopolymères et Surfaces, UMR 6270 & FR 3038 CNRS, Bd. Maurice de Broglie, 76821 Mont Saint Aignan Cedex, France
[2] Université de Rouen, laboratoire L.E.C.A.P., BP 12, 76801 Saint-Etienne du Rouvray cedex - France
[3] CREAGIF Biopolymères, 18, avenue de la voie aux coqs, 14760 Bretteville-sur-Odon, France

nadege.follain@univ-rouen.fr

Polyhydroxyalkanoates (PHA – Polyester synthetized by bacteria) have been attracting more and more attention in industrial and academic fields due to the global growing conscience relating to the preservation of ecological systems. The specific properties of PHA such as biodegradability, biocompatibility, high renewable carbon content and thermoplasticity with high crystallinity make them interesting for short-lived industrial applications, in replacement of non-degradable petroleum based plastics.

Today, tailoring new eco-friendly plastics represents a wide field of investigation. In this context, polyhydroxybutyrate (PHB), which is the first isolated PHA, and its copolymers such as polyhydroxy(butyrate-co-valerate) (PHBV) are the most produced and investigated biopolymers of this family. Their properties come from their monomer composition depending on carbon source and on the microorganisms used for their production. In addition, the molecular structure differences between PHB and PHBV involved more ductile and processable copolymers compared to PHB properties. The random bio-copolyesters present a lower melting point and a relative lower crystallinity compared to PHB. Consequently, the better processing characteristics of PHBV improved their mechanical properties. Beyond that, depending on the packaging applications requirement, the water vapor permeability comparable to that of LDPE represents an interesting property of PHA.

The purpose of this study dedicated to the water transport properties [1-2] is to evaluate the potential of these bio-copolyesters for film packaging applications. To our knowledge, investigation on barrier properties of PHA are few considered in the literature [3] despite some devoted to physical and thermal properties of PHA. When compared to common polymers such as polyethylene or polypropylene, PHBV copolymers showed a very good balance of barrier properties [4]. In addition, theses bio-copolymers have another advantage which is their low moisture sensitivity with a hydrophobic behavior against water molecules. The results on PHBV films are presented: a dependence of barrier properties against to the film preparation (thermocompression, solvent casting) and to the addition of additives is observed. The low-formulated films present increased gas barrier properties related to the crystallinity index of films. The water vapor sorption measurements proved the reduced ability to sorb water vapor of these biodegradable films, correlated to the gas permeabilities measurements. The tortuosity concept explains that barrier properties are related to the increase in the migration pathways which leads to limited permeability. Despite interesting barrier properties, few extensive applications to replace conventional plastic materials have been found although various production sources not compete with human or animal alimentation can be even envisaged.

References:

[1] C. Joly, D. Le Cerf C. Chappey, D. Langevin, G. Muller, « Residual solvent effect on the permeation properties of fluorinated polyimide films", Separation and Purification technology 16 (1999) 47-54.
[2] S. Marais, M. Métayer, M. Labbé, "Water diffusion and permeability in unsaturated polyester resin films characterized by measurements performed with a water-specific permeameter: analysis of the transient permeation", Journal of Applied Polymer Science 74(14) (1999) 3380–3395.
[3] O. Miguel, M.J. Fernandez-Berridi, J.J. Iruin, "Survey on Transport Properties of Liquids, Vapors, and Gases in Biodegradable Poly(3-hydroxybutyrate) PHB", Journal of Applied Polymer Science 64 (1997) 1849-1859.
[4] N. Follain, N. Jouen, E. Dargent, F. Chivrac, F. Girard, S. Marais, « Transport mechanism of small molecules through bacterial polyester films", 2nd International Conference on Natural Polymers, Bio-Polymers, Bio-Materials, their Composites, Blends, IPNs, Polyelectrolytes and Gels: Macro to Nano Scales, Kottayam, Kerala, Inde (2010)

Isothermal crystallisation study of P3HT:PCBM blends as used in bulk heterojunction solar cells based on fast scanning calorimetry techniques

N. Van den Brande [a], *F. Demir* [a], *S. Bertho* [b], *B. Van Mele* [a], *D. Vanderzande* [b], *J. Manca* [b], *G. Van Assche* [a]

[a] Department of Physical Chemistry and Polymer Science, Vrije Universiteit Brussels, Pleinlaan 2, 1050 Brussels Belgium.
[b] Institute for Materials Research, Hasselt University, Wetenschapspark 1, 3590 Diepenbeek, Belgium.

e-mail: npvdbran@vub.ac.be

Introduction

Post-production annealing is an important step in the preparation of bulk heterojunction solar cells, improving the efficiency [1-2]. It is important to define appropriate annealing temperatures and times, therefore the isothermal crystallisation of a poly(3-hexyl thiophene) (P3HT) and [6,6]–phenyl C_{61} – butyric acid methyl ester (PCBM) blend is investigated in this study in order to better understand the annealing process. In order to achieve this, fast scanning calorimetry techniques are required that allow for high cooling rates, avoiding crystallisation during cooling and achieving a glassy blend. It is then possible to study isothermal crystallisation closer to the glass transition temperature (T_g) than by conventional DSC techniques.

Materials and methods

This study was performed on a 50/50 wt% or 1:1 blend of P3HT (Merck, M_w=35 000 g mol^{-1}, M_w/M_n = 1.8; regioregularity greater than 98.5%) and PCBM (Solenne). A first technique used is "Rapid Heat-Cool" Calorimetry (RHC), that contains a millimeter-sized furnace for operation at scan rates of up to 2000 $K.min^{-1}$ [3]. In addition, ultra fast scanning chip calorimetry (UFSC) was used, based on a chip with a 100 µm x 100 µm heating area, which allows to study 100 nm layers at scan rates of 10^3-10^6 $K.s^{-1}$ [4].

Results and discussion

As annealing and the deterioration of the long-term stability of P3HT:PCBM active layers both involve crystallisation, the crystallisation rate of the 1:1 blend was investigated at temperatures in between the glass transition and melting. The evolution of the crystallisation rate with temperature was compared for annealing from the glassy state and from the melt state. The melting enthalpy after isothermal crystallisation was taken as a measure for isothermal crystallisation and plotted as a function of annealing time. The resulting crystallinity curves were then analysed using Avrami kinetics [5], yielding rates of crystallisation. When plotting the isothermal crystallisation rate versus crystallisation temperature (T_c) ,both from the melt and from the glassy state, bimodal bell-shaped curves are obtained with two maxima, one at lower temperature (70 or 80°C) and the second at higher temperature (110 or 125°C) , as can be seen in figure 1.

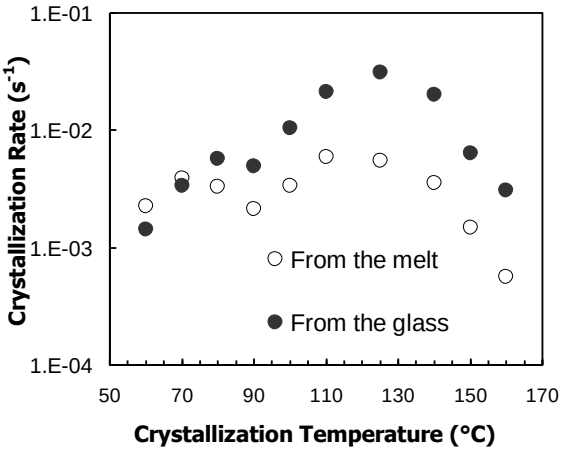

Figure 1: Isothermal crystallisation rates of a 1:1 P3HT/PCBM blend as calculated from Avrami kinetics as a function of temperature. A bimodal behaviour is seen when crystallizing both from the glass and from the melt.

Conclusion

The isothermal crystallisation rate of a 1:1 P3HT:PCBM blend was evaluated at several temperatures. The crystallisation rate curve as a function of temperature shows bimodal behaviour, attaining two maxima. The results found in this study could lead to a more optimised annealing procedure for the P3HT/PCBM devices.

References

1. Erb T., Zhokhavets U., Gobsch G., Raleva S., Stuhn B., Schilinsky P., Waldauf C., and Brabec C.J., Advanced Functional Materials, 2005. **15**(7): p. 1193.
2. Hoppe H. and Sariciftci N.S., Journal of Materials Chemistry, 2006. **16**(1): p. 45.
3. Danley R.L., Caulfield P.A., and Aubuchon S.R., American Laboratory, 2008. **40**(1): p. 9.
4. Minakov A.A., van Herwaarden A.W., Wien W., Wurm A., and Schick C., Thermochimica Acta, 2007. **461**(1-2): p. 96.
5. Avrami M., Journal of Chemical Physics, 1940. **8**(3): p. 212.

Solvent And Substrate Contributions To The Formation Of Breath Figure Patterns In Polystyrene Films

Elisa Ferrari, Paola Fabbri, Francesco Pilati

Department of Materials and Environmental Engineering, University of Modena and Reggio Emilia, Strada Vignolese 905/a, 41125 Modena, Italy

elisa.ferrari@unimore.it

When moist air is blown over a polymer solution, evaporative cooling can lead to the formation of water droplets on the liquid surface. These droplets can be arranged into a highly ordered hexagonal array because of different thermofluidodynamic mechanisms such as, for instance, Marangoni convection. Complete evaporation of both solvent and water results in formation of 2D or even 3D arrays of holes, often ordered hexagonally, the so-called BREATH FIGURES (BF).

The generation of BF has long been described as a complex phenomenon, in which several parameters combine in a fairly unknown way.

This work reports a detailed investigation over the role played by the solvent in the process of BF generation from polystyrene (PS, MW 192000g/mol) solutions spread over different substrates, and discuss the geometrical aspects of the pores by a quantitative point of view by using a purposely developed software for image analysis.

PS solutions (1% wt/vol) were prepared at room temperature using the following as solvents: acetone, carbon disulfide, chloroform, ethyl acetate, methyl ethyl ketone, dichloromethane, tetrahydrofuran, toluene. PS solutions were spread onto substrates having different surface energy, under humid conditions (RH 75± 2%): glass (43.1 mN/m), glass treated with piranha solution (62.8 mN/m), silicon wafer trated with RCA1 solution (48.1 mN/m), silicon wafer trated with piranha solution and then silanized with 3-glycidoxypropyltrimethoxysilane (49.0 mN/m), silicon wafer trated with piranha solution and then silanized with octyltriethoxysilane (61.5 mN/m), fluorinated glass treated with piranha solution (13.8 mN/m), polyethylene (34.5 mN/m), polyvinylchloride (38.0 mN/m) and polyethylene terephthalate (41.0 mN/m).

Effect of the solvent:

Chloroform and dichloromethane allowed the formation of regular BF, differently from carbon disulfide, that did not allow the formation of an extended hexagonal array of pores on hydrophilic glass GW; it seems that a too fast solidification of the polymer film occurred, favoured by the relatively low boiling point and high vapour pressure of carbon disulfide. The other solvents used were unable to generate porous structures, independently from the substrate. Interestingly, after solvent evaporation, the surface of samples prepared from acetone, methyl ethyl ketone and THF was characterized by the presence of polymer microspheres rather than porous polymer films. This last behaviour, which leads to morphologies quite similar to those recently described and named Reverse Breath Figures, will be discussed in more detail in an upcoming work.

Effect of the substrate:

According to our findings, there is no a quantitative correlation between the substrate surface energy or wettability and pore size and order. From a qualitatively point of view, however, the effect of the substrate (nature, hydrophilicity, wettability) is clear.

All the above reported results suggest that the role of the substrate in the overall mechanism of BFs formation is strictly related to the type of solvent used. In particular the combined effect of solvent and substrate could affect the nucleation of water droplets. Water adsorbed on the substrate before the deposition of the polymer can be removed after the application of the polymer solution and transported to the surface by the Marangoni convective movements. More hydrophilic substrates are able to bind higher amounts of water and this can make the formation of water nuclei faster when the solution is able to remove efficiently this water from the substrate surface.

Figure 1 (a-d) shows SEM micrographs of porous films generated from 1% wt/vol PS/dichloromethane on: (a) PET; (b) PVC; (c) Silanized glass - GWO; (d) pirañha treated glass - GW.

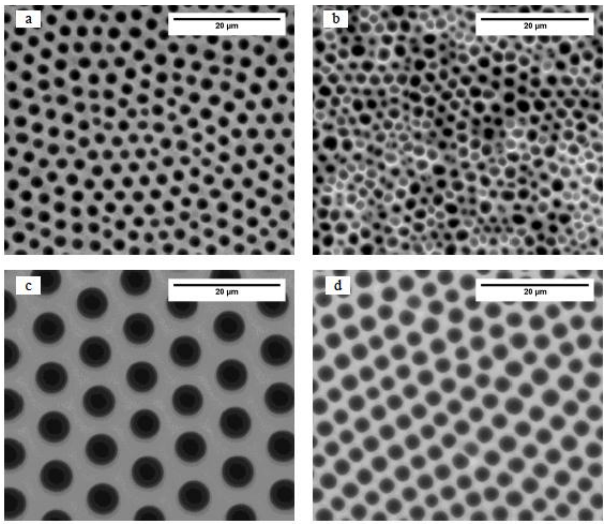

Results show that thermodynamic affinity between polymer and solvent is the key parameter for BFs formation, along with other solvent characteristics such as water miscibility, boiling point and enthalpy. According to our findings, the role played by the substrate is strictly related to the type of solvent used in the generation of BFs.

References.

E. Ferrari, P. Fabbri, F. Pilati, Langmuir (2011) DOI: 10.1021/la104500j, in press

Collapse of polyelectrolyte star. Theory and modeling

Oleg V. Rud[1], Anna A. Mercurieva[2], Tatiana M. Birshtein[1]

[1]Institute of Macromolecular Compounds RAS, [2]Saint-Petersburg State University

helvrud@gmail.com

Collapse of a hydrophobic polyelectrolyte star is considered using Self-Consistend Field theory and numerical Scheutjens-Fleer method [1, 2]. Star consists of several polyelectrolyte chains, each of these in turn is composed of identical monomers. Monomers can be ionized, and are hydrophobic by itself. For example it can be a polyacid, implying that its chain monomers can be either neutral or negatively charged and all of these have the lateral hydrophobic group.

The aim was to study the interplay between two forces that determine the conformation of polyelectrolyte stars in the solution. These are the hydrophobicity of the polymer and the electrostatic interaction between polyelectrolyte and the dissolved ions. The first one makes the chain monomers stick each other and avoid contact with the solvent molecules, which leads to compression (collapsing) of the polymer. The second one is contrary to swelling of the polymer by increasing the osmotic pressure in the interior region of the polymer coil. Osmotic pressure in turn is caused by the attraction of charged chain groups and oppositely charged low molecular weight counter- and salt ions.

The situation is much more complicated in heterogeneous systems, such as PE brushes or polyelectrolyte stars. Parameters: pH of the solvent, ionic strength turn out local and related to the local concentration of the star PE.

We have shown that the locality of parameters determine the nature of the star collapse process. The transition from swollen to collapsed star goes through an intermediate state. There is a local area in the star, where that is profitable for star chains to be collapsed, and the area where that is profitable to be swollen. As a result we have a microphase segregated star. The inner part of the star is a dense and relatively uncharged core and the outer is swollen strongly charged shell (corona). Large enough corona can support the collapsed core dissolved (or correctly speaking weighted) in a solution.

This state we call quasi-micelle.

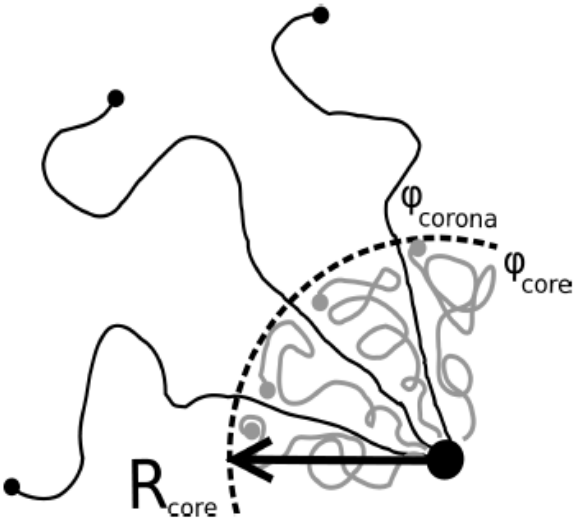

Figure: quasi-micelle state.

A quasi-micell is organised as follows. Each arm of the star can fall either into a collapsed phase or into a swolen one and thus participate in forming either a dense core or a low-density soluble star corona. A number of arms fallen into collapsed phase depends on the solution features, that is by varying solvent parameters one can control relative sizes of a core and a corona.

The possibility to be weighted opens up the prospect to use such systems in well known drug delivery problem.

Substances, soluble in the matter of star core, might be delivered inside the core in the place that we want,where would be released either through star destruction or its transition into the swollen state.

References:

1. van Male, J.; Leermakers, F. A. M. “sfbox”, 2001 A Computer Program.

2. Fleer, G. J.; Cohen Stuart, M. A.; Scheutjens, J. M. H. M.; Cosgrove, T.; Vincent, B. Polymers at Interfaces; Chapman & Hall; London, 1993.

Polylactide and β-Tricalcium Phosphate Composite Fibers by Electrospinning Technique for Tissue Engineering Applications

Loredana Tammaro[1*], *Ralf Wyrwa*[2], *Juergen Weisser*[2], *Ulrike Müller*[2], *Matthias Schnabelrauch*[2]

[1]Department of Chemical and Food Engineering, University of Salerno, Via Ponte Don Melillo 1, Fisciano (SA), 84084 - ITALY

[2]Biomaterials Department, INNOVENT e. V., Pruessingstrasse 27B, D-07745 Jena - GERMANY

* e-mail: ltammaro@unisa.it

Introduction

A wide variety of biocompatible and biodegradable polymers have been developed for medical applications including synthetic polymers, such as poly(lactide), poly(glycolide), poly(ε-caprolactone), and natural polymers including proteins such as collagen, and fibrogen, and polysaccharides like chitosan. Among them, poly(L-lactide-co-D,L-lactide) (PLDLA) has been widely studied for biomedical applications including substrates for tissue engineering. Although polymeric materials alone have shown some positive results for bone regeneration, efforts have been made to enhance and stimulate their bone response by introduction of fillers similar to the mineral bone phase such as hydroxyapatite, tricalcium phosphate, calcium carbonate. Recently several investigations for producing nanofiber matrices have been performed using electrospinning technique. Nowadays nanofibers are gaining a lot of attention and are being explored as scaffold in bone tissue engineering applications, due to their properties that can modulate cellular behavior.

Materials and Methods

PLDLA was chosen in this study for production of electrospun microfiber non-woven membranes with and without a bone-like β-tricalcium phosphate (β-TCP).

The structure, the morphology and the thermal properties of the obtained membranes have been investigated by X-ray diffraction (XRD), scanning electron microscopy (SEM), thermogravimetric analysis (TGA) and differential scanning calorimetry (DSC). The feasibility of combining β-TCP with PLDLA nanofibers mats for in vitro tissue engineering was examined using the MC-3T3-E1 osteogenic cell line. The in vitro degradation of the fibers has been tested in a simulated body fluid medium.

Results and Discussion

Microfibers of PLDLA and PLDLA/β-TCP have been successfully produced using the electrospinning method in acetone solvent. The X-ray data indicated that the electrospinning process led to a mixture of PLDLA and β-TCP. The SEM analysis showed very similar diameter values of the fibers with a distribution centered at value less than 1.0 µm and generally uniform thickness along the fibers. The TGA analysis confirmed the amount of β-tricalcium-phosphate in the composite fibers and showed good and similar thermal properties of all membranes (by TGA and DSC). Using the MC-3T3-E1 an excellent cytocompatibility was found for both PLDLA and PLDLA/β-TCP non-wovens.

Conclusions

Taking into account all the results together, it is clearly demonstrated that the obtained PLDLA/β-TCP electrospun fibers form a favorable physical and biological environment suitable in advanced applications as scaffold for bone tissue engineering.

References

1. Joon-Pyo Jeun, Yun-Hye Kim, Youn-Mook Lim, Jae-Hak Choi, Chan-Hee Jung, Phil-Hyun Kang, and Young-Chang Nho, Electrospinning of Poly(L-lactide-co-D, L-lactide), *J. Ind. Eng. Chem.*, Vol. 13, No. 4, (2007) 592-596.
2. Yi Zuo, Fang Yang , Joop G.C. Wolke, Yubao Li , John A. Jansen, Incorporation of biodegradable electrospun fibers into calcium phosphate cement for bone regeneration, *Acta Biomaterialia* 6 (2010) 1238–1247.
3. Cevat Erisken, Dilhan M. Kalyon, Hongjun Wang, Functionally graded electrospun polycaprolactone and β-tricalcium phosphate nanocomposites for tissue engineering applications, *Biomaterials*, 29 (2008) 4065–4073.
4. Bora Mavis, Tolga T. Demirtaş, Menemşe Gümüşderelioğlu , Güngör Gðündüz , Üner Colak, Synthesis, characterization and osteoblastic activity of polycaprolactone nanofibers coated with biomimetic calcium phosphate, *Acta Biomaterialia* 5 (2009) 3098–3111.
5. Young You, Byung-Moo Min, Seung Jin Lee, Taek Seung Lee, Won Ho Park, In Vitro Degradation Behavior of Electrospun Polyglycolide, Polylactide, and Poly(lactide-co-glycolide), *Journal of Applied Polymer Science*, Vol. 95, (2005),193–200.

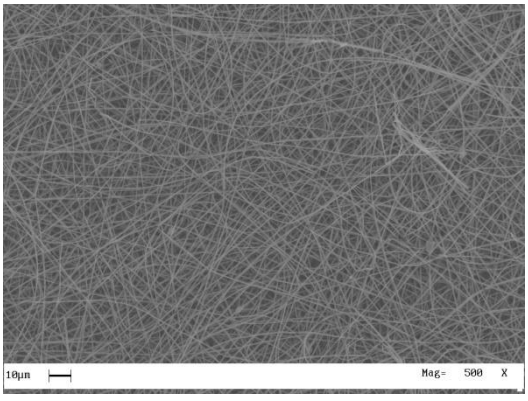

SEM micrograph of the electrospun fibers from PLDLA-β-TCP solution (Electric voltage: 20 KV; Needle-screen distance: 20 cm; Solution flow-rate: 0.5 ml/h; Solution concentration: 2.5wt% in acetone solvent, β-TCP concentration: 5 wt%

Azobenzene block copolymers and blends: microstructure, photoinduced anisotropy and holographic storage

Cristina Berges[1], Eva Blasco[2], Nélida Gimeno[2], Patricia Forcén[1], Luis Oriol[2], Milagros Piñol[2], Carlos Sánchez[1], Rafael Alcalá[1]

[1]Departamento de Física de la Materia Condensada. Facultad de Ciencias
[2]Departamento de Química Orgánica. Facultad de Ciencias
Instituto de Ciencia de Materiales de Aragón, Universidad de Zaragoza-CSIC, 50009 Zaragoza, Spain.

berges@unizar.es

The interest on polymers containing azobenzene moieties in the side chain has increased in the last years due to the optical anisotropy induced by *trans-cis-trans* photoisomerisation and reorientation of azobenzene molecules using polarized light. This phenomenon makes this kind of materials suitable for optical applications[1-3]. However, due to the optical absorption of azo units at the wavelengths of the exciting light (488nm), thick films, needed for some applications (such as volume holographic storage[4]) cannot be illuminated through the complete film thickness.

Lower optical absorption, while keeping the interactions among azo, units can be achieved by using di-block copolymers in which a block contains the azo units while the other block is made of a polymer that does not absorb at the recording wavelength. To further reduce the azo content, blends can be made by mixing these diblock copolymers with the same homopolymer of the transparent block. In this way thick films, in which the exciting light is able to go through them with low attenuation, can be made. Good photoinduced response in di-block copolymers with azo-contents down to 20% in weight, as well as in some blends of these polymers with PMMA has been presviously reported[5,6].

In this communication we present the results of a study comparing the photoinduced response of two methacrylic diblock copolymers with different azo content (Block 24-14 with a 24% wt, and Block 12-30 with a 12% wt) and their blends. The reduction of azo content has been achieved both by increasing the molecular weight of the methacrylic block of Block12-30 and by blending with PMMA of different molecular weights.

Both block copolymers developed a well defined microstructure which has been characterized by Transmission Electron Microscopy (TEM). Block 24-14 shows a lamellar like structure, while for Block 12-30, the observed microstructure is spherical, with an average diameter of the azobenzene microdomain of 25-30nm, as it can be seen in Fig. 1 (the size of the black bar is 200nm).

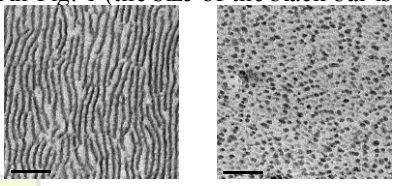

Fig. 1

Blends of Block 24-14 with PMMA of molecular weight 11500, changed the lamellar microdomains into spheres, as the azo content decreased from 24%wt to 12%wt (Blend 1) and to 3%wt (Blend 2). However, blends of Block 12-30, with a decrease in the azo content down to 3%wt (Blend 3), showed the same spherical microstructure as Block 12-30.

Photoinduced anisotropy has been studied in these materials in terms of birefringence (Δn) and dichroism. Since Δn is mainly associated with azobenzene units, the saturation value of /Δn/ decreases when the azo content goes from 24%wt to 12%wt and 3%wt in the case of Block 24-14, and from 12 %wt (Block 12-30) to 3 %wt (Blends 5) in the case of Block 12-30, as it can be seen in Fig. 2. However, values of birefringence normalized to the azo content ($/\Delta n/_{norm}$), are similar in the two block copolymers and in blends of Block 12-30 while lower values are got in blends of Block 24-14.

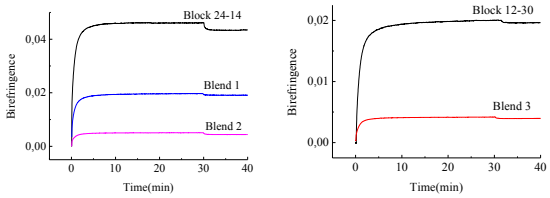

Fig. 2

This can be associated with the lower order achieved in these blends, which was checked by dichroism measurements. The photoinduced orientation was defined by an in plane order parameter η. The values obtained for Blends 1 and 2 are $\eta = 0.47$ and $\eta = 0.40$ respectively, which are smaller than the order parameter measured for Block 24-14 ($\eta = 0.51$). This decrease in the order parameter can be due to the change from lamellar to spherical microstructure. However, Block 12-30 and Blend 3, show η values of approximately 0.51.

We can conclude that Block 12-30 and Blend 3 allow us to maintain values of $/\Delta n/_{norm}$ and η similar to that of Block 24-14, although the azo content is lower; while Blends 1 and 2 have a worse optical response than Block 24-14. Holographic recording has also been studied in blends of Block 12-30 with an azo content reduced down to 0.1%. Stable holographic gratings have been stored in this material.

1. Shibaev V.; Bobrovsky A.; Boiko N.; Prog. Polym. Sci. 2003, 28, 729.
2. Yanamoto T.;Yoneyama S.; Tsutsumi O.; Kanazawa A.; Shiono T.; Ikeda T.; J. Appl. Phys. 2000, 88, 2215.
3. Matharu A. S.; Shehzad J.; Ramanujam P.S.; Chem. Soc. Rev. 2007, 36, 1868.
4. Hvilsted S.; Sánchez C.; Alcalá R.; J. Mater. Chem. 2009, 19, 6641.
5. Forcén P.; Oriol L.; Sánchez C.; Alcalá R.; Hvilsted S.; Jankova K.; Loos J.; J. Pol. Sci. A: Pol. Chem. 2007, 45, 1899.
6. Gimeno S.; Forcén P.; Oriol L.; Piñol M.; Sánchez C.; Rodríguez F. J.; Alcalá R.; Jankova K.; Hvilsted S.; Eur. Pol. J. 2009, 45, 262.

Diastereoselective synthesis of azanorbornenes from enantiomerically pure precursors and subsequent polymerizations

Elisabeth Rossegger,[1] *Franz Stelzer*,[2] *Frank Wiesbrock*[2,*]

[1] Polymer Competence Center Leoben GmbH PCCL,
Roseggerstrasse 12, AT-8700 Leoben, Austria.
[2] Graz University of Technology, Institute for Chemistry and Technology of Materials,
Stremayrgasse 9/V, AT-8010 Graz, Austria.

e-mail: f.wiesbrock@tugraz.at

Introduction

Azanorbornenes are optically active nitrogen-containing compounds that are ideal synthetic precursors for a large variety of natural products like amino acids.[1,2] Consequently, azanorbornenes are of topical interest for the synthesis of various active agents.

Furthermore, there is an increasing demand for the fine-tuning of properties of highly functionalized polymers in virtually all application fields. However, catalytic polymerization methods using transition metal based initiators are limited by the functional-group tolerance. Concomitant with the introduction of 3rd generation Grubbs initiator, state of the art ROMP (ring opening metathesis polymerization) offers the advantage of paramount functional group tolerance these days. Hence, the incorporation of highly diverse chemical groups into the targeted materials is greatly facilitated.

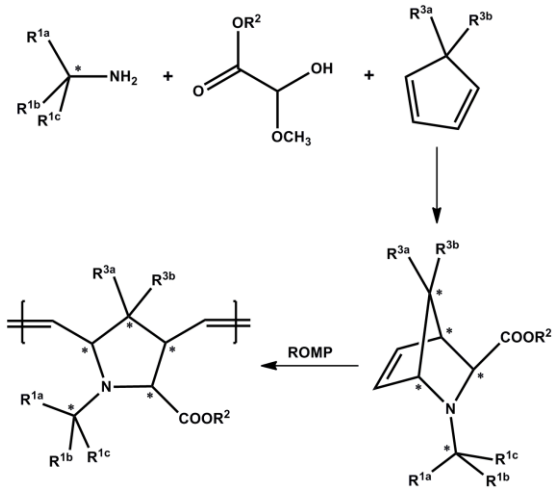

Scheme 1: Synthesis of azanorbornenes by ROMP.

The objective of this research work was to develop synthetic strategies towards well-defined polymers that meet a plethora of requirements; high glass-transition temperatures (T_g) were additionally favored: high T_g materials are attractive for various applications in industry. Until now, only isolated examples of ROM polymers with high T_g are known. A further step in the direction of material design concerns the control of the stereochemistry of the polymers obtained by a hetero-Diels-Alder reaction.

Materials and Methods

Asymmetric Diels-Alder reactions of cyclopentadiene and the phenyl-methyl imine of methyl glyoxylate yielded azanorbornenes (Scheme 1). The following ROM polymerization was initiated by a ruthenium complex. Four structures of poly(azanorbornene)s are possible (Figure 1).

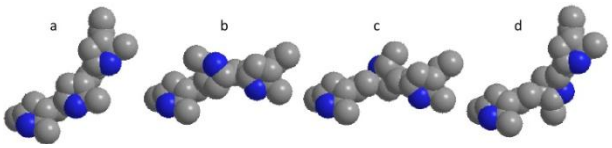

Figure 1: Four possible regular structures of poly(2-azanorbornene) derivatives.[3] (a) cis, HT, isotactic; (b) cis, TT, syndiotactic; (c) trans, HT, isotactic; (d) trans, TT, syndiotactic.

Results and Discussion

Diastereoselective poly(azanorbornene)s were synthesized via ROMP[3] from monomers prepared by aza-Diels-Alder reactions. In general, 16 stereoisomers of the monomers are possible. The ruthenium complexes as initiators for ROM polymerization exhibited sufficient functional group tolerance for polymerizing azanorbornenes.

Conclusions

A general design principle for monomers leading to high T_g ROM polymers is under current investigation. In this poster presentation, the structure characterization of azanorbornenes as well as the subsequent ROM polymerizations will be reported. Furthermore, the characterization of the poly(azanorbornene)s will be presented.

References

[1] H. Sunden, I. Ibrahem, L. Eriksson, A. Cordova, *Angew. Chem. Int. Ed.* **2005**, *44*, 4877-4880.
[2] A. A. Ruggiu, R. Lysek, E. Moreno-Clavijo, A. J. Moreno-Vargas, I. Robina, P. Vogel, *Tetrahedron* **2010**, *66*, 7309-7315.
[3] R.M.E. Schitter, T. Steinhäusler, F. Stelzer, *J. Mol. Cat.* **1997**, *115*, 11-20.

Screening of New Developed Copolymers as Potential Antidotes Against Radionuclides.

Farmazyan Z.[1], *Harutyunyan G.*[1], *Sargsyan V*[1]., *Hayriyan L.*[1], *Stepanyan K.*[2], *Pogosyan A.*[2]

1. CJSC "Yerevan SRI "Plastpolymer"Arshakunyats 127, Yerevan 0007, Armenia
2. Scientific Center of Radiation Medicine and Burns, SCRMB, Davidashen, m/b 25 Yerevan 0108, Armenia

zoefa2000@yahoo.com

Introduction. Risk of internal and external radiation injury exists everywhere where radioactive substances are used or produced. Now these risks are increased because of terrorism attacks and possibilities of using "dirty" bombs [1,2].

In case of penetration of radionuclides in human organism the primary task is their fast removing. At present for this purpose various low-molecular chelating compounds (pentacinum, ferrocinum, trimephacinum) are used in practice. However, almost all of them possess a number of negative properties and can cause headache, nausea, decrease of calcium level in serum, etc [2,3].

We are developing new grades of copolymers that showed high effectiveness in binding and removing of radio nuclides (^{137}Cs, ^{60}Co and ^{90}Sr) from different surfaces [4].

In this connection a possibility of using some of these copolymers (water-soluble) as potential polymeric antidotes with high effectiveness and low toxicity has been examined.

Materials and Methods.Three series of copolymers modified polyvinyl alcohol (MPVAL), derivatives of vinylacetate (VA) - acrylic acid (AC) and N-vinylpyrrolidone – maleic acid (VPMA) have been investigated. The functional compositions of copolymers were examined by methods of chemical, conductometric titration, IR-, NMR spectroscopy. Surface tension of solutions and critical concentration of micelle formation were determined with CAM-101 apparatus

For each series in model conditions (water solutions of non -radioactive salts) functional composition of copolymers providing the maximum binding of Cs, Co and Sr was verifiied [5].

Cytogenetic activities (proliferative activity, chromosomal aberration) of the selected samples of copolymers have been studied *in vivo* (bone marrow cells of white rats).

Results and Discussion.

First the principle possibility of using some of the developed copolymers for binding of radionuclides (^{90}Sr) in blood was verified *in vitro*.

Since in the reactions of strontium binding both blood protein and co-polymers, injected into the blood, may participate, the experiments to find out their role and the share were carried out in the reactions with non-radioactive ions.

To reveal competitiveness between developed copolymers and blood proteins in binding of metals ions the comparative researches by using of albumen were conducted. It is revealed, that efficiency of metals binding in the presence of albumen depends both on polymer type and on its functional composition. It was shown, for example, that mixture of albumen and copolymer VA-AC-16 (1: 0,5) binds 90% of Co^{2+} in water solution, while VA-AC-16 copolymer alone binds 85% of Co^{2+}. MPVAL is more effective in binding of Co^{2+} than albumin. However these copolymers exhibit different citogenetic activity (Table1, substance dose 60 mg/kg).

Table1. Cytogenetic changes of bone marrow cells

Samples	PA (amount)	ChA (%)
MVAL26/05	591.6±48.7	2.08±0.44
VPMA	718.0±90.8	2.0±0.28
VA-AC-16	778±19.8	2.0±0.09
VA-AC-19	1317.0±30.6	1.0±0.1
Control	654.75±55.11	3.31±0.57

Despite the difference in performance, these polymers are considered to be cytogenetically inactive and can be used in *vivo* studies.

Conclusion. The results, received up to now, show that developed copolymers have potentiality to be used in further testing as antidotes in *vivo* with using ^{137}Cs, ^{60}Co and ^{90}Sr radionuclides.

References

1. Kuna P. et al. How serious is threat of radiological terrorizm? ACTA MEDICA, 2009, 52 (3), 85-89
2. Armin Ansari, Dirty Bomb Pills, Shots, Weeds and Spells, Health Physics News, Vol.32, 11, 2004
3. Mashkovskiy M.D. Medicinal agents. Moscow, "Novaya volna", 2002, vol. 2, p. 202-209
4. Farmazyan Z., Harutyunyan G., Dalalyan N., Hayriyan L., Hakobyan E., Sargsyan V., "Strippable Deactivating Coatings on the Basis of Modified Polyvinylalcohol", 33rd AMOP Technical Seminar on Environmental Contamination and Response, 7 - 9 June, 2010 , Halifax, Nova Scotia, Canada
5. Sargsyan V., Farmazyan Z., Hayriyan L.,Harutyunyan G. «Mechanism of binding of non-rarioactive cobalt and cesium with polymeric compounds», «Plasrmassi», Moscow, rus, in press.

Poly(ferrocenylsilane) Hydrogels

Mark A. Hempenius,[1] *Xiaofeng Sui*,[1] *Concetta Cirmi*,[2] *Jing Song*[3] *and G. Julius Vancso*[1]

[1]Faculty of Science and Technology, MESA+ Institute for Nanotechnology,
University of Twente, P.O. Box 217, 7500 AE Enschede, The Netherlands
[2]Faculty of Engineering, Department of Industrial and Mechanical Engineering,
University of Catania, Viale A. Doria 6, 95125 Catania, Italy
[3]Institute of Materials Research and Engineering (IMRE)
3, Research Link, Singapore 117602

m.a.hempenius@utwente.nl

Introduction

Stimulus-responsive hydrogels are attracting much attention due to their potential use in controlled release systems[1] where drugs or cosmetics can be released upon receiving a specific stimulus, or as actuators, artificial muscles or valves.[2,3] Typical stimuli used to date include temperature, pH, ionic strength, light and to a much lesser extent redox stimuli.[4] Redox stimuli may offer fast and reversible switching between states and can be applied externally. We recently reported redox-responsive poly(ferrocenylsilane) (PFS)[5] polyion hydrogels[6] based on water-soluble PFS polyelectrolyte chains.[7] PFS hydrogels may undergo redox-induced[8] volume changes or changes in viscoelastic properties due to alterations in chain conformation, charge density and polarity of the constituent polymer chains. Networks based on PFS chains soluble in regular organic solvents have been reported.[9] Making use of the PFS redox activity, full-color displays based on the electrical actuation of photonic crystals have been fabricated.[10] However, there are, to our knowledge, no accounts of PFS hydrogels in the literature. Here we report on the synthesis of two distinct types of poly(ferrocenylsilane) hydrogel, featuring PFS chains with negatively charged side groups and a hydrogel based on organic solvent-soluble PFS chains.[11]

Results and Discussion

Poly(ferrocenyl(3-iodopropyl)methylsilane) **1** (Scheme 1) was synthesized as described earlier.[7b] A desired amount of 4(1-adamantyl)phenol was attached to PFS **1** by nucleophilic substitution, followed by reaction of the resulting **2** with α-lithio isobutyl methanesulfonate anion.[7b] Deprotection of the isobutylsulfonate side groups and subsequent ion exchange led to PFS polyanion **3** which possessed a tunable amount of adamantyl side groups. PFS polyanion **3** will then be combined with a *β*-CD-derivatized 8-arm star-shaped poly(ethylene glycol) (Scheme 1), employed earlier by W.E. Hennink *et al.* to form a hydrogel by self-assembly.[12] Side group modification of PFS **1** with sodium acrylate anions yielded a PFS that could be crosslinked using α,ω-poly(ethylene glycol)dithiol via thiol-Michael addition click reaction. A water-swellable network was obtained. The equilibrium swelling ratio, morphology, rheology, and redox responsive properties of this PFS-PEG-based hydrogel were investigated.

Conclusions

PFS hydrogels, composed of water-soluble PFS polyions or of organophilic PFS chains, were produced. The hydrogels could be oxidized and reduced reversibly by chemical and electrochemical means. Their redox-responsive behavior is currently under study.

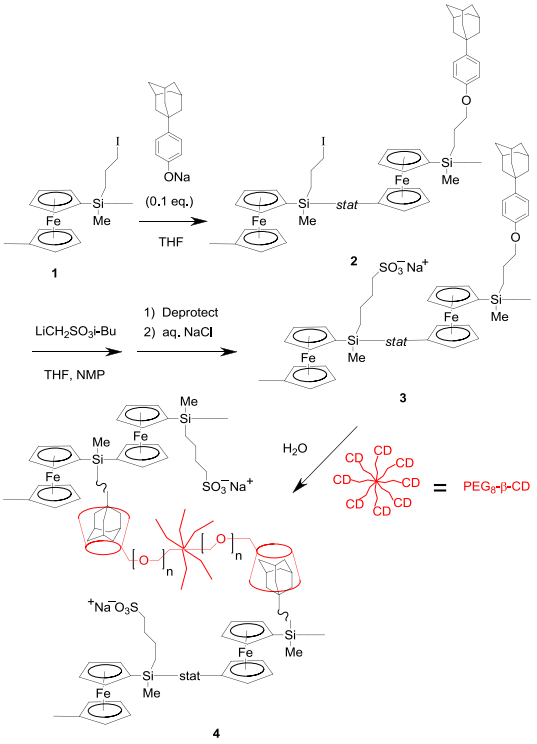

Scheme 1. PFS polyanion hydrogel formation by self-assembly, using *β*-CD/adamantane host-guest complexation for creating crosslinks.[12]

References

1. Franssen, O.; Vandervennet, L.; Roders, P.; Hennink, W. E. *J. Contr. Release* **1999**, *60*, 211.
2. Zhang, Y.; Kato, S.; Anazawa, T. *Smart Mater. Struct.* **2007**, *16*, 2175.
3. Liu, Z.; Calvert, P. *Adv. Mater.* **2000**, *12*, 288.
4. Peng, F.; Li, G.; Liu, X.; Wu, S.; Tong, Z. *J. Am. Chem. Soc.* **2008**, *130*, 16166.
5. Whittell, G. R.; Manners, I. *Adv. Mater.* **2007**, *19*, 3439.
6. Hempenius, M. A.; Cirmi, C.; Song, J.; Vancso, G. J. *Macromolecules* **2009**, *42*, 2324.
7. (a) Wang, Z.; Lough, A.; Manners, I. *Macromolecules* **2002**, *35*, 7669. (b) Hempenius, M. A.; Brito, F. F.; Vancso, G. J. *Macromolecules* **2003**, *36*, 6683.
8. Rulkens, R.; Lough, A. J.; Manners, I.; Lovelace, S. R.; Grant, C.; Geiger, W. E. *J. Am. Chem. Soc.* **1996**, *118*, 12683.
9. Kulbaba, K.; MacLachlan, M. J.; Evans, C. E. B.; Manners, I. *Macromol. Chem. Phys.* **2001**, *202*, 1768.
10. Arsenault, A. C.; Puzzo, D. P.; Manners, I.; Ozin, G. A. *Nature Photonics* **2007**, *1*, 468.
11. Sui, X.F.; van Ingen, L.; Hempenius, M.A.; Vancso, G.J. *Macromol. Rapid Commun.* **2010**, *31*, 2059.
12. van de Manakker, F.; Braeckmans, K.; el Morabit, N.; De Smedt, S. C.; van Nostrum, C. F.; Hennink, W. E. *Adv. Funct. Mater.* **2009**, *19*, 2992.

Synthesis and Characterization of Stimuli-responsive Amphiphilic Block Copolymers

E. Blasco,[1] C. Berges,[2] R. Alcalá,[2] C. Sánchez,[2] L. Oriol,[1] M. Piñol[1]

[1]Departamento de Química Orgánica. Facultad de Ciencias
[2]Departamento de Física de la Materia Condensada. Facultad de Ciencias
Instituto de Ciencia de Materiales de Aragón, Universidad de Zaragoza-CSIC, 50009 Zaragoza, Spain

mpinol@unizar.es

Stimuli-responsive block copolymers have received an increased attention in recent years. One of the most well-known thermal-responsive polymers is PNIPAM. However, alternative polymers such as copolymers containing short oligo(ethylen glycol) methacrylates have being investigated. Their lower solution critical temperature (LSCT) can be tuned by adjusting the monomers ratio.[1] On the other hand, functionalization of amphiphilic copolymers with azobenzene derivates allows obtaining interesting photoresponsive materials.[2]

In this work, block copolymers consisting of a thermoresponsive block linked to an aliphatic polyester fourth-generation dendron functionalized with azobenzene moieties have been synthesized (*Figure 1)*.
The linear block is composed by a copolymer of 2-(2-methoxyethoxy)ethyl methacrylate (MEO_2MA) and oligo(ethylene glycol) methacrylate (OEGMA).

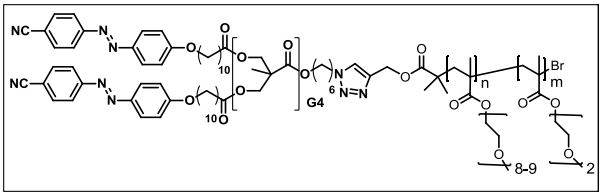

Figure 1. Chemical structure of the block copolymers.

Controlled radical polymerization, in particular ATRP, has been employed to obtain well-defined thermosresposive blocks. An efficient coupling of the preformed blocks has been achieved using copper(I)-catalyzed azide-alkyne cycloaddition (CuAAC).

Chemical structures of the linear-dendritic block copolymers were confirmed by IR, ^{1}H NMR, and ^{13}C NMR espectroscopies. Purity and molecular weight determination were performed by gel permeation chromatography (GPC).

Cloud points of the thermoresponsive linear bock were measured on a photometer. Transmitance of polymer solution in water at 670 nm was monitored as a function of temperature.

Thermal transitions were studied by differential scanning calorimetry (DSC) and polarized optical microscopy (POM).

Morphological study is going to be performed by using electronic microscopy.

This work was supported by the MICINN (Spain) under the project MAT2008-0625-C02-01 and DGA founding.

References

1. J.F.Luzt, A. Hoth . *Macromolecules* **2006**, 39, 893-896
2. J.Del Barrio, L.Oriol, C.Sánchez, J.L.Serrano, A.Di Cicco, P.Keller, M.H. Li, *J.Am. Chem. Soc.* **2010**,*132*, 3762-3769.

Development of Active Flexible Packages by the Incorporation in Bulk of Antimicrobial Natural Additives

R. González-Leyba, B. Galindo-Galiana, C. Gadea-Tomás, F. Martí-Ferrer

AIMPLAS, Gustave Eiffel, 4. Parque Tecnológico, 46980 Paterna (Valencia), Spain. Tel. +34 96 136 60 40, Fax +34 96 136 60 41

rgonzalez@aimplas.es

Introduction

Active packaging is referred to packaging systems where the package has active functions beyond containing and protecting the product inside. The interaction produced between the package and the product helps to extend its shelf-life. Different systems of active packaging are well-known, consisting usually in the incorporation of an active agent inside the package in a separated bag or as a coating, interacting with the package head-space or directly with the food. The active package has to be designed specifically to the product to be packed.

In this study, different natural additives were used as antimicrobials by their incorporation into the polymer matrix of flexible packages in order to study their effectiveness on different types of food.

Extracts from grape seeds and garlic were selected among several natural additives due to their good thermal stability, allowing their incorporation in bulk during the extrusion process.

Protection of food against microbial degradation should take place by additive migration from the polymer matrix to the food inside the package.

The two keys of the active packages development are both the correct incorporation of the natural additives into the polymer matrix, withstanding temperature and shear conditions given at a conventional extrusion process, and migration of the additives from the polymer matrix that should take place.

This type of active packages would differ from the current ones on the market as the active additive is incorporated directly into the polymer matrix.

Materials and methods

The natural antimicrobials studied were garlic extract from DOMCA, grape seeds and onion extracts both from NATUREX. The polymeric matrix was polypropylene (PP), grades from REPSOL (standard grade) and BASELL (low melt temperature grade).

The thermal stability of the natural antimicrobials was studied by Thermal Gravimetric Analysis (TGA).

Compounds of PP with natural antimicrobials were prepared by compounding using a co-rotating extruder. Monolayer films of PP containing different amounts of the active additive were obtained by flat film extrusion.

Results and discussion

Results from TGA showed that garlic and grape seed extracts had the best thermal properties, being thermal degradation initiated above 200 ºC. The most stable was the garlic extract. Onion extract showed thermal degradation initiation at 100 ºC, taking place the most part at 160 ºC.

Garlic and grape seeds extracts were selected for the PP compounds preparation. Due to their different thermal stability, a low melt temperature PP grade was used in the preparation of grape seed extract compounds, whereas a standard PP grade was used for garlic extract compounds. Extract compounds containing 10% (w/w) of the antimicrobial additives were prepared in a co-rotating extruder. A specific screw configuration was designed to avoid degradation of the natural additives by shear during the compounding process. The compounds were used in flat film extrusion to obtain PP films with different amounts of each extract. Figure 1 shows a film of PP containing grape seed extract. Temperatures were optimised in order to avoid degradation of the natural extracts. The antimicrobial character of the extruded films is being studied with different types of food like salmon, cheese, jam, avocado and apple.

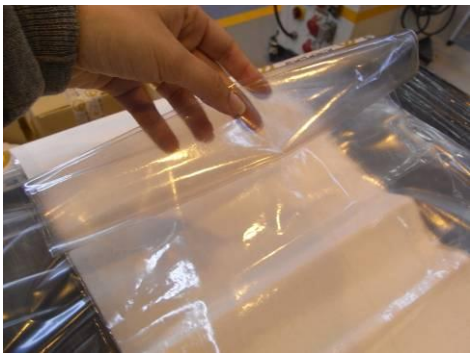

Figure 1: Extruded PP film with grape seed extract incorporated

Conclusions

Natural additives can be incorporated in PP by the conventional processing techniques for polymeric materials. The selection of the most suitable polymer grade in combination with the extrusion equipment and conditions is crucial to maintain the antimicrobial character of the natural additive in the PP matrix.

Acknowledgements

This study is part of the project “Desarrollo de envases activos con aditivos naturales obtenidos de residuos agroindustriales”, a Consortium Project between Research Technological Centres, co-funded by the Science and Innovation Ministry of Spain (PID-600200-2009-18), Generalitat Valenciana (ACOMP/2010/210), IMPIVA and European Regional Development Fund (ERDF).

Synthesis of Superparamagnetic Magnetite/Poly(butylcyanoacrylate) (Core/Shell) Nanoparticles for Drug Delivery Purposes

Daniele Alioto, Margarita López-Viota, Eva Sáez-Fernández, Mª Adolfina Ruiz, José L. Arias

Department of Pharmacy and Pharmaceutical Technology, University of Granada, Spain.

jlarias@ugr.es

Introduction. Drug delivery to severe diseases can be based on nanomaterials sensitive to external stimuli. Such advanced nanoplatforms (stimuli-sensitive nanocarriers) are capable to experience alterations in their structure and physical properties under small changes in the environment. The consequence will be a controlled delivery of the nanomedicine and/or triggered drug release into the disease site. In this way, one of the major approaches is the use of magnetic nanoparticles (NPs). Such advanced nanomaterials can specifically deliver drugs to targeted sites under the guidance of magnetic gradients. Iron oxide NPs are primarily used in their formulation. However, due to the poor drug loading capacity and uncontrollable drug release frequently exhibited by iron oxides, it is also needed to embed them into a biodegradable shell (mainly a polymer or a lipid vesicle). The shell will play the role of transporting the drug to the non-healthy tissue (controlling its release). At the same time, the iron oxide core will allow the magnetic guidance of the nanomedicine towards the site of action [1, 2].
In this work, we describe the synthesis and characterization of magnetic NPs composed of a core of superparamagnetic magnetite (Fe_3O_4) and a shell of poly(butylcyanoacrylate) (PBCA).

Materials and Methods. Superparamagnetic Fe_3O_4 (size ≈ 10 nm) and PBCA (size ≈ 250 nm) were synthesized following the chemical co-precipitation process [3] and the emulsion/polymerization method [4], respectively. The formulation of the Fe_3O_4/PBCA nanocomposites was possible by anionic polymerization of the BCA monomer (1 %, w/v) in a Fe_3O_4 aqueous suspension (0.4 %, w/v) with a concentration of 10^{-4} N of HCl, during 3 hr under mechanical stirring. Particle size was determined by PCS. The presence of the shell onto the magnetic nuclei was checked by HRTEM.
The characterization of the chemistry and internal structure of the NPs was achieved by FTIR spectrometry and X-ray diffractometry, respectively. Surface electrical properties were analyzed by zeta potential (ζ) determinations as a function of pH and ionic strength. Surface thermodynamics of the nanocomposites were investigated by contact angle measurements of standard liquids (water, formamide, and diiodomethane) on pellets of the NPs.
Finally, the determination of the hysteresis cycle and the way of variation of the first magnetization of the samples with the external applied field were useful tools to completely characterize (at the macroscopic level) the magnetic behavior of these nanosystems.

Results and Discussion. The synthesis procedure followed for the preparation of Fe_3O_4/PBCA NPs allowed the formation of a well-stabilized nanocarrier with an average diameter of ≈ 200 nm. HRTEM photographs proved that Fe_3O_4 cores were well-covered by the biodegradable shell. X-ray diffractograms of composite and Fe_3O_4 NPs showed excellent coincidence with the ASTM pattern of Fe_3O_4. This was an indication of the high crystalline nature of the synthesized magnetic nuclei. All the bands of the polymer were present in the FTIR spectrum of the composite NPs, a clear prove that the shell observed by HRTEM was indeed PBCA coating.
The efficiency of the polymer coating was further demonstrated by comparing ζ values of core/shell NPs with those of the nucleus and of pure PBCA particles. ζ of the nanocomposites were similar to the ones for the PBCA, and clearly different to the ones of the Fe_3O_4 core, this suggesting the efficiency of the coating. The fact that the surface properties of the magnetic core/shell NPs mimic those of the pure polymer was additionally confirmed by thermodynamic analysis. It was determined that the originally hydrophilic Fe_3O_4 changes to hydrophobic when coated by the polymer.
The magnetic responsiveness was completely defined by the determination of the hysteresis cycle. It was observed that both Fe_3O_4 and Fe_3O_4/PBCA NPs were soft magnetic materials, with a very narrow hysteresis cycle. This behavior is useful for our purpose of controlling their magnetization and, eventually, the rate of drug release by application of not very intense magnetic fields.

Conclusions. In this work we have shown that it is possible to reproducibly coat magnetite NPs with a shell of PBCA. Although the existence of the polymer shell was observable under the electron microscope, the efficiency of the coating was demonstrated by the chemical characterization and the surface analysis of the nanocomposites compared to that of their components. The very important magnetic responsiveness of these core/shell NPs opens promising possibilities to improve drug delivery to severe diseases.

Acknowledgements. Financial support from Junta de Andalucía, Spain, under Project PE-2008-FQM-3993.

References. [1] Ciofani, G., et al., Med. Hypotheses 73 (2009) 80. [2] Arias, J.L., et al., J. Control. Rel. 77 (2001). [3] Massart, R., IEEE Trans. Magn. 17 (1981), 1247. [4] Arias, J.L., et al., J. Colloid Interface Sci. 299 (2006) 599

Batch foaming and cellular structure of biodegradable PLA/Graphene Nanocomposites

Enrique Giménez[1], *Alfonso Cárcel*[1], *Luis Cabedo*[2], *Wentao Zhai*[3], *Chul B. Park*[3]

[1]Instituto de Tecnología de Materiales, Universidad Politécnica de Valencia (UPV), 46022 Valencia (SPAIN)
[2]Departamento de Ingeniería de Sistemas Industriales y Diseño, Universitat Jaume I, 12071, Castellón (SPAIN)
[3]Microcellular Plastics Manufacturing Laboratory, Department of Mechanical & Industrial Engineering. University of Toronto, M5S 3G8, Ontario (CANADA)

enrique.gimenez@mcm.upv.es[1]

Introduction

Considerable efforts have been devoted to the development of nanocomposite foams with good mechanical properties and reduced density[1]. The use of nanoparticles as nucleant agents, especially organoclays, in nanocomposites based on PLA have been reported previously by several research groups[2-4].

Since its discovery in 2004[5], graphene has become of intense interest as fillers in polymeric nanocomposites with novel functional and structural properties.

In this work, the performance potential of the PLA/graphene nanocomposites in foam application was studied. In particular, the main objective was to understand the effect of graphene sheets on both cell morphology (e.g., cell density and cell size) and volume expansion ratio of PLA/graphene nanocomposite foams obtained.

Materials and Methods

A commercial poly(L-lactide) (2002D, NatureWorks®, USA) with approximately 4% of D-lactic acid monomer was used in this work. Graphite fillers with an average particle size of 3 µm were supplied from Avanzare Co. Graphene nanosheets were obtained by chemical reduction of graphite oxide. A co-rotating twin-screw microcompounder (15-cm^3, DSM Xplore, Netherlands) with two conical screws and a bypass was used for the preparation of the PLA/graphene hybrids. The processing temperature was set at 180ºC. The rotor speed and mixing time were fixed at 150 rpm and 8 min, respectively. The foam processing was conducted on PLA/graphene nanocomposites in an autoclave by using supercritical CO_2.The pressure in the chamber was monitored by a connected pressure gauge and adjusted by an ISCO syringe pump (ISCO 260D Syringe Pump). The polymer nanocomposite samples were then foamed by rapid depressurization. Various foaming temperatures (100ºC~140ºC) were investigated. Scanning electron microscopy (SEM) and transmission electron microscopy (TEM) were utilized to investigate the cellular foam structure of neat PLA as a referent material and PLA/graphene having different nanographene loadings.

The cellular structure analysis of foams was examined by SEM. The effect of the dispersion capability of grapheme layer on the final properties was investigated. Experimental results demonstrated that low additions of graphene induced homogeneous nucleation of extra-cells during foaming at temperatures above 125ºC, while the neat PLA foam shows non-uniform cell structure (Figure 1).

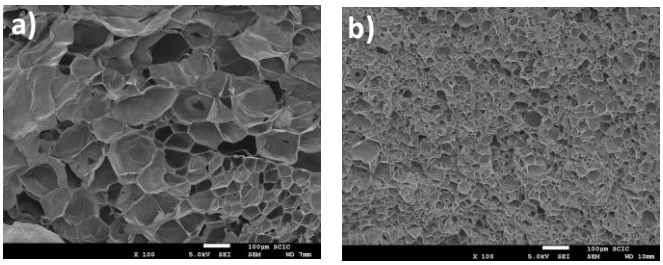

Fig.1. *SEM photographs of the freeze-fracture surface of (a) neat PLA and (b) nanocomposite foams*

Acknowledgments

The authors would like to acknowledge the Ministerio de Ciencia e Innovación (MAT2010-21494-C03) and PAID program of the UPV for financial support. The authors also express their gratitude to Avanzare S.L. for supplying graphite fillers.

References

[1] Fujimoto Y., Sinha SR, Okamoto M., Ogami A. Ueda K.; Macromol Rapid Commun. (2003), 24, 457

[2] Ema Y, Ikeya M, Okamoto M, Polymer (2006), 47, 5350

[3] Di Y, Iannace S, Di Maio E, Nicolais L; J Appl. Polym. Sci. (2005), 43, 689

[4] Zhai W, Ko Y, Zhu W, Wong A, Park C.B; Int. J. Mol. Sci. (2009), 10, 5381

[5] Novoselov, K.S, Geim A.K. et al., Science (2004), 306, 666

Synthesis and Photopolymerization of Hydrolytically Stable Crosslinkers for Dental Composites

Ayse Altin, *Duygu Avci*

Department of Chemistry, Bogazici University 34342 Bebek Istanbul Turkey

Introduction:

Commonly used dental composites are composed of dimethacrylate monomers such as 2,2-bis[4-(2-hydroxy-3-methacryloyloxy propyloxy)phenyl]propane (Bis-GMA), an inorganic filler coated with methacrylate-functional silane coupling agents and a polymerization initiator system (1,2). A comonomer such as triethylene glycol dimethacrylate (TEGDMA) is added to adjust the viscosity of the dental resin. Dental monomers should have rigid structures and be able to form a crosslinked polymer matrix for good mechanical properties. Biostability, low polymerization shrinkage, low viscosity, adhesion to tooth material and high polymerization reactivity are other characteristics that an ideal monomer should have. Many approaches have been developed to improve these properties. In this study, we develop new dental crosslinkers based on alkyl α-hydroxymethacrylates with improved adhesion, volume shrinkage and stability and investigate their photopolymerization behavior.

Materials and Methods:

Monomer and polymer characterization involved FTIR, ^{1}H-, ^{13}C-NMR. The photo-polymerizations were performed on a TA Instruments Q100 differential photocalorimeter (DPC).

Synthesis of Monomer 1

To a solution of diethyl 1-aminomethylphosphonate (0.0990 g, 0.59 mmol) and anhydrous pyridine (0.0470 g, 0.59 mmol) in 1.13 mL of dry dichloromethane, 2,2'-(4,4'-(propane-2,2-diyl)bis(4,1 phenylene))bis(oxy)bis(methylene)diacryloyl chloride (0.1161 g, 0.268 mmol) was added dropwise in an ice bath under N_2. After stirring overnight at room temperature, 5 mL of chloroform was added and the solution was extracted with water (2x2 mL), 2M HCl (2x3 mL), 2M NaOH (2x 3 mL) and brine (3 mL). After drying the organic phase with anhydrous Na_2SO_4, the solvent was evaporated. The dark yellow viscous product was obtained. ^{1}H-NMR (400 MHz, $CDCl_3$, δ, ppm): 1.29 (t, 12H, CH_3-CH_2), 1.59 (s, 6H, CH_3-C), 2.0 (m, 4H, CH_2-P), 3.6 (m, 4H, CH_2-CH_2), 4.0 (m, 4H, CH_2-CH_3), 4.7 (s, 4H, CH_2-O), 5.65 (s, 2H, CH=C), 5.97 (s, 2H, CH=C), 6.8 (d, 4H, Ar-CH), 7.1 (d, 4H, Ar-CH).

FTIR (cm^{-1}): 3308 (NH), 2966-2868 (C-H), 1660 (C=O), 1616 (C=C), 1180 (C-O), 1243 (P=O), 1014 (P-O-Et) cm^{-1}.

Synthesis of Monomer 2

Thrimethylsilyl bromide (TMSBr) (0.43 g, 2.78 mmol) was added dropwise to a solution of monomer **1** (0.3346 g, 0.463 mmol) in 2 mL dry dichloromethane in an ice bath and under N_2. Then the solution was refluxed for 4 hours at 40 ^{0}C. After evaporation of the solvent, methanol was added and the mixture was stirred at room temperature overnight. The methanol was evaporated.

Results and Discussion:

The monomer synthesis involved the following steps: i) synthesis of t-butyl-α-hydroxymethyl acrylate (TBHMA) from the reaction of t-butyl acrylate and paraformaldehyde in the presence of 1,4-diazobicyclooctane, ii) synthesis of t-butyl-α-bromomethyl acrylate (TBBr) from the reaction of TBHMA and PBr_3, iii) synthesis of TBBr-Bisphenol A Diester from the reaction of TBBr and Bisphenol A, iv) conversion to diacid by cleavage of t-butyl groups using trifluoroacetic acid, v) conversion to dicid chloride using oxalyl chloride vi) reaction of the diacid chloride and diethyl 2-aminoethylphosphonate to give monomer **1**, vii) hydrolysis of phosphonate groups using trimethylsilyl bromide to give monomer **2** (Figure 1).

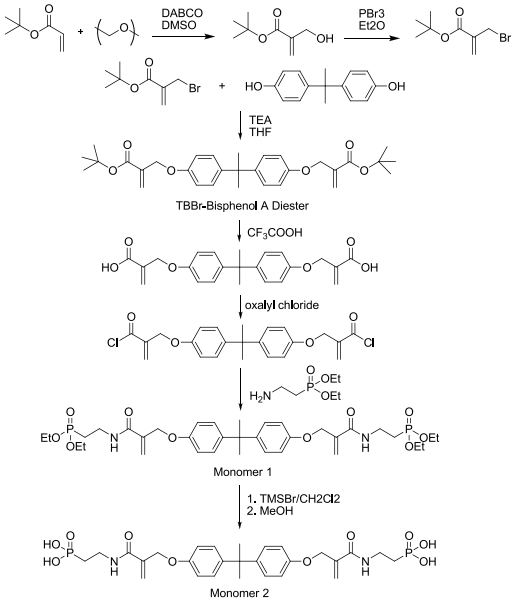

Figure 1. Synthesis of monomers.

^{1}H-NMR and FTIR spectra of the monomers confirmed their structures. The homopolymerization and copolymerization behaviors of these monomers were also examined with Bisphenol A glycolate dimethacrylate (BISGMA) using photo differential scanning calorimeter at 40 ^{0}C with 2,2'-dimethoxy-2-phenylacetophenone (Irgacure 651) as initiator.

Conclusions:

Two novel monomers containing phosphonate or phosphonic acid groups have been prepared. The hydrolytic stability, binding efficiency and copolymerization studies of these monomers are continuing.

Acknowledgements:

This work was supported by Bogazici University Research Fund (BAP 5697)

References:

[1] Anseth, K. S.; Newman, S. M.; Bowman, C. N. Adv. Polym. Sci. 1995, 122, 177.

[2] Moszner,N.; Salz, U. Prog. Polym. Sci. 2001, 26, 535.

Plasma Modification of MWCNTs and Their Use in the Preparation of PA6/MWCNT Nanocomposites

R. Scaffaro, A. Maio

Dipartimento di Ingegneria Industriale, Università di Palermo, Viale delle Scienze, Ed. 6, 90128 Palermo, Italy

e-mail: roberto.scaffaro@unipa.it

Introduction

Carbon nanotubes (CNTs) are suitable as reinforcing fillers for nanocomposites because of their excellent mechanical and electrical properties.[1] Since their bad dispersion in almost all solvents and polymer matrices, CNTs are usually functionalized. Among the several functionalizations, plasma treatment provides a rapid, easy and solvent-free modification of CNT surface.

Plasma treatment was adopted to generate oxygenated moieties on the sidewalls of multi-walled CNTs (MWCNTs). The reaction mechanism of plasma treatment on CNTs can be essentially divided into two steps: (1) ablation of less stable carbonaceous compounds of the CNTs that volatilize as CO_2 and (2) formation of oxygenated functional groups (tipically –COOH and –OH). [2]

Aim of this work is the realization of high performance nanohybrids materials based on polyamide 6 (PA6) and MWCNTs functionalized via plasma. In particular, the possibility to obtain nanocomposites in a rapid, cheap and practicable on industrial scale way was investigated. The process was optimized through the investigation of the role that three parameters, namely plasma power, type of gas and reaction time, played in the surface modification of CNTs.

Materials and methods

A commercial grade of MWCNTs was supplied by Sigma Aldrich (L= 5-9 μm, D=100-170 nm, purity ≥ 90%). The PA6 (Radilon S35 100 NAT, supplied by Radicinova, Italy) has an inherent viscosity (sulfuric acid) equal to 3.4 dl/g. PA6 was dried in a vacuum oven overnight to prevent hydrolytic scission of polymer chains. MWCNTs were used as received.

The functionalization level was measured via Raman and XPS spectroscopy, dispersion tests in water and iso-propyl alcohol.

Nanocomposites were obtained by melt processing. Neat and modified MWCNTs (0, 0.5, 1 and 2% wt/wt) were added to PA6 and mixed in a batch mixer. The specimens were obtained by compression-moulding in order to perform tensile and Izod tests, according to ASTM D882 and ASTM D256, respectively.

Results and Discussion

The XPS and Raman results indicated that the highest content in polar moieties was exhibited by the CNTs modified under the following conditions: 120 W, 10 minutes, oxygen plasma.

The dispersion tests in water and iso-propyl alcohol revealed that neat CNTs precipitated after a few minutes, while air-treated (A-MWCNTs) and oxygen-treated CNTs (O-MWCNTs) remained in suspension, thus confirming the achievement of a more hydrophilic surface. SEM and TEM observations confirmed that functionalized CNTs have less tendency to aggregate in bundles and that plasma treatment did not destruct excessively the CNTs structure. Moreover, TEM observations confirmed that oxygen-plasma treatment removes amorphous carbon by the MWCNTs surface.

A-MWCNTs and O-MWCNTs obtained were selected as fillers for the manufacturing of PA6-based nanocomposites.

Tensile tests demonstrated the higher performance of functionalized MWCNTs-based materials, likely due to a better dispersion and/or a stronger interfacial adhesion. The SEM micrographs of the nanocomposites put into evidence that the wettability of A-MWCNTs and O-MWCNTs in PA6 is better than that observed for neat MWCNTs.

The impact strength (IS) measurements indicate that adding neat MWCNTs to the PA6 induces fragility, so the IS for specimens containing 1% in MWCNT is lower than neat PA6. Otherwise, the use of A-MWCNTs or O-MWCNTs as fillers leads to values of IS up to 2 times higher than PA6+1%CNTs.

Conclusions

The pathway consisting of plasma activation of CNTs and melt blending permits an easy, cheap and rapid fabrication of nanocomposites having improved mechanical properties, achieved at relatively low loading of nanofillers. As process gas, oxygen (more than air) induced the best degree of functionalization in the range investigated. In general, by changing the process parameters it is possible to tune the performances of the materials obtained and XPS and Raman analysis are power tools in order to verify the characteristics of the nanoparticles and to predict their role into the polymer matrix.

References

1. N.G. Sahoo, S. Rana, J.W. Cho, L. Li and S.H. Chan, *Prog. Polym. Sci.* **35** (2010), pp. 837–867

2. Wang Shenggao *et al* 2007 *Plasma Sci. Technol.* **9** 194

Flexible Nanoskin-Core Poly(Ethylene-co-Acrilic Acid)/Polyaniline Hybrids

Roberto Scaffaro[1], *Giada Lo Re*[1], *Clelia Dispenza*[1], *Maria A. Sabatino*[1], *Lidia Armelao*[2]

[1] Dipartimento di Ingegneria Industriale, University of Palermo, Viale delle Scienze, ed. 6, 90128 Palermo, Italy
[2] ISTM-CNR and INSTM, Department of Chemistry, University of Padova, Via Marzolo 1, 35131 Padova, Italy

roberto.scaffaro@unipa.it

Introduction

Several strategies have been adopted to overcome the limitations associated to the bad processability of the inherently conductive form of PANI. Unfortunately, these approaches resulted not particularly effective in obtaining PANI-based composite materials with acceptable mechanical and electrical properties. In this study, we present a general methodology to covalently attach PANI onto a modified polyolefin flexible substrate. Aim of this work is the development of a new polymeric conductive-insulating hybrid material prepared by a simple process, conceptually based on "grafting from" approach, by which the substrate is first activated, then “primed” with suitable reactive groups under mild reaction conditions. A sample of modified ethylene-acrylic acid copolymer (EAA) was selected as a substrate, both in the form of films and fibres. Carboxyl groups of EAA have been first converted into acyl chloride (EAA-Cl) via facile wet chemistry method [1-3]. Later, the acyl groups of EAA-Cl substrates have been first converted by reaction with aniline or para-phenyldiamine (priming) and then coated with "in situ" grown PANI.

Materials and Methods

EAA (Escor 5001, Exxon Chemical) films with 6.2 % by weight of acrylic acid were prepared using a single screw extruder (Brabender PLE 651, L/D=25, D=19) equipped with a film blowing unit. The thermal profile adopted for the operation was 120–140–160–190 °C, the screw speed 70 rpm and the drawing speed 3 m/min. Wires were obtained by capillary extrusion (Rheologic, CEAST, Italy) at T=190° C and v=10 rpm.

The surface modification consists of three-steps: 1. Activation of the substrate as acyl chloride intermediate (EAA-Cl); 2. Priming of the activated substrate with aniline or para-phenyldiamine (EAA-Cl-A and EAA-Cl-pPDA, respectively); 3. Synthesis of PANI onto primed substrates. The final hybrid materials and corresponding intermediates were fully characterized via FT-IR (Perkin Elmer) Spectroscopy, X-ray Photoelectron Spectroscopy (XPS), SEM-EDAX (FEI QUANTA 200F). Conductivity measurements were carried out via Impedance Spectroscopy (IS) by means of a Frequency Response Analyser and Tensile test, according to ASTM D882, by using a Zwik/Roell Z005.

Results and Discussion

The tensile test on hybrid PANI films, carried out to evaluate their mechanical properties showed that substitution of carboxylic acid groups in acyl groups via wet chemistry promoted a slight increase of the elongation at break value with a slight reduction of Young's modulus and tensile stress values. The second modification, i.e. the conversion of acylic groups into aril substituted amides, caused the decrease of tensile stress and elongation at break, even if the Young's modulus remains pratically constant. Nevertheless, after PANI polymerization, the mechanical properties of the hybrid systems seem to be slightly improved and the elongation at break shows a slight increase, with concomitant increases of tensile stress. EAA is an insulant material with a σ'(1Hz) of ~4 x 10^{-13}, the same film primed with aniline and further coated with PANI shows an increase of bulk conductivity (at 1 Hz) of four orders of magnitude, while when priming is operated with pPDA the increase of conductivity is of eight orders of magnitude. Considering that, by the morphological evaluation, the thickness of the coating is smaller in the case of priming with pPDA, this result is either correlated to a superior electrical conductivity of the PANI grown out from the pPDA-primed films and/or to a deeper penetration of PANI inside the EAA core when reacted with pPDA.

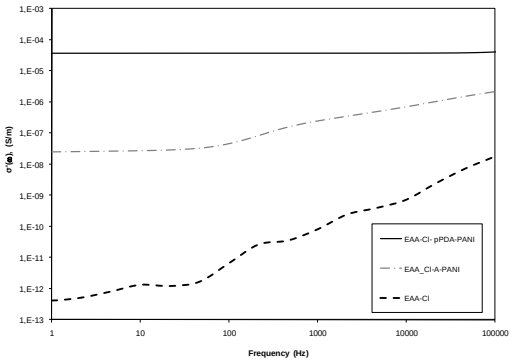

Conclusion

We demonstrated that PANI was successfully polymerized and covalently grafted onto flexible EAA substrates, previously activated. There are no significant differences after each treatment in the mechanical properties, except a faint decrease of the elongation at break. The electrical conductivity shows values of 10^{-4} S/m for the PANI-based hybrid systems drastically enhanced if compared with 10^{-13} S/m value of the neat EAA. The PANI particles obtained have a typical average size of a few tens of nanometers and are thus often regarded as nanogranular typical morphology of PANI polymerized in a strongly acidic solution. All the characterization data strongly suggest that PANI was successfully polymerised and covalently grafted onto the flexible EAA substrates.

References

1. Scaffaro, R. *et al.*, Reactive and Functional Polymers, 70 (3): 189-200, 2010
2. Luo, N. *et al.*, J. Appl. Polym. Sci., 92: 1688, 2004
3. Zhang, C. *et al.*, Polymer, 46: 9257, 2005

Associative and segregative phase behaviour of poly(N-diethylacrylamide)/poly(4-vinylphenol) mixtures. Effect of solvent.

L. Ruiz[1], N. Rioja[1], M.T. Garay[1], M. Rodríguez[1], E. Bilbao[2] y J.E. Figueruelo[3]

[1]Laboratorio de Química Macromolecular (Labquimac). Dpto. Química Física. Facultad de Ciencia y Tecnología. Universidad del País Vasco (UPV/EHU). Barrio Sarriena s/n. 48940-Leioa.
[2] Dpto Ing. Química y Medio Ambiente. E.U. I.T. de Minas y Obras Públicas. Colina de Beurko s/n 48902 Barakaldo
[3]Dpto de Química Física, Facultad de Químicas. Universidad de Valencia.
c/ Dr. Moliner 50. 46100 Burjasot, Valencia

E-mail: leire.ruiz@ehu.es

Introduction

Polymer-polymer complexes are the result of favourable specific interactions between two dissimilar polymers. The main factors governing their formation are the specific interaction between the component polymers and the solvent in which complex formation takes place. When polymer-polymer interaction outweighs polymer-solvent interaction, the two polymers coprecipitate as highly associated materials, the polymer-polymer complexes. Additional factors such as functional group accessibility, self association of component polymers[1] and differences in the polymer-solvent interactions[2] can prevent interpolymer complexation, and a miscible or inmiscible polymer blend or even a segregative phase separation[3] can be observed.

The influence of solvent on complexation of poly(N-diethylacrylamide) (PNDEAm) and poly(4-vinylphenol) (PVPh) has been studied using methanol, acetone and tetrahydrofuran (THF) as solvents.

Materials and Methods

PVPh used was a commercial sample and PNDEAm sample was obtained by radical polymerization. Complexes were prepared by mixing separate polymer solutions in the selected solvent, at concentration 0.2 mol monomeric unit.L^{-1}.

Differential scanning calorimetry (DSC), Fourier transform infrared spectrometry (FTIR) and Elemental Analysis are the techniques used.

Results and Discussion

Several mixtures for the system PDEAm/PVPh have been prepared for different compositions in methanol. (Table 1)

Table 1.Data of complexes in methanol

Solvent Methanol	35/65	50/50	65/35
Complex yield (% w)	63.8	84.5	69.2
Complex composition (mol% PVPh)	48	46	41
Tg (ºC)	177	170	164

Elemental analysis measurements of the precipitates obtained, once isolated, indicate the formation of interpolymer complexes of composition close to 50% mol PVPh. A single glass transition temperature is observed for the complexes and though not much higher than those of the polymer components (96ºC and 167ºC for PNDEAm and PVPh respectively), as usually occurs in hydrogen bonded complexes, they present positive deviations from additivity.

When using THF and acetone as solvent, the precipitates obtained for 50/50 mixtures present compositions of aprox. 10% mol PVPh, indicating that PNDEAm segregates from the mixture. Tg values obtained for both phases, the precipitate and the solution once evaporated, are 96ºC and 149ºC respectively, making evident the PNDEAm segregation. FTIR measurements confirm these results.

The behaviour of this system contrast to the one observed for the system Poly(N-t-butylacrylamide) /PVPh for which, when using THF as solvent, interpolymer complexes of high stability and very high Tg values, around 190ºC are observed.

Conclusion

Poly(N-diethylacrylamide) and poly(4-vinylphenol) form interpolymer complexes in methanol whereas PNDEAm is segregated from the mixture, as a precipitate, when using acetone and tetrahydrofuran as solvents, as shown by Fourier transform infrared spectrometry and elemental analysis studies.

The fact that a change of solvent causes the disruption of the complex could be interesting for technical applications as, for example, in surfaces modification.

Acknowledgements

Financial support provided by the Gobierno Vasco (Actimat, Etortek project), technical and human support provided by SGIker (UPV/EHU, MCINN, GV/EJ, ERDF and ESF) is gratefully acknowledged.

References

1.-Coleman, M.M., Pehlert, G.J. and Painter, P.C., Macromolecules, 1996, **29**, 6820-6831.
2.-Bergfeldt, K., Piculell, L. and Linse, P., J. Phys. Chem., 1996, **100**(9), 3680-3687.
3.-Garay, M.T., Ruiz, L., Marín, J.R., Laza, J.M., Rodriguez, M. and León, L.M., Colloid. Polym. Sci., 2010. **288**, 1593-1599.

Formation Study of Biocomposite Films Synthesized from Chitosan

Jesica A. Cavallo[1], Mar López-González[2], Miriam C. Strumia[1], E. Riande[2], Cesar G. Gomez[1]

[1]Dpto. de Química Orgánica, Facultad de Ciencias Químicas (IMBIV-CONICET), Universidad Nacional de Córdoba, Argentina; [2]Dpto. de Química Física de Polímeros, Instituto de Ciencia y Tecnología de Polímeros, CSIC, Madrid, España.

mar@ictp.csic.es; gom@fcq.unc.edu.ar

Introduction

The use of synthetic polymers for packaging has evolved to the preparation of films by combining natural and synthetic polymers. Some properties such as hydrophilicity and biocompatibility improve, while maintaining good mechanical properties. Since chitosan (CS) is a biocompatible polysaccharide and its backbone presents electrolyte moieties, CS is ranked among the most widely used natural polymers. However, this polymer has weak mechanical properties that limit its use. Therefore, the enhancement of CS properties is an issue that has gained a great interest lately [1-3]. In this work, the synthesis of biocomposite films from CS and poly(acrylic acid) (PAAc) was studied in order to obtain a material with the best properties.

Materials and Methods

CS, M_w 120 kDa, and an acetylation degree of 85 % (Sigma, USA); PAAc, p.a., Mw 450 KDa (Sigma, USA), acrylic acid (AAc), p.a., (Sigma, USA). Films of CS and PAAc were obtained through different casting methods. Thus, a CS-PAAc blend was obtained from the mixture of 1 wt% aqueous solutions of each polymer, at pH 5, the ratio of moles of CS to PAAc being 4. Interpenetrating films of CS-PAAc were attained by radical polymerization of AAc in a 1% aqueous solution of CS, at pH 5. As initiators sodium persulfate (NaPS) or azo-bis-isobutyronitrile (AIBN) were used. Moreover, films containing 10 % molar of sorbitol as plasticizer were also prepared. Finally, the films were characterized by studying the mechanical properties and gas permeation.

Results and Discussion

Values of permeability (*P*, **eq. 1**), diffusion (*D*, **eq. 2**) and solubility (*S*, **eq. 3**) coefficients for hydrogen, helium, oxygen and carbon dioxide in CS modified films are shown in **Table 1**.

$$P = \frac{273}{76}\frac{Vl}{ATp_0}\lim_{t\to\infty}\frac{dp(t)}{dt} \qquad (1)$$

$$D = \frac{l^2}{6\theta} \qquad (2)$$

$$S = \frac{P}{D} \qquad (3)$$

In eq 1, V is the volume of the downstream chamber, A the area of the film of thickness l through which the flux of gas take place, $p(t)$ is the evolution of the pressure of the permeating gas with time in the downstream chamber, T the absolute temperature at which the measurements were performed and p_0 the pressure of the gas at the upstream chamber. The results for the permeation coefficient, collected in **Table 1,** show that the films exhibit good barrier properties for oxygen and carbon dioxide. However, its behavior towards the hydrogen permeation depends on the nature of the film. The greater diffusion of hydrogen in the interpenetrated films obtained with NaPS as initiator is responsible for the increase in the permeability coefficient of this gas in the films. The permeability decrease in interpenetrated films polymerized with AIBN due to an increase in the membrane tortuosity, presumably arising from crosslinking. Both films exhibit the same behavior towards the helium diffusivity, regardless of the initiator used in acrylic acid polymerization.

Table 1. Gas transport properties of CS-modified films at 30 ºC and 1 bar

Gas	Sample	P x 10^2 (barrer)	D x 10^9 (cm^2/s)	S x 10^5 (cm^3/(cm^3 cm Hg))
H_2	CS	1.92	2.29	83.9
	Blend	0.46	3.79	12.0
	Interp. (NaPS)	6.57	261	2.52
	Interp. (AIBN)	1.92	11.6	17.1
O_2	CS	NP	NP	NP
	Blend	NP	NP	NP
	Interp. (NaPS)	1.08	5.38	20.3
	Interp. (AIBN)	NP	NP	NP
CO_2	CS	NP	NP	NP
	Blend	NP	NP	NP
	Interp. (NaPS)	NP	NP	NP
	Interp. (AIBN)	NP	NP	NP
He	Interp. (NaPS)	10.4	180	5.77
	Interp. (AIBN)	10.9	184	5.9

NP: no evidence of gas permeation. 1 barrer=10^{-10} $cm^3cmcm^{-2}s^{-1}(cm\,Hg)^{-1}$

Table 2 displays the films mechanical properties, where it can be seen that the Young´s modulus (E´) of the CS-PAAc is higher than that of CS. The inclusion of PAAc in the film leads to an increase in the elastic modulus due to electrostatic interactions. Moreover, the presence of sorbitol in the samples decreases the modulus caused by the reduction of polymer backbones interactions.

Table 2. Young´s modulus of the obtained films.

Sample	E´(MPa)
CS	588
CS + sorbitol	9
Blend	2309
Blend + sorbitol	86
NaPS film	6242
NaPS film + sorbitol	836
AIBN film	4808
AIBN film + sorbitol	247

Conclusion

CS-based films were synthesized and characterized by gas permeation and mechanical properties. These materials provide good barrier properties and different behavior to hydrogen transport. The incorporation of PAAc into the films improves their mechanical properties. This behavior was mostly attributed to the formation of electrostatic interactions between polymer chains. Sorbitol also decreases the film crystallinity due the fact that it solvates the polymer chains.

Acknowledgements

The authors thank CONICET-CSIC (Luis Santaló), FONCYT, and SECYT-UNC for their financial support. J. Cavallo thanks CONICET for her Doctoral Scholarship.

Reference

[1] H. Moller. J. Agric. Food Chem. 52 (2004) 6585
[2] Y.Umasankar. Anal. Biochem. 388 (2009) 288
[3] M. Ye. Food Microbiol. 25 (2008) 260

Self-curable PDMS-containing PU Oligomers for Water Repellent Textile Treatment

*Rei-Xin Wu, Jing-Zhong Hwang, Kan-Nan Chen**

Department of Chemistry, Tamkang University, Tamsui, New Taipei, Taiwan 251

E-mail: knchen@mail.tku.edu.tw

ABSTRACT: A moisture-curable NCO-terminated polyurethane (PU) prepolymers and fluoro- or polydimethylsiloxane (PDMS) containing PU oligomers are synthesized, respectively. The coating materials are obtained by blending of these PU oligomers and PU prepolymers, in different ratios. These coating materials are spray coated onto cotton and polyethylene terephthalate (PET) textiles, aiming for hydrophobic surface of textiles. The spray coating on textile surface by blending of these PU prepolymer, fluorinated PU prepolymer or/and PDMS PU oligoemers, an inter-penetrating polymeric network (IPN) system will be resulted and anchored into on textile fibers upon drying and moisture-curing raction at ambient temperature. The resulted IPN coating system with highly cross-linked polymer anchored into fabric fibers that enhance water washing durability of treated textiles. The treated textile surface with fluoro- or/and PDMS containing PU system that demonstrates the long lasting water repellency characters.

Keywords: PU, water repellency, Self-curing, PDMS

Introduction: Polyurethanes (PUs) are proved widely accepted materials for various applications in our life. PU means a polymer material including urethane group, produced by various kinds of polyisocyanates and polyols via polyaddition process and form different performance characters [1]. The soft segments have various characters can be easily modified by introducing distinct function [2]. The chemical modification of a surface can alone lead to water contact angles of up to 120° by using fluoropolymer or silane containing layer[3-5].

Experimental: NCO-terminated PU prepolymer was prepared by polytetramethylene-ether-glycol-2000 (PTMEG-2000) and isophorone diisocyanate (IPDI). This PDMS-containing oligomer was prepared by a reaction of polydimethylsiloxane diol (PDMS) with excess amount of IPDI, the fluorinated oligomer was prepared by PU prepolymer and fluorinated compound. The reaction was carried out and kept for 12 hours (according to ASTM D1638 NCO determination method). The contact angle of de-ionized water droplet on PU treated cotton and PET textile was measured at room temperature after 30 second after dropping water droplet. Five measurements of each sample were performed, and the closest results were chosen and averaged for the mean value.

Results and Discussion

NCO-terminated PU prepolymer was prepared as the conventional process and FT-IR was used to confirm the product by the absorption of NCO group. When the FT-IR figure of PTMEG prepolymer shows the –NCO group still appeared at 2260 cm^{-1}, –C=O group of urethane produced at 1720 cm^{-1} was used to confirm the reaction was completed. And the FT-IR figure of PDMS oligomer shows the –NCO group still appeared at 2264 cm^{-1}, –C=O group of urethane produced at 1708 cm^{-1} was used to confirm the reaction was completed. Effect the blending of PU prepolymer, PDMS-containing and fluorinated oligomer on the contact angle for water and diiodomethane on the cotton or PET textiles (Table 1-2).

Table 1. Contact Angle of Water (°)

Sample	PU-1		PU-2		PU-3	
Fibers	Cotton	PET	Cotton	PET	Cotton	PET
Contact Angle^{1st}	140	137	140	134	138	130
Contact Angle^{2nd}	141	138	141	134	138	132
Contact Angle^{3rd}	141	138	142	135	139	132
Contact Angle^{4th}	142	139	142	135	140	132
Contact Angle^{5th}	143	140	143	136	140	133
Average(°)	143	140	142	140	142	140

Table 2. Contact Angle of Diiodomethane (°)on treated textiles

Sample	PU-1		PU-2		PU-3	
Fibers	Cotton	PET	Cotton	PET	Cotton	PET
Contact Angle^{1st}	110	108	108	100	111	109
Contact Angle^{2nd}	111	108	108	102	112	111
Contact Angle^{3rd}	111	109	110	102	112	111
Contact Angle^{4th}	112	109	111	103	113	112
Contact Angle^{5th}	113	109	112	104	114	113
Average(°)	111	109	110	102	112	111

Conclusions: The self-curable fluorinated PU oligomer with PDMS coated on hydrophilic cotton and PET textile, then successfully turned them into superhydrophobic. The static water contact angle is 143° of PU-1 on the PU treated cotton textile, and the diiodomethane contact angle is 118° of PU-3 on the modified cotton textile. When the blending of PU prepolymer, PDMS prepolymer and fluorinated oligomer modified the surface of cotton or PET textile, it becomes highly hydrophobic and that demonstrated as water-repellency characters.

References:

1. Dieterich, D., In Polyurethane Handbook (Ed: G. Oertel), Hanser, New York, Chapt 2(1985).
2. G. N. Chen, K. N. Chen, *J. Appl. Polym. Sci.*, **71**, 903(1999).
3. Shafrin, E. G.; Zisman, W. A. In Contact Angle, Wettability, and Adhesion; Fowkes, F. M., Ed.; Advances in Chemistry Series; American Chemical Society: Washington, p 145(1964).
4. W. H. Chen, Y. T. Yeh, C. Y. Huang, K. N. Chen, *J. Polym. Eng.*, **28**, 517 (2008) .
5. W. H. Chen, P. C. Chen, S. C. Wang, J. T.Yeh, C. Y. Huang, K. N. Chen, *J. Polym. Research* **16**, 601 (2009)

Novel Reactive Polymeric Supports for Synthesis of Polymer Drug Conjugates

Gamze Tanriver, Rana Sanyal

Bogazici University, Department of Chemistry, Bebek, 34342, Istanbul, Turkey.

email: rana.sanyal@boun.edu.tr

Polymer drug conjugates i.e. covalent combination of macromolecules with small drug molecules are attractive tools for drug delivery since such conjugates offer increased drug efficiency via the enhanced permeation and retention (EPR) effect.[1] Conjugation of the drug molecule to a polymer also provides increased water solubility, reduced toxicity and prolonged half life owing to the slower clearance. Water soluble, non-toxic and biodegradable polymers that can be appended with drug molecules are in demand to design such delivery systems. Novel biocompatible and biodegredable polymers based on poly(ethyleneglycol) (PEG) reactive towards amine and alkyne containing small molecules have been synthesized.[2] These reactive polymeric supports must be biodegradable in order to allow elimination of the polymeric substances from the body after delivery of the drug molecule to the desired site. Synthesis and in vitro biodegradation behaviors of these PEG based copolymers in acidic and neutral medias and release studies of small molecules from these polymeric conjugates will be presented.

1 Liu S., Maheshwari R., and Kiick K. L., *Macromolecules*, 42, 3-13, 2009

2 Cengiz N.; Kabadayioglu H.; Sanyal R ,Journal of Polymer Science: Part A: Polymer Chemistry, Vol. 48, 4737–4746, 2010.

Thiol Reactive Hydrogels for Biomolecular Immobilization via Photopolymerization

Tugce Nihal Gevrek, Eun-Ju Park, Amitav Sanyal

Bogazici University, Department of Chemistry, Bebek, 34342, Istanbul, Turkey.

email: amitav.sanyal@boun.edu.tr

Poly(ethylene glycol)-based 3D hydrogel patterns containing thiol reactive maleimide functional groups have been prepared using a novel Diels-Alder/retro Diels-Alder strategy.[1] Bulk-hydrogels and hydrogel micro patterns containing varying amounts of the thiol reactive maleimide functional group were synthesized by photo polymerization. A novel methacrylate based monomer containing a furan protected maleimide group was utilized during the gelation process.[2] The maleimide functional groups were unmasked to their reactive form via the retro-Diels-Alder reaction. These novel reactive hydrogels could be efficiently derivatized with thiolated biotin derivatives under mild condition. Immobilization of FITC-streptavidin onto the biotinylated hydrogel patterns was performed to demonstrate successful efficient biomolecular immobilization.

1 Sanyal, A. Macromol. Chem. Phys. 2010, 211, 1417–1425

2 Dispinar, T.; Sanyal, R.; Sanyal A. Journal of Polymer Science Part A: Polymer Chemistry 2007, 45, 4545- 4551

Dynamic Covalent Reorganization of Polymer/Polymer Systems: Alcoholysis Catalyst Effect on Kinetic and Secondary Reactions

Touhtouh S, Becquart F, Taha M

Université de Lyon, F-42023, Saint Etienne ;
CNRS, UMR 5223, Ingénierie des Matériaux Polymères, 42023, Saint-Etienne, France;
Université de Saint-Etienne, Jean Monnet, F-420023, Saint-Etienne, France;
Samira.Touhtouh@univ-st-etienne.fr, Frederic.Becquart@univ-st-etienne.fr, Mohamed.Taha@univ-st-etienne.fr

Abstract - Dynamic covalent chemistry concept is fully applied to polymer-polymer systems where reversible exchange reactions occurs with a sufficient fast equilibration process under thermodynamic control. This concept takes place here when alcoholysis reaction is involved to prepare graft copolymers and/or to compatibilize polymer/polymer systems bearing alcohol and ester functions. No systematic comparative studies concerning different catalyst effects onto polymer covalent organization by alcoholysis conducted in melt was found in literature. This study first presents kinetic studies on model reactants with different common organometallic catalysts classically used to polymer/polymer systems at 110°C without solvents. A reversible second order kinetic model was applied. The effect of reaction conditions on secondary reactions was analyzed. No secondary reaction were observed, with the most efficient 1,5,7-Triazabicyclo[4.4.0]dec-5-ene (TBD), until 180°C. The obtained results were used for a correct choice of reaction conditions of EVOH/PCL and PMMA/PCL dynamic covalent reorganization. Reactions leaded to graft copolymers synthesis. Compatibilization of the used immiscible polymers was obtained. Important structural changes involve a total disappearance of the EVOH cristallinity and leaded, in all cases, to an elastomer. The effect of shear rate on reaction kinetics of reactions conducted on polymer was also studied.
In the molten state, the reaction was applied to the EVOH/PCL polymer/polymer system. Both these polymers being immiscible and working in a viscous state, the quality of the mixing, directly in relation with the shear of mixing, is an important parameter which affects the reactivity between the involved functions.
For the chosen conditions or mixing, in a reactor with an anchor, it was found a significant and better efficiency of the 1.5.7-triazabicyclo[4.4.0]dec-5-ene controlled by the rate of substitution of the methane protons of EVOH by ^{1}H-NMR spectroscopy.
In all cases, the reactive system aspect really changes during the process. First, the polyester is seriously degraded and its molecular weights fast decrease. This catalyzed degradation systematically happens whatever the chosen catalyst. Slower, the alcoholysis reaction takes places. This typical evolution is observed when the torque to agitate the system at a constant rate, is recorded. The interest of this reaction applied to polymer/polymer system is observed when about 5 - 6% of substitution is reached onto EVOH whatever the chosen catalyst. Indeed, the viscosity of the system seriously increases for around two minutes. At this moment, the properties of the materiel totally changes. The immiscible blend controlled by the poor properties of the PCL at room temperature becomes an interesting elastomer with good mechanical properties.
At this moment, the EVOH cristallinity has totally disappeared.

Introduction

Dynamic covalent reorganization is a class of reaction who was proposed and very described by Stuart J. Rowan and al. [1] in 2002. Takeshi Maeda [2] also contributed by a review in 2009. Dynamic covalent chemistry has a central role in the development of conformational analysis ability to re-adjust the product distribution of a reaction. In the presented study, the dynamic covalent chemistry is applied to polymer/polymer systems with one polyol and one polyester by the alcoholysis reaction, commonly called transesterification. New copolymers with comb structures are synthesized in molten state without solvent. The kind of system is in a continuous evolution with the randomness of the grafting onto the polymer backbone and the free homopolymer remaining in the reactive system. Consequently, important changes in physical and chemical properties of the system are expected. First, a preliminary model study was investigated to define the catalytic system. Well-known organometallic catalysts and more original guanidines, applied to polymers, were tested.

Experimental

Alcoholysis on model reactants and EVOH-g-PCL synthesis in melt processing:

Reactions were made in a 250mL, 90mm diameter glass reactor with a three necked steel cover with a steel anchor stirrer under a dried nitrogen flow.

Results and Discussion

Before applying alcoholysis reaction in dynamic covalent reorganization of polycaprolactone and poly(ethylene-co-vinyl alcohol), model reactions were used to determine reaction parameters effects, particularly on kinetics and side reactions (Figure 1). tin(II) bis(2-ethylhexanoate) and TBD were found as the most efficient and a reversible second order mechanism is confirmed with TBD.

References

1. S. J. Rowan, S. J. Cantrill, G. R. L. Cousins, J. K. M. Sanders, J. F. Stoddart Angew. Chem. Int. Ed. 2002, 41, 898
2. T. Maeda, H. Otsuka, A. Takahara, Progress in Polymer Science 2009, 34, 581

Mechanical Properties of Crosslinked Hybrid PVA Membranes for DEFCs Applications

Aílton de Souza Gomes and José Carlos Dutra Filho

Instituto de Macromoléculas Professora Eloisa Mano, Universidade Federal do Rio de Janeiro. Cidade Universitária, Av. Horácio Macedo, 2.030, Centro de Tecnologia, Prédio do Bloco J, CEP 21941-598, Rio de Janeiro, RJ, Brazil. Tel.: +55 021 2562 7210; fax: +55 021 2270 1317.

asgomes@ima.ufrj.br

Introduction: In the last years, many studies involving the synthesis and characterization of polymer electrolytes presenting proton conductivity at room temperature, allowing their potential use in direct alcohol fuel cells (DAFCs), have been performed. Direct ethanol fuel cells (DEFCs) have recently gained a great deal of attention for their highly potential applications in terms of electric vehicles, stationary applications, and portable power sources, such as cellular phones and notebook computers, etc [1]. Thus, many new materials have been studied for the manufacture of proton conducting membranes for DEFCs. A particularly interesting polymer is poly(vinyl alcohol) (PVA) due to its good chemical and mechanical resistance, reduced ethanol permeability and low cost. The mechanical properties of the polymer membranes used in fuel cells are extremely important to the performance and lifetime of the cell [2]. PVA is a versatile polymer and has been proved to be commercially viable in many fi elds spanning from surface coatings to biomedical applications. But, pristine PVA alone does not meet the required properties and needs to be tailored according to the application. Phosphotungstic acid (HPW) has been described in the literature as a good proton conductor, but the main drawback of its use in membranes is its high solubility in water, leading to HPW loss together with water at medium temperature [3]. The extent and velocity of membrane water uptake depend on the membrane viscoelastic mechanical properties, which are they dependent on membrane hydration, and increased hydration improves proton conductivity and fuel cell performance. Membrane mechanical properties also affect durability and cell longevity, preventing membrane failure from stresses induced by changing temperature and water content during operational cycle. Among the modifications that are viable for PVA, introduction of acid groups such as HPW into PVA matrix and crosslink with diethylenetriamine pentaacetic acid (DTPA) will be discussed in this work, for direct ethanol fuel cells (DEFCs) applications.

Materials and Methods: Poly(vinyl alcohol) (PVA-p) 86,5 – 88,5 % hydrolyzed as supplied by Vetec Química Fina. Poly(vinyl alcohol) (PVA-f) 99% hydrolyzed and phosphotungstic acid hydrate H3PW12O40.xH2O (HPW) 99 % of purity were purchased from Sigma-Aldrich Co. Diethylenetriaminepentaacetic acid (DTPA) 99 % of purity as supplied by Dow Chemical Co. All chemicals were used as received without further puri cation.

Proton conducting hybrid membranes have been prepared by solution casting and all components were dissolved in deionized water under magnetic stirring and heating in a closed system. The hybrid membrane uptake was tested in deionized water and ethanol solution 20 wt.% in deionized water, separately, by measuring the change in the weight before and after the hydration. The ATR-FTIR spectra were recorded i n transmittance mode using a Perkin Elmer FTIR spectrometer model 1720X. Electrochemical impedance spectra (EIS) of the membranes were recorded using an Autolab PGSTAT-30 instrument. PVA partially hydrolyzed and fully hydrolyzed were used as polymer matrix and mechanical properties of this new material will be evaluated by dynamic mechanical analysis (DMA) using a Q800 DMA-Thermal analyzer (T A Instruments).

Results: Results using PVA-p as polymer matrix show that water and ethanol uptake decreases with doping of HPW and addition of DTPA. From the FTIR spectra can be observed a progressive shift corner-shared octahedral band (W -Oc -W) with increasing of PVA-p content. The best conductivity (8.6 x 10-3 Scm-1) at room temperature was obtained for membranes containing 50 wt.% of HPW and crosslinked with 2 wt.% of DTPA by electrochemical impedance spectroscopy (EIS).

Conclusions: The results of dynamic mechanical analysis are being fi nalized and is expected to increase in Young's modulus with increasing content of HPW and DTPA. Moreover, it is expected that the use o f PVA-f promotes better mechanical, barrier and proton conductive properties. The conductivity of the samples also depends of nanostructure and is promoted by the increase on connectivity between the hydrophilic nanodomains.

References:

[1] E.D. Wang, T.S. Zhao and W.W. Yang, Poly (vinyl alcohol)/3-(trimethylammonium) propyl-functionalized silica hybrid membranes for alkaline direct ethanol fuel cells, *Inter J Hydro Ener* 35 (2010), pp. 2183-2189.

[2] Y.P. Patil, W.L. Jarret and K.A. Mauritz, Deterioration of mechanical properties: A cause for fuel cell membrane failure, *J Membr Sci* 356 (2010), pp. 7-13.

[3] M.J. Janik, R.J Davis and M. Neurock, A first principles analysis of the location and affinity o f protons in the secondary structure of phosphotungstic acid, *J Phys Chem B* 108 (2004), pp. 12292-12300.

Study of Natural Aging of PVC Flat-plate Absorber Used for Low Cost Solar Collectors

Julio Roberto Bartoli, Bruna Rosa Prado, Renato Cesar Pereira

Dept. of Polymer Technology, School of Chemical Engineering, State University of Campinas-UNICAMP

bartoli@feq.unicamp.br

Introduction:

Regardless the excellent amount of solar irradiation in Brazil, the development and production of solar water heating systems did not reach the low-income families yet. The relatively high cost of conventional solar water heaters is still the main reason to prevent it. The electrical shower is the main system for bath water heating; it consumes 8.5% of the electric energy produced in the country[1].

The development of a low cost solar water heater (around US$ 200), easy technology, was the scope of previous work[2]. All-plastic solar collector prototypes were developed using unplasticized Polyvinyl chloride (PVC) ceiling panels and tubes, commodities from building engineering. PVC is one of the most important plastics used in various industries like building and construction (around 50%). Despite of common solar collectors, these whole plastic do not use the "greenhouse effect" (transparent cover). This innovative concept allows this solar collector to meet requirements of simplicity, easy manufacturing, low cost and thermal performance. It was measured a thermal efficiency of 67% (hot water reaches 55°C on a sunny day), compared to the 75% of conventional solar collectors made of copper tubes and glass cover[3]. Nevertheless, the main thermal and photo degradation mechanisms for PVC are well known[4]; the unusual application of PVC as solar collector materials should need a specific investigation on environmental aging. Therefore, this work presents a natural aging study of PVC flat-plate absorber of solar collectors after 5 years on use at the State University of Campinas.

Materials and Methods:

Figure 1: Low cost solar collector system for 100 L

Each PVC flat-plate (0.75 m^2) has two pipes connected at the ends. The water enters the cross section of the flat-plate (black painted) from the inlet pipe, then flows up along the internal cavities of the plate and exits at the outlet pipe to the reservoir (Figure 1). The solar collector prototypes were removed after 27, 36, 48 and 60 months of use and test specimens were cut from the PVC panel for mechanical (ASTM D 638, Standard Test Method for Tensile Properties of Plastics) and physico-chemical characterization (FTIR-ATR and SEM analyses).

Results:

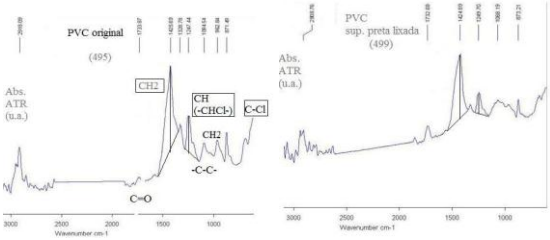

Figure 2: FTIR-ATR spectra of PVC original (left) and after 27 months exposed to sun.

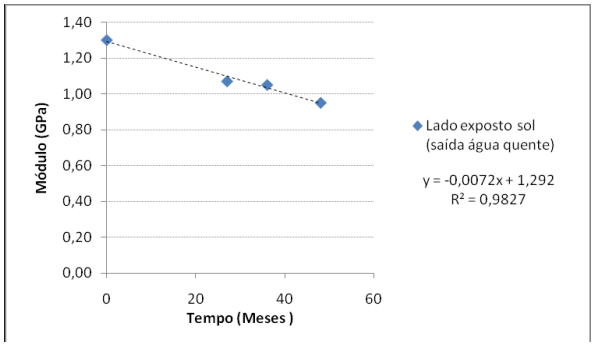

Figure 3: Young Modulus vs Time (month)

Conclusions:

The mechanical properties of PVC flat-plate were significantly modified after 5 years, Young modulus was reduced around 20% and PVC photodegradation was observed as dehydrochlorination. Even that, these low cost solar collectors performed very well, heating water to 50°C and no leakage were found, until being removed for PVC characterization. The linear regression of the PVC Young modulus estimates that a reduction of 50% (0.65 GPa) would take 7.5 years.

[1] Balanço Energético Nacional 2008, EPE, Ministério de Minas e Energia, www.epe.gov.br.

[2] Bartoli, J. R., et al.; Int. Conf. Renewable Resources and Renewable Energy: A Global Challenge, Trieste, 2004

[3] Bartoli, J.R., et al.,17º Cbecimat, Foz Do Iguaçu, 2006

[4] Braun, D. et al:Theory of degradation and stabilization mechanisms, Encyclopedia of PVC, M.Dekker, NY, 1986

Acknowledgments: Tatiane Pinto, Brino R. Negri, Valdir Assis Jr.; Rhodia, CAPES, FAPESP and CNPq.

Synthesis of organic/inorganic composite hydrogels with embedded clay particles

*Manja Kurecic**, Silvo Hribernik*,+, Majda Sfiligoj-Smole*,+

*Faculty of Mechanical Engineering, University of Maribor, Smetanova 17, Maribor, Slovenia
+Centre of Excellence PoliMat, Tehnoloski park 24, Ljubljana, Slovenia

manja.kurecic@uni-mb.si

Cross-linked organic/inorganic composite gels are widely used in different areas of modern industry. Polymeric hydrogels present very interesting and versatile materials, being sensitive to various environmental stimuli, such as temperature, pH, pressure, ionic strength and electric fields. Hydrogels with incorporated clay particles are a very specific class of such composite materials.

Presented research deals with the preparation of polymeric hydrogels with organically-modified clay particles, distributed in the gel matrix. Hydrogels were obtained by UV polymerization of N-isopropylacrylamide (NIPPAM) crosslinked with N,N`-methylenebisacrylamide (BIS); organically-modified montmorillonite particles (as an active component) were included into the hydrogel formulation. Process parameters (particle concentration, dispersing medium, monomer, cross-linker concentrations and drying procedure) were varied with the aim to thoroughly study the formation of particle-embedded hydrogels. In addition to functional properties of nanocomposites conditioned by the preparation process were analysed.

Scanning electron microscopy was used to evaluate the morphology of synthesized composite hydrogels and to determine the particles distribution in the matrix. Hydrogels with different morphological structure were observed dependent on surfactant addition and drying procedure (vacuum drying and freeze drying, respectively). Swelling behaviour of hydrogels depends on the ratio of cross-linker/monomer concentrations as well as the amount of embedded clay particles and was determined by monitoring the water uptake. Functional properties of nano-hydrogels were determined by organic dyes adsorption on composites. The efficiency of dye-adsorption was studied as a function of time and particle concentration and was correlated to the degree of particles' agglomeration in the polymerized gels.

SEC-MALS and Molecular Dynamics Characterization of an Amphiphilic Poly(Acrylic Acid-*b*-Styrene-*b*-Styrene-*b*-Acrylic Acid) Symmetric Block-Copolymer Synthesized by RAFT

M. Pilar Tarazona[a], *Gema Marcelo*[b], *Enrique Saiz*[a], *José Gaspar Martinho*[b], *José Paulo Farinha*[b]

[a]Departamento de Química Física, Facultad de Farmacia, Universidad de Alcalá (Madrid, Spain)
[b]Centro de Química Física Molecular, Instituto Superior Técnico (Lisbon, Portugal)

mpilar.tarazona@uah.es

Introduction: Controlled radical polymerization techniques have become increasingly popular for the production of polymers and block-copolymers with predetermined molecular weight, narrow molecular weight distributions and well-defined architecture, from a much larger variety of monomers and under simpler polymerization conditions compared to anionic polymerization. These polymers have attracted much attention because of their versatile self-assembly behavior and potential applications in many areas. The assembly can be controlled by different factors, among them the composition of the solvent. In order to obtain structures by controlled self-assembly, one has to characterize different aspects of the copolymers, namely in terms of composition, structure, molecular weight and molecular weight distribution.

The use of size exclusion chromatography (SEC) with a mass sensitive detector, a multiangle laser light scattering (MALS), has become a polymer characterization standard method and is advantageous since it offers the possibility of obtaining both absolute molecular weights and chain dimensions along the chromatogram.

In this work, a sequential reversible addition-fragmentation chain transfer (RAFT) polymerization strategy was used to prepare a symmetric amphiphilic block-copolymer composed by a poly(acrylic acid-*b*-styrene-*b*-styrene-*b*-acrylic acid) unit with a bridge of trithiocarbonate between the two blocks of styrene (**Scheme 1**).

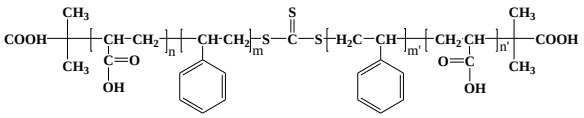

Scheme1. Block copolymer structure.

Poly(styrene-*b*-acrylic acid) copolymers with different block compositions have been previously prepared and several supermolecular structures were observed in solution. The molecular weight and polydispersity of these polymers has been determined by SEC-MALS in THF, DMF, and 1,4-dioxane solvents.

Materials and methods: SEC measurements were carried out using a Waters Associates equipment with a 510 pump, a 7725 Rheodyne injector and a differential refractive index detector (model 410).

The Amber molecular modelling package, including the Amber force field, was employed for all the Molecular Dynamics (MD) simulations.

Results and discussion: By performing a similar analysis to the bibliography study, SEC-MALS was used to study the aggregation behavior of the copolymer in different solvents: 1,4-Dioxane; THF; THF with different salts, DMF; and DMF with LiBr. To evaluate the influence of acrylic acid, the polymer was methylated and further analyzed in THF. Molecular weights and polydispersity values (**Table 1**) larger than those estimated from the synthetic procedure were obtained in THF, THF with salts, DMF and DMF with salts. However, in 1, 4-dioxane the values are similar to those expected and agree with those obtained to the methylated polymer in THF.

Solvent	M_w / 10^5 (g/mol)	$\langle s^2 \rangle^{1/2}$ (nm)	M_w / M_n
THF	7.58	21.9	1.50
THF/NaCl 0.04 M	1.68	11.4	1.12
THF/LiBr 0.1 M	6.12	21.9	1.56
THF/LiCl 0.2 M	1.85	11.8	1.26
DMF	2.68	74.8	1.69
DMF/LiBr 0.15M	0.343	13.0	1.24
Dioxane	0.161	---	1.13
Methylated copolymer in THF	0.234	---	1.04

Table1. Average molecular weight (M_w), polydispersity (M_w / M_n) and root mean square radii of gyration $\langle s^2 \rangle^{1/2}$ of the copolymer in SEC-MALS solvents.

Molecular Dynamics simulations have been performed on systems formed by one oligomer having a central trithio carbonate unit, -S-(CS)-S- flanked on each side by a block of styrene units followed by a block of either acrylic acid or methyl acrylate ester in the same solvents as used in the SEC measurements. The calculations allowed us to evaluate the correlations among rotational angles over the chain backbone and among distances between different groups that were used to rationalize the experimental results.

Conclusions:

The RAFT polymerization technique allowed us to copolymerize acrylic acid and styrene with very good control of molecular weight and architecture. The copolymer is both water- and organo-soluble and can self-assemble to form different structures and materials.

We also found out that the copolymer in 1,4-dioxane or the methylated copolymer exhibit isolated chains in solution because similar molecular weight distributions are obtained in both systems, and in good agreement with the predicted value for the synthesis. The experimental results obtained for the methylated polymer show that the acrylic acid units are the main cause of inter-chain interactions leading to aggregation.

The results obtained by SEC-MALS were rationalized by performing MD simulations in similar oligomers. The agreement between the experimental results for the polymers and MD simulations for the oligomers in the different solvents is very good.

Development of conducting nanofillers based on polypyrrole and nanoclays

Luis Cabedo[1], *Izabela Mróz*[1], *José M. Lagarón*[2], *Enrique Giménez*[3]

1. Polymers and Advanced Materials Group (PIMA). ESID, Universidad Jaume I, 12071 Castellón
2. Laboratorio de Nuevos Materiales y Nanotecnología. IATA, CSIC, Burjassot, 46100 Valencia.
3. Instituto de Tecnología de Materiales, Universidad Politécnica de Valencia, 46022 Valencia

lcabedo@esid.uji.es

Nanocomposites based on the addition of modified nanofillers with conducting polymers have attracted the attention of researches lately due to its potential in a broad variety of applications such as antistatic coatings, electromagnetic shielding, semiconductors, batteries, etc. The intercalation of conducting polymers in the interlaminar region of the nanoclays can lead to a nanocomposite having properties which differ from both original materials, such as an increase in the electric conductivity and mechanical performance.

In this work, two kinds of clays have been utilized: montmorillonite (MMT) and vermiculite (WMT). Nanocomposites of these two clays have been obtained by oxidative polymerization of the polypyrrole (PPy) in an aqueous solution of the clays following several methods and conditions[1,2,3,4]. The resulting materials have been evaluated by different techniques hence studying the influence of the clay type and processing route on the final performance of the nanofillers.

The so-obtained nanofillers have been characterized morphologically by means of wide angle X-ray scattering (WAXS) and electron microscopy. High degree of intercalation of the polymer chains within the interlaminar gallery has been found, being this intercalation higher for the vermiculite. Thermogravimetric analysis of the nanocomposites showed an increase in the thermal stability of the PPy nanocomposites with respect to the pristine polymer.

Finally, the conductive properties of the PPy/clay were evaluated and compared with the ones of the pure PPy using for so the 4-point Van der Pauw technique for measuring the surface conductivity. These experiments proved that the conductivity of the resulting nanocomposites is extremely dependent on the polymerization conditions as well as on the measuring method. Among others, the final conductivity varies with the catalyst, reaction time, clay modifier, temperature and clay concentration. Figure 1 shows the surface electrical dependence with the PPy content in the vermiculite/PPy nanocomposites.

References

1. Mravcakova, M., Omastová, M., Poetschke, P., Pozsgay, A., Pukánszky, B., Pionteck J.; Polym. Adv. Technol. 2006;17:715-726

2. Pomposo, J.-A., Ochoteco E., Pozo, C., Carrasco, P.-M., Grande, H-J. Rodríguez F.-J.;Polym. Adv. Technol. 2006;17:26-29

3. Jakab, E., Mészáros, E., Omastova, M., J. ; Polym. Adv. Technol. 2006;17:715-726. J. Therm. Anal. Calorim. 2007;88:515-521

4. Boukerma, K., Piquemal, J.-Y., Chehimi, M. M., Mravcakova, M., Omastová, M., Beaunier P.; Polymer 2006;47:569-576

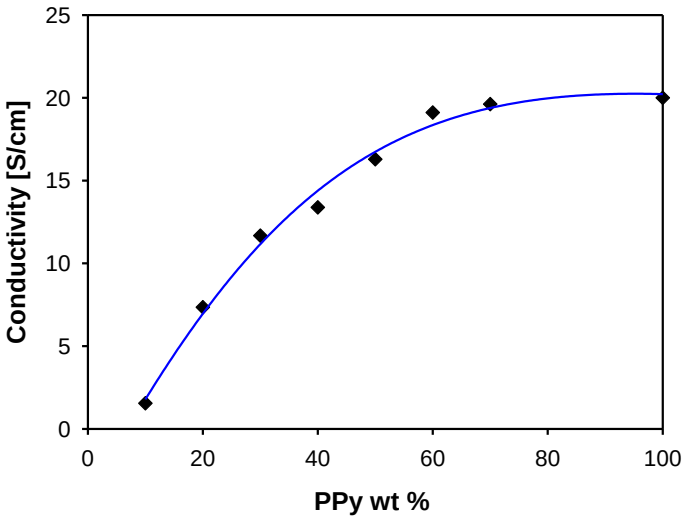

Figure 1: Conductivity measurements of the vermiculite/PPy nanocomposites.

Acknowledgements: This work has been financially supported by the Spanish Ministry of Science and innovation and the ERDF (IPT MAT2009-14533-C02-02).

Strippable Deactivating Coatings: Case of Modified Polyvinylalcohol.

Farmazyan Z.[1], Harutyunyan G.[1], Hayriyan L.[1], Sargsyan V[1]., Dalalyan N[1]., Stepanyan K.[2], Pyuskyulyan K.[3], D.G.Abramyan[4], I.V.Shahazizyan[4]

1. CJSC "Yerevan SRI "Plastpolymer"Arshakunyats 127, Yerevan 0007, Armenia
2. Scientific Center of Radiation Medicine and Burns, SCRMB, Davidashen, m/b 25 Yerevan 0108, Armenia
3. Armenian NPP, Armavir Marz, Metsamor, Armenia
4. Faculty of Biology, Yerevan State University, Alek Manukyan 1, Yerevan, Armenia

Introduction. Polyvinyl alcohol (PVAL) is known to be one of the most applicable polymers in water compositions for strippable deactivating coatings. However in these compositions the polymer serves only a film- forming functions and in order to provide the demanded operational properties, some plasticizers, chelating agents, etc. are added into compositions [1]. Through the modification of PVAL with chelating functional groups (FG) it is possible to vary many of its characteristics and correspondingly properties and by this to simplify content of compositions and make them more stable, available and cheaper [2]. With this purpose PVAL modified with different content of derivatives of maleic anhydride (MA) have been elaborated and studied (MPVAL).

Materials and Methods. MPVAL-s have been synthesized through two various methods of vinylacetate(VA)-MA loading which provides different distribution of FG: alternating (samples 27/05,1-09/2, 2/06-2MEF) or random (block) (26/05, 2/09-2, 12/08 MAMEF). The ratio of the comonomers was VA:MA=95:5, 90:10 and 93:7(mass.%).

Content and types of FG were determined by methods of chemical analysis, IR and NMR spectroscopy. MM was defined by SEC (Waters). Viscosities of 10-11% solutions were studied by Brookfield viscosimeter.

DF (decontamination factor) and β_F (% of removed contaminations) were examined at SCRMB and Armenian NPP on separate radioactive isotopes (^{60}Co and ^{137}Cs) and in real conditions of radiation contamination (^{137}Cs, ^{110m}Ag, ^{58}Co, ^{60}Co, ^{54}Mn) at one of facilities of Armenian NPP. Testing copolymers solutions were coated over a contaminated plate or floor and were left to be dried. Then the radioactivity of the surface with a polymeric film and after its removing was measured.

Dispersion ALARA-1146 was used as analogues [3].

Testing by fungi resistance was conducted by the use of a set of mycromycites: *Aspergillus flavus, A.niger, A.ochraceus, Penicillium duclauxii, P.cyclopium, Alternaria alternata, Cladosporium herbarum, Trichoderma viride.*

Results and Discussion.

The main parameters allowing to use MPVAL as deactivating strippable films are an ability to bind different RN and to form films with predetermined properties. These properties mainly are stipulated by type, content, distribution of FG and MM of co-polymers.

Data in Table 1 show variation in content of FG depending on MPVAL synthesis methods. Moreover these data considerably deviate from their theoretical values. The reason of this is reactions of cyclization and lactonization, the extent of which is stipulated by FG distribution in a macromolecule.

Film-forming properties of copolymers depend on MM, MMD and type of super-molecular formation.

Table 1. Functionslity of MPVAL sample

Samples (% of comonomer)	$OCOCH_3$ % mass.	COONa % mass.	[η], dl/g
26/05(5%)	9,7	5,5	1.34
2/09-2 (7%)	8.8	9.7	Electrolyte effect
12/08 (10%)	13.1	11.4	2.63
27/05(5%)	8,6	8,2	2.52
1/09-2(7%)	10.5	10.3	1.43
2/06-2(10%)	10,5	17,6	2.12

Comparative studies of M_w, M_n, [η] and Huggins constant K_x, have shown that super-molecular order is realized at least by 3 factors - polyelectrolyte effect, polymer-solvent interaction, hydrophilic-hydrophobic balance of macromolecule. Hence, set of FG, their distribution and type of super-molecular formation are responsible for decontamination efficiency (Fig.1).

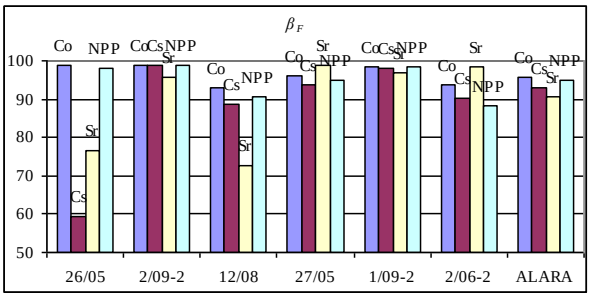

Fig.1 β_F for MPVAL samples

From presented data follows, that independently of synthesis methods, 7% of MA is preferable for creation of copolymers providing high level of deactivation.

Other very important criteria to select grade of MPVAL is storage of radioactive films (there is not a publication about this issue). Evaluation of fungi resistance carried out till now reveals that samples with MEF are the most resistant to fungi damage.

Conclusions. Characteristics of MPVAL allowing to use their solutions for deactivation of contaminated surfaces without addition special chelating agents are revealed.

The technology of MPVAL synthesis at laboratory scale is developed.

References.

1. US Patent 50061357, Strippable PVA coatings, 2005
2. Harutyunyan G., Farmazyan Z., Dalalyan N., Hayriyan L., Hakobyan E., Sargsyan V.The strippable polymeric coatings for deactivation of various surfaces from radionuclides, Worshop on Response to Chemical, Biological and Radiological/Nuclear Terrorist Attacks in Ottawa, 28-30 April 2009.
3. ALARA 1146 Strippable coatings, Summary Report, US Department of Energy, April 2000

Production and Characterization of Starch and Starch Based Composite Biodegradable Films Crosslinked By Glutaraldehyde

Ilknur Gonenc, Ferhunde Us**

* Hacettepe University, Department of Food Engineering, 06800, Beytepe, Ankara, Turkey.

ilknur@hacettepe.edu.tr
ferosh@hacettepe.edu.tr

Plastics made from petroleum that are not degradable in the soil has become a serious environmental pollution problem. Therefore development of starch and starch based composite novel plastics can be interesting solution.

In this study, films composed of corn starch, corn starch-methyl cellulose (MC), corn starch-poly(vinyl)alcohol (PVA) and corn starch-carboxymethyl cellulose (CMC) were prepared. Glutaraldehyde (GLU) was used as crosslinking reagent. The films were plasticized by glycerol and polyehyleneglycol 400 (PEG400). Films prepared without GLU were used as the control group. It was found that starch was not compatible with PEG400 therefore 14 film samples were studied in this study. Tensile strength (TS), %elongation (%E) and water vapor permeability (WVP) of the films were investigated. Water adsorption capacity and opacity of the films were also determined.

The WVP of the films was determined to be $0.25x10^{-10}$ – $1.28x10^{-10}$ g/m.s.Pa, depending on the plasticizer type and GLU. Films prepared with PEG and without GLU had the higest WVP values than the other film samples. The cross linking effect of GLU caused a decrease in film water vapor permeability and %E and caused an increase in film TS. Composite films showed beter flexibility than starch based films.

The whole results, including adsorption capacity and opacity will be presented and discussed.

Validation of an elasto -viscoplastic model for polyvinilidene fluoride (Pvdf)

Viviane Goncalez1, Ilson Paranhos Pasqualino2, Marysilvia Ferreira da Costa3

1,2 Naval and Ocean *Engineering Program*, COPPE, Federal University of Rio de Janeiro; 3 *Materials and Metallurgical Engineering Program*, COPPE, Federal University of Rio de Janeiro.

Email: viviane@lts.coppe.ufrj.br

Introduction

Polyvinylidene fl uoride (PVDF) copolymer is a thermoplastic of great potential to structural applications, such as internal pressure barriers of flexible risers used in offshore petroleum industry and also for lining of corroded onshore oil pipes [1,2]. The time-dependent properties of PVDF are still a subject of concern when higher temperatures are considered. Mechanical properties of polymers are strongly influenced by strain, temperature and time or frequency [3], thus it is important to study the viscoplastic behavior to assess the response of a polymeric structure in structural engineering applications. The aim of this study is to test a constitutive model to be employed in the numerical simulation of PVDF under time dependent thermo-mechanical loading.

Materials and Methods

In this case, the two layer visco-plastic model of Abaqus Software will be tested. For model implementation, several mechanical parameters must be obtained through tensile and relaxation tests in different conditions. The model parameters, such as elastic, viscous and plastic modulus were determined through tensile tests at 25, 40 and 60 °C and strain r ates from
1.2 10-5 s-1 to 1.2 10-1 s-1.

Results and Discussion

Tensile results showed a decrease of elastic modulus and maximum stress with increasing temperature or decreasing strain rate. The relaxation tests were made at 25, 40 and 60°C and initial strains from 3 to 20%. Through these results it was possible to establish a theoretical stress -strain curve for almost zero strain rate to be used in the constitutive model. Also, the time dependent stresses under different temperatures were proposed through the Norton-Hoff equation. The relaxation tests were correlated with the numerical results using a nonlinear finite element modeling under the proposed constitutive model.

Conclusions

The employed methodology generated good correlation within the beginning of the relaxation tests but showed an increasing discrepancy with time for the predicted stresses. These discrepancies were reduced with the manipulation of the convergence parameters and time increments.

References

[1]D.M., Abraham; S.A. Gillani. *Tunneling and Underground Space Technology*; 14, 43, 1999.
[2]S. Hellinckx, J. C. Bauwens. *Colloid Polym. Sci*.; 219-226, 1995.
[3]L.J. Findley, K. Onaran in *Creep and Relaxation o f Nonlinear Viscoelastic Materials*: Dover Publications, Inc., New York, 1989.

Characterization of poly(lactide-co-glycolide) (PLGA) obtained via ring-opening polymerization: effect of the LA/GA molar ratio

Jorge C. Ramirez[1], *Edna Vargas-Reyes*[1], *Perla Hernández-Belmares*[2], *Juan C. Ortiz-Rodríguez*[2]

[1]Departamento de Procesos de Polimerización, Centro de Investigación en Química Aplicada (CIQA), Blvd. Enrique Reyna 140, 25253, Saltillo, Coahuila, México.
[2]Universidad Autónoma de Coahuila, Blvd. Venustiano Carranza s/n col. República Oriente, 25000, Saltillo, Coahuila, México.

E-mail address: jramirez@ciqa.mx

Abstract: Ring-opening polymerization of lactide/glycolide (LA/GA) using different molar ratio at 130°C was studied. Stannous octoate ($Sn(Oct)_2$) was used as catalyst and 1-dodecanol (ROH) as cocatalyst. LA/GA, (LA/GA)/$Sn(Oct)_2$ and ROH/$Sn(Oct)_2$ molar ratios used during the bulk polymerizations were from 100/0 to 75/25, 2000 and 1, respectively. All the polymers synthesized were purified prior to characterizations. The results obtained by ^{1}H-NMR indicated that is possible to obtain copolymers with an experimental composition of LA/GA from 100/0 to 80/20 molar ratio, where the weight-average molecular weight (M_w) decreased (from ≈100,000 to 35,000 Da) conform the GA unit in the backbone structure of copolymer was higher. In addition, the thermograms obtained by differential scanning calorimetry (DSC) also shows that the tg value decreased from ≈50 to 42°C conform the GA unit in the copolymer chain was increased. Finally, the copolymers also were analyzed by infrared spectroscopy (FTIR) in order to obtain more information about these polymerizations.

Internal and external gelling method for alginate hydrogels preparation with planar geometry

E. Papajová,[1] Z. Kroneková,[1] M. Stach,[1] D. Chorvát Jr.,[2] C. Hoesli,[3] D. Horne,[3] J. Piret,[3] I. Lacík[1*]

[1]Polymer Institute of Slovak Academy of Sciences, Dúbravská cesta 9, 845 41 Bratislava 45, Slovak Republic
[2]International Laser Centre, Ilkovičova 3, 841 04 Bratislava 4, Slovak Republic
[3]University of British Columbia, 2185 East Mall, Vancouver BC, V6T 1Z4, Canada

eva.papajova@savba.sk@savba.sk; igor.lacik@savba.sk

Introduction: Sodium alginate (SA) is a polysaccharide extracted from natural sources brown algae and bacteria. SA is composed of guluronic (G) and mannuronic (M) acid units arranged in homopolymeric blocks or blocks of alternating units. SA forms three- dimensional hydrogel structures by electrostatic interactions with divalent metal ions (e.g. Ca^{2+} or Ba^{2+}) [1]. In spite of the broad knowledge about SA hydrogel, the research is still needed to provide information on SA hydrogel properties and new applications.

This contribution deals with preparation of externally gelled SA hydrogel slabs with planar geometry. Planar geometry is commonly obtained by internal gelling method [2] based on dispersing the source of gelling cation (commonly $CaCO_3$) within SA alginate solution. A decrease of pH results in slow dissolving of $CaCO_3$ particles, which initiates the gelling process. In the case of external gelling method [1], the preparation of hydrogel starts with diffusion of Ca^{2+} cations into SA solution. Preparation of SA hydrogels with planar geometry by external gelling method needs controlled and slow exposure of SA solution for avoiding the shape distortion. In our approach, the SA planar hydrogel slabs were prepared by slow exposure of SA solution to aerodispersion of $CaCl_2$ following the methodology described for preparation of SA films [3].

Materials and methods: SA with high content of G units (Protanal LF10/60) was purchased from FMC BioPolymer (Norway). All inorganic salts for gelling process and for preparation of solutions were of analytical grade. *External gelling:* A mold with dimensions of 19×19×1 mm filled with SA solution (SA concentration range 1-3 wt.%) was put 40 cm under the airbrush (Rich, AB 200). Airbrush was spraying $CaCl_2$ solution of concentration from 0.5 to 4 wt.% $CaCl_2$ on the surface of SA solution in the mold with flow rate around 7.0 mg/min·cm^2 in the time range from 2.5 to 20 min. *Internal gelling:* $CaCO_3$ particles were homogenously dispersed in SA solution. D-glucono-δ-lactone (GDL) was added into the dispersion. The mixture containing 2 wt.% SA, 20 mM $CaCO_3$, 60 mM GDL was poured between glass plates seprated by 1 mm distance. Hydrogel was formed for 24 hours at 6°C. Saline solution was used as a solvent for preparation of all solutions in both gelling methods. For both types of SA hydrogels, gelling process was followed by treating hydrogel in solution containing 1 mM $BaCl_2$, 50 mM $CaCl_2$, 0.2 M NaCl for 20 min. Then hydrogels were stabilized in storage solution (0.9 wt.%, 5 mM $CaCl_2$, 100 ppm NaN_3) for at least 24 hours at 6°C before characterization.

Mechanical properties of SA hydrogels were determined in a compression mode (Young's modulus). Dimensional stability during hydrogel formation and after stabilization in storage solution was characterized by gravimetry. Permeability was determined by an inverse size exclusion chromatography (iSEC). Internal structure of hydrogels was analyzed by cryo–scanning electron microscopy (cryoSEM) and confocal laser scanning microscopy (CLSM) with SA chains covalently labeled by fluorescein.

Results and discussion: Results are discussed in terms of (1) effect of experimental conditions used for preparation of externally gelled SA, and (2) comparison between internally and externally gelled SA hydrogels.

(1) For the concentration range of SA from 1 to 3 wt.% and 20 min exposure to 2.5 wt.% $CaCl_2$ solution, the syneresis decreased with increased SA concentration from 15% for 1 wt.% SA to 0% for 3 wt.% SA. The Young's modulus increased in this SA concentration range from 40 to 200 kPa. For 2 wt.% SA, these characteristics were neither significantly influenced by changing the $CaCl_2$ concentration nor by changing the exposure time.

(2)The conditions for internal and external gelling processes (2 wt.% SA in both cases) were adjusted to the same stochiometry ratio Ca^{2+}:COO^- = 0.5:1 related to the COO^- groups on GG and MG diads. The Young's modulus of around 80 kPa was determined for both hydrogels. A difference was seen in the dimensional stability after gelling. The internal gelling method resulted in 15% of syneresis while the external one only in 5% syneresis. CSLM revealed a homogeneous distribution of SA chains for both hydrogels in spite of different directions of Ca^{2+} diffusion during internal and external gelling process. Also cryo-SEM analysis showed regular porous structure. The pore size and pore size distribution quantified by iSEC showed for that both hydrogels exhibit rather broad pore size distribution with the molecular weight cut-off of around 450 kDa (viscosity radius ~ 20 nm) determined by pullulan standards.

Conclusion: The methodology for preparation of planar alginate hydrogel slabs by external gelling was developed. It is advantageous in terms of shorter preparation time and physiological conditions maintained throughout the gelling process compared to the internal gelling. The properties of both gels are similar.

References:

[1] Mørch et al. *Biomacromolecules* **2006**, *7*, 1471.
[2] Draget et al. *Carbohyd Polym* **1991**, *14*, 159.
[3] Cathell et al. *Biomacromolecules* **2007**, *8*, 33.

Acknowledgement. *This work has been supported by the Scientific Grant Agency of the Ministry of Education of Slovak Republic under the Grant VEGA No. 2/0152/10 and by the Slovak Research and Development Agency under the contract No APVV-0486-10.*

Porous methacrylate copolymers as stationary phases for HPLC

Marta Grochowicz, Małgorzata Maciejewska

Department of Polymer Chemistry, Maria Curie Sklodowska University,
Gliniana Street 33, 20-614 Lublin, Poland

mgrochowicz@umcs.pl

Introduction

Porous polymeric particles are important materials used as column packings in different chromatographic methods. The most popular are macroporous copolymers of styrene crosslinked with divinylbenzene (ST-DVB) but growing interest of new copolymers obtained by polymerization of methacrylate monomers is observed. Highly crosslinked polymeric microspheres for chromatographic purposes can be prepared by the polymerization of multifunctional monomers in the presence of thermoinitiator. Among crosslinking monomers multifunctional (meth)acrylate compounds are often used [1,2]. Methacrylate copolymers synthesized from monomers possessing polar functional groups are less hydrophobic than the traditional ST-DVB stationary phases [3]. The electron-donating ability of these functional groups additionally contributes to the adsorption analytes with electron-withdrawing groups. In this work we present new group of methacrylate monomers: 2-hydroxy-3-methacryloyloxypropoxybenzene (1,3-, and 1,4-di(2-hydroxy-3-methacryloyloxypropoxy)benzene) applicable for synthesis of polymeric microspheres. They were synthesized with the intention to use them as polymeric stationary phases in high performance liquid chromatography.

Materials and Methods

The copolymers in a form of porous microspheres were produced by suspension-emulsion polymerization of aromatic methacrylate monomers and TRIM. Copolymerization was made in the aqueous medium, as a surfactant bis (2-ethylhexyl) sulfosuccinate sodium salt was used. In each case, to the water solution of surfactant, the solution containing mixture of pore forming diluents (toluene and decan-1-ol), 15 g of aromatic methacrylate ester and TRIM (molar ratio 1:1), and 0.1 g of α,α'-azoisobisbutyronitrile (initiator) were added while stirring. Copolymerization was performed for 10 h at 80°C. Porous beads of MPH-TRIM, 1,3DMH-TRIM, 1,4DMH-TRIM formed in these processes were sucked off, washed with distilled water, dried and extracted in a Soxhlet apparatus with boiling acetone. The obtained particles (5-15µm) used in further studies were isolated by sedimentation and decantation from acetone.

To determine the textural properties of the studied microspheres nitrogen adsorption–desorption and inverse sized exclusion chromatography measurements were used. To compare the chromatographic properties of porous copolymers the method proposed by Smith et al [4, 5] was applied. The retention indices of five sets of homologous compounds and the selectivity test compounds (toluene, nitrobenzene, p-cresol, 2-phenylethanol, N-methylaniline) were measured. Retention index scale was based on alkyl aryl ketones. Methanol-phosphate buffer pH 7 (70:30; v/v) and acetonitrile-phosphate buffer pH 7 (50:50; v/v) were used as mobile phases.

Results and Discussion

MPH-TRIM, 1,3DMH-TRIM, 1,4DMH-TRIM polymeric microspheres (Fig. 1) are characterized by developed porous structure. Comparison of surface parameters obtained by nitrogen adsorption-desorption and inverse size exclusion chromatography methods shows some differences. Pore volumes for the swollen copolymers are significantly larger than that for the dry copolymers. In the swollen state micropores are revealed in their internal structure, whereas for dry copolymers they are absent.

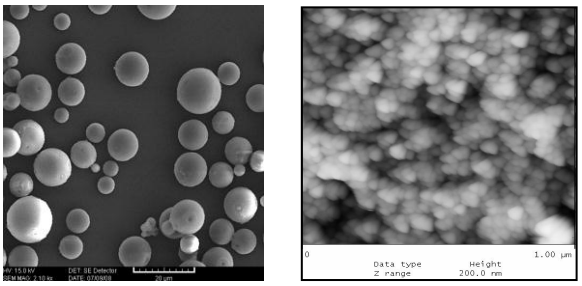

Figure 1. SEM and AFM images of porous MPH-TRIM microspheres.

The lowest value of the retention indices of the test compounds obtained on the studied porous copolymers is observed for 2-phenylethanol whereas the highest – for nitrobenzene. Better separations of homologous compounds are obtained in mobile phase containing acetonitirle.

Conclusions

Polymerization reaction of aromatic methacrylate monomers with TRIM in the presence of pore forming dilutents allows obtaining permanently porous microspheres. In their chemical structures ester and hydroxyl groups are present. They allow using obtained microspheres as polymeric stationary phases in high performance liquid chromatography.

References

1. T. Rohr, S. Knaus, H. Gruber, D. C. Sherrington, Macromolecules 35 (2002) 97-105
2. Viklund, E. Ponten, B. Glad, K. Irgum, P. Horstedt, F. Svec, Chem. Mater., 9 (1997) 463-471
3. T. Rohr, S. Knaus, D. C. Sherrington, H. Gruber, Acta Polym. 50 (1999) 286-292
4. Smith, R. M. Chem Anal 1984, 56, 256.
5. Smith, R. M.; Garside, D. R. J Chromatogr 1987, 407, 19

Crosslinked Membranes of PVA/MMT for Direct Ethanol Fuel Cells

Aílton de Souza Gomes, José Carlos Dutra Filho and Gabriel Medeiros Gomes

Instituto de Macromoléculas Professora Eloisa Mano, Universidade Federal do Rio de Janeiro. Cidade Universitária, Av. Horácio Macedo, 2.030, Centro de Tecnologia, Prédio do Bloco J, CEP 21941-598, Rio de Janeiro, RJ, Brazil. Tel.: +55 021 2562 7210; fax: +55 021 2270 1317.

asgomes@ima.ufrj.br

Introduction: The direct ethanol fuel cells (DEFCs) have recently received a lot of attention due to their high-energy density and low emission of pollutants. Many studies involving the use of poly(vinyl alcohol) (PVA) in the preparation of membranes polymer electrolyte have been performed in order to optimize the DEFC's efficiency and circumvent the limitations of Nafion® membranes use [1]. Some studies show the addition of inorganic fillers to improve the barrier properties of PVA polymer. Montmorillonate (MMT) is a well known layered silicate, which was used as the nano-fillers added into the Nafion polymer membrane. The layer structure and high aspect ratio of MMT clays are expected to be able to decrease the ethanol permeability owing to a winding diffusion path. The addition of MMT-H+ in PVA polymer matrix will also increase its ionic conductivity [2-3]. This work aims to develop nanocomposite membranes of PVA/MMT- H+ crosslinked with a melanine/formaldehyde resin and evaluate the changes in different concentrations of inorganic filler and crosslinking agent (CA), in properties such as proton conductivity and mechanical properties

Materials and Methods: Poly(vinyl alcohol) (PVA) 86,5 – 88,5 % hydrolyzed as supplied by Vetec Química Fina. Montmorillonate (MMT-H+) was purchased by Bentonita do Nordeste S.A. Melanine/formaldehyde resin was supplied by Cytec Industries Inc. All chemicals were used as received without further purification. The PVA/MMT nanocomposite polymer membranes were prepared using a solution casting method. PVA was dissolved in deionized water with magnetic stirring, heating and ultrasonic stirring for a better homogenization of inorganic filler.

Membrane uptake was tested in ethanol solution 20 wt.% in deionized water by measuring the change in the weight before and after the hydration. X-ray diffraction measurements were recorded using a Rigaku X-ray diffractometer model Miniflex (30kV, 15mA). Electrochemical impedance spectra (EIS) of the membranes were recorded using an Autolab PGSTAT- 30 instrument and the measurements were made in ethanol solution 20 wt.% in deionized water.

Results: The uptake measurements in ethanol solutrion show that the crosslinked material exhibits chemical resistance to ethanol at temperatures of 30, 50 and 80 °C. X-ray diffraction showed the possible formation of nanocomposite due to the absence of the characteristic peak of MMT (Fig.1). The conductivity measurements show that the addition of inorganic filler confers conductivities of the order of 10-1 mS.cm-1 to the polymer matrix.

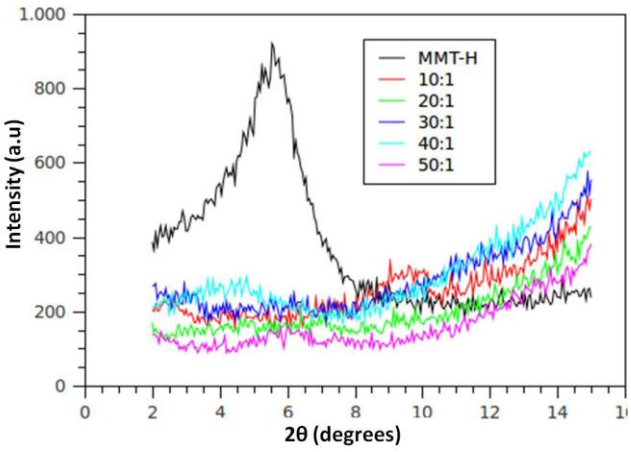

Figure 1. X-ray diffractograms of PVA/MMT-H+ composite membranes.

Conclusions: The absence of the characteristic peak of MMT in the polymer matrix observed by X-ray diffraction measurements is an indication of the formation of nanocomposite by good dispersion of inorganic filler in PVA. The membranes uptake behavior was significantly reduced with decreasing content of MMT and with increasing of CA content. The proton conductivity of membranes increased with decreasing content of MMT mainly in the samples at 80 °C. The conductivity of the samples depends on the nanostructure and are promoted by increased connectivity nanodomains between hydrophilic. The results favor the use of these membranes in direct ethanol fuel cells.

References:

[1] M. Higa *et al*, Poly(vinyl alcohol)-based polymer electrolyte membranes for direct methanol fuel cells. *Electroch Acta* 55 (2010), pp. 1445-1449.

[2] C.-C. Yang and Y.-J. Lee, Preparation of the acidic PVA/MMT nanocomposite polymer membrane for the direct methanol fuel cell (DMFC). *Thin Solid Films* 517 (2009), pp. 4735-4740.

[3] C.-C. Yang, Y.-J. Lee and J.M. Yang, Direct Methanol Fuel Cell (DMFC) based on PVA/MMT composite polymer membranes. *J Power Sources* 188 (2009) pp. 30-37.

Synthesis and Characterization of Polymeric Microspheres Based on Styrene / Divinylbenzene Containing Silver Nanoparticles

Karen Segala[1], Deborah C. Cruz[1], Lívia Cordi[2], Osmar R. Bagnato[3], Nelson Duran[4], Liliana M. F. Lona[1], Lucia H. I. Mei[1]*

[1*]Faculdade de Engenharia Química – UNICAMP, Av. Albert Einstein, 500, C.P. 6066, Campinas/SP
[2] Instituto de Biologia – UNICAMP, Rua Monteiro Lobato, 255 CEP 13083-970 Campinas/SP
[3] Laboratório de Microscopia Eletrônica (LME) - LNLS – C. P. 6192, 13083-970 Campinas/SP
[4] Instituto de Química – UNICAMP, C.P. 6154, 13083-862 Campinas/SP

ksegala@feq.unicamp.br; deborahccruz@gmail.com; cordi@unicamp.br ; osmar@lnls.br ; duran@iqm.unicamp.br; lumei@feq.unicamp.br

Introduction

The synthesis of novel materials with improved properties and performance is a continually expanding frontier at the interface of chemistry and materials science. While materials possessing structural complexity are common in nature, the development of versatile methods to prepare synthetic nanocomposites remains an exciting challenge that is currently being tackled by research groups around the world. [1,2,3]. Advances in the development of nanotechnology, especially in the use of colloidal silver, have been attracted the attention of researchers worldwide. In this work we described preliminary results about the influence of the nanosilver in the preparation of the polymeric microspheres.

Materials and Methods

Polymeric microspheres were prepared in the system composed by two phases: an aqueous phase (AP) and organic phase (OP). The AP was prepared by addition of gelatin, 2-Hydroxyethycelullose (HEC) and NaCl, in relation to water, while the OP was composed by styrene and divinylbenzene copolymerizations, toluene and benzoyl peroxide as initiator. The reaction was maintained in reflux condenser with mechanical stirrer, at 70 °C for 24 hours. After that, the resin bead was thoroughly washed with hot water and with propanone and dried at 60 °C. The AgNPs were synthesized in an aqueous media by chemical reduction of $AgNO_3$ using $NaBH_4$ as reducing agent and sodium citrate as stabilizer. The nanometric dimension of the Ag particles was monitored by UV–vis and confirmed through Transmission Electron Microscopy (TEM).

Results and Discussion

FEG image of the colloidal silver nanoparticles revealed the presence of nearly spherical particles with diameters ranging 50 nm (Figure 1). The image obtained by an optical microscope (OM) of microspheres sty/DVB is shown in Figure 2. It is observed in this picture the formation of a material with spherical appearance of various sizes. The literature shows that the stirring speed during emulsion polymer synthesis constitutes an important parameter in controlling the size of the microspheres. [4]

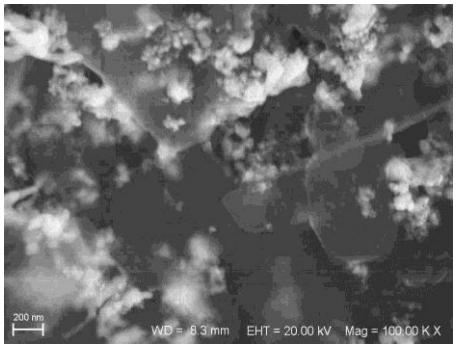

Figure 1. Image obtained by FEG of the nanosilver in aqueous medium.

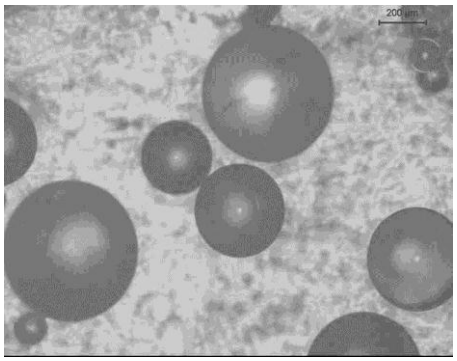

Figure 2. Image obtained by optical microscopy of polymeric type sty/DVB.

Conclusions

The synthesis of the polymeric microspheres in the presence of the silver nanoparticles was done successfully. Antimicrobial aspects from this material were studied. Studies assessing on the release of Ag+ in the culture medium and other issues relating to the understanding of this material is under way in our laboratories

References

[1] Y. Chujo, *Curr. Opin. Sol. State Mater. Sci*. **1996**, *1*, 806.
[2] M. J. MacLachlan, I. Manners, G. A. Ozin, *Adv. Mater.* **2000**, *12*, 675.
[3] J. Pyun, K. Matyjaszewski, *Chem. Mater.* **2001**, *13*, 3436.
[4] L.C. Santa Maria, M.C.A.M. Leite, M.A.S. Costa, J.M.S. Ribeiro, L.F. Senna, M.R. Silva. *Mater. Letters* **2004**, *58*, 3001.

Photorresponsive bifunctional side chain polymers

J. Royes[1], L. Oriol[1], M. Piñol[1], R.M. Tejedor[2]

[1]Facultad de Ciencias-Instituto de Ciencia de Materiales de Aragón, Universidad de Zaragoza-CSIC, 50009 Zaragoza, Spain.
[2]Centro Universitario de la Defensa, Academia General Militar, Carretera de Huesca s/n, 50090 Zaragoza, Spain.

rtejedor@unizar.es

Materials with a controlled molecular architecture have been deeply investigated because it is possible to establish better relations structure-properties, leading to a new generation of materials rationally designed in function of the desired properties. Moreover, photoactive materials have been an area of interest due their capability of respond to a light stimulus and generate a determinate response, such changes on the material alignment, catalysis of a reaction or macroscopic moves[1]. Specifically, azobenzene side chain polymers has also been hardly studied because their optical and electro-optical applications[2].

Here, we present the properties of a series of bifunctional polymers that have been obtained by combining controlled radical polymerization and 'click chemistry' tools. Therefore, by this tandem approach a polymer skeleton with alkyne groups has been modified with dual functional azides giving rise to a family of functional materials were the final properties can be modulated by the nature of the functional units and the regularity on their position, frequency and distribution along the polymeric main chain. Side-chain polymers with pendant units containing photo-addressable azobenzene moieties, cinnamate units and classical liquid crystal moieties have been prepared.

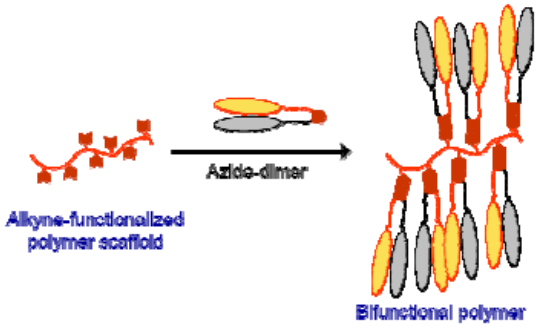

In particular, our interest is focussed on the photoinduction of chirality in polymeric achiral materials when they are put under a chiral stimulus, a phenomena that was recently described. This photoinduction of chirality can be achieved irradiating a photoactive material with circularly polarized light (CPL)[3]. In this family of materials, a switchable phototransference of chirality from the CPL to the material has been achieved. The effect of a precise alternation of the functional units as well as the possible cooperative motion of the liquid crystalline units in the supramolecular chirality is also evaluated.

References

[1] H. F. Yu, T. Kobayashi, *Molecules* **2010**, *15*, 570.
[2] J. Del Barrio, L. Oriol, R. Alcalá, C. Sánchez, *J. Polym. Sci. Pol. Chem.* **2010**, *48*, 1538.
[3] R. M. Tejedor, L. Oriol, J. L. Serrano, T. Sierra, *J. Mater. Chem.* **2008**, *18*, 2899.

Acknowledgements: Financial support by the Ministerio de Ciencia e Innovación (project MAT-2008- 0625-C02-01) and by the Diputación General de Aragón.

Characterization of the functional properties of commercial Polyhydroxyalkanoates (PHA)

Yves-Marie CORRE, Stéphane BRUZAUD, Yves GROHENS

Laboratoire d'Ingénierie et Matériaux de Bretagne (UBS), Université Européenne de Bretagne, Centre de Recherche Christiaan Huygens, Rue de Saint Maudé, 56321, Lorient, France

yves-marie.corre@univ-ubs.fr

Abstract

Bio sourced and/or biodegradable polymers attract growing interest in the polymer community since a few decades. Replacing durable petroleum based polymers by biodegradable ones would drastically reduce land and water pollution. Polyhydroxyalkanoate (PHA) is one of the promising materials to reach such an objective as it is a polyester synthesized and accumulated by specific bacteria. This living synthesis results in a biodegradable polymer with specific chemical structure depending on the strain of bacteria and the substrate used.

The aim of this study is to characterize some commercially available PHAs in term of functional properties such as mechanical, thermal and gas and water vapour transmission capacity. The mechanical study first positions PHAs compared to conventional polymers in order to evaluate the applications field for such biopolymer. Glass transition temperature and crystallization behaviour investigations then bring some information about the heat resistance and the process limitation induced by the crystallization completion during a process cycle such as injection moulding. The evaluation of oxygen and water vapor transmition capacity complete this investigation in term of functional properties dedicated to specific application such as food or medical packaging.

Keywords Polyhydroxyalkanoates, PHA, Mechanical properties, Crystallization, Oxygen transmission rate, Water vapor transmission rate.

Preparation and characterization of polystyrene-*graft*-polyethylene glycol copolymers as solid–solid phase change heat storage material

Alper Biçer, Cemil Alkan, Ahmet Sarı, Ali Karaipekli*

Department of Chemistry, Gaziosmanpaşa University, 60240, Tokat, Turkey

In this study, graft copolymers of polystyrene with different PEG6000 content as novel polymeric solid-solid phase change materials (PCMs) were synthesized.

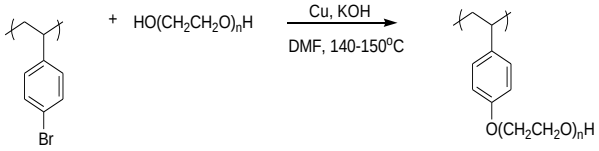

Fig. 1 Synthesis scheme for the preparation of graft copolymers of polystyrene

In these new materials, polystyrene is the skeleton and PEG is a functional side chain that stores and releases heat during its melting and freezing process. The heat storage mechanism of copolymers is the transfer between crystalline and amorphous states of the soft segment PEG in copolymer, and the hard segment polystyrene restricted the free movement of molecular chains of the soft segments at high temperature.

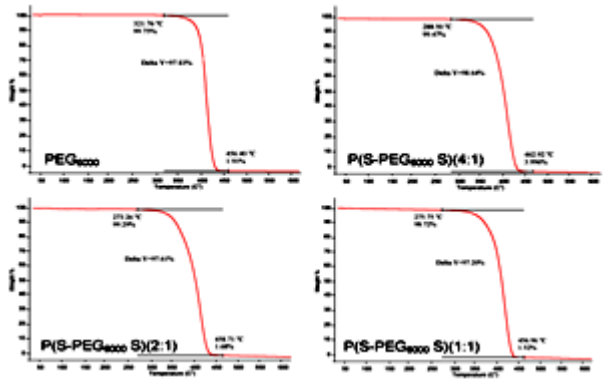

Fig. 2 TG curves of graft copolymers of polystyrene

Thus, these copolymers can keep them solid state in the phase transition processing and were described as form-stable PCM.

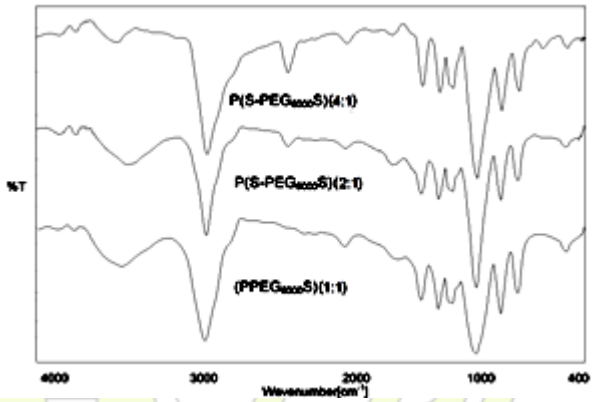

Fig. 3 FT-IR spectra of graft copolymers of polystyrene

To investigate ingredients, thermal properties, thermal reliability and crystalline morphology of the synthesized copolymers, fourier transform infrared spectroscopy (FT-IR), differential scanning calorimetry (DSC), thermogravimetric analyses (TGA), and polarization optical microscopy (POM) analyses were performed.

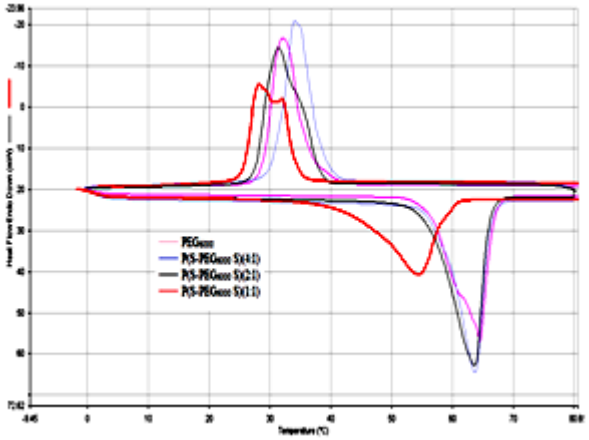

Fig. 4 DSC thermograms of graft copolymers of polystyrene

The results indicated that the PEG chains were successfully grafted onto the polystyrene backbone and the copolymers have typical solid-solid phase transition properties. The synthesized P(S-PEG_{6000}S)(4:1), P(S-PEG_{6000}S)(2:1) and P(S-PEG_{6000}S) (1:1) have solid-solid phase transition temperature of 44.9, 56.5 and 58.0 °C, respectively, and latent heat values of 111.48, 130.98, and 179.47, J/g, respectively.

Moreover, thermal cycling test showed that the copolymers have good thermal reliability and chemical stability although they were subjected to 5000 melting/freezing cycling. Based on all results, it was concluded that the polystyrene-*graft*- PEG copolymers as novel solid-solid PCMs have potential applications for thermal energy storage and temperature control.

References

Cao Q, Liu P, Hyperbranched polyurethane as novel solid–solid phase change material for thermal energy storage, European Polymer Journal, 42, 2931-2939, 2006.

Su J.C, Liu P.S, A novel solid–solid phase change heat storage material with polyurethane block copolymer structure, Energy Conversion and Management, 47, 3185-3191, 2006.

Li Y, Liu R, Huang Y, Synthesis and Phase Transition of Cellulose-graft-Poly(ethylene glycol) Copolymers, Journal of Applied Polymer Science, 110, 1797-1803, 2008.

Synthesis and Characterization of Poly (alkyloyloxyethylmethacrylate-co-methylacrylate) as Solid-Solid Phase Change Materials for Thermal Energy Storage

Tuğba Güngör Ertuğral1, Ömer Faruk ENSARİ2, Cemil ALKAN2

1Giresun University, Şebinkarahisar Vocational School, Department of Food Technology, Giresun, Turkey
2Gaziosmanpaşa University Department of Chemistry 60240 Tokat, Turkey

tuba.gungr@hotmail.com

Phase change material is a substance with a high heat of fusion which, melting and solidifying at a certain temperature, is capable of storing and releasing large amounts of energy. Heat is absorbed or released when the material changes from solid to liquid and vice versa; thus, PCMs are classified as latent heat storage (LHS) units. Total amount of energy absorbed or released by a phase change material can be calculated by equation 1.

$$Q = m\Delta H_M + \int_i^M mC_p dT + \int_M^f mC_p dT \quad (1)$$

PCMs should be encapsulated for usage and they are mostly encapsulated in polymers for the ease of application. Polymeric solid solid phase change materials are promising for their easy applicability and expected long lasting property. In this work, 2- hydroxyethyl methacrylate esterified with acyl chlorides of three different fatty acids to obtain monomers with phase changing property at convenient temperatures with high storage density so that copolymerization of these monomers with methylacrylate will result in polymers with solid solid phase changing property at variable phase change temperatures. 9 different polymers have been synthesized as a result of the reaction between produced monomers and methylacrylate at 3 different weight ratios. Produced copolymers were characterized by structural and thermal aspects. For the synthesis of the novel PCMs, myristic acid, palmitic acid, and stearic acid were chosen and they were transformed to acyl chlorides by thionyl chloride in the presence of dimethylformamide catalyst. Fatty acid acyl chlorides were bound to 2-hydroxyethylacrylate monomer from hydroxyl group as shown in the following Figure.

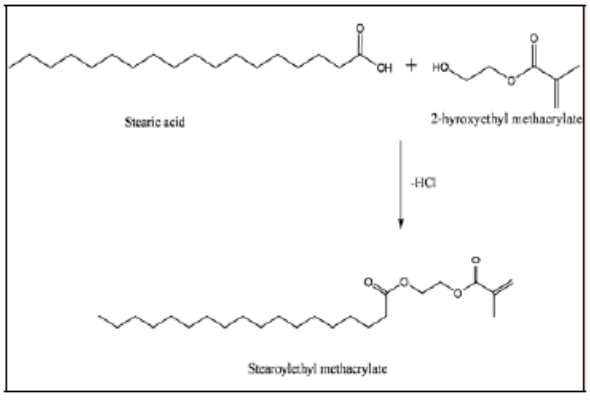

FT-IR and NMR spectroscopy techniques were used to characterize the produced PCMs structurally as molecular weight measurements were done using Gel Permeation Chromatography (GPC) technique. Molecular weight of the polymers produced decreased by the fatty alkyloylethylmethacrylate monomer content

and with increasing paraffinic side length. Phase change temperatures and enthalpies and degradation temperatures of the synthesized PCMs were investigated using Differential Scanning Calorimetry (DSC) and Thermal Gravimetric Analysis instruments respectively and it was found that produced polymers have potential to be used as thermal energy storage materials and stable up to considerably high temperatures. On the other hand structural and thermal consistency of the polymers was confirmed by FT-IR and DSC measurements after accelerated thermalcyclings.

Thermal conductivity of the polymers was found to be in the range of the thermal conductivities of fatty acids.

Besides polarize optical microscopy was used for morphology investigation of polymers below and above phase transition temperatures.

Key words: 2-hydroxyethyl methacrylate, methylacrylate, phase change material, fatty acid

References

Baran, G., Sarı, A., 2003. Phase change and heat transfer characteristics of a eutectic mixture of palmitic and stearic acids as PCM in a latent heat storage system. Energy Conversion and Management 44: 3227–3246.

Feldman, D., Khan, M. A. Banu, D., 1989. Energy storage composite with an organic PCM, Solar Energy Materials, 18(6), 333-341

Feldman D., M.M. Shapiro, D. Banu and C.D. Fuks, Fatty acids and their mixtures as phase change materials for thermal energy storage, *Solar Energy Materials* 18 (1989), pp. 201–216.

Hong K., Park S., Preparation of polyurethane microcapsules with different soft segments and their characteristics. Reactive and Functional Polymers 42, (1999) 193.

Jiang Y., Ding E. Y., Li G. Study on transition characteristics of PEG/CDA solid-solid phase change materials Polymer 43 (2002) 117–122.

Su J. C., Liu P. S. A novel solid-solid phase change heat storage meaterial with polyurethene blok copolymer structure Energy Conversion and Management 47, (2006) 3185.

Yuan X. P., Ding E. Y. Synthesis and Characterization of Storage Energy Materials Prepared from Nano Crystalline Cellulose/Polyethylene Glycole Chinese Chemical Letters 17(8), (2006) 1129.

Polyethers As Phase Change Materials for Passive Thermal Energy Storage

Derya Kahraman, Cemil Alkan, Mukaddes Ülkü Önder

Gaziosmanpaşa University, Department of Chemistry, 60240, Tokat / TURKEY

dkahraman@gop.edu.tr

Polyethylene glycols (PEGs) are the most promising polymers for thermal energy storage applications due to their high storage densities and variable phase change temperatures. They are also considered in preparation of solid solid polymeric phase change materials for their functional OH groups at chain ends. In this work it was aimed to determine the physicochemical properties of some of the other aliphatic polyethers for their feasibility to be used as phase change materials for thermal energy storage. For this purpose, polytetrahydrofurane at two different molecular weights were obtained commercially as poly(1,3-dioxolane) and poly(1,3,5-trioxane) polymers at 3 different molecular weights were synthesized and characterized as shown in the Figure 1. 1,3-dioxolane and 1,3,5-trioxane were polymerized with ethylene glycol initiator and $BF_3.Et_2O$ catalyst.

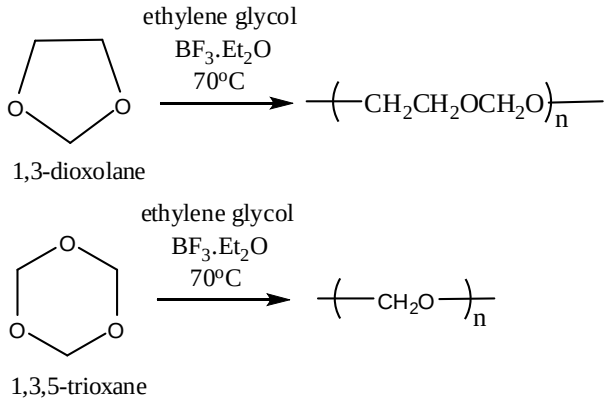

Figure 1: Synthetic route for the synthesis of poly(1,3-dioxolane) and poly(1,3,5-trioxone)

The chemical characterization of poly(1,3-dioxolane) and poly(1,3,5-trioxane) polymers were made by fourier transform infrared radiation (FT-IR) spectroscopy (Figure 2) as their molecular weight analysis were done using gel permeation chromatography (GPC).

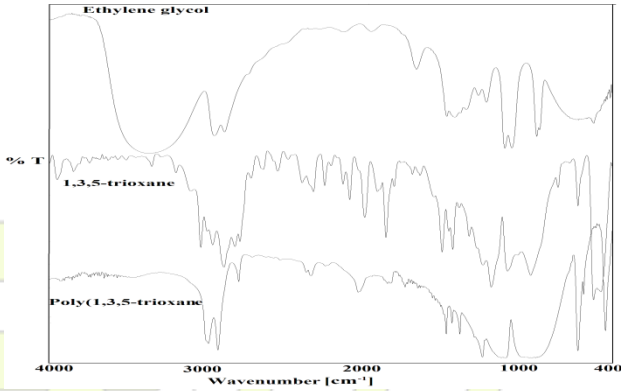

Figure 2: Ethylene glycol, 1,3,5-tioxane, and poly(1,3,5-tioxane) FT-IR spectrum

The melting and freezing temperatures and latent heats of the polyethers as phase change materials were measured using DSC instrument and it was found that polyethers

having different phase change temperatures can be considered as novel phase change materials for some other applications due to their variable phase change temperatures and high thermal energy storage densities. They are also found thermally stable and they have potential for both to be used as solid-liquid phase change material and to be used in the preparations of polymeric solid-solid phase change materials for thermal energy storage. Thermal gravimetric analysis (TGA) indicated that both commercially obtained and synthesized polyethers had good thermal stability up to high temperatures (Figure 3).

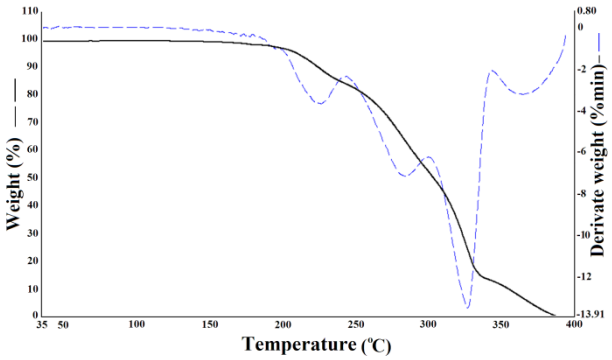

Figure 3: TGA thermogram for one of the poly(1,3,5-trioxane) produced in this research

Polytetrahydrofurane, poly(1,3-dioxolane)s and poly(1,3,5-trioxane)s have also been considered as counterparts of eutectic mixtures of poly(ethylene glycol)s so that polyether mixtures with different phase change temperatures could be obtained. Eutectic temperatures were calculated using following Schröder equation theoretically.

$$lnx_B = -\frac{\Delta H_B}{R}\left(\frac{1}{T^*}+\frac{1}{T_B}\right)$$

References:

Li, J., Yan, D., Inclusion Complexes Formation between Cyclodextrins and Poly(1,3-dioxolane), Macromolecules, 2001, 34, 1542-1544.

Kajiwara, A., Matyjaszewski, K., Formation of Block Copolymers by Transformation of Cationic Ring-Opening Polymerization to Atom Transfer Radical Polymerization (ATRP), Macromolecules, 1998, 31, 3489-3493.

Pielichowski, K., Flejtuch, K., Differential scanning calorimetry studies on poly(ethylene glycol) with different molecular weights for thermal energy storage materials, Polymers for advanced Technologies 13,2002, 690-696.

Synthesis of Paramagnetic Polymers Using Ionic Liquid Chemistry"

Markus Döbbelin,[a,*] *Vasko Jovanovski*,[a] *Luis J. Claros Marfil*,[b] *Germán Cabañero*,[a] *Javier Rodriguez*[a] *and David Mecerreyes*[a]

[a] New Materials Department, CIDETEC, Center for Electrochemical Technologies, Parque Tecnológico de San Sebastián, Paseo Miramón 196, Donostia-San Sebastián, 20009, Spain. Fax: +34 943309136; Tel: +34943309022
[b] ACCIONA Infraestructuras, Centro Tecnológico I+D+i, Valportillo II, nº8, Alcobendas 28108, Spain

[*] mdobbelin@cidetec.es

Herein, the synthesis of polymeric ionic liquids (PILs) with paramagnetic anions based on tetrachloroferrate(III) ($FeCl_4^-$) and tetrabromoferrate(III) ($FeBr_4^-$) is presented. The formation of the novel polymers encompassing the paramagnetic anions is proven by UV-VIS and Raman spectroscopy. Paramagnetic properties are analyzed using a SQUID measuring system. Some of the obtained PILs show higher magnetic susceptibility values than previously measured for paramagnetic ionic liquids. It is further found that the magnetic susceptibility can be tailored by controlling the iron content in the anion. Interestingly, casted films of the PILs show a strong response to a neodymium magnet. As a potential application, a microgel based on a paramagnetic PIL is used as reusable catalyst in aromatic Friedel–Crafts alkylation. The PIL microgel can be easily removed and reused after the reaction making these new materials interesting for green chemistry processes.

The pictures in **Figure 1** show the response of a polymeric film of poly(1-vinyl-3-ethyl-imidazolium $FeBr_4^-$) (obtained by casting from acetone solution) to a neodymium magnet. The film showed a good response to the magnet field and eventually sticked to the magnet when close enough. Similar behaviour was observed for films of the other paramagnetic PILs.

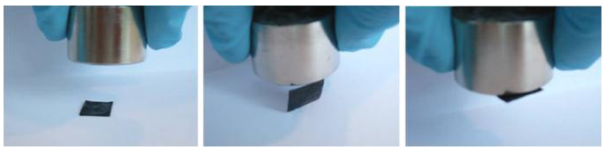

Figure 1. Response of a film of $pViEtIm^+$ $FeBr_4^-$ to a neodymium magnet.

The paramagnetic/Lewis acid character of the presented PILs make them interesting candidates to be applied as "reusable catalyst" in Friedel-Crafts reactions. For this purpose, a microgel of paramagnetic PIL was synthesized. The magnetic response can be beneficial to overcome difficulties in separation/recovery of the catalyst as it can be simply removed by a magnet or by centrifugation, washed and reused. Hence, a microgel of poly(1-vinyl-3-butyl-imidazolium $FeCl_4^-$) was used as reusable catalyst in Friedel-Crafts alkylation. **Figure 2** shows the reaction scheme of the aromatic Friedel-Crafts alkylation and a SEM micrograph of the reusable polymeric microgel. The isomers of benzyl-4-methylbenzene were obtained from toluene and benzyl chloride. The procedure was repeated 10 times without any loss in catalytic performance of the paramagnetic microgel. The product yield ranged constantly above 99%.

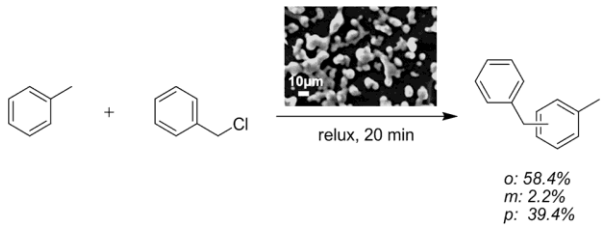

Figure 2. Synthesis scheme of the aromatic Friedel-Crafts alkylation. The SEM micrograph shows the paramagnetic microgel.

Relevant references:

1) S. Hayashi, H. Hamaguchi, *Chem. Lett.*, 2004, 33, 1590.
2) J. Tang, M. Radosz, Y. Shen, *Macromolecules*, 2008, 41, 493.
3) G. Wang, N. Yu, L. Peng, R. Tan, H. Zhao, D. Yin, 4) H. Qiu, Z. Fu and D. Yin, *Catal. Lett.*, 2008, 123, 252.
5) M. Döbbelin, V. Jovanovski et al., *Polymer Chemistry* 2011, submitted.

Environmentally Friendly Polyurethane Foams

Yu. Savelyev, L.Markovskaya, I.Yanovych, E.Akhranovych

Institute of macromolecular chemistry, NAS of Ukraine, Kharkovskoe shosse, 48, o2160, Kiev, Ukraine

The most of the synthetic polymer materials posses the low degradability in environment due to stability of their chemical structure to external influences, therefore they are a considerable source of environmental pollution. The decision of this problem is not so much removal of such challenges to environment as their prevention that is the aim of the "Green chemistry", the principle of which in increasing frequency have been considered. The best solution of the problem of "polymer wastes" is the creation of polymers retaining their exploitation characteristics only during period of usage, whereupon such polymers undergo physic-chemical and biochemical transformation (hydrolytic, oxidative, photo-, thermo-, mechanic- and biodestruction) under the influence of different factors of environment and are easily enter into metabolism processes of natural biosystems.

The main biological systems damaging polymers are microorganisms (especially mould fungi and bacteria). That is why the commonly used method of giving the polymers an ability to degradation is their combination / blending with biodegradable components (di-, polysaccharides) which are the sours of food for different microorganisms. However, such composite materials are just conditionally degradable, since only carbohydrates, but synthetic polymers in the most cases are not being decomposed.

Polyurethane foams (PUF) are the widespread class of macromolecular compounds used as the base for creation of variety modern polymer materials due to their polyblock structure, which determine unrestricted abilities of their structure and physical properties. The distinctive feature of PUF is their hypothetic biocompatibility as the result of their heterogeneous structure.

Taking into account preceding, the aim of this work is the creation of novel degradable under environment conditions PUF on the basis of saccharid-containing precursors and polysaccharides

Synthesis of PUF was carried out using ethers and esters, activators of the process and water. As diisocyanate component we used saccharid-containing precursors with reactive NCO groups, received by reaction of lactose (mannose, sucrose) with 2,4(2,6)-toluenediisocyanate (TDI). The following polysaccharides were used: starch, cellulose derivatives (hydroxymethyl-, carboxymethyl-), Na-alginate. Spuming was made owing to carbon dioxide, which exude at decomposition of unstable aminoformic acid, formed as the result of interaction between diisocyanate and water.

The character of degradation of PUF has been studied under the influence of different destructive factors: a) long action of heightened humidity (up to 87%) and temperature (37°C); b) mould fungi (*Aspergillus* and *Penicilium*); c) 0,1N solution of KOH and HCl; d) incubation of polymers into the soil for 3, 6, and 9 months. Definition of the soil microflora has shown the presence of *Rhizopus, Aspergillus, Penicillium.*

The degree of destruction is 40-50%, that essentially exceeds the actual content of natural compounds in polymer composition. The mass lost by reference template of PUF (without carbohydrates) even after 270 days' incubation is insignificant (2,4 %). I. e. the introduction of these compounds contributes to degradation of polymer materials.

Thus, the FPU creation using the introduction of nature compounds into the polymer structure serve as the way of the obtaining materials with given properties, biodegradable under the action of different environmental factors.

Effect Of Salt Concentration On Strength And Morphology Of Natural Degradable Additive PP Film Upon Immersion in water.

Rahmah Mohamed[1], *Zarith Sofia Mohd Bakri, AmirFakhrul Islam Abdullah.*

[1]Polymer Technology Programme, Faculty of Applied Sciences(FSG)
University Technology MARA(UiTM) Shah Alam, 40450 Shah Alam, MALAYSIA.

Email: rahmahmd@salam.uitm.edu.my, greenkayangan@gmail.com

Due to preservation of our valuable environment, use of natural degradable additive is an important solution to discarded plastics material. Use of degradant additive for non biodegradable plastics such as polyethylene (PE) and polypropylene(PP), are preferred due to their low cost. In this work, natural additive, RM is used as the degradant to impart oxidative degradation and enhanced chain scission to PP before fragmentation. Film are immersed to different pH and two salt concentration. From this study, the greatest degradation for degraded film from PP filled RM additive was at pH value of 7 with 3.5% salt concentration. Tensile strength of PP filled additive at pH 7 (neutral environment) showed lowest strength compared to PP blank.Carbonyl index and surface roughness of film were determined. Presence of chloride ion in salt had enhanced oxidation and degrade PP film. Surface roughness visualized through Atomic Force Microscopy (AFM) of PP filled RM additive with dione was highest and tensile strength was found to be lowered.

Keyword: Degradation, Non degradable PE and PP, Natural Additive, Tensile Strength, Carbonyl index, Atomic force microscopy(AFM)

INTRODUCTION

Current state of global warming and threats to the environment had caused plastics to be blamed and banned in some countries. Plastics for packaging are being scrutinized due to its resistance to degrade. Polymer degradation may occur through thermal, light oxygen and uv degradation or weathering (Singh and Sharma, 2007). Additives had being used as degradant such as metal stearates and cobalt which may affect the environment.(Chiellini 2006) This study differ from others studies whereby natural additive formulations of oil and dione (named RM) are chosen as a pro-oxidant and photosensitizer respectively for Polypropylene (PP). In this study, PP filled with RM additives are studied and investigated.

MATERIALS AND METHODS

Polymer compounding using twin screw, PRISM with L/D ratio of 16:1 were perfomed using Propylene, I102 from *MTBE, Petronas* with MI of 10 and different ratios of RM additives, namely *RM1 and dione*. Films cut according to ASTM D882 were placed in water of three pH, 3,5 and 0 with sodium chloride salt of 3.5% and 5%. Films were immersed for one and three weeks. All film samples were being tested for tensile strength, carbonyl index using Fourier Transform Infrared (FTIR) and morphology using Atomic Force Microscopy (AFM).

RESULTS AND DISCUSSION.

The tensile strength(TS) of PP filled RM at pH 7 were significantly reduced compared to PP Blank. Presence of RM oil had actually accelerated degradation process as this formulation had the lowest tensile strength..

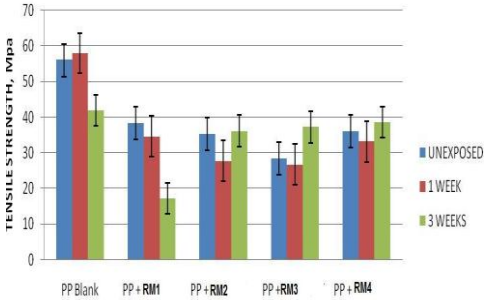

Figure 4.1 Tensile strength versus formulation at pH 7 and 3.5% salt concentration.

The degradation of the PP samples was followed by FTIR. A sharp increase in absorption in the carbonyl region was recorded with time in all the samples exposed. Among films studied, PP filled palm oil at pH 7 with 3.5% salt concentration resulted in higher CO_i.(carbonyl index). Roughness $_{RMS}$ of PP filled palm oil after exposure for three weeks was significantly increased. Obvious changes of PP filled additives was due to more chain scission occurred and the oil could be oxidized by chloride ion resulting in lower TS and CO_i.

REFERENCES

1. Baljit Singh and Nisha Sharma, (2007). *Polymer Degradation and Stability, 93*, pp 561-584.
2. E. Chiellini , A. Corti , S. D'Antone , R. Baciu, (2006). *Polymer Degradation and Stability, 91*, pp 2739-2747.
3. F.Gugumus. *Polym Degrad Stab*, **76**, 329-340, 2002.
4. P.K. Roy , P. Surekha , C. Rajagopal , S.N. Chatterjee , V. Choudhary, (2006). *Polymer Degradation and Stability 9*, pp 1791-1799.
5. L.F.Doty (2005). Oxo-biodegradable Plastics Institute . *A Brief Overview of Degradable Plastics.*
6. Loo, C. Y., W. H. Lee, T. Tsuge, Y. Doi and K. Sudesh, (2005). *Biotechnol. Lett*, Vol 27, No. 18, pp 1405-1410.

Synthesis of flexible polymer-ceramic composites for RFID tagging of people

C. Ortiz[1], *M. Suárez*[1,2], *S. Ver Hoeye*[3], *E. de Cos*[3], *M. Fernández*[3], *C. Vázquez*[3], *R. Camblor*[3], *G. Hotopan*[3], *R. Hadarig*[3], *F. Las Heras*[3], *J. L. Menéndez*[2], *S. García-Caso*[4].

[1] Fundación ITMA, Parque Tecnológico de Asturias, 33428, Llanera, Spain.
[2] Department of Nanostructured Materials, Centro de Investigación en Nanomateriales y Nanotecnología (CINN). Principado de Asturias – Consejo Superior de Investigaciones Científicas (CSIC) – Universidad de Oviedo (UO). Parque Tecnológico de Asturias, 33428 Llanera, (Asturias), Spain.
[3] University of Oviedo, Department of Electrical Engineering, E-33203 Gijón, Spain.
[4] Treelogic, Parque Tecnológico de Asturias, 33428, Llanera, Spain.

m.ortiz@itma.es

Introduction

The identification of people and the monitoring of their history is still issue of great interest today in our society. Radio Frequency Identification (RFID) has a diverse and wide application potential to use in this field. RFID tags require substrates that meet strict requirements in terms of their properties (electromagnetic, mechanical and chemical), this is they should be flexible, biocompatible and with high dielectric constant. Nowadays, the major barrier in the implementation of RFID is the high cost of the system due to the existing conformal antennas is still printed on rigid laminate substrates with curved shapes. Polymers are rapidly getting important among materials for this kind of applications whether used in pure form or combined with ceramic powders. In the present work, polymer-ceramic flexible tags containing ethylene vinyl acetate (EVA) and $SrTiO_3$ were synthesized. Using the optimized substrate and Perfect Magnetic Conductors (PMC) design, a high performance RFID tag were obtained.

Materials and Methods

Polymer-ceramic flexible tags containing ethylene vinyl acetate (EVA) and different percentages of $SrTiO_3$ (4-60% v/v) were synthesized by extrusion and subsequent forming. The chemical characteristics of the different compositions were characterized by Termogravimetric analysis (TGA). Structural characteristics of the composites were investigated using a FTIR spectrometer in the range of 400–4000 cm^{-1} by the KBr pellet method. The microstructure was analyzed by Field Emission Scanning Electron Microscopy (FESEM). The electrical parameters (permittivity and loss tangent) of polymer-ceramic composites were measured with a broadband probe 0.2-20 GHz after depositing a layer of copper on the surface of the samples by Chemical Vapour Deposition (CVD).

Results and Discussion

Flexible tags based on polymer and ceramic composites were obtained. Ethylene Vinyl Acetate was chosen as polymer since it approaches an elastomeric material in softness and flexibility and it is biocompatible with the body. To achieve higher dielectric constant, ceramic powders were introduced into the polymer matrix during the extrusion process. Figure 1 shows the FT-IR absorption spectra for the pure polymer and the composite prepared with 25% v/v $SrTiO_3$. A Sr-O stretching band is seen in the composite spectra at 596 cm^{-1} which is not visible in the pure spectra, indicating the presence of $SrTiO_3$ particles into the polymer matrix. FE-SEM characterization image demonstrate that composites show a homogeneous morphology with the $SrTiO_3$ particles being embedded within the EVA matrix (Figure 2). Polymer-ceramic composites show a high dielectric constant value and great flexible to be used as substrates for RFID tags as is shown in Figure 3.

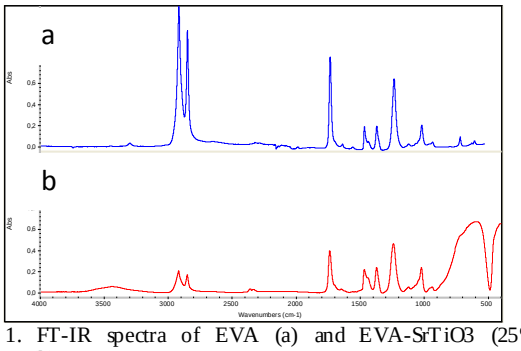

Figure 1. FT-IR spectra of EVA (a) and EVA-SrTiO3 (25%v/v) composite (b)

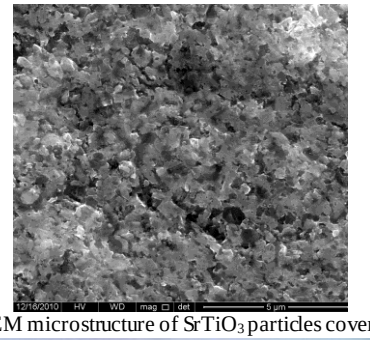

Figure 2. FE-SEM microstructure of $SrTiO_3$ particles covered by polymer

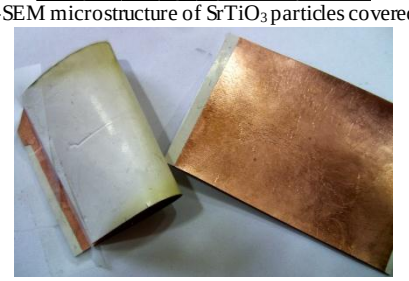

Figure 3. Photograph of polymeric-ceramic flexible tags for using in RFID applications

Multifunctional properties of PLA composites based on silver nanoparticles and crystalline cellulose: role of crystal micro and nano-dimension.

E. Fortunati[1], I. Armentano[1], Q. Zhou[3], A. Iannoni[1], E. Saino[5], L. Visai[6], L.A. Berglund[4], J.M. Kenny[2]

[1]Materials Engineering Center, UdR INSTM, University of Perugia, Italy
[2]Institute of Polymer Science and Technology, CSIC, Spain
[3]School of Biotechnology, Royal Institute of Technology, Stockholm, Sweden
[4]Wallenberg Wood Science Center, Royal Institute of Technology, Stockholm, Sweden
[5] Department of Biochemistry, Medicine Section, and Center for Tissue Engineering (C.I.T), Pavia, Italy
[6] Salvatore Maugeri Foundation IRCCS, Pavia, Italy and International Centre for Studies and Research in Biomedicine (I.C.B.), Luxembourg

elena.fortunati@unipg.it; kenny@ictp.csic.es

Introduction

Biodegradable polymers have been investigated during the last few decades as alternatives to non-degradable polymers.[1] PLA is becoming popular as a biodegradable engineering plastic owing to its high mechanical strength, easy processability compared to other biopolymers. The preparation of micro- and nano-composites represents a promising method to improve the physical properties of biopolymers. The incorporation of antimicrobial substances in food-packaging materials to control undesirable growth of microorganisms on the surface of foods, represents a great challenge.[2] Microcrystalline cellulose (MCC) has been used as additive to improve the properties of polymer in several applications, while nanocrystalline cellulose (CNC), produced from the acid hydrolysis of MCC and properly modified, presents increased crystalline phase. CNC shows high mechanical properties, great biodegradability and biocompatibility, high stiffness, and low density.[3-5]

Materials and Methods

Poly-Lactide Acid (PLA) 3051D, supplied by Nature Works®, was used as polymer matrix and commercial silver (Ag) nanopowder were added in order to provide antibacterial properties to the system. Microcrystalline cellulose (MCC, dimensions of 10-15 µm) was supplied by Sigma Aldrich and cellulose nanocrystal (CNC) suspension was prepared from MCC by sulphuric acid hydrolysis.[6] Cellulose nanocrystals were modified with an acid phosphate ester of ethoxylated nonylphenol (s-CNC). Binary and ternary films with 5%wt of MCC, 5%wt of pristine CNC or surfactant modified s-CNC and with 1%wt of Ag were prepared by a melt extrusion followed by a filmature process. New multifunctional materials were characterized in terms of morphology, mechanical, thermal and antibacterial properties and the effect of cellulose crystal micro- and nano-dimension, the presence of surfactant, and the combination with silver nanoparticles were investigated.

Results and Discussion

Cellulose nanocrystals produced by acid hydrolysis appear individualized, with the typical dimensions ranging from 100 to 200 nm in length and 15 nm in width, highlighting the success of the process.

Morphology studies of PLA composite films prepared combining MCC and Ag nanoparticles revealed a well dispersion of silver and the presence of microcrystalline cellulose aggregates, while the mechanical properties demonstrated the MCC reinforcing effect. The presence of surfactant on the CNC surface, favors their dispersion in the polymer and the nucleation effect was remarkably enhanced compared to both MCC and pristine CNC based systems, supporting the positive effect of nanoscale and of surface modifications on the thermal and mechanical properties of resulting PLA composite films.

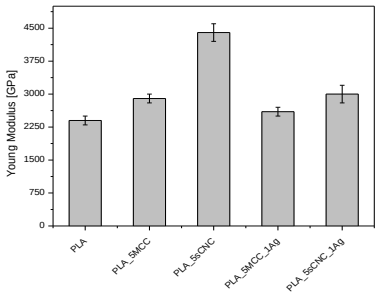

Fig. 1: Mechanical properties of PLA composite films.

Moreover, a bactericidal effect of all the analyzed PLA composites on *S.aureus* and *E.coli* was detected suggesting possible applications which requires an antibacterial effect constant over time.

Conclusions

PLA composites reinforced with micro- and nano-crystalline cellulose combined with silver nanoparticles offer a good perspective for food packaging applications which requires high mechanical performances, good transparency, thermal stability, and an antibacterial effect.

References

1. Davis et al., *Prog Polym Sci*, **2009**,34,125.
2. Vermeiren et al., *Trends Food Sci Tech*, **1999**,10,77.
3. Ma et al., *Carbohyd Polym*, **2008,** 72, 369.
4. Fortunati et al., *Polym Degrad Stab*, **2010,** 95,2200.
5. Bondeson et al., *Compos Interfaces*, **2007**,14,617.
6. Zhou et al., *Macromolecules*, **2009**,42,5430.

Acknowledgements: The authors gratefully acknowledge the financial support from INSTM.

Solid-State Polymerized Conducting Polymers for Highly Efficient, Iodine-Free Dye-Sensitized Solar Cells

*Jeonghun Kim, Jong Kwan Koh, Byeonggwan Kim, Jong Hak Kim,*and Eunkyoung Kim**

Department of Chemical and Biomolecular Engineering, Yonsei University, 262 Seongsanno, Seodaemun-gu, Seoul 120–749, South Korea

e-mail: eunkim@yonsei.kr

Introduction

In solid-state dye sensitized solar cells (ssDSSCs), hole transporting materials (HTMs) and the control of interfacial properties between the nanoporous TiO_2 layer and HTM are critical to the photo conversion efficiency of the cells. Recently, HTMs have been extensively investigated as potential replacements for conventional I_3^- /I^- redox electrolyte systems using iodine (I_2) in DSSCs due to the leakage of electrolyte and corrosion of electrode by I_2. Recently, we have developed the iodine (I_2)-free ssDSSC with high efficiency of 5.4 % using solid-state polymerized conductive polymer conductive polymer as HTM to enhance the penetration of HTM to thick TiO_2 layer.[1] Herein, we present about the application of highly conductive polymers to the I_2 free ssDSSCs with a facile fabrication method.

Materials and Methods

The ssDSSCs were constructed by drop-casting of electrolyte solution onto the photoelectrode and covering with Pt coated counter electrode, using the previously reported procedure.[2-5] The commercial TiO_2 paste (solaronix D20) was casted onto the glass using a doctor-blade technique, followed by successive sintering at 450 °C for 30 min. Nanocrystalline TiO_2 films were immersed into N719 solution (0.5 mM in ethanol) for 24 hr at R.T. The DBEDOT (2,5-dibromo-3,4- ethylene dioxythiophene) was dissolved in anhydrous ethanol (1 wt and 3 wt %) and a few drops of the solution were directly casted onto the TiO_2 photoelectrode and counter electrode. After drying the solvent, the DBEDOT onto the photoelectrode was thermally polymerized at 60 °C for 24 hr in an oven (fig. 1). Then, a drop of the acetonitrile solution consisting of MPII (1.0 M), TBP (0.2 M) and Li salt (0.2 M) was casted onto the photoelectrode. After evaporation of the solvent in a vacuum oven, sandwich-type DSSCs were fabricated by clipping two electrodes. The active area was 0.16 cm^2.

Results and Discussion

SSP, yielding highly conductive polymers, has been reported using halogenated crystalline heterocyclic monomers.[6] The synthesized crystalline monomer (DBEDOT) showed good solubility in many common solvents and was polymerizable in the solid-state upon heating. The crystal DBEDOT is small enough to penetrate into the nanopores of nanocrystalline TiO_2 layers where SSP occurs upon heating without additives.

Successful penetration of DBEDOT and SSP were also confirmed using FT-IR, XRD, SEM, and TEM study. The cell fabricated using the PEDOT/MPII/LiTFSI/TBP system exhibited effective electron lifetime of 30.2 ms, V_{oc} of 0.64 V, J_{sc} of 14.2 mA/cm^2 with excellent energy conversion efficiency of 5.4 %, which is the highest value in iodine-free ssDSSCs with N719 dye.

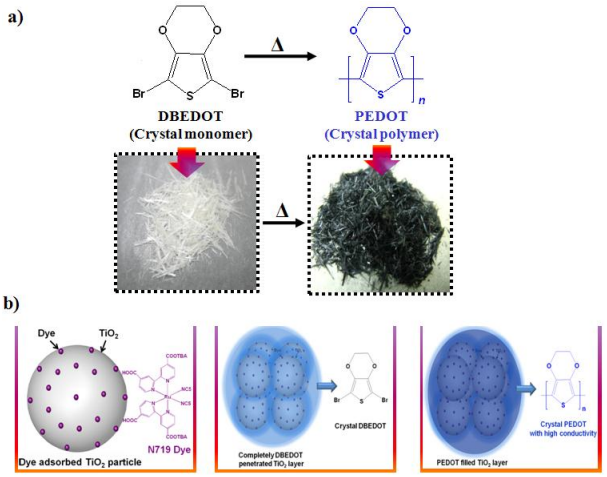

Figure 1. Schematic representation for a) the solid-state polymerization of DBEDOT and b) facile fabrication process of highly efficient iodine-free ssDSSC using N719 dye and conductive polymer as HTM.

Conclusions

We developed a facile method for the preparation of iodine-free ssDSSC with excellent performance and improved electrode/HTM interfacial properties based on the SSP of a conductive polymer. The solid-state polymerizable monomer was small enough to effectively penetrate into the nanopores of TiO_2 film, improving interfacial contact between the electrode and HTM. Importantly, this approach allowed deep penetration of HTM into 11 μm thick TiO_2 film, allowing for enhanced dye adsorption and resulting in high performance. We believe that this SSP approach introduces a new and simple route toward the synthesis of conducting polymer as the HTM in iodine-free ssDSSCs serve as an alternative to the conventional photoelectrochemical polymerization method.

References

1. J. K. Koh, J. Kim, B. Kim, J. H. Kim, E. Kim, *Adv. Mater*. in press. DOI: 10.1002/adma.201004715
2. S. H. Ahn, J. H. Koh, J. A. Seo, J. H. Kim, *Chem. Commun*. **2010**, *46*, 1935.
3. J. T. Park, D. K. Roh, R. Patel, E. Kim, D. Y. Ryu, J. H. Kim, *J. Mater. Chem*. **2010**, *20*, 8521.
4. J. H. Koh, J. K. Koh, N. G. Park, J. H. Kim, *Sol. Energy Mater. Sol. Cells* **2009**, *94*, 436.
5. M.-S. Kang, J. H. Kim, J. Won, Y. S. Kang, *J. Phys. Chem. C* **2007**, *111*, 5222.
6. H. Meng, D. F. Perepichka, M. Bendikov, F. Wudl, G. Z. Pan, W. Yu, W. Dong, S. Brown, *J. Am. Chem. Soc*. **2003**, *125*, 15151.

Towards innovating polymer materials for a new generation of organic laser sources

F. Lincker[a], V. Barret-Vivin[a], D. Kreher[a], F. Mathevet[a], A. Barsella[b], A. Boeglin[b], A. Fort[b] and A.-J. Attias[a]

[a] LCP, Laboratoire de Chimie des Polymères, Université Pierre et Marie Curie (UPMC), 3 rue Galilée, 94200 Ivry sur Seine, France
[b] DON, Institut de Physique et Chimie des Matériaux de Strasbourg, 23 rue du Loess, BP 43, 67034 Strasbourg Cedex 2, France.

David.kreher@upmc.fr

The goal of this multidisciplinary project is the design and synthesis of novel (macro)molecular materials for a new generation of organic laser sources emitting light in the blue/near UV part of the spectrum. Our approach relies on the use of unique Non Linear Optical (NLO) fluorophores, *i.e.* a new class of push-pull molecules associating fluorescence with strong quadratic hyperpolarizabilities. Such "bifunctional" NLO-phores will be able to generate both laser emission in the visible range as well as frequency-doubling of their own laser emission (self-doubling), thus providing a single-element near-UV laser source. (1)

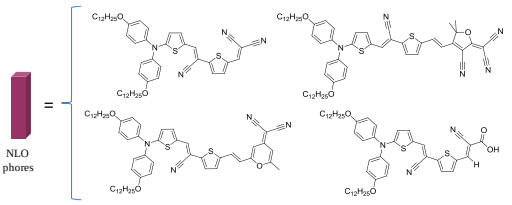

Unfortunately, despite the high-value of the hyperpolarizability, it seems problematical to translate microscopic nonlinearity to macroscopic electro-optic activity. (2) In order to minimize the intermolecular electrostatic interactions between NLO-phores and control the distance between them along the polymer backbone, we propose a new approach combining ATRP controlled radical polymerisation and Click Chemistry to obtain first "macromonomers" and second sequence-ordered polymers (figure below). (3)

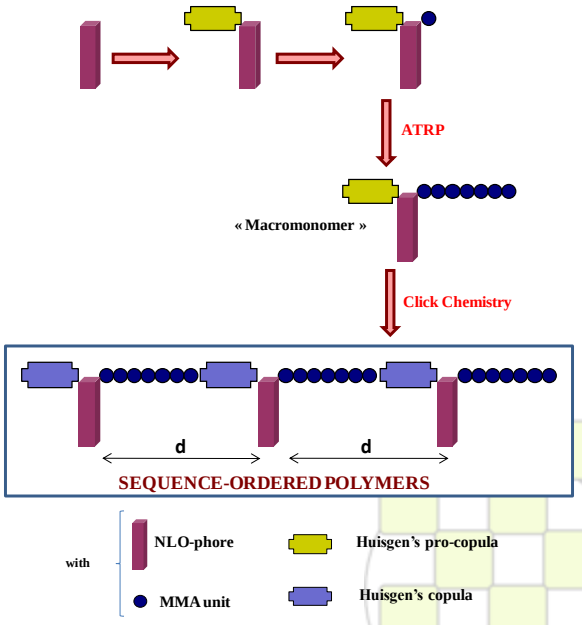

More precisely, we report here the preliminary results concerning the synthesis and characterization of a series of model sequence-ordered polymers based on methyl methacrylate (MMA) backbone and bearing Disperse Red derivatives (DR19) as pendant model chromophores. As an example, by controlling the kinetics of the ATRP stage, we can obtain the following macromonomer :

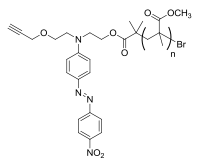

DR19:PMMA = 7.8 w% (n = 57)
As an example, at t = 55 min :
Ip = 1.1, Mn = 6220 g.mol^{-1}
Tg = 94°C

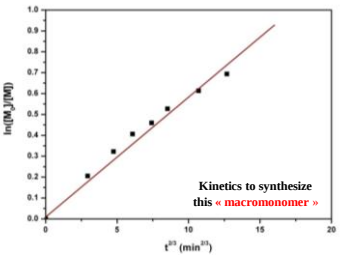

Then, we made a systematic study of the experimental conditions to realize the ultimate Click Chemistry step, modifying for example the solvent and/or of the type of Huisgen's copula, …, in order to see the impact of such parameters on optical properties already (see an illustration below) before to make films with these materials to measure their NLO response.

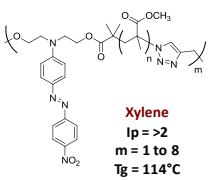

Toluene
Ip = 1.1
m = 2 to 4
Tg = 116°C

Xylene
Ip = >2
m = 1 to 8
Tg = 114°C

Mesitylene
Ip = >2
m = 1 to 8
Tg = 111°C

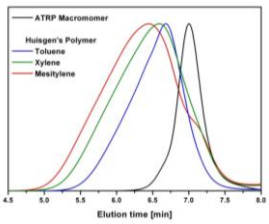

To conclude, our approach based on the combination of ATRP and Click Chemistry allowed us to obtain model sequence-ordered polymers, these latter being chemically and structurally fully characterized. Now we try to take advantage of this strategy to attach our innovating NLO-phores to the PMMA matrix in order to reach, we hope, innovating and efficient (macro)molecular self-doubling materials.

(1) (a) F. Hide et al., *Science*, Vol.273, n°.5283, 1833-1836 (1996); (b) J. Heeger et al., *Acc. Chem Res.*, 30, 430 (1997).
(2) (a) L. R. Dalton et al., *Chem. Rev.*, 110, 25-55 (2010). (b) H. Kang et al., *J. Am. Chem. Soc.*, 129, 3267-3286 (2007). (c) H. S. Nalwa and S. Miyata : "*Nonlinear Optics of Organic Molecules and Polymers*", CRC Press: Boca Raton, FL, (1997). (d) S. M. Budy et al., *J. Phys. Chem. C*, 112, 8099–8104 (2008). (e) T.D. Kim et al., *Adv. Mater.*, 18, 3038-3042 (2006). (f) P.A. Sullivan et al., *J. Am. Chem. Soc.*, 129 7523-7530 (2007). (g) Y.V. Pereverzev et al., *J. Chem. Phys.* C, 112 4355-4363 (2008).
(3) (a) Y. Morisaki et al., *Prog. Pol. Sci.* 33, 346-364 (2008). (b) K. Matyjaszewski et al., *QSAR Comb. Sci.*, 26, n°11-12, 1116-1134 (2007). (c) J. E. Moses et al., *Chem. Soc. Rev.*, 36, 1249-1262 (2007). (d) D. Fournier et al., *Chem. Soc. Rev.*, 36, 1369-1380 (2007). (e) B. S. Summerlin et al., *Macromolecules*, 43, 1-13 (2010).

Preparation and Characterization of waste Leather reinforced polymeric composite

Authors: Shamsun Nahar[1,3], Mubarak Ahmed Khan[2], Fazlul Karim[1], Riadul Islam[1], Shamim Hussain[1], Amol Kanti Deb[1], Hira Lal Paul[1], Fahmida Pervin[2], Saifur Rahman[1]*

[1]Bangladesh College of Leather Technology
[2]Institute of Radiation and Polymer Technology,AEC
[3]Bangladesh University of Engineering & Technology

*E-mail-shamshilpi@yahoo.com

Abstract: Leather is natural polymer of amino acid monomer. For tanning of raw leather a lot of chemical process are involved. As result a huge amount of solid waste are coming from the leather industry. In this study an attempt was taken to use solid leather waste as reinforcing agent with polymeric substance such as polyester resin. Leather fiber reinforced polyester resin based composites were prepared by Wet layup method. Resin content in the composite was varied from 100 ml to 40 ml. After mixing the matrix with the reinforcement, benzoyl peroxide was used as a radical initiator to induce polymerizations. Tensile strength(TS) ,Young modulus and elongation at break (E_b) was measured were measured and found to increase TS and Young modulus up to certain ratio and also found to decrease after certain level. Elongation at break was found to decrease with increasing leather materials upto certain level and again found to increase with increasing leather materials. Leather waste reinforced matrix was found to better result compare to polyester matrix. As a result it will reduce the environmental pollution and also reduce of polymeric pollution . So it can be concluded that natural amino acid fiber, leather can be used as a reinforcing material and found to have better result than matrix and reinforced material.

Key: leather waste, polyester resin, tensile strength, environmental pollution.

Studying PMMA/PVC polymer blend for its use as lithium polymer electrolyte

Leire Zubizarreta[a], *Abel García-Bernabé*[a], *Mayte Gil-Agustí*[a], *Pedro Llovera*[b]

[a]Instituto Tecnológico de la Energía (ITE), Avenida Juan de la Cierva, 24 46980 Paterna, Valencia, Spain
[b]Instituto de Tecnología Eléctrica, Universidad Politécnica de Valencia, Spain

e-mail: leire.zubizarreta@ite.es

1. Introduction

The ever increasing effort for the development of storage systems for sustainable energy supplies make the lithium (Li) ion battery technology one of the most promising future energy resources. This technology has tremendous scope to be used in many applications from modern hi-tech devices to electric vehicle. Polymer electrolyte has been attractive for developing Li batteries due to its advantages respect to liquid electrolytes. It not only promises better safety as the polymer electrolyte do not ignite easily but also the possibility of making battery cells very thin [1].
Currently, poly (methyl methacrylate) (PMMA) and polyvinyl chloride (PVC) are polymers extensively studied for this application due to its ability to solvate inorganic salts to form a polymer salt complex, and its good mechanical properties, respectively [2]. Preparation of PMMA/PVC blends could allow taking the advantages that these polymers have separately in a new polymer blend electrolyte. However, in spite of these good properties, the ionic conductivity of lithium salt solution in these polymers is still low to use in Polymer-Li Batteries applications. The addition of some plasticizers such as ethylene carbonate (EC), propylene carbonate (PC) or γ-butyrolactone (BL), in PMMA/PVC composites could increase the ionic conductivity of polymer electrolytes.
The objective of this work is to study the effect of the amount of different Li salts and organic plasticizers on ionic conductivity of PMMA/PVC polymer blend electrolyte.

2. Materials and methods

All reagents were used without any further purification, and they were obtained from Sigma-Aldrich. Dry and gel polymer electrolytes were prepared. $LiCF_3SO_3$ lithium salt and a mixture of PC:EC (1:1) plasticizer were used for this study. PMMA, PVC, Li salt and plasticizers were dissolved in 15 ml of tetrahydrofuran (THF). The polymer solution was cast as film and THF was allowed to evaporate slowly at room temperature. Obtained films were regular and with a thickness of 100µm. Ionic conductivity was determined by sandwiching of the sample between two gold electrodes. The measurements were realized using a Potentiostat from AUTOLAB in the frequency range of 10^{-3} to 10^{6} Hz at room temperature.

3. Results and discussions

Different series of membranes were synthesised varying the amounts of Li salt and plasticizers. Figure 1 shows how the ionic conductivity of PMMA/PVC synthesized with a 5wt. % of Li salt varies with the amount of plasticizer. It can be seen that the conductivity increases with the amount of plasticizer used, especially when a 35 and 45 wt. % of plasticizer is used. It should be noted that the consistency of the membranes with this amount of plasticizer is good.

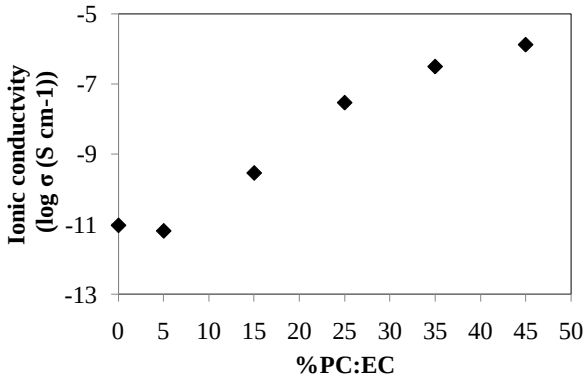

Figure 1. *Variation of ionic conductivity with amount of plasticizer in PMMA/PVC membranes with 5% of* $LiCF_3SO_3$

In addition, the effect of the Li salt amount was studied. In dry polymer electrolytes (without plasticizer) it was observed that conductivity increased considerably with the amount of Li salt. However, in case of gel polymer electrolytes (with plasticizer) the influence of this parameter is lower.

4. Conclusions

In this work, the effect of the amount of plasticizer and lithium salt on the ionic conductivity of PMMA/PVC based membranes have been study. The effect of the amount of plasticizer on ionic conductivity is strong and it seems a very good strategy to increase considerably the ionic conductivity of this type of membranes without alter the good mechanical properties of the blend. The increase of the Li salt amount also increases the conductivity of the PMMA/PVC blend, especially, in dry PMMA/PVC polymers blend electrolytes.

5. Acknowledgements

This work is granted by the 7FP of the EC (SOMABAT: Grant Agreement No. NMP3-SL-2010-266090).

6. References

[1] Diganta Saikia, Hao-Yiang Wu, Yu-Chi Pan, Chi-Pin Lin, Kai-Pin Huang, Kan-Nan Chen,
George T.K. Fey, Hsien-Ming Kao, Journal of Power Sources 196 (2011) 2826-2834
[2] Nam-Soon Choi, Jung-Ki Park, Electrochimica Acta 46 (2001) 1453–145.

Ionic conductivity vs. thickness on the cast Nafion® polymer

Mayte Gil-Agustí, Leire Zubizarreta, Jessica Calleja-Langa, Rosa Iserte

Instituto Tecnológico de la Energía (ITE), Avenida Juan de la Cierva, 24 46980 Paterna, Valencia, Spain
Instituto de Tecnología Eléctrica, Universidad Politécnica de Valencia, Spain

e-mail: mayte.gil@ite.es

1. Introduction

Perfluorosulfonic acid membranes such as the Nafion are currently used as the electrolyte due to their favourable chemical and mechanical stabilities together with their high proton conductivity [1]. The conductivity of fully hydrated Nafion® membranes plays a key role in the performance of PEM fuel cells.

Many groups have previously studied the conductivity of Nafion® membranes and a large quantity of data has been published. The main difficulty in the analysis and comparison of these works is related with the utilization of different measuring methods. It is very difficult to rationalize all these data, but it appears clear that conductivity measurements are influenced by a number of parameters such as: (a) cell geometry, (b) technique employed, (c) electrolyte and (d) sample preparation method [2]. Moreover, the hydration of the material has also introduced differences that are well known in the conductivity measurements. So, the method to obtain the conductivity has to be taken into account.

On the other hand, there are several strategies to provide satisfactory proton conductivity and fuel cell performance. In the optimization to reduce the resistance of the membranes is usual to reduce the thickness.

The purpose of the present work was to study and to rationalize the experimentally observed increase of Nafion conductivity with membrane thickness that has also been obtained by other authors [2-4].

2. Materials and methods

Nafion polymer iso-propanol solutions were obtained from Ion-Power (USA). Adequate amounts of the solution were cast on Petri dish in order to obtained adequate thickness of the membranes. Solvent evaporation at 70ºC during 24 h, and annealing of the membrane at 125 ºC during 90 min were followed.

To measure the ionic conductivity of the membranes, they were conditioned by washing with water, H2O2 and diluted HCl, in hot conditions.

Ionic conductivity measurements were performed in a Zahner IES, in a frequency range of 1 Hz – 499 kHz, by sandwiching of the sample between two gold electrodes of 20mm of diameter at 2 bars of pressure and 90 ºC.

3. Results and discussions

Ionic conductivity of one-hundred membranes was studied. Measurements were obtained following Eq. 1,

$$\sigma = L / (R * S) \qquad Eq.1$$

where, σ (S/cm) is the conductivity, L (cm) is the thickness of the membrane, R (Ω) is the resistance, and S (cm2) the measured area.

Obtained results are in agreement with those recently published by Tsampas *et al*. [4]. They were found that the conductivity of Nafion contains two components, one due to proton migration in the aqueous phase, the other due to proton tunneling between adjacent sulfonate groups in narrow pores.

In the present study, several membranes with different thickness were synthesised and their ionic conductivity was measured. In Fig.1 is shown the correlation between ionic conductivity and thickness of cast membranes. Results were fit to a liner regression with a coefficient of adjustment of R = 0.94.

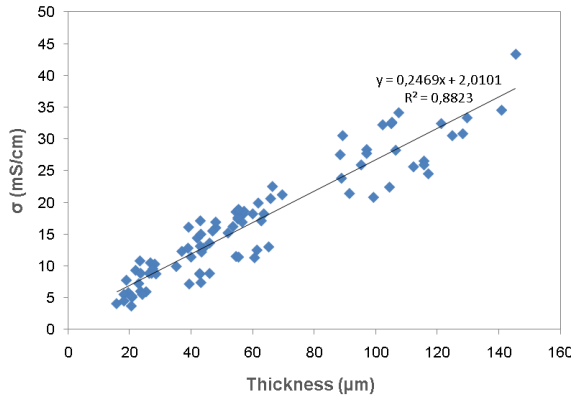

Fig.1. Variation of ionic conductivity with the thickness of the Nafion cast membrane.

4. Conclusions

The ionic conductivity value of Nafion cast membranes increases linearly with the membrane thickness in the range of 20 to 150 µm. This effect shows that a skin conductivity layer could be produced.

5. Acknowledgements

This work was supported by the Ministry of Science and Innovation (Spain) in the context of the National Plan for Scientific research, Development and Innovation 2008-2011 with the aid of FEDER funds from EC (project ref. PS-120000-2009-3).

6. References

[1] B. Yang, Y.Z. Fu, A. Manthiram, J. Power Sources 139 (2005) 170–175.

[2] R.F. Silva, M. De Francesco, A. Pozio. Journal of Power Sources 134 (2004) 18–26

[3] A. Katsaounis, S.P. Balomenou, D. Tsiplakides, M. Tsampas, C.G. Vayenas Electrochimica Acta 50 (2005) 5132–5143.

[4] M.N. Tsampas, A. Pikos, S. Brosda, A. Katsaounis, C.G. Vayenas. Electrochim. Acta 51 (2006) 2743–2755.

Chitosan-collagen sponge-like 3d scaffolds as potential biomaterials For tissue engineering

Maikol Ramos[1], Vanessa Zamora-Mora[1], Sergio Madrigal-Carballo[1], M. Lopretti[2], María Sibaja[1]

[1] Polymers Research Laboratory, School of Chemistry, National University, 86-3000 Heredia, Costa Rica
[2] Biotechnology CIN , Universidad de la Republica, Facultad de Ciencias ,Uruguay

smadriga@una.ac.cr

Introduction: Collagen is the most abundant extracellular matrix (ECM) constituent of nature, dermis and scaffolds made from collagen exhibit weak antigenicity, biodegradability, and superior biocompatibility (haemostatic and cell-binding properties) by comparison to the synthetic polymers, such as poly(lactic acid) (PLA), poly(glycolic acid) (PGA), and polyethylene terephthalate (PET). As a scaffold, collagen-based materials in the form of a sponge have been considered the most popular 3D scaffolds for dermal regeneration. Recently, much attention has been given to utilize chitosan in biomedical applications, for example, a wound healing agent, bandage material, skin grafting template, hemostatic agent, hemodialysis membrane and drug delivery vehicle. Chitosan has been applied to conduct ECM formation in tissue regenerative therapy. The superior tissue compatibility of chitosan may primarily be attributed to its structural similarity to glycosaminoglycan in ECM. Chitosan has been reported to be biocompatible, bioabsorbable and particularly, is considered a good wound-healing accelerator. Importantly, the oligomers of chitosan degraded by tissue enzymes were found to be of benefit to regeneration of the skin tissue of wound areas.
We isolated chitosan from native shrimp waste streams and collagen from tilapia skin waste; composite materials were successfully obtained by mixing chitosan with collagen at different molar ratios. Chitosan-collagen composites were formulated as a 3D sponge-like scaffold, applying previously developed methodologies involving solvent casting and freeze drying. Chitosan-collagen 3D scaffolds were characterized according to its water uptake capacity, thermal behavior (DSC) and morphology (SEM).

Materials and Methods: *Scaffold preparation:* Chitosan solution (2%, w/v) was slowly dropped into collagen suspension to make a chitosan-collagen composite mixture with a final chitosan concentration of 10% (wt chitosan/wt collagen). After driving out the air bubbles under vacuum, the collagen-chitosan blend was poured into glass molds and then freeze-dried to produce a porous composed matrix of collagen and chitosan.

Results: Chitosan binds physically to collagen by hydrogen bonding interactions, driven by their available amino and hydroxyl groups. This interaction allows for developing stable biomaterials, such as nanoparticles biomembranes, biofoams and tissue scaffolds. Figure 1 shows a picture, for illustrative purposes, of a chitosan-collagen sponge-like 3D scaffold. Thermal analysis of the chitosan-collagen 3D scaffolds by TG showed that chitosan-collagen biocomposite behavior was intermediate between both of its constituents (figure 1).

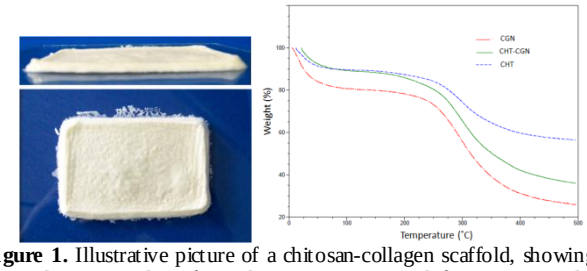

Figure 1. Illustrative picture of a chitosan-collagen scaffold, showing its crossed (top) and surface (bottom) sections (*left picture*) and TG thermogram for chitosan (CHT), collagen (CGN) and CHT-CGN composite 3D-scaffold (*rightfigure*).

SEM micrographs showed a change on the surface morphology of chitosan biomembranes when conjugated to collagen (figure 2), as evidence by the irregular surface appearance and the increase in porosity of the composed 3D-scaffold. Chitosan bioconjugation to collagen may provide a greater crosslink density; this effect may be driven by the higher number of potential interactions available between both macromolecules (hydrogen bonding and/or electrostatic interactions).

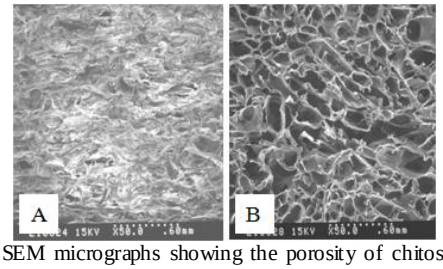

Figure 2. SEM micrographs showing the porosity of chitosan (A) and chitosan-collagen (B) 3D-scaffolds.

Conclusions: Chitosan-collagen 3D porous scaffolds for tissue engineering have been successfully optimized and characterized according to its thermal behaviour (TGA and DSC), porosity and morphology (SEM). We are currently starting cell growth studies on the scaffolds using model epithelial cells. On the other hand, chitosan-collagen hydrogels have been formulated with different active agents (drugs, natural and cosmetic compounds). Results obtained so far indicate that chitosan-collagen sponge-like bioconjugates can be considered as suitable 3D scaffold systems for tissue engineering and drug delivery. In general, biopolymers research by POLIUNA allows concluding that shrimp and tilapia waste streams are suitable sources for added-value derivatives with potential for innovative biomedical applications.

Studies on toughening of polylactic acid by melt-blending with thermoplastic polyurethanes

Kuo-Huang Hsieh[1,2], *Chih-Kai Huang*[1], *Yi-Sheng Lai*[1], *Jin-Lin Han*[3]

1) Institute of Polymer Science and Engineering, National Taiwan University, Taipei, Taiwan. 2) Chemical Engineering, National Taiwan University, Taipei, Taiwan.3) Department of Chemical and Materials Engineering, National Ilan University, I-lan, Taiwan

khhsieh@ntu.edu.tw

Poly(lactic acid) (PLA) is a widely used polymer in our daily life which has received increasing attention in the recent decade for its originating from renewable resources and its potential biodegradability. PLA exhibits high tensile strength (~58MPa) fulfils the packaging industry's requirements for most of the rigid objects but its low elongation at break (4~7%) limited the polymer to be utilized to form bags from blow-molding process or used as tough materials.

In this study, a series of thermoplastic polyurethanes (TPUs) were synthesized from reacting 1,6-hexamethylene diisocyanate (HDI) with three different types of polyols (Poly(ethylene glycol) adipate (PEA), Poly(butylene glycol) adipate (PBA) and Polycaprolactone (PCL)) and 1,4-butanediol. The obtained TPUs were utilized to toughen the commercial polylactic acid (PLA) through melt-blending process in the Brabender at 175°C. Mechanical properties, thermal properties and toughening mechanism of the polymer blends were investigated. The polymer blends were characterized as an immiscible system due to their two separate glass transition temperatures obtained from the differential scanning calorimeter (DSC) analyzer. The mechanical properties of the PLA/TPUs blends were found to be influenced by the crystallinity and crystallization speed of the added TPUs. The PLA/TPUs blends were more flexible and tough materials during the tensile testing and the necking-formation also can be observed.

When PBA derived TPUs was blended into the PLA at 10wt% content, the tensile strength and elongation at break was increased from 58MPa to 81.6MPa and 7% to 144% respectively. Therefore, the proposed PLA/TPUs blends were almost promising for fabrication of biodegradeable blow-molding bags and tough materials.

Keywords: Poly(lactic acid) (PLA), thermoplastic polyurethanes (TPUs), biodegradeable, melt-blending process

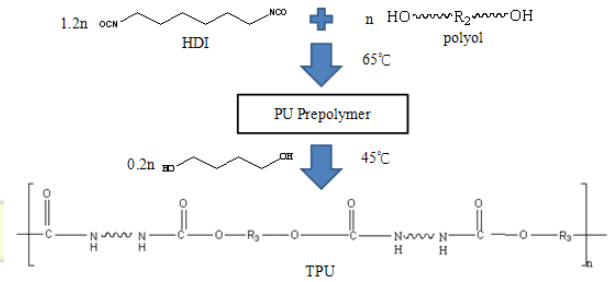

Figure1. The preparation of thermoplastic polyurethanes.

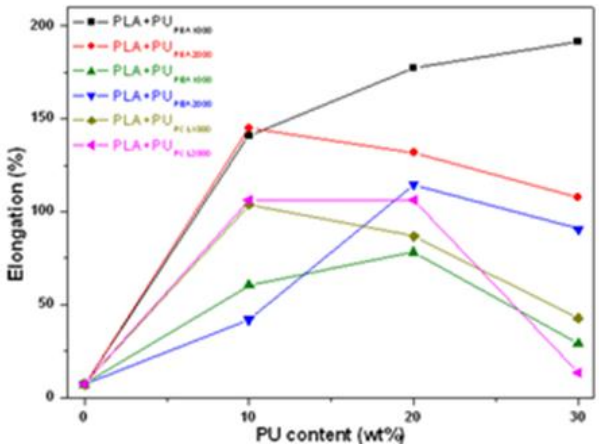

Figure2. The elongation at break of different PLA/TPUs blends.

Multifunctional PDMS-PEG Coatings for the Finishing of Cotton

Ramona Ronge, *A. Körner*, *M. Möller*

DWI an der RWTH e.V., Aachen (Germany)

ronge@dwi.rwth-aachen.de

Their extraordinary combination of hydrophobic properties with low glass temperature, high elasticity and chain flexibility distinguishes silicones significantly from other synthetic polymers. Due to these properties they provide surfaces with low surface tension, low adhesion and high dewetting potential and therefore, they are widely used in the textile industry to improve the garments´ performance and to enhance soft handle, silk like gloss, soft and graceful flow and water repellence. Furthermore, silicones can improve sewability, abrasion resistance and crease recovery of the treated textiles.[1] Classical silicone softeners provide an unmatched soft handle but they also contribute to the water repellency of the surface and impair the moisture management of the garments. Another important aspect is the permanence of the silicone finishing both on textiles.[2],[3]

Aim of this work therefore was to design hydrophilic polydimethylsiloxanes (PDMS) endowed with reactive groups to provide a covalent attachment to the surfaces of cotton fibres. Commercially available PDMS with a comb like structure bearing hydrophilic ethylene- and propylene oxide side chains with hydroxyl end groups were used to implement the combination of hydrophilic properties and provision of soft handle. Functional groups were inserted in a polymer analogous reaction into the side chains by reaction with isocyanatotriethoxysilane.[4] Triethoxysilane groups are then available to react either with the hydroxyl groups on the cotton surface or with other triethoxysilanes to build a network at the fibre surface (see figure 1).

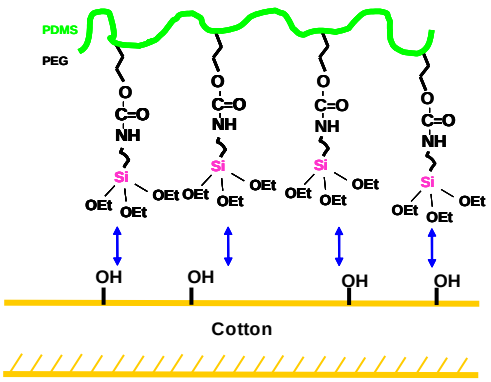

Figure 1: Concept of covalent attachment.

The successful conversion of the commercially available PDMS-PEG copolymers with isocyanatotriethoxysilane was confirmed by infrared spectrometry. ^{1}H-NMR spectroscopy proved that the degree of functionalization was nearly complete.

Cotton fabrics were finished with the functionalized silicone. For this purpose, an aqueous emulsion of the silicone with the surfactants Imbentin T060 and T120 was prepared. The cotton fabric was immersed in the emulsion for 20 min at 60°C with a liquor ratio of 1:20.

To check the permanence of the treatment the fabrics were twice washed with water. The composition of the elements on the fibre surface was analyzed by XPS. The results before and after washing are shown in figure 2. The data shown were corrected by subtraction of the blank values.

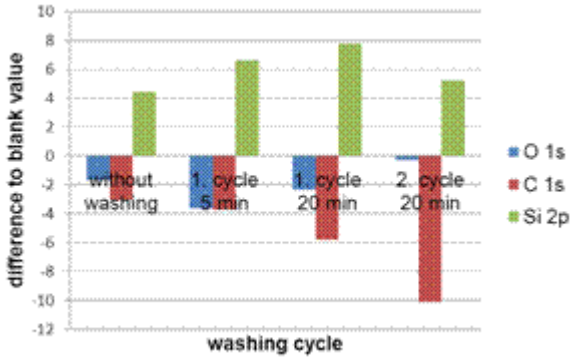

Figure 1: Permanence of the functionalized silicone on cotton.

The silicium content on the surface serves as a measure of both the presence and the permanence of the finishing. A decrease in the silicium content after washing was not determined. Thus a permanent modification was achieved.

The hydrophilic characteristic of the finished cotton were proved in a wetting test. Depending on the portion of PDMS in the copolymers, an increase of the hydrophobic character after washing was found.

The PDMS-PEG copolymer functionalized with isocyanatotriethoxysilane was proven to achieve a covalent attachment on the cotton surface. It is possible to apply the reactive silicone from aqueous emulsion. The functionalization of silicone with triethoxysilane has a positive impact on the substantivity and permanence of the finishing. However the desired hydrophilic character of the functionalized PDMS-PEG still has to be designed by variation of the PEG portion.

References:

[1] P. Habereder, A. Bereck, *Rev. Prog. Color. Relat. Top.* **2002**, *32*, 125.
[2] T. Hohberg, *Melliand Textilberichte* **2005**, *86*, E118.
[3] T. Hohberg, *Textilveredlung* **2005**, *40*, 10.
[4] X. Elias, R. Pleixats, M. W. C. Man, J. J. E. Moreau, Advanced Synthesis & Catalysis 2007, 349, 1701.

Osteoconductive and Bioresorbable Composites Based on Poly(L,L-lactide) and Pseudowollastonite

D.T-J Barone[a], Z.Luklinska[b], O. Persenaire[a], J-M. Raquez[a], Ph. Dubois[a]

[a]Centre d'Innovation et de Recherche en Matériaux Polymères CIRMAP, Service des Matériaux Polymères et Composites, University of Mons, Place du Parc 20, 7000 Mons, Belgium
[b] Queen Mary University of London, Department of Materials, E.M.Unit, Mile End Road, London E14NS , Great-Britain.
[c]Service de Chimie Organique et Biomédicale, University of Mons, Place du Parc 20, 7000 Mons, Belgium

(email: jean-marie.raquez@umons.ac.be)

Introduction

In osseointegration applications, pseudowollastonite (psW), a silica-based polycrystalline ceramic (α-$CaSiO_3$)[1,2] has been suggested as a bone substitute material for bone regeneration. psW is bioactive in physiological solutions as SBF or in cell-culture media by forming a bioactive HA layer onto its surface. However, during the dissolution of psW in physiological medium, a fast alkalization of the medium occurs due to the important release of Ca^{2+} and $(SiO_4)^{4-}$ ions, being harmful for the *in-vitro* or *in-vivo* applications. Hence, **this contribution aims at reporting the osseointegration studies composites made of psW and poly(L,L-lactide) (PLLA) in osseointegration**[3]. Design of such composites combining a bioresorbable semi-crystalline PLLA with psW offers an exceptional opportunity to tailor the release of the bioactive ions and also their physical and mechanical properties. These composites were straightforwardly prepared by melt-blending in a microcompounder. To modulate their bioactivity, amphiphilic poly(ethylene oxide-*b*-L,L-lactide) (PEO-*b*-PLLA) block copolymers were added to these composites. The bioactivity of the composites was evaluated by soaking them in a physiological fluid, followed by *in-vitro* and *in-vivo* studies.

Results & Discussion

Bioactivity Studies

The bioactivity and osteoconductivity of PLLA/psW(20%)-based composites is studied in view of a future application in osseointegration. Initial psW-based composites (20 wt% psW) were successfully prepared from PLLA and psW by a melt-blending process. These composites are found to be bioactive as they form an HA-like layer at the composite surface after 16 weeks of immersion in SBF. Hence, an amphiphilic copolymer was added to the initial composites to increase the hydrophilicity of the composite surface and to accelerate the HA formation and adhesion. The compatibilization of PLLA/psW(20%)-based composites with 15 wt% PEO-*b*-PLLA block copolymer **(**M_{nPEO} = 5000 g/mol; M_{nPLLA} = 7000 g/mol**)** allows to significantly reduce the time to form in vitro an HA top layer (~10µm) to 1 week (Figure 1). The enhanced hydrophilicity of the composites also improves the adhesion of the HA layer.

Figure 1. SEM image of a cross-section of the PLLA-based composite with 15 wt% PEO-b-PLLA block copolymer after

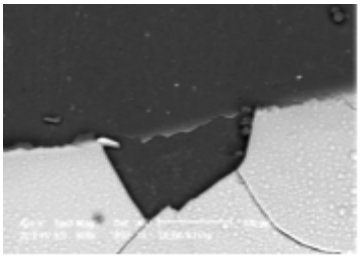

In vitro Studies

The PLLA/psW(20%) composite added with 15wt% PEO-*b*-PLLA block copolymer nor its degradation products are not toxic for osteoblastic SaOS-2 cells under the studied experimental conditions. Only a limited number of dead cell are observed, attesting that the presence of the by-products of degradation has no negative effect on cell viability *in-vitro*.

In vivo Studies

The effect on bone growth was studied *in vivo* using a rat tibia model, showing that the PLLA/psW(20%) composite added with 15wt% PEO-*b*-PLLA block copolymer is a biocompatible material as no inflammation occurs when implanted *in vivo*. Moreover, the composite shows to be permissive as it supports the formation of new bone (Figure 2).

Figure 2. Histological section of the composite when implanted in tibia's of rats (the implant is highlighted).

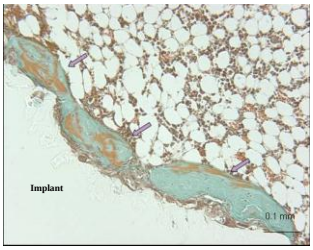

Conclusions

In conclusion, these composites show to be permissive for bone-regeneration results. These promising in vitro and in vivo results are encouraging to perform further studies to improve these bioactive

References.

[1]Yoneda M et al. *Biomaterials* **2005,** 26, 5145-5152. [2]Li H et al. *J Mater Sci Mater Med.* **2004**, 15, 1089-1095. [3]Roether J.A et al. *Biomaterials* **2002**, 23, 3871-3878. [4]Raquez JM et al. *Biomacromolecules* **2011**, accepted.

Onion-Like Superabsorbent Microspheres with PS-DVB Core and PAA-b-Crosslinked(PMMA) Capsules via SI-ATRP

Ahmet Ince, Bunyamin Karagoz, Niyazi Bicak

Istanbul Technical University, Department of Chemistry, Maslak 34469 Istanbul, Turkey

ahmetince85@gmail.com

Introduction: Superabsorbent hydrogels are loosely crosslinked polyelectrolyte's capable of water sorption as high as 100-1000 times of their own weights[1]. Having extensive use in our day-life, these materials found billion dollars of global market. Although sanitary napkins and baby diapers are the main areas of their use, these also have many potential applications in other fields. Production these materials is largely based on poly (acrylic acid)'s or its salts. Optimization of water diffusion and gel-blocking effects are problematic and crucial issues in their large-scale manufacturing. To avoid these difficulties in the present work, we have targeted to prepare crosslinked PS-DVB (10%) microspheres surrounded by bilayer-capsules consisting of poly(acrylic acid)-*b*-crosslinkedpoly(methyl methacrylate). Such a structure was generated by the reaction sequences outlined in Scheme-1.

Swelling ratios of the hydrogels is inversely proportional to the crosslinking densities. In this work we have targeted to attain maximum swelling ratios without using additional crosslinker for the poly (acrylic acid) segments. The resulting structure so obtained was expected to behave as micro-pools accommodating large amounts of water.

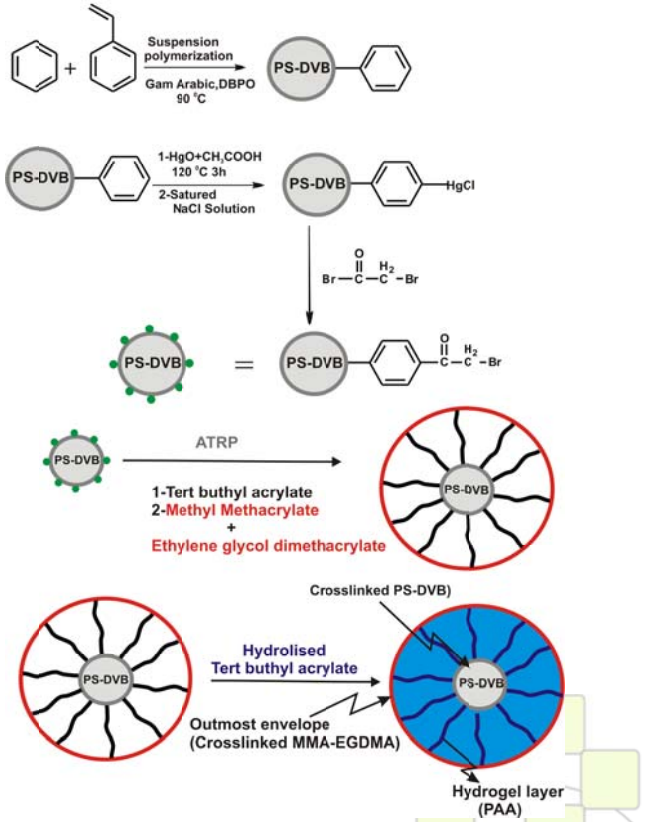

Scheme-1 Reaction sequences for preparing onion like water sorbent.

Result and Discussion: In the first step bromoacetyl groups were introduced to ST-DVB microspheres as ATRP initiator to create non-hydrolysable linking with surface brushes[2]. Sequential ATRP of *tert*-butyl acrylate and MMA and following selective hydrolysis of PBA block yielded superabsorbent capsules.

Experiments showed that, swelling of the resulting material is pH-dependent and equilibrium swelling ratios in neutralized form is proportional to thickness of PAA block and reaches to 200-220. Swelling rate of the onion-like superabsorbent did not change practically, upon standing in air atmosphere, indicating anti-gel blocking effect of the outmost PMMA layer.

Conclusion: Since block lengths of the poly(acrylic acid) layer can tuned up by surface density of the initiation sites and polymerization time, one can attain onion like superabsorbent materials with predetermined swelling capabilities.

References

1- S. Korpe, B. Erdoğan, G. Bayram, S. Ozgen, Y. Uludag, N. Bicak, *Reactive & Functional Polymers* 69 660–665(2009)

2- B Karagoz,G Bayramoglu, Begum Altintas, N.Bicak, M. Y Arica. *Ind. Eng. Chem. Res*.49, 9655–9665(2010)

ABSTRACTS

POSTER PRESENTATIONS

Topic 5: Chemistry and Physics of Nanomaterials and Nanotechnologies

Morphology and fracture behaviour of Phenoxy/layered silicate nanocomposites

M. Corres[1], *A. Mugica*[1], *M. Zubitur*[2], *M. Cortázar*[1]

1- Polymer Science and Technology Department, University of The Basque Country
2- Chemical Engineering and Environment Department, University of The Basque Country

marian.corres@ehu.es

The improvement of polymer matrix properties based on synergetic advantage that offer the addition of fillers of nanoscale dimensions is an area of primary interest. In the field of polymer fillers, clays have an outstanding position, because they have a structure of parallel layers that, in suitable conditions, can be delaminated into layers of nanometric size (1). The extent of compatibility between clay and matrix seems to be the most important factor that determines the delamination degree. For this purpose the inorganic surface of the clays can be organically modified to have more affinity with the organic polymeric matrix. In these sense the organic modifier has a double role, for one side it can expand the interlaminar space providing polymer chains diffusing into clay galleries and for other side it can favour specific interactions with polymer matrix. Consequently, the election of organic modifier is of primary importance to reach a good degree of dispersion and finally, to achieve improvement of properties derived of extremely high surface contact between filler and polymer resulting of nanoscale dispersion.

Attending to the above request the poly(hydroxy ether of bisphenol A) also known as phenoxy resin was selected as polymer matrix. It is an amorphous thermoplastic of linear chain containing a pendant hydroxyl group in its repeat unit, so phenoxy resin exhibits proton donor characteristics when interacting with fillers.

As layered clay was selected the vermiculite (VMT) and as organic modifier methyl, tallow, bis-2-hydroxyethyl, quaternary ammonium salt (known as Ethoquad) with the aim of promote specific interactions with host polymer.

Nanocomposites of phenoxy resin and VMT/Ethoquad with different clay content (2, 5, and 10 wt%) were prepared by melt extrusion using a co-rotating twin-screw extruder-kneader. The rotating speed of the rotor, the mixing time, and the temperature were fixed, respectively, at 200 rpm, 10 min, and 180 ºC.

Differential Scanning Calorimetry (DSC) of VMT/Ethoquad and nanocomposites was carried out to understand the clay dispersion in the polymer matrix. The quaternary alkyl ammonium salt exhibits endothermic peak, corresponding to melt transition during first heating (2). Therefore, analysing the thermal behaviour of the surfactant could aid to prove if the organic modification has taken place.

The DSC scans corresponding to Ethoquad sample show multiple endothermic peaks that confirm the heterogeneity of surfactant crystalline structures. Regarding the scans of the organically modified vermiculite the melting transition persist; indicating the possible intercalation of ETO into the clay layers where the tallow chain remain in a ordered packing (form). However the scan corresponding to matrix filled with 2%, 5% and 10% of organically modified vermiculite do not show any melting peak. This behaviour can be explained assuming that some exfoliation has been reached in the phenoxy matrix and Ethoquad is not constrained into vermiculite layers.

In order to prove the level of dispersion of VMT-Ethoquad within phenoxy matrix, a phenoxy/VMT-Ethoquad nanocomposite prepared by melt extrusion and a simple mixture of phenoxy and VMT were dissolved in chloroform, respectively. Whereas the simple mixture exhibits a precipitated phase, the nanocomposite shows a more transparent dispersion, proving that VMT-Ethoquad is well dispersed within the matrix.

Nanocomposite morphology was directly observed by Transmission Electron Microscopy (TEM). Microphotographs show that compositions of 2%, 5% and 10% of VMT-Ethoquad were homogeneously dispersed in the phenoxy matrix. Intercalated and exfoliated morphology were observed indicating that abundant delamination has taken place, however some tactoids were also present principally in 10 wt% composition nanocomposite. Probably the organic modifier containing hydroxyl groups promote the compatibility

The freeze-fractured surfaces of pure phenoxy and the nanocomposites were comparatively examined using SEM. Pure phenoxy resin exhibits a relatively smooth fracture surface. The SEM pictures of nanocomposites show a rougher surface, indicating that the presence of nanoclay layers forced the cracks to propagate along a very tortuous path. This result indicates that there is good interfacial adhesion between the clays and polymer and the transfer of stress to the clay layers.

Acknowledgements Financial support is acknowledged from Gobierno Vasco: SAIOTEK (project 2010-2011) and Subvención a Grupo Consolidado (IT330-10).

Bibliography

1- Ke Y.C., Stroeve, P. *Polymer-Layered Silicate and Silica Nanocomposites*. Elsevier, Amsterdam (2005).
2- Carretero-González J., Retos H., Verdejo R., Toki S.,Hsiao B. J., Giannelis E. P., López-Manchado M. A. *Macromolecules*. 41(18), 6763 (2008).
3- Abraham T. N., Siengchin S., Ratna D., Karger-Kocsis. *Journal of Applied Polymer Science*, 118, 1297 (2010).

Quantum-chemical study of the low molecular polyethylene fluorination

*Lidia Ignat'eva, Vyacheslav Bouznik

[a]Institute of Chemistry, FEB RAS, pr. 100-letia Vladivostoka 159, Vladivostok, 690022 Russia A.A. Baykov Institute of Metallurgy and Material Science RAS, Moscow, Russia

ignatieva@ich.dvo.ru

Fluoropolymers occupy an important place among polymer materials and are assigned to functional materials due to their many applications. The low molecular specimens, that already have practical applications for coatings, nanofilms, composites and nancomposites, have attracted considerable interest among varying fluoropolymers. One of ways to obtain the low molecular fluoropolymers is fluorination of hydrocarbon materials, such as paraffin and low molecular polyethylene. Quantum chemical calculations can be a good tool to study the processes of formation of these polymers. With a high degree of confidence you can get information on how to modify material, topological parameters of these systems, the preferred configurations and, finally, to a great extent help in the interpretation of experimental data obtained by the methods of vibration spectroscopy, NMR, and XPS which are commonly used to control the process of preparation of such polymers and study the molecular structure of the resulting materials. The results of quantum chemical calculations of the model system $C_{10}H_{22}$ with successive substitution of hydrogen by fluorine atoms are presented in this work. The energy of fluorination process, topological parameters, $NMR^{19}F$, $NMR^{13}C$, $NMR^{1}H$ and vibration spectra of model systems of $C_{10}F_nH_{22-n}$ (n = 1-22) were calculated. The nature of the signals in the $NMR^{19}F$, $NMR^{13}C$ spectra and band assignments in IR spectra of the calculated model molecules were made. *Ab initio* Hartree-Fock (HF, basis of 6-31G)
and density functional (DFT (B3LYP, basis of 6-311+G(d)) methods was used for calculations. The calculation method was adopted by the carried out test (molecules with known parameters) calculations. The obtained results are very close to experimental data for compounds which these molecules simulated.

Conclusion

The obtained calculations showed.
- At the fluorination of the polymer chain the intrachain substitution of hydrogen to fluorine gives the most stable configuration and the both fluorine atoms belong to the common carbon.
- At a partial fluorination of the polymer the new bands corresponding to vibrations of the CF, CF_2, and CF_3 groups appear in the vibration spectra. The structure and position of the bands, that characterize the vibrations of hydrocarbon groups, change due to redistribution of electron density in the whole molecule at substitution of hydrogen to fluorine. Noticeable changes in the IR spectrum occur even in the region of stretching vibrations of C-H at 3000-2800 cm^{-1} (Fig.1), therefore, one can easily discern whether the system has formed by a composite of the core-shell, or modified form of the polymer is created.
- $NMR^{19}F$ and $NMR^{13}C$ spectra differ at changing in number of substituted hydrogen atoms and the place of substitution in the polymer chain. Differences are rather obvious and in the $NMR^{19}F$ spectra and $NMR^{13}C$ spectra (Fig.2), therefore the NMR spectra can be an indicator of the configuration of the studied system and degree of chain fluorination.

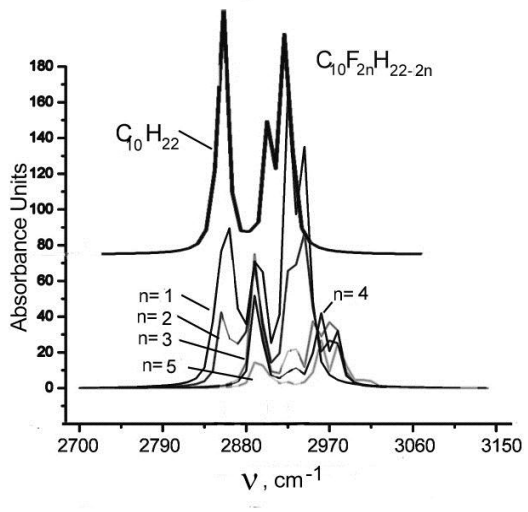

Fig.1. Calculated IR spectra of model molecules: $C_{10}H_{22}$ and $C_{10}F_nH_{22-2n}$

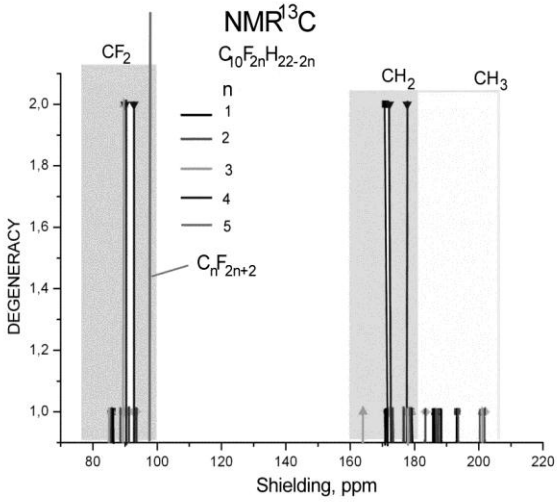

Fig.2. $NMR^{13}C$ spectra of model molecules: C_nF_{2n+2n} and $C_{10}F_{2n-2n}$

Characterization and thermal properties of Poly(L-lactid acid)/clay bionanocomposites

A. Oyarzabal[1], A. Mugica[1], M. Zubitur[2], M. Cortázar[1]

1- Polymer Science and Technology Department, University of The Basque Country
2- Chemical Engineering and Environment Department, University of The Basque Country

andreaoiarzabal@hotmail.com

The poly(L-lactide) (PLLA) is a biodegradable and a biocompatible material that can be produced from renewable resources, and that exhibit mechanical properties comparable to those of commercial thermoplastics. PLLA is a semicrystalline polymer whose bioresorption and mechanical properties depend on the crystalline morphology and crystallinity degree (1). One of the most interesting ways to modify the polymer properties is the addition of nanoclays. This addition improves polymer properties, and in some cases, it leads to a unique combination of properties. The property improvement is highly dependent on the degree of dispersion in the polymeric matrix (2). However, the organophilic character or many semicrystalline polymers prevents sufficient interaction between the polymer and clay resulting in poor dispersion of the naturally polar clay within the hydrophobic polymer matrix. The increase of the clay dispersion degree can be achieved by means of organic modification of the clay. The election of the organic modifier is of primary importance to obtain a good level of matrix-clay interactions. These interactions affect chain mobility and consequently, the crystallization kinetics can be strongly affected (3). In addition to the nature of both, clay and polymer, components the obtained nanocomposite morphology depends on the preparation conditions.

In this study, nanocomposites based on poly(L-lactic acid) (PLLA) and an organomodified vermiculite (OMVMT) were prepared by melt processing. The effect of melt processing conditions on the degree of dispersion and thermal properties of the nanocomposites was analyzed. The melt processing was carried out at two different rotating speeds: 80 and 150 rpm.

The morphology of nanocomposites was analyzed by X-ray diffraction (XRD) and transmission electron microscopy (TEM) and their thermal properties by differential scanning calorimetry (DSC) and thermogravimetric analysis (TGA).

The XRD pattern of the nanocomposites were interpreted taking into account the position of the basal peak which depends on the distance between two adjacent layers. The basal peak of the OMVMT appears at 2θ=2.08 º, whereas the nanocomposite basal peak shows a shift to lower angle degree and in adition the peak decreases in intensity and broadens in peak breadth. This result suggests that there are interactions in between the polymer and clay that can lead to intercalation or exfoliation.

The morphology of OMVMT within the polymer matrix was characterized by TEM. The TEM micrographs reveal a mixed intercalated-exfoliated morphology without significant differences in the nanocomposites obtained at the two melt-mixing processing conditions.

The thermal stability of neat PLLA and its nanocomposites was analysed by TGA. The nanocomposites showed a slight increase in thermal stability comparing with neat PLLA. The enhancement of the thermal stability could be attributed to the exfoliated OMVMT layers dispersed randomly in PLLA matrix at nanoscale level, which are impermeable to volatiles, rendering more difficult the diffusion of volatiles from thermally decomposed products. DSC scans reveal that T_g and T_m are not influenced by the presence of clay. However, the nanocomposites show a significant increase in the enthalpy of crystallization and melting comparing with the pure PLLA (Fig.1). The fact that the crystallization is favoured by the organomodified clay can be a consequence of the good dispersion level achieved that enhances the nucleant effect promoted by the clay. No significant differences were observed in crystallization and melting enthalpies with the different melt-mixing processing conditions employed.

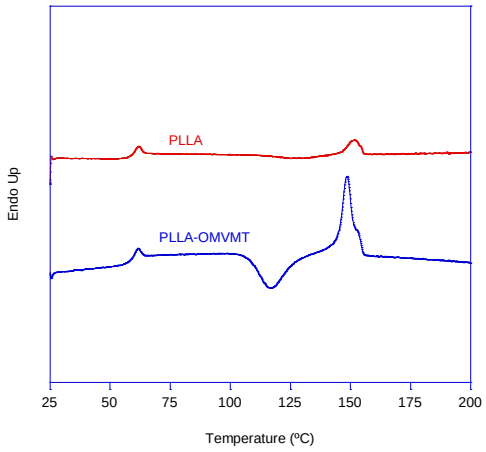

Figure 1. DSC heating scan of pure PLLA and PLLA with OMVMT.

Acknowledgements Financial support is acknowledged from Gobierno Vasco: SAIOTEK (project 2010-2011) and Subvención a Grupo Consolidado (IT330-10).

Bibliography

1- Gupta A.P., Kumar V. *European Polymer Journal*, 43, 4053 (2007).
2- Suprakas S. R., Okamoto S. *Progress in Polymer Science*. 28, 1539 (2003).
3- Miri V., Elkoun S., Peurton F., Vanmansart, C., Lefebvre, J. M., Krawczak, P., Seguela, R. *Macromolecules*, 41, 9234 (2008).

Textile Strain Sensors Based on Conductive Polymer Nano-Composite

C. Cochrane[1,2], *M. Lewandowski*[1,2], *V. Koncar*[1,2]

[1] ENSAIT, GEMTEX, F-59100 Roubaix, France
[2] Univ Lille Nord de France, F-59000 Lille, France

cedric.cochrane@ensait.fr

Introduction

The aim of this work is to develop a smart flexible sensor adapted to textile structures, able to measure strain deformations of a parachute canopy during a drop test. It is therefore important that the integration of this sensor does not modify the general behaviour of the parachute.

Materials and Methods

A piezoresistive sensor based on a Conductive Polymer Nano-Composite (CPC), fully compatible with a textile substrate and its general properties, has been developed in our laboratory. The material used for the sensor is based on a thermoplastic elastomer (Evoprene)/carbon black nano-composite.

The optimized preparation procedure of the sensor and its deposition on a parachute canopy (Polyamide 6.6 lightweight fabric, Figure 1) are fully described.

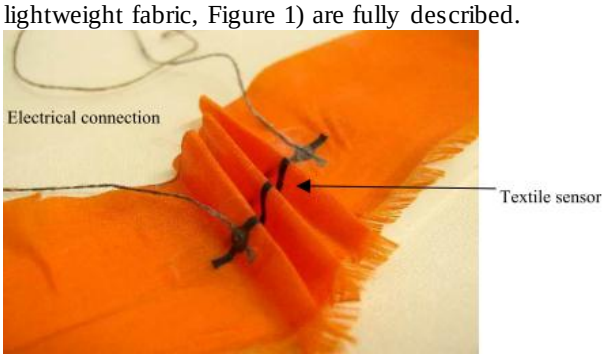

Figure1: CPC sensor on fabric.

Results and discussion

The electromechanical characterization (i.e. electrical response to mechanical stress) is performed to demonstrate the adaptability and the correct functioning of the sensor as a strain gauge on the fabric. In particular the effects of strain rate (ranging from 10 to 1000 mm/min, Figure 2) and of repeated elongation cycles (up to 5) on the sensor behaviour are investigated. The results show that strain rate (up to 1000 mm/min) seems to have only little influence on sensor response.

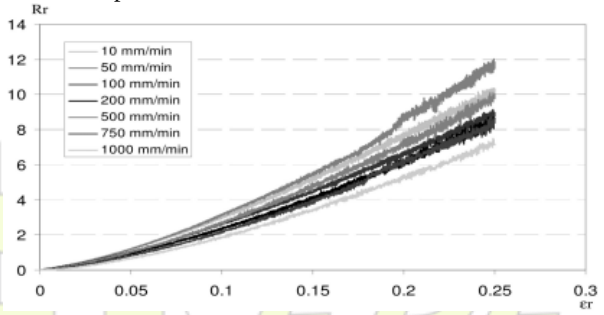

Figure 2: Relative resistance of sensors vs. elongation for different strain rates.

The average (linear) gauge factor K obtained in the strain range $0<\varepsilon r<0.1$ is 31. This is a very high value for a piezoresistive sensor. Recorded data can be fitted with better accuracy by a simple power law relation (Equation 1):

$$Rr = r.\varepsilon r^{p} \qquad \text{Equation 1}$$

Where Rr is relative electrical resistance of the sensor (Equation 2) and εr, elongation of the sensor.

$$Rr = (R-R_0)/R_0 \qquad \text{Equation 2}$$

Where R_0 is initial electrical resistance of the sensor.

This calibration law (Equation 1) will be used to evaluate the canopy fabric deformation during the real drop test.

As expected, when submitted to repeated tensile cycles, the CPC sensor is able to detect accurately fabric deformations over each whole cycle, taking into account the mechanical behaviour of the textile substrate.

Finally, the influence of environmental factors, such as temperature and atmospheric humidity, on the sensor performance is investigated. The results show that the sensor's electrical resistance is particularly affected by the humidity factor. Complementary information is given concerning the non-effect of aging on the global resistivity of the CPC sensor.

Finally, our sensor was tested on a parachute canopy during a real drop test: the canopy fabric deformation during the critical inflation phase was successfully measured.

Conclusion

The use of the CPC sensor in a real flight test has demonstrated that the deformation of a parachute canopy could be successfully measured with CPC sensor. This flexible sensor proved to resist the particularly drastic packing conditions of the parachute, the drop, the inflation, and the landing phases. Data from the CPC sensor were coherent with data provided by other conventional sensors and with literature. The results showed that elongation of the fabric during inflation was less than 0.09 mm/mm.

The CEV / DGA Institute (Toulouse) is acknowledged for the financial support of this research project.

Influence of the aminopropylisobutyl POSS nanoparticles on the thermal behavior of isotactic polypropylene

R. Bouza, C. Ramírez, L. Barral, B. Montero, R. Bellas

Grupo de Polímeros, Dpto. de Física, E.U.P. Ferrol, Universidad de A Coruña, Avda. 19 de Febrero s/n, 15405 Ferrol, Spain

labpolim@udc.es

Introduction

Design of new composites based on polyhedral oligomeric silsesquioxane (POSS)/thermoplastic nanostructure blends is receiving a great attention from the plastic industries. The use of POSS cages as reinforcement into thermoplastic matrixes is very interesting; hence it allows obtaining new materials that may result in increase temperature usage, surface hardening or increased flame resistance. These enhancements have been found to apply to a wide range of thermoplastics and some thermosets systems [1].

Material and methods

In this work, the aminopropylisobutyl POSS was added by melt blending with isotactic polypropylene (iPP) at several concentrations and the dynamic crystallization behavior was studied by means of differential scanning calorimeter. Nevertheless, the poor interfacial adhesion between the matrix and the filler makes get worse the final properties of the nanocomposites. In order to improve this behavior, a coupling agent was added to the formulations. The maleic anhydride – modified PP (MAPP) was used as coupling agent to increase the affinity between the POSS and the matrix and improve the dispersion of the filler.

Results and discussion

The figure 1 shows the non-isothermal crystallization behavior of iPP and iPP/POSS composites as function of POSS content at a cooling rate of 10 ºC/min. It was observed an increase in the crystallization temperature in composites. The POSS acts as nucleating agent when it is incorporated into the iPP matrix in small amounts.

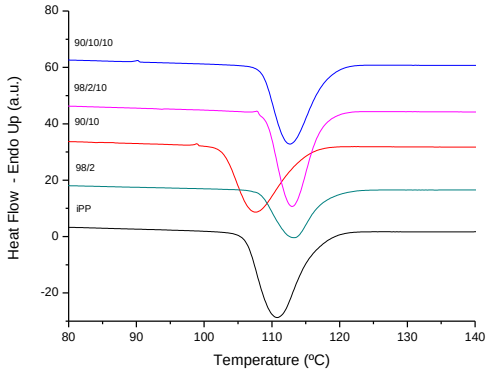

Figure 1: Crystallizations exotherms for the indicated samples.

However, the incorporation of greater amounts of POSS means to loss of nucleating effect. This may be due to the formation of clusters in the 90/10 binary system, as can be seen by SEM. In ternary systems with MAPP, this coupling agent does not affect the nucleation effect, since the crystallization temperature in the cooling rate studied, does not vary with respect to binary mixtures. But, it is important to note, that the MAPP provides more regular and stable morphologies, so that the POSS is better distributed in the polypropylene matrix and thus, there is an effect of nucleation in the sample 90/10/10. In this sense, several authors [2] indicated that a good dispersion of POSS was obtained particularly at low loadings of POSS.

The evolution of the crystallization process from the melt state to the organized state was followed by means of the variation in conversion, figure 2.

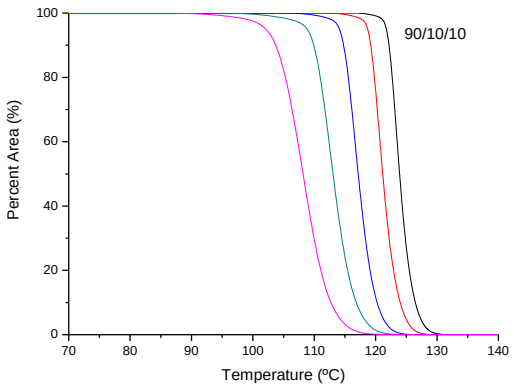

Figure 2: Variation of the conversion for 90/10/10 blend at the cooling rate specified.

The tendency of the conversion curves shows a much accelerated primary crystallization even at the lowest cooling rates. In the ternary blends the presence of the MAPP induces the compatibilization of iPP and POSS acting as an interfacial agent.

Conclusions

The crystallization of the iPP is affected by the presence of the compatibilizing agent. This presence leads to a slightly reduction in the crystallization temperature, indicative of an increase in compatibility.

References

[1] C. Ramírez, M. Rico, L. Barral, J. Díez, S. García-Garabal, B. Montero J. Therm. Anal. Calor., 87, 69 (2007).

[2] A. Fina, D. Tabuani, A. Frache and G. Camino, Polymer 46, 7855 (2005).

Financial support XUGA 10TMT172009PR

Microstructural and morphological analysis of SBR/nanoclay composites

R. Bellas, R. Bouza, J.Díez, J. López, C. Ramírez, M. Rico

Grupo de Polímeros, Departamento de Física, E.U.P., Universidade da Coruña, Avda. 19 de Febrero s/n, 15405, Ferrol, Spain

labpolim@udc.es

Introduction

Recently, there is a large scientific and industrial interest in the development of rubber nanocomposites with layered silicates as reinforcements. Due to the nanometric scale of the layered silicate with high aspect ratio and high surface area, good reinforcement is possible at low filler loading compared to conventional fillers. In general, there are two idealized morphologies that can be developed using nanosilicate fillers: (a) intercalated (i.e., silicate layers are partially separated by polymer chains but ordered structure is still retained, and (b) exfoliated (i.e., silicate layers are totally delaminated and disordered). The basic principle of the formation of rubber/clay nanocomposites is that the rubber should penetrate into the intergalleries of clay, so the space between the galleries of the silicate should be accessible to the rubber chains. This is usually achieved by replacing the interlayer cations with ammonium salts. The distance between the silicate layers is greatly enlarged, and the clay becomes organophilic and more compatible with the rubber matrix.

In this work the state of intercalation and exfoliation in styrene-butadiene rubber (SBR) nanocomposites was investigate using infrared spectroscopy (IR), transmission electron spectroscopy (TEM) and X-ray diffraction.

Materials and methods

SBR 1502 (Dow Chemical) and Nanomer® I.30E (Nanocor, USA) were used as the elastomeric matrix and nanoclay, respectively. Nanomer® I.30E contains 70-75% montmorillonite and 30-25% octadecylamine. The curatives used for vulcanization (stearic acid, zinc oxide, 2-mercaptobenzothiazole and sulphur) were of analytical grade.

SBR nanocomposites with 2.5, 5, 10 and 15 phr nanoclay were prepared by compounding procedure followed by a compression-molding at 160ºC. The optimum cure time was determined by rheometry.

Infrared spectra were obtained using an *i*-Series IMAGE infrared microscope coupled to a Spectrum GX 2000 FTIR spectrometer. The spectra were obtained using an attenuated total reflectance (ATR) objective.

Transmision electron microscopy images were taken with a JEOL 1010 microscope with an accelerator voltage of 80 kV.

XRD analysis was carried out with a Siemens diffractometer using a Cu target, with a tube voltage of 40 kV and current of 30 mA.

Results and discussion

The infrared spectra of SBR and its composites contain information both of the component of vulcanized styrene butadiene rubber system as well as the clay filler. The most strongly absorbing region for the momtmorillonite corresponds to a broad feature between 1000 to 1200 cm^{-1} attributed to silicon-oxygen stretching modes. These bands in the Si-O region increase in relative intensity with increasing content of the nanofiller. However, the bands which appear to vary most significantly are three sharp features at around 1536, 1640 and 1397 cm^{-1} which can be attributed to zinc stearate. This component is originated from the reaction of zinc oxide with stearic acid and we have found some evidence that this component migrates during processing. No clear evidence for the formation of new component in the rubber was found, which suggest that the nanoclay does not form any new components. However, the spectral information from the nanofiller was different when it was located in the polymer matrix. A significant variation in the profile of Si-O stretching region was observed. This fact indicates strong evidence for significant exfoliation and intercalation [1, 2]. X-ray patterns and TEM microphotographs confirmed these results. For the SBR/nanoclay composites the diffraction peak corresponding to the clay shifted to lower angles as a result of an increase in the interlayer distance attributed to the intercalation of SBR into the organoclay galleries. Partially exfoliated structures and the formation of aggregates were also observed from TEM micrographs. The length and the thickness of the clay structures were measured as 123 and 8 nm, respectively.

Conclusions

Infrared spectroscopy provided clear evidence for clay exfoliation and migration of zinc stearate to the surface of the samples. The dispersion of the clay and the spacing between the silicate layers revealed the presence of intercalated, aggregated and partially exfoliated structures.

References

1. W. L. Ijdo, S. Kemnetz and D. Benderley, Polym. Eng. Sci., 46, 1031 (2006).

2. S. Tzavalas and V.G. Gregoriou, Vibrational Spectroscopy, 51, 39 (2009).

Financial support XUGA 10TMT172009PR

Preparation and characterization of polyethylene nanocomposites including titanium oxide nanoparticles

Paula A. Zapata [a], *Franco M. Rabagliati* [a]

a) Grupo Polímeros, Facultad Química y Biología, Universidad de Santiago de Chile, USACH. Casilla 40, Correo 33, Santiago, Chile.

E.mail paula.zapata@usach.cl

Introductions

It has been reported that polymer with inorganic materials is considered a powerful method to produce new materials called polymer composites or filled polymers. However, due to the significant development in nanotechnologies in the recent years, nanoscale inorganic materials such as SiO_2, Al_2O_3 and ZrO_2 have brought much attention to this research field. [1] So nanocomposites usually have improved properties compared to neat polymers, such as better mechanical, barrier properties and higher thermal stability. [2,3]

Basically, there are three methods used to produce the polymer nanocomposites: (i) melt mixing; (ii) solution blending; and (iii) in situ polymerization. This late method is perhaps considered the most powerful technique to produce polymer nanocomposites with good distribution and dispersion of the fillers inside polymer matrix.

On the other hand metallocene catalyst has become an important class of catalyst for olefin polymerization of polyethylene, due to the possibility of modelling the molecular structure of the polymers and offers a great versatility and flexibility in the synthesis and control of the polyolefin structure.

In this study, we described the preparation of polyethylene nanocomposites by in situ polymerization using TiO_2 nanospheres synthesized by Sol-Gel method. TiO_2 nano-particles have unique properties such as higher stability, long lasting, safe and broad-spectrum anti-biosis. TiO_2 nano-particles have been especially the center of attention for their photo-catalytic activities. This makes TiO_2 nano-particles applicable in many fields such as self-cleaning, anti-bacterial agent, UV protecting agent and environmental purification. [4]

The TiO_2, monomer and catalyst system (metallocene/MAO) were added to the reactor at the same time, therefore the polymerization was made in the presence of the TiO_2. The effect of the different amount of TiO_2 on the catalytic activity, the thermal, mechanical and antimicrobial properties will be studied.

Results

STEM image and light scattering analysis (**Figure 1**) reveal spherical particles with average diameters of ca. 50 nm with relatively narrow size.

The polymerization results and polymer properties (viscosity, melting temperature) of the synthesized polyethylene with and without TiO_2 nanoparticles are shown in **Table 1**. The catalytic activity for ethylene polymerization in presence TiO_2 nanoparticles presented a slight decreasing in comparison with the resulting for polyethylene without nanoparticles.

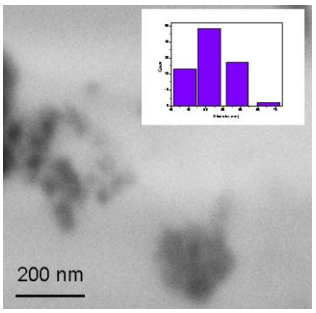

Figure 1. STEM image of TiO_2 particles.

Table 1. Results of ethylene polymerizations using TiO_2 as filler

Reaction	TiO_2 Nps (g)	Catalytic activity (kg mol^{-1} Zr^{-1} h^{-1}bar^{-1})	Tp (°C)	n (dL/g)
1	none	3100	65-68	1.31
2	0.2	1700	60	1.02
3	0.4	2600	60	--

Tp: polymerization temperature, n:viscosity, Polymerization conditions: mol Zr: $3x10^{-6}$; Al/Zr: 1400;T:60 °C. Pressure: 1 bar; reaction time: 30 min.

The incorporation of TiO_2 nanoparticles into polyethylene matrix can generated changes in the final thermal, mechanical and antimicrobials properties which will be studied.

Acknowledgments

The authors acknowledge partial financial support from FONDECYT, grant 108.5061 and Conicyt. P. Zapata. acknowledge the partial financial support insertion project CONICYT 79100010

References

1.Chaichana E, Jongsomjit B, Praserthdam P.,Chem. Eng. Sci., 62, 899-905, 2007.
2.Zapata, P.; Quijada, R.; Benavente R.; J. Appl. Polym. Sci. 2010. (In press)
3. Zapata, P.; Quijada, R.; Covarrubia, C.; Moncada, E.; Retuert, J.; J Appl Polym Sci 2009, 113, 2368.
4. Dastjerdi R., Montazer M., Colloids and Surfaces B: Biointerfaces 79 (2010) 5–18

A new way to improve PC/ABS blends: use of nano-sepiolite

Félix C. Basurto[1], *David García-López*[2], *Norky Villarreal-Bastardo*[2], *Juan Carlos Merino*[1,2], *José María Pastor*[1,2]

[1] Departament of Condensed Matter, EII, University of Valladolid, Paseo del Cauce 59, 47011, Valladolid, Spain.
E-mail: felbas@cidaut.es

[2] CIDAUT – Foundation for Research and Development in Transport and Energy, Parque Tecnológico de Boecillo, Boecillo, 47151, Valladolid, Spain.

INTRODUCTION

Blends of PC and ABS offer a wide field of applications to automotive industry, as automobile parts: instrument panels, air-bag covers, consoles, door handles, mirror housings, etc. As a well-known fact, PC possesses interesting properties, such as high heat distortion temperature and impact strength, but shows poor results in strength at low temperatures, chemical resistance and processability; in turn, ABS could provide low cost, good processability and impact strength in a large range of temperatures[1]. The combination of the best properties of ABS and PC has resulted in the development of commercially available blends.

Sepiolite is employed as a reinforcing nanoparticle to improve the thermo-mechanical properties of the polymeric materials[2]. The idea of using sepiolite is to reduce the PC percentage and obtain very similar properties.

The aim of this work is to obtain the best methodology to obtain these nanocomposites. In particular, it is investigated the effect of the modification of sepiolite, the ABS and PC percentages and the best mixing order of polymers and nanoparticle.

MATERIALS AND METHODS

In this work, PC LEXAN 223R matrix was supplied by SABIC, ABS HI-100H matrix was supplied by LG Chem., and both sepiolites, standard without modification and modified with a quaternary ammonium salt (BM2TH) were supplied by TOLSA S.A. (Spain).

Characterisation of microstructural properties of nanocomposites has been carried out by means of microscopic techniques, such as optical and scanning electron microscopy (SEM). The morphology was related to thermo-mechanical properties such as Young's modulus, heat distortion temperature (HDT) and notched Izod impact strength at room temperature. Thermogravimetric analysis (TGA) has been done in order to know the residue left by clay in the nanocomposites.

RESULTS AND DISCUSSION

Several factors could affect the resulting morphology, and hence, the final properties of PC/ABS nanoblends: PC and ABS viscosities, percentages of both polymers in the blend, and processing conditions, among others[3]. These parameters are of great importance in phase inversion, and this phenomenon could be studied by means of scanning electron microscopy (SEM).

SEM microphotographs in sepiolite nanocomposites were also employed to elucidate the real location of clay, because sepiolite fibres could be located in ABS, PC or in the interphase, depending on the method followed during compounding.

Those different methods were designed to obtain PC/ABS nanocomposites, according to four different orders of mixing:

- (ABS + sepiolite) + PC
- (PC + sepiolite) + ABS
- (ABS + PC) + sepiolite
- ABS + PC + sepiolite

All these nanocomposites were elaborated and characterized, in order to define the best way to mix the raw materials, trying to reduce the PC percentage in the blend, with similar properties in nanocomposites.

REFERENCES

1. Tjong S.C., Meng Y.Z. Effect of reactive compatibilizers on the mechanical properties of polycarbonate / poly(acrylonitrile – butadiene – styrene) blends. European Polymer Journal, 2000, 36, 123-129.

2. García-López D., Fernández J.F., Merino J.C., Santarén J., Pastor J.M. Effect of organic modification of sepiolite for PA 6 polymer/organoclay nanocomposites. Composites Science and Technology, 2010, 70, 1429-1436.

3. Tan Z.N., Xu X.F., Sun S.L., Zhou C., Ao Y.H., Zhang H.X., Han Y. Influence of rubber content in ABS in wide range on the mechanical properties and morphology of PC/ABS blends with different composition. Polymer Engineering and Science, 2006, 46, 1476-1484.

In situ Formation of Polystyrene Magnetic Particles via Batch Suspension Polymerization

Juliete S. Neves[1], *Fernando G. de Souza Jr.*[2], *Paulo A. Z. Suarez*[1], *Alexandre P. Umpierre*[1], *Fabricio Machado*[1,*]

[1]Instituto de Química, Universidade de Brasília, CP 04478, Brasília, DF, Brazil
[2]Instituto de Macromoléculas Professora Eloisa Mano – UFRJ, CP 68525, Rio de Janeiro, Brazil

*fmachado@unb.br

Introduction

The magnetic nature of the polymeric material is closely associated to the magnetic nanoparticle size. In this scenario, special attention is given to superparamagnetic magnetite (Fe_3O_4) nanoparticles due to its remarkable features, such as biocompatibility, low susceptibility to changes due to oxidation, magnetic retention only when exposed to an external magnetic field and strong ferromagnetic behavior.[1-4]

It is well-known that in suspension polymerization processes each aqueous-dispersed monomer droplets behaves as a bulk microreactor.[5] For this reason, the surface modification of Fe_3O_4 magnetic particles with oleic acid permits a good dispersion of these inorganic nanocharges within the final polymeric particles, which leads to the formation of materials with uniform magnetic properties.

This work focuses on the synthesis of micro-sized polystyrene magnetic beads by *in situ* incorporation of surface modified Fe_3O_4 nanoparticles through suspension polymerization process intended for biotechnological applications.

Materials and Methods

Styrene (polymer grade) was used as monomer in the polymerizations. The suspending agent DENKA POVAL B-24 was kindly supplied by DENKA, Tokyo, Japan. The initiator LUPEROX® 78 (99.4%) was kindly donated by Arkema Química Ltda, São Paulo, Brazil. Nitrogen (99.5%) was supplied by White Martins Ltda, Rio de Janeiro, Brazil. Sodium hydroxide (97%) was provided by F. MAIA (Rio de Janeiro, Brazil), ferric chloride hexahydrate (97%) and ferrous sulfate heptahydrate (99%) were provided by VETEC (Rio de Janeiro, Brazil), hydrochloric acid (36.5-38.0% w/w) was provided by ISOFAR (São Paulo, Brazil) and oleic acid extra pure was provided by Merck (Rio de Janeiro, Brazil). All chemicals were used as received, without further purification.

Synthesis of Magnetic Nanoparticles

Magnetite (Fe_3O_4) nanoparticles were prepared by chemical coprecipitation of aqueous Fe^{2+} and Fe^{3+} salt solution and NaOH solution.[6] Initially, 6.1 g of $FeCl_3 \cdot 6H_2O$ and 3.1 g of $FeSO_4 \cdot 7H_2O$ were dissolved in 125 mL of distilled water and 5 mL of hydrochloric acid and heated to 60 ºC with bubbling of nitrogen gas. The salts and basic solution (60 g/L NaOH) were mixed under vigorous stirring. The temperature was kept constant and equal to 60 ºC for 30 min under atmosphere of nitrogen.

Surface Modification of Magnetic Nanoparticles

The surface of Fe_3O_4 nanoparticles was modified by using oleic acid.[7] 5 g of magnetic nanoparticles were dispersed in 170 mL of distilled water under nitrogen gas and heated to 85ºC. Then, 5.6 mL of oleic acid were added dropwise at a constant rate 0.5 $mL \cdot min^{-1}$ under an inert nitrogen atmosphere. The resulting mixture was maintained under stirring for 30 min at 85ºC.

In-Situ Formation of Magnetic Nanocomposites

The polymerization reactions were carried out in a 250-mL glass reactor (Quickfit®, England) at 85 °C, with a total organic load of 25 wt-%, 3.5 wt-% of initiator (in relation to styrene) and 0.5 wt-% of suspending agent (in relation to water), under an inert nitrogen atmosphere with a constant agitation of 1000 rpm for 4.5 hours. A hotplate IKA® C-MAG HS 7 (IKA® Works, Inc.) equipped with an integrated temperature control, including a Pt1000 temperature probe was used to heat the reaction medium.

Results and Discussion

The weight fraction of nanoparticles determined by thermogravimetric measurements (Shimadzu Scientific Instruments, Maryland, USA) was 1.7, 4.8 and 10.1 wt-%, respectively. It was observed that the thermal stability of the polymers was not improved by magnetic nanoparticles distributed in the polymeric matrix.

Based on the susceptibility classification (Johnson Matthey magnetic susceptibility balance, Pennsylvania, USA), the magnetic nanocomposites behave as paramagnetic materials. It was noted that the magnetic susceptibility increases as the concentration of Fe_3O_4 nanoparticles dispersed in the polystyrene matrix is increased.

It was also observed that the magnetic force is proportional to the amount of Fe_3O_4 nanoparticles dispersed in the polystyrene matrix. When the relative magnetic force is considered, one can observe that the polymeric sample with 1.7 wt-% of Fe_3O_4 nanoparticles presents the best response to the employed magnetic field.

Conclusions

Micro-sized polystyrene magnetic beads by *in situ* incorporation of oleic acid-modified Fe_3O_4 magnetic nanoparticles were obtained via suspension polymerization process. The obtained polymeric materials presented good magnetic behavior, indicating that the modified Fe_3O_4 nanoparticles were successfully dispersed in the polystyrene particles.

References

[1] C. T. Yavuz, A. Prakash, J. T. Mayo, V. L. Colvin, *Chem. Eng. Sci.* **2009**, *64(10)*, 2510.
[2] F. G. De Souza Jr., J. A. Marins, J. C. Pinto, G. E. D. Oliveira, C. M. Rodrigues, L. M. T. R. Lima, *J. Mater. Sci.* **2010**, *45(18)*, 5012.
[3] J. Vidal-Vidal, J. Rivas, M. A. López-Quintela, *Coll. Surf A Physicochem. Eng. Asp.* **2006**, *288(1-3)*, 44.
[4] A. Aqil, S. Vasseur, E. Duguet, C. Passirani, J. P. Benoit, A. Roch, R. Muller, R. Jerome, C. Jerome, *Eur. Polym. J.* **2008**, *44(10)*, 3191.
[5] F. Machado, E. L. Lima, J. C. Pinto, *Polímeros* **2007**, *17(2)*, 166.
[6] H. T. Pu, F. J. Jiang, Z. L. Yang, *Mat. Chem. Phys.* **2006**, *100(1)*, 10.
[7] A. Pich, S. Bhattacharya, A. Ghosh, H. J. P. Adler, *Polymer* **2005**, *46(13)*, 4596.

Cracking in Thin Polymer Films Promoted through Physical Ageing

Mithun Chowdhury[1], Christophe Calers[1], Arnold Chang–Mou Yang[2], Ullrich Steiner[3,4] and Günter Reiter[1,3]

[1] Physikalisches Institut, Albert-Ludwigs-Universität Freiburg, 79104, Freiburg, Germany. [2] Department of Materials Science and Engineering, National Tsing Hua University, Hsinchu, Taiwan. [3] Freiburg Institute for Advanced Studies (FRIAS), 79104, Freiburg, Germany. [4] Cavendish Laboratory, University of Cambridge, Cambridge CB3 0HE, UK

mithun.chowdhury@physik.uni-freiburg.de

Introduction: Dynamics of polymers in ultrathin films is a long standing yet ever stimulating topic of polymer physics. Being inspired by unintentionally observed cracking of such films, we performed systematic studies of crack growth as a function of physical ageing at a temperature close to the glass transition temperature T_g. Cracking/ crazing occurred only after cooling from this elevated ageing temperature to room temperature. AFM inspection showed nano/micro-structures within the cracks consisting of voids and fibrils, indicating plastic deformation similar to crazing. The role of residual stresses was examined by following crack growth and dewetting dynamics through varying molecular weight (M_w).

Materials and Methods: Our results are based on experiments performed on thin polystyrene (PS) films of M_w ranging from 52 to 16800 kg /mol with a low index of polydispersity between 1.04 and 1.15 and of thicknesses varying between 40 and 100 nm. T_g of PS in the bulk is about 103°C. Thin films were obtained by spin-coating polymer solutions directly onto silicon substrates that were coated with PDMS, acting as a non-wettable layer. Cracking experiments were performed at room temperature after ageing at 90°C, i.e. T= T_g-13°C, under vacuum. Isothermal dewetting was studied at 125°C, i.e. T=T_g +22°C. Both processes were followed in real time by optical microscopy. Details of the craze microstructures were inspected by atomic force microscopy (AFM).

Results and Discussion: Cracking/crazing was taking place only after elevated temperature ageing. This has to be contrasted to freshly prepared films which never showed any cracks, even when stored at room temperature for several months. The morphology of voids and fibrils within the cracks largely resembles previous observations of crazes in deformed thin polymer films of similar thickness, probably related to the lack of plastic constraint along the film normal [1,2]. A clearly detectable tip of the craze (Fig. 1b) was found. A stripe-pattern orthogonal to the craze direction hints at periodic 'stiffening' tentatively attributed to heterogeneous stress distribution or possibly strain-hardening close to the craze boundary [3]. For low M_w (52 kg/mol), fibrils within the crazes were closely packed, without noticeable interfibrillar voids (Fig. 1d). In close agreement with previous results[4,5], a linear dependence with a slope of 0.28±0.05 of craze depth with film thickness was found (Fig. 1e) for 4060 kg/mol PS, while the short chain polymer (PS 52 kg/mol) exhibited a slope of about 1, implying that the craze cuts through the whole film. Craze depth and thickness were simultaneously measured by AFM [6], consistent with film thickness values determined by ellipsometry. Interestingly, an extrapolation of craze width vs. film thickness for the shorter polymer intersects the film thickness axis around 30 nm, coinciding with the threshold thickness below which our experiment never resulted in any crack formation, irrespective of molecular weight.

For the higher molecular weight PS (4060 and 16800 kg/mol), a systematic study of crack growth velocity showed a progressive increase with increasing ageing time while for the same films the dewetting velocity decreased with increasing ageing, consistent with earlier findings[7]. In contrast, for 52 kg/ mol PS a decrease in crack growth velocity with increasing ageing time was found while the dewetting velocity was unaffected by ageing, probably indicating the absence of residual stresses for such low molecular weight polymers.

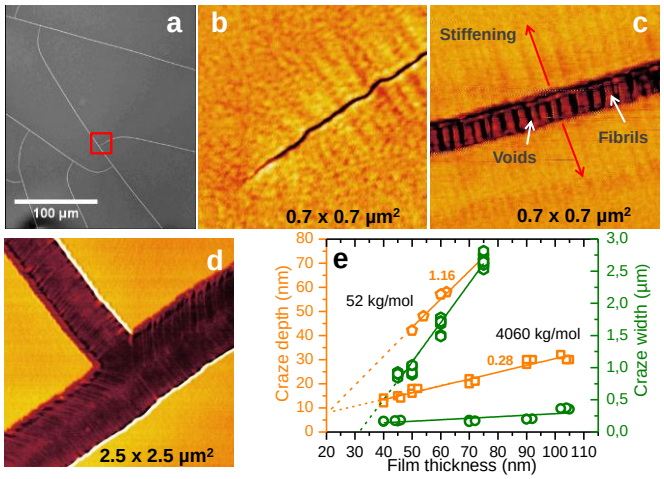

Fig. 1(a) Optical micrograph showing crack patterns formed in a 45 nm thick film of 52 kg/mol PS, aged for 24 hours at 90°C and 3 min at room temperature after quenching. AFM phase images of a 40 nm thick film of 4060 kg/mol PS, aged for 24 hours at 90°C and 2 hours at room temperature after quenching are showing: (b) a crack-tip, (c) that the two sides of a crack are interconnected by regularly spaced fibrils separated by voids and that this craze is bounded by 'stiffening' pattern of perpendicular stripes. (d) AFM phase image corresponding to the marked area in (a). (e) Plot showing the variation of craze depth and craze width with film thickness. Symbols are representing: Craze depth (□, □) and craze width (□, ○) for 52kg/mol and 4060 kg/mol PS, respectively.

Conclusions: We tentatively conclude that physical ageing of such films causes segmental relaxations of non-equilibrated polymer chains. Relaxations are easier and thus faster at the free surface. This introduces a gradient in lateral tension within the film in the direction normal to the film surface. Considering the possibility of generating strong mechanical tension at the film surface due to the formation of a 'crust' during film preparation [8], we may have to consider two antagonistic origins for crack growth: a gradient in stress induced by film preparation, with the highest lateral tension close to the free surface, and the building up of an inverted stress gradient after physical ageing and cooling the film to room temperature. Both gradients are potentially causing the formation of cracks.

References:

[1] Chan, T., Donald, A. M., Kramer, E. J., J. Mater. Sci., 16, 676 (1981)
[2] Krupenkin, T. N., Fredrickson, G. H., Macromolecules, 32, 5029 (1999)
[3] Reiter, G., Eur. Phys. J. E., 8, 251-255 (2002).
[4] Crosby, A. J., Fasolka, Michael, J. & Beers, K. L., Macromolecules, 37, 9968 (2004)
[5] Yang, A. C. M., Kunz, M. S., Logan, J. A., Macromolecules, 26, 1767 (1993)
[6] McGraw, J. D, Dalnoki-Veress, K., Phys. Rev. E, 82, 021802 (2010)
[7] Reiter, G. et. al., Nature Mater. 4, 754 (2005)
[8] De Gennes, P. G., Eur. Phys. J. E., 7, 31 (2002)

Strategy to improve the mechanical properties of electroactive materials: preparation of PEDOT-montmorillonite and multilayer PEDOT/poly(*N*-methylpyrrole)/Montmorillonite exfoliated nanocomposites

Francesc Estrany[1,3], David Aradilla[2,3], Denise S. Azambuja[4], María T. Casas[2], Carlos A. Ferreira[5] and Carlos Alemán[2,3]

[1]Departament d'Enginyeria Química, Escola Universitària d'Enginyeria Tècnica Industrial de Barcelona, Universitat Politècnica de Catalunya, Comte d'Urgell 187, 08036, Barcelona, Spain.
[2]Departament d'Enginyeria Química, E. T. S. d'Enginyers Industrials, Universitat Politècnica de Catalunya, Diagonal 647, 08028 Barcelona, Spain.
[3]Center for Research in Nano-Engineering, Universitat Politècnica de Catalunya, Campus Sud, Edifici C', C/Pasqual i Vila s/n, Barcelona E-08028, Spain
[4] Institute of Chemistry, Federal University of Rio Grande do Sul, Av. Bento Gonçalves 9500 – CEP 91501-970, Porto Alegre, RS Brazil.
[5] Universidade Federal do Rio Grande do Sul – DEMAT - Av. Bento Gonçalves, 9500 - setor 4- prédio 74 - Cep. 91501-970 - Porto Alegre - RS – Brazil

Francesc.estrany@upc.edu, denise@iq.ufrgs.br and carlos.aleman@upc.edu

Introduction

Exfoliated nanocomposites [1] formed by poly(3,4-ethylenedioxythiophene) and multilayer PEDOT/ poly(N-methylpyrrole), with different concentrations of non-modified montmorillonite or bentonite (MMT), from 1% to 50% w/w, have been prepared by anodic electropolymerization in aqueous solution. Analyses of the electrochemical and electrical properties reveal that the electroactivity of the nanocomposites is higher than that of the individual homopolymer, and that of the multilayer without bentonite. The exfoliated distribution of the clay in the polymeric matrix and the morphology of the prepared materials have been characterized using TEM, X-ray diffraction, SEM and AFM. Standard Sellotape Test [2] has been used to verify the improvement in the adherence of nanocomposites.

Materials and Methods

Monomers and MMT (bentonite) were purchased from Aldrich. Both nanocomposites were prepared by chronoamperometry (CA) under a constant potential of 1.10 V, on a VersaStat II potenciostat-galvanostat using a three-electrode two-compartment cell under nitrogen atmosphere at 25 ºC, from a 10 mM monomer solution in distilled water containing 0.1 M $LiClO_4$ as supporting electrolyte. Steel AISI 316 sheets (4 cm^2 area) were employed as working and counter electrodes, and the reference electrode was an Ag|AgCl electrode. The electroactivity of both the nanocomposites were determined by cyclic voltammetry (CV). A scan rate of 100 $mV \cdot s^{-1}$ was used. The structure and distribution of the clay in the nanocomposites were examined using a Phillips TECNAI 10 transmission electron microscope at an accelerating voltage of 100 kV. X-ray diffraction (XRD) spectra of PEDOT-MMT films were recorded using a Bruker D8 Advance model to 40 kV and 40 mA (λ= 1.5406 Å). SEM images were analyzed using a Focused Ion Beam Zeiss Neon40 scanning electron microscope at 3 kV. Topographic AFM images were obtained with a Molecular Imaging PicoSPM using a NanoScope IV controller in ambient conditions.

Results and Discussion

In the electropolymerization, the current density stabilizes at higher values for nanocomposites that for de polymers without bentonite, indicating that the flow of monomer during the electrogeneration process increases upon the addition of MMT.

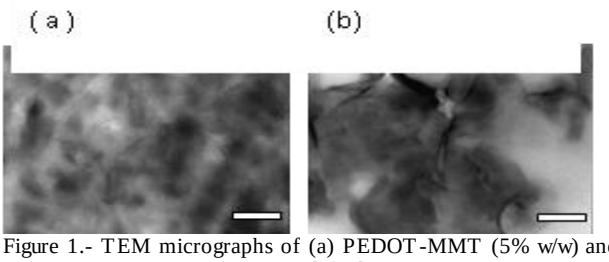

Figure 1.- TEM micrographs of (a) PEDOT-MMT (5% w/w) and (b) PEDOT-MMT (10% w/w). Line length: 100 nm.

TEM micrographs of the nanocomposites reveal that, independently of the clay concentration, MMT is exfoliated into individual platelets within the polymeric matrix. This is illustrated in Figure 1 for the PEDOT-MMT (5% w/w) and PEDOT-MMT (10% w/w).

In some cases, the electroactivity of the nanocomposite is higher than that of the homopolymer and that the multilayer PEDOT/poly(N-methylpyrrole), indicating that the addition of clay can enhanced the ability to store charge of the polymers. It has also been determined that the adhesion of the nanocomposites increases with the percentage of clay.

Conclusions

Conducting polymers-MMT nanocomposites have been prepared by anodic electropolymerization. Structural characterization indicates that the clay is exfoliated in the polymers matrix, which represents a significant improvement with respect to the intercalative structure usually found in conducting polymer-clay nanocomposites. The electroactivity and the adhesion of the nanocomposites, which increases with the concentration of clay, is higher than that of polymers without MMT. This fact indicate that PEDOT-MMT nanocomposites are potential candidates for the fabrication of devices able to store charge.

Acknowledgements

This work has been supported by MICINN and FEDER funds (project MAT2009-09138), and by the International Cooperation Program from Brazilian and Spanish CAPES-MICINN (PHB2007-0038-PC)

References

1) D. Aradilla, F Estrany, D. S. Azambuja et al. *European Polymer Journal*. 46 (2010). 977-983.
2) J. I. Martins, M. Bazzaoui, T. C. Reis et al. *Synthetic Metals*. **129** (2002). 221-228

Effect of Binary Organoclay Mixture on the Properties of ABS-Clay Nanocomposites Prepared by Melt Intercalation

Danieli Galvan[1], *Julio Roberto Bartoli*[1], *Marcos Akira D'Ávila*[2], *Mateus Mazzuco*[1], *Felipe Massucato*[1].

[1]DTP, School of Chemical Eng.; [2]DEMa, School of Mechanical Eng.; State University of Campinas –UNICAMP

bartoli@feq.unicamp.br

Introduction:

Polymeric nanocomposites exhibits improved physical proprieties compared to conventional materials as metals, polymeric alloys and thermoplastic composites. This new class of materials has large impact in various industrial segments, mainly in automotive sector due to its low density. This benefit is explained by the small amount of nanoclay added to the polymer matrix compared to common reinforced agents. Because of easy processing, most of the research activities have focused on preparation by melt compounding. Some parameters can influence nanocomposite formation, as: clay surface treatment, processing conditions and polymer matrix. ABS poly(acrylonitrile-butadiene-styrene) is a large volume engineering plastic and relatively low cost. Nanocomposites of ABS are being studied to improve mechanical and flammability properties[1,2]. The aim of this work is to investigate the effect of a binary mixture of organically modified montmorillonite (OMMT) on the properties of ABS.

Materials and Methods:

Two commercial OMMTs (Southern Clay), one with methyl, tallow, bis-2-hydroxyethyl quaternary ammonium (Cloisite 30B) and one with dimethyl, dehydrogenated tallow quaternary ammonium (Cloisite 20A) were used in single and binary mixture with ABS (Terluran GP35, BASF). The MFR measured was 10.5 g/10 min (ASTM D1238, 230°C/3.8 kg). All the materials were dried at 80°C for 4 h. The ABS/OMMTs (4 wt%) were prepared by melt intercalation on a co-rotating twin-screw extruder (Figure 1), Coperion ZSK 26Mc, L/D 44, screw speed 120 rpm (170 to 210°C), and two feeding rates 4 and 8 kg/h to obtain two levels of torque (40 and 75%, respectively). XRD analyses were done in a Rigaku DMAX 2200m Cu-Kα (40kV, 30mA), step of 0.05, 1s time and 2θ from 1.6° to 10°.

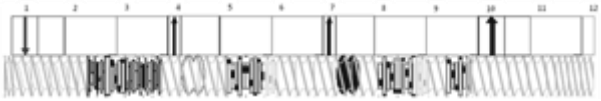

Figure 1: Twin-screw extruder design.

The factorial experimental design[3] (Table 1) for the binary OMMT mixtures study is a two block designs for screw torque factor (low and high level).

Table 1: Factorial experimental design for clay and torque.

Independent variables	Torque	C20A	C30B
Levels	-1	1	0
		½	½
		0	1
	1	1	0
		½	½
		0	1

Results:

Figure 2 shows XRD results of the OMMT (Cloisite 20A and 30B) and the two OMMT/ABS composites with a binary mixture of these organoclays, at 40% and 75% of screw torque. The XRD difratograms of the others OMMT/ABS, either OMMT 20A or 30B, were very similar. The interlayer spacing of the OMMT and for all the OMMT/ABS composites are shown in Table 2. These distances were significantly increased for all the OMMT/ABS, which is related to some intercalation of the polymer into the galleries of the clays. It seems that the torque did not have any significant effect on the dispersion of clay in the ABS matrix.

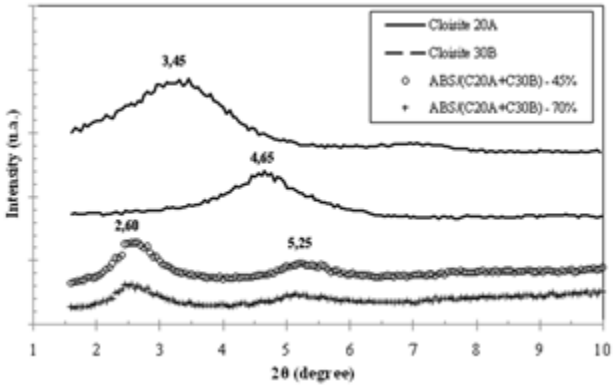

Figure 2: XRD analyses of OMMT and ABS/OMMT.

Table 2: Diffraction angles and interlayer spacing.

	2θ (°)	d001 (nm)
C20A	3,45	2,57
C30B	4,65	1,91
ABS/C20A - 45%	2,60	3,41
ABS/C20A - 70%	2,55	3,47
ABS/C30B - 45%	2,60	3,41
ABS/C30B - 70%	2,65	3,34
ABS/ (C20A+C30B) - 45%	2,65	3,34
ABS/ (C20A+C30B) - 70%	2,55	3,47

Conclusions:

The DRX analyses of the ABS/OMMT binary mixture presented the similar pattern observed in other works **¡Error! Marcador no definido.¡Error! Marcador no definido.** with the same commercial single OMMT, indicating that polymer intercalation was achieved. Rheological, TEM and DMTA analyses, as well flammability and mechanical tests are in progress.

References:

[1]Karahaliou,E.;Tarantili,P.;J.Polymer Sci.,13,p.2271-81, 2009
[2]Patiño-Soto, A.P. et.al. J. Polymer Sci., 46, p.190-200, 2008.
[3]Barros Neto, B.; et al., Campinas, Editora Unicamp, 2007.

Acknowledgments: F. Carneiro (Positron);Dr. C.Schuch, G. Lago and R. Nascimento (Rhodia); *Unicamp*: Prof. C.K. Suzuki and C.R. Silveira (FEM), Prof. M.A.de Paoli and R. Gadioli (IQ), D. Thomazelli (FEQ); and the financial support of CNPq, PIBIC, CAPES, FAPESP 2004/15084-6

Synthesis, Characterization and Nonlinear Optical Properties of Micellar Nanohybrids Based on Pd Nanoparticles and Carbazole-Containing Block Copolymers

Maria Demetriou[a], *Theodora Krasia-Christoforou*[a], *George Chatzikyriakos*[b], *Irene Papagiannouli*, *Stelios Couris*[b]

[a]Department of Mechanical and Manufacturing Engineering, University of Cyprus
[b] Institute of Chemical Engineering and High Temperature Chemical Processes (ICEHT), Foundation for Research and Technology-Hellas (FORTH), Patras

[a]demmaria@hotmail.com, krasia@ucy.ac.cy

Introduction:

It is strongly believed that the future optoelectronic and photonic devices will be comprised of organic-inorganic hybrid materials with nonlinear optical (NLO) response [1]. Most of the reported work refers to gold and silver nanoparticles embedded in organic matrices [2]. Palladium nanoparticles have been only rarely investigated towards their NLO properties [3].

Herein we report the synthesis, characterization and experimental investigation of the NLO properties of novel organic-inorganic hybrid materials based on functional amphiphilic block copolymers (ABCs) and palladium nanoparticles.

Results and Discussion:

Well-defined ABCs consisting of 2-(N-carbazolyl) ethyl methacrylate (CzEMA) and 2-(acetoacetoxy) ethyl methacrylate (AEMA) (Fig.1) were synthesized by RAFT controlled radical polymerization and their molecular characteristics were determined.

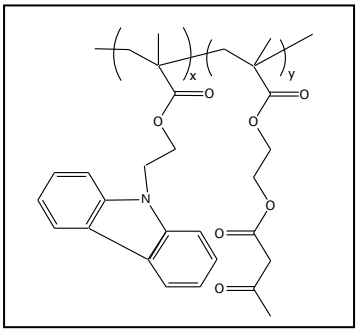

Figure 1: *Molecular structure of CbzEMA-b-AEMA ABCs.*

Micellar nanohybrids based on CzEMA-*b*-AEMA combined with Pd^o were fabricated in tetrahydrofuran (THF) as illustrated in Fig. 2.

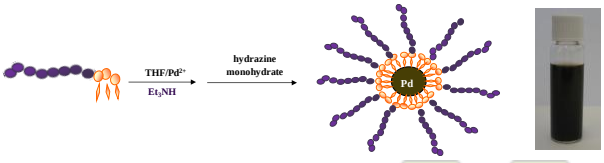

Figure 2: Schematic representation of the methodology followed for the preparation of CbzEMA-b-AEMA/Pd^o micelles.

Dynamic Light Scattering was employed to obtain information on the hydrodynamic size of the hybrid systems. In the absence of Pd^o, only unimers exist in solution; micellization is induced upon complexation followed by reduction.

Sample	λ (nm)	Conc. (mM)	$Re\chi^{(3)}$ 10^{-13} esu	$Im\chi^{(3)}$ 10^{-13} esu	$\chi^{(3)}$ 10^{-13} esu
$CzEMA_{104}$-*b*-$AEMA_{44}$ AEMA:Pd 2:1	532	1.43	0.795±0.033	-0.34±0.16	0.864±0.16
		1.067	0.502±0.033	-0.3±0.2	0.584±0.2
		0.72	0.185±0.0385	-0.23±0.13	0.294±0.135
		0.36	0.074±0.038	-0.134±0.068	0.152±0.077
		THF	0.24±0.022	-	0.24±0.022
	1064	4.096	0.121±0.0092	0.611±0.085	0.622±0.085
		1.68	0.045±0.015	0.242±0.034	0.245±0.037
		1.3	0.0037±0.015	0.212±0.057	0.212±0.059
		0.794	-	0.129±0.041	0.129±0.041
		THF	0.187±0.0072	-	0.187±0.007

Furthermore, their NLO response has been investigated by employing the Z-scan technique (35ps).

Table 2: Third-order NLO parameters of the $CzEMA_{104}$-*b*-$AEMA_{44}$/Pd^o measured in THF.

The originality of this work lies on the fact that it constitutes the first systematic work in which the NLO properties of novel hybrid systems consisting of carbazole-containing ABCs and Pd nanoparticles were investigated in detail.

References:

[1] D. M. Schaadt, B. Feng, E. T. Yu *Applied Physics Letters* **2005**, 86, 063106-1-3.

[2] (a) Mitsuishi, M. et al. *Polymer Journal*, **2007**, *39*, 411-422. (b) Adhyapak, P. V. et al. *Journal of Nanoscience and Nanotechnology*, **2006**, *6*, 2141. (c) Wang, Y.; Xie, X. B.; Goodson, T. *Nano Letters*, **2005**, *5*, 2379.

[3] Ebothe, J.; Kityk, I. V.; Chang, G.; Oyama, M.; Plucinski, K. J. *Physica E* **2006**, *35*, 121.

Inducing Microdomain Orientation of Thermoplastic Elastomer in As-spun Electrospinning Fibers through Study Cases of SEBS Triblock Copolymer

Wonchalerm Rungswang[1], *Masaya Kotaki*[3], *Shinichi Sakurai*[4], *and Suwabun Chirachanchai*[1,2]

[1]The Petroleum and Petrochemical College, Chulalongkorn University, Soi Chula 12, Phyathai Road, Pathumwan, Bangkok, Thailand 10330.
[2]Center for Petroleum, Petrochemicals, and Advanced Materials, Chulalongkorn University, Bangkok, 10330, Thailand
[3]Department of Advanced Fibro-science and [4]Department of Macromolecular Science & Engineering, Kyoto Institute of Technology, Matsugasaki, Sakyo-ku, Kyoto 606-8585, Japan.

Thermoplastic Elastomer (TPE) isone the well-known block copolymers composing of soft and hard segments in a single chain.Due to immiscibility of those soft and hard parts, TPE simultaneously performs nano-phase separation, so-called microdomains. An orientation of those microdomains has been extensively studied in films and sheets, especially based on the stretching force. In the case of fibers, electrospinning is a good technique to generate the confined fiberat nanometer to sub-micrometer level under ultimate stress and at the same time in combining additional disk collector, it can control the fiber alignment[1] which allows us to understand the polymer at molecular level.In the past, electrospun TPEs were investigated and only peculiar and short shape of the microdomains as observed by TEM were reported [2]It comes to our question whether the ordered microdomainsand their orientation are existed in the TPEs, and how can we identify it? In addition, if the microdomain can be generated, is there any possibility to direct the microdomain orientation?

This present work, thus, for the first time, clarifies an existence of the short-range ordered microdomains including directing their orientation through the as-spun electrospinning fibers ofpolystyrene-*block*-poly(ethylene-co-butylene)-*block*-polystyrene triblock copolymer (SEBS).[3] Two dimensional small angle X-ray scattering (2D-SAXS) technique was applied to reveal the microdomain in details. The important result is that theelectrospun SEBS showed both elliptic pattern,referring to distorted lamella, and four-point patternobliquely oriented to the stretching direction (SD), regarding to the rapture of microdomain to tiny grains.

In our related work, we already reported about the molecular interaction betweenbenzoxazines monomer (BZ) and SEBSvia π-πstacking with PS segments.[4] Here, an addition of BZ in SEBS chain initiated the electrospun fibers to perform a unique orientation of which the microdomain is almost parallel to SD as evaluated from μ angle (the angle between vector normal to the lamellar microdomain and SD) ~ 80° and ϕ angle (the angle between vector normal the grain of lamellar microdomain and SD) ~90°.

The authors would like to acknowledge the Royal Golden Jubilee Program (the Thailand Research Fund (PHD/0058/2550)), and the Japan Student Services Organization (JASSO)for financial support. SEBS was kindly supported from Asahi Kasei Chemical Corporation, Japan and the SAXS measurements were conducted at Spring-8 under the approved number 2009A1153.

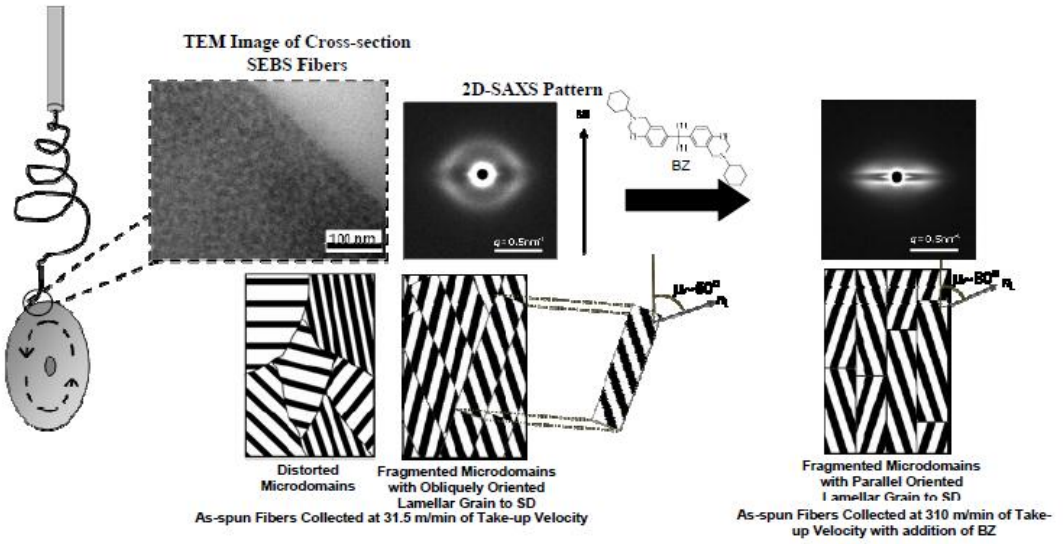

Selected References

1. Kongkhlang, T., Tashiro, K.,Kotaki, M. and Chirachanchai, S. *J. Am. Chem. Soc.***2008**, 130 (46), 15460-15466.
2. Fong H, Reneker DH. *J. Polymer. Sci. B Polymer Phy.*,**1999**, 37, 3488-3493.
3. Rungswang, W., Kotaki, M., Shimojima, T., Kimora, G., Sakurai, S. and Chirachanchai, S. *Polymer*, In Press (doi: 10.1016/j.polymer.2010.12.019)
4. Rungswang, W. and Chirachanchai, S. *Macromol. Mater. Eng.*, In Press, (doi: 10.1002/mame.201000315).

Computational Modeling of Nanocomposites' Mechanical Behavior at Different Environments Parameters (Moisture and Thermal Loadiing)

Katya Marinova Simeonova, PhD, Civil Engineer, Engineer-mathematician,

Associate Professor, Institute of Mechanics, Bulgarian Academy of Sciences,

e-mail: katyas@bas.bg

Discovering of carbon nanotubes (CNTs) by S. Iijima, [1] put the beginning of a revolution in nanoscience (nanomaterials). Carbon nanotubes, possess extraordinary physico-mechanical, electronic, electrical properties, transport, chemical, thermal etc. properties. These nanomaterials have nanoscale sizes and chirality structure. Moreover CNTs could be used as a very useful reinforcement for relatively novel materials, so called nanocomosites. In many cases nanocomposites have a matrix from different polymer materials (for example epoxy, resin, or other ones). Regarding nanocomposites, may be mentioned that because of so good properties of reinforcement (Carbon nanotubes), they are better than only CNTs. So, nanotubes and nanocomposites, find applications in many fields of technique, electronics, optoelectronics, transistors, engineering etc., [2]. Recently has been proved that these nanoscale materials are very good tool in molecular and cellular biology and clinic medicine too. The aim of the paper, presented below, could be formulated as follows: to develop a modified theoretical (computational) model for study of the effects of moisture and thermal loading on the stress state of nanocomposites at different types of reinforcements carbon nanotubes-single walled carbon nanotubes (SWCNTs) and multiwalled carbon nanotubes and (MWCNTs). Computational model, has been developed on the basis of classical mechanics theories, and experimental data, [3]. Numerical algorithms and FORTRAN programs, designed by authors, have been presented as well in the work. Comparison of the results, obtained and experiments in literature, shows a good agreement.

Key words: carbon nanotubes, nanocomposites, moisture, shear stress, computational models, FORTRAN programs

[1]. S. Iijima, Nature, 354, 56-58, (1991)
[2]. K. Simeonova, G. Milanova, A REVIEW ON THE MECHANICAL BEHAVIOR OF CARBON NANOTUBES (CNTs), AS SEMICONDUCTORS, ISCOM2007, Spain, 24-30 September 2007, Poster, ISCOM'07, Grant from ISCOM2007, Book of Abstracts, p. 136
[3]. L. Chunyu, T. Chou, A Structural Mechanics Application for Analysis of Carbon Nanotubes, Int. J. of Solids and Structures, Nature, 381 (1996)

Fluoroalkyl End-Capped Oligomers/Polyaniline and /Phenyl-Capped Aniline Dimer Nanocomposites: Controlling Photochromism between These Nanocomposites Induced by UV-Light-Responsive Titanium Oxide Nanoparticles

Hideo Sawada[1)], *Taiki Tsuzuki-ishi*[1)], *Mari Iizuka*[2)], *and Masato Yoshida*[2)]

[1)]Department of Frontier Materials Chemistry, Graduate School of Science and Technology, Hirosaki University, Bunkyo-cho, Hirosaki 036-8561, Japan
[2)]School of Medicine, Shimane University, Izumo, Shimane 693-8501, Japan

e-mail: hideosaw@cc.hirosaki-u.ac.jp

Polyanilne (**PAn**)/inorganic composites have been considered as new class of materials due to their improved properties compared with those of pure conducting polymers and inorganic materials. For example, the combination of electrical conductivity of **PAn** and UV sensitivity of anatase TiO_2 are expected to find applications in electochromic devices, nonlinear optical system, and photochemical devises.[1] It is in general difficult to prepare conducting polymers/inorganic nanoparticle composites by conventional blending or mixing in solutions or melt form, because, polymers are not molten in nature and generally insoluble in common solvents.[2] On the other hand, partially fluoroalkylated polymers, especially fluoroalkyl end-capped oligomers are attractive polymeric surfactants, because they exhibit various unique properties such as high solubility, surface active properties, biological activities and nanometer size-controlled molecular aggregates which cannot be achieved by the corresponding non-fluorinated and randomly fluoroalkylated ones.[3] Therefore, it is in particular interest to develop novel fluoroalkyl end-capped oligomers/**PAn** nanocomposites, especially fluoroalkyl end-capped oligomers/**PAn**/titanium oxide nanoparticles composites have high potential applications imparted by not only fluorine but also **PAn** or titanium oxide toward a variety of areas such as conductive coating, charge storage, electocatalyst, electrochromic devices, and photovoltaic cells.

Here we report that fluoroalkyl end-capped acrylic acid oligomer [R_F-$(ACA)_n$-R_F]/, 2-methacryloyloxyethanesulfonic acid oligomer [R_F-$(MES)_n$-R_F]/, 2-acrylamido-2-methylpropanesulfonic acid oligomer [R_F-$(AMPS)_n$-R_F] /polyaniline [**PAn**] nanocomposites are prepared by the polymerization of aniline initiated by ammonium persulfate in the presence of the corresponding oligomers, respectively. These fluorinated oligomers were also applied to the preparation of the corresponding fluorinated oligomers/phenyl-capped aniline dimer (**An-dimer**: *N,N'*-diphenyl-1,4-diphenyldiamine) nanocomposites by the interaction of the fluorinated oligomers with **An-dimer**, which is considered to be an excellent model of **PAn**. In these nanocomposites, R_F-$(MES)_n$-R_F/**PAn** nanocomposites and R_F-$(MES)_n$-R_F/**An-dimer** nanocomposites were effective for the preparation of colloidal stable fluorinated oligomer/**PAn**/TiO_2 and /**An-dimer**/TiO_2 nanocomposites. These two types of fluorinated TiO_2 nanocomposites can exhibit quite different photochromic behaviors: R_F-$(MES)_n$-R_F/**PAn**/TiO_2 nanocomposites can exhibit a reversible wavelength change for polaron absorptions around 760 ~ 820 nm by alternation of UV-irradiation and storage in the dark; in contrast, R_F-$(MES)_n$-R_F/**An-dimer**/TiO_2 nanocomposites can exhibit a reversible color change from blue to colorless (a reversible absorbance change) by the similar treatment.

References:

1. S.-J. Su, N. Kuramoto, Synthetic Metals, 114 (2000) 147 – 153.
2. M. D. Butterworth, R. Corradi, J. Johal, S. F. Laschelles, S. Maeda, S. P. Armes, J. Colloid Interface Sci., 174 (1995) 510 – 517.
3(a)H. Sawada, Prog. Polym. Sci. 32 (2007) 509 - 533;
(b) H. Sawada, J. Fluorine Chem. 121 (2003) 111 - 130;
(c) H. Sawada, Polym. J. 39 (2007) 637 - 650.

Hybrid materials based on unsaturated polyester resins and polyhedral oligomeric silsesquioxanes (POSS)

Floriana Constantin, Sorina-Alexandra Gârea, Horia Iovu

University POLITEHNICA of Bucharest, Faculty of Applied Chemistry and Materials Science, Department of Polymer Science and Technology, 149 Calea Victoriei, 010072, Bucharest, Romania

c_floriana2005@yahoo.com

Introduction:

The polyhedral oligomeric silsesquioxanes are hybrid molecules with the structure $(RSiO_{1,5})_n$.

Unsaturated polyester resin is one of the most used thermosetting resins thanks to relatively low cost, adaptability to many fabrication processes and good properties, so it was used as matrix resin for polymeric composites [1-2].

The main purpose of this research was to study the influence of different types and concentrations of polyhedral oligomeric silsesquioxanes (POSS) on the thermal properties of unsaturated polyester resin (UPR) using several techniques like Dynamical Mechanical Analysis (DMA), Thermogravimetric Analysis (TGA) and Differential Scanning Calorimetry (DSC)[3-5].

Materials and Methods

The polymeric matrix was unsaturated polyester resin and benzoyl peroxide (5%wt. against UPR) was used as crosslinking agent.

As reinforcing agents two types of POSS were used, one with eight reactive vinyl groups and the other with one reactive vinyl group and seven unreactive groups, isopropyl (Scheme 1).

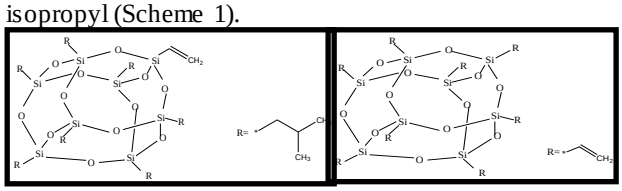

Scheme 1. The chemical structure of monovinylPOSS and octavinylPOSS

Results and Discussion

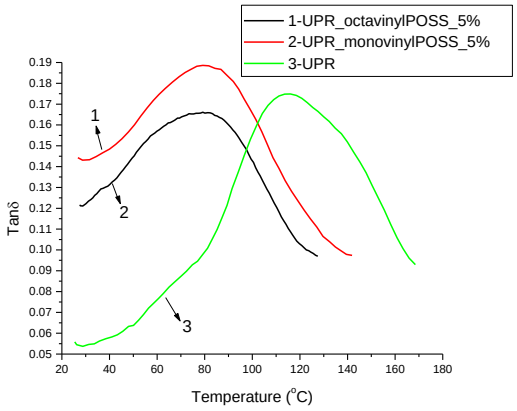

Fig.1 – The DMA curves of the (1) UPR – octavinylPOSS (5wt.%);
(2) UPR – monovinylPOSS (5 wt.%); (3) UPR.

From the DMA results (Fig. 1) it can be observed that the addition of the octa- and monovinylPOSS to the UPR decreased the glass transition temperature value with about 30°C which is probably caused by the plastifier effect of the POSS molecules.

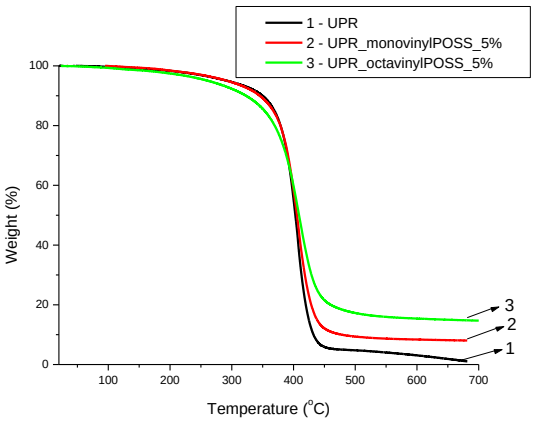

Fig. 2 TGA curves for the (1) UPR; (2) UPR – monovinylPOSS 5wt.%); (3) UPR – octavinylPOSS (5wt.%);

From the TGA curves (Fig. 2) one may observe that the thermal behavior of the UPR is not influenced by the addition of octa- or monovinylPOSS.

Also, the DSC tests confirmed that the addition of POSS compound to the UPR does not significantly modify the crosslinking temperature of the polyester resin.

Conclusions:

The glass transition temperature of the hybrid materials decreased due to the plastifier effect of POSS.

The termostability of the hybrid materials is not influenced by the POSS molecules.

References:

[1] – Y. Feng, Y. Jia, S. Guang, H. Xu – J Appl Polym Sci, 2010, 115, 2212-2220;

[2] – J. Gao, C. Dong, Y. Du – Int J Polym Mater, 2010, 59, 1-14;

[3] – C-H. Su, Y-P. Chiu, C-C. Teng, C-L. Chiang - J. Polym. Res., 2010, 5, 673-681

[4] –E.S.A Rashid, K. Ariffin, C.C. Kooi, H.M. Akil- Materials and Design, 2009, 30, 1-8

[5] – Y-L. Liu, G-P. Chang, K-Y. Hsu, F-C. Chang-J. Polym. Sci.:Part A: Polym. Chem., 2006, 44, 3825-3835

Aknoledgement

The work has been funded by the Sectoral Operational Programme Human Resources Development 2007-2013 of the Romanian Ministry of Labour, Family and Social Protection through the Financial Agreement POSDRU/6/1.5/S/16.

Micellization and gelation of PEO/PPO block copolymers and their carboxyl-terminal derivatives

Jiří Dybal, Adriana Šturcová, Alena Braunová, Michal Pechar, Alexander Jigounov, Jaroslav Kříž

Institute of Macromolecular Chemistry AS CR, v. v. i.,
Heyrovský Sq. 2, 162 06 Prague 6, Czech Republic

e-mail: dybal@imc.cas.cz

Introduction

Micellization and gelation of water soluble tri-block copolymers PEO-PPO-PEO (Pluronics) is relevant in view of possible wide applications in pharmacy, bioprocessing and separation. Carboxyl-terminal derivatives were shown to micellize thermoreversibly and to bind multivalent cations. In the present work, Raman spectroscopy, attenuated total reflectance Fourier transform infrared (ATR FTIR) spectroscopy, NMR spectroscopy, and density functional theory (DFT) model calculations have been used to explore micellization and gelation processes in Pluronics at molecular level.

Materials and Methods

ATR FTIR spectra were collected on a Nicolet Nexus 870 FTIR spectrometer purged with dry air and equipped with a horizontal micro-ATR Golden Gate unit (SPECAC). Raman spectra were obtained on a Renishaw In-Via Raman micro-spectrometer with Ar^+ ion laser with excitation line at 514.5 nm. At given temperature, vibrational spectra of pure water were subtracted from spectra of Pluronic/water solutions. ^1H and ^{13}C NMR spectra and relaxations were measured with a 600 MHz Bruker 600 Avance III spectrometer. PFG diffusion experiments and dynamic relaxation experiments were done on a 300 MHz Bruker Avance DPX300 spectrometer. The model calculations were carried out at the density functional theory (DFT) level employing the Gaussian 03 program package.[2] All the structures were fully optimized with the B3LYP functional and the 6-31G(d) basis set.

Results and Discussion

We have studied a series of macromolecules with the same length of more hydrophobic PPO block (31 structure units) and varying length of more hydrophilic PEO blocks (5 to 84 structure units)[3,4] together with Pluronic P85 (EO26–PO39–EO26) and its carboxyl-end modification denoted as CAE-85 and low-molecular-weight model compounds.

Vibrational spectra of Pluronics in water and quantum chemical calculations showed that analogous coordination types of water molecules are detected in interacting water as in bulk water. Hydrophobic contacts prefer tetra-coordinated water and hydrophilic contacts induce di-coordinated water.[5] PPO chain was shown to reversibly coil in the pre-association stages as a result of its partial dehydration and this process is shifted to higher temperatures by the hydrophilic pull of PEO blocks.

While gelation of Pluronic P85 takes place when the concentrations are above the critical gelation concentration, carboxyl-terminal derivative CAE-85 displays significant differences. Formation of micelles corroborated by the shifts of the CH_3 deformation and C-O stretching vibrational bands due to dehydration of both hydrophobic and hydrophilic groups. Micelles of CAE 85 may be further stabilized by negative charge appearing at temperatures above critical micellization temperature, and it probably prevents the micelles from forming gel.

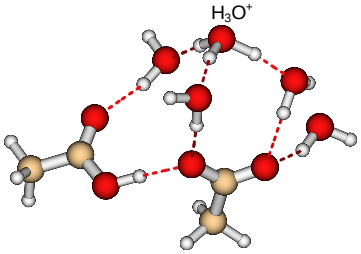

Figure 1. DFT optimized geometry of the dissociated carboxylic group.

DFT model calculations indicate that dissociated ion pair $COOH \rightarrow COO^- + H^+$ may be stabilized due to hydration and interaction with other carboxylic groups (Figure 1). The effects of multivalent cations on the CAE-85 micellization and micelle stability were also studied.

Acknowledgement. This work was supported by the Grant Agency of the Czech Republic under Projects 203/09/1478 and 203/08/0543.

References

1. Batrakova, E. V.; Kabanov, A. V. *J. Control. Release* **2008**, *130*, 98.
2. Frisch, M. J. et al. Gaussian 03, Revision C.02; Gaussian, Inc.: Wallingford CT, 2004.
3. Schmidt, P.; Dybal, J.; Šturcová, A. *Vib. Spectrosc.* **2009**, *50*, 218.
4. Kříž J.; Dybal J. *J. Phys. Chem. B* **2010**, *114*, 3140.
5. Šturcová, A.; Schmidt, P.; Dybal, J. *J. Colloid Interface Sci.* **2010**, *352*, 415.

A Plasma reactor for the surface modification of silica based fillers: description and the apparatus and EPR investigation of reactive intermediates

Armando Buttafava, Daniele Dondi, Damiano Grassi, Fabio Pepori, Antonio Faucitano

Dipartimento di Chimica Generale, Università di Pavia, V.le Taramelli 12, 27100 Pavia (ITALY)

armando.buttafava@unipv.it

Introduction

Low pressure plasma in nonthermal conditions, possess an high temperature of electrons while conserving a low temperature for atoms and ions. In these conditions, it's possible to generate highly reactive species (radicals, ions) while studying the primary radical reactions having low or no activation energies. This permits either to investigate the thermal behavior of generated radicals or to study the reaction with suitable radical traps. For this purpose, an RF inductive plasma apparatus was designed for the EPR study of radicals at liquid nitrogen temperature. The radical chemistry of polymer fillers (silica, polybutadiene-coated silica and organoclays) and some polymers (polybutadiene, SBR and polystyrene) was studied with this method.

Materials and Methods

The inductive plasma apparatus consist of a radiofrequency generator at 13.56 MHz with a maximum power of 300W (Dressler Cesar III 133) coupled with a impedance matching unit (Dressler VM 1500W-ICP). The whole apparatus was shielded in order to avoid environmental radiofrequency dispersion. The plasma was generated in a specially-designed glassware (Figure 1) suitable for transferring the sample in a quartz EPR tube while keeping the sample at 77K. The internal gas pressure was set up in the range (0.1- 0.5 Torr). Nitrogen, oxygen and argon were used for the plasma generation.

Silica Zeosil 1165 with a surface area 160 m^2/g was used as received from Rhodia. Polibutadiene-coated silica was obtained according to literature data [1]. Organically modified montmorillonite with alkyl ammonium salts were purchased from Nanocor.

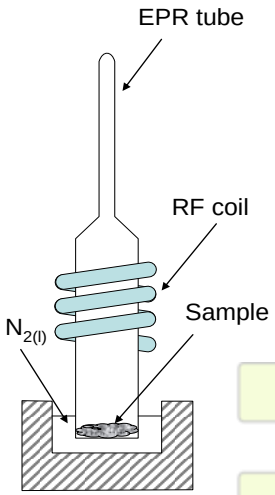

Figure 1. Schematic representation of the RF-plasma apparatus used.

Results and Conclusion

Plasma irradiation of silica lead to the formation of E' centres (b, Figure 2) and paramagnetic species attributed to zeosil impurities (c). The plasma treatment under nitrogen atmosphere lead also to the formation of H atoms (a), feature not visible in the oxygen plasma-treated sample. The presence of H atoms is an indirect evidence of the low temperature maintained by the sample. In fact, these signals usually decay, in the χ irradiated zeosil, at a temperature of 177 K [1]. Moreover, the EPR spectrum of silica treated in oxygen plasma shows that E' centres are produced in higher yields, as described for silica glass implanted with oxygen ions [2]

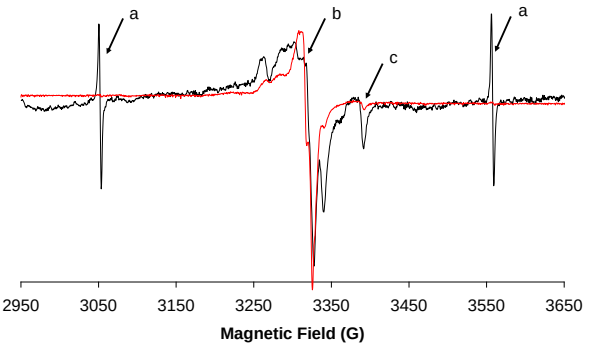

Figure 2. EPR spectrum of Zeosil silica plasma-treated with nitrogen (black) and oxygen (red).

The evolution of paramagnetic centers was investigated by recording EPR spectrum at different temperatures. Their thermal stability will be discussed and compared between different experimental setup.

The reactions of generated radicals in silica, clays and polymers with radical traps (volatile olefins, oxygen) were studied by introducing the reactants at low temperature and then increasing the temperature in the EPR cavity.

Bibliography

1) D. Dondi, A.Buttafava, P.Stagnaro, A.Turturro, A.Priola, S.Bracco, P.Galinetto, A.Faucitano "The radiation-induced grafting of polybutadiene onto silica" *Rad. Phys. And Chem.* 78, (2009), 525-530.

2) Y. Morimoto, R. A. Weeks, R. H. Magruder, R. A. Zuhr "Optical and electron paramagnetic resonance spectra of silica glass implanted with oxygen ions" *J. of Non-Cryst. Solids* 203, (1996), 55-61.

Effect of Sodium Dodecylbenzene Sulfonate on Carbon Nanotubes Dispersion

Ghamgosar khorshidi V., Bakhshandeh G.R., Salimi A., Naderi Gh*

Iran Polymer and Petrochemical Institute, P. O. Box: 14965/115, Tehran, Iran

a.salimi@ippi.ac.ir

Introduction

To achieve the best properties of Carbon Nanotubes (CNTs) in polymer matrixes, the filler must be dispersed effectively. Due to the strong van der Walls interactions in CNT, there is tendency to CNT agglomerations especially in non-polar polymer matrix [1]. A wide variety of surfactants have been used for dispersion of CNTs in aqueous media [2, 3]. In this work, we study the effect of sodium dodecylbenzene sulfonate (SDBS) as surfactant for dispesion of functionalized and non-functionalized Multi walled carbon Nanotubes in aqueous media.

Materials and Methods

Functionalized and non-functionalized Multi walled carbon Nanotubes (diameter 10-30 nm, length 10 µm, purity 95%) was supplied by Institute of Petroleum Industry (Tehran, Iran). The surfactant SDBS from Fluka was used as received. All dispersions were prepared in deionized water for constant 1wt% of each CNT. The samples were ultrasonicated for 5 minutes using (Bandelin HD 3200, Germany) and then filtered after centrifuging at 3000 rpm for 20 min. The dispersion of CNTs was characterized using UV-vis spectrophotometer model UV-1650 PC (SHIMADZU, Japan).

Results and Discussions

The UV spectra of non-functionalized and functionalized MWNTs are shown in Fig 1a and b, respectively. As shown in Fig. 1 a, the absorption increases as the surfactant concentration increases from 0.5 g/L to 1.5 g/L. This indicates that the SDBS can be adsorbed on CNT surface resulting to more dispersion of the CNTs in media. Besides, the existing benzene ring in SDBS structure provides higher attraction to CNTs surface [3]. As shown in Fig.1 b, the increase in absorption is more pronounced for the functionalized CNTs. Due to hydrogen bonding between the hydrophilic head of surfactant and the existing –OH group of functionalized CNTs, higher dispersion for CNT-OH can be obtained for the same level of surfactant loading.

Conclusions

The use of SDBS for CNT dispersion in aqueous media is an effective way. The increase in SDBS loading resulted to higher dispersion may be due to attraction of existing benzene ring in SDBS to CNT surface. The increase in dispersion was more pronounced for the functionalized CNTs mainly because of the hydrogen bonding between the hydrophilic head of surfactant and the existing –OH group of functionalized CNTs.

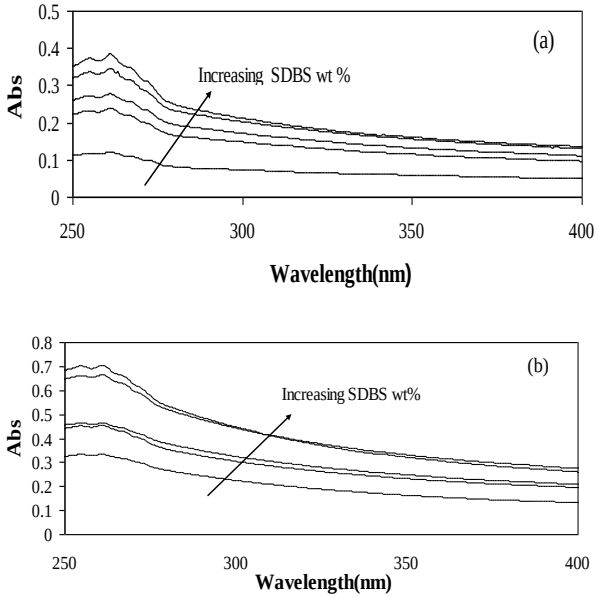

Fig 1. UV–vis spectra of (a) non-functionalized MWNT (b) functionalized MWNT

References

1- Lin, D., Liu, N., Yang, K., Xing, B., Wu, F., Enviromental Pollution, 158 (2010) 1270-1274.
2- Rastogi R., Kaushal R., Tripathi S. K., Sharma A. L., Kaur I., Bharadwaj L. M., Journal of Colloid and Interface Science, 328 (2008) 421- 428.
3- Bystrzejewski M., Huczko A., Lange H., Gemming T., Buchner B., Rummeli M. H., Journal of Colloid and Interface Science, 345 (2010) 138- 142.

Optical and electrochemical properties of temperature fractions of nanodispersed polytetrafluoroethylene Forum®

Tsvetnikov[1], L. Matveenko[1], S. Suchoverchov[1], V. Kuryaviy[1], D. Opra[1], K. Galkin[2], S. Gnedenkov[1]

[1]Institute of Chemistry and [2] Institute for Automation and Control Processes Far-East Branch of the Russian Academy of Science 159, Prospect Stoletiya Vladivostoka, Vladivostok, 690022, Russia

e-mail: tsvetnikov@ich.dvo.ru

The original thermo-gas-dynamic (TGD) method of nanofluoropolymers (Forum®) synthesis based on the thermal destruction of bulk polytetrafluoroethylene (PTFE) under special gas-dynamic conditions was developed in the Institute of Chemistry FEBRAS [1]. PTFE FORUM® is the material consisting of polymer molecules of various molecular weights (Fig. 1).

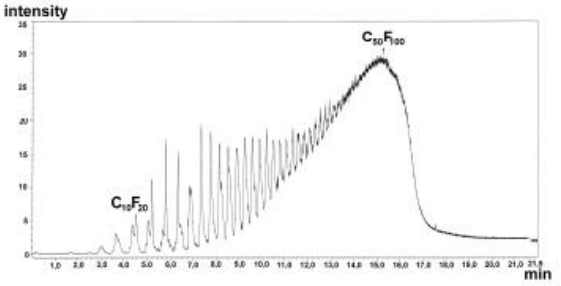

Fig. 1. Chromatography-mass spectrometry of PTFE low-molecular phase up to 400o C. At the temperature up to 400o C the molecules with molecular weights from 338 to 3000 transfer into the gas phase.Heating FORUM® powder in the defined temperature ranges allows generating fractions with defined molecular weights. Researches show that these fractions have different physical-chemical properties of practical interest. For example, film which is transparent in the optical band and generated from the PTFE FORUM® powder is able to absorb ultraviolet radiation. The degree of absorption is inversely proportional to the fraction's molecular weight (Fig. 2).

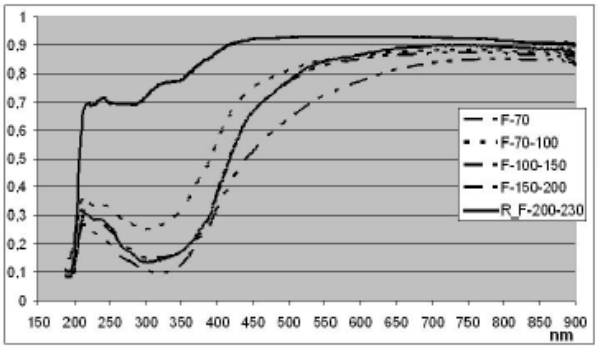

Fig. 2. Experimental light-spectrums of PTFE Forum® temperature fractions' reflection.

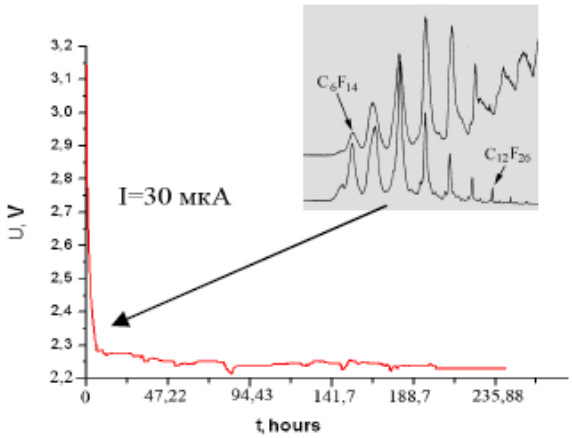

Fig. 2. The LCB discharge curve on the C_8F_{16} cathode

This paper contains the results of physical-chemical, structural and morphological researches of different PTFE FORUM® temperature fractions.

References:

1. A.K. Tsvetnikov, Thermo-gradientional and thermoimpact methods of synthesis of nano-and microdispersed fluorocarbons materials. Properties and applicatio, Bulletin FEB RAS. 2009. - №2. – pp. 18-22.

Influence of dopants on properties of polypyrrole nanocoated poly(styrene-*co*-methacrylic acid particles)

I. Carrillo[1], *M.J. González-Tejera*[2], *J.L.G. Fierro*[3], *E. Sánchez de la Blanca*[2], *M.I. Redondo*[2], *M.V. García*[2], *E. Enciso*[2]

[1]Dpto. Química Industrial y Polímeros, E.U.I.T. Industrial, Univ. Politécnica de Madrid, C/. Ronda de Valencia 3, 28012 Madrid, Spain

[2]Dpto. Química Física I, Fac. Ciencias Químicas, Univ. Complutense, Avda. Complutense s/n, 28040 Madrid, Spain

[3]**Instituto de Catálisis y Petroleoquímica, CSIC, Madrid, Spain**

isabel.carrillo@upm.es

During the last decades, polypyrrole (PPy) has been one of the most studied conducting polymers because its easy synthesis, good electrical conductivity, redox properties, and environment stability make it a very promising material for technological applications.

The aim of this work was to study the influence of different dopants on the morphology and structure of composites of PPy coated polystyrene-co-methacrylic acid (PS-MMA) spherical particles.

Spherical particles of PS-MMA were prepared form surfactant free emulsion as it was described in [1]. PPy was chemically synthesized and deposited onto PS-MMA particles (PPy/PS-MMA) using different dopants such us $FeCl_3$, sodium p-toluensulfonate hexahydrate (NaTS), 5-sulfosalicylic acid dehydrate (SSA). The PPy amount in the samples was determined by elemental analysis. The influence of the dopant anion on the PPy morphology observed by scanning electron microscopy at the particle surface and the electric conductivity, at room temperature, of pellets obtained from dried suspensions are discussed. X-ray photoelectron and infrared spectroscopy were also used to analyze the structure of the samples. Their conductivities were also measured.

Uniform and continuous PPy coating is deposited on the samples with MMA. A relationship between morphology and size and conductivity was found. Samples with the highest sphere size and a smooth PPy coating showed higher conductivity than those smaller and with an irregular PPy distribution.

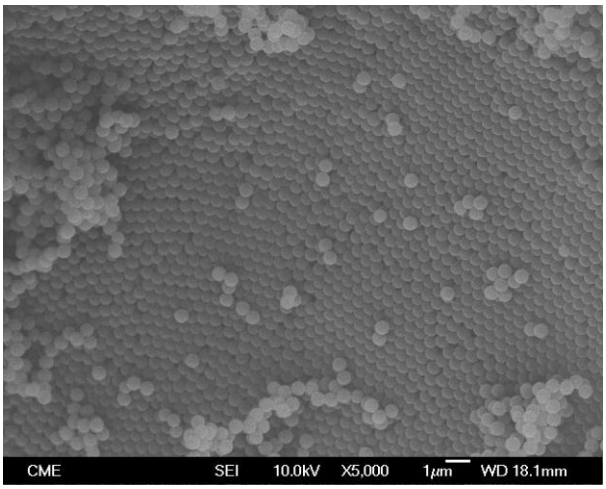

Figure 1. Scannning electron micrograph of (Ppy/PS-MAA) doped with FeTS.

Conductivity values from 5.84 S cm^{-1} for the most conducting coated latex to 0.50 S cm^{-1} for the less one have been found.

XPS experiments allow us to determine the contribution of C, O, Cl and S to the surface composition. The fraction of nitrogen atoms with positive charge excess (N_{ox}/N_{tot}) is equivalent to the doping level. One positive nitrogen atom to four (or three) total nitrogen was found in all the studied samples.

PPy deposition onto MMA/PS samples was followed by infrared spectra. FTIR spectra showed the strong high frequency absorption characteristic of conducting polymers in addition to bands assigned to latex and PPy vibrations. No signals of carbonyl group bands appear in the spectra indicating that degradation of PPy was low or non-existent.

REFERENCES

[1] M.I. Redondo, M.V. García, E. Sánchez de la Blanca, M. Pablos, I. Carrillo, M.J. González-Tejera, E. Enciso, Polymer 51 (2010) 1728-1736.

Effect of Silane Grafting and Post Cross-linking of HDPE on Compatibilization and Oxygen Barrierity of HDPE/Clay Nanocomposite

Ali Sharifpakdaman, Jalil Morshedian, Yousef Jahani

Iran polymer and petrochemical institute

a.pakdaman@ippi.ac.ir

Introduction:

Due to several advantages, polyethylene is the most widely used polymer in food packaging industries. However, the use of neat PE is restricted because of some of its inherent properties such as relatively high oxygen and aroma permeability which weakens long shelf life property required for these applications.[1-3] Recently, polymer-clay nanocomposite materials have attracted attention as alternative route to improve polymer barrierity as well as other properties.[2] It has been found that these superior properties of nanocomposites are attributed to the dispersion and orientation of clay and interactions between clay and polymer. Consequently, in the case of PE because of its non-polar backbone, modification of clay surface or polyethylene molecules is highly required.[3,4]

In this work silane grafting of HDPE is done by reactive extrusion to improve hydrophilic property of polymer molecules. Furthermore other objective of this modification was creation of post cross-linkability of composite matrix for further enhancement of barrierity as well as stabilization of microstructure. As a result HDPE-g-silane/montmorillonite nanocomposites were successfully prepared by melt compounding with acceptable exfoliation and considerable reduction of oxygen transmission rate (OTR).

Materials and methods:

The polymer (HDPE–BL3) with MFR of 1.2 g/min (5Kg, 190^{o}C) and density of 0.954 g/cm^{3} was purchased from Jam Co., Iran. Vinyl trimethoxy silane (VTMO) with commercial name of Silfin-25 was supplied from Evonik (Degussa). Dicumyl peroxide 99% (DCP) from concord Co. was used as an initiator. And finally nano clay (org-MMT) was Cloisite 15A from Rockwood Co.

Appropriate amount of DCP was dissolved in silane (4 phr) and this solution was adsorbed in polyethylene granules in turbo mixer during about an hour. These granules were fed into twin screw extruder (Brabender) where grafting reaction was done. Then the prepared HDPE-g-silane was blended with org-MMT and again melt compounded in twin extruder. Finally cast film by Thermo Haake Reomix (200 micron thickness) and sheets by compression moulding (1 mm thickness) were prepared as test specimens. The samples were exposed to moisture whenever the cross-linking required.

Results and discussion:

The silane grafting of HDPE was examined using FTIR by visiting a peak around wavenumber1080cm^{-1}. In addition decreased MFR of grafted samples and attaining about 38 percent gel content after moisture curing confirmed successfully grafting of silane on PE backbones.

The XRD data obviously demonstrated the effect of grafting on compatibilization of HDPE and org-MMT (Fig 1). Intercalation occurred as a result of insertion of polymer chains between the clay layers. This could be seen in curves by shifting diffraction peak to smaller 2Θ which implied higher d-spacing according to Bragg equation.[5] Exfoliated morphology could be achieved by smaller amount of MMT in highly grafted PE. TEM micrographs also confirmed the XRD results by visiting good dispersion and widely intercalated systems.

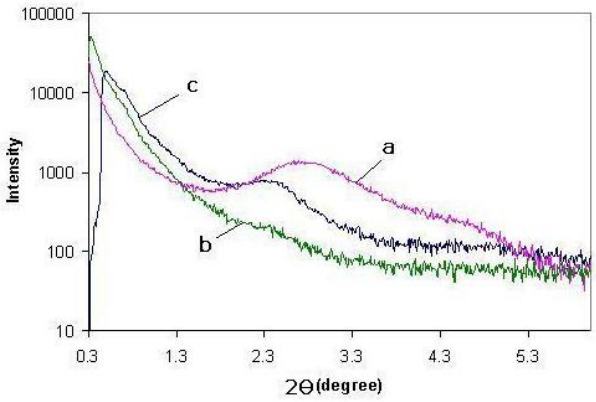

Figure 1. XRD patterns of (a) MMT (b) HDPE-g-silane (2 phr clay) and (c) HDPE-g-silane (4 phr clay)

Finally the oxygen transport properties of samples were measured. These data showed that barrierity of HDPE against oxygen was strongly improved in intercalated and exfoliated nanocomposite samples. In addition a slight improvement was observed by cross-linking of all specimens. Whereas, the crystallinity remained almost unchanged in compounding (examined by DSC), the changes of permeation were attributed to incorporation of nano clay and also cross-linking of final products.

Conclusions:

Silane grafting of HDPE was successfully performed to improve the miscibility of clay with PE. The oxygen permeability was strongly decreased in compatibilized nanocomposites. Furthermore, cross-linking of samples showed further improvement in barrierity.

References:

1- Baldev Raj, R.S. Jagadish; J. of applied polymer Science, Vol. 96, 1193-99, 2005.
2- A. Sorrentino, M. Tortora; J. of polymer science, Vol. 44, 265-274, 2006.
3- M. A. Osman, J. E. P. Rupp; Macromol. Rapid Commun., Vol. 26, 880-884, 2005.
4- Zhongzhong Qian, Hu Zhou; Polymer composites, Vol. 30, 1234-42, 2009.
5- Hongmei Wang, Pengfei Fang; polymer international, Vol. 57, 50-56, 2008.

PLA/PCL/montmorillonite nanocomposite systems: morphology and properties

V. Vascotto, A. Brunetin**, R. Sulcis**, P. Schiavuta***

* Nanofab, Via delle Industrie 5 Marghera (VE) Italy
** CIVEN, Via delle Industrie 5 Marghera (VE) Italy

v.vascotto@nanofab.it

Nowadays, biopolymers have attracted great attention by industry due to the more and more growing interest for environment and the possibility to replace the conventional polymer produced by petroleum sources.

Poly(lactic acid) (PLA) is a biodegradable thermoplastic material characterized by good barrier properties to gases, and it could be used in different fields, ranging from packaging to agriculture or medicine. PLA is usually hard and brittle and for this reason its fracture properties can be improved by adding a ductile polymer, like Poly(ε-caprolacton) (PCL). PCL is a biodegradable polymer too but PLA and PCL are immiscible, with formation of phase separation. Moreover, PCL is characterized by poor barrier to gases, which limit some industrial applications of the blend. In order to overcome this drawback, we studied the possibility to add layered silicates to the PLA/PCL blend.

In the last years, the utility of inorganic nanoparticles as additives to enhance the polymer performances has been well established. Of particular interest are polymers added with small amount (1-5 wt%) of organically modified layered silicates (OMLS); these nanocomposites demonstrated significant enhancement, relative to an unmodified polymer, of a large number of physical properties, including barrier to gases and vapour, flammability resistance, thermal and environmental stability, solvent uptake, and rate of biodegradability of biodegradable polymers.

In the case of PLA/PCL blends, the possibility to use nanoclays for the increase of the barrier properties in particular of PCL is of particular interest.

The aim of this paper is to study the preparation and the characterization of PLA/PCL/nanoclay composites for packaging applications. The materials were all prepared by melt blending the polymers and the nanoclays in a Brabender discontinuous mixer. Before the mixing process, PLA, PCL and the clays were dried under vacuum. Nanocomposites were obtained by melt blending polymers with nanofillers in the Brabender discontinuous mixer at 190 °C for 15 min.

Because PLA and PCL are not miscible, the study of the phases distribution in the blend is fundamental; for this reason Raman spectroscopy and Atomic Force Microscopy were used. In particular the confocal μ-Raman spectrometry was used to study the distribution of the phases, with and without nanofiller. The 514.5 nm line of an Ar-ion laser was used as excitation source; the spectrometer used is a 300mm focal length, equipped with a 600 lines/mm grating and images are collected by means of a 100x microscope objective (0.90NA). Phase mapping has been performed by measuring μ-Raman spectra during surface scanning of the sample over a selected area of a sample (40 μm x 16 μm). Since the μ-Raman spectra of the two components are quite similar, we exploited a characteristic peak of the PLA at 380 cm^{-1} (absent in the PCL spectrum) to map its distribution in the material. Another peak at 1430 cm^{-1} was chosen for comparison, being present in both materials (Fig. 1). The comparison between the distribution of the two peaks on the surface is used to tentatively identify phase separation of matrix and dispersed phase.

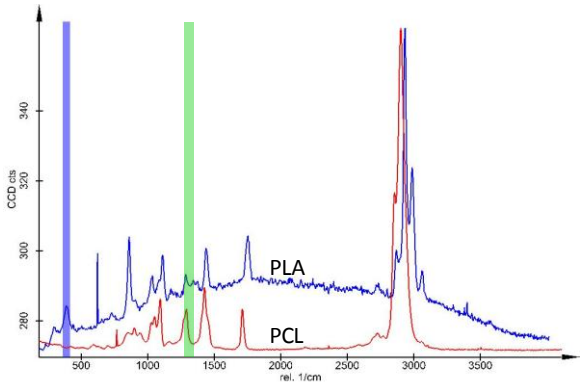

Fig. 1. μ-Raman spectra of PLA and PCL .

AFM topographic and phase images reveal the presence of small aggregates of few μm inside the polymer matrix, that could be attributed to the PCL dispersed phase. This is consistent with what we observed in μ-Raman maps, where the resolution is of the order of 0.5 μm. The results can suggest that modified montmorillonite preferentially forms aggregates of 1-2 μm inside the Poly(ε-caprolacton) domains.

Mechanical characterizations were performed and gas and vapour barrier properties were evaluated.

The addition of PCL on PLA caused, even at low amount, a decrease of tensile and barrier properties, in agree to the plasticizing effect of poly(ε-caprolacton).

However, by using nanoclay it was possible to overcome this drawback and in some cases it was possible to increase the properties of pure PLA.

Synthesis and Characterization of Superparamagnetic and Thermoresponsive Hydrogels Based on Functional Methacrylates and Oleic Acid-Coated Magnetite Nanoparticles

Theodora Krasia-Christoforou[1], *Petri C. Papaphilippou*[1], *Antonis Pourgouris*[1], *Oana Marinica*[2], *Alina Taculescu*[3], *George I. Athanasopoulos*[1] *and Ladislau Vekas*[3]

[1]Department of Mechanical and Manufacturing Engineering, University of Cyprus, Nicosia, CYPRUS
[2]National Center for Engineering of Systems with Complex Fluids, University "Politehnica" Timisoara,Timisoara, ROMANIA
[3] Center for Fundamental and Advanced Technical Research, Romanian Academy, Timisoara Branch, Timisoara, ROMANIA

e-mail: krasia@ucy.ac.cy

Introduction: Magneto-responsive composites belong to the broad category of "intelligent" materials capable of responding to external stimuli such as temperature, pH, the presence of an electric or a magnetic field etc. Among others, magnetic polymer conetworks in which magnetic (nano)particles are embedded, is a new class of "soft" composite materials, exhibiting great interest in nanotechnology and in biomedicine since they could be potentially used in magnetic drug delivery, cell sorting, catalysis, as sensors and actuators [1]. This study deals with the preparation of novel magnetoresponsive and thermoresponsive nanocomposite conetworks consisting of: (a) oleic acid coated magnetite nanoparticles ($OA.Fe_3O_4$) and (b) hydrophilic/thermoresponsive and hydrophobic (ligating) units namely hexa(ethylene glycol) methyl ether methacrylate (HEGMA) and 2-(acetoacetoxy)ethyl methacrylate (AEMA), respectively [2].

Materials and Methods:

Oleic acid-coated magnetite nanoparticles. The oleic acid-coated magnetite nanoparticles ($OA.Fe_3O_4$) were prepared by following an experimental procedure developed by Bica *et al.* [3]. Briefly, magnetite nanoparticles, Fe_3O_4, were obtained by the chemical co-precipitation of Fe^{2+} and Fe^{3+} cations in an aqueous solution in the presence of NH_4OH, at 80–82 °C.

HEGMA-co-AEMA/EGDMA random conetworks and $OA.Fe_3O_4$-containing nanocomposite conetworks. Free radical copolymerization was employed for the synthesis of the conetworks. Random cross-linking copolymerizations of HEGMA and AEMA were performed in either ethyl acetate (EA) or tetrahydrofuran (THF) in the presence of 2,2'-azobis(isobutylnitrile) that served as the radical initiator. For the preparation of the magnetoresponsive polymer conetworks the same synthetic methodology was followed in the presence of $OA.Fe_3O_4$.

Results and Discussion: Two series of hydrogel nanocomposites have been prepared in EA (Series A) and THF (Series B) in which the organic content was kept constant and only the inorganic content varied. In Fig. 1 a schematic presentation of the synthetic pathway followed for the preparation of the nanocomposite magnetoresponsive conetworks is given. The degrees of swelling (DSs) of all conetworks (in the absence and presence of $OA.Fe_3O_4$) were determined in organic (EA, THF) and in aqueous media. Deswelling kinetic studies that were carried out at ~ 60 °C in water, demonstrated the thermoresponsive properties of the nanocomposites, attributed to the presence of the hexa(ethylene glycol) side chains within the conetworks.

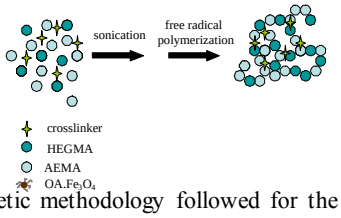

Fig. 1: Synthetic methodology followed for the preparation of $OA.Fe_3O_4$-containing nanocomposite conetworks [2].

Furthermore, the nanocrystalline phase adopted by the embedded magnetic nanoparticles was investigated by X-ray diffraction spectroscopy. The obtained diffraction patterns indicated the presence of magnetite (Fe_3O_4). Thermal gravimetric analysis (TGA) measurements showed that the $OA.Fe_3O_4$-containing conetworks exhibited superior thermal stability compared to the pristine conetworks. Further to the characterization of compositional and thermal properties, assessment of magnetic characteristics by vibrational sample magnetometry (VSM) disclosed tunable superparamagnetic behavior, depending on the magnetic content within the conetwork as presented in Fig. 2.

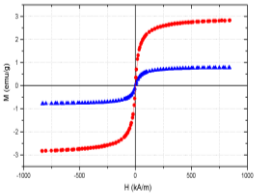

Fig. 2: Magnetization curves of $OA.Fe_3O_4$-containing nanocomposite conetworks measured at 300K [2].

Conclusions: A novel approach for the fabrication of nanocomposite conetworks exhibiting temperature- and magnetoresponsive behavior is reported. The tunable superparamagnetic behavior demonstrated by these materials combined with their thermoresponsive properties may allow for their future exploitation in the biomedical field.

References:

[1] (a) A. M. Schmidt, Macromol. Rapid Commun. 27 (2006) 1168. (b) T.Y. Liu, S.H. Hu, K.H. Liu et al., J. Controlled Release 126 (2008) 228.

[2] P. Papaphilippou et al. J. Magn. Magn. Mater. 323 (2011) 557.

[3] D. Bica, Rom.Rep.Phys., 47 (1995) 265.

Biosensory Function of Self-Assembled Fluorescent Nanotubes

Chulhee Kim, Jeonghun Lee, Sang Kyu Park, Hyun Soo Kim

Department of Polymer Science and Engineering, Inha University, Incheon 402-751, Korea

chk@inha.ac.kr

Nanotubes have been a subject of great interests due to their innovative properties and potential applications in a variety of areas of nanoscience. In particular, for organic nanotubes, the precise functionalization and interconnection of the building blocks provided a vision that they could exhibit not only unprecedented architectures but also valuable functions for applications such as electronics and biomedicine.

Even though various self-assembling building blocks for nanotubes have been developed, a molecular recognition motif has not been employed for controlling the self-organization of building blocks into organic nanotubes. Recently, we have reported that the cyclodextrin (CD)-covered dendron nanotubes (Den-CD-NTs) were obtained by a hierarchical self-assembly process derived from a host-guest complexation between the amide dendrons with the focal pyrene moiety and cyclodextrins.[1,2] The smaller rim of CD is exposed to the surface of the nanotube upon inclusion of the focal pyrene groups into the cavity of CD. We reasoned that this type of hierarchical self-assembly approach would provide a facile methodology for the construction of diverse nanotube architectures via the host-guest interaction between the dendron and the C-6 modified CDs. The tunability in the surface functionalization would enable us to construct the hybrid of the nanotubes with metal nanoparticles. Furthermore, we also reasoned that the fluorescence characteristics of the nanotube in response to the change of the surface environment for the application of the nanotube as a biosensory vehicle.

In the primary building block, amide Dendron, the focal pyrene group was introduced not only as the guest moiety for a CD host but also as a fluorescent probe. Dendron self-organizes into vesicles in aqueous solution. Upon addition of CDs into the vesicular solution, the CD-pyrene complexation occurs through the inclusion of the hydrophobic focal pyrene unit into the cavity of CD. This supramolecular recognition transforms the self-assembled structures from the vesicle to the CD-covered nanotubes.

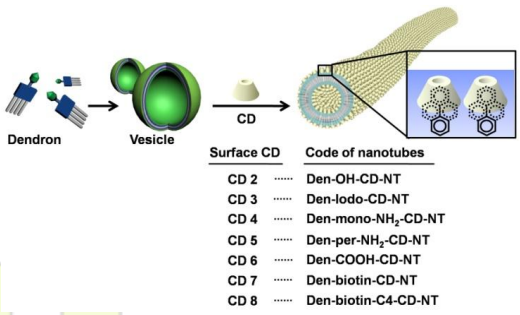

The fluorescent nature of Den-CD-NTs with the tunable surface functionality described in this work provides an opportunity for utilizing the nanotubes as a biosensing platform when the surface functional groups of the nanotubes are designed to interact specifically with the analytes. The sensitive emission property of the pyrene unit in the cavity of CDs of the nanotube toward the change in local environment would allow such binding of the biomolecules on the nanotube to trigger the change in the fluorescence emission of the nanotubes. For that purpose, we prepared the biotin-covered nanotubes (Den-biotin-CD-NT and Den-biotin-C4-CD-NT) as a biosensing platform for utilizing the specific binding of biotin with receptor proteins such as streptavidin and avidin. When streptavidin-AuNP conjugate (SA-AuNP) was added to the Den-biotin-C4-CD-NT solution, the fluorescence was quenched due to proximity of the pyrene moiety to the AuNP of SA-AuNP which binds to the biotin unit on the tube surface. These fluorescence characteristics of Den-CD-NTs along with well-defined surface architecture suggest that Den-CD-NTs can be utilized as a biosensor. To demonstrate the possibility of Den-CD-NT as a biosensory vehicle, an inhibition assay was carried out between streptavidin, avidin, and biotin as a proof-of-concept experiment.[3]

In the inhibition assay with Den-biotin-C4-CD-NT, SA-AuNP, and avidin, the fluorescence intensity of pyrene in Den-biotin-C4-CD-NT increased with increasing the concentration of avidin, because SA-AuNP binds less strongly to biotin than avidin so that the concentration of SA-AuNP bound on Den-biotin-C4-CD-NT decreases with increasing the avidin concentration. As shown in Figure 6e, the I_t/I_0 ratio increased with increasing the avidin concentration. I_0 denotes the fluorescence intensity of Den-biotin-C4-CD-NTs, and I_t is the fluorescence intensity of SA-AuNP/Den-biotin-C4-CD-NT depending on the avidin concentration. The detection limit for avidin was in the range of ~ 1 nM.

The tunability of the structure and function of Den-CD-NTs demonstrated the substantial advantage of our supramolecular approach for development of unique biomaterials.

Acknowledgment

This work was supported by the National Research Foundation of Korea (NRF) grant funded by the Korea government (MEST) (No. 2009-0079739).

References

1. C. Park, I. H. Lee, S. Lee, Y. Song, M. Rhue, C. Kim, *Proc. Natl. Acad. Sci. U. S. A.* **2006**, *103*, 1199.

2. C. Park, M. S. Im, S. Lee, Jino Lim, C. Kim, *Angew. Chem. Int. Ed.*. **2006**, *103*, 1199.

Luminescent Gold–poly(thiophene) Nanoaggregates prepared by One-step Oxidative Polymerization

Jung Hyun Kim [1,], Yeon Jae Jung [1], Sun Jong Lee [1], Seung Mo Lee [1], Hongkwan Park [1], and In Woo Cheong [2]*

[1]Department of Chemical and Biomolecular Engineering, Yonsei University, 134 Shinchon-Dong, Seodaemoon-Gu, Seoul 120-749, Republic of Korea

[2]Department of Applied Chemistry, Kyungpook National University, 1370 Sankyuk-dong, Buk-gu, Daegu 702-701, Republic of Korea

e-mail : jayhkim@yonsei.ac.kr

We report the facile synthesis, formation mechanism, and photoluminescent (PL) properties of gold–poly(thiophene) (Au–PTh) nanoaggregates. They were prepared by one-step oxidative polymerization, in which Au3+ ion was utilized as an oxidizing agent for the polymerization of thiophene. Transmission electron microscopy (TEM) and high-resolution TEM (HR-TEM) analyses demonstrated that the raspberry-like Au–PTh nanoaggregates consist of individual Au NPs covered by PTh and stabilized by Tween 80. For Au–PTh nanoaggregates, a clear red shift in the SP peak was observed in the UV absorption spectra as compared with pristine Au nanoparticles (NPs). This red shift of the SP band is a consequence of the location of p-conjugated PTh on the surface of Au NPs, resulted from a strong binding between sulfur atoms of PTh and the Au NPs (sulfur–gold interaction). The strong interaction between the gold and sulfur atoms of PTh in the Au–PTh nanoaggregates was observed by X-ray photoelectron spectroscopy (XPS) analysis. The SP effect contributes to the PL intensity enhancement of the Au–PTh nanoaggregates and was confirmed by confocal laser scanning microscopy (CLSM).

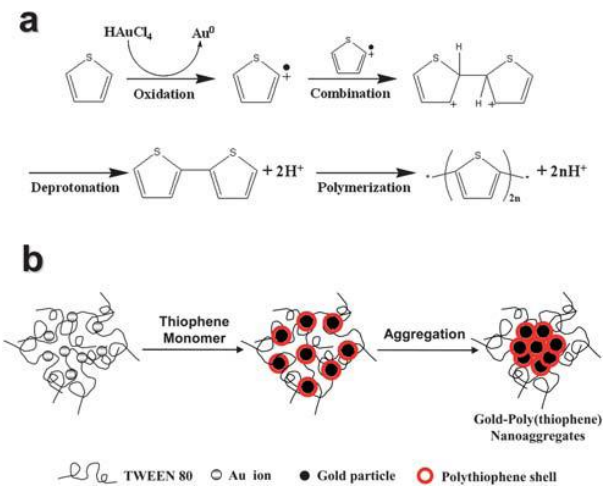

Fig.1 (a) Reaction mechanism of oxidative polymerization of thiophene monomers via Au^{3+}-catalysis. (b) Schematic illustration of the mechanism for preparation of Au–PTh nanoaggregates.

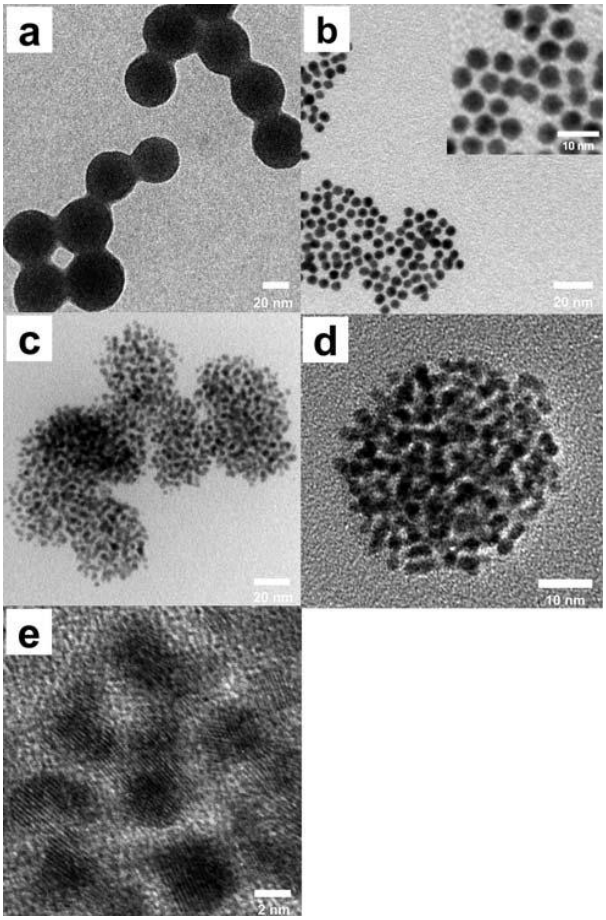

Fig. 2 TEM images of (a) pristine PTh NPs, (b) Au NPs, and (c) Au–PTh nanoaggregates, and (d and e) high-resolution TEM images of Au–PTh nanoaggregates.

The Influence of Thermodynamic Quality of Solvent on Properties of Molecular Nanoobjects

Alina Amirova [1], Elena Belyaeva [1], Anna Kovina [1], Elena Tarabukina [1], Natalia Sheremet'eva [2], Aziz Muzafarov [2], Alexander Filippov [1]

[1] Institute of Macromolecular Compounds of the Russian Academy of Sciences, Bolshoy, 31, Saint Petersburg, 199004 Russia
[2] Institute of Synthetic Polymer Materials of the Russian Academy of Science, Profsoyuznaya, 70, Moscow, 117393 Russia

aliram@rambler.ru

The present abstract is devoted to the investigation of hyperbranched macromolecules behavior dependence on thermodynamic quality of solutions.

In our work we study the hydrodynamic and conformational characteristics of hyperbranched polydi(allyl)carbosilanes with butyl (PCS-But) and tris-γ-trifluoropropyl (PCS-F) terminal groups and polydi(undecenyl)carbosilane (PCS-Und). All samples were characterized by equal degree of branching DB = 0.5. The dilute solutions of unfractionated polymers in toluene were examined by viscometry and light scattering methods. The intrinsic viscosity [η] and second virial coefficient A_2 values were determined in the range of temperature from 15 to 60°C. The hydrodynamic radius $R_{h[\eta]}$ magnitudes were computed using Einstein equation:

$$R_{h[\eta]} = \left(\frac{[\eta]M}{2.5\, N_A \frac{4}{3}\pi} \right)^{1/3}$$

Although rather significant changes of the A_2 magnitudes were found in the case of PCS-But, we did not see increase or decrease of intrinsic viscosity for hyperbranched PCS-But and PCS-Und.

It is expected the fluorinated substitutes can make the hyperbranched macromolecules more sensitive to thermodynamic quality changes. Our previous work [1] shows the role of thermodynamic quality of solvent in conformational and hydrodynamic properties of PCS-F. The decrease of molecular sizes and its asymmetry in poor solvent was found. We hoped to discover dependence of [η] and $R_{h[\eta]}$ on thermodynamic quality of solution under different temperature. However, PCS-F displayed the same behavior as unfluorinated PCS. This fact can be linked with relatively small temperature range, and the coil swelling effect could be observed at higher temperatures.

[1]. A.M. Muzafarov, A.P. Filippov et al. *Polymer Science, Ser. C.* **2010.** 52 (1) 70–78.

Colloidal Crystallization of Poly(*N*-isopropylacrylamide) Microgels

H. Takeshita, S. Nakano, M. Miya, K. Takenaka and T. Shiomi

Nagaoka University of Technology, Japan
takeshita@mst.nagaokaut.ac.jp

Introduction: Colloidal particles with monodispersed size distribution can form *crystal* at a volume fraction beyond a certain level. When colloidal particles are formed from thermosensitive gels such as poly(*N*-isopropylacrylamide) (PolyNIPA), colloidal crystallization can be caused by temperature-controlled reversible size change of the particles. In such systems, because gels have almost the same density with solvent, crystallization of microgel colloids can be a good model for colloidal crystallization of hard spheres in a microgravity condition. In this study, crystallization and glass transition behavior of PolyNIPA microgels were investigated by using ultraviolet-visible spectroscopy (UV-Vis), optical microscopy, and light scattering techniques.

Experimental: PolyNIPA microgels were synthesized by a precipitation polymerization technique. In the presence of sodium dodecyl sulfate (SDS), NIPA and *N*,*N*'-methylenebisacrylamide was polymerized at 40 °C using potassium persulfate as an initiator. The resulting aqueous microgel dispersion was dialyzed in deionized water for a week. The size and the size distribution of the microgel, which can be controlled by the amount of SDS, were measured by a dynamic light scattering technique. Colloidal crystallization behavior was measured by UV-Vis spectroscopy, in which crystal diffraction reduces intensity of transmitted light at a characteristic wavelength depending on lattice spacings of colloidal crystals.

Results and Discussion: The PolyNIPA microgels reduced their diameter with increasing temperature especially at around 40 °C, which coincides with the volume phase transition temperature of the ordinary PolyNIPA gels. The aqueous dispersion of the microgels with appropriate concentration formed colloidal crystal. The crystallization process was monitored by UV-Vis spectroscopy. Diffraction by the crystal structure formed causes absorption peaks at wavelengths corresponding to the lattice spacing. Crystallization temperature, T_c, and melting temperature, T_m, were determined from the behavior of the absorption peaks in cooling and heating processes. Concentration dependence of T_c and T_m is shown in Fig. 1. Based on this phase diagram, crystallization kinetics was investigated. Fig. 2 shows the double logarithmic plots of the time evolution of the degree of crystallization estimated from the peak heights of the absorption spectra. The slopes of the plots are about 2 for all T_c's, which coincides to the colloidal crystallization behavior of hard spheres under microgravity. Crystallization rate was estimated as an inverse of time for the transmission to decrease by 1%. In Fig. 3, T_c dependence of the crystallization rate is shown for microgel concentration of 4.53tw %. The bell-shaped dependence indicates that, the dispersion may become glassy state when quenched below 25 °C.

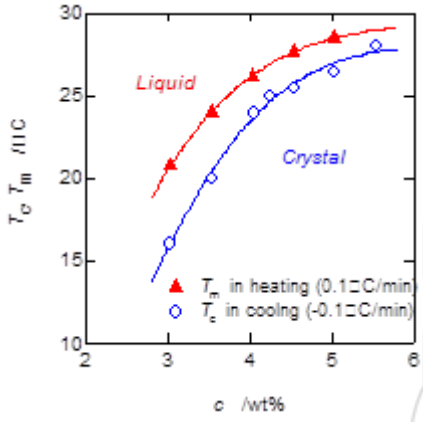

Fig. 1 Phase diagram of the aqueous polyNIPA microgel dispersion

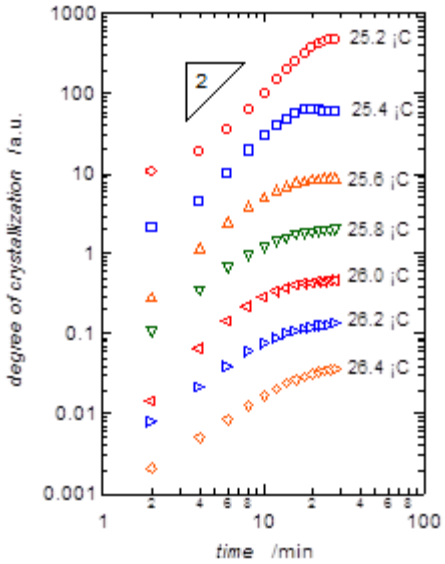

Fig. 2 Time evolution of degree of crystallization in isothermal crystallization.

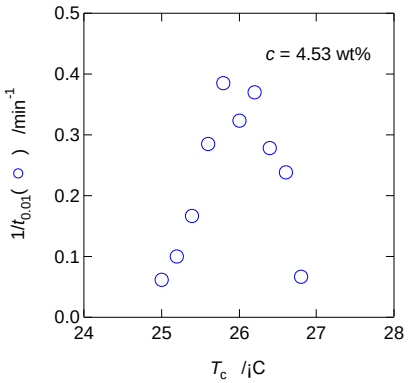

Fig. 3 T_c dependence of the crystallization rate

Effect of orientation on structure and thermal properties of constrained polypropylene nanocomposite fibres

Anton Marcincin, Konstantin Marcincin, Marcela Hricova, Anna Ujhelyiova, Eberhard Borsig

Slovak University of Technology in Bratislava, FCHFT, Institute of Polymer Materials, Radlinskeho 9, 812 37 Bratislava, Slovakia

anton.marcincin@stuba.sk

Introduction: The development of polypropylene (PP) composites and composite fibres containing inorganic fillers with nano-size of primary particles such as montmorillonites, boehmites, carbon nanotubes (CNT) and others is focused in particular on improving their mechanical properties [1], barrier properties, electrical conductivity and thermal stability [2].

Experimental: The commercially available kinds of polypropylene (PP), organically treated montmorillo-nites Cloisite 15A (C15A) and Cloisite 30B (C30B), boehmites Disperal 40 (D40), Disperal 60 (D60) and modified Disperal (DUN and DAM), further multiwall carbon nanotubes (MWCNT) Nanocyl 7000, as well as the non-reactive compatibiliser-dispersants based on polyoxyalkyl-enoxide and polyalkylsiloxane, were used in the experimental work. The PP multifilaments were prepared by spinning of PP and PP masterbatch blend using a laboratory spinning plant. The spinning temperature was 250-280°C. Fibres were drawn using a laboratory drawing machine at various draw ratios λ at a draw temperature of 120°C.

Method used: The DSC analysis was performed using Perkin Elmer DSC 7. The measurements were carried out with the cut fibres with length 1-2 mm using conventional method (CM) and with the fibres with constant length, which was achieved through winding of fibres on a small spool, later placed in a DSC pan – constant length (constrained) method (CLM) [3]. The Instron (Type 3343) was used for the measurements of the mechanical properties of fibres. The average factor of orientation of fibres (fα) was evaluated by sonic velocity measurements. Wide-angle scattering (WAXS) method was used for evaluation of total crystallinity Xα and the content of the mesophase Xm. Small-angle scattering (SAXS) method was used for evaluation of the d-spacing of organoclay in PP fibres.

Results and Discussion: Majority effects of nanofillers on supermolecular structure, thermal and mechanical properties of polypropylene fibres were very similar for layered silicates (plates), boehmites (more spherical) and CNT (fibrous) particles. To obtain high dispersion degree (exfoliation of silicates) the treatment with organic phase and/or suitable compatibiliser-dispersant was needed. Besides, the mechanical forces at drawing were helpful in this process (Figure 1). Similarly, the same conditions were convenient also for mechanical properties of fibres. The maximum tenacity and Young's modulus were achieved for nanofiller concentration about 0.1 wt% regardless of filler nature. DSC-CLM method showed as very sensitive for evaluation of thermal properties of oriented fibres. The melting temperature of constrained fibres significantly increased proportionally with orientation of fibres compared with CM method (Figure 2). It corresponds with their draw ratio (Figure 3). Nanofillers act as weak nucleation agents in PP; the highest effect was found for CNT. Unambiguous straight-line dependence was found for melting temperature vs. tensile strength (Young's modulus) of composite fibres (Figure 4). The analysis of the width and asymmetry of DSC-CLM thermograms related to non-uniformity of mechanical properties and processing are discussed in the paper as well.

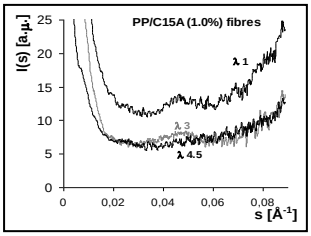

Figure 1 SAXS curves for evaluation the d-spacing of PP/C15A (1.0 wt%) composite fibres in dependence on draw ratio

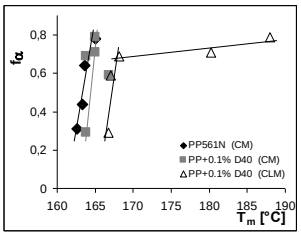

Figure 2 The correlation between the average factor of orientation fα and melting temperature T_m of the PP/D40 (0.1 wt%) composite fibres for various draw ratio

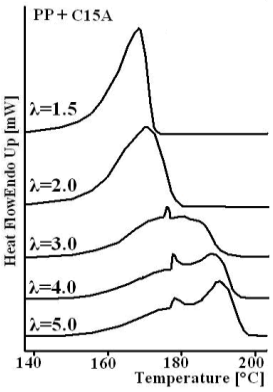

Figure 3 CLM – DSC melting thermograms of the PP/C15A (1.0 wt%) composite fibres

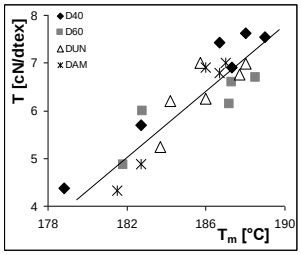

Figure 4 The correlation between the tensile strength T and melting temperature T_m of the PP/Boehmite composite fibres drawn for maximum draw ratio λ_{max}

References

[1] Chatterjee A., Deopura B.L.: Composites Part A: Applied Science and Manufacturing, Volume 37, Issue 5, May 2006, Pages 813-817

[2] S.C. Tjong: Mater. Sci. Eng. R 53, 2006, p. 73-197

[3] Samuels, R.J.: Journal of Polymer Science Part A-2: Polymer Physics, Vol. 6 (1968) No 12, pp. 2021 – 2041.

Polyurethanes from Agroindustrial Wastes: Pineapple Case.

Vega-Baudrit, J[1]*., Madrigal, S*[2]*., Benavides, L*[2]*., Sibaja-Ballestero, M*[2]

1. Laboratorio Nacional de Nanotecnología LANOTEC-CeNAT, Costa Rica
2. Laboratorio de Polímeros POLIUNA, Universidad Nacional, Costa Rica

e-mail: jvegab@hotmail.com

Abstract

Kinetics of thermal degradation of chitin and chitosan using thermogravimetric technique (TGA) in dynamic mode were studied.

TGA analysis was carried out in an inert atmosphere of nitrogen, using a range of temperatures from 30 to 600ºC, in addition to rapidly heating values (β) of 5, 10, 15, 20, 25 and 30 degree/min.

Kinetic models were applied degradation *Ozawa*, *Friedman*, *Kissinger* and *Broido*. For the degradation of chitosan all models applied presented good adjustment, on the other hand for the chitin behavior was different, as the only model that presented a good adjustment linear was that of *Broido*.

From the termogramas obtained was determined that the decomposition temperature is higher for the chitin that for the chitosan, this is due to the greater crystallinity and a lower level of polymerization of the chitin.

However, in the values kinetic, was obtained greater activation energy for the chitosan, a product of interbreeding led by the group amino free. In the implementation of the model of *Ozawa* for chitosan expressed the effect of compensation kinetics, so that to be an increase of the activation energy, the factor preexponencial increases, maintaining the value of the rate constant change.

Hybrid Block Copolymer Precursors Carrying Reactive Triethoxy Silyl Side Groups : Synthesis, Micellar Behaviour and Hydrolysis-Condensation

CG Gamys[1], E. Beyou[1], E. Bourgeat-Lami[2]

[1] Ingénierie des Matériaux Polymères, CNRS UMR5223,: Laboratoire des Matériaux Polymères et Biomatériaux, Université de Lyon, Université Lyon 1, 15 boulevard Latarget, F-69622 Villeurbanne, France
[2] Université de Lyon, Université Lyon 1, CPE Lyon, CNRS, UMR 5265, Laboratoire de Chimie, Catalyse, Polymères et Procédés (C2P2), LCPP group, 43, Bd. du 11 Novembre 1918, F-69616 Villeurbanne, France

beyou@univ-lyon1.fr

Among the several ways to obtain organic–inorganic hybrid materials, the sol-gel process, which relies on base- or acid-catalyzed hydrolysis and condensation reactions of metal alkoxides, is frequently used. This technique can be easily combined with organic polymerization to produce a variety of organic/inorganic nanostructured materials. Along this line, block copolymers with reactive alkoxysilyl groups has recently attracted much interest within the polymer community.[1-4] Herein, a series of poly(acryloxy propyl triethoxysilane)-*b*-poly(styrene) (PAPTES-*b*-PS) diblock copolymers of various compositions and molecular weights was prepared by nitroxide-mediated polymerization. We observed two clearly distinct T_gs for all the block copolymers, with values close to those of the corresponding pure homopolymer segments, suggesting that the PS and PAPTES blocks are phase-separated into two distinguished domains. Then, micelle formation was carried out by first dissolving the PAPTES-*b*-PS diblock copolymer in a solvent suited to both blocks (dioxane) and then adding methanol as a precipitant of the PS block. As seen in Figure 1a, the scattered light intensity suddenly increased when the methanol content reached a critical amount for which the PS block started aggregating.

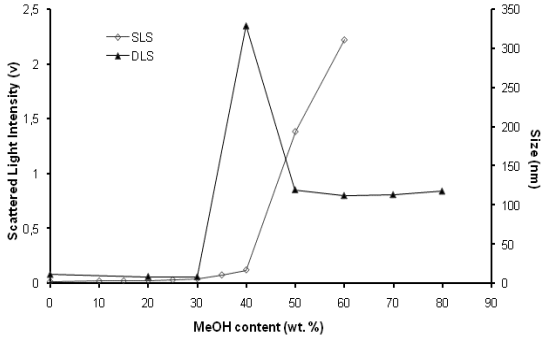

Figure 1. *a) Scattered light intensity as a function of added methanol content in $PAPTES_{91}$-b-PS_{175} / 1,4 dioxane solutions at different concentrations and b) Dynamic light scattering measurements and scattered light intensity as a function of added methanol content in a $PAPTES_{91}$-b-PS_{175} / 1,4 dioxane solution at a concentration of 2 mg.mL^{-1}.*

The micelle diameters, determined by dynamic light scattering, were in the range 50-109 nm depending on the PS molar fraction and the copolymer molecular weight. Regular spherical micelles were clearly seen in the TEM image (Figure 2).

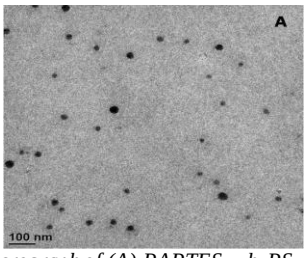

Figure 2. *TEM micrograph of (A) $PAPTES_{91}$-b-PS_{34} micelles in 40/60 (w/w) dioxane/MeOH solutions (C_0=30 mg.mL^{-1}).*

In order to permanently fix the micellar morphology of the aggregates, the PAPTES chains in the shell were cross-linked through hydrolysis/condensation of the alkoxysilyl groups in acidic medium (scheme 1).

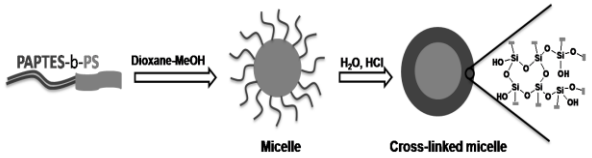

Scheme 1. *Crosslinking of the PATES-b-PS micelles through hydrolysis-condensation*

A decrease of the hydrodynamic diameter of 10-15 nm was observed after the cross-linking process whatever the copolymer composition which was tentatively attributed to shrinkage of the corona induced by cross-linking. Similar particle sizes were observed by TEM before and after cross-linking suggesting that the cross-linking reaction mainly involved silanol groups located at the periphery of the corona on polymer chain ends. SAXS and SANS experiments carried out on these cross-linked core-shell particles will be also discussed.

References

1. Brinker, C.; Scherer, G. Sol–gel science: the physics and chemistry of sol–gel processing, Academic Press, Boston 1990.
2. Wen, J.; Wilkes, G.L. Chem Mater 1996, 8, 1667.
3. Mellon, V.; Rinaldi, D.; Bourgeat-Lami, E.; D'Agosto, F. Macromolecules 2005, 38, 1591.
4. Gamys, C.G.; Beyou, E.; Bourgeat-Lami, E., J Polym Sci Part A 2010, 48, 784.

Mechanical and Thermal Properties of Nanocomposites based on Heterophasic Polypropylene/Multiwalled Carbon Nanotubes Functionalized with Itaconic Acid or Monomethylitaconate

M. Yazdani-Pedram [1], J. Miranda [1], R. Quijada [2], P. Toro [2], R. Benavente [3]

[1] Facultad de Ciencias Químicas y Farmacéuticas, Universidad de Chile, S. Livingstone 1007, Independencia, Santiago, Chile.
[2] Facultad de Ciencias Físicas y Matemáticas, Universidad de Chile, Santiago, Chile.
[3] Instituto de Ciencia y Tecnología de Polímeros, CSIC, Madrid, Spain.

mypedram @gmail.com

Introduction: Recently, there has been increasing interest in the use of PP as matrix for the preparation of PP/MWCNTs nanocomposites [1-5]. This is due to the fact that PP has a good balance of mechanical and thermal properties, as compared with other polyolefins, which has made it a fast growing commodity. It has been observed that the mechanical and other properties of PP/MWCNTs depend on the degree of the dispersion of the MWCNTs in the polymeric matrix [1-5]. Strong interaction between nanotubes results in the formation of large aggregated bundles preventing their homogenous dispersion in the polymer matrix and therefore composites with poor mechanical properties are obtained due to the poor load transfer from the polymer matrix to the nanotubes [1-5]. The modification of MWCNTs reduces these interactions allowing a better degree of dispersion of the nanotubes in the polymeric matrix. The aim of this work was to study the effect of the modification of MWCNTs with IA and its derivative MMI on the morphology, mechanical and thermal properties of PP/MWCNTs nanocomposites.

Materials and Methods: MWCNTs were Baytubes® 150 CP from Bayer, Germany. High impact polypropylene copolymer with melt flow index of 0.8 g/10 min at 230 ºC and 2.16 kg was obtained from Petroquímica Cuyo, Argentina. IA was perchased from Sigma-Aldrich, USA. MWCNTs was oxidized by refluxing for 1 hour in a mixture of 2:1 of HNO_3 (58%) : H2SO4 (98%) followed by washing with water and drying under reduced pressure. FTIR and TGA were used to characterize the functionalized nanotubes.

The nanocomposites were prepared by melt mixing using a Brabender-Plasticorder batch mixer at 190 °C during 30 minutes at a rotor speed of 75 rpm and under nitrogen atmosphere to prevent polymer oxidation. The resulting composite was grinded and then pressed at 200 ºC to form a plaque of 1.5 mm thickness. The specimens for tensile mechanical measurements were obtained from the plaque as 1.5 x 90 x 120 mm according to the ASTM D 638-95.

Results and Discussion: The oxidation of MWCNTs mainly resulted in nanotubes with hydroxyl groups as well as carboxyl groups. The oxidized nanotubes were functionalized by using either IA or MMI and characterized by FTIR and thermogravimetric analysis (TGA). New absorption bands from MMI Carbonyl ester and acid at 1744, 1726 and 1716 cm^{-1} were observed, respectively. The vinyl C=C absorption band of MMI is also observed at 1633 cm^{-1}. An absorption band due to the carbonyl groups from IA was also observed in the FTIR spectrum of the IA-functionalized MWCNTs at 1695 and 1710 cm^{-1}. Figure 1 shows TGA of unmodified, oxidized and functionalized MWCNTs with IA and MMI. Considerable weight loss is observed at around 200 °C corresponding to the loss of functional groups from oxidized and functionalized nanotubes. All nanocomposites showed better thermal stability than polypropylene due to presence of carbon nanotubes. This major stability was attributed to the capacity of the nanotubes to restrict the thermal agitation of the polymer as well as to the major stability and thermal conductivity of the carbon nanotubes. The mechanical properties of PP was improved when 0.5 wt.% of MWCNTs was incorporated, specially nanotubes functionalized with itaconic acid, where an increase of up to 40 % of the elastic modulus was observed.

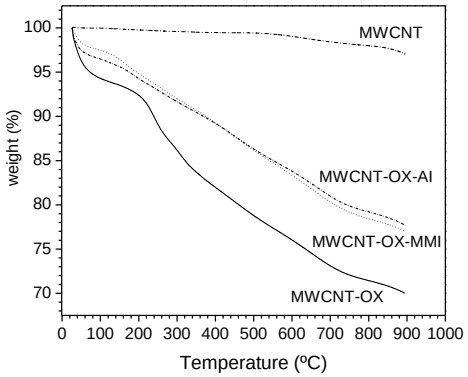

Figure 1. TGA thermograms of MWCNTs, oxidized MWCNTs and functionalized MWCNTs with IA and MMI.

Conclusions: The mechanical and thermal properties of PP were improved by incorporation of MWCNTs, especially those functionalized with IA, where a 40% increase of tensile modulus and higher thermal stability of PP was observed.

References:

1. S. Choi, Y. Jeong, G.-W. Lee, D. H. Cho, Fibers & Polym., 10(4), 513-518 (2009)
2. L. Liu, Y. Wang, Y. Li, J. Wu, Z. Zhou, C. Jiang, Polymer, 50, 3072–3078 (2009)
3. S. P. Bao, S. C. Tjong, Mat, Sci. Engin. A, 485, 508–516 (2008)
4. B. X. Yang, J. H. Shi, K. P. Pramoda, S. H. Goh, Comp. Sci. Technol., 68, 2490–2497 (2008)
5. M. Ganß, B. K. Satapathy, M. Thunga, R. Weidisch, P. Po¨tschke, D. Jehnichen, Acta Materialia, 56, 2247–2261(2008)

Acknowledgements: Financial support of Conicyt through Project FONDECYT 1090260 and Vicerectoria de Investigación y Desarrollo (VID), Universidad de Chile, are greatly appreciated.

Microspherical Aniline Oligomers and their Nitrogen-containing Carbon Analogues

Zuzana Rozlívková, Miroslava Trchová, Elena N. Konyushenko, and Jaroslav Stejskal

Institute of Macromolecular Chemistry, Academy of Sciences of the Czech Republic, Heyrovsky Sq. 2, 162 06 Prague 6, Czech Republic

E-mail: rozlivkova@imc.cas.cz

Introduction

Polyaniline is probably the most studied conducting polymer because of a variety of morphologies that are displayed [1], nanotubes being the most interesting [2–4]. Aniline oligomers are generally believed to be responsible for the self-assembly that guides the growth of polymeric structures [3]. The chemical nature of such oligomers is still open to discussion.

The oligomers are produced at the early stages of aniline oxidation at higher pH [4]. Only at lower pH < 2, polymeric products are produced in addition to oligomers originated earlier. The oxidations, which are started and finished above pH 2.5, produce aniline oligomers only [5].

Methods

Oligomers were dissolved in various solvents, dropped on silicon wafers and left to dry.

In the present study aniline oligomers prepared at alkaline conditions have been studied by FTIR and Raman spectroscopy in combination with UV–visible spectroscopy, gel-permeation chromatography, and electron microscopic techniques.

Conclusions

Aniline oligomers have ion-exchange and redox properties that can have a potential usefulness. In some cases the self-assembling is observed. We illustrate that they may also be used as carbonization precursors in the preparation of nitrogen-containing carbons.

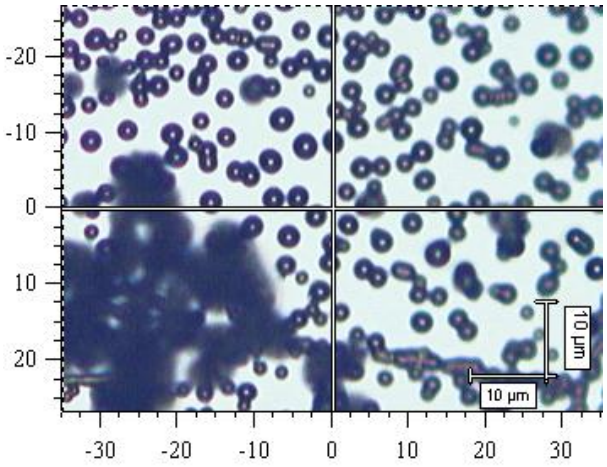

Figure 1. A drop of methanol-soluble part of oligomers evaporated on silicon support.

References

[1] Stejskal J., Sapurina I., Trchová M., *Prog. Polym. Sci.* 2010, *35*, 1420.

[2] Konyushenko, EN; Stejskal, J; Šeděnková, I; Trchová, M; Sapurina, I; Cieslar, M; Prokeš J. *Polym. Int.* 2006, *55*, 31.

[3] Stejskal, J; Sapurina, I; Trchová, M; Konyushenko, EN; Holler, P. *Polymer* 2006, *47*, 8253.

[4] Trchová, M; Šeděnková, I; Konyushenko, EN; Stejskal, J; Holler, P; Ćirić-Marjanović, G; *J. Phys. Chem. B* 2006, *110*, 9461.

[5] Stejskal, J; Sapurina, I; Trchová, M; Konyushenko, EN. *Macromolecules* 2008, *41*, 3530.

Porous titanium dioxide nanocomposite materials

O. Gaer, J. U. Wieneke, M. Ulbricht

Universität Duisburg-Essen, Lehrstuhl für Technische Chemie II, 45177 Essen, Germany
oxana.gaer@uni-due.de

To meet the future energy needs in an appropriate way and to prevent further climate damage, new environmentally friendly alternatives are in demand. Fuel cell technology provides an alternative energy; however, for the everyday consumer it has so far been too expensive. By linking fuel technology with nanotechnology innovations, it is intended to extend the life span of fuel cells and to reduce their production costs.

Here we present a concept for the synthesis and characterization of porous composite materials comprising nanoparticles (NPs) and styrene copolymers which are cross-linked with divinylbenzene (DVB). The materials are intended to be further pyrolyzed to yield new NP carbon composite materials. Here, polystyrene as reference and a copolymer obtained from 90 % styrene and 10 % 1,4-cyclohexanedimethanolmonovinylether were used. As starting material latex particles were synthesized by suspension polymerization of the monomers according to *Goodwin et al.* [1]. By swelling the latex particles with DVB and dilution with organic solvents and thinner (*Ugelstad* method [2]), it was possible to obtain porous copolymer particles. Pore sizes and pore size distributions and the resulting specific surface area were controlled by the systematic changes of process parameters (crosslinker and thinner composition). Characterization of the products was carried out by ATR-IR spectroscopy and BET measurements. In parallel to the polymer synthesis, dispersions of titanium dioxide NPs, for instance in toluene, were produced using an ultrasonic sonotrode. The quality of the dispersions was investigated using dynamic light scattering. The composites were prepared by impregnation of the styrene copolymers with the stable dispersion of titanium dioxide nanoparticles. The morphology of the materials and the distribution of titanium dioxide NPs were investigated with scanning electron microscopy. Overall, titanium dioxide nanoparticles could be incorporated into the porous polymer matrix in well defined distribution and relatively high loading. However, further studies are needed to find suitable pyrolysis conditions to achieve NP carbon composite materials for the use in fuel cell technology.

Acknowledgements. Financial support of the "NETZ" project in the frame of the program "NanoMikro + Werkstoffe.NRW" is gratefully acknowledged.

[1] Goodwin J., Ottewill R., Pelton R., *Colloid & Polymer Sci.*, **1979**, 257, 61-69.

[2] Ugelstad J., Kaggerud K. H., Hansen F. K., *Makromol. Chem.*, **1979**, 180, 737-744.

Nitrate remove from drinking water using polymer/MWCNTs nanocomposites

Mohammad Reza Nabid[1], Roya Sedghi[1,2], Roghayye Sharifi[1] and Nayerehossadat Mousavi Rad[1]

[1]Department of Chemistry, Faculty of Science, Shahid Beheshti University, 1983963113 Tehran, Iran
[2]Department of Chemistry, School of Sciences, Alzahra University, Vanak, Tehran, Iran

m-nabid@sbu.ac.ir

Introduction:

The nitrate ion in groundwater is becoming an environmental problem of major concern due to its high toxicity that causing cancer and nethemoglobinemia [1,2]. The important sources of nitrate can be inorganic fertilizer, industrial and sanitary waste waters, vegetable residues and compost, as well as rainfall and spontaneous nitrification of atmospheric nitrogen by nitrification bacteria. The dissolved nitrates filtrate through the ground by rainfall or irrigation and contaminate phreatic waters that feed wells from which drinking water is taken. Nitrates consumed with drinking water can be converted into nitrites in human body and may cause health problem. The increasing rigorousity of the drinking water quality standard, 50 mg/L in the European Union or 25 mg/L in USA, generates the urgent need to develop a new technology for nitrate removal from aqueous solutions. Recently, the catalytic reduction of nitrate by platinum and palladium metals is attracting considerable interest [3] **Experimental and Methods:**

The nanocomposites of polymers/MWCNTs were synthesized via in situ chemical oxidation polymerization method. These nanocomposites synthesized in different mass proportions of monomer to MWCNTs.

Results and Discussion:

In this research, we prepared nanocomposites of multiwalled carbon nanotubes (MWCNTs) with different polymers (such as: polyaniline (PANI), polypyrrole (PPY), poly(1,8-diaminonaphthalene) (poly(1,8-DAN)), poly (3,4-ethylenedioxythiophene) (PEDOT)) and poly (vinyl pyridine) (PVP), as effective and reusable nanocomposites for nitrate removal from drinking water. The nitrate removed from water with toxic concentration using ion-exchange mechanism with synthesized polymers counter ions without any toxic byproducts. We used different dopants as polymers counter ions and results shown that effective exchange of nitrate with Cl^- ions.

The different experimental parameters such as pH of the sample, polymers ion-pairs or dopants, temperature, nanocomposite loading, and ratio of polymer versus MWCNTs in nanocomposites, affect the amount of nitrate removal.

In order to examination of different nanocomposites in nitrate removal, every nanocomposite with different proportion in mass of polymer/MWCNTs was used. Results shown that effective nanocomposite with lower concentration of polyaniline is 3:1 and 4:1 nanocomposite. Since the pH of the aqueous solution is an important analytical factor in nitrate ions removal, the influence of pH on removation was examined in the pH range of 2-12 for each nanocomposite.

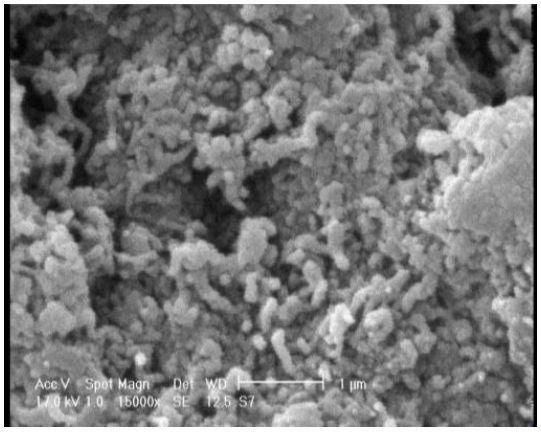

Fig. 1. SEM image of PANI/MWCNTs nanocomposite in 3:1 proportion.

In nanocomposite with higher concentration of PANI more remove percent has never been seen. For optimization of other factors that affecting nitrate removal the 3:1 portion selected because of higher physical stabilization in reusing for several times. In higher polymer concentration in nanocomposite the processability shows decrease.

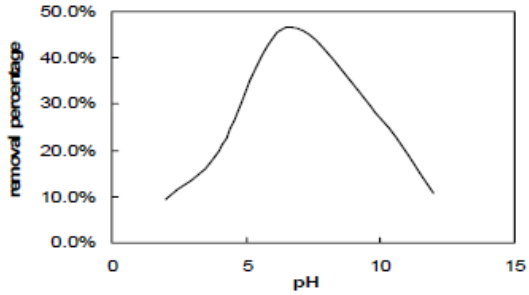

Fig. 2. Effect of water acidity on nitrate removal percent with PANI/MWCNTs.

Since the pH of the aqueous solution is an important analytical factor in the nitrate ions removal, the influence of pH on removing was examined in the pH range of 2-12 for each nanocomposite. The effect of solution acidity was investigated under prior found optimum condition. The results for PANI nanocomposite are shown in figure 2. It is obvious that the best removal of nitrate was done in pH= 6.5.

Conclusions:

The better performances explain by high degree of doping for PANI that allows the more exchange between nitrate and dopant anion of the conducting polymer.

References:

1. A. Pintar, Catal. Today 77(2003)451.
2. L.W. Canter, Nitrates in Groundwater, CRC Press, Boca Raton, 1996.
3.I. Dodouche, D. Pereira Barbosa, M. Rangel, F. Epron, Appl. Catal. B: 93 (2009) 50.

Spherulite Growth Rate in Polypropylene/Silica Nanoparticle Composites: effect of particle Morphology and Compatibilizer

H. Palza[1], *J. Vera*[1], *M. Wilhelm*[2], *P. Zapata*[3]

1 Departamento de Ingeniería Química y Biotecnología, Facultad de Ciencias Físicas y Matemáticas, Universidad de Chile, Beauchef 850, Santiago, Chile.

2 Institut für Technische Chemie und Polymerchemie, Karlsruhe Institute of Technology (KIT), Engesserstrasse 18, 76131 Karlsruhe, Germany

3 Grupo Polímeros, Facultad de Química y Biología, Universidad de Santiago, Av. Alameda Libertador B. O'Higgins 3363, Santiago, Chile.

hpalza@ing.uchile.cl

By adding small amounts of nanoparticles relevant modifications of the polymer behaviour can be obtained justifying the extraordinary research in the field of nanocomposites during the last years [1]. It is well known today, although not completely understood, that these fillers can change the main polymer properties such as: crystallization, mechanical strength, electrical and thermal conductivity, melt processing, permeability, thermal degradation, and viscoelasticity, among others [1,2,3]. In this context, the addition of spherical silica nanoparticles modifying the crystallization and crystal morphology of the polymer matrix is highlighted as any final property of the material depends on these characteristics.

Despite several articles showing that silica nanoparticles produce both faster crystallization rates and an nucleating effect, an opposite effect has been recently published with outstanding consequences in the polypropylene properties [4,5]. Nitta et al. showed that the spherulite growth rate is drastically reduced when silica nanoparticles are added becoming zero at higher filler content [5]. These results stress the need of more studies about how the kind of nanoparticles and its dispersion affect the morphological behaviour of the matrix.

The main goal of the present article is to study the effect of adding spherical and tube-like silica particles on the spherulite formation of polypropylene under isothermal conditions. The effect of the particle size and morphology, and of the presence of a compatibilizer is further characterized.

Spherical (15 and 80 nm) and tube-like silica nanoparticles were melt blended with an isotactic polypropylene matrix and its effect on the isothermal spherulite growth rate was analyzed by polarized optical microscope. The addition of low amount (~ 1 wt%) of either 15 nm spherical or tube-like particles raises the spherulite growth rate and the nucleation density (see Figure 1), the latter in more than one order of magnitude. Samples prepared with silica spheres of 80 nm otherwise do not show any change in the crystallization behaviour. By adding a compatibilizer, both the nucleation density and the spherulite growth rate of the pure polymer are increased. Noteworthy, although the nanoparticles do not further increase the nucleation density of the polypropylene/compatibilizer blend, independent of its form and size, they cause a decrease in its spherulite growth rate. Therefore, the kind of nanoparticles and the compatibilizer are relevant variables controlling the spherulite formation processes of polypropylene composites.

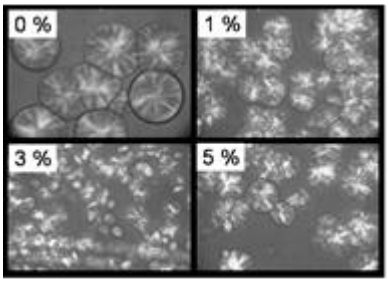

Figure 1. Optical micrographs showing the nucleating effect of S15 particles on polypropylene crystallization at 135 ºC. The number in the left-up corner represents the filler content in wt%.

Based on our results, we can conclude that by adding silica nanoparticles is possible to modify the spherulite growth of a polypropylene under isothermal conditions. The size and aspect-ratio of these particles are relevant variables controlling the crystallization processes.

Acknowledgments

The authors gratefully acknowledge the financial support of CONICYT, project FONDECYT 1100058. It is also expressed the thanks to Dr. R. Quijada for the support and discussions during this research.

References

1.- D.R. Paul, L.M. Robeson. Polymer 2008,49,3187.
2.- H. Palza, B. Reznik, M. Kappes, F. Hennrich, I.F.C. Naue, M. Wilhelm. Polymer 2010,51,3753.
3.- H. Palza, R. Vergara, P. Zapata. Macromol. Mat. Engin. 2010,295,899.
4.- K. Asuka, B. Liu, M. Terano, K. Nitta K. Macromol. Rapid Commun. 2006,27,910.
5.- K. Nitta, K. Asuka, B. Liu, M. Terano. Polymer 2006,47,6457.

Supramolecular Assembly of End-functionalized Polymer Mixture Confined in Nanospheres

June Huh,[1] *Cheolmin Park*,[1] *Won Ho Jo*[2]

[1]Department of Materials Science and Engineering, Yonsei University, Seoul, Korea
[2]Department of Materials Science and Engineering, Seoul National University, Seoul 151-742, Korea

junehuh@yonsei.ac.kr

Introduction: Supramolecular assembly of functionalized polymers, capable of forming block copolymer-like molecular clusters, has emerged as a promising alternative for creating nanoscopically ordered structures. Here, we demonstrate that nanospheres, which have intriguing internal nanodomains and controllable surface functionality, can be fabricated by supramolecular assembly of complementarily end-interacting two species of mono-end-functionalized polymers using the self-organized precipitation (SORP) method.[1,2] An exotic internal morphology, hierarchically organized structure of perforated spherical layers, was formed inside the nanosphere prepared from the stoichiometric mixture of the end-functionalized polymers, which is due to the formation of diblock-like supramolecules and their packing frustration in the spherically confined nanospace. When the mixing ratio of the two end-functionalized polymers differs from the stoichiometric ratio, the nanoparticle surface is enriched with excess of unpaired functionalized groups, which therefore provide us with a useful way to precisely control the surface functionality of the nanoparticles.

Materials and Methods: Our method for preparing nanospheres is based on the SORP of mono-end-sulfonated polystyrene (SPS) and mono-end-aminated poly(1,2-butadiene) (APB) at room temperature. A mixed solute consisting of SPS (M_n=10.5 kg/mole, polydispersity index =1.05) and APB (M_n=15.0 kg/mole, polydispersity index =1.05) with a weight fraction of SPS (Φ) is first dissolved in tetrahydrofuran (THF) chosen as a good solvent for both polymers. Subsequently, water drops are slowly added to the end-functionalized polymer solution, which provides a driving force for the polymers to form temporal aggregates nearby each of water droplets. The formation of these fluctuating, temporal aggregates become stabilized more and more by the steady addition of water droplets and the simultaneous evaporation of volatile THF. While the added water gradually becomes a majority solvent, the minority THF solvent, miscible both with polymers and water, plays a role similar to colloidal stabilizer preventing polymer aggregates from excessive growth. During this gradual change of solvent quality leading to the polymer assembly into nanospheres, the 1:1 end-associations between SPS and APB chains occur due to strong ionic interaction between a proton-donating sulfonic acid group of SPS and a proton-accepting amino group of APB ($SO_3^-\cdots NH_3^+$), which determines the morphological structure within the nanoparticle in combination with other interactions including the nonspecific repulsion between styrene and butadiene segments.

Results and Discussions: The transmission electron microscopy (TEM) images of the nanoparticles prepared from mixed solute of SPS and APB with Φ = 0.40 and their cryotommed section are shown in Figure 1, where the darker phase corresponds to the APB domains stained by osmium tetraoxide (OsO_4) and the lighter phase to SPS domains. The TEM image and its simulated morphologies reveal that the dashed circle-like SPS domains shown in Figure 1 are spherical layers perforated by several APB struts connecting concentric APB layers at different level.

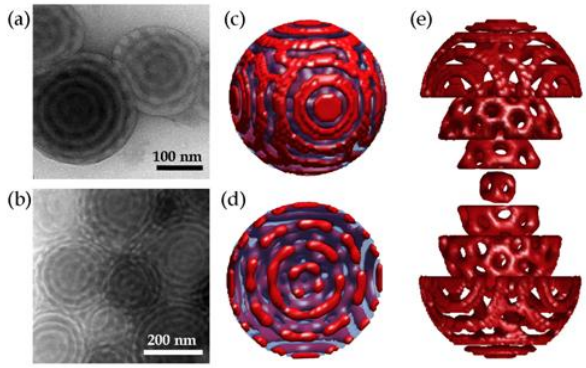

Figure 1. Nanoparticles prepared from mixed solute of SPS and APB with Φ = 0.40. (a) TEM image of the produced nanoparticles and (b) TEM image of cryo-sectioned nanoparticles. (c) The simulated nanosphere and (d) its internal structure represented by a radial cross section. Regions of high density of SPS and APB are colored opaque red and transparent blue, respectively. (e) The decomposed representation of hierarchical perforated spheres.

Conclusions: Nanospheres comprised of complementarily end-interacting two species of polymers have been fabricated by the SORP method. An exotic internal morphology, hierarchically organized perforated spheres, was formed inside the nanosphere prepared from the stoichiometric mixture, resulting from the formation of diblock-like supramolecules and their packing frustration in the spherically confined nanospace.

References

1. H. Yabu, T. Higuchi, K. Ijiro, M. Shimomura *Chaos 15*, 047505 (2005).
2. T. Higuchi, A. Tajima, K. Motoyoshi, H. Yabu, M. Shimomura *Angew. Chem. Int. Ed. 48*, 1-5 (2009).

Graphene-wrapped conductive nanospheres

Sang-Soo Lee[1], Kyunghee Kim[1], Sang Ah Ju[1,2]*

[1] Polymer Hybrid Center, Korea Institute of Science and Technology, Seoul 136-791, Korea
[2]Yonsei University, Department of Chemical Engineering, Seoul 120-749, Korea

(s-slee@kist.re.kr)

Introduction: As well known, graphene, two-dimensional graphite, exhibits remarkable, electronic properties that quantify it for applications in future optoelectronic devices. To date, most of researches concerning the applications of graphene have been poured into the evaluation of natural properties of graphene itself, mass production of well crystalline graphene nanosheets or the two-dimensional device applications, such as transparent conductive films. Recently, our group found that the simple modification of graphene surface without loss of the conductivity can be adapted to fabricate three-dimensional functional materials such as conductive micro/nanospheres, which have been highly requested due to the environmental problems induced by highly toxic chemicals during the metal-plating process.
Herein, we present a simple approach for the fabrication of monodisperse nanospheres with outstanding electro-conductivity, as an alternative to the conventional metal-plated conductive particles.

Materials and Methods: Negatively charged graphene sheets were prepared through chemical oxidation of expandable graphite flake (Graftech) using a modified Hummer's method, followed by reduction using hydrazine hydrate as noted in references [1, 2]. Positively charged polystyrene beads of two different sizes (cationic microsphere and nanosphere) were prepared by emulsifier-free emulsion copolymerization. The mixture of styrene (10.42 g, 0.1 mol) and MATMAC (0.05 mol) were added into the reactor, followed by addition of 0.1 g KPS dissolved in 10 ml deionized water. The polymerization was carried out under mechanical stirring at 400 rpm under nitrogen atmosphere at 70 oC for 8 hrs. Products were purified through dialysis. Positively charged PS spheres (0.08 g) and negatively charged graphene sheets (0.05 g), respectively dispersed in deionized water, were mixed on sonicator for 30 min and then were vigorously shaken for 12 hr at room temperature on vortex shaker (Maxi Mix II, Fisher). Subsequently, the coagulates were collected by centrifugation of 5000 rpm and dispersion in water at least three times, and finally dried on freeze dryer for 24 hrs.

Results and Discussion: In order to obtain hybrid spheres of electrical conductivity, assembly of graphene sheets containing anion charge with cationic polymer spheres (micro and nanospheres, respectively) was performed by simply mixing them together in deionized water medium. We found a spontaneous change of dispersion from respective colloidal states of graphene and polymer spheres to irreversible agglomerates, indicating the formation of graphene-polymer sphere assembly accompanied by spontaneous anion-cation coupling reaction. Electron microscopic examination was performed to analyze the assembly behavior between polymer spheres and graphene sheets. In Figure 1, SEM images obviously show that the polymer spheres were successfully decorated by graphene nanosheet patch. While the pristine colloidal polymer spheres don't exhibit any notable feature except smooth surface, the surface of polymer spheres after assembly with graphene sheets showed very rough texture, as shown in Figure 1(a), implying that there are adsorbed layer of texturing molecules on polymer spheres. In this system, the ionic interaction drove the graphene sheet to anchor on the polymer surface. Deposition of graphene sheets on polymer sphere is supported by transmission electron microscopy examination, showing that thin layer of graphene sheet was well deposited on the surface of polymer spheres to thickness of 5 to 16 nm, as shown in Figure 1(b).
In order to assess the electrical conductivity of graphene-wrapped hybrid spheres, the suspension of hybrid spheres in ethanol medium was sprayed on a fresh slide glass heated at 150 ^{o}C to form a translucent cell coated with the hybrid spheres, which exhibited an electrical conductivity of 1.33 S/m under four-probe method. For comparison, a pristine graphite-coated cell was fabricated and evaluated with the same procedure, showing an electrical conductivity of 15.5 S/m. The somewhat lower electrical conductivity of the cells made with graphene-wrapped hybrid spheres might be possibly due to the partial lack of ohmic contact in the cell as well as the electronic interfacial change. Nevertheless, it can be told that the electron transfer behavior found in graphene sheets is preserved even after the formation of hybrid with insulating polymer spheres.

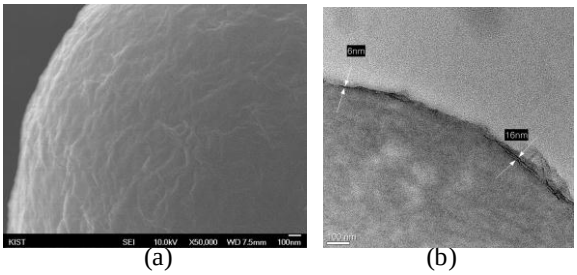

(a) (b)

Figure 1. Electron microphotographs of polymer spheres coated with graphene; by (a) SEM and (b) TEM

References

1. D. Li, M. B. Müller, S. Gilje, R. B. Kaner, G. G. Wallace, *Nat. Naotech*. **2008**, 3, 101.
2. W. S. Hummers, R. E. Offeman, *J. Am. Chem. Soc*. **1958**, 80, 1339.

Behavior of ZrO_2/SiO_2 Nanoparticles on the Properties of the PVC/ABS Blend

M.A. Reyes-Acosta[1], A. Flores-Vela[1], J.L. Rivera-Armenta[2], A.M. Torres-Huerta[1], M.A. Domínguez Crespo[1]

[1]Centro de Investigación en Ciencia Aplicada y Tecnología Avanzada-IPN, Carretera Tampico-Puerto Industrial Km. 14.5, C.P. 89600, Altamira, Tamps., MÉXICO.

[2]División de Estudios de Posgrado e Investigación, Instituto Tecnológico de Ciudad Madero, Juventino Rosas y Jesús Urueta S/N Col. Los Mangos, C.P. 89440, Cd. Madero Tamps., MÉXICO.

afloresv@ipn.mx

Introduction

The inorganic nano-sized particles (1 to 20 nm) into polymer matrix at very low concentrations (<10 wt%) can lead to obtain composite materials with superior properties[1]. The nanoparticles have high surface area and develop more contact with the polymer matrix[2]. In this study, nanoparticles, ZrO_2/SiO_2 were introduced in the blends PVC/ABS (70/30) in order to obtain a composite material of high mechanical performance.

Materials and methods

Nanoparticles of zirconia/silica (ZrO_2/SiO_2) ratio at 80:20 were synthesized by the sol-gel process. Later it was incorporated into the PVC/ABS (70/30) polymer matrix to obtain a composite material. Nanoparticles treated at 400 °C were added to the matrix PVC/ABS (70/30) at 1, 2.5 and 5 wt% and processed in a two-roll mill. The film was obtained compression molded. Subsequently, we studied by DSC and DMA, tensile test and Izod impact strength.

Results and Discussion

By DSC showed a glass transition temperature (T_g) in the blend PVC/ABS, approximately 125.24 °C, corresponding to the rigid SAN phase present in the ABS and a melting temperature (T_m) to 188.4 °C. The decomposition temperatures (T_d) of PVC and ABS were observed at 282.85 and 305.64 °C, respectively. The variation of T_g of all material PVC/ABS-ZrO_2/SiO_2 (80/20) with respect to the T_g of the matrix PVC/ABS pure was at least ± 1 °C. Also the T_d was great than PVC/ABS pure matrix with 1%. However the events greater T_m shows the concentration effect when reach 5% of ZrO_2/SiO_2. In DMA, the use *E''* (loss modulus) and tan δ (loss factor) decided displays maxima at T_g[3]. In between-mixtures can be T_g detected two, one from each phase, but it shows shifts in their positions if some miscibility is present[4]. Figure 1 show the pattern of loss factor for mixing PVC/ABS (70/30) with ZrO_2/SiO_2 to different percentages and heat treated at 400 ºC. Noted that is the introduction of ZrO_2/SiO_2 (80/20) treated at 400 °C, produces an increase in T_g and at the same time a approach to the T_g present in the polymer matrix, improving the homogeneity in the composite.

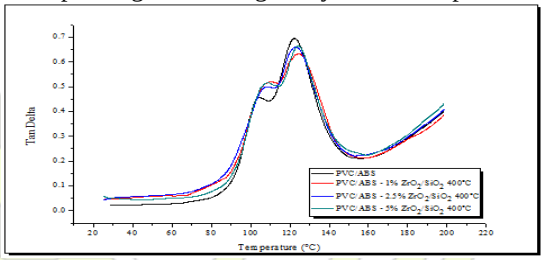

Figure 1. Loss factor matrix PVC/ABS (70/30) with ZrO_2/SiO_2 treated at 400 ° C.

Figure 2 show the tensile and impact strengths of the PVC/ABS with ZrO_2/SiO_2 to different concentrations. Figure 2(a) indicated the maximum resistance and the matrix increases slightly to 2.5% of the system. This can be due to greater compatibility between phases promoted by the system. With 1% is not a significant change in the maximum resistance of the matrix. On the other hand with 5% decrease slightly possibly due to overcrowding of the system ZrO_2/SiO_2 in the matrix.

Figure 2(b) show the impact strength of PVC/ABS blends as a function of ZrO_2/SiO_2 content. It could be seen that with the presence of 1% of the system treated at 400 °C gives an increase in impact strength with 258.50 J / M. The difference was 66.23% compared to the resistance of the pure matrix, indicating that there is a better interaction with the phases with the presence of 1% ZrO_2/SiO_2. It was noted that the presence of this system, the impact gradually decreased strength with more incorporation of ZrO_2/SiO_2.

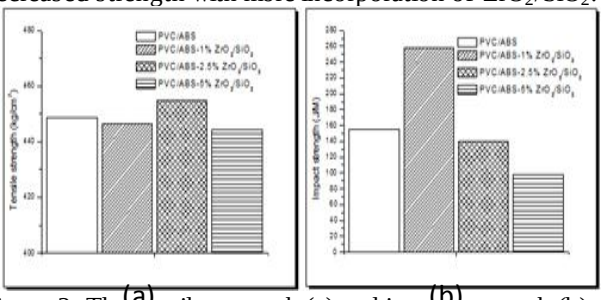

Figure 2. The tensile strength (a) and impact strength (b) of ABS/PVC (70/30, wt%) blends as a function of ZrO_2/SiO_2 content treated at 400 ° C.

Conclusions

According to the results of the DMA, the ZrO_2/SiO_2 system can act as a coupling agent for mixing PVC/ABS (70/30).A small amount of system has an influence on the tensile strength and impact. The tensile and impact of the blends increases with 1% of the system treated at 400 ° C due to the good dispersion and high degree of interaction between the nanoparticle and the polymer matrix.

References

1. S. Varghese, J. Karger-Kocsis, Layered silicate/rubber nanocomposites *via* latex and solution intercalations. Polymer Composites, Springer Science+Busines Media, Inc. USA, (2005) 77

2. Bernd-Wetzel, Reinforcement of thermosetting polymers by the incorporation of micro and nanoparticles. Polymer Composites, Springer Science+Busines Media, Inc. USA, (2005) 45-46

3. L. H. Sperling, Introduction to Physical Polymer Science, John Willey and Sons, (1986) 236-238

4. S. Krause, in Polymer Blends, D. R. Paul and S. Newman, Ed., Academic Press, Vol. 2, (1978) 25-27

Coarse-Grained Molecular Dynamics Simulations of Nylon-6 Nanofibers

Alberto Milani, Mosè Casalegno, Chiara Castiglioni, Guido Raos

Dip. Chimica, Materiali, Ing. Chimica "G. Natta", Politecnico di Milano,
P.zza Leonardo da Vinci, 32 - 20133 Milano, Italy

alberto.milani@polimi.it

Introduction In recent years, the electrospinning technique has been shown to provide a promising route to the production of nanostructured polymeric materials and nanofibers in particular[1]. These nanofibres have found applications in many fields such as template materials synthesis, catalysis, active filtering, nanocomposites, cell growth, tissue engineering and controlled drug release. There is currently a lot of interest in gathering information about the properties and the internal structure of electrospun nanofibers. Experimentally, it has been found that these depend crucially on processing conditions and post-processing treatments. Molecular simulations (MD or MC) have already been successfully applied to this aim[2].

Materials and Methods Because of the large size of nanofiber model systems, we carried out coarse-grained (CG) MD simulations of nylon-6 (NY6) nanofibers by means of the GROMACS 4 package [3]. Using the MARTINI force field by Marrink et al.[4] for the description of all intermolecular non-bonding interactions, we represent NY6 as an alternating copolymer consisting of apolar (C1) and polar (P4) spherical beads, respectively representing the $-(CH_2)_4-$ and the $-CO-NH-CH_2-$ units. As for the intramolecular stretching and bending terms, we generated our potentials by Boltzmann inversion of an all-atoms simulation of a short NY6 model chain.

We simulated isolated NY6 nanofibers of different radii and infinite length by suitably adopting full three-dimensional periodic boundary conditions. Initially, the chains were fully extended along the fiber axis. The simulations have been carried out at different temperatures until the occurrence of melting and each nanofiber was subjected to a whole heating-cooling cycle.

Results and Discussion All the fibers show a qualitatively similar evolution as shown in the figure.

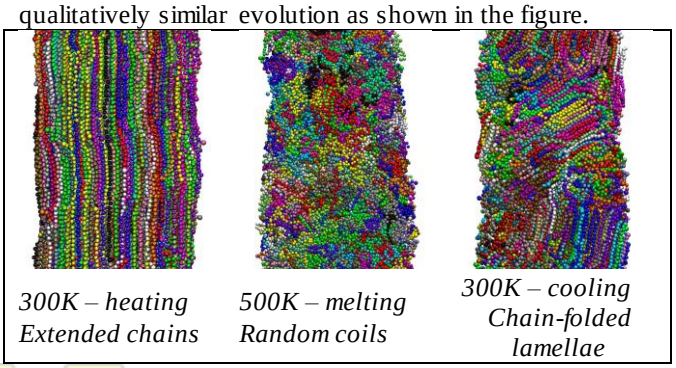

300K – heating Extended chains | *500K – melting Random coils* | *300K – cooling Chain-folded lamellae*

The initial configurations (extended chains) are retained almost completely when running the simulation at 300 K. The fiber surface itself is quite uniform and does not show any appreciable disordering during the simulation. When the temperature is raised up to 500 K, the fibers undergo a very substantial disordering: they loose their preferential orientation and adopt a random coil conformation, thus indicating a molecular level melting. A kind of re-crystallization takes place upon cooling to 300K, without leading back to the original oriented chain-extended order; indeed lamellar-like domains are formed by chain-folded molecules. The folds appear to be fairly regular and tight, without long loops between the crystallized segments and there seems to be a fairly well-defined characteristic thickness for the lamellae. These domains do not have a well-defined orientation but they are randomly oriented with respect to the fiber axis. Finally, at intermediated temperature, the fibers may be in a nematic liquid-crystalline state or in an undercooled amorphous state. The structural and conformational features observed can be confirmed quantitatively by analysing density profiles, radial distribution functions, end-to-end distances, radii-of-gyrations and P2 orientation parameter for all the systems investigated.

The dynamics of the polymer chains have been also discussed by analysing the mean-square displacements of the chains along the fiber axis: the polymer chains do not diffuse at 300 K, both in the original chain-extended state and in the final chain-folded one, thus confirming that these states are indeed "solid". At 500 K, the chains are fairly free to translate along the fiber axis, despite of their mutual entanglements while at intermediate temperature a "liquid-like" state is obtained. Furthermore, the dynamics depends strongly on the radius of the oriented fibers during heating: the chains in the thinnest fiber are much more mobile than those in thicker ones as a result of different dynamics at the core and on the surface of the fibers.

Conclusions A coarse-grained force field has been implemented for the simulation of nylon-6 nanofibers. Similarly to the experimental evidence, in our simulations the nanofiber structure depends markedly on the thermal history and phase transitions are observed during heating and cooling from a melted state. In particular, a recrystallization in chain-folded crystalline domains takes place upon cooling as observed experimentally [5].

References

[1] Li, D. et al. Adv. Mater. 2004, 16, 1151; Greiner, A. et al. Angew. Chem. Int. Ed. 2007, 46, 5670; Rutledge, G.C. et al. Adv. Drug. Del. Rev. 2007, 59, 1384; Reneker, D.H. et al Polymer 2008, 49, 2387.

[2]Curgul S. et al. Macromolecules 2007, 40, 8483; Buell, S. et al. Macromolecules 2009, 42, 4887; Vao-soongnern, V. et al. Macromol. Theory Simul. 2000, 9, 1; Vao-soongnern, V et al. Langmuir 2000, 16, 6757.

[3] Van der Spoel, D.et al.. *J. Comput. Chem.* **2005**, *26*, 1701

[4] Marrink, S.J. et al.. *J. Phys. Chem. B* **2007**, *111*, 7812; Monticelli, L.et al. *J. Chem. Theory and Comput.* **2008**, *4*, 819.

[5] Liu, Y. et al. *Macromolecules* **2007**, *40*, 6283

Testing 'Double Percolation' of Carbon Nanotubes in Copolymer Latexes by means of Reverse Addition Fragmentation Transfer Polymerisation.

Gavin TH Hill[1], *Guy Van Assche*[1], *Bruno Van Mele*[1], *Cor E. Coning*[2] *and Marie-Claire Hermant.*

[1] Vrije Universiteit Brussels (VUB), Physical Chemistry and Polymer Science (FYSC), Pleinlaan 2, B-1050 Brussels, Belgium.
[2] Technische Universiteit Eindhoven (TUE), Laboratory of Polymer Chemistry, 5600 MB Eindhoven, The Netherlands.

Gavin.hill@vub.ac.be

Introduction Polymer composites containing carbon nanotube (CNT) networks have undergone extensive study over the last few years[1,2]. Electronic conductance in these films relies on a connected network of nanotubes or by saturation of CNT's into the polymer matrix. Recent studies on latex systems and polymer blends have revealed that conductivity at lower NT loadings can be achieved by a concept known as 'Double Percolation'(figure 1) where the threshold is controlled by the composition and morphology of the polymers. In this way the percolation threshold may be reduced by preferentially dispersing the NT's into the more compatible minor phase.

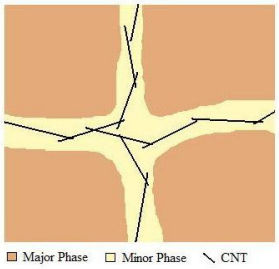

Figure 1 illustrating a percolated network in a copolymer.

This concept of double percolation is being applied to copolymers where the major and minor blocks can be produced in a latex (controlled morphology) using controlled radical polymerisation methods such as RAFT (Reverse Addition Fragmentation Transfer) followed by dispersion of the CNT's therein. Owing to studies by Van den Brande and Van Mele[3], Koning et. al.[4,5] and Hermant[6]; several candidate co-polymers have been identified, notably copolymers containing blocks of polystyrene (PS), poly-t-butylmethacrylate (PtBMA), polymethylmethacrylate (PMMA), polydimethylsiloxane (PDMS) and poly(2-dimethylamino)ethyl methacrylate (PDMAEMA).

Experimental Block Copolymers are prepared using emulsion RAFT polymerization and bulk RAFT polymerization. ATRP was carried out for some PDMAEMA-co-PS or PMMA copolymers.

Block copolymers and composites are analysed using Differential Scanning Calorimetry, Thermal Gravimetric Analysis and Gel Permeation Chromatography utilizing Universal Calibration and Triple detection. Latexes and solutions are analysed by Dynamic Light Scattering and UV-vis spectroscopy. Percolation thresholds are acquired by 2 and 4 point conductivity measurements on Nanocomposite thin films.

Discussion RAFT polymerization offers a flexible route to well defined block copolymers latexes. A significant challenge was using PDMS in emulsion systems, which was unrealistic for R-ATRP due to emulsion stability and catalyst/ligand problems. In the case of blocks where block A and block B are both miscible phases for CNT's 'Double Percolation' does not hold and a higher threshold is obtained (Figure 2).

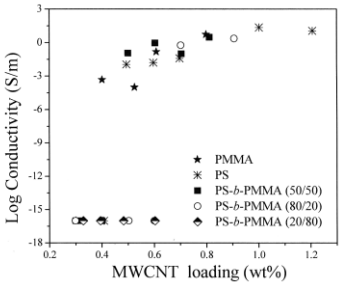

Figure 2 Conductivity measurements of films of PS, PMMA and PMMA-*b*-PS.

Co-polymer blocks consisting of PDMS-*b*-hydrophilic polymer can be used as a CNT dispersing surfactant. MWCNT's can be dispersed by these surfactants at lower concentrations than sodium dodecyl sulfate, SDS can have undesirable effects on compression molded films. Aqueous dispersion directly into a block-copolymer can offer an improved compatibility route to CNT dispersion into latexes or a direct route to nancocomposite polymer films.

References

[1] O. Breuer and U. Sundararaj, *Polymer Composites*, **2004**, 25(6), 630-645

[2] N. Grossiord, J. Loos, L. Van Laake, M. Maugey, C. Zakari, C.E. Koning and A.J. Hart, *Advanced Materials*, **2008**, 18, 3226-3234

[3] N. Van den Brande, B. van Mele, P Geerlings and G van Lier, (Thesis) *Experimental and Theoretical Investigation of novel (semi-)conducting nanocomposites based on carbon nanotubes*, **2009**, Vrije Universiteit Eindhoven.

[4] O. Regev, P.N.B ElKati, J. Loos and C.E. Koning, *Advanced Materials*, **2004**, 16(3), 248-251.

[5] N. Grossiord, H.E. Miltner, J. Loos, J. Meuldijk, B. Van Mele and C.E. Koning, *Chemistry of Materials*, **2007**, 19(15), 3787-3792.

[6] M-C. Hermant, L. Klumperman and C.E. Koning, (Thesis) *Manipulating the Percolation Threshold of Carbon Nanotubes in Polymeric Composites*, **2009**, Technische Universiteit Eindhoven.

Aqueous Microgels Modified by Wedge-Shaped Amphiphilic Molecules:Hydrophilic Microcontainers with Hydrophobic Nanodomains

Lei Li; Cheng Cheng; Xiaomin Zhu; Andrij Pich; Martin Möller

DWI at RWTH Aachen University, Aachen, Germany

Email: li@dwi.rwth-aachen.de, cheng@dwi.rwth-aachen.de, zhu@dwi.rwth-aachen.de,pich@dwi.rwth-aachen.de, moeller@dwi.rwth-aachen.de

Introduction: In the field of biology and pharmaceutics, various polymeric drug delivery and drug targeting systems are currently developed or under development in order to improve the specific delivery of drugs with low therapeutic index. In recent years, micelles self-assembled by amphiphilic polymers are the most used carriers for the encapsulation and transport of hydrophobic molecules[1].Meanwhile, the superior colloidal stability and flexible chemical composition of polymer-based microgelsalso attract more attention[2, 3]. Recentlywe developed a simple route to design hydrophilic microgels comprising inner hydrophobic nanodomains by complexationwithwedge-shaped amphiphilic molecules containingcomplementary functional groups[4]. Poly(N-vinylcaprolactam-co-acetoacetylethyl methacrylate) (PVCL/AAEM)-based microgel systems functionalized with vinylimidazole (VIm) groups were transferred into an organic medium, where they were neutralized by water-insoluble wedge-shaped sulfonic acid molecules. The loading of the wedge-shaped molecules into microgels can be controlled by varying the amount of imidazole groups integrated into the microgel network as well as the neutralization degree. In this work, a series of hydrophobic wedge-shaped sulfonic acid molecules with different alkyl chain length weresynthesized and used to modifythe PVCL/AAEM/Vimmicrogels. The structures as well as the uptake ability of the hydrophobizedmicrogels were addressed.

Materials and Methods: The synthesis of 4-N-[3',4',5'-tris-(dodecyloxy)benzamido]benzene-4-sulfonic acid (C12-H), 4-N-[3',4',5'-tris-(decyloxy)benzamido]benzene-4-sulfonic acid (C10-H) and 4-N-[3',4',5'-tris-(octyloxy)benzamido]benzene-4-sulfonic acid (C8-H)wasdescribedelsewhere[5].PVCL/AAEM/VImmicrogel was prepared using a literature procedure[6].VCL/AAEM/Vimmicrogelswith5mol-%vinylimidazolegoupswere separated from water bycentrifugationand dispersed in THF, where the complexationwith C12-H, C10-H and C8-Htook place. Afterwards the modified microgels were re-dispersed in water. Different amountsof Nile Red (0.97 mg/ml in a 1:2THF/acetone mixture) were added to eachmodified microgel solution (0.2 mg/ml in THF) to evaluate the dye uptake capacity.The dye uptake by the modified microgel particles was proved by means of fluorescence microscopy.The optical properties of the dye-loaded microgelsand the loading capacity were studiedusing UV-vis spectroscopy.Hydrodynamic diameter and zeta-potential were measured with Zetasizer Nano Series. Scanningforce microscopy (SFM) andtransmission electron microscopy (TEM) wereemployed to study the distribution ofhydrophobic domains formed by wedge-shaped moleculeswithin the microgel particles.

Results and Discussion: Independently on the degree of neutralization and the alkyl chain length all modified microgelparticles showed excellent colloidal stability and narrow size distribution after re-dispersion into the aqueous phase. Microscopicinvestigations confirmed the presence of nanodomains formed by wedge-shaped sulfonic acid molecules inside the microgel.At room temperature the microgelparticles modified with C12-Hat 100 % degree of neutralization exhibited smaller size than the original particles, while the modification with C10-H and C8-H increased the particle sizes.Note that after the complexationwith C12-H and C10-H the microgels lost completely their thermal sensitivity. However, the microgel modified with C10-H showed a slight linear shrinkage from the size of the C8-H microgel to the one with C12-H, while the temperature increased from 20 to 60 °C. This is possibly due to the different thermal behavior of the nanodomains formed by different wedge-shaped molecules. On the other hand, all the modified microgels lost their pH-sensitivity and exhibited strong negative surface charge even at degree of neutralization as low as 10 %. When hydrophobic Nile Red dyemolecules were loaded in the modified microgels, strong absorption and fluorescence in the visible range was observed. Meanwhile, all of them exhibited a clear temperature dependence of the maximum absorption wavelength.

Conclusions:A series of wedge-shaped sulfonic acid molecules with different alkyl chain length were incorporated into the PVCL/AAEM/Vimmicrogels. The modified microgelscontaining hydrophobic nanodomains in their interior could retain their colloidal stability in water. The varied structure affects both the particle size and the environmental sensitivity. The ability of the modified microgels to encapsulate hydrophobic molecules in water was confirmed by the uptake experiment of a hydrophobic dye monitored by UV-visspectroscopy and fluorescence microscopy.The dye-loaded microgel particles showed a thermochromism that allows them to be used as a temperature sensor.

References:

[1] Torchilin, V.P.*Journal of Controlled Release*, **2001**. 73(2-3),137-172.
[2] Nolan, C.M., et al. *Biomacromolecules*, **2006**. 7(10), 2918-2922.
[3] Wu, J.Y., et al. *Journal of Controlled Release*, **2005**. 102(2), 361-372.
[4] Cheng, C., et al. *Langmuir*. **2010**. 26(7), 4709-4716.
[5] Zhu, X.M., et al.*Chemistry – a European Journal*, **2004**. 10(16), 3871-3878.
[6]Pich, A., et al.*Macromolecules*,**2006**.39(22). 7701-7707.

Simulation of End-Coupling Reactions at a Polymer-Polymer Interface: The Kinetics and Mechanism of Interfacial Roughness Development

Anatoly V. Berezkin[1], *Daria V. Guseva*[2], *Yaroslav V. Kudryavtsev*[3]

[1]Max-Planck Institut für Eisenforschung GmbH, Max-Planck str. 1, 40237 Düsseldorf, Germany
[2]Physics Department, Lomonosov Moscow State University, Leninskie gory, 119991 Moscow, Russia
[3]Topchiev Institute of Petrochemical Synthesis, RAS, Leninsky prosp. 29, 119991 Moscow, Russia

yar@ips.ac.ru

Design of commercial polymer composites is based on combining different species to tailor material properties. One of the most promising strategies is the reactive compatibilization, when copolymers are formed *in situ* at interfaces just where they are needed to improve thermodynamic and mechanical properties of a composite.

In this work, an end-coupling between immiscible melts of two monofunctionalized macromonomers (Fig. 1) is modeled by dissipative particle dynamics starting from a flat interface and up to the formation of a mature microstructure (Fig. 2). The study is focused on understanding reasons of interface roughening and describing the subsequent self-assembling process. Influence of the reaction rate, chain length and polydispersity, blend composition and incompatibility of its components on the kinetics of copolymer formation and morphology development is investigated.

Simulations are performed with DPDChem freeware package [2] combining coarse-grained molecular dynamics with probabilistic treatment of chemical reactions. Time scales are attained that are two orders of magnitude as large as the interface saturation time making it possible to study the development of interface roughening in detail. Regimes of linear and logarithmic conversion growth are observed before the flat interface becomes unstable (Fig. 3), as predicted in theory [3].

It is demonstrated that overcrowding the interface with the copolymer product causing its phase separation plays the main role in spontaneous interface distortion. The instability leads to autocatalytic interface growth with exponential kinetics, when each new portion of the product creates more area for further reactions. It is followed by a slower terminal regime including formation and ripening of the lamellar microstructure. The late stage kinetics of end-coupling is strongly influenced by depletion of reactants and formation of ordered product layers. At certain conditions, it becomes asymptotically diffusion controlled in agreement with experimental data [4].

The role of diffusion is revealed in polydisperse systems, where the dependence of the copolymer average length on conversion goes through a minimum due to the competition of macromonomers of a same kind but different lengths. If the length ratio of dissimilar macromonomers is varied, self-assembling into different non-lamellar structures takes place. However, increasing this ratio results in a pronounced slowdown of the process at the autocatalytic stage, presumably, due to the formation of dense layers by longer blocks of the copolymer. Thus, an interfacial instability appears to be quite common in reacting melts of end-functionalized polymers but it does not ensure spontaneous formation of an ordered microstructure.

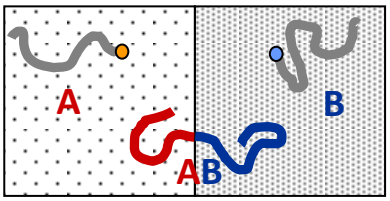

Fig. 1. Model melt of macromonomers A and B with an initially flat interface. Shown are active ends A (orange) and B (light blue), copolymer blocks A (red) and B (dark blue).

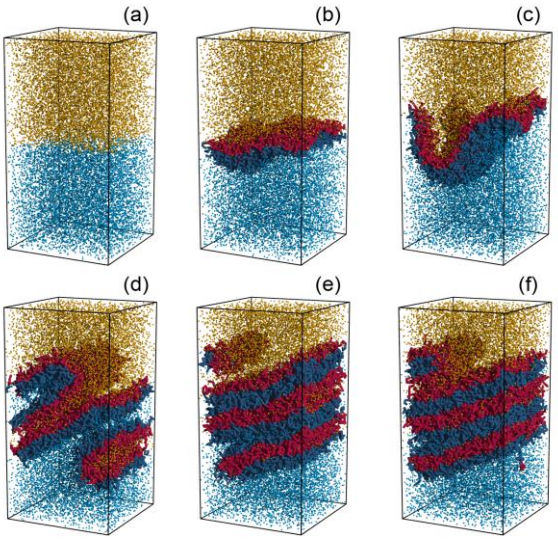

Fig. 2. Interface evolution: (a) the initial equimolar system, (b) saturated layer, (c) perturbed interface, (d-f) forming lamellar microstructure. The macromonomer lengths $N_A = N_B = 5$, reaction probability at contact $p_R = 0.25$, repulsion parameter $a_{AB} = 50$ [1].

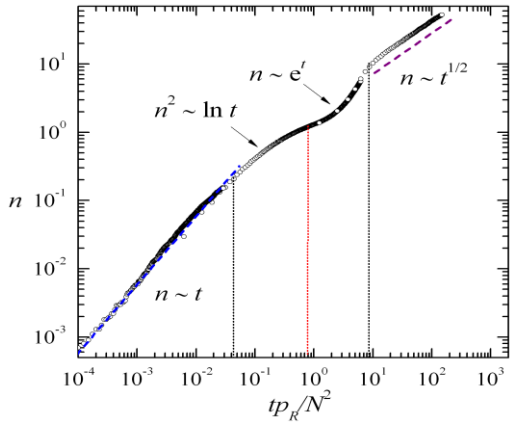

Fig. 3. End-coupling kinetics: the copolymer interfacial coverage n versus time t. $N_A = N_B = 2$, $p_R = 0.025$, $a_{AB} = 50$.

1. Berezkin A.V., Kudryavtsev Y.V. *Macromolecules* 2011, 44, 112
2. http://polymer.physik.uni-ulm.de/~khalatur/exchange/DPD_Chem
3. Fredrickson G.H., Milner S.T. *Macromolecules* 1996, 29, 7386
4. Yin Z., Koulic C., Pagnoulle C., Jérôme R. *Langmuir* 2003, 19, 453

Low temperature process of Inkjet-printed ZnO Oxide transistor

Sang Chul Lim[1], *Seong Youl Kang*[1], *Ji Young Oh*[1], *Seong deok Ahn*[1], *Hee-Ok Kim*[1], *and Kyoung Ik Cho*[1]

[1]IT Convergence and Components & Materials Research Laboratory, Electronics and Telecommunications Research Institute 138, Gajeongno, Yuseong-gu, Daejeon 305-700, Korea

On the way towards wide-spread flexible large-area electronics, several features are of particular interest. With focus on low-cost applications, the manufacturing requires high throughput, preferably realized by simple methods on large-area flexible substrates, for example spin coating, inkjet-printing or roll-to-roll techniques.

For solution processed ZnO field-effect transistor (FET) devices, the highest electron mobility values are currently 1.65 cm^2/Vs, however obtainable only after annealing at temperatures >300 ℃. Here we report our investigation on the formation, characterization, room temperature processing and inkjet printing behavior of a molecular precursor and adherence of such films in an FET device. ZnO nanoparticles were synthesized using a facile sonochemical method with modification of previously conditions. The ZnO active channel layer was patterned with drops using a piezo ink-jet device. A single piezo-dispenser with a 50 μm orifice was used for ink-jet printing.

The appropriate active channel region was successfully formed on the substrate at a resolution of 200 dpi and a head frequency of 300 Hz. For film synthesis, inkjet printed ZnO was annealed at 150 ^oC for 30 min in air. The TFTs device has a channel width (W) of 100 μm and a channel length (L) of 10 μm. The I_{DS}-V_{DS} curves showed well-defined transistor characteristics with saturation effects at V_G>-10 V and V_{DS}>-20 V for the inkjet printing ZnO device. The carrier charge mobility was determined to be 0.162 cm^2 V^1s^{-1} with FET threshold voltage of -4 V and on/off current ratio 10^4

Electrospinning of poly(γ-benzyl-L-glutamate) nanofibres: the effect of polymer molecular weight and spinning conditions in various solvents

Jana Svobodová, *František Rypáček*

Institute of Macromolecular Chemistry AS CR, Heyrovsky sq. 2, Prague 6, 162 02, Czech Republic

jsvobodo@imc.cas.cz

Introduction: Natural and synthetic polypeptides belong to important biocompatible and biodegradable materials, which are being studied for biomedical applications. While the natural polymers, including proteins such as gelatin, collagen and silk fibrinogen are difficult to electrospin, because of their high viscosity and low solubility in organic solvents, the synthetic poly(α-amino acid)s can be prepared with properties suitable for this type of processing. In the presented work, the electrospinning of poly(γ-benzyl-L-glutamate) (PBLG), as an example of versatile poly(α-amino acid)s with many options for post-processing modification of spun fibres, was studied.

Current electrospinning research effort has focused on understanding the formations and morphology of electrospun fibres depending on process parameters as well as on finding suitable application of nanofibrous matrix. The main experimental parameters for successful electrospinning include applied voltage, tip-to-collector distance, solution concentration, viscosity, solvent conductivity and surface free energy. The feasibility of electrospinning often depends on the molecular weight of polymers, concentration and viscosity of polymer solutions and these parameters have also a dominant effect on the diameter and morphology of resulting fibres [1,2].

In this work three solvents (tetrahydrofuran (THF), dichloromethane (DCM) and dichloromethane/ trifluoroacetic acid (DCM/TFA) mixture) were used to prepare PBLG nanofibres. Electrospinning of all solutions was carried out at identical conditions to reveal the effects of molecular weight, solution concentration and viscosity on the PBLG fibre formation and morphological features of the electrospun material.

Materials and Methods: The PBLG samples were prepared by the ring opening polymerization of γ-benzyl-L-glutamate *N*-carboxyanhydride in dry dioxane, initiated with sodium methoxide [3]. The degree of polymerization was determined by viscometry in *N*,*N*-dimethylformamide, using Mark-Howink equation $[\eta] = 2.9 \times 10^{-7} M_v^{1.7}$. Intrinsic viscosities [η] of PBLG solutions were measured using Ubbelohde viscometer VS2004 (Vistec, Czech Republic) at 25 °C.

The electrospinning was performed using a standard jet apparatus with stainless steel nozzle having an inner diameter of 0.6 mm and copper plate with aluminum foil as the collector. The electrospinning parameters such as flow rate, applied voltage and tip-to-collector distance were fixed at 1 ml/h, 12 kV and 12 cm, respectively.

The morphology of the electrospun fibres was observed with scanning electron microscope VEGA Plus TS 5135 (Tescan, Czech Republic).

Results and Discussion: The molecular weights of the synthesized PBLG samples were 50 000, 120 000 and 270 000 g/mol. Bead-free, uniform fibres were successfully prepared of all the tested solvents from the PBLG samples with higher molecular weight (120 000 and 270 000 g/mol). The highest molecular weight (270 000 g/mol) produces thinner fibres with narrower fibre diameter distribution at the lower concentrations. The PBLG with the lowest molecular weigh (50 000 g/mol) did not produce uniform fibres.

The intrinsic viscosity of PBLG solutions decreases in the order DCM, THF, DCM/ TFA mixture. This is due to the fact, that DCM and THF are known as helicogenic solvents, in which the rod-like α-helix PBLG molecules aggregate to larger head-to-tail complexes [4]. The higher PBLG viscosity in these solvents lead to formation of thicker electrospun fibres (average diameters were higher than 1 μm) with broader diameters distribution. As the content of TFA in DCM/TFA mixtures increases (DCM/TFA = 90/10, 80/20, 70/30), the head-to-tail aggregation of chains decreases with PBLG conformation changing single α-helix and random coil, the solution viscosity decreases and the electrospun fibres become thinner and more homogeneous.

This results indicate, that for successful preparation of PBLG nanofibres, not only the molecular weight, and solution concentration and viscosity is important, but also the chain conformation of PBLG in electrospun solutions must be considered.

Acknowledgment: Support from Academy of Sciences of the Czech Republic (Grant No: KJB400500904) and Research Centres Programme (MEYS, no.: 1M0538) is gratefully acknowledged.

References:

1. Gupta P., C. Elkins., T.E. Long, G.L. Wilkes, (2005) *Macromolecules* **37** (24):9211-9218
2. Shenoy S.L., W.D. Bates, H.L. Frisch, G.E. Wnek, (2005), *Polymer* **46** (10):3372-3384
3. Daly W.H., D. Poche, (1988), *Tetrahedron Lett*. **29**: 5859–5862

P. Doty, J.H. Bradbury, A.M. Holtzer, (1956) *J. Am. Chem. Soc*. **78**: 947

Investigation of Structure and Resistance of Electroless Copper Sulfide NanoParticles in Different Deposition Time

NSC 99-2221-E-036-002-MY3

Chi-Yuan Huang[*], *Yu-Min Fan*, *Ching-Shan Tsai*, *Keng-Yu Tsao* and *Chien-Pang Chang*

Department of Materials Engineering, Tatung University, Taipei, Taiwan

E-mail: cyhuang@ttu.edu.tw

In this investigation, the conductive filler of copper sulfide nanoparticles (CSNP) were prepared by the method of electroless deposition. Results showed that the CSNP transformed from flake-like columnar to ball shape from 0 minute to 60 minutes by SEM morphology analysis. The XRD analysis showed that the powder of CSNP fit in JCPDS card (PDF 11-0240) as Chevreul's salt at deposition time of 0 minute. When the deposition time increased from 20 to 40 minutes, the CSNP had the production of phase transitions. After deposition of 40 minutes, the phase of CSNP changed to Cu_2S, and the surface resistances of CSNP decreased from $>10^9$ Ω to 10.33 mΩ.

Experimental

The cupric source was from Copper Sulfate $CuSO_4 \cdot 5H_2O$ made by Wako, Japan. The weak reducing agent was Sodium Bisulfite $NaHSO_4$ made by Wako, Japan, and the strong reducing agent was Sodium thiosulfate $Na_2S_2O_3 \cdot 5H_2O$ made by Wako, Japan. The electroless bath carried on 75°C with nitrogen stir, separated to 0、20、40 and 60 minutes. After complete deposition, the precipitation carried on the steps of water wash、filtration and dry. The powder was measured by field emission scanning electron microscope (JEOL JSM-6700F and Hitachi S4700), the surface of the sample was coated with platinum and viewed with FESEM at voltage 3.0 KV. The powder was carried out by X-ray Diffractometer utilizing CuKα radiation of wavelength 1.54 angstrom. The resistance of powder was measured by 4-point-probe method (QT-50, Quatek, Taiwan), the precipitation of powder was pressed by 400 kgf/cm^2 as circular ingot (diameter 5mm) by compression machine.

Results and discussion

Fig.1 showed the SEM photographs of CSNP in different deposition time was from 0 minute to 60 minutes. The particle morphology at 0 minute was flake-like columnar shape of Chevreul's salt [1~2], and then 20 minutes the particle morphology was changed to laminated and ball-like shape coexisting. When the deposition time was 40 minutes, the flake shape was nearly vanished. At the deposition time of 60 minutes, the ball-like shape was decreased from 400 nm to 100 nm. Fig. 2 showed that the electroless plating time was longer, the phase of the copper sulfide was stronger. When the deposition time was 40 minutes, the phase was nearly Cu_2S. The powder at 0 minute fit in JCPDS card (PDF 11-0240), and powder at 40、60 minutes fit in with JCPDS card (PDF 02-1284). There were three characteristic peaks (2 Theta) at 46.29°、32.30°、27.99° which was (220)、(200)、(110) plane of Cu_2S (PDF 02-1284) [3]. Fig. 3 showed that the precipitation at deposition time of 60 minutes could be obtained the optimum surface resistances value of 10.33mΩ.

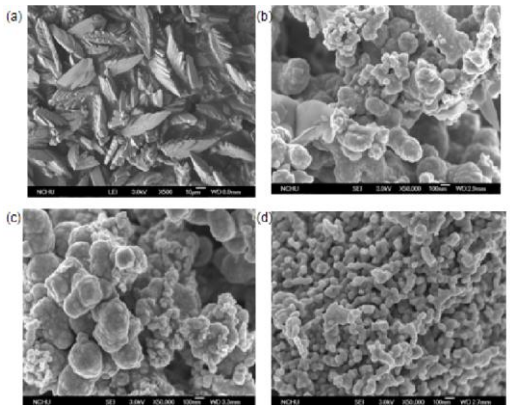

Fig. 1 Scanning electron microscope photographs analysis of electroless copper sulfide nanoparticles in different deposition time. (a) 0 minute; (b) 20 minutes; (c) 40 minutes; (d) 60 minutes.

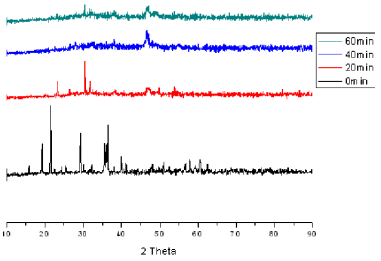

Fig. 2 X-ray Diffraction pattern of electroless copper sulfide nanoparticles in different electroless deposition time. (a) 0 minute; (b) 20 minutes; (c) 40 minutes; (d) 60 minutes.

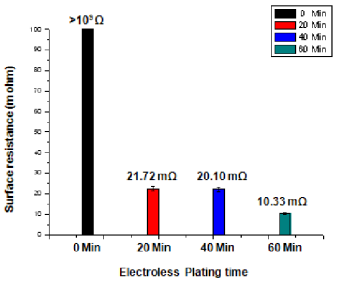

Fig. 3 Surface resistance of electroless copper sulfide nanoparticles in different electroless deposition time.

References

[1] Turan Calban, Soner Kuslu, Sabri Colak, *Chem. Eng. Comm.*, 196, 1018 (2009).

[2] M. E. Chevreul ; *Ann. Chim.*, 83, 187, (1812).

[3] Y. H. Chen, and C. Y. Huang, *e-polym*, L1616, Jun. (2004).

Study of the film formation and mechanical properties of the latexes obtained by miniemulsion co-polymerization of the butyl acrylate, methyl acrylate and 3-methacryloxypropyltrimethoxysilane.

José Manuel Ramos-Fernández, Celia Guillem, Ángel Lopez-Buendía

AIDICO, Polymer research unit C\ Camí de castellan Nº4 Novelda (Alicante) 03660

Water-based emulsion polymers are used in many applications such as latex paint, paper coatings and adhesives. Thermoplastic polymers are commonly selected because these kinds of materials can easily deform, coalesce and form coherent films. These kinds of films usually have low performance because, high glass transition temperature (Tg) (high cross-linking degree) polymer particles do not give coherent films at room temperature, (the coalesce and polymer chain interdiffusion is restricted) and low Tg (low cross-linking degree) polymer particles do not give hard and strength films. Therefore, high performance films based on waterborne thermoplastic polymers synthesis still remains a challenging issue. For many applications, the mechanical properties can be increased by introduction of cross-linking chemistry into latex-based coating. Thus, the latex particles remain with relatively low cross-linking degree in the dispersion but undergo the cross-linking once they have formed the coating on the substrate. Among the different alternatives, the incorporation of alkosysilanes into latex particles is an interesting alternative.

The general formula for an alkoxysilane shows two different kinds of chemical groups attached to the silicon atom. One is a nonhydrolyzable organic group, this group provides the functional group which reacts with the monomers commonly used in the coating formulation, and the second one represents the alkoxy moieties, which can react with hydroxyl groups and liberate methanol or ethanol. The alkoxy moieties provide the self-cross-linking ability to the copolymer. Thus after the film formation, the hydrolysis and condensation reactions of the alkoxysilane moieties, at room temperature, would lead to the film cross-linking.. Thus, premature hydrolysis and the subsequence cross-linking must be avoided during the latex synthesis in order to obtain the desired cross-linking degree after the film formation. Several strategies can be tackled to reduce the premature cross-linking: the use of sterically hindered alkoxysilane would produce a reduction in the hydrolysis rate, besides, good pH control is required since the lower hydrolysis rate occurs at neutral pH. On the other hand, the selection of an adequate polymerization technique can be a powerful tool to avoid the premature cross-linking. Semicontinuous addition of the alkoxysilane in the late states of polymerization reaction would avoid the prolonged contact between the alkoxysilane and water and therefore the hydrolysis can be efficiently avoided. One different approach is to carry out a miniemulsion polymerization instead of conventional emulsion polymerization. Miniemulsion polymerization consists of the polymerization of a stable dispersion of monomer droplets in the aqueous phase. The dispersion is formed by using an adequate dispersion device in order to break down the monomer droplets and reduce their size to the required value, usually below 500 nm. In properly

formulated miniemulsion, the alkoxysilane monomers are protected from the aqueous phase by a waterproof oil droplet, therefore the hydrolysis reactions can be dramatically reduced.

This work will be focussed in the miniemulsion co-polymerization of butyl acrylate, metyl acrylate and two different alcoxysilanes. The influence of the experimental parameters in the latex features will be evaluated. These latexes will be used to protect natural stone against external physical and chemical attacks; therefore the mechanical properties of the film obtained using these latexes will be evaluated, focussing the studies in the influence of the alcoxysilane in the mechanical properties.

Nanoindentation test will carried out to select the adequate amount of alcoxysilane. Under our knowledge, few nanoindentation tests have been carried out to evaluate the mechanical properties of this kind of cross-linked latexes. It is now widely recognized that the composition and properties of the material near the surface of a given coating may be quite unlike the composition and properties of the bulk of the film. Surface physical properties can have major effects on important coating performance properties such as appearance, adhesion, mar and scratch resistance, and wetability. Therefore an important effort will be made in order to asset the mechanical properties of the coating over the substrate (marble tiles).

Investigation of porous structure and thermal properties of sulphur containing copolymers

Beata Podkościelna

Faculty of Chemistry, MCS University, pl. M. Curie-Skłodowskiej 5,
20-031 Lublin, Poland; tel/fax: +48 81 524 22 51

*email: beatapod@poczta.umcs.lublin.pl

Introduction

Porous polymers have been used in several applications like HPLC packings, catalysis, enzyme immobilization, as adsorbents and many others. These applications are a consequence of their physico-chemical and morphological properties such as dilution and cross-linking degree, porosity, pore volume, capability of modification, thermal resistance etc. Polymeric packing materials especially the most popular styrene/divinylbenzene copolymers seem to be great alternatives to silica based supports and to the alkyl bonded phases. These polymeric sorbents are chemically stable in solvents in the entire pH range, but have also drawbacks associated with the presence of micropores in the polymeric matrix. For this reason, the attention of scientists and producers is focused on designing their porosity.

Materials and Methods

Copolymerization of two pairs of tetrafunctional monomers bis[4(2-hydroxy-3-acryloyloxypropoxy)-phenyl]sulfide with divinylbenzene S.A-DVB and bis[4(2-hydroxy-3-methacryloyloxypropoxy)-phenyl]-sulfide with glycidyl methacrylate S.M-GMA are described. Porous microspheres were obtained by suspension-emulsion copolymerization in the presence of pore-forming diluents: toluene and decan-1-ol, using α,α'-azoiso-*bis*-butyronitrile (AIBN) as an initiator. In the syntheses constant concentrations of toluene in the mixture with decan-1-ol (1:1, w/w) were used. Porous structure of the obtained microspheres in dry (calculated by the BET method from the nitrogen adsorption-desorption measurements) and swollen (the inverse SEC method) states was studied and compared with that of bis[4(2-hydroxy-3-methacryloyloxypropoxy)phenyl]-sulfide with divinylbenzene S.M-DVB copolymers previously studied [1]. Swelling properties of the obtained copolymers as well as thermal properties studied by differential scanning calorimetry (DSC) and thermogravimetric analysis (TG) were discussed in detail. The surface texture of the obtained microspheres was controlled by the AFM analysis.

Porous structure characterization

In the dry state, porous structure of copolymers was characterized by nitrogen adsorption at 77K using an adsorption analyzer ASAP 2405 (Micrometrics Inc., USA). Before measurements the copolymers were outgassed at 150 ^{o}C for 2 h. Specific surface areas were calculated by the BET method, assuming that the area of a single nitrogen molecule in the adsorbed state is 16.2 Å^2. Pore volumes and pore size distributions were determined by the BJH method. In a swollen state the beads were characterized by the inverse size exclusion chromatography (SEC) technique introduced by Halász and Martin [2].

Results and Discussion,

The copolymer (S.A-DVB) has the narrowest pore size distribution with most probable pores of a diameter ~ 200 Å (calculated by the BET method from the nitrogen adsorption-desorption measurements) (Fig.1). Compared with the reference S.M-DVB both copolymers are characterized by monodispersive pore size distribution. Porous structure of these copolymers was also studied by the inverse SEC. Pore volumes determined by the inverse SEC method are significantly larger for all the studied copolymers. Additionally, the inverse SEC method reveals micropores in the internal structure of polymeric beads. The results obtained from the DSC and TG data indicate that the highest thermal resistance is found for the copolymer S.A-DVB which has the most crosslinked chemical structure. To investigate swelling behaviour microspheres were swollen in typical solvents, in all polar solvents the swellability coefficients vary from 16 to 40 %. The largest swellability coefficient in THF is observed for the S.M-GMA copolymer.

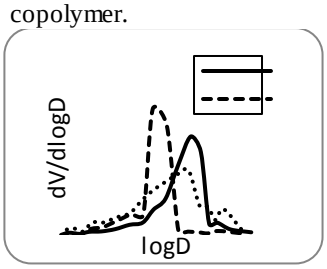

Fig.1 Differential pore size distributions as a function of the logarithm of the pore diameter (D)

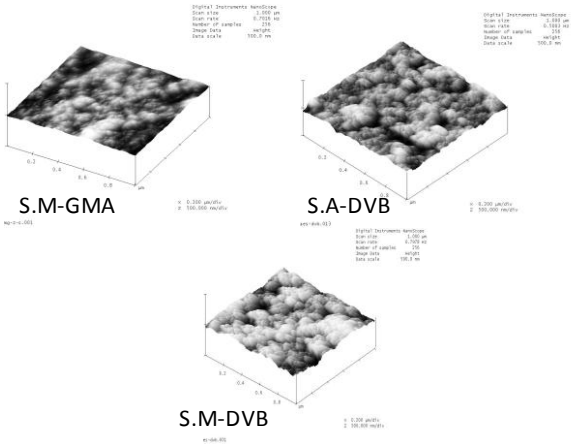

Fig. 2 Contact-mode AFM images

References:

1. B. Podkościelna, A. Bartnicki, B. Gawdzik, J. Appl. Polym. Sci. 2009 **111** 1257-1267.
2. L. Halasz, K. Martin, Ber. Busenges Phys. Chem. 1975 **79** 731-732.

"Unexpected Enhancement of Polymerization Rate in Solution Polymerization with nanoCeO$_2$ particles "

Miren Aguirre, Maria Paulis, J.R. Leiza

POLYMAT

miren.aguirre@ehu.es

Introduction

Wood has the potential for being a competitive and sustainable material. However, for outdoor use it is necessary to enhance its performance and long term durability. The main problem is its high sensitivity to UV degradation. It is common knowledge that wood is affected by light either by color change or by degradation of the surface.

To protect wood from sunlight spectrum, UV-VIS (250-440nm), the light should be cut off or filtered before it reaches the wood surface. Traditionally, organic UV absorbers were used but these substances tend to degradate upon outdoor weathering. Several inorganic fillers, such as TiO_2, ZnO and CeO_2 have been proposed as alternative candidates.

The aim of this work is to synthesize clear-coat wood coating based on hybrid acrylic/nanoCeO$_2$ latexes by miniemulsion polymerization. In this work however, the effect of the nanofiller in the solution polymerization of the typical acrylic monomers used in the coating applications was be investigated.

Materials and Methods

The solution polymerization reactions were carried out batchwise at 70ºC. The solids content of the reactions was 25 wt%. The solvent (Toluene), the monomers (MMA/BA/AA) and the nanoceria (0-3 wt% with respect to the monomer) were charged in the reactor and after reaching 70ºC a initiator (AIBN) shot was added to start the polymerization.

Homopolymerizations of MMA and BA and copolymerizations of MMA/BA with and without AA were carried out, under the presence or not of the nanoceria.

The evolution of the conversion was followed gravimetrically and the molecular weight by GPC.

Results and Discussion

Figure 1 presents the time evolution of conversion for three different runs carried out with MMA monomer, for different nanoceria amounts. According to the data in Figure 1 the polymerization rate increases with the presence of 1% of nanoceria in the polymerization medium. However, increasing the concentration of nanoceria from 1 wt% to 3 wt% did not have an additional effect on the polymerization rate.

Table1. Conversion, molecular weight and polymerization rate results. *With respect to the monomer.

Run	nanoCeO$_2$ (%)	Conversion (%)	Mw (g/mol)	Rp (mol/s)
1	0	76.7	62000	0.205
2	1	99.6	28200	0.284
3	3	100	29300	0.291

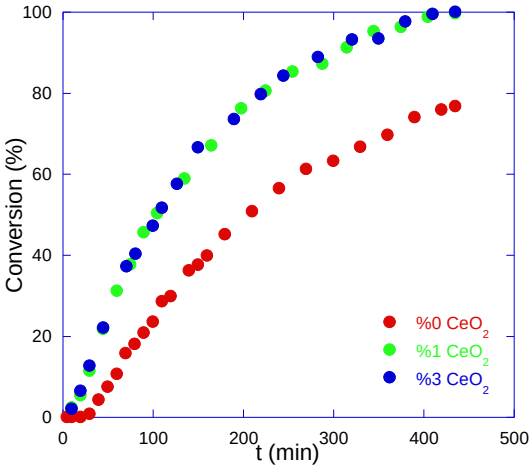

Figure 1. Time evolution of conversion for the batch solution polymerization experiments of MMA carried out with and without nanoceria.

The molecular weights of PMMA produced significally decreased in presence of nanoCeO$_2$. This was expected because in classical free-radical polymerization, increasing the polymerization rate the molecular weights of the polymer decreases. That might be due to the fact that more (AIBN) radicals are generated in the presence of the nanoceria, producing shorter polymer chains. Similar effect in the polymerization rates and molecular weights were also observed for the homopolymerization of BA and the copolymerization of MMA/BA. Nevertheless, the presence of small amounts of AA in the polymerization counteracts the enhancement effect provided by the nanoceria.

Whether the enhanced radical concentration is due to an increased decomposition of the AIBN in the presence of nanoceria or to the formation of new radicals is being investigated.

It will be investigated if this effect is similar in a compartmentalized system as miniemulsion polymerization.

Acknowledgments

This work was supported by Woodlife Project (NMP-2009-1.2-2; Project Number: 246434). Miren Aguirre acknowledges the Ph. D. fellowship given by the Basque Goverrnment (*Ikertzaileak prestatzeko eta hobetzeko laguntzak*).

Stimuli-responsive and electically conductinghydrogel nanocomposites from *N*-isopropylacrylamide and polyaniline.

Katarzyna Depa, Adam Strachota, Patrycja Bober, Jaroslav Stejskal*

Institute of Macromolecular Chemistry Academy of Sciences of the Czech Republic in Prague, Heyrovského nám. 2, 162 06 Praha 6, Czech Republic

(depa@imc.cas.cz, strachota@imc.cas.cz, bober@imc.cas.cz, stejskal@imc.cas.cz)

Introduction

Stimuli-responsive hydrogels are subject of great scientific interest due to their unique properties and rich field of applications. Among thermoresponsive hydrogels one of the most popular are those based on Poly(N-isopropylacrylamide). They are highly swollen at temperatures below the so-called lower critical solution temperature and shrink at higher ones. This strong volume trermo-responsivity makes from Poly-NIPA hydrogels a very attractive matterial for many applications. Most popular uses are drug delivery systems, enzyme immobilizations, nano-valves, electrophoresis or mechanical actuators. Our attention is focused on the latter application.

Results and discussion

In the first part of this contribution, we modified our previously developed highly porous, silica-filled poly-NIPA nanocomposite hydrogels [1,2], characterized by a short time of response to temperature. Our goal was to obtain materials with markedly higher moduli as well as with fast and strong force response to external stimuli, while keeping the fast responsivity and the original volume ratio of the swollen and deswollen states. This type of material could be potentially used in mechanical actuators. We managed this by synthesizing new highly porous gels with thicker pore walls and also by variation of nanofiller: silica nonopaticles, titanium dioxide nanopowder and hectorite clay were tested. The mechanical properties, the morphology, the kinetics of the volume- and force-response to temperature and to pH will be discussed.

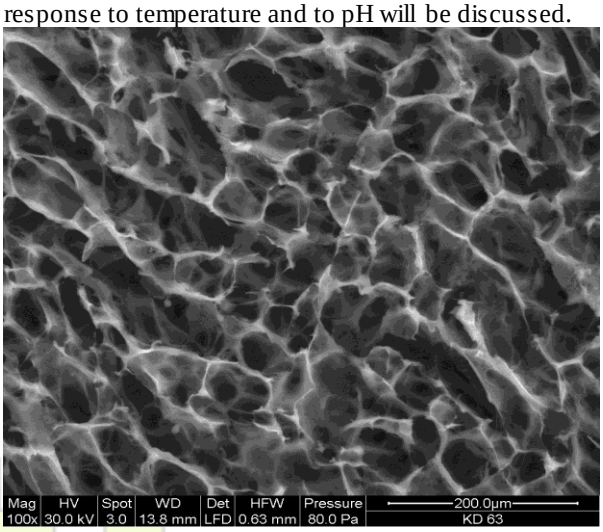

Figure 1. SEM picture of porous gel sample with 14 % of monomers concentration

Secondly, we prepared conductive hydrogels composites based on N-isopropylacrylamide and polyaniline (PANI). Polyaniline is one of the most

famous conducting polymers. It displays high electrical conductivity, environmental stability, ease of preparation from common chemicals, good processibility, in addition to a relatively low cost [3]. Highly porous specimens of poly-NIPA based hydrogels containing varying amounts of sodium methacrylate were covered by polyaniline via oxidation of aniline hydrochloride with ammonium peroxydisulfate, in aqueous medium at room temperature. To obtain homogenous distribution of the polyaniline in pore system, the gels were at first swollen with peroxodisulfate for five days and then subsequently treated with an aniline hydrochloride solution. The final products display a dark green color typical for PANI. Morphology, conductivity and mechanical properties of those composites will be presented.

References:

1. M. Lutecki, B. Strachotová, et al., Polymer Journal **2006**, 38, 527.
2. B. Strachotová, A. Strachota, M. Uchman, et al., Polymer **2007**, 48, 14713
3. I. Sapurina, J. Stejskal, *Polym. Int.* **2008**, 57, 1295.

Acknowledgement:
The authors thank the Grant Agency of the Czech Republic, Grant Nr. 106/09/1101, and the Charles University in Prague, Faculty of Science, for financial support of this work

Instantaneous Electric Dipole Moment in Conjugated Polymers

Luiz F. Roncaratti, Ricardo Gargano, Pedro H. de Oliveira Neto, Wiliam F. da Cunha, Geraldo Magela e Silva

Instituto de Física, Universidade de Brasília, Brasil

gargano@fis.unb.br

Introduction

Conjugated polymers has two degenerated ground states called A and B phases. The kink is a defect where these two phases have a "misfit". This is the basic signature of a soliton state [1]. We consider a zero charge spin ½ soliton on a thermalized one-dimensional lattice. In this case we found an oscillatory electric dipole at the kink induced by the thermal phonons on the lattice.

Methods

Our system is defined by a model Hamiltonian containing an interaction potential that depend on relative atomic coordinates [2], plus a Tight-Binding term as approximation for the π electrons-phonons interaction [3]. The last term includes also a modified hopping term to take into account an external electric field [4]. Each atom is also coupled to a set of reservoir oscillators representing a thermal bath.

To time evolve the system, we prepare a stationary state fully self-consistent with the degrees of freedom of electrons and phonons. To perform the dynamics we solve the Schrödinger one-particle equations coupled with the Euler-Lagrange equations to treat the lattice. Since our main objective is to characterize the dynamics under a temperature regime we eliminate the reservoir degrees of freedom in the usual way and obtain a quantum Langevin equation [5]. These equations are defined by an exponential correlated noise and its respective memory kernel [6]. The set of equation of motion was integrated numerically [7] using a fourth-order Runge–Kutta method.

Results and Conclusion

We used the parameters of a perfectly dimerized *trans*-polyacetylene [2] and characterized the instantaneous electric dipole at the kink as function of the lattice temperature. Our results shows a stable oscillating dipole over a large range of temperature values. This unveils a new and unexpected characteristic of solitons in conjugated polymers.

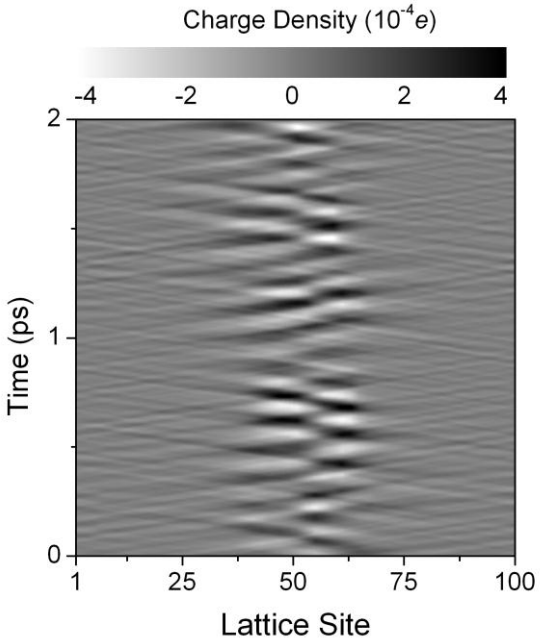

References

[1]Y. Lu, *Solitons & Polarons in Conducting Polymers* (World Scientific, Singapore, 1988).

[2]W. P. Su, J. R. Schrieffer, A. J. Heeger, Phys. Rev. B **22**, 2099 (1979).

[3]G. M. e Silva, Phys. Rev. B **61**, 10777 (2000).

[4]G. W. Ford, J. T. Lewis, R. F. O'Connell, Phys. Rev. A **37,** 4419 (1988).

[5]D. Banerjee, B. C. Bag, S. K. Banik, D. S. Ray, J. Chem. Phys. **120**, 8960 (2004).

[6]R. F. Fox, I. R. Gatland, R. Roy, G. Vemuri, Phys. Rev. A **38**, 5938 (1988).

[7]L. F. Roncaratti, R. Gargano, G. M. e Silva, J. Phys. Chem. A **113**, 14591 (2009).

Effect of reaction parameters on the conductivity of nano polyaniline particles using Taguchi experimental design

Reza Arefinia [a], *Akbar Shojaei* [a], *and Homeira Shariatpanahi* [b]

a) Department of Chemical and Petroleum Engineering, Sharif University of Technology, P. O. Box 11155-9465, Tehran, Iran, reza_arefinia@yahoo.com

b) Coating Research Center, Research Institute of Petroleum Industry (RIPI), Tehran, Iran

Abstract

Polyaniline (PANI) as a conductive polymer was successfully synthesized via inverse microemulsion polymerization. The effect of four main reaction parameters including aniline (AN, as monomer) concentration, molar ratio of dodecylbenzenesulfonicacid (DBSA, as surfactant) to AN, molar ratio of ammonium peroxydisulfate (APS, as oxidant) to AN and reaction temperature were well studied on the PANI volume conductivity. For this purpose, an experimental schedule was made according to Taguchi experimental design. SEM and TEM images of the prepared PANI showed a spherical morphology having less than 70 nm particle size diameter the all samples. The analysis of experimental results indicates that volume conductivity of PANI particles increases with increasing of AN concentration and APS/AN molar ratio. The PANI conductivity decreases continuously with increasing DBSA/AN molar ratio while the reaction temperature does not show a distinct trend on the conductivity of nano PANI particles.

Introduction

Intrinsically conductive polymers have been attracted much research especially due to their applications such as rechargeable batteries, solar control, optical property and anticorrosion coatings. Among these polymers, PANI has been greatly investigated because of its low cost, easy synthesis and environmental stability compared to the other conductive polymers. Indeed, electrical conductivity of PANI is resulted from its structural conjugated double bonds that can easily change from oxidized to reduced state and vise versa. Many parameters such as polymerization method, particle size, morphology and reaction parameters can affect the electrical conductivity of PANI[1]. However, according to our knowledge, there is no comprehensive investigation in this field.

In this work, the effect of four main reaction parameters all in four levels (Table 1.) was well investigated on the PANI conductivity which is the most important property of PANI. To do this, an experimental design was utilized according to Taguchi approach suggesting a standard L_{16} orthogonal array. Subsequently, the analysis of results was performed with analysis of variance (ANOVA) technique.

Table 1. Chosen reaction parameters and their levels for Taguchi experimental design

Parameters	Level 1	Level 2	Level 3	Level 4
AN (mol/lit.)	0.05	0.1	0.15	0.20
DBSA/AN	1.5	2.0	2.5	3.0
APS/AN	0.2	0.4	0.6	0.8
T (°C)	0	10	20	30

Materials and methods

AN, APS and hexane (as reaction environment) were purchased from Merck and DBSA was received from a local company. The AN was distilled twice in reduced pressure while the other chemicals were used as received. PANI was well synthesized through inverse microemulsion polymerization according to literature[2]. In this procedure, DBSA and AN were consecutively added into the hexane and the solution was kept under sonication which was leading to formation of nano micelles (as nano reactors). At the end, water dissolved APS was introduced drop wise into the system to initiate the polymerization reaction.

Results

SEM and TEM images showed a spherical morphology having less than 70 nm diameter indicating the nano size of the micelle structures.

The relative influence of each parameter on the PANI conductivity take into account with the ANOVA technique and the results are shown in Fig. 1. As can be seen, the electrical conductivity is improved with increasing AN and APS/AN ratio due to formation of longer PANI polymer chain and more oxidation of PANI, respectively. However, the conductivity decreases with increasing DBSA/AN molar ratio. This behavior could be related to the excess protonation of PANI polymer chains. This is because of the fact that the half doped structure of PANI is the most suitable structure for charge transfer through the polymer chains.

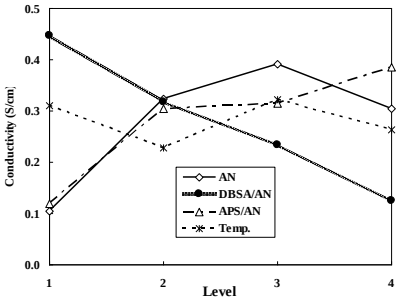

Fig. 1. Average influence of four reaction parameters on the electrical conductivity of PANI particles

Conclusion

The reaction parameters could be greatly affected the conductivity of PANI. Furthermore, they could be easily controlled during the PANI polymerization. To increase the conductivity of PANI, one can increase AN and APS/AN ratio and decrease DBSA/AN ratio.

References

1. Bhadra S., Khastgir D., Singha N.K., Lee J. H., Progress in Polymer Science Vol.34 (2009) 783–810.

2. Han Y.G. Kusunosea T., Sekinob T., Synthetic Metals vol.159 (2009) 123-131.

Influence of Different Nanofillers on the Phase Behavior of Epoxy/Polystyrene Blends

Mario Culebras, Isidro S. Monzó and Clara M Gómez

Dpertment of Physical Chemistry/ICMUV, University of Valencia, Burjassot (Valencia) Spain

clara.gomez@uv.es

Introduction

Brittle thermosets materials, like epoxy resins, can be toughened by the incorporation of an elastomer or thermoplastic additive [1,2]. This modifier forms a homogeneous solution with the epoxy precursor. Addition of a curing agent increases the molar mass of the thermoset and a liquid-liquid phase separation occurs at a certain level of conversion [2]. The ultimate properties of these materials depend on the morphology generated during the build-up of the epoxy matrix. In order to predict or explain morphologies and properties, we must begin with a reasonable phase separation thermodynamic description of the system. The lattice theory of Flory and Huggins [3] is the best known theory used to describe the phase separation of polymeric solutions and blends and has been applied to study phase separation in thermoset/thermoplastic blends. A detailed phase-separation thermodynamic description of the system, starting with the thermoset precursor, thus establishing the basis of the thermodynamic treatment aids to better understand morphology development and final properties.

In the last years, there has been significant interest in the effect of nanoparticles on the properties of polymer systems. Nanoparticle addition can dramatically change the properties of polymers or polymer blends, or act as potential nanocompatibilizers for mixtures of immiscible blends. Much work has been devoted in obtaining improved matrices with very well-dispersed nanoparticle. However, the factors that control the formation of such hybrids are not well-understood. It is not clear under what conditions the different components will become intermixed to yield thermodynamic stable materials. An intense research can be carried out in this direction since the properties improvement will depend on the thermodynamic stability of the mixture and on the overall morphology of the material.

The aim of this paper is to study the influence of different nanoparticles on the phase separation and morphology development of an epoxy/polystyrene blend before curing and after polymerization with a diamine. The aspect ratio of the nanoparticles has been varied thus employing, fiber-like particles like sepiolite, spherical particles as silica and platelet like particles as montmorillonite.

Experimental Part

The epoxy prepolymer DER336 is based on diglycidyl ether of bisphenol A, kindly provided by Dow Chemical Company. The polystyrene Lacqrene PS1450N supplied by Atofina. Unmodified (S9) and organically modified (B5) sepiolite, different montmorillonites and modified SiO_2 were used as nanofillers.

Cloud-point temperatures of the different mixtures were determined using a light transmission device that detects the light transmitted as a function of temperature.

Results and Discussion

Figure 1 shows as an example of the experimental data the cloud point temperatures for epoxy/polystyrene in presence of different montmorillonite (MMT) type laminar silicates. It is observed that the organic modification of the MMT increases the cloud point temperatures of the epoxy/polystyrene blends, thus decreasing miscibility.

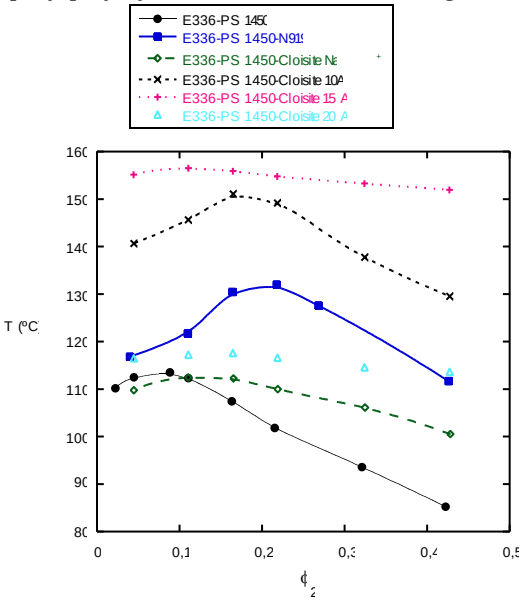

Figure 1. Phase diagram of epoxy DER336 and polystyrene in presence of different laminar nanofillers.

Systems modified with sepiolite show a decrease in miscibility when using organically modified one, however in the case of the silica the epoxy modified one increases miscibility.

Addition of an aromatic diamine as a curing agent decreases considerably the cloud point temperature, thus increasing the overall compatibility.

The Flory-Huggins theory has been used to theoretically represent the experimental cloud point curves. Binodal, spinodal as well as critical temperatures and interaction parameters concentration and temperature dependent have been determined.

References

[1] CK Riew, AJ Kinloch, "Toughened Plastics I:Science and Engineering", Adv. Chem. Ser. No 233, American Chemical Society, Washington, DC 1993.

[2] RJJ Williams, BA Rozenberg, JP Pascault, Adv. Polym. Sci.1997;128:95.

[3] PJ Flory, J Chem Phys 1942;10:21 and L Huggins, J Phys Chem 1942;46:151.

Successive AGET ATRP of Cationic Methacrylate and PEO Macromonomer Yielding Water Soluble Stiff Cylindrical Molecular Brushes with Cationic Tail

C.Visnevskij, A.Baceviciute, R.Makuska

Vilnius University, Naugarduko 24, LT-03225 Vilnius, Lithuania

ricardas.makuska@chf.vu.lt

Introduction. One of the most successful controlled/living radical polymerization (CRP) techniques is atom transfer radical polymerization (ATRP) which allows the synthesis of copolymers with different architecture, such as block, gradient and brush, between others [1]. Activators generated by electron transfer (AGET) is an initiating process for ATRP in which the active Cu^{1+}/L_m complex is formed by the reaction of reducing agents, such as ascorbic acid or tin(II) 2-ethylhexanoate, with an oxidatively stable Cu^{2+}/L_m precursor prior to normal initiation with the added alkyl halide initiator [2].

In the present work, we aimed to synthesize diblock copolymers in which one block is charge carrying and composed of [2-(methacryloyloxy)ethyl]trimethyl ammonium chloride (METAC) units, and the another one is molecular brush and composed of poly(ethylene oxide) methyl ether methacrylate (PEOMEMA, M_n = 2080) units. Such diblock copolymers are envisaged as polymeric brushes containing cationic tail through which they could adsorb effectively to negatively charged surfaces and modify surface properties in extreme manner.

Materials and Methods. Components of AGET ATRP system was ethyl 2-bromoisobutyrate (EBrB), copper (II) chloride ($CuCl_2$), tris[2-(dimethylamino)ethyl] amine (Me_6TREN) and ascorbic acid (AscA). AGET ATRP was carried out at 35 °C in closed cells under mixing by magnetic stirrer. Poly-METAC was purified by double precipitation to acetone, and poly-PEOMEMA and diblock copolymers METAC$_x$-*block*-PEOMEMA$_y$ by ultrafiltration and freeze-drying. ^{1}H NMR spectra of the copolymers in D_2O or $CDCl_3$ were recorded at 30 °C using UNITY INOVA VARIAN 300 MHz spectrometer. For monitoring of the progress of polymerization, WATERS 600 series SEC instrument equipped with TSK-GEL column GMPW$_{XL}$ and RI detector Waters 410 was used. Molecular weight of the polymers was determined by both ^{1}H NMR spectroscopy and SEC combined with WYATT DAWN-DSP light-scattering photometer.

Results and Discussion. Under ATRP of METAC in methanol-water mixture (85/15 wt/wt), hydrolysis of the monomer was very fast far bypassing polymerization process. The AGET system containing Cu^{2+} and AscA helped to avoid hydrolysis and prepare pure poly-METAC. Reproducibility of the results of AGET ATRP of METAC in methanol-water (85/15 wt/wt) was improved significantly by automatic injection of the reducing agent using chromatographic pump. Optimal conditions for AGET ATRP of METAC were established from which the most important was periodic dosing of the reducing agent AscA. High conversion of METAC was achieved (more than 80%), and poly-METAC with degree of polymerization (DP) 15, 30, 50 and 100 (molecular weight M_n up to 20 000) and low polydispersity was synthesized. These polymers with living chain ends were used as macroinitiators for the synthesis of diblock copolymers.

AGET ATRP of PEOMEMA from EBrB was very slow and lasted 1–2 weeks. Moreover, the polymerization proceeded only in the presence of a certain excess of the ligand Me_6TREN (2-fold) and reducing agent AscA (1.75-fold) in respect to [Cu^{2+}]. Although maximal conversion of PEOMEMA was 40% only, poly-PEOMEMA with DP 15, 30, 50, 100, 160, 210 and 240 (molecular weight up to 500 000) and low polydispersity was synthesized.

Previously synthesized poly-METAC was used as macroinitiators for AGET ATRP of PEOMEMA. Conditions of polymerizations of PEOMEMA from poly-METAC were similar to those described before, i.e. a certain excess of the ligand and the reducing agent. Two series of diblock copolymers METAC$_x$-*block*-PEOMEMA$_y$ were obtained (Fig. 1), one with varying length of the cationic block, and another one with varying length of the brush block.

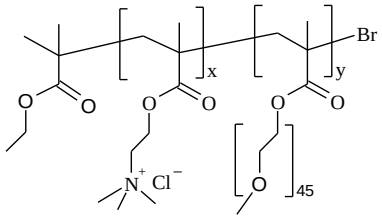

Fig. 1. Diblock copolymers METAC$_x$-*block*-PEOMEMA$_y$

Although diblock copolymers METAC$_x$-*block*-PEOMEMA$_y$ were soluble in water, they had a tendency to self-association (aggregation). The most intense aggregation in pure water was characteristic for the long-chain poly-PEOMEMA. The presence of the block of poly-METAC reduced aggregation of the molecular brushes or even removed it at all. Aggregation of the molecular brushes was removed also by addition of strong electrolytes, e.g. in 0.8 M $NaNO_3$.

Conclusions. Two series of diblock copolymers METAC$_x$-*block*-PEOMEMA$_y$ differing in the length of the both blocks were synthesized and characterized. Molecular brushes containing cationic tail will be tested as surface modifiers providing friction-reducing or protein-repelling properties.

Acknowledgement. Financial support from the Research Council of Lithuania (Contract MIP-50/2010) is gratefully acknowledged.

References

1. W. A. Braunecker, K. Matyjaszewski, *Prog. Polym. Sci.*, **32**, 93-146 (2007).
2. H. Gao, K. Matyjaszewski, *Prog. Polym. Sci.*, **34**, 317-350 (2009).

Preparation and Optical Properties of Novel Bioactive Photonic Crystals Obtained from Core-shell Hydrophilic Microspheres

Teresa Basinska[1], *Monika Gosecka*[1], *Nebewia Griffete*[2], *Claire Mangeney*[2], *Mohamed M. Chehimi*[2], *Stanislaw Slomkowski*[1]

[1] Center of Molecular and Macromolecular Studies, Polish Academy of Sciences, Sienkiewicza 112, 90-363 Lodz, Poland

[2] Interfaces, Traitements, Organisation & Dynamique des Systèmes (ITODYS), Université Paris Diderot-CNRS (UMR 7086), 15 rue Jean de Baïf, 75013 Paris, France

basinska@cbmm.lodz.pl

Introduction.

Recently, nano- and microsphere assemblies with crystalline morphology found applications in various optical devices. It was revealed that the colloidal crystal arrays diffract visible light according to the Bragg law.[1] Diameters of microspheres in this kind of materials should be in a range 100-400 nm and their dispersity should be narrow. The high uniformity of particles allows to avoid defects in the colloidal crystals. Our studies were directed towards preparation and characterization of core-shell hydrophilic microspheres containing α-tert-butoxy-ω-vinylbenzyl-polyglycidol in the surface layer with properties needed for formation of colloidal crystals with thermoresponsive properties.

Materials and Methods.

Microspheres were prepared by a soap free emulsion polymerization of styrene and α-tert-butoxy-ω-vinylbenzyl-polyglycidol macromonomer (PGL) in water and initiated by $K_2S_2O_8$.[2] PGL (with M_n=2700, M_w/M_n=1.05) was prepared by anionic polymerization of 1,1-ethyl-ethoxyglycidyl ether and terminated by p-chloro-methylstyrene with potassium *tert*-butoxide and subsequent hydrolysis of ethyl ethoxy groups by oxalic acid.[3]

Diameters of microspheres (D_n and D_w/D_n) were determined by analysis of scanning electron microscopy (SEM) microphotographs registered using a JEOL 5500LV apparatus.

Chemical composition of interfacial layer of P(S/PGL) microspheres was determined by X-ray photoelectron spectroscopy.[4]

Hydrodynamic diameters of P(S/PGL) microspheres were determined by photon correlation spectroscopy measurements (PCS) in the range of temperatures from 15 to 65°C. The colloidal assemblies were prepared by gentle deposition of the suspension of P(S/PGL) particles (around 0.1 ml) onto the glass plates and subsequent drying at various temperatures.

The angle-resolved UV-VIS spectra were recorded using SPECORD S600 Analytik Jena spectrophotometer equipped with a variable angle reflectance attachment, operated in the range 20-60°. Water drop static contact angles were measured by Rame-hart NRL goniometer.

Results and Discussion.

The emulsion polymerizations yielded particles with very uniform diameters in the range 230-400 nm, depending on the concentration of macromonomer used in polymerization. It was found that particles are composed from polystyrene cores, and shells enriched with hydrophilic polyglycidol.

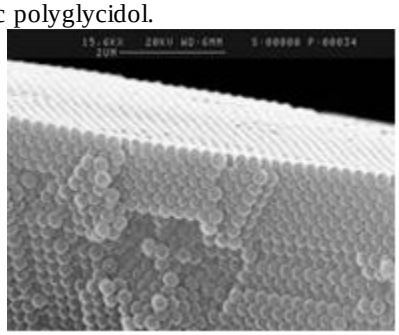

Figure 1. Colloidal array of P(S/PGL) microspheres The dependence of hydrodynamic diameter of particles suspended in water on temperature indicated that shells of particles shrank above the critical temperature equal 45 °C. This critical temperature did depend on composition of particle interfacial layer and on the ionic strength of solution.

The microspheres were used for preparation of colloidal crystals. Studies of light diffraction revealed that colloidal crystals formed above 45°C were composed of particles with diameters smaller than diameters of particles in crystals formed below 45°C. We found that with increased temperature the refractive index of material in colloidal crystals also did increase. Presumably, above the critical temperature polymer chains in the interfacial layer do collapse what leads to expulsion of water and to the higher hydrophobicity of the crystals (water contact angles increased from *ca*. 50° at 25°C to *ca*. 110° at 70°C.

Conclusions.

We did show that optical properties of colloidal crystals from P(S/PGL) particles could be tuned by changing temperature. Such crystals containing particles with ─OH groups are superior to thermosensitive crystals from poly(*N*-isopropylacrylamide) and poly(ethylene-glycol) particles with only functional end groups.

References.

1.Asher SA, Holtz J, Liu L, Wu Z (1994) J Am Chem Soc 116:4997-4998

2.Basinska T, Slomkowski S, Dworak A, Panchev I, Chehimi MM (2001) Colloid Polym Sci 279:916-924

3. Dworak A, Panchev I, Trzebicka B, Walach W (1998) Polym Bull 40:461-468

4. Briggs D (1990) in Briggs D, Seah MP (eds), Practical Surface Analysis, vol.1, Auger and X-ray photoelectron spectroscopy, 2nd edn. Wiley New York pp 437-483.

Microspheres of poly(3-hydroxybutyric acid-co-3-hydroxyvaleric acid) loaded with holmium-166 for braquitherapy.

Jaime Roberto de Souza, José Roberto Martinelli[b], João Alberto Osso Junior[c], Nanci Nascimento[a], Mariangela de Burgos M. de Azevedo[a]*

[a]Centro de Biotecnologia, [b]Centro de Ciência e Tecnologia de Materiais, [c]Centro de Radiofarmácia, Instituto de Pesquisas Energéticas e Nucleares -IPEN;

email: jrsouza@ipen.br

Abstract: This project proposes the development of microspheres (**MS**) size raging between 20 to 50 microns of biodegradable polymer poly(3-hydroxybutyric acid) (PHB) and its copolymer, the poly(3-hydroxybutyric acid-co-3-hydroxyvaleric acid) (PHB-HV), loaded with ^{165}Ho, as holmium acetylacetonate (**HoAcAc**), to be used in brachytherapy procedure to liver cancer treatment. At the first glance this study aims to confirm both the feasibility of the microsphere formation with these biopolymers and their ^{165}Ho incorporation capability. Further ahead, the influence of the amount of co-3-hydroxyvaleric acid in the in the PHB-HV-**MS** loaded and unloaded with Ho, will be evaluated in terms of thermal degradation, holmium encapsulation efficacy, microspheres size and morphology and resistance to the neutron irradiation. Therefore, initially, we are testing PHB-HV with HV contents of 8 and 5% (wt). Initial attempts to use the homopolymer PHB failed due to its lack of solubility in the process used to form the microspheres.

Introduction: The polyhydroxyalkanoates (PHAs) comprise a family of biodegradable and biocompatible polyesters produced by wide variety of microorganism. The general PHA chemical structure is depicted in **Figure 1**.

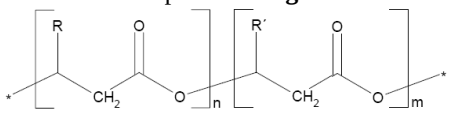

Figure 1: PHA chemical structure

The HoAcAc is depicted in **Figure 2**.

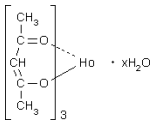

Figure 2: Holmium acetylacetonate (HoAcAc)

Brachytherapy is an internal radiotherapy treatment and presents an alternative treatment with promising results in relation to the usual procedures of chemotherapy or radiotherapy The brachytherapy treatment with yttrium-90 microspheres (^{90}Y-MS), with a glass matrix is well established in the treatment for patients with unresectable liver malignancies. Like ^{90}Y, ^{166}Ho is a high energy beta-emitter. However, considering its physical properties, ^{166}Ho is the ideal radionuclide for such therapies. Namely, holmium is the only element that can be both neutron-activated to a beta- and gamma-emitter with a logistically favorable half-life and visualized by MRI. Microspheres formed for some biopolymers have being found to be the best candidates to overcome the glass matrixes inherent problems. The microspheres of some biopolymers are capable to resist the neutron radiation from the atomic reactor and moreover they are biocompatible and after the irradiation treatment they can be further biodegraded.

Stable ^{165}Ho can be incorporated into the biodegradable microspheres and irradiated later in a nuclear reactor to be converted into the high-energy negatron emitter. The radioactive holmium-166 loaded PHB or PHB-HV microspheres are promising systems for the treatment of liver malignancies.

Results and discussions: The microspheres have been prepared by solvent evaporation technique, where through out a microemulsion stabilized by polyvinyl alcohol (PVA), the HoAcAc is incorporated into the polymer matrix, then subsequent sieving in order to separate the microspheres in the required sizes and further drying by lyophilization. In order to check the size and morpholoy the microspheres were analysed by confocal laser scanning microscopy (CLSM) and scanning electron microscopy (SEM), **Figures 3 and 4**, respectively.

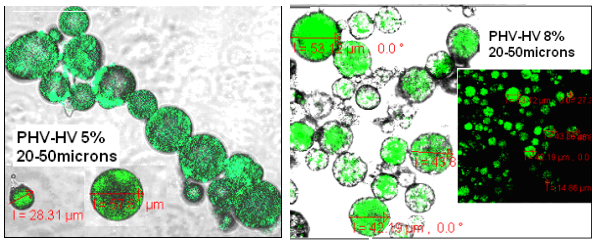

Figure 3: CLSM of PHV-HV loaded with HoAcAc

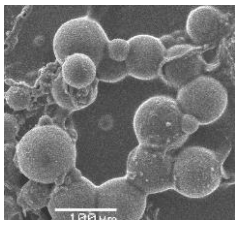

Figure 4: SEM of unloaded PHB-HV.

We are reporting the first results of this project which attempts to show the feasibility of microspheres formation using the PHB-HV through the o/w emulsion, stabilized by PVA by the solvent evaporation technique, a well established approach for the system widely studied poly(L-Lactic acid) HoAcAc. The results of CLSM and SEM confirm the formation of microspheres by the process used. Moreover, the images of CLSM show the incorporation of HoAcAc in the PHB-HV microspheres by the fluorescence of HoAcAc (the green areas of the figure). Although, this project is in its early stages of development, one has not seen yet significant differences between the HV content in the PHB-HV, just slight difference in the yield of microspheres preparation. Thus, the overall microspheres yield (between 70-20microns) was practically the same, however the PHB-HV 8% has shown about 13% more of microspheres sizing between 20-50 microns, which are the ones of interest. The presence of HV in the PHB it is well established and has remarkable influence in the PHB properties as, for instance, the crystallinity. Therefore, in the course of this project, the HV influence on the PHB will be evaluated more properly.

References

[1] Renata F. Costa, Mariangela B. M. Azevedo, Nanci Nascimento, Frank F. Sene, José R. Martinelli, João A. Osso ***International Nuclear Atlantic Conference - INAC 2009; ASSOCIAÇÃO BRASILEIRA DE ENERGIA NUCLEAR - ABEN ISBN:*** 978-85-99141-03-8. **[2]** M. A. D. Vente, T. C. de Wit, M. A. A. J. van den Bosch, W. Bult, P. R. Seevinck, B. A. Zonnenberg, H. W. A. M. de Jong, G. C. Krijger, C. J. G. Bakker, A. D. van het Schip, J. F. W. Nijsen - ***Eur Radiol (2010) 20: 862–869***.

Microspheres of poly(lactic acid) loaded with holmium-166 for braquitherapy.

Geovanna Pires[a], Jaime Roberto de Souza[a], José Roberto Martinelli[b], João Alberto Osso Junior[c], Nanci Nascimento[a], Mariangela de Burgos M. de Azevedo[a]*

aCentro de Biotecnologia, bCentro de Ciência e Tecnologia de Materiais, cCentro de Radiofarmácia, Instituto de Pesquisas Energéticas e Nucleares -IPEN;

email: geovannapires@gmail.com

Abstract: This study describes the development of poly(lactide) (PLA) microspheres by an emulsion method for brachytherapy. The effects of both PLA and PDLA polymers on holmium encapsulation efficacy were evaluated. Microspheres containing holmium were prepared and characterized by thermal analysis, X-Ray diffraction, Scanning Electron Microscopy, FTIR spectroscopy and zeta potential measurements. Experimental data show that both polymers were converted into microspheres. However, PLLA1 with small inherent viscosity has formed higher amount of microspheres with size distribution smaller as compared with PLLA2 and PDLA.

Introduction

Three different types of material substrates have been investigated, i.e., biodegradable polymer-based, glassbased and resin-based microspheres. Currently, there is a project being developed at the IPEN coordenated by the radiopharmacy department, related to the labeling of three materials with ^{166}Ho. The nuclide ^{166}Ho($t_{1/2}$=26.8h) is a beta particle emitter (E_{max}=1.84 MeV), with suitable properties for radiotherapy and it can be produced with the relatively low neutron flux from the Brazilian Nuclear Reactor IEA-R1m. As an initial experience we used resin-based microspheres, a cation exchange resin labeled with ^{166}Ho, which showed the essential characteristics for liver cancer therapy.

Preliminary results concerning the preparation of glassbased microspheres labeled with ^{165}Ho showed that 5% of Ho_2O_3 was incorporated in an aluminosilicate glass, through the process of spheronization by flame, which produced spherical microspheres with 20-40 μm particle size. The preparation of biodegradable material, polymerbased microspheres, is in its initial stage and the objective is to prepare and label with 165Ho different polymer-based microspheres. These combined efforts have been done to offer a radiotherapeutic product for the Brazilian nuclear medicine community at reasonable cost and also to offer a viable possibility of treatment for patients affected by liver malignances [1]. In the present study, we report the effects on the PDLA e PLLA polymers after the Ho encapsulation efficacy and the characterization of the materials by different techniques: SEM, Thermal analyses, EDX, zeta potential, porosity and infrared spectroscopy (IR) [2].

Experimental

The PLLA1 (M_w 101,700), PLLA2 (M_w 152,000), PDLA polymers, and polyvinyl alcohol (PVA, MW = 31 KDa, hydrolyzation degree = 88%) were provided by Sigma Aldrich. Holmium acetylacetonate trihydrate (HoAcAc) was prepared as described previously [2]. The microspheres with HoAcAc were prepared by solvent evaporation as described previously (Fig.1) [2]. The HoAcAc and the polymer were dissolved in chloroform. The resulting homogeneous solution was added to an aqueous solution of PVA. The mixture was stirred at 500rpm, and the formed microspheres were were separated by sieving.

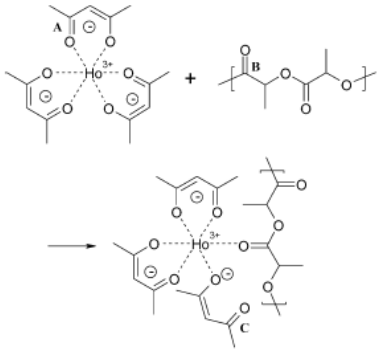

Fig. 1. Reaction of the formation of holmium microspheres.

Results and discussions

Microspheres were prepared by solvent evaporation and sieved to retain particles in a suitable size range. Fig. 2 shows the SEM micrographs of microspheres without holmium in different polymers. As it can be seen, they are spherical with a relatively small index of polydispersity according to the zeta potential results.

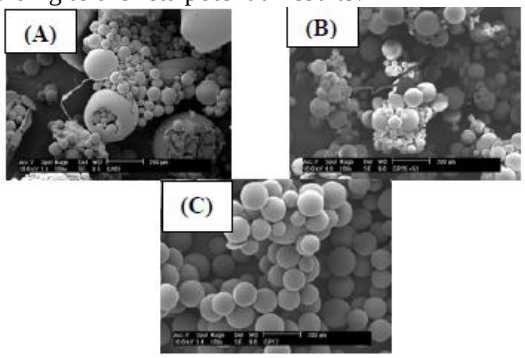

Fig. 2. SEM of PDLA (A) PLLA1 (B) and PLLA2 (C) microsphere without holmium.

The results showed that there was significant difference between the FTIR spectra of the microsphere-Ho when compared to the spectra of individual components. Thermal analysis curves showed that both PLLA samples have the characteristic melting points of the crystalline polymers, indicating that the crystallinity was maintained. EDX analysis showed the concentration of Ho in the material.

Conclusion

This study showed that microspheres were formed with and without holmium, and that the microspheres containing holmium present promising results for brachytherapy application.

References

[1] Renata F. Costa, Mariangela B. M. Azevedo, Nanci Nascimento, Frank F. Sene, José R. Martinelli, João A. Osso; *2009 International Nuclear Atlantic Conference - INAC 2009; ASSOCIAÇÃO BRASILEIRA DE ENERGIA NUCLEAR - ABEN* **ISBN: 978-85-99141-03-8**

[2] Nijsen J.F.W., Zonnenberg B.A., Woittiez J.R., Rook D.W., Swildens-van Woudenberg I.A., Van Rijk P.P., Van Het Schip A.D. Eur. J. Nucl. Med. 26, 699-704, 1999

Exciton Diffusion Length in Conjugated Polymers

P. H. O. Neto, W. F. da Cunha, L. F. Roncaratti, F. V. Moura, R. Gargano and G. M. e Silva

University of Brasilia

pedrohenrique@unb.br

Introduction:

Recently, optical electronic devices based in semiconducting conjugated polymers are attracting a huge attention of scientific community. Particularly, the formation, transport and recombination process of excitons are fundamental when concerning performance. It is known that the presence of triplet excitons further enhances solar cell efficiency over singlet-state-only cells [1]. However, the direct optical studies of triplet states are very difficult once singlettriplet transitions are forbidden. In this sense, this work investigates the dynamic of both singlet and triplet excitons in conjugated polymers samples under a presence of thermal effects to determined the diffusion length and to estimate the diffusivity. Our approach consists on a semi-empirical tight binding method with lattice relaxation in a first order expansion. Concerning the Ehrenfest molecular dynamics, the lattice degrees of freedom was treated by Euler Lagrange equations while the pi-electrons are described by the time dependent Schrodinger equation.

Thermal effects are incorporated on the method by means of a typical Langevin equation.

Methods:

The used hamiltonian was:

$$H = -\sum_{n,s} t_{n,n+1}(C^{\dagger}_{n+1,s}C_{n,s} + H.c) + \sum_n \frac{K}{2}y_n^2 + \sum_n \frac{p_n^2}{2M},$$

with $C_{n,s}$ being the annihilation operator of a pi-electron with s spin in the nth site; M isthe isthemassofaCH group; K is the harmonic constant; $y_n \equiv u_{n+1} - u_n$ where u_n is the displacement coordinate of the molecule site from the completely non dimerised configuration; p_n is the momentum conjugated to u_n. The hopping integral is $t_{n,n+1}$, given by $t_{n,n+1}=[1+(-1)^n D_0](t_0-ay_n)$ where a is the electron-phonon coupling; t_0 is transfer integral betweem nearest neighbor site in the undimerized chain; and D_0 is the Brazovskii-Kirova symmetry breaking parameter responsible for simulating a cis conjugated polymer symmetry.

In the scope of the Unrestricted Hartree-Fock Approximation, we first prepare a stationary state fully self consistent with the degrees of freedom of both the electrons and phonons.

Results and Discussion:

The parameters values used in this work are the usually adopted for cis-polyacetylene chains [2] and the results are expected to be valid for other conjugated polymers[3]. The systems are composed of 100 sites of cis-conjugated polymer under several temperature regimes. The figure presents the time evolution of bonding pattern order parameter at 300 K. It is observed

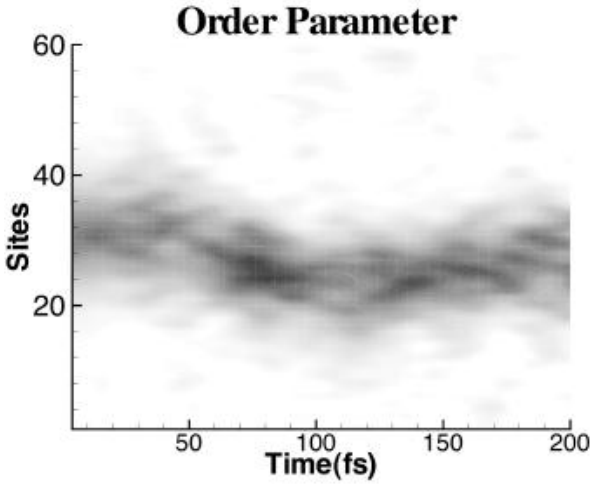

a phenomenological quasi-one-dimensional random walk of a polaron-exciton on the first excited state. The occupation electrons were chosen to set a triplet polaron-exciton. Our results are in good agreement with photo absorption spectroscopy data [4].

Conclusions:

In this work we studied the exciton dynamic on cis conjugated polymers. Specifically, we determined the diffusion length of both triplet and singlet polaronexciton under several temperature regimes. The used method was a semi-empirical tight binding with lattice relaxation. In the scope of the Unrestricted Hartree-Fock Approximation we performed the Ehrenfest molecular dynamic. Our results are in good agreement with experimental observations.

References:

[1] W. A. Luhman and R. J. Holmes, Appl. Phys. Lett. 94 153304 (2009)

[2] P. H. O. Neto, *et al*, J. Phys. Chem. A 113 14975 (2009)

[3] Coropceanu *et al*, Chem Rev 107, 926 (2007)

[4] Mohammad Samiullah *et al*, Phys Rev B 82 205211 (2010)

Bamboo Charcoal Supported Silver Particle by Polyol Process

Tzu Hsuan Chiang[1], Guan-Ting Lai*

[1]Department of Energy and Resources, National United University, Taiwan

thchiang@nuu.edu.tw

Authors Instructions

The structure of 1500°C carbonization bamboo charcoal approach face-centered cubic (FCC) of graphite that had excellent electric and thermal conductivity. For enhance thermal and electric conductivity of materials and the investigation was utilize bamboo charcoal supported silver particle by polyol process.

Introduction

Bamboo charcoal have electric and thermal conductivity when carbonization temperature upper 1000°C. Increase with carbonization temperature cause decrease proportion unregulated carbon structure that can form regulated graphite structure. Ishihara [1] reported the carbonization temperature with 600°C the electric resistance as 10^{12}-$10^{8}\Omega$, 600-800 °C is 10^{8}-10^{1} Ω, upper 800°C is $10^{-2}\Omega$. Many studies reported to synthetize silver particle [2-4] and CNT supported metal [5-6] by polyol process. But there is not study to about bamboo charcoal supported silver particle by polyol process. Therefore, the study used 1500°C carbonization bamboo charcoal that investigate influence on silver particle for different reaction temperature, reaction time and content of silver nitrate.

Materials and Methods

The study used materials such as 1500°C carbonization bamboo charcoal, silver nitrate and reducing agent as tripropylene glycol.

The 1g silver nitrate dissolved to tripropylene glycol then put 0.5g bamboo charcoal (modified by nitrate acid) and heating 120°C at 1hr.

Results and Discussion

Different reaction temperature was effect form silver particle size on bamboo charcoal as shown in Figure 1. The reaction temperature at 100°C formed smaller silver particle onto bamboo charcoal and larger silver particle as reaction temperature with 120°C. In the other hand, the increase with content of silver nitrate react with reducing agent that formed more silver particle which help enhance thermal and electric conductivity of bamboo charcoal.

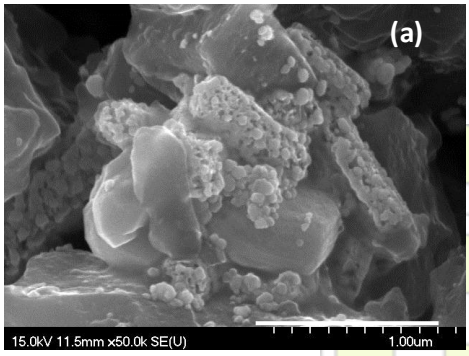

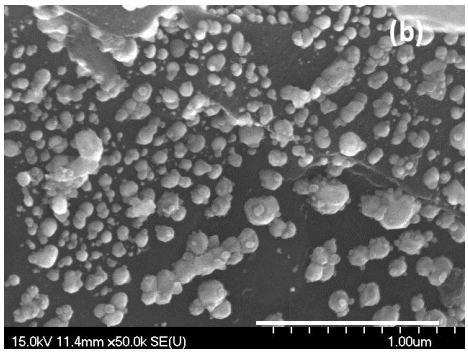

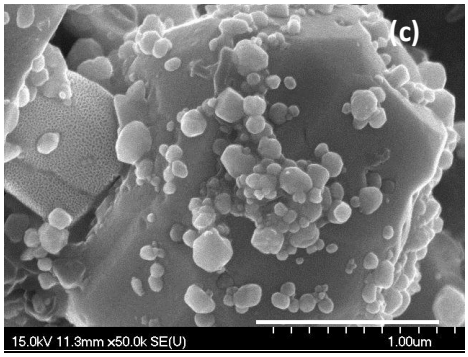

Figure 1: Bamboo charcoal supported silver particle for reaction temperature with (a) 100°C (b)110°C (c)120°C

Conclusions

The bamboo charcoal supported silver particle by polyol process which enhance thermal and electric conductivity.

References

1. S. Ishihara, K. Nishimiya, K. Yamane, I. Ide, Proceedings – 22nd Biennial Conference Held at the University of California, San Diego, CA, 1995, 738-739.
2. D.W. Kim, J.M. Lee, J.J. Lee, P.Y. Kang, Y.C. Kim, S.G. Oh, *Surface & Coatings Technology*, 2007, 201, 7663-7667.
3. D. Kim, S. Jeong, J. Moon, Nanotechnology, 2006, 17, 4019-4024.
4. J. Bregado-Gutie'rrez, A. J. Saldı'var-Garcı'a, H. F. Lo'pez, *Journal of Applied Polymer Science*, 2008, 107, 45-53.
5. X. Wang, B. Xia, X. Zhu, J. Chen, S. Qiu, J. Li, , *Journal of Solid State Chemistry*, 2008, 181, 822-827.
6. Ying Yu, L.L. Ma, W.Y. Huang, J.L. Li, P.K. Wong, J.C. Yu, *Journal of Solid State Chemistry*, 2005, 178, 1488-1494.

Theory of Polyelectrolyte Solutions

Argyrios Karatrantos

Department of Chemistry, University of Durham, Durham DH1 3LE, United Kingdom

argyrios.karatrantos@durham.ac.uk

Soft matter systems, such as polymers, membranes, and proteins, usually contain objects that are electrically charged. The driving force behind the different physical phenomena that appear in charged materials such as liquid crystal ordering, self-assembly, and macroion complexation is the electrostatic interaction. For instance, in a solution it is possible to have a mixture of polyelectrolytes ranging from weak to very strongly charged (Fig. 1). From a theoretical point of view, salt free polyelectrolyte solutions have been studied greatly over the last years [1-4]. However, all these theories fail to qualitatively and quantitatively predict the properties of systems with strong correlations (strong coupling regime).
A theory for salt free polyelectrolyte systems is proposed based on a modified Debye-Huckel approach. The electrostatic interactions are inserted through random phase approximation. Moreover, counterion condensation is accounted for to determine the effective number of charges along the polyelectrolyte as well as of free counterions. The theory is applied to predict the thermodynamic behaviour of flexible polyelectrolytes, such as the osmotic coefficient of a salt free solution in weak and strong coupling regimes. The theory is in agreement with Monte Carlo simulations [4].

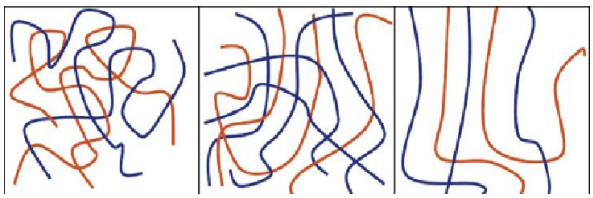

Fig. 1: Charged polyelectrolytes of different coupling strengths. Increasing coupling strength from left to right.

References:

[1] N. von Solms, Y.C. Chiew; *J. Chem. Phys.;* **1999**, 111, 4839.
[2] J.W. Jiang, L. Blum, O. Bernard, J.M. Prausnitz; *Mol. Phys.;* **2001**, 99, 1121.
[3] A.V. Ermoshkin, M.O. de la Cruz; *Phys. Rev. Lett;* **2003**, 90, 125501.
[4] A. Yethiraj; *J. Phys. Chem B*, **2009**, 113, 1539.

A New Method for Size Controlled Synthesis of Zinc Oxide Nanocrystallites and Their Nanocomposite Films

Bunyamin Karagoz, Niyazi Bicak

Istanbul Technical University, Department of Chemistry, Maslak 34469 Istanbul, Turkey

karagozb@itu.edu.tr

Introduction: Control of particle size is critical issue in preparing nanostructured materials. A number of methods, such as controlled-nucleation growth and microemulsion techniques have been developed to attain desired particle sizes[1]. These approaches, however have limited success for precise control of the particle sizes. The inorganic nanoparticles such as ZnO nanoparticles generated by these methods are generally amorphous. The most common method of crystalline nanoparticles is the hydrothermal technique, in which the nanospecies are generated from dissolved reagents[2].

In this work, we described a chemical method, "ligand exchange method", for size-controlled synthesis of zinc oxide nanoparticles in crystalline form at ambient temperatures.

Result and Discussion: In the present procedure size-controlled synthesis of ZnO nanoparticles was achieved by slow exchange of ammonia of the zinc complex with dodecylamine (DDA) in alcohol-water solution.

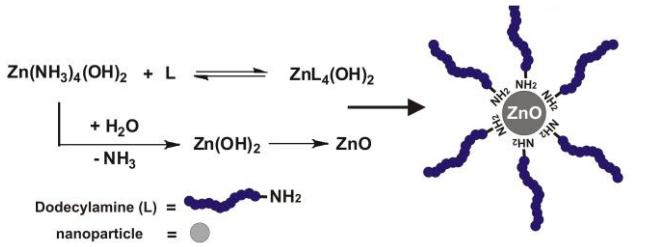

Fig-1 : size controlled ZnO nanoparticle formation in aqueous alcohol solution by simultaneous ligand exchange with DDA

The overall process gave ZnO nanoparticles with surface tethered amine molecules (Fig-1). A series of nanoparticles was prepared using various [DDA] /[Zn (II)] ratios (1/3-1/15 and characterized by UV, FT-IR, TGA, DLS, PL and ESEM techniques. Those investigations implied that, the particle size is directly proportional to M/L ratio (Fig-2).

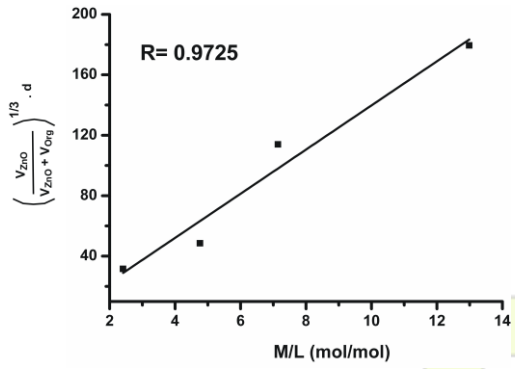

Figure-2: The particle size- M/L relationship for ZnO nanocrystals.

Surprisingly, XRD patterns indicated 30-200 nm size of rod like nanoparticles having hexagonal crystalline (Wurtzite) structure for ZnO nanoparticles.

The resulting nanoparicles were reacted with poly (glycidyl methacrylate)-*block*-poly(methlymethacrylate) in toluene solution to encapsulate in a crosslinked matrix.

The PMMA block was considered as shell forming component to provide miscibility in organic matrix. DLS measurements of the resulting core-shell nanoparticles with L/M: 0.44 indicate considerable increases their sizes (from 62 nm to 212 nm) after treatment with the block copolymer.

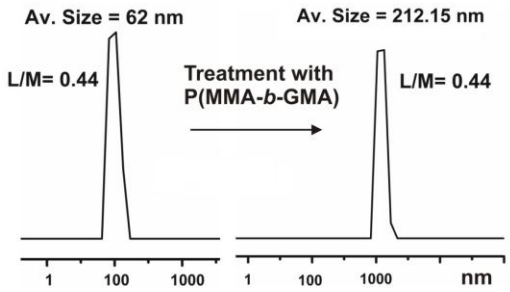

Figure-3: DLS of ZnO nanoparticle (with L/M:0.44) showing size increment after treatment with PMMA-*b*-PGMA

Nearly transparent dispersions of the resulting the core-shell nanoparticles in acetone solutions of poly (methylmetacrylate-*co*-butylacrylate) gave homogenous freestanding films (40-60 μm) with good homogeneities upon casting on glass substrates.

Conclusion: The ligand exchange method presented provides size controlled (60-210 nm) synthesis of ZnO nanoparticles in crystalline forms. Action of poly (glycidyl methacrylate)-*block*-poly(methlymethacrylate) in toluene solution yields core-crosslinked nanocrystallites with PMMA shells.

References

1- Guido Kickelbick Prog. Polym. Sci. 28 83–114(2003)
2- Cheng, H.; Ma, J.; Zhao, Z.; Qi, L. *Chem. Mater. 7*, 663(1995).

Influence of SiO_2 Nanoparticles on Ionic Conductivity of PEI-LiTFSI Electrolytes

İ. Bayrak Pehlivan[1]*, *C. G. Granqvist*[1], *P. Georen*[2], *R. Marsal*[2], *G. A. Niklasson*[1]

[1]Department of Engineering Sciences, The Ångström Laboratory, Uppsala University, P O Box 534, SE-75121 Uppsala, Sweden

[2]ChromoGenics AB, Märstagatan 4, SE-75323, Uppsala, Sweden

*ilknur.pehlivan@angstrom.uu.se

Polymer electrolytes are used in electrochemical devices such as batteries, fuel cells, super capacitors, and electrochromic devices. Some of the most attractive electrolytes for these applications are based on poly (ethylene oxide) (PEO) and its nitrogen analogue poly (ethylene imine) (PEI).

In a previous study [1], we discussed the influence of ion pair concentration and mobility on the molar conductivity of PEI-LiTFSI electrolytes. The influence of the segmental motion of the polymer chains was inferred from comparisons between molar conductivity, glass transition temperature and, viscosity of the electrolyte.

In the present study we used the same methods to investigate the ion conduction mechanism of PEI- LiTFSI electrolytes containing SiO_2 nanoparticles. The ionic conductivity of the electrolytes was examined at different salt concentrations and temperatures and with certain amounts of SiO_2 nanoparticles having a particle size of 7 nm. The electrolytes were characterized by impedance spectroscopy, differential scanning calorimetry, and viscosity measurements. The ionic conductivity was noticeably enhanced as a result of the SiO_2 nanoparticles. A comparison of the latter results with those of the previous study allows us to discuss the influence of ion pairs and the mobility on the conductivity as well as the temperature dependence of the ionic conductivity.

References

[1] İ. Bayrak Pehlivan, P. Georen, R. Marsal, G. A. Niklasson, C. G. Granqvist (2010) Ion conduction of the branched PEI-LiTFSI electrolytes, Electrochimica Acta, accepted.

Keywords: polymer electrolyte, conductivity, poly ethylene imine, nanoparticle, SiO_2.

Disiloxyl and Dihydroxyl Functionalized Polymers by Controlled/Living Polymerization Methods

Nomfusi A Mputumana[1] and Gabriel J Summers[2]

[1]Department of Chemistry, Tshwane University of Technology, Arcadia Campus, Nelson Mandela Drive, PO Box X680, Pretoria, South Africa, 0001

[2]Department of Chemistry, University of South Africa, PO Box 392, UNISA, Pretoria, South Africa, 0003

email: summegj@unisa.ac.za

Introduction:

The atom transfer radical polymerization of styrene provides an efficient method for the synthesis of polystyrene with controlled number average molecular weight, molecular weight distribution, chain functionality, polymer topology and composition1. ATRP entails the reversible homolytic cleavage of a carbon-halogen bond of an alkyl halide initiator molecule in the presence of a transition metal/ligand catalyst complex, such as CuBr/2,2'-dipyridyl, followed by the successive monomer addition to form the resultant polymer1. The present research involves the extension of the ATRP method to the synthesis of chain end functionalized polymers by utilizing functionalized initiators based on substituted 1,1-diphenylethylene derivatives2.

Experimental:

1,1-Bis(4-t-butyldimethylsiloxyphenyl)ethylene was prepared according to the procedure outlined by Quirk and Wang3. The preparation of α-disiloxyl functionalized polystyrene was performed according to the general ATRP method2. α-Dihydroxyl functionalized polystyrene was prepared by the acid catalyzed hydrolysis of α-disiloxyl functionalized polystyrene3. The initiator precursor and functionalized polymers were characterized by size exclusion chromatography, spectroscopy and non-aqueous titration measurements.

Results, Discussions, Conclusions:

By ATRP methods, the initiation of the polymerization of styrene with a functionalized initiator adduct, formed *in situ* by the reaction of (1-bromoethyl)benzene with 1,1-bis(4-t-butyldimethylsiloxyphenyl)ethylene in the presence of CuBr/bpy catalyst in solution, proceeded via a controlled/living fashion to afford α-disiloxyl functionalized polystyrene. Quantitative yields of α-siloxyl polystyrenes with predictable molecular weights and narrow molecular weight distributions were obtained in high initiator efficiency reactions.

Polymer kinetic measurements show that the polymerization reaction follows first order rate kinetics with respect to monomer consumption and the number average molecular weights of the polymers increase linearly with monomer conversion.

Deblocking of the siloxyl group by acid hydrolysis provides the corresponding α-dihydroxyl functionalized polystyrene in quantitative yields.

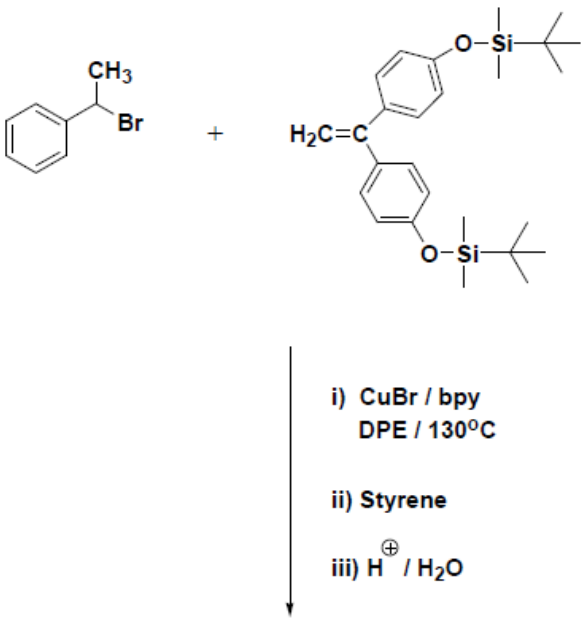

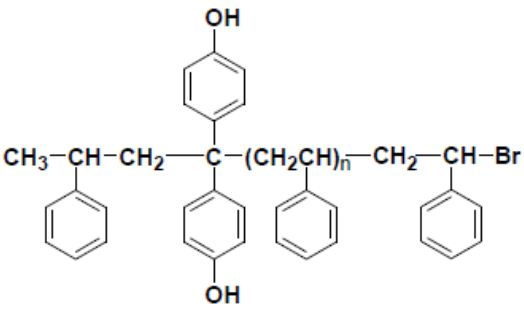

Similarly, preliminary results show that the use of functionalized 1,1-diphenylethylene derivatives as initiator precursors in RAFT polymerization methods produces well defined chain end functionalized polymers.

References:

1K. Matyjaszewski, J. Xia, *Chem. Rev.* **2001**, *101*, 292

2G.J. Summers, M.P. Ndawuni, C.A. Summers, *J. Polym. Sci. Polym. Chem. Ed.* **2001**, *39*, 2058

3R.P. Quirk and Y.C.Wang, *Polym. Intl*, ***1993,*** *31, 51*

Structures of the Thermo-Responsive Poly(*N*-isopropylacrylamide) Grafted from Cotton Fabric Substrate

*Hengrui Yang[1], Haijin Zhu[2], Dujin Wang[2], John H. Xin[1]**

[1] Institute of Textiles & Clothing, Hong Kong Polytechnic University, Hong Kong, PR. China
[2] Beijing National Laboratory for Molecular Sciences, CAS Key Laboratory of Engineering Plastics, Institute of Chemistry, Chinese Academy of Sciences, Beijing 100190, China

e-mail: hr.yang@polyu.edu.hk

Authors Instructions: Hengrui Yang is a PhD student of institute of textiles & clothing, Hong Kong Polytechnic University. Her research focus on the smart multifunctional block copolymer for textile applications.

Introduction: In the last few decades, a lot of interest in both industry and academic circle has been directed towards the modification of the chemical and physical properties of cellulose-based nature fibers, with the aim of obtaining new functional materials or preparing highperformance composites based on renewable resources.1-5 For this purpose, great efforts have been devoted to control properties such as wettability, hydrophobicity, and adhesion of the cellulose fibers by surface modification.6,7 . ATRP has previously been utilized for surface modification of silicon, gold, silica and porous substrates, etc. In this work, ATRP "grafting from" technique was used to polymerize a stimuliresponsive, smart polymer, Poly(Nisopropylacrylamide) (PNIPAAm), from initiators immobilized on cotton fabric substrate.

Results: A temperature responsive homopolymer brushes poly(N-isopropylacrylamide) (PNIPAAm) were fabricated on the surface of cotton fibers by the typical surface-initiated atom transfer radical polymerization in water/methanol. The success of grafting was confirmed by fourier transform infrared spectroscopy (FTIR), Xray photoelectron spectroscopy (XPS). Scanning electron microscope (SEM) images (Fig. 1) was used to study the surface morphology of the bare cotton and cotton-PNIPAAm.1H solid-state NMR techniques were applied to characterize the molecular structure and covalent bond between PNIPAAm and cotton surface.

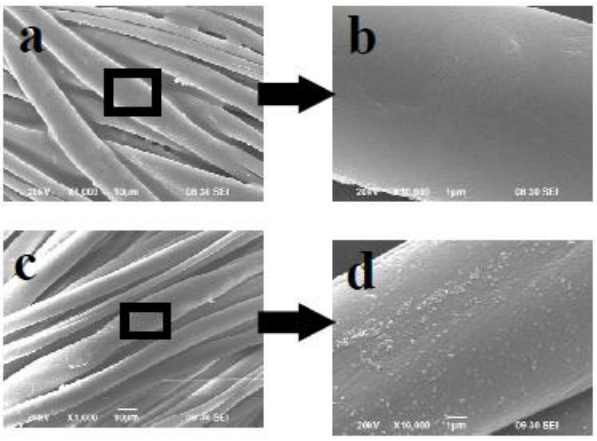

Figure 1. SEM images of (a) bare cotton fabric and (c) cotton-PNIPAAm. (b) and (d) are the magnified image of (a) and (c), respectively. The rectangles in (a) and (c) represent typical areas selected for magnification.

Reference:

(1)Carlmark, A.; Malmstrom, E. E. Biomacromolecules 2003, 4, 1740.

(2)Kono, H.; Yunoki, S.; Shikano, T.; Fujiwara, M.; Erata, T.; Takai, M. J. Am. Chem. Soc. 2002, 124, 7506.

(3)Kono, H.; Erata, T.; Takai, M. J. Am. Chem. Soc. 2002, 124, 7512.

(4)Carlmark, A.; Malmstrom, E. J. Am. Chem. Soc. 2002, 124, 900.

(5)Fujita, M.; Shoda, S.; Kobayashi, S. J. Am. Chem. Soc. 1998, 120, 6411.

(6)Singh, B.; Gupta, M.; Verma, A.; Tyagi, O. S. Polym. Int. 2000, 49, 1444.

(7)Botaro, V. R.; Gandini, A.; Belgacem, M. N. J. Thermoplast. Compos. 2005, 18, 107.

Raspberry–like silica particles to design superhydrophobic surfaces.

Raquel de Francisco, Nuria García and Pilar Tiemblo

Instituto de Ciencia y Tecnología de Polímeros (CSIC)

rdefranciscorivas@ictp.csic.es

Nowadays, the design of surfaces with special wetting behaviour such as superhydrophobicity[1,2] arises much interest because of their applications as self-cleaning and antifouling surfaces. Superhydrophobic surfaces are those with water contact angle (CA) over 150º and hysteresis of 10º or lower.

It is well known that for a surface to show superhydrophobic behaviour both the chemistry of the surface and its topography have to be controlled and roughness at the micro and/or nanoscale has to be introduced. On flat surfaces, a maximum CA of 120º can be achieved by chemical means. Lotus leaves[3], for instance, evidence the need for a dual size roughness to obtain superhydrophobic surfaces.

On the other hand, transparency is a desired property for many of superhydrohobic surfaces applications. However the requirements for transparency and superhydrophobicity are in conflict since the demand micro/nanoroughness for the particular wetting behaviour induces light scattering and therefore opacity. Thus, there are only few examples in the literature which manage both, optical transparency and superhydrophobic behaviour. These works are based on controlled rough structures smaller than the wavelength of visible light.[4]

In this work we present a strategy based on a combination of both low-surface energy compounds and hierarchical topographic features to try imitating raspberry structures.

First, silica particles of different sizes ranging from 50 to 800 nm in diameter have been synthesised by the Stöber[5] method. These particles are dispersed in ultra-pure water using mechanical stirring. Methyltrimethoxysilane (MTMS) was afterwards added to the dispersion to form the nanometric spheres which are grafted to the silica surface. This MTMS condensation reaction is catalysed by ammonium. The final whitish mixture was lyophilized to prevent the agglomeration of the decorated silica nanoparticles.

Reaction conditions such as reaction time, MTMS and catalyst concentrations and post-treatments were studied and optimized to render the raspberry-like structures. These particles were characterized by microanalysis to calculate the MTMS content, solid-state NMR to estimate the MTMS condensation ratio, dynamic light scattering to determine the particle size, specific surface measurement to evaluate the surface coverage, and microscopic techniques, SEM, TEM, and AFM, to elucidate the surface structure. A SEM micrograph showing the particular rough surface of the as-obtained silica particles is shown in Figure 1.

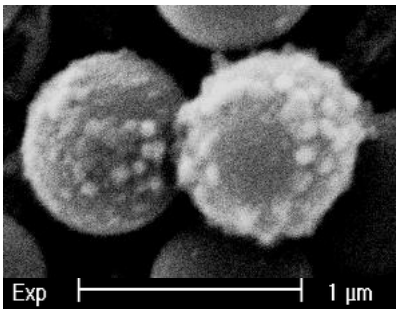

Figure 1: SEM micrograph of raspberry-like silica particles.

These decorated silica particles were dispersed in polymer matrixes of different nature (hydrophilic such as polymethylmethacrylate, PMMA, or hydrophobic as polydimethylsiloxane, PDMS). The dispersions were made using a high shear lab dissolver. The polymer/silica suspensions were used to prepare the final coatings on glass and silicon supports with a spin coater and bar coater. The wetting behaviour, optical transparency, surface roughness and scratch resistance of the resulting surface coatings were critically analyzed.

The results show that using these particular raspberry-like structures it is possible to improve the hydrophobicity of polymer coatings without detrimental effects on transparency and the mechanical properties.

Acknowledgements

We acknowledge financial support from the Spanish Science and Innovation Ministry (MAT2008-06725-C03-01) and CSIC (JAE-Doc grant to R.d.F).

References

[1]Feng, X.; Jiang, L. Adv. Mater. 2006, 18, 3063

[2] Zhang, X.; Shi, F.; Nit, J.; Wang, Z. J. Mater. Chem. 2008, 18, 621

[3]W. Barthlott and C.Neinhuis, Planta ,1997,202,1

[4] P. A. Levkin, F. Svec, J. M. Fréchet. Adv. Funct. Mater. 2009, *19*, 1993-1998.

[5] W. Stöber, A.Fink, E. Bohn: J. Colloid Interface Sci., Nr. 26, 1968, 62–69

Preparation and Characterization of Polyester Resin-Layered Silicate Containing Reactive Groups

Calvo S[1]., Arribas C[1]., Masegosa R. M[2]., Prolongo M[1]. and Salom C[1].

[1] E.T.S. I. Aeronáuticos and [2] E.U.I.T. Aeronáutica. Universidad Politécnica de Madrid. Madrid. Spain

catalina.salom@upm.es

In the last years the area of nanocomposites has received considerable attention with expectation that nanoclay filled polymers can be used as matrix material for high temperature composite application. In addition, unlike traditional filled polymer systems, nanocomposites require relatively low dispersant loadings to achieve significant property enhancements, which make them a key candidate for aerospace applications. These enhancements are primarily a consequence of the interfacial effects that result from dispersing the silicate nanolayers in the polymer matrix and the high in-plane strength, stiffness and aspect ratio of the lamellar nanoparticles. The clay known as montmorillonite (MMT), modified with organic onium ions with long alkyl chains, has been widely used in order to obtain nanocomposites. In previous works (1,2) it has been reported that the presence of reactive groups in organic onium ions can form chemical bonds with the polymer matrix which favours a very high exfoliation degree of the clay platelets in the nanocomposite. In this work nanoclays from MMT have been modified using cationic exchange and characterized. Then, polyester (PE) nanocomposites have been prepared from unsaturated polyester resin (UPE). The effect of the type of reactive alkyl ammonium ion clay modifier (RAA) on the microstructure and on the thermal mechanical behaviour has been analyzed. The results are also compared with PE/C30B MMT previously studied.

Materials and Methods

The materials used in the preparation of PE thermosetting nanocomposites are listed in Table 1

Table 1 Materials used in PE nanocomposites

UPE	Norsodyne 44233
MMT	Na^+ montmorillonte
C30B	$CH_3T(CH_2CH_2OH)_2N^+Cl^-$
RAA1	Di-allyl-dimethyl ammonium chloride
RAA2	[2-(acryloyloxy) ethyltrimethyl ammoniun] chloride

Preparation of reactive nanoclays

Reactive nanoclays (RN) were prepared using the cationic exchange reaction between MMT and RAA´s modifiers. Thus, 3 g of MMT in 250 ml of distilled water was stirred at 300 rpm during 2.5 h (T=60 ºC). A separate solution with 1ml of RAA1 or RAA2 in 20 ml of water + ethanol was kept under vigorous stirring during 45 min at room temperature. The modifier solution was slowly added to MMT solution (1 h), stirred at 300 rpm and T=30 ºC. The ion exchange reaction was then carried out by stirring de mixture for 2 h at 60ºC and 15 h at room temperature to obtain the reactive nanoclay. The reactive nanoclay was washed repeatedly with distilled water. RN powder was obtained by freeze-drying the product.

Preparation of PE/RN nanocomposite. A mixture of UP resin+RAA1 or RAA2 (4% weight fraction) was stirred at 300 rpm at 50ºC during 7 h. In both cases, well-dispersed mixtures and stable suspensions of the RAA´s in UPE were obtained. Then, crosslinking reaction was initiated adding 1.5 wt% of benzoyl peroxide to UP/RAA mixtures. The mixture was achieved by stirring at 400rpm at room temperature. Next the reactive mixtures were pressed in aluminum moulds and cured in an oven at 80 ºC for 1 h. Postcuring was also performed for 3 h at 110 ºC.

Results and Discussion

Figure 1 shows the wide angles X-ray diffraction patterns (WAXD) of PE/RN nanocomposites

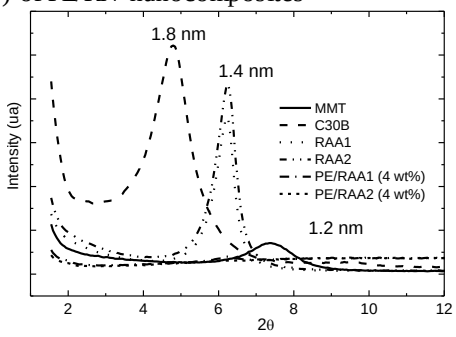

Figure 1. WAXD patterns for PE/RN nanocomposites

The reactive MMT (MMT-RAA1 and MMT-RAA2) shows an interlayer distance d_{001} of 1.4 nm placed between the corresponding ones to MMT-Na^+ and commercial organic modified MMT (C30B). This behaviour indicates that de reactive organic modifier RAA1 and RAA2 are less effective in diffusing into the clay gallery than the non reactive organic modifiers of C30B. However PE/RN nanocomposites show no peaks in WADX patterns in the $1.5º<2\theta<10$ region which is in accordance with a fully exfoliated structure for PE/RN nanocomposites.

The thermal characterization of the nanocomposites by means of DSC measurements (Mettler Toledo mod 821 DSC calorimeter) indicates that the glass transition temperatures, T_g, of RN nanocomposites are similar to those obtained for PE/C30B. However the thermo-mechanical properties determined by DMTA (DMTA V Rheometric Scientific instrument) are significantly improved. It has been observed an increase of 30% in the value of the elastic modulus, E´ in the glassy region, respect to the E´ value of PE/30B nanocomposites. This increment reaches up to 70% in the rubber region.

Conclusion

Exfoliated structures of polyester nanocomposites have been obtained using reactive nanoclays as organic modifiers. A significant improvement in the mechanical behaviour has been observed.

References

1- Chen-Yang YW, Lee YK, Chen YT, Wu JC. Polymer 2007;48:2969
2- Lu H, Hu Y Li M Cheng Z, Fan W, Compos Sci Technol 2006;66:3035

Analysis of Polyhedral Oligomeric Silsesquioxanes, POSS, influence in properties of epoxy thermoset materials

B. Montero[2], *A. Serra*[1], *C. Ramírez*[2], *X. Ramis*[3]

[1] Department of Analytical and Organic Chemistry, University Rovira i Virgili, C/ Marcel lí Domingo s/n, 43007 Tarragona, Spain.
[2] Group of Polymers, Department of Physics, University of A Coruña, Avda. 19 Febrero s/n, 15405 Ferrol, Spain.
[3] Thermodynamics Laboratory, ETSEIB Universitat Politècnica Catalunya, Diagonal 647, 08028 Barcelona, Spain

angels.serra@urv.cat

Introduction

This study is focussed on the use of a new class of organic-inorganic hybrid as modifier of epoxy networks. These hybrids, the polyhedral oligomeric silsesquioxanes, POSS, are nanosized cage structures, that can be chemically incorporated into linear or thermosetting polymers.[1] These compounds are based on a Si-O central cage, which have different organic chains linked on it. If some of these chains have any active group, it can react with the epoxy rings of the resin becoming covalently linked to the network structure.

Material and methods

Mixtures of diglycidylether of bisphenol A resin (DGEBA Araldite GY240, provided by Hunstman) and two different POSS, the glycidylisobutyl-POSS (GIb) and the glycidylcyclohexyl-POSS (GCh), provided by Hybrid Plastics were cured with methyltetrahydro-phtalic anhydride (MTHPA) from Sigma-Aldrich by means of a catalyzed mechanism using N,N-dimethyl benzylamine (BDMA) from Fluka.

Epoxy nanocomposites with 1, 3 and 5 wt% of both POSS were prepared. The curing procedure was studied by differential scanning calorimetry with a Mettler Toledo DSC-821e thermal analyzer and FTIR spectrophotometer FTIR-680PLUS from Jasco. This device is equipped with an attenuated-total-reflection accessory with thermal control and diamond crystal (Golden Gate heated single-reflection diamond ATR, Specac Tecnokroma).

Thermal-dynamic-mechanical analyses were carried out with DMTA 2980 from TA Instruments.

Results and discussion

The presence of both POSS slows down the reaction as observed by DSC. In mixtures containing GIb, the deceleration is higher with increasing of POSS content but, in samples with GCh higher contents of POSS this has a minor effect on the reaction rate. GIb shows a glass transition at -13 ºC and three melting points at 51 ºC, 112 ºC and 135 ºC respectively, while, GCh only shows a glass transition at -37 ºC. The curing of samples with GIb starts at a lower temperature than the third melting point of this POSS and therefore the delay in the start of curing with higher contents of GIb can be attributed to the presence of unreacted crystalline POSS agglomerates. In samples with GCh, the curing shows a slight delay in reference to the neat formulation because of the presence of the rigid cage structures of Si-O. However, the higher reactivity of epoxy cycloaliphatic groups and the greater size of these nanoparticles, which increases the free volume, lead to an improvement of the reactivity.

Isoconversional kinetic analysis and Coats-Redferns method were applied to DSC scans in order to determine the kinetic parameters and the kinetic model.

An autocatalytic procedure with reaction orders m + n = 2 was selected as the kinetic model that better explains the experimental results.

IR analyses at a temperature of 150 ºC is used to follow the disappearance of the bands corresponding to epoxy and anhydride groups and the appearance of the ester band produced during the curing process. The results obtained confirm that the reaction occurs even in the presence of POSS with the same trend than the observed by DSC. [2]

Finally, thermo-mechanical properties analyzed by DMTA show a decreasing of glass transition temperature, T_g, of the samples when POSS is added, (fig. 1). This fact is attributed to the higher free volume of mixtures when the cage of POSS is present in the structure.

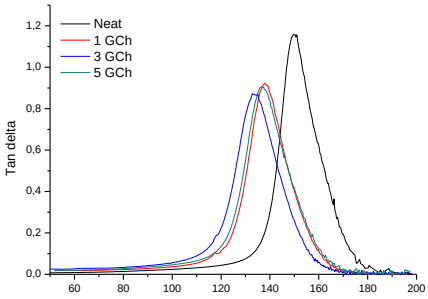

Fig.1. Tan δ determined by DMTA of thermosets modified with GCh.

The storage moduli in the rubbery state are higher in all the POSS modified thermosets, which is attributed to the rigidity that the inorganic nanoparticles provides to the structure.

Conclusions

The presence of POSS in the neat epoxy resin slows down the reaction in different ways, depending on the thermal behavior of the POSS used and its structure. However, the reaction can completed and the materials obtained have a higher stiffness than the neat material in the rubbery state.

References

[1] S. A. Pellice, D. P. Fasce, R. J. J. Williams. J. Polym. Sci.: Polym. Phys. 41 (**2003**) *1451-1461*.

[2] M. Morell, X. Ramis, F. Ferrando, Y. Yu, A. Serra. *Polymer* 50 (**2009**) *5374-5383*.

Acknowledgements

To MICINN, FEDER, Xunta de Galicia and Generalitat de Catalunya (MAT2008-06284-C03-01, MAT2008-06284-C03-02, XUGA IN809A, 2009-SGR-1512)

Obtaining of biodegradable polymer films containing silver nanoparticles

Kh. E.Yunusov, A. A. Atakhanov, A. A.Sarymsakov, S. Sh.Rashidova

Institute of Polymer Chemistry and Physics, Academy of Sciences of Uzbekistan
7-"b" Abdulla Kadyri Str. Tashkent, Uzbekistan, Ind:100128

e-mail:haydar-yunusov@rambler.ru

Introduction

Synthesis of silver clusters and nanoparticle in solution of polymers and polymeric matrixes are en intensively developing direction of reception of nanostructures systems containing metal nanoparticles with unusual physico-chemical and medico-biological properties [1]. Researches in this area show, that macromolecules not only stabilize the disperse systems, but also participate in their formation, controlling the size and the form of growing nanoparticles [2-3].

The aim of this work is to obtain of biodegradable bactericidal polymer films, containing nanoparticles of silver on the basis of derivatives of cellulose.

Materials and Methods

The following samples as research objects were selected: Na-carboxymetilcellulose (Na-CMC), microcrystalline cellulose (MCC) and nanocellulose (NC).

In 2% solution of Na-CMC and suspensions of MCC, NC solutions of polymers, under ultrasound dispersion 0,01-0,1M the solution of nitrate silver was added.

Films with the thickness of 20-40 microns were obtained by the method of overflow from the polymer, containing $AgNO_3$. The process of nanosized silver particles formation in polymer was initiated by ultra-violet irradiation.

Results and Discussion

The formation of spherical silver nanoparticles and clusters has been observed in the course of photochemical restoration of CMC salts the content silver ions. It has been established, that containing of free Ag^+ ions in a reactionary blend is no more than~5%, the formation of nanoparticle take place only at the expense of photorestoration of cations, connected with CMC carboxylate-anions. Therefore with rather high concentration of carboxylate-anions the complex of $Ag^+ \cdot$CMC represents as a nanoreactor at formation of silver nanoparticles. It has been established, that, at low 0.01 M concentration of silver nitrate the form of silver nanoparticles are spherical with diameter of 8-25nm. (fig. 1a)

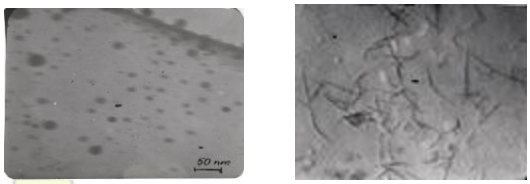

а) б)

Fig.1. TEM images of *films* CMC *containing spherical (a) and rod nanoparticles silver(b).*

At increasing the concentration of silver nitrate up to 0,1M solution CMC the nanoparticles silver.were formed in form of nanorods with length of 500 nm and thickness of 30-50 nm. (fig. 1b)

At fig.2 shows TEM images of the obtaining samples nanocomposite on the basis of NC and MCC.

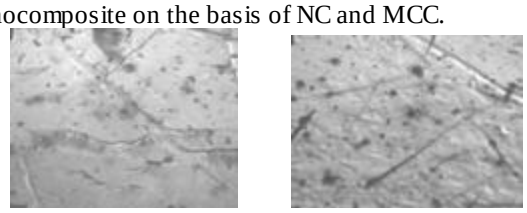

а) б)

Fig. 2. TEM images of NC *(a) and* MCC *(b) films containing spherical and rod nanoparticles silver.*

The samples containing spherical nanoparticle of silver with the size of about 35-60 nanometers were obtained with the addition of 0,01 M aqueous $AgNO_3$ solution to 2 % water suspension of NC under ultra sound and UF-irradiations.(fig. 2a)

In the same concentration of $AgNO_3$ in the suspension of MCC it is observed more accurately rod silver clusters. In this case the range of the size and the form of particle nanosilver is very great. Spherical and linear forms of silver nanoparticles with various sizes are observed,.

The increase in concentration of a solution of nitrate of silver leads to transformation of spherical particles into nanorods having the length till several microns at width of 50-70 nanometers. (fig. 2b)

In this case on the surface layer of MCC elastic resistance of a matrix is possibly less, that, apparently, and it defines the formation of nanoparticle of big sizes.

Conclusions

The possibility of reception of the films containing nanoparticle of silver on the basis of biodecomposed polymers, such as CMC, MCC and NC is studied.

It is shown, that depending on structure and molecular characteristics of used polymeric matrix and concentration of silver ions it is possibility regulated the sizes and forms of silver nanoparticles. Obtained biodegradable, antimicrobic and bactericidal films can be used as a covering agent for the treatment of wound and burns.

References

1. Pomogaylo A. D., Rozenberg A. S., Uflyand I. E. Nanoparticle of metals in polymers. M, 2000.
2. Litmanovich A. A., Papisov I. M. / Vysokomolek. Soed. A series. 1997. 39. P. 323.
3. Huang H. H., Ni X. P., Loy G. L. et. al. // Langmuir. 1996.12. P. 909.

First-Principles Simulations of IR Spectra of Polymers: Nylon-6 Polymorphs

Alberto Milani, Claudio Quarti, Chiara Castiglioni

Dip. Chimica, Materiali, Ing. Chimica "G. Natta", Politecnico di Milano,
P.zza Leonardo da Vinci, 32 - 20133 Milano, Italy

alberto.milani@polimi.it

Introduction In addition to their use in the everyday life, many advanced applications in polyamides science and technology are still investigated: the development of nanocomposites, the application of the electrospinning technique and even applications in the field of biomaterial and nanomedicine are promising fields of research. Moreover, the detailed study of structure/property correlations is required in these perspectives. Polymorphism in particular is the key feature ruling at a nanoscale the properties shown by these materials and nylon-6 is probably the most significant example, due to the existence of two main crystalline forms (α and γ). The characterization of nylon polymorphs has been experimentally carried out by means of X-ray diffraction and IR spectroscopy and sometimes by molecular mechanics simulations. In the case of vibrational spectroscopy, however, a reliable simulation requires suitable first-principles techniques, which became available only in very recent years. Therefore, their spectroscopic characterization is often left to fully experimental works whose results are now routinely used also for the characterization of new systems based on polyamides. However, no validation of these results has been so far presented based on accurate molecular calculations. To this aim, we here present state-of-the-art first-principles simulations of the IR spectra of nylon-6 (NY6) α and γ polymorphs.

Materials and Methods Density Functional Theory (DFT) calculations of the NY6 polymorphs were carried out by using the CRYSTAL09 code [1]. The functional B3LYP was used with 6-31G** basis set; the correct description of Van der Waals forces was guaranteed by application of Grimme's correction. A full geometry optimization of the two crystal structures was carried out by taking into account properly the space group symmetry of the systems; based on the optimized structures so obtained, IR spectra were calculated and compared with the available experimental spectra for both the forms.

Results and Discussion We report in the figure the comparison between the DFT computed and experimental IR spectra of the two crystalline forms of NY6, showing separately the two frequency ranges where spectroscopic markers of the two structures can be found. A very good agreement is found between experimental and computed spectra: we can confirm that the bands at 930, 960 and 1030 cm^{-1} are indeed clear markers of the α form while the bands at 915, 973 and 1002 cm^{-1} are markers of the γ form. This conclusion is in agreement with previous experimental studies where these assignment are accepted on the basis of empirical spectral correlations [2]. It should be noted that some authors [3] assigned the band 973 cm^{-1} to the metastable β form: our investigation does not support this results.

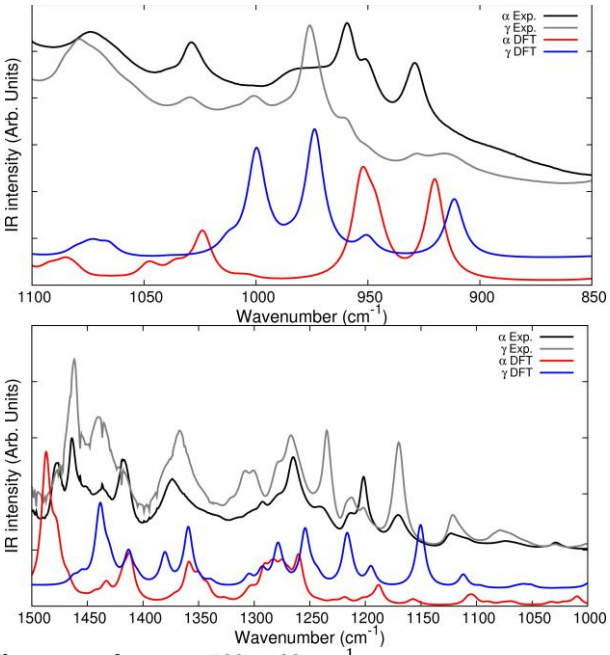

The spectral range 1500-1100 cm^{-1} is even more interesting since some ambiguities are present in the previous studies and marker bands in this range have been rarely identified or used when investigating the different crystal phases of NY6. Based on our calculations, the band at 1170 cm^{-1}, sometimes assigned to the amorphous phase and sometimes to crystalline forms [3], should be attributed mainly to the γ form as for the bands at 1234 and 1440 cm^{-1}. On the other side, we can assign the bands at 1202, 1416 and 1478 cm^{-1} to the α form. For all these bands, assignments in terms of phonon eigenvectors can be now proposed unambigously. A deeper and complete characterization of the IR spectra of NY6 can be thus obtained based on DFT calculations, thus providing new basis for the characterization of NY6-based materials by means of vibrational spectroscopy.

Conclusions DFT calculations have been used to simulate the IR spectra of two NY6 polymorphs by using the state-of-the-art techniques of computational solid state chemistry. A very good agreement is found between experimental [2] and computed spectra: on this basis previous experimental analysis have been discussed, confirming some of the previous assignment, introducing new evidences and settling some of the existing ambiguities.

References

[1] R. Dovesi et. Al, CRYSTAL09 (CRYSTAL09 User's Manual. University of Torino, Torino, 2009).

[2] H. Arimoto J. Polym. Sci. A **1964**, 2, 2283; N. Vasanthan et al. **2001**, 39, 536 ; K.H. Lee et al. Macromol. **2008**, 41, 1494

[3] O. Persyn et al. Polym. Eng. Sci. **2004**, 44, 261; V. Miri et al. Polymer **2007**, 48, 5080.

Covalent Modification of MWCNT for Styrene-Isoprene-Styrene Block Copolymer-Based Nanocomposites

M. Ilčíková,[a] *M. Mrlík,*[b] *A. Juhari,*[c] *K. Koynov,*[c] *T. Sedláček* [b], *K. Csomorová,*[a] *J. Mosnáček* [a]

[a]Polymer Institute of Slovak Academy of Sciences, Dúbravská cesta 9, 845 41 Bratislava, Slovakia
[b]Polymer Centre of Faculty of Technology, TGM 275, 762 72 Zlín, Czech Republic
[c]Max Planck Institute for Polymer Research, Ackermannweg 10, D-55128 Mainz, Germany

upolmail@savba.sk

Introduction: Since their discovery, carbon nanotubes (CNT) have attracted particular attention for their unique structural, mechanical and electrical properties. However, thank to strong van der Waals interactions, CNT tend to aggregate and their not uniform dispersion limits their applications. Functionalization of CNT with long molecules and polymer chains enables suppressing the interactions between CNT and their aggregation.
In this work, Nanocyl multiwall carbon nanotubes (MWCNT) were covalently modified in order to achieve better dispersion and their location in one phase of styrene-isoprene-styrene block copolymer (Kraton). The modification is expected to cause significant changes in mechanical and electrical properties of final composite materials.
Materials and methods: Surface of MWCNT was modified by a) polymerization of styrene from MWCNT surface (MWCNT-PS), or b) covalent bonding of cholesteryl groups (MWCNT-chol). In both cases, MWCNT surface was first modified by 4-(2-hydroxyethyl)nitrobenzene to introduce hydroxyl groups onto MWCNT surface (MWCNT-OH). MWCNT-PS were prepared by reaction of MWCNT-OH with 2-bromopropionyl bromide and subsequent atom transfer radical polymerization of styrene from the surface of MWCNT by ATRP using CuBr/PMDETA as a catalytic system. MWCNT-chol were prepared by esterification of MWCNT-OH by reaction with cholesteryl chloroformate. The modified MWCNT were characterized by scanning electron microscopy (SEM), transmission electron microscopy (TEM), thermal gravimetric analyses (TGA), and Fourier transmission infrared spectroscopy (FTIR).

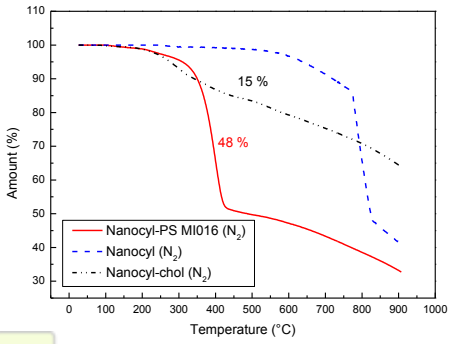

Figure 1: TGA of neat MWCNT, MWCNT-PS and MWCNT-chol under nitrogen atmosphere

Results and discussion: According to conversion determined by NMR and GC, the molecular weight of PS grafted from the MWCNT surface was 4500 g/mol. The average content of grafted PS determined by TGA in nitrogen atmosphere was about 48 ± 3wt. % (Fig. 1). FTIR spectra (ATR, Ge) proved the presence of peaks corresponding to PS. The modification was confirmed also by TEM, where white layer of PS was observed around the MWCNT (Fig. 2).

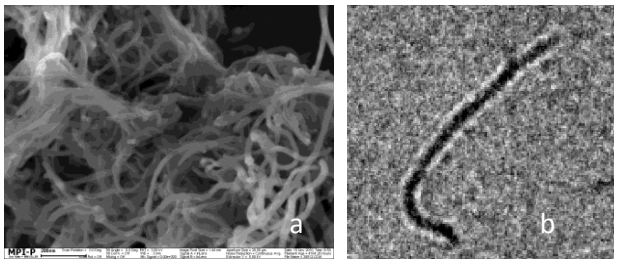

Figure 2 a) SEM image of MWCNT-PS b) TEM image of 0.1 wt. % MWCNT-PS/Kraton cast from chloroform, solution concentration 3mg/ml

The content of grafted cholesteryl groups in MWCNT-chol determined by TGA in nitrogen atmosphere was about 15 wt %. The modified MWCNT were used for composite preparation by casting from solution method.

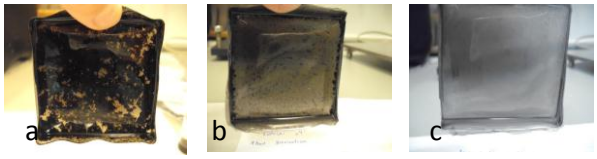

Figure 3 The composite films of Kraton containing 0.1 wt. % of a) neat MWCNT, b) MWCNT-chol, and c) MWCNT-PS.

The best films were obtained as follows: The carbon nanotubes were sonicated for 1 hour in chloroform and subsequently mixed with dissolved polymer matrix and sonicated for 10 minutes. The films were prepared by slow evaporation of the solvent.

Conclusion: MWCNT were successfully covalently modified. The modification significantly improved positive influence on carbon nanotubes dispersion, what was best observable at concentration of 0.1 wt. %.

Acknowledgement. The authors thank for the financial support to the Centre for materials, layers and systems for applications and chemical processes under extreme conditions Stage II supported by the Research & Development Operational Programme funded by the ERD, the European Commission within 7th Frame Program (project NOMS, contract no. 228916) and the Grant Agency VEGA through Grant 2/0074/10.

Influence of montmorillonite (Cloisite 30B) content on water and oxygen barrier properties of polylactic acid films

Nadine TENN[1], Nadège FOLLAIN[1], Kateryna FATYEYEVA[1], Sébastien ALIX[2], Jérémie SOULESTIN[2], Stéphane MARAIS[1]

[1] Université de Rouen, Laboratoire Polymères, Biopolymères et Surfaces, UMR 6270 & FR 3038 CNRS, Bd. Maurice de Broglie, 76821 Mont Saint Aignan Cedex, France

[2] Department of Polymers and Composites Technology & Mechanical Engineering, Ecole des Mines de Douai, 59508 Douai Cedex, France

nadine.tenn@univ-rouen.fr

Barrier properties of polymers are currently in great demand, particularly in packaging industry, where they are replacing many traditional materials [1]. However, in comparison with traditional materials (metals, glass and paper) plastic packaging are more permeable to gases, water vapor and aroma compounds. The ingress of water leads to a permanent change in the nature of food products. Thus, the protection of the packaged goods against oxygen and water vapor is an essential prerequisite for achieving a long shelf-life [2].

With growing environmental awareness, the use of biodegradable polymers is seen as one of many important strategies to minimize the environmental impact of petroleum-based plastics. Therefore, the research of biodegradable polymers has gained considerable attention in recent years. Among all biodegradable polymers, polylactic acid (PLA) is the most promising polymer which in addition to its biodegradable characteristics shows good mechanical, thermal and barrier properties, comparable to those of polystyrene or poly(ethylene terephtalate) [3,4]. However, PLA gives rise to degradation, mainly caused by hydrolysis reactions in the presence of water. Different solutions were proposed in order to solve this problem, for example melt blending with other polymers or nanoparticles.

In this work a serie of PLA based nanocomposites containing organomodified montmorillonite (Cloisite 30B) was prepared. The influence of montmorillonite content (5, 10, 15 and 20 wt. %) in the nanocomposite film on water and oxygen permeabilities, on phase morphology and on thermal behavior was investigated. Atomic force microscopy (AFM) images confirmed well the homogeneous distribution of montmorillonite nanoparticles in the composite films up to 15 wt. % of Cloisite 30B. The presence of Cloisite 30B agglomeration was observed for nanocomposite films with particle content higher than 15 wt. %. The dispersion of clay nanoparticles in composite films was revealed by X-ray diffraction measurements. Besides, the increase of the crystallinity degree with the increasing of nanoparticle content (up to 15 wt. %) was found by means of DSC measurements. An important decrease of water (about 70 %) and oxygen (about 60 %) permeabilities was observed for nanocomposite film with 15 wt. % of Cloisite 30B. This high barrier effect may be explained by good dispersion and orientation of nanoparticles and, also, by the increase of the crystallinity degree of the nanocomposite film.

Therefore, the obtained results show the interest of using such nanocomposites for packaging application, especially due to the important improvement of their barrier properties.

References:

[1] J. Lange, Y. Wyser, “Recent innovations in barrier technologies for plastic packaging-review”, Packaging Technology and Science 16 (2003) 149-158.

[2] S. Marais, Y. Hirata, C. Cabot, S. Morin-Grognet, M.-R. Garda, H. Atmani, F. Poncin-Epaillard, “Effect of a lower-pressure plasma of polyethylene films”, Surface & Coating Technology 201 (2006) 868-887.

[3] J.-W. Rhim, S.-I. Hong, C.-S. Ha, “Tensile, water vapor barrier and antimicrobial properties of PLA/nanoclay composite films”, LWT-Food and Technology 42 (2009) 612-617.

[4] R.A. Auras, B. Harte, S. Selke, R. Hernandez, “Mechanical, Physical, and Barrier Properties of Poly(Lactide) Films”, Journal of Plastic Film & Sheeting, 19 (2003) 123-135.

Organo modified clay - Biodegradable PHB/PCL nanocomposites: morphology, mechanical and barrier properties evaluation as function of blend composition

Botana, Adrián[º]; Mollo, Mariana[º]; Eisenberg, Patricia[º]**

[º] INTI-Plásticos, San Martín, Argentina; * 3iA – UNSAM, San Martín, Argentina

patsy@inti.gob.ar

Introduction

Polymer blending is an alternative approach to obtaining new materials with desirable properties based on available polymers rather than to design and synthesize completely new polymers. Blends obtained from polycaprolactone (PCL) and polyhydroxybutyrate (PHB) are immiscible polymer. Researchers show organo-modified clay changes blend morphology in different immiscible polymer blends [1,2]. In a previous work we studied the preparation of nanocomposite materials from PHB and organic modified clay [3].

In the present study, we evaluate blend nanocomposite films morphology, mechanical and barrier properties in order to study the effect of organic modified clay on PHB/PCL blends, as function of its composition. Films were obtained by cast film extrusion.

Materials and Methods

Commercial grade PCL FB 100 was supplied by Solvay Chemical and PHB homopolymer by PHB Industrial S.A.. "Cloisite^{TM} 30B"(MMT30B) was supplied by Southern Clay Products.

PHB /PCL (20/80 and 50/50 w/w) blends and their composites (5% MMT30B) were prepared in a Werner & Pfleiderer ZSK25 intermeshing twin screw extruder. Films were obtained in a Killion KL-100 single screw extruder with flat die and take off unit. PHB/PCL blend and nanocomposite films morphology (fractures surface) was studied by SEM (Philips 505). Mechanical properties were measured in machine direction using INSTRON 5569A (Test Method ASTM D882). Oxygen permeability was measured using OX-TRAN 2/61(MOCON) (Test Method ASTM D3985) and water vapor permeability (WVP) was determined using a modified ASTM E96 procedure at RH 52%.

Results

SEM images (Figure 1) show that incorporation of MMT30B organo modified clay to PHB/PCL (20/80) does not change blend morphology. The size of PHB disperse phase in PHB/PCL/MMT30B nanocomposite was smaller. For PHB/PCL 50/50 a co-continuous morphology was clearly formed (Figure 2). Occlusions of PCL within the PHB continuous phase and occlusions of PHB within PCL continuous phase were observed. MMT30B incorporation changes the blend morphology from a co-continue to a ¨disperse phase into matrix¨ morphology. The disperse phase domain size decreased drastically when MMT30B was incorporated to PHB/PCL blend, as it was shown for different polymer blends by other authors [2, 3]. MMT30B intercalation/exfoliation was effective due to a better interaction with the polymeric matrixes (PHB and PCL). The organic modified clay was localized at the interfacial polymer region [4]. Nanocomposite blend films mechanical and barrier properties are shown in Table I. For PHB/PCL 20/80 blend no significant difference was observed for the properties evaluated in this study, when MMT30B was added. For nanocomposites films obtained with PHB/PCL 50/50, better mechanical and barrier properties were observed. The change in blend morphology could explain the highest mechanical and gas barrier performance of PHB/PCL 50/50/ MMT30B nanocomposite film.

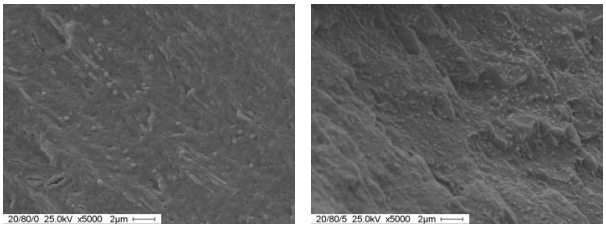

Figure 1:PHB/PCL 20/80 (left) and PHB/PCL 20/80/MMT30B (right)

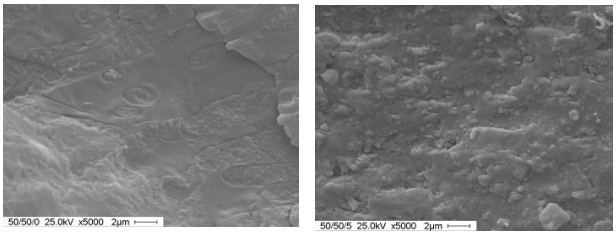

Figure 2:PHB/PCL 50/50 (left) and PHB/PCL 50/50/MMT30B (right)

Table I: Mechanical and barrier properties

PHB/ PCL/ MMT30B film	Elastic Mod (GPa)*	Tensile Max.(MPa)*	O_2 permeability**	WVP ***
20/80/0	0.7 (0.1)	19 (2)	202	--
20/80/5	0.9 (0.1)	17 (1)	167	--
50/50/0	0.9 (0.1)	11 (1)	112	3.1×10^{-14}
50/50/5	1.8 (0.1)	12 (1)	61	8.3×10^{-16}

*Crosshead rate 50mm/min. **(10^{-3}cm^{3}um/m^2/d/atm). ***(g/m/seg/Pa)

Conclusion

Nanocomposite films from PHB/PCL 50/50 and 20/80 (w/w) and MMT30B, were prepared by cast film extrusion. Morphology, mechanical and barrier properties were evaluated in order to study the effect of MMT30B incorporation for different blend composition. The incorporation of MMT30B changes the blend morphology and, as a consequence of this, PHB/PCL 50/50/5 films showed better mechanical and barrier properties.

References

[1] Lepoittevin, B; Devalckenaere, M; Pantoustier, N; Alexandre, M; Kubies, D; Calberg, C; Jérôme, R; Dubois, P. Polymer, 43 (2002) 4017-4023.

[2] Qiu, Z; Yang, W; Ikehara, T; Nishi, T. Polymer, 46 (2005) 11817.

[3] Botana, A; Mollo, M: Eisenberg, P; Torres Sanchez, RM. Applied Clay Science, 47 (3-4), (2010) 263-270

[4] Botana, A; Mollo, M; Reborí, T; Eisenberg P. V Simposio Chileno-Argentino de Polímeros Archipol´09. P.1.C.24-GP

Behavior of Polyelectrolyte Solutions in a Wide Temperature Range

S.K. Filippov[a], *Thomas A.P. Seery*[b,c], *Peter Černoch*[a], *Jiří Pánek*[a], *Stepanek*[a]

[a] Institute of Macromolecular Chemistry, Academy of Sciences of the Czech Republic, Heyrovský Sq. 2, 162 06 Prague 6, Czech Republic

[b]Department of Chemistry, University of Connecticut, Storrs, Connecticut 06269 [c]Polymer Program, Institute of Materials Science, University of Connecticut, Storrs, Connecticut 06269

e-mail:filippov@imc.cas.cz

We exploit the strong temperature dependence of dielectric constant of N-methylformamide to vary the Bjerrum length of a polyelectrolyte, sodium polystyrene sulfonate, and investigate the dynamic properties of salt-free solutions over a broad temperature range, from 54 to -58 °C.

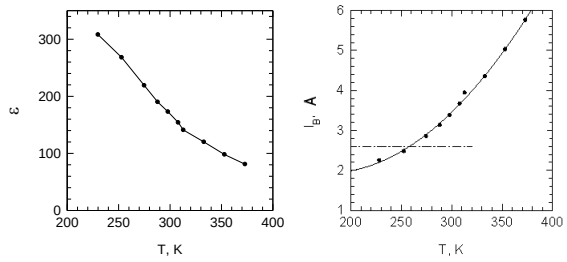

Fig. 1. (a).Temperature dependence of dielectric constant ε of NMF (b)Temperature dependence of Bjerrum length l_B for NaPSS. The dotted line indicates the distance of the neighboring charges on the polyelectrolyte chain.

Dielectric constant, ε for NMF (ε = 160 at 25°C) is much higher than that of water (ε = 85 at 25°C) and strongly depends on temperature (Fig. 1a). This feature of the solvent can be exploited to vary the Bjerrum length (Fig. 1b), to make it possibly larger or smaller than the charge spacing a of the polyion. The purpose of this paper is to investigate, by dynamic light scattering, whether the transition between the ordinary and extraordinary regime in salt-free polyelectrolyte solutions can be achieved only by a change of temperature.

For PSSA in salt-free solution in NMF, DLS experiments were performed in broad temperature range from -58 to 54 °C (Fig. 2). One can see that intensity correlation functions $g_2(t)$ are clearly bimodal with a fast and slow relaxation processes.

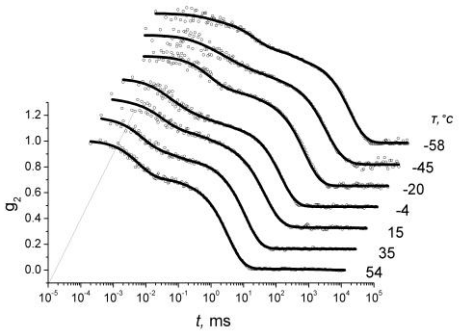

Fig. 2. Correlation functions $g_2(t)$-1 measured at a scattering angle of 90° together with the fitted curves, for the indicated temperatures T(°C).

Therefore we have selected the model of double Williams-Watts stretched exponential function to analyze the intensity correlation functions. The temperature dependence of the diffusion coefficients and the amplitude of the fast and slow modes is shown in Fig. 3a,b.

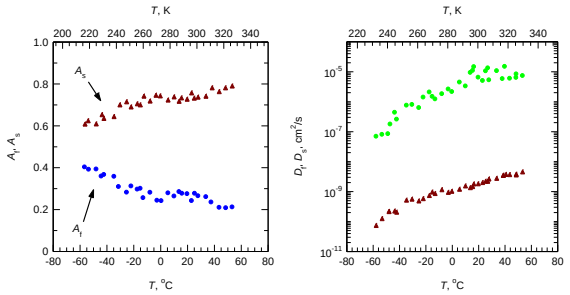

Fig. 3. (a)Temperature dependence of the amplitude of the fast (A_f) and slow (A_s) modes. Indeed the relative amplitude of the slow mode decreases from 0.8 at 54 °C to 0.6 at -58°C. (b)Temperature dependence of the diffusion coefficients of the fast (D_f) and slow (D_s) modes for a solution of NaPSS in NMF.

In order to suppress the effect of temperature variation of viscosity on diffusion, the ratio D_s/D_f of fast and slow diffusion coefficients was examined. As temperature is decreased from 54 to -58°C, D_s/D_f increases by a factor of 2, *i.e.*, follows a trend equivalent to adding salt to a polyelectrolyte solution at constant temperature (Fig. 4a). The same tendency is observed of the ratio A_s/A_f.

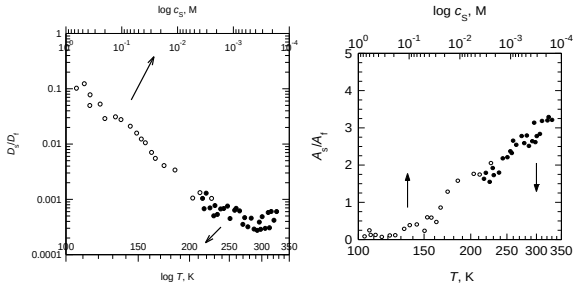

Fig. 4. (a) Dependence of the ratio of the slow and fast diffusion coefficients D_s/D_f (full symbols) on absolute temperature (logarithmic axis) and dependence of D_s/D_f (open symbols) measured on the same polymer/solvent system at 25°C as a function of concentration c_s of added salt (NaCl) obtained in a previous publication. (b) The same for amplitudes.

We conclude that the polyelectrolyte solution approaches the O-E transition as temperature decreases, but even at the lowest temperature that we could reach, A_s did not decrease below 0.5. Comparison with results reported earlier shows that a salt-free NaPSS/NMF solution at a temperature of -58°C corresponds to a solution with 0.001 M salt (NaCl) at 25°C. These results confirm the expected variation of the Bjerrum length of a polyelectrolyte chain.

The influence of nanoparticles on the crystallization behaviour and the local deformation mechanism of poly(ε-caprolactone)

Maria Eriksson[1,2], *Pascal Pichon*[2,3], *Ton Peijs*[1,2,3], *Han Goossens*[1,2]

[1]Laboratory of Polymer Technology, Department of Chemical Engineering and Chemistry, Eindhoven University of Technology, P.O. Box 513, 5600 MB Eindhoven, the Netherlands,
[2] Dutch Polymer Institute DPI, P.O. Box 902, 5600 AX Eindhoven, the Netherlands,
[3]Centre for Materials Research, School of Engineering and Materials Science, Queen Mary University of London, Mile End Road, E1 4NS London, UK

Email: m.eriksson@tue.nl

Polymer nanocomposites have recieved a lot of attention over the last few years. The nano-sized fillers have, due to their large specific surface area, a potentional to influence the whole bulk of the nanocomposite already at very low filler content and could therefore induce changes in the properties of the polymer that are very different from conventional composites[1]. However, there is a lack of understanding on what the exact mechanisms behind these changes are. Fillers can affect the nanocomposites in different ways, a.o. they can act as nucleation agents for crystallization[2], change the entanglement density in the amorphous phase[3], give pure reinforcement[4] and/or change the morphology of the obtained composite[5].

The main objective of our study is to investigate the influence of different nano-sized fillers on the morphology and the crystallization behaviour of a semi-crystalline polymer, i.e. poly(ε-caprolactone) (PCL), and to link this to the mechanical properties and the local deformation mechanism of the obtained composites. Special focus will be on how the orientation of the polymer chains is affected by the presence of the fillers and their orientation upon deformation and an attempt will be made to indentify the different mechanisms that are responsible for the observed changes. The state of dispersion of the filler in the matrix, the aspect ratio and the surface treatment of the filler will be discussed. Next to the results of standard measurments like DSC, DMTA and tensile tests more indept studies of the crystallization and deformation behaviour via in situ SAXS and WAXD measurments will also be presented.

Two different systems will be discussed; PCL/silica nano-composites, prepared via solution dispersion of premade silica nanoparticles and PCL/cellulose nanowhiskers composites. The nanowhiskers are needle-like structures with a length of 150-250 nm and a diameter comparable to the radius of the silica particles, i.e. 15-20 nm[6]. These fillers can be more easily oriented in the direction of deformation and they have a very distinct effect on the polymer matrix, compared to silica particles. The matrix/filler interaction is changed via grafting of PCL of different length to the surface of the fillers, and its influence on the properties of the composite will also be discussed.

Acknowledgement
This study is part of the Research Program of the Dutch Polymer Institute (DPI) project # 623. We acknowledge prof. F. Dubois (University of Mons, Belgium) for supplying the cellulose nanowhiskers.

References

[1] L. Schadler, L. Brinston, W. Sawyer, JOM, 2007, **59**, 53-60.
[2] S. Jain, H. Goossens, M. van Duin, P. Lemstra, Polymer, 2005, **46**, 8805-8818.
[3] C. Sun, PhD-thesis, Eindhoven University of Technology, Eindhoven, the Netherlands, 2010.
[4] Z. Wang, P. Ciselli, T. Peijs, Nanotechnology, 2007, **18**, 455709.
[5] E. Bilotti, H. Deng, R. Zhang, D. Lu, W. Bras, H.R. Fischer, T. Peijs, Macromol. Mater. Eng. 2010, **295**, 37–47.
[6] Y. Habibi, A.L. Goffin, N. Schiltz, E. Duquesne, P. Dubois, A. Dufresne, J. Mater. Chem. 2008, **18**, 5002–5010.

Preparation and Characterization of PLA-Hydrotalcite Nanocomposites

R. Scaffaro, L. Botta

Dipartimento di Ingegneria Industriale, Università di Palermo, Viale delle Scienze, 90128 Palermo (Italy)

roberto.scaffaro@unipa.it; luigi.botta@unipa.it

Introduction

Over the past years, the interest in polymeric materials from renewable sources has been continuously growing both in the academia and in industry, due to the increasing need for differentiation of energy resources and reducing their environmental impact. In this context, poly(lactid acid) (PLA) becomes highly attractive for a substitution of fully petrochemical based polymers.

On the other hand, the large scale application of PLA is often limited by its mechanical and its barrier to gases and vapours. The addition of small amounts of lamellar nanoparticles in a polymer matrix (polymer nanocomposites) can remarkably improve the mechanical properties of the matrix and enhance the barrier properties of these materials. However, the improvements of these properties depend on the nature of the final morphology of the material, the control of the dispersion and on the dimensions of the particles.

Among inorganic materials, smectite clays have received considerable attention because their structure exhibits the required stiffness, strength, and dimensional stability. However, very recently, attention has been turned to layer double hydroxides, also known as hydrotalcites (HT), as inorganic filler materials.

HT consist of brucite-like layers of zinc hydroxide, where some Zn(II) cations are isomorphically substituted with Al(III) cations to confer net positive charges to the layers. These charges are balanced by inter-layered hydrated anions, resulting in a multi-layer of alternating host layers and gallery anions [1].

The possibility of replacing these anions by simple ion-exchange procedures makes HT a unique class of layered solids to be used as hosts of polymers bearing a negative charge or polymers copolymerized with a small amount of a negatively charged monomer.

Aim of this work was to study the effect of the compounding methods on the morphology and on the properties of PLA-hydrotalcite nanocomposites prepared by melt extrusion. Moreover the influence of two different kinds of hydrotalcites – organically modified and not modified – and their concentration were evaluated too.

Materials and Methods

The polymer used in this work was an extrusion grade poly(lactid acid) (PLA Polymer 2002D) supplied by NatureWorks.

Two commercial hydrotalcites, supplied by AkzoNobel, were used as nanofillers: a unmodified type, Perkalite LD and an organically modified type, fully ion exchanged with fatty acid, Perkalite F100S.

The filled materials have been prepared using either a single screw extruder, a counter rotating twin-screw compounder or a corotating twin-screw extruder.

The top processing temperature adopted in all the extruders was 200 °C. The PLA has been compounded with both the hydrotalcites at different concentrations: 1%, 2% and 5% wt/wt.

Neat PLA was processed under the same conditions as the nanocomposites and used for all the further comparison with the other materials.

The prepared materials were characterized by SEM, mechanical and rheological measurements.

Results and Discussion

SEM analyses showed that the best morphology is exhibited by materials prepared with the corotating twin-screw extruder while the worse one by the samples processed with the single screw extruder. The increase of the hydrotalcite concentration led to a worsening of the morphology, i.e. an increase of aggregates and worse dispersion. However the materials containing the organic modified filler showed a better morphology. The rheological measurements revealed that the viscosity of all the materials containing the HT is lower in comparison with the viscosity exhibited by neat matrix in particular when the modified HT is used. It could be hypothesized that this behavior is due to degradation phenomena occurring during the processing of the materials. In particular, the products of the organic modifier degradation could act as a promoter/initiator of polymer degradation.

As regards the mechanical properties, the addition of HT caused only a slight increase of elastic modulus of filled materials even if the 5% of filler was incorporated. The tensile strength of the filled materials decreased if compared with the neat PLA, while the elongation at break is almost the same. Probably, the improvements that should be related to dispersion of the nanofiller in the systems are counterbalanced by degradation of matrix as reported for similar systems [2].

However, in full agreement with morphological analyses, the best performances were exhibited by materials prepared with the corotating twin-screw extruder while the worse ones by the samples processed with the single screw extruder.

Conclusions

PLA-hydrotalcite nanocomposites were prepared using either a single screw extruder, a counter rotating twin-screw compounder or a corotating twin-screw extruder.

The filled materials showed only a slight improvement of mechanical properties probably due degradation phenomena occurring during the processing of the materials.

References

1. V. Rives, Layered Double Hydroxides: Present and Future; Ed.; Nova Science: New York, 2001.
2. R. Scaffaro, L. Botta, M. Ceraulo, F.P. La Mantia. *J Appl Polym Sci* (2011). Accepted.

Investigation of Relationship between Morphology and Thermal Stability of Polystyrene & Polymethylmethacrylate/Na-MMT Nanocomposites Prepared by Emulsion Polymerization

Mahdiyeh Rezaie[1], *Hossein bouhendi*[1], *Vahid Haddadi-Asl*[2] & *Mahdi Nekomanesh-Haghighi*[1]

[1]Iran Polymer and Petrochemical Institute, [2]Amirkabir University of Technology

m.rezaei@ippi.ac.ir

Introduction: Recently, polymer/layered silicate nanocomposites have been studied in details, because of significant improvement in total properties. Also the effect of 2-acrylamido-2-methyl-1-propane sulfonic acid (AMPS), a reactive surfactant that has amido and sulfonic groups in the molecule in achievement and stability of exfoliated morphology of nanocomposites produced by emulsion polymerization have been studied[1]. In the current work we prepared some polymer nanocomposites with styrene and methylmethacrylate (MMA), AMPS as reactive surfactants and two amount of Na-MMT (4 and 8 weight percent) via emulsion polymerization and investigated relationship between morphology and thermal stability of nanocomposites.

Materials and Methods: Na-MMT was from Southern clay Co. MMA, styrene, AMPS and potassium persulfate (KPS) were purchased from Merck Co. Before polymerization step, Na-MMT was dispersed in deionized water and stirred at room temperature for 4days. Table 1 shows the sample codes. At first step, 10g of monomers, Na-MMT/water suspension, AMPS (0.6g) and deionized water was poured in the 1L reactor. Under nitrogen atmosphere and at 65^{O}C, KPS/water solution was injected. In second step the rest of the monomers were fed into the reactor at the rate of 19.2ml/h, using a syringe pump. In the last step, while keeping the temperature constant at 85^{o}C, the polymerization was continued to reduce un-reacted monomers for 2 hours. Finally the latex was dried under vacuum at ambient temperature for 5days.

Table1: Formulation of samples

Sample Code	MMA(g)	Styrene(g)	Na-MMT/Water(ml)
SAT4	-	40	40
SAT8	-	40	80
MAT4	40	-	40
MAT8	40	-	80

Results and Discussion: Figure 1 shows XRD patterns of samples. All PMMA/nanocomposites did not show any peak. Consequently they have the exfoliated structures. However, for polystyrene nanocomposites containing 4 and 8 Wt% Na-MMT, two peaks exist at 4.15^{o} and 5.5^{o}, respectively. This shows that polymerization of styrene in the presence of AMPS, has led to intercalated morphology. About thermal stability of nanocomposites (Figure 2) high weight residue and less thermal stability at temperatures below 385^{o}C for PS/nanocomposites can be observed. High amount of weight residue of PS nanocomposites which prepared with AMPS has been attributed to reduction of monomer conversion in emulsion polymerization [2]. When the monomer conversion decreases, relative amount of Na-MMT to monomer increases and intercalated morphology achieves. Different phenomena control thermal behavior of nanocomposites. Dispersed nanoscale Na-MMT layers can prevent the evaporation of small molecules

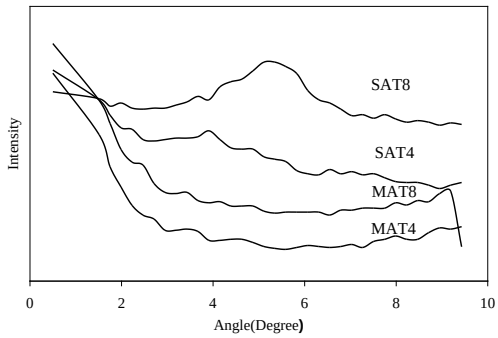

Figure1: X-ray diffraction patterns of samples

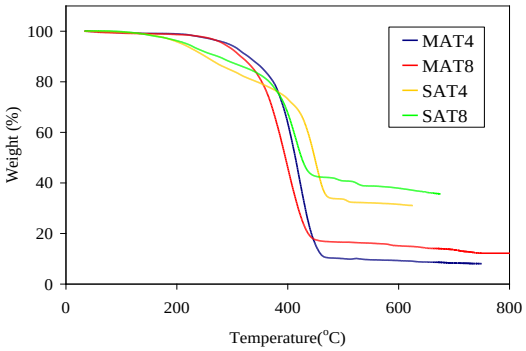

Figure2: TGA curves of samples

generated in thermo-oxidative degradation process and effectively inhibit decomposition of polymer molecules; therefore thermal stability of polymeric nanocomposites improves. In contrast, the stacked Na-MMT layers can hold accumulated heat that can be used as an internal heat source to accelerate the decomposition process, in conjunction with the heat flow supplied by the outside heat source; therefore the thermal stability is decreased [3]. Our results showed intercalated morphology may affect these two opposite phenomena on thermal stability, but the active temperature ranges are different: in temperature rang before 400^{o}C heat accumulation by Na-MMT layers is dominant factor to control thermal stability, but in temperature rang above 400^{o}C Na-MMT layers are more effective as gas barrier and thermal stability is improved.

Conclusion: Our results showed that AMPS has a significant effect on monomer conversion, especially in case of styrene, and monomer conversion reduction is a driving force to achievement intercalation morphology. From results of TGA analysis it can be concluded that intercalation morphology can considerably change thermal stability behavior of nanocomposites.

References:

1- Y.S. Choi et al, *Macromolecules*, 34 (2001) 8978-8985.
2- Y.K. Kim et al, *Chem. Mater.*, 14 (2002) 4990-4995.
3- J.W. Gilman et al, "*Flammability properties of polymer-layered silica nanocomposites*" in: Chemistry and Technology of Polymer Additives, Oxford Blackwell Science, UK, 1999.

Viscoelasticity of graphite oxide based suspensions in PDMS

Aline Guimont[1], Emmanuel Beyou[1], Gregory Martin[2], Philippe Sonntag[2], Philippe Cassagnau[1]

[1]Ingénierie des Matériaux Polymères, CNRS UMR 5223, Université Lyon1, Villeurbanne, F-69622 Lyon, France
[2]Hutchinson S.A., Centre de Recherche, Rue Gustave Nourry, BP 31, 45120 Chalette-sur-Loing, France

philippe.cassagnau@univ-lyon1.fr

Introduction

We report the rheology of PDMS based suspensions with solvent-dispersed graphite oxide (GO) and decorated GO with 3-(acryloxypropyl) trimethoxy silane (GOM) sheets. The aim is to study both the dispersion of these carbon nanofillers in PDMS fluids from viscoelastic measurements (Rouse regime) and their rearrangement in terms of complex shear modulus recovery under non-linear deformation. Finally, the dispersion stability and aggregation/agglomeration structural formation of such 2D sheets is discussed.

Experimental

Graphite, graphite oxide (GO) and graphite oxide functionalized with 3-(acryloxypropyl) trimethoxy silane (GO-M) were dispersed in low molar mass PDMS (no entangled chains, viscosity: η = 0.6 Pa.s). These suspensions have been characterized from a linear and non-linear viscoelasticity point of view. First of all, Transmission Electron Microscopy and X-Ray diffraction showed an intercalated morphology of graphite and functionalized graphite oxide. In PDMS suspensions, GO-M and graphite oxide have been assumed to be exfoliated by the short PDMS chains.

Results and Discussion

Only the PDMS suspension filled with the graphite oxide showed a drastic change in the viscoelastic properties for weight fractions up to 6.5 wt % (Fig 1). Actually, for GO concentrations higher than 1.5wt%, the viscoelastic behavior does not show any terminal flow zone and the elastic character of this suspension becomes dominant at low frequencies with the appearance of a secondary plateau. Furthermore, the low percolation threshold of GO sheets is attributed to their macro-scale aggregation/agglomeration driven by their Brownian motion in these low viscosity PDMS suspensions. It was further concluded that the surface modification of graphite oxide by 3-(acryloxypropyl) trimethoxy silane prevents the aggregation of GO sheets.

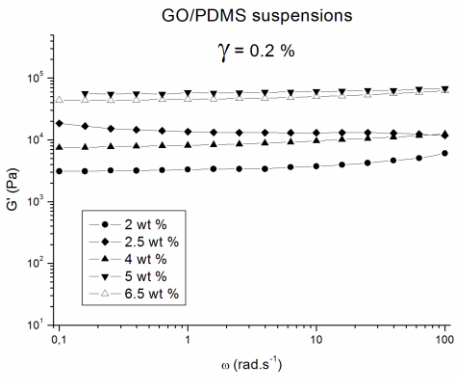

Fig 1: Storage modulus variation of GO/PDMS suspensions

The non-linear behavior of the GO/PDMS suspensions revealed that the increase of strain amplitude leads to a high modification of the network structure out of the equilibrium state. Nevertheless, the critical strain (transition between the linear and non-linear) regime was observed not to depend on GO concentration ($\gamma_c \approx 0.2$ %) as shown in Fig2. This result means that a fractal structure cannot be associated to the aggregation of GO sheets. Actually, GO sheets aggregate into agglomerates that span through the gap between the plates of the rheometer. Finally, recovery tests carried out by subsequent strain sweep proved that the initial equilibrium network structure can be completely and instantaneously restored, and this within the time necessary to start the subsequent non-linear test i.e., a few seconds. Compared with literature works, this particular behavior originates from the low viscosity of the suspension that allows Brownian motion of graphene oxide sheets within the magnitude order of a few seconds. Future work will consist in grafting polymethylhydrogenosiloxane onto APTMS-grafted GO sheets in order to check if functionalization with a polysiloxane backbone offers the possibility to tailor the viscoelastic properties of GO/PDMS suspensions.

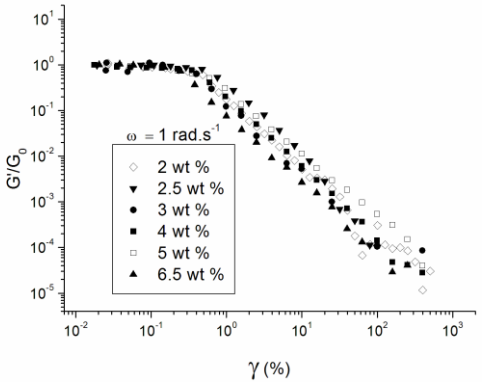

Fig 2: Variation of the normalized storage modulus versus strain for different GO weight fractions: 2, 2.5, 3, 4, 5 and 6.5 % (ω = 1 rad.s^{-1})

Synthesis and Characterization of New Polyamides Bearing 2,2'-Thio, Sulfinyl and Sulfoxobis(1-naphthoxy) Units in the Main Chain under Microwave Irradiation

Esmael Rostami

Faculty of Science, Department of Chemistry, Bushehr Payame Noor University,
P.O. Box 1698, Bushehr, Iran; Payame Noor University (PNU), Iran.

e-mail: Esmaelrostami@gmail.com

Keywords: Poly(sulfide-ether-amide)s; Poly(sulfinyl-ether-amide)s; Poly(sulfoxo-ether-amide)s; 1-Naphthol; Improved solubility; Thermal stability; Microwave Irradiation (MW).

Polyamides constantly attract much interest because of their unique property combination. Although they show exceptional thermal and oxidative stability, chemical resistance and low flammability, their insolubility in common organic solvents and high glass and softening temperature make these polymers difficult to process and fabrication [1,2]. Therefore, much effort has been concentrated on synthesizing soluble, processable polyamides without scarifying their desired properties.

In this research work new high thermal resistance polyamides, bearing naphthalene, sulfide, sulfoxide and sulfone units in the polymer backbone were prepared under microwave (MW) irradiation. Improved solubility together with retained high thermal stability could be achieved by introduction of bulky naphthalene rings. The thermal stability, solubility and viscosity of polyamides were obtained. The sizes of polymer species were evaluated using Scanning Electron Microscopy (SEM) images.

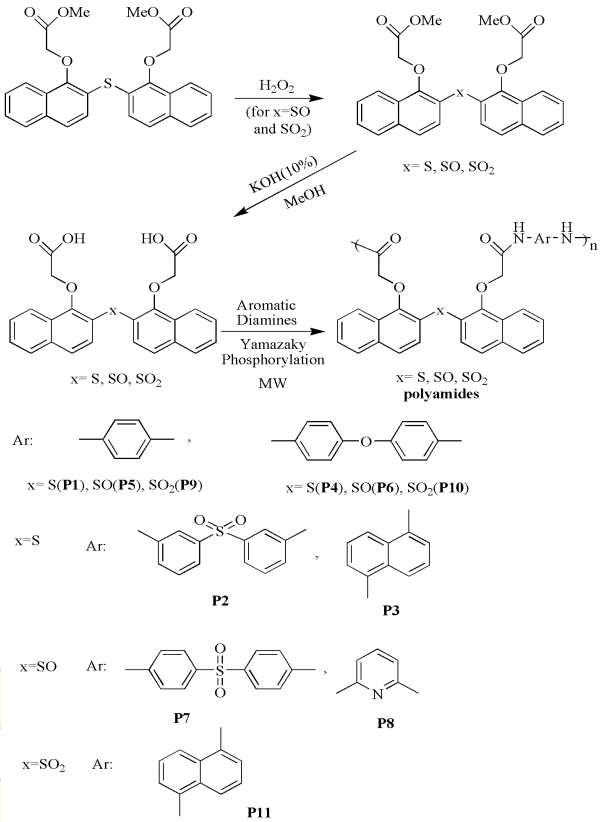

Scheme 1 Synthesis of polyamides (**P1-P11**).

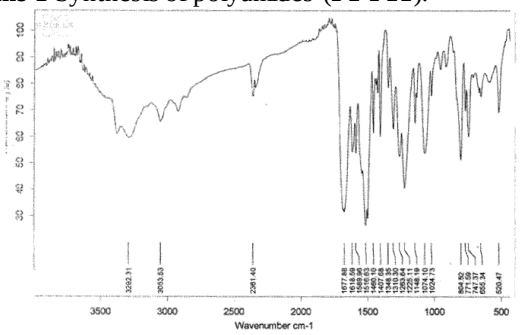

Figure 1 FT-IR spectrum of **P1**.

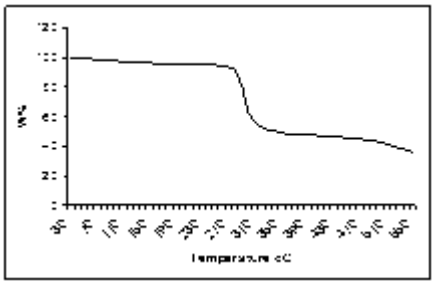

Figure 2 TGA of **P1**.

Polymer[a]	NMP	DMAc	DMSO	THF
P1	++	++	++	+
P2	++	++	++	+
P3	++	++	++	+
P4	++	++	++	+
P5	++	++	++	±
P6	++	++	++	±
P7	++	++	++	±
P8	++	++	++	±
P9	++	++	++	-
P10	++	++	++	±
P11	++	++	++	-

(++) Soluble at room temperature; (+) soluble upon heating; (±) partially soluble; (-) insoluble; [a]Solubility measured at a polymer concentration of 0.05 g/ml.

Table 1 The solubility of polyamides (**P1-P11**).

References

[1] Fink, J. K. *High performance polymers*, William Andrew, New York, **2008**, pp.423-442.

[2] Mallakpour, S.; Kowsari, E. *Iran. Polym. J.* **2006**, *15*, 239.

Optical properties of 83 Titanium mono layers on glass substrate by Kramers Kronig method

[1] Haleh Kangarlou, [2] Maryam Motalebi Aghdam

[1] *Faculty of Science, I.A.U Urmia Branch*
[2] *Faculty of Science, I.A.U Urmia Branch*

h.kangarlou@iaurmia.ac.ir

Titanium mono layers were deposited on glass substrate under HV conditions, at 373 K temperature, in vertical, 10, 15 and 20 degree deposition angles. Other deposition rates were same for all layers.
Transmittance and Reflectance of layers were determined by spectrophotometer in 300-1100 nm wave length range (visible range). Optical constants were calculated by Kramers_Kronig method. The relation between deposition angle and optical constants were investigated.

Key words: Titanium, Optical constants, Kramers-Kronig

Production and investigation of optical and structural properties of $MgF_2 / Tio_2 / glass$ and $MgF_2 / Ag / glass$ multi layers

Haleh Kangarlou[1] and Elnaz sattarpoor Isa Kan[2]

1- Faculty of Science, I. A. U, Urmia Branch.
2- Faculty of Science, I. A. U, Mahabad Branch.

$MgF_2 / Tio_2 / glass$ and $MgF_2 / Ag / glass$ multi layers were produced by physical vapor deposition method in HV conditions at 100 Celsius degree temperature by rotating substrate. Each of layers have same thickness. Their optical and structural properties were investigated by spectrophotometer in the spectral range of 300-1100 nm, atomic force microscopy and X-ray diffraction. Produced multi layers were amorphous and topography of multi layers showed different structures, that we can use them for different industrial applications. Transmittance of the multi layers were different and they can be use in different optical devises .

Key words: Titanum Di Oxide, AFM, XRD, Spectrophotometer

Synthesis of thermoresponsive nanocomposite hydrogels by alternative methods

Bernhard Ferse, Anna Große, Karl-Friedrich Arndt

Technische Universität Dresden, Physikalische Chemie der Polymere, 01062, Dresden, Germany

Bernhard.Ferse@chemie.tu-dresden.de

Introduction: In the last three decades, hydrogels have attracted increasing attention in many applications. The mechanical stability plays a decisive role to use hydrogels as actuators in microfluidics, tactile communication and others. HARAGUCHI *et al*. [1] synthesized novel polymer-clay nanocomposite gels (NC-gels), which possess very large deformability, amazing toughness, and high optical transparency. They consist of poly(*N*-isopropylacrylamide) (PNIPAAm), a temperatureresensitive polymer, and the synthetic clay Laponite. The inorganic clay, a synthetic hectorite, belongs to the 2:1 phyllosilicates.
The polymerization of NIPAAm using a free radical thermal initiator was studied extensively in the past. But this method cannot be used for the preparation of thin films or hydrogel structures. Patterned hydrogels in the µm-range or sensitive layers can find applications as sensors and actuators in microfluidic devices.

Materials and Methods: The here presented nanocomposite hydrogels were prepared by in-situ free radical polymerization of NIPAAm in the presence of inorganic, exfoliated clay without the need of an organic crosslinking agent. The initiation was carried out by UV-light ($\lambda < 360$ nm) using a photoinitiator 2-hydroxy-4'-(2-hydroxyethoxy)-2-methylpropiophenone. Irradiation through a mask results in pattern of a sensitive polymer with enhanced mechanical properties even in the swollen state. [2]

Results and Discussion: To understand the photopolymerization process of PNIPAAm-Clay nanocomposite hydrogels in aqueous solutions the gelation reaction was monitored by rheometry using oscillatory deformation tests. Tensile mechanical properties of photopolymerized NC-gels were investigated in order to get information about the gelation mechanism. Additional microscopic analyses (SEM, TEM, AFM) complete the results concerning the network structure of NC-gels

Conclusions: A discussion of the results of different analytical methods come to the realization, that the main process of network formation is the adsorption of the formed polymer chains on the clay surface. Consequently, a simple additive free mixing process of linear PNIPAAm and clay solutions leads to homogenous, thermosensitive mix-hydrogels without any chemical reaction. The obtained mix-gels show good mechanical stability and transparency.[3]

References:

[1] K. Haraguchi, T. Takehisa, *Adv. Mater*. **2002**, *14*, 1120
[2] B. Ferse, S. Richter, F. Eckert, A. Kulkarni, Ch. M. Papadakis, K.-F. Arndt, *Langmuir* **2008**, *24*, 12627

[3] B. Ferse, *Ph.D. Thesis*, Technische Universität Dresden 2010

PVDF/Copper Nanocomposites: Preparation and Properties

J. Arranz-Andrés, E Pérez , M. L. Cerrada

Institute of Polymer Science and Technology, CSIC, Juan de la Cierva 3, 28006 Madrid, Spain,

jarranz@ictp.csic.es

Introduction

The insertion of nanometric inorganic compounds in polymeric matrices provides an interesting method to improve some polymers properties, such as electric, thermal, optic or the magnetic ones. On the other hand the resulting materials present the advantages from polymers regarding processability[1], flexibility or less weight and price in comparison with traditional metals. The nanometric structure sometimes shows properties different from those of the same material in a higher level structure[2,3]. For example, polymer composites with conductive metallic particles can be used as antistatic or in electromagnetic interference shielding applications[4]. As a result, this methology has a lot of applications depending upon the inorganic material incorporated within the polymers.

Materials and Methods

Composites of poly(vinylidene fluoride), PVDF, with copper nanoparticles (with a nominal average particle size of 25 nm) have been prepared at different compositions via melt blending. The films obtained were characterized from a morphological and thermal standpoint by transmission and scanning electron microscopies, synchrotron radiation, thermogravimetry and differential scanning calorimetry. Synchrotron X-ray measurements were performed at the CRG beamline BM16 of the ESRF (Grenoble, France). In addition, the molecular dynamic and mechanical properties of the samples have been evaluated.

Results and Discussion

Scanning electron micrographs of cryofractured specimens show a homogeneous dispersion of copper nanoparticles within the polymer matrix without significant aggregation.

An increase in the mechanical parameters related to rigidity, such as young modulus or microhardness, is found when the content of metal does. However, an opposite effect is observed for the properties related to the deformation of the polymer.

The effectiveness of a shield and its resulting electromagnetic interference attenuation depend on the frequency, the distance of the shield from the source, the thickness of the shield, and the shield material. In the present samples, shielding effectiveness is expressed as a function of the ratio of the incident and transmitted X-ray radiation (with a wavelength of 0.098 nm). Figure 1 shows a decrease in more than four orders of magnitude of the incident electromagnetic radiation when the sample with 20 vol% copper is used as shield.

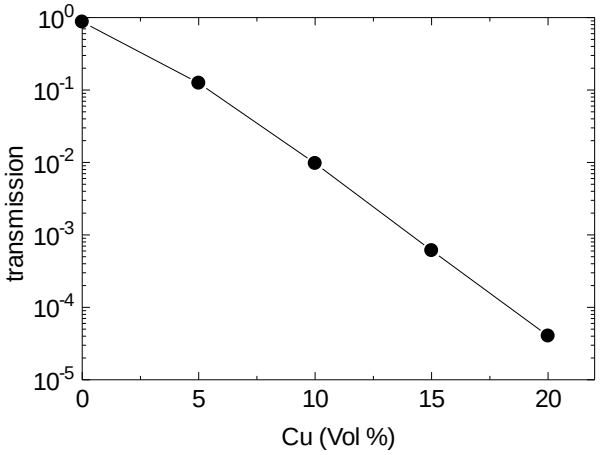

Figure 1. Normalized transmission of X-ray radiation as a function of Cu content in the PVDF/copper nanocomposites.

Conclusions

The dependence of different physical properties on copper nanoparticles concentration has been studied for poly(vinylidene fluoride) nanocomposites. A good distribution of nanoparticles is observed in these PVDF-based materials independently of their composition. On the other hand, a significant improvement is found in some of the properties evaluated.

References

1. S.K. Bhattacharya, Ed.; Metal-Filled Polymers: Properties and Applications; Marcel Dekker: New York, 1986.

2 . Y. Voloktin, *Nature* **1996**, *384*, 621.

3. J. L. Dorman, D. Fiorani (Eds.), Magnetic Properties of Fine Particles, Elsevier, Amsterdam, 1992.

4. J. Delmonte, Metal/Polymer Composites; Van Nostrant Reinhold: New York, 1990.

Acknowledgements

The authors are grateful for the financial support of Ministerio de Ciencia e Innovación (project MAT2010-19883). We also thank ARKEMA for the supply of the poly(vinylidene fluoride). The synchrotron work was also supported by MCIN through specific grants for the access to the CRG beamline BM16 of the ESRF.

J. Arranz-Andrés thanks to the CSIC JAE-Doc Program for his financial support.

The Effect of Organoclay Nature on the Nanostructure and Mechanical Properties of Polyamide-12 Nanocomposites

N. Aranburu, J. I. Eguiazábal, J. Nazabal

Dpto. de Ciencia y Tecnología de Polímeros and Instituto de Materiales Poliméricos, POLYMAT
Facultad de Ciencias Químicas, UPV/EHU, Paseo Manuel de Lardizabal 3, 20018 Donostia, Spain

e-mail: naramburu003@ikasle.ehu.es

Introduction

For the last decade, polymer/organoclay nanocomposites (NC´s) have attracted the academic interest, due to their clearly superior properties relative to those of conventional composites. Addition of low clay contents to a polymer matrix (2-5%) leads to the enhancement of different properties, such as mechanical properties, thermal stability, barrier properties or flame retardancy. The properties improvement of the NC´s is related to the high aspect ratio and rigidity of the silicate layers, and also to its degree of dispersion and delamination in the polymer matrix [1]. The affinity between the polymer matrix and the organoclay is the main factor achieving a good dispersion. It can be enhanced by optimizing the structure of the organoclay for a given polymer matrix [2].

Among the different NC´s, those based on polyamide matrices obtained by melt processing have been the most studied. For common polyamide/organoclay NC´s, montmorillonite modified with one alkyl tail has been shown to be the most effective achieving a good dispersion [3]. The highest exfoliation levels have been observed for polyamide-6/organoclay NC´s, while high dispersion levels have been observed also for other polyamide based NC´s. However, in polyamide-12 NC´s, where the aliphatic content is bigger, the role of the organoclay modifier is not still clear.

In this work, we have analysed the effect of the modifier structure of the organoclay on the phase behaviour, the nanostructure, and mechanical and thermal properties of NC´s based on polyamide-12 (PA12).

Experimental

The PA12 was Rilsan AMNO-TLD from Arkema and the fillers were three montmorillonites (MMT) modified with dimethyl dehydrogenated tallow quaternary ammonium (Cloisite® 20A, Southern Clay Products), bis-2-hydroxyethyl methyl tallow quaternary ammonium (Cloisite® 30B, Southern Clay Products), and octadecylamine (Nanomer® I30 TC, Nanocor). The NC´s were prepared in the melt state using a twin screw extruder, and injection molded to obtain standard testing specimens. The phase behaviour and the thermal properties of the NC´s were characterized by differential scanning calorimetry (DSC) and dynamic mechanical-thermal analysis (DMTA). The nanostructure was determined by transmission electron microscopy (TEM) and X-ray diffraction (XRD). The mechanical properties were measured by tensile and impact tests.

Results and Discussion

The melting and crystallization temperatures and the crystallinity of the PA12 measured by DSC, as well as the glass transition temperature measured by DMTA, remained unaffected in the nanocomposites, regardless of the organoclay nature.

In Figure 1 it can be observed that the best results in terms of Young´s modulus improvement of the NC´s were achieved with the organoclay containing hydroxyl groups (30B) and the organoclay modified with two alkyl tails (20A). The Young´s modulus values of the NC´s obtained with one alkyl tail modified organoclay (I30) were unexpectedly lower than those of the other NC´s, regardless of the MMT content. These mechanical properties results are in good agreement with the TEM micrographs of the PA12 NC´s (Figure 2), where higher dispersion levels are observed for NC´s obtained using 30B and 20A organoclays as fillers.

It is suggested that, unlike polyamide-6 based NC´s, organic modifiers with higher molecular volume facilitate the organoclay dispersion in the PA12 matrix. This is related to the higher aliphatic content of the PA12.

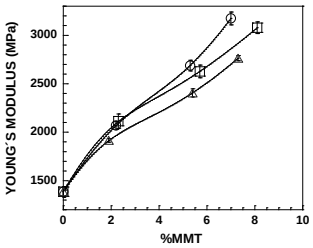

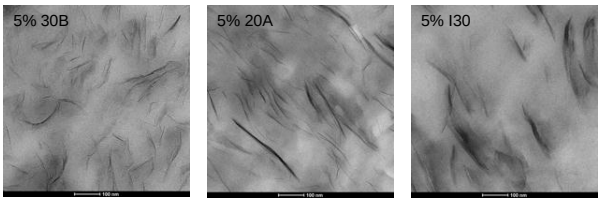

Figure 1. Young´s modulus of the PA12 NC´s as a function of the 30B (○), 20A (□) and I30 (Δ) organoclay content.

Figure 2. TEM micrographs of PA12 based NC´s containing 5% 30B, 20A and I30 organoclays.

References

[1] Utracki, L. A. Clay-Containing Polymeric Nanocomposites, Rapra Technology, Shropshire (2004).

[2] Fornes, T. D., Yoon, P. J.; Hunter, D. L.; Keskkula, H.; Paul, D. R. Polymer 43, 5915-5933 (2002).

[3] Fornes, T. D.; Hunter, D. L.; Paul, D. R. Macromolecules 37, 1793-1798 (2004).

Acknowledgements

The financial support of the Spanish "Ministerio de Ciencia e Innovación" (project n. MAT2010-16171) is gratefully acknowledged. N. Aranburu acknowledges the grant awarded by the Basque Government.

Crystallization Studies on Clay Nanocomposites of Nylon 47

L. Franco, L. Morales, M.T. Casas, J. Puiggalí

Departament d'Enginyeria Química/Centre de Recerca en Nanoenginyeria, Universitat Politècnica de Catalunya, ETSEIB, 08028-Barcelona

lourdes.franco@upc.edu

The α and β crystalline structures of even-even nylons are based on a stacking of sheets composed of hydrogen-bonded molecular chains with a planar zig-zag conformation. The corresponding diffraction patterns are characterized by the presence of two strong reflections at spacings close to 0.44 and 0.38 nm. In general, a not completely well understood reversible phase transition is detected on heating/cooling processes. In the first case, the two indicated reflections gradually merge on a single one indicative of a pseudohexagonal arrangement at the so called Brill transition temperature. Peculiar structures based on the establishment of hydrogen bonds along two different directions have recently been postulated in some even-odd nylons, which fibers rendered also two strong equatorial reflections at similar spacings than reported for the α/β conventional structures. Synchro-tron radiation experiments (Figure 1) indicated that the new structure can also be found in nylon 47, which in addition showed complex polymorphic transitions.

Nanocomposites of nylon 47 and different organo-modified clays (i.e. C25A and C30B) were prepared by both melt mixing and solution intercalation film-casting methods. TEM micrographs (Figure 1) and X-ray diffraction data showed exfoliated and intercalated structures for nanocomposites with C30B (melt mixing) and C25A (film-casting) clays, respectively.

DSC calorimetric data indicated that the structure of the nanocomposite had a remarkable influence on both isothermal (Figure 3) and non-isothermal hot crystallization processes. Thus, the crystallization rate decreased or increased when the added clay adopted an exfoliated or an intercalated structure, respectively.

Nylon 47 crystallized from the melt giving rise to different types of morphologies with distinctive features than observed in conventional even-even nylons. Thus, spherulites with a fibrilar texture and a negative birefringence were always observed at low crystallization temperatures, whereas spherulitic aggregates were typical at high crystallization temperatures (> 228 ºC). These aggregates had a birefringence (positive or negative) that depended on the temperature of the sample and changed on a reversible way (Figure 3).

Overall crystallization rate depends on the primary nucleation density and the crystal growth rate. These two effects could be independently evaluated by means of optical microscopy. Thus, primary nucleation density increased and decreased respect to the neat polymer when clay particles gave rise to intercalated and exfoliated structures, respectively. The crystal growth rate was lower in both nanocomposite samples since clay particles had a disturbing effect that was more significant when an exfoliated organization was attained. The degree of crystallinity decreased also significantly in the exfoliated nanocomposite sample.

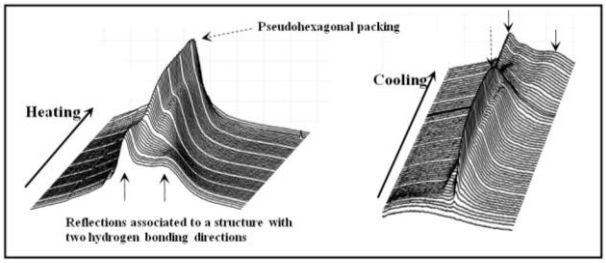

Figure 1. 3-D diffraction profiles of nylon 47 taken during heating and cooling processes.

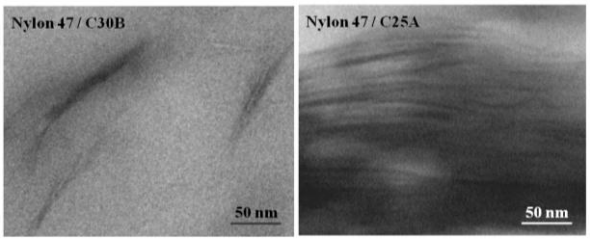

Figure 2. TEM micrographs showing exfoliated (left) and intercalated (right) nanocomposite structures.

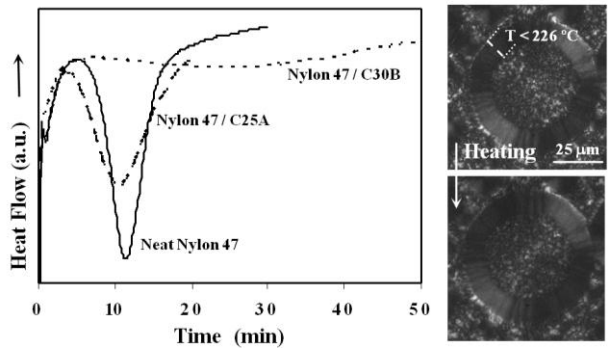

Figure 3. DSC isothermal crystallization exotherms (230 ºC) of nylons 47 and its nanocomposites with the C30B and C25A clays (left). Change of the birefringence properties of non-isothermally grown spherulites during heating (right).

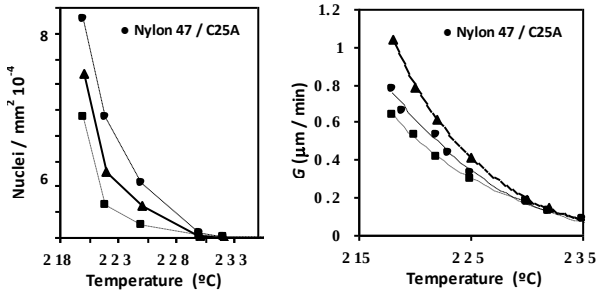

Figure 4. Temperature dependence of the nucleation density (left) and the crystal growth rate (right) for nylon 47 and its nanocomposites with the C30B and C25A clays.

Acknowledgements: This research has been supported by a grant from CICYT/FEDER (MAT2009-11503).

Characterisation and Cure Kinetics of Epoxy-Clay Nanocomposites Cured using an Anionic Initiator

F. Román, Y. Calventus, P. Colomer, J. M. Hutchinson

Thermodynamics Laboratory, ETSEIAT, Polytechnic University of Catalonia,
Colom 11, 08222 Terrassa, Spain

calventus@mmt.upc.edu

Introduction

One of the problems in the fabrication of epoxy polymer layered silicate (PLS) nanocomposites cured with diamines is that stoichiometric conditions cannot be achieved in the inter- and intra-gallery regions [1]. This has a detrimental effect on the nanostructure and properties of the cured nanocomposites. In the present work we investigate an alternative approach, which involves the anionic homopolymerisation of the epoxy monomer, which avoids the problems of stoichiometry. This approach will be shown to result in PLS nanocomposites with improved properties.

Materials and Methods

The homopolymerisation reaction is initiated by 4-N,N-dimethylaminopyridine (DMAP), which is added, in a proportion of 3 phr with respect to the resin [2], to the resin/clay mixture. The resin is diglycidyl ether of bisphenol-A (DER331, Dow Chemical Company) and the clay is a commercial organically modified montmorillonite (MMT) (I.30E, Nanocor Inc.). We investigate the influence of the MMT content on the homopolymerisation reaction and on the nanostructure and properties of the nanocomposite.

The cure reaction is studied by differential scanning calorimetry (DSC) under isothermal conditions at temperatures from 80ºC to 110ºC and under non-isothermal conditions at rates between 2 and 20 K/min. The glass transition temperature (T_g) and thermal stability of the cured material are determined by DSC and Thermogravimetry (TGA), respectively, and the nanostructure is assessed by Small Angle X-ray Scattering (SAXS) and Transmission Electron Microscopy (TEM). We present here the results for three different systems, with the following approximate wt% of epoxy, initiator and clay, respectively: 97, 3, 0 (ED); 95, 3, 2 (EDM2); 92, 3, 5 (EDM5).

Results and Discussion

There are some important differences between the results obtained here and those obtained earlier for the same epoxy-clay system cured with a diamine [1]. First, whereas for the amine-cured system T_g decreases with increasing clay content, here the T_g of sample EDM2 is higher than that of the neat resin (ED), as shown in the Figure below. The reduction in T_g for sample EDM5, seen in the same Figure, could be due to a poorer dispersion of the clay in the resin.

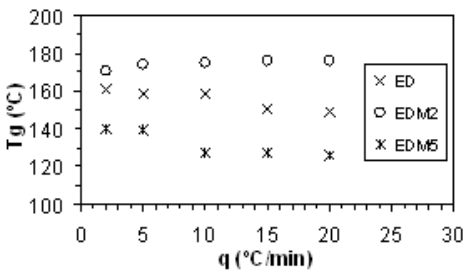

In addition to the increase in T_g, the TGA results also show that EDM2 has significantly improved thermal stability with respect to 2 wt% systems thermally homopolymerised without DMAP or amine-cured.

In the kinetic analysis, the experimental cure curves have been fitted with an autocatalytic model. For the non-isothermal experiments, a good fit is obtained, as can be seen in the Figure below, while for the isothermal experiments the cure curves can be fit only up to vitrification. The isoconversional activation energy for EDM2 is lower than for both ED and EDM5.

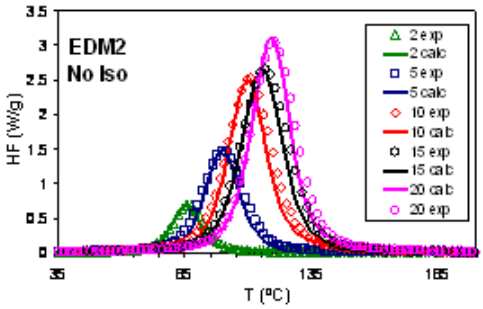

The DSC results have been complemented with nanostructural studies. SAXS indicates an improved degree of exfoliation for EDM2 compared with an amine-cured sample, but there remains some intercalation with a d-spacing of 1.5 nm. When examined by TEM, the 2 wt% sample presents a much greater degree of exfoliation than the 5 wt% sample. Typically it consists of some small agglomerates, about 2 μm in size, with layers separated by 1.5 nm, but with evidence of considerable exfoliation outside these agglomerations, as seen in the micrograph below (scale bar 20 nm).

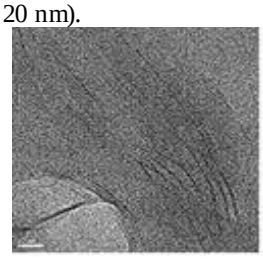

Conclusions

In the light of these results, EDM2 presents an interesting possibility for the development of an optimum nanostructure.

References

1. S. Montserrat, F. Román, J. M. Hutchinson, L. Campos, J. Appl. Polym. Sci., **108**, 2008, 923
2. I. E. Dell'Erba, R. J. J. Williams, Polymer Eng. Sci., **46**, 2006, 351

Acknowledgements

We are grateful to the CICYT for a research grant (MAT2008-06284-C03-03) and to the Dow Chemical Company for the provision of the epoxy resin DER331

Biocompatible nanofibrous constructs targeted for controlled delivery of selected drugs

Jiri Michalek[1], *Jakub Sirc*[1], *Radka Hobzova*[1], *Martin Pradny*[1], *Nina Kostina*[1], *Vladimir Holan*[2], *Marcela Munzarova*[3]

1) Institute of Macromolecular Chemistry AS CR, v.v.i., Heyrovskeho Sq. 2, Prague 6, 162 06, Czech Republic
2) Institute of Molecular Genetics AS CR, v.v.i., Videnska 1083, Prague 4, 142 20, Czech Republic
3) ELMARCO ltd., V Horkach 76/18, Liberec, 460 07, Czech Republic

e-mail: jiri@imc.cas.cz

Introduction

The use of nanofibers in tissue engineering is rapidly growing in several last years. The random nanofibrous structure is suitable to form three-dimensional scaffolds with selected seeding cells and/or various constructs with bioactive compounds or drugs. The main goal in tissue engineering is to regenerate a function or part of a damaged tissue. The combination of cell cultivation and control delivery of suitable drugs or bioactive motifs seems to be good way to fulfill requirements for this purpose. To assess the controlled release of model drugs from nanofibrous constructs we decided to study three different approaches: 1) incorporation of drug (model drug gentamycin) into multilayer nanofibrous construct; 2) binding of drugs to linear polymer carriers with increasing molecular weight; 3) control the release of drug by its solubility in aqueous environment (model drug cyclosporine).
The comparison of individual procedures (1-3) is shown and discussed in the presentation.

Materials and Methods

Recent advances in the preparation of nanofiber layers, especially using the Nanospider™ technology, allow the preparation of a sufficiently large area of nanofibrous layer with reproducible thickness and structure. Subsequently, it is possible to employ these layers as drug carriers and evaluate their efficiency in laboratory scale by physical and chemical methods and by *in vitro* tests in tissue culture.

Nanospider technology

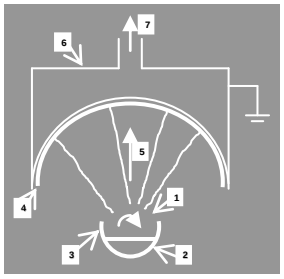

Photo picture of Nanospider TM

Scheme 1. Principle of NanospiderTM
1- electrode metal roller, 2 - fiber-forming polymer solution, 3 - reservoir, 4 - textile substrate, 5 - nanofiber formation direction, 6 –electrode earthing shield, 7 – air suction

Nanofibers were prepared from polycaprolactone (PCL), polylactide (PLA) and polyvinyl alcohol (PVA). Some of the PVA layers were covered from the both sides by polyurethane (PUR) nanofibrous layers of various thicknesses (PVA/PUR). Wide range antibiotic gentamycin and immunosuppressant cyclosporine were incorporated to the nanofiber samples.

The set of linear polyethylene glycols with molecular weights 2000, 6000, 10000 and 20000 was terminated by phenyl groups (detectable by spectral methods) by reaction of end hydroxy groups with phenylisocyanate.
Concentration of studied compounds released to the surrounding solution (water) was determined by HPLC/MS and UV spectroscopy.

Results and Discussion

PVA nanofibers containing 10 % (w/w) of gentamycin overlapped from both sides by PUR nanofibers of various thicknesses were immersed into 10ml of distilled water and shaken at 37°C. After a particular time period, 2.5ml of solution was withdrawn and replaced by fresh water. The concentration of gentamycin was determined by HPLC/MS.
Overlapping of the PVA layer containing gentamycin by layers of stable PUR nanofibers apparently decreased the influence of diffusion and convection in the process of gentamycin release and its washing out was prolonged.
Synthesized polyethylene glycols were incorporated into polymer nanofibers (PVA, PCL, PLA) in a amount of 3 wt%.
It appeared that the rate of release of model molecules is affected by their size (chain length) and the polarity of polymer nanofibers into which they were incorporated.
Samples of PLA nanofibers with incorporated 10 % (w/w) of cyclosporine were immersed to 10ml of distilled water and shaken at 37 °C. After a particular time period the concentration of cyclosporine in solution was determined by HPLC/DAD.
The concentration of cyclosporine increased at about 0.6-0.8 μg/ml within approx. 30 hours and than steadied. Apparently, the release of cyclosporine is considerably influenced by its low solubility in aqueous medium.

Conclusions

The retention of biologically active compound in the nanofibrous structure, kinetic of its release respectively, is affected by a number of factors such as thickness of the nanofibrous layer, interaction of the drug with polymeric nanofibers and the size of the molecules incorporated to the nanofibrous structure. The relationship of these factors and kinetics of the drug release was observed and evaluated for 3 different procedures. In all cases, the ability to control the rate of the release of model compounds was demonstrated.

Acknowledges:
This work was supported by AS CR, KAN 200520804 and MEYS 1M 0538

Effect of Dispersed Phase Modulus on Brittle/Tough Transition of Toughened Polypropilene Based Nanocomposites

A. Zabaleta[a], I. González[b], J. I. Eguiazábal[a] and J. Nazabal[a]

a Dpto. de Ciencia y Tecnología de Polímeros and Instituto de Materiales Poliméricos POLYMAT. Facultad de Ciencias Químicas UPV/EHU, Paseo Manuel Lardizábal 3, 20018, San Sebastián, Spain.
b Nanoscience Cooperative Research Center CIC nanoGUNE. Avenida de Tolosa 76, 20018 San Sebastian, Spain.

asier.zabaleta@ehu.es

Introduction: The achievement of super-toughness in polymers that are ductile but notch-sensitive is clearly one of the most significant advances in the development of new polymeric materials [1]. Different theories are used to explain the brittle/tough (B/T) transition in rubber-toughened blends. Among them, those which relate the B/T transition with a particle size or with an interparticle distance or ligament thickness (τ) are the most used. However, the τ is increasingly used to asses the B/T transition in detriment of the particle size because similar impact strength values may be obtained when the particle size changes, whereas the relation between τ and impact strength is bidirectional.

The critical interparticle distance (τ_c) was firstly considered to be a characteristic of a given matrix, but subsequent studies showed that it depended both on extrinsic (impact speed, test temperature and mode of deformation) and intrinsic parameters (interfacial adhesion (γ), modulus of the matrix (E_m), type and modulus of the rubber (E_d)). However, the influence of the intrinsic parameters on the B/T transition, is often difficult to understand, since the change of one parameter usually supposes the change of at least another. For that reason, the true effect of E_d on τ_c is far from being understood [2].

Therefore, the aim of this paper is to examine the influence of the modulus of the rubber on the B/T transition of toughened polypropylene (PP) nanocomposites (PNs). Maleic anhydride modified poly(ethylene-octene) (mPEO) was mixed with a minority amount of organically modified montmorillonite (OMMT) (10%) in order to increase the modulus of mPEO from 10 MPa to around 90 MPa. This allows us to change the modulus of the dispersed phase without changing other intrinsic parameters.

Materials and Methods: The toughened PNs were obtained in two extrusion steps. Firstly, the mPEO was mixed with 10% OMMT in a twin screw extruder. Subsequently, this PN was added up to 30% to a PP matrix in a second extrusion step before injection moulding. The PP/mPEO blends were prepared as a reference in one step. The characterization of the nanostructure was carried out by transmission electron microscopy (TEM), the surfaces of cryogenically fractured specimens were observed by scanning electron microscopy (SEM) and the phase structure was analyzed by dynamic mechanical analysis (DMA). The mechanical properties were determined by Izod impact and tensile tests.

Results and discussion: The phase structure analysis indicated that both the high temperature glass transition (T_g), which corresponds to the PP phase, and the low temperature T_g, corresponding to mPEO, remained practically constant with the OMMT addition; indicating its pure nature.

The nanostructure analysis revealed that the clay layers stayed in the mPEO dispersed phase and that the additional processing, required to incorporate the rubber to PP, did not lead to any compaction of the widely dispersed layers. Moreover, the SEM micrographs showed that the particle size of the dispersed phase of the PNs was similar to that of the corresponding blends. This indicates that both the nature of the matrix and the interface were preserved and therefore, the addition of OMMT only influenced on E_d.

The impact strength values of the PNs and blends have been plotted against τ in Fig. 1. The B/T transition of PNs occurred at a τ_c smaller than that of the blends. Taking into account that the extrinsic parameters (testing conditions) that influence τ_c were the same both in PNs and blends, and among intrinsic parameters only the dispersed phase modulus varied, this lower τ_c value of the PNs, compared with that of the corresponding blends indicated that τ_c depends on the modulus of elasticity of the dispersed phase, and that a higher modulus leads to a lower τ_c.

References: [1] D.R. Paul, C.B. Bucknall. Polymer Blends, John Wiley & Sons, (2000).

[2] A. Aróstegui, J. Nazábal. Journal of Polymer Science: Part B: Polymer Physics, 41 (2003) 2236-2247.

Acknowledgements: The financial support of Spanish "Ministerio de Ciencia e Innovación" (Project Number MAT2007-60153) is gratefully acknowledged. A. Zabaleta acknowledges the grant awarded by the Ministerio de Ciencia e Innovación.

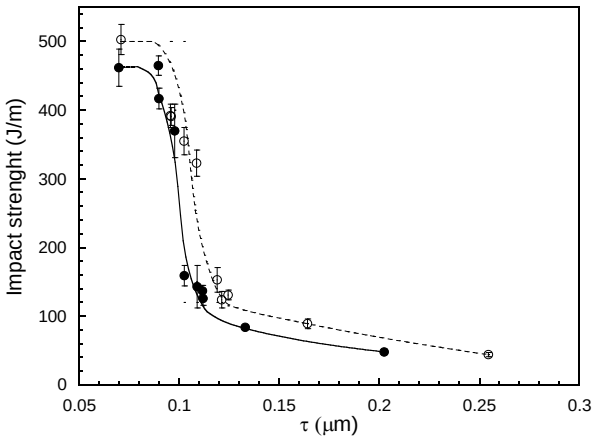

Figure 1. Notched Izod impact strength of the PNs (solid symbols) and reference blends (open symbols) versus τ.

A Low-Temperature Preparation of Polymer-ZnO Hybrid Materials and/or ZnO Nanoparticles from Poly(zinc methacrylate)

Gabriela Ambrožič,[a] *Srečo D. Škapin*,[b] *Majda Žigon*[a] *and Zorica Crnjak Orel*[a]

[a] National Institute of Chemistry, Hajdrihova 19, SI-1000 Ljubljana, Slovenia.
[b] Jožef Stefan Institute, Jamova cesta 39, SI-1000 Ljubljana, Slovenia.

gabriela.ambrozic@ki.si

The use of polymers as additives in the solution-phase synthesis of ZnO nanoparticles has been shown to be an excellent way of controlling the crystallites' size, shape and dispersibility. The polymers do not only prevent the agglomeration of the inorganic nanoparticles in the given solvent, but also control the particle growth by adsorbing selectively through functional groups on the surface of the ZnO crystals.[1, 2] However, in order to obtain pure ZnO, a follow-up removal of the polymer template by calcination or long-term UV-radiation exposure is needed.

On the other hand, the polymer can be used not only as an additive but also as a macromolecular ZnO precursor. In such a case the ZnO was obtained by a post-calcination of Zn-coordinated polymers.[3, 4]

In this investigation we focus on a simple, robust and low-temperature synthesis of pure ZnO nanoparticles and polymer-ZnO hybrid materials formed by the NaOH-mediated conversion of poly(zinc dimethacrylate) in 1-butanol, without a post-calcination.

Although the synthesis and properties of poly(zinc dimethacrylate) have already been the subject of some research investigations[5-7], there is, however, only one example reported on its conversion into ZnO particles incorporated inside the native polymer-forming nanocomposite.[8] ZnO/ZnS polymer nanocomposites were prepared by exposing the fibers of poly(zinc dimethacrylate), pre-synthesized by solid-state γ-ray polymerization, to 180 ^{o}C and a H_2S gas flow.

In our work for the first time we used poly (zinc dimethacrylate) to prepare neat ZnO particles. The polymer in this case acts as a template for controlling the crystal growth as well as a precursor of neat ZnO nanoparticles formed under defined reaction conditions, which ensure that the degradation of the polymer chain or the formation of insoluble $Zn(OH)_2$ does not occur.

The obtained single-crystalline ZnO nanorods show a low tendency to aggregate and can be effectively re-dispersed once they are isolated and dried (Figure 1).

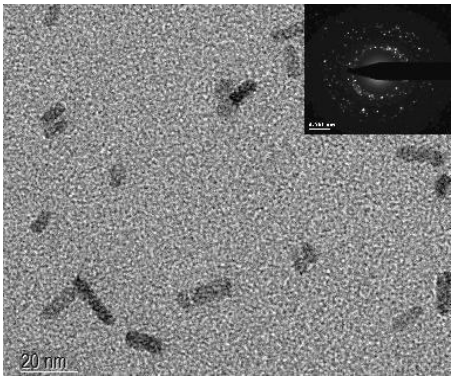

Figure 1: TEM image of ZnO nanorods formed by exposing poly(zinc methacrylate) to NaOH

References:

[1] C.H. Brown, T.V. Richter, F. Schacher, A.H.E. Müller, E.J.W. Crossland, S. Ludwigs, Macromol. Rapid Commun. 31 (2010) 729.
[2] R. Muñoz-Espí, Y. Qi, I. Lieberwirth, C.M. Gómez, G. Wegner, Chem. Eur. J. 12 (2006) 118.
[3] X. Liu, Angew. Chem. Int. Ed. 48 (2009) 3018.
[4] S. Jung, W. Cho, H.J. Lee, M. Oh, Angew. Chem. Int. Ed. 48 (2009) 1459.
[5] I.C. McNeill, M. Zulfiqar, Polym. Deg. And Stab. 9 (1984) 239.
[6] I.C. McNeill, A. Alston, Angew. Makromol. Chem. 261/262 (1998) 157.
[7] C.F. Parrish, G. L. Koceanny, Makromol. Chem. 115 (1968) 119.
[8] S.- W.Kuo, Y.- C. Chung, K.- U. Jeong, F.- C. Chang, J. Phys. Chem. C 112 (2008) 16470.

Thermal stability of PMMA/ZnO nanocomposites

A. Anžlovar, Z. Crnjak Orel, M. Žigon

National Institute of Chemistry, Hajdrihova 19, SI-1000, Ljubljana, SLOVENIA

e-mail:alojz.anzlovar@ki.si

Introduction

Zinc(II) oxide - ZnO is a widely used semiconducting material with an exceptional combination of physical properties having a wide range of potential applications[1]. PMMA is widely used thermoplastic polymer well known for its optical properties. It is reported that inorganic nanofiller enhances the thermal stability of the polymer matrix in composite materials[1,2,3]. Therefore, by combining nano ZnO filler and PMMA polymer it is possible to prepare transparent composite materials which show, besides exceptional UV absorption and sun light resistance, also enhanced thermal stability of the PMMA matrix[4,5].

Experimental

Organophilic nano ZnO powders were synthesized by the hydrolysis of zinc(II) acetate in various diols[6,7] using p-toluene sulphonic acid - pTSA as an end capping agent and without pTSA. Particles were characterized by SEM microscopy, IR spectroscopy and XRD diffraction confirming the presence of crystalline ZnO. Thermal properties of PMMA/ZnO nanocomposites were studied by thermogravimetric analysis - TGA and differential thermogravimetry - DTG.

Results

It is known that nano ZnO can enhance the thermal stability of the PMMA matrix[1,2,3]. Results of TGA and DTG analysis showed that significant shift of T_d – 5% weight loss (20 – 40 °C) was achieved by adding 1 wt. % of nano ZnO. At lover concentrations of ZnO filler the thermal stability enhancement is much smaller. DTG curves also showed that nano ZnO particles have more intense effect on thermal stability enhancement than submicrometer ZnO particles (Figure 1) [8].

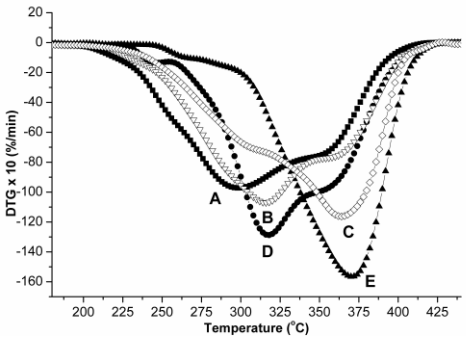

Figure 1: DTG curves of PMMA/ZnO nanocomposites in dependence of ZnO content and particle size:A) PMMA, B) 0.1%ZnO–340nm, C) 1.0%ZnO–340nm, D) 0.1% ZnO–75nm, E) 1.0% ZnO–75nm..

The thermal decomposition course of PMMA studied by DTG curves also indicates that the chemical structure of PMMA is changed (reduced concentration of vinylidene chain end double bonds) when MMA is polymerized in the presence of nano ZnO. This was confirmed by ^{1}H NMR spectroscopy which showed significant reduction of double bond signals at 5.54 and

6.18 ppm by increasing the concentration of nano ZnO, while by adding sub micrometer ZnO no changes were observed (Figure 2) indicating that the main mechanism of thermal stabilization is reduced concentration vinylidene double bonds[8].

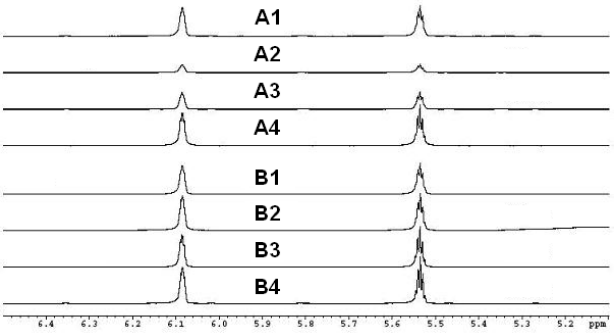

Figure 2: The intensity of vinylidene proton peaks in ^{1}H NMR spectra of PMMA in dependence of the ZnO concentration and size: A-ZnO(75nm); A1) 0%, A2) 1%, A3) 0.1%, A4) 0.01% and B-ZnO(340nm); B1) 0%, B2) 1%, B3) 0.1%, B4) 0.01%.

Conclusion

Themal stability of PMMA matrix in composite materials is enhanced by admixing nano ZnO in concentration of 1 wt. % and higher while submicrometer ZnO shows much less intense effect. DTG and ^{1}H NMR spectroscopy showed that the main mechanism of thermal stabilization of PMMA is changed mechanism of MMA radical chain polymerization causing reduced concentration of vinylidene double bonds

Literature

1. M.M. Demir, M. Memesa, P. Castignolles, G. Wegner, Macromol. Rapid Commun., 27 (2006) 763-770
2. Y. Ding, Z. Gui, J. Zhu, Z. Wang, Y. Hu, L. Song, J. Mater. Res., 22 (2007) 3316–3323
3. M.M. Demir, P. Castignolles, Ü. Akbey, G. Wegner, Macromolecules, 40 (2007) 4190-4198
4. E. Tang, G. Cheng, X. Pang, X. Ma, F. Xing, Colloid Polym. Sci., 284 (2006) 422-428
5. V. Khrenov, M. Klapper, M. Koch, K. Mullen, Macromol. Chem. Phys., 206 (2005) 95-101
6. Jezequel D., Guenot J., Jouini N., Fievet F., J. Mater. Res., 10 (1995) 77–83
7. C. Feldmann, Scripta Materialia, 44 (2001) 2193-2196
8. A. Anzlovar, Z. Crnjak Orel, M. Zigon, Eur. Polym. J.,46 (2010) 1216-1224

Influence of the epoxy /amine stoichiometry on the thermomechanical properties of nanocomposites based on high T_g epoxy and organophilic clays

MA. García del Cid, M.G. Prolongo, R.M. Masegosa, C. Arribas, C. Salom

Escuela de Ingeniería Aeronáutica y del Espacio. Universidad Politécnica de Madrid

mg.prolongo@ upm.es

In epoxy-layered silicate nanocomposites two main steps govern the morphology: the intercalation in which epoxy monomers diffuse into clay galleries, leading to an increase of the d-spacing and the exfoliation in which the silicate layers are delaminated and fully dispersed. Organic modification of the silicate layers makes it compatible with the polymer. The mechanical properties improvement of epoxy-organophilic clay nanocomposites and their correlation with the intercalated or exfoliated morphologies, are object of study nowadays. For epoxy thermosets having low glass transition temperature (T_g), improvements of the elastic modulus and increases in T_g have been reported, both when intercalated or exfoliated morphologies are formed. However, the effect of organophilic clay dispersion on epoxies of high T_g, that are cured using aromatic diamines, is not clear, thus increases as well as decreases of the epoxy T_g in the nanocomposite have been reported.

In previous works (1,2) we have studied the thermal and mechanical properties of epoxy-clay nanocomposites prepared with organically modified montmorillonites (Cloisites: C93A, C15A and C30B). The different effects of clays on epoxy curing are related to the chemical structure of the onium cations. Both C30B and C15A are modified with quaternary alkyl onium cations, C30B has two hydroxyls in the onium cations. C93A is modified with alkyl ammonium cations having one acidic hydrogen. Moreover epoxy/Nanomer I.30E nanocomposites were prepared, Nanomer I.30E is a montmorillonite modified with primary alkyl ammonium cations. The three epoxy/cloisite nanocomposites show intercalated clay structures. The epoxy/I.30E nanocomposites present exfoliated structures according to the catalytic effect of the acidic onium cations that promotes the intragallery curing.

The nanocomposites show improved mechanical properties i.e. they show higher elastic modulus than the neat epoxy thermoset. However all clay-epoxy nanocomposites have lower T_g than the neat epoxy thermoset, regardless of the clay used, with no significant differences between exfoliated or intercalated nanocomposites. The lowering of T_g is usually attributed to a plastizasing effect of the alkyl ammonium ions or sometimes to the formation of an imperfect -no totally crosslinked- network. If the homopolymerization of the epoxy is favored between the layers, this may cause a displacement of stoichiometry so that the T_g would be reduced. Another hypothesys is that there occurs thermal dissociation of the alquyl onium on curing at high temperatures.

The objective of this work is to study if there is a relation between the decrease in T_g and a possible imbalance of the stoichiometry caused by the clay.

The epoxy resin was diglycidyl ether of bisphenol A (DGEBA) and the curing agent 4,4'-

diaminodiphenylmethane (DDM). Stoichiometric ratio: r = HN/-O- = 1 and non stoichiometric r = 0.94, r = 0.85 were studied. The nanocomposites were prepared with Cloisites: C30B, C93A and Nanocor I.30E. The clay was dispersed in DGEBA at 120ºC, the dispersion was degassed, mixed with DDM at 80ºC, sonicated and cured. The curing protocol was: 1h at 120º + 2h at 180ºC. The experimental techniques used were: DSC, DMTA, WAXD, FTIR, and Testing Machine.

Firstly the effect of the clays on the homopolymerization of DGEBA without DDM was studied . It was found that the clays act as catalysts for the self-polymerization. The effect is more pronounced for I.30, and C93A is less effective than C30B.Then the curing by DSC, the DMTA properties and the structure by WAXS of the nanocomposites having different stoichiometric ratios were investigated.

The figure shows tanδ-temperature isochrones obtained from DMTA for some of the nanocomposites studied. For nanocomposites having r=1, the T_g decreases with the clay content. For nanocomposites having r < 1, T_g increases with the clay content. This opposite behavior indicates that organophilic clay offsets the effect of the stoichiometry imbalance.

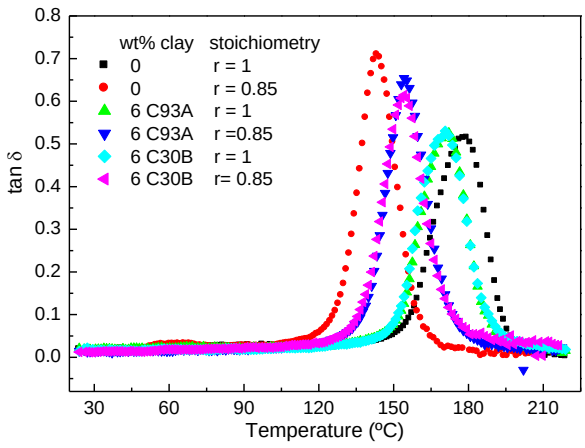

FTIR was used to confirm the presence of amine, glycidyl moieties in the nanocomposites. Mechanical properties obtained from DMTA and from testing mechanical tests were correlated with the nanocomposite structure.

1- M. G. Prolongo, F. J. Martínez-Casado, R. M. Masegosa, C. Salom. J. Nanosci. Nanotech, 2010. 10: 2870M.

2- M.G. Prolongo, MA. García del Cid, R.M. Masegosa, C. Salom, J. Baselga , R.G. Rubio. EPF´09. Graz. July 2009. Abstr: PC1-112

Biodegradable Polyesters Reinforced With Mesoporous Silica Particles

J. M. Campos[a], *M. R. Ribeiro*,[a] *A. Deffieux*[b], *F. Péruch*[b], *J. P. Lourenço*[c], *M. L. Cerrada*[d]

[a] Instituto de Ciência e Engenharia de Materiais e Superfícies & Departamento de Engenharia Química e Biológica, Instituto Superior Técnico, Lisboa, Portugal;
[b]Laboratoire de Chimie des Polymères Organiques, Université Bordeaux I UMR CNRS 5629 16 avenue Pey Berland 33607 Pessac Cedex France
[c] Centro de Investigação em Química do Algarve, Departamento de Química, Bioquímica e Farmácia, Universidade do Algarve, Faro, Portugal
[d] Instituto de Ciencia y Tecnología de Polímeros (CSIC), Juan de la Cierva 3, Madrid

rosario@ist.utl.pt

Introduction: In recent years, the development of mechanically reinforced nanocomposites based on biodegradable polyester matrices has gained a strong incentive due to their potential use as biomaterials and to growing worldwide environmental concerns.

Objectives: This work aims to pursue this goal, and combines polycaprolactone matrices (PCL) with mesostructured silicas, by means of surface initiated acid-catalysed Ring Opening Polymerisation (ROP). Mesoporous silica materials are known as adequate carriers for hosting many types of molecules [1], and they were used here simultaneously as reinforcement filler and as carrier for ROP initiators. Metal-free ROP catalysts, based on organic derivatives of sulfonic acid, are used [2, 3] which will constitute an additional benefit from the environmental standpoint.

Methods: The reinforced polymers were prepared using high surface area SBA-15 and MCM-41 mesoporous silicas functionalised with OH groups (initiators). Methane sulfonic acid was used as catalyst for the surface-initiated ring-opening polymerisation of CL and LA.

Results and Discussion: Preliminary physical characterisation data show that for a PCL sample with moderate molecular weight (Mn~20000) and containing around 3.5% mesoporous silica (SBA-15), the mechanical properties are drastically improved, with the reinforced polymer being much tougher than neat PCL. Melt rheology measurements show that this reinforced PCL has a zero-shear viscosity nearly 5 times higher than for neat PCL, with shear-thinning visible at higher shear rates.
In spite of an expected initiation by the hydroxyl attached to the mesoporous silica framework, it was found that nearly all the PCL chains are not attached to the silica particles. MALDI-TOF results hint that this is due, in part, to the formation of cyclic PCL species by back-biting transesterification reaction.

References:

[1] K. Tajima and T. Aida, Polymerization with Mesoporous Silicates, in Nanostructured Catalysts, S.L. Scott, C.M. Crudden and C.W. Jones, Editors. 2003, Kluwer Academic / Plenum Publishers: New York. p. 231-255.
[2] S. Gazeau-Bureau, D. Delcroix, B. Martin-Vaca, D. Bourissou, C. Navarro and S. Magnet, Macromolecules, 2008. 41 (11): p. 3782-3784.

[3] D. Bourissou, B. Martin-Vaca, A. Dumitrescu, M. Graullier and F. Lacombe, Macromolecules, 2005. 38 (24): p. 9993-9998.

Fluorinated epoxy resin nanocomposites reinforced with amine functionalized MWNTs

Celina Maria Damian [1*], *Sorina Alexandra Gârea*[1], *Corina Andronescu*[1], *Andreea Madalina Pandele*[1], *Eugeniu Vasile*[2], *Horia Iovu*[1]

[1] Politehnica University of Bucharest, Faculty of Applied Chemistry and Materials Science
[2] METAV Research Institute, Bucharest, Romania

[*] petrea_celina@yahoo.com

Introduction: Nanosized fillers such as carbon nanotubes, clay and nanofibers have been considered suitable reinforcing materials for epoxy resins to produce high performance composites with enhanced properties. Carbon nanotubes (CNTs) are excellent candidates for improvement of thermo-mechanical properties of epoxy resins [1]. Raw CNTs have a tendency to aggregate because of their large surface area and strong resultant van der Waals forces. The dispersion of CNTs is very important in order to fully realize improvement in epoxy based CNT composites, this being improved considerably by functionalization [2] Aiming the enhancement of the dielectric properties and the moisture resistance of classic DGEBA epoxy resins, the present research proposes fluorinated epoxy nanocomposite systems reinforced with amine modified Multiwalled Carbon Nanotubes (*MWNT*).

Materials and methods: Fluorinated epoxy resin was synthesized from epichlorhydrine and 4,4′-(Hexafluoroisopropylidene)diphenol by a method described in the literature [3]. Amine modified nanotubes have been obtained by a two step reaction: first step is the interaction between carboxylated MWNTs and thyonil chloride ($SOCl_2$) to obtain acylated groups on the nanotubes surface, second step was the interaction between acylated MWNTs and the amines modifying agents: benzylamine (*BA*) and a polyetheramine (*B100*). Functionalization was proved by TGA, FT-IR, XPS and SEM analysis. The modified CNTs were dispersed in diglycidylether of hexafluorinated bisphenol A (DGEFBA) by tip sonication, cured with an aromatic polyamine (Poly(m-xylylenediamine-alt-epichlorohydrin) diamine terminated) by a two step temperature schedule to obtain the final composites. Composite samples were characterised by TGA, DMA, DSC and SEM analysis.

Results and disscusion: XPS surface characterization of functionalized MWNTs showed a decrease of the oxygen content for MWNT-BA and subsequent appearance of nitrogen bonds from the amine groups. Amine groups were present also in the MWNT-B100, but due to the ether groups from the B100 backbone, the O1s content was slightly increased as shown in table 1.

Table 1 XPS data for functionalized MWNTs

Nanotubes Type	At. C1s %	At. O1s %	At. N1s %
MWNT-COOH	83.8	16.2	0
MWNT-BA	88.3	9.7	2.0
MWNT-B100	81.8	16.9	1.3

Thermostability of the DGEFBA composites systems, defined as the temperature of 3% weight loss ($Td_{3\%}$), was obtained using TGA technique. Compared with the neat DGEFBA, the composites reinforced with only 0.3% of functionalized MWNTs showed a ~20°C improvement of $Td_{3\%}$ (figure 1), meaning that the epoxy network was strengthened by the one formed through the good dispersion of the nanotubes.

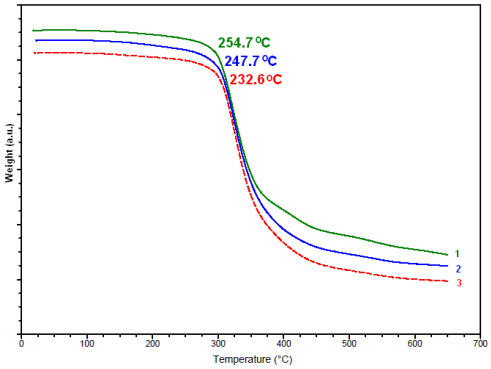

Fig. 1 TGA curves of 1) DGEFBA/MWNT-B100 2) DGEFBA/MWNT-BA; 3) neat DGEFBA;

The curing process of the initial composite systems was studied by dynamic DSC, resulting that 0.3% of functionalized MWNTs do not affect significantly the reaction enthalpy (~290 J/g) and the maximum cure temperature (~ 99°C).

Fluorinated epoxy resins are known as hydrophobic materials with high resistance to the moisture environment. Due to this fact it was noticed a low compatibility with the carboxylic groups from the MWNTs surface resulting in agglomerates. The SEM images for amine functionalized MWNTs (Fig.2.B) showed well dispersed nanotubes in the DGEFBA resin, which is responsible for the enhancement of the new composites.

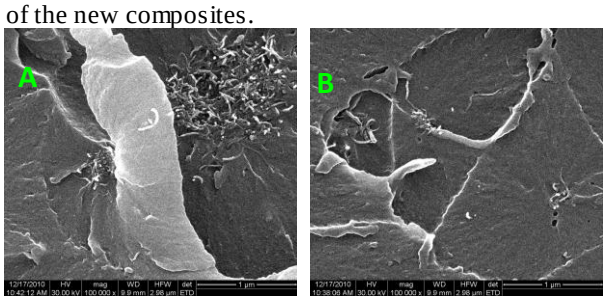

Fig. 2 SEM images of DGEFBA composites with A) MWNT-COOH and B) MWNT-B100

Conclusions: MWNTs were functionalized with two aromatic amines in order to improve their compatibility with fluorinated epoxy resin. The new composites showed improved thermal stability and good dispersion.

Aknowledgrments: This work was kindly supported by CNCSIS –UEFISCSU through project number PNII – IDEI 1718/2008

References: [1] Xianhong Chen, JianfengWang, Ming Lin,Wenbin Zhong, Tao Feng, Xiaohua Chen, Jianghua Chen, Feng Xue, Materials Science and Engineering A 492 (2008) 236–242; [2] Yumi Kwon, Byung-seung Yim, Jong-min Kim, Jooheon K, doi:10.1016/j.microrel.2010.11.005; [3] Mosznet N. et al., US Patent Application 0287458A1, Dec. 21,2006

Fluorescent Polynorbornene/Oxazine-1 Loaded Fluoromica Nanocomposites by *In Situ* Polymerization for Solution Processable Electronics

Giuseppe Leone, Umberto Giovanella, William Porzio, Chiara Botta, and Giovanni Ricci

CNR-Istituto per lo Studio delle Macromolecole (ISMAC), via E. Bassini 15, I-20133 Milano (Italy)

giovanni.ricci@ismac.cnr.it

In the growing world of nanotechnologies, a particular interest has been given to the synthesis of hybrid supramolecular assemblies, arranged into ordered nano-scaled architectures embedding photofunctional dyes, for the development of optoelectronic devices. [1]

A common limitation of organic dyes is their susceptibility to chemical and photochemical degradation. Moreover, their tendency to aggregate induces multichromophoric interactions that alter the color quality and give unfavorable non-fluorescent species. In order to overcome these drawbacks, many researchers began investigating hybridization of the dye by addressing these molecules into different organic or inorganic hosts. Among host–guest assemblies, layered silicates belonging to the family of 2:1 phyllosilicate clays have proved to be very convenient hosts, especially because they offer unique two-dimensional expandable interlayer spacing to yield organized intercalated guest species. [2] To date, several luminous dye-clays have been extensively studied to prepare functional assemblies. However, the fabrication of optoelettronic devices with these hybrids is still a challenging task because of the still poor film quality.

We thought that a possible way to find a solution to the above critical points could have been the incorporation of dye doped clays into a flexible polymeric matrix, allowing to maintain the dye luminescence properties and to improve the film processability at the same time.

Following this idea, we have now prepared fluorescent polynorbornene/oxazine-1 (Ox1) loaded fluoromica nanocomposites by *in situ* polymerization via Ziegler-Natta catalysis.

Sodium-fluoromica is modified with cationic Ox1 dye by ion-exchange: at higher Ox1 loading the dye adopts a much more perpendicular orientation of the long-molecular axis with respect to the clay layer surface. As a result of this tilted geometrical arrangement the clay *d*-spacing increases and minimizes the area covered per a monolayer intercalated Ox1 molecules. These features facilitate the entry of the incoming polymerizable monomers (*i.e.*, norbornene and ethylene) in between the clay galleries, and thus the interlayer growth of the macromolecular chains (see Scheme 1). [3] When the polymerization is initiated within the layers, where the slabs of the inorganic host act as a template, an ordered and well-dispersed multicomponent polymeric hybrid, in which dyes are highly oriented in the inorganic framework, is formed.

Nanocomposites exhibit an improved solubility with respect to the dye/clay compounds, which made the polynorbornene composite easy processable by spin-coating technique. Absorption and photoluminescence studies show that the nanohybrids exhibit the presence of dye species having features of both Ox1 monomer molecules and J-dimers.

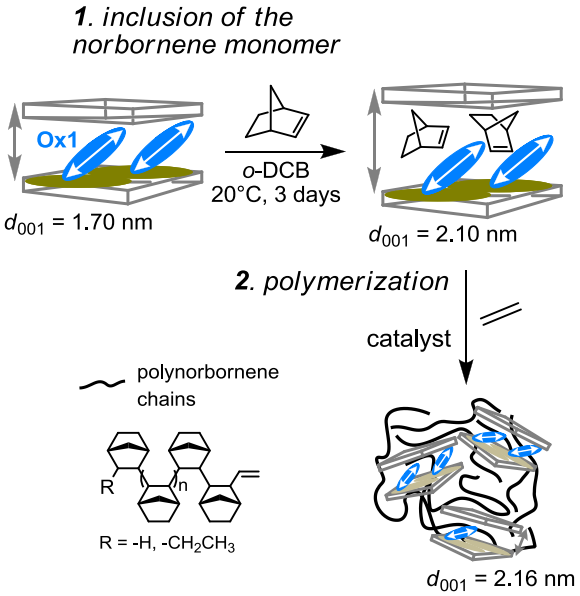

Scheme 1.

The nanocomposites show four main advantages: (*i*) a high dye concentration can be achieved avoiding non-fluorescent dye aggregate formation; (*ii*) the clay aggregation is hampered by the polymer chains that wrap the clay platelets; (*iii*) the solubility is improved with respect to the dye/clay compounds, making the polymer composites easy processable by spin-coating technique; (*iv*) the presence of the hydrophobic poorly–polar polymer in between the clay layers affords a phase segregation which drives the dye molecules to adopt less conformational degrees of freedom until to increase the head-to-tail interaction (J-aggregates) between them.

In conclusion, the results obtained open up unprecedented prospects for the synthesis of novel luminescent polymer hybrids which can be used to fabricate functional devices with unique photoluminescence properties.

[1] S. Förster, T. Plantenberg, *Angew. Chem. Int. Ed.* **2002**, *41*, 688.

[2] M. Ogawa, K. Kuroda, K. *Chem. Rev.* **1995**, *95*, 399.

[3] G. Leone, A. Boglia, A. C. Boccia, S. Taglialatela Scafati, F. Bertini, G. Ricci, *Macromolecules* **2009**, *42*, 9231.

Novel rheological and electrical results of polyamide/graphene nanocomposites

Jorge Canales[1], *Mercedes Fernández*[1], *Maria Eugenia Muñoz*[1], *Antxon Santamaría*[1]

1- Polymer Science and Technology Department, University of the Basque Country

antxon.santamaria@ehu.es

Introduction

The number of papers on polymer nanocomposites based on layered silicates and carbon nanotubes has increased exponentially in recent years. However, publications about the use of graphene to obtain polymer nanocomposites are still relatively scarce, although its number is also increasing[1,2,3]. Yet, the excellent electrical, thermal and mechanical properties of graphenes open sound prospects for the dispersions of such nano thin carbon sheets in thermoplastic or thermoset polymers. In this contribution we investigate rheological and electrical features of polyamide/graphene nanocomposites.

Results

A commercial amorphous polyamide, with a processing temperature in the range 220-290ºC, is used as the polymer matrix where carbon sheets are dispersed. For comparison purposes, graphite, a commercial graphene and graphene prepared in our laboratory are employed. With the aim of approaching to industrial processes, the dispersions are performed in the molten state, in a mini extruder which works either in corotational or contrarotational mode. Adequate mixing conditions are selected according to a feedback procedure involving rheological and electrical data of the dispersions Dynamic viscoelastic measurements are used to evaluate the effect of temperature on the complex viscosity of the nanocomposites. Besides, the analysis of the terminal zone, in particular the variation of the loss factor with frequency, allows determining the percolation threshold or the minimum volume fraction of nano sheets to constitute a physical network. These rheological results are linked with electrical conductivity results, leading to discuss the connection between rheological and electrical percolation. Pressure-Volume-Temperature experiments are also carried out to investigate the effect of pressure on viscosity, in concordance with rheological data obtained by dynamic viscoelastic measurements.

The following scheme reflects the *road-map* of the research involved in the work:

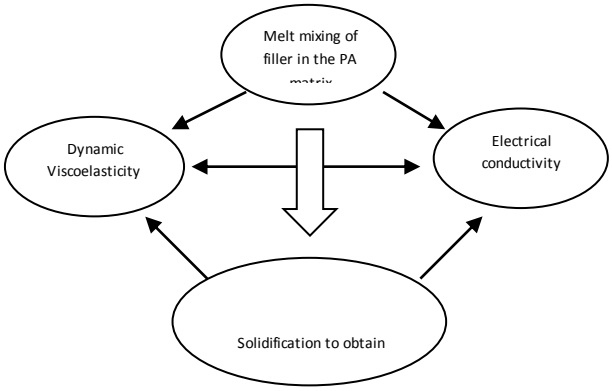

Acknowledgements

Financial support is acknowledged from GIC IT-441-10 (Basque Government) and MICIN (MAT 2010-16171) (Spanish Government). One of us J.C. acknowledges a Thesis grant from Basque Government.

Bibliography

1- Kim H., Abdala A.A., Macosko C.W. *Macromolecules*, 43, 6515-6530 (2010).

2- Potts J.R., Dreyer D.R., Bielawski C.W., Ruoff R.S. *Polymer*, 52, 5-25 (2010).

3- Kuilla T., Bhadra S., Yao D., Kim N.H., Bose S., Lee J.H., *Progress in Polymer Science*, 35, 1350–1375 (2010).

Evaluation of polymeric micelles as potential carriers of antifungal agents

A. F. Olea[1], *I. Fuentes*[1], *H. Carrasco*[1], *R. Martínez*[1], *I. Montenegro*[2]

1 Universidad Andrés Bello, Faculta de Ecología y Recursos naturales, Departamento de Ciencias Químicas, República 275, Santiago, Chile.

2 Universidad de Valparaíso, Escuela de Química y Farmacia, Valparaíso, Chile

aolea@unab.cl

Introduction. Polymeric micelles are created by spontaneous self-assembly of individual amphiphilic polymeric molecules (unimers) at a critical micelle concentration (CMC) and above the critical micelle temperature (CMT). Most of the polymeric micelles used for drug delivery are spherically shaped core-shell structures where the hydrophobic segments of an amphiphilic polymer form the core of the micelle while the hydrophilic parts form the corona or outer shell. The hydrophobic micelle core serves as a microenvironment for the incorporation of lipophilic drugs, while the hydrophilic shell helps to avoid micelle aggregation and to ensure micelle solubility. The most commonly used hydrophilic blocks has been poly(ethylene oxide) (PEO) that has the monomer subunit –CH2-CH2-O-. Water-soluble triblock copolymers of PEO and poly(propylene oxide) (PPO) are commercially available in a range of molecular weights and PPO/PEO composition ratios. Commercial names for these copolymers are Poloxamers and Pluronic®. These molecules are widely used in industrial applications such as detergency, dispersion stabilization, foaming, emulsification, and recently in drug solubilization and controlled release. In aqueous solution, these amphiphilic copolymers form micelles with hydrophobic PPO blocks as the core and hydrated PEO blocks as the corona.
Therefore, in this work we have studied from a physicochemical standpoint, polymeric micelles formed by Pluronic® with the aim to get information on the factors that control the incorporation and delivery of antifungal agents.

Materials and Methods. Two different Pluronic®, F-127 and F-68, were used as received. Aqueous solutions, with polymer concentration in the range $1 \times 10^{-2} - 1 \times 10^{-3}$, were prepared by direct solubilization of polymer in distilled and deionized water. Polygodial extracted from *drymis winteri* was dissolved in acetonitrile and incorporated to the micelle solution by either injection or sonication methods. Antifungal activity was evaluated against *Saprolegnius*.
The micelle critical concentration, cmc, was determined by measuring the ratio monomer/excimer intensities in pyrene fluorescence spectra, as a function of polymer concentration.

Results and Discussion. The cmc of block copolymers was determined by fluorescence probing. Typical results are shown in figure 1. The obtained values are similar to those found in literature, i.e. 2.8×10^{-6}M and 4.8×10^{-4}M, for F127 and F68, respectively.

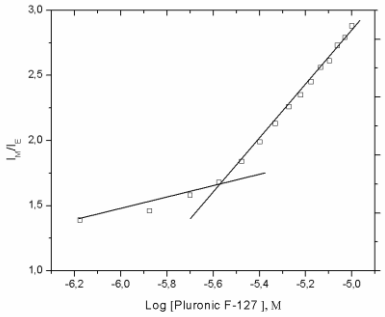

Figure 1. Plot of the ratio of monomer to excimer intensities, against log of Pluronic concentration.

The maximum amount of polygodial incorporated to these polymeric micelles is 0.69 mg/mL, and it is independent of the solubilization method. At this concentration the aqueous solution of poygodial in micelles exhibit large zones of inhibition growth for *Saprolegnius* (see figure2)

Figure 2. Growth of Saprolegnius in the presence of different concentrations of polygodial solubilised in polymeric micelles.

The results are interpreted in terms of the distribution constant and the liberation rate of polygodial.

Conclusions. Polygodial has been solubilised in aqueous solution of triblock copolymers. The anti-Saprolegnius activity of this agent is not affected by the polymer carrier.

Acknowledgments. This work has been funded by UNAB DI-44-10/R and InnovaChile grant 09MCSS-6683

Isothermal Titration Calorimetry as a Tool for Elucidating the Cobalt bis(dicarbollide) Interaction with Hydrophilic Polymers

Mariusz Uchman,[1] *Karel Prochazka*,[1] *Michael Gradzielski*,[2] *Pavel Matejicek*,[1]

[1]Department of Physical and Macromolecular Chemistry, Faculty of Science, Charles University in Prague, Hlavova 2030, 128 40 Prague 2, Czech Republic

[4]Stranski-Laboratorium für Physikalische Chemie und Theoretische Chemie, Institut für Chemie, TU Berlin, Sekr. TC 7, Strasse des 17. Juni 124, D-10623 Berlin, Germany

qqryk@o2.pl

Introduction: Sodium cobalt bis(dicarbollide), COSAN, is water soluble despite the fact that the boron cluster itself is strongly hydrophobic. These and other features lead to peculiar behavior of the metallacarborane in water, such as aggregation and surface activity despite a lack of amphiphilic topology.[1] It is also known that metallacarboranes can interact with several biocompatible polymers that could be exploited in preparation of nanoparticles for drug delivery.[2,3] To obtain a deeper insight into the cobalt bis(dicarbollide) behavior in aqueous solutions and its interaction with water soluble polymers consisting of poly(ethylene oxide), PEO, and poly(2-ethyl oxazoline), PEOX, we employed isothermal titration calorimetry.

Materials: Sodium salt of metallacarborane anion [3-cobalt(III) bis(1,2-dicarbollide)](-1) was a kind gift of Dr. Bohumír Grüner and Dr. Jaromír Plešek (Institute of Inorganic Chemistry, ASCR, Řež near Prague). Poly(ethylene oxide) was purchased from Fluka (M_w is 41.5×10^3 and PDI 1.10). Poly(2-ethyl-2-oxazoline) was purchased from Aldrich (M_w is 50.0×10^3). Poly(ethylene oxide)-*block*-poly(2-ethyl oxazoline) was purchased from Polymer source, Inc. (Dorval, Quebec, Canada), (M_w of PEO and PEOX: 5.0×10^3 and 6.5×10^3, respectively, PDI 1.10).

Results and Discussion: The ITC results show fairly complex behavior even of pure sodium bis(dicarbollide). The heat of dilution is both endo- and exothermic depending on starting concentration of metallacarborane. When PEO solution is titrated by metallacarborane in 0.1 M NaCl solution, we observed exothermic contribution with the sharp exothermic peak (see Figure 1) that can be attributed to rearrangement of the boron clusters within the PEO matrix of the creating composite. We also observed that the interaction with PEOX and PEO-PEOX is more complex than simple one-binding-site approach and requires using of more sophisticated models. The binding sites of cobalt bis(dicarbollide) with PEO and PEOX chains were estimated by 2D NMR experiments. From appropriate fits of the experimental ITC curves we calculated heat of formation, stoichiometry and binding constants of the metallacarborane/polymer complexes.

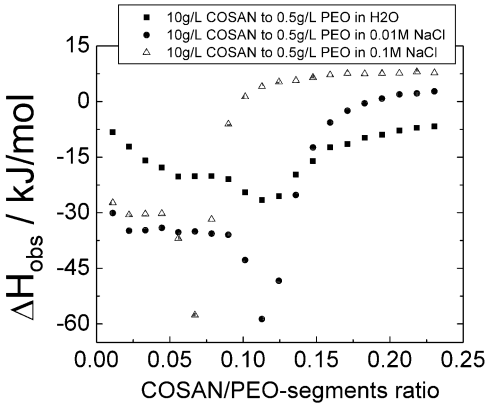

Figure 1: The ITC isotherms of PEO solutions titrated by COSAN as indicated.

References: (1) Matejicek, P.; Cigler, P.; Prochazka, K.; Kral, V. *Langmuir* **2006**, *22*, 575.

(2) Matejicek, P.; Zednik, J.; Uselova, K.; Plestil, J.; Fanfrlik, J.; Nykanen, A.; Ruokolainen, J.; Hobza, P.; Prochazka, K. *Macromolecules* **2009**, *42*, 4829.

(3) Uchman, M.; Cigler, P.; Gruner, B.; Prochazka, K.; Matejicek, P. *J. Colloid Interface Sci.* **2010**, *348*, 129.

Synthesis of Polymeric Nanoparticles by Miniemulsion Evaporation for the Development of Optical Sensing Phases

M. Marín Suárez del Toro[1*], *J.F. Fernández Sánchez*[1], *T. Galeano Díaz*[2], *A. Fernández Gutiérrez*[1]

[1] Department of Analytical Chemistry, University of Granada, Avda. Fuentenueva s/n, 18071 Granada (Spain)
[2] Department of Analytical Chemistry, University of Extremadura, Avda. de Elvas s/n, 06071 Badajoz (Spain)

*mmarinst@ugr.es

Introduction: Molecular oxygen is one of the most important gases in our environment. Oxygen sensors are usually based on the quenching of luminescent dyes by paramagnetic oxygen. Therefore, the incorporation of luminescent dyes into polymeric nanoparticles makes them an interesting platform for oxygen optical sensing. Miniemulsion solvent evaporation and the influence of different variables have been already studied by G. Mistlberger *et al.*[1] for the production of optical sensing nanoparticles. However, due to the complex medium and the multiple physic processes involved, the relation between all the variables is not yet clear. Statistical design offers a tool to find out this influence by using a minimum number of experiments. In this work a preliminary screening test has been carried out to choose which are the most relevant parameters leading to a monodisperse size distribution.

Materials and Methods: polymer nanoparticles were prepared by the emulsification of a water insoluble cocktail and the consequent evaporation of the solvent. Poly(styrene-co-maleic anhydride) of three different molecular weights and maleic contents, chloroform, polyvinyl alcohol (PVA) and sodium dodecyl sulfate (SDS) were used. The parameters studied to characterize the nanoparticles were size (d, in nanometers) and polydispersion index (PdI), both measured with a Zetananosizer (Malvern Instrument).

Results and Discussion: Factors able to affect the nanoparticles are related to either the processes or the raw materials. Main factors regarding to the process are time and amplitude of sonication. It seems clear that factors influencing size and polydispersity are also related with polymer weight and concentration, surfactant type and concentration and o/w relation. In other to evaluate the most relevant ones a screening test was proposed covering the range shown in Table 1 for each variable.

Table 1. Codes for the different variables and range selected

Codes	Variable	Range Min	Range Max
W	Molecular Weight ($g \cdot mol^{-1}$)	14400	240000
C_p	Polymer concentration (mg/ml)	10	160
V	Percentage of organic phase (%)	1	20
C_{SDS}	SDS concentration (mg/ml)	0.14	2.88
A	Amplitude of sonication	20	90
t	Time of sonication	5	10

Since one of the challenges is to produce small, monodisperse nanoparticles, the response function was designed to penalize the values of PdI and d over 0.2 and 200 nm, respectively. Therefore, three different response functions were proposed, and the effects were calculated. Following an analysis of variance criteria (ANOVA), the most significant variables were: polymer type and concentration, and organic phase percentage. This is in concordance to considering significant those variables whose effect exceeds the percentage of error, corresponding to a sample prepared in triplicate, as can be

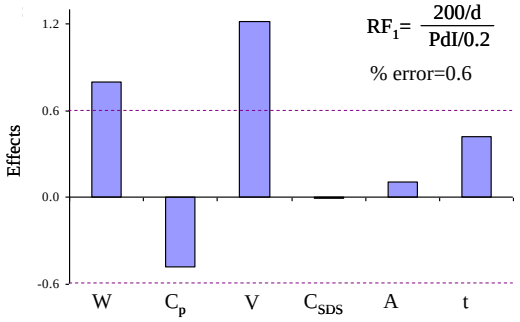

Fig. 1. Effects for the variables according to response function RF_1.

As expected, the most relevant parameters are those related to the raw materials. However, it is worth mentioning that although SDS does not appears as a significant variable, the surfactant role is very important in the particle formation. Thus, this variable has a significant effect over the particle size, but seems not to be so critical in the RF_1 defined above, for the range selected. In fact, two experiments were repeated using PVA instead of SDS and in both cases, the result was a highly polydisperse solution of nanoparticles exceeding 1 μm. This can be explained by the high molecular weight of PVA, which leads to the incomplete formation of micelles for the concentration used in the experience.

Conclusions: Miniemulsion evaporation was performed to study the effect of variables. The preliminary results show that for the range studied, the SDS amount does not affect size and size distribution, when both responses are combined in a function which represents the result considered as optimum: small and narrow distributed particles. Therefore, these parameters may be controlled by means of polymer type and concentration, and o/w relation. Further studies will be carried out to completely optimize the system.

References: [1]Mistlberger, G., Medina-Castillo, A.L., Borisov, S.M., Mayr, T., Fernández-Gutiérrez, A., Fernandez-Sanchez, J.F., Klimant, I.; *Microchimica Acta* (2010) 1-10.

Acknowledgment: This research is funded by Spanish Ministry of Education (Project CTQ2008-01394) and Regional Government of Andalusia (Excellence projects P07-FQM-2625 and P07-FQM-2738 and Marín-SuárezdelToro's grant).

NAOB® – Nanocomposites of Natural Rubber Filled with Organophillic Clay and other reinforcers carbonous materials

Guillermo R. Martín Cortés[1], Fabio J. Esper[2], Adriana A. Cutrim[3], Alexandre A. Dantas[4], Wildor T. Hennies[5], Francisco Rolando Valenzuela Díaz[6].

[1-6] Metallurgic & Materials Eng. Dept. – Polytechnic School – Univ. of São Paulo; [2]Esper Ltda.; [3-4]Bentonisa – Bentonita do Nordeste S.A.; [5] Mining & Petroleum Engineering Dept. – Polytechnic School – Univ. of São Paulo.

frrvdiaz@usp.br

Introduction. Natural rubber (NR) is commonly reinforced with carbon black (CB) to produce vulcanized material. CB is derived from the oil refining process polluting the environment. Replacing CB by a little among of modified clays mixed with a complementary volume of some carbonous materials (CM) turns it into a new environmentally friendly nanocomposite. CB substitution in this industrial process must contribute to diminish the oil dependence and the environment pollution. This paper shows the application results of organophilic clay (OC) blended with CM substituting CB as rubber fillers. OC is the organic modification of smectite clay by ammonium quaternary (AQ). CM are very little sized particulate minerals obtaining as byproducts of the mining process with today poor economical applications because it's very little grain size. In the blend CM act as a supplement to volume and as reinforcers too.

Industrial rubber products commonly use, at least 40% of CB filler. Products tested in this work use 10% OC + 30% CM as maximum filler. Weights in % referring to the NR total mass.

Materials. Bentonites. An absorbent aluminum phyllosilicate generally impure clay consisting mostly of montmorillonite, $(Na,Ca)_{0,33}(Al,Mg)_2Si_4O_{10}(OH)_2(H_2O)_n$ Two types exist: swelling bentonite, or Na-bentonite and non-swelling bentonite or Ca-bentonite. Originated from weathering of volcanic ash often in presence of water. [1]. Some Ca-bentonites from the Paraiba State, Brazil were selected to modify them with sodium carbonate transforming the same ones into Na-bentonites that swell in water. These synthesized Na-bentonite were modified using AQ to produce hydrophobic OC. OC reacts with the polymer materials collaborating in its structure during the mass preparation and in the vulcanization, transferring to the end product technological properties the same or better than the traditionally CB filler.[2]

CM are finest grain of coal shale (black dust) with high-C level or of limestone (nearly white) with CO_3^{-2} from the mining excavation activities.

NR: Product obtained from the Hevea Brasiliensis tree.

Additives: Traditionally used substances for rubber vulcanization as sulphur (S), Zinc Oxide; Stearic Acid and the rubber accelerators: TMTD; MBTS; MBT.

AQ: Alkyl – Trimethyl - Ammonium chloride.

Methods. OC production: The clay fraction below 325 meshes characterized by X-ray diffraction, Foster swelling test, Scanning electronic microscope, Thermal Analyses, and others were modified by Na and AQ to OC trough a new "dry" process described by Silva (2006) [2]. It is a small water addition to the clay followed by homogenization, cure, addition of AQ, cure, homogenization, drying, milling and classification by a 200# sieve. Depending use / type of the end product, the CM is selected and blended with the OC.

Plates vulcanization, conformation and characterization of the test samples. OC+CM added to mass by a mixer. Plates were produced according the Esper Ltd. process and standard ASTM D 3182 for the carpet for cars and synthetic floors production.

For characterizations the reinforcement fillers were 0%, and 40% of CB; and 10% OC + 30%CM. After 2 min of lamination of sulfur with the rubber blanket, verified homogeneous visual aspect, being, directed for the plate vulcanization effected in steel form under action of Thermo-Hydraulic Press Marconi Mark Model MA098 warm to 160°C ± 5°C.

Universal test machine model EMIC DL3000 was used for **evaluation of the mechanical properties** of rupture lengthening and rupture tension according ASTM D412 standard [3]. Hardness was evaluated for each plate according to the ASTM D2240 standard [4].

Results.

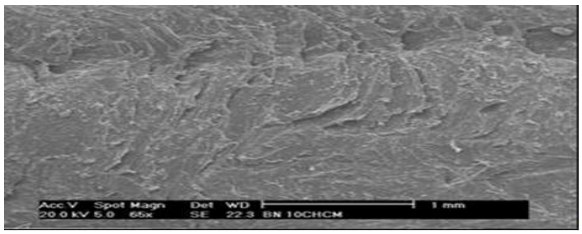

Fig. 1 Micrograph of a nanocomposite vulcanized plate

Table 1 – Results of the Mechanical assays

Sample	Rupture tension (MPa)	Rupture lengthening (%)	Shore A
NR	03,2	700,0	43
NR + 40% CB	11,2	315,0	52
NR+10%OC+30%CM	29,5	757,0	58

Conclusions: 1. The OC-CM/NR nanocomposites show normal aspect at the micrograph. 2. The OC-CM/NR nanocomposites mechanical results show greater values than the composite with CB as filler.

References:

[1]M.A.F. Monteiro, A.P. Ribeiro, A.T. Machado, S.M. Toffoli, G.R. Martín-Cortés, H. Wiebeck, F.R. Valenzuela-Díaz. Brazilian bentonites for geosynthetic clay liners (GCL). 2007. In Proceeding 6th. Int. Latin-American Conf. Powder Technology, Búzios, RJ, Brazil. p1316-1323 In CD-Rom.

[2] SILVA, A. A. Estudo de argilas organofílicas destinadas à separação óleo/água. Dissertação apresentada à Univ. Federal de Campina Grande, Campus I, Campina Grande, 2006.

[3] ASTM D412. Standard Test Methods for Vulcanized Rubber and Thermoplastic Elastomers-Tension. Dec-2006.

[4] ASTM D2240 Standard Test Method for Rubber Property - Durometer Hardness.

Hierarchical Structure and Its Formation Process in Liquid Crystalline Block Copolymers

Tomoo Shiomi, Hiroki Takeshita, Shunsuke Adachi, Shin-ichi Taniguchi, Katsuhiko Takenaka

Department of Materials Science and Technology, Nagaoka University of Technology

shiomi@vos.nagaokaut.ac.jp

1. Introduction

Block copolymers containing a side-group liquid crystalline (LC) block have a potential to exhibit hierarchical phase structure, which consists of several ten nanometers of microphase separation (MS) structure and a few nanometers of liquid crystalline (LC) structure. Such hierarchical structure may be formed in the interplay between microphase separation and liquid crystallization. Therefore, main interests are as follows: (1)[1,2] in liquid crystallization from microphase separated melts, whether the microphase separation structure is disrupted or kept, or how is the formation process, (2) how is the liquid crystalline structure within the microdomain, and (3) how is the orientation of the mesogen axis to the interface of the microdomain. In this paper, we will present the formation process as well as the hierarchical structure in liquid crystalline -amorphous block copolymers.

2. Experimental

Block copolymers composed of a cyanobiphenyl-type liquid crystalline block (PCB) and poly(*n*-butyl acrylate) (PBA), shown in Fig. 1, were prepared by atom transfer radical polymerization (ATRP). The length of spacer between the main chain and mesogenic group was controlled by the number *x* of methylene groups to be *x*=6, 8, 11. The characteristics of the samples employed are listed in Table 1. Phase structure and its formation process were observed using time-resolved small-angle X-ray scattering (SAXS) techniques employing synchrotron radiation at beam lines BL-10C and BL-15A for 1D and 2D experiments, respectively, at the Photon Factory in the High Energy Accelerator Research Organization in Tsukuba, Japan. The orientation of mesogenic groups was observed by 2D-SAXS together with polarized optical microscopy (POM), and LC-isotropic transition temperatures were determined by DSC.

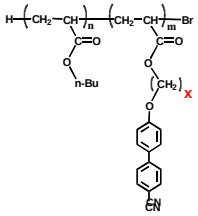

Fig. 1. Block copolymer

3. Results and Discussion

The liquid crystalline structure of the PCB homopolymer was bilayer smectic (Sm) for *x*=8 and 11 and nematic (Nm) for *x*=6.

For block copolymers, the MS structure and LC structure were characterized as shown in Table 1: Sm in the lamellar domain except for *x*=6 whose structure was Nm even for the homopolymer, while Nm in the cylindrical domain. Fig. 2a and 2b show SAXS profiles of the isotropic and liquid crystalline states and the temperature dependence of the peak position q_m of the 1st-order peak of the SAXS curve due to the MS structure, respectively, in the liquid crystallization from lamellar MS structure. The liquid crystallization process from cylindrical MS structure is shown in Fig. 3a and 3b. As shown in BA08OCB and BA11OCB44 of Fig. 2b, the peak position shifted discretely in the Sm formation. This suggests that the MS structure is reorganized by the liquid crystallization. Also, the coexistence of Sm and Nm is observed in the transition region, which means that Sm structure is formed via Nm formation. On the other hand, as seen in BA06OCB_35 of Fig. 2a and BA11OCB_20 of Fig. 3b, the peak position of MS structure is not discretely changed in the Nm formation.

The orientation of mesogenic groups was parallel to the interface of microdomain, regardless of LC structure and MS structure.

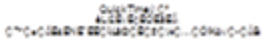

Fig. 2. In the liquid crystallization from lamellar structure, (a) SAXS profiles and (b) change of the 1-st order peak

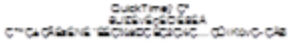

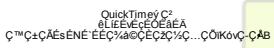

References

(1) S. Taniguchi et al., *Polymer*, 2008, 49, 4889.
(2) H. Takeshita et al., *Polymer*, 2009, 50, 271.

Polyimide/Silica Nanocomposite Thin Films for Advanced Applications

C. Hamciuc[1], E. Hamciuc[1], I. Bacosca[1] and L. Okrasa[2]

[1]"Petru Poni" Institute of Macromolecular Chemistry, Aleea Gr. Ghica Voda 41A, Iasi-700487, Romania
[2]Department of Molecular Physics, Technical University of Lodz, 90-924 Lodz, Poland

email: chamciuc@icmpp.ro

Introduction

Polyimide/silica nanocomposites were extensively studied as materials with improved thermal, mechanical and electrical properties [1-2]. The compatibility between polyimides and silica generated in the sol-gel process is limited because of weak interactions between the pure organic and inorganic phases. A way to improve the compatibility between polyimide and silica is by functionalizing the polymer chains at their ends, including comonomers that contain appropriate functional groups or adding a coupling agent to bond the polyimide chains and inorganic oxide network. Introduction of polydimethylsiloxane segments into polyimide may prevent the phase separation of hybrid composites and the formation of high-molecular weight silicate. The siloxane segment interacts with silica because of the similarity of its structure with the sol-gel glass matrix of the silica precursor, indicating that polyimide-polydimethylsiloxane/silica might be a good material for organic/inorganic hybrid composites [3].

Materials and Methods

(3,4-Dicarboxyphenoxy)phenyl]phthalide dianhydride (DAFT) and α,ω-bis(3-aminopropyl)oligodimethyl-siloxane (PDMS) were prepared according to [4, 5]. Two series of polyimide nanocomposites thin films containing 10%, 20% and 30% silica were prepared starting from a poly(amic acid) and tetraethoxysilane via sol-gel technique and thermal cyclodehydration. The first series was obtained using a poly(amic acid) resulting from polycondensation reaction of 1,3-bis(4-aminophenoxy)-benzene (DAB) with DAFT, (molecular ratio: 10/11) in NMP as solvent. For the second series the poly(amic acid) was synthesized from 4,4′-oxydiphthalic anhydride and a mixture of DAB and PDMS in NMP/THF as solvent. 3-Aminopropy-ltriethoxysilane (APTES) was used as coupling agent.

Results and Discussion

The structure of the nanocomposites was confirmed by FTIR spectroscopy. The films, having the thickness in the range of tens of micrometers, were flexible and showed good thermal and mechanical properties. Effects of inorganic particles on primary and secondary relaxations and on the overall dielectric behavior were also studied. The surface morphology and the roughness were investigated by atomic force microscopy (AFM) and scanning electron microscopy. The AFM images of films having siloxane segments showed high light points related to the microphase-separated areas in the polymer. All samples exhibited good thermal stability having the initial decomposition temperature above 400°C. They showed high glass transition temperature in the range of 240-248°C for the first series of hybrid films, and 216-223°C for the second series of samples containing siloxane segments in the polymer matrix. The dielectric spectroscopy of the samples containing siloxane segments revealed a primary α_1 relaxation due to the siloxane segments, and three subglass transitions: γ, β_1 and β_2. At higher temperature an α_2-relaxation that corresponds to the upper glass transition and a conductivity process appeared. The dynamic mechanical analysis showed relaxation processes similar to those observed by means of dielectric spectroscopy (Figure 1).

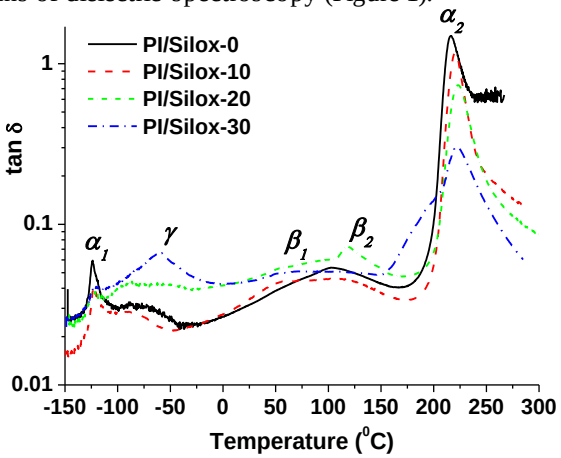

Figure 1. Temperature dependence of *tan δ* for samples having siloxane segments in the polymer matrix

Conclusions

Nanocomposite thin films containing different amount of silica were prepared by sol-gel technique, using a polyimide or a polyimide-polydimethylsiloxane as polymer matrix. APTES was used in order to obtain chemical bonding between silica and polymer matrix, and thus a better compatibility of the organic and inorganic phases. The influence of silica content on hybrid film properties was evidenced by dynamic mechanical analysis and dielectric spectroscopy.

References

1. V.Y. Kramarenko, T.A. Shantalil, I.L. Karpova, K.S. Dragan, E.G. Privalko, V.P. Privalko, D. Fragiadakis, P. Pissis, *Polym. Adv. Techn.*, **15**, 144, 2004
2. S. Chen, D. Shen, X. Zhu, X. Tian, D. Zhou, L. Fan, *Eur. Polym. J.*, **45**, 2767, 2009
3. H.B. Park, J.H. Kim, J.K. Kim, Y.M. Lee, *Macromol. Rapid Commun.*, **23**, 544, 2002
4. C.P. Yang, Y.Y. Su, *J. Polym. Sci. Part A: Polym. Chem.*, **44**, 3140, 2006
5. M. Cazacu, A. Vlad, M. Simionescu, C. Racles, M. Marcu, *J. Macromol. Sci.- Chem.*, **39**, 1487, 2002

Acknowledgements: This work was supported by CNCSIS–UEFISCDI, project PNII–IDEI code ID_997/2008. The dielectric investigations were financed by Department of Molecular Physics of Technical University of Lodz, Poland. We thank Dr. M. Cazacu at "Petru Poni" Institute of Macromolecular Chemistry, Iasi, Romania, for supplying siloxane oligomer.

Dynamic mechanical relaxations and free-volume holes in polypropylene/carbon nanotubes composites

G. Zamfirova[1], N. Djourelov[2], J.M. Pereña[3], R. Benavente[3], E. Pérez[3], M.L. Cerrada[3], S. Peneva[2], V. Gaydarov[1]

[1]Transport University "T. Kableshkov", Sofia, Bulgaria
[2]Institute for Nuclear Research and Nuclear Energy, Sofia, Bulgaria
[3]Instituto de Ciencia y Tecnología de Polímeros (CSIC), Madrid, Spain

gzamfirova@mail.bg; perena@ictp.csic.es

Introduction

The main feature of polymeric nanocomposites, in contrast to conventional composites, is their immense reinforcement effect. The carbon nanotubes as reinforcing nanofibers affect the structure and consequently the properties of the polymer matrix. Dynamic Mechanical Thermal Analysis (DMTA) and Positron Annihilation Lifetime Spectroscopy (PALS) as methods for studying the polymer structure are adequate tools and complementary approaches for investigating the nanocompositions in a nanostructural level.

DMTA is most useful for studying the viscoelastic behavior of polymers, locating their glass transition temperature as well as identifying secondary transitions corresponding to other macromolecular motions, which can be attributed to the temperature-dependent activation of a wide variety of chain movements. Moreover, PALS is one of the most sensitive and non-destructive methods for investigation of the free volume in materials.

The aim of this work is to establish the structural changes in isotactic plypropylene (iPP) caused by addition of different quantities of carbon nanotubes in the presence or absence of maleic anhydride as compatibilizer.

Materials and methods

The materials investigated were the virgin iPP (density = 901 kg/m^3) and iPP nanocomposites containing multiwalled carbon nanotubes, MWCNTs, (diameter 10-15 nm, length 1-10 μm) as filler. Initially it was in the form of a masterbatch based on iPP and 20 wt.% of MWCNTs. This masterbatch was mixed with virgin iPP at 200°C, preparing compositions of different filler content. (0.05; 0.1; 0.5; 1, wt.% MWCNTs) The technology of sample preparation consists of extrusion, followed by calendering at 230°C. Therefore, the sheet about 1.5 mm thick was the experimental material including a control sheet of virgin iPP. A sample series with addition of maleic anhydride as compatibilizer was also measured.

DMTA measurements were carried out with a Polymer Laboratories MK II apparatus working in the tensile mode. The complex modulus and tan δ of the sample were determined at 1Hz over a temperature range from –150 to 150 ºC. The heating rate was 1.5 ºC min^{-1}.

The used PALS spectrometer was a standard fast-fast coincidence system. The source was $^{22}Na_2CO_3$ with activity of 30 μCi, between two 7.5 μm-thick Kapton foils. The analysis of the PALS spectra were performed by LT v.9.

Results and discussion

The composites with low contents of nanofiller (0.05 % and 0.1 %) show a shift of the alpha relaxation of iPP to lower temperatures and higher intensities. Further increases of filler concentration (0.5 % and 1 %) decrease the intensity of this relaxation and increase its temperature location. The values of storage modulus E' for all samples investigated almost coincide for temperatures higher than Tg (β relaxation). At lower temperatures also coincide E' values for pure PP and for composites with 1% filler. However, the composite with filler concentration 0.1% shows the highest values for E' (Figure 1).

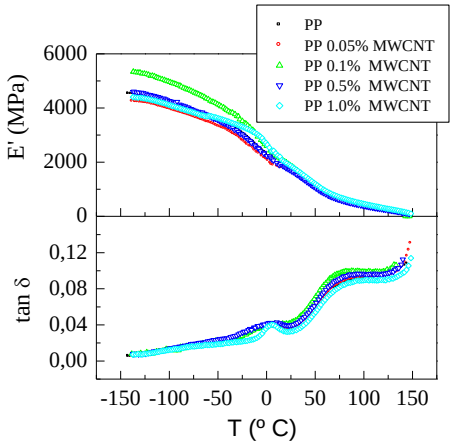

Figure 1. Storage modulus (E') and loss tangent (tan δ) as a function of temperature for virgin iPP and different iPP/carbon nanotubes composites.

Microhardness studies confirm the particular behavior of the sample with 0.1% of nanotubes, content near to the beginning of the strengthening mechanism [1].

Loss tangent exhibits a widened beta relaxation for compositions containing higher than 0.1% nanotubes. This could be interpreted in two ways:

a) Increasing nanotubes content leads to a rise of agglomeration and then the distribution of relaxation times is considerably broadened.

b) Nanotubes grouping leads to nanovacancies arising which could be reflected in easier motions of the PP macromolecular segments. As a consequence, the intensity of the low-temperature gamma relaxation, occurring at around -80 ºC, increases.

On the other hand, the addition of maleic anhydride (MAN) does not have a significant influence on DMTA results and does not influence the free volume holes (FVH) dimensions obtained from PALS measurements. Moreover, for these compatibilized samples the o-Ps intensity rapidly decreases, which could be due to the increase of the crystallinity degree or to the possibility that MAN acts as an inhibitor of Ps formation.

References

1. G. Zamfirova, Nanocsience &Nanotecnology, 10, 215-218 (2010)

Acknowledgments

We acknowledge the financial support from the NSF-Bulgaria (project D002-138/2008-2011) and MICIIN (projects PET2008-0108, MAT2007-65519-C02-01 and MAT2010-19883).

New nanocomposites based on unsaturated polyester resin and modified halloysite

A. Ghebaur[1], *S.A. Gârea*[1], *H. Iovu*[1]

[1]Polytechnic University of Bucharest, Faculty of Applied Chemistry and Materials Science, Department of Polymer Science and Engineering, 149 Calea Victoriei, 010072, Bucharest

ghebauradi@yahoo.com

Introduction

Halloysite in the natural state exhibits a high hydrophilic behavior and therefore shows a low compatibility with polymer matrix like epoxy resin, unsaturated polyester resin (UPR). The compatibilization step of inorganic compound with organic matrix was done by a cationic exchange process between silicate and protonated organic agents. This compatibilization method is not suitable for halloysite due to its low CEC value [1-3].

The goal of this study was to synthesize new hybrid materials based on UPR and modified halloysite with two different coupling agents which contain amine and vinyl functional groups.The hybrid materials were analyzed using different methods like FTIR, XPS, XRD, DMA, DSC and TGA.

Materials and Methods

Unsaturated polyester resin (UPR) was supplied by Vianova under the trade name VIAPAL UP 52 YE and used as received. Benzoyl peroxide (BP) was used as crosslinking agent (5 wt. % against UPR). Halloysite (HNT) was provided by Sigma–Aldrich and used without further purification. The HNT exhibit a diameter of 30 nm and a length between 0.25 - 4 μm. The specific surface area is 65 m^2/g and specific gravity 2.53 g/cm^3, the CEC being 8.0 meq/100g..

The silanization (coupling) agents, Triethoxyvinylsilane (TEVS) and Aminopropyltriethoxysilane (APTES) were received from Sigma-Aldrich. X-Ray Diffraction (XRD) analysis was performed on a XRD 6000 SHIMADZU diffractometer.

The DMA tests were run on a TRITEC 2000 equipment using 5°C/min heating rate at three different frequencies (0.316, 1 and 3.16 Hz) in the temperature range 25-240°C.

Results and Discussion

In case of modified HNT with coupling agents, the XRD results showed that the peak corresponding to the basal distance exhibits the same position as for unmodified HNT, indicating that the reactions of HNT with coupling agents occurred on the external surface. The results of dynamic mechanical analyses showed that the glass transition temperature value of hybrids was influenced by the halloysite's modifier agents.

Conclusions

The properties of the final hybrids based on modified HNT are influenced by the concentration and type of modifier. Thus Vinyl-HNT will lead to a higher T_g value and also a higher thermostability especially at lower concentration used which is caused by the direct involving of the vinylic groups from the HNT surface into the crosslinking process with UPR carbon-carbon double bonds. Amine-HNT lead to a low compatibility to the UPR matrix, the T_g value and thermostability of

the final composites decrease, the modified HNT act more like a plasticizer.

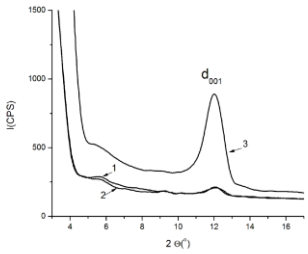

Figure 1. XRD spectra of 1-Vinyl-NHT, 2-Amine-HNT, 3-unmodified-HNT

Table 1. The T_g value of different HNT-based hybrid materials

System	T_g (°C)
UPR	116
UPR/Vinyl-HNT (1 wt. %)	120
UPR/Vinyl-HNT (2 wt. %)	118
UPR/Vinyl-HNT (5 wt. %)	112
UPR/Amine-HNT (1 wt. %)	107
UPR/Amine-HNT (2 wt. %)	101
UPR/Amine-HNT (5 wt. %)	103
UPR/Unmodified-HNT (1 wt. %)	116
UPR/Unmodified-HNT (2 wt. %)	117
UPR/Unmodified-HNT (5 wt. %)	117

Acknowledgement

The work has been funded by the Sectoral Operational Programme Human Resources Development 2007-2013 of the Romanian Ministry of Labour, Family and Social Protection through the Financial Agreement POSDRU/88/1.5/S/61178.

References

1. Shiqiang Deng, Jianing Zhang, Lin Ye, Jingshen Wu, Polymer, 2008, 49, 5119–5127.

2. Yueping Ye, Haibin Chen, Jingshen Wu, Lin Ye, Polymer, 2007, 48, 6426-6433.

3. Shiqiang Deng, Jianing Zhang, Lin Ye, Composites Science and Technology, 2009, 69, 2497–2505.

Influence of Silane Treatment on the Filler-Coupling Agent Interactions

Adriana Lungu, Nicoleta M. Florea, Cristian Parvu, Eugeniu Vasile, Horia Iovu

University Politehnica of Bucharest, Romania

adriana_lungu2006@yahoo.com

Introduction:

Dental resins composites are composed of a polymeric matrix and a silane treated reinforcing inorganic filler. The filler usually consists of glass, quartz, or ceramic particles of different compositions and size distribution. Adhesion between the polymeric matrix and the inorganic particles is accomplished using a silane coupling agent. In the literature, two main silanization mechanisms for silica nanoparticles are described: direct condensation path and hydrolyzation and condensation path. According to the first mechanism, silane would chemically bond to the surface of filler particles via direct condensation of the $–OCH_3$ groups of the silane with the surface –OH groups of the filler, in an anhydrous environment. For the second mechanism, the presence of water is required in order to hydrolyze $–OCH_3$ groups from silane to silanol groups, and the silanol groups condense with surface –OH groups on the inorganic particles to form a covalent bond [1-3].

Materials and Methods:

The purpose of the present study was to compare the efficiency of the chemical grafting of fumed nanosilica with the same organosilane (methacryloxypropyl-trimethoxysilane (MPS)) using each mechanism already mentioned. The interaction of the MPS with silica particles was extensively studied but the best method or mechanism of silanization does not emerge from the literature.

Hydrophilic fumed silica having an average particle diameter of 7 nm and a specific area about 400 m^2/g was purchased from Aldrich. The advantage of fumed silica is that many chemical and spectroscopic analyses can be carried out because of the high specific area. Prior to silanization, silica particles were dried for 24 h at 150^{0}C in an oven and were used immediately.

Different solvents were tested, but anhydrous toluen and acetone were finally selected to perform the comparative grafting reaction of MPS on nanosilica. Fumed silica was silanated with 5% MPS either in toluene and acetone and triethylamine (TEA) was used as catalyst for both reactions. After sylanization, MPS physically adsorbed was removed by washing and UV-VIS spectroscopy confirms the gradually MPS removal. Particles sylanization was proved using FTIR, TGA and XPS. ^{29}Si-NMR and TEM were also performed.

Results and discussion:

FTIR spectra show the expected characteristic bands of the grafted silane (C–H stretching bands in the 2900 cm^{-1} region and free C=O stretching band at 1720 cm^{-1}). The peak at 1700 cm^{-1} attributed to C=O group hydrogen bonds with silanol groups is almost completely overlapped by the strong peak at 1720 cm^{-1}. The native silica exhibits the Si-OH and O-H stretching at 3400 and 1630 cm^{-1} and the Si-O-Si network vibration at 1090 cm^{-1}.

TGA curves prove that the weight loss at 800^{0}C is 23% for silica sylanized in acetone, and only 12% for silica sylanized in toluene. Both results are significantly greater than native fumed silica which exhibits 3% weight loss.

XPS wide-scan spectrum revealed that, after the sylanization occurred, C1s peak was detected, assigned to MPS covalently linked to silica surface. According to the XPS data, the carbon atomic percent is almost double for the silica sylanized in acetone than in toluene.

Fig. 1 shows the TEM images of silica nanoparticles whose surface had been coated with organosilane using the two methods. Native fumed silica exhibits a three-dimensional nano-scale chain-like aggregated structure, while sylanated silica is covered by a thin film.

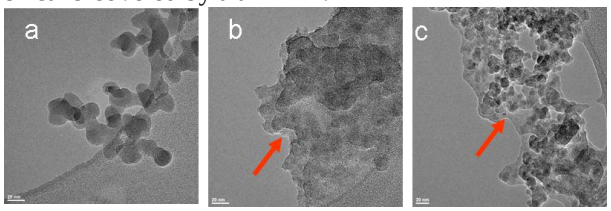

Fig. 1. TEM micrographs of native silica particles (a); silica sylanated in acetone (b) and in toluene (c)

AFM was carried out for further characterization of the silica nanoparticles. The AFM analysis reveal a slightly increase of the roughness for silica modified in toluene.

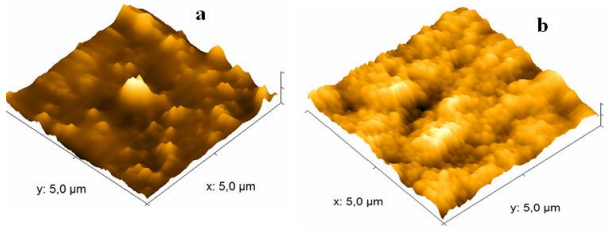

Fig. 2 AFM surface plot of unmodified (a) and modified silica particles in toluene (b)

Conclusions:

The chemical grafting of silanes at the surface of fumed silica is one of the main steps of the dental composites synthesis. The main aim of our future work is to obtain dental composite materials with improved properties.

References:

[1] Q. Liu, J. Ding, D. E. Chambers, S. Debnath, S. L. Wunder, G. R. Baran, *J. Biomed Mater Res*, 57, 384-393, 2001

[2] I. D. Sideridou, M. M. Karabela, *Dent Mater*, 25, 11, 1315, 2009

[3] I. D. Sideridou, M. M. Karabela, *J. Appl Polym Sci*, 110, 507, 2008

Acknowledgements:

Authors recognize the financial support from the European Social Fund through POSDRU/89/1.5/S/54785 project: "Postdoctoral Program for Advanced Research in the field of nanomaterials".

Sphere-to-cylinder transition in mixed PS-*b*-PEO/TiO_2 micellar systems

Dominique Scalarone,[1] *Massimo Lazzari,*[2] *Fabrizio Caldera,*[1] *Oscar Chiantore*[1]

[1] Department of IPM Chemistry and NIS Centre of Excellence, University of Torino, 10125 Torino, Italy
[2] Department of Physical Chemistry, Faculty of Chemistry and Centre for Research in Biological Chemistry and Molecular Materials (CIQUS), University of Santiago de Compostela, 15782 Santiago de Compostela, Spain

e-mail: dominique.scalarone@unito.it; massimo.lazzari@usc.es

In recent years great efforts have been directed toward the synthesis of metal and metal oxide nanoparticles and their assemblies within block copolymer templates.[1,2]
In particular, polar compounds, such as metal oxide precursors, exhibit preferential interactions with hydrophilic blocks that, as a consequence, are able to guide metal oxides to a variety of structures according to the morphologies and dimensions accessible by block copolymers.
Among the variety of metal oxides, TiO_2 has been receiving much attention because of its non-toxicity, chemical stability, low cost, high refractive index and especially because of its photoactivity.
The research described in this contribution focuses on the preparation of mixed micellar solutions obtained by adding proper amounts of a polar solution of TiO_2 nanoparticles to benzene solutions of polystyrene-*block*-poly(ethylene oxide) (PS-*b*-PEO) copolymers. TiO_2 nanoparticles were synthesized by sol-gel reaction of titanium tetraisopropoxide (TTIP) in 2-propanol under acidic conditions (HCl, 37%).
The existence of specific interactions between TiO_2 nanoparticles and PEO guides the nanoparticle distribution within micellar solutions according to the block copolymer self-assembling. While benzene is a good solvent for both PS and PEO, HCl_{aq} and 2-propanol are non-solvent for the hydrophobic PS block. As a consequence PS-*b*-PEO molecules in solution self-assemble in direct or inverse micelles depending on the solvent/co-solvent ratio.
The inorganic content was varied in a wide range of compositions, focusing on micellar systems with PS cores and PEO/TiO_2 coronas, that in a further step were used as scaffolds in order to fabricate nanostructured titania films.
Micelle morphologies were mostly studied by Atomic Force Microscopy after spin coating of the micellar solutions. The spin coating conditions used, the composition and the low concentration of the solutions ensure fast evaporation of solvents and the freezing of micelles in the solid state.
Apart from fully spherical micellar structures (Figure 1a) also mixed morphologies (Figure 1b), mainly spheres with diameter of about 35 nm, but also some cylindrical micelles 200 nm long, were obtained.
In particular, micelle shape was tuned by adding small amounts of homopolymer of the same nature of the core forming block (PS), which surprisingly forced the sphere-to-cylinder transition (Figure 1c). This finding is especially remarkable because the formation of such micelles occurs for a limited range of compositions.[3,4]

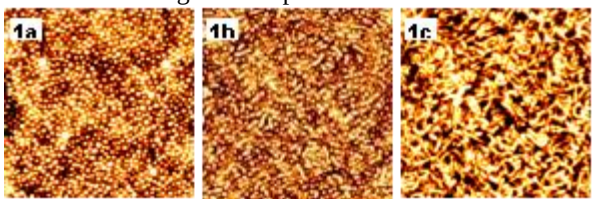

Figure 1. AFM images (2X2 mm) of different PS-*b*-PEO/ TTIP micellar morphologies

In a following step of the research thin PS-*b*-PEO/TiO_2 hybrid films with different morphologies were prepared by spin-coating micellar solutions and were transformed into the corresponding nanostructured titania, either in the form of nanoporous thin films or challenging worm-like shapes. The degradation of the polymer template in form of dried micelles and the simultaneous crystallization of TiO_2 was achieved by thermal treatments without collapsing the nanostructures.[5]

Acknowledgments. M.L. thanks the financial support by the Spanish "Ministerio de Ciencia e Innovación" (MAT2008-06503) and the Xunta de Galicia (PX2010/168-2 and PX2010/152-2)

References

1. Haryono A., Binder W.H., "Controlled Arrangement of Nanoparticle Arrays in Block-Copolymer Domains", *Small* **2** (2006) 600.
2. Lopes W.A., Jaeger H.M., "Hierarchical Self-Assembly of Metal Nanostructures on Diblock Copolymer Scaffolds", *Nature* **414** (2001) 735
3. Song L., Lam Y.M., Boothroyd C., Teo P.W., "One-step Synthesis of Titania Nanoparticles form PS-P4VP Diblock Copolymer Solution", *Nanotechnology* **18** (2007) 135605.
4. Chen Y.-J., Gutmann J.S., "Morphology Phase Diagram of Ultrathin Anatase TiO_2 Films Templated by a Single PS-*b*-PEO Block Copolymer", *J. Am. Chem. Soc.* **128** (2006) 4658.
5. D. Scalarone, J. Tata, F. Caldera, M. Lazzari, O. Chiantore, "Porous and Worm-like Titanium Dioxide Nanostructures from PS-*b*-PEO Block Copolymer Micellar Solutions", *Materials Chemistry and Physics* (submitted).

Microstructure analysis of the layers containing nanoparticles hybrids $ZnO-SiO_2$, TiO_2-SiO_2 on textile fabrics

SÓJKA-LEDAKOWICZ Jadwiga[1], WALAWSKA Anetta[1], OLCZYK Joanna[1], JESIONOWSKI Teofil[2]

[1]Textile Research Institute, 5/15 Brzezinska Str., Lodz, Poland
[2]Institute of Chemical Technology and Engineering, Poznan University of Technology, M. Sklodowskiej-Curie 2 Str., Poznan, Poland,

e-mail: ledakowicz@iw.lodz.pl

Keywords: *textile composites, nanoparticle hybrids, microstructure analysis, coating*

Introduction

The development of materials in the nano scale is a base of the production of many modern composite products. This kind of products based on textiles can be widely applied thanks to new properties imparted to them. Very interesting modifiers are micronized particles of metals, such as: zinc oxide (ZnO), titanium dioxide (TiO_2) [1]. Metal oxides have not got the chemical affinity for fibres. They can be incorporated into the textiles in the form of coatings containing appropriate binding agents based on organic compounds. The oxide composites TiO_2-SiO_2 and $ZnO-SiO_2$, characterised by high thermal stability and excellent mechanical strength, have been recently more and more used [2]. The addition of silica can improve the dispersion of metal oxide particles in composite as well as increase their adhesion, reduce tendency to agglomeration and also contribute to the increase of surface activity of a final product. The research works have focused on developing a methodology of obtaining nanostructured textile composites with barrier properties against UV radiation and microorganisms with the use of nanoparticles hybrids TiO_2-SiO_2 and $ZnO-SiO_2$. The aim of studies was the microstructure analysis of layers obtained on textile carriers as a result of modification with metal oxides. The impact of low temperature plasma pre-treatment of textiles on the chemical bonding of nanostructured layers with fibres was analysed.

Materials and Methods

Polyester non-woven obtained with aqua-jet technology and cotton and polyester fabrics were modified. The modifiers incorporated into the structure of textile products were: oxide composites TiO_2-SiO_2 and $ZnO-SiO_2$. In order to characterize their adsorption-desorption properties, the adsorption-desorption izoterms of nitrogen were determined as well as the specific surface area with BET method using AUTOSORB-1 apparatus was found. Morphology and microstructure of micronized particles of oxide hybrids were tested with TEM method (JOEL 1200 EX II microscope) while the assessment of modified surface microstructure of textiles was done using SEM method (SEM Zeiss VO40 microscope). The plasma pre-treatment of textile materials was carried out in TETRA 30 reactor (Diener Electronic) in the RF (frequency of 13.56 MHz) and AF (40kHz) discharge. Plasma was generated in the environment of Ar and CO_2. The preparations of metal oxides nanoparticles were incorporated into the textile structure by coating with pastes based on acrylic resins, characterized by homogeneous dispersion and suitable viscosity. Obtained textile composites were evaluated in the scope of protective properties against UV radiation and antibacterial effect for selected colonies of bacteria and fungi.

Results and Discussion

The analysis of the microstructure morphology and particle size distribution showed that the particles of TiO_2-SiO_2 and $ZnO-SiO_2$ hybrids have a nanometric size and are characterized by the shape resembling the spherical one. These preparations have a well developed specific surface area (especially $ZnO-SiO_2$) and are characterized by high homogeneity (especially TiO_2-SiO_2). Analysis of SEM microscopic images of modified textile products showed the presence of thin, often discontinuous coatings containing micronized particles of metal oxides on their surfaces.

Application of low temperature plasma pre-treatment of textile materials contributes significantly to the increased incorporation of coating pastes, especially it increases the amount of attached nanoparticles of hybrids (TiO_2-SiO_2 and $ZnO-SiO_2$) to textile surface.

SEM images of polyester fabric: a) unmodified b) modified with TiO_2-SiO_2

a) 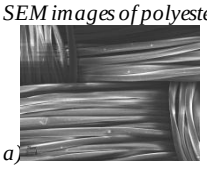 b) 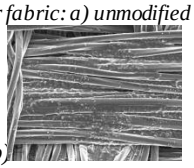

Conclusion

Introduction of coatings containing TiO_2 nanoparticles-SiO_2 hybrids or $ZnO-SiO_2$ to textile surface is an effective way to obtain added value textile materials. Obtained nanostructural textile composites exhibit good barrier properties against UV radiation (UPF> 40) and the inhibition effect for selected bacteria and fungi colonies.

References:

1. Sójka-Ledakowicz J., Lewartowska J., Kudzin M., Leonowicz M., Jesionowski T., Siwińska-Stefańska K., Krysztafkiewicz A., *„Functionalization of textile materials by alkoxysilane-grafted titanium dioxide”,* Journal of Materials Science, 44, 3852-3860, 2009

2. Siwińska-Stefańska K., Przybylska A., Jesionowski T., Sójka-Ledakowicz J. Olczyk J., Walawska A *„The effect of oxide composite on the barrier properties of textile fabrics”* . Chemical Review nr 89(12); 2010; s. 1189-1194 ISSN: 0033-2496

The research work was financed by Ministry of Science and Higher Education in 2007-2011 as a special project EUREKA/308/2006-Eureka E!3776 NANOTEX

Synthesis of Multi-walled Carbon nanotubes using hydrocarbon as carbon sources in an arc discharge

[1] Mehrdad Teymourzade, [2] Haleh Kangarlou, [3] Kave Kazemikia

[1] *Faculty of Science, I.A.U Urmia Branch*
[2] *Faculty of Science, I.A.U Urmia Branch*
[3] *Faculty of Science, Payamenoor university, Bonan Branch*

[1] tanar_mehr@yahoo.com
[2] h.kangarlou@iaurmia.ac.ir

Abstract

The influence of starting carbon materials on the synthesis of carbon nanotubes (CNTs) is investigated. Comparisons are made between graphite rods and polycyclic aromatic hydrocarbons (PARs) as carbon sources in helium arc discharge. The major parameters are also evaluated in order to obtain high-yield and high-quality carbon nanotubes. The cathode deposits are examined using scanning electron microscopy (SEM) and scanning probe microscopy (SPM) in AFM mode to determine the microstructure and nanostructure of carbon nanotubes.

The SEM investigation of the carbon nanotube deposits formed on the cathode provides evidence that PARs can serve as building blocks for nanotube formation. The high-temperature graphitization process induced by the arc plasma enables the hydrocarbons to act as carbon sources and changes the aromatic species into the layered graphite structure of CNT. These polycyclic aromatic hydrocarbons not only act as the precursors but also enhance the production rate of carbon nanotubes. The PAR precursors thus play an important role in the mass production of carbon nanotubes.

Keywords: Carbon nanotube (CNT); Arc discharge; Precursor; Polycyclic aromatic hydrocarbons; Field emission

Synthesis of Novel Macroporous Copolymer Resins via Aggregation/ Breakage and Post-Polymerization

Alexandros Lamprou1, Itir Köse2, Giuseppe Storti1, Massimo Morbidelli1

1 Inst. for Chemical & Bioengineering, Department of Chemistry & Applied Biosciences, ETH Zurich, Switzerland
2 Department of Chemical & Biological Engineering, Koç University, Turkey

alexandros.lamprou@chem.ethz.ch

Introduction: The synthesis of macroporous crosslinked polymeric resins has been extensively investigated for half a century, with numerous target applications, from solid-phase synthesis and ionexchange to chromatographic columns, pollutant adsorbents and catalysts. Irrespective of how sophisticated the procedure is, a pore-forming agent is typically applied, be it a template or a traditional porogen. Herewith we put forth a novel, porogen-free approach towards rigid macroporous microclusters combining the colloidal concepts of Controlled Aggregation and Breakage with the emerging "Reactive Gelation"[1] technique.

Materials and Methods: In our work, primary latex Poly(Styrene-co-Divinylbenzene) nanoparticles were produced by a 3-step core-shell semi-batch miniemulsion polymerization. Following swelling of the primary particles with monomer mixture containing radical initiator, salt was introduced under defined rates of addition and mixing. Aggregation was induced due to latex destabilization, while the resulting aggregates were simultaneously broken due to shear. After reaching equilibrium between aggregation and breakage the temperature was increased, inducing polymerization inside the monomer-swollen, interpenetrated particles, thus anchoring the structure of the formed aggregates. The resulting microclusters were thoroughly characterized by SEM, Dynamic Light Scattering, Nitrogen sorption and Mercury Intrusion Porosimetry.

Results and Discussion: These microparticles were found to be irregularly shaped, yet monodisperse in size and mechanically rigid, with compact internal structure, relatively small specific surface area, high internal porosity, with very large macropores and negligible amount of micropores.

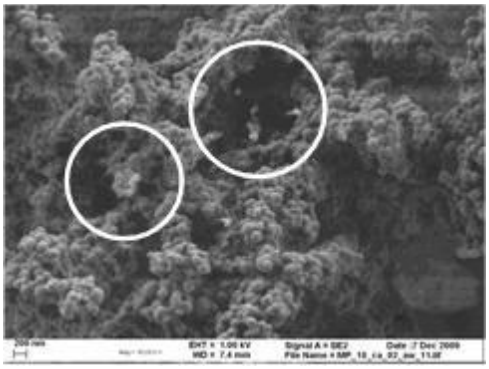

Figure 1: SEM image of aggregate produced.

The effects of initial latex properties and operating parameters on the final microclusters were investigated. Namely, the primary particle size, crosslinking density along the outer particle shell and shear rate during salt addition were varied. We concluded that it is qualitatively possible to control the final cluster size and pore size distribution, while the internal structure remains essentially unaffected. For the sake of comparison a monolith was also produced under static aggregation for one group of experimental conditions.

Conclusions: Alongside the fundamental conclusions, by introducing proper functionalizations, a vast range of applications may be addressed.

References: 1 N. Marti, F. Quattrini, A. Butté and M. Morbidelli, Macromol. Mater. Eng., 2007, **290**, 221-229

Crystallization Kinetics of Polypropylene Nanocomposites

Helton P. Nogueira[1], Evandro M. Alexandrino[2] and Maria I. Felisberti[3]

Chemistry Institute, University of Campinas (UNICAMP), P.O. Box 6121, Zip Code 13083-970, Campinas - SP, Brazil –

[1] helton.nogueira@iqm.unicamp.br;[2]evaalexandrino@iqm.unicamp.br; [3] misabel@iqm.unicamp.br

Introduction

The development of polymeric nanocomposites by the Toyota's Research group has opened a new dimension on materials science field, being the most different systems polymer/nanoparticles obtained.[1]

One of the most studied system is the polymer/nanoclay system. For instance, the use of montmorillonite as filler for polymer matrixes such as polypropylene, polyethylene, polyamide, and others, has resulted in nanocomposites with enhanced mechanical properties and improved characteristics such as gas permeability barrier, and thermal stability. [2]

The properties of semi-crystalline polymers depend on chemical structure, molecular weight, polydispersity and crystallization conditions. The crystallization conditions and the mechanisms involved in it directly influence the material properties. Therefore, controlling crystallization allows to control various characteristics of the material, such as crystallite size, degree of crystallinity, the molecular arrangement of the lamellae of the crystallites and interfacial interactions, *i.e.* the morphology of the semicrystalline material.[3] In this work the Hoffman-Lauritzen theory was used to describe the non-isothermal crystallization kinetics of polypropylene and its nanocomposites containing organophilic montmorillonite (OMMT). Differential Scanning Calorimetry analysis (DSC) provided the crystallization data for this purpose.

Materials and Methods

Polypropylene (PP) nanocomposites with OMMT were prepared by melt compounding in a twin screw compounder with or without poly(propylene-co-maleic anidryde) (PP-g-MA) as compatibilizer. Samples from the central region of the injection molded specimens (3 to 7 mg), were used in DSC experiments performed under non-isothermal conditions at constant cooling rate (β) from the molten state. Experiments were carried out at different cooling rates 2, 4, 6 and 8 °C min^{-1} allowing the construction of conversion or crystallization degree (α) curves as a function of temperature (T).

In order to determine the activation energy (Ea) for different crystallization degree of PP and its nanocomposites Ozawa-Flynn-Wall Isoconversional Method[4] (OFW) was applied (equation 1). Hoffmann-Lauritzen's parameters a constant U^* and the growing rate K_g, were determined from Ea x T curves using the method proposed by Vyazovkin's[5], (equation 2).

$$ln\beta = -1{,}0516\,\frac{E_\alpha}{RT} + constant \qquad \text{Equation 1}$$

$$E = U^*\frac{T^2}{(T-T_\infty)^2} + K_g R\frac{T_m^2 - T^2 - T_m T}{(T_m - T)^2 T} \qquad \text{Equation 2}$$

Results and Discussion

Ea curves as a function of the conversion degree (α) were obtained and the equations to describe the dependence of Ea on the conversion for each material were obtained by fitting these curves.

These activation energies were not constant in overall conversion range due to the complex crystallization process, which depends on a number of variables such as nucleation, growing rates and viscosity. These factors affect the polymeric chain mobility.

(E_a x T) curves were obtained from (α x T) and (E_a x α) curves. Hoffmann-Lauritzen's parameters (HF parameters were obtained from the non-linear regression method applied to (E_a x T) curves, according to Vyazovkin's method. Table 1 summarizes the HF parameters for polypropylene and its nanocomposites.

Table 1 – Hoffmann-Lauritzen's parameters

Cooling rate (8°C min^{-1})	U* (kJ mol^{-1})	K_g (K^2)
PP_{neat}	4.7±0.4	(3,31±0,03)x10^5
PP/OMMT (95/5) %wt	39.0±0.6	(5.70±0.04)x10^5
PP/PP-g-MA/OMMT (90/5/5) %wt	21.0±0.4	(4.00±0.03)x10^5
PP/PP-g-MA/OMMT (85/10/5) %wt	31.0±0.4	(5.00±0.03)x10^5

From table 1, it is observed that PP growing rate constant result was in agreement with the literature reports [6]. With the addition of OMMT, the Kg values were increased, showing that this filler influenced the PP crystallization kinetics.

Conclusion

Thermal analysis were successfully carried out to obtain the Hoffmann-Lauritzen parameters, which were mainly measured only by optical microscopy under isothermal crystallization conditions.

From the results it was possible to describe the crystallization kinetics of polypropylene nanocomposites in a non-isothermal condition, with a good precision.

References

[1]–Okada, A., *et al.*; Polymer based molecular composites, Vol. 171, Materials Research Society 1990 45-50

[2]–Benetti, E. M., *et al.*; Polymer 46 (2005); 8275-8285

[3]–K. Tashiro, *et al.;Encyclopedia of Polymer Science and Engeneering*, John Willey e Sons, N. Y., 2nd ed., 1989, 231-288

[4]–Pratap, A., *et al.;* Journal of Thermal Analysis and Calorimetry, Vol. 89 (2007) 2, 399-405.

[5]–Vyazovkin, S., *et al.*; Macromol. Rapid Commun. 2004, 25, 733–738

[6]–Ke Wang, *et al.*; European Polymer Journal 39 (2003) 1647–1652

Magnetite-Montmorillonite Hybrid Materials for Wastewater Treatment

Gema Marcelo, Iñigo Larraza, M. Mar López, Carmen Peinado, Teresa Corrales

Departamento de Fotoquímica. Instituto de Ciencia y Tecnología de Polímeros (CSIC), Juan de la Cierva 3, 28006 (Madrid)

gema.marcelo@ictp.csic.es

Introduction

During the last few decades, magnetite (Fe_3O_4) nanoparticles have attracted increasing attentions in the field of enviroment remediation due to the fact that magnetite can be easily separated and collected by an external magnetic field. However, one of its main limitations is the coaggregation of magnetite nanoparticles. Motmorillonite is a kind of natural 2:1 type layered clay mineral with high cation exchange capacity, swelling and high surface area. In nature MMT forms agglomerates, making delamination essential. In order to exfoliate it, it is necessary to swell it in water and make it react with a molecule that increases the interlayer space.

Montmorillonite has been shown to be a suitable support for the dispersion of magnetite nanoparticles and avoid the aggregation of the particles [1].

In the present study, Montmorillonite-supported modified magnetite nanoparticles with a polymeric shell were prepared. Positive charged hyperbranched polymers such as polyethyleneimine (PEI) was chosen for this work because PEI can change the magnetite nanoparticle surface and at the same time react with the clay platelets, exchanging with the metallic cations present between the layers. Among the different polymers used in order to modify magnetite particles and to exchange with the cations of Montmorillonite interlayer galleries we have chosen PEI because it has been established as a good adsorbent for removal of chromium from water. Therefore, Montmorillonite-PEI-magnetite hybrid material was further investigated for the removal of hexavalent chromium from aqueous solutions.

Materials and Methods

Magnetite nanoparticles were prepared as reported in bibliography [3] and characterized by TEM. They have a cubic shape and 40± 15 nm of diameter.

The characterization of the resulting hybrid material was performed through TEM, XRD, FTIR and gas diffusion through a polymeric membrane.

Chromium adsorption experiments were carried out in a Perkin Elmer spectrophotometer according to the determination procedure described in the literature [2].

Results and Discussion

Incorporation of magnetite particles in the Montmorillonite material yielded to a magnetic material easy to treat with a magnet. **Figure 1** shows two TEM images of the hybrid Montmorillonite-PEI-magnetite system. As it can be seen Montmorillonite sheets have been well exfoliated and magnetite particles are dispersed between Montmorillonite sheets.

Chromium adsorption experiments were performed at different pHs and Cr (VI) concentrations, the amount of Cr(VI) adsorbed per unit mass of the adsorbent, q and the removal efficiency of Cr (VI), *E* (%), for several pHs are shown in **Figure 2.** As can be observed removal of our material is close to 100% for a long range of pHs.

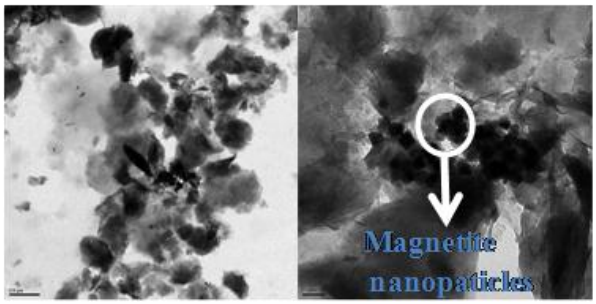

Figure 1. TEM images of montmorillonite-magnetite material.

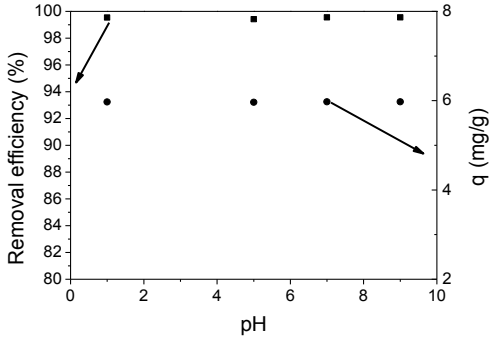

Figure 2. Removal efficiency and amount of Cr adsorbed per mass of the adsorbent.

Conclusions

The use of MMT as a support is useful to control the dispersion and the aggregation behaviour of magnetite nanoparticles. Also, compatibilization of magnetite nanoparticles with montmorillonite through PEI surface modification of magnetite nanoparticles provides a good exfoliation of montmorillonite sheets that increases the effective surface to interact with the magnetite nanoparticles.

Adsorption experiments seem not to be affected by pH and present high values of removal efficiency therefore showing promising applications for the removal of Cr(VI) from aqueous solutions.

References

[1] Journal of Hazardous materials 2009, 166, 821-829.

[2] Standar methods for the examination of waterand wastewater 16th ed., American Public Health Association, New York, 1975.

[3] J. Am. Chem. Soc. 2009, 131, 454-455

Analysis of the dispersion of nanofillers in PVC plastisols via rheological and morphological characterizations

Claire Barrès, Abdoulaye Gueye, Jannick Duchet-Rumeau

Université de Lyon, F-69361, Lyon, France;
CNRS, UMR 5223, Ingénierie des Matériaux Polymères, F-69621, Villeurbanne, France;
INSA Lyon, F-69621, Villeurbanne, France

claire.barres@insa-lyon.fr

Introduction

PVC plastisols are polymer particle suspensions in plasticizers. In such systems, PVC volume fraction, particle size and size distribution, plasticizer type and interactions among particles and between particles and plasticizers strongly influence the rheological properties of the plastisol. Plastisol processing involves the gelation of the material, which turns it into a homogeneous solid.

Polymer nanocomposites generally surpass conventional microcomposites, with same filler content, in terms of thermal and mechanical properties. Very few studies have been devoted so far to the dispersion of nanofillers in PVC plastisols. The present study is aimed at better understanding the effect of nanofillers on the final properties of gelled PVC plastisols, especially by characterizing the micro/nanostructure resulting from the nanofiller distribution among the PVC network.

Materials and Methods

Model PVC plastisols, i.e. simplified formulations, were prepared by mixing PVC resin in di-isononyl phthalate (DINP) so that to obtain polymer volume fractions ranging from 0.1 to 0.65.

Cation-exchanged montmorillonite with dimethyl benzyl hydrogenated tallow (MMT2MBHT), or untreated silica with a specific surface area of 200 m2/g were added to the plastisols, with variable volume fractions of inorganic material.

Measurements of viscoelastic and flow properties were carried out on controlled stress rotational rheometers (MCR300, Anton Paar; AR1000, TA Instruments) in cone-and-plate geometry. The gelation process was monitored using a parallel-plate geometry by multi-frequence analysis in the linear viscoelastic domain, while raising the temperature of the sample at 2°C/min from 45 to 120°C. Plots of tan δ (tan δ =G"/G') vs. temperature for different angular frequencies ω of the oscillations yield a single intersection point which, according to Winter [1],[2] or Aoki [3] defines the beginning of gelation. The temperature at which cross-over of all plots occurred was considered as the "pre-gel" temperature. It actually consists in a liquid-solid transition due to the formation of a percolated particles network, and must be distinguished from the complete gelation/fusion of PVC grains [4].

Complementary morphological characterization (by SEM and TEM), allowed to document the PVC and filler network(s) formation.

Results and Discussion

As displayed in figure 1, a clear yield stress appears upon nanofiller addition, which expresses the buildup of a physical network of particles. This network "rigidity" increases with filler fraction.

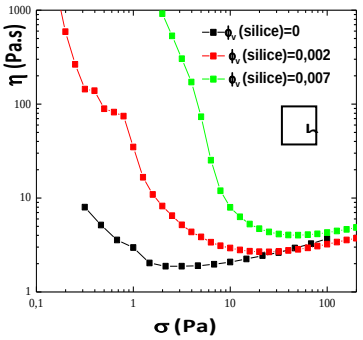

Fig. 1 : flow curves for the 65 vol% PVC plastisol with different volume fractions of silica.

The pre-gelation temperature of PVC suspensions is affected by volume fraction. The achievement of a good dispersion of the nanofiller and the buildup of a nanofiller percolated network significantly decreases the pre-gel temperature by comparison with PVC-only plastisols or with plastisols with lower nanofiller content (a drop of ~10-12°C can be observed).

Micrographs of gelated samples show specific features of the suspensions with percolated filler: the filler particles form a network which fills the "free" space left by the PVC particles after their percolation (example in fig.2). So, the pre-gel temperature reduction can the be interpreted as a consequence of the nanofiller promoting PVC particle-to-particle contact by a steric effect.

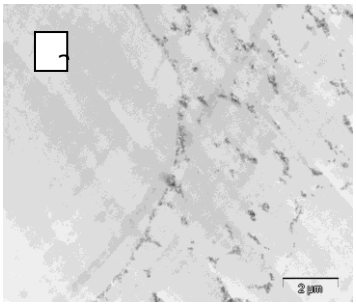

Fig. 2: TEM micrograph of a silica-filled, gelled plastisol.

Conclusions

Rheology and microstructural analysis are complementary in characterizing the structures of complex suspensions such as nanofilled PVC plastisols.

Different morphologies were obtained for the 2 types of nanofillers (organophilic MMT and silica), which reveals different dispersion and network formation mechanisms.

References

[1] Winter HH (1986) J Rheol 30, 367-382
[2] Winter HH (1992). Macromolecules 25, 2492
[3] Aoki (1997). Macromolecules 30, 7835
[4] Boudhani H, Cassagnau P (2006) Rheologica Acta 46 (6) 825-838

Intermolecular Interactions in Polyacrylic Acid Solutions and Gels

D.B.Shaltykova[1], *E.Kalacheva*[2], *E.I. Shadrova*[3], *D.Kaldybekov*[2], *Zh.Konyrbayeva*[2]

[1]National Engineering Academy of Kazakhstan
[2]al-Faraby Kazakh National University
[3]Almaty University of Power Engineering and Telecommunications

dina_65@mail.ru

Introduction

Investigations of nonelectrostatic intermolecular interactions in polymers solutions are of considerable interest for understanding of interpolymer complexes formation mechanisms, including ones of biological origin [1]. Among objects emerging as a result of polymer-polymer interactions, are least studied hydrophilic associates [1], intermediate between noninteracting macromolecules and stable interpolymer complexes. Associates formed by the molecules of one definite polymer are even less studied. At the same time studying of such associates is interested for understanding of formation mechanisms of supramolecular structures, tertiary and quaternary structure of protein, etc. [1]. New approach to research of interactions between macromolecules of identical chemical nature, but essentially different on the molecular mass (MM) is proposed in present report. It is shown that intermolecular interactions influence even on parameters of such well studied systems as water solutions of polyacrylic acid (PAA).

Experimental

Behavior of water solutions containing PAA of two MM M_w=2000 (PAA_1) and M_w=750 000 (PAA_2) at various temperatures and total concentrations, as well as behavior of PAA in crosslinked form were investigated. Dependences of pH of solution from a parity of macromolecules concentration of two various M_w and total concentration, as well as dependences of swelling degree of crosslinked analogues on temperature at various neutralization degrees of crosslinked polyacid were registered.

Results

It is known that ionization ability of polyacids macromolecules decreases with increase in their molecular weight/3/. Really, direct pH measurements of PAA's water solutions, executed in the given work, have shown that transition from PAA with low molecular weight M_w=2000 to polyacid with M_w=750000 is accompanied by pH increase on 0,9÷1,1 units of pH-meter scale approximately. Examples of pH dependences of PAA's water solution of two various M_w from mixture composition x (x - ratio of [PAA1] mole concentration to total mole concentration [PAA1] + [PAA2]) for the various total concentrations of polyacids are presented on fig. 1 ($T=27^0C$). It is seen that noticeable deviation of the received dependences on additive straight line, which corresponds to a case of absence of intermolecular interactions takes place at rather high general total PAA concentrations.

pH dependences of the aqueous solutions of PAA of different MM and the swelling degrees of crosslinked PAA on the temperature were obtained also. These dependencies demonstrate opposite behavior of mentioned above systems. The measured pH value of solutions of PAA of high MM with increasing temperature is shifted to the alkaline region (decreasing of average concentration of hydrogen ions), and at the same time the swelling degree of crosslinked PAA increases (increase the degree of ionization polyacid.)

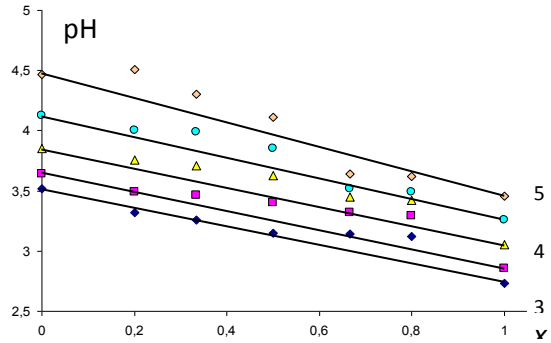

Fig.1. Dependences of pH of water solution of PAA_1 and PAA_2 mixture on composition of solution at different dilutions; curve 1: $c_{0\Sigma}$ = 0,05 mole/l, curves 2-5, $c = c_{0\Sigma}/2$, $c_{0\Sigma}/4$, $c_{0\Sigma}/8$, $c_{0\Sigma}/16$.

Discussion

The observed deviations from additivity are evidence of the existence of interactions both between individual molecules PAA and between their segments. The amplitude of these interactions increases with increasing of the local concentration of links in a certain region of the solution. These interactions, as shown in present report, make core of coils more compact, which leads to significant inhomogenity of solution. There are the areas filled relatively dense associates, and the regions corresponding to the periphery of the friable coils in the solution (a modified model "globule with a loose periphery" for a theoretical description of the observed phenomena was used).

Conclusions

Pronounceable interactions of non-electrostatic nature between both individual macromolecules and their segments take place in solutions of polycarbon acids proceed as expressed in the These interactions, particularly, lead to the anomalous behavior of acidity of polyacid solution, which shifts to higher pH values with increasing temperature, despite the fact that this factor increases the degree of ionization of carboxyl groups.

References

1. Ergozhin E.E., Zezin A.B., Suleimenov I.E., Mun G.A. Hydrophilic polymers in nanoelectronics (in Russian), Almaty – Moscow, LEM, 2008, 214 p.

Polymeric Ionic Liquids: Homo- and Copolymers in Water

Erno Karjalainen & Heikki Tenhu

University of Helsinki, Finland

heikki.tenhu@helsinki.fi

Introduction. A methacrylate substituted with an ionic liquid has been polymerised using RAFT. The obtained homopolymer has been further used as an macro chain transfer agent with which poly(N-isopropylacrylamide) (PNIPAM) blocks with varying lengths were constructed.

Scheme 1. Polymer synthesis

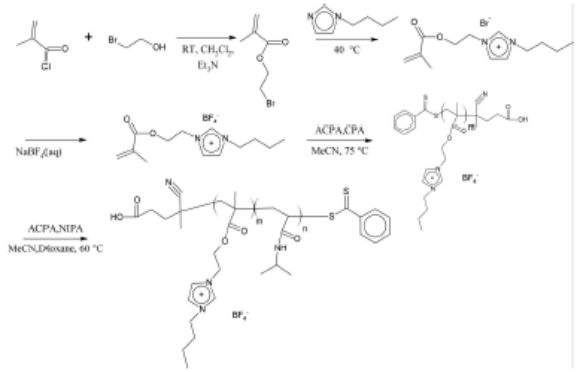

Results and discussion. The solubility of the polymeric ionic liquid (PIL) block depends on the counterion. In the case shown below, the PIL block is not soluble in water. However, both the homoPIL and the block copolymers may be transferred from an organic solvent into water. In aqueous surroundings all polymers form nanoscopic particles, micelles or aggregates. Block copolymers show thermal behaviour typical for micelles with an outer shell of thermoresponsive PNIPAM. The emperature dependence of the zeta potentials of the ationic polymers is most interesting. In the case of homopolymeric PIL the potential keeps more or less constant with temperature. On the other hand, the block copolymers show a considerable and discontinuous increase of the potential, the temperature range of which matches that of the collapse of the PNIPAM blocks. Because the change in the zeta potential probably results from the release of the counterions, the phenomenon has been further studied by fluorescence spectroscopy using a fluorescent probe 1,8-ANS. The detachment of the probe from the polymer with increasing temperature occurs differently in the case of homo and copolymers. A tentative way to rationalize the observations is that the BF4- counterions are more strongly bound to the homopolymer than to the thermosensitive block copolymer.

Figure 1. Zeta potential vs temperature for two block copolymers with varying PNIPAM block lengths.

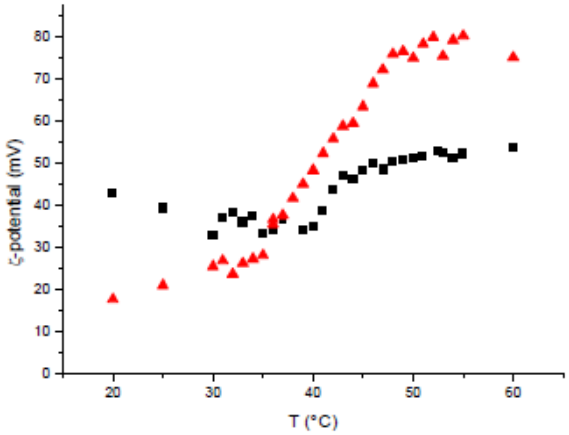

Functional poly(vinylpyrrolidone)s for the controlled synthesis of Ag nanoparticles

A. Ledo-Suárez, I. Rielo-Rodríguez, M. A. López-Quintela, M. Lazzari

Department of Physical Chemistry, Faculty of Chemistry and Centre for Research in Biological Chemistry and Molecular Materials (CIQUS), University of Santiago de Compostela, 15782 Santiago de Compostela, Spain

M. G. Tardajos, H. Reinecke, A. Gallardo

Inst. de Ciencia y Tecnologia de Polimeros (CSIC), 28006 Madrid, Spain

e-mail: ana.ledo@usc.es

Synthesis of metal nanoparticles has been widely studied and many preparative methods have been developed in the last decades. Particularly, gold and silver nanoparticles have received a special attention because of their peculiar catalytic, electronic or optic properties.

One of the most frequently used protective agent for the synthesis of metal nanoparticles is poly(N-vinyl-2-pyrrolidone) (PVP), which has recently been demonstrated to act not only as protection against aggregation but also as reducing agent of the metal ions. Several synthesis of silver nanoparticles in presence of this polymer were carried out at low temperatures by means of a one-step process, without the presence of any reducing agent. Kinetics of the reaction, shape and size of nanoparticles could be tuned by changing PVP/metal salt ratio (R) or temperature. With high values of R, slow and well controlled reactions with formation of small and homogeneous nanoparticles take place, whereas lower values, or high temperatures, give the opposite situation, i.e. faster reactions, bigger dimensions and worse polydispersity [1].

In the framework of a comprehensive project aiming to investigate the effect of diverse functionalized polymers on the synthesis of noble metal nanoparticles in solution, herein we report preliminary results of a further investigation focused on the potential of functional PVP for the controlled synthesis of silver nanoparticles, namely poly(1-vinylpyrrolidin-2-one-3-carboxylate) (PVP-COONa), poly(3-(3-Sulfopropyl)-1-vinyl-2-pyrrolidone) (PVP-RSO3), and their random copolymers with PVP. The preparation of these polymers has been recently described [2,3].

Functional PVP-capped silver nanoparticles were produced in a controlled fashion in absence of any other reducing agent, working at rather low values of R (i.e. at low polymer concentration). PVPs containing lateral chains with -COONa or -SO_3Li groups, clearly provide a better stability to the colloids because of the interactions between the side chain groups, and nanoparticles. As a consequence, the rates of formation are slower and a better control of silver nanoparticle size and distribution may be obtained.

In particular, a better stabilization was observed in the case of PVP-SO3 due to the more effective electrostatic interactions with the nanoparticle precursors.

Acknowledgments. M.L. thanks the financial support by the Spanish "Ministerio de Ciencia e Innovación" (MAT2008-06503 and MAT2010-20001) and the Xunta de Galicia (PX2010/168-2 and PX2010/152-2)

References

6. Hoppe, C. E., Lazzari, M.; Pardiñas-Blanco, I.; Lopez-Quintela, M.A. *Langmuir* 22, 7027-7034, 2006.
7. Pérez M, Navarro R, Gómez M, Gallardo A, Reinecke H. *Eur. Polym. J.* 46 (7), 1557-1562, 2010.
8. Bencini M, Ranucci E, Ferruti P, Oldani C, Licandro E, Maiorana S. *Macromolecules* 38, 8211-8219, 2005.

Study of Nanocomposites Processing containing Polyaniline and Carbon Nanotube as use with Radar Absorbing Structures.

Luiza de C. Folgueras and Mirabel C. Rezende

Departamento de Ciência e Tecnologia Aeroespacial / Instituto de Aeronáutica e Espaço / Divisão de Materiais

luiza@ita.br; mirabelmcr@iae.cta.br

Introduction: Due to the unique properties of the carbon nanotubes (CNTs), several new usage possibilities and applications have impelled the development of new materials. Among the attractive properties of the CNTs we may quote the good mechanical resistance and excellent heat conductors and are capable of transporting electricity [1]. The use of conducting polymers in the processing of radar absorbing materials is increasing due to the large chemical versatility of these polymers, especially polyaniline, which allows the control and the modeling of its physical-chemical properties [2]. The present work shows the processing of structural microwave absorbing materials. Polyaniline and carbon nanotubes formulations were used and a simulating the preparation of the structural material.

Materials and Methods: In the processing of absorbing nanocomposites, first, the substrates of glass fiber woven (20 cm x 20 cm) were individually impregnated with polyaniline formulations (PAni) (15% (w/w)), multiwalled carbon nanotubes (MWNT) (formulations with 0.1, 0.3, 0.5, 0.8, 1.0 and 1.2% (w/w), each one named of material 1 up to 6) in polyurethane matrix. The polyaniline was synthesized by using dodecylbenzene sulphonic acid, at chemical route; and the multiwalled carbon nanotubes were acquired from Bayer – Baytubes C 150 P. The impregnation of the PAni/NTC in the wovens was done using the conventional painting method. Aiming at forming the structural and radar absorbing composite, the impregnated wovens were piled up and then, the layers were positioned, beginning with the woven impregnated with the formulation 0,1% of NTC. For the electromagnetic characterization (frequency range of 8-12 GHz) were carried out using the Naval Research Laboratory (NRL) arch method. A flat aluminum plate was used as a reference for the measurements (100% reflectivity and 0% absorptivity).

Results and Discussion: Fig. 1 shows the aspects of the woven processed and the evaluation of the materials by scanning electron microscopy. Fig. 1(a-b) shows the aspects of the fiber glass woven impregnated individually with the different formulations; it can also be noticed that there has been a good dispersion of the PAni/CNT powders in the polyurethane matrix. Fig. 1(c-d) shows both the polyaniline dispersed in the polyurethane matrix and the region where the carbon nanotubes are agglomerated, respectively.

Fig. 2 shows the results of the absorption of the radiation of the materials processed (named from 1 to 6) and piled in two forms of multilayers, placed one above the other: materials from 1 to 6 (Fig. 2(a)), and materials from 1 to 5 (Fig. 2(b)). Then, one woven at a time was removed from the multilayer formation, reducing the total amount in the piling, and the electromagnetic behavior was evaluated.

This way, the performance of the materials concerning the quantity of polyaniline and carbon nanotubes present in each multilayer assembly can be evaluated. We observe that, as the impregnated fiber glass wovens are removed from the multilayer formation, the behavior of absorption of the radiation reduces, and it begins to behave as a transparent to radar material, for smaller concentrations of the formulation. In this case, it is a typical behavior of the materials formed with fiber glass and without any impregnation of absorbing center. The average attenuation of both materials is of up to 50% of the incident microwave radiation.

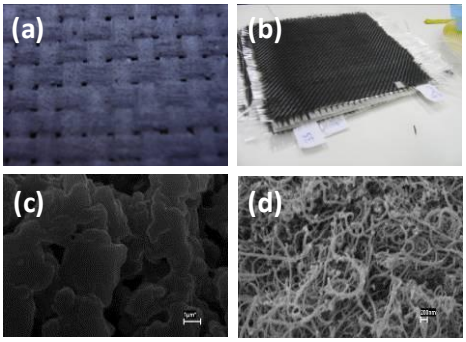

Fig. 1 – Aspects of materiais.

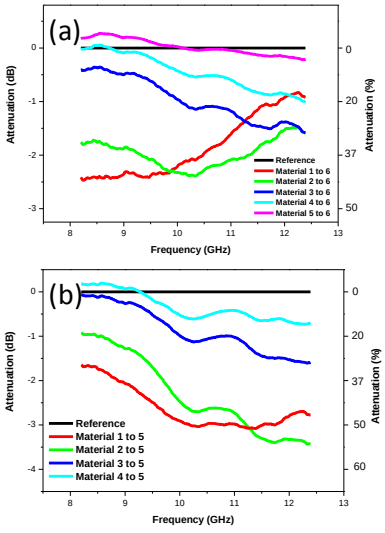

Fig.2 – Attenuation of materials.

Conclusions: The best multilayer formation aiming at processing structural absorbing materials is the composition that contains the materials from 1 to 5, because they attenuate the radiation and also have a behavior of broadband material in frequencies higher than 12 GHz.

References

[1] A.L. Chun *Nature Nanotechnology*, jun., 2008.

[2] L.C.Folgueras, M.A.Alves, M.C.Rezende *J. Aerospace Tech. an Manag.*, 2010.

Single Macromolecule as Neural Network

Sergey Panchenko, Ibragim Suleimenov

Almaty University of Power Engineering and Telecommunications

esenych@yandex.ru

Introduction

Information aspects of polymer based systems behavior are of a considerable interest from both academic and practical points of view. The problem of "generation of information" during the evolution that preceded the biological one remains unresolved in many respects because of poor understanding of mechanisms of evolutionary transition toward the macromolecules able to store and process information. From the practical point of view, the data recording onto systems of macromolecular and submolecular levels are also of a considerable interest for development of qasi-biological base of nanoelectronics [1]. Accordingly, it is relevant whether an individual synthetic polymer molecule in a liquid phase can be considered "a memory cell" or its analogue. At first sight, it is unequivocally not, so as the macromolecular coils represents statistical and, moreover, strongly fluctuating system. However, viewing the macromolecule as analogue of the neural network reveals that synthetic hydrophilic macromolecules even of an elementary structure are capable both to store and process information.

Numerical modeling of a macromolecule as a neural network

Two versions of the structures modeling behavior of real macromolecules were generated numerically. The plane model structure was generated as sequence of random steps on a grid made of regular hexagons (fig. 1).

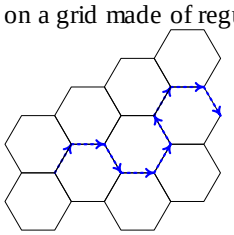

Fig.1. Plane model structure

The modeling 3D structure was generated similarly using the tetrahedral structures of C-C bonds. It is supposed, that each of the knots of the outcome structure can obtain individual electrostatic charge (which corresponds to the maximum simplified model of a partially dissociating polyelectrolyte). The point where the knot is located is impacted by the field generated by both the chain charges and the cloud of counterions (such potentials as dipole-dipole and Coulomb interactions are used at modeling). It is supposed, that the structure knots are also impacted by a heterogeneous external field, which physically corresponds to, for example, interaction of a macromolecule with other one or to internal interactions between macromolecular fragments.

It is shown that each knot of the structure can be considered as an element of the artificial neural network of Hopfield in present report. A Hopfield network is described by a formal Hamiltonian having the same structure as the functional whose minimization allows receiving distribution of charges along the model of polymeric chain. Comparison of the Hamiltonians allows obtaining mentioned above conclusion.

It is of importance, that each configuration of an external field corresponds to a certain set of input signals of the neural network. This brings along the conclusion that external fields impacting the macromolecule form definite set of images which the macromolecule as an analogue of a neural network is able to distinguish.

Results of numerical modeling

In searching of images distinguished by the macromolecular neural network, their representation in the form of a set of binary numbers, which then were translated into decimal form, was used. Reaction of the network to all the images totally was investigated using the method of consecutive search. The example of result for a case of 10 neurons (10 monomer units) is shown on fig. 2, the decimal number of an image N is on the axis of abscissas and frequency of its recognition f is on the axis of ordinates. The distinct peaks testifying the presence of stable image distinguishing (of charges sequence) are visible.

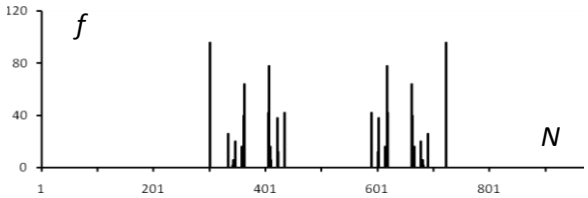

Fig.2. Images recognized by molecular neural network

With use of the various randomly generated structures, it is shown that there are certain steadily distinguished images whose character does not depend on conformation of the modeling macromolecule. The conclusion also remains true at transition to the 3D structures, as well as while using various modeling potentials of interaction between knots. In other words, **each macromolecule generates its own "alphabet" itself**; this **native** alphabet may be used for data storage and processing in quasi-biological nanoelectronics.

Conclusion

The isolated macromolecule in a liquid phase can be considered as an object able to store information, the statistical nature of the coil not being an obstacle for this purpose due to the well-known property of neural networks, namely, their tolerance to errors.

1. Ergozhin E.E., Zezin A.B., Suleimenov I.E., Mun G. A. Hydrophilic polymers in nanotechnology and nanoelectronics, Almaty-Moscow: LEM, 2008, p.214. (in Russian)

Novel fluorescence properties of syndiotactic polystyrene and its derivative

Tomohiro Sago[1*] *and Hideyuki Itagaki*[1,2]

Department of Chemistry, [1]Graduate School of Science and Technology, and
[2]School of Education, Shizuoka University, 836 Ohya, Suruga-ku, Shizuoka 422-8529, Japan

f5944001@ipc.shizuoka.ac.jp

Introduction

Studies on fluorescence of high molecular weight atactic polystyrene (aPS) have been carried out by many authors since early 1960's. In addition to its monomeric fluorescence at 280 nm, aPS shows strong excimer fluorescence at 330 nm not only in solid state but also in fluid solution, because the excimer of aPS is formed between adjacent side-chain phenyl groups whose main conformer has been assigned to be tt in a meso diad [1]. Thus, most fluorescence of isotactic polystyrene (iPS) is of excimer since iPS consists of meso diads. On the other hand, the racemo diad of aPS and oligostyrenes are known to have quite low efficiency of excimer formation [1]. However, the fluorescence behavior of syndiotactic polystyrene (sPS) that consists of all racemo diads have not been published much.

Thus, we tried to show the novel fluorescence behavior of sPS solids and to explain the origin of the fluorescence by comparing it with the behavior of another syndiotactic polystyrene derivative, syndiotactic poly(*p-tert*-butyl-styrene) (sPTBS) in the present study.

Experimental Section

THF solutions of sPS, iPS, aPS and sPTBS were used for the measurement of uv/vis and fluorescence spectrum and the preparation of films (~3%). These films with various thicknesses were prepared by a spin-coating method on quartz disks or by casting the THF solutions on glass plates.

Results and Discussion

First, we measured the uv/vis absorption spectra of sPS, iPS, aPS and sPTBS in THF. The absorption peak of sPS was slightly red-shifted compared with aPS and iPS, but this is due to the change of the fraction of two vibrational bands.

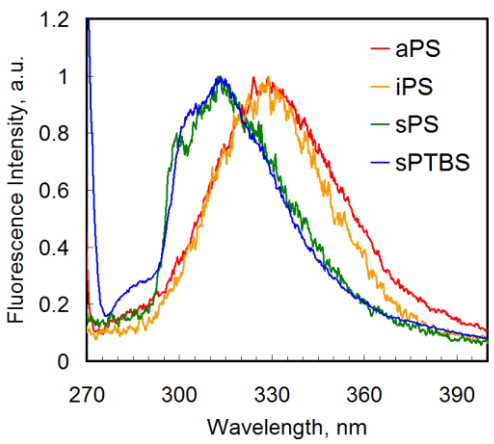

Figure 1. Fluorescence spectra of aPS, iPS, sPS and sPTBS thin films on quartz prepared from THF solutions by a spin-coating method. They are normalized to their peaks.

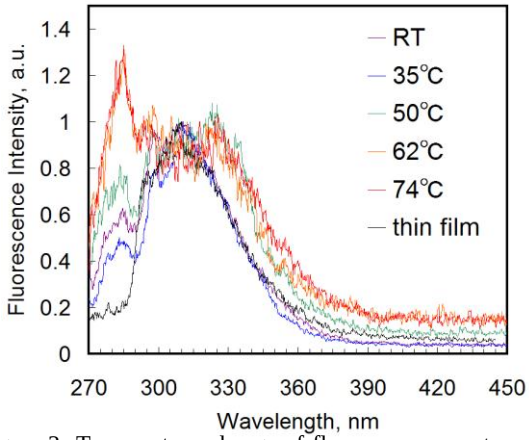

Figure 2. Temperature change of fluorescence spectra of sPS in THF when they were heated. All of them are normalized to the fluorescence peaks at 315 and 330nm.

Figure 1 shows the fluorescence spectra of each thin film. aPS and iPS demonstrated strong excimer fluorescence whose peak was at 330 nm. However, the fluorescence of sPS thin films showed one component whose peak was at 315 nm, which was different from phenyl monomer (at 280 nm) and excimer. The same fluorescence was observed for thick sPS films, so this was found to be of the main fluorescence of sPS solids. Interestingly, the similar fluorescence was observed for sPTBS, though it also showed its monomer fluorescence around 290 nm. Then, we examined the excitation spectra of sPS and sPTBS films of various thicknesses for 315-nm fluorescence. The absorption peak corresponding to the 315-nm emission was not the same as usual phenyl monomer, but did not change with film thicknesses. Consequently, the 315-nm emission of sPS and sPTBS was concluded to be of a ground state dimer formed between side-chain phenyl groups of different chains in solid state.

THF solution of sPS at higher concentrations turned out to form partially pre-gel at room temperature. The fluorescence of sPS was monitored during the pre-gel being gradually heated (Figure 2). Because the ground state dimer dissociate at higher temperatures, the peak at 315 nm was found to decrease while the phenyl monomeric fluorescence at 280 nm began to appear and increased with an increase in temperature.

Finally, we have succeeded to clarify the fluorescence behavior of sPS and sPTBS solids and to demonstrate that they are useful for monitoring their states such as aggregation or pre-gel.

References

[1] H. Itagaki, in "Experimental Methods in Polymer Science: Modern Methods in Polymer Research and Technology", ed. T. Tanaka, Academic Press, chapter 3, **2000**, 155.

Polymers as Nanocarbon Presursors in Template Method Characterization and Sorption Properties of the Obtained Products

M. Sobiesiak, B. Podkościelna, M. Podgórski, A.M. Puziy[a], O.I. Poddubnaya[a], C.A. Reinish[a], M.M. Tsyba[a]

Faculty of Chemistry, Maria Curie-Sklodowska University, pl. M. Curia-Sklodowskiej 3, 20-031 Lublin, Poland
[a] Institute for Sorption and Problem sof Endoecology, Naumov ST. 13, 03164 Kiev, Ukraine

magdalena.sobiesiak@umcs.pl

Introduction

Porous carbons are attractive materials for adsorption, separation, catalysis, energy storage devices due to their characteristic properties like porosity, chemical stability, heat resistance and electrical conductance. Template method is advanced technique using ordered structure of inorganic materials for formation carbonaceous products with determined and homogenous porosity. In creating porous structure of the carbon choosing of appropriate type of template plays important role. Another important feature is surface chemistry. From practical point of view surface chemistry is equally important as porous structure, since functional groups have principal influence on interactions between solid surface and molecules in fluid phase.

Polymers are especially promising in this field, because their properties can be modified in wide range e.g. hydrophobic or hydrophilic character, thermal stability, ability to carbon formation.

In our work we have studied three polymers as carbon precursors and their influence on properties of the obtained carbon materials.

Materials and Methods

Nanocarbons were prepared using template method. Furfuryl alcohol (FA) – P1, 4,4'-bismaleimidediphenyl methane (BM) – P4 and its copolymer with divinylbenzene (BM-DVB) – P5 were used as a source of carbon. A hard template was silica gel. Acetone solutions of each precursor (FA, BM, BM-DVB) were applied to impregnate the template. After total pore volume was filled, an obtained composites were heated in order to polymerize precursors inside porous structure of the template. Then carbonization process was performed. Temperature was gradually elevated up to 800ºC and maintained for 30 min. To prevent oxidizing reactions heating was carried in argon atmosphere. The silica template was removed by dissolution in 40% HF. The obtained products were washed with water and dried.

Elemental analyses, nitrogen sorption experiments (at 77K), thermal analyses, FTIR spectra, Boehm titrations, and solid phase extractions (SPE) for phenolic compounds were performed to characterize porous and chemical structure of the obtained carbon products.

Results and Discussion

Some of the obtained results are presented in the Table. Elemental analysis reveal FA (P1) is the precursor that give product the richest in carbon, percentage contents of H, N and other elements (mainly oxygen) is rather poor. Then P1 has relatively small amount of functional groups. P4 and P5 possess chemically differentiated surfaces. The presence of DVB (P5) in the polymer structure caused that the obtained carbon has two times less basic functional groups, as showed results of Boehm titration. The differences in surface functional groups are also confirmed by FTIR analyses (not presented here). Polymeric precursor has influence on thermal stability of the carbon products, as well. Initial decomposition temperature for analysed samples (IDT) are in the range of 130-180ºC, but carbons (P4 and P5) are much more thermally resistant. They possess in their structures substantial quantity of nitrogen.

Table

Sample	%C	%H	%N	% other	S_{BET} m^2/g	V_{tot} cm^3/g	IDT ºC	Basic mmol/g	Acidic mmol/g
P1	93.54	0.48	0.33	5.65	1785	1.56	130	0.35	0.44
P4	85	0.71	4.43	9.86	1013	1.34	170	0.37	0.69
P5	86.3	0.85	3.03	9.82	836	1.26	180	0.14	0.54

Results of nitrogen sorption experiment, specific surface area (S_{BET}), total pore volume (V_{tot}) and pore size distribution (PSD) are shown in Fig1. Porosity parameters (S_{BET} and V_{tot}) decrease in the following order P1, P4 and P5. Very interesting information can be obtained from Fig1. Although the silica template in all cases was the same the differences in pore size distribution are visible. In the case of P1 pore width is 3 nm, whereas for P4 and P5 pore widths are identical and equal 3.7nm. High and sharp peak for P4 indicates a narrow range of pore sizes. Peaks for P1 and P5 have similar shapes. These peaks are a little wider than that for P4 peak, what means the structures of P1 and P5 carbons are more heterogeneous than P4.

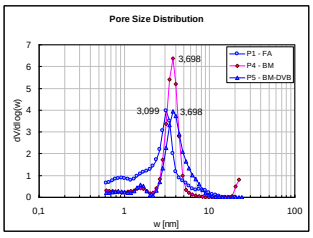

Fig1

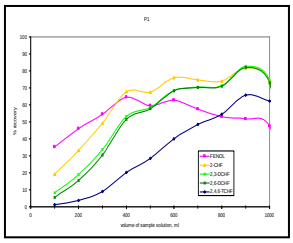

Fig2

In Fig2 example of sorption properties of P1 carbon in SPE method is presented. Different affinity of phenol and four its chlorinated derivatives towards the surface is proved. Breakthrough of most compounds takes place at volume of 1000mL and recovery reaches 80%.

Conclusions

These studies revealed that:

- the most homogenous porous structure was obtained from BM precursor
- the most developed surface was obtained from FA precursor
- the most thermally resistant product was obtained from BM-DVB precursor.

How affect the shape and modifier of clay on polymer blends?

R. Gallego[1], *D. García-López*[1], *J.C. Merino*[1,2], *J.M. Pastor*[1,2]

[1] CIDAUT - Foundation for Research and Development in Transport and Energy, Parque Tecnológico de Boecillo, Boecillo, 47151,Valladolid, Spain
E-mail: raugal@cidaut.es

[2] Department of Condensed Matter, EII, University of Valladolid, Paseo del Cauce 59, 47011, Valladolid, Spain.

INTRODUCTION

Nowadays, the development of new materials with balanced properties between stiffness and toughness are required in sector such as automotive to develop some parts like bumpers, hub cups, tail gates, doors handle, etc. Thus, the addition of an elastomeric phase to polymer nanocomposites usually could improve the toughness, but a detrimental of the stiffness properties will be obtained[1]. Then, the challenge is achieve a good balance between stiffness and toughness

From our knowledge, all studies based on polymer nanoblends used clay with a platelet-like shape such us smectite. Furthermore, the study of the microstructure and macrostructure of polymer blends with fibrilar clay shape, i.e., sepiolite, offers a unique opportunity to know how the properties are influenced by the clay shape.

In that sense, the main purpose of this work is to compare the effect of clay shape on polymer nanoblends based on PA6 and EPDM using montmorillonite and sepiolite modified with the same organic surfactant, in this case an ammonium salt. Also along this study we will explore the effect of change the surfactant employed in sepiolite, because the modification degree of clay could affect both the inorganic/organic compatibility and the dispersion of the sepiolite in the polymer matrix. In that sense, the sepiolite employed was organically modified with silanes, because of the high affinity between silane groups and amide groups of PA6[2]. Furthermore, in this paper we have used a theoretical relation EPDM-g-MA:Clay 5:1, where the amount of clay was 3 and 5 wt%, because blends with that relationship showed good balanced properties for automotive parts as can be seen in our previous work.[3]

MATERIALS AND METHODS

In this work, PA6 Akulon F130C matrix was supplied by DSM, mEPDM nordel IP3722P was supplied by Dupont, EPDMgMA Roylatuf 498 was supplied by Crompton, motmorillonite Nanofil® 8 was supplied by Süd Chemie and both sepiolites, standard without modification and modified with a quaternary ammonium salt (2M2TH) and a silane (HS06) were kindly supplied by TOLSA S.A. (Spain).

Characterization of microstructural properties of nanocomposites has been carried out by means of microscopic techniques, such as scanning and transmission electron microscopy (SEM & TEM). The morphology was related to thermo-mechanical properties such as Young's modulus, heat distortion temperature (HDT) and notched Izod impact strength at room temperature. Thermogravimetric analysis (TGA) has been done in order to know the residue left by clay in the nanocomposites.

RESULTS AND DISCUSSION

The results have shown that sepiolite has a lot of influence, not only in the morphology, but also in the mechanical properties.

In that sense, the blends with 3 wt% of sepiolite has reached a best balanced properties than its homologous with MMT and even higher mechanical properties than blends with higher MMT content as could be compared with our previous work.[3]

Nevertheless, the blends with 5 wt% of sepiolite have not reached best balanced properties than its homologous with 5 wt% of MMT, indicating that the relationship EPDMgMA:MMT is not valid for fibrous clays as sepiolite.

In reference to the surface functionalization of sepiolite, the blends reinforced with 3 wt% have not shown differences in the mechanical properties. However, the blends with 5 wt% of sepiolite modified with silanes have reached better properties than those reinforced with sepiolite modified with ammonium salts. That indicates that the Si-OH groups of sepiolite, interact with the amide groups of the matrix and this improves the stiffness of the blends with a slight loss in toughness.

REFERENCES

1. González I, Eguiazabal JI and Nazabal J, J Polym Sci Part B: Polym Phys 43: 3611-3620 (2005).
2. Cárdenas M., PhD Thesis, University of Valladolid, Spain (2007).
3. Gallego R., García-López D., Merino JC and Pastor JM, Polym Inter 59: 472-478 (2009).

Role of polymer-to-filler grafting in dispersion of CNTs in rubbers.

Pierre Verge[1], Sophie Peeterbroeck[2], Leila Bonnaud[2] and Philippe Dubois[1,2].

[1]Center of Innovation and Research in Materials&Polymers CIRMAP, University of Mons-UMONS, Place du Parc 20, B-7000 Mons, Belgium

[2]Materia Nova, Parc initialis, Avenue Copernic 1, B-7000 Mons, Belgium

sophie.peeterbroeck@materianova.be

Abstract

This contribution reports on the dispersion by simple meltblending of tinyamounts of carbon nanotubes (CNT) in nitrile butadienerubbers (NBR). Acrylonitrile (ACN) units of NBR are known to generate free radicalsuponheating and/or shearing. This studyhighlightselementsevidencingapossibility for NBR polymerchains to react by a free-radical mechanism and to graft onto CNT surface all along the process of mechanicalblending of NBR withCNTs. More precisely and since the formation of the free-radicalstakesplace on the ACN units, the influence of the ACN relative content in NBR on the grafted CNT amount has beenstudied. It comes out that the polymer-grafting rate onto the CNT surface increaseswith the ACNcontent in NBR. Interestingly, the nanotubes proved more finelydispersed in NBR containinghigherrelative ACN content as evidenced by morphological observations as well as electricalmeasurements.

Introduction

Various NBR samplescharacterized by increasing content in ACN have been chosen for the production of conductingelastomernanocompositesfilledwithmultiwallCNTssurfacegraftedby NBR chains. Firstly, wewillhighlightthat the thermooxidativeand/or thermo-mechanicaldegradation of the polymertaking place during the meltblendingprocess leads to the covalentgrafting of elastomerchains onto the nanotube surface.

Wewill show that the content in surface-graftedCNTsincreaseswiththe ACN relative content spreadalong the NBR chains. Finally,transmissionelectronmiscroscopy (TEM) and electricalmeasurementswillbeapproached for highlighting the effect of the ACNcontent on the extent of dissociation of the native nanotube bundlesand the quality of the nanofillers distribution and dispersionthroughout the NBR matrix.

Processing conditions

NBR/CNT composites werepreparedusing a two-step process.
The components (i.e. NBR, CNTs and vulcanization agents, if any)were mixed simultaneously in a Brabenderinternalmixer.
Exceptwhenindicated, all the compounds werepreparedat 50°C for 10 min at 60 rpm and werethenvulcanizedat 190°C under50 bars for 15 min.

Results and Discussion

During the meltblending of NBR withCNTs, the graftingreactionof somepolymerchains onto the nanotubes surface has beenevidenced. This grafting more likelyresultsfrom the formation offree-radicalsalong the polymerchains as generated by thermooxidationand/or thermo-mechanicaldegradationmechanisms.
Interestingly the vulcanization, i.e., a free-radical reaction, involvesthe CNTsreducing the number-averagemolar mass between thecrosslinkingnodesathigher nanotubes content. Sinceitiswellacceptedthatboth thermo-oxidative and thermo-mechanicaldegradationsof NBR chainstake place on ACN units[1–3], it has alsobeendecided to study the effect of ACN relative content of NBR on thepolymer-grafting rate in NBR/CNT blends.
Reducing the ACN relative content in NBR also leads to a decrease of the amount of surface-graftedCNTs, shiftingfrom 1.4% to 0.2%, respectively, for rubberscontaining 44 and18 wt.% ACN units. The more the NBR elastomercontainsACN groups, the more the CNTs in the NBR/CNT blends aresurface-grafted. Such an observation mightbeexplained by the relativelyhigheramount of free-radicalsthusgenerated on the ACNgroups and the affinitybetween the acrylonitrile functions andthe nanotubes.

Conclusion

It wasshownthatduring the blendingprocess, the polymerchains are graftedonto the CNT surface via a free-radical mechanism. Indeed, NBRgenerates free-radicalsfromits ACN unitsuponheating and/orshearing. As a result of the highinherentaffinitybetween the CNTsand ACN units, and due to the formation of ACN-based free-radicalsleading to NBR-grafting on CNTs, increasing the ACN relativecontent along NBR chains triggers higherpolymer-grafting on thenanotube surface.

[1] Grassie N, Heaney A. EurPolymer J 1974;10(5):415–24.
[2] Budrugeac P. PolymDegradStab 1992;38(2):165–72.
[3] Budrugeac P. PolymDegradStab 1995;47(1):129–32.

Synthesis of Colloidal Stable Silica Containing Blockcopolymer-Nanoparticles

Nesrin Köken Öz[1], *Klaus Tauer*[2], *Nancy Weber*[2]

[1]Istanbul Technical University, Faculty of Science, Chemistry Department,34469-Maslak-Istanbul/Turkey
[2] Max-Planck Institute of Colloids and Interfaces, Am Mühlenberg, D-14476 Golm, Germany

nesrin@itu.edu.tr, klaus.tauer@mpikg.mpg.de, nancy.weber@mpikg.mpg.de

Introduction

The heterogeneous nature of aqueous heterophase polymerizations is the base for an easy route to unique block copolymers, for the development of new and more effective polymerization strategies. [1-5] The aim of this project is to produce inorganic - polymeric nanocomposites in a one-step procedure and to carry out studies regarding the synthesis and the properties of block copolymers and double hydrophilic block copolymer particles which are easily and only accessible by a special aqueous heterophase polymerization technique. Water-soluble hydrolytic precursor polymers with hydroxymethyl end groups such as poly(ethylene glycols) m-PEG 5 (methoxy terminated PEG a molecular weight of 5000g/mol) and various hydrophobic monomers such as VTMEOS (vinyl trimethoxysilane), VTEOS(vinyl triethoxysilane), VTISOPOS(vinyl triisopropoxysilane), VTISOPREnOS (vinyl triisopropenoxysilane), NIPAM (N-isopropyl acrylamide) were used to synthesize silica containing triblock copolymer particles by radical polymerization with ceric ion redox initiation mechanism in water.

Materials and Methods

Chemicals. The monomers were either carefully distilled or at least two times re-crystallized prior to use. Methoxy-terminated PEG with a molecular weight of 5000 g/mol (mPEG 5000, Aldrich), vinyl trimethoxy silane(VTMeOS,Aldrich),Vinyltriethoxysilane (VTeOS, ABCR), Vinyl triisopropoxysilane(VTISOPOS, ABCR) and Vinyl tri phenoxysilane(VPhEOS,ABCR), were used as received. Cerium ammonium nitrate from (Fluka) was used as ceric ion source. All block copolymers were synthesized in a CPA200 reaction calorimeter (ChemiSens AB, Lund, Sweden). Before any analysis the final latexes were purified by ultrafiltration through a YM-100 membrane (regenerated cellulose) with a cut-off of 100 kDa until the conductivity of the eluate reached a constant value. Then, the block copolymers were isolated by freeze drying (Beta 1-16, Christ, Germany). FT-IR spectra were recorded with a Varian 1000 Scimitar in ATR mode (Pike Miracle ATR cell). Transmission and scanning electron microscopy (TEM, SEM) was performed with a Zeiss EM 912 Omega microscope operating at 100 kV and a Leo Gemini 1550 according to standard procedures, respectively.

Results and Discussion

The silica containing triblock copolymer particles (peg-pnipam-pvteos, peg-pnipam-pvtmeos, peg-pnipam-pvtisopos,peg-pnipam-pvtisoprenos) were characterized regarding morphology by TEM and SEM. FT-IR spectroscopy was used to characterize the chemical composition. The results revealed a strong influence of the nature of the siloxane. After ultrafiltration and freeze drying the solid triblock copolymers are easily redispersable in water. The SEM image (Fig.1a) clearly shows regions which suggest the presence of silica at the particles. The solid triblock copolymers were, in a further reaction step, calcined at 550 °C for 7 hours. If the solid triblock copolymers are treated with a high temperature flame (~2000 °C) the residual organic parts burn away and the remaining SiO_2 melts and forms quartz pearls (Fig.1b). After calcination the silica is porous as proven by SEM images (Fig.1c). The structure of the triblock copolymer is proven by FT-IR spectroscopy (Fig 1d). The vibration spectrum of the triblock copolymer unambiguously shows, besides the characteristic bands of the PNIPAM and the PEG blocks, the existence of SiO_2 units already in the triblock copolymer.

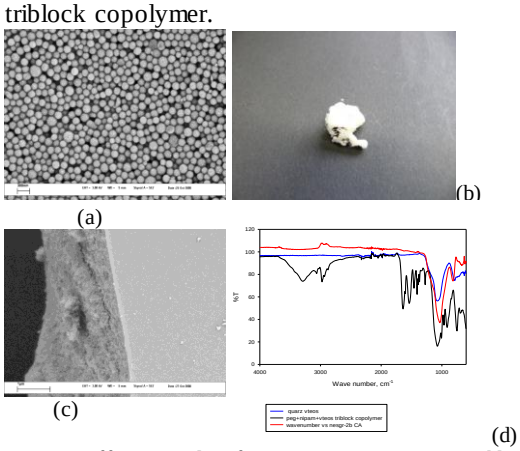

Fig. 1. Different results of PEG-PNIPAM-PVTEOS triblock copolymer a) SEM images, (b) quartz pearls after burning the solid polymer in a high temperature flame, (c) SEM images of the calcinated block copolymer, (d) FT IR spectra

Conclusions

The established strategy for the synthesis of block copolymer particles via aqueous heterophase polymerization is versatile and could be successfully applied to produce novel silica-containing block copolymer particles in an effective one step procedure.

References

[1]K. Tauer, V. Khrenov, *Macromol. Symp.* **2002**, 179, 27-52

[2]K.Tauer,V.Khrenov,N.Shirshova,N.Nassif, *Macromol. Symp.***2005,** 226, 187-201

[3]K.Tauer, M.Mukhamedjanova, C.Holtze, P. Nazaran, J. Lee, *Macromol. Symp.* **2007**, 248, 227-238

[4]K. Tauer, N. Weber, S. Nozari,K. Padtberg, R. Siegel, A. Stark, A. Völkel, *Macromol. Symp.* **2009**, 281, 1-13

[5]N.Nassif, N.Pinna, N.Gehrke, K. Tauer, N.Shirshova M.Antonietti, H.Cölfen, *Angew. Chem. Int. Ed.* **2005**, 44, 2-6

Characterization of Conducting Polymer Nanocomposites with Poly(vinylidene fluoride) Used in Devices Electroluminescents

Alex L. Gomes, [1,2,3] João Sinézio de C. Campos, [1] Elaine Armelin, [2] Carlos Alemán, [2] Reinaldo A. Ricci Jr., [1,3] Maria Beny P. Zakia, [3] Mara A. Canesqui, [3] Alfredo R. Vaz, [3] Jose G. Filho, [3] José A. Diniz [3].

[1] Department of Polymer Technology, State University Of Campinas, Av. Albert Einstein, 500, 13083-852, Campinas-SP-Brazil
[2] Departament d'Enginyeria Química, E.T.S d'Enginyers Industrials de Barcelona, Universitat Politècnica de Catalunya, Av. Diagonal 647, Barcelona E-08028, Spain
[3] Center of Semiconductor Components, St. João Pandia Calógeras, 90, P.O.Box 6061,13083-870- Campinas-SP-Brazil

e-mail: alexgomes@feq.unicamp.br and sinezio@feq.unicamp.br

Introduction: It is well known the concern of scientists in producing devices for conversion and clean power generation. Among the devices studied stand out the organic light emitting diodes (OLEDs), the polymer light emitting diodes (PLEDs) and light emitting devices based in luminophors components. The efficiency of these devices has increased in recent years; however, more studies should be conducted to enlarge it. This paper presents the construction and characterization of components of an electroluminescent device consisting of: Monolayers of composites of various thicknesses (4 µm-20 nm) containing poly (3-thiophene methyl acetate) PT3MA doped with ferric chloride ($FeCl_3$), the polymer poly (vinylidene fluoride) and the luminophor $ZnSiO_4$: Mn (zinc silicate doped with manganese), which were dissolved in dimethylformamide (DMFA) and deposited by spinner or drop casting techniques on Indium Titanium Oxide (ITO) and silicon wafers. The film formed was then taken to evaporation of metals and in its opposite face deposited aluminum to form external contacts. The samples were characterized with the techniques of atomic force microscopy (AFM), focused ion beam (FIB) scanning electron microscopy, ellipsometry, perfilometry and I-V characteristic curve.

Materials and Methods

Figure 1: Device fabrication process

The steps for assembling and preparing the device (Figure 1) are: 1) partial removal of the ITO by corrosion process using Zn powder and HCl 1:1 [1], 2) clean of substrate with solvents (acetone, water and isopropyl alcohol using ultrasound) [1], 3) deposition of the composite by drop casting or spinner, 4) evaporation of the solvent in the vacuum oven, 5) deposition of aluminum by sputtering with the aid of mask

Results and discussion: The average thickness determined by Perfilometry and FIB to the composite deposited on the substrate by drop casting was 4 µm. In the tests evidence of depositions by spinner, nanocomposites of the material can be obtained and their values of thicknesses determined by ellipsometry. The solutions spin coated at 1000 rpm and 2000 rpm formed membranes with thicknesses near 20 nm. The SEM images showed an excellent distribution of luminophors in the films thicker, however low their distribution in the nanocomposites deposited by spinner resulting in an increase of the agglomeration of luminophors particles in the extremities of the ITO surface.

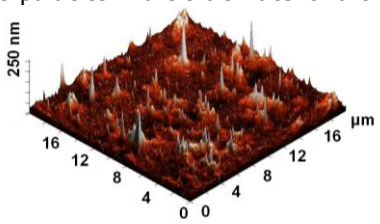

Figure 2: AFM images of nanocomposite

AFM images were performed to determine quantitatively the average roughness of the composites deposited on the substrates. Figure 2 shows the surface topography of the composite deposited on ITO substrate by spinner at 2000 rpm with a value of average roughness of 11 nm. Composites with values of 450 nm and 14 nm of roughness were obtained respectively by drop casting and spinner at 1000 rpm. The I-V characteristic curve of composite PT3MA / PVDF / ZnSiO4: Mn with 2µm of thickness and 0,3 cm² of area is presented in Figure 3. The measurements were performed for a sample polarized with direct current (DC) voltage using a slope of 93 mV/dec.

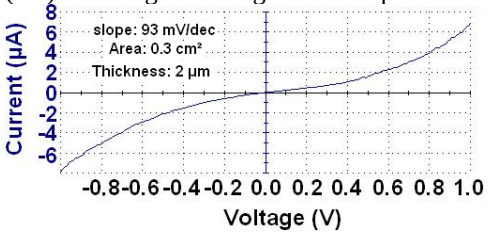

Figure 3: I-V characteristic curve voltage x current

Analyzing the curve is possible to observe that the device presents a behavior characteristic of a semiconductor diode. However for voltages greater than 3 volts a new behavior is observed, because the curves show the formation of hysteresis (graph not reported in this paper). These results are similar to those reported for blends of PVDF-PT3MA [2].

Conclusion: The films obtained this work presented low roughness, excellent distribution of luminophors, especially the thicker films. The electrical characteristic voltage versus current (VxI) showed a diode behavior and not resistive for the device.

References

1. KIM, J.S.*et al*, *J. Appl. Phys.*, **84**(12), 1998, 6859-70.
2. MANNA, S.; NANDI, K.A.; MANDAL, A.; *J. Phys. Chem. B*, **114**, 2010, 2350-2351.

*This work was supported by CNPq

Formation and Size Tuning of Colloidal Microcapsules via Host-Guest Molecular Recognition at the Liquid-Liquid Interface

K. Merve Türksoy, Fırat Özdemir, Amitav Sanyal

Bogazici University, Department of Chemistry, Bebek, 34342, Istanbul, Turkey

email: amitav.sanyal@boun.edu.tr

Microcapsules are classes of functional materials that have recently aroused great interest. They can be utilized as containers as an alternative to micelles and vesicles for applications such as drug delivery devices. A strategy based on the host-guest complexation ability of cyclodextrins, the formation of stimuli-responsive colloidal microcapsules due to crosslinking via specific non-covalent 'host-guest' chemistry was examined. Unlike covalently cross-linked microcapsules, the reversible nature of these bridging interactions can be used to manipulate the size of these capsules via introduction of competing amphiphilic guest molecules. Partial disruption of interfacial cross-linking allows microcapsules to coalesce with each other to form larger capsules.

References.

[1]D. Patra, F. Ozdemir, O. R. Miranda, B. Samanta, A. Sanyal, V. M. Rotello Langmuir 2009, 25(24), 13852–13854

Characterization, bioactivity and *in vitro* cellular response of sol-gel silica-polymer hybrid nanocomposites

S. Iváshchenko[1], D. M. García Cruz[2,1], A. Campillo Fernández[3], M. Monleón Pradas[1,2,4], J. L. Escobar Ivirico[1,2], G. Gallego Ferrer[1,2,4]

[1]Centro de Biomateriales e Ingeniería Tisular, Universitat Politècnica de València, 46022, Valencia, Spain
[2]Centro de Investigación Príncipe Felipe, Autopista del Saler 16, 46013 Valencia, Spain
[3] Metis Biomaterials, Parc Tecnològic, Av. Franklin, 12, 46980 Paterna, Valencia, Spain
[4]CIBER en Bioingeniería, Biomateriales y Nanomedicina (CIBER-BBN), Spain

seriv@etsia.upv.es; dgarcia@cipf.es; alcamfer@metisbiomaterials.com; mmonleon@upvnet.upv.es, joresciv@ter.upv.es, ggallego@ter.upv.es

Introduction

Caprolactone derived materials are good candidates for tissue engineering. Although previous works demonstrate that methacrylate-endcapped caprolactone (CLMA) and 2-hydroxyethyl acrylate (HEA) copolymer networks present good response when cultured with chondrocytes [1], they lack of sufficient mechanical properties for hard tissue engineering applications like bone. The hybridation of the organic matrix with silica (SiO_2) by the polymerization of the organic phase during the simultaneous in situ sol-gel polymerization of a silica precursor has been presented as and strategy for mechanical reinforcement and bioactivity improvement [2]. The aim of the present work is the synthesis, characterization and evaluation of the cellular response of new CLMA-co-HEA/SiO_2 hybrids.

Materials and Methods

The hybrids were obtained through the co-polymerization reaction of CLMA and HEA in monomers ratio 60/40% (w/w) and the simultaneous acid-catalyzed sol-gel polymerization of TEOS as described elsewhere [2]. 1 mm thickness sheets were obtained with different proportions of SiO_2 (up to 30 wt.%). Effective silica network formation was confirmed by infrared spectroscopy (FTIR). Thermogravimetry (TGA) allowed determining the real quantity of SiO_2 in the hybrids. The glass transition temperature of the samples was assessed by differential scanning calorimetry (DSC). Dynamic mechanical measurements (DMA) allowed measuring the storage modulus as a function of temperature. The ability of the samples to form a layer of hydroxyapatite (HAp) on their surface was tested *in vitro* by soaking them in a simulated body fluid (SBF) [3]. MC3T3-E1 pre-osteoblastic cells were cultured *in vitro* on the materials to evaluate their osteogenic potential.

Results and Discussion

The weights of the inorganic residual at 650ºC of the TGA curves agree well with the nominal ones. FTIR spectra show the characteristic peaks of the silica network: at 1060–1100 and 800 cm^{-1} (attributed to the Si-O-Si asymmetric and symmetric stretching vibration, respectively) and at 950 cm^{-1} (characteristic of the Si-OH stretching vibration). Their intensities increase proportionally to the silica content, mainly at silica contents above 15%. This abrupt increase is correlated with the percolation of the silica network. The copolymer is amorphous and random showing a single glass transition at -23ºC. It monotonously shifts to higher temperatures with the increase of the silica content, up to 9.48ºC for the 30% SiO_2 sample. The rubbery modulus does not vary significantly up to 15% SiO_2 content when it markedly increases due to the formation of a continuous inorganic network. Scanning electron microscopy (SEM) images of the samples after 7 days of immersion in SBF show few hydroxyapatite nuclei grown on their surface. After 14 and 21 days the copolymer and the hybrid with a 15% SiO_2 are completely covered by a layer of HAp (formed by the typical needle-shape crystals) with aggregates of a second and third layer (Figure 1 left). On the contrary, although the sample with a 30% SiO_2 is bioactive it presents a HAp layer with some imperfections. Electron dispersive X-ray spectroscopy shows that the coatings are mainly composed of calcium and phosphorous, with Ca/P atomic ratio close to the stoichiometric apatite, 1.67. The MTS proliferation assay shows an increment in the number of cells at 7 days of culture, being the number of cells independent of the silica content. Confocal laser scanning microscopy images of the immuno-histochemistries (Figure 1 right) show cells producing osteocalcin and collagen type I, typical markers of osteoblastic differentiated cells.

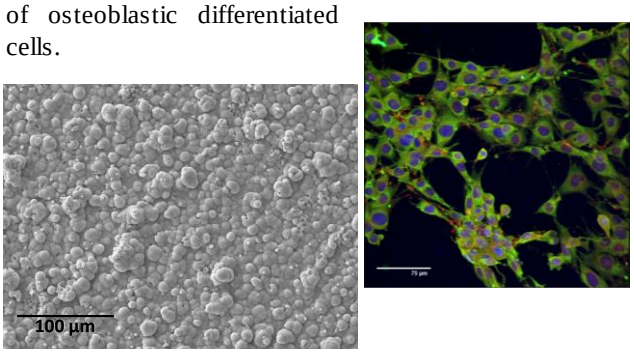

Figure 1. Left: SEM image of the hydroxyapatite layer grown on the 15% SiO_2 hybrid, 14 days immersed in SBF; right: double immunofluorescence image showing staining of osteocalcin (green) and collagen type I (red) of pre-osteoblastic cells cultured on the 15% SiO_2 hybrid at 14 days. Cell nucleus is stained with Dapi (blue). Bar equal to 75 µm.

Conclusions

The new silica hybrids have improved mechanical properties in comparison to pure copolymers, are bioactive and induce the osteoblastic differentiation as good candidates for bone tisuue engineering.

Acknowledments: this work is supported by the Spanish Ministry of Science and Innovation trough the DPI2010-20399-C04-03 and PTQ08-08-06321 projects.

References

[1] Escobar Ivirico J.L. *et al.* J Biomed Mater Res Part B: Appl Biomater, 2007;83B:266-75
[2] Vallés-Lluch A. *et al.* Eur Polym J, 2010;46:1446-55
[3] Kokubo T. Biomaterials, 1991;12:155–63

Unusual blue-shifted photoluminescence of MDMO-PPV films

H. Méndez[1,*], *C. Hernández*[1,2], *B.A. Páez-Sierra*[1] *and J.C. Salcedo-Reyes*[1]

[1] *Thin films group, Physics Department, Javeriana University. Bogotá, Colombia.*
[2] *Electronics Engineering Department, Javeriana University. Bogotá, Colombia*

h.mendez@javeriana.edu.co

Introduction

The mechanisms of radiative processes taking place in spin coated thin films of the electroluminescent polymer MDMO-PPV, were identified through photoluminescence (PL) spectra.

Materials and methods

Thin films of poly[2-methoxy-5-(3′,7′-dimethyloctyloxy)-1,4-phenylene vinylene] (MDMO-PPV) [1], were deposited by spin coating and its optoelectronic properties were explored by a combination of transmittance, photoluminescence and conductivity measurements as a function of temperature (13K-410K) [2].

Results and discussion

A temperature dependent blue shift of the Q band was observed (See figs. 1 and 2).

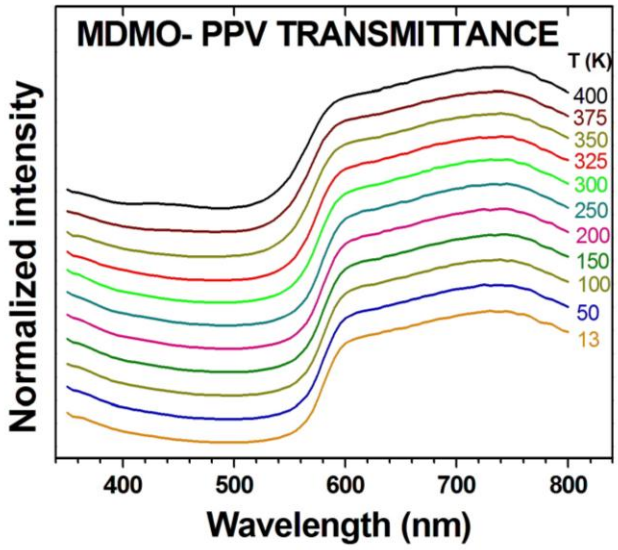

Figure 1. Transmittance of a MDMO-PPV film in the temperature range 13K-410K.

This behavior was investigated by combining optical and electrical measurements in a wide range of temperatures (13K to 410K). Both, transmittance and PL spectra show an unusual shift of the optical bandgap towards shorter wavelengths as the temperature increases. Further analysis of the temperature dependency in optical spectra and electrical conductivity data, suggests segmentation and self-ordering of the polymer chains.

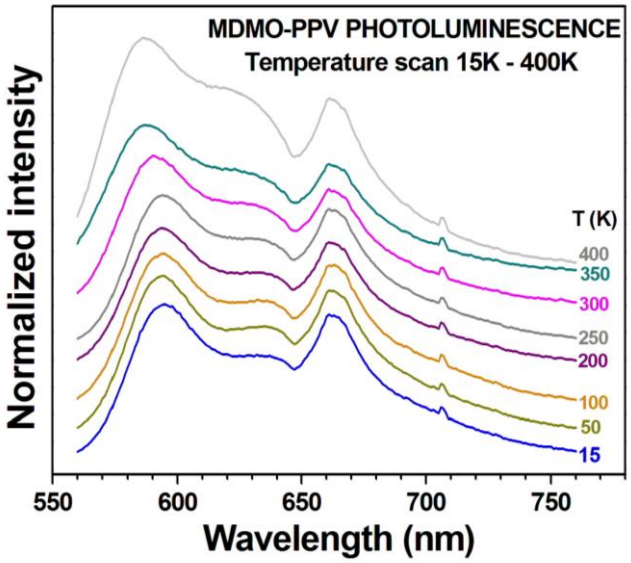

Figure 2. Temperature dependent Photoluminescence measurements on MDMO-PPV films, in approximately 50K intervals.

Conclusions

The results allow deducing a phenomenological model for the observed structural changes in the organic film. Thus, the heating process results in an improvement of the molecular order and therefore, according to the model, an enhancement of the electroluminescence is expected.

References

[1] Sigma-aldrich webpage. http://www.sigmaaldrich.com . Visited on January 31st .
[2] C. Hernández. Propiedades opto electrónicas de materiales utilizados en la construcción de OLEDs. Thesis work, Electronics engineering department, Pontificia Universidad Javeriana.

The Thermodynamics of Formation and Structure Peculiarities of Nanostructured Polyurethane/Poly(2-Hydroxyethyl Methacrylate) Interpenetrating Polymer Networks

L.V. Karabanova[a]* *Yu.P.Gomza* [a], *S.D.Nesin* [a]

[a] Institute of Macromolecular Chemistry of National Academy of Sciences of Ukraine, Kharkov Road 48, Kiev 02660, Ukraine;

email: abrosim@mail.kar.net

Interpenetrating polymer networks (IPNs) based on polyurethane (PU) and poly(2-hydroxyethyl methacrylate) (PHEMA) were synthesized by sequential method. The thermodynamic miscibility and structure peculiarities by SAXS have been investigated. A study of the thermodynamics of the process of a multicomponent polymer system formation was carried on. It was shown that the values of free energy of mixing of the polymer's components Δgx (Gibbs free energy) are positive for all compositions under investigation. It means that polymeric components of the system are thermodynamically incompatible. The synthesized IPNs have a structure of incomplete phase separation. A study of the particular structure of interpenetrating polymer networks by methods of small angle and wide-angle scattering was done. It was shown (Fig.1) that SAXS curve of initial PU shows intensity maximum that evidences nanophase separated structure of such a component. The SAXS curve of PHEMA is completely structureless and has low level of intensity that evidences homogeneity of morphology.

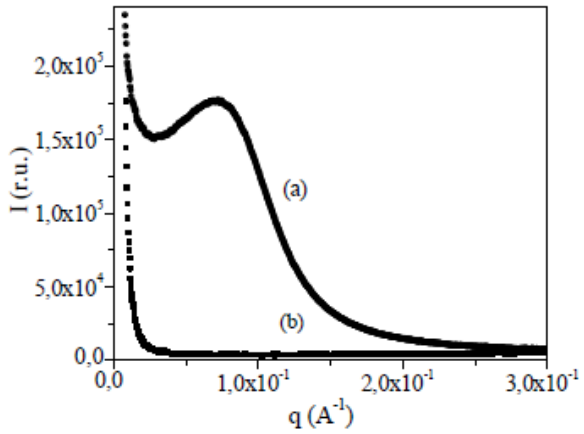

Fig.1. Scattering intensity I(q) . q2 versus scattering vector q, for Polyurethane network (a) and for PHEMA (b).

The curves of all the IPNs show two set of interference maxima. They are located at the wave vector values corresponding characteristic lengths in the ranges 6 – 9 nm and 26 – 28 nm, respectively (Fig.2).

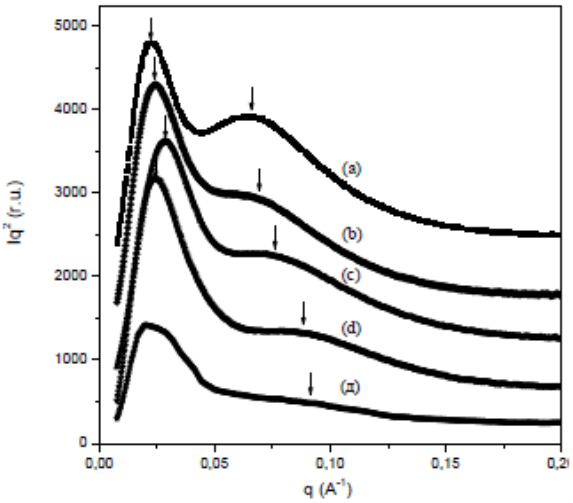

Fig.2. Scattering intensity I(q) . q2 versus scattering vector *q* curves of PU/PHEMA semi-IPN's for different PHEMA contents:16.2 (a), 21.4 (b), 31.9 (c), 40.4 (d); 57.7% (e).

The first set maxima reflect a presence of PU nanophase structure and the second ones are attributed to the frozen nanophase separated structure of IPNs formed by nanodomains which are rich by one of the components. The first type maximum in the IPNs curves reflect an existence of spinodal decomposition type anophaseseparated structure induced by chemical reaction. The second interference maxima are connected to the PU nanophase separated structure and evidence the presence of the PU-rich domain. The presence of two hierarchical levels of heterogeneity in the IPNs was established and the features of each of them was analyzed. The first level of heterogeneity is recorded in the early stages of spinodal decomposition, the fluctuations of concentration with size of 30 - 40 Å were found. The second level of heterogeneity corresponds to later stages of microphase separation and is characterized by highlighting almost pure polyurethane and PHEMA domains, which include crosspassing chains of polyurethane.

This research was supported by project N 6.22.7.21
of the SGSTP "Nanotehnology and Nanomaterials"

Polyurethane urea Nanocomposites: Synthesis and Characterization

A. Cuellar-Burgos[a], F.A. Mesa-Rueda[a], J.E. Perilla-Perilla[b]

[a]Laboratorio de Polímeros y Materiales Compuestos, Universidad Nacional de Colombia, Manizales, Colombia
[b]Departamento de Ingeniería Química y Ambiental, Universidad Nacional de Colombia, Bogotá, Colombia

acuellarb@unal.edu.co

Polyurethane urea (*PUU*) elastomers are formed by joining blocks of two chemically dissimilar segments along the polymer backbone. These polymers have the general structure $(A\text{-}B)_n$, where *B* is the soft segment. The hard segment (*A*) is formed by extending a diisocyanate with a low molecular diol or diamine. Organically modified clays play an important role in the formation of the structure and morphology of polymer/clay nanocomposites, and thus significantly influences material properties [1-3]. Therefore, the choice of modifiers used to treat clay is crucial to prepare polymer/clay nanocomposites with enhanced properties [4]. Thermoplastic polyurethane urea (*PUU*)/Clay nanocomposites were prepared via solution processing using ether type *PUU* and a modified organoclay. The *PUU* was prepared from isomer mixture of methylene diisocyanate (*MDI*), polyether polyol (*PTMG*) and ethylenediamine (*EDA*) as chain extender. The hard segment concentration of the final copolymer was 36 wt % (by reaction stoichiometry), assuming all *MDI* and *EDA* contribute to the hard segments. Two differently modified organoclays (denoted as 93, 10) and pristine montmorillonite (*MT*) were intercalated and exfoliated in the *PUU* matrix using an intercalation technique for solution and subsequently characterized by X-ray diffraction (*XRD*), atomic force microscopy (*AFM*) and *DSC*.

The figure 1 shows *PUU360*, *PUU365_10* and *PTMG*, where nanocomposite containing final concentration of 5 w/w%. The pure *PUU* (*PUU360*) exhibits an amorphous halo near 2θ = 20°, consistent with the result of Dai et al. [5] and is found at the same location for the composite. This is implying that *PUU* is intercalated into layered silicates, exfoliated and dispersed in *PUU* matrix amorphous.

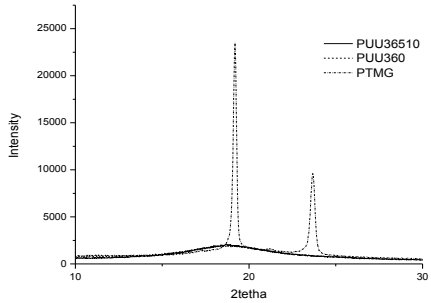

Figure 1. *XRD* patterns of *PUU*: 0.0 w/w % clay (PUU360); 5.0 w/w % clay (PUU365-10) and PTMG.

Finally, morphological changes induced by the addition of clays were analyzed using *DSC* and *AFM*. The *DSC* melting curves of copolymer pristine and nanocomposite show the thermal behavior of *PUU* at a scanning rate of 10°C/min, the curves had an exothermic peak (cold crystallization, at about -20°C) and an endothermic peak (melting of crystallization, at about 20°C), while there was crystallization peak on the cooling. After adding nucleating agents organically modified clays, the exothermic peak decrease on the heating curve. It can be concluded that in the course of heating less crystal was formed [6].

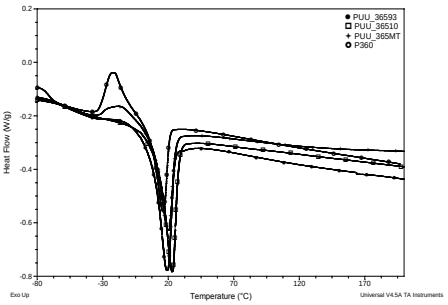

Figure 2. *DSC* melting curves of pure *PUU* and nanocomposite with clay modifiers 10, 93 and *MT*.

Figure 3 shows the hard domains light and soft dark by noncontact *AFM*. Pure *PUU* of left is amorphous with aggregation of hard domains (*PUU360*), while nanocomposite of the right has a slight crystallization. The other modified presented different morphologies without crystallization.

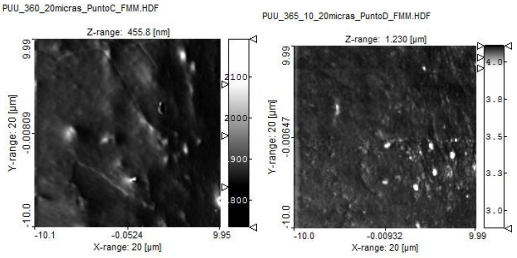

Figure 3. Ambient temperature tapping *AFM* force image of *PUU360* and *PUU365-10*.

In conclusion, the cold crystallization presents in pure polyurethane is reduced by the effect of clay modifiers addition. Furthermore, the modifier affects the morphology obtained by crystallization soft domains or segregation of the hard domains.

References:

[1] C.B. Wang, S.L. Cooper, Macromolecules. 16 (1983) 775-786.
[2] A. Cuellar, F.A. Mesa, J.E. Perilla, Rev. Fac. Ing. Univ. Antioquia. 54 (2010) 57-64.
[3] J.T. Garrett, C.A. Siedlecki, J. Runt, Macromolecules. 34 (2001) 7066-7070.
[4] J. Xiong, Z. Zheng, H. Jiang, S. Ye, X. Wang, Composites Part A: Applied Science and Manufacturing. 38 (2007) 132-137.
[5] X. Dai, J. Xu, X. Guo, Y. Lu, D. Shen, N. Zhao, X. Luo, X. Zhang, Macromolecules. 37 (2004) 5615-5623.
[6] R. Liao, B. Yang, W. Yu, C. Zhou, Journal of Applied Polymer Science. 104 (2007) 310-317.

Applications of Broadband Dielectric Spectroscopy in Polymer Nanoscience

A. Serghei[1], F. Kremer[2], and T.P. Russell[3]

[1] Université Lyon 1, CNRS, UMR 5223, Ingénierie des Matériaux Polymères, F-69622 Villeurbanne, France
[2] University of Leipzig, Faculty of Physics and Geosciences, Leipzig, Germany
[3] University of Massachusetts Amherst, Polymer Science and Engineering, Amherst MA 01003, USA

anatoli.serghei@univ-lyon1.fr

The present contribution aims to review the applications of Broadband Dielectric Spectroscopy in polymer nanoscience. The broad frequency and temperature range of this technique allows one investigations on a variety of physical phenomena taking place on different time- and length-scales: density fluctuations[1] (and thus phase transitions), polymer dynamics (molecular fluctuations, glass transition, chain dynamics, capillary flow[2-3]), charge transport phenomena in the bulk and at interfaces[4]. Its high accuracy in measuring low signals enables one measurements on extremely small amounts of matter, down to the level of attograms (1 attogram=10^{-18} gram). The present contribution will exemplify the strengths of Broadband Dielectric Spectroscopy in measuring polymer systems having one, two or three dimensions on the nanometric length scales (ultra-thin layers, monolayers and sublayers, polymer nanorods, nanowires and nanotubes, single polymer chains). A special emphasis will be placed on polymer nanofluidics[2-3], in particular, on investigations of capillary flow of polymers into cylindrical nanopores (Fig. 1).

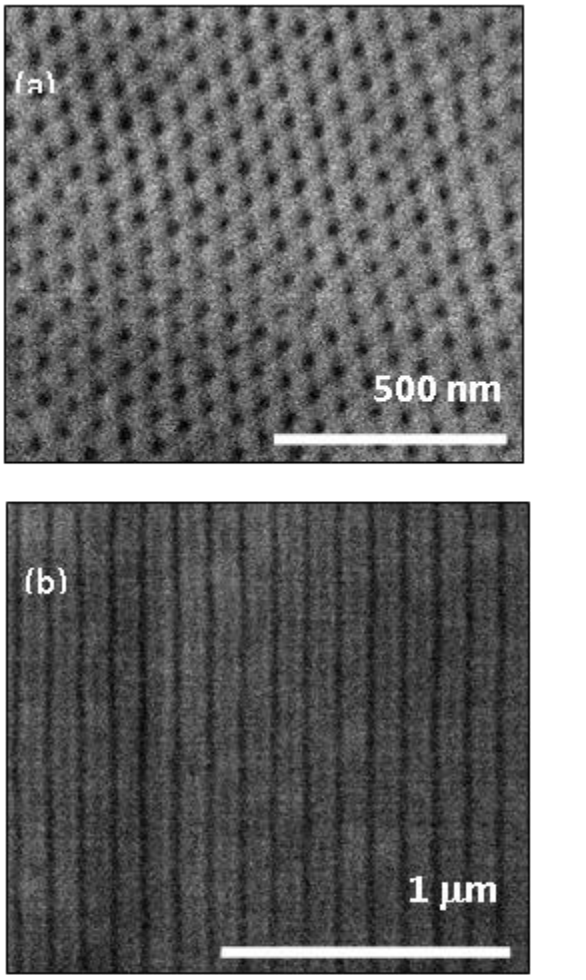

Fig. 1: SEM images of ordered nano-porous media: (a) top view (b) cross-section view; (c) measurement cell for experiments in the field of nanofluidics. Thin electrodes of gold are deposited onto both sides of the porous membrane and connected to the measurement device. The capillary flow of polymers into nanometric channels is continuously monitored in time by measuring the dielectric response of the sample cell[2-3].

References:

[1] A. Serghei, J. Lutkenhaus, D. Miranda, K. McEnnis, F. Kremer, and T.P. Russell, Small **6**, 1822 (2010).
[2] A. Serghei, D. Chen, D.H. Lee, and T.P. Russell, Soft Matter **6**, 1111 (2010).
[3] A. Serghei, W. Zhao, X. Wei, D. Chen, and T.P. Russell, Eur. Phys. J. Special Topics **189**, 95 (2010)
[4] A. Serghei, M. Tress, and F. Kremer, Phys. Rev. B **80**, 184301 (2009).

Charge transport mechanism and thermal properties of novel Polycyanurates/MWCNTs nanocomposites

Liubov Bardash[1,2], Gisèle Boiteux[1], Jacek Ulanski[3], Remigiusz Grykien[3], Ireneusz Glowacki[3], Alexander Fainleib[2], Philippe Cassagnau[1]*

[1]Université de Lyon, Université Lyon 1, Ingénierie des Matériaux Polymères, UMR CNRS 5223, 15 Boulevard A. Latarget, F-69622 Villeurbanne, France
[2]Institute of Macromolecular Chemistry of the National Academy of Sciences of Ukraine, 48, Kharkivske Chaussee, 02160 Kiev, Ukraine
[3]Department of Molecular Physics (K-32), Technical University of Lodz, 116, ul. Zeromskiego, 90-924 Lodz, Poland
philippe.cassagnau@univ-lyon1.fr

During the last decade a lot of attention in polymer science was focused on polymer nanocomposites formation that offers a combination of properties generally notavailable in polymers. Recently much interest h as been given to the use of carbon nanotubes (CNTs) in polymer composite materials to improve their mechanical and electrical properties. CNT-filled plastics are used already in several commercial applications. The electronic packaging industry, for example, uses CNTs-filled plastics to protect sensitive electronic parts such as integrated circuits and hard disc drives from antistatic shock during fabrication and handling. The automobile industry uses CNTs filled nanocomposites to prevent electrostatic discharge in fuel lines and pumps. CNTs-filled polymers are very promising material for antistatic shielding in airplane wings and fuselages. However, such materials require also the complex of properties such as resistance to low temperatures, semiconductivity behavior and good mechanical properties [1].

Polycyanurate Networks (PCN) originating from Cyanate Ester Resins are perspective high-performance materials for use in industrial applications especially for space and aircraft building. They are the most romising group of high-temperature thermosetting polymers [2,3].

In this work we have studied the PCN composites containing from 0.02 to 1.2 wt. % of multiwall-CNTs (MWCNTs) prepared using sonication technique followed by thermal curing. The structure of MWCNTs was investigated using Raman spectroscopy and Transmission Electron Microscopy. The glass transition temperatures (determined by differential scanning calorimetry) is higher than 265 °C for all the nanocomposites and do not change significantly with variation of the MWCNTs content. The dependence of the electrical conductivity on the MWCNTs content was analyzed using percolation theory [4] yielding the percolation threshold *pc* = 0.0038 (0.38 wt. %). The temperature dependence of conductivity was investigated in very broad temperature range. The results were discussed in terms of different models of electrical conductivity in heterogeneous materials [5] and it was found, that the Fluctuation Induced Tunneling model [6] is the most appropriate. The samples above *pc* show very weak temperature dependence of the conductivity what is related to high connectivity of the MWCNTs network.

Such nanocomposites can find potential applications as antistatic materials of automobile parts and in electronics; their good performance at low temperatures makes also possible using such materials in aircraft and space constructions.

Acknowledgements :
The authors would like to acknowledge French Government grant for grant for PhD students as well as to Région Rhône- Alpes (the grant of international mobility for PhD students EXPLO'RA DOC 2007) for the financial support.

References:
[1] Robertson, J. Materials Today, 7, 2004 pp. 46-52.
[2] Hamerton I., Ed. Glasgow: Chaman & Hall, 1994, 254 p.
[3] Fainleib A., Ed. Nova Science Publishers, Inc., New York, 2010, 370 p.
[4] Sahimi M., Taylor & Francis, London, 1994, 258 p.
[5] Ulanski J., Kryszewski M., Polish J. Chem., 69, 1995 pp. 1-23
[6] P.Sheng L., Phys. Rev. B, 21, 1980 pp. 2180-2195

Templating Functional Nanoporous Materials with Macromolecular Architectures of Controlled Degradability

Rim Majdoub, Daniel Grande

"Complex Polymer Systems" Laboratory, Institut de Chimie et des Matériaux Paris -Est, 2 rue Henri Dunant, 94320 Thiais, France

E-mail : grande@icmpe.cnrs.fr

It is a great challenge to produce nanoporous polymeric membranes with a simultaneous control of porosity and functionality (surface chemistry),[1,2] while maintaining mechanical properties and a chemical stability. There is a need to obtain such functional porous systems by simple and highly reproducible approaches, being cost-effective and compatible with the production of materials at an industrial scale.[3,4]

The main thrust of this communication is to address two original routes to (meso)porous frameworks with a simultaneous control over the porosity and functionality. The first approach relies on the synthesis of well -defined polystyrene-*block*-poly(D,L-lactide) (PS-*b*-PLA) diblock copolymers with a functional group (*e.g.* carboxylic or sulfonic acid groups) at the junction point between the two blocks. By the proper design of initiating systems and copolymer composition, as well as a good control over the polymerization processes, copolymers with a preferentially cylindrical morphology (PLA cylinders in a PS matrix) could be obtained.[5-7] By taking advantage of the well-known hydrolytic degradability of aliphatic polyesters, the PLA block was subsequently removed by basic hydrolysis, leaving behind a porous PS membrane with functional groups located along the walls of the channels. The second synthetic strategy entails the preparation of acidfunctionalized PS/PLA-based (semi-)Interpenetrating Polymer Networks (IPNs), where the styrenic subnetwork served as the future membrane material while the polyester partner could be selectively removed under mild conditions in a subsequent step.[8,9]

This communication will examine the scope and limitations of both complementary routes to meso- or macro-porous polymeric materials with defined porosity and functionality. It essentially focuses on the investigation of the correlations between the nanoscale solid-state organization of the precursors and the morphology of the resulting porous frameworks, as examined by different physico-chemical techniques, *e.g.* Differential Scanning Calorimetry (DSC), Scanning Electron Microscopy (SEM) and Small -Angle X-ray Scattering (2-D SAXS). The newly prepared (nano)porous materials were also analyzed by nitrogen sorption porosimetry. Obtained functional porous materials are of potential interest for heterogeneous supported catalysis, and selective transport applications.

Acknowledgements

Financial support by the French National Agency for Research through the "POLYNANOCAT-ANR-05-NANO-025" project is gratefully acknowledged. The authors are indebted to T Antoun for his assistance, as well as P. Davidson (Orsay, France) and R. Denoyel (Marseille, France) for their expertise in SAXS and nitrogen porosimetry, respectively.

References

[1] Hillmyer, M. A. *Adv. Polym. Sci.* **2005**, *190*, 137.
[2] Balaji, R.; Boileau, S.; Guérin, Ph.; Grande, D. *Polymer News* **2004**, *29*, 205.
[3] Rohman, G.; Grande, D.; Lauprêtre, F.; Boileau, S.; Guérin, Ph. *Macromolecules* **2005**, *38*, 7274.
[4] Rohman, G.; Lauprêtre, F.; Boileau, S.; Guérin, Ph.; Grande, D. *Polymer* **2007**, *48*, 7017.
[5] Gorzolnik, B.; Penelle, J.; Grande, D. *Polym. Mater. Sci. Eng.* **2007**, *97*, 223.
[6] Antoun, T.; Gorzolnik, B.; Davidson, P.; Beurroies, I.; Denoyel, R.; Grande, D. *Journal of Nanostructured Polymers and Nanocomposites* **2009**, *5*, 44-51.
[7] Grande, D.; Penelle, J.; Davidson, P.; Beurroies, I.; Denoyel, R. *Micropor. Mesopor. Mater.* **2011**, *140*, 34-39.
[8] Grande, D.; Mamache, S.; Lacoudre, N.; Denoyel, R. *Polym. Mater. Sci. Eng.* **2007**, *97*, 430.
[9] Grande, D.; Beurroies, I.; Denoyel, R. *Macromol. Symp.* **2010**, *291*, 168.

Preparation and Characterization of EVA Nanocomposites Obtained from Montmorillonite and Methylene-blue

M.I. Beltrán, A. Marcilla, V. Marchante, V. Benavente and I. Pelaez

Chemical Engineering Department, Alicante University, Spain

e-mail:maribel.beltran@ua.es

Introduction: Polymer/nanoclay nanocomposites are innovative materials that show interesting mechanical, chemical, and physical properties (1). Nanopigment are a new type of pigments that present some of the organic colorant properties and better light and environmental stability than conventional pigments and dyes (2). Moreover, they are prepared from nanoclays and they are expected to improve the mechanical properties of the materials that include them. To our knowledge, there are no commercial applications of nanopigments with polymers and they have only been used with polyethylene at a lab scale (3). Nanocomposites are usually prepared via melt mixing at high shear stress conditions in order to achieve the adequate dispersion of the nanoclay in the polymer matrix since exfoliation is essential to benefit from the excellent nanoscale properties that nanoclays confer (4).

In this work nanocomposites based on EVA containing different quantities of montmorillonite nanoclay and nanopigment (montmorillonite/methylene blue) were prepared by melt mixing. The caharacterization of the samples was performed by different techniques.

Materials and Methods: EVA (18%VA) from trithene was employed, the monmorillonite (MO) was the EXM 757 grade (gently supplied by Süd Chemie) with a cation exchange capacity (CEC) of 95mg/100g and the methylene blue (MB) (C.I. Basic Blue 9). Nanopigments (NP) were sinthesized at a lab scale with the method described elsewhere (3).

The formulations included EVA plus 0.1 to 5 phr (part per hundred of resin) of unmodified montmorillonite (0.1MO, 1MO and 5MO), 1phr of nanopigment synthesized with different quantities of MB, from 5 to 100% of the total CEC of the MO (NP5, NP20 and NP100) and 1 phr of unmodified montmorillonite plus the same quantity of MB introduced in the nanopigments (MO0.02MB, MO0.07MB and MO0.28MB). An EVA reference was also processed under the same conditions than the other samples. Ingredients were mixed in a Banbury GUIX-2P batch mixer at 90ºC and 8 min and in a Brabender Plasticorder PL2000 under the same temperature and time conditions. Obtained samples were compression molded at 130ºC and 100 bar for 10 min to obtain 1 mm thickness sheets.

The properties of the nanocomposites were analyzed trough differential scanning calorimetry (Pyris 6 DSC), thermogravimetric analysis (TGA Netzch TG 209), oscillatory rheometry (Bohlin CS-50), mechanical behavior (Instrom 4411) and transmission electron microscopy (TEM-Jeol JEM-2010). The micro- and nano-dispersions were analyzed through XRD (Seifert JSO-DEBYEFLEX 2002). To assess the colorimetric behavior of the samples, their spectral reflectances over black and white substrate have been measured (spectrophotometer Konica Minolta CM-2600d).

Results and Discussion: The rheological behavior and thermal properties of the samples prepared with and without the additives did not show important modifications due to the low concentrations employed. A remarkable increase in the Young's Moduli of the samples including the nanopigments have been obtained (up to 20% at 1phr), specialty in those cases where intercalation and/or partial exfoliation was attained, as shown in Figure 1 (those samples including NP and specially those processed at the higher shear rates). Respect to the color performance, much higher levels of transparency and coloring power was observed for the samples containing the nanopigments than for the corresponding references with the same proportion of the pigment.

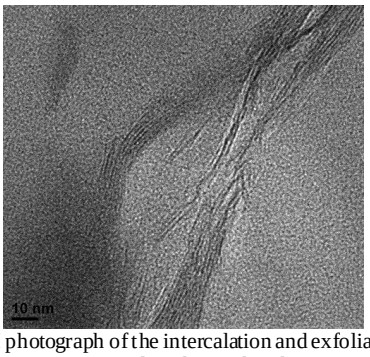

Figure 1. SEM photograph of the intercalation and exfoliation attained by NP20 processed in the Brabender mixer.

Conclusions: Intercalation and/or partial exfoliation were found to occur for the formulations based on the nanopigments and specially for those processed under the higher shear rates. No intercalation took place with samples obtained with the unmodified montmorillonite. The mechanical properties were clearly improved when intercaled and or exfoliated structures appeared, and a higher transparency and coloring power was observed for the samples containing the nanopigment than for the corresponding references.

The nanopigments appear as a promising alternative to conventional pigments and dyes in applications with polymers.

References:

1. J. Morawiec, A. Pawlac, M. Slouf, A. Galeski, E. Piorkowska, N. Krasnikowa, Eur. Polym. J., 41 (2005) 1115-1122.
2. H.R. Fischer, *Mater. Sci. Eng.*, 23 (2003) 763-772.
3. V. Marchante, F. M. Martínez-Verdú, A. Marcilla, M.I. Beltrán, Pigment & Resin Technology, Manuscript ID PRT-09-2010-0084.
4. W. Gianelli, G. Camino, N. T. Dintcheva, S. Lo Verso, F.P. La Mantia, Macromol. Mater. Eng., 289 (2004) 238-244.

Nanostructures in Polymer Surfaces Controlled by Mechanical Orientation

C. Fuentes, J. P. Fernández-Blázquez, A. del Campo

Max-Planck-Institut für Polymerforschung. Ackermannweg 10, 55128 Mainz, Germany

fuentes@mpip-mainz.mpg.de

We have recently shown that plasma-based roughening can be exploited as a low-cost method for producing useful nanopatterns.[1] Here we present the correlation between the mechanical pretreatment of the polymer film and the resulting plasma-etched surface topography in semycristalline polymers. PET, PE, PEO or PP samples with known thermal history are stretched under different experimental conditions (T, rate) have been prepared, analyzed and treated with oxygen plasma. The resulting topography was examined by SEM and AFM. Our results provide insight into the pattern formation mechanism and into the possibility of defining the pattern geometry and dimensions by the thermal and mechanical properties of the polymer sample.

References:

(1) E. Wohlfart, J.P. Fernández-Blázquez, E. Knoche, A. Bello, E. Pérez, E. Arzt, A. del Campo*, Macromolecules 43(23), 9908-9917 (2010)

Estimation of Cross-link Density into Networks in the Polymerization of Acryl-furanic Compounds by Mathematical Modelling

J.Lange

Centro de Biomateriales, Universidad de La Habana
jurgen@biomat.uh.cu

E. Lozano

Departamento de Química Macromolecular, Instituto de Ciencia y Tecnología de Polímeros (CSIC)
lozano@ictp.csic.es

Introduction and objectives

Free radical polymerization of acryl-furanic compounds (Figure 1), Furfuryl acrylate (FA) and methacrylate (FM) leads to cross-linked polymeric networks, which can be employed to make biomaterials [1]. Moreover, the copolymerization of these compounds with hydrophilic comonomers such as vinylpyrrolidone and 2-hydroxyethyl methacrylate produces cross-linked hydrogels, which have shown to be useful as coating agents in bioactive compounds controlled delivery system [2]. In the case of these intricate polymerizing systems in which insoluble gels are obtained, the values of the parameters characterizing network structure (e.g cross-link density) are not easily obtained experimentally. However, they can be readily be theoretically estimated, for instance, by means of mathematical models using kinetic schemes [3-5] In this way, the aim of this work is focused in the estimation of average cross-link density ($\bar{\rho}$) of the networks formed in the bulk thermopolymerization of FM through two mathematical models (Tobita's model [3] and cross-linked model [3-5]). In turn, by means of values of $\bar{\rho}$ given for both models, the influence of polymerization temperature on the network formation is studied.

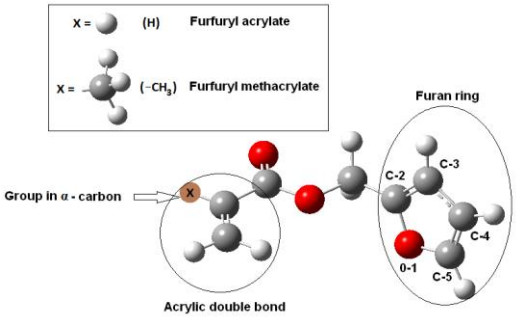

Figure 1: Molecular estructure of furfuryl acrylate (FA) and methacrylate (FM)

Simulation

For simulation of the experiments with cross-linked model, a numerical multi-step integration subroutine **ODE15S** [6] of non-linear ordinary differential equations system was used. The validity of values of kinetics constants involved in cross-linking process was corroborated by means of frontier orbital theory using Density Functional Theory [7]

Results and Discussion

In order to compute the values of $\bar{\rho}$ for both models, the values of kinetic constants involved in network cross-linking were obtained by means of Arrhenius's equations [5]. It was also possible to obtain the values of pseudo-kinetic rate constants by means of the Tobita's model. Also, the values of $\bar{\rho}$ in polymeric network at a given monomer conversion were calculated using the radical and pendant group concentrations into primary chains as estimated by cross-linked model (Fig. 2).

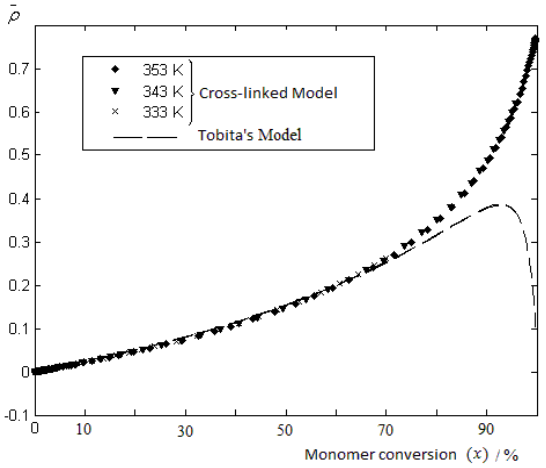

Figure 2: Evolution of average cross-link density of the network ($\bar{\rho}$) with monomer conversion at different temperatures.

As shown in Fig. 2, the results computed for both models are computationally equivalent until 70% of monomer conversion. This equivalence has also been proved for the photopolymerization of FM at low conversions and when low polymerization temperatures are employed [3]. The practical importance of this result is that, known the values of the pseudo-kinetics constants, is possible to simply predict the values of $\bar{\rho}$ by the Tobita's model, without solving complicated non-linear ordinary differential equations. On the other hand, polymerization temperature do not influence upon the values of average cross-link density in networks during all polymerization.

References
[1] Davidenko, N.; Zaldivar D. ; Peniche C.; Sastre R.; San Roman J. ; J. Polym. Sci., A: Polym. Chem. 1996, 34, 2759.
[2] Zaldivar, D.; Peniche, C.; San Roman J.; Biomaterials 1993,14, 14.
[3] Lange, J. Rieumnot, J.; Davidenko, N.; Sastre, R.; Polymer 2002, 43, 1003.
[4] Lange, J. Rieumnot, J.; Davidenko, N.; Sastre R.; Macromol. Chem. Theo. Simul. 2004, 13, 641.
[5] Lange, J.; Davidenko, N.; Sastre R.; Macromol. Chem. Theo. Simul. 2009, 18, 511.
[6] Matrix Laboratory (MATLAB v 6.5), MathWorks, Inc. 2002.
[7] Gaussian 03, Revision E.01, Inc., Wallingford CT, 2004.

Acknowledgments

Jurgen Lange gratefully acknowledges the financial support provided by MAEC-AECID.

Polymer shell nanocapsules for footwear applications

[1]M Sánchez, [1]F. Arán, [1]C. Orgilés, [2]A. Marcilla

[1]INESCOP. Footwear Research Institute. 253. 03600 Elda, Alicante, (SPAIN)
[2] Chemical Engineering Department, Alicante University, San Vicente del Raspeig, Alicante, (SPAIN).

msanchez@inescop.es

Introduction

Nanoencapsulation presents a new option for the shoe industry as its application can transform traditionally used materials or products into smart ones capable of interacting with feet. For instance, they can improve quality of life by incorporating products for foot care such as properly dosed essential oils or other products. The nanoencapsulation of active substances to be incorporated in different footwear components in order to obtain an "active shoe" presents an opening up of a new way of innovation.
The *in situ* polymerization allows the formation of micro and nanocapsules containing a water-immiscible dispersed phase, with improved mechanical properties and thermal stability. The properties of the membrane depend not only on its chemical structure but also on all the synthesis conditions. In the case of melamine-formaldehyde nanocapsules, the polycondensation of the amino resin occurs in the continuous phase, and the phase separation is linked to the pH and the melamine-formaldehyde resin molar ratio.
In this study a series of melamine-formaldehyde (MF) nanocapsules containing essential oils with different polymer to oil ratio was prepared to be applied to footwear materials (lining, insoles, etc…) by an *in situ* polymerization (O/W) method. Their physicochemical properties have been characterized by different experimental techniques.

Materials and Methods

Synthesis of melamine-formaldehyde nanocapsules containing essential oil. First of all, a melamine-formaldehyde (MF) resin to be used as nanocapsules shell was prepared from the monomers, melamine and formaldehyde. After that, an O/W emulsion was prepared. The oil phase was composed of the active substance, and the aqueous phase was constituted of distilled water and sodium dodecyl sulfate (SDS) as surfactant. Next the above prepared prepolymer is added and the pH adjusted, which causes the coagulation of the polymer around the oil droplets. Subsequently, hardening of the polymeric membrane was attained by raising the temperature. Finally, it was allowed to cool down to room temperature and the pH was adjusted to basic.

Characterization of nanocapsules. Physicochemical properties of the synthesized nanocapsules containing the oil have been characterized by different experimental techniques. The average size distribution of the nanocapsules was determined using a particle size meter Coulter LS 230. The thermal decomposition behavior was studied by thermogravimetic analysis (TGA). Finally, the nanocapsules morphology was analyzed by scanning electron microscopy (SEM).

Results

Nanocapsules containing an essential oil showed a narrow particle size distribution in number with a medium particle size around 100 nm. The higher resin ratio the higher the nanocapsule size.
The thermogravimetric analysis (TGA), showed the thermal decomposition behavior of the microcapsules. Three main decomposition zones can be observed. The first one (around 150ºC) corresponding to the oil volatilization or decomposition. The second and third ones correspond to the resin decomposition. The first resin decomposition process is around 240ºC and the second between 300-450ºC. As the resin/oil ratio increases in the nanocapsule the oil decomposition temperature moves towards higher temperatures, possibly due to the wall shell growth, according to the previous particle size measurements. The area of the resin decomposition peaks changes as the resin/oil ratio increases may be due to the oil interaction with the resin.
Finally, the morphology of the nanocapsules containing essential oil was studied by Scanning Electronic Microscopy (SEM). There are several interesting changes in the nanocapsules morphology as the resin/oil ratio increases. The nanocapsules formation is observed only for resin/oil ratio over four, thus ensuring the encapsulation of the oil.

Conclusions

Regarding the nanocapsules synthesis containing oils, the relationship between the resin mass that forms the shell and the active substance contained in the core largely determines the efficiency of the nanoencapsulation process and the morphology of the nanocapsules and the particle size distribution thereof. Themogravimetry provides valuable information regarding the structure of the nanocapsules.

References

1. Wang H.P. et al. Advanced Materials Research 47-50 286 (2008).
2. Luo W et al Polym. Degrad. Stabil. **92**(7): 1359 (2007).
3. Fabien Salaün et al.. European Polymer Journal **44** 849 (2008).
4. Li Wei et al. Materials Chemistry and Physics **106** 437 (2007).

Aknowledgments: The Research was partially funded by MICINN (project CTQ2010/16551).

Stable dispersions of chemically functionalized carbon nanofibers in waterborne polyurethanes

Elena Orgilés-Calpena, Francisca Arán-Aís, Ana M. Torró-Palau, César Orgilés-Barceló

INESCOP. Innovation and Technology Centre.
Industrial Zone Campo Alto. 03600 Elda, Alicante (Spain).

eorgiles@inescop.es

Introduction

Carbon nanofibers (CNFs) are considered as ideal reinforcing fibers for polymer matrices in many technological applications due to their unique structure and properties: high aspect ratio, high Young's modulus, excellent mechanical strength and good thermal conductivity. They are excellent nanofillers in polyurethane matrices originating a new polymeric material, exhibiting the same chemical properties as organic polymers, whereas the rheological and thermal properties may be greatly improved. However, the incorporation of carbon nanofibers to waterborne polyurethanes implies a great difficulty because of their tendency to form aggregates, which sometimes prevents an efficient dispersion [1]. In this sense, it is necessary to insert functional groups on the surface of the nanofibers, either to induce a repulsive force between the particles or to improve their interaction with the polymer in aqueous phase, thus obtaining a stable dispersion and the subsequently sedimentation [2,3]. Therefore, to improve the dispersion of nanofibers in the waterborne polymer, they must undergo a pre-oxidation, thus increasing the number of surface functional groups with oxygen, such as C=O, COOH, OH, NH_2, etc.

Materials and Methods

From the primal polyurethane dispersion (WBPU), four adhesives were prepared with a different amount of carbon nanofibers (0.10, 0.25, 0.50 and 1 wt%). Previously, a chemical treatment based on acids was carried out and the nanofibers oxidation was produced in order to improve the compatibility between the polymer matrix and the nanofiller. Finally, stable mixtures of carbon naofibers in the polyurethane dispersion were achieved.

Results and Discussion

Although the addition of the carbon nanofibers does not affect the segmented WBPU structure monitored by DSC, the kinetics of crystallization of the soft segments is decelerated [4], indicating the formation of a reinforced structure, being more noticeable as the content of the carbon nanofiber increases. Regarding the rheological properties, the addition of the carbon nanofibers produces a noticeable increase in both elastic and viscous moduli of the WBPU, indicating again the existence of nanofiber-polyurethane interactions.

This increase is more pronounced as the content of the nanofiber increases [5], due to the existence of a great number of CNFs-polyurethane interactions.

Furthermore, DMA results confirm the existence of polyurethane–CNFs interactions and a more enhanced structure, in agreement with DSC and plate–plate rheometry results.

Conclusions

The obtained results indicate that chemical functionalization method enables the dispersion of the carbon nanofibers in the polyurethane matrix, contributing to the stability of the adhesive. The addition of the carbon nanofibers to the polyurethane dispersions influences in its rheological and viscoelastic properties, producing an increase in the moduli (storage and elastic), which indicates the existence of a more enhanced structure after the addition of these nanofibers. Additionally, an increase of crystallization time is observed, indicating also the formation of a more reinforced structure that difficult the interactions between polyurethane chains during the crystallization process.

References

[1] J. Ryszkowska, M. Jurczyk-Kowalska, T. Szymborski, K. J. Kurzydlowski. Physica E , 39, 124 (2007).
[2] T. G Kim, D. Ragupathy, A. I. Gopalan, K. P. Lee. Nanotechnology, 21,1 (2010).
[3] S. Bose, R. A. Khareb, P. Moldenaersa. Polymer 51, 5,975 (2010).
[4] C.X. Zhao, W.D. Zhang, D.C. Sun. Polymer Composites (2008). DOI 10.1002/pc.
[5] M. Chapartegui, N. Markaide, S. Florez, C. Elizetxea, M. Fernandez, A. Santamaría. Composites Science and Technology 70, 5, 879 (2010).

This research was supported by the Institute for Small and Medium Industry of the Generalitat Valenciana (IMPIVA) through its R&D Program for Technologic Institutes 2011. Thanks to GRUPO ANTOLÍN (Burgos, Spain) for providing carbon nanofibers (GANF) and to INSOCO S.L. (Alicante, Spain) for the polyurethane dispersion.

Conformation and aggregation behavior of polymer-coated gold nanoparticles studied by dynamic light scattering experiments and Monte Carlo computer simulation

Ramón Pamies, José Ginés Hernández Cifre, and José García de la Torre

Departamento de Química Física, Facultad de Química, Universidad de Murcia, Spain

jgt@um.es

Introduction:

Gold nanoparticles (AuNPs) are known to be biocompatible and non-toxic materials and the modification of their surface has opened a wide range of uses in biomedicine such as cancer therapy or drug delivery. In biological or high-ionic-strength media, the stabilization of the colloidal nanoparticles is required since the screening of the electrostatic repulsion may result in aggregation. Physisorption of macromolecules is one of the strategies used to coat the surface of the AuNPs and thus flocculation is avoided. It has been proved that, generally, oppositely charged polyelectrolytes have a stronger tendency to form a core-shell complex with AuNPs than neutral polymers. In this work, we have performed Dynamic Light Scattering (DLS) experiments and Monte Carlo (MC) computer simulations to evaluate the behavior of hybrid nanoparticles with a gold core and a polymeric corona made with a positively charged polusaccharide, hydroxyethylcellulose (HEC).

Materials and Methods:

The charged HEC samples with 7 mol % (HEC(+)7) and 60 mol % (HEC(+)60) charges were prepared directly from HEC as it is described in [1]. The preparation of the hybrid nanoparticles is done just by mixing HEC(+) solutions with AuNPs solution.

The DLS experiments were conducted with the aid of an ALV/CGS-8F multidetector compact goniometer system, with eight off-fiber optical detection units, from ALV-GmbH, Langen, Germany. The beam from a Uniphase cylindrical 22 mW He−Ne laser, operating at a wavelength of 632.8 nm with vertically polarized light.

MC simulations were performed with the program MONTEHYDRO [2], which is freely available at http://leonardo.inf.um.es/macromol/ and implements the rigid-body treatment to calculate hydrodynamic properties. With this approach, the polymeric chains are treated as having instantaneous rigid conformations to calculate their overall hydrodynamic properties. Thus, a set of conformations of the model chain is generated randomly following certain statistical rules (i.e., a MC procedure), and then the conformational properties of each conformation are evaluated using the procedures applicable to rigid particles and the final results are taken just as sample averages. Therefore, a simple and convenient way to build the polymeric chain is the usage of beads as elements. Springs with a suitable potential energy have been employed to connect these beads, , in the so-called bead-and-spring model.

Results and Discussion:

Two different driving forces for adsorption have been evaluated: the electrostatic interaction between the positive charges on the polymers and the negatively charged gold surfaces and the affinity of the polymers for gold due to hydrophobic interactions. The comparison between the data obtained from curved and planar surfaces suggests a strong correlation between surface curvature and adlayer conformation in the formation of the hybrid polymer−gold nanoparticles. The influence of particle size on the amount of adsorbed polymer has been evaluated for the different polymers. The impact of the ionic strength on polymer adsorption has been explored, and the adsorbed polymer layer has been found to protect the gold nanoparticles from aggregation when salt is added to the solution. The addition of salt to a mixture of gold particles and a charged polymer can induce a thicker adsorbed layer at low salinity, and desorption was found at high levels of salt addition.

Regarding the simulations, in a previous work we used the bead-and-spring model to simulate the behavior of star polymers in equilibrium and under different kinds of flow. Based on this, we have designed the core-shell structures as star-shaped chains containing a big core and several arms consisting on linear chains which elements have a much smaller size than the central bead. Thus, two different kinds of elements can be found in the model: a big sphere which represents the hard core and several small beads forming the arms which simulate the polymeric shell. Therefore, these linear chains mimic the behavior of the polymers coating the metallic nanoparticle.

Conclusions.

Positively charged hydroxyethylcellulose derivatives have been found to be useful for the formation of hybrid polymeric−inorganic nanoparticles when solutions of these polymers are mixed with citrate-coated gold nanoparticles. The thickness of the adsorbed layer for these systems depends on the nature and concentration of the polymer and on the ionic strength of the solution. MC simulations of a bead-and-spring star shaped structure were found to mimic the behavior of core-shell nanoparticles in solution.

References.

[1] R.Pamies, S. Volden, A.-L. Kjoniksen, K. Zhu, W. R. Glomm, B. Nystrom, *Langmuir*, 26, 15925-15932, 2010.

[2] J. García de la Torre, A. Ortega, H. Pérez Sánchez, J.G. Hernández Cifre. *Biophys. Chem.* 2005, 116, 121– 128

Chain Dimensions, Entanglement Features and Linear Rheology of Short Chain Branched Polyethylene Models: Simulations and Experiments

J.F. Vega, J. Ramos, J. Martínez-Salazar

Departamento de Física Macromolecular, Instituto de Estructura de la Materia, CSIC, Serrano 113 bis, 28006 Madrid, Spain

e-mail: jfvega@iem.cfmac.csic.es

A combined study including computer simulations, dilute solution experiments, and rheological properties is presented for molecular models of ethylene/1-hexene copolymers with different short chain branching content obtained from single-site catalyst polymerization.

For the computer simulations, a series of linear and branched C_{1000} polymer chains were equilibrated using advanced Monte Carlo moves,[1] and Molecular Dynamics trajectories were then calculated.[2] From these simulations the melt entanglement nanoscale features as the molecular weight between entanglements, M_e, and the entanglement equilibration relaxation time, τ_e, were directly obtained. The values of M_e and τ_e obtained from the simulations, together with the molecular weight distribution obtained from dilute solution experiments have been used within the reptation framework to explain the experimental melt linear viscoelastic properties (storage and loss moduli) of a set of model ethylene/1-hexene copolymers.[3,4]

The results can be summarized as follows: **(i)** the chain dimensions obtained from both the simulations and the experiments account for a molecular size contraction and a dilated tube (or increased M_e values) as the amount of short chain branches increases;[5] **(ii)** a slowing down in chain dynamics is obtained as the amount of short chain branches increases, characterized by increased τ_e values and a decrease of the Rouse segmental rate;[6] and **(iii)** the curves derived of the dynamic shear modulus using the simulated values of M_e and τ_e and the reptation theory nicely coincide with the experimental ones (see Figure 1 for the linear case).

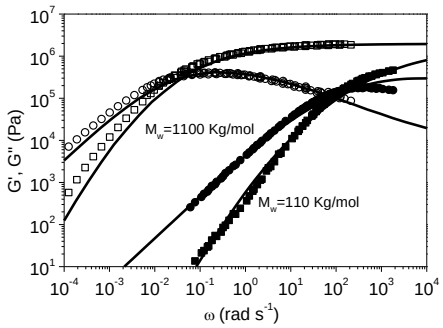

Figure 1. Comparison of calculated (lines) and experimental (symbols) dynamic moduli for two linear polyethylene samples of different molecular weight at 160 ºC. The simulated values of M_e and τ_e, together with the molecular weight distribution have been used to compute the dynamic moduli.

References

[1]Ramos, J.; Peristeras, L.D.; Theodorou, D.N. Macromolecules 2007, 40, 9640.
[2]Ramos, J.; Vega, J.F.; Theodorou, D.N.; Martínez-Salazar, J. Macromolecules 2008, 41, 2959.
[3]Doi, M. and S.F. Edwards, The Theory of Polymer Dynamics (Clarendon, Oxford, 1986)
[4]de Gennes, P.G., Scaling Concept in Polymer Physics (Cornell University Press, Ithaca, New York, 1979)
[5]Vega J.F., Martín S., Expósito M.T., Martínez-Salazar J., J. Appl. Polym. Sci. 2008, 109, 1564.
[6]Chen, X.; Stadler, F.J.; Münstedt, H.; Larson, R.G. J. Rheol. 2010, 54, 393.

Particles Composed of Oppositely Charged Polyelectrolytes: Effect of Polymer Molecular Weight.

Filipe Lima[1], Carmen Moran[2,3], Filipe E. Antunes[2,], Hernan Chaimovich[1], Maria G. Miguel[2], Björn Lindman[2,3]*

[1]Institute of Chemistry, University of São Paulo, São Paulo, Brazil
[2]Department of Chemistry, University of Coimbra, 3004-535 Coimbra, Portugal
[3] Departament de Fisiologia, Facultat de Farmàcia, Universitat de Barcelona, E-08028, Barcelona, Spain

*filipe.antunes@ci.uc.pt

Motivation

Gel particles are promising delivery vectors that are formed by local phase separation of oppositely charged species. They can be used to carry drugs and other molecules of biological interest. Viral infection and synthetic vectors are today the most used tools for gene delivery.

The species used for gel particle formation are usually a polyelectrolyte droplet that is complexed by an oppositely charged surfactant. The success of the preparation of such particles by a mixture of a polyelectrolyte and a surfactant is attributed to the fast complexation rate of the droplet compared to the dissolution rate of the polymer droplet.

The motivation of this study is to build stable gel particles by using two (or more) oppositely charged polyelectrolytes. JR400, a cationic cellulose based polymer, is here combined with polyacrylates of different molecular weights.

Materials

Polyelectrolytes used are polyacrylic acid 450KDa (PAA 450), polyacrylic acid 2KDa (PAA 2) and JR400, a cellulose derivative polycation with 500KDa. A nonionic polymer, Polyethylene oxide, with 1000KDa was also tested.

Methods

Particles were prepared by dropwise addition method, where drops composed of 2-7wt% of aqueous solution of JR400 were added to 2mL of oppositely charged polymer solutions.

The particles were kept in the polyelectrolyte solution until they reached maximum swelling. This takes 30 minutes for PAA 2 solutions, 4 hours for PAA 450 and 1 hour for PAA 2/PAA 450 mixed solution.

Rheological measurements were carried out in a Stress Tech Rheometer with automatic gap in a bob and cup measurement system.

Achievements

Polyelectrolyte-based particles can be formed at sufficiently high polymer concentrations. Temperature plays an important effect on particle formation but the major contribution comes from the balance between droplet dissolution rate and complexation rate. In agreement to this, the particles are more stable by using two polyelectrolytes with different molecular weights as complexing agents.

References

1. Burey, P.; Bhandari, B. R.; Howes, T.; Gidley, M. J. Critical Reviews in Food Science and Nutrition 2008, 48, 361–377.

2. Morán, M. C.; Miguel, M. G.; Lindman, B. Langmuir 2007, 23, 6478–6481.

3. Babak, V. G.; Merkovich, E. A.; Galbraikh, L. S.; Shtykova, E. V.; Rinaudo, M. MendeleeV Commun. 2000, 3, 94–95.

4. Morán, M. C.; Miguel, M. G.; Lindman, B. Biomacromolecules 2007, 8, 3886–3892.

5. Lapitsky, Y.; Kaler, E. W. Colloids Surf. A 2004, 250, 179-187.

6. Lapitsky, Y.; Kaler, E. W.; Eskuchen, W. J. Langmuir, 2006, 22, 6375-6379.

Transparent Flexible Electrodes using Carbon Nanotubes

Jordi Figueras, Jordi Pérez-Puigdemont, Oriol López, Angel Fabregas, Aida Abiad-Monge, Nuria Ferrer-Anglada

Applied Physics Department, Universitat Politècnica de Catalunya, Barcelona, Spain

nuria@fa.upc.edu

Abstract: Thin films of conductive, transparent and flexible structured single walled carbon nanotubes (SWCNTs) network can be used for electronic devices, sensors and solar cells [1]. We prepared a thin SWCNT network on transparent and flexible substrate (PC) with different SWCNT densities using a simple spray method [2]. We measured the electric impedance at different frequencies Z(f) by two different techniques: 1) two probes contact method, in the frequency range from 40 Hz to 110 MHz, and 2) a Corbino (coaxial) geometry, in the range from 10MHz to 20GHz [3]. We measured the optical absorption and electrical conductivity in order to optimize the conditions for obtaining optimum performance, films with both high electrical conductivity and transparency. **Figure 1** shows the transparency (%Transmittance at 550nm) versus the resistance per square, R□. We observe a square resistance from 8,5 to 2 kOhm for samples showing 85% to 65% optical transmittance respectively.

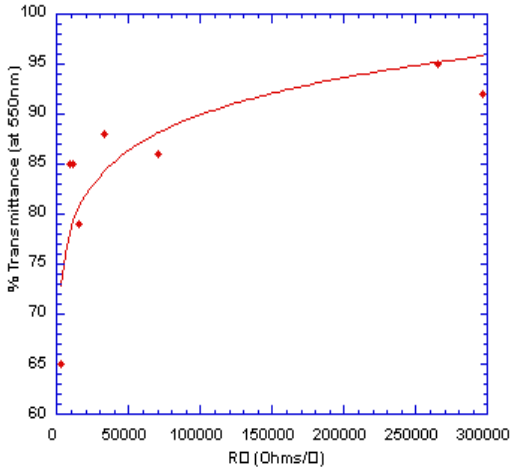

Figure 1. Optical transmittance (at 550 nm) versus sheet resistance R□ of SWCNTs network with different carbon nanotubes densities

Moreover for some applications we need flexibility and not transparency. By the same method we obtained random network films of single-wall carbon nanotubes (SWCNTs) on a flexible silicone substrate by spraying an aqueous SDS carbon nantotubes suspension. At high SWCNT density, the samples are quite conductive and flexible, the square resistance is as low as 200Ω, and it can be bended and stretched. We stretched uniaxialy the samples at different elongations up to 20 percent the original length and we measure the electrical conductivity. The **electrical resistance** increases slightly with the stretching, recovering the initial value for small elongations, up to 10%. We realised **Raman spectroscopy** on the same stretched and non stretched samples, **Figures 2, 3**. We could observe a shift on the

RBM mode, the G line is practically not changed, indicative that we are not introducing defects when stretching [4], the tubes are elongated and maybe deformed on the silicone substrate but not damaged or broken. Polarized Raman spectroscopy could be indicative of a partial alignment of single-wall carbon nanotubes on the elongated samples.

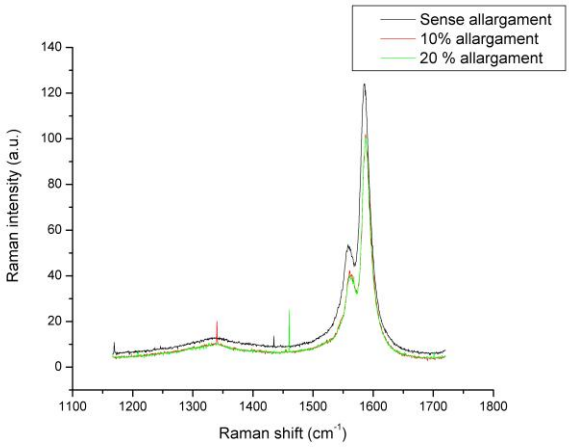

Figure 2. The Raman G line spectra from unstretched and stretched samples is nearly not changed. Laser excitation is 514,5nm, non polarized.

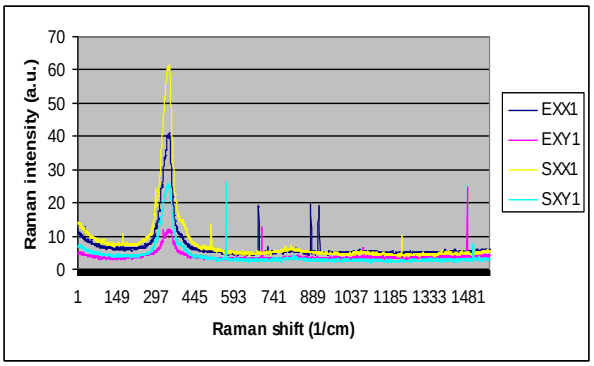

Figure 3. Polarized Raman RBM (radial breathing mode) spectra on the unstretched SXX1, SXY1 and stretched EXX1, EXY1 samples.

References:

[1] S. Bae, S. Iijima, et al., Nature Nanotechnology 5(2010) pp 574–578.
[2] N. Ferrer-Anglada, J. Pérez-Puigdemont, S. Roth, et al., Phys. Stat. Sol. (b) 245 (2008) pp.2276-2279.
[3] H. Xu, G.Gruner, et al., Appl. Phys. Lett. 90 (2007) pp. 183119(1-3).
[4] S. Reich, C. Thomsen, J. Maultzsch, "Carbon Nanotubes", Wiley-VCH.

Mesoporous CuO as New Catalyst for Advanced Energetic Composites of Polyurethane Matrix

José Luis de la Fuente

Instituto Nacional de Técnica Aeroespacial "Esteban Terradas", INTA.
Ctra. de Ajalvir, Km 4. 28850 Torrejón de Ardoz. Madrid. Spain.

e-mail: fuentegj@inta.es

In the past few years the development of organicinorganic hybrids and nanocomposites has attracted much interest because of the superior engineering properties compared to neat polymers [1]. The polymer composite materials have been regarded as a new generation of high performance materials, combining the advantages of inorganic moiety and those of the organic polymer matrix. As a clear example, transition metal oxides (TMOs) based materials are of great interest in many areas of modern science and technology, and in particular in (photo)catalysis, sensors, optics, separation, and smart coatings [2]. In addition, nanoporous materials are now widely applied in many technological fields due to their defined pore structure and size distribution. In most of applications, the pore structure, especially the pore size, size distribution and pore volume have become the crucial factors determining the applicability of these materials. Recently there has been an intense interest in preparing mesoporous TMOs. Several mesoporous TMOs have been prepared with large specific surface area due to their possible uses in the areas mentioned previously, being mesoporous copper oxides of particular interest. Thus for example, CuO has been studied as a unique and attractive monoxide material, due to its both fundamental investigations and practical applications. CuO is a well-known component of catalysts, and is widely employed commercially for the direct decomposition of N2O to N2, CO oxidation, and the complete combustion of hydrocarbons. However, an
application much less known is as combustion catalyst in highly energetic materials of polymeric matrix, such as composite solid propellants.

Composite propellants are highly particle-filled elastomers, which are made by embedding a finely divided solid oxidizing agent, generally ammonium perchlorate (AP) in a plastic, resinous, or elastomeric matrix. The matrix material usually provides the fuel for the combustion reaction, although solid reducing agents are frequently included in the compositions, such as aluminium. Composite solid propellants based on hydroxyl-terminated polybutadiene (HTPB) have become the workhorse propellants in the present-day aerospace solid propulsion technology world-wide. The polyurethane network obtained by curing HTPB with a suitable diisocyanate provides a matrix for inorganic oxidizer and metallic fuel which are dispersed in the propellant grain. Others ingredients are plasticizers, bonding agents, stabilizers and catalysts. The main objective of this study is to broaden the knowledge of the use of mesoporous fillers as combustion catalysts. Thus, the effect of mesoporous copper (II) oxide particles on the burning rate and on the thermal and combustion properties of composite solid propellants based on HTPB has been deeply studied. To do that, mesoporous CuO particles were incorporated in AP/Aluminium/HTPB-based composite propellants by using the slurry cast technique.

Mesoporous CuO particles with high surface area are expected to possess better catalytic activity than those of micro- and nano-meter sized with low surface area. This is due to the catalytic reactions taking place on the surface of catalysts, so the reaction rates are greatly related to the surface area of the catalyst. Therefore, it is worthwhile to use mesoporous CuO with a relatively large surface area in this application. The total surface areas of the different CuO samples selected in the present study were evaluated using the Brunauer-Emmett-Teller (BET) method, and the found values are collected in **Table 1**. The calculated BET surface area for the mesoporous CuO, denominated as CuO-3, was 32 m2/g, being logically much higher than the others CuO samples; fifteen and five times over the BET surface areas of CuO-1 (micrometric particles) and CuO-2 (nanometric particles), respectively. Besides, the adsorption pore-diameter distribution plot exhibited a broad maximum around 3 nm for the CuO-3 sample. The morphology and particle size of the raw powders were also determined by scanning and transmission electron microscopy and laser diffraction, respectively; and the crystallographic properties were analyzed by Xray diffraction. The thermal and combustion characteristics of these highly energetic composite materials with differently CuO powders, in terms of steady burning rates, showed how better is the performance of mesoporous CuO compared to non-porous and traditional CuO propellants. The thermal characterization of these advanced composites was also carried out, by differential scanning calorimetry and thermogravimetry analysis, demonstrating that the incorporation of mesoporous CuO particles in the formulations improves their combustion behaviours, shifting the temperature decomposition peak toward lower temperature, and decreasing the activation energy.

Table 1. Physical characteristics of the CuO used in the preparation of energetic composites based on HTPB.

CuO sample	Particle size (nm)	BET (m^2/g)
CuO-1	11250	2.1
CuO-2	42	5.9
CuO-3	44300	32

REFERENCES

[1] P.M. Ajayan, L.S. Schadler, P.V. Braun, Nanocomposite Science and Technology. 1st Ed., Wiley-VCH, Weinheim, 2003.

[2] J.L.G. Fierro, Metal Oxides: Chemistry and Applications, Chemical Industries Series Vol. 108. CRC Press & Francis Group; Boca Raton, FL, 2006.

Evaluation of the Phase Inversion in HIPS/Silver Nanoparticles Nanocomposites through UV-Vis spectrophotometry

Graciela Morales and Florentino Soriano

Centro de Investigación en Química Aplicada

gmorales@ciqa.mx

Introduction

UV-Vis spectrophotometry and transmission electron microscopy (TEM) are the most important techniques to characterize metallic nanoparticles as they present free conduction electrons which in the presence of an electromagnetic field (i.e. UV-Vis) oscillate collectively at a specific wavelength[1]. This optical phenomenon, known as surface resonance Plasmon (SRP), depends on the size, concentration, geometry[2], distance between nanoparticles and the refraction index (*n*) of the surrounded media where some changes in the substrate color can take place[3].

On the other hand, during the polymerization of styrene in the presence of a rubber to obtain high impact polystyrene, (HIPS) several events take place: i) initially the reaction medium consists of a homogeneous solution of rubber dissolved in styrene (St), ii) phase separation and as the PS increases, iii) a co-continuous phase is formed followed by iv) the phase inversion (PI) phenomenon where the morphology of the rubber phase is established[4]. The generation of PS and graft copolymer (PS-*g*-PB) provokes these changes and modifies the *n* values that reaches a maximum in the co-continue stage due to the periodical arrangement in the system's morphology.

This work deals with the evaluation of the PI phenomenon in HIPS/silver nanoparticles (AgNP´s) nanocomposites through the evolution of SRP as a function of conversion by UV-Vis spectrophotometry and TEM.

Materials and Methods

For the synthesis of HIPS/AgNP´s nanocomposites: St monomer, benzoyl peroxide (Aldrich Co.), Styrene-Butadiene block copolymer (Dynasol Elastómeros), and spherical silver nanoparticles (4-30 nm) (Servicios Industriales Peñoles) were added in a steel reactor with anchor-turbine stirrer at 40 rpm and 90 °C. Conversion was evaluated gravimetrically. The SRP was carried out using a Shimadzu UV-2401 (λ=200-700nm) spectrophotometer. PI phenomenon was corroborated by TITAN transmission electron microscope.

Results and Discussion

Phase inversion can be estimated from the values of SRP wavelength (λ) as a function of X (Fig. 1) where a sudden decrease in the λ, after reaching a maximum value, indicates that phase inversion (PI) occurs. This behavior can be interpreted as follows: the first stage of the curve relates to a reaction mixture presenting a rubber rich continuous phase with an slightly increase in the amount of graft copolymer, b) λ reaches a maximum and then decreases; during this period a co-continuous phase is present and the increase of the λ can be attributed to the increase in the *n*. At the end of this period the phase inversion occurs and the λ values decrease due to a decrease in the *n* values. The increase in λ at X>0.33can be attributed to the increase of PS volume and to new grafting reactions that take place at the occlusions into the rubber particles. Then, the reaction mixture presents a rich PS continuous phase and *n* and λvalues increase. The changes in color during the different reaction steps, as a function of X are shown in Fig.1, where color shifts from strong blue to strong red.

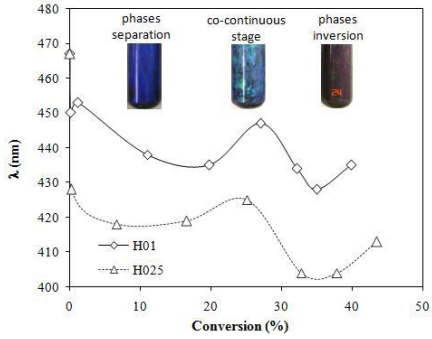

Figure 1. Evolution of λ as a function of X for HIPS with 0.1 (H01) and 0.025 (H025) wt-% of AgNP´s.

TEM micrographs corresponding to X=0.1, 0.28 and 0.32 are shown in Fig. 2 where the PI interval was corroborated. At X=0.1(rubber rich region) micelles and extended structures were observed (phase separation), followed by co-continuous stage (X=0.28) in the form of lamellas characteristic of the rubber copolymer used [6]. At X=0.32 the PI phenomenon was reached.

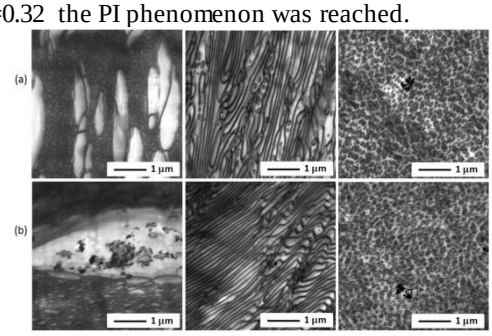

Figure 2. TEM micrographs for a) H025 and b)H01, both at X=0.1, 0.28 and 0.32.

Conclusions

The evaluation of PI through of UV-Vis spectrophotometry was successful as it is closed to that evaluated by TEM.

References

[1] Liz-Marzan L. M, *Materials Today*, 27-31 (2004)
[2] Mock J. J., Barbic M., Smith D. R., Schultz D. A., Schultz S., *J. of Chem.Phys.* **116**, 6755-6759 (2002)
[3] Underwood S.,Mulvaney P., *Langmuir*, **10**, 3427-3430 (1994)
[4] G. E. Molau, H. Keskkula, *J. Polym. Sci., Part A: Polym. Chem.*, 4, 1595(1966).
[6] Sardelis K., Michels H. J., Allen G., F. R. S. *Polymer*, **28**, 244-250 (1987)

Acknowledgments

The authors would like to thank Pablo Acuña and Adán Herrera for their technical support.

Biopolymers / Clays Nano-Biocomposites: Impact of Clay Organo-Modification on the Morphology and Properties of these Hybrid Materials

E. Pollet, L. Avérous

Université de Strasbourg, France

eric.pollet@unistra.fr

Introduction: Nano-biocomposites are a combination of biodegradable polymer matrices and nanosized fillers, such as nanoclays. Interestingly, relatively small amounts (less than 5 wt%) of these nanoclays are required to obtain the best properties. To achieve such improvement, the filler has to be homogeneously dispersed into the matrix and for that nanoclays are often organo-modified. Thus, numerous parameters such as the type of clay, clay modifier, plasticizer, process… may influence the morphology and thus the materials final properties [1-2].

This study focus on the "formulation-processing-morphology-properties" relationships of nano-biocomposites based on plasticized starch and polyhydroxyalkanoates (PHB & PHBV) matrices filled with different nanoclays (montmorillonite, sepiolite).

Results and discussion:

First, the impact of the clay/matrix affinity is highlighted through the difference in clay dispersion quality achieved in plasticized starch with different nanoclays. Indeed, our results show the great benefits of montmorillonite organo-modification performed with cationic starch, resulting in nano-biocomposites with exfoliated morphology and thus greatly improved properties[3].

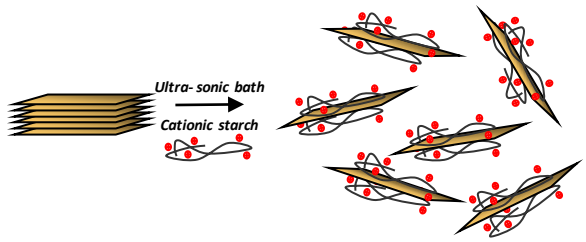

Besides, the morphologies obtained with montmorillonite and sepiolite clays evidence a possible negative impact of glycerol as starch plasticizer that may induce phase separation phenomena, heterogeneous clay dispersion [4-5] and thus poor barrier properties [6].

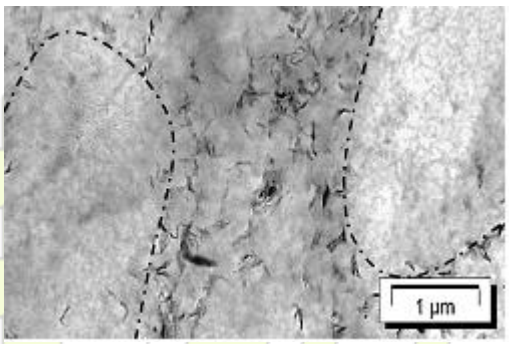

In addition, the influence of clay organo-modification on polyhydroxyalkanoates based nano-biocomposites is detailed in terms of thermal stability of the obtained materials. The results highlight the dramatic influence of some ammonium salts, used as clay organo-modifiers, on the PHB and PHBV thermal stability.

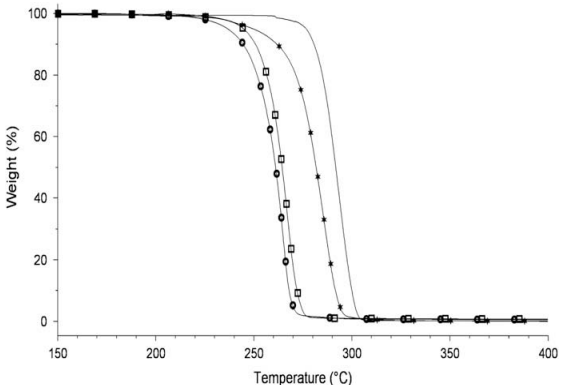

Indeed, our results evidenced that the ammonium salts degradation products catalyze the thermal degradation of polyhydroxyalkanoates [7]. As a consequence, clay exfoliation is difficult to reach and thus the obtained nanocomposites do not present significantly improved properties [8].

Conclusions:

The various biopolymer/clay systems presented here give a broad overview of the "products-process-morphology" relationships for these nano-biocomposites. The great impact of clay organo-modification and plasticizer addition on the mechanical, thermal and barrier properties of such hybrid materials is more particularly evidenced.

References:

1. P. Bordes, E. Pollet, L. Avérous, Progr. Polym. Sci., 2009, 34, 125
2. F. Chivrac, E. Pollet, L. Avérous, Mater. Sci. Eng. R-Rep., 2009, 67, 1
3. F. Chivrac, E. Pollet, M. Schmutz, L. Avérous, Biomacromolecules, 2008, 9, 896
4. F. Chivrac, E. Pollet, P. Dole, L. Avérous, Polym. Adv. Technol., 2010, 21, 578
5. F. Chivrac, E. Pollet, M. Schmutz, L. Avérous, Carbohydr. Polym., 2010, 80, 145
6. F. Chivrac, H. Angellier-Coussy, V. Guillard, E. Pollet, L. Avérous, Carbohydr. Polym., 2010, 82, 128
7. P. Bordes, E. Hablot, E. Pollet, L. Avérous, Polym. Degrad. Stabil. 2009, 94, 789
8. P. Bordes, E. Pollet, S. Bourbigot, L. Avérous, Macromol. Chem. Phys., 2008, 209, 1474

ABSTRACTS

POSTER PRESENTATIONS

Topic 6: Bioinspired Polymers, Bioengineering and Biotechnology

Production of poly(lactic acid) microsphere loaded with holmium-166 for braquitherapy.

GeovannaPires[a]*, *José Roberto Martinelli*[b], *João Alberto Osso Junior*[c], *Nanci Nascimento*[a], *Mariangela de Burgos M. de Azevedo*[a]

[a]Centro de Biotecnologia, [b]Centro de Ciência e Tecnologia de Materiais, [c]Centro de Radiofarmácia, Instituto de Pesquisas Energéticas e Nucleares -IPEN; email: geovannapires@gmail.com

Abstract: This study describes the development of poly(lactide) (PLA) microspheres by an emulsion method for braquitherapy. The effects of both PLA and PDLA polymers on holmium encapsulation efficacy were evaluated. Microspheres containing holmium were prepared and characterized by thermal analysis, X-Ray diffraction, Scanning Electron Microscopy, FTIR spectroscopy, and zeta potential measurements. The experimental data showed that both polymers formed microspheres, however the PLLA1 of small viscosity inherent formed more microspheres with size distribution smaller when comparable with PLLA2 and PDLA.

Introduction

Three different types of material substrates have been investigated, i.e., biodegradable polymer-based, glass-based, and resin-based microspheres. Nowadays there is a project concerning the labeling of these 3 materials with ^{166}Ho being developed at IPEN-CNEN/SP and coordinated by the Radiopharmacy Directory. The nuclide ^{166}Ho($t_{1/2}$=26.8h) is a beta particle emitter (E_{max}=1.84 MeV), with suitable properties for radiotherapy and it can be produced with the relatively low neutron flux from theBrazilian Nuclear Reactor IEA-R1m. As an initial experience we used resin-based microspheres, a cation exchange resin labeled with ^{166}Ho, which showed the essential characteristics for liver cancer therapy. Preliminary results concerning the preparation of glass-based microspheres labeled with ^{165}Ho showed that 5% of Ho_2O_3 was incorporated in an aluminosilicate glass, through the process of spheronization by flame, which produced spherical microspheres with 20-40 µm particle size. The preparation of biodegradable material, polymer-based microspheres, is in its initial stage and the objective is to prepare and label different polymer-based microspheres with ^{165}Ho. These combined efforts have been done to offer a radiotherapeutic product for the Brazilian nuclear medicine community at reasonable cost and also to offer a viable possibility of treatment for patients affected by liver malignances [1]. In the present study, we report the effects on the PDLA e PLLA polymers after the Ho encapsulation efficacy and the characterization of the materials by different techniques: SEM, Thermal analyses, EDX, zeta potential, porosity and infrared spectroscopy (IR) [2].

Experimental

The PLLA1 (M_w 101,700), PLLA2 (M_w 152,000), PDLA polymers, and polyvinyl alcohol (PVA, MW = 31 KDa, hydrolyzation degree = 88%) were provided by Sigma Aldrich. Holmium acetylacetonatetrihydrate (HoAcAc) was prepared as described previously [2].

The microspheres with HoAcAc were prepared by solvent evaporation as described previously (Fig.1) [2]. The HoAcAc and the polymer were dissolved in chloroform. The resulting homogeneous solution was added to an aqueous solution of PVA. The mixture was stirred at500rpm, and the formed microspheres were filtered through sieves.

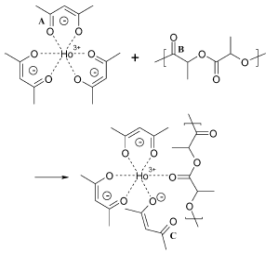

Fig. 1.Reaction of the formation of holmium microspheres.

Results and discussions

Microspheres were prepared by solvent evaporation and sieved to retain particles in a suitable size range.

Fig. 2 shows the SEM micrographs of microspheres without holmium in different polymers. As it can be seen, they are spherical with a relatively small index of polydispersity according to the zeta potential results.

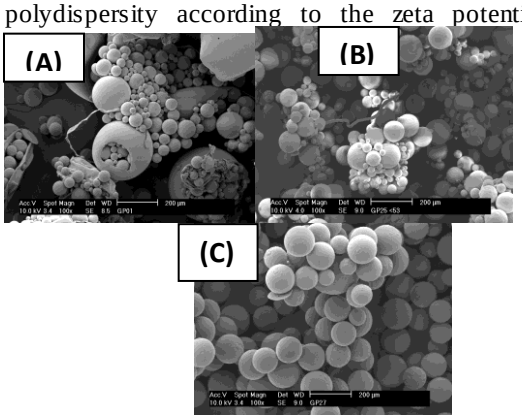

Fig. 2.SEM of PDLA (A) PLLA1 (B) and PLLA2 (C) microsphere without holmium.

The results showed that there was significant difference between the FTIR spectra of the microsphere-Ho when compared to the spectra of individual components.

Thermal analysis curves showed that both PLLA samples have the characteristic melting points of the crystalline polymers, indicating that the crystallinity was maintained. EDX analysis showed the concentration of Ho in the material.

Conclusion

This study showed that microspheres were formed with and without holmium, and that the microspheres containing holmium present promising results for braquitherapy application.

References

[1] Renata F. Costa, Mariangela B. M. Azevedo, Nanci Nascimento, Frank F. Sene, José R. Martinelli, João A. Osso; *2009 International Nuclear AtlanticConference - INAC 2009; ASSOCIAÇÃO BRASILEIRA DE ENERGIA NUCLEAR - ABEN* **ISBN: 978-85-99141-03-8**

[2] Nijsen J.F.W., Zonnenberg B.A., Woittiez J.R., Rook D.W., Swildens-van Woudenberg I.A., Van Rijk P.P., Van HetSchip A.D. Eur. J. Nucl. Med. 26, 699-704, 1999

Morphology and properties of porous thermosensitive cryogels based on poly(*N*-isopropilacrylamide) systems

H. Peniche[1], F. Reyes[2], G. Rodriguez[2], M. R. Aguilar[2], C. Peniche[1], J. San Román[2]

[1] Centro de Biomateriales, Departamento de Química Macromolecular, Universidad de La Habana, La Habana, Cuba
[2] Instituto de Ciencia y Tecnología de Polímeros (ICTP), Departamento de Biomateriales, CSIC, Madrid, España

hazel@biomat.uh.cu

Introduction

Cryogels are polymeric macroporous materials obtained by cryotropic gelation of monomers or polymer precursors in moderately frozen state (liquid microphase). The gel formation occurs in liquid microphase, where the concentration of monomer and other dissolved substances is higher. Crystals frozen solvent act as porogen during gel formation giving rise after defrost system to a three-dimensional maze interconnected macropores allowing diffusion without impairments of solutes of practically any size throughout the volume of the gel [1].

Poly(*N*-isopropylacrylamide) crosslinked is a typical temperature-sensitive gel, which exhibits a volume phase transition at about 34°C. Below this temperature, p-NIPA gels are swollen, hydrated, and hydrophilic, temperatures above the gels shrink.

Sensitivity temperature p-NIPA gels have attracted much attention for their usefulness in drug delivery systems sensitive to temperature, separation techniques in biotechnology, agricultural processing and as sensors. These applications require a quick response of the hydrogel against external stimuli. To increase the response speed of the gels p-NIPA, various techniques have been proposed [2]. In the case of "smart materials" such as p-NIPA, the speed of response to temperature change increases significantly when prepared as macroporous gels compared to gels obtained by in bulk polymerization [3].

Synthesis of the p-NIPA cryogels

Poly(*N*-isopropylacrylamide) (p-NIPA) cryogels were synthesized by free radical polymerization of NIPA under freezing conditions. Polymerization reaction was carried out by dissolving the monomer NIPA in water. N,N'-methylenebisacrylamide (NNMBAM) was added to the solution and N_2 gas was bubbled for 15 min. For the initiation of the reaction *N*,*N*,*N'*,*N'*-tetrametiletilendiamina (TEMED) was added and the solution was placed in an ice bath for 5 min. Ammonium persulfate (APS) was added to the reaction mixture and stirring was maintained for 1 min. 2 mL aliquots of the reaction mixture was poured into plastic tubes.

The tubes containing the reaction mixture were placed in to cryostat for 1 hour at - 20 °C and after 16 hours at - 12 °C. The cryogels obtained were freeze-dried.

The preformed cryogels were loaded with previously obtained and characterized chitosan/bemiparin nanoparticles in suspension at 0%, 5% and 15%.

The lyophilized samples were cut into disks and weighed before and after loading with nanoparticles.

Swelling study of p-NIPA cryogels

Swelling kinetics was performed in PBS buffer (pH= 7.4) at 15 °C and 37 °C. Three replicates of each sample (0%, 5%, 10%) were made.

Results and Discussion

Cryogels showed thermoresponsive swelling behavior at 15 ºC, below the lower critical solution temperature (LCST) of p-NIPA and de-swelling at 37 ºC, above its LCST.

Similar behavior was obtained for cryogels charged at 5% and 15% with nanoparticles.

Cryogels of p-NIPA have a highly porous structure. As shown in Figure 1.

Nanoparticles loading of cryogels is evidence by SEM and ATR analysis.

ATR spectrum of cryogels loaded with nanoparticles showed a band corresponding to stretching vibration of S=O bond of bemiparin at 1235 cm^{-1}.

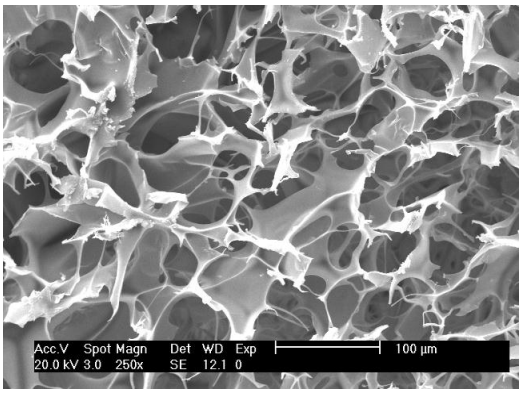

Figure 1 SEM photography of p-NIPA cryogel

Conclusions

The p-NIPA cryogels were successfully synthesized. They have a highly porous morphology and were able to incorporate chitosan/bemiparin nanoparticles. Swelling kinetics of cryogels of p-NIPA was studied at two temperatures (above and below the LCST), obtaining an expected behavior for this type of system temperature dependent.

References

[1] Mohand Chalal, Franc¸oise Ehrburger-Dolle, Isabelle Morfin, Jean-Claude Vial, Maria-Rosa Aguilar de Armas, Julio San Roman, Nimet Bölgen,Erhan Pişkin,| Omar Ziane, and Roger Casalegno *Macromolecules 42*:2749-2755(2009).

[2] Paloma Perez, Fatima Plieva, Alberto Gallardo, Julio San Roman, Maria Rosa Aguilar, Isabelle Morfin, Françoise Ehrburger-Dolle, Francoise Bley *Biomacromolecules, 9:* 66–74 (2008).

[3] Yucel Dogu, Oguz Okay Journal of Applied Polymer Science, 99: 37–44 (2005).

Biologically Inspired Polymer Scaffold Development for Artificial Skin

Mohana Marimuthu[1], Jeongho An[2], and Sanghyo Kim[1]

[1]College of Bionanotechnology, Kyungwon University, Seongnam-si, Gyeonggi-do, 461-701, SOUTH KOREA, [2]Department of Polymer Science & Engineering, SungKyunKwan University, Suwon, Gyeonggi-do, 440-146, SOUTH KOREA

samkim@kyungwon.ac.kr

By utilizing polymeric materials integrated microfluidic technology, we have developed a novel porous microfiber (MF) scaffold embedded with Poly(D,L-lactic-*co*-glycolic acid)-Glucosamine (PLGA-GlcN) microparticles (MPs) to minimize post implant inflammatory effect spontaneously and to produce controlled protein release simultaneously. Previously, ketoprofen as non-steroidal anti-inflammatory drug (NSAID) delivery system was studied based on the electrospunpolycaprolactone based fiber scaffold. A microfluidic apparatus has been developed by Lee *et al.* that creates a continuous process for the production of protein loaded MF by employing the "on the fly" phase inversion processes. Present method differs from that of Lee group in bringing the microfluidic technology for porous fiberfabrication by altered dual mechanisms: precipitation by evaporation and immersion precipitation, and in the development of new anti-inflammatory drug based on naturally occurring GlcN, an amino monosaccharide evinced as natural COX-2 inhibitor , and their encapsulation into MF scaffold in order to prevent the adverse effects caused by NSAIDs.

Chemical grafting of the PLGA-g-GlcN was prepared with EDC system. Briefly, the GlcN solution was mixed to the PLGA/DMAP and EDC solution at room temperature. After 3 h, the mixed solution was poured into excess of acetone to produce precipitates, and were dissolved in PBS and dialyzed for two days to remove the ungraftedGlcN. Later, the sample lyophilized to dryness and stored. PLGA GlcNMPs were made using W/O/W double emulsion technique. Amphiphilictriblock copolymer, poly (p-dioxanone-co- caprolactone)-block-poly (ethylene oxide)-block-poly(p-dioxanone-co-caprolactone)(PPDO-co-PCL-b-PEG-b-PPDO -co-PCL) MF loaded with MPs with/without fibronectin werefabricated using a modified microfluidic device reported previously by our group. Microfluidic system differs from the established method in such a way that, inner diameter of the core inlet micropipette (200µm and 50 µm diameter at outer and at pulled end, respectively) was twice larger than outlet micropipette (100 µm at both ends). The core solution (10% PPDO-co- PCL -b-PEG- b-PPDO- co -PCL copolymer in CH2Cl2) and sheath solution (DI water with or without PLGA-GlcN MPs) were injected through the micropipette inlet and 12-guage needle inlet using infusion pumps and their flow rate were controlled at 10 µl/min and 100ml/hr respectively. The extruded porous fibers were collected in precleanedpetridish (Figure 1).

The morphology of all 3 samples obtained from FE-SEM images. Cell viability of all scaffolds were evaluated using cell proliferation reagent WST-1 kit (Figure 2). Cytocompatability for MPs containing MF are reasonably higher than that of MPs and MF alone. This may be due to synergistic activity of higher surface roughness for both MF and MPs. These results support and confirm that the MPs loaded microfibers could be potentially used as a candidate for drug delivery and tissue regeneration applications with minimized post-implant inflammatory response due to PLGA-GlcN.

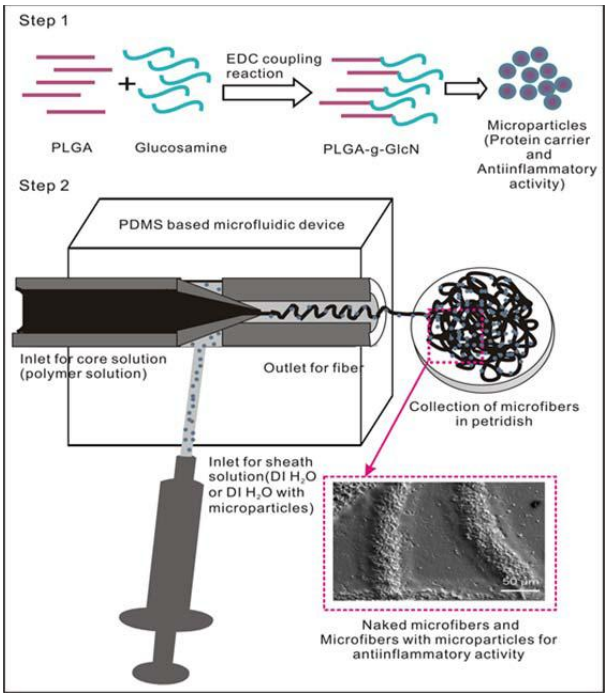

Figure. Schematic of PLGA-GlcNmicroparticle synthesisand loading into microfiber

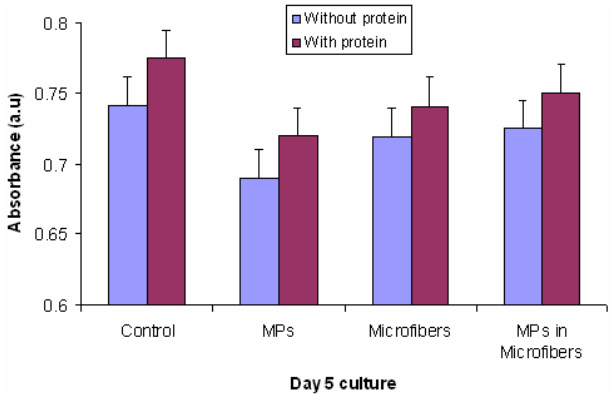

Figure 2. WST-1 results of 5 day culture of L929 cells

Phenol biosensor based on electrochemically controlled integration oftyrosinase in a redox polymer

HuseyinBekir Yildiz[1], *Jaime Castillo*[2], *Dmitrii A. Guschin*[3], *Levent Toppare*[4], *Wolfgang Schuhmann*[3]

[1] Department of Chemistry, KaramanogluMehmetbey University, 70100 Karaman, Turkey.
[2]MIC – Institut for Mikro- ogNanoteknologi DTU, Bygning 345Ø, DK-2800 Kgs. Lyngby, Denmark.
[3]Faculty of Chemistry RuhrUniversiteat Bochum, Universiteatsstrasse 150, D-44780 Bochum, Germany.
[4]Department of Chemistry, Middle East Technical University, 06531 Ankara, Turkey.

yildizhb@kmu.edu.tr, yildizhb@gmail.com

Introduction: In this study, we propose a sensor architecture for the preparation of tyrosinase-based biosensors using the non-manual electrochemically controlled integration of tyrosinase within Os-complex functionalized electrodeposition paints. An Os complex functionalized cathodic electrodeposition polymer was used to entrap tyrosinase in a simple, controlled and reproducible way on a platinum electrode surface. A modified bi-layer architecture of the sensor was designed to reduce ascorbic acid interferences by entrapping ascorbate oxidase within a second outer polymer layer. Polymer thickness, enzyme-polymer volume ratio, applied potential, and sensor stability were optimized aiming on the design of sensitive and selective biosensors for catechol and phenol determination.

Materials and Methods: Tyrosinase (EC 1.14.18.1, lyophilized power, _1000 unitsmg_1 solid, from mushroom), ascorbate oxidase (AscOx, EC 1.10.3.3, lyophilized power, 1000–3000 unitsmg_1 protein, from Cucurbita sp.) were obtained from Sigma (Deisenhofen, Germany). Constant potential amperometry, differential pulse voltammetry (DPV) and cyclic voltammetry (CV) were performed using an Autolab PGSTAT12 potentiostat (Eco Chemie, Utrecht, The Netherlands) controlled by the GPES 4.7 software (Metrohm, Filderstadt, Germany) in a three-electrode configuration with a Ag=AgCl (3M KCl) reference electrode, a Pt-wire counter electrode and a Pt disk (1mm) working electrode.

The cathodic electrodeposition polymer (EDP) was synthesized following a strategy reported previously [1, 2]. In a miniaturized electrochemical cell the cathodic paint was precipitated on the electrode surface using a potentiostatic pulse sequence of -1200mV for 0.8 s and 0mV for 5 s. The pulse sequence was continuously applied up to 80 times.

Results and Discussions: An amperometric biosensor for the detection of phenolic compounds was developed based on the immobilization of tyrosinase within an Os-complex functionalized electrodeposition polymer. Integration of tyrosinase within the redox polymer assures efficient catechol recycling between the enzyme and the polymer bound redox sites. The non-manual immobilization procedure improves the reproducibility of fabrication process, greatly reduces the desorption of the enzyme from the immobilization layer, and, most importantly prevents fast inactivation of the enzyme by its substrate due to fast redox cycling.

A two-layer sensor architecture was developed involving ascorbic acid oxidase entrapped within an electrodeposition polymer in a second layer on top of the redox polymer=tyrosinase layer. Using this sensor architecture it was possible to eliminate the current interference arising from direct ascorbate oxidation up to a concentration of 630 mM ascorbic acid. The effects of the polymer thickness, the enzyme= polymer ratio, and the applied potential were evaluated with respect to optimal sensor properties. The sensitivity of the optimized sensors for catechol was 6.1 nA mM_1 with a detection limit of 10 nM, and for phenol 0.15 nA mM_1 with a detection limit of 100 nM [3].

Conclusion: The electrochemically induced deposition of an Osmium-complex modified electrodeposition polymer under simultaneous entrapment of tyrosinase is a straight forward way for the non-manual fabrication of catechol and phenol sensors. The developed sensor architecture can be optimized by adjusting the volume ratio of the enzyme and polymer stock solutions. Moreover, the polymer film thickness can be modulated by changing the number of potential deposition pulses.
The sensor architecture can be further extended to additional layers by a sequence of pH-induced polymer precipitation steps. The successful formation of an anti-interference layer containing ascorbate oxidase could be demonstrated. Fast substrate recycling within the polymer layer does not only lead to high sensitivity but obviously contributes to the preservation of the tyrosinase activity and hence to an improved longterm stability. Future work will be directed to the determination of phenolic compounds in real samples.

References

1)Neugebauer S., Isik S., Schulte A., Schuhmann W. *Anal. Lett*. 36 (2003) 2005-2020.
2)Ngounou B., Neugebauer S., Frodl A., Reiter S., Schuhmann W., *Electrochim. Acta* 49 (2004) 3855-3863.
3) Yildiz H.B., Castillo J., Guschin D.A., Toppare L., Schuhmann W., Microchim. Acta 159 (2007) 27-34.

Characterization and Properties of PCL / PDIPF Matrices for Biomedical Applications

Fernández, JM[1,2]; Cortizo, SM[1]; Cortizo, AM[2]; Abraham, GA[3]

[1]Instituto de Investigaciones Fisicoquímicas Teóricas y Aplicadas (INIFTA), CCT-La Plata, UNLP-CONICET [2]GIOMM, Departamento de Cs. Biológicas, Facultad de Cs. Exactas, UNLP, La Plata, Argentina
[3]Instituto de Investigaciones en Ciencia y Tecnología de Materiales (INTEMA), (UNMdP-CONICET), Mar del Plata, Argentina

E-mail: jmfernandez33@yahoo.com.ar

Introduction: Currently there is a high interest in the study of synthetic biodegradable polymers for use as biocompatible scaffolds in different areas of tissue engineering and regenerative medicine. Poly(epsilon-caprolactone) (PCL) and poly(diisopropilfumarato) (PDIPF) have proven to be good substrates for adhesion, growth and differentiation of two osteoblastic cell lines, mouse calvaria derived MC3T3E1 and rat osteosarcoma UMR106, suggesting that these polymers can be useful in bone tissue regeneration. A blend material with better mechanical properties, intermediate degradation rate between the two homopolymers and demostrated biocompatibility was prepared and compatibilized by high intensity ultrasound starting from PCL and PDIPF(1). The aim of this study was to characterize and to evaluate the activity of MC3T3E1 cells compared to porous and non porous matrices of PCL/PFIP compatibilized.

Materials and Methods: The compatibilized sample was obtained according to previously described method (1). Non-porous films were obtained by casting of 4%w/v solutions on Petri dishes (5.5 cm diameter). Solvent was evaporate at ambient conditions in a fume hood and finally dried under vacuum until constant weight. Porous films were obtaining by electrospraying (flow rate = 1.5 ml / h, applied voltage = 0.7 kV / cm) and collected on glass slides (2.6 cm x 1.8 cm). The morphology of both kind of films was evaluated by scanning electron microscopy (SEM) and optical microscopy (OM). The hydrophobicity of films was determined by contact angle measurement. Adhesion and proliferation test: MC3T3E1 cells cultured on the films for 1 or 24 h, washed with PBS, fixed with methanol and stained with Giemsa. The number of cells was evaluated by counting the cells in 10 fields/films using an inverted microscope. Alkaline phosphatase activity (ALP), a markers of osteoblastic phenotype associated with bone-forming capacity was evaluated as previously reported (2). The control experiments were performed on plastic petri dishes for cell culture. The results are expressed as mean ± SEM obtained from experiments. Differences between groups were evaluated by a linear model with Tukey post-hoc using GraphPad in Stat version 3.00. A p value <0.05 was considered significant for all statistical analysis.

Results and Discussion: SEM images (Fig. 1 A,B) shows the morphology of the membranes obtained by electrospraying consist of a highly porous structure with interconnected pores, formed by polymer droplets of a size 6.7 µm ± 0.1 µm. In contrast, the films obtained by casting display a smooth surface, only few pores can be observed.

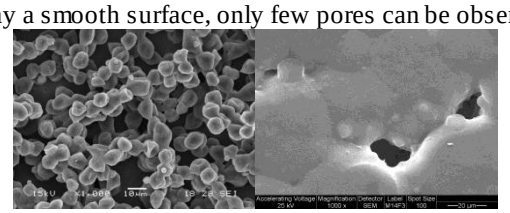

Figure 1: SEM micrographs of PCL/PDIPF matrices obtained by electrospraying (left), and solvent casting (right).

Biocompatibility studies showed that both adhesion and cell proliferation as well as ALP increased significantly in cells cultured on the porous matrix with respect to non-porous scaffold ones (Fig.2).

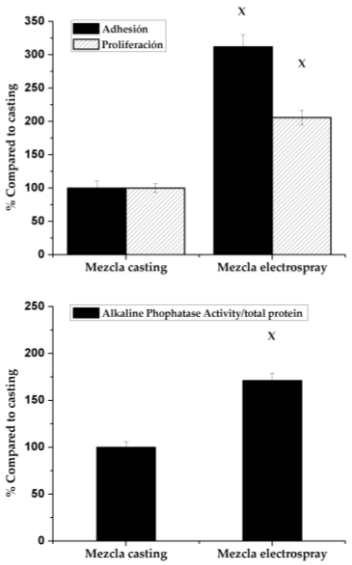

Figure 2: Cell adhesion and proliferation (upper graph) and Alkaline phosphatase specific activity (lower graph).

Conclusions: Matrices obtained by deposition of droplets by the method of electrospraying allow us to obtain polymeric matrices with structures of interest in the field of bone tissue engineering.

References

1) J.M. Fernadez, M.S. Molinuevo, A.M. Cortizo, A.D. McCarthy, M.S. Cortizo. J. Biomater. Sci. Polym. Ed. 21, 1297-1312 (2010).
2) A.M. Cortizo, M.S. Molinuevo, D.A. Barrio and L. Bruzzone, Int. J. Biochem. Cell Biol. 38, 1171-1180 (2006).

Reducing Fibrillation Tendency of Polyvinyl Alcohol Fiber by Incorporating Cellulose Nanowhiskers

Ahmed Jalal Uddin, Jun Araki, YasuoGotoh

Faculty of Textile Science and Technology, Shinshu University, 3-15-1 Tokida, Ueda, Nagano 386-8567, Japan

Email: jalal@shinshu-u.ac.jp

Introduction: Polyvinyl alcohol (PVA) has a broadrange of industrial and technical applications, especiallyin fiber-reinforced concrete. High strength PVA fiberreinforces the strength, toughness and crack resistanceof concrete due to its high strength, high modulus andgood adhesion to the matrix but it suffers in poorbending and compressive strength [1]. Moreover, highlyoriented PVA fiber fibrillates when subjected toabrasion or agitation due to its high orientation and lackof lateral cohesion between fibrils.

With a view to reducing the fibrillation behaviour offibres, several methods have been attempted in order toenhance the lateral interactions of molecular chains viacross-linkers [2], but they have not been shown toreduce the fibrillation tendency of fibres to the desiredlevels. In the present work, we explored a newtechnique to reduce the fibrillation properties of PVAfibres by inserting cellulose nanowhiskers (CWs) in theinter-fibrillar regions in a highly oriented form. Due toabundant surface hydroxyl groups, highly oriented CWscan be considered to create strong hydrogen bondingwith the surrounded PVA microfibrils and reinforceagainst fibrillation. Since CWs exhibit very highmechanical properties along their longitudinal axis,highly oriented CWs interlinked with PVA fibrils areexpected to contribute greatly to enhance themechanical properties of PVA fibres.

Materials and Methods: The CWs suspension wasobtained by hydrolysis of cotton powder by 65%sulfuric acid at 70°C for 10 min under vigorous stirringfollowed by washing with distilled water using acombination of centrifugation and dialysis. The stablecolloidal suspension of prepared CW (5 wt%) wasincorporated into the spinning dope of PVA (DP:ca.1500) aqueous solution various whisker contents (5-30wt% against the solid PVA). The spinning dopeswere extruded into cold methanol to form gel fibers. Asspunfibers were then undergone hot-drawing to their maximum possible draw ratio.

Results and Discussion: Fig.1 shows the SEM images of the fibers after pulverization test through a laboratory blender at 14,500 rpm for 30 sec. The images reveal that the introduction of a small amount of CWs drastically enhances the fibrillation resistance of PVA fibers. This reason may be attributed to the reinforcing of interfibrillar phase by whisker network. The fibrillationresistance of fibers results in a remarkable improvementin knot-pull strength as shown in Figure 2.

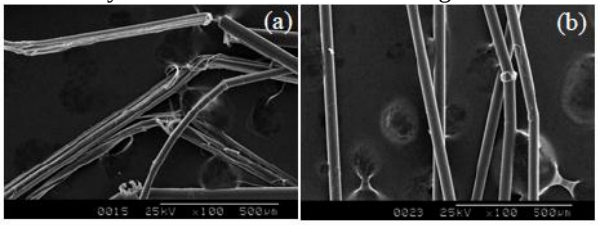

Fig 1. SEM images of fibers after fibrillation test. (a) Neat PVA, and (b) PVA-CW 5%.

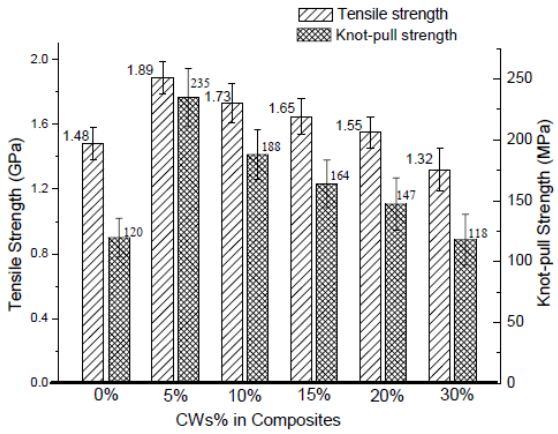

Fig 2. Tensile and knot-pull strength of neat PVA and PVA-CW composite fibers.

We consequently examined the knot configuration ofPVA-CW fibres to study their response againstcompressive and shear stresses. In the knot or loopstate, the fibre configuration turns out to be highly bent.The fibre undergoes severe axial stress in the outer layerand high compressive stress at its buckled inner layer[3]. As seen in Fig. 3, it is clear that the fibrillated PVA fibre cannot withstand such a high stress differenceimposed between the outer and inner layers, andconsequently the fibre shows a dilapidated appearance.Conversely, in case of PVA-CW fibres, possibleinteraction of the CWs with the PVA fibrils causesgeneral chain slippage and homogeneous shearing offibrils. Therefore, the PVA-CW fibres nearly retainedtheir original structures in the bent state.

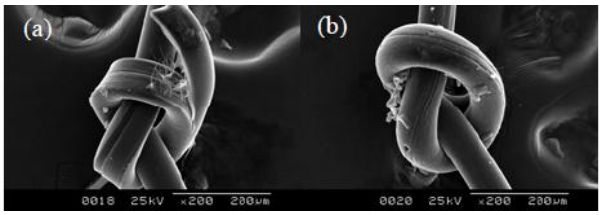

Fig. 3. The structure of knotted (a) neat PVA and (b) PVA-CW 5% fibers.

References:

1. Lyoo, W.S., Ha, W.S., Polymer, 40, 497-505 (1999).
2. Knijnenberg, A., Bos, J., Dingemans, T.J., Polymer, 51, 1887-1897 (2010).
3. Morton, W.E., Hearle, J.W.S., Physical properties of textilefibres. London: Buttersworth; 1962. p. 383.

Synthesis and Characterisation of Well-Defined Optically Active Methacrylate-Based Block Copolymers

MarilizAchilleos,[1] DemetrisKafouris,[2] Simon J. Holder[3] and Theodora Krasia-Christoforou[1]

[1] Department of Mechanical and Manufacturing Engineering, University of Cyprus
[2] Department of Chemistry, University of Cyprus
[3] Functional Materials Group, School of Physical Sciences, University of Kent

achilleos.mariliz@ucy.ac.cy

Introduction. The synthesis of optically active artificial biomimic materials has been of great interest to modern polymer science in the past years.[1-5] This is due to the fact that their resemblance to naturally occurring optically active polymers makes them good candidates as chiral and molecular recognition systems, enantiomeric separation materials, specific catalysts and vehicles for drug delivery.[1,2,6] The synthesis of such materials required polymerisation conditions employing specialised catalysts or monomers.[7] Up to date a number of optically active methacrylic monomers has been reported containing functional moieties such as amino acids, urea and cholesteryl groups in order to induce optical activity.[8-11] The synthesis of optically active methacrylic monomers, characterised by structural simplicity has not been reported so far. Herein we report for the first time the synthesis of a new, simple and optically active methacrylic monomer using conventional methods. The respective homopolymers and water-soluble diblock copolymers are also synthesised and characterised. Micellisation of diblock copolymers possessing an optically active block segment may lead to nanoparticles with size and shape that can be tuned to match biological constructs.

Results and Discussion.*Synthesis of a new optically active monomer.* The new optically active monomer, (*S*)-(-)-2-methyl-1-butyl methacrylate [(S)-(-)-MBuMA] was synthesised*via* a typical methodology reported in literature.[12] The corresponding optically active alcohol was allowed to react with methacryloyl chloride in THF in the presence of triethyl amine at. The monomer structure was confirmed by ^{1}H NMR analysis spectroscopy.

Synthesis of homopolymers. (*S*)-(-)-MBuMAhomopolymers were synthesised using conventional RAFT polymerisation in benzene in the presence of AIBN. Two chain transfer agents were used for the synthesis of these polymers, namely cumyldithiobenzoate (CTA1) and 2-cyano-2-propylbenzodithioate (CTA2). All polymers appeared as pink solids soluble in most common organic solvents in which typically *n*-butyl methacrylate dissolves. Even though it has been reported in literature that there is no difference in the reactivity of the above mentioned CTAs [12] we observed that polymers using CTA1 gave much lower yields (30%) than those synthesised using CTA2 (65%). All polymers were characterised using Gel Permeation Chromatography (GPC) with an Refractive Index (RI) detector calibrated with PMMA standards and ^{1}H NMR spectroscopy. All polymers gave unimodal molecular weight distributions with polydispersity indices (PDI) ranging from 1.12-1.27. The specific optical rotation values of the homopolymers determined by polarimetry were found to be independent on the molecular weights of the polymers. This is in agreement with results reported in literature.[8,10]

*Synthesis of block copolymers.*Amphiphilic block copolymers were generated by chain growth of the poly[(*S*)-(-)-(MacroCTA1) via the addition of the hydrophilic and ionisable 2-(dimethyl amino)ethyl methacrylate (DMAEMA). The polymerisation degrees (DP) of DMAEMA were 104, 230 and 475 respectively whereas the DP of (S)-(-)-MBuMA was in all cases 55. The resulting block copolymers were characterised by a unimodal molecular weight distribution indicating that complete extension has occurred providing further evidence for the "living" nature of the polymerisation under these conditions.[8,12]

Micellisation of (S)-(-)-MBuMA-b-DMAEMA. The (*S*)-(-)-MBuMA-*b*-DMAEMA amphiphilic block copolymers were dissolved in a selective for the DMAEMA block solvent (water) to form micelles. It should be noted at this point that the optically active block segment [(*S*)-(-)-MBuMA] of the diblock copolymers constructed the micelle's core whilst the hydrophilic segment (DMAEMA) formed the shell of the micelle. The morphological characteristics of the micelles were determined using dynamic light scattering (DLS) and atomic force microscopy (AFM).

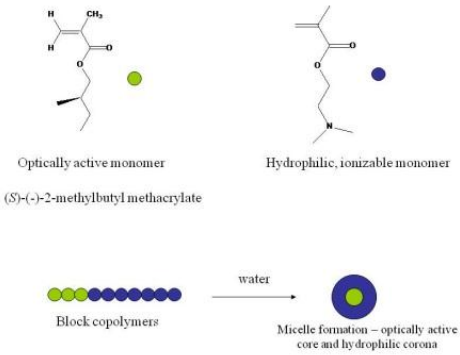

Fig. 1: Chemical structures of the monomers used for the synthesis of optically active block copolymers and their micellisation in aqueous media.

References.1.J. J. L. M. Cornelissen*et al*. *Chem. Rev*. **2001**, *101*, 4039 **2.**M. Fujiki, *J. Organomet. Chem*.**2003**, *685*, 15 **3.**M. Farina *Top.Stereochem.***1987**, *17*, 1 **4.** Y. Okamoto *et al.Chem. Rev*.**1994**, *94*, 3021, **5.**M. M. Green *et al*. *Science***1995**, *268*, 1860 **6.** M. Fujiki, *Macromol. Rapid Commun*.**2001**, *22*, 539 **7.** Y. Okamoto *et al.J. Am. Chem. Soc*. **1979**, *101*, 4768 **8.**J. Skey*et al.J. Polym. Sci. Part A Polym. Chem.* **2008**, *46*, 3690 **9.**Y.–K. Lee *et al. J. Appl. Polym.Sci*.**2003**, *90*, 1018 **10.** H. Mori *et al.Macromolecules*, **2005**, *38*, 9055 **11.**Y. –K. Lee *et al.J. Polym. Sci. Part A Polym Chem.***2000**, *38*, 4315 **12.**J. E. Keams*et al.J. Macromol. Sci. Part A***1974**, *4*, 673 13.G. Moad*et al.Austral. J. Chem.***2009**, *62*, 140.

Immobilization of Soy Bean Peroxidase into Nanotubes of Natural Halloysite and Its Application in the Polyaniline Synthesis

Romero-Garcia Jorge[1], *Tierrablanca-Maldonado Elisa*[1] *and Cruz-Silva Rodolfo*[2]

[1]Centro de Investigación en Química Aplicada, Blvd. Enrique Reyna # 140, Saltillo, Coahuila, México, 25253
[2]ResearchCenter for Exotic NanoCarbon, 6FEngineeringResearchCenter, Faculty of Engineering, 4-17-1 Wakasato, Nagano 380-8553, Japan

jromero@ciqa.mx

Introduction. Polyaniline (PAni) is one of the most intensively studied electronically conducting polymers because of its potential commercial applications in microelectronics, electrochromic displays devices, etc. PAni can be synthesized either by chemical or electrochemical oxidation of aniline monomer in acidic aqueous medium. Enzymatic polymerization of aniline has been proposed as environmentally and friendly alternative using Horseradish Peroxidase (HRP) and Soy Bean Peroxidase (SBP)[1,2]. In any case, like all other enzymes, there are some disadvantages that have to be considered for practical applications; among others is the instable nature of these biomacromolecules. The immobilization of enzymes in natural inorganic hosts has merge as interesting approach, due to its promising potential in improving enzyme thermal or pH stability, at the same time work as nanoreactors[3]. Halloysite is a naturally occurring aluminosilicate nanotube, chemically similar to kaolin. The size of halloysite particles vary between 1-15 micrometers and have an inner diameter of 10-150 nm.

Few papers on the use of the inner lumen of halloysite particles as nanoconfined reactors have been published. Herein, we employ halloysite tubules as hollow enzymatic nanoreactors for the polyaniline synthesis.

Materials and Methods. Soy Bean Peroxidase (SBP) was purchased from Organic Technoligies (Coshocton, OH, USA). Aniline, N-methyl-2 pyrrolidinone (NMP), (2,2-azino-bis(3-ethylbenzothiazoline-6-sulfonic acid) diammonium salt) (ABTS) and ptoluenesulfonic acid monohydrate (TSA) were purchased from Sigma–Aldrich. Halloysite nanotubes (HNTs) were from NaturalNano, (Rochester, NY, USA). Deionized water (DW) was used in all experiments.

SBP was immobilized in the HNTs suspension (HNTs/SBP) by dissolving 40 mg of SBP in 100 mL of DW (pH 3.0, using PTSA). Then 200 mg of HNTswas added to this solution.HNTs/SBP, was lyophilized and stored for further studies. The peroxidise activity in the HNTs/SBP was measured by spectrophotometry, using ABTS as substrate (λ_{max}= 405 nm, 36.8 mM^{-1} cm^{-1} extinction coefficient). Polyaniline synthesis was carried out using the HNTs/SBP. HNTs/SBP (240 mg) and aniline (400 µL) were added to 100 mL of DW. The pH (2.0) was adjusted with 800 mg of PTSA. The reaction was initiated by adding H_2O_2 and after that washed with methanol, centrifuged and freeze-dried.

Results and discussion. The peroxidise activity in the HNTs/SBP was measured by spectrophotometry, using ABTS as substrate (λ_{max}= 405 nm, 36.8 mM^{-1} cm^{-1} extinction coefficient) and show that the SBP was successfullyimmobilized inside the lumen of the HNTs. The HNTs/SBP at pH 2.0 was catalytically more active than the free SBP.

The spectrum of the HNT/SBP/PAni in acid media shows the characteristic two polaron bands (400nm and 775nm) of the electrically conductive form of polyaniline. Figure 1 shows the XRD patterns of the halloysite before and after aniline polymerization. Because not appreciable differences were found between the difractograms of HNTs/SBP and (HNTs/SBP/PAni (Fig. 1A. and Fig. 1B, respectively), both shows a diffraction pattern typical for halloysite. Therefore, the HNTs nanotubes were eliminated with HF. The new XRD pattern at (100) and (111) are signals corresponding to 21° and 26.2°, characteristic of a pseudorombic cell, associated with the structure of the emeraldine salt for the PAni (Fig. 1C).

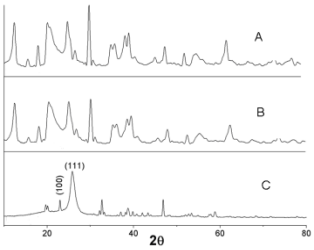

Fig. 1. Powder X-ray diffraction patterns of a). HNTs/SBP, b). HNTs/SBP/PAni and c). HNTs/SBP/PAni after HNTs were eliminated with HF.

Morphologies by STEM analysis of HNTs/SBP and HNTs/SBP/PAnidid not show major differences with the original HNTs sample (Fig b,c and a respectively). However, after removing the HNTs with HF is evident the complete filling of the inner halloysite space with the synthesized polyaniline in the form of nanowires (Fig. 2d). The electrical conductivity using the four point of this material was 1 Scm^{-1}.

Fig. 2. STEM images of: original HNTs (a), HNTs/SBP (b), HNTs/SBP/PAni and HNTs/SBP/PAni after HNTs were eliminated with HF.

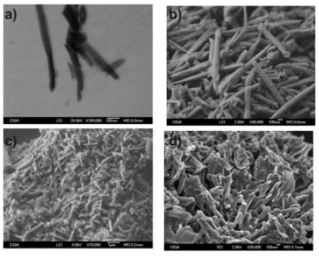

Conclusions.HNTs were successfully used as SBP support in a physical immobilization process. Using this supported SBP was possible to obtain electrically conductive PAni.

References.1).Liu W, *et al*. *J. Am. Chem. Soc.* 1999; **121:**71-78; 2).Cruz-Silva R, *et al*. *Eur. Polym. J.* 2005;**121:**1129- 3). Shchukin, GD, *et. al.Small*.2005; **5:**510-513.

Acknowledgments: Funded by CONACYT, Mexico under project CB-2008-01-103123.

Bioactive Alginate-Nanosilver-Anthocyanin Hybrid Composite

JinHyun Choi,[1,2] *SongYi Seo*,[2] *Ga Hyun Lee*,[3] *Se Guen Lee*,[3] *Eun Jung Oh*,[4] *Ho Yun Chung*,[4] *Jeong Hyun Yeum*,[1,2] *Sang Ik Han*[5]

[1]Department of Natural Fiber Science,Kyungpook National University, Korea
[2]Department of Advanced Organic Materials Science and Engineering,Kyungpook National University, Korea
[3]Division of Nano & Bio Technology,DaeguGyungbuk Institute of Science & Technology,Korea
[4]Department of Plastic & Reconstructive Surgery, Kyungpook National University Hospital, Korea
[5]Division of Functional Crop Resource Development, Department of Functional Crop, National Institute of Crop Science, Korea

jinhchoi@knu.ac.kr

Introduction: Biopolymers have received increased attention as excipientsin pharmaceutical formulations as they are derived from natural sources [4]. Silver has a long history of use in human healthcare and medicine [11]. A number of healthcare products such as wound dressing materials, body wall repairs, augmentation devices, tissue scaffolds, and antimicrobial filters now contain silver [16]. In this study, alginate-nanosilver-anthocyanin hybrid sponges (ANAHS) were prepared by in-situ synthesis of silver nanoparticles in an aqueous alginate solution. Antimicrobial activity and pro-inflammatory cytokine inhibition of ANAHS were investigated.

Materials and Methods: A solution of 1.0 wt/v% alginate and anthocyanin was prepared by dissolving alginate and anthocyanin in a 100ml of distilled water. Silver nitrate (2ml, 5.0 wt/v% in water) was dropped in 100ml of the alginate and anthocyanin solution. After 1 hour, freshly prepared sodium borohydride solution (2ml, 1.0 wt/v% in water) was slowly added under magnetic stirring. A rapid color change to dark brown indicated the formation of silver nanoparticles. The mixture was stirred for 3 hours at room temperature in order to lead entire reduction. And then, the solution was dialyzed for 2 days to eliminate the salts which were formed while alginate and silver nitrate were synthesized. The alginate-nanosilver-anthocyanin solutions were freeze-dried. Finally, the ANAHS were prepared by cross-linking of the freeze-dried matrices, washing, and freeze-drying.

The ANAHS were characterized by transmission electron microscopy (TEM), X-ray diffraction (XRD), and ultraviolet-visible (UV) spectroscopy. Cytotoxicity of the ANAHS were checked by 3-(4,5-dimethylthiazol-2-yl)-5-(3-carboxymethoxy phenyl)-2-(4-sulfophenyl)-2H-tetrazolium (MTS) assay. Pro-inflammatory cytokines 9 (IL-1β, IL-6, and TNF-α) were measured by cell culture of RAW 264.7 cells and enzyme-linked immunosorbent assay (ELISA).

Results and Discussion: The size of nanoparticles in the TEM images of the alginate solution are about 5-20 nm. Figure 1 is TEM images of the ANAHS. Nano-sized silver crystals were spread in the sponge.

We confirmed the presence of silver in the ANAHS by XRD as shown.

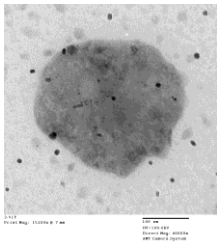

Figure 1. TEM images of silver nanoparticles in the ANAHS.

The ANAHS revealed the 97-99% reduction of number of colonies of staphylococcus auseus and klebsiellapneumonia.

From results in Figure 3, we confirmed that the ANAHS inhibited the production of IL-1β, IL-6, and TNF-α

Conclusively, the ANAHS had a good microbial activity and anti-inflammatory property. They are considered a candidate for the application as wound dressing material.

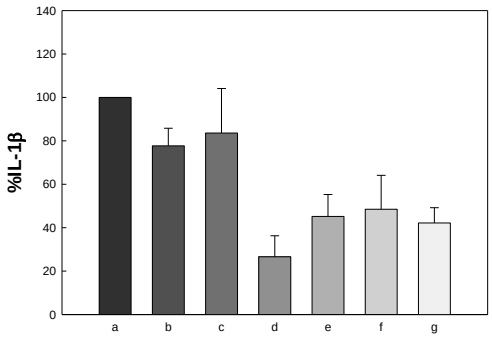

Figure 2. Relative amount of IL-6 produced by RAW264.7 cells cultured with the sponges of (a) alginate, (b) alginate-anthocyanin (0.05%), (c) alginate-anthocyanin (0.1%), (d) alginate-nanosilver (0.1%), (e) alginate-nanosilver (0.1%)-anthocyanin (0.05%), (f) alginate-nanosilver (0.05%)-anthocyanin (0.1%), and (g) alginate-nanosilver (0.1%)-anthocyanin (0.1%).

Acknowledgement: This work was supported in part by grants from Agenda Program (PJ0073852010) ofNational Institute of Crop Science, Rural Development Administration (RDA), Republic of Korea.

Degradation of polyethylene by a thermophilc bacterium

*YeunSugJeong and*Mal Nam Kim

Department of Biology, Sangmyung University, Seoul, Korea

mnkim@smu.ac.kr

Introduction

Polyethylene is one of the most consuming plastics due to its durability and excellent mechanical properties. It is being widely used for many single use applications. However due to the recently grown up environmental pressure, eventual fate of plastics after use became more and more important.

It has been admitted that the molecular weight of polyethylene should be lower than 500, otherwise it should be at least formulated with transition metal pro-oxidants and then oxidized to low molecular weight so as to be biodegraded. A lot of researches have been carried out to examine biodegradation of polyethylene containing pro-oxidants and to explore microorganisms degrading polyethylene having deliberately been oxidized [1-3].

Few studies have been devoted to exploring biodegradation of PE free from pro-oxidants. The molecular structure of PE formulated with pro-oxidants should be different from that of neat PE after the pretreatment, and thereby this should lead to different biodegradation behavior.

In this study, a thermophilc bacterium able to degrade LMWPEs was isolated from compost. LMWPEs were prepared by thermal degradation of HDPE and LDPE under strict nitrogen atmosphere. Biodegradation of LMWPEs whose average molecular weights were well above 500 was examined by using the isolated strain.

Results and Discussion

A microorganism isolated from the compost made from aminal fodder formed clear zone with about 4mm of diamenter at 58℃. The isolated strain was a rod shaped Gram negative bacterium. Analysis of 16S rDNA coding gene sequence resulted in the phylogenetic tree as shown in Fig. 1.

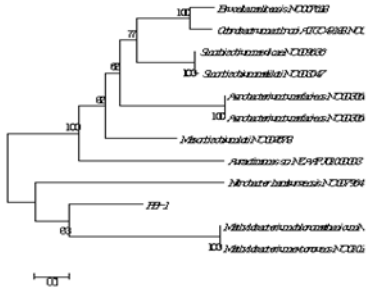

Fig 1: Phylogenic tree of the isolate

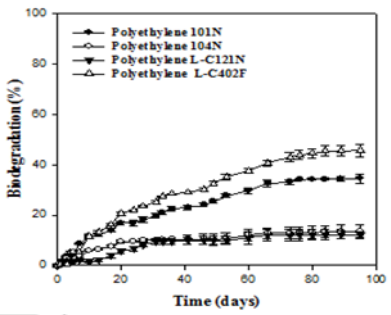

Fig. 2: Biodegradation rate of polyethylenes

Based on the results of the 16S rDNA analysis, the present strain was identified as *Methylobacteriumchloromethanicum.*

Mineralization of polyethylenes with different molecular weights was examined at 58℃, as shown in Fig. 2.It can be seen that the bacterium acclimated with the low molecular weight PE1 was active not only for the degradation of PE1 but also for the other higher molecular weight LMWPEs, PE2, PE3 and PE4. However the biodegradability decreased with increase in the molecular weight of the LMWPEs.

Contrary to the expectation that the biodegradation should reduce the molecular weight of PE1, the weight-average-molecular weight (Mw) of PE1 increased from 1,700 to 2,400 during the biodegradation. This should be attributed to the preferential assimilation of the low molecular weight fraction of PE1 by the microorganism.

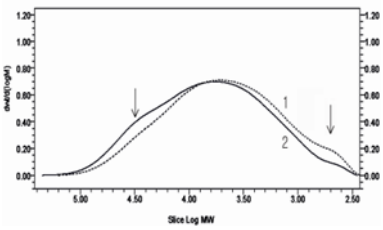

Fig. 3: GPC profile of PE4 before and after the biodegradaion

Fig. 3 shows the GPC chromatogram of PE4, having the highest molecular weight among the LMWPEs tested. The biodegradation also raised both Mn and Mw of PE4. However the shoulder peak at $10^{2.6}$ appearing in the chromatogram of PE4 before biodegradation vanished and the new shoulder peak at $10^{4.5}$ showed up after the biodegradation. As a result, the polydispersity of PE4 remained almost unchanged in spite of the differences in Mn and Mw.

Acknowledgement

This research was supported by the Basic Science Research Program through the National Research Foundation of Korea(NRF)funded by the Ministry of Education, Science and Technology(2010-A001-0021).

References

1. Ojeda T F M, Dalmolin E, Forte M M C, Jacques R J S, Bento F M, Camargo F A O (2009) *Polym. Degrad. Stab.*94: 965-970

2. ChielliniEmo, Corti Andrea, Swift Graham (2003) *Polym. Degrad. Stab.*81:341-351

3. Fontanella S, Bonhomme S, Koutny M, Husarova L, Brusson J-M, Courdavault J-P, Pitteri S, Samuel G, Pichon G, Lemaire J, Delort A-M (2010) *Polym. Degrad. Stab.*95: 1011-1021

Stimuli-responsive Hydrogels for Recognition of Ions and Biomolecules

Tobias Hennecke[1], *Nadia Adrus*[1,2], *Dana M. Balster*[1], *Mathias Ulbricht*[1]

[1] Lehrstuhl für Technische Chemie II, Universität Duisburg-Essen, Universitätsstrasse 5, Essen, 45141, Germany
[2] Polymer Engineering Department, Universiti Teknologi Malaysia, UTM Skudai, Johor 81310, Malaysia

e-mail: tobias.hennecke@uni-due.de

Smart molecularly imprinted polymer (MIP) hydrogels can combine both responsivity to external stimuli and recognition properties towards guests such as biomolecules including proteins or antibodies.[1] The key motivation is to mimic biological functions and natural feedback systems.
In our work we synthesized and investigated poly(acrylamide) (PAAm) and poly(*N*-isopropyl-acrylamide) (PNIPAAm)-based MIP and non-imprinted (NIP) hydrogels for protein recognition via photo initiated free radical crosslinking copolymerization (15 min irradiation, intensity ~ 30 mW/cm^2, $\lambda > 300$ nm). We used lysozyme as template protein. Two different template-selective monomers were used; i.e. 2-acrylamido-2-methylpropane sulfonic acid (AMPS) and methacrylic acid (MAA), along with *N*,*N'*-methylene-bisacrylamide (MBAAm) as crosslinker and Irgacure 2959® as photoinitiator. After polymerization, all hydrogels were washed with NaCl solution. The washing solutions were analyzed with TOC in order to quantify monomer conversion and to monitor the removal of template protein.
Based on previous experiments,[2] it was necessary to wash P(AAm-co-AMPS)-based hydrogels with at least 1.0 M NaCl in order to remove the template protein. After that, swelling experiments were done at room temperature (RT) for up to 24 h. However, under this extreme condition, the hydrogels were partially collapsed and this contributed to a lower binding capacity (Table 1).

Table 1: P(AAm-co-AMPS)-based hydrogels

	Conversion [%]	Swelling ratio (-)	Binding capacity* [mg/g]
NIP	84	5.0	30.4
MIP	80	4.8	24.4

**(100 mg dried gel in 100 ml 0.5 g/l lysozyme, RT, 24 h)*

Table 2: P(NIPAAm-co-MAA)-based hydrogels

	Conversion [%]	Swelling ratio (-)	Binding capacity# [mg/g]
NIP	97	13.4	111
MIP	92	12.9	441

#(10 mg dried gel in 10 ml 0.5 g/l lysozyme, RT, 24 h)

Therefore, P(NIPAAm-co-MAA)-based hydrogels were washed in both 1.0 M (results not shown) and 0.3 M NaCl (Table 2). In this case, the washing conditions with lower salt concentration were already sufficient. The hydrogels had high swelling degree and very high binding capacity. Note that in this case, the gel dimension was 10 times smaller. This may have influenced the measured binding capacities and must be reconfirmed.

The sorption experiments with the P(AAm-co-AMPS)-based hydrogels showed a higher binding capacity for the NIP than the MIP (Table 1). This was related to the comonomer AMPS leading to an ion exchanger gel, which causes specific binding for the imprinted gel and also non-specific binding for both the imprinted and the non-imprinted gel. Judged by the much higher capacities for MIP than NIP, the effect of non-specific binding was reduced with MAA (Table 2). More important, for P(NIPAAm-co-MAA) the protein binding selectivity (lysozyme over cytochrome C) was much higher for MIP than for NIP. Nevertheless, the template removal has emerged as the major problem; a complete protein removal could not be obtained during the washing step, even through solvent and washing condition variations. Hence, hydrogels with entrapped lysozyme were obtained. This seemed to contribute to a densification of the polymer network, causing a reduced swelling ratio at increasing fraction of entrapped protein (Tables 1 and 2).
In ongoing studies these preparations are optimized and adapted in order to fill macropores with such MIP hydrogels to obtain a size- and protein-selective membrane.
Another approach is the preparation of ion-sensitive stimuli-responsive hydrogels for the detection and quantification of potassium concentrations in the human blood. These hydrogels are PNIPAAm-based and containing crown ether units. This leads to a pronounced change in the swelling degree, depending on the concentration of specific ions. This will enable the detection of these ion's concentration via swelling pressure measurement in a sensor system.
Our first results showed that the ion sensitivity depends on the content of benzo-18-crown-6 units in the hydrogel, a higher content caused a higher sensitivity. Furthermore a significant change in the swelling ratio depending on the ion concentration was observed; the effect decreased in the order $Ba^+ > K^+ > Na^+$. In the ongoing work these hydrogels have to be optimized with focus on the potassium selectivity and sensitivity.

Acknowledgements: This work is partially supported by the German Ministry for Education and Research (BMBF; grant 16SV5460).

[1] C. Alexander, H. S. Andersson, L. I. Andersson, R. J. Ansell, N. Kirsch, I. A. Nicholls, J. O'Mahony, M. J. Whitcombe, *J. Mol. Recognit.* **2006**, *19*, 106-180.
[2] T. Hennecke, Master Thesis, Universität Duisburg-Essen, **2010**.

Novel pH-sensitive hydrogel for nano-pearl powder delivery

Hong-Ru Lin, Yu-Chaio Chen, Yiu-Jiuan Lin[1] and Ming-Hung Ling

Department of Chemical and Materials Engineering, Southern Taiwan University, Tainan 710, Taiwan
[1]Department of Nursing, Chung Hwa University of Medical Technology, Tainan 717, Taiwan

hrlin@mail.stut.edu.tw

Introduction

To protect the protein drugs from the harsh environment in the stomach before they can be absorbed in the intestine, pH-sensitive polysaccharides like chitosan and alginate have attracted increasing attention due to their favorable properties including biocompatibility, biodegradability, pH sensitivity, and mucoadhesive property. In this study, a novel pH-sensitive hydrogel system composed of chitosan and alginate was developed for delivering of nano-pearl powder.

Experimental

Alginic acid (3 wt%) was dissolved in distilled water and stirred continuously with a homogenizer (Polytron; Kinematica, AG, Switzerland) at 26,000 rpm for the desired amount of time. During homogenization, nano-pearl powder was added to the solution in order to prepare hollow hydrogel beads for the drug-release experiments. Calcium chloride (0.25 M) was dissolved in distilled water and N, O-carboxymethyl chitosan was added to the solution during homogenization to prepare $CaCl_2$ solution. The alginic acid/ nano-pearl powder solution was then dropped using a hypodermic syringe into $CaCl_2$/ N, O-carboxymethyl chitosan solution to obtain the hydrogel beads. The in vitro release profiles of hydrogel beads were studied in simulated gastric and intestine mediums, respectively. IEC-6 cells were seeded and cultured on the hydrogel beads to examine the biocompatibility of the carrier. In the in vivo studies, the nano-pearl powder levels (percentage oral dose) in blood with time after the oral administration of hollow hydrogel beads loaded with nano-pearl powder was compared with the levels after the oral administration of an aqueous nano-pearl powder solution in mice.

Results and discussion

As shown in Fig. 1, the hollow hydrogel beads incorporated nano-pearl powder exhibited low release profile and no erosion in SGF (pH 1.2). Such behavior is contributed to hydrogen bonding between –COOH from alginate and –OH from chitosan, leading to dense structure of hydrogel beads. The amount of nano-pearl powder released from hollow hydrogel beads was lower than 28 % at acidic environment. As the beads transferred to SIF (pH 7.4), their release was faster than in SGF. Since the –COOH groups from alginate were deprotonated to -COO^- when the buffer pH was high than its pKa (3.3~3.5), leading to loose structure of hydrogel beads. Under basic environment, the amount of nano-pearl powder released from hollow hydrogel beads was increased up to 36~84 %.

Fig. 2 shows the result of the IEC-6 cells culturing in the well, containing different kinds of hydrogel beads after 1, 3, 5, 7 days culture. The result shows the viable cells number increased slowly from 1 to 5 day, because the samples were acidic. The viable cells number increased obviously at day 7. We confirmed that the hollow hydrogel beads made from alginate-chitosan should not be cytotoxic.

Fig. 3 shows the means release rate of nano-pearl powder after oral administration of nano-pearl powder solution and loaded nano-pearl powder beads. At 6 hr, the release rate of nano-pearl powder solution was already reached maximum (81.7 %) and the release was terminated at 12 hr. However, the release rate of loaded nano-pearl powder beads was sustained for the next 6 hr (67.1 %) in comparison with solution. The in vivo release studies confirmed that hollow hydrogel beads have the controlled and sustained release ability.

Conclusions

The results suggest the pH-sensitive alginate-chitosan hydrogel system can be used as a promising vehicle for oral delivery of health nutrients.

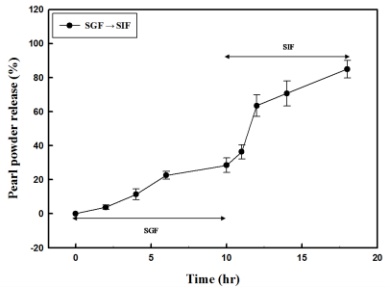

Fig.1 In vitro release studies in simulating the human gastrointestinal tract.

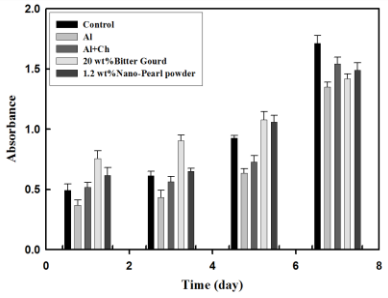

Fig. 2 MTS cytotoxicity test of the hollow hydrogel beads.

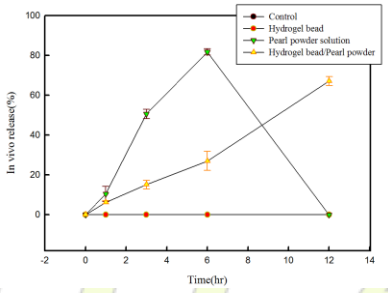

Fig. 3 In vivo release of nano-pearl powder from the hollow hydrogel beads.

Reinforced Composites Based on Biodegradable Polymer Matrix and Microcrystalline Cellulose

Fernanda A. dos Santos[1]*, *Maria Inês B. Tavares*[2], *Roberto P.C. Neto*[3]

Instituto de Macromoléculas Professora Eloísa Mano (IMA)
Universidade Federal do Rio de Janeiro (UFRJ)

[1*]fabbate@ima.ufrj.br; [2]mibt@ima.ufrj.br; [3]robertoneto@ima.ufrj.br

Introduction: Polylactic acid (PLA) is a biodegradable material that has a great potential to replace petroleum-based plastics [1]. The reinforcement of PLA using biomaterials like cellulose has been studied with the goal of obtaining fully bio-based composites [2].

Cellulose has been used largely like reinforcement in polymers matrix. The goal of the present study was to produce PLA based composites using microcrystalline cellulose (MCC) and characterize the obtained materials by NMR, DRX and SEM.

Experimental:

Materials: PLLA 2002D (NatureWorks LLC product), MCC PH 102 (Viapharma), Chloroform (Merck)

Methods: MCC suspensions containing an adequate amount of reinforcement were mixed in PLA solutions and run in a Blender for 24 h. The formulations were then casted in Petri dishes and left to evaporate in room temperature for one day. One formulation containing just PLA and three others with PLA and 3%, 5% and 7% wt MCC were obtained.

Results and Discussion:

The XRD spectra for MCC, PLLA neat (film and pellet) and PLLA/MCC system with 5 wt % MCC are presented in Figure 1.

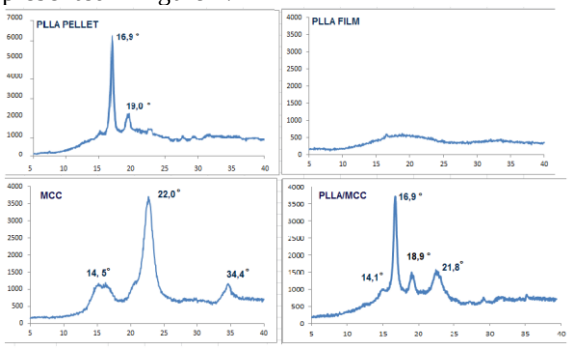

Figure 1: X-ray spectra for PLLA, MCC and PLLA/MCC

The X-ray diffraction patterns of neat PLA shows that the PLA FILM exhibits no peaks showing an amorphous nature. However, the result of x-ray experiment for PLLA in a pellet form shows that the material appears semi-crystalline. In the result of x-ray for the system PLLA/MCC appears diffraction peaks related to cellulose and PLLA.

Figure 2 shows the SEM micrograph of PLA/MCC system. It is possible to see from figure 2 that the MCC dispersion on the polymeric matrix is reasonable, presenting some aggregates.

Proton spin-lattice relaxation times (T_1H) obtained to the PLLA was 650 ms and 184ms for MCC. For the systems PLA/MCC with 3, 5 and 7% wt, T_1H was 592, 580 and 538 µs respectively. Analyzing PLLA resin, one value for the relaxation parameter was found. It was attributed to mobile region, which is constituted by amorphous phase. This result indicates that there was an increase in the molecular mobility of the polymeric chains with MCC addition.

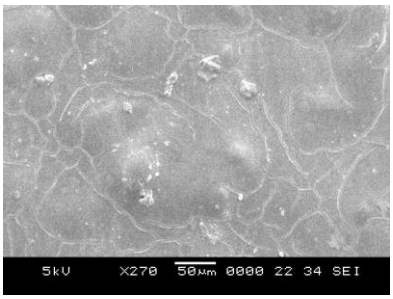

Figure 2: SEM image of PLLA/MCC film with 5% wt MCC

Figure 3 shows the domain curves for PLLA, MCC and for each system PLLA/ MCC obtained. Composites showed no change in the baseline width for the neat polymer and there was also no denotative displacement of the domains, indicating that addition of MCC did not affect the structural organization of the polymer and also that there was good dispersion of the load in the matrix.

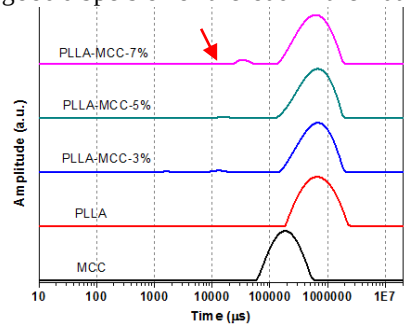

Figure 3: Domains Curves for MCC, PLLA and composites

However, in the PLLA with 7% wt of cellulose appeared a second domain (red arrow), which indicates that from this cellulose content begins to occur filler dispersion impairment in the matrix.

Conclusions: The X-ray diffraction (XRD) studies on the materials showed that cellulose can act as nucleating agent on the crystallization of PLLA. The morphology study on composites showed that the MCC were reasonable well dispersed in the PLA matrix due to the MCC particle self-aggregation. T_1H value decrease with MCC addiction, indicating increase in molecular mobility of PLLA chains. MCC decreased the stiffness of the PLA polymer chains, reducing the relaxation times of the pure polymer, ie, increasing its molecular mobility, indicating that weak intermolecular interactions were formed between MCC and PLLA. Despite the tendency of self-aggregation of cellulose, the results show that it is possible to obtain a good dispersion of MCC until 7 wt%, without adding any coupling agent or having to undergo any type of cellulose treatment.

References: 1. L. Suryanegara; A. N. Nakagaito; H. Yano Comp. Sci. Technol. 2009, 69, 1187.
2. A.K. Mohanty; M. Misra; L.T. Drzal J. Polym. Environ. 2002, 9, 19.

Combined Effect of Temperature and Humidity on the Biodegradation Behaviour of Polylactic Acid (PLA) and its Nanocomposites

Kontou E., P. Georgiopoulos, M. Niaounakis

Department of Applied Mathematical and Physical Sciences, Section of Mechanics, National Technical University of Athens 5 Heroes of Polytechnion, GR-15773, Athens, Greece

ekontou@central.ntua.gr

Polylactic Acid (PLA) is biodegradable polymer with an expanding range of potential applications. However, its poor thermal and mechanical resistance, limited barrier properties and relatively higher production costs hinder the penetration of PLA across a wide range of industrial sectors. The addition of a small amount -up to 4 wt.%- of nanosized fillers leads to the enhancement of the thermomechanical and barrier properties of pristine PLA [1]. So far, the biodegradability of PLA and PLA/nanocomposites has been tested in terms of storage under atmospheric conditions [1,2], while a large number of works has been performed on the hydrolytic degradation behavior of PLA films in neutral media [3]. Little work has been done on the variation of the thermal and tensile properties (Young's modulus and yield stress) of PLA and its nanocomposites with ageing. Moreover, the role of the nanofillers in the degradation procedure of PLA is an open issue. The aim of the present work is to study the effect of specific environmental conditions, namely exposure to 80% relative humidity at 40 °C for a period of up to six months, on the thermomechanical properties of PLA and PLA/nanocomposites.

Two different types of nanofillers and their mixtures were introduced in pristine PLA: Silica (Si) particles with an average size of 16 nm and Montmorillonite clay (MMT) both surface modified. Based on PLA and the two nanofiller-types, three series of PLA nanocomposites were prepared by melt mixing, namely PLA/Si and PLA/MMT nanocomposites with a filler content of 2, 3 and 5 wt.% of silica (Si) and montmorillonite clay (MMT), respectively; as well as PLA nanocomposites with a filler content of 4 wt.% based on MMT/Si ratio of 60/40 and 40/60. Experimental techniques including Scanning Electron Microscopy (SEM), Differential Scanning Calorimetry (DSC), Dynamic Mechanical Analysis (DMA), and tensile measurements were employed to analyze both the degree of thermomechanical enhancement of PLA due to nanofillers and their influence on the biodegradability of PLA and PLA/nanocomposites.

Both nanofiller types acted as nucleating agents, leading to an increment of crystallinity content, varying from 50 to 57% for the PLA/Si and from 32 to 50% for the PLA/MMT nanocomposites. On the other hand, the mixture of the two nanofillers showed no effect on the crystallinity content. Regarding Young's modulus, the higher degree of enhancement was observed at 2 wt.% and 3 wt.% of silica and MMT, respectively. The PLA/Si nanocomposite with a filler content of 3 wt.% silica gave the highest yield stress. The concurrent addition of both nanofillers caused the yield stress to decrease and the Young's modulus to increase compared to pristine PLA matrix. After exposure to the ageing conditions, a distribution of holes in the PLA/Si and cracks in the PLA/MMT intercalated nanocomposites was detected by SEM, related directly to the selective hydrolytic degradation of PLA matrix and removal of the chains in the amorphous regions. Crystallinity content was initially decreased with ageing time, and hereafter increased, effect which was interpreted by the molecular weight reduction. This was further supported by the lowering of the cold crystallization temperature. The same trend was observed in Young's modulus and yield stress, while the strain at break was decreased dramatically. MMT appears to have a higher impact on yield stress in comparison with silica. On the other hand, silica has a greater effect in Young's modulus and strain at break, compared to MMT. On the basis of the experimental results, it can be concluded that both nanofillers accelerate the degradation process of PLA. In addition, the degradation mechanism of PLA is greatly affected by the quality of nanofillers dispersion, due to the creation of aggregates.

References

1. Fukushima, K. , Abbate C., Tabuani D., Gennari M., Camino G., Polym Degrad Stab 2009, 94, 1646.
2. Pluta M, Murariu M, Alexandre M, Galeski A, Dubois P, Polym Degrad Stab, 2008, 93, 925-931. 3.Saha S.K, H. Tsuji, Polym Degrad Stab 2006, 91, 1665-1673.

New copolymers derived from pyrrolidine and cyclodextrin with applications in Gene Therapy

J. A. Redondo[1], D. Velasco[1], A. Gallardo[1], H. Reinecke[1], A. Fernández-Mayoralas[2], G. Corrales[2], E. García-Doyagüez[2], A. Pandit[3], C. Elvira[1]

[1]Instituto de Ciencia y Tecnología de Polímeros (ICTP), CSIC
[2]Instituto de Química Orgánica General (IQOG), CSIC
[3]Network of Excellence for Functional Biomaterials (NFB), National University of Ireland, Galway

jaredondo@ictp.csic.es

Introduction

Cationic polymers, such as the poly-methacrylamide of [*N*-(2-aminoethyl pyrrolidine)] (EPA) (**Fig. 1**) are not only interesting due to their pH sensitivity and their application in controlled release, but also for their ability to complex with another systems, of anionic nature, such as drugs or nucleic acids. Cationic polymers are being evaluated as alternative vectors to viruses in Gene Therapy, due to some advantages like the absence of immunogenicity or patogenicity risk, or their lack of limitation in the length of the nucleic acid that is going to be delivered. Nevertheless, the transfection levels observed are significantly lower than using viral vectors *(a)*. The low transfection efficiency could be, in part, due to some excess of positive charge, aspect that could be improved by copolymerization with some neutral and hydro soluble monomers, such as dimethylacrylamide (DMA) or the methacrylamide of N-(2-hydroxypropyl) (HPMA), that are biocompatible, nontoxic, and non immunogenic. In our previous works, some of these copolymers were evaluated, and the results showed that the biocompatibility and transfection efficiency of these non viral vectors was significantly improved with respect to the EPA homopolymer.

In the present work the systems were prepared using another biocompatible and more complex monomer, a permethylated monomer derived from β-Cyclodextrin (βCD), a cyclic oligosacharide, that was copolymerized with EPA and the resulting copolymers were evaluated as non viral vectors (**Fig 1**).

Materials and methods

The EPA monomer was synthesized as previously described *(b)*, and the βCD monomer was prepared by the Química Bio-orgánica Group (IQOG-CSIC).

The EPA-CD copolymers were prepared by free radical polymerization using two different molar ratios of βCD, 5% and 10% molar. These polymeric systems were characterised by ^{1}H-NMR. The molecular weights were determined by GPC and the sensitivity to pH was measured by an acid-base titration. Polymers complexation ability with plasmidic DNA, at different N/P ratios (w/w) was studied by Gel Retardation Electrophoresis. Alamar Blue assay and an haemolysis assay were carried out in order to check their toxicity and biocompatibility. The particle size of the polyplexes and their superficial charge were measured, in order to check if they were suitable for the internalization into the cells. Finally transfection experiments were carried out using 3T3 cells in serum free media and luciferase as reporter gene. The transfection levels were determined by measuring the luciferase activity after 48 hours of incubation, using Polyethylenimine (PEI) (25000 kDa, hyperbranched) as positive control.

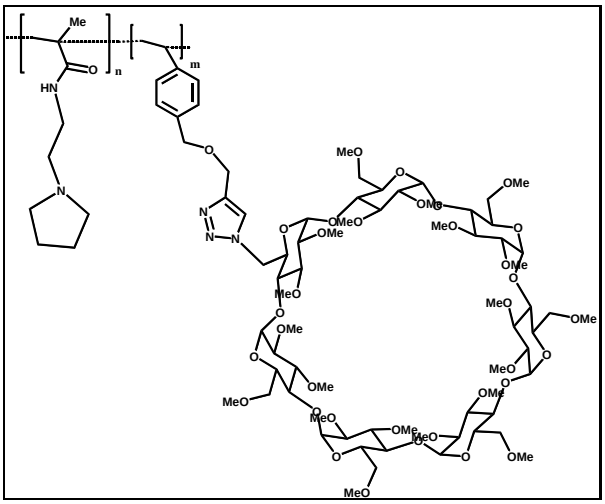

Fig 1. Chemical structure of the EPA-CD copolymers.

Results and Discussion

The ^{1}H-NMR spectra of the prepared copolymers confirmed the chemical structure and high purity grade.

The Gel Retardation Electrophoresis shows that all copolymers were able to complex with the plasmidic DNA at different N/P ratios (w/w), obtaining polyplexes with a proper size for internalization into the cells (200 nm), that are also stable in solution (Z-potential around 30 mV). The Alamar Blue results indicate that these systems are biocompatible. Finally, the transfection levels obtained after 48 hours in serum free media are significantly higher than the levels reported with the PEI, and also significantly higher than the results in our previous study with the copolymers of EPA with HPMA or DMA.

Conclusions

New cationic systems EPA-βCD were prepared and characterized. These copolymers exhibited low levels of toxicity and better transfection efficiency than the systems previously studied, and the obtained by the positive control PEI.

References

a. S. Y. Wong, *et al. Prog. Polym. Sci.* 2007, 32, 799–837
b. D. Velasco, C. Elvira, J. San Román. *J Mater Sci: Mater Med* 2008, 19, 1453–1458
c. A. Rasheed *et al. Sci. Pharm.* 2008, 76, 567-598

Aknowledgement

This project is made possible by the pre-doctorate grant *JAE Pre_09_02225*, from the Consejo Superior de Ivestigaciones Científicas (CSIC).

Biomimetic Block Copolymer Membranes for Functionalized Surfaces

S. Toughraï, E. Rakhmatullina, V. Malinova, N. Bruns, W. Meier

Department of Chemistry, University of Basel, Klingelbergstrasse 80, CH-4056 Basel, Switzerland.

Smahan.toughrai@unibas.ch

Introduction: The functionalization of surfaces using biomimetic block copolymer membranes aims at developing smart surfaces for biotechnological applications such as biosensing. Instead of lipid membranes, amphiphilic block copolymer membranes were chosen as mimics of biological membranes due to properties such as tunable thickness, chemical and mechanical stability, lower permeability, fluidity, mobility, etc. Upon insertion of membrane proteins, these systems could allow for the preparation of mechanically and chemically robust and air-stable biosensor devices.

Materials & Methods: Surface-initiated atom transfer radical polymerization (ATRP) provides good control of brush thickness by controlling polymer molecular weight and by initiating polymerization of a second monomer from the free end of the first chain. Poly(2-hydroxyethyl methacrylate)-*block*-poly(n-butyl methacrylate)-*block*-poly(2-hydroxyethyl methacrylate), PHEMA-*b*-PBMA-*b*-PHEMA block copolymers were synthesized with the first PHEMA block anchored to a self-assembled monolayer of initiators on a gold surface, while the other PHEMA block was exposed to the outer surface. To achieve this, a self-assembled monolayer of ($BrC\text{-}(CH_3)_2COO(CH_2)_{11}S)_2$) initiator was formed by disulphide − gold covalent bonding. This initiator was synthesized as previously reported[1]. HEMA monomer was then polymerized by ATRP. The first PHEMA block initiated the polymerization of BMA. Subsequently, the PBMA block initiated HEMA polymerization, thus resulting in a triblock copolymer membrane anchored to the gold substrate. Gold surfaces were prepared according to Naumann et al.[2]. Block copolymer brushes of differing block lengths were prepared and characterized, both on the gold surfaces and – after detaching from the solid support – in solution.

Results and Discussion[3]: The grafted triblock copolymer brushes exhibit an amphiphilic structure where hydrophilic (PHEMA) and hydrophobic (PBMA) blocks of the polymer chain that have the potential to respond variably to solvent treatment. To test the solvent response behaviour of the triblock copolymer, block-selective solvent as well as an effective, common solvent for the entire triblock system were used for swelling experiments. Ethanol was chosen as a solvent for the triblock copolymer chains, whereas hexane and water selectively swell PBMA and PHEMA blocks, respectively. The PHEMA blocks swell considerably in water, whereas the hydrophobic PBMA block minimizes its contact with aqueous surroundings. However, the phase segregation was shown to be reversible because re-immersion of the sample into one of three tested solvents resulted in reproducible morphologies. Figure 1(a) shows the 3D topography image of the wet copolymer chains on the gold surface. After drying, the sample acquired nanodomain surface topography [Fig. 1(b)].
Upon swelling in water, the brush-like structure of the macromolecules assumes a stretched conformation of the PHEMA chains. Drying most probably causes a collapse of the polymer brushes and thus formation of nanodomains. The reversibility of the phase segregation proves the covalent attachment of the block copolymer layer and shows the potential use of these block copolymer membranes as responsive surfaces.

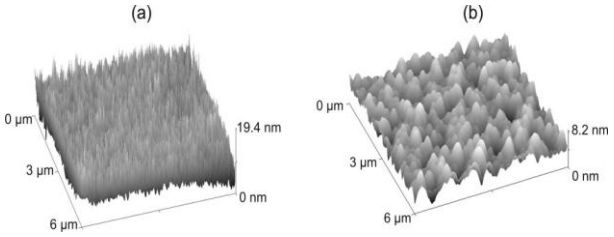

Fig. 1: Contact mode AFM analysis of the amphiphilic triblock copolymer membrane in water (a) and after sample drying (b).

Conclusion: ATRP was successfully applied to the grafting of ABA-triblock copolymer membranes from gold supports. The length of each individual block was controlled by varying the polymerization time. The amphiphilic character of the triblock copolymer brushes provided a responsive surface that showed a solvent-dependent arrangement of the block copolymer chains, which was also reflected in the morphologies of the dried films. Polymer brushes such as these, exhibiting a hydrophilic-hydrophobic-hydrophilic sequence, could be regarded as the first example of solid supported, biomimetic block copolymer membranes prepared by a "grafting-from" approach.

References: [1] S.Belegrinou, et al., *Synth. Comm.*, **2010**, **40**:3000-3007. [2] R.Naumann, et al., *Langmuir*, **2003**, **19**:5435-5443. [3] E.Rakhmatullina, et al., *J. Polym. Sci. A*, **2009**, **47**:1-13.

Acknowledgements: The authors thank Hans-Peter Lang for help with the preparation of gold substrates, and Dr. Serena Belegrinou and Dr. Raffaello Masciadri for helpful discussions on the synthesis and characterization of the triblock copolymer brushes. This work is supported by the Swiss National Science Foundation within the framework of the National Research Programme NRP 62.

Biodegradable Micellar Polymer Drug Carriers Based on *N*-(2-Hydroxypropyl)methacrylamide Copolymers

Petr Chytil, Tomáš Etrych, Karel Ulbrich

Institute of Macromolecular Chemistry, Academy of Sciences of the Czech Republic, v.v.i.
Heyrovský Sq. 2, 162 06, Prague 6, Czech Republic

e-mail: chytil@imc.cas.cz

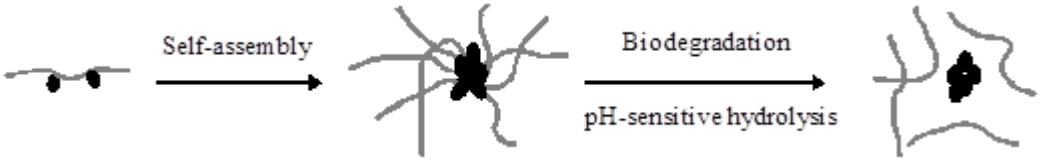

Introduction

N-(2-Hydroxypropyl) methacrylamide (HPMA) copolymers are used as polymer precursors in the synthesis of water-soluble polymer-drug conjugates. The conjugates containing anticancer drug, e.g. doxorubicin or dexamethasone, bound through a pH-sensitive hydrazone bond exhibited a significant therapeutic effect in the treatment of mouse lymphomas[1]. While the hydrazone bond is relatively stable at neutral pH (modeling blood pH), drug is released under mild acid conditions imitating intracellular environment (endosomes in tumour cells).

Introduction of hydrophobic cholesterol moieties into the HPMA copolymer structure resulted in an amphiphilic copolymer self-assembling into micelles in aqueous solutions[2]. The conjugate of such high-molecular-weight drug carrier with doxorubicin showed enhanced tumour accumulation and significant anti-tumour activity (with up to 100 % of long-term survivors) in the treatment of EL-4 lymphoma due to the EPR (enhanced permeability and retention) effect.

Here, we present the synthesis and physico-chemical properties of biodegradable micellar polymer drug carriers. While the former micellar system was nondegradable, the new one is designed as hydrolytically degradable. Micelles are formed by self-assembly of amphiphilic HPMA copolymer bearing hydrophobic cholesterol-derived moieties, bound by pH-sensitive hydrazone bond. Degradation of the linkages in mildly acidic environment of tumour cells followed by disassembling of the supramolecular structure might facilitate renal removal of polymers forming micelles from the body.

Result and Discussion

A set of amphiphilic polymer drug carriers was prepared by conjugation of linear water-soluble HPMA copolymer bearing free hydrazide groups (5.7 mol%) with hydrophobic cholesterol-like moieties, i.e. 5*a*-cholestan-3-one, cholest-4-en-3-one, cholest-5en-3*β*-yl 4-(2-oxopropyl)benzoate and cholest-5en-3*β*-yl 4-oxopentanoate. Formation of hydrazone bond did not significantly influence molecular weight of the copolymers, which was aprox. $2.5 \cdot 10^4$. However, introduction of hydrophobic substituents (1 – 3 mol%) resulted in self-assembly of the copolymers in aqueous solutions and formation of micelles. Hydrodynamic radii (R_H) and apparent molecular weights (M_{app}) of the micelles were growing with increasing content of hydrophobic moieties. These findings are in agreement with results of our previous study using cholesterol-bearing HPMA copolymers with cholesterol bound by ester bond almost stable in body fluids[2]. Presence of doxorubicine attached to the carrier by hydrazone bond influenced neither R_H nor M_{app}.

The amount of cholesterol-derived moieties released from the micelles incubated in phosphate buffers of pH 5.0 or 7.4 at 37°C was determined by HPLC or GC after their extraction into chloroform. 5*a*-Cholestan-3-one and cholest-5en-3*β*-yl 4-oxopentanoate were released at pH 5.0 with the highest rate while cholest-4-en-3-one or cholest-5en-3*β*-yl 4-(2-oxopropyl) benzoate were released more slowly as a result of stabilization of hydrazone bond situated in vicinity of aliphatic or aromatic double bonds. The rates of release of all cholesterol derivatives at pH 7.4 were significantly slower.

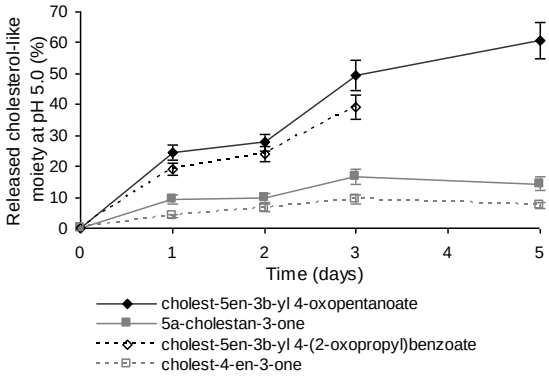

The direct observation of hydrolysis was performed by DLS. During hydrolysis R_H increased with time from ~13 nm up to 30 – 60 nm while their distribution became narrower. Probably, in this static settings of experiment the released cholesterol-like moieties did not escape from micelles, rearranged their hydrophobic core forming new and larger micelles.

Conclusion

HPMA copolymer-cholesterol micelles are promising polymer drug carrier with high potential for solid-tumour-targeting and polymer elimination after fulfilling its carrier role.

References

[1] Etrych T. et al., *J. Appl. Polym. Sci.* 2008, *109(5)*, 3050-3061.; Šírová M. et al., *Pharm. Res.* 2010, *27 (1)*, 200-208.; Kostková H. et al., *J. Bioact. Compat. Polym.*, accepted for publication

[2] Chytil P. et al., *J. Controlled Release* 2008, *127*, 121-130

Acknowledgements

This work was supported by Grant Agency of Academy of Sciences of the Czech Republic, grants No. IAAX00500803 and No. IAA400500806.

PEG and Tartaric Acid: crosslinking agents and spacers for targeting delivery of chitosan nanogels

Leyre Pérez, Maite Artetxe and L. Carlos Cesteros

New Materials and Supramolecular Group. Department of Physical Chemistry, Faculty of Science and Technology, University of the Basque Country 48940 Leioa, Vizcaya, Spain

leyre.perez@ehu.es

Introduction: Chitosan is a renewable polysaccharide widely used in pharmaceutical and medical areas because of its favorable biological properties[1]. A limiting factor in the application of chitosan is its low solubility in aqueous media at neutral conditions. Due to the presence of reactive amino groups, chitosan can be modified easily to achieve the desired moieties, create crosslinked structures or get improved properties. The toxicity of the most used chitosan covalent crosslinker, glutaraldehyde, has supposed a need of developing non-toxic and biocompatible crosslinking agents for chitosan. Only a few studies[2] have proposed this dual-purpose chemical modification of chitosan with a biocompatible hydrophylic crosslinkers in order to generate biocompatible chitosan networks and, simultaneously, impart water-solubility properties to the gel.

Besides, chitosan was found to be an attractive targeting nanodevice for drug and gene delivery because of its high positive charge density and relatively low cytotoxicity[3]. In this regard, it has been roughly accepted that the introduction of a spacer molecule among the nanodevice and the targeting agent enhances the cellular association of nanocarrier.

According to the previous information, the aim of this work was to synthesize chitosan nanogels by modification with biocompatible dicarboxylic acids which play a triple role: first as biocompatible crosslinking agent, second improving hydrophilicity of the nanogels and third playing as spacer molecule for posterior targeting reaction.

Materials and Methods: The chitosan and crosslinker agent microemulsions were separately prepared mixing their aqueous solution with cyclohexane, n-hexanol and by adding Triton X-100 until the mixed emulsion became transparent. The W/O microemulsion of crosslinker was previously activated with *N*-(3-Dimethylaminopropyl)-*N´*-ethylcarbodiimide hydrochloride (EDC) and *N*-hydroxysuccinimide (NHS). The crosslinking reaction took place after the addition of the crosslinker microemulsion into the chitosan microemulsion during 24 hours at room temperature. The nanoparticles were isolated and washed by dispersion in ethanol and posterior centrifugation. Finally, the obtained nanogels were dispersed in acetic acid solution, ultrafiltred and dried.

Results and Discussion: Chitosan was crosslinked with two dicarboxylic acids with different chain length, such as, tartaric acid and Poly(ethylene glycol) bis(carboxymethyl)ether $PEG(COOH)_2$, by inverse microemulsion with different chitosan/crosslinking ratios in order to obtain simultaneously crosslinked and activated nanogels as Figure 1 shows.

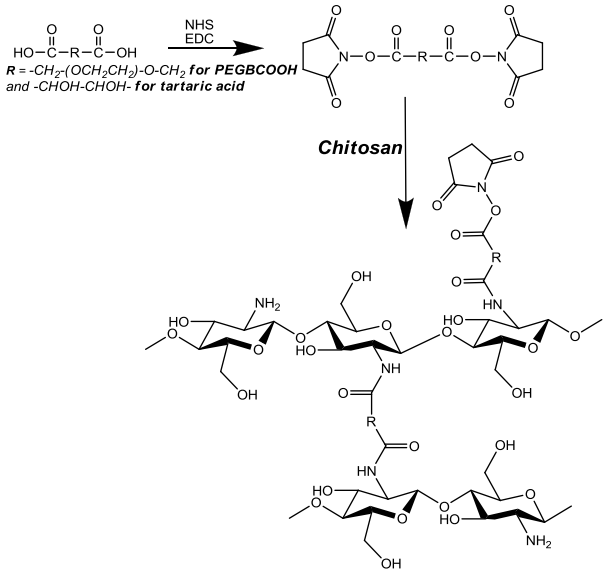

Figure 1. Chitosan modification reaction

The structure of modified chitosan was clearly confirmed by IR and ^1H NMR spectroscopy. The qualitative study of the evolution of the crosslinking reaction was performed by IR spectroscopy. The amide C=O stretching at 1655 cm^{-1} and amide N-H stretching at 1560 cm^{-1} was increasing in the spectra of chitosan while crosslinking proportion increased. In the case of tartaric acid, the closed nature of the network was confirmed by the presence of the band at 1730. cm^{-1} in IR spectra at long time of reaction corresponding to the ester bond of NHS-pendant groups unable to react. The crosslinking reactions could be quantitative evaluated by the decreased of the peak located at 3.2 ppm in the ^1H NMR spectra assigned to the proton of H-2 protons of glucosamine moieties. In all the cases maleic acid was used as internal standards (D_2O, δ = 6.0 ppm).

TEM images of chitosan nanogels indicated that the particles are spherical and have a mean particle size closed to 50 nm.

The pH dependence of the water dispersability of synthesized nanogels was studied by turbidimetry and, in most cases, improved properties were obtained respect to chitosan as crosslinker ratio increases.

Conclusions: Chitosan nanoparticles have been obtained by partial modification with $PEG(COOH)_2$, and tartaric acid resulting in activated systems for potential applications in targeting therapy.

References:

1.- Rinaudo M. *Prog.Polym.Sci.* 2006; **31**: 603-632
2.- Bodnar M.,Hartmann J. F., Borbely J. *Biomacromol.* 2006; **7**: 3030-3036
3.- Ravi Kumar MNV, Muzzarelli RAA, Muzzarelli C, Sashiwa H, *Chem Rev.* 2004;104:6017–84.

Immobilization of glucose oxidase in conducting graft copolymers and determination of glucose amount in orange juices with enzyme electrodes

Huseyin Bekir YILDIZ[1], Senem KIRALP[2], Levent TOPPARE[2], Yusuf YAGCI[3]

[1] Department of Chemistry, Karamanoglu Mehmetbey University, 70100 Karaman, Turkey
[2] Department of Chemistry, Middle East Technical University, 06531 Ankara, Turkey
[3] Department of Chemistry, Istanbul Technical University, Maslak, 34469 Istanbul, Turkey

yildizhb@kmu.edu.tr, yildizhb@gmail.com, toppare@metu.edu.tr

Introduction: Biosensors containing enzymes have been widely applied in chemistry and biology due to their high sensitivity and potential selectivity, in addition to low cost and possibility of miniaturization or automation. In this study, immobilization of glucose oxidase was done via entrapment within three different polypyrrole/poly(methyl methacrylate (PMMA)-co-thienyl methacrylate (PMTM)) matrices (Scheme 1). The types of PMMA-co-PMTM random copolymers were coded as MT1, MT2, and MT3. Although they have the same segments, they have different copolymer
compositions (Table 1). These random copolymers were synthesized and characterized previously [1]. Optimu conditions for immobilized glucose oxidase, such as pH, temperature, and kinetic parameters (Km and Vmax) were investigated. The operational stability studies of these enzyme electrodes were done. The amount of glucose in two orange juices of Turkey were determined using these enzyme electrodes.

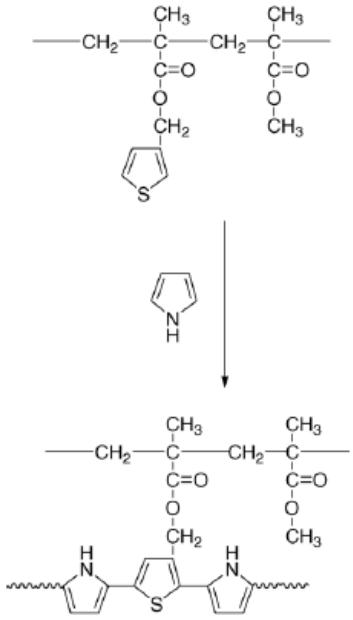

Scheme 1: Synthesis of conducting polymer of PMMA-co-PMTM/PPy.

Table 1
Random copolymers

Code	Mn	Copolymer composition (mol%)	
		PMTM	PMMA
MT1	1.1×10^5	17	83
MT2	1.1×10^5	25	75
MT3	1.2×10^5	45	55

Materials and Methods: Glucose oxidase, (37,700 U/g) Type II-S, (GOD, EC:1.1.3.4), peroxidase, Type II, (POD, EC: 1.11.1.7), *o*dianisidine, and sodium dodecyl sulfate (SDS) were purchased from Sigma. Pyrrole (Merck) was distilled before use and stored at 4 °C. Sulfuric acid and hydrogen peroxide were supplied by Merck. Potentioscan Wenking POS-73 potentiostat and Shimadzu UV-160 model spectrophotometer were used.

Immobilization process was achieved by electropolymerization of pyrrole on bare or any one of MT1-, MT2-, MT3-coated platinum electrodes (1 cm2). Polymerization reactions were carried out by applying 1.0V for 20 min at 25 ◦C. In order to determine maximum velocity of the reaction (V_{max}) and the Michaelis–Menten constant (K_m) for each electrode, activity assay was applied for different concentrations of glucose. The reaction temperature was changed between 10 and 80 ◦C while glucose concentration was kept constant at 10Km for every case. For pH optimization at 25 ◦C, the pH of the reaction was altered between pH 4 and 11 while glucose concentration was kept constant at 10 Km. The activities were determined as previously described [2].

Results and Discussion: This study shows that GOD can be successfully immobilized in PPy, MT1/PPy, MT2/PPy, and MT3/PPy matrices. As regards to temperature, pH and operational stability MT1/PPy/, MT2/PPy, and MT3/PPy enzyme electrodes yield very good results. Only other hand, PPy electrode reveals the best Km and Vmax values among enzyme electrodes. Immobilization of glucose oxidase enzyme in conducting polymer electrodes was studied as an alternative method.

Conclusion: The enzyme electrodes can be used with a considerable activity for determination of glucose. Their wide working ranges observed for temperature and pH and biosensing advantages over conventional methods such as their simplicity, rapidity and low cost make them very useful. For the determination of glucose amount in fruit juices and results show that this significant development can successfully replace the classical methods.

References:

1. Yildiz H.B., Kiralp S., Toppare L., Yagci Y., *J. Appl. Polym. Sci.*, 96 (2005) 502-507.
2. Yildiz H.B., Sahmetlioglu E., Boyukbayram A.E., Toppare L., Yagci Y., Int. J. Biol. Macrom., 41 (2007) 332-337.

Elaboration of Functionalized Polylactide Nanoparticles from *N*-Acryloxysuccinimide-Based Block Copolymers for Drug Delivery Applications

Nadège Handké,[1] *Thomas Trimaille*, [1] *Elsa Luciani*, [2] *Marion Rollet*, [1] *Thierry Delair*, [3] *Bernard Verrier*, [2] *Denis Bertin*, [1] *and Didier Gigmes*[1]

[1] Laboratoire Chimie Provence - UMR 6264, Universités d'Aix-Marseille I, II et III - CNRS, Case 542, Av. Escadrille Normandie-Niemen, 13397 Marseille Cedex 20, France

[2] Institut de Biologie et de Chimie des Protéines - UMR 5086, Université Lyon 1 - CNRS, 7 Passage du Vercors, 69367 Lyon, France

[3] Laboratoire des Matériaux Polymères et Biomatériaux - UMR 5223, Université Lyon 1 - CNRS, 15 Boulevard Latarjet, 69622 Villeurbanne, France

nadege.handke@univ-provence.fr

Introduction

Polylactide (PLA) nanoparticles are attractive candidates for drug delivery systems because of their biocompatibility and biodegradability properties.[1,2] Their potential could be further increased through the coupling of appropriate receptor ligands at the particle surface. However, such coupling can hardly be performed due to the lack of functional groups on PLA. In this context, we focused on the synthesis of poly(D,L-lactide)-*b*-poly(*N*-acryloxysuccinimide-*co*-*N*-vinylpyrrolidone) (PLA-*b*-P(NAS-*co*-NVP)) and their use as surface modifier in the PLA particle preparation process, for further coupling of amino-bearing biomolecules of interest through the *N*-succinimidyl ester moieties of the NAS units

Results and Discussion

For this purpose, nitroxide mediated polymerization (NMP) of NAS and NVP was performed from a SG1 functionalized poly(D,L-lactide) (PLA-SG1) macro-alkoxyamine as initiator, in the presence of free SG1 nitroxide (*N*-(2-methylpropyl)-*N*-(1-diethylphosphono-2,2-dimethylpropyl)-*O*-(2-carboxylprop-2 yl)hydroxylamine), in DMF at 120°C. The PLA-SG1 macro-alkoxyamine was previously obtained by 1,2-intermolecular radical addition (IRA) of the MAMA-SG1 alkoxyamine (BlocBuilder MA) onto acrylate end-capped PLA previously prepared by ring opening polymerization (ROP) (scheme 1).[3]

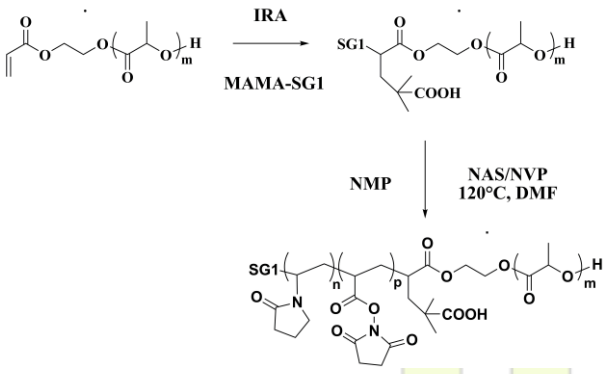

Scheme1. Strategy of synthesis of PLA-b-P(NAS-co-NVP), using PLA-SG1 macro-alkoxyamine as initiator for NAS/NVP NMP.

The reactivity ratios of NAS and NVP were determined to be r_{NAS}=0.17 and r_{NVP}=0,02, when copolymerization was conducted from PLA-SG1 macroinitiator, indicating a strong alternating tendency for the P(NAS-*co*-NVP) block, and were very similar to those obtained for a P(NAS-*co*-NVP) initiated from a molecular alkoxyamine as initiator (MAMA-SG1). The PLA-*b*-P(NAS-*co*-NVP) block copolymer was characterized by GPC in DMF and ^{1}H NMR.

This copolymer was then further used as a surface modifier for the PLA diafiltration and nanoprecipitation processes to achieve biodegradable nanoparticles in the range of 450 nm and 150 nm, respectively, without aggregates, as shown in figure 1. The presence of the *N*-succinimidyl ester moieties at the particle surface was evidenced by ethanolamine derivatization and zeta potential measurements.

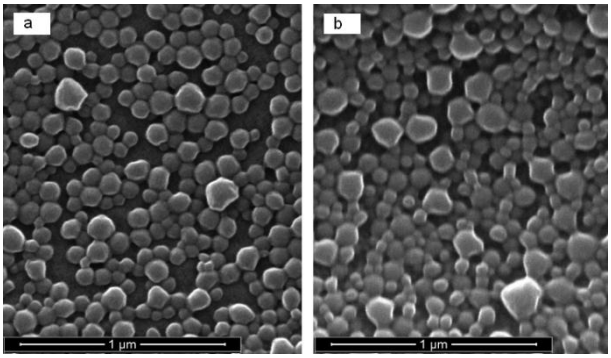

Figure 1. SEM images of functionalized (a) and naked (b) nanoparticles PLA particles obtained by nanoprecipitation

Conclusions

These particles with highly functional surface properties represent a generic system of high interest in drug delivery applications for coupling of amino-bearing ligands.

References

1. Jalil, R.; Nixon, J. R. *J. Microencapsul.* **1990,** 7, (3), 297-325.

2. Mundargi, R. C.; Babu, V. R.; Rangaswamy, V.; Patel, P.; Aminabhavi, T. M. *J. Controlled Release* **2008,** 125, (3), 193-209.

3. Clément, B.; Trimaille, T.; Alluin, O.; Gigmes, D.; Mabrouk, K.; Féron, F.; Decherchi, P.; Marqueste, T.; Bertin, D. *Biomacromolecules* **2009,** 10, (6), 1436-1445.

Preparation of Pluronic Micelles for Ophthalmic Delivery Using Ethyl Acetate as a Dispersion Agent

Hong-Ru Lin, Pei-Csang Chang, Huei-Jen Kao[1]

Department of Chemical and Materials Engineering, Southern Taiwan University, Tainan 710, Taiwan
[1]Department of Pharmacy, Chia-Nan University of Pharmacy and Science, Tainan 717, Taiwan

E-mail: hrlin@mail.stut.edu.tw

Introduction

Pluronic is a class of block copolymers, consisting of poly(oxyethylene) (PEO) and poly(oxypropylene) (PPO) units. Once blocks of PEO and PPO are combined, one can expect amphiphilic characteristics and aggregation phenomena at higher temperatures. In this study, ethyl acetate used as a dispersion agent was added to the pluronic solution to prevent gel formation. One the other hand, the surface of the pluronic micelles was modified by poly (ethylenglycol) methyl ether (MPEG) to improve their surface hydrophilicity. The improvement in hydrophilicity is expected to improve the encapsulation efficiency of loading hydrophilic drug.

Experimental

Two drops of span 80 were added to pluronic solution with fast agitation, and then ethyl acetate solution with MPEG was slowly added and was stirred completely until completely dispersed. Finally, the completely mixed solution was freeze-dried to obtain micelle particles. The particle size and its distribution of the micelles were investigated. The morphology of the micelles was observed by transmission electron microscopy (TEM). Turbidity test of the micelle solution was investigated.

Results and discussion

When the Pluronic concentration and the characteristic temperature are above a critical point, this block copolymer forms micelles. These micelles will aggregate to form gel by the chain entanglement between the micelles. In order to prevent gel formation, ethyl acetate used as a dispersion agent was added to the pluronic solution. The hydrophobic chains in both ends of ethyl acetate may interfere with the chain entanglement between micelles, thus preventing the gel formation. Figure 1 shows the photographs of pluronic solution at critical micelle concentration (28 wt %). The solution formed gel without the addition of ethyl acetate (Fig. 1 (A)), however, no gel formation was found when the ethyl acetate was incorporated (Fig. 1 (B)).

Figure 2 shows the typical morphology of micelles observed by TEM. The micelle with a spherical shape (Fig. 2 (A)) has a core-shell like structure with hydrophobic segments in the core (light region in the photograph) and hydrophilic segments in the shell (dark region in the photograph). The particles of micelles were well distributed as shown in Fig. 2 (B). The average size of pluronic micelles is about 200 to 350 nm. In this study, the surface of the pluronic micelles was modified by MPEG to improve their surface hydrophilicity. The improvement in hydrophilicity is expected to improve the encapsulation efficiency of loading hydrophilic drug. The size of pluronic micelles was increased (300 to 500 nm) after surface modification by MPEG.

Different amount (0.05 and 0.1 g) of micelles was soaked in the PBS and was observed by UV-Visible to investigate their turbidity (Fig. 3). The result indicates both amounts of micelles had constant turbidity during 5 h investigation. This suggests the micelles prepared in this study were very stable in the PBS environment. In the case of 0.05 g of micelles, the penetration was higher than 90% even after 5 h investigation; the blurred vision can be avoided after topical administration of the micelles suspension.

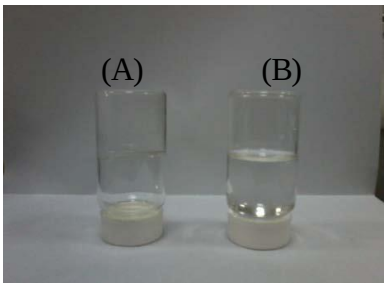

Fig. 1 The photographs of pluronic solution at critical micelle concentration (28 wt%). The solution formed gel without the addition of ethyl acetate (Fig. 1 (A)), however, no gel formation was found when the ethyl acetate was incorporated (Fig. 1 (B)).

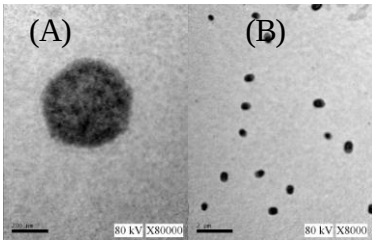

Fig. 2 The morphology (A) and distribution (B) of micelles observed by TEM.

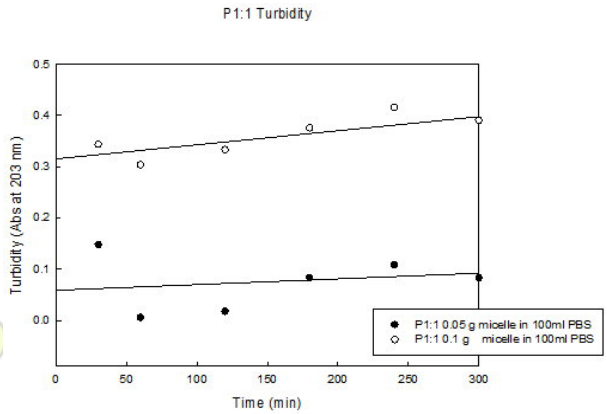

Fig. 3 The turbidity test of pluronic micelles under PBS environment

Effect of the crosslinker in Molecularly Imprinted Polymers

I. Iturralde, M. Paulis, J. R. Leiza

POLYMAT-Grupo de Ingeniería Química. Fac. Química SS, EHU/UPV

ibon.iturralde@ehu.es

Introduction: Molecularly Imprinted Polymers (MIP) are synthetic materials with high molecular recognition capacity that mimic the functions of enzymes and biological antibodies. Molecularly Imprinted Polymers present higher robustness to temperature, pH, solvents or impurities of the reaction and molecular recognition media than the enzymes and biological antibodies.

The art of molecularly imprinted polymer synthesis involves the self-assembly between a functional monomer and a template molecule in presence of a crosslinking monomer and a solvent that acts as porogen. Typically, molecularly imprinted polymers synthesis is carried out by bulk polymerization in which MAA is used as functional monomer and EGDMA as crosslinking agent.

The following work involves the synthesis of molecularly imprinted polymers of Propranolol with different crosslinking agents bearing different chain lengths. The influence of the different swelling capacities produced by each crosslinker on rebinding capacity and specificity of the MIP was also studied.

Materials and Methods: Methacrylic Acid (MAA) (0.02 mmol), used as functional monomer, was purchased by Sigma Aldrich. The crosslinking agents (1 mmol) Ethylene Glycol Dimethacrylate (EGDMA), 1, 6 Hexanodiol Dimethacrylate (HDDMA), 200-Poly Ethylene Glycol Dimethacrylate (PEGDMA) and Allyl Methacrylate (AMA) were obtained from Sigma Aldrich. The R, S-Propranolol Hydrochloride was used as template (Sigma Aldrich). The R, S-Propranolol was hydrophobized by an aqueous solution of NaOH and extracted in presence of Chloroform. The initiator used was 2, 2′-Azobisisobutyronitrile (0.025 mmol) supplied, by Wako. Toluene was employed as porogen. The polymerization took place in vials at 70ºC. In order to establish the amount of template specifically adsorbed, the same recipes without template were polymerized in order to obtain the non-imprinted polymers (NIP). The resulting monoliths were grounded and cleaned in AcOH NH_4/MeOH/AcOH/H_2O solution, followed with several cleanings with MeOH/AcOH (90/10 volume ratio) in order to extract the R, S-Propraonolol. L-[4-3H]- Propranolol, purchased by Perkin Elmer, was used for rebinding experiments according to the procedure developed by Andersson [1]. The experiments were carried out in a Packard liquid sparkle detector, Tricarb 2000 CA model. The swelling experiments were performed using the methodology proposed by Lu et al.[2] and Tan et al.[3]. Surface BET analysis was carried out to determine the structural characteristics of the MIPs and NIPs (ASAP 2020 apparatus).

Results and discussion: MIPs having different chain length crosslinker were used in rebinding trials. MIPs synthesized with AMA rebound the highest amount of L-[4-3H] – Propranolol, while PEGDMA MIPs presented the lowest rebinding capacity. Regarding to the specificity, the difference between the template rebound in MIP and NIP, surprisingly AMA samples showed the highest value. HDDMA and EGDMA samples presented quite similar high specificity and PEGDMA MIP had poor selectivity for L-[4-3H] – Propranolol.

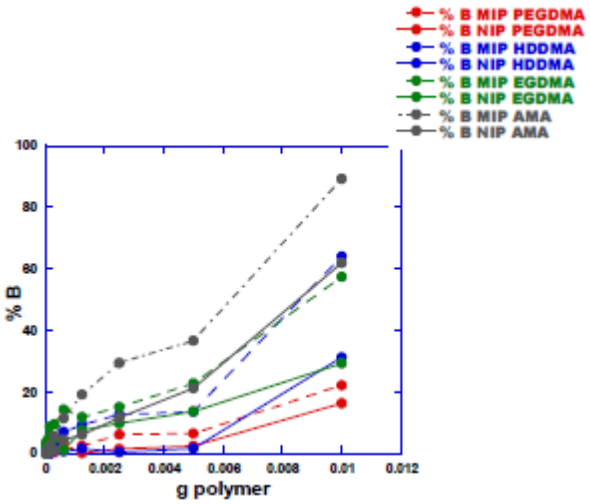

Swelling and specificity results were compared in order to establish a relationship between structure and template affinity. The highest swelling was related to the less specific MIP, the one synthesized with PEDGMA. The lowest swelling was obtained for the MIP with AMA. Quite similar values were observed for MIPs synthesized with EGDMA and HDDMA.

Conclusions: MIPs having different branch length crosslinkers were synthesized. Surprisingly, the highest imprinting capacity and specificity was observed for MIPs synthesized with AMA and HDDMA. MIPs with EGDMA, widely used in the literature, showed a slightly lower specificity. PEGDMA did not present any specificity for Propranolol. High swelling ratios were related with to imprinting capacity.

Acknowledges:

I. Iturralde acknowledges the scolarships by the Ministerio de Educación (BES2007-16021) and the Ministerio de Ciencia e Innovación (TME2009-0081).

References:

1. Andersson, L.I. Analytical Chemistry, 1996. **68**(1): p. 111-117.
2. Lu, S., G. Cheng, and X. Pang,Journal of Applied Polymer Science, 2006. **100**(1): p. 684-694.
3. Tan, C.J. and Y.W. Tong. Analytical Chemistry, 2006. **79**(1): p. 299-306.

Chitosan based microspheres with good swelling characteristics

Małgotzata Maciejewska, *JoannaOsypiuk-Tomasik*

Faculty of Chemistry, Maria Curie-Skłodowska University, Gliniana 33, 20-614 Lublin, Poland

e-mail: mmacieje@umcs.pl

Introduction

Polymer microspheres are broadly defined as spherical polymer particles in the size range of about 20 nm to 2,000µm. They can be derived from numerous inorganic and organic monomers as well as naturally occurring polymers e.g. chitosan. Chitosan, [poly-β(1-4)-2-amino-2-deoxy-D-glucose], is a polymer derived from chitin in the process of deacetylation. Commercially available preparations have degrees of deacetylation ranging from 50 to 90%. Chitosan is inexpensive, biodegradable, and biocompatible. The main applications concerns agriculture and water treatment, food and cosmetic industries and biopharmaceutical uses[1]. Because of the stable, crystalline structure, chitosan is normally insoluble in aqueous solutions above pH 7. However, in dilute acids, the free amino groups are protonated and the molecule becomes fully soluble below ~pH 5. The lack of solubility in higher pH creates great numbers of limitation in many kind of applications. An addition of suitable amount of hydrosoluble polymer can improve the hydrophilicity of the system. Due to its nontoxicity, biocompatibility and good complexing properties 1-vinyl-2-pyrrolidone can be a good choice. In this work we present the preparation of crosslinked microspheres based on chitosan and 1-vinyl-2-pyrrolidone(VP).

Materials and Methods

Preparation of crosslinked chitosan microspheres

0.8g of chitosan was dispersed in 30ml of 3% acetic acid. The mixture was stirred for 5 h and then sonificated for 15 min. The crosslinker (ethylene glycol dimetacrylate) and the mixture of 1-vinyl-2-pyrrolidone with the initiator (2,2'-azobisisobutyronitryle) were directly added the solution. Different ratios of crosslinker/chitosan and VP/chitosan were used to modulate the crosslinking extent and hydrophilicity of the final product.

The above solution was strirred for 7 h and then poured into a syringe equipped with a micro-pipette tip and dropped into 50mL solution containing 70% of ethanol and 30% of aqueous amomonia solution at 35w/w %.

The droplets give rise to microspheres suspended in the coagulant. They were left under low stirring for 6 h in 65ºC to complete the reaction of crosslinking.

The obtained microspheres were filtred out, washed with deionised water to neutral pH and dried under vacuum. In this way we obtained regular beads with diameter ranging between 300 – 500 µm. The SEM micrograph of the disscused microspheres is presented in Fig. 1.

Swelling

In order to determine the swelling behaviour a suitable number of microspheres was placed into a stainless steel basket containing various buffer solution at 25ºC. The swellability coefficient (B) was expressed as:

$$B = \frac{W_s - W_d}{W_d} \times 100\%$$

where:

W_s-weight of the swollen polymer

W_g- weight of the dry polymer

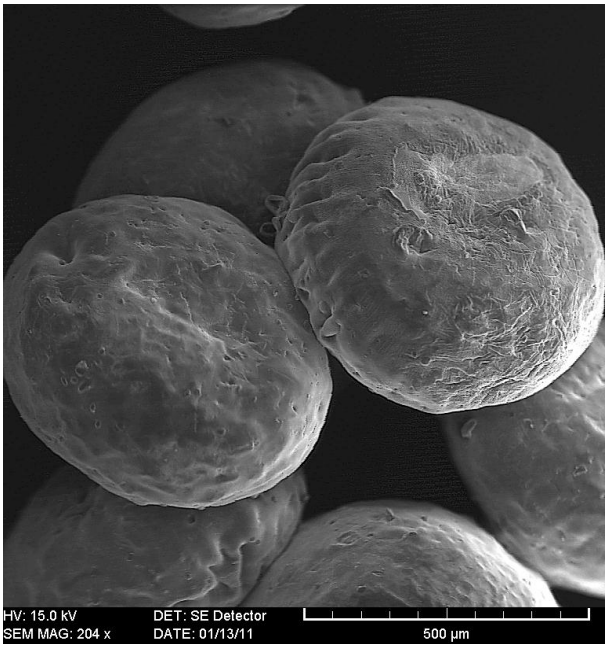

Fig1. SEM micrograph of the obtained microspheres.

Results and Discussion

In contrast to neat chitosan gels, which swell only in acid solution, the chitosan-vinylpyrrolidone microspheres posses the capability of reversible swelling in water at room temperature at pH 7. The swellability coefficient determined in water is strongly dependent on the crosslinking extent and amount of VP incorporated into chitosan matrix. The value of B changes from 0 to 200 and it takes 240min to reach equilibrium swelling, whilethe time necessary to reach the half of the equilibrium is about 60min. Also the pH of the solution influences the value of swellability coefficient. The high value of B in acid environment dropped dramatically after increasing the value of pH above 5.5. The sensitive behaviour ofchitosanmicrospheres is connected with the ioniztation of $-NH_2$ groups.

References

[1] L. Yu, ed. Biodegradable Polymer Blends and Composites, John Wiley & Sons, Inc., Hoboken, New Jersey, 2009

Purification and Characterization of Adhesive Proteins for Footwear

N. Cuesta, M.J. Escoto, C. Orgilés

INESCOP. Footwear Research Institute. 253. 03600 Elda (Alicante)

ncuesta@inescop.es

Introduction

Nowadays, several legislative, economic and environmental awareness factors make necessary the introduction of new industrial production systems that without losing competitiveness were increasingly more and more environmentally friendly.

In response to this need, INESCOP is working on a research line focused on the application of protein adhesives with microbial origin, as the base polymer for the formulation of industrial adhesives.

One of the advantages of using these polymers, compared to other with a non-renewable synthetic origin, lies on the reduction of the risk of environmental pollution which favors the elimination of their waste without harming the environment. Moreover, its composition makes these proteins to be soluble in aqueous medium, avoiding the use of organic solvents in the formulation of adhesives.

Materials and Methods

The study has been focused on a protein from *Bacillus subtilis*, Gram-positive, non-pathogenic and biofilm-forming bacteria, capable of producing high amounts of proteins. According to a sequence alignment analysis (BLAST), this protein has a high percentage of homology with sequences of proteins with known adhesive function.

The involvement of selected protein in biofilm formation mechanisms has been assessed by carrying out bioadhesion assays.

The gene that encodes for the protein was subcloned into a commercial expression vector, pQE60, adding in the carboxyl tail a 6 histidines tag which has been used to purify the target protein throughout a column with a nickel resin bed.

Once the protein had been purified, several tests were conducted to characterize the possible adhesive properties of the protein for its possible use as an adhesive in the shoe industry.

Results

After over-expressing the protein of interest, an increase in the amount of biofilm was determined and a greater affinity for the test surface was observed. In addition, the target protein was purified obtaining remarkable concentration. Finally, the wettability and adhesive ability have been analyzed, showing surprising results that could be improved incorporating leveling and moisturizer additives.

Conclusions

The overexpression of the target protein promotes the biofilm adhesion.

It has been established a protocol for protein purification at laboratory scale.

The purified protein has a good wettability for different substrates representative of materials used in the manufacture of footwear.

The target protein shows remarkable adhesion on the surface. However, the adhesive suffers from a low cohesive strength, which should be improved for its application.

References

1. K. Inoue, et al. J Mol Evol, 43:4, 348-356 (1996).
2. Mélanie A. Hamon and Beth A. Lazazzera. Molecular Microbiology 42 (5), 1199 (2001).
3. Masaaki Morikawa. Journal of Bioscience and Bioengineering 101 (1), 1 (2006).
4. Jessica C Zweers, Imrich Barák, Dörte Becher, Arnold JM Driessen, Michael Hecker, Vesa Kontinen, Manfred J Saller, Ludmila Vavrova and Jan Maarten van Dijl. Microbial Cell Factories 7, 10 (2008).
5. Haeshin Lee, Norbert F. Scherer, and Phillip B. Messersmith. PNAS 13 (35), 12999 (2006)
6. Heather G. Silverman, Francisco F. Roberto. Marine Biotechnology 9, 661 (2007).

Flocculation by Cationic Amphiphilic Polyelectrolytes: Relating Efficiency with Polymer Characteristics and Concentration

Luminita Ghimici, *Marieta Nichifor*

"Petru Poni" Institute of Macromolecular Chemistry, Aleea Grigore Ghica Voda, 41A Iasi, Romania

e-mail: lghimici@icmpp.ro

Introduction

Ionic polymers are widely used to improve the flocculation process efficiency which is of considerable importance in the wastewater treatment. Theoretical and experimental data revealed that the flocculation activity of a polyelectrolyte is strongly sensitive to the polymer characteristics and environment.[1] Although a considerable range of flocculants is now available, new types have to be introduced either to reduce the cost or to provide special functional groups to match the surfaces on which they are required to adsorb. In this context, the current work centers on the flocculation properties of some amphiphilic polyelectrolytes based on dextran carrying pendent quaternary ammonium groups randomly distributed along the polymer backbone (Fig. 1). These polycations varied in hydrophobicity (by variation of the length of the alkyl substituent at the quaternary nitrogen, alkyl= ethyl, butyl, octyl, dodecyl), molar mass (M=40, 200, 400 kg mol^{-1}) and charge density (X= 0.42 and 0.96) and are therefore useful in probing the competitive effect between electrostatic and hydrophobic interactions on the flocculation efficiency.

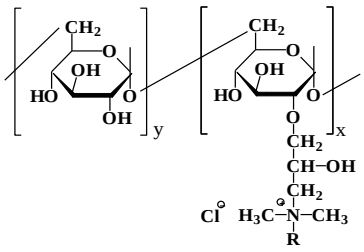

Fig. 1: DM-RX
R= Et (ethyl); Bu (butyl); Oct (octyl); Dod (dodecyl)

Materials and Methods

Cationic polysaccharides with pendent quaternary ammonium groups were synthesized by chemical modification of dextran samples.[2] Each sample was purified by repeated precipitation and dialysis, and finally recovered as a white powder by liofilization. The chemical structure was proved by ^{1}H-NMR, elemental analysis (nitrogen content) and potentiometric titration with 0.02N $AgNO_3$ aqueous solution (chloride ion content). Clay dispersions with concentration of 1g L^{-1} were prepared in distilled water, sonicated for 30 min, followed by vigorous stirring during 15 min.

Turbidity measurements were carried out using a HACH 2100 AN turbidimeter. The zeta potential of clay suspensions in the presence and absence of polycation was measured with a Zetasizer Nano-ZS, ZEN-3500 model (Malvern Instruments). Measurement of particle dimensions was done using laser diffraction technology with a Mastersizer 2000 system (Malvern Instruments, Malvern, England).

Results and Discussion

Influence of polymer dose and hydrophobicity.

Examination of the residual turbidity-polycation dose plots for D40-R30 (Fig. 2) demonstrated a downwards trend of the residual turbidity with increasing polycation dose until a minimum was reached, followed by an increase with a further increase in polycation dose.

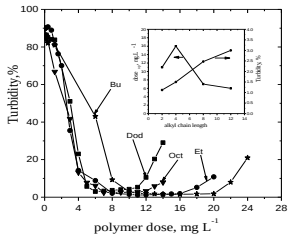

Fig. 2: Residual turbidity dependence on the polymer dose; settling time =15 min.

The alkyl chain length greatly influenced the polymer dose where the maximum clarity degree was reached (Fig. 2, inset) as well as the width of the flocculation window since these parameters increased when the ethyl group was replaced by a butyl group and decreased for longer R. The different behavior of D40-R30 could have resulted from the various conformations of their macromolecular chains in solution: extended for R=ethyl and butyl and more compact coils for R=octyl and dodecyl. The magnitude of the zeta potential increased significantly as the polycation dose increased for all amphiphilic polysaccharides. The negative value of ζ at the optimum polycation dose and floc size measurements point to contributions from both patch and bridging mechanisms for the flocculation process

Influence of the charge density molar mass

The maximum clarity degree was shifted to a lower polymer dose when the charge density increased.

Influence of the molar mass

The dextran derivative with higher molar mass flocculated better, but no dramatic effect was observed in the range of molar mass investigated.

Conclusions

Flocculation of clay dispersion by some amphiphilic polyelectrolytes based on dextran is strongly influenced by the polymer hydrophobicity and charge density, but less by molar mass. The combined information supplied by turbidity, zeta potential and laser diffraction measurements were consistent with destabilization of clay suspension by the combined mechanisms of electrostatic patch and bridging.

References

1. B. Bolto, J. Gregory, Water Res. 41, 2301, 2007.
2. M. Nichifor, M.C. Stanciu, B.C. Simionescu, Carbohydr. Polym., 82, 965, 2010.

Composting of some biodegradable synthetic polyesters can be influenced by sample shape and surface quality

Marek *Koutny*[1,2], *Petr Stloukal*[1], *Sophie Commereuc*[3], *Vincent Verney*[3]

[1]Environmental Protection Engineering, Faculty of Technology and
[2]Centre of Polymer Systems, Polymer Centre, Tomas Bata University in Zlín, T.G.M sqr. 5555, 760 01 Zlín
[3]Clermont Université, UBP, Laboratoire de Photochimie Macromoleculaire, F-63000 Clermont-Ferrand

mkoutny@ft.utb.cz

Introduction: Presently, polymer scientists are looking for the possible replacement of conventional polyolefins by biodegradable alternatives [1,2]. The perspective materials are represented by synthetic copolyesters with content of aromatic and aliphatic components [3,4]. Changing the component ratio one is able to balance processing properties of the copolyester and its biodegradability [5,6,7]. Several these materials were already commercialized and they are available on the market [8]. Another candidate appears to be polylactide, which is a synthetic polymer but the corresponding monomer can be obtained from renewable resources. In general, these materials especially well comply with composting technologies of waste treatment but, as we show here, biodegradation of such materials can be greatly affected by the form of the sample specimen.

Material and methods: The polymers used throughout the study were:
P1, aromatic aliphatic copolyester containing units of terephtalic acid, adipic acid and 1,4-butane-diol (producer 1).
P2, aromatic aliphatic copolyester containing units of terephtalic acid, adipic acid and 1,4-butane-diol (producer 2).
P3, polylactide (3251D, Natureworks).
Polymer processing. Raw polymer in the form of pellets was processed to obtain different forms of the polymer with different specific surfaces.
Films. Films were prepared by compression molding at 140°C. According to the inserted steel frame films of 100 μm and 300 μm were prepared.
Powder. Chloroform solution of polymer (50 mg/ml) was poured into four volumes of ethanol and the mixture was vigorously stirred. Obtained precipitate was filtered out and dried on air.
Thin coating on inert surface. Calculated volume (4 ml) of the chloroform solution of polymer (50 mg/ml) was applied on the surface of pre-weighed porous inert material (perlite, 7 g) and stirred. Then the solvent was stripped out with air leaving the polymer coating on the surface of perlite.
Biodegradation experiment. Three components were weighed into 500 ml biometric flasks: polymer samples (200 mg), mature compost or any of tested soils (5 g of dry weight) and perlite 7 g. Biometric flasks were equipped with septa on stoppers. Sample flasks were incubated at 58°C. Head space gas was sampled at appropriate intervals through the septum with a gastight syringe and then injected manually into a GC instrument (Agilent 7890).

Results and discussion: Investigated copolyester was designed to be a biodegradable material with potential applications in agriculture. Preliminary experiments showed (data not presented) that biodegradation of relatively thick compression (100 μm) molded polymer films appeared to be relatively slow. We decided to test whether this phenomenon was caused by low specific surface of the films. To answer the question we prepared two other forms of the polymer with higher specific surfaces, solvent precipitated powder of the polymer and deposition of the polymer on high specific surface inert material (perlite).
Copolyesters (P1 and P2) of both producers showed quite similar properties. Samples in forms of thin and thicker films behaved almost equally and end up with about 20-40% carbon mineralization after 90 days of incubation. However for the two forms of samples with higher specific surfaces the results are clearly more optimistic with results from 45% to more than 80% at the end of the observation period. The copolymers proved its good biodegradability under composting conditions. However, our experiments clearly showed that specific surface of polymer specimens affects greatly the rate of biodegradation. Experiments with polylactide (P3) are still on the way. The results will be added to the final poster presentation together with a general conclusion.
This contribution was created with support of Operational Program Research and Development for Innovations co-funded by the European Regional Development Fund (ERDF) and national budget of Czech Republic, within the framework of project Centre of Polymer Systems (reg. number: CZ.1.05/2.1.00/03.0111).

References:
[1] E. Rudnik, Compostable Polymer Materials. Amsterdam, Elsevier Science 2008.
[2] L. S. Naira and C. T. Laurencin, Prog Polym Sci 2007 32, 762–98.
[3] V. Sasek, J. Vitásek, D. Chromcová, I. Prokopová, J. Brožek and J. Náhlík, Fol Microbiol 2006 51(5) 425-30.
[4] L. Han, G. Zhu, W. Zhang and W. Chen, J of Appl Polym Sci, 2009 113(2) 1298–306.
[5] T. Nakajima-Kambe, F. Ichihashi, Ryoko Matsuzoe, S Kato and N. Shintani, Polym Degrad Stab 2009 94(11) 1901–5.
[6] E. Marten, R.-J. Muller and W.-D. Deckwer, Polym Degrad Stab 2005 88 371-81.
[7] F. Trinh Tan, D. G. Cooper, M. Maric and J. A. Nicell, Polym Degrad Stab 2008 93 1479-85.
[8] W. Amass, A. Amass and B. Tighe. Polym Int 1998 47(2) 89-144.

Synthesis and Characterization of Organic-Inorganic Hybrid Biomaterials Based on 2-Hydroxyethylmethacrylate/Triethoxyvinylsilane Composites

Łukasz John, Marta Bałtrukiewicz, and Piotr Sobota

University of Wrocław, Faculty of Chemistry, 14 F. Joliot-Curie, 50-383 Wrocław, Poland

e-mail: john@eto.wchuwr.pl

Introduction. Research and developments in the area of organic-inorganic hybrid materials based on silica bioceramics and polymeric biocomposites increased rapidly over the past decade.[1] Demands in bone tissue engineering have promoted various synthetic materials that interact with biological systems (cells, tissues, organs, body fluids, growth factors, peptides, hormones, etc.). Since the beginning of the 21st century, a very special interest is related to so-called second- and third-generation biomaterials which are allowed to induce tissue repair and regeneration through the bionic approach.[2]
Poly(2-hydroxyethylmethacrylate) (pHEMA) constitu-tes a biocompatible polymer widely used in bio-medicine.[3] There are also known some examples of pHEMA-based biocomposites that demonstrates the attractive in vitro activity in biological fluids.[4] Here we report our previous studies on organic-inorganic hybrid biomaterials based on 2-hydroxyethylmethacrylate/ triethoxyvinylsilane (HEMA/TEVS) systems – pure and doped by Ca^{2+} and PO_4^{3-} ions. The present topic is devoted to the design of biohybrids that can bond to living bone via hydroxyapatite (HAp)-layer formation and appropriate architecture which allows bone tissue penetration. Surface structure of the samples were examined by powder X-ray diffraction, Fourier-transformed infrared and physisorption analysis.

Materials and Methods. *Chemical reagents:* HEMA (2-hydroxyethylmethacrylate), TEVS (tri-ethoxyvinylsilane), calcium dichloride, and triethyl phosphate were used as starting materials without further purification.
Experimental: Mixture of HEMA/TEVS with various molar ratio was dissolved in EtOH. The mixture was polymerized by heat treatement at 70°C with tert-butyl hydroperoxide as initiator. In case of Ca^{2+} and PO_4^{3-}-doped materials, obtained polymer solution was mixed with calcium dichloride and triethyl phosphate. Then, solution was cast in PP mold and dried in the range of RT to 70°C. Homogenous and transparent gels were obtained for all synthesized materials.
In vitro assays: A small amount (~ 60 mg) of a hybrid material was immersed at 37°C for 0.5h, 1h, 6h, 12h, 1d, 2d, 3d, 4d, and 7 days in ca. 10 ml of a standard Dulbecco's modified Eagle medium (DMEM, Biochrom AG, Germany). After interaction, the samples were removed from the fluid and air-dried.
Measurements: powder XRD, FT-IR, ICP-AES, TEM-EDS, DSC, physisorption analysis.

Results and Short Discussion. In the body environment, the hydrophylic nature of HEMA-based organic and inorganic composites enables them to interact well with cells and have been used for variety of applications such as drug delivery. From this perspective we have synthesized a series of promising hybrids with the general compositions: HEMA-TEVS, HEMA-TEVS-Ca and HEMA-TEVS-Ca-P (where: HEMA/TEVS = x/(1-x), x = 0.1, 0.5, and 0.9; Ca = Ca^{2+}, and P = PO_4^{3-}). TEVS has alkoxysilane groups that may provide silanol moieties ≡Si-OH after hydrolysis, whereas HEMA may provide hydrophilic polymer matrix in the materials.

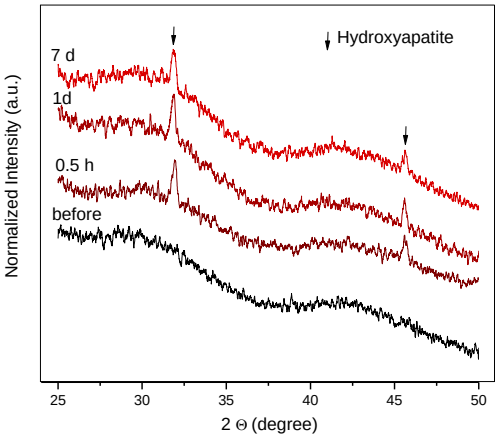

Figure 1. X-ray diffraction patterns of the sample of 0.9HEMA-0.1TEVS-Ca(15 mol%), before and after soaking in DMEM solution for various periods.

In vitro studies conducted in the Dulbecco's modified Eagle medium (DMEM) have shown that formation of a bone-like apatite layer occurs on material surface after exposure to the biological fluid. All of the samples were immersed for 0.5h – 7 days at 37°C. The formation of the HAp surface is induced both by dissolution of calcium ions, and by silanol groups in the hydrated silica gel formed on the surface. Surprisingly, in the case of 0.9HEMA-0.1TEVS-Ca, nanocrystalline HAp-layer formation is observed after 30 minutes of exposure in DMEM (Figure 1).

Conclusions. The organic-inorganic hybrids derived from HEMA-TEVS-based composites doped by Ca^{2+} and PO_4^{3-} ions have a potential as a bioactive material for bone repairing and replacing agents.

References

1. Vallet-Regí, M.; Colilla, M.; González, B. *Chem. Soc. Rev.* **2011**, DOI: 10.1039/c0cs00025f.
2. Craelius, W. *Science* **2002**, *295*, 1018.
3. (a) Uchino, T.; Kamitakahara, M.; Otsuka, M.; Ohtsuki, C. *J. Ceram. Soc. Japan* **2010**, *118*, 57. (b) Giordano, C.; Causa, F.; Di Silvio, L.; Ambrosio, L. *J. Mater. Sci.: Mater. Med.* **2007**, *18*, 653.
4. (a) Juhasz, J. A.; Best, S. M.; Bonfield, W. *Sci. Technol. Adv. Mater.* **2010**, *11*, 014103. (b) Ohtsuki, C.; Miyazaki, T.; Tanihara, M. *Mater. Sci. Eng. C* **2002**, *22*, 27.

Controlled delivery of gentamicin antibiotic from bioactive electrospun polylactide-based ultrathin fibers

Sergio Torres-Giner, Antonio Martinez-Abad, Maria J. Ocio and Jose M. Lagaron

Novel Materials and Nanotechnology Group, IATA, CSIC, Avda. Agustín Escardino 7, 46980, Burjassot, Spain

e-mail: lagaron@iata.csic.es

Abstract Body: Post-surgical infection is an emerging problem, which frequently develops after surgical procedures. This kind of infections may even require secondary surgical intervention, which is not only time-consuming and costly, but also increases the potential for further infections, scar tissue formation, and even later rejections. Prevention of infections can thus decrease the overall hospital costs and the severity of complications, and can also ease the technical complexity and/or need for subsequent surgery. Wound healing currently not only aims to restore the milieu required for tissue regeneration but also to protect the wound from environmental threats and penetration of bacteria. Novel bioresorbable wound dressings successfully avoid clinical changing since they do not need to be removed from the wound surface once they have fulfilled their role [1,2].

The purpose of the present study was to investigate the use of PLA and collagen electrospun blends to develop antibiotic-loaded fibrilar structures which, in addition to biocompatibility, display adjustable release characteristics in functional dressings for wound healing applications. For this purpose, gentamicin was chosen as the incorporated drug since this is a well-known antibiotic that can inhibit or kill bacteria of most typical post-surgical infections. Therefore, electrospun ultrathin fibers containing gentamicin of PLA, PLA-collagen blend, and co-axial PLA-collagen-PLA fibers were produced. It was investigated how the choice of polymer chemistry and antibiotic distribution within the fibers influenced the morphology and release properties of the biomedical fibers. Preliminary antibacterial effectiveness against Staphylococcus epidermis, Pseudomonas aeruginosa and Escherichia coli were also tested to establish the appropriateness of these electrospun fibers to be applied for decreasing frequency and severity of post-surgery infections.

From the results, it was found out that incorporation of gentamicin antibiotic in ultrathin fibers of PLA, uniaxial PLA-collagen and coaxial PLA-collagen-PLA was successfully performed by electrospinning. The study recognized that the drug location within the electrospun morphology largely determined the delivery characteristics. This also showed that release rates were extremely correlated with the hydrophilicity of the polymer fibers. Resultant fibers not only displayed high antibacterial performance but also cell biocompatibility.

The present results provide a basis for further design to generate ultrathin electrospun antibiotic-loaded fibers in order to achieve highly sustainable, controllable, and effective antibiotic-releasing kinetics.

References:

(1) Jürgens, C.; Schulz, A.P.; Porté, T.; Faschingbauer, M.; Seide, K. Eur. J. Trauma. 2006, 32, 160-171.

(2) Torres-Giner, S.; Gimeno-Alcañiz, J.V.; Ocio, M.J.; Lagaron, J.M. ACS Appl. Mater. Interfaces 2009, 1, 218-223.

Stress-Strain Analysis Of Poly (Lactic-Co-Glycolic) Acid / Poly (Isoprene) Blend For Use As Implants

Douglas Ramos Marques[1], Luis Alberto dos Santos[1]

1- Biomaterials Laboratory, Engineering School , Federal University of Rio Grande do Sul, Porto Alegre - Brasil.

E-mail: dougmarques@ibest.com.br

The development of a raw material to an implantable medical device that approach the ideal behavior requires a plausible combination of mechanical properties and tissue response. With this sight, the polymeric blend of Poly(Lactic-Co-Glycolic) Acid (PLGA) and natural latex rubber – or Polyisoprene (IR) – was idealized, uniting the good biocompatibility and absorption capacity by the organism of the PLGA with the specific mechanical characteristics promoted by IR. To determine the mechanical behavior of blend in the compositions 100% PLGA, 50%PLGA+50%IR, 60%PLGA+40%IR, 75%PLGA+25%IR, tensile test was performed with the compositions. The test aims generate the stress vs strain curves for the different compositions, to determinate the influence of IR amount in the mechanical properties of blend, specially observing variations in materials tenacity. To perform the test, the polymeric blend was obtained by the polymers' solubilization (PLGA and IR) in organic solvent, following 24 hours drying in 30°C stove for volatilize solvent. Three samples for each composition were made by injection molding (model Haake Minijet II, Thermo Scientific, Netherlands). These samples were submitted to tensile test (model Autograph AG-X 50KN, Shimadzu, Japan) in proceedings based on standard ISO 527-1. As results, we can observe that the IR presence in the blend modifies significantly its mechanical properties, and the tenacity can be raised approximately 90% in compositions with bigger IR proportion, as well as increase in total tensile at break in the samples with increasing in the rubber's proportion.

Comparative Study of the Polymer – Lipase Complexes

D.O. Soloveva, S.Yu. Zaitsev, E.V. Tulskaya

Moscow State Academy of Veterinary Medicine and Biotechnology;

e-mail: d.solovieva@mail.ru

Introduction:

One of the modern methods of polymer and biological chemistry, nanotechnology and biotechnology is the method of enzyme immobilization on polymeric carriers.

Such systems as polymer - enzyme have several advantages that making them more convenient for the effective applications:

Increasing the stability of the enzyme in time to various denaturing agent;

It became possible to reuse the enzyme;

More simple and rapid separation of the reaction medium [1,2].

The purpose of this study was to prepare complexes of PE-240 and lipase from various sources possessing high catalytic activity.

Materials and Methods:

We used the following reagents: lipase from porcine pancreas, triacylglycerols, Na-polystyrenesulfonate (PSS), polydiallildimethylammonium chloride (PAMA), copolymer based on polypropylene oxide (PE-240). The lipase activity was measured using the method of potentiometric titration on an automatic titrator of the "Radiometer" Company (Copenhagen). It was measured by the rate of hydrolysis of the substrate. The main advantages of this method are high accuracy, high sensitivity and the ability to carry out the titration in the more dilute solutions than it allows visual indicator methods.

Results and Discussions:

It was found that the lipase activity in the PSS presence was higher than the control at 17 and 15 % at a ratio of 1:10 and 1:100 (lipase:PSS). It can be explained by increasing of the microheterogeneity system due to the interaction of lipase with polyelectrolytes (fig. 1). At a ratio 1:1 the lipase activity was decreased to 77% due to the insufficient number of PSS for the formation of microheterogeneous systems.

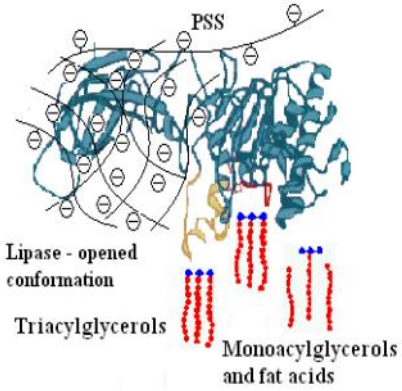

Figure 1. - Model of lipase:PSS 1:1 complexes with "low activity".

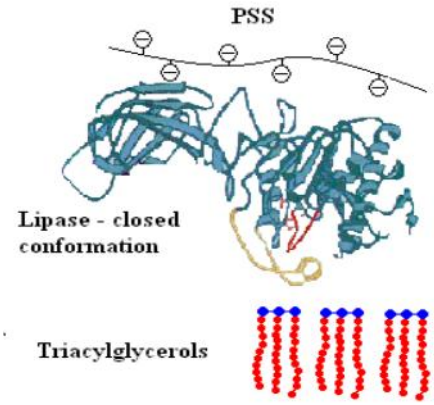

Figure 2. - Models of lipase:PSS 1:10 complexes with "high activity".

In the presence of PAMA the lipase activity was decreased to 94% at a ratio 1:10 (lipase:PAMA). It can be explained by that the lipase is negatively charged at neutral pH during complex formation is located inside the globule of a positively charged polymer and becomes less accessible to substrate.

In the presence of PE-240 the lipase activity was decreased to 88% at a ratio 1:5 (lipase:PE-240) and was higher than the control at 12% at a ratio 5:1.

Conclusions:

Thus, the lipase activity depends on polyelectrolyte parameters (molecular mass, charge, chain flexibility etc.) and ratio of polyelectrolyte to enzyme. The best systems are the following: lipase:PSS 1:10 and 1:100, lipase:PE-240 5:1 and 1:1, which are promising for application in bioengineering and biotechnology.

Acknowledgments:

The authors are grateful to Yu.G. Shtyrlin from Kazan (Volga Region) Federal University for PE-240 preparation and Russian Foundation for Basic Research for financial support.

References:

1. Jaeger K.E., Eggert T. Lipases for biotechnology. // Curr. Opin. Biotechnol. – 2002. – Vol. 13. – P. 390-397.

2. Zaitsev, S.Y. Supramolecular Nanodimentional Systems at the Interfaces: Concepts and Perspectives for Bionanotechnology; LENAND: Moscow, Russia, 2010; p. 208. (in Russia)

Magnetic Nanoparticles Coated with a Molecularly Imprinted Polymer Synthesized by RAFT Polymerization

Carlo Gonzato, Pamela Pasetto and Karsten Haupt

Compiègne University of Technology

karsten.haupt@utc.fr

Molecularly imprinted polymers (MIPs) are tailor-made biomimetic receptors that are obtained by polymerization of interacting and cross-linking monomers in the presence of molecular templates. They contain binding sites for target molecules with affinities and specificities on a par with those of natural receptors such as antibodies, hormone receptors, or enzymes. One of their main application areas is as artificial antibodies in pseudo-immunoassays and in chemical sensors[1].

Superparamagnetic nanoparticles are attracting increasing interest in bioanalysis because they can easily be separated from a matrix by using a magnetic field without retaining residual magnetism[2]. If the magnetic nanoparticles are functionalized with a MIP layer, the specific recognition properties of the polymer can be combined with a magnetic response.

The aim of this research work is therefore to synthesize magnetic hybrid nanoparticles composed of iron oxide cores and a molecularly imprinted polymer shell.

Examples of magnetic MIPs are already known in the literature[2;3]. The originality of our approach consists in the controlled synthesis of these materials, starting the polymerization from the iron oxide surface using a controlled/"living" radical polymerization technique instead of the conventional free radical polymerization.

The use of the Reversible Addition-Fragmentation chain Transfer (RAFT) technique allows to build a more regular polymer network and to preserve living chain ends, giving access to hierarchical structures, core-shell materials and composites.

The first step of the synthesis of the hybrid nanoparticles was the grafting of a RAFT agent onto the iron oxide nanoparticles, and the second to fine-tune the polymerization process parameters. An ultrasonic bath was used to stir our system during synthesis, and a number of solvents were tested for the synthesis of the imprinted layer, based on their different ability to stabilize the dispersion of RAFT-modified Fe_3O_4. In that way we obtained nanocomposites with different sizes and morphologies.

The thus obtained materials were characterized using FTIR, thermogravimetric analysis, energy dispersive X-rays spectroscopy (EDS) and superconducting quantum interference device magnetometer (SQUID) measurements, as well as transmission electron microscopy. For example, nanocomposite particles synthesized in heptyl cyanide had diameters of 50nm, with MIP layers of 7nm thickness. The absence of hysteresis curves confirmed that the superparamagnetic properties were preserved in the nanocomposites. Moreover, radioligand binding experiments were performed to evaluate the binding ability of the nanocomposites. Selective binding of the radiolabeled target molecule, here the beta-antagonist propranolol, was demonstrated. While molecularly imprinted particles showed a considerable binding of the target, the non-imprinted control particles (chemically identical but synthesized in the absence of template) showed virtually no binding.

Finally the presence of "living" fragments on their surface has was demonstrated to further functionalize them by polymerizing an additional monomer, ethyleneglycol methacrylate phosphate . This showed the versatility of our approach for fine-tuning the surface properties.

(1) Haupt Karsten. Imprinted polymers: the next generation. *Anaytical Chemisty* **2003** 75, 376A-383A.

(2) Ansell Richard J.; Mosbach Klaus. Magnetic molecularly imprinted polymer beads for drug radioligand binding assay. *Analyst* **1998** 123 1611-1616**.**

(3) W. Xiaobin; D. Xiaobin; Z. Zhaohui; H. Xinhua; C. Xu; P. Yuxing. *Macromol. Rapid Comun.*. **2006** 27 1180-1184.

Novel biodegradable copolyesters of poly(butylene succinate containing ether-oxygen atoms: correlation between chemical and architectural modification and enzymatic hydrolysis

M. Gigli, A. Negroni, M. Soccio, G. Zanaroli, N. Lotti, F. Fava, A. Munari

Dipartimento di Ingegneria Civile, Ambientale e dei Materiali, Università di Bologna, Via Terracini 28, 40131 Bologna, Italy.

matteo.gigli@unibo.it

Introduction.

In recent years, biodegradable polymers have gained much attention as green materials and biomaterials. Aliphatic polyesters, due to their favorable features of biodegradability and biocompatibility, are one of the most important classes of synthetic biodegradable polymers: polycaprolactone, poly(hydroxybutyrate), poly(L-lactide), poly(butylene succinate) (PBS), etc. are nowadays available commercially [1]. Among all, PBS is used in a wide range of applications, such as packaging film, bags, flushable hygienic products and garden mulch [2], but shows a quire slow rate of degradation [1]. As is well known enzymatic biodegradation of a polymer is controlled by several factors: the most important one is the nature of the polymer itself, i.e. its chemical structure; hydrophilicity and consequently water uptake increases degradation rate; moreover, the degree of crystallinity is a crucial factor, since enzymes preferably attack the amorphous domains of a polymer. Conditions like temperature, pH and concentration of enzyme also play a important role [1]. In our study, the effect of chemical modification as well as of molecular architecture on PBS biodegradation rate has been investigated. In addition, different enzymes and different operating conditions have been explored.

Materials and methods.

Copolymers of PBS containing diethylene succinate sequences with different molecular architecture have been prepared in our laboratories via reactive blending in the presence of Ti-based catalyst (PBSPDGS). In particular, a block copolymer with long sequences and the random one have been considered. For comparison the parent homopolymer PBS has been also synthesized by the usual two-stage melt polycondensation. Four different commercially available lipases were tested from *Candida rugosa*, *Candida cylindracea*, *Aspergillus niveus* and hog pancreas and a serine protease (alpha-chymotrypsin from bovine pancreas) (50U/ml in 0.1M phosphate buffer pH 7.4, 30°C, 100 rpm). To evaluate the biodegradability of the polymers under investigation, two kind of tests were carried out: i) turbidimetric film assay, which has high sensitivity to very small extents of degradation and ii) weight loss measurements. ATRIR analysis and DSC measurements have been performed to correlate degradation rate with crystallinity degree. Lastly, NMR analysis was performed to follow changes in composition of the copolymers under investigation.

Results and Discussion.

The molecular and thermal characterization data of the polymers under investigation are reported in Table 1.

Table 1: Molecular and thermal characterization data.

Polymers	M_n	*BS* (mol %) (^{1}H-NMR)	L_{BS}	*b*	T_g (°C)	T_m (°C)	ΔH_m (J/g)
PBS	38300	100	-	-	-36	114	82
PDGS	28200	0	-	-	-21	-	-
PBSPDGS*block*	28200	52.5	22.7	0.12	-30	112	44
PBSPDGS*random*	27000	49.9	1.85	1.03	-32	51	29

Preliminary results based on turbidimetric film assay, indicate that the most active enzyme is the lipase from *Candida cylindracea*, and that the best operative conditions are: [E]=50 U/ml (at higher [E] biodegradation is too fast for correct monitoring), T= 30°C (close to ambient temperature; high degradation rate) and pH =7.0 (highest degradation rate). Copolymers degrade to a much higher extent than PBS (see Figure 1). Moreover, random copolymer degrades faster than the block one, probably due to its lower degree of crystallinity (see Figure 1).

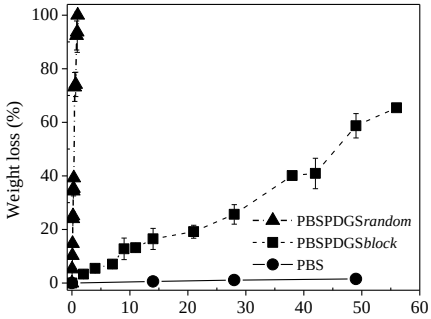

Figure 1. Weight loss (%) as a function of incubation time

ATRIR and DSC analyses confirm that the amorphous phase is the region attacked first by enzyme. Lastly, in the case of PBSPDGS*block* an evident decrease of DGS content is observed by means of NMR analysis with the proceeding of degradation, indicating that enzyme hydrolysis involves preferentially ester groups of DGS sequences, probably because of their higher hydrophilicity.

Conclusions.

Relevant results have been obtained from the present research. They can be summarized as follow:

1. Copolymerization is an efficacious way to increase PBS biodegradability.
2. Biodegradation rate can be modulated changing the molecular architecture, which affects the crystallinity degree.

References

[1] Bikiaris *et al*., (2005). Polymer Degradation and Stability **91**: 31.

Synthesis and characterization of hydrogels based on copolymers 2-hydroxyethyl methacrylate –*co*- zwitterionic carboxybetaine (meth)acrylamide for tissue engineering

Nina Yu. Kostina, Cesar Rodriguez-Emmenegger, Jiri Michalek, Eduard Brynda

Institute of Macromolecular Chemistry AS CR, Heyrovskeho Sq. 2, Prague 6, 162 06, Czech Republic

E-mail: kostina@imc.cas.cz

Introduction

The main goal of tissue engineering is to regenerate a function or part of a damaged tissue. For this purpose, scaffolds based on advanced materials with controlled properties are required.[1] Hydrogels are excellent scaffolds owing to their mechanical properties, high water content, and structural similarity to macromolecular-based components of the body. The attachment of bioactive molecules interacting specifically with cells as well as a protection against changing these interactions by non-specific fouling in cell cultivation media or physiological environment are essential for a successful cell growth on a material surface. Highly wettable zwitterionic polymer brushes have been shown to suppress protein fouling[2] and provide functional groups for covalent immobilization of bioactive molecules. So far, no attempts to use them as hydrogel components has been made. Herein the preparation of hydrogels based on copolymer of 2-hydroxyethyl methacrylate (HEMA) and zwitterionic carboxybetaine acrylamide (CBAA) or newly synthesized carboxybetaine methacrylamida (CBMAA) is presented.

Materials and Methods

Hydrogel films from copolymer of HEMA and CBAA (poly(HEMA–*co*-CBAA)) or HEMA and CBMAA (poly(HEMA–*co*-CBMAA)) with different molar ratios of the monomer units were prepared by radical polymerization between glass and Teflon plates initiated with UV-light irradiation for 30 min at room temperature.

Chemical composition, morphology and mechanical properties were studied by FTIR, transmission electron microscopy, and measuring compressive and tensile moduli. Wettability and swelling degree were studied by sessile bubble contact angle measurement and gravimetry. The data were correlated with the non-specific protein adsorption studied by FTIR. Model systems based on polymer brushes were also synthesized using surface initiated atom transfer radical polymerization. Non-specific protein adsorption on the brushes was determined using surface plasmon resonance and compared with that on hydrogels.

Results and Discussion

Chemical composition of the hydrogels was confirmed by FTIR. All the hydrogels containing zwitterionic betaines showed a much higher hydration and wettability than that from HEMA homopolymer. Hydrogels with low molar content of betaines showed good mechanical properties while high betain content considerably impaired the mechanical properties. Importantly, even low content of carboxybetaines provided excellent antifouling properties while keeping good mechanical properties.

The increase in wettability of co-polymeric hydrogels of poly(HEMA–*co*-CBAA) and poly(HEMA-*co*-CBMAA) seemed to correlate with the decrease in the fouling.

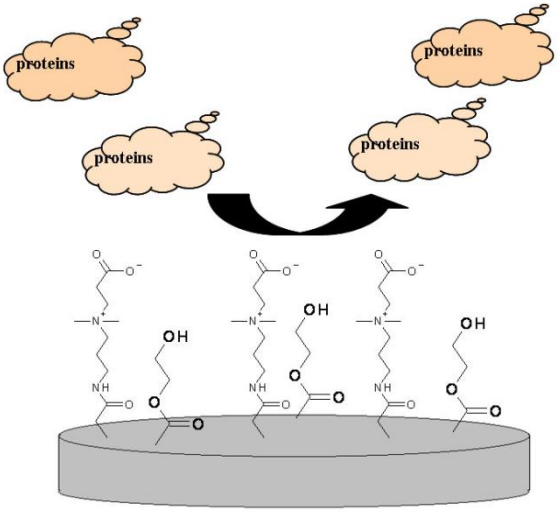

Conclusions

Poly(HEMA–*co*-CBAA) and poly(HEMA-*co*-CBMAA) hydrogels with different molar content of zwitterionic monomer units were synthesized and characterized. Good anti-fouling properties associated with a high wettability and electroneutrality of the zwitterionic betaines and the presence of carboxylic groups capable of easy functionalization make these hydrogels a promising platform for tissue engineering.

References

1. Williams, D. F. *Biomaterials* **2009,** 30, (30), 5897-5909.

2. Rodriguez Emmenegger, C.; Brynda, E.; Riedel, T.; Sedlakova, Z.; Houska, M.; Alles, A. B. *Langmuir* **2009,** 25, (11), 6328-6333.

Acknowledges:

This work was supported by KAN 200520804

Norfloxacin-impregnated intraocular lenses: supercritical fluids technology *vs.* aqueous immersion

C. González-Chomón[a], M.E.M. Braga[b], H.C. de Sousa[b], A. Concheiro[a], C. Alvarez-Lorenzo[a]

[a] Departamento de Farmacia y Tecnología Farmacéutica, Facultad de Farmacia, Universidad de Santiago de Compostela, 15782-Santiago de Compostela, Spain.

[b] CIEPQPF, Chemical Engineering Department, FCTUC, University of Coimbra, Rua Sílvio Lima, Pólo II–Pinhal de Marrocos, 3030-790 Coimbra, Portugal

e-mail: clara.gonzalez@rai.usc.es

Introduction

Cataracts treatment usually involves the extraction of the opaque crystalline lens and its replacement by an implanted intraocular lens (IOL) [1,2]. A serious problem associated to this procedure is the appearance of a post-surgery infection called endophthalmitis which is mainly caused by *Staphylococcus epidermidis*, *Staphylococcus aureus* and *Pseudomonas aeruginosa* [3,4]. To overcome these issues, acrylate-based IOLs having the ability to load and to release norfloxacin in a controlled way and at efficient therapeutic levels were synthesized. Different acrylate-based copolymers were prepared. Norfloxacin was loaded from aqueous drug solutions as well using a supercritical CO_2 ($scCO_2$) impregnation/loading method [5]. Prepared samples were characterized by different methods. Loading capacities and drug release profiles were obtained, compared and discussed in terms of copolymer composition and of the employed drug-loading method.

Materials and methods

Hydrogels synthesis - 2-hydroxyethyl methacrylate (HEMA) and 2-butoxyethyl methacrylate (BEM) mixtures (100:0, 80:20, 60:40, 40:60, 20:80, 0:100) were prepared and ethyleneglycol dimethacrylate (EGDMA) was added as cross-linker. Methacrylic acid and 2,2´-azo-bis(isobutyronitrile) (AIBN) were added to different aliquots of comonomer mixtures. After polymerization (at 50ºC/12 h and at 70ºC/24 h), obtained hydrogels were boiled in water, cut into 10 mm diameter discs and dried at 70ºC/12h.

Hydrogels characterization - Glass transition temperatures (T_g, ºC) were determined by DSC (TA Instruments, Q100, UK). Water sorption capacities (S, %) were obtained by gravimetry. Water contact angles and surface free energy were determined by an OCA 20 contact angle apparatus (Dataphysics Instruments GmbG, Germany). Hydrogels IR spectra were obtained in a FTIR-ATR (Jasco, model 4000, Japan) after being dried at 40ºC until constant weight. Optical transparency of hydrated hydrogels was evaluated spectrophotometrically at 600 nm.

Norfloxacin loading experiments – Norfloxacin loading with $scCO_2$ was carried out at 40 ºC and at two pressures: 150 and 300 bar. Processing time was 14 h and depressurization rate was 1 bar min^{-1}. Loading from norfloxacin aqueous solutions (0.0096 g/L) was carried out by discs immersion and soaking. Drug-loaded amounts were determined spectrophotometrically for both drug-loading methods.

Norfloxacin release experiments – Norfloxacin-loaded discs were immersed in artificial lachrymal fluid at 37ºC, under orbital stirring and release solution absorbance (at 273 nm) was measured continuously for 8h. Other measurements were performed after 48h.

Results and discussion

As expected, DSC results showed that T_g decreased as the BEM composition increased. Same trend was observed for water sorption capacities while water contact angles showed the opposite behavior (table 1).

Table 1. IOLs polymer physical characterization

Hydrogel	Tg (ºC)	S (%)	Contact angle, H_20 (º)
100:0	111.9	54.4	50.6
80:20	84.2	28.5	72.8
60:40	64.5	12.1	75.2
40:60	41.1	5.6	75.8
20:80	17.2	2.9	77.5
0:100	-14.7	0.6	81.1

Total norfloxacin released amounts from those hydrogel discs processed with $scCO_2$ were almost twice the released amounts that were obtained by the immersion loading method. Although release rates were faster for samples containing higher HEMA compositions, all norfloxacin release experiments presented controlled release profiles. An example is presented in Figure 1.

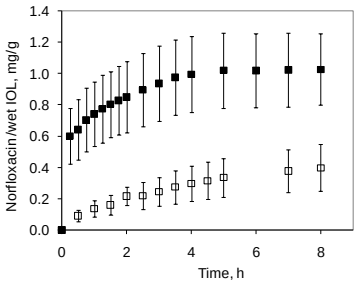

Figure 1. Norfloxacin release profiles from loaded hydrogels (100:0): ■ SSI □ immersion

Conclusions

Cross-linked HEMA:BEM-based hydrogels were synthesized, characterized and loaded with norfloxacin by soaking in aqueous drug solutions and by a $scCO_2$ loading method. Total norfloxacin released amounts from discs impregnated using $scCO_2$ were almost twice those released from hydrogels loaded by the soaking method. For most prepared and processed hydrogels, obtained thermomechanical, water-sorption, wettability and optical properties seemed to be adequate for their potential application as IOL materials.

References

[1] Lloyd AW et al. Biomaterials 2001; 22: 769-785.
[2] Duarte ARC et al. Current Drug Del. 2008; 5: 1-6.
[3] Anderson EM et al. Biomaterials 2009; 30: 5675-5681.
[4] Parsons C et al. Biomaterials 2009; 30: 597-602.
[5] Yañez F et al. Acta Biomater. 2010.

Acknowledgements
MICINN (Acción integrada PT2009-0038), FEDER and Xunta de Galicia (10CSA203013PR), FCT-MCTES (PTDC/SAU-FCF/71399/2006).

Synthesis of biodegradable polymer and evaluation of its elastic properties available for stent coating layer

Min Ji Kim, Jeongho An, Dong June Chung

Department of Polymer Science & Engineering, Sungkyunkwan University

Tel:+82-31-290-7302, Fax: +82-31-292-8790, e-mail: djchung@skku.edu

Introduction

The implantation of a stent in coronary artery is widely practiced for the treatment of patients with coronary artery disease. Several kinds of commercialized bare metal stents have been used for clinic, but it has some risk such as inflammation, late thrombosis or restenosis due to the low biocompatibility and toxicity. To reduce the problems, surface treated stent were developed. These are typically made by coating a metallic stent with a biodegradable polymer. In this work, we examined the electrospray coating poly(glycerol-co-sebacate)(PGS) on metal surface. PGS was synthesized by condensation polymerization and it has biocompatibility, biodegrability and suitable mechanical strength. After coating on the stent, we checked the durability, surface morphology and thickness of coated polymer.

Experiments

The PGS prepolymer was synthesized by polycondensation of equimolar glycerol(Aldrich) and sebacic acid(Aldrich). Both elements were mixed together in a three-necked flask at 130℃ under argon for 3 h. The reaction was continued for 36 h at 40 mtorr and 130℃. The bare metal stents used in this study were nitinol stents. The stent was placed in a electrospray machine, polymer solution of each concentration in acetone was sprayed on the stent. For the process of cross linking, coated stents were placed in vacuum oven at 120℃ in a day. The surface morphologies and thickness of coated stents were observed by SEM.

Result

At first, we checked that PGS polymers have biocompatibility, biodegrability and suitable mechanical strength. And the surface morphologies of coated stent were smoother than bare stents. We can control the surface and thickness by changing the solution parameters and conditions of electro spraying. The thickness of polymer film which used high concentration(10wt%) was thicker than one which used low concentration(1wt%). It is expected that drug-eluting stent(DES) coated with drug and PGS polymers can be applied practically for clinical applications.

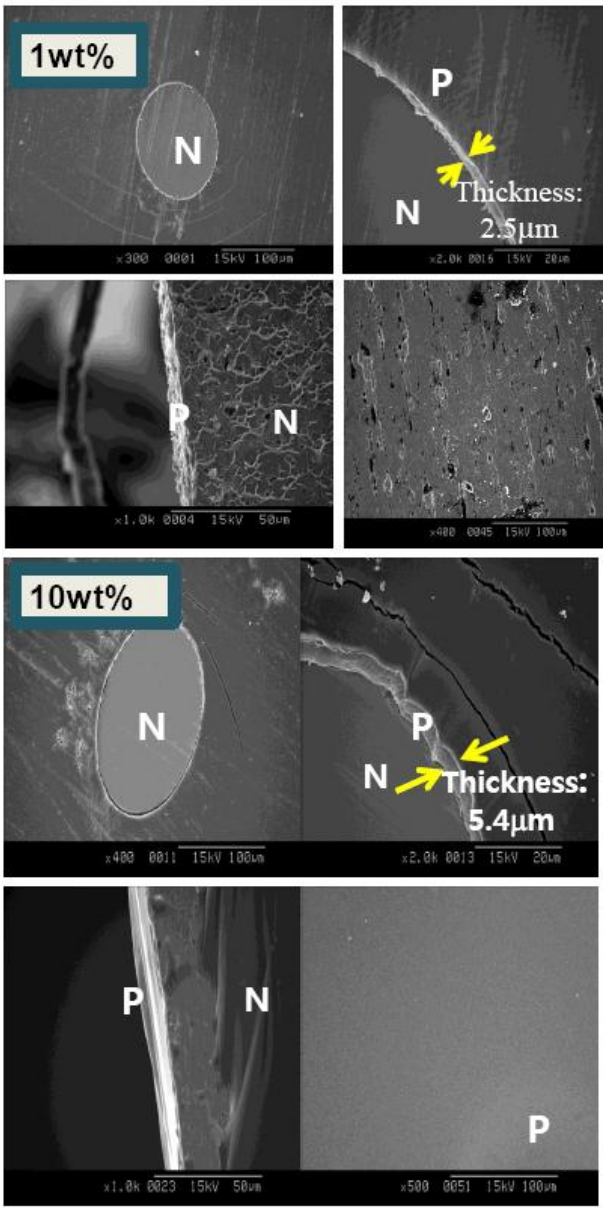

Fig 1.) SEM observation of PGS coating with EtOH solutions (a) 1wt% (b) 10wt% (polymer concentration) on nitinol stent at 15cm of working distance, 0.6mL/h of flow rate(N; nitinol stent, P; PGS polymer).

Bio-FET using biotinylated F8T2

Seong Hyun Kim, Sang Chul Lim, Yong Suk Yang, and Hyun Tak Kim

Electronics and Telecommunications Research Institute, Daejeon, 305-700 Korea

Recently, there has been much interest in OTFT new biological, chemical, and environmental applications. One example of such device is a biologically sensitive field-effect-transistor (BioFET) to detect specific protein. We present the effects of electrochemical and chemoresistive changes on the electrical performance of organic thin-film transistors (OTFTs). 0.8 wt % of biotinylated F8T2(poly(9.9-dioctylfuorene-co-bithiophene)) in p-xylene were spin coated for a channel layer of OTFTs, and it has functional group with biotin hydrazide.binding of avidin (from egg white)to the biotin moieties caused drastic changes to photoluminescence of the polymer in solution, and to the electrochemistry and conductivity of the polymer in thin films. We have demonstrated a bio-organic-FET, or BioFET, in which the current was modulated over three orders of magnitude from the 2-terminal resistor(I-V) measured.

Correlation of physical and surface properties of polyurethane films with their chemical structure

Cansu Citak, Ahmet Sirkecioglu, F. Seniha Guner

Istanbul Technical University, Department of Chemical Engineering, Maslak 34469 Istanbul, Turkey

e-mail: guners@itu.edu.tr

Polymeric materials are widely used in biomedical applications due to their desired properties. Among these, polyurethanes are one of the most important classes of polymers due to their segmented (hard and soft) polymeric character.

The aim of the study is to correlate some physical and surface properties of the polyurethane (PU) films with their chemical structure. The study is performed in two steps; (a) synthesis of the films and determination of their chemical structure and some physical properties, (b) treatment of the film surfaces by plasma and determination of their performance in view of protein adsorption.

In the preparation of the films castor oil (CO) and polyethylene glycol (PEG) are used as polyol sources, and hexamethylene diisocyanate (HDI) is used as diisocyanate component. The films are prepared in various CO/PEG weight ratios (50/50, 60/40, 70/30, 90/10 and 100/0) without using any solvent and catalyst. The samples are characterized by Fourier transform infrared (FTIR) spectroscopy, differential scanning calorimeter (DSC), thermal gravimetric analysis (TGA) and dynamic mechanical analysis (DMA). Crosslink density and molecular weight between crosslinks are determined by Flory-Rehner method. Swelling behavior of the films is investigated in phosphate buffer solution (PBS) medium. Gel content is determined by Soxhlet extraction. Densities of the films are also determined.

For surface modification the films prepared with the CO/PEG weight ratio of 50/50, 70/30 and 100/0, are priorly exposed to radio frequency low-pressure argon plasma treatment at working power of 50 W for 2 min, and then acrylic acid (AA) plasma treatment is applied at 50 W for 5 min. The effect of plasma polymerization on protein adsorption is determined by using bovine serum albumin (BSA) and bovine serum fibrinogen (BSF). The adsorption experiments are performed by the batch process. Protein is analyzed by UV spectrophotometer at 280 nm and the specific adsorption rate constant is calculated for each polymer surface. The water contact angle and surface free energy are measured by a goniometer. Scanning electron microscopy (SEM) and atomic force microscopy (AFM) are used for inspecting surface topology. The existence of the polyacrylic acid layer on PU surface is observed by x-ray photo spectrometer (XPS) analysis.

The glass transition temperature (T_g), loss tangent (tan δ), crosslink density and gel content of the films increase with increasing CO/PEG ratio. On the other hand, the molecular weight between crosslinks, swelling ratio, density and transparency of the films decrease with increasing CO/PEG ratio.

As shown in Figure 1, the water contact angles are determined to be c.a. 91, 68 and 61° for the films prepared with the CO/PEG ratio of 100/0, 70/30and 50/50, respectively. After plasma polymerization, the water contact angles for all films are c.a. 43°. Before plasma treatment, protein adsorption increases with decreasing CO/PEG ratio (Figures 2 and 3). After plasma polymerization the content of protein adsorbed decreases for each films. XPS results are given in Table 1 for the PU film before and after plasma treatment and after protein adsorption.

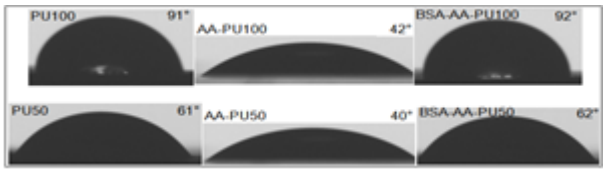

Figure 1: Water contact angle of the PU films

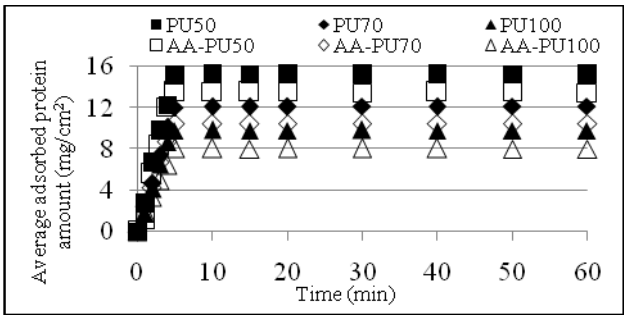

Figure 2: BSA adsorption for the PU films

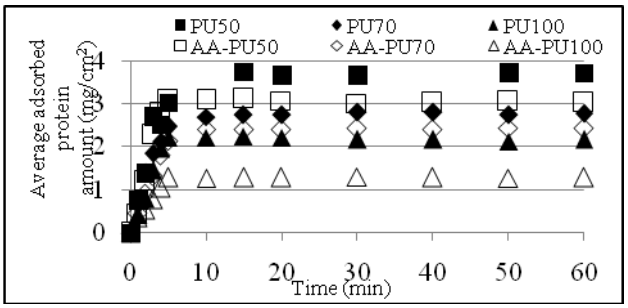

Figure 3: BSF adsorption for the PU films

Table 1: Surface composition of the PU films obtained by XPS analysis

Sample	C	O	N	O/C	N/C
PU	74.6	22.2	3.2	0.298	0.04
AA-PU	62.4	34.8	2.8	0.56	0.045
F-AA-PU	69.4	25.6	5.0	0.37	0.072

Aging of a Medical Device Surface after a Cold Plasma Treatment

O.Mrad[1], J.Saunier[1], C.Aymes-Chodur[1], V.Mazel[1], V.Rosilio[2], F.Agnely[2], J.Vigneron[3], A.Etcheberry[3], N. Yagoubi[1]

[1] Univ Paris-Sud , EA 401, Faculté de pharmacie. F-92296 Châtenay Malabry – France
[2] Univ Paris-Sud , UMR 8612, Faculté de pharmacie. F- 92296 Châtenay Malabry - France
[3] Univ. Versailles, IREM CNRS UMR 8637, Institut Lavoisier – F-78035 Versailles – France

Johanna.saunier@u-psud.fr

Introduction: For polymeric medical devices, the surface plays an important role for the biocompatibility. The invasive devices have to be sterile and are thus subjected to a sterilization treatment that can change the surface properties by modifying the chemistry and the topography of the surface [1]. Moreover, the treated surface may evolve with time [2]. In this work, polyurethane catheters were treated with a cold nitrogen plasma dedicated to the decontamination of medical devices and the post treatment aging of the catheter surface was studied for several storage conditions (temperature, humidity…). As commercial polymers contain additives that can bloom onto the surface [3, 4], a specific care was taken to characterize the behavior of these low molecular weight compounds during the post-treatment aging.

Material and methods: Pellethane 2363 80AE ® (Dow Chemical), a poly (ether urethane), was the major constituent of the catheters that contained also two additives, a lubricant (ethylene bis stearamide) and an antioxidant (Irganox 1076®). Plasma [5] was obtained using a pulsed corona discharge (voltage: 10 kV, frequency : 10 kHz, mean power : 15 W) on a pure nitrogen gas at atmospheric pressure. Samples were subjected to treatment during 40 minutes. To characterize the surface, contact angle measurements were carried out with different liquids (diiodomethane, ethylene glycol, water and formamide), and X ray photoelectron spectroscopy (Thermo Electron VG Escalab 220iXL) was performed. Additives and polymers were moreover characterized by differential scanning calorimetry (Q1000 TA instrument), thermostimulated current analysis (Setaram TSC) and powder X-ray diffraction (PANalytical X-ray).

Results and discussion: Evolution toward a hydrophobic surface state was observed for the stored treated material. The kinetic depended on temperature and relative humidity: a faster evolution was observed for higher temperatures and higher relative humidity. At 25°C a fast evolution of the surface energy and polarity was observed during the first two days following treatment, but then the evolution was slow. At 45 °C, the evolution was complete after 24 hour storage, with a surface energy of the catheter surface that was in the same range than that of the non treated samples. A study of the phase transitions and relaxations of the polymer and of the additives, associated to contact angle measurements on the different constituents (polymer, antioxidant and lubricant) showed that the additive phase transitions might governed the post treatment aging process on the catheter surface and explained in this particular case the difference in aging at 25°C and 45°C.

Conclusion: To understand the evolution of a surface after a cold plasma treatment, conditions of storage must be controlled. Moreover, the polymer relaxations and phase transitions and the surface chemistry have to be characterized: if additives bloom onto the surface, they can influence in an important way the kinetic of the post treatment surface aging, depending on their transitions and relaxation temperatures, and on their polymorphic form.

1. Wilson, D.J., N.P. Rhodes, and R.L. Williams, *Surface modification of a segmented polyetherurethane using a low-powered gas plasma and its influence on the activation of the coagulation system.* Biomaterials, 2003. **24**(28): p. 5069-5081.
2. Gerenser, L.J., *XPS studies of in situ plasma modified polymer surfaces.* J.Adhesion Sci.Technology, 1993. **7**(10): p. 1019-1040.
3. Spatafore, R. and L.T. Pearson, *Migration and blooming of stabilizing antioxidant in polypropylene.* Polymer Engineering and Science, 1991. **31**: p. 1610-1617.
4. Tyler, B.J., et al., *Variations between biomer lots : I.significant differences in the surface chemistry of two lots of a commercial polyetherurethane.* Journal of Biomedical Materials Research, 1992. **26**: p. 273.
5. Ganciu, M., et al., *Method for decontamination Patent 10/610158 - n° 7,229,589 (US).* 2007, CNRS, Université Paris Sud.

A Comparative Kinetic Study of the Controlled Drug Release Ability of the Hydrogels Synthesized from Diepoxy-Terminated Poly(Ethylene Glycol)s and Aliphatic Polyamines

Bogdan Cursaru, Mircea Teodorescu, Cristian Boscornea, Paul O. Stanescu, Stefania Stoleriu

Polytechnic University of Bucharest, Faculty of Applied Chemistry and Material Science, 149 Calea Victoriei, 010072, Bucharest, Romania ,
e-mail: bogdancursaru@yahoo.com

Introduction

The present work describes a comparative kinetic study of the controlled release of diclofenac sodium (DCF-Na) and 5-fluorouracil (5-FU) from PEG-based hydrogels with various structures and properties, synthesized from diepoxy-terminated poly(ethylene glycol)s of different molecular weights (600, 1000, 2000 and 4000 Da, $DEPEG_X$) and aliphatic polyamines of different chain length and functionality: ethylenediamine (EDA), 1,8-octanediamine (ODA), 1,12-dodecanediamine (DADD), diethylenetriamine (DETA) and triethylenetetramine (TETA).[1,2] DCF-Na and 5-FU were used as model drugs, as we expected them to interact in a different manner with the PEG chains.

Materials and methods

The $DEPEG_X$-polyamine hydrogels (epoxy groups/H_{amine} = 1/1) were synthesized as previously described.[1,2] The hydrogels were loaded by swelling into the drug solution of known concentration, followed by drying at room temperature to constant weight. The drug release experiments were carried out at 37°C in PBS (pH = 7.4).

Results and discussion

The drug release experiments showed a much slower discharge of DCF-Na as compared to 5-FU (Fig. 1), which was ascribed to a stronger interaction of DCF-Na with the PEG chains.

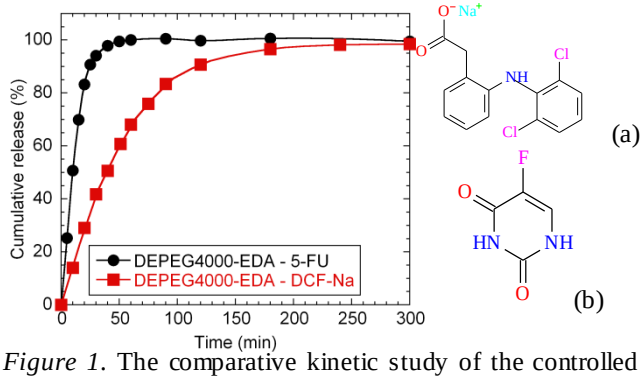

Figure 1. The comparative kinetic study of the controlled release of DCF-Na (a) and 5-FU (b) from the $DEPEG_{4000}$ – EDA hydrogels.

This supposition was supported by SEM analysis, which revealed smaller and deep inside located crystals on the surface of the DCF-Na loaded xerogels as compared with the 5-FU xerogels (Fig. 2).

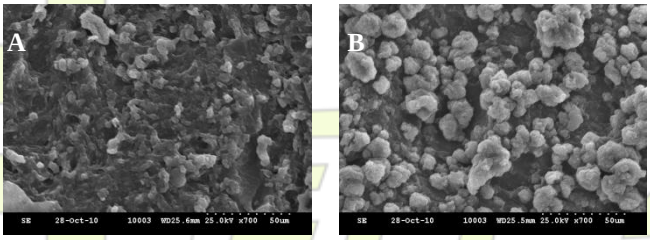

Figure 2. SEM micrographs of $DEPEG_{4000}$ xerogels loaded with DCF-Na (A) and 5-FU (B).

The mechanism of drug diffusion was also investigated according to the Ritger-Peppas equation, and it was anomalous (non - Fickian) in all cases, as indicated by the values of the diffusion exponent n ranging between 0,81 and 0,97.

The influence of the network structure (molecular weight of the PEG chains and amine functionality and chain length – Figure 3) upon the release rate of the drug was also investigated in the case of DCF-Na.

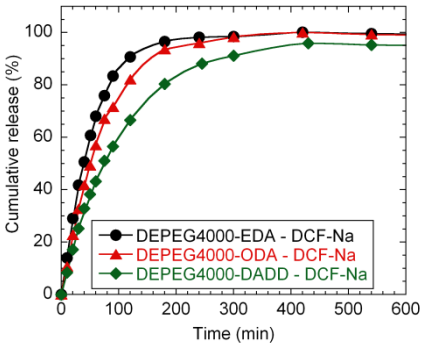

Figure 3. The influence of the amine chain length upon the controlled release of DCF-Na.

Conclusions

The hydrogels loaded with DCF-Na displayed a lower release rate as compared to 5-FU due to the presence of the sodium cation, which presumably promotes the formation of some structures similar to the crown ethers complexes, leading to a stronger interaction with the network. Both hydrogels with the shortest PEG chain and the longest amine hydrocarbon chain showed the smallest release rate of DCF-Na.

References

1. M. Teodorescu, B. Cursaru, P. Stanescu, C. Draghici, N. D. Stanciu, D. M. Vuluga, Novel hydrogels from diepoxy-terminated poly(ethylene glycol)s and aliphatic primary diamines: synthesis and equilibrium swelling studies, Polym. Adv. Technol., 2009, **20**, p. 907-915

2. M. Teodorescu, B. Cursaru, P. O. Stanescu, Swelling and diffusion characteristics of hydrogels synthesized from diepoxy-terminated poly(ethylene glycol)s and aliphatic polyamines, Soft Materials, 2010, **8,** p. 288-306

ACKNOWLEDGEMENT: The financial support of the National University Research Council in Romania through the PNII – IDEAS grant no.389/2007 is gratefully acknowledged.

Computer Simulation of Lysine Based Peptide Dendrimers

I.Neelov, S.Falkovich, A.Darinsky, H.Tenhu

Institute of Macromolecular Compounds, RAS, St.Petersburg, Russia
University of Helsinki, Helsinki, Finland

i.neelov@mail.ru

Introduction: Dendrimers are star-like molecules, with regular spherically symmetric branching in each arm (dendron). Dendrimers are widely used in industry and biomedical applications. Many dendrimers (PAMAM, PEI, carbosilane and others) have spherically symmetric branched backbone with two (or three) spacers of the same chemical structure (and thus the same number of chemical bonds (for example, seven bonds for PAMAM)) originating from each branching point. At the same time there are some dendrimers with non symmetrical branching of backbone. For example for poly-L-Lysine dendrimer there are two spacers with different chemical structure and different lengths (three and seven bonds) originating from each branching point. The lysine dendrimers are less toxic than widely used PAMAM and PEI dendrimers and thus are very promising for different biomedical applications. Our goal is to investigate the structure of such asymmetric dendrimers and their conjugates with short peptides.

Materials and Methods: In present work we performed simulation of lysine based dendrimers Method of molecular dynamic simulation with full atomic details (Amber99 forcefield) was used for this goal. One lysine dendrimer of generations g=3, 4 and 5 (or 3.5 generation conjugate with KFFE peptides) were placed in periodic box with 7000-8000 explicit water molecules (TIP3P model). The same number of negative counterions Cl- were added to system for compensation of dendrimer charge. All calculations were performed at temperature T=300K. The length of each molecular dynamics trajectory was equal to 100ns. Computational package OpenMM [1] for computer simulation of molecular systems with full atomic details on graphical processor units (GPU) was used.

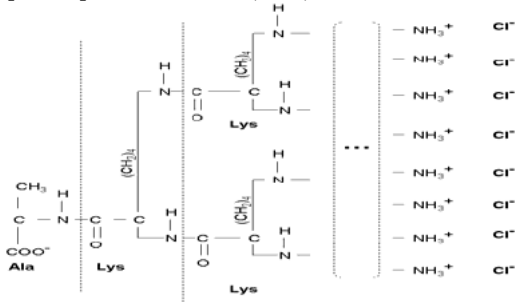

Fig.1 Schematic representation of lysine dendrimer

Results and Discussion: Main global characteristics of dendrimers are their gyration radius, asymmetry and distribution of density (for all atoms and for terminal groups) around the centre mass of molecule.. We calculated these characteristics for all lysine dendrimers and conjugate of dendrimer with KFFE tetrapeptides Time dependence of gyration radius of dendrimer was used to distinguish the relaxation and equilibrium parts of trajectory. 20ns was usually enough for full relaxation of system while the rest 80 ns were used for calculation of average values and distribution functions. We obtained that lysine dendrimer of generation g=3 after relaxation has rather asymmetric shape while dendrimers

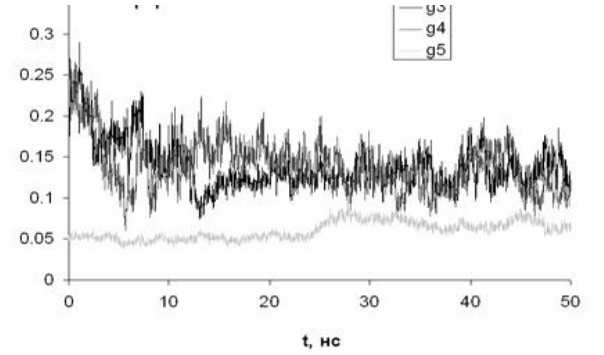

of generation g=4 and 5 are more spherical.
Fig.2 Tine dependence of asphericity of lysine dendrimers of generation g=3, 4 and 5

Dendrimers of g=4 and 5 have rather extended tails of radial density distribution while distribution of terminal groups has significant plateau-like region. Chemical attachment of KFFE peptides in hybrid structure doesn't influence the general dendrimer structure but slightly increase distance of terminal group from centre.

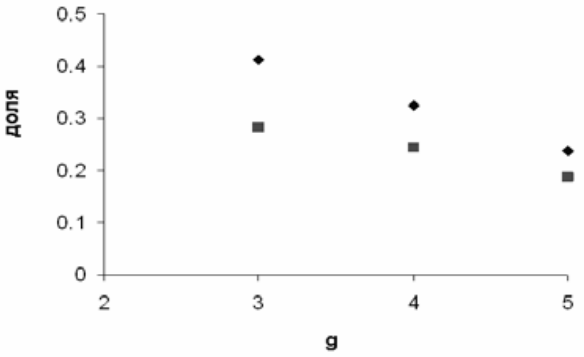

Fig. 3 Dependence of part of terminal groups of dendrimer not connected with counterions (diamonds) and part of counterions not connected to terminal groups of dendrimer (squares)

Conclusions

Lysine dendrimers of small generation has rather asymmetric shape which become more spherical for dendrimers of larger generations. Counterions play important (generation dependent role) in structuring the dendrimers. Short KFFE peptides attached to terminal groups of dendrimer doesn't influence its internal structure.

References:

[1] Friedrichs, M., et all J. Comp. Chem., **2009**, 30, 864-872

Improved Properties of Cross-Linked Sodium Hyaluronate Films

Calles J. A.[1], Ressia J.A.[1,2], Llabot J. M.[3], Chetoni P.[4], Palma S. D.[3], Vallés E. M.[1]

[1]Planta Piloto de Ingeniería Química (UNS-CONICET), Cam. La Carrindanga, Km. 7, Bahía Blanca, Argentina.
[2]Comisión de Investigaciones Científicas de la Provincia de Buenos Aires (CIC), La Plata, Argentina.
[3]Departamento de Farmacia, Facultad de Ciencias Químicas, Universidad Nacional de Córdoba, Córdoba, Argentina.
[4]Dipartimento di Scienze Farmaceutiche, Università di Pisa, Italy.

e-mail: jcalles@plapiqui.edu.ar

Introduction

The hyaluronan (HA) or hyaluronic acid sodium salt is a naturally occurring biopolymer, composed of a repeating disaccharide that consists of alternating units of N-acetyl-β-D-glucosamine and β-D-glucuronic acid. It's widely distributed in the human body composing the extracellular matrix of biological tissues. The biocompatibility and biodegradability of HA have made of it a material commonly used in treatment of osteoarthritis, drug delivery, ophthalmic surgery and tissue engineering (1-5). Despite these benefits, its fast water dissolution and a short residence times in biological tissues make necessary some structural modifications in order to overcome this drawbacks. The crosslinking process is the key to ensure better mechanical integrity in aqueous environments. Crosslinking heterogeneous methods have been reported (6) where reactions are carried out on solid HA, cast in the form of films or membranes, using glutaraldehyde (GTA) as crosslinker agent.

Polymer crosslinking processes not only improve the strength of materials, also make it more rigid and fragile. In this work we propose the use of triacetin (TA) during the formulation to mitigate this unwanted effect, leading to more ductile materials.

Materials and Methods

HA/GTA and HA/GTA + TA solutions were prepared using bidistilled water as solvent. The amount of each reactive was adjusted to achieve (1:2) and (1:4) HA/GTA molar ratios. The plasticizer, TA, was used in order to attain a 20% of the solid weight in the casted films.

Crosslinking reactions have been accomplished under acidic conditions, pH adjusted with 0.01M HCl. HA molecular weight was 1.56 x 10^6, and solution concentration was 1 wt %. After 24-h reaction time stirring at room temperature, the gels were casted at room temperature under extractive hood. Different size Petri dishes were used to obtain variety on film thicknesses.

Contact angle (CA) was tested on a Kruss, EasyDrop Standard, DSA 15 goniometer. Mucoadhesive studies were performed using mucin as simulated biological substrate. Stress-strain tests were obtained in an Instron 3369 tester in traction mode at 2 mm/min at room conditions.

Results and Discussion

The table 1 summarizes the amount of each reactant and some of the most important results obtained in this work.

The contact angle measurements clearly show the increment of this parameter with the use of more GTA as crosslinker agent in the reaction process. CA is also incremented with the incorporation of TA to the mixture.

Table 1: Contact angle and mucoadhesive strength.

HA/GTA*	TA%	C. Angle	Mucoadh. (kgf/cm^2)
1:0	0	-	153,241
1:2	0	43.025	198,781
1:4	0	47.075	226,744
1:2	20	56.419	220,431

*molar ratio

A marked increment is also evidenced in the mucoadhesive strength needed to unstick the films from the mucin layer, both for using GTA and TA in the formulation. This is attributed to the increment in the chain mobility favored by the presence of the plasticizer.

In the stress strain studies the crosslinked films exhibit fragile behavior. The specimens break before the reaching the yield point. The incorporation of TA to the formulations changes the stress-strain performance from fragile to ductile. All the plasticized samples attained the yield point and had a plastic deformation.

Conclusions

The use of GTA as crosslinker agent for HA films significantly improves the integrity of HA films in aqueous environments incrementing the bioadhesiveness of HA to mucin and reducing the wettability of the material.

Incorporation of TA as plasticizer to the formulation not only enhances the strength and the bioadhesiveness of the material, but also made it more ductile and less rigid.

Acknowledgements

The authors thank financial support from Universidad Nacional de Sur (UNS), the Consejo Nacional de Investigaciones Científicas y Técnicas (CONICET), and the Comisión de Investigaciones Científicas de la Provincia de Buenos Aires (CIC) .

References:

(1) E. A. Balazs, J. L. Denlinger, J. Rheumatol. 1993, 20, 3.
(2) E. A. Balazs, in: ''Healon (Sodium Hyaluronate).'', D. Miller, R. Stegmann, Eds., Wiley, N. Y. 1983, p. 5.
(3) S. K. Hahn, S. J. Kim, M. J. kim, C. H. Chung, D. B. Moon, Y. P. Lee, J. Control Release 2005, 104, 323.
(4) S. K. Hahn, E. J. Oh, H. Miyamoto, T. Shimobouji, Int. J. Pharm. 2006, 322, 44.
(5) R. Ohri, S. K. Hahn, P. S. Stayton, A. S. Hoffman, M. Giachelli, J. Biomed. Mater. Res. 2004, 70A, 159.
(6) Tomihata, K.; Ikada, Y. Biomaterials 1997, 18, 189.

Thermoset biodegradable elastomers with tunable mechanical properties and degradations.

A. Harrane, H. Nouailhas, A. Leroy, B. Nottelet and J.Coudane

IBMM, Artificial Biopolymers Group, UMR-CNRS 5247, UM1-UM2, 15 Av. C. Flahault, 34093 Montpellier, France

Benjamin.Nottelet@univ-montp1.fr

Introduction: Biodegradable elastomers have recently attracted growing attention. Indeed, for the regeneration of soft tissues such as blood vessels their ability to provide a structural support with similar mechanical properties to those of native tissues in dynamic environment makes them of a particular interest.[1] Among them, thermoset elastomers have the ability to degrade by combination of bulk and surface erosion which guarantee a constant shape during degradation as well as a linear drug release profile.[2] We describe here the preparation of degradable elastomers based on short photo-cross-linkable PLA-PEG-PLA triblocks with chosen amphiphilic balance to provide intermediate degradation times and linear degradation profiles. In addition, we would like to illustrate the possibility to obtain various mechanical behaviours from the same initial tribloc depending on the presence and the nature of the cross-linker. Finally degradation and biocompatibility are discussed.

Materials and Methods: PLA_9-PEG_{45}-PLA_9 was synthesized according to a methodology developed in our group.[3] Methacrylation was carried out in dry CH_2Cl_2 with methacryloylchloride and triethylamine. Irgacure® 184, 2,4,6-triallyloxy-1,3,5-triazine (TAC), and pentaerythritol triallyl ether (PETAE) were used in conjunction with a PentaFUSION UV system for UV-cross-linking. Mechanical properties were evaluated on an "Instron 4444". Degradation was followed in PBS at 37°C. Biocompatibility was evaluated with MTT tests.

Results and Discussion: PLA_9-PEG_{45}-PLA_9 was obtained with a 90% yield. ^{1}H NMR analyses confirmed a ratio EO/LA of 2.5 and a polymerization degree of PLA blocks of 9 in agreement with the expected theoretical values. Methacrylation reaction was conducted for 72 h at room temperature under nitrogen (yield 88%). Each elastomer was then prepared by UV-curing of mixtures containing i) the tribloc copolymer (TC) ii) Irgacure® 184 (I) or no photo-initiator and iii) TAC or PETAE (0 to 100% with respect to alkene groups) or no cross-linker. After soaking of the resulting elastomers in CH_2Cl_2, the cross-linking efficiency was calculated and ranged from 80 to 90% without significant influence of the composition on the grafting efficiency.

Figure 1. Picture of elastomer $TC_{I\text{-}PETAE100}$

Thermal properties of the ed. The glass transition temperature (Tg) increased with the cross-linking. For TC Tg is -38.2°C but increased to -11.7 °C for the elastomer cross-linked with TAC ($TC_{I\text{-}TAC100}$) and -13.4 °C for the one cross-linked with PETAE ($TC_{I\text{-}PETAE100}$). In accordance with known elastomers behaviours, Tgs increased with the cross-linking ratio. Elastomers were found to be soft and amorphous **(Figure 1)**. TAC and PETAE have very different structures, the first one being much more rigid and hydrophobic than the second one. **Figure 2** demonstrates the influence of the cross-linker nature on the elastomers mechanical properties, $TC_{I\text{-}TAC100}$ being the stiffest one (E = 4.45 MPa) whereas $TC_{I\text{-}PETAE100}$ is the most deformable one (ε_{break} = 60 %). As expected when considering the hydrophilicity of TAC *vs.* PETAE, this difference was even more pronounced in the hydrated state (not shown here).

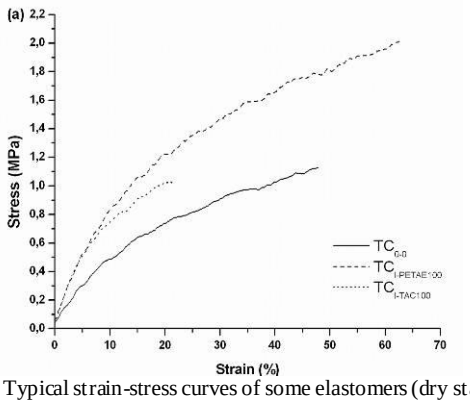

Figure 2. Typical strain-stress curves of some elastomers (dry state)

All elastomers degraded linearly and at the same rate up to 30 days, with for all samples a weight loss of 30%. Beyond, while degradation continued, degradation rates changed as a result of the elastomers structures. The higher the hydrophilicity, the faster and more complete the degradation was **(Figure 3)**. MTT tests were done on the various elastomers and demonstrated that all compositions led to biocompatible materials.

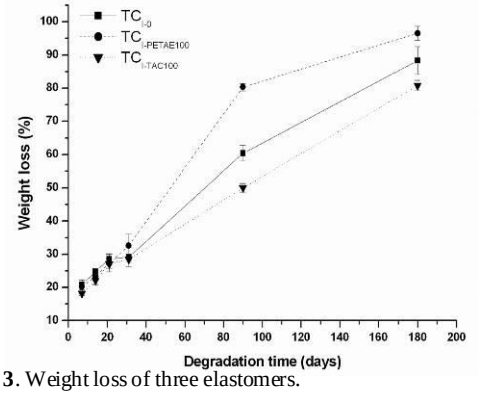

Figure 3. Weight loss of three elastomers.

Conclusion: Design of soft degradable elastomers having defined mechanical properties and degradability can be achieved by the careful choice of the amphiphilic character of pre-polymers and the nature of the cross-linkers.

References: **1.** *Serrano M. et al. Adv. Func. Mater.2010, 20, 19.* **2.** *Barrett D. et al. Polym. Chem., 2010, 1, 296* **3.** *Nouailhas, H. et al. Polym. Int. 2010, 59, 1077.*

Synthesis, characterization and application in controlled drug release of chitosan hydrogels obtained from *aspergillus niger*

N.E. Valderruten[1], E. Ruiz[1], H.F. Zuluaga[2], Z. Lentini[1], G.A. Muñoz[2], E.L. Romero[2], G. Alvarez[1], C. Suárez[1], L. Trujillo[1], J. De la cruz[1]

[1] Facultad de Ciencias Naturales, Universidad ICESI, A.A. 25608, Cali, Colombia
[2] Departamento de Química, Universidad del Valle, A.A. 25360, Cali, Colombia

nevalderruten@icesi.edu.co

Introduction:

In the industrial production of citric acid from sugar cane using *Aspergillus niger*, big amounts of the fungi's mycelia is obtained as a byproduct. Most of the mycelia is sold, at a very low price, as food supplement for cattle.

The chitin contained in the mycelia can be transformed into chitosan by enzymatic or chemical processes. Chitosan is a biodegradable and biocompatible polymer with many applications.

Commercial chitosan is also obtained from crustaceans. Cross-linking of chitosan affords three-dimensional networks known as hydrogels. Hydrogels are polymers that exhibit the ability to absorb a considerable amount of water without dissolving. This behavior is usually achieved by a low degree of cross-linking.

Different types of hydrogels sensitive to temperature, pH, ionic force, and other stimuli have been synthesized. A particular characteristic of chitosan hydrogels is their sensibility to pH changes. This behavior could allow their use in intelligent systems for substances release. In this work chitosan was extracted from *Aspergillus niger* in order to produce hydrogels using dialdehydes and dicarboxylic acids as cross-linking agents. Kinetic studies of drug release were carried out.

Method and Materials:

Chitosan was extracted by basic hydrolysis at 110ºC, followed by washings with water and ethanol. The filtrate was dissolved with HCl and then precipitated with 30% NaOH. The extracted chitosan was characterized by FTIR (Shimadzu FTIR-8400 spectrophotometer) and ^{1}H NMR in a 400 MHz Bruker instrument. Chitosan molecular weight was measured with a capillary reverse flow viscometer, applying the Mark-Houwink-Sakurada equation.

Chitosan deacetylation degree was calculated by elemental analysis and potentiometry. Hydrogels were prepared using dialdehydes as cross-linking agents at 30 ºC. Alternatively, dicarboxylic acids were used as cross-linking agents. The synthesis was carried out at room temperature, using a carbodiimide (EDC) and N-hidroxysuccinimide. The hydrogels were characterized by thermal (DSC y TGA), spectroscopic (FTIR) and mechanical tests (DMA). Some swelling and controlled drug release studies were performed.

Results and discussion:

Chitosan extraction was favored using hydrochloric acid and concentrated solutions of sodium hydroxide, reaching a yield of 6,0%. The FTIR spectrum of chitosan revealed the strong absorption band at 3300 cm^{-1} attributed to the O-H and N-H groups, and at 1650 cm^{-1} the stretching vibrations of C=O group. The ^{1}H-NMR spectrum of chitosan revealed a signal at 2.02 ppm corresponding to the mehyl groups of N-acetylglucosamine; signals between 3 and 4 ppm were assigned to carbons C2-C6 from glucosamine and N-acetylglucosamine subunits, 4.7 ppm signals from C1 from N-acetylglucosamine, and at 4.8 ppm the signal of C1 from glucosamine. Deacetylation degree was 76.33% and the molecular weight was 1.15 x 10^5 Da. This results show that a good percentage of chitin was converted into chitosan. The experimental data suggest that the swelling process follows a second-order kinetics. The swelling rate constant and the equilibrium water content of hydrogels were dependent on the cross-linking degree and pH in the swelling medium. The hydrogels transitions and their decomposition were determined by differential scanning calorimetry, DSC, and termogravimetric analysis, TGA. Drug release kinetics was followed by UV/Vis. Some differences in the release speed related with the percentage of cross-linking and the dicarboxilic acid type used in each case were observed.

Conclusions:

The use of concentrated basic solutions increases the percentage of chitosan isolated from *Aspergillus niger*. Variations in cross-linking agent type (dialdehyde or diacid) and the percentage itself, modified hydrogels properties. The hydrophilic character from hydroxyl and amino groups also modifies the swelling behavior of hydrogles and the controlled drug release at different pHs.

References:

1. Abdou, E; Nagy, K; Elsabee, M., *Bioresource Technology*. 2008, 99, 1359
2. Kumirska, J; Czerwicka, M; Kaczyński, Z; Bychowska, A; Brzozowski, K; Thöming, J; Stepnowski, *Mar. Drugs*. 2010, 8, 1567
3. Sánchez, A; Sibaja, M; Vega-Baudrit, J; Madrigal S., *Revista Iberoamericana de Polímeros*. 2007, 8, 241
4. Bodnar, M; Hartmann, J; Borbely, J., *Biomacromolecules*. 2005, 6, 2521
5. Narayan B., Jonathan G., Miqin Z., *Advanced Drug Delivery Reviews*, 2010, 62, 83

The Use of a Novel Polymer to Measure and Classify Plantarsurface Skin Stresses

Samantha Stucke, Daniel McFarland*, Brian Davis PhD*, Larry Goss PhD[+], Sergey Fonov PhD[+], Robert Forlines[+], Necip Berme PhD[°], Hasan Cenk Guler PhD[°], Chris Bigelow[°]*

*The Austen BioInnovation Institute in Akron, Akron, Ohio, [+]Innovative Scientific Solutions Inc., Dayton, Ohio and [°]Bertec Corporation, Columbus, Ohio

bdavis@abiakron.org

Introduction:

Diabetic foot ulceration is the prime reason for limb amputation in the USA. As a result, considerable efforts are being implemented to both understand the etiology of foot ulcers, and predict patients who are at elevated risk.Our team is using a novel polymer that has been patented (US 7127950 B2) for measuring and understanding mechanical stresses at the foot-ground interface. The so-called "Surface Stress Sensitive Film" (S3F), holds special promise for not only quantifying plantar surface skin stresses but also for evaluating biomedical implant interfaces in general.

Material and Methods:

S3F is a polymer film-based optical measurement system that provides a force map over the entire contact surface. It records the vertical pressure gradients and lateral (shear) forces being produced by a foot, tire, air, water, or other force generating activities. Examples of shoe contact measurements are shown in Figure 1.

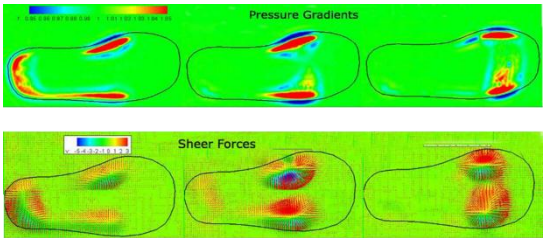

Figure 1. Pressure gradients and shear force maps produced by a child's shoe, at three walking motion time points, on the S3F Measurement System.

The response of the film to a tangential force is depicted in Figure 2. The response of the film may be visualized by considering a series of markers on the surface on the film. The markers will be displaced as the film shears, where the displacement is a function of the film thickness and shear modulus. The response of S3F to a normal force is depicted in Figure 3.

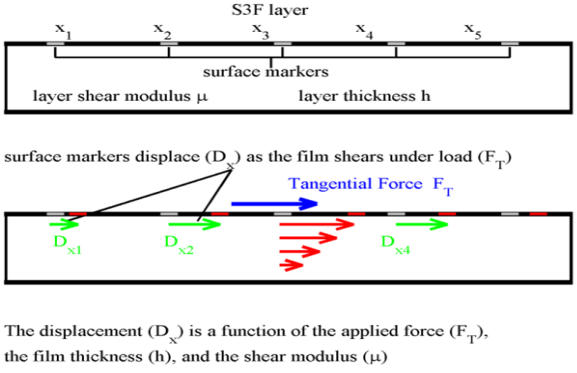

Figure 2. Response of the S3F to a tangential load.

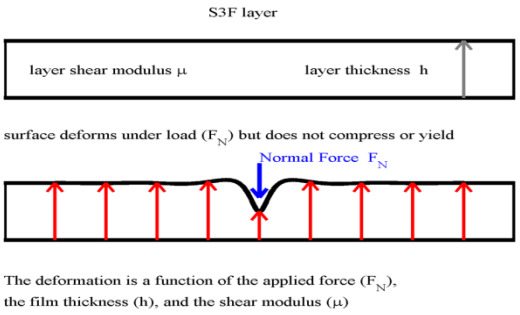

Figure 3. Response of the S3F polymer to a normal load applied to the top surface.

The *Foot Pressure and Shear Mapping System* integrates (i) the S3F polymer film for contact force analysis and (ii) a force plate system (Bertec Corporation) for human gait analysis and biomechanics research. Shear distributions can be extracted from a pair of unloaded and loaded images taken by a single hi-resolution CCD camera. The force plate provides combined measures of the six forces and moments (Fx, Fy, Fz, Mx, My, Mz) which are used for global force comparisons. For this study, data were collected on 12 subjects walking at a self-selected speed.

Results and Discussion

Currently the system is being clinically tested and statistical analysis of a preliminary study was conducted to determine the level of repeatability associated with this system. As illustrated in Figure 4. Interclass Correlation Coefficients where calculated, as a function of trails, for the peak normal (pressure) and shear displacement in each region of the foot. The results of the ICC analysis showed excellent repeatability between trails for each foot region.

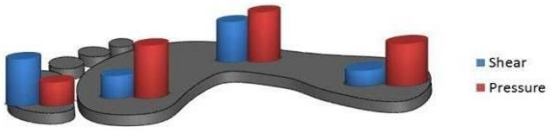

Figure 4. ICC values as a function of trials.For peak pressure the ICC's in the four regions where 0.966 (Heel), 0.844 (Midfoot), 0.892 (Forefoot) and 0.944 (Hallux). The ICC's for peak shear in the four regions where 0.924 (Heel), 0.709 (Midfoot), 0.839 (Forefoot) and 0.948 (Hallux).

Acknowledgment

This study was funded by a grant (1R44DK084844-01) from the National Institutes of Health (NIH) awarded to Dr. Hasan Cenk Guler. The participation of the control subjects is also acknowledged.

Removal of Heavy Metals from Waste Water by Naturally Occurring Bio-waste

Fares D Alsewailem and Saad A Aljlil

King Abdualziz City for Science and Technology (KACST), P.O.Box 6086, Riyadh 11442, Saudi Arabia

fsewailm@kacst.edu.sa

Abstract

Biomass materials, which may be considered natural polymers, such as nut shells, rice hulls, and sugar canes remaining are known to have good adsorption affinity towards heavy metal ions. In the current research we are reporting initial results of the adsorption isotherms of lead and cooper on two types of date pits grown largely in the arabian peninsula region. Figure 1 below showed that one of the two types of date pits has a good adsorption capacity for lead ions even at lower concentrations. We believe that date pits surface characteristics, e.g. functional groups and pore size, had able lead ions to attach to the surfaces in an efficient manner.

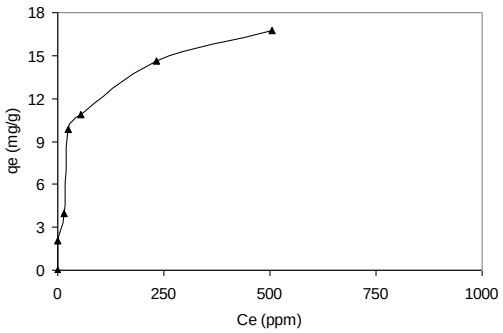

Fig(1): Equilibrium isotherm of lead ions adsorption on sucaray date pits

Amphiphilic Segmented Elastomeric Polyurethane Bio-Based on PLLA: Synthesis and Characterization

Jonathan M. Bergamaschi[1] *and Maria I. Felisberti*

Physical-Chemistry Department, Chemistry Institute, State University of Campinas (UNICAMP), P.O. Box 6121, Zip Code 13083-970, Campinas - SP, Brazil

[1] jmb_jj@yahoo.com.br

Introduction

Poly(L-lactide) (PLLA) is a very important synthetic material widely used in tissue engineering due to its biodegradability, biocompatibility and excellent shaping and molding properties [1]. However, interaction between the polymers, as PLLA, and cells can not be adequate, leading to in vivo foreign body reactions, such as inflammation, infections, local tissue necrosis etc [2]. Moreover, due to lack of functional groups, they cannot be modified easily with biologically active moieties.

Recently, many investigations have attempted to improve the hydrophilicity of polyester. Copolymers based on poly(ethylene glycol) is often introduced because of its hydrophilicity, nontoxcity, biocompatibility and nonimmunogenicity. Segmented Polyurethanes (SPUs) are very important strategic macromolecules and suitable for biomedical applications such as sutures, artificial tissues, implants and drug delivery because of their excellent physical properties, biocompatibility and biodegradability. SPU is generally synthesized by incorporating soft segments susceptible to hydrolysis, such PLLA, into PU [3]. Poli(lactic acid) is synthesized via two different polymerization mechanisms, direct polycondensation of lactic acid and ring-opening polymerization (ROP) of the cyclic dimer, lactide [4]. In either case, the lactoyl units may possess a single stereo-configuration, usually L, leading to semicrystalline poly(L-lactic acid), or they may be the racemic mixture, leading to amorphous poly(D,L-lactic acid) (PDLLA). ROP provides more precisely targeted and potentially higher molecular weight [5]. Therefore the PLLA diol was synthesized by ROP from L-lactide using stannous di-octoate as initiator and ethylene glycol as co-initiator. In this study, amphiphilic segmented polyurethanes based on hydrophobic poly(L-lactide) diol – PLLA-diol (Mn ~ 2,500 g mol^{-1}) and hydrophilic multiblock copolymers poly(propylene glycol)-*block*-poly(ethylene glycol)–*block*–poly(propylene glycol) - PPO-PEO-PPO (Mn ~ 2,700 g mol^{-1}) were synthesized. The SPUs were characterized by proton nuclear magnetic resonance spectrometry (^{1}H-NMR), attenuated total reflection Fourier transform infrared spectroscopy (ATR-FTIR), gel permeation chromatography (GPC), differential scanning calorimetry (DSC), dynamic mechanical analysis (DMA) and X-ray diffraction (XRD).

Material and Methods

Equimolar ratio of diols and toluene diisocyanate (TDI) was used for the polyurethanes synthesis and stannous octanoate was used as catalyst (0.05 wt% relation to diol). The reaction was carried out in chloroform under reflux and under nitrogen atmosphere. TDI was added slowly to the reaction at 0.1 mL h^{-1} rate, for 3.5 hours. The resulting polyurethane was precipitated in ethyl ether, filtered and vacuum oven-dried for air renewal at 35 ° C for 12 h. Finally, the SPUs were dried in the vacuum oven (35 ° C) for 6 h. The global composition of the synthesized SPUs was: 100; 70; 50; 30 and 0 wt% of PLLA-diol, named PU-PLLA100; PU-PLLA70; PU-PLLA50; PU-PLLA30 and PU-PLLA0, respectively. Molar mass of these polyurethanes varies from 20,000 g mol^{-1} for PU-PLLA0 to 70,000 g mol^{-1} for PU-PLLA100.

Results and Discussion

^{1}H NMR as well as ATR-FTIR spectra show evidences of the SPUs formation. X-ray difractograms and second DSC heat scans of the segmented polyurethanes revealed that the crystallization of both PPO-PEO-PPO and PLLA segments was mutually restricted. The SPUs present only one glass transition which is dependent on the composition. The glass transition temperatures (Tg) occur at values between the Tg of PU-PLLA100 and PU-PLLA0, suggesting miscibility of the blocks awarded by randomly-distributed blocks. Storage modulus at higher temperatures than Tg of SPU increases as the amount of PLLA blocks increases, while the peak in the Loss modulus curves corresponding to glass transition is broader for PU-PLA100 due to the presence of different microambients: amorphous and crystalline phases and interface. Water swelling tests show that the equilibrium water content (EW%) of PU-PLLA100 is 5,5% and increases as the amount of the hydrophilic block contents increases up to 164% for PU-PLLA0. The EW% values for the other SPU are intermediate, indicating the amphiphilic character of the segmented PUs.

Conclusions

The amphiphilic elastomeric segmented polyurethanes bio-based on PLLA diol and PPO-PEO-PPO diol were synthesized. SPUs compositions influence the physical-chemistry properties and the swelling tests show an increase in mass gain with the increase of hydrophilic multiblock copolymers percentage, it was one of the factors that determined the level of cytocompatibility of samples.

References

[1] Chen S, Pieper R, Webster DC, Singh J. *Int. J. Pharmac.* **2005,** 2, 207–218

[2] Hersel, U.; Dahmen, C.; and Kessler, H. *Biomat.* **2003**, 24, 4385–4415;

[3] K. Gisselfalt, B. Edberg, P. Flodin, *Biomacromol.* **2002**, 3, 951– 958;

[4] Dechy-Cabaret, O.; Martin-Vaca, B.; Bourissou, D. *Chem. Rev.* **2004**, *104*, 6147-6176;

[5] Mehta, R.; Kumar, V.; Bhunia, H.; Upadhyay, S. N. *J. Macromol. Sci., Part C: Polym. Rev.* **2005**, *43*, 325-349.

Polyhydroxyalkanoates (PHAs) produced by *Cupriavidus necator* employing by-products from industrial biodiesel production as carbon source

Jimmy A. López[1], *Isabel López*[2], *Apostolis Koutinas*[3], *Marcelo A. Villar*[1]

[1]Planta Piloto de Ingeniería Química, PLAPIQUI (UNS-CONICET), Departamento de Ingeniería Química, Universidad Nacional del Sur, Camino "La Carrindanga" Km. 7, (8000) Bahía Blanca, Argentina
[2]Department of Chemical Physics and Applied Thermodynamics, E.P.S. Campus Universitario de Rabanales, University of Cordoba, 14071, Cordoba, Spain
[3]Department of Food Science and Technology, Agricultural University of Athens, Iera Odos 75, 118 55, Athens, Greece

e-mail: jlopez@plapiqui.edu.ar, mvillar@plapiqui.edu.ar

Introduction: Polyhydroxyalkanoates (PHAs) are bio-polyesters produced by a wide variety of bacteria as intracellular carbon and energy storage materials. The most commonly bio-synthesized PHAs are short-chain-length (SCL) copolymers containing 3-5 carbon atoms such as poly(3-hydroxybutyrate) (PHB)) and poly(3-hydroxybutyrate-*co*-3-hydroxyvalerate) (P(HB-*co*-HV)) [1]. The versatility of these microbial polyesters in terms of physical properties and therefore of commercial and biomedical applications, is increased when more carbon atoms are presented in their molecular structure [2]. Thus, medium-chain-length (MCL) PHA copolymers containing 6-14 carbon atoms represent a great commercial alternative for more specific biopolyesters with a range of additional favorable material properties [3].
This work studies the production and characterization of short-chain-length and medium-chain-length (MCL, 6-14 carbon atoms) PHAs produced by bacterial bioconver-sions of *Cupriavidus necator* via bioprocessing strategies using crude glycerol and rapeseed residues generated from industrial biodiesel production. Chemical structures and physical properties of produced PHA copolymers were analyzed by using Fourier Transform Spectroscopy (FTIR), ^{1}H- and ^{13}C-Nuclear Magnetic Resonance (^{1}H- and ^{13}C-NMR), Differential Scanning Calorimetry (DSC), and Termogravimetric analysis (TGA).

Results and Discussion: Biopolymers extraction was carried out by dispersion with sodium hypochlorite and chloroform [4]. A standard PHB sample was also included during the analysis in order to compare the properties of obtained copolymers. ^{1}H- and ^{13}C-NMR results shown that SCL copolymer correspond to P(HB-*co*-HV), while the other sample can be identified as a medium-chain-length PHA copolymer.
Thermal properties of PHB and PHA copolymers are presented in Table 1. It should be stressed that marked differences between melting point (T_m), and degree of cristallinity (X_c) confirms the incorporation of higher carbon atom monomers into original PHB structure.

Table 1. Thermal properties of PHB, SCL- and MCL-PHA copolymers

Sample	T_m (ºC)	ΔH_m (J/g)	X_c (%)
PHB	170.6	91.83	61.5
SCL-PHA	155.0	72.61	48.6
MCL-PHA	140.9	44.11	29.5

TGA profiles for the three studied biopolyesters are shown in Fig. 1. TGA results indicate that MCL-PHA has a lower degradation temperature than PHB and P(HB-*co*-HV) due to the incorporation of higher carbon atom monomers.

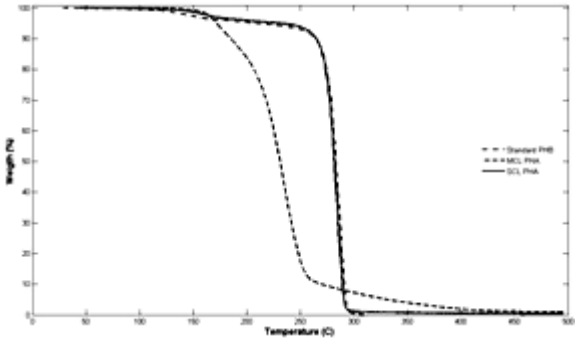

Figure 1. Thermogravimetric analysis (TGA) for standard PHB, SCL- and MCL-PHA copolymers.

FTIR and ^{1}H- and ^{13}C-NMR (data not shown) also indicate that MCL-PHA copolymer has at least three different monomeric units such as 3-hydroxybutyrate, 3-hydroxyvalerate, and other higher carbon atom monomer which is being identified by comparing its experimental ^{1}H- and ^{13}C-NMR spectra with theoretical predicted one.

Conclusions: Complex media generated from by-products of the biodiesel manufacture used as carbon source by bacterial bioconversions of *Cupriavidus necator* give different SCL- and MCL-PHA copolymers. The main goal of this work is the biosynthesis and characterization of PHA copolymers with a bigger spectrum of commercial applications obtained from agroindustrial residues of biodiesel manufacture.

Acknowledgements: Authors thank to Consejo Nacional de Investigaciones Científicas y Técnicas (CONICET), Universidad Nacional del Sur (UNS), and Greek State Scholarships Foundation (IKY) for financial support.

References

1. Steinbüchel, A., Bernd, F. *Trends Biotechnol.* **1998**, *16*, 419-427.
2. Anderson, A.J., Williams, D.R., Taidi, B., Dawes, E.A., Ewing, D.F. *FEMS Microbiol. Rev.* **1992**, *103*, 93-101.
3. Dai, Y., Lambert, L., Yuan, Z., Keller, J. *J. Biotechnol.* **2008**, *134*, 137-145.
4. Hahn, S.K., Chang, Y.K., Kim, B.S., Chang, H.N. *Biotechnol. & Bioeng.* **1994**, *44*, 256-261

Synthesis of Caffeic Acid Molecularly Imprinted Polymer Microspheres and HPLC Evaluation of their Sorption Properties

Ángel Valero Navarro[1*], *María Gómez Romero*[1], *Jorge F. Fernández Sánchez*[1], *Antonio Segura Carretero*[1], *Peter A.G. Cormack*[2], *Alberto Fernández Gutiérrez*[1]

[1]Department of Analytical Chemistry, University of Granada, Avd. Fuentenueva s/n, 18071 Granada, Spain
[2]WestCHEM, Department of Pure and Applied Chemistry, University of Strathclyde, 295 Cathedral Street, Glasgow, UK

*angvana@ugr.es

Introduction

Caffeic acid (CA) is a well-known and important phenolic antioxidant present in many plants and beverages, including coffee, apple juice and white wine. It is usually found in the presence of many other related compounds so its isolation and preconcentration from such complex matrices, although of genuine of interest, can be complicated. However, this isolation and preconcentration aim can potentially be realised by using molecularly imprinted polymers (MIPs) to bind the target molecule (CA) in a selective manner even although CA is present in a complex matrix. In this context, MIPs are biomimetic materials which function as antibody binding mimics. In the present work, we present the first example of a caffeic acid molecularly imprinted polymer which has been synthesised in the form of well-defined polymer microspheres.

Materials and Methods

The polymers were prepared by precipitation polymerisation in a fashion similar to the procedure described by Wang et al.[1] For the preparation of MIP, CA (0.66 mmol), 4-vinylpyridine (2.65 mmol), divinylbenzene-80 (13.23 mmol) and α,α'-azobisisobutyronitrile (0.58 mmol) were dissolved in a mixture of acetonitrile and toluene (100 ml, 75/25 v/v) in a 250 ml, polypropylene bottle. The mixture was degassed with oxygene-free nitrogen for 10 minutes while cooling on an ice bath, sealed under nitrogen atmosphere and left to polymerise on a low-profiler roller housed inside a temperature-controlable incubator. Reaction temperature was raised from 25ºC to 60ºC for 2 h and then kept at 60ºC for a further 24 h.

Results and Discussion

The morphological characterisation of the polymer was carried out by means of scanning electron microscopy (Fig. 1) (narrow size distribution: ~ 5 and 1.5 µm for MIP and NIP [non-imprinted polymer], respectively) and nitrogen sorption porosimetry: specific surface area of 340 and 350 $m^2\ g^{-1}$ for MIP and NIP and average pore volume of 0.17 and 0.19 $cm^3\ g^{-1}$, for MIP and NIP, respectively.

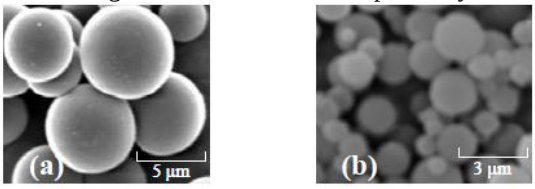

Fig. 1. Scanning electron micrographs of MIP (a) and NIP (b).

The polymers were evaluated by batch rebinding analysis and the derived Freundlich isotherm (number of binding sites (N_K) = 0.6 and 0.3 mmol/g for the MIP and NIP, respectively, and apparent average adsorption constant (K_N) = 10.0 and 1.6 L/mmol for MIP and NIP, respectively). The molecular recognition character of the MIP was evaluated by packing it into a stainless steel LC column (50 mm x 4.6 mm i.d.) and exploiting the MIP as an LC stationary phase. These experiments corroborated the imprinting phenomenon and selective recognition of CA by the imprinted material since very good selectivity was achieved when CA was perfectly isolated in a matrix with eight structurally related compounds. The performance of the imprinted microspheres was proven superior to conventionally prepared bulk and solution polymers when the imprinted column was used directly with juice samples without any clean-up step allowing an efficient removal and recovery of CA from such complex samples.

The CA recoveries obtained were quantitative in all cases and higher than 81 %. It is worthwhile to mention that reproducible responses were noted for both NIP and MIP materials for the template over a 12-month-time-period.

Conclusions

In this work, the technique of molecular imprinting by precipitation polimerisation has been successfully used to produce the first CA MIP in the form of well-defined microspheres. The binding properties of the MIP and the NIP were evaluated by batch rebinding studies and using the derived adsorption isotherms. From the fitting parameters we calculated the affinity distributions for MIP and NIP demonstrating the imprinting phenomenon and strong adsorption ability of the MIP towards CA. Finally, when the imprinted LC column was used for the selective recognition of CA over eight related compounds, a very good selectivity was obtained and it allowed an efficient removal of CA from apple juice samples.

Acknowledgments

The authors thank the Spanish Ministry of Education (FPU grant reference AP2006-01147 and Project CTQ2008-01394) and the Regional Government of Andalucia (Excellence projects P07-FQM-2738, P07-FQM-2625 and P09-CTS-4564) for their financial support.

References

[1]Wang, J.F. *et al.*, 2003. Angew. Chem. Int. Ed. 42(43), 5336-5338.

Nano and Micro Phospholipid/Block Copolymer Hybrid Vesicles: a new approach for the design of carriers for cancer therapy

Chemin M.[1], *Brun PM.*[1], *Sandre O.*[1], *Lecommandoux S.*[1], *Le Meins JF.*[1]

[1] Université de Bordeaux, ENSCBP, 16 avenue Pey Berland, 33607 Pessac Cedex, France
CNRS Laboratoire de Chimie des Polymères Organiques, (UMR CNRS 5629), Pessac Cedex,

lemeins@enscbp.fr

Introduction: Liposomes or lipid vesicles are known for a long time. They are largely used in cosmetics and pharmaceutics applications but suffer from a lack of stability. Polymer vesicles also called polymersomes are quite recent supramolecular structures discovered in the nineties. These promising structures exhibit tremendous properties but their high stability might be a drawback in applications where a transient carrier is required (for instance in drug delivery). Therefore, we propose to elaborate a new type of vesicles, namely hybrid vesicles assembled from both phospholipids and polymers which will bring novelty in terms of vesicular membrane properties (permeation, elasticity, stability…) and membrane nano-structuration (creation of domains in analogy to lipid rafts in cell's membrane) which plays a significant role for future therapeutic applications.

To the best of our knowledge only three papers have been published so far in this field.[1-3] Up to now, only membranes in which block copolymers and lipids are homogeneously distributed have been obtained. The creation of "spot like" lipid rich domain have been achieved only in one particular case, using an external driving force to perturb the initial equilibrium homogeneous state of the vesicles. We show in this study that spontaneous membrane structuration can occur provided an appropriate choice of copolymers and lipids.

Materials and methods: We have used models copolymers well described in the literature for their ability to form polymersomes. One provided by Dow Corning is a grafted copolymer with Poly (dimethylsiloxane) backbone and poly (ethyleneoxide) as pendant chains (PDMS-*g*-PEO). Its average molar mass is in the range of 3000 g/mol and a 5 nm membrane core thickness has been reported, close to the value reported for liposomes. Another available block copolymer is poly(butadiene)-b-poly(ethyleneoxide) (PBut-b-PEO) with a number-average molar mass of 3800 g/mol and a 9.0 ± 1 nm membrane core thickness. As phospholipids we used the synthetic ones POPC and DPPC from Avanti Polar Lipids. A fluorescent lipid was used as a marker to reveal lipid phases in the membrane. Giant vesicles were prepared by electroformation.

Results and discussion: All the vesicles observable by optical phase contrast microscopy (Fig 1-a) were also observable using epi-fluorescence microscopy (Fig 1-b) whatever the molar content of phospholipid (10-80%) attesting to the presence of block copolymer and phospholipids in all vesicles. Interestingly, in one particular case (PBut-*b*-PEO/DPPC (90/10)) vesicles are obtained but no fluorescence could be detected. In all other combinations of lipid and polymer, the fluorescence signal was clearly visible at 10% molar ratio of lipid.

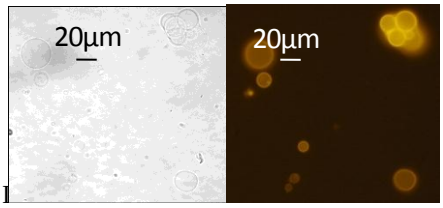

Figure 1 Vesicle formed from PDMS-g-PEO/POPC (90/10).Phase contrast. b) Fluorescence mode

This particular situation may be ascribed to a self quenching effect resulting from a compaction of DPPC phase induce by block copolymer in analogy to what has been reported for DPPC/cholesterol vesicles[4,5]. This has to be confirmed by further experiments.

Preliminary Cryo-TEM experiments have been performed on hybrid vesicles with PDMS-*g*-PEO choosen for its hydrophobic thickness (5nm) commensurate with lipid bilayer thickness (~4nm). Hybrid vesicle (PDMS-*g*-PEO/POPC 75/25) were reduced to a size close to 100nm by extrusion process and compared to pure PDMS-*g*-PEO vesicles. In both cases the vesicular structures are clearly seen. The enveloppe appears as thick line of electron scattering matter for PDMS-g-PEO polymersomes, while for the hybrid vesicles, areas with two lines (inset of figure 3) characteristic of lipid bilayer structures coexist with areas with one single line (in contact with the carbon film). This attest the presence of lipid bilayer domains in the vesicles.

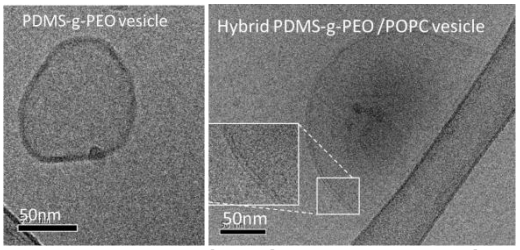

Figure 2: Cryo-TEM images obtained on PDMS-g-PEO polymersomes (left) and hybrid vesicles (right).

Conclusions On the basis of these results it is clear that we can obtain hybrid vesicles at micro and nanoscale and that depending on the nature and molar mass of the block copolymer as well as the nature of phospholipids, complex membrane structuration can be realized. Further experiments will be devoted to a full characterization of the membrane structure (Confocal Microscopy, FRAP…) their resulting properties (permeability, elasticity…) and evaluation of the ability of these hybrid vesicles to encapsulate and release anticancer drugs (Doxorubicin)

References

1. Cheng, Z. et al., *Langmuir* **2008,** 24, (15), 8169-8173.
2. Ruysschaert, T. et al. *JACS* **2005,** 127, (17), 6242-6247.
3. Nam, J. et al. *Langmuir* **2010,** 27, (1), 1-6.
4. MacDonald, R. I., *J. Biol.Chem.* **1990,** 265, (23), 13533-13539.
5. Xu, X. L.; London, E., *Biochem.* **2000,** 39, (5), 843-849.

Removal of textile dyes with Chitosan-Polyacrylic acid (PAA) polymer conjugates

Mithat Celebi[1,2] *Zafer Omer Ozdemir*[2] *Huseyin Yildirim*[1,3]

[1]Yalova University, Faculty of Engineering, Polymer Engineering Department, 77100, Yalova, Turkey
[2]Yildiz Technical University, Bioengineering Department, 34220, Istanbul, Turkey
[3]Yildiz Technical University, Department of Chemistry, 34220 Istanbul, Turkey

mithatcelebi@yalova.edu.tr

Chitosan is a partially acetylated glucosamine biopolymer which exists in the cell wall of some fungi such as the Mucorales strains (1). It mainly results from deacetylation of chitin, a major component of arthropod and crustacean shells such as lobsters, shrimps, crabs and cuttlefishes. Chitosan is an excellent biosorbent presenting abundance, non-toxicity, hydrophilicity, biocompatibility, biodegradability, anti-bacterial property, inexpensiveness and effective sorbtive ability for all classes of dyes, except for basic. Coagulation and flocculation have their place among the conventional processes that are frequently cited for treating dye-containing effluents(2).

In this study; a coagulation/flocculation process was employed for the treatment of model reactive (Remazol Brillant Blue R-RBBR) and acid (Napthol Blue Black-NBB) dye solutions. A semi-natural biopolymer flocculant synthesized from chitosan and polyacrylic acid in organic media with microvawe irradiation. The flocculants (Chitosan and Chitosan-PAA) were tested for synthetic wastewater containing dyes (NBB, RBBR). For the synthetic RBBR dye solution, color removal carried out about 80 % with flocculant (chitosan-PAA).

Keywords: flocculant, chitosan, dye

Acknowledge: This research is supported by Yildiz Technical University Project number 29-07-04-GEP01 and Istanbul Chamber of Industry.

References

1. George Z. Kyzas, Nikolaos K. Lazaridis., Journal of Colloid and Interface Science 331 (2009) 32–39.
2. Agata Szyguła, Eric Guibal, Montserrat Ruiz , Ana Maria Sastre, Colloids and Surfaces A: Physicochem. Eng. Aspects., 330 (2008) 219–226.

Effect of redox mediator (HOBT) on biodecolorization of textile dyes

Mithat Celebi[1,2] Melda Altikatoglu [3] Zeynep Akdeste [2]
[1]Yalova University, Faculty of Engineering, Polymer Enginneering Department, 77100, Yalova, Turkey
[2]Yildiz Technical University, Bioengineering Department, 34210, Istanbul, Turkey
[3]Yildiz Technical University, Department of Chemistry, 34220 Istanbul, Turkey
mithatcelebi@yalova.edu.tr

Treatment of synthetic dyes in wastewater is a matter of great concern. Extensive research has been directed towards developing processes in which enzymes are employed to remove dyes from polluted water (1). A large amount of chemically different synthetic dyes are used for various industrial purposes and significant proportions of it appear in the form of wastewater and are spilled into the environment. Synthetic dyes which are normally employed in textile and dyeing industries. Biodecolorization of dyeing wastewaters by microbial enzymes is a promising, eco-friendly and cost competitive alternative (2). Free radicals mediators have been used to enhance the oxidation activity of peroxidase (1).

In the present study the ability of Lignin peroxsidase (LiP) on decolorization of Naphtol Blue Black (NBB) and Remazol Brillant Blue R (RBBR) has been investigated. Various concentrations of HOBT (1,5-20 mM) were prepared from a stock solution of 450 mM HOBT in DMSO. At different incubation times optimum HOBT and enzyme (LiP) concentration was determined at pH 5.0 (50 mM asetate buffer) in lab. temperature. The synthetic solutions of textile dyes were prepared in distilled water to examine their decolorization by LiP. The efficiency of color removal was expressed as the percentage ratio of the decolorized dye concentration to that of initial one. Dye decolorization rates (%) of NBB and RBBR increase at the presence of mediator HOBT. At optimum enzyme and HOBT concentration dye decolorization carried out almost (%) 95 for two weeks.

Acknowledge: This work is supported by Istanbul Chamber of Industry and Yildiz Technical University Project number: 29-01-02-GEP01.

References

1. S. Sadhasivam, S. Savitha, K. Swaminathan.World J Microbiol Biotechnol (2009) 25:1733–1741.
2. M. Matto, Q. Husain., Ecotoxicology and Environmental Safety 72 (2009) 965– 971.

Novel synthetic route for covalent coupling of biomolecules on super-paramagnetic hybrid nanoparticles

Antonio L. Medina-Castillo[1,], Julia Morales- Sanfrutos[2], Alicia Megia-Fernandez[2], Jorge F. Fernández Sánchez[1], Francisco Santoyo-Gonzalez[2], Alberto Fernández-Gutiérrez[1]*

[1]Department of Analytical Chemistry, University of Granada, Avd. Fuentenueva s/n, 18071 Granada.
[2]Department of Organic Chemistry, Faculty of Sciences, University of Granada C/Fuentenueva s/n.

*antonioluismedina@ugr.es

Introductions: In the last years, there has been an increasing interest in the design and fabrication of super-paramagnetic polymeric nanoparticles (SPHNPs). Many efforts have also been done in order to multifunctionalise these SP-HNPs. The immobilization of biomolecules1 is a feasible way to introduce different functionalities on the SP-HNP surface, and, in addition, the immobilization of biomolecules could provide an increase of their performances. The covalent coupling of biomolecules on the surface of SP-HNPs allows the design of multifunctional nanoparticles which have important properties: (1) very high magnetic susceptibility to an external magnetic field; (2) the capacity of co-immobilize other compounds (drug, dyes, etc…) in the core of these nanoparticles; (3) the properties of the attached biomolecule on the shell: e.g. enzymatic activity or antibodies specificity.

Materials and methods

A novel monomer A was synthesized:

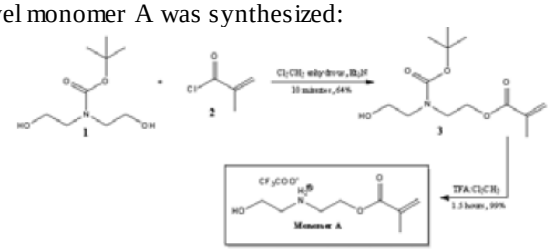

Fig.1. synthesis of a novel polymerisable monomer

The monomer A was used for synthesis amine functionalized SP-HNPs by two step miniemulsion polymerization, then SP-HNPs were functionalized with bis-vinyl sulfone (SP-HNPs-VS).

The vinyl group of the SP-HNPs-VS was used to covalent attach of different (bio)molecules by a Micheltype reaction. The (bio)molecules used were: (1) aminodamsyl (AMD), (2) avidin, (3) Invertase, (4) peroxidase. The fluorescent of avidin-biotin system was measured using a 1.5 mm optical fiber, coupled into magnetic collector. The catalytic activities of invertase and peroxidase on SP-HNPs-VS were also measure. **Result and discussions:** We describe herein a new strategy to immobilize biomolecules on superparamagnetic crosslinked nanoparticles based on the reactivity of vinyl sulfone groups with naturally occurring functional groups present in biomolecules (amine and thiol). A new monomer containing a polymerizable methacryloyl group and a secondary amine group was synthesized and characterized (see Fig.1.). It was used to prepare super-paramagnetic hybrid nanoparticles (SP-HNPs) by two-step miniemulsion polymerization using ethyleneglicol dimethacrylate (EDMA) as cross-linker (see Fig.2.). By this way, were achieved SP-HNPs with amino secondary groups in its surface. Then, these nanoparticles (SP-HNPs) were modified by a Michael addition reaction between bis-vinyl sulfone and the secondary amine groups localized on the nanoparticles surface, and thus was introduced the vinyl sulfone function on the SP-HNPs (SP-HNPs-VS).

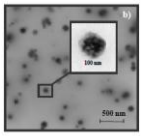

Fig.2. HRTEM picture of SP-HNPs.

In order to demonstrate that the interactions between (SP-HNPs-VS) and biomolecules is covalent and, that the catalytic activity of biomolecules is maintained after immobilization aminodamsyl and three different enzymes were used. Amino-functionalized SP-HPNs were used as negative control and were treated exactly in the same conditions that the vinyl sulfone modified nanoparticles. The Fig.3. shows the high catalytic activity of Invertase and peroxidase after its immobilization on SP-HNPs-VS. The catalytic activity for the controls (SP-HNPs) was practically cero.

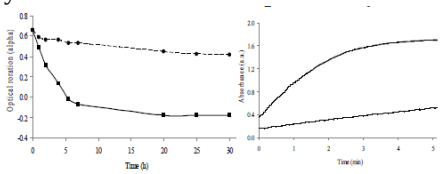

Fig.3. Catalytic activity of SP-HNPs-VS (□; solid line) and SP-HNPs (---; dashed line) incubated with a) invertase and b) peroxidase.

Conclusions: We have synthesized and characterized a novel monomer to develop a new and attractive route in the design of bio-active super-paramagnetic nanoparticles. The developed SP-HNPs show a relatively narrow size distribution and have very high magnetic susceptibility to an external magnetic field; they are completely collected in less than 1 min under magnetic field. In addition, we demonstrate that the SPHNPs functionalized with DVS react with biomolecules

in mild conditions by means of a Michael-type reaction. The only prerequisite is the presence of amine and/or thiol groups which are naturally present in most of the biomolecules. In this work we have demonstrated the high efficiency of the covalent coupling between SPHNPs- VS and biomolecules, which maintains their catalytic activity after their immobilization.

References: **1**Wong, L. S.; Khan, F.; Micklefield, J Chemical Reviews 2009, 109, (9), 4025-4053.

Acknowledgments: The authors express their thanks to the Spanish Ministry of Education (FPU grant reference AP2006-01144, AP2006-01145, and Project CTQ2008-01394) and the Regional Government of Andalusia (Excellence projects P07-FQM-02738 and P07-FQM-02625).

Thermal Degradation of Poly(hexamethylene terephthalate-*co*-dioxanone) Copolyesters

G. Giammanco, A. Martínez de Ilarduya, A. Alla, and S. Muñoz-Guerra

Dept d'Enginyería Química, Universitat Politècnica de Catalunya, ETSEIB, Diagonal 647, 08028 Barcelona

antxon.martinez.de.ilarduia@upc.edu

Introduction

Since aromatic polyesters are quite resistant to hydrolytic degradation under physiological conditions, the insertion of aliphatic ester units by copolymerization opens the possibility to obtain materials combining the excellent thermal and mechanical properties and biodegrability of both aromatic and aliphatic polyesters respectively.[1] Taking this fact into account, a series of new random copolyesters derived from poly(hexamethylene terephthalate) and containing 1,4-dioxan-2-one units *(PHT_xDO_y)* (Figure 1) were obtained by ring opening polymerization and their thermal properties were studied.[2] In this work we would like to report on their thermal degradation under inert atmosphere which has been evaluated by combining thermogravimetry, NMR and viscosimetry analysis.

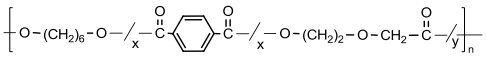

Figure 1. Chemical structure PHT_xDO_y copolyesters.

Materials and Methods

PHT_xDO_y were obtained by ring opening polymerization of cyclic hexamethylene terephthalate oligomers and 1,4-dixoxan-2-one.[2] NMR spectra were recorded on a Bruker AMX-300 in $CDCl_3$. TGA analysis was carried out under nitrogen atmosphere within a temperature range from 30 to 600 ºC. Viscosimety measurements were performed in dichloroacetic acid using an Ubbelhode viscosimeter.

Results and Discussion

The dynamical thermogravimeric analysis of these copolyesters showed a two step degradation process, with maximum degradation rates at 300 and 420 ºC, similar to that reported in a recent work on block terpolyesters containing ethylene-*co*-hexamethylene terephthalate and 1,4-dioxan-2-one.[3]

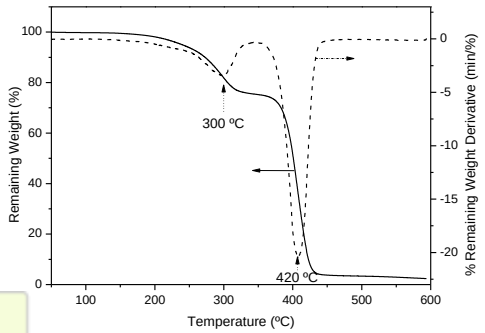

Figure 2. TGA traces of $PHT_{57}DO_{43}$ copolyester.

In order to elucidate the mechanism of degradation, isothermal studies were performed on PHT_xDO_y at 180, 220, 300 and 350 ºC, studying the residues and volatile products by NMR and viscosimetry. It was observed that the copolyesters isothermally treated at 180 and 200ºC lost different amounts of 1,4-dioxan-2-one units and the molecular weight of the residual copolyester increased two or three times when samples were treated for one or two hours respectively. Samples heated at 300 ºC showed that 1,4-dioxan-2-one units were lost in 10 minutes. The spectrum of the residue was essentially poly(hexamethylene terephthalate) (PHT) whereas the volatile was pure 1,4-dioxan-2-one (Figure 3).

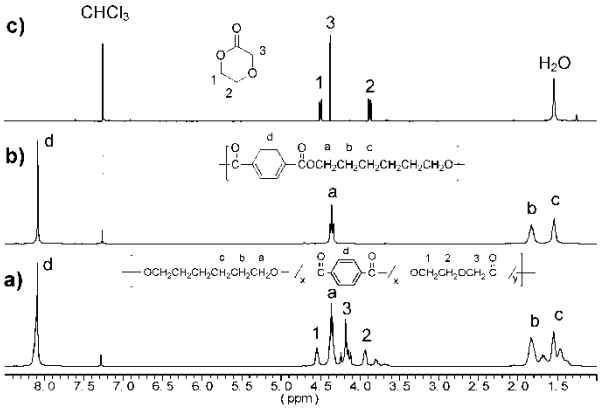

Figure 3. ^{1}H NMR spectra of (a) $PHT_{57}DO_{43}$, (b) residue and (c) volatile left from sample treated at 300 ºC for 10 min.

When the PHT_xDO_y copolyesters were treated at 350 ºC, it was observed in the ^{1}H-NMR spectra of both residue and volatiles, the presence of vinyl end groups, indicating that a β-elimination process takes place, similarly to that observed in PET and PBT, with generation of carboxylic and vinyl end groups.

Conclusions

The mechanism proposed for the thermal degradation of PHT_xDO_y copolyesters at 200-300 ºC happens with elimination of dioxanone due to an intramolecular cyclation process accompanied by esterification of end carboxylic and hydroxyl groups and subsequent formation of high molecular weight PHT. At higher temperatures a β-elimination process takes place which implies chain scission and generation of vinyl and carboxylic end groups accompanied by volatilization when low molecular weights fragments are reached.

Financial support given by MICINN with grant MAT-2009-14053-CO2-01 is acknowledged. Our thanks to the Venezuelan government (FONACIT) for the Master Thesis grant awarded to G.G.

References

[1] Müller R.J. in *Handbook of Biodegradable Polymers*; Bastioli, C., Ed.; Smither Rapra Publishing: Shorphire, U.K., 2005; p. 303.

[2] Giammanco, G.; Martínez de Ilarduya, A.; Alla, A.; Muñoz-Guerra, S. *Biomacromolecules* **2010**, *11*, 2512.

[3] Gong J.; Lou, X.-J.; Li, W.-D.; Jing, X.-K.; Chen H.B.; Zeng J.B.; Wang X.L.; Wan, Y.Z.; *J. Polym.Sci. Polym. Chem.* **2010**, 48, 2828.

Microwave Assisted Conjugation of BSA & Chitosan

Zafer Omer Ozdemir

Yildiz Technical University,
Faculty of Chemical & Metallurgical Eng.Bioengineering Dept.

ozdemirz@yildiz.edu.tr

Chitin is the second most important natural polymer in the world[1]. Chitosan is deacetylation product of chitin. Chitosan has a unique properties because of holding NH_2 group in chemical structure. There is no other polysaccahryde which contains NH_2 functional group. Chitosan is linear, hydrophilic, positively charged and has mucoadhesive property. It is an excellent biopolymer for preparation of microparticles and nanoparticles owing to its excellent biocompatibility and biodegradability[2].

BSA is the carrier protein. Its role is very functional for organism. Also BSA is very beneficial protein for conjugation reactions[3].

In this research Chitosan BSA conjugation reaction was investigated. Conjugation reactions were done with activators (HBTU, EDC) in organic (DMF) and aqueus media.

Acknowledgments

This research is supported by Yildiz Technical University. Project number 29-07-04-GEP01.

References

1) M. Rinaudo, *Prog. Polym. Sci.* **31** (2006) 603–632.
2) S. Sundar, et al., *Sci. Technol. Adv. Mater.* **11** (2010) 1-13.
3) J. P. Magnusson, *Polym. Chem.*, 2011, **2**, 48.

Investigation of Cellulase-Dextran Conjugates

Lutfi Karagoz, Zafer Omer Ozdemir

Yildiz Technical University,
Faculty of Chemical & Metallurgical Eng.Bioengineering Dept.

ozdemirz@yildiz.edu.tr

Cellulose is the major polysacharide in plants and is most abundant biological material on earth. In addition to this great amounts of wastes include cellulose, because of this reason cellulose-degrading enzymes become very important. Cellulose–degrading enzymes, which exhibit three types of activities are called as cellulases[1]. (1) Endonuclease hydrolyse internal bonds in cellulose molycule. (2) Cellobiohyrolase hydrolyse terminal bonds and (3) β-glucodisase hydrolyse cellobiose and little olisaccarides to D-glucose.

In this study, cellulase from *Aspergillus niger*[2] was examined. Dextran is oxidated to its aldehyde derivative[3] by using $NaIO_4$. The amount of aldehyde groups at dextran molecule was determined FT-IR.

Acknowledgments

The authors wish to commemorate this study to beloved professor Huriye Kuzu.

References

1) Okada, G., *Methods in Enzymology*, **1988**, 160,259-264.
2) Dobrechenko, S., et. al., *Carbohydrate Research*, **1993**, 241, 189-199.
3) Kang, S.W., et al., *Biosource Technology*, **2004**, 91, 153-156.

Thermal Degradation of Polyuronic Acids and their Ionic Complexes

Ainhoa Tolentino, Abdelilah Alla, Antxon Martínez de Ilarduya and Sebastián Muñoz-Guerra

Departament d'Enginyeria Química, Universitat Politècnica de Catalunya, ETSEIB, Diagonal 647, 08028 Barcelona

abdel.alla@upc.edu

Introduction

Comb-like polymers consisting of a stiff backbone with long flexible side chains are able to form supramolecular assemblies of interest to prepare materials for novel practical applications.[1] Our research is currently addressed to comb-like systems based on ionic complexes of biotechnological polyacids and alkyltrimethyl-ammonium surfactants bearing long alkyl groups. In this work we report on the thermal degradation under inert atmosphere of the polyuronic acids and their alkylammonium ionic complexes.

Materials and Methods

Alginic acid sodium salt (Na·*co*PGuMnA), polygalacturonic acid (PGaA) and the octadecyl trimethylammonium bromide (18ATMA·Br) were purchased from Sigma-Aldrich. 20 and 22ATMA·Br were obtained using the procedure described in the literature.[2] ^{1}H and ^{13}C NMR spectra were recorded on a Bruker AMX-300 spectrometer at 25.0 °C operating at 300.1 and 75.5 MHz, respectively. TGA analysis was carried out under inert atmosphere within a temperature range of 30 to 800 ºC.

Results and Discussion

The ionic complexes were obtained following the method used by Pérez-Camero *et al*.[3]

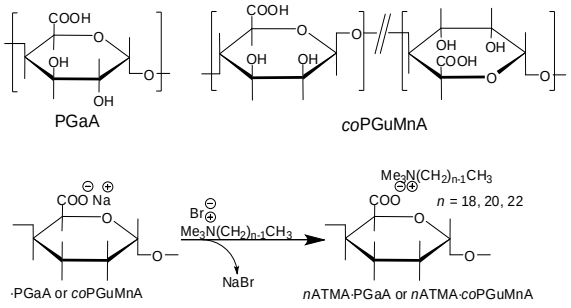

Figure 1. Polyuronic acids and their ionic complexes.

Thermal stability of the polyuronic acids and their ionic complexes was investigated through thermogravimetric analysis; the results of the non isothermic TGA analysis of these polymers are compared in Table 1.

The TGA traces revealed that these polymers are highly hygroscopic with an initial loss of water near to 90 °C. The polyuronic acids present one-step degradation process that starts at about 230 °C with a maximum degradation rate around 250 °C. On the contrary, the ionic complexes showed a three-step degradation process. ^{1}H-NMR analysis of the volatiles arising from isothermal degradation treatment at different temperatures reveals, in the case of the polyuronic acids, the occurrence of formic and acetic acids, and furfural at amounts increasing with the time of treatment.

Table 1. Thermal parameters of Na·*co*PGuMnA and PGaA and their ionic complexes.

Compound	T_o[a] (ºC)	T_d[b] (ºC)	W[c] (%)
PGaA	232	95/252	90/16
18ATMA·PGaA	211	100/229/270/381	93/65/17/0
20ATMA·PGaA	212	100/227/281/398	97/66/18/0
22ATMA·PGaA	207	99/219/301/411	97/71/22/0
Na·*co*PGuMnA	227	100/237	90/23
18ATMA· *co*PGuMnA	204	84/210-217/266/381	88/58/13/0
20ATMA· *co*PGuMnA	206	94/211-220/289/392	88/58/16/0
22ATMA· *co*PGuMnA	202	82/209/301/400	89/65/20/0

[a] Onset decomposition temperature.
[b] Maximum rate decomposition temperature.
[c] Remaining weight at the end of each step.

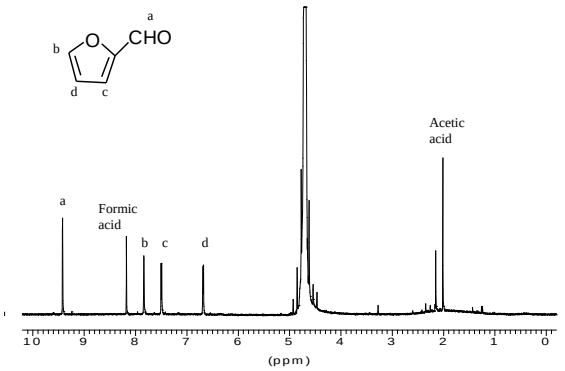

Figure 2. ^{1}H-NMR in D_2O of volatile compounds obtained from PGaA after heating at 250 ºC for 15 min in a nitrogen atmosphere.

The ionic complexes degraded through a much more complicated process implying several parallel and successive decomposition reactions. The ^{1}H-NMR spectra revealed in the volatiles the presence of methanol, *N*,*N*-dimethylalkylamine and trimethylamine. These results suggest that dissociation of the ionic complex occurred at the first stage of decomposition followed by a simultaneous degradation of the alkylammonium surfactant and the polyuronic acid.

Acknowledgements

Authors acknowledge the MICINN of Spain for grant MAT2009-14053-CO2-01 and the Basque Government for the PhD grant awarded to A. Tolentino.

References

[1] Loos, K.; Muñoz-Guerra, S., In *"Supramolecular Polymers"*, Ed. A. Ciferri, CRC Press, Taylor & Francis Group, second edition, 2005, p. 393

[2] Hendrix, W.T.; von Rosenberg, J.L. *J. Am. Chem. Soc.* **1976**, *98*, 4850.

[3] Pérez-Camero, G.; García-Alvarez, M.; Martínez de Ilarduya, A.; Campos, L.; Muñoz-Guerra, S. *Biomacromolecules* **2004**, *5*, 144.

Electrospun fibrous scaffolds from novel poly(ester urethane urea) and poly(dioxanone) for vascular tissue regeneration

Inessa Stanishevskaya[1], Vinoy Thomas[2], Pablo C. Caracciolo[3], Gustavo A. Abraham[3], Yogesh K. Vohra[2]

[1]Rensselaer Polytechnic Institute, Troy NY 12180, USA,
[2]CNMB, University of Alabama at Birmingham, Birmingham, Alabama 35294, USA
[3]INTEMA (UNMdP-CONICET), B7608FDQ Mar del Plata, Argentina

pcaracciolo@fi.mdp.edu.ar

Introduction

Electrospinning is an enabling fabrication technique for creating micro/nanofibrous tissue-scaffolds having extracellular matrix-like environment with tailored properties for tissue engineering and drug delivery applications [1]. The scaffolds intended for use in cardiac and vascular tissue regeneration have to undergo repeated cyclic flexing with respect to blood flow with little or no hysteresis. Segmented poly(ester urethane urea)s are elastomeric polymers with good biocompatibility, soft-tissue mechanical properties and controlled degradation characteristics. The preparation and characterization of an aliphatic segmented poly(ester urethane urea) (PHH) was recently reported [2,3]. Polydioxanone (PDO) is a semicrystalline, flexible and biodegradable polymer whose mechanical strength is capable of withstanding pulsatile blood flow and that possesses shape memory, preventing kink formation in vascular structures. In this study, electrospun fibrous of PHH/PDO blends were obtained and its properties were compared with the corresponding scaffolds prepared with the single components. The meshes were characterized for their biomechanical properties, in both dry and hydrated conditions, and structural and morphological properties for soft-tissue engineering applications.

Materials and methods

The novel PHH was synthesized from polycaprolactone, hexamethylene diisocyanate and an aliphatic diurea-diol chain extender according to previously reported procedures [2,3]. Electrospun scaffolds were obtained by electrospinning technique using PHH (25 % w/v), PDO (15 % w/v), and PHH/PDO blend (1/1) (15 % w/v) in 1,1,1,3,3,3-hexafluoro-2-propanol. The setup consisted of a syringe pump (2 mL/h), a power supply (25 kV), and a rotating mandrel (400 rpm). The scaffolds were characterized by scanning electron microscopy, atomic force microscopy (AFM) in contact mode, and differential scanning calorimetry (DSC). The porosity was calculated from the apparent density measurements. PBS uptake was determined to evaluate the hydrophilicity. Uniaxial tensile properties of dry and hydrated tubular specimens were tested using a Bose Electroforce LM1 machine.

Results and Discussion

The scaffolds show randomly oriented bead-free fiber meshes with relatively narrow distribution of fiber diameters (PHH/PDO: 758.9 ± 169.4 nm). The fiber diameters of PHH and PHH/PDO are comparable to the typical diameters of collagen fibers found in natural arteries (50 nm to 500 nm). AFM was performed on the individual fibers, obtaining the highest roughness for PDO fibers (788.8 nm), followed by PHH/PDO (257.3 nm) and PHH (154.1 nm). This could be attributed to a high crystallinity of PDO fibers, leading to a high surface waveness. The increase in surface area favors the cell attachment and proliferation. DSC tests displayed that PHH, PDO and also PHH/PDO blend have semicrystalline morphology. Very high porosities with interconnected pore network and very high surface area-to-volume ratio are characteristics for electrospun meshes. The porosity values showed that the PDO samples were the most porous (79.2 %), followed by the PHH/PDO (71.7 %) and the PHH scaffold (66.4 %). Interestingly, the PBS uptake ability of the PHH/PDO (852.5 %) scaffold was higher than that of the one component scaffolds (PHH: 197.1 % and PDO: 503.3 %). This could be due to a favorable combination of high interconnected porosity and decreased crystallinity. The addition of PHH to PDO conduced to mechanical properties values intermediates between those of the two pure scaffolds. The ultimate tensile strength value was 2.0 ± 0.47 MPa while the Young's modulus was 3.9 ± 1.05 MPa, both measured in hydrated conditions, resulting lower than the dry-sample values. As for the elongation at break, the blend had approximately the same value as the PDO under hydrated conditions (150.2 ± 44.4 %). The mechanical properties of electrospun PHH and PHH/PDO scaffolds are comparable to those of elastomeric polymeric materials reported for cardiac tissue engineering in the literature [4]. Studies on the protein adsorption, platelet adhesion and thrombus formation showed excellent blood compatibility of the PHH for potential blood contacting applications [2,3]. Degradation behavior and cell-scaffold interactions should be undertaken to warrant its potential use in this soft-tissue engineering.

Conclusions

Electrospun PHH/PDO scaffolds showed high porosity and tensile properties comparable to that of cardiac or vascular tissues, demonstrating the feasibility to prepare cardiac patch that mimic the nanoscale structure and mechanical properties of native tissues.

References

1. Thomas V, Dean D, Vohra YK. Curr Nanosci, 2, 155, 2006.
2. Caracciolo PC, de Queiroz AAA, Higa OZ, Buffa F, Abraham GA. Acta Biomater, 4, 976, 2008.
3. Caracciolo PC, Buffa F, Abraham GA. J Mater Sci Mater Med, 20, 145, 2009.
4. Chen CH, *et al*. Cardiovascular Research, 80; 88, 2008.

Hydrophilic Nanoparticles Based On A Three Star Poloxamer For Ophthalmic Applications

J. Marinich[1] , I. T. Molina-Martínez[1] , F. J. Parra[2] , V. Andrés-Guerrero[1] , M. B. Vázquez-Lasa[2], R. Herrero-Vanrell[1], J. San Román[2]

1. Department of Pharmacy and Pharmaceutical Technology, Faculty of Pharmacy, Complutense University. Plaza Ramón y Cajal s/n. 28040 Madrid, Spain
2. Institute of Polymer Science and Technology, CSIC. Juan de la Cierva 3, 28006- Madrid, Spain

bvazquez@ictp.csic.es

Introduction

Polymeric nanoparticles (NPs) have been widely studied as particulate carriers in the pharmaceutical and medical fields as drug delivery systems [1]. Nanoparticles have the capacity to deliver ocular drugs to specific target sites and therein, provide solutions in the therapy of many eye diseases [2]. Recently, we have synthesized copolymers based on 2-hydroxyethyl methacrylate (HEMA) and a methacrylic derivative of a three star poloxamer (Bayfit® 10WF15) (Bayfit-MA) which had thermosentive behavior in an interval temperature close to that of cornea [3], suggesting that the proposed systems can have application as carriers in ocular drug delivery, e.g. for topical ophthalmic administration. Here, we report the preparation and characterization of NPs of these copolymers and the biocompatibility studies of the particulate systems by in vitro and in vivo experiments.

Experimental

HEMA-co-Bayfit-MA copolymers with HEMA:Bayfit-MA ratios of 99:1, 95:5 and 90:10 (w/w) were used for NPs preparation, named as NP1, NP5 and NP10, respectively. NPs were obtained by dialysis of 50 ml of DMSO copolymeric solutions in distilled water (2 mg/ml). Aqueous dispersions were concentrated to 10 ml by rotary evaporation. Particle size distributions were determined by light scattering (Coulter Electronics). *In vitro* tolerance was assessed by the MTT assay in presence or not of trehalose (T) using immortalized human corneal-limbal epithelial cells (HCLE), normal human conjunctival cells (IOBA-NCH) and macrophages from Swiss male mice. In order to simulate chronic therapies, in which the formulations are in contact with the ocular surface for short and long periods of time, times of contact were 15 minutes (short term exposure) and 1 and 4 hours (long term exposures).

In vivo tolerance was studied with New Zealand rabbits. Each rabbit received 10 µl of one of the formulations in the right eye every 30 min for 6 h. The left eye was used as a control.

Results and Discussion

NPs dispersions in water were obtained by the dialysis method. The aqueous dispersions were concentrated up to values of 1.58±0.1, 2.20±0.7 and 1.88±0.5 mg/ml, for copolymers containing 1, 5 and 10% Bayfit-MA. Size distributions of the NP1 samples after concentration were bimodal, with average diameter of 0.24±0.06 µm and 1.91±0.17 µm respectively. For NP5 and NP10 samples size distributions showed a main peak, which gave average particle diameters of 0.14±0.01 and 0.15±0.02 µm respectively, and a slight tendency to present a small fraction of aggregates. In all cases these concentrated aqueous dispersions were used for tolerance assays.

In vitro tolerance of the NP formulations was carried out by means of cellular viability measurements. For topical ophthalmic administration, the osmolarity of the solutions must be adjusted and firstly *in vitro* tolerance studies in macrophages were carried out with four trehalose (T) concentrations. Results revealed that a trehalose concentration of 72 mg/ml, corresponding to a hypotonic solution, produced the less cytotoxicity in all cases and it was chosen to test NPs in further cell culture experiments. In general, cellular viability of HCLE cells in presence of or not of trehalose was around 100% and results are shown in Figure 1. Values of cellular viability in normal human conjuntival (IOBA-NCH) cells ranged between 85 and 97% after 15 min and 1 h of exposure, but at longer times (4 h) IOBA-NCH cells viability decreased to values around 80% for NP tested in absence of trehalose and around 70% for assays containing trehalose, independently of NP composition.

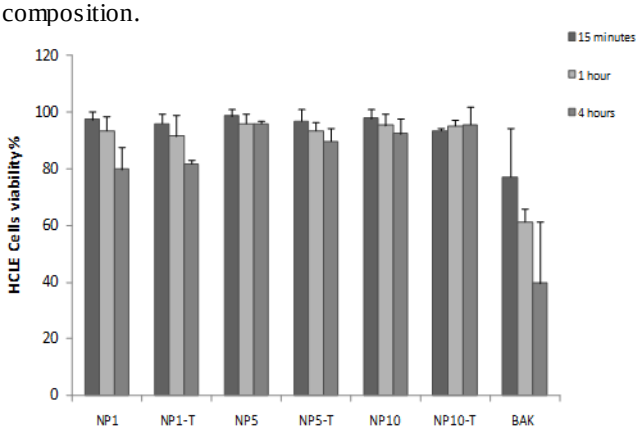

Figure 1. HCLE cells viability in percentage (coefficient of variation, c.v.) for different NPs formulations.

Macrophages viability was higher than 80% after 15 min and 1 h for all samples but it decreased to values between 34 and 67% after 4 h depending on NP composition. The best result at this time was obtained for the NP10-T sample. *In vivo* tolerance assays revealed no significant differences between control and treated eyes for each formulation and all rabbits showed no signs of discomfort during the 24 h assay.

References

[1] Adibkia K, et al. Pharmaceutical Sciences 15, 303, 2009.

[2] Diebold Y, Calonge M. Progress in Retinal and Eye Research 29, 596, 2010

[3] Parra FJ, et al. Journal of Biomaterials Science Polymer Edition 2010, in print.

Erythrocyte aggregation induced by cationically-modified biopolymers

Kamil Kaminski [1], Monika Plonka [1], Justyna Ciejka [1], Krzysztof Szczubialka [1], Maria Nowakowska [1], Barbara Lorkowska [2], Ryszard Korbut [2]

1.Jagiellonian University, Faculty of Chemistry, Ingardena 3, 30-060 Krakow, Poland;
2. Jagiellonian University, Medical College, Chair of Pharmacology, Grzegorzecka 16. 31-531 Krakow, Poland,

e-mail: kaminski@chemia.uj.edu.pl

Introduction:

Biopolymers and their cationic derivatives are increasingly important in pharmacological sciences. One of the possible applications is related to their impact on blood coagulation. Protamine sulfate is an example of cationic biopolymer which have found clinical applications. It is important to find out the factors governing the interactions between the cationic biopolymers and blood components, erythrocytes in particular. Cationic polymers interact strongly with the phospholipid bilayer of the erythrocytes due to its negative charge which may result in erythrocyte aggregation, which is an undesired and potentially dangerous effect.

Materials and Methods

In our studies we have studied the cationic derivatives of dextran, HPC, and chitosan with different degree of modification. Determination of the cationic polymers concentration which results in the erythrocyte aggregation was carried out using optical microscope. Full blood samples were inspected after addition of excess of polymer solution.

Results and Discussion

We are reporting results showing that the aggregation induced by the cationic polymers depends strongly on the structure of the biopolymer, positive charge density of the of the polymeric chain and the zeta potential of the macromolecules. The greater value of the zeta potential the lower was the concentration of the polymer necessary to start aggregation.

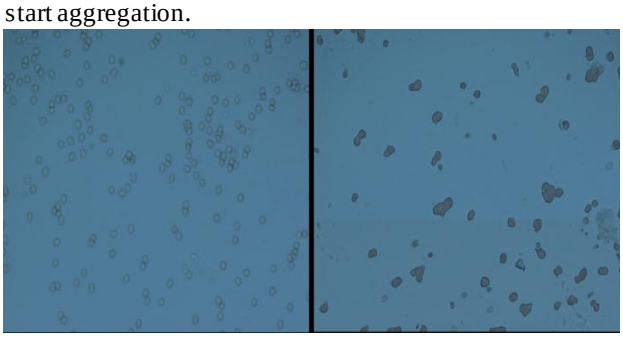

Figure 1. Human erythrocytes under the influence of protamine sulfate (PS). Left Picture: 2,52 ug PS in 1 ul human blond,; right picture: 2,88 ug PS in 1 ul human blood

Conclusions

It was found that for some cationic biopolymers the aggregation of erythrocytes occurs at similar concentration as for clinically-applied protamine. That means that they may be potentially used intravenously for heparin reversal during emergency medicinal procedures.

Acknowledgment:

The project was operated within the Foundation for Polish Science Team Programme (TEAM/208-2/6) and Ventures Programme (VENTURES/2009-4/4) cofinanced by the EU European Regional Development Fund

Polymer-Cooperative Blocking the Viruses: *in silico* Modeling the *in vitro* HIV-1 Entry Inhibitors

Vladimir B. Tsvetkov[1,2], *Alexander V. Veselovski*[2], *Alexander V. Serbin*[1,3]

[1]Biomodulators RC, Health RDF, Moscow, Russia
[2]Orehovich Institute of Biomedical Chemistry, RAMS, Moscow, Russia
[3]Topchiev Institute of Petrochemical Synthesis, RAS, Moscow, Russia

e-mail: serbin@ips.ac.ru

Introduction

Early the alternating copolymers of structure series **1**:

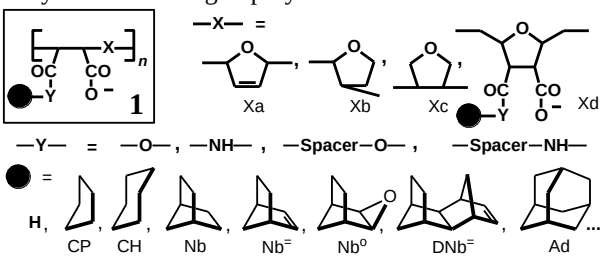

containing the controlled combinations of variable alicyclic and anionic side groups have been designed, synthesized and evaluated as anti-viral agents. On the experimental models *in vitro* of cells infected by the human immunodeficiency virus type 1 (**HIV-1**), among the polymers **1**, the potent inhibitors of the viral entry, most probably fusion step (fig.1), were discovered [1].

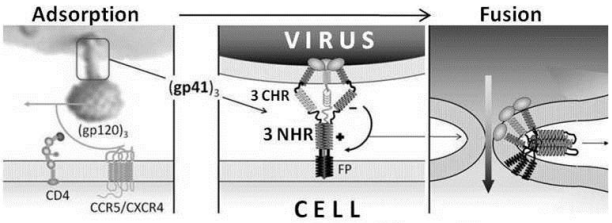

Fig. 1. HIV-1 entry:
Adsorption removes the $[gp120]_3$. The [FP of $gp41]_3$ anchors into cell membrane, and the $[CHR]_3$ hairpin-like rearranges to $[NHR]_3$ forming the six-helices bundle and inducing the virus - cell membranes fusion

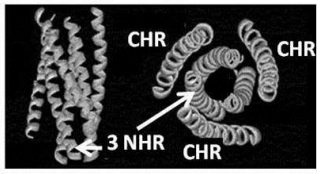

The six-helices bundle of heptade repeat regions (NHR and CHR) of three macromolecules of HIV envelope protein gp41 (fig.1) is starting switch for the fusion, and the $[NHR]_3$ pre hairpin core prevention against contacts with CHR is key mode for the fusion (entry) blockage. Predicting a selective tropism (via electrostatic-co-hydrophobic manner) of **1** to the $[NHR]_3$ tri-helices core we undertook a computational modelling *in silico* of the synthetic (**1**) – viral ($[NHR]_3$) polymers inter-actions as the most expected mechanism of the HIV-1 entry inhibition experimentally observed *in vitro*.

Objects and Methods

Taken from the open PDB 3D structures of the $[NHR]_3$ were used as target. The fragmentary models **M1.i** step-by-step approximated to the real structures of the investigated polymers **1** (fig.2) were applied for docking

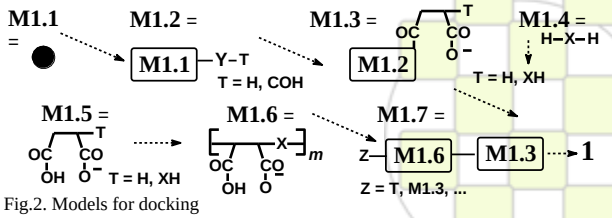

Fig.2. Models for docking

Results and Discussion

The target constructed by three equal NHR regions α-helices is a nano-object (~2x7nm) of trimer-adequate symmetry. Locations of H-bond-active, ionized, and hydrophobic/-philic points/sites were mapped.

The M1.1, lipophil spheroid ● models docked to the target surface by wide distribution in accordance with the hydrophobic sites location. But next generation **models M1.2** (with polar atoms of –Y–) corrected this distribution toward concentration within the ~ nine hydrophobic cavities of target, predominantly to 3 main cavities (**MC**) around target at the inter-helices triplet of hydrophobic amino-acid clusters $(Leu565,568, Val570, Thr571)_3$. **Models M1.4-5**, single fragments of polymer **1** backbone, also were widely distributed on the target surface, but at H-bonds enriched positions, exhibiting similar accumulation nearly the MC, but due to co-clustered triplet of (ionized Lys+574 and H-bond active $Gln567,575,577)_3$. **M1.6**, the anion-oligomer fragments (free of ●) actively docked for lengthwise directions (A, fig.3) along the α-helices (from C-terminal to MC and N-terminal cavities between the parallel helices).

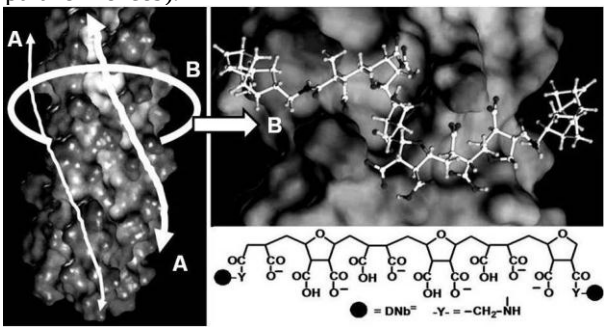

Fig.3. *The $[NHR]_3$ 3D state wit axial (A) and belting (B) directions for docking, and an example of the belting capable minimal fragment*

Unlike M1.6 the **M1.7**, models "equipped" by the ● -sensors become more mobile for complex adaptation to the target configuration. At the optimal chain flexibility and distance between the ● -sensors the **M1.7** models possessed capacity to effective docking by both axial, and "belting" (B, fig.3) mode, predominantly around the mentioned MC triplet. The calculated *in silico* hierarchy of the ● effectiveness (CP,CH << Nb, $Nb^{=}$, Nb^{O} < $DNb^{=}$ ~ Ad) correlated with the anti-HIV efficiency *in vivo* (especially by Chem-Score usage). The X, Y, m, n parameters-efficiency relationship was estimated too.

Conclusion

In contrast with the known small-molecular (mono-point/site) or peptide related (axial) blockers of NHR the newly studied polymers **1** possess the unique adaptability to combined axial-co-belting (from pocket to pocket) multi-blockage for the HIV entry prevention.

Reference: *1. Macromol Symp 2010,296:466; PMID:10320046, 12803048, 12968467, 15954475.*

Novel bioactive resin adhesives inhibit dentin MMPs mediated collagen degradation.

Osorio R,Yamauti M, Sauro S, Watson TF, Quintana M, Toledano M.

Aim of the study: Bonding to dentin requires an etching step and subsequent resin infiltration. Effective inhibitors of matrix metalloproteinases (MMPs) may be included in resin-dentin bonded interfaces to protect the seed crystallite-sparse collagen fibrils of the scaffold, from degradation. Bioactive parcticles, able to release minerals, may also be included in order to facilitate dentin remineralization. MMPs mediated collagen degradation in the different bonded interfaces has to be determined.

Methods: An in vitro assay with dentin beams was performed. Dentin beams were obtained and immersed in: 1) 10% phosphoric acid (PA); 2) 0.5 M EDTA and 3) no demineralized. Dentin beams were resin impregnated with four prototypes of bioadhesives containing a light curing resin (HEMA and BisGMA mixture) and bioactive microparticles (tricalcium phosphate and tricalcium silicate). In some resin mixtures 1% of $ZnCl_2$ or 20% of ZnO particles were added. Four dentin beams were tested for each condition. Dentin beam specimens were incubated in 500 µl of media artificial saliva at 37°C for 24 h, 1 and 3 wk. Supernatants were analyzed for the release of collagen degradation product (C-terminal telopeptide of type I collagen -ICTP-) using a radioimmunoassay. Values were analyzed by ANOVA and SNK multiple comparison ($P<0.05$).

Results: Mean ICTP values and multiple comparisons results are in the table. Identical numbers in each row indicate no significant difference. In each column values with identical letters indicate no difference.

Conclusions: Addition of 20% of zinc oxide particles alone or combined with 1% $ZnCl_2$ provide a stable dentin MMPs inhibition at the resin/dentin hybrid layers created with the tested resin mixtures, regardless of the previous dentin treatment. MMPs degradation of collagen is strongly reduced in all tested resin infiltrated dentin beams.

Acknowledgments: CICYT/FEDER MAT2008-02347, JA-P07-CTS2568 and JA-P08-CTS-3944.

References:

1. Toledano M, Nieto-Aguilar R, Osorio R, Campos A, Osorio E, Tay FR, Alaminos M. Differential expression of matrix metalloproteinase-2 in human coronal and radicular sound and carious dentine. J Dent. 2010;38(8):635-40.

2. Toledano M, Osorio R, Osorio E, Aguilera FS, Yamauti M, Pashley DH, Tay F. Effect of bacterial collagenase on resin-dentin bonds degradation. J Mater Sci Mater Med. 2007a;18(12):2355-61.

3. Osorio R, Yamauti M, Osorio E, Ruiz-Requena ME, Pashley DH, Tay FR, Toledano M. Zinc reduces collagen degradation in demineralised human dentin explants. J Dent 2011;39:148-153.

4. Osorio R, Yamauti M, Osorio E, Ruiz-Requena ME, Pashley DH, Tay FR, Toledano M. Effect of dentin etching and clorhexidine application in MMPs mediated collagen degradation. Eur J Oral Sci 2011, 119(1):79-85.

	Dentin Treatment	24 h	1 wk	3 wk
No Adhesive	Mineralized	1.80 (0.02) 1A	5.73 (0.50) 2A	6.85 (1.72) 2A
	Phosphoric acid	53.44 (4.20) 1B	199.21 (31.72) 2B	202.32 (26.78) 2B
	EDTA	60.57 (5.30) 1B	198.77 (34.22) 2B	205.56 (24.56) 2B
Adhesive 1	Mineralized	0.39 (0.01) 1C	0.61 (0.02) 1C	0.82 (0.02) 1C
	Phosphoric acid	3.29 (0.30) 1D	9.20 (1.21) 2D	13.40 (2.34) 3D
	EDTA	1.75 (0.10) 1A	4.81 (0.70) 2A	8.30 (2.30) 3A
Adhesive 2 1% ZnCl	Mineralized	0.43 (0.02) 1C	1.42 (0.2) 2E	1.60 (0.48) 2E
		2.40 (0.10) 1A	7.19 (1.20) 2AD	10.93 (1.76) 3D
	EDTA	2.09 (0.21) 1AD	4.76 (0.30) 2A	6.91 (1.23) 3A
Adhesive 3 20% ZnOx	Mineralized	0.21 (0.01) 1C	0.37 (0.01) 1C	0.59 (0.01) 1C
	Phosphoric acid	1.38 (0.42) 1A	2.15 (0.20) 1E	3.74 (0.53) 2F
	EDTA	1.07 (0.20) 1A	1.68 (0.10) 1E	2.24 (0.76) 2EF
Adhesive 4 1% ZnCl 20% ZnOx	Mineralized	0.72 (0.03) 1C	0.54 (0.01) 1C	0.67 (0.01) 1C
	Phosphoric acid	0.77 (0.04) 1C	0.72 (0.02) 1C	0.49 (0.02) 1C
	EDTA	0.88 (0.10) 1C	0.42 (0.01) 1C	0.17 (0.01) 1C

Actin Networks at Interfaces: Microrheology of Reconstituted Cell Cortex

Dmitry Ershov1; vander Gucht, Jasper1

Wageningen University Lab of Physical Chemistry and Colloid science1

dmitry.ershov@wur.nl

Although there have been quite a number of promising attempts to investigate mechanical and structural properties of cells' actin cortex in vivo, the factors that determine the properties of the cortical actin network are not well understood. A first step towards reaching such understanding is the development of an in-vitro reconstituted actin cortex. In our attempt to develop an actin system that would be analogous to the cell cortex and closely mimicking its structure, we attach actin filaments to lipids lining the surface of an oil droplet using biotin-streptavidin bonds; we show that in this way we can form a very thin actin network that could be visualized and studied by confocal microscopy

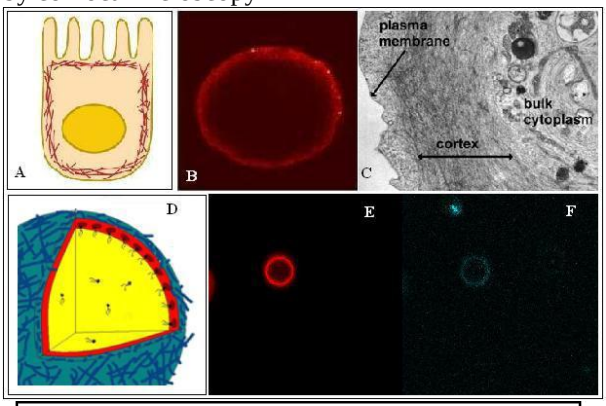

Animal cells' cortex sketch (A, cortical actin filaments are shown in red) and images obtained from different types of microscopy (B, C) and a sketch of our system (D, streptavidin is shown in red and actin filaments in blue) and confocal microscope images (E –streptavidin signal, F – filaments signal).

To measure the visco-elastic properties of this reconstituted actin cortex, we use microrheology based on multi-particle tracking, which allows extracting storage and loss moduli from the mean square displacement of the traced particles moving in the cortex. Our approach allows incorporating different actin-binding proteins or even motor proteins into this "2D-network" with an opportunity to quantitatively characterize their effect on the mechanical properties of the actin cortex. We show that adding cross-linkers to this network increases its elasticity similarly to "3D" cases, and addition of myosin in the presence of ATP causes a quick and sharp stiffening of the cortex.

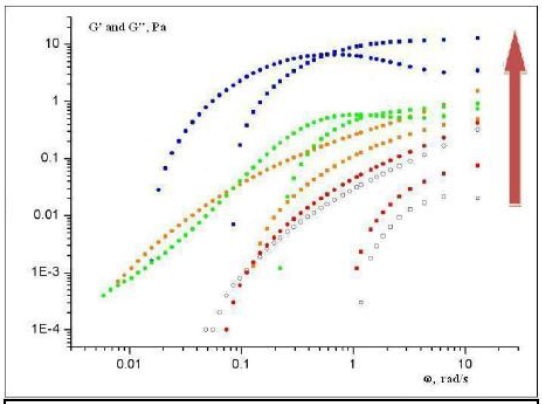

Storage (G', squares) and loss (G'', circles) moduli of the reconstituted cortex. Different colors for different cross-linker concentrations. Arrow indicates the direction in which the cross-linker concentration (streptavidin) incorporated into network increases. Blank datapoints characterize an interface with no actin network on it.

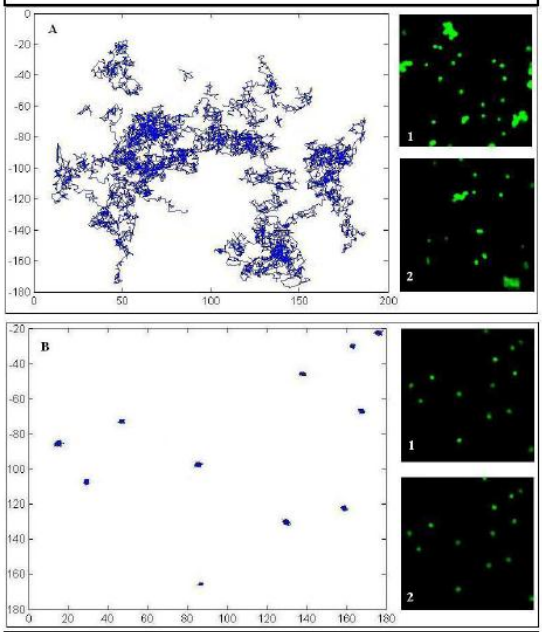

Mean square displacement of tracked particles before (A) and after (B) stiffening caused by motor proteins upon addition of ATP. Insets show the position of particles in the beginning (1) and in the end (2) of observation.

We believe that our approach opens a variety of possibilities to study visco-elastic properties of the cell cortex in vitro even in the non-linear regime, allowing incorporating any protein of interest into the system.

Surface Nanostructuring and Biofunctionalization through PAMAM Chemical Immobilization

A. Lungu, D.M. Dragusin, E. Rusen, A. Mocanu, E. Vasile, I.C. Stancu, H. Iovu

University Politehnica of Bucharest, Romania

adriana_lungu2006@yahoo.com

Introduction:

Bio-inspired materials and increased bioactivity of the biomaterials represent two top challenges in hard tissue engineering (HTE). Providing macro- and micro-organized scaffolds with surface nano-features remains very important when aiming HTE [1-2]. This work refers to the engineering of polymer-based surface-nanostructured smart biomaterials with cluster-like architecture and functionality. Polyamidoamine (PAMAM) dendrimers were selected as surface modifiers, their multifunctional reactive shell providing increased efficiency for the delivery of various bioactive species [3-4].

In the first part the surface chemical nano-texturing with PAMAM molecules is described. The second part of this study presents the set up of a new strategy for the chemical loading of the dendrimer-modified scaffolds with bioactive species. The technique is highly thiol-specific and it leads to multibiofunctional materials. The influence of the dendrimer generation is also emphasized.

Materials and Methods:

Generations 2 and 4 of amino-ended PAMAM were chemically immobilized on solid polymer substrates, consisting in poly(hydroxyethyl methacrylate) (PHEMA) – based compact scaffolds and microparticles, coated with (2,3-epoxypropyl)-methacrylate (GMA). The coupling occurred through the direct reaction between epoxy groups of the substrate and amines from the reactive shell of PAMAM molecules. The chemical immobilization was studied through FT-IR, XPS, UV-VIS. Moreover, the morphology of the obtained materials was investigated through SEM and AFM. Roughness analysis was also performed in order to quantitatively prove the nano-texturing of the surfaces. The resulted materials were biofunctionalized through specific bioconjugation leading to thiol-reactive conjugates. Glutathione (GSH) was then used as a model peptide for the highly selective immobilization of thiol-ended species.

Results and Discussion:

The chemical modification of the substrate with dendrimer macromolecules was successful. The PAMAM immobilization led to surface nano-texturing of the studied materials. Both roughness and chemical functionality increased with the dendrimers generation. Nano-structures with the size between 50 and 70 nm were visible and homogeneously spread onto the PAMAM-grafted materials (Figure 1).

Dendrimers formed multifunctional clusters on which GSH was efficiently linked. GSH successful coupling was firstly qualitatively evidenced through FT-IR. The coupling efficiency has been also proved through UV-VIS detection of the Py-2-thione formed during the coupling reaction.

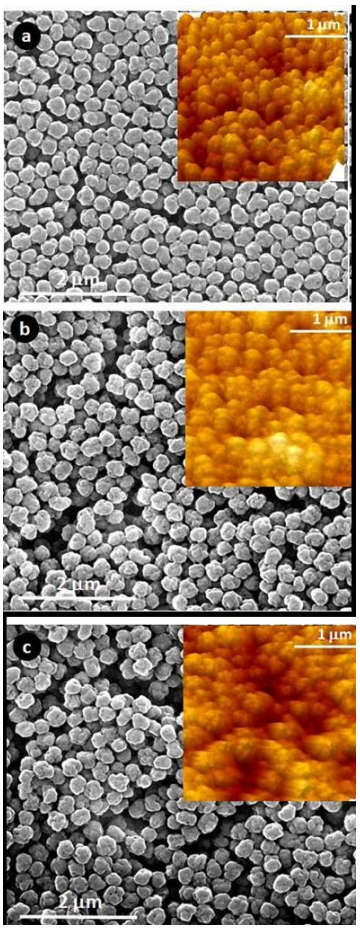

Figure 1. Surface morphology through SEM and AFM for polymer microparticles modified with PAMAM:
a) control sample without PAMAM,
b) particles modified with PAMAM-2 and
c) particles modified with PAMAM-4.

Conclusions:

Multifunctional nanorough surfaces were created. The selective reactivity with respect to thiol-ended species was demonstrated. The dendrimer-modified structures are promising candidates for biofunctionalization and further loading into biomaterials for HTE.

References:

[1] B.C. Ward, T.J. Webster, Biomaterials **27**, 3064, 2006;
[2] B.C. Ward, T.J. Webster, Mater. Sci. Eng.: C. **27**, 575 (2007);
[3] I.C. Stancu, React. Funct. Polym. **70,** 5, 314, 2010;
[4] I. C. Stancu, A. Lungu, E. Rusen, A. Mocanu, P. Z. Iordache, D. M. Dragusin, C. Cotrut, E. Vasile, H.Iovu, Dig. J. Nanomater. Biostruct., **5**, 4, 1077, 2010.

Acknowledgements:

This work was supported by CNCSIS – UEFISCSU, project number PNII – IDEI code 248/2010.

Transport properties in plasticized biodegradable polymers.

A. Chaos, E. Agirrezabal, A. Gonzalez, A. Etxeberria.*

Polymer Science and Technology Departament and Institute for Polymer Materials (POLYMAT). UPV/EHU. P.O. Box 1072. 20080 Donostia-San Sebastián (Spain).

* To whom all correspondence should be addressed to e-mail address: a.chaos@ehu.es.

1. Introduction:

The similar structure of the general biodegradable polymers, usually esters in the main chain, makes it share the same disadvantages, like its hydrofilicity, its thermal instability and difficulties in their processability due to its rigidity and brittleness[1341]. A large number of substances have been blended with this kind of polymers in order to increase its flexibility.

The compatibility of the two or more components, affects physical properties such as T_g, T_m, crystallinity and morphology. Consequently, other properties of the macroscopic material are also modified.

In the present work the modification of transport properties of PHB has been studied by the addition of a low molecular weight additive, tributyl citrate.

In the same way, a large amount of research was devoted to the plasticization of PLA[2]. PEG was found to be an effective plasticizer, but phase separation and its migration to the surface over time results in an unstable blend[3]. Blends of PLA and PEG chains of different molecular weights (630, 1500 and 4600) are being studied. Films were prepared by solution-casting from chloroform on glass plates. In both systems, the study has been focused on the permeability of the blends to carbon dioxide, oxygen and water vapour.

2. Results and discussion.

2.1. PHB-Tributyl citrate blends.

The decrease of T_m and crystallinity is related to the effect of the plasticizer in PHB´s neat with increasing molecular mobility.

Content (%wt)	T_m (°C)	% Degree of crystallinity	% Degree of crystallinity PHB
PHB 100	170	70.1	70.1
TbC 2.5	170	67.0	68.7
TbC 5	168	64.5	67.9
TbC 10	169	66.4	73.8
TbC 20	168	60.6	75.6

Table 1. Thermal data obtained by DSC measurements for films of neat and plasticized PHB.

As was observed in Table 1, the melting peaks were slightly shifted to lower temperature from the neat PHB.

The permeability of the blends is directly related with the values of crystallinity. As it can be seen, the plasticization increased all the values for the different compositions, especially the 5 % in weight of TbC.

A larger reduction of the PHB crystallization has been observed for the 5% TbC composition. This effect is reflected on a higher permeability for all the penetrans, see Figure 1.

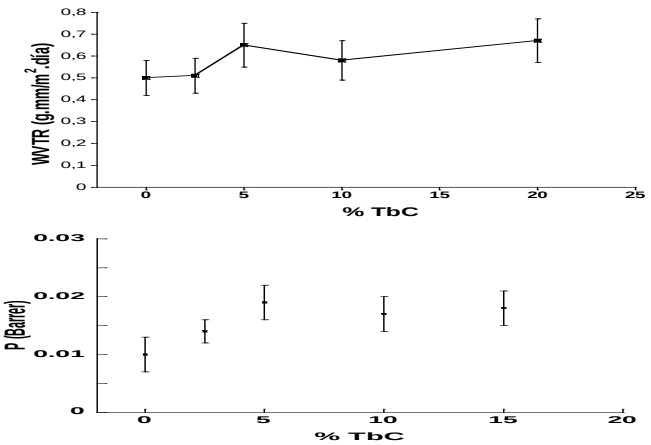

Figure 1: Permeability for water vapour and O_2 of PHB/TbC blends.

2.2. PLA-PEG blends.

This system consists of two semi-miscible crystalline phases dispersed in an amorphous matrix[4]. In our samples, even at low concentration of PEG, both components crystallize.

In table 2, permeability of PLA/PEG samples are summarized. In the case of oxygen, surprisingly, an increase in the barrier property has been found. The opposite behaviour is observed in the water vapour case, as it can be expected when plasticizers are present, where the barrier property suffers a progressive decrease.

Content (% wt) Mw= 4600	MOCON Permeability O_2 (Barrer)	WVTR (g mm/ m^2 dia)
PLA	0.24 ± 0.00	4.3 ± 0.3
PEG 5%	0.22 ± 0.00	6.2 ± 0.3
PEG 7.5%	0.22 ± 0.02	7.2 ± 1.8
PEG 10%	0.19 ± 0.01	10.3 ± 1.3
PEG 15%	0.16 ± 0.01	19.9 ± 3.3

Table 2. Permeability values for blends of PLA/PEG 4600.

References

1. Meinander K, Niemi M, Hakola J S, Selin J-F. Macromol Symp 1997; 123:147-153.
2. Ljungberg N, Wesslen B. J Appl Polym Sci 2002; 86(5): 1227-1234.
3. Hu Y, Rogunova M, Topolkaraev V, Hiltner A, Baer E. Polymer 2003; 44(19): 5701-5710.
4. Younes H, Cohn D. Eur Polym J 1988; 24:765-773.

Development of PVA-based Polyurethane Microparticles for Enzyme Immobilization

S. Budriene, A. Straksys, T. Romaskevic

Department of Polymer Chemistry, Vilnius University, Naugarduko 24, LT-03225, Vilnius, Lithuania

saulute.budriene@chf.vu.lt

Introduction. There are some basic ways for synthesis of polyurethane (PU) particles. One of the most popular methods is the one-step polyaddition polymerization of in organic medium [1]. Another way of synthesis of PU particles is one step or two step procedure in aqueous medium [2]. Only few reports were found where PVA was used instead of polyols in synthesis of PU [3]. Crosslinked PVA found promising application in the preparation of biomedical materials as films [4] and magnetic-field-sensitive gels [5]. Maltogenase, an exo-acting enzyme, which hydrolyzed 1,4-α-glucosidic linkages in starch, is used for production of high maltose syrups.

In the present work the preparation of PU microparticles derived from PVA and blend of 1,6-hexamethylene diisocyanate (HMDI) and 2,4-toluene diisocyanate (TDI) in dimethyl sulfoxide (DMSO) solution was studied. PU microparticles were used for immobilization of maltogenase by covalent binding.

Materials and Methods. PVA-based PU microparticles were synthesized by one-step method according to our previous works [6-8]. Content of isocyanate and hydroxyl groups and nitrogen in PU was determined by chemical methods. Molar composition of PU was evaluated from quantity of functional groups. The morphology and size of the microparticles was investigated by using the optical microscopy measurements. The structure of PU was characterized using FT-IR analysis.

Results and discussion. PU microparticles were synthesized from PVA and blend of diisocyanates HMDI and TDI when initial molar ratio of PVA and diisocyanates was from 1:0.5 to 1:1 and initial molar ratio of HMDI and TDI in the blend was: 1) 0.25:0.25; 2) 0.35:0.35; 3) 0.50:0.50; 4) 0.40:0.60; 5) 0.75:0.25; 6) 1.00:0.00). Influence of ratio of components, their reactivity, reaction temperature and time on structure of PU microparticles was investigated. Increasing of molar amount of diisocyanates in initial molar ratio of PVA and (HMDI:TDI) and molar amount of HMDI in the blend of diisocyanates resulted in increasing yield of PU and quantity of isocyanate groups. Increasing reaction temperature resulted in increasing yield of PU and decreasing quantity of NCO groups. The highest yield of PU microparticles and quantity of NCO groups was in the case when molar ratio of PVA:(HMDI:TDI) was 1:(0.75:0.25). The isocyanate groups of 2.4-TDI have different reactivities with the 4-position approximately four times the reactivity of the 2-position and at least two orders higher than isocyanate group in HMDI. Structure of PU has been proven by FT-IR spectra. FT-IR spectra of PU microparticles, shows ν N-H at 3394 cm^{-1}, amide I (ν C=O) at 1625 cm^{-1}, amide II (δ N-H, ν C=N) at 1569 cm^{-1}, amide III (ν C=N, δ N-H) at 1251 cm^{-1} and ν C-O-C at 1020 cm^{-1} absorption bands. Obtained PU microparticles consist of macromolecules with three types of monomeric units: non-reacted hydroxyethylene monomeric unit (type I), monomeric unit with one urethane group after reaction of hydroxyethylene monomeric unit with one isocyanate group from either of diisocyanates (HMDI or TDI) (type II) and monomeric unit with two urethane groups after crosslinking reaction of two hydroxyethylene monomeric units with two isocyanate groups from either of diisocyanates (type III). The increasing amount of diisocyanates in initial reaction mixture resulted in decreasing quantity of monomeric units of type I and increasing quantity of monomeric units of type II and III. Increasing of quantity of HMDI in HMDI-TDI blends resulted in increasing units of type II and decreasing units of type III in PU. PU microparticles are tended to agglomeration, however single PU particles are in the narrow size distribution (10-30 μm).

MG was immobilized onto PU microparticles. Efficiency of immobilization (EI) of MG depends on content of NCO groups in PU and it was increased with increasing quantity of diisocyanates in initial mixture of synthesis of carrier. Prolongation of reaction time and increasing of temperature of synthesis of PU was resulted in decreasing of EI of MG. The highest EI of MG was 111 %. Immobilized MG is stable in time and after 28 days more than 95 % of initial activity of MG was remained.

Conclusions. The increasing amount of diisocyanates in initial reaction mixture as well as increasing quantity of HMDI in HMDI-TDI blends resulted in increasing of isocyanate groups and crosslinks in PU. PU microparticles have relatively narrow size distribution in the range from 10 μm to 30 μm. High efficiency of MG immobilization onto PU microparticles and storage stability of immobilized preparations was obtained. MG immobilized onto PU microparticles could be used in biotechnological industry.

References

1. P. G. Shukla et al., US Patent 5859075. 1999.
2. E. Jabbari, M. Khakpour, Biomaterials. 2000; 21, 2073–2079.
3. M. Krumova et al., Polymer. 2000; 41, 9265-9272.
4. V. Caro et al., J. Appl. Polym. Sci. 1976; 20, 3241-3254.
5. M. Zrinyj et al., Polym. Gels Networks. 1997; 5, 415-427.
6. A. Zubriene et al., Chemistry 2003, 6th National Lithuanian Conference, Vilnius, 2003, 107-108.
7. S. Budriene et al., Proceedings of Baltic Polymer Symposium. Kaunas. 2004; 41-42.
8. T. Romaskevic et al., J. Mol. Cat. B: Enzym. 2010; 64, 172-176.

Preparation of Polyurethane-Gold and Polyurethane-Silver Nanoparticles Conjugates for Immobilization of Enzyme

T. Romaskevic[a], *S. Budriene*[a], *A. Ramanaviciene*[b], *N. Ryskevic*[b]

[a]Department of Polymer Chemistry, [b]Center of Nanotechnology and Material Science,
Vilnius University, Naugarduko 24, 03225 Vilnius, Lithuania

tatjana.romaskevic@chf.vu.lt

Introduction. Gold and silver nanoparticles have been used for various technological solutions within past three decades. The silver nanoparticles (Ag-NPs) have aptly investigated for their antibacterial property. The gold nanopartilces (Au-NPs) demonstrate not susceptible photobleaching, they are not cytotoxic and show excellent biocompatibility to biomolecules [1]. Au-NPs and Ag-NPs are excellent candidates for bioconjugation with proteins because amine groups and cysteine residues in the proteins are known to bind strongly with gold and silver colloids. Although the Au-NPs bioconjugates with proteins showed excellent catalytic activity, a major drawback was that their reusability was extremely poor [2]. It was primarily due to the difficulty in separating the bioconjugate material from the reaction medium. In this report, functionalized Au-NPs and Ag-NPs embedded on the surface of porous poly(vinyl alcohol)-based polyurethane (PU) microparticles were prepared and investigated. Obtained conjugates were applied as carriers for immobilization of starch hydrolyzing enzyme – maltogenase.

Materials and methods. PU microparticles in the range of 20-60 □m were obtained from poly(vinyl alcohol) and hexamethylene diisocyanate according to our previous works [3, 4]. The Au-NPs and Ag-NPs were synthesized by reduction of tetrachloroauric acid and silver nitrate with sodium citrate, respectively [5, 6]. It was estimated from AFM measurements that shape of height histograms of formed nanoparticles are near monodispersed. Distribution in diameter is narrow, within the range of 12-16 nm for Au-NPs and 20-40 nm for Ag-NPs. The PU was modified with Au-NPs and Ag-NPs by two different methods: (I) adsorption onto polymer surface of Au-NPs and Ag NPs from prepared colloidal solutions and (II) formation of Au-NPs or Ag-NPs from tetrachloroauric acid solution or silver nitrate via reduction with sodium citrate, respectively.

Results and discussions. Modification of PU by Au-NPs or Ag-NPs could be very attractive because of extremely high surface-to-volume ratio of conjugates. Binding of colloidal Au-NPs or Ag-NPs to the PU through nitrogen atoms in polyurethane backbone obviates the need for additional surface modification of PU. It was estimated, that higher amount of Au-NPs was remained in conjugates in the case when adsorption method of Au-NPs and Ag-NPs onto PU surface was applied. Total saturation of Au-NPs onto PU surface was obtained when Au-NPs and PU weight ratio was 1:500 and 1:800 for PU/Au-NPs samples, obtained by adsorption and formation of nanoparticles onto PU surface, respectively. In the case with PU/Ag-NPs conjugates total saturation of Ag NPs onto PU surface was obtained when Ag NPs and PU weight ratio was 1:950 and 1:2300, for I and II modification methods, respectively.

It was determined from TEM and SEM measurements that Au-NPs and Ag-NPs in the range of size 12-17 and 18-42 nm are well dispersed on PU.

Structures of PU-nanoparticles conjugates were proven by FT-IR spectra. It was estimated, that Au-NPs and Ag-NPs were attached to PU surface due to interaction between nitrogen atom of the –NH– of PU and Au-NP. FT-IR results were confirmed absorption of Au-NPs onto PU surface resulted in hydrogen bond formation. Comparable results were achieved in study of PU with Ag-NPs.

Fluorescence spectra of PU, PU/Au-NPs and PU/Ag-NPs conjugates were obtained under 266 nm YAG:Nd^{3+} laser excitation. The fluorescence spectrum of PU contained one broad band peaked at 2,73 eV (corresponds to 454 nm). It was supposed, that fluorescence of PU could be caused by formation of higher aggregates with intramolecular and intermolecular hydrogen bonds between urethane groups. Fluorescence of PU/Au-NPs conjugates shows fluorescence quenching, which is caused by change of nonradiative rate. In the case with PU/Ag-NPs conjugates, fluorescence enhancing with slight peak shift to 2.78 eV (447 nm) was determined.

Using PU/Au-NPs or PU/Ag-NPs conjugates for immobilization enzyme was bound through amine groups to the Au-NP or Ag-NP in the carrier. High catalytic activity (about 89 %) of immobilized biocatalyst was observed when PU/Au-NPs conjugates were used. No maltogenase activity was found in the solution after immobilization; however activity of immobilized enzyme on carrier was reduced. During immobilized enzyme stability assay was found that part of enzyme was leached to the solution after 40 days of storage, though almost all activity of enzyme (about 98%) on the carrier was remained. It is supposed, that part of enzyme was immobilized into PU/Au-NPs conjugate structure and could not be reached by substrate. Efficiency of maltogenase immobilization onto PU/Ag-NPs conjugates reached over 100 %. Immobilized maltogenase remained 61 % of initial catalytic activity after 35 days.

Conclusion. It is predicted that PU/Au-NPs as well as PU/Ag-NPs conjugates have immense potential for the immobilization of enzymes and it could be suitable for biotechnological applications.

References

1. S.M.Nasir et al. J. Fundam. Sci. 4 (2008) 245.
2. A.Gole et al. Colloids Surf. B. 25 (2002) 129.
3. S.Budriene et al. Polym. Adv. Technol. 18 (2007) 67.
4. T.Romaskevic et al. J. Mol. Catal. B: Enzym. 64 (2010) 172.
5. A.Ramanaviciene et al. Sensor. Actuat. B-Chem. 137 (2009) 483.
6. A.Sileikaite et al. Mater. Sci. 12 (2006) 287.

Nanoparticles of Glycopolymers as Tumor-Specific Polymeric Drugs

M.L. López-Donaire[1], M. Fernández-Gutierrez[1], B. Vázquez-Lasa[1], E. Sussman[2], B.D. Ratner[2], J. San Román[1].

1. Institute of Polymer Science and Technology, CSIC. Juan de la Cierva 3, 28006 - Madrid, Spain.
2. Department of Bioengineering, University of Washington, Seattle, WA 98195-5061, USA.

marisalop@ictp.csic.es

Introduction

Nowadays, the concept of self-assembled nano structures plays an important role in the cancer treatment. Nanoparticles (NPs) are used as tumor-specific drug delivery to provide an enhanced therapeutic efficacy and the reduction of adverse side effects. Nanoparticles can passively accumulate [1] in tumours as a result of the enhanced permeability and retention effect. Due to their small size, they can be efficiently internalized by tumor cells and subsequently released the loading active drug [2]. In the present work, self-assembled nanoparticles have been prepared with polymeric drugs obtained previously [3] by radical copolymerization of a hydrophilic monomer, vinyl pyrrolidone (VP), with a glycomonomer, oleyl -2-acetamide -2-deoxy -α-D-glucopiranoside methacrylate (OAGMA) which has demonstrated antimitotic activity against glioma cells. Biological assays were designed in order to investigate the activity of the NPs in cell cultures using human glioblastoma (A-172) and human fibroblasts cell lines and the qualitative evaluation of NPs invagination.

Materials and Methods

Nanoparticles of a OAGMA:VP copolymer [2] of composition 80:20 (mol-%) (NP) were obtained by nanoprecipitation of a dioxane solution in distilled water, in concentrations between 1 and 0.02 mg/ml. Particle size distribution and zeta potential of nanoparticles were determined by dynamic light scattering (DLS) and morphology analyzed by transmission electron microscopy (TEM). Surface chemical structure was analyzed by X-ray photoelectron spectroscopy (XPS).

Cytotoxicity of nanoparticles was assessed by MTT assay. NP dispersions were obtained in water at concentrations in the range 1 to 0.1 mg/ml. Afterwards, 100 µl of each dispersion was mixed with 100 µl of DMEM and the resulting 200 µl dispersions were used for cytotoxicity assays. Assays based on fluorescence were performed for internalization studies. Coumarin-6 loaded NPs were obtained by applying the same procedure except that 0.01 wt% coumarin 6 was added to the dioxane copolymeric solution.

Results and Discussion

Self-assembled nano structures based on the statistical copolymer OAGMA:VP 80:20 (mol-%) were obtained in a dilute aqueous medium mainly due to the amphiphilic "blocky sequences" microstructure. Size of these self-assembled aggregates was analyzed by dynamic light scattering getting an unimodal distribution and narrow P.D.I. values as it is shown in Figure 1A for a NPs suspension of 1 mg/ml. It is worth noting that the nanoaggregates showed a drop in their size when the concentration of NPs suspension decreased. The apparent hydrodynamic diameter (D_h) of the copolymeric nanoaggregates oscillated between 106.8±0.5 and 208.9± 1.9 nm. The zeta potential (ξ) value of -20 mV revealed the presence of negative charge on the NPs surface. The ξ absolute value of these nanoparticles is considered to be enough to ensure their stability. TEM characterization of nanoparticles showed a spherical morphology and confirmed the NPs size obtained by DLS. The surface chemical structure analyzed by XPS revealed that the experimental percents of C1s, O1s and N1s were in close agreement with the stoichiometry percents. On the other hand, the C1s high resolution spectrum (Figure 1B) was deconvoluted into three peaks attributed to hydrocarbon species (BE = 285.0 eV), C-C=O, C-OH/OR and C-N species (BE = 286.24 eV) and N-C=O, O-C=O and O-C-O functional groups (B.E. = 288.12 eV).

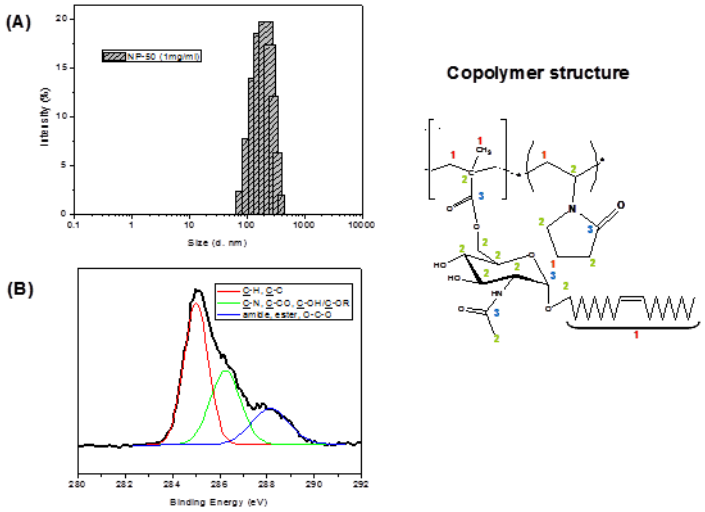

Figure 1. (A) Particles size distribution by DLS and (B) High resolution C 1s XPS spectrum of NPs obtained form a suspension of 1 mg/ml.

Biological activity of nanoparticles at different suspension concentrations was evaluated in human glioblastoma cells and human fibroblasts. At any NP concentration, an inhibition of glioblastoma cells around 45% was observed. However, cell viability of fibroblasts remained between 80 and 100 %.

Endocytosis of nanoparticles by the tumour cells was evaluated with coumarin 6 loaded nanoparticles. The fluorescence images of A-172 cells after incubation with the water:DMEM 50:50 dispersion showed the presence of coumarin 6 loaded nanoparticles mainly inside the cells or attached to the cellular membrane.

References

1. Matsumura Y, et al. Cancer Research 1986;46(12 I):6387-6392.
2. Zhang BS, et al. Adv. Mater. 2009;21:419-424.
3. López Donaire ML, et al. Biomaterials 2009;30(8):1613-1626

Self-Assembling Enzyme-Polyelectrolyte Nanofilms for Sensor Applications

Larisa V. Sigolaeva[1], Hanna A. Tarhonskaya[1], Natalia A. Krainova[1], Marya S. Gromova[1], Alina V. Kondrashina[1], Arkadi V. Eremenko[1], Axel H.E. Mueller[2], Ilya N. Kurochkin[1]

[1]Department of Chemical Enzymology, School of Chemistry, Moscow State University, 119991 Moscow, Russia
[2]Makromolekulare Chemie II, Universitaet Bayreuth, 95440 Bayreuth, Germany

lsigolaeva@genebee.msu.ru

Introduction

The preparative techniques to build up multilayer films via the alternative adsorption of polyelectrolytes and biomolecules is one of the most important subjects in biomaterials sciences due to the potential application for the construction of bioreactors, biomedical devices, and biosensors. Requirements for their sensitivity and selectivity force to look for new polymer objects with non-linear topology compared to conventional linear polyelectrolytes. Such non-linear polymers are expected to provide enhanced adsorption and improved fixation of biomaterial.

This work deals with multilayered films obtained by self-assembling method of polyelecrolyte deposition (layer-by-layer technique), which are composed from electrochemically active tyrosinase or choline oxidase electrostatically complexed with the star-like polyionic species. As star-like polyionic species we have used (i) star-shaped poly(N,N-dimethylaminoethyl methacrylate)s with the relatively small number of arms (6, 9, and 17 arms) as well as (ii) star-like micelles of poly(styrene)-block-poly(N,N-dimethylaminoethyl methacrylate)s and poly(butadiene)-block-poly(N,N-dimethylaminoethyl methacrylate)s characterized by the larger number of arms, as well as their quaternized with methyl iodide derivatives.

Materials and Methods

Self-assembled films were deposited on graphite supports via layer-by-layer technique for the formation of biosensing surfaces for phenol and choline detection. The films were constructed via subsequent stages of deposition of the polyelectrolyte component onto graphite substrate, washing, adsorption of enzyme molecules via their complexation with the adsorbed oppositely charged polyelectrolyte component, washing and so on. The electrochemical activity of the incorporated enzymes, their kinetic parameters (K_M, V_M) and the stability of self-organized films were studied amperometrically. Electrochemical data were compared with surface topography characteristics obtained by Atomic Force Microscopy and Scanning Electron Microscopy.

Results and discussion

Spatial organization of the polyelectrolyte component appears to have an influence on the properties of self-assembled films containing incorporated enzymes. The comparison between the enzymatic activities of the films constructed from star-like polyionic species and of the films built up from their linear analogues (reference homopolyelectrolytes) demonstrates an increase in enzymatic activities of the films containing polyphenol oxidase and choline oxidase. The effect becomes stronger with the increasing number of arms of the star-like polyionic species.

Enzymatic activities of the films can also be modulated by the small ion composition (Cl^- vs I^-) of the solution of the polyelectrolyte component, which is used at the stage of its deposition. According to amperometrical measurements, pronounced enhance in the enzymatic activity of films was observed with the increasing iodide-anion concentration. This effect appears to strengthen in the series: short linear polycation < star-like polycationic species ~ long linear polycation and, as supposed, is determined by the flexibility of polyelectrolyte chains and their ability to undergo salt-induced change of conformation from expanded to compact one. The adsorption of macromolecules in compact conformation is thought to result in the increasing amount of the polyelectrolyte component adsorbed on the substrate surface, which therefore can potentially bind more enzyme molecules at the following enzyme adsorption stage. The latter leads to higher amount of the adsorbed enzyme in the films, thereby resulting in the increase of their enzymatic activity.

The analytical characteristics of resulting sensor coatings for phenol and choline detection (linear ranges, detection limits, operational stability, sensitivity, etc.) were described in detail and biomedical applications are demonstrated for the analysis of biochemically important enzymes in the samples of whole blood of humans and experimental animals.

Conclusion

The enzymatic activity of self-assembled polyelectrolte-enzyme films built up via layer-by-layer technique can be controlled by varying topology of the polyelectrolyte component and conditions (such as the type of small ions and their concentration), at which its deposition is performed. This finding is thought to be in demand by modern sensor technologies creating highly active and stable sensor coatings.

Acknowledgements

This research was supported by the Russian Foundation for Basic Research (project numbers 08-08-12081-ofi and 11-03-00712-a).

Bioactive Alginate-Nanosilver-Anthocyanin Hybrid Composite

Jin Hyun Choi,[1,2] Song Yi Seo,[2] Ga Hyun Lee,[3] Se Guen Lee,[3] Eun Jung Oh,[4] Ho Yun Chung,[4] Jeong Hyun Yeum,[1,2] Sang Ik Han[5]

[1]Department of Natural Fiber Science, Kyungpook National University, Korea
[2]Department of Advanced Organic Materials Science and Engineering, Kyungpook National University, Korea
[3]Division of Nano & Bio Technology, Daegu Gyungbuk Institute of Science & Technology, Korea
[4]Department of Plastic & Reconstructive Surgery, Kyungpook National University Hospital, Korea
[5]Division of Functional Crop Resource Development, Department of Functional Crop,National Institute of Crop Science, Korea

jinhchoi@knu.ac.kr

Introduction: Biopolymers have received increased attention as excipients in pharmaceutical formulations as they are derived from natural sources. Silver has a long history of use in human healthcare and medicine. A number of healthcare products such as wound dressing materials, body wall repairs, augmentation devices, tissue scaffolds, and antimicrobial filters now contain silver. In this study, alginate-nanosilver-anthocyanin hybrid sponges (ANAHS) were prepared by in-situ synthesis of silver nanoparticles in an aqueous alginate solution. Antimicrobial activity and pro-inflammatory cytokine inhibition of ANAHS were investigated.

Materials and Methods: A solution of 1.0 wt/v% alginate and anthocyanin was prepared by dissolving alginate and anthocyanin in a 100ml of distilled water. Silver nitrate (2ml, 5.0 wt/v% in water) was dropped in 100 ml of the alginate and anthocyanin solution. After 1 hour, freshly prepared sodium borohydride solution (2ml, 1.0 wt/v% in water) was slowly added under magnetic stirring. A rapid color change to dark brown indicated the formation of silver nanoparticles. The mixture was stirred for 3 hours at room temperature in order to lead entire reduction. And then, the solution was dialyzed for 2 days to eliminate the salts which were
formed while alginate and silver nitrate were synthesized. The alginate-nanosilver-anthocyanin solutions were freeze-dried. Finally, the ANAHS were prepared by cross-linking of the freeze-dried matrices, washing, and freeze-drying. The ANAHS were characterized by transmission electron microscopy (TEM), X-ray diffraction (XRD), and ultraviolet-visible (UV) spectroscopy. Cytotoxicity of the ANAHS were checked by 3-(4,5-dimethylthiazol-2-yl)-5-(3-carboxymethoxyphenyl)-2-(4-sulfophenyl)-2H-tetrazolium (MTS) assay. Pro-inflammatory cytokines 9 (IL-1β, IL-6, and TNF-α) were measured by cell culture of RAW 264.7 cells and enzyme-linked immunosorbent assay (ELISA).

Results and Discussion: The size of nanoparticles in the TEM images of the alginate solution are about 5-20 nm. Figure 1 is TEM images of the ANAHS. Nano-sized silver crystals were spread in the sponge. We confirmed the presence of silver in the ANAHS by
XRD as shown

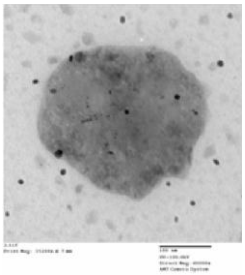

Figure 1. TEM images of silver nanoparticles in the ANAHS

The ANAHS revealed the 97-99% reduction of number of colonies of staphylococcus auseus and klebsiella pneumonia. From results in Figure 3, we confirmed that the ANAHS inhibited the production of IL-1β, IL-6, and TNF-α Conclusively, the ANAHS had a good microbial activity and anti-inflammatory property. They are considered a candidate for the application as wound dressing material.

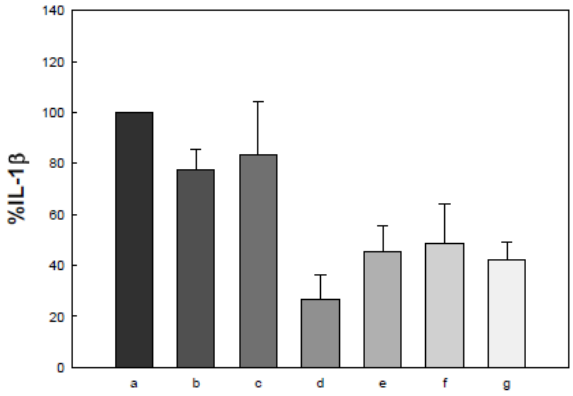

Figure 2. Relative amount of IL-6 produced by RAW264.7 cells cultured with the sponges of
(a) alginate, (b) alginate-anthocyanin (0.05%),
(c) alginate-anthocyanin (0.1%),
(d) alginate-nanosilver (0.1%),
(e) alginate-nanosilver (0.1%)-anthocyanin (0.05%),
(f) alginate-nanosilver (0.05%)-anthocyanin (0.1%), and
(g) alginate-nanosilver (0.1%)-anthocyanin (0.1%).

Acknowledgement: This work was supported in part by grants from Agenda Program (PJ0073852010) of National Institute of Crop Science, Rural Development Administration (RDA), Republic of Korea.

Characterization and biocompatibility evaluation of novel segmented polyurethanes based on poly(ε-caprolactone)-poly(dimethylsiloxane)-poly(ε-caprolactone)

Marija V. Pergal[1], Vesna V. Antić[2], Gordana Tovilović[3], Jelena Nestorov[3], Jasna Djonlagić[4]

[1]Center of Chemistry, ICTM, Studentski trg 12-16, Belgrade, Serbia; [2]Faculty of Agriculture, Nemanjina 6, Belgrade, Serbia; [3]Department of Biochemistry, Institute for Biological Research, Bul. Despota Stefana 142, Belgrade, Serbia; [4]Faculty of Technology and Metallurgy, Karnegijeva 4, Belgrade, Serbia

Thermoplastic polyurethane elastomers (TPUs) are widely used as biomaterials because of their excellent mechanical properties and good biocompatibility. They are employed in a wide range of medical applications including implantable medical devices, drug-controlled release systems or scaffolds for tissue engineering.[1] TPUs are multiblock copolymers composed of short, rigid polyurethane sequences, hard segments (HS) connected *via* long and flexible chains of soft segments (SS). The thermodynamic incompatibility of the HS and and SS segments at low temperatures results in phase separation and, consequently, in the formation of a domain structure. Their two-phase microstructure imparts excellent mechanical properties. The introduction of poly(dimethylsiloxane) (PDMS) into the polymer chain has the advantage of imparting some of the attractive properties of PDMS to polyurethanes such as high flexibility, excellent thermal, oxidative and hydrolytic stability and low surface energy. [2-4]

In this study a series of novel TPUs based on *α,ω*-dihydroxy-[poly(*ε*-caprolactone)-*block*-poly(dimethyl siloxane)-*block*-poly(*ε*-caprolactone)] (PCL-PDMS-PCL) triblock copolymer, 4,4′-methylenediphenyl diisocyanate (MDI) and 1,4-butanediol (BD), is presented. TPUs were synthesized by a two-step solution polymerization and evaluated for biomedical applications. The triblock prepolymer contained terminal crystallizable PCL blocks and a central PDMS block. PCL is particularly interesting due to excellent water resistance, slow hydrolytic and enzymatic degradation, good biocompatibility and very high flexibility. The combination of the properties of PCL and PDMS makes these block copolymers excellent candidates for surface modifying additives, pharmaceutical and biomedical applications. In the synthesis of the TPUs, the PCL blocks served as a compatibilizer between the non-polar PDMS blocks and the polar comonomers, MDI and BD. The content of hard MDI/BD segments in the polymer chains was varied from 9 to 63 wt%.

The influences of the content and length of the hard segments on the thermal, surface, mechanical properties and biocompatibility were investigated. The structure, composition and HS length were examined using ^{1}H and quantitative ^{13}C NMR spectroscopy. The degree of hydrogen bonding and its influence on the microstructure of synthesized TPUs was analyzed by means of FTIR spectroscopy.

DSC results implied that the synthesized TPUs were semicrystalline polymers in which both the hard MDI/BD and soft PCL-PDMS-PCL segments participated. It was found that an increase in the average HS length (from 1.2 to 14.4 MDI/BD units) was accompanied by an increase in the crystallinity of the HS, storage moduli, hydrophilicity and degree of microphase separation of the copolymers.

Depending on the HS content, a gradual variation in polyurethane surface properties was revealed by AFM and static water contact angle measurements. The *in vitro* biocompatibility of copolymers was evaluated using endothelial EA.hy926 cell line. The cell adhesion and morphology were analyzed by light microscopy. In order to investigate the cell viability and cytotoxic effect of polyurethanes, MTT and LDH assays were used. Protein adsorption on the polyurethane films was also investigated.

Studies of protein adsorption onto polymeric surfaces showed that the adsorption ratio of fibrinogen/albumin for the TPUs, which was adopted as the indicator of biocompatibility, was in the range from 0.306 to 0.513. Since the surface of all samples has adsorbed larger amount of albumin compared to fibrinogen, it can be concluded that all synthesized copolymers have good biocompatibility.

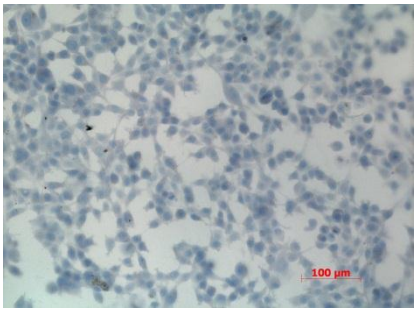

Fig. 1 Photographs of endothelial EA.hy926 cells on the surface of TPU film with 50 wt% soft segment

The copolymer films with high HS content exhibit the best biocompatibility due to a combination of cellular affinity, non-toxic effects to cells and good microphase morphology (Fig. 1). Therefore, their non-cytotoxic chemistry makes TPUs with rougher surface and good microphase separation promising biomaterials for use in implantable medical devices.

References:

1. S. Gogolewski, *Colloid Polym. Sci*. 267, 757 (1989).
2. D. J. Martin, L. A. Poole Warren, P. A. Gunatillake, S. J. McCarthy, G. F. Meijs, K. Schindhelm, *Biomaterials* 21, 1021 (2000).
3. E. Briganti, P. Losi, A. Raffi, M. Scoccianti, A. Munaò, G. Soldani, *J. Mater. Sci.: Mater. Med.* 17, 259 (2006).
4. N. Roohpour, J. Wasikiewicz, D. Paul, P. Vadgama, I. Rehman, *J. Mater. Sci.: Mater. Med*. 20, 1803 (2009).

Amphiphilic bioactive polymers and preparation of self assembled nanostructures

Patricia Suárez[1], *Álvaro González-Gómez*[1], *Luis Rojo*[2], *Julio San Román*[1]

[1] Biomaterials Department, ICTP-CSIC, C/Juan de la Cierva 3, 28006, Madrid, Spain.
[2]Department of Materials, Imperial College London, Prince Consort Rd. SW7 2AZ, London, UK.

alggomez@ictp.csic.es

Amphiphilic copolymers have attracted a great deal of attention in terms of their ability to form self assembled nanosized structures. These polymers are obtained by the polymerization of two or more types of monomers, typically one hydrophobic and one hydrophilic, so that the resulting macromolecule is composed of regions that have opposite affinities for an aqueous environments. Therefore, these systems offer a unique methodology to prepare structures such us polymeric-drug conjugates nanospheres, in which a hydrophobic drug, covalently bound to the macromolecule and isolated from the surrounded aqueous medium by a hydrophilic shell, enhancing the control of the therapeutic action and the biostability of the drug.

The aim of this work has been the incorporation of the ibuprofen (Ibu), ketoprofen (Keto) or naproxen (Nap) molecule onto self assembling 1-vinylimidazole (VI) based macromolecules which led in stable aqueous nanoparticles to be used as controlled drug delivery systems for biomedical applications.

Acrylic derivatives of Ibu, Keto and Nap were synthesised in accordance with the literature[1]. Each acrylic monomer was copolymerized with VI, through free radical polymerization in a range of feed compositions from 20:80 to 80:20. The reaction products were characterized by ^{1}H-NMR, ATR-FTIR, DSC and SEC. The reactivity ratio values for all the comonomer pairs and copolymer compositions of the product obtained were determined by in situ ^{1}H-NMR[2], showing a higher reactivity for the three acrylic derivatives in comparison to the observed for the VI monomer indicating that the polymeric backbones grow with a gradient distribution of the molecular units along the macromolecular chains. These heterogeneous triads distribution of the hydrophobic and hydrophilic segments provide amphiphilic properties to the copolymers synthesised.

The polymeric nanoparticles were prepared by nanoprecipitation method in water (Figure 1).

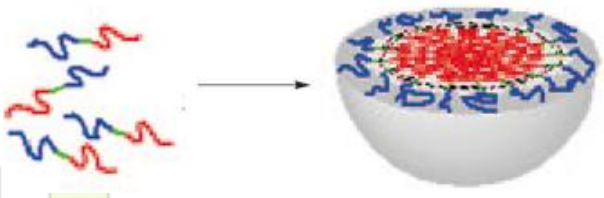

Figure 1. Amphiphilic copolymer micelle formation transforming into a nanoparticle.

Morphology and mean diameter of the particles obtained were determined by Scanning Electron Microscopy (Figure 2) and by Polarization Intensity Differential Scattering respectively. Spherical nanosized particles were observed with mean diameters in a range of 50 to 200 nm, dependent on the microstructure and molar composition of each copolymer system.

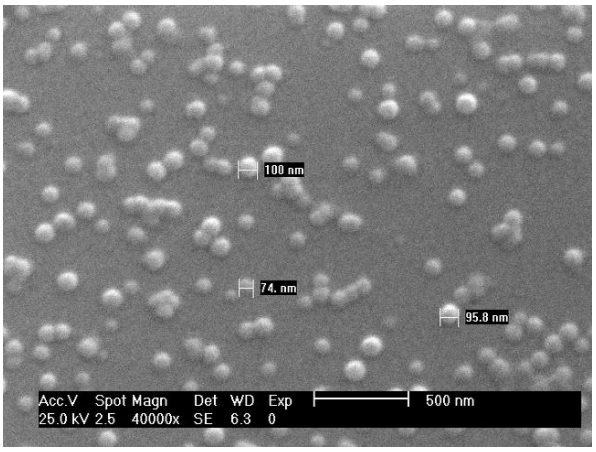

Figure 2. SEM images of p(HKT-co-VI) (20:80).

In vitro drug released from the nanoparticles were determined in pH 7.4 and 10.0 buffers at 37 ºC by HPLC-UV. Both the kinetics and total amount of drug released shown a noticeable dependant on the micelle composition and the physicochemical properties of the surrounding media as a consequence of the existing balance between the chemical natures of the imidazole ended units and the drug molecule content within the polymer backbones.

Finally, the biocompatibility studies analysed through the MTT assay, showed absence of toxicity as a consequence of the release of leachables to the medium in any of the copolymer formulations, which permitted a cellular activity greater than 95% from the second to the seventh day.

All these results shown in this work indicate the potential of these copolymers for obtaining nanoparticles through self-assembling mechanisms which provide a very interesting approach to the preparation of polymer-drug systems for biomedical applications.

[1] C. Parejo, A. Gallardo, J. San Roman. J. Mater. Sci.-Mater. Med. (1998) 9, 803-809.
[2] M.R. Aguilar, A. Gallardo, M.D. Fernandez, J. San Roman. *Macromolecules* (2002), *35* (6), 2036-2041.

Viability and proliferation analysis of culture from human mesenchymal stem cells onto bioinspired collagen membranes for guided tissue regeneration.

Fraga, AF[1]; Tavares, HS[1]; Marques, RFC[1]; Tómas, H[2]; Santos, JL[2];

[1]PROCELL/Brasil; [2]Universidade da Madeira (CQM)/Portugal.

Introduction and Objective: Human mesenchymal stem cells (hMSC) have several advantages in practical and experimental uses due to its easy isolation and purification protocols and principally its capability to differentiate into cells of different tissue. Biomaterials like collagen barriers are current employed in guided tissue regeneration (GTR) for plastic and reconstructive surgery, dental implants and bone graft procedures. Recently, drug and gene delivery systems based on collagen membranes appear as a new promissory treatment for sportive traumas such as muscle and tendon lesions. Human mesenchymal stem cells cultures provide excellent model for these evaluations because have many advantages when compared to *in vivo* methods, and reliable results without unnecessary animal sacrifices. The actual challenges of sportive medicine are trauma in muscle, tendon and cartilage structures where clinical and surgical treatment shows many controversies. The aim of this preliminary study was to evaluate the behavior of human stem cells and proliferation after the initial stage of cell adhesion among collagen matrices, with different compositions, nanostructures and mechanical properties. **Materials e Methods**: After local ethical committee approbation, hMSC from fourth passage with density of $5x10^4$ cells/sample were seeds onto collagen membranes manufactured by PROCELL BIOLOGICS LTDA. The experiments were realized in hex-plicate (n=6) for all biological barrier studied. The cell adhesion and proliferation was analyzed by fluorescent method using Alamar Blue assay. This sensitive method is extremely stable and nontoxic to the cells allowing its continuous cells cultures monitoring over time. Mainly for this reason, this test has been considered superior to classical tests for cell viability such as the MTT test. In order to evaluate morphological aspects, fluorescent labeling by Alexafluor were performed. **Results:** Good cell adhesion behavior of cells on all barriers was observed without any citotoxicity. The best performance for Bilayer group was found after 24h. The cells were monitored every 24h until day 5, when was performed the expression of enzyme Alkaline Phosphatase and the quantification of total protein. These evaluations were also realized at day 10, when was determinate the initial cell differentiation. The proliferation results shows decrease of RFU (Relative Fluorescence Units) after 24h due to environment changing and cell adaptation on the morphologies of each collagen membrane. The results of resasurin increases after 72h and 96h by the proliferation into the porous surfaces (see Fluorescence Microscopy day 3) and decrease after 120h when the cell differentiation starts. The ends of these evaluations are the comparison between Alcaline phosphatase expression and amount of protein for 5 and 10 days. **Conclusions**: The biodegradable collagen membranes Bilayer and Hydroxyapatite coated showed excellent morphology for cell growing. These biomaterials have presented good properties for tissue engineering as scaffold for cells culture from human mesenchymal stem cells as.

Modular And Tunable Polymeric Systems Containing Dual Biologically Active Ions

F. J. Parra [1,2], *M. Fernández-Gutiérrez* [1], *B. Vázquez-Lasa* [1,2*], *N. Dinjaski* [3], *A. Prieto* [3], *J. San Román* [1,2]

1. Institute of Polymer Science and Technology, CSIC. C/ Juan de la Cierva, 3, 28006 Madrid, Spain.
2. CIBER-BBN. Ebro River Campus, Building R&D, Block 5, 1st Floor, Poeta Mariano Esquillor s/n, Zaragoza 50017, Spain
3. Centre of Biological Research, CSIC. C/ Ramiro de Maeztu 9, 28040 Madrid, Spain.

fparra@ictp.csic.es

Introduction

A successful new approach for the treatment of diseases is the combined therapy in which two or more active pharmaceutical ingredients (APIs) that act on the same or different therapeutic target are combined. In the particular case of infectious diseases the success is relatively big because by this way it has managed to reduce the resistance to the treatment as well as other associated diseases [1]. It is well known that quaternary ammonium polymers have antibacterial activity and they have found application in the biomedical field for prophylaxis or treatment of implant associated infections. So, recently we have synthesized hydrophilic quaternary ammonium copolymers for application as foldable intraocular lenses [2].

Here, we report the synthesis, characterization and the bactericidal behaviour of dual biologically active quaternary ammonium monomers bearing active pharmaceutical ingredients, like broad-spectrum antibiotics (BSAs) or non-steroidal anti-inflammatory drugs (NSAIDs), as well as their polymeric derivatives. The anti-inflammatory activity and the biocompatibility studies of copolymers and homopolymers by *in vitro* cell cultures were also studied.

Experimental

Monomers were synthesized by applying established procedures [3] as shown in Scheme 1. Polymerization reactions were carried out in solution of dimethylformamide (1M) using AIBN (0.5 wt-%) as a free radical initiator at 50ºC. Copolymers of the dual functional monomer and 2-hydroxyethyl methacrylate (HEMA) were obtained in bulk. Chemical characterization was carried out by nuclear resonance spectroscopy. Drug release profiles from polymeric systems were studied at 37ºC and pH = 7.4 by UV spectroscopy. Antimicrobial activity of monomers and polymers was analyzed against Gram-negative strains of *Pseudomona aeruginosa* PAO1 and *Salmonella typhimurium* LT2, and Gram-positive strains of *Staphylococcus epidermidis* and *Staphylococcus aureus*. The anti-inflammatory activities of extracts of polymeric samples were performed according to the method of Wang et al [4] using macrophages from Swiss male mice. The *in vitro* tolerance cytotoxicity was assessed by the MTT assay using human skin dermal fibroblasts

Results and Discussion

The monomeric compounds were synthesized by one-step ion exchange reaction from the corresponding monomeric quaternary ammonium halide and the sodium salt of the API to give the dual biologically active quaternary ammonium compound in quantitative yield (Scheme 1).

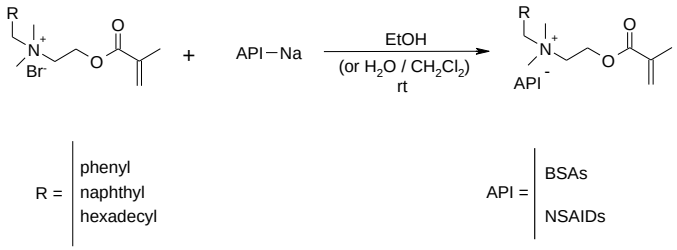

Scheme 1. Synthesis of dual functional monomers.

Polymerization of representative monomers, e.g. the benzyl ammonium ketoprofenate derivative monomer (BK), was successful in giving a corresponding polymer, e.g. poly-BK, and the polymerization yields were in the range 40 to 70 %. Bulk copolymerization reactions of the BK monomer and HEMA with a BK:HEMA ratio of 20:80 (wt %) were carried out to obtain transparent and hydrophilic discs. Ketoprofen release amounted to 80% from poly-BK after 10 days and around 15% from BK-co-HEMA copolymer after 8 days. In the bactericide assays of monomers or polymers it was found that the NSAID counterion had little effect on the anti-microbial activity, giving MIC and MBC values similar to those of the halide counterion. The benzyl ammonium derivative monomers had the highest MIC values and the hexadecyl ammonium derivatives the lowest MIC values, independently of the strain although they were more effective against gram-positive bacteria.

Cellular viability of human fibroblasts in presence of extracts of poly-BK was around 60% indicating that the biocompatibility is compromised; however, fibroblasts viability in presence of the extracts of the copolymer BK-co-HEMA (20:80) at any time was 100% (Figure 1). Anti-inflammatory activity of extracts of the copolymer taken during the first week was around 80% and it decreased for longer times. Macrophages viability was of 100% during the whole period studied.

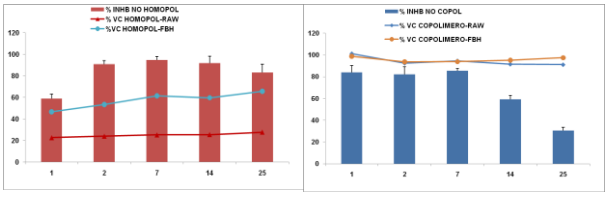

Figure 1. NO release and cytotoxicity against macrophages and fibroblast of poly-BK (left), and BK-co-HEMA (20:80) (right).

References

[1] Clarke T et al. Nature 2003, 422, 791.
[2] Parra FJ et al. Biomacromolecules 2009, 10, 3055.
[3] Caillier L et al. Eur J Med Chem 2009, 44, 3201.
[4] Wang SY et al. Phytother Res 2008, 22, 213.

Surfactante influence in obtaining hyaluronic acid micro and nanoparticles for *Arrabidaea chica* encapsulation and its effects on cicatrization.

Ferre-Souza, V.[1], *Giacobbe, D.*[1], *Lima, J.*[1], *Jorge, M. P.*[2,3], *Ruiz, A. L. T. G.*[3], *Sousa, I. M. O.*[3], *Rodrigues, R. A. F. R.*[3], *Carvalho, J. E.*[3], *Foglio, M. A.*[3], *Santana, M. H. A.*[1*].

[1]Departamento de Desenvolvimento de Processos Biotecnológicos, Universidade Estadual de Campinas, Campinas (SP), Brasil. *Responsible author.
[2]Departamento de Clínica Médica, Universidade Estadual de Campinas, Campinas (SP), Brasil.
[3]CPQBA, Universidade de Campinas, Paulínia, SP, Brasil.

vivianeferre040@gmail.com

Introduction - *Arrabidaea chica* is a scrambling shrub which occurs in tropical America whose extract of their leaves contains a 3-desoxiantocianidina, carajurina, which presents activities anti-inflammatory, scarring and antioxidant. The efficiency of crude extract of *A. chica*, involves the stimulus to growth of fibroblasts and collagen synthesis, as demonstrated "in vitro" and "in vivo". Hyaluronic acid (HA) is a glycosaminoglican anionic and non sulfated, widely distributed in connective, epithelial and neural tissues. Several studies suggest that the HA participates in processes that promote the cellular proliferation and migration in the growth of tissues and favors the hydration, which has beneficial effects in cicatrization. These properties, associated to the effects of encapsulation and controlled release produced by hyaluronic acid nano and microparticles, descry more efficient actions in the various stages of the process of healing and their effects in cicatrization.

Matherials and Methods - In this work was studied the influence of two surfactants, Span 80® and Tween 80® in obtaining hyaluronic acid micro and nanoparticles using the method of w/o emulsion, for encapsulation the *A. chica* leaves extract and testify the healing activity. Span 80® was evaluated free and together with Tween 80®, in the proportion 9:1, in both conditions, the concentrations tested were 1 to 5 %. The particles were characterized through its average diameter, polidispersity and morphology. The effects of *A. chica* extract encapsulated were studied in the mouse back tegument through the subcutaneous injection of the same and blood vessels were count to evaluate the healing ability.

Results and Discussion - Was verified that the saturation of the surface of the particles occurred more rapidly when used the lipophilic surfactante Span 80®, better stability of emulsions in the presence of free surfactant was in the concentration of 1% and together with Tween 80®, in the concentration of 3%. Span 80® 1% was choose to produce the HA particles, confirming the utilization already described in the literature. Tests carried out in a culture of human fibroblasts showed that the extract of *A. chica* and empty HA particles had no toxic effect, allowing their use in the testing of healing. In mouse back tegument was find out an increase of blood vessels number when the particles with the *A. chica* extract was employed.

Conclusion – It showed more interesting use Span 80® 1% to obtain the HA micro and nanoparticles. The association between the HA and *A. chica* extracts properties to obtain micro and nanoparticles present characteristics to be employed as inductors in healing process through the increase of blood vessels number.

References –

*****Segura, T., Anderson, B. C., Chung, P. H., Webber, R. E., Shull, K. R., Shea, L. D. Crosslinked hyaluronic acid hydrogels: a strategy to functionalize and pattern. Biomaterials, 26: 359-371, 2005.

*****Peattie, R. A., Nayate, A. P., Firpo, M. A., Shelby, J., Fisher, R. J., Prestwich, G. D. Stimulation of in vivo angiogenesis by cytokine-loaded hyaluronic acid hydrogel implants. Biomaterials, 25: 2789-2798, 2004.

*****Yun, Y. H., Goetz, D. J, Yellen, P., Chen, W. Hyaluronan microspheres for sustained gene delivery and site-specific targeting. Biomaterials, 25: 147-157, 2004.

*****Prestwich, G. D. Biomaterials from chemically-modified. Glycoforum; 2001. Available in: /http//:www.glycoforum.gr.jp. Access: May, 2006.

*****Barbosa, W. L. R., Pinto, L. N., Quignardi, E., Vieira, J. M. S., Silva Jr., J. O. C., Albquerque, S. Arrabidaea chica (HBK) Verlot: phytochemical approach, antifungal and trypanocidal activities. Brazilian Journal of Pharmacognosy, 18, 544-548, 2008.

*****Jorge, M. P., Madjarof, C., Ruiz, A. L. T. G., Fernandes, A. T., Rodrigues, R. A. F., Sousa, I. M. O., Foglio, M. A., Carvalho, J. E. Evaluation of wound healing properties of Arrabidaea chica Verlot extract. Journal of Ethnopharmacology, 118; 361-366; 2008.

Synthesis and Characterization of Porous Hydroxyapatite/Polymer Biocomposite Scaffolds

Dajana Kranzelic, Marica Ivankovic, Hrvoje Ivankovic

University of Zagreb, Faculty of Chemical Engineering and Technology, Marulićev trg 19, 10000 Croatia

dkranzel@fkit.hr

Scaffold materials designed from highly porous hydroxyapatite, HAp, derived from cuttlefish bone, and natural (gelatin, alginate) and synthetic (polycaprolactone) biopolymers were prepared and characterized.

In the first stage, complete hydrothermal conversion of aragonite ($CaCO_3$) originated cuttlefish bone (*Sepia Officinalis L.*) to pure HAp, maintaining the original highly porous micro-architecture of bone, was achieved. In the second stage, different concentration of polymer solutions (2-20 wt. %) were impregnated into the HAp scaffolds.

The hydrothermal conversion of aragonite from cuttlefish bone into HAp was confirmed by XRD analysis. The FTIR spectra of HAp/biopolymer composite contain only the characteristic bands of HAp and polymers. There is no evidence of formation of new chemical bonds between HAp and polymers.

In vitro treating with Hank's balanced salt solution (HBSS) for period up to 28 days at 37°C was performed.

Morphological investigations of the prepared composite scaffold performed by SEM revealed the appearance of much more regular sponge-like microspheres (5-10µm) deposited on the original microstructure of HAp converted cuttlefish bone.

The SEM-EDX analysis of the composite surface showed the precipitation of calcium deficient hydroxyapatite (CDHA) and amorphous calcium phosphate (ACP) depending on the nature of precipitation substrate. The chemical analysis of HBSS solution, performed after *in vitro* treating by ionic chromatography method, also indicated calcium phosphate precipitation on the composite surface.

After initial weight increase, HAp scaffold was partially crumbled with weight loss ~6.7 % during 28 days while HAp/polymer composite samples showed weight increase ~7.0 % due to the Ca-P precipitation on composite surface.

These biocomposite materials can be used in delivery of drugs and as growth factors stimulating cellular adhesion, proliferation, and differentiation thus promoting bone and cartilage regeneration.

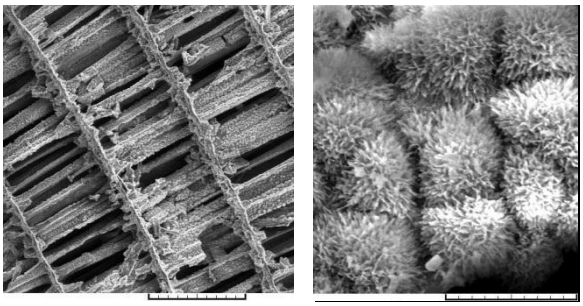

Fig.1. SEM micrograph of cuttlefish bone after HT conversion into HAp (a) and microspheres of plate-like HAp crystals (b).

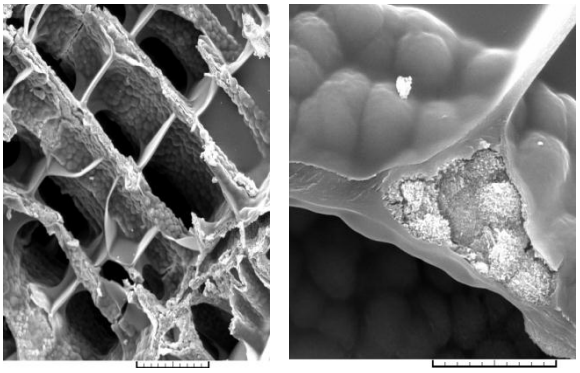

Fig.2. SEM micrographs of gelatin coated hydroxyapatite scaffold.

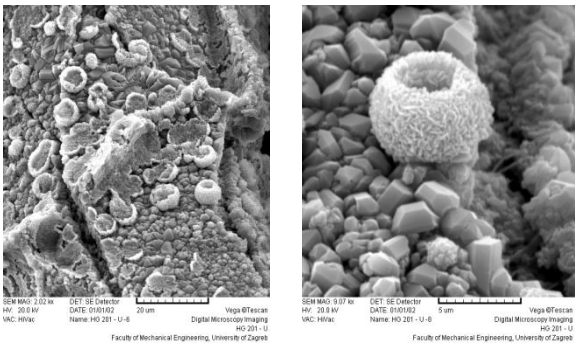

Fig.3. SEM micrographs of the surfaces of the HG20 after soaking in HBSS for 28 days.

References:

1.H. Ivankovic, G. Gallego Ferrer, E. Tkalcec, S. Orlic and M. Ivankovic: Preparation of highly porous hydroxyapatite from cuttlefish bone, *Journal of Materials Science: Materials in Medicine*, 20(2009) 1039-1046.

2.H. Ivankovic, E. Tkalcec, S. Orlic, G. Gallego Ferrer, Z. Schauperl: Hydroxyapatite formation from cuttlefish bones: Kinetics, *Journal of Materials Science: Materials in Medicine* ; 21(2010) 10, 2711-2722.

Polymer Brushes Grafted on Polymer Foils as Platforms for Enzyme Immobilization

Sonja Neuhaus[1,2], *Celestino Padeste*[1], *Nicholas D. Spencer*[2]

[1]Laboratory for Micro- and Nanotechnology, Paul Scherrer Institut, 5232 Villigen PSI, Switzerland
[2]Laboratory for Surface Science and Technology, ETH Zurich, 8093 Zurich, Switzerland

sonja.neuhaus@psi.ch

Introduction

Grafting of polymer brushes is a versatile method for surface modification, as the thickness and functionality of the created layer can be varied over a wide range. The flexible extended interface created by the polymer brush significantly enhances the possibilities for enzyme immobilization compared to modified flat surfaces. With the strategy presented in this contribution, polymer brushes with a large variety of functional groups can be produced on an inert but flexible substrate. Different strategies for the immobilization of horseradish peroxidase (HRP) or microperoxidase (MP) were evaluated by assaying the enzymatic activity with colorimetry (Figure 1).

Materials and Methods

Polymer brushes were grown from poly(ethylene-*alt*-tetrafluoroethylene) (ETFE) foils. (Hydro)peroxide radicals for the initiation of a free radical polymerization were created by exposure of the foils to EUV light at the Swiss Light Source (SLS) or by activation with cold, atmospheric-pressure helium plasma [1]. The strong covalent attachment of the grafted chains and the excellent chemical stability of the substrate allowed for modification of the functional groups when necessary. For instance, poly(vinylformamide) brushes were hydrolyzed to yield a weak positively charged polyelectrolyte (PEL) brush and poly(glycidyl methacrylate) (PGMA) brushes were derivatized with metal chelating groups via ring opening of the epoxide.

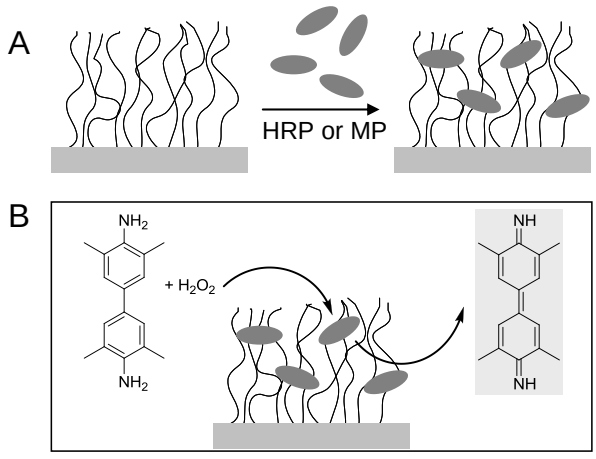

Figure 1: Strategy for testing the activity of HRP immobilized in polymer brushes. A) Immobilization; B) addition of the substrate (tetramethylbenzidine, TMB); enzymatic activity yielded a coloured product which can be quantified colorimetrically.

Results and Discussion

In a first approach, polymer brushes of different wettability and polyelectrolyte character were prepared in order to study the physisorption of enzymes. As an example, MP was loaded into a poly(acrylic acid) brush of variable thickness (Figure 2). Strong enzymatic activity was observed and the polymer brush was stained blue by the reaction product, while the adjacent area consisting of pristine ETFE remained colourless. Therefore, immobilization occurred exclusively in the brush. Moreover, thicker brushes were more intensely stained, indicating that a larger amount of enzyme was immobilized.

Another strategy was focused on the exploitation of metal affinity binding of proteins [2]. To this end, PGMA brushes were derivatized with strong metal chelating groups for the complexation of Cu^{2+} or Ni^{2+}. The contribution of metal affinity interactions to the immobilization of HRP will be assessed by conducting tests in the presence and absence of complexed metal cations.

Conclusion and Outlook

The versatility of the presented polymer brush preparation method was used for studying different parameters affecting enzyme physisorption or enzyme binding via metal affinity interactions. The influence of the local chemistry in the polymer brush on the activity of the immobilized enzyme will be investigated in further studies.

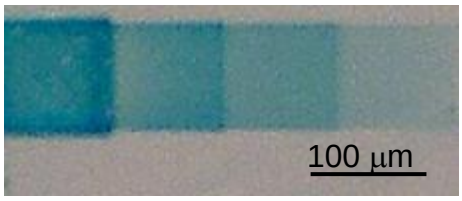

Figure 2: Microscopy image of an array of squares grafted with poly(acrylic acid) brushes. MP was immobilized in the brush and assayed with TMB whereby the brush was stained by the blue reaction product. The staining of the brush decreased with brush thickness from left to right.

References

[1] S. Neuhaus, C. Padeste, H. H. Solak, N. D. Spencer, *Polymer* **2010**, *51*, 4037.

[2] J. H. Dai, Z. Y. Bao, L. Sun, S. U. Hong, G. L. Baker, M. L. Bruening, *Langmuir* **2006**, *22*, 4274.

Photochemicaly promoted degradation of poly(epsilon-caprolactone)

Katarina Borska, Martin Danko, Ivica Janigova, Jaroslav Mosnacek

Polymer Institute, Center of Excellence GLYCOMED, Slovak Academy of Sciences, Dubravska cesta 9,845 41 Bratislava, Slovakia

e-mail: katarina.borska@savba.sk

Introduction: Studies aimed at controlling of degradation rate of biodegradable polymer materials are of great importance for biomedical or environmental applications[1,2]. Photochemical effects of low molecular weight benzil (1,2-diphenylethandion) doped in biodegradable polyester poly (ε-caprolactone) (PCL) have not yet been studied. The aim of this work was to monitor the photochemical degradation of PCL in the presence of benzil as photoactive dopant using infrared spectroscopy and gel permeation chromatography (GPC).

Materials and methods: Polymer films of 40 μm thickness were casted from chloroform solution on a 10 cm^2 glass plate. The concentration of doped benzil (BZ) in PCL matrix was 7 wt%. Irradiation of polymer films with light of λ> 400 nm was carried out by medium pressure mercury lamp in Spectramate (Ivoclar AG, Schaan, Liechtenstein, 350 to 530 nm) in combination with UV CL SR HPR plastic filter (LLumar, USA). Samples were inserted into the glass finger cooled with water to prevent heating of the sample during irradiation.

The PCL/bz samples were characterized by gel permeation chromatography (GPC) and Fourier transmission infrared spectroscopy (FTIR).

Results and discussion: Benzoyl peroxide is product of photooxidation of benzil in solid polymer matrices after irradiation with light at wavelength λ> 400 nm [3-5]. During the irradiation of the polymer at this wavelength in the air a decreasing of the characteristic stretching band of 1,2-dicarbonyl groups of BZ at 1660-1690 cm^{-1} in the IR spectra was observed (Fig.1).

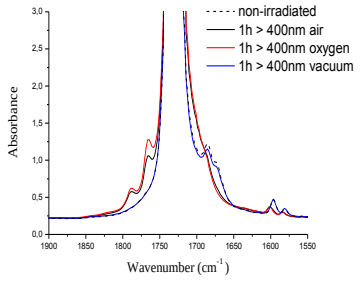

Figure 1: FTIR spectra of PCL/bz films after 1 h irradiation in Spectramate at λ> 400 nm at room temperature.

Nearly quantitative conversion of benzil was visible after 1 h of irradiation. Decay of vibration band of dicarbonyl groups at 1660-1690 cm^{-1} in FTIR spectra was accompanied by the appearance of two new vibrational bands at 1750-1800 cm^{-1} corresponding to benzoyl peroxide.

From FTIR spectra of the films irradiated at λ> 400 nm in the air or under oxygen atmosphere was clear that at higher oxygen concentration the amount of formed benzoyl peroxide was higher. On the other hand, in the film irradiated under vacuum, the benzoyl peroxide related bands did not arise at all. Comparing the elution curves (Fig. 2) showed that the extent of degradation of the PCL increased with increasing oxygen concentration. In contrast, increase in molecular weight with partial gellation due to the recombination of polymer radicals was observed during irradiation under vacuum.

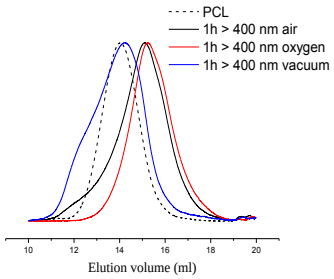

Figure 2: GPC elution curves of PCL/bz films after 1 h irradiation in Spectramate in air, oxygen, vacuum at λ> 400 nm at room temperature.

Based on these observations, we assume that under vacuum the abstraction of hydrogen from PCL chain by benzil in the excited state with subsequent recombination of created macroradicals was occurred. In the presence of oxygen two competitive processes could take place – photoperoxidation of benzil and hydrogen abstraction from the PCL chain. Results showed that increasing oxygen concentration led to higher yield of benzoyl peroxide and thus lower extent of hydrogen abstraction. However, the extent of degradation of PCL was higher. The reason is that even though less macroradicals is formed by hydrogen abstraction by benzil in excited state, in the presence of higher oxygen concentration the macroradicals reacts with the oxygen and subsequent degradation of polymer is occurred. During this process new macroradicals are formed which leads to multiplying the effect of degradation.

References: [1] Nair L. S., Laurencin C. T.: Prog. Polym. Sci., 32 (2007), 762 – 798.
[2] Han C., Ran X., Su X., Zhang K., Liu N., Dong L.: Polym. Int., 56 (2007), 593 – 600.
[3] Lukáč I., Kósa Cs.: Macromol. Rapid Commun., 15 (1994), 929 – 934.
[4] Kósa Cs., Lukáč I., Weiss R.: Macromol. Chem. Phys., 200 (1999), 1080 – 1085.
[5] Mosnáček J., Weiss R. G., Lukáč I.: Macromolecules, 37 (2004), 1304 – 1311.

Acknowledgement. This contribution is the result of the project implementation: Centre for materials, layers and systems for applications and chemical processes under extreme conditions Stage II supported by the Research & Development Operational Program funded by the ERDF. The authors thank Grant Agency VEGA for funding projects 2/0097/09 and 2/0074/10.

Gene Vectors with Anticancer Drugs Based on DNA-Polycationic Complexes

N. Kasyanenko[1], L. Lysyakova[1], O. Nazarova[2], E. Panarin[2]

[1] Department of Molecular Biophysics, Faculty of Physics, Saint Petersburg State University, 198504 St. Petersburg, Peterhof, Ulianovskaya str. 1, Russia;

[2] Institute of Macromolecular Compounds, Russian Academy of Science, 199004 St. Petersburg, Bolshoy pr. 31, Russia

nkasyanenko@mail.ru

Introduction

DNA complexes with synthetic polycations are the well-known objects for the manipulation in biotechnology. They are perspective for gene therapy of different diseases, including cancer. Most anticancer drugs have serious negative side effects. The combining of drug efficiency and targeted delivery by means of gene vectors opens up new perspectives in cancer therapy. DNA is the main target for one of the best anticancer drugs cisplatin, *cis*-$PtCl_2(NH_3)_2$. The construction of gene vectors with coordination platinum compounds is of great interest. The use of gene vectors allows avoiding the drug binding to other biological components on the way to reach DNA thus enhancing the selectivity of chemicals.

Materials and methods

Calf thymus and plasmid DNA binding with the coordination platinum compound cis-diamminedichloroplatinum (cis-DDP) in the presence of polycations and DNA-polycation interaction in 0,005 M NaCl were studied by Viscometry, Circular Dichroism, UV spectroscopy, Dynamic Light Scattering, Atomic Force Microscopy, Electrophoresis. Linear polymer polyallylamine (PAA) and graft-copolymer of N-methacryloilamino-D-glycose and N, N-dimethylaminoethylmethacrylate (MAG-g-DMAEM) 30:70 mol. % were used.

Results and Discussion

It was shown that the coordination of cis-DDP to DNA does not prevent the formation of interpolyelectrolyte complex DNA-polycation and the construction of gene vectors. The size of formed nanoparticles estimated by atomic force microscopy and dynamic light scattering showed that the complexation of DNA with cis-DDP does not affect the size of gene vectors.

Conclusions

The formation of gene vectors with the inclusion of anti-cancer drug cisplatin was regarded revealing the new potential in antitumor treatment. Besides, this result indicates that any modification of DNA by the linkage with coordination compounds is possible for further application in nanotechnologies based on DNA packaging.

Cisplatin PAA

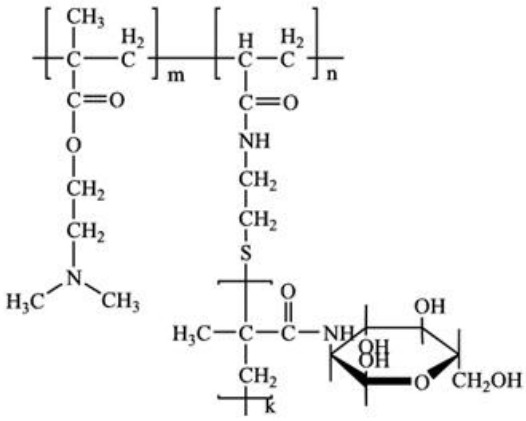

MAG-g-DMAEM

Structures of compounds under the study

Synthesis and the Characterization of Poly(L,L-lactide)-b-Poly(ethylene glycol) diblock copolymers as plasticizers and their effect on the hydrophilicity of the polymer matrix to promote cellular affinity

Giada Lo Re[1], Franck Meyer[2], Jean-Marie Rasquez[2], Philippe Dubois[2], Roberto Scaffaro[1]

[1] Dipartimento di Ingegneria Industriale, University of Palermo, Viale delle Scienze, ed. 6, 90128 Palermo, Italy
[2] Service des Materiaux Polymeres et Composites, University of Mons-Hainaut, Place du Parc 20, B-7000 Mons, Belgium

roberto.scaffaro@unipa.it

Introduction

Biopolymer-based scaffolds can stimulate isolated cells to regenerate tissue with defined size and shape. Consequently, they have been studied as supports for cell transplantation both *in vitro* and *in vivo* [1]. Due to their known biocompatibility and their modular kinetics of degradation, polylactides (PLA) are currently studied as potential materials to obtain three-dimensional structures for tissue engineering applications. In order to enhance their flexibility and resilience, to tune the degradation rate and to promote the surface hydrophilicity of the PLA-based scaffold, studies have been carried out on the possible modification of PLA bulk and surface, including blending and copolymerization with polyethylene glycol (PEG) [2]. In addition to biocompatibility, PEG can be also used to eliminate or at least to minimize the adsorption of proteins via steric repulsion [3]. The study includes the synthesis and the characterization of poly(L,L-lactide)-b-poly(ethylene glycol) diblock copolymers as plasticizers and their effect on the leaching properties and on the hydrophilicity of the polymer matrix to promote cellular affinity. These diblock copolymers were obtained by metal-free ring-opening polymerization of lactide from a ω-hydroxy PEG macroinitiator at room temperature [4].

Materials and Methods

To synthesize PEG-PLA block copolymers, ring opening polymerization (ROP) of L,L-lactide (LA) was initiated from a monohydroxylated PEG segment (polyethylene glycol monomethyl ether, CH3PEG5000 Mn=5 kDa, polyethylene glycol monomethyl ether, CH3PEG2000, Mn = 2 kDa) or dihydroxylated PEG (PEG4600 Mw = 4.6 kDa and PEG200 Mw = 2 kDa) using organic DBU as catalyst. L,L-lactide was gifted by PURAC. The monohydroxylated PEG segment were supplied by Fluka-Chemicals. The dihydroxylated PEG segment and DBU were supplied by Sigma-Aldrich. MALDI-ToF, MS, 'H NMR spectrometry and Gel Permeation Chromatography (GPC) were adopted to estimate the molar ratio between both blocks, the polymerization degree and the molecular weight of the block copolymers. The coexistence and the interactions between the different phases have been evaluated by Differential Scanning Calorimetry (DSC) and Thermogravimetric Analysis (TGA). The morphological characterization of the materials produced was performed by Scanning Electron Microscope (SEM).

Results and Discussion

The GPC results suggest that the polymerization takes place rapidly and that it is possible to achieve the desidered polymerization degree in less than than 30 mins. The polydispersity index, very close to 1.0, indicates that the experimental conditions adopted for performing the synthesis are appropiate to obtain almost single molecular weight copolymers.

Looking at the calorimetric results, it can be observed a strict correspondence between the glass transition temperatures of monohydroxylated CH3PEGs and the corresponding copolymers. In particular, the Tg recorded for CH3PEG5000 is -34.7 °C, close to that found for CH3PEG5000-b-PLLA5000. For CH3PEG2000-b-PLLA2000 it was observed a Tg of -46.4 °C while the Tg of the corresponding PEG is -47.8 °C. As regards the melting temperatures, there is a correspondence between the values recorded for the commercial monohydroxylated PEG used in the synthesis and the values of the first peak of the heating curves of the copolymers. These results indicate that the macroinitiator did not undergo any degradation/modification during the synthesis. TGA data show two distinct degradation peaks associated with the two blocks. In particular, a first peak at 326.3 °C for CH3PEG5000-b-PLLA5000 and at 290.8 °C for CH3PEG2000-b-PLLA2000 that can be attributed to the block of lactide. The onset values recorded for the copolymer with lower molecular weight are, as expected, lower. The second degradation step occurs at about the same temperatures of onset, and may be attributed to the PEG block. The residues measured at 360 °C and at 600 °C confirm the correct proportion between the two blocks.

Conclusions

The copolymers synthesized in the frame of the present work presents properties that are compatible with applications in tissue engineering. Preliminary studies to assess the cytotoxicity of the materials produced are ongoing to evaluate the vitality of SK-Hep1 cells seeded and grown *in-vitro*.

References

1. Shoichet, M., Macromolecules, 4: 581–591, 2010
2. Rasal, R. *et al.*, Progress in Polymer Science, 35, 338–356, (2010).
3. Jeon, S.I. *et al.*, J Colloid Interf Sci, 142: 149-158, 1991
4. Jerome, C. *et al.*, Advanced Drug Delivery Reviews, 60 (9): 1056-1076, 2008

The Role of Poly(ethylenglycol) Molecular Weight on Viability and Cell Adhesion in Polylactide-based Scaffolds

Giada Lo Re[1], *Roberto Scaffaro*[1], *Silvia Rigogliuso*[2], *Giulio Ghersi*[2]

[1]Dipartimento di Ingegneria Industriale, University of Palermo,Viale delle Scienze, ed. 6, 90128 Palermo, Italy
[2]Dipartimento di Biologia Cellulare e dello Sviluppo, University of Palermo,Viale delle Scienze, ed. 16, 90128 Palermo, Italy

roberto.scaffaro@unipa.it

Introduction

The purpose of this study is to evaluate a method combining melt-blending and leaching techniques for the preparation of a highly interconnected three-dimensional polymeric porous scaffold [1]. More specifically, sodium chloride (NaCl) and poly(ethylenglycol) (PEG) will be used as water soluble porogens to form porous Poly(L,D-lactide) (PLA) and plasticized PLA-based scaffolds, solvent free, designed for applications in field of tissue engineering [2]. This study set out to investigate the effect of processing of polylactide-based blends, on the simultaneous bulk and surface modifications and different pore architectures obtained. The effects on the viability and cell adhesion will be assured too.

Materials and Methods

Blends of PLA and PEG in the presence of NaCl were prepared by Brabender PLE-330 (operating conditions with T=190°C, t=10 minutes, composition PLA:PEG:NaCl=20:5:75 by weight) and then leached in boiling distilled water for 3 hours. We correlated the pores architecture with the preparation of the materials by changing the molecular weight of PEG. Image analysis - based on the elaboration of SEM micrographs detecting back secondary electrons diffusion (BSED) - were coupled with other analysis methods to ascertain the real pores architecture of the scaffolds. The morphological results were therefore correlated with in vitro adhesion, proliferation and viability tests on human SK-Hep1 hepatocarcinoma cells.

Results and Discussion

The SEM results obtained confirm the feasibility of a method of preparing three-dimensional porous and interconnected structures that combines the techniques of working with molten mixtures of polymeric and composite materials of thermoplastic and leaching.

In order to evaluate the effects performed by different PLA-PEG scaffolds on SK-Hep1 cells viability we have firstly tested if morphological exchange in direction to apoptotic/necrotic phenotypes occur. As shown in Fig. A Sk-Hep 1 cells cultured together scaffolds containing PLA (Fig. A-c) with different molecular weight of PEG (Fig. A-d, e and f) did not show difference with respect to the control (Fig. A-a) in which cells were cultured in absence of scaffolds; on the contrary SK-Hep 1 cultured together Doxorubicin (apoptotic inducer) shown (Fig. A-b) classical morphological exchanges of apoptotic cells. However, a minimal of cell died (<3%), evaluated by Tripan Blue, physiologically occur during SK-Hep 1 cell culture in absence or presence of scaffolds as shown in Fig. B. To further validate this data, was performed an enzymatic assay using a specific substrate for Caspase 3. Fluorocrome extinction kinetic value, here not reported for the sake of brevity, shows that cells grown in the presence of the respective scaffolds do not exhibit caspase activity, because they have not been able to cut the substrate as it has been able to do the positive control, cells SK-Hep 1 in which apoptosis was induced by Doxorubicin 10 μM.

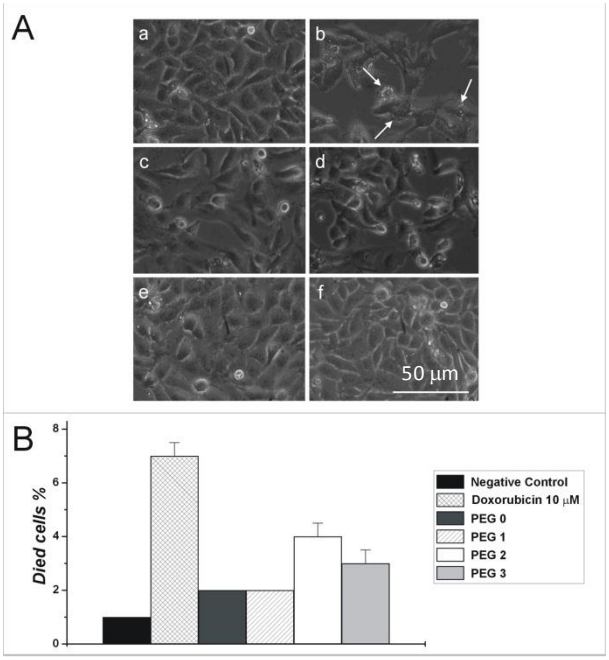

Conclusion

The solubilization of crystalline phase (NaCl) and phase hydrophilic polymer (PEG) has made porous and interconnected matrix biocompatible polylactide (PLA), without the help of toxic solvents, making, therefore, the resulting three-dimensional structures suitable for applications in the field of tissue engineering. Viability and adhesion assays demonstrate that PEG-based scaffolds are well biocompatible to SK-Hep 1. Moreover the treatment of scaffolds with PEG shown to change the adhesive capability, thar are comparable to those obtained when scaffolds are treated with ECM components as type-I collagen.

References

1. Reignier, J. *et al*., Polymer, 47:4703-4717, 2006

2. Shoichet, M., Macromolecules, 4:581-591, 2010

PLA nanocomposites reinforced by cellulose nanowhiskers: Influence of the preparation on the final properties

B. Ruelle, L. Bonnaud and Ph. Dubois

CIRMAP – Materia Nova

Benoit.ruelle@materianova.be

Keeping in mind environmental problems and the consequence of the fossil resources rarefaction, a new category of materials has been developed over the last years: the cellulosic bionanocomposites which designate biopolymer combinated with cellulosic nanofillers. Besides the low cost of the raw material, the use of cellulose nanoparticles as a reinforcing phase in nanocomposites has numerous advantages such as low density, high availability through the world, high specific properties, reactive surface or biodegradability of the cellulose [1]. However, the cellulose nanoparticles present also some disadvantages, mainly, high moisture absorption, relative low degradation temperature and incompatibility with hydrophobic polymers due to strong hydrophilic interactions between nanoparticles.

The main focus of this work is to characterize polylactide (PLA) nanocomposites reinforced by cellulose nanowhiskers extracted from ramie (CNW) prepared through different ways such as chloroform casting, reactive extrusion and compatibilization of the cellulose surface with PLA chains grafting. The mechanical properties of the different (nano)composites were characterized by DSC and DMA. Their barrier properties were also determined and the degree of CNW dispersion was evaluated by high resolution transmission microscopy.

[1] G. Siqueira, J. Bras and A. Dufresne, "Cellulosic Bionanocomposites: A Review of Preparation, Properties and Applications," Polymers, vol. 2, n°. 4, 728-765, 2010.

Novelty linear (N-ethyl pyrrolidine methacrylamide-co-1-vinylimidazole) copolymers for gene therapy applications

D. Velasco[1], G. Réthore[2], B. Newland[2], J. Parra[4], C. Elvira[1], A. Pandit[2], L. Rojo[3], J. San Román[1]

[1]Instituto de Ciencia y Tecnología de Polímeros (ICTP), CSIC, Madrid, Spain
[2]Network of Excellence for Functional Biomaterials (NFB), NUI Galway, Ida Business Park, Galway, Ireland
[3]Department of Materials, Imperial College London, London, SW7 2AZ, United Kingdom
[4]Unidad de Investigación CHA-CSIC. Hospital Provincial de Ávila (SACYL). CIBER-BBN, Jesús del Gran Poder, Ávila, Spain

Introduction

Proton-sponge polymers are known to be part of the best available off-the-shelf materials for gene delivery [1]. However, they suffer from several drawbacks due to their high cytotoxicity. In this sense, it is primordial to design enhanced biocompatible materials which mimic proton-sponge mechanism necessary for buffering the pH and improving endosomal escape efficiency without increasing toxicity.

Our approach is based on the combination of a cationic polymer derived from pyrrolidine and imidazole moieties in order to increase the biocompatibility and the transfection efficiency. For these reasons, it has been developed novel linear copolymers combining *N*-ethyl pyrrolidine methacrylamide (EPA) and 1-vinilimidazole (VI) properties (Figure 1). Throughout this presentation, synthesis, characterization, composition-cytotoxicity relationship and blood compatibility studies of these novel linear copolymers will be reported as well as their evaluation as possible carriers for gene delivery.

Materials and methods

The EPA monomer was prepared as previously reported [2] and the 1-vinilimidazole monomer was purchased from Sigma. Poli(EPA-co-VI) copolymers were obtained by free radical polymerization from molar ratio feed of EPA/VI monomers of 80:20, 50:50 and 20:80 respectively. Microstructural analysis were carried out by ^{1}H-NMR and ATR-FTIR spectroscopy whereas molecular weight, glass transition temperature (Tg) and pH buffering capacity of the (EPA-co-VI) copolymers were determined by Size Exclusion Chromatography (SEC), Differential scanning Calorimetry (DSC) and acid-base titration respectively. *In vitro* cytotoxicity and blood compatibility of the (EPA-co-VI) copolymers were evaluated by MTT, platelet activation, complement system, plasma clotting time, red blood cells aggregation and haemolysis essays following standardized protocols. Finally, w/wo serum media DNA complexation ability with plasmid gaussian luciferase (pGLuc) and transfection efficiency of the pGLuc-(EPA-co-VI) polyplexes were evaluated using 3T3 cells, after 48 hours of incubation. Linear poly (dimethylaminoethyl methacrylate) (10 kDa, PDI: 1.097) [p(DMAEMA)] [3] was used as positive control.

Results and Conclussions

High conversion Poli(EPA-co-VI) copolymers were obtained by free radical polymerization reactions with 70% yield. The ^{1}H-NMR spectra confirmed the structure shown in *Figure 1* for the copolymeric systems with calculated molar fractions of 0.84/0.16, 0.57/0.43 and 0.19/0.43 for 80:20, 50:50 and 20:80 EPA:VI monomeric units respectively. The pK_a values of the copolymers indicate that it was possible to increase the buffering capacity compared to the homopolymer of EPA and are partially protonated at physiological pH.

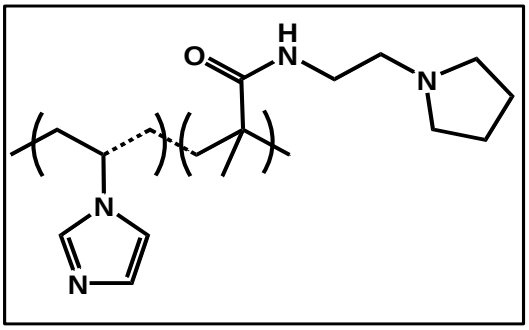

Fig 1. Structure of (*N*-ethyl pyrrolidine methacrylamide-co-1-vinylimidazole) copolymer [Poly (EPA-co-VI].

Finally the Tg values obtained are remarkable higher than the physiological temperature. The Gel Retardation Electrophoresis shows that the copolymers were able to complex with DNA at different N/P ratios, obtaining polyplexes with a proper size for internalization into the cells (200-300 nm), which are stable in solution (10-25 mV). Blood compatibility (data not shown) studies revealed that the copolymers are biocompatible. In addition, MTT assay (data not shown) showed that the cytotoxicity increases when EPA monomer increased in the composition of the copolymer. Finally, the transfection levels (data not shown) obtained after 48 hours in serum free media are higher than the levels reported with the p(DMAEMA), and also significantly higher at high N/P ratios when transfection experiments were carried out in serum media which make these copolymers an attractive transfection reagent for serum-sensitive cell lines.

References

[1] Sh. Asayama, T. Sekine, H. Kawakami, Sh. Nagaoka. Design of aminated poly (1-vinylimidazole) for a new pH-sensitive polycation to enhance cell-specific gene delivery, Bioconjugate Chem., 2007, 18, 1662-1667.

[2] D. Velasco, C. Elvira, J. San Román. New stimuli-responsive polymers derived from morpholine and pyrrolidine. J Mater Sci: Mater Med 2008, 19, 1453–1458.

[3] B. Newland, H. Tai , Y. Zheng, D. Velasco, A. Di Luca, S. M. Howdle, C. Alexander, W. Wang, A. Pandit, A highly effective gene delivery vector-hyperbranched poly (2-(dimethylamino) ethyl methacrylate) from in situ deactivation enhanced ATRP. Chem. Co

Polymer-Cooperative Blocking the Viruses: Cholesten Modified Polyanions for Raft-tropic Antivirals

Alexander V. Serbin1,2, Yuri A. Egorov 1, Ekaterina N. Karaseva1,2, Olga L. Alikhanova1, Vladimir B. Tsvetkov1,2

1Biomodulators RC, Health RDF, Moscow, Russia
2Topchiev Institute of Petrochemical Synthesis, RAS, Moscow, Russia

e-mail: serbin@ips.ac.ru

Introduction

An analysis of the modern evidence of cholesterol enriched micro(nano)domains of plasma membrane, the so-called **rafts**, leads to understanding a crucial role of the rafts in viral entry into cells for no less than 80% cases of known human viruses infections. Since the rafts are natural epicenters (portals) of the enhanced risks for viral interventions, we accept the raft-targeting macromolecular design as one of key strategy for the viral entry prevention [1]. Here we report a synthesis and evaluation of the cholesterol-related anchors (***Chol***) containing polyanions derived from graft-modified alternating copolymers of maleic anhydride within the general formula **1**, fig.1.

Synthesis

The purposed synthesis was carried out by scheme:

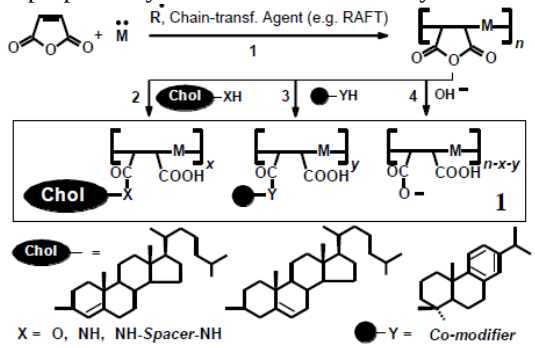

Fig.1. Scheme of synthesis

The **step 1** (free radical alternating copolymerization) assigned the –M– nature, polymerization degree and polydispersity; the **steps 2-3** (grafting in anhydrous media) determined the degree of the modification by the ***Chol*** (*x/n*, step2) and, if it was required, by co-modifiers (*y/n*, step3). The **step 4** (hydrolysis in aqueous $NaHCO_3$) resulted in acid salts, the water-soluble anionic polyelectrolytes **1**. The needed ***Chol*** content (>1< several units per macromolecule) was controlled on the step 2. For the etherification (X = O) the *x/n* grade was predictable from the early studied kinetic data [2]. The aminolysis (X = NH/NH-Spacer-NH) provided the needed grade by the initial concentrations $[RNH_2]_0$: [Anhydride units]$_0$ = *x/n* due to a quantitative yield. To regulate a distance between the ***Chol*** and polymeric chain the various spacers were inserted in the ***Chol*** reagents, using, for example, the pre-synthesis:

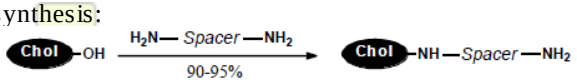

The products **1** were characterized by element analysis, IR, NMR, GPC data. Final products were carefully purified by multi-cyclic ultra filtration and separated as lyophilized samples suitable for bio-testing

Safety and Antiviral Effectiveness

The evaluations of the synthesized products series **1** demonstrated, that grafting the one ***Chol*** unit per anionic macromolecule (*x* ~ 1-2) resulted in minimal toxicity *in vitro* (CC_{50} >1500 μg/ml, MT4, Hella cells), comparable with one of the non-modified (*x* = 0) precursors, whereas the *x* ~2-4 leaded to ~6-fold more high toxicity. Similar effects were observed at the too much extended hydrophobic chain of the spacer bridge between ***Chol*** and polymer backbone. From the other hand even the minimal content of ***Chol*** at optimal spacers turned the **1** into strong inhibitors of viral infection, in particular, the human immunodeficiency type 1 virus (**HIV-1**). This fact has been confirmed from independent laboratories on experimental models *in vitro* of various viral strains (see the table).

Structure (n~40, -X- = O; *y* =0)		Tox. CC_{50} μg/ml	Activity **IS**= CC_{50}/EC_{50} against the **HIV**-1 strains*				
-M-	*x*		EVK	899	AD8	NL4.3	SF162
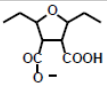	0	1500	14	76	95	63	38
	0.9	1500	-	125	-	-	-
	1.7	1500	-	**300**	**960**	**375**	240
	3.0	600	-	140	-	-	-
	3.6	250	-	< 25	125	100	80
	0	1500	260	-	-	-	-
	1.6	1500	**470**	174	240	190	170
	2.8	370	-	-	160	110	120

**The experimental data were obtained from the laboratories of: Dr. Igor V. Timofeyev (EVK strain SRBC Vector, Koltsovo, Russia); Prof. Alla G. Bukrinskaya (899 strain, Ivanovski Inst. Virol., Moscow, Russia), and Prof. Paul Clapham (AD8, NL4.3, and SF162 strains, Univ. Massachussets Med. Schoool, USA)*

The represented in the table indexes of antiviral selectivity (**IS**), as integrative criteria of antivirals safety-efficiency, reflected the antagonistic tendencies: 1) the safety lowering (enhancement of toxicity for cells), but 2) the antiviral potency amplification with enriching the polymeric molecules by the ***Chol***. It is very interesting, that maximum of IS (5-10-fold increasing) were achieved at very moderate content of the ***Chol***: ~ 1-2 units per polymer **1** molecule. Probably just 1 or 2 cholesten anchor(s) is/are optimum for virus entry blocking without detriment for cells. To understand the specifics of the polymers **1** interactions with the HIV entry mediators (viral env proteins gp120, gp41 and cell receptors CD4, CCR5, CXCR4) within the raft locus, we initiate a computational modeling on base on molecular dynamics and docking techniques.

Conclusion

The proposed raft targeting strategy through the cholesten – modified polymers synthesis is promising way toward new antiviral agent developments.

References: 1. *A.Serbin, et al., Antivir Res 2003; 57(3):50; 2007, 74(3):49.* **2**. *A.Serbin, et al., Polym Sci (Moscow) 1989, A31(9):1975-81*

Protein Nanoreactors for Atom Transfer Radical Polymerization

K. Renggli, G. Kali, N. Bruns

Department of Chemistry, University of Basel, Klingelbergstrasse 80, CH-4056 Basel, Switzerland.

Kasper.Renggli@unibas.ch

Chemical reactions can be confined to nanoscale compartments by encapsulating catalysts in hollow nanoobjects. Such reaction compartments effectively become nanoreactors when substrate and product are exchanged between bulk solution and cavity (Figure 1). Nanoreactors hold promise for applications ranging from selective and size-constrained organic synthesis to biomedical advances (e.g., artificial organelles, biosensing) and as analytical tools to study reaction mechanisms.[1]

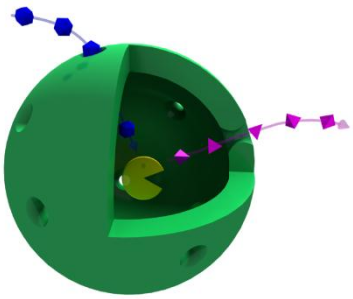

Fig. 1: Schematic of a nanoreactor, where substrate and product are exchanged between bulk solution and cavity.

Atom transfer radical polymerization (ATRP) has emerged as one of the most powerful synthetic techniques in polymer science. Similarly to other controlled radical polymerization (CPR) methods, it allows the synthesis of polymers with predetermined molecular weight, narrow molecular weight distribution, as well as desired composition and molecular architecture.[2] ATRP is a metal complex-mediated reaction with copper-based catalysts being most commonly used. Recent advances have provided access to polymers with protein-reactive end groups synthesized by ATRP and other CPR methods. Conjugates have also been prepared by polymerizing directly from the proteins. To the best of our knowledge, preparation of protein catalyst conjugates for ATRP have not yet been reported.

In our work we successfully grafted ATRP catalysts into the thermosome (THS), an archaeal chaperonin, and used the resulting conjugates as nanoreactors for ATRP polymerization. THS possesses built-in lids that cover the central cavities (Figure 2). The gated pore is large enough (up to approximately 10 nm in diameter) to allow the uptake of guest molecules into the cavity. The lids are formed by helical protrusions at the tip of the apical domain of the subunits. Their opening and closing proceeds in a two stroke-cycle, in which one ring opens in a cooperative movement while the other ring closes. The conformational changes are driven by the hydrolysis of ATP. Depending on the experimental conditions, fully closed or open conformations are obtained as well. THS uses an iris-like conformational change, where apical and intermediate domains rotate in a coordinated manner to close off access to the central cavity.

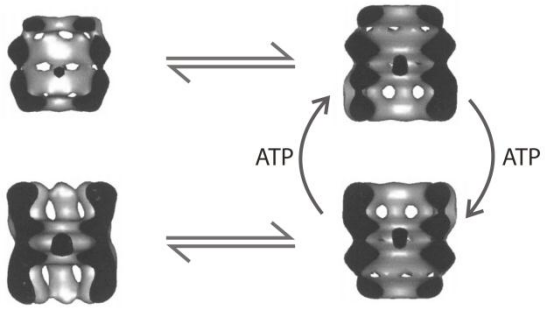

Fig. 2: Cut away models of a thermsosome based on cryo-electron microscopy data.[3]

Here we present an easy and efficient way to couple copper-based catalysts to THS. The resulting nanoscale catalyst enables ATRP in pure water and greatly enhances control over the polymerization.

References: [1] Renggli et al. *Adv. Funct. Mater.* **2011,** in press. [2] N. Tsarevsky and K. Matyjaszewski, *Chem. Rev.* **2007, 107**:2270-2299. [3] G. Schoehn et al. *J. Mol. Biol.* **2000, 301:**323–332.

Acknowledgements: We thank Farzad Seidi, Martin Rother and Severin Sigg for helpful discussions on the synthesis and characterization of the polymers. Nico Bruns gratefully acknowledges the Marie Curie Actions of the European Commission for an Intra-European Fellowship.

Amino functionalization of poly(lactic-co-glycolic acid) (PLGA) films with low-temperature plasma treatments

Claudia Riccardi[1]; Stefano Zanini[1]; Elisa Grimoldi[1]; Elisabetta Ranucci[2]; Amedea Manfredi[2]; Silvia Maria Doglia[3]; Antonino Natalello[3]

[1] Dipartimento di Fisica "G. Occhialini", Università degli Studi di Milano-Bicocca, p.za della Scienza, Milano Italy
[2] Dipartimento di Chimica Organica e Industriale, and Centro Interdisciplinare Materiali e Interfacce Nanostrutturati (CIMAINA) Università di Milano, via Venezian 21, Milano, Italy
[3] Dipartimento di Biotecnologie e Bioscienze, Università degli Studi di Milano-Bicocca, p.za della Scienza, 2 Milano ITALY

Introduction

Poly(α-hydroxy acids), which includes poly(lactic acid) (PLA), poly(glycolic acid) (PGA) and their copolymer poly(lactic-*co*-glycolic acid) (PLGA), are some of the most widely used synthetic polymers in biomedical applications. Due to its biocompatibility and biodegradability, PLGA has been widely employed in the areas of surgical sutures, controlled release and tissue engineering (for example in orthopedic devices, where high mechanical strength and toughness are required). However, the hydrophobicity and the lack of functional groups on the surface of PLGA are general drawbacks, which restrain its applications. For example, the absence of recognition sited for cells on its surface, which affect cell attachment and growth, represents a limitation for the use of PLGA in tissue engineering. Furthermore, the lack of functional groups prevents the use of unmodified PLGA in directed adhesion and targeted drug delivery applications. Recent works on different poly(α-hydroxy) acids have demonstrated that both oxygen and ammonia plasma treatments modify their hydrophilicity and morphology, leading to an enhanced cell affinity.

Materials and Methods

This work deals with the surface modification of PLGA films by means of nitrogen/hydrogen mixtures plasmas. N_2/H_2 plasmas are often utilized for the introduction of amino groups onto polymeric substrates such as poly(ethylene) and poly(styrene). However, the effect of such kind of plasmas on biodegradable poly(α-hydroxy acids) has not been studied. Chemical modifications were monitored by contact angle measurements, attenuated total reflection Fourier transform infrared spectroscopy (ATR-FTIR) and X-ray Photoelectron Spectroscopy (XPS). Morphological modifications were assessed with atomic force microscopy (AFM) analyses. Finally, the density of the inserted primary amino groups was determined by means of fluorescence labeling with fluorescamine.

Results and Discussion

XPS analysis confirms the introduction of N-containing functional groups owing to plasma exposure of the PLGA films. In fact, the N1s peak appears in the spectrum of the treated sample. From XPS results, some considerations about the efficiency of the plasma treatments can be drawn:

1. The N/C ratio (which is equal to zero for untreated PLGA) ranges between 0.027 and 0.045, depending on the adopted operating parameters. From a quantitative point of view, these results are similar to that obtained previously with NH_3 plasma.
2. The N/C ratio increases by increasing the N_2 flow, the power input and the treatment time

The introduction of nitrogen containing functionalities results in an increased hydrophilicity of the PLGA films, as assessed by the decrease of the water contact angle.

A reliable methodology for the quantification of primary amino groups onto plasma treated polymeric materials is their labelling with fluorescamine, a non-fluorescent compound that selectively reacts with primary amino groups yielding a fluorescent product. The fluorescence intensity of the treated sample (measured at 475 nm) allow us to determinate, by difference with that of the untreated one, the surface density of primary amino groups. As previously reported, mixtures with N_2/H_2 ratios of 1:2 and 1:3 are more efficient for the introduction of primary amino groups. For these mixtures we obtained an amino groups surface density of about 1.3 groups/nm^2.

The morphological changes on the PLGA film surface owing to the plasma treatment were evaluated by means of AFM analyses. A surface patterning owing to the plasma exposure can be easily detected. The formation of such surface structures, probably deriving from differential etching of the PLGA surface, is potentially interesting for biomedical applications because of, for example, surface roughness and topography can influence cell attachment and proliferation onto solid substrates.

Conclusions

We investigated the chemical and morphological changes owing to N_2/H_2 plasma treatments of PLGA films, with particular attention to the quantification of the inserted primary amino groups. Our results demonstrates the possibility of a chemical functionalization of PLGA with NH_2 groups, which can influence the cell behavior on the modified polymer or can be exploited for chemical grafting of bioactive molecules. Morphological changes owing to the plasma treatment were also detected.

Effect of Photo, Thermal and Biodegradation on Molar Mass and Crystallization of Polylactide

L. Santonja-Blasco[a-b], *A. Ribes-Greus*[b], *R. G. Alamo*[a]

[a]FAMU/FSU College of Engineering, Chemical and Biomedical Engineering Department, 2525 Pottsdamer St., Tallahassee, FL 32310-6046, USA.

[b]Instituto de Tecnología de Materiales. Universidad Politécnica de Valencia, 46022 Valencia, Spain.

lausanbl@upvnet.upv.es, alamo@eng.fsu.edu

Introduction. A large number of external agents can affect the degradation of polylactide (PLA) such as temperature, water, weathering, microorganisms, radiation etc. Degradation occurs mainly via chain excision, monitored by the decrease in molar mass. The present work investigates the effect of a thermal treatment on the crystallization kinetics of PLA in reference to those of the virgin resin. The temporal decrease of molar mass and crystallization kinetics are also investigated as a function of exposure to both photo and soil-degradation processes for extended times. A major feature of this work, with respect to prior studies, is the simultaneous study of the three major degradation routes in the same specimen for longer degradation times than previously reported.

Materials and Methods. The material studied is a commercial polylactide copolymer with ~ 4% D-content manufactured by Natureworks, PLA2002D (Minnetonka, USA). Different types of samples were analyzed, the original pellets, melt pressed plates, photodegraded plates and plates degraded in soil. The plates were prepared from the original pellets by melt compression in a Collin 6300P hydraulic press at 210ºC in five pressure steps. The biodegradation was studied in soil for up to 60 months according to ISO 846-1997. Test specimens were collected from 1 to 60 months exposure and kept in a desiccator for 2 days before analyzing. Photodegradation test was carried out using an accelerated exposure system, Suntest XLS+ (Atlas) at 478 W/m^2 with a Xenon lamp with solar filter for simulating sunlight exposure in a maximum of 5100 hours of sample exposure. Specimens were collected from 400 to 5100 hours (corresponding to the Spanish average radiation exposure from 1.7 to 21.4 months) The molar mass was measured by Gel Permeation Chromatography (GPC), the crystallization and melting of the samples by Differential Scanning Calorimetry (DSC), and the linear growth rates by Optical Microscopy (OM) coupled with a Linkam hot stage.

Results and Discussion. The decrease of the number-average molar mass (M_n) with the degradation time has been assessed for all the degradation processes. The first degradation step is thermal, it takes place during melt compression of the initial pellets. The pressing procedure at 210 °C caused a very large reduction of the initial molecular weight, ~ 40% decrease (from 222K to 135K). Interestingly, the time dependence of the decrease of molar mass during biodegradation is different than for photodegradation. The temporal variation of the molar mass of soil-degraded specimens follows an exponential behavior ($M_n = M_{no}\, e^{-kt}$) where M_{no} is the initial molar mass and k the rate constant of degradation. In spite of different biodegradation conditions, the same exponential temporal functionality was reported for hydrolysis and compost biodegradation studies (1,2). Conversely, the molecular weight of specimens tested during photodegradation follows a power law relation with molecular weight ($M_n = M_{no} - At^k$). Although the algebraic variation of M_n with time in PLA photodegradation was not given in prior works, literature data obtained in similar conditions were fitted with equivalent power law functionality, in support of a difference in rate dependence between the soil and photodegradation processes. The photodegradation of PLA is faster than via soil degradation.

The effect of decreasing molar mass from both bio and photo degradation on cold crystallization temperatures (T_c) and on the linear growth rates (G) of specimens crystallized isothermally from the melt has been also studied. T_c obtained from the second DSC heating scan displays the same slight decreasing dependence with increasing time or decreasing molar mass for bio and photodegraded samples, indicative of a faster crystallization. Moreover, the linear growth rates of isothermally crystallized samples from the melt in a large range of T_c are increasing with molecular weight, as expected from the main contribution of the transport term in nucleation. The change of G with molecular weight follows for both processes a power law, characteristic of semicrystalline polymers in a wide range of molecular weights ($G = K\, M^{-1.4}$). A slightly lower value of K for photodegraded samples indicates that although chain excision is the major degradation mechanism, the functional groups generated differ in some extent. Lower values of G for photodegraded samples than for bio at equivalent molecular weights conforms to the presence of anhydride groups in specimens from the former degradation type (evidence obtained by FTIR) (3). These groups act as defects lowering the crystallization rate. Anhydride groups are absent in the biodegraded specimens. The kinetic G data have been analyzed according to secondary crystallization theory.

Conclusions. Photodegradation is a faster process than biodegradation. Differences in linear growth rates at equivalent molecular weights give evidence for characteristic functional groups in photodegraded samples, absent in other types of degradation.

References

1. Kale et al. Polymer Testing 26 (2007) 1049–1061.
2. Saha et al. Polymer Degradation and Stability 91 (2006) 1665-1673
3. Bocchini et al. Biomacromolecules 11, (2010), 11, 2919-2926.

Acknowledgements: Funding of this work by Ministerio de Ciencia e Innovación, Project ENE2007-67584-C03-02, and a FPI scholarship to LSB is gratefully acknowledged.

Chitosan and layered silicates bionanocomposites of preparation to be used as drug carrier vehicle

Itamara F. Leite[1], Samilla F. de Oliveira[2], Thaís Maria A. Marinho[3], Oscar L. Malta[4] e Suédina M. de L. Silva[5]

[1,2,3,5]Universidade Federal de Campina Grande, [4]Universidade Federal de Pernambuco

Biopolymers (chitosan) and clay minerals (montmorilonite) are common ingredients in pharmaceutical products. Although they are frequently used in their pure form, a single polymer or clay mineral often does not meet all the requirements. A way to further extend their applications is to modify biopolymers by incorporation of inorganic fillers to obtain bionanocomposites with improved properties, especially for pharmaceutical applications. Recently, the field of polymer layered silicate bionanocomposites has attracted much attention for drug delivery applications. The unique properties of the polymer layered silicate bionanocomposites such as easy degradation, biocompatibility and tunable mechanical properties are essential for pharmaceutical applications.

Chitosan (CS) is widely used as a drug delivery vehicle for control release of therapeutic agents. This polymer has been extensively used in recent years due to be non toxic and exhibit high mechanical strength, hydrophilic character, good adhesion beyond its low cost. On the other hand, the montmorillonite (MMT) is widely used in the modification of the biopolymer chitosan, since this mineral belongs to smectite family and is a promising layered silicate as delivery carrier for various drug molecules. Moreover, the negatively charged edges on the layers of MMT could interact with cationic polymer like chitosan (CS) to form unique polymer layered silicate materials having a large inter-planar spacing; and superior capability to intercalate drug molecules into the interlayer space of the (001) plane. Recently, synthesis of micro and nanocomposites with clay minerals was proposed as a novel approach to modify some of the properties of polysaccharide (chitosan), including swelling, hydrophilicity, mechanical and thermal behavior and bioadhesion. These modifications permit to obtain films of chitosan/layered silicates bionanocomposites with improved thermal and mechanical properties for use as a drug carrier vehicle.

Chitosan was obtained from Polymar (Fortaleza/Brazil) with degree of deacetylation at about 86%. A sodium Bentonite named Argel 35 was supplied by Bentonit União Nordeste (Campina Grande/Paraíba/Brazil) to the form powder with the cation exchange capacity (CEC) of 92 meq/100g.

In this work, bionanocomposites of chitosan and natural bentonite were prepared by solution intercalation using different concentrations, 5:1 and 10:1, respectively. At first a chitosan aqueous solution was prepared by dissolving powdery chitosan corresponding to desired weight ratio in 300mL of 1% (v/v) acetic acid and stirring for about 2h/45°C. A 1wt% clay suspension was also prepared by dispersing clay powder in distilled water and stirring for 10min at 50°C prior to use. The chitosan solution was then slowly added to the clay suspension at about 50°C and 1200 rpm. During the mixing process, the weight ratio of chitosan to clay was from 5:1 and 10:1 in order to control the chitosan loading level in the silicate layers. The reaction mixture was stirred for 4h, separated by filtration three times. Then the bionanocomposites films were dried at 50°C for 24h.

The influence on the amount of bentonite in the morphology, thermal and mechanical properties of the chitosan bionanocomposites were evaluated. Pure chitosan and chitosan/bentonite bionanocomposites films were characterized by infrared spectroscopy, X-ray diffraction, thermogravimetric analysis and mechanical tests. The morphology of the nanocomposites was affected by the ratio of chitosan/bentonite. Nanocomposites with intercalated morphology were obtained predominantly when the ratio of chitosan to bentonite was 5:1, while that the ratio 10:1 of chitosan/bentonite favored the formation of nanocomposites with exfoliated morphology predominantly.

References

HAN, Y.; LEE, S.; CHOI, K.; PARK, I. Preparation and characterization of chitosan–clay nanocomposites with antimicrobial activity, **Journal of Physics and Chemistry of Solids** 71 (2010) 464–467.

PILLAI, C.K.S.; PAUL, W.; SHARMA, C. P. Chitin and chitosan polymers: Chemistry, solubility and fiber formation, **Progress in Polymer Science** 34 (2009) 641–678.

VASSILIOU, A.A.; CHRISSAFIS, K.; Bikiaris, D.N. In situ prepared PET nanocomposites: Effect of organically modified montmorillonite and fumed silica nanoparticles on PET physical properties and thermal degradation kinetics, **Thermochimica Acta** 500 (2010) 21–29.

SINHA, V.R.; SINGLA, A.K.; WADHAWAN, S.; KAUSHIK, R.; KUMRIA, R.; BANSAL, K.; DHANWAN, S. Chitosan microspheres as a potential carrier for drugs, **International Journal of Pharmaceutics** 274 (2004) 1–33.

Plasma polymerization of methyl methacrylate on zirconium oxide particles for use in the preparation of bone cements

Escamilla-Coral Martin1, Ávila-Ortega Alejandro1, Cervantes-Uc José Manuel2

1. Facultad de Ingeniería Química, Campus de Ingenierías y Ciencias Exactas, Periférico Norte Kilómetro 33.5, Tablaje Catastral 13615, Col. Chuburná de Hidalgo Inn, C.P. 97203. Mérida, Yucatán, México
2. Centro de Investigación Científica de Yucatán, A.C.
Calle 43 No. 130. Col. Chuburná de Hidalgo, C.P. 97200, Mérida, Yucatán, México

1. miec_3205@hotmail.com

Introduction

Bone cements, or surgical cements, are polymeric biomaterials which are tolerated by the human body. These materials are used in clinical applications such as prosthesis fixation or procedures to treat spinal fractures (Percutaneous Vertebroplasty and Kyphoplasty). These cements are made mostly of two phases: a solid phase of Poly (methyl methacrylate) PMMA powder, benzoyl peroxide (BPO) and a contrast agent for X-rays as zirconium oxide and, a liquid phase formed by methyl methacrylate monomer (MMA), which polymerizes in situ during surgery, hydroquinone and an activator such as N, N-dimethyl-p-toluidine. A very important element in the conformation of this kind of cements is the contrast agent used, which is essential for the bone cement to be radiologically detectable. The addition of inorganic molecules within the polymer matrix produces that the mechanical strength and fracture toughness of cement decreases due to the incompatibility between them. These problems can be overcome by superficial modifications of zirconium oxide with plasma polymerization of MMA. Plasma polymerization can be used to modify diverse substrates without altering the bulk mechanical properties of the substrates although polymers obtained by this technique are significantly different from those produced by conventional techniques.

Materials and Methods

Zirconium oxide particles were modified with plasma polymer of methyl methacrylate (PPMMA). The modification was performed in an inductively coupled methyl methacrylate plasma reactor with 50 W (13.56 MHz) for 4 h and, 100 W for another 4 h at 5 X 10-1 Torr. The modified zirconium oxide particles were characterized by water contact angle, Fourier transform infrared (FT-IR), thermo gravimetric (TGA) analysis and Scanning Electron Microscopy.

Results and Discussion

The water contact angle results shows that surface of modified zirconium oxide particles were slight hydrophobic (56°+ 5) compared to the unmodified particles (0°). This behavior is due to the deposition of PPMMA. The FT-IR analysis of modified particles showed the presence of carbonyls at 1726 cm-1 (Figure 1) which indicates the presence of PPMMA; this was confirmed with TGA analysis which shows a 1 % of mass weight loss between 450°C and 340 °C which can be addressed to the degradation of the PPMMA (Figure 2).

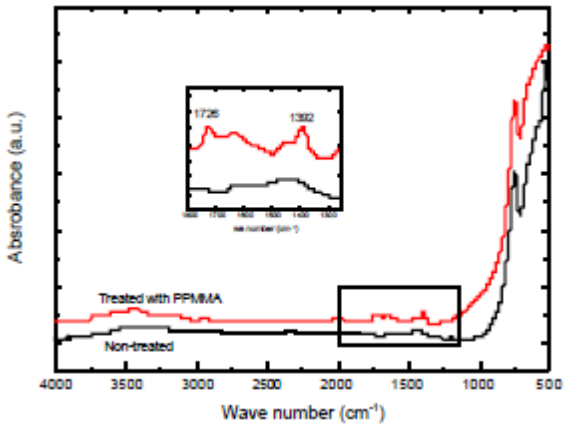

Figure 1. FT-IR analysis of zirconium oxide particles without and with modification with PPMMA

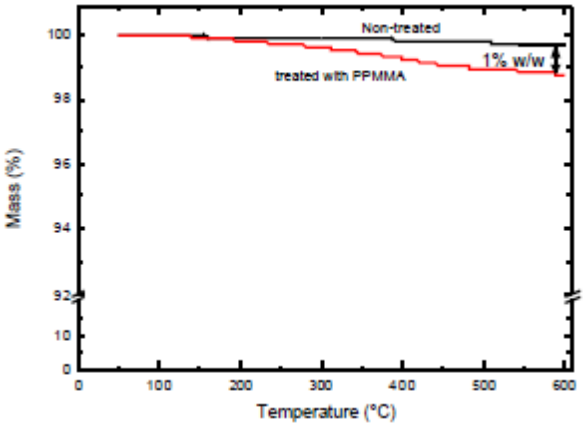

Figure 2. TGA analysis of zirconium oxide particles without and with modification with PPMMA

References.

1. P.K. Chua et al., Plasma-surface modification of biomaterials, Materials Science and Engineering R 36.
2. O. Cisneros, Preparación y caracterización de cementos óseos acrílicos con monómeros alcalinos para la preparación VPP y CP, Tesis, 2008.
3. M. P. Ginebra et al., Mechanical performance of acrylic bone cements containing different radiopacifying agents, Biomaterials 23, 2002.
4. H. K. Yasuda et al., Improvement of Fatigue Properties of Poly(methyl methacrylate) Bone Cement by Means of Plasma Surface Treatment of Fillers, J Biomed Mater Res.

Three-Dimensional Porous Biocompatible and BiodegradableScaffolds Based on PHAs

Julien Ramier, Estelle Renard, Valérie Langlois, Daniel Grande

"Complex Polymer Systems" Laboratory, Institut de Chimie et des Matériaux Paris -Est, 2 rue Henri Dunant, 94320 Thiais, France

E-mail: grande@icmpe.cnrs.fr

Introduction

Polyhydroxyalkanoates (PHAs) represent a class of aliphatic biopolyesters produced by different microorganisms as energy and carbon supply when they are subjected to stress conditions (limiting oxygen, nitrogen or other compounds)1,2. These biopolyesters possess interesting properties for various applications in the biomedical field as sutures, drug carriers, but also as scaffolds for tissue engineering, thanks to their tunable mechanical properties, and mainly due to their biocompatibility and biodegradability. Among the family of PHAs, poly(3-hydroxybutyrate) (PHB), poly(3-hydroxybutyrate-co-3-hydroxyvalerate) (PHBHV), and poly(3-hydroxybutyrate-co-3-hydroxyhexanoate) (PHBHHx) are increasingly used as bio-based systems involving in vitro and in vivo studies.

To engineer three-dimensional scaffolds with thin fibers as the extracellular matrix, the electrospinning technology is generally used to produce nanofibrous mats (Figure 1, as an example). Under the action of a strong electrical field, a jet of a concentrated solution is formed, stretched and the as-made fibers are collected3.

Three-dimensional nanofibrous scaffolds exhibit a high porosity, and a high specific surface which leads to better interactions with cells4. In our work, PHB, PHBHV, and PHBHHx have been electrospun in order to investigate the biological properties associated with the corresponding fibers. Additionally, block copolymers of PHBHV and PLA have been synthetized under microwave irradiation in order to develop different mats with tunable degradation properties.

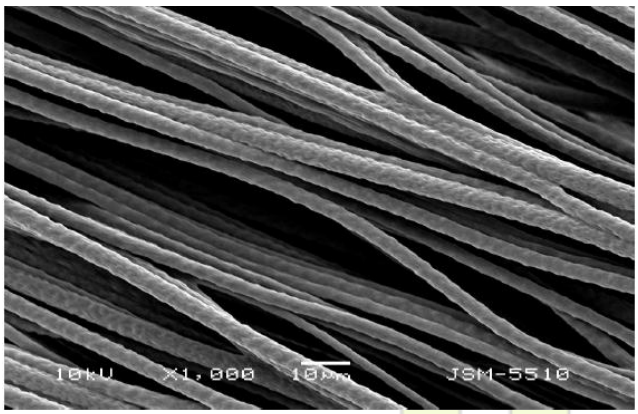

Figure 1. SEM micrograph of PHA nanofibers produced by electrospinning

Results and discussion

Nanofibrous PHA-based scaffolds were engineered by the electrospinning technique with concentrated solutions of the different PHAs in $CHCl_3$ and a $CHCl_3$/DMF mixture. Due to the low dielectric constant of $CHCl_3$ (4.8), highly viscous solutions were used, thus leading to the formation of fibers with a diameter between 3 and 4 µm. Because of a higher dielectric constant (36.7), DMF was added as a cosolvent to the $CHCl_3$ solution: the conductivity of the solution was significantly increased, and one such system enhanced the effect of the electrical field.

Indeed, the more conductive the solution, the higher the charge capacity of the solution, and the stronger the stretching forces, thus leading to the decrease of the fiber diameter. SEM analyses display PHB, PHBHV, and PHBHHx nanofibers with an average diameter of 900 nm. These mats with oriented nanofibers were formed with a smooth surface and a very homogeneous structure.

Among the different properties that distinguish a nanofibrous three-dimensional polymer scaffold and a polymeric film, wettability is of paramount importance.

Because of the higher specific surface of a nanofibrous mat, the water droplet is in contact to a larger surface. Therefore, the hydrophobicity of the PHA surface associated with a three-dimensional fibrous scaffold was higher than that of a two-dimensional flat surface.

This assertion was illustrated through the increase of the water contact angles of all PHAs.

In order to develop different scaffolds with tunable degradation properties, block copolymers based on PHBHV and PLA with various compositions were synthesized under micro-wave irradiation5,6. The LA polymerization was initiated by a PHBHV macroinitiator (M_n = 12000 g.mol^{-1}, I_p = 1.9). Using alow [LA]0/[PHBHV]0 initial ratio, the complete melting of the mixture turned out to be difficult, thus leading to quite moderate conversions. After a polymerization time higher than 5 minutes, the monomer conversion did not increase. Microwave-assisted procedures allow for fast and efficient reactions: in the system under investigation, the initiation efficiency was higher than 0.9.

Acknowledgements

The authors are indebted to Prof. I. Rashkov, Prof. N. Manalova, and Dr. O.Stoilova (Institute of Polymers, Sofia, Bulgaria) for their collaboration in the electrospinning technique.

References

[1] Vert, M. Biomacromolecules 2005, 6, 538-546.
[2] Zinn, M. et al. Adv. Drug Delivery Rev. 2001, 53, 5-21.
[3] Still, T. J. et al. Biomaterials 2007, 29, 1989-2006.
[4] Sombatmankhong, K. et al. Polymer 2007, 48,1419-1427.
[5] Zhang, C. et al. Macromol. Rapid Commun 2007, 28422-427.
[6] Ebner, C. et al. Macromol. Rapid Commun. 2011, 32, 254-288.

Preparation of polyvinylpyrrolidone (PVP) /polyethyleneglycol dimethacrylate (PEGMA) scaffolds for tissue engineering

B. Fernández-Montes Moraleda, L. M. Rodríguez-Lorenzo, M. Fernández-Gutierrez, J. San Román.

Institute of Polymer Science and Technology, CSIC. Juan de la Cierva 3, 28006 - Madrid, Spain.

bfernandezmontes@ictp.csic.es

Introduction

Tissue engineering has failed, up to date, to provide with satisfactory devices for bone regeneration. Two of the main factors that are hampering the general application of tissue engineering devices are:

i) Adverse effects of degradation products

ii) Long times required to produce an implantable construct

Inorganic filled polymer matrices have the potential to overcome these shortcomings. Inorganic components allow the tailoring of the resorption kinetics of the polymer matrix to the desired rate while improving the biocompatibility and promoting a faster integration with the hard tissue.

In this paper we propose the fabrication of porous scaffolds that include a polymeric matrix based on polyvinylpyrrolidone (PVP) with polyethyleneglycol dimethacrylate (PEGMA) and an inorganic filler based on hydroxyapatite (OHAp).

Materials and Methods

1-Vinyl-2-pyrrolidone (VP) (Aldrich) and polyethyleneglycol dimethacrylate (EGMA) (Acros) were chosen as the organic components for the preparation of the copolymer system. Composites materials have been prepared through a bulk polymerization induced thermally at 40°C using 1wt% azobis(isobutyronitrile) (AIBN) as free-radical initiator and a solution of chitosan as crosslinker under nitrogen atmosphere. OHAp particles were added to the monomer mixture prior to induce the polymerization.

The ceramic component added in different ceramic/polymer weight ratios: 0/100, 15/85 and 30/70. After washing the composites, the highly porous scaffolds were produced using a freeze-drying technique.

The prepared composites were frozen at a controlled rate (0.9 °C min^{-1}) to −20 °C and held for 90 min, The frozen suspensions were subsequently sublimed at 0 C for 20h under a vacuum of less than 100mTorr

The specimens were characterized by thermogravimetric analysis (TGA), ^{1}H nuclear magnetic resonance (NMR), attenuated total reflectance Fourier transformed infrared spectroscopy (ATR-FTIR), X-ray diffraction (XRD), and scanning electron microscopy (SEM).

Results and Discussion

TGA was the first analysis performed on the specimens, a weight loss between 316 and 480ºC can be observed for each of the compositions analyzed which corresponded to the decomposition and volatilization of the polymer component on heating. From the weight loss ceramic/polymer final ratio of the specimens were calculated. Ceramic/polymer weight ratios obtained are: 17/83 and 34/66. The deviation from the ratios utilized for the synthesis was lower than 3% confirming the reliability of the employed system.. FTIR was used to study the incorporation of both VP and PEGMA and OHAP in the system while NMR spectra confirmed the formation of the crosslinked polymers. XRD spectra of the specimens confirm that the only crystalline phase was hydroxyapatite. No secondary phases were formed during the processes of polymerization and frezze drying.

Development of highly porous scaffolds by a freeze-drying approach was used in this work due to the advantage of this method in employing only water upon freezing as a porogen. Freeze-drying conditions consisting of a relatively high freezing temperature (−20°C) and a rather slow rate of cooling (less that 1°C/min) were chosen to achieve the formation of highly connected ice crystals of rather large size. After sublimation of these ice crystals under vacuum at 0°C, sponges with an inner morphology (pore size, shape, distribution, interconnectivity, etc.) that mirrored the structure of these ice crystals were obtained

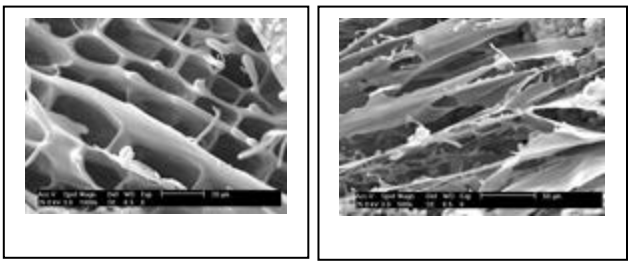

Left. Polymeric porous scaffolds(0/100). Right. Composite scaffold (15/85).

All scaffolds were highly porous and interconnected, and appeared to be relatively homogeneous throughout the bulk of the scaffold. A fairly uniform pore structure can be observed for ceramic free specimens (0/100) while the introduction of the ceramic seems to yield specimens with smaller pore interconnections.

Conclusions

Highly porous PVP/PEGMA/OHAp scaffolds containing different amounts of OHAp, with an interconnected pore structure, were produced in this study.

The freeze-drying technique proved to be an easy, versatile, effective and contaminant-free technique to produce scaffolds for tissue engineering

Chitosan and layered silicates bionanocomposites of preparation to be used as drug carrier vehicle

Itamara F. Leite, Samilla F. de Oliveira, Thaís Maria A. Marinho, Oscar L. Malta e Suédina Maria de L. Silva

Biopolymers (chitosan) and clay minerals (montmorilonita) are common ingredients in pharmaceutical products. Although they are frequently used in their pure form, a single polymer or clay mineral often does not meet all the requirements. A way to further extend their applications is to modify biopolymers by incorporation of inorganic fillers to obtain bionanocomposites with improved properties, especially for pharmaceutical applications. Chitosan (CS) is widely used as a drug delivery vehicle for control release of therapeutic agents. This polymer has been extensively used in recent years due to be non toxic and exhibit high mechanical strength, hydrophilic character, good adhesion beyond its low cost. Recently, synthesis of micro and nanocomposites with clay minerals was proposed as a novel approach to modify some of the properties of polysaccharide (chitosan), including swelling, hydrophilicity, mechanical and thermal behavior and bioadhesion. These modifications permit to obtain films of chitosan/layered silicates bionanocomposites with improved thermal and mechanical properties for use as a drug carrier vehicle. In this work, bionanocomposites of chitosan and natural bentonite were prepared by solution intercalation and the influence on the amount of bentonite in the morphology, thermal and mechanical properties of the chitosan bionanocomposites were evaluated. Pure chitosan and chitosan/bentonite bionanocomposites films were characterized by infrared spectroscopy, X-ray diffraction, thermogravimetric analysis and mechanical tests. The morphology of the nanocomposites was affected by the ratio of chitosan/bentonite. Nanocomposites with intercalated morphology were obtained predominantly when the ratio of chitosan to bentonite was 5:1, while that the ratio 10:1 of chitosan/bentonite favored the formation of nanocomposites with exfoliated morphology predominantly.

Synthesis and biocompatibility studies of P(HEMA-co-DMAEMA) based scaffolds obtained by cryopolymerization

Tiago Volkmer[1], Materials Lab, UNIFRA, Brazil

Joana Magalhães, Francisco Blanco, Elena F. Burguera J. Osteoarticular and Aging Research Lab, INIBIC, Spain

Vania Sousa, Luis Alberto Santos Biomaterials Lab, UFRGS, Brazil

Luis M. Rodríguez-Lorenzo, Julio San Román. Institute of Polymer Science and Technology, CSIC

[1]- Biomaterials Laboratory, Engineering School, Federal University of Rio Grande do Sul, Porto Alegre - Brasil.

E-mail: tiagovolkmer@unifra.br

Introduction

Cryopolymerization is a clean processing technique that produces highly hydrophilic and elastic porous materials. The method consists in the polymerization by a cryogenic treatment of a system potentially capable of forming a gel where the crystals of the frozen solvent are used as porogen agents. Structures obtained with this technique posse an elevated chemical and mechanical stability. A variety of polymeric cryogels have been prepared but the cryopolymerization technique has not been applied for the preparation of composite scaffolds for bone/cartilague tissue engineering up to date.

Scaffolds for tissue engineering should combine mechanical properties that resemble those of the tissue to be regenerate, porosity that allows cell seeding, cell migration and proliferation and extracellular matrix production and the ability to carry and release signaling molecules that induce or maximize cell phenotype

The goal of this project is the production of scaffolds that spread the range of applications of the cryopolymerization technique into the field of tissue engineering. The preparation of composite scaffolds based on 2-(Dimethylamino) ethyl Methacrylate (DMAEMA), 2-hydroxyethyl methacrylate (HEMA) and α-tricalcium phosphate (α-TCP) and the response of cultured human osteoblastic cells and human mesenchymal stem cells to the prepared cryogels are described in the current paper.

Materials and Methods

The selected monomers, 2-hydroxyethyl methacrylate (HEMA,) and 2- (Dimethylamino) ethyl Methacrylate (DMAEMA,), were purified through sequential extraction steps and vacuum distillation to remove impurities. Sodium persulfate, $Na_2S_2O_8$ was used as a REDOX initiator, and N,N,N´,N´-Tetramethylethylene diamine (TEMED) as an activator. α-TCP with an average particle size of 7.8 μm, was chosen as ceramic component.

Cryogels were prepared by free radical copolymerization in an aqueous solution at -20ºC. Drying of the cryogels was performed by direct freeze-drying. The obtained specimens were washed by immersion in distilled water for 2 h.

Total monomer amount was optimized at 10%. HEMA/DMAEMA ratio (25/75-50/50-75/25) were prepared with and without a 5% weight of TCP. Biocompatibility was tested with osteoblasts and MSCs isolated from bone marrow stroma. They were expanded until 90% confluent, then cultured on the different cryogels for 7, 14 and 21 days. Cell viability was assessed, after 96h, through the alamar blue assay. The cell distribution and morphology were determined by histological techniques. Expression of type-I collagen and alkaline phosphatase (ALP) were analyzed by immunohistochemistry.

Results and Discussion

This study explores the use of the cryopolymerization technique for the manufacture of scaffolds for bone tissue engineering. The challenge is to produce an appropriate pair surface-structure that favours new tissue ingrowth while maintains the integrity of the scaffold. The obtained dry scaffolds are rigid porous bodies with pore sizes up to 1 mm. Greater porosity (75%) and pore sizes (1 mm) were obtained for specimens containing a 25% of HEMA. Swelling ability is greater for 25/75 specimens, up to 500%, than for any other composition. DMAEMA is a pH sensitive monomer and conferred this property to all the prepared compositions influencing their swelling ability. i.e. 25/75 specimens swelled 5 times more at pH 2 than at pH 10. The Molecular weight between crosslinks decreased with the increase of the HEMA amount. α-TCP content did not affect significantly the aforementioned properties. However XRD diagrams shows that α-TCP did not converted into HA during the preparation of the cryogels

Cell response to scaffolds is strongly dependent on the material composition as well as on the cell type, for that reason, in this work, the biocompatibility of the manufactured scaffolds was studied using two different types of cells. After 96h, human osteoblasts and mesenchymal stem cells, had adhered and proliferated on the materials' surface. Material colonisation could be observed along the 21 days of culture, inferring their biocompatible profile. Expression of type-I collagen could be detected whilst the early osteogenic differentiation marker- ALP, expression appeared to be positively correlated with the increase of α-TCP.

Conclusions

Scaffolds with a 75% of porosity and pore sizes up to 1mm can be obtained with the cryopolymerization technique. It is possible to incorporate highly reactive α-TCP into these scaffolds.

Biocompatibility assays indicate that the materials tested are biocompatible, showing vital cells adhering to the materials, proliferating and giving evidence of early expression of biochemical markers of osteoblastic phenotype.

Cryopolymerization is a clean technique that yields promising porous structures for scaffold based bone engineering applications

DOPA Crosslinked Biopolymers

L. Pastor-Pérez, Z. Shafiq, V. San Miguel and A. del Campo

Max Planck Institute for Polymer Research, Ackermannweg 10, Mainz, 55128, Germany

e-mail: lourdes.pastor@mpip-mainz.mpg.de

Abstract : *3,4*-Dihydroxyphenylalanine (DOPA) residue and its derivatives are known to play a crucial role in the adhesive and hardening properties of mussel adhesive proteins. As such, DOPA can be regarded as an effective and biocompatible crosslinker that can replace chemically synthesized cross-linking reagents to form stable and biocompatible hydrogels. We report about the crosslinking reactions of DOPA with different biopolymers under different experimental conditions (type of polymer, pH and oxidant concentration).

Novel caged RGDs for photocontrol of cell attachment to artificial surfaces

M. Wirkner[(1)], *A.J. García*[(2)], *A. del Campo*[(1)]

[(1)]Max-Planck-Institut für Polymerforschung. Ackermannweg 10, 55128 Mainz, Germany
e-mail: wirkner@mpip-mainz.mpg.de

[(2)] Woodruff School of Mechanical Engineering and Petit Institute for Bioengineering and Bioscience, Georgia Institute of Technology, 315 Ferst Drive, Atlanta, GA 30332-0363, USA

The ability to trigger or turn 'on/off' material properties with external stimuli in order to control biological responses is critically important to biotechnological and biomedical applications. One such application is the use of light to trigger cell adhesion to synthetic materials by controlling the presentation of the bioadhesive arginine-glycine-aspartic acid (RGD) oligopeptide.
New caged cyclo[RGDfK] peptides, able to phototrigger cell attachment at defined volumes, have been developed. Cyclo[RGDfK] cell-adhesive peptide was modified by introducing a 3-(4,5-dimethoxy-2-nitrophenyl)-2-butyl or a 7-(diethylamino)-4-(hydroxymethyl)-coumarin ester photolabile caging groups at the carboxylic side chain of the aspartic acid. In their caged forms, the peptides do not show affinity for binding integrins at the cell membrane. Light of different wavelengths allows the selective release of the cages from the peptide structures and hence restores their activity, allowing in-situ site and temporal control of cell attachment. Cell-repellent materials modified with the caged peptides (OFF state) can therefore become cell-adhesive after irradiation (ON state) with the appropriate wavelength and intensity.

In a different approach, we focus on light-triggered cell release from surfaces based on the use of photocleavable linkers which couple the RGD ligand to the surface. Upon light exposure, the linker is cleaved by means of a photolytic reaction, thereby un-tethering the RGD peptide from the surface and releasing adhering cells (OFF state). Therefore we are able to specifically promote cell adhesion to materials with the ability to precisely deactivate or detach the cells at later time points or spatial locations. Our approach represents a more specific and controlled alternative to enzymatic or temperature-driven changes in substrate hydrophobicity. It is applicable to any material, provided proper linker design, and provides direct control over the molecular interactions involved in cell adhesion.

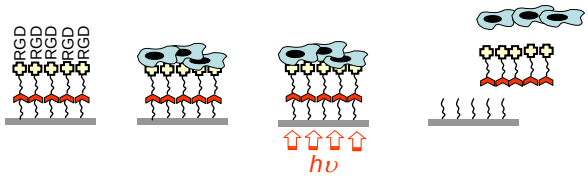

Figure 1: Working principle of phototriggered release particularized to cell detachment from surfaces using photocleavable linkers with an intercalated cage.

Two novel Poly-ether-ether-ketone (PEEK) applications for bone repair: assessment of dental implants and craniotomy closure devices.

Bárbara Pérez-Köhler[1], *Alberto Cifuentes-Negrete*[1], *Ana Rodríguez*[2], *Salvador Llas*[2], *Juan Manuel Aragoneses*[3], *Julia Bujan*[1], *Natalio García-Honduvilla*[1].

[1]Department of Medical Specialities, Faculty of Medicine, University of Alcalá, Madrid, Spain. Networking Research Centre on Bioengineering, Biomaterials and Nanomedicine (CIBER-BBN). Spain.
[2]Neos Surgery SL, Barcelona, Spain.
[3]Mississippi Institution, Madrid, Spain.

barbara.perez@uah.es

Introduction

Poly-ether-ether-ketone (PEEK) is a non-absorbable biopolymer widely used in the manufacture of several medical devices, such as trauma, orthopaedic or spinal implants. Due to its mechanical properties (e.g. elastic modulus), which are similar to bone, this biocompatible material has been tested in two possible clinical applications, involving opposite mechanical stress: closure of craniotomies and dental implants.

Material and Methods:

New Zealand white rabbits (n=6) underwent a 1.5 cm^2 craniotomy, and PEEK device (FC05, NEOS Surgery SL) was used to fix the removed bone fragments in their anatomical sites. Intracranial part of the device was in direct contact with the dura, and the subcutaneous part was placed over the dome. Bone healing was monitorized at day 30 (n=3) and 60 (n=3). Histopathologic studies were carried out to analyze the effects on the dura, and immunohistochemical techniques were performed to study the presence of macrophages. PEEK dental implants (Ilerimplant) were placed on 12 patients and Osstell values were measured to assess the performance of the device, according to the standard odontological procedures.

Results:

Despite of the common nature of both devices, PEEK dental implants did not accomplish the experiment. All patients showed an Osstell value below the acceptable limits, commiting the long-term-viability of the implants.

All animals reached the end of study, while only 1 of 6 presented subcutaneous infection, being attributable to surgical procedures. Histopathological examination at 30 and 60 days showed a good behaviour of PEEK, with normal morphology and dura without significant changes. The device allowed proper bone healing, evidenced at day 30 by the appearance of normal trabecular bone in the defect area, surrounded by a connective tissue from the subcutaneous area. Osteoid substance and new bone formation were observed, especially at day 60. Immunohistochemical studies confirmed the presence of macrophages surrounding the biomaterial.

Conclusions:

-PEEK dental implants are not as efficient at long term as traditional devices, probably due to the strong mechanical forces that occur in the jaw. However, these implants could be a low-cost alternative to temporal devices.

-The use of PEEK for bone fixing after craniotomy maintains the normal morphology of the meninges, and allows proper bone healing.

Acknowledgments:

Bone fixation devices have been granted by NEOS Surgery SL (Barcelona, Spain). Dental implants have been granted by Ilerimplant (Spain).

The present work was supported by grant BIOAVAN PSS-300000-2008-01

Sol-gel synthesis of silica-chitosan hybrids for bone regeneration

M. Suarez[1,2], *E. M. Valliant*[3], *Julian R. Jones*[3]

[1] Fundación ITMA, Parque Tecnológico de Asturias, 33428, Llanera, Spain.
[2] Department of Nanostructured Materials, Centro de Investigación en Nanomateriales y Nanotecnología (CINN). Principado de Asturias – Consejo superior de Investigaciones Científicas (CSIC) – Universidad de Oviedo (UO). Parque Tecnológico de Asturias, 33428 Llanera, (Asturias), Spain
[3] Department of Materials, Imperial College London, SW7 2AZ, UK.

m.suarez@cinn.es

Introduction

Bone and cartilage injuries compromise significantly the quality of life and significant socio-economic increasing problem, rising from an increasingly aged population and degenerative diseases or traumatic accidents. Chitosan is a copolymer of linked β(1→ 4), 2-amino 2-deoxy-D-glucose, and 2-acetamidodeoxy-D-glucan, which has been used for these applications as it is biodegradable, non-toxic and possesses antibacterial properties. For bone regeneration, polymers alone do not have sufficient compressive strength. Ceramic and glasses are too brittle. Interactions between inorganic and organic components are necessary to obtain a bioactive material that will degrade congruently. Hybrids provide this potential.

In this work, silica-chitosan hybrid biomaterials were synthesized by a sol-gel technique. Chitosan was covalently crosslinked with 3- glycidoxyproyltri-methoxysilane (GPTMS) in order to improve its physical and mechanical properties. The influence of the synthesis pH on the interaction between chitosan and GPTMS and on the bioactivity behavior was studied. Organic-inorganic hybrid with good mechanical properties was obtained and a clear effect of the pH value on these properties was found.

Materials and Methods

Chitosan (CS) solutions were prepared in wt% in distilled water at pH 2 and 5 fixed with 2 M hydrochloric acid. Then GPTMS (crosslinking agent) was added into the solution in a 1: 0.25 molar ratio of chitosan: GPTMS. Structural characteristics of the hybrid were investigated using FTIR. The chemical shifts of the ^{29}Si of powdered samples were measured with a solid-state nuclear magnetic resonance (NMR) spectrometer. The morphology of the surface and the cross-section of the hybrids were characterized using FEG-SEM. Hybrid samples were immersed in simulated body fluid (SBF) for up to 672 h and the solutions were analyzed by Inductively Coupled Plasma optical emission spectrometer (ICP-OES) to determine the Si, Ca and P concentrations in solution. Compression tests were performed using an Instron-type tensile testing machine (Instron 5866).

Results and Discussion

Chitosan is one of the most widely known natural polymers for biomedical applications due to its biocompatibility, biodegradability and low toxicity. In this study organic-inorganic hybrids were prepared using a sol-gel process since it is an effective method to be used for the synthesis of an inorganic network in an organic matrix at low temperature. Hybrids were formed with a range of mechanical properties from rigid to flexible depending on the content of polymer used (Figure 1). All of them were completely transparent, indicating a good integration of the organic and inorganic components. From the FTIR spectra (Figure 2), Si-O stretching bands were observed for chitosan-GPTMS-TEOS hybrids at 1110-1000 cm^{-1}, suggesting the formation of Si-O-Si bridging bonds on hybridization. The appearance of the Si-O-C bands at 795 cm^{-1} is seen in the hybrid monolithic spectra but are not visible in the pure chitosan spectrum, indicating that there is a definite interaction between the polymer and the silica components. The SEM image demonstrated that the hybrids were organized on the nanoscale with a homogeneous morphology and with silica nanoparticles being embedded within the chitosan matrix. This microstructure was dependent on the polymer content. The amount of soluble silica released from the hybrids after 1 month of soaking in SBF is shown in Figure 3. The physical interaction exists between GPTMS and chitosan at pH 2 produce a larger amount of silica releasing from the hybrid. The working pH influences in the mechanical properties. Compressive testing showed a Young´s modulus up to 2 times greater at pH 5 than at pH 2.

Figure1. Images for rigid (a) and flexible (b) materials

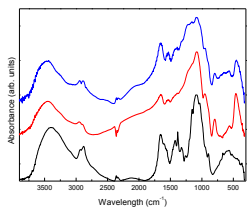

Fig. 2. FT-IR spectra of pure CS (black line), SiO_2: CS (65:35) (red line) and SiO_2: CS (35:65) (blue line).

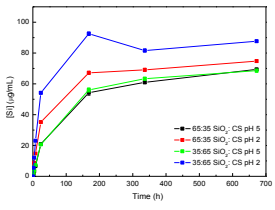

Fig. 3. Dissolution profiles for monoliths SiO_2: CS (65:35) pH 5 (black line), SiO_2: CS (65:35) pH 2 (red line), SiO_2: CS (35:65) pH 5 (green line) and SiO_2: CS (35:65) pH 2 (blue line) after soaking in SBF up to 672 h.

Conclusions

Class II organic-inorganic hybrids based on silica and a natural polysaccharide, chitosan, have described. The kind of interaction between chitosan and GPTMS has an influence in the degradation behavior and in the mechanical properties of the hybrids.

Hemoglobin Binding From Human Blood Hemolysate With Poly(glycidyl methacrylate) Beads

*Evrim Banu Altıntaş, Deniz Türkmen, Veyis Karakoç, Handan Yavuz and Adil Denizli**

Hacettepe University, Department of Chemistry, Biochemistry Division, Ankara, Turkey

denizli@hacettepe.edu.tr

Introduction: Hemoglobin (Hb), a tetrameric protein composed of two pairs of different subunits, is the iron-containing oxygen transport metalloprotein in the red blood cells in mammals and other animals[1]. The proteomic studies to identify low-abundance protein profiles and biomarkers in human blood have been largely affected by the high abundance of some proteins like Hb. It is estimated that 85% of the protein mass in human serum is comprised of only a few proteins[2]. The high-abundance proteins make detection of low-abundance proteins difficult, no matter which proteomic method is used[3,4]. Typical methods that have been published to bind Hb include tangential flow filtration, fast performance liquid chromatography, hydrophobic interaction chromatography, ion exchange chromatography and molecular recognition[5-10]. Recently, immobilized metal affinity binding has shown great potential in the binding studies and several types of metal affinity carriers have been applied to binding studies[11]. So far, no one study has been published using IMAC to deplete Hb from human blood for analyzing the proteome of human blood.

We used iminodiacetic acid (IDA) immobilized poly(glycidyl methacrylate) [PGMA] beads with chelated Cu^{2+} ions as a model carrier capable of selective binding of Hb from human plasma. PGMA was used as the basic matrix because of its known good mechanical strength, stability at neutral pH values even in wet conditions and high reactivity of the epoxy groups for surface immobilization. Epoxy-derived carriers seem to be almost ideal systems to develop very easy protocols for biomolecule immobilization[12,13].

Materials and Methods: IDA was covalently attached to the PGMA beads (1.6 µm in diameter). Cu^{2+} ions were chelated via IDA groups on PGMA beads for affinity binding of hemoglobin (Hb) from human blood hemolysate. The PGMA beads were characterized by scanning electron microscopy (SEM). The PGMA-Cu^{2+} beads were used in the Hb binding-elution studies. The effect of Hb concentration, pH and temperature on the binding efficiency of PGMA-Cu^{2+} beads was performed in a batch system.

Results and Discussion: Non-specific binding of Hb to PGMA beads in the absence of Cu^{2+} ions was very low (0.39 mg/g). The maximum Hb binding was 130.3 mg/g. The equilibrium Hb binding increased with increasing temperature. The negative change in Gibbs free energy ($\Delta G° < 0$) indicated that the binding of Hb on the PGMA-Cu^{2+} beads was a thermodynamically favorable process. The ΔS and ΔH values were 102.2 J/mol.K and -2.02 kJ/mol, respectively. Significant amount of the bound Hb (up to 95.8%) was eluted in the elution medium containing 1.0 M NaCl in 1 h. The binding followed Langmuir isotherm model with monolayer binding capacity of 80.3-135.7 mg/g. Consecutive binding-elution experiments showed that the PGMA-Cu^{2+} beads can be reused almost without any loss in the Hb binding capacity. To test the efficiency of Hb depletion from blood hemolysate, eluted portion was analyzed by fast protein liquid chromatography. The depletion efficiency for Hb was above 97.5%.

Conclusion: Proteomics research is a long-established part of biochemistry[14]. The depletion of high abundant proteins is often significant in diagnosis and therapy. The results obtained in this depletion study are consistent with published studies. We reached the Hb depletion amount up to 95.8%. In the light of this study we believe that the PGMA-IDA-Cu^{2+} beads offered the promising strategy with good depletion specificity and efficiency of Hb.

References:

1. B.J. Bain, R.J. Amos, D. Bareford, C. Chapman, S.C. Davies, J.M. Old, B.J. Wild, Br. J. Haem., 101 (1998) 783.
2. N.L. Anderson, N.G. Anderson, Mol. Cell Proteomics, 1 (2002) 845.
3. E. Tamahkar, C. Babaç, T. Kutsal, E. Pişkin, A. Denizli, Process Biochem., 45 (2010) 1713.
4. N. Bereli, G. Şener, E.B. Altıntaş, H. Yavuz, A. Denizli, Mater. Sci. Eng. C, 30 (2010) 323.
5. J. Elmer, P.W. Buchler, Y. Jia, F. Wood, D.R. Harris, A.I. Alayash, A.F. Palmer, Biotechnol. Bioeng., 106 (2010) 76.
6. M.L. Dimino, A.F. Palmer, J. Chromatogr. B., 856 (2007) 353.
7. X. Lu, D. Zhao, G. Ma, Z. Su, J. Chromatogr. A., 1059 (2004) 233.
8. C.T. Andrade, L.A.M. Barros, M.C.P. Lima, E.G. Azero, Int. J. Biol. Macromol., 34 (2004) 233.
9. A. Derazshamshir, G. Baydemir, M. Andaç, R. Say, I.Y Galaev, A. Denizli, Macromol. Chem. Phys., 211 (2010) 657.
10. Z.Y. Ma, Y.P. Guan, X.Q. Liu, H.Z. Liu, Langmuir, 21 (2005) 6987.
11. M. Karataş, S. Akgöl, H. Yavuz, R. Say, A. Denizli, A., Int. J. Biol. Macromol., 40 (2007) 254.
12. D. Horak, P. Shapoval, Polym. Sci. Polym. Chem., 38 (2000) 3855.
13. Y.X. Bai, Y.F. Li, M.T. Wang, Enzym. Microb. Technol., 39 (2006) 540.
14. L. Qin, X.W. He, W. Zhang, W.Y. Li, Y.K. Zhang, Anal. Chem., 81 (2009) 7206.

Biodegradable Fibrous Polymer Materials and Composites Prepared on the Basis of Plant Biomass

Andrzej Okruszek

Institute of Technical Biochemistry, Faculty of Biotechnology and Food Sciences, Technical University of Lodz, Stefanowskiego 4/10, 90-924 Lodz, Poland

andrzej.okruszek@p.lodz.pl

Within the Project "Utilization of biomass for the preparation of environmentally friendly polymer materials" various kinds of plant biomass are employed for the preparation of biodegradable fibrous polymer materials and composites by biotechnological methods, involving enzymatic or microbial processess. The major intermediates in the preparation of final products are cellulose nanofibres, tactical polylactide and biodegradable aliphatic-aromatic copolyesters.

For the preparation of cellulose nanofibres, a cellulose rich plant biomass is being utilized, including grass and straw of various cereals or other agriculture useful plants, as well as waste fibres from textile industry (cotton, linen). The biomass is first pretreated with physical and/or chemical methods including boiling, steam-explosion or treatment with certain chemicals. Multienzyme complex obtained from *Aspergillus* niger mould is utilized as the main enzymatic tool.

The synthesis of tactical polylactide is being performed by chemical polymerization of L,L-lactide, prepared from L-lactic acid. The latter is obtained by stereoselective fermentation of plant biomass, after its saccharidification by appropriate enzymes (*Aspergillus niger* preparations). The stereoselective microorganisms (bacteria) used for the fermentation were selected by classical microbiology methods from the environment. In this case patatoes, cereal grains or beet pulp are utilized as starting biomass.

The third path involves utilization of various oil-plant biomass, which on sequential treatment with lipase preparations obtained from *Mucor circinelloides* and *Mucor racemosus* moulds (structurization, hydrolysis) and appropriate chemical reactions (cycloaddition process, catalytic hydrogenation) are transformed into oligodiols/polyols with glyceride backbone. These will be copolymerized with appropriate reagents in order to produce new biodegradable aliphatic-aromatic copolyesters. The polyesters will be utilised for preparation of various fibrous polymers and composites.

The fibrous materials and composites prepared within this Project on the basis of abovementioned intermediates will be further utilized for obtaining new functional textiles and nonwovens with potential sanitary or technical applications, such as sweat-absorbing textile inserts, sanitary textiles, filtration materials, geotextiles and agrotextiles. Within this Project the processes of ageing and controlled biodegradation of prepared materials will be studied, as well as the conditions of their recycling and possible use of degradation products in agriculture.
The poster presents information about Project "BIOMASS" which is being realized within the time
frame 2009-2013 by the Consortium composed of eight research groups from Poland.
The Project (POIG 01.01.02-10-123/09) is partially financed by the European Union within the European Regional Development Fund

Bioactive Alginate Based Drug Delivery Microgels For Skeletal Tissue Engineering

Luis Rojo[1], *Helene Autefage*[1], *Seth McCullen*[1], *Eileen Gentleman*[1], *Molly M. Stevens*[1,2]

[1]Department of Materials and [2]Department of Bioengineering, Imperial College London, UK.

l.rojo-del-olmo@imperial.ac.uk m.stevens@imperial.ac.uk

Introduction: Development of musculoskeletal tissue requires the orchestration of cells, growth factors, scaffold, and physiological stimuli within a highly defined 3D architecture[1]. There is significant interest in the development of novel systems that can control the temporal-spatial delivery of soluble factors, whilst maintaining a 3D structure in which the cell population can receive appropriate physiological stimulation[2]. This work is focused on the preparation of bioactive alginate-poloxamer interpenetrating microparticles loaded with recombinant human transforming growth factor β3 (TGFβ3) to be used in musculoskeletal tissue regeneration. *In vitro* studies were performed to assess the viability of chondrocytes (C), chondroprogenitors (CP) and mesenchymal stem cells (MSCs) growing within pelleted alginate-poloxamer condensates. We also assessed the formation of cartilaginous matrix by culturing cells in alginate-poloxamer condensates for 3 weeks *in vitro*.

Materials and methods: Sodium alginate macromolecules were grafted with GRGDS pentapeptide and the microstructure and degree of modification was determined by ^{1}HNMR. Alginate-poloxamer microparticles loaded with model protein or TGFβ3 growth factor were prepared by w/o inverse emulsion and external gelation using $CaCl_2$ and $SrCl_2$ as crosslinking agents. Morphology and particle size distribution were examined by SEM and laser scattering respectively. *In vitro* model protein bioactivity, encapsulation efficiency and release profiles were determined by Ghaderi-Carlfors and BCA assays, respectively. Pelleted cell-microgel condensates were prepared by centrifugation of precultured bovine CP (10^6cells/ml) mixed with the alginate particles and cultured for three days. Cell viability was assessed using the LIVE/DEAD assay. Effect of cell type and alginate-poloxamer condensates on *in vitro* chondrogenesis was assessed via histological examination, by embedding condensates in paraffin, and staining 10 µm sections for proteoglycan production with Alcian Blue (AB) and for cell nuclei and extracellular matrix deposition via Hematoxylin and Eosin (H&E).

Results: GRGDS peptide prepared by conventional solid-phase was obtained in 87% yield and > 95% purity. The experimental efficiency of alginate modification was calculated by considering the resonance signals of the corresponding GRGDS protons (14H, 3.76 – 1.01 ppm) and alginate protons (2H, 4.46-3.82 ppm). The molar fraction of GRGDS moieties was found to be 0.09 indicating that the macromolecular chains consist mainly in guluronic-co-manuronic units with carboxylate groups available for the characteristic crosslinking reactions mediated by divalent cations, with 9 % of pendant GRGDS peptide moieties.

Alginate-poloxamer microparticles were prepared by a w/o emulsion method and model protein encapsulated within. As observed by SEM imaging, spherical and fairly homogeneous particles were observed with average size of 5 µm (Figure 1). Reconstituted particles in PBS showed swollen morphology during soaking leading to an enlarged particle diameter up to 25 µm as determined by laser diffraction measurements.

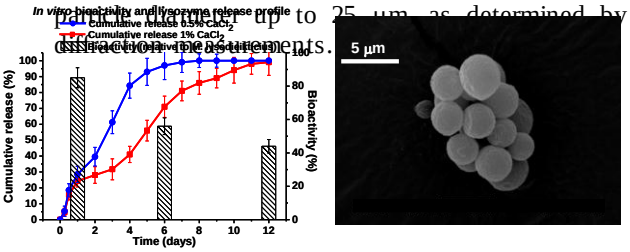

Figure 1. Bioactivity and lysozyme release profile (left) and SEM examination (right) from alginate-poloxamer particles prepared by w/o inverse emulsion method.

Drug release studies showed a 64% loading efficiency for the model protein with a tunable release profile during the first month. Additionally, protein released showed that 85% of the natural protein activity was conserved (Figure 1). Histological staining revealed significant differences in AB staining in a cell-specific manner, indicating that CP cells were able to synthesize a rich proteoglycan matrix compared to both C and MSCs cells (Figure 2). MSC-alginate poloxamer condensates yielded a poor cartilage like tissue with minimal matrix deposition.

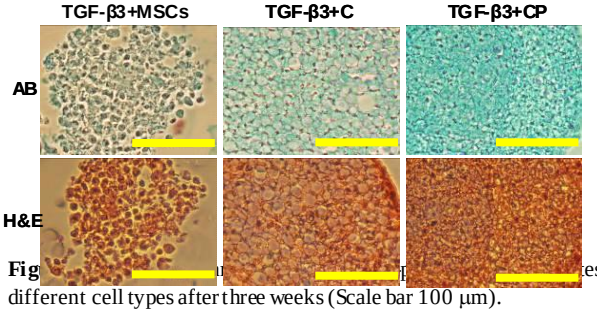

Figure 2. [illegible] with different cell types after three weeks (Scale bar 100 µm).

Conclusions: GRGDS cell adhesion peptides were covalently grafted onto alginate molecules for the preparation of novel poloxamer-alginate micro-scaffolds that deliver soluble factors in a temporal-spatial manner. These are potentially promising growth factors delivery systems enabling high encapsulation efficiency, tuneable protein release profiles and viability of entrapped cell condensates as useful for skeletal tissue engineering applications. Histological examination revealed cell-specific differences in proteoglycan staining intensity and distribution, suggesting that CP cells may be an optimal cell source of musculoskeletal repair and regeneration of cartilage.

Acknowledgment: Financial support from BBSRC Strategic longer and larger grants (LoLas). We thank C. Archer for advice on CP isolation.

References:

[1]Stevens MM et al. Science (2005) 310, 1135-1138.
[2]Stevens MM. Mater Today (2008) 11, 18-25.

Preparation of Protein-like Amphiphatic Polymers with Antimicrobial Activity

Angela Plum, Elisabeth Heine, Helmut Keul, Martin Möller

Institute of Technical and Macromolecular Chemistry, RWTH Aachen
and DWI an der RWTH Aachen e.V., Pauwelsstr. 8, D-52056 Aachen (Germany)

plum@dwi.rwth-aachen.de, keul@dwi.rwth-aachen.de

Introduction

Multi-resistant bacteria are nowadays an increasing problem especially in the medical sector. Therefore the demand for new antibacterial solutions is rising. To overcome the problem of excessive bacterial growth and contamination, one approach may be, to equip surfaces with antibacterial coatings.

The problem with common antimicrobial coatings is that these coatings often release their active compound into the environment. This causes two negative effects: 1. the antimicrobial effect is lost over time and 2. the long term effect resulting from the development of bacterial resistance and associated health risks etc. is not known. Therefore it is desirable to develop non-leaching coatings. Antibacterial polymers may be one solution.

The polymers developed herein are able to overcome these problems and can be used as non-leaching antimicrobial coatings.

Materials and Methods

In this work we present the functionalisation of poly(vinyl amine) (PVAm) to generate new non leaching antibacterial candidates. PVAm is a weak cationic polyelectrolyte and possesses the highest known cationic charge density for a technical polymer. Due to the high cationic charge density it shows very good adsorption behaviour to glass, metal and negatively charged surfaces (e.g. cellulose). Here, PVAm was further derivatised to display antibacterial properties.

The resulting products were characterised on the molecular level using NMR and Raman spectroscopy. The modified amphiphilic polymers were then coated onto surfaces and the antimicrobial effect was studied. Through variation of the degree of functionalisation of the amine groups with alkyl chains and quaternary ammonium groups, the influence of the hydrophilic/hydrophobic balance on the antimicrobial effect was investigated.

We assume that the alkyl chains and cationic groups self-assemble during the reaction and build up microstructures in the polymer. Samples with the same composition and different microstructure were prepared by simultaneous or sequential addition of functional epoxides to poly(vinyl amine) (PVAm).

Results and Discussion

Amphiphilic multifunctional poly(vinyl amine)s were synthesised and characterised by ^{1}H-, ^{13}C-NMR and Raman spectroscopy. The degree of functionalisation was adjusted by changing the ratio of functional epoxides to amine groups. The amphiphilic polymers thus obtained showed a good antibacterial effect against *E. coli*. From the antibacterial tests it can be concluded that the antibacterial action takes mainly place during the cell division (under growth conditions). It was found that the antibacterial activity increased with increasing degree of functionalisation with quaternary ammonium groups, and decreasing degree of functionalisation with alkyl chains.

The antimicrobial effect was investigated in dependence of the polymer microstructure.

Acknowledgment

This work is part of the NMP Project NanoBond which is funded by the European Commission (Grant agreement No. CP-TP 228490-2; 7th Framework Programme) (www.nanobond.org).